F 1103

R

REFERÁLVA

REVUE ROUMAINE DE CHIMIE

TOME 14

N° 1

Janvier 1969

ÉDITIONS DE L'ACADÉMIE DE LA RÉPUBLIQUE SOCIALISTE DE ROUMANIE

Rev. Roumaine Chim. 14, 1–146 (1969), Bucarest

COMITÉ DE RÉDACTION

Rédacteur en chef :

C. D. NENIȚESCU, membre de l'Académie de la République Socialiste de Roumanie.

Rédacteurs en chef adjoints :

A. T. BALABAN et V. E. SAHINI, membres correspondants de l'Académie de la République Socialiste de Roumanie.

Collège de rédaction :

C. DRĂGULESCU, RALUCA RIPAN, CR. SIMIONESCU, membres de l'Académie de la République Socialiste de Roumanie ; EM. BRATU, membre correspondant de l'Académie de la République Socialiste de Roumanie, Pr G. OSTROGOVICH, MARG. AVRAM, F. BADEA, D. MARCHIDAN, D. NEGOIU et D. SĂNDULESCU.

Les manuscrits, les livres et les revues proposés en échange, ainsi que toute correspondance seront envoyés à la rédaction :

REVUE ROUMAINE DE CHIMIE

23, str. Dumbrava Roșie, Bucarest, Roumanie.

REVUE ROUMAINE
DE
CHIMIE

ORSZÁGOS MŰSZAKI KÖNYVTÁR 1883

Tome 14, N° 1 Janvier 1969

Page

I. G. MURGULESCU, D. OANCEA and G. MINCU, Reactions between benzyl chloride and alkali alcoxides . . . . 3–15 ✓
V. E. SAHINI and A. O. FULEA, The force constants of $PH_4^+(T_d)$ 17–21
O. RADOVICI and N. TOTIR, Some kinetic aspects of anodic oxidation of methanol . . . . 23–27 ✓
D. CISMARU and ANGELA GEANGU-MOISIN, The oxidation of tungsten at high temperatures. The system $W + CO_2$ . . . . 29–34 ✓
ŞT. ZĂMÂRCĂ, LUCIA GANOVICI and I. GANOVICI, Self-diffusion of indium in liquid indium-aluminium alloys 35–43
E. SEGAL, Modèle du gaz électronique bidimensionnel dans la chimisorption sur métaux 45–55
CONST. GH. MACAROVICI et L. CZEGLÉDI, Combinaisons complexes avec des hydroxyacides. VII. Étude spectrophotométrique du système $TiO(ClO_4)_2$ – acide D-gluconique 57–66
N. PETRESCU, Viscosity and density of the molten InBi compound 67–77
A. POPESCU, E. SEGAL, A. IONESCU and A. SZABO, D.T.A., electrical conductivity and activity of some $Bi_2O_3-MoO_3$ catalysts 79–85
I. V. NICOLESCU and OLGA ŞERBAN, Study on the intermediates occurring in the octylation reaction of the aromatic nucleus with the catalysts $AlEt_2Cl$-RCl 87–94
J. SIECHOWSKI and J. SLIWIOK, The role of Cr^{+5} ions in the catalytic oxidation of soja oil . . . . 95–99 ✓
MARGARETA AVRAM, GH. D. MATEESCU and C. D. NENITZESCU, Investigations in the cyclobutane series. XX. Stereoisomeric 1.2.3.4-tetrabromocyclobutanes by the Hunsdiecker reaction 101–110
A. B. SUSAN and A. T. BALABAN, Reaction of pyrylium salts with nucleophiles. VIII. Triphenylpyrylium and methylamine: thermal degradation of N-methyl-2,4,6-triphenylpyridinium halides to methyl halides and 2,4,6-triphenylpyridines 111–120
F. HODOŞAN and N. ŞERBAN, Steroids in the adsorbed state. II. Reductions with sodium borohydride under heterogeneous conditions 121–124
H. H. MANTSCH, W. SEIFFERT and V. ZANKER, π-Electronic structure of acridine-N-oxide 125–133
C. CRISTESCU and VERONICA BADEA, 6-Azauracil derivatives with potential cytostatic activity. VII. Thionation of 5-benzylthio-6-azauracil 135–140
V. TĂMAŞ and C. BODEA, $TiCl_4$-carotenoid complexes. III. Action of $TiCl_4$ on carbonylcarotenoids (canthaxanthin, rhodoxanthin, β-apo-8′-carotenal) . . 141–145

Rev. Roumaine Chim. **14, 1–146 (1969). Bucarest**

Revue Roumaine de Chimie, **14**, 3–15 (1969)

REACTIONS BETWEEN BENZYL CHLORIDE AND ALKALI ALCOXIDES

I. G. MURGULESCU, D. OANCEA and G. MINCU

Faculty of Chemistry of Bucharest University, Physical Chemistry Department,
Bd. Republicii 13

Received April 22, 1968

The reactions between benzyl chloride and alkali alcoxides in alcoholic solutions were studied using methyl, ethyl, n propyl, n butyl, n amyl and n hexyl alcohols. The rate constants of these reactions were measured at different temperatures between 45° and 90°. The energies of activation and A factors were calculated. The dependence of the rate constants upon dielectric constants of the solvents was studied, regarding these reactions as ion-dipole reactions.

The reactions between benzyl chloride and alkali alcoxides have been little studied. Experimental data determined by different authors are not in agreement and interpretations are contradictory. Thus, Franzen [1] has found for the reaction between sodium ethoxide and benzyl chloride a rate coefficient equal with 6.88 l mol^{-1} min^{-1} at 50.6°. For the same reaction, von Brown and Engel [2] have found a rate coefficient equal with 7.86 l mol^{-1} min^{-1} at 31.6° and later Kindler [3] has found, at the same temperature, other value equal with 8.70 l mol^{-1} min^{-1}.

The discrepancy between specified experimental data can be correlated with different experimental conditions. Especially the presence of water can influence sensibly on the kinetic results because, as Farinacci and Hammet[4] have proved, water reacts in turn with benzyl chloride. In a comparative study on reactions of benzyl chloride, benzyl bromide and chloropicrine with pyridine and sodium methoxide, Tronov and Gerschewitsch [5] have found that benzyl chloride reacts 2.5 times faster with sodium methoxide than with pyridine. The kinetics of reactions between benzyl chloride and alkali alcoxides, just like the kinetics of SN reactions, generally speaking, raised some problems which have remained unsolved up to now.[6]

---

[1] H. Franzen, *J. prakt. Chem.*, (2), **97**, 61 (1918).

[2] F. von Brown and H. Engel, *Ann. Chem.*, **436**, 320 (1924).

[3] K. Kindler, *Ann. Chem.*, **452**, 119 (1927).

[4] N. Farinacci and L. Hammet, *J. Amer. Chem. Soc.*, **59**, 2547 (1937).

[5] B. Tronov and A. Gerschewitsch, *Chem. Zentr.*, **1928**, II, 771 and **1927**, II, 1145.

For a better characterization of these reactions and for contributing to the knowledge of SN reactions, we aim in this paper to study the kinetics of reactions between benzyl chloride and sodium alcoxides.

EXPERIMENTAL

Riedel benzyl chloride redistilled under low pressure was used. In order to dry the alcohols which were used, these were refluxed and distilled over calcium oxide and then over magnesium and iodine, according to the method indicated by Lund and Bjerrum.[7] Anhydrous methyl and ethyl alcohols were obtained in a column filled with molecular sieve of 4 Å. The residual water content was determined by Karl Fischer's method and was always found to be less than 0.01 %. Alkali alcoxides were prepared by dissolving metallic sodium in the appropriate alcohols in an inert gas (N_2) atmosphere.

Precautions were taken to remove the oxygen traces because alkali alcoxides suffer slight self-oxidations.[8] Metallic sodium, after having been washed in anhydrous alcohols, in two separated vessels, was introduced quickly in the reaction vessel, where it dissolved. The determination of the concentration of alcoxides thus obtained was made by titrating with salicylic acid in isoamyl alcohol in the presence of phenolphthalein.

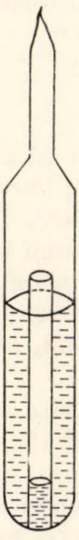

Fig. 1. — Sealed ampoule with two concentric compartments used as reaction vessel.

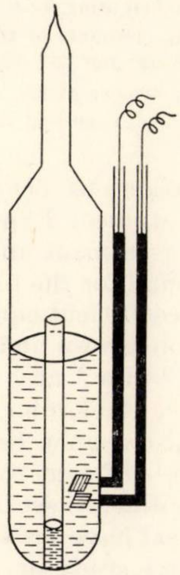

Fig. 2. — Sealed cell with two concentric compartments used for conductometric determinations.

The reactions were studied at different temperatures between 45° and 90° in a Höppler thermostat (±0,02°) up to a 80—90 % conversion. As reaction vessels, calibrated flasks directly introduced in the thermostat were used. After the solution of alcoxide has taken the temperature of the thermostat, benzyl chloride was added and the flask was strongly agitated, and then again introduced in the thermostat.

---

[6] O. A. Reutov, "Probleme teoretice ale chimiei organice", Ed. Acad. Bucharest, 1964. Translation from Russian, p. 134.

[7] H. Lund and N. Bjerrum, *Ber. dtsch. chem. Ges.*, **64**, 210 (1931).

[8] A. Le Berre, *Bull. Soc. Chim. France*, **1961**, 1198.

For analysis, aliquots were withdrawn from the flask at known times and discharged into a cooled Berzelius glass and titrated with salicylic acid (0.1 m).

Reagents were kept in Pellet burettes protected from atmospheric humidity by tubes filled with anhydrous $CaCl_2$.

At higher temperatures which exceed boiling points of inferior alcohols, sealed ampoules with two concentric compartments were used (fig. 1).

After the reagents have taken the temperature of the thermostat, these ampoules were strongly agitated and, at known times, one of them was suddenly cooled and broken. Measured amounts were titrated with salicylic acid.

Alcoholysis of benzyl chloride in methanol and ethanol was studied in sealed ampoules (fig. 1). Withdrawn aliquots were titrated with sodium alcoxides in the presence of phenolphthalein. The data obtained from these reactions were verified by a conductometric method using a sealed cell with two concentric compartments (fig. 2).

Electric conductivity of the system was measured by the a.c. Wheatstone-bridge method. The concentrations of HCl at different times were determined by using a curve of calibration. The curve of calibration was obtained using titrated solutions of dry HCl in the respective alcohols. Kinetic data obtained by both methods are in agreement.

For a better characterization of the reactions between benzyl chloride and sodium alcoxides, an examination of the dependence of the rate coefficient upon dielectric constants of the solvents (respective alcohols) was necessary.

For this purpose, dielectric constants were determined for the same range in which rate coefficients were measured (40–90°), using a DK 600 RL apparatus.

RESULTS

Simultaneous reactions occur between benzyl chloride and sodium alcoxides in the respective alcohols, according to the following scheme :

$$C_6H_5CH_2Cl + RO\,Na \rightarrow C_6H_5CH_2OR + NaCl \qquad (a)$$

$$C_6H_5CH_2Cl + ROH \rightarrow C_6H_5CH_2OR + HCl \qquad (b)$$

$$RO\,Na + H\,Cl \rightarrow ROH + NaCl \qquad (c)$$

$$(R \equiv CH_3,\ C_2H_5,\ C_3H_7,\ C_4H_9,\ C_5H_{11},\ C_6H_{13})$$

Reaction (b) has a much smaller rate as compared to reaction (a) and consequently can be neglected. In order to justify this simplification, rate constants for reaction (b) were given in table 1. Their values range from 10^{-4} to 10^{-3} $cm^3\ mol^{-1}\ sec^{-1}$ and really can be neglected in comparison with rate constants for reaction (a) which, as will be seen further on, are comprised in the range from 10^{-1} to 10^{1} $cm^3\ mol^{-1}\ sec^{-1}$. The other alcohols react still slower with benzyl chloride.

Table 1

Rate constants of alcoholysis reactions of benzyl chloride at 80°

System	k_2 (cm^3 mol^{-1} sec^{-1})	
	literature [9]	our values
$C_6H_5CH_2Cl + CH_3OH$	—	1.03×10^{-3}
$C_6H_5CH_2Cl + C_2H_5OH$	2.96×10^{-4}	3.57×10^{-4}

The reactions between benzyl chloride and sodium alcoxides in the respective alcohols can be now reduced to the simpler scheme:

$$C_6H_5CH_2Cl + RONa \rightarrow C_6H_5CH_2OR + NaCl$$

Experimental data showed that up to 80—90% conversion, the process is always bimolecular and verifies the kinetic equation:

$$k_2 = 2.303/t\,(a - b) \log b\,(a - x)/a\,(b - x) \tag{1}$$

where a and b are initial concentrations of reagents, x is the decrease in the concentration after time t, and k_2 is the second-order rate constant for the reaction. When $a = b$, equation (1) becomes:

$$k_2 = 1/t\,(1/a - x - 1/a) \tag{2}$$

Tables 2 and 3 show typical results for two rate constants. For each reaction, the obtained values are invariable, deviations being within the range of experimental errors.

At the same temperature, rate constants do not depend upon the initial concentrations of reagents. Also, as shown in table 4, rate constants do not depend upon the ratio between the initial concentrations of reagents.

Table 2

Rate constant of reaction $C_6H_5CH_2Cl + CH_3ONa$

$T = 60°$; $a = b = 0.1$ mol l^{-1}

t (minutes)	$(a - x)$ (mol l^{-1})	k_2 (cm^3 mol^{-1} sec^{-1})
0	0.1000	—
10	0920	1.44
20	0850	1.46
40	0750	1.38
60	0675	1.34
90	0565	1.42
120	0485	1.47
150	0445	1.38
185	0405	1.32
210	0365	1.38
240	0345	1.32
400	0240	1.32
500	0195	1.35
		Average 1.38

---

[9] B. Bensley and G. Kohnstam, *J. Chem. Soc.*, **1957**, 4747.

Table 3

Rate constant of reaction $C_6H_5CH_2Cl + C_6H_{13}ONa$

$T = 80°$; $a = b = 0.1$ mol l^{-1}

t (minutes)	$(a - x)$ (mol l^{-1})	k_2 (cm^3 mol^{-1} sec^{-1})
0	0.1000	—
5	0930	2.51
15	0800	2,78
30	0680	2.61
45	0570	2.79
60	0500	2.78
90	0415	2.61
120	0340	2.70
180	0245	2.85
240	0205	2.75
375	0135	2.85
		Average 2.72

Table 4

Rate constants of the reactions between benzyl chloride and sodium alcoxides for different proportions between the initial concentrations of the reagents (a is the concentration of sodium alcoxide)

T	a (mol.l^{-1})	$a : b$	k_2 (cm^3 mol^{-1} sec^{-1})
	$C_6H_5CH_2Cl + CH_3ONa$		
60	0.1	1 : 2	1.39
	0.1	1 : 1	1.37
	0.2	2 : 1	1.45
	0.3	3 : 1	1.39
	$C_6H_5CH_2Cl + C_2H_5ONa$		
70	0.1	1 : 2	4.02
	0.1	1 : 1	4.09
	0.2	2 : 1	3.92
	0.3	3 : 1	4.10
	$C_6H_5CH_2Cl + C_3H_7ONa$		
70	0.1	1 : 2	2.96
	0.1	1 : 1	2.96
	0.2	2 : 1	2.92
	0.3	3 : 1	2.78
	$C_6H_5OH_2Cl + C_4H_9ONa$		
70	0.1	1 : 2	2.38
	0.1	1 : 1	2.33
	0.2	2 : 1	2.30
	$C_6H_5CH_2Cl + C_5H_{11}ONa$		
70	0.1	1 : 2	1.72
	0.1	1 : 1	1.77
	0.2	2 : 1	1.79
	$C_6H_5CH_2Cl + C_6H_{13}ONa$		
80	0.1	1 : 2	2.83
	0.1	1 : 1	2.72
	0.2	2 : 1	2.77

Rate constants for investigated reactions at different temperature are given in table 5.

Table 5

Rate constants, k_2 ($cm^3\ mol^{-1}\ sec^{-1}$), of the reactions between benzyl chloride and sodium alcoxides at different temperatures

T	$C_6H_5CH_2Cl + RONa$					
	CH_3ONa	C_2H_5ONa	C_3H_7ONa	C_4H_9ONa	$C_5H_{11}ONa$	$C_6H_{13}ONa$
45	0.33	—	—	—	—	—
50	0.56	0.60	0.53	0.46	0.35	0.27
55	0.86	—	—	—	—	—
60	1.37	1.50	1.31	1.02	0.83	0.62
65	—	2.50	—	—	—	—
70	3.23	4.09	2,96	2.33	1.77	1.33
80	8.27	9.55	6.39	4.96	3.65	2.77
90	15.78	13.53	—	10.00	7.43	5.67

The reactions between benzyl chloride and sodium alcoxides can be regarded as ion-dipole reactions. In this case ($z = 1$), the rate constant is given by :

$$\ln k_2 = \ln A - E/RT - \mathrm{Ne}\,\mu \cos \theta / D r_0^2\, RT \qquad (3)$$

where A is the constant of the Arrhenius equation, E is Arrhenius energy of activation, D is the dielectric constant of the solvent, μ is the dipole moment of the polar molecule, r_0 is the distance between the ion and the dipole, and θ is the angle of inclination of the polar axis to the line joining its centre to that of the ion.

In order to prove dependency of the rate constants upon the dielectric constants, the folowing data are used (table 6) :

Table 6

Dielectric constants of the alcohols at different temperatures

T	D^{10}	D^{11}	D^{12}	D^{13}	D exp (our values)	D calc.
			CH_3OH $c = 196.4;\ L = 6.035 . 10^{-3}$			
0	37.92	37.5	—	37.92	—	37.82
10	34.05	—	—	—	—	35.57
20	33.58	33.7	—	—	—	33.49
25	31.50	—	32.63	—	32.50	32.51
30	—	—	—	—	31.50	31.53
40	—	—	—	—	29.70	29.58
50	—	—	—	—	28.00	27.95
60	—	—	—	—	26.25	26.31

---

[10] H. LANDOLT — R. BÖRNSTEIN, "Physikalisch-Chemische Tabellen", Verlag von Julius Spinger, Berlin, 1912, p. 1214.

[11] INTERNAT. CRIT. Tables, vol. VI, 1st Editor, McGraw Hill Book Co., New York, 1929, p. 83.

[12] "Handbook of Chemistry and Physics", 41st edition, Chemical Rubber Publishing, 1959—1960.

[13] "Spravochnik Khimica", Tom I, II. Izd. Gosudarstvennoe Nauchno-Tehnicheskoe Izdatelstvo khimicheskoi Literatury. Leningrad-Moscow, 1962, p. 956.

Table 6 (continued)

T	D^{10}	D^{11}	D^{12}	D^{13}	D exp. (our values)	D calc.
C_2H_5OH $c = 117.72$; $L = 5.285.10^{-3}$						
0	—	28.9	—	—	—	27.80
10	26.41	—	—	26.4	—	26.37
20	25.09	25.7	—	—	25.10	25.02
25	24.30	—	24.3	—	—	24.36
30	—	—	—	—	23.75	23.72
40	—	22.70	—	—	22.50	22.50
50	—	—	—	—	21.25	21.34
60	—	20.20	—	—	20.20	20.24
70	—	—	—	—	19.25	19.20
n C_3H_7OH $c = 162.12$; $L = 7.083.10^{-3}$						
0	—	24.5	—	—	—	23.43
20	21.7	21.8	—	—	20.30	20.32
25	19.7	—	20.1	19.7	—	19.62
30	—	—	—	—	19.00	18.96
40	—	—	—	—	17.76	17.65
50	16.6	—	—	—	16.40	16.44
60	—	—	—	—	15.25	15.31
70	—	—	—	—	14.25	14.26
80	—	—	—	—	13.30	13.07
97.12	—	11.83	—	—	—	11.56
n C_4H_9OH $c = 156.96$; $L = 7.515.10^{-3}$						
20	—	17.8	17.1	17.7	—	17.75
30	15.68	—	—	—	16.00	16.17
40	15.36	—	—	—	14.87	14.91
50	—	—	—	—	13.85	13.85
60	—	—	—	—	12.83	12.84
70	—	—	—	—	11.90	11.91
80	—	—	—	—	11.10	11.06
n $C_5H_{11}OH$ $c = 186.50$, $L = 8.582\ 10^{-3}$						
20	15.27	15.8	—	—	15.00	15.08
25	14.40	—	13.9	—	—	14.44
30	—	—	—	—	13.80	13.83
40	—	—	—	—	12.70	12.70
50	—	—	—	—	11.75	11.65
60	—	11.2	—	—	10.77	10.70
70	—	—	—	—	9.80	9.81
80	—	—	—	—	8.95	9.01
n $C_6H_{13}OH$ $c = 159.05$; $L = 8.607.10^{-3}$						
20	—	—	—	—	12.75	12.77
25	12.5	—	13.3	12.5	—	12.23
30	12.9	—	—	—	11.75	11.71
40	—	—	—	—	10.75	10.75
50	—	—	—	—	9.88	9.86
60	—	—	—	—	9.00	9.04
70	—	—	—	—	8.25	8.29
75	8.53	—	—	—	—	7.95
80	—	—	—	—	7.65	7.61

The variation with the temperature of the dielectric constants is given by the following equation :[14]

$$D = C \exp(-LT) \tag{4}$$

C and L having specific values.

Taking data from table 6 we have determined these constants for the alcohols used by us. The dielectric constants computed by using equation (4) are given in the last column of table 6. When a comparison is possible, it has been found that data of different sources are in good agreement. Figure 3 shows that the dependence of log D upon the temperature is perfectly linear.

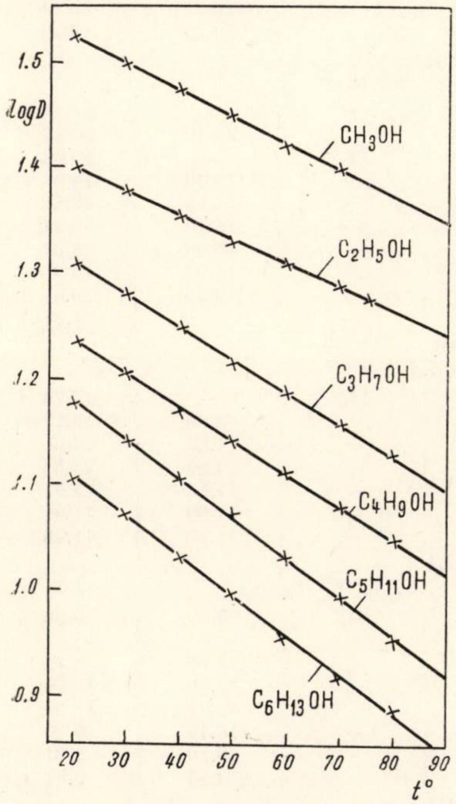

Fig. 3. — Influence of temperature on the dielectric constants of alcohols.

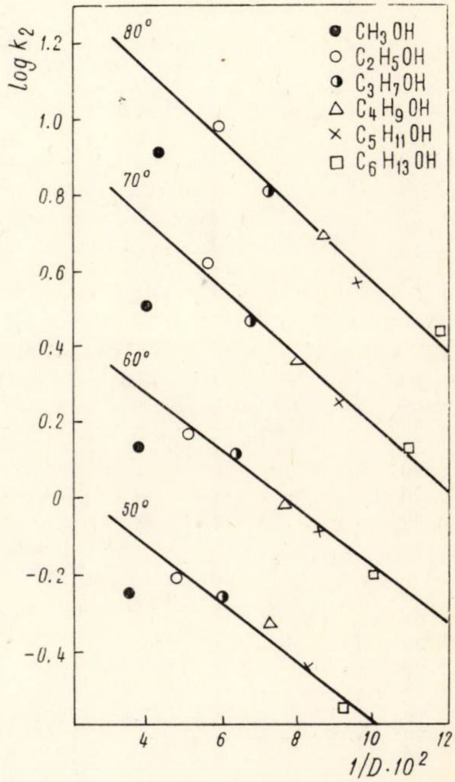

Fig. 4. — Influence of dielectric constants on the rate of reactions.

By plotting log k against $1/D$, it has been found a linear dependence at each temperature (Fig. 4).

The reactions with sodium methoxide have a smaller rate constant than expected. The variation of the rate constant upon the dielectric constant shows that the reactions between benzyl chloride and sodium alcoxides are really ion-dipole reactions. The curves plotted in figure 4 can be expressed in the following form:

---

[14] E. A. Moelwyn-Hughes, "The Kinetics of Reactions in Solution". 2nd edition, Oxford University Press, Amen House, London, 1947, p. 90.

$$\log k_2 = \log k_0 - B/D \tag{5}$$

By comparing with equation (3), we can obtain now the meaning both of the slopes of the curves and of the intercepts on the ln k axis:

$$\log k_0 = \log A - E/2.303\ RT \tag{6}$$

$$B = \mathrm{N\ e}\ \mu \cos\theta/2.303\ r_0^2\ RT \tag{7}$$

It has been found that B do not vary sensibly in the range of the temperature in which determinations were made (table 7).

Table 7

The values of B, r_0 and $\log k_0$ graphically determined

T	B	r_0 (Å)	$\log k_0$
50	6.667	2.91	0.160
60	6.601	2.88	0.540
70	6.596	2.84	0.945
80	6.539	2.81	1.290

By means of equation (7), the distance between ion and dipole can be estimated (the dipole moment of benzyl chloride is 1.82 Debye [15] and $\cos\theta$ can be replaced by its mean value in the range $-\pi/2 - +\pi/2$: $\overline{\cos\theta} = 2/\pi \approx 2/3$). In the 3rd column of table (7) are given the distances r_0 thus obtained. Their reasonable values about 3 Å are the same for all reactions.

The Arrhenius energy of activation E, and A constant of Arrhenius equation can be estimated with the help of equation (6). For this purpose, the data in the last column of table 7 can be used (the intercepts on the ln k axis in figure 5), or k_0 can be estimated directly from experimental data by means of equation (5). We have preferred this last method. The results thus obtained are given in table 8, and the mean values (the last column of table 8) are in good agreement with those found graphically (the last column of table 7).

Table 8

The values of $\log k_0$ (cm^3 mol^{-1} sec^{-1}) calculated by using equation (5)

T	$C_6H_5CH_2Cl + RONa$						Average
	CH_3ONa	C_2H_5ONa	C_3H_7ONa	C_4H_9ONa	$C_5H_{11}ONa$	$C_6H_{13}ONa$	
45	(−0.251)	—	—	—	—	—	—
50	(−0.014)	0.0854	—	0.151	0.110	0.106	0.113
55	(0.180)	—	—	—	—	—	—
60	(0.388)	0.506	0.550	0.523	0.532	0.527	0.528
65	—	0.732	—	—	—	—	—
70	—	0.954	0.934	0.922	1.021	0.923	0.951
80	—	—	1.309	1.285	1.293	1.296	1.296

---

[15] O. A. Reutov, loc. cit. Annex, Table 9.

When the mean values were calculated, the data regarding sodium methoxide were left out, since sodium methoxide has an abnormal behaviour.

The energies of activation and A factors can be graphically estimated by using the data given in table 8. The results thus obtained are given in table 9.

Table 9

Experimental and calculated kinetic parameters

Reaction	E (cal mol^{-1})	log A_{exp}	log A (calc. for RO$^-$)	log A (calc. for Na$^+$)
$C_6H_5CH_2Cl + CH_3ONa$	20 370	13.83	14.38	14.24
$C_6H_5CH_2Cl + C_2H_5ONa$	21 760	14.86	14.36	
$C_6H_5CH_2Cl + C_3H_7ONa$	20 570	14.12	14.36	
$C_6H_5CH_2Cl + C_4H_9ONa$	20 780	14.27	14.35	
$C_6H_5CH_2Cl + C_5H_{11}ONa$	21 000	14.41	14.35	
$C_6H_5CH_2Cl + C_6H_{13}ONa$	20 970	14.48	14.35	
		14.49	14.36	

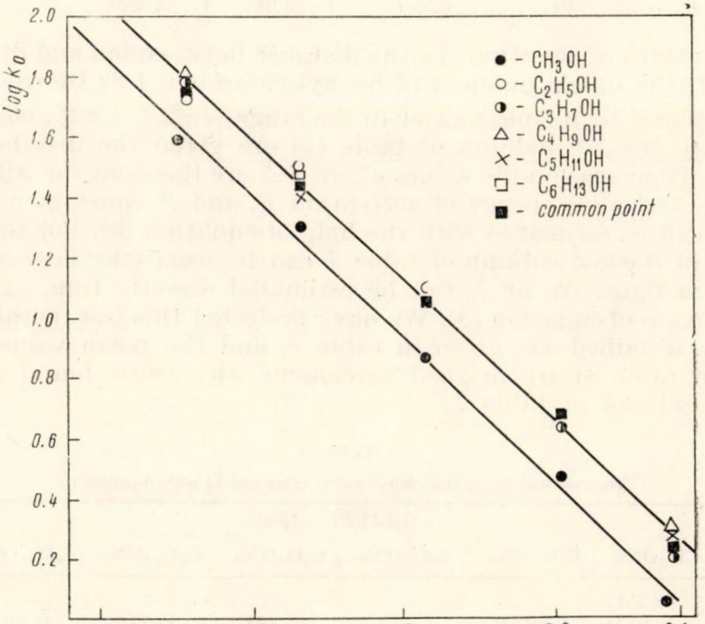

Fig. 5. — Influence of temperature on the rate of reactions.

The energy of activation has the same value for all reactions and its mean value is 20900 cal mol $^{-1}$. This result is drawn in figure 5.

Within the range of experimental errors, all the points are on the same line except those regarding sodium methoxide. At the same time, the line obtained for sodium methoxide by plotting log k against $1/T$, is fairly parallel with the first line ; hence, the energy of activation is roughly the same for all systems which have been investigated. The points regarding benzyl chloride-sodium ethoxide system are situated on a line with a slope which is a little greater than those regarding the other systems. A factors, given in the 3rd column of table 9 by their logarithms, have close and reasonable values ($1.5 - 3.0 \times 10^{14}$ cm^{3}mol^{-1} sec^{-1}), except the figure regarding sodium methoxide which has a smaller value. In the last column of table 9 are given A factors, computed by using the following equation :

$$A = N\sigma_{12}^2\,[8\pi \mathrm{RT}\,(1/\mathrm{M}_1 + 1/\mathrm{M}_2)]^{1/2} \tag{8}$$

which is fundamental in the collision theory.

The results are given at 60° (the mean working temperature). A factors found in this manner are in good agreement with those found experimentally.

In order to estimate molecular diameters, molecular volumes were used, which were related to the molecular diameters by the equation :

$$N\sigma^3 = Vm \tag{9}$$

which gives :

$$\sigma = 1.184 \times 10^{-8}\, Vm^{1/3} = 1.184 \times 10^{-8}\,(M/d)^{1/3} \tag{10}$$

where M is the molecular weight and d is the density of the liquid. Also, we assumed that molecular diameters of the alcohols in the liquid state do not differ from those of the appropriate alcoxide ions.

Table 10

Data regarding the alcohols used as solvents

	d 25° (g cm^{-3})	M	σ (Å)	σ_{12} (Å)
CH_3OH	0.7886	32.03	4.07	4.90
C_2H_5OH	0.7891	46.05	4.59	5.16
C_3H_7OH	0.7997	60.07	5.00	5.37
C_4H_9OH	0.8057	74.10	5.35	5.55
$C_5H_{11}OH$	0.8110	88.12	5.65	5.69
$C_6H_{13}OH$	0.8153	102.14	5.93	5.83
$C_6H_5CH_2Cl$	1.1030	126.51	5.74	—

In table 10 are given required data and ionic diameters thus obtained. The densities of the alcohols were taken from an earlier paper. [16]

In the last column, the mean diameters σ_{12} are given. Obtained values are reasonable and, introduced in the equation (7), give fairly good results.

---

[16] I. G. Murgulescu and Fl. Bărbulescu, *Rev. Roumaine Chim.*, **8**, 153 (1963).

DISCUSSION

According to the experimental results, the reactions between benzy chloride and sodium alcoxides are reactions between polar molecules and ions.

All these reactions require the same energy of activation equal with 20 900 cal mol^{-1}.

Also, *A* factors have a constant value, except the value regarding the reaction with sodium methoxide which is a little smaller.

This behaviour seems to be due to the strong molecular association of the methanol which diminishes the rate of reaction because of the "cage" effect.

Experimental values of the *A* factors ($1.3-2.5 \times 10^{14} cm^3 mol^{-1} sec^{-1}$) harmonize with those found by other investigators [17] for the analogous reactions in alcoholic solutions.

These regularities prove that the dimensions of RO^- do not influence the kinetics of the reactions between sodium alcoxides and benzyl chloride.

By inserting the dielectric constants of the alcohols into the equation of the rate constant (3) it is possible to explain satisfactorily the effect of solvent on the kinetic mechanism. This behaviour results from the chemical similitude of the different primary alcohols used as solvents. When the chemical features of solvents are very different, their influence on the kinetic mechanism cannot be explained only by their dielectric constants, as proved by the reaction between $(C_2H_5)_3N$ and C_2H_5I, studied by Mentschutkin. [18]

From the kinetic point of view, the reactions between benzyl chloride and alkali alcoxides can be regarded either as SN_2 reactions which occur by nucleophilic attack of RO^- on saturated carbon :

$$C_6H_5CH_2Cl + RO^- \longrightarrow C_6H_5CH_2OR + Cl^-,$$

or as systems of consecutive reactions :

$$C_6H_5CH_2Cl + Na^+ \xrightarrow[\text{slow reaction}]{} C_6H_5\overset{+}{C}H_2 + NaCl$$

$$C_6H_5\overset{+}{C}H_2 + RO^- \xrightarrow[\text{fast reaction}]{} C_6H_5CH_2OR$$

where the rate-determining step is the first reaction.

The rates of these reactions are determined by both the difference between bond energy of $C_6H_5CH_2$-OR and dissociation energy of $C_6H_5CH_2$-Cl, and the difference between electron affinity of Cl and RO^- according to the following decomposition into partial processes [19]:

---

[17] E. A. Moelwyn—Hughes, loc. cit., p. 123.

[18] Mentschutkin, *Z. phys. Chem.*, **6**, 41 (1890).

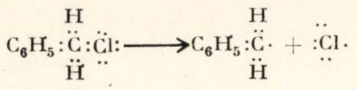

$$C_6H_5:\overset{H}{\underset{H}{\ddot{C}}}:\ddot{\underset{\cdot\cdot}{Cl}}: \longrightarrow C_6H_5:\overset{H}{\underset{H}{\ddot{C}}}\cdot + :\overset{\cdot\cdot}{\underset{\cdot\cdot}{Cl}}\cdot \qquad (a)$$

$$R:\underset{\cdot\cdot}{\ddot{O}}:^{-} \longrightarrow R:\underset{\cdot\cdot}{\ddot{O}}\cdot + e^{-} \qquad (b)$$

$$:\underset{\cdot\cdot}{\ddot{Cl}}\bullet + e^{-} \longrightarrow Cl^{-} \qquad (c)$$

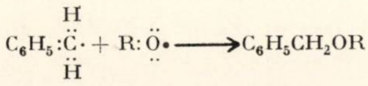

$$C_6H_5:\overset{H}{\underset{H}{\ddot{C}}}\cdot + R:\underset{\cdot\cdot}{\ddot{O}}\bullet \longrightarrow C_6H_5CH_2OR \qquad (d)$$

Since the mean values of the partial reactions (a) and (d) are comprised between 66.5 – 78 $kcal.mol^{-1}$ and 70 – 79 $kcal\ mol^{-1}$,[20] their difference is small. The remarkable nucleophilic reactivity of benzyl chloride-alkali alcoxides systems seems to be due to the great electron affinity of Cl, by comparison with the small affinity of RO^-.

In the 4th column of table 9, are given *A* factors computed by using the classical theory of collisions between reactant molecules for reactions between benzyl chloride and alkali alcoxides assumed to be SN_2 reactions.

The results are in good agreement with experimental values. In the last column of table 9 is given the *A* factor computed by admitting that these reactions occur always between benzyl chloride and sodium ion. The agreement with experimental values is also good.

The second explanation seems to be more plausible because all reactions occur with the same activation energy and RO^- does not influence on the rates of reactions, but the alcohols exert such an influence by their dielectric constants. The result seems to be due to the fact that, in any case, there occurs the same reaction – between benzyl chloride and sodium ion.

---

[19] C. D. NENITZESCU, "Chimie Organică", vol. I, 5th edition, Bucharest, 1960, p. 173.

[20] H. A. STAAB, "Einführung in die theoretische organische Chemie", Wernsuim, 1966, p. 172.

Revue Roumaine de Chimie, **14**, 17 – 21 (1969)

THE FORCE CONSTANTS OF PH_4^+ (T_d)

V. E. SAHINI and A. O. FULEA

Physical Chemistry Department, Bucharest University, Bd. Republicii 13

Received June 18, 1968

From the isotopic effect in the vibration spectrum of PH_4^+ and PD_4^+ the anharmonicity factors, the harmonic wave numbers, all the symmetry force constants and all the seven constants of the most general square potential are calculated.

The object of the present paper is the calculation of the anharmonic corrections and of the force constants of the PH_4^+, using the vibration spectra of PH_4^+, respectively PD_4^+.

In contrast with the case of the isotopic pair XY_4, X^*Y_4 (T_d), where isotopic splittings are not sufficient for the determination of all anharmonicity constants, in the case of the isotopic pair XY_4, XY_4^*(T_d) all four normal vibrations are different for XY_4 and respectively XY_4^* and there is a possibility to compute all the anharmonicity constants. An evaluation without application of the anharmonic correction leads to errors of about 10% or even more.[1]

The calculation of force constants with the anharmonicity correction after Dennison have been effected for NH_4^+[2] and BH_4^-.[3,4]

In the first two columns of table 1 are given the wave numbers for the normal vibrations of PH_4^+ respectively PD_4^+. As shown in table 1, two

Table 1

Wave numbers [(a)] in cycles/cm of the normal vibrations

Vibration	PH_4^+	PD_4^+	PD_4^+
σ_1 (A_1)	2 304	(1625)	1 625
σ_2 (E)	1 040	777	777
σ_3 (F_2)	2 370	1740 (E)	1 740
		1658 (B_2)	
	930	701 (B_2)	683
σ_4 (F_2)		683 (E)	

[(a)] The numerical values are taken from K. Nakamoto, Infrared and Coordination Compounds, John Willey, New York, 1964, page 104.

---

[1] D. M. Dennison, *Rev. Modern Phys.*, **12**, 175 (1940).

[2] S. Sundaram, *J. Chem. Phys.*, **33**, 708 (1960).

[3] N. Brearly and S. Sundaram, *Z. phys. Chem.* (*Frankfurt*), **32**, 219 (1962).

[4] K. V. Venkateswarlu and M. Radhakrishnan, *Czech. J. Phys.* **14**, 848 (1964).

values are given for the wave numbers of the treble degenerate vibrations of the PD_4^+ ion, due to the mode of obtaining the vibration spectrum of this ion.[5] In comparison with the ion PH_4^+ spectrum, effected under the same conditions, we chose — as being closest to the real value of a vibration F_2 — the wave number of the vibration E, corresponding in the symmetry V_d.

As a matter of fact, for PH_4^+ in table 2 [5] the vibration E for the pellet spectrum differs very little from vibration F_2, whilst vibration B_2 differs much. In the last column of table 1 we put down the values we shall use in this article.

Considering an isotopic couple XY_4, XY_4^* according to,[1] we may write :

$$\omega_i = \sigma_i (1 + x_{ii}) \tag{I}$$

$$\omega_i^* = \sigma_i^* \left(1 + x_{ii} \frac{\omega_i^*}{\omega_i}\right) \simeq \sigma_i^* \left(1 + x_{ii} \frac{\sigma_i^*}{\sigma_i}\right) \tag{II}$$

where : ω_i = the harmonic wave number,
σ_i = the observed wave number,
x_{ii} = the anharmonicity factor.

The relation $\frac{\omega_i}{\omega_i^*}$ is given [6] for each symmetry species. Out of this relation and of the relation $\frac{\sigma_i}{\sigma_i^*}$ we can easily obtain x_{ii}.

The wave numbers ω (cycles/cm) and the values of the anharmonicity factors are given in table 2.

Table 2 shows that for the vibration E an unusually high value of the anharmonic correction is obtained. According to table 1 the vibration E is the only normal one of the PD_4^+ ion for which a sure value is given in the literature. Yet, it might be that the assigning of the value of the wave number σ_2^* (E) as 777 be erroneous. That would account for the too high value of x_{ii} for this vibration. If assigning of the value 777 cm^{-1} is erroneous, the value we have to calculate for F_{22} will be higher by about 20% than the real one, affecting however little enough the values of f_α, $f_{\alpha\alpha}$, $f'_{\alpha\alpha}$ as can easily be seen from their expressions and from the value of F_{22}.

Table 2

Anharmonicity factors and harmonic wave numbers

Vibration	$\frac{\sigma_i}{\sigma_i^*}$	PH_4^+		PD_4^+	
		x_{ii}	ω (cycles/cm)	x_{ii}	ω (cycles/cm)
A_1 stretching	1.395	0.070	2 465	0.050	1 735
E bending	1.338	0.271	1 322	0.196	932
F_2 stretching	1.362	0.040	2 465	0.029	1 790
F_2 bending	1.362	0.040	967	0.029	703

---

[5] J. V. Martinez and E. L. Wagner, *J. Chem. Phys.*, **27**, 1110 (1957).

As the other four force constants to be calculated are not functions of F_{22}, they will not change at an eventual redistribution of σ_2^*.

The secular equation we have to solve is :

$$|FG-\lambda| = 0 \tag{III}$$

The matrix F is given,[6] for G one may see,[7] and $\lambda = 4\pi^2 c\omega^2$. We will work with the matrixes F and G in symmetry coordinates. The significance of the force constants F_{ij} we work with is given below :

vibration A_1 $$\begin{array}{c|c} & S_r^{(A_1)} \\ \hline S_r^{(A_1)} & F_{11} \end{array}$$

vibration E $$\begin{array}{c|c} & S_\alpha^{(E)} \\ \hline S_\alpha^{(E)} & F_{22} \end{array}$$

vibrations F_2 $$\begin{array}{c|c|c} & S_r^{(F_2)} & S_\alpha^{(F_2)} \\ \hline S_r^{(F_2)} & F_{33} & rF_{34} \\ \hline S_\alpha^{(F_2)} & & r^2F_{44} \end{array}$$

The secular equation is divided into the following equations :

$$F_{11} = 4\pi^2c^2m_Y\omega_1^2 \tag{IV}$$

$$F_{22} = 4/3\pi^2c^2m_Y\omega_2^2 \tag{V}$$

$$\left(m_x + \frac{4}{3}m_Y\right)F_{33} + \left(2m_x + \frac{16}{3}m_Y\right)F_{44} - \frac{16}{3}m_YF_{34} = 4\pi^2c^2m_xm_Y(\omega_3^2 + \omega_4^2) \tag{VI}$$

$$(2m_x + 8m_y)\ (F_{33}F_{44} - F_{34}^2) = [4\pi^2c^2]^2\ \omega_3^2\omega_4^2m_xm_Y^2 \tag{VII}$$

Considering also the isotopic effect, we obtain from equation (VI) :

$$\left(m_x + \frac{4}{3}m_Y^*\right)F_{33} + \left(2m_x + \frac{16}{3}m_Y^*\right)F_{44} - \frac{16}{3}m_Y^*F_{34} = 4\pi^2c^2m_xm_Y^*(\omega_3^{*2} + \omega_4^{*2}) \tag{VIII}$$

where m_x, m_Y = the atomic masses in g.

From the equation (VII) and (VIII) we obtain F_{33} and F_{44}, functions of F_{34}, all expressed in mdyn/Angstrom :

$$F_{33} = 2.534 - 4F_{34}$$

$$F_{44} = 0.688 + 2F_{34}.$$

---

[6] E. B. Wilson, J. C. Cross and P. C. Decius, "Molecular vibrations", McGraw-Hill, New York, Toronto, London, 1955, p. 303.

[7] V. E. Sahini and A. O. Fulea, *Rev. Roumaine Chim.*, **11**, 1045 (1966).

Substituting F_{33} and F_{34} in (VII) we obtain :

$$F_{34} = -0.207\,;\ +0.477.$$

Table 3

Symmetry constants of PH_4^+ in mdyn/Ansgtrom

Force constant	Solution 1	Solution 2
F_{11}	3.585	3.585
F_{22}	0.344	0.344
F_{33}	3.362	0.626
F_{34}	−0.207	0.477
F_{44}	0.274	1.642

The two sets of symmetry force constants are given in table 3.

According to the physical significance of the force constants, we chose solution 1 as being closest to reality.

By the aid of the relations between the symmetry force constants and the valency force constants given below,[2] we can obtain all the seven valency force constants. These are given in the first column of table 4, and their physical significance may be seen in work.[7]

$$f_r = \frac{F_{11}+3F_{33}}{4};\quad f_{rr} = \frac{F_{11}-F_{33}}{4}$$

$$f_{\alpha r} = \frac{F_{34}}{\sqrt{8}} = -f'_{\alpha r}$$

$$f_{\alpha} = \frac{2F_{22}+3F_{44}}{6};\quad f_{\alpha\alpha} = -\frac{F_{22}}{6};\quad f'_{\alpha\alpha} = \frac{2F_{22}-3F_{44}}{6}$$

Table 4

Valency force constants of PH_3 and PH_4^+ in mdyn/Angstrom

Valency force constant	PH_4^+	PH_3^8
f_r	3.418	3.32847
f_{rr}	0.056	0.05482
$f_{\alpha r}$	−0.073	−0.051551
$f'_{\alpha r}$	+0.073	−0.005323
f_{α}	0.299	0.361587
$f_{\alpha\alpha}$	−0.057	−0.014171
$f'_{\alpha\alpha}$	+0.045	—

Sundaram and his co-workers [8] have calculated all the force constants for PH_3. Since the constants for the interactions between stretchings and bendings, for the bendings and for the interactions between bendings are given in other units than those used by us in the present work, we have transformed them all to be expressed in mdyn/Angstrom. Thus expressed, the force constants determined in work [8] are gathered in the second column of table 4. As may be seen in table 4, there is a very good concordance for f_r, f_{rr}, $f_{\alpha r}$ and a good enough one for f_α and $f_{\alpha\alpha}$. Reassigning of the spectrum band E would diminish $f_{\alpha\alpha}$ in absolute value up to approx. -0.04.

---

[8] S. Sundaram, F. Suszek and F. F. Cleveland, *J. Chem. Phys.*, **32**, 251 (1960).

As for PH_3 $f_{\alpha r}$ is much differing from $f'_{\alpha r}$ and $f_{\alpha r}$ of the same molecule is close to the $f_{\alpha r}$ of the PH_4^+ ion, it results that we cannot obtain a concordance between the force constant $f'_{\alpha r}$ of PH_4^+ and respectively $f'_{\alpha r}$ of PH_3.

Revue Roumaine de Chimie, **14**, 23–27 (1969)

SOME KINETIC ASPECTS OF ANODIC OXIDATION OF METHANOL

O. RADOVICI and N. TOTIR

Institute of Physical Chemistry of the Academy, Bucharest, str. Galaţi 31

Received April 5, 1968

The anodic oxidation of methanol on platinized-platinum electrodes in acid and alkaline media has been studied. The experiments were carried out by cyclic voltametry. Our results have shown that the first step of anodic oxidation of methanol is the process of chemisorption, which depends to a great extent on the electrochemical treatment of the electrodes.

INTRODUCTION

Considerable work was devoted to the study of the mechanism of anodic oxidation of methanol on platinum or catalytic metals. This mechanism is very complex and is strongly influenced by the surface condition of the electrode, and by the nature and concentration of the reacting species.

Pavela [1] was the first to establish direct experimental evidence for the adsorption of methanol on Pt electrodes. In his interpretation, Pavela has shown that the hydroxylic hydrogen atom is expelled far easier in this process.

However Bellinger and Long [2] have found only 3% CH_3O^- radical in the alkaline solutions of methanol.

Bagotzky [3] and co-workers concluded that only adsorbed species are oxidized and that the catalytic activity of the electrode is modified by the formation of various kinds of surface oxides. The works of Frumkin [4] and co-workers lead to the conclusion that the potentials of a platinized-platinium electrode in methanol solutions are determined by the adsorbed hydrogen, resulting from the chemisorption of methanol.

The present work is concerned with the influence of the electrochemical treatment of the platinized-platinum electrode, on methanol chemisorption.

---

[1] T. O. Pavela, *Ann. Acad. Sci. Fennicae*, A II, **59**, 1 (1954).

[2] P. Ballinger and F. A. Long, *J. Amer. Chem. Soc.*, **82**, 795 (1960).

[3] V. S. Bagotzky and Yu. B. Vassiliev, *Electrochim. Acta*, **9**, 869 (1964).

[4] O. A. Petry, B. I. Podlovchenko, A. N. Frumkin and Hira Lal, *J. Electroanalyt. Chem.*, **10**, 253 (1965).

EXPERIMENTAL

A glass cell with separated anodic and cathodic compartments was used, containing in the anodic compartment the working electrode of platinized-platinum (Pt/Pt) electrode sealed in glass to expose a geometric area of $10.2 \cdot 10^{-2}$ cm^2, and an auxiliary Pt/Pt electrode in the cathodic compartment. The electrodes were platinized for 15 minutes by means of a 3% chloroplatinic acid + 0.025% lead acetate at a current density of 10 mAcm^{-2}. As reference electrode a saturated calomel electrode was used. The arrangement of the electrode in the cell is shown in figure 1.

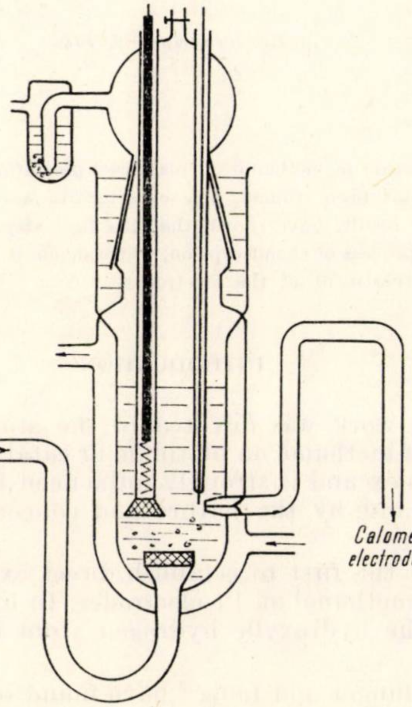

Fig. 1. – Electrolytic cell.

The supporting electrolyte (H_2SO_4 or NaOH) was prepared from p. a. reagents and conductivity water. Spectroscopic grade methanol was used. Before measurements the solutions were deaerated by bubbling pure argon for 3 hours, and the methanol was introduced into the anode compartment under argon flow. The solution was stirred before measurements by strong bubbling of argon.

The experiments were carried out by cyclic voltametry using a Tacussel instrumentation. The triangular voltage sweep had a sweep rate of 18 mV/s.

All measurements were performed at 25 ± 0.1°.

RESULTS AND DISCUSSIONS

We have studied the behaviour of a platinized-platinum electrode treated and untreated electrochemically.

The idea of the electrochemical treatment of platinum electrodes derived from the work of Bagotzky and Vassiliev [3] who utilized in their experiments electrodes activated by means of cathodic anodic activation, and from the fact that the process of chemisorption and oxidation of methanol is very much accelerated by the presence of different oxides in the catalyst, (platinized-platinum electrode).

The procedure of our electrochemical treatment was as follows : the platinized-platinum electrodes were anodically polarized in supporting electrolyte solutions (H_2SO_4 or NaOH) by a triangular sweep or saw tooth sweep with a sweep rate of 18 mV/sec. In this process some active species are formed on the electrode surface. After this treatment methanol was introduced in the supporting electrolite and a new triangular sweep (cyclic voltametry) was applied on the electrode. The kinetic current was recorded simultaneously.

An anodic triangular sweep was also applied on the Pt/Pt electrodes immersed in acid or alkaline methanol solutions without a previous electrochemical treatment.

In figure 2 are presented the anodic polarization curves of Pt/Pt electrodes with and without a previous treatment obtained by cyclic voltametry in a NaOH supporting electrolyte in the presence of methanol. Only the peaks for adsorbed hydrogen oxidation are shown.

Figure 3 presents the same curves as described in figure 2 for H_2SO_4 solutions as supporting electrolyte. In this figure the first two small peaks are for adsorbed hydrogen oxidation and the next for anodic oxidation of methanol.

Figure 4 shows the oxidation curves of adsorbed hydrogen and methanol at different concentrations of methanol in the supporting electrolyte (NaOH). The curve 1 represents the supporting electrolyte only.

The behaviour of platinized-platinum electrodes treated by saw tooth anodic sweep are shown in figure 5, which presents the anodic oxidation curves in NaOH as supporting electrolyte.

The significance of the peaks are the same as for triangular sweep treatment of the electrodes.

The phenomena observed depend on the conditions of the surface treatment of the electrode. If, for example, the anodic curve is measured using electrodes which were not treated previously the peaks for adsorbed hydrogen oxidation and the peaks for methanol oxidation present lower values as compared to the peaks of the anodic curve obtained with electrochemical treated electrodes. All this convincingly shows that the oxidation products obtained on the platinized-platinum electrodes during the electrochemical treatment in (H_2SO_4 or NaOH) as supporting electrolyte are responsible for the increase of the kinetic current of anodic oxidation of adsorbed hydrogen or methanol, according to the well known kinetic equation :

$$i = k \cdot a_{\varphi} c^{\alpha} \exp (\beta F \varphi_r / RT)$$

It is interesting to point out that the maxima obtained with electrodes treated by saw tooth sweep potential are nearly as high as the

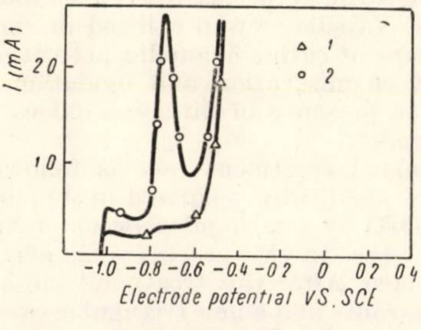

Fig. 2. — Potentiostatic curves (from cyclic voltammograms) at 18 mV/s in 0.4 M NaOH and 0.4% CH_3OH : *1* — without previous treatment ; *2* — with previous treatment.

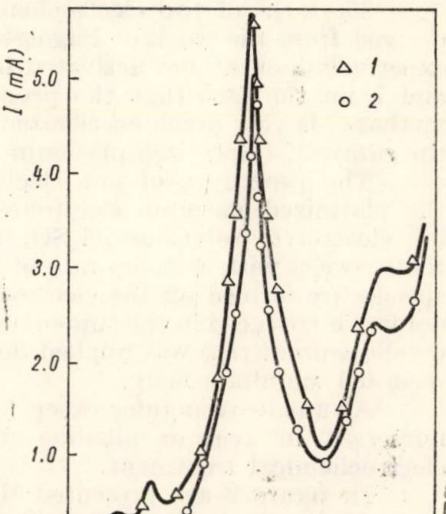

Fig. 3. — Potentiostatic curves (from cyclic voltammograms) at 18 mV/s in 1 N H_2SO_4 and 0.4% CH_3OH : *1*—with previous treatment ; *2* — without previous treatment. →

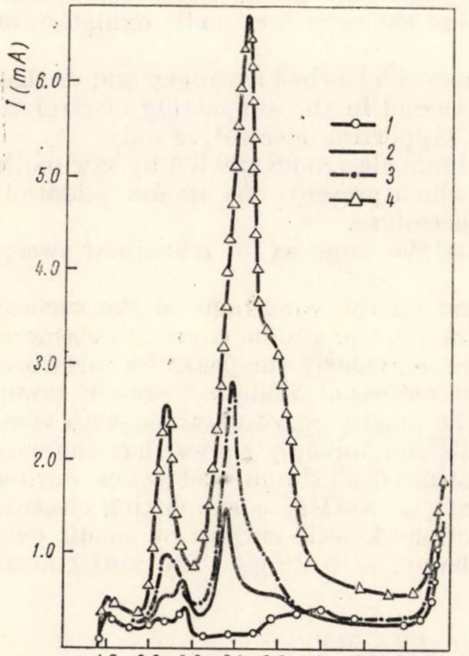

Fig. 4. — Potentiostatic curves (from cyclic voltammograms) at 18 mV/s in 0.4 M NaOH and : II — 0,1%CH_3OH ; III — 0.2% CH_3OH ; IV — 0.4% CH_3OH ; I — supporting electrolyte.

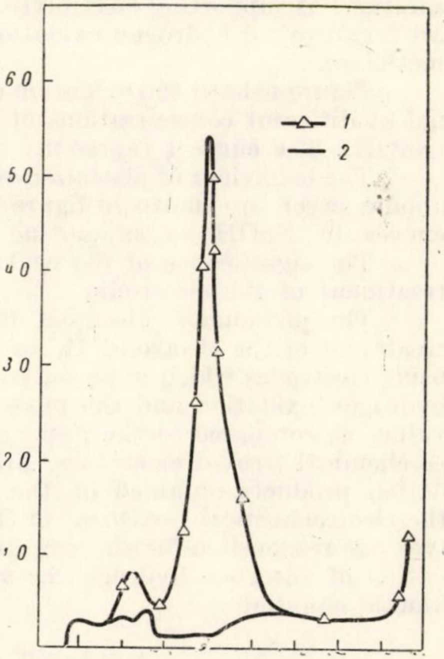

Fig. 5. — *1* — curves of the saw-tooth pulse in 0.4 M NaOH and 0.4% CH_3OH ; *2* — supporting electrolyte.

The graduations on the abscissa axis should read as: — 1.0; — 0.8; — 0.6; — 0.4; — 0.2; 0; 0.2; 0.4; 0.6

maxima of the electrodes treated by triangular sweep potential. This behaviour indicates that the species absorbed on the platinum surface during the increasing part of the triangular sweep are not completely reduced during the descending part of the sweep.

It is necessary to point out that taking into account the regions of anodic polarization curve of the platinized electrode (hydrogen oxidation, charging of the double layer, anodic oxidation of platinum, oxygen overvoltage) the electrochemical treatment consisting of anodizing only in the region of Pt oxidation does not give an active surface for methanol chemisorption.

Our results which clearly show the increase of adsorbed hydrogen on platinized-platinum electrodes is in very good agreement with the methanol oxidation mechanism proposed by many authors.[1-4] Taking into consideration this mechanism, the first step of anodic oxidation of methanol is the process of chemisorption. This process occurs at open circuit potential, i. e. it is not an electrochemical process. The chemisorption is a dissociative process and involves the dehydrogenation of the methanol molecule, i. e. the breaking of C—H bonds and the formation of new C—Pt and H—Pt bonds according to the probable scheme:

$$CH_3OH_{ads} \longrightarrow CHO_{ads} + 3H_{ads}$$

CHO_{ads} radical has a probable structure.

The rate of this dissociative process is markedly influenced by our anodic treatment of the platinized-platinum electrode in the supporting electrolite be it acid or alkaline.

The following processes in anodic oxidation described by anodic curves are: the oxidation of adsorbed hydrogen

$$H_{ads} \longrightarrow H^+ + e$$

and the oxidation in successive steps of methanol adsorbed species. The amount of adsorbed species on platinized-platinum electrodes depends to a great extent (as was shown by our results) on the electrochemical treatment of the electrodes.

Revue Roumaine de Chimie, 14, 29–34 (1969)

THE OXIDATION OF TUNGSTEN AT HIGH TEMPERATURES. THE SYSTEM W + CO_2

D. CISMARU and ANGELA GEANGU-MOISIN

Institute of Physical Chemistry of the Academy, Bucharest, str. Dumbrava Roşie 23

Received March 28, 1968

Studies were made on the oxidation of tungsten from 700° to 1000° in CO_2 at $p_{CO_2} = 150$ mm Hg. We intended to determine the composition of the oxide scales formed during the oxidation of this metal. To this purpose we have made the X-ray analysis of the reaction products. Our results are different from those obtained at the oxidation of tungsten in air or oxygen.

I. INTRODUCTION

The tungsten oxidation, both from the viewpoint of the kinetic reaction and of the crystal structure of the oxide scales formed during this process, under different conditions of temperature and pressure, was studied by many authors. [1–11]

In two previous papers [10, 11] the kinetics of tungsten oxidation in CO_2 at different pressures and from 500° to 1000° was studied.

In the present paper we intend to complete these studies with the determination of the nature and composition of the oxide layers formed during the tungsten oxidation in CO_2.

Studying the oxidation of tungsten in air or oxygen, different authors [5, 7, 8, 9] concluded that during this process two oxide layers are formed. At the beginning of the oxidation a thin, black, adherent layer is formed and at higher temperatures is eventually overlain by a bright yellow scale.

---

[1] E. A. Gulbransen and W. S. Wysong, *Amer. Inst. Min. Met. Eng.*, **175**, 611 (1949).

[2] K. M. Gorbunova and V. A. Arslambekov, *J. Chim. Phys.*, **53**, 871 (1956).

[3] J. S. Dünn, *J. Chem. Soc.*, **11**, 49, (1929).

[4] E. Scheil, *Z. Metallkunde*, **29**, 209 (1957).

[5] W. W. Webb, J. T. Norton and C. Wagner, *J. Electrochem. Soc.*, **103**, 107 (1956).

[6] E. A. Gulbransen and K. F. Andrew, *J. Electrochem. Soc.*, **107**, 619 (1960).

[7] E. A. Kellett and S. E. Rogers, *J. Electrochem. Soc.*, **110**, 502 (1963).

[8] V. S. Arkharov and Yu. D. Kozmanov, *Fiz. Metal i Metalloved., Akad. Nauk SSSR, Ural Filial*, **2**, 361 (1956).

[9] J. W. Hickman and E. A. Gulbransen, *Trans. AIME*, **171**, 371 (1947).

[10] D. Cismaru and A. Geangu-Moisin, *Rev. Roumaine Chim.*, **11**, 777 (1966).

[11] D. Cismaru and A. Geangu-Moisin, *Rev. Roumaine Chim.*, **12**, 1425 (1967).

All the authors [5, 7, 8, 9] generally accepted that the yellow layer is formed by WO_3. The composition and the structure of the black oxide layer made the object of several investigations in the recent years, especially by means of X-ray diffraction method.

Thus according to some authors [8] the black film has been claimed to be of γ-form while according to others [9] of the δ-form. It was also surmised to be a metastable modification of one of the intermediate oxide phases. [5]

In their paper on the composition and crystal structure of the oxide layers formed during the tungsten oxidation in air or oxygen, Kellett and Rogers [7] concluded that the essential difference between the black and the yellow oxide layers is related to structural perfection and orientation rather than to composition.

For the oxides of tungsten there has been established the existence of the following phases :

α WO_3 triclinic, yellow

β $WO_{2.90}(W_{20}O_{58})$, light blue

γ $WO_{2.72}$ ($W_{18}O_{49}$ or W_4O_{11}), monoclinic, violet

δ WO_2, monoclinic, brown.

In the present paper we tried to establish the composition of the oxide layers formed on tungsten during the oxidation in CO_2, with X-ray analysis.

II. EXPERIMENTAL

For oxidation tungsten sheets were used which had the same provenience and purity like those reported by us in previous papers.[10,11] The preparation of the tungsten surfaces for oxidation, the preparation of CO_2 and the working technique, are also the same as those described by us in the two mentioned papers.[10,11]

We employed the X-ray diffraction method for our studies with the following type of samples :

— oxide layers formed on the tungsten sheets during the oxidation (*in situ*) ;

— coatings removed as a whole of the oxidized tungsten sheets ;

— powder of the tungsten oxides which had evaporated and covered the quartz suspension thread during the oxidation in kinetic determination carried out at 1000° and $p_{CO_2} = 150$ mm Hg. The samples of tungsten for oxidation had their surfaces chemically pickled, described in our previous papers.[10,11] In addition, at 1000°, we worked with samples whose surface was not chemically pickled, in order to observe if the treatment of the surface influences the nature of the oxide layers.

The samples have been oxidized in CO_2 at $p_{CO_2} = 150$ mm Hg, from 700 to 1000°. We chose this range of temperature because the rate of oxidation is lower in CO_2 than in air or oxygen. All samples have been oxidized for 24 hours, a large period of time, for obtaining a great amount of oxides necessary for X-ray examinations.

The X-ray examinations were all carried out at room temperature and for the samples *in situ* with a difractometer TUR M-61.

Instrumental conditions : -Ni-filtered CuK_α radiation ; — work voltage : 35 kv at 20 mA ; — scanning speed 1/4° 2θ per/min ; — voltage counter 1380 V ; — horizontal divergence slight

1 mm ; — receiving slight width : 0.3 mm ; — vertical divergence slight : 9 mm ; — impulsion scale : 18,000 impulsions/min.

The analysis of the stripped oxides as well as the analysis of the oxide covering the quartz suspension thread at 1000° during the reaction were performed through the powders recording method. In this case the instrumental conditions were the following :

— Ni-filtered Cu K_α radiation ; — work voltage 50 kv at 12 mA ; — recording time : 6 hours ; — Laue film : ORWO RF 44.

III. RESULTS

In all range of temperature the formation of two oxide layers of different colours is observed. At 700° one observes the existence of a first brown protective layer. In proportion as the temperature rises, a second, violet layer becomes visible. For the same time of oxidation the second layer grows with the rising of the temperature. The way in which the second layer is growing on the first layer is presented in figures 1—3.

Figure 1 presents the oxidation at 800° ; figures 2 and 3 present the tungsten oxidation at 1000° in two cases : a) samples with chemically pickled surfaces ; b) samples without chemically pickled surfaces.

Tables 1—3 present the data obtained by the difractometer. These

Table 1

The values of d Å and I% calculated from the diffraction patterns for tungsten oxidation at 800°

N_c	d Å	I %
1	4.620	5
2	4.459	8
3	3.784	100
4	3.748	50
5	3.657	42
6	3.459	80
7	3.405	40
8	3.241	9
9	3.167	9
10	3.050	9
11	3.022	7
12	2.957	10
13	2.918	20
14	2.785	7
15	2.753	20
16	2.660	10
17	2.620	10
18	2.526	10
19	2.477	5
20	2.446	10
21	2.425	20
22	2.397	10
23	2.336	6
24	2.313	6
25	2.231	10
26	2.213	6
27	2.005	6

results have an error probability of ± 0.002 in determining the Θ and of ± 2% in determining the intensity.

Table 2

The values of d Å and I% calculated from the diffraction patterns for tungsten oxidation at 1000°. The surfaces of the samples were chemically pickled before oxidation

N_c	dÅ	I%
1	4.52	9
2	4.34	10
3	4.165	3
4	3.803	8
5	3.72	100
6	3.66	65
7	3.57	60
8	3.41	50
9	3.37	85
10	3.27	9
11	3.21	6
12	3.17	20
13	3.026	12
14	2.975	17
15	2.93	25
16	2.89	30
17	2.837	5
18	2.775	12
19	2.720	55
20	2.630	35
21	2.600	30
22	2.553	4
23	2.507	36
24	2.463	8
25	2.412	20
26	2.343	7
27	2.311	16
28	2.295	17
29	2.239	5
30	2.213	20
31	2.143	5
32	2.070	5
33	2.000	14
34	1.980	9
35	1.952	5
36	1.934	16

The data obtained by us have been compared to those existing in literature (A.S.T.M.; Difraction Data Cards):

$W_{18}O_{49}$ A.S.T.M. 5 — 0.392; $W_{20}O_{58}$ A.S.T.M. 5 — 0.386

WO_2 A.S.T.M. 5 — 0.431; WO_3 A.S.T.M. 5 — 0.363.

Oxidation at 700°. Under work conditions the oxide layer is very thin and the X-ray determination of the oxides is practically impossible.

Oxidation at 800°. The patterns obtained for the sheets which have been oxidized at this temperature show the existence of a mixture of two oxides: WO_2 and $W_{18}O_{49}$. From the data of the table 1 one can see that

Fig. 1. — The aspect of tungsten oxidized at 800° and $p_{CO_2} = 150$ mm Hg.

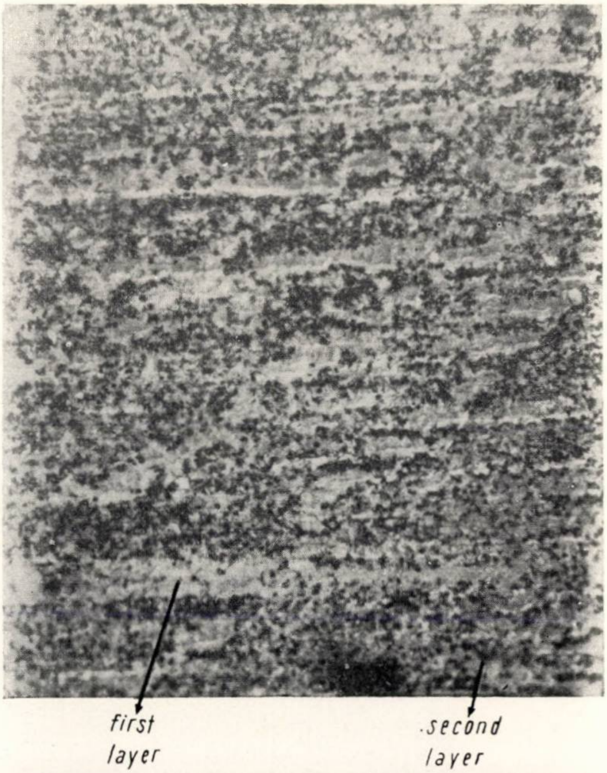
first layer
second layer

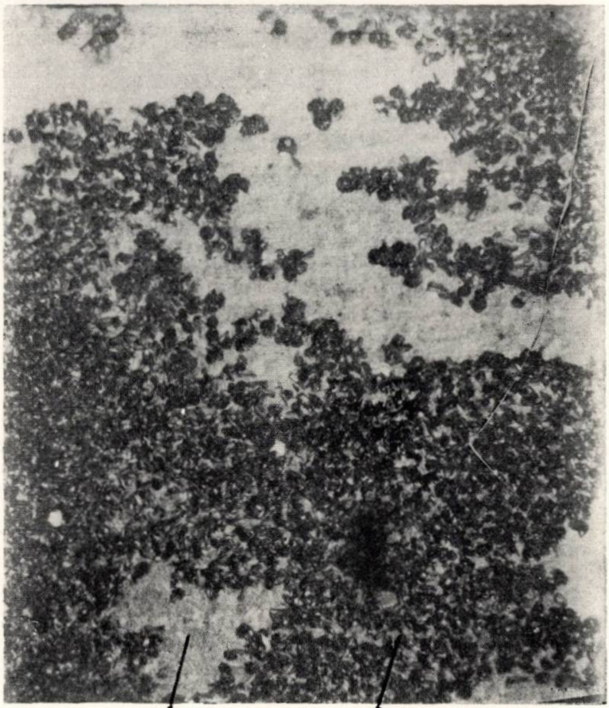
first layer
second layer

Fig. 2. — The aspect of tungsten oxidized at 1000°. The surface of the tungsten sheet was chemically pickled.

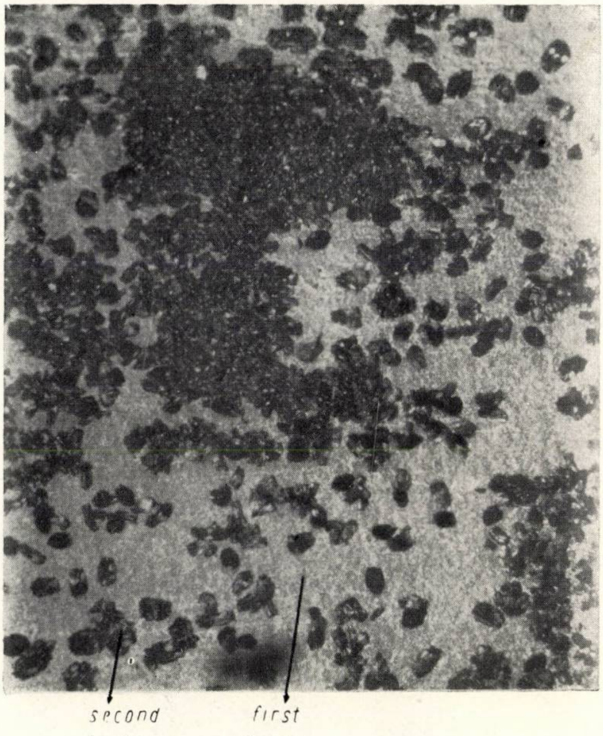
second layer
first layer

Fig. 3. — The aspect of tungsten oxidized at 1000°. The surface of the tungsten sheet was not chemically pickled.

there is not a perfect concordance between all the d and the I of our samples and those from A.S.T.M. These differences are probably due to superposition of the lines of the two oxides from mixture, as well as to the preferential orientation of the oxide crystals and their irregular sizes. In proportion as the temperature rises, the samples show the existence of $W_{18}O_{49}$ in the oxides mixture.

Table 3

The values of d Å and I% samples oxidated at 1000°. The surfaces were not chemically pickled

N_c	d Å	I%
1	4.84	3
2	4.398	1
3	3.950	22
4	3.800	22
5	3.669	10
6	3.465	100
7	3.401	11
8	3.198	4
9	3.072	3
10	3.038	2
11	2.971	4
12	2.941	6
13	2.858	2
14	2.818	3
15	2.770	10
16	2.679	8
17	2.635	3
18	2.545	6
19	2.460	13
20	2.431	26
21	2.331	4
22	2.333	5
23	2.013	2
24	1.999	2

Oxidation at 1000°. At this temperature we studied the samples with chemically pickled surfaces before oxidation and the samples without chemically pickled surfaces. Both table 2 and 3 show that at this temperature two oxides are present: WO_2 and $W_{18}O_{49}$. On the nonpickled samples the presence of WO_2 is more evident. The modification of the d and I% at this temperature shows that in this case too, there exist a more accentuate preferential orientation of the oxides as compared to those formed at 800°.

The oxide samples stripped off the sheets of tungsten also show the presence of $W_{18}O_{49}$. Further on, there has been made the analysis of the oxides which covered the quartz suspension thread during the kinetic determination at 1000° and $p_{CO_2} = 150$ mm Hg. The time of oxidation in this case was about 5 hours.

The diffraction patterns indicate in this case only the presence of $W_{18}O_{49}$. The concordance between dÅ calculated from our patterns, and d from A.S.T.M. is very good. This can be explained by the presence in this case only of a single oxide. The results are indicated in table 4.

Table 4

Comparison between $d_{calc.}$ and $d_{W_{18}O_{49}}$ for samples obtained on quartz suspension thread at 1000°

N_c	$dÅ_{comp.}$	$dÅ_{W_{18}O_{49}}$
1	4.529	4.54
2	3.787	3.78
3	3.412	3.40
4	2.965	2.958
5	2.675	2.654
6	2.528	2.522
7	2.221	2,218
8	2.005	2.005
9	1.897	1.888

These results agree with the data obtained by us in previous kinetic determinations [10,11] and with the properties of $W_{18}O_{49}$ (this oxide beginning to sublimate over 900°).

IV. CONCLUSIONS

We tried to establish the nature of the oxides formed during the oxidation of tungsten in CO_2.

We found that a mixture of at least two oxides : WO_2 and $W_{18}O_{49}$ is formed in our working conditions. The oxides found by us are different from those found during tungsten oxidation in air or oxygen. In our case the oxidation is incomplete ; we could not outline the presence of WO_3.

It is left for us to test if this fact could be due to the reduction of the WO_3 at the intermediate oxides.

Revue Roumaine de Chimie, **14**, 35–43 (1969)

SELF-DIFFUSION OF INDIUM IN LIQUID INDIUM-ALUMINIUM ALLOYS

ŞT. ZĂMÂRCĂ, LUCIA GANOVICI and I. GANOVICI

Institute of Physical Chemistry of the Academy

Bucharest, str. Galaţi 31

Received March 19, 1968

Self-diffusion coefficients of In in homogeneous molten In-5.5 wt % Al alloy have been measured by the capillary-reservoir method on a temperature range from about 748 to 500°. A conventional counting technique was used to determine the In^{114} content of the integral capillary samples after diffusion. The results indicate that diffusivity of In is affected by "clustering" in the neighbourhood of immiscibility curve since a sensitive deviation of data from the linearity on a log D versus l/T plot was found.

INTRODUCTION

Very little work has been done on diffusivities in molten alloys which exhibit miscibility gaps; this is also shown in the recent Wilson's study [1] on the structure and properties of liquid metals and alloys. Until now only the experimental results of Ma and Swalin's investigations [2] regarding the application of the fluctuation theory in the case of solute diffusion in liquid tin may be quoted. Their study indicated that those solutes which have a large repulsive interaction with the solvent tend to diffuse faster than the solvent itself.

Thus, for the diffusion of aluminium in liquid tin (dilute solutions ranging from 0.2 to 0.7 wt% Al) was found that aluminium which has a large positive relative partial molar enthalpy diffuses 5 times faster than tin does in tin at 347°.

The Ma and Swalin's results have also been confirmed by Kassner *et al.* [3] for the typical "pure-size factor" system Pb–Zn which exhibit miscibility gap in liquid state. On the basis of free-volume model for self-diffusion first used by Cohen and Turnbull ,[4,5] Kassner *et al.* have found an increase of the self-diffusion coefficients of Zn with temperature (from about 400 to 500°) as well as with increasing Zn content in liquid dilute Pb–Zn alloys on a concentration range from 0.1 to 1.5 wt% Zn. Due to the close connection between diffusion and viscosity [6], diffusivities should exhibit the same dependence on factors reflecting the bond strength and free-volume of the liquid as the viscosities.

---

[1] J. C. Wilson, *Metall. Rev.*, **10**, 509 (1965).

[2] C. H. Ma and R. A. Swalin, *Acta Met.*, **8**, 388 (1960).

[3] T. F. Kassner, R. J. Russell and R. E. Grace, *Trans. Amer. Soc. Metals*, **55**, 858 (1962).

[4] M. H. Cohen and D. Turnbull, *J. Chem. Phys.*, **31**, 1164 (1959).

[5] M. H. Cohen and D. Turnbull, *J. Chem. Phys.*, **34**, 120 (1961).

Recently Budde and Sauerwald [7] for the systems Bi—Zn and Pb—Zn, Zămârcă *et al.* [8] for Al—In system have determined an important structural modification in the neighbourhood of the immiscibility curve by viscosity measurements. "Cluster formation" that was already shown to be present in organic liquids near the critical point seems to preclude the separation of homogeneous molten alloys in two layers. This subject is worth being also carefully studied by diffusivities measurements; it seems that no attempts have been done in this direction so far, probably due to extreme experimental difficulties.

EXPERIMENTAL

A. *Purity of metals and the investigated alloy*

Aluminium 99.995% (Johnson, Mathey) and indium 99.995% (Institute of Chemical Research, Bucharest) were used for diffusivities measurements on a liquid alloy from In—Al systems. Alloy of 5.5 wt % Al near the limit 2.8 wt % Al of the miscibility gap at the monotectic temperature (638.6°) as reported by Campbell *et al.*[9] was chosen for determinations. Thus, we have been interested in the phenomena above the immiscibility curve, although the increased content of aluminium introduces some difficulties in interpreting the diffusivity data as well as their correlation with the viscosity of the same alloy, difficulties which will be presented further.

B. *Capillary Filling*

Measurement of self-diffusion coefficients in high temperature melts by means of a radioactive tracer is usually carried out using one of the following two methods. In the first, diffusion takes place between two cylindrical samples of the same material, one of which is radioactive. Self-diffusion coefficient is computed from the radioactivity penetration curve in the solidified sample after the diffusion. In the second method, samples contained in capillaries of an inert substance are immersed in an infinite reservoir of the same material. Either the material in capillary or that in the reservoir is radioactive, the self-diffusion coefficient is computed from the change of the radioactivity of the capillary samples after diffusion. The second method is more simple because a radioactivity penetration curve is not needed for the computation of diffusivity. During the experiments no convection occurred into the sample; this condition was achieved by using capillaries with diameters smaller than 1 mm and by rigorously controlling the temperature (±2°). It is recalled that no thermal gradient occurred since Ludwig-Sorret effect might have produced an important scattering or forgeing of data.

The experimental technique employed in the present investigation is the capillary-reservoir technique.

---

[6] H. J. Saxton and O. D. Sherby, *Trans. Amer. Soc. Metals*, **55**, 826 (1962).

[7] J. Budde and F. Sauerwald, *Z. phys. Chem.* (Leipzig), **3**, 42 (1965).

[8] St. Zămîrcă, N. Petrescu, I. Ganovici and Lucia Ganovici, *Rev. Roumaine Chim.*, **13**, 1 011 (1968).

[9] A. N. Campbell, L. B. Buchanan, J. M. Kuzmak and R. H. Tuxworth, *J. Amer. Chem. Soc.*, **74**, 1962 (1952).

A special attention must be paid to capillary filling for avoiding the separation of the molten In—Al alloy as well as the segregation during freezing ; this careful attention was maintained all through the experiments including the self-diffusion measurements.

For that reason we have adopted for capillary filling the direct-sampling technique used by Campbell and co-workers to establish Al—In equilibrium diagram.

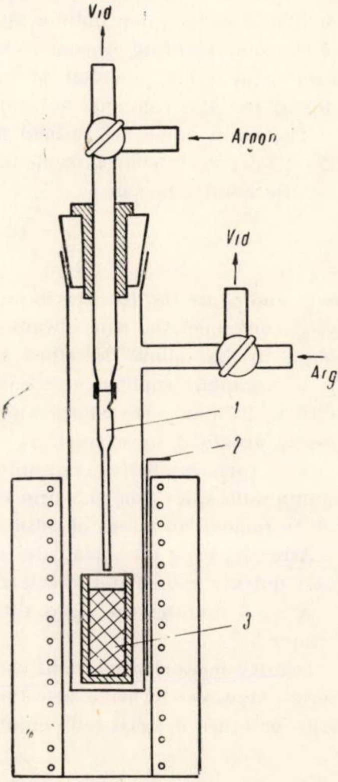

Fig. 1. — Draft of the apparatus for the direct-sampling method :
1 — silica pipette; *2* — Pt — 10% Rh — Pt thermocouple; *3* — the graphite crucible with molten indium — aluminium alloy.

Preliminary attempts were made to achieve the best conditions for capillary filling. Non-radioactive indium and aluminium were mixed in suitable portions for obtaining approximately 9 cm^3 liquid alloy in a pure graphite crucible 70 mm high and 17 mm in inner diameter. This crucible was then placed in a long silica tube with one end sealed, as shown in figure 1.

This cell was alternatively pumped out after loading and filled with pure argon. The molten alloy was kept for homogenizing in an argon atmosphere at 950° for 26 hours, the temperature of the furnace being set with a $\pm$ 2° precision by means of a potentiometric device. A Pt-10 % Rd-Pt thermocouple was calibrated in the usual way according to freezing points of pure metals : In, Zn, Sb, Ag.[10]

All samples were rapidly extracted from the molten alloy with a thin silica pipette also shown in figure 1. Immediately after extraction, the pipette was removed from the cell and immersed in cold water or cooler mixture of natrium chloride and ice, the whole operation requiring less than 30 sec. The silica capillaries were cracked then, metallic samples removed and cut into small pieces for density measurements, chemical analysis and for filling the graphite capillaries used in the diffusivity experiments.

---

[10] "Etudes de pyrométrie pratique", Collection de l'ANRT, Eyrolles, Paris, 1959, p. 57.

As shown by Campbell and Wagemann, [11] in density measurements the results are within 0.002 g/cc accuracy, corresponding to an error in composition of about ± 0.002% In for high concentration indium alloys. We determined the density of In—Al samples in a 25 ml pycnometer using ethanol as inert liquid, the temperatures of all determinations being measured with ± 0.2° precision, in the range from 22 to 24°. No significant scattering of data was found for the top and bottom parts of the samples.

The mean value determined for density of In — 5.5 wt % Al alloy was 6.875 g/cm³ (6.895—6.855 g/cm³ being extreme limits), similar to that computed using the following expression of the additivity rule :

$$\rho^{20^\circ}_{\text{In Al}} = \frac{100\,\rho_1\rho_2}{a\,\rho_2 - (100 - a)\,\rho_1} \tag{1}$$

where ρ_1 and ρ_2 are the densities of pure components, a and $(100 - a)$ wt % of these. Chemical analysis* confirmed the data obtained by density measurements. In capillary filling a similar technique to that above described was used.

The graphite capillaries of 5 mm o.d. and 1 mm i.d. with the capillary length ranging from 19 to 21 mm were charged with small pieces of In—Al alloy cut from the thin rods previously obtained by extraction.

Two such capillaries containing twice the needed filling quantity were introduced in a long thin walls silica tube (5.5 mm i.d.) ; the silica tube was then pumped out for 30 minutes at 120° to remove all traces of adsorbed gas.

After degasing the silica tube was placed in a different furnace at 950°, the metal charge was very quickly melted and forced into capillaries by addmiting pure argon gas over pressure.

After 3 minutes the silica tube was removed from the furnace and rapidly cooled in cold water.

Density measurements and chemical analysis proved that no segregation took place in capillaries. However to make sure that no other disturbances occurred during capillary filling (porosity or other defects) radiographs of all samples were taken.

C. *Diffusion experiments*

The diffusion experimental system and the accessories were generally similar to those described in a previous paper.[12] A graphite crucible loaded with approximately 64 g In—5.5 wt % Al alloy (with radioactive In^{114}) was placed in a long silica tube connected to the diffusion system. Samples (two samples at a time) were held in a graphite sample holder and then rapidly lowered in the radioactive molten bath. In order to minimize the convection effects, the temperature of the reservoir and samples was kept within ± 2° precision by means of a potentiometric device.

Before the diffusion run takes place, the liquid radioactive bath was homogenized during about 26 h at 950° in a purified argon atmosphere ; the samples were held in a vertical position with the open end of capillaries at the top.

---

* The chemical analysis was carried out at the Institute of Chemical Research — Bucharest.

[11] A. N. Campbell and R. Wagemann, *Canad. J. Chem.*, **44**, 657 (1966).

[12] N. Petrescu, St. Zămărcă, Lucia Ganovici and I. Ganovici, *Rev. Roumaine Chim.*, **13**, 865 (1968).

The diffusion time was 2 hours for all samples. Since the same diffusion bath was used for all runs, its specific radioactivity C_0 was determined before and after each diffusion experiment. Samples were extracted from the radioactive reservoir with special graphite rods in a vacuum-argon system similar to that described in the quoted previous paper.

The self-diffusion of In in liquid In$-$5.5 wt % Al alloy has been investigated within the temperature range 748° to 900°, above the immiscibility curve.

D. *Determination of self-diffusion coefficients*

After diffusion the radiographs of all samples were also made to be sure that no disturbance in the structure of metallic samples occurred.

Diffusion under the conditions previously described follows Fick's law:

$$\frac{\partial c}{\partial t} = \mathrm{D}\,\frac{\partial^2 c}{\partial x^2} \qquad (2)$$

with initial and boundary conditions:

$$t = 0\,;\ c = 0\,;\ 0 < x < 1$$

$$t > 0 \begin{cases} \dfrac{\partial c}{\partial x} = 0\,;\ x = 1 \\ C = C_0\,;\ x = 0 \end{cases} \qquad (3)$$

the solution of Fick's second law being as follows:

$$\frac{\overline{C}}{C_0} = 1 - \frac{8}{\pi^2}\,\frac{1}{(2n+1)^2}\,e^{-\frac{(2n+1)^2\pi^2\theta}{4}} \qquad (4)$$

where $\overline{C}$ is the average specific radioactivity of the metallic samples after diffusion, C_0 is the specific radioactivity of the samples extracted from the bath during diffusion runs and $\theta = \dfrac{Dt}{l^2}$, D being the self-diffusion coefficient in cm^2/s, t is the time of diffusion in seconds and l the length of capillary in centimeters.

After diffusion run, the metallic rods were separated mechanically from the graphite container and weighed on an analytical balance.

Since a rapid cooling was not possible when the samples were raised out of the melt, as performed during capillary filling, the segregation was not wholy avoided. In this case a radioactivity penetration curve was not possible to be drawn, and a conventional counting technique was used to determine radioactive In^{114} content of the integral capillary diffusion samples.

Correct evaluation of $\overline{C}$, an important element in the precise determination of the diffusion coefficients,[13] proved to be extremely difficult in our experimental conditions: a small drop of molten alloy was drawn out of the molten bath through the top of graphite capillaries; a relative slow cooling by comparison to capillary filling was achieved; volume changes due to cooling of homogeneous alloy, to passing through miscibility gap (ΔV^M) and to freezing in two stages followed by continuous cooling up to 25°.

In the case of a very slow cooling, in a similar way to that necessary for establishing the equilibrium diagram, the computation of $\overline{C}$ can be carried out using the corrected capillary length. So, for the studied alloy an equation established for the purpose by these authors was used :

---

[13] E. V. Vasilenko and S. I. Harkov, *Fiz. Met. i Metallovedenie*, **18**, 203 (1964).

$$l^{25}_{\text{corrected}} = l_{\text{capillary}} \frac{\rho^{t^\circ}_{\text{InAl}}}{\rho^{725-0}_{\text{InAl}}} \left\{ \varphi_{\text{In}} \frac{\rho^{725-0}_{\text{In}}}{\rho^{156.3-0}_{\text{In}}} \sqrt[3]{\frac{\rho^{156.3-0}_{\text{In}}}{\rho^{25}_{\text{In}}}} + \varphi_{\text{Al}} \frac{\rho^{725-0}_{\text{Al}}}{\rho^{638.6-0}_{\text{Al}}} \sqrt[3]{\frac{\rho^{638.6-0}_{\text{Al}}}{\varphi^{25}_{\text{Al}}}} \right\} \qquad (5)$$

where

$\rho^{t^\circ}_{\text{In}} = 7.1896 - 1.00854.10^{-3}\ t^\circ$ was experimentally determined,[14] $\rho^{156.3-0}_{\text{In}}$, $\rho^{638.6-0}_{\text{Al}}$, $\rho^{t^\circ}_{\text{Al}}$, was computed from Wilson's data and $\rho^{t^\circ}_{\text{InAl}} = 6.2505 - 0.7406 \cdot 10^{-3}\, t^\circ$ was experimentally determined in a previous work.[8]

φ_{In} and φ_{Al} are volumetric fractions in the miscibility gap. The data from table 1 were computed with the corrected length using the last relationship. It could be seen that the correction for capillary length is about 2.5 mm.

However the values of the self-diffusion coefficient of In in molten In—Al alloy are probably by about 10—20% greater than those computed with the corrected length, since the experimental solidified conditions of the metallic samples from capillaries are not almost the same with those required for the equilibrium diagram.

E. *Results and discussion*

The results concerning self-diffusion of indium in In — 5.5 wt% Al alloy above the immiscibility curve are shown in table 1 and plotted on figure 2.

Table 1

Self-diffusion coefficients of In in liquid In—5.5 wt% Al alloy

Temperature	First series of experiments					Second series of experiments				
	Time s	Length diff. — cm	Length corr. — cm	c/c_0	D.10^{-5} cm²/s	Time s	Length diff. — cm	Length corr. — cm	c/c_0	D.10^{-5} cm²/s
900	7 200	1.907	1.634	0.3965	6.24	7 200	1.991	1.706	0.3676	5.84
	7 200	1.928	1.652	0.4019	6.55	7 200	2.030	1.740	—	—
850	7 200	1.914	1.651	0.3794	5.75	7 200	2.023	1.745	0.2955	3.90
	7 200	2.017	1.740	0.3618	5.81	7 200	1.994	1.720	0.3942	6.74
806	7 200	1.966	1.706	0.3465	5.06	7 200	2.027	1.759	0.3335	4.99
	7 200	1.975	1.714	0.3410	4.95	7 200	2.011	1.745	—	—
768	7 200	1.988	1.734	0.3123	4.21	7 200	1.935	1.688	—	—
	7 200	2.027	1.768	0.3025	4.10	7 200	2.050	1.788	0.3042	4.24
748	7 200	1.993	1.743	0.2833	3.49	7 200	2.027	1.772	—	—
	7 200	2.022	1.768	—	—	7 200	2.022	1.768	—	—

From those data two significant points emerge. First, the aspect of the log *D* versus *l*/*T* plot with a more stressed curvature towards the immiscibility line, seems to indicate an influence of the structural changes from the molten alloy on the self-diffusion on indium. The possible interpretation of these results could be similar to that given for the viscosity changes near the critical curve by Budde and Sauerwald for Bi—Zn and Pb—Zn systems as well as by the authors of the present study for In — 5.5 wt% Al alloy. "Cluster formation" pointed out by McLaughlin and Ubbelohde [15] and Ubbelohde [16] as a disputable phenomenon for the variation of viscosity in the pre-freezing of organic and metallic liquids, here seems the only true element to be considered undoubtedly. Recently an important decrease of diffusivity towards the critical temperature was reported for organic liquids, [17] so that for metallic alloys exhibiting miscibility gap in liquid state a similar phenomenon may be now observed since a sort of very finely divided emulsion is also possible to occur as a prelude of the gravitational segregation with the separation into two layers.

---

[14] I. Ganovici and Lucia Ganovici, *Rev. Roumaine Chim.*, **13**, 879 (1968).

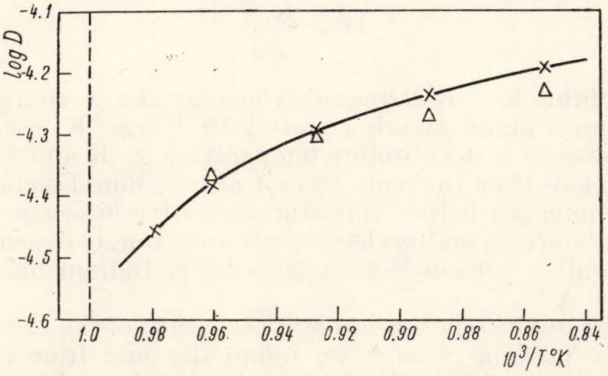

Fig. 2. — Temperature dependence of indium self-diffusion in homogeneous molten indium-aluminium alloy as $\log_{10}D$ versus l/T plot.

At first glance it might be expected that self-diffusion of indium in the presence of indium and aluminium clusters (equally large or greater than $10^2 - 10^3$ atomic dimensions such as was reported for the pre-freezing phenomenon in liquid eutectic alloys [18]), should occur much less than in pure liquid indium.

It must be emphasized that the mechanism of self-diffusion is probably more complicated and it is difficult to assess the relative importance of the factors involved so that more data would be welcome in order to clarify this problem.

Secondly, from the examination of the data regarding self-diffusion of indium in molten In — 5.5 wt % Al alloy, results the relationship between diffusivity and viscosity data, in order to obtain some knowledge about the mechanism of diffusion.

---

[15] E. McLaughlin and A. Ubbelohde, *Trans. Faraday Soc.*, **56**, 989 (1960).

[16] A. Ubbelohde, "Melting and Crystal Structure", Clarendon Press, Oxford, 1965, p. 260.

[17] I. A. Baltsevich, V. G. Martinets and E. V. Matizen, *Zhur. exp. teor. Fiz.*, **51**, 983 (1966).

[18] G. M. Barteniev, "Struktura i svoistva zhidkikh metallov", Izd. Inst. Metallurghii A. N. SSSR, 1959.

According to Saxton and Sherby[6] for pure liquid metals and Ma, and Swalin[2] for solute diffusion, the Sutherland's relationship may be used taking into account that the dimensions of diffusion particles and medium are small enough. The general form of this is the following :

$$D = \frac{S \cdot T}{\eta \, \mathrm{d_i}} \tag{6}$$

where S (including K — Boltzmann's constant and a configurational parameter) for pure liquid metals equals 2.10^{-17} ergs/°K, η is the dynamic viscosity in poise, T is the absolute temperature in °K and $\mathrm{d_i}$ is the diameter of metallic ions from the melt. In case of pure liquid metals the Pauling univalent diameter is a better indicator of relative ionic size than multivalent values size since all multivalent values are strongly dependent upon the amount of bonding deformation in ionic salts. Indium has $r_i^{3+} = 0.81$ Å and $r_i^{+} = 1.04$ Å[19].

Using the above relationship and the results of the viscosity measurements from a previous work[8] we found the data from table 2 at two temperatures (850° and 748°) for both cases of molten alloy : homogeneous liquid and liquid in the neighbourhood of the immiscibility curve. The data we obtained for the radii of diffusing particles are 2—3 times greater than the radius of indium univalent ion ; this value cannot be thought as a true one since the ionic character of diffusion mechanism in liquid metals is well established. However, the values seem to indicate that the mechanism of diffusion is affected by "clusters" formed as a prelude of the segregation and separation of homogeneous liquids in two layers.

Table 2

Comparison of atomic radii calculated on the basis of experimental results using the Sutherland's equation with Pauling ionic radii

Temp. °K	D In in In-5.5% Al cm²/s	η In-5.5% Al poise	r_i computed Å	r_i In + Pauling Å
1 123	$5.796 . 10^{-5}$	$7.569 . 10^{-3}$	2.55	1.04
1 021	$3.48 . 10^{-5}$	$8.28 . 10^{-3}$	3.55	1.04

Meanwhile, the results acquired by correlating diffusivities and viscosities data for molten indium-aluminium alloy seem to indicate that the Sutherland's relationship still used to liquid metals and dilute alloys does not allow to obtain more precise data in case of concentrated liquid alloys since it fits to unexpanded liquid, with interatomic distance equal to the atomic diameter (ΔV^M at the formation of the liquid metallic solutions with the variation of the coordination number as well as the free-expansion of liquids with temperatures were not considered). As was shown by

---

[19] A. F. Wells, "Structural Inorganic Chemistry", Oxford, Clarendon Press, 1945, p. 69, 975.

Petrescu and co-workers [12] in a comprehensive discussion concerning the self-diffusion of indium in liquid In Sb compound, a better correlation beween viscosity and diffusivity can be acquired by taking into account the thermodynamic factor (activity coefficient) for the non ideal behaviour of the particular diffusion system as well as structural data with respect to the type of packing and the coordination number (that can be obtained by X-ray diffraction, untrasounds).

Such data have not been available so far for the molten indium-aluminium alloys.

CONCLUSIONS

In the present work some new information concerning the self-diffusion in liquid metallic system which exhibit miscibility gap is obtained. It seems to be possible to evidence "clustering phenomenon" by extreme careful diffusivities measurements and little attempt was made on liquid In — 5.5 wt % Al alloy.

However reliable information in this field is still scanty and additional experimental work should be carried out.

Revue Roumaine de Chimie, 14, 35—43 (1969)

Revue Roumaine de Chimie, **14**, 45–55 (1969)

MODÈLE DU GAZ ÉLECTRONIQUE BIDIMENSIONNEL DANS LA CHIMISORPTION SUR MÉTAUX

E. SEGAL

Institut de Chimie physique de l'Académie, Bucarest, 23, str. Dumbrava Roșie

Reçu le 15 février 1968

On reconsidère de façon critique le modèle du gaz électronique bidimensionnel, en tenant compte du phénomène de variation de la chaleur de chimisorption avec le degré de recouvrement de la surface. On obtient ainsi une formule de type Temkine modifiée, dont l'application a fourni des résultats vérifiés de manière satisfaisante par les données expérimentales.

La chimisorption des gaz sur des surfaces solides est accompagnée d'effets thermiques généralement exothermiques. Ceux-ci faiblissent à mesure qu'augmente le degré de recouvrement de la surface. L'interprétation de ce phénomène de variation de la chaleur de chimisorption avec le degré de recouvrement, θ, a constitué l'objet de nombreuses recherches, dirigées surtout sur l'interaction des gaz avec les métaux. Certains résultats peuvent être éventuellement généralisés, de façon à embrasser aussi les interactions gaz-semi-conducteur. L'étude de la variation de la chaleur de chimisorption avec le degré de recouvrement a permis la cristallisation de certaines conceptions qui tendent à expliquer ce phénomène, en l'attribuant principalement aux causes suivantes :

1. *Hétérogénéité de la surface.* D'après Constable[1] et Taylor[2] la diminution de la chaleur de chimisorption avec le degré de recouvrement est due à la hétérogénéité de la surface. Sur une surface hétérogène, les centres d'adsorption sont successivement occupés dans l'ordre de l'affaiblissement de leur activité. Suivant Taylor, la hétérogénéité est due au fait que les pointes et les arêtes des cristaux, les défauts du réseau et les pores, possèdent une capacité d'adsorption beaucoup plus élevée que les surfaces idéales. Des nombreuses expériences qui confirment cette théorie, nous nous bornerons à rappeler celles concernant la désorption de l'oxyde de carbone sur wolfram. Sur une surface polycristalline de wolfram, on a réussi à mettre en évidence quatre modes différents de liaison de l'oxyde

---

[1] F. H. Constable, *Proc. Roy. Soc.*, **A 108**, 355 (1925).
[2] H. S. Taylor, *Proc. Soc. Roy.*, **A 108**, 105 (1925).

de carbone, auxquels correspondent quatre valeurs de la chaleur d'adsorption. [3,4]

On considère que les différences élevées entre les valeurs de la chaleur initiale de chimisorption et celles de la chaleur de chimisorption correspondant à un degré de recouvrement égal à l'unité ne peuvent être dues uniquement à la hétérogénéité de la surface. C'est pourquoi Roberts [5] soutient que la variation de la chaleur d'adsorption est produite aussi par d'autres causes, groupées sous le nom général de :

2. *Interactions superficielles.* La diminution de la chaleur de chimisorption avec le degré de recouvrement est conditionnée par les forces de répulsion agissant entre les corpuscules représentés par les dipôles de la couche adsorbée, même si la surface est homogène.

3. *Variation du travail d'extraction des électrons comme suite de la chimisorption.* D'après Boudart [6] et de Boer, [7] l'apparition d'une couche électrique double, formée par les dipôles superficiels, est cause, d'une part, de la variation de la chaleur de chimisorption avec le degré de recouvrement, et d'autre part, de la variation du travail d'extraction en fonction du même paramètre. Autrement dit, la variation de la chaleur de chimisorption avec le degré de recouvrement est égale, en valeur absolue, avec la variation du travail d'extraction en fonction du degré de recouvrement. Ce type spécial de hétérogénéité est dénommée par Boudart « hétérogénéité induite », tandis que de Boer la définit comme un effet du potentiel de surface.

4. *Variation du type de liaison entre les molécules adsorbées et la surface.* Les liaisons réalisées par les molécules ou les atomes du corps adsorbé changent de caractère à mesure qu'augmente le degré de recouvrement. Ainsi, on sait que le sodium et le cæsium adsorbés sur des surfaces de platine, de cuivre, d'aluminium ou de wolfram, pour des valeurs réduites du degré de recouvrement, forment des liaisons d'un caractère ionique accentué. A mesure que le degré de recouvrement augmente, la liaison d'adsorption change de caractère et se transforme en liaison métallique. [8–10]

5. *Variation de la distribution des électrons dans le métal comme suite de la chimisorption.* Dans la littérature on trouve aussi quelques études qui essaient d'expliquer la diminution de la chaleur de chimisorption avec le degré de recouvrement par le changement de la distribution des électrons dans le métal, changement qui accompagne le phénomène

---

[3] G. Ehrlich, *J. Chem. Phys.*, **34**, 29 (1961).
[4] P. A. Redhead, *Trans. Faraday Soc.*, **57**, 641 (1961).
[5] J. K. Roberts, *Proc. Roy. Soc.*, A **152**, 445 (1935).
[6] M. Boudart, *J. Amer. Chem. Soc.*, **74**, 1531, 3556 (1952).
[7] J. H. de Boer, «Chemisorption», Ed. W. E. Garner, Butterworths, 1957, p. 27.
[8] H. Mayer, *Phil. Mag.* (7), **16**, 594 (1933).
[9] J. H. de Boer et C. F. Voenemans, *Physica*, **2**, 521 (1935).
[10] R. Gomer, *Discuss. Faraday Soc.*, **41**, 14 (1966).

de chimisorption.[11–13] Dans un essai de traiter quantitativement la variation de la chaleur de chimisorption avec le degré de recouvrement, Temkine[14] présente un calcul effectué dans l'hypothèse que cette variation soit due à la variation de l'énergie cinétique des électrons dans le métal. Dans ce but, l'auteur précité a utilisé le modèle du gaz électronique d'après Sommerfeld, avec la différence que ce gaz est considéré bidimensionnel, pour tenir compte du caractère superficiel du phénomène. Par un raisonnement statistique relativement simple, on est arrivé à la relation suivante entre la chaleur de chimisorption, Q, et le degré de recouvrement

$$Q = Q_0 - \frac{h^2 \sigma_0}{4\pi m} \theta \qquad (1)$$

où

Q_0 = chaleur initiale de chimisorption ;
σ_0 = nombre maximum d'atomes adsorbables par cm^2 ;
h = constante de Planck ;
m = masse de l'électron.

Etant donné que :

$$\theta = \frac{\sigma}{\sigma_0}$$

où σ represénte le nombre d'atomes adsorbés par l'unité de surface, l'équation (1) peut être exprimée sous la forme

$$Q = Q_0 - \frac{h^2}{4\pi m} \frac{N}{S} \qquad (1')$$

en notant avec N le nombre total d'atomes adsorbés par la surface S. On retrouve ainsi une bien connue loi linéaire de variation de la chaleur d'adsorption avec le degré de recouvrement

$$Q = Q_0 - a\theta \qquad (1'')$$

valable pour les gaz dont l'adsorption est décrite par l'isotherme logarithmique.

En calculant la valeur approximative du terme $\frac{h^2}{4\pi m} \frac{N}{S}$ pour le recouvrement total de la surface avec une couche monoatomique, on trouve 3,8.10^{12} erg/atome, c'est-à-dire 56 kcal/atome gramme. La valeur expérimentale de la chimisorption de l'hydrogène sur wolfram est, d'après Roberts, [15] de 13,5 kcal/atome gramme H. Pour la chimisorption de l'azote

---

[11] G. M. Schwab, *Trans. Faraday Soc.*, **42**, 689 (1946).

[12] D. D. Eley, *J. Phys. Chem.*, **55**, 1017 (1951).

[13] J. C. P. Mignolet, *J. Chem. Phys.*, **23**, 753 (1955).

[14] M. I. Temkine, « Voprosy Khimitcheskoi kinetiki, cataliza i reaktsionnoi sposobnosti », Izdatelstvo Akademii Nauk S.S.S.R., Moscou, 1955, p. 484.

[15] J. K. Roberts, « Some Problems in Adsorption », 1939, p. 19 (cité par Temkine).

sur fer,[16] la chaleur différentielle de chimisorption varie entre 53 et 39 kcal/mole, donc de 7 kcal/atome gramme d'azote. En analysant ces exemples, on remarque que les valeurs calculées pour la variation totale de la chaleur d'adsorption avec le degré de recouvrement sont de quelques fois plus grandes que les valeurs expérimentales.

On a critiqué le modèle du gaz électronique bidimensionnel, d'une part, à cause des différences entre les valeurs calculées et celles expérimentales, et d'autre part, parce que la variation de la chaleur de chimisorption avec le degré de recouvrement, calculée d'après ce modèle, ne reflète point le caractère spécifique de la chimisorption.[17,18]

Boudart[6] aussi a commenté le fait que l'effet thermique qui accompagne le dissolution de l'hydrogène dans certains métaux, par exemple le βtitane, ne dépend pas de la concentration de ce gaz.[19] La dissolution de l'hydrogène n'exclue pas l'échange d'électrons avec le métal, mais ce processus ne se manifeste point dans la variation de la chaleur de dissolution avec la concentration de l'hydrogène. Il en résulte que, ni dans le cas de la chimisorption, la variation de l'effet thermique avec le degré de recouvrement ne doit être attribuée à l'échange d'électrons entre la phase adsorbée et le métal. D'autre part, Temkine cite l'ouvrage où Fedorova et Frumkine[20] ont démontré que l'effet thermique qui accompagne la dissolution de l'hydrogène (Q_s) dans la phase β du système Pd—H dépend de la concentration de l'hydrogène supplémentaire dissous dans cette phase, d'après la formule

$$Q_s = 46{,}7 - 55{,}2 \frac{[\mathrm{H}]}{[\mathrm{Pd}]} \text{ kcal/mole} \tag{2}$$

où [H] et [Pd] représentent les concentrations atomiques de l'hydrogène, et respectivement du palladium.

Tenant compte, d'une part, des phénomènes décrits ci-dessus, et d'autre part, du fait que la variation de la chaleur de chimisorption avec le degré de recouvrement, pour l'adsorption de certains gaz sur des surfaces métalliques, est décrite par la loi linéaire,[5,21] l'auteur considère qu'il est nécessaire de réanalyser de façon critique le modèle du gaz électronique bidimensionnel, dans le but de le perfectionner, afin de le faire embrasser les données expérimentales.

Commençons par analyser l'indication de Temkine, conformément à laquelle on peut améliorer les résultats, en introduisant la masse effective de l'électron dans la relation (1). La masse effective de l'électron de nickel, d'après les données de Seitz,[22] a une valeur égale à 28 m. En introduisant cette valeur dans la formule (1), on obtient, pour la variation totale de la chaleur de chimisorption de l'hydrogène sur nickel, une valeur égale à 2 kcal/atome gramme, valeur de beaucoup inférieure à celle de 14 kcal/atome gramme, déterminée expérimentalement par Klemperer et Stone, [23] d'où il résulte qu'en tenant compte de la masse effective de l'électron, les résultats obtenus sont loin de se rapprocher des données expérimentales.

---

[16] A. E. Romanushkina, S. L. Kiperman et M. I. Temkine, *Zhur. fiz. Khim.*, **27**, 1181 (1953).

[17] J. H. de Boer, *Adv. Catalysis*, **8**, 18 (1956).

[18] P. M. Gundry et F. C. Tompkins, *Quart. Rev.*, **14**, 257 (1960).

[19] A. D. Mc Quillan, *Proc. Roy. Soc.*, **A 204**, 309 (1952).

[20] A. J. Fedorova et A. N. Frumkine, *Zhur. fiz. Khim.*, **27**, 247 (1953).

[21] G. C. A. Schuit et J. H. de Boer, *Rev. Trav. chim.*, **72**, 909 (1953).

[22] F. Seitz, «The Modern Theory of Solids», Mc Graw-Hill, New York-Londres, 1940, p. 159.

En principe aussi, il est discutable s'il est opportun d'utiliser la masse effective de l'électron. En effet, les valeurs des masses effectives dont nous disposons caractérisent le comportement des électrons dans les corps solides massifs, tandis que dans les phénomènes de chimisorption ce sont les électrons superficiels qui interviennent. D'autre part, les liaisons réalisées sur des surfaces métalliques par les gaz, dont nous allons nous occuper, ont un caractère covalent accentué ; les électrons appartiennent donc presque en égale mesure à la surface et à la couche chimisorbée. C'est pourquoi nous tâcherons de maintenir dans les calculs la valeur de la masse réelle de l'électron.

En analysant le calcul statistique présenté par Temkine, on remarque que celui-ci s'est tacitement basé, dans son raisonnement, sur l'hypothèse que les électrons dont l'énergie cinétique varie à la suite de la chimisorption se trouvent dans l'état quantique *s*. C'est pourtant un fait bien connu, et Temkine lui-même ne manque de le rappeler, que dans le cas des métaux de transition, ce sont les électrons ***d*** ceux qui se trouvent en interaction avec les molécules de gaz, réalisant ainsi le phénomène de chimisorption.

L'auteur se propose de réanalyser le modèle du gaz électronique bidimensionnel, en tenant compte des faits susmentionnés, et de déduire une formule de calcul suffisamment générale pour comprendre l'interaction entre les métaux de transition et les gaz.

On développe la suite des calculs en supposant que le gaz électronique bidimensionnel est dégénéré, la condition de dégénération étant

$$\zeta \gg k_0 T \tag{3}$$

où ζ représente le potentiel chimique de l'électron ;
k_0 = la constante de Boltzmann ;
T = la température absolue.

D'après la mécanique statistique de Fermi-Dirac, la probabilité $f(\varepsilon_k)$ d'occuper un niveau s'exprime comme suit [24]

$$f(\varepsilon_k) = \frac{1}{e^{\frac{\varepsilon k - \zeta}{k_0 T}} + 1} \tag{4}$$

Le nombre d'électrons sur l'unité de surface, $dn_s(\varepsilon)$, ayant des énergies comprises dans l'intervalle ε et $\varepsilon + d\varepsilon$ est, en tenant compte de la dégénération orbitale et du spin, le suivant

---

[23] D. F. Klemperer et F. S. Stone, *Proc. Roy. Soc.*, A **243**, 375 (1957).

[24] A. I. Anselm, «Vvedenie v teoriu poluprovodnikov», Gossudarstvenoe Izdatelstvo fizico-matematicheskoi literatury, Moscou — Leningrad, 1962, p. 202.

$$\mathrm{d}n_s(\varepsilon) = 2\ g\ f(\varepsilon)\ g(\varepsilon)\ \mathrm{d}\varepsilon \tag{5}$$

où g représente le degré de dégénération initiale du niveau atomique duquel provient la bande d'énergie du métal et $g(\varepsilon)\,\mathrm{d}\varepsilon$ le nombre d'états de l'électron correspondant à un intervalle d'énergie compris entre ε et $\varepsilon + \mathrm{d}\varepsilon$.

Dans le cas de l'approximation des électrons libres, pour des valeurs de l'énergie potentielle situées à l'origine ($U = 0$), l'énergie de l'électron se réduit pratiquement à la forme cinétique et s'exprime par la relation

$$\varepsilon\, k = \frac{\hbar^2 k^2}{2m} \tag{6}$$

où k, le soi-disant nombre d'onde, représente le module du vecteur d'onde $\bar{k}$. Etant donné le caractère bidimensionnel du problème, on peut considérer

$$k^2 = k_x^2 + k_y^2 \tag{7}$$

En tenant compte de la condition cyclique[25]

$$\left|\begin{aligned} k_x &= \frac{2\pi}{\mathrm{Na}}\, r_1 \\ k_y &= \frac{2\pi}{\mathrm{Na}}\, r_2 \end{aligned}\right. \qquad r_1 r_2 = 0, \pm 1, \pm 2, \ldots \tag{8}$$

dans laquelle N peut être approximé par le nombre d'atomes du cristal et a représente la période du réseau, on obtient pour k^2 l'expression suivante

$$k^2 = \left(\frac{2\pi}{\mathrm{Na}}\right)^2 (r_1^2 + r_2^2) \tag{9}$$

Les états stationnaires des électrons dans l'espace du réseau inverse (l'espace k) sont représentés par les différents nœuds d'un réseau quadratique ayant une période égale à $\frac{2\pi}{\mathrm{Na}}$. Le nombre d'états, égal au nombre de nœuds de ce réseau, est aussi égal au nombre de cellules élémentaires. Dans ces conditions, une certaine surface σ, située dans l'espace du réseau inverse, contient un nombre d'états égal au nombre de cellules qui se trouvent dans le domaine délimité par celle-ci, c'est-à-dire égal à $\sigma \Big/ \left(\frac{2\pi}{\mathrm{Na}}\right)^2$. Il en résulte que la densité des états dans l'espace bidimensionnel du réseau inverse est égale à $\left(\frac{\mathrm{Na}}{2\pi}\right)^2$ ou bien à $\frac{S}{(2\pi)^2}$, l'expression $(\mathrm{Na})^2$ étant égale à la surface géométrique du réseau bidimensionnel. Les points figuratifs des états correspondant aux valeurs d'énergie comprises entre ε et $\varepsilon + \mathrm{d}\varepsilon$ se trouvent dans le domaine de l'espace bidimensionnel du réseau inverse, situé entre deux cercles concentriques ayant le centre dans l'origine et les rayons k, respectivement $k + \mathrm{d}k$. La surface correspondant à ce domaine est égale à $2\pi\, k\, \mathrm{d}k$. Dans ces conditions, le nombre d'états correspondant aux valeurs des énergies comprises entre ε et $\varepsilon + \mathrm{d}\varepsilon$ est obtenu comme résultat du produit entre la densité des états et cette surface.

---

[25] V. SERGIESCU, «Introducere în fizica solidului», Bucarest, 1956, p. 63.

En calculant ce nombre pour une unité de surface géométrique ($S = 1$), et tenant compte de (6), on obtient

$$g(\varepsilon)\, \mathrm{d}\varepsilon = \frac{m}{2\pi \hbar^2}\, \mathrm{d}\varepsilon \tag{10}$$

ou bien

$$g(\varepsilon) = \frac{m}{2\pi \hbar^2} \tag{11}$$

Pour le cas particulier du mouvement bidimensionnel, le nombre d'états correspondant à un intervalle d'énergie égal à l'unité ne dépend pas de la valeur de l'énergie. On continuera pourtant à le noter avec $g(\varepsilon)$, pour le distinguer du degré de dégénération initiale des niveaux atomiques g.

En intégrant l'équation (5), on obtient la valeur de la concentration superficielle des électrons n_s

$$n_s = 2g \int_0^\infty f(\varepsilon)\, g(\varepsilon)\, \mathrm{d}\varepsilon \tag{12}$$

qui, en tenant compte de (11), devient

$$n_s = \frac{gm}{\pi \hbar^2} \int_0^\infty \frac{1}{e^{\frac{\varepsilon - \zeta}{k_0 T}} + 1}\, \mathrm{d}\varepsilon \tag{13}$$

Pour calculer la concentration superficielle des électrons dans l'hypothèse du gaz électronique dégénéré, on observe que, en tenant compte de l'inégalité (3), la fonction $f(\varepsilon_k)$ de la relation (4), pour des valeurs très élevées ou très réduites de l'énergie, devient respectivement $f(0) = 1$ et $f(\infty) = 0$. De même, on remarque que dans ces conditions le quotient différentiel $\left(-\frac{\partial f}{\partial \varepsilon}\right)$ est différent de zéro seulement pour les valeurs de l'énergie situées autour de $\varepsilon = \zeta$

$$-\frac{\partial f}{\partial \varepsilon} = \delta(\varepsilon - \zeta) \tag{14}$$

et

$$\int_0^\infty \left(-\frac{\partial f}{\partial \varepsilon}\right) \mathrm{d}\varepsilon = -\int_0^\infty \mathrm{d}f = f(0) - f(\infty) = 1 \tag{15}$$

Pour évaluer l'intégrale

$$I = \int_0^\infty \frac{d\varepsilon}{e^{\frac{\varepsilon-\zeta}{k_0 T}} + 1} \tag{16}$$

qui figure dans (13), on doit intégrer par parties. Il en résulte

$$I = \int_0^\infty \varepsilon \delta(\varepsilon - \zeta)\, d\varepsilon = \zeta \tag{17}$$

Introduisant cette relation dans (13), on obtient

$$n_s = \frac{gm}{\pi \hbar^2} \tag{18}$$

d'où

$$\zeta = \frac{\pi \hbar^2}{gm} n_s \tag{19}$$

Pour le cas des systèmes dégénérés, l'expression (5) se simplifie devenant

$$dn_s(\varepsilon) = 2g\, g(\varepsilon)\, d\varepsilon = \frac{gm}{\pi \hbar^2}\, d\varepsilon \tag{20}$$

et l'énergie cinétique totale des électrons de l'unité de surface est exprimée par

$$E = \int_0^\zeta \frac{gm}{\pi \hbar^2} \varepsilon\, d\varepsilon = \frac{gm}{\pi \hbar^2} \frac{\zeta^2}{2} \tag{21}$$

Introduisant dans cette relation l'expression du potentiel chimique de l'électron ζ de (19) on obtient

$$E = \frac{1}{2} \frac{\pi \hbar^2}{gm} n_s^2 \tag{22}$$

A la suite de l'adsorption d'un atome, on gagne une quantité d'énergie μ qui n'est pas totalement libérée sous forme de chaleur d'adsorption, étant donné qu'une partie en est consommée pour la modification de l'énergie cinétique du gaz. Si, à la suite de l'adsorption d'un atome, la variation du nombre d'électrons est égale à l'unité, le changement de l'énergie cinétique deviendra

$$\frac{dE}{dn_s} = \frac{h^2}{4\pi\, gm} n_s \tag{23}$$

Il en résulte que l'adsorption d'un atome sera accompagnée du dégagement d'une quantité de chaleur q, exprimée par

$$q = u - \frac{h^2}{4\pi gm}\,\frac{N}{S} \tag{24}$$

Pour le cas particulier du $g = 1$, on retrouve la formule de Temkine. Il en résulte que le raisonnement de Temkine s'applique seulement aux électrons provenant des niveaux *s* des atomes individuels. L'échange d'électrons avec les gaz dans le cas des métaux de transition est réalisé par les électrons *d* pour lesquels $g = 5$. C'est pourquoi, dans la suite des calculs, on utilise la relation (24) *pro mole*, comme suit

$$\Delta H = \Delta H_0 - \frac{\mathcal{N} h^2}{20\pi\, m}\,\frac{N}{S} \tag{24'}$$

dans laquelle $\mathcal{N}$ représente le nombre d'Avogadro, le reste des grandeurs ayant les significations connues.

Il reste ensuite à vérifier expérimentalement la relation (24′), en comparant les variations totales de la chaleur de chimisorption calculées (jusqu'à $\theta = 1$) avec celles obtenues expérimentalement. Etant donné les approximations de calcul, aussi bien que les erreurs expérimentales, une comparaison avec les valeurs de la chaleur de chimisorption déterminées pour des recouvrements intermédiaires ne serait point concluante. Dans ces conditions, le rapport $\frac{N}{S}$ devient égal au nombre total d'atomes adsorbés sur l'unité de surface, ou, plus exactement, au nombre maximum de liaisons formées entre la surface et les molécules adsorbées par cm^2.

Si à la suite de l'adsorption dissociative d'un gaz, la surface retient des atomes de dimensions inférieures, tout au plus égales aux dimensions des centres d'adsorption, à chaque centre correspondra un atome et le rapport $\frac{N}{S}$ pour le recouvrement complet de la surface sera égal au nombre de centres d'adsorption sur l'unité de surface. On a évalué ce nombre en tenant compte du fait qu'en général les facettes des métaux exposées aux gaz sont caractérisées par des indices réduits (100), (110) et (111),[26] et que la surface correspondant à un centre d'adsorption sur les facettes (100) est proche de la valeur moyenne des surfaces des centres d'adsorption correspondant aux trois facettes. Il sera donc suffisant d'utiliser dans les calculs, en première approximation, les valeurs correspondant aux facettes (100). Pour évaluer ces surfaces, on a utilisé les valeurs des rayons atomiques existant dans la littérature. [27]

L'application de la formule (24′) à différents systèmes gaz-métal a conduit aux résultats suivants :

Système hydrogène-wolfram. En calculant on trouve la valeur 14,2 kcal/atome gramme H pour la variation totale de la chaleur de chimisorption, en accord satisfaisant avec la valeur expérimentale de 13,5 kcal/atome gramme H.[15]

---

[26] B. M. W. Trapnell, « Khemosorbtsia », Izdatelstvo inostrannoi literatury, Moscou, 1958, p. 225.

[27] « Spravochnik khimika », Moscou, 1962, p. 380.

Système hydrogène-tantale. On trouve des résultats satisfaisants aussi dans ce cas, la valeur calculée étant de 13,1 kcal/atome gramme H, par rapport à la valeur de 12 kcal/atome gramme H obtenue expérimentalement.[28]

Système hydrogène-nickel. La concordance entre la valeur calculée pour la variation totale de la chaleur de chimisorption, 18,1 kcal/atome gramme H, et la valeur expérimentale, 14 kcal/atome gramme H,[23] peut encore être considérée satisfaisante.

Système hydrogène-fer. La valeur calculée pour la variation totale de la chaleur de chimisorption est de 17,6 kcal/atome gramme H, tandis que la valeur expérimentale est de 11,5 kcal/atome gramme H.[29] Cette différence est probablement due à la sensibilité des surfaces de fer aux diverses impuretés.

Système azote-fer. Les données expérimentales relatives à la variation totale de la chaleur de chimisorption de l'azote sur des couches minces [30] et des poudres [16] de fer avec le degré de recouvrement sont comprises entre 12 kcal/atome gramme N et 7 kcal/atome gramme N. La chimisorption est supposée de nature atomique et le complexe superficiel créé entre l'azote et le centre actif est probablement de la forme $N \equiv Fe$. [31] On sait encore que l'adsorption de saturation de l'azote sur des surfaces de fer correspond à un atome d'azote pour cinq atomes superficiels [31] de fer, ce qui est dû aux dimensions relativement élevées des atomes d'azote et à l'immobilité de la couche. En calculant la variation totale de la chaleur de chimisorption en fonction des faits susmentionnés, on obtient la valeur de 10,6 kcal/atome gramme N, comprise entre les deux valeurs expérimentales précitées.

Système azote-wolfram. L'adsorption de saturation correspond à un atome d'azote pour deux atomes de wolfram.[32] Supposant l'existence du même type de liaison qu'au cas antérieur, en utilisant la relation (24′) on trouve la valeur de 21,4 kcal/atome gramme N. La valeur expérimentale est de 15 kcal/atome gramme N.[33] On peut attribuer la différence des deux valeurs au fait d'avoir négligé d'autres formes d'adsorption de l'azote, par exemple

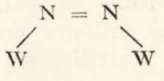

ou

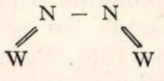

quoique l'existence de celles-ci soit relativement improbable.

Système azote-tantale. Etant donné le diamètre relativement élevé de l'atome de tantale ($d = 2{,}92$ Å), on peut supposer que le nombre maximum d'atomes adsorbés est égal au nombre des centres d'adsorption.

---

[28] O. Beeck, *Discuss. Faraday Soc.*, **8**, 118 (1950).

[29] J. Bagg et F. C. Tompkins, *Trans. Faraday Soc.*, **51**, 1071 (1955).

[30] B. M. W. Trapnell, *op. cit.*, p. 230, 231.

[31] O. Beeck, *Adv. Catalysis*, **2**, 151 (1950).

[32] B. M. W. Trapnell, *Trans. Faraday Soc.*, **48**, 160 (1952).

[33] M. Boudart, *J. Amer. Chem. Soc.*, **74**, 3559 (1952).

En supposant qu'il y a le même type de liaison que dans les cas antérieurs, on trouve avec la relation (24') la valeur de 39 kcal/atome gramme N. La valeur expérimentale est de 35 kcal/atome gramme N, la dépendance de la chaleur d'adsorption du degré de recouvrement n'étant cependant pas parfaitement linéaire.[34]

Système éthylène-wolfram. La valeur de la variation totale de la chaleur d'adsorption de l'éthylène sur wolfram est de 80 kcal/mole.[28] En supposant que la molécule d'éthylène peut engager six liaisons avec la surface du wolfram, conformément au schéma suivant

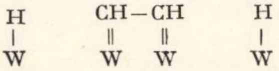

$$\begin{array}{cccc} H & CH{-} & CH & H \\ | & \| & \| & | \\ W & W & W & W \end{array}$$

l'application de la formule (24') nous conduit à la valeur de 85,2 kcal/mole. Dans ce cas aussi, la concordance de la valeur calculée et de celle expérimentale est satisfaisante.

La conclusion qui se dégage de cette étude est que la reconsidération critique du modèle du gaz électronique bidimensionnel conduit à des résultats en accord satisfaisant avec les données expérimentales.

---

[34] O. BEECK, W. A. COLE et A. WHEELER, *Discuss. Faraday Soc.*, **8**, 314 (1950).

Revue Roumaine de Chimie, **14**, 45–55 (1969)

Revue Roumaine de Chimie, **14**, 57—66 (1969)

COMBINAISONS COMPLEXES AVEC DES HYDROXYACIDES. VII

ÉTUDE SPECTROPHOTOMÉTRIQUE DU SYSTÈME $TiO(ClO_4)_2$ — ACIDE D-GLUCONIQUE

Const. GH. MACAROVICI et L. CZEGLÉDI

Institut de Chimie de l'Académie, Filiale de Cluj, 59—65, str. Donath

Reçu le 23 février 1968

Dans l'interaction de l'ion titanyle avec l'acide D - gluconique, on a constaté l'existence dans la solution de trois espèces de complexes, en fonction du pH. Dans le domaine au pH = 3—6 le complexe est du type $1TiO^{2+} : 1\ HGH_4$, mononucléaire, de stabilité moyenne. La constante de dissociation apparente est $K_c = 2{,}2 \cdot 10^{-5}$ moles/l, au pH = 3 ($\lambda = 220$ mμ). Le comportement du complexe permet de doser par voie spectrophotométrique le titane en présence d'acide D-gluconique.

Différents travaux comparatifs ont mis en évidence l'effet complexant de l'acide D-gluconique[1—2].

Les recherches sur l'action complexante de l'acide D-gluconique avec des cations bi- et trivalents[3] ont montré une tendance de formation de complexe plus prononcée envers les ions trivalents qu'envers les ions bivalents. Etant donné l'affinité très prononcée des ions métalliques tétravalents pour l'oxygène comme élément donneur d'électrons, on peut supposer que ces ions seront plus fortement complexés.

Compte tenu de la grande importance accordée par la science et la technique moderne aux éléments du sous-groupe 4 ainsi que de la vaste applicabilité qu'offre l'acide D — gluconique comme agent de chélation, on a étudié potentiométriquement l'action complexante de cet acide sur les ions Ti(IV) Zr(IV) et Th(IV) en solutions aqueuses.[4]

En partant du fait connu que l'ion perchlorique ne tend pas à former des complexes et n'absorbe pas en UV, on étudie dans ce travail par voie spectrophotométrique le système perchlorate de titanyle—acide D-gluconique

Le but du présent travail est d'obtenir une orientation générale sur le système en fonction du pH et de connaître le rapport de combinaison générale entre l'ion titanyle et l'anion acide D-gluconique.

---

[1] C. L. Mehltretter, B. H. Alexander et C. E. Rist, *Ind. Eng. Chem.*, **45**, 2782 (1953)

[2] H. Leopold et Zd. Valter, *Naturwiss.*, **44**, 558 (1957).

[3] D. I. Sawyer, *Chem. Rev.*, **64**, 633 (1964).

[4] Const. Gh. Macarovici, H. Roth et L. Czeglédi, *Studii și Cercetări Chim. Acad. Fil. Cluj*, **12**, 229 (1961).

PARTIE EXPÉRIMENTALE

Appareillage. Les mesures d'absorption ont été effectuées au spectrophotomètre Beckmann-DK-2A, en utilisant des cuves de quartz de 0,5 cm.

Le pH a été mesuré au potentiomètre LP-5 avec des électrodes en verre et du calomel saturé.

Solutions. a) La solution de 0,1 M $TiO(ClO_4)_2$ a été préparée à partir du $TiCl_4$ *p.a.*, par évaporation avec de l'acide perchlorique jusqu'à la formation de la fumée blanche. Dans ces conditions, il reste un excès de $HClO_4$ libre. On a contrôlé l'absence de l'ion chlore à l'aide du nitrate d'argent.[5] La concentration en perchlorate de titanyle a été établie gravimétriquement et la teneur en $HClO_4$ libre a été déterminée par voie volumétrique.

b) On a préparé les solutions d'acide D-gluconique de différentes concentrations, en utilisant des échangeurs d'ions (par ex. Amberlite IR 120, forme hydrogène et gluconate de calcium *p.a.*).

c) A l'établissement des pH souhaités on a employé 0,5M NaOH.

d) La force ionique a été fixée avec du $HClO_4$.

SPECTRES D'ABSORPTION EN FONCTION DU pH

Trois séries de solutions ont été préparées, dans chaque série, la concentration du perchlorate de titanyle étant de 2.10^{-4} M et la force ionique de $\mu = 0,035$. Dans la première série, on n'a pas ajouté d'acide D-gluconique (1 : 0) ; dans la deuxième série, la concentration de l'acide D-gluconique était de 2.10^{-4} M (1 : 1) et dans la troisième série elle était de 1.10^{-3} M (1 : 5). Le pH des solutions a été ajusté avec 0,5 M NaOH. Toutes les solutions ont été maintenues à la température de la chambre pendant plusieurs jours, afin de leur faire atteindre l'équilibre. On a effectué des spectres d'absorption chaque jour, au bout d'un jour, les spectres d'une série étant identiques à ceux d'après trois jours. Les solutions au pH > 2, qui ne contenaient pas de l'acide D-gluconique, étaient instables et, au repos, l'hydroxyde de titane précipitait immédiatement ou après quelques heures. L'acide D-gluconique et l'acide perchlorique, aux concentrations utilisées, absorbant moins de $E = 0,05$, leur concentration n'a pas été prise en considération.

Dans la figure 1 sont représentés les spectres d'absorption des mélanges de 1 :1 titanyle — acide D-gluconique (15 échantillons au pH variant entre 1,53 et 13).

Les spectres aux différents pH n'indiquent pas un maximum d'absorption en UV. L'accroissement de l'absorption des échantillons de pH = = 1,53 — 3,10 à une longueur d'onde donnée représente le domaine de formation du complexe. Deux points isosbestiques sont évidents, dont le premier à $\lambda \cong 240$ mμ et le second à $\lambda \cong 223$ mμ qui indiquent la présence dans la solution de trois espèces de complexes. Pareillement se comporte la série de mélanges au rapport 1 : 5 titanyle — acide D-gluconique.

Vu que les spectres d'absorption aux différents pH représentés en fonction de la longueur d'onde ne se sont pas signalés par un maximum

---

[5] A. K. Babko et L. I. Dubovenko, *Zhur. neorg. Khim*, *4*, 372 (1959).

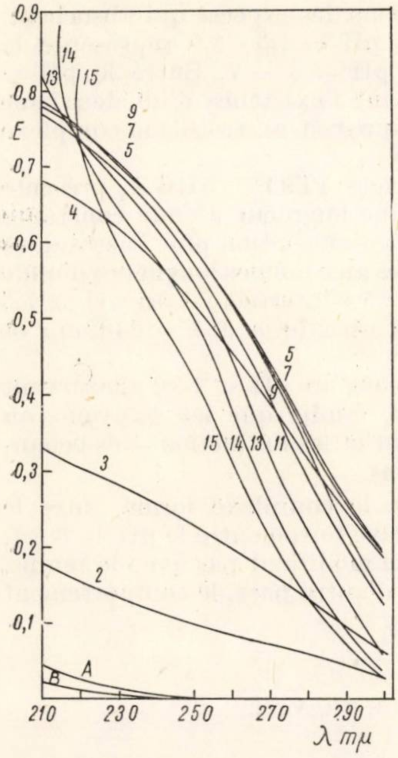

Fig. 1. — Spectres d'absorption des mélanges de concentration $[TiO(ClO_4)_2] = [HGH_4] = 2.10^{-4}$ M, à différents pH ; 2 : pH = 2,04 ; 3 : pH = 2,18 ; 4 : pH = 2,52 ; 5 : pH = 3,10 ; 7 : pH = 4,23 ; 9 : pH = 6,79 ; 11 : pH = 8,58 ; 13 : 1.10^{-3}M NaOH ; 14 : 1.10^{-2} M NaOH ; 15 : 1.10^{-1} M NaOH ;
A : $[TiO(ClO_4)_2] = 2.10^{-4}$ M, pH = = 1, 48 ; B : $[HGH_4] = 2.10^{-4}$ M, pH = 1,5 — 8,5.

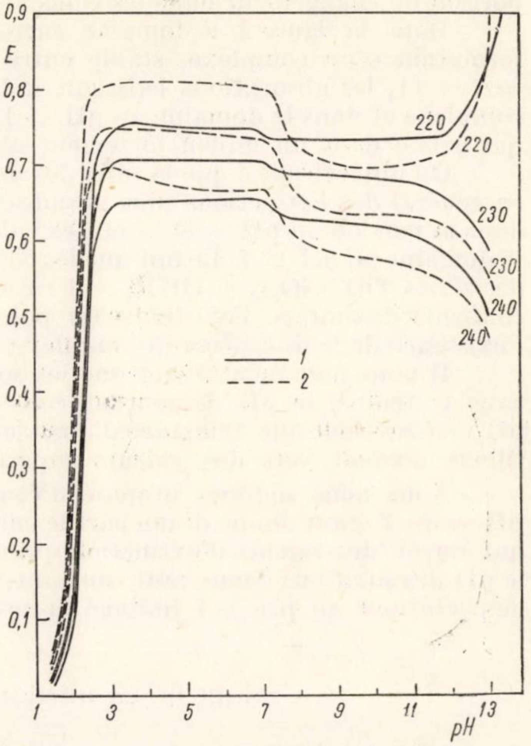

Fig. 2. — Absorption à une longueur d'onde constante (représentée en mμ dans la partie droite de la figure), en fonction du pH: *1*, $[TiO^{2+}] : [HGH_4] = 1:1$; *2*, $[TiO^{2+}] : [HGH_4] = 1:5$.

prononcé, on a passé à la représentation de l'extinction en fonction du pH à une longueur d'onde constante, afin de pouvoir formuler des conclusions plus précises.[6] Les courbes sont représentées dans la figure 2. Dans la région comprise entre le pH = 3 et 7, les courbes d'absorption se présentent comme des lignes parallèles. Dans les régions où ces courbes ont une pente maximum, les spectres se modifient dans la proportion la plus grande. S'il existe des points isosbestiques, les courbes pour ces longueurs d'onde doivent avoir une pente zéro. Les points d'inflexion qui apparaissent représentent donc les valeurs du pH où il y a la plus grande proportion de changement dans les concentrations des espèces qui absorbent.

---

[6] R. L. Pecsok et J. Sandera, *J. Amer. Chem. Soc.*, **77**, 1489 (1955).

Dans la figure 2, le domaine entre le pH = 1,5—3,0 représente la formation d'un complexe, stable entre le pH = 3 — 7. Entre le pH = = 7 — 11, les absorptions baissent, indiquant l'existence d'un deuxième complexe et dans le domaine au pH > 11, apparaît un troisième complexe qui existe dans un milieu fortement alcalin.

On observe aussi que la série des mélanges $1TiO^{2+} : 5HGH_4$ présente en général des extinctions plus grandes à une longueur d'onde constante dans la portion au pH = 3—7 et des valeurs d'extinction plus basses dans le domaine au pH > 7. Le fait que les courbes aux mêmes longueurs d'onde des séries $TiO(ClO_4)_2 + HGH_4 = 1 : 1$ et 1 : 5 s'intersectent au pH ≅ 7,5 confirme davantage l'existence du point isosbestique à $\lambda = 240$ mμ et l'existence de trois espèces de complexes.

Il nous faut mentionner que les solutions au pH < 7 se conservent avec le temps, le pH demeurant constant, tandis que les solutions au pH > 7 révèlent une tendance d'abaissement et les extinctions des échantillons tendent vers des valeurs supérieures.

Nous nous sommes proposé d'étudier le complexe formé entre le pH = 3—7 étant donné d'une part le complexe formé entre le pH = 3—7, qui fournit des valeurs d'extinction qui ne se modifient pas avec le temps, le pH des solutions demeurant constant, et, d'autre part, le comportement des solutions au pH > 7 indiqué ci-dessus.

CHOIX DE LA MÉTHODE DE TRAVAIL

Afin de mettre en évidence le complexe formé dans la solution, dans le domaine du pH = 3—7, entre l'ion TiO^{2+} et l'acide D-gluconique, on a mis à profit trois méthodes spectrophotométriques, à savoir : la *méthode du principe des variations continues*, la *méthode des pentes* et la *méthode du rapport molaire.*

La méthode du principe des variations continues [7–9] s'applique seulement au cas de la formation des composés très stables, à constante de dissociation basse ; la composition du complexe est difficile à établir s'il existe plusieurs ligands. Dans notre cas, le fait que, à un petit excès d'ion central, il se produit une hydrolyse, à la suite de laquelle l'absorption des échantillons augmente, sans provoquer toutefois la précipitation, empêche sensiblement l'évaluation du rapport de combinaison.

La méthode des pentes [10] n'a pas non plus pu être appliquée dans notre cas, parce que l'utilisation de la concentration de l'ion central, en excès important constant, ne permet pas d'évaluer les extinctions réelles, en raison de l'hydrolyse de l'ion central.

La méthode du rapport molaire [11] fournit des résultats satisfaisants seulement au cas où les combinaisons sont très stables. L'aspect des

---

[7] I. Ostromyslenski, *J. Russ. Phys. Chem. Soc.*, **42**, 1332, 1500 (1910).

[8] P. Job, *Compt. rend.*, **180**, 928 (1925).

[9] W. C. Vosburgh et C. R. Cooper, *J. Amer. Chem. Soc.*, **63**, 437 (1941).

[10] A. E. Harvey Jr. et D. L. Manning, *J. Amer. Chem. Soc.*, **72**, 4488 (1950).

[11] J. H. Yoe et A. E. Harvey Jr., *J. Amer. Chem. Soc.*, **70**, 648 (1948).

courbes obtenues, qui représentent le module d'extinction en fonction du volume du ligand pour les complexes plus faibles ou fortement dissociés, ne donne pas des résultats concluants en ce qui concerne le rapport de combinaison entre l'ion central et le ligand.

En raison des difficultés de l'hydrolyse de l'ion central, lors de l'application de la méthode du principe des variations continues et de la méthode du rapport molaire, nous avons appliqué la méthode des droites,[12] fondée sur l'équation de Asmus, valable pour les complexes pas trop stables et dans des solutions suffisamment diluées

$$\frac{1}{v^n} = \frac{a_0 v_0 b_0^n \varepsilon}{V^{n+1} \cdot K_c} \cdot \frac{1}{m} - \left(\frac{b_0}{V}\right)^n \cdot \frac{1}{K_c} \qquad (1)$$

où :

n = nombre des ligands.

K_c = constante de dissociation apparente

$$\mathrm{A} + n\mathrm{B} = \mathrm{AB}_n\,;$$

$$K_c = \frac{[\mathrm{A}] \cdot [\mathrm{B}]^n}{[\mathrm{AB}_n]}\,;$$

ε = coefficient molaire d'extinction à une longueur d'onde bien définie ;

m = module d'extinction ; $m = \frac{E}{d}$ (E = extinction, d = épaisseur de la couche) ;

a_0, b_0 = concentration des solutions ;

v_0 (constant) = volume de la solution de concentration a_0 dans le volume total de V ml ;

v (variable) = volume de la solution de concentration b_0 dans le volume total de V ml.

L'équation (1) représente une droite de la forme $y = Mx - N$.

Le mode opératoire est le même que dans le cas de la méthode du rapport molaire : on lit l'extinction d'une série de solutions qui contiennent dans le même volume final des volumes constants d'ion métallique et des volumes variés, croissants, de ligand, et on représente graphiquement dans un système de coordonnées 1/m en abscisse en cm et $\frac{1}{v^n} \cdot 10^{-3n}$, exprimé en l^{-n}.

On transpose les points sur une ligne droite seulement au cas où « n » est égal au nombre des ligands de la combinaison complexe. On opère donc par tâtonnements, en faisant varier le « n » jusqu'à l'obtention d'une droite.

---

[12] E. Asmus, U. Hinz, K. Ohls et W. Richley, *Z. analyt. Chem.*, **178**, 104 (1960).

La méthode s'applique au cas où K_c a une valeur moyenne, quand le complexe n'est pas trop fortement dissocié.

La droite $\frac{1}{v^n} = f\left(\frac{1}{m}\right)$ — de la relation (1) — intersecte l'ordonnée dans

$$-\left(\frac{b_0}{V}\right)^n \cdot 1/K_c \text{ et donc } K_c = -\left(\frac{b_0}{V}\right)^n \cdot v^n. \qquad (2)$$

DÉTERMINATION DE LA COMPOSITION ET DE LA CONSTANTE DE DISSOCIATION DU COMPLEXE

A la détermination de la composition et de la constante de dissociation du complexe, on a procédé de la façon suivante : dans des ballons jaugés de 50 ml, on prend 1 ml de solution 0,01 M $TiO(ClO_4)_2$ et 1,75 M $HClO_4$ et des volumes croissants de la solution 0,01 M acide D-gluconique ; après une dilution proche du volume final, on ajuste le pH avec du NaOH 0,5 n et on complète le volume à 50 ml avec de l'eau distillée. A l'ajustement du pH, on n'a pas utilisé des solutions tampon, afin de ne pas faire baisser la sensibilité de la réaction.

Pour observer le comportement du complexe en fonction du pH, on a effectué deux séries de mesures à des pH différents. Parmi les valeurs obtenues, on n'a utilisé dans la représentation graphique (figures 3 et 4) ni les valeurs basses, affectées d'erreurs, ni celles qui correspondent aux solutions saturées.

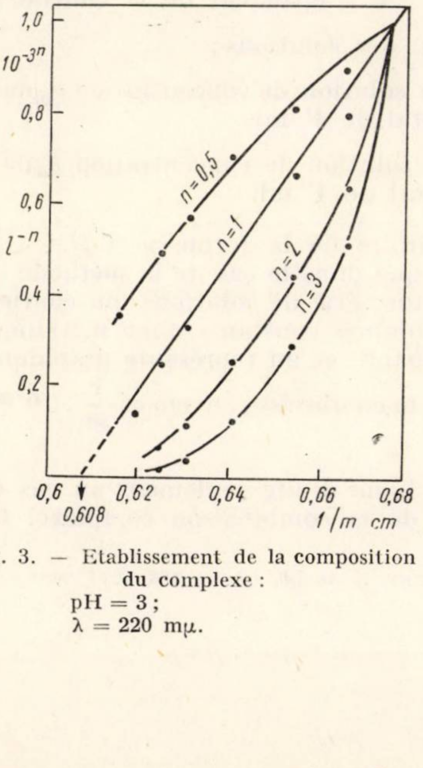

Fig. 3. — Etablissement de la composition du complexe :
pH = 3 ;
λ = 220 mμ.

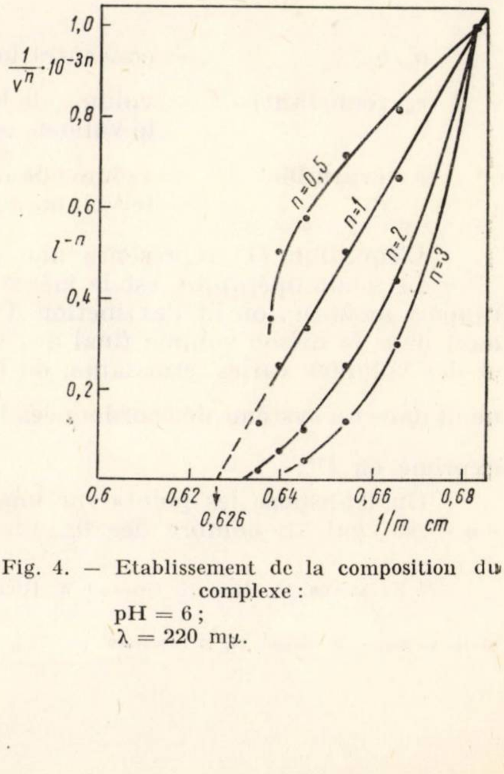

Fig. 4. — Etablissement de la composition du complexe :
pH = 6 ;
λ = 220 mμ.

Il ressort des figures 3 et 4 que, quel que soit le pH de la série (pH = 3 ou 6), seulement la courbe qui correspond pour $n = 1$ est une droite. Il résulte de ces données qu'il y a dans la solution un seul complexe au rapport de combinaison 1 : 1.

On peut calculer la valeur de la constante de dissociation apparente (K_c) de l'intersection de la droite obtenue avec l'axe de l'ordonnée (respectivement la valeur négative de l'ordonnée), où

$$-1/v^n = -(b_0/V)^n \,.\, 1/K_c \quad \text{d'où} \quad K_c = (b_0/V)^n . v^n$$

Dans notre cas, $1/v^n$ ayant une valeur très grande, il est plus avantageux de le calculer de la valeur de la pente de la droite M. On obtient la valeur $-1/v^n$, qui entre dans le calcul de K_c, en multipliant la valeur de la pente M par la valeur $1/m$ pour $-1/v^n = 0$, c'est-à-dire par la valeur de l'intersection de la droite avec l'abscisse déduite du graphique. De la première partie de l'équation (1) on a pu calculer la valeur du coefficient d'extinction molaire (ε = apparent), connaissant la valeur de la K_c. On a aussi calculé la valeur du module d'extinction (m) de la valeur de M, correspondant à la complexation total des ions titanyle, respectivement au rapport de ligand, qui correspond à la complexation totale. Le tableau 1 contient les données susmentionnées.

Tableau 1

Termes qui interviennent lors du calcul de la constante de dissociation

pH	λ mμ	M l^{-1} cm^{-1}	$-\dfrac{1}{v^n}$ l^{-1}	m cm^{-1}	ε l/mole cm	K$_c$ mole/l
3	220	$14{,}93.10^3$	$9{,}07.10^3$	1,644	$8{,}22.10^3$	$2{,}20.10^{-5}$
6		$17{,}60.10^3$	$11{,}01.10^3$	1,598	$7{,}99.10^3$	$1{,}82.10^{-5}$
3	230	$18{,}08.10^3$	$11{,}89.10^3$	1,520	$7{,}60.10^3$	$1{,}68.10^{-5}$
6		$29{,}67.10^3$	$20{,}36.10^3$	1,457	$7{,}28.10^3$	$0{,}98.10^{-5}$

Il ressort des données du tableau 1 que la pente M croît avec l'augmentation du pH ; plus la pente est grande, plus K_c sera petit. Etant donné que ε est fonction de pH, conformément aux courbes d'absorption $E = f$ (pH), les valeurs E baissent un peu du pH = 3 vers le pH = 6 ; par conséquent, les valeurs de ε doivent également diminuer. On a trouvé que le volume de la solution de ligand correspondant à la complexation totale des ions titanyle est de $v = 10$ ml, c'est-à-dire qu'il correspond au rapport ion métallique — ligand de 1 : 10.

La valeur relativement basse de la constante de dissociation à $\lambda = 220$ mμ entre les pH = 3 et 6 ($Kc_{(\mathrm{pH}=3)} = 2{,}20 \,.\, 10^{-5}$ moles/l et $Kc_{(\mathrm{pH}=6)} = 1{,}82.10^{-5}$ moles/l) révèle qu'on a affaire à un complexe de stabilité moyenne.

La valeur de la K_c est donc déterminée par la grandeur de la pente droite, respectivement par l'intersection de la droite avec l'ordonnée. Parallèlement à l'accroissement de la longueur d'onde, croît la valeur de M, et K_c sera de plus en plus petite, pour que, à une valeur donnée de la longueur d'onde, la pente soit parallèle à l'ordonnée et que K_c soit infiniment petite. Cette valeur correspond à un point isosbestique. Dès que la longueur d'onde continue à augmenter, la pente commence à décroître et K_c acquiert des valeurs négatives, ce qui révèle la présence d'un autre complexe.

Dans notre cas, dans la série de $[Ti] = 2.10^{-4}$ M (constant) et $[HGH_4]$ = variable ; le pH = 6,0 — K_c a une valeur de $1,82.10^{-5}$ moles/l à $\lambda = 220$ mμ, décroît à la valeur de $0,98.10^{-5}$ moles/l à $\lambda = 230$ mμ. Le point isosbestique se trouve à la valeur de $\lambda = 235$ mμ, où K_c a une valeur très basse, pour que, à des valeurs de longueur d'onde plus grandes, la pente de la droite, respectivement l'intersection avec l'ordonnée, acquière des valeurs plus basses qui décroissent avec l'accroissement de la longueur d'onde, ce qui indique la présence d'un autre complexe.

D'ailleurs, ce fait s'observe aussi d'après l'aspect des courbes, qui représentent l'extinction par rapport au volume du ligand, où, à un volume de solution d'ion métallique constant, on a ajouté des volumes croissants de ligand, de la même concentration (série au pH = 6). A $\lambda = 220-230$ mμ, les courbes révèlent des valeurs croissantes de l'extinction en fonction du volume d'acide D-gluconique ajouté. A $\lambda = 235$ mμ, on obtient des extinctions approximativement constantes (point isosbestique) et à $\lambda = 240-260$ mμ, les extinctions décroissent en fonction du volume du ligand ajouté.

POSSIBILITÉ DE DOSAGE SPECTROPHOTOMÉTRIQUE DU TITANE EN PRÉSENCE D'ACIDE D-GLUCONIQUE

On a constaté que, à la dilution des mélanges au pH = 3—6, où le rapport entre l'ion métallique et le ligand était de 1 : 1 et 1 : 5 ($[TiO(ClO_4)_2] = 2.10^{-4}$ M) et le pH constant, il ne se produisait pas de modification des extinctions jusqu'à la dilution d'environ 8 fois, si les mesures étaient effectuées avec des cuvettes de dimensions correspondantes, ce qui dénote une stabilité suffisante du complexe.

Le fait qu'un grand excès de réactif est nécessaire (au moins 10 : 1 rapport molaire) pour l'engagement dans le complexe de la quantité totale d'ion métallique nous a suggéré l'idée de vérifier l'applicabilité de la loi de Beer au domaine des concentrations d'ion métallique 2.10^{-5} M — 2.10^{-4} M, en présence de l'acide D-gluconique de concentration 1.10^{-3}M

On a procédé de la façon suivante : dans des ballons jaugés de 50 ml, on prend des volumes croissants (0,1—1,0 ml) de solution 0,01 M $TiO(ClO_4)_2$ en solution de 1,75 M $HClO_4$ et on y ajoute de l'acide perchlorique, tel que, finalement, la force ionique soit de $\mu = 0,035$, et 5 ml d'acide D-gluconique 0,01 M. Après dilution par de l'eau distillée proche du volume final, on ajuste le pH au pH = 3 avec 0,5 M NaOH, on complète le volume jusqu' à 50 ml avec de l'eau distillée et on lit les extinctions des échantillons après 24 heures.

Les résultats obtenus, reportés à la figure 5, représentent graphiquement l'extinction des échantillons en fonction de la quantité d'ion métallique.

La figure 5 permet de constater que pour les deux longueurs d'onde on a obtenu des droites, ce qui signifie que la loi de Beer s'applique et que la méthode se prête au dosage du titane par voie spectrophotométrique dans l'intervalle de 50—500 μg TiO^{2+}.

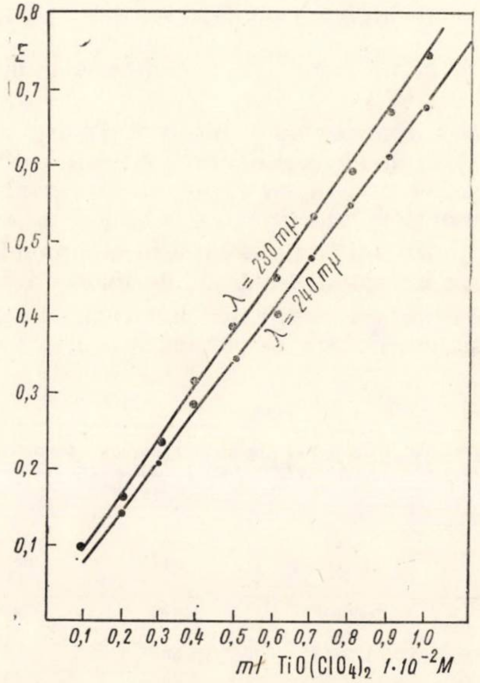

Fig. 5. — Courbe d'étalonnement du dosage du titane par de l'acide D-gluconique ; 1.10^{-2} M TiO $(ClO_4)_2$ et 1,75 MH ClO$_4$ (v = 0,1 — — 1,0 ml) et 5 ml d'acide D-gluconique 1.10^{-2} M ; V = 50 ml ; pH = 3,0 ; cuve 0,5 cm ; référence eau.

Il faut remarquer qu'à des dilutions de 10 fois des échantillons' l'extinction mesurée avec la cuve de 5 cm se superpose dans la plupart des points aux échantillons non dilués (mesurés avec la cuve de 0,5 cm), indifféremment si la dilution a été faite avec une solution au pH = 3 et μ = 0,035 (dans de l'acide perchlorique) ou si les épreuves ont été diluées avec de l'eau. Dans ce dernier cas, le pH augmente presque d'une unité ; par conséquent, l'accroissement du pH = 3 au pH $\cong$ 4 ne dérange pas le dosage.

Klausen et ses collaborateurs [13] discutent l'applicabilité de la méthode de la ligne droite à la détermination de la composition des complexes polynucléaires et soutiennent que la méthode n'est pas capable de faire la distinction entre les espèces mono- et polynucléaires.

---

[13] K. S. Klausen et F. J. Langmyhr, *Analyt. Chim. Acta*, **28**, 501 (1963).

On obtient expérimentalement la valeur du nombre des ligands « n » du complexe $A_m B_n$, en utilisant des concentrations constantes de A et des concentrations variables de B. En prenant la concentration du B constante et différentes quantités de A, on obtient une ligne droite pour la valeur exacte de « m » du complexe $A_m B_n$, lorsqu'on représente graphiquement $\frac{1}{v^m}$ en fonction de $1/E$. Si, dans les deux séries de solutions il ne prédomine qu'un complexe, la composition de celui-ci est donnée par la valeur de « m » et « n ».

En utilisant les données du tableau 2 (figure 5), qui représentent les valeurs d'extinction de la série ligand constant — ion central variable, au pH = 3 et $\lambda = 240$ mμ, et en représentant graphiquement $1/v^m$, en fonction de $1/E$, on obtient une droite à la valeur de « m » = 1.

Cela indique qu'il s'agit d'un complexe mononucléaier où le rapport de l'ion central avec le ligand est 1 : 1, de forme AB.

Cette constatation est confirmée aussi par l'examen des courbes des variations continues, où, sur la portion $x = 0...0{,}5$ (fraction molaire $x = \frac{[\mathrm{TiO}^{2+}]}{[\mathrm{TiO}^{2+}] + [\mathrm{HGH}_4]}$), on obtient une droite sans inflexions,[14] ce qui dénote la présence dans la solution du complexe AB avec $m = n = 1$.

Tableau 2

1.10^{-2} M TiO $(ClO_4)_2$ et 1,75 M $HClO_4$ (vml) + 1.10^{-3} M acide D-gluconique (5 ml) : volume total 50 ml : pH = 3 : cuve d = 0,5 cm : référence eau ; λ = 240 mμ ; μ = 0,035

v	E	$\frac{1}{E}$	$\frac{1}{(10\,v)}$	$\frac{1}{(10\,v)^2}$	$\frac{1}{(10\,v)^3}$
0,08	0,058	17,24	1,250	1,56	1,95
0,1	0,077	12,99	1	1	1
0,2	0,140	7,14	0,50	0,25	0,125
0,3	0,207	4,83	0,333	0,111	0,037
0,4	0,283	3,53	0,250	0,060	0,015
0,5	0,351	2,83	0,200	0,040	0,008
0,6	0,407	2,46	0,166	0,028	0,004
0,8	0,544	1,84	0,125	0,015	0,002
0,9	0,613	1,63	0,111	0,012	0,001
1,0	0,680	1,47	0,1	0,01	0,001

---

[14] K.S. Klausen et F. J. Langmyhr, *Analyt. Chim. Acta*, **28**, 335 (1963).

Revue Roumaine de Chimie, **14**, 67 – 77 (1969)

VISCOSITY AND DENSITY OF THE MOLTEN InBi COMPOUND

N. PETRESCU

Institute of Physical Chemistry of the Academy, Bucharest, str. Galaţi 31

Received April 24, 1968

The viscosity and the density of the molten InBi compound were studied in the pre-freezing range, from the melting point up to a superheating of 110°. The density was measured through a dilatometric method ; it varies with temperature according to relation : $\rho = 8.873 - 1.074 \cdot 10^{-3}\ t°$. The mixing volume is positive (+0.87 % at the melting point) and it increases as temperature rises. The viscosity was measured through the oscillating cylinder method. It depends on temperature according to Arrhenius relation : $\ln \eta = 679.5 \frac{1}{T} - 5.500$, except a temperature range of 10° above the melting point, where the viscosity presents positive deviations from the above relationship. The free activation energy of viscous flow was calculated ; its temperature dependence presents a minimum at 115°. The positive deviations of viscosity and the minimum in the free energy of viscous flow can be ascribed to the existence of a short-range order in the melt, at temperatures near the solidification point.

At present, there is general agreement about the fact that in the metallic melts, at least for certain compositions and in the vicinity of the freezing point, structural modifications are taking place ; these changes are pronounced enough to be detected experimentally by means of determinations on the structure and on the properties of the melts. As regards the fundamental understanding of these processes which are taking place in the metallic melts, no considerable advances have been made. Though certain explanations which have been given are intellectually satisfying, they do not yet permit a quantitative evaluation of the influence of the structural modifications in the properties of the melt. Even if the amount of experimental evidence obtained up to now has allowed certain correlations suited to several types of alloys in the liquid state to be established, there are always exceptions. Many experimental and theoretical studies are still needed, in order that the prediction of the properties of metallic melts in the pre-freezing region becomes feasible.

The molten InBi compound and generally the liquid alloys in the In–Bi system have formed the object of a series of studies regarding their structure and physical properties. However the conclusions arrived at are far from being concordant. Though the structure of the molten In–Bi alloys was systematically studied by means of different investigation methods,[1–7] still the opinions about the existence in the melts of distinctive structural characteristics susceptible to be related to the structure of the compounds In_2Bi and InBi are controversial. For instance one of the papers [2] concerning the X-ray investigation of the molten In—Bi eutectic with 47.28 at % In (situated in the close proximity of the InBi compound) leads to the conclusion about the existence in the eutectic melt of micro-regions having the structure of the InBi compound, respectively of pure Bi. But in another paper [3] based also on X-ray diffraction technique, the conclusion is that the structure of the liquid alloy with the composition of the InBi compound is characterized by a quasi-eutectic distribution of the atoms in micro-regions comprising essentially the pure components of the alloy.

The liquid In—Bi alloys have formed the object of structural studies carried out by means of the nuclear magnetic resonance method, till now scarcely applied to this purpose. By means of this method the values of the ratio $\Delta k/K$ for both kinds of nuclei in the alloy have been determined (where K is the Knight shift in the pure metal melt and Δk is the difference between the Knight shift in the pure metal melt and in the alloy melt). From the study of the variation of the Knight shift with the composition ,[4] it appears that in the melts of the In—Bi system there is not a linear variation with composition of the ratio $\Delta k/K$ as it was observed in a series of other liquid alloy systems which comprise no intermetallic compound or in the range of solid solution of alloys in solid state. By analysing the experimental data, the idea was advanced [4] that the Knight shift is sensitive to the short-range order, and in the particular case of the In—Bi system it provides evidence that the compounds persist in liquid state. Another investigation [5] of the nuclear magnetic resonance in the liquid In—Bi system, carried out in the temperature range 200—285°, reaches the conclusion that a mechanical mixture of In and Bi is present in the liquid.

The examination of some other physical properties of the liquid alloys in the In—Bi system does not contribute supplemental clearings up about the structure of the molten InBi compound. So, when determining the thermo-electro-motive force[8] in the melts of the In—Bi system, at the composition of the InBi compound a maximum was present; this was more persistent when the temperature was risen than the maximum corresponding to the In_2Bi compound. Still, on the other hand, when

---

[1] Ia. I. Dutcheak, N. M. Klym and A. G. Mikolaichiuk, *Fiz. Metal. i Metalloved.*, **14**, 787 (1962).

[2] Ia. I. Dutcheak and N. M. Klym, *Zhur. fiz. Khim.*, **39**, 766 (1965).

[3] A. V. Romanova and R. M. Kuchiak, *Ukrain. fiz. Zhur.*, **9**, 428 (1964).

[4] E. F. W. Seymaur and G. A. Styles, *Proc. Phys. Soc.*, **87**, 473 (1966).

[5] Setty Radhakrishma and B. D. Mungurwadi, *Current Sci.* (*India*), **35**, 405 (1966).

[6] N. V. Alekseev, Ia. I. Gerasimov and A. M. Evseev, *Doklady Akad. Nauk SSSR*, **129**, 563 (1959).

[7] Ia. I. Dutcheak, A. G. Mikolaichiuk and N. M. Klym, *Fiz. Met. i Metalloved.*, **14**, 548 (1962).

[8] Ia. I. Dutcheak and O. P. Stetskiv, *Zhur. fiz. Khim.*, **15**, 718 (1966).

determining the electrical conductivity[9] of the In–Bi system melts, the InBi compound was not marked on the curve dρ/dt versus composition, in contrast with the In_2Bi compound for which a pronounced maximum was manifest.

In the present paper are given the results of the viscosity study made on the InBi compound, which, at least in solid state, can be considered the most stable compound of the system. About its stability in liquid state quite different opinions were expressed.

We chose the viscosity as investigation method on account of the following considerations : viscosity is esteemed to be a precise method, more sensitive than other transport properties to the structural anomalies which may occur in the vicinity of the freezing point. Of course other methods, e.g. the direct structural methods, may give more penetrating information about the structural modifications, but the interpretation of the results is more complex than for the viscosity and more largely subject to discussion. The relatively large number of viscosity studies carried out on different metallic systems, allowed establishing of some relationships between the variation of the viscosity and the specific interactions among the components.

EXPERIMENTAL. INTERPRETATION OF RESULTS

The viscosity and the density of the molten InBi compound have been determined on a material whose stoechiometry and purity were rigorously observed. These careful precautions were necessary because of the existence of the eutectic InBi–Bi (at 52.7 at %Bi) situated on the phase diagram in the close proximity of the InBi compound. The preparing operations comprised the synthesis of the compound from pure indium (99.999 %) and from bismuth of an alike purity produced by Johnson-Mathey Comp. Because of the oxide present on the bismuth surface, the bismuth was used after melting and reducing; these operations were carried out in a boat of spectrally pure graphite, at 600° in pure hydrogen.

The synthesis of the compound was performed at a temperature scarcely higher than the melting point of bismuth in a Pyrex vacuum sealed ampoule.

The compound in the form of an ingot 1 cm^2 cross-section and 25 cm length was zone refined through ten passes of the molten zone ; the length of the liquid zone was 2 cm and its travelling speed 2.5 cm/hour. After zone melting not only a high purity was attained but also the exact stoichiometric composition of the compound was ensured. To verify this, a detailed metallographic examination of several samples was performed. Up to 600 field magnification, in the microscope's image field a single phase (e.g. the compound) was visible.

The density measurements of the molten compound have been carried out by an improved dilatometric method.[10] By the statistical analysis of our experimental results, relation (1) was obtained for the temperature dependence of the density of the molten InBi compound.

---

[9] Franco Gauzzi and Umberto Bernabai, *La Ricerca Sci.*, **36**, 548 (1966).

[10] N. Petrescu, St. Zămîrcă, L. Ganovici and I. Ganovici, *Rev. Roumaine Chim.*, **13**, 865 (1968).

$$\rho = 8.873 - 1.074 \cdot 10^{-3} t^\circ \qquad (1)$$

On the basis of the density values obtained from relation (1) as well as on the basis of the extrapolated density of the pure components,[11,12] the excess volume of the molten compound was computed. The calculated values are given in table 1.

Table 1

The density and the mixing volume of the molten InBi compound

Temp.	ρ_{InBi}	ΔV^M	$\frac{\Delta V^M \cdot 100}{V_{id}}$
115	8.750	+0.318	+0.867 %
150	8.712	+0.323	+0.877 %
185	8.674	+0.328	+0.887 %
220	8.637	+0.333	+0.896 %
350	8.497	+0.360	+0.953 %

One may observe that the excess volume is positive and has a slight tendency to increase as the temperature rises. This behaviour is difficult to explain when taking into account the mixing enthalpy of the molten alloy and the structural characteristics of the solid compound. In liquid state, most of the compounds have negative mixing enthalpies and negative mixing volume. The molten InBi compound has also a negative mixing enthalpy, but a positive mixing volume. A series of compounds, e.g. InSb, have alike as InBi a negative mixing enthalpy and a positive mixing volume, but in most cases the explanation of their behaviour can be found in the open structure of the solid compound. So, we calculated for the InSb compound, from the density data in the literature,[12,13] a mixing volume in solid state at 20° of +20 % and in liquid state at 700° of +3 %. As can be seen from these data, the positive mixing volume of the molten InSb can be ascribed to the persistency, to some extent, of the characteristics of the open structure of the solid compound, in which directional interatomic bonds are present.

For the InBi compound, the explanation cannot be this. From our density measurements on the InBi compound in solid state, the mixing volume at 20° is −2.4 %. The mixing volume of the compound in liquid

---

[11] S. W. Strauss and L. E. Richards, *J. Nuclear Materials*, **1**, 12 (1963).

[12] A. Schneider and G. Heymer, *Z. anorg. Chem.*, **286**, 118 (1956).

[13] N. P. Makovski and A. R. Regel, *Zhur. tekhn. Fiz.* **12**, 1281 (1952).

state was calculated in table 1. From this point of view the behaviour of the InBi compound resembles more to that of the Mg_3Bi_2 compound, which has a mixing volume of -2.1% in solid state and of $+2\%$ in liquid state. For the InBi compound, just as in the case of the Mg_3Bi_2 compound, the negative mixing volume in solid state can result from the open structure with covalent bonds of the solid bismuth and from the compact metallic structure of the liquid bismuth. As compared with the open structure of the solid bismuth, the structure of the compound, owing to its heteropolar bonds, appears more compact (negative mixing volume) but as compared with the compact metallic structure of the liquid bismuth, the molten compound can preserve a sufficient amount of heteropolar bonds to afford itself a more open structure (positive mixing volume). As regards an other explanation which can be given, we shall discuss it later, after having presented the viscosity determinations.

The viscosity measurements have been carried out by means of the oscillating cylinder method. The oscillations have been photographically recorded and the amplitudes have been measured with ± 0.1 mm accuracy. The times of oscillation were measured by means of an electronic device, with the accuracy of ± 1 msec. The determinations have been carried out, in high vacuum (5.10^{-5} thorrs). The temperature was kept constant with ±1° accuracy by thermostating the system with a liquid in circuit with an ultrathermostat. The distancee between the movable system of the crucible and the thermostating liquid, e.g. the size of the evacuated room, was kept at a minimum. The logarithmic decrement of the damping of the oscillations was computed by least square analysis of the values of all the recorded oscillations. To account for the errors due to the meniscus of the metal in the crucible, to the state of the free surface of the molten metal (eventual oxides traces), or to the geometry of the crucible's bottom, the determinations were carried out at two and sometimes even at three different levels of the metal in the crucible. On the basis of these determinations the correction factor h introduced by Armbruster [14] was calculated by means of relation (2).

$$h = \frac{H_1 H_2(\sqrt{\nu_1} - \sqrt{\nu_2})}{H_2\sqrt{\nu_2} - H_1\sqrt{\nu_1}} \tag{2}$$

In relation (2), ν_1 and ν_2 are the kinematic viscosities determined at level 1 and 2; H_1 and H_2 represent the heights of the liquid metal in the crucible in the respective determinations. The viscosity was computed by means of relation (3), and the auxiliary relation (4), both comprising the correction factor h.

$$\nu = \frac{1}{\pi}\left(\frac{k}{MR\,\dfrac{H_0 - h}{H_0}}\right)^2 \frac{(\delta - \tau/\tau_0\cdot\delta_0)^2}{\tau\sigma^2} \tag{3}$$

$$\sigma = A - \frac{3}{2}\left(\frac{\delta}{2\pi}\right) + \frac{2nR}{H_0 + h}\left(B - C\frac{\delta}{2\pi}\right) \tag{4}$$

The significance of the magnitudes entering relations (3) and (4) is :

M = mass of metal in the crucible ; K = axial moment of inertia of the movable system, determined experimentally by means of two standard weights[14] ; R = inner radius of the crucible ; H_0 = height of metal in the crucible ; δ, δ_0 = logarithmic decrement of oscillations of the crucible filled with the molten metal, respectively of the empty crucible ; τ, τ_0 = time of one oscillation of the movable system comprising the filled, respectively the empty crucible ; A, B, C = numerical coefficients, determinable as a function of a parameter $y = 2\pi R^2/\tau\nu$. Because ν enters the expression of the viscosity through the parameter y, the computation is performed by means of successive approximations. The factor n stands for the number of horizontal friction surfaces, and has a value comprised between 1 (upper surface of the melt absolutely free — absence of oxides —) and 2 when the upper surface is rigidized (for instance by means of rigid oxide films).

The right choice of n affects the value of the viscosity if calculated through the relation without the correction h, but has a very small importance if relation (3) is used, where h assumes the eventual errors in the choice of n. The computations made for $n = 1$ and $n = 2$ proved that.

Table 2

Kinematic and dynamic viscosity of the molten InBi compound

Temp.	112	115	120	130	150	170	180	185	220
ν cst.	0.2981	0.2819	0.2663	0.2536	0.2330	0.2172	0.2105	0.2090	0.1879
η cps.	2.609	2.466	2.329	2.215	2.030	1.888	1.827	1.813	1.623

Since the viscosity determinations aimed at detecting the transformations in the pre-freezing interval, the measurements were made in a temperature range of 110° above the freezing point. At each temperature the measurement was made only after attainment of the thermal equilibrium (four hours to this purpose).

The results of the determinations of the kinematic viscosity as function of temperature are presented in table 2. On the graph in figure 1 the peculiarities of the variation of the viscosity cannot be seized. In order to make evident the anomalies of the viscosity in the neighbourhood of the freezing point, it is necessary to choose a temperature dependency supposed to be normal, and to extrapolate it in the pre-freezing range ; the values which do not agree with this dependence will be esteemed as deviations. As a normal dependence one chooses a relation which correlates well the experimental data in the range of higher temperatures. The most general relation of this kind, resulting from many structural models and which was often successfully applied to represent the experimental data, is an Arrhenius type relation. To ascertain the agreement with this relation, our experimental data were plotted in figure 2 in coordinates $\ln \eta = f\left(\frac{l}{T}\right)$. It is obvious that down to about 120° the experimental points are situated on a straight line according to the Arrhenius equation; at lower temperatures, that is below 120°, the experimentally determined viscosity is greater than the viscosity resulting from the linear temperature dependence of $\ln \eta$. The analytical expression of the linear portion of the experimental curve in figure 2, calculated through the least square treatment of the experimental data is:

---

[14] J. C. Armbruster, "Thèses", Faculté des Sciences, Paris, 1961.

$$\ln \eta = 679.53 \frac{l}{T} - 5.500 \qquad (5)$$

From relation (5), a value of $4.083 \cdot 10^{-3}$ ps. was computed for the pre-exponential factor in the Arrhenius equation; the activation energy of the viscosity calculated from the same relation was equal to 1,350 cal/grd, mol.

In the temperature range below 120°, the modification of the slope of the curve means an increase of the activation energy of the viscosity up to 5,562 cal/grd, mol in the interval of our last measurements. Owing to the narrowness of this temperature range, it is difficult to state if the activation energy varies according to a curve, or if another fixed value of the activation energy settles, as suggested in some papers. [15,16]

Other information about the particularities in the viscosity variation can be obtained by interpreting the experimental data according to the model proposed by Eyring, in treating the transport properties on the basis of the theory of absolute reaction rates. In this theory, the vis-

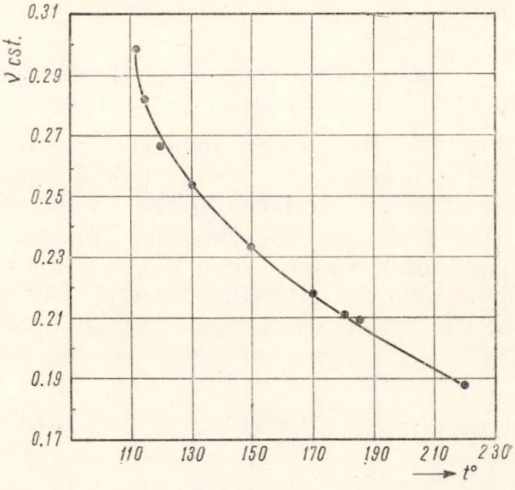

Fig. 1. — Kinematic viscosity of the molten InBi compound.

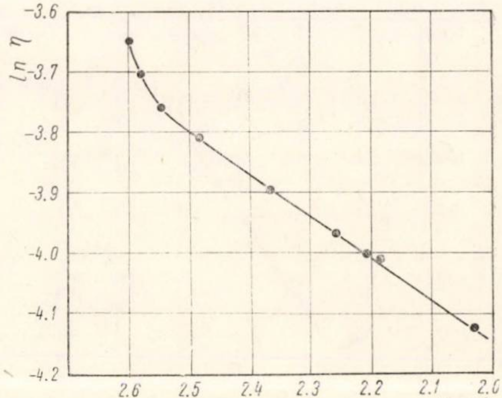

Fig. 2. — Representation of viscosity experimental data in coordinates of the Arrhenius type relation.

---

[15] L. I. Cesnokov, *Zhur. fiz. Khim.*, **39**, 699 (1965).
[16] M. M. Qurashi, *J. Phys. Chem.*, **67**, 955 (1963).

cosity is expressed in terms of the free energy of activation of the viscous flow, according to relation :

$$\Delta G = RT \ln \frac{V\eta}{hN} \quad (6)$$

where :

ΔG = free energy of activation of viscous flow ; V = molar volume ; h = Planck's constant ; N = Avogadro's number.

The free energy of activation is a linear function of temperature, in the absence of structural modifications in the liquid. This behaviour was verified for pure molten metals, e.g. Al and Cu.

From the experimental data on the viscosity of the molten InBi compound, we computed the free energy of activation, whose temperature dependence is given in figure 3. The free energy of activation decreases in the temperature range from the melting point to 115°, where a minimum is reached ; henceforth as the temperature rises the free energy of activation increases in a continuous and uniform manner.

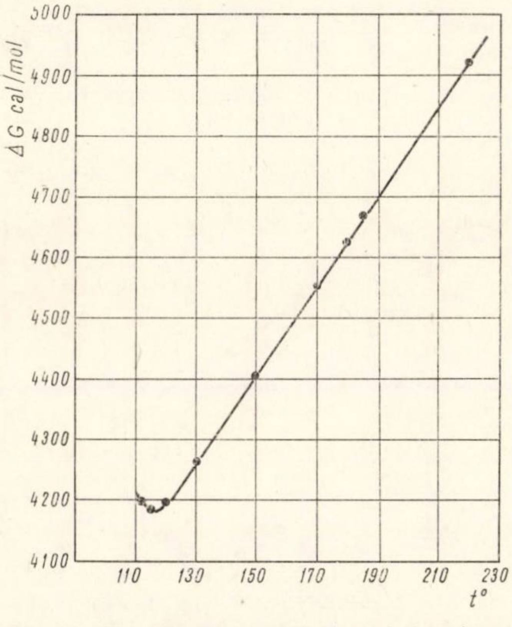

Fig. 3. — Free energy of activation of the viscous flow of the molten InBi compound.

Usually the minimum of the free energy of the viscous flow is taken as indicating a transformation which occurs in the structure of the liquid. For most molten compounds this minimum is found at 25—50° above the melting temperature. For instance for the In_2Bi compound it is situated at 30° above the melting point. [1]

The minimum of the free energy of the viscous flow found at a temperature only 5° above the freezing point, may be taken as indicating a trend towards instability of the preferential bonds between unlike atoms in the molten InBi compound, as compared with other compounds. This agrees with the estimation that is to be attached to the magnitude of the viscosity values obtained, as compared with the viscosities of the components. A comparison between the viscosity of the compound and the viscosities of the components is useful, since many of the attempts to derive an expression for the viscosity of an alloy from the viscosities of its components involve a term that is dependent on the energy of the interatomic bonds. For the ideal solutions the viscosity can be calculated through the simple or the logarithmic additivity rule (6) or (7).

$$\eta = x_1\eta_1 + x_2\eta_2 \tag{7}$$

$$\ln \eta = x_1 \ln \eta_1 + x_2 \ln \eta_2 \tag{8}$$

In the melts of the intermetallic compounds, where a great affinity among the components is manifest (negative mixing enthalpy, negative mixing volume) large positive deviations of the viscosity from the above relations are observed.

The difficulties encountered in the calculation of the viscosities of the mixtures directly from the interatomic potentials (e.g. through the Born-Green theory [17]) have given rise to the attempts to extend the additivity relations by taking into account the excess enthalpy,[18] the partial molar enthalpy [19] or the volumetric changes ;[20] however the resulting relations can be successfully applied only for liquids which do not deviate much from the behaviour of regular solutions. Yet it is still interesting to analyse, even if from a qualitative standpoint, the ratio between the viscosity of the compound and that of the components.

When comparing the experimental values of the viscosity of the InBi compound with those calculated from the pure components viscosities [21,22] by means of relation (7) or (8), one must take into account that the least temperature above which both components and compound are in liquid state is 271° (the melting point of bismuth) ; at this temperature the molten compound is in a pronounced state of superheating (160° above its melting point). At such temperatures the viscosity of the InBi compound determined experimentally is less than the viscosity calculated through relations (7) and (8). The negative excess viscosity observed for the molten InBi compound represents a particular case among the metallic liquid solutions with negative mixing enthalpy. However, organic systems are known [23] in which the excess viscosity changes its sign throughout the system, while the excess enthalpy keeps its sign constant. At some extent the negative excess viscosity could be ascribed to the positive excess volume exhibited by the molten InBi compound, according to the idea expressed in Bachinski's equation that viscosity is dependent on density (eq. 9) : $V = a + \frac{C}{\eta}$ (9) (where V = specific volume, a and C = constants).

---

[17] M. Born and H. S. Green, "A General Kinetic Theory of Liquids". 1949, Cambridge, University Press.

[18] J. Vander, *Acta Chim. Acad. Sci. Hung.*, **6**, 1 (1955).

[19] L. A. Koledov, A. P. Liubimov, *Izvest. V.U.Z. Chiorn. Metallurg.* **1963**, 136.

[20] L. I. Gvozdeva and A. P. Liubimov, *Izvest. V.U.Z., Chiorn. Metallurg.*, **1965**, 13.

[21] M. F. Culpin, *Proc. Phys. Soc.*, **70**, 1069, (1957).

[22] D. Ofte and L. J. Wittenberg, *Trans. A.I.M.E.* **227**, 706 (1963).

[23] M. Rother and H. Y. Bittrich, *Z. phys. Chem. (Leipzig)*, **235**, 195 (1967).

However, in the case of other compounds, e.g. InSb compound equally having a positive excess volume, and for equally high superheatings, the excess viscosity is positive. From the data of the viscosity of the InSb compound, [24] we have calculated at 700° an excess viscosity of $+60\%$ through relation (7) and $+62.5\%$ through relation (8). The excess viscosity of the InBi compound at 350° is -10.3%. The mixing enthalpies of these compounds in liquid state are not too much different.[25,26] ($\Delta H = -600$ cal/g. atom for InSb and $\Delta H = -440$ cal/g. atom for InBi).

The differences between the viscosities of these compounds at high temperatures suggest some structural difference being present in their melts. As compared with the InSb compound whose stability in liquid state was evinced through several investigation methods, the InBi compound appears, obviously, less stable. The results of the present paper argue for the persistence of a short range order in the molten InBi, only at low temperatures.

Arguments in favour of the persistence of a short-range order in the liquid are brought by the positive deviations of the viscosity from the Arrhenius law, below 120° (figure 2) and by the dependence on temperature of the free energy of activation for viscous flow, which shows a minimum at 115° (figure 3).

By comparing our viscosity determinations on the InBi compound with the determinations made on the In_2Bi compound,[1] it results that the viscosity of the molten In_2Bi compound is greater than that of the InBi compound; this can mean a greater stability of the interatomic bonds in the In_2Bi compound in liquid state as compared with the InBi compound.

The results of several investigations carried out by means of different experimental methods seem to argue for that. Such a confirmation is brought by the X-ray study performed by Romanova and Kuchak [3] on the molten intermetallic compounds in the In–Bi system. The conclusions of this study, at least for temperatures which surpass by 10° the liquidus, show that there is not a direct connection between the structure of the solid compounds and the structure of their melts. However at 120° this study admits a certain probability of existence in the molten compound of clusters with a short range order related to the atomic distribution in the solid phases. While for the molten InBi compound it is estimated that a proportion less than 20% of the atoms in the alloy can participate in clusters whose short range order distribution corresponds with the atomic distribution in the crystalline lattice, for the In_2Bi molten compound it is estimated that $30-40\%$ of the atoms in the alloy take part into clusters whose atomic distribution is related to that of the crystalline lattice. Even if other papers give larger probability of conservation of the compound type interatomic bonds in the melts of the two compounds, we feel that, as regards the ratio between the structural stabilities of the InBi and of the In_2Bi, this paper [3] is quite conclusive.

---

[24] V. M. Glazov and D. A. Petrov, *Izvest. Akad. Nauk S.S.S.R., Otdel. tekhn. Nauk,* **1958**, 125.

[25] H. Hoshino, Y. Nakamura, M. Shimoji and K. Niwa, *Ber. Bunsenges. Physik. Chem.,* **69**, 114 (1965).

[26] Bruno-Predel, *Z. Metallkunde,* **55**, 97 (1964).

Further explanations can be obtained from the investigation of the dependence of the viscosity on composition in this system, and from the study of the self-diffusion of the components in the molten InBi compound; both these studies are now in progress.

Revue Roumaine de Chimie, **14**, 79–85 (1969)

D. T. A., ELECTRICAL CONDUCTIVITY AND ACTIVITY OF SCME $Bi_2O_3 - MoO_3$ CATALYSTS

A. POPESCU, E. SEGAL, A. IONESCU and A. SZABO

University of Bucharest, Faculty of Chemistry, Laboratory of Catalysis
Spl. Independenţei 89

Received January 13, 1968

$Bi_2O_3-MoO_3$ catalysts of different composition were studied by means of the D.T.A. and electrical conductivity method. We have also followed the real activity of these catalysts during the oxidation of MeOH via formaldehyde. The crystallization of the compounds $BiO_3 \cdot 3MoO_3$ and $Bi_2O_3 \cdot MoO_3$ at 300° and respectively 380° has been pointed out. The electrical conductibility and the real activity of these catalysts are discussed with respect to their structure and chemical composition.

Recent works concerning the joint catalysts of $V_2O_5 - MoO_3$, $V_2O_5 - Co_2O_3$, $MoO_3 - Co_2O_3$, $WO_3 - Bi_2O_3$, show peculiar activity and selectivity of the listed catalysts in several oxidation reactions.[1-8] The $Bi_2O_3 - MoO_3$ system was especially studied, as it is used for the partial oxidation of olefines.[7-17] The activity and selectivity of the joint catalysts

---

[1] I. I. Ioffe, I. Z. Ezhkova, and A. G. Lyubarski, *Zhur. fiz. Khim.*, **35**, 2348 (1960).

[2] Yu. D. Kernos and B. L. Moldavski, *Zhur. priklad. Khim.*, **33**, 2593 (1960).

[3] I. I. Ioffe, I. Z. Ezhkova and A. G. Lyubarski, *Kinetica i Kataliz*, **3**, 194 (1962).

[4] L. Ya. Margolis, E. H. Enikeev, O. V. Isaev and M. Ya. Kusherev, *Kinetica i Kataliz*, **3**, 181 (1962).

[5] I. Z. Ezhkova, I. I. Ioffe, V. B. Kzanski, A. V. Krylova, A. G. Lyubarski and I. Ya. Margolis, *Kinetica i Kataliz*, **5**, 861 (1964).

[6] I. K. Kolchin, E. L. Galperin, S. S. Bobkov and L. Ya. Margolis, *Neftekhimia*, **5**, 111 (1965).

[7] L. Ya. Margolis, A. V. Krylova and I. L. Aleksandrova, *Kinetica i Kataliz*, **7**, 69 (1966).

[8] S. S. Stroeva, A. I. Gelbstein, N. V. Kulkova, G. G. Skelova, I. Z. Ezhkova, and Yu. E. Roginskaia, *Neftekhimia*, **6**, 412 (1966).

[9] G. Z. Gattow, *Z. anorg. Chem.*, **B 298**, 64, 71 (1959).

[10] E. L. Galperin, L. M. Ernan, I. K. Kolchin, I. F. Dobronski and K. S. Chernishev, *Zhur. neorg. Khim.*, **9**, 2174 (1964).

[11] I. N. Beliaev and N. P. Smoleaninov, *Zhur. neorg. Khim.*, **7**, 1127 (1962).

[12] A. I. Gelbstein, S. S. Stroeva, N. V. Kulkova, Yu. M. Baksi, V. L. Lapidus, I.B. Vasilieva and I. G. Sevasteanov, *Neftekhimia*, **4**, 906 (1964).

[13] C. R. Adams, H. H. Voge, C. Z. Morgan and W. E. Armstrong, *J. Catalysis*, **3**, 379 (1964).

[14] A. C. A. M. Bleijenberg, B. C. Lippens and G. C. A. Schuit, *J. Catalysis*, **4**, 581 (1965).

[15] Ph. A. Batist, B. C. Lippens and G. C. A. Schuit, *J. Catalysis*, **5**, 55 (1966).

[16] J. A. Rashkin and E. D. Pierron, *J. Catalysis*, **6**, 332 (1966).

[17] Ph. A. Batist, C. J. Kapteijns, B. C. Lippens and G. C. A. Schuit, *J. Catalysis*, **7**, 33 (1967).

have been explained by some authors by the presence in their composition of some chemical combination between the two oxides. Systematical studies of $Bi_2O_3 - MoO_3$ system-structure have shown the possible formation of solid solutions, multiphase systems or compounds of the type : $3Bi_2O_3 \cdot MoO_3$,[14-16] $2Bi_2O_3 \cdot MoO_3$,[9-16] $Bi_2O_3 \cdot MoO_3$,[7,10,14,16] $Bi_2O_3 \cdot 2MoO_3$,[7] $Bi_2O_33MoO_3$.[7,10,14,16]

Literature data, which show the existence of various combinations between Bi_2O_3 and MoO_3, differ probably due to the different methods and preparations used, as well as to the various ratios between the constituent oxides.

In order to obtain more data concerning the behaviour of these catalysts also in the oxidation reaction of MeOH via formaldehyde — a fact not yet recorded in the literature — in the present paper the results concerning their catalytical activity in this reaction are shown, as well as data concerning their electrical conductivity and structure.

EXPERIMENTAL

The bismuth oxide and the molybdenum oxide catalysts characterized by ratio value of numbers of atoms R = Mo/Bi shown in table 1, were obtained by the coprecipitation of the solutions of ammonium molybdate and bismuth nitrate by means of an ammonia solution at 80° and pH = 4 (constant). The catalysts precipitates 2, 3 and 4 were washed on the filter with hot distilled water, MeOH, acetone and ether. The precipitates were then dried on a vacuum desiccator. The precipitates of the catalysts 5, 6 and 7 without being filtered were evaporated. The dry samples, regardless of the way they have been prepared, were calcinated for 3 hours at 300° and then for 5 hours at 420° and formed in tablets 2 mm in diameter and 1 mm in height.

The chemical analysis of the calcinated catalysts was carried out by gravimetric method after the molybdenum has been removed from the bismuth. The molybdenum was measured by means of α-benzoinoxime [18] and bismuth by means of phosphate.[19]

Bismuth oxides and molybdenum oxides shown in table 1, have been prepared by the calcination of the ammonium molybdate and bismuth nitrate.

Table 1

The composition of the studied catalysts

No.	The chem. comp.		R = Mo/Bi
	%Bi_2O_3	%MoO_3	
1	100	—	—
2	84.27	15.73	0.30
3	75.71	24.29	0.52
4	58.16	41.84	1.16
5	44.70	55.30	2.00
6	35.75	64.25	2.91
7	24.45	75.55	5.00
8	—	100	—

---

[18] H. B. Knowles, *Bur. Standards Research*, **9**, 1 (1932); *C. A.*, **26**, 5273 (1932).

[19] W. C. Blodsdale and W. C. Parle, *Ind. Eng. Chem.-Anal. Ed.*, **8**, 352 (1936).

The D.T.A. analysis of these catalysts was carried by means of the derivatograph MOM-Budapest, type Paulik, Paulik, Erdely. The D.T.A. plots were recorded at heating rates of 10°/min. Debyegrams of the catalysts were carried by means of TUR M60 diffractometer which use K_α radiation of a copper anticathode.

Electrical conductivity was performed in an original installation upon catalyst tablets of known size. The sample is introduced between two platinum electrodes. The whole system is introduced in a tubular reactor of silica glass, heated by means of an electrical furnace fitted with an automatic heating device. The installation provides different media in the reactor. The electrical resistances were measured by means of the electrical bridge Tesla type BM 283 and TM 393, supplied by an electrical stabilizer. In order to avoid disturbances due to magnetical and electrical external fields, all the leads were shrouded.

The catalytic activity was measured by means of the oxidation reaction of MeOH via formaldehyde. The experiments were carried out in a laboratory installation which includes an isothermal reactor of silica glass 18 mm in diameter provided also with a unit for purifying the air, device for feed rates, pressure and temperature measurements. The formaldehyde absorbed in water was measured gravimetrically with dimedone.

D. T. A. ANALYSIS

The measurements were carried on samples dried at 110°, with exception of sample 2 which was calcinated at 900°. The results obtained are plotted in figures 1 and 2, where on the ordinate is the temperature difference between the sample and the standard one expressed in arbitrary units, and on the abscissa, the temperature. On the D.T.A. curve of the catalyst 2 no important thermic effect is observed because the melting point of the mixture which corresponds to $R = 0.30$ is higher than the maximum temperature at which the samples were heated.[14] The catalyst 3 shows two endothermic effects at 600° and 860° corresponding to the melting of eutectic mixture formed from the system $Bi_2O_3 \cdot 3MoO_3 - Bi_2O_3 \cdot MoO_3$ and melting of solid solution of $Bi_2O_3 \cdot 3MoO_3$ in $Bi_2O_3 \cdot MoO_3$.[11,14] On the same D.T.A. curve one may observe also two exothermic effects of which the one at 380° may be assigned to the combination $Bi_2O_3MoO_3$ and the other at 460° to the crystallization of another intermediate combination from the series $Bi_{1-x}Mo_xO_{1.5(1-x)}$.[12] The catalyst 4 shows one exothermic effect at 300° due to crystallization of the combination $Bi_2O_33MoO_3$. Also the two effects at 620° and 650° correspond to the melting of the eutectic mixture of the type $Bi_2O_3 \cdot 3MoO_3 - Bi_2O_3 \cdot MoO_3$ and respectively of the solid solution of $Bi_2O_3 \cdot MoO_3$ in $Bi_2O_3 \cdot 3MoO_3$. For the samples 5, 6 and 7 which have been obtained directly by evaporation it is shown that in the range of the temperatures between 60° and 360° endothermic effects occur which correspond to water losses. In the catalyst 5 the endothermic effect at 620° may be assigned to the solid solution of $Bi_2O_3 \cdot 3MoO_3$ in MoO_3. The endothermic effects at 600° plotted on the D.T.A. curve of the catalysts 6 and 7 are due to the melting of an eutectic of the type $MoO_3 - Bi_2O_3 \cdot 3MoO_3$. The two exothermic effects of the D.T.A. curves of the catalysts 6 and 7 at 500° are connected with the crystallization of unidentified intermediary phases.

Figure 2 shows some D.T.A. curves of mechanical mixtures formed from bismuth nitrate and ammonium molybdate which correspond to the amount of bismuth and molybdenum oxides of the catalysts in table 1. One may observe that the samples 4a, 5a, 6a and 7a show an endothermic effect between 60° and 360° which may be assigned to water losses. The sample 4a loses much more water, therefore the heat absorbed in this process partially masks the exothermic effect of the $Bi_2O_3 \cdot 3MoO_3$ crystallization at 320° which effect is obvious with the catalyst 4. The crystallization effect of the combination $Bi_2O_3 \cdot 3MoO_3$ takes place also in samples 5a, 6a, and 7a. The exothermic effects at 400° and 500° of samples 6a and 7a correspond to some unidentified combinations. The endothermic effects at 600° and 620° observed with the samples 4a, 5a, 6a and 7a correspond to the melting of an eutectic mixture formed from the system $Bi_2O_3 \cdot 3MoO_3 - Bi_2O_3 \cdot MoO_3$ and respectively to the solid solution of $Bi_2O_3 \cdot MoO_3$ in $Bi_2O_3 \cdot 3MoO_3$.

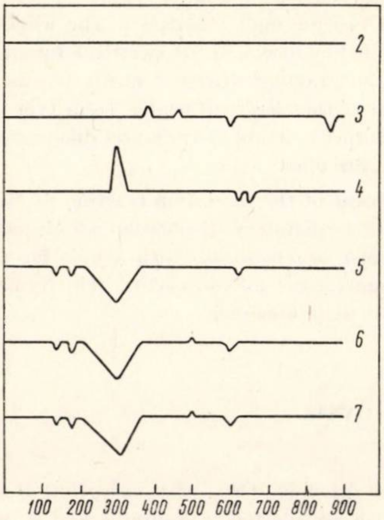

Fig. 1. — D.T.A. curves of the catalysts 2, 3, 4, 5, 6 and 7.

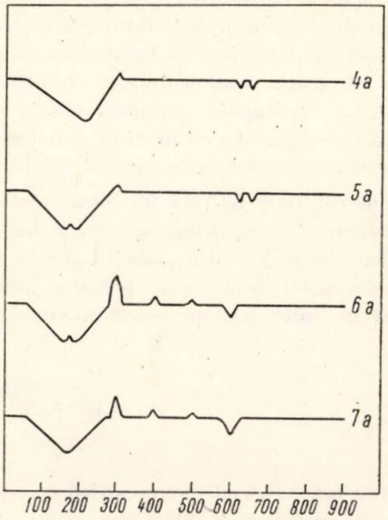

Fig. 2.— D.T.A. curves of the mechanical mixtures 4a, 5a, 6a and 7a.

The Debye-Scherer analysis of the catalysts 6 and of the sample 6a as well as the combination which results by crystallization at 300° show that irrespective of the thermic treatment (dry precipitate or mechanical mixture) one obtains the same compound ($Bi_2O_3 \cdot 3MoO_3$) which exhibit the same crystallin-lattice.

The data shown in figures 1 and 2 make evident the crystallization of the compounds $Bi_2O_3 \cdot 3MoO_3$ and $Bi_2O_3 \cdot MoO_3$, phenomena which are pointed out on the D.T.A. curves by an exothermic effect at 300° and respectively at 380°. The exothermic effect at 300° may be concealed when the mechanical mixture of the bismuth nitrate and ammonium molybdate contain a large amount of water, whose removal is associated with a strong endothermic effect.

ELECTRICAL CONDUCTIVITY

The measurements of electrical conductivity were carried for all the studied samples in the temperature range 200—500° in air at normal pressure or in a current of nitrogen at a constant flow rate of 20 l/h.

In order to obtain data concerning the semiconductor type of the samples, variations of the electrical conductivity versus the temperature

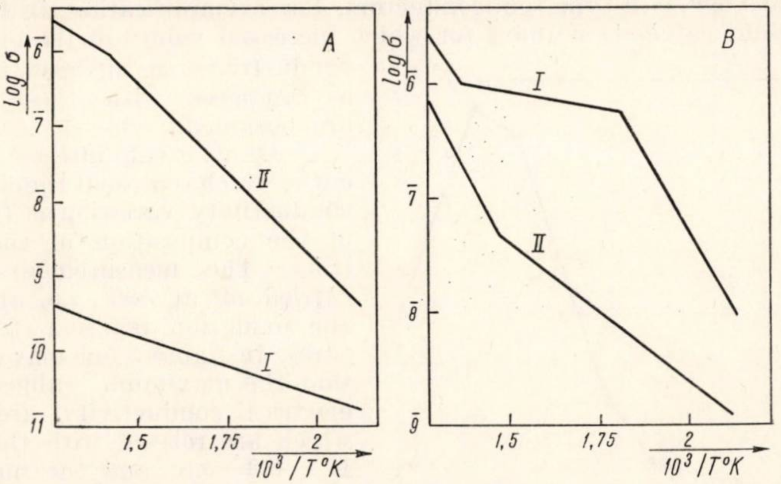

Fig. 3. — The variation of the electrical conductibility as function of the inverted absolute temperature for the catalysts MoO_3 and Bi_2O_3 : A — for Bi_2O_3 ; B — for MoO_3 ; I — in nitrogen ; II — in air.

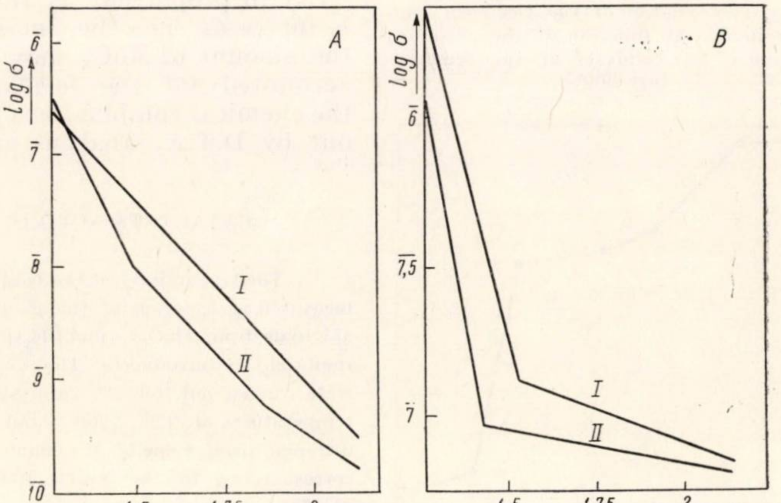

Fig. 4. — The variation of the electrical conductivity as function of the inverted absolute temperature of the catalysts 2 and 7. A—for catalyst 7 ; B — for catalyst 2 ; I — in nitrogen ; II — in air.

and the medium of measurements (air, nitrogen) were determined. The measurements in air and nitrogen flow show that MoO_3 and Bi_2O_3 behave as an n- and respectively p-type semiconductor (fig. 3).

The variation of electrical conductivity in the same conditions as for catalysts indicated in table 1 shows that all behave from the electrical point of view as n-type semiconductors. For exemplification, in figure 4 we present catalysts 2 and 7 for which increased values of the electrical conductivity in nitrogen medium as compared with those in air are obtained.

Of a great interest is the curve which represent the electrical conductivity variation as function of the composition of the catalysts. The measurements were carried out at 300°, i.e. at one of the oxidation reaction temperatures. In figure 5 one may observe that the maximum values of the electrical conductivity are those which are related with the ratio R = 0.3 – 0.5, and the minimum in the catalysts the ratio of which ranges between 2 and 5. The decrease in the electrical conductivity in proportion as the ratio R increases, i.e. the increase in the amount of MoO_3, may be also accounted for the formation of the chemical combinations pointed out by D.T.A. analysis (fig. 1).

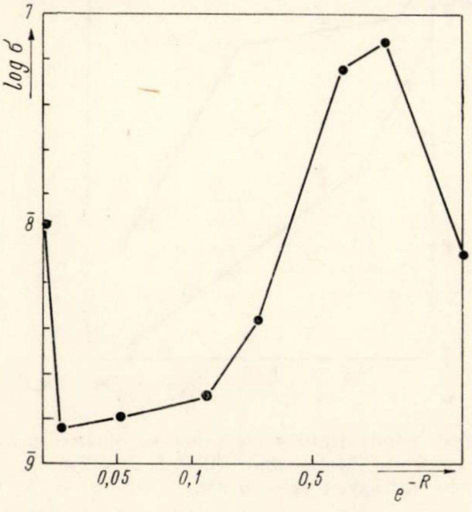

Fig. 5. — The variation of the electrical conductivity in air, as function of the chemical composition of the catalysts at the temperature 300°.

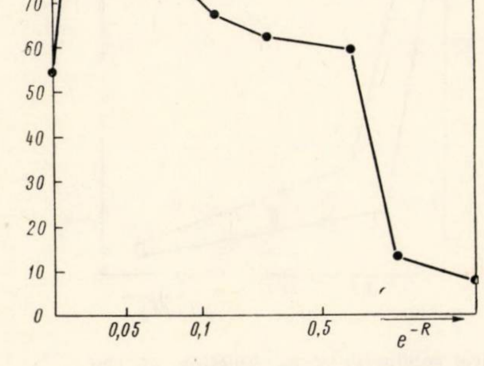

Fig. 6. — The variation of the real activity of the catalysts as function of the chemical composition, at the temperature 300°.

CATALYSTS ACTIVITY

The real activity of the catalysts was measured as function of the yield of formaldehyde from MeOH (mol.CH_2O obtained /mol.CH_3OH introduced). The experiments were carried out for all catalysts at the temperatures of 220°, 260°, and 300° at different space velocity of reactant mixture corresponding to the g.air/g.MeOH ratio of 15/1.

The experimental data show that the optimum activity is performed by catalysts with an increased amount of MoO_3. The activity variations of the catalysts versus the chemical composition is plotted in figure 6. The experimental data show that when MoO_3 itself is used as catalyst one may obtain yields ranging from 50 – 55 % formaldehyde, whereas for

Bi_2O_3, the yields are below 10%. From figure 6 one may observe that the increased activity is due to a ratio R = 2.91 and 5. As soon as the ratio R decreases the catalysts real activity decreases also : namely from values ranging from 80—90% to values below 15%.

The different behaviour of the active catalysts versus those less active may be accounted for by the presence or the absence of the MoO_3 excess as against the stoichiometric combination $Bi_2O_3 \cdot MoO_3$ pointed out by the D.T.A. analysis. For the catalysts containing an excess of MoO_3 the activity may be explained by the presence of the $Bi_2O_3 \cdot 3MoO_3$ combination also pointed out by the D.T.A. analysis. It is very interesting to remark that as a function of the chemical composition of the catalysts, the variation of real activity runs vice-versa to the electrical conductivity.

Revue Roumaine de Chimie, **14**, 87–94 (1969)

STUDY ON THE INTERMEDIATES OCCURRING IN THE OCTYLATION REACTION OF THE AROMATIC NUCLEUS WITH THE CATALYSTS $AlEt_2Cl$-RCl

I. V. NICOLESCU and OLGA ŞERBAN

Department of Technological Chemistry and Catalysis
University of Bucharest, Spl. Independenţei, 89

Received February 16, 1968

The present paper deals with the octylation reaction of benzene in the presence of catalytic systems consisting of halides of alkyl aluminium complexed with alkyl chlorides reacting also with the aromatic solvent. The catalytic properties of the systems under study are influenced by the structure of the complexing component and by the nature of the solvent. The formation of ionized intermediate compounds as "ion groups" is emphasized by spectral studies as well as by studies of electrical conductivity. The activity of the catalytic systems is correlated to the ionization degree of the intermediate compounds.

The ethylation reaction of the aromatic nucleus in the presence of catalytic systems made up of diethyl-aluminium monochloride complexed with alkyl chlorides was described in a previous contribution.[1]

Continuing these researches, the present paper brings a series of results related to the study of the activity of the same catalytic systems as against the octylation reaction of the aromatic nucleus.

We found the study of these catalytic systems to be of interest for the following reasons :

a) The ternary compounds obtained by the interaction $AlEt_2Cl$-ArH-RCl are soluble within certain concentration ranges in the aromatic hydrocarbon since they are formed in a wholly aprotic medium and in the absence of oxygen.

b) This behaviour enables one to investigate their properties and structure by means of spectrophotometrical, electrical and other methods.

Thus, a further advance of our knowledge as to the nature of intermediates occurring in aromatic alkylation may be obtained.

EXPERIMENTAL

For the preparation of the catalytic systems we used benzene as well as 1-octene L.R. dried over metallic sodium and on a molecular sieve Linde 4 A. Purity was checked chromatographically.

---

[1] **I. V. Nicolescu, O. Şerban, *Rev. Roumaine Chim.*, 10, 515 (1965).**

The n- and t-butyl chlorides were purified and dried on a molecular sieve (Linde 4 A); the $AlEt_2Cl$ used was provided by "Montecatini".

The reactions have been performed in an installation suited for working conditions in inert gas, pure and dried argon.

The octylation reactions have been carried out under isothermal conditions, within the temperature range 10—70°.

A constant catalyst amount i.e. 2×10^{-2} moles of $AlEt_2Cl$ has been used in all experiments. The ratio of aromatic hydrocarbon : 1-octene was 4 : 1 mole.

In the reaction product distilled up to 72° at 1 Torr, 2-phenyl-octane and 3-phenyl-octane were identified.

The analysis of the reaction products was performed chromatographically using a Perkin Elmer F 11 apparatus. The original D.E. 210 column was used.

The structure of these isomers was checked up also by means of IR spectra.

The spectrophotometric study of the catalytic systems was performed using a spectrophotometer Beckman D.B., and the extinction values were also determined by a Carl Zeiss V.S.U. 10 spectrophotometer.

The electrical conductivity of the catalytic systems with and without 1-octene was measured with a Tesla Terra-Ohmmeter, and a 100 V current.

The activity of the catalyst was expressed in per cent total alkylate obtained as against the amount of 1-octene introduced into the reaction.

The specific activity was calculated as per cent moles phenyl octanes (monoalkylate) as against the amount of catalyst in grammes introduced into the reaction. Run time : 3 hrs.

RESULTS AND DISCUSSIONS

a) *Activity of the catalytic systems within the octylation reaction*

As catalytic system we considered the compound which is formed from the catalytic components and the aromatic hydrocarbon (solvent):

$AlEt_2Cl$-n.C_4H_9Cl-ArH (denoted by K_1)

$AlEt_2Cl$-t.C_4H_9Cl-ArH (denoted by K_2)

The diethylaluminium chloride alone does not catalyze the alkylation reaction.

When the alkyl chloride C_4H_9Cl is introduced into the reaction medium, a coloured compound which is soluble in benzene (solvent) and which catalyzes the octylation reaction is formed. Generally, this compound is little stable and may decompose into aluminium chloride and by hydrogen disproportionation into ethane and butyl-benzene.[2]

However, in a large excess of aromatic hydrocarbon the initial compound stabilizes by interaction with the solvent and yields an ionized and coloured ternary compound of the type of Brown's σ complex [3] under the form of an "ion group".

[2] A. G. Pozamantîr and M. L. Genusov, *Zhur. obshchei Khim.*, **32**, 1175 (1962).

[3] H. C. Brown and M. Grayson, *J. Amer. Chem. Soc.*, **75**, 6285 (1953).

Such compounds under the form of "ion pairs" are well described by Olah,[4,5] Nenitzescu [6,7] and other researchers.[8,9]

Intermediate I, a weak Lewis acid, may be considered the proper catalytic compound sufficiently stable for the study.

This intermediate I, from the following scheme, interacts with the alkene (1-octene), when a new charge transfer between the alkene and the benzenonium ion of the "ion group" takes place, producing intermediate II, which is in equilibrium with the system products

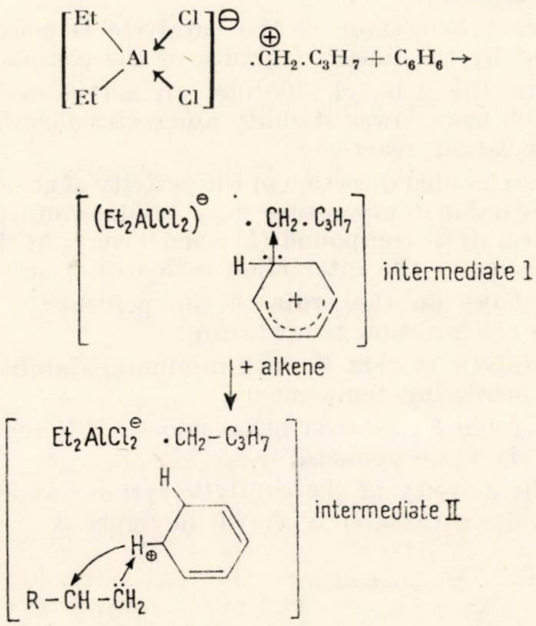
Et
Cl
Al
Et
Cl
$\overset{\oplus}{.CH_2}.C_3H_7 + C_6H_6 \rightarrow$
$(Et_2AlCl_2)^{\ominus}$ · $CH_2.C_3H_7$
H
+
intermediate I
+ alkene
$Et_2AlCl_2^{\ominus}$ · $CH_2-C_3H_7$
H
H⊕
R – CH – CH₂
intermediate II

The ionized catalytic compound I, in whose formation the "solvent" is also involved, is at the same time the first intermediate within the aromatic alkylation reaction under study.

---

[4] G. A. Olah and S. J. Kuhn, *J. Amer. Chem. Soc.*, **80**, 6541 (1958); G. A. Olah, S. J. Kuhn and S. H. Flood, *J. Amer. Chem. Soc.*, **84**, 1688 (1962).

[5] G. A. Olah, S. H. Flood, S. Kuhn, M. Moffat and N. Overchuck, *J. Amer. Chem. Soc.*, **86**, 1046 (1964).

[6] C. D. Nenitzescu, *Rev. Roumaine Chim.*, **9**, 1 (1964).

[7] V. Ioan, D. Săndulescu, S. Ţiţeica and C. D. Nenitzescu, *Tetrahedron*, **19**, 323 (1963).

[8] S. V. Pasynkiewicz, *Vysokomol. Soedineniya*, **10**, 1585 (1963).

[9] B. A. Dolgopolsk, *Vysokomol. Soedineniya*, **10**, 1587 (1963).

In what follows, figure 1 shows the experimental results within the octylation reaction of the benzene in the presence of the above mentioned catalytic systems (K_1 and K_2).

Analysis of the results leads to the following remarks:

— The maximum activity, 94 per cent alkylate, is shown by the catalyst complexed with n-butyl chloride and mainly at 10°;

— In return, the activity of the catalyst decreases with increasing temperature for the system complexed with n-butyl chloride.

Generally, the catalyst complexed with t-butyl chloride exhibits a more reduced activity.

This different behaviour of the catalysts is considered by us as being determined by the linear structure of the complexing component.

As concerns the n-butyl chloride, an active catalytic compound is obtained, which has a lower stability and a steric configuration favourable to the alkylation reaction.

The opposite handed direction of the activity of the catalyst (figure 1) related to the reaction temperature may be determined by the greater stability of the catalytic compound (I) when it contains the t-butyl carbocation, which decreases the interaction rate with 1-octene.

Figure 2 shows on the ordinate the percentage variation of the selectivity as to the reaction temperature.

For the catalytic system K_1 with minimum stability, the selectivity decreases with increasing temperature.

The more stable K_2 catalyst behaves quite differently, although the overall activity is more reduced.

The specific activity of the catalytic systems expressed in per cent moles monoalkylate/g catalyst is shown in figure 3.

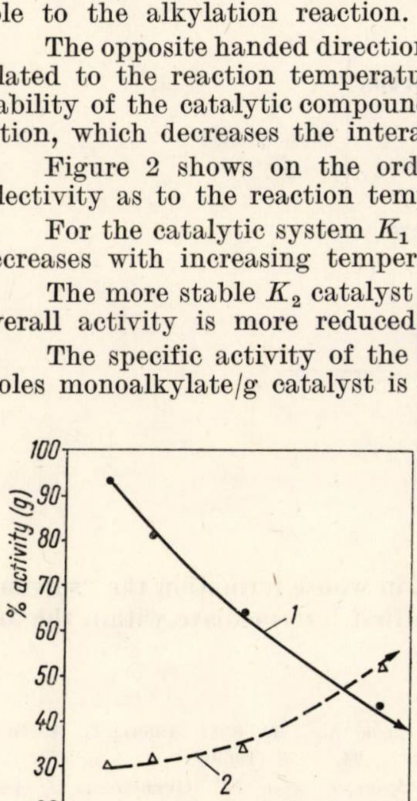

Fig. 1. — Variation of catalytic activity related to temperature. *1*, catalyst K_1; *2*, catalyst K_2.

We mention that the experimental data are plotted on straight lines, thus showing the proportionality of the specific activity to the reaction temperature. The symbatic character of the curves in figures 1 and 3 is also to be noticed.

b) *Spectrophotometric study and electrical conductivity of the reaction intermediates*

In order to evidence both the formation and the nature of the above mentioned intermediary compounds, the absorption spectra as well as the electrical conductivity of the systems as such and in the presence of octene have been studied.

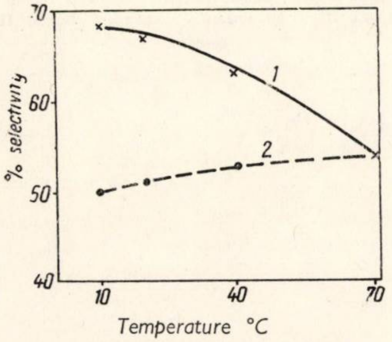

Fig. 2. — Variation of catalytic selectivity related to temperature. *1*, catalyst K_1; *2*, catalyst K_2.

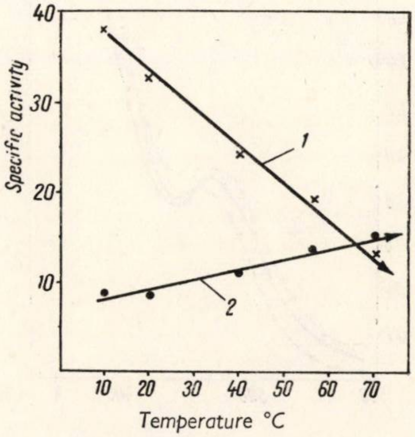

Fig. 3. — Variation of specific activity of the catalysis related to temperature. *1*, catalyst K_1; *2*, catalyst K_2.

These measurements were carried out with special caution as to the air-tightness of the cells in order to avoid atmospheric contact.

The main problem for us was to evidence within the system the existence of intermediate I as well as that of intermediate II (I + octene).

The spectrophotometrical determinations yielded the following result:

The absorption spectra of the coloured compounds among the components of the system (catalysts K_1 and K_2) without octene and with octene remain unchanged and present two absorption maxima at 450 mμ and 368 mμ [10,11] (fig. 4).

This shows that the overall structure of the compound $AlEt_2Cl$-C_4H_9Cl-aromatic solvent, which is intermediate I of the process, is analogous to that of the intermediate in which alkene (intermediate II) takes part.

We determined further the extinction values of the systems under study, referred to the concentration either of 1-octene or of $AlEt_2Cl$.

---

[10] O. Şerban, S. Moldoveanu and I. V. Nicolescu, *Anal. Univ. Buc.*, **11**, 147 (1966).
[11] O. Şerban and S. Moldoveanu, *Anal. Univ. Buc., Seria Şt. Chim.*, (in print).

Table 1 shows the extinction variation of the system $AlEt_2Cl$-$n.C_4H_9Cl$ (or $t.C_4H_9Cl$)-benzene, as well as of the alkylation component 1-octene for $E = 380$ mμ.

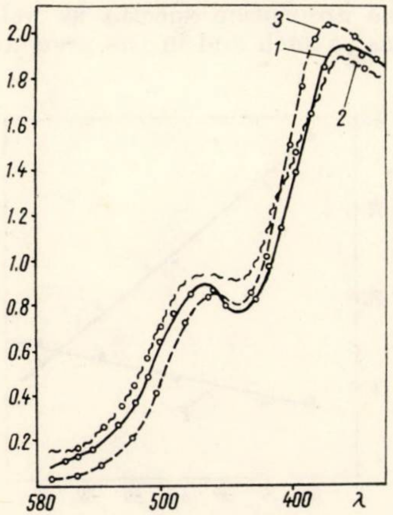

Fig. 4. — Visible absorption spectra, *1*. system: $AlEt_2Cl$-nC_4H_9Cl-C_6H_6; *2*. system: $AlEt_2Cl$-$t.C_4H_9Cl$-C_6H_6; *3*. system: $AlEt_2Cl$-nC_4H_9Cl-C_6H_6-octene.

In this case we modified the $AlEt_2Cl$ concentration from 0.6 to 1.6 mol $\times 10^{-3}$ and maintained constant the 1 : 10 complexing ratio to the butyl chloride, as well as the octene concentration.

Table 1

Extinction variation of the system $AlEt_2Cl$-C_4H_9Cl-C_6H_6; E 380 mμ

Moles $AlEt_2Cl \times 10^{-3}$	$AlEt_2Cl$-nC_4H_9Cl-C_6H_6		$AlEt_2Cl$-$t.C_4H_9Cl$-C_6H_6	
	without 1-octene	with 1-octene	without 1-octene	with 1-octene
0.6	1.12	1.80	1.2	1.4
0.8	1.2	1.90	2.0	∞
1.0	1.33	2.00	∞	∞
1.2	1.44	∞	∞	∞

In table 2 the octene concentration has been altered, and the concentration in $AlEt_2Cl$ (1×10^{-3} mol) as well as the RCl (n-C_4H_9Cl) amount have been kept constant.

Table 3 shows the extinction variation at $E = 480$ mμ for the same systems and for constant concentrations of catalytic component.

A study of the extinction shows (tables 1—3) that the values obtained are considerably modified both by the structure of the complexing agent, the alkyl chloride (normal or tertiary) and by the presence of octene within the system.

In both cases the introduction of 1-octene brings about an increase in the extinction values as compared to the extinction value of the basic system $AlEt_2Cl\text{-}nC_4H_9Cl\text{-}C_6H_6$ for the same wavelength.

Table 2

Extinction variation of the system $AlEt_2Cl\text{-}n\text{-}C_4H_9Cl\text{-}C_6H_6$-1-octene; *E* 480 mμ

1-octene moles 10^{-3}	*E* 480 mμ
0	0.035
3	0.130
6	0.270
12	0.520
31	1.250

This result confirms the existence of two different structural formations which exhibit a determined ionization degree.

The remark on the ionization degree of the "ion group" forming intermediates I and II may be also related to the data on the variation of the electrical conductivity listed in table 4.

This table also includes the values of the electrical conductivity at 20° ($\sigma_{20°}$) of the same samples used in the spectrophotometric study.

A sensible variation of the electrical conductivity, function of the nature of the alkyl chloride as well as of the presence of octene within the system is remarked.

Table 3

Extinction variation of the system $AlEt_2Cl\text{-}C_4H_9Cl\text{-}C_6H_6$; *E* 480 mμ

Moles $AlEt_2Cl \times 10^{-3}$	$AlEt_2Cl\text{-}n.C_4H_9Cl\text{-}C_6H_6$; *E* 480 mμ			$AlEt_2Cl\text{-}t.C_4H_9Cl\text{-}C_6H_6$; *E* 480 mμ		
	without 1-octene	with 1-octene	$+\Delta E_0$	without 1-octene	with 1-octene	$+\Delta E_0$
1.0	0.035	0.520	0.485	0.850	0.900	0.050

Table 4

Correlation of catalytic activity *versus* the electrical conductibility of the catalytic systems

Moles $AlEt_2Cl \times 10^{-3}$	$AlEt_2Cl\text{-}n.C_4H_9Cl\text{-}C_6H_6$ $\sigma_{20°}$ $ohm^{-1}.cm^{-1} \times 10^{-9}$			$AlEt_2Cl\text{-}t.C_4H_9Cl\text{-}C_6H_6$ $\sigma_{20°}$ $ohm^{-1}.cm^{-1} \times 10^{-9}$		
	without 1-octene	with 1-octene	$\Delta\sigma_0$	without 1-octene	with 1-octene	$\Delta\sigma_0$
1	2	3	4	5	6	7
1.0	0.65	17.0	16.35	1.3	4.1	2.8
activity % (20°)		83.0			32.0	

If we refer the catalytic activity to the difference between the electrical conductivities of intermediates II and I, columns 4 and 7, table 4, $\Delta\sigma_0 = \sigma$ int. II $- \sigma$ int. I. a good correlation results between the maximum values of $\Delta\sigma_0$ and of the activity of the catalytic system with $n.C_4H_9Cl$ and the minimum values for the system with $t.C_4H_9Cl$.

For a better estimation of the relationship : extinction — electrical conductivity — activity, we also supplemented the above experiments with systems where the aromatic hydrocarbon (i.e. the benzene) has been replaced by other aromatics such as toluene and *p*-xylene, with increasing basicity.

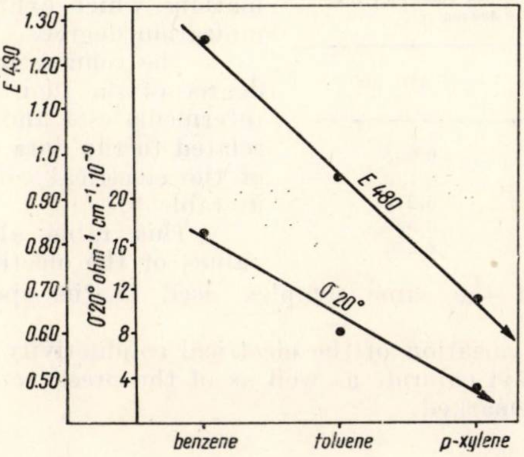

Fig. 5. — Variation of extinction and electric conductivity as a function of the basicity of the aromatic hydrocarbon.

The activity of these systems varies according to the following order : benzene > toluene > *p*-xylene.

E 480 mμ as well as σ_{20} = varies in accordance with the same order for the systems comprising the intermediate II, as it results from figure 5.

Thus, the participation of the solvent (the aromatic component within the system) in the formation of the intermediate compound II is confirmed, which means the stage determining the rate of the process. There results also an interesting correlation between the ionization degree of these compounds (ion groups) expressed by the values of the electrical conductivities and of the extinction with the yield in alkylated product respectively with the catalytic activity of the systems under study.

CONCLUSIONS

The catalytic properties of the systems under study are influenced by the structure of the complexing component and by the nature of the solvent.

The formation of ionized intermediate compounds as "ion groups" has been emphasized by spectral studies as well as by studies of electrical conductivity. The activity of the catalytic systems is correlated to the ionization degree of the intermediate compounds.

We gratefully acknowledge Dr. Emilian Angelescus contribution.

Revue Roumaine de Chimie, **14**, 95–99 (1969)

THE ROLE OF Cr^{+5} IONS IN THE CATALYTIC OXIDATION OF SOJA OIL

JERZY SIECHOWSKI and JÓZEF SLIWIOK

Uniwersytet Slaski Katowice, Poland

Received January 13, 1968

The oxidation process of fats depends on many factors, among others on storing conditions, kind of tested product, as well as on the presence of a trace amount of metals such as copper and iron, which considerably accelerate the oxidation process. The present paper tries to show the influence of Cr^{+5} ions, resulting from the thermal treatment of the $Al_2O_3-CrO_3$-system, on the catalytic oxidation of soja oil.

CATALYST CHARACTERISTICS

The catalysts have been obtained by impregnation of $\theta-Al_2O_3$ with a water solution of CrO_3 of different concentrations.[1] Products thus obtained are subjected to drying and then to calcination at temperatures from 100° to 700° every 100°. The actual calcination amounted to 5 hours. The finished product was subjected to determination of the oxidation state of chromium ions by the Bunsen-method.[2] Results of these analyses are shown in figure 1, which indicates the mean oxidation number of chromium ions depending on the calcination temperature. For small concentrations of chromium, the temperature increase causes an insignificant reduction of the medium state of oxidation even at a calcination up to 700°. Greater alterations of the mean oxidation number of chromium ions have been noticed at total increase of chromium concentration. Great concentrations of chromium show alterations of the mean oxidation number of chromium ions even at a temperature of 100°. In this case a mild temperature increase up to 50°, at which the catalytic preparation had been subjected to drying, already causes a slow decrease in the chromium ions' valences. The most important changes in the mean oxidation number of chromium ions occur in the 200°–300° temperature range. The concentrations of chromium (6.5% Cr and 8% Cr) at the highest temperatures are showing a mean oxidation number of chromium ions at the level + 3. The described effect – as earlier tests have shown – depends on the dispersion degree of chromium ions on the carrier surface. Thus the specific surface of the carrier, on which the catalyzing factor settles, plays here a part. The specific surface area of the carrier and the catalytic preparations were calculated by means of the BET equation [3] $\left(\theta - Al_2O_3 : 95 \frac{m^2}{g}\right)$. Our tests as well as the tests of Cosse and Van Reijen [4] have shown that this carrier stabilizes to the greatest extent the oxidation number of chromium ions at + 5. This stabilizing influence depends, however, on the dispersion degree of chromium ions : for a small chromium concentration this oxide appears in a monomolecular dispersion and the stabilizing influence of the carrier is considerable.[1]

---

[1] J. DEREN, J. HABER and J. SIECHOWSKI, "Proc. IIIrd Intern. Congress on Catalysis", Amsterdam, 1965, p. 993.

[2] G. JANDER and K. F. JAHR, "Maßanalyse", 8 Aufl., Berlin, 1959.

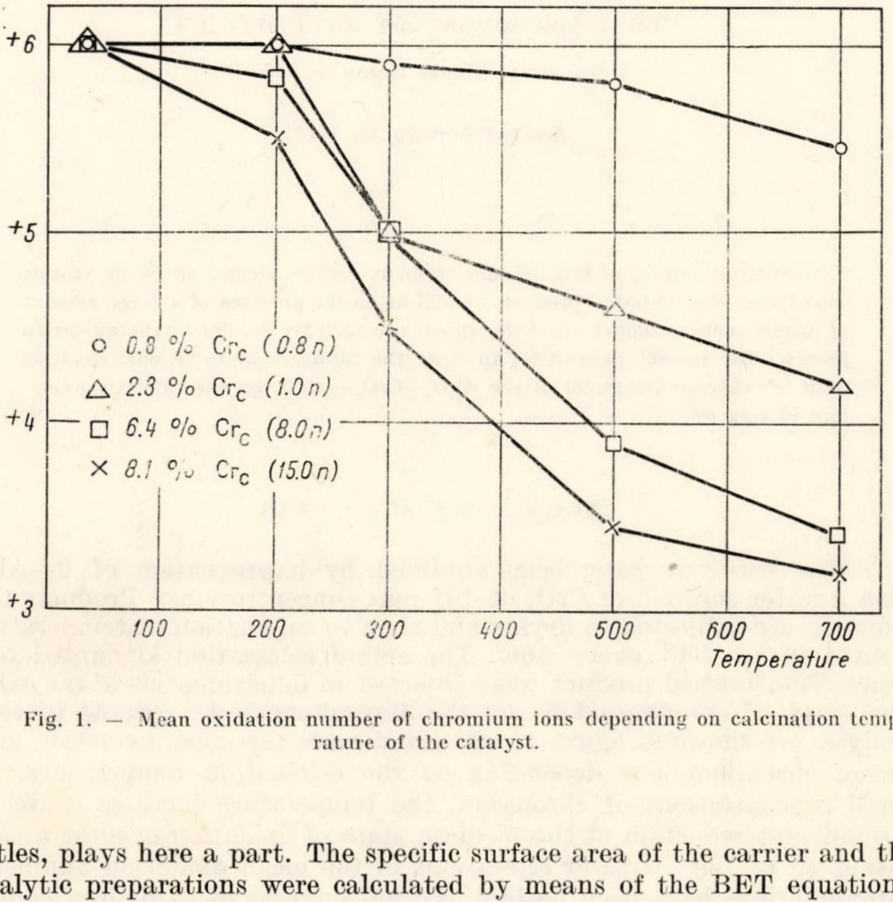

Fig. 1. – Mean oxidation number of chromium ions depending on calcination temperature of the catalyst.

---

[3] S. Brunauer, "The Adsorption of Gases and Vapors", Princeton, 1945.

[4] P. Cosse and L. L. Van Reijen, "Actes du IIe Congrès Intern. Catalyse", Paris, 1960, p. 1679.

As the chromium concentration increases, this oxide is already collecting on the carrier surface under the form of multilayers, and consequently its stabilizing influence is decreasing. On calcination, a new Cr_2O_3 phase may now arise.

EXPERIMENTAL

Soja oil with iodine value = 131.2, neutralization value = 189.2 and acid value = 0.1, has been tested. The percentage composition of fatty acids has been determined by meano fs the paper chromatography method.[5] For the measurements, 40 g oil have been used which have been poured out into Petri dishes of 10 cm diameter. To each, 40 mg catalyst have been added, carefully distributed and from this quantity 1 g has been taken every 24 hours for the determination of the peroxide volume by iodometry. The method's accuracy did not exceed 3 p.c. of a relative error. The averages indicated by the determinations constituted the bases for further computations. This process has been carried out at a constant temperature of 30° (+0.2°). In parallel, test analyses have been also carried out without a catalyst.

RESULTS AND DISCUSSION

The rate constants of the reaction for the respective chromium concentrations and the calcination temperatures of the catalysts have been determined. The obtained values of rate constants have been ascribed to the unit of chromium ions concentration Cr^{+6}, Cr^{+5}, Cr^{+3}. Results shown in figures 2, 3 and 4 enable us to ascertain that not all ions are catalyzing this process in the same way. The greatest influence is exerted by ions on the +5 mean oxidation number of chromium ions, for at all sectional concentrations of chromium the rate of this process on a unit concentration of Cr^{+5} is the greatest. Its distinct amount may be ascertained beginning from 200°, i.e. at the temperature in which the distinct process of CrO_3 reduction is already beginning. This also causes a distinct increase in the oxidation rate of the soja oil. As asserted by many authors, the selectivity and activity of this system may also depend on the ratio $\frac{Cr^{+6}}{Cr^{+5}}$.[6] The results of these computations are shown in figures 5, 6, 7 and 8. The rate alterations of soja oil oxidation are parallel to the ratio change $\frac{Cr^{+6}}{Cr^{+5}}$. The rate constant of the investigated process corresponding to the concentration unit of Cr^{+3} is a constant value in the whole range of applied Cr concentrations and catalyst calcination temperatures. We assume therefore that these ions practically do not take part in the examined process.

---

[5] Z. KWAPNIEWSKI, J. SLIWIOK and J. ZAREBA, *Zeszyty Naukowe W.S.P. Katowice Sekcja Chemii*, 6, 7, (1965).

[6] K. W. TOPCHIEVA. *Neftkhimia* 1, 760 (1961); 2, 18 (1962).

The present knowledge concerning catalytic processes does not allow substantiating the specific role of the Cr^{+5} ion in its catalytic activity although many empirical results confirm the importance of this ion in the catalytic processes.

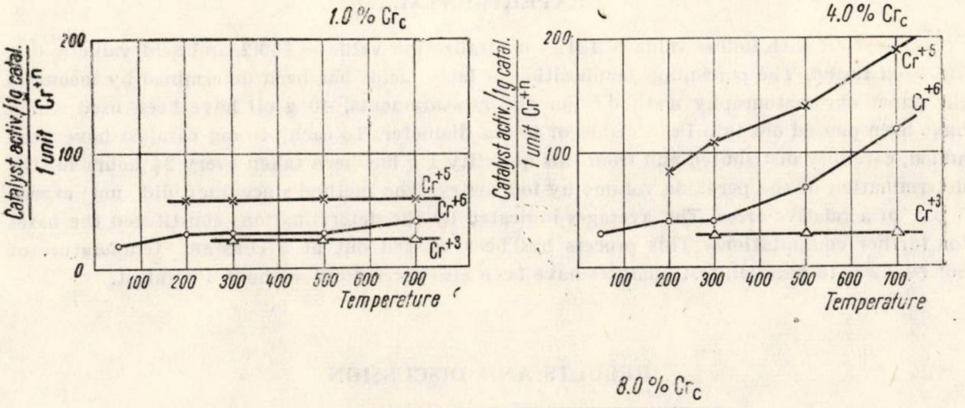

Figs. 2—4. — The rate constants of oxidation of soja oil corresponding to a unit of ions concentration Cr^{+6}, Cr^{+5}, Cr^{+3} depending on calcination temperature of the catalyst.

Analysis of this process on the basis of other systems is in progress.

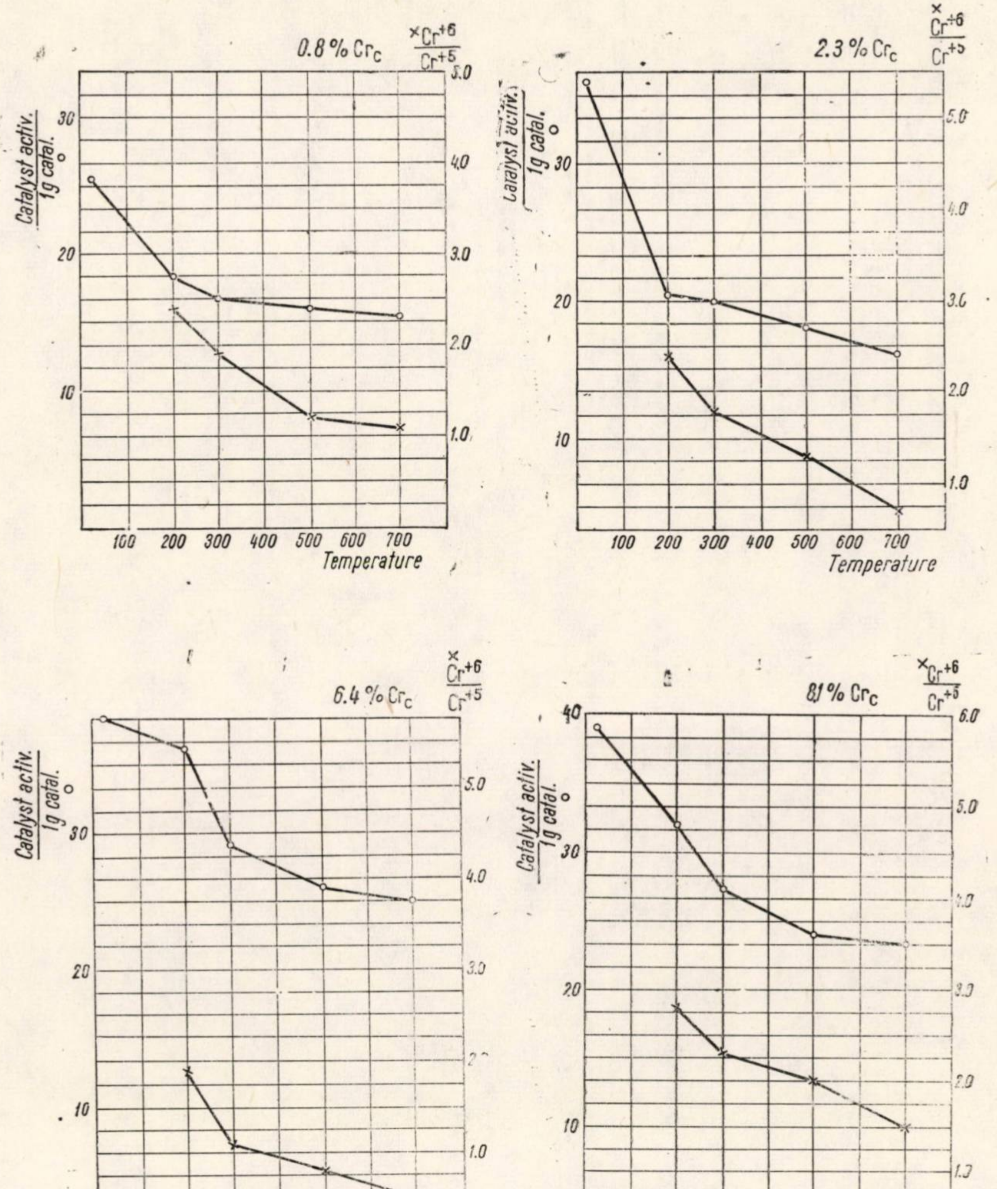

Figs. 5–8. — Summary of rate constants with ratio of concentrations depending on calcination temperature of the catalyst.

Revue Roumaine de Chimie, **14**, 95–99 (1969)

Revue Roumaine de Chimie, **14**, 101–110 (1969)

INVESTIGATIONS IN THE CYCLOBUTANE SERIES. XX[1]

STEREOISOMERIC 1.2.3.4-TETRABROMOCYCLOBUTANES BY THE HUNSDIECKER REACTION

MARGARETA AVRAM, GH. D. MATEESCU and C. D. NENITZESCU

Institute of Organic Chemistry of the Academy, Bucharest, Str. Polizu 1

Received July 9, 1968

On the basis of infrared and nuclear magnetic resonance spectra it was established that the three resulted 1.2.3.4-tetrabromocyclobutanes obtained from the *trans*-3.4-dibromocyclobutane-*cis*-1.2-dicarboxylic acid, by the Hunsdiecker reaction, possess the following steric configurations : *all-trans* (6), *cis, cis, trans* (7) and *cis, trans, cis* (8).

The Hunsdiecker reaction has been studied a great deal up to the present.[2] In the aliphatic series the homolitic, nonstereospecific substitution of the COOAg group by bromine was proved by using the silver salts of the optically active monocarboxylic acids.[2c]

In the case of the cycloalkanecarboxylic acids the literature data are less conclusive.[3-8] The *cis*- and *trans*-alkylcycloalkanemonocarboxylic acids gave a mixture of *cis*- and *trans*-bromoalkylcycloalkanes in which the *trans*-isomer is prevailing. From both the conformationally pure *cis*- and *trans*-4-tert-butylcyclohexanecarboxylic acids, Eliel[6] obtained a mixture of *cis*- and *trans*-1-bromo-4-tert-butylcyclohexane in which the *trans* isomer represents 65%. The isomer ratio is more close to an equilibrium mixture (77% of *trans*) than to a racemic mixture. A similar behaviour was observed in the case of the stereoisomeric *cis*- and *trans*-1-methylcyclopropyl-2-carboxylic acids.[7] Here also, in both cases the *trans*-

---

[1] Part XIX : M. Avram, Gh. D. Mateescu, M. Rențea, I. G. Dinulescu and C. D. Nenitzescu, *Rev. Roumaine Chim.*, **13**, 1097 (1968).

[2] *a*. J. Kleinberg, *Chem. Rev.*, **40**, 381 (1947) ; *b*. R. G. Johnson and R. K. Ingham, *Chem. Rev.*, **56**, 219 (1956) ; *c*. C. V. Wilson, in R. Adams "Organic Reactions", vol. 9, John Wiley Inc., New York, 1957, p. 332 ; *d*. H. Henecka, in "Methoden der organischen Chemie (Houben-Weyl)" vol. 8, Ed. E. Müller, Georg Thieme Verlag, Stuttgart, 1952, p. 496.

[3] P. I. Abell, *J. Org. Chem.*, **22**, 769 (1957).

[4] D. E. Applequist and A. S. Fox, *J. Org. Chem.*, **22**, 1751 (1957).

[5] M. Avram, E. Marica and C. D. Nenitzescu, *Rev. Roumaine Chim.*, **4**, 253 (1959).

[6] E. L. Eliel and R. V. Acharya, *J. Org. Chem.*, **24**, 151 (1959).

[7] D. E. Applequist and A. H. Petersen, *J. Amer. Chem. Soc.*, **82**, 2372 (1960).

[8] D. E. Applequist and N. D. Werner, *J. Org. Chem*,. **28**, 48 (1963).

isomer appears in the proportion of 65%, indicating a predominant conformational control.

With the cycloalkane-1.2-dicarboxylic acids the results are quite different from those obtained with the monocarboxylic acids. Thus from the Hunsdiecker reaction applied to the *cis*- and *trans*-cyclohexane-1.2-dicarboxylic acids, Abell [3] and Applequist [8] isolated as sole reaction product the *trans*-1.2-dibromocyclohexane. It has been proved [8] that the 1.2-dibromocyclohexane obtained beside the racemic product is formed with inversion of configuration. Taking into account the imperfections of the utilized analytical methods, the authors indicate 85% as a limit of the stereospecificity of the reaction, considering that possible traces of *cis*-1.2-dibromocyclohexane could not be detected.

In the case of the cyclobutane-1.2-dicarboxylic acids from both isomers *cis* and *trans*, the *trans*-1.2-dibromocyclobutane was exclusively obtained.[4] From the silver salt of the optically active *trans*-cyclobutane-1.2-dicarboxylic acid the optically active 1.2-dibromocyclobutane was isolated. On the basis of this result the authors drew the conclusion that the probable intermediate of the reaction is a radical of the type **1** or **2** and not an intermediate of the type **3** or **4**:

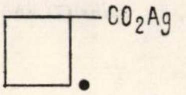

1

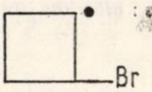

2

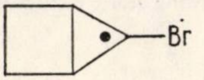

3

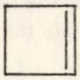

4

The exclusive formation of the *trans*-dibromo compound from the cyclobutane-1.2-dicarboxylic acids seems to indicate a clear stereospecific course of the reaction, quite different in the case of the monocarboxylic acids.

During the course of our work in the cyclobutane field, the Hunsdiecker reaction was used with preparative purposes in order to obtain the dibromo-[5] and tetrabromo-[9] derivatives of the cyclobutane. In a previous work [5] we showed that by the degradation of the silver salts of the *cis*- and *trans*-cyclobutane-1.2-dicarboxylic acids, a mixture of stereoisomeric *cis*- and *trans*-1.2-dibromocyclobutanes is obtained. By the gas-chromatographic analysis of the crude product, it was established that from the *trans*-cyclobutane-1.2-dicarboxylic acid a mixture of 64% of *trans* and 26% of *cis*-1.2-dibromocyclobutane, while from the *cis*-cyclobutane-1.2-dicarboxylic acid a mixture of 78% of *trans* and 14% of *cis*-1.2-dibromocyclobutane were obtained.

The discrepancy between our results and those described in literature [4] in the case of the cyclobutane-1.2-dicarboxylic acids brought us about to study quantitatively also the Hunsdiecker reaction products of the *trans*-3.4-dibromocyclobutane-*cis*-1.2-dicarboxylic acid (**5**).[9] The gas-chromatographic analysis of the reaction crude product shows the presence of three isomeric tetrabromo-derivatives in the proportion of 55.7%, 20.1% and 24.2%. The main reaction product is the 1.2.3.4-

---

[9] M. Avram, E. Marica and C. D. Nenitzescu, *Chem. Ber.*, **92**, 1088 (1959).

tetrabromocyclobutane **6**, with m.p. 104° and b.p. 115–120°/2 mm, after recrystallization from methanol.[9] The other two isomers were obtained by chromatography on an alumina column or by vacuum fractional distilation of the fraction left after the separation of the isomer **6**. Thus the tetrabromocyclobutane **7** with m.p.86° and b. p. 140–145°/2 mm and the isomer **8** with m.p. 38–40° were isolated.

CONFIGURATION OF THE STEREOISOMERIC TETRABROMOCYCLOBUTANES

Theoretically from acid **5** three isomeric tetrabromocyclobutanes **6**, **7** and **8** can be formed :

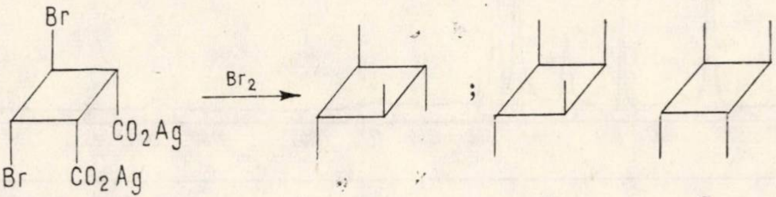

5 **6** **7** **8**

The three possible configurations belong to the point groups D_{2d} (**6**), C_s (**7**) and C_{2h} (**8**).

The number and activity of the normal modes of vibration corresponding to these configurations are recorded in table 1.

The isomer possessing the symmetry D_{2d} has 12 normal vibration modes in the infrared region ($5B_2$ and $7E$) ; all vibrations of the asymme-

Table 1

Normal modes of vibration of $C_4H_4Br_4$

Point group	Species of vibrations	Number of normal vibrations	Activity in IR	Total number of normal vibrat.	Number of active vibrations in IR
D_{2d} (**6**)	A_1	6	—	23	12
	A_2	2	—		
	B_1	3	—		
	B_2	5	M		
	E	7	M		
C_s (**7**)	A′	18	M	30	30
	A″	12	M		
C_{2h} (**8**)	A_g	8	—	30	15
	A_u	8	M		
	B_g	7	—		
	B_u	7	M		

tric isomer C_s are active in the infrared region (30) and the isomer with a symmetry C_{2h} has 15 active modes ($8A_u$ and $7\ B_u$).

The infrared spectrum of the compound with m.p. 104° (fig. 1a) exhibits 9 bands of medium intensity. It results that this compound possesses the configuration **6**. This interpretation is also confirmed by the NMR spectrum in which the four equivalent protons gave rise to only one signal at δ 4.28 ppm.

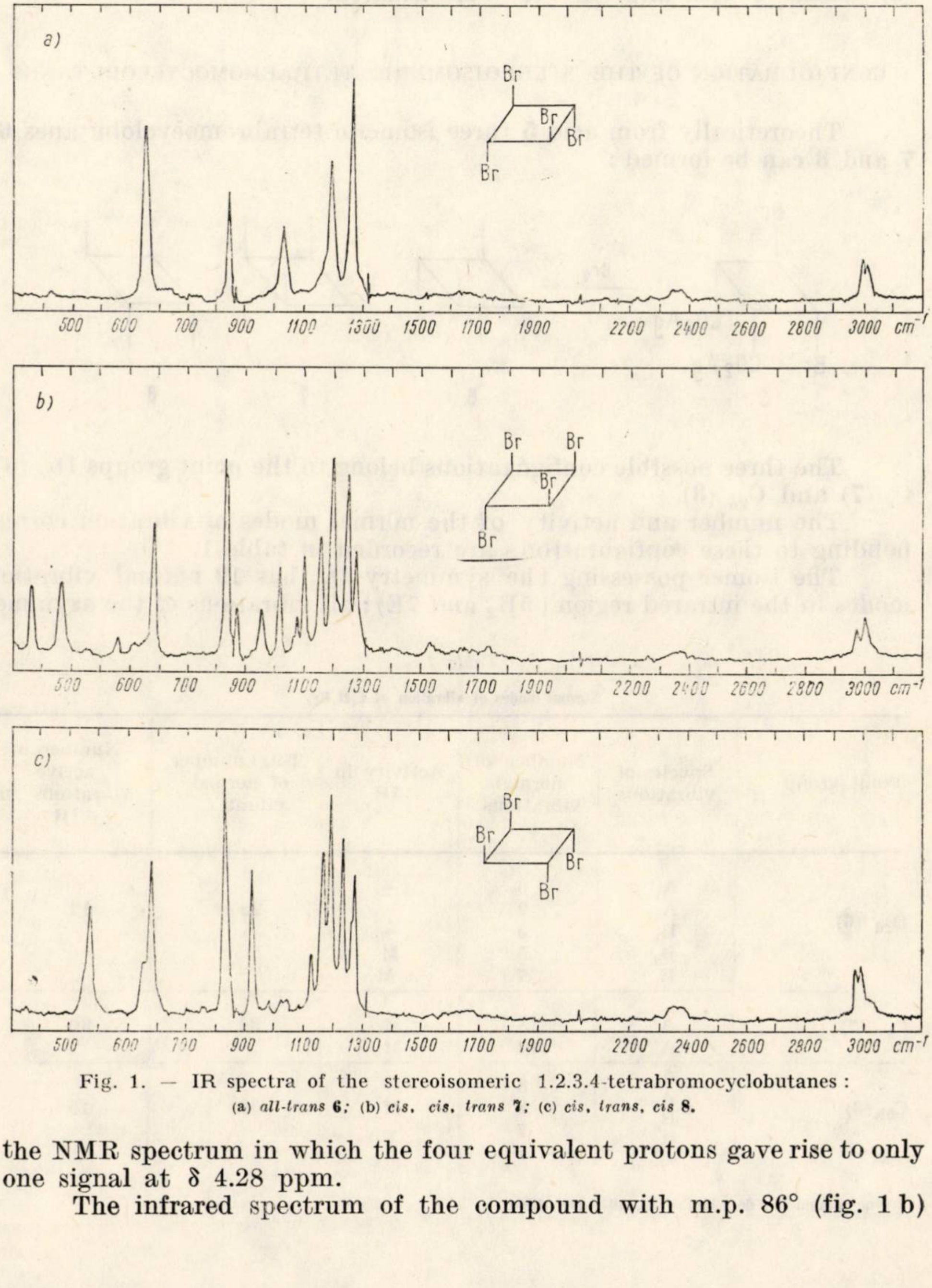

Fig. 1. — IR spectra of the stereoisomeric 1.2.3.4-tetrabromocyclobutanes : (a) *all-trans* **6**; (b) *cis, cis, trans* **7**; (c) *cis, trans, cis* **8**.

The infrared spectrum of the compound with m.p. 86° (fig. 1 b) is much more complex. In this spectrum 20 medium-strong bands can be set off what is to suggest the asymmetric configuration **7**. The NMR spectrum (fig. 2) shows two signals with fine structure centered at δ 5.17 and δ 4.65 ppm. The ratio of the corresponding integrated intensities is 1 : 3. The spectrum of the type AB_2C confirms the structure **7** assigned on the basis of the IR spectrum.

The third isomer is relatively poor in absorption IR bands. From the 15 active bands corresponding to configuration **8** only 12 medium-strong bands were identified. The NMR spectrum shows one signal at δ 4.92 ppm.

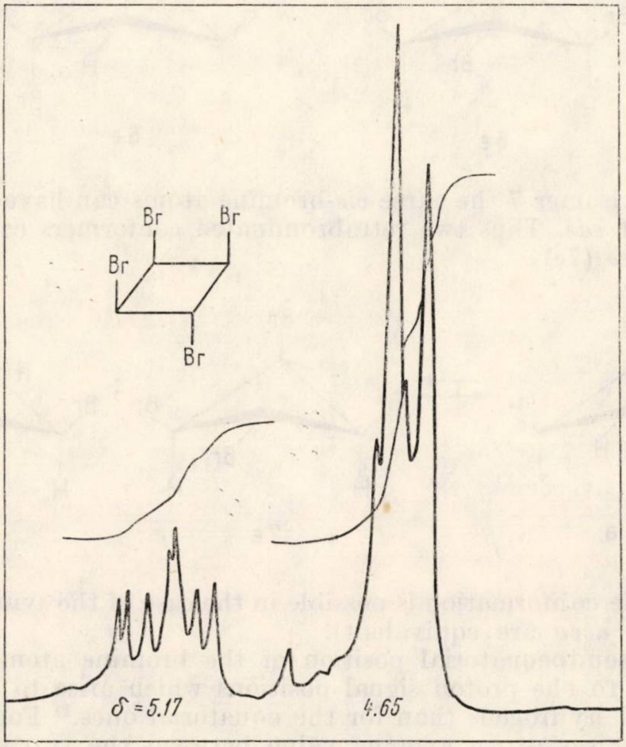

Fig. 2. — NMR spectrum of *cis, cis, trans*-1.2.3.4-tetrabromocyclobutane (**7**).

The stronger deshielding of the protons in configurations **7** and **8** than in the isomer *all-trans* **6** can be possibly attributed to conformational effects.

In the nonplanar ring of the isomeric tetrabromocyclobutanes **6**, **7** and **8** the bromine atoms can take pseudoaxial (*a*) or pseudoequatorial (*e*) conformations.[10]

---

[10] N. L. Allinger and L. A. Tushaus, *J. Org. Chem.*, **30**, 1945 (1965); J. B. Lambert and J. D. Roberts, *J. Amer. Chem. Soc.*, **87**, 3884 (1965).

The stereoisomer **6**, *all-trans*, could possess two conformations: either with pseudoaxial hydrogens and pseudoequatorial bromine atoms, **6e** or with pseudoequatorial hydrogen atoms and pseudoaxial bromine atoms, **6a**:

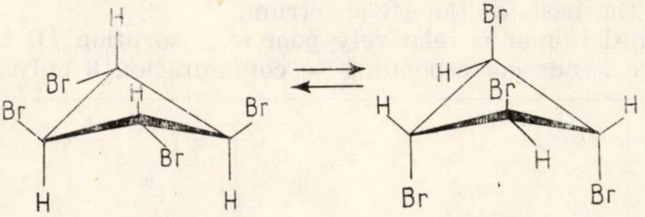

6e **6a**

In the isomer **7** the three *cis*-bromine atoms can have the positions either *aea* or *eae*. Thus two tetrabrominated conformers can exist: *aeaa* (**7a**) and *eaee* (**7e**):

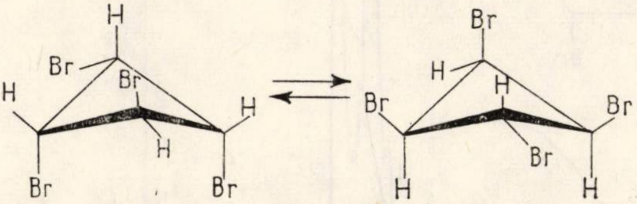

7a **7e**

;

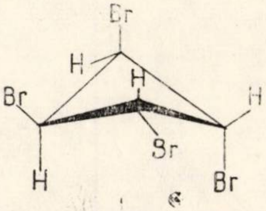

8

A single conformation is possible in the case of the symmetric isomer **8** (*eaae* and *aeea* are equivalent).

The pseudoequatorial position of the bromine atoms (**6e** and **7e**) corresponds to the proton signal positions which arise to a higher field for the axial hydrogens than for the equatorial ones.[11] For the isomer **8** the signal arises at an average value between the two extremes. The prevalence of conformations of the type **7e** were observed also in the case of the corresponding tetrachlorocyclobutanes.[12]

DISCUSSION

There is a complete agreement [2c], in considering the primary product of the reaction, between the silver salt of the carboxylic acid and bromine as being an acylhypobromide. In the second step of the reaction the decomposition of the hypobromide leads to the formation of the brominated compound with evolution of carbon dioxide:

---

[11] N. S. Bhacca and D. H. Williams, "Application of NMR Spectroscopy in Organic Chemistry", Holden Day Inc., San Francisco, 1964.

[12] M. Avram, Gh. D. Mateescu, I. G. Dinulescu, A. Juvara and C. D. Nenitzescu *Rev. Roumaine Chim.*, **13**, 1075 (1968).

$$RCOOAg + Br_2 \rightarrow RCOOBr + AgBr$$
$$RCOOBr \rightarrow R - Br + CO_2$$

It was demonstrated [2c] that the decomposition reaction has a chain homolytic mechanism; the steps of the chain propagation are not yet unambiguously established. In the case of a monocarboxylic acid they can be formulated as follows:

$$RCOO\cdot \rightarrow R\cdot + CO_2$$
$$R\cdot + RCOOBr \rightarrow R - Br + RCOO\cdot$$

or

$$R\cdot + Br_2 \rightarrow R - Br + Br\cdot$$
$$Br\cdot + RCOOBr \rightarrow RCOO\cdot + Br_2$$

The neighbourhood of the two reacting carboxyl groups of the cycloalkane-1.2-dicarboxylic acids gives rise to the possibility of bromine shift intramolecular reactions between the two neighbouring groups.[8] In this way the inversion of configuration of the 1.2-dibromocyclohexane obtained from the silver salt of the optically active *trans*-cyclohexane-1.2-dicarboxylic acid could be explained.[8]

The formation of a nonstereospecific mixture of *cis*- and *trans*-1.2-dibromocyclobutanes from the silver salts of the *cis*- and *trans*-cyclobutane-1.2-dicarboxylic acids (**9** and **10**) can be rationalized by the intermediate formation of the radical **11**, common to both stereoisomers (Scheme 1).

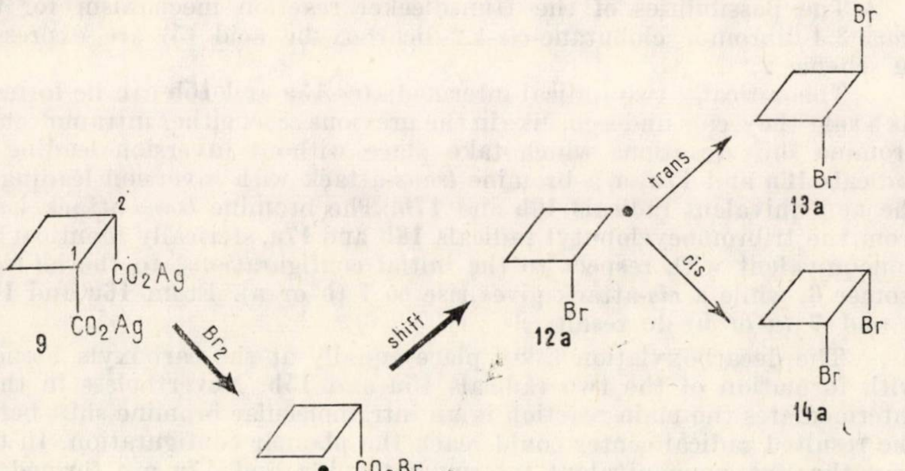

Scheme 1

In intermediate **11**, the intramolecular bromine shift can take place before the radical center could reach a planar conformation; **12a** results which can attach the bromine atom in either the *trans* or the *cis* position with respect to the first bromine atom. The former case is sterically favoured. If the radical **11** reaches a planar form the reaction propagation can take place by a bromine attack from the opposite side of the COOBr group in the molecule; it results **12b** from which the dibromocyclobutanes **13b** and **14b** can be formed.

Compounds **13a** and **13b** are enantiomers. The *trans*-1.2-dibromocyclobutane **13a** is formed with inversion of the configuration, while **13b** should have a configuration identical to that of the *trans*-cyclobutanedicarboxylic acid (**10**).

The formation of the common intermediate **11** both from the *cis*-acid **9** and the *trans*-acid **10** explains the formation of the *trans*-dibromocyclobutane as a main product also from the *cis*-acid. The formation of the *cis*-dibrominated product **14**, in proportion of 15–25% from both isomers is in agreement also in this case with a nonstereospecific homolytic course of the reaction. The large percentage of *trans*-isomer suggests a prevailing conformation control also observed in the case of the methylcyclopropanedicarboxylic acids.[7] The formation of *cis*-isomer in the homolytic additions to alkenes was also observed in many cases of strongly stereospecific reactions.[12,13]

The possibilities of the Hunsdiecker reaction mechanism for the *trans*-3.4-dibromocyclobutane-*cis*-1.2-dicarboxylic acid (**5**) are expressed in scheme 2.*

Theoretically two radical intermediates **15a** and **15b** can be formed. As a rule they can undergo, like in the previous case, either intramolecular bromine shift reactions which take place without inversion leading to radicals **16a** and **17a** or a bromine *trans*-attack with inversion leading to the nonequivalent radicals **16b** and **17b**. The bromine *trans*-attack leads from the tribromocyclobutyl radicals **16b** and **17a**, sterically identical but nonequivalent with respect to the initial configurations, to the *all-trans* isomer **6**, while a *cis*-attack gives rise to **7** (**b** or **a**). From **16a** and **17b**, **8** and **7** (**a** or **b**) do result.

The decarboxylation takes place equally at the carboxyls 1 and 2 with formation of the two radicals **15a** and **15b**. Nevertheless in these intermediates the main reaction is an intramolecular bromine shift before the resulted radical center could reach the plannar configuration. In this way the two nonequivalent intermediates **16a** and **17a** are formed. It should be pointed out that in the nonsymmetrical tribromocyclobutyl radical **16a**, the bonding of the bromine *trans* with respect to one adjacent halogen atom becomes *cis* with respect to the other one and reversely.[12] This leads to approximately equal proportions of **7a** and **8**.

The reaction mixture is composed, as previously shown, of 50% of **6** and almost equal amounts of **7** and **8**. This suggests a course of the reaction in the way indicated in scheme 2 with thick arrows.

---

[13] H. L. Goering and L. L. Sims, *J. Amer. Chem. Soc.*, **77**, 3465 (1955).

* The bromine atoms are indicated only by their valence lines, corresponding to their steric configuration.

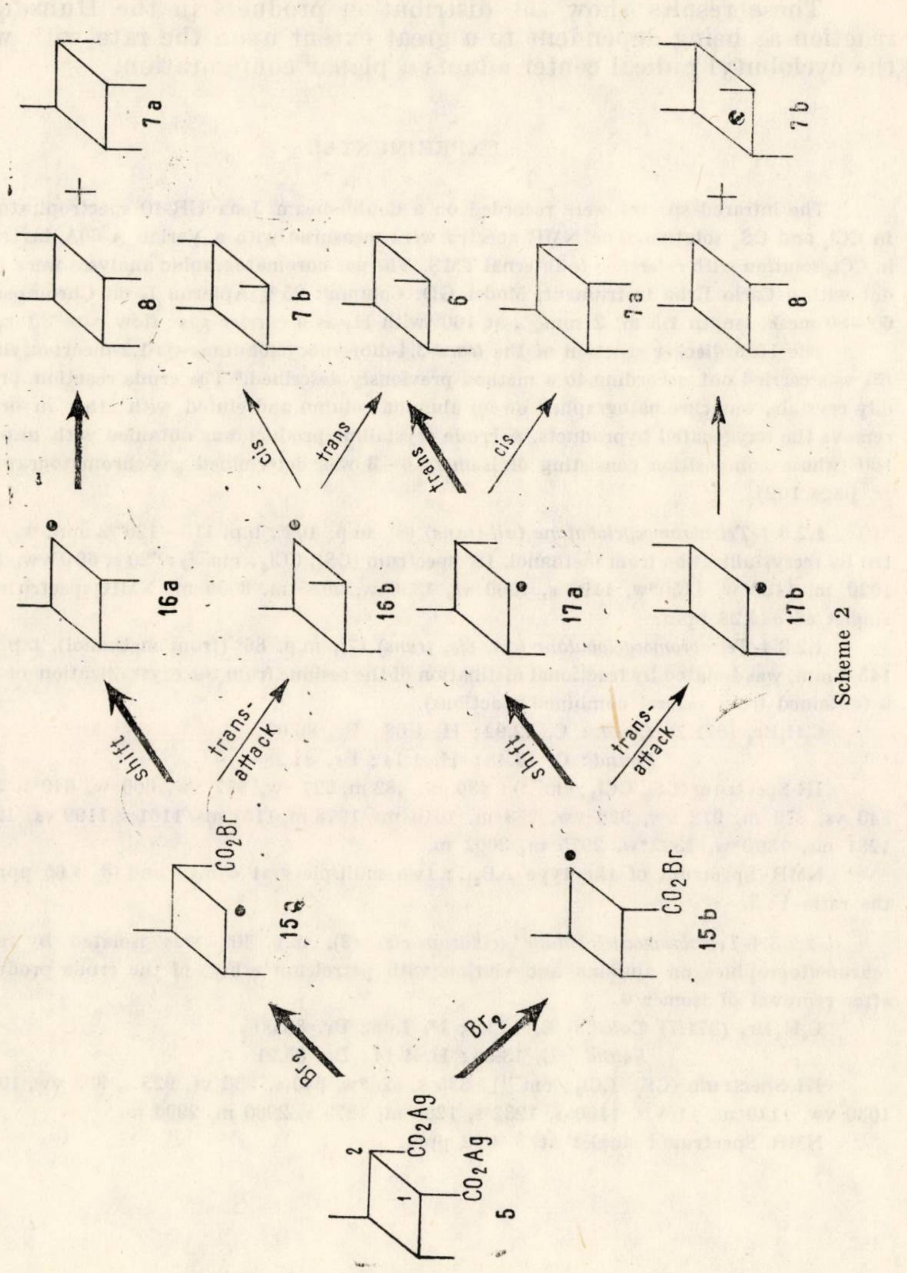
7a
7b
8
7b
6
7a
8
cis
trans
trans
cis
16a
16b
17a
17b
shift
trans-attack
shift
trans-attack
CO_2Br
15a
CO_2Br
15b
Br_2
Br_2
CO_2Ag
CO_2Ag
1
2
5

Scheme 2

These results show the distribution products in the Hunsdiecker reaction as being dependent to a great extent upon the rate with which the cyclobutyl radical center adopts a planar configuration.

EXPERIMENTAL

The infrared spectra were recorded on a double-beam Jena UR-10 spectrophotometer in CCl_4 and CS_2 solution. The NMR spectra were measured with a Varian A-60A instrument in CCl_4 solution with reference to internal TMS. The gas-chromatographic analyses were carried out with a Carlo Erba instrument, Model GD. Column: 25% Apiezon L on Chromosorb P, 60–80 mesh, length 1.5 m, 2 mm∅, at 160° with H_2 as a carrier gas; flow rate 30 ml/min.

The Hunsdiecker reaction of the *trans*-3.4-dibromocyclobutane-*cis*-1.2-dicarboxylic acid (**5**) was carried out according to a method previously described.[9] The crude reaction product, oily crystals, was chromatographed on an alumina column and eluted with ether in order to remove the oxygenated byproducts. A crude crystalline product was obtained with m.p. 90–100° whose composition consisting of isomers **6**–**8** was determined gas-chromatographically (s. page 102).

1.2.3.4-*Tetrabromocyclobutane* (*all-trans*) (**6**), m.p. 104°, b.p. 115–120°/2 mm, was isolated by recrystallization from methanol. IR spectrum (CS_2, CCl_4; cm^{-1}): 620 s, 660 vw, 835 m, 1020 m, 1130*w, 1150*w, 1190 s, 1260 vs, 1330 w, 2985 m, 3005 m. NMR spectrum: one singlet at δ 4.28 ppm.

1.2.3.4-*Tetrabromocyclobutane* (*cis, cis, trans*) (**7**), m.p. 86° (from methanol), b.p. 140–145/2 mm, was isolated by fractional distillation of the residue from the crystallization of isomer **6** (obtained from several combined reactions).

$C_4H_4Br_4$ (371.7) *Calcd.*: C, 12.92; H, 1.08; Br, 86.00
Found: C, 13.48; H, 1.14; Br, 84.28

IR Spectrum (CS_2, CCl_4; cm^{-1}): 430 m, 482 m, 527 vw, 577 vw, 606 w, 640 s, 831 vs, 840 vs, 870 m, 912 vw, 928 vw, 958 m, 1010 ms, 1078 m, 1101 ms, 1161 s, 1199 vs, 1253 vs, 1281 ms, 1300*w, 1322*w, 2975 m, 3002 m.

NMR Spectrum of the type AB_2C: two multiplets at δ 5.17 and δ 4.65 ppm with the ratio 1 : 3.

1.2.3.4-*Tetrabromocyclobutane* (*cis-trans-cis*) (**8**), m.p. 40°, was isolated by repeated chromatographies on alumina and elution with petroleum ether, of the crude product left after removal of isomer **6**.

$C_4H_4Br_4$ (371.7) *Calcd.*: C, 12.92; H, 1.08; Br, 86.00
Found: C, 13.55; H, 1.14; Br, 85.21

IR Spectrum (CS_2, CCl_4; cm^{-1}): 535 s, 625*w, 640 s, 830 vs, 925 s, 985 vw, 1020 vw, 1030 vw, 1130 m, 1165 s, 1190 s, 1232 s, 1260 m, 1275 s, 2980 m, 2990 m.

NMR Spectrum: singlet at δ 4.92 ppm.

Revue Roumaine de Chimie, **14**, 111–120 (1969)

REACTION OF PYRYLIUM SALTS WITH NUCLEOPHILES. VIII*

TRIPHENYLPYRYLIUM AND METHYLAMINE: THERMAL DEGRADATION OF N-METHYL-2,4,6-TRIPHENYLPYRIDINIUM HALIDES TO METHYL HALIDES AND 2,4,6-TRIPHENYLPIRIDINES

A. B. SUSAN and A. T. BALABAN

Institute of Atomic Physics, P. O. Box 35, Bucharest

Received June 27. 1968

The reaction of 2,4,6-triphenylpyrylium perchlorate with methylamine was studied. No definite evidence for a keto-dienimine was obtained; the major product was 1-methyl-2,4,6-triphenylpyridinium salt. Two unexpected products were also obtained: 1-methyl-2,4,6-triphenylpyridinium chloride when the solvent was carbon tetrachloride (the anion originating from the solvent) and 2,4,6-triphenylpyridine. The last product is also obtained on thermal degradation, at the melting (decomposition) point of 1-methyl-2,4,6-triphenylpyridinium halides along with methyl halide.

A. INTRODUCTION

The reaction of pyrylium salts (I) with primary amines, leading to N-substituted pyridinium salts (IV) which can be obtained with difficulty by direct quaternization of pyridines, was discovered by Baeyer and Piccard[1] and was studied later by Lombard and co-workers. [2,3] We reinvestigated this reaction in an attempt to isolate a tautomeric ketone-iminic — iminoenol intermediate (III), similar to the amino analogue of the pseudobase (II) previously reported for the reaction of 2,4,6-triphenylpyrylium perchlorate with ammonia, [4] the intermediate product in the conversion of 2,4,6-triphenylpyrylium (I) into 2,4,6-triphenylpyridine (V). This study ought to complete the previous reports on the reaction of 2,4,6-trimethyl- and -triphenylpyrylium with ammonia,[4] and of 2,4,6-trimethylpyrylium with primary amines.[5]

---

* Previous part in the series: A. T. BALABAN, *Tetrahedron*, **24**, 5059 (1968).

[1] A. BAEYER and J. PICCARD, *Liebigs Ann. Chem.*, **384**, 217 (1911).

[2] R. LOMBARD and J. P. STEPHAN, *Bull. soc. Chim. Fr.*, **1958**, 1458.

[3] R. LOMBARD and A. KRESS, *ibid.*, **1960**, 1528.

[4] A. T. BALABAN and C. TOMA, *Tetrahedron*, **22**, suppl. 7,1 (1966).

[5] C. TOMA and A. T. BALABAN, *Tetrahedron*, **22**, suppl. 7, 9 (1966).

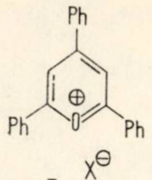

I

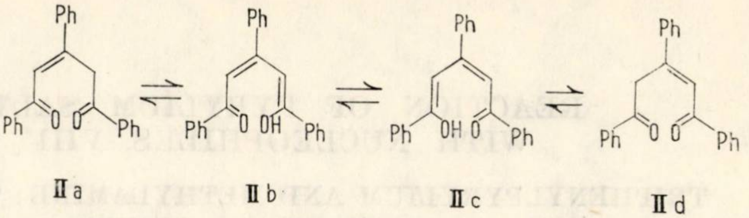

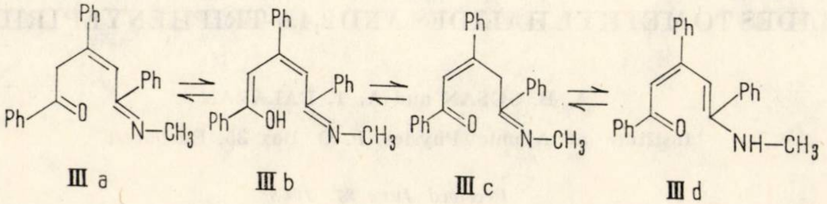

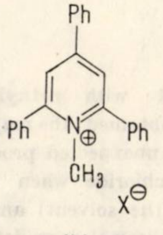

IV

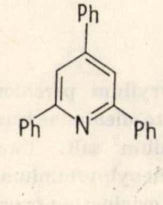

V

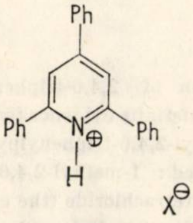

VI

B. 1-METHYL-2,4,6-TRIPHENYLPYRIDINIUM SALTS (IV, X = ClO_4 OR I)

Agitation of a suspension of crystalline 2,4,6-triphenylpyrylium perchlorate or iodide (1 mole) with 2 moles of an aqueous methylamine solution in ether or ethanol or with a solution of methylamine in carbon tetrachloride as reaction medium, at room temperature, leads to the disappearance of the fluorescence due to the pyrylium salt and to the apparition of an intense coloration in red of the solution. After a few minutes of shaking, slightly exothermally, the suspension became homogeneous and then deposited a solid substance. This was filtered off and after recrystallization from ethanol it was identified as 1-methyl-2,4,6-triphenylpyridinium perchlorate (IV) (X = ClO_4), m.p. 214° or respectively the corresponding iodide, m.p. 178—9°. The red filtrate deposited after standing for a few hours some more perchlorate IV which was removed by filtration. The pseudobase II does not react with methylamine in the same conditions.

C. TAUTOMERIC N-METHYL-KETO-DIEN-AMINE (III)

Previous reports mentioned red oils formed in poor yields in the reaction of 2,4,6-triphenyl substituted pyrylium salts with primary aliphatic and aromatic amines.[2,4,5] We attempted to isolate such an intermediate which could have a structure like III.

Taking into account the presumed instability of III on the basis of previous works,[2,4,5] we performed the reaction not only in ether or ethanol but also in dry carbon tetrachloride. This last solvent was expected to be suitable for the rapid identification of the tautomeric N-methyl-keto-dienamine compound III by means of infrared spectra. As it could be seen from the infrared spectra of the carbon tetrachloride solution of the red oil, measured immediately after the two reactants, 2,4,6-triphenylpyrylium salt and methylamine were mixed, no sure evidence of such an intermediate can be made; although some runs gave a product exhibiting carbonyl stretching bands at 1685, or 1685 and 1740 cm^{-1}, the yield was too low to allow a chemical characterization. This can be explained by the instability of the red solution containing the N-methyl-keto-dien-amine compound III, evidenced by the rapid change in time of the i.r. spectra of the same sample followed by the deposition, after about 5 minutes, of the main product of the reaction, 1-methyl-2,4,6-triphenylpyridinium salt IV. The red colour can be due to a charge-transfer complex between the amine as donor, and pyrylium (or pyridinium) cations as acceptor.[5a]

D. 1-METHYL-2,4,6-TRIPHENYLPYRIDINIUM CHLORIDE (IV, X = Cl)

An unexpected substance, 1-methyl-2,4,6-triphenylpyridinium chloride IV (X = Cl) was isolated as a by-product formed in about 10% yield when the reaction between 2,4,6-triphenylpyrylium perchlorate I ($X = ClO_4$) and methylamine was carried out in dry carbon tetrachloride. After filtering off the main product of this reaction, 1-methyl-2,4,6-triphenylpyridinium perchlorate IV ($X = ClO_4$), another solid substance crystallized, identified as the chloride (X = Cl), the yield being much higher when the clear filtrate was allowed to stand overnight.

The structure of the white substance, m.p. 148—9° (after repeated recrystallization from acetone — ether) was found by analysis to correspond to the 1-methyl-2,4,6-triphenylpyridinium chloride IV (X = Cl) and was proved by i.r. and n.m.r. spectra, mixed melting points, chemical reactions and thermogravimetric analysis. The i.r. and n.m.r. spectra of the substance with m.p. 148—9° are identical to those of 1-methyl-2,4,6-triphenylpyridinium iodide IV (X = I) prepared from 2,4,6-triphenylpyrylium iodide I (X = I) and methylamine in aqueous ethanolic solution, under similar conditions: in the infrared spectrum of IV characteristic bands appear at 1632 (vs), 1610 (w) and 1577 (s) cm^{-1}, enabling the easy differentiation from I, V, or VI*; the n.m.r. spectrum contains three main peaks at τ 6.05 (3 methyl protons), 2.30 (15 phenyl protons) and 1.90 (2 pyridinium protons) in agreement with the literature data for related systems.[5]

---

* Along with other bands at 1504 (m), 1450 (m), 1420 (m), 1268 (ms), 1183 (m), 900 (s), 779 (vs), 733 (s), 705 (vs) cm^{-1}.

[5a] M. FĂRCAȘIU and D. FĂRCAȘIU, *Tetrahedron Letters*, **1967**, 4833, A. LEDWITH and D.H. ILES, Chem. Brit., **1968**, 266.

The chloride anion was identified (as AgCl) with silver nitrate and determined volumetrically by titrating with silver nitrate in a potassium hydroxide solution in the presence of potassium chromate.

Treatment of the substance with m.p. 148–9° with potassium iodide in aqueous ethanolic solution led to a solid substance melting at 179–80° which was identified as 1-methyl-2,4,6-triphenylpyridinium iodide IV (X = I) by mixed melting points and i.r. spectrum. This metathetic reaction is another structure proof for the compound with m.p. 148–9°.

The formation of 1-methyl-2,4,6-triphenylpyridinium chloride IV (X = Cl) along with the expected perchlorate IV ($X = ClO_4$) can be interpreted by the presence of hydrochloric acid in the reaction medium explaining the replacement of the perchlorate anion by the chloride anion. As all reactants were proved to be free from hydrogen chloride, the formation of 1-methyl-2,4,6-triphenylpyridinium chloride IV (X = Cl) can be understood as following a reaction between the excess of methylamine with the carbon tetrachloride solvent. Such a reaction is not unprecedented ; similar behaviour was reported for mixtures of carbon tetrachloride with aniline, alkyl amines, ammonia [6,7] or benzylamine. [8,9] According to these reports the formation of hydrogen chloride in the reaction media can be assigned to the following reaction path owing to the nucleophilic attack of the amine on carbon tetrachloride :

$$CH_3NH_2 + CCl_4 \longrightarrow CH_3NHCCl_3 + HCl$$

This assignment is supported by the isolation in our experimental conditions of methyl- and benzylamine hydrochlorides (characterized by m.p. and i.r. spectra) when a mixture of the corresponding amine and carbon tetrachloride was allowed to stand a few hours at room temperature in the daylight.

E. THERMAL DEGRADATION OF IV, X = Hal

It is interesting to mention the unusual behaviour of 1-methyl-2,4,6-triphenylpyridinium chloride IV (X=Cl) and the corresponding iodide IV (X = I) at the melting point, leading to 2,4,6-triphenylpyridine V, besides methyl chloride and methyl iodide respectively.

Such a thermal degradation of 1-alkyl-2,4,6-trisubstituted pyridinium halides was briefly described by Ziegler and Fries.[9a] The behaviour of such quaternary pyridinium compounds is quite different from

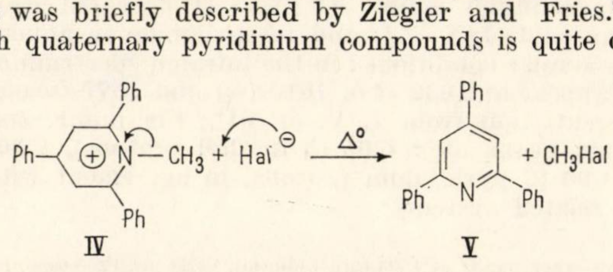

---

[6] H. E. ANDERSOHN, *J. Amer. Chem. Soc.*, **74**, 1421 (1952).

[7] G. DREFAHL and G. HEUBLEIN, *J. Prakt. Chem.*, **20**, 323 (1963).

[8] M. ASHER, *Chem. and Ind.*, **1965**, 1430.

[9] T. G. BONNER and R. A. HANCOCK, *Chem. and Ind.*, **1965**, 257.

[9a] K. ZIEGLER and F. A. FRIES, Ber. dtsch. chem. Ges., **59**, 242 (1926).

the usual Hofmann degradation, but can be easily understood as a nucleophilic substitution of the triphenylpyridine moiety by the anions Cl^- or I^-, yielding the corresponding methyl chloride and iodide. It is likely, but this point has not yet been experimentally checked, that the process is an S_N2 reaction. *

This path of the reaction was proved by the isolation of reaction products : 2,4,6-triphenylpyridine V (characterized by melting point, i.r. spectrum, perchlorate and picrate derivatives and elementary analyses) and the corresponding methyl halides (characterized as the corresponding methylmercuric halides). The reaction was carried out by sublimation (or melting) of the 1-methyl-2,4,6-triphenylpyridinium halides IV (X = Cl, I) followed by trapping the corresponding methyl halides. A good confirmation of the above mentioned reaction path was the thermogravimetric analysis of the 1-methyl-2,4,6-triphenylpyridinium halides IV (X = Cl, I) as shown in table 1 and figure 1.

Table 1

Thermogravimetric analyses of some quaternary pyridinium halides

Sample analysed / Experimental conditions	IV X = Cl m.p.148°	IV X = I m.p.178–9°
Weight of substance (mg)	34.5	151.3
Thermal weight loss (mg)	4.9	47.5
Thermal weight loss (%)	14.2	31.4
Theoretical weight loss (%) calculated for CH_3X	14.1	30.9

The pattern of the thermogravimetric curve of 1-methyl-2,4,6-triphenylpyridinium perchlorate IV ($X = ClO_4$) is different, i.e. no change until the temperature of 330° is attained, then a rapid (almost explosive) decomposition with an inflection corresponding to a weight loss of 43%. This is a deep fragmentation of the molecule, not a simple methyl splitting, which can be rationalized by the low nucleophilicity and the high oxidizing power of the perchlorate anion.

F. 2,4,6-TRIPHENYLPYRIDINE V

Treatment with perchloric acid of the red ethanolic or carbon tetrachloride solution, obtained after 1-methyl-2,4,6-triphenylpyridinium perchlorate IV ($X = ClO_4$) and chloride IV (X = Cl) were separated, yielded white crystals, m.p. 196–8°, of 2,4,6-triphenylpyridinium perchlorate VI, identified by mixed melting points and i.r. spectrum. Alkalinization of this compound affords 2,4,6-triphenylpyridine V.

As the formation of perchlorate VI could be interpreted as originating from traces of ammonia in the methylamine as previously reported,[3] a v.p.c. analysis proved the absence of the ammonia in the commercial

---

* Cf. D. Hellwinkel and H. Seifert, *Chem. Commun.*, **1968**, 1683, and further references therein.

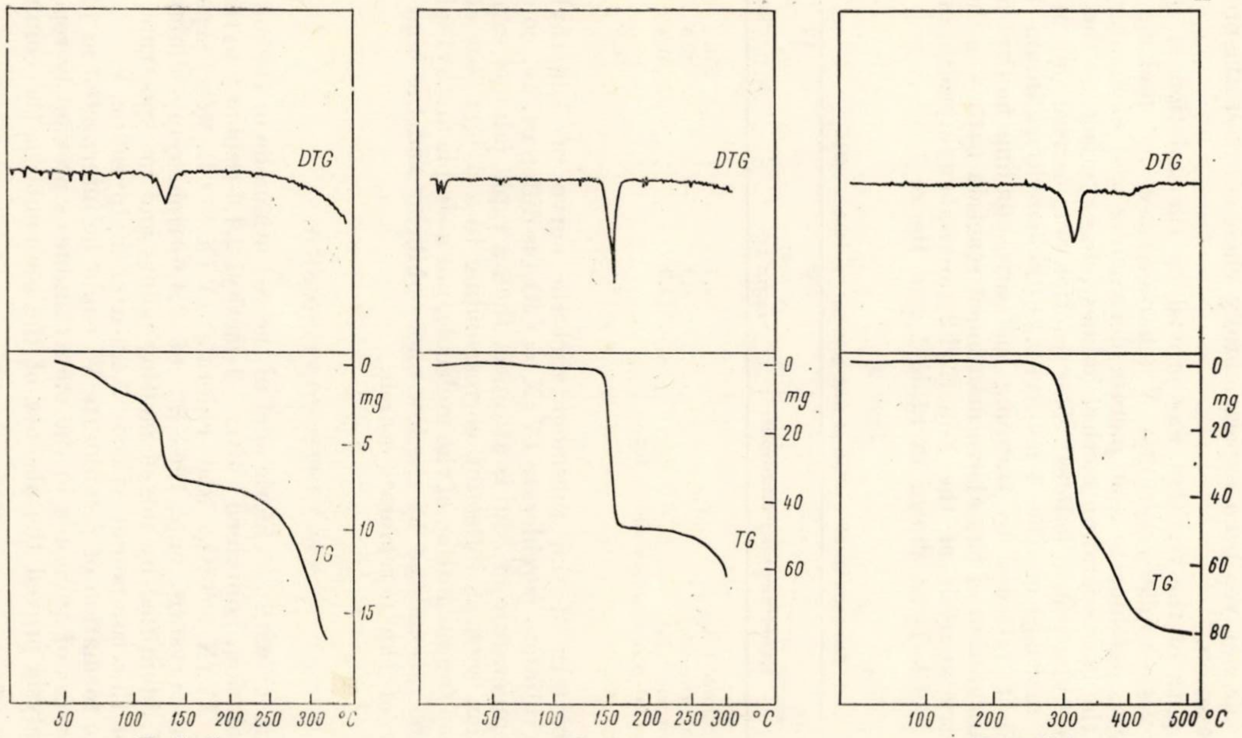

IV, X = Cl IV, X = I IV, X = ClO4

Fig. 1. — Thermogravimetric analysis of quaternary pyridinium salts (IV).

methylamine solution. Therefore this reaction can be explained as occurring in the reaction medium in a similar manner with the above mentioned thermal degradation of 1-methyl-2,4,6-triphenylpyridinium chloride IV (X = Cl). Another possible path for the reaction is the nucleophilic attack on the methyl group by the methylamine in the solution, similarly to previously reported reactions of N-2,4-dinitrophenyl pyridinium compounds with bases like aniline.[10] No dimethylamine could be isolated from the reaction mixture. However, both reactions of this kind are essentially the reverse of those by which pyridinium salts are formed. The reverse course of the reaction in the present case is probably due both to steric factors (relief of steric strain in IV), and to electronic factors (the nucleophilicity of 2,4,6-triphenylpyridine being very low). When 1-methyl-2,4,6-triphenylpyridinium perchlorate IV was refluxed with a strongly alkaline solution of sodium hydroxide no fission of the methyl-nitrogen bond could be detected, though hydroxyl is more nucleophilic than the halide anion.

G. CONCLUSION

The newly found thermal degradation of 1-alkyl-2,4,6-triphenylpyridinium halides is expected to be useful especially for works with isotopically labelled compounds: the reaction of methylamine with 2,4,6-triphenylpyrylium iodide and the degradation of the intermediate N-methyl-2,4,6-triphenylpyridinium iodide to methyl iodide are practically quantitative. In such a case the usual path (*i*) for the obtention of an alkyl iodide from a nitrile can be changed (*ii*) and the yields improved as shown below:

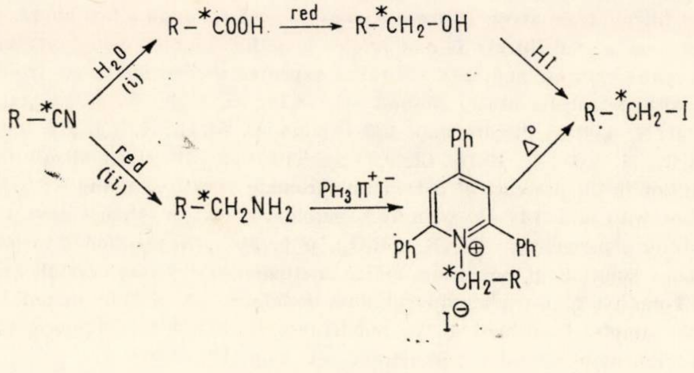

EXPERIMENTAL

In the present paper, i.r. spectra were recorded with a Jena UR-10 apparatus, the n.m.r. spectra with a JEOL JNM-3H-60 apparatus, the thermogravimetric analyses with an ORION Derivatograph.

---

[10] A. F. Vompe and N. F. Turitsyna, *Dokl. Akad. Nauk S.S.S.R.*, **64**, 341 (1949); *Chem. Abstr.*, **43**, 4671 (1949).

2, 4, 6-Triphenylpyrylium perchlorate I ($X = ClO_4$) was prepared [11] from 2 moles chalcone [12] and 1 mole acetophenone by heating on the steam bath at 100° with 1.5 moles 70% perchloric acid under stirring for 7 hours, then refluxing 5 minutes with 0.5 l ethanol and precipitating, after cooling, all the perchlorate with ether. After filtration, the perchlorate was washed with ether and recrystallized from 60% acetic acid, m.p. 290°.

Pseudobase of 2,4,6-triphenylpyrylium was prepared [13] from a solution of 2,4,6-triphenylpyrylium perchlorate (13 g) in 200 ml ethanol to which a solution of crystallized sodium acetate (22.75 g) in 50 ml water was added continuously in small portions with good stirring and heating on the steam bath. After cooling almost pure crystals were filtered off (10.6 g, yield 98%), m.p. 118°.

2,4,6-Triphenylpyrylium iodide I ($X = I$) was prepared [14] from the corresponding pseudobase (3.65 g) and 9 ml (18 g) of a commercial grade concentrated hydriodic solution in water, diluted with 15 ml ethanol and 35 ml water. By bubbling SO_2 gas through this solution a dark red solid substance deposited. More ethanol (200 ml) was then added to solubilize the solid, the solution was heated and more SO_2 gas passed through the solution. The dark red substance precipitated after cooling was recrystallized[15] from hot ethanol saturated with SO_2, by precipitating with ether or petroleum ether, yielding a bright red substance (4.5 g, yield 99%), m.p. 223–4° (lit.[16] 224°).

Reaction of 2,4,6-triphenylpyrylium perchlorate with methylamine.

2,4,6-Triphenylpyrylium perchlorate I (7.96 g, 20 mmoles) was shaken a few minutes at room temperature with a solution of about 1.86 g (60 mmoles) methylamine gas absorbed in 35 ml cold dry carbon tetrachloride. A sample of the clear red carbon tetrachloride solution was immediately checked for i.r. spectrum. The substance which crystallized in about ten minutes was filtered off and recrystallized from ethanol yielding 6.1 g (75% yield) of 1-methyl-2,4,6-triphenylpyridinium perchlorate, white crystals, m.p. 216° (Found: C, 68.61; H, 4.87; N, 3.57. $C_{24}H_{20}ClNO_4$ requires: C, 68.52; H, 4.97; N, 3.82%).

The red filtrate from above (filtrate A) was allowed to stand a few hours, yielding after repeated filtrations a red filtrate B and crude 1-methyl-2,4,6-triphenylpyridinium chloride IV ($X = Cl$), white crystals m.p. 148–9° (after repeated recrystallizations from acetone and precipitation with petroleum ether) (Found: C, 78.10; H. 6.23; N, 4.96.$C_{24}H_{20}NCl$ requires C, 80.5; H, 5.60; N, 4.00%). Picrate, m.p. 182 (Found: C, 65.41; H, 4.80; N, 9.99. $C_{30}H_{22}N_4O_7$ requires C, 65.45; H, 4.03; N, 10.18; Cl, 9.90%). Titration with silver nitrate in a potassium hydroxide solution in the presence of potassium chromate gave 10.3% and 9.8% Cl. Treatment of this substance with m.p. 148–9° with 70% perchloric acid in ethanol gave 1-methyl-2,4,6-triphenylpyridinium perchlorate IV ($X = ClO_4$), m.p. 214°; the reaction of the same substance with an aqueous solution of potassium iodide in ethanol gave yellow crystals, m.p. 179–80°, identified as 1-methyl-2,4,6-triphenylpyridinium iodide IV ($X = I$) by mixed melting points with an original sample. Treatment of the red filtrate B with 70% perchloric acid in ethanol lead to 2,4,6-triphenylpyridinium perchlorate VI, m.p. 196–198°.

The red filtrate from above (filtrate A) can be worked up also in a different manner. Evaporation to dryness in vacuum on the water bath at 60°, extraction of the residue with warm benzene, drying on magnesium sulphate and evaporation of the solvent lead to a red oil which gave by distillation or sublimation in vacuum, white crystals, m.p. 137°, which was identified as 2,4,6-triphenylpyridine V (lit.[16,17] m.p. 139°) by mixed melting point with an original sample, i.r. spectrum and formation of 2,4,6-triphenylpyridinium perchlorate VI by treatment with perchloric acid. The solid residue left after extraction with benzene as mentioned above was identified, after recrystallization from acetone and precipitation with ether, as 1-methyl-2, 4, 6-triphenylpyridinium perchlorate, m.p. 148°.

---

[11] A. T. Balaban, *Compt. rend.*, **256**, 4239 (1963).

[12] E. P. Kohler and H. M. Chadwell, "Organic Syntheses" (2nd Edition), Coll. vol. I, 78 (1941).

[13] A. T. Balaban, C. N. Rențea and M. Băcescu-Roman, *Rev. Roumaine Chim.*, **10**, 865 (1965); J. A. Berson, *J. Amer. Chem. Soc.*, **74**, 358 (1952).

[14] A. T. Balaban, *Compt. rend.*, **256**, 4041 (1963).

[15] A. T. Balaban, M. Mocanu and Z. Simon, *Tetrahedron*, **20**, 119 (1964).

[16] W. Dilthey, *J. Prakt. Chem.*, **94**, 53 (1916).

Reaction of 2, 4, 6-triphenylpyrylium iodide with methylamine.

2,4,6-Triphenylpyrylium iodide I (X = I) (4.3 g, 10 mmoles) was vigorously shaken for about ten minutes with a solution of 5 ml 33% aqueous methylamine (1.65 g, 53 mmoles) in 50 ml ethanol. After the solubilization of the pyrylium iodide, a yellow substance deposited which was recrystallized from ethanol and precipitated with ether yielding 1.4 g of 1-methyl-2,4,6-triphenylpyridinium iodide IV (X = I), m.p. 178—9°. More substance was obtained from the crude filtrate by allowing it to stand a few hours (1.4 g) followed by evaporation to dryness in vacuum of the red filtrate from above, yielding a third portion of 0.8 g crude 1-methyl-2,4,6-triphenylpyridinium iodide, the total yield being 3.6 g (81%)

Thermal degradation and behaviour at the melting point temperature of the N-methyl-2,4,6-tri phenylpyridinium halides IV (X = Cl, I).

By means of a Boetius micro hot stage, a net change of the crystalline form of the 1-methyl-2,4,6-triphenylpyridinium halides IV (X = Cl, I) can be observed together with a drop to 136—8° of the melting point of the above pyridinium halides after resolidification, i.e. 148—9° for the chloride and 178—9° for the corresponding iodide. Mixed melting points with authentic samples of 2,4,6-triphenylpyridine (m.p. 138°) of the above mentioned substance with m.p. 136—8° showed no depression.

The chemical change of the above mentioned substances at the melting point due to a thermal degradation was proved by means of thermogravimetric analysis as shown in the first part of this paper and also by i.r. spectra and chemical methods.

After an infrared spectrum of a potassium bromide pellet of 1-methyl-2,4,6-triphenylpyridinium chloride was registered, the pellet was heated in an air stream to 150° for 5 minutes, the i.r. spectrum of the pellet showed a net change in the structure of the substance, identical to a potassium bromide pellet of an authentic sample of 2,4,6-triphenylpyridine.

Vacuum sublimation of N-methyl-2, 4, 6-triphenyl-pyridinium iodide, m.p. 178—9° at a temperature of about 180° gave a solid residue, 2,4,6-triphenyl-pyridine, m.p. 138—9°, identified by means of i.r. spectrum and mixed melting point. A few grams of 1-methyl-2,4,6-triphenylpyridinium iodide were warmed at a temperature of about 180—200°, under a slight vacuum and trapping of the gas evolved in a trap cooled at about —20°. The solid substance remaining in the distillation flask was identified as 2, 4, 6-triphenylpyridine and the liquid substance trapped as methyl iodide by means of refractive index ($n_D^{20} = 1.5293$) and also by chemical methods as follows : a Grignard reagent was made from 0.15 g magnesium in 8 ml of dry ether with about 0.5 ml of the substance trapped, in a dry test tube. After the reaction was started by adding of a crystal of iodine the solution was filtered and allowed to flow in a test tube containing 3 g of mercuric iodide. The reaction mixture wa

---

[17] R. L. Frank and R. P. Seven, *J. Amer. Chem. Soc.*, **71**, 2629 (1949); L. Amoros-Marin and R. B. Carlin, *ibid.*, **81**, 733 (1959); Z. S. Ariyan and H. Suschitzky, *J. Chem. Soc.*, **1961**, 2242.

shaken vigorously, warmed on the steam cone a few minutes and evaporated to dryness. Crude methyl mercuric iodide was obtained after the residue was boiled with 15 ml of 95% ethanol, followed by filtration, dilution with water of the filtrate and cooling in an ice bath. The solid substance, collected and recrystallized from 60% ethanol, yielded pure methyl mercuric iodide, m.p. 143° (lit.[18] m.p. 145°).

Reaction of methylamine with carbon tetrachloride.

An equimolar mixture of methylamine gas and dry carbon tetrachloride free from hydrogen chloride was allowed to stand at room temperature in the daylight. After one hour colourless crystals (plates) separated, were filtered off and dried over phosphorus pentoxide, m.p. 225–228°. By infrared spectrum, identification of ionic chloride with silver nitrate, and mixed melting points with an authentic sample of methylamine hydrochloride, this substance with m.p. 225–228° was identified as methyl-ammonium chloride.

V.p.c. proof for the absence of ammonia in methylamine.

Gas samples of methylamine collected in a separatory funel at atmospheric pressure (by heating an aqueous solution of methylamine and sodium hydroxide) were analysed on a Willy Giede Model GCF-18 gas chromatograph, in a column packed with Carbowax 1500 on Celite C22, at 30° with a flow of hydrogen gas of 100 ml/min. Only the peak corresponding to methylamine was obtained. The sensitivity of the instrument was checked with a gas mixture of 1% ammonia in methylamine gas, when two peaks were obtained in the above mentioned conditions.

Aknowledgement – Infrared spectra were taken by Mrs. E. Romaş and thermogravimetric analyses were made by Mr. H. Paraschiv to whom our thanks are given.

---

[18] R. L. Shriner, R. C. Fuson and D. Y. Curtin, "Systematic Identification of Organic Compounds", 5th Edition, John Wiley a. Sons, New York, 1965.

Revue Roumaine de Chimie, **14**, 121–124 (1969)

STEROIDS IN THE ADSORBED STATE. II

REDUCTIONS WITH SODIUM BOROHYDRIDE UNDER HETEROGENEOUS CONDITIONS

F. HODOŞAN and N. ŞERBAN

Institute of Chemistry of the Academy, Cluj, Str. Donath 59–65

Received April 13, 1968

Alumina treated with aqueous sodium borohydride and dried *in vacuo* is a useful reagent for the reduction of ketones in nonpolar solvents or in the solid state. Alkali sensitive groups are not affected under these conditions, as it was demonstrated by the conversion of Δ^4-androstene-3,17-dione into testosterone via the 3-enol acetate.

Sodium borohydride is used with considerable success in the reduction of ketosteroids owing to its selectivity, its marked stereospecificity and stability in hydroxylic solvents.[1] Most part of borohydride reductions are carried out in methanol, ethanol or aqueous alcoholic solutions. The choice of the reaction medium is dictated by the water or alkali sensitivity of the compound to be reduced. Side reactions due to the alkalinity of the reagent can be depressed by using less polar solvents, such as dioxane or tetrahydrofuran. There is no mention concerning the utilization of sodium borohydride in nonpolar solvents.

In the present paper we wish to describe a new reduction procedure which permits the use of sodium borohydride in solvents such as dry benzene. Under the conditions reported here, ketones possessing highly alkali sensitive functional groups can be reduced too. The reagent employed can be readily prepared by treating neutral alumina with a concentrated aqueous sodium borohydride solution; the excess water is then removed by gentle heating *in vacuo* over P_2O_5. It is noteworthy that a spontaneous heating occurs when the aqueous sodium borohydride is added to the support. Evolution of hydrogen is observable during the preparation and storage of the reagent, which indicates a slow decomposition of the borohydride. Therefore, the reagent is recommended to be freshly prepared just before utilization.

---

[1] N. G. Gaylord, "Reduction with Complex Hydrides", Interscience Publishers, New York, 1956, p. 100, 288, 1013; L. F. Fieser and M. Fieser, "Steroids", Reinhold Publishing Corporation, New York, 1959, p. 268; H. J. E. Loewenthal, *Tetrahedron* **6**, 269 (1959); E. Schenker, *Angew. Chem.*, **1961**, 81; C. Djerassi, "Steroid Reactions", Holden Day, Inc., San Francisco, 1963, p. 135.

The reduction of steroidal ketones can be carried out at room temperature, in dry benzene, with an excess of $NaBH_4-Al_2O_3$ reagent, under vigorous stirring. The reaction times do not differ appreciably from those in hydroxylic solvents under usual conditions.

The $NaBH_4-Al_2O_3$ reagent is effective in the solid state reactions too. In this case, the ketone previously adsorbed on alumina is reduced by mixing for 3—4 hours in a mechanical grinder with the $NaBH_4-Al_2O_3$ reagent.

Investigations carried out on a series of five ketosteroids indicated that the steric course of the reductions with $NaBH_4-Al_2O_3$ seems to be essentially the same as that in solution under usual conditions. Thus, the chief reduction products of 17-ketones as well as those of 3- and 6-ketones of 5α series are β-alcohols, whereas a 3-ketone of the 5β series yields mainly the 3α-alcohol.

The usefulness of the borohydride-alumina reagent in the reduction of ketones possessing alkali sensitive functional groups was demonstrated by conversion of Δ^4-androstene-3,17-dione (I) into testosterone (IV) via the 3-enol acetate II. As it is well known, the initial step in the action of borohydride on an enol acetate under usual conditions consists in its solvolysis to yield the free ketone which is then reduced to the corresponding epimeric alcohols.[2] In turn, the reduction of the 17-oxo-3-enol acetate II according to our procedure afforded almost exclusively 3-acetoxy-$\Delta^{3,5}$-androstadien-17 β-ol (III). Thin layer chromatography of the crude reduction product showed that the enol acetate group was affected

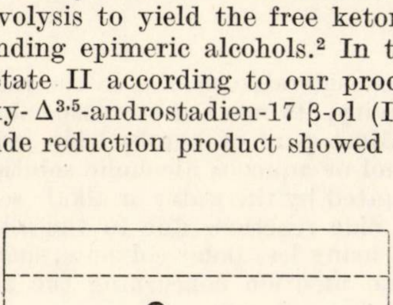

Fig. 1. — **A**: Δ^4-androstene-3,17-dione (I) ($R_F = 0.50$) ;**B**: 3-acetoxy-$\Delta^{3,5}$-androstadien-17-one (II) ($R_F = 0.90$) ; **C** : 3-acetoxy-$\Delta^{3,5}$-androstadien-17β-ol (III) ($R_F = 0.65$) ; **D** : testosterone (IV) ($R_F = 0.37$). *Adsorbent* : silica gel G (Merck). *Solvent* : benzene — ether 1 : 2.

---

[2] W. G. Dauben and J. F. Eastham, *J. Amer. Chem. Soc.*, **73**, 4463 (1951); B. Belleau and T. F. Gallagher, *J. Amer. Chem. Soc.*, **73**, 4458 (1951).

only insignificantly during the reduction. The chromatographic behaviour of the pure compounds involved in these transformations are pictured in figure 1.

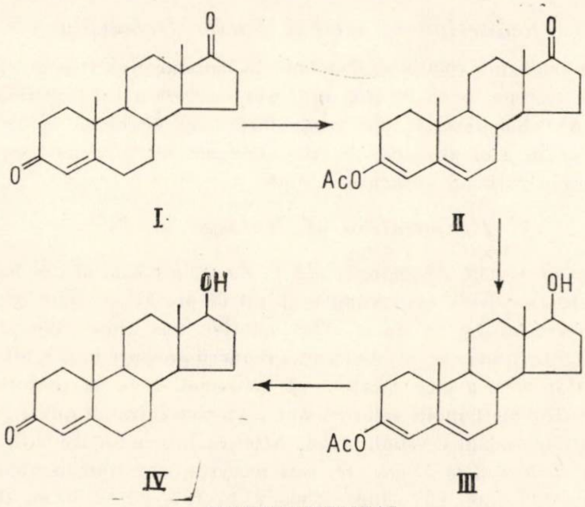

EXPERIMENTAL

General procedure

A solution of 1 part of $NaBH_4$ in 2 parts of water is added to 20 parts of neutral Al_2O_3. The mixture is shaken until the mass becomes homogeneous. The flask is then connected with a tube containing P_2O_5 and heated under reduced pressure (5—10 mm) at 40—50° in a water bath, under occasional shaking, until the water evolvement appears to be complete. Two parts of monoketone are then dissolved in 50—60 parts of dry benzene and poured onto the reagent. The reduction is carried out at room temperature, under vigorous stirring; its progress is controlled by thin layer chromatography and IR spectrometry. After the reaction is complete, the solution is filtered and the alumina washed thouroughly with a suitable solvent (benzene, ether, methanol, etc.). If methanol is used*, the residue obtained by removal of the solvent has to be washed with water prior to its purification.

Unless otherwise stated, in the examples given below the reaction time was 1 hour.

5α-Androstane-3β, 17β-diol, from 1.5 g of 5α-androstan-17β-ol-3-one. Yield : 1.1 g of pure diol, m. p. 165—167° (from ethanol) (Lit.[3] m.p. 168°).

Methyl 3α-hydroxy-6α-tosyloxy-5β-cholanate, from 2 g of methyl 3-oxo-6α-tosyloxy-5β-cholanate. The crude alcohol was dissolved in 10 ml of benzene, 20 ml of isopropyl ether was added and allowed to crystallize overnight at about —10°. Yield : 1.1 g ; m.p. 155—158°.

$C_{32}H_{48}O_6S$ (560.8) *Calcd.* : C, 68.63 ; H, 8.62.

Found : C, 68.66 ; H, 8.79.

5α-Cholestane-3β, 6β-diol 3-acetate, from 590 mg of 5α-cholestane-3β-ol-6-one acetate. The crude reaction product (470 mg) was adsorbed on 20 g of alumina (activity IV). Elution with petrol ether — benzene 1 : 1 and 1 : 2 gave 250 mg of a crystalline product, which was purified from ethanol; m.p. 158—160° (Lit.[4] m.p. 155—156°).

---

* Take care of hydrogen evolution!

[3] L. Ruzicka, A. Goldberg and E. Rosenberg, *Helv. Chim. Acta*, **18**, 1487 (1935).

[4] D. H. R. Barton and W. J. Rosenfelder, *J. Chem. Soc.*, **1949**, 2459.

Δ^5-Androstene-3β, 17β-diol, from 1 g of Δ^5-androsten-3β-ol-17-one. Yield : 965 mg of crude diol, which after recrystallization from aqueous acetone gave 650 mg of pure substance melting at 181—183° (Lit.[5] m.p. 182—183°).

Reduction of methyl 3-oxo-Δ^4-cholenate

The starting substance (900 mg) dissolved in benzene was stirred with the reagent for 4 hours. The crude reaction product (750 mg) was converted by refluxing with methanolic HCl[6] into methyl $\Delta^{3,5}$-choladienate. The crude diene was dissolved in dry benzene, filtered through a column of 25 g of alumina (activity IV) and recrystallized from methanol. M.p. 97—99°; no depression with an authentic sample.

Preparation of testosterone IV

a) A solution of 4 g of Δ^4-androstene-3,17-dione in 65 ml of dry benzene was treated with 16 ml of acetic anhydride containing 0.01 ml of perchloric acid 70%, and allowed to stand at room temperature for 2 hours. The solution was then washed three times with water, dried over $MgSO_4$, and concentrated under reduced pressure in CO_2 atmosphere to a small volume. After dilution with a large amount of methanol, 1 ml of pyridine was added and refluxed for 1 hour. The methanolic solution was then concentrated under reduced pressure in CO_2 atmosphere until abundant crystallization. After cooling in an ice bath and filtration, the crude *3-acetoxy-$\Delta^{3,5}$-androstadien-17-one* (II) was recrystallized from methanol. Yield : 2.5 g; m.p. 135—137° (Lit.[7,8,9] m.p. 137—139°, 130—133°, 127—129°). From the mother liquors a second crop (500 mg, m.p. 125—127°) could be isolated by evaporation and repeated crystallizations from methanol.

UV absorption (in MeOH) : $\lambda_{max} = 235$ nm ($\log \varepsilon = 4.27$);

IR spectrum (in CCl_4) : 1760 (enol acetate carbonyl), 1750 (17-oxo group), 1672, 1640 cm^{-1} ($\Delta^{3,5}$).

b) A solution of 1 g of compound II in 30 ml of dry benzene was treated with 10 g of $NaBH_4$-Al_2O_3 and stirred for 70 minutes at room temperature. The suspension was then filtered, the alumina washed with 60 ml of dry benzene and the filtrate evaporated to dryness. The crystalline residue was recrystallized from methanol and dried *in vacuo*. The pure *3-acetoxy-$\Delta^{3,5}$-androstadien-17β-ol* (III) (600 mg) melted at 144—147°.

UV absorption (in MeOH) : $\lambda_{max} = 235$ nm ($\log \varepsilon = 4.26$);

IR spectrum (in CCl_4) : 3630, 1055 (17β-hydroxyl), 1760, 1220, 1127, 1113 (enol acetate group), 1675, 1640 cm^{-1} ($\Delta^{3,5}$).

$C_{21}H_{30}O_3$ (330.5) *Calcd.* : C, 76.32 ; H, 9.16,

Found : C, 76.50 ; H, 9.47.

c) A solution of 650 mg of compound III in 100 ml of methanol was treated with 50 ml of H_2SO_4 4N and refluxed for 40 minutes. After cooling, 50 ml of water was added and most part of the acid neutralized with solid sodium bicarbonate. The solution was treated with charcoal, filtered and the ethanol removed under reduced pressure in an inert gas atmosphere. The precipitate was filtered, washed with water, dried and recrystallized from aqueous acetone. Yield : 450 mg of *testosterone* (IV), m.p. 151—153° ; after a second recrystallization from the same solvent m.p. 153—155°.

IR spectrum identical with that of an authentic sample.

IV-Acetate, m.p. 141—142°.

---

[5] L. Ruzicka and A. Wettstein, *Helv. Chim. Acta,* **18,** 1264 (1935).

[6] G. Rosenkranz, S. Kaufmann and J. Romo, *J. Amer. Chem. Soc.,* **71,** 3689 (1949).

[7] A. Ercoli and R. Gardi, *Ger.* 1, 159, 940 ; *Chem. Abstr.,* **61,** 7086 b (1964).

[8] K. Ysuda, *Chem. Pharm. Bull.* (Tokyo), **11,** 1167 (1963) ; *Chem. Abstr.,* **59,** 12864 g (1963).

[9] L. Ruzicka and W. H. Fischer, *Helv. Chim. Acta,* **19,** 1371 (1936).

Revue Roumaine de Chimie, **14**, 125–133 (1969)

π-ELECTRONIC STRUCTURE OF ACRIDINE-N-OXIDE

H. H. MANTSCH*, W. SEIFFERT and V. ZANKER

Physikalisch-Chemisches Institut, Technische Hochschule
München, Arcis Str. 21

Received August 6, 1968

State energies, charge densities and bond orders are calculated for acridine-N-oxide by a β-variable SCF method within the PPP formalism including configuration interaction. The computed transition energies and reactivity indices are in good agreement with experimental data and chemical evidence.

INTRODUCTION

In spite of various shortcomings, the Pariser-Parr-Pople (PPP) method (or modifications of it), is still the wide-most used procedure for the interpretation of π-electron structures of complex aromatic and heteroaromatic molecules, especially as its computational bakground is now quite well established. Mainly the variable β-procedure within this semiempirical PPP-approximation, developed by Nishimoto and Forster [1] has been applied rather successfully to molecules which contain more heteroatoms. There is a number of theoretical investigations concerning the basic nitrogen heterocycles, particularly in connection with testing parameters on azaaromatic compounds within various SCF-procedures,[2] but quite few reports have been made yet on heterocyclic N-oxides. Some time ago Kubota [3] reported on the electronic structure of several heterocyclic N-oxides including acridine-N-oxide for the ground state configuration, but only in the approximation of SMO calculations. Since acridine-N-oxide shows a peculiar photochemical behaviour,[4] we have been interested primarily in the lower excited states, particularly in the calculation of the charge distribution in the lowest excited singlet and triplet states.

---

* On leave from the Institute of Chemistry, Cluj, Romania.

[1] K. Nishimito and L. S. Forster, *Theor. Chim. Acta*, **4**, 155 (1966); *J. Chem. Phys.*, **71**, 409 (1967).

[2] K. Nishimoto, *Theor. Chim. Acta*, **10**, 65 (1968); also earlier papers. G. W. Puganic, D. R. Forshey, B. J. D. Wegener and J. B. Greenshields, *Theor. Chim. Acta*, **10**, 240 (1968); B. Tinland, *Theor. Chim. Acta*, **8**, 361 (1967); E. Clementi, *J. Chem. Phys.*, **46**, 4731 (1967); J. S. Dewar and G. J. Gleicher, *J. Chem. Phys.*, **44**, 759 (1966).

[3] T. Kubota, *Bull. Chem. Soc. Japan*, **35**, 946 (1962).

[4] H. Mantsch and V. Zanker, *Tetrahedron Letters*, **35**, 4211 (1966).

METHOD OF CALCULATION AND PARAMETER ESTIMATION

The electronic system of acridine-N-oxide was treated as 16 π-electrons on 15 centers. In this planar molecule with C_{2v}-symmetry the dative $N \rightarrow O$ bond is directed along the twofold symmetry axis, the coordinate system is shown in the Table.

The SCF-procedure within the Pariser-Parr-Pople framework was used, in which the resonance integrals $\beta\mu\nu$ are expressed in terms of π-bond orders and adjusted iteratively until selfconsistency is obtained, by means of the following relations :

$$\beta_{CC} = -0.51\,p - 2.04\,eV$$
$$\beta_{CN} = -0.53\,p - 2.34\,eV$$
$$\beta_{NO} = -0.56\,p - 2.00\,eV.$$

An initial set of orthogonalized eigenvectors obtained from a Hückel approximation was used to construct the starting MO's. Convergence to ± 0.0003 in the bond order-charge density matrix has been reached always in less than eight iteration steps. These SCF molecular orbitals were used then as the basis for a configuration interaction treatment which included all possible configurations arising from single electron excitations between the five highest occupied and the six lowest empty orbitals.

The one-center repulsion integrals $\gamma_{\mu\mu}$ were evaluated as follows :

$$\gamma_{CC} = 8.25\ eV\,;^{5} \quad \gamma_{NN} = 12.00\ eV \quad \text{and} \quad \gamma_{OO} = 10.60\ eV.$$

The two-center repulsion integrals $\gamma\mu\nu$ have been approximated by the method of Nishimoto-Mataga,[6] where the internuclear distances $r_{\mu\nu}$ are originally taken from a conventional geometry, i.e. all intraring bond lengths were set at 1.40 Å, while the exocyclic NO bond was assumed initially to 1.22 Å.

As to the diagonal core integrals α_μ, Klessinger's formalism was used with :[7]

$$\alpha_\mu(X) = \delta\omega_x - \sum_{\nu\neq\mu} n_\nu \gamma\,\mu\nu$$

since $W_c - \sum_{\mu'} (\mu|U_{\mu'}|\mu)$ is taken as zero point of energy, for a certain heteroatom X , $\delta\omega_x \simeq W_x - W_c$ and perhaps $\delta\omega_c = 0$.

A quite difficult problem is the estimation of the actual contribution of the oxygen atom from the dative NO bond to the π-electronic system i. e. the adequate choice of the semiempirical parameter $\delta\omega_0$. For the present calculations we have used the values $\delta\omega_N = 10.5$ eV and $\delta\omega_0 = 5.0$ eV ($Z_0 = 1$). In previous calculations [8] we treated the NO-group slightly different, namely with a negative charge at the oxygen ($Z_0 = 2$), i. e. with other one-center repulsion integrals and $\delta\omega_x$-values for the oxygen and nitrogen. However, the calculated transition energies and charge distributions are quite similar for both treatments. Figure 1 shows the

---

[5] This low γ-value for carbon was used to obtain reasonable triplet states ; see : F. DÖRR, G. HOHLNEICHER and S. SCHNEIDER, *Ber. Bunsenges. physik. Chem.*, **70**, 803 (1966).

[6] K. NISHIMOTO and N. MATAGA, *Z. phys. Chem. (Frankfurt)*, **12**, 335 (1957) ; **13**, 140 (1957).

[7] M. KLESSINGER, *Theor. Chim. Acta*, **5**, 236 (1966).

[8] H. MANTSCH, W. SEIFFERT and V. ZANKER, *Tetrahedron Letters*, 3161 (1968).

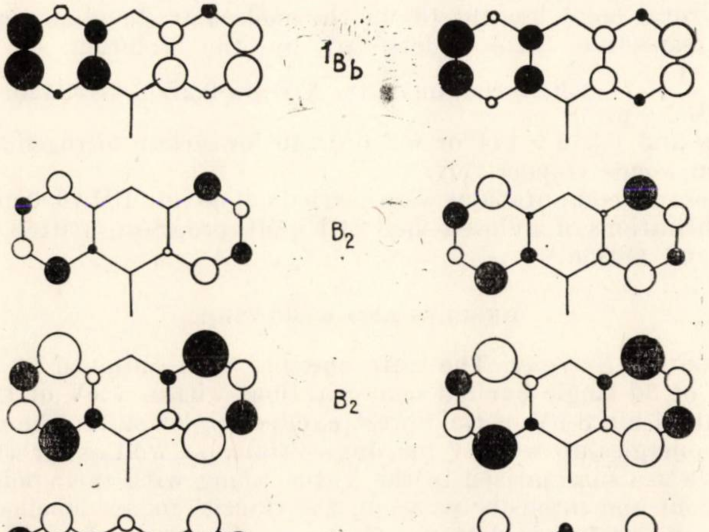
^1B_b
B_2
B_2
A_1
^1L_b
^1L_a
$Z_O = 2;\ Z_N = 1$
$Z_O = 1;\ Z_N = 2$

Fig. 1. — Transition-charge densities for acridine-N-oxide.

corresponding transition-charge densities — which actually are characterizing the various transitions best — for the first six bands, which are practically identical for both cases (Z_0 and Z_N represent the corresponding cores for the two heteroatoms). These results once again remind us that the PPP-method represents only a π-electron approximation.

The total bond lengths (d) in the molecular diagrams are derived from the respective bond orders (p) by the relation of Jenkins[9] $d^2 = \frac{1}{A+B(1+p)}$ where the constants A/B are 0.2868/0.1334 for pure carbon bonds and 0.316/0.144 or 0.216/0.240 for carbon-nitrogen and nitrogen-oxygen bonds respectively.

The actual computations were carried out on an IBM 7090 instrument using modifications of a closed-shell SCF—MO program, written originally by Bloor and Gilson.[10]

RESULTS AND DISCUSSION

Transition Energies. The state energies were obtained by including a number of 30 single excited configurations within 7 eV of the lowest singlet and within 8 eV of the lowest excited triplet state. The computed transition energies up to 6 eV for singlet states as well as for the lowest triplet state are summarized in the Table, along with their polarization, dipol moment and intensity pattern; the transitions are labelled S_n with increasing energy for singlets and T_1 for the lowest triplet.

We have been able also to correlate these transitions on the basis of the nodal pattern map with the corresponding transitions for acridine and anthracene; however the most important single feature in the relationship among the electronic spectra of these three compounds is the fact that the first excited singlet state originates from an almost pure ψ_{+1}^{-1} configuration ($\simeq$97 %), which in the Platt classification scheme, based on the perimeter model, corresponds to the ^1L_a-transition. Figure 2 shows the eigenfunctions and symmetries of those SCF—MO's which determine this transition nearly exclusively for all three compounds; they show the same nodal pattern map, only in the case of the N-oxide there is an additional nodal plan between the oxygen and nitrogen.

Bond Order, π-Electron Densities and Reactivity. The calculations were carried out first with the assumption that all bonds have a common "aromatic" lengths (1.40 Å), and by an iterative procedure, allowance is made for variations in the various integrals with bond lengths. Figure 3G indicates that the most stable form of this molecule is one with significant bond alternation in the outer annelated rings, in particular the "double" bonds are predicted to be short ($\simeq$1.38 Å), while the adjacent "single" bonds are long ($\simeq$1.43 Å). These results agree closely with the corresponding figures for acridine, where X-ray diffractions were available to be correlated with the calculations[11]; yet it is interesting to mention that

---

[9] H. O. Jenkins, *J. Amer. Chem. Soc.*, **77**, 3168 (1955).

[10] Quantum chemistry program exchange, Indiana University, Chemistry Department, Bloomington, Indiana 47401, USA.

[11] A. Albert, "The Acridines", Arnold Publ., London 1966, p. 236.

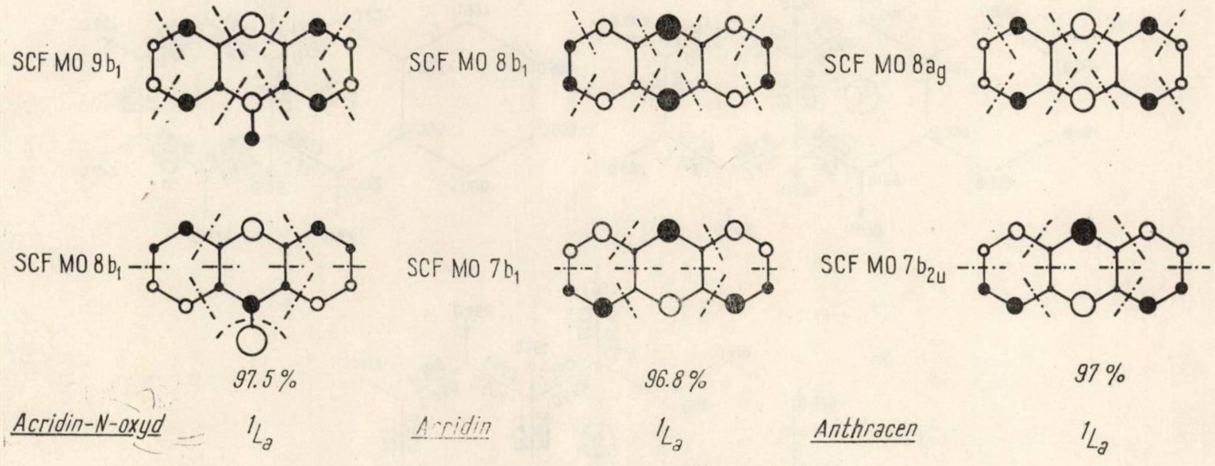
SCF MO 9b₁
SCF MO 8b₁
SCF MO 8a_g
SCF MO 8b₁
SCF MO 7b₁
SCF MO 7b_2u
97.5 %
96.8 %
97 %
Acridin-N-oxyd
¹L_a
Acridin
¹L_a
Anthracen
¹L_a

Fig. 2. — SCF-Eigenfunctions for anthracene, acridine and acridine-N-oxide.

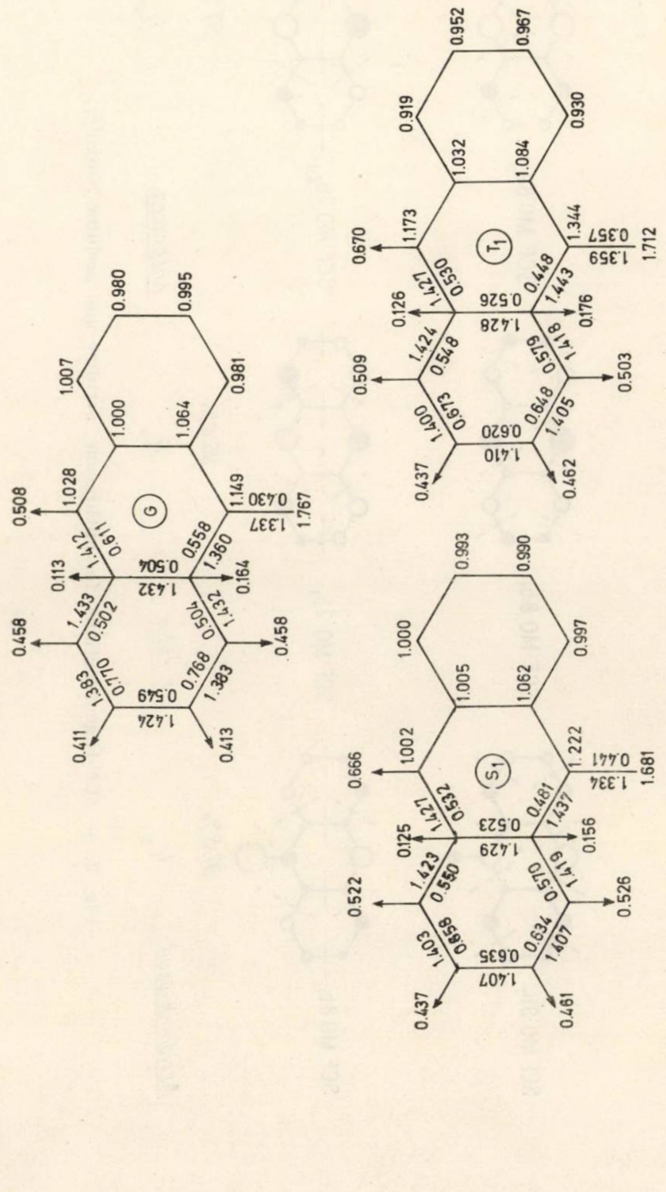
G
0.508
1.028
1.412
0.611
0.113
1.433
0.502
0.458
1.383
0.710
0.411
1.424
0.549
0.768
1.383
0.413
0.458
0.504
1.432
1.432
0.504
0.164
0.558
1.360
1.149
0.430
1.337
1.767
1.000
1.064
1.007
0.980
0.995
0.981
S1
0.522
0.125
0.666
1.002
1.427
0.532
1.423
0.550
1.403
0.658
0.437
1.407
0.635
0.634
1.407
0.461
0.570
1.419
0.526
1.429
0.523
0.156
0.481
1.437
1.222
0.441
1.334
1.681
1.005
1.062
1.000
0.993
0.990
0.997
T1
0.509
0.126
0.670
1.173
1.427
0.530
1.424
0.548
1.400
0.673
0.437
1.410
0.620
0.648
1.405
0.462
0.579
1.418
0.503
1.428
0.526
0.176
0.448
1.443
1.344
0.357
1.359
1.712
1.032
1.084
0.919
0.952
0.967
0.930

Fig. 3. — Molecular diagrams of acridine-N-oxide for the ground (G) — and lowest excited states (S_1 and T_1).

Table

Computed transition energies, polarisation, oscillator strength, dipol moment and CI-coefficients

Notation and Symmetry	Transition Energy eV (cm^{-1})	Pol.	D. calc. Debye	f. 100 calc.	Coefficients*
$S_1\,(^1A_1)$	3.03 (24422)	Z	3.65	41.5	Ψ'^{9}_{3} (0.986)
$S_2\,(^1B_2)$	3.48 (28060)	Y	2.10	14.0	Ψ'^{10}_{8} (0.871), Ψ'^{9}_{7} (0.433)
$S_3\,(^1B_2)$	4.21 (33920)	Y	2.41	1.3	Ψ'^{11}_{8} (0.984)
$S_4\,(^1A_1)$	4.38 (35308)	Z	1.90	0.4	Ψ'^{9}_{5} (0.972)
$S_5\,(^1B_2)$	4.44 (35795)	Y	5.46	16.3	Ψ'^{9}_{6} (0.716), Ψ'^{9}_{7} (0.645)
$S_6(^1B_2)$	4.64 (37423)	Y	4.68	187.8	Ψ'^{9}_{7} (0.597), Ψ'^{10}_{8} (0.443)
$S_7\,(^1A_1)$	4.94 (39839)	Z	4.16	0.1	Ψ'^{13}_{8} (0.447), Ψ'^{10}_{6} (0.430) Ψ'^{12}_{8} (0.429), Ψ'^{11}_{7} (0.377)
$S_8\,(^1A_1)$	5.07 (40900)	Z	1.55	0.5	Ψ'^{11}_{6} (0.880)
$S_9\,(^1B_2)$	5.52 (44492)	Y	0.46	38.8	Ψ'^{10}_{5} (0.921)
$S_{10}\,(^1A_1)$	5.66 (45692)	Z	3.18	13.9	Ψ'^{10}_{5} (0.605), Ψ'^{10}_{6} (0.526)
$S_{11}(^1A_1)$	5.70 (45992)	Z	3.06	8.8	Ψ'^{13}_{8} (0.761), Ψ'^{10}_{7} (0.580)
$S_{12}\,(^1A_1)$	5.88 (47400)	Z	3.05	3.9	Ψ'^{9}_{4} (0.806), Ψ'^{10}_{6} (0.428)
$T_1\,(^3A_1)$	1.402 (11307)				

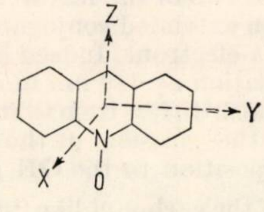

* This column gives the CI coefficients with the main configurations which build up that particularly excited state.

with acridine-N-oxide the CN-bonds become slightly longer as compared with acridine. Upon excitation however, a pronounced trend to bond length equalization is observed(figures $3S_1$ and $3T_1$) for both excited states, where a benzene-like structure is achieved.

The distribution of the π-electron charges associated with the ground state configuration shown in Figure 3G, is seriously modified as compared with that of the parent acridine and the theoretical predictions are consistent with the molecular properties of acridine-N-oxide. As with other heterocyclic N-oxides the position *para* to the NO group becomes the richest one in π-electron density and experience shows that electrophilic reagents like nitro or bromine readily substitute this position; indeed, at electrophilic substitution acridine-N-oxide yields 9-nitro, and 9-bromo-acridine-N-oxide.[12]

This ground state molecular constants can be correlated also with other spectroscopical measurements. Such, in acridine-N-oxide the chemical-shift of H_9 (-488 cps)[13] is significantly lower than in acridine (-517 cps), which also shows that the pronounced reactivity of this position towards anionic (nucleophilic) reagents in the latter case, has been changed now into reactivity towards electrophilic reagents for the N-oxide, as predicted from the MO calculations. It is possible to correlate the chemical-shift pattern with the π-electron densities, however after the chemical shifts have been adjusted by considering the anisotropy effect of the NO group. The smaller coupling constant between positions 2 and 3 ($J = 6.6$ cps; $d = 1.42$ Å) if compared to those between positions 1 and 2 ($J = 8.2$ cps; $d = 1.38$ Å) or 3 and 4 ($J = 9.0$ cps; $d = 1.38$ Å) is also in good agreement with the previously discussed bond alternation.

The investigation of the infrared spectrum of acridine-N-oxide shows that the NO group is stabilized by the two annelated benzene rings i. e. the $N \rightarrow O$ stretching frequency which was associated to a very strong absorption band at 1330 cm^{-1},[14] possesses an increased double bond character if compared with pyridine-N-oxide ($\nu NO = 1265$ cm^{-1}).

To calculate the total π-electron moment, localized atom charges were used with the usual reservation in mind (point charge approximation). The calculated π-dipol moment for the ground state of acridine-N-oxide is 5.56 Debye and upon excitation it is always lowered (Table).

Acridine N-oxide contains two of the features common to potentially-photoreactive molecules i. e. an extended conjugated system of π-electrons and a number of nonbonding n-electrons. Indeed acridine-N-oxide is quite photoreactive and upon irradiation at 440 nm in diluted alcohol it undergoes easily a photoreduction which differs from that of acridine and assumes a hydrogen abstraction by the scission of the OH bond of the alcohol and not of a CH bond (in α-position to the OH group) as with acridine.

As the photochemistry of the carbonyl-like "nitronyl-group" $\left(> N \rightarrow O \right)$ is governed primarily by the electronic distribution of the lowest excited triplet state, whereas the photochemistry of the heteroaromatic acridine residue is determined by the reactive singlet state, a comment regarding the charge distribution both in the lowest excited singlet and triplet is appropriate; a first glance at the calculated π-electron charges (Figs. $3S_1$ and $3T_1$) reveals a serious charge transfer from the oxygen to the ring system and especially to the adjacent nitrogen. Such the photoreduction of this N-oxide group can be described as an attack by the electron-deficient oxygen atom either in the singlet or triplet state, probable by an molecular mechanism as the reaction is quite insensitive to the presence of oxygen.

---

[12] R. M. Acheson, B. Adcock, G. M. Glover and L. E. Sutton, *J. Chem. Soc.*, **1960**, 3367.

[13] H. H. Mantsch, W. Seiffert and V. Zanker, *Rev. Roumaine Chim.*, **12**, 1137 (1967).

[14] M. Ionescu, I. Goia and H. H. Mantsch, *Rev. Roumaine Chim.*, **11**, 243 (1966).

Actually the conversion of a molecule from its ground state to an excited state alters the electronic distribution to such an extent that the excited state often may be considered to be a species that is even chemically different from the ground state. Perhaps also the basicities or acidities of the molecules are quite different in their excited states as it was shown initially by Förster.[15] If the π-electron charge at the heteroatom would be considered a measure of basicity (as it is done usually), an examination of the charge distribution for acridine-N-oxide shows that the π-electron density at the oxygen (q_O), and herewith its basicity decreases considerably in the fluorescence state but also in the phosphorescence state, whereas the charge at the nitrogen (q_N) and its basicity increases in both cases. These findings agree well with the actual photoreduction-scheme of acridine-N-oxide.

We have carried out also SCF—CI—MO calculations on the azaaromatic series : quinoline, acridine, 2.3-benz- and 2.3.6.7.-dibenz-acridine [16] as well as for 9.10-dihydro-acridine[17]. In the latter case — which is a diphenylamine-like compound — the charge density at the nitrogen decreases upon excitation both in the singlet and triplet state as it is expected for aliphatic amines. For the first mentioned series however, we found an overall migration of charge towards the nitrogen on excitation both for the singlet and triplet and could not reproduce the decrease on charge density in the triplet state quoted by Tyutylkov [18] for pyridine, quinoline and acridine. In our view it is due to a different parametrization (which can affect the triplet drastically) and in this connection it should be noted that in the literature quite different values have been assigned to the ground state configurations of these heterocycles and these values surely will affect the magnitude of change of charge produced upon excitation and hence to the ascribed basicities.

Acknowledgments. We are grateful to the Alexander von Humboldt-Stiftung for a fellowship for one of us (H.H.M.), and to the Verband der Chemischen Industrie and the Deutsche Forschungsgemeinschaft for support.

---

[15] K. Breitschwerdt, Th. Förster and A. Weller, *Naturwiss.*, **43**, 443 (1956).
[16] W. Seiffert, V. Zanker and H. H. Mantsch, *Tetrahedron Letters*, 3437 (1968).
[17] Unpublished work from this laboratory.
[18] N. Tyutylkov, F. Fratev and D. Pelkov, *Theor. Chim. Acta*, **8**, 236 (1967).

Revue Roumaine de Chimie, **14**, 135–140 (1969)

6-AZAURACIL DERIVATIVES WITH POTENTIAL CYTOSTATIC ACTIVITY. VII *)

THIONATION OF 5-BENZYLTHIO-6-AZAURACIL

C. CRISTESCU and VERONICA BADEA

Chemical Pharmaceutical Research Institute, Bucharest, Şos. Vitan, 112

Received March 5, 1968

Thionation with P_2S_5 in pyridine of 5-benzylthio-6-azauracil occurs selectively in the 4 position, yielding 4-thioxo-5-benzylthio-6-azauracil, a compound which can be alkylated either at S_4 or at N_1. S_4-alkyl- and S_4, N_1-dialkyl-derivatives thus obtained, yield with ammonia 5-substituted- or 1-alkyl-5-substituted-6-azacytosine.

6-Azauracil derivatives show a particular interest because of their biological activity as the analogues of naturally occurring pyrimidines. Recent works have shown that analogous derivatives of other pyrimidines, essential in the synthesis of nucleic acids have cytostatic action. Thus 6-azacytosine, analogue of cytosine, has proved to be an efficient antimetabolite and 6-azacytidine has shown a high activity toward E. coli and a high cytostatic action. [1, 2]

A possible intermediate in the synthesis of 6-azacytosine is 4-chloro-6-azapyrimidine,[3] a very unstable compound. The drawback of using this compound is its tedious synthesis, which calls for the examination of other possible routes to obtain 6-azacytosine derivatives.

In the present paper, besides the preparation of an intermediate for the synthesis of 5-substituted -6-azacytosine, we have studied a blocking method for the 4 position of 5-substituted-6-azauracils.

It is known that 6-azauracil with P_2S_5 in molar ratio 1 : 2 gives the thionation product in low yield. Lately Mizuno et al.[4] have improved the yield using a molar ratio 6-azauracil : P_2S_5 of 2 : 1 and pure reactants.

In our laboratory we found that 5-benzylthio-6-azauracil [5] (I) with phosphorus pentasulphide in pyridine is selectively thionated at the 4 position to give 4-thioxo-5-benzylthio-6-azauracil (II). The yield is 80%

---

*) Part VI, *Rev. Roumaine Chim.*, **12**. 365 (1968).

[1] S. Bresnik, S. Singer and G. H. Hitchings, *Biochem. Biophys. Acta*, **37**, 251 (1960).

[2] F. Šorm, *Experientia*, **17**, 64 (1961).

[3] P. K. Chang and T. V. Ulbricht, *J. Amer. Chem. Soc.*, **80**, 976 (1958).

[4] Y. Mizuno, M. Ikehara and K. A. Watanabe, *Chem. Pharm. Bull.* (*Japan*), **10**, 647 (1962).

[5] C. Cristescu and J. Marcus, *Pharmazie*, **16**, 135 (1961).

at a molar ratio substance : P_2S_5 of 2 : 1.06, and decreases with increasing amount of P_2S_5.

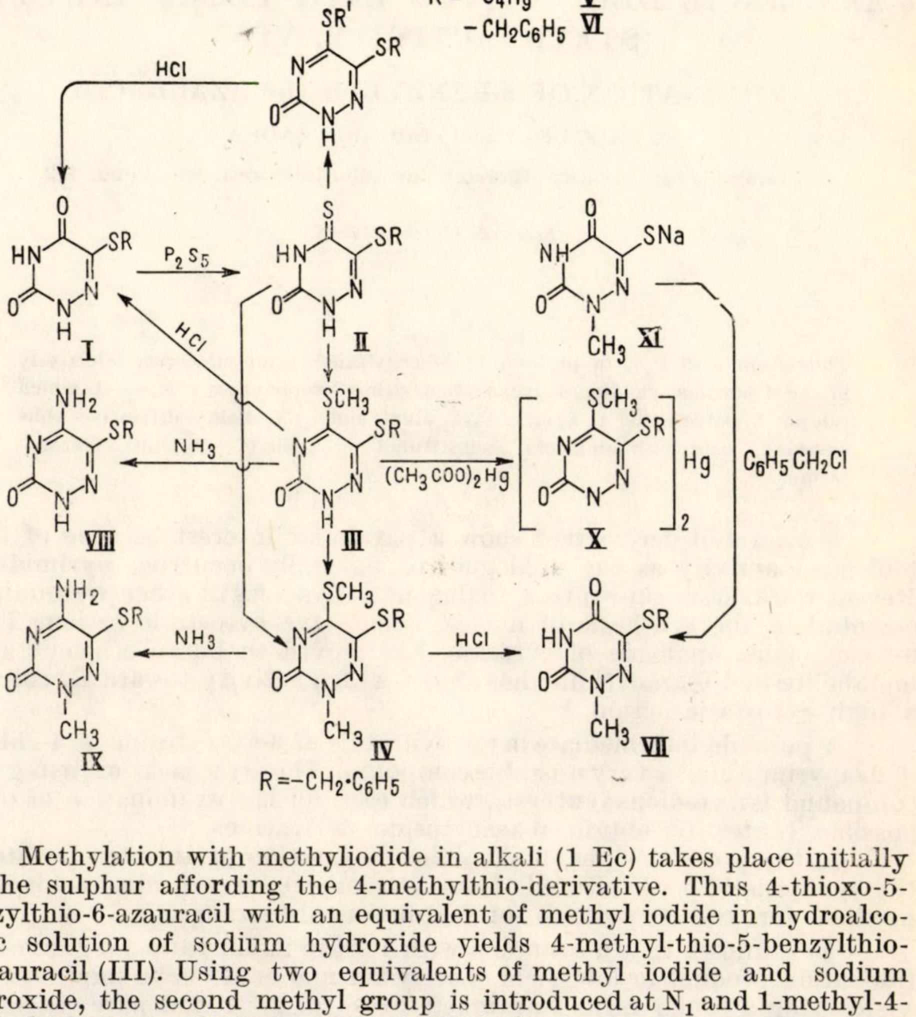

Methylation with methyliodide in alkali (1 Ec) takes place initially at the sulphur affording the 4-methylthio-derivative. Thus 4-thioxo-5-benzylthio-6-azauracil with an equivalent of methyl iodide in hydroalcoholic solution of sodium hydroxide yields 4-methyl-thio-5-benzylthio-6-azauracil (III). Using two equivalents of methyl iodide and sodium hydroxide, the second methyl group is introduced at N_1 and 1-methyl-4-methylthio-5-benzylthio-6-azauracil (IV) is obtained as the unique product.

In this reaction two similar ambidient ions II-A and III-A are produced. It is interesting to note that in the first of these ions, alkylation does not take place at the nitrogen atom, but this atom is preferred in the reaction of the second ion.

It was recently stressed by Gompper[6] that the reaction of ambidient ions with poor electrophiles takes place at the most polarizable atom of the ambidient systems. For the atoms of the same period, the polarizabi-

---

[6] R. Gompper, *Angew. Chem.*, **76**, 412 (1964).

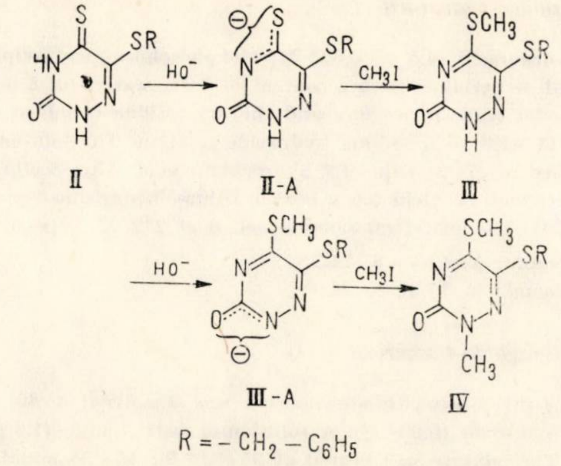

lity decreases toward the right-hand side of Mendeleyev's periodic system. For atoms of different periods, the atoms with higher atomic numbers are more polarizable.[7] Thus, in the ambidient ion II-A , the sulphur atom is more polarizable than the nitrogen atom ; alkylation takes place at the sulphur. In the ambidient ion III-A, the nitrogen atom being more polarizable than the oxygen atom, alkylation takes place at the nitrogen atom.

Compound IV may be subjected to acid hydrolysis to give 1-methyl-5-benzylthio-6-azauracil (VII). Reaction conditions did not affect the 5-benzylthio-group. This procedure is the most convenient route for the synthesis of VII, the product being obtained with a 95% yield.

To check the alkylation at N_1, compound VII was obtained by an alternative route. 1-Methyl-5-mercapto-6-azauracil[8] (XI) was treated with benzylchloride yielding a compound identical in all respects with the product isolated from the acid hydrolysis of compound IV.

The S-substituted products V – VI of the compound II were prepared in a similar way.

4-Methylthio-5-benzylthio-6-azauracil treated with ammonia in methanol yielded 5-benzylthio-6-azacytosine (VIII). Compound IV treated in the same conditions yielded 1-methyl-5-benzylthio-6-azacytosine (IX).

4-Methylthio-5-benzylthio-6-azauracil treated with mercuric acetate gives a mercuric salt (X), which may be used in the synthesis of N_1-glycosides.

EXPERIMENTAL

Melting points were determined on a heating microscope stage. Analytical samples were dried at 20°/5 Torr or 8 hours over P_2O_5.

---

[7] C. K. INGOLD, "Structure and Mechanism in Organic Chemistry", Ithaca, New York 1953, 72.

[8] C. CRISTESCU and V. BADEA, *Rev. Roumaine Chim.*, **12**, 913 (1967).

4-Thioxo-5-benzylthio-6-azauracil (II)

5-Benzylthio-6-azauracil[5] (6.5 g; 0.028 M) and phosphorus pentasulphide (4 g; 0.018 M) were boiled in 150 ml of pyridine, with a content of 0.3% water, for 5 hours. The pyridine was distilled off under reduced pressure and the dry residue dissolved in water (60 ml) and adjusted to pH 11 with 10% sodium hydroxide solution. The solution was filtered and the filtrate was acidified to pH 3 with 10% hydrochloric acid. After cooling, the product was recrystallized from ethanol to yield 5.6 g (80%) 4-thio-5-benzylthio-6-azauracil, orange-red needles, m.p. 269–271°. The analytical sample melted at 272–273° from ethanol.

$C_{10}H_9N_3OS_2$ *Calcd.*: N, 17.1; S, 24.7%;
(251.32) *Found*: N, 17.2; S, 24.9%.

4-Methylthio-5-benzylthio-6-azauracil (III)

1 g (0.004 M) 4-thio-5-benzylthio-6-azauracil was dissolved at 40° in 20 ml ethanol and 4 ml N sodium hydroxide (0.004 M). A solution of methyliodide (1.8 g; 0.012 M in 5 ml ethanol) was added. The mixture was heated at 35–40° for 15–20 minutes, under stirring, then cooled at 0° and filtered. The product was recrystallized from water-ethanol (1.5 : 1) to yield 0.85 g (80%) 4-methylthio-5-benzylthio-6-azauracil with m.p. 182–184°. The analytical sample melted at 184–186° from ethanol.

$C_{11}H_{11}N_3OS_2$ *Calcd.*: N, 15.83; S, 24.16%;
(265.35) *Found*: N, 16.0; S, 24.2%.

Hydrolysis: 4-methylthio-5-benzylthio-6-azauracil (0.106 g) was boiled for 30 minutes with 1 ml ethanol and 1 ml hydrochloric acid. 5-Benzylthio-6-azauracil precipitated after cooling. Yield 0.067 g (90%), m.p. 224–226° (water-ethanol), without depression when mixed with an authentic sample.

1-Methyl-4-methylthio-5-benzylthio-6-azauracil (IV).

N_1-methylation: 4-methylthio-5-benzylthio-6-azauracil (1.06 g, 0.004 M) was dissolved at 40° in 50 ml ethanol and 4 ml N sodium hydroxide (0.16 g, 0.004 M). A solution of methyl iodide (1.8 g, 0.012 M) in 5 ml ethanol was added. The mixture was heated at 40° for 3 hours under stirring. The solution was evaporated *in vacuo* and the oil residue was dissolved in chloroform (20 ml). The chloroformic solution was extracted with 2× 10 ml N sodium hydroxide, washed with water, dried and evaporated *in vacuo*. The oily residue was dissolved in isopropanol, n-hexane was added to the cloud point, and the solution was maintained at 4° over night. After recrystallization from cyclohexane 0.96 g (80%) of IV was obtained with m.p. 93–95°. A sample for analysis recrystallized from cyclohexane had m.p. 95–97°.

$C_{12}H_{13}N_3OS_2$ *Calcd.*: N, 15.04; S, 22.95%;
(279.37) *Found*: N, 15.1; S, 23.1%.

N_1, S_4-methylation. 4-Thio-5-benzylthio-6-azauracil (1 g, 0.004 M) was dissolved at 40° in 70 ml ethanol and 8 ml N sodium hydroxide (0.32 g, 0.008 M). A solution of methyl iodide (3.6 g, 0.025 M in 10 ml ethanol) was added in the course of 20 minutes. The mixture was heated for 4 hours at 40°, under stirring. The solution was evaporated *in vacuo* and the oily residue was dissolved in chloroform. The chloroformic solution was extracted with 2× 10 ml N sodium hydroxide, washed with water and dried. After evaporation *in vacuo*, the oil residue was dissolved in isopropanol and n-hexane was added to the cloud point and the

solution was maintained at 4° over night. Yielding 0.72 g (60%) with m. p. 95—97° from cyclohexane without depression when mixed with an authentic sample.

Hydrolysis. 1-Methyl-4-methylthio-5-benzylthio-6-azauracil (0.9 g) was boiled for 30 minutes with 7.5 ml ethanol and 7.5 ml 10% hydrochloric acid. 1-Methyl-5-benzylthio-6-azauracil (VII) precipitated after cooling. The product was recrystallized from water-ethanol (1 : 2) to yield 0.76 g (95%) with m.p. 172—174°. The analytical sample melted at 173—175° from ethanol-water (1 : 1), without depression when mixed with an authentic sample.

$C_{11}H_{11}N_3O_2S$ *Calcd.* : N, 16.85 ; S, 12.86% ;
(249.28) *Found* : N, 17.0 ; S, 12.9%.

4-Butylthio-5-benzylthio-6-azauracil (*V*)

The compound II (0.5 g, 0.002 M) was dissolved at 50° in 25 ml ethanol and 2 ml N sodium hydroxide (0.002 M). A solution of butyl bromide (0.274, 0.002 M in 2 ml ethanol) was added and the mixture was heated at 60° for 6 hours under stirring. The solution was evaporated under reduced pressure at 5 ml, cooled at —10° and the filtered precipitate crystallized from ethanol-water (1.5 : 1); yield 0.43 g (70%) with m.p. 126—128°. A sample for analysis recrystallized from isopropanol water (1 : 1) had m.p. 128—130°.

$C_{14}H_{17}N_3OS_2$ *Calcd.* : N, 13.66 ; S, 20.86% ;
(307.43) *Found* : N, 14.0 ; S, 21.0%.

Hydrolysis. 0.1 g of V was boiled with 2 ml ethanol-water (2 : 1) and 0.1 ml hydrochloric acid conc., for 30 minutes ; 5-benzylthio-6-azauracil precipitated after cooling. Yield 0.07 g (90%), m.p. 224—226° (water-ethanol), without depression when mixed with an authentic sample.

4,5-Dibenzylthio-6-azauracil (*VI*)

4-Thio-5-benzylthio-6-azauracil (1 g, 0.004 M) was dissolved at 40° in 50 ml ethanol and 4 ml N sodium hydroxide (0.004 M). Benzyl chloride (0.25 g, 0.004 M) was added and the mixture was heated under reflux for 5 hours with stirring. The solution was evaporated *in vacuo* at 10 ml and cooled at —10°. The resulting solid crystallized from ethanol-water (4 : 1) to yield 1.1 g (62%) 4,5-dibenzylthio-6-azauracil with m.p. 157—159°. A sample for analysis recrystallized from isopropanol-water (5 : 1) had m.p. 159—161°.

$C_{17}H_{15}N_3OS_2$ *Calcd.* : N, 12.30 ; S, 18.77% ;
(341.43) *Found* : N, 12.4 ; S, 19.0%.

Hydrolysis. 0.1 g of VI was boiled with 5 ml ethanol and 0.5 ml 10 per cent hydrochloric acid, for 30 minutes. The solution was evaporated under reduced pressure. The residue melted at 224—226° after recrystallization from water-ethanol. Yield 0.065 g (95%) 5-benzylthio-6-azauracil without depression when mixed with an authentic sample.

1-Methyl-5-benzylthio-6-azauracil (*VII*)

1-Methyl-5-mercapto-6-azauracil sodium salt (2.16 g, 0.01 M) was dissolved in 150 ml water-ethanol (1 : 1) and a solution of benzyl chloride (1.26 g, 0.01 M in 4 ml ethanol) was added at 50°. After 30 minutes at this temperature, the reaction mixture was cooled and 1-methyl-5-benzylthio-6-azauracil precipitated. After recrystallization from ethanol-water (1 : 2), yield 2.2 g (90%) with m.p. 172–174°. The analytical sample melted at 173–175° from ethanol-water (1 : 1).

$C_{11}H_{11}N_3O_2S$ *Calcd.* : N, 16.85 ; S, 12.86% ;
(249.28) *Found* : N, 16.9 ; S, 12.9%.

5-Benzylthio-6-azacytosine (*VIII*)

4-Methylthio-5-benzylthio-6-azauracil (3.6 g, 0.0136) was placed into a steel autoclave chilled to 0° and treated with absolute methanol (100 ml) previously saturated at 0° with dry ammonia. The mixture was kept standing at room temperature for 3 days. The solvent was evaporated on a water bath at reduced pressure. The residue was recrystallized from ethanol. Yield, 2.86 g (90%) 5-benzylthio-6-azacytosine with m.p. 249–251° (dec.) . The analytical sample melted at 250–252° (dec.) after recrystallization from ethanol.

$C_{10}H_{10}N_4OS$ *Calcd.* : N, 23.0 ; S, 13.68% ;
(234.27) *Found* : N, 23.8 ; S, 13,9%.

1-Methyl-5-benzylthio-6-azacytosine (*IX*)

By treating 1-methyl-4-methylthio-5-benzylthio-6-azauracil (2.79 g, 0.01 M) with absolute methanol (100 ml), previously saturated at 0° with dry ammonia, in a sealed tube at room temperature for 3 days, 1-methyl-5-benzylthio-6-azacytosine is produced. Recrystallization from ethanol gave 2.12 g (85%) of pure material with m.p. 174–176°. A sample for analysis recrystallized from ethanol had m.p. 175–177°.

$C_{11}H_{12}N_4OS$ *Calcd.* : N, 22.56 ; S. 12.91% ;
(248.30) *Found* : N, 22.8 ; S, 12.7%.

A warm solution of 1.59 g (0.05 M) mercuric acetate in 100 ml methanol was added to.a warm solution of 2.65 g (0.01 M) 4-methylthio-5-benzylthio-6-azauracil in 300 ml methanol. The mixture was stirred for 20 minutes at 40–50°. After cooling, the precipitate was filtered and washed successively with water, ethanol, and finally with ether. The salt was dried over P_2O_5 at diminished pressure, at 50–60°. A white powder m.p. 164–165° (dec.) was obtained. The product weighed 3.27 g (90%) and had a good analysis for a compound containing a ratio of 2 moles of triazine and one mole of mercury.

$C_{22}H_{20}N_6S_4Hg$ *Calcd.* : N, 11.53 ; S, 17.58% ;
(729.27) *Found* : N, 11.6 ; S, 17.8%.

The analyses were carried out by Mrs. Cornelia Ioan in the Analytical Laboratory of this Institute.

Revue Roumaine de Chimie, **14**, 141–145 (1969)

$TiCl_4$-CAROTENOID COMPLEXES. III

ACTION OF $TiCl_4$ ON CARBONYLCAROTENOIDS (CANTHAXANTHIN, RHODOXANTHIN, β-APO-8′-CAROTENAL)

V. TĂMAŞ and C. BODEA

Institute of Agronomy, Department of Biochemistry, Cluj, Str. Mănăştur 3

Received April 15, 1968

In the reaction of $TiCl_4$ with carbonylcarotenoids like canthaxanthin, rhodoxanthin and β-apo-8′-carotenal, titanochloro-carotenoid complexes are formed in which the Ti atom is attached to the carbonylic oxygen acting as electron donor. By acetonolysis the starting carotenoids are regenerated.

In previous papers [1,2] we have described $TiCl_4$-carotenoid complexes of some cyclic, half-cyclic and acyclic C(40) carotenoids, the acetonolysis of which had led to dehydrocarotenoids and to cyclization reactions.

We report in this paper the action of $TiCl_4$ on carbonylcarotenoids with keto- and aldehyde groups. It is known that $TiCl_4$ reacts with oxygenated organic compounds, among others with amides,[3,4,5] to form complexes in which the oxygen of the amide is coordinated with the titanium atom.

Acting with $TiCl_4$ in benzene solution on carbonylcarotenoids with the $>C=O$ group conjugated with the polyene system, like canthaxanthin (4, 4′-diketo-β-carotene), rhodoxanthin (3, 3′-diketoretrodehydro-β-carotene) and β-apo-8′-carotenal, we have stated that the $TiCl_4$ molecule is attached to the carbonyl group. In the so formed complexes of the general type

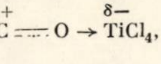

$$>\overset{\delta+}{C}\text{=}\overset{\delta-}{O}\rightarrow TiCl_4,$$

the oxygen atom acts as electron donor.

The structure of the complexes was studied by means of electron and infrared spectroscopy, chlorine analysis and cleavage by acetonolysis.

---

[1] V. TĂMAŞ and C. BODEA, *Rev. Roumaine Chim.*, **12**, 1517 (1967).

[2] V. TĂMAŞ and C. BODEA, *Tetrahedron*, (in press).

[3] J. ARCHAMBAULT and R. RIVEST, *Canad. J. Chem.*, **36**, 1461 (1958).

[4] J. ARCHAMBAULT and R. RIVEST, *Canad. J. Chem.*, **38**, 1331 (1960).

[5] D. SCHWARTZ and R. HEYER, *J. Inorg. Nuclear Chem.*, **29**, 1384 (1967).

The chlorine analyses shown in table 1 indicate in the case of the canthaxanthin-$TiCl_4$ complex (I) the ratio 1 : 1, even on treating with a large excess of $TiCl_4$ (1 : 50). Rhodoxanthin and β-apo-8′-carotenal each gives two complexes in which the ratio carotenoid : $TiCl_4$ is 1 : 1 (II and IV) and 1 : 2 (III and V).

Table 1

Chlorine analysis of the $TiCl_4$ carotenoid complexes

Complex	Cl %	
	calculated	found
Canthaxanthin. $TiCl_4$ (I)	18.66	18.00
Rhodoxanthin. $TiCl_4$ (II)	18.62	18.92
Rhodoxanthin. 2 $TiCl_4$ (III)	33.00	31.80
β-Apo-8′-carotenal. $TiCl_4$ (IV)	23.58	22.55
β-Apo-8′-carotenal.2 $TiCl_4$ (V)	27.88	27.19

The electron spectra of the complexes, recorded in dimethylformamide, compared to those of the starting carotenoids, show in the case of the complexes I and IV no structural modifications and no significant hypso- or batochrome shift of λ_{max}. In the spectra of the complexes II there appears a hypsochrome shift of λ_{max} of 6 nm and in those of complexes III and V a hypsochrome shift of 9–10 nm (table 2).

Table 2

λ_{max} in the electronic spectra

Carotenoid	λ_{max}, nm	$TiCl_4$-Complexes	λ_{max}, nm
Canthaxanthin	481	I	479
		II	488
Rhodoxanthin	494	III	484
		IV	459
β-Apo-8′-carotenal	459	V	450

The results of the chlorine analyses and the electron spectra are consistent with the structures of the complexes shown in figure 1.

The hypsochrome shift of 6, respectively 10 nm of λ_{max} in the spectra of the complexes II and III is probable due to a partial deconjugation of the carbonyl and the double bond of the cycle with regard to the conjugated polyene system, as shown in figure 2. A 6 or 10 nm amount of the shift is consistent with the coordination taking place through one of the carbonyl groups or through both of them.

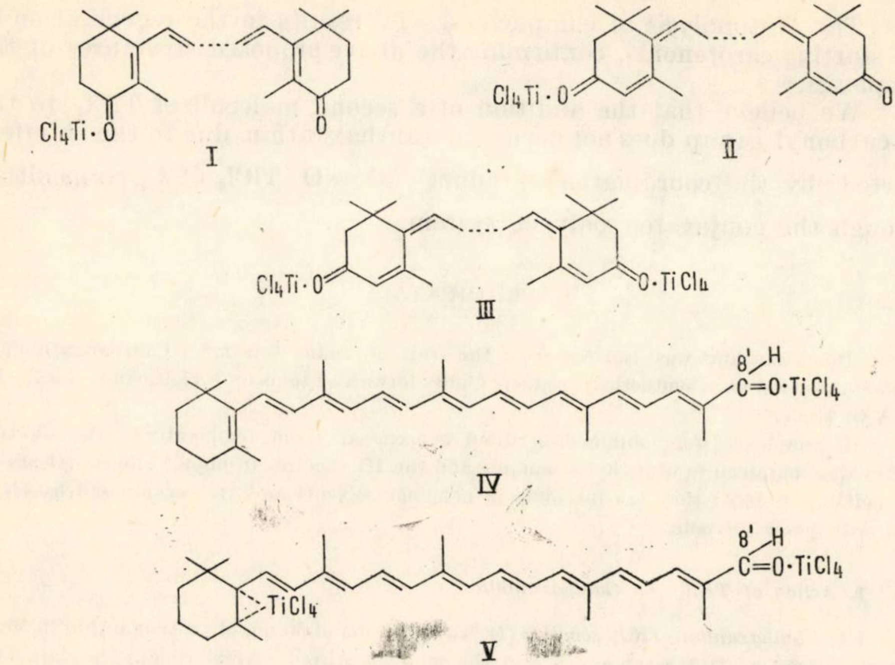
Cl$_4$Ti·O
O
I
Cl$_4$Ti·O
O
II
Cl$_4$Ti·O
O·TiCl$_4$
III
8′ H
C=O·TiCl$_4$
IV
8′ H
C=O·TiCl$_4$
TiCl$_4$
V

Fig. 1

The hypsochrome shift of 9 nm in the spectrum of complex V indicates the addition of a second TiCl$_4$ molecule to the double bond of the β-ionone ring.

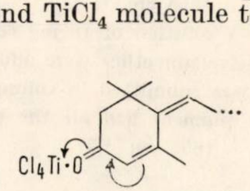

Fig. 2

In the IR spectra of the complexes the carbonyl band involved in the coordination shows a shift of 45–50 cm^{-1} to a lower frequency as compared to the carbonyl band of the free carotenoids, as it is presented in table 3.

Table 3

Carbonyl band in the IR spectra (cm^{-1})

Carotenoid	$\nu_1(C = O)$	TiCl$_4$-Complex	$\nu_1(C = O)$	$\nu_2(C = O.TiCl_4)$	$\Delta\nu = \nu_1 - \nu_2$
Canthaxanthin	1655	I	1655	1610	45
		II	1670	1625	45
Rhodoxanthin	1670	III	—	1625	45
		IV	—	1615	50
β-Apo-8′-carotenal	1655	V	—	1615	50

The acetonolysis of complexes I—IV results in the regeneration of the starting carotenoids, confirming the above proposed structures of the complexes.

We believe that the addition of a second molecule of $TiCl_4$ to the C_4 carbonyl group does not occur in canthaxanthin due to the -I effect exerted by the coordination product $\rangle C = O. TiCl_4$ of C_4 transmitted through the conjugated polyene system.

EXPERIMENTAL

Rhodoxanthin was isolated from the fruit of *Taxus baccata*[6,7]. Canthaxanthin and β-apo-8′-carotenal were synthetical products kindly forwarded to us by F.Hoffmann—La Roche, Co. A.G. Basle.

All complexes were obtained in dried benzene at room temperature. The electron spectra were obtained in dimethylformamide and the IR spectra, in nujol.[8] The complexes do not melt up to 355°; they are insoluble in nonpolar solvents and are decomposed by treatment with polar solvents.

1. *Action of $TiCl_4$ on Canthaxanthin*

1.1. *Canthaxanthin $TiCl_4$ complex (I).* To a solution of 50 mg of canthaxanthin in 50 ml benzene, 0.3 ml of $TiCl_4$ were added and the mixture stirred several times. The dark blue reaction mixture was kept during 15 min , then the precipitate filtered off and washed with benzene till the solvent remained incolor. 45 mg of dark powder containing 17.37 % Cl were obtained. $\lambda_{max} = 480$ nm ; $\nu_{(C = O)} = 1655$ cm^{-1}, $\nu_{(C=O.TiCl_4)} = 1610$ cm^{-1}.

Cleavage of complex I. To a solution of 10 mg complex I in 15 ml dimethylformamide, 10 ml benzene and 20 ml petroleum ether were added. After washing with water and drying with Na_2SO_4 the solution was submitted to column chromatography. The chromatogram showed a single zone. The pigment had all the properties characteristic to canthaxanthin ($\lambda_{max} = 480$ nm ; $\nu_{(C=O)} = 1655$ cm^{-1}).

2. *Action of $TiCl_4$ on Rhodoxanthin*

2.1. *Rhodoxanthin. $TiCl_4$ complex (II).* A solution of 20 mg rhodoxanthin in 30 ml of benzene was treated with 0.05 ml $TiCl_4$ and worked up as complex I. 19 mg black powder containing 18.90 % Cl were obtained . $\lambda_{max} = 488$ nm ; $\nu_{(C=O)} = 1670$ cm^{-1}; $\nu_{(C=O.TiCl_4)} =$ $= 1625$ cm^{-1}.

Cleavage of complex II. The cleavage was carried out as that of complex I. The pigment obtained by chromatography showed in the electron spectrum a maximum at 492 nm and in the IR spectrum a band at 1670 cm^{-1}. Hydrogenation with $NaBH_4$ resulted in the formation of Eschscholtzxanthin.

2.2. *Rhodoxanthin. 2 $TiCl_4$ complex (III).* 10 mg rhodoxanthin were solved in 20 ml benzene and 0.15 ml $TiCl_4$ were added. The mixture was worked up as in the case of complex I. 12 mg of complex III containing 30.00 % Cl were obtained. ($\lambda_{max} = 484$ nm ; $\nu_{(C=O.TiCl_4)} = 1625$ cm^{-1}).

[6] R. Kuhn and H. Brockmann, *Ber. dtsch. chem. Ges.*, **66**, 828 (1933).

[7] C. Bodea, E. Nicoară and T. Salontai, *Rev. Roumaine Chim.*, **9**, 517 (1964).

[8] C. Bodea, E. Nicoară, V. Tămaş and H. Mantsch, *Liebigs Ann. Chem.*, **666**, 189 (1963 ·(

Cleavage of complex III. The cleavage was carried out as that of complex II. A mixture of pigments was obtained, consisting of rhodoxanthin and small quantities of degradation products.

3. *Action of $TiCl_4$ on β-apo-8′-carotenal*

3.1. *β-Apo-8′-carotenal. $TiCl_4$ complex (IV).* To a solution of 50 mg β-apo-8′-carotenal in 15 ml benzene 0.1 ml $TiCl_4$ were added, the mixture stirred several times and worked up as discribed for complex I. 56 mg of complex IV containing 22.55% Cl were obtained. In the electron spectrum appeared a maximum at 459 nm and in the IR spectrum a band at 1615 cm^{-1}.

Cleavage of complex IV. The cleavage was performed as above for complex I. The pigment proved to be β-apo-8′-carotenal by $\lambda_{max} = 457$ nm and $\nu_{(C=O)} = 1665\ cm^{-1}$.

3.2. *β-Apo-8′-carotenal. 2 $TiCl_4$ (V).* A solution of 50 mg β-apo-8′-carotenal in 15 ml benzene was treated with 0.3 ml $TiCl_4$ and the mixture worked up as in the case of complex I. 58 mg of complex V containing 27.12 Cl were obtained. $\lambda_{max} = 450$ nm, $\nu_{(C=O)} = 1615\ cm^{-1}$.

Cleavage of complex V. The cleavage carried out as above for complex I, led to a mixture of pigments. The main pigment showed $\lambda_{max} = 454$ nm, $\nu_{(C=O)} = 1665\ cm^{-1}$. In co-chromatography with authentical β-apo-8′-carotenal there was a separation by interzone, the cleavage product being stronger adsorbed. The structure of this product could not be determined.

Cleavage of complex [illegible] was carried [illegible] complex II. A mixture of ligands was obtained, consisting of [illegible] and small quantities of [illegible] products.

2. Action of $FeCl_3$ on π-complexes

2.1 [illegible] $FeCl_3$ complex (IV). To a solution [illegible] in [illegible] the mixture [illegible] several times and worked up as described for complex I. [illegible] mg of complex IV containing 22.8% Cl were obtained. In the [illegible] appeared [illegible] in the IR spectrum a band at 1615 cm⁻¹.

[illegible] complex [illegible] was performed as above for complex [illegible] λ_{max} [illegible] $\nu_{C=O}$ [illegible] 1650 cm⁻¹.

2.2 [illegible] $FeCl_3$ [illegible] solution of [illegible] mg [illegible] was treated with 0.3 ml [illegible] Cl_2 and the mixture worked up as in the case of complex I. [illegible] mg of complex [illegible] containing 17.13% [illegible] were obtained. λ_{max} = 350 nm, $\nu_{C=O}$ 1683 cm⁻¹.

[illegible] complex [illegible] The cleavage was carried out as above for complex I [illegible] a mixture of [illegible]. The main product showed λ_{max} [illegible] 1690 cm⁻¹ [illegible] There was [illegible] the [illegible] product being [illegible] The structure of this product was not [illegible]

La REVUE ROUMAINE DE CHIMIE paraît 12 fois par an. Le prix d'un abonnement annuel est de £ 5,—; $ 12,—; FF 60,—, DM 48,—. Toute commande de l'étranger (fascicules ou abonnements) sera adressée à CARTIMEX, Boîte postale 134—135, Bucarest, Roumanie, ou à ses représentants à l'étranger :

R.P. d'ALBANIE, **Ndermarja Shtetnore e Botimeve,** Tirana; R. D. ALLEMANDE, **Deutscher Buch-Export und -Import,** Leipzig, 701, Leninstrasse 16 ; R. P. de BULGARIE, **Hemus,** Place Slaweikov, 11, Sofia; R. P. de CHINE, **Waiwen Shudian,** P.O.B. 88, Peking ; R.P.D. COREENNE, **Chulphanmul,** Phenian ; RÉPUBLIQUE CUBA, **Cubartimpex,** Simón Bolivar 1, Palacio Aldamo, Habana ; R. P. de HONGRIE, **Kultúra,** P.O.B. 149, Budapest 62; R. P. MONGOLE, **Mongolgosknigotorg,** Ulan Bator ; R. P. POLOGNE, **Ruch,** Ul. Wronia 23, Warszawa ; R. S. TCHÉCOSLOVAQUE, **Artia,** Ve Smeckach 30, Praha II ; U.R.S.S., **Mejdunarodnaïa Kniga,** Moskva G-200 ; R. D. VIETNAM, **So Xuat Nhap Khau Sach Bao,** 32 Hai Ba Trung, Hanoï ; R. S. F. YOUGOSLAVIE, **Jugoslovenska Knjiga,** Terazije 27, Beograd; **Prosveta** 16/1, Terazije, Beograd; **Forum,** Voïvode Misica, Novi Sad ; ARGENTINE, **Editorial Sudaminter S.A.,** Alsina 500, Buenos Aires ; AUSTRALIE, **Current Books Ltd.,** Distributors 168—174, Day Street, Sydney ; AUTRICHE, **Globus Zeitungs-, Drucks- und Verlagsanstalt GmbH,** 1200 Wien, Höchstädplatz 3 ; BELGIQUE, **Du Monde Entier,** 5, Place St.-Jean, Bruxelles, Agence Messageries de la Presse 14—22, Rue du Persil, Bruxelles ; CANADA, **Progress Books,** 44 Stafford St., Toronto, Ontario, W. M. Dawson Subscriptions Service Ltd., Six Thorneliffe Park Drive, Toronto 17, Ontario ; COLOMBIE, **Libreria Buchholz Galeria,** av. Jiménez de Quesada 8—40, Bogotá ; DANEMARK, **Ejnar Munksgaard,** Noregade 6, Kobenhavn ; ESPAGNE, **Librería Herder,** Calle de Balmés 26, Barcelona 7 ; ÉTATS-UNIS, **Fam Book Service,** 69, Fifth Avenue, Suite 8. F., New York, 10003 N. Y.; **Continental Publications,** 111, South Mermanee Ave., St.-Louis, Missouri 63105, **Turner Subscription Agency** 235, Park Avenue South, New York 3, N. Y.; FINLANDE, **Akateeminen Kirjakauppa,** P.O.B. 10128, Helsingfors, 10 ; FRANCE, **Nouvelles Messageries de la Presse Parisienne,** 111, Rue Réaumur, Paris II, **Europériodiques S. A.,** 72, Boul. Senard, 22 Saint-Cloud ; GRANDE-BRETAGNE, **Collet's Holdings Ltd.,** Dennington Estate, Wellingborough, Northants, **Central Books Ltd.,** 37, Inn Road, London W. C. 1 ; ISRAEL, **Lepac Ltd.,** P.O.B., 1136 Tel-Aviv, **Haiflepac Ltd.,** P.O.B. 1794, Haïfa ; ITALIE, **So. Co. Lib. Ri.,** Piazza Margana 33, Roma; **Messagerie Italiane Sp. A.,** Milano, Via Priv. Renzo e Lucia 7; JAPON, **Nauka Ltd.,** 30—19 Minami — Ikebukuro 2 ohome Toshima Ku, Tokyo ; PAYS-BAS, **N. V. Martinus Nijhoff,** P.O.B. 269, Den Haag; **Swets & Zeitlinger,** Keizersgracht 471—487, Amsterdam C. ; NORVÈGE, **Tryggve Juul Moller-Boekhandel Øvre,** Slottsgate 15, Oslo 1 ; R. F. ALLEMANDE, **Kubon & Sagner,** P.O.B. 68, München 34, **Presse Vertriebsgesellschaft GmbH,** 6, Frankfurt/Main, Börsenstrasse 13 — 15 ; **Kunst und Wissen,** Erich Biber, P.O.B. 46, 7 000 Stuttgart 1 ; SUISSE, **Pinkus & Cie,** Froschaugasse 7, Zürich, **Fachbücherei Berne,** P.O.B. 397, 3001 Berne.

NOUS VOUS PRIONS DE RENOUVELER VOTRE ABONNEMENT POUR
L'ANNÉE 1969

ORSZÁGOS MŰSZAKI KÖNYVTÁR ÉS DOKUMENTÁCIÓS KÖZPONT 1969

[illegible] CHINE [illegible] par an [illegible] Toutes commandes de [illegible] ou abonnements sont envoyées à [illegible] postale [illegible] ou à ses représentants à l'étranger.

[illegible] Buchhandlung und Import [illegible] Sofia [illegible] Peking [illegible] Budapest [illegible] Moscou [illegible] Progress Books, 81 Simcoe St. Toronto, Ontario. W. M. Dawson Subscription Service [illegible] Ejnar Munksgaard, Nørregade 6, Copenhague [illegible] Libreria Herder [illegible] Barcelona [illegible] Fam Book Service [illegible] New York [illegible] Continental publications [illegible] Turner Subscription Agency [illegible] Akateeminen Kirjakauppa [illegible] Helsinki [illegible] FRANCE Nouvelles Messageries de la Presse Parisienne [illegible] Paris [illegible] GRANDE-BRETAGNE Collet's Holdings Ltd. Dennington Estate, Wellingborough, Northants. Central Books Ltd. 37 Gray's Inn Road, London W.C.1 [illegible] Hellenique Ltd [illegible] Messaggerie Italiane Sp. A. Milano [illegible] JAPON Nauka Ltd. [illegible] Tokyo [illegible] PAYS-BAS N. V. Martinus Nijhoff P.O.B. 269, Den Haag. Swets & Zeitlinger, Keizersgracht 471—487, Amsterdam C. NORVÈGE Tryggve Juul Møller Bokhandel, Oslo, Slottsgate 15, Oslo 1 [illegible] ALLEMAGNE Kubon & Sagner, P.O.B. 68, München 34. Presse Vertriebs gesellschaft GmbH [illegible] Frankfurt [illegible] Kunst und Wissen, Erich Bieber [illegible] SUISSE Pinkus & Co. [illegible] Zürich. Fachbuchcenter Ernst [illegible] Bern.

[illegible]

NOTE POUR LES AUTEURS

La *Revue Roumaine de Chimie* publie des articles en anglais, français, russe,

publie des articles dus aux collaborateurs roumains ou étrangers. Les auteurs recevront 50 tirés à part.

CORRECTION

The readers are kindly asked to consider figure 3, published within the paper "Molecular orbital calculations in the 2,5-diamino-1,4-benzoquinone series. II" by A. Balint and Z. Simon, p. 1635 in *Revue Roumaine de Chimie*, vol. 13, no. 12, 1968 as correctly belonging to the paper "Effect of oxygen chemisorption on the electrical resistance of thin copper films" by I. G. Murgulescu and N. I. Ionescu, p. 1533.

PRINTED IN ROMANIA

1969 APR 2 3

1969 APR 2 3

TRAVAUX PARUS AUX ÉDITIONS DE L'ACADÉMIE DE LA RÉPUBLIQUE SOCIALISTE DE ROUMANIE

CORNEL BODEA et collab. **Tratat de biochimie vegetală**, partea I, **Fitochimie** (Traité de biochimie végétale, Ire partie, Phytochimie), Ier vol., 1964, 747 p.+4 annexes +2 pl., 41 lei ; IIe vol., 1965, 1262 p., 1 pl., 56 lei ; IIIe vol., 773 p., 35 lei.

V. GHEŢIE et V. MICUŞAN, **Analiza imunochimică. Teorie şi practică** (Analyse immunochimique. Théorie et pratique), 1966, 369 p., 28 lei.

SILVIA IONESCU, **Reacţii chimice induse de radiaţiile ionizante** (Réactions chimiques produites par les radiations ionisantes), 1963, 271 p., 15 lei.

MARIETA NICOLAE, **Fizico-chimia proceselor fotografice** (Physico-chimie des processus photographiques), 1964, 426 p. + 4 pl., 35 lei.

R. PORTOCALĂ et L. POPA, **Acizii ribonucleici celulari şi virali** (Les acides ribonucléiques cellulaires et viraux), 1966, 375 p. + 8 pl., 26 lei.

D. PURDELA et R. VÎLCEANU, **Chimia compuşilor organici ai fosforului şi ai acizilor lui** (La chimie des composés organiques du phosphore et de ses acides), 1965, 540 p., 37 lei.

CRISTOFOR SIMIONESCU, MARGARETA GRIGORAŞ et AGATA CERNĂTESCU-ASANDEI, **Chimia lemnului în R.P.R.** (La chimie du bois en Roumanie), 1964, 239 p.+6 pl., 27 lei.

CRISTOFOR SIMIONESCU et CLEOPATRA VASILIU-OPREA, **Mecanochimia compuşilor macromoleculari** (La mécanochimie des composés macromoléculaires), 1967, 344 p., 23,50 lei.

I. P. „Informaţia" – c. 6036

43426

Lei 15.—

F 1103

R REFERÁLVA

REVUE ROUMAINE DE CHIMIE

TOME 14
N° 2
Février 1969

ÉDITIONS DE L'ACADÉMIE DE LA RÉPUBLIQUE SOCIALISTE DE ROUMANIE

Rev. Roumaine Chim. 14, 147–272 (1969), Bucarest

COMITÉ DE RÉDACTION

Rédacteur en chef :

C. D. NENIŢESCU, membre de l'Académie de la République Socialiste de Roumanie.

Rédacteurs en chef adjoints :

A. T. BALABAN et V. E. SAHINI, membres correspondants de l'Académie de la République Socialiste de Roumanie.

Collège de rédaction :

C. DRĂGULESCU, RALUCA RIPAN, CR. SIMIONESCU, membres de l'Académie de la République Socialiste de Roumanie ; EM. BRATU, membre correspondant de l'Académie de la République Socialiste de Roumanie ; Pr G. OSTROGOVICH, MARG. AVRAM, F. BADEA, D. MARCHIDAN, D. NEGOIU et D. SĂNDULESCU.

Les manuscrits, les livres et les revues proposés en échange, ainsi que toute correspondance seront envoyés à la rédaction :

REVUE ROUMAINE DE CHIMIE

23, str. Dumbrava Roşie, Bucarest, 9, Roumanie.

REVUE ROUMAINE DE CHIMIE

ORSZÁGOS MŰSZAKI KÖNYVTÁR ÉS DOKUMENTÁCIÓS KÖZPONT 1883

Tome 14, N° 2 **Février 1969**

Page

I. G. MURGULESCU and IOANA DEMETRESCU, The kinetics of the reactions between benzoil chloride and normal alcohols . . . . 149 – 155 ✓
V. E. SAHINI and LILIANA TELEA, On the electronic spectra of Co(III) halogeno pentaammines . . . . 157 – 158
O. RADOVICI and M. MACOVSCHI, Hydrogen overvoltage on thin evaporated metal films. I. Gold films . . . . 159 – 165 ✓
GH. VASU, On the mechanism of viscous flow in ionic liquids . . . . 167 – 171
ST. ZĂMÂRCĂ, I. GANOVICI and LUCIA GANOVICI, Evidence of the ternary miscibility gap in indium-aluminium-silver system by viscosity measurements . . . . 173 – 181
D. FĂTU et E. SEGAL, Cinétique de la décomposition de l'hydrazine sur des couches minces de germanium . . . . 183 – 188 ✓
C. DRĂGULESCU, I. JULEAN and ANA NIMARĂ, Basic permanganates of bismuth. Investigations in solution on the $[Bi_6(OH)_{12}](OH)_2(MnO_4)_4$-complex . . . . 189 – 195 ✓
RALUCA RIPAN und V. CORDIŞ, Chemische Bestimmung der Basizität des $[PV_{12}O_{36}]^7$ – Heteropolyanions . . . . 197 – 200 ✓
P. SPACU and ELENA ANTONESCU, Complexes of lanthanide halogenoacetates with 1-10-phenanthroline and 2-2′-dipyridyl (II) . . . . 201 – 207
A. ŞUTEU et GH. CRISTEA, Étude du $H_5[PW_{10}V_2O_{40}]$ par la méthode RÈS 209 – 216
LUCREŢIA POPA et IOANA ARSENIE, Étude de la solubilité de l'oxyde de zirconium . . . . 217 – 223
L. FEY and N. BODOR, Electronic spectra of the substituted α-oximinoalkylbenzenes. I. Steric effects on electronic absorption spectra of the substituted *o*-nitro-α-oximinoalkylbenzenes . . . . 225 – 234
I. OLARU, H. CHARCOSSET, Y. TRAMBOUZE et M. PRETTRE, Étude des catalyseurs oxyde de chrome – alumine – potassium par analyse thermique différentielle et mesures de chimisorption . . . . 235 – 245
EUGENIA GÂRD, ILEANA STĂNOIU, A. T. BALABAN and F. CHIRALEU, Isotopic exchange of active methyl hydrogens. VI. Deuteration of 2,4,6-triphenyl-, 2,3,5,6-tetramethyl- and 2,3,6-trimethyl-4-phenyl-pyrylium salts 247 – 252 ✓
A. BARABÁS, ELENA IŞFAN, ELENA ROMAŞ and ALICE TRESTIANU, Heterocyclic organoboron compounds. XI. Boronium chelate salts and beryllium chelates of 2-substituted 1,3-diketones; methyl-acetylacetone, phenyl-acetylacetone and methyl-dibenzoylmethane . . . . 253 – 264
A. M. EL-ABBADY, M. EL-ASHRY and S. H. DOSS, Further studies on the Stobbe condensation with 2-methyl-cyclohexanone . . . . 265 – 271

Rev. Roumaine Chim.

14, 147–272 (1969), Bucarest

Revue Roumaine de Chimie, **14**, 149 – 155 (1969)

THE KINETICS OF THE REACTIONS BETWEEN BENZOIL CHLORIDE AND NORMAL ALCOHOLS

I. G. MURGULESCU and IOANA DEMETRESCU
Physical Chemistry II Department, Bucharest University,
Bd. Republicii 13

Received July 15, 1968

The system $C_6H_5COCl + ROH \rightarrow C_6H_5COOR + HCl$, with $R = CH_3$, C_2H_5, C_3H_7, C_4H_9, C_6H_{13}, was studied. The rate constants at various temperatures between 0° and 50° have been determined. In order to follow up the evolution of the reactions, the resulting HCl was determined by a direct conductometric method; for each alcohol, at various temperatures, calibration curves were plotted, from which HCl concentrations corresponding to measured specific conductivities were made evident. It was found that the rate constants for all alcohols do not depend on the benzoil chloride initial concentration. For each reaction both energy of activation and the pre-exponential factor were determined by the least squares method.

INTRODUCTION

The reactions between benzoil chloride and normal alcohols have been the subject of several kinetic studies. Thus, Norris *et al.* [1,2,3] determined the rate constants of the reactions $C_6H_5COCl + CH_3OH$ and $C_6H_5COCl + C_2H_5OH$ at 0° and 25°. The results were analysed in the Moelwyn-Hughes' book.[4]

In studying some alcoholysis reactions of benzoil chloride, Peeling[5] utilized acetone as solvent, having mainly in view the kinetic influence of the substituents within the benzenic nucleus. We mention also the work of Bluestein Hybl and Nishioka,[6] in which determinations are made in aqueous solutions.

The present work was carried out in order to find a more complete kinetic characterization of reactions between benzoil chloride and normal alcohols.

---

[1] J. F. Norris, E. V. Fasce and C. J. Staud, *J. Amer. Chem. Soc.*, **57**, 1415 (1935).

[2] J. F. Norris and H. H. Young, *J. Amer. Chem. Soc.*, **57**, 1420 (1935).

[3] J. F. Norris and E. Haines, *J. Amer. Chem. Soc.*, **57**, 1425 (1935).

[4] E. A. Moelwyn-Hughes, "The Kinetics of Reactions in Solution", Oxford, Clarendon Press, second edition, 1947, p. 204.

[5] E. R. A. Peeling, *J. Chem. Soc.*, **1959**, 2309.

[6] B. R. Bluestein Hybl and Y. Al. Nishioka, *Proc. Yowa Acad. Sci.*, **61**, 225 (1954); *Chem. Abstr.*, **1955**, 3629 f.

EXPERIMENTAL

The utilized benzoil chloride, Reanal, was kept in the original phial, which has been closed every time after the needed quantities have been taken out.

Austranal p.a. alcohols were used. 4 Å molecular sieves were applied for removing water traces out of methyl and ethyl alcohols. The remaining water was dosed by titration with the Karl Fischer's reagent.

In order to follow up the evolution of the reactions, the resulting HCl was determined by a direct conductometric method; for each alcohol, at various temperatures, calibration curves were plotted, from which HCl concentrations corresponding to measured specific conductivities were evinced. The diminution in the concentration of the benzoil chloride resulted from the HCl concentration. The calibration curves were in perfect agreement with those obtained through the same method by other authors.[7,8,9] For example, the HCl in ethyl alcohol calibration curves are plotted in figure 1.

The conductivity cell, provided with a tight taper, was directly introduced in the thermostat. Platinum platinized electrodes were used.

Resistance measurements were made by means of a Wheatstone bridge, utilizing a cathode-ray oscilloscope as null indicator.

RESULTS

The reactions between benzoil chloride and primary alcohols taking place according to the scheme

$$C_6H_5COCl + ROH \rightarrow C_6H_5COOR + HCl,$$

the equation of the reaction velocity is:

$$\frac{dx}{dt} = k(a-x)(b-x),$$

where x is the diminution of concentration of the reactants and a and b their initial concentrations. Since the diminution x is negligible with respect to the alcohol concentration b, the rate equation takes the simple form

$$\frac{dx}{dt} = kb(a-x),$$

which on being integrated gives:

$$k = \frac{2.303}{bt} \log \frac{a}{a-x} \cdot \qquad (1)$$

In the following, we will make use of this equation for the presentation of results.

---

[7] H. Goldschmidt, *Z. phys. Chem.*, **89**, 129 (1915).

[8] H. Goldschmidt and P. Dahl, *Z. phys. Chem.*, **108**, 121 (1924).

[9] F. Bărbulescu and A. Greff, *Rev. Roumaine Chim.*, **10**, 387 (1965).

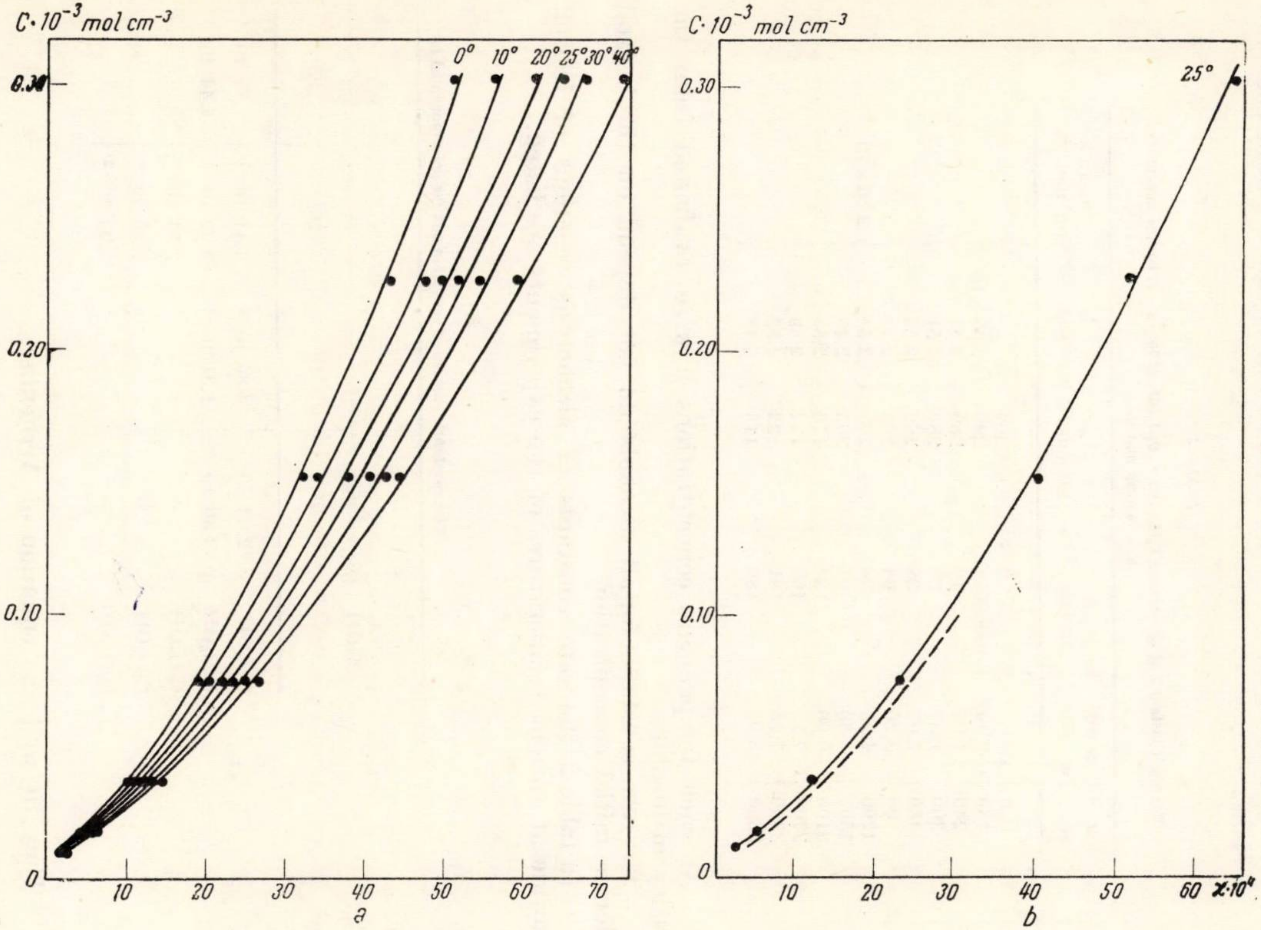

Fig. 1. — HCl in ethyl alcohol calibration curves (1*a*). Comparison with Goldschmidt's results[8] (dashed line) (1*b*).

To exemplify the validity of equation (1), we give in table 1 the evolution of the measurements we have performed to find a kinetic constant.

Table 1

The rate constant k of the reaction $C_6H_5COCl + C_4H_9OH$, at 20°. $a = 0.000304$ molcm^{-3}; $b = 0.0109$ molcm^{-3}

t sec.	$\varkappa \cdot 10^4$ ω^{-1}cm^{-1}	x molcm^{-3}	a − x molcm^{-3}	k cm^3 mol^{-1}s^{-1}	mean k cm^3 mol^{-1}s^{-1}
0		0	0.000304	—	
180	0.797	0.000014	290	2.40×10^{-2}	
240	1.06	19	285	2.47	
300	1.37	24	280	2.51	
480	2.07	38	266	2.55	
900	3.26	64	240	2.41	
1200	4.23	86	218	2.54	2.50×10^{-2}
1500	4.80	101	203	2.47	
2100	6.06	134	170	2.54	
2700	7.13	162	142	2.59	
3300	7.75	181	123	2.52	
3600	8.01	189	115	2.48	

At each temperature concentrations b were evaluated from the density of alcohol.

The rate constants for all alcohols do not depend on the benzoil chloride initial concentration.

In table 2 the rate constants of alcoholysis reactions of benzoil chloride at various temperatures of the experiments are listed.

Table

Rate constants, energies of activation and the pre-exponential factors

ROH	k,			
	0°	10°	20°	25°
CH_3OH	$2.03\ 10^{-2}$	$4.80\ 10^{-2}$	$1.17\ 10^{-1}$	$1.79\ 10^{-1}$
C_2H_5OH	$3.80\ 10^{-3}$	$1.31\ 10^{-2}$	$2.70\ 10^{-2}$	$4.44\ 10^{-2}$
C_3H_7OH	—	—	$2.54\ 10^{-2}$	—
C_4H_9OH	—	—	$2.50\ 10^{-2}$	—
$C_6H_{13}OH$	—	—	$2.44\ 10^{-2}$	—

They fit well the equation of Arrhenius:

$$k = Ae^{-\frac{E}{RT}}, \tag{2}$$

as one can easily see in figure 2.

According as the R radical increases, the representing straight lines tend to superpose each other and the differences between the corresponding energies of activation decrease.

In the last two columns of table 2 energies of activation E, and pre-exponential factors A, determined by the least squares method, are listed. One can see that both energy of activation and pre-exponential factor are the greatest in the case of reactions in which methyl and ethyl alcohols are involved; for the other reactions the values are smaller, with very slight differences between them.

The experimental values of A listed in table 2 are much smaller than those calculated, for instance, by means of the well known relation:

$$A = N\sigma_{12}^2 \left[8\pi RT\left(\frac{1}{M_1}+\frac{1}{M_2}\right)\right]^{1/2} \mathrm{cm^3 mol^{-1} s^{-1}}, \tag{3}$$

the symbols of which have the current meanings. To evaluate the molecular diameters we used, fault of other data, the relation:

$$\sigma = \left(\frac{M}{N\rho}\right)^{1/3}, \tag{4}$$

ρ representing density.

In table 3 the experimental values of A are given together with those calculated through the equation (3). By comparing the columns 4 and 5, one can see that the experimental values are 10,000–100,000 times smaller than the calculated ones. Hence the reaction between benzoil chloride and normal alcohols is a slow one.

2

corresponding to the reactions $C_6H_5COCl + ROH$

$\mathrm{cm^3\ mol^{-1}\ s^{-1}}$			E $\mathrm{calmol^{-1}}$	A_{exp} $\mathrm{cm^3 mol^{-1} s^{-1}}$
30°	40°	50°		
$2.72\ 10^{-1}$	—	—	14270	$5.26\ 10^9$
$5.75\ 10^{-2}$	$1.36\ 10^{-1}$	—	14730	$2.60\ 10^9$
$5.30\ 10^{-2}$	$1.16\ 10^{-1}$	$2.33\ 10^{-1}$	13780	$4.69\ 10^8$
$5.26\ 10^{-2}$	$1.13\ 10^{-1}$	—	13610	$3.54\ 10^8$
$5.24\ 10^{-2}$	$1.11\ 10^{-1}$	$2.13\ 10^{-1}$	13450	$2.64\ 10^8$

One comes to the same conclusion when applying other formulae to evaluate the factor A, like [4]:

$$A_{\mathrm{exp}} = \frac{3\pi\sigma\eta}{2m}, \tag{5}$$

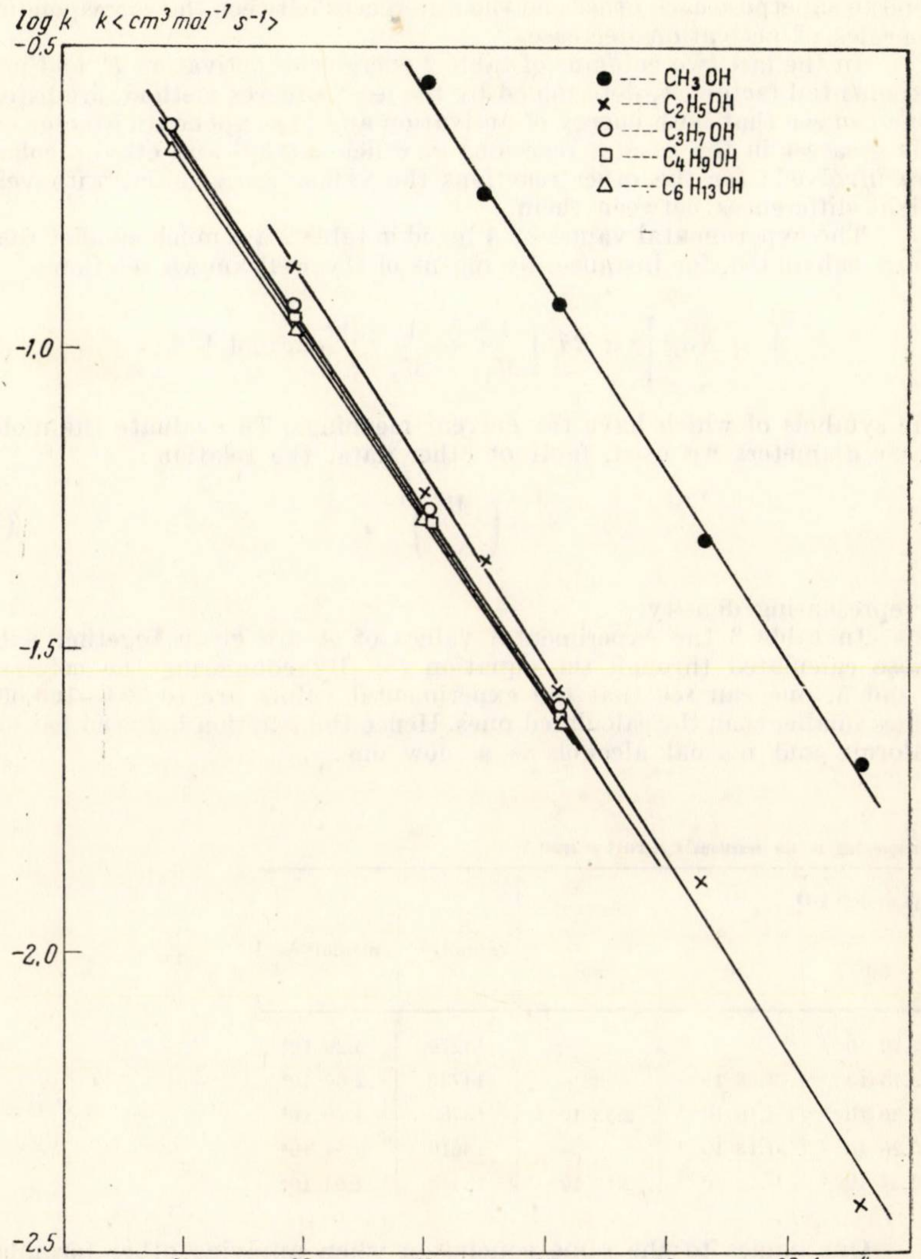

Fig. 2. — Alcoholysis reactions of benzoil chloride.

Table 3

The pre-exponential factors and the entropies of activation corresponding to the reactions $C_6H_5COCl + ROH$

$\sigma_{C_6H_5COCl} = 2.68$ Å; $T = 293.15$ °K

ROH	ρ gcm^{-3}	σ_{12} Å	A, $cm^3mol^{-1}s^{-1}$		$\frac{A_{exp.}}{A_{calc.}}$	ΔS^*
			exp.	calc.		
CH_3OH	0.7923	2.28	$5.26\ 10^9$	$4.80\ 10^{13}$	$1.09\ 10^{-4}$	-15.68
C_2H_5OH	0.7893	2.41	$2.60\ 10^9$	$4.64\ 10^{13}$	$5.60\ 10^{-5}$	-17.40
C_3H_7OH	0.8035	2.50	$4.69\ 10^8$	$4.54\ 10^{13}$	$1.03\ 10^{-5}$	-20.80
C_4H_9OH	0.8090	2.58	$3.54\ 10^8$	$4.52\ 10^{13}$	$7.83\ 10^{-6}$	-21.36
$C_6H_{13}OH$	0.8204	2.71	$2.64\ 10^8$	$4.50\ 10^{13}$	$5.42\ 10^{-6}$	-21.95

η being the viscosity of the solvent, and m and σ the mass and the diameter of molecules of the dissolved substance. A is found to be as great as about $10^{13} cm^3mol^{-1}s^{-1}$. Likewise, by means of the equation

$$A = N \frac{kT}{h} \cdot \frac{F^*}{F_1F_2} \ cm^3mol^{-1}s^{-1}, \tag{6}$$

known from the activated complex theory, one obtains values between $10^{12} - 10^{13}$ $cm^3mol^{-1}s^{-1}$.

The slowness of the studied reactions is also reflected in the activation entropy ΔS^*, which is defined by

$$A_{exp} = e \cdot \frac{kT}{h} \cdot e^{\frac{\Delta S^*}{R}} \tag{7}$$

As we can see from the last column of table 3, the entropy of activation is markedly negative, which is a characteristic feature of the very slow reactions.

The fact that the reactions between benzoil chloride and normal alcohols are slow ones could be accounted for by lost of the efficiency of collisions between the molecules of the reactants, as a result of some steric impediments. Thus one could suppose that only the collisions involving directly the reactive zones of molecules, $-COCl$ and $-OH$, result in chemical reactions, while the other collisions are effectless from the chemical point of view. Also, we may suppose, according to the activated complex conception, that the coefficient of the transmission over the potential barrier is much less than the unity. Finally, we can not rule out the possibility that the solvent exercises a strong desactivation action on the reactant molecules.

The reactions between benzoil chloride and normal alcohols are of the intermolecular dipol—dipol type and develop following a nucleophilic SN_2 substitution mechanism. Because of the chemical similarity of these reactions, both energies of activation and pre-exponential factors have neighbouring values.

Revue Roumaine de Chimie, **14**, 157 –158 (1969)

ON THE ELECTRONIC SPECTRA OF Co(III) HALOGENO PENTAAMMINES

V. E. SAHINI and LILIANA TELEA

Institute of Physical Chemistry of the Academy
Bucharest, str. Dumbrava Roşie 23

Received July 15, 1968

The paper deals with the localization of the two maxima of the first electronic absorption band of $[Co(NH_3)_5Cl]^{2+}$ and $[Co(NH_3)_5Br]^{2+}$ ions, using a corrected Gauss function (a cubic equation with two parameters). The results are in good agreement with the band splittings and shifts of the ions of the $[Co(NH_3)_5X]^{2+}$ type and in close connection with the spectrochemical serie.

Electronic absorption spectra of $[Co(NH_3)_5X]^{2+}$ ions (X=halogen) have been extensively studied, both experimentally and theoretically,[1–4] special attention being paid to the splittings and shifts of the first electronic bands, as compared to that of $[Co(NH_3)_6]^{3+}$. The exchange of one NH_3 molecule with one halogen ion as ligand has as one of the results the splitting of the longest wave-length electronic band of $[Co(NH_3)_6]^{3+}$ in two components presenting a marked bathochromic shift, the value of which is proportional to the polarisability of the halogen ion. Since previously published results [1] concerning the position of the maximum of this band have led only to a partial agreement to the above statement, we have considered of interest to carefully examine the position of these bands.

EXPERIMENTAL PART

$[Co(NH_3)_6]Cl_3$, $[Co(NH_3)_5Cl]\,Cl_2$ and $[Co(NH_3)_5Br]Br_2$, obtained and analysed according to literature,[5–9] have been repeatedly recrystallized from ethanol. The spectra were obtained with a UNICAM SP 500 spectrophotometer. Special care has been taken in order to prevent the effects of hydrolysis.[1]

---

[1] M. Linhard and M. Weigel, *Z. anorg. Chem.*, **266**, 49 ; 73 (1951) ; *Z. phys. Chem. (Frankfurt)*, **11**, 308 (1957).

[2] L. E. Orgel, *J. Chem. Soc.*, **1952**, 4576 ; *J. Chem. Phys.*, **23**, 1004 (1955).

[3] J. S. Griffith and L. E. Orgel, *J. Chem. Soc.*, **1956**, 4981.

[4] H. Yamatera, *Naturwiss.*, **13**, 375 (1957) ; *Bull. Chem. Soc. Japan*, **31**, 95 (1958).

[5] J. Bjerrum, *Inorg. Synth.*, **2**, 216 (1946).

[6] K. Jörgensen, *J. prakt. Chem.*, **2**, 417 (1887).

[7] S. Sörensen, *Z. anorg. Chem.*, **5**, 369 (1894).

[8] W. Harkins, *J. Amer. Chem. Soc.*, **38**, 2646 (1916).

[9] S. M. Jörgensen, *Z. anorg. Chem.*, **17**, 463 (1898).

RESULTS

The bands of the pentaammine ions have been analysed graphically in order to establish the correct value of the maximum, owing to the strong overlap of the two bands. The following corrected Gauss function has been used[10] :

$$\varepsilon = \varepsilon_{0\ \mathrm{exp}} \{-a(\nu_0 - \nu)^2 [1 + b(\nu_0 - \nu)]\}$$

where ε and ε_0 are the molar extinction coefficients, respectively at the ν and ν_0 wave numbers, a and b being constants related to the half band width and to the band asymmetry. In each case an iteration of the wave number value of the low intensity band has been considered, the rapid convergence enabling us to use only three steps of the iteration processes. Our experimental results and Linhard's are given in table 1, the analytically found data being enclosed in brackets.

Table 1

Wave-numbers of the first absorption band

Ion	Wave-numbers			
	Lit. [1]		Present paper	
	I_a	I_b	I_a	I_b
$[Co(NH_3)_6]^{3+}$	21.05		21.05	
$[Co(NH_3)_5F]^{2+}$	19.45	21.95	—	—
$[Co(NH_3)_5Cl]^{2+}$	18.72	(21.35)	18.72	(21.36)
$[Co(NH_3)_5Br]^{2+}$	18.23	(21.47)	18.25	(20.83)

The $^1A_{1g} \rightarrow {}^1T_{1g}$ transition of $[Co(NH_3)_6]^{3+}$ is responsible for the first absorption band. In $[Co(NH_3)_5X]^{2+}$ ($X = Cl$, or Br, in our case), the symmetry being lowered from O_h to C_{4v}, the theoretical treatments of the further splittings of energy levels in a tetragonal field reveal that the energy differences corresponding to those transitions which are leading to the two components of this first electronic band depend on some properties which vary monotonously from one ligand to other. [2-4] Then we may expect to record a monotonous modification of the maximum wave-number of the bands according to the same monotonous variation of these properties of the corresponding halogens and of their position in the spectrochemical series. Our results presented in table 1 are in good agreement with this consequence of the theoretical treatment and the same order of modification recorded in the wave-number of the I_a band has also been obtained in the wave-number of the I_b band. Passing from $[Co(NH_3)_5F]^{2+}$ to $[Co(NH_3)_5Br]^{2+}$ the frequency modification of the I_b is more important than that of the I_a band.

---

[10] H. Siebert and M. Weigel, *Z. phys. Chem.* (*Frankfurt*), **11**, 318 (1957).

Revue Roumaine de Chimie, **14**, 159–165 (1969)

HYDROGEN OVERVOLTAGE ON THIN EVAPORATED METAL FILMS. I

GOLD FILMS

O. RADOVICI and M. MACOVSCHI

Institute of Physical Chemistry of the Academy,
Bucharest, Str. Galaţi 31

Received April 9, 1968

Using a potentiokinetic method, the cathodic polarization curves of evaporated gold films of different thickness in 2N H_2SO_4 are determined. It was found that Tafel slope of the curves, the exchange current density and the overvoltage at 10 $mA.cm^{-2}$ depend on the thickness of the film.

INTRODUCTION

Thin metal films are very important for the study of the adsorption and catalysis processes and a great number of studies on gases adsorption on different evaporated metal films were carried out in order to explain the mechanism of these processes. Though chemosorption processes are of great importance in electrochemical reactions, there are few works concerning electrode processes on evaporated films.[1-4]

The present paper deals with the hydrogen overvoltage on thin gold films.

EXPERIMENTAL

The procedure for obtaining the working surface of the electrode is very important to obtain reproducible experimental data. According to Gossner,[5] the reproducibility of the experimental data is still inadequate, in spite of the real efforts displayed for obtaining as clean surfaces as possible. Moreover, in most cases electron diffraction studies make evident foreign substances on the processed surfaces. Using a scraping technique, Gossner[5] obtained a good reproducibility. From his data it results that as long as the investigated electrode is scraped, its steady state voltage, at a given value of the current, is constant. When

---

[1] A. Matsuda and T. Ohmori, *J. Res. Inst. Catalysis, Hokkaido Univ.*, **10**, 203 (1962).

[2] A. Matsuda and T. Ohmori, *J. Res. Inst. Catalysis, Hokkaido Univ.*, **10**, 215 (1962).

[3] H. Shimizu, *Electrochim. Acta*, **13**, 27 (1968).

[4] H. Shimizu, *Electrochim. Acta*, **13**, 45 (1968).

[5] K. Gossner, *Z. phys. Chem (Frankfurt)*, **36**, 392 (1963).

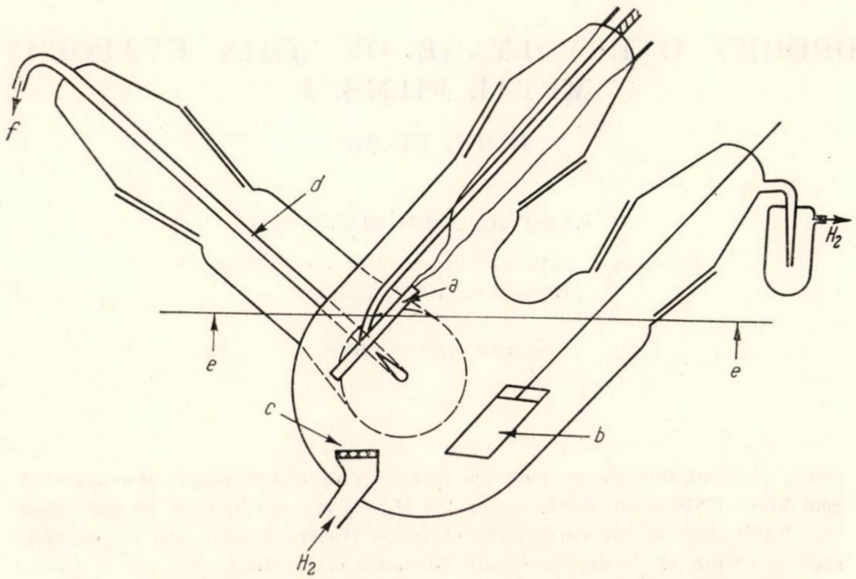

Fig. 1. — The glass cell. *a* — working electrode ; *b* — auxiliary electrode ; *c* — sintered glass for H_2 bubbling ; *d* — Luggin capillary ; *e* — level of the solution ; *f* — electrolytic contact toward reference electrode.

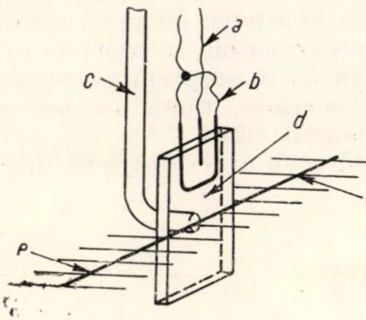

Fig. 2. — Working electrode. *a* and *b* — platinum contacts ; *c* — supporting rod ; *d* — polished glass surface ; *e* — level of the solution.

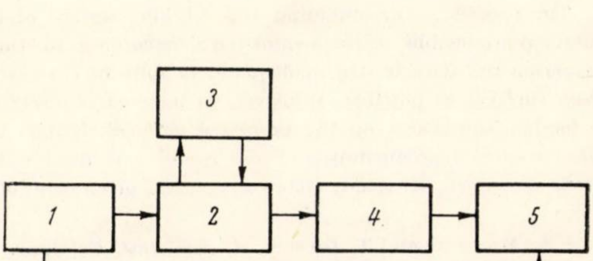

Fig. 3. — Blok-diagram of the recording equipment of polarization curves. *1* — pilot voltage ; *2* — potentiostat ; *3* — cell ; *4* — logalex ; *5* — recorder ; *6* — start/stop synchronization.

scraping ceases, the electrode voltage is changed from its constant value, the deviation increasing with time.

A different situation is encountered in experiments with thin films :

1. A scraping technique cannot be used ;

2. The films being obtained by vacuum evaporation of the pure metals, their surface may be considered clean enough ;

3. The errors may be considered small if measurements are made immediately after films introduction into the solution.

Taking into account that the smallest degree of dissolution of the films could influence the measurements (because of the film thickness variation), the metal tested at the beginning was gold, an inert metal toward dissolution in many media.

A glass cell, presented in figure 1, was used for experimental measurements. The special building of the Luggin capillary allows the capillary top to explore the electrode surface at different depths from the air-solution surface.

The working electrode were obtained by pure gold evaporation (99.99 %) on a polished glass surface in a high vacuum equipment. Before evaporation, the glass surface was heated at 350° for 4 hrs at a pressure of 10^{-5} torr to withdraw the gas traces on the surface ; the evaporation was carried out at the same pressure with a rate of 150—175 Å/min. The electric contacts were realized by means of two platinum wires introduced in the glass. The electrodes were disposed in such a manner that the bimetal couples Au—Pt remain outside the solution. The electrodes assembly is shown in figure 2.

The film thickness was calculated from the total amount of gold, determined by an original method.[6]

Non-stabilized (thermically) films were used. The films were transferred quickly from the evaporation equipment to the working cell.

A saturated calomel electrode was used as reference electrode ; as auxiliary electrode served a platinum plate.

2N sulfuric acid solution were used as working electrolyte under aerated or deaerated conditions. All the experiments were carried out at room temperature.

In order to reduce the errors due to the high electrode potential changes during the experiments, the time necessary to the measurements was reduced to a minimum by using the potentiokinetic technique. The blok-diagram of the equipment for the recording of the polarization curves is described in figure 3. The time influence upon these curves is illustrated in figure 4.

RESULTS AND DISCUSSION

Hydrogen overvoltage is an important kinetic characteristic of the metals and is expressed by the known kinetic equation of Tafel :

$$\eta = \frac{RT}{\alpha F} \ln i_0 + \frac{RT}{\alpha F} \ln i$$

or

$$\eta = a + b \lg i$$

---

[6] M. Macovschi, *Talanta*, in press.

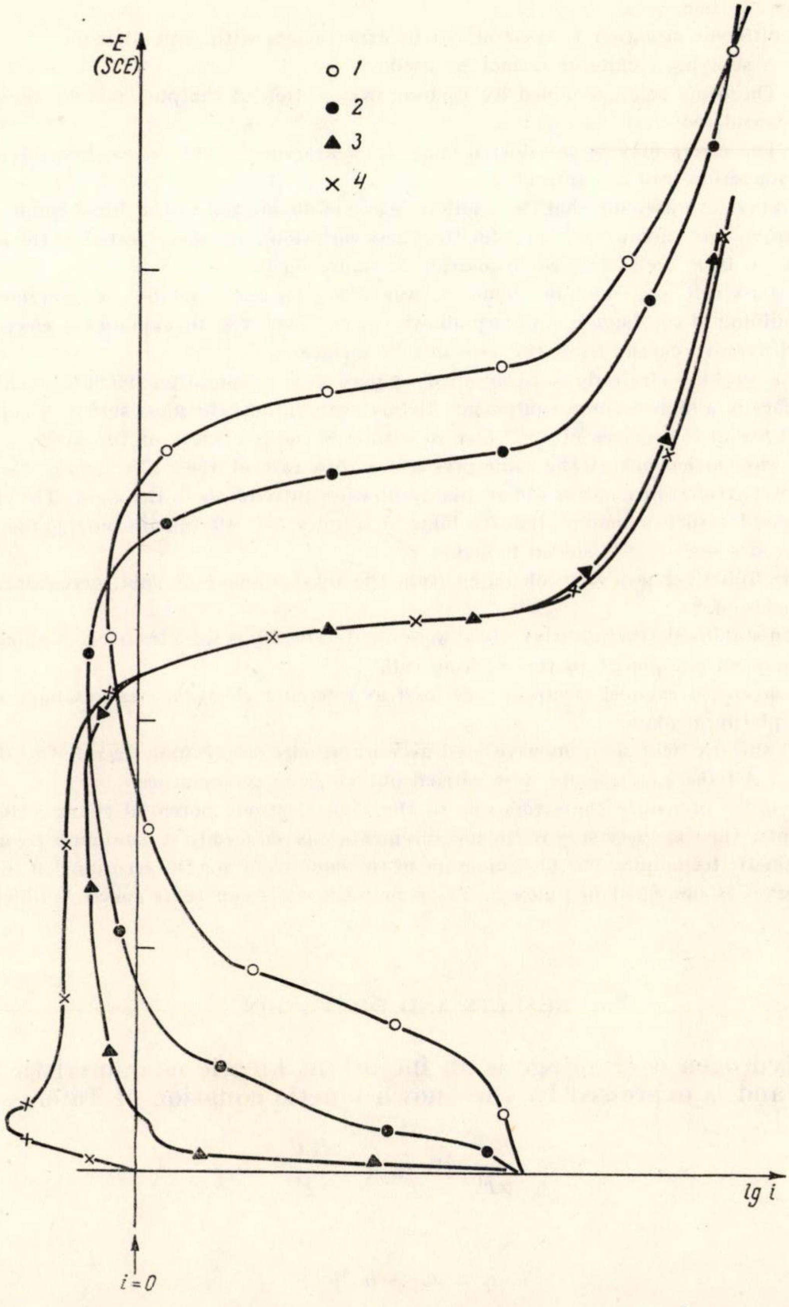

Fig. 4. — Curves $E = E_{(\lg i)}$ for the same film ; time influence, film 750 Å, sweeping rate 500 mV/min, non-aerated solution, experiment start at : *1.* 2 min ; *2.* 8 min ; *3.* 15 min ; *4.* 29 min after film immersion in the solution.

where a represents the overvoltage for the unity value of the current density, b is the Tafel constant, and i_0 is the exchange current density.

Different authors determined the hydrogen overvoltage on massive gold or monocrystals. Some results concerning experimental data on hydrogen overvoltage on gold are shown in table 1. As can be seen in table 1, no agreement can be reported regarding the hydrogen overvoltage data obtained by different authors. For example b values vary between 27 and 123 mV; a high dispersion for the overvoltage values can also be observed, which for current density of 10 mA.cm^{-2} (η_{10}) vary between −60 and −430 mV.

Table 1

Some experimental data concerning hydrogen overvoltage on gold

No.	b (mV)	$-\eta_{10}$ (mV)	Electrolyte	Current density domain (A.cm^{-2})	Observations	Authors
1	27	60	H_2SO_4 2N	$10^{-3}-1$		Schuldiner, Hoare (1957)[7]
2	45	160	HCl 1N	$10^{-3}-10^{-1}$	electrolytically deposed gold	Bockris, Parsons (1948)[8]
3	80	190	sulphamic acid 0.1 M	$10^{-4}-10^{-1}$	monocrystal face (110)	Bicelli, Romagnani (1966)[9]
4	70−80	250	HCl 1N	$10^{-3}-1$	electrolytically deposed gold	Hickling, Salt (1940)[10]
5	116	390	H_2SO_4 2N	$10^{-2}-10^{-1}$	scraping technique	Gossner, Löfler (1963)[11]
6	123	430	HCl 0.1N	$10^{-6}-10^{-3}$		Ives (1959)[12]

In the present paper determination of b, i_0 and η_{10} values and their dependence on the film thickness were studied.

Shape of current-voltage curves in deaerate solutions is presented in figure 5*a*. On the same figure can be seen the values of b, i_0 and η_{10}. Figure 5*b* shows the shape of a current-voltage curve obtained in aerated solution. Because of oxygen influence, the equilibrium potential of the electrode cannot be determined and hence only Tafel constants were obtained for this particular case.

The results of these preliminary experiments are presented in figure 6. As comparison values for the massive gold were considered Gossner and Löfler [11] data ($b = 116$ mV, $\eta_{10} = -390$ mV, $i_0 = 4.4.10^{-6}$ A.cm^{-2}), that present a better certainty because of their reproducibility. For films not

---

[7] S. Schuldiner and I. P. Hoare, *J. Phys. Chem.*, **61**, 705 (1957).

[8] J. O'M. Bockris and R. Parsons, *Trans. Faraday Soc.*, **44**, 860 (1948).

[9] L. Peraldo-Bicelli and C. Romagnani, *Electrochim. Metalorum*, **1**, 102 (1966).

[10] A. Hickling and F. W. Salt, *Trans. Faraday Soc.*, **36**, 1226 (1940).

[11] K. Gossner and C. Löfler, *Z. phys. Chem.* (*Frankfurt*), **37**, 115 (1963).

[12] D. J. G. Ives, *Canad. J. Chem.*, **37**, 213 (1959).

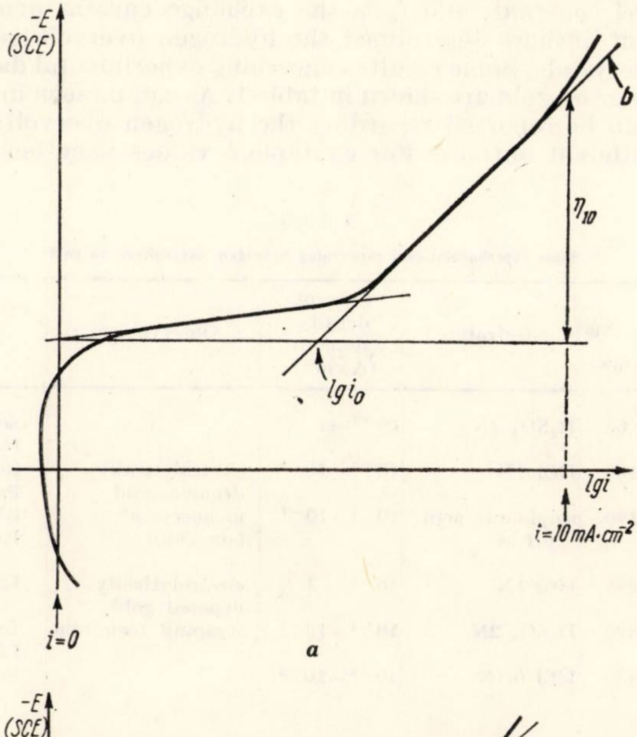

Fig. 5. — Polarization curves. *a* — non-aerated ; *b* — aerated solution. *a* — shows the graphic calculus of *b*, i_0 and η_{10}.

too thin — i. e. 500 to 900 Å — a decrease of the overvoltage and of Tafel slopes and an increase of the exchange current density is observed, when the thickness of the film decreases. We suggest that this phenomenon may be due to the film surface energy, which increases as the film thickness decreases. For thinner films, under 500 Å, a limitation of the current occurs; for example, for a film of 127 Å thickness, at an imposed voltage of -2500 mV (SCE), the current density hardly reaches a value of 7 mA.cm^{-2}. Further investigations by our team will try to clear up this phenomenon.

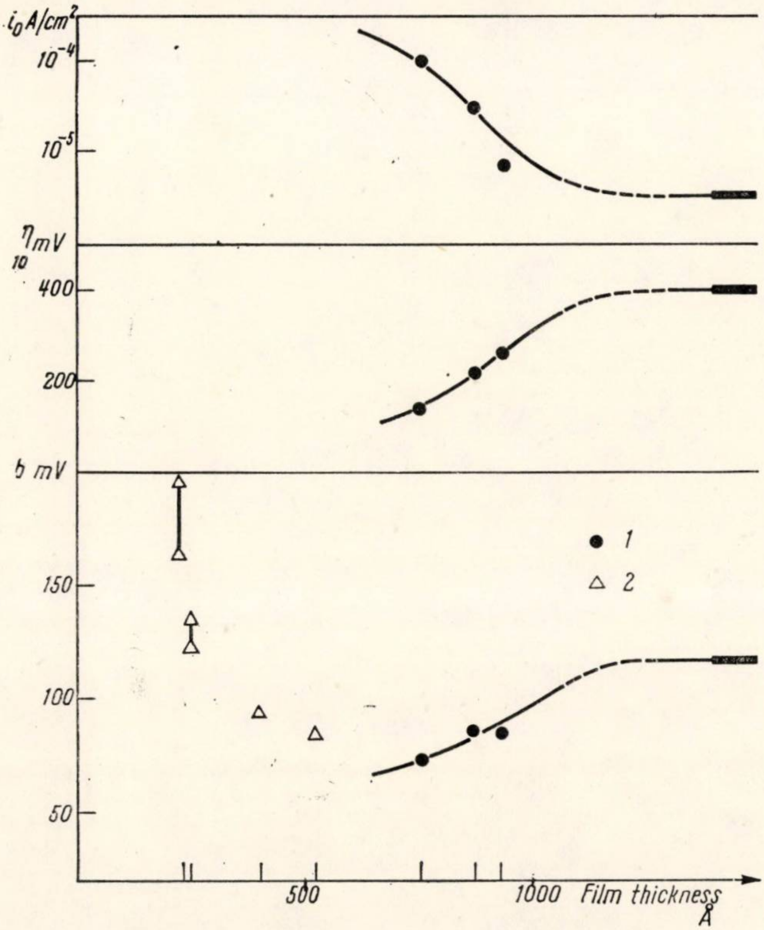

Fig. 6. — Change of the value of b, η_{10} and i_0 as function of films thickness. 1. non-aerated solutions, 2. — aerated solutions.

Revue Roumaine de Chimie, 14, 167–171 (1969)

ON THE MECHANISM OF VISCOUS FLOW IN IONIC LIQUIDS

GH. VASU
Institute of Physical Chemistry of the Academy,
Bucharest, str. Galați 31

Received April 24, 1968

Based on Enskog's method, an interpretation is given of the viscosity coefficients of fused salts. Two hypotheses are considered: of the coupled motion of ion pairs, and of the independent motion of ions. It is shown that whereas the last hypothesis is conducive to difficulties, the hypothesis of coupled motion of ion pairs allows a very natural interpretation of the viscosity of fused alkali halides.

In a theoretical study on the viscosity of molten salts, Murgulescu and Zuca [1] have shown that the pre-exponential factors of the viscosity of fused alkali halides may be interpreted by ascribing the viscous flow to the motion of ion pairs and applying Eyring's [2] theory of the reaction rates.

Recently Dymond and Alder [3] have suggested a very attractive method for the computation of transport phenomena in simple liquids (the so-called van der Waals method). Actually, this consists in applying Enskog's method to the dense gas of hard spheres [4], corrected by using the value of the radial distribution function at the contact distance[5] ; for real molecules, an effective diameter determined from the van der Waals constant is introduced in the formulas obtained.

Undoubtedly, the Eyring and the Chapman-Enskog methods represent the two extreme models in the theory of liquids ; the real situation should be somewhere midway. From this point of view it would be interesting to see whether the Chapman-Enskog method (applied as the "van der Waals theory of dense fluids") leads also to the mechanism of viscous flow by the motion of ion pairs, proposed by Murgulescu and Zuca [1] as basis for an interpretation of viscosity within the frame of Eyring's theory.

---

[1] I. G. Murgulescu and St. Zuca, *Rev. Roumaine Chim.*, **10**, 123 (1965).

[2] S. Glasstone, K. I. Laidler and H. Eyring, "The Theory of Rate Processes", McGraw-Hill, London, 1941, p. 485.

[3] J. H. Dymond and B. J. Alder, *J. Chem. Phys.*, **45**, 2061 (1966).

[4] S. Champman and T. J. Cowling, "The Mathematical Theory of Non-Uniform Gases", Cambridge University Press, London, 1960, chap. 16.

[5] See for general, discussion and references H. Reiss, in *Adv. in Chemical Physics*, **9**, 1 (1965).

THE HYPOTHESIS OF INDEPENDENT IONS

Let us assume that in an ionic melt of the NaCl type there does not exist any kind of association of ions. As it is known the thermodynamic characteristics of such systems may be described by a model of hard spheres where the difference of charge of the ions is neglected.[4] Whe shall consider here that the same hypothesis is valid with respect to viscous flow. As a model of ionic melt we shall consider an equimolar mixture containing two species of hard spheres with the diameters σ_1 and σ_2 and the masses m_1 and m_2 equal to the ion masses.

Under these conditions the viscosity may be immediately computed by Enskog's method using Thorne's formulas[4]; however, a higher precision is attained if the correlation factors χ_1, χ_2 and χ_3 which appear in these formulas are replaced by the values of the correlation function of the molecular densities at the contact distance — the factors G_{11}, G_{22} and G_{12} — of which sufficient accurate values are known at present.[6]

A substantial simplification of Thorne's formulas occurs in the case of an equimolar mixture of spherical molecules with identical diameters but different masses. In that case, by Eq. (58) of ref. 6, the three correlation functions take values given by the equations

$$G_{11} = G_{22} = G_{12} = G \tag{1}$$

where G may be written

$$G = \frac{1 - \dfrac{\pi x}{12} + \left(\dfrac{\pi x}{12}\right)^2}{\left(1 - \dfrac{\pi x}{6}\right)^3} \tag{2}$$

Here $x = 2N\sigma^3/V$, V denotes the molar volume, N is Avogadro's number and σ is the common diameter of the two species of particles.

In the present simple case of an equimolar mixture containing N molecules of mass m_1 and N molecules of mass m_2 and having a common diameter σ, Thorne's[4] expression reduces after a few algebraic operations to the more compact relation

$$\eta = \frac{1.9\cdot 10^{-5}\, \rho^{2/3} T^{1/2}}{(M/2)^{1/6}} \, \frac{1}{x^{2/3}} \left\{ A_{-1} G^{-1} + A_0 \frac{B}{V} + A_1 G \left(\frac{B}{V}\right)^2 \right\}, \tag{3}$$

where, as usual, ρ is the density, T is the temperature and $M = N(m_1 + m_2)$ is the mass of a mol of the compound. The other symbols are given by the expressions :

$$B = \frac{4\pi N \sigma^3}{3}, \tag{4}$$

$$A_{-1} = 3\sqrt{2}\, \frac{a_{-1-1} - 2a_{1-1} + a_{11}}{a_{11}\, a_{-1-1} - a_{1-1}^2}, \tag{5}$$

---

[6] J. L. LEBOWITZ, E. HELFAND and E. PRAESTGAARD, *J. Chem. Phys.*, **43**, 777 (1965).

$$A_0 = \frac{6\sqrt{2}}{5}\,\frac{(1+2M_2)\,a_{-1-1} - 4a_{1-1} + (1+2M_1)\,a_{11}}{a_{11}\,a_{-1-1} - a_{1-1}^2}\,, \tag{6}$$

$$A_1 = \frac{3\sqrt{2}}{25}\left\{\frac{(1+2M_2)^2\,a_{-1-1} - 2(3+4M_1M_2)a_{1-1} + (1+2M_1)^2 a_{11}}{a_{11}a_{-1-1} - a_{1-1}^2} + \right.$$

$$\left. + \frac{4}{\pi}\left(\sqrt{M_1} + 2\sqrt{2M_1M_2} + \sqrt{M_2}\right)\right\}. \tag{7}$$

In these relations $M_1 = m_1/(m_1 + m_2)$, $M_2 = m_2/(m_1 + m_2)$ and a_{11}, a_{-1-1}, a_{1-1} are defined by

$$a_{11} = \frac{1}{M_1}\left[3\sqrt{M_1} + (3 + 2M_1)\sqrt{2M_1M_2}\right], \tag{8}$$

$$a_{-1-1} = \frac{1}{M_2}\left[3\sqrt{M_2} + (3 + 2M_2)\sqrt{2M_1M_2}\right], \tag{9}$$

$$a_{1-1} = -2\sqrt{2M_1M_2}. \tag{10}$$

Let us consider cesium chloride. In that case the ionic diameters are $\sigma_{\mathrm{Cl}} = 3.62$ Å, $\sigma_{\mathrm{Cs}} = 3.34$ Å. These values are obtained from intercrystalline distances. However, as it has been shown by Dymond and Alder, [3] these values cannot be adopted as diameters of the corresponding hard spheres; such hard spheres represent a kind of "effective" hard core; the diameter of the hard cores must be considered as the mean distance up to which the ions approach in the course of their impacts in the system at the given temperature. Consequently, the diameters of the hard cores of chlorine and cesium are smaller than those indicated above (the smaller in proportion as the temperature of the system increases). The ionic diameters of chlorine and cesium are fairly close in magnitude, the chlorine diameter being slightly greater. At the same time chlorine is more deformable than cesium; for this reason the hard cores of the two ions must take closer values such that expression (3) established for mixtures of hard spheres of different masses but equal diameters should be applicable, at least approximately. Introducing the values of the masses of chlorine and cesium atoms, the expressions (3)—(10) reduce to the following contracted relation for the viscosity of cesiun chloride

$$\eta_{\mathrm{CsCl}} = 0.91\cdot 10^{-5}\rho^{2/3}T^{1/2}x^{-2/3}\left[1\,G^{-1} + 0.716\,\frac{B}{V} + 0.677\,G\left(\frac{B}{V}\right)^2\right], \tag{11}$$

where G and B are defined by (2) and (4).

Naturally, one would be tempted to use eq. (11) for computing the viscosity. By relation (2), eq. (11) expresses viscosity as a function of the diameter of the particles; the function is far from being linear: the diameter appears at the third power in the parameter x while relation (2) includes higher powers of x, hence still higher powers of σ. Consequently, according to (11), at a given density, the viscosity is a very fast varying function of the diameter. But σ is an "effective" diameter, the diameter of the "hard core", which can be determined if the interaction potential of the particles is known.[3] But in the case of fused salts there does not exist up to now a sufficiently precise method for determining the effective diameter. Consequently it seems more rational to use Eq. (11) together with viscosity data for computing the effective diameter. Based on considerations of plausibility we may then evaluate the validity of the mechanism of viscous flow which constitutes the premise of Eq. (11).

THE HYPOTHESIS OF ASSOCIATED IONS IN MOLECULES

Fused salts are characterized by a strong force which acts upon the component particles. Hence the idea of an associated motion of the ions seems very natural. Taking up again the view stated by Murgulescu, [1] namely that the viscous flow of fused alkali halides is due to the motion of pairs of ions of opposite charges, we consider the molecule as the essential element of viscous flow. Let then $m = m_1 + m_2$ be the mass of the molecule. Evidently the molecules are not spherical. However, we shall assume in a first approximation that they are spherical; let σ be the corresponding effective diameter. In this case viscosity is expressed by [3]

$$\eta = 1.936 \cdot 10^{-5} \rho^{2/3} T^{1/2} M^{-1/6} x^{-2/3} \left[G^{-1} + 0.8 \frac{b}{V} + 0.761\, G \left(\frac{b}{V} \right)^2 \right] \qquad (12)$$

where G is again given by (2) but the definitions of x and b are different; now we have

$$x = \frac{N\sigma^3}{V},\ b = \frac{2\pi}{3}\ N\sigma^3 \qquad (13)$$

We shall use the above relations for determining the effective diameter from viscosity data. Below we give the results thus obtained.

RESULTS AND CONCLUSIONS

The experimental data on the viscosity and density of fused salts are summed up in table 1. Using the values for cesium chloride, Eq. (11) can be solved with respect to σ and we obtain $\sigma = 3.70$ Å. But in accordance with the significance of Eq. (11) this value should be equal to the effective diameter of the hard core of the ions. Clearly, the value obtained is not consistent with such an interpretation; indeed, this value exceeds both the diameter of the chlorine ion (3.62 Å) and the diameter of the cesium ion (3.34 Å) while the "hard core" should have been smaller than these values.

In the simple hypothesis of viscous flow by the motion of ion pairs, the values obtained for the effective diameter of the pair, σ_{visc}, computed from viscosity data with relation (12), are given in column V of table 1.

For comparison purposes, the values computed additionally $\sigma_{add} = \sqrt[3]{\sigma_1^3 + \sigma_2^3}$, according to the model developed by Murgulescu and Zuca [1], are given in column VI. A surprisingly good agreement has been found : the diameters determined from the viscosity data are only slightly greater than those determined additionally. In fact they verify the relation $\sigma_{visc} = 1.057\ \sigma_{add}$. The fact that in this case the effective diameter of the hard core is slightly greater than the "additional diameter" is not objectionable. On the one hand the ion pair is not really of a spherical form ; for the purpose of simplifying the calculation it may be assumed to be a sphere, but the diameter of this sphere is not determined *a priori*. On the other hand a similar situation occurs in the case of diatomic substances, e. g. oxygen and nitrogen molecules. Taking into account the interatomic distances and the van der Waals radii of atoms [7], the "exact" volume of these molecules can be computed ; equating this volume to $(4\pi/3)\ (\sigma_{add}/2)^3$ we obtain the diameter σ_{add}. This diameter may be compared with σ_{visc}, the diameter determined from viscosity measurements. [8] One obtains for nitrogen $\sigma_{visc} = 1.07\ \sigma_{add}$ and for oxygen, $\sigma_{visc} = 1.05 . \sigma_{add}$ (these are only approximate values, they vary slightly with temperature). It should be observed that these results are in perfect agreement with those obtained for fused salts.

Consequently, within the frame of Enskog's theory, as well as in the frame of Eyring's one [1], the model based on the motions of ion pairs offers a simple and plausible interpretation of viscous flow. A more complete description, based on the hypothesis of independent motion of the ions has not been advanced yet in the present stage of the theory. An improvement could be achieved only by introducing certain correlation functions G_{ij} where the ion charges are explicitly taken into account. So far such correlation functions have not been determined for fused salts.

Table 1

Experimental data and computed diameters. The diameters given in column V have been computed from viscosity by using relation (12). The diameters computed "additioally", $\sigma_{add} = \sqrt[3]{\sigma_1^3 + \sigma_2^3}$, where the ionic diameters have been used, are given in column VI

Salt	T (°K)	η (cP)	ρ g/cm³	σ_{visc} (Å)	σ_{add} (Å)	$\frac{\sigma_{visc}}{\sigma_{add}}$
NaCl	1 100	1.32	1.542	4.02	3.80	1.057
KCl	1 070	1.10	1.512	4.34	4.05	1.073
CsCl	950	1.28	2.7575	4.49	4.19	1.072
RbCl	1 010	1.29	2.2290	4.64	4.37	1.063
NaBr	1 060	1.28	2.309	4.18	4.08	1.025
KBr	1 030	1.14	2.108	4.51	4.29	1.051
RbBr	980	1.41	2.689	4.70	4.43	1.061

Acknowledgements. The author wishes to express his thanks to Professor I. G. Murgulescu, Member of the Academy, for the valuable guidance in the field of the theory of liquids and the permanent scientific assistance offered.

---

[7] M. W. Wolkenstein, "Struktur- und physikalische Eigenschaften der Moleküle", B. G. Teubner Verlagsgesellschaft, Leipzig, 1960, p. 141, 151.

[8] J. O. Hirschfelder, C. F. Curtiss and R. B. Bird, "Molecular Theory of Gases and Liquids", John Wiley Sons, Inc., NewYork, 1954, p. 1111.

Revue Roumaine de Chimie, **14**, 173–181 (1969)

EVIDENCE OF THE TERNARY MISCIBILITY GAP IN INDIUM-ALUMINIUM-SILVER SYSTEM BY VISCOSITY MEASUREMENTS

ST. ZĂMÂRCĂ, I. GANOVICI and LUCIA GANOVICI

Institute of Physical Chemistry of the Academy,
Bucharest, Str. Galați 31

Received March 25, 1968

The viscosity of In – 5.3 wt % Al – 3.7 wt % Ag alloy at a temperature range from 580 to 850° was studied, making use of the oscillating cylindrical crucible method. Important modifications of the logarithmic decrement of the damped oscillations at the transformation $L \rightarrow L_1 + L_2$ as well as at the transition in the $L_1 + L_2 + S$ field under the ternary miscibility gap were found. Log $_{10}\eta = f\left(\frac{1}{T}\right)$ dependency for the homogeneous liquid alloy changes the linear character in the neighbourhood of the immiscibility curve due to the "clustering" phenomenon.

INTRODUCTION

Experimentally, the binary metallic system which exhibit miscibility gap in liquid state as well as the effect of the third element on this domain, have hardly been studied. Several metallic alloys which exhibit total or partial immiscibility in liquid state, by the association of physical and mechanical properties of their components, have an outstanding interest in engineering practice. New methods as powder metallurgy, the utilization of the ultrasounds for homogenizing alloys, special cast technologies with rapid cooling of the finely divided emulsion have already been developed and also applied in order to obtain pieces with relatively homogeneous structure. The trend in recent investigations seems to be the combination of the last two methods listed above or their combination with alloying a third element.

On the basis of such a combination, Sushkin and co-workers [1] have studied the alloys of Pb–Zn–Sn system in view of extending it to the refractory alloy systems Co–Cu, Mo–Cu and Cr–Cu with Ni or Fe as the third element.

From the above considerations it can be noted that the decreasing or the removing of the liquid immiscibility range for a given pair of metals by alloying with a third element is often of scientific and technological importance.

---

[1] E. D. Sushkin, Z. M. Zanozina, V. I. Likhtman and P. A. Rebinder, *Doklady Akad. Nauk S.S.S.R.*, **160**, 1355 (1965).

If many years ago the Ni, Sn, Ag additions to Cu–Pb bronzes, much appreciate das antifriction alloys in both motorcar and aeronautics industries, were made on an empirical basis, the theoretical investigations [2–4] in the last 10–15 years established in this direction few rules which enable one to choose the third element with a certain degree of certainty.

Starting from the conventional theory of nonelectrolytic mixtures, Hildebrand and Scott found that the excess free energy of formation of a liquid solution is very similar to the theoretical expression for the energy of mixing of a regular solution

$$\Delta F^M \simeq \Delta H^M \simeq V^M (\delta_A - \delta_B)^2 \cdot \Phi_A \cdot \Phi_B \tag{1}$$

where V^M is the average atomic volume of the solution, Φ_A and Φ_B the volume fractions of the two components, of the form:

$$\Phi_A = \frac{x_A V_A}{x_A V_A + x_B V_B} \tag{2}$$

while δ_A and δ_B are so-called "solubility parameters", characteristic of the two pure components. For van der Waals force we have also $\delta_A \simeq \left(\frac{\Delta E_A^{\text{vap}}}{V_A}\right)^{1/2}$ where ΔE_A^{vap} is the energy of vaporization and V_A the atomic volumes of component A.

Hildebrand and Scott postulated that when the heat of mixing is sufficiently great, separation into two liquid phases occurs. The complete condition for immiscibility deduced from the theoretical expression for the energy of mixing (1) combined with the critical mixing condition for regular solutions $\lambda = 2\ RT_{\text{critic}}$ (established from "zero approximation of quasi-chemical theory"

$$\Delta F^E \simeq \Delta H^M \simeq \Delta F^M \simeq x_A x_B Z N_0 [W_{AB} - 1/2 (W_{AA} + W_{BB})] = x_A x_B \lambda$$

is the following:

$$1/2\ (V_A + V_B)(\delta_A - \delta_B)^2 > 2\ RT_{\text{critic}} \tag{3}$$

Further, Mott modified Hildebrand's inequality by taking into account the difference in electronegativity between the two components, since the tendency toward immiscibility is compensated by a tendency toward chemical bonding. For this purpose he introduced a correction term $- E_B$, which on the basis of Pauling electronegativity concept [5] may be evaluated from the expression

$$E_B = 23\,060\ n\ (X_A - X_B)^2 \tag{4}$$

---

[2] J. H. HILDEBRAND and R. L. SCOTT, "The Solubility of Non-Electrolytes", Reinhold Publishing Corporation, New York, 1950.

[3] B. W. MOTT, *Phil. Mag.*, **20**, 259 (1957).

[4] M. SHIMOJI, "International Symposium on Physical Chemistry of Process Metallurgy", Part. I, A.I.M.E. Met. Soc. Conf., **7**, 421 (1961).

[5] L. PAULING, *J. Amer. Chem. Soc.*, **54**, 3570 (1932).

where n should be of the order of $z/2$, z is the coordination number in the mixture, and X_A and X_B are the electronegativities of the two components respectively. Finally, the condition for immiscibility in liquid state is thus the following:

$$1/2\ (V_A + V_B)(\delta_A - \delta_B)^2 - 23\,060\, n\, (X_A - X_B)^2 > 2RT \qquad (5)$$

This relationship allowed Mott to explain the observed liquid immiscibilities or miscibilities in 426 out of a total of 529 systems considered.

He also showed that in order to decrease the immiscibility of two metals A and B, the choice of the third element C should be such that its solubility parameter δ_C should preferably be in the range of $\delta_A \rightarrow \delta_B$ or not greatly different from δ_A and δ_B, and the electronegativity X_C should be as different as possible from X_A and X_B.

In–Al–Ag *system*

The values of the solubility parameters and the electronegativities of the three components of the ternary system are presented in table 1.

Table 1

Electronegativities and solubility parameters at 25°

Element	Solubility parameter $(\mathrm{cal/cm^3})^{1/2}$	Electronegativity
In	60	1.5
Al	86	1.5
Ag	82	1.8

The solubility parameters at 25° are those listed by Mott while the electronegativities have been taken from Gordy's compilation[6].

On the basis of the previous considerations as well as from the examination of data in table 1, one may observe that the addition of silver to the In–Al alloy decreases the immiscibility range in liquid state.

As a matter of fact, establishing of the effect of the third element is actually the problem of tracing the ternary equilibrium diagram.

As it was shown by Campbell and Wagemann [7] in their recent study regarding the equilibrium diagram of In–Al–Ag system, determined by the direct-sampling method, followed by density determinations in solid state, a true ternary critical point does not exist, i. e. the binary critical temperature is lowered continuously by addition of silver.

Additions of silver to the binary system In–Al increase the mutual solubility and progressively lower the temperature of complete miscibility as well as the starting point of solidification (Fig. 1).

The lowest temperature at which two liquid layers can coexist in absence of a solid phase, is 590°. The critical composition at 650° is approximately 26 wt % Ag, 47% In, 27% Al. Attempts at detecting by thermal analysis the boundaries of the three-phase region $L_1 + L_2 + S$, which lies bellow the ternary miscibility gap, failed, no doubt, on account of the smallness of the heat effect.

---

[6] J. Gordy, *J. Chem. Phys.*, **24**, 439 (1956).

[7] A. N. Campbell and R. Wagemann, *Canad. J. Chem.*, **44**, 657 (1966).

In a previous investigation [8] we have shown the possibility of evidencing by density and viscosity measurements the immiscibility line in the system Al—In.

At the same time we will consider here the experimental results of Glazov and Kizhevskaia's investigations [9] regarding the determination of the starting point of freezing by viscosity measurements. This method has been recommended by the quoted authors as a useful method, particularly when freezing takes place with small heat effect so that the thermal analysis failed (does not allow sure results).

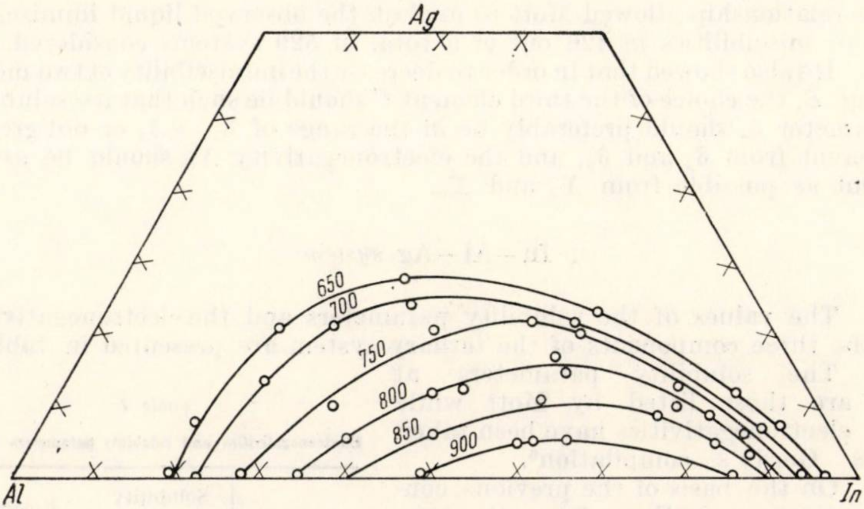

Fig. 1. — Isotherms through liquid-liquid immiscibility system In—Al—Ag (according to Campbell and Wagemann).

We have studied the In—5.3 wt% Al—3.7% Ag alloy in order to evidence the structural changes in this molten alloy, to establish the equilibrium diagram in such ternary system with miscibility gap, and to study the effect of the third element in liquid state.

EXPERIMENTAL

A. *Determination of the density*

The calculation of the viscosity of the ternary In—Al—Ag alloy has required the accurate determination of the density in the homogeneous liquid state. To this end a dilatometric method [10] similar to that of Glazov [11] was used. The density determinations have been carried out on the molten In—Al—Ag alloy in a cylindrical fritted alumina crucible, also used for the viscosity measurements. To avoid errors due to the volatility of the indium and the silver from the liquid alloy in high vacuum conditions, the experiments were carried out in pure argon atmosphere, obtained by passing it through platinized asbestos [12] at 450° in a mixture with 10% H_2, drying and finally bubbling in molten aluminium at 900°.

---

[8] St. Zămârcă, N. Petrescu, I. Ganovici and L. Ganovici, *Rev. Roumaine Chim.*, **13**, 1011 (1968).

[9] V. M. Glazov, S. N. Kizhevskaia, *Zavodskaya Lab.*, **26**, 721 (1960).

[10] N. Petrescu, St. Zămârcă, L. Ganovici and I. Ganovici, *Studii și Cercetări în Chim. Acad. R. S. România* (under print).

[11] V. M. Glazov and D. A. Petrov, *Zavodskaya Lab.*, **1**, 8 (1958).

Before measuring the density, the alloy was kept for 17 hours at 1000° for homogenizing, and for $2^1/_2$ to 3 hours at each working temperature, which were adjusted within ± 2° accuracy by means of a potentiometric device. The results obtained are shown in table 2.

If the density of the components are known for a certain temperature, one can calculate at a first approximation the density of the liquid alloy by means of the linear additivity relationship:

$$\rho_{\text{alloy}} = \Phi_A \rho_A + \Phi_B \rho_B + \Phi_C \rho_C \qquad (6)$$

Table 2

Density of liquid In–Al–Ag alloy

t°	690	700	720	760	800	900
g/cm³	6.069	5.971	5.901	5.867	5.834	5.757

where ρ_i is the density of the pure components and Φ_i is their volumetric fractions in liquid alloy.

The density of liquid indium, aluminium and silver have been computed from data given by Wilson[13].

The data experimentally obtained and then extrapolated at 1000° show an approximate difference of 3.5% as compared to the ones computed by the additivity rule at the same temperature.

This difference is near to that of 3% also experimentally determined by the authors in a previous work [8] on a In – 5.5 wt % Al alloy.

As a consequence, the homogeneous liquid ternary alloy has a positive ΔV^M, in full agreement with the theoretical considerations concerning the immiscible liquids.[14]

B. *Determination of the viscosity*

The kinematic viscosity of the indium-aluminium-silver alloy was obtained by the oscillating cylindrical crucible method (with filled crucible), using the installation described in a previous paper, [15] the maximum error being smaller than 2%.

The working conditions have been generally similar to those in the density measurements. To avoid the scattering of the results and to eliminate the introduction of correction terms regarding the viscosity of the protective atmosphere, the viscosity measurements were carried out in vacuum of 10^{-4} torr, the loses of indium and silver through volatilization being small (of milligramme order).

The important elements in the viscosity computation — the logarithmic decrement of the damped oscillations and the oscillation period — were experimentally determined with a 10^{-4} and 10^{-3} sec precision.

From Campbell and Wagemann's investigations [7] regarding the system In—Al—Ag as well as from our previous work on a In — 5.5% Al alloy [8], we have approximately estimated the temperature range 590—800°, covering homogeneous and heterogeneous liquid domains for the chosen In—Al—Ag alloy.

---

[12] G. Cavalier, *Compt. rend.*, **244**, 2608 (1957).

[13] J. R. Wilson, *Metallurgical Reviews*, **10**, 558 (1965).

[14] O. J. Kleppa, "Liquid Metals and Solidification", Amer. Soc. Metals, Ohio, 1958, p. 60.

[15] St. Zămârcă, N. Petrescu, I. Ganovici and L. Ganovici, *Studii şi Cercetări Chim. Acad. R. S. România*, **15**, 657 (1967).

RESULTS AND DISCUSSION

The curve representing the dependency of the logarithmic decrement on temperature for the damped oscillations takes the "λ" shape, similar to that determined by Budde and Sauerwald[16] for the flowing time in the viscosity measurements on the systems Bi–Zn, Pb–Zn, carried out by horizontal capillary methods.

The peaks on both curves I and II, showing dependency of the decrement on temperature at the two filling levels of the crucible ($H_{II} > H_I$) coincide for the same temperature on the immiscibility line. This temperature is similar to that obtained by density measurements and it seems to be in agreement with Campbell and Wagemann's data[7] obtained by the direct-sampling method followed by density measurements in the solid state. By comparing with our previous data on a In – 5.5 wt% Al alloy (the 3rd curve in fig. 2) one may observe that the transition temperature from homogeneous to heterogeneous liquid T_i, shifts from $T_i = 725°$

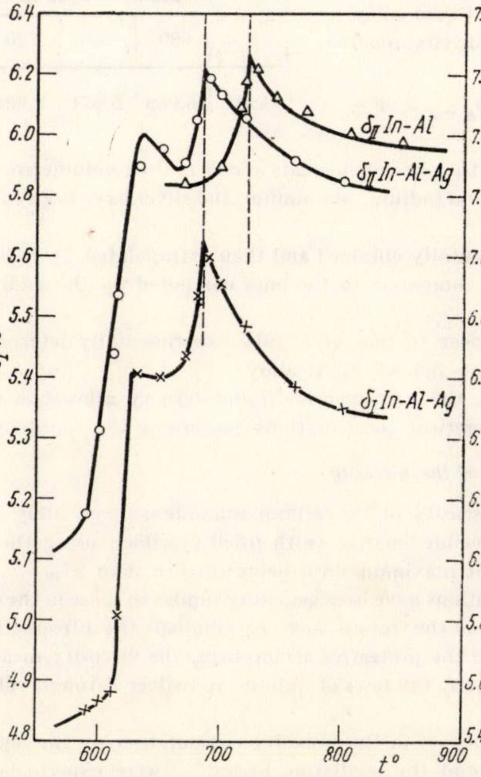

Fig. 2. — Dependency of the logarithmic decrement on the temperature of the damped oscillations in two liquid alloys from the systems: In–Al–Ag and In–Al.

---

[16] I. Budde and F. Sauerwald, *Z. phys. Chem.* (Leipzig), 3, 42 (1965).

of In — 5.5% Al alloy to $T_i = 700°$ of In — 5.3 wt% Al — 3.7% Ag alloy. Furthermore, the curve of the dependency of the logarithmic decrement on temperature for the damped oscillations as well as the oscillation period (Fig. 3) show important changes within the heterogeneous domain or the ternary miscibility gap.

Thus, at 665—670° an increase of the logarithmic decrement (more marked at the second level) was found up to 625°, when a sudden decrease which seems to diminish at 590° occurs. The oscillation period shows similar but contrary changes.

As it was shown by Glazov and Kizhevskaia, [9] if a second phase in a binary homogeneous liquid is formed through the intersection of liquidus line, the initial freezing stage will give rise to a rapid increase of the viscosity. If at a given temperature within the molten alloy in $L_1 + S$ state a solid crust was formed, the decrement would rapidly decrease since the system by its properties approaches the solid state. Taking into account the above, the possible interpretation with regard to the decrement change

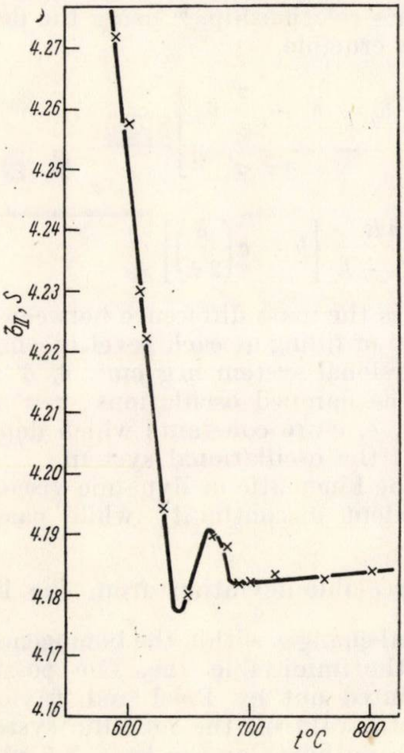

Fig. 3. — Dependency of the oscillation period on temperature for In — Al — —Ag alloy.

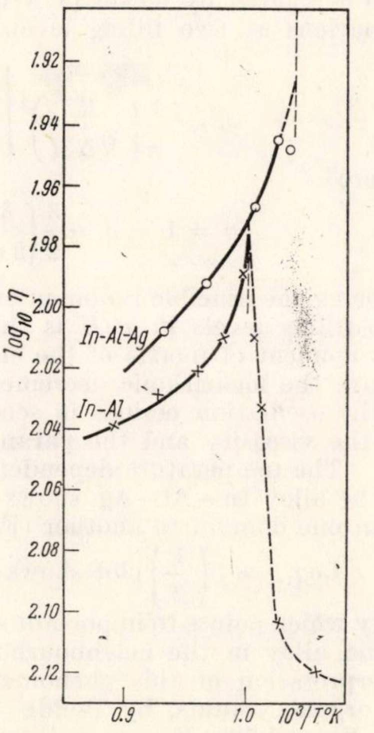

Fig. 4. — Dependency of the dynamic viscosity on temperature in two liquid alloys from the systems : In — Al — Ag and In — Al.

The values on the ordinate are negative.

for the In—Al—Ag alloy studied by us, is the following : the range from about 700 to 665° is probably the ternary miscibility gap $L_1 + L_2$ (liquid indium with aluminium and silver solutes, and liquid aluminium with indium and silver solutes). Within the range from about 665° to 625° (630°), the small increase of the decrement would probably correspond to a small viscosity increase of the ternary alloy, a common phenomenon for liquid metals and alloys in the neighbourhood of the freezing point. At the temperature of about 625—630°, taking into account the gravitational segregation with the separation into two layers of the liquid alloy In—Al—Ag, the initial freezing stage leads to the formation of an aluminium alloy crust. This is shown by the drop in the decrement as well as by the increase of the oscillation period, a process which seems to diminish just at the temperature of about 590°.

The kinematic viscosity of the homogeneous alloy In—Al—Ag was computed by means of Armbruster's relationship, [15] using the determinations at two filling levels of the crucible.

$$\nu = \frac{1}{\pi}\left(\frac{K}{R\,\Delta M}\right)^2 \left[\frac{\delta - \frac{\tau}{\tau_0}\delta_0}{\sqrt{\tau}\,\sigma} - \frac{\delta' - \frac{\tau'}{\tau_0}\delta_0}{\sqrt{\tau'}\,\sigma'}\right] \tag{7}$$

where

$$\sigma = 1 - a - \frac{3}{2}\left(\frac{\delta}{2\pi}\right) + \frac{2nR}{2H \pm h}\left[b - c\left(\frac{\delta}{2\pi}\right)\right] \tag{8}$$

R being the crucible radius in cm, ΔM is the mass difference between the two filling levels in g, H is the height of filling at each level in cm, K the moment of inertia of the empty torsional system in g·cm², δ, δ' and δ_0 are the logarithmic decrements of the damped oscillations ; τ, τ' and τ_0 the oscillation periods in seconds ; a, b, c are constants which depend on the viscosity and the parameters of the oscillational system.

The temperature dependency of the kinematic or dynamic viscosity of the alloy In—Al—Ag shows an evident discontinuity while passing from one domain to another (Fig. 4).

$\mathrm{Log}_{10} = f\left(\frac{1}{T}\right)$ plot shows an appreciable deviation from the linearity which points to important structural changes within the homogeneous liquid alloy in the neighbourhood of the immiscible line. The possible interpretation of this phenomenon pointed out by Reed and Taylor [17] on organic liquids, by Budde and Sauerwald on the metallic systems Bi—Zn and Pb—Zn, as well as by the authors [8] on the In — 5.5 wt % Al liquid alloy migh be similar to that given by Laughlin and Ubbelohde [18] and Ubbelohde [19] for the variation of the viscosity in the pre-freezing phenomena : "cluster formation" as well as on organic liquids is a true element to be considered in the case of liquid alloys which exhibit miscibility gaps, since a sort of finely divided emulsion is also possible to occur as a prelude of the gravitational segregation with the separation into two stratified layers. It follows that near the immiscibility line the viscosity of the liquid alloy grows due to the greater dimensions acquired by the "flowing unity" though, owing to the positive, ΔV^M, a decrease of the viscosity according to Batshinsky's relationship might be expected.

---

[17] T. M. Reed and T. E. Taylor, *J. Phys. Chem.*, **63**, 58 (1959).

[18] McLaughlin and A. R. Ubbelohde, *Trans. Faraday Soc.*, **56**, 989 (1960).

[19] A. R. Ubbelohde, "Melting and Crystal Structure", Oxford, Clarendon Press, 1965, p. 260.

CONCLUSIONS

The variation of the viscosity and density on ternary alloys which exhibit miscibility gaps in liquid state might show the structural changes : $L_{\text{homogeneous}} \rightarrow L_1 + L_2$ and $L_1 + L_2 \rightarrow L_1 + L_2 + S$.

The satisfactory agreement of the data obtained in the present study with Campbell and Wagemann's results regarding the In—Al—Ag alloy confirms the fact that precise viscosity and density measurements are direct continuous methods which justify their use in studying ternary alloys which exhibit miscibility gaps. The viscosity and density measurements on such liquid ternary alloys can also lead to defining their structural particularities to obtain data on the effect of the third element upon immiscibility in liquid state, as well as to draw the equilibrium diagrams in such ternary systems.

Revue Roumaine de Chimie, **14**, 183–188 (1969)

CINÉTIQUE DE LA DÉCOMPOSITION DE L'HYDRAZINE SUR DES COUCHES MINCES DE GERMANIUM

D. FĂTU et E. SEGAL

Université de Bucarest, Laboratoire de Chimie physique,
13, Bd. Republicii

Reçu le 28 mars 1968

On présente une étude cinétique de la décomposition de l'hydrazine sur des couches minces de germanium, obtenues par évaporation dans le vide et on détermine aussi la variation de la résistance électrique de ces couches pendant la réaction. La valeur réduite de l'énergie d'activation, ainsi que l'ordre de réaction égal à l'unité constituent des indications sur la marche de la réaction en régime de diffusion externe.

Le comportement catalytique du germanium a constitué l'objet de recherches commencées dès l'année 1932 par Hogness et Johnston [1] qui ont étudié l'activité catalytique de cet élément au cours de la réaction de décomposition du germanium. Des études concernant cette réaction, ainsi que d'autres travaux dédiés à une série de réactions d'oxydo-réductions catalysées par le germanium ont été publiés beaucoup plus tard, après l'année 1955, par Tamaru, Boudart et Taylor, [2–5] Roguinski, Frolov et Krylov, [6–8] Schwab, [9] Liashenko et Gorohovatski. [10] L'intérêt accordé aux propriétés catalytiques du germanium s'explique par le fait que celles-ci ne dépendent point de l'existence de niveaux *d* inoccupés (le germanium est un semi-conducteur typique qui ne contient point de tels niveaux [11]).

---

[1] T. K. Hogness et W. S. Johnston, *J. Amer. Chem. Soc.*, **54**, 3583 (1932).

[2] H. Taylor, *Canad. J. Chem.*, **33**, 838 (1955).

[3] K. Tamaru, M. Boudart et H. Taylor, *J. Phys. Chem.*, **59**, 801, 806 (1955).

[4] K. Tamaru, *J. Phys. Chem.*, **60**, 612 (1956).

[5] K. Tamaru, *J. Phys. Chem.*, **61**, 647 (1957).

[6] O. V. Krylov, S. Z. Roguinski et V. M. Frolov, *Doklady Akad. Nauk S.S.S.R.*, **111**, 63, 623 (1956).

[7] O. V. Krylov, S. Z. Roguinski et V. M. Frolov, „Fizica i fizico-khimia Kataliza", Izdatelstvo Akademii Nauk S.S.S.R., Moscou, 1960, p. 102.

[8] V. M. Frolov, *Kinetica i Kataliz*, **6**, 149 (1965).

[9] G. M. Schwab, *Adv. Catalysis*, **9**, 229 (1957).

[10] L. V. Liashenko et I.V. Gorohovatski, *Kinetica i Kataliz*, **8**, 694 (1967).

[11] S. Z. Roguinski, „Fizica i fizico-khimia Kataliza", Izdatelstvo Akademii Nauk S.S.S.R, Moscou, 1960, p. 5.

L'étude de la réaction de la décomposition de l'hydrazine sur des poudres de germanium et du germanium massif a été commencée par l'école soviétique.[6-8,10]

Dans cette note les auteurs présentent une étude cinétique de la décomposition de l'hydrazine sur des couches minces de germanium. Grâce à l'utilisation des couches minces, on peut effectuer en même temps des mesures cinétiques et des déterminations de la conductibilité électrique de la couche, en obtenant ainsi, dans certains cas, des informations supplémentaires sur le mécanisme du processus étudié.

PARTIE EXPÉRIMENTALE

L'hydrazine utilisée a été préparée suivant la méthode proposée par Audrieth,[12] à partir de l'hydrate d'hydrazine BDH, de pureté 99 %. Les couches minces ont été obtenues en évaporant le germanium polycristallin d'une spirale conique de wolfram, à la pression de 10^{-5} – 10^{-6} torr.

La variation de la résistance de la couche pendant l'évaporation dans le vide, ainsi que pendant la réaction, a été mesurée avec un voltohmmètre électronique Tesla de type BM–289, classe de précision 1,5. Les indications de l'instrument ont été vérifiées à l'aide des résistances étalon Métra. Pour le contrôle du vide, on a utilisé un vacuomètre de type Penning, la mesure de la pression dans le réacteur étant effectuée au moyen d'un manomètre à colonne de mercure. La variation de la hauteur de la colonne de mercure, due au changement de pression provoqué par la réaction, a été mesurée avec un cathétomètre, dont la précision a été augmentée jusqu'à 10^{-2} mm, à l'aide d'une vis micrométrique. La température du réacteur, déterminée avec un thermocouple Chromel-Alumel, est maintenue constante moyennant un régulateur de température de type Automatica, de précision ± 0,5°.

DESCRIPTION DE L'INSTALLATION

L'installation, représentée dans la figure 1, comporte trois parties :

a) *l'installation de vide* formée par : pompe rotative (*1*), pompe de diffusion (*2*), pièges de refroidissement (*3*) et vacuomètre (*4*) ;

b) *le dispositif d'introduction contrôlée* de l'hydrazine dans le réacteur, composé par l'ampoule (*5*) qui contient la substance, le ballon (*6*) dans lequel on introduit les vapeurs d'hydrazine, le manomètre à mercure (*7*) qui contrôle la pression dans le ballon (*6*), le tube capillaire (*8*) utilisé pour régler la pression initiale dans le réacteur, le manomètre (*9*) et le cathétomètre (*10*) qui mesurent la pression dans le réacteur ;

c) *le réacteur* 11 *et ses annexes*. Le réacteur comprend un ballon en verre razotherme, muni d'une résistance d'échauffement, isolé avec de l'asbeste et relié à l'installation par le rodage (*12*). Pour éviter l'échauffement du rodage, on utilise un serpentin de refroidissement, traversé par de l'eau. Le piège (*13*) est destiné à capter les gaz condensables du réacteur. Dans le réacteur se trouvent aussi un filament de wolfram (*14*) et une cellule (*15*) fixée près de la paroi du réacteur, utilisée pour mesurer la résistance de la couche mince et formée par un support rectangulaire en verre razotherme, poli optiquement, dans lequel on a encastré deux électrodes en platine. La résistance d'échauffement est alimentée par un autotransformateur (*16*), à travers un régulateur de température (*17*), monté en parallèle avec une résistance variable (*18*), destinée à améliorer la stabilisation de la température. Pour mesurer la température on a utilisé un thermocouple (*19*).

---

[12] L. F. Audrieth et B. Acherson Ogg., „Khimia guidrazina", Moscou, IL, 1954, p. 50.

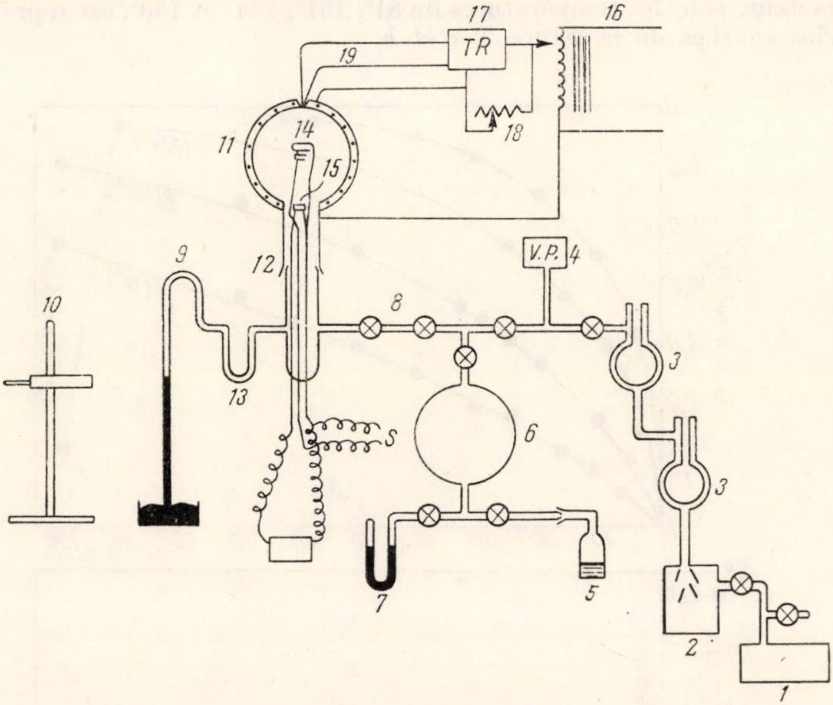

Fig. 1. — Schéma de l'installation :
1, pompe rotative ; *2*, pompe de diffusion ; *3*, pièges de refroidissement ; *4*, vacuomètre ; *5*, ampoule ; *6*, ballon ; *7*, manomètre à mercure ; *8*, cathétomètre ; *9*, tube capillaire ; *10*, manomètre ; *11*, réacteur ; *12*, rodage ; *13*, piège de condensation ; *14*, filament de wolfram ; *15*, cellule de mesure de la résistance ; *16*, autotransformateur ; *17*, régulateur de température ; *18*, résistance variable ; *19*, thermocouple.

RÉSULTATS ET DISCUSSIONS

A la pression de $10^{-5}-10^{-6}$ torr, on a déposé sur la surface intérieure de 348 cm^2 du réacteur une couche mince de germanium de densité superficielle égale à $4{,}5.10^{-4}$ g/cm^2, ce qui correspond à une épaisseur de $5{,}7.10^{-5}$ cm, si on considère la densité de la couche approximativement égale à celle du germanium massif.

Pendant l'évaporation, la température à la paroi du réacteur a été de 50° et pour sa stabilisation, la couche mince a été chauffée jusqu' à 250°.

L'hydrazine a été introduite dans le réacteur à une pression de 10 mm Hg. La variation de la pression et de la résistance de la couche mince, comme suite de l'introduction et de la décomposition de l'hydrazine dans le réacteur, pour les températures de 81°, 101°, 134° et 150°, est représentée par les courbes de la figure 2 *a* et *b*.

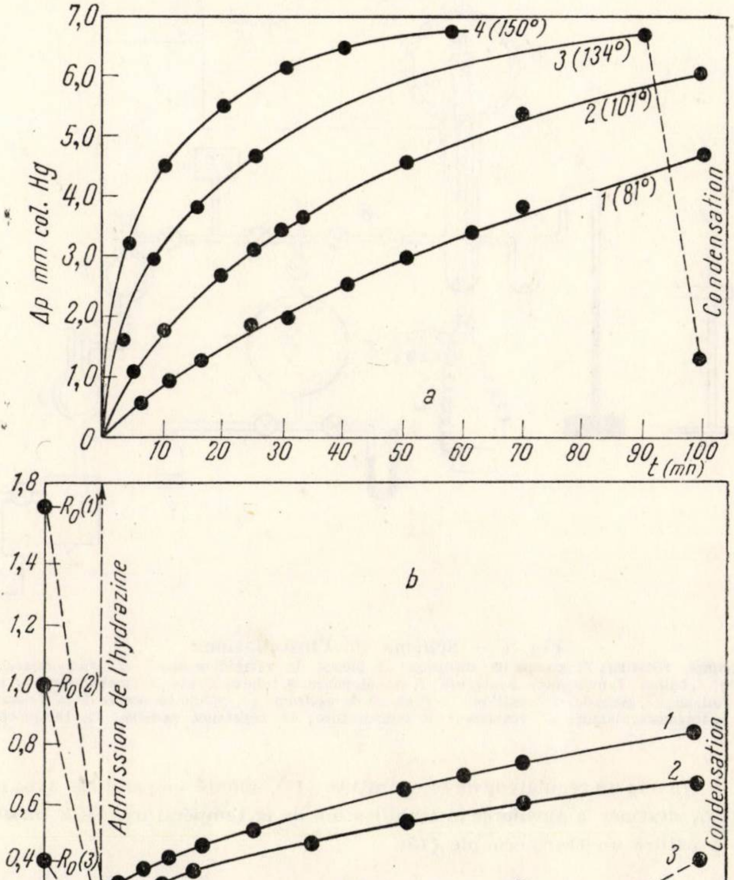

Fig. 2. — Variation de la pression totale (2*a*) et de la résistance électrique de la pellicule de germanium (2*b*), pendant la réaction, pour les températures de 81° (courbes *1*), 101° (courbes *2*), 134° (courbes *3*) et 150° (courbes *4*).

La réaction de décomposition de l'hydrazine sur divers catalyseurs peut être exprimée par l'équation chimique[12]

$$3N_2H_4 = 4(1-x)NH_3 + (1+2x)N_2 + 6xH_2$$

Pour vérifier cette équation, on a refroidi les produits de réaction à la température de l'azote liquide ; le rapport entre la pression totale et celle partielle des gaz non condensables résulte à peu près égal à 5 (fig. 2).

Vu que parmi les produits de réaction on n'a pas trouvé d'hydrogène, il résulte que $x = 0$ et l'équation chimique devient

$$3N_2H_4 = 4NH_3 + N_2$$

La réaction (fig. 2 *b*) est accompagnée d'une augmentation de la résistance de la couche mince de germanium, jusqu'à une certaine valeur inférieure à la valeur initiale. On revient à la valeur initiale par l'évacuation ou bien par la condensation des gaz dans le piège, à la température de l'azote liquide. Après chaque expérience, la couche a été dégazéifiée par échauffement à 250° et par évacuation. L'introduction de l'hydrazine dans le réacteur sans couche mince de germanium ne produit pas une variation mesurable de la pression, ce qui démontre que la vitesse de la réaction homogène en absence du catalyseur est négligeable.

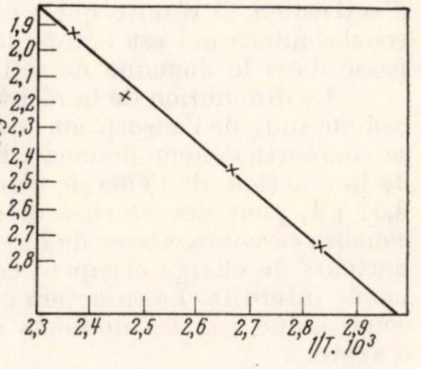

Fig. 3. — Variation de la constante cinétique k_1 avec la température. La droite d'Arrhénius.

Pour évaluer l'ordre de réaction on a utilisé la méthode intégrale. Les données expérimentales vérifient l'équation cinétique correspondant à un ordre de réaction égal à l'unité.

$$k_1 = \frac{2,303}{t_2 - t_1} \log \frac{P\infty - P_1}{P\infty - P_2}$$

où

k_1 — la constante cinétique ;

t_1, t_2 — deux valeurs successives du temps ;

P_1,P_2 — les pressions du mélange de gaz correspondant aux valeurs t_1 et t_2 du temps ;

$P\infty$ — la pression du mélange de gaz à la fin de la réaction.

Les constantes cinétiques, ainsi calculées pour les quatre valeurs de température auxquelles on a effectué des mesures, vérifient l'équation d'Arrhénius (fig. 3).

De la pente de la droite $\log k_1 = f(1/T)$ et de son ordonnée en origine, on obtient les valeurs apparentes suivantes pour l'énergie d'activation E, respectivement pour le coefficient préexponentiel A

$$E = 9\,000 \text{ cal/mole}$$
$$A = 5,87 \cdot 10^2 \text{ s}^{-1}$$

Etant donné la variation brusque de la résistance électrique de la couche mince de germanium à l'introduction de l'hydrazine dans le réacteur, on peut éliminer la chimisorption de celle-ci comme étape limitante.

De même, la réaction superficielle de décomposition de l'hydrazine avec libération d'azote

$$3N_2H_4\,(ads) \rightarrow 4NH_3\,(ads) + N_2(g)$$

ne peut être considérée comme étape limitante si on tient compte des conditions de la réaction. En effet, étant donné la pression et la température relativement élevées dans lesquelles a eu lieu la réaction, la valeur égale à l'unité de l'ordre de réaction, ainsi que la valeur réduite de l'énergie d'activation, il résulte que c'est le processus de diffusion du gaz vers la couche mince qui est l'étape limitante, ce qui signifie que la réaction se passe dans le domaine de diffusion externe.[13]

La diminution de la résistance électrique de la couche de germanium comme suite de l'adsorption de l'hydrazine (fig. 2 *b*) prouve que l'hydrazine se comporte comme donneur. En effet, la diminution, au moment initial de la réaction, de l'énergie d'activation de la conductibilité électrique de 0,37 eV, pour des couches de germanium pur, jusqu'à 0,21 eV, pour des couches en contact avec de l'hydrazine non décomposée, démontre que des porteurs de charge occupent certains niveaux additionnels situés dans la bande interdite. Le caractère de donneur de l'hydrazine est probablement conditionné par les doublets électroniques non participants des atomes d'azote.

La libération de l'azote (qui ne peut demeurer chimisorbé dans les conditions analysées [14]) diminue le nombre des porteurs de charge occupant ces niveaux, à mesure que la réaction avance. Il s'ensuit que la résistance électrique augmente, tout en continuant à rester inférieure à la valeur initiale, dû au fait que seulement une partie de l'ammoniac résulté de la réaction demeure dans la phase adsorbée.[15]

CONCLUSIONS

1. On a étudié la cinétique de la décomposition de l'hydrazine sur des couches minces de germanium.
2. Simultanément avec les mesures cinétiques, on a déterminé la variation de la conductibilité électrique des couches de germanium pendant la réaction.
3. Les données expérimentales obtenues, surtout la valeur réduite de l'énergie d'activation, ainsi que l'ordre de réaction égal à l'unité constituent des indications sur la marche de la réaction en régime de diffusion externe.

[13] S. L. Kiperman, „Vvedenie v kineticou gueteroguenykh kataliticheskikh reactzii", Izdatelstvo Akademii Nauk S.S.S.R., 1964, Moscou, p. 401.

[14] J. T. Low, *J. Phys. Chem.*, **59**, 543 (1955).

[15] W. H. Bratain et J. Bardeen, *Bell. syst. Tehn.*, **32**, 1 (1953).

Revue Roumaine de Chimie, 14, 189–195 (1969)

BASIC PERMANGANATES OF BISMUTH INVESTIGATIONS IN SOLUTION ON THE $[Bi_6(OH)_{12}](OH)_2(MnO_4)_4$-COMPLEX

C. DRĂGULESCU, I. JULEAN and ANA NIMARĂ

Centre for Chemical Research of the Academy
Timişoara, Bd. Mihai Viteazul 24

Received April 19, 1968

The reaction between bismuthyl perchlorate and potassium permanganate was radiometrically and spectrophotometrically investigated, and a soluble red-coloured combination was identified having the combination ratio BiO^+/MnO_4^- equal to 6/4. Based on this combination, a spectrophotometrical method was worked out in order to determine bismuth from oxides and alloys.

Investigations performed in the last time have shown that the bismuthyl ion is to be found in bismuthyl perchlorate solutions in a hexacondensed form of $Bi_6O_6^{6+}$ and $Bi_6(OH)_{12}^{6+}$ respectively.[1–6] It has an octahedral structure, and it can keep its condensation degree and even its structure in solid salts, too.[7] There have been identified also more basic products of this polycation in which one or several anions are replaced by groups of OH^- : $Bi_6O_6(OH)(NO_3)_5$, $Bi_6O_6(OH)_3(NO_3)_3$,[8] and $Bi_6O_6(OH)_3(ClO_4)_3$[5] respectively.

Among the basic combinations of bismuth, the permanganates seem to approach perchlorates as to their properties, forming like these a series of basic soluble and insoluble salts.

Among basic bismuth perchlorates the following may be mentioned : $(BiO)_2OHClO_4$; $Bi_3O_2(OH)_3(ClO_4)_2$,[9] while among the permanganates the following : $Bi_2O_2(OH)MnO_4 . 1.5\ H_2O$ and $Bi_3O_3(OH)_2MnO_4$.[10,11] Recent papers on basic bismuthyl perchlorates define them as products of the hydrolyzed hexamer $Bi_6(OH)_{12}^{+6}$.[2,5]

---

[1] F. Graner, A. Olin and L. G. Sillen, *Acta Chem. Scand.*, **10**, 476 (1956).

[2] A. Olin, *Acta Chem. Scand.*, **11**, 1445 (1957); **13**, 1971 (1959).

[3] R. W. Holmberg, K. A. Kraus and J. S. Johnson, *J. Amer. Chem. Soc.*, **78**, 5506 (1956).

[4] J. S. Johnson, G. Scatchard and K. A. Kraus, *J. Phys. Chem.*, **63**, 787 (1959).

[5] R. S. Tobias, *J. Amer. Chem. Soc.*, **82**, 1070 (1960); **82**, 3244 (1960).

[6] H. A. Devy, M. D. Danford and P. A. Agron, *J. Chem. Phys.*, **31**, 1458 (1959).

[7] V. A. Maroni and T. C. Spira, *J. Amer. Chem. Soc.*, **88**, 1410 (1966).

[8] G. Gattow and D. Schott, *Z. anorg. Chem.*, **324**, 31 (1963).

[9] M. Prytz and P. Nagel, *Z. anorg. Chem.*, **227**, 65 (1936).

[10] Fr. Hein and H. Holzapfel, *Z. anorg. Chem.*, **248**, 77 (1941).

[11] W. Klemm, *Ber. dtsch. chem. Ges.*, **75**, 1600 (1942).

Considering the similar composition of permanganates and perchlorates it would seem quite normal that also the basic permanganates might be defined as products of hexacondensed bismuthyl ion hydrolysis having the formulae : $[Bi_6O_6](OH)_3(MnO_4)_3$ and $[Bi_6O_6](OH)_4(MnO_4)_2$.

Hein and Holzapfel [10] showed in their papers concerning the basic bismuth permanganates that prior to the precipitation of the two basic permanganates a cherry-red colour appeared which was not yet investigated by them.

Since the two insoluble basic permanganates may be easily inserted into the series of hexamer bismuthyl ion hydrolysis, we considered it would be interesting to investigate whether the red colour which appears at the beginning in the mixture of a bismuthyl perchlorate solution with sodium or potassium permanganate is also due to a basic but soluble bismuth combination appearing prior to the precipitation as an intermediate product.

The aim of the present paper is to investigate this soluble combination, both as to its properties and possibilities of utilization.

EXPERIMENTAL

Working method. In order to observe the precipitation mechanism in time, we performed a radiometrical investigation by marking bismuthyl perchlorate with Bi^{210} ; the coloured soluble product was investigated spectrophotometrically.

Reagents. The bismuthyl perchlorate $BiOClO_4 . H_2O$ was prepared from bismuth oxide p. a. by dissolving in 35 per cent perchloric acid and by crystallizing in vacuum. Bismuthyl perchlorate solutions were prepared by dissolving in distilled water and by cheking the factor complexometrically. In the same way the marked bismuthyl perchlorate was prepared by starting from Bi_2O_3, marked with Bi^{210}.

Potassium permanganate. Volumetrical standard BDH solutions were used.

Apparatus. Electronical counter "Vakutronik VAM–16 D" with "VAZ 410" G.M.tubes Spectrophotometer "UNICAM SP–800". and PH-meter "Radiometer" with a glass electrode "G –202 C".

RESULTS AND DISCUSSIONS

The papers by Hein and Holzapfel [10] as well as our own previous observations show that the forming reaction of insoluble basic permanganates depends on the reactant concentration and on time. It is rather difficult to establish the reactant equilibrium. This fact determined Hein and Arway [12] to suggest the separation of the product 8 hours after mixture.

In order to investigate the separated products, the radiometrical measurements on the solutions were performed 3 days after mixture. A number of 20 samples were carried out, and the permanganate concentration was to be maintained constantly (0.004 M) also when adding increasing amounts of bismuthyl perchlorate from 0 up to 0.04 M.

---

[12] Fr. Hein and V. Arway, *Angew. Chem.*, **A–60**, 157 (1948).

Figure 1 presents the results.

The figure shows that for values of the ratio BiO^+/MnO_4^- between 2 and 3 which correspond to insoluble products $Bi_2O_2(OH)MnO_4$ and $Bi_3O_3(OH)_2MnO_4$, bismuth is completely separated from the solution. The fact that from samples where the ratio between BiO^+/MnO_4^- is smaller than 1.5 no precipitate is separated but appears only a red colour, shows that in this field a soluble basic bismuth permanganate is formed whose composition could perhaps agree with a ratio between $BiO^+/MnO_4^- = 1.5$.

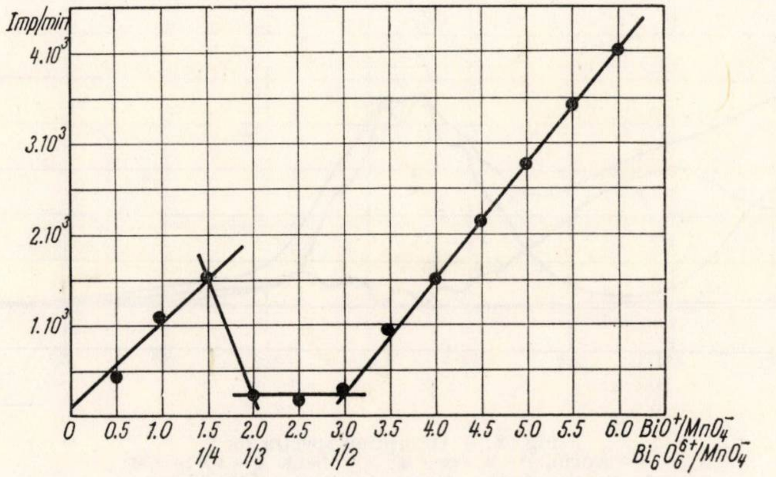

Fig. 1. — Radioactivity of solutions for $BiOClO_4.H_2O + KMnO_4$ mixtures at various ratios.

In order to establish more exactly the combination ratio between bismuthyl perchlorate and potassium permanganate in the soluble coloured product, the performed spectrophotometrical determinations with a solution whose ratio between BiO^+ and MnO_4^- is greater than 1.5 were carried out immediately after mixing, in order to avoid the separation of insoluble basic permanganates. In this way we could observe that even at a very great bismuthyl excess versus permanganate, the Lambert-Beer's law was observed within the spectrophotometrical measurements.

In order to be able to characterize the absorbant which at the beginning is specific for the complex, we traced the absorption spectrum of the reactants and of the coloured product versus water and permanganate. The absorption curves are represented in figure 2.

From the figure it results that the absorption spectrum of the complex is roughly similar to that of permanganate, however distinguishable from it by a series of maxima of which the greatest is to be found at the wavelength of 400 mμ. Therefore all the spectrophotometrical measurements performed on the complex were carried out *versus* permanganate at this wavelength.

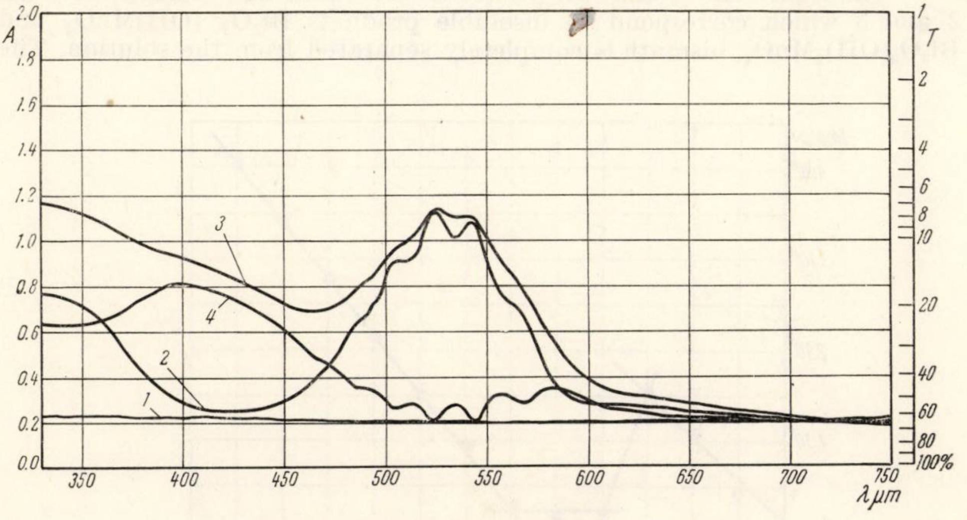

Fig. 2. — Absorption spectra for:
1 – $BiOClO_4$ $C = 6 \times 10^{-4}$ M; *2* – MnO_4K $C = 4 \times 10^{-4}$ M;
3 — Complex of water reference; *4* – Complex of MnO_4^- reference.

Determination of the combination ratio

In order to determine the combination ratio between permanganate and bismuthyl ion, we used : *1)* the molar ratio method,[13] *2)* the slope ratio method,[14] and *3)* the Job's method.[15]

By expressing the results, although normally it would have been necessary to report permanganate *versus* $Bi_6(OH)_{12}^{6+}$ (this being the ion which is in the solution) because of the easiness of representing, we preferred to report MnO_4^- *versus* BiO^+. The determination results are shown in figures 3, 4 and 5.

By all the three methods the same conclusion results, namely that at an immediate mixing of bismuthyl perchlorate with potassium permanganate a soluble product is formed which is red coloured with a composition corresponding to the ratio $BiO^+/MnO_4^- = 3/2$. This product may be compared from the composition viewpoint with bismuthyl perchlorate $Bi_3O_2(OH)_3(ClO_4)_2$ syntesized by Prytz and Nagel.[9]

The compound can be expressed assuming as a basis the existence of hydrolyzed hexamer products $Bi_6(OH)_{12}^{6+}$ as $[Bi_6(OH)_{12}]$ $(OH)_2(MnO_4)_4$ or $[Bi_6O_6](OH)_2(MnO_4)_4.nH_2O$.

---

[13] H. J. Yoe and A. L. Jones, *Ind. Eng. Chem. Anal.*, **Ed. 16**, 111 (1944).

[14] A. E. Harwey and D. L. Manning, *J. Amer. Chem. Soc.*, **72**, 4488 (1950).

[15] P. Job, Compt. Rend., **180**, 928 (1925).

The reaction through which this product is formed can be expressed as follows:

$$Bi_6(OH)_{12}^{6+} + 6ClO_4^- + 4(K^+ + MnO_4^-) + 2H_2O \rightleftharpoons$$
$$[Bi_6(OH)_{12}](OH)_2(MnO_4)_4 + 2(H^+ + ClO_4^-) + 4(K^+ + ClO_4^-).$$

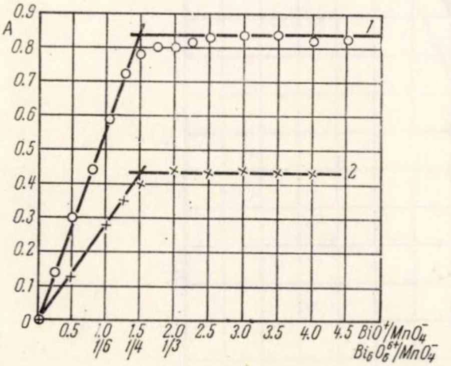

Fig. 3. — Molar ratio method.
— $c_{MnO^-} = \times 10^-$; — $c_{MnO_4^-} = 2 \times 10^{-4}$ M

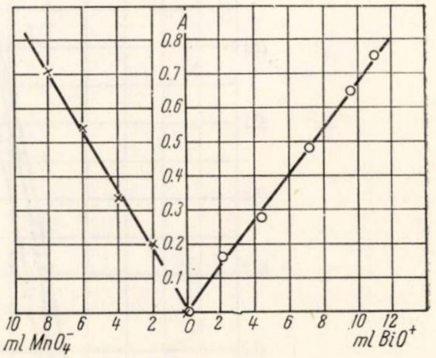

Fig. 4. — Slope ratio method.

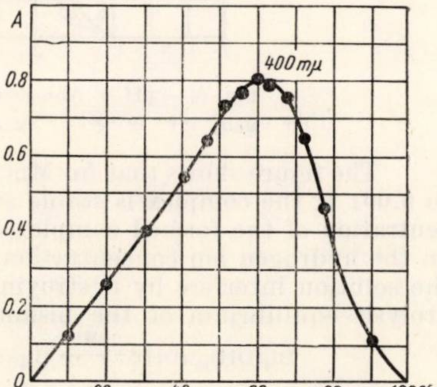

Fig. 5. — Job curves for equimolecular $BiOClO_4$ and $KMnO_4$ solutions. Concentration of the ions BiO^+ and $MnO_4^- = 1 \times 10^{-3}$ M.

From the above reaction it results that the forming of this complex depends, besides on the reactant concentration, also on the hydrogen ion concentration of the solution. In order to observe the influence of the hydrogen ion concentration and the influence of the pH-value respectively, upon the formed complex concentration, a series of determinations were performed with the aim of observing the variation of the complex concentration (the solution absorbent respectively) function of the pH-value and of the permanganic anion concentration. The results are graphically presented in figure 6.

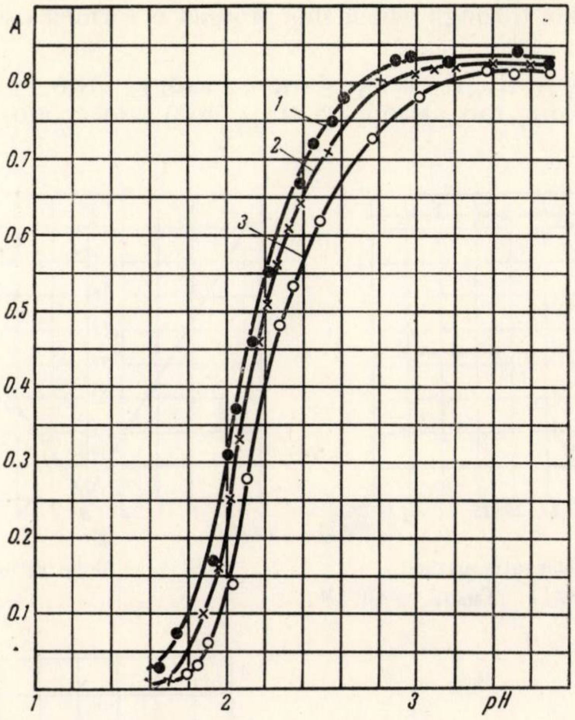

Fig. 6. — pH — Absorbance curves for $C_{BiO^+} = 8 \times 10^{-4}M$:
$1 - C_{MnO_4^-} = 6 \times 10^{-4}$ M; $2 - C_{MnO_4^-} = 8 \times 10^{-4}$ M; $3 - C_{MnO_4^-} = 1 \times 10^{-3}$M

The figure shows that for MnO_4^- concentrations ranging from 0.0006 to 0.001 M the complex is stable at a pH-value greater than 3. If the concentration of the formed complex has a value smaller than 3, it depends on the hydrogen ion concentration of the solutions. The hydrogen ions of the solution interfere by destroying the complex; they act upon the hydrolysis equilibrium of the bismuth ion by shifting it as follows:

$$\begin{array}{l} Bi_6(OH)_{12}(OH)_2^{4+} \xrightarrow{2H^+} Bi_6(OH)_{12}^{6+} \\ \qquad\qquad\qquad\qquad\qquad \downarrow\uparrow \\ \qquad\qquad\qquad\qquad 6Bi(OH)_2^+ \xrightarrow{6H^+} 6BiOH^{2+} \xrightarrow{6H^+} 6Bi^{3+}. \end{array}$$

Thus, the $[Bi_6(OH)_{12}](OH)_2(MnO_4)_4$ complex is formed by the reaction between bismuthyl perchlorate and permanganate at a pH-value greater than 3 provided that the permanganate should be in excess. Since in this reaction phenomena of hydrolysis, condensation and complexion interfere, the calculation of the stability constant of this complex becomes complicate because of the necessity to know also the relationship among them.

Spectrophotometrical determination of bysmuthyl as $[Bi_6(OH)_{12}](OH)_2(MnO_4)_4$

The previously presented results allow to show that bismuth can be very easily determined spectrophotometrically in the form of the above described complex. The method is very sensitive, fast and needs reagents available in any laboratory. The method can be easily applied in case of bismuth determination from oxides and alloys. In case of determination from salts it is necessary to remove the anions which precipitate with the bismuthyl ion (Cl^-, NO_3^-, SO_4^{2-}, etc.).

Reaction conditions. To determine 0.1 mg BiO^+, 10 ml KMO_4 2×10^{-3} M were used in an aqueous medium. The optimal time to measure the absorbant is up to 10 minutes after preparation of the solutions. The Lambert-Beer's law is observed in a range within 0.002 g/l — 0.3 g/l BiO^+ at a pH-value, greater than 3.

The average molar absorption coefficient calculated on the calibration curve is 7.10^4.

Influence of foreign ions. Foreign coloured ions absorbing at $\lambda = 400$ mμ, e. g. Cu, Fe, Co, Ni interfere and hinder the determinations. Therefore they must be removed. In the determination also the effect of colourless ions such as Pb^{2+}, Zn^{2+}, Cd^{2+} and Sn^{2+} was observed in solutions containing 0.1 mg bismuth. The results obtained are shown in table 1.

Table 1

Influence of foreign ions on bismuth determination

Foreign ion				
Nature	Added quantity mg	X/Bi[a]	Absorption	Interference[b] %
Cd^{2+}	0.12	1.2	0.94	+42
	0.04	0.4	0.74	+12
	0.02	0.2	0.66	0
Zn^{2+}	0.06	0.6	0.77	+16
	0.04	0.4	0.74	+12
	0.02	0.2	0.68	+ 3
Pb^{2+}	0.04	0.4	0.82	+24
	0.02	0.2	0.72	+ 9
	0.01	0.1	0.67	+1.5
Sn^{2+}	0.04	0.4	0.83	+25
	0.02	0.2	0.69	+4.5
	0.01	0.1	0.67	+1.5

[a] X/Bi represents the ratio between the foreign ion and bismuth.

[b] The interference was calculated by means of the relation 100 $\Delta A/A_0$ where A_0 represents the corresponding absorbants only for the bismuth ion, being $A_0 = 0{,}66$. and Δ A is the absorbant variation when a foreign ion is added.

CONCLUSIONS

By radiometric and spectrophotometric method a new basic bismuth permanganate was identified in solution to which the following formula $Bi_6(OH)_{12}$ $(OH)_2$ $(MnO_4)_4$ could be attributed. The spectrophotometric determination of the bismuth, based on the formation of this compound, s disturbed by the coloured ions and by the Cd^{2+}, Zn^{2+}, Pb^{2+} and Sn^{2+} ions.

Revue Roumaine de Chimie, **14**, 189–195 (1969)

Revue Roumaine de Chimie, 14, 197–200 (1969)

CHEMISCHE BESTIMMUNG DER BASIZITÄT DES $[PV_{12}O_{36}]^{7-}$-HETEROPOLYANIONS

RALUCA RIPAN und V. CORDIŞ

Aus dem Chemischen Institut der Akademie, Zweigstelle Cluj,
Str. Donath, 59–65

Eingegangen am 11. Juni 1968

Vorliegende Arbeit befaßt sich mit der Bestimmung der Basizität des Phosphor-12 Vanadin-Heteropolyanions anhand seiner Reaktion mit Ag- und Tl-Salzen einer Reihe von null-, mono-, di- und tribasischen Komplexamminen des Co^{3+}, sowie mit einigen organischen Basen verschiedenen Molekulargewichts. Die Synthese oben genannter Verbindungen zeigte eine zwischen 3 und 7 liegende Basizität des Phosphor-12 Vanadin-Heteropolyanions.

Das Studium der Basizität des $[PV_{12}O_{36}]^{7-}$-Heteropolyanions wurde sowohl potentiometrisch[1] als auch chemisch durch die Bildung schwerlöslicher Ag- und Tl-Salze in wässerigen Lösungen sowie der Salze einer Reihe null-, mono-, di- und tribasischer Komplexammine des Co^{3+} und einer Reihe organischer Basen mit verschiedenem Molekulargewicht verfolgt.

EXPERIMENTELLES

Bei der Synthese der in Tabelle 1 angegebenen Verbindungen könnte sowohl die Phosphor-12 Vanadinsäure ($H_7PV_{12}O_{36}$) als auch ihr Natriumsalz ($Na_3H_4PV_{12}O_{36}$) angewendet werden, da kein unterschiedliches Verhalten festgestellt wurde. Natrium-Phosphor-12 Vanadat wurde nach dem in der Literatur[2] beschriebenen Verfahren dargestellt, Phosphor-12 Vanadinsäure durch das Passieren der Natriumsalzlösung über eine Amberlytesäule IR–120, Form H.

Dadurch, daß der Stabilitätsbereich der Phosphor-12 Vanadinsäure zwischen pH = = 1,5–2,5 liegt und das in Wasser gelöste Natriumsalz dieser Säure einen pH-Wert von 2,5 besitzt,[1] mußte der pH-Wert aller Fällungsreagenzien mit Hilfe von HCl auf 2,0–2,5 eingestellt und das Auswaschen der Niederschläge mit gesäuertem Wasser von gleichem pH durchgeführt werden. In allen Fällen wurden kristalline verschiedenfarbige Niederschläge erhalten.

Aufgrund der Analysenergebnisse der erhaltenen Salze (s. Tabelle 1) wurden die entsprechenden Formeln festgesetzt. Vanadin wurde gravimetrisch mit O-Oxychinolin[3] sowie maß-

---

[1] R. Ripan, A. Duca und V. Cordiş, *Rev. Roumaine Chim.*, **12**, 375 (1967).

[2] A. B. Bekturow und A. K. Iliasowa, *Izvest. Akad. Nauk Kasakh. S.S.R., Trud. Inst. Khim. nauk*, **10**, 1964.

[3] L. Erdey, „Theorie und Praxis der gravimetrischen Analyse'', II. Band, Akadémiai Kiadó, Budapest, 1964, S. 570.

Tabelle 1

Salze des Phosphor-12 Vanadin-Heteropolyanions

Lfd. Nr.	Angewendete Salze zur Fällung dem $[PV_{12}O_{36}]^{7-}$- Anion		%										Erhaltene Verbindungen
			V	P	Co	N	C	H	H_2O	Cl	Ag	Tl	
1	$AgNO_3$	*Gef.* :	27,63	1,38					8,15		33,48		$Ag_7PV_{12}O_{36}.10H_2O$
		Ber. :	28,42	1,43					8,36		35,07		
2	$TlOOC\text{-}CH_3$	*Gef.* :	23,15	1,12					1,93			53,93	$Tl_7PV_{12}O_{36}.3H_2O$
		Ber. :	22,64	1,14					1,99			52,93	
3	$\left[Co(NH_3)_3(NO_3)_3\right]$	*Gef.* :	34,01	1,72	7,36	7,25		3,24	9,59				$\left[Co(NH_3)_3NO_3(H_2O)_2\right]_2H_3PV_{12}O_{36}9H_2O$
		Ber. :	34,01	1,77	6,50	6,22		2,26	9,11				
4	$\left[Co(NH_3)_4(NO_2)_2\right]Cl$ *trans*	*Gef.* :	26,30	1,31	10,99	15,34		3,29	16,15				$\left[Co(NH_3)_4(NO_2)_2\right]_4H_3PV_{12}O_{36}.14H_2O$
		Ber. :	26,09	1,31	10,34	14,30		3,36	17,9				
5	$\left[Coen_2Cl_2\right]Cl$ *trans*	*Gef.* :	25,83	1,31	10,14	9,84	8,99	3,79	4,99	13,05			$\left[Coen_2Cl_2\right]_4H_3PV_{12}O_{36}.6H_2O$
		Ber. :	26,28	1,33	10,12	9,61	8,24	3,39	4,64	12,18			
6	$\left[Coen_2CO_3\right]Cl$	*Gef.* :	26,30	1,29	10,25	9,69	8,86	4,25	10,02				$\left[Coen_2CO_3\right]_4H_3PV_{12}O_{36}.13H_2O$
		Ber. :	25,38	1,28	9,77	9,29	7,96	3,85	9,71				
7	$\left[Co(NH_3)_5NO_2\right](NO_3)_2$	*Gef.* :	34,75	1,63	7,27	11,42		3,10	7,43				$\left[[CoNH_3)_5NO_2\right]_2H_3PV_{12}O_{36}.7H_2O$
		Ber. :	35,43	1,79	6,22	9,72		3,69	7,30				
8	$\left[Coen_2ClPy\right]Cl_2$	*Gef.* :	31,07	1,52	6,68	7,70	11,41	3,55	7,96	4,50			$\left[Coen_2ClPy\right]_2H_3PV_{12}O_{36}.8H_2O$
		Ber. :	33,04	1,67	6,36	7,56	11,66	3,29	7,78	3,88			
9	$\left[Co(NH_3)_6\right]Cl_3$	*Gef.* :	35,71	1,69	7,18	9,72		3,59	9,17				$\left[Co(NH_3)_6\right]_2HPV_{12}O_{36}.9H_2O$
		Ber. :	35,95	1,82	6,92	9,86		3,22	8,92				
10	Pyridin C_5H_5N	*Gef.* :	32,34	1,53		5,84	20,82	2,77	3,09				$(C_5H_5N)_7PV_{12}O_{36}.3H_2O$
		Ber. :	33,51	1,69		6,45	23,00	2,24	2,95				
11	Anilinchlorhydrat C_6H_8NCl	*Gef.* :	31,10	1,53		5,31	25,70	3,47	7,63				$(C_6H_8N)_7PV_{12}O_{36}.8H_2O$
		Ber. :	30,28	1,53		4,84	24,93	3,56	7,13				
12	Guanidinchlorhydrat CN_3H_6Cl	*Gef.* :	35,10	1,70		16,71	4,52	3,24	4,50				$(CN_3H_6)_7PV_{12}O_{36}.4H_2O$
		Ber. :	35,78	1,81		17,19	4,91	2,92	4,21				
13	O-Oxychinolin C_9H_7ON	*Gef.* :	32,52	1,53		3,26	25,70	3,13	5,96				$(C_9H_7ON)_4H_3PV_{12}O_{36}.6H_2O$
		Ber. :	33,22	1,67		3,03	23,39	2,33	5,85				
14	O-Phenantrolin $C_{12}H_8N_2$	*Gef.* :	31,59	1,37		5,65	31,53	3,07	5,55				$(C_{12}H_8N_2)_4H_3PV_{12}O_{36}.6H_2O$
		Ber. :	30,00	1,51		5,46	28,09	2,20	5,26				
15	Chininchlorhydrat $C_{20}H_{24}O_2N_2.2HCl$	*Gef.* :	26,13	1,33		3,55	29,03	4,06	4,30				$(C_{20}H_{24}O_2N_2H_2)_3H_4PV_{12}O_{36}.6H_2O$
		Ber. :	26,50	1,34		3,63	31,13	4,07	4,68				

analytisch durch Titration mit Mohrsalz, Phosphor kolorimetrisch,[4] Stickstoff, Kohlenstoff und Wasserstoff durch die Mikromethode nach Dumas bestimmt. Der Wassergehalt wurde durch 3stündiges Trocknen der Verbindungen bei 110° bestimmt.

DISKUSSION UND ERGEBNISSE

Allgemein sind Heteropolysäuren durch zweierlei Basizitätsarten charakterisiert : eine starke Basizität entsprechend der Basizität der Säure, deren zentrales Atom komplexbildend wirkt und eine schwache Basizität, die bei der Bildung des Heteropolyanions erscheint. Die Gesamtbasizität des Heteropolyanions ist die Summe dieser beiden Basizitäten.

Tabelle 2

Molekulargewichte der angewendeten Kationen und organischen Basen zur Fällung des $[PV_{12}O_{36}]^{7-}$-Heteropolyanions

Lfd. Nr.	Kationen und organische Basen	Molekulargewicht
1	Ag^{+}	107.88
2	Tl^{+}	204.39
3	$[Co(NH_3)_3NO_3(H_2O)_2]^{2+}$	208.07
4	$[Co(NH_3)_4(NO_2)_2]^{2+}$	219.06
5	$[Co\,en_2Cl_2]^{+}$	249.90
6	$[Co\,en_2CO_3]^{+}$	238.99
7	$[Co(NH_3)_5NO_2]^{2+}$	190.10
8	$[Co\,en_2ClPy]^{2+}$	293.54
9	$[Co(NH_3)_6]^{3+}$	161.13
10	C_5H_5N	79.10
11	C_6H_8N	94.12
12	CN_3H_6	60.09
13	C_9H_7ON	145.15
14	$C_{12}H_8N_2$	180.22
15	$C_{20}H_{24}O_2N_2H_2$	326.41

Aus Tabelle 1 und 2 ist ersichtlich, daß die Fällung des $[PV_{12}O_{36}]^{7-}$-Heteropolyanions von Molekulargewicht und Molekularvolumen abhängt. Ag- und Tl-Ionen, sowie organische Basen mit relativ kleinem Molekulargewicht, wie z. B. Pyridin, Anilin und Guanidin bilden mit dem Phosphor-12 Vanadin-Heteropolyanion heptabasische Salze. Das dreiwertige Kobaltkomplexkation $[Co(NH_3)_6]^{3+}$, dessen Molekulargewicht in der Reihe der angewandten Kobaltkomplexkationen am kleinsten ist, bildet ein hexabasisches Phosphor-12 Vanadat. Die ein- und zweiwertigen Komplexkationen, sowie die organischen Basen *o*-Oxychinolin und *o*-Phenantrolin bilden tetrabasische Salze. Mit Chinin, welches das größte Molekulargewicht von allen bisher erwähnten Kationen und organischen Basen hat, bildet das Phosphor-12 Vanadin-Heteropolyanion ein tribasisches Salz. Daraus folgt, daß bei der Bildung dieser Salze nur die erste Basizität

---

[4] Iu. N. Knipowich und Iu. V. Morachewski, „Analis mineralnowo syria", Leningrad, 1956, S. 329–331.

(die starke Basizität) des Phosphor-12 Vanadin-Heteropolyanions mitwirkt.

Im Falle des $[Co(NH_3)_3(NO_3)_3]$-Nichtelektrolyten findet in der Lösung eine Hydratationsisomerie statt, da er sich wie ein dibasisches Kobaltkomplexammin $[Co(NH_3)_3NO_3(H_2O)_2](NO_3)_2$ verhält.

SCHLUSSFOLGERUNGEN

— Die durch die Synthese einer Reihe von Salzen des Phosphor-12 Vanadin-Heteropolyanions bestimmte Basizität liegt zwischen 3 und 7, wobei die höchste mit der potentiometrisch bestimmten in Übereinstimmung ist.

— Die Molzahl der an das Phosphor-12 Vanadin-Anion gebundenen Kationen, beziehungsweise organischen Basen nimmt mit wachsendem Molekulargewicht ab.

Revue Roumaine de Chimie, **14**, 201–207 (1969)

COMPLEXES OF LANTHANIDE HALOGENOACETATES WITH 1-10-PHENANTHROLINE AND 2-2′-DIPYRIDYL (II)

P. SPACU and ELENA ANTONESCU

Centre of Inorganic Chemistry, Bucharest, Spl. Independenţei 89

Received May 25, 1968

The paper presents 26 new compounds of tripositive rare earths (lanthanides) with mono-, di- and trichloroacetic acids and with ligands containing heterocyclic nitrogen as: 2-2'-dipyridyl, 1-10-phenanthroline, and 4-7-diphenylphenanthroline. For characterizing the new prepared compounds, visible, ultraviolet and infrared spectrophotometric studies were performed as well as a thermogravimetric study. Under the action of ultraviolet rays, europium compounds manifest an intense red fluorescence.

The coordination compounds of tripositive rare earths (lanthanides) with ligands containing heterocyclic nitrogen acquired special interest because of their unexpected stability, fluorescence characteristics and possible applications in laser devices. [1–4]

In carrying on our studies [5] we prepared a new series of halogenoacetic compounds of rare earths with 1-10-phenanthroline and 2-2′-dipyridyl as well as with some of their derivatives, in order to observe on the one hand their chemical and physico-chemical behaviour and on the other hand the influence of substituents on the characteristics of these compounds.

The compounds already prepared have the general form $[Ln(HalAc)_3B]$, where:

$$Ln = La, Ce, Pr, Nd, Sm, Eu, Dy, Er.$$
$$HalAc = CClH_2COO^-, CCl_2HCOO^-, CCl_3COO^-$$

B = 1-10-phenanthroline, 2-2′dipyridyl, 4-7-diphenylphenanthroline. The experimental results led to the ratios 1 : 3 : 1 for Ln : halogenoacetate : chelating agent, irrespective of the amount of chelating agent added. It is quite possible that this situation was due to steric impediments. Literature moreover indicates some compounds of the same type we prepared with rare earth acetates, where phenanthroline and dipyridyl interfere only in the ratio of 1 : 1.[6] Even in the case of rare earth chlorides,

---

[1] F. A. Hart and F. P. Lamming, *J. Inorg. Nuclear Chem.*, **27**, 1825 (1965).
[2] R. G. Charles and E. P. Riedel, *J. Inorg. Nuclear Chem.*, **28**, 3005 (1966).
[3] N. I. Lobanov and V. A. Smirnova, *Zhur. neorg. Khim.*, **10**, 1593 (1956).
[4] S. P. Sinha, *J. Inorg. Nuclear Chem.*, **27**, 115 (1965).
[5] P. Spacu and E. Antonescu, *Z. Chem.*, **7**, 163 (1967).
[6] F. A. Hart and F. P. Lamming, *J. Inorg. Nuclear Chem.*, **27**, 1605 (1965).

there are found for the last four elements only compounds in which phenanthroline and dipyridyl are in the same 1 : 1 ratio. [7]

The compounds we obtained are generally anhydrous except some dichloroacetates and trichloroacetates from dipyridylic series containing one or two water molecules, as follows

$$[Ln(CCl_2HCOO)_3\ dip].H_2O \text{ where } Ln = Ce, Dy, Eu, Er$$
$$[Ln(CCl_3COO)_3dip].2H_2O \text{ where } Ln = Sm, Eu, Dy, Er$$

except cerium, whose both compounds crystallize with a molecule of water.

All compounds we prepared are solid, non-hygroscopic and very stable in time, unlike rare earth halogenoacetates which can be obtained in the solid state solely by evaporation of the solvent and by long-time drying on P_2O_5 .[8] The colour of either compound series is similar to that of the corresponding lanthanide ion except cerium compounds which are characterized by a light yellow colour. As concerns the solubility, some differences between the three compound series were stated. All of them are insoluble in alcohol, ether, benzene and dioxane. A certain solubility in alcohol is however observed for dipyridylic compounds whose preparation is, for this reason, less efficient. For avoiding this drawback, a certain amount of ether was added on their preparation. A much higher solubility was observed for dipyridylic complexes in pyridine and piperidine. The difference from the other compound series is more marked in this case : thus the phenanthrolinic compounds are soluble only by heating in pyridine and not at all in piperidine, whereas the diphenylphenanthrolinic ones are insoluble in both solvents. Even in the dipyridylic series some differences as concerns the solubility in piperidine were observed. Whereas dichloroacetates and trichloroacetates are generally easyly soluble, monochloroacetates are insoluble in piperidine. These differences concerning solubility of dipyridylic halogenoacetates of rare earths in piperidine coincide with the amount in crystallization water of the same compounds. As we showed, only the dipyridylic di- and trichloroacetates of Ce, Eu, Sm, Dy and Er contain crystallization water, and even these compounds are easy to solve in piperidine. The corresponding anhydrous derivates of lanthanum are however not soluble in piperidine.

By evaporating the excess of piperidine from the yellow solution resulted after solving, a viscous liquid is obtained in a first stage; after a long standing this liquid crystallizes in acicular yellow crystals. Several tests led to the assumption that some adducts of dipyridylic halogenoacetates of rare earths with piperidine could be formed.

Both phenanthrolinic and dipyridylic series, and less the diphenylphenanthrolinic one, are easy to solve in dimethylformamide and dimethylsulphoxide.

---

[7] N. I. Lobanov and V. A. Smirnova, *Zhur. neorg. Khim.*, **12**, 473 (1967).

[8] P. Spacu, E. Antonescu, M. Mavrodin and S. Şerban, *Studii şi Cercetări Chim. Acad. Rom.*, **10**, 163 (1962).

SPECTROPHOTOMETRY

For characterizing the new prepared compounds a visible and ultraviolet spectrophotometric study was performed both in solution and in reflection of powders, as well as an infrared study. In figures 1 and 2 absorption spectra are given between 250 and 400 nm wavelengths for $[Eu(CCl_2HCOO)_3\ dip]\ H_2O$ and $[Eu(CCl_2HCOO)_3$ 4-7-diphenylphen] in DMFA solution. In table 1 the absorption peaks of the compounds towards their respective components are presented by comparison.

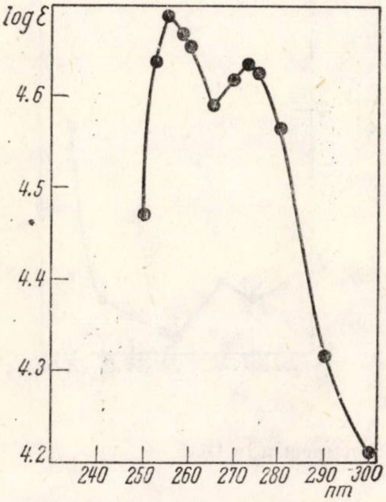

Fig. 1. — Absorption spectra of $[Eu\ (CCl_2HCOO)_3$ 4-7-diphenylphenanthroline]

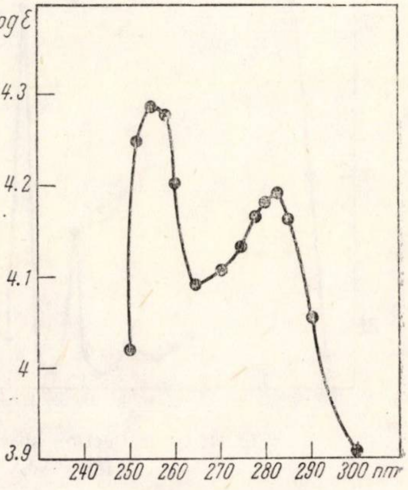

Fig. 2. — Absorption spectra of $[Eu\ (CCl_2HCOO)_3\ dip].\ H_2O$.

Table 1

Absorption maxima of the compounds in DMF solution

Formula of the compound	λ Max nm	ν Max (cm^{-1})	Log ε
$[Eu(CCl_2HCOO)_3dip]$	255	39220	4.29
	282	35460	4.183
$Eu(NO_3)_3.6H_2O$	255	39220	2.321
2-2′-dipyridyl	282	35460	4.209
$[Eu(CCl_2HCOO)_3$4-7-diphenylphen]	255	39220	4.697
	272	36760	4.634
4-7-diphenylphenanthroline	272	36760	4.631

In both situations the characteristic absorption peak of europium ion at 255 nm is maintained also in complexes, but in a much higher intensity. Similarly at 272 nm for the diphenylphenanthrolinic compound, and at 282 nm for the dipyridylic one, chracteristic peaks occur, corresponding to the respective bases and having almost equal intensities to those of uncomplexed bases.

It may be concluded that the bonding between rare earth ions and the respective ligands is rather weak.

Reflection spectra led to similar conclusions. For erbium, praseodymium, and neodymium compounds both ultraviolet and visible spectra were recorded. In figure 3 absorption spectra in DMFA and in reflection of $[Er(CCl_3COO)_3dip]2H_2O$ are represented.

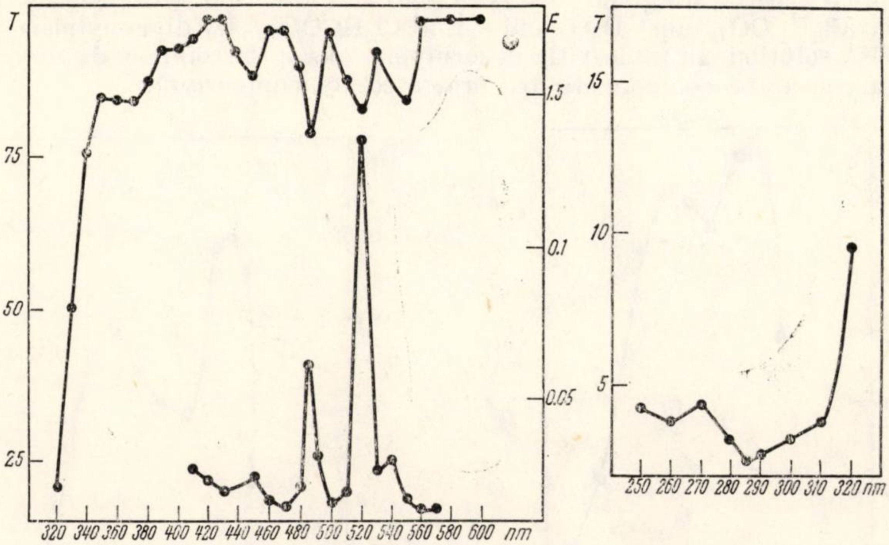

Fig. 3. — Reflection spectra and absorption spectra in DMF of $[Er\ (CCl_3COO)_3\ dip].\ 2H_2O$

It may be observed that each reflection spectrum contains the characteristic bands of rare earth ion which occur in the visible range, whereas in the ultraviolet range the characteristic bands of phenanthroline, dipyridyl, and diphenylphenanthroline are to be found.

Even if spectrophotometry does not indicate a very tight bond between metals and the mentioned bases, qualitative tests showed that an addition of a base to europium halogenoacetates leads to a very pronounced increase in the fluorescence properties. The whole series of europium compounds present an intense red fluorescence under the action of ultraviolet rays.

Infrared studies were performed only for phenanthrolinic compounds. The spectra do not show any significant dependence on the nature of the metal. The two strongest absorption bands in the spectra of free phenanthroline,[9] appearing at 730 and 840 cm^{-1} and which are attributed to C—H out-of-plane bending vibrations, generally appear without positional changes but with an increased intensity in the compounds too. An interesting feature consists in the splitting up, in the complex compounds, of the characteristic ring stretching vibration band of the phenanthroline — at 1565 cm^{-1} — when complexed, into two very intensive bands, the lower at 1525 cm^{-1} and the upper one at 1590 cm^{-1}. The band at 1430 cm^{-1}, due to the vibration of Ln-halogenoacetate bond, appears unchanged in the studied compounds.

---

[9] S. S. Krishnamurthy and S. Soundararajan, *Z. anorg. Chem.*, **348**, 309 (1966).

THERMOGRAVIMETRY

In figure 4 and 5 the thermograms of [Er($CCl_2HCOO)_3$ phen] and [Ce($CCl_3COO)_3$ phen] are given.

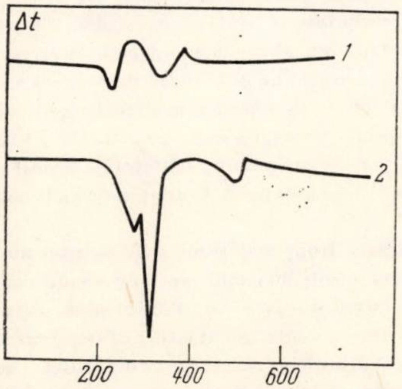

Fig. 4. — DTG curve of:
1. — [Ce($CCl_3COO)_3$phen];
2. — [Er($CCl_2HCOO)_3$phen].

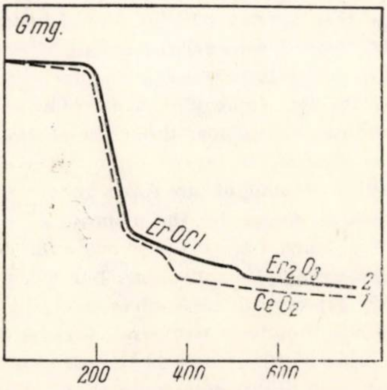

Fig. 5. — Thermograms for decomposition of:
1. — [Ce($CCl_3COO)_3$ phen]:
2. — [Er($CCl_2HCOO)_3$ phen].

The behaviour of compounds by groups of halogenoacetate is almost the same, the major difference being the temperatures at which the different products are formed. For dipyridyl compounds the removal of crystallization water is observed at about 80°. In all other cases, the eduction of phenanthroline starts at 200° [10] and that of dipyridyl at about 150°. This process is however complicated by an almost simultaneous decomposition of halogenoacetic ions. The literature [11] moreover indicates that rare earth trichloroacetates are decomposed in open air into : oxychloride between 210° and 240°, according to the respective rare earth; then, at higher temperatures, i. e. 475°—950° (except La and Pr where temperatures exceed 1000°), the oxychlorides turn into the corresponding oxides.

More clearly for dihalogenoacetates, our results indicate over 200° two processes which are occurring one close to the other, rendered evident also in the differential thermogram by an endothermic effect followed by an exothermic one, weaker for monochloroacetates and more pronounced for trichloroacetates, which correspond to base eduction and to oxychloride formation. At temperatures indicated by literature, a strong exothermic effect due to oxide formation is evidenced also for the compounds we have prepared. Owing to the greater stability of CeO_2, the temperature at which cerium compounds attain a constant weight is much lower than that needed for other rare earths.

---

[10] V. A. Smirnova, N. I. Lobanov and A. I. Vlasov, *Zhur. neorg. Khim.*, 12, 2419 (1966)
[11] B. S. Mathur and T. R. Bhat, *Z. anorg. Chem.*, **343**, 220 (1966).

EXPERIMENTAL

The complexes in the form of $[Ln\,(HalAc)_3B] \times H_2O$ were prepared by adding the solid ligands (1-10-phenanthroline, 2-2′ -dipyridyl, 4-7-diphenyl 1-10-phenanthroline) in the ratio of 1 mol/1 mol of lanthanide halogenoacetate (monochloroacetate, respectively dichloroacetate, trichloroacetate) dissolved in absolute ethylic alcohol at room temperature. By stirring and then leaving still for several hours a crystallized precipitate is formed ; it is then filtered and washed with small portions of warmed alcohol. Obtaining of monochloroacetic derivates from all the three series of compounds proved difficult enough for the first three rare earths La, Ce, Pr. For diphenylphenanthroline and phenanthroline series, by working in slightly modified conditions as compared to common procedure, good results were obtained ; a different situation occurred in case of diphyridylic series where every time compounds containing almost a double amount of rare earth and a half amount of base were obtained, so that no conclusion could be drawn for the moment.

Some attempts were made for obtaining compounds from 6-6′-dimethyldipyridyl and 2-9-dimethylphenanthroline, but every time, with various solvents and working conditions, only non-crystallizable glues were obtained. It is moreover unlikely to obtain some compounds from these two bases, because the two methylic substituents are in either of these cases in *ortho* position towards the nitrogen atoms from phenanthroline, respectively dipyridyl. The very good results obtained with 4-7-diphenylphenanthroline (Bathophenanthroline), where substituents are in *para* position towards nitrogen, seem to confirm this assumption.

Analytical data :

Table 2

Analytical data

No.	Formula of the compound	Me %		C %		H %	
		Calculated	Found	Calculated	Found	Calculated	Found
1	$La(CClH_2COO)_3C_{12}H_8N_2$	23.17	23.31	36.06	36.09	2.35	2.40
2	$La(CCl_2HCOO)_3C_{12}H_8N_2$	19.76	19.98	30.76	30.28	1.69	2.03
3	$La(CCl_3COO)_3C_{12}H_8N_2$	17.23	17.29	26.82	26.96	0.99	1.06
4	$Sm(CCl_2HCOO)_3C_{12}H_8N_2$	21.05	21.10	30.27	30.15	1.54	2.09
5	$Sm(CCl_3COO)_3C_{12}H_8N_2$	18.39	18.40	26.44	26.50	0.97	1.32
6	$Sm(CCl_2HCOO)_3C_{10}H_8N_2.H_2O$	21.23	21.31	27.14	27.05	1.83	2.02
7	$Sm(CCl_3COO)_3C_{10}H_8N_2.2H_2O$	18.12	18.21	23.17	23.30	1.77	1.65
8	$Eu(CCl_2HCOO)_3C_{12}H_8N_2$	21.23	21.25	30.20	30.29	1.53	1.75
9	$Eu(CCl_3COO)_3C_{12}H_8N_2$	18.56	18.59	26.39	26.15	0.97	1.05
10	$Eu(CCl_2HCOO)_3C_{10}H_8N_2.H_2O$	21.41	21.52	26.90	26.87	1.99	1.89
11	$Eu(CCl_3COO)_3C_{10}H_8N_2.2H_2O$	18.29	18.32	23.12	23.21	1.44	1.55
12	$Dy(CClH_2COO)_3C_{10}H_8N_2$	27.12	27.32	32.07	32.10	2.33	2.55
13	$Dy(CCl_2HCOO)_3C_{10}H_8N_2.H_2O$	22.56	22.63	26.68	26.83	1.80	1.95
14	$Dy(CCl_3COO)_3C_{10}H_8N_2.2H_2O$	19.30	19.27	22.83	22.57	1.42	1.61
15	$Er(CCl_2HCOO)_3C_{12}H_8N_2$	22.87	22.84	29.57	29.61	1.51	1.76
16	$Er(CCl_2HCOO)_3C_{10}H_8N_2.H_2O$	23.06	23.07	26.50	26.29	1.79	1.65
17	$Er(CCl_3COO)_3C_{10}H_8N_2.2H_2O$	19.76	19.73	22.71	22.85	1.41	1.50
18	$Nd(CClH_2COO)_3C_{24}H_{16}N_2$	19.06	19.16	47.60	47.76	2.90	3.05
19	$Nd(CCl_2HCOO)_3C_{24}H_{16}N_2$	16.77	16.78	41.88	41.98	1.67	1.73
20	$Nd(CCl_3COO)_3C_{24}H_{16}N_2$	14.97	14.93	37.39	37.40	1.66	1.65
21	$Dy(CClH_2COO)_3C_{24}H_{13}N_2$	20.96	20.68	46.48	46.81	2.83	2.95
22	$Dy(CCl_2HCOO)_3C_{24}H_{16}N_2$	18.50	18.64	41.01	41.23	2.16	2.26
23	$Dy(CCl_3COO)_3C_{24}H_{16}N_2$	16.55	16.34	36.69	36.82	1.63	1.85
24	$Eu(CClH_2COO)_3C_{24}H_{16}N_2$	19.83	19.57	47.12	47.21	2.87	3.20
25	$Eu(CCl_2HCOO)_3C_{24}H_{16}N_2$	17.51	17.65	41.50	41.59	2.18	2.28
26	$Eu(CCl_3COO)_3C_{24}H_{16}N_2$	15.64	15.72	37.09	37.23	1.64	1.75

Spectrophotometry

The ultraviolet and visible study was performed with a VSU-1 Zeiss Jena spectrophotometer equipped with a diffuse reflection attachment for reflection spectra, using MgO as standard at room temperature.

The infrared study was performed with a UR–10 spectrophotometer in KCl pellets.

Thermogravimetry

Thermal properties were established by thermogravimetric and differential thermal analyses with a OD 102 Paulik-Erdey derivatograph in air atmosphere, using Al_2O_3 as standard. An amount of approx. 0.1 g was taken for each sample.

Revue Roumaine de Chimie, **14**, 209–216 (1969)

ÉTUDE DU $H_5[PW_{10}V_2O_{40}]$ PAR LA MÉTHODE RES

A. ŞUTEU et GH. CRISTEA

Université «Babeş-Bolyai», Faculté de Chimie, Cluj, 11, str. Arany János

Reçu le 2 février 1968

Dans le présent travail on démontre par la RES que les deux atomes vanadium du $H_5[PW_{10}V_2O_{40}]$ occupent deux positions non équivalentes, non-équivalence due au fait que les axes de symétrie du champ cristallin local de ces ions forment des angles θ différents, par rapport au champ magnétique constant *H*. A cause de cette non-équivalence on peut considérer que la structure est exprimée plus clairement par la formule : $H_5[(VW_2O_{10})_2P(W_3O_{10})_2]$. A l'aide du spectre RES on a déterminé aussi les constantes de structure hyperfine et les facteurs *g*, tant pour l'orientation parallèle, que pour l'orientation perpendiculaire.

L'acide phosphowolframovanadique $H_5[PW_{10}V_2O_{40}]$. 26 H_2O a été synthétisé par nous par la méthode de Kokorin,[1] l'analyse de la substance démontrant que le rapport des constituants correspond à la formule indiquée.

Le dosage du wolfram a été effectué par gravimétrie sous forme d'oxynate, le vanadium étant, au préalable, réduit jusqu'au vanadium tétravalent et puis complexé avec l'EDTA, afin d'empêcher sa précipitation sous forme d'oxynate.[2]

Le vanadium a été déterminé dans un autre aliquote et calculé par soustraction de la valeur totale des oxynates de wolfram et de vanadium.

On a déterminé le phosphore par colorimétrie, d'après la méthode de Chareton et ses collaborateurs,[3] et l'eau par thermogravimétrie.

La substance a été obtenue sous forme de monocristaux, par cristallisation d'une solution aqueuse concentrée, l'étude cristallographique montrant que les cristaux obtenus relèvent du système cubique (octaédron).

Le cristallohydrate est instable dans l'atmosphère ; il peut accepter ou perdre de l'eau en fonction de l'humidité atmosphérique, c'est pourquoi nous avons protégé les cristaux par une couche mince de polystyrène.

L'acide $H_5[PW_{10}V_2O_{40}]$ dérive de l'acide phospho-12-wolframique $H_3[PW_{12}O_{40}]$ par substitution de deux ions W^{6+} par deux ions V^{5+}.

L'étude röntgénographique effectuée par Keggin [4] sur l'acide $H_3[PW_{12}O_{40}]$ a démontré que :

---

[1] A. H. Kokorin et N. A. Polothebnova, *Uch. Zap. Khishn. Univ.*, **6**, 63 (1953).

[2] L. Erdey, "A kémiai analizy sulyszerinti modszerei", vol. II, Acad. Kiadó, Budapest, 1960, p. 527.

[3] B. Chareton, F. Chauveau, G. Bertho et P. Courtin, *Chem. analyt.*, **47**, 17 (1965).

[4] I. F. Keggin, *Proc. Roy. Soc.*, **144**, 75 (1934).

L'atome P forme le centre d'un tétraèdre central PO_4 autour duquel sont disposés douze octaèdre déformés de WO_6, répartis en quatre groupes, dont chacun est constitué de trois WO_6, qui s'ordonnent tétraédriquement autour de l'atome central. Ces données nous indiquent pour l'acide phosphowolframique la formule suivante : $H_3[P(W_3O_{10})_4]$. La structure de l'acide phosphowolframique est représentée dans la figure 1.

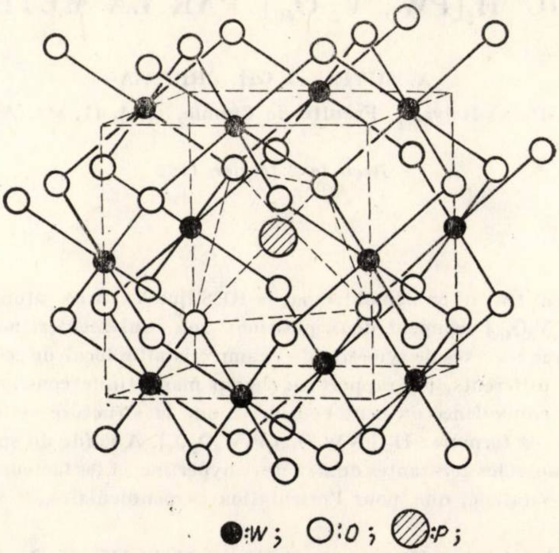

Fig. 1. — Structure röntgénographique du $H_3P(W_3O_{10})_4$.

Les axes de symétrie des octaèdres de WO_6 correspondant au même groupe sont parallèles entre eux. Entre les axes de symétrie des octaèdres appartenant à divers groupements il y a un angle égal à 109° (angle de coordination tétraédrique).

Dans le $H_5[PW_{10}V_2O_{40}]$ deux octaèdres de WO_6 ont été substitués par deux octaèdres de VO_6. On doit élucider si les deux octaèdres de VO_6 appartiennent au même groupement constitué par trois octaèdres, ou s'ils appartiennent à deux groupes différents.

Ainsi que nous avons démontré, par la méthode RES nous pouvons obtenir des informations tant sur la position, que sur la déformation des octaèdres de VO_6. Jusqu'ici la méthode RES n'a pas été utilisée à l'étude de cette classe de substances.

Il est bien connu qu'une partie des ions W^{6+} et Mo^{6+} des hétéropolyacides sont aisément réductibles, sans que l'édifice cristallin en soit modifié.

Dans nos expériences nous avons supposé que le V^{5+} aussi se réduit très aisément à V^{4+}, d'autant plus que c'est un oxydant plus fort que le W^{6+} et le Mo^{6+}.

Cette hypothèse a été confirmée par l'existence du spectre RES caractéristique de l'ion V^{4+}, qui résulte de la réduction du V^{5+} des hétéropolyacides sous l'action de la lumière.

L'hypothèse que la réduction a eu lieu par une réaction photochimique est soutenue par la croissance de l'intensité du spectre RES, après une irradiation par UV.

TECHNIQUE EXPÉRIMENTALE

Les mesures ont été effectuées à l'aide d'un spectromètre RES JES-3^B, en bande X, au Laboratoire des Corps Solides de l'Université de Cluj.

Du fait que la substance contient une grande quantité d'eau de cristallisation qui empêche les mesures RES à la température de la chambre, les mesures ont été effectuées à la température de l'azote liquide.

Le monocristal de $H_5[PW_{10}V_2O_{40}]$, aux dimensions de 3 mm, a été fixé tel qu'il soit orienté au bout d'une baguette en verre introduite dans un récipient Dewar, rempli d'azote liquide et situé dans la cavité de spectrophotomètre.

Les mesures en fonction de l'angle formé par l'axe de symétrie du champ cristallin local et l'axe du champ magnétique constant H ont été effectuées par la rotation du cristal à l'aide d'un dispositif attaché à la cavité.

Nous notons l'angle entre l'axe [111] et la direction du champ magnétique constant H par Φ, parce que cet angle ne coïncide pas toujours avec θ pour tous les groupements des ions.

THÉORIE DU SPECTRE RES

L'état fondamental de l'ion V^{4+} est $^2D_{3/2}$, ce qui résulte de la configuration électronique de la couche incomplète $3d^1$. Dans cet état, le spin électronique et nucléaire est $S = 1/2$ et $I = 7/2$.[5]

On introduit l'ion dans un champ cristallin de symétrie cubique (O_h). Son terme fondamental, cinq fois dégénéré d'après l'orbite se fend dans un triplet inférieur et un doublet supérieur.

Sous l'action perturbatrice du champ cristallin de symétrie plus réduite et sous l'action du couplage spin-orbite, la dégénération se réduit encore, l'orbital inférieur devenant un singlet.[6]

En considérant aussi le spin d'électron, nous pouvons constater qu'après celui-ci chaque orbital est doublement dégénéré. Les signes plus

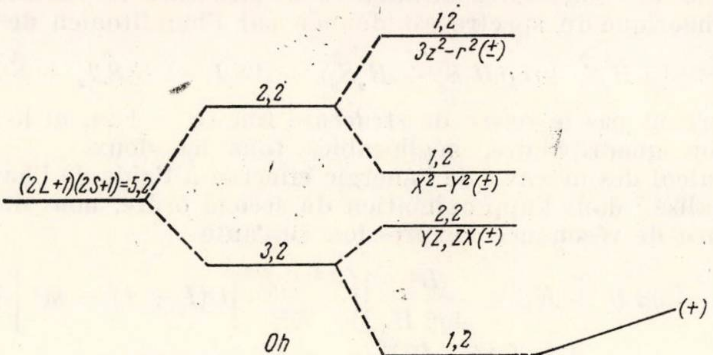

Fig. 2. — Niveau d'énergie et fonctions d'onde des ions 3d'dans les champs cristallins de différentes symétries, ainsi que dans le cas $H \neq 0$.

---

[5] I. Ursu, ,,Rezonanţa electronică de spin'', Ed. Acad., Bucarest, 1965, p. 186.

[6] I. L. Van Rejen, ,,Electron spin resonance studies of pentavalent and trivalent chromium'', Multhype Amsterdam, 1964, p. 44.

et minus de la figure 2 indiquent l'état du spin. Pour l'élévation de la dégénération du spin on doit intervenir avec un champ magnétique extérieur H, qui produit une séparation de Zeeman

$$\hat{H} = g \times \beta H \times \hat{S}x + gy\, \beta\, Hy\hat{S}y + g_z\, \beta\, H_z\, \hat{S}_z \tag{1}$$

décrite par l'hamiltonien du spin.

La contribution du moment magnétique orbital à la croissance du fendage de Zeeman est exprimée par les relations connues

$$g_{\parallel} = 2 - \frac{8\lambda}{E_{x^2-y^2}} \text{ et } g_{\perp} = 2 - \frac{8\,\lambda}{E_{zx \cdot zy}} \tag{2}$$

λ étant la constante du couplage spin-orbite.

Pour une coordination octaédrique fortement déformée (qui apparaît au V^{4+} dans les composés de vanadyl), $E_{x^2-y^2}$ et $E_{zy \cdot zx}$ sont de l'ordre de 10 000 cm^{-1}. Pour les ions du groupement de fer, à la configuration électronique $3d^1$, λ aussi est de l'ordre de 200 cm^{-1}.

Dans ces conditions il est clair que $g_{\parallel}$ et $g_{\perp}$ ne s'écartent pas beaucoup de la valeur du g pour l'électron libre.

Comme on pourra voir, les valeurs que nous avons obtenues dans le cas de V^{4+} de l'acide $H_5[PW_{10}V_2O_{40}]$ pour $g_{\parallel}$ et $g_{\perp}$ confirment la théorie susmentionnée.

Dans le cas d'une orientation du champ magnétique constant suivant la direction [111] (orientation qui coïncide avec l'axe de symétrie du champ cristallin local H, de l'un des quatre groupements d'octaèdres, le spectre de résonance électronique de spin de l'ion V^{4+} de l'acide $H_5[PW_{10}V_2O_{40}]$ est constitué de 16 lignes de structure hyperfine qui représentent deux spectres (I) et (II), composés chacun de 8 lignes séparées par des constantes différentes de structure hyperfine. La description théorique du spectre est donnée par l'hamiltonien de spin

$$\hat{H} = \beta[g_{\parallel} H_z \hat{S}_z + g_{\perp}(H_x \hat{S}_x + H_y \hat{S}_y) + A\hat{S}_z I_z + B(\hat{S}_x I_x + \hat{S}_y I_y) \tag{3}$$

qui ne contient pas le terme de structure fine ($S = 1/2$), ni le terme de l'interaction quadripolaire, négligeables tous les deux.

Le calcul des niveaux de l'énergie effectué à l'aide de l'hamiltonien (3) diagonalisé [7] dans l'approximation du second ordre, nous donne pour la fréquence de résonance l'expression suivante

$$h\nu = g\beta\, H + K_m + \frac{B^2}{4g\beta\, H_0}\left[\left(\frac{A^2 + K^2}{K^2}\right) I\,(I + 1) - m^2\right] + \\ + \frac{1}{2g\beta\, H_0}\left[\frac{A^2 - B^2}{K}\right]^2 \left(\frac{g_{\parallel}\;\, g_{\perp}}{g^2}\right)^2 \sin^2\theta \cos^2\theta\; m. \tag{4}$$

où

$$g^2 = g_{\parallel}^2 \cos^2\theta + g_{\perp}^2 \sin^2\theta$$
$$K^2 g^2 = A^2\, g^2{}_{\parallel} \cos^2\theta + B^2 g_{\perp}^2 \sin^2\theta$$

θ est l'angle formé par l'axe de symétrie du champ cristallin et la direction du champ magnétique constant ; A, B, $g_{\parallel}$ et $g_{\perp}$ sont les paramètres du spectre RES notés selon les notations consacrées.

---

[7] A. Nicula, I. Ursu et S. Nistor, *Rev. Roumaine Phys.*, **10**, 229 (1965).

En partant du cas simple $\Phi = 0$, quand pour l'un des quatre groupements d'ions $\theta = 0$, nous obtenons de l'équation (4) pour la valeur du champ

$$H(m) = H_0 - Am - \frac{B^2}{2H_0}[I(I+1) - m^2] \tag{5}$$

Cela représente le champ magnétique où il doit apparaître les lignes correspondant à la valeur donnée m, de la projection du moment cinétique du spin nucléaire. La formule 5 explique aussi la croissance du fendage spectroscopique vers les champs plus grands.

H_0 est déterminé à partir de la condition de résonance $h\nu = g\beta H_0$.

Les valeurs expérimentales des paramètres des spectres RES sont

$$A = 162 \pm 2G_s\,;$$
$$B = 68 \pm 2G_s\,;$$
$$g_{\parallel} = 1{,}951 \pm 0{,}002\,;$$
$$g_{\perp} = 2{,}003 \pm 0{,}002.$$

Pour vérifier si l'hamiltonien adopté décrit correctement le spectre RES obtenu, nous avons calculé les valeurs du champ magnétique Hm données par (5), pour le spectre correspondant au groupement parallèle ($\theta = 0$), à l'aide de la valeur expérimentale des constantes de la structure hyperfine et nous les avons confrontées avec les valeurs du champ magnétique mesuré sur le spectre.

Tableau 1

Valeurs des champs magnétiques mesurées expérimentalement et calculées selon la théorie

m	7/2	5/2	3/2	1/2	−1/2	−3/2	−5/2	−7/2
$H_{\text{mesuré}}$	2816	2970	3127	3288	3448	3612	2780	3951
$H_{\text{calculé}}$	2819	2972	3128	3287	3448	3612	3778	3948

Comme il ressort du tableau 1, les déviations sont comprises entre les limites d'erreur de la mesure.

DISCUSSION DES RÉSULTATS

Les deux spectres séparés par des constantes de structure différente s'expliquent par le fait que dans la cellule élémentaire, quand $\Phi = 0$, le vanadium occupe deux positions non équivalentes.

La non-équivalence des ions vanadium est déterminée par les angles θ différents, formés entre le champ magnétique constant H et les axes de symétrie du champ cristallin local de ces ions.

Le spectre (I) a été attribué aux ions V^{4+} qui substituent le W^{6+} dans les groupements d'octaèdre à l'axe de symétrie parallèle au champ magnétique constant H.

Nous avons attribué le spectre (II) aux ions V^{4+} qui substituent le W^{6+} dans les trois autres groupements d'octaèdre dont l'axe de symétrie forme avec le champ magnétique extérieur l'angle $\theta = 109°$ (angle de coordination tétraédrique).

Cette affirmation est soutenue par :

a) la variation de l'intensité des lignes de résonance en fonction de l'angle Φ ;

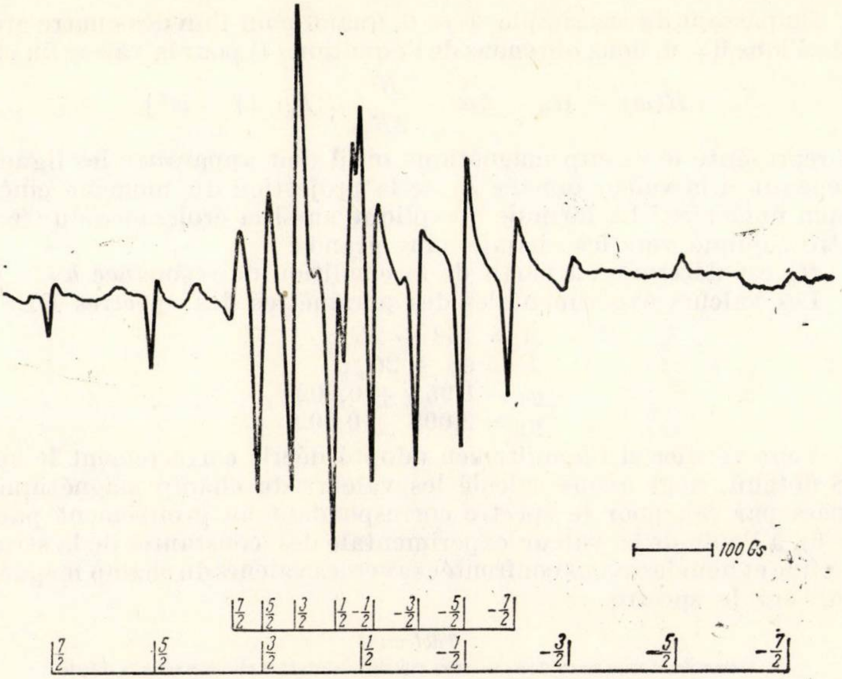

Fig. 3. — Le spectre RES quand $\Phi = 0$.

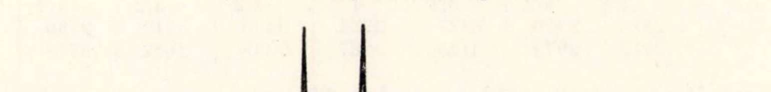

Fig. 4. — Le spectre RES quand $\Phi \neq 0$.

b) l'apparition dans le spectre, pour $\Phi \neq 0$, d'un troisième spectre (III), provoqué par la formation d'une troisième position non équivalente sur la cellule élémentaire.

Dans les figures 3 et 4 nous avons donné les spectres RES au cas où $\Phi = 0$, respectivement $\Phi \neq 0$.

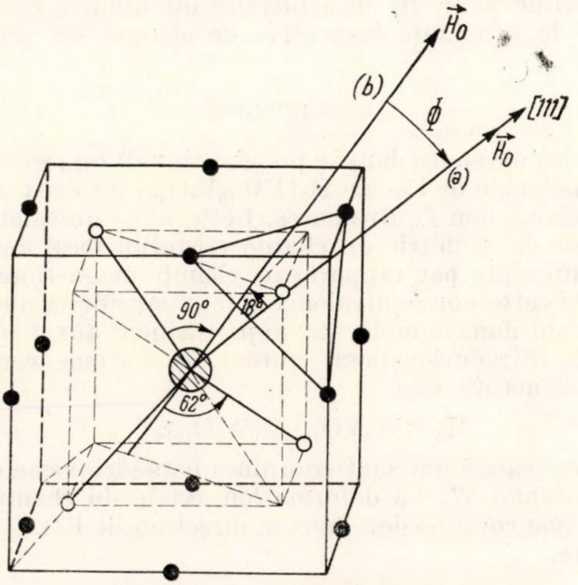

Fig. 5. — Direction du champ magnétique constant H par rapport à l'axe [111] dans les cas suivants : a) deux ions non équivalents; b) trois ions non équivalents.

Pour ce qui est de l'observation a), on peut constater un rapport 1 : 3 entre l'intensité du spectre (I) et l'intensité du spectre (II). La figure 5 rend cela parfaitement intelligible si nous admettons avec la même probabilité une distribution de ces deux ions V^{4+} de la cellule élémentaire entre les quatre positions non équivalentes susceptibles d'être substituées. A $\Phi = 0$,1/4 du nombre total des ions paramagnétiques seront orientés parallèlement avec le champ magnétique constant et 3/4 de manière à former un angle de $\theta = 109°$, étant situés symétriquement par rapport à la direction du champ.

Une rotation dans le plan [110] avec $\Phi = 19°$ amène l'un des groupements d'ions à $\theta = 90°$. Dans cette position le groupement d'ions orienté auparavant parallèlement aura maintenant un angle $\theta = 19°$; les autres groupements seront orientés symétriquement à $\theta = 62°$ (fig. 5).

Dans ces positions le spectre devrait être constitué de trois spectres (I), (II), (III), correspondant à ces trois orientations différentes, mais à cause de la superposition de quelques lignes cela peut être observé, plus clairement, seulement aux lignes extrêmes du spectre (I) qui se brise.

Après une rotation$=109°$, le spectre RES se reproduit, ce qui confirme le fait que tant dans le cas de l'acide phosphowolframovanadique, que dans celui de l'acide phosphowolframique, les quatre groupements constitués de trois octaèdres sont situés autour de l'atome central *P*, dans une coordination tétraédrique.

Le spectre RES est très peu anisotrope à cause de l'anisotropie réduite du facteur *g* et en raison du fait que la valeur des constantes de structure hyperfine pour un Φ arbitraire est donnée par une moyenne des valeurs de la constante respective de chaque ion paramagnétique.

CONCLUSIONS

Des données obtenues dans le présent travail on peut constater que :

Dans la molécule de l'acide $H_5[PW_{10}V_2O_{40}]$ les deux atomes V occupent deux positions non équivalentes. Cette non-équivalence est due au fait que les axes de symétrie du champ cristallin local des ions forment des angles θ différents par rapport au champ magnétique constant *H*.

À cause de cette non-équivalence il faut considérer que les deux atomes V, se trouvant dans la molécule, appartiennent aux deux groups différents coordinés tétraédriquement autour de l'atome central *P*. Ainsi la formule de structure sera

$$H_5\ [(W_2VO_{10})_2P(W_3O_{10})_2]$$

Les atomes vanadium sont coordinés octaédriquement, de la même façon que les atomes W. La déformation axiale du champ cristallin est provoquée par une compression dans la direction de l'axe [111] de la cellule élémentaire.

Nous remercions le professeur Ioan Ursu de nous avoir autorisés à effectuer des mesures au Laboratoire des corps solides de l'Université, Alexandru Nicula, maître de conférences et V. Lupei, chercheur, pour les discussions précieuses qui ont contribué à l'élucidation des problèmes apparus pendant la rédaction de ce travail.

Revue Roumaine de Chimie, **14**, 217–223 (1969)

ÉTUDE DE LA SOLUBILITÉ DE L'OXYDE DE ZIRCONIUM

LUCREŢIA POPA et IOANA ARSENIE
Institut de Physique Atomique, Bucarest, Şos. Măgurele

Reçu le 15 mars 1968

On étudie la solubilité de l'oxyde de zirconium monoclinique provenu des concentrés roumains, la dissolution étant effectuée par deux voies :

- voie humide, dans les acides et dans les alcalis ;
- voie ignée (sèche).

I. INTRODUCTION

L'oxyde de zirconium, cristalisé sous forme monoclinique, est l'un des plus importants produits stables du zirconium. L'énergie de formation de ce composé, $\Delta H = -261,5$ kcal/mole,[1] indique une très grande stabilité (à 2300 °K il n'y a aucune dissociation du produit). Grâce à sa stabilité, l'oxyde de zirconium est très utilisé dans l'industrie, à côté du zirconium métallique.

Dans la technologie de séparation de zirconium, de hafnium (tous les deux utilisés dans la technique nucléaire), on constate fréquemment que l'oxyde de zirconium précipite des solutions, si celles-ci ne sont pas utilisées immédiatement.

C'est pourquoi, nous avons considéré nécessaire de mettre au point une méthode pour la dissolution de l'oxyde de zirconium, en vue de le récupérer.

Dans le présent travail on étudie la solubilité de l'oxyde de zirconium, cristallisé sous forme monoclinique, dans les acides et les solutions concentrées des alcalis, ainsi que la dissolution de ce composé par chauffage, en présence d'un fondant.

Par cette étude on contribue à résoudre le problème de la récupération du zirconium, déposé sous forme d'oxyde de zirconium, particulièrement dans les solutions concentrées (90–110 g/l Zr), qu'on utilise couramment. Mentionnons, par exemple, que 25 jours après avoir préparé les solutions (chlorures, azotates, sulfates), à peu près 5,5% de la quantité totale de zirconium se dépose sous forme d'oxyde.

---

[1] G. L. Humphrey, *J. Amer. Chem. Soc.*, **76**, 978 (1954).

Les essais de dissolution ont été effectués sur oxyde de zirconium roumain, chimiquement pur, dont la composition (en impuretés) est la suivante :

Hf = 2% (rapporté à Zr.) Ti = 10^{-2}%, Si = 10^{-3}%
Ca = 10^{-2}% Pb = 10^{-3}% Cu = $10^{-3} - 10^{-4}$%
Fe = 10^{-3}% Al = 10^{-3}% Mg = 10^{-3}%

L'analyse de l'oxyde de zirconium a été faite par voie spectrale.

On a effectué des essais quant à la dissolution de l'oxyde de zirconium tant avec des acides concentrés, qu'avec des acides dilués, ainsi que dans des solutions concentrées d'alcalis, en variant la température et le temps de réaction entre l'oxyde et les acides.

Les résultats des expériences sur la dissolution de l'oxyde de zirconium par voie humide sont donnés dans les tableaux 1—5.

On a continué les expériences par fonte avec des fondants, tels que : sulfate de sodium, mélange de carbonates, sulfate acide de potassium, les résultats étant représentés dans les tableaux 6—8.

II. STADE DU PROBLÈME

Dans les travaux relativement récents [2] on indique que l'oxyde de zirconium est pratiquement insoluble dans tous les acides.

Les auteurs mentionnent [3] l'obtention de solutions d'azotate de hafnium et zirconium par l'attaque prolongée et à chaud de l'acide azotique fumant sur l'oxyde respectif et mentionnent aussi que l'attaque même prolongée est incomplète.

On affirme [4] qu'aucun réactif n'est capable de dissoudre l'oxyde de zirconium calcinéet on précise également qu'il y a une attaque très lente de l'acide sulfurique concentré à chaud, et que les vapeurs de l'acide fluorhydrique à la température d'environ 250° attaquent, lentement, l'oxyde de zirconium.

Fassel et Anderson [5] ont obtenu des échantillons (de zirconium nucléaire et hafnium nucléaire) pour l'analyse dans différents concentrés, par la fonte de l'oxyde de zirconium avec du sulfate acide de sodium.

Dans le travail précité on n'indique pas les détails de la fonte.

III. RÉSULTATS EXPÉRIMENTAUX

Les essais sur la solubilité de l'oxyde de zirconium ont été effectués par deux voies :

1. voie humide, par attaque des acides et des alcalis ;
2. voie sèche, par fonte à différents fondants.

---

[2] J. Huré, M. Rastoix et R. Saint-James, *An. Chim. Ac.*, **25**, 118 (1961).

[3] J. Huré, M. Rastoix et R. Saint-James, *Rapport du Commissariat d'Energie Atomique*, n° 1771 (1961).

[4] P. Pascal, „Nouveau traité de chimie minérale", tome IX, 1963, Masson et Cie, Ed. Paris, p. 494.

[5] V. A. Fassel et Ch. Anderson, *J. Opt. Soc. Am.*, **11**, 742 (1950).

1. *Essais par voie humide*

Les expériences par voie humide ont été effectuées en conditions de température, temps et concentrations d'acides différentes.

Dans le tableau 1 sont présentés les résultats des expériences sur la solubilité de l'oxyde de zirconium à 100°C, le temps de réaction étant de 150 heures dans les acides concentrés et dans les solutions concentrées d'alcalis.

Toutes les expériences sur la dissolution par voie humide ont été effectuées avec 1 g d'oxyde de zirconium, traité avec 50 ml de solution réactif.

Nous précisons que les solutions obtenues par la dissolution n'ont pas été stables dans le temps.[6-8]

Les données inscrites au tableau 1 indiquent que l'oxyde de zirconium est peu soluble dans l'acide sulfurique (65 %), tandis que dans l'acide sulfurique concentré il est à peu près complètement soluble (98 %), dans d'autres acides concentrés, ou dans leurs mélanges n'étant pas soluble.

On a obtenu la dissolution partielle dans des solutions concentrées de sulfate acide de sodium, ou de potassium.

On a essayé d'effectuer la dissolution avec des échantillons d'oxyde de zirconium maintenus, au préalable, dans de l'eau (24 heures), et ensuite traités par l'attaque avec les réactifs indiqués au tableau 1.

Tableau 1

Dissolution de l'oxyde de zirconium dans les acides concentrés

Nº échant.	Réactif	Température °C	Temps de réaction	% Zr solubilisé
1	2	3	4	5
1	Acide azotique 65 %	100	150	0,89
2	Acide chlorhydrique 37,2 %	100	150	0,87
3	L'eau régale directe	100	150	0,87
4	L'eau régale inverse	100	150	0,11
5	Acide sulfurique 65 %	100	150	2,26
6	Acide sulfurique 98 %	100	150	98
7	Solution de KOH conc.	100	150	Ne se dissout pas.
8	Solution de NaOH conc.	100	150	,,
9	Solution de carbonates conc.	100	150	,,
10	Solution de sulfate acide de potassium	100	150	17,45
11	Solution de sulfate acide de sodium	100	150	17,40

---

[6] M. J. Farah et I. S. El. Jammani, «Conf. Appl. PAC Energ. Atom,» Geneva, 9, P — 131 — (1964).

[7] R. E. Connick et W. N. Mc. Veg. *J. Amer. Chem. Soc.*, **91**, 3182 (1949).

[8] R. L. Nickok et R.D. Cannon, «Report 1960 U. S. Atomic Energy Commission».

On a enregistré les mêmes résultats que ceux indiqués au tableau 1.

Les mêmes essais ont été effectués sur un oxyde maintenu, au préalable dans de l'eau oxygénée, les résultats étant identiques à ceux mentionnés ci-dessus.

Dans une autre série d'expériences effectuées sur un oxyde de zirconium, finement broyé au préalable dans un mortier, on a enregistré la même solubilité.

On a continué les essais, avec des acides dilués (sulfurique, azotique, chlorhydrique), les résultats obtenus étant présentés dans le tableau 2.

Tableau 2

Dissolution de l'oxyde de zirconium en fonction de la concentration de l'acide (% Zr en fonction de la conc. de l'acide)

Nº échant.	Réactif	Température °C	Temps de réact. h	% Zr en fonction de la conc. de l'acide		
				2N	4N	8N
1	Acide chlorhydrique	100	150	0,82	0,83	0,83
2	Acide azotique	100	150	0,64	0,71	0,86
3	Acide sulfurique	100	150	1,11	2,03	2,16

Pour élucider l'influence de la témperature sur la dissolution de l'oxyde de zirconium on a effectué des expériences de solubilité, à différentes températures, dans les milieux suivants : acide chlorhydrique 37,2%, acide azotique 65%, acide sulfurique 65%.

L'oxyde de zirconium a été maintenu dans les acides mentionnés, pendant 10 heures. Les résultats sont présentés dans le tableau 3.

Tableau 3

Dissolution de l'oxyde de zirconium en fonction de la température

Nº échant.	Réactif	% Zr dissous en fonction de la température				
		20°	50°	75°	100°	132°
0	1	2	3	4	5	6
1	Acide chlorhydrique (37,2%)	0,11	0,27	0,35	0,35	0,35
2	Acide azotique (65%)	0,44	0,61	0,63	0,63	0,64
3	Acide sulfurique (65%)	0,36	0,37	0,37	0,38	0,38

Dans la série suivante d'expériences, effectuées à 100°C, par l'augmentation du temps de réaction des acides concentrés sur l'oxyde de zirconium, on n'a pas obtenu une meilleure dissolution, la solubilité étant inférieure à 1%, à l'exception des échantillons traités avec de l'acide sulfurique 65% et 98%. Les résultats sont donnés dans les tableaux 4 et 5.

Il résulte des données ci-dessus que l'oxyde de zirconium est pratiquement insoluble dans l'acide chlorhydrique et dans l'acide azotique concentrés, ou dans leurs mélanges, tant à chaud qu'à froid, même après une réaction prolongée.

Il y a une solubilité partielle dans les solutions aussi bien dans de l'acide sulfate de sodium ou de potassium que dans de l'acide sulfurique 65%.

Dans l'acide sulfurique, 98%, la solubilité est à peu près totale.

Tableau 4

Dissolution de l'oxyde de zirconium en fonction du temps

Nº échant.	Réactif.	% Zr dissous en fonction du temps		
		50 h	100 h	150 h
0	1	2	3	4
1	Acide chlorhydrique (37,2%)	0,35	0,35	0,35
2	Acide azotique (65%)	0,63	0,63	0,67
3	Acide sulfurique (65%)	0,38	2,0	2,20

Tableau 5

Dissolution de l'oxyde de zirconium, en fonction du temps dans de l'acide sulfurique 98%

Nº échant.	Réactif	% Zr dissous en fonction du temps			
		5 h	15 h	25 h	150 h
0	1	2	3	4	5
1	Acide sulfurique (98%)	15	60	98	98

2. *Essais de dissolution par voie sèche*

Parallèlement avec les essais de dissolution de l'oxyde de zirconium par *voie humide* on a effectué une série d'expériences de dissolution par fonte avec des fondants.

Les fontes ont été réalisées avec du sulfate acide de sodium, du mélange de carbonates et du sulfate acide de potassium. Les conditions de travail sont représentées dans les tableaux 6–8.

Dans le tableau 6, on donne les résultats des fontes avec le sulfate acide de sodium. Les deux derniers échantillons du tableau 6 sont totalement solubles.

Tableau 6

Dissolution de l'oxyde de zirconium par fonte, en fonction du rapport SO_4H Na/ZrO_2

Nº échant.	Rapport poids SO_4HNa/ZrO_2	Température °C	Temps mn	% Zr solubilisé	
				Trouvé dans la solution	Zr résulté de l'échant. initial
0	1	2	3	4	5
1	5	400	20	10,6	14,38
2	10	400	20	53,9	72,46
3	15	400	20	64,2	86,20
4	20	400	20	66,2	89,80
5	25	400	20	74,0	100,00
6	30	400	20	74,0	100,00

Les essais de dissolution du zirconium par fonte avec des mélanges de carbonates donnent de bons résultats (1 partie CO_3Na_2 et 1,3 parties CO_3K_2), arrivant jusqu'à la solubilité totale de l'oxyde.

Les résultats des expériences de dissolution avec des mélanges de carbonates sont donnés dans le tableau 7.

Tableau 7

Dissolution de l'oxyde de zirconium par fonte, en fonction du rapport $\frac{CO_3Na_2+1,3\ CO_3K_2}{ZrO_2}$

N° échant.	Rapport poids $\frac{CO_3Na_2+1,3\ CO_3K_2}{ZrO\ 2}$	Température °C	Temps (mn)	% Zr sobulilisé	
				Trouvé dans la solution	Zr résulté de l'échant. initial
0	1	2	3	4	5
1	5	960	20	2,68	3,6
2	10	960	20	52,5	70,5
3	15	960	20	68,4	91,8
4	20	960	20	68,8	92,5
5	25	960	20	74,0	100,0
6	30	960	20	74,0	100,0

Les échantillons fondus sont solubilisés dans de l'acide chlorhydrique (les deux derniers totalement, et les autres partiellement).

Dans le tableau 8, sont donnés les résultats des expériences de dissolution avec du sulfate acide de potassium.

Les fontes ont été réalisées à 300° et 400°, les résultats enregistrés étant les mêmes que ceux du tableau 8.

Tableau 8

Dissolution de l'oxyde de zirconium par fonte, en fonction du rapport $\frac{SO_4HK}{ZrO_2}$

N° échant.	Rapport poids SO_4HK/ZrO_2	Température °C	Temps (mn)	% Zr solubilisé	
				Trouvé dans la solution	Zr résulté de l'échant. initial
0	1	2	3	4	5
1	5	400	20	8,89	12
2	10	400	20	22,70	30,30
3	15	400	20	37,80	50,90
4	20	400	30	37,80	50,90
5	25	400	20	37,85	51,20
6	30	400	20	42,40	57,0

IV. ANALYSES

Les résultats des essais de dissolution donnés dans la IIIe partie du présent travail ont été établis par trois méthodes :

1. On a déterminé la teneur en zirconium et hafnium dans la solution, par précipitation (gravimétrique) avec de l'acide mandélique [9] et de la tartrazine.[10]

2. On a pesé le résidu de l'oxyde de zirconium [11] resté après l'attaque avec les réactifs indiqués, dans les conditions mentionnées.

3. On a effectué des mesures radiométriques. Les solutions obtenues par la dissolution des échantillons ont été marquées avec du Zr^{95}. Le zirconium et le hafnium ont été précipités avec de l'acide mandélique, ensuite le précipité a été séché et mesuré à l'aide d'un compteur d'impulsions — Scintillateur (I Na).

Zr^{95} a été obtenu par activation de l'azotate de zirconium spectralement pur, irradié à un flux de 1.10^{13} $n^1/cm^2.s$, pendant 122 heures.

V. CONCLUSIONS

1. L'oxyde de zirconium est pratiquement insoluble dans les acides chlorhydrique, azotique et dans leurs mixtures, ainsi que dans les solutions concentrées des alcalis, et partiellement soluble (2,2 %) dans l'acide sulfurique 65 % et dans les solutions concentrées de sulfate acide de sodium ou de potassium. La solubilité est approximativement 17,4 % de l'oxyde initial.

Dans l'acide sulfurique (98 %) on obtient une solubilité pratiquement complète (98 % de la teneur en zirconium initiale).

2. Par la fonte de l'oxyde de zirconium avec du sulfate acide de sodium ou avec les carbonates de sodium et de potassium on obtient la solubilité totale pour le rapport suivant (en poids) :

$$\frac{\text{Fondant}}{\text{oxyde de zirconium}} = \frac{25 \div 30}{1}$$

La dissolution par fonte est rapide (20 mn), c'est pourquoi elle est préférée à la dissolution par voie humide dans de l'acide sulfurique concentré, opération de longue durée.

---

[9] Cl. J. Rodden, « Analysis of Essential Nuclear Reactor Materials », Ed. Washington U.S.A.E.C., 1964.

[10] Gh. Băiulescu et L. Turcu, *Analyt. Chim. Acta,* **21**, 33 (1959).

[11] Const. Gh. Macarovici, « Chimie analitică cantitativă », Ed. tehnică, Bucarest, 1959, p. 95.

IV. ANALYSE

Les résultats [illegible] de la [illegible] dans les deux méthodes.

[illegible] la solution.

[illegible]

[illegible]

[illegible]

1. [illegible]

2. [illegible]

[illegible]

[illegible]

[illegible]

[illegible]

Revue Roumaine de Chimie, 14, 225–234 (1969)

ELECTRONIC SPECTRA OF THE SUBSTITUTED α-OXIMINOALKYLBENZENES. I.

STERIC EFFECTS ON ELECTRONIC ABSORPTION SPECTRA OF THE SUBSTITUTED *o*-NITRO-α-OXIMINOALKYLBENZENES

L. FEY and N. BODOR

Chemical Pharmaceutical Research Institute, Cluj, Str. K. Marx 93–97

Received March 19, 1968

On account of the *ortho*-steric effect between the α-oximinoalkyl and nitro groups, the electronic spectra of these oximes can be interpreted as a simple superposition of the relatively independent spectra of the steric hindered phenyl-nitro and phenyl-α-oximinoalkyl systems. A comparative study of the steric effects in the cases of undissociated and ionized forms of these oximes was carried out. It was demonstrated that the apparent contradiction observed in the case of *o*- nitro-acetophenonoxime, namely the unexpected hypsochromic and hyperchromic shift which followed the dissociation, is in fact the result of the significant bathochromic displacement from the far UV-region of the band of the steric deviated phenyl-α- oximinoethyl system, the decreased phenyl-nitro band being completely included in this displaced, high-intensity maximum. The effects of some chromophore *p*-substituents on this phenomenon are investigated.

In some previous papers [1,2] we have studied the effects of the *ortho*-nitro group on the reactivity of the alkyl groups (ethyl-, propyl-, isobuthyl-) in the isonitrozation, as well as on the physical and chemical properties (pK, $E_{1/2}$) of the corresponding oximes, resulted from this reaction.

It is evident that the *ortho*-steric effects of the nitro group must be significantly manifest also in the electronic absorption spectra of these oximes. The purpose of the present paper is to give a satisfactory explanation on the mode the *ortho*-steric effects of the nitro group affect the energetical and spectral properties of the substituted *o*-nitro-α-oximinoalkylbenzenes, in their ionized and undissociated forms. To this end, the following compounds were studied:

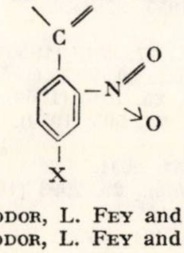

$R = H, CH_3$

$X = H, Cl, Br, I, CH_2OC_2H_5.$

$CH_2OC_6H_5, CH_2{-}\overset{\frown}{\underset{\smile}{N\quad(CH_2)}}_5,$

$SO_2C_6H_5, SO_2N(CH_3)_2.$

---

[1] N. Bodor, L. Fey and A. Kövendi, *Rev. Roumaine Chim.*, **11**, 405 (1966).

[2] N. Bodor, L. Fey and A. Kövendi, *Rev. Roumaine Chim.*, **11**, 421 (1966).

The absorption spectra of these compounds were studied in aqueous solutions, our main problem being to prepare a comparative study of the undissociated molecules and the corresponding anions.

Beside these oximes, we have studied the spectra of some structurally related compounds (nitro-alkylbenzenes [3] and *o*-substituted benzaldoximes), which were used as references in interpretation of the observed shifts.

Steric effects on electronic spectra of some related compounds (aromatic oxo-compounds) were reported and studied by several authors. Thus, Braude and Sondheimer[4,5] have accomplished a detailed study on the spectra of the mono-, di-, and tri-methyl benzaldehydes and acetophenones. Supposing the absence of any appreciable steric hindrance to the coplanarity of the $\mathrm{Ph{-}\overset{|}{C}=O}$ group in the unsubstituted benzaldehyde and acetophenone, they have calculated the angles of twist (θ) for the *o*-mono-, and *o*, *o'*-dimethyl derivatives, from the spectral data. However, Suzuki [6] suggests that acetophenone itself is slightly hindered, therefore the obtained angles[4,5] must be reconsidered.

The existence of *ortho*-steric effects in the substituted benzaldehydes and acetophenones were reported also by other authors,[7-10] but from the point of view of the present paper, the most important are the works of Grammaticus,[11] Welkar [12] and Lutzki[13,14] referring to the spectra of *o*-, *m*-, and *p*-nitro-benzaldehydes and -acetophenones. In these cases hypsochromic shifts of the corresponding bands were observed concomitantly with the decrease of their intensities, because the concurrent effects of the two antiauxochrome (electron-withdrawing) substituents. In the case of the *o*-nitro-derivatives the *ortho*-steric effects are superposed on these shifts.

The UV-spectra in isooctan and 94% sulphuric acid of some substituted acetophenonoximes, such as: 2-, 3-, 4-, methyl; 3,5-, 2, 4-dimethyl; 3, 4, 5-trimethyl; 4-t-buthyl; 2-, 4- chloro; 4-bromo; 4-iodo; 2-, 3-, 4-nitro- and 2-, 4-, methoxy-derivatives were described by Pearson and Watts. [15] The hypsochromic and hypochromic effects observed in spectra of all *ortho*-derivatives were attributed by these authors to steric hindrance of coplanarity.

Taking into account that the spectra of the *o*- and *p*-nitro-acetophenonoximes were given only in isooctan and sulphuric acid solutions,[15] we have repeated these spectra in water and in alkaline solution, because our main purpose was to make a comparative study concerning the *ortho*-steric effects in ionized and undissociated forms of these oximes.

---

[3] W. M. Schubert and J. Robins, *J. Amer. Chem. Soc.*, **80**, 559 (1958).

[4] E. A. Braude, F. Sondheimer and W. F. Forbes, *Nature*, **173**, 117 (1954).

[5] E. A. Braude and F. Sondheimer, *J. Chem. Soc.*, **1955**, 3754.

[6] H. Suzuki, *Bull. chem. Soc. Japan*, **33**, 613 (1960).

[7] D. D. Clarke and F. F. Nord, *J. Amer. Chem. Soc.*, **77**, 6618 (1955).

[8] W. J. Horton and J. T. Spence, *J. Amer. Chem. Soc.*, **80**, 2453 (1958).

[9] W. J. Horton and D. E. Robertson, *J. Org. Chem.*, **25**, 1016 (1960).

[10] D. J. Cram and F. W. Cranz, *J. Amer. Chem. Soc.*, **72**, 595 (1950).

[11] A. Grammaticus, *Bull. Soc. chim. France*, **1953**, 821.

[12] E. A. Welkar and J. R. Young, *J. Chem. Soc.*, **1957**, 2041.

[13] A. J. Lutzki and V. T. Alexejeva, *Zhur. obsch. Khim.*, **29**, 2998 (1959).

[14] A. J. Lutzki and V. T. Alexejeva, *ibid.*, **29**, 3248 (1959).

[15] D. E. Pearson and E. D. Watts, *J. Org. Chem.*, **20**, 494 (1955).

For the same reason were registered in water the reference spectra of the *o*- and *p*-nitro-ethylbenzenes.

RESULTS AND DISCUSSIONS

A. o-*Nitro-benzaldoxime* (I) (*trans*-phenyl-/-OH)

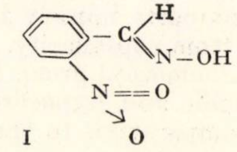
I

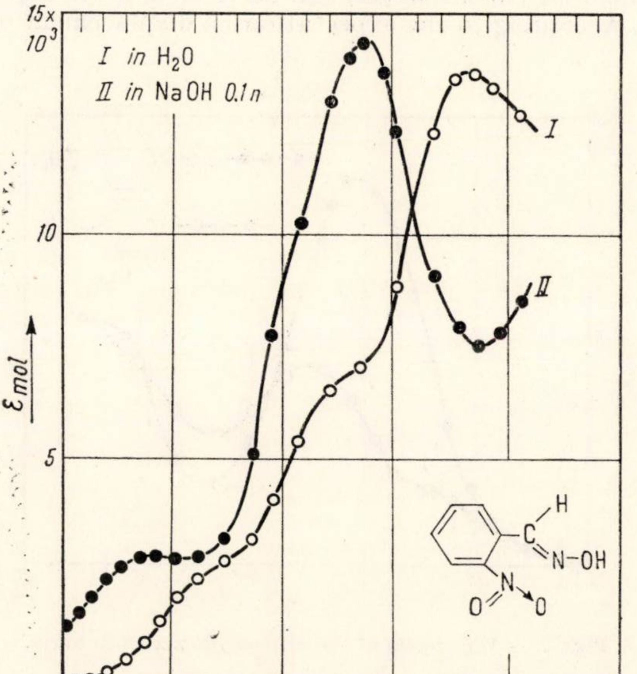

Fig. 1. — UV spectra of the *o*-nitro-benzaldoxime.
I - in water; *II*— in NaOH 0.1 N.

(In a previous work [1] we have demonstrated that the nitro-α-oximino-alkylbenzenes are completely dissociated in sodium hydroxide 0.1 N, however in water only the undissociated molecules are extant.)

The spectrum of the undissociated form (curve I in fig. 1.) has a high-intensity band at 43,200 cm^{-1} and two lower-intensity shoulders at 37,500 and 32,000 cm^{-1}, therefore this spectrum becomes more complex than the spectra of the corresponding mono-substituted derivatives (nitrobenzene,[16] benzaldoxime[17]). On account of the *ortho*-steric effects existing between the auxochrome-antiauxochrome substituent-pair, a certain independence from the spectral point of view of the two component systems may be expected. In this way, we have attempted to derive the spectrum of *o*-nitro-benzaldoxime as an algebraic summation of the spectra of the structurally constituent parts, namely from the: (*a*) spectrum of a nitrobenzene steric hindered from coplanarity, and (*b*) spectrum of a benzaldoxime, in which the oximinomethyl group is also deviated from coplanarity. Evidently, hypsochromic and hypochromic displacements can be expected in these spectra, comparative to the unhindered mono-substituted derivatives.

The *o*-nitro-ethylbenzene (II) can serve as a steric hindered phenylnitro system. According to the expectations, a displacement of the characteristic band toward shorter wavelength, accompanied with a decrease of its intensity can be observed, comparative to the *p*-nitro-derivative (III) (Fig. 2). This hypsochromic displacement causes that the secondary band (L_b^1 according to Platt[18]) becomes visible at 32,000 cm^{-1}, which does not appear with the unhindered nitro-benzene derivatives.

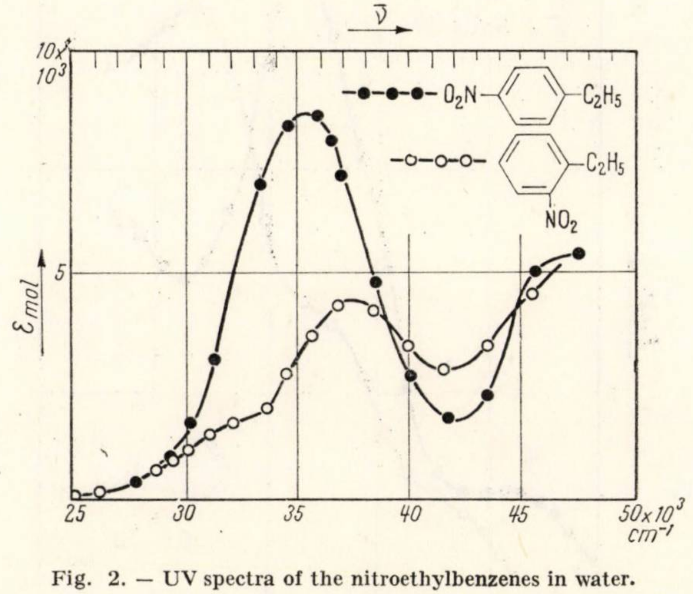

Fig. 2. — UV spectra of the nitroethylbenzenes in water.

o-Nitro-ethylbenzene (II) was chosen in our study as the reference compound because the bulky ethyl group has practically the same steric effect as that of oximinomethyl ($-CH=N-OH$) group. This presumption is supported by the obtained results, namely both *o*-nitro-benzaldoxime and *o*-nitroethylbenzene have absorption bands at 37,500 and 32,000 cm^{-1}, which implies that these bands can be attributed to the system phenyl-nitro, deviated from coplanarity.

---

[16] L. Doub and J. M. Vandenbelt, *J. Amer. Chem. Soc.*, **69**, 2714 (1947); *ibid.*, **71**, 2414 (1949).

[17] "Absorption Spectra of the UV and Visible Region", Ed. by Hungarian Acad. of Sciences, Budapest, 1964, vol. II, p. 109.

[18] J. R. Platt, *J. Chem. Phys.*, **17**, 484 (1949).

Now substracting the spectrum (II) in figure 3 from the spectrum of *o*-nitro-benzaldoxime (spectrum I in fig. 3) the hypothetical spectrum of the steric hindered benzaldoxime (spectra I—II) is obtained, which has a single maximum. The similarity between the character of this hypothetical spectrum and that of the benzaldoxime (curve III in fig. 3)[17] is categorical, on the other hand the hypsochromic and hypochromic displacement of the hypothetical spectrum is to be expected precisely because the *ortho*-steric effect.

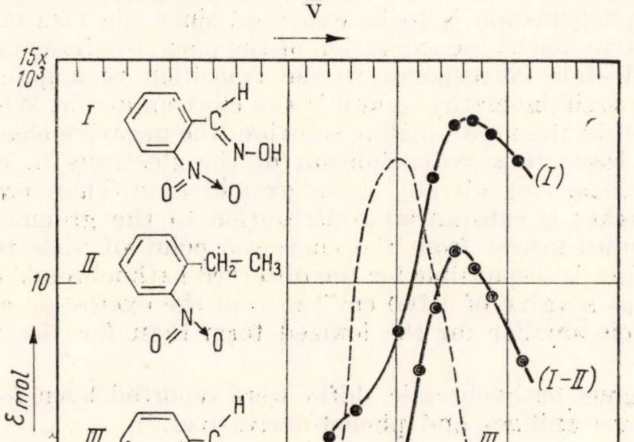

Fig. 3. — Modelation of the spectrum of *o*-nitro-benzaldoxime.

I — *o*-nitrobenzaldoxime in water; *II* — *o*-nitroethylbenzene in water; *III* — benzaldoxime in water; (*I*—*II*) hypothetical spectrum of the steric hindered benzaldoxime.

Consequently, the spectrum of *o*-nitro-benzaldoxime can be considered as an algebraic sum of the relative independent spectra of the steric hindered phenyl-nitro and phenyl-oximinomethyl systems.

The attempts at using the *o*-chloro-bezaldoxime (IV) and *o*-methylbenzaldoxime (V) to model of steric deviated phenyl-oximinomethyl system, do not give satisfactory results, because these small *o*-substituents do not lead to large deviations from coplanarity, contrary to the bulky nitro-group.

The analysis of the spectrum of ionized species (Fig. 1, spectrum II) shows a significant bathochromic displacement of the high-intensity band initially found at 43,200 cm^{-1}, masking in this way the shoulder at 37,500 cm^{-1}. This phenomenon is to be expected since the maximum at 43,200 cm^{-1} was attributed to the excitation of the phenyl-oximinomethyl system. This excited state corresponds to the transition to a quinoid structure in which the oximinomethyl group is the electron donor. When the oxime is dissociated in the used alkaline solution, the negative charge formed on the oxygen leads to a redistribution of the electrons (i. e. of charges) towards benzene ring already in the ground-state. Therefore, the quinoid structure makes a substantial contribution to the ground state, which this way comes nearer from the energetic point of view to the excited state. This fact is responsible for the observed bathochromic displacement. This shift has a value of 4,700 cm^{-1} so that the excitation energy is with 13.4 kcal/mole smaller for the ionized form than for the undissociated oxime.

Analogous bathochromic shifts were reported even for the ionized forms of some aniline- and phenol-derivatives.[16]

B. o-*Nitro-acetophenonoxime* (VI)

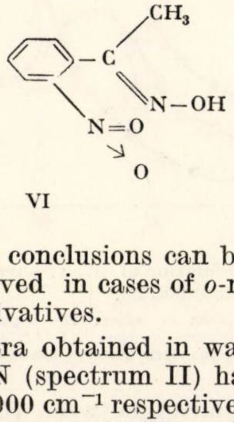

VI

Most of the previous conclusions can be used for the interpretation of the steric effects observed in cases of *o*-nitro-acetophenonoxime (VI) and its *p*-substituted derivatives.

However, both spectra obtained in water (spectrum I, fig. 4) and in sodium hydroxide 0.1 N (spectrum II) have only a single maximum, at 37,500 cm^{-1} and at 40,000 cm^{-1} respectively. Yet, apparently, a significant hypsochromic displacement (2,500 cm^{-1}) following the dissociation can be observed. Evidently this is in all an unexpected and unusual phenomenon, which cannot be justified energetically. On the contrary, a considerable bathochromic shift can be expected, such as in case of *o*-nitro-,*o*-methyl- and *o*-chloro-benzaldoximes. The important increasse in the intensity of the hypsochromic shifted band (hyperchromic effect) is another paradoxical phenomenon.

There is a single explanation of these inconsistent phenomena, namely that the maximum obtained at 37;500 cm^{-1} for the undissociated oxime is not the result of the same transition, as the band of anion, obtained at 40,000 cm^{-1}.

On account of the newly introduced methyl group, it would have been anticipated that the steric effects are more important in *o*-nitro-acetophenonoxime, than in analogous o-nitro-benzaldoxime. In the spectrum of *o*-nitro-benzaldoxime, the absorption band of the hindered phenyl-oximinomethyl system was situated at 43,200 cm^{-1}. The analogous phenyl-α-oximino-ethyl system, due to the additional methyl group, is more deviated from coplanarity, so that the corresponding band must be hypsochromic shifted, thus situated in the far UV-region, being not available in our conditions. Consequently, in the spectrum of the undissociated *o*-nitro-acetophenonoxime only the absorption band of the hindered phenyl-nitro system appears naturally moderately hypsochromic shifted, in comparison with the spectra of *o*-nitro-benzaldoxime and *o*-nitro-ethylbenzene, because of the increased steric hindrance of this system.

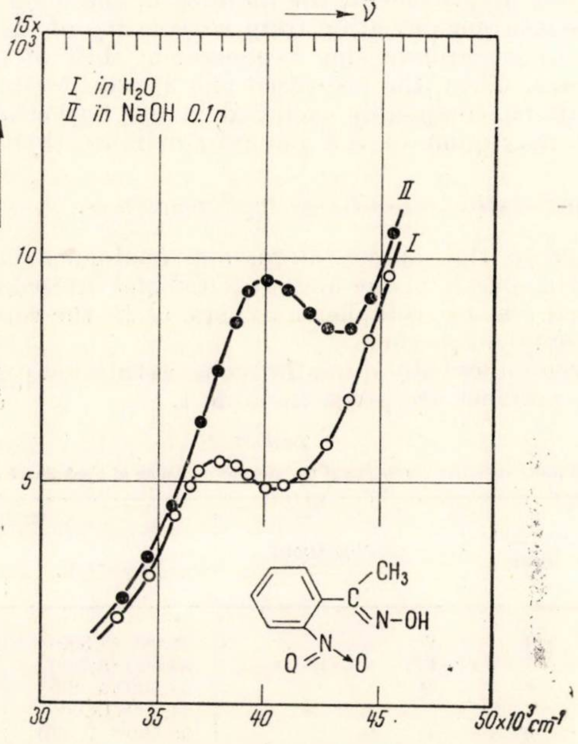

Fig. 4. — UV spectra of the *o*-nitro-acetophenonoxime.
I — in water; *II* — — in NaOH 0.1N

Thus, the similarity is compliant between the spectra of the undissociated *o*-nitro-acetophenonoxime and of *o*-nitro-ethylbenzene from the point of view of the position and of the intensity of absorption bands, because in both cases only the absorption band of the steric deviated phenyl-nitro system appears.

However, in alkaline solution the maximum of the phenyl α-oximinoethyl system also appears, shifted significantly bathochromic. Simultaneously with this displacement, the increase of the bond order of C_1-C_α bond produces a larger deviation from coplanarity of the nitro group, so that a slight hypsochromic and hypochromic shift of the phenyl-nitro band takes place. Thus, the decreased and hypsochromic shifted phenyl-nitro band will be completely included in the bathochromic displaced, high-intensity maximum of the phenyl-α-oximinoethyl system.

C. p-*Substituted* o-*nitro-acetophenonoximes.*

According to the above discussion, analogous bands and shifts were obtained in spectra of the undissociated and ionized forms of a series of *p*-substituted *o*-nitro-acetophenonoximes, as in the case of unsubstituted *o*-nitro-acetophenonoxime.

The wavenumber values and the molar extinction coefficients of the corresponding maxima are given in table 1.

Table 1

Wavenumber values and molar extinction coefficients of the absorption maxima of *p*-substituted *o*-nitro-acetophenonoximes

No. of comp.	No. of[a] figure	*p*-Substituent	$\bar{\nu}\,cm^{-1}\ (\varepsilon_{mol})$	
			in water[c]	in NaOH 0.1 N[d]
VI	4	H	38,000 (5,500)	40,000 (9,500)
VII	7	Cl	39,000[b](5,700)	39,500 (10,500)
VIII	8	Br	38,500[b](5,700) 44,500 (18,000)	39,500 (11,00)
IX	9	I	38,500[b](7,700) 42,000 (19,900)	40,000[b](13,700) 43,000 (17,300)
X	10	$-CH_2OC_2H_5$	37,800 (5,300)	39,500 (10,200)
XI	11	$-CH_2OC_6H_5$	38,000 (6,500)	39,200 (12,000)
XII	12	$-CH_2\overset{\frown}{\underset{\smile}{N\ (CH_2)}}_5$	39,000[b](5,700)	39,500 (10,300)
XIII	13	$-SO_2-C_6H_5$	39,200[b](13,100) 42,100 (21,700)	34,200[b](6,300) 38,500[b](8,800)
XIV	14	$-SO_2-N(CH_3)_2$	38,500[b](8 ,000) 42,600 (14,800)	45,000 (21,000) 38,000 (8,800)

a) Given in the experimental part.
b) Shoulders (inflections).
c) Undissociated oximes.
d) Anions.

Significant differences as compared to the unsubstituted reference compounds were observed only in such cases when the newly introduced substituents are themselves chromophores, and their absorption bands are superposed on the spectrum of the basic system. This phenomenon can be observed in the case of *p*-halo(VII, VIII, IX)-and *p*-sulphonyl-(XIII, XIV)-derivatives.

The comparative study of the *p*-halo-*o*-nitro-aceto-phenonoximes and the corresponding *p*-halo-*o*-nitro-ethylbenzenes (XV, XVI, XVII) demonstrated that the high-intensity bands obtained at low wavelengths can be attributed to the additional chromophores. Thus, the shoulder at 45,000 cm^{-1} obtained for *p*-chloro-derivative (VII) indicates a high - intensity band in the far UV-region. The *p* - bromo - derivative (VIII) already has a maximum at 44,500 cm^{-1}, while this band appears at 42,000 cm^{-1} for *p*-iodo-derivative (IX) covering partly the spectrum of the initial *o*-nitro-α-oximinoethyl system. In the cases of *p*-chloro-and *p*-bromo-derivatives these additional bands have little effect on the remainder parts of the spectra, therefore these are quite similar with that of *o*-nitro-acetophenonoxime.

Similar additional bands can be observed at the corresponding *p*-halo-*o*-nitro-ethylbenzenes which can serve as reference compounds to support these conclusions. The additional high-intensity band is shifted in the same order as in the case of corresponding oximes, this band being

Table 2

Compounds studied

No. of comp.	Compounds	Purified	Characteristics	Ref.
I	*o*-nitro-benzaldoxime	R :dil.acetic acid	m.p.101–102°	(1)
II	*o*-nitro-ethylbenzene	Fract.dist.	n_D^{22} = 1.5352	(19)
III	*p*-nitro-ethylbenzene	Fract.dist.	n_D^{22} = 1.5452	(19)
IV	*o*-chloro-benzaldoxime	R :dil. Ethanol	m.p.75–76°	(20)
V	*o*-methyl-benzaldoxime	R :peth.ether	m.p.49°	analogically to (21)
VI	*o*-nitro-acetophenonoxime	R :dil. ethanol	m.p.119–120°	(19)
VII	*p* chloro-*o*-nitro-AcO	R :ethanol	m.p.155–156°	(22)
VIII	*p*-bromo-*o*-nitro-AcO	R :acetic acid 50%	m.p.147–148°	(22)
IX	*p*-iodo-*o*-nitro-AcO	R :ethanol	m.p.164–165°	(22)
X	*p*-ethoxymethyl-*o*-nitro-AcO	R :benzene	m.p.103–104°	(2)
XI	*p*-phenoxymethyl-*o*-nitro-AcO	R :CCl_4	m.p.124–125°	(2)
XII	*p*-pyperidylmethyl-*o*-nitro-AcO	R :ethanol 80%	m.p.127–129°	(2)
XIII	*p*-phenylsulphonyl-*o*-nitro-AcO	R :ethanol	m.p.159–160°	(22)
XIV	*p*-dimethylaminosulphonyl-*o*-nitro-AcO	R :dil. ethanol	m.p.145–146°	(22)
XV	*p*-chloro-*o*-nitroethylbenzene	Fract. dist.	b.p.100.5–102.5/3 mm	(23)
XIV	*p*-bromo-*o*-nitroethylbenzene	Fract. dist.	b.p.111.5–113.5/3mm	(23)
XVII	*p*-iodo-*o*-nitro-ethylbenzen	Fract. dist.	b.p.125.5–127/3 mm	(23)

R : = recrystallized from...
AcO = acetophenonoxime.

---

[19] N. BODOR and A. KÖVENDI, *Rev. Roumaine Chim.*, **11**, 393 (1966).

[20] "Dictionary of Organic Compounds", Ed. by I. HEILBRON and H. M. BUNBURY, London, 1946, vol. III, p. 778.

[21] A. H. BLATT, "Organic Syntheses", coll. vol. 2, p. 323.

[22] A. KÖVENDI and M. KIRCZ, *Chem. Ber.*, **97**, 1896 (1964).

[23] N. BODOR and A. KÖVENDI, *Rev. Roumaine Chim.*, **11**, 412 (1966).

only well formed in spectrum of *p*-iodo-*o*-nitro-ethylbenzene, at 44,000 cm^{-1}.

The maxima at about 38,000 cm^{-1}, found in all these spectra, evidently can be attributed to the deviated phenyl-nitro system.

EXPERIMENTAL

Compounds used. Compounds described in our previous works, or prepared according to other literature data were used, attention being given to a high purity of the products. These compounds are given in table 2.

UV spectra of the compounds studied. A "Zeiss VSU–1" ultraviolet spectrophotometer was used, in the region of 210–400 nm (47,000 – 25,000 cm^{-1}). On account of the small solubility in water of the compounds studied, initially ethanolic solutions were prepared (1 mg/ml). One ml of these solutions was completed to 100 ml with the corresponding solution (water or sodium hydroxide 0.1 N). One ml ethanol completed to 100 ml with water or NaOH 0.1 N respectively, was used as reference solution.

The extinction values were determined every 10 nm interval, respectively every 5 nm interval at inflections or maximum values. The molar extinction coefficients were calculated from all these values, and plotted on a wavenumber scale.

Revue Roumaine de Chimie, **14**, 235-245 (1969)

ÉTUDE DES CATALYSEURS OXYDE DE CHROME-ALUMINE-POTASSIUM PAR ANALYSE THERMIQUE DIFFÉRENTIELLE ET MESURES DE CHIMISORPTION

I. OLARU*, H. CHARCOSSET, Y. TRAMBOUZE et M. PRETTRE

Institut de Recherches sur la Catalyse du C.N.R.S., France, 39, boulevard du 11 novembre 1918, 69, Villeurbanne

Les diagrammes d'ATD montrent que l'alumine-γ modifie les caractères de la décomposition thermique de l'anhydride chromique en supprimant, en particulier, l'étape intermédiaire de formation du bichromate de chrome. Les mesures de chimisorption d'oxygène permettent de préciser l'état de dispersion de l'oxyde de chrome, Grâce à elles, on a pu montrer que l'effet de l'alumine se transmet, en s'atténuant progressivement, jusqu'à la cinquième couche environ d'ions chrome. Par les mêmes méthodes, on a établi que l'imprégnation par le nitrate de potassium s'accompagne de la formation d'une couche unimoléculaire de biochromate à la surface de l'oxyde de chrome. Le nitrate, lorsqu'il est en excès, se dépose sous forme de sel libre, qui réagit en partie lors des traitements thermiques avec le bichromate pour donner du chromate. Il existe des corrélations très nettes entre les résultats de l'ATD et ceux des mesures de chimisorption.

INTRODUCTION

Le système oxyde de chrome-alumine est connu depuis longtemps pour être un catalyseur très efficace, notamment en déshydrogénation et déhydrocyclisation des paraffines. Il n'est donc pas surprenant que de nombreuses études dont les résultats principaux sont rassemblés dans un article récent de Poole et Mc Iver [1] lui aient été consacrées.

Toutefois, les catalyseurs industriels contiennent toujours un promoteur alcalin, introduit par imprégnation, généralement sous forme de nitrate de potassium ou de potasse. Les interactions chimiques éventuelles de ces sels avec la matrice d'oxyde de chrome et d'alumine demandent à être précisées. En effet, Voltz et Weller,[2] Rubinshtein et ses collaborateurs,[3] Bridges et ses collaborateurs [4] ont émis l'hypothèse de la formation de complexes superficiels de type chromate ou bichromate, mais n'appor-

---

* Institut de Recherches, « Petrochim » 291, Bul. Republicii, Ploieşti, Roumanie.

[1] C. P. Poole et D. S. Mac Iver, *Adv. Catalysis*, **17**, 226 (1967).
[2] S. E. Woltz et S. W. Weller, *J. Phys. Chem.*, **59**, 569 (1955).
[3] A. M. Rubinshtein, N. A. Pribytkova, V. A. Afanasev et A. A. Slinkin, *Kinetika i Kataliz*, **1**, 129 (1960).
[4] J. M. Bridges, G. T. Rymer et D. S. Mac Iver, *J. Phys. Chem.*, **66**, **5**, 870 (1962).

tent pas de preuves formelles. Nicolescu et ses collaborateurs [5] envisagent la création d'une non-stœchiométrie dans le réseau d'oxyde de chrome par suite de l'incorporation d'une partie du potassium.

Afin d'apporter des éléments nouveaux sur la nature de ces phénomènes, nous avons employé deux techniques ; l'analyse thermique différentielle et la détermination de la surface accessible de l'oxyde de chrome par chimisorption.

A. TECHNIQUE EXPÉRIMENTALE

I. *Préparation des catalyseurs*

A 15 g d'alumine-γ, bien agités, on ajoute, goutte à goutte, une solution aqueuses d'anhydride chromique, en quantité telle qu'il y ait absorption totale (7 cm^3).

La concentration de la solution est calculée de façon à obtenir la teneur voulue en chrome. Une partie du solide, destinée à l'ATD, est séchée sous vide à la température ambiante. Le reste est séché 24 h à l'étuve, à 110°, puis placé dans un four à circulation d'air. Il y subit des traitements thermiques successifs d'une heure, à 200, 300 et 400°, avant d'être porté à 500°, température à laquelle il est maintenu durant 24 h.

Ce sont les catalyseurs ainsi traités qui subissent l'imprégnation avec le nitrate de potassium en suivant exactement le mode opératoire décrit à propos de l'anhydride chromique. Comme précédemment, la quantité de solide prélevée pour l'ATD est séchée sous vide à la température ambiante, tandis que le reste subit l'activation dans l'air à 500°, déjà décrite.

II. *Analyses chimiques*

1. *Dosage du chrome*. Après la mise en solution de l'échantillon dans de l'acide sulfurique à 50 %, le chrome est amené dans sa totalité à l'état de Cr^{+6} par oxydation au persulfate d'ammonium, en présence d'ions Ag^+. Il est ensuite titré par du sel de Mohr.

2. *Dosage du potassium*. Il est réalisé par photométrie de flamme sur la solution sulfurique.

III. *Analyse thermique différentielle*

L'appareil est décrit, en détail, par ailleurs. [6] On utilise un thermocouple différentiel Chromel-Alumel. On place 250 mg d'échantillon dans une cellule de 4 mm de profondeur, 4 mm de large et 17 mm de long. Une telle disposition permet un bon contact entre le catalyseur et l'air. Celui-ci est desséché par passage sur anhydride phosphorique, puis dans un piège à carboglace. Son débit est de 3 l/h. Le produit de référence est le kieselguhr à 1 000°. La vitesse de chauffage est de 10°/mn.

IV. *Mesure de la surface occupée par l'oxyde de chrome*

L'adsorbat utilisé est l'oxygène. Le principe et l'application volumétrique de la méthode ont été décrits par Bridges, Mc Iver et Tobin. [7]

---

[5] I. V. Nicolescu, M. Gruia, A. Papia et V. Dumitrescu, *Rev. Roumaine Chim.*, **10**, 523 (1965) et **11**, 363 (1966).

[6] D. Fouque, P. Fouilloux, P. Bussière, D. Weigl et M. Prettre, J. *Chim. phys.*, **62**, 1088 (1965).

[7] J. M. Bridges, D. S. Mac Iver et H. H. Tobin, « Actes du Deuxième Congrès international de Catalyse », Paris, IIe Vol., 1960, p. 2161.

Son adaptation à des mesures gravimétriques et des arguments complémentaires confirmant sa validité ont été présentés par Charcosset, Revillon et Guyot [8] et par Charcosset, Trambouze et ses collaborateurs[9] dans des publications récentes. Nous résumons ici l'ensemble de ces données.

La microbalance est de type Sartorius Electrono Vacuum. Un traitement de 13h par l'hydrogène, sous une pression de 500 torr a pour but de réduire le catalyseur. Il est précédé et suivi d'une désorption de 3h sous pression réduite de 10^{-5} torr à la même température. L'échantillon est ensuite refroidi à $-78°$, sous pression d'argon de l'ordre de 10 torr. L'argon est alors évacué et une pression d'oxygène voisine de 100 torr est introduite. L'équilibre de poids est atteint en 1/2h environ puis l'échantillon est remis sous vide. Il en résulte la désorption de l'oxygène adsorbé physiquement et un nouvel équilibre de poids correspondant à l'oxygène chimisorbé est obtenu en 1/4h environ. Le résultat est indépendant de la pression d'oxygène dans un large domaine de variation de celle-ci.

Théoriquement, le recouvrement maximal correspond à l'existence d'un film bidimensionnel d'oxyde de chrome à la surface du support. Selon cette hypothèse et compte tenu de la structure cristalline de α-Cr_2O_3, des calculs ont montré qu'à une teneur de 1% en chrome correspond une aire maximale de 12 m^2. [7-10]

Le recouvrement réel, $S_{(Cr)}$, est obtenu grâce à un étalonnage effectué sur oxyde de chrome Cr_2O_3 pur. Celui-ci est issu de la décomposition thermique du bichromate d'ammonium suivie de calcination dans l'air, à 700°. Sa surface spécifique déterminée par la méthode BET à l'argon ($\sigma = 14{,}4$ Å^2; P_0 obtenue par extrapolation des données de Born [11] relatives au liquide), à l'aide des mesures gravimétriques, est de 23 m^2/g. Il chimisorbe 3,293 mg/g d'oxygène. A 1 mg d'oxygène chimisorbé correspond donc une surface de 7 m^2 en oxyde de chrome. Le rapport de l'aire théorique maximale définie ci-dessus à l'aire expérimentale $S_{(Cr)}$ donne le nombre moyen de couches d'oxyde de chrome.

La validité de la détermination suppose évidemment que l'adsorption par le support est négligeable, ce qui a été vérifié pour l'alumine-γ.

De plus, elle suppose qu'à une surface égale, la quantité d'oxygène chimisorbée est la même que l'oxyde de chrome, soit pur soit déposé sur le support. A l'appui de cette hypothèse notons que des valeurs de $S_{(Cr)}$, voisines de la valeur théorique ou égales à elle, ont été plusieurs fois observées, tandis que des valeurs supérieures, qui correspondraient à un non-sens physique n'ont jamais été enregistrées. Enfin, lorsque les mesures d'adsorptioin sont faites à 0° au lieu de $-78°$, l'étalonnage effectué sur de l'oxyde de chrome pur condurt à la valeur de 8 m^2/mg au lieu de 7 m^2/mg ; mais compte tenu de cette différence, les valeus de $S_{(Cr)}$ sont pratiquement identiques.

B. SYSTÈME OXYDE DE CHROME-ALUMINE

I. *Surface recouverte par l'oxyde de chrome*

La courbe de variation de $S_{(Cr)}$ en fonction de la teneur en chrome est donnée sur la figure 1. Son allure générale est tout à fait conforme aux résultats de Bridges et ses collaborateurs. On note cependant un écart relativement important de certains points expérimentaux par rapport à la courbe moyenne. Nous l'attribuons à des irréproductibilités dans les conditions d'élaboration des solides, plutôt qu'à une imprécision des mesures de chimisorption. A une teneur en crome de 1,50 %, la valeur de $S_{(Cr)}$ trouvée est égale à la valeur calculée en supposant tous les ions chrome accessibles. A une teneur supérieure, elle s'en écarte progressivement.

---

[8] H. Charcosset, A. Revillon et A. Guyot, *J. Catalysis*, **8**, 326 (1967).

[9] H. Charcosset, D. Barthomeuf, R. Nicolova, A. Revillon, L. Tournayan et Y. Trambouze, *Bull. Soc. chim., France*, **1967**, 4555.

[10] P. W. Selwood, *Bull. Soc. chim., France*, **1949**, D 489.

[11] A. Born, *Ann. Physique*, **69**, 473 (1922).

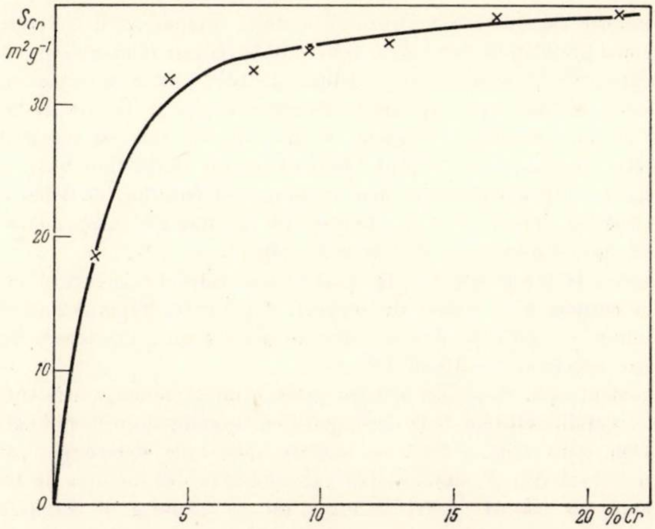

Fig. 1. — Variation de la surface accessible de l'oxyde de chrome, en fonction de la teneur en chrome

Corrélativement, le nombre moyen de couches d'ions chrome croît de 1,6 pour 4,25 % Cr, à 4,5 pour 12,5% Cr et à 6,8 pour 21,1 % Cr.

Il est dès lors logique de penser que pendant l'imprégnation, les premières fractions d'anhydride chromique qui se déposent sur l'alumine forment une pellicule bidimensionnelle sur une partie de la surface de celle-ci. Les fractions suivantes se déposent soit sur une partie libre de l'alumine, en augmentant la surface recouverte, soit sur la première couche d'ions chrome précédemment formée. Au fur et à mesure que la teneur en chrome croît, une proportion de plus en plus grande se fixe sur le sel de chrome déjà déposé, plutôt que sur l'alumine. Ainsi, au-delà d'une teneur en chrome de l'ordre de 7 %, toute quantité supplémentaire ne provoque qu'un accroissement très faible de $S_{(Cr)}$; elle se traduit essentiellement par une augmentation du nombre de couches d'ions chrome. Ce modèle est en bon accord avec les conclusions de Eischens et Selwood [12] déduites des mesures magnétiques.

II. *Analyse thermique différentielle*

La figure 2 reproduit les diagrammes obtenus. Ils présentent tous un pic endothermique vers 120°, dont l'intensité est voisine de celle observée avec l'alumine pure. Ce pic peut être attribué sans ambiguïté à la déshydratation de l'alumine. A 9,5% Cr et au-delà, se manifestent d'autres effets liés à la présence de l'anhydride chromique.

---

[12] R. P. Eischens et S. W. Selwood, *J. Amer. Chem. Soc.*, **69**, 1590, 2698 (1947); **70**, 2271 (1948).

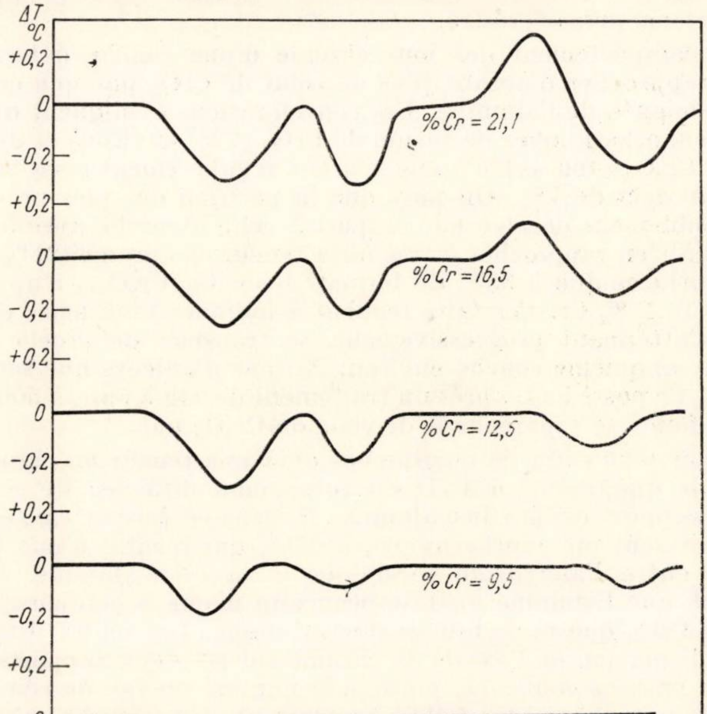

Fig. 2. — Diagrammes d'ATD de l'alumine imprégnée de CrO_3.

Nous avons vérifié que le diagramme fourni par CrO_3 pur est conforme aux données de Lorthioir et Michel. [13] Il présente des pics endothermiques intenses à 200 et 400°, attribués par ces auteurs à la fusion et à la décomposition en Cr_2O_3, ainsi que deux pics exothermiques. L'un, intense, à 330°, correspond à une réduction partielle en bichromate de chrome $Cr_2(Cr_2O_7)_3$ et l'autre, très faible, à 410°, à la formation d'un polychromate $Cr_4(Cr_7O_{27})$.

L'absence totale de ces pics pour des teneurs en chrome inférieures à 9,5 % est due à l'accroissement déjà signalé [14] de la stabilité thermique de l'anhydride chromique, en présence d'alumine. A cet égard, on peut noter que les solides de faible teneur en chrome traités 24h à l'air à 500° conservent la coloration jaune des solides imprégnés. De plus, l'effet du support doit s'exercer avec une intensité maximale sur la première couche d'ions chrome, puis décroître.

---

[13] G. Lorthioir et A. Michel, *Compt. rend.*, **258**, 4560 (1964).

[14] J. Deren, J. Haber et J. Siechowski, «Proceedings of the Third International Congress of Catalysis», Amsterdam, Ier vol., 1964, p. 993.

Le comportement des ions chrome d'une couche déterminée doit donc se rapprocher d'autant plus de celui de CrO_3 pur que cette couche est plus éloignée de l'alumine. Ces considérations expliquent que les aires des pics endothermiques de fusion de CrO_3 (225° environ) et de décomposition en Cr_2O_3 (400 à 420°) augmentent régulièrement avec la teneur en chrome au-delà de 7%. On note que la position des pics précédents est assez sensiblement décalée par rapport à celle observée avec le CrO_3 pur. Elle tend à s'en rapprocher à très forte teneur en chrome (21%). De plus, le pic exothermique à 330° de formation de $Cr_2(Cr_2O_7)_3$ n'apparaît qu'à partir de 16,5 % Cr. Ces faits tendent à indiquer l'influence du support, tout en s'atténuant progressivement, se transmet de proche en proche jusqu'à la cinquième couche environ. Notons d'ailleurs que seuls les solides à 21% Cr possèdent, après un traitement de 24h à l'air, à 500°, une couleur vert foncé se rapprochant de celle de Cr_2O_3 pur.

Il convient enfin de mentionner qu'à une teneur en chrome voisine (12,5%), le diagramme d'ATD est totalement différent de celui obtenu quand le support est la silice-alumine. [15] Dans ce dernier cas, en effet, on observe un seul pic exothermique, à 270°, qui résulte d'une interaction chimique entre l'anhydride chromique et la silice-alumine. Il apparaît clairement que l'alumine modifie beaucoup moins le comportement thermique du CrO_3 que ne le fait la silice-alumine. Les seules différences de l'état de dispersion de l'oxyde de chrome sur ces deux supports devraient intervenir en sens contraire, puisque le nombre moyen de couches d'ions chrome est nettement plus faible sur alumine. En fait, il semble que l'interaction chimique entre l'anhydride chromique et l'alumine-γ est nulle ou très limitée. Les effets observés résulteraient plutôt d'autres phénomènes, telle une orientation du réseau cristallin de l'anhydride chromique par celui de l'alumine.

C. SYSTÈME OXYDE DE CHROME-ALUMINE-POTASSIUM

Trois séries de solides à teneurs variables en potassium ont été préparées. Elles concernent respectivement les catalyseurs oxydes de chrome-alumine à 3, 10 et 20% Cr. Nous décrivons tout d'abord les résultats relatifs à la série à 10% Cr qui a fait l'objet de l'étude la plus détaillée.

I. *Etude par ATD des catalyseurs à 10 % Cr et K variable*

Les diagrammes obtenus sont représentés sur la figure 3. Outre le pic endothermique à 120°, dû à la déshydratation de l'alumine, apparaissent, au moins, 5 pics, tous endothermiques, à 126, 200, 265, 330 et 400°.

---

[15] A. Guyot, H. Charcosset, A. Revillon et G. Vuillaume, *J. Macromol. Science* (sous presse).

Au-delà de cette dernière température et jusqu'à 600°, on n'observe pas de phénomène net. L'attribution des pics a été faite à l'aide d'expériences témoins notamment sur le nitrate et le bichromate de potassium purs, complétées par des indications bibliographiques.[16] Nous avons pu établir de cette façon que les phénomènes observés à 126, 200, 330 et 400° sont dus respectivement à la transformation allotropique de KNO_3 et aux fusions de CrO_3, KNO_3 et $K_2Cr_2O_7$. L'interprétation du pic situé à 265° s'est avérée plus délicate. En effet, $K_2Cr_2O_7$ subit bien à cette température un changement de phase cristalline, mais la chaleur mise en jeu est trop faible pour rendre compte, à elle seule, de la totalité du phénomène. Par contre, il est logique de penser que cette transformation se traduit par une augmen-

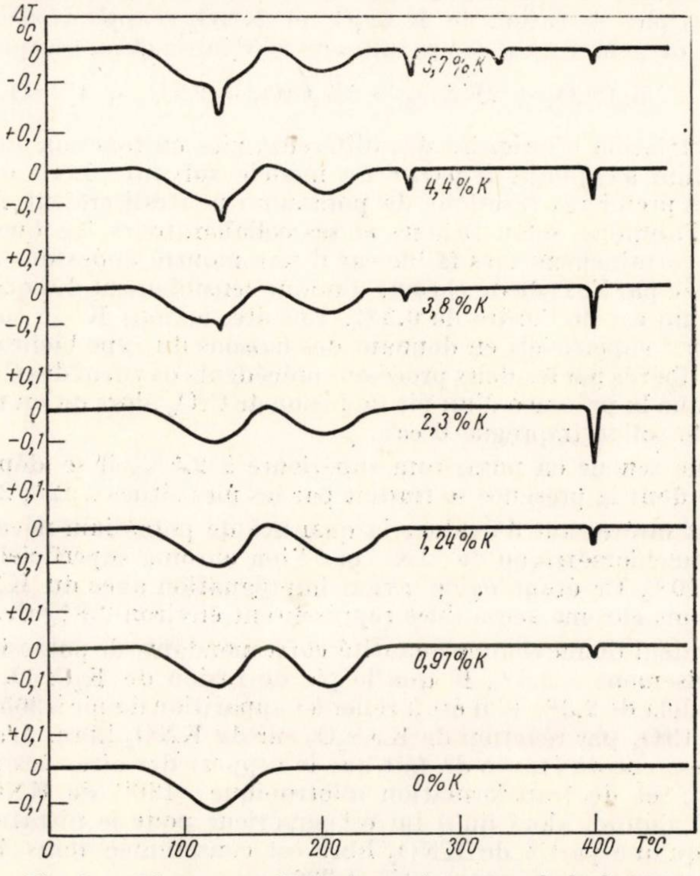

Fig. 3. — Diagrammes d'ATD des catalyseurs oxyde de chrome-alumine (10 % Cr) imprégnés de KNO_3.

---

[16] I. Langmuir, *J. Amer. Chem. Soc.*, **42**, 274 (1920) ; D. J. Hissink, *Z. phys. Chem.*, **32**, 541 (1900) ; E. Groschuff, *Z. anorg. Chem.*, **58**, 102 (1908).

tation de réactivité de $K_2Cr_2O_7$, conforme à l'effet Hedwall,[17] qui pourrait faciliter sa réaction avec le KNO_3. Effectivement, un mélange à teneur égale en potassium de $K_2Cr_2O_7$ et de KNO_3 donne seulement deux pics endothermiques, le premier à 126° et le second, très intense, à 268°. Puisque les pics de fusion de $K_2Cr_2O_7$ et KNO_3 n'apparaissent pas, il y a tout lieu de penser qu'il se produit vers 265° la réaction complexe

$$K_2Cr_2O_7 + 2KNO_3 \rightarrow 2K_2CrO_4 + 2NO_2 + 1/2\ O_2$$

La variation d'intensité des différents pics en fonction de la teneur en potassium s'explique à partir du modèle suivant. Lors de l'imprégnation, les premières fractions de potassium neutraliseraient des centres acides de l'alumine, selon Bridges et ses collaborateurs. La quantité mise en jeu est certainement très faible car il sera montré ci-dessous que la surface occupée par l'oxyde de chrome diminue sensiblement dès que la teneur en potassium est de l'ordre de 0,3 %. Ensuite, les ions K^+ se combinent à des ions Cr^{+6} superficiels en donnant des liaisons du type bichromate. Les ions NO_3^- libérés par les deux processus précédents oxydent des Cr^{+3} en Cr^{+6}. Ceci explique la présence d'un pic de fusion de CrO_3 alors qu'on n'en décèle pas pour le solide imprégné d'eau.

A une teneur en potassium supérieure à 2,5 %, il se dépose du nitrate libre dont la présence se traduit par les pics situés à 126, 265 et 330°.

Il est intéressant d'évaluer la quantité de potassium nécessaire à la fixation stœchiométrique de $1K^+$ par l'ion chrome superficiel. La valeur de $S_{(Cr)}$ à 10 % Cr étant égale avant imprégnation avec du KNO_2 à 33,4 m^2/g, les ions chrome accessibles représentent environ 2,8 % Cr.

Le calcul donne comme quantité correspondante de potassium 21,1 %. C'est précisément à 2,3 % K que le pic de fusion de $K_2Cr_2O_7$ est maximal et au-delà de 2,3 % K il est à relier à l'apparition du pic à 265° de formation de K_2CrO_4 par réaction de $K_2Cr_2O_7$ sur du KNO_3 libre. L'attribution de ce pic est encore étayée du fait que le rapport des aires des pics de fusion (330°) et de transformation allotropique (126°) de KNO_3 est ici inférieur à l'unité, alors qu'il lui est supérieur pour le nitrate pur. Ceci confirme qu'une partie de KNO_3 libre est consommée dans le domaine de température compris entre 126° et 330°.

II. *Etude par l'ATD des catalyseurs à 20 % et 3 % Cr et % K variable*

A une teneur égale en potassium, les solides à 20 % Cr donnent des diagrammes identiques à ceux obtenus avec les catalyseurs à 10 % Cr, ce qui n'est pas surprenant puisque la fixation du potassium semble être, dans nos conditions de préparation des solides, un phénomène essentiellement superficiel et vu que la surface occupée par l'oxyde de chrome est sensiblement la même (33,8 au lieu de 33,2 m^2/g). Les diagrammes relatifs aux solides à 3 % Cr sont représentés sur la figure 4. On constate tout d'abord que le pic de transformation allotropique de KNO_3 apparaît dès 2,2 % K, c'est-à-dire un peu plus tôt que pour les séries à 10 à 20 % Cr. Ceci est à relier au fait que la surface occupée par l'oxyde de chrome a une valeur un peu plus faible (29,4 m^2/g). On peut donc penser que la formation de $K_2Cr_2O_7$ se produit comme précédemment. Mais les pics de fusion de ce composé (400°) et de réaction avec le KNO_3 libre (265°) n'apparaissent en aucun cas. La même observation a été faite en imprégnant l'alumine directement de $K_2Cr_2O_7$. A 3% Cr, le bichromate se trouve directement

---

[17] J. A. Hedwall, „Einführung in die Festkörperchemie", 1952, p. 182.

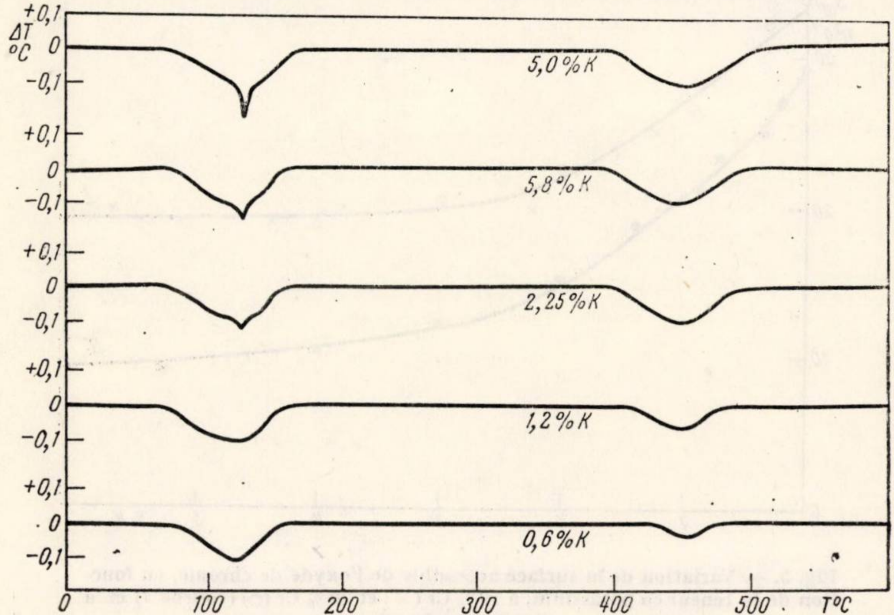

Fig. 4. — Diagrammes d'ATD des catalyseurs oxyde de chrome-alumine (3% Cr) imprégnés de KNO_3.

au contact du support au lieu d'être situé sur une couche d'oxyde de chrome comme c'était le cas à 10 et 20% Cr. Il est probable que l'alumine exerec pour le $K_2Cr_2O_7$ une stabilisation vis-à-vis des traitements thermiques, comparable à celle déjà mentionnée à propos de l'anhydride chromique.

Le pic endothermique situé entre 400 et 500° a une intensité qui augmente avec la teneur en potassium jusqu'à 2%, puis reste sensiblement constante. Il ne semble pas dû à une réaction du bichromate mais relié plutôt à la présence d'ions nitrates. Il apparaît, en effet, avec l'alumine imprégnée de KNO_3(5%K) ou d'acide nitrique de concentration équivalente. Il est vraisemblablement dû à la décomposition du nitrate d'aluminium formé lors de l'imprégnation du solide à 3% Cr avec du KNO_3. L'acide nitrique libéré ne peut en effet oxyder ici des ions Cr^{+3} puisque le chrome se trouve déjà, au moins dans sa presque totalité, au degré d'oxydation +6.

III. *Surface occupée par l'oxyde de chrome*

La figure 5 donne les courbes de variation du $S_{(Cr)}$, en fonction de la teneur en potassium pour les trois séries de solides examinées. Aux erreurs expérimentales près, les points relatifs à 10 et 20 % Cr conduisent à la même courbe moyenne. De plus la diminution de $S_{(Cr)}$ est rapide jusqu'à une teneur en potassium de l'ordre de 2 %, puis plus lente, principalement à forte teneur en chrome (courbe *1*).

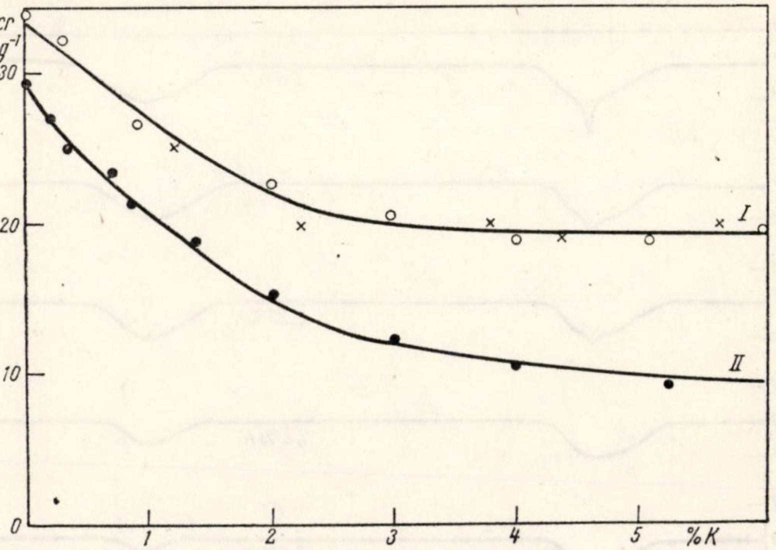

Fig. 5. — Variation de la surface accessible de l'oxyde de chrome, en fonction de la teneur en potassium, à 10 % Cr (×) et 20 % Cr (○) (courbe *1*) et à 3 %Cr (courbe *2*).

Ces résultats corroborent les conclusions des expériences d'analyse thermique différentielle. En effet, l'analogie des diagrammes d'ATD à 10 et 20 % Cr a montré qu'à une teneur donnée en potassium, l'état superficiel des solides est sensiblement le même ; il est donc normal que les valeurs de $S_{(Cr)}$ soient très voisines. Quant au changement de pente observé dans les courbes de variation de $S_{(Cr)}$ pour des teneurs en potassium inférieures à 2 %, il est à relier au dépôt de nitrate libre lors de l'imprégnation avec du KNO_3. Il est logique de penser que le produit issu des transformations du KNO_3 libre a un effet de blocage plus faible que le potassium lié à l'oxyde de chrome sous forme de complexe superficiel.

CONCLUSIONS

1. L'aire recouverte par l'oxyde de chrome déposé sur alumine augmente jusqu'à 5 % Cr, puis tend vers un palier. L'alumine modifie les caractères de la décomposition thermique de l'anhydride chromique. Son effet, maximal pour la première couche d'ions chrome, s'atténue progressivement pour s'annuler à partir de la sixième couche environ. Il se traduit en particulier par la suppression de l'étape intermédiaire de formation de bichromate de chrome.

2. Lors de l'imprégnation avec le nitrate de potassium il se forme à la surface de l'oxyde de chrome une couche unimoléculaire de bichromate. Le nitrate de potassium en excès se dépose sous forme de sel libre et réagit, en partie, lors des traitements thermiques, avec le bichromate pour former du chromate. La surface libre de l'oxyde de chrome, déterminée après des traitements à 500°, diminue rapidement jusqu'à une teneur en potassium de 2%, puis très lentement. C'est précisément à une teneur en potassium supérieure à 2% que se manifeste la présence du nitrate libre.

Les auteurs expriment leurs remerciements à Monsieur H. Urbain et à ses collaborateurs, Messieurs M. Galley et R. Bacaud, auxquels ils doivent les résultats des analyses chimiques.

Revue Roumaine de Chimie, **14**, 247–252 (1969)

ISOTOPIC EXCHANGE OF ACTIVE METHYL HYDROGENS. VI[1]

DEUTERATION OF 2,4,6-TRIPHENYL-, 2,3,5,6-TETRAMETHYL- AND 2,3,6-TRIMETHYL-4-PHENYL-PYRYLIUM SALTS

EUGENIA GÂRD, ILEANA STĂNOIU, A. T. BALABAN

Institute of Atomic Physics, Bucharest, P.O.Box 35

and F. CHIRALEU

Centre of Organic Chemistry, Bucharest, Spl. Independenţei 89

Received September 11, 1968

2,3,5,6-Tetramethylpyrylium perchlorate is deuterated in D_2O only at the α-standing methyl groups, in a fast reaction. 2,4,6-Triphenylpyrylium perchlorate is slowly deuterated in the β-position on heating in CH_3COOD. 2,3,6-Trimethyl-4-phenylpyrylium perchlorate in D_2O exchanges rapidly the α-methyl hydrogen atoms and slowly the β-standing pyrylium hydrogen. The reaction mechanism is discussed.

I. INTRODUCTION

Previous papers in this series have reported the isotopic exchange between D_2O or CH_3COOD, in neutral or acidic conditions, and alkyl-substituted pyrylium salts. It was found that for 2,4,6-trimethylpyrylium perchlorate in D_2O, γ-methyl hydrogens are exchanged very fast, α-methyl hydrogens fast, and β-standing hydrogens slowly.[1] The reactivity order of α- and γ-methyl hydrogens is the same in 2-methyl-4,6-diphenyl- and 4-methyl-2,6-diphenylpyrylium perchlorate,[2] which have only one kind of methyl group.

So far, no study had been made to see whether an exchange is possible for hydrogens of β-methyl groups in pyrylium salts, or for hydrogens bonded to γ- or α-carbon atoms in pyrylium salts. The present study of the deuteration of 2,3,5,6-tetramethylpyrylium perchlorate gives negative answers to the first two questions. Also, we now report the isotopic exchange between CH_3COOD and 2,4,6-triphenylpyrylium perchlorate where the only exchangeable hydrogens are in the β-position of the pyrylium ring. Lastly, 2,3,6-trimethyl-4-phenylpyrylium perchlorate combines structural features of the former two salts (rapidly exchangeable α-methyl protons, slowly exchangeable β-hydrogen, non-exchangeable β-methyl protons).

---

[1] Previous part, E. Gârd, A. Vasilescu, G. D. Mateescu and A. T. Balaban, *J. Labelled Comp.*, **3**, 196 (1967).

[2] E. Gârd, I. Bally, A. Vasilescu, A. Arsene and A. T. Balaban, *ibid.*, **1**, 182 (1965).

II. EXPERIMENTAL PART

2,4,6-Triphenylpyrylium perchlorate was prepared from acetophenone (1 mole) and halcone[3] (2 moles) in the prese nce of perchloric acid[4]; the condensation to 1,3,5-triphenylpentane-1,5-dione, its dehydrogenation by the conjugate acid of chalcone, and the dehydration to a pyrylium salt are merged in one step.[4-6] The purification was effected by recrystallization from acetic acid; m.p. 290°.

2,3,5,6-Tetramethylpyrylium perchlorate was prepared by diacetylation of 2-pentene with acetic anhydride and perchloric acid, [7] and recrystallized from *n*-butanol; m.p. 83°. The dehydration of 2-pentanol (b.p. 121°) to 2-pentene (b.p. 39.9–40°) was effected by the action of sulphuric acid. [8]

2,3,6-Trimethyl-4-phenylpyrylium perchlorate was obtained by a method similar to that employed for preparing 2,4,6-trimethyl-3-phenylpyrylium perchlorate.[9] From acetophenone and ethylmagnesium bromide, decomposing the reaction mixture with a solution of ammonium chloride, ethyl-methyl-phenyl-carbinol was obtained. This carbinol (25 g) and acetic anhydride (100 ml) were treated gradually, under reflux and stirring, with 25 ml 72% perchloric acid. After cooling, ether was added, and the lower layer was left overnight to crystallize. Recrystallization from water acidified with perchloric acid gave the perchlorate m.p. 148°. (*Found* : C, 56.05; H, 4.82. $C_{14}H_{15}O^+ClO_4^-$ requires: C, 56.29; H, 5.06%). The infrared spectrum of the perchlorate presents strong I. R. bands [10] at 1625 (ν8a Π^+), 1592 (ν8a Ph), 1516, 1483, 1452, 1392, 1330, 1234, 800 and 740 cm^{-1}. On deuteration, the weak CH stretching bands at 2927 and 2973 cm^{-1} disappear and are replaced by weak bands at 2100, 2127, 2230, 2260 and 2305 cm^{-1}.

Deuterations were effected by heating the perchlorate in deuterium oxide or in CH_3COOD,[2] and deuterium analyses were performed by combustion and refractometry of the condensed water. [2]

Nuclear magnetic resonance spectra were recorded with a Varian A–60 A spectrometer in liquid sulphur dioxide. Infrared absorption spectra were recorded with a Jena UR–10 apparatus in potassium bromide pellets.

III. RESULTS

III.1. *Isotopic exchange between deuterium oxide and 2,3,5,6-tetramethylpyrylium perchlorate* (I). The nuclear magnetic resonance spectrum of I in liquid sulphur dioxide [11] presents three peaks at τ : 1.51 (1 H) due to the γ-hydrogen, 7.09 (6H) due to the α-methyl hydrogens and 7.48 (6H) due to the β-methyl hydrogens. Besides integration giving relative intensities 1.06 : 5.95 : 5.95 of these peaks, in agreement with formula I, a count of the hydrogens was also made (cf. [1]) by adding to A mg I in SO_2 a known amount B of tetramethylammonium bromide (mol. weight 154.1 g/mole) whose peak at τ 6.75 due to 12 hydrogen atoms serves as an internal intensity standard.

---

[3] E. P. Kohler and H. M. Chadwell, Org. Synth. Coll., Vol. 1, 2nd Ed., p. 78 (1941).

[4] A. T. Balaban, *Compt. rend.*, **256**, 4239 (1963).

[5] J. A. Van Allen and G. A. Reynolds, *J. Org. Chem.*, **33**, 1102 (1968).

[6] A. T. Balaban, A. R. Katritzky and B. Semple, *Tetrahedron*, **23**, 4001 (1967).

[7] P. F. G. Praill and L. Whitear, *J. Chem. Soc.*, **1961**, 3573.

[8] J. F. Norris and F. C. Whitmore, "Org. Synth. Coll.", Vol. 1, 2nd Ed., p. 430 (1941).

[9] A. T. Balaban, *Tetrahedron Letters*, **1963**, 91.

[10] A. T. Balaban, G. D. Mateescu and M. Elian, *Tetrahedron*, **18**, 1083 (1962).

[11] A. T. Balaban, G. R. Bedford and A. R. Katritzky, *J. Chem. Soc.*, **1964**, 1646.

If the integrated intensities of the Me_4N^+ peak at τ 6.75 and of a pyrylium proton peak are y and x mm respectively, the number of pyrylium protons is 12 MB x/154.1 Ay, where the molecular weight M is 236.5 g/mole for the non-deuterated (I) and 242.5 g/mole for the deuterated pyrylium salt (IV).

Deuterations were performed by heating at 100° solutions of 1 g perchlorate I in 20 ml 99.6% deuterium oxide; after a prescribed time the solvent was distilled off in vacuum. Several successive deuterations can be carried out with fresh portions of deuterium oxide. Results of NMR and refractometric deuterium oxide analyses indicate already after 5 hrs complete deuteration of the α-methyl groups. In order to force deuteration of the β-methyl groups or of the γ-hydrogen, the samples were heated longer times in deuterium oxide.

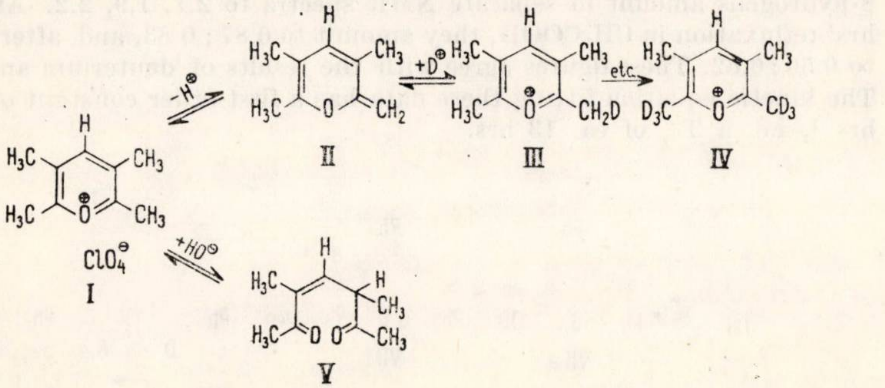

Table 1

Deuteration of 2,3,5,6-tetramethylpyrylium perchlorate in deuterium oxide at 100°

Product	Time hrs	Amount, mg		NMR integrated intensities, mm				No. of protons		
		I	$Me_4N^{\oplus}Br^{\ominus}$	$Me_4N^{\oplus}Br^{\ominus}$	γ-H	α-CH_3	β-CH_3	γ-H	α-CH_3	β-CH_3
		A	B	y	x					
Initial	—	67.5	16.9	46	10	56	56	1.0	5.6	5.6
Deuterated	40	85.8	14.2	57	15	0	111	0.82	0	6.08
Deuterated	70	99.0	12.1	61	25	0	157	0.94	0	5.95

As seen from table 1, the peak at τ 7.09 disappears completely on deuteration whereas the other two peaks remain practically constant. Therefore no deuteration can be observed of the γ-hydrogen or of the β-methyl hydrogens in these conditions.

III.2. *Isotopic exchange between 2,4,6-triphenylpyrylium perchlorate (VI) and CH_3COOD.* The NMR spectrum of VI in SO_2 consists in two multiplet peaks at τ ca. 2.2 (due to the 9 *p*- and *m*-protons of the phenyl groups) and 1.7 (due to the 6 *o*-protons of the phenyl groups), and in a singlet peak at τ 1.39 due to the two protons bonded to the β positions of the pyrylium ring. On refluxing 0.5 g VI in 70 ml CH_3COOD at 118°, the latter peak slowly decreases indicating isotopic exchange of the β-protons. Owing to partial overlapping with the phenyl multiplet centered at τ 1.7, and to the limited solubility of the pyrylium perchlorate in liquid sulphur dioxide, integral curves are imprecise. No internal standard for counting hydrogens was employed because the phenyl hydrogens do not exchange and serve as standard. For the non-deuterated pyrylium salt, the number of β-hydrogens amount in separate NMR spectra to 2.1, 1.9, 2.2. After 18 hrs' refluxation in CH_3COOD, they amount to 0.87 ; 0.83, and after 23 hrs to 0.50 ; 0.62. These figures agree with the results of deuterium analyses. The kinetic equation fitting these data has a first-order constant of 0.055 hrs^{-1}, i.e. a $T_{1/2}$ of ca. 13 hrs.

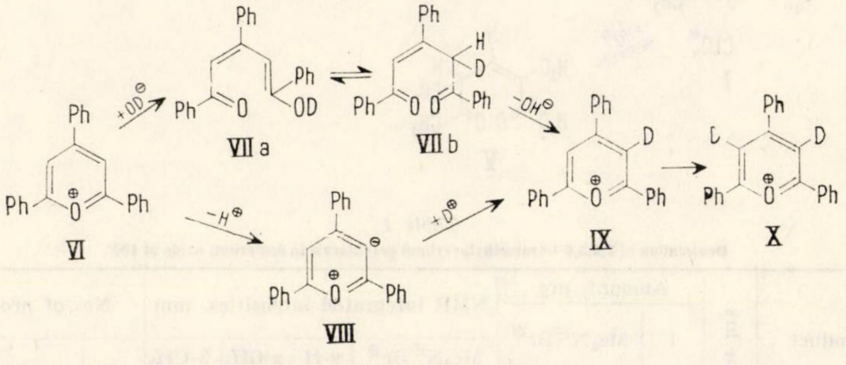

III.3. *Isotopic exchange between deuterium oxide and 2,3,6-trimethyl-4-phenylpyrylium perchlorate (XI).* The NMR spectrum of XI (not recorded previously) contains five peaks at τ : 7.52 (3H) due to the β-methyl group, 7.03 and 7.00 (3H each) due to the α-methyl groups, 2.36 (5H, fairly sharp multiplet) due to the phenyl group and 2.29 (1H) due to the β proton. On heating at 100° in deuterium oxide, the peaks due to the α-methyl groups decrease with a first order constant of ca. 0.1 min^{-1}, i.e. $T_{1/2} = 7$ min. Then, much more slowly, the peak at τ 2.29 also decreases indicating β-deuteration and is no longer visible after 140 hrs' heating ;

because of overlapping with the phenyl multiplet integrated curves are imprecise : $T_{1}/_{2}$ is 20−25 hrs. Isotopic exchanges in AcOD proceed appreciably more slowly than in D_2O, in agreement with previous data.[2]

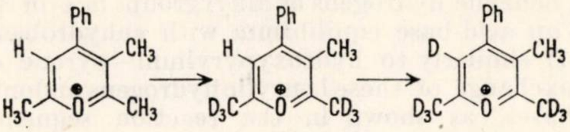

XI XII XIII

IV. DISCUSSION OF THE RESULTS

On the basis of the present and previous data, the following conclusions can be drawn on the isotopic exchange of pyrylium salt with D_2O or AcOD :

(*i*) benzylic hydrogens of alkyl groups in γ position are exchanged very fast ;

(*ii*) benzylic hydrogens of alkyl groups in α positions are exchanged fast ;

(*iii*) other hydrogen atoms of alkyl groups are not exchanged ;

(*iv*) β-standing hydrogen atoms are exchanged slowly ;

(*v*) γ-standing hydrogen atoms are not exchanged ;

(*vi*) addition of bases increases the rate of exchange ;

(*vii*) there are as yet no data for exchange of α-standing hydrogen atoms.

These findings agree with data for the isotopic exchange of pyridines, [12,13] pyridine-N-oxides[14] or pyridinium salts,[14] and their methyl-derivatives, [15,16] in strongly basic media. Similar isotopic exchange reactions were observed for other six-membered heterocyclic systems like pyrazines[17] or pyrimidines [18] where benzylic hydrogens are exchanged in relatively mild conditions. 4-Pyrones can be considered as pyrylium salts with a 4-oxide substituent ; being strongly activated towards electrophilic

---

[12] J. A. Zoltewicz and C. L. Smith, *J. Amer. Chem. Soc.*, **89**, 3358 (1967) ; J. A. Zoltewicz and J. D. Meyer, *Tetrahedron Letters*, **1968**, 421.

[13] A. R. Katritzky and B. J. Ridgewell, *J. Chem. Soc.*, **1953**, 3753 ; A. R. Katritzky and C. D. Johnson, *Angew. Chem.*, **79**, 629 (1967).

[14] R. A. Abramovitch, G. M. Singer and A. R. Vinutha, *Chem. Commun.*, **1967**, 55 ; R. A. Abramovitch and J. B. Davis, *J. Chem. Soc.*, in press.

[15] T. I. Abramovich, I. P. Gragerov and V. V. Perekalin, *Zhur. obshchei Khim.*, **31**, 1962 (1961) ; *Doklady Akad. Nauk. SSSR*, **121**, 295 (1958).

[16] N. N. Zatsepina, A. V. Kirova and I. F. Tupitsyn, *Organic Reactivity* (*Tartu*), **5**, 70 (1968).

[17] R. L. Lichter, *Diss. Abs.*, **28**, 841−B (1967).

[18] T. J. Batterham, D. J. Brown and M. N. Paddon-Row, *J. Chem. Soc.*, (B), **1967**, 171 ; L. A. Paquette and L. D. Wise, *J. Amer. Chem. Soc.*, **90**, 807 (1968).

substitutions, they exchange easily the 3- and 5-protons [19-21] (correcting previous erroneous data [22]).

Unlike pyridines, pyrylium salts cannot exist in the prevailing reaction conditions both as a free and/or a protonated species; however, pyrylium salts with benzylic hydrogens of alkyl groups in α- or γ-positions (e.g. I, III) present an acid-base equilibrium with anhydrobases (methylenepyrans) (e.g. II) similarly to hydroxypyrylium—pyrone equilibria. The rapid isotopic exchange of these benzylic hydrogens undoubtedly involves these anhydrobases, as shown in the reaction sequence I→IV. The absence of exchange of benzylic hydrogens of β-standing alkyl groups agrees with the non-existence of β-methylenepyrans.

So far, attempts to trap such methylenepyrans by reaction with 1,3-dipolar reagents have been unsuccessful.

The isotopic exchange of β-hydrogens attached to the pyrylium ring can involve (*i*) electrophilic protonation—deprotonation of methylenepyrans, when these are possible; (*ii*) ring-opening of the pyrylium nucleus by addition of anions such as hydroxy, acetoxy, etc. with formation of enolic 1,5-enediones (pseudobases) e. g. VII; (*iii*) deprotonation of the pyrylium ring with formation of betaines, such as VIII, as argued for azaaromatics, [12,14] or (*iv*) a plurality of mechanisms. Taking into account the oxygen exchange, [23] we favour pathway (*ii*); when data for the isotopic exchange of α-hydrogens will become available, pathway (*iv*) will be able to be evaluated more exactly.

[19] P. Beak and G. A. Carls, *J. Org. Chem.*, **29**, 2678 (1964).

[20] D. W. Mayo, P. J. Sapienza, R. C. Lord and W. D. Phillips, *ibid.*, **29**, 2682 (1964); R. C. Lord, D. W. Mayo and W. D. Phillips, *Analyt. Chem.*, **26**, 429 (1954).

[21] P. Bellingham, C. D. Johnson and A. R. Katritzky, *Chem. Commun.*, **1967**, 1047.

[22] R. C. Lord and W. D. Phillips, *J. Amer. Chem. Soc.*, **74**, 2429 (1952).

[23] E. Gârd, A. Runge, A. Barabas and A. T. Balaban, *J. Labelled Comp.*, **3**, 151 (1967).

Revue Roumaine de Chimie, **14**, 253–261 (1969)

HETEROCYCLIC ORGANOBORON COMPOUNDS. XI*)

BORONIUM CHELATE SALTS AND BERYLLIUM CHELATES OF 2-SUBSTITUTED 1,3-DIKETONES; METHYL-ACETYLACETONE, PHENYL-ACETYLACETONE AND METHYL-DIBENZOYLMETHANE

A. BARABÁS, ELENA IŞFAN, ELENA ROMAŞ and ALICE TRESTIANU
Institute of Atomic Physics, Bucharest, P. O. Box 35

Received April 30, 1968

Boronium salts of the formula $[(1,3\text{-diket})_2B]^+X^-$, (I) were prepared and characterized, in which the 1,3-diketones were: methyl-acetylacetone (R_1, R_2, R_3 = = Me), phenyl-acetylacetone (R_1, R_3 = Me, R_2 = Ph) and methyl-dibenzoylmethane (R_1, R_3 = Ph, R_2 = Me). Salts with the following anions were prepared: $X = Cl^-$, $FeCl_4^-$, $SbCl_6^-$, ClO_4^- and I_3^-. The beryllium chelates of the same 1,3-diketones were also prepared and characterized. Ultraviolet, infrared and nuclear magnetic resonance spectra of the prepared complexes were recorded and discussed.

INTRODUCTION

In a previous paper,[1] several chelated boronium salts of the most common 1,3-diketones, acetylacetone, benzoylacetone and dibenzoylmethane were described. For all these compounds I, R_2 = H. In the present paper we report the preparation of analogous chelate salts starting from 1,3-diketones in which the central methlyene group bears an alkyl or aryl substituent.

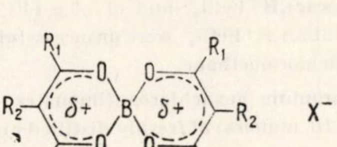

I

Derivatives of the following 1,3-diketones were prepared: 3-methyl-2,4-pentanedione (methyl-acetylacetone, meacacH), 3-phenyl-2,4-pentanedione (phenyl-acetylacetone, phacacH) and 2-methyl-1,3-diphenyl-1,3-propanedione (methyl-dibenzoylmethane, medbmH). The anions X^- used were Cl^-, $FeCl_4^-$, $SbCl_6^-$, ClO_4^-, and I_3^-.

---

*) Paper X: I. Bally, E. Ciornei and A. T. Balaban, *Revue Roumaine Chim.*, **13**, 1507 (1968).

[1] A. Barabás, E. Işfan, M. Roman, M. Paraschiv, E. Romaş and A. T. Balaban, *Tetrahedron*, **24**, 1133 (1968).

EXPERIMENTAL PART

1. *Preparation of the starting materials* : Tri-*n*-butylborate and anhydrous perchloric acid in dichloromethane were prepared as described previously.[1] In the preparation of the 2-substituted 1,3-diketones procedures starting from the unsubstituted compound were consciously avoided. Acylation procedures were selected from the comprehensive review available on the synthesis of 1,3-dicarbonyl compounds. [2] Methyl acetylacetone [3] and phenyl-acetylacetone[4] were prepared from methyl-ethyl ketone and phenylacetone, respectively, through acylation by acetic anhydride and boron trifluoride. Boron trifluoride was generated in the very moment of the reaction by heating a mixture of 180 g boric acid, 200 g CaF_2 and 700 ml oleum [5] to 160—200° and bubbling the evolved gas through concentrated sulphuric acid before being left in the reaction flask. From the above amounts of reactants enough BF_3 evolves to obtain literature yields in acylation runs calculated for 0.5 mole of 1,3-diketone. Methyl-dibenzoylmethane was obtained from propiophenone and phenyl benzoate with sodium amide. [6]

2. *Syntheses of the boronium salts* : Synthetic methods were analogous to those used in the previous paper. [1]

a) Preparation of the boronium chlorides : these were prepared by total synthesis from 1,3-diketones, tri-*n*-butyl-borate and dry hydrogen chloride.

The 1,3 diketone (20 mmoles, namely 2.3 g meacacH, 3.2 g phacacH and 4.6 g medbmH respectively) was dissolved in 10 ml of dry dichloromethane, 2.8 ml (2.2 g, 10 mmoles) of tri-*n*-butyl borate were added and the mixture cooled to —40°. Dry hydrogen chloride was bubbled through the solution with stirring for about 1 hr.

These solutions were used directly in the preparation of the salts of other anions. Attempts to isolate the chlorides by evaporation of these solutions in dry conditions were unsuccessful for $(meacac)_2\,B^+Cl^-$ and surprisingly also for $(medbm)_2B^+Cl^-$; $(phacac)_2B^+Cl^-$ was obtained in crystalline form by bubbling HCl in the reaction mixture at —55°, until it precipitated. The solvent was evaporated in vacuo, and the crystals filtered off from the oil in which they were contained. They were too hygroscopic to be handled or analysed but they could be converted into the corresponding perchlorate $(phacac)_2\,B_4^+ClO_4^-$, as will be shown below.

b) Preparation of the boronium tetrachloroferrates : to the solution of the corresponding chloride 1.6 g (10 mmoles) of dry ferric chloride was added with continuous stirring. The solution was left overnight to reach room temperature, then evaporated in vacuo, obtaining yields of 1.5 g (35%) for $(meacac)_2B^+FeCl_4^-$ and of 3.3 g (40%) for $(phacac)_2B^+FeCl_4^-$. Analogous attempts to prepare $(medbm)_2B^+FeCl_4^-$ were unsuccessful. For analysis the chloroferrates were recrystallized from dry dichloromethane.

c) Preparation of the boronium hexachloroantimonates : to the solutions of the corresponding chloride, 1.3 ml (3g, 10 mmoles) of freshly distilled antimony pentachloride in 2 ml of dichloromethane was added dropwise with stirring. The solution was allowed to reach room temperature, then concentrated in vacuo nearly to dryness. The resulting crystals were recrystallized for analysis from dichloromethane. $(Medbm)_2B^+SbCl_6^-$ was prepared also by synthesis from its components in glacial acetic acid, as follows : 1 g (5 mmoles) of medbmH was dissolved in 2 ml glacial acetic acid and 0.7 ml (0.55 g, 2.5 mmoles) tri-*n*-buthyl-borate was added. Into this solution, another solution formed by 0.3 ml (0.7 g, 2.5 mmoles) $SbCl_5$ and a drop of concentrated hydrochloric acid in 2 ml of glacial acetic acid was added. The chelate salt precipitated on seeding. Yield : 0.5 g. The formation of the boronium salt is parallel with the formation of the *n*-butyl-acetate which can be detected by its characteristic odour.

---

[2] C. R. Hauser, F. W. Swamer and J. T. Adams, *Org. Reactions*, **8**, 59 (1954) ; R. Adams editor, J. Wiley & Sons Inc., New York.

[3] C. R. Hauser and J. T. Adams, *J. Amer. Chem. Soc.*, **66**, 345 (1944).

[4] C. R. Hauser and R. M. Manyik, *J. Org. Chem.*, **18**, 590 (1953).

[5] A. T. Balaban, *Rev. Chim.* (Bucharest), **14**, 603 (1963).

[6] C. R. Hauser, B. J. Ringler, F. W. Swamer and D. F. Thompson, *J. Amer. Chem. Soc.*, **69**, 2649 (1947).

d) Preparation of the boronium perchlorates : an amount of anhydrous perchloric acid containing 10 mmoles of $HClO_4$ was added dropwise into the cold (−40°) and stirred solution of the corresponding chloride. It was left to reach room temperature, then evaporated, yielding 1.6 g (50%) $(meacac)_2B^+ClO_4^-$ and 2.5 g (45%) $(phacac)_2B^+ClO_4^-$ respectively. For analysis the perchlorates were recrystallized several times from dichloromethane. $(phacac)_2B^+ClO_4^-$ was prepared also from crystalline $(phacac)_2B^+Cl^-$, by dissolving it in dichloromethane, adding anhydrous perchloric acid and concentrating near to dryness. $(meacac)_2B^+ClO_4^-$ was prepared also by synthesis from its components : 2.5 ml (2.5 g, 20 mmoles) of meacacH and 2.8 ml (2.2 g, 10 mmoles) of tri-*n*-butyl-borate were dissolved in 10 ml dichloromethane, cooled with stirring to −40° and anhydrous perchloric acid containing 10 mmoles of $HClO_4$ was added dropwise. The mixture was left overnight to reach room temperature, then concentrated in vacuo in successive steps, until no more crystals can be obtained from the residual oil.

Attempts to prepare $(medbm)_2B^+ClO_4^-$ either from the solution of the corresponding chloride or from components were not successful.

e) Preparation of the *bis*-(methyl-dibenzoylmethanato)-boronium triiodide, $(medbm)_2B^+I_3^-$: to the solution of the corresponding chloride a mixture of 1 ml 67% hydroiodic acid (1.4 g, 10 mmoles) and 2.6 g iodine (10 mmoles) was added with stirring. After several hours' stirring, the product was filtered off and washed with ethanol. The triiodide, which is sparingly soluble in ethanol, was recrystallized from dry chloroform.

3. *Synthesis of the beryllium bis-(1,3-diketonates)* : $(meacac)_2Be$, m.p. 170°,[7] $(phacac)_2Be$, m.p. 244°, found C, 73.33 ; H, 6.13 ; Be, 2.58 ; ($C_{22}H_{22}O_4Be$ requires C, 73.51 ; H, 6.17 ; Be, 2.51%), and $(medbm)_2Be$, m. p. 282°, found C, 79.21 ; H, 5.15 ; Be, 1.75, ($C_{32}H_{26}O_4Be$ requires C, 79.48 ; H, 5.42 ; Be, 1.86%) were prepared by adding the calculated amount of the 1,3-diketone to a solution of anhydrous beryllium chloride in ethyl acetate and refluxing until no more HCl evolves, followed by evaporation and recrystallization from n-heptane. $(phacac)_2Be$ and $(medbm)_2Be$ had been studied with respect to their stability constants[8] but not yet isolated as pure substances.

4. *Analytical.* Carbon and hydrogen were determined by combustion, halogens by decomposition in KOH solution, followed by titration with $AgNO_3$ in the presence of K_2CrO_4 as reported in the previous paper.[1] Beryllium and sometimes boron could be determined from the combustion residue calculated as BeO or B_2O_3, respectively. Results are shown in table 1.

5. *Spectra.* UV-spectra (Table 2) were recorded in 1,2-dichloroethane solution by means of an Optica Milano CF 4 spectrophotometer. IR-spectra (Tables 3, 4, 5) were recorded with a Jena UR−10 double beam spectrophotometer in KBr disks. NMR-spectra (Table 6) were recorded by an JEOL−60−3H apparatus at 60 Mc in $CDCl_3$ solution, using TMS as internal standard. Part of the spectra were recorded also at 100 Mc.

---

[7] E. S. Prjevalskii and L. M. Moiseeva, *Vestn. Mosk. Univ., Ser. mat. mekh., astron., fiz. khim.*, **14**, *1*, 203 (1959).

[8] D. F. Martin and B. B. Martin, *Inorg. Chem.*, **1**, 404 (1962).

Table 1

bis-(1,3-Diketonato)-boronium salts (I)

No.	Formula				M. p. (corr.) °C	Analyses %					
						C		H		Cl	
	R_1	R_2	R_3	X		Found	Calc.	Found	Calc.	Found	Calc.
1	Me	Me	Me	Cl		not isolated					
2				$FeCl_4$	72	32.68	33.15	4.32	4.17	32.70	32.62
3				$SbCl_6$	140	25.04	25.22	3.55	3.12	37.30	37.22
4				ClO_4^a	184	42.47	42.83	5.49	5.39	—	10.53
5	Me	Ph	Me	Cl		not isolated pure					
6				$FeCl_4$	186	47.42	47.28	3.88	3.97	25.40	25.28
7				$SbCl_6$	140		37.98	3.40	3.19	30.50	30.58
8				ClO_4^b	230	57.52	57.35	5.32	4.81	—	7.70
9	Ph	Me	Ph	$SbCl_6$	206	46.50	46.88	3.11	3.19	25.00	25.95
10				$J_3^{c,d}$	215	43.88	44.38	3.05	3.03	—	—

[a] boron found as combustion residue 3.10%, calc. 3.21%.
[b] boron found as combustion residue 2.27%, calc. 2.35%.
[c] boron found as combustion residue 1.13%, calc. 1.24%.
[d] iodine found by titration 43.0%, calc. 43.96%.

Table 2

UV-Absorption maxima of the 1,3-diketones, and of their beryllium and boronium chelates in 1,2-dichloroethane solution

Compound	λ max mμ			
	1	2	3	4
meacacH				289
$meacac_2Be$				311
$meacac_2BFeCl_4$[a]				311
$meacac_2BSbCl_6$		273s		310
$meacac_2$ $BClO_4$		268s		312
phacacH			262s	297
$phacac_2Be$				307
$phacac_2BFeCl_4$[a]			286s	312
$phacac_2BSbCl_6$			282	311
$phacac_2BClO_4$			296	310
medbmH	246	281		
$medbm_2Be$			255	351
$medbm_2BSbCl_6$	247	281	319	382
$medbm_2BI_3$			296	380

[a] additional UV-band due to the anion at 366 mμ

Table 3

IR-Spectra of the methyl-acetylacetone chelates

meacacH	meacac$_2$Be	meacac$_2$BSbCl$_6$	meacac$_2$BClO$_4$	meacac$_2$BFeCl$_4$	Assignments
		3015 vvw	3000 shvw	3015 vw	
2990 s	2990 m	—	2970 vw	2990 mw	
2940 s	2960 mw	2920 w	2935 w	—	ν (C−H)
2885 m	2910 m	2880 shvw	2890 shvw	2880 shw	
1720−40 vvs	1690 shw	1700 shw	1700 shw	1700 shw	νfree (C=O)
1620 vs	1640 ms	—	—	—	ν (C=O−H)
—	1580 vvs	1570 vvs	1575 vs	1570 vvs	ν (C=O−M)
—	1485 vvs	1525 vvs	1525 vvs	1530 vvs	ν Chelate (C=C)
1460 vs	1470 vs	—	1460 ms	—	
1430 v	1420	1435 m	—	1435 ms	δas (CH$_3$)
	1460 shvs				
—	—	1400 ms	1400 ms	1400 s	
1370 vvs	1375 vvs	—	1370 m	—	
	1350 shvs	—	—	—	
1330 s	1320 vs	1330 vvs	1335 vs	1337 vvs	δs (CH$_3$)
1285 s	1267 w	—	—	—	
1240 ms	—	—	—	—	
1195 s	1193 s	1212 vvs	1210 vs	1210 vvs	
1170 s	—	—	—	—	
—	—	1120 shms	1100 vvs	1110 shs	ν (^{10}B−O) ClO$_4^-$
1090 s	—	1095 vs	—	1090 vvs	
	1018 s	1002 ms	1005 ms	1002 s	
990 vs	990 vs	—	—	—	
—	—	985 shm	950 shm	970 ms	
		948 m	938 m	945 ms	ν (^{11}B−O)
890 m	906 m	899 mw	890 mw	890 mw	
—	—	—	—	885 mw	
—	845 vvs	—	—	—	ν (Be−O)
810 m	790 ms	—	—	—	
—	759 m	750 vw	750 vw	750 vw	
—	723 w	—	—	—	
685 mw	670 ms	662 vw	662 vvw	660 vw	
635 mw	—	—	—	—	
—	—	—	625 ms	—	ClO$_4^-$
620 w	—	—	—	—	
605 m	—	—	—	—	
570 ms	—	555 w	—	555 w	
528 m	510 vw	510 w	—	—	
490 w	—	503 mw	500 w	502 m	
—	466 ms	—	—	—	(Be−O)
455 w					
430 vw					

Table 4

IR-Spectra of the phenyl-acetylacetone chelates

phacacH	$phacac_2Be$	$phacac_2BSbCl_6$	$phacac_2BClO_4$	$phacac_2BFeCl_4$	Assignments
3080 mw	3078 vw	3085 w	3090 vvw	3080 vvw	νarom. (C−H)
3067 mw	3050 mw	3065 w	3060 vw	3050 w	
3022 mw	3020	3030 w	3040 shvw	3035 vvw	νaliph. (C−H)
2920 vvw	2925 vw	2920 mw	2920 vw	2910 w	
—	—	1595 shms	1610 shm	1610 shm	νPh (C=C)
1612 vs	1582 vvs	1570 s	1570 s	1560 vs	ν (C=O−M)
1505 s		1505 vvs	1505 vs	1510 vvs	νChelate (C=C)
1450 shs	1465 vs	1450 ms	1450 m	1450 ms	δas (CH_3)
1415 vs	1440 shs	1425 ms	1425 m	1420 ms	
1370 shs	1370 vvs	1370 mw			
1340 vs	1335 vs	1350 vvs	1340 vs	1345 vvs	δs (CH_3)
		1330 vvs			
		1290 vs	1290 s	1290 vs	
	1258 m				
	1182 vw				
1165 w	1160 vw	1130 shs		1160 w	
		1100 vvs	1100 vvs	1120 vs	ν $(^{10}B-O)$ ClO_4^-
				1095 vvs	
1080 m	1075 mw				
	1046 s	1040 m	1035 shms	1035 m	
	1024 s	1025 m		1025 m	
		1010 m	1010 ms	1010 ms	
990 shms	990 mw		1000 shm	1000 m	
	938 ms	952 ms	955 ms	952 s	
	920 m	930 m	920 m		
		910 ms		908 m	ν $(^{11}B-O)$
	850 vs				ν (Be−O)
	785 w		785 m	785 ms	
770 m	755 ms	765 ms	775 ms	775 ms	δ Ph (C−H)
		745 mw		750 w	
710 vs	710 s	710 shms	720 ms	710 s	
		705 s			δ Ph (C−H)
	682 w		678 w	685 shw	
	660 m				
			625 ms		ClO_4^-
560 m	554 mw	580 m	580 mw	575 mw	
520 vw		528 vw	528 vvw	525 vw	
		478 mw	475 w	478 m	
	450 mw				
	440 mw				

RESULTS AND DISCUSSION

The present study was undertaken in order to get further information about the influence exercised on the chelates by substituents of the chelate ring II (M=B, Be).

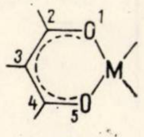

II

Table 5

IR-Spectra of the methyl-dibenzoylmethane chelates

medbmH	medbm$_2$Be	medbm$_2$SbCl$_6$	medbm$_2$BJ$_3$	Assignments
3105 w				
3095 vvw	3087 vw			ν (C−H)
3065 mw	3060 w	3065 w	3060 vvw	
3042 w	3020 w			
2990 mw	2980 w	2990 vvw		
2940 mw	2955 w	2970 vvw		
2878 vw	2870 vw	2930 vvw		
1700 vs		1700 mw		ν (C=O) (non-chelated)
1670 vs		1680 w		
1603 s	1601 m	1608 ms	1605 s	ν Ph (C=C)
1590 ms	1580 ms	1590 shm	1590 shm	
	1550 vs			ν (C=O−M)
1500 vw	1502 s	1510 vvs	1510 vvs	Chelate ν (C=C)
	1472 vs	1490 vvs	1485 vvs	
1460 vs	1450 shs	1460 vs	1460 vs	
	1430 vs	1443 vvs	1440 vvs	δ as (CH_3)
1380 m				
1355 vs	1360 vs	1370 s	1370 vs	δ s (CH_3)
		1335 s	1330 vs	
1312 ms	1315 ms	1320 shms	1320 shms	
1290 s	1297 ms	1295 s	1292 vs	
1240 vs				
1212 vs	1219 ms	1212 vs	1215 vs	
1190 ms	1180 m	1185 vs	1185 vs	
	1160 w			
1110 mw		1110 shm	1110 shm	ν (^{10}B−O)
1085 m	1080 mw	1088 m	1088 ms	
		1060 ms	1060 s	
		1040 ms	1040 s	
1022 mw	1020 vs	1020 s	1020 vs	
1010 m		1005 ms	1005 s	
978 vs		980 w	980 shm	
950 s	930 m	930 mw	930 mw	
		910 mw	910 m	ν (^{11}B−O)
	880 vs			ν (Be−O)
855 w		860 mw	850 w	
	810 w	802 w	802 w	
798 s	798 w	790 w	782 w	δPh (C−H)
770 mw	768 w	755 shw		
755 s	758 w	740 s	735 s	
	740 mw			
715 vs	728 m	728 shm	720 s	
690 vs	707 s	690 ms	690 s	δPh (C−H)
670 s	683 m			
655 m				
	617 vw	612 w	617 vw	
578 ms	594 m	595 ms	585 ms	
	565 ms			
	542 m			
480 mw	482 vw	480 w	480 m	

Table 6

NMR-Spectra of the beryllium and boronium chelates [9]

Compound	Solvent	τ-relatively to internal TMS		
		2-CH_3	3-H	3-CH_3
$acac_2Be$	$CDCl_3$	7.89	4.37	—
$meacac_2Be$[a]	$CDCl_3$	7.85	—	8.12
$phacac_2Be$[b]	$CDCl_3$	8.08	—	—
$bzac_2Be$	SO_2	7.75	3.59	—
dbm_2Be	SO_2	—	2.89	—
$medbm_2Be$	$CDCl_3$	—	—	8.04
$acac_2BClO_4$	SO_2	7.53	3.54	—
$meacac_2BClO_4$	SO_2	7.50	—	7.88
$phacac_2BClO_4$	SO_2	7.65	—	—
$bzac_2BClO_4$	SO_2	7.35	2.88	—
dbm_2BClO_4	SO_2	—	$\leqslant 2.30$	—
$medbm_2BSbCl_6$	SO_2	—	—	7.50

[a] Lit.[10] data in $CDCl_3$ 2−CH_3 : 7.85 τ, 3-CH_3 : 8.12 τ
[b] J.A.S. SMITH, private communication.

The information in this respect obtained from previous work [1,9] can be summarized as follows: substitution of 2-methyl groups by phenyl groups (as in the series acetylacetone, benzoylacetone and dibenzoylmethane) causes an important enhancement of the hydrolytic and thermal stability of the corresponding boronium salts, as reflected by thermal decomposition temperatures: e. g. 180, 250 and 335° for the boronium perchlorates in the above series. [1] This stabilization is due to electronic factors as shown by UV and NMR spectra. UV spectra of the chelates in the above series show an increasing batochromic shift of the main absorption band assigned to an $\pi - \pi^*$ transition in the delocalized electron system of the chelate ring (296, 355 and 400 mμ respectively [1]), indicating thus an extension of this delocalized electron system by conjugation with the phenyl groups in 2-position. Downfield shifts of the NMR signals, especially those of the ring protons in 3-position in the same series (3.54, 2.88 and $< 2.30\,\tau$, see Table 6) indicates also a progressive electron delocalization as a source of this deshielding effect. [9] Then one can conclude that phenyl groups in the 2-position are conjugated with the chelate ring. This implies coplanarity of these groups with the chelate ring which is possible without difficulty for benzoylacetone and dibenzoylmethane, as was shown by models.

The beryllium chelates of the same 1,3-diketones (which are isoelectronic to the corresponding complex boronium cations discussed above) are subject of a similar delocalization effect due to phenyl substitution in 2-position; wavelengths of the absorption bands assigned to the $\pi \rightarrow \pi^*$ transition are 294, 329 and 378 mμ for *bis*-(acetlyacetonato)-, -(benzoylacetonato)- and -(dibenzoylmetanato)-beryllium respectively,[1] whereas chemical shifts of the 3-proton of the chelate ring are 4.37, 3.59 and 2.89τ in the same series [9] (Table 6).

---

[9] A. Trestianu, H. Niculescu, I. Bally, A. Barabás and A. T. Balaban, *Tetrahedron*, 24, 2499 (1968).

[10] J. A. S. Smith and E. J. Wilkins *J. Chem. Soc. A*, **1966**, 1749.

In the present paper, the influence of a similar substitution in the 3-position was studied. The effect of substituents in this position in less unambiguous and is determined rather by steric than electronic factors.

For boronium chelates (I) with R_1R_3 = Me the substitution in the series R_2 = H (acetylacetone), Me (methyl-acetyl-acetone) and Ph (phenyl-acetylacetone) has little effect on the chelates. Boronium chelates of the methyl-acetylacetone are very similar in their above mentioned properties (thermal decomposition temperature, UV bands and proton resonance signals) with those of acetylacetone. Phenyl substitution in the 3-position causes an increase of the thermal decomposition temperature of the boronium perchlorate, but leaves the major UV-band esentially in the same position and causes a slight upfield shift of the proton resonance signal of the 2-methyl groups (See Table 1, 2 and 6). This was interpreted [9] as being due to the position of the phenyl group tilted out of the plane of the chelate ring. Models show that a *cis*-enol configuration of the phenyl-acetylacetone with the phenyl group coplanar to the chelate ring encounters considerable steric hindrance.

Striking is the effect of substitution in the 3-position of the dibenzoylmethanato-boronium salts (I, R_1, R_3 = Ph). Dibenzoylmethane (R_2 = H) is known to give the thermically and hydrolytically most stable boronium salts among all 1,3-diketones tested so far. On the contrary, methyl-dibenzoylmethane afforded only two boronium salts of low stability, as evidenced by the presence of bands due to the free ligand in the UV and IR spectra of the $(medbm)_2BSbCl_6$ (see Table 2 and 5). Any attempts to prepare $(medbm)_2BClO_4$, whose analogue with (R_2 = H) is known as the most stable *bis*-(1,3-diketonato)-boronium salt,[1] failed.

This marked difference in the behaviour of these so closely related 1,3-diketones is due to steric factors. Methyl-dibenzoylmethane in the planar *cis*-enol configuration necessary for chelation exhibits an important steric hindrance between the methyl and the two phenyl groups, as shown by models. This conclusion is supported by the IR, UV and NMR spectra of the two 1,3 diketones which differ significantly from one another. Dibenzoylmethane has no free C = O streching band in its IR spectrum in the solide state or in solution, [1] showing that it is in both states completely chelated by intramolecular hydrogen bonds, i. e. quantitatively in the planar *cis*-enol configuration. Methyl-dibenzoylmethane shows very strong absorption peaks at 1670 and 1700 cm^{-1} (see Table 5), indicating the presence of non-chelated C = O groups. The UV spectra of both 1,3-diketones are shown in table 7. They can be interpreted as follows: Dibenzoylmethane shows a spectrum which is very similar to those of its chelates. The intense longest-wavelength band can be assigned to a $\pi \rightarrow \pi^*$ transition in the delocalized electron system of the planar *cis*-enol form,

Table 7

UV-Absorption spectra of dibenzoylmethane and methyl-dibenzoylmethane

	Dibenzoylmethane		Methyl-dibenzoylmethane	
λ max ;	252	344	246	281
ε max ; 1/mole.cm	7,500	22,500	23,300	2,200
f	0.053	0.332	0.399	0.011

chelated by hydrogen bonding; the weak band at shorter wavelengths can be an n→π* transition at the oxygen atom of the chelated carbonyl group. For methyl-dibenzoylmethane the intense band at short wavelengths is due probably to π→π* transitions of the two equivalent free C = O groups and the weak absorption band at longer wavelength by the phenyl groups. The spectrum of the methyl-dibenzoylmethane free ligand is completely different from those of its beryllium and boronium chelates (whereas all other 1,3-diketones studied so far give spectra which are similar to those of their chelates), showing that chelation implies an important structure change in this case. Finally the NMR spectra of the two diketones show clearly that dibenzoylmethane has structure III and methyl-dibenzoylmethane structure IV in $CDCl_3$ solution. Thus dibenzoylmethane showed, in fair agreement with literature data, [11-13] signals at

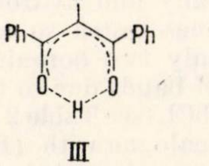

III

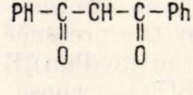

$$\mathrm{PH-\underset{\underset{O}{\|}}{C}-\overset{\overset{CH_3}{|}}{CH}-\underset{\underset{O}{\|}}{C}-Ph}$$

−6.78 τ (0.75 H, broad : O---H---O); 1.90−2.80τ (10.0 H : phenyl multiplet) and 3.20τ (1.0 H, sharp singlet CH), whereas methyl-dibenzoylmethane showed signals at 1.80−2.80τ (9.3 H : phenyl multiplet) along with a coupled quartet-doublet, characteristic to $> CH-CH_3$ groups : an 1:3:3:1 quartet centered on 4.66 τ (1.0 H, J = 7.2 cps : > CH − group) and an 1:1 doublet centered on 8.43τ (2.75 H, J = 7.2 cps : $-CH_3$ group).

Methyl- and phenyl-substitution in the 3-position of the *bis*-(acetylacetonato)-beryllium H has very little effect on the longest wavelength UV and on the proton-resonance signal of the 2-methyl group. Contrary to the boronium analogues, methyl-dibenzoylmethane affords easily a very stable beryllium chelate, whose m.p. 282° is considerably higher than that of the R_2 = H analogue (m.p. [1] 217°).

It is interesting to note the position of the Be−O stretching bands in the IR-spectra of the studied beryllium 1,3-diketonates (Table 8).

---

[11] J. L. Burdett and M. Rogers, *J. Amer. Chem. Soc.*, **86**, 2105 (1964).

[12] R. L. Lintvedt and H. F. Holtzclaw Jr., *ibid.*, **88**, 2713 (1966).

[13] D. C. Nonhebel, *Tetrahedron*, **24**, 1869 (1968).

Table 8

Be-O stretching frequencies of the beryllium 1,3-diketonates

Chelate	$(acac)_2Be$	$(meacac)_2Be$	$(phacac)_2Be$	$(bzac)_2Be$	$(dbm)_2Be$	$(medbm)_2Be$
$\nu(Be-O)$; cm^{-1}	830 s	845 vvs	850 vs	820 s	865 mw	880 vs

The conclusion which can be drawn from this table is that 3-substitution shifts this IR band to higher frequencies, making Be-O bonds shorter and stronger. One can suppose that the bulky substituents cause the oxygen atoms of the 1,3-diketone in its planar *cis*-enol configuration to approach closer to one another.*

The effect of the substituents in positions 2 and 3 could be deduced from the stability constants of the chelates. These values are available from the literature for the beryllium compounds discussed here. A compilation of data is shown in table 9.

Table 9

Stability constants of beryllium 1,3-diketonates and acidity constants of the ligands determined by potentiometric titration [8,14,15]

	$(acac)_2Be$	$(meacac)_2Be$	$(phacac)_2Be$	$(bzac)_2Be$	$(dbm)_2Be$	$(medbm)_2Be$
lgK_1	12.36	11.36	pp.	12.59	13.62	12.36
lgK_2	10.94	10.15	pp.	11.42	12.41	pp.
pk_a	12.70	14.32	13.76	12.85	13.75	14.76

Thus 2-substitution, extending electron delocalization, causes an enhancement of the acidity of the ligands and of the stability of the complex. The effect of 3-substitution cannot be determined because the compounds are not suitable to potentiometric measurements.

Finally we should like to comment on the observed chemical shifts of the 3-methyl groups in the chelates having meacacH and medbmH as ligands. Contrary to 2-methyl groups which undergo only weak influences due to chelation,[9] 3-methyl groups are much more sensitive to it, as shown in table 6.

Chelation causes an important downfield chemical shift of the 3-methyl signal relatively to the keto form of the free ligand; from 8.75τ in meacacH (keto form)[11] to 8.16 τ in meacacH (enol form)[11] or 8.12 τ in $meacac_2Be$, respectively from 8.43 τ in medbmH (IV, keto form) to 8.04 τ in $(medbm)_2Be$. The 2-methyl signal is much less sensitive to chelation : it lies at 7.83τ in meacacH (keto form),[11] at 7.92 τ in meacacH (enol form)[11] and at 7.85τ in $(meacac)_2Be$.

---

* Analogous considerations for the corresponding boronium salts are difficult to be made, because the assignments of the B-O vibrations in their IR spectra are somewhat less unambiguous.

[14] L. G. Van Uitert, W. C. Fernelius and B. E. Douglas, *J. Amer. Chem. Soc.*, **75**, 2736 (1953).

[15] A. Barabás, *Studii și Cercetări Chim. Acad. Rom.*, **14**, 87 (1966); Russian translation, Preprint IFA−CO−30−1965.

A further downfield shift results by passing from the beryllium to the boronium chelates. This shift can be assigned to the apparition of an overall positive electric charge in the complex molecule [9,10] and affects equally the 2-methyl and the 3-methyl signals (see Table 6). The calculated effect (after ref. [10]) of a positive charge localized at the central boron atom on the chemical shift of the 3-methyl group afforded a $\Delta\tau$ value of cca. -0.2 ppm ; the measured difference between $(meacac)_2Be$ and $(meacac)_2B^+ClO_4^-$ was $\Delta\tau = -0.24$ ppm. The difference between the chemical shifts of the 3-methyl groups in $(medbm)_2B^+SbCl_6$ relative to $(medbm)_2Be$ has a much larger value : $\Delta\tau = -0.54$ ppm ; the unusual low value of the 3-methyl chemical shift in this boronium compound allows us to suppose an important ring current effect exercised by the neighbouring phenyl groups ; this fact implies the ligand molecule to have a planar configuration.

Aknowledgements. Thanks are expressed to Mr. S. Murakami from JEOLCO (EUROPE) S. A., Paris, for recording part of the NMR spectra and commenting them. The authors also thank Mrs. M. Roman for elementary analyses.

Revue Roumaine de Chimie, **14**, 265–271 (1969)

FURTHER STUDIES ON THE STOBBE CONDENSATION WITH 2-METHYL CYCLOHEXANONE

A. M. EL-ABBADY, M. EL-ASHRY and S. H. DOSS

Department of Chemistry, University College for Girls
Ain Shams University, Cairo, U.A.R.

Received April 27. 1968

2-Methyl cyclohexanone is condensed with dimethyl succinate in the presence of potassium tertiary butoxide giving an isomeric solid mixture of the corresponding alkylidene and alkyenyl half-esters. This gives on alkaline hydrolysis a homogeneous unsaturated dibasic acid which is found to be β-carboxy-β-(2-methyl cyclohex-1-enyl) propionic acid. Cyclization of the half-ester to keto-ester is carried out using both the stannic chloride and zinc chloride methods. The keto-ester on acid hydrolysis and decarboxylation yields the corresponding unsaturated ketone. Clemmensen's reduction of the keto-ester affords the corresponding β-unsaturated ester. Both the unsaturated ketone and ester are easily hydrogenated in the presence of platinum oxide to the corresponding saturated ketone and ester. These two methyl perhydroindane compounds are useful intermediates for the synthesis of steroid-like compounds.

Cook and Phillip,[1] and Chatterjee and Bhattacharyya[2] reported the Stobbe condensation of 2-methyl cyclohexanone with diethyl and dimethyl succinate respectively in the presence of potassium tert-butoxide showing that the half-esters β-carbethoxy-β-(2-methyl cyclohex-1-enyl)-propionic acid (I_c ; $R = C_2H_5$) as a solid, and β-carbmethoxy-β-(2-methyl cyclohex-1-enyl)-propionic acid (I_c ; $R = CH_3$) as an oil were obtained.

In the present investigation the above reaction was repeated for further study and for the preparation of a methyl perhydroindane nucleus which can be regarded as an intermediate for the synthesis of steroid-like compounds.

2-Methyl cyclohexanone was condensed with dimethyl succinate in the presence of potassium tert-butoxide [3] to yield the corresponding half-ester as an oil. The yield was found to be greatly increased from 71%[2] to 90% by increasing the molarity of potassium tert-butoxide. This oil on keeping for few days in the refrigerator was solidified giving glittering colourless crystals which were proved to be an isomeric mixture (I_a, I_b and I_c ; $R = CH_3$). The ultraviolet absorption spectrum showed one strong band at 225 mμ (ϵ 10000), characteristic of β-unsaturated esters.[4a] This indicated the presence of the half-ester (I_a; R = CH_3) as one isomer of the mixture. It seems that this isomer is present in a small amount as indicated by the low value of the molecular extinction coefficient. Moreover no 2-methyl cyclohexanone could be isolated from a mild oxidation of the half-ester mixture using alkaline permanganate at room temperature, but instead a neutral carbonyl compound was only obtained which gave a 2,4-dinitrophenyl hydrazone. This substance is still under investigation. Repeating the oxidation at 0° it failed to give any neutral carbonyl substance. The infrared spectrum of the half-ester showed bands at 2800—2500 (w), 1750 (S), 935 (V) and 810 (S) cm^{-1}, characteristic of the stretching frequencies of hydroxyl and carbonyl groups of saturated acids and esters, the hydroxyl deformation (out of plane) of acids and the CH out-of-plane deformation vibrations of trisubstituted alkenes respectively.[5] These vibrations strongly suggest the presence of the isomer (I_b ; R = CH_3). Finally the n.m.r. spectrum showed signals at 1.6 and 5.1 ppm (δ), characteristic of a methyl group attached to unconjugated double bonds and a vinyl proton respectively.[4b] This indicated the presence of the two isomers (I_b and I_c; R = = CH_3).

---

[1] J. W. Cook and R. Phillip, *J. Chem. Soc.*, **1948**, 162.

[2] R. C. Chatterjee and B. K. Bhattacharyya, *J. Indian Chem. Soc.*, **34**, 515 (1957).

[3] W. S. Johnson, W. Petersen and W. P. Schneider, *J. Amer. Chem. Soc.*, **64**, 74 (1947).

The half-ester mixture on alkaline hydrolysis gave one homogeneous crystalline dibasic acid, m.p. 157°, which probably does the structure of one of the three possible isomers (I_a, I_b and I_c; R = H). This acid showed no ultraviolet absorption in the characteristic region of the αβ-unsaturated acids (220—260 mμ), thus excluding structure (I_a; R = = H). Its infrared spectrum showed bands at 2800—2500 (w), 1740 (S) and 930 (v) cm^{-1}, characteristic of the stretching frequencies of hydroxyl and carbonyl groups of saturated acids and the hydroxyl deformation (out-of-plane) of acids respectively.[5] The disappearance of the strong band at 810 cm^{-1} characteristic of γ-CH of trisubstituted alkenes (shown by the half-ester) excluded structure (I_b; R = H) and confirmed structure (I_c; R = H) for this unsaturated dibasic acid. However, the presence of the olefinic linkage was chemically proved by catalystic hydrogenation, using platinum oxide, where one mole of hydrogen was absorbed to give the known 2-methyl cyclohexy-1-succinic acid (II), m.p. 163—4° (Lit.[2], m.p. 155—6°).

The crude methyl half-ester was converted into its acid chloride by the action of thionyl chloride in the presence of one molecular proportion of pyridine.[6] Cyclization of this acid chloride was achieved by anhydrous stannic chloride.[7] The neutral oily product thus obtained after washing with carbonate solution (to remove any acidic substances) then with dilute alkali solution (to break and remove any lactone) was found to be the keto-ester (III) in 37% yield. It gave a 2,4-dinitro-phenyl hydrazone and a semicarbazone. The carbonate washings afforded probably a trace of unreacted half-ester, and the alkali washings gave a small amount of a

---

[4] J. C. P. SCHWARZ, "Physical methods in organic chemistry". Oliver and Boyd, London, 1465, pp. (a) 32, (b) 175, (c) 139, (d) 143.

[5] L. J. BELLAMY, "The infrared spectra of complex molecules". Methuen & Co. Ltd., London, 1958, pp. 140, 152, 31.

[6] J. W. COOK and C. A. LAWRENCE, *J. Chem. Soc.*, **1935**, 1637.

[7] M. ELLIOTT, *J. Chem. Soc.*, **1956**, 2231.

colourless solid which was found to be the unsaturated dibasic acid (I_c; $R = H$).

Cyclization of the half-ester was also carried out using acetic anhydride and a catalytic quantity of fused zinc chloride in glacial acetic acid,[8] but a lower yield (31.6%) of the keto-ester was obtained.

Acid hydrolysis and decarboxylation of the keto-ester was effected by refluxing with a mixture of glacial acetic acid, constant boiling hydrobromic acid and water to give the corresponding unsaturated ketone (IV) in a good yield as a pale yellow oil. It gave a 2,4-dinitrophenyl hydrazone in addition to the known semicarbazone.[1]

The ultraviolet spectra of the keto-ester and the unsaturated ketone in ethanol had maxima at 237 mμ (ε 6162) and 236 mμ (ε 11000) respectively. These values confirm the presence of α-β-unsaturated ketone grouping.[4c]

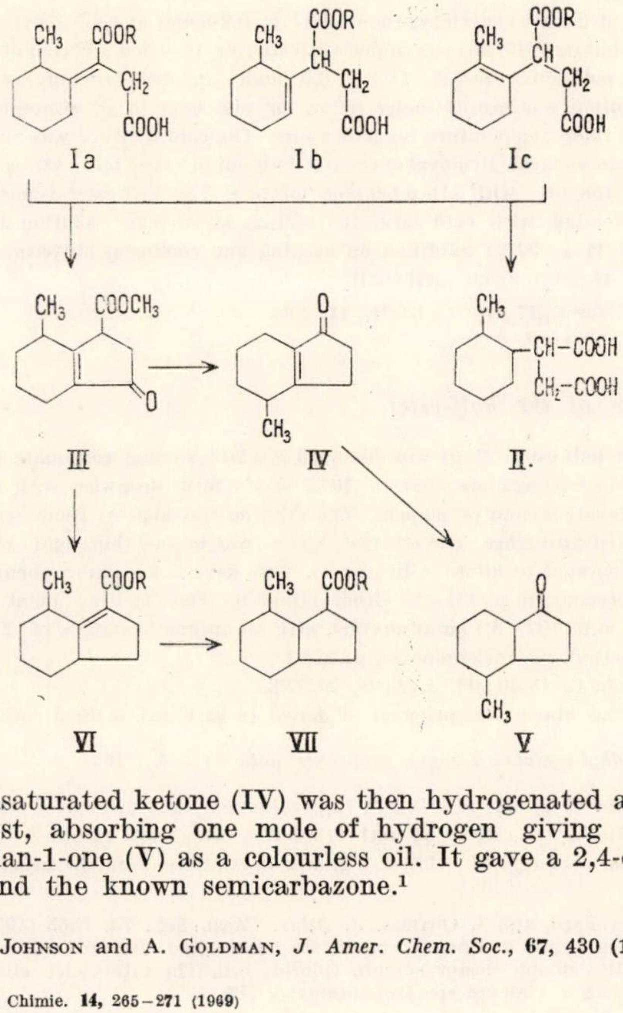
CH₃
COOR
CH₂
COOH
Ia
CH₃
COOR
CH
CH₂
COOH
Ib
CH₃
COOR
CH
CH₂
COOH
Ic
CH₃
COOCH₃
O
III
O
CH₃
IV
CH₃
CH-COOH
CH₂-COOH
II.
CH₃
COOR
VI
CH₃
COOR
VII
O
CH₃
V

The unsaturated ketone (IV) was then hydrogenated at a platinum oxide catalyst, absorbing one mole of hydrogen giving 4-methyl-*cis*-perhydro-indan-1-one (V) as a colourless oil. It gave a 2,4-dinitrophenyl hydrazone and the known semicarbazone.[1]

---

[8] W. S. Johnson and A. Goldman, *J. Amer. Chem. Soc.*, **67**, 430 (1945).

Clemmensen's reduction of the keto-ester (III) afforded mainly a neutral oil, which is more probably the αβ-unsaturated ester (VI ; R=CH_3) since its observed absorption band $\lambda_{max}^{ethanol}$, 230 mμ (ε 6021) fairly agrees with those reported for αβ-unsaturated esters in alcoholic solution.[9,4d] Alkaline hydrolysis of the unsaturated ester afforded the corresponding αβ-unsaturated acid (VI ; R = H) as a colourless oil.

The methyl unsaturated ester was then hydrogenated in the presence of platinum oxide to yield the corresponding saturated ester (VII) ; (R = CH_3) as a colourless oil, whence alkaline hydrolysis gave 7-methyl perhydroindan-1-carboxylic acid (VII ; R = H) as a colourless solid.

EXPERIMENTAL[10]

Condensation of 2-methyl cyclohexanone with dimethyl succinate

A solution of 2-methyl cyclohexanone (22.4 g, 0.2 mole) and dimethyl succinate (44 g, 0.3 mole) in tert-butanol (40 ml) was added with stirring to a hot solution of potassium tert-butoxide (from potassium metal, 11.7 g, 0.3 mole, in dry tert-butanol 200 ml). The brownish red solution was heated under reflux for one hour in an atmosphere of nitrogen and then kept at room temperature for four hours. The cold mixture was acidified with ice-cold dilute hydrochloric acid. Removal of the tert-butanol in vacuo left a straw yellow oil which was extracted thoroughly with ether-benzene mixture. The half-ester isomeric mixture (I ; R = CH_3) was isolated with cold saturated sodium bicarbonate solution and the resulting viscous oil (about 41 g, 90%) solidified on keeping and cooling as glittering colourless crystals, m.p. 126—9° (from aqueous methanol).

Anal. calcd. for $C_{12}H_{18}O_4$: C, 63.71 ; H, 7.96
Found : C, 63.92 ; H, 7.73%.

Oxidation of the half-ester

The methyl half-ester (1 g) was dissolved in a 20% sodium carbonate solution (10 ml). Aqueous potassium permanganate solution 10% was added dropwise with stirring till the colour of permanganate became permanent. The solution was kept at room temperature for 2 hours then extracted with ether. The ethereal layer was washed thoroughly with water, dried (Na_2SO_4) and evaporated to afford a brown oil. This gave a 2,4-dinitrophenyl hydrazone as glittering yellow crystals, m.p. 151—2° (from ethanol). This melting point was depressed markedly (mixed m.p. 107—8°) on admixture with an authentic sample of 2,4-dinitrophenyl hydrazone of 2-methyl cyclohexanone (m.p. 128°).

Anal. Found : C, 43.39 ; H, 3.72 ; N, 24.57%.

Repeating the above oxidation at 0° failed to give any neutral carbonyl substance.

β-Carboxy-β-(2-methyl-cyclohex-1-enyl) propionic acid (I_c; R=H)

The half-ester (2 g) was refluxed in 10% sodium hydroxide solution (20 ml) for 3 hr. The reaction mixture after extraction with ether was cooled and acidified. The precipitated unsaturated dibasic acid (I_c ; R = H), 1.7 g, was crystallized from benzene, m.p. 157°.

---

[9] H. E. Ungrade and I. Ortega, *J. Amer. Chem. Soc.*, **73**, 1565 (1951).

[10] All melting points and boiling points are uncorrected. Infrared spectra were recorded on a Beckmann IR4 double beam sodium chloride cell. The ultraviolet absorption spectra were determined with a Unicam spectrophotometer 700.

Anal. calcd. for $C_{11}H_{16}O_4$: C, 62.26 ; H, 7.54.
Found : C, 62.07 ; H, 7.78 %.

2-Methyl cyclohexyl succinic acid (II)

The unsaturated dibasic acid (1 g) dissolved in glacial acetic acid (15 ml) was shaken with hydrogen in presence of platinum oxide (0.1 g) until uptake of hydrogen (one mole) was complete ($3^1/_2$hr). The solid product was crystallized from water yielding the known saturated diacid (II) as colourless crystals, m.p. 163–164° (Lit. [2], m. p. 155–6° from ether-petroleum ether).

Anal. calcd. for $C_{11}H_{18}O_4$: C, 61.68 ; H, 8.41.
Found : C, 61.90 ; H, 8.29 %.

Cyclization of the half-ester

(a) *Stannic chloride method.* The methyl half-ester (5 g) in dry benzene (50 ml) was treated with pyridine (2.3 ml) and redistilled thionyl chloride (2 ml) at 0° for half an hour. The benzene solution of the acid chloride was decanted from the solid cake, which was then pulverized and washed by decantation with dry benzene. The acid chloride solution and washings were treated with stannic chloride (2 ml) for 15 hr at 0°, the benzene solution was then poured on ice and concentrated hydrochloric acid (15 ml) and shaken. The benzene layer was separated and the aqueous layer washed with ether. The combined ether-benzene extract was washed with saturated sodium bicarbonate solution. Acidification of the bicarbonate washings gave both a small amount of a solid (0.4 g), m.p. 124–6°, undepressed with a sample of the solid half-ester. The organic layer was then re-extracted with cold 5 % sodium hydroxide solution. Acidification of the alkaline solution afforded a colourless solid (0.8 g), m.p. 155–7° (from benzene) undepressed with a sample of the unsaturated dibasic acid obtained directly from the alkaline hydrolysis of the half-ester. The organic layer after washing with water, drying (Na_2SO_4) and evaporation of the solvent gave a brown oil (1.7 g). This oil in distillation afforded 3-carbmethoxy-4-methyl-4,5,6,7-tetrahydroindan-1-one (III) as a pale yellow liquid, b.p. 110° at 0.6 mm.

Anal. calcd. for $C_{12}H_{16}O_3$: C, 69.23 ; H, 7.69.
Found : C, 69.98 ; H, 7.65 %.

It gave a semicarbazone as pale yellow crystals, m.p. 227–228° (decomp.) (from ethanol).

Anal. calcd. for $C_{13}H_{19}O_3N_3$: C, 58.86 ; H, 7.17 ; N, 15.84.
Found : C, 58.70 ; H, 7.12 ; N, 15.73 %.

Its 2,4-dinitrophenyl hydrazone melted at 201–202° (decomp.) (from ethanol).
Anal. calcd. for $C_{18}H_{20}O_6N_4$: C, 55.67 ; H, 5.15 ; N, 15.6.
Found : C, 55.45 ; H, 5.12 ; N, 15.33 %.

b) *Zinc chloride method.* The methyl half-ester (10 g) in freshly distilled acetic anhydride (180 ml) was refluxed (under nitrogen) with 2 % solution of fused zinc chloride in glacial acetic acid (90 ml) for 6 hr. Excess anhydride and acid were removed in vacuo and the dark brown residue poured into crushed ice (100 g). The resulted aqueous mixture was then made alkaline with solid sodium carbonate. The ethereal extract after washing with cold 5 % sodium hydroxide solution then water, and drying gave on evaporation a brown oil (2.8 g), which on distillation gave the keto-ester (III).

4-Methyl-4,5,6,7-tetrahydroindan-1-one (IV)

The keto-ester (3.4 g) was refluxed with glacial acetic acid (45 ml), constant-boiling hydrobromic acid (26 ml) and water (13 ml) for 1 hr, during which carbon dioxide evolved. The acidic mixture was cooled and poured carefully on crystalline sodium carbonate (125 g) in sufficient water to form a slurry. The product was extracted with ether and dried over anhydrous Na_2SO_4. Removal of the solvent gave an oily residue (2.4 g). This after distillation yielded 4-methyl-4,5,6,7-tetrahydroindan-1-one as a pale yellow liquid, b.p. 84° at 0.4 mm.

Anal. calcd. for $C_{10}H_{14}O$: C, 79.95 ; H, 9.39.

Found : C, 79.72 ; H, 9.12 %.

It gave a semicarbazone, m.p. 240° (decomp.) from ethanol (Lit.[1], m.p. 240.5°).

Anal. calcd. for $C_{11}H_{17}ON_3$: C, 63.74 ; H, 8.27 ; N, 20.27.

Found : C, 63.46 ; H, 8.25 ; N, 19.27 %.

Its 2,4-dinitrophenylhydrazone melted at 208° (from acetic acid).

Anal. calcd. for $C_{16}H_{18}O_4N_4$: C, 58.17 ; H, 5.49 ; N, 16.96.

Found : C, 58.07 ; H, 5.56 ; N, 16.96 %.

4-Methyl perhydroindan-1-one (V)

A solution of the unsaturated ketone (1.2 g) in glacial acetic acid (10 ml) was shaken with hydrogen in presence of Adams platinum oxide (0.15 g) until the absorption of hydrogen ceased. After filtration, the acetic acid was neutralized with sodium carbonate solution. The neutral product was extracted with ether and dried (Na_2SO_4). The solvent was evaporated to give an oily residue. This on distillation yielded the saturated ketone as a colourless liquid (0.8 g), b.p. 65–67° at 0.5 mm.

Anal. calcd. for $C_{10}H_{16}O$: C, 78.95 ; H, 10.53.

Found : C, 78.70 ; H, 10.42 %.

It gave a semicarbazone as colourless crystals, m.p. 210–212° (decomp.) from ethanol (Lit.[1], m.p. 210–211°).

Anal. calcd. for $C_{11}H_{19}ON_3$: C, 63.20 ; H, 9.10 ; N, 20.10 ; N, 20.10.

Found : C, 63.41 ; H, 8.92 ; N, 19.88 %.

Its 2,4-dinitrophenyl hydrazone as orange crystals, melted at 205–206° from methanol.

Anal. calcd. for $C_{16}H_{20}O_4N_4$: C, 57.83 ; H, 6.02 ; N, 17.39.

Found : C, 57.97 ; H, 5.93 ; N, 17.18 %.

7-Methyl-$\Delta 1^8$-hexahydroindan-1-carboxylic acid (VI ; $R=H$) and its methyl ester (VI ; $R = CH_3$)

To amalgamated zinc wool (20 g) in water (20 ml) and conc. hydrochloric acid (40 ml) was added the methyl keto-ester (5 g) in toluene (35 ml). The mixture was refluxed for 30 hr with addition of conc. hydrochloric acid (10 ml) every 6 hr. After cooling, the toluene layer was separated and the aqueous layer extracted with ether. The combined toluene and ether extracts after washing with sodium bicarbonate solution, water and drying (Na_2SO_4) afforded mainly the unsaturated ester (VI ; $R = CH_3$) as a pale yellow oil (3.1 g), b.p. 85° at 0.04 mm.

Anal. calcd. for $C_{12}H_{18}O_2$: C, 74.26 ; H, 9.28.

Found : C, 74.43 ; H, 9.54 %.

A mixture of this oil (1 g) and 5 % sodium hydroxide solution (20 ml) was refluxed for 3 hr. The alkaline solution after washing with ether was cooled in ice and acidified to give the unsaturated acid (VI ; $R = H$) as a colourless oil, b.p. 92° at 0.05 mm.

Anal. calcd. for : $C_{11}H_{16}O_2$: C, 73.33 ; H, 8.90.
Found : C, 72.97 ; H, 9.35%.

7-Methyl perhydroindan-1-carboxylic acid (VII; R=H) and its methyl ester (VII; R = CH$_3$)

A solution of the unsaturated ester (VII ; R = H) (2 g) in absolute ethanol (30 ml) was shaken with hydrogen in presence of Adams platinum oxide (0.2 g), until the absorption of hydrogen ceased. Filtration and removal of the solvent afforded the saturated ester (VII ; R = CH_3) as a colourless oil, b.p. 142° at 0.05 mm (1.8 g).

Anal. calcd. for $C_{12}H_{20}O_2$: C, 73.47 ; H, 10.20.
Found : C, 73.22 ; H, 10.09%.

The saturated ester (1 g) was refluxed for 6 hrs with 10% sodium hydroxide solution (10 ml) and ethanol (10 ml). Removal of the alcohol, washing the aqueous residue with ether, then acidification gave the saturated acid (VII ; R = H) as a colourless oil (0.8 g), b. p. 88—90° at 0.5 mm, which solidified on keeping. This was crystallized from benzene as colourless crystals, m.p. 157—8°.

Anal. calcd. for $C_{11}H_{18}O_2$; C, 72.52 ; H, 9.89.
Found : C, 72.22 ; H, 9.91%.

Acknowledgement

The authors thank Dr. Leigh C. Anderson, Professor of Organic Chemistry, Department of Chemistry, University of Michigan, U.S.A. for measuring the n.m.r. spectra.

ORSZÁGOS MŰSZAKI KÖNYVTÁR ÉS DOKUMENTÁCIÓS KÖZPONT 1883

La *Revue Roumaine de Chimie* paraît 12 fois par an. Le prix d'un abonnement annuel est de $ 14, — ; FF 69, — ; DM 56, — .

Toute commande de l'étranger (fascicules ou abonnements) sera adressée à CARTIMEX, Boîte postale 134—135, Bucarest, Roumanie, ou à ses représentants à l'étranger :

R.P. d'ALBANIE, Ndermarja Shtetnore e Botimeve Tirana ; R.D. ALLEMANDE, Deutscher Buch Export und Import Leipzig, 701, Leninstrasse 16 ; R.P. de BULGARIE, Hemus, Place Slaweikov, 11, Sofia ; R.P. de CHINE, Waiwen Shudian P.O.B. 88, Peking ; R.P.D. COREENNE, Chulphanmul, Phenian ; REPUBLIQUE CUBA, Cubartimpex Simón Bolivar 1 Palacio Aldamo, Habana ; R.P. d'HONGRIE, Kultúra, P.O.B. 149 Budapest 62 ; R.P. MONGOLE, Mongolgosknigotorg, Ulan Bator ; R.P. POLOGNE, Ruch, Ul. Wronia 23, Warszawa ; R.S. TCHECOSLOVAQUE, Artia, Ve Smeckach 30-Praha II ; U.R.S.S., Mejdunarodnaia Kniga, Moskva G-200; R.D. VIETNAM, So Xuat Nhap Khau Sach Bao, 32 Hai Ba Trung, Hanoï ; R.S.F. de YOUGOSLAVIE, Jugoslovenska Knjiga Terazije 27, Belgrad ; Prosveta, 16/1, Terazije, Belgrad ; Forum Voïvode Misica, Novi Sad ; ARGENTINE, Editorial Sudaminter S.A., Alsina 500, Buenos Aires; AUSTRALIE, Current Books Ltd. Distributors 168—174, Day Street Sydney ; AUTRICHE, Globus Zeitungs Drucks und Verlagsanstalt GmbH, 1200, Wien, Höchstädplatz 3; BELGIQUE, Du Monde Entier 5, Place St. Jean — Bruxelles, Agence Messageries de la Presse 14—22, Rue du Persil, Bruxelles ; CANADA, Progress Books 44 Stafford St. Toronto, Ontario, W.M. Dawson Subscriptions Service Ltd., Six Thorneliffe Park Drive, Toronto 17, Ontario ; COLOMBIA, Librería Buchholz Galeria, av Jiménez de Quesada 8—40 Bogotá; DANEMARK, Einar Munksgaard, Noregade 6, Kobenhavn ; ESPAGNE, Librería Herder, Calle de Balmés 26, Barcelona 7 ; ETATS-UNIS, Fam Book Service 69, Fifth Avenue, Suite 8 F., New York, 10003 N.Y. ; Continental Publications, 111, South Mermanec Ave., St. Louis Missouri 63105 ; Turner Subscription Agency 235, Park Avenue South, New York 3 N.Y.; FINLANDE, Akateeminen Kirjakauppa P.O.B. 10128, Helsingfors, 10 ; FRANCE, Nouvelles Messageries de la Presse Parisienne, 111, Rue Réaumur, Paris II, Europériodiques S.A. 72, Boul. Senard, 22 Saint-Cloud ; GRANDE-BRETAGNE, Collet's Holdings Ltd. Dennington Estate, Wellingborough, Northants Central Books, Ltd., 37, Inn Road London W.C. 1 ; ISRAEL, Lepac Ltd., P.O.B., 1136 Tel-Aviv ; Haiflepac Ltd. P.O.B. 1794, Haifa ; ITALIE, So. Co. Lib. Ri. Piazza Margana 33 — Roma ; Messagerie Italiane Sp. A. Milano, Via Priv. Renzo e Lucia 7 ; JAPON, Nauka Ltd. 30—19 Minami — Ikebukuro 2 chome Toshima Ku, Tokyo ; PAYS-BAS, N.V. Martinus Nijhoff, P.O.B. 269, Den Haag; Swetz & Zeitlinger Keizersgracht471—487, Amsterdam C.; NORVÈGE, Tryggve Juul Moller—Boekhandel Øvre Slottsgate 25 Oslo 1 : R.F. ALLEMANDE, Kubon & Sagner, P.O.B. 68, München 34; Press Vertriebsgesellschaft GmbH, 6, Frankfurt/Main Börsenstrasse 13—15 ; Kunst und Wissen, Erich Biber P.O.B. 46, 7000 Stuttgart 1 ; SUISSE, Pinkus & Cie Froschaugasse 7 Zürich, Fachbücherei Berne, P.O.B. 397, 3001 Berne.

En Roumanie vous pourrez vous abonner por les bureaux de poste, chez votre facteur ou directement par les services de presse des entreprises et institutions.

NOTE POUR LES AUTEURS

La *Revue Roumaine de Chimie* publie des articles en anglais, français, russe, allemand ou espagnol. Les auteurs sont priés d'envoyer des articles, notes, communications et comptes rendus inédits.

Les manuscrits seront dactylographiés à deux intervalles. Les tableaux seront dactylographiés sur feuilles séparées, de même que la légende des figures. Les diagrammes seront tracés à l'encre de Chine sur papier calque. Les tableaux et les figures seront numérotés par des chiffres arabes, en nombre strictement nécessaire. Prière de ne pas inscrire les mêmes données dans les tableaux et les figures. Les formules chimiques seront incluses dans le texte ; en outre, elles seront transcrites sur des feuilles séparées. L'ordre des références bibliographiques sera celui de leur mention dans le texte ; le nom de l'auteur sera précédé de l'initiale du prénom ; les publications périodiques seront présentées suivant les prescriptions internationales. Les références seront ajoutées à la fin de l'article ; elles paraîtront comme des notes, au bas de la page. Le texte sera précédé d'un résumé, comprenant 15 lignes au maximum.

L'entière responsabilité du contenu des articles appartient aux auteurs. On publie des articles dus aux collaborateurs roumains ou étrangers. Les auteurs recevront 50 tirés à part.

PRINTED IN ROMANIA

1969 MAJ 1 4

TRAVAUX PARUS AUX ÉDITIONS DE L'ACADÉMIE DE LA RÉPUBLIQUE SOCIALISTE DE ROUMANIE

CORNEL BODEA et collab., **Tratat de biochimie vegetală**, partea I, **Fitochimie** (Traité de biochimie végétale, Ire partie, Phytochimie), Ier vol., 1964, 747 p. + 4 annexes + 2 pl., 41 lei ; IIe vol., 1965, 1262 p., 1 pl., 56 lei ; IIIe vol., 1967, 773 p., 35 lei.

V. GHEȚIE et V. MICUȘAN, **Analiza imunochimică. Teorie și practică** (Analyse immunochimique. Théorie et pratique), 1966, 369 p., 28 lei.

SILVIA IONESCU, **Reacții chimice induse de radiațiile ionizante** (Réactions chimiques produites par les radiations ionisantes), 1963, 271 p., 15 lei.

MARIETA NICOLAE, **Fizico-chimia produselor fotografice** (Physico-chimie des processus photographiques), 1964, 426 p. + 4 pl., 35 lei.

R. PORTOCALĂ et L. POPA, **Acizii ribonucleici celulari și virali** (Les acides ribonucléiques cellulaires et viraux), 1966, 375 p. + 8 pl., 26 lei.

D. PURDELA et R. VÎLCEANU, **Chimia compușilor organici ai fosforului și ai acizilor lui** (La chimie des composés organiques du phosphore et de ses acides), 1965, 540 p., 37 lei.

CRISTOFOR SIMIONESCU, MARGARETA GRIGORAȘ et AGATA CERNĂTESCU-ASANDEI, **Chimia lemnului din R.P.R.** (La chimie du bois en Roumanie), 1964, 239 p. + 6 pl., 27 lei.

CRISTOFOR SIMIONESCU et CLEOPATRA VASILIU-OPREA, **Mecanochimia compușilor macromoleculari** (La mécanochimie des composés macromoléculaires), 1967, 344 p., 23,50 lei.

I. P. „Informația" –c. 6131

43426

Lei 15

F 1103

R

REFERÁLVA

REVUE ROUMAINE DE CHIMIE

TOME 14
N° 3
Mars 1969

ÉDITIONS DE L'ACADÉMIE DE LA RÉPUBLIQUE SOCIALISTE DE ROUMANIE

Rev. Roumaine Chim.

14, 273–408 (1969), Bucarest

COMITÉ DE RÉDACTION

Rédacteur en chef :

C. D. NENIŢESCU, membre de l'Académie de la République Socialiste de Roumanie.

Rédacteurs en chef adjoints :

A. T. BALABAN et V. E. SAHINI, membres correspondants de l'Académie de la République Socialiste de Roumanie.

Collège de rédaction :

C. DRĂGULESCU, RALUCA RIPAN, CR. SIMIONESCU, membres de l'Académie de la République Socialiste de Roumanie ; EM. BRATU, membre correspondant de l'Académie de la République Socialiste de Roumanie, Pr G. OSTROGOVICH, MARG. AVRAM, F. BADEA, I.D. MARCHIDAN, D. NEGOIU et D. SĂNDULESCU,

Les manuscrits, les livres et les revues proposés en échange, ainsi que toute correspondance seront envoyés à la rédaction :

REVUE ROUMAINE DE CHIMIE
23, str. Dumbrava Roşie, Bucarest, Roumanie.

REVUE ROUMAINE DE CHIMIE

Tome 14, N° 3 Mars 1969

Page

V. E. SAHINI and C. I. GHIRVU, On the electronic structure and spectra of the monosubstituted naphthalenes 275–282

RODICA VÎLCU und ELENA LUCINESCU, Assoziationslösungen. I (Essigsäure-Wasserlösungen) 283–290

D. CISMARU and ELISABETA DOBROGHIU, The oxidation of zirconium at high temperatures. The oxidation kinetics of zirconium powder in O_2 and CO_2 atmosphere 291–296

O. RADOVICI and SULTANA CIOLAC, Influence of halogenide ions on electrochemical behaviour of titanium and alloys 297–302

S. STERNBERG and LUCIA BEJAN, Thermodynamic properties of the reciprocal system of fused silver iodide and potassium chloride 303–309

R. NUŢIU and Z. SIMON, Molecular orbital studies on tautomers of dilituric Acid. II. Correlation with some IR and X-ray diffraction data 311–318

L. FEY and N. BODOR, Electronic spectra of the substituted α-oximinoalkylbenzenes. II. MO calculations of the bathochromic shifts produced by the dissociation of benzaldoxime and *p*-nitro-benzaldoxime. 319–327

SIMONA BĂDILESCU and I. I. BĂDILESCU, Hydrogen bonds. II. The infrared study of the strength of hydrogen bond in some dihydroxyacetophenones 329–332

F. BUNUŞ and I. MATEI, Contributions to the uranium content determinations in solutions based on ^{238}U daughter radioactivity measurements 333–337

IOANA ZAMFIR et C. N. ŢURCANU, Le marquage par échange isotopique de la thioacétamide et du 6-méthyl-2-thiouracile avec ^{35}S . . . . 339–344 ✓

D. A. TOTOESCU, Equations and interpretation of osmotic pressure 345–352

RALUCA RIPAN, I. EGER et N. BOJAN, Étude des nitrates métalliques en mélanges de solvants. II. 1. Les systèmes : le nitrate de nickel et de cobalt hexahydraté-acétone-tétrachlorure de carbone ; le nitrate de nickel et de cobalt dihydraté-acétone-tétrachlorure de carbone 353–356

CONST. GH. MACAROVICI and RODICA MICU-SEMENIUC, Complex combinations with dyphenilic derivatives. XXIII. On the structure of some Cu(I) and Cu(II) complex thiocyanates 357–364

I. FLOREA, Sur le chromate, le bichromate, le molybdate et le wolframate de 2-éthoxy-6,9-diaminoacridine . . . . 365–372 ✓

Rev. Roumaine Chim. **14**, 273–408 (1969), Bucarest

I. POINESCU, Transformations chimiques du chlorure de polyvinyle. I. Synthèses des polyélectrolytes réticulés sulfoniques à base de chlorure de polyvinyle arylé avec du benzène 373–383

P. T. FRANGOPOL, MARIA FRANGOPOL, N. NEGOIŢĂ and A. T. BALABAN, Factors affecting stability and equilibria of free radicals. IV. t-Butyl-cyanonitroxide 385–387

C. GREFF et S. MOLDOVEANU, Détermination des constantes de dissociation de certaines 1-alcoyl-3,5-bis-(*p*-dialcoylamino-benzyliden)-4-pipéridones en solution aqueuse 389–394

I. I. BĂDILESCU, Acetoacetanilides. II. Preparation of some acetoacetanilides and derivatives 395–398

F. HODOŞAN and N. ŞERBAN, Preparation of 3α,6α-dihydroxy-5β-etianic acid and its conversion into methyl 3β-thiocyano- and 3β-isothiocyano-Δ^5-etienate 399–403

V. TĂMAŞ and C. BODEA, $TiCl_4$-Carotenoid complexes. IV. Action of $TiCl_4$ on cryptoxanthin and cryptoxanthin-palmitate 405–408

Revue Roumaine de Chimie, **14**, 275–282 (1969)

ON THE ELECTRONIC STRUCTURE AND SPECTRA OF THE MONOSUBSTITUTED NAPHTHALENES

V. E. SAHINI and C. I. GHIRVU *

Institute of Physical Chemistry of the Academy, str. Dumbrava Roşie 23, Bucharest

Received September 10, 1968

The π-electronic energy levels of methylnaphthalenes (α and β) and of naphthalenesulphonic acids were calculated using both Hückel's and the ASMO-CI methods. The electronic spectra of these compounds have been interpreted in terms of the Dewar and Longuet-Higgins approach, the orbitals obtained by the HMO approximation method-inductive model, being used as starting orbitals.

INTRODUCTION

The monosubstituted naphthalenes offer interesting theoretical problems arising from the interpretation of the differences between the spectral properties of the α and β isomers. Related to this question, in the framework of the simple LCAO-MO method there are some investigations [1,2] and also some papers in which the π-energy levels calculation has been performed by improved methods. [3,4]

In the present paper the electronic structure of both α and β-methylnaphthalenes and naphthalenesulphonic acids is investigated using Hückel's and ASMO-CI methods. For the simple LCAO-MO calculations, in the case of the methylnaphthalenes the calculation schemes of toluene have been extended, namely the conjugation, [5] the heteroatom [6] and the inductive [7] models, using Streitwieser's parameters. [8] For the α and β-naphthalenesulphonic acids we used the same calculation schemes, the calculation parameters being those previously used in the case of the benzenesulphonic acid.[9] The ASMO-CI calculation is performed by a semiempirical variant due to Baba [10] and to Baba and Suzuki, [3] but we used as starting orbitals those obtained by Hückel's treatment of the inductive model.

---

* Permanent address : The "Al. I. Cuza" University, Physical Chemistry Laboratory Calea 23 August 11, Jassy, Romania.

[1] D. Peters, *J. Chem. Soc.*, **1957**, 646, 1993, 4182.

[2] K. Nishimoto and R. Fujishiro, *Bull. Chem. Soc. Japan*, **32**, 445 (1959).

[3] H. Baba and S. Suzuki, *Bull. Chem. Soc. Japan*, **34**, 82 (1961).

[4] L. Forster and K. Nishimoto, *J. Amer. Chem. Soc.*, **87**, 1459 (1965).

[5] C. A. Coulson and V. A. Crawford, *J. Chem. Soc.*, **1953**, 2502.

[6] F. A. Matsen, *J. Amer. Chem. Soc.*, **72**, 5243 (1950).

[7] G. W. Wheland and L. Pauling, *J. Amer. Chem. Soc.*, **57**, 2086 (1935).

[8] A. Streitwieser, Jr., "Molecular Orbital Theory for Organic Chemists", John Wiley and Sons Inc., New York, 1961, p. 131.

THEORETICAL CONSIDERATIONS

In spite of some differences between spectral characteristics of the α- and β-monosubstituted naphthalenes, both these compounds retain the general spectral features of the pattern molecule, naphthalene.

Dewar's and Longuet-Higgins' interpretation [11] of the electronic spectra of the aromatic hydrocarbons is based on the limited configuration interaction as introduced by Moffitt, [12] the interaction being considered only between the degenerate configurations with the same symmetry.

In the present paper it is assumed that the electronic spectra of the monosubstituted naphthalenes may be interpreted in terms of the same scheme as the pattern molecule.

By using as starting orbitals those of the inductive model, the calculation presents a slight modification of that of naphthalene. Let us denote by Φ_1, Φ_2, Φ_3, ..., Φ_{10} the starting orbitals, the order being that of increasing energy. The ground state of the molecule can be described by the following wave function:

$$\Psi_0 = |\, \Phi_1 \bar{\Phi}_1 \Phi_2 \bar{\Phi}_2 \Phi_3 \bar{\Phi}_3 \Phi_4 \bar{\Phi}_4 \Phi_5 \bar{\Phi}_5 \,| \qquad (1)$$

The excited states are obtained by jumping one electron from the latest occupied orbitals (Φ_4 and Φ_5) to the lowest vacant ones (Φ_6 and Φ_7). From the above considerations the first three excited simple singlet configurations will be:

$$\left.\begin{aligned}
\Psi_{56} &= \frac{1}{\sqrt{2}}\{|\Phi_1\bar{\Phi}_1\Phi_2\bar{\Phi}_2\Phi_3\bar{\Phi}_3\Phi_4\bar{\Phi}_4\Phi_5\bar{\Phi}_6| + |\Phi_1\bar{\Phi}_1\Phi_2\bar{\Phi}_2\Phi_3\bar{\Phi}_3\Phi_4\bar{\Phi}_4\Phi_6\bar{\Phi}_5|\}\\
\Psi_{57} &= \frac{1}{\sqrt{2}}\{|\Phi_1\bar{\Phi}_1\Phi_2\bar{\Phi}_2\Phi_3\bar{\Phi}_3\Phi_4\bar{\Phi}_4\Phi_5\bar{\Phi}_7| + |\Phi_1\bar{\Phi}_1\Phi_2\bar{\Phi}_2\Phi_3\bar{\Phi}_3\Phi_4\bar{\Phi}_4\Phi_7\bar{\Phi}_5|\}\\
\Psi_{46} &= \frac{1}{\sqrt{2}}\{|\Phi_1\bar{\Phi}_1\Phi_2\bar{\Phi}_2\Phi_3\bar{\Phi}_3\Phi_4\bar{\Phi}_6\Phi_5\bar{\Phi}_5| + |\Phi_1\bar{\Phi}_1\Phi_2\bar{\Phi}_2\Phi_3\bar{\Phi}_3\Phi_6\bar{\Phi}_4\Phi_5\bar{\Phi}_5|\}
\end{aligned}\right\} \qquad (2)$$

Since the energies of the Ψ_{57} and Ψ_{46} configurations are very close to one another, we shall take into consideration only their interaction and, finally, shall consider the following configurations:

$$\left.\begin{aligned}
\Psi'_0 &= \Psi_0\\
\Psi'_{56} &= \Psi_{56}\\
\Psi'_{57(46)} &= A\Psi_{57} + B\Psi_{46}
\end{aligned}\right\} \qquad (3)$$

---

[9] V. Em. Sahini, C. I. Ghirvu and V. P. Macovei, *Rev. Roumaine Chim.*, **12**, 237 (1967).

[10] H. Baba, *Bull. Chem. Soc. Japan*, **34**, 76 (1961).

[11] M. J. S. Dewar and H. C. Longuet-Higgins, *Proc. Phys. Soc.*, **A67**, 795 (1954).

[12] W. Moffitt, *J. Chem. Phys.*, **22**, 320 (1954).

the coefficients A and B being obtainable by the usual variational method.[13] Thus from the wave functions Ψ_{57} and Ψ_{46} we shall obtain other two Ψ'_1 and Ψ'_2 corresponding to the lower energy configuration and to the higher one, respectively. Now the three electronic absorption bands from the near ultraviolet spectrum can be interpreted as due to the following transitions

$$\Psi'_0 \rightarrow \Psi'_{56} \text{ (p band)}$$
$$\Psi'_0 \rightarrow \Psi'_1 \text{ } (\alpha \text{ band})$$
$$\Psi'_0 \rightarrow \Psi'_2 \text{ } (\beta \text{ band})$$

THE CALCULATION OF MATRIX ELEMENTS AND THE CHOOSING OF PARAMETERS

The necessary matrix elements may be calculated in the usual way.[14] For the energy of the ground state we have:

$$E(\Psi_0) = 2\sum_{i=1}^{5} I_i + \sum_{i=1}^{5}\sum_{j=1}^{5}(2J_{ij} - K_{ij}) \tag{4}$$

where

$$\left.\begin{aligned} I_i &= \langle \Phi_i|\hat{H}|\Phi_i\rangle \\ J_{ij} &= \langle \Phi_i(1)\,\Phi_j(2) \mid \Phi_i(1)\,\Phi_j(2)\rangle \\ K_{ij} &= \langle \Phi_i(1)\,\Phi_j(2) \mid \Phi_j(1)\,\Phi_i(2)\rangle \end{aligned}\right\} \tag{5}$$

In a straightforward manner we obtain:

$$\left.\begin{aligned} E(\Psi_{56}) - E(\Psi_0) = {} & I_6 - I_5 + 2J_{16} + 2J_{26} + 2J_{36} + 2J_{46} + 2J_{56} - \\ & - 2J_{15} - 2J_{25} - 2J_{35} - 2J_{45} - J_{55} + K_{15} + K_{25} + \\ & + K_{35} + K_{45} - K_{16} - K_{26} - K_{36} - K_{46} + K_{56}. \\ E(\Psi_{57}) - E(\Psi_0) = {} & I_7 - I_5 + 2J_{17} + 2J_{27} + 2J_{37} + 2J_{47} + J_{57} - \\ & - J_{55} - 2J_{15} - 2J_{25} - 2J_{35} - 2J_{45} + K_{15} + K_{25} + \\ & + K_{35} + K_{45} - K_{17} - K_{27} - K_{37} - K_{47} + K_{57}. \\ E(\Psi_{46}) - E(\Psi_0) = {} & I_6 - I_4 + 2J_{16} + 2J_{26} + 2J_{36} + J_{46} + 2J_{56} - \\ & - 2J_{45} - 2J_{14} - 2J_{24} - 2J_{34} - J_{44} + K_{14} + K_{24} + \\ & + K_{34} + K_{45} - K_{16} - K_{26} - K_{36} + K_{46} - K_{56}. \end{aligned}\right\} \tag{6}$$

Besides the above matrix elements, we must calculate the following one nondiagonal:

$$\langle \Psi_{57}|\hat{H}|\Psi_{46}\rangle = 2\langle \Phi_4\Phi_7|\ \Phi_6\Phi_5\rangle - \langle \Phi_4\Phi_7|\Phi_5\Phi_6\rangle \tag{7}$$

---

[13] A. Messiah, "Quantum Mechanics", vol. 2 (translated from French), North-Holland Publishing Company, Amsterdam, 1965, p. 762.

[14] R. G. Parr, "The Quantum Theory of Molecular Electronic Structure", W. A. Benjamin, Inc., New York, Amsterdam, 1964, p. 21.

where $\hat{H}$ is the Hamiltonian indicated by Pariser and Parr[15]

$$\hat{H} = \sum_{\mu} \hat{H}_{\text{core}}(\mu) + 1/2 \sum_{i,j}{}' \frac{e^2}{r_{ij}} \tag{8}$$

For the calculation of the indicated matrix elements it would be necessary to introduce the numerical values for the involved integrals. To calculate the integrals over the molecular integrals it is necessary to reduce them to those over the atomic orbitals. Such scheme has been applied earlier by us for the benzenesulphonic acid.[16] In the case of substituted naphthalenes this scheme needs tedious calculations. For this reason in the present paper was considered a scheme due to Baba and Suzuki,[3,10] in which the configuration interaction is used as indicated by Dewar and Longuet-Higgins[11] and the diagonal matrix elements are calculated in the semiempirical approximation due to Goodman and Shull.[17] Our calculation of the nondiagonal matrix element is different with respect to Baba and Suzuki's, as are different our starting orbitals.

To obtain a set of parameters with the Goodman and Shull's approximation, we used the Gelus, Bonnier and Traynard's experimental data for the naphthalene spectrum.[18]

EXPERIMENTAL DATA

The electronic spectra of naphthalene and methylnaphthalenes (α and β) have been recorded by Gelus, Bonnier and Traynard in cyclohexane as solvent.[18]

In the present paper the electronic spectra of naphthalene, β-methylnaphthalene and naphthalenesulphonic acids (α and β) (Na salts) have been recorded using ethyl alcohol as solvent and a Beckman DK–2 instrument. Our data for naphthalene and β-methylnaphthalene are slight modifications of Gelus' *et al.*

RESULTS AND DISCUSSIONS

A. *Hückel type calculations*

The parameters we used for the Hückel type calculations are given n table 1, the marking of the atoms being given in figure 1.

---

[15] R. Pariser and R. G. Parr, *J. Chem. Phys.*, **21**, 466, 767 (1953).

[16] V. Em. Sahini and C. I. Ghirvu, *Rev. Roumaine Chim.*, **13**, 851 (1968).

[17] L. Goodman and H. Shull, *J. Chem. Phys.*, **23**, 33 (1955).

[18] M. Gelus, J. M. Bonnier and Ph. Traynard, *Compt. rend.*, **255**, 2576 (1962).

Making use of the parameters given in table 1 the corresponding molecular diagrams are calculated.

The charge distributions obtained by all calculation schemes we used are in good agreement with the electrophylic substitution,[19] but the reactivity problem is more complex[20] and is no longer discussed here. It is

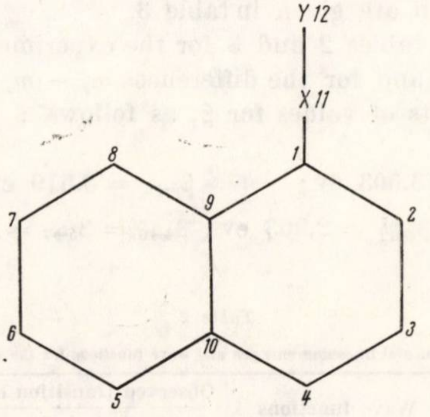

Fig. 1. — Marking of the atoms for monosubstituted naphthalenes.

worth, however, to remark that in all calculation schemes the order of the charge distribution is the same.

Table 1

The parameters used for the Hückel type calculations

Model	Parameters $\alpha_X = \alpha + h_X\beta$, $\beta_{XY} = k_{XY}\beta$									
	Methylnaphthalenes [a]					Naphthalenesulphonic acids [b]				
	h_{12}	h_{11}	$h_{1(2)}$	$k_{11.12}$	$k_{1(2)11}$	h_{12}	h_{11}	$h_{1(2)}$	$k_{11.12}$	$k_{1(2).11}$
Conjugation	−0.5	0.0	−0.1	3	0.8	0.2	0.1	0.1	2	0.8
Heteroatom		2	−0.2		0.7		−2.7	0.2		0.6
Inductive			−0.5					0.6		

a) Parameters indicated by STREITWIESER.[8]

b) Our parameters, reference.[9]

---

[19] L. F. FIESER and M. FIESER, "Advanced Organic Chemistry", Reinhold Publishing Corporation, New York, Chapman and Hall, Ltd., London, 1961, chap. 27.

[20] H. H. GREENWOOD and R. MCWEENY, *Adv. in Phys. Org. Chem.* (edited by V. GOLD), 4, 73 (1966).

B. *ASMO-CI calculations*

The diagonal matrix elements are calculated by the semiempirical manner indicated above using naphthalene as starting molecule (Table 2).

The differences $m_j - m_i$, in β units, obtained in the inductive model approximation are given in table 3.

The data from tables 2 and 3 for the experimental transition energies of naphthalene and for the differences $m_j - m_i$, respectively, allow us to obtain two sets of values for β, as follows*:

$$\left.\begin{aligned} \beta_{\mathrm{GBT}}^{5\to6} &= 3.503 \text{ ev}; \qquad \beta_{5\to6} = 3.519 \text{ ev} \\ \beta_{\mathrm{GBT}}^{4\to6} &= \beta_{\mathrm{GBT}}^{5\to7} = 2.963 \text{ ev}; \ \beta_{4\to6} = \beta_{5\to7} = 2.954 \text{ ev} \end{aligned}\right\} \qquad (9)$$

Table 2

The experimental transition energies and wave functions for the naphthalene

Band	Wave functions	Observed transition energies, ev. a	Observed transition energies, ev. b
α	$\frac{1}{\sqrt{2}}(\Psi_{46} - \Psi_{57})$	3.99	3.95
p	Ψ_{56}	4.33	4.35
β	$\frac{1}{\sqrt{6}}(\Psi_{46} + \Psi_{57})$	5.60	5.62

[a] GELUS, BONNIER and TRAYNARD's results. [18]
[b] Our results.

Table 3

The differences $m_j - m_i$

Difference $(m_j - m_i)$	The value of difference $m_j - m_i$ in β units: Naphthalene	α-methyl-naphthalene	β-methyl-naphthalene	α-naphthalene-sulphonic acid (Na salt)	β-naphthalene-sulphonic acid (Na salt)
$m_6 - m_5$	1.2360	1.2304	1.2219	1.2279	1.2160
$m_7 - m_5$	1.6183	1.5271	1.6536	1.7185	1.5563
$m_6 - m_4$	1.6183	1.7033	1.5661	1.5094	1.6565

---

* We denoted by $\beta_{\mathrm{GBT}}^{i\to j}$ the value obtained from Gelus, Bonnier and Traynard's experimental data (GBT) and by $\beta_{i\to j}$ those obtained making use of our experimental data.

These two sets of values are slightly different to one another perhaps due to the solvent effect.

To calculate the nondiagonal matrix element given by eq. (7), the integrals over molecular orbitals have been reduced to those over atomic orbitals and for the latter the Pariser's values have been used.[21] The experimental and calculated transition energies are given in table 4.

As comparison criterion we used as previously[16] the differences between the calculated and experimental values.

The results we obtained (table 4), in satisfactory agreement with the experimental data, may be compared with those obtained by Baba and Suzuki (table 5), the starting orbitals being obtained using the heteroatom model.

Table 4

The calculated and experimental transition energies (ev)

Molecule	Band	Transition energies		Difference
		Experimental	Calculated	
α-methyl-naphthalene	α	3.95	3.90	0.05
	p	4.23	4.31	0.08
	β	5.52	5.67	0.15
β-methyl-naphthalene	α	3.89 (3.90) [a]	3.86 (3.84)	0.03 (0.06)
	p	4.33 (4.32)	4.28 (4.30)	0.05 (0.02)
	β	5.52 (5.52)	5.67 (5.66)	0.15 (0.14)
α-naphthalene-sulphonic acid	α	3.91 [b]	3.79 [b]	0.12 [b]
	p	4.21	4.32	0.11
	β	5.44	5.75	0.31
β-naphthalene-sulphonic acid	α	3.88	4.03	0.15
	p	4.35	4.28	0.07
	β	5.30 5.45	5.45	0.15 0.00

a) The results in brackets are those obtained using $\beta_{i \to j}$.

b) For the naphthalenesulphonic acids we used only our data, the others being not available.

---

[21] R. Pariser, *J. Chem. Phys.*, **24**, 250 (1956).

Table 5

Baba and Suzuki's experimental and calculated transition energies for some monosubstituted naphthalenes [3]

Molecule	Band	Transition energies (ev)		Difference
		Experimental	Calculated	
α-Naphthol	α	3.86	3.82	0.04
	p	4.29	4.32	0.03
	β	5.41 5.81	5.64	0.23 0.17
β-Naphthol	α	3.78	3.71	0.07
	p	4.54	4.37	0.17
	β	5.53	5.47	0.06
α-Naphthylamine	α	3.73	3.71	0.02
	p	3.91	4.06	0.15
	β	5.12 5.89	5.52	0.40 0.37
β-Naphthylamine	α	3.56	3.71	0.15
	p	4.44	4.10	0.34
	β	5.52	5.13	0.12

(As pointed out by Pariser and Parr [15] in the case of a limited configuration interaction, the starting orbitals play an important role).

Revue Roumaine de Chimie, **14**, 283–290 (1969)

ASSOZIATIONSLÖSUNGEN. I

ESSIGSÄURE-WASSERLÖSUNGEN

RODICA VÎLCU und ELENA LUCINESCU

Physikalisch-Chemisches Laboratorium der Universität Bukarest, Bd. Republicii, 13

Eingegangen am 23. März 1968

Man versucht den Molekularzustand der Essigsäure-Wasserlösungen mit verschiedenen Konzentrationen durch die Ramanspektroskopie, Kryoskopie und Brechungsindex-Messungen zu charakterisieren.

Man hat für die Arbeitsbedingungen die Gleichgewichts-Assoziationskonstante, den Assoziationsgrad und die Dimerisationsenthalpie berechnet. Es wurden die Essigsäurehydrate hervorgehoben.

EINLEITUNG

Das physikalisch-chemische Verhalten der reinen Essigsäure und ihrer Lösungen in polaren und unpolaren Lösungsmitteln hat die Möglichkeit der Bildung von Assoziationskomplexen durch Wasserstoffbindungen bestätigt.

Wie alle organischen Säuren kann auch die Essigsäure mit der Karbonylgruppe (Protonannehmer) und mit der Hydroxylgruppe (Protonabgeber) Wasserstoffbindungen bilden.

Die Struktur der Assoziationskomplexe in reiner Säure, in Wasserlösungen oder in inerten Lösungsmitteln (CCl_4, C_6H_6 usw.) wurde von verschiedenen Forschern oft mit unterschiedlichen Ergebnissen verfolgt.

Obwohl die Selbstassoziation der Essigsäuredämpfe, in reinen Flüssigkeiten oder in inerten Lösungsmitteln gut bekannt ist, ist die Essigsäureassoziation in Wasserlösungen noch sehr strittig.

Die Essigsäure-Selbstassoziation wurde durch die Bestimmung eines doppelten Molekulargewichtes und einer Schwingungsfrequenz zwischen 1656 und 1674 cm^{-1} [1–6, 7] infolge der Karbonylverbindungen mit der Wasserstoffbindung bestätigt.

Die wahrscheinliche Struktur ist die dimerzyklische [3, 5, 8, 9]

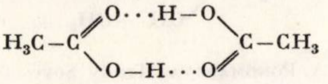

---

[1] P. Koteswaran, *Indian J. Phys.*, **14**, 340 (1941).

[2] Ph. Traynard, *Bull. Soc. Chim. France*, **(1947)**, 316.

[3] S. Fénéant, a) *J. Ph. et Radium*, **4**, 325 (1954).
b) *Compt. rend.*, **235**, 240 (1952); *ibid.*, 1292.

[4] M. I. Batuev, *Compt. rend. Acad. Sci. URSS*, **53**, 507 (1947).

[5] I. Cucurezeanu, *Studii şi Cercetări Fiz. Romania*, **9**, 269 (1958).

[6] P. Simova, *Izvest. Bulgar. Akad. Nauk. Ser. Fiz.*, **2**, 107 (1951).

[7] H. Dunken, *Z. Chem.*, **2**, 117 (1962).

Außer dieser vorherrschenden Struktur wird auch die Anwesenheit von offenen Dimeren[3,5,8, 0] und sogar Hochpolymerketten vermutet.[6,7,11]

Die Zerlegung des zyklischen Dimers in lineare Dimere steigt mit dem Verdünnungsgrad. Zwischen diesen zwei Formen entsteht das folgende Gleichgewicht :

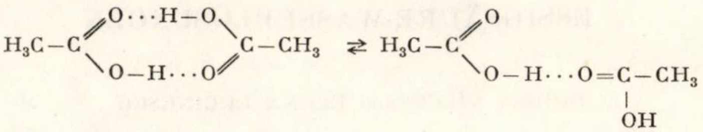

Da in der Anwesenheit der Dimerbande von 1660 cm^{-1} auch eine andere Bande erscheint mit einer Frequenz zwischen 1730 und 1770 cm^{-1}, [1—4,7] und welche das freie Karbonyl charakterisiert, kann man die Dissoziation der Dimere (A_2) in Monomere (A_1) annehmen.

Dieser Prozeß nimmt mit der Temperaturerhöhung zu

$$A_2 \rightleftarrows 2\,A_1$$

Die Raman- oder Infrarotspektren bezeugen die Anwesenheit der Essigsäure-Wasser-Assoziationskomplexe.

Durch die Säureverdünnung mit Wasser erscheint eine neue Bande ($\bar{\nu}$ 1690 — 1715 cm^{-1}) [1, 2, 3, 5, 12]

Diese Bande wird mit der Verdünnung intensiver und bleibt unbeweglich [1, 2,3] ; die Banden bei 1660 cm^{-1} und 1760 cm^{-1} verschwinden allmählich. Da die Assoziation zu einer Frequenzabnahme des Karbonyls führt,[13] folgt, daß sich der Komplex mit Wasser durch eine Wasserstoffbindung mit dem Karbonyl bildet ($\bar{\nu}$ nimmt von 1750 cm^{-1} bis 1710 cm^{-1} ab). Die wahrscheinlichste Struktur des Komplexes ist durch folgende Formel ausgedrückt [3,5].

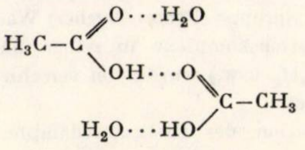

Diese Struktur entspricht den spektroskopischen Messungen der Äquimolarlösungen. Sie wurde auch durch Dichte und Viskositätsmessungen [14] bestätigt. Die von Traynard [2] angegebene Struktur des Molekularkomplexes

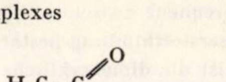

---

[8] K. P. MISCHENKO und A. PONOMAREVA, Trudy Soveschiania po Termodinamiki, 27—30 ianvaria 1958, Moskau.

[9] W. M. LATIMER und W. H. RADEBUSH, *J. Amer. Chem. Soc.* **42**, 1419 (1920).

[10] M. I. BATUEV, *Izvest. Akad. Nauk. SSSR, Ser. Fiz.*, **12**, 611 (1948).

[11] M. HAURIE, *J. Chim. phys.*, **62**, 137 (1965).

[12] A. A. GLAGOLEVA und A. A. FERKHIM, *Zhur. obshchei Khim.*, **28**, 289 (1958).

[13] P. KOTESWARAN, *Z. Physik*, **110**, 118 (1938).

[14] H. LANDOLT-R. BÖRNSTEIN, „Physikalisch-Chemische Tabellen'', Springer Verlag, Berlin, 1912, S. 296.

ist nicht bewährt, denn das Spektralband des freien Karbonyls ($\bar{\nu} \cong 1750\ \mathrm{cm}^{-1}$) erscheint nicht.

Bei größerer Verdünnung wird sich wahrscheinlich auch ein Dihydrat [2, 5, 8] bilden

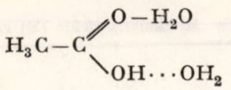

Die Lösungen mit weniger als 25 % Essigsäurekonzentration weisen spektral die Frequenzen des freien Wassers auf [3b] und die elektrolytische Dissoziation wächst mit der Verdünnung.

Die strukturellen Forschungen berichten über das Verhalten der Essigsäure in verschiedenen Arbeitsbedingungen. Es wurden aber keine einheitlichen Forschungen für einen ganzen Konzentrationsbereich, durchgeführt.

In vorliegender Arbeit versuchen wir, die Molekularassoziation in Essigsäure-Wasserlösungen für einen großen Konzentrationsbereich zu charakterisieren.

Zu diesem Zweck haben wir die Spektralmethoden mit den auf kolligativen und konstitutiven Eigenschaften der Lösungen beruhenden Methoden kombiniert.

Auf diese Weise haben wir die Assoziationskomplexe und das thermodynamische Gleichgewicht mit Ramanspektroskopie, kryoskopischer Methode und Brechungsindexmessungen charakterisiert.

EXPERIMENTELLE ERGEBNISSE UND DISKUSSIONEN

Die Lösungen wurden durch Verdünnung mit doppeltdestilliertem Wasser der durch wiederholte Kristallisation erhaltenen 98 %igen Essigsäure aufbereitet.

a. *Die kryoskopische Methode*

Die Gefrierpunkte wurden mit einem Beckmann-Kryoskop bestimmt.

Über die Essigsäure-Wasser-Assoziation wurden schon verschiedene Arbeiten [15–18] veröffentlicht. Die aufschlußreichsten Ergebnisse erzielte Grimaux. [18] Das Minimum in dem Gleichgewichtdiagramm entspricht einem Gemisch mit 37 – 38 % Wasser.

Diese Beobachtung ließ den Verfasser die Entstehung eines Essigsäurehydrates voraussetzen.

Auf Grund unserer kryoskopischen Messungen haben wir dann die scheinbaren Molekulargewichte der Essigsäure und des Wassers durch die klassische Gleichung der idealen Lösungen berechnet.

Durch Erstreckung dieser Berechnungen auf die konzentrierten Lösungen, die sich nicht ideal verhalten, ergaben sich Orientierungswerte für diesen Konzentrationsbereich.

---

[15] S. Arrhenius, *Z. phys. Chem.*, **2**, 491 (1888).
[16] E. Beckmann, *Z. phys. Chem.*, **2**, 715 (1888).
[17] E. R. Jones und C. R. Bury, *Phil. Mag.*, **7**, 841 (1927).
[18] E. Grimaux, *Ann. Chim. Physique*, **1899**, 275.

Die Tabellen 1 und 2 enthalten die Berechnungsergebnisse :

Tabelle 1

Die scheinbaren Molekulargewichte (M) der Essigsäure

g. Essigsäure (%)	5	10	25	45	98
M	57	59	71	84	113

Tabelle 2

Die scheinbaren Molekulargewichte (M) des Wassers

g. Wasser(%)	2	10	15	23	28	40
M	20	30	35	41	47	60

Die Veränderung des scheinbaren Molekulargewichtes der Komponenten mit der Lösungskonzentration ist von den Assoziationserscheinungen verursacht. Die Analyse der Berechnungswerte führte zu folgenden Schlußfolgerungen :

— Bei kleinen Konzentrationen bleibt die Essigsäure frei.

— Die Essigsäure-Wasser-Assoziation ist von der Zunahme der Säurekonzentration begünstigt (die scheinbaren Wasser- und Essigsäure-Molekulargewichte nehmen zu).

— Bei Konzentrationen von über 95% Essigsäure dimerisieren die Säuremoleküle, und die Wassermoleküle bleiben praktisch frei (die Assoziation mit Wasser ist vernachlässigbar).

Der kryoskopische Effekt widerspiegelt die Partikelanzahl in der Lösung und die Strukturerforschung dieser Molekülarten wurde ramanspektroskopisch durchgeführt.

b. *Die Brechungsindex-Methode*

Die Brechungsindexmessungen bei 20° wurden mit einem Abbéschen Refraktometer (Zeiss, Modell G) durchgeführt.

Das Verbindungsverhältnis Essigsäure-Wasser kann man durch die Gilessche Methode[19] auf Grund der Brechungsindexmessungen hervorheben.

Diese Methode besteht aus der Darstellung des Quadrates der Brechungsindex-Mittelwerte, in Abhägigkeit von dem Molarprozent einer Komponente. Wenn sich in dem erforschten System kein Komplex bildet, oder seine Konzentration vernachlässigbar ist, wird dann die graphische Darstellung durch eine Linearabhängigkeit wiedergegeben.

Die Veränderung des Gefälles in der Darstellung bei einer bestimmten Zusammensetzung der Lösung hebt die Bildung eines Assoziationsmoleküls zwischen den Systemkomponenten hervor.

---

[19] C. H. GILES, *J. Chem. Soc.*, **1952**, 3799.

Die Tabelle 3 enthält die von der Lösungszusammensetzung abhängigen Brechungsindexwerte.

Tabelle 3

Brechungsindex verschiedener Lösungen

Wasser (mol %)	27	37	42,4	45,5	52,8	56,4	61,4	69	77	83
n^2	1,9010	1,8997	1,8988	1,8983	1,8953	1,8930	1,8881	1,8799	1,8659	1,8512

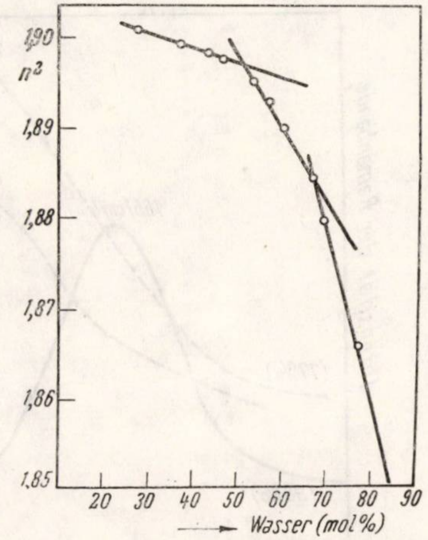

Abb. 1 — Brechungsindex verschiedener Lösungen.

Die in der Abb. 1 für einen Essigsäure-Konzentrationsbereich von 10% — 80% Mol. aufgetragenen Angaben, zeigen deutlich die Veränderung des Gefälles für Essigsäurekonzentrationen von 50% Mol. und 31% Mol. und demnach die Bildung der Essigsäure-Wasser-Verbindungen von 1 : 1 und 1 : 2.

c. *Die Ramanspektroskopie*

Die Ramanspektren hat man mit einem Spektrograph I.S.P.51 mit Lineardispersion von 19 Å/mm für die Wellenlänge 4 000 Å, erhalten. Als Erregungsstrahlung wurde die Linie 4358 Å (in Hg-Spektrum) benützt.

Für die Spektralbestimmung haben wir folgende Lösungen gewählt : eine hochkonzentrierte Lösung (98% Essigsäure), eine Äquimolarlösung (77% Essigsäure) und eine Verdünnungslösung (25% Essigsäure).

Die Messungen wurden bei Temperaturen von 20° und 80° durchgeführt. Bei 80° konnten wir aber die Spektrogramme nicht deuten, denn die Spektralbanden waren sehr diffus.

Die Bestimmung der charakteristischen Spektralbanden der verschiedenen Molekularformen wurde auf Grund der analysierten Ergebnisse in unserer Arbeitseinleitung durchgeführt.

Die bei 20° analysierten Lösungen mit 98% Essigsäure (Gewichtsprozent), bestätigen durch das Spektralband 1661 cm^{-1}, die Anwesenheit der Dimerform. Das Spektralband von 1735 cm^{-1} hebt die Anwesenheit der Monomerform hervor.

Diese Werte stehen im Einklang mit den von Traynard [2] bestimmten Werten – die Assoziation mit Wasser kann man bei dieser Essigsäurekonzentration weglassen; die charakteristische Frequenz (1710 cm^{-1}) wird von dem absteigenden Zweig der Dimerbande bedeckt.

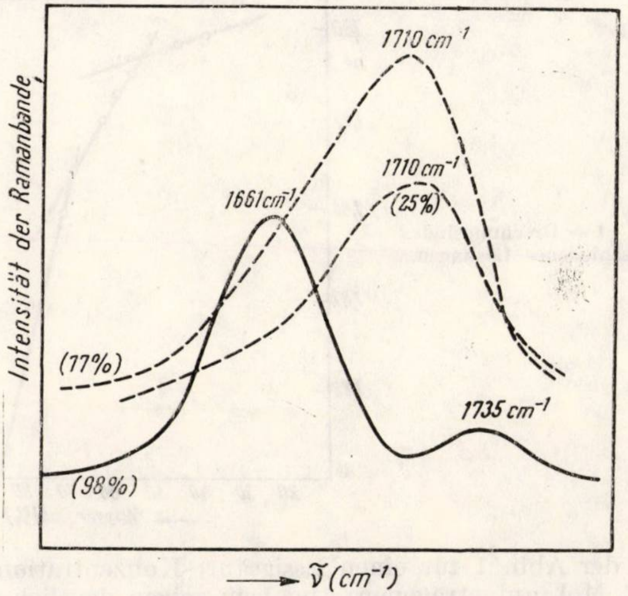

Abb. 2. – Ramanspektren einiger Essigsäurelösungen.

Unter diesen Bedingungen ist das Dissoziationsgleichgewicht eines Dimers in zwei Monomermoleküle möglich. Die Dissoziationsgleichgewichtskonstante kann man aus Spektralmessungen berechnen, unter Berücksichtigung der Proportionalität zwischen der Intensität der Ramanbande und der Konzentration der betreffenden Molekülart. [20,21]

Diese Methode gestattet die Berechnung des absoluten Prozentes einer Molekülart nicht, sie ermöglicht es aber, die relative Proportion abzuschätzen, was ausreicht um die Gleichgewichtskonstante zu bestimmen.

Die von uns erhaltene Beziehung zwischen der Monomer- und Dimerzahl (n_{A_1}, n_{A_2}) ist folgende:

$$\frac{n_{A_1}}{n_{A_2}} = \frac{1}{8}$$

---

[20] Ramakrishma Rao, *Proc. Roy. Soc.*, **A 92**, 496 (1931).
[21] Rajeswara Rao, *Indian J. Phys.*, **14**, 143 (1940).

Die Berechnung der Gleichgewichtskonstante hat man mit der Gleichung [22] der Dissoziation der Polymere zu Monomeren durchgeführt:

$$A_i \rightleftarrows iA_1$$

$$K = \frac{n_A^{(i-1)}\left(\frac{i}{\alpha}-1\right)^i}{(i-1)^{(i-1)}\left(1-\frac{1}{\alpha}\right)} \tag{1}$$

Es wurde das Allgemeinverhältnis des Dissoziationsgrades berücksichtigt

$$\alpha = \frac{n_A}{\sum\limits_i n_{Ai}}$$

wo bei n_A die Molzahl in der Lösung gleich $\sum in_{A_i}$ ist. In unserem Fall ist $i = 2$ und die Gleichung (1) verwandelt sich in:

$$K = \frac{n_A\left(\frac{2}{\alpha}-1\right)^2}{\left(1-\frac{1}{\alpha}\right)} \tag{2}$$

Mit Hilfe der Ramanspektroskopie haben wir bei 20° einen Assoziationsgrad von 1,88 und eine Gleichgewichtskonstante von $1{,}3 \cdot 10^{-1}$ mol/1 bestimmt.

Das mittlere Essigsäure-Molekulargewicht betrug 113. Die Gleichgewichtskonstante nimmt mit der Temperatur zu und der Assoziationsgrad nimmt stark ab, was auf die Dissoziation des Dimers in den Monomer hinweist. Traynard bestimmte bei 100° die Gleichgewichtskonstante $K_{100} = 8{,}1$ mol/1 und den Assoziationsgrad $\alpha = 1{,}45$.

Die von uns bei 20° und die von Traynard bei 100° bestimmten Werte erlaubten durch die Integration folgender Gleichung

$$\left(\frac{\partial \ln K}{\partial T}\right)_P = \frac{\Delta H}{RT^2} \tag{3}$$

die Berechnung der Dissoziationsenthalpie ΔH (Temperaturgrenzen von 293°K bis 373°K).

Der thermische Effekt welcher die Dimerdissoziation begleitet, betrug 11,200 kcal/mol. Dieser Wert wurde auch von Traynard bestätigt ($\Delta H = 11{,}50$ kcal/mol).

Die erhaltenen Werte des Assoziationsprozesses durch Wasserstoffbindungen sind annehmbar. (Zum Beispiel beträgt die Dimerisationswärme von HCOOH $-14{,}12$ kcal/mol).

---

[22] I. Prigogine und R. Defay, "Chemical Thermodynamics", Longmans, Green and Co. Ltd., London, 1954, S. 422.

Die Dissoziationswärme der Essigsäuredämpfe beträgt 15,05 kcal/ /mol [23] und unterscheidet sich selbstverständlich von unseren Werten für die flüssige Essigsäure.

Die spektroskopischen Untersuchungen mit Essigsäure-Wasserlösungen 77 % und 25 % konnten nicht in derselben Weise wie die der konzentrierten Lösungen durchgeführt werden, weil die breite Frequenzbande des entsprechenden Hydrates von 1710 cm^{-1}, die Dimer- und Monomerbanden ganz bedeckt (Abb. 2).

---

[23] W. Weltner, *J. Amer. Chem. Soc.*, **77**, 3941 (1955).

Revue Roumaine de Chimie, **14**, 291 – 296 (1969)

THE OXIDATION OF ZIRCONIUM AT HIGH TEMPERATURES

THE OXIDATION KINETICS OF ZIRCONIUM POWDER IN O_2 AND CO_2 ATMOSPHERE

D. CISMARU and ELISABETA DOBROGHIU

Institute of Physical Chemistry of the Academy, str. Dumbrava Roșie 23, Bucharest

Received July 19, 1968

Studies were carried out on the oxidation of Zr powder with O_2 from 125° to 175° at normal pressure and with CO_2 from 350° to 500° at reduced pressure (0.368, 0.197, 0.0986 atm).

1. INTRODUCTION

The kinetics of Zr oxidation in O_2, air and CO_2 was the topic of an important number of works.

Taking into account the results obtained regarding Zr oxidation in sheets or rods in several gases and the influence on oxidation of different conditions such as : the purity of metal and metal surface, the thickness of the sample, the pressure of the oxidizing atmosphere, the temperature of oxidation, etc., several authors [1-8] reached the conclusion that the oxidation law is influenced by these conditions.

The oxidation takes place according to a law of the form :

$(\Delta m)^n = kt$, when the values of n are greater than the unit in the early stage of oxidation but have a tendency to equal the unit in time.

---

[1] E. A. Gulbransen and K. F. Andrew, *Trans. A.I.M.E.*, **185**, 515 (1949).

[2] D. Cubiciotti, *J. Amer. Chem. Soc.*, **72**, 138 (1950).

[3] J. Belle and M. W. Mallet, *J. Electrochem. Soc.*, **101**, 329 (1954).

[4] A. C. Phalnikar and W. H. Baldwing, *Proc. Amer. Soc. Test. Mat.*, **51**, 1035 (1951).

[5] W. M. Maldwin, H. M. Green and H. E. Tuchschmid, *U. S. Atomic Energy Commission, Report AECN*, **1955**, 3013.

[6] D. J. Garibolli, H. H. Green and W. M. Baldwin, *U. S. Atomic Energy Commission, Report AECN*, **1955**, 3013.

[7] D. Whitwham, J. Boghan and J. Herenguel, *J. Rev. Aluminium*, **34**, 611 (1957).

[8] W. G. O'Driscoll, C. Tyzack and T. Raine, *II-e Conf. Genève sur Energ. Atom.*, Mémoire no. 1450.

For the oxidation carried out on bulk Zr in atmosphere of CO_2 and pure O_2 and temperatures over 600°, some authors[8-12,13] found a series of similar phenomena which suggest a similar oxidation mechanism.

The research works regarding the oxidation of Zr powder encounters a series of difficulties since the powder catches fire and burns in O_2 at normal pressure at about 200° and also because at high temperatures the gas solves in metal.[8-10]

Taking into account these assumptions we considered interesting to study the Zr powder oxidation with O_2 and CO_2.

This experiment tries to explain the kinetics mechanism of the solid-gas reaction when the solid is a powder.

2. EXPERIMENTAL

The oxidation kinetics of zirconium powder has been studied by gravimetric method by means of a microbalance with quartz thread of 2×10^{-5} g sensitivity.

The zirconium powder *p.a.* employed was from Germany (Serva). The particle size was of about 0.002 mm diameter determined by adsorption method.

The sample studied was put into a little quartz flat cup in a very thin layer and was hanged to the balance by a quartz thread.

The oxidation of Zr powder was carried out in a flow system of O_2 purified when the flow rate was of 3.2 l/h.

The oxidation kinetics of Zr powder in CO_2 as performed the static system employing a vacuum apparatus permitting to obtain a vacuum of 1×10^{-5} mm Hg.

Heating was secured by an electric oven with temperature adjustment to a ± 2° precision.

Temperature measurements have been made by means of a thermocouple cromel-alumel placed in the reaction zone very near to the sample (about 0.5 cm distance).

After introduction into the reaction chamber, the sample was submitted for an hour to a baking in vacuum.

The oxidation chamber has been introduced by a gliding operation into the electric oven previously heated to the experimental temperature.

The CO_2 was obtained by dissociation of dry $CaCO_3$ *p.a.* (Merck) in a reaction tube, connected to the experimental device, then introduced at the experimental pressure. The weight increase has been traced by means of the microbalance.

---

[9] L. W. Doyle, B. J. Conway and V. A. Grasse, *J. Inorg. Nuclear Chem.*, **6**, 138 (1958).

[10] S. Dravniecks, *J. Phys. Chem.*, **55**, 540 (1951).

[11] G. W. Guldner and A. C. Wooton, *Trans. Electrochem. Soc.*, **93**, 223 (1948).

[12] R. S. Ambertsumyan, R. V. Kiselev, R. V. Grabennikov, V. A. Nyshkin, L. J. Tsupran and A. V. Nikulina, *II-e Conf. Genève sur Energ. Atomique* (1958) A/conf. 115/ p. 2044.

[13] H. Loriers, R. Danas and P. Bague, *Colloque sur la thermodynamique de matière nucléaire et le transport atomique dans les solides,* Vienne, 1965, S.M.—66/48.

3. RESULTS

Kinetic law

System $Zr-O_2$

The oxidation of zirconium powder with O_2 has been performed at the following temperatures : 125°, 150°, 175° and at 1 atm pressure.

We have not worked at greater temperatures because at about 200° the powder catches fire and burns.

If we use the cubic law of oxidation :

$$(\Delta m)^3 = K_c'' t \tag{1}$$

in which K_c'' is the rate constant, t is the time in minutes and Δm is the growth in weight related to one gram; by representing the results obtained by means of the $(\Delta m)^3$ and t coordinates, one obtains straight lines. From the slopes of these lines we have calculated the rate constants.

The rate constants are given in table 1.

Table 1

The values of rate constants K_c''

Temperature in °C	$K''_c \cdot 10^8$ min^{-1}
125	2.5
150	4.37
175	6.2

System $Zr-CO_2$

The oxidation kinetics of Zr powder in atmosphere of CO_2 was carried out at the temperatures : 350°, 400° and 500° and pressures of 0.368, 0.197 and 0.0986 atm.

If we used the parabolic equation of the form :

$$(\Delta m)^2 = K''t \tag{2}$$

where Δm and t have a similar significance as in equation (1) and K'' is the parabolic rate constant and representing the results obtained by means of the $(\Delta m)^2$ and t coordinates, one obtains some straight lines; from the slopes of these lines we have calculated the rate constants.

Using the equation Ghinstling-Brounshtein [14] and Cismaru [15] for the reactions powder-gas :

$$I = 1 - (1 - z)^{2/3} - 2/3\, z = K_G'' t \tag{3}$$

where z is ratio of Zr which has reacted, K_G'' is the rate constant and t is the time in minutes and representing the results obtained by means of the I and t coordinates, one obtains straight lines; from the slopes of these lines we have calculated the rate constants.

---

[14] A. M. GHINSTLING and B. I. BROUNSHTEIN, *Zhur. priklad. Khim.*, **23**, 1249 (1950).

[15] D. CISMARU, *Studii şi Cercetări Fiz. Acad. R.S. Romania*, 3, 435 (1955).

It may be then noticed that this equation is valid for the description of the phenomenon.

One finds that these two equations are applicable confirming the identity of the oxidation mechanism for both Zr bulk and Zr powder as a mechanism controlled by diffusion.

The values of the rate constants K'' and K''_G obtained are shown in table 2.

Table 2

The values of rate constants K_G and K''

Temperature in °C	$K''_G.10^6\mathrm{min}^{-1}$			$K''.10^6\mathrm{min}^{-1}$		
	Pressure in atm			Pressure in atm		
	0.368	0.197	0.0986	0.368	0.197	0.0986
350	2.2	2.00	1.33	2.00	1.78	1.2
400	3.5	3.2	2.5	3.34	2.57	2.2
500	76.5	47.8	28.5	79.0	47.0	24.2

Consequently the oxidation of Zr powder in O_2 atmosphere in the range of temperature 125—175° follows the cubic oxidation law as noticed also by other authors for the bulk Zr.[1,3]

In CO_2 atmosphere in the range of temperatures 350—500° the oxidation law is parabolic as shown also by other authors for the oxidation of Zr in rods or sheets.[8,12]

Pressure effect

We have studied the pressure effect on the oxidation reaction kinetics for the CO_2—Zr powder system.

The range of the pressure is 0.368—0.0986 atm. Representing K'' versus p_{CO_2} one obtains some plots and to these plots there corresponds the relationship:

$$1/K'' = \frac{1}{a\sqrt{p}} + b \tag{4}$$

This is true because representing $1/K''$ versus $1/\sqrt{p}$ one obtains straight lines as seen in figures 1 and 2.

The relationship (4) may be written:

$$K'' = K''_0 \frac{\alpha\sqrt{p}}{1+\alpha\sqrt{p}} \tag{5}$$

where

$$\begin{aligned} a &= K''_0\,\alpha \\ b &= 1/K''_0 \end{aligned} \tag{6}$$

The constant K_0'' is determined by extrapolation of the plots on the figures 1 and 2 and has the following values :

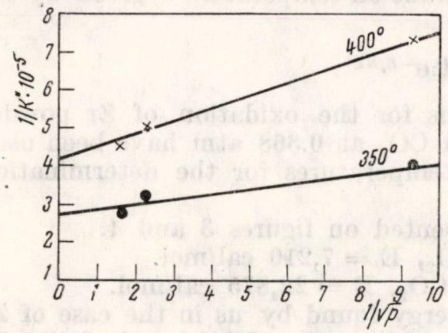

Fig. 1. — Variation of $1/K''$ *versus* $1/\sqrt{p}$; $T = 350°$ and $400°$.

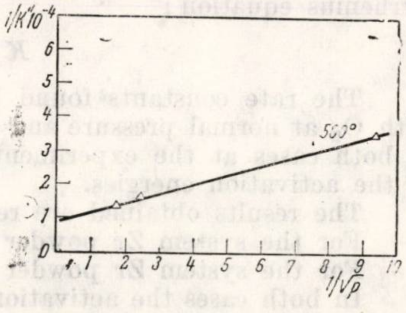

Fig. 2. — Variation of $1/K''$ *versus* $1/\sqrt{p}$ $T = 500°$.

$$\text{for } 350° : K_0'' = 2.38 \times 10^{-6} \ \text{min}^{-1}$$
$$400° : K_0'' = 3.45 \times 10^{-6} \ \text{min}^{-1}$$
$$500° : K_0'' = 1.11 \times 10^{-5} \ \text{min}^{-1}$$

Using the relationships (4) and (5) and the values of K_0'' we can consider the values :

$$\text{for } 350° : \alpha = 19.7 \ \text{atm}^{-1/2}$$
$$400° : \alpha = 18.3 \ \text{atm}^{-1/2}$$
$$500° : \alpha = 3.77 \ \text{atm}^{-1/2}$$

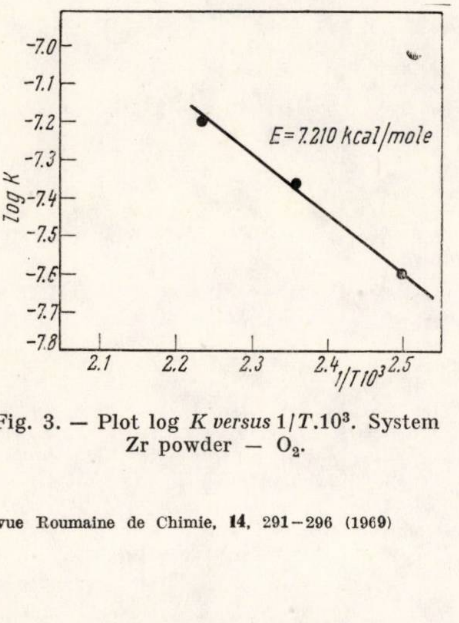

Fig. 3. — Plot log K *versus* $1/T.10^3$. System Zr powder — O_2.

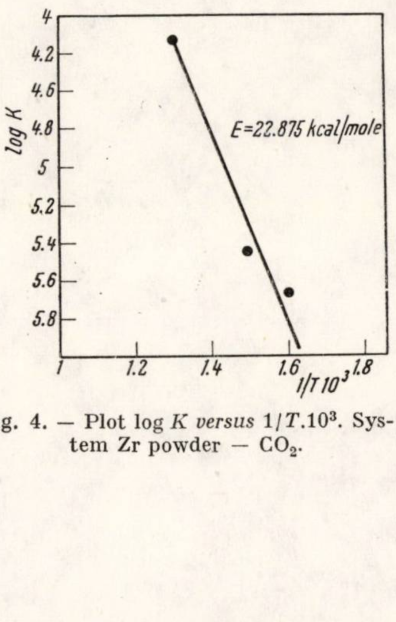

Fig. 4. — Plot log K *versus* $1/T.10^3$. System Zr powder — CO_2.

Temperature effect

The dependence of the rate constant on temperature is given by the Arrhenius equation :

$$K = A.e^{-E/RT}$$

The rate constants found by us for the oxidation of Zr powder with O_2 at normal pressure and with CO_2 at 0.368 atm have been used in both cases at the experimental temperatures for the determination of the activation energies.

The results obtained are represented on figures 3 and 4.

For the system Zr powder — O_2, E = 7,210 cal/mol.

For the system Zr powder — CO_2, E = 22,875 cal/mol.

In both cases the activation energy found by us in the case of Zr powder is smaller than that found by other authors[3,16,17] for the bulk Zr oxidized at higher temperature than ours.

[16] N. A. Porter and J. G. Schnizlein, *J. Electrochem. Soc.*, **107**, 506 (1960).

[17] R. G. Charles, S. Barnort and E. A. Gulbransen, *Trans. Met. Soc. A.I.M.E.*, **212**, 101 (1958).

Revue Roumaine de Chimie, **14**, 297–302 (1969)

INFLUENCE OF HALOGENIDE IONS ON ELECTROCHEMICAL BEHAVIOUR OF TITANIUM AND ALLOYS

O. RADOVICI and SULTANA CIOLAC

Institute of Physical Chemistry of the Academy, str. Galaţi 31, Bucharest

Received April 15, 1968

Experiments were carried out by potentiokinetic techniques in order to study the pitting corrosion of titanium and some titanium alloys in complexing media. The results have shown that the pitting potential is dependent on the nature of halogenide ions and on the temperature of reacting media.

1. INTRODUCTION

Different authors have shown that titanium has an electrochemical behaviour similar to that of other passivating type metals. However, the results obtained concluded that titanium presents typical potentiostatic polarization curves which do not show transpassive behaviour in this range as other metals.[1] It does, however, show breakdown (dielectric) at several hundreds volts depending on the environment.[2] For example in formic acid solutions the passivity film of titanium can stand 400 V before dielectric breakdown. Breakdown voltage in strong noncomplexing acid solutions is ranging between 80–150 V.

Rüdiger and Fischer[3] found breakthrough phenomena on the passive titanium which give rise to localized attack of the metal. This process appears at higher potentials in solutions containing chloride, bromide, iodide and fluoride ions. The potential at which the breakthrough occurs depends on a number of factors as temperature, concentration and the nature of halogenide ions.

In a recent report[4] we have presented some results on the rate of dissolution of titanium in oxalic acid and in the presence of Cl^- and F^- ions at different temperatures.

The present paper is dealing with the behaviour of titanium passivation films in oxalic acid in the presence of halogenide ions.

[1] M. Stern and H. Wissenberg, *J. Electrochem. Soc.*, **109**, 755 (1959).

[2] E. E. Millaway, *Materials protection*, **4**, 16 (1965).

[3] O. Rüdiger and W. R. Fischer, *Z. Electrochem*, **62**, 803 (1958).

[4] O. Radovici and S. Ciolac, *Rev. Roumaine Chim.*, **13**, 31 (1968).

2. EXPERIMENTAL

The experiments were carried out in a glass cell with separate anodic and cathodic compartments. 10% oxalic acid in the presence of different amounts of KF, KCl, KBr and KI was used as working electrolyte. All solutions were prepared from analytic grade reagents and double distilled water.

Commercial grade titanium Ti + 0.01% Fe, titanium-palladium (Ti+0.16% Pd), titanium-molybdenum (Ti + 15.51% Mo) and titanium-aluminium-vanadium (Ti + 6% Al + +4% V) alloys were used as working electrodes.

All the electrode potential values were recorded against calomel electrode.

The potentiostatic analysis of the anodic behaviour of titanium and of the alloys was achieved by means of a conventional potentiokinetic instrumentation.

The experiments were carried out at 75° in a thermostat bath in deaerated solutions.

3. RESULTS AND DISCUSSION

3.1. *Titanium.* The anodic behaviour of commercial grade titanium in oxalic acid is shown in figure 1. The curve in the figure indicates a typical active, passive and transpassive behaviour. No similar behaviour was observed for titanium in inorganic acids, bases or salts in low potential range. The increase of the anodic current in transpassive region occurs at + 2.8 V. It is interesting to point out that this phenomenon can be observed only at elevated temperatures (75°). No transpassive behaviour of titanium in oxalic acid was observed at 25°. The breakthrough phenomenon of the passive film in transpassive region is due to the reactivity of the passive oxide film in the presence of the complexing agent (oxalic acid) and a consequent formation of a soluble complex compound.

The anodic polarization curve of Ti in oxalic acid + NaF is shown in figure 2. No transpassive behaviour can be observed from the figure, but a relatively high passivity current density, which indicates the adsorption of F^{-}_{ions} on the passive film. No pitting of the electrode was observed during anodic polarization of the metal.

A completely different anodic behaviour of titanium was observed when Cl^-, Br^-, I^- ions are present in oxalic acid solutions.

Figure 3 illustrates this behaviour, which is characterized by the increase of the anodic current starting from a potential value which can be considered a pitting potential, because in this potential range the breakdown of the film and pitting of the metal was observed.

It is interesting to emphasize that the pitting potential depends on the nature of halogenide ions and on the temperature. No pitting was observed at room temperature and low potential polarization. The values of the breakdown potential and of pitting potential for titanium and some titanium alloys in oxalic acid or in oxalic and halogenide ions are shown in table 1.

This table shows that the lowest value for the pitting potential is obtained for I^- ions. The pitting corrosion of titanium is described by means of the limiting current-potential curve.

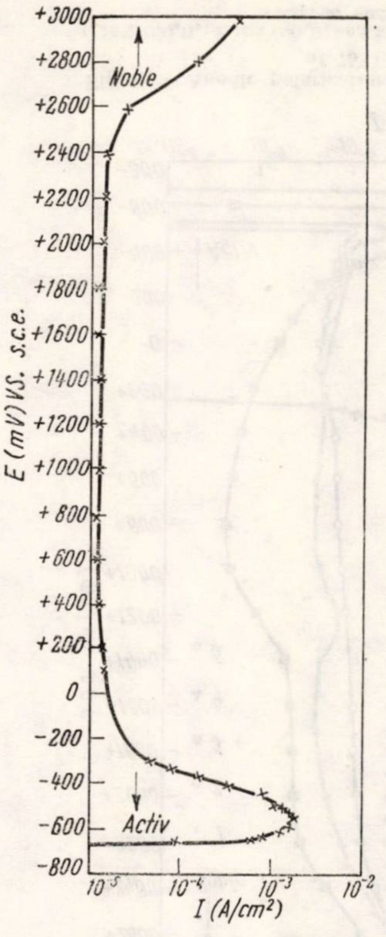

Fig. 1. — 1 — × Anodic polarization curves of Ti in 10% $C_2O_4H_2$ at 75°.

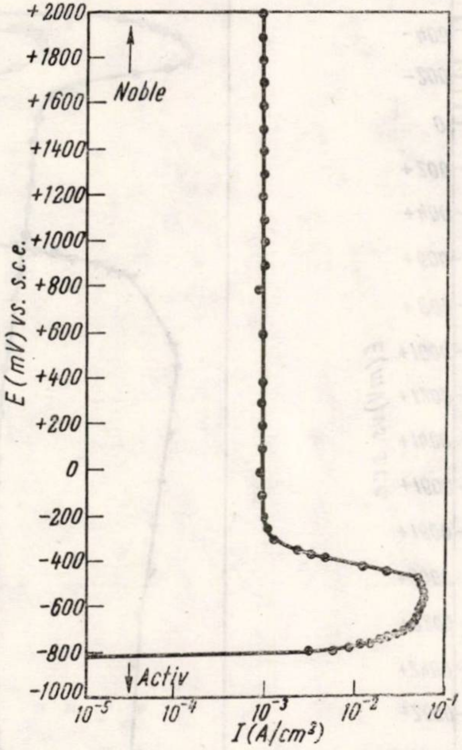

Fig. 2. — 5 — ● Anodic polarization curves of Ti in 10% $C_2O_4H_2$ + 0.2 NaF at 75°.

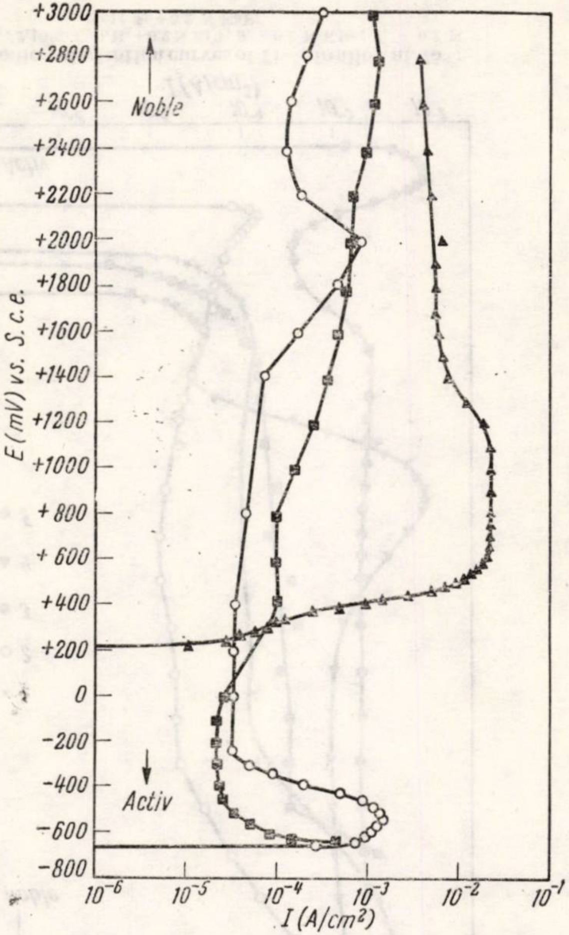

Fig. 3. — Anodic polarization curves of Ti at 75° in: 2. — ○ 10% $C_2O_4H_2$ + 0.2 N KCl; 3. — ▨ + 0.2 N KBr; 4. ▲ + 0.2 N NaI.

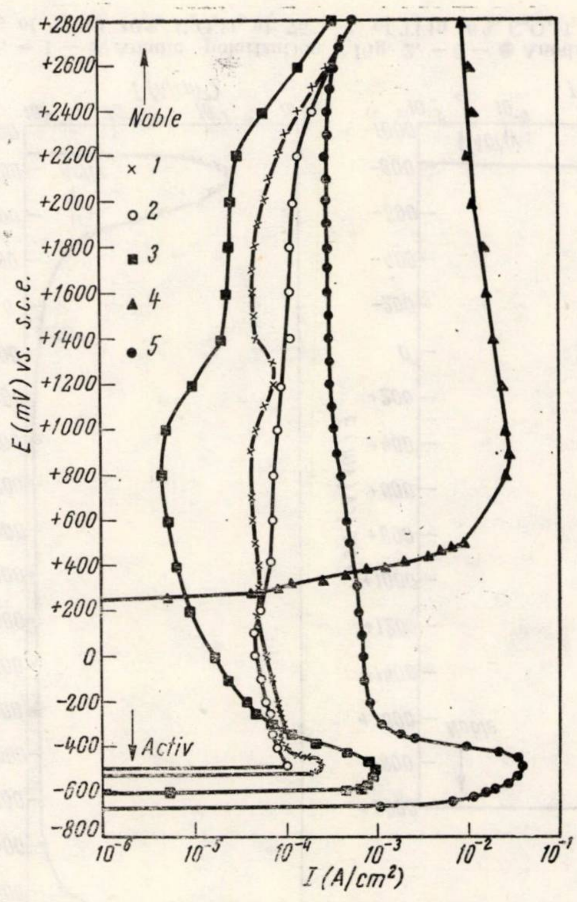

Fig. 4. — Anodic polarization curves of Ti — Pd alloy at 75° in :

1, 10% $C_2O_4H_2$; *2*, 10% $C_2O_4H_2$ + 0.2 N KCl ; *3*, + 0.2 N KBr ; *4*, + 0.2 N NaI ; *5*, + 0.2 N NaF.

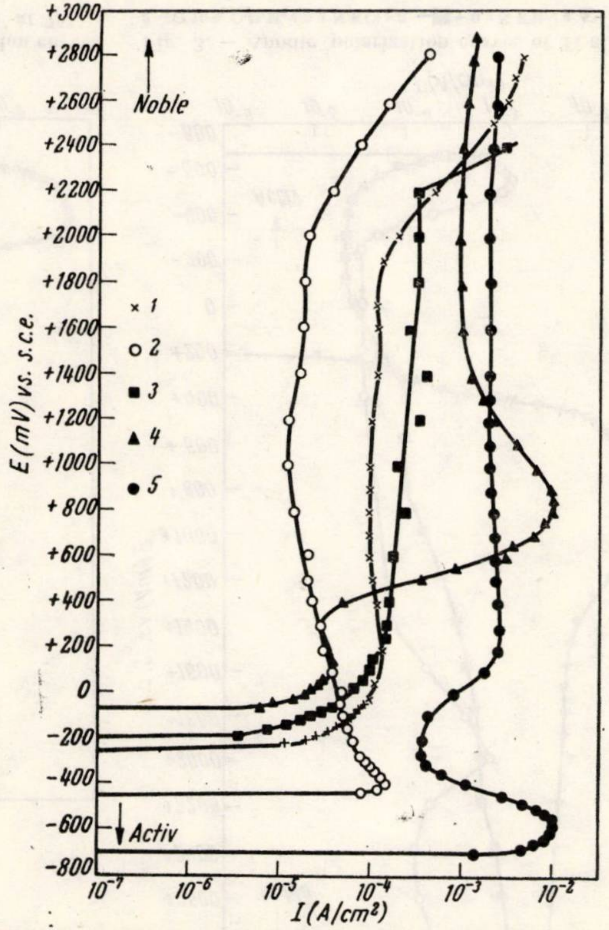

Fig. 5. — Anodic polarization curves of Ti — Mo alloy at 75° :

1, 10% $C_2O_4H_2$; *2*, 10% $C_2O_4H_2$ + 0.2 N KCl ; *3*, + 0.2 N KBr ; *4*, + 0.2 N NaI ; *5*, + 0.2 N NaF.

Its behaviour shows that the process is diffusion-controlled according to the equation:

$$I_{x^-} = nFAC_{x^-}\sqrt{\frac{D}{\pi t}}$$

where: I_{x^-} = diffusion current density; A = surface area; C_{x^-} = concentration of halogenide ions; D = diffusion constant; t = time

Table 1

Breakdown and pitting of titanium and alloys at 75°

Alloy	Breakdown potential (mV) in 10% $C_2O_4H_2$	Pitting potential mV			
		10% $C_2O_4H_2$ +0.2N NaF	10% $C_2O_4H_2$ +0.2 N KCl	10% $C_2O_4H_2$ +0.2 N KBr	10% $C_2O_4H_2$ +0.2N NaI
Commercial titanium	+2.400	—	+1400	+ 800	+600
Ti + 0.16% Pd	+2.400	—	+2000	+1000	+600
Ti + 15.5% Mo	+1.900	—	+2000	+2000	+900
Ti + 6% Al + 4% V	+2.000	—	+1600	+1600	+300

The mechanism of pit formation on titanium electrode may be explained supposing that some soluble complex compounds are formed in the presence of oxalic acid, halogenide ions and passive film. No data are available so far in the literature concerning the chemical composition and the structure of such complex compounds.

The forming potential of such complex compounds depends on the nature and concentration of halogenide ions. The ability of halogenide ions to form such soluble compounds decreases from $I^- > Br^- > Cl^-$.

Our results show that in complexing media such as oxalic acid, the pitting corrosion of titanium can be started at very low potential i.e. the corrosive resistance of the metal is low especially at elevated temperature.

The influence of alloying element on the pitting corrosion of titanium can be observed from the next figures.

Titanium-paladium alloy. Anodic behaviour of this alloy is shown in figure 4 which shows that the alloys behave in similar manner as pure titanium in oxalic acid in absence or in presence of halogenide ions.

Titanium-molybdenum alloy. Figure 5 shows the limiting current density-potential relationship of the oxalic acid. This indicates that the process is diffusion-controlled.

Transpassive region is observed too. Pitting potential is observed for Cl^-, Br^-, I^- ions and not for F^- ions. Titanium-molybdenum alloy presents the highest value of pitting potential in the presence of I^- ions, i.e. it is the most resistant alloy against pit formation by I^- ions in complexing media.

Titanium-aluminium-vanadium alloy presents potentiostatic polarization curves (see fig. 6) which resembles the curves of titanium metal but with higher values for critical current densities and passive current densities. The values of pitting potential are shown in table 1.

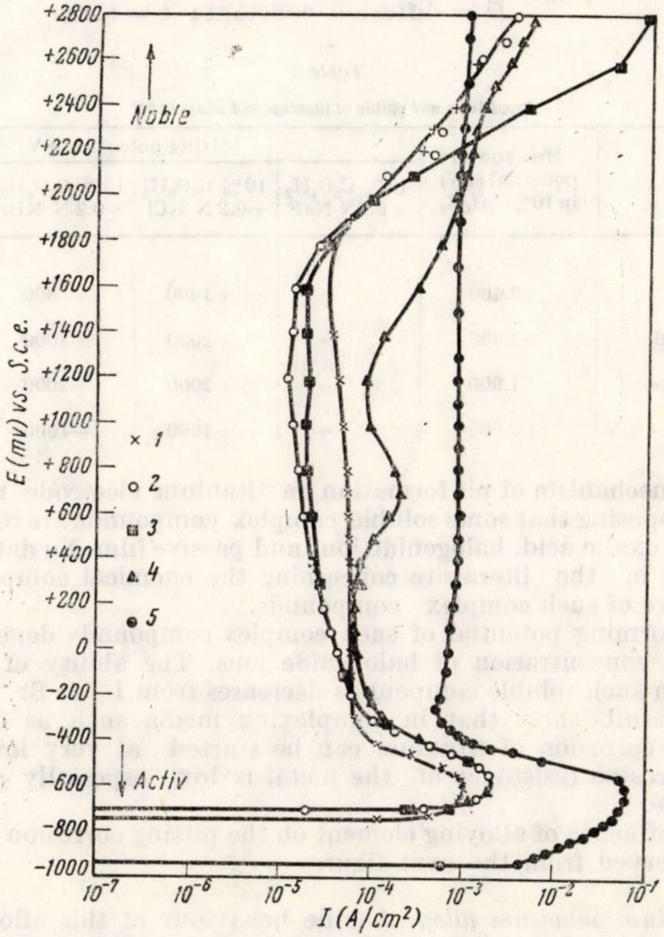

Fig. 6. — Anodic polarization curvesof Ti — Alalloy at 75° in : *1*, 10% $C_2O_4H_2$; *2*, 10% $C_2O_4H_2$+0.2 N KCl; *3*, +0.2 N KBr; *4*, +0.2 N NaI; *5*, +0.2 N NaF.

Titanium-aluminium-vanadium alloy does not present a limiting current potential dependence in the presence of I^- ions as titanium shows.

From the results which we obtained may be concluded that the most resistant against pitting corrosion in the presence of oxalic acid and halogenide ions is the titanium-molybdenum alloy followed by titanium and titanium-palladium alloy.

Revue Roumaine de Chimie, **14**, 303 – 309 (1969)

THERMODYNAMIC PROPERTIES OF THE RECIPROCAL SYSTEM OF FUSED SILVER IODIDE AND POTASSIUM CHLORIDE

S. STERNBERG and LUCIA BEJAN
Institute of Physical Chemistry of the Academy, str. Galaţi 31, Bucharest

Received June 4, 1968

The e.m.f. of the formation cells :

$$\mathrm{Ag(s)\,|\,\underset{x_1}{AgI}\,(l),\ \underset{x_2}{KCl}\,(l)\,|\,I_2\,(g,\ 1\,At)\ graphite}$$

has been measured and the excess thermodynamic properties of silver iodide in the reciprocal mixture have been computed. The excess thermodynamic properties have been computed from the exchange heat of the ionic exchange reaction taking also into account the deviations from the random distribution. Computed and experimental values have been found to be in good agreement.

The thermodynamic properties of reciprocal mixtures of fused salts of the type AX + BY have been investigated theoretically by Flood, Førland and Gryotheim [1,2] and Blander.[3]

The different theories have been verified mostly with the help of the cooling curves of reciprocal systems. However the cryoscopic method has a limited applicability since many reciprocal systems form solid solutions. More comprehensive results may be obtained by the formation cell method.

Quite recently Førland and Ostwald[4] have studied the thermodynamic properties of the system AgBr + NaCl by this method.

For the study of reciprocal systems it is very convenient to use formation cells with iodine electrode, since the equilibrium :

$$\mathrm{Me_IX} + 1/2\,\mathrm{I_2} \rightleftharpoons \mathrm{Me_I\,I} + 1/2\ \mathrm{X_2}$$

is practically completely shifted to the left.

The method for obtaining a reversible iodine electrode has been described recently. [5,6]

---

[1] H. Flood, T. Førland and K. Gryotheim, *Z. anorg. Chem.*, **276**, 289 (1954).

[2] T. Førland in "Fused Salts", Editor B. R. Sundheim, McGraw-Hill, Book Company, New York, 1964, p. 63–164.

[3] M. Blander, Editor, "Molten Salt Chemistry", Interscience Publishers, New York, 1964, p. 127–237.

[4] T. Førland and T. Ostwald in "Selected Topics in High-Temperature Chemistry", Universitetsforlaget, Oslo, 1966, p. 15.

[5] S. Sternberg, I. Adorian and I. Galasiu, *J. Chim. phys.*, **62**, 63 (1965).

[6] S. Sternberg, I. Adorian and I. Galasiu, *Electrochim. Acta*, **11**, 385 (1966).

In the present paper a study on the thermodynamic properties of the system AgI + KCl based on e. m. f. measurements of the following formation cells :

$$\mathrm{Ag(s)}\,|\,\underset{x_1}{\mathrm{AgI(l)}} + \underset{x_2}{\mathrm{KCl(l)}}\,|\,\mathrm{I_2(g,\ 1\ At.)\ graphite}$$

is reported.

EXPERIMENTAL

The experimental determinations have been carried out with the help of quartz cell, a detailed description of which was given in a previous paper.[5] The cathode consisted of a 1.5 mm diameter silver wire and the anode of a 6 mm diameter spectral carbon rod. The temperature was measured with a Pt—Pt, Rh thermocouple introduced into the melt and protected by a quartz sheath.

The reversible iodine electrode was achieved by the continuous bubbling of a stream of gaseous iodine. Gaseous iodine was obtained from an iodine generator consisting of a razotherm glass flask filled with solid iodine and heated at 230° in an electric furnace. Gaseous iodine was introduced into and ejected from the cell through quartz tubes heated by electric resistors.

In order to obtain the reproducibility of the e.m.f. it was necessary to saturate with iodine the carbon electrode. Preliminary experiments have shown that about 10 hours were required to obtain a reversible potential with a new carbon electrode. The e.m.f. was measured as a function of temperature with a "Solartron" digital voltmeter type LM 1440.2 ; the measurement error was ± 0.1 mV and the reproducibility was 1 — 1.5 mV.

The AgI and KCl salts were previously dried, fused and purified by bubbling off with gaseous acids.

RESULTS AND DISCUSSION

Table 1 gives the e. m. f. as a function of molar fraction and temperature. The equations E = f(T) have been obtained by the method of least squares from a number of about 30 — 40 points for every molar fraction.

Table 1

Experimental e.m.f. values and computed thermodynamic functions for AgI + KCl mixtures

X_{AgI}	e. m. f. V	$\Delta\overline{G}_{AgI}$ cal/mole	$\Delta\overline{S}_{AgI}$ cal/grad. mole	$\overline{G}^E_{AgI}$ cal/mole	$\overline{S}^E_{AgI}$ cal/grad. mole	$\overline{H}^E_{AgI}$ cal/mole
1	$0.5238-0.272\times10^{-3}\,(T-973)$	—	—	—	—	—
0.9	$0.5376-0.254\times10^{-3}\,(T-973)$	− 318	0.415	−114	0.205	86
0.8	$0.5488-0.223\times10^{-3}\,(T-973)$	− 576	1.130	−159	0.687	509
0.65	$0.5626-0.199\times10^{-3}\,(T-973)$	− 895	1.844	− 63	0.827	742
0.5	$0.5715-0.175\times10^{-3}\,(T-973)$	−1100	2.237	+238	0.860	1075
0.4	$0.5833-0.144\times10^{-3}\,(T-973)$	−1372	2.952	+397	1.131	1497
0.3	$0.5984-0.096\times10^{-3}\,(T-973)$	−1720	4.059	+606	1.666	2227
0.2	$0.6192-0.0513\times10^{-3}(T-973)$	−2200	5.050	+907	1.899	2756

The molar partial free enthalpy of silver iodine has been computed by relation (1)

$$\Delta\,\overline{G}_{AgI} = -\,\mathfrak{F}\,(E - E^0) \qquad (1)$$

where E^0 refers to cells with pure silver iodide and E to those with mixtures.

The partial molar entropy is obtained from relation

$$\Delta \bar{S}_{AgI} = \mathcal{F}\left[\left(\frac{\partial E}{\partial T}\right)_P - \left(\frac{\partial E^0}{\partial T}\right)_P\right] \tag{2}$$

The respective excess functions have been computed from the relations :

$$\bar{G}^E_{AgI} = \Delta\bar{G}_{AgI} - \Delta\bar{G}^{id}_{AgI} \tag{3}$$

$$\bar{S}^E_{AgI} = \Delta\bar{S}_{AgI} - \Delta\bar{S}^{id}_{AgI} \tag{4}$$

where

$$\left.\begin{aligned}\Delta\bar{G}^{id}_{AgI} &= RT \ln x_1\\ \Delta\bar{S}^{id}_{AgI} &= -R \ln x_1\end{aligned}\right. \tag{4 bis}$$

The heat of mixing has been computed from relation

$$H^E = G^E + TS^E \tag{5}$$

The thermodynamic functions thus computed are also given in table 1. As may be seen, both the heat of mixing and the excess entropies show positive deviations from the ideal behaviour.*

The thermodynamic properties of reciprocal mixtures of fused salts of the AY + BX type may be explained by taking into account the ion exchange reaction

$$AX_{pair} + BY_{pair} = AY_{pair} + BX_{pair}$$

the Temkin model of "ideal solutions of fused salts", and the deviations from the random distribution caused by the existence of relatively large ionic exchange energies.

According to Temkin [7] the partial molar entropy of the component AY is given by the relation

$$\Delta\bar{S}_{AY} = -R \ln x_A x_Y$$

where x_A and x_Y are :

$$x_A = \frac{n_A}{n_A + n_B}; \quad x_Y = \frac{n_Y}{n_X + n_Y}$$

n_A, n_B, n_X and n_Y representing the number of ion grams of each ion species.

Førland suggests for the entropy of configuration a corrected relation where account is taken of the deviations from the random distribution :

$$\Delta\bar{S}_{AY} = -R \ln x_A x_Y - 1/2\, x_B x_X (x_A + x_Y - 3\, x_A x_Y)\, E'^2/zRT^2 \tag{6}$$

---

* The authors previously quoted[1-4] take usually as standard state for reciprocal mixtures of molten salts the "ideal ionic solutions" according to Temkin's definition. In the present paper the standard state was taken according to the usual convention given by equation 4 bis. This treatment is purely formal and was introduced to allow a uniform "language" for all molten salts mixtures.

[7] M. Temkin, *Acta Physicochim. U.R.S.S.*, **20**, 411 (1945).

where E'/Nz is the exchange energy of the reaction mentioned above, N is Avogadro's number and z the coordination number.

According to Flood, Førland and Grjotheim the first component of the partial molar heat of mixing $\overline{H}^E_{AY}$ is

$$\overline{H}^E_{AY} = x_B x_X \, \Delta E$$

where $\Delta E = - \Delta H^0$. The heat of reaction ΔH^0 refers to the exchange reaction

$$AX(l) + BY(l) = AY(l) + BX(l)$$

where all the components are taken in the pure fused state.

Førland considers also the existence of certain variations of the energies of ionic interactions, similar to those occurring in binary mixtures of fused salts, and he obtains the relation:

$$\overline{H}^E_{AY} = x_B x_X \Delta E + x_B^2 (x_X b_X + x_Y b_Y) + x_X^2 (x_B b_B + x_A b_A) + \\ + x_B x_X [x_Y (b_A - b_B) + x_A (b_Y - b_X)] \tag{7}$$

where b_A, b_B, b_X, b_Y are the interaction parameters in equations of the type

$$H^E = b \, x_1 x_2$$

of the four binary mixtures

$$AX + AY, \ BX + BY, \ AX + BX \text{ and } AY + BY,$$

the lower index referring to the common ion.

Further, Førland computes also the deviations from the random distribution and he obtains the relation:

$$\overline{H}^E_{AY} = \overline{H}^E_{AY} \text{ (rel 7)} - x_B x_X (x_A + x_Y - 3 \, x_A x_Y) \, E'^2/zRT$$

The Førland and Temkin relations may be written in a more suitable form for computation.

Starting from a mixture AY + BX and denoting by x_1 and x_2 the weighed molar fractions of the two components, we have:

$$x_A = x_1, \ x_Y = x_1, \ x_B = x_2 \text{ and } x_X = x_2$$

For the excess entropy we obtain the relations:

$$\overline{S}^E_{AY} = - R \ln x_1 \tag{8}$$

$$\overline{S}^E_{AY} = - R \ln x_1 - 1/2 \, x_2^2 (2x_1 - 3x_1^2) \, E'^2/zRT^2 \tag{9}$$

For the heat of mixing we obtain the relations:

$$\overline{H}^E_{AY} = x_2^2 \, \Delta E \tag{10}$$

$$\overline{H}^E_{AY} = x_2^2 \, \Delta E + x_2^2 [(x_2 - x_1)(b_X + b_B) + 2 \, x_1 (b_A + b_Y)] \tag{11}$$

$$\overline{H}^E_{AY} = \overline{H}^E_{AY} \text{ (rel 11)} - x_2^2 (2x_1 - 3x_1^2) \, E'^2/zRT \tag{12}$$

Assuming a random distribution, the excess partial molar free enthalpy can be computed with the relations :

$$\overline{G}^E_{AY} = \overline{H}^E_{AY}\,(\text{rel } 10) - T\overline{S}^E_{AY}\,(\text{rel. } 8) \tag{13}$$

$$\overline{G}^E_{AY} = \overline{H}^E_{AY}\,(\text{rel } 11) - T\overline{S}^E_{AY}\,(\text{rel. } 8) \tag{14}$$

If deviation from the random distribution are admitted, the following relation may be used

$$\overline{G}^E_{AY} = \overline{H}^E_{AY}\,(\text{rel } 12) - T\overline{S}^E_{AY}\,(\text{rel. } 9) \tag{15}$$

The relations (8)—(15) have been applied to the computation of the excess thermodynamic properties of AgI in the system AgI + KI. x_1 refers to the weighed molar fraction of silver iodide and x_2 to that of potassium chloride.

The heat of reaction for

$$AgCl(l) + KI(l) = AgI(l) + KCl(l)$$

has been computed from the thermochemical data presented in table 2 according to Kubaschewski.[8] Since data concerning the heat capacities of liquid AgI and KI are lacking, it has been considered that $\sum \int_{T'}^{T''} \Delta C_p dt \simeq 0$, an approximation which may be admitted in ion exchange reactions, and has been justified by a preliminary orientative computation. The following values have been obtained : $\Delta H^0 = -9250$ cal/mol and $\Delta E = 9250$ cal/mol.

Table 2

Thermochemical data

Substance	$-\Delta H^0_{298}$ kcal/mole	Transition points °K	ΔH_{tr} kcal/mole	melting points °K	ΔH_f kcal/mole
AgI	14.9	420	1.47	831	2.25
KI	78.3	—	—	958	5.75
AgCl	30.3	—	—	728	3.1
KCl	104.2	—	—	1043	6.41

The constants B have been taken as follows : for the system AgCl + AgI, $B_{Ag} = 380$ cal/mol according to Sternberg, Adorian and Galasiu[9]; for the system AgCl + KCl, $B_{Cl} = -2212$ cal/mol according to Kleppa and Hersh[10]; for the system AgI + KI, $B_I = -2040$ cal/mol, according to Sternberg, Adorian and Galasiu.[6] For the system KI + KCl no experimental determinations were available. Since in all the binary systems of fused salts with a common alkali cation the heat of mixing has very small positive values,[11] it has been approximated by $B_K = 50$ cal/mol.

---

[8] O. Kubaschewski, E. Ll. Evans and C. Alcock, "Metallurgical Thermochemistry", Pergamon Press, London, 1967, p. 303.

[9] S. Sternberg, I. Adorian and I. Galasiu, *Rev. Roumaine Chim.*, **11**, 581 (1966).

[10] O. J. Kleppa and L. Hersh, *J. Chem. Phys.*, **42**, 1309 (1965).

For the evaluation of the energy E′ Førland recommends to choose a value of the same order of magnitude as ΔE and which introduced in relation (9) should satisfy the experimental values of the entropy.

Thus, in the system AgBr + NaCl, ΔE computed by Førland is 5435 cal/mol and E′ is taken 8000 cal/mol.

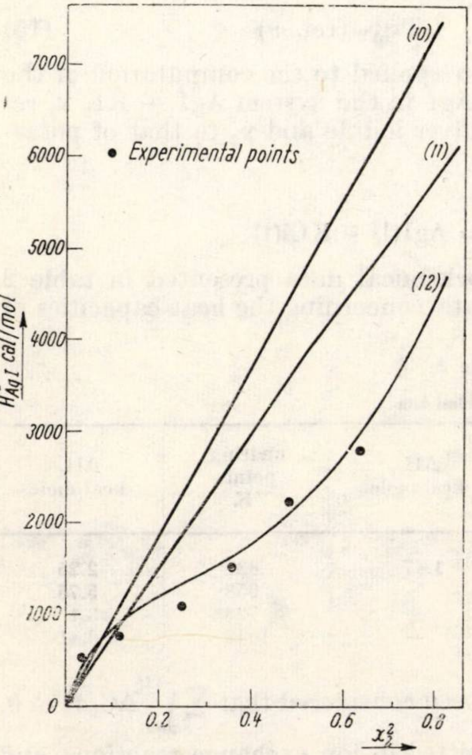

Fig. 1. — Partial molar excess enthalpy of silver iodide in mixtures AgI + KCl. Numbers of curves refer to corresponding equations in the text.

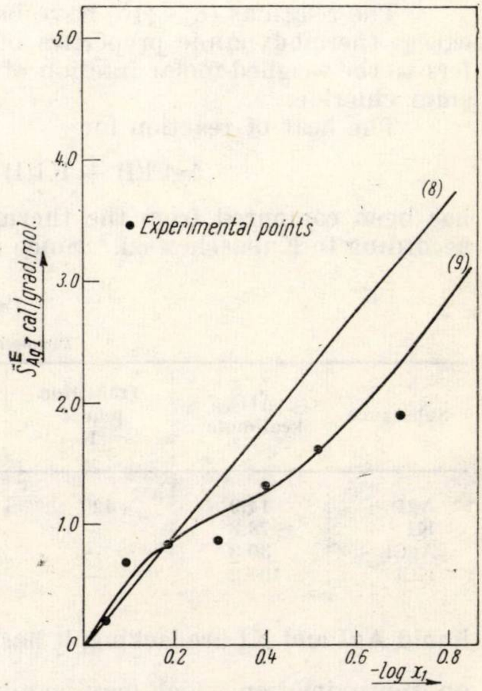

Fig. 2. — Partial molar excess entropy of silver iodide in mixtures AgI + KCl. Numbers of curves refer to corresponding equations in the text.

For the system AgI + KCl and by the same method we have obtained E′ = 9500 cal/mol, a value closely approaching that of ΔE computed from thermochemical data. The coordination number was taken as $z = 5$.

In figures 1, 2 and 3 the computed magnitudes and the experimental data are compared. The equations by which each curve has been computed are also given.

The endothermic heats of mixing are explained by the existence of a positive exchange energy ΔE. In order that from AgI and KCl new bonds AgCl and KCl may be formed, an absorption of energy from the surrounding medium is necessary. But besides this "chemical" interaction energy which is specific for reciprocal mixtures, there is also a "simple interaction" which is similar to that of mixtures with a common ion and is introduced through the constants b forming thus the second component of the heat of mixing.

---

[11] S. Sternberg and C. Herdlicka, *Rev. Roumaine Chim.*, **13**, 13 (1968).

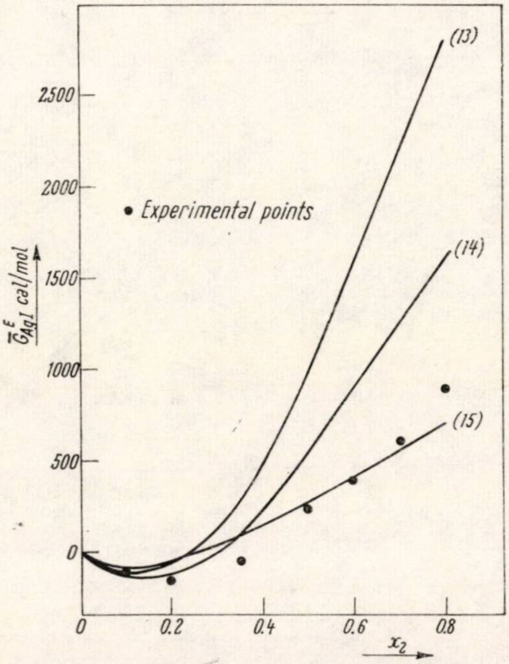

Fig. 3. — Partial molar excess free enthalpy of silver iodide in mixtures AgI+ KCl. Numbers of curves refer to corresponding equations in the text.

In the case of the system investigated it may be stated that the second component of the heat of mixing is due mainly to the polarization energy of the anions by the two cations. This phenomenon is exothermic and reduces the value of the heat of mixing. As may be seen from figure 2 the correction introduced by this term brings closer together the computed values and the experimental data.

The positive excess entropies are explained by the "Temkin model". But the AgI and KCl bonds are favoured from the energetic point of view because formed with heat evolving. This causes a deviation from random distribution. The number of AgCl and KI pairs is smaller than required by the law of random distribution. Hence an ordering effect occurs and both the heat of mixing and excess entropy become smaller.

As may be seen by taking into account the deviation from random distribution, the agreement between computed and experimental results is considerably improved.

ing medium is necessary, but besides this "chemical" interaction energy which is specific for reciprocal mixtures, there is also a Coulomb interaction which is similar to that of mixtures with a common ion and is introduced through the constants belonging into the second component of the heat of mixing.

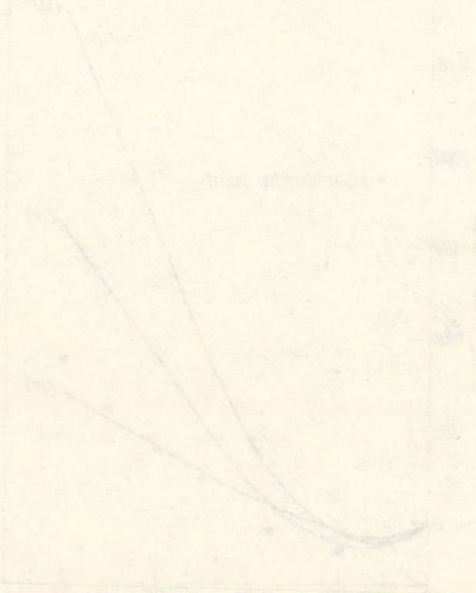

Fig. 3. — Partial molar excess heat of mixing of silver halide in mixtures AgCl + KCl. Numbers at curves refer to corresponding equations in the text.

In the case of the system investigated it may be stated that the second component of the heat of mixing is due mainly to the polarization energy of the anions by the two cations. This phenomenon is exothermic and reduces the value of the heat of mixing. As may be seen from figure 3 the correction introduced by this term brings closer together the computed values and the experimental data.

The positive excess entropies are explained by the "Temkin model" but the AgCl and KCl bonds are favoured from the energetic point of view because formed with heat evolution. This causes a deviation from random distribution. The number of AgCl and KCl pairs is smaller than required by the law of random distribution. Hence an ordering effect occurs and both the heat of mixing and excess entropy become smaller.

As may be seen by taking into account the deviation from random distribution, the agreement between computed and experimental results is considerably improved.

[illegible] 14, pp. 249 (1959).

Revue Roumaine de Chimie, **14**, 311–318 (1969)

MOLECULAR ORBITAL STUDIES ON TAUTOMERS OF DILITURIC ACID

II.[1] CORRELATION WITH SOME IR AND X-RAY DIFFRACTION DATA

R. NUŢIU and Z. SIMON

University of Timişoara, Department of Chemistry,
Bd. V. Pârvan 4

Received June 4, 1968

In this paper, which continues the HMO-study on tautomers of dilituric (5-nitrobarbituric) acid, the results for the di-anion and tri-anion of this acid are given. For the most stable tautomers the Hückel molecular diagrams are given, and for the anhydrous acid and its trihydrate, they are compared with interatomic distances obtained by X-ray diffraction. A satisfactory correlation is obtained between the maximal bond order and the maximal IR frequency of the carbonyl in the stable tautomers. The HMO calculations concerning the stability of tautomers were generally extended to the aci-nitro tautomery.

In a previous note[1] a molecular orbital study was performed on the tautomers and limiting structures of dilituric (5-nitrobarbituric) acid and of the mono-anion. The relative stability of the various theoretically possible tautomers was evaluated thereby. In table 4 of note [1] the spectral transitions, calculated for the di-anion and tri-anion, were anticipated.

In this note the molecular orbital study is continued in order to estimate the stability for the tautomers of the di-anion and the tri-anion of the dilituric acid. The calculations were extended also to the general aci-nitro tautomery. The theoretical considerations were completed with the results of UV and IR spectral determinations.

THEORETICAL DISCUSSION ON THE STABILITY OF THE TAUTOMERS OF THE DI-ANION AND TRI-ANION OF THE DILITURIC ACID

The di-anion of the dilituric acid has four tautomers, listed below and numbered continuously to our previous note. The tri-anion has a single tautomer.

The numbering of the atoms and the α and β parameters are the same as for the previous note. In table 1 the total energies, in kcal/mol, are given for the structures (XVI)-(XX), as well as the resonance energies, the energy of the highest occupied molecular orbital (ε_{HO}) and of the lowest empty one (ε_{LE}), the double bond order (π) of the C-NO_2 bond and the π-electronic charge (q) of the nitro-group. The energy of the localized bonds is denoted by C for the di-anion and by D for the tri-anion.

---

[1] Z. Simon, Fr. Mihai and R. Nuţiu, *Rev. Roumaine Chim.*, **13**, 147 (1968).

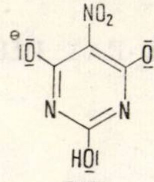

XVI

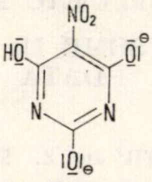

XVII

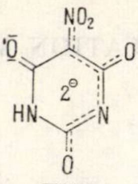

XVIII

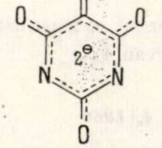

XIX

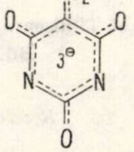

XX

The most stable tautomer of the di-anion is (XVIII) with a percent of (unprotonated) aci-nitro valence bond structure of 54%. The energy levels and the molecular orbitals of the most stable tautomer of the di-anion (XVIII) and of the tri-anion (XX) are given in table 2.

Table 1

Hückel parameters for the tautomers of the dilituric acid di-anion and tri-anion

Tautomer	E (kcal/mol)	R (β-units)	ε_{HO}	ε_{LE}	π	q
XVI	C−92.5	3.458	$\alpha+0.958\beta$	$\alpha-0.406\beta$	0.529	−0.257
XVII	C−97.5	3.458	$\alpha+0.918\beta$	$\alpha-0.404\beta$	0.521	−0.252
XVIII	C−105.9	3.336	$\alpha+0.920\beta$	$\alpha-0.426\beta$	0.537	−0.262
XIX	C−80	2.464	$\alpha+0.967\beta$	$\alpha+0.227\beta$	0.843	−1.212
XX	D−97	3.682	$\alpha+0.909\beta$	$\alpha-0.426\beta$	0.541	−0.266

THEORETIC DISCUSSION OF THE ACI-NITRO TAUTOMERY

The results of calculations for the relative stability of the dilituric acid tautomers are now available for both the undissociated acid and its three dissociation steps. We will now compare these results with those for the simpler systems :

$R-CH_2-NO_2$ and

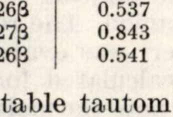

$$\underset{NO_2}{R-\underset{|}{CH}}-\underset{O}{\overset{}{\underset{\|}{C}}}-R$$

(1) (2)

For the simplest system (1) in which the aci-nitro tautomery may appear, only two tautomers can be written:

$$\underset{(1)}{R-CH_2-NO_2} \rightleftarrows \underset{(1a)}{R-CH=NO_2H}$$

Table 2

Molecular orbitals and energy levels for the stable tautomers

Structure		C_1	C_2	C_3	C_4	C_5	C_6	C_7	C_8	C_9	C_{10}
XVIII	$\alpha-2.026\beta$	0.5246	−0.4829	0.3087	−0.2970	0.2040	−0.4222	−0.2258	0.1319	0.0812	0.1153
	$\alpha-1.215\beta$	0.3718	0.0467	−0.4110	0.6582	−0.1411	−0.2750	−0.3193	−0.0160	−0.2252	0.0941
	$\alpha-0.910\beta$	0.0641	−0.5682	0.2164	0.2631	−0.3463	+0.5715	−0.0881	0.2148	−0.0995	−0.2161
	$\alpha-0.426\beta$	−0.0310	−0.2834	0.0103	0.2739	0.0097	−0.2925	+0.8417	0.1285	+0.1242	0.1326
	$\alpha+0.920\beta$	−0.5976	−0.0508	0.4941	0.2581	0.0325	−0.2770	−0.3170	0.0517	−0.2629	0.2821
	$\alpha+1.231\beta$	−0.3777	−0.3409	−0.5788	−0.0825	0.3474	−0.0108	−0.1621	0.4879	0.1180	0.0155
	$\alpha+1.794\beta$	−0.0742	−0.0917	−0.0919	−0.0972	−0.6535	−0.0949	−0.0237	0.1157	0.5190	0.5067
	$\alpha+2.569\alpha$	0.1544	0.0670	−0.1246	−0.3249	−0.0195	+0.3041	0.0364	0.1295	−0.6279	0.5896
	$\alpha+2.614\beta$	0.1057	0.4283	0.1696	−0.0698	−0.2145	−0.1691	0.0246	0.7675	−0.1250	−0.3031
	$\alpha+3.049\beta$	0.2028	0.2330	0.2387	0.3754	0.4726	0.3564	0.0412	0.2444	0.3938	0.3739
XX	$\alpha-2.088\beta$	0.4910	−0.4413	0.2998	−0.3346	0.2998	−0.4413	−0.2036	0.1187	0.0900	0.1187
	$\alpha-1.259\beta$	0.4216	−0.1451	−0.2929	0.6602	−0.2929	−0.1451	−0.3437	0.0490	−0.2229	0.0490
	$\alpha-1.045\beta$	—	−0.5680	0.3677	—	0.5680	−0.3677	—	0.2052	—	−0.2052
	$\alpha-0.426\beta$	−0.0311	−0.2875	0.0101	0.2781	0.0101	−0.2875	0.8404	0.1304	−0.1261	0.1304
	$\alpha+0.909\beta$	0.6433	0.1721	−0.2959	−0.2932	−0.2959	0.1721	0.3439	−0.1735	0.2957	−0.1735
	$\alpha+0.967\beta$	—	−0.2729	−0.5839	—	0.2729	0.5839	—	0.2908	—	−0.2908
	$\alpha+1.482\beta$	0.2950	0.1802	0.3932	0.2059	0.3932	0.1802	0.1097	−0.3828	−0.4374	−0.3828
	$\alpha+2.568\beta$	0.1623	0.1950	−0.0773	−0.3548	−0.0773	0.1950	0.0383	0.3778	−0.6876	0.3778
	$\alpha+2.577\beta$	—	0.3207	0.1544	—	−0.3207	−0.1544	—	0.6110	—	−0.6110
	$\alpha+2.914\beta$	0.2304	0.3185	0.2758	0.3472	0.2758	0.3185	0.0487	0.3836	0.4180	0.3836

With the method used in the previous note (bond energies and HMO calculations) we calculated the relative energies of the two isomers. The parameters used in the calculations are those given in table 3.

Table 3

Hückel parameters for heteroatom in the tautomeric structures

Coulomb integrals	Exchange integrals
$\alpha_0 = \alpha + 2\beta$	$\beta_{C-C(cycle)} = \beta_{C-N(cycle)} = \beta$
$\alpha_N = \alpha + 0.5\beta$	$\beta_{C=O} = 1.4\ \beta$
$\alpha_{N_H} = \alpha + 1.5\ \beta$	$\beta_{C-O} = 0.8\ \beta$
$\alpha_{NO_2} = \alpha - 0.4\beta$	$\beta_{C-O} = 1.1\ \beta$
$\alpha_{NO_2H} = \alpha + \beta$	$\beta_{C-NO_2} = 0.7\ \beta$
$\alpha_{CH_2} = \alpha + 2\beta$	$\beta_{C=NO_2H} = \beta$
	$\beta_{CH_2-NO_2} = 0.6\ \beta$

For the compound (1) the CH_2 group was considered, according to Streitwieser,[2] as a heteroatom with two π electrons ($\alpha_{CH_2} = \alpha + 2\ \beta$; $\beta_{CH_2-NO_2} = 0.6\ \beta$). The calculation indicates the nitro-tautomer (1) with 22 kcal/mol stabler than the aci-tautomer (1a) in good agreement with the instability of this type of aci-nitro derivatives.[3]

System (2) presents the same main types of tautomers as the diliturie acid and the ω-nitro-acetophenone[4]:

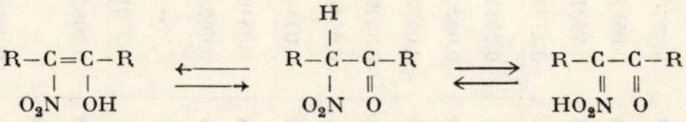

(2a) (2) (2b)

With the method used in our previous note and taking also into account the stabilizing effect of the hydrogen bond for the tautomers (2a) and (2b) and of the electrostatic repulsion between the dipoles of the NO_2 and $>C=O$ groups in the tautomer (2), the following results are obtained. The nitro-enolic tautomer (2a) is also in this case the stablest one, but the aci-tautomer (2b) and the nitro-ketonic tautomer (2) are by only 6 kcal/mol and respectively 5 kcal/mol less stable. The more pronounced stability of the nitro-enolic tautomer is probably due to the conjugation between the nonparticipating p-electron pair at the oxygen atom, with the carbon-carbon double bond and the nitro-group, and to the hydrogen bond between the OH and NO_2 groups. These data permit to explain the data available on ω-nitro-acetophenone. Our opinion is that these calculations can be considered as a generalization for all combinations of this type.

---

[2] A. STREITWIESER, JR., "Molecular Orbital Theory for Organic Chemists", John Wiley, New York, 1961, chap. 5.

[3] N. KORNBLUM and R. A. BROWN, *J. Amer. Chem. Soc.*, **85**, 1359 (1963).

[4] a) F. ARNDT and I. D. ROSE, *J. Chem. Soc.*, **1935, 1**;

b) G. W. WHELAND, "Advanced Organic Chemistry", ed. 3, John Wiley Sons, Inc., New York, 1960, p. 713.

DOUBLE BOND ORDERS AND CORRELATIONS WITH SOME X-RAY AND IR DATA

The π-bond orders were calculated for the most stable tautomers (II, V, XIII, XVIII and XX; figure 1) in order to correlate our HMO calculations with X-ray diffraction data and with IR spectra.

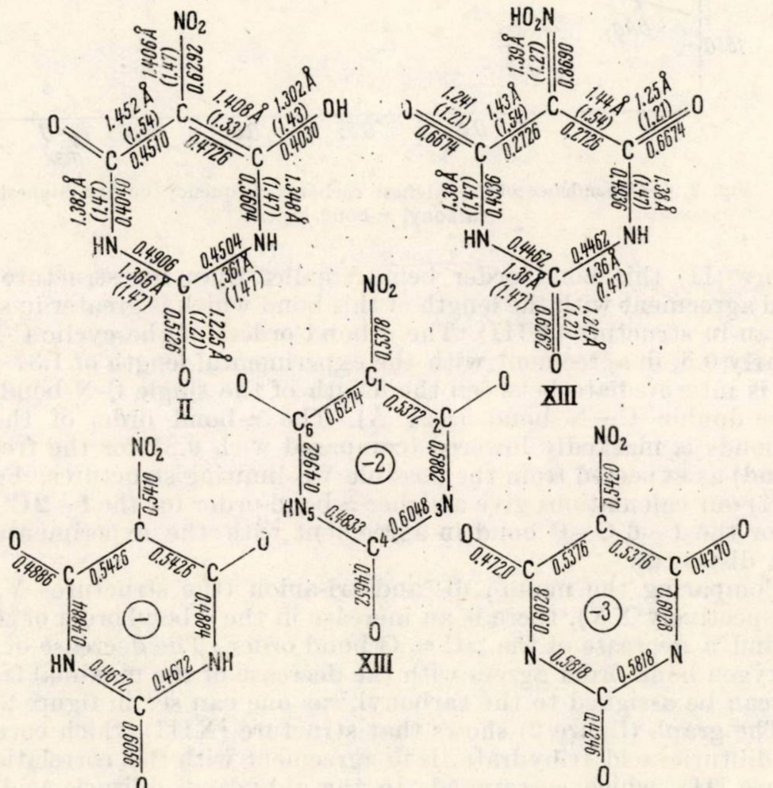
NO2
1.406 Å
(1.47)
0.6292
1.452 Å
(1.54)
0.4510
1.408 Å
(1.33)
0.4726
1.302 Å
(1.43)
0.4030
OH
1.382 Å
(1.47)
0.4040
0.5604
1.348 Å
(1.47)
HN
0.4906
1.366 Å
(1.47)
0.4504
1.361 Å
(1.47)
NH
1.225 Å
(1.21)
0.5126
II
HO2N
1.39 Å
(1.27)
0.8690
1.241
(1.21)
0.6674
1.43 Å
(1.54)
0.2726
1.44 Å
(1.54)
0.2726
1.25 Å
(1.21)
0.6674
1.38 Å
(1.47)
0.4336
0.4336
1.38 Å
(1.47)
HN
0.4462
1.36 Å
(1.47)
0.4462
1.36 Å
(1.47)
NH
1.24 Å
(1.21)
0.6262
XIII
NO2
0.5378
C1
0.6274
0.5372
C6
2C
0.4962
0.5088
HN5
0.4833
0.6048
3N
C4
0.2374
XIII
NO2
0.5410
0.4886
0.5426
0.5426
0.4884
0.4884
HN
0.4672
0.4672
NH
0.6036
V
NO2
0.5400
0.4720
0.5376
0.5376
0.4270
0.6028
0.6028
N
0.5818
0.5818
N
0.4246
XX

Fig. 1. — Bond orders of the main tautomers of the dilituric acid and his anions.

Structure (II)—corresponding to the anhydrous 5-nitrobarbituric acid, and structure (XIII) — corresponding to the trihydrate, contain the π-bond orders (underlined), given also for the other structures, but also the interatomic distances as determined by X-ray diffraction[5] and the mean distances for the simple and double bonds[6] (in parantheses). For structures (II) and (XIII) the calculated C-NO_2 π-bond orders indicate those bonds as intermediate between simple and double bond, for structure (II) this bond order being smaller than for structure (XIII), in good agreement with the length of this bond which is greater in structure (II) than in structure (XIII). The π-bond orders of the cyclic C-N bonds are nearly 0.5, in agreement with the experimental length of 1.37 ± 0.01 Å which is intermediate between the length of the single C-N bond (1.47Å) and the double C=N bond (1.27 Å). The π-bond order of the carbonylic bonds is markedly lowered (compared with 0.81 for the free carbonyl bond) as expected from the possible VB-limiting structures. For structure (II) our calculations give a higher π-bond order for the 1−2 C−C bond than for the 1−6 C−C bond in agreement with the experimental interatomic distances.

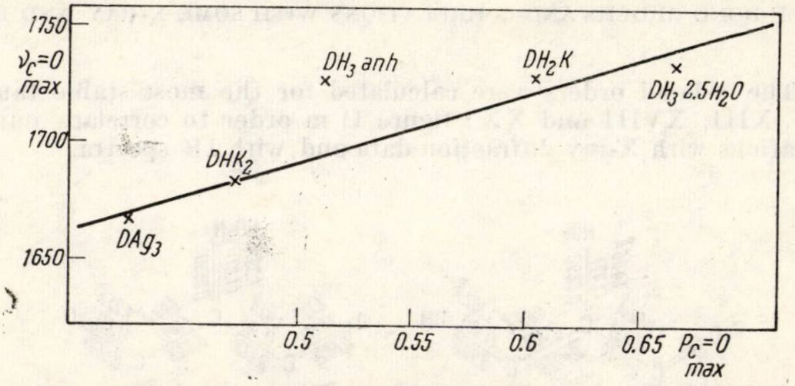

Fig. 2. — Dependence of the highest carbonyl frequency on the highest carbonyl π-bond order.

Comparing the mono-, di- and tri-anion (the structures V, XVIII and respectively XX), there is an increase in the π-bond order of the C−N bond and a decrease of the $>C=O$ bond order. The decrease of the carbon-oxygen bond order agrees with the decrease of the maximal frequency which can be assigned to the carbonyl,[7] as one can see in figure 2.

The graph (figure 2) shows that structure (XIII) which corresponds to the dilituric acid trihydrate, is in agreement with this correlation while structure (II), which corresponds to the anhydrous dilituric acid, gives a point far away from the correlation line.

NEW UV AND IR DATA

In our previous note,[1] the UV absorption spectra (given in table 4) were considered identic for the mono- and di-potassic salts. This identity is due to the hydrolysis of the di-potassic salt, hydrolysis accompanied by the precipitation of the mono-potassic salt and described also by Baeyer.[8] Although the di-potassic diliturate (described first by Schlieper[9]) contains also some mono-potassic diliturate, its IR spectrum (done in a KBr pellet as described in a previous note [7]) contains the characteristic bonds for the symmetric and antisymmetric valence vibrations of the NO_2 group at 1362 cm^{-1} and respectively 1580 cm^{-1}. Thus, the IR spectrum is clearly different from that of the mono-potassic salt. These results demonstrate that the structure of the di-potassic salt could be identic with structure (XVIII) indicated by our calculations concerning the stability of the various structures. The highest frequency in the IR spectrum of this substance, which can be assigned to the carbonyl, is the 1682 cm^{-1} frequency and it is in good agreement with the correlation given in figure 2. In the IR spectrum of the tri-argentic diliturate the NO_2 bands at 1350 cm^{-1} and 1580 cm^{-1} clearly exist, while the bonds characteristic to the amidic carbonyl are at low frequencies (1655 – 1665 cm^{-1}) where they may be assigned also to the carbon-nitrogen double bond. [7,10]

---

[5] a) W. Bolton, *Acta Cryst.*, **16**, 950 (1963);
b) B. M. Craven, S. Martinez-Caressa and G. A. Jeffrey, *Acta Cryst.*, **17**, 891 (1964).

[6] C. D. Nenițescu, "Chimie organică", vol. 1, Bucharest, 1966, p. 77.

[7] Fr. Mihai and R. Nuțiu, *Rev. Roumaine Chim.*, **13**, 39 (1968).

A discussion of the work of Professor Dr. M. P. Poni et al.[11] concerning the IR spectra of 5-nitrobarbituric acid and its complex salts seems now suitable. These authors give a spectrum for the dilituric acid in which characteristic bands for both the anhydrous and the hydrated form are available (for example 1260 m, 1300 ws, 1392 ws, ..., 1594 ws, ... 1664 cm^{-1} ws...). The intense 1594 cm^{-1} band was assigned in this work[11] to a "harmonic of the NO_2-valence vibration" and the authors were surprised at not finding it in the spectra of the complex salts. We consider the 1594 cm^{-1} band to be characteristic of the antisymmetric valence vibration of the NO_2 group which appears in the spectrum of the anhydrous acid. Also, the intense 1392 cm^{-1} band, assigned to the antisymmetric NO_2 valence vibration by Poni et al. corresponds rather to a vibration of the cycle, as shown by Mihai.[12] This last assignement is demonstrated by the presence of this band in the spectra of barbiturates, for example of the 5,5-diethylbarbituric acid.[7] This band appears also in the spectrum of the di-potassic salts (1390 cm^{-1}) and of the tri-argentic salts (1400 cm^{-1}).

The work[11] probably neglected the fact that the anhydrous and the hydrated forms of the dilituric acid have markedly different structures as demonstrated by the X-ray diffraction [5] and by UV and IR spectra.[7] In the anhydrous form, which is a 2,6-diketo-4-hydroxi-5-nitro-1,2,3,6-tetrahydropyrimidine the characteristic bands for the symmetric and antisymmetric NO_2 valence vibration are found at 1318 cm^{-1} and 1585 $\pm$ ± 5 cm^{-1}, while in the hydrated dilituric acid which is an aci-tautomer

---

[8] A. Baeyer, *Liebigs Ann. Chem.*, **127**, 215 (1863).

[9] A. Schlieper, *Liebigs Ann. Chem.*, **56**, 26 (1845).

[10] Fr. Mihai, *Rev. Roumaine Chim.*, **11**, 657 (1966).

[11] a) M. P. Poni, M. Bostan, N. Iorga and I. Gabe, *Rev. Roumaine Chim.*, **9**, 575 (1964);
b) M. Bostan and M. Poni, *Rev. Roumaine Chim.*, **12**, 493 (1967).

[12] Fr. Mihai, "Contribuţii la studiul unor dilituraţi metalici", Dissertation, 1964, Universitatea Babeş-Bolyai, Cluj, p. 108.

(and not nitro), these bands disappear. The bands of the aci-group ($=NOO^{\ominus}$) for the hydrated acid are not so clear as for the simple salts (for example the potassium dilituratebands at 1291 cm^{-1} and 1260 cm^{-1}) but they are comparable with the bands of the alkaline salts of certain nitro-derivatives.[13]

The bands in the spectra of the complex salts of dilituric acid which were assigned to the dilituric anion[11] are identic with those of the simple salts. Our opinion is, for this reason, that the dilituric acid in these complexes exists as an aci-tautomer and as such, the normal NO_2 group is absent, the metal atom is not bound to the C_5 carbon atom as proposed by Poni et al.[11] We consider also difficult to assign frequencies separately to the interacting, carbonylic bonds of position 4 and 6, as in.[11a] The strong frequency in the 1650 cm^{-1} region in the spectrum of the complex salts of dilituric acid should be assigned rather to a ($\nu_{C=N}$) vibration of the dilituric cycle.

CONCLUSIONS

The HMO calculations indicate for the undissociated dilituric acid the 2,6-diketo-4-hydroxi-5-nitro-1,2,3,6-tetrahydropyrimidine structure as the stablest tautometric structure. For the anhydrous dilituric acid the X-ray diffraction data and the IR spectrum are in good agreement with this theoretical result, but for the trihydrate the experimental data favour an aci-nitro structure. In the trihydrate, the dilituric acid, a strong acid, will exist as a mono-anion, in agreement with the observation of Novikov et al.[14] that the aci-forms of nitro derivatives are dissociated. The distribution of the electrons in the anion is very similar to that of the aci VB-structure.

The results of the HMO-calculations generally agree with the characteristics of the IR spectra and with the interatomic distances. Some discordances which appear could be due to specific effects of the crystalline lattice and to approximations inherent to the HMO method.

[13] A. Buczkowski and T. Urbanski, *Spectrochim. Acta*, **18**, 1187 (1962).

[14] S. S. Novikov, V. I. Slovetskii, A. A. Fainzilberg, S. A. Shevelev, V. A. Shlyapochnikov, A. I. Ivanov and V. A. Tartakovskii, *Nitro Compds.-Proc., Intern. Symp., Warsaw*, **1963**, 119, (*Chem. Abstr.*, **63**, 14665 (1965)).

Revue Roumaine de Chimie, **14**, 319–327 (1969)

ELECTRONIC SPECTRA OF THE SUBSTITUTED α-OXIMINOALKYLBENZENES. II[1]

MO CALCULATIONS OF THE BATHOCHROMIC SHIFTS PRODUCED BY THE DISSOCIATION OF BENZALDOXIME AND *P*-NITRO-BENZALDOXIME

L. FEY and N. BODOR

Chemical-Pharmaceutical Research Institute,
Cluj, str. Karl Marx 93–97

Received March 19, 1968

Molecular orbitals, energy levels, electron densities and bond orders of the undissociated benzaldoxime, *p*-nitro-benzaldoxime and their anions were calculated, using the simple LCAO-MO method (Hückel's approximation). The calculated bathochromic shifts of the primary bands corresponding to the intramolecular charge transfer are in good agreement with the experimental values. On the basis of the MO data of the formaldoxime (undissociated and ionized forms) and of nitrobenzene, the change produced by dissociation on the vertical resonance energy (delocalization energy) was evaluated in the first approximation.

In the previous paper [1] we have studied and interpreted the displacements of the absorption bands, which take place as a result of the transition of the undissociated *o*-nitro-α-oximino-alkylbenzenes in their anions. It was demonstrated that the observed bathochromic shifts are produced, on the one hand, by the redistribution of the electrons (i. e., of charges), on the other hand, by the change of the steric effects (steric hindrance of resonance).

In the present work, the bathochromic shifts produced only by the changes of electron distributions, in consequence of the ionization of benzaldoxime (I) and *p*-nitro-benzaldoxime (II) were investigated, therefore when no steric hindrance of resonance takes place.

The spectrum of the undissociated benzaldoxime in various organic solutions has been given by several authors[2,3]; however for our study, the spectra in water and alkaline solution had to be registered, according to the procedure given in our previous work.[1]

The observed bathochromic shifts of the primary bands, corresponding to the intramolecular charge transfer, have the following values:

---

[1] L. FEY and N. BODOR, *Rev. Roumaine Chim.*, (under print).

[2] R. F. REKKER and J. U. WEELAND, *Rec. Trav. chim.*, **78**, 379 (1959).

[3] *"Absorption Spectra in the UV and Visible Region"*, Ed. by Hungarian Acad. of Sciences, Budapest, Vol. II. p. 109.

3000 cm^{-1} for benzaldoxime and 5300 cm^{-1} for *p*-nitro-benzaldoxime.

On the other hand we have studied to what extent the simple LCAO-MO method (in Hückel's approximation) is suitable to express these displacements. For the calculation of the MO values, the following sets of Coulombian and resonance integrals were found as the most suitable :

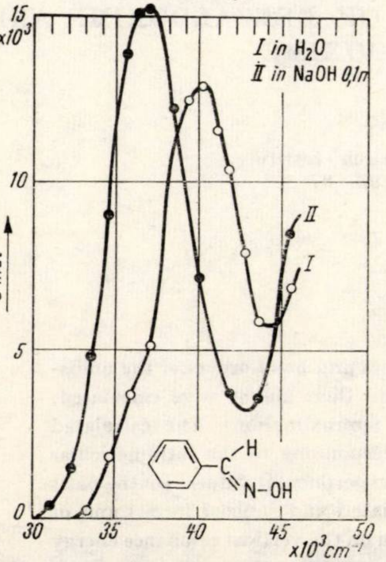

Fig. 1. — UV spectra of benzaldoxime.
I, in water ; *II*, in NaOH 0.1 N.

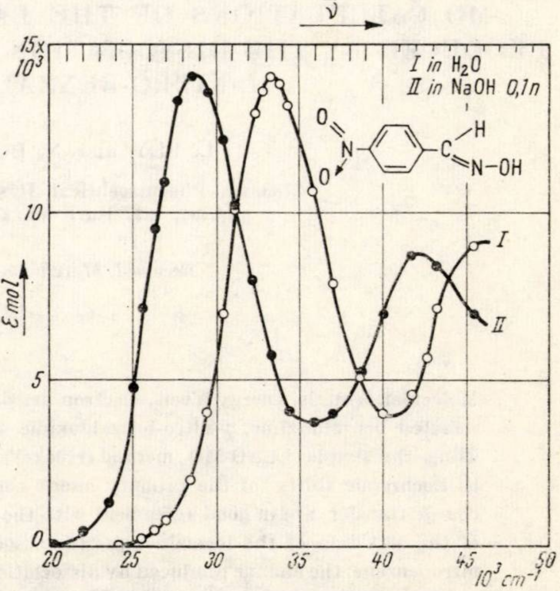

Fig. 2. — UV spectra of p-nitro-benzaldoxime.
I, in water ; *II*, in NaOH 0.1 N.

For the oximinomethyl grouping $(-\overset{|}{C}=N-\ddot{O}-H)$:

Undissociated molecule, Anion

$$\alpha_{\ddot{O}} = \alpha_C + 1.5\ \beta \qquad \alpha_{\ddot{O}} = \alpha + \beta$$
$$\alpha_N = \alpha_C + 0.5\ \beta \qquad \alpha_N = \alpha + 0.5\ \beta$$
$$\beta_{C-N} = 1.2\ \beta \qquad \beta_{C-N} = 1.2\ \beta$$
$$\beta_{N-O} = 0.7\ \beta \qquad \beta_{N-O} = 0.7\ \beta$$

For the nitro group (according to[4]) :

$$\alpha_O = \alpha + \beta \qquad \beta_{C-N} = 0.7\ \beta$$
$$\alpha_N = \alpha + \beta \qquad \beta_{N-O} = 1.2\ \beta$$

and

$$\beta_{C-C} = -\ 2.8\ \text{eV}$$

Electron distributions and bond orders of the ground state and the first excited states of the undissociated and ionized forms are given in figures 3 and 4.

---

[4] V. E. Sahini, E. Keplinger and M. Hillebrand, *Rev. Roumaine Chim.*, **12**, 361 (1967).

The corresponding orbital coefficients and energy levels are given in tables 1, 2, 3 and 4.

From these data, the following bathochromic shifts of the primary bands were calculated : 2700 cm^{-1} for benzaldoxime and 6200 cm^{-1} for *p*-nitro-benzaldoxime.

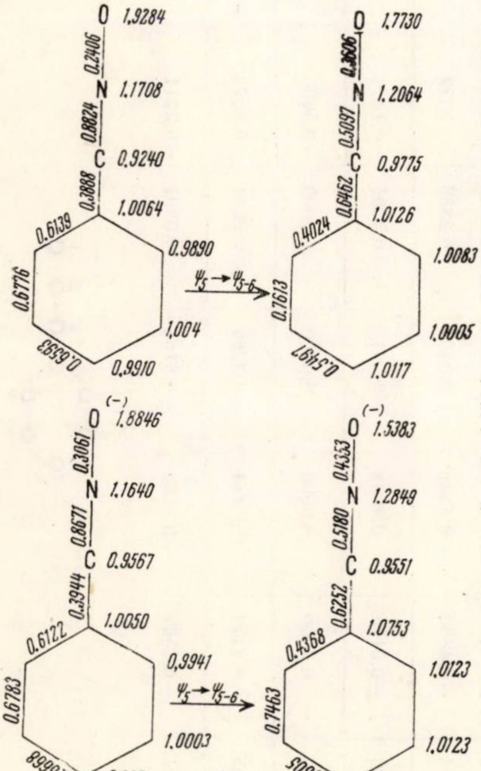
O 1.9284
0.2406
N 1.1708
0.8824
C 0.9240
0.3888
1.0064
0.6139
0.9890
0.6776
1.004
0.6583
0.9910
ψ5→ψ5-6
O 1.7730
0.3606
N 1.2064
0.5097
C 0.9775
0.6462
1.0126
0.4024
1.0083
0.7613
1.0005
0.5497
1.0117
(−)
O 1.8846
0.3061
N 1.1640
0.8671
C 0.9567
0.3944
1.0050
0.6122
0.9941
0.6783
1.0003
0.6668
0.9973
ψ5→ψ5-6
(−)
O 1.5383
0.4353
N 1.2849
0.5180
C 0.9551
0.6252
1.0753
0.4368
1.0123
0.7463
1.0123
0.5805
1.0688

Fig. 3. — Molecular diagrams of benzaldoxime (undissociated and anion).

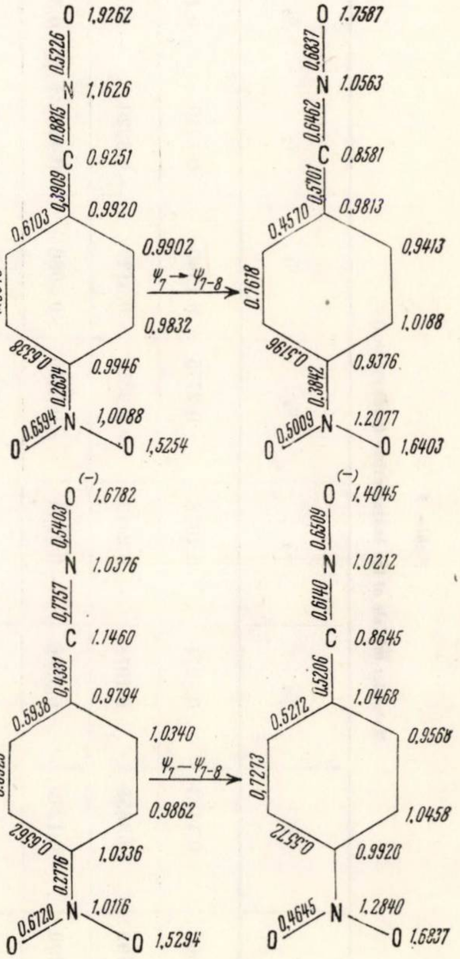
O 1.9262
0.5226
N 1.1626
0.8815
C 0.9251
0.3909
0.9920
0.6103
0.9902
0.6840
0.9832
0.6238
0.9946
0.2634
N 1.0088
0.6594
O
O 1.5254
ψ7→ψ7-8
O 1.7587
0.6837
N 1.0563
0.6462
C 0.8581
0.5701
0.9813
0.4570
0.9413
0.7618
1.0188
0.5196
0.9376
0.3842
N 1.2077
0.5009
O
O 1.6403
(−)
O 1.6782
0.5403
N 1.0376
0.7757
C 1.1460
0.4331
0.9794
0.5938
1.0340
0.6923
0.9862
0.6662
1.0336
0.2776
N 1.0116
0.6720
O
O 1.5294
ψ7—ψ7-8
(−)
O 1.4045
0.6509
N 1.0212
0.6140
C 0.8645
0.5206
1.0468
0.5212
0.9568
0.7273
1.0458
0.5572
0.9920
N 1.2840
0.4645
O
O 1.6837

Fig. 4.— Molecular diagrams of *p*-nitro-benzaldoxime (undissociated and anion).

Consequently, the simple HMO-method was suitable not only to express the direction of the displacements, but also to estimate quantitatively these shifts with satisfactory precision.

Table 1

Molecular orbitals of the benzaldoxime (undissociated)

ψ_i	$\frac{\alpha - \varepsilon}{\beta}$	c_1	c_2	c_3	c_4	c_5	c_6	c_7	c_8	c_9
1	−2.2738	0.4065	0.4493	0.4271	0.4318	0.2775	0.1990	0.1750	0.1990	0.2775
2	−1.9421	0.5792	0.3658	0.1018	−0.2413	−0.2852	−0.3127	−0.3220	−0.3127	0.2852
3	−1.3319	0.5290	−0.1270	−0.3966	−0.3759	−0.0520	0.3066	0.4604	0.3066	−0.0520
4	−1.0000	0.0000	0.0000	0.0000	0.0000	0.5000	0.5000	0.0000	−0.5000	−0.5000
5	−0.7102	0.4284	−0.4833	−0.3346	0.3423	0.2889	−0.1372	−0.3863	−0.1372	0.2889
6	0.6669	0.1676	−0.5188	0.4068	0.3513	−0.3205	−0.1374	0.4122	−0.1374	−0.3205
7	1.0000	0.0000	0.0000	0.0000	0.0000	0.5000	−0.5000	0.0000	0.5000	−0.5000
8	1.4445	0.0825	−0.3472	0.5144	−0.3265	−0.0214	0.3574	−0.4949	0.3574	−0.0214
9	2.1466	0.0301	−0.1567	0.3282	−0.5164	0.3901	−0.3211	0.2992	−0.3211	0.3901

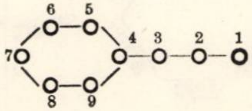

Table 2

Molecular orbitals of the benzaldoxime (anion)

ψ_i	$\frac{\alpha-\varepsilon}{\beta}$	c_1	c_2	c_3	c_4	c_5	c_6	c_7	c_8	c_9
1	−2.2281	0.2185	0.3834	0.4247	0.4861	0.3992	0.2475	0.2221	0.2475	0.3292
2	−1.8037	0.4510	0.5178	0.2994	−0.0813	−0.2230	−0.3210	−0.3559	−0.3210	−0.2230
3	−1.1782	0.5464	0.1391	−0.2408	−0.4498	−0.1449	0.2790	0.4737	0.2790	−0.1449
4	−1.0000	0.0000	0.0000	0.0000	0.0000	0.5000	0.5000	0.0000	−0.5000	−0.5000
5	−0.5709	0.6266	−0.3841	−0.3882	0.2393	0.2624	−0.0895	−0.3135	−0.0895	0.2624
6	0.6850	0.2152	−0.5181	0.3861	0.3572	−0.3154	−0.1411	0.4121	−0.1411	−0.3154
7	1.0000	0.0000	0.0000	0.0000	0.0000	0.5000	−0.5000	0.0000	0.5000	−0.5000
8	1.4487	0.1009	−0.3529	0.5141	−0.3214	−0.0243	0.3566	−0.4923	0.3566	−0.0243
9	2.1472	0.0353	−0.1585	0.3291	−0.5163	0.3898	−0.3207	0.2987	−0.3207	0.3898

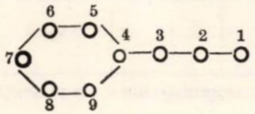

Table 3

Molecular orbitals of the p**-nitro-benzaldoxime (undissociated)**

ψ_i	$\frac{\alpha-\varepsilon}{\beta}$	c_1	c_2	c_3	c_4	c_5	c_6	c_7	c_8	c_9	c_{10}	c_{11}	c_{12}
1	−2.8264	0.4583	0.6979	0.4533	0.2485	0.1072	0.0543	0.0462	0.0543	0.1072	0.0221	0.0135	0.0071
2	−2.2631	0.0818	0.0861	0.0818	−0.1251	−0.1717	−0.2635	−0.4246	−0.2635	−0.1717	−0.4339	−0.4645	−0.4261
3	−1.9216	0.1162	0.0892	0.1162	−0.2809	−0.3011	−0.2978	−0.2710	−0.2978	−0.3011	0.0747	0.3455	0.5735
4	−1.3201	0.1347	0.0359	0.1347	−0.4454	−0.3066	0.0407	0.3603	0.0407	−0.3066	0.3942	0.1335	0.5195
5	−1.0000	0.0000	0.0000	0.0000	0.0000	0.5000	0.5000	0.0000	−0.5000	−0.5000	0.0000	0.0000	0.0000
6	−1.0000	0.7071	0.0000	−0.7071	0.0000	0.0000	0.0000	0.0000	0.0000	0.0000	0.0000	0.0000	0.0000
7	−0.7176	0.1133	−0.0267	0.1133	−0.3777	−0.1262	0.2871	0.3322	0.2871	−0.1262	−0.3359	−0.4777	0.4274
8	0.4830	0.3616	−0.4468	0.3616	−0.2930	0.2271	0.1833	−0.3157	0.1833	0.2271	−0.2142	0.3492	−0.1233
9	0.8595	0.3036	−0.4704	0.3036	0.2087	0.0750	−0.2731	0.1598	−0.2731	0.0750	0.4089	−0.4261	0.1264
10	1.0000	0.0000	0.0000	0.0000	0.0000	0.5000	−0.5000	0.0000	0.5000	−0.5000	0.0000	0.0000	0.0000
11	1.5374	0.1197	−0.2531	0.1197	0.5071	−0.3012	−0.0440	0.3688	−0.0440	−0.3012	0.4818	0.3064	−0.0706
12	2.1689	0.0399	−0.1055	0.0399	0.3405	−0.3324	0.3804	−0.4926	0.3804	−0.3324	0.3077	−0.1456	0.0278

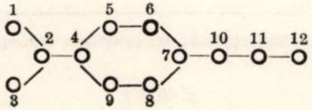

Table 4

Molecular orbitals of the *p*-nitro-benzaldoxime (anion)

ψ_i	$\frac{\alpha-\varepsilon}{\beta}$	c_1	c_2	c_3	c_4	c_5	c_6	c_7	c_8	c_9	c_{10}	c_{11}	c_{12}
1	−2.8261	0.4580	0.6971	0.4580	0.2486	0.1074	0.0549	0.0478	0.0549	0.1074	0.0253	0.0197	0.0130
2	−2.4030	0.0590	0.0689	0.0590	−0.0640	−0.1010	−0.1787	−0.3285	−0.1787	−0.1010	−0.4312	−0.5913	−0.5057
3	−1.9667	0.1330	0.1071	0.1330	−0.3080	−0.3404	−0.3614	−0.3704	−0.3614	−0.3404	−0.0057	0.2994	0.3716
4	−1.2137	0.1514	0.0269	0.1514	−0.5108	−0.3194	−0.1231	0.4689	0.1231	−0.3194	0.3228	−0.0643	−0.3610
5	−1.0000	0.0000	0.0000	0.0000	0.0000	0.5000	0.5000	0.0000	−0.5000	−0.5000	0.0000	0.0000	0.0000
6	−1.0000	0.7071	0.0000	0.7071	0.0000	0.0000	0.0000	0.0000	0.0000	0.0000	0.0000	0.0000	0.0000
7	−0.3766	0.1040	−0.0540	0.1040	−0.3085	−0.0392	0.2938	0.1498	0.2938	−0.0392	−0.5312	−0.2915	0.5611
8	0.5497	0.4063	−0.5247	0.4063	−0.2314	0.2472	0.0955	−0.2997	0.0955	0.2472	−0.0263	0.2618	−0.2027
9	0.9751	0.2392	−0.3937	0.2392	0.2908	−0.0040	−0.2869	0.2837	−0.2869	−0.0040	0.2971	−0.4779	0.2903
10	1.0000	0.0000	0.0000	0.0000	0.0000	0.5000	−0.5000	0.0000	0.5000	−0.5000	0.0000	0.0000	0.0000
11	1.5846	0.1072	−0.2309	0.1072	0.4850	−0.3034	−0.0041	0.3100	−0.0041	−0.3034	−0.4830	0.3794	−0.1762
12	2.1771	0.0386	−0.1022	0.0386	0.3314	−0.3250	0.3761	−0.4938	0.3761	−0.3250	0.3228	−0.1742	0.0658

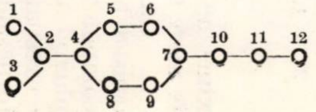

It seems necessary to mention, that the electron distributions and especially the bond orders calculated for the anions (see molecular diagrams), make obvious the increased contribution of the quinoid structure already in the ground state, the energy difference (required for transition to the excited state) between this ground state and the corresponding first excited state being thus smaller, than in the case of undissociated oximes. This phenomenon is more pronounced for the *p*-nitro-benzaldoxime, and, according to the above explanation, the bathochormic shift is more significant in this case.

Table 5

Molecular orbitals of the formaldoxime

	Undissociated				Anion			
ψ_i	$\frac{\alpha-\varepsilon}{\beta}$	c_1	c_2	c_3	$\frac{\alpha-\varepsilon}{\beta}$	c_1	c_2	c_3
1	−2.0649	0.3428	0.5898	0.7309	−1.8523	0.4477	0.6911	0.5675
2	−0.9908	0.5802	0.4790	−0.6585	−0.7230	0.5212	0.3140	−0.7936
3	1.0557	0.7388	−0.6500	0.1780	1.0753	0.7266	−0.6511	0.2197

$$\overset{1}{C}-\overset{2}{N}-\overset{3}{O}$$

On the other hand, we have intended to estimate the changes caused by dissociation on the delocalization energies between the two-component resonance systems (oximinomethyl-phenyl; oximinomethyl-phenyl-nitro). For this reason we have calculated the MO values of the corresponding simple systems, which build up our compounds, namely formaldoxime (III) (undissociated and anion), (table 5), and nitrobenzene (IV), the data of benzene (V) are well known, using the preceding sets of parameters. Molecular orbitals of nitrobenzene have been calculated by several authors,[5] using various methods and parameters. From these data, Trotter's calculations[5d] are comparable with ours, because he has used also the HMO-method, and the same α and β values, except the β_{N-O} (1.41 β instead of 1.2 β used by us). Naturally, we have obtained quite similar electron distribution and bond orders, although for the evaluation of delocalization energies, it was necessary to use our MO-data, calculated with the parameters employed at *p*-nitro-benzaldoxime.

Possessing now all required π-energy values (table 6), the delocalization energies were calculated in the following manner:

a., *Benzaldoxime*:

Undissociated,

$$DE_{(I)} = E_{(I)} - (E_{(V)} + E_{(III)}) = 0.405\ \beta\,;$$

---

[5] a) S. NAGAKURA and J. TANAKA, *J. Chem. Phys.*, **22**, 236 (1954); b) T. N. REKASCHEWA, *Zhur. fiz. Khim.*, **35**, 638 (1961); c) A. F. TERPUGOWA, *Optika i Spektroskopija*, **7**, 581 (1959); d) J. TROTTER, *Canad. J. Chem.*, **37**, 905 (1959).

Anion,

$$DE_{(I)}(-) = E_{(I)}(-) - (E_{(V)} + E_{(III)}(-)) = 0.411\ \beta;$$

b., p-*Nitro-benzaldoxime* :

Undissociated,

$$DE_{(II)} = E_{(II)} - (E_{(IV)} + E_{(III)}) = 0.407\ \beta;$$

Anion,

$$DE_{(II)}(-) = E_{(II)}(-) - (E_{(IV)} + E_{(III)}(-)) = 0.843\ \beta;$$

Table 6

π-energy values of the studied compounds

No of compounds in text	Compound	$E_\pi = \sum 2\cdot E^{occ}$	
		Undissociated E_n	Anion $E_{n(-)}$
I.	Benzaldoxime	$10\alpha+14.516\beta$	$10\alpha+13.562\beta$
II.	*p*-Nitrobenzaldoxime	$14\alpha+22.098\beta$	$14\alpha+21.573\beta$
III.	Formaldoxime	$4\alpha+6.111\beta$	$4\alpha+5.151\beta$
IV.	Nitrobenzene	$10\alpha+15.579\beta$	—
V.	Benzene	$6\alpha+8\beta$	—

$n = I, II, \ldots V$

Obviously, in both cases an increase of delocalization energy takes place owing to the dissociation, which is more significant in the case of *p*-nitro-benzaldoxime, evidently because of the considerable electron-withdrawing effect of the *p*-nitro group.

Acknowledgments. The authors wish to express their thanks to Mr. L. Negrescu, for valuable mathematical contributions, as well as to Prof. V.E. Sahini for helpful discussions.

Revue Roumaine de Chimie, **14**, 329–332 (1969)

HYDROGEN BONDS. II*

THE INFRARED STUDY OF THE STRENGTH OF HYDROGEN BOND IN SOME DIHYDROXYACETOPHENONES

SIMONA BĂDILESCU and I. I. BĂDILESCU

Research Department, Petrochemical Works, Piteşti

Received June 4, 1968

The strength of the hydrogen bonds in some dihydroxyacetophenones was investigated by infrared spectroscopy. The C=O stretching frequencies of the investigated dihydroxyacetophenones are lower than that of 2-hydroxyacetophenone (I) except for 2,5-dihydroxyacetophenone (IV) whose positive $\Delta\nu_{C=O}$ value indicates an intramolecular hydrogen bond weaker than that in I.

Intramolecular hydrogen bonding in *o*-substituted phenols has long been studied by many workers and some n.m.r. and infrared spectral studies were also reported in the past decade. [1-5] Recently, Yoshida and Haruta [6,7] reported the effects of various substituents on the intramolecular hydrogen bonds of 4- and 5-substituted 2-hydroxyacetophenones.

In the previous paper of this series [8] we reported the results of an infrared study of the strength of the hydrogen bond in some polyhydroxyacetyl-benzenes. The shifts in the C=O frequency in the spectra of such compounds with respect to that in 2-hydroxyacetophenone (I), in the same solvent, was defined as $\Delta\nu_{C=O}$, which measures the strength of the hydrogen bond in the investigated compound relatively to that in 2-hydroxyacetophenone. In this paper we wish to report the results of the infrared investigation of the strength of the hydrogen bond in the following hydroxy-substituted 2-hydroxyacetophenones : 2,3- (II), 2,4- (III), 2,5- (IV) and 2,6-dihydroxyacetophenone (V). The spectrum of 2-hydroxy-6-methoxy-

---

[*] Part I : S. Bădilescu and I. Bădilescu, *Rev. Roumaine Chim.*, **10**, 103 (1965).

[1] I. M. Hunsberger, *J. Amer. Chem. Soc.*, **72**, 5626 (1950).

[2] A. L. Porte, H. S. Gutowsky and I. M. Hunsberger, *J. Amer. Chem. Soc.*, **82**, 5057 (1960).

[3] N. M. Cullinane, R. A. Woolhouse and V. V. Bailey-Wood, *Rec. Trav. chim.*, **80**, 116 (1961).

[4] R. W. Hay and P. P. Williams, *J. Chem. Soc.*, **1964**, 2270.

[5] D. J. Ringshaw and H. J. Smith, *Chem. and Ind.*, **1965**, 1383.

[6] Z. Yoshida and M. Haruta, *Tetrahedron Letters*, **1964**, 2631.

[7] Z. Yoshida and M. Haruta, *Tetrahedron Letters*, **1967**, 1966.

[8] S. Bădilescu and I. Bădilescu, *Studii Cercetări Chim.*, **14**, 101 (1965).

acetophenone (VI) was also recorded in order to clear up if the double chelation of the carbonyl group occurs in the parent compound V. Table 1 records the frequencies of the carbonyl absorption band of compounds I—VI in carbon tetrachloride, chloroform and acetonitrile, along with the $\Delta\nu_{C=O}$ values for II—VI.

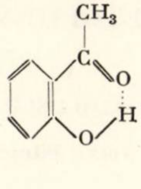
I

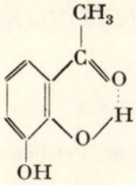
II

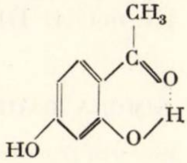
III

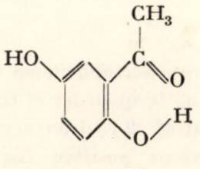
IV

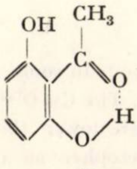
V

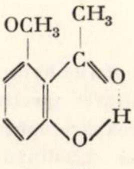
VI

Table 1

Frequencies of the carbonyl absorption bands

Compound	M.p. °C	M.p. lit.	Frequency, cm^{-1}, in			$\Delta\nu_{C=O}$ cm^{-1} [a]
			CCl_4	$CHCl_3$	CH_3CN	
2-Hydroxyacetophenone (I)[b]	—	—	1647	1645	1644	—
2,3-Dihydroxyacetophenone (II) [9,10]	—	97	1633[c]	—	—	−14
2,4-Dihydroxyacetophenone (III)[12,13]	144.5	144−145	1638	1638	1639	− 9
2,5-Dihydroxy-acetophenone(IV)[14]	203	202−3	1655	1651	1651	+ 8
2,6-Dihydroxy-acetophenone (V)[15,16]	157	156−7	1629	—	—	−18
2-Hydroxy-6-methoxy-acetophenone(VI) [15]	59	60	(1630)	—	—	(−17)

[a] As against 2-hydroxyacetophenone (I); CCl_4 solutions.

[b] B. p. 100−105°/25 Torr; n_D^{20} 1.5583.

[c] Value reported by AWAD *et al.* [11]

[9] H. V. Krannchfeldt, *Chem. Ber.*, **46**, 4017 (1913).

[10] W. I. Awad, M. F. El-Neweihy and S. F. Selim, *J. Org. Chem.*, **23**, 1783 (1958).

[11] W. I. Awad, M. F. El-Neweihy and S. F. Selim, *J. Org. Chem.*, **25**, 1333 (1960).

[12] K. C. Gulati and K. Venkataraman, *J. Chem. Soc.*, **1931**, 2378.

[13] J. B. Lal, *J. Indian Chem. Soc.*, **16**, 296 (1939).

[14] G. C. Amin and N. M. Shah, *Organic Syntheses*, **28**, 42 (1948).

[15] W. Baker, *J. Chem. Soc.*, **1934**, 1953.

[16] A. Russell and J. R. Frye, "Organic Syntheses", Coll. vol. 3, New York, John Wiley and Sons, 1955, p. 281.

Data recorded in table 1 indicate the strongest intramolecular hydrogen bond in 2,6-dihydroxyacetophenone (V), with $\Delta\nu_{C=O}$ equal to $-18\ cm^{-1}$. The low frequency of the carbonyl absorption band at 1629 cm^{-1} might be accounted for by assuming that the carbonyl oxygen in V is hydrogen-bonded to both 2- and 6-OH groups. However, the infrared spectrum of 2-hydroxy-6-methoxy-acetophenone (VI) shows the carbonyl absorption near 1630 cm^{-1} as in the parent compound V and, consequently, the carbonyl group must be involved in a single chelation in both V and VI compounds. Further evidence of the single chelation in 2,6-dihydroxyacetophenone (V) gives ultraviolet spectral data [17,18] which indicate that C=O bonds are coplanar to the benzene ring in both V and VI compounds.

The intramolecular hydrogen bonds in 2,3- (II) and 2,4-dihydroxyacetophenone (III) are also stronger than that in 2-hydroxyacetophenone (I) but the positive $\Delta\nu_{C=O}$ value of 2,5-dihydroxyacetophenone (IV) indicates a chelated ring with hydrogen bond weaker than that of all investigated compounds. As it is seen in table 1 the strength of the hydrogen bond in the investigated compounds increases in the order $IV < I < III < II < VI < V$.

Some considerations may be made in order to explain the observed $\nu_{C=O}$ absorption band shifts in the spectra of such chelated compounds. As it is well known, the mesomeric effect defines the relative importance of the canonical forms VII and VIII in the chelated conjugated molecules. Thus, a decrease in the $\nu_{C=O}$ absorption band value results from an increasing contribution from form VIII, which in turn increases as the double-bond character of the C=C bond in VII increases. Taken in conjunction with Pauling's assumption [19] on the different contribution of one Kekulé structure to the normal state of the molecules, it becomes obvious that $\Delta\nu_{C=O}$ values are a measure of the strength of the intramolecular hydrogen bonds in such compounds and would be also proportional to the percent double bond character of the ring carbon-to-carbon bond holding the substituents.

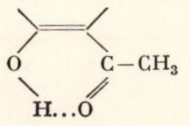

VII

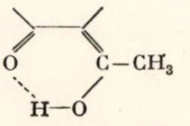

VIII

Although the results of this work cannot be interpreted quite easily as those for polyhydroxyacetyl-benzenes,[8] it is clear that the intramolecular interaction between O−H and C=O group is enhanced by introducing a second hydroxyl group in the aromatic ring of 2-hydroxyacetophenone (I) and the resulting dihydroxyacetophenones, except IV, showed $\nu_{C=O}$ absorption bands lower than that of I. Consequently, the different strength

---

[17] W. Baker, *J. Chem. Soc.*, **1939**, 956.

[18] D. J. Cram and F. W. Crantz, *J. Amer. Chem. Soc.*, **72**, 595 (1950).

[19] L. Pauling, "The Nature of the Chemical Bond", 2nd ed., Oxford University Press, London, 1948, p. 321.

of the hydrogen bonds in the chelated dihydroxyacetophenones II—V may be explained by the changes in electronegativities of hydroxyl oxygen and carbonyl carbon atoms corresponding to changes of the positions of the other non-chelated, hydroxyl in the benzene ring. The effect of this hydroxyl group on the strength of the intramolecular hydrogen bond in compounds II—V will be further studied, and molecular orbital calculations are in progress in order to correlate molecular bond orders with $\Delta\nu_{C=O}$ values obtained in our studies.

EXPERIMENTAL

Dihydroxyacetophenones used in this work were prepared according to known procedures (reference in table 1) and purified by recrystallization from suitable solvents until melting points were constant.

Infrared work. All spectra were determined with a UR—10 Carl Zeiss-Jena spectrophotometer with NaCl and LiF prisms. The data in table 1 were recorded with a probable error of about $\pm$ 2 cm^{-1}. The solvents were used without supplementary purifications : carbon tetrachloride and chloroform, "for infrared spectroscopy" (Union Chimique Belge) and acetonitrile, a Chinoin "pro analysi" reagent.

The $\Delta\nu_{C=O}$ values were estimated from the $\nu_{C=O}$ absorption bands in 0.001—0.005 molal solutions in carbon tetrachloride.

Revue Roumaine de Chimie, **14**, 333–337 (1969)

CONTRIBUTIONS TO THE URANIUM CONTENT DETERMINATIONS IN SOLUTIONS BASED ON ^{238}U DAUGHTER RADIOACTIVITY MEASUREMENTS

F. BUNUŞ and I. MATEI

Technological Research Department, Ministry of Mines, Bucharest str. Dionisie Lupu 68

Received June 3, 1968

In this paper a study related to the applicability of a fast uranium content determination in solution has been carried out. This method is based on uranium (daughters) radioactivity measurements in solutions. In doing so the uranium radioactive daughters have been taken into consideration as the influence upon the precision and the limited field of applications involved. Measurements on standard solutions and samples were made. The method described here appeared to be suitable for our scope.

1. PRINCIPLE OF THE METHOD

Uranium natural radioactivity was an important subject in the attention of many studies concerning uranium and its daughters behavior.[1–3] Using as starting point the natural radioactivity, intensive work was carried out to find mathematical relations between this and uranium content[1]. This procedure was extended to uranium ores.[1] Most of these methods are based on α and γ measurements.

It should be stressed that almost all measurements are carried out in solid (powder) form.

Extrapolation of this principle to the uranium content determination in solutions seems to be difficult either due to the very low ^{238}U radioactivity or to the imprecision on estimating the radioactive ^{238}U daughters attending it. There are two limiting alternatives. Uranium solutions obtained in a chemical proces may have no ^{238}U daughters at all or a secular equilibrium between ^{238}U and its daughters could be found.

It is perhaps worth to remind the general relation of radioactive decay[4]:

$$N = N_0 \exp(-\lambda t)$$

---

[1] A. Soroiu, *Tehnica Nucleară*, **2**, 11 (1964).

[2] G. Friedlender, J. W. Kennedy and I. M. Miller, "Nuclear and Radiochemistry", 2nd ed., J. Wiley, New York, London, Sydney, 1964, p. 10.

[3] M. Hayssinsky, "La Chemie Nucléaire et ses Applications", Ist ed., Masson et Cie., Paris, 1957 p. 169.

[4] R. D. Evans, "The Atomic Nucleus" 1st ed. McGraw-Hill Book Co., New York, Toronto, London, 1955, p. 477.

where N is the number of radioactive atoms at time t and N_0 at $t = 0$; λ is the disintegration constant and at $t = T_{1/2}$ when $N = N_0/2$ we have:

$$\lambda = 0.693/T_{1/2}$$

For two radioactive species A and B the secular equilibrium is attained when $T^A_{1/2} \gg T^B_{1/2}$; thus the following relation appears:

$$\lambda_A N_A = \lambda_B N_B$$

where the number of nuclei decayed is the same per unit time.

For more than two radioactive components at secular equilibrium the last equation becomes:

$$\lambda_A N_A = \lambda_B N_B = \lambda_C N_C \ldots$$

A similar situation occurs with ^{238}U and its decay products.

It should be reminded that uranium in nature is a mixture of three isotopes with abundances as follows: ^{238}U 99.27%, ^{235}U 0.72%, and ^{234}U 0.0056%. Because of the low abundances for the scope of this work, the last two isotopes may be neglected.

^{238}U is a starting component of a radioactive series with half-life 4.5×10^9 yr. All its daughters are α, β γ emitters till the last member ^{206}Pb which is stable.

Series ^{238}U,[5] may be divided into three subseries, each with a head long-lived component in secular equilibrium with all the members of the same subseries. Thus, we can write the following three subseries:

$$^{238}U \xrightarrow{\alpha} {}^{234}Th(22d) \xrightarrow{\beta^-} {}^{234}Pa(6.6h) \rightarrow$$

$$^{226}Ra \xrightarrow{\alpha} {}^{222}Rn(3.8d) \xrightarrow{\alpha} {}^{218}Po(3.05min) \rightarrow$$

$$^{210}Pb \xrightarrow{\beta^-} {}^{210}Bi(5d) \xrightarrow{\beta^-} {}^{210}Po(138d) \xrightarrow{\alpha} {}^{206}Pb \text{ stable.}$$

Comparing the decay schemes of all these radioactive components, the following remarks on the type of radiation emitted can be made[4,5]:

From the beginning, α emission is neglected, because all measurements are carried out with a G-M end window counter (mica window thickeness 2.6 mg/cm^2).

For an eventual contribution of gamma emission (however low) to the G-M counter measurements, the following remarks are to be reminded:

— $\beta - \gamma$ emission[2,3,5].

Within ^{238}U subseries, ^{234}Pa is a β^- emitter with $E_{max} = 2.3$ MeV and 0.32 MeV. ^{234}Th β^- emission is of low energy $E_{max} = 0.19$ MeV. The contribution of γ emission within the whole subseries is about 5%.

— ^{226}Ra subseries have two β^- emitters with complex decay schemes, ^{214}Pb and ^{214}Bi with energetic β^- rays of $E_{max} = 3$ MeV. The γ emission contribution to ^{238}U series is important, i. l. 95%.

— The last subseries can be neglected for both β and γ emission.

---

[5] "Nuklidkarte", Bundesministerium für Atomkernenergie und Wasserwirtschaft, GFR, 1963.

We must bear in mind that with this type (G-M counter) of detector gamma rays efficiency is much lower than β^- one.

In our measurements radium and its daughters are absent.

These last two factors make gamma rays contribution negligible.

FIELD OF APPLICATION AND RESULTS

It was our intention, based on previous discussion, to apply this principle to solutions where radioactive equilibrium for the first subseries is attained.

$$^{238}U \rightarrow {}^{234}Th \rightarrow {}^{234}Pa$$

We found these conditions fulfilled by nitric acid solutions obtained in the dissolution of natrium diuranate (calcium or magnesium) yellow cake — from the chemical processing of uranium ores. It is worth reminding that uranium ores are processed following two chemical ways :

— acid treatment (acid leaching)

— alkaline treatment (sodium carbonate leaching).

The application of one or other is a function of ore characteristics and is reflected in the economicity of the procedure. These methods exclude the presence, in aqueous solution of radium (and its daughters). In uranium ores processing a diuranate finally results. In a next industrial stage this concentrate is solubilized in a view of being purified. Uranium purification is carried out in a refining unit where uranium in aqueous nitric solution is treated with TBP. Since a uranium refining plant can process the diuranate from several uranium ores processing plants the first one is almost always located elsewhere. Thus from the obtaining of the uranium concentrate till its refining an appreciable time interval elapses. During this time the ^{238}U daughters accumulate and an equilibrium may be reached. It is important to insist on the absence of ^{226}Ra and ^{210}Pb subseries because of the initial chemical treatment of the ores.

If the time interval does not permit the equilibrium to be attained, the manufacturing date printed on each bag (barrel) easily allows a time correction.

Application of this method to the nitric solution (diuranate dissolution) used in the uranium refining plant seems to be relatively simple, and a continuous determination of uranium content before TBP extraction is easily done.

This method might be also used elsewhere, when ^{234}Th and ^{234}Pa have accumulated so as to permit a β counting.

The method is based on β-activity measurements of a solution in the conditions mentioned. (^{238}U in equilibrium with its subseries daughters). A G–M counter associated with an electronic scaler has been used. Previous measurements carried out on standards allow the plotting of an activity-uranium content curve which later is used to find out the uranium content in a sample.

For each set of determinations the geometry is observed.

Corrections for background, dead time and a factor which takes into account the time interval related to the equilibrium time, are carried out. Measurements are made on solutions deposited on plastic trays, the liqiud thickness is always the same. Generally speaking a infinite thickness layer is attained when inferior layers contribution to β counting is negligible. When other ions are present, corrections are made when necessary (the same for densities). The counting time is selected to attain the precision desired.

Our results are given in the following four figures :

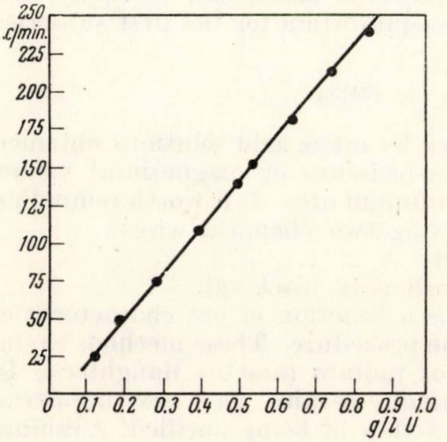

Fig. 1. — Uranium content plot within the concentration range 0—1 g/l U.

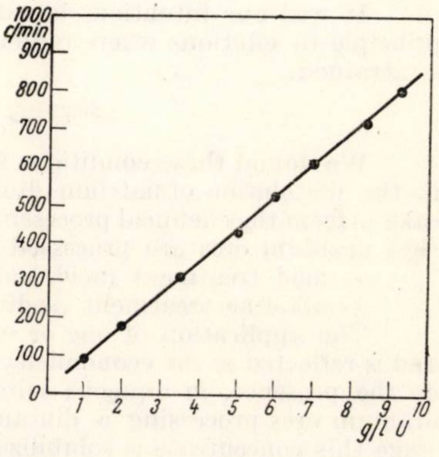

Fig. 2. — Uranium content plot within the concentration range 0—10 g/l U.

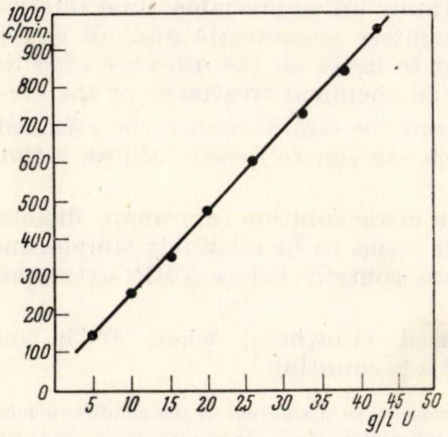

Fig. 3. — Uranium content plot within the concentration range 0—50 g/l U.

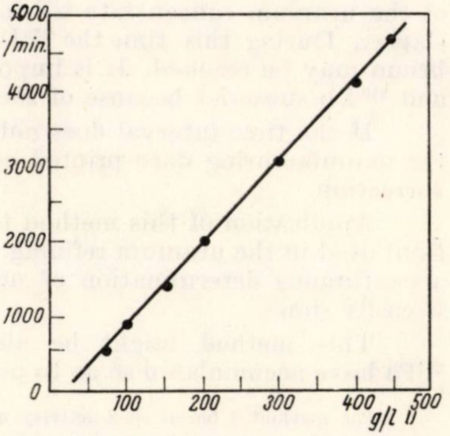

Fig. 4. — Uranium content plot within the concentration range 0—500 g/l U.

All these plots were based on uranium content determined chemically *versus* the activity, and are used as references for the estimation of uranium in an unknown sample (with all corrections just mentioned). Of course all samples used as standards respect the conditions imposed, therefore ^{238}U and its decay products (the first subseries) are in equilibrium.

The acidity of the solution was 2.5 normal nitric acid.

Geometry was not maintained the same among the figures but for one figure it was respected.

When uranium content was lower than 1 g/l the measurements have been performed on dried samples. Here care should be given to uniform residues, selfabsorption, and backscattering.

CONCLUSIONS

This method has been used in uranium content determinations for nitric aqueous solutions which provide the feed for TBP solvent extraction in view of obtaining uranium nuclear purity grade.

This method proved to be very simple, fast and needs no previous chemical treatment so that no reagent is required.

The precision is good enough and depends on the counting time which should be appropriate.

The field of application might be extended but care should be taken in estimating the presence of radioactive daughters.

Revue Roumaine de Chimie, 14, 333–337 (1969

therefore [illegible] and its decay products (the first ones) are in equilibrium.

The quality of the solution was [illegible] nitric acid.

[illegible] obtained the same [illegible] but for one figure it was expected.

When [illegible] all the measurements have been [illegible] on [illegible]. This [illegible] should be [illegible] solution, and [illegible].

CONCLUSIONS

This method has been used in a plant to control determinations for [illegible] which provide the feed for TBP solvent extraction in view of obtaining [illegible] quickly possible.

This method proved to be very simple, fast and needs no previous chemical treatment so that no reagent is required.

The precision is good enough and depends on the counting time which should be appropriate.

The field of application might be extended but care should be taken in estimating the presence of radioactive daughter.

[illegible]

[illegible]

Revue Roumaine de Chimie, **14**, 339–344 (1969)

LE MARQUAGE PAR ÉCHANGE ISOTOPIQUE DE LA THIOACÉTAMIDE ET DU 6-MÉTHYL-2-THIOURACILE AVEC ^{35}S

IOANA ZAMFIR et C. N. ŢURCANU

Institut de Physique Atomique Bucarest, P. O. Box 35

Reçu le 5 juin 1968

On présente l'étude du marquage au ^{35}S élémentaire, par échange isotopique, de la thioacétamide (TAA) et du 6-méthyl-2-thiouracile (6M2TU) dans un milieu de naphtalène fondu et solvants organiques. La répartition de la radioactivité entre les produits qui participent à l'échange a été déterminée par radiochromatographie sur papier. Pour la TAA on a obtenu de bons rendements de marquage par échange isotopique en milieu de solvants organiques et pour le 6M2TU par échange isotopique dans du naphtalène fondu à 250°. On a obtenu des produits de haute pureté radiochimique.

INTRODUCTION

La thioacétamide 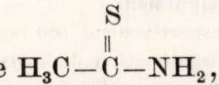 $H_3C-\overset{\overset{\displaystyle S}{\|}}{C}-NH_2$, grâce aux propriétés de l'atome de soufre et du groupe $-NH^2$, est utiliseé dans la chimie analytique,[1–6] la physique moléculaire,[7] la pharmacodynamie[8·9] la biochimie générale,[10] etc.

Le 6-méthyl-2-thiouracile 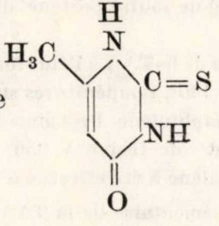 est utilisé au traitement

---

[1] L. D. Zinoveva, K. F. Gladysheva et A. I. Lazakova, *Zavodskaya Lab.*, **32**, 1460 (1966).

[2] S. Petri et T. Lipies, *Roczniki Chem.*, **40**, 1795 (1966).

[3] J. Halinka et S. Petri, *Chem. Analit.*, **11**, 1007 (1966).

[4] E. C. Mallory, *Amer. Chem. Soc. Div. Water Waste Chem. Preprints*, **7**, 126 (1967); *Chem. Abstr.*, **66**, 118702 W (1967).

[5] M. Pryszczewska, *Talanta*, **13**, 1700 (1966).

[6] K. A. Chaubal, B. P. Gothoskar et K. S. Korgaonkar, *Indian J. Exp. Biol.*, **5**, 61, appendix 64 (1967).

[7] M. M. Gerbier et J. Gerbier, *Compt, rend.*, **263**, 1067 (1966).

[8] R. G. Kleinfeld, *Nat. Cancer. Inst. monogr.*, **23**, 369 (1966).

[9] A. Vorbrodt, Z. Steplewski et S. Krzyzowska Gruca, *Folia Histochem. Cytochem.*, **4**, 7 (1966).

[10] R. H. Burdon, *Biochem. J.*, **104**, 186 (1967).

des thyréotoxicoses [11] et dans la synthèse de quelques composés à l'action antitumorale.[12]

La littérature mentionne le marquage de la thioacétamide (TAA) au ^{35}S par échange isotopique avec du $H_2{}^{35}S$, en éthanol absolut ($Ba{}^{35}S + H_3PO_4$).[13]

Ce procédé nous semble difficile, étant donné les conditions spéciales de travail qu'il exige (exclusion complète de l'oxygène pour empêcher l'oxydation de l'hydrogène sulfuré).

Le 6-méthyl-2-thiouracile (6M2TU) a été marqué par synthèse en partant de la thio-urée ^{35}S, avec rendements radioactifs de 20–45 %.[14,15]

Le marquage par échange isotopique au ^{35}S élémentaire à l'état fondu a permis l'obtention des produits de haute pureté radiochimique et des rendements d'échange élevés, dans le cas d'autres substances, telles que : tebezone I, thio-urée et phényl-thio-urée[16] thioxanthine, thioguanine et 2 thiouracile (2TU).[17]

PARTIE EXPÉRIMENTALE

a) *Préparation des échantillons.* On a utilisé des substances de base de qualité *p.a.* et les solvants organiques ont été fraîchement distillés.

Pour le marquage à l'état fondu sans addition d'autre substance, on a préparé des mélanges contenant la substance à marquer et du ^{35}S élémentaire avec addition de 1,6 mg de soufre porteur, dissous dans du trichloroéthylène (TCE).

Dans les cas de marquage dans du naphtalène fondu, les échantillons contenaient, en plus, 200 mg de naphtalène pour la TAA, respectivement 100 mg pour le 6M2TU. Après évaporation, à sec, du solvant, séchage et homogénéisation du mélange, les échantillons ont été introduits dans des ampoules en verre « Supremax », vidées et fermées à flamme.

Dans le cas d'échange dans les solvants organiques, les échantillons contenaient 500 mg de TAA, ^{35}S élémentaire et 2,4 mg de soufre porteur dissous en 25 ml de solvant.

b) *Chauffage.* Le marquage de la TAA à l'état fondu a été étudié par échange isotopique, aux températures de 120°, 130° et 140°, températures supérieures au point de fusion de la TAA (117°), tandis qu'en présence du naphtalène, l'échange à été étudié à 120°.

Pour le 6M2TU—au point de fusion à 350° — avec décomposition — le chauffage du mélange en présence du naphtalène à été effectué à 250°.

Pour le marquage au ^{35}S élémentaire de la TAA par reflux en milieu de solvants, on a utilisé de l'alcool butylique tertiaire (p éb 82,9°), de l'alcool butylique secondaire (p éb. 99,5°), de l'alcool isobutylique (p éb 108°), de la pyridine (p éb. 115°) et de l'alcool butylique normal (p éb 117°).

---

[11] R. Hazard, « Précis de thérapeutique et de pharmacologie », Masson et Cie, Paris, 1953, 1177 p.

[12] M. Florkin, « Introduction biochimique à la médecine », Masson et Cie, Paris, 1959, 309 p.

[13] A. Nygaard, L. Eldjarn et K. F. Nakken, *Cancer. Res.*, **14**, 625 (1954).

[14] H. L. Wheeler et D. F. Mc. Farland, *J. Amer. Chem. Soc.*, **42**, 101 (1909).

[15] A. Murray, et D. L. Williams, « Organic Synthesis with Isotopes », Interscience Publishers Inc., New York, 1958, IIe vol., 1974 p.

[16] C. Chiotan et I. Zamfir, *Rev. Roumaine Chim.*, **11**, 961 (1966).

[17] C. Chiotan et I. Zamfir (sous presse)

c) *Traitement des échantillons: l'analyse chromatographique.* Après avoir ouvert les ampoules, le contenu a été dissous à chaud en TCE et éthanol absolu pour la TAA, et la même mixture de solvants avec quelques gouttes de NH_3 25 %, pour le 6M2TU.

Les solutions claires ont été pipettées sur papier chromatographique sur la ligne de start où on a déposeé préalablement une goutte d'une solution de 2 % soufre élémentaire, dissous dans TCE.

Pour le marquage par échange isotopique en milieu homogène, après reflux, la solution a été déposée directement sur du papier chromatographique préparé comme pour les échantillons fondus.

Pour établir la répartition de l'activité du ^{35}S, on a effectué l'analyse par chromatographie ascendante, en utilisant du papier Schleicher-Schull 2045 a. Pour la TAA ^{35}S on a utilisé un mélange formé d'alcools : isobutylique, éthylique et eau (1/2/10 en volumes), la durée de développement étant de 18 heures, et pour le 6M2TU on a utilisé du NH_3 25 %, de l'éthanol et de l'eau (1/10/10 en volumes) et la même durée de développement.

Les résultats des séparations chromatographiques sont représentés sur la figure 1.

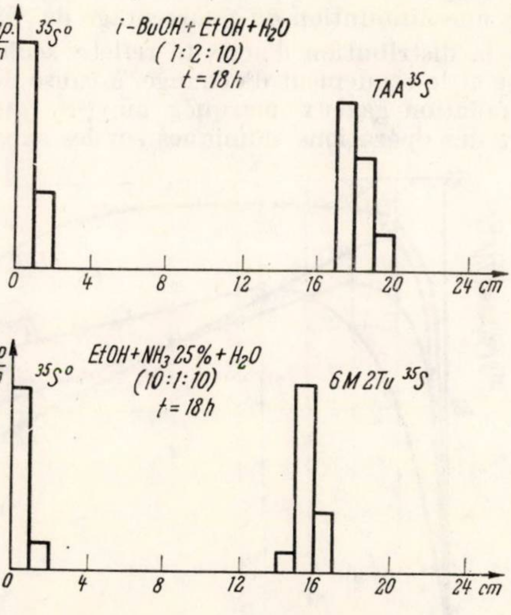

Fig. 1.— Séparations chromatographiques pour les mélanges TAA $^{35}S-^{35}S^{\circ}$ et 6M2TU$^{35}S-^{35}S^{\circ}$.

d) *Séparation chimique.* Pour la séparation des produits actifs, on dissout les substances fondues dans des mélanges de TCE et d'éthanol absolu, auxquels on ajoute du soufre inactif, on chauffe lentement jusqu'à dissolution complète des substances, on dilue avec de l'eau, on évapore la TCE et puis on filtre la solution aqueuse.

On distille l'eau à pression réduite jusqu'au sec et on obtient ainsi des cristaux de TAA ^{35}S et respectivement de 6M2TU ^{35}S.

Dans le cas de l'échange isotopique dans des solvants organiques, après reflux, les solvants ont été distillés à sec et puis on a procédé à la purification des produits actifs, de la même manière, que dans le cas des substances fondues.

Les rendements d'échange ont été déterminés du rapport entre les activités spécifiques obtenues et celles théoriques calculées pour le cas d'équilibre.

Parallèlement on a calculé aussi les rendements chimiques des produits purifiés (tabl. 1).

RÉSULTATS ET DISCUSSIONS

La répartition de l'activité entre le soufre élémentaire et la TAA fondue, sans addition de naphtalène, en fonction de la température et du temps de chauffage, est montrée dans la figure 2. On voit que le pourcentage de ^{35}S dans la TAA croît avec la température.

A 140°, le maximum de distribution (92 %) est atteint après environ 10 minutes de chauffage, tandis qu'à 120° il est atteint après 40 minutes (77 %). Avec l'échange ont lieu des réactions de dégradation pyrolytique qui conduisent à une diminution du pourcentage de ^{35}S dans la TAA.

L'étude de la distribution d'activité reflète seulement d'une façon relative la vitesse et le rendement d'échange, à cause de la formation des produits de dégradation gazeux marqués au ^{35}S, qui sont perdus du système au cours des opérations chimiques sur les substances à étudier.

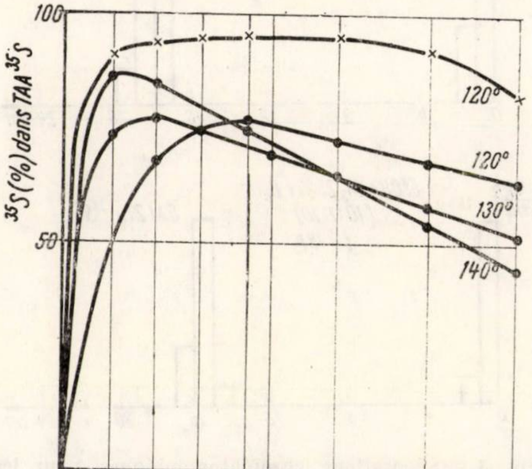

Fig. 2. — Répartition de l'activité entre le soufre élémentaire ($^{35}S^{\circ}$) et la TAA ^{35}S fondue, avec et sans addition de naphtalène.

Les pertes de radioactivité peuvent atteindre des valeurs de 50 à 60 % de l'activité initiale du ^{35}S, ce qui fait que ce procédé de marquage de la TAA ne soit pas convenable pour les conditions de production. De plus, le produit final marqué n'est pas pur, gardant une couleur jaune-brune, même après de multiples recristallisations.

Dans les cas de la substance marquée dans du naphtalène fondu (fig. 2) à 120°, on enregistre après environ 20 minutes de chauffage un pourcentage maximum (95 %), qui se maintient même après une heure de chauffage. La TAA ^{35}S obtenue, s'est avérée être pure. La marquage dans le naphtalène fondu favorise l'échange et empêche, dans une certaine mesure, la dégradation thermique de la TAA active.

Pour le 6M2TU les résultats obtenus à l'état fondu, sans addition de naphtalène, ne sont pas satisfaisants, car le produit se décompose et prend une couleur brune.

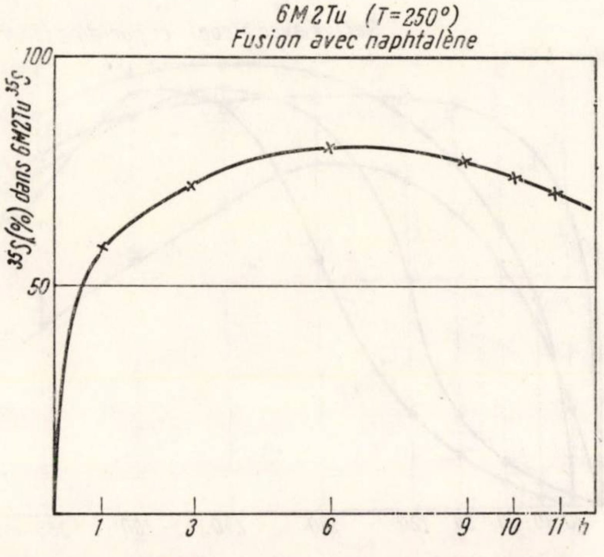

Fig.3. — Répartition de l'activité entre le soufre élémentaire ($^{35}S^{\circ}$) et le 6M2TU^{35} S fondu, avec addition de naphtalène.

Les essais de marquage dans du naphtalène fondu et chauffé à 250° (fig. 3) montrent qu'après 6 heures d'échauffement on atteint la valeur maximale de 80 %, comportement identique à celui du 2TU^{35}S, constaté dans un travail antérieur.[17] La répartition de l'activité après l'échange, sans pertes d'activité au marquage, se trouve dans le milieu de naphtalène fondu.

La réactivité du groupe aminique pour le ^{35}S élémentaire, au cas de la TAA, chauffée à une température élevée, a été aussi observée dans d'autres cas de marquage par ce procédé.[16,17] Au cas du marquage de la TAA en solution, la répartition du ^{35}S sur les radiochromatogrammes (fig. 4) montre qu'elle varie avec le temps d'échauffement pour la pyridine et les quatre alcools utilisés. La répartition maximale des activités est atteinte aux températures d'ébullition respectives, après 3–4 heures, apparaissant des phénomènes de décomposition.

En ce qui concerne les différences de comportement de la TAA au marquage par l'échange isotopique, dans les solvants étudiés, nous considérons qu'elles ne sont pas dues exclusivement aux températures d'ébullition différentes, mais aussi aux compositions des solvants.

CONCLUSIONS

L'étude de la répartition du ^{35}S entre le soufre élémentaire et la TAA, respectivement 6M2TU, effectuée par radiochromatographie a permis d'établir de nouvelles méthodes de marquage de ces substances non mentionnées dans la littérature (tabl. 1).

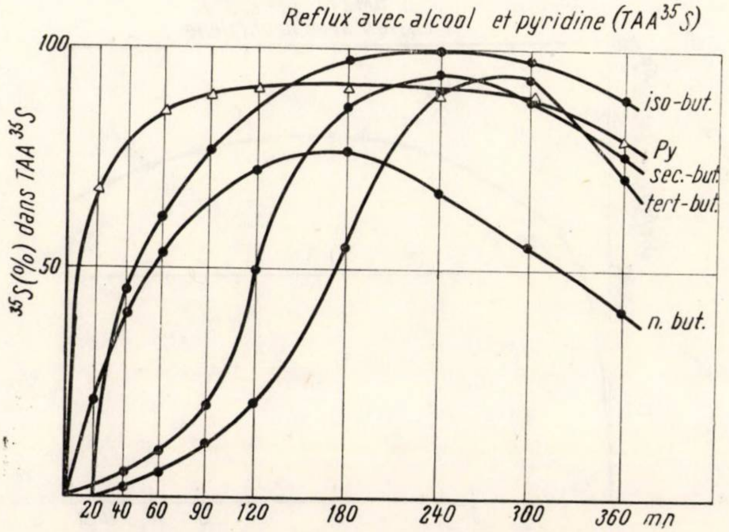

Fig.4. — Répartition de l'activité entre le soufre élémentaire ($^{35}S°$) et la TAA ^{35}S pour l'échange, en milieu de solvants organiques.

Les auteurs remercient M. le Dr C. Chiotan pour les suggestions précieuses données, et pour la discussion critique du présent travail et Mmes A. Croitoru et S. Popescu, pour l'assistance technique.

Tableau 1

Résultats du marquage au ^{35}S élémentaire par échange isotopique de la TAA ^{35}S et du 6M2TU^{35}S purifiés

Produits	Conditions de marquage	produit mg	porteur mg S	Activité totale µCi	Activité spéc. initiale µCi/mg S	Activité spéc., expérim. µCi/mg S	Rendement de marquage %	Rendement chimique %
TAA	Reflux dans l'alcool butylique tertiaire 5 heures à 82,9°	500	6	1 280	5,9	4,5	76	70
6M2TU	Fusion en milieu de naphtalène à 250°	100	1,2	289	12,2	9,8	80	70

Revue Roumaine de Chimie, **14**, 345—352 (1969)

EQUATIONS AND INTERPRETATION OF OSMOTIC PRESSURE

D. A. TOTOESCU

Institute of Petroleum, Gas and Geology, Bucharest
str. Av. Traian Vuia no 6

Received May 21, 1968

In a former paper a new definition of perfect solutions was given based on two models, a quasi-gaseous and a quasi-crystalline, and equations for determining the osmotic pressure in perfect as well as in real solutions were deduced. In the present study, by introducing the term "molecular density" instead of the "average molar volume" (a parameter utilized in the former paper) identical equations are obtained, whereby a more accurate demonstration is made that the phenomena which take place in solutions may be interpreted according to the laws of perfect gas. The new equations, which as the former, were verfied in water-sucrose solutions, give results in agreement with the experimental data for the whole range of concentrations.

Although the osmotic pressure equations, except those of van't Hoff[1] have been directly deduced using thermodynamic considerations by van Laar[2], and later by Lewis[3] the interpretation of the phenomenon continued to be the object of numerous research works. Thus, scientists like Mayer[4], Ostwald[5], Planck[6], Eucken,[7] more recently Vasilescu Karpen[8] and others [9] deal with the same subject.

In spite of the fact that osmotic pressure and vapour pressure (like the freezing and boiling temperatures) of solutions are related phenomena, their definition involves in principle (or at least historically) different conceptions. Thus, Raoult's equation regarding the vapour pressure does not take into account the change of the molecular density of the solution as against the pure solvent and van't Hoff's equation disregards the ratio of the solvent and solute molecules (referring only to the volume occupied by the dissolved substance). According to Raolut's [10] all the components of a solution play an active role (since in the equations the molar fraction intervenes). From the van't Hoff's[11] equation it follows that the solvent plays a passive role (since the ratio between the solvent and solute molecules is immaterial) as in Nernst's[12] view, which holds that the solute is in a kind of void space.[13]

---

[1] J. H. van't Hoff, *Z. phys. Chem.*, **1**, 481, (1887).

[2] J. J. van Laar, *Z. phys. Chem.*, **15**, 497 (1894).

[3] G. V. Lewis, *J. Amer. Chem. Soc.*, **30**, 668, (1908).

[4] L. Mayer, *Z. phys. Chem.*, **5**, 33, (1890).

[5] W. Ostwald, *Z. phys. Chem.*, **159 A**, 375, (1938).

[6] J. Fredenhagen and Fl. Traunitz, *Z. Physik.*, **87**, 62, (1934).

[7] A. Eucken, *Z. phys. Chem.* (A), **168**, 309, (1934).

[8] N. Vasilescu Karpen, *Bul. Acad. R.P.R. secția științe matematice și fizice*, **8**, 205, (1956).

[9] M. Bodenstein, K. K. Bohnhoeffer and M. G. Joos, *Z. phys. Chem.* (B), **47**, **288**, (1940).

In this paper a new equation is deduced which allows the determination and at the same time the theoretical interpretation of the mechanism of the osmotic pressure.

I. PERFECT SOLUTIONS

Besides the definition of ideal solutions based on rigorous thermodynamic principle, more or less complete enunciations have been formulated.[14] According to Schröder [15] in perfect solution the components should dissolve without any thermal effect and volume change.

The water-sucrose solutions fulfil approximately the conditions of perfect solution from the point of view of volume, as stated by Schröder, practically for the whole range of concentrations (from 0 to 70 % sugar). The maximum contraction of these solutions as against the joint volume of the two components amounts to less than 0.5 %.[16] Nevertheless, the experimental departures of the vapour pressure as compared to the data obtained from Raoult's equation, are much smaller than those of osmotic pressure values as against van't Hoff's equation. Both fluid and gaseous bodies may be characterized also by molecular density instead of molar volume. We formulated the following definition of perfect solutions : assuming isothermal conditions the molecular density of the solution (D_s) should be equal to the molecular density of the pure solvent (D) :^{0}

$$D_s = D^0 \tag{1}$$

A similar definition has been given in a previous paper[13] with the difference that there it was stated that the average molar volume of perfect solution should be equal to the molar volume of pure solvent.

Equation (1) puts strict conditions for perfect solutions (which represent only a limiting case of Schröder's definition). This conclusion is in agreement with experimental practice since only a small number of systems with close molar volumes and generally with related chemical composition (as for instance the isobuthylic alcohol-isoamylic alcohol system)[17], follow Raoult's equation strictly.

---

[10] F. M. Raoult, *Z. phys. Chem.*, **15**, 497, (1894).

[11] J. H. van't Hoff, *Z. phys. Chem.*, **9**, 485, (1898).

[12] W. Nernst, "Theoretische Chemie", 15th ed. 1920.

[13] D. A. Totoescu, *Studii și Cercetări Chim., Acad. Romania*, **15**, 561 (1967).

[14] G. N. Lewis and M. Randall, "Thermodynamics" 2nd ed., McGraw-Hill Book. Comp., New York, 1961, p. 224.

[15] I. Schröder, *Gornyi Zhur.*, **2**, 272 (1890).

[16] Landolt-Börnstein, "Physikalisch-chemische Tabellen" vol. I, Berlin, Springer Verlag, 1923, p. 467.

[17] V. V. Udovenco and T. V. Fried, *Zhur. fiz. Khim.*, **22**, 1126, (1948).

II. EQUATIONS DEFINING OSMOTIC PRESSURE

In order to explain the osmotic pressure, van't Hoff[18] used the similar behaviour of solutions to gas mixtures separated by membrane permeable for only one of the components. The significance of the notion "gas pressure" might be assimilated, in the case of solutions, to "thermic pressure", a term used also by other investigators[19,20]. In perfect solutions, the difference between the thermic pressure of the pure solvent (p^0) and that of the solvent used (p) (taking into account that $D_s = D^0$ and consequently $p = p^0 x_1$) will result from an equation expressed like Raoult's equation:

$$\Delta_p = \pi_t = p^0 - p = p^0 - p^0 x_1 = p^0(1 - x_1) = p^0 x_2 \tag{2}$$

where $x_1 x_2$ are the molar fractions of the solvent and of the solute.

If in the equation (2) p^0 is replaced by the expression resulting from the ideal gas equation ($p^0 V^0 = n_1 RT$) it follows:

$$\pi_t = X_2 p^0 = \frac{n_2}{n_1 + n_2} \cdot \frac{nRT}{V^0} = X_1 \frac{n_2 RT}{V^0} \tag{3}$$

where V^0 is the volume unit containing n_1 moles of pure solvent.

In real solutions the osmotic pressure (π_r) is different from that of the perfect solutions (π_t) with the same molar concentration, since $D \neq D^0$.

The term π_t (which may be calculated also in real solutions) as well as the term π_r (which actually represents a variation of the π_t) being due to the concentration (molar fraction) and not to molecular density, may be considered as pressure and not as pressure difference, from the Boyle-Mariotte's law point of view. However, the correlation between the four amounts (π_t, π_r, D^0 and D_s) cannot be expressed by the equation: $(\pi_r - \pi_t)/\pi_t = (D_s - D^0)\ D^0$ which would follow from Boyle-Mariotte's law, since the term D^0 does not correspond to only one, but to an infinity of π_t values. The molecular density value of fluids is much higher than that of gaseous bodies and supposing that as against gas the terms D^0 and D_s increase by the same amount (k) then the following equation may be written:

$$(\pi_r - \pi_t) / \pi_t \approx (D_s - k - D^0 + k) / (D^0 - k) \approx (D_s - D^0)/(D^0 - k)$$

Thus, the relative variation of the osmotic pressure (which is proportional to the molecular density change) will increase as function of the correction value (k), but the limit of this increase or in other words the limit of the difference decrease ($D - k$) will equal the arithmetic mean: $(D^0 + D_s)/2 = D_m$ (average molecular density) since in perfect solutions (which correspond to this limit) the same requirement is fulfilled owing to the fact that $D_m = D^0 = D_s$.

---

[18] J. H. VAN'T HOFF, *Z. phys. Chem.*, **5**, 174 (1890).

[19] G. JÄGER, "Handbuch der Physik" vol. 9, Springer Verlag, Berlin, 1927, *Theorie der Wärme*, p. 463.

[20] K. FREDENHAGEN, "Für den Aufbau einer Theorie der Zweistoffsysteme", Akademie Verlag, Berlin, 1950, p. 92.

Taking into account that $D_{\text{fluid}} \gg D_{\text{gas}}$ ($D_{\text{gas}} / D_{\text{fluid}} \approx 1/1000$) it may be approximated fairly well that the corresponding value of the term π_t is D_m, and of the term π_r is D_s (both terms D_m and D_s change in different solutions).

Similarly to the first equation (derived from Boyle-Mariotte's law) the following equation may be written : $(\pi_r - \pi_t)/\pi_t = (D_s - D^0)/D_m$, which in limiting conditions evolves to the Boyle-Mariotte's equation, when D_m approaches D^0 (in perfect solutions $D_m = D^0 = D_s$). Considering that osmotic pressure actually is a depression and in order to give it a pressure significance (which was introduced owing to the interpretation of van't Hoff's equation) in equation (2) an inversion was performed by subtracting the p value from p^0 (according to a well known interpretation [21]). The same inversion should be made also in the equation deduced above, so that :

$$\frac{\pi_r - \pi_t}{\pi_t} = \frac{D^0 - D_s}{D_m} \tag{4}$$

Thus in equation (4) actually the same inversion was made as in equation (1), in both the afferent term of the solution being subtracted from that of the solvent (in this way depression acquires pressure significance).

By usual transformation, equation (4) yields the equation for assessement of osmotic pressure of real solutions :

$$\pi_r = \pi_t \left(1 + \frac{D^0 - D_s}{D_m}\right) \tag{5}$$

From the quasi-gaseous and quasi-crystalline model of the solutions, the following equality [13] was deduced :

$$\frac{\pi_r - \pi_t}{\pi_t} = \frac{V_s - V^0}{\dfrac{V_s + V^0}{2}} = \frac{2\,(V_s - V^0)}{V_s + V^0} = \frac{V_s - V^0}{V_m} \tag{6}$$

whence :

$$\pi_r = \pi_t \left(1 + \frac{V_s - V^0}{V_m}\right) \tag{7}$$

where V^0 and V_s are the volume of solvent and of the solution with the same number of particles. $V_m = (V_s + V^0)/2$ the average molar volume.

The volumes V^0 and V_s and V_m with the same number of particles are inversely proportional to their molecular densities : $(V_1' = 1/D_1')$. By adequate substitutions we can write the equation :

$$\frac{2\,(V_s - V^0)}{V_s + V^0} = \frac{2\left(\dfrac{1}{D_s} - \dfrac{1}{D^0}\right)}{\dfrac{1}{D_s} + \dfrac{1}{D^0}} = \frac{D^0 - D_s}{\dfrac{D^0 + D_s}{2}} = \frac{D^0 - D_s}{D_m} \tag{8}$$

---

[21] O. Sackur, *Z. phys. Chem.*, **70**, 477 (1910).

Thus, equations (6) and (7) have proved to be identical to equations (4) and (5) since $(V_s - V^0)/V_m = (D^0 - D_s) / D_m$. Equations (5) and (7) are valid for real as well perfect solutions since when their molecular densities, respectively their molar volumes, are equal, the correction value : $\pi_t (D^0 - D_s)/ D_m$ or $\pi_t (V_s - Vt)/ V_m$ becomes zero.

III. EXPERIMENTAL CHECKING OF OSMOTIC PRESSURE EQUATIONS

As in the former study,[13] the equation (5) deduced for osmotic pressure determination was verified by means of a great range of experimental values (π_{exp}) taken from many reliable works.[22–25] Table 1 shows samples at different temperatures (0°, 30°, 55.7°) and with a wide range of concentrations (0,20% – 68.65%). The concentration was expressed in different ways : as grams sugar per 1 kilo water (column 2), as molality (sucrose moles per kilo water) (col. 3), and in weight percentage (col. 4) : col. 5 shows density values (d) of solutions[26] required the calculation of osmotic pressure by means of equations (5) and (7), and of van't Hoff's equation (π_{vH}). The values of osmotic pressure were given as calculated using the empirical equation of Morse-Fraser[27] (π_{MF}) most widely used at present, and also those obtained by means of van Laar's equation (π_{vL})[2], deduced thermodynamically. Some of the equations being inferred for ideal solutions, in order to apply them to real solutions, some approximations are necessary. Thus in van Laar's equation it has been assumed that the solutions follow Raoult's law, and in equation (3) the same approximation was made assuming that the resulting solution is perfect (although $D_s \neq D^0$). In order to illustrate the difference between the results obtained by means of various equations and to show the value of different terms used, the calculation of a sample is given : (table 1 no 24).

– van't Hoff equation (π_{vH})

$$\pi_{\text{vH}} = \text{CRT} = 2.624 \cdot 0,8205 \cdot 328.85 = 71.36 \text{ atm.}$$

C – moles sugar per volume unit as calculated from W – kg sugar per 1 kg. water

$$\left(C = \frac{n_2 d}{1+W} = \frac{6.395 \cdot 1.319}{1+2.190} = 2.624 \text{ mol/1}\right)$$

– Morse and Fraser's equation: (π_{MF}):

$$\pi_{\text{MF}} = \frac{n_2 RT}{V^0} = \frac{6.398 \cdot 0.08205 \cdot 328.85}{1.015} = 170.10 \text{ atm.}$$

V^0 = volume of 1 kg water ($V^0_{273.15} = 1.0001$ l; $V^0_{303.15} = 1.004$ l; $V^0_{328.85} = 1.015$ l).

---

[22] H. M. Morse and J. C. Fraser, *J. Amer. Chem. Soc.*, **36**, 39 (1906) ; **36**, 667 (1908) ; **41**, 1257 (1909) ; **45**, 554 (1911) ; **49**, 91 (1912) ; Landolt-Börnstein "Physikalisch-chemische Tabellen", vol. 2, Springer Verlag, Berlin, 1923, p. 1420.

[23] Earl Of Berkely and E. G. J. Hartley, *Proc. Roy. Soc. London*, **82**, 271 (1909) ; **92**, 480 (1916) ; *Phil. Trans. Roy. Soc. London A*, **206**, 499 (1906) ; Landolt-Börnstein "Physikalisch-chemische Tabellen" vol. 2, Springer Verlag, Berlin, 1923, p. 2826.

[24] J. C. W. Fraser and R. T. Myrich, *J. Amer. Chem., Soc.* **38**, 1915 (1916) ; Landolt-Börnstein "Physikalisch-chemische Tabellen", vol. 2, Springer Verlag, Berlin, 1923, p. 1420.

[25] P. Lotz and J. C. Fraser, *J. Amer. Chem. Soc.*, **43**, 2504, (1921) ; Landolt-Börnstein "Physikalisch-chemische Tabellen" vol. 3, Springer Verlag, Berlin, 1936, p. 2826.

[26] Landolt-Börnstein, "Physikalisch-chemische Tabellen", vol. 1, Springer Verlag, Berlin, 1923, p. 1420.

[27] H. N. Morse and J. C. Fraser, *J. Amer. Chem. Soc.*, **28**, 1 (1906).

Table 1

Values of osmotic pressure as calculated by means of different equations

Sample no	Concentrations			Density values d	Temperature ^{0}C	Osmotic pressure in atmospheres						Relative error %	Authors indices*
	g sugar per kilo-water W	molality n/kilo-water	weight percentage			Van't Hoff π_{VH}	Morse and Fraser π_{MF}	Van Laar π_{VL}	Equation (3) π_t	Equation (5) π_{r5}	Experimental values π_{exp}		
1	2	3	4	5	6	7	8	9	10	11	12	13	14
1	2.02	0,0059	0.1996	1.0007	0	0.129	0.132	0.322	0.132	0.132	0.134	+ 1.21	23
2	10.0	0,029	0.9921	1.0038	0	0.644	0.649	0.649	0.649	0.652	0.66	+ 1.12	23
3	20.0	0,058	1.961	1.0078	0	1.290	1.300	1.298	1.297	1.314	1.32	+ 0.46	23
4	34.2	0,100	3.31	1.0085	30	2.426	2.477	2.475	2.472	2.514	2.47	− 1.58	22
5	64.4	0,200	6.05	1.0245	0	4.325	4.48	4.47	4.466	4.630	4.72	+ 1.43	22
6	171.1	0.500	14.61	1.0612	0	10.20	11.20	11.17	11.10	12.09	11.89	− 1.66	22
7	171.1	0.500	14.61	1.0544	30	11.20	12.38	12.34	12.27	13,39	12.97	− 3.04	22
8	300.0	0.876	23.08	1.0996	0	16.62	19.64	19.47	19.23	22.26	26.80	+20.08	23
9	342.3	1.000	25.51	1.111	0	18.56	22.42	22.22	22.01	25.77	24.82	− 3.19	23
10	342.3	1.000	25.51	1.1023	30	20.43	24.77	24.56	24.33	28.56	27.22	− 4.69	22
11	664.9	1.942	39.94	1.1718	30	330.99	48.10	47.29	46.47	60.71	57.16	− 5.84	24
12	680.0	1.987	40.48	1.1746	30	34.48	49.21	48.36	47.50	62.50	57.50	− 8.00	25
13	685.0	2.001	40.65	1.1628	55.7	37.26	53.20	52.30	51.36	67.70	63.10	− 6.80	25
14	812.6	2.374	44.85	1.2093	0	35.50	52.97	52.06	51.02	69.33	67.74	− 2.30	23
15	1000.0	2.921	50.00	1.2115	55.7	47.75	77.76	75.76	73.78	105.39	97.40	− 5.32	24
16	1018.8	2.974	50.47	1.2330	30	44.96	73.66	72.85	69.91	100.26	94.75	− 5.50	24
17	117.3	3.264	52.76	1.2535	0	43.29	73.14	71.06	69.07	100.76	100.13	− 0.63	23
18	1284.0	3.751	56.22	1.2456	55.7	55.20	99.73	96.57	93.42	141.48	133.50	− 5.86	25
19	1327.1	3.877	57.03	1.2642	30	52.39	96.02	92.80	89.75	136.93	133.95	− 2.18	24
20	1411.0	4.121	58.77	1.2883	0	49.37	92.34	89.01	86.00	132.54	134.84	+ 1.71	23
21	1610.5	4.704	61.70	1.2924	30	57.93	116.50	111.90	107.39	171.72	172.38	+ 0.39	24
22	1796.0	5.247	64.23	1.3065	30	60.98	129.94	124.16	118.73	195.01	206.10	+ 5.69	25
23	1982.4	5.790	66.47	1.3200	30	63.75	143.39	136.40	129.87	218.55	217.00	− 0.71	24
24	2190.0	6.398	68.65	1.3187	55.7	71.36	170.10	161.10	152,55	263.20	265.60	+ 0.91	25

* With reference to the experimental value given in column 12

— van Laar's equation π_{vL} assuming that the solution follows Raoult's law and the partial molar volume V is equal to the solvent's molar volume

$$\pi_{vL} = -\frac{RT}{V}\cdot\ln\frac{P}{P^0} = -\frac{RT}{V}\ln x_1 = \frac{RT}{V}2.303\,\lg\frac{n_1+n_2}{n_1} =$$

$$= \frac{0.08205\cdot 328.85\cdot 2.303}{0.01827}\lg\frac{55.51+6.398}{55.51} = 161.10 \text{ atm.}$$

$V_{273\cdot 15} = 0.01802$ l; $V_{307.15} = 0.01810$ l; $V_{328\cdot 85} = 0.01827$ l).
— the equation (3) (π_t) assuming the solutions to be perfect (that is to say $V_s = V^0$)

$$\pi_t = \frac{n_2RT}{{}_0}\,x_1 = \frac{6.398\cdot 0.08205\cdot 328.85}{1.015}\cdot\frac{55.51}{55.51+6.398} = 152.55 \text{ atm.}$$

V^0 has the same value as in the Morse-Fraser equation.
— Equation (5) (π_{r5}):

$$\pi_{r5} = \pi_t^0\left(1+\frac{D_0-D_s}{D_m}\right) = 152.55\left(1+\frac{55.51-30.54}{42}\right) = 263.2 \text{ atm.}$$

$$D_s = \frac{55.51+6.398}{V_s} = \frac{55.51+6.398}{2.169} = 30.54 \text{ mol/l}$$

—Equation (7) (π_{r7}):

$$\pi_{r7} = \pi_t\left(1+\frac{2\,(V_s-V^0)}{V_s+V^0}\right) = 152.55\left(1+\frac{2.169-1.014}{2.169+1.048}\right) = 263.2 \text{ atm.}$$

$$V_s = \frac{1.00 \text{ kg water} + W \text{ kg sugar}}{\text{d}}\,X_1 = \frac{1.00+2.190}{1.319}\cdot\frac{55.51}{55.51+6.398} = 2.169 \text{ l.}$$

The results obtained prove at the same time the identity of equations (5) and (7) so that the results of column 11 from table 1, are valid for both equations. Table 1 gives the experimental values (col.12) as well as the relative error (col.13) with respect to equation (5).

IV. INTERPRETATION OF OSMOTIC PRESSURE

The conclusion that the osmotic pressure represents a difference of pressure between the solvent molecules in the two fluids is in agreement with the view of a great number of scientists, such as Mayer, [4] Konovalov, [28] Iakovkin, [29] Vasilescu-Karpen, [8] Fredenhagen, [20] and others. [9]

Among the equations used for osmotic pressure determination in ideal solutions, when applied to real solutions, van't Hoff's equation gives the greatest departures as compared to experimental data (in concentrated water-sucrose solutions departures amount to as much as 300%). The criterion on which this equation is theoretically based gives no explanation as to such a decisive role of volume changes. On the other hand, when using equation (3) for real solutions (when no account is taken that $D_s \neq D^0$) much smaller departures result (in sucrose-water solutions they do not exceed 100%). The conclusion that equation (3) is better grounded is confirmed also thermodynamically. Thus, by making about the same approximation in equation (3) and in van Laar's equation (obtained thermodynamically), very close results are obtained (Morse-Fraser's[29] empirical equation leads to nearly the same but slightly higher results).

---

[28] D. P. Konovalov, *Ann. Phys.*, **10**, 376 (1903).
[29] A. A. Jakovkin, *Z. phys. Chem.*, **70**, 158 (1910).

The surprising fair agreement between experimental and calculated by means of equation (7) values, represents a confirmation of the validity of both deduced relationships and theoretical interpretation of phenomena.

In perfect solutions the value of osmotic pressure (π_t) is determined only by molar fraction. The osmotic pressure of real solutions (π_r) is dependent both on molar fraction, which represents the main factor, and on molecular density changes, which are a secondary factor (associated effect). The osmotic pressure due to molar fraction is accounted for by the law of partial pressure of gas and the difference between the terms π_r and π_t ($\pi_r - \pi_t$) due to molecular density variation is interpreted according to the law of Boyle-Mariotte. It is noteworthy that departures of real solutions as against perfect ones may be explained by a law of deal gas (Boyle-Mariotte's law).

Revue Roumaine de Chimie, **14**, 353–356 (1969)

ÉTUDE DES NITRATES MÉTALLIQUES EN MÉLANGES DE SOLVANTS. II

1. LES SYSTÈMES : LE NITRATE DE NICKEL ET DE COBALT HEXAHYDRATÉ-ACÉTONE-TÉTRACHLORURE DE CARBONE ; LE NITRATE DE NICKEL ET DE COBALT DIHYDRATÉ-ACÉTONE-TÉTRACHLORURE DE CARBONE

RALUCA RIPAN, I. EGER et N. BOJAN
Institut de Chimie de l'Académie, Filiale de Cluj, 59–65, str. Donath

Reçu le 9 août 1968

On a étudié la solubilité du nitrate de nickel hexahydraté, du nitrate de nickel dihydraté, du nitrate de cobalt hexahydraté et du nitrate de cobalt dihydraté en mélange d'acétone-tétrachlorure de carbone à 25°. La limite de solubilité du sel dans le mélange de solvants – quand la séparation des composants de la phase organique n'a pas lieu, – a été déterminée pour un domaine « continu » du mélange de ces deux composants. Les isothermes de solubilité indiquent la solubilité différente de ces deux hydrates du nitrate de nickel et du nitrate de cobalt dans le mélange d'acétone-tétrachlorure de carbone, respectivement les sels dihydratés du nitrate de nickel et du nitrate de cobalt sont plus solubles que les sels hexahydratés.

Dans une note antérieure [1] nous avons démontré l'existence d'un phénomène de ségrégation en deux phases distinctes des composants d'un mélange de solvants organiques, quand on dissout dans ce mélange une quantité de nitrate d'uranyle qui dépasse la concentration limite.

Ce phénomène, d'ailleurs peu étudié, est connu seulement aux cas où le mélange de solvants organiques se trouve en équilibre avec la phase aqueuse de laquelle on extrait les sels inorganiques. [2–6]

Nous avons utilisé une seule phase initiale, le mélange « continu » d'acétone-tétrachlorure de carbone auquel on a ajouté des sels inorganiques jusqu'à l'obtention de la solubilité limite, respectivement jusqu'à la séparation des deux solvants organiques en deux phases distinctes, ce phénomène étant la conséquence d'une interaction entre le sel et le solvant actif organique.

---

[1] Note I : R. Ripan, I. Eger et N. Bojan, *Rev. Roumaine Chim.*, **13**, 421 (1968).

[2] T. V. Healy et H. A. C. McKay, *Trans. Faraday Soc.*, **52**, 633 (1956).

[3] A. S. Solovkin, N. S. Povitzkei et K. P. Lunitchikina, *Zhur. neorg. Khim.*, **5**, 2115 (1960).

[4] V. M. Vdodenko, T. V. Kovaleva et M. A. Riazov, *Radiokhimiya*, **4**, 609 (1962).

[5] M. L. Good et S. E. Bryan, *J. Amer. Chem. Soc.*, **82**, 5636 (1960).

[6] M. L. Good et S. E. Bryan, *J. Amer. Chem. Soc.*, **83**, 140 (1961).

Dans ce travail on a étudié le nitrate de nickel hexahydraté et dihydraté, le nitrate de cobalt hexahydraté et dihydraté en mélange d'acétone — tétrachlorure de carbone à 25°.

Réactifs utilisés : Le nitrate de nickel hexahydraté produit Merck *p.a.*. Le nitrate de nickel dihydraté a été préparé par la déshydratation thermique du sel hexahydraté.[7] Le nitrate de cobalt hexahydraté utilisé était un produit Merck *p.a.* Le nitrate de cobalt dihydraté a été préparé en traitant le sel hexahydraté indiqué ci-dessus par la méthode de Clarck et Buckner.[8] L'acétone et le tétrachlorure de carbone utilisés ont été des produits *p.a.* anhydres. Le nickel a été déterminé par la méthode de Tschugaeff avec diméthylglyoxime, [9] l'eau étant dosée par la méthode de Karl Fischer améliorée. [10] La cobalt a été déterminé avec l'oxine (8-*ortho*-oxyquinoline) et par la méthode de Spacu-Dick.[11–12]

Pour obtenir l'isotherme de solubilité des hydrates (du hexahydrate et du dihydrate) du nitrate de nickel et du nitrate de cobalt, on a utilisé des mélanges continus d'acétone et de tétrachlorure de carbone, les volumes étant variés ainsi : 1 p. acétone + 9 p. tétrachlorure de carbone ; 2 p. acétone + 8 p. tétrachlorure de carbone ... 9 p. acétone + 1 p. tétrachlorure de carbone.

Les épreuves ont été thermostatées dans un ultrathermostat Wobser à 25°.

Dans toutes les épreuves dans lesquelles la substance solide était présente comme corps de fonds, la séparation des mélanges de solvants a eu lieu en deux phases : la phase active (l'acétone), qui contenait le nitrate de nickel ou de cobalt à une concentration rapprochée de la concentration de saturation de ces deux sels dans l'acétone pure, et la phase inerte (le tétrachlorure de carbone) qui contenait des quantités fortement réduites de nitrate de nickel , respectivement de nitrate de cobalt.

Ce phénomène diffère de celui observé dans le cas du nitrate d'uranyle, parce que dans ce cas, la séparation des phases, respectivement la solubilité des sels, présente des valeurs déterminables seulement dans le mélange dans lequel la teneur en acétone dépasse 30% vol.

Dans les mélanges homogènes acétone — tétrachlorure de carbone, dans lesquels la teneur en acétone est moindre que 30% vol., la teneur en nickel est si réduite qu'on ne peut pas la doser par la réaction avec la diméthylglyoxime, la teneur en cobalt n'étant déterminable ni par réaction avec l'oxine ni par réaction Spacu-Dick.

Les isothermes de solubilité, indiquées sur les figures 1—4 et les tableaux 1—4 correspondants, montrent la solubilité limite, respectivement la concentration limite des sels dans le mélange de solvants, qui ne peut être dépassée sans que les deux solvants ne se séparent en phases distinctes.

Le procédé utilisé par nous pour déterminer la solubilité limite de ces quatre hydrates dans les mélanges de solvants indiqués a été le suivant : on a prélevé chaque fois un volume déterminé de la solution saturée du sel en acétone à 25°.

---

[7] A. Eieverts et L. Schreiner, *Z. anorg. Chem.*, **219**, 105 (1934).

[8] G. L. Clarek et H. K. Bruckner, *J. Amer. Chem. Soc.*, **44**, 230 (1922).

[9] L. Tschugaeff, *Ber. dtsch. chem. Ges.*, **38**, 2520 (1905).

[10] E. Eberius et H. Bohnes, *Z. analyt. Chem.*, **168**, 330 (1959).

[11] R. Berg, *J. prakt. Chem.*, **115**, 178 (1927).

[12] G. Spacu et J. Dick, *Z. analyt. Chem.*, **71**, 97 (1927).

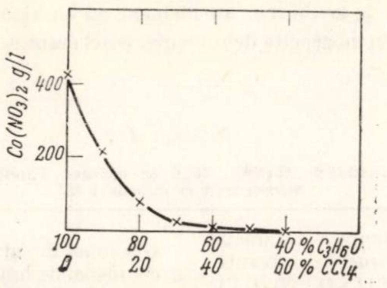

Fig. 1. — Isotherme de solubilité du nitrate de cobalt hexahydraté en mélange d'acétone et de tétrachlorure de carbone.

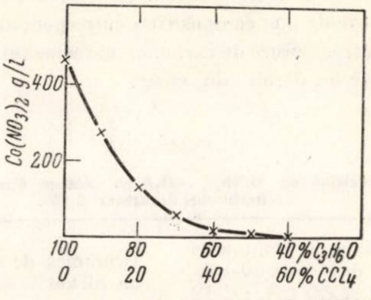

Fig. 2. — Isotherme de solubilité du nitrate de cobalt dihydraté en mélange d'acétone et de tétrachlorure de carbone.

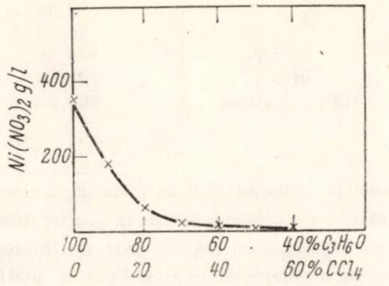

Fig. 3. — Isotherme de solubilité du nitrate de nickel hexahydraté en mélange d'acétone et de tétrachlorure de carbone.

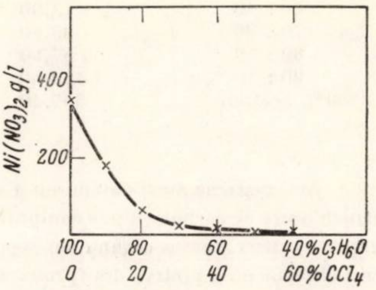

Fig. 4. — Isotherme de solubilité du nitrate de nickel dihydraté en mélange d'acétone et de tétrachlorure de carbone.

Tableau 1

Solubilité du $Co(NO_3)_2$ en mélange d'acétone – tétrachlorure de carbone à 25°

Rapport volumétrique des solvants $CH_3CO\,CH_3 : C\,Cl_4$	Grammes de nitrate de cobalt par litre de solution
10 : 90	—
20 : 80	—
30 : 70	—
40 : 60	1,34
50 : 50	7,70
60 : 40	13,20
70 : 30	24,20
80 : 20	78,80
90 : 10	212,50
100 % acétone	423,80

Tableau 2

Solubilité du $Co(NO_3)_2\ .2H_2O$ en mélange d'acétone – tétrachlorure de carbone à 25°

Rapport volumétrique des solvants $CH_3CO\,CH_3 : C\,Cl_4$	Grammes de nitrate de cobalt par litre de solution.
10 : 90	—
20 : 80	—
30 : 70	—
40 : 60	1,87
50 : 50	10,25
60 : 40	15,81
70 : 30	53,30
80 : 20	124,37
90 : 10	275,60
100 % acétone	466,40

A cette solution on a ajouté le volume de tétrachlorure de carbone nécessaire pour obtenir une composition correspondant à un point de la courbe. Au moment où on ajoute le tétrachlorure de carbone, se forme un mélange sans homogénéité de solvants, le sel étant déposé sur les parois du vase .

Tableau 3

Solubilité du $Ni(NO_3)_2 . 6H_2O$ en mélange d'acétone – tétrachlorure de carbone à 25°.

Rapport volumétrique des solvants $CH_3CO\,CH_3 : C\,Cl_4$	Grammes de nitrate de nickel de solution
10 : 90	—
20 : 80	—
30 : 70	—
40 : 60	1,42
50 : 50	4,17
60 : 40	12,30
70 : 30	23,60
80 : 20	57,90
90 : 10	180,30
100% acétone	347,40

Tableau 4

Solubilité du $Ni\,(NO_3)_2 .2H_2O$ en mélange d'acétone – tétrachlorure de carbone à 25°

Rapport volumétrique des solvants $CH_3CO\,CH_3 :C\,Cl_4$	Grammes de nitrate de nickel de solution
10 : 90	—
20 : 80	—
30 : 70	—
40 : 60	1,85
50 : 50	4,48
60 : 40	12,31
70 : 30	36,02
80 : 20	134,26
90 : 10	231,56
100% acétone	369,23

Au système ainsi obtenu on a ajouté des quantités croissantes d'un mélange d'acétone-tétrachlorure de carbone d'une composition correspondante du même point de la courbe, jusqu'à ce que les deux phases organiques séparées deviennent homogènes. De la solution homogène ainsi obtenue on a prélevé des épreuves dans lesquelles on a déterminé le nickel par la méthode de Tschugaeff et des épreuves dans lesquelles on a dosé le cobalt comme oxinate ou sous forme de complexe Spacu-Dick.

En examinant les isothermes de solubilité des hydrates du nitrate de nickel et de cobalt et les tableaux correspondants, on observe que le dihydrate du nitrate de nickel et du nitrate de cobalt présentent une solubilité plus grande que les sels correspondants hexahydratés.

En même temps on remarque que la solubilité des hydrates, des nitrates de nickel et de cobalt dans les mélanges d'acétone-tétrachlorure de carbone présente des valeurs discernables à peine à une teneur en acétone qui dépasse 30% volumes dans le mélange susmentionné.

Revue Roumaine de Chimie, **14**, 357–364 (1969)

COMPLEX COMBINATIONS WITH DYPHENILIC DERIVATIVES. XXIII*.

ON THE STRUCTURE OF SOME Cu(I) AND Cu(II) COMPLEX THIOCYANATES

CONST. GH. MACAROVICI and RODICA MICU-SEMENIUC
Inorganic Chemistry Department, University of Cluj
Str. Arany János 11

Received May 21, 1968

The IR spectra of some Cu (I) and Cu(II) complex inorganic thiocyanates with different aromatic amines have been recorded between 3600–400 cm^{-1}. The characteristic absorption bands are assigned and their shifts are disscused. The correlation between the absorption bands frequencies and the ligands bonding in complexes has been made by reference to complexes having a known crystalline structure. The studied complexes are polymers, or, at least dimers linked with the bifunctional radical –SCN– or/and by the diamines used in their synthesis.

In the present paper the structure of a few Cu (I) and Cu (II) complex thiocyanates with aromatic amines and diamines was studied by means of the IR spectra. The mode of bonding of the –SCN– group in the complex thiocyanates was established according to the conclusions of different authors on simple or complex metallic thiocyanates. [1–9]

EXPERIMENTAL

The IR spectra of the following substances were recorded for a comparative study (with a UR–10 Zeiss Jena spectrograph) though some of them are already known in the literature.

---

* Part XXII. A. Nicula, R. Micu-Semeniuc and Const. Gh. Macarovici, *Rev. Roumaine Chim.*, **14**, 1329 (1968).

[1] K. Nakamoto, "Infrared Spectra of Inorganic and Coordination Compounds", John Wiley Inc., New York, London, 1963, p. 173 (see also the literature indicated).

[2] G. S. Jdanov and Z. V. Zvancova, *Uspekhi Khim.*, 22, 3 (1953).

[3] L. Pauling, "The Nature of the Chemical Bond and the Structure of Molecules and Crystals. An Introduction to Modern Structural Chemistry", ed. III. Ithaca, New York, Cornell University Press, London, Oxford University Press, 1960, p. 274.

[4] J..Fujita, K. Nakamoto and M. Kobayashi, *J. Amer. Chem. Soc.*, **78**, 3295 (1956).

[5] Y. Takéuchi and J. Saito, *Bull. Chem. Soc. Japan*, **29**, 319 (1957).

[6] * * * "Theory and Structure of Complex Compounds". Proceedings of the Symposium held at Wroclaw, 1962, Pergamon Press Book, Macmillan Company, New York, 1964, **p.** 225.

[7] S. M. Nelson, *Proc. Chem. Soc.*, **1961**, 372.

[8] O. Kinell and B. Strandberg, *Acta Chem. Scand.*, **13**, 1607 (1959).

[9] F. Basolo, J. L. Burmeister and A. J. Poë, *J. Amer. Chem. Soc.*, **85**, 1700 (1963).

Organic Bases

1. Aniline (An)
2. Benzidine (Bzd)
3. m,m′-diaminodiphenyl (m,m′—DADF)
4. 0,0′ — —,,— (0,0′—DADF)
5. 2,7-diaminofluorene (2,7—DAF)
6. Pyridine (Py)

Simple and Complex Thiocyanates

I. NH_4 NCS colourless
II. KNCS colourless
III. AgSCN white
IV. CuSCN white
V. [CuPySCN] white

VI. [$CuPy_2$ $(NCS)_2$] green
VII. [$CuAn_2$ $(NCS)_2$] olive
VIII. [CuBzd $(NCS)_2$] brown-black
IX. [$CuBzd_2$ $(NCS)_2$] dark-blue
X. [Cu(m,m′—DADF) $(NCS)_2$] olive
XI. [Cu(o,o′—DFDF)$_2$$(NCS)_2$] brown-red
XII. [Cu(2,7—DAF)$(NCS)_2$] blue

The studied samples were either obtained by purifying the commercially available substances or synthetized by us, following the methods given in the literature.

Substance (V), [Cu(SCN)Py], was synthetized as follows : to 0,5 g $Cu(NO_3)_2 \cdot 6H_2O_2$, dissolved in very little water, a solution of SO_2 in excess was added. After the mixture was heated to its boiling point an aqueous solution of NH_4 SCN and pyridine was added. The white preci-

Table 1

IR absorption bands of the SCN group in some simple thiocyanates and in Cu(I), Cu(II) complex combinations

No	Sample	ν_{1C-NS} cm^{-1}	ν_3 S—CN cm^{-1}	ν_2 δ_{SCN} cm^{-1}	$2\nu_2$ cm^{-1}
1	NH_4NCS	2 050	750	485	972
		2 003		470	954
2	KNCS	2 050	750	485	972
		2 002		470	955
3	AgSCN	2 169	743	446	901
			723	423	861
IV	CuSCN	2 175 v.s	748w	430v.w	880 v.w
		2 078 v.w			
V	[CuSCNPy]	2 172 m		448	910w(?)
		2 120v.s	750 m(?)	410	895 w(?)
		2 068w			
VI	[$CuPy_2(NCS)_2$]	2 095v.s	828 m	477 m	960 w
		2 050 sh		467 w	948 w
VII	[$CuAn_2(NCS)_2$]	2 120 v.s	830 m	464 w	935 w(?)
		2 077 m			
VIII	[$CuBzd(NCS)_2$]	2 120 v.s	—	—	942 w(?)
		2 075 sh			
IX	[$CuBzd_2(NCS)_2$]	2 120 v.s			
		2 095 m	—	—	922 w(?)
		2 070 m			
X	[Cu(m,m′-DADF)$(NCS)_2$]	2 120v.s	832 m	460 w	930 w
		2 078 sh			
XI	[Cu(0,0'—DADF)$_2$$(NCS)_2$]	2 102 v.s.	822 m	470 w	938 w(?)
XII	[Cu(2,7-DAF) $(NCS)_2$]	2 090 v.s	850 m(?)	915 m(?)	

v.s. = very strong
m = medium
w = weak
v.w. = very weak

pitate yiealded was filtered off and washed with water and alcohol. This substances is stable in air, insoluble in water and organic solvents.

Analysis [Cu(SCN)Py] (200.7) Calcd. : Cu 31,68% N 13.96%;

Found : Cu 32.12% N 14.17%.

In table 1 the IR absorption band values of the—SCN— group were listed and in table 2 those of the $-NH_2$ group in the free organic bases and complexes studied in the present paper

The IR spectra of the IV, V and VII—XII combinations have not been studied so far.

Table 2

IR absorption bands of the free amines and of the Cu(II) complexes with these amines

No	Sample	Range cm^{-1}			
		3500—3200 ν_{aNH_2} and ν_{sNH_2}	1660—1550 δ_{NH_2}	1300—1200 ν_{CN}	1100—100 $\delta^{*}_{NH_2}$
1	Aniline	3 440 s 3 355 s 3 210 s	1 620 v.s	1 278 s	
2	Benzidine	3 390 s 3 320 v.s 3 200 v.s	1 615 v.s	1 268 v.s	
3	*m, m'*-DADF	3 432 s 3 400 s 3 325 v.s 3 200 m	1 620 v.s	1 262 m	
4	*o,o'*-DADF	3 395 s 3 378 s 3 280 s	16 25 v.s	1 295 s	
5	2,7-DAF	3 380 s 3 305 v.s 3 210 s	1 610 v.s	1 250 s	
VII	$[CuAn_2(NCS)_2]$	3 305 v.s 3 218 s	1 588 m (bonded)	1 235 m	1 080 v.s
VIII	$[CuBzd(NCS)_2]$	3 290 v.s 3 220 v.s	1 588 m (bonded)	1 243 m	1 060 v.s
IX	$[CuBzd_2(NCS)_2]$	3 360s(free) 3 335 s 3 290 v.s (bonded) 3 220 v.s (bonded)	1 660 m 1 622 s 1 590 m 1 556 s	1 282 m 1 245 m (bonded)	1 062 v.s
X	[Cu(*m,m'*-DADF)$(NCS)_2$]	3 298 v.s (bonded) 3 207 s (bonded)	1 590 s (bonded)	1 233 w (bonded)	1 072 v.s
XI	[Cu(*o,o'*-DADF)$_2(NCS)_2$]	3 370 s 3 330 s 3 305 s (bonded) 3 260 s 3 215 s (bonded)	1 618 s (free) 1 585 s (bonded)	1 295 w (free) 1 240 w (bonded)	1 052 m
XII	[Cu(2,7-DAF) $(NCS)_2$]	3 320 v.s 3 200 v.s	1 580 v.s	1 222 s	

$\delta^{*}NH_2$ = twist; v.s = very strong w = weak
s = strong
m = medium

RESULTS AND DISCUSSIONS

The Cu (I) combinations

IV. *CuSCN* : According to different authors [1-9] and considering the absorption bands at 2175, 2078, 748, 430 and 880 cm^{-1} of the CuSCN IR spectrum (see table 1) it can be deduced that in this compound the Cu^+ ion is bound to sulfur and that between Cu^+ and $-SCN-$ group there is a "bridge" type bond.

$$- - - - CU-SCN-Cu- - - -$$

Since the electronic configuration of Cu^+ resembles that of Ag^+ and the IR absorption spectra of both thiocyanates have close values (see table 1), we assigned the zig-zag chain structure to copper I thiocyanate, i.e. $(CuSCN)_n$, as well as to silver thiocyanate. [8,10-13]

V. *[Cu (SCN) Py]* : By comparing the IR spectrum of this combination to that of $(CuSCN)_n$ it was ascertained that besides the two common vibrations, at 2172 cm^{-1} and 2068 cm^{-1} respectively, another very intensive absorption at 2120 cm^{-1} , was recorded probably due to the influence of the Py ligand in the molecule. The other absorption bands concerning the $-SCN-$ group, are superposed on the pyridine absorption bands. The majority of pyridine absorption bands in the complex are less intensive and they are shifted with 20—25 cm^{-1} to greater wave numbers as compared to the IR absorption bands of the free base. It is most likely that the [CuSCNPy] combination obtained by us, is a chained polymer :

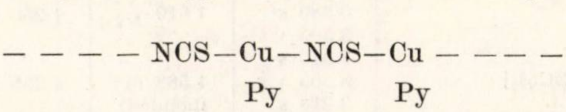

$$- - - - NCS-\underset{Py}{Cu}-NCS-\underset{Py}{Cu} - - - -$$

As it was expected both $(CuSCN)_n$ and [CuSCNPy] are diamagnetic substances.

The Complex Combinations of Cu (II)

In the IR spectra of copper (II) complex thiocyanates with the already mentioned organic bases, a large and extremely intensive absorption band, due to the antisymmetrical vibration ν_1 (see table 1) was recorded in the 2120—2090 cm^{-1} range. This would attest a metal-nitrogen bond, M—NCS, having larger values on account of the "bridge" bond. In the IR spectra of VIII—XII combinations, the symmetrical vibrations ν_3 are of a medium intensity and located within 832—822 cm^{-1}. The ν_2 vibrations evidently appear in VI, VII, X and XI conbinations while $2\nu_2$ vibrations are present in VI and X combinations. In several substances (VIII, IX and XII) ν_2 vibrations, in the other $2\nu_2$ vibrations, are superposed on of the base vibrations.

---

[10] A. Turco and C. Pecile, *Nature*, **191**, 66 (1961).
[11] A. Turco, *Nature*, **187**, 772 (1960).
[12] J. Lindquist, *Chem. Abstr.*, **51**, 4793b (1957).
[13] C. Panattoni and E. Frasson, *Gazz. Chim. Ital.*, **93**, 601 (1963).

As it results from table 2 the characteristic bands $\nu_{a\,NH_2}$, $\nu_{s\,NH_2}$ and ν_{CN} of the complexes are shifted toward lower frequencies as compared to those of the free amines which indicate that they are involved in coordinative bonds.[14-16]

VI. [*Cu Py*$_2$(*NCS*)$_2$]. Porai-Koshits[17] found by X-ray studies on this complex that the copper atom is in the center of a lengthened octahedron, surrounded by four SCN groups and two Py. The bonds are accomplished by two nitrogen atoms of two SCN groups, two nitrogen atoms of 2 Py and two sulphur atoms of the other two SCN groups. Thus, a polymer chained by —NCS— bridges between the copper atoms, which appears hexacoordinated, is formed.

The pyridine absorption bands have the same behaviour as in combination V, their shifts being due to the loosening of C—N bond in pyridine as a consequence of its involving in the complex.[18]

VII. [*Cu An*$_2$(*NCS*)$_2$] : We assigned for this combination a structure similar to other results in the literature.[17,19] However, a "dimeric" form $[CuAn_2(NCS)_2]_2$ analogues to those proposed by Chatt for platinum II complex thiocyanates with different ligands, can also be imagined :

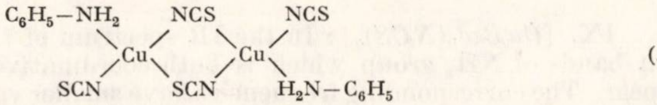

(A)

VIII. [*CuBzd*(*NCS*)$_2$]. As results from tables 1 and 2, in the IR spectrum of this substance only two vibrations are recorded for SCN group, one at 2120 cm^{-1} (v.s.) and a shoulder at 2075 cm $^{-1}$, while the other vibrations ν_3, ν_2 and $2\nu_2$ are superposed on the benzidine absorption bands.

The vibrations of the aminic functions are shifted toward lower frequencies indicating their coordinative bond.[14,15,18] A "dimeric" structure might be considered for this substance.

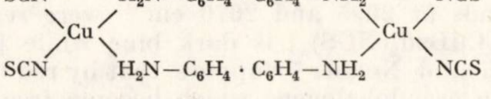

(A)

or a chain polymer structure, like :

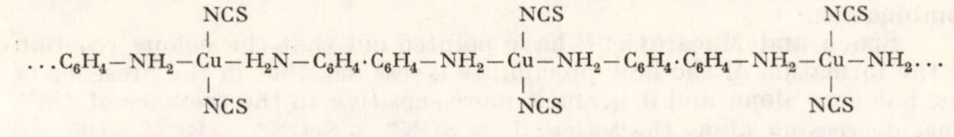

$$\ldots C_6H_4-NH_2-\underset{NCS}{\overset{NCS}{Cu}}-H_2N-C_6H_4\cdot C_6H_4-NH_2-\underset{NCS}{\overset{NCS}{Cu}}-NH_2-C_6H_4\cdot C_6H_4-NH_2-\underset{NCS}{\overset{NCS}{Cu}}-NH_2\ldots$$

---

[14] L. J. Bellamy, "The Infrared Spectra of Complex Molecules", ed. II, Methuen Co. Ltd., New York, John Wiley Sons, Inc., 1960, p. 249—58 and p. 269.

[15] C. Gh. Macarovici, G. Schmidt and E. Hamburg, *Rev. Roumaine Chim.*, **9**, 51 (1964) (see also the literature indicated).

[16] L. Marion, D. A. Ramsay and N. Jones, *J. Amer. Chem. Soc.*, **73**, 306 (1951).

[17] M. A. Porai-Koshits and G. N. Tishchenko, *Kristallografiya* **4**, 239 (1959).

[18] O. A. Osipov and I. M. Semenova, *Zhur. obshchei Khim.*, **33**, 720 (1963).

[19] J. Garaj, *Chem. Zvesti*, **18**, 488 (1963).

Even a similar structure to that given for $[CuPy_2(NCS)_2]$[17] is not ruled out, the more so as the ESR studies[20] show that the central copper atom has here an axial symmetry and we suppose it to be hexacoordinated. In this sense its structure can be written as follows :

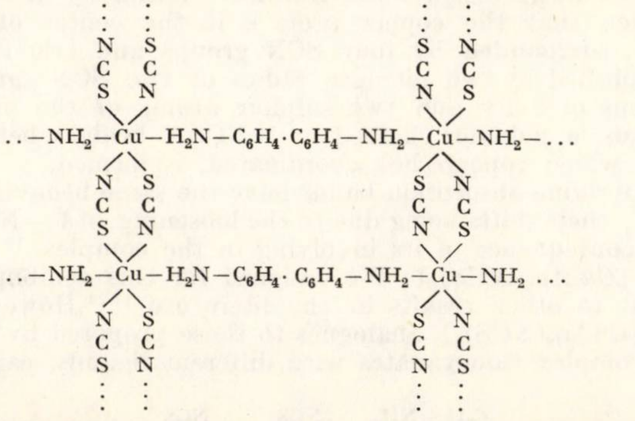
N S
C C
S N
...—NH₂—Cu—H₂N—C₆H₄·C₆H₄—NH₂—Cu—NH₂—...
N S
C C
S N
...—NH₂—Cu—H₂N—C₆H₄·C₆H₄—NH₂—Cu—NH₂ ...

(B)

IX. $[CuBzd_2(NCS)_2]$: In the IR spectrum of this complex, absorption bands of NH_2 group which is both coordinatively bounded and free appear. The corresponding frequencies have smaller values than 3400 cm^{-1} (see table 2) as in the case of free benzidine where a molecular association is supposed.

The analysis of this spectrum reveals evidently three bands of medium intensity at 1556, 1390 and 1165 cm^{-1} . These bands do not appear in the spectrum of combination VIII with one benzidine molecule, and the first two of them do not appear either in the free benzidine spectrum. The same absorption bands are to be found in the spectrum of the blue product obtained by oxidizing the benzidine with gaseous chlorine, at 1542, 1385 and 1155 cm^{-1} , respectively.

For the —SCN— group a larger and very intensive band at 2120 cm^{-1} and two bands at 2095 and 2070 cm^{-1} were recorded (see table 1). The complex $[CuBzd_2(NCS)_2]$ is dark blue while $[CuBzd(NCS)_2]$ is brown-black. Feigh and Neuber[21] suppose that by reducing Cu^{2+} to Cu^{+}, the halogens or the pseudohalogens which become free oxidize the benzidine. A blue substance results which could be a "partially chinoidic" combination.

Spacu and Macarovici[22] have pointed out that the colour reaction or the formation of the blue precipitate is less sensible in the presence of free halogens alone and it is much more sensitive in the presence of Cu^{2+} ions, decreasing along the series : $J^- > SCN^- > SeCN^- > Br^- > Cl^-$.

But it was proved that, according to ESR spectra,[20] in the resulting blue compound the copper is bivalent beside a benzidine semiqui-

---

[20] A. Nicula, R. Micu-Semeniuc and C. Macarovici, *in press*.

[21] F. Feigl, "Qualitative Analyse mit Hilfe von Tüpfelreaktionen", 2nd ed., Akademische Verlagsgesellschaft, Leipzig, 1935, p. 170.

[22] G. Spacu and C. Gh. Macarovici, *Atti della Reale Accademia delle Scienze di Torino*, **72**, 3 (1936—37).

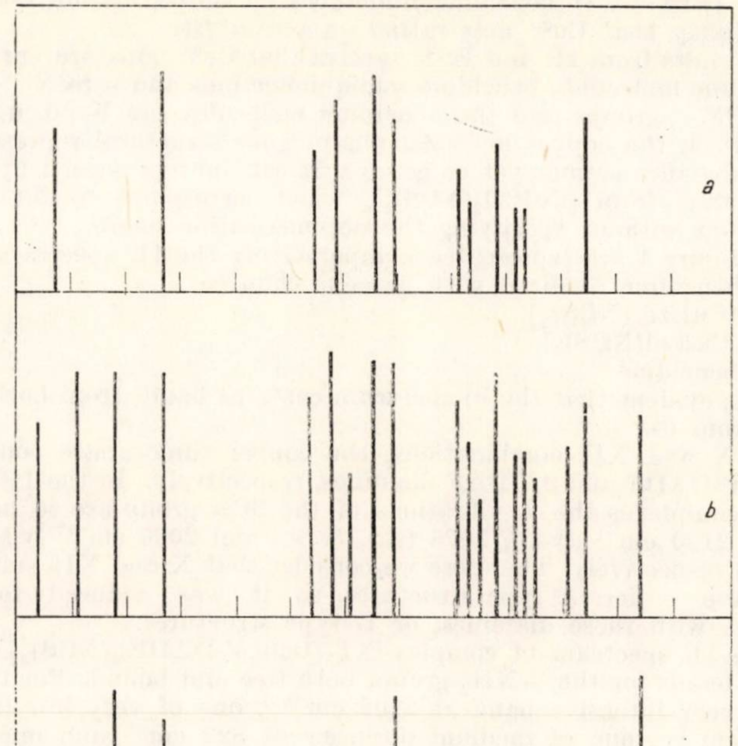

Fig. 1. — Absorption bands of IR spectra of :
a, oxidized benzidine; *b*, $[CuBzd_2(NCS)_2]$; *c*, $[CuBzd(NCS)_2]$; *d*, benzidine.

none ion $[Bzd.]^+$. If benzidine undergoes an autooxidation reaction it is most likely that Cu^{2+} acts rather as a catalyst.

It results from IR and ESR spectra that Cu^{2+} ions are surrounded by benzidine molecules, benzidine semiquinone ions and $-SCN-$ groups. The $-SCN-$ groups and the benzidine molecules can build up ''bridges'' between the copper ions. An unambigous structural representation of this substance cannot yet be given . It can be represented by the general polymer from $[CuBzd_2(NCS)_2]_n$ which corresponds to the chemical analysis but without specifying the polymerization degree.

In figure 1 are represented comparatively the IR spectra of :

a) benzidine oxidized with gaseous chlorine
b) $[CuBzd_2(NCS)_2]$
c) $[CuBzd(NCS)_2]$
d) benzidine

It is evident that the b) spectrum contains bands from both a) and c) and from d).

In X and XII combinations, the copper thiocyanate coordinates the m, m'-DADF and 2,7-DAF diamines, respectively. In the IR spectra of these complexes the ν_1 vibrations of the SCN group are to be found at 2115, 2120 cm^{-1} (v.s.), 2078 (sh), (v.w.) and 2090 cm^{-1} (v.s.), 2172 cm^{-1} (w) respectively. Therefore we consider that X and XII substances might have either. A type structures, as it was deduced for $CuCl_2$ complexes with these diamines, or B type structures.

The IR spectrum of complex XI $[Cu(o,o'\text{-DADF})_2(NCS)_2]$ has absorption bands for the $-NH_2$ group, both free and bound. For the SCN group a very intensive band at 2102 cm^{-1} , one of very low intensity at 2170 cm^{-1} , one of medium intensity at 822 cm^{-1} and one of low intensity at 470 cm^{-1} were recorded. These results would make possible the assumption that substance XI has a B type structure. It is to be noticed that in the $[Cu(o,o'\text{-DADF})_2Cl_2]$ [15] complex the diamine binds both $-NH_2$ groups forming two heptacycles around the copper ion, though the two $-NH_2$ groups are not in same plane. In the XI complex the same diamine is binding only one aminic function most likely due to the thiocyanate bridge bond which is a sterical impediment in closing the heptacycles.

As a conclusion it can be stated that all studied complexes are polymers or at least dimers linked by the bifunctional radical SCN or by the diamines used in their synthesis.

In CuSCN and [CuSCNPy] the SCN group is bound whith Cu (I) through the sulfur atom and forms a strong ''bridge'' by means of the nitrogen atom. The pyridine is coordinatively bound and so the copper appears tetracoordinated. [11] Both substances are polymers.

In the copper II thiocyanates complex the SCN group is bound through the nitrogen atom and a weak ''bridge'' is formed through the sulfur atom.

All these substances with Cu (II) are paramagnetical ones as proved by ESR study, [20] that is to say in the VI–XII combinations copper exists only as a bivalent ion, whereas in the IX combination a benzidine free radical $[Bzd.]^+$is also present.

Revue Roumaine de Chimie, **14**, 365–372 (1969)

SUR LE CHROMATE, LE BICHROMATE, LE MOLYBDATE ET LE WOLFRAMATE DE 2-ÉTHOXY-6,9-DIAMINO-ACRIDINE

I. FLOREA

Laboratoire de Chimie générale de l'Institut Polytechnique, 14, str. Remus, Timişoara

Reçu le 22 avril 1968

On a suivi conductométriquement la réaction entre les anions CrO_4^{2-}, $Cr_2O_7^{2-}$, $Mo_7O_{24}^{6-}$, WO_4^{2-} et le lactate de 2-éthoxy-6,9-diaminoacridine (Rivanol)-BHL. Les substances formées pendant les titrages conductométriques ont été séparées, analysées, étudiées thermogravimétriquement et on a déterminé leur solubilité dans l'eau à 20°. D'après les données obtenues on a établi leurs formules chimiques : $(BH)_2CrO_4$, $(BH)_2Cr_2O_7$, $(BH)_6Mo_7O_{24}$ et $(BH)_2WO_4$. L'étude conductométrique de la réaction de bichromate de potassium et lactate de 2-éthoxy-6,9-diaminoacridine a établi que les ions $Cr_2O_7^{2-}$ et BH^+ peuvent être dosés par cette voie.

Dans le présent article on a suivi si les anions CrO_4^{2-}, $Cr_2O_7^{2-}$, $Mo_7O_{24}^{6-}$ et WO_4^{2-} forment, de manière analogue aux autres anions dont nous nous sommes occupés auparavant, [1–5] des composés chimiques avec le lactate de 2-éthoxy-6,9-diaminoacridine et si leurs propriétés les indiquent, éventuellement, pour des utilisations analytiques.

Auerbach [6] a utilisé le $K_2Cr_2O_7$ au dosage indirect du lactate de 2-éthoxy-6,9-diaminoacridine. La méthode consiste dans le traitement du lactate de 2-éthoxy-6,9-diaminoacridine avec un excès de bichromate de potassium N/10. On filtre le précipité formé, et dans la solution filtrée et acidulée avec de l'acide clorhydrique, on ajoute une solution d'iodure de potassium 10%. Après agitation, on titre l'iode libéré avec thiosulfate de sodium 0,1 N.

---

[1] C. Drăgulescu et I. Florea, *Studii şi Cercetări Şti., Chim. Baza Cercetări Şti., Timişoara*, **9**, 205 (1962).

[2] C. Drăgulescu et I. Florea, *Studii şi Cercetări Şti., Chim. Baza Cercetări Şti., Timişoara*, **9**, 219 (1962).

[3] C. Drăgulescu et I. Florea, *Studii şi Cercetări Şti., Chim. Baza Cercetări Şti., Timişoara*, **9**, 247 (1962).

[4] C. Drăgulescu et I. Florea, *Studii şi Cercetări Şti., Chim. Baza Cercetări Şti., Timişoara*, **9**, 227 (1962).

[5] C. Drăgulescu et I. Florea, *Studii şi Cercetări Şti., Chim. Baza Cercetări Şti., Timişoara*, **10**, 31 (1963).

[6] M. E. Auerbach, *J. Amer. Pharm. Assoc.*, **26**, 321 (1937).

Les anions CrO_4^{2-}, $Cr_2O_7^{2-}$, $Mo_7O_{24}^{6-}$ et WO_4^{2-} forment avec le BHL des composés ayant une couleur jaune jusqu'au jaune brun.

Les composés chimiques qui se forment par le mélange des solutions mentionnées ont été étudiés conductométriquement, en titrant les solutions de chromate de potassium, bichromate de potassium, molybdate d'ammonium et wolframate de sodium avec des solutions de lactate de 2-éthoxy-6,9-diaminoacridine.

Les titrages ont été effectués avec des solutions de K_2CrO_4, $(NH_4)_6Mo_7O_{24}$, Na_2WO_4 0,1 M et $K_2Cr_2O_7$, BHL 0,2 M, leurs concentrations étant établies par la pesée exacte.

Pour la préparation des solutions on a employé : K_2CrO_4, $K_2Cr_2O_7$, $(NH_4)_6Mo_7O_{24}$, Na_2WO_4 Merck *p.a.* et BHL chimique pur, recristallisé.

1. TITRAGES CONDUCTOMÉTRIQUES

Les résultats des titrages conductométriques sont représentés dans les figures 1 et 2.

Les données montrent que dans le titrage conductométrique représenté dans le diagramme de la figure 1, du K_2CrO_4 avec le BHL, à la suite du remplacement des anions CrO_4^{2-} par les anions L^-, la conductivité de la solution reste constante jusqu'à l'équivalence. La conductivité équivalente de l'anion lactique Λ_{L^-} semble être approximativement égale à $1/2\ \Lambda_{CrO_4^{2-}}$ $[\Lambda_{L^-} \simeq 1/2\ \Lambda_{CrO_4^{2-}}]$. Après l'équivalence, la conductivité de la solution augmente, grâce à l'excès du réactif additionné.

Dans le titrage conductométrique, donné dans le diagramme 2 de la figure 1, du $K_2Cr_2O_7$ avec le BHL, on voit une diminution de la conductivité de la solution jusqu'à l'équivalence, au remplacement des anions $Cr_2O_7^{2-}$ par les anions L^-, $[\Lambda_{L^-} < 1/2\ \Lambda_{Cr_2O_7^{2-}}]$. Après l'équivalence, la conductivité de la solution augmente, grâce à l'excès du réactif additionné.

Au titrage conductométrique, présenté dans le diagramme 3 de la figure 1, du $(NH_4)_6Mo_7O_{24}$ avec le BHL on enregistre une diminution de la conductivité de la solution jusqu'à l'équivalence, due au remplacement des anions $Mo_7O_{24}^{6-}$ par les anions L^-, $[\Lambda_{L^-} < 1/6\ \Lambda_{Mo_7O_{24}^{6-}}]$.

Après l'équivalence, la conductivité de la solution augmente grâce à l'excès du réactif additionné.

Dans le titrage conductométrique, présenté dans le diagramme 4 de la figure 1, du Na_2WO_4 avec le BHL, jusqu'à l'équivalence, a lieu une augmentation de la conductivité de la solution grâce au remplacement des anions WO_4^{2-} par les anions L^-, $[\Lambda_{L^-} > 1/2\ \Lambda_{WO_4^{2-}}]$. Après l'équivalence, la conductivité de la solution augmente, grâce à l'excès du réactif additionné.

Les diagrammes 1, 2, 3 et 4 de la figure 2 représentent des solutions de BHL, titrées avec K_2CrO_4, $K_2Cr_2O_7$, $(NH_4)_6Mo_7O_{24}$ et Na_2WO_4. Jusqu'à l'équivalence a lieu une augmentation de la conductivité de la solution, grâce au remplacement des cations BH^+ par les cations de K^+, NH_4^+ et Na^+, $[\Lambda_{BH^+} < \Lambda_{K^+}$, $\Lambda_{BH^+} < \Lambda_{NH_4^+}$ et $\Lambda_{BH^+} < \Lambda_{Na^+}]$. Après l'équiva-

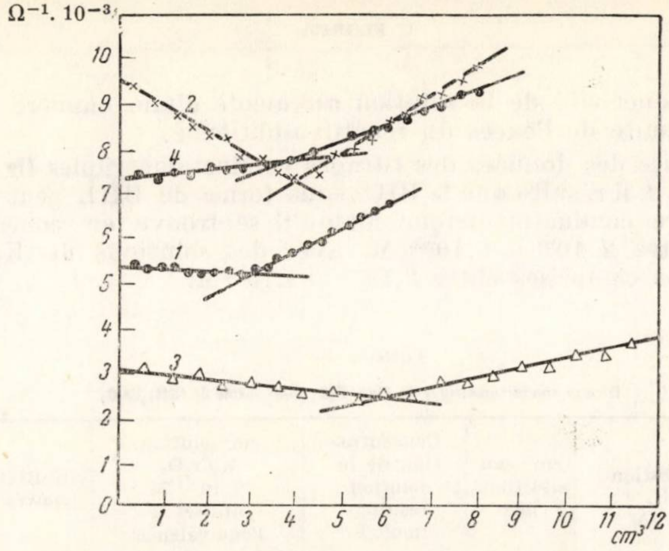

Fig. 1. — 1) 1,5 cm^3 de K_2CrO_4 $1.10^{-1}M$+13,5 cm^3 d'eau sont titrés avec du BHL $1.10^{-1}M$; 2) 2 cm^3 de $K_2Cr_2O_7$ 1.10^{-1} M+9 cm^3 d'eau sont titrés avec du BHL 1.10^{-1} M ; 3) 1 cm^3 de $(NH_4)_6Mo_7O_{24}$ 1.10^{-1} M + 49 cm^3 d'eau sont titrés avec du BHL 1.10^{-1} M ; 4) 2 cm^3 de Na_2WO_4 1.10^{-1} M +8 cm^3 d'eau sont titrés avec du BHL 1.10^{-1} M.

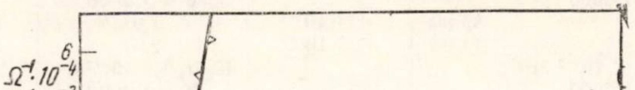

Fig. 2. — 1) 6 cm^3 de BHL 1.10^{-1} M + 4 cm^3 d'eau sont titrés avec du K_2CrO_4 1.10^{-1} M ; 2) 2 cm^3 de BHL 1.10^{-1} M + 28 cm^3 d'eau sont titrés avec du $K_2Cr_2O_7$ 1.10^{-1} M ; 3) 6 cm^3 de BHL 1.10^{-1} M + 24 cm^3 d'eau sont titrés avec du $(NH_4)_6Mo_7O_{24}$ 1.10^{-1} M ; 4) 4 cm^3 de BHL 1.10^{-1} M + 16 cm^3 d'eau sont titrés avec du Na_2WO_4 1.10^{-1} M.

lence, la conductivité de la solution augmente d'une manière plus prononcée, par suite de l'excès du réactif additionné.

A la suite des données des titrages conductométriques figurées aux tableaux 1 et 2 il résulte que le BH^+ sous forme de BHL peut être dosé d'une manière conductométrique lorsqu'il se trouve en concentrations comprises entre $2.10^{-1} - 1.10^{-3}$ M, avec des solutions de $K_2Cr_2O_7$ de concentrations comprises entre $2.10^{-1} - 1.10^{-2}$ M.

Tableau 1

Dosage conductométrique de l'ion BH^+ sous forme de $(BH)_2Cr_2O_7$

N°	cm³ solution BHL 2.10^{-1}M	cm³ eau additionnée	Concentration de la solution résultée mole/l	cm³ solution $K_2Cr_2O_7$ 2.10^{-1} M utilisés à l'équivalence	cm³ BHL trouvés	E %
	F = 1,0000			F = 1,0000		
1	6,00	39,00	$2,6.10^{-2}$	2,99	5,98	−0,33
2	6,00	54,00	$2,10^{-2}$	3,02	6,04	+0,66
3	6,00	74,00	$1,5.10^{-2}$	3,03	6,06	+1,00
	BHL 1.10^{-1} M F = 1,0000			$K_2Cr_2O_7 1.10^{-1}$ M F = 1,0000		
4	6,00	39,00	$1,3.10^{-2}$	3,01	6,02	+0,33
5	6,00	74,00	$7,5.10^{-3}$	2,97	5,94	−1,00
	BHL 1.10^{-2} M F = 1,0000			$K_2Cr_2O_7 1.10^{-2}$M F = 1,0000		
6	6,00	24,00	2.10^{-3}	2,94	5,88	−2,00
7	6,00	14,00	3.10^{-3}	2,96	5,92	−1,33
8	6,00	9,00	4.10^{-3}	3,01	6,02	+0,33
9	6,00	19,00	$2,4.10^{-3}$	2,96	5,92	−1,33
10	6,00	11,00	$3,5.10^{-3}$	2,99	5,98	−0,33
11	6,00	48,00	1.10^{-3}	3,94	5,88	−2,00
12	6,00 12,00	42,00	1.10^{-3}	2,95	5,90	−1,66
13	6,00 6,00	48,00	1.10^{-3}	2,99	5,98	−0,33
14	6,00 12,00	42,00	1.10^{-3}	3,02	6,04	+0,66
15	6,00 6,00	48,00	1.10^{-3}	2,95	5,90	−1,66
16	6,00 12,00	42,00	1.10^{-3}	3,03	6,06	+1,00
17	6,00 6,00	48,00	1.10^{-3}	2,94	5,88	−2,00
18	6,00 12,00	42,00	1.10^{-3}	3,02	6,04	−0,66

On peut doser également l'ion $Cr_2O_7^{2-}$, sous forme de $K_2Cr_2O_7$, de manière conductométrique, lorsqu'il se trouve en concentrations comprises entre $2.10^{-2} - 1.10^{-3}$ M, avec des solutions de BHL-lactate de 2-éthoxy-6,9-diaminoacridine, de concentrations comprises entre $2.10^{-1} - 1.10^{-2}$ M.

Dans le tableau 1, les échantillons notés avec 11 et 12 représentent des titrages de BHL avec le bichromate de potassium, en présence de glucose, dans des solutions de la même concentration avec du BHL (échantillon 11) et dans des solutions deux fois plus concentrées que la solution de BHL (échantillon 12). Les échantillons 13 et 14 ont été titrés en présence de l'urée, les échantillons 15 et 16 en présence d'acide borique, et les échantillons 17 et 18 en présence de glycérine. Dans tous ces cas, on a utilisé le lactate de 2-éthoxy-6,9-diaminoacridine en concentrations égales à celles employées à son titrage en présence de glucose.

Tableau 2

Dosage conductométrique de l'ion $Cr_2O_7^{2-}$ sous forme de $(BH)_2Cr_2O_7$

N°	cm^2 solution $K_2Cr_2O_7$ 2.10^{-1} M utilisés	cm^3 eau additionnée	Concentration de la solution résultée mole/l	cm^3 solution BHL 2.10^{-1} M utilisés à l'équivalence	cm^3 $K_2Cr_2O_7$ trouvés	E%
	F = 1,0000			F = 1,0000		
1	1,50	28,50	1.10^{-2}	2,98	1,49	−0,66
2	1,50	21,00	$1,33.10^{-3}$	3,06	1,53	+2,00
3	1,50	18,50	$1,5.10^{-2}$	2,94	1,47	−2,00
4	1,50	13,50	2.10^{-2}	3,02	1,51	+0,66
	$K_2Cr_2O_7$			BHL		
	1.10^{-1} M			1.10^{-1} M		
	F = 1,0000			F = 1,0000		
5	1,50	13,5	1.10^{-2}	3,04	1,52	+1,33
6	1,50	50,5	$2,9.10^{-3}$	2,96	1,48	−1,33
7	1,50	78,5	$1,9.10^{-3}$	3,04	1,52	+1,33
8	1,50	43,5	$3,3.10^{-3}$	2,96	1,48	−1,33
9	1,50	18,5	$7,5.10^{-3}$	2,98	1,49	−0,66
	$K_2Cr_2O_7$			BHL		
	1.10^{-2} M			1.10^{-2} M		
	F = 1,0000			F = 1,0000		
10	1,5	13,5	1.10^{-3}	2,96	1,48	−1,33

Les erreurs enregistrées au dosage du lactate de 2-éthoxy-6,9-diaminoacridine avec bichromate de potassium , ainsi que le dosage du bichromate de potassium avec le lactate de 2-éthoxy-6,9-diaminoacridine ne dépassent pas ±2%.

La méthode instituée par nous présente par rapport à celle indiquée par Auerbach [6] les avantages suivantes : elle est plus rapide et elle nécessite un seul réactif, le bichromate de potassium.

2. PRÉPARATION ET ANALYSE DES COMPOSÉS FORMÉS

Mélangeant les réactifs en proportions d'équivalence des titrages conductométriques, on a obtenu des composés avec le BHL des ions $Cr_2O_7^{2-}$ et $Mo_7O_{24}^{6-}$ sous forme de précipités qui ont été lavés à l'eau distillée et séchés dans l'étuve à 110°, jusqu'à un poids constant. Les composés $(BH)_2CrO_4$ et $(BH)_2WO_4$ ont été préparés de manière analogue , après une évaporation préalable des solutions à volume petit.

La composition des composés a été déterminée en dosant d'une manière gravimétrique les Cr, Mo et W, sous forme d'oxydes, par calcination de la substance. L'ion BH^+ a été déterminé photométriquement. [7-9]

a. $(BH)_2CrO_4$ (624,63)

Analyse :

trouvé : Cr 8,45 ; 8,09 ; BH^+ 81,20 ; 81,81 %
calculé : Cr 8,20 BH^+ 81,47 %

b. $(BH)_2Cr_2O_7$ (724,63)

Analyse :

trouvé : Cr 14,04 ; 14,27 ; BH^+69, 78 ; 69,98 %
calculé : Cr 14,35 BH^+ 70,19 %

c. $(BH)_6Mo_7O_{24}$ (2581,55)

Analyse :

trouvé : Mo 25,77 ; 26,18 ; BH^+ 58,80 ; 59,43 %
calculé : Mo 25,95 BH^+ 59,10 %

d. $(BH)_2WO_4$ (756,48)

Analyse :

trouvé : W 24,16 ; 24,54 ; BH^+ 66,90 ; 67,40 %
calculé : W 24,31 BH^+ 67,23 %

3. SOLUBILITÉ DES SUBSTANCES OBTENUES

La solubilité du chromate, du bichromate, du molybdate et du wolframate de 2-éthoxy-6,9-diaminoacridine a été déterminée photométriquement [7-9] en dosant de chaque composé l'ion BH^+.

Les substances étudiées ont été conservées jusqu'à saturation en fioles Erlenmeyer, dans un mouvement perpétuel, à 20°, température maintenue avec un thermostat Wöbser. Les résultats obtenus sont les suivants :

$$S_{(BH)_2CrO_4} = 4{,}5 \cdot 10^{-5} \text{ mole/l}$$
$$S_{(BH)_2Cr_2O_7} = 9 \cdot 10^{-5} \text{ mole/l}$$
$$S_{(BH)_6Mo_7O_{24}} = 9{,}80 \cdot 10^{-4} \text{ mole/l}$$
$$S_{(BH)_2WO_4} = 3{,}66 \cdot 10^{-5} \text{ mole/l}$$

4. COMPORTEMENT THERMOGRAVIMÉTRIQUE

Pour l'étude thermogravimétrique du chromate, du bichromate, du molybdate et du wolframate d'éthoxy-6,9-diaminoacridine on a utilisé une thermobalance, dont on a mesuré la température dans l'intervalle de 30 à 800°. Le régime d'échauffement a été choisi à 10°/mn. Les résultats obtenus sont représentés dans les diagrammes de la figure 3.

---

[7] J. M. Schulte, *Pharm. Weekblad*, **67**, 601 (1930), dans: *Chem Zentr.*, **2**, 2020 (1930)

[8] J. Ssolz, *Farmacia*, **11**, 20 (1940), dans : *Chem. Zentr.*, **2**, 23 (1941).

[9] Maizelis et A. Miasuicova, *Farmatsija*, 4, **617**, 26 (1941), dans : *Chem. Abstr.*, **38**, 2453 (1944).

a. *$(BH)_2CrO_4$*. Le diagramme 1 de la figure 3 représente le thermogramme obtenu. La substance est stable jusqu'à 110°. Au-dessus de cette température, elle se décompose graduellement et à 730° elle est totalement transformé en Cr_2O_3. Le résidu pèse 25,6 mg et il est formé de Cr_2O_3. De la substance mise en œuvre on calcule 24,7 mg de Cr_2O_3. L'erreur de la détermination thermogravimétrique est de +2,40%.

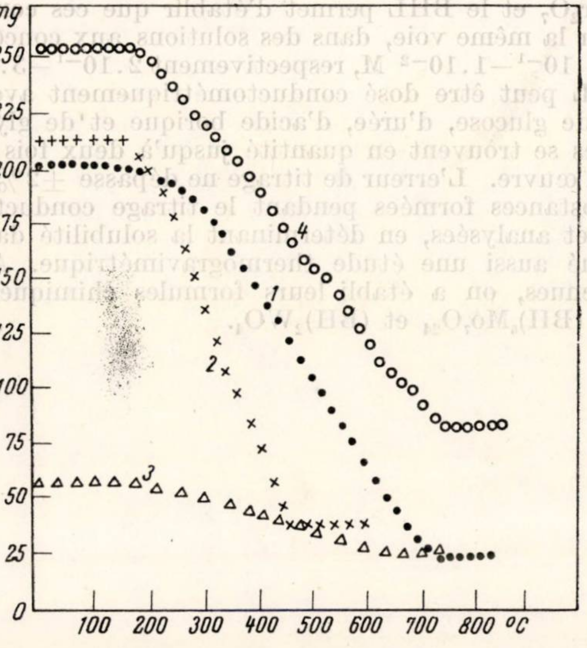

Fig. 3. — *1*, Thermolyse $(BH)_2CrO_4$; *2*, thermolyse $(BH)_2Cr_2O_7$; *3*, thermolyse $(BH)_6Mo_7O_{24}$; *4*, thermolyse $(BH)_2WO_4$.

b. *$(BH)_2Cr_2O_7$*. Le diagramme 2 de la figure 3 représente le thermogramme obtenu. La substance est stable jusqu'à 170°. Au-dessus de cette température elle se décompose graduellement et à 490° la décomposition est finie. Le résidu pèse 45,7 mg et il est formé de Cr_2O_3. De la substance mise en œuvre on calcule 45 mg de Cr_2O_3. L'erreur de la détermination thermogravimétrique est de + 1,62%.

c. *$(BH)_6Mo_7O_{24}$*. Le diagramme 3 de la figure 3 représente le thermogramme obtenu. La substance est stable jusqu'à 210°. Au-dessus de cette température elle se décompose graduellement, et à la température de 650° elle est totalement transformée en MoO_3. Le résidu pèse 25,9 mg et il est formé de MoO_3. De la substance mise en œuvre on calcule 25,5 mg de MoO_3. L'erreur de la détermination thermogravimétrique est de + 1,68%.

d. *$(BH)_2WO_4$*. Le diagramme 4 de la figure 3 représente le thermogramme obtenu. La substance est stable jusqu'à 170°. Au-dessus de cette température elle se décompose graduellement et à 760° elle est totalement transformée en WO_3. Le résidu pèse 81,0 mg et il est formé de WO_3. De la substance mise en œuvre on calcule 80,3 mg de WO_3. L'erreur de la détermination thermogravimétrique est de + 1,30%.

5. CONCLUSIONS

Par le traitement du chromate de potassium, du bichromate de potassium, du molybdate d'ammonium et du wolframate de sodium avec le lactate de 2-éthoxy-6,9-diaminoacridine, on forme des précipités de couleur jaune jusqu'à jaune brun. L'étude conductométrique de la réaction entre le $K_2Cr_2O_7$ et le BHL permet d'établir que ces composés peuvent être dosés par la même voie, dans des solutions aux concentrations comprises entre $2.10^{-1}-1.10^{-2}$ M, respectivement $2.10^{-1}-3.10^{-2}$ M.

Le BHL peut être dosé conductométriquement avec du $K_2Cr_2O_7$, en présence de glucose, d'urée, d'acide borique et de glycérine, lorsque ces substances se trouvent en quantité jusqu'à deux fois la quantité de BHL mise en œuvre. L'erreur de titrage ne dépasse $\pm 2\%$.

Les substances formées pendant le titrage conductométrique ont été séparées et analysées, en déterminant la solubilité dans l'eau à 20°. On a effectué aussi une étude thermogravimétrique. A la suite des données obtenues, on a établi leurs formules chimiques : $(BH)_2CrO_4$; $(BH)_2Cr_2O_7$; $(BH)_6Mo_7O_{24}$ et $(BH)_2WO_4$.

Revue Roumaine de Chimie, **14**, 373–383 (1969)

TRANSFORMATIONS CHIMIQUES DU CHLORURE DE POLYVINYLE. I

SYNTHÈSES DES POLYÉLECTROLYTES RÉTICULÉS SULFONIQUES À BASE DE CHLORURE DE POLYVINYLE ARYLÉ AVEC DU BENZÈNE

164

I. POINESCU
Institut de Chimie macromoléculaire « Petru Poni », Secteur
des polymères réactifs, Jassy, 41 A, Aleea Grigore Ghica Vodă

Reçu le 24 avril 1968

Dans ce travail on présente les conditions de synthèse des polyélectrolytes réticulés, obtenus par sulfonation à l'acide chlorosulfonique, en présence d'un solvant inerte (1,2-dichloréthane), du chlorure de polyvinyle arylé avec du benzène. Les capacités d'échange des polyélectrolytes réticulés sont en fonction du degré de substitution du chlore avec des noyaux benzéniques dans le chlorure de polyvinyle. Les polyélectrolytes réticulés, ainsi obtenus, contiennent également des groupements sulfoniques, de même que des groupements carboxyliques, par suite de l'action oxydante de l'acide chlorosulfonique.

Le problème de la synthèse des polyélectrolytes réticulés à base de chlorure de polyvinyle et de ses copolymères présente une importance scientifique et pratique toute particulière.

Ces derniers temps on a publié une série de travaux sur la synthèse des polyélectrolytes réticulés — échangeurs d'ions — à base de chlorure de polyvinyle.

Vasiliev et Vansheidt [1,2] ont montré la possibilité de synthétiser des échangeurs de cations sulfoniques en partant du chlorure de polyvinyle, du polyacétate et des copolymères de ceux-ci, par sulfonation à l'oléum ou à l'acide chlorosulfonique en présence du 1,2-dichloréthane. Par ce procédé on a obtenu des échangeurs de cations avec une capacité d'échange de 2–4 méq/g.

Wolkober,[3] en sulfonant le chlorure de polyvinyle avec l'acide chlorosulfonique en présence de l'acide azotique, ou en l'absence de celui-ci, a montré qu'on obtient des produits qui ont la propriété d'échanger les cations.

Kan Hak Min [4], a sulfoné le chlorure de polyvinyle avec l'acide chlorosulfonique à la température de 60–100°.

---

[1] A. A. Vasiliev et A. A. Vansheidt, *Zhur. priklad. Khim.*, **32**, 150 (1959).

[2] A. S. Vansheidt et A. A. Vasiljev, U.S.S.R. Pat., 114 196, 30 Juillet, 1958; *Chem. Abstr.*, **53**, 11718 (1959).

[3] Z. Wolkober, *J. Polymer. Sci.*, **58**, 1311 (1962).

[4] Kan Hak Min, *Zhur. Khim. i Khim. prom.-sti.*, **7**, 225 (1963); Ref. *Zhur. Khim.*, **8**, 8c 534 (1964).

Hooker[5] a synthétisé des membranes échangeuses d'ions par la sulfonation du chlorure de polyvinyle avec un mélange d'acide sulfurique et chlorosulfonique en présence du trixylénilfosfate.

Dima et ses collaborateurs, [6-13] ont effectué une étude systématique concernant la synthèse des échangeurs de cations sulfoniques en partant du chlorure de polyvinyle. Vu que les échangeurs de cations obtenus du chlorure de polyvinyle possèdent une grande capacité d'échange (approx. 5,0 méq/g), des résistances mécanique et chimique satisfaisantes, les auteurs mentionnés ci-dessus ont entrepris l'étude détaillée des conditions de synthèse et de l'influence de celles-ci sur la structure et les propriétés des échangeurs de cations obtenus.

Kiichi Takemoto et ses collaborateurs[14] ont synthétisé des polyélectrolytes à structure linéaire, avec des groupements sulfoniques, par la copolymérisation du chlorure de vinyle avec l'acide vinyl-propylsulfonique.

Dans le présent travail nous nous sommes proposé de synthétiser les polyélectrolytes insolubles du type des copolymères du chlorure de vinyle avec du styrène, en partant du chlorure de polyvinyle modifié chimiquement.

On sait qu'à cause de la différence très grande entre les valeurs des constantes de copolymérisation r_1 et r_2 du chlorure de vinyle et du styrène, [15] on ne peut pas obtenir des copolymères du type chlorure de vinyle — styrène.

Teyssié et Smets[16] ont synthétisé des produits avec une composition chimique rapprochée de celle des copolymères du chlorure de vinyle avec du styrène (alkyl-styrène) par l'arylation du chlorure de polyvinyle avec des hydrocarbures aromatiques, en présence du chlorure d'aluminium anhydre.

La structure chimique du produit obtenu et le degré de substitution du chlorure dans la chaîne de chlorure de polyvinyle sont en fonction des conditions de synthèse.

Ces composés macromoléculaires constituent le point de départ dans la synthèse des nouveaux polyélectrolytes réticulés avec des groupements sulfoniques, présentés dans notre travail.

---

[5] P. D. Hooker, Brit. Pat. 942 814, 12 nov., 1963 ; *Chem. Abstr.*, **60**, 6997 (1964).

[6] M. Dima, I. Scondac, Ig. Poinescu, A. Carpov et Gh. V. Cotruţ, *Studii şi Cercetări Şti., Chim. Fil. Iaşi*, **14**, 233 (1963).

[7] Ig. Poinescu, I. Scondac et M. Dima, *Studii şi Cercetări Şti., Chim. Fil. Iaşi*, **14**, 255 (1963).

[8] I. Scondac, Ig. Poinescu et M. Dima, *Studii şi Cercetări Şti., Chim. Fil. Iaşi*, **14**, 265 (1963).

[9] M. Dima, I. Scondac, Ig. Poinescu, A. Carpov et Gh. V. Cotruţ, *Colecţia Omagiu Acad. Prof. Raluca Ripan*, **1966**, 213.

[10] A. Carpov, Ig. Poinescu, I. Scondac, Fl. Popescu, Gh. V. Cotruţ et M. Dima, *Studii şi Cercetări Chim. Acad.*, **13**, 555 (1965).

[11] M. Dima, I. Scondac, Gh. V. Cotruţ, A. Carpov et Ig. Poinescu, *Studii şi Cercetări Chim. Acad.*, **13**, 567 (1965).

[12] I. Scondac, Ig. Poinescu, A. Carpov, Gh. V. Cotruţ et M. Dima, *Studii şi Cercetări Chim. Acad.*, **13**, 659 (1965).

[13] M. Dima, I. Scondac, Ig. Poinescu et A. Carpov (travail non encore publié).

[14] Kiichi Takemoto, Michio Otsuda, Kimiaki Matsuoka et Minoru Imoto, *Chem. High Polymers (Japan)*, **23**, 574 (1966).

[15] E. C. Chapin, G. E. Ham et R. G. Fordyce, *J. Amer. Chem. Soc.*, **70**, 538 (1948).

[16] Ph. Teyssié et G. Smets, *J. Polymer Sci.*, **20**, 351 (1956).

PARTIE EXPÉRIMENTALE

Le chlorure de polyvinyle a été arylé avec du benzène selon la méthode indiquée par Teyssié et Smets, [16] à la température de 0°. En raison des conditions de réaction on a obtenu des produits à différents degrés de substitution du chlore, à partir de 0% (le chlorure de polyvinyle non substitué) jusqu'à 100% (totalement substitué).

Les polymères ainsi obtenus ont été sulfonés par l'acide chlorosulfonique , en présence du 1,2-dichloréthane, aux températures de 20° et 90°. L'opération de sulfonation a été effectuée dans un ballon à trois tubulures, muni de thermomètre, d'agitateur et de réfrigérant ascendant et fermé à l'aide d'un tube à chlorure de calcium anhydre. Après la sulfonation, on refroidit et on verse, sous agitation énergique et refroidissement extérieur, le contenu du ballon dans un becher contenant de l'eau refroidie. Ensuite, on rince le produit obtenu jusqu'à ce que l'acidité soit complètement éliminée. Les échangeurs d'ions *sous forme hydrogène* ont été séchés sous vide à 50° pendant 10 heures et puis caractérisés du point de vue physico-chimique.

Détermination de la teneur en chlore et en soufre. La minéralisation du polyélectrolyte réticulé a été réalisée par la méthode de combustion en oxygène, [17,18] le chlore étant dosé par voie potentiométrique. Le soufre est dosé par voie complexométrique. [19]

En comparant les valeurs de la teneur en soufre, déterminées par expérience, et les valeurs calculées de la capacité d'échange sulfonique, selon l'équation de Moralli, [20] on ne constate pas l'existence du soufre inactif.

Les capacités d'échange ont été déterminées par la méthode dynamique — en colonne — avec une solution de chlorure de calcium $2^0/_{00}$, pour la capacité d'échange sulfonique, $-K_{SO_3H}$, et avec une solution d'acétate de calcium $2^0/_{00}$, pour la capacité d'échange totale, $-K_T$, [21] qui représente la somme des capacités d'échange sulfonique et carboxylique. La détermination du calcium a été faite complexométriquement. [22] La différence entre la capacité d'échange totale et celle sulfonique donne la capacité d'échange carboxylique, $-K_{COOH}$.

RÉSULTATS ET DISCUSSIONS

Les résultats obtenus dans l'étude des paramètres de la synthèse (le rapport polymère/acide chlorosulfonique, la quantité de solvant, la température, la durée et la teneur en chlore du polymère) sont représentés dans les figures qui suivent.

Pour la sulfonation — à l'exception des épreuves appartenant à l'étude de l'influence de degré de substitution — on a utilisé le chlorure de polyvinyle préalablement arylé avec du benzène, dont la teneur en chlore après l'arylation était de 23,47%.

Capacité d'échange sulfonique, $-K_{SO_3H}$. En examinant la figure 1, on constate que la valeur de la capacité d'échange sulfonique

---

[17] W. Schöniger, *Mikrochim. Acta*, **1955**, 123 ; **1956**, 869.

[18] J. Haslam, J. B. Hamilton et D. C. Squirrell, *J. Appl. Chem.*, **10**, 97 (1960).

[19] N. H. Wilson, M. R. Pearson et M. D. Fitzgerald, *J. Appl. Chem.*, **4**, 488 (1958).

[20] T. G. Moralli, *J. Rech. C.N.R.S.*, **26**, 265, (1954).

[21] M. Dima et M. Mavrodin, *Studii şi Cercetări Şti., Chim. Fil. Iaşi*, **10**, 55 (1959).

[22] R. Pribil, « Complexonii în chimia analitică », Ed. Tehnică, Bucarest, 1961, p. 255.

est peu influencée par la quantité d'acide chlorosulfonique utilisé dans la réaction de sulfonation, à la température de 20°. La capacité d'échange croît de 2,65 méq/g pour le rapport polymère : acide chlorosulfonique 1 : 1, à 2,87 méq/g, pour le rapport polymère : acide chlorosulfonique 1 : 25.

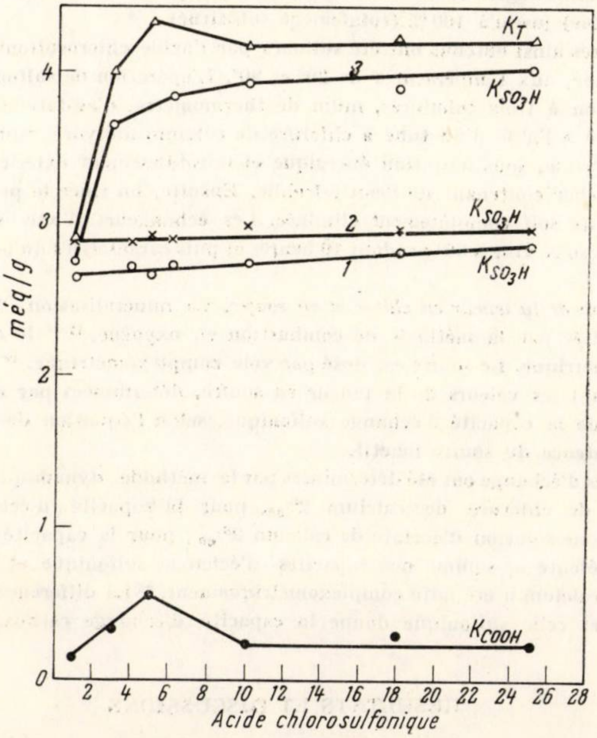

Fig. 1. — Influence de la quantité d'acide chlorosulfonique sur la capacité d'échange sulfonique, carboxylique et totale.
1, sulfonation à 20° pendant 6 heures; *2*, sulfonation à 20° pendant 8 heures; *3*, sulfonation à 90° pendant 6 heures.

Cet accroissement, exprimé en pourcentage, est approximativement de 8,3%. Il est probable que le groupement sulfonique se fixe seulement sur le noyau benzénique. Cette hypothèse est confirmée par les constatations suivantes :

— Le chlorure de polyvinyle ne réactionne pas avec l'acide chlorosulfonique (en présence du 1,2-dichloréthane) à la température de 20°.[6-8]

— Le copolymère styrène – divinylbenzène (8% DVB) est complètement sulfoné avec l'acide chlorosulfonique à la température de la chambre.[23]

La capacité d'échange sulfonique du polyélectrolyte réticulé est peu influencée par la durée de la sulfonation pour les mêmes rapports polymère : acide chlorosulfonique (figure 1, courbes *1* et *2*).

---

[23] R. M. Wheaton et L. E. McMahon (to Dow Chemical Co.), 3 133 030, 12 mai, 1964 ; *Chem. Abstr.*, **62**, 5407 (1965).

La réaction de sulfonation à température élevée (90°) est accompagnée d'autres réactions secondaires par exemple ; réactions d'oxydation-dégradation, la déhydrochloruration des segments de chaîne de chlorure de polyvinyle non substitué, cette dernière réaction étant très avancée.

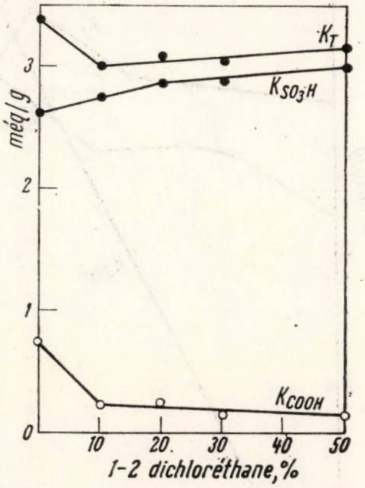

Fig. 2. — Influence de la quantité de solvant sur la capacité d'échange sulfonique, carboxylique et totale.

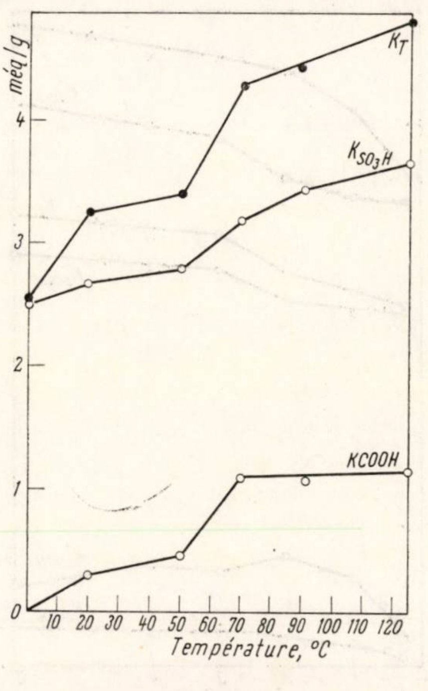

Fig. 3. — Influence de la température sur la capacité d'échange sulfonique, carboxylique et totale.

La capacité d'échange sulfonique est supérieure de plus d'une unité au cas antérieur (figure 1, courbe *3*). Cet accroissement de la valeur de la capacité d'échange sulfonique est dû aux réactions de sulfonation simultanée des noyaux benzéniques et des segments de chaînes de chlorure de polyvinyle non substitué du polymère. On remarque également dans le cas de la sulfonation à la température de 90°, comme une conséquence des réactions d'oxydation, la présence, dans les eaux de rinçage des échangeurs de cations, une quantité appréciable de substances solubles.

La capacité d'échange sulfonique dépend pratiquement très peu de la quantité de solvant qu'on a employée (figure 2). On remarque que la sulfonation du chlorure de polyvinyle arylé en présence du 1,2-dichloréthane freine les réactions secondaires d'oxydation-dégradation, la quantité de substances solubles diminuant à mesure que la quantité de solvant inerte augmente. La valeur de la capacité d'échange sulfonique est de 3,05 méq/g pour une concentration du polymère en 1,2-dichloréthane d'approximativement 4%.

Un autre paramètre qui influence beaucoup la valeur de la capacité d'échange sulfonique est la température (figure 3). L'influence de la température a été poursuivie pour l'intervalle de 0° jusqu'à 125°. La courbe qui représente la dépendance de la température a l'allure représentée sur la figure 3. La vitesse de la réaction de sulfonation, à la température au-dessus de 50°, croît beaucoup, comme une conséquence de la participation à la réaction de sulfonation aussi des unités de chlorure de vinyle. Dans la phase finale du processus de sulfonation (au-dessus de 90°), la vitesse de réaction croît très peu. Les échangeurs d'ions obtenus à la température de 125° ont la capacité d'échange sulfonique de 3,69 méq/g.

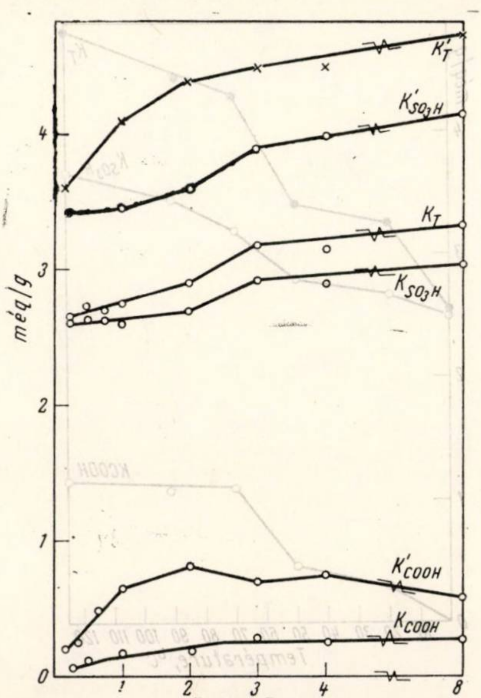

Fig. 4. — Influence de la durée (τ minutes) sur la capacité d'échange sulfonique, carboxylique et totale. sulfonation à 20° (K_{SO_3H}· K_{COOH}· K_T); sulfonation à 90° (K'_{SO_3H}· K'_{COOH}, K'_T).

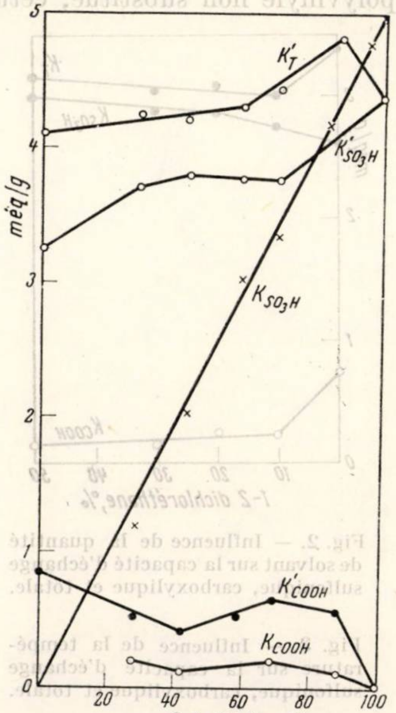

Fig. 5. — Influence du degré de substitution du chlore provenant du chlorure de polyvinyle aux noyaux benzéniques sur la capacité d'échange sulfonique, carboxylique et totale. sulfonation à 20° (K_{SO_3H}· K_{COOH}· K_T); sulfonation à 90° (K'_{SO_3H}· K'_{COOH}· K'_T).

L'influence de la durée du processus de sulfonation a été étudiée pour un intervalle d'approximativement 480 minutes aux températures de 20° et 90° (figure 4). Dans les deux cas on constate une dépendance presque linéaire entre la capacité d'échange sulfonique et la durée.

Pour les mêmes durées du processus de sulfonation, les valeurs des capacités d'échange sulfonique des échangeurs de cations obtenus par la sulfonation à 90° augmentent de 0,80—1,10 méq/g, par rapport aux produits sulfonés à 20°. Ceci s'explique par une sulfonation simultanée des noyaux benzéniques et de la chaîne aliphatique, mentionnée ci-dessus.

La dépendance de la capacité d'échange sulfonique du degré de substitution du chlorure de polyvinyle est très intéressante (figure 5).

Cette dépendance de la capacité d'échange sulfonique est marquée par une droite qui passe par l'origine. Par extrapolation de la droite à une substitution de 100% (le cas du chlorure de polyvinyle complètement substitué), on obtient la valeur de 5,0 méq/g, valeur caractéristique pour les échangeurs de cations obtenus par sulfonation du copolymère styrène-divinylbenzène (8% DVB). Pour conclure, la capacité d'échange peut être exprimée par l'équation

$$K_{SO_3H} = f\,(\text{substitution } \%)$$

Cette relation ne s'applique pas aux échangeurs de cations obtenus par sulfonation du chlorure de polyvinyle arylé avec du benzène, aux températures dépassant 20° (figure 5).

Capacité d'échange carboxylique, $-K_{COOH}$. Pendant la sulfonation du chlorure de polyvinyle arylé avec du benzène, apparaissent des groupements carboxylique, à côté des groupements sulfoniques, à cause des réactions d'oxydation. Ceux-ci ont été mis en évidence de manière indirecte — par échange ionique — avec une solution d'acétate de calcium

$$K_{COOH} = K_T - K_{SO_3H}$$

La capacité d'échange carboxylique dépend beaucoup de la température à laquelle a eu lieu le processus de sulfonation du polymère (figure 3).

La valeur de la capacité d'échange carboxylique, pour les échangeurs de cations par sulfonation à la température de 20° est d'approximativement 0,25 méq/g et monte jusqu'à 1,15 méq/g pour les produits sulfonés aux températures plus élevées (figure 3).

Capacité d'échange totale, $-K_T$. La valeur de la capacité d'échange totale $K_T = K_{SO_3H} + K_{COOH}$ dépend du degré de substitution du chlore du chlorure de polyvinyle et des conditions de synthèse (figures 3—5).

Titrage potentiométrique. Les déterminations potentiométriques pour établir les courbes de titrage ont été faites selon les méthodes connues, [24] les déterminations du pH étant effectuées 24 heures et sept jours plus tard. Pour l'Amberlite IR — 120 utilisé (comme témoin) les déterminations ont été effectuées seulement après 24 heures (figure 6).

L'allure des courbes confirme clairement la présence des groupements carboxyliques à côté des groupements sulfoniques. Entre les courbes tracées après 24 heures et sept jours, on remarque une différence dans la zone du pH 7—12, domaine où les groupements carboxyliques participent à la réaction d'échange d'ions. La réaction atteint l'équilibre après un intervalle de temps plus long. Avec l'accroissement du nombre des groupements carboxyliques les courbes de titrage ont aussi une inclinaison accentuée.

Tel que nous l'avons mentionné ci-dessus à côté de la réaction principale — la sulfonation — il y a aussi des réactions secondaires. Parmi celles-ci la déhydrochloruration du chlorure de polyvinyle arylé avec du benzène est très importante. Elle a lieu en même temps que le processus de sulfonation non seulement à des températures relativement élevées, mais aussi à la température de 20°. Les résultats expérimentaux sont

---

[24] F. Helfferich, «Ionenaustauscher», Band 1, Verlag Chemie, Weinheim, 1959, p. 84.

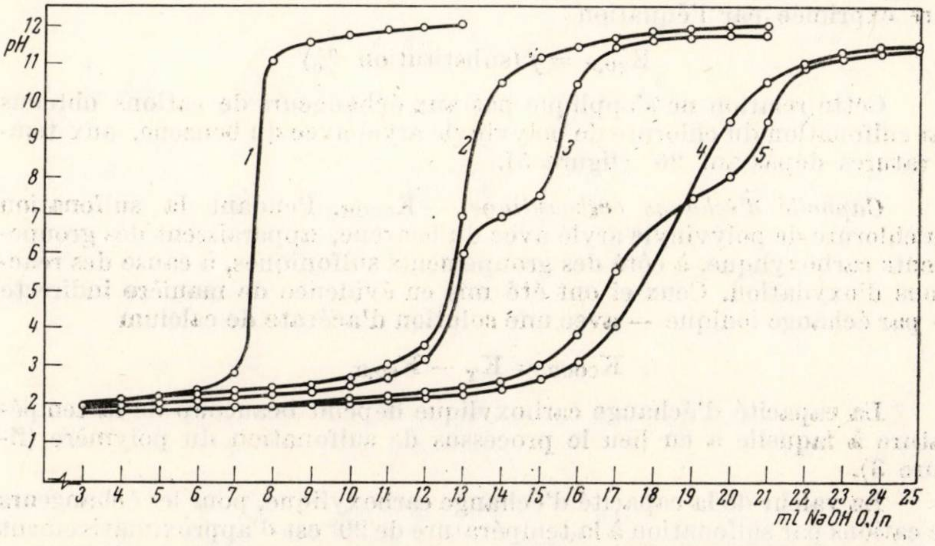

Fig. 6. — Courbes de titrage de l'échangeur de cations à base de chlorure de polyvinyle arylé avec du benzène.

1, courbe de titrage de l'échangeur de cations Amberlite IR—120 ; *2*, courbe de titrage de l'échangeur de cations synthétisé à 20°, après 24 heures ; *3*, courbe de titrage de l'échangeur de cations synthétisé à 20°, après sept jours ; *4*, courbe de titrage de l'échangeur de cations synthétisé à 90°, après 24 heures ; *5*, courbe de titrage de l'échangeur de cations synthétisé à 90°, après sept jours.

représentés graphiquement dans les figures 7—12. En examinant les figures, on peut conclure :

— Les pertes en chlore calculées en pour-cent dépendent beaucoup du rapport polymère : acide chlorosulfonique et sont maximales pour le rapport 1 : 6 (figure 7).

Egalement, pour le même rapport polymère : acide chlorosulfonique, les pertes en chlore sont beaucoup plus grandes si l'opération de sulfonation a été effectuée à une température élevée.

— Les pertes en chlore sont peu influencées par la quantité de solvant utilisé (figure 8).

— La variation des pertes en chlore en fonction de la température de sulfonation présente un point d'inflexion à 50° (figure 9). Ceci marque, probablement, la température à laquelle a lieu une modification de la vitesse de réaction durant le processus de déhydrochloruration. A cette température l'acide chlorosulfonique réagit avec le chlorure de polyvinyle en obtenant des polyélectrolytes réticulés avec des propriétés d'échange ionique. [6-8]

— Les réactions de déhydrochloruration dépendent de la durée du processus de sulfonation (figure 10). Les valeurs maximales de la déhydrochloruration sont obtenues après environ 4 heures à la température de 20° (33,66%, courbe *1*) et après 2,5 heures 3 à la température de 90° (85%, courbe *2*).

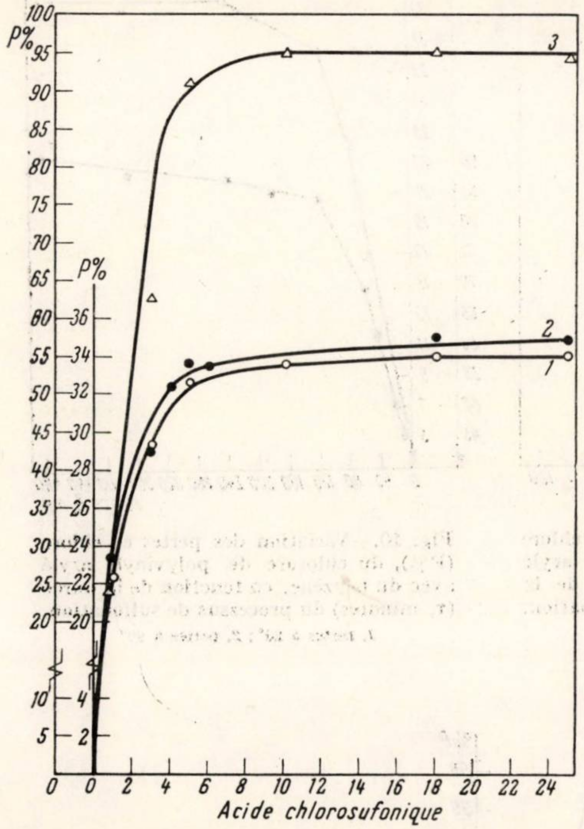

Fig. 7. — Variation des pertes en chlore (P%), du chlorure de polyvinyle arylé avec du benzène en fonction de la quantité d'acide chlorosulfonique.

1, température 20°, durée de la réaction de sulfonation six heures; *2*, température 20°, durée de la réaction de sulfonation huit heures; *3*, température 90°, durée de la réaction de sulfonation six heures.

Fig. 8. — Variation des pertes en chlore (P%), du chlorure de polyvinyle arylé avec du benzène, en fonction de la quantité de solvant.

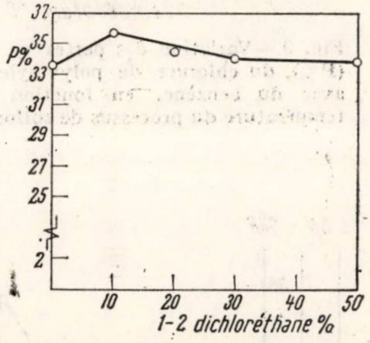

— Les pertes en chlore qu'on peut suivre dans la figure 11, sont les plus grandes quand le degré de substitution du chlorure de polyvinyle est de 58—70% (figure 11, courbe *1*). Les pertes en chlore ($\Delta P = Cl_i - Cl_f$), rapportées au degré de substitution pour les polyélectrolytes réticulés obtenus par sulfonation à 20°, se placent sur une droite (figure 11, droite 3), qui intersecte l'ordonnée à la valeur de 50, 61 et l'abscisse à la valeur de substitution de 100%. C'est le cas du chlorure de polyvinyle dont le chlore a été complètement substitué par des noyaux benzéniques.

— Les pertes en chlore, exprimées en pour-cent, ont été calculées par la formule

$$P\% = 100\left(1 - \frac{Cl_f\ \%}{Cl_i\ \%}\right)$$

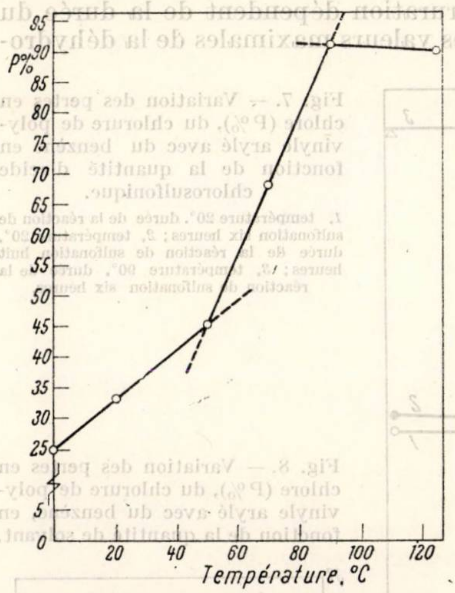

Fig. 9. — Variation des pertes en chlore (P%), du chlorure de polyvinyle arylé avec du benzène, en fonction de la température du processus de sulfonation.

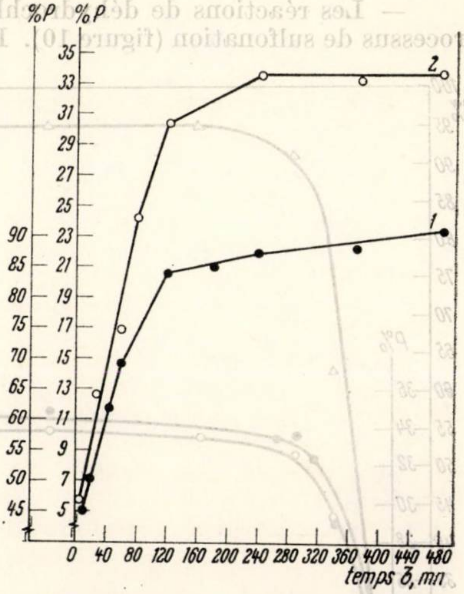

Fig. 10. — Variation des pertes en chlore (P%), du chlorure de polyvinyle arylé avec du benzène, en fonction de la durée (τ, minutes) du processus de sulfonation.

1, pertes à 20° ; 2, pertes à 90°

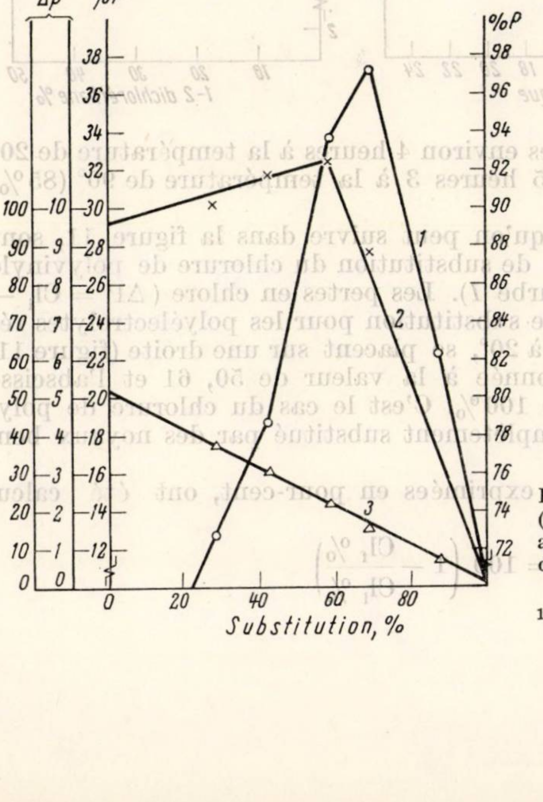

Fig. 11. — Variation des pertes en chlore (P%, ΔP), du chlorure de polyvinyle arylé avec du benzène, en fonction du degré de substitution du chlore provenu du chlorure de polyvinyle.

1, température 20° (P%) ; 2, température 90° (P%) ; 3, température 20° (ΔP).

où

Cl_i % = la teneur en chlore du polymère avant la réaction;

Cl_f % = la teneur en chlore du polymère après la réaction.

CONCLUSIONS

1. On a synthétisé de nouveaux échangeurs de cations, dont les capacités d'échange dépendent :

— du degré de substitution du chlore dans le chlorure de polyvinyle avec du benzène;

— des conditions de synthèse.

2. Les échangeurs de cations obtenus contiennent des groupements sulfoniques et des groupements carboxyliques.

3. Pendant le processus de sulfonation ont lieu des réactions d'oxydation-dégradation des chaînes macromoléculaires et la déhydrochloruration des segments de chaîne de chlorure de polyvinyle non substitué.

4. On a établi les conditions de synthèse des échangeurs de cations à base de chlorure de polyvinyle arylé avec du benzène.

Revue Roumaine de Chimie, **14**, 373–383 (1969)

Cl_i % = la teneur en chlore du polymère avant la réaction ;

Cl_f % = la teneur en chlore du polymère après la réaction.

CONCLUSIONS

1. On a synthétisé de nouveaux échangeurs de cations, dont les capacités d'échange dépendent :

— du degré de substitution du chlore dans le chlorure de polyvinyle avec du benzène ;

— des conditions de synthèse.

2. Les échangeurs de cations obtenus contiennent des groupements sulfoniques et des groupements carboxyliques.

3. Pendant le processus de sulfonation ont lieu des réactions d'oxydation-dégradation des chaînes macromoléculaires et la déshydrochloruration des segments de chaîne de chlorure de polyvinyle non substitué.

4. On a établi les conditions de synthèse des échangeurs de cations à base de chlorure de polyvinyle acylé avec du benzène.

Revue Roumaine de Chimie, **14**, 385–387 (1969)

FACTORS AFFECTING STABILITY AND EQUILIBRIA OF FREE RADICALS. IV[1]

t-BUTYL-CYANONITROXIDE

P. T. FRANGOPOL, MARIA FRANGOPOL, N. NEGOIŢĂ and A. T. BALABAN [2]
Institute of Atomic Physics, P.O.B. 35, Bucharest, Romania

Received October 9, 1968

The preparation and the ESR spectrum of the new free radical t-butyl-cyanonitroxide is described.

The importance of the electronic delocalization and of the steric shielding for the stability of free radicals, advocated in the preceding parts of the series, [1, 3, 4] has found some confirmations in the structure determination of α, α-diphenyl-β-picrylhydrazyl [5] and in the preparation of α, α-diphenyl-β-(2,4,6-tricarbomethoxy phenyl)-hydrazyl. [6]

1,2-Di-t-butyl-1,2-dicyanohydrazine (I) with the two bulky t-butyl groups in *s-trans* conformation can be constructed strain-free from molecular models, therefore it is expected that this compound would not dissociate at room temperature into free radicals. However, the corresponding nitroxide (IV) in which the sterically shielded nitrogen atom is bonded to donor and acceptor groups, is expected to be stable.

t-Butylcyanamide (III) [7–9] was prepared [10] from t-butylamine (II)[11] and cyanogen bromide. [12]

---

[1] Part III: A. T. Balaban, P. T. Frangopol, M. Frangopol and N. Negoiţă, *Tetrahedron*, **23**, 4661 (1967).

[2] Present address: International Atomic Energy Agency, Kärntnerring 11, Vienna 1010, Austria.

[3] A. T. Balaban, P. T. Frangopol, M. Mărculescu and I. Bally, *Tetrahedron*, **13**, 258 (1961).

[4] A. T. Balaban, M. Mărculescu, I. Pascaru, M. Rotaru, A. Valeriu and M. Weiner, *Z. physik. Chem. (Leipzig)*, **219**, 285 (1962).

[5] D. E. Williams, *J. Amer. Chem. Soc.*, **89**, 4280 (1967).

[6] D. Braun, G. Peschk and E. Hechler, *Chimia*, **21**, 536 (1967).

[7] T. Mukaiyama, S. Ohishi and M. Takamura, *Bull. Chem. Soc. Japan*, **27**, 416 (1954).

[8] E. Schmidt, D. Ross, J. Kittl and H. H. Von Düsel, *Liebigs Ann. Chem.*, **612**, 11(1958).

[9] N. M. Bortnick, U. S. Pat. 2, 606, 923, Aug. 12, 1952; *Chem. Abstr.*, **47**, 5432 (1953).

[10] R. Kitawaki, M. Yamashita and K. Sugino, *Nippon Kagaku Zasshi*, **78**, 567 (1957); *Chem. Abstr.*, **53**, 5124 (1959).

[11] K. N. Campbell, A. H. Sommers and B. K. Campbell, Org. Synth. Coll. Vol. 3, p. 148, 1955.

[12] W. H. Hartman and E. E. Dreger, Org. Synth. Coll. Vol. 2, p. 150, 1943.

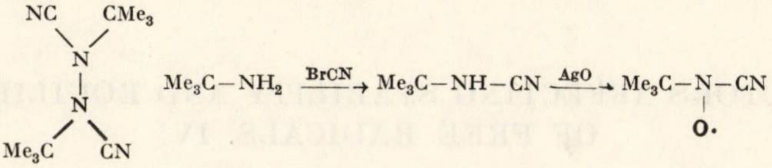

I II III IV

Attempts to oxidize (III) with lead dioxide,[3,4] silver oxide,[1] phosphowolframic acid and hydrogen peroxide failed; lead tetraacetate resulted in a very weak ESR signal. However, treatment of t-butylcyanamide (III) (0.2 ml) in 0.4 ml benzene with 50 mg silver (II) oxide[13] in a special vial[1] with 1 mm diameter of the tube inserted into the ESR cavity afforded a paramagnetic solution (half life about 10 min. at 28°). The ESR spectrum in deaerated solution (Fig. 1) is a triplet of triplets with equal intensity of all nine lines due to interaction of the odd electron with the two nitrogen nuclei. Coupling constants are 1.67 gauss for the cyano nitrogen and 9.34 gauss for the other nitrogen.

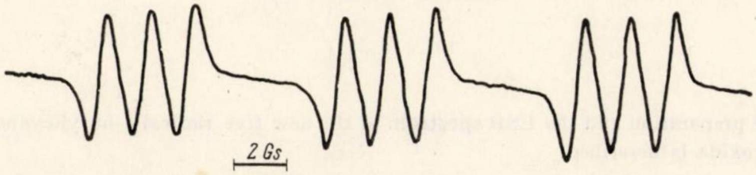

Fig. 1. — ESR spectrum of t-butyl-cyanonitroxide at 25° in deaerated benzene solution 1.5×10^{-3} moles/l. (Field decreases from left to right).

No hyperfine structure due to the coupling of the odd electron with the t-butyl protons[14–17] is apparent; the corresponding coupling constant must therefore be smaller than 0.1 gauss. The g-value of $2.0066 \pm$ ± 0.0003, determined by reference to sodium peroxylaminedisulphonate, clearly indicates[1,18–21] that the radical is t-butyl-cyanonitroxide (IV), and not t-butyl-cyano-nitrogen formed by dissociation of (I), when the g-factor would have been lower than 2.004.

---

[13] L. Syper, *Tetrahedron Letters*, 4193 (1957).

[14] C. Trapp, C. A. Tyson and G. Giacometti, *J. Amer. Chem. Soc.*, **90** 1394 (1968).

[15] C. Lagercrantz and S. Forshult, *Nature*, **218**, 1247 (1968).

[16] J. T. Weil and J. J. Windle, *ibid.*, **217**, 842 (1968).

[17] C. Lagercrantz and K. Torssell, *Arkiv Kemi*, **29**, 203 (1968).

[18] A. T. Balaban, P. J. Halls and A. R. Katritzky, *Chem. and Ind.*, 651 (1968).

[19] J. H. Osiecki and E. F. Ullman, *J. Amer. Chem. Soc.*, **90**, 1074 (1968).

[20] K. Volkamer, H. Baumgärtel and H. Zimmermann, *Angew. Chem.*, **79**, 941 (1967).

[21] H. Lemaire, Y. Marechal, R. Ramasseul and A. Rassat, *Bull. Soc. Chim. France*, **372** (1965).

The similar formation of diarylnitroxide free radicals on oxidation of darylamines is well documented.[22–28]

The oxidation of methylcyanamide in analogous conditions failed to afford a stable free radical. The investigation of other cyanamides withont hydrogen attached to the carbon bonded to the nitroxide group (cf. diarylnitroxides,[27–29] di-t-butylnitroxide[30] and aryl-t-butylnitroxides[27,31,32]) is under way.

Acknowledgement. Thanks are expressed to prof. dr. Erich Schmidt (München) for a sample of t-butylcyanamide, to dr. I. Pascaru (Bucharest) for ESR spectrum and discussions and to dr. Friedrich Bär (Marburg/Lahn) for a high resolution ESR spectrum.

---

[22] R. Hoskins, *J. Chem. Phys.*, **25**, 788 (1956).

[23] K. Hirota and I. Kagayama, *Bull. Chem. Soc. Japan*, **36**, 875 (1963).

[24] J. R. Thomas and C. A. Tolman, *J. Amer. Chem. Soc.*, **84**, 2930 (1962).

[25] G. A. Abakumov, A. A. Abramova and G. A. Razuvaev, *Doklady Akad. Nauk, S.S.R.*, **163**, 579 (1936)

[26] A. L. Buchachenko, *Optika i Spektroskopia*, **13**, 795 (1962).

[27] G. Chapelet-Letourneux, H. Lemaire and A. Rassat, *Bull. Soc. Chim. France*, 3283 (1965).

[28] F. A. Neugebauer and P. H. H. Fischer, *Chem. Ber.*, **98**, 844 (1965); *Z. Naturforsch.*, **21** b, 1036 (1966);
P. H. H. Fischer and F. A. Neugebauer, *ibid.*, **19**a, 1514 (1964).

[29] Y. Deguchi, *Bull. Chem. Soc. Japan*, **35**, 260 (1962).

[30] A. K. Hoffmann, W. G. Hodgson and W. H. Jura, *J. Amer. Chem. Soc.*, **83**, 4675 (1961);
A. K. Hoffmann and A. T. Henderson, *ibid.*, 4671;
A. K. Hoffmann, A. M. Feldman, E. Gelbum and W. G. Hodgson, *ibid.*, **86**, **639** (1964).

[31] A. Calder and A. R. Forrester, *Chem. Commun.*, 682 (1967).

[32] H. Lemaire, A. Rassat and A. M. Ravet, *Bull. Soc. Chim., France*, 1380 (1963).

Revue Roumaine de Chimie, 14, 385–387 (1969)

Revue Roumaine de Chimie, **14**, 389–394 (1969)

DÉTERMINATION DES CONSTANTES DE DISSOCIATION DE CERTAINES 1-ALCOYL-3,5-BIS-(*p*-DIALCOYLAMINO-BENZYLIDEN)-4-PIPÉRIDONES EN SOLUTION AQUEUSE

C. GREFF et S. MOLDOVEANU

Université de Bucarest, Faculté de Chimie, Laboratoire de Chimie organique et de Chimie analytique, 89, Spl. Independenţei

Reçu le 6 novembre 1967

Dans ce travail on détermine les constantes de dissociation de certaines 1-alcoyl-3,5-bis-(*p*-dialcoyl-amino-benzyliden)-4-pipéridones, en solution aqueuse, par une méthode spectrophotométrique. L'erreur des déterminations pour les valeurs pK_a est comprise entre ± 0,01 et ± 0,04.

Dans la littérature , on connaît de nombreuses méthodes pour la détermination des constantes de dissociation des bases organiques. [1-3]

Le présent travail s'occupe de la détermination des constantes de dissociation des composés I—IV [4, 5]

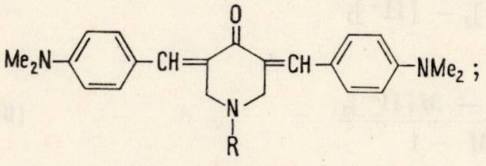

I R = Et
II R = n-Bu

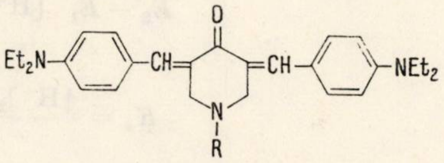

III R = Et
IV R = n-Bu

Ces composés sont différemment colorés pour les valeurs diverses du pH, se comportant donc comme des indicateurs, ce qui a permis de faire la détermination des constantes de dissociation par la méthode spectrophotométrique, en accord avec la méthode de Colleter. [6]

---

[1] B. B. Owen, *J. Amer. Chem. Soc.*, **60**, 2229 (1938).
[2] R. G. Bates, *J. Amer. Chem. Soc.*, **70**, 1579 (1948).
[3] H. v. Halban et J. Brül, *Helv. Chim. Acta*, **27**, 1719 (1944).
[4] N. Bărbulescu et C. Greff, *Rev. Chim.* (*Bucureşti*), **17**, 202 (1966).
[5] N. Bărbulescu, C. Greff et N. Giurescu (non publié).
[6] J. C. Colleter, « Thèse», Paris, 1964.

La méthode est basée sur les considérations suivantes :

Si une base B est dissoute dans l'eau, un équilibre s'établit entre la forme B et son acide conjugué BH$^+$

$$BH^+ (aq.) \rightleftharpoons B + H^+ (aq.)$$

d'où :

$$K_a = \frac{[B] \cdot [H^+]}{[BH^+]} \tag{1}$$

Si les formes B et BH$^+$ sont colorées, par le choix d'une longueur d'onde convenable, elles absorberont les radiations choisies suivant la loi de Lambert-Beer. Dans ce cas, pour l'extinction E on a la relation (2)

$$E_\lambda = \varepsilon_{(B)} \cdot [B] \cdot l + \varepsilon_{(BH^+)} \cdot [BH^+] \cdot l \tag{2}$$

où on peut prendre, arbitrairement, $l = 1$.

Si dans la solution la concentration de la base est c, c'est-à-dire

$$[B] + [BH^+] = c \tag{3}$$

alors, en partant des relations (1), (2) et (3), on obtient

$$E_\lambda = \varepsilon_{(BH^+)} c - c\,(\varepsilon_{(BH^+)} - \varepsilon_{(B)}) \cdot \left(1 + \frac{[H^+]}{K_a}\right)^{-1} \tag{4}$$

La relation (4) contient trois inconnues : $\varepsilon_{(B)}$, $\varepsilon_{(BH^+)}$ et K_a. En attribuant trois valeurs à $[H^+]$ et en lisant les valeurs correspondantes d'E- on obtient un système de trois équations à trois inconnues, d'où il résulte

$$\frac{E_3 - E_1}{E_2 - E_1} \cdot \frac{[H^+]_2 - [H^+]_1}{[H^+]_3 - [H^+]_1} = M \tag{5}$$

e

$$K_a = \frac{[H^+]_2 - M[H^+]_3}{M - 1} \tag{6}$$

PARTIE EXPÉRIMENTALE

Par l'augmentation de la valeur du pH pour les solutions aqueuses des composés I—IV, on constate que de l'incolore, la couleur passe dans un milieu fortement acide, au rouge, ensuite au jaune-orange, pour qu'enfin, dans un milieu basique la couleur devienne jaune, verdâtre, avec une forte fluorescence verte.

En effectuant les spectres d'absorption sur un spectrophotomètre Beckmann, modèle DB, on a constaté que ces composés présentent trois maximums d'absorption à 498 mμ, 472 mμ et 435 mμ et trois points isosbestiques à 362 mμ, 455 mμ et 488 mμ.

L'existence de ces trois points isosbestiques indique l'existence de quatre formes, ce qui est en concordance avec nos expectatives car les composés I—IV possèdent trois atomes azote, donc les formes B, BH$^+$, BH$_2^{2+}$ et BH$_3^{3+}$ peuvent exister.

Dans ce cas nous aurons trois constantes K_a, à savoir

$$K_{a_1} = \frac{[B]\cdot[H^+]}{[BH^+]} \tag{7}$$

$$K_{a_2} = \frac{[BH^+]\cdot[H^+]}{[BH_2^{2+}]} \tag{8}$$

$$K = \frac{[BH_2^{2+}]\cdot[H^+]}{[BH_3^+]} \tag{9}$$

Ces trois constantes ont été déterminées conformément aux relations (5) et (6), en supposant que dans la solution il n'y avait pas plus de deux formes à la fois. Cette supposition est basée sur les différences importantes entre les valeurs du pH où on a constaté des changements de couleur et elle a prouvé sa justesse par la constance des valeurs K_a.

Pour déterminer les constantes K_a, on a effectué la lecture des extinctions pour chaque valeur des maximums d'absorption sur un spectrophotomètre Carl Zeiss VSU 1, à des valeurs différentes du pH, mesurées à un pH-mètre du type MV 11 S. Le mesurage a été effectué à la température de 23°. On a étalonné le pH-mètre approximativement aux valeurs auxquelles, par des essais préliminaires, on a constaté l'intervention de l'inflexion de la courbe caractéristique des composés I–IV, ayant le caractère d'indicateurs.

Si pour la courbe caractéristique d'un indicateur, représentée par la relation (4), on note $[H^+] = 10^{-pH}$, $\varepsilon_{(B)}\cdot K_a\cdot c = b$ et $\varepsilon_{(BH^+)}\cdot c = a$, on obtient

$$E = \frac{a.10^{-pH} + b}{10^{-pH} + K_a} \tag{10}$$

qui est l'équation de la courbe de dépendance E – pH, c'est-à-dire la courbe de l'indicateur. En partant de la relation (10), on peut écrire

$$E' = (b - a\cdot K_a)\cdot \ln 10 . \frac{10^{-pH}}{(10^{-pH} + K_a)^2} \tag{11}$$

et

$$E'' = (b - a\cdot K_a)\cdot(\ln 10)^2 \cdot \frac{10^{-pH}\cdot(10^{-pH} - K_a)}{(10^{-pH} + K_a)^3} \tag{12}$$

On constate donc que la seconde dérivée de E, par rapport au pH, est annulée pour $K_a = 10^{-pH}$, ce qui indique le fait que pour la valeur pH = pK_a il existe une inflexion de la courbe.

Par l'étalonnage du pH-mètre aux valeurs pH = 2,8, 3,4, 4,8, 5,4 et 9,4, on est arrivé à une erreur de moindre importance dans la détermination du pH.

Pendant les déterminations, la teneur ionique des solutions a été maintenue relativement constante en leur ajoutant du chlorure de potassium, la concentration des solutions étant 0,2 M KCl.

La concentration des solutions des indicateurs a été de 10 mg/l, au maximum, à cause de la faible solubilité des formes B et BH^+ dans l'eau.

Les courbes caractéristiques des quatre indicateurs, pour un intervalle pH = 1–4, sont représentées dans la figure 1, pour le pH = 4–7 dans la figure 2 et pour le pH = 8–11 dans la figure 3.

En partant des valeurs de ces courbes, on a déterminé les valeurs – log K_a, c'est-à-dire pK_a, représentées dans le tableau 1.

Tableau

Valeurs des pK_{a1}, pK_{a2}, pK_{a3}

Détermination	Composé I			Composé II		
	pK_{a3}	pK_{a2}	pK_{a1}	pK_{a3}	pK_{a2}	pK_{a1}
1	2,86	4,80	9,40	2,87	4,81	9,48
2	2,82	4,86	9,46	2,82	4,86	9,40
3	2,85	4,87	9,30	2,80	4,85	9,46
4	2,80	4,75	9,52	2,84	4,81	9,36
5	2,78	4,80	9,45	2,80	4,76	9,30
6	2,81	4,83	9,32	2,78	4,83	9,41
7	2,85	4,79	9,33	2,79	4,86	9,32
8	2,79	4,86	9,50	2,86	4,78	9,35
Moyenne	**2,82±0,01**	**4,82±0,015**	**9,41±0,04**	**2,82±0,01**	**4,82±0,015**	**9,39±0,04**

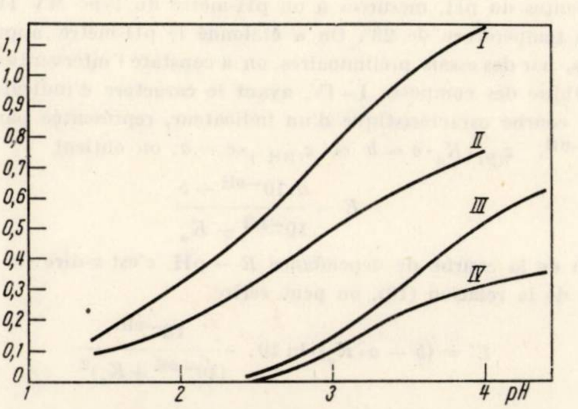

Fig. 1. — Courbes caractéristiques des composés :

I, concentration 10 mg/l
II, concentration 7,2 mg/l
III, concentration 6,8 mg/l
IV, concentration 5 mg/l
} au pH = 1–4

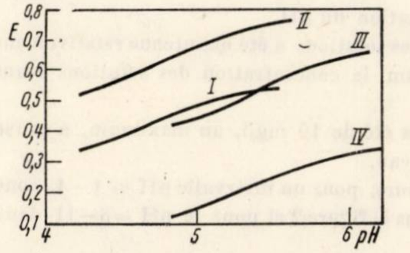

Fig. 2. — Courbes caractéristiques des composés :

I, concentration 5,5 mg/l
II, concentration 7 mg/l
III, concentration 10,8 mg/l
IV concentration 5 mg/l
} au pH = 4–7

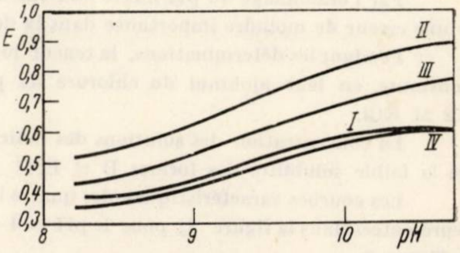

Fig. 3. — Courbes caractéristiques des composés :

I, concentration 5 mg/l
II, concentration 7 mg/l
III, concentration 6,8 mg/l
IV, concentration 5 mg/l
} au pH = 8–11

1
our les composés I–IV, à 23°

Composé III			Composé IV		
pK_{a3}	pK_{a2}	pK_{a1}	pK_{a3}	pK_{a2}	pK_{a1}
3,40	5,28	9,42	3,47	5,40	9,41
3,40	5,40	9,48	3,40	5,41	9,49
3,42	5,42	9,52	3,42	5,29	9,33
3,46	5,39	9,34	3,40	5,36	9,55
3,47	5,41	9,38	3,47	5,40	9,29
3,40	5,39	9,29	3,49	5,36	9,41
3,41	5,44	9,41	3,39	5,40	9,42
3,48	5,31	9,38	3,40	5,50	9,31
3,43±0,015	5,38±0,02	9,40±0,03	3,43±0,015	5,39±0,02	9,40±0,03

CONCLUSIONS

En comparant les données du tableau 1, on constate que les deux constantes, pK_{a_2} et pK_{a_3} sont dues aux groupements aminiques tertiaires attachés aux noyaux benzéniques, et la constante, pK_{a_1} est due à l'atome azote hétérocyclique.

En se basant sur les données expérimentales, on peut considérer que dans les solutions des substances I–IV on trouve les équilibres suivants.

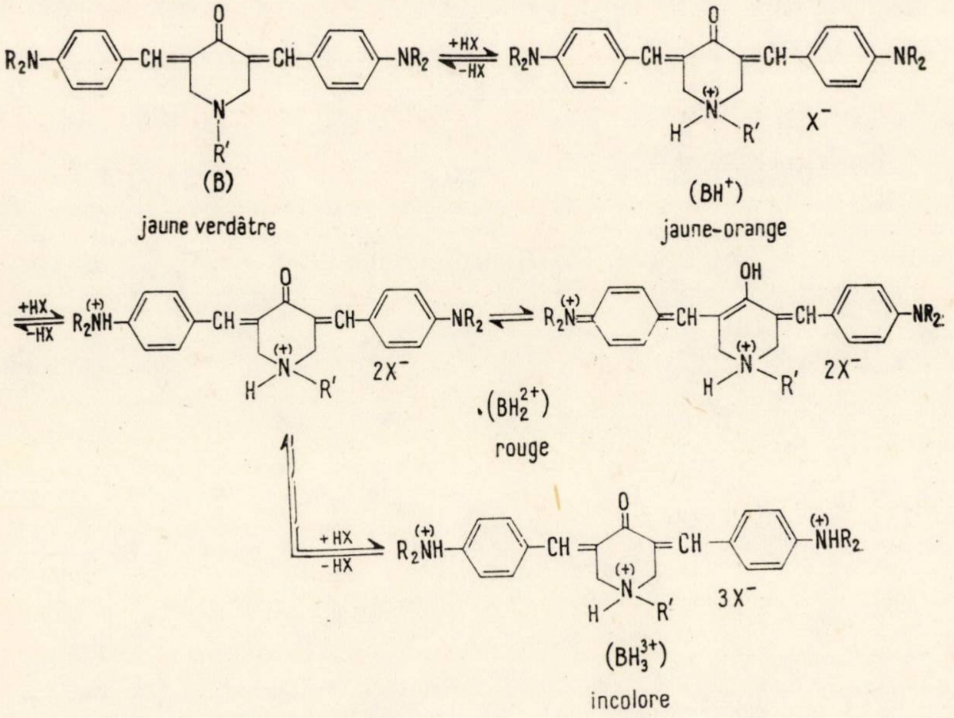

On constate, aussi, que par l'augmentation du radical aliphatique du groupement aminique attaché au noyau benzénique, les constantes de dissociation varient sensiblement, tandis que l'amplification du radical aliphatique attaché à l'atome azote hétérocyclique n'a pas d'influence sur la constante de dissociation, la valeur pK_{a_1} étant pratiquement la même pour les quatre substances.

Revue Roumaine de Chimie, **14**, 395–398 (1969)

ACETOACETANILIDES. II[1]

PREPARATION OF SOME ACETOACETANILIDES AND DERIVATIVES

I. I. BĂDILESCU

Research Department, Petrochemical Works, Pitești

Received April 29, 1968

The preparation of some substituted acetoacetanilides and derivatives is described. A modified synthesis for several acetoacetanilides is presented.

In a previous paper[1] the preparation of *p*-iodo-acetoacetanilide was described. In this paper, we wish to report the preparation of both unreported *meta*- and *ortho*-iodoacetoacetanilides, and also the preparation of some other substituted acetoacetanilides and derivatives.

The procedure of Fierz-David and Ziegler[2] for acetoacetylation of aromatic amines was used in this work for the preparation of most substituted acetoacetanilides. This procedure (*A*) leads to pure compounds and good yields (Table 1). However, using this procedure, from *o*-iodoaniline and ethyl acetoacetate in xylene, a complex mixture was obtained from which the attempted *o*-iodoacetoacetanilide was isolated in poor yield. Alternatively, when *o*-iodoaniline was added to boiling, freshly distilled, ethyl acetoacetate (molar ratio 1 : 10) which contains three drops of pyridine, the mixture heated at 150–160° for further ten minutes, then cooled and the excess ethyl acetoacetate removed in vacuo, *o*-iodoacetoacetanilide was obtained in high yield. This procedure (*B*) was also used for the preparation of some acetoacetanilides and the results are recorded in table 1.

For both *A* and *B* procedures we have noted that high yields of acetoacetanilide are obtainable when the resulted ethyl alcohol was removed by continuous distillation, using a five to twenty fold amount of diluent and freshly purified materials, and when the arylamine solution was slowly added to the ethyl acetoacetate. The above observations are in

---

[1] I. Bădilescu, *Rev. Roumaine Chim.*, **9**, 887 (1964). *Studii și Cercetări Chim., Acad. R. S. România*, **13**, 931 (1964).

[2] H. E. Fierz-David and E. Ziegler, *Helv. Chim. Acta*, **11**, 776 (1928).

Table 1

Acetoacetanilides and their copper complexes

Substituent	Procedure	Yield	M.p.*)	Lit. m.p. °C	Copper complex		
		%	°C		Colour	Decopn. p. °C	Lit. decopn. p. °C
None (H)	A B	87 93	85.5a)	85–86 [2,3]	olive-green	212	212 [4,5]
o-CH_3	A	83	106.5b)	106 ; 107 [2]	green	160–162	161–163[5]
m-CH_3	A	58	59–60c)	57–58 [6]	dark-green	194	192 [4,5]
p-CH_3	A	91	95–95.5b)	94–96 [2,6]	green	220	220 [4,5]
o-Cl	B	94	105–106d)	107–108 [2,6,7]	green	215	—
m-Cl	A	90	106.5d)	105–106 [7]	dark-green	223–234	—
p-Cl	A	94	133–133.5c)	132–133 [6,7,8]	green	234	232–233[5]
o-Br	B	85	83.5d)	86 [8]	green	200	—
m-Br	A	91	107–109d)	108–110 [6]	green	217–218	—
p-Br	A	90	140–141c)	137–138 [6]	green	222	223–225[5]
o-J	B	94	83–84.5e)	—	green	216	—
m-J	A	64	109.5–110a)	—	green	219	—
p-J	A	72	144.5a)	144.5 [1]	dark-green	224 [1]	224 [1]
	B	79	143–144d)				
p-NO_2	A	32	124.5c)	123–124 [2,6,7]	yellow	251	250–252[5]
p-OC_2H_5	A	60	105–106c)	101–102 [9]	light-green	209–210	—
p-OC_6H_5	A	71	98d)	96 [10]	olive-green	216	—
p-$COCH_3$	A	35	117–118c)	110 [6]	green	219	
bis-(*o*-tolidin)	A	96	204.5f)	204–205 [11]	—	—	—

*) Recrystallization solvents : *a)* EtOH, *b)* $(Et)_2O$, *c)* C_6H_6, *d)* xylene, *e)* ligroine and *f)* acetone.

agreement with the results of Talpade and Gadgil [12–14] which have shown that the rate of acetoacetarylide formation decreases in the presence of

---

[3] H. Pfeiffer, *J. prakt. Chem.*, **111**, 240 (1925).

[4] L. Wolf and K. Wetzel, *Chem. Ber.*, **90**, 1007 (1957).

[5] H. O. Chaplin and L. Hunter, *J. Chem. Soc.*, **1939**, 484.

[6] L. Monti and V. Cirelli, *Gazz. chim. ital.*, **66**, 723 (1936).

[7] G. V. Jadhav, *J. Indian Chem. Soc.*, **7**, 669 (1930).

[8] Y. Hamada, H. Sugihara and T. Isobe, *Yakugaku Zasshi*, **82**, 1592 (1962).

[9] S. Arikawa, A. Kashioka and T. Kawamata, *Yûki Gôsei Kagaku Kyôkaishi*, **16**, 29 (1958) ; *Chem. Abstr.*, **52**, 6272 (1958).

[10] A. Arcoria, *Boll. sedute Accad. Gioenia Sci. Nat. Catania* [4], **4**, 304 (1958).

[11] A. Zitscher and R. Schmitt, **U.S. 1, 594, 864**, *Aug. 3, 1926* ; *Chem. Abstr.*, **20**, 3822 (1926).

[12] C. R. Talpade and L. H. Gadgil, *J. University Bombay*, **28**, 32 (1959).

[13] C. R. Talpade and L. H. Gadgil, *J. University Bombay*, **29**, 20 (1961).

[14] C. R. Talpade and L. H. Gadgil, *J. University Bombay*, **29**, 27 (1961).

water, ethyl alcohol and of the synthesized acetacetarylide itself. Indeed, the different products obtained by the interaction of an aromatic amine and ethyl acetoacetate are : (*i*) — ethyl β-arylaminocrotonate ($CH_3C(NHR):CH{\cdot}COOC_2H_5$), (*ii*) — acetoacetarylide ($CH_3CO{\cdot}CH_2{\cdot}CO{\cdot}NHR$), and (*iii*) — β-arylamino-crotonarylamide ($CH_3C(NHR):CH{\cdot}CO{\cdot}NHR$), (where R is an aromatic nucleus). It is obvious that the presence of ethyl alcohol in the reaction mixture favoures the formation of (*i*) but an arylamine excess and the presence of acetoacetarylide (*ii*) leads to compounds of type (*iii*).

The course of the reaction is also influenced by the nature of the substituent and its position in the aromatic nucleus. Thus, *p*-nitro,- and *p*-acetyl-aniline react slowly with ethyl acetoacetate and give mixtures containing about 20—35% of the corresponding acetoacetanilide. Alternatively, *o*-nitro-acetoacetanilide could not be isolated from the reaction mixture which was obtained by a standard treatment of *o*-nitroaniline with ethyl acetoacetate. Similar results were reported by several workers [2,6,15] and the following order of reactivity of anilines can be noticed :

$$CH_3 > H > OC_2H_5 > OC_6H_5 > Cl > Br > J > COCH_3 > NO_2.$$

The *ortho* substituted anilines are not taken into consideration, since in *ortho* compounds steric hindrance is operative and the behaviour of *ortho* substituted anilines could be explained on the basis of steric hindrance and the formation of chelated rings by hydrogen bonds. However, the general order of activity is : *para* > *meta* > *ortho*.

Some substituted *bis*- (acetoacetanilidato) copper compounds were therefore obtained from copper acetate and the corresponding acetoacetanilide by the procedure of Hunter and Chaplin. [5] The structure of such complexes is well established to be all-oxygen-coordinated; the oxygen is the only coordinating element in complexes of acetoacetamide derivatives, and the nitrogen is not bonded to copper. [16–19] Accordingly, preliminary results of a study of the infrared spectra [20] of such compounds, give strong evidence for the above mentioned all-oxygen-coordination.

EXPERIMENTAL

Table 1 contains the data on the acetoacetanilides prepared. Freshly purified materials were used in all the cases and the purity of ethyl acetoacetate and xylene was proved by v.p.c. Melting and decomposition points recorded in the table are uncorrected. The preparation of *m*-iodo-and *o*-iodo-acetoacetanilide are representative for both *A* and *B* procedures.

---

[15] W. A. Sexton, *J. Chem. Soc.*, **1942**, 303.

[16] R. L. Belford, A. E. Martell and M. Calvin, *J. Inorg. Nuclear Chem.*, **2**, 11 (1956).

[17] H. J. Harries, *J. Inorg. Nuclear Chem.*, **25**, 519 (1963).

[18] E. P. Dudek and M. Barber, *Inorg. Chem.*, **5**, 375 (1966).

[19] E. P. Dudek and M. L. Snow, *Inorg. Chem.*, **5**, 395 (1966).

[20] S. Bădilescu and I. Bădilescu, (in preparation).

Procedure A. *m-Iodoacetoacetanilide.* A mixture of 4.3 g (0.033 mole) of ethyl acetoacetate, 20 ml of xylene and three drops of pyridine (as catalyst), was heated at 135–138° and then a solution of 6.57 g (0.03 mole) of *m*-iodoaniline (Schuchardt, *puriss.*) in 50 ml of xylene was dropwise added to the boiling mixture at a rate which assures a slow distillation, over half an hour, of excess xylene and the resulting ethyl alcohol. The reaction mixture was heated under reflux for further two hours, cooled, and the product filtered off, washed with xylene and recrystallized to give 5.85 g (64%) of *m*-iodoacetoacetanilide, m.p. 108–109.5°.

An analytical sample, melting at 109.5–110.0°, is obtained by twice recrystallization from ethyl alcohol.

Calculated for $C_{10}H_{10}INO_2$, (M.W. 303.1); C, 39.63%, H, 3.32%, N, 4.62%.
Found : C, 40.20%, H, 3.40%, N, 5.00%.

2,4-Dinitrophenylhydrazone, orange needles, m.p. 186.0–186.5° (from EtOH). *Found* : N, 14.81 %, $C_{16}H_{14}IN_5O_5$ *requires:* N, 14.46%.

Procedure B. *o-Iodoacetoacetanilide.* A solution of 1 g of *o*-iodoaniline (Schuchardt, *puriss.*), in 5 ml of freshly distilled ethyl acetoacetate, is added dropwise, during ten minutes, to 5 ml boiling ethyl acetoacetate which contains three drops of pyridine. The resulting ethyl alcohol is removed by distillation continuously. The reaction mixture is heated for further ten minutes at 150–160° then cooled to 100° and the excess ethyl acetoacetate removed in vacuo. By cooling 1.4 g of crude product is obtained which by recrystallization from ligroine gives 1.26 g (94%) of *o*-iodoacetoacetanilide as needles, melting at 83.0–83.5°.

Further recrystallization from ligroine gives an analytical sample m.p. 83.5–84.5°

Calculated for $C_{10}H_{10}INO_2$, (M.W. 303.1): C, 39.63%, H, 3.32%, N, 4.62%.
Found : C, 40.10%, H, 3.20%, N, 4.86%.
2,4-Dinitrophenylhydrazone, m.p. 181° (orange needles).
Found: N, 14,21 %. $C_{16}H_{14}IN_5O_5$ *requires* : N, 14.46 %

Cupric complexes of acetoacetanilides. [5]

Copper acetate (1.0 g), dissolved in the least amount of water, was poured into a warm alcoholic solution of acetoacetanilide (1.8–3.0 g). A green granular deposit soon formed, which crystallized from acetone, methylpropylketone or dioxan-methylpropylketone mixtures.

Cupric complexes are very soluble in dioxane, pyridine, N-methyl-2-pyrrolidone, forming green solutions. It was slightly soluble in benzene, chloroform, ether and alcohol, fairly soluble in acetone and methylpropylcetone.

Revue Roumaine de Chimie, **14**, 399–403 (1969)

PREPARATION OF 3α,6α-DIHYDROXY-5β-ETIANIC ACID AND ITS CONVERSION INTO METHYL 3β-THIOCYANO- AND 3β-ISOTHIOCYANO-Δ^5-ETIENATE

F. HODOŞAN and N. ŞERBAN

Institute of Chemistry of the Academy, Cluj, Str. Donath 59–65

Received April 22, 1968

The degradation of 5β-pregnane-3α,6α-diol-20-one via the 21-benzylidene derivative gave 3α,6α-dihydroxy-5β-etianic acid along with 5β-androstane-3α,6α-diol-17-one. Methyl 3α,6α-ditosyloxy-5β-etianate treated with potassium thiocyanate in dimethylformamide yielded methyl 3β-thiocyano- and 3β-isothiocyano-Δ^5-etienate as well as methyl $\Delta^{3,5}$ -etiadienate.

There are no data in the literature concerning the degradation of 5β-pregnane-3α,6α-diol-20-one (I) into the corresponding etianic acid III, except a mention encountered in the abstract of a US patent elaborated by Marker;[1] it reports only the melting point of the presumed end-product.

Being interested in the preparation of the etianic acid III, we converted 5β-pregnane-3α,6α-diol-20-one (I) into the corresponding 21-benzylidene derivative II. The latter could not be purified by the usual methods and was transformed into the readily crystallizable diacetate IIa.

Oxidation of compound IIa with chromic acid in acetic acid at 65–70° and subsequent hydrolysis gave a mixture of two substances. One of them had m.p. 315–317° and was found to possess acidic properties. It could be converted into a methyl ester and thereafter into a ditosylate. These results, corroborated with the elemental analyses data and IR absorptions, demonstrated that this oxidation product is 3α,6α-dihydroxy-5β-etianic acid (III); accordingly, its above-mentioned derivatives must have the formulae IIIa and IIIb.

The second compound isolated had m.p. 250°; its chemical and spectral properties pointed to the presence of a keto group in a cyclopentane ring. This compound was found to be identical with 5β-androstane-3α,6α-diol-17-one (IV), already prepared by one of us following a quite different route.[2] The formation of this ketone is very probably due to the partial enolization of the side chain as follows:

$$\rangle CH-CO-CH=CH-C_6H_5 \rightleftarrows \rangle C=C(OH)-CH=CH-C_6H_5$$

---

[1] R. E. MARKER, U.S. **2,337,563**; *Chem. Abstr.*, **38**, 3423 (1944).

[2] F. HODOŞAN, I. JUDE, N. ŞERBAN and A. BALOGH, *Chem. Ber.*, **95**, 1094 (1962).

Consequently, Marker's substance with m.p. about 252° cannot be the etianic acid III[1]; very probably he confused it with the 17-ketone IV.

As reported in a series of papers,[3] the $3\alpha,6\alpha$-ditosyloxy-5β-steroids are readily convertible under the action of nucleophiles into the corresponding 3β-substituted Δ^5-derivatives. Employing potassium thiocyanate as nucleophile in dimethylformamide, the ditosylate IIIb could be transformed into a mixture whose chromatographic work-up afforded methyl 3β-thiocyano-Δ^5-etienate (V) as main product, along with smaller amounts of methyl 3β-isothiocyano-Δ^5-etienate (VI) and methyl $\Delta^{3,5}$-etiadienate (VII).

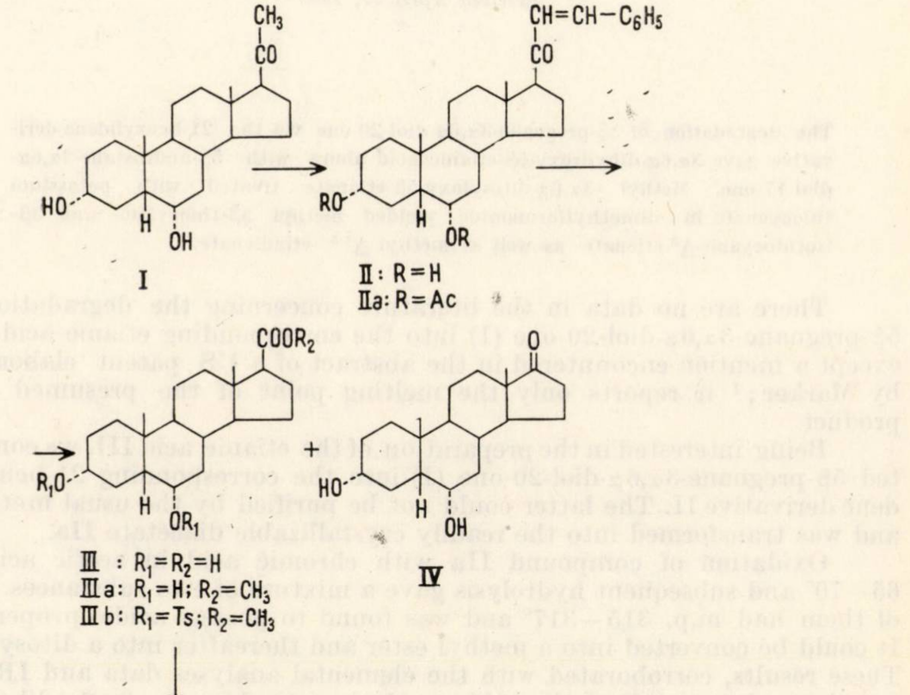
CH3
CO
HO
H
OH
I
CH=CH−C6H5
CO
RO
H
OR
II : R=H
IIa: R=Ac
COOR2
R1O
H
OR1
+
O
HO
H
OH
III : R1=R2=H
IIIa: R1=H; R2=CH3
IIIb: R1=Ts; R2=CH3
IV
COOCH3
NC−S
V
+
COOCH3
S=C=N
VI
+
COOCH3
VII

---

[3] K. R. Bharucha, G. C. Buckley, C. K. Cross, L. J. Rubin and P. Ziegler, *Canad. J. Chem.*, **34**, 982 (1956); F. Hodoşan, N. Şerban, A. Balogh and I. Jude, *Z. Chem.*, **1**, 29 (1961); F. Hodoşan, N. Şerban, A. Balogh and I. Jude, *Bull. Soc. Chim. France*, **1962**, 713; F. Hodoşan, N. Şerban, I. Jude, A. Pop-Gocan and A. Balogh, *Rev. Roumaine Chim.*, **9**, 637 (1964).

EXPERIMENTAL *

21-Benzylidene-5β-pregnane-3α,6α-diol-20-one diacetate (IIa)

To a solution of 10 g of 5β-pregnane-3α,6α-diol-20-one (I) in 400 ml of dry ethanol were added 8 ml of freshly distilled benzaldehyde and a solution of sodium ethoxide prepared from 6 g of sodium and 150 ml of ethanol. It was allowed to stand for 42 hours at room temperature. The solution was then concentrated *in vacuo* to 300 ml and neutralized with dil. HCl. After removal of the unreacted benzaldehyde by steam distillation, the crude reaction product was extracted with benzene, the organic layer separated, dried, and the solvent evaporated *in vacuo*. The residue was dissolved in 127 ml of dry pyridine, treated with 38 ml of acetic anhydride, and allowed to stand for 18 hours at room temperature. The solution was then poured into 1500 ml of water. The precipitate was extracted with dichloromethane and washed with water. The solvent was then removed *in vacuo* and the residue recrystallized twice from ethanol. Yield : 7 g; m.p. 209–214°.

UV spectrum (in methanol) : 222, 226sh, 291 nm

$C_{32}H_{42}O_5$ (506.6) *Calcd.:* C, 75.85; H, 8.36. *Found:* C, 76.25; H, 8.72.

Oxidation of the 21-benzylidene derivative IIa

A solution of 6 g of compound IIa in 750 ml of acetic acid was heated at 65–70° and treated dropwise under stirring with a solution of 12 g of CrO_3 in 40 ml of water and 400 ml of acetic acid. The addition required about $6^1/_2$ hours. Stirring at 65–70° was continued for 1 hour more; the solution was then allowed to stand at room temperature for 24 hours. The excess chromic acid was destroyed with a $NaHSO_3$ solution and the solvent removed *in vacuo* almost completely. A NaCl solution (about 400 ml) was added and the precipitate formed was extracted with ether. After washing with a $NaHCO_3$ solution and finally with water, the ethereal extract was dried and evaporated to dryness. The residue (5.6 g) was refluxed with 100 ml of 7% methanolic KOH for 6 hours. After removal of the solvent *in vacuo*, the residue was treated with 50 ml of water and extracted with ether and finally with chloroform.

The water layer was treated with dil. HCl and the crystals formed separated by filtration. The crude *3α, 6α-dihydroxy-5β-etianic acid* (III) (2 g) melted at 290–300° ; it was purified by repeated crystallizations from methanol. M.p. 315–317° with previous softening at about 300°.

IR spectrum (in KBr) : 1725 cm $^{-1}$

$C_{20}H_{32}O_4$ (336.4) *Calcd.:* C, 71.39; H, 9.59. *Found:* C, 71.66; H, 9.68.

The neutral oxidation product was obtained from the ethereal and chloroformic extracts. After removal of the solvents, the residue (0.6 g) was macerated with methanol, filtered, and recrystallized from acetone. The pure *5β-androstane-3α, 6α-diol-17-one* (IV) melted at 250°. Mixed m.p., IR spectra, and R_F values were used for comparing this compound with that prepared following a different route. [2]

IR spectrum (in KBr) : 1725 cm^{-1}

$C_{19}H_{30}O_3$ (306.2) *Calcd.:* C, 74.46; H, 9,87. *Found:* C, 74.38; H, 9.72.

Methyl 3α,6α-dihydroxy-5β-etianate (IIIa)

The crude etianic acid III (1.6 g) was esterified with 90 ml of methanol and 1 ml of $POCl_3$ by standing overnight at room temperature. The crude ester IIIa was recrystallized twice from benzene, then dissolved in methanol, poured in water, filtered, and dried. Yield: 0.75 g; m.p. 170–173°. $[\alpha]_D^{22} = +37°$ (in methanol).

---

* The melting points were determined using a "Mikroheiztisch Boetius".

IR spectrum (in KBr): 1735 cm^{-1}

$C_{21}H_{34}O_4$ (350.5) *Calcd.:* C, 71.96; H, 9.77. *Found:* C, 72.11; H, 10.04.

Methyl 3α,6α-ditosyloxy-5β-etianate (IIIb)

The methyl etianate IIIa (1.66 g) was dissolved in 6 ml of dry pyridine and 2.8 g of tosyl chloride was added. After standing at room temperature for 48 hours, the reaction mixture was worked up as usually. The crude ditosylate IIIb (2.9 g) had m.p. 159–160° (decomp.) with previous softening at 120°. An analytic sample was obtained by chromatography on a silica gel column. M. p. 162—164° (decomp.).

$C_{35}H_{46}O_8S$ (658.8) *Calcd.:* C, 63.80; H, 7.04; S, 9.73. *Found:* C, 63.70; H, 7.08; S, 9.97.

The action of potassium thiocyanate on the ditosylate IIIb

The ditosylate IIIb (1.5 g) was treated with 1.8 g of KSCN (previously dried at 130°- in 11 ml of freshly distilled DMFA. After heating in a boiling water bath for 3 hours, the solution was diluted with 150 ml of water and extracted with chloroform. The residue (0.94 g) obtained after removal of the solvent was chromatographed on 80 g of neutral alumina (activity II-III).

Fractions of 40 ml were collected as follows:

Fractions	1– 4	benzine	
,,	5–11	benzine-benzene	10 %
,,	12–18	,, ,,	15 %
,,	19–28	,, ,,	20 %
,,	29–33	,, ,,	30 %
,,	34–46	,, ,,	50 %
,,	47–56	benzene	
,,	57–59	benzene-dichloromethane	10 %
,,	60–64	,, ,,	20 %
,,	65–69	,, ,,	30 %
,,	70–71	,, ,,	50 %
,,	72–74	dichloromethane	
,,	75–80	dichloromethane-methanol	20 %
,,	81	methanol	

The fractions were combined according to the indications of the thin layer chromatographic determinations (Fig. 1).

Methyl $\Delta^{3,5}$ -etiadienate (VII) (33 mg) was isolated from the fractions 10–12. M.p. 134—140° (from methanol).

UV spectrum (in ethanol): 228, 235, 243 nm

$C_{21}H_{30}O_2$ (314.4) *Calcd.*: C, 80.21; H, 9.62. *Found*: C, 80.40; H, 9.74.

Methyl 3β-isothiocyano-Δ^5-etienate (VI) (70 mg) was obtained from the fractions 18–22. M.p. 133–135° (from methanol).

IR spectrum (in KBr): 2090, 2170 (—N=C=S); 798, 818 (Δ^5)

$C_{22}H_{31}O_2NS$ (373.5) *Calcd.*: C, 70.73; H, 8.37. *Found*: C, 71,16; H, 8.32.

Methyl 3β-thiocyano-Δ^5-etienate (V) (408 mg) was obtained from the fractions 32—41. M.p. 143—145,5° (from benzine).

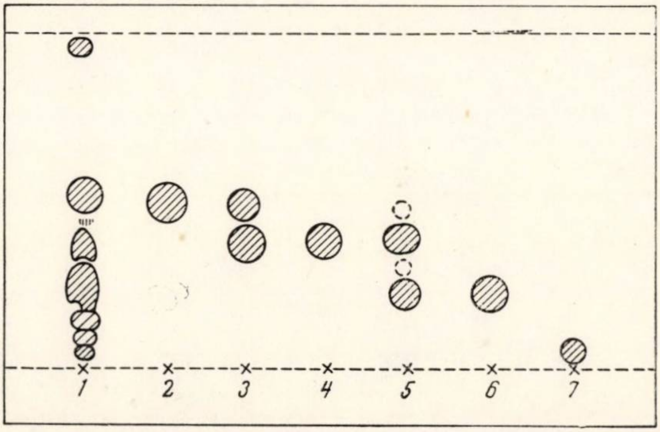

Fig. 1. — **1**: crude reaction product; **2**: methyl $\Delta^{3,5}$-etiadienate (VII) (fractions 10—12); **3**: mixture VII + VI (fractions 13—17); **4**: methyl 3β-isothiocyano-Δ^5-etienate (VI) (fractions 18—22); **5**: mixture VI + V (fractions 23—31); **6**: methyl 3β-thiocyano-Δ^5-etienate (V) (fractions 32—41); **7**: unknown product (fractions 68—75). — *Adsorbent*: silica gel G (Merck). *Solvent*: benzine-dichloromethane 1 : 1. *Reagent*: phosphomolybdenic acid.

IR spectrum (in KBr): 2150 (—S—CN); 807, 818, 837 (Δ^5) cm^{-1}

$C_{22}H_{31}O_2NS$ (373.5) *Calcd.*: C, 70.73; H, 8.37; S, 8.58. *Found*: C, 70.99; H, 8.07; S, 8.85.

[illegible] was obtained from the fractions [illegible] M.p. 144–145° (from benzene).

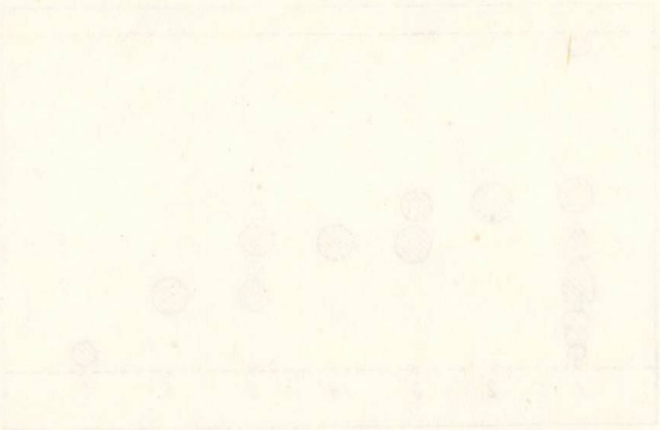

Fig. [illegible] 2 – methyl [illegible] mixture [illegible] methyl [illegible] (fraction [illegible]); 4 – mixture [illegible] fraction [illegible]; 6 – methyl [illegible] (fractions [illegible]); 7 – unknown [illegible] (fractions [illegible]) [illegible]

IR spectrum [illegible]

[illegible] Found: C, 70.00 [illegible]

Revue Roumaine de Chimie, **14**, 405–408 (1969)

$TiCl_4$-CAROTENOID COMPLEXES. IV[1]

ACTION OF $TiCl_4$ ON CRYPTOXANTHIN AND CRYPTOXANTHIN-PALMITATE

V. TĂMAŞ and C. BODEA

Institute of Agronomy "Dr. Petru Groza", Department of Chemistry and
Biochemistry, Cluj, Str. Mănăştur 3

Received May 21, 1968

The action of $TiCl_4$ on cryptoxanthin and cryptoxanthin-palmitate yields carotenoid-titanochloro-complexes like cryptoxanthin-$TiCl_4$ and cryptoxanthin-palmitate-$TiCl_4$. By acetonolysis of the first complex retrodehydro-cryptoxanthin and retrobisdehydro-β-carotene and of the second retrodehydro-cryptoxanthin-palmitate were obtained.

It has been previously shown [1-3] that by the action of $TiCl_4$ on C_{40}-carotenoids, hydrocarbons and oxygenated carotenoid-titanochloro-complexes are formed. By the acetonolysis of these complexes retrodehydro-carotenoids are obtained in large yields, superior to other methods.

Following our studies about the action of $TiCl_4$ on carotenoids we have examined the products that result from the action of this reactant on cryptoxanthin and cryptoxanthin-palmitate. We have found that and in this case carotenoid-titanochloro-complexes also are formed. In this way by the action of $TiCl_4$ on cryptoxanthin and cryptoxanthin-palmitate complexes were isolated in benzene solution, in which the molar carotenoid : $TiCl_4$ ratio is 1 : 1, as it results from the data presented in table 1.

Table 1

Chlorine analysis and λ_{max} of $TiCl_4$-carotenoid complexes

Compound	Cl %		λ_{max}, nm
	Calculated	Found	
Cryptoxanthin.$TiCl_4$	19.13	18.50	456
Cryptoxanthin-palmitate.$TiCl_4$	14.02	14.86	456
Cryptoxanthin, cryptoxanthin-palmitate	—	—	460,488

---

[1] Part III. V. TĂMAŞ and C. BODEA, *Rev. Roumaine Chim.*, **14**, 141 (1969)
[2] V. TĂMAŞ and C. BODEA, *Rev. Roumaine Chim.*, **12**, 1517 (1967).
[3] V. TĂMAŞ and C. BODEA, *Tetrahedron*, (in press).

Comparing the electronic spectra of the $TiCl_4$-carotenoid complexes, recorded in dimethylformamide, to these of the starting carotenoids, we found a disappearance of the fine structure of the spectrum and the appearance of only one maximum (see Table 1). This structural modification indicates that in the formation of these complexes, $TiCl_4$ is added to the end of the double band C = C of the polyene system.

The intimate mechanism of formation of the $TiCl_4$-carotenoid complexes is the same with that one shown in our previous papers. [2,3]

On the basis of the data presented in table 1 we can formulate the structures of the obtained complexes. From cryptoxanthin (Ia) results the complex IIa and from cryptoxanthin-palmitate (Ib) the complex IIb.

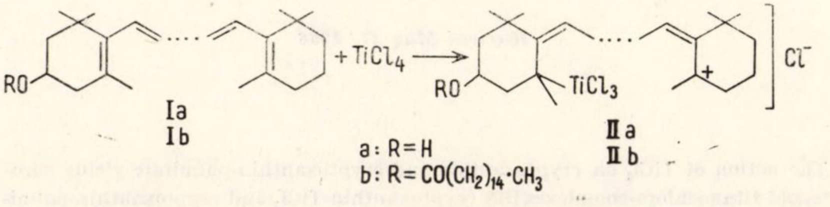

By the acetonolysis of these complexes we have obtained hydrocarbons and oxygenate retrodehydro-carotenoids. From IIa complex a mixture of retrodehydro-carotenoids were obtained, namely: retrodehydro-cryptoxanthin (IIIa) with a yield of 22% and retrobisdehydro-β-carotene (IV) with a yield that may reach 35%.

The reactions that take place are:

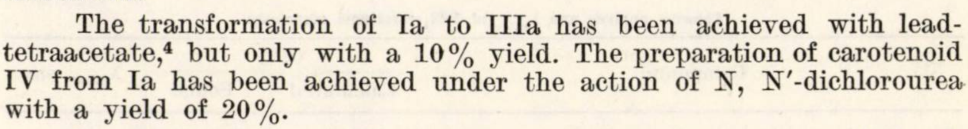

In the case we have used a larger quantity of $TiCl_4$, the yield in the product IV could be increased up to 50%, but with a decrease in IIIa carotenoid.

The transformation of Ia to IIIa has been achieved with lead-tetraacetate,[4] but only with a 10% yield. The preparation of carotenoid IV from Ia has been achieved under the action of N, N′-dichlorourea with a yield of 20%.

By acetonolysis of IIb complex, retrodehydro-cryptoxanthin-palmitate (IIIb) with a yield of 30% was obtained.

The structure of the dehydro-carotenoids was studied by means of electronic and infrared spectroscopy and cochromatography with authentic carotenoids.

---

[4] C. Bodea and V. Tămaş, *Liebigs Ann. Chem.*, **671**, 51 (1964).

EXPERIMENTAL

Cryptoxanthin and cryptoxanthin-palmitate were isolated from calices of *Physalis alkekengi* and flowers of *Curcubita pepo*.

The complexes were obtained in dried benzene at room temperature and dehydro-carotenoids in benzene or chloroform solution. The electronic spectra of the $TiCl_4$-carotenoids were obtained in dimethylformamide, while those of the dehydro-carotenoids in neophaline (b.p. = =70°). The absorbent used was a mixture of MgO and sand. The elution of the pigments was performed with a mixture of ether-acetone-ethanol (9 :3 :1).

1. *Preparation of $TiCl_4$-carotenoid complexes*

Cryptoxanthin. $TiCl_4$ (IIa). To a solution of 100 mg cryptoxanthin (Ia) in 30 ml benzene, 0.3 ml $TiCl_4$ were added and the mixture stirred for 10 min. The precipitate was filtered off and washed with benzene till the solvent remained colourless. 120 mg IIa, containing 18.50 % Cl, were obtained. The electronic spectrum, in dimethylformamide, shows an absorption maximum at 456 nm.

Cryptoxanthin-palmitate. $TiCl_4$ (IIb). 150 mg cryptoxanthin-palmitate (IIb) in 20 ml benzene was treated with 0.2 ml $TiCl_4$ and worked up as the complex IIa. 160 mg IIb, containing 14.86 %, were obtained. $\lambda_{max} = 456$ nm (in dimethylformamide).

2. *Preparation of dehydro-carotenoids*

2.1. *Dehydro-carotenoids from cryptoxanthin.* 0.2 ml $TiCl_4$ were added to a solution of 100 mg cryptoxanthin in 10 ml benzene or in 10 ml chloroform and the mixture stirred for one min. After this time interval, to the dark blue solution, 75 ml acetone were added, then after 10 min 100 ml petroleum ether. The solution of pigments was washed with water, dried with Na_2SO_4 and chromatographed. The chromatogramme ((column 5× 20 cm) obtained after developing with a mixture of petroleum ether-benzene in which the ratio of benzene was increased up to 20 %, appeared, as follows :

2.5 cm	orange-red	retrodehydro-cryptoxanthin
0.5 cm	interzone	
3 cm	orange	cryptoxanthin
0.3 cm	interzone	
4 cm	rose-red	retrobisdehydro-β-carotene

Retrodehydro-cryptoxanthin (IIIa). 22 mg red crystals were obtained from ether. The maxima of electronic spectrum were at 500, 470, 445 nm (in neophaline). In the IR-spectrum, in nujol, IIIa, showed an absorption band at 1030 cm^{-1} which is attributed to HO allylic[5] and a doublet, characteristic for the retro form[6,7] at 964 and 982 cm^{-1}. In a mixture of petroleum ether-methanol 95 % IIIa had a hypophasic partition of 45 %. Treating IIIa with chloroform containing-HCl IV was obtained.

---

[5] C. Bodea, E. Nicoară, V. Tămaş and H. Mantsch., *Liebigs Ann. Chem.*, 189 (1963).

[6] H. H. Strain, M. R. Thomas and J. J. Katz, *J. Org. Chem.*, **26**, 5061 (1961).

[7] E. Nicoară, V. Tămaş, G. Neamţu and C. Bodea, *Liebigs Ann. Chem.*, **697**, 201 (1966).

Retrobisdehydro-β-carotene (IV). 35 mg dark red crystals were obtained from ether. The electronic spectrum, in neophaline, showed λ_{max} at 517, 488, 460 nm and the IR-spectrum, in nujol, a doublet at 960 and 980 cm^{-1}. In the chromatography with authentic retrobisdehydro-β-carotene [8] there was no separation.

In the case when 0.3 ml $TiCl_4$ were added to a solution of 100 mg cryptoxanthin, 50 mg IV were obtained.

2.2. *Dehydro-carotenoids from cryptoxanthin palmitate.* A solution of 150 mg cryptoxanthin-palmitate in 20 ml benzene was treated with 0.15 ml $TiCl_4$ and worked up as at 2.1. After developing with a mixture of petroleum ether and 10% benzene the column appeared as follows :

4 cm	orange-red	retrodehydro-cryptoxanthin-palmitate
0.5 cm	interzone	
1 cm	orange	cryptoxanthin-palmitate

Retrodehydro-cryptoxanthin-palmitate (IIIb). 45 mg red powder were obtained from ether $\lambda_{max} = 500, 470, 444$ nm (in neophaline). The saponification of pigment IIIb with a solution of ethanolic potassium hydroxide, yields IIIa.

---

[8] C. Bodea, V. Tămaş and G. Neamţu, *Rev. Roumaine Chim.*, **11**, 739 (1966).

La REVUE ROUMAINE DE CHIMIE paraît 12 fois par an. Le prix d'un abonnement annuel est de : £ 5.0.0; $ 12,—; FF 60,—; DM 48,—. Toute commande de l'étranger (fascicules ou abonnements) sera adressée à CARTIMEX, Boîte postale 134 — 135, Bucarest, Roumanie, ou à ses représentants à l'étranger.

R.P. d'ALBANIE, Ndermarja Shtetnore e Botimeve Tirana; R.D. ALLEMANDE, Deutscher Buch Export und Import Leipzig, 701, Leninstrasse 16; R.P. de BULGARIE, Hemus, Place Slaweikov, 11, Sofia; R.P. de CHINE, Waiwen Shudian P.O.B. 88, Peking; R.P.D. CORÉENNE, Chulphanmul, Phenian; RÉPUBLIQUE CUBA, Cubartimpex Simón Bolivar 1, Palacio Aldamo, Habana; R. P. de HONGRIE, Kultúra, P.O.B. 149, Budapest 62; R.P. MONGOLE, Mongolgosknigotorg, Ulan Bator; R.P. POLOGNE, Ruch Ul. Wronia 23, Warszawa; R.S. TCHÉCOSLOVAQUE, Artia, Ve Smeckach 30-Praha II; U.R.S.S., Mejdunarodnaia Kniga, Moskva G-200; R.D. VIETNAM, So Xuat Nhap Khau Sach Bao, 32 Hai Ba Trung, Hanoï; R.S.F. de YOUGOSLAVIE, Jugoslovenska Knjiga Terazije 27, Belgrad; Prosveta 16/1, Terazije, Belgrad; Forum Voïvode Misica, Novi Sad; ARGENTINE, Editorial Sudaminter S.A., Alsina 500, Buenos Aires; AUSTRALIE, Current Books Ltd. Distributors 168—174, Day Street Sydney; AUTRICHE, Globus Zeitungs Drucks und Verlagsanstalt GmbH, 1200, Wien, Höchstädplatz 3; BELGIQUE, Du Monde Entier 5, Place St. Jean-Bruxelles, Agence Messageries de la Presse 14—22, Rue du Persil, Bruxelles; CANADA, Progress Books 44 Stafford St. Toronto, Ontario, W.M. Dawson Subscriptions Service Ltd., Six Thorneliffe Park Drive, Toronto 17, Ontario; COLOMBIE, Librería Buchholz Galeria, av. Jiménez de Quesada 8—40 Bogotá; DANEMARK, Ejnar Munksgaard, Noregade 6, Kobenhavn; ESPAGNE, Libreria Herder, Calle de Balmés 26, Barcelona 7; ÉTATS-UNIS, Fam Book Service 69, Fifth Avenue, Suite 8 F., New York, 10003 N.Y.; Continental Publications, 111, South Mermanec Ave., St. Louis Missouri 63105; Turner Subscription Agency 235, Park Avenue South, New York 3 N.Y.; FINLANDE, Akateeminen Kirjakauppa P.O.B. 10128, Helsingfors, 10; FRANCE, Nouvelles Messageries de la Presse Parisienne, 111, Rue Réaumur, Paris II, Europériodiques S.A. 72, Boul, Senard, 22 Saint-Cloud; GRANDE-BRETAGNE, Collet's Holdings Ltd. Dennington Estate, Wellingborough, Northants Central Books, Ltd., 37, Inn Road London W.C.1; ISRAËL, Lepac Ltd., P.O.B., 1136 Tel-Aviv; Haiflepac Ltd. P.O.B. 1794, Haifa; ITALIE, So. Co. Lib. Ri. Piazza Margana 33 — Roma; Messagerie Italiane Sp. A. Milano, Via Priv. Renzo e Lucia 7; JAPON, Nauka Ldt. 30 — 19 Minami—Ikebukuro 2 chome Toshima Ku, Tokyo; PAYS-BAS, N.V. Martinus Nijhoff, P.O.B. 269, Den Haag; Swetz & Zeitlinger, Keizersgracht 471—487, Amsterdam C.; NORVÈGE, Tryggve Juul Moller—Boekhandel Øvre Slottsgate 15 Oslo 1; R.F. ALLEMANDE, Kubon & Sagner, P.O.B. 68, München 34; Presse Vertriebsgesellschaft GmbH, 6, Frankfurt/Main Börsenstrasse 13—15; Kunst und Wissen, Erich Biber P.O.B. 46, 7000 Stuttgart 1; SUISSE, Pinkus & Cie Froschaugasse 7 Zürich, Fachbücherei Berne, P.O.B. 397, 3001 Berne.

En Roumanie vous pourrez vous abonner par les bureaux de poste, chez votre facteur ou directement par les services de presse des entreprises et institutions.

NOTE POUR LES AUTEURS

La *Revue Roumaine de Chimie* publie des articles en anglais, français, russe, allemand ou espagnol. Les auteurs sont priés d'envoyer des articles, notes, communications et comptes rendus inédits.

Les manuscrits seront dactylographiés à deux intervalles. Les tableaux seront dactylographiés sur feuilles séparées,de même que la légende des figures. Les diagramnes seront tracés à l'encre de Chine sur papier calque. Les tableaux et les figures seront numérotés par des chiffres arabes, en nombre strictement nécessaire. Prière de ne pas inscrire les mêmes données dans les tableaux et les figures. Les formules chimiques seront incluses dans le texte ; en outre, elles seront transcrites sur des feuilles séparées. L'ordre des références bibliographiques sera celui de leur mention dans le texte ; le nom de l'auteur sera précédé de l'initiale du prénom ; les publications périodiques seront présentées suivant les prescriptions internationales. Les références seront ajoutées à la fin de l'article ; elles paraîtront comme des notes, au bas de la page. Le texte sera précédé d'un résumé, comprenant 15 lignes au maximum.

L'entière responsabilité du contenu des articles appartient aux auteurs. On publie des articles dus aux collaborateurs roumains ou étrangers. Les auteurs recevront 50 tirés à part.

PRINTED IN ROMANIA

F 1103

REVUE ROUMAINE DE CHIMIE

TOME 14
N° 4
Avril 1969

ÉDITIONS DE L'ACADÉMIE DE LA RÉPUBLIQUE SOCIALISTE DE ROUMANIE

Rev. Roumaine Chim.

14, 409–554 (1969), Bucarest

COMITÉ DE RÉDACTION

Rédacteur en chef :

C. D. NENIŢESCU, membre de l'Académie de la République Socialiste de Roumanie.

Rédacteurs en chef adjoints :

A. T. BALABAN et V. E. SAHINI, membres correspondants de l'Académie de la République Socialiste de Roumanie.

Collège de rédaction :

C. DRĂGULESCU, RALUCA RIPAN, CR. SIMIONESCU, membres de l'Académie de la République Socialiste de Roumanie; EM. BRATU, membre correspondant de l'Académie de la République Socialiste de Roumanie, Pr G. OSTROGOVICH, MARG. AVRAM, F. BADEA, D. MARCHIDAN, D. NEGOIU et D. SĂNDULESCU.

Les manuscrits, les livres et les revues proposés en échange, ainsi que toute correspondance seront envoyés à la rédaction :

23, str. Dumbrava Roşie, Bucarest, Roumanie.

F 1103

REVUE ROUMAINE DE CHIMIE

Tome 14, N° 4 Avril 1969

Page

I. G. MURGULESCU et I. VLAGIU, Détermination des constantes $Q_{tr} - e_{tr}$ des valeurs des constantes de transfert, dans le cas de la polymérisation radiochimique de l'acrylonitrile dans des solvants de filage 411–417

RODICA BELDIE and V. E. SAHINI, Raman spectra of beryllium oxalate complexes 419–422

O. RADOVICI and E. ROMAN, The mechanism of the action of lauril-amine on the corrosion of iron in HCl solutions . . . . 423–427 ✓

RODICA VÎLCU and I. CIOCĂZANU, Alkaline hydrolysis of the methyl and ethyl acetates. I. Calorimetrical determination of the standard thermal effects during the evolution of the chemical reactions 429–439

E. ANGELESCU and MINODORA RADU, Electrical conductivity and dispersion degree of lyophilic colloids relationship. X. 0.2 M sodium stearate, palmitate and laurate in the presence of electrolytes with different anions. 441–450

Z. GROPŞIANU, D. KOHN und A. IOVI, Wärmeübergangszahlen beim Verdampfen von Ammoniumnitratlösungen 451–457

CONST. GH. MACAROVICI und C. STANISAV, Die Entfernung der störenden Wirkung des Eisens, Kobalts, Nickels und Kupfers bei der kolorimetrischen Bestimmung des Titans . . . . 459–461 ✓

P. TRIBUNESCU et M. CRISTEA, Structure des hexacyanocobaltiates de zinc, cadmium, nickel et manganèse 463–467

ADELINA LUPU, LEONTINA NASTA, I. BALTOG and BRÎNDUȘA BRĂILEANU, Light scattering and viscosity measurements on unfractionated polyvinylchloride 469–472

I. VELEA, VICTORIA DIMONIE, E. MELEGA, P. BLENKE and VALENTINA PROVINCEANU, Stereospecific polymerization of 1,3 butadiene. I. Some kinetic aspects of 1,3 butadiene polymerization with soluble catalysts on the basis of cobalt complex compounds, diethylaluminium monochloride, water 473–480

L. FEY and N. BODOR, Electronic spectra of the substituted α-oximinoalkylbenzenes. III. Steric effects on electronic absorption spectra of the *o*-substituted *p*-nitro-α-oximinoalkylbenzenes 481–493

Rev. Roumaine Chim. **14**, 409–554 (1969), Bucarest

Page

LUCREŢIA ALMASI, A. HANTZ und ERIKA HAMBURG, Über heteroorganische Verbindungen. XXXVI. Infrarot-spektroskopische Untersuchungen der Addukte der 0,0-Dialkylthiophosphorsäuren mit sekundären und tertiären Aminen 495–501

M. ARSHAD A. BEG, Correlation of the physical properties of organophosphorus compounds. II Refractivity and boiling point of phosphines 503–508

F. HODOŞAN and FELICIA TEODOR, Spectral studies on steroidal nitrate esters. III. UV spectra in concentrated sulfuric acid 509–516

MARIA IONESCU and MARIA VĂGĂONESCU, Contributions to the study of octanesultone 517–521

C. BODEA, V. FĂRCĂŞAN and TEODORA PANEA, Synthetical phenothiazine glycosides. II. 0-Glucosides of 3-hydroxy-1,9-dibromo-7-chloro-phenothiazine and 3-hydroxy-7-chloro-phenothiazine 523–526

P. T. FRANGOPOL, MARIA FRANGOPOL, N. NEGOIŢĂ et E. ROMAŞ, Radicaux libres stables diarylazote avec un groupe sulfonique dans la molécule 527–534

I. NICULESCU-DUVĂZ, V. FEYNS, V. SAVANIU, M. IONESCU, A. ŞERBAN and A. CAMBANIS, Potential anticancer agents. VI. New aromatic nitrogen mustards with good antitumor activity 535–547

H. H. MANTSCH, The mass spectrum of acridine-N-oxide 549–553

Revue Roumaine de Chimie, **14**, 411–417 (1969)

ORSZÁGOS MŰSZAKI KÖNYVTÁR ÉS DOKUMENTÁCIÓS

DÉTERMINATION DES CONSTANTES $Q_{tr} - e_{tr}$ DES VALEURS DES CONSTANTES DE TRANSFERT, DANS LE CAS DE LA POLYMÉRISATION RADIOCHIMIQUE DE L'ACRYLONITRILE DANS DES SOLVANTS DE FILAGE

I. G. MURGULESCU et I. VLAGIU

Institut de Chimie Physique de l'Académie
Bucarest, 23, str. Dumbrava Roşie

Reçu le 25 mai 1958

Des valeurs des constantes de transfert ($C_{tr,\,s}$) dans le cas de la polymérisation radiochimique de l'acrylonitrile en diméthylformamide et en carbonate d'éthylène on a évalué les constantes $Q_{tr} - e_{tr}$ de l'équation de Fuhrman-Mesrobian, en obtenant les valeurs $4{,}53.10^{-5}$; $2{,}10.10^{-5}$; $2{,}05.10^{-5}$ et $+0{,}30$; $+0{,}71$ et $0{,}55$. Les valeurs des constantes de transfert ($C_{tr,\,s}$) à 40° et 50° (dans le cas du carbonate d'éthylène) pour les solvants énumérés ci-dessus sont : $32{,}40.10^{-5}$; $8{,}12.10^{-5}$ et $5{,}11.10^{-5}$.

L'évaluation des constantes $Q_{tr} - e_{tr}$ comme mesure de la réactivité et de la polarisation du solvant, de l'équation de Mayó[1] a été généralisée par Fuhrman-Mesrobian[2]. Tenant compte du schéma général de copolymérisation proposé par Mayó

$$- A^{\bullet} + A \xrightarrow[k_{12}]{k_{11}} - AA^{\bullet}$$

$$- A^{\bullet} + B \xrightarrow{k_{12}} - AB^{\bullet}$$

$$- B^{\bullet} + A \xrightarrow{k_{21}} - BA^{\bullet}$$

$$- B^{\bullet} + B \xrightarrow{k_{22}} - BB^{\bullet}$$

La formule finale, qui définit la composition du copolymère (conformément aux détails donnés plus haut) est la suivante

$$\frac{\mathrm{d}(A)}{\mathrm{d}(B)} = \frac{(A)\, r_1\, (A) + (B)}{(B)\, (A) + r_2\, (B)} \tag{1}$$

---

[1] F. R. Mayó, *J. Amer. Chem. Soc.*, **66**, 1594 (1944).

[2] N. Fuhrman-Mesrobian, *J. Amer. Chem. Soc.*, **76**, 9281 (1954).

où (A), (B) représentent la concentration des monomères participant à la relation de copolymérisation et r_1 et r_2 la réactivité des deux monomères, définie par la relation

$$k_{11} = r_1 k_{12}$$
$$k_{22} = r_2 k_{21}$$

Si l'on considère le cas particulier de la copolymérisation, où $A = M$ (le monomère) et B (le solvant), alors $r_2 = 0$, parce que le solvant ne polymérise pas et l'équation (1), conformément aux calculs de Küchler-Ulbricht [3], devient

$$\frac{\mathrm{d}(M)}{\mathrm{d}(S)} = \frac{(M)}{C_{tr,s}(S)} + 1 \tag{2}$$

$$C_{tr,s} = \frac{1}{r_1} = \frac{k_{12}}{k_{11}} = \frac{k_{11tr}}{k_{11}} = \frac{k_{tr,s}}{k_p} = C_1 \tag{2'}$$

Fuhrman-Mesrobian propose l'extension du schéma $Q - e$ aux réactions de transfert de chaîne au solvant $S - X$ du radical en augmentation $R - M_n^{\cdot}$, conformément au schéma

$$R - M_n^{\cdot} + M \xrightarrow{k_p} R - M_{n+1}$$

$$R - M_n^{\cdot} + S - x \xrightarrow{tr,s} R - M_n - x + S$$

et la constante de transfert au solvant $(C_{tr,s})$ peut être exprimée à l'aide des termes $Q - e$ (pour le monomère) et $Q_{tr} - e_{tr}$ (pour le solvant) conformément à l'équation [2]

$$\begin{aligned} C_1 &= \frac{k_{11\,tr}}{k_{1,1}} = \frac{Q_{tr}}{Q_1} \exp\{-e_1(e_{tr} - e_1)\} \\ C_2 &= \frac{k_2 tr}{k_2 2} = \frac{Q_{tr}}{Q_2} \exp\{-e_2(e_{tr} - e_2)\} \end{aligned} \tag{3}$$

où K_p = la constante de vitesse de propagation ; $K_{tr,s'}$ = la constante de vitesse de transfert au solvant ; C_1, C_2 = les constantes de transfert pour le monomère 1 et pour celui de référence 2, Q_1, Q_2 = la réactivité et la polarité des monomères 1, 2 ; e_1, e_2 ; e_{tr}, Q_{tr} = la réactivité et la polarité du solvant.

Pour déterminer la constante de transfert du solvant on a utilisé la relation connue

$$\frac{1}{P} = \frac{k_t V_g}{\underbrace{k_p^2 (M)^2}_{R}} + C_{tr,s} \frac{(S)}{(M)} \tag{4}$$

---

[3] J. Ulbricht, *Faserforsch. u. Textiltechnik*, **11**, 62 (1960).

Par la représentation graphique du degré de polymérisation $\left(\frac{1}{P} - R\right)$, en fonction du rapport solvant/monomère : $\left(\frac{1}{P} - \underbrace{\frac{k_t V_g}{k_2^2 (M)^2}}_{R}\right) f \frac{(S)}{(M)}$, on obtient la valeur constante de transfert[4] qui a été introduite après dans l'équation (3) pour évaluer $Q_{tr} - e_{tr}$, conformément au procédé de Fuhrman-Mesrobian. Dans les tableaux 1 et 2 sont représenteés les caractéristiques cinétiques de la polymérisation radiochimique de l'acrylonitrile en diméthylformamide, diméthylsulfoxyde et carbonate d'éthylène.

Il résulte de l'étude cinétique que l'acrylonitrile a des comportements bien différents dans les trois solvants (DMF, Me_2SO et EtC).

De la détermination du rapport des constantes relatives de vitesse obtenues de la pente des droites comme suite de la représentation graphique de la vitesse d'amorçage (V_i), en fonction du rapport de la vitesse de réaction (concentration du monomère au carré) on obtient les valeurs suivantes[5]

a) diméthylformamide $\frac{k_t}{k_p^2} = 162$; $\frac{k_p}{k_t^{1/2}} = 0{,}074$ $(1/\text{mole.s})^{1/2}$

Tableau 1

Dépendance du $C_{tr,s}$ du degré de polymérisation et du rapport solvant/monomère dans le cas de la polymérisation radiochimique de l'acrylonitrile

M	S	$[M]$ mole/l	$\frac{[S]}{[M]}$	$\frac{1}{P} \cdot 10^4$	$Vg \cdot 10^5$ mole/l.s	$\left(\frac{1}{P} - \frac{k_t}{k_p^2} \frac{V_g}{[M]^2}\right) \cdot 10^4$	$C_{tr,s} \cdot 10^5$
AN	DMF	5,40	1,10	10,29	11,02	4,30	
		4,60	1,55	11,71	9,10	4,75	
		3,50	3,30	14,94	6,37	6,68	
		2,60	4,00	17,38	4,12	7,50	
		1,80	4,80	19,30	2,23	8,29	
		1,60	6,30	21,09	1,77	9,75	32,40
AN	Me_2SO	5,40	1,20	3,71	17,24	1,94	
		4,60	1,45	4,42	15,81	2,20	
		3,50	3,50	7,50	13,40	4,30	
		2,60	4,70	8,50	11,60	5,40	
		1,80	5,00	14,58	9,60	5,71	
		1,30	5,38	21,53	8,82	5,90	8,12
AN	EtC	5,40	0,90	3,43	18,60	0,91	
		4,60	2,84	5,12	16,18	2,08	
		3,50	4,21	6,84	13,00	2,60	
		2,60	5,05	9,24	10,39	3,12	
		1,80	5,77	13,32	8,00	3,48	
		1,30	6,48	19,92	6,78	3,88	5,11

---

[4] I. Vlagiu et J. Păun, *Rev. Roumaine Chim.*, **9**, 1085 (1967).

[5] M. Hayssinski, «Actions chimiques et biologiques des radiations», Maison de Paris, IIIe vol., 1958, p. 82.

b) diméthylsulfoxyde $\frac{k_t}{k_p^2} = 0{,}30$; $\frac{k_p}{k_t^{1/2}} = 0{,}18$ $(1/\text{mole.s})^{1/2}$

c) carbonate d'éthylène $\frac{k_t}{k_p^2} = 0{,}40$; $\frac{k_p}{k_t^{1/2}} = 0{,}15$ $(1/\text{mole.s})^{1/2}$

Tableau 2

Caractéristiques cinétiques de la polymérisation radiochimique de l'acrylonitrile en DMF, Me_2SO et EtC

M	*S*	$[M]$ mole/l	$\frac{[S]}{[M]}$	$V_g \cdot 10^5$ mole/l.s	$[M]^2$	$V_g^2 \cdot 10^{10}$ $(\text{mole/l.s})^2$	$\frac{V_g^2}{[M]^2}$	$V_i \cdot 10^8$	$\frac{k_t}{k_p^2}$	$\frac{k_p}{k_t^{1/2}}$
AN	DMF	5,40	1,10	11,02	29,16	121,44	4,16	6,94		
		4,60	1,55	9,10	21,16	82,81	3,91	6,52		
		3,50	3,30	6,37	12,25	40,58	3,31	5,52		
		2,60	4,00	4,12	6,76	16,97	2,51	4,19		
		1,80	4,80	2,23	3,24	4,97	1,53	2,55		
		1,60	6,30	1,77	2,56	3,13	1,22	2,03	162	0,077
,,	Me_2SO	5,40	1,20	17,24	29,16	297,21	10,19	3,05		
		4,60	1,45	15,81	21,16	248,95	11,76	3,52		
		3,50	3,50	13,40	12,25	179,56	14,65	4,39		
		2,60	4,50	11,60	6,76	134,56	19,90	5,97		
		1,80	5,00	9,60	3,24	92,16	28,45	8,53		
		1,30	5,38	8,82	1,69	77,79	46,03	13,80	30	0,18
,,	EtC	5,40	0,90	18,60	29,16	345,96	11,86	4,74		
		4,60	2,84	16,18	21,16	267,79	12,65	5,06		
		3,50	4,21	13,00	12,25	169,00	13,78	5,51		
		2,60	5,05	10,39	6,76	107,95	15,97	6,38		
		1,80	5,77	8,00	3,24	64,00	19,75	7,30		
		1,30	6,48	6,78	1,69	45,96	27,31	10,92	40	0,15

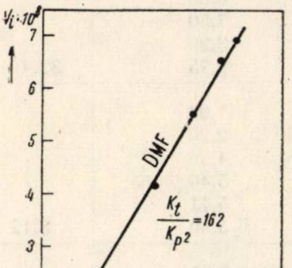

Fig. 1. — Variation de la vitesse d'initiation en fonction du rapport $\left(\frac{V_g}{[M]}\right)^2$ dans le diméthylformaldéhyde.

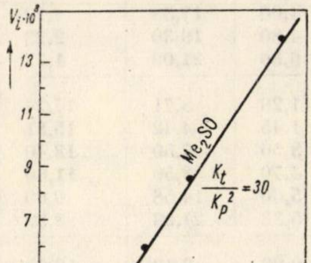

Fig. 2. — Variation de la vitesse d'initiation en fonction du rapport $\left(\frac{V_g}{[M]}\right)^2$ dans le diméthylsulfoxyde.

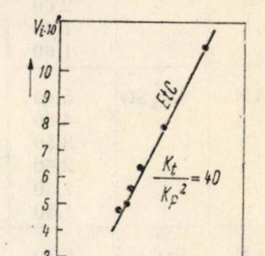

Fig. 3. — Variation de la vitesse d'initiation en fonction du rapport $\left(\frac{V_g}{[M]}\right)^2$ dans l'éthylènecarbonate.

Les valeurs obtenues par nous n'ont pu être comparées à d'autres données que dans le cas de polymérisation chimique de l'acrylonitrile en diméthylformamide en additionnant du $FeCl_3$, déduites par Dainton[6] d'après la méthode du secteur rotatoire.

On a obtenu la valeur de $k_t/k_p^2 = 198$.

Conformément aux données susmentionnées il résulte que le comportement de l'acrylonitrile dans les trois solvants utilisés est différent tant dans le système de polymérisation, que dans le système de filage du polyacrylonitrile. La vitesse de réaction est moindre en DMF en comparaison du Me_2SO et de l'EtC.

En même temps il résulte encore, que l'éventuelle utilisation industrielle du procédé de polymérisation en DMF n'est pas rentable, étant radiolysé à côté du monomère.

La constante de transfert au solvant, dans ces conditions, favorise l'interruption de la chaîne macromoléculaire, en obtenant un polymère d'un poids trop réduit pour être filé[7,8].

Lors de l'étude cinétique de la polymérisation radiochimique de l'acrylonitrile en DMF, Dainton[6] tire la conclusion de la scission du solvant en deux radicaux primaires $H\dot{C}O$ et $(CH_3)_2\dot{N}$, qui pourraient éventuellement former avec le monomère un radical du type :

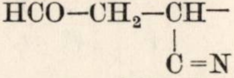

$$HCO-CH_2-\underset{\displaystyle C\equiv N}{\underset{|}{CH}}-$$

On a établi aussi, outre la détermination du rapport relatif des constantes absolues de réaction (k_t / k_p^2), les valeurs $Q_{tr} - e_{tr}$ de l'équation (3) de Fuhrman-Mesrobian, valeurs qui mettent en évidence par une autre voie aussi, le comportement bien différent des trois solvants dans la marche cinétique de la réaction.

Dans ce sens-là on a adopté le procédé de Ulbricht en utilisant comme moment de référence le styrène dont les paramètres $Q_{tr} - e_{tr}$ sont connus en comparaison de ($Q = 1$ et $e = -0{,}8$) qui a les valeurs connues aussi ($Q = 0{,}44$ et $e = +1{,}2$) et en utilisant pour le rapport la valeur de 880 obtenue par Ballantine lors de la polymérisation radiochimique du styrène avec des radiations γ Co^{60}.

Les valeurs des constantes de transfert au solvant dans le cas du styrène, nécessaires au calcul des valeurs pour Q_{tr} et e_{tr}, sont données dans le tableau 3.

Dans le tableau 4 on a donné les valeurs obtenues pour $Q_{tr} - e_{tr}$, conformément à l'équation (3) en partant des valeurs de la constante de transfert au solvant.

Il en résulte la conclusion, qu'une fois en baisse les valeurs de Q_t, (DMF, Me_2SO et EtC), le degré de polymérisation obtenu augmente dans le même sens avec les valeurs de Q_{tr} et les valeurs constantes de transfert varient dans le sens contraire.

---

[6] N. Colebourne, E. Collinson, D. J. Currie et F. S. Dainton, *Trans. Faraday Soc.*, **159**, 1357 (1963).

[7] I. H. Peebles, *J. Polymer. Sci.*, A_3, **353**, 361 (1965).

[8] L. Kücheler, « Polymerisationskinetik », Springer Verlag, Berlin, 1951, p. 150.

Tableau 3

Dépendance du $C_{tr,s}$ du degré de polymérisation et du rapport solvant/monomère dans le cas de la polymérisation radiochimique du monomère

M	S	$[M]$ mole/l	$\frac{[S]}{[M]}$	$\frac{1}{\overline{P}} \cdot 10^4$	$V_g \cdot 10^6$ mole/l.s	$\left(\frac{1}{\overline{P}} - \frac{k_t}{k_p^2} \frac{1}{[M]^2} V_g\right) \cdot 10^4$	C°	$C_{tr,s} \cdot 10^5$
St	DMF	3,50	9,59	8,63	3,25	6,30	40	
		5,00	6,50	6,39	4,81	4,70	40	
		6,04	3,90	4,51	5,82	3,11	40	
		7,02	1,75	3,16	6,55	2,00	40	10,92
St	Me_2SO	3,50	10,00	6,51	3,50	4,00	40	
		5,00	6,99	4,85	5,01	3,08	40	
		6,04	4,00	3,45	6,02	2,03	40	
		7,02	2,29	2,68	7,00	1,44	40	6,93
St	EtC	3,50	10,21	5,66	3,60	3,09	50	
		5,00	7,20	3,98	5,11	2,20	50	
		6,04	3,60	2,70	6,20	1,21	50	
		7,02	2,00	2,13	7,45	0,80	50	2,35

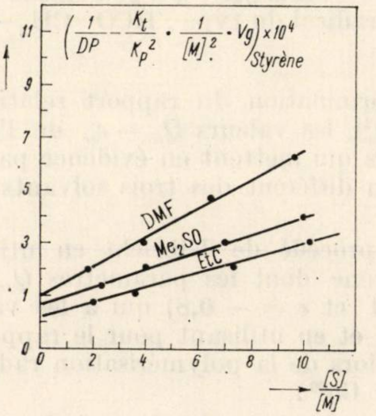

Fig. 4. — Dépendance de la constante de transfert $C_{tr,s}$ en fonction du rapport $\frac{[S]}{[M]}$ du styrène dans le DMF Me$_2$SOEtC.

Tableau 4

Dépendance des valeurs C_{tr} et Q_{tr} de $e_{tr,s}$

(S)	$C_{tr,s} \cdot 10^5$ (AN)	$C_{tr,s} \cdot 10^5$ (St)	$Q_{tr} \cdot 10^5$	e_{tr}
DMF	32,40	10,92	4,53	+ 0,30
Me_2SO	8,12	6,93	2,10	+ 0,71
EtC	5,11	2,53	2,05	+ 0,55

Les valeurs obtenues pour e_{tr} font différencier les trois solvants. Les valeurs obtenues pour l'acrylonitrile par voie théorique (d'une manière indirecte) prouvent que le polymère obtenu aura un poids moléculaire plus grand en Me$_2$SO et EtC en comparaison de DMF (chose constatée et expérimentée par nous aussi).

Dans le cas de la polymérisation radiochimique, par le mécanisme radicalaire, à la suite de la réaction de transfert au solvant l'augmentation des chaînes cesse et à cause de celà le degré de polymérisation décroît.

A la différence des procédés classiques de polymérisation, dans le cas du procédé radiochimique, étant donné le fait, qu'en général, le solvant est fortement radiolysé, en comparaison du monomère qui favorise l'obtention de quelques valeurs élevées de la constante de transfert au solvant, les expériences ont une valeur surtout théorique parce que (par exemple) dans le cas des polymères qui peuvent être filés on obtient des polymères inférieurs.

En conclusion on tient à préciser que des valeurs $Q_{tr} - e_{tr}$ aussi on peut tirer des conclusions (dans le cas de la polymérisation radiochimique) de la rentabilité ou du manque de rentabilité de ce procédé qu'on a étudié.

Revue Roumaine de Chimie, **14**, 411 – 417 (1969)

Revue Roumaine de Chimie, **14**, 419–422 (1969)

RAMAN SPECTRA OF BERYLLIUM OXALATE COMPLEXES

RODICA BELDIE and V. E. SAHINI

Institute of Physical Chemistry, Bucharest, str. Dumbrava Roşie, 23

Received October 17, 1968

The Raman spectra of the complex compounds $K_2[Be(C_2O_4)_2]$ and $Na_2\ [Be(C_2O_4)_2]\ .\ H_2O$ in solid state are investigated.

The beryllium oxalate complexes have been investigated hitherto from different points of view.[1-6] Only the last three of the quoted papers dwell on problems concerning vibrational spectra of these complexes. A qualitative study of the infrared spectra of the complex compounds $Na_2\ [Be(C_2O_4)_2]$, $Na_2\ [Be\ (C_2O_4)_2]\ .\ H_2O$, $K_2\ [Be\ (C_2O_4)_2]$ and $(NH_4)_2\ [Be(C_2O_4)_2]$ was carried out by Drăgulescu *et al.* [4] while Graddon [5] studied only the vibrational frequency of the $C = O$ group in the complex. The aim of the present paper is to complete these information with the Raman spectra of the complex compounds $Na_2\ [Be(C_2O_4)_2]\ .\ H_2O$ and $K_2\ [Be(C_2O_4)_2]$.

EXPERIMENTAL

The Raman spectra of the beryllium complex oxalates were recorded using a Zeiss-Jena three glass prism spectrograph on 68 A 56 Gavaert spectral plates. The pellets of crystalline powder (0.6–1.3 mm thick) were irradiated in transmittance with the Hg 436 nm line. The exposer method mentioned in our previous paper [7] was used. The frequencies were measured with an Abbe comparator.

The infrared spectra of the same complexes were recorded using the UR 10 Zeiss-Jena spectrophotometer.

The syntheses of the complexes were performed in accordance with the indications given in paper. [5]

---

[1] C. Drăgulescu, P. Tribunescu and I. Menessy, *Studii și Cercetări Şti. Chim. Acad. R. P. Române. Baza cercetări Şti. Timișoara*, **9**, 197 (1962).

[2] C. Drăgulescu, P. Tribunescu and I. Menessy, *Bul. Şti. Tehn. Inst. Politeh. Timișoara*, **7**, 257 (1962).

[3] T. Sekine, *Bull. Chem. Soc. Japan*, **40**, 261 (1967).

[4] C. Drăgulescu, P. Tribunescu and I. Menessy, *Rev. Roumaine Chim.*, **10**, 913 (1965).

[5] D. P. Graddon, *J. Inorg. Nucl. Chem.*, **3**, 308 (1956).

[6] J. Menessy, *Thesis*, Timişoara, 1966.

[7] V. E. Sahini, R. Beldie and M. Damaschin, *Rev. Roumaine Chim.*, **11**, 1361 (1966).

RESULTS AND DISCUSSION

Table 1 includes the vibrational frequencies of the complexes, measured with an accuracy of ± 0.7 — 3.0 cm^{-1}. A microphotometric recording of one of our Raman plates for $K_2[Be(C_2O_4)_2]$ is illustrated in figure 1. Assignments are based on the results of Fujita *et al.* [8] The complex oxalates of various metals studied by Fujita show nearly the same infrared spectra.[8] This allowed for an assignment of their bands (and of those of the oxalates studied in this paper) based on the calculation performed on the 1 : 1 model of $K_3[Cr(C_2O_4)_3] . 3H_2O$, for which

Table 1

Vibrational frequencies (cm^{-1}) of beryllium complex oxalates

$K_2[Be(C_2O_4)_2]$			$Na_2[Be(C_2O_4)_2] . H_2O$			Assignments	
Raman	IR[4]	IR*	Raman	IR[4]	IR*		
1726	1730	1738	1730	1732	1738	$\nu_a(C=O)$	ν_7, ν_{18}
1697	1700	1700, 1710	1698	1700	1702	$\nu_s(C=O)$	ν_1, ν_{12}
1395	1395, 1387	1402	1398	1402, 1390	1412	$\nu(C-O)+\nu(C-C)$	ν_2, ν_{13}
	1280	1282	—	1282	1295	$\nu(C-O)$	ν_8, ν_{19}
905	935	940, (920)	904	935	940	$\nu(C-O)+\nu(Be-O)+$ $+\delta(O-C=O)$	ν_3, ν_{14}
	860, 826	870, 835		860, 826	865, 830	$\delta(O-C=O)+\nu(Be-O)$	ν_9, ν_{20}
	592, 580	592, 582	—	588, 570	588, 573	$\nu(Be-O)$	ν_4, ν_{15}
	485	502, (485)		510, 485	510, 487	def. ring. $+\delta(O-C=O)$ $+\nu(Be-O)$	ν_{10}, ν_{21}

* Our values.
Values in brackets are measured only for some samples.

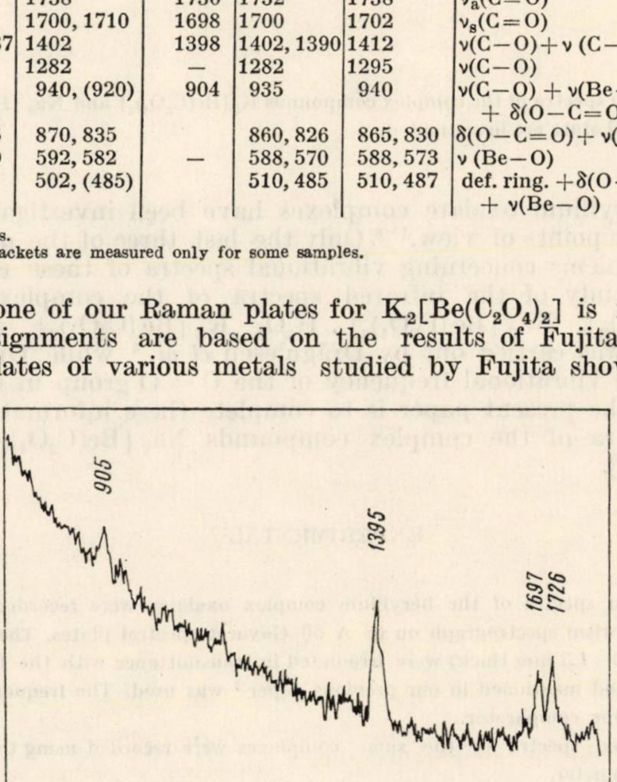

Fig. 1. — Microphotometric recording of the $K_2[Be(C_2O_4)_2]$ Raman spectrum.

---

[8] J. Fujita, K. Nakamoto and A. Martell, *J. Chem. Phys.*, **36**, 324, 331 (1962).

X-ray data were also available. On the other hand comparison between the spectra of 1 : 1 and 1 : 2 platine complexes as well as comparison between the results of their normal coordinate treatment shows that:

— above 1000 cm^{-1} the spectra are similar and the calculation is leading to the same value for both 1 : 1 and 1 : 2 models.

— below 1000 cm^{-1} the bands of the 1 : 1 complex split into two maxima for the 1 : 2 complex (separation 5—15 cm^{-1}). The calculation agrees with the presence of two vibrations (u and g type) in the 1 : 2 model, their mean frequency being nearly equal to the corresponding calculated frequency of the 1 : 1 model.

The Raman frequency assignment in table 1 was carried out in accordance with the above mentioned facts. The two bands around 850 cm^{-1} correspond to $\nu_9(B_{1g})$ and $\nu_{20}(B_{3u})$, attributed to the $\delta(O=C-O)$ $+ \nu(Be-O)$ vibration.[8] For the $\nu(Be-O)$ vibration near 550 cm^{-1} we found a similar splitting corresponding to $\nu_4(A_g)$ and $\nu_{15}(B_{2u})$. It should be however mentioned that Drăgulescu *et al.*[4,6] found in this region of the IR-spectrum of anhydrous $Na_2[Be(C_2O_4)_2]$ a single band (575 cm^{-1}).

All our IR-spectra show in the 620—635 cm^{-1} region bands which have been found previously in,[4,6] but which cannot be assigned to any of the in-plane vibrations of the complex oxalate.[8] One of these bands might indicate the presence of simple oxalate traces.

The 15 fundamental vibrations of the 1 : 1 model of the complex oxalate (C_{2v} symmetry) are grouped in four symmetry classes: $6A_1 + 5B_2$, IR- and Raman-active in-plane vibrations and $2A_2$ Raman-active $+ 2B_1$ IR- and Raman-active out-of-plane vibrations. Accordingly, all the observed Raman frequencies of the investigated beryllium complex oxalates (Table 1) coincide with the frequencies of the corresponding IR bands. It should be mentioned that the strong background caused by the long exposal times prevented us from measuring the Raman frequencies below 800 cm^{-1}.

We introduced our results in Fujita's empirical diagrams[8] in which the (C=O) and (C—O) stretching frequencies are plotted against the (M—O) stretching frequency for different divalent metals. As can be seen in figure 2, the beryllium point lies nearly on Fujita's straight line, but above the Pt point.

In the other two diagrams (Fig. 3), the beryllium points do not lie on either of the two experimental straight lines. This deviation was previously stated also by Drăgulescu *et al.*[4] on the basis of complex stability considerations.

The marked differences between the beryllium complex and the complex oxalates of the other divalent metals consist in the small mass of the Be atom and the comparatively small Be—O distance (1.72 Å). The frequency modifications are consequently understandable. In order to check quantitatively these deviations as compared with the regularities observed in the other divalent complex oxalates, one has to start with a quantitative relation between spectral and thermodynamic data. In view of their independence as to the bond distance and mass, the force constants are the only spectroscopic quantities to be used for this purpose. That is why in the divalent oxalates series one has to compare the M—O stretching force constant with the heat of reaction of the (M—O) bond formation.[9] If on this basis a good correlation between force constants and the corresponding bond strengths is supposed to exist (see [9] for the series of acetylactetonate complexes), then a correlation of the latter with the corresponding frequencies would obviously appear only if metals with similar covalent radii and masses are compared.[9]

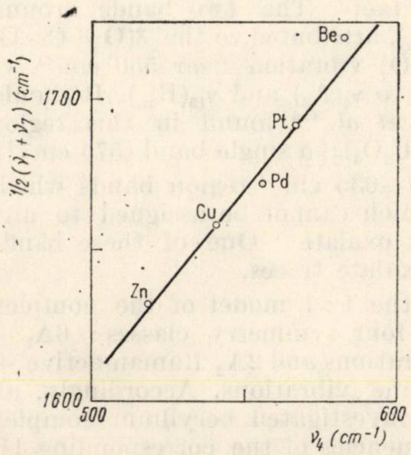

Fig. 2. — Fujita's diagram of ν(C=O) plotted against ν(M—O).

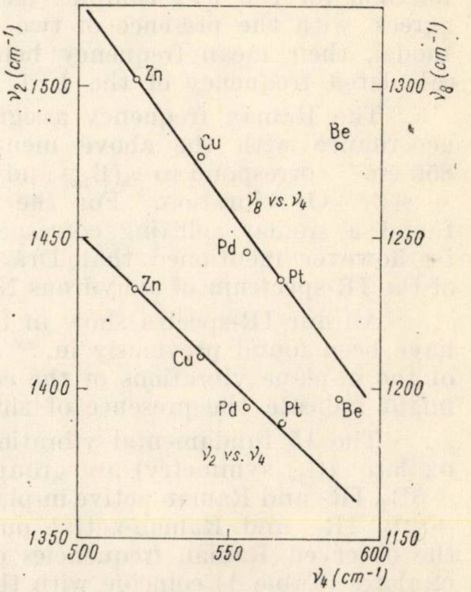

Fig. 3. — Fujita's diagrams of ν(C—O) plotted against ν(M—O).

That explains why an empirical relation was found between ν (C=O) or ν(C—O) and ν(M—O) for divalent complex oxalates of Zn, Cu, Pd, Pt but not for the beryllium oxalate complex. Only a normal coordinate treatment of that complex and implicitely the calculation of potential energy distribution on each normal vibration with respect to each symmetry coordinate would allow solving of the problem quantitatively and would lead to a correct assignment of all the observed vibrational frequencies.

---

[9] K. Nakamoto, P. J. McCarthy and A. E. Martell, *J. Amer. Chem. Soc.*, 83, 1272 (1961).

Revue Roumaine de Chimie, **14**, 423–427 (1969)

THE MECHANISM OF THE ACTION OF LAURIL-AMINE ON THE CORROSION OF IRON IN HCl SOLUTIONS

O. RADOVICI and E. ROMAN
Institute of Physical Chemistry, Bucharest, str. Galaţi, 31

Received March 30, 1968

The corrosion inhibition efficiency of lauril-amine at different concentrations in deaerated HCl solutions has been determined. It was observed that the increase of temperature reduces the inhibitor efficiency between 25–70°. The experimental results permitted the calculation of activation energy in the absence and in the presence of lauril-amine. The surface coverage of the metallic surface with inhibitor has been calculated and the adsorption isotherm has been investigated.

INTRODUCTION

The mechanism of corrosion inhibition by organic inhibitors is a subject under discussion in the corrosion science.[1-3] The action of these compounds is closely related to their adsorption at metal-solution interface.[4]

The adsorption of the organic molecules causes changes in the differential capacity of the double layer. The change of the shape of the $C-\varphi$ curves when the inhibitor is added allows the determination of the surface coverage with organic molecules and of the adsorption isotherm of the system.[5]

The present work deals with the influence of lauril-amine on the corrosion rate or iron in HCl solutions, as well as the influence of temperature upon the action of the compound.

EXPERIMENTAL

Filiform electrodes of pure iron of 20 mm² area have been employed. Initially, electrodes were mechanically polished and then degreased in benzene and cleaned in acetone. The electrodes were sealed in teflon gasket.

---

[1] I. N. Poutilova, S. A. Balezin and V. P. Barranik, "Metallic Corrosion Inhibitors", Pergamon Press, New York, London, Oxford, Paris, 1960, p. 43.

[2] S. A. Balezin, 2ème *Symposium Européen sur les Inhibiteurs de Corrosion.* Comptes rendus, I, Ferrara, 1966, p. 278.

[3] M. F. Donahue and Ken Nobe, *J. Electrochem. Soc.*, **110**, 509 (1963).

[4] Z. A. Jofa, 2ème *Symposium Européen sur les Inhibiteurs de Corrosion.* Comptes rendus, I, Ferrara, 1966, p. 92.

[5] B. B. Damaskin, *Electrochim. Acta*, **9**, 231, (1964).

Saturated calomel electrode was used as reference.

A 5% HCl solution has been used as working electrolyte. Before starting the experiments, the solution was pre-electrolysed and deaerated.

The lauril-amine $C_{11}H_{23}NH_2$ was used as a corrosion inhibitor.

The electrochemical determination of the inhibitor efficiency was performed in a glass cell with cathode and anode separate compartments. A special cell, shown in figure 1, was used for the measurements of the electrode capacities.

The polarization measurements were performed by means of a potentiostatic arrangement. The experiments were carried out in a thermostated bath at 25°, 40°, 55° and 70°.

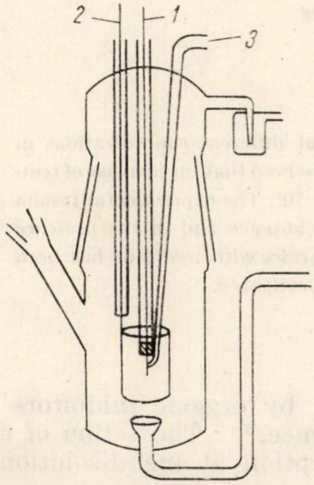

Fig. 1. — Cell for capacity measurements.
1. Test electrode; 2. Auxiliary electrode; 3. Luggin capillary.

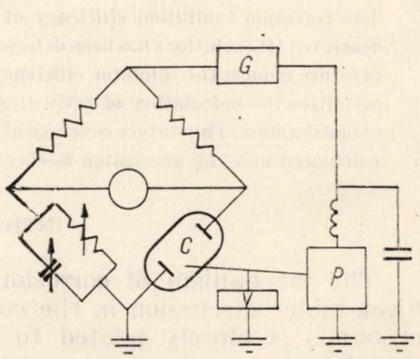

Fig. 2. — Block scheme of the apparatus.
C. — cell; P. — potentiostat; V. — voltmeter; G. — a–c generator.

A capacitance bridge with an external source of variable frequency was used for the determination of the electrodes capacities. The block scheme of the experimental instrumentation is shown in figure 2.

The capacity measurements were carried out at 25°.

RESULTS AND DISCUSSIONS

The cathodic and anodic behaviour of iron in HCl 5% solutions in the absence and the presence of lauril-amine at 25° and 70° is exemplified in figure 3.

As can be seen from the figure, the inhibitor has a kinetic effect on the cathodic curves only by rising the hydrogen overvoltage, according to the kinetic equation:

$$i_k = k' \, [H_3O] \exp\left\{-\frac{F}{RT}\,[\alpha\varphi_c + (1-\alpha)\psi_1]\right\}. \qquad (1)$$

where ψ_1 is the adsorption potential of the organic compound. The adsorption of the organic molecules produces a decrease in the corrosion currents and a modification of Tafel slopes. The corrosion currents and the Tafel slopes for four temperatures in the absence and the presence of the inhibitor are shown in table 1.

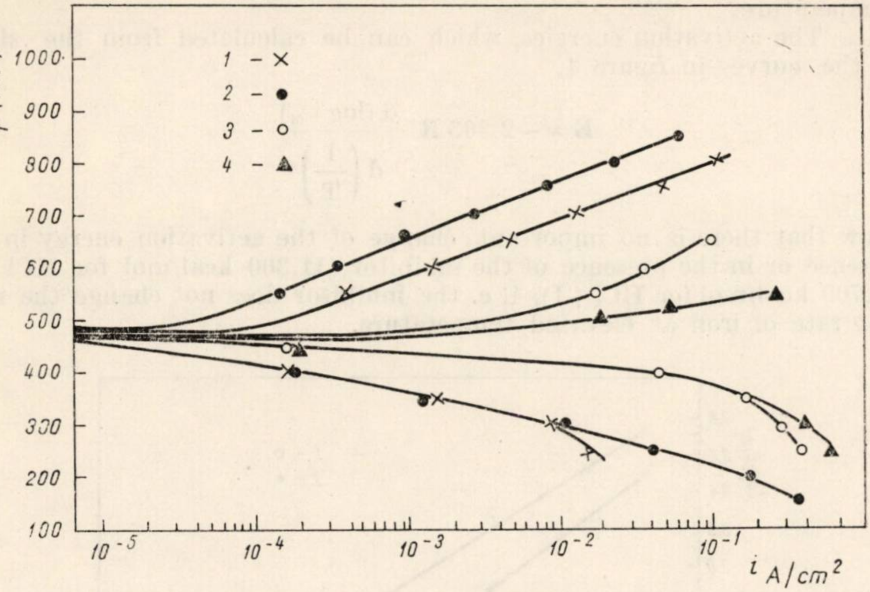

Fig. 3. — Cathodic and anodic curves in the absence and in the presence of the inhibitor at 25° and 70°.

1, 25° HCl; 2, 25° HCl + I; 3, 70° HCl; 4, 70° HCl + I.

Table 1

Tafel slopes and the corrosion currents at 25, 40, 55 and 70°C

Solution	25°		40°		55°		70°	
	I_{A/cm^2}	b_+ mV	I_{A/cm^2}	b_+ mV	I_{A/cm^2}	b_+ mV	I_{A/cm^2}	b_+ mV
HCl 5%	1.16×10^{-4}	104	4.1×10^{-4}	115	2.14×10^{-3}	125	5.5×10^{-3}	73
HCl 5% + 0.002% I	2.8×10^{-5}	110	1.07×10^{-4}	115	7.55×10^{-4}	81	3.25×10^{-3}	20

The results allow the calculation of the inhibitor efficiency I% according to the relation:

$$I\% = \frac{i_{cor} - i'_{cor}}{i_{cor}} 100 \tag{2}$$

The following results were obtained: 75.86% at 25°, 74.83% at 40°, 64.71% at 55° and 40.91% at 70° that show a decrease in the inhibitive action of lauril-amine with increasing temperature. This behaviour is explained by a desorption process of the organic molecules with increasing temperature.

The activation energies, which can be calculated from the slopes of the curves in figure 4,

$$E = -2.303\,R\,\frac{d\,(\log i_{cor})}{d\left(\frac{1}{T}\right)} \tag{3}$$

show that there is no important change of the activation energy in the absence or in the presence of the inhibitor (11.300 kcal/mol for HCl and 10.700 kcal/mol for HCl+I), i. e. the inhibitor does not change the reaction rate of iron at elevated temperature.

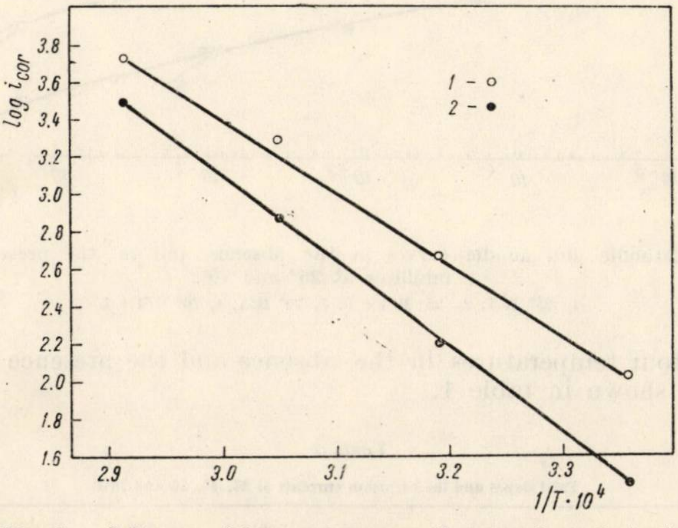

Fig. 4. – Influence of temperature upon the corrosion rate in the absence and in the presence of the inhibitor.
1, HCl; 2, HCl + I.

The surface coverage was measured only at 25°, because at higher temperature the inhibitor is desorbed. In this case, the surface coverage will be given by the relative diminution of the capacity of the double layer, produced by the adsorption of the inhibitor.

$$\theta = \frac{C_0 - C_i}{C_0 - C_\infty} \tag{4}$$

where C_0, C_i and C_∞ are the differential capacities in the absence of the inhibitor, at a given concentration and at its boundary concentration.

The measurements were achieved at three frequencies (800, 2000 and 5000 Hz) and the double layer capacities for cathodic range were calculated by extrapolation for infinite frequencies. C_∞ was determined from the curves C—c.

The adsorption isotherm, shown in figure 5, is a Frumkin isotherm

$$Bc = \frac{\theta}{1-\theta} e^{-2a\theta}. \tag{5}$$

where a — the interaction parameter — is, in this case, 2.5.

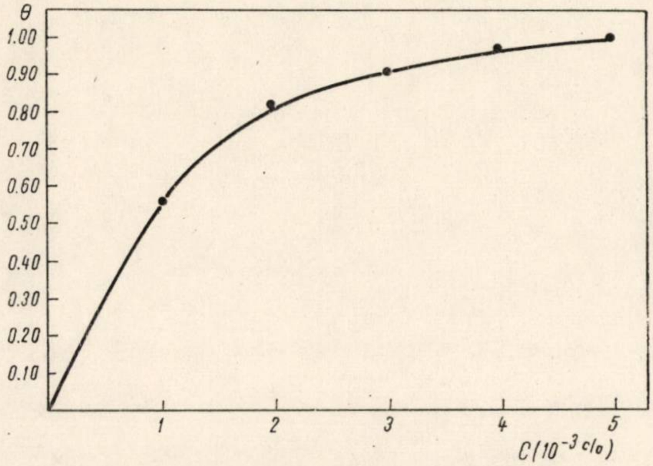

Fig. 5. — Adsorption isotherm at —450 mV.

The values of surface coverage for cathodic potentials, as well as the values of the inhibition are shown in table 2.

Table 2

Surface coverage and the inhibition

c %	I %	—450 mV	—500 mV	—550 mV	—600 mV
0	0	0	0	0	0
0.001	50.30	0.56	0.58	0.58	0.59
0.002	75.86	0.82	0.87	0.88	0.87
0.003	83.25	0.90	0.93	0.93	0.93
0.004	90.17	0.97	0.96	0.97	0.96
0.005	91.84	0.99	0.98	0.99	0.98

The results show that the inhibitor efficiency is determined by the surface coverage of the electrode by molecules of inhibitor.

Revue Roumaine de Chimie, **14**, 423—427 (1969)

Revue Roumaine de Chimie, **14**, 429—439 (1969)

ALKALINE HYDROLYSIS OF THE METHYL AND ETHYL ACETATES. I

CALORIMETRICAL DETERMINATION OF THE STANDARD THERMAL EFFECTS DURING THE EVOLUTION OF THE CHEMICAL REACTIONS

RODICA VÎLCU and I. CIOCĂZANU

Laboratory of Physical Chemistry III, University of Bucharest
Bdul. Republicii 13

Received May 20, 1968

By calorimetric measurements, the rate constants were determined for the alkaline hydrolysis reactions of the methyl acetate and of the ethyl acetate at 25°. The thermokinetics of the process was studied with the help of a calorimeter designed and constructed by the authors.

INTRODUCTION

The kinetic characterization of the alkaline hydrolysis reactions of the alkyl esters was made ninety years ago in the works of Warder [1], Reicher [2], van't Hoff [3], Trautz [4], Olsson [5], etc., nearly exclusively by means of volumetric methods, though equally, in a few cases, by means of conductivity measurements. [6] Considering that they were well substantiated by the large number of works devoted to reactions of the type

$$R - COOR' \,(aq) + OH^{-}(aq) \rightarrow R'OH \,(aq) + RCOO^{-}(aq)$$

these studies were resumed lately [7, 8] so as to ascertain the possibility of applying thermochemical determinations to the study of the reaction kinetics. The method of estimating the kinetic parameters from thermochemical data, initiated by Ducleaux[9] and by Guggenheim,[10] is based on the proportionality between the amount of transformed substance in the course of a reaction and the thermal effect due to the chemical process development[11].

---

[1] R. B. Warder, *Ber. dtsch. chem. Ges.*, **14**, 1361 (1881).

[2] L. Th. Reicher, *Liebigs. Ann. Chem.*, **232**, 103 (1886).

[3] J. H. van't Hoff, „Vorlesungen III", 138 (1903).

[4] M. Trautz and K. T. Volkmann, *Z. phys. Chem. (Leipzig)*, **64**, 53 (1908).

[5] H. Olsson, *Z. phys. Chem. (Leipzig)*, **118**, 107 (1925).

[6] J. Walker, *Proc. Roy. Soc.*, *A* **78**, 160 (1906).

[7] F. Becker and F. Spalnik, *Z. phys. Chem. (Frankfurt)*, **26**, 1, (1960).

[8] P. Baumgartner and P. Duhant, *Bull. Soc. chem. France*, **1960**, 1187.

CORRELATION BETWEEN THE KINETIC PARAMETERS AND THE THERMOCHEMICAL QUANTITIES

In this paper the correlation is studied between the rate constants and the reaction enthalpies of the alkaline hydrolysis of the methyl and ethyl acetates. The alkaline hydrolysis of the considered esters represents a process of the second order, characterized — on the assumption of the initial concentrations of equal reactants — by the following formula of the velocity reaction

$$\frac{dx}{dt} = k_T(a - x)^2. \tag{1}$$

The integral form of equation (1) defines the velocity constant k_T

$$k_T = \frac{1}{t}\left(\frac{1}{a-x} - \frac{1}{a}\right) \tag{1a}$$

where

t is the reaction time,
a — the initial concentration of the reactant,
x — the concentration decrease in the course of time.

The equation connecting the kinetic and thermodynamic quantities of the system is based on the proportionality between the reaction rate and the thermal effect Q due to the process evolution

$$\frac{dQ}{dt} = \Delta H \frac{dn}{dt} = \Delta H. V. \frac{dx}{dt} \tag{2}$$

where

n is the mole number
V — the solution volume,
ΔH — the molar heat of the reaction

If Q_∞ denotes the heat amount developed by the reactant transformation ($a\,V$ moles) and Q_0 denotes the heat amount accompanying the forerunning reaction processes (the crushing of test tube, the reactants mixing), then the initial concentration and the concentration diminution in regard to thermal quantities of the system can be expressed as follows

$$a = \frac{Q_\infty - Q_0}{V \cdot \Delta H} \tag{3}$$

---

[9] J. Duclaux, *Compt. rend.*, **146**, 120 (1908).
[10] E. A. Guggenheim, *Phil. Mag.*, **2**, 538 (1926).
[11] J. Barthel, E. Barker and N. G. Smahl, *Z. phys. Chem. (Frankfurt)*, **29**, 58 (1961).

and

$$x = \frac{Q_{t_r} - Q_0}{V \cdot \Delta H} \tag{4}$$

where Q_{t_r} represents the thermal effect due to the reaction at the moment t_r, when a concentration decrease x is recorded.

By substituting relations (2), (3), (4) into the kinetic equation (1a) and by making explicit the obtained expression with respect to Q_{t_r}, we have the time dependance of the reaction heat

$$Q_{t_r} = \frac{Q_0 + a k t_r Q\infty}{1 + a k t_r}. \tag{5}$$

After performing the division we obtain

$$Q_{t_r} = Q_0 + a k t_r (Q_\infty - Q_0) \sum_{i=0}^{\infty} (-a k t_r)^i. \tag{6}$$

Index r denotes a given moment t_r to which corresponds a determinate thermal effect Q_{t_r}. If the sum of the series in equation (6) is replaced by its value, there results the formula

$$Q_{t_r} = Q_0 + (Q_\infty - Q_0) \frac{a k t_r}{1 + a k t_r}. \tag{7}$$

This formula confirms directly the physical reality under boundary conditions: at the initial moment ($t = 0$), before the reaction is started, we have $Q_{t_r} = Q_0$ (no thermal effect due to the reaction is recorded and Q_{t_r} is identical to the mixing effect of the reactants, forerunning the chemical process). At the end of the reaction period ($t \to \infty$), $Q_{t_r} = Q_\infty$. If equation (7) is reversed and if $\frac{1}{Q_{t_r} - Q_0}$ represents the ordinate in a system of rectangular axes against the reciprocal time value as its abscissa, a straight line is obtained having the slope $\operatorname{tg} \alpha = \frac{1}{a k (Q_\infty - Q_0)}$. The average value of the reaction rate constant

$$k_T = \frac{1}{\operatorname{tg} \alpha} [a (Q_\infty - Q_0)]^{-1} \tag{7a}$$

is estimated simultaneously with the determination of the angle α trigonometric tangent. If the successively represented points describe a perfect straight line, there results that the quantity k_T is kept at an invariable value all along the reaction development, which confirms the validity of the computation basic elements.

ESTIMATION OF QUANTITIES Q_{t_r}, Q_0 AND Q_∞

In the non-adiabatic working conditions offered by the calorimeter within which the temperature variations recorded during the process evolution were measured, we took into account both the outward heat transfer $C \cdot \beta \cdot \Delta T$ (β being the cooling constant of the calorimeter) and the thermal agitation effect (l_0). In this manner, the variation in time of the thermal effect $\frac{dQ}{dt}$ is expressed as a function of the temperature variation, during the chemical process, corrected as follows

$$\frac{dQ_t}{dt} = C\left[\frac{d\Delta T_m}{dt} + \beta \Delta T_m\right] - l_0 \tag{8}$$

where

C is the heat capacity of the system,

ΔT_m, the temperature difference between the calorimeter and the medium.

The integration of equation (8) from $t = 0$ to a moment t_r gives the heat amount Q_{t_r} spent during this time interval

$$Q_{t_r} = C\left[\Delta T_m - (\Delta T_0)_m + \beta \int_0^{t_r} \Delta T_m \, dt\right] - l_0 t_r, \tag{9}$$

$(\Delta T_0)_m$ has the same signification as ΔT_m, but for $t = 0$ and is assimilated with zero. The integral in equation (9) is solved by measuring with a planimeter the surface delimited by the representative curve, figured in temperature-time coordinates within the integral limits.

The cooling constant β can be computed either with the help of the Newton cooling law,[7] or by solving the linear differential equation (9) by considering its left hand side null, according to the method proposed by Guggenheim.[10] In the first case, the mathematical treatment of Newton's law leads to the following relation

$$\beta = \frac{2.303}{t_{r+1} - t_r} \log \frac{T_{r+1} - T_e}{T_r - T_e}, \tag{10}$$

where T_e is the temperature of the external medium, constant during the experience, while index r applied to the time parameter t or to temperature T indicates the number of the determination.

In the second case, Guggenheim's method, by using the solution of the linear differential equation (8), gives the expression

$$\log[\Delta T_m(t + \Delta t) - \Delta T_m(t)] = -\frac{\beta}{2.303} t + \log\left(\frac{l_0}{\beta C} - \Delta T_{0,m}\right)(1 - e^{\beta \Delta t}). \tag{11}$$

The left hand side of this equation is a linear function of time. Its slope is $-\beta/2.303$.

The quantity Q_0, in equation (7) is determined directly from calorimetric measurements, by fulfilling the conditions of the reaction evolution.

For determining the quantity Q_∞,[7] an equation is proposed which expresses the rate constant as a function of temperature

$$k_T = k_{T_0}\left[1 + \frac{E_R}{RT_0} \cdot \frac{\Delta T_m}{T_0} + \frac{E_a}{RT_0}\left(\frac{E_a}{2RT_0} - 1\right)\left(\frac{\Delta T_m}{T_0}\right)^2\right]^{*)} \tag{12}$$

---

*) The second power term of ΔT_m is negligible if to ΔT_m is attributed a value of about 1°, under standard conditions and if for the activation energy we take into consideration $E_a \approx 12$ kcal/mole. Under these conditions the error is less than 0.5% when the above mentioned term is disregarded.

where,

k_{T_0}, is the reaction rate constant at a reference temperature T_0,

E is the activation energy of the reaction.

By identifying the expressions of the rate constant as given by equation (12) — from which only the term at the first power of ΔT is considered — with the following formulation

$$k_T = \frac{\frac{\mathrm{d}Q}{\mathrm{d}t}(Q_\infty - Q_0)}{a(Q_\infty - Q_t)^2} \tag{13}$$

which results easily from equations (1), (2), (3) and (4) and, by integrating the resulted relation within the time interval $0 - t_r$, we obtain

$$\frac{1}{a}\,\frac{Q_{t_r} - Q_0}{Q_\infty - Q_{t_r}} = k_{T_0}\left(t_r + \frac{E_a}{RT_0^2}\int_0^{t_r} \Delta T\,\mathrm{d}t\right). \tag{14}$$

Equation (14) allows to calculate Q_∞ by forming the differences for two of the equations obtained above and making use of three pairs of Q_{t_r} and t_r values

$$Q_\infty = \frac{(t_3 - t_2)(Q_{t_2} - Q_{t_1})\,Q_{t_3} - (t_2 - t_1)(Q_{t_3} - Q_{t_2})\,Q_{t_1}}{(t_3 - t_2)(Q_{t_2} - Q_{t_1}) - (t_2 - t_1)(Q_{t_3} - Q_{t_2})}. \tag{15}$$

The conditions to be fulfilled by times t_1, t_2 and t_3 is that the average values of the integrals such as

$$\frac{1}{t_r - t'_r}\int_{t'_r}^{t_r} \Delta T\,\mathrm{d}t$$

for the pairs of values of the parameter be identical, that is

$$\frac{1}{t_2 - t_1}\int_{t_1}^{t_2} \Delta T\,\mathrm{d}t = \frac{1}{t_3 - t_2}\int_{t_2}^{t_3} \Delta T\,\mathrm{d}t. \tag{16}$$

This condition is fulfilled if the experimental curve $\Delta T = \Delta T(t)$ has a maximum, while the values t_1 and t_3 are situated on both its sides.

The apparatus, adapted to follow the reactions developed in the liquid phase, at temperatures of 10—80°, consists of the calorimeter proper A, based on the working principle of the anisothermal calorimeters [12] and of a cylindric container B immersed into a Höppler ultrathermostat W, type U10 (Fig. 1).

In the thermostat, the liquid is kept at a constant temperature, within $\pm 2 \times 10^{-2}$°. The calorimeter A, having a capacity of about 150 cm^3 is made of stainless steel V_2A and is hermetically closed with a lid of the same material with a teflon packing. The lid is provided with three apertures one for the thermometer T, one for the stirrer glass-rod M centered on two ball bearings P against friction, and a third one to let pass the device I for the test tube crushing. The stirrer is set to work by an electric motor. The test tube crushing device is made of a stainless steel rod, prolonged by an insulating rod so as to prevent heat exchanges between the calorimeter container and the medium. Under an external action, the rod I crushes the test tube F spilling its content into the second reactant held in the calorimeter. The test tube F made of thin glass contains the ester and is borne by a support D.

---

[12] R. VÎLCU, I. CIOCĂZANU and A. UZUM, *Studii și cercetări chimie Acad. Romania*, **12**, 823 (1966).

The temperature within the calorimeter is measured either with a Beckmann thermometer, or with a platinum thermoresistive transductor (100 Ω at 0°, with a thermal coefficient of 3.8×10^{-3} Ω /deg) mounted in a Wheatstone bridge[13].

In the last case, the variation of thermal effects can be recorded.

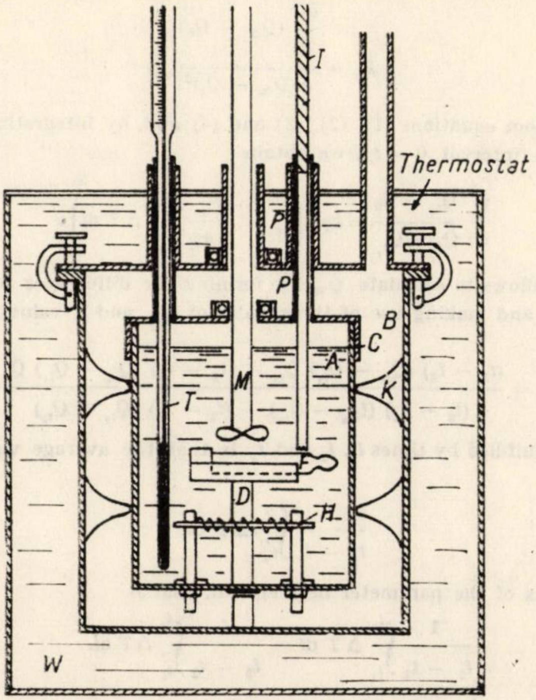

Fig. 1. — Diagram of the reaction calorimeter.

A — calorimeter proper; *B* — cylindric container;
M — stirrer; *P* — bearings; *T* — Beckmann thermometer;
I — device for test tube crushing; *F* — test tube;
D — support for test tube; *W* — ultrathermostat U 10;
H — heater; *K* — suporters.

The heat capacity of the system is determined with the help of the heater *H*, immersed into the calorimeter liquid. Its platinum winding, having a resistance of about 2 Ω and a 0.1 mm diameter, is fed from a d. c. source (4 V) with both its intensity and its voltage under control. The resistance winding is made on a teflon rod.

Calorimeter *A* is borne, in the center of the brass container *B* (with a 3 mm thick wall), by supporters *K*. Between the calorimeter and the container there is an air lager whose thickness can be reduced, according to the necessities, by metallic filling. The container lid *B* is fastened, with the help of a rubber packing at three points, by pressing clamps. Three of its apertures correspond to the three ones of the calorimeter lid, while the 4-th one is used for the passage of the electric wires system. The whole assembly described above is immersed into the ultrathermostat *W*.

[13] R. VÎLCU and F. STANCIU, *Rev. Roumaine Chim.*, **9**, 686 (1964).

EXPERIMENTAL RESULTS AND DISCUSSIONS

The thermal effects accompanying in time the alkaline hydrolysis of the methyl acetate and ethyl acetate were calorimetrically determined under standard conditions. The initial mole number of the esters made use of (supplied by Merck for chromatographic purposes) was taken equal to the mole number of the sodium hydroxide, contained in a 0.1 m solution. The NaOH solution is contained in calorimeter A and the ester in the test tube F. The reaction starts after the thermal stabilization of the system. The transition from the thermal equilibrium (the initial period) towards the principal period is marked by the sudden temperature increase, represented, according, to figure 2, by means of the experimental data from columns 1 and 2 of Tables 1 and 2. The thermal effects Q_{t_r}, at the various moments t_r of the process evolution were calculated with equation (9). The corrections applied to quantity Q_{t_r} relate to heat transfer losses, enthalpy variations due to the mixing of the reactives as well as to the thermal accumulation resulting from the mechanical stirring of the solutions and from the test tube crushing, etc. These secondary effects were determined by distinct measurements and their average values (obtained by repeated determinations) are recorded in Table 3. For instance, the mixing heat and the test tube crushing heat Q_0 were determined on a blind test: instead of the 0.1 m NaOH solution, an equal water volume, was introduced, taking into account the solution dilution as well as the possibility of estimating its density and specific heat in regard to those of the water. Q_∞ was estimated by means of equation (15) from several pairs of Q_{t_r} and t_r values. The

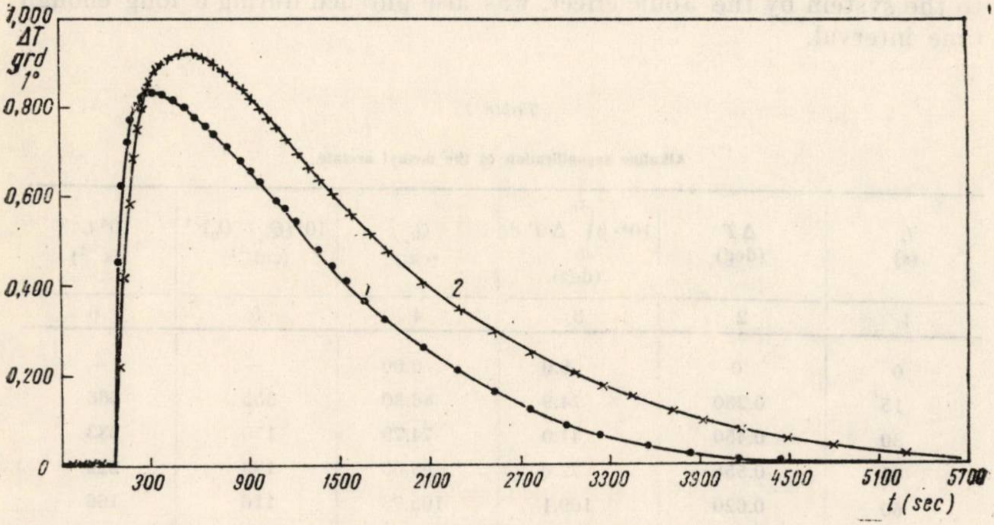

Fig. 2. — Variation of temperature with time in the process of the alkaline hydrolysis of the methyl acetate (1) and of the ethyl acetate (2).

average values recorded in the tables do not differ from the individual values by more than ± 0.2%. The thermal effect l_0 due to the liquid stirring, was determined by pursuing the temperature variation of the calorimetric medium during a long enough time interval and by taking into account the heat capacity of the system. For determining the cooling constant of the calorimeter the loss of a known heat amount, transmitted to the system by the Joule effect, was also pursued during a long enough time interval.

Table 1

Alkaline saponification of the methyl acetate

t_r (s)	ΔT (deg)	$10^4 \cdot \beta \int_0^{t_r} \Delta T \, dt$ (deg)	Q_{t_r} (cal)	$10^4 (Q_{t_r} - Q_0)^{-1}$ (cal^{-1})	$10^4 t_r^{-1}$ (s^{-1})
1	2	3	4	5	6
0	0	0.0	0.00	—	—
15	0.280	14.9	46.30	355	666
30	0.450	41.0	74.79	176	333
45	0.558	72.0	93.05	133	222
60	0.620	109.1	103.73	116	166
75	0.685	159.5	113.22	105	133
90	0.720	207.2	121.77	96.4	111
105	0.750	257.6	127.49	91.4	95.2
120	0.770	311.7	131.73	88.0	83.3
133	0.787	365.7	135.17	85.4	74.0
150	0.798	421.1	138.07	83.3	66.6
165	0.800	473.8	139.17	82.6	60.6
180	0.817	529.2	142.75	80.2	55.5
195	0.821	588.6	144.35	79.2	51.2
210	0.825	647.2	145.95	78.2	47.6
225	0.828	706.0	147.34	77.3	44.4
240	0.829	764.7	148.49	76.7	41.6
255	0.829	822.3	149.48	76.1	39.2
270	0.828	880.0	150.25	75.6	37.0
300	0.827	994.1	151.65	74.8	33.3
315	0.824	1052.3	152.30	74.5	31.7
360	0.818	1220.8	153.86	73.6	27.7
390	0.810	1332.7	154.40	73.2	25.6
465	0.795	1606.5	156.23	72.4	21.5
—	—	—	—	—	—
∞(4800)	0.005	6228.9	—	—	—

Table 2

Alkaline saponification of the ethyl acetate

t_r (s)	ΔT (deg)	$10^4 \cdot \beta \int_0^{t_r} \Delta T\, dt$ (deg)	Q_{t_r} (cal)	$10^4 (Q_{t_r} - Q_0)^{-1}$ (cal^{-1})	$10^4\, t_r^{-1}$ (s^{-1})
1	2	3	4	5	6
0	0.000	0.0	0.00	—	—
60	0.420	53.7	69.91	190	166
75	0.508	87.5	84.87	148	133
90	0.580	125.2	97.36	125	111
105	0.635	167.3	107.04	111	95.2
120	0.685	222.7	116.23	101	83.3
135	0.720	269.8	122.61	95.1	74.0
150	0.750	319.7	128.33	90.2	66.6
165	0.775	369.6	133.23	86.4	60.6
180	0.795	421.7	137.47	83.3	55.5
210	0.834	530.9	145.62	78.0	47.6
240	0.854	642.3	150.63	75.1	41.6
270	0.875	756.4	155.81	72.2	37.0
300	0.890	872.2	160.16	70.0	33.3
330	0.903	990.9	164.19	68.1	30.3
360	0.908	1111.6	166.89	66.9	27.7
390	0.915	1232.4	169.92	65.6	25.6
420	0.917	1352.7	172.13	64.6	23.8
480	0.921	1595.4	176.55	62.5	20.8
510	0.920	1717.3	178.26	62.0	19.6
540	0.917	1837.6	179.65	61.6	18.5
555	0.914	1896.9	180.09	61.4	18.0
600	0.904	2078.7	181.26	61.2	16.6
—	—	—	—	—	—
∞(5400)	0.005	8328.0	—	—	—

Table 3

Thermochemical quantities and computation data for the alkaline hydrolysis reactions

Ester	$10^2 \cdot a$ (mol. l^{-1})	Q_0 (cal)	Q_∞ (cal)	$Q_\infty - Q_0$ (cal)	$10^2 \cdot l_0$ (Watt)	β (s^{-1})
1	2	3	4	5	6	7
Methyl acetate	9.96	18.14	163.56	145.42	1.40	$5.08 . 10^{-4}$
Ethyl acetate	8.15	17.50	200.70	183.20	1.40	$5.08 . 10^{-4}$

The heat capacity of the system (about 165 cal/deg) was determined by the electric technique. The value read ΔT_c of the temperature variation was corrected according to the temperature fluctuations during the initial and final periods, thus obtaining the actual temperature difference ΔT

$$\Delta T = \Delta T_c - \frac{1}{2}\left[\left(\frac{\Delta T}{\Delta t}\right)_i + \left(\frac{\Delta T}{\Delta t}\right)_f\right] \cdot t_p \tag{17}$$

where Δt is the time interval during which the temperature raises by ΔT. Index i refers to the initial period and index f to the final period. The quantity t_p represents the initial period length.

The values of the rate constants k_T, obtained from experimental data, are recorded in Table 4 alongside with the reference values for reactions pursued either under similar conditions [7] or conductometrically.[6] Columns 1 and 2 of this table give the computation data for k_T from equation (7a). Between the literature data and those of the present paper there are differences of up to ± 3% in the rate constant values of the considered reactions.

Table 4

Rate constant at 25° of the alkaline hydrolysis reactions of the methyl and ethyl acetates

Ester	$10^4\,a(Q_\infty - Q_0)^{-1}$ $\mathrm{l \cdot mole^{-1}\,cal^{-1}}$	$(\mathrm{tg}\,\alpha)^{-1}$ $\mathrm{cal.\ s^{-1}}$	k $(\mathrm{l \cdot mole^{-1}\,s^{-1}})$ Present paper	k $(\mathrm{l \cdot mole^{-1}\,s^{-1}})$ Literature [6, 7]
1	2	3	4	5
Methyl acetate	690	3.125	0.215	0.209
Ethyl acetate	669	1.629	0.109	0.112

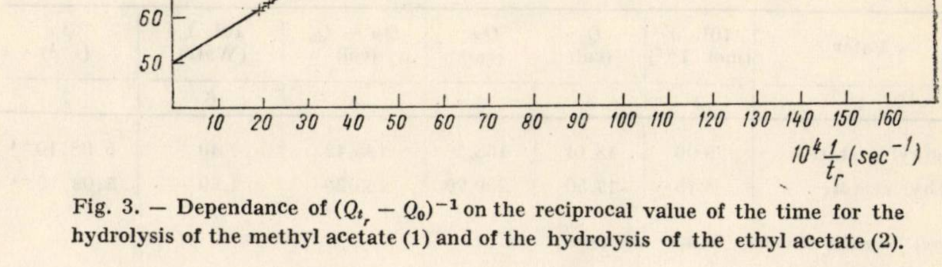

Fig. 3. — Dependance of $(Q_{t_r} - Q_0)^{-1}$ on the reciprocal value of the time for the hydrolysis of the methyl acetate (1) and of the hydrolysis of the ethyl acetate (2).

In the case of the considered temperature, owing to the perfect linearity of the dependence between the quantities represented in figure 3, no fluctuation appears in the values of the rate constants.

In the whole time interval during which the reaction evolution was studied, the straight line slope obtained is invariable.

The present study will be extended also to other temperatures with the object of establishing the thermal coefficients of the rate constants and, implicitely, the kinetic elements characterizing the reactions under study. Owing to the continuous character of the determinations, the calorimetric method obviates the errors inherent to the methods based on periodical sample extraction.

The calorimetric method as applied to this study can be extended with good results to the chemical reactions proceeding at reduced rates where temperature variations smaller than 1 deg are recorded in order to be able to warrant to a certain extent the isothermal character of the process and hence the exact value of the rate constant.

Revue Roumaine de Chimie, **14**, 429–439 (1969)

Revue Roumaine de Chimie, **14**, 441–450 (1969)

ELECTRICAL CONDUCTIVITY AND DISPERSION DEGREE OF LYOPHILIC COLLOIDS RELATIONSHIP. X*

0.2 M SODIUM STEARATE, PALMITATE AND LAURATE IN THE PRESENCE OF ELECTROLYTES WITH DIFFERENT ANIONS

E. ANGELESCU and MINODORA RADU

Institute of Macromolecules of the Academy
Macromolecular physical chemistry and colloids division
Bucharest, Splaiul Independenţei, 89

Received June 28, 1968

Electrical conductivity of 0.2 M sodium stearate, palmitate and laurate with addition of $NaNO_3$, Na_2SO_4 and Na_2CO_3 of various concentrations ranging from 0.02–0.1 M, in the temperature range 20–80° has been determined. The viscosity of the same colloidal systems at the temperatures 60, 70 and 80° has also been measured. The data obtained lead to the conclusion that regardless of the electrolytical colloid nature, the effects of electrolytes upon the emphasizing of lyophobic character of the system differ according to the anion nature of electrolytes and are as follow : $CO_3^{=} > SO_4^{=} > NO_3^{-}$. The longer the hydrocarbon chain of electrolytical colloid is, the more effective are the electrolytes.

The effect of added electrolytes on the behaviour of electrolytical association colloids has been noticed, ever since first investigations of these systems began.

The practical and theoretical interest which the addition of the electrolytes presents is the reason for which, nowadays, this problem is very often studied.

First it has been noticed that the addition of electrolytes causes a diminution of the soap solubility. In certain conditions, this insolubility can complete leading to the "salting-out" phenomenon.

The research led, in several cases, to the conclusion that the addition of electrolyte to an association electrolytical colloid solution, decreases its critical micelle concentration, [1–5] and increases the micellar weight ,[6,7] as well as the gelation temperature [8–10] of the colloidal system.

---

* Previous part (IX), E. Angelescu and M. Radu, *Rev. Roumaine Chim.*, **12**, 1359 (1967).

[1] M. L. Corrin and W. D. Harkins, *J. Amer. Chem. Soc.*, **69**, 679, 683 (1947).

[2] E. L. Colichman, *J. Amer. Chem. Soc.*, **73**, 3385 (1951).

[3] H. Lange, *Kolloid-Z.*, **121**, 66 (1951).

[4] K. Shinoda and K. Kinoshita, *Bull. Chem. Soc. Japan*, **27**, 73 (1954).

[5] P. A. Demchenco, Doctoral thesis, Kiev, U.R.S.S., 1964.

[6] W. D. Harkins and R. Mittelmann, *J. Colloid Sci.*, **4**, 367 (1949).

[7] H. B. Klevens, *J. Amer. Chem. Soc.*, **72**, 3780 (1950) ; **72**, 3581 (1950) ; **74**, 4624 (1952).

[8] E. Angelescu and D.M. Popescu, *Kolloid-Z.*, **66**, 175 (1934).

[9] E. Angelescu and M. Radu, *Studii şi Cercetări Chim. Acad. Romania*, **6**, 403 (1958) ; **6**, 503 (1958).

[10] G. Popescu, *Studii şi Cercetări Chim. Acad. Romania*, **6**, 465 (1958).

Continuing our earlier researches[9] and based on conclusions obtained in this respect, the present paper deals with the action of electrolytes which enhance the hydrophoby of the electrolytical colloid and, in certain cases, lead even to the formation of coagels (microcrystalline structure).

Furthermore, we intended to observe the effects of electrolytes with different anions, added to salt solutions of higher fatty acids having hydrocarbon chain of various lengths, in solution as well as during the sol to gel transition.

Considering that the above effects are revealed by the electrical transport, we measured the electrical conductivity of 0.2 M sodium stearate, palmitate and laurate aqueous solutions, in the presence of Na_2SO_4, $NaNO_3$ and Na_2CO_3. Electrolytes have been added in various concentrations ranging from 0.02 to 0.1 M at the temperature 20–80° for every 10°.

The temperature was maintained with a $\pm$ 0.05° accuracy.

Furthermore we measured the viscosity of those systems at 80, 70° and in some cases also at 60°.

Only the values which presented a time constancy were taken into account.

EXPERIMENTAL RESULTS

Sodium stearate pure BDH, sodium palmitate *p. a.* "Reanal" and sodium laurate *purum* "Heidelberg" have been used and as electrolytes, $NaNO_3$ *puriss.* "Spolek", Na_2CO_3 anh. *p. a.* "Chinoin" and Na_2SO_4 *puriss.* "Gliwice".

Solutions concentration has been expressed in moles per kg solution.

The installation used for determining the electrical conductivity has been described in a previous paper.[11]

The viscosity has been determined by means of an Ostwald viscosimeter (flow time for water at 80, 70 and 60° being 47.5, 52.9 and 58.9 sec., respectively), with an accuracy of about 1 %, and the density by means of a picnometer.

The solutions are quite clear in sol and the gelation obtained by temperature lowering, leads to a sudden decrease of the electrical conductivity. We may conclude that coagels are obtained.

It has been noticed that the addition of electrolytes to the solutions of sodium stearate and palmitate, reduces the transition period from sol to gel (from 8–9 hours till almost 10 minutes).

Solutions of sodium laurate do not form gels regardless of the nature or concentration of the added electrolyte. The electrical conductivity values obtained for the colloidal systems which form gels in the studied temperature range, are shown in tables 1–6.

---

[11] E. Angelescu and M. Radu, *Rev. Roumaine Chim.*, **11**, 131 (1966).

Table 1

Electrical conductivity ($\lambda \times 10^4\ \Omega^{-1}\ cm^{-1}$) of 0.2 M sodium stearate + $NaNO_3$

Electrolyte conc. / °C	0.02 M	0.04 M	0.06 M	0.08 M	0.1 M
80	171.4	206.7	249.0	292.4	343.6
70	148.8	180.8	218.7	259.6	305.8
60	126.8	155.9	191.0	226.9	268.1
50	60.5	83.7	111.0	140.4	159.1
40	48.33	69.4	94.7	119.4	135.6
30	39.80	56.6	78.3	98.0	120.2
20	31.84	44.97	62.5	79.8	98.2

Table 2

Electrical conductivity ($\lambda \times 10^4\ \Omega^{-1}\ cm^{-1}$) of 0.2 M sodium stearate + Na_2SO_4

Electrolyte conc. / °C	0.02 M	0.04 M	0.06 M	0.08 M	0.1 M
80	167.3	204.7	253.1	274.7	310.5
70	145.2	178.6	224.0	242.6	274.7
60	123.6	153.4	194.1	211.5	240.6
50	57.7	80.0	115.2	127.7	148.6
40	46.25	66.1	97.6	107.0	125.0
30	37.72	54.2	80.4	87.2	101.7
20	29.30	42.9	63.6	70.0	81.9

Table 3

Electrical conductivity ($\lambda \times 10^4\ \Omega^{-1}\ cm^{-1}$) of 0.2 M sodium stearate + Na_2CO_3

Electrolyte conc. / °C	0	0.02 M	0.04 M	0.06 M	0.08 M	0.1 M
80	127.3	167.3	204.7	253.1	274.7	310.5
70	108.7	145.2	178.6	224.0	242.6	274.7
60	90.6	123.6	153.4	194.1	211.5	240.6
50	32.67	57.7	80.0	115.2	127.7	148.6
40	21.46	46.25	66.1	97.6	107.0	125.0
30	16.97	37.72	54.2	80.4	87.2	101.7
20	13.27	29.30	42.9	63.6	70.0	81.9

Table 4

Electrical conductivity ($\lambda \times 10^4$ Ω^{-1} cm^{-1}) of 0.2 M sodium palmitate + $NaNO_3$

Electrolyte conc. °C	0.02 M	0.04 M	0.06 M	0.08 M	0.1 M
80	219.9	253.6	298.5	335.5	372.2
70	193.3	224.4	264.6	296.6	330.9
60	166.9	194.8	229.8	259.8	289.7
50	141.1	165.4	195.2	220.8	248.7
40	76.7	99.2	122.3	144.0	165.2
30	62.4	81.8	101.2	119.4	137.6
20	50.0	65.6	81.6	96.7	112.3

Table 5

Electrical conductivity ($\lambda \times 10^4$ Ω^{-1} cm^{-1}) of 0.2 M sodium palmitate + Na_2SO_4

Electrolyte conc. °C	0.02 M	0.04 M	0.06 M	0.08 M	0.1 M
80	219.9	248.7	287.4	320.5	350.3
70	193.7	219.6	253.6	284.3	310.5
60	167.5	190.3	220.1	247.7	271.1
50	140.6	161.6	187.0	211.5	231.6
40	77.3	93.5	113.1	134.1	153.2
30	62.8	76.4	92.9	110.4	126.4
20	49.8	60.8	74.4	87.9	100.0

Table 6

Electrical conductivity ($\lambda \times 10^4$ Ω^{-1} cm^{-1}) of 0.2 M sodium palmitate + Na_2CO_3

Electrolyte conc. °C	0	0.02 M	0.04 M	0.06 M	0.08 M	0.1 M
80	179.7	210.2	252.9	283.3	319.5	355.5
70	157.0	184.5	222.6	250.2	281.2	314.2
60	134.4	158.9	192.6	216.5	243.5	272.6
50	112.2	134.3	162.9	183.5	207.0	231.1
40	53.8	70.2	91.4	105.6	124.6	144.3
30	43.4	56.9	74.3	86.3	102.2	118.0
20	34.3	44.8	58.9	68.4	81.6	93.7

As one may observe from figure 1 in which the conductivity variation of 0.2 M sodium stearate with an addition of $NaNO_3$ *versus* temperature is plotted, the electrical conductivity of the colloidal solution, in gel, tends to that of the added electrolyte. The more it tends to, the greater is the electrolyte amount (similar to the Na stearate with added NaCl system [9])

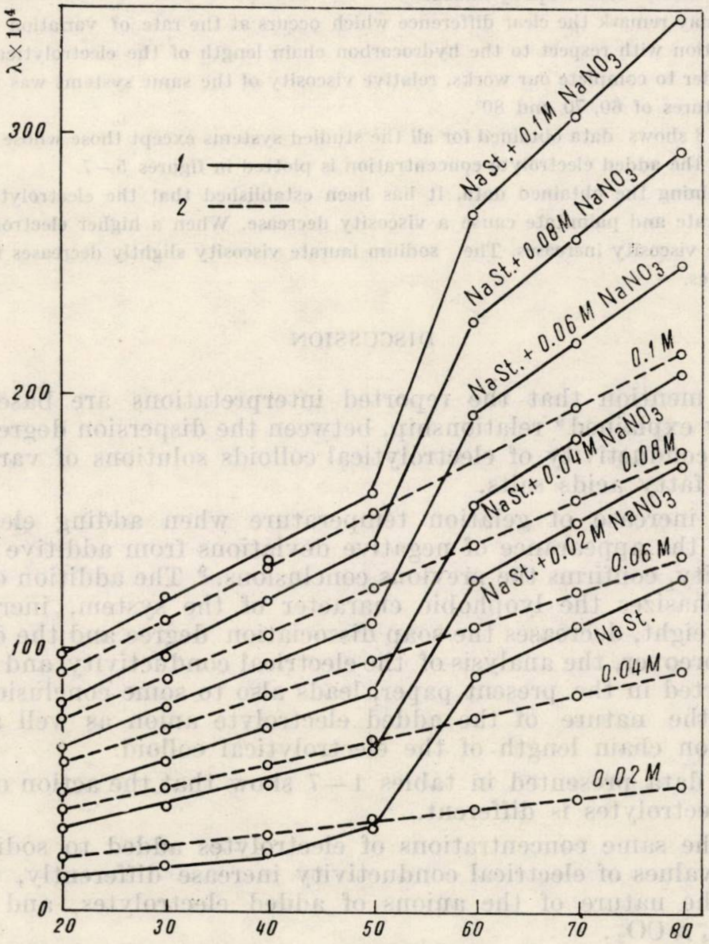

Fig. 1. — Electrical conductivity *versus* temperature of 0.2 M sodium stearate + $NaNO_3$ (1) and $NaNO_3$ (2).

Since the electrical conductivity of the Na laurate solutions mixed with three studied electrolytes as well as those of the respective electrolytes, varies linearly *versus* temperature, in table 7 are shown only the electrical conductivity values measured at the two ends of the studied temperature range (20 and 80°).

In order to obtain further information connected with electrolytes effects on the studied electrolytical colloids, the percentage deviation of the electrical conductivity from the additive electrical conductivity was calculated as shown in the previous paper.[9]

It may be established that all the systems show negative deviation from additivity. Since the curves which represent the deviation of electrical conductivity *versus* temperature have the same shape for the same soap, in figures 2—4 are plotted only the diagrams for each type of electrical colloid with Na_2CO_3 added.

One may remark the clear difference which occurs at the rate of variation of the additivity deviation with respect to the hydrocarbon chain length of the electrolytical colloid.

In order to complete our works, relative viscosity of the same systems was measured at the temperatures of 60, 70 and 80°.

Table 8 shows data obtained for all the studied systems except those whose relative viscosity *versus* the added electrolyte concentration is plotted in figures 5—7.

Examining the obtained data, it has been established that the electrolytes added to sodium stearate and palmitate cause a viscosity decrease. When a higher electrolyte amount is added, the viscosity increases. The sodium laurate viscosity slightly decreases for any kind of electrolytes.

DISCUSSION

We mention that the reported interpretations are based on the previously explained[9] relationship, between the dispersion degree and the electrical conductivity of electrolytical colloids solutions of various type of higher fatty acids salts.

The increase of gelation temperature when adding electrolytes, as well as the appearance of negative deviations from additive electrical conductivity, confirms the previous conclusions.[9] The addition of electrolytes emphasizes the lyophobic character of the system, increases the micellar weight, decreases the soap dissociation degree and the dispersion degree. Moreover, the analysis of the electrical conductivity and viscosity data reported in the present paper, leads also to some conclusions which refer to the nature of the added electrolyte anion as well as of the hydrocarbon chain length of the electrolytical colloid.

The data presented in tables 1—7 show that the action of various studied electrolytes is different.

At the same concentrations of electrolytes added to sodium stearate, the values of electrical conductivity increase differently, with respect to the nature of the anions of added electrolytes, and namely: $NO_3^- > SO_4^= > CO_3^=$.

At higher temperatures (80°) and lower concentrations of electrolyte, the increase of electrical conductivity caused by $NaNO_3$ and Na_2SO_4 is the same, but remains higher than that caused by Na_2CO_3.

Owing to the addition of electrolytes to sodium laurate solution, the increase of electrical conductivity, caused by the electrolytes added in large quantities, varies as follows: $NO_3^- > SO_4^= > CO_3^=$.

The negative values of deviations from additive electrical conductivity, for all systems, constitute an argument for the dissociation degree diminution of micelles when adding electrolytes with the same cations as micelle counterions.

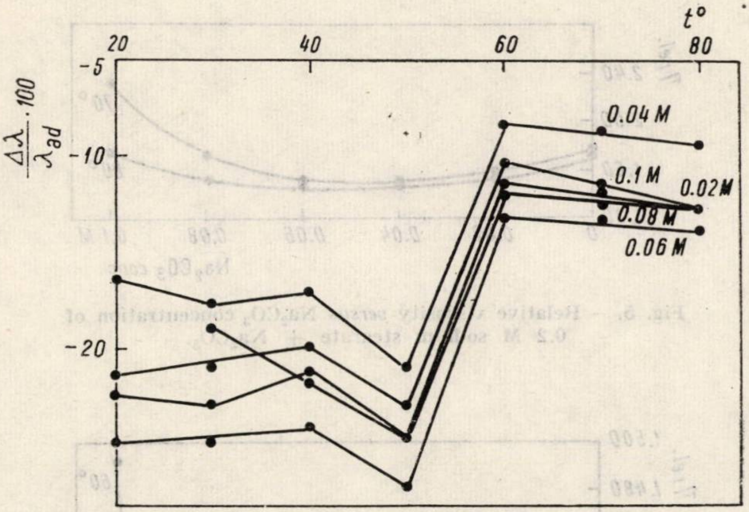

Fig. 2. — Electrical conductivity deviations $\left(\frac{\Delta\lambda}{\lambda_{ad}}\cdot 100\right)$ from additivity *versus* temperature of 0.2 M sodium stearate + Na_2CO_3.

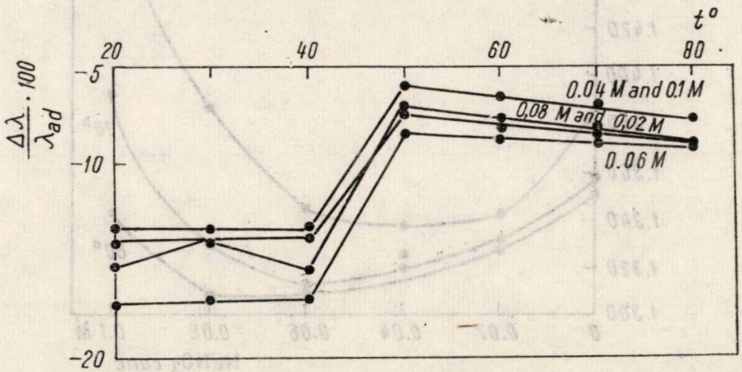

Fig. 3. — Electrical conductivity deviations $\left(\frac{\Delta\lambda}{\lambda_{ad}}\cdot 100\right)$ from additivity *versus* temperature of 0.2 M sodium palmitate + Na_2CO_3.

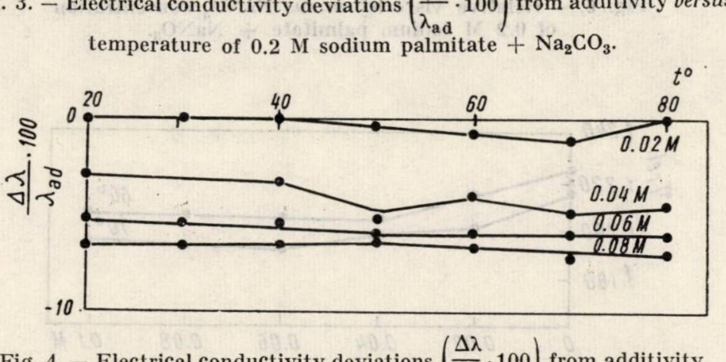

Fig. 4. — Electrical conductivity deviations $\left(\frac{\Delta\lambda}{\lambda_{ad}}\cdot 100\right)$ from additivity *versus* temperature of 0.2 M sodium laurate + Na_2CO_3.

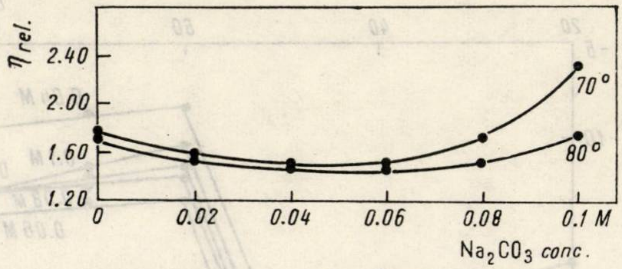

Fig. 5. — Relative viscosity *versus* Na_2CO_3 concentration of 0.2 M sodium stearate + Na_2CO_3.

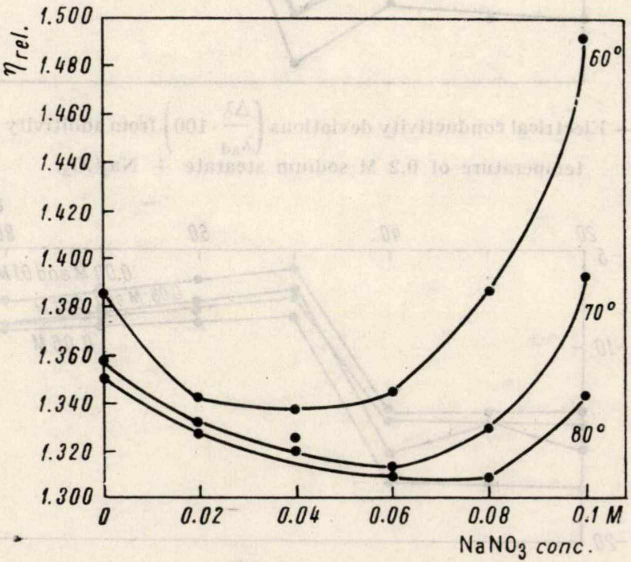

Fig. 6. — Relative viscosity *versus* $NaNO_3$ concentration of 0.2 M sodium palmitate + $NaNO_3$.

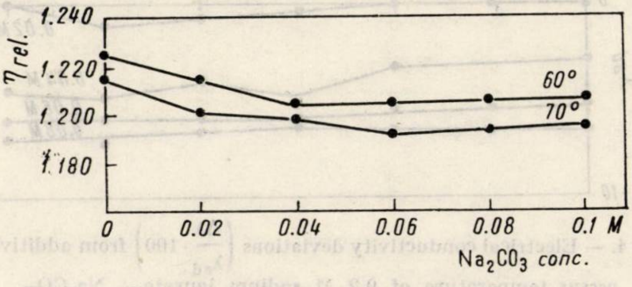

Fig. 7. — Relative viscosity *versus* Na_2CO_3 concentration of 0.2 M sodium laurate + Na_2CO_3.

Table 7

Electrical conductivity ($\lambda \times 10^4$ Ω^{-1} cm^{-1}) of electrolytes solutions and 0.2 M sodium laurate + electrolytes

°C / Electrolyte conc. mole/Kg.	$NaNO_3$		Na_2SO_4		Na_2CO_3		Na laurate 0.2M + $NaNO_3$		Na laurate 0.2M + Na_2SO_4		Na laurate 0.2M + Na_2CO_3	
	20	80	20	80	20	80	20	80	20	80	20	80
0	—	—	—	—	—	—	—	—	73.9	209.5	—	—
0.02	20.12	47.96	19.43	48.51	18.01	51.2	93.8	248.0	89.7	246.4	92.1	260.3
0.04	38.54	91.6	36.21	90.6	33.64	94.5	108.1	290.3	104.6	277.9	104.3	290.2
0.06	56.8	135.8	51.6	128.7	48.50	132.9	124.4	326.2	118.7	317.3	115.6	320.9
0.08	73.7	176.4	66.3	165.2	62.1	169.1	139.8	364.5	132.1	349.7	127.2	351.9
0.1	91.7	214.6	80.6	199.7	75.5	203.8	157.5	400.1	146.0	384.8	132.0	363.0

Table 8

Relative viscosity of 0.2 M electrolytical colloids + electrolytes

°C / Electrolyte conc. mole/Kg	0.2 M Na stearate + $NaNO_3$		0.2 M Na stearate + Na_2SO_4		0.2 M Na palmitate + Na_2SO_4			0.2 M Na palmitate + Na_2CO_3			0.2 M Na laurate + Na_2SO_4		0.2 M Na laurate + $NaNO_3$	
	70	80	70	80	60	70	80	60	70	80	60	70	60	70
0	1.720	1.695	—	—	1.386	1.359	1.351	—	—	—	1.224	1.214	—	—
0.02	1.528	1.516	1.519	1.504	1.367	1.345	1.333	1.348	1.319	1.305	1.225	1.204	1.212	1.194
0.04	1.567	1.515	1.540	1.528	1.350	1.334	1.321	1.330	1.308	1.302	1.222	1.200	1.193	1.171
0.06	2.165	1.874	2.313	2.035	1.355	1.327	1.314	1.329	1.298	1.299	1.212	1.206	1.200	1.181
0.08	2.274	2.286	2.817	2.249	1.356	1.321	1.306	1.323	1.295	1.286	1.205	1.196	1.200	1.188
0.1	—	—	—	—	1.421	1.359	1.332	1.353	1.316	1.303	1.207	1.180	1.193	1.190

The negative deviations from additivity speak also in favour of a dispersion degree decrease and of the emphasis of the hydrophobic character of the respective electrolytical colloid.

In the case of systems which form gels, the deviation is maximum in gel or near the gelation temperature, which proves that in this range, the electrolyte has a stronger action on the micelles and on the formation of microcrystalline structure than in sol, where the deviations are smaller.

In the case of sodium laurate, the deviation is practically constant, since the system does not form gels.

It may be remarked that the highest deviation from the additive electrical conductivity is shown by that electrolytical colloid which has the longest hydrocarbon chain (sodium stearate) and the lowest one, by the more lyophilic colloid, with the smallest carbon number in its molecule (sodium laurate).

Consequently, the effect of electrolytes is the stronger, the more emphasized the lyophobic character of the respective colloid (the longer its hydrocarbon chain).

It is also noticed, that the highest deviation value appears, in the case of every colloidal system, to which Na_2CO_3 is added.

Hence, regardless of the electrolytical colloid nature, the electrolytes effects upon the lyophilic character lowering of the system and those of the dispersion degree and dissociation degree of micelles, are as follow: $CO_3^= > SO_4^= > NO_3^-$.

These transformations which a colloidal system undergoes after the introduction of electrolytes may lead to the following assumption. There is a possibility — special temperature conditions — of the change of micelle structure. The viscosity decrease of the colloidal system due to the electrolyte addition obtained by one of us when adding other electrolytes to K or Na stearate[12] may be attributed to the micelle dehydration, produced by the presence of electrolytes in the colloidal solution (9) and facilitated by the high temperature (60—80°). For higher concentrations of electrolytes, the effect on the colloidal solution dispersion degree prevails over the dehydration effect; the micellar volume increases, so that viscosity increases. The longer the hydrocarbon chain of electrolytical colloid is, the better pronounced are both effects of electrolytes through the viscosity variation.

The effects of electrolytes with respect to the anion nature, in the studied temperature range, are not evidenced by the viscosity behaviour.

It is noticed that the effect of the micelle dehydration exerted by the electrolytes added to colloidal solution, in sol (at high temperatures) is corroborated by the fact that within this temperature range — in the case of all colloidal systems — the deviations from the additive electrical conductivity have the smallest values.

---

[12] E. Angelescu and St. Szasz, *Kolloid-Z.*, **90**, 302 (1940).

Revue Roumaine de Chimie, **14**, 451–457 (1969)

WÄRMEÜBERGANGSZAHLEN BEIM VERDAMPFEN VON AMMONIUMNITRATLÖSUNGEN

Z. GROPŞIANU, D. KOHN und A. IOVI

von der Fakultät für Angewandte Chemie an der Technischen Hochschule, Timişoara,
str. Bocşa 6

Eingegangen am 15. Juni 1968

Auf Grund experimenteller Untersuchungen wurden die Wärmeübergangszahlen beim Sieden für wäßrige Ammoniumnitratlösungen in Abhängigkeit zur Heizflächenbelastung und Temperaturdifferenz bestimmt. Es wurden Gleichungen zur Berechnung dieser Wärmeübergangszahlen bei atmosphärischem Druck und bei 260 Torr aufgestellt. Gleichfalls wurden für Ammoniumnitratlösungen verschiedener Konzentrationen die Siedetemperaturen in Abhängigkeit zum Druck bestimmt.

Ammoniumnitrat ist ein sehr wichtiges Stickstoffdüngemittel, das als solches oder zur Herstellung konzentrierter, komplexer, fester oder flüssiger Düngemittel verwendet werden kann. Dies hat zu einer ständigen Zunahme seiner Erzeugung geführt,[1] so daß es gegenwärtig eine vorherrschende Stellung unter den Stickstoffdüngemitteln einnimmt.[2]

Ammoniumnitrat wird aus Salpetersäure und Ammoniak hergestellt. In Abhängigkeit von dem verwendeten Verfahren erhält man gewöhnlich Lösungen, die eine Konzentration von 60—80% haben, [2–4] welche zwecks Überführung in ein festes Produkt, durch Verdampfen im Falle der Erzeugung von kristallisiertem Ammoniumnitrat auf ungefähr 95%, bzw. im Falle eines körnigen Produktes auf 98,5% konzentriert werden[3,5–7] (in einigen neueren Anlagen sogar bis zu 99% [4] oder 99,8% [2]). Die Lösungen werden bei einem Druck von 0,2—0,3 ata konzentriert. [4,6,7] Da diese Phase bei der Erzeugung des Produktes von großer Bedeutung ist, wird es als notwendig erachtet, die Daten über den Wärmeübergang vom Erwärmungsmittel zu den im Sieden befindlichen Lösungen zu kennen.

Andererseits gibt es im Fachschrifttum ziemlich wenig Angaben über die Bestimmung der Wärmeübergangszahlen beim Sieden der Lösungen im allgemeinen.[8–11] Vollständigere Angaben gibt es für Zweistoffgemische einiger organischer Lösungsmittel.[12–16]

---

[1] R.F. Muns, *Chem. Eng.*, **74**, 108 (1967).

[2] J. Landet und I. Bouchou, *Génie chim.*, **97**, 632 (1967).

[3] M.E. Pozin, „Tekhnologia mineralnykh solei", Goskhimizdat, Leningrad, 1961.

[4] *Nitrogen*, **1967**, 36.

[5] *Rev. Chim.* (*Bucarest*), **16**, 316 (1965).

[6] V.A. Klevke, N.N. Poliakov und L.Z. Arsenieva, „Tekhnologia azotnykh udobrenii", Goskhimizdat, Moskau, 1963.

[7] N.V. Boguslavski, „Proizvodstva ammiachinoi silitry", Izd. Tekhnika, Kiev, 1967.

Obwohl eine Gleichung zur Berechnung der Wärmeübergangszahlen bei siedenden Lösungen vorhanden ist, kann diese nicht verwendet werden, weil dazu die Kenntnis einiger physikalischer Konstanten notwendig ist, welche für die meisten Lösungen gänzlich oder teilweise fehlen. Deshalb ist es zweckmäßiger, diesen Koeffizienten und einige spezifische, einfache Gleichungen auf experimentellem Wege zu bestimmen. In der vorliegenden Arbeit wurde auf Grund von Versuchen die Bestimmung der Wärmeübergangszahlen und einiger Gleichungen zur Berechnung derselben beim Sieden von wäßrigen Ammoniumnitratlösungen verfolgt.

Die verwendete Vorrichtung war aus Glas, wobei als Erwärmungskörper ein rostfreies Stahlrohr mit einem Durchmesser von 10,14 mm und einer Wandstärke von 0,55 mm diente. Das Rohr wurde durch den Anschluß an einen die Spannung vermindernden Umspanner erhitzt. Das Funktionsprinzip ist dem im Fachschrifttum beschriebenen ähnlich.[17]

Die Wärmeübergangszahl beim Sieden, α, wurde mit Hilfe folgender Gleichung berechnet:

$$\alpha = \frac{q}{\Delta t}$$

wo α — Wärmeübergangszahl beim Sieden W/m^2. Grad
q — Heizflächenbelastung W/m^2
Δt — Temperaturunterschied zwischen der Wandtemperatur und der Siedetemperatur der Lösung.

Die Bestimmung der Wärmeübergangszahl beim Sieden, α, wurde für Ammoniumnitratlösungen in einem Konzentrationsbereich von 20—90%, bei atmosphärischem Druck und bei einem Druck von 260 mmHg im intensiven Siedebereich $q = 85 \cdot 10^3 - 57 \cdot 10^4$ W/m^2 durchgeführt.

Die Versuchsergebnisse wurden in den Abbildungen 1—6 dargestellt.

Aus Abbildung 1, welche die Veränderung von α in Abhängigkeit von q bei verschiedenen Konzentrationen und bei atmosphärischem Druck aufzeigt, ergibt sich, daß bei gleichbleibender Konzentration der Koeffizient α mit der Zunahme der Heizflächenbelastung q wächst, bzw. für dieselbe Heizflächenbelastung mit dem Anstieg der Konzentration C fällt.

---

[8] M. Miheev, „Osnovy teploperedachi", Gosenergizdat, Moskau-Leningrad, 1956.

[9] Z. Gropşianu, D. Kohn und A. Iovi, *Rev. Roumaine Chim.*, **12**, 485 (1967).

[10] I. Curievici, D. Peretz und V. Macri, „Îndrumar pentru calcule de transmitere a căldurii", Ed. didactică şi pedagogică, Bukarest, 1962.

[11] R.I. Ladiev, „Teploobmen i gidrodinamika v dvukhfaznykh sredakh", Izd. Naukova Dumka, Kiev, 1967, p. 63.

[12] D.A. Huber und J.C. Hoehne, *J. Heat Transfer*, C, **85**, 215 (1963).

[13] S.J.D. van Stralen, *Brit. Chem. Eng.*, **4**, 8 (1959).

[14] W.R. van Wijk und S.J.D. van Stralen, *Ned. Tijdschr. Natuurk.*, **29**, 287 (1962).

[15] A.J. Lovery und J.W. Westwater, *Ind. Eng. Chem.*, **49**, 1445 (1957).

[16] Th. Dunskus und J.W. Westwater, *Chem. Eng. Progr., Symp.*, **57**, 173 (1962).

[17] B.S. Petuhov, „Studiul experimental al proceselor de transmitere a căldurii", (a.d. Russ.), Ed. tehnică, Bukarest, 1956.

Auf Grund der Versuchsergebnisse (Abb. 1) wurde zwischen α und q folgende Beziehung festgesetzt:

$$\alpha = \varepsilon q^{0.7}$$

wo ε ein Koeffizient ist, der von der Konzentration der Lösung abhängt. Die Konzentrationsabhängigkeit von ε ist in Abb. 2 (Kurve *1*) dargestellt. Aus diesem Schaubild ergibt sich das Vorhandensein zweier Variationsbereiche von ε, in Abhängigkeit von der Konzentration C;

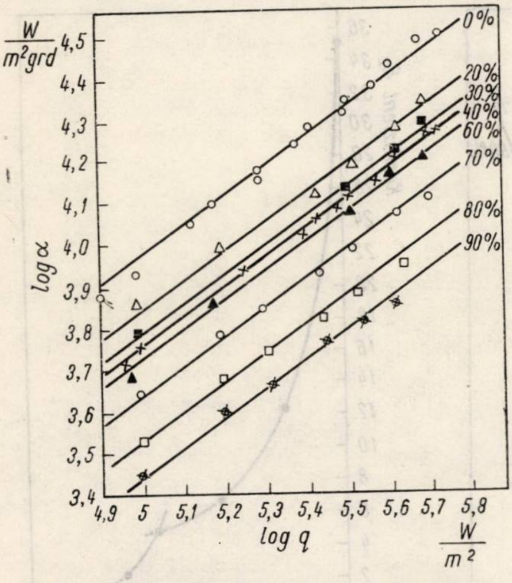

Abb. 1. — Veränderung von α in Abhängigkeit von q bei atmosphärischem Druck für wäßrige Ammoniumnitratlösungen.

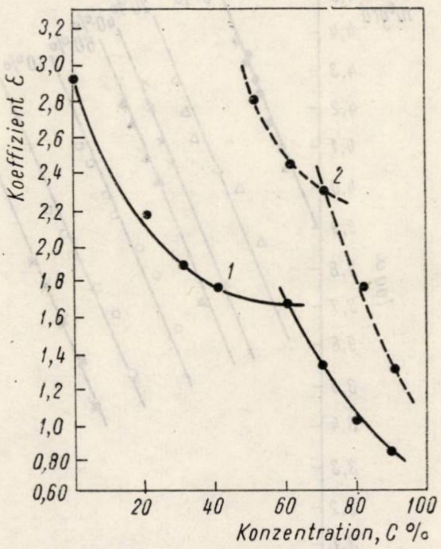

Abb. 2. — Abhängigkeit des Koeffizienten ε von der Konzentration der Ammoniumnitratlösungen.

1, experimentelle Kurve; *2*, berechnete Kurve.

— der eine Bereich, von 0% bis ungefähr 60%

$$\varepsilon = 4{,}27 \cdot C^{-0{,}23}$$

— der andere, über 60%

$$\varepsilon = 1{,}175 \cdot 10^3 \cdot C^{-1{,}6}$$

Die Werte der Wärmeübergangszahl beim Sieden, α, die für Lösungen von 60% bestimmt wurden, stimmen gut mit den im Fachschrifttum nur für diese Konzentration vorhandenen Werten überein.[11]

Die Diskontinuität der Kurven im dem Schaubild, welches die Veränderung von ε in Abhängigkeit von C enthält, wurde auch bei der Kurve wiedergefunden (Abb. 2, Kurve *2*), die durch Berechnung dieser Funktion mit Hilfe der theoretischen Gleichung von Kruzhilin[8] erhalten worden war, wobei die physikalischen Konstanten dem Fachschrifttum entnommen wurden.[6, 7, 18, 19]

---

[18] I. Moldovan und G. Chivu, „Tehnologia îngrăşămintelor minerale", 2. Bd., Ed. tehnică, Bukarest, 1964.

[19] I.V. Efremov und I.F. Golubev, Trudy G.I.A.P., XIV, Khimia i tekhnologia azotnykh udobrenii, Moskau, 1963, S. 5.

Die für den Koeffizienten α mit Hilfe dieser Gleichung erhaltenen Werte sind größer als die, welche auf experimentellem Wege bestimmt wurden.

Aus Abb. 3, in welcher die Veränderung der Wärmeübergangszahl beim Sieden in Abhängigkeit von dem Temperaturunterschied Δt zwischen der Wandtemperatur und der Siedetemperatur der Lösung dargestellt ist, kann man ein betontes Anwachsen von α mit der Zunahme von Δt für alle Konzentrationen beobachten.

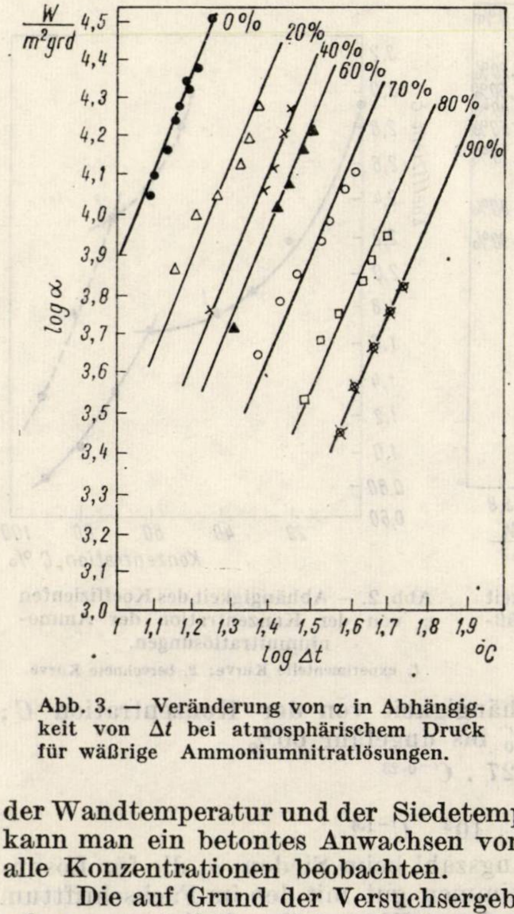

Abb. 3. — Veränderung von α in Abhängigkeit von Δt bei atmosphärischem Druck für wäßrige Ammoniumnitratlösungen.

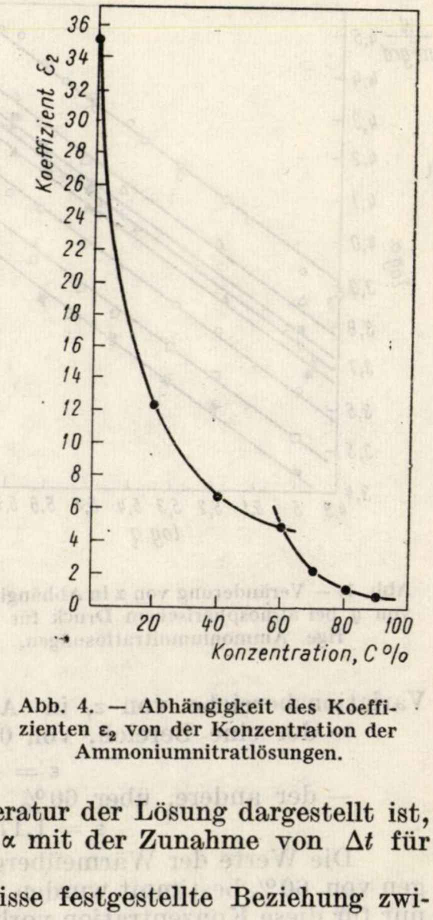

Abb. 4. — Abhängigkeit des Koeffizienten ε_2 von der Konzentration der Ammoniumnitratlösungen.

Die auf Grund der Versuchsergebnisse festgestellte Beziehung zwischen α und Δt hat folgende Form:

$$\alpha = \varepsilon_2 \Delta t^{2,33}$$

wo ε_2 ein Koeffizient ist, der von der Konzentration der Lösung abhängt.

Wie im Falle der Beziehung $\alpha = f(q)$, wird das Vorhandensein einer Diskontinuität der Kurve festgestellt, welche die Veränderung von ε_2 in Abhängigkeit von der Konzentration aufweist (Abb. 4).

Für die beiden Konzentrationsbereiche gibt es folgende Beziehungen zwischen ε_2 und C:

— für Konzentrationen bis zu 60%,

$$\varepsilon_2 = 1,39 \cdot 10^2 \cdot C^{-0,81}$$

— für Konzentrationen über 60%,

$$\varepsilon_2 = 2{,}665 \,.\, 10^9 \cdot C^{-4{,}9}$$

Zwecks Bestimmung der Wärmeübergangszahl beim Sieden, α, wurden Bestimmungen bei einem Restdruck von 260 mmHg durchgeführt. Die Veränderung von α in Abhängigkeit von der Heizflächenbelastung q ist in Abb. 5 wiedergegeben. Auf Grund der Versuchsergebnisse wurden Beziehungen folgender Form festgesetzt:

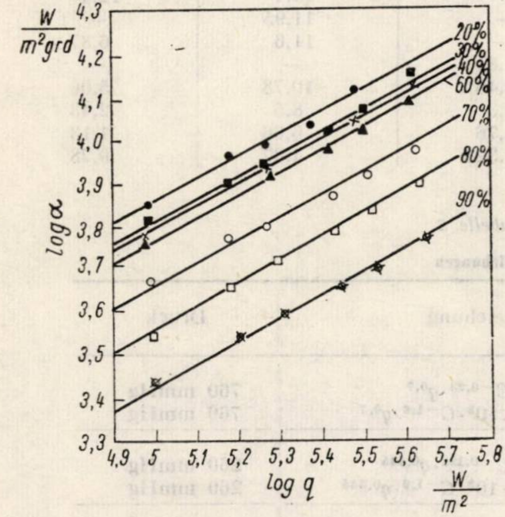

Abb. 5. — Veränderung von α in Abhängigkeit von q bei einem Druck von 260 mmHg für wäßrige Ammoniumnitratlösungen.

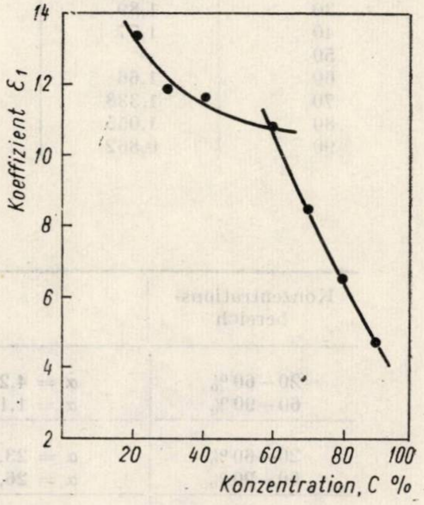

Abb. 6. — Abhängigkeit des Koeffizienten ε_1 von der Konzentration der Ammoniumnitratlösungen.

$$\alpha = \varepsilon_1 \cdot q^{0{,}545}$$

wo ε ein von der Konzentration abhängender Koeffizient ist.

Die Konzentrationsabhängigkeit von ε_1 (Abb. 6) zeigt ebenfalls zwei Variationsbereiche. Folgende Beziehungen wurden festgesetzt:

— für Konzentrationen bis zu 60%

$$\varepsilon_1 = 23{,}4 \cdot C^{-0{,}192}$$

— für Konzentrationen über 60%

$$\varepsilon_1 = 26{,}35 \cdot 10^3 \cdot C^{-1{,}9}$$

Die Werte von ε, ε_1 und ε_2, sowie die Gleichungen zur Berechnung der Wärmeübergangszahlen beim Sieden, α, die auf Grund der Versuchsergebnisse festgestellt wurden, sind in den Tabellen 1 und 2 angeführt.

Tabelle 1

Werte der Koeffizienten ε, ε_1 und ε_2

Konzentration %	Koeffizient ε bestimmt	Koeffizient ε berechnet	Koeffizient ε_1	Koeffizient ε_2
0	2,915	—	—	35,5
20	2,165	—	13,4	12,4
30	1,89	—	11,95	—
40	1,77	—	11,6	6,87
50	—	2,81	—	—
60	1,66	2,45	10,78	5,06
70	1,338	2,3	8,5	2,43
80	1,055	1,76	6,66	1,13
90	0,862	1,323	4,87	0,78

Tabelle 2

Gleichungen

Konzentrationsbereich	Gleichung	Druck
20–60%	$\alpha = 4{,}27 \cdot C^{-0{,}23} \cdot q^{0{,}7}$	760 mmHg
60–90%	$\alpha = 1{,}175 . 10^3 \cdot C^{-1{,}6} \cdot q^{0{,}7}$	760 mmHg
20–60%	$\alpha = 23{,}4 \cdot C^{-0{,}192} \cdot q^{0{,}545}$	260 mmHg
60–90%	$\alpha = 26{,}35 \cdot 10^3 \cdot C^{-1{,}9} \cdot q^{0{,}545}$	260 mmHg
20–60%	$\alpha = 1{,}39 \cdot 10^2 \cdot C^{-0{,}81} \cdot \Delta t^{2{,}33}$	760 mmHg
60–90%	$\alpha = 2{,}665 . 10^9 \cdot C^{-4{,}9} \cdot \Delta t^{2{,}33}$	760 mmHg

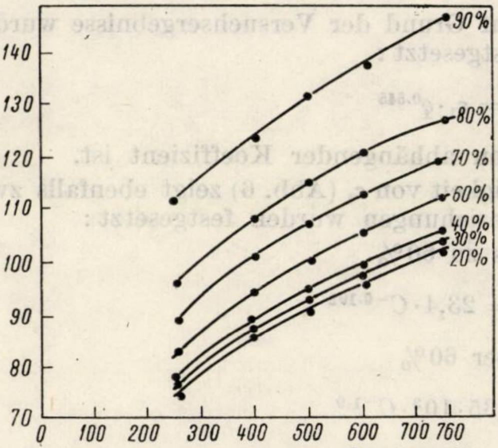

Abb. 7. — Siedetemperaturen der Ammoniumnitratlösungen in Abhängigkeit vom Druck bei verschiedenen Konzentrationen.

Desgleichen wurden die Siedetemperaturen der Ammoniumnitratlösungen in Abhängigkeit vom Druck bestimmt. Die Ergebnisse sind in Abbildung 7 dargestellt.

Schlußfolgerungen

— Auf Grund von Versuchsergebnissen wurden Gleichungen zur Berechnung der Wärmeübergangszahl beim Sieden von wäßrigen Ammoniumnitratlösungen unter atmosphärischem Druck und unter einem Druck von 260 mmHg aufgestellt.

— Die Wärmeübergangszahl beim Sieden nimmt gleichzeitig mit zunehmender Konzentration der Lösungen ab.

— Es wurden die Siedetemperaturen der Ammoniumnitratlösungen in Abhängigkeit vom Druck bei verschiedenen Konzentrationen bestimmt.

Revue Roumaine de Chimie, **14**, 451–457 (1969)

Revue Roumaine de Chimie, **14**, 459–461 (1969)

DIE ENTFERNUNG DER STÖRENDEN WIRKUNG DES EISENS, KOBALTS, NICKELS UND KUPFERS BEI DER KOLORIMETRISCHEN BESTIMMUNG DES TITANS

CONST. GH. MACAROVICI und C. STANISAV

aus dem Laboratorium für Anorganische Chemie der Babeş-Bolyai-Universität, Cluj, str. Arany János 11

Eingegangen am 11. Juni 1968

Bei der photokolorimetrischen Bestimmung des Titans(IV) mit H_2O_2 in einer Lösung die auch Fe(III), Co(II), Ni(II) und Cu(II) enthält, wurde Natriumpolyphosphat verwendet. Es bilden sich lösliche Polyphosphate der oben genannten Ionen. Diese Lösung wird über eine, mit Kationit Dowex — 50W × 12 H Form gefüllten Säule, geführt. Titan(IV)- und Eisen(III)-polyphosphat gehen in das Laufmittel über. Die Kobalt-, Nickel- und Kupferpolyphosphate zersetzen sich und Co^{2+}, Ni^{2+}, Cu^{2+} werden vom Kationit quantitativ zurückgehalten. Das Eisen(III)-polyphosphat ist farblos und stört die kolorimetrische Bestimmung des Titans nicht.

In der einschlägigen Literatur werden mehrere kolorimetrische Methoden für die Bestimmung des Titans beschrieben. Unter diesen, die Bestimmung mit Sulfosalicylsäure,[1,2] mit Tiron,[3,4] mit Chromotropsäure, [5,6] mit Gallussäure, [7] Katechin,[8,9] Salicylsäure [10,11] und mit Askorbinsäure .[12,13]

Die am häufigsten angewandte Methode bei der kolorimetrischen Bestimmung des Titans(IV) besteht darin, daß unter Einwirkung von H_2O_2 und Schwefelsäure, eine gelbe Färbung auftritt. [14–16] Die Färbung

---

[1] M. Ziegler und O. Glemser, *Z. analyt. Chem.*, **139**, 92 (1953).

[2] K. Saazni und G. Snikkanen, *Z. analyt. Chem.*, **143**, 112 (1954).

[3] P. Szerves und B. Csiszár, *Acta Chim. Acad. Sci. Hung.*, **7**, 7 (1955).

[4] J.H. Yoe und A.R. Armstrong, *Analyt. Chem.*, **19**, 100 (1947).

[5] W.W. Brandt und A.E. Preiser, *Analyt. Chem.*, **25**, 25 (1953).

[6] A.V. Endredy und F. Brugger, *Z. anorg. Chem.*, **249**, 263 (1942).

[7] P.N. Das-Gupta, *J. Indian Chem. Soc.*, **6**, 855 (1929).

[8] J. Piccard, *Ber. dtsch. chem. Ges.*, **42**, 4343 (1909).

[9] R.N. Pike, J.B. Fricklen und I.L. Newell, *Ber. dtsch. chem. Ges.*, **68**, 1023 (1935).

[10] J.H. Müller, *J. Amer. Chem. Soc.*, **33**, 1506 (1911).

[11] M. Schenk, *Helv. Chim. Acta*, **19**, 1127 (1936).

[12] E. Hines und D.F. Boltz, *Analyt. Chem.*, **24**, 947 (1952).

[13] R. Castagnon und G. Dudéon, *Chem. Abstr.*, **48**, 6908 (1954).

[14] P.G. Melikov und L.V. Pisarejevski, Izbranye trudy, izd. A.N. U.S.S.R., 1949, S. 482.

[15] E.B. Sendel, „Kolorimetricheskie metody opredelenia sledov metalov", Izdatelstvo „Mir", 1964, S. 782.

[16] A.K. Babko und A.T. Pilipenko, „Kolorimetricheskii analiz", Goskhimizdat, 1951, S. 228, 290–93.

folgt dem Absorptionsgesetz und ermöglicht Bestimmungen des Titans bis zu 0,05 mg/mg.[17]

Die gelbe Färbung wird von einigen Forschern durch die Bildung des $[TiO_2(SO_4)_2]^{2-}$ Ions erklärt. Neuere Untersuchungen[18] deuten auf die Bildung einiger der Kationen : $[TiO(H_2O_2)_2]^{2+}$ [16] oder $[Ti\,H_2O_2]^{4+}$.[19] Für die Gleichgewichtskonstante $K = [Ti^{4+}][H_2O_2]/[Ti\,H_2O_2]^{4+}$ werden folgende Werte angegeben: 10^{-4}, [20] 10^{-5}, [21] 9.10^{-5} und $4{,}5.10^{-5}$.[22]

Die gelbe Farbe der Titanlösung mit H_2O_2, bleibt zwei Jahre unverändert.[23] Elemente die farbige Ionen bilden, wie zum Beispiel Eisen(III), Kobalt, Nickel und Kupfer stören die kolorimetrische Bestimmung des Titans. Man entfernt daher diese Elemente durch Elektrolyse mit Quecksilberkathode.[17]

Um die störende Wirkung der oben genannten Ionen zu verhindern, haben wir makromolekuläres Natriumpolyphosphat — Grahamsches Salz — mit der Gesamtformel $Na_nH_2P_nO_{3n+1}$ angewendet. Das Natriumpolyphosphat läßt sich durch Erhitzen auf 900° des primären Natriumphosphats, in einem Platintiegel und raschem Abkühlen der gläserigen Schmelze, erhalten. Versetzt man die Probelösung mit überschüssigem Natriumpolyphosphat, so bilden sich lösliche Polyphosphate des Titans(IV), Eisens(III), Kobalts(II), Nickels(II) und Kupfers(II). Leitet man nun die so erhaltene Lösung durch eine chromatographische Säule, die mit Kationit Dowex—50W×12 (50—100 mesh) H Form gefüllt ist, so zersetzen sich die Kobalt-, Nickel- und Kupferpolyphosphate und die gebildeten Ionen Co^{2+}, Ni^{2+}, Cu^{2+} werden quantitativ zurückgehalten. Der Abfluß enthält nur noch Titan(IV) und Eisen(III). Das farblose Eisen(III)-polyphosphat stört die kolorimetrische Bestimmung des Titans nicht.

Arbeitsmethode. Die mit Schwefelsäure angesäuerte Lösung, die Titan(IV), Eisen(III), Kobalt(II), Nickel(II), Kupfer(II) enthält, wird mit einer wässerigen, molaren Natriumpolyphosphatlösung versetzt, bis sich der am Anfang gebildete Niederschlag löst. Sollte sich am Anfang kein Niederschlag bilden, so sind die notwendigen Mengen des Natriumpolyphosphates aus Tabelle 2 zu entnehmen. Das Auftreten eines Niederschlages ist von der Konzentration der Ionen und vom pH-Wert der Lösung abhängig. Die erhaltenen löslichen Polyphosphate wurden über eine chromatographische Säule geführt. Die Säule ist mit Kationit Dowex—50W × 12 (50—100 mesh) H Form gefüllt. Der Durchmesser beträgt 4 cm, die Höhe des Kationits 7 cm. Die Durchlaufgeschwindigkeit beträgt 10—15 ml Lösung/Min. Das Titan(IV)- und Eisen(III)-polyphosphat werden nicht zurückgehalten.[24,25] Da wahrscheinlich bei diesen zwei Polyphosphaten eine kovalente Bindung vorwiegt und das Polyphosphatanion makromolekulär ist, hat die elektrische Ladung einen negativen Wert und demzufolge geht Titan(IV) und Eisen(III) mit dem Polyphosphatanion in das Laufmittel über. Die zweiwertigen Metallionen sind ionisch an das Polyphosphatanion gebunden und werden deshalb von dem Trägermaterial zurückgehalten.

---

[17] I.P. Alimarin und B.I. Frid, „Microanaliza chimică anorganică cantitativă", Edit. tehnică, Bukarest, 1962, S. 152.

[18] R. Schwartz, *Z. anorg. Chem.*, **210**, 303 (1933).

[19] A.K. Babko und A.I. Volkova, *Zhur. obshchei Khim.*, **21**, 1949 (1951).

[20] M. Bending und H. Hirschmüller, *Z. analyt. Chem.*, **120**, 385 (1940).

[21] Y. Schaeppi und W.D. Treadwell, *Helv. Chim. Acta*, **31**, 577 (1948).

[22] E. Gastinger, *Z. anorg. Chem.*, **275**, 331 (1954).

[23] G.H. Ayers und E.M. Vienneau, *Ind. Eng. Chem. Anal. Ed.*, **12**, 96 (1940).

[24] R. Ripan und C. Stanisav, *Stud. Univ. Babeş-Bolyai, Chem.*, **1**, 131 (1963).

[25] Const. Gh. Macarovici und C. Stanisav, *Rev. Roumaine Chim.*, **11**, 823 (1966).

Der Lösung, die Titan(IV)- und Eisen(III)-polyphosphat enthält, fügt man 3–5 ml 3%iges Wasserstoffsuperoxid bei, füllt einen 250 ml-Kolben und mißt die Extinktion der erhaltenen Lösung.

Die Bestimmungen wurden mit einen Fotokolorimeter FEK-M mit blauem Filter (3), der im Bereich 410 nm absorbiert, durchgeführt. Hier zeigt auch unsere Lösung den maximalen Absorptionswert. Die Schichtdicke betrug 10,084 mm.

Die Ergebnisse der Bestimmungen sind in Tabelle 1 und 2 zusammengefaßt. Tabelle 1 enthält die Extinktionswerte einer reinen Titanlösung(IV). Tabelle 2 enthält die Extinktionswerte einer Titanlösung(IV), die ursprünglich auch Eisen, Kobalt, Nickel und Kupfer enthielt.

Tabelle 1

Die Ergebnisse der photokolorimetrischen Bestimmung des Titans(IV)

Nr.	Extinktion	Ti mg	Ti M/l
1	0,023	0,6882	$5{,}747.10^{-5}$
2	0,023	0,6882	$5{,}747.10^{-5}$
3	0,218	6,882	$5{,}747.10^{-4}$
4	0,218	6,882	$5{,}747.10^{-4}$
5	0,313	10,32	$8{,}617.10^{-4}$
6	0,313	10,32	$8{,}617.10^{-4}$
7	0,482	17,20	$1{,}436.10^{-3}$
8	0,482	17,20	$1{,}436.10^{-3}$

Tabelle 2

Die Ergebnisse der photokolorimetrischen Bestimmung des Titans(IV) neben Eisen. Kobalt Nickel und Kupfer

Nr.	Extinktion	Ti mg	Fe mg	Co mg	Ni mg	Cu mg	Summe Fe, Co, Ni, Cu mg	Na-Polyphosphat molar ml
1	0,024	0,6882	165,7	125,9	115,6	157,7	561,9	20
2	0,024	0,6882	165,7	125,9	115,6	154,7	561,9	20
3	0,219	6,882	66,2	50,36	46,25	61,91	224,81	15
4	0,219	6,882	66,2	50,36	46,25	61,91	224,81	15
5	0,313	10,32	33,1	25,18	23,12	30,95	112,39	10
6	0,313	10,32	33,1	25,18	23,12	30,95	112,39	10
7	0,479	17,20	6,629	5,036	4,625	6,191	22,481	15
8	0,480	17,20	6,629	5,036	4,625	6,191	22,481	15

Aus den beiden Tabellen ist ersichtlich, daß die Extinktionswerte große Ähnlichkeit aufweisen. Tabelle 2 zeigt, daß man einerseits kleine Mengen Titan in Gegenwart großer Mengen Eisen, Kobalt, Nickel und Kupfer, andererseits aber auch große Mengen Titan in Gegenwart kleiner Mengen Eisen and anderer Ionen bestimmen kann.

Revue Roumaine de Chimie, **14**, 459—461 (1969)

Revue Roumaine de Chimie, **14**, 463–467 (1969)

STRUCTURE DES HEXACYANOCOBALTIATES DE ZINC, CADMIUM, NICKEL ET MANGANÈSE

P. TRIBUNESCU et M. CRISTEA
Laboratoire de Chimie physique, Faculté de Chimie industrielle, Timişoara
6, str. Bocşa

Reçu le 22 juin 1968

Dans le présent travail, on s'est proposé d'étudier la structure cristalline des combinaisons : $Zn_3[Co(CN)_6]_2$, $Cd_3[Co(CN)_6]_2$, $Ni_3[Co(CN)_6]_2 \cdot 3H_2O$ et $Mn_3\,[Co(CN)_6]_2 \cdot 3H_2O$. L'étude röntgénographique — complétée avec des données thermogravimétriques — par la méthode des poudres (Debye-Scherrer) indique que les combinaisons étudiées sont isomorphes, en possédant un réseau cubique à faces centrées.

Sur la structure des combinaisons complexes avec des anions $[Me\,(CN)_6]^{x-}$, où le cation central peut être le Fe^{2+}, le Fe^{3+} ou même le Cr^{3+} et le Mn^{3+}, on a effectué des études ayant trait particulièrement aux combinaisons à cations mono- ou bivalents, [1,4] tandis que les études structurales concernant les combinaisons de l'anion complexe $[Co\,(CN)_6]^{3-}$ sont plus réduites. [5,9]

Dans l'étude de la structure des combinaisons complexes du type mentionné — particulièrement dans le cas des combinaisons à cations bivalents — outre le problème structural proprement dit, on pose également le problème d'établir si ces combinaisons peuvent donner ou non des hydrates, d'autant plus que pour les mêmes combinaisons certains auteurs [10] à l'encontre d'autres [11] admettent la possibilité de la formation des cristallohydrates. La controverse est favorisée par l'isomorphisme des combinaisons anhydres avec leurs hydrates. C'est pour cette raison que dans le présent travail, où nous nous sommes proposé d'étudier la structure

[1] R. Rigamonti, *Gazz. chim. Ital.*, **67**, 137 (1937).
[2] R. Rigamonti, *Gazz. chim. Ital.*, **68**, 803 (1938).
[3] M. A. Rollier et E. Arreghini, *Gazz chim. Ital.*, **69**, 499, (1939).
[4] M. A. Rollier et G. Cesoni, *Gazz. chim. Ital.*, **69**, 674, (1939).
[5] P. Pascal, « Nouveau traité de chimie minérale », tome 18, Masson, Paris, 1959 p. 686
[6] E. M. Miller et J. A. Mathews, *Chem. Zentr.*, I, 754 (1901).
[7] C. Drăgulescu et P. Tribunescu, *Rev. Chim. Minérale*, **2**, 119 (1965).
[8] C. Drăgulescu et P. Tribunescu, *Rev. Roumaine Chim.*, **11**, 705 (1966).
[9] C. Drăgulescu et P. Tribunescu, *Rev. Roumaine Chim.*, **12**, 943 (1967).
[10] A. K. Bever, *Rec. Trav. chim.*, **57**, 1259 (1938).
[11] W. B. Weser, W. O. Milligan et J. B. Bates, *J. Phys. Chem.*, **42**, 945 (1938.

des combinaisons de l'anion $[Co(CN)_6]^{3-}$ avec les cations bivalents Zn^{2+}, Cd^{2+}, Ni^{2+} et Mn^{2+}, les études röntgénographiques ont été complétées avec des données thermogravimétriques.

PARTIE EXPÉRIMENTALE

Les combinaisons $Zn_3[Co(CN)_6]_2$, $Cd_3[Co(CN)_6]_2$, $Ni_3[Co(CN)_6]_2 \cdot 3H_2O$ et $Mn_3[Co(CN)_6]_2 \cdot 3H_2O$ ont été obtenues selon les indications de la littérature,[5, 6] par précipitation, en employant des solutions de $K_3[Co(CN)_6]$ 0,5 N et des solutions de chlorures des cations Mn^{2+}, Ni^{2+} et Cd^{2+}, respectivement de $ZnSO_4$, de la même concentration. Les précipités, lavés et séchés à 25° contiennent de l'eau, ainsi qu'on peut voir des courbes thermogravimétriques des quatre combinaisons.

Pour constater, si l'eau contenue dans les précipités est éliminée intégralement dans les mêmes conditions de température, on a effectué, à l'aide d'une thermobalance, une série de pyrolyses, pour des quantités de produits de 100 mg, avec des vitesses d'échauffement variant entre 2°/mn et 10°/mn (courbes *1*) et à la température constante — jusqu'au poids constant — et ensuite à la température croissante, avec la même vitesse de chauffage (courbes *2*).

La figure 1 représente deux courbes de pyrolyse obtenues pour le $Zn_3[Co(CN)_6]_2$, d'où il résulte que cette substance retient 12,5 % de l'eau qu'elle perd continuellement, dans une seule étape, entre 50 et 130° (courbe *1*), et après 10 minutes au chauffage isotherme — à 110° — (courbe *2*). Les paliers horizontaux des deux courbes caractérisent la substance anhydre, dont la décomposition commence autour de 330°. L'allure des courbes montre que toute la quantité d'eau s'élimine aisément et provient de l'adsorption.

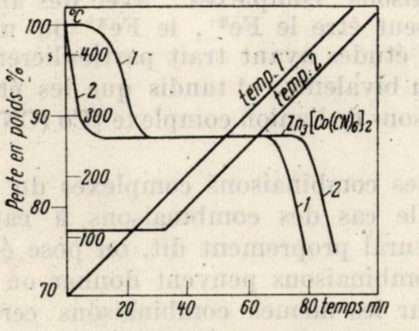

Fig. 1. — Courbes thermogravimétriques de la combinaison $Zn_3[Co(CN)_6]_2$.

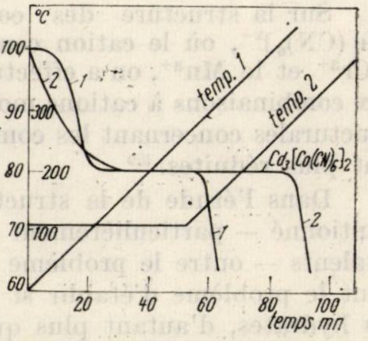

Fig. 2. — Courbes thermogravimétriques de la combinaison $Cd_3[Co(CN)_6]_2$.

La figure 2 représente deux courbes obtenues pour le $Cd_3[Co(CN)_6]_2$. Le précipité retient un peu plus d'eau — 20 % — mais l'eau est éliminée aisément et dans une seule étape, tout comme dans le cas de la combinaison antérieure, d'où on peut conclure que l'eau est adsorbée à la surface des particules.

Les deux courbes thermogravimétriques de la combinaison $Ni_3[Co(CN)_6]_2 \cdot 3H_2O$ — présentées dans la figure 3 — montrent deux paliers horizontaux, l'un pour une perte en poids égale à 29 %, palier qui caractérise la combinaison anhydre, dont la décomposition commence autour de 330°, et l'autre pour une perte en poids égale à 22 %.

Vu que la perte de 22 % d'eau a lieu continuellement jusqu'à la température de 130—140° (courbe *1*), et qu'au chauffage isotherme à 140° on arrive au poids constant après 30—40 mn, on peut attribuer cette quantité d'eau à l'adsorption. Le reste de l'eau, éliminé entre 150 et 240° — donc plus difficilement — et correspondant exactement à trois molécules pour une molécule de la combinaison respective, peut être considéré comme de l'eau de cristallisation.

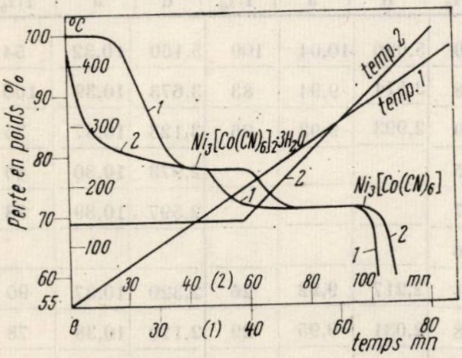

Fig. 3. — Courbes thermogravimétriques de la combinaison $Ni_3[Co(CN)_6]_2 \cdot 3H_2O$.

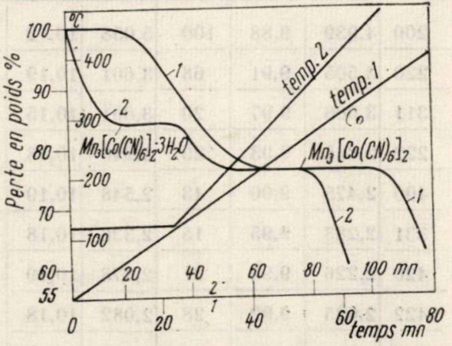

Fig. 4. — Courbes thermogravimétriques de la combinaison $Mn_3[Co(CN)_6]_2 \cdot 3H_2O$.

Les courbes de la déshydratation, obtenues pour le $Mn_3[Co(CN)_6]_2.3H_2O$, données dans la figure 4, représentent aussi deux paliers (courbe *2*), dont le premier — la courbe *1* accuse seulement une faible modification de pente — montre une perte en eau égale à 16 %, pendant que le deuxième — qui survient au-dessus de 210° et caractérise la substance anhydre — accuse une perte en poids égale à 24 %. La différence de poids entre les deux paliers correspond ici de même à trois molécules d'eau, molécules qui peuvent être considérées comme appartenant au réseau cristallin.

L'étude röntgénographique de ces quatre combinaisons a été effectuée par la méthode Debye-Scherrer, en employant une chambre cylindrique — au diamètre de 57,5 mm — dans l'appareil TuR-M-60 et la radiation $Fe_{K\alpha}$ (filtre de Mn), et aussi un appareil TuR-M-61, muni d'un goniomètre horizontal HZG-1 et d'un enregistreur linéaire d'impulsions VAD-53. Les données structurales obtenues sont représentées dans le tableau 1, pour toutes les quatre combinaisons.

L'identité des diagrammes montre que toutes les combinaisons étudiées possèdent aussi la même structure cristalline, qu'elles sont isomorphes. Les réflexions trouvées correspondent à un réseau cubique à faces centrées, satisfaisant les conditions de limitation [12] des réflexions possibles : $h + k$; $h + 1$; $1 + k = 2\ n$.

Compte tenu des conditions de limitation des réflexions possibles, auxquelles se soumettent les combinaisons étudiées, il résulte que leur réseau cristallin appartient à la classe de symétrie O_h^5 (Fm 3m).

Dans la maille élémentaire de ce réseau cubique à faces centrées, des positions équivalentes occupent les quatre anions $[Co(CN)_6]^{3-}$ (4 *a* positions : 000 → 0 1/2 1/2) et quatre cations Me^{2+} (4 *b* positions : 1/2 0 0 → 1/2 1/2 1/2), les premiers placés dans les nœuds et les centres

---

[12] International Tables for X-Ray Crystallography, tome I, Kynoch Press, Birmingham, 1965, p. 338.

Tableau 1

Données röntgénographiques des combinaisons étudiées

hkl	$Ni_3[Co(CN)_6]_2 \cdot 3H_2O$			$Mn_3[Co(CN)_6]_2 \cdot 3H_2O$			$Zn_3[Co(CN)_6]_2$			$Cd_3[Co(CN)_6]_2$		
	d	a	I/I_0	d	a	I/I_0	d	a	I/I_0	d	a	I/I_0
200	4,939	9,88	100	5,058	10,12	100	5,020	10,04	100	5,160	10,32	54
220	3,505	9,91	68	3,601	10,19	88	3,514	9,94	83	3,673	10,39	100
311	3,006	9,97	20	3,061	10,15	19	2,993	9,93	26	3,128	10,37	25
222	2,868	9,93	25	2,940	10,18	25				2,973	10,30	40
400	2,475	9,90	43	2,548	10,19	67				2,597	10,39	78
331	2,283	9,95	15	2,336	10,18	16						
420	2,226	9,95	21	2,278	10,19	21	2,217	9,92	26	2,320	10,37	90
422	2,025	9,92	28	2,082	10,18	48	2,031	9,95	29	2,119	10,38	78
511				1,961	10,19	13	1,915	9,95	21	1,997	10,37	19
440	1,755	9,93	38	1,802	10,19	37	1,756	9,98	38	1,835	10,38	38
531				1,715	10,15	14						
600	1,655	9,93	20	1,703	10,22	28	1,645	9,87	24	1,731	10,39	21
620	1,576	9,97	36	1,610	10,18	36	1,563	9,89	26	1,641	10,38	28
533				1,551	10,17	10				1,571	10,30	8
622				1,536	10,19	22	1,506	9,87	18	1,554	10,31	22
444	1,431	9,91	32	1,470	10,19	36	1,446	10,02	20	1,502	10,41	28
711				1,423	10,16	7						
640				1,418	10,22	18	1,374	9,91	15	1,439	10,38	20
642	1,330	9,95	24	1,369	10,24	28				1,387	10,38	32
553										1,352	10,38	5
800				1,275	10,20	22				1,300	10,40	18
733				1,295	10,19	8						

des faces du cube élémentaire, tandis que les cations Me^{2+} occupent les milieux des arêtes et le centre de la maille élémentaire. Les deux autres cations Me^{2+} se trouvent placés dans des positions inéquivalentes envers les premiers (2 *c* positions des huit existantes : 1/4 1/4 1/4 → 3/4 3/4 3/4). Comme les cations métalliques des positions *c* — les centres des octants — laissent libres six telles positions, il résulte que celles-ci peuvent être occupées par six molécules d'eau, ainsi qu'on peut voir dans le cas des combinaisons des cations Ni^{2+} et Mn^{2+}.

L'identité structurale des quatre combinaisons montre que l'occupation des six positions libres par les molécules d'eau ne conduit pas à la modification de la structure réticulaire, les huit *c* positions pouvant être considérées des vides dans le réseau spatial. Mais d'autre part, on constate que l'occupation, au moins de deux de ces positions s'impose pour qu'un tel type de réseau se forme et se stabilise ; les combinaisons de tels anions avec des cations trivalents, lesquels laisseraient libres toutes ces positions, n'ont pu être obtenues à l'état solide.

La disposition spatiale des particules dans le réseau est confirmée par l'intensité des réflexions obtenues. Ainsi, l'intensité maximale est détenue par les réflexions correspondant à $4n$; moins intenses sont celles correspondant à $4n+2$ et les plus faibles sont les réflexions impaires. D'ailleurs on peut constater que les particules des positions *a* et *b* ont la plus grande contribution à l'intensité des réflexions, ce qui s'explique pour les combinaisons étudiées.

Vu que, d'une part, le degré de cristallisation de ces combinaisons est réduit et par conséquent les réflexions, particulièrement celles d'ordres plus élevés, présentent de faibles intensités et peuvent être difficilement évaluées avec exactitude, et que, d'autre part, la force de diffusion des molécules d'eau est aussi faible, en comparaison de celle des ions métalliques, avec lesquels les molécules d'eau occupent des points identiques, la contribution de l'eau, aux réflexions correspondant à $4n$ et à $4n+2$ — dans les hydrates — n'est pas mise en évidence.

A l'aide des données du tableau 1, on obtient pour les constantes réticulaires les valeurs suivantes

Combin.	$Zn_3[Co(CN)_6]_2$	$Cd_3[Co(CN)_6]_2$	$Ni_3[Co(CN)_6]_2 \cdot 3H_2O$	$Mn_3[Co(CN)_6]_2 \cdot 3H_2O$
a (Å) ±0,05	9,94	10,37	9,93	10,18

Dans le tableau 2 sont représentées, comparativement, les densités röntgénographiques — calculées pour deux molécules/maille — et celles expérimentales, les deux valeurs de chaque combinaison étant comparables, dans la limite des erreurs de mesure. Les densités expérimentales ont été mesurées à 22°, avec le pychnomètre, employant comme liquides d'immersion de l'alcool éthylique absolu et du toluène, dans lesquels les substances respectives sont pratiquement insolubles.

Tableau 2

Densités röntgénographiques expérimentales

Comb.	$Zn_3[Co(CN)_6]_2$	$Cd_3[Co(CN)_6]_2$	$Ni_3[Co(CN)_6]_2 . 3H_2O$	$Mn_3[Co(CN)_6]_2 . 3H_2O$
ρ calc.	2,103	2,270	2,030	2,224
ρ exp.	2,098	2,219	2,150	1,983

CONCLUSIONS

En vertu des données présentées il résulte une identité structurale pour les combinaisons étudiées, celles-ci formant une série isomorphe, appartenant à la classe de symétrie O_h^5 (Fm 3m). Il résulte aussi que pendant que les combinaisons du zinc et du cadmium sont anhydres, celles de nickel et manganèse forment des hydrates à trois molécules d'eau, ces molécules occupant, dans le réseau cristallin, six octants libres — deux étant occupés par des ions métalliques.

Revue Roumaine de Chimie, **14**, 469–472 (1969)

LIGHT SCATTERING AND VISCOSITY MEASUREMENTS ON UNFRACTIONATED POLYVINYLCHLORIDE

ADELINA LUPU, LEONTINA NASTA, I. BALTOG and BRÎNDUȘA BRĂILEANU

Faculty of Physics, University of Bucharest, Str. Academiei, 14 and Institute of Physics of the Academy, Bucharest, Calea Victoriei, 114

Received July 5, 1968

By correlated intrinsic viscosity and weight-average molecular weight (determined by light scattering) it was established that the unfractionated PVC samples, obtained in suspension under similar conditions, follow satisfactorily a relation of the Mark-Kuhn-Houwink type. The shifts of some unfractionated samples from this relation were ascribed to some structural modifications of the polymer.

The data in the literature, concerning the constants K and α in the Mark-Kuhn-Houwink relation for polyvinyl chloride (PVC) which are given in table 1, show a great dispersion which is certainly — at least in part — due to differing characteristics of the PVC samples analysed by various authors.

Consequently, viscosity measurements alone (e.g. *K* Fikentscher's viscosity constant) cannot provide sufficient information regarding the average molecular weight of a polymer, if the straight line log $[\eta]$ as a function of log $\overline{M}$ has not been traced using PVC samples with features similar to those of the examined material.

That is why we proposed to study whether for commercial unfractionated materials, which were obtained under comparable polymerization conditions, and are hence likely to show similar characteristics in terms of the degree of ramification and polydispersity, a relation of the Mark-Kuhn-Houwink type may be established by means of which quite precise information may be obtained concerning the average molecular weight of industrial products.

With this end in view, measurements have been performed on 7 PVC samples — which we shall consider as standards — obtained in suspension from the firms Solvic, Dow, Danuvil, Dinamit and Corvic.

The weight-average molecular weights were obtained by light scattering using Zimm's double extrapolation method. The measurements were carried out with a SOFICA instrument in cyclohexanone solutions of PVC, which had been optically purified by centrifugation.

Table 1

$\overline{M}$ and $[\eta]$ values on P. V. C. reported in the literature

Authors	Solvent		Type of the used polymers	Constants in the law $[\eta]=K.\overline{M}^{\alpha}$ ($[\eta]$ in dl. g^{-1})		$\overline{M}$	Range of $\overline{M}\times 10^{-3}$
	in $[\eta]$ measurements	in $\overline{M}$ measurements		K	α		
Fournier, Thiesse [1]	cyclohexanone	cyclopentanone	fractionated	1.558×10^{-4}	0.76	$\overline{M}_n$	13–137
Mead, Fuoss [2]	cyclohexanone	methylamylketone	fractionated	1.12×10^{-5}	1	$\overline{M}_n$	
Hengstenberg [3] and	cyclohexanone	cyclohexanone	fractionated	1.95×10^{-4}	0.79	$\overline{M}_n$	20–90
Breitenbach, Forster, Renner [4]	cyclohexanone	cyclohexanone	unfractionated	1.16×10^{-4}	0.85	$\overline{M}_n$	25–100
Staudinger, Häberle [5]	cyclohexanone	cyclohexanone	fractionated	1.6×10^{-5}	1	$\overline{M}_n$	30–130
		tetrahydrofuran	fractionated	2.15×10^{-4}	0.76	$\overline{M}_n$	50–200
Danusso, Moraglio, Gazzera [6]	cyclohexanone	cyclohexanone	unfractionated	2.4×10^{-3}	0.77	$\overline{M}_n$	30–140
Menčík [7]	cyclohexanone	tetrahydrofuran	fractionated	2.04×10^{-3}	0.56	$\overline{M}_n$	19–150
Bier, Krämer [8]	cyclohexanone	cyclohexanone	fractionated	1.4×10^{-5}	1	$\overline{M}_n$	34–125
Ciampa, Schwindt [9]	cyclohexanone	cyclohexanone	unfractionated	2.4×10^{-4}	0.77	$\overline{M}_n$	16–140
				1.1×10^{-5}	1	$\overline{M}_w$	19–200
Batzer, Nisch [10]	tetrahydrofuran	tetrahydrofuran	fractionated	3.65×10^{-5}	0.92	$\overline{M}_n$	30–100
Freeman, Manning [11]	tetrahydrofuran	tetrahydrofuran	fractionated	1.63×10^{-4}	0.766	$\overline{M}_w$	25–300

$\overline{M}_n$ = number average, $\overline{M}_w$ = weight average

---

[1] M. Fournier and X. Thiesse, *Compt. rend.*, **222**, 1437 (1946).

[2] D. Mead and P. Fuoss, *J. Amer. Chem. Soc.*, **64**, 277 (1942).

[3] J. Hengstenberg, *Angew. Chem.*, **62**, 26 (1950).

[4] J. Breitenbach, E. Forster and A. Renner, *Kolloid Z.*, **127**, 1 (1952).

[5] H. Staudinger and M. Häberle, *Makromol. Chem.*, **9**, 35 (1953).

[6] F. Danusso, G. Moraglio and S. Gazzera, *Chimica e Industria*, **36**, 883 (1954).

[7] Z. Menčík, *Coll. Czech. Chem. Comm.*, **21**, 517 (1956).

[8] G. Bier and H. Krämer, *Makromol. Chem.*, **19**, 151 (1956).

[9] G. Ciampa and H. Schwindt, *Makromol. Chem.*, **21**, 169 (1956).

[10] H. Batzer and A. Nisch, *Makromol. Chem.*, **22**, 131 (1957).

[11] M. Freeman and P. Manning, *J. Polymer Sci.*, **2**, 2017 (1964).

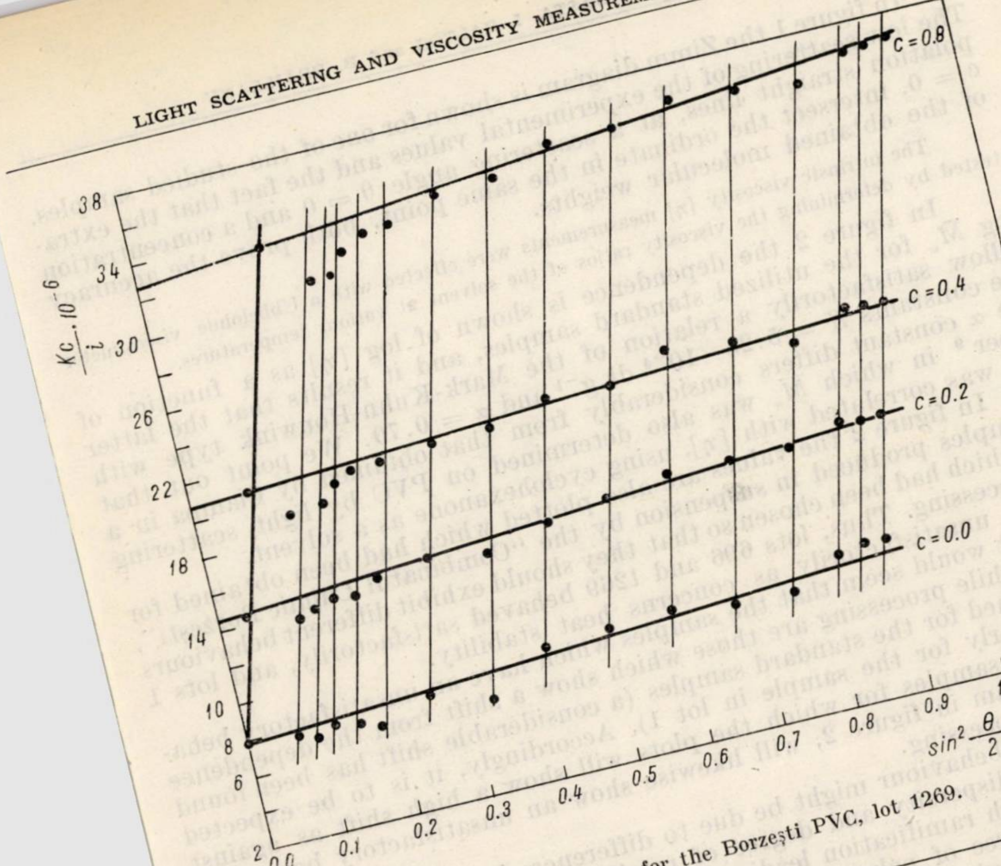

Fig. 1. — Zimm Diagram for the Borzești PVC, lot 1269.

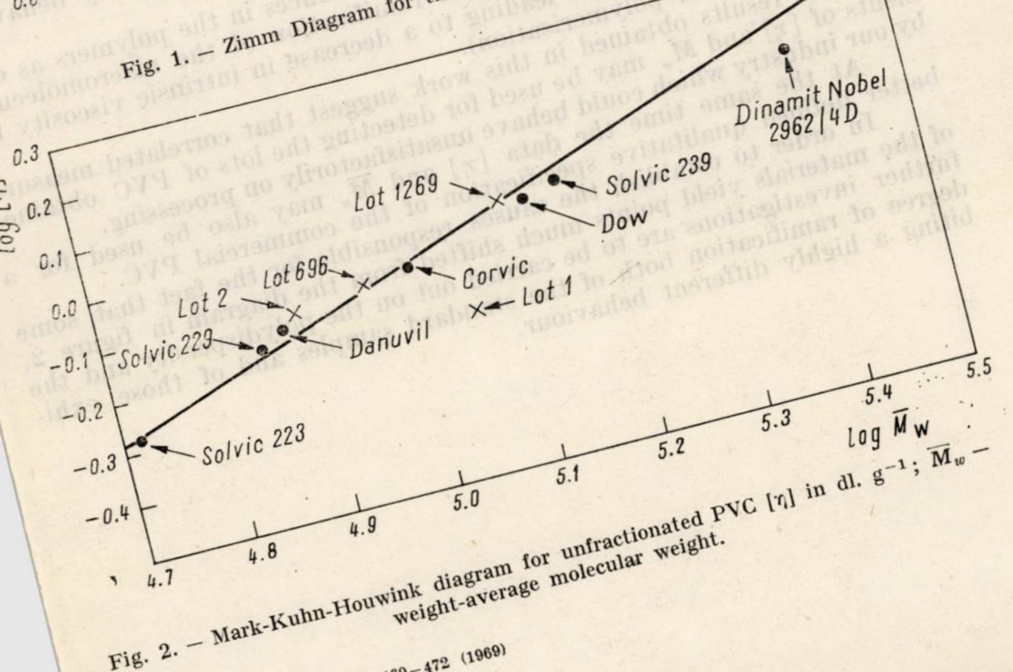

Fig. 2. — Mark-Kuhn-Houwink diagram for unfractionated PVC [η] in dl. g^{-1}; $\overline{M}_w$ — weight-average molecular weight.

In figure 1 the Zimm diagram is shown for one of the studied samples. The low scattering of the experimental values and the fact that the extrapolation straight lines, at a scattering angle $\theta = 0$ and a concentration $c = 0$, intersect the ordinate in the same point, both prove the accuracy of the obtained molecular weights.

The intrinsic viscosity $[\eta]$ measurements were effected with a Ubbelohde viscosimeter tested by determining the viscosity ratios of the solvent at various temperatures.

In figure 2 the dependence is shown of log $[\eta]$ as a function of log $\overline{M}_w$ for the utilized standard samples, and it results that the latter follow satisfactorily a relation of the Mark-Kuhn-Houwink type with the constants $K = 5.25 \times 10^{-4}$ dl.g^{-1} and $\alpha = 0.70$. We point out that the α constant differs considerably from that obtained by Ciampa in a paper [9] in which $\overline{M}_w$ was also determined on PVC by light scattering and was correlated with $[\eta]$, using cyclohexanone as a solvent.

In figure 2 the values are also plotted which had been obtained for 4 samples produced in suspension by the "Combinatul Chimic Borzeşti", and which had been chosen so that they should exhibit different behaviours at processing. Thus, lots 696 and 1269 behaved satisfactorily, and lots 1 and 2 unsatisfactorily as concerns heat stability.

It would seem that the samples which have an unsatisfactory behaviour while processing are those which show a shift from the dependence established for the standard samples (a considerable shift has been found particularly for the sample in lot 1). Accordingly, it is to be expected that the samples for which the plots will show a high shift as against the diagram in figure 2, will likewise show an unsatisfactory behaviour during processing.

This behaviour might be due to differences in the polymers as concerns polydispersity and degree of ramification of the macromolecular chain (a high ramification leading to a decrease in intrinsic viscosity for a given degree of polymerization).

The results obtained in this work suggest that correlated measurements of $[\eta]$ and $\overline{M}_w$ may be used for detecting the lots of PVC obtained by our industry which could behave unsatisfactorily on processing.

At the same time the data $[\eta]$ and $\overline{M}_w$ may also be used for a better defined qualitative specification of the commercial PVC.

In order to establish the causes responsible for the fact that some of the materials yield points much shifted from the diagram in figure 2, further investigations are to be carried out on the polydispersity and the degree of ramification both of the standard samples and of those exhibiting a highly different behaviour.

Revue Roumaine de Chimie, 14, 473–480 (1969)

STEREOSPECIFIC POLYMERIZATION OF 1,3 BUTADIENE. I

SOME KINETIC ASPECTS OF 1,3 BUTADIENE POLYMERIZATION WITH SOLUBLE CATALYSTS ON THE BASIS OF COBALT COMPLEX COMPOUNDS, DIETHYLALUMINIUM MONOCHLORIDE, WATER

I. VELEA, VICTORIA DIMONIE, E. MELEGA, P. BLENKE
and VALENTINA PROVINCEANU

Polytechnic Institute "Gh. Gheorghiu-Dej", Laboratory of macromolecular technology, Bucharest, Calea Victoriei, 149

Received June 26, 1968

The kinetics of butadiene polymerization in benzene media, with homogeneous catalyst on the basis of $AlEt_2Cl$, $CoCl_2.MeEtPy$ and H_2O was investigated. The reaction order related to the concentration of the monomer, the catalyst, as well as the influence of each catalytic component on the molecular weight was determined. The influence of the temperature on the polymerization was carried on. The polymer structure was practically not influenced by the studied parameters. On the basis of the obtained data a reaction mechanism is proposed.

In 1961, the selective catalytical activity of cobaltous salts in butadiene polymerization was first put into evidence, by obtaining a high stereospecific polybutadiene, with a content over 98% *cis* 1–4 structure.[1,2]

Subsequently the cocatalytical influence of the water and oxygen,[2–9] the influence of the nature of the organoaluminic compounds,[10–13] has

---

[1] C. LONGIAVE, R. CASTELLI and G. F. CROCE, *Chimica e Industria*, **43**, 625 (1961).

[2] M. GIPPIN, *Ind. Eng. Chem. Prod. Res. Develop.*, **1**, 32 (1962).

[3] V. N. ZGONIC and B. A. DOLGOPLOSK, *Doklady Akad. Nauk S.S.S.R.*, **145**, 1285 (1962).

[4] V. N. ZGONIC and B. A. DOLGOPLOSK, *Vysokomol. Soedineniya*, **6**, 1000 (1962).

[5] V. N. ZGONIC, B. A. DOLGOPLOSK, N. I. NICOLAEV and V. A. KROPACEV, *Vysokomol. Soedineniya*, **7**, 308 (1965).

[6] U. YU. KIRCHEVSKAIA and S. S. MEDVEDEV, *Doklady Akad. Nauk S. S. S. R.*, **153**, 1116 (1964).

[7] I. DIACONESCU and S. S. MEDVEDEV, *Doklady Akad. Nauk S.S.S.R.*, **155**, 890 (1964).

[8] I. DIACONESCU and S. S. MEDVEDEV, *J. Polymer Sci. A*, **3**, 31 (1965).

[9] E. J. TINIACOVA and B. A. DOLGOPLOSK, *Doklady Akad. Nauk S. S. S. R.*, **152**, 1376 (1963).

[10] C. LONGIANE and R. CASTELLI, *J. Polymer Sci. C*, **4**, 387 (1963).

[11] E. SUSA, *J. Polymer Sci. C*, **4**, 399 (1963).

[12] M. GIPPIN, *Ind. Eng. Chem. Prod. Res. Develop.*, **4**, 160 (1965).

[13] V. A. GRECHIANOVSKY and B. A. DOLGOPLOSK, *Doklady Akad. Nauk S. S. S. R.*, **144**, 792 (1962).

been noticed and the necessity of a halogen atom presence in these compounds in order to obtain a polybutadiene with a preponderant *cis* 1—4 structure has been underlined.

In the present paper, some kinetic aspects of the butadiene polymerization with catalyst on the basis of $AlEt_2Cl$ — $CoCl_2$.methyl ethylpyridine (MeEtPy) complex and H_2O, have been studied in order to obtain information about the reaction mechanism.

EXPERIMENTAL

Having in view the great sensitivity of the catalytic system based on organometallic compounds towards moisture, oxygen, CO_2, etc. as well as the fact that in the above mentioned catalytic system, a most important part has the water, the purification of reagents and the working method needed a high degree of purity.

All the reagent manipulations as well as the polymerizations were carried out in a dry and oxygen-free argon atmosphere, also the apparatus for polymerization and reagent collecting were emptied up to a 10^{-3} mmHg vacuum, heated at 200° and after vacuumating filled with purified argon.

All reagents were previously refluxed on the metal sodium wire or on calcium hydride, distilled on high efficiency columns and finally dried on molecular sieves.

The catalyst compounds were used in benzene solutions.

The cobaltous catalyst was prepared by complexing $CoCl_2$ with pyridine or 2methyl-5ethyl pyridine, both perfectly anhydrous, in a molar ratio $CoCl_2 : Py = 1 : 2$. The $CoCl_2.6H_2O$ was anhydrized being kept for 24 hours at 150° under a 10^{-3} mmHg vacuum.

The three catalyst compounds: the diethylaluminium monochloride solution, the $CoCl_2$.2MeEtPy complex solution and the water benzenic solution were measured in sealed glass bubbles.

The polymerizations were dilatometrically followed. The dilatometer is connected to the charging vessel (which is provided with a stirrer for breaking the bubbles and for homogenizing the mixture) by a capillary, to avoid liquid leakage before the opening of the stop-cock.

The obtained polymers were coagulated in isopropyl alcohol, washed with a 5% hydrochloric acid methanol solution for the removal of catalyst traces, then washed with much methanol, swollen in pentane and dried under vacuum at 50°. Like antioxidating agent was used phenyl-β-naphtyl-amine, 1% as against the polymer.

The molecular weight of polymers was measured in toluene solutions in a Ubbelohde viscosimeter, using for calculation the formula [1]:

$$\overline{M} = 1.53 \times 10^{-4} (\eta)^{0.8}$$

The polymer structure was obtained by infrared spectroscopy according to the method indicated by Kimmer and Schmaltz. [14]

All the results reported in tables and figures represent the arithmetical average of at least two runs which differ between them with maximum 3%.

---

[14] W. Kimmer and E. O. Schmalz, *Plaste und Kautschuk*, **2**, 18 (1965).

RESULTS AND DISCUSSIONS

The butadiene polymerization with the catalytic system $AlEt_2Cl$ $CoCl_2.2MeEtPy-H_2O$ occurs in homogeneous medium, without induction period, at the end of the process the conversion being maximum.

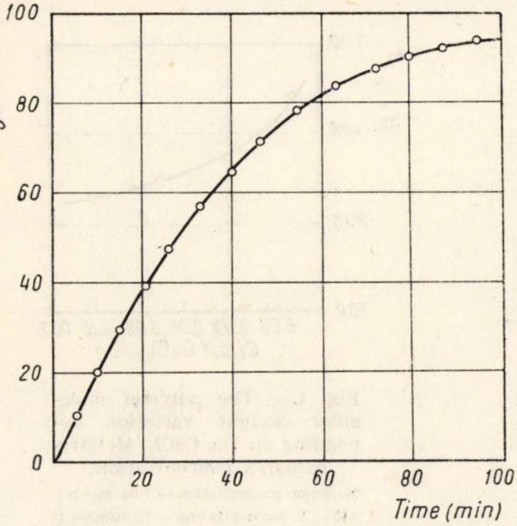

←Fig. 1. — The conversion variation in time.

Monomer concentration — 1.91 moles/l.

Fig. 2. — The dependence of polymerization initial rate on $AlEt_2Cl$ concentration.

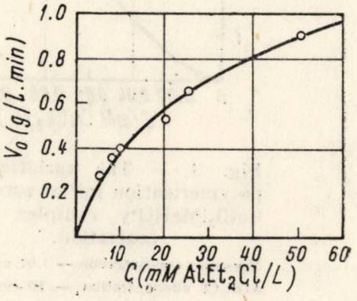

A curve characteristic of the polymerization process with time is shown in figure 1.

The polymerization reaction takes place only in the simultaneous presence of the three catalyst compounds, whose concentrations influence differently the reaction rates as well as the molecular weight of polymers.

As one can see from table 1, the $AlEt_2Cl$ concentration does not influence greatly the polymerization process and the characteristics of

Table 1

The influence of diethyl aluminium monochloride

Monomer concentration = 1.91 moles/l
$CoCl_2 \cdot MeEtPy$ concentration = 0.02 mmoles/l
H_2O ,, = 1 mmoles/l
Polymerization temperature = 5°

No	$AlEt_2Cl$ concentration mmoles/l	Initial rate V_0 g/l. min	$\overline{M}$	Structure %		
				cis 1,4	*trans* 1,4	vinyl 1,2
1.	5	0.28	—	—	—	—
2.	8	0.35	532,000	98.4	1.2	0.4
3.	10	0.39	518,000	97.5	1.6	0.9
4.	20	0.54	490,000	97.8	1.7	0.5
5.	25	0.66	470,000	97.3	1.8	0.9
6.	50	0.91	458,000	97.0	2.1	0.9

the obtained polymers (molecular weight and structure). The reaction order towards $AlEt_2Cl$ concentration is 0.5 (fig. 2) in a large field of concentrations (5 mmoles/l till 50 mmoles/l).

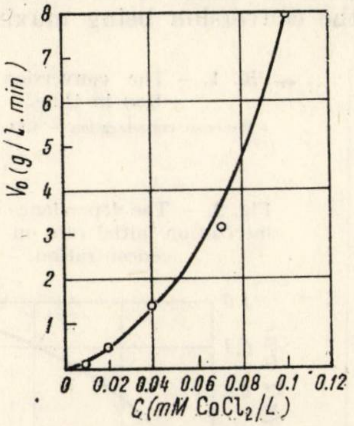

Fig. 3. — The variation of polymerization initial rate on $CoCl_2$.MeEtPy complex concentration.

Monomer concentration — 1.91 moles/l;
$AlEt_2Cl$ concentration — 10 mmoles/;
H_2O concentration — 1 mmoles/l;
Polymerization temperature = 5°.

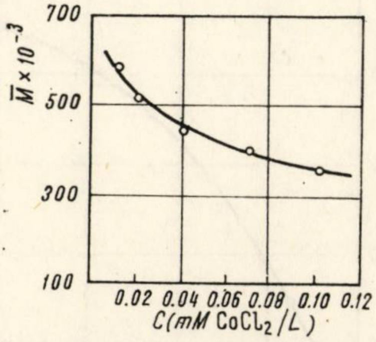

Fig. 4. — The polymer molecular weight variation depending on the $CoCl_2$. MeEtPy complex concentration.

Monomer concentration — 1.91 moles/l;
$AlEt_2Cl$ concentration — 10 mmoles/l;
H_2O concentration — 1 mmoles/l;
Polymerization temperature — 5°.

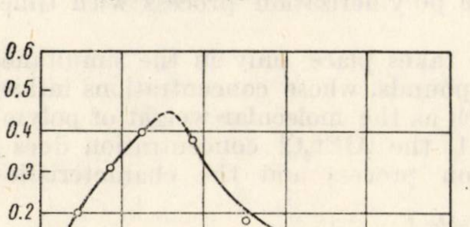

Fig. 5. — The variation of polymerization initial rate depending on water concentration.

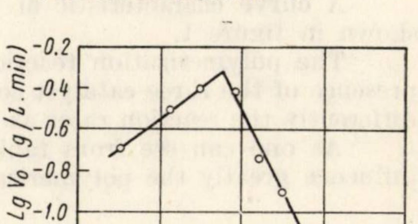

Fig. 6. — The dependence of polymerization initial rate on water concentration.

The polymerization rate changes substantially with the $CoCl_2$. 2MeEtPy complex concentration, for concentrations between 1×10^{-2} mmoles/l and 1×10^{-1} mmoles/l (fig. 3).

At the same time with the increase in the amount of cobalt in the catalytic system a remarkable decrease in the polymer molecular weight was observed (fig. 4).

The third of the catalytic compounds, the water, plays a decisive part in the polymerization process. As one can see from figure 5, the reaction rate increases at the same time with the increasing of water concentration up to values of 1.1 mmoles/l, after which the rate suddenly decreases.

The polymerization rate order related to water is equal to 0.75, in the field of concentrations in which water has the role of increasing the rate of the polymerization process (fig. 6).

The molecular weight increases at the same time with the amount of water in the whole field of concentrations (table 2).

Table 2

The influence of water concentration

Monomer concentration = 1.91 moles/l
$AlEt_2Cl$ concentration = 10 mmoles/l
$CoCl_2MeEtPy$ concentration = 0.02 mmoles/l
Polymerization temperature = 5°

No	Water Concentration mmoles/l	Initial rate V_0 g/l.min	$\overline{M}$	Structure %		
				cis 1,4	*trans* 1,4	vinyl 1,2
1.	0.4	0.20	302,000	—	—	—
2.	0.7	0.31	381,000	97.9	1.6	0.5
3.	1.0	0.39	518,000	97.5	1.6	0.9
4.	1.5	0.37	550,000	98.4	1.2	0.4
5.	2.0	0.18	—	98.0	1.6	0.4
6.	2.5	0.13	590,000	97.3	1.5	1.2
7.	4.0	0.05	616,000	96.9	1.7	1.4
8.	6.0	Lack polymer				

The part of water in this process is probably somewhat similar to the role of cocatalyst, played by water generally in cationic polymerization processes. The decrease of reaction rate with the increase of water concentration is due most probably to the disappearance of active centers under the influence of the water excess.

The continuous molecular weight increase at the same time with the increase of the water amount from the catalytic system can be explained as follows: for concentrations smaller than 1.1 mmoles/l the water stabilizes the active centers and therefore limits the termination reactions; at concentrations higher than 1.1 mmoles/l, the excess of water destroys the active centers, which leads to the increase in the molecular weight.

In a series of runs the influence of catalyst concentration was followed maintaining constant the ratio between the catalytic compounds and varying the amount of catalyst introduced into the system.

As one can see from figure 7, the polymerization rate is directly proportional with the overall amount of catalyst.

The molecular weight as well as the polymer structure do not practically depend on the catalyst concentration (fig. 8, table 3).

In all cases under consideration, the polymerization reaction development in time represents a first order process related to the concentration of unreacted monomer (fig. 9).

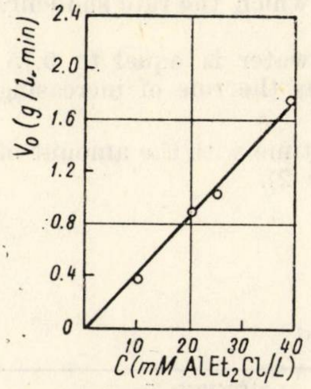

Fig. 7. — The variation of polymerization initial rate depending on catalyst concentration.

Monomer concentration — 1.91 moles/l; Molar ratio Al : Co : H_2O — 500 : 1 : 50.

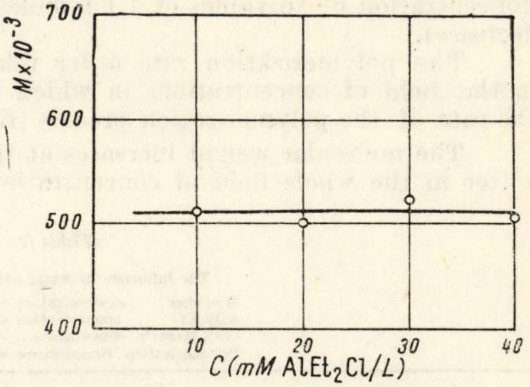

Fig. 8. — The polymer molecular weight dependence on the catalyst concentration.

Monomer concentration — 1.91 moles/l; Molar ratio Al : Co : H_2O — 500 : 1 : 50.

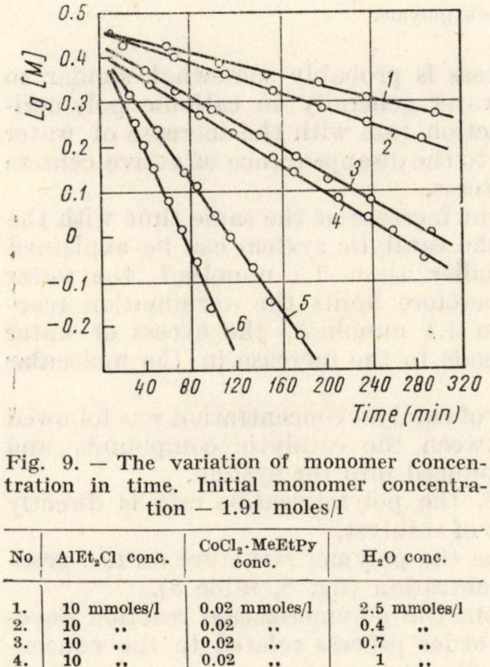

Fig. 9. — The variation of monomer concentration in time. Initial monomer concentration — 1.91 moles/l

No	$AlEt_2Cl$ conc.	$CoCl_2 \cdot MeEtPy$ conc.	H_2O conc.
1.	10 mmoles/l	0.02 mmoles/l	2.5 mmoles/l
2.	10 ..	0.02 ..	0.4 ..
3.	10 ..	0.02 ..	0.7 ..
4.	10 ..	0.02 ..	1 ..
5.	50 ..	0.02 ..	1 ..
6.	10 ..	0.04 ..	1 ..

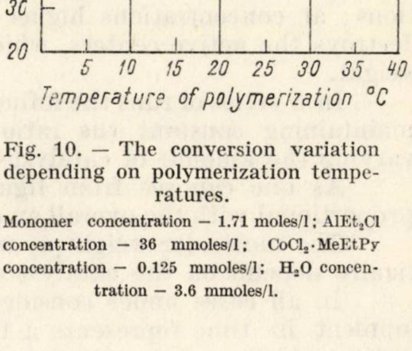

Fig. 10. — The conversion variation depending on polymerization temperatures.

Monomer concentration — 1.71 moles/l; $AlEt_2Cl$ concentration — 36 mmoles/l; $CoCl_2 \cdot MeEtPy$ concentration — 0.125 mmoles/l; H_2O concentration — 3.6 mmoles/l.

The temperature influence on the polymerization process was studied in a temperature range between 5° and 30°. The polymerization time in all cases was 1 hour.

As it is seen from figures 10 and 11, the conversion as well as the molecular weight are deeply influenced by temperature.

Table 3

The influence of catalyst concentration

Monomer concentration = 1.91 moles/l
Molar ratio Al : Co : H_2O = 500 : 1 : 50
Polymerization temperature = 5°

No	Catalyst concentration $AlEt_2Cl$ m moles/l	Structure %		
		cis 1,4	*trans* 1,4	vinyl 1,2
1.	10	97.5	1.6	0.9
2.	20	98.2	1.4	0.4
3.	25	97.2	1.3	1.5
4.	40	98.3	1.2	0.5

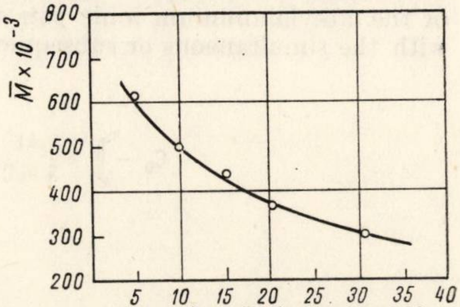

Fig. 11.— The polymer molecular weight variation depending on the polymerization temperatures.

Monomer concentration — 1.71 moles/l; $AlEt_2Cl$ concentration — 36 mmoles/l; $CoCl_2 \cdot MeEtPy$ concentration — 0.125 mmoles/l; H_2O concentration — 3.6 mmoles/l.

The fact that the polymer molecular weight presents a strong dependence on temperature (fig. 11), but practically does not depend on catalyst concentration (fig. 8), points out a monomolecular termination mechanism and a high value of the termination reaction activation energy. The constant maintaining of the first order related to the monomer concentration during the whole process (fig. 9) proves that during polymerization the active center concentration remains constant. This constant concentration of active centers suggest two possible reaction schemes : the first scheme implies the existence of a stationary state in which the initiation rate is equal to the rate of termination. The second scheme supposes a rapid initiation in which all the active centers are formed at the beginning of the polymerization process and the termination reaction takes place at the same time with the remaking of the active centers. For the last assumption also plead Dolgoplosk's and coworker's [13] data ; they found that the polymerization of a new amount of butadiene introduced into the reaction medium 48 hours after the first process conversion has reached the highest value, takes place with an almost equal rate like that of the initial reaction.

Thus, the butadiene polymerization process with soluble catalyst based on $AlEt_2Cl - CoCl_2.2MeEtPy - H_2O$ can be represented by the following scheme :

$$\begin{aligned} &\text{Initiation} &&: C^x + M \longrightarrow M^x \\ &\text{Growth} &&: M^x + nM \longrightarrow M^x_{n+1} \\ &\text{Termination} &&: M^x_{n+1} \longrightarrow C^x + P_n \end{aligned}$$

The nature of active centers in the butadiene polymerization process cannot be firmly stated but the kinetic data obtained by us are in accordance with the reaction mechanism proposed by Gippin[12] who considers the butadiene polymerization as a two-step process.

The formation of butadiene—cobalt complex in which the monomer is coordinated in *cis* position, followed by the addition, in position 1,4, of the alkylaluminium ionic pair to the coordinated butadiene molecule, with the simultaneous or subsequent expulsion of the cobalt atom.

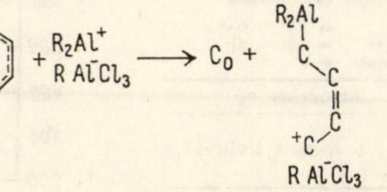

The role of cobalt is that of a carrier of butadiene molecule, sterically arranged in *cis* position, conferring to it at the same time a higher reactivity as a consequence of electron delocalization with the coordination complex formation.

Revue Roumaine de Chimie, **14**, 481–493 (1969)

ELECTRONIC SPECTRA OF THE SUBSTITUTED α-OXIMINOALKYLBENZENES. III[1]

STERIC EFFECTS ON ELECTRONIC ABSORPTION SPECTRA OF THE *o*-SUBSTITUTED *p*-NITRO-α-OXIMINOALKYLBENZENES

L. FEY and N. BODOR

Chemical-Pharmaceutical Research Institute,
Cluj, str. Karl Marx 93–97

Received June 10, 1968

On the basis of the spectral data and of the approximated potential functions of the torsion of C_1-C_α-bond, the electronic transition energies depending on the angles of torsion were estimated for the undissociated molecules and their anions. It is demonstrated that the potential curves of the ortho-substituted derivatives have two minima, corresponding to the two rotation isomers. However, the calculated differences between the excitation energies of these two isomers appear only in anions sufficiently great, so that two distinct bands in the electronic spectra may become visible, which statement is in good agreement with the experimental data.

In our previous papers [1,2] we have studied the orthosteric effects on the electronic spectra of *p*-substituted-*o*-nitro-acetophenonoximes, as well as the bathochromic shifts which followed the dissociation of these molecules.

In the present work, our previous study was extended to the following *o*-substituted *p*-nitro-acetophenonoximes :

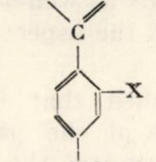

X = Cl, Br, I, $SO_2N(CH_3)_2$,
(I) (II) (III) (IV)
$SO_2N(C_2H_5)_2$
(V)

p-Nitroacetophenonoxime (VI) and *p*-nitro-propiophenonoxime (VII) were used as reference for the interpretation of the observed steric effects. These compounds give quite equal absorption spectra (Fig. 10), the bands being nearly similar as to position and intensity. The dissociation causes significant bathochromic displacements in these spectra, which were to be expected and quantitatively estimated by the LCAO-MO calculations. [2]

---

[1] Previous paper : L. Fey and N. Bodor, *Rev. Roumaine Chim.*, **14**, 319 (1969).

[2] L. Fey and N. Bodor, *Rev. Roumaine Chim.*, **14**, 225 (1969).

In the spectra of the *o*-substituted derivatives an important hypsochromic shift of the primary band corresponding to the intramolecular charge transfer was observed (see Table 5, Fig. 9) as compared to the unsubstituted reference compound (VI). This shifted maximum is situated in the proximity of the nitrobenzene maximum, which indicates a strong torsion of the $C_1-C\alpha$ bond. Thus, on account of the deviation from coplanarity of the α-oximinoethyl grouping by the ortho-substituent, the auxochrome-anti-auxochrome couple (oxime-phenyl-nitro) is almost completely repealed, and consequently only the phenyl-nitro resonance system remains untouched.

However, in the spectra of the ionized forms there appear two maxima placed at 4–5,000 cm^{-1} intervals. The band placed at shorter wavelengths cannot be attributed to the second transition of the *p*-nitro-acetophenonoxime, because in this case an unjustifiable strong bathochromic displacement of the corresponding band would be supposed. Thus, supposing that the secondary band of the undissociated form was placed in the far UV-region at about 38,000 cm^{-1}, this displacement must be more than 7,000 cm^{-1} .Such a very significant displacement was not observed however even in the unhindered systems. This phenomenon can neither be explained by the chromophore properties of the corresponding ortho-substituents, because their own-absorption bands are placed at much shorter wavelengths. [1]

The forms and the changed intensities of the absorption curves of anions suggest that actually a splitting of the band of undissociated molecules takes place. This presumption is confirmed by the evaluation of the integral intensities ($\int \varepsilon d\nu$). First, we have established that practically no change takes place in the integral intensity values of the primary bands of reference, sterically unhindered compounds (VI, VII and *p*-nitrobenzaldoxime), by their transformation into the corresponding anions. This result implies that the transition moments as well as the vibrational and rotational transitions — which determine the aspect of the bands — remain practically unchanged.

On the other hand, we have established that in the cases of *o*-substituted derivatives, the integral values of the primary bands of undissociated molecules are equal with the sum of the integrals of the two bands obtained for the corresponding anions. Evidently, this result supports the presumption referring to the splitting in two of the characteristic band of the undissociated oxime, when this becomes transformed into its anion.

The integral values of the primary bands of the studied compounds are given in table 1.

Table 1

The integral intensities of the oximes studied [a)]

Compounds	$I = \int \varepsilon d\nu$ (10^{10} cm/mol)	
	Undiss.	Anion sum of the 2 bands
p-nitro-benzaldoxime	9.4	9.4
p-nitro-acetophenonoxime	8.2	8.2
p-nitro-propiophenonoxime	8.6	8.4
p-nitro-izobutirophenonoxime	7.4	6.8
o-chloro-*p*-nitro-acetophenonoxime	7.2	7.2
o-bromo-*p*-nitro-acetophenonoxime	7.0	7.4
o-iodo-*p*-nitro-acetophenonoxime	5.2	5.2
o-dimethylaminosulfonyl-*p*-nitro-acetophenonoxime [b)]	5.1–5.7	5.1–5.7
o-diethylaminosulfonyl-*p*-nitro-acetophenonoxime [b)]	6–7	6–7

a) The integral values were evaluated by planimetry, after the extrapolation of the extinction curves, according to fig. 1.

b) The complexity of the spectra obtained for the *o*-dialkylaminosulfonyl derivatives, due to the chromophore properties of these substituents, make uncertain the correct extrapolation of these curves.

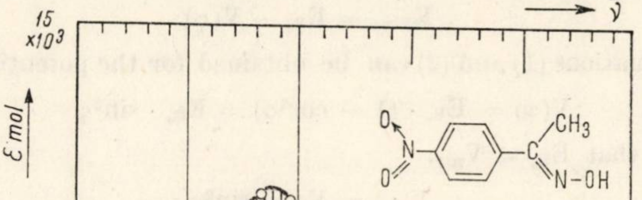

Fig. 1. — Evaluation of the integral intensity of the primary band by planimetry.

Still it is necessary to explain, how the ortho-steric effect causes the splitting of the primary band and why this phenomenon becomes visible only in the spectra of the ionized forms.

Taking into account that this phenomenon appears together with the torsion of the C_1-C_α-bond, the existence of two population maxima depending on the angles of torsion must be presumed, maxima corresponding to the two minima on the potential curves.

For the estimation of the potential curve of torsion $V(\varphi)$, we have started from the relationship proposed by several authors [3,4] for the variation of the extraresonance energy in an R—S resonance system, depending on the measure of its deviation from coplanarity :

$$E_{R(\varphi)} = E_{R_0} \cdot \cos^2\varphi \tag{1}$$

where φ is the angle of torsion.

The validity of this equation in the whole interval of torsion (0—90°) of the nitro grouping has been demonstrated by Trotter [5] for aromatic nitro-derivatives.

The extraresonance energy decreases simultaneously with the increase due to the torsion of the potential energy, so we can write :

$$E_{R(\varphi)} = E_{R_0} - V(\varphi) \tag{2}$$

From the equations (1) and (2) can be obtained for the potential function :

$$V(\varphi) = E_{R_0} \cdot (1 - \cos^2\varphi) = E_{R_0} \cdot \sin^2\varphi$$

or knowing that $E_{R_0} = V_{\pi/2}$,

$$V(\varphi) = V_{\pi/2} \cdot \sin^2\varphi \tag{3}$$

This expression is valid both for the undissociated molecules and anions, the only difference being the $V_{\pi/2}$ value, which is greater for anions due to the increase of the C_1-C_α-bond order.

The energy of the torsioned system in the ground as well as in the excited states can be obtained assuming the energy of coplanar molecule and the corresponding potential energy of torsion :

$$\begin{aligned} E_\varphi &= E_0 + V(\varphi) \\ E^*_\varphi &= E^*_0 + V^*(\varphi) \end{aligned} \tag{4}$$

where $V(\varphi)$ and $V^*(\varphi)$ are the potential functions in the ground and in excited states respectively. According to Franck-Condon's principle, the angle of torsion remains unchanged during the electronic transition (vertical transition between the two potential curves), thus the absorbed energy will be :

$$\Delta E_\varphi = \Delta E_0 + \Delta V(\varphi) \tag{5}$$

---

[3] M. J. S. Dewar, *J. Amer. Chem. Soc.*, **74**, 3345 (1952).

[4] H. H. Jaffé and M. Orchin, "Theory and Application of UV Spectroscopy". Ed. John Wiley, New York, 1964, p. 390.

[5] J. Trotter, *Canad. J. Chem.*, **37**, 905 (1959).

where $\Delta E_\varphi = E^*_\varphi - E_\varphi$ — the excitation energy of the system torsioned by the angle/φ,

$\Delta E_0 = E^*_0 - E_0$ — the excitation energy of the coplanar model,

$\Delta V(\varphi) = V^*(\varphi) - V(\varphi)$ — the potential function difference between the two states.

Admitting that the expression (3) is valid also in the excited state,

$$\Delta V(\varphi) = \Delta V_{\pi/2} \cdot \sin^2\varphi \tag{6}$$

where

$$\Delta V_{\pi/2} = V^*_{\pi/2} - V_{\pi/2}$$

In the case of the orthogonal torsion, the expression (5) becomes:

$$\Delta E_{\pi/2} = \Delta E_0 + \Delta V_{\pi/2}$$

and

$$\Delta V_{\pi/2} = \Delta E_{\pi/2} - \Delta E_0 \tag{7}$$

Including the expressions (6) and (7) in (5) we obtain the following expression for the variation of the excitation energy, depending on the angle of torsion:

$$\Delta E_\varphi = \Delta E_0 + (\Delta E_{\pi/2} - \Delta E_0) \cdot \sin^2\varphi$$

respectively

$$\Delta E_\varphi = \Delta E_{\pi/2} \cdot \sin^2\varphi + \Delta E_0 \cdot \cos^2\varphi \tag{8}$$

The values ΔE_0 and $\Delta E_{\pi/2}$ can be obtained from the spectral data both for the undissociated and ionized forms. Thus, ΔE_0 — the transition energy of the coplanar model — corresponds to the maxima of the *p*-nitro-acetophenonoxime (33,500 cm^{-1} = 96 kcal/mole for the undissociated and 28,500 cm^{-1} = 81 kcal/mole for the ionized forms). $\Delta E_{\pi/2}$ is the transition energy of the orthogonal torsioned model, which in our case is the nitrobenzene (37,250 cm^{-1} = 107 kcal/mole).[6]

Introducing these values in equation (8) we have obtained for the undissociated molecule:

$$\Delta E_\varphi = 107 \cdot \sin^2\varphi + 96 \cdot \cos^2\varphi \tag{9}$$

and for the anion:

$$\Delta E^{(-)}_\varphi = 107 \cdot \sin^2\varphi + 81 \cdot \cos^2\varphi$$

In absence of any ortho-steric effect, the potential function (3) only has a single minimum, so the repartition function has a single maximum corresponding to the coplanar molecule. Consequently, the primary electronic transition appears as a single band in the spectrum.

---

[6] L. Doub and J. M. Vandenbelt, *J. Amer. Chem. Soc.*, **69**, 2714 (1947); **71**, 2414 (1949).

It was demonstrated that the population of the potential curves is practically continuous, as the energy levels of the oscillation are placed very close to each other,[7] the ground frequency having only some tens of cm^{-1}.

In the case of a steric hindered molecule, the potential minimum will be placed at angles different from zero, depending on the interaction forces (above all van der Waals forces). The sizes of these forces are determined by the dimensions of the substituents and by their direct distances depending on the angles of torsion.

In our case, the ortho-X grouping takes place in two interactions: on the one hand with the oximino-nitrogen, and on the other with the methyl grouping from the oximinoethyl side chain.

For evaluation of the distances between groups in the above interactions, the following geometrical problem must be solved:

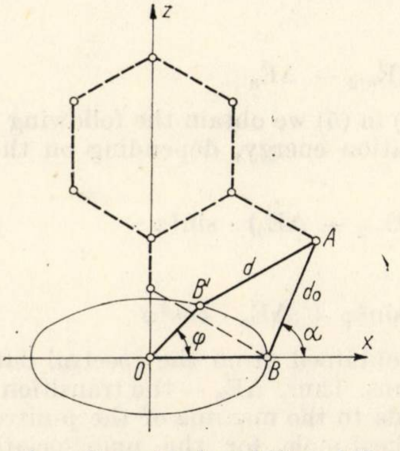

Fig. 2. — Geometrical modelling of the *ortho*-steric effect.

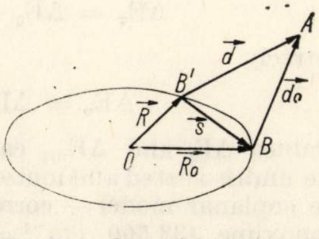

Fig. 3. — Vectorial scheme of the *ortho*-steric effect.

The circle O is placed in the x, y-plane. A(x, y, z), which represents in fact the ortho-X grouping, is a point placed in space, and B(x, y) (oximino-nitrogen or CH_3- respectively), on the circle. The distance $d = AB$ should be determined in function of the angle Φ, knowing the angle α, as well as the one when $\Phi = 0$, $d = d_0$. The problem can be modelled by the following vectorial scheme, which makes its solution easier:

$$|\vec{d}| = d$$

$$|\vec{d}_0| = d_0$$

$$\vec{s} = \vec{R}_0 - \vec{R}$$

$$\vec{d} = \vec{s} + \vec{d}_0 = \vec{R}_0 - \vec{R} + \vec{d}_0 \qquad (10)$$

[7] G. Kortüm and G. Dreesen, *Chem. Ber.*, 84, 182 (1951).

Our orthogonal coordinate system was choosen in such a manner as to place the circle in the x, y plane and R_0 vector (radius) on the X-axis. Thus :

$$\vec{R}_0 = R \cdot i$$
$$\vec{R} = R \cdot \cos\varphi \cdot i + R \cdot \sin\varphi \cdot j$$
$$\vec{d}_0 = d_0 \cdot \cos\alpha \cdot i + d_0 \cdot \sin\alpha \cdot k$$

and the expression (10) becomes :

$$\vec{d} = [R.(1 - \cos\varphi) + d_0 \cdot \cos\alpha] \cdot i - R.\sin\varphi.\, j + d_0 \cdot \sin\alpha \cdot k$$

and

$$|\vec{d}| = d = \sqrt{[R \cdot (1 - \cos\varphi) + d_0 \cdot \cos\alpha]^2 + R^2 \cdot \sin^2\varphi + d_0^2 \cdot \sin^2\alpha}$$

By several simple trigonometric transformations, the following expression was obtained :

$$d = \sqrt{d_0^2 + 4R \cdot \sin^2(\varphi/2) \cdot (R + d_0 \cdot \cos\alpha)} \qquad (11)$$

The d_0, R and $d_0 \cdot \cos\alpha$ values can be calculated from the bond lengths and bond angles of the hypothetical coplanar molecules ; thus the values of d for any angles of torsion can be obtained using the equation (11).

The bond lengths applied in our calculations were obtained according to Bikov's theory, [8] taking into account the electron charges of the bonds, by the following expression :

$$L' = L - \Delta^{1\pi} \cdot A^{\pi} \qquad (12)$$

where :

L' — the real bond lengths
L — the standard σ-bond lengths
$\Delta^{1\pi}$ — the specific contraction of the bonds in Å/e
A^{π} — π-electron charges of the bonds in e.

The corresponding values are given in table 2.

Table 2

The standard σ-bond lengths and the corresponding real bond lengths calculated by equation (12)

Bond	L(Å)	$\Delta^{1\pi}$	A^{π}	L′(Å)
(Ar) ⟩C − C	1.542	0.15−0.16	0.6	1.45
(Ar) ⟩C − Cl	1.782	0.210	0.5	1.68
(Ar) ⟩C − Br	1.938	0.188	0.4	1.82
(Ar) ⟩C − I	2.140	0.185	0.5	2.047
C = N (oximinic)	1.474	0.095	1.9	1.29
C = C (aryl)	—	—	—	1.397

---

[8] G. V. Bikow, "Electronnije zarjadi svjazei v organitcheskikh soedinenjakh", Ed. Acad. Sci. USSR, Moscow, 1960, p. 51−58.

The calculated d values for the different angles of torsion are given in table 3.

Table 3

The calculated "d"-values for several angles of torsion

$\varphi°$	$d_{X/N}$ (Å)			$d_{X/methyl}$ (Å)		
	Cl	Br	I	Cl	Br	I
0	2.50	2.52	2.58	2.47	2.48	2.52
20	2.56	2.58	2.65	2.56	2.58	2.61
30	2.65	2.66	2.74	2.66	2.67	2.72
45	2.82	2.88	2.92	2.84	2.89	2.94
60	3.03	3.07	3.16	3.10	3.14	3.21
75	3.26	3.31	3.40	3.36	3.42	3.50
90	3.48	3.54	3.64	3.62	3.68	3.78
100	3.64	3.70	3.80	3.79	3.86	3.96

The repulsive interactions begin at the distances corresponding to the van der Waals radii, which are:

$$R_{CH_3} = 2.00 \text{ Å}; \; R_N = 1.50 \text{ Å}; \; R_{Cl} = 1.80 \text{ Å}; \; R_{Br} = 1.95 \text{ Å}; \; R_I = 2.15 \text{ Å}.$$

The van der Waals function for the interaction between the atoms bromine and hydrogen have been estimated by several authors. [9,10] Thus, Westheimer [9] proposed an exponential relationship the value of which is near zero at distances corresponding to van der Waals radii, and which suddenly increases towards infinite at distances smaller than 0.6—0.7 Å. Our case (when CH_3 and Br enter into interaction) is similar with the H/Br interaction; consequently the given approximation can be used. Taking into account the exponential character of the curves, in the first approximation these can be replaced by rigid barriers, at distances smaller by 0.6—0.7 Å than the sum of the van der Waals radii. Neglecting the electrostatic interactions, we can generalize this treatment for each of the studied ortho-steric interactions. Thus, the potential barriers are placed at the following angles of deviation from coplanarity (rounded values):

N-oximino/Cl 30° (2.65 Å); CH_3/Cl 60° (3.15 Å);
,, /Br 35° (2.80 Å); ,, /Br 65° (3.30 Å);
,, /I 45° (3.00 Å); ,, /I 75° (3.50 Å).

In the first approximation, the potential torsion function can be estimated by the superposition of the van der Waals barriers on the function $V = V_{\pi/2} \cdot \sin^2\varphi$, which will be limited consequently to the interval determined by the above angles. The character of the potential curves is given in figure 4.

This presentation reproduces only the character of the curves, the exact form, positions and values of the minima being influenced by several factors which are neglected, such as the electrostatic interactions (inductive and field effects) and the bond elasticity-forces. The main finding of this approximation is that there are two minima on the potential curves, placed asymmetrically as compared to the orthogonal torsion. Even these minima correspond to torsions with the greatest population. Granted that there is no considerable difference between the energies of these torsioned forms, the number of the particles corresponding to the two rotation isomers would be conmeasurable.

---

[9] F. H. Westheimer and J. E. Mayer, *J. Chem. Phys.*, **14**, 733 (1946).

[10] J. Dostrowsky, E. D. Hughes and C. K. Ingold, *J. Chem. Soc.*, **1946**, 173.

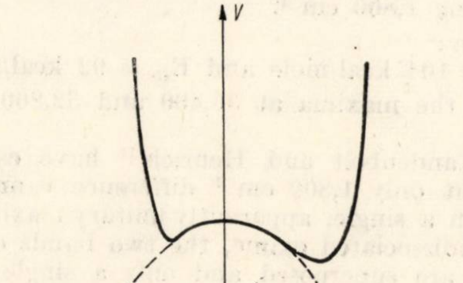

Fig. 4. — The potential curve of *ortho*-steric effect in the case of *o*-halo-*p*-nitro-acetophenon-oximes.

In order to estimate how the changed potential curves affect the electronic spectra, we resort to equation (5). In this case, the potential function V(φ) must be corrected with the steric effect. This correction can be considered as a simple superposition of the van der Waals barriers on the function V(φ), corresponding to the unhindered form, it being the same for the ground and for the excited states. Consequently, in the energy difference expression (ΔE_φ) this correction does not take part. Thus, the absorbed energy can be expressed by (8) and (9), similarly to the sterically unhindered case. Only the repartition function is changed, the population maxima being the angles corresponding to the minima of the potential functions. In such a way, in the electronic spectra, the absorption bands corresponding to the angles of torsion can be expected. We demonstrate in the case of the *o*-bromoderivative the calculation of the position of the expected absorption bands which represent in fact approximately the medium of the *o*-halo-derivatives (on the other hand, the differences of the corresponding values are so small that no considerable deviation of bands position was obtained for the other *o*-halo-derivatives).

As in ortho-bromo-derivative the van der Waals barriers are placed at the 65° and 35° angles, the minima of the potential curves will be placed at torsions of about 70° and 40° respectively. Using equation (9), the excitation energies depending on the torsion can be obtained in the following manner:

a) For undissociated molecule:

$$E_{70} = 107\cdot\sin^2 70 + 96\cdot\cos^2 70 = 106 \text{ kcal/mole}$$
$$E_{40} = 107\cdot\sin^2 40 + 96\cdot\cos^2 40 = 101 \text{ kcal/mole}$$

These energy values correspond to the maxima at 37,100 and 35,300 cm^{-1}, the difference being 1,800 cm^{-1}.

b) For anion:

$$E_{70} = 104 \text{ kcal/mole and } E_{40} = 92 \text{ kcal/mole},$$

corresponding to the maxima at 36,400 and 32,200 cm^{-1}, outdistanced by 4,200 cm^{-1}.

However, Vandenbelt and Henrich[11] have established that two maxima placed at only 1,800 cm^{-1} difference cannot be distinguished they being fused in a single, apparently unitary maximum. Consequently, in the case of undissociated oxime, the two bands corresponding to the rotation isomers are superposed and only a single maximum appears. On the other hand, in the case of anion, the distance between the two maxima is sufficiently great to become both visible and well outlined. For graphical exemplification of the preceeding conclusions, we give in figure 5 the superposition of the two bands at 37,100 and 35,300 cm^{-1}, their intensities being approximately the same as the corresponding experimental values obtained for *o*-bromo-*p*-nitro-acetophenonoxime. On the other hand, figure 6 gives the superposition of two bands situated at 36,400 cm^{-1} and 32,200 cm^{-1}.

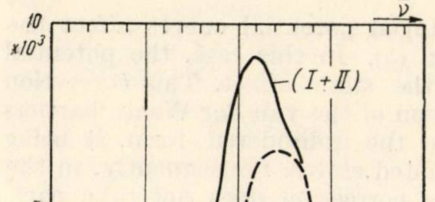

Fig. 5. — Superposition of two bands outdistanced by 1,800 cm^{-1}.

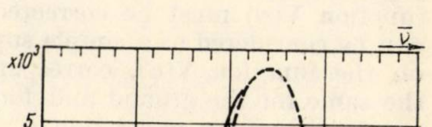

Fig. 6. — Superposition of two bands outdistanced by 4,200 cm^{-1}.

These curves are evidently similar to those obtained experimentally, from which initially we have substracted by extrapolation the slopes obtained at shorter wavelengths, which can be attributed to other transitions (see Figs 7 and 8).

---

[11] J. M. Vandenbelt and C. Henrich, *Appl. Spectroscopy*, **7**, 173 (1953).

In conclusion, it was established that whilst the unsubstituted *p*-nitro-acetophenonoxime exists only in a single stable form, namely the coplanar structure, in which the oximinoethyl side chain oscillates freely around the equilibrial position, its ortho-halo-derivatives (or other derivatives substituted with bulky groups in ortho position) can exist in two rotation isomers which are in termodynamic equilibrium. These isomers are conspicuous in the electronic spectra of the corresponding anions.

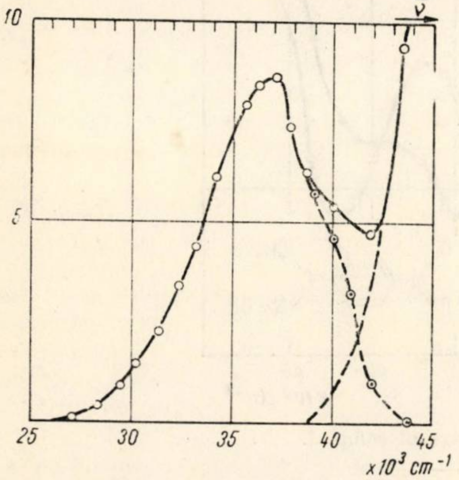

Fig. 7. — The superposed bands of the rotation izomers of the undissociated *o*-bromo-*p*-nitro-acetophenonoxime.

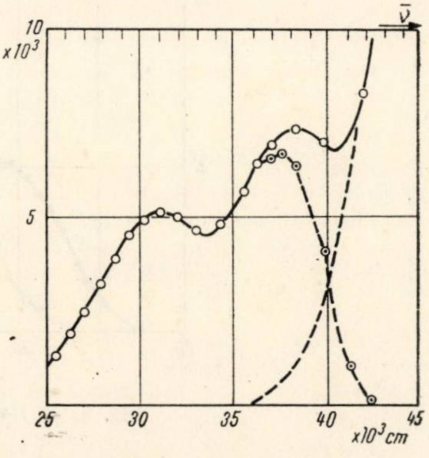

Fig. 8. — Splitting of the primary band into the corresponding bands of rotation izomers, due to dissociation.

EXPERIMENTAL

Compounds used. Compounds used and some characteristic physico-chemical properties are given in table 4.

Table 4

Compounds studied

No. of comp.	Compounds	Recryst. from	m.p.	Ref.
I	*o*-chloro-*p*-nitro-AO	dil.acetic acid	129–130°	12
II	*o*-bromo-*p*-nitro-AO	dil.acetic acid	144–145°	12
III	*o*-iodo-*p*-nitro-AO	dil.acetic acid	163°	12
IV	*o*-dimethylaminosulphonyl-*p*-nitro-AO	dil.acetic acid	138°	12
V	*o*-diethylaminosulphonyl-*p*-nitro-AO	dil.acetic acid	154–155°	12
VI	*p*-nitro-acetophenonoxime	dil. ethanol	176–178°	13
VII	*p*-nitro-propiophenonoxime	benzene+ethanol	143–145°	14

AO = acetophenonoxime

---

[12] A. Kövendi and M. Kircz, *Chem. Ber.*, **97**, 1902 (1964).

[13] N. Bodor, L. Fey and A. Kövendi, *Rev. Roumaine Chim.*, **11**, 405 (1966).

[14] N. Bodor and A. Kövendi, *Rev. Roumaine Chim.*, **11**, 393 (1966).

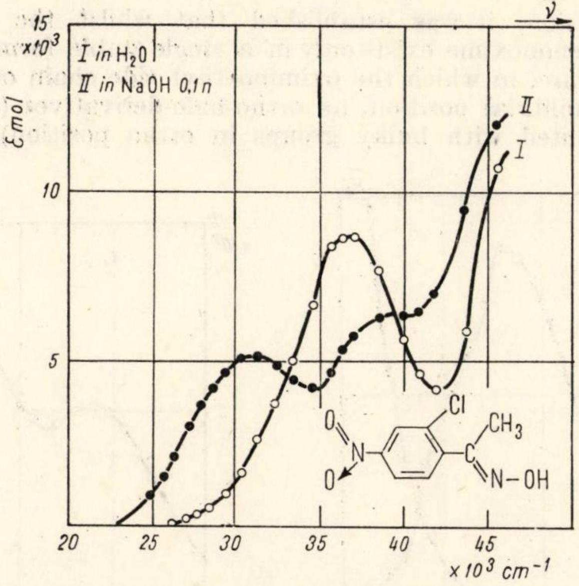

Fig. 9. — UV Spectra of comp. I.

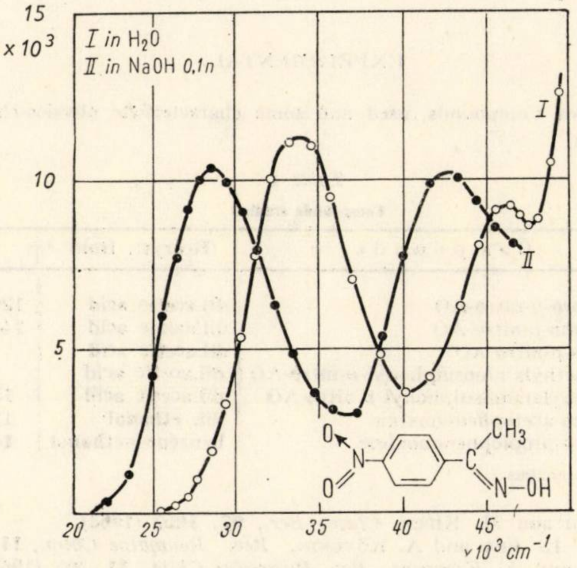

Fig. 10. — UV Spectra of comp. VI.

UV-spectra of the compounds studied. The spectra were registred according to the procedure given in our previous work.[1] The spectral data obtained for the ortho-substituted *p*-nitro-acetophenonoximes are given in table 5, and the spectra of two representative substances in figs. 9 and 10.

Table 5

Absorption maxima of the ortho-X-substituted *p*-nitro-acetophenon-oximes

Substituent X	In water $\bar{\nu}_{max}$	In water (ε_{max})	In NaOH 0.1 n I $\bar{\nu}_{max}$	In NaOH 0.1 n I (ε_{max})	In NaOH 0.1 n II $\bar{\nu}_{max}$	In NaOH 0.1 n II (ε_{max})
Cl	37,000	(8,700)	31,000	(5,100)	38,500	(6,300)
Br	37,000	(8,500)	31,200	(5,100)	38,500	(7,300)
I	37,000	(8,400)	31,200	(4,200)	38,200	(7,600)
$SO_2-N(CH_3)_2$	40,000	(9,400)	30,000	(2,300)	40,000	(9,500)
$SO_2-N(C_2H_5)_2$	40,200	(9,800)	30,100	(2,600)	40,200	(10,100)

Revue Roumaine de Chimie, 14, 495–501 (1969)

ÜBER HETEROORGANISCHE VERBINDUNGEN. XXXVI[1]

INFRAROT-SPEKTROSKOPISCHE UNTERSUCHUNGEN DER ADDUKTE DER O,O-DIALKYLTHIOPHOSPHORSÄUREN MIT SEKUNDÄREN UND TERTIÄREN AMINEN

LUCREŢIA ALMASI, A. HANTZ und ERIKA HAMBURG
Aus dem Chemischen Institut der Akademie, Cluj, str. Donath 59–65

Eingegangen am 27. April 1968

Es wird festgestellt, daß Addukte der O,O-Dialkylthiophosphorsäuren mit sekundären und tertiären Aminen (aliphatische, cykloparaffinische, aromatische und π-deffekt heterocyklische), deren ΔpK* zwischen 9,6 und 3,6 schwanken, intermolekulare Wasserstoffbrückenbindungen darstellen, bei welchen Protonenübergang stattfindet. Die Struktur der Anionen entspricht einem Zustand folgender Grenzstrukturen 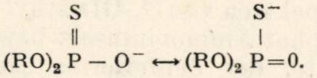 $(RO)_2\overset{\overset{S}{\|}}{P}-O^- \longleftrightarrow (RO)_2\overset{\overset{S^-}{|}}{P}=0$. Mit abnehmender Basicität des Protonenakzeptors (bei gleichem Protonendonator) verschiebt sich die Struktur des mesomeren Anions in die Richtung der Thionstruktur.

In Fortsetzung unserer früheren Arbeit[2] bezüglich der Struktur der Addukte thiophosphororganischer saurer Ester mit organischen Basen, wird in der vorliegenden Arbeit über die Addukte der O,O-Dialkylthiophosphorsäuren mit sekundären und tertiären Aminen berichtet, deren ΔpK-Werte zwischen 9,6–3,6 schwanken.

Es ist bekannt,[3,4] daß O,O-Dialkylthiophosphorsäuren eine Thion-Thioltautomerie $(RO)_2P(S)OH \rightleftarrows (RO)_2P(O)SH$ darstellen; ihre Alkalisalze wurden von einigen Autoren[5,6] als O-Abkömmlinge (Thionstruktur) betrachtet, während in einer anderen Arbeit[7] dem Anion eine mesomere Struktur (Resonanzhybrid) 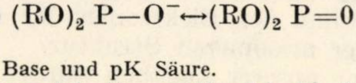 $(RO)_2\overset{\overset{S}{\|}}{P}-O^- \longleftrightarrow (RO)_2\overset{\overset{S^-}{|}}{P}=0$ zugeschrieben wird.

---

* Differenz zwischen pKa Base und pK Säure.

[1] XXXV. Mitt.: L. Almasi und A. Hantz, *Monatsh.*, **99**, 1045 (1968).

[2] L. Almasi, A. Hantz, E. Weissmann und E. Hamburg, *Rev. Roumaine Chim.*, **12**, 1269 (1967).

[3] M. I. Kabatchnik, S. T. Zhoffe und T. A. Mastrukowa, *Zhur. obshchei Khim.*, **25**, 684 (1955).

[4] M. I. Kabatchnik, T. A. Mastrukova, A. E. Shipow und T. A. Melentiewa, *Tetrahedron*, **9** 10 (1960).

[5] R. C. Gore, *Disc. Farad. Soc.*, **1950**, 138.

[6] M. I. Kabatchnik, T. A. Mastrukowa, N. P. Rodionowa und E. M. Popow, *Zhur. obshchei Khim.*, **26**, 120 (1956).

[7] T. W. Mastin, G. R. Norman und E. A. Weilmuenster, *J. Amer. Chem. Soc.*, **67**, 1662 (1945).

In neuesten Arbeiten[8,9] wurde auf Grund eingehender Untersuchungen der IR-Spektren alkalischer und nicht alkalischer Salze der O,O-Dialkylthiophosphorsäuren, wie auf Grund des Vergleiches der gefundenen IR-Frequenzen mit den für die drei Modelle (Thionstruktur, Thiolstruktur und Mesomerstruktur des Anions) berechneten Frequenzen, festgestellt, daß das Anion der Alkali- und Ammoniumsalze mesomere Struktur hat, während andere Salze assoziiert sind und von dem Kation abhängig die Thiol- bzw. Thionstruktur überwiegt.

Die von uns synthetisierten Addukte, stellen erwartungsgemäß intermolekulare Wasserstoffbrückenbindungen dar, so daß die Verwendung von IR-Spektroskopie zur Untersuchung dieser Verbindungen geeignet ist. Alle erhaltenen Addukte (I—VIII) sind 1 : 1 Komplexe, kristalline oder flüssige Verbindungen, deren physikalische Konstanten, Analyse und ΔpK-Werte in Tabelle 1 angegeben sind.

Leider ist es uns nicht gelungen das Addukt der O,O-Diäthylthiophosphorsäure mit Diphenylamin (sehr schwache Base) zu erhalten, so daß die ΔpK-Werte der untersuchten Verbindungen zwischen 9,6—4,6 schwanken, ein Gebiet, in welchem die Pyridinbenzoesäureaddukte ionisch sind.[10]

Um Angaben über die Struktur der von uns untersuchten Addukte zu erhalten, wurden die IR-Spektren von O,-ODiäthyl-S-äthyl-thiolphosphat, O,O,O-Triäthylthionphosphat Ammoniumsalz bzw. Natriumsalz der Säure, der Säure-Base-Addukte, der deuterierten Addukte der freien Basen und protonierten Basen untereinander verglichen.

Die Frequenzen[8] der P=O- und P—S-Gruppen in 0,0-Diäthyl-S-äthyl-thiolphosphat sind bei 1256 cm^{-1} bzw. 608 cm^{-1}, die Frequenz der P=S-Gruppe befindet sich im Bereich 629—615 cm^{-1}. Im Ammonium- bzw. Natriumsalz der O,O-Diäthylthiophosphorsäure befindet sich die P=O-Frequenz im Bereich 1130—1146 cm^{-1} und die P=S-Frequenz im Bereich 604—613 cm^{-1}. Die Struktur, des Anions dieser Salze wird als mesomer betrachtet 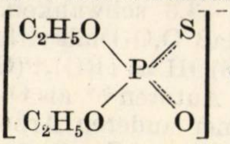 da ihre Frequenzen nicht einer vollen P=O-Gruppe (Differenz ~110 cm^{-1}) und nicht einer vollen P=S-Gruppe (Differenz ~20 cm^{-1} * entsprechen); die Verteilung der Ladungen und der Elektronen der π-Bindung im System der Triade entspricht der mesomeren Struktur.

Zur Auswertung unserer Angaben wurden folgende Spektralbereiche in Betracht gezogen: Gebiet I 550—1700 cm^{-1}, Gebiet II 1700—2300 cm^{-1}, Gebiet III 2300—2800 cm^{-1}.

In Tabelle 2 sind die uns interessierenden charakteristischen Frequenzen in den drei Spektralbereichen für die Addukte (I—VIII) IR

---

* Es ist bekannt, daß die Differenz zwischen den Banden der P=S- und P—S-Gruppen etwa 20 cm^{-1} beträgt während die der P=O- und P—O-Gruppen viel größer ist.

[8] M. I. Kabatchnik, T. A. Mastrukowa, E. I. Matrosow und B. Fisher, *Zhur. strukt. Khim.*, **6**, 691 (1965).

[9] E. I. Matrosow, *Zhur. strukt. Khim.*, **8**, 540 (1967).

[10] S. L. Johnson und K. A. Rumon, *J. Phys. Chem.*, **69**, 1 (1965).

Spektren Ia—VIIIa, für die deuterierten Addukte IR Spektren Ib—VIIIb angegeben.

Es ist aus der Literatur bekannt, daß manchen anorganischen sauren Salzen [11] wie auch Säure-Base-Addukten [12-19] eine Wasserstoffbrückenbindung vom Doppelminimumpotentialtypus zugeschrieben wird, was sich IR-spektroskopisch in der Aufspaltung der Protonenvalenzschwingung ausdrückt d.h. in einem gleichzeitigen Auftreten des Systems von Absorptionsbanden im Gebiet II und III. Auch diese Annahme wird bei der Auswertung der IR-Spektren unserer Addukte in Betracht gezogen.

AUSWERTUNG DER IR SPEKTREN

Das IR-Spektrum Ia enthält Banden bei 612 cm^{-1}, 1138 cm^{-1}, die für die mesomere Struktur des Anions sprechen. Eine neue Bande erscheint bei 1632 cm^{-1}, die im Spektrum der freien Base und Säure nicht vorhanden ist, sich aber im Spektrum der protonierten Base befindet. Diese Bande 1632 cm^{-1} ist der Scherenschwingung der NH_2-Gruppe zuzuschreiben, da es bekannt ist, daß diese Gruppe im Gebiet 1600 cm^{-1} absorbiert. Diese Behauptung ist auch dadurch unterstützt, daß in Ib diese Bande verschwindet und eine neue Bande bei 1298 cm^{-1}, die in Ia nicht vorhanden ist, erscheint, welche wahrscheinlich der ND_2-Scherenschwingung entspricht. Das Verhältnis ν_H/ν_D beträgt 1,26 und zeigt, daß es sich um eine Schwingung handelt, die mit anderen Schwingungen wenig gekoppelt ist. In Gebiet III befindet sich eine strukturierte Bande (Maxima bei 2310, 2360, 2425, 2525, 2650, 2735 cm^{-1}), deren Intensität mit abnehmenden Frequenzen abnimmt. Diese Banden sind den NH_2-Valenzschwingungen zuzuschreiben. Dies ist auch dadurch bewiesen, daß die Banden vom Bereich 2310—2800 cm^{-1} in Ib an Intensität sehr abnehmen und eine breite intensive Bande zwischen 1800—2380 cm^{-1}, die den ND_2-Valenzschwingungen entspricht, erscheint. Die Anwesenheit der NH_2-Scherenschwingung und der NH_2-Valenzschwingungen in Ia zeigt, daß Protonentransfer stattfindet und die Verbindung (I) ionisch ist.

Auf Grund der obigen Betrachtungen gestattet der Vergleich von IIa, IIb, bzw. IVa, IVb die Schlußfolgerung, daß die Verbindungen (II) bzw. (IV) ionische Struktur besitzen: Anwesenheit von Scherenschwingungen der NH_2-Gruppen bei 1638 bzw. 1630 cm^{-1}, Verschwinden dieser Banden beim Deuterieren (IIb, IVb) und Erscheinen in IVb einer Bande bei 1290 cm^{-1}; in IIb ist sie nicht aufweisbar, da sich die Bande 1180

---

[11] M. A. Kowner und W. N. Kapstahl, *Izvest. Akad. Nauk S. S. S. R., Otdel. fiz. Nauk*, **17**, 561 (1953)

[12] D. Hadzi, A. Novak und E. Gordon, *J. Phys. Chem.*, **67**, 1118 (1963).

[13] D. Hadzi, *J. Chem. Soc.*, **1962**, 5128.

[14] G. M. Barrow und E. A. Jergen, *J. Amer. Chem. Soc.*, **76**, 5211 (1954).

[15] G. M. Barrow, *J. Amer. Chem. Soc.*, **78**, 5802 (1956).

[16] S. Iwata, H. Tsubomura und S. Nagakura, *Bull. Chem. Soc. Japan*, **37**, 1506 (1964).

[17] G. Ramaichak und L. Sobshik, *Zhur. strukt. Khim.*, **6**, 262 (1965).

[18] Ch. L. Bell und G. M. Barrow, *J. Chem. Phys.*, **31**, 300 (1959)

[19] R. H. Nutall, D. W. A. Sharp und T. C. Waddington, *J. Chem. Soc.*, **1960**, 4965.

cm^{-1} bis 1300 cm^{-1} verbreitert. In IIa bzw. IVa befinden sich die Banden der Gruppen $P{=}S \leftrightarrow P{-}S^-$ und $P{=}O \leftrightarrow P{-}O^-$ bei 615 bzw. 617 cm^{-1} und 1120—1140 cm^{-1} bzw. 1132 cm^{-1}; die letzteren erscheinen als ein Schulter der breiten Bande vom Gebiet 1110—1190 cm^{-1}. Im Gebiet III von IIa befinden sich die Maxima bei 2390, 2500 und 2730 cm^{-1} entsprechend in IVa bei 2460—80, 2660, 2735 cm^{-1}. In IIb bzw. IVb erscheinen neue Banden bei 1890, 2090, 2200 cm^{-1} bzw. 1940—2000, 2050, 2140 cm^{-1} während die Banden vom Bereich 2300—2800 cm^{-1} fast verschwinden. Diese Banden entsprechen den assoziierten NH_2-Valenzschwingungen. Alle diese Angaben sprechen für die ionische Struktur der Verbindungen (II und IV).

Im IR-Spektrum VIa finden wir im Vergleich zu VIb dieselbe regelmäßige Änderungen, wie bei den oben besprochenen IR-Spektren, nur ist in diesem Fall die Frequenz der NH_2-Scherenschwingung schwerer zu erkennen, da sie sich in demselben Gebiet wie die Skelettschwingung des Benzolkerns befindet. Trotzdem war es möglich, sie zu entdecken, da von den in diesem Bereich erscheinenden Banden in VIa 1610 und 1632 cm^{-1} nur die Bande 1632 cm^{-1} beim Deuterieren verschwindet (VIb). Die Bande 1632 cm^{-1} entspricht also der NH_2-Scherenschwingung, während die Bande 1610 cm^{-1} der Skelettschwingung des Benzolkerns entspricht.

Im Gebiet III von VIa erscheinen strukturierte deuterierungsempfindliche Banden bei 2400, 2520 und 2700 cm^{-1}, die den NH_2-Valenzschwingungen entsprechen. Nennenswert ist die Tatsache, daß die $P{=}S \leftrightarrow P{-}S^-$- bzw. $P{=}O \leftrightarrow P{-}O^-$-Schwingungen sich bei 625 cm^{-1} bzw. 1120 cm^{-1} befinden, was für die sehr große Teilnahme der Thionstruktur des Anions (im Vergleich zu den anderen Addukten und zum Ammoniumsalz) spricht; Äthylanilin ist die schwächste von den von uns verwendeten Basen. Alle diese Angaben sprechen für die ionische Struktur der Verbindung VI.

Das IR-Spektrum IIIa hat im Gebiet I die Maxima 615 cm^{-1}—1125 cm^{-1}, im Gebiet II eine unstrukturierte Bande von sehr kleiner Intensität (1900—2300 cm^{-1}) und im Gebiet III eine intensive strukturierte Bande bei 2400—2500 und eine bei 2625 cm^{-1} die deuterierungsempfindlich sind. In IIIb erscheinen neue Banden 1700—2200 cm^{-1} mit Maxima bei 1860, 1940, 2040 und 2200 cm^{-1}, die den N-D-Schwingungen entsprechen. In IIIa erwarteten wir bei 1410 cm^{-1} ein Maximum, welches der $\overset{+}{N}H$-Deformationsschwingung entsprechen sollte. Dieses Maximum fehlt aber, möglicherwiese deshalb, weil die C-H-Deformationsbande bei 1380 cm^{-1} sich bis 1410 cm^{-1} verbreitert. Die Anwesenheit der Banden 615 und 1125 cm^{-1} (sehr nahe an denen des Ammoniumsalzes der 0,0-Diäthylthiophosphorsäure), wie auch die Absorption im Gebiet III, die dieselbe ist wie in Triäthylammoniumhydrochlorid (welche den N-H-

Valenzschwingungen entsprechen) zeigen, daß die Verbindung (III) ionische Struktur besitzt.

Im Gebiet I von Va finden wir Absorptionsbanden bei 640 cm^{-1} und 1142 cm^{-1} wie auch drei Banden bei 1470, 1595, 1660 cm^{-1}. In diesem Gebiet des IR-Spektrums der protonierten Base (Akridiniumhydrochlorid) befinden sich Maxima bei 1648, 1590 und 1475 cm^{-1} deren Intensitätsverhältnisse zu einander dieselben sind wie in Va. *

Alle diese Angaben sprechen dafür, daß die 1470-, 1595- und 1660 cm^{-1}-Banden der Pyridiniumringschwingung entsprechen. Im IR-Spektrum Vb ist in diesem Gebiet folgendes zu bemerken: die Bande 1660 cm^{-1} nimmt an Intensität sehr ab und verbreitert sich bis 1640 cm^{-1}, aus der Bande 1598 cm^{-1} bleibt eine verbreiterte kleine Schulter zurück, während die Bande bei 1470 cm^{-1} stark an Intensität zunimmt. Im Gebiet II von Va befindet sich eine unstrukturierte Bande zwischen 1800—2100 cm^{-1} und eine strukturierte Bande zwischen 2260—2470 cm^{-1} mit zwei Maxima 2300 und 2400 cm^{-1}. Die Anwesenheit von Banden im Bereich II bzw. III, d.h. die Aufspaltung der Protonenvalenzschwingung in diese voneinander entfernten Bereiche, könnte eventuell einem Doppelminimum der Potentialkurve der Wasserstoffbrückenbindung zugeschrieben werden.

Im Gebiet I von VIIa finden wir Absorptionsbanden bei 618, 1141 und vier Banden bei 1490, 1540, 1615 (Schulter) und 1639 cm^{-1}. In VIIb vergrößert sich die Intensität der 1490 cm^{-1}-Bande, die 1540 cm^{-1}-Bande verschwindet, eine Bande sehr kleiner Intensität erscheint bei 1590 cm^{-1}, während die Bande bei 1639 cm^{-1} sehr stark an Intensität abnimmt. Dasselbe geht im IR-Spektrum des deuterierten Pyridiniumchlorides vor, wobei das Verhältnis ν_H/ν_D 1,02 bzw. 1,04 beträgt, d.h. sehr nahe an dem des Benzols bzw. deuterierten Benzols liegt. [20]

Im Gebiet II und III von VIIa befinden sich zwei breite und unstrukturierte Banden zwischen 1800—2180 cm^{-1} und 2450—2800 cm^{-1}. Beim Deuterieren (VIIb) verschwindet die Bande 2450—2800 cm^{-1} und eine sehr breite unstrukturierte Bande erscheint zwischen 1700—2260 cm^{-1}. Alle diese Angaben sprechen für eine ionische Struktur der Verbindung VI und für eine Wasserstoffbrückenbindung, die möglicherweise vom Doppelminimumpotentialtypus ist.

Aus unseren Ergebnissen geht hervor, daß alle untersuchten Addukte ionisch sind, und daß die Struktur des Anions mesomer ist; im Vergleich aber mit den Frequenzen des Ammoniumsalzes der O-O-Diäthylthiophosphorsäure bezüglich der $P{=}S \leftrightarrow P{-}S^-$-Gruppe und $P{=}O \leftrightarrow \leftrightarrow P{-}O$-Gruppe sind diese in die Richtung der Thionstruktur verschoben, was mit der Verminderung der Basicität des Protonenakzeptors (bei gleichem Protonendonator) noch mehr in Erscheinung tritt.

---

* Es wurde das IR-Spektrum vom Addukt des Akridins mit O,O-Diäthyldithiophosphorsäure (Schmp. 156°) aufgenommen und mit Va im Gebiet 1450—1700 cm^{-1} verglichen. Auch in diesem Spektrum erscheinen nur die Maxima bei 1476, 1595 und 1655 cm^{-1}.

[20] D. Cook, *Canad. J. Chem.*, **39**, 2009 (1961).

Tabelle 1

Physikalische Konstanten, Analyse und ΔpK-Werte der untersuchten Addukte (I–VII)

Addukte Nr.	$(RO)_2P(O)SH \rightleftarrows (RO)_2P(S)OH$ R	Base	Schmp. °C	n_D^{20}	d_4^{20}	P % ber.	P % gef.	ΔpK
I.	C_2H_5	Piperidin	—	1,4965	1,1237	12,14	12,30	9,63
II.	C_2H_5	Diäthylamin	—	1,4747	1,0862	12,73	12,70	9,51
III.	C_2H_5	Triäthylamin	—	1,4839	1,0809	10,90	11,03	9,23
IV.	C_2H_5	Morpholin	52	—	—	12,04	11,80	7,21
V.	i-C_3H_7	Akridin	99	—	—	8,21	8,16	4,01
VI.	C_2H_5	Äthylanilin	65	—	—	10,63	10,40	3,62
VII.	C_3H_7	Pyridin	—	1,4990	1,1423	11,18	11,24	3,60

Tabelle 2

Frequenzen (cm^{-1}) der IR-Spektren Ia–VIIa (Addukte) Ib–VIIb (deuterierte Addukte)

IR Spektren	Gebiet I	Gebiet II	Gebiet III
Ia	612, 1138, 1632	—	2310, 2360, 2425, 2525, 2650, 2735
Ib	612, 1138, 1298	1800–2380	—
IIa	615, 1120–1140, 1638	—	2390, 2500, 2730
IIb	615, 1135	1890, 2090, 2200	—
IIIa	615, 1125	1900–2300	2400, 2500, 2625
IIIb	616, 1125	1860, 1940, 2040, 2200	
IVa	617, 1132, 1630	—	2460–80, 2660, 2735
IVb	617, 1135, 1290	1940–2000, 2050, 2140	—
Va	640, 1142, 1470, 1595, 1660	1800–2100	2260–2470
Vb	640, 1142, 1470, 1600, 1660	1800–2200	—
VIa	625, 1120, 1610, 1632	—	2400, 2520, 2700,
VIb	625, 1120, 1610,	1800–2300	—
VIIa	618, 1141, 1490, 1540, 1615, 1639	1800–2180	2450–2800
VIIb	617, 1140, 1490, 1590, 1639	1700–2260	—

VERSUCHSTEIL

Darstellung der Säure-Base-Addukte (I—VII)

Äquimolare Mengen der Basen (in benzolischer Lösung) und der O,O-Dialkylthiophosphorsäuren (in benzolischer Lösung) werden miteinander bei 10° versetzt. Die benzolische Lösung wird mit Petroläther versetzt bis sich ein Niederschlag (im Falle der Verbindungen IV, V, VI) oder ein Öl (im Falle der anderen Verbindugen) ausscheidet. Die Verbindungen (IV, V, VI) werden aus Benzol-Petroläther umkristallisiert. Die anderen Verbindungen werden mehrmals mit Petroläther gewaschen, der Petroläther dann bei 10 Torr entfernt und die Substanz über Phosphorsäureanhydrid in einem Vakuumexsikkator 24 Std. aufbewahrt.

Deuterierung der Säure-Base-Addukte (Allgemeine Methode)

0,1 g des Adduktes wird mit 0,5 ml Deuteriumoxid (99,5%) gelöst und auf 60° erwärmt, dann die Flüssigkeit bei 5 Torr bei Zimmertemperatur entfernt (bei diesem Druck und dieser Temperatur wird nur das Wasser verjagt). Diese Operation wird 8—10mal wiederholt und bei der letzten Entfernung des Wassers i. Vak. wird die Temperatur auf 70° erhöht um die letzten Wasserspuren zu entfernen.

Die IR-Spektren werden mit einem Spektralphotometer UR-10 (VEB Carl Zeiss, Jena) mit KBr-, NaCl- und LiF-Optik im Bereich 400—3200 cm^{-1} in KBr-Preßling bzw. Nujol und Flüssigkeitskuvetten aufgenommen. Der KBr-Preßling, wie auch die Nujolprobe, wird über Phosphorsäureanhydrid in einem Exsikkator 24 Std. lang aufbewahrt. Die deuterierten Addukte werden rasch nach ihrer Erhaltung spektrophotometriert.

Revue Roumaine de Chimie, **14**, 495—501 (1969)

Revue Roumaine de Chimie, **14**, 503–508 (1969)

CORRELATION OF THE PHYSICAL PROPERTIES OF ORGANOPHOSPHORUS COMPOUNDS. II

REFRACTIVITY AND BOILING POINT OF PHOSPHINES

M. ARSHAD A. BEG

Central Laboratories, P.C.S.I.R., Karachi-32, Pakistan

Received July 29, 1968

Refractivity and the boiling point of phosphines having different substituents have been measured. The two properties have been correlated through the equation :

$$K = \frac{T_b \cdot n_D}{M^{1/2}}$$

On the basis of the value of K it is possible to distinguish between the normal and associated phosphines.

In the previous paper [1] a correlation was sought for the boiling points of phosphines with the molecular weight and the cohesive energy given by $M\rho^2$. The variations were noted to be dependent on the type of substituent on the phosphorus atom. Since the refractivity of a particular class of compounds also varies uniformly, it may be possible to classify the different phosphines on this basis. The refractivity of the organophosphorus compounds has been discussed by Sayre [2] in order to extend the concept of bond and molar refraction to these compounds. This paper describes such a relation for the different phosphines and also correlates the molar refractivity with their boiling point.

EXPERIMENTAL

The phosphines were prepared as described earlier. The refractive indices of the solid aromatic phosphines were determined in solution and those of the liquid phosphines were measured as such on the Abbe refractometer, care being taken to minimize the access of air by flushing the environment of the sample with nitrogen.

---

[1] M. A. A. Beg, *Bul. Chem. Soc. Japan*, **40**, 15 (1967).

[2] R. Sayre, *J. Amer. Chem. Soc.*, **80**, 5438 (1958).

DISCUSSION

The boiling point T_b has been correlated with the refractive index using the formula[3]

$$\frac{T_b \cdot R_L^{1/2}}{M - R_L} = K \tag{1}$$

where R_L is the molar refraction as obtained from the expression of Lorenz and Lorentz. Another form of equation (1)

$$\frac{T_b \cdot R_L}{M^{3/2}} = K \tag{2}$$

has been found to hold in the case of slightly polar compounds and the boiling point also seems to be well related.[4] Organophosphorus compounds have been found to follow the molar refractivity coefficient as determined by Vogel.[5] A critical study of the Mn_D values of the different classes of triply connected phosphorus compounds also supports this point. In equation 2, therefore, R_L may be substituted by Mn_D which then becomes:

$$\frac{T_b \cdot Mn_D}{M^{3/2}} = K \tag{3}$$

or simply

$$\frac{T_b \cdot n_D}{M^{1/2}} = K \tag{4}$$

The R_L values also require the knowledge of the densities of the compounds and thus the advantages of Mn_D are obvious. In table 1 the calculated values for the different phosphines have been obtained from Vegel's

Table 1

Calculated values for the different phosphines

S. No.	Compound	Molecular weight	Boiling point °K	Mn_D		$K = \frac{Mn_D \cdot T_b}{M^{3/2}}$	Ref.
				Obsd.	Calcd.		
1	2	3	4	5	6	7	8
1.	PH_3	34	185.6		48.48	45.38	2
2.	PCl_3	137.5	351	207.75	205.72	45.24	2
3.	PBr_3	271	446	459.9		45.97	
4.	$MePCl_2$	117	354.5	175.1	174.41	49.03	
5.	$EtPCl_2$	131	385	195.6	194.04	50.19	6
6.	n-PrPC'$_2$	145	407.5	215.3	215.53	50.23	6
7.	n-$BuPCl_2$	159	433	235.9	235.70	50.96	6
8.	n-$AmPCl_2$	173	457	256.3	256.74	51.47	6
9.	n-$HexPCl_2$	187	481	276.8	277.38	52.07	6
10.	n-$HeptPCl_2$	201	501.5	297.2	298.03	52.30	6
11.	n-$OctPCl_2$	215	520	317.6	318.71	52.40	6

---

[3] B. Nekrassow, *Z. phys. Chem.*, **A 141**. 378 (1939).

[4] B. Nekrassow, *Z. phys. Chem.*, **A, 148,** 216 (1930).

[5] A. I. Vogel, W. T. Cresswell, G. H. Jeffery and J. Leicester, *J. Chem. Soc.*, **1952,** 531.

[6] R. B. Fox, *J. Amer. Chem. Soc.*, **72,** 4148 (1950).

Table 1 (continued)

1	2	3	4	5	6	7	8
12.	$PhPCl_2$	179	495	285.8	279.89	59.06	7
13.	$p\text{-}TolPCl_2$	193	518	306.3	299.40	59.15	7
14.	$EtC_6H_4PCl_2$	207	524	326.6	320.78	57.08	7
15.	$i\text{-}PrC_6H_4PCl_2$	221	542	346.4	340.27	57.15	7
16.	Me_2PCl	96.2	350.2	143.1	143.11	52.87	
17.	$MeEtPCl$	110.5	374	162.9	162.74	52.47	
18.	Et_2PCl	124.5	404.5	185.69	182.37	54.09	
19.	$EtPH_2$	62	298	90.88	89.22	55.55	
20.	$PrPH_2$	76	327	110.71	110.7	54.61	
21.	$n\text{-}BuPH_2$	90	360	127.3	130.88	53.67	
22.	$i\text{-}BuPH_2$	90	351.5	131.0	131.0	53.94	
23.	$s\text{-}BuPh_2$	90	350	131.67	131.6	53.99	
24.	$t\text{-}BuPh_2$	90	333	128.1	131.1	49.96	
25.	$AmPH_2$	104	375	150.1	151.92	53.07	
26.	$HexPH_2$	118	401	171.4	172.56	53.49	
27.	$HeptPH_2$	132	442.5	193.1	193.21	56.34	
28.	$OctPH_2$	146	442	212.4	213.89	53.20	
29.	$NonPH_2$	160	466	233.1	234.26	53.00	
30.	$C_6H_{11}PH_2$	116	419.8	172.4	173.9	57.91	
31.	$PhPH_2$	220	433	174	174.98	64.29	
32.	$BzPH_2$	124	453	191.8	194.58	62.93	
33.	$p\text{-}EtC_6H_4PH_2$	138	473	214.1	215.96	62.47	
34.	Et_2PH	90	358	133.28	129.96	55.90	
35.	$BuEtPH$	118	405	173.67	171.62	54.86	
36.	Bu_2PH	146	456	212.8	213.28	54.99	
37.	$i\text{-}Bu_2PH$	146	443	219.52	213.52	55.10	
38.	$s\text{-}Bu_2Ph$	146	437	214.81	214.86	53.21	
39.	$Pr(n\text{-}C_6H_{13})PH$	160	466.5	233.3	234.79	53.80	
40.	Ph_2PH	186	545	301.55	301.48	64.80	
41.	Me_3P	76	311.4	111.81	111.81	52.54	
42.	Me_2EtP	90	344.2	133.1	133.1	53.67	
43.	Et_3P	118	400	170.7	175.68	53.26	
44.	Pr_3P	160	458.5	235.17	235.2	32.30	
45.	Bu_3P	202	513	295.7	295.68	53.14	
46.	$i\text{-}Bu_3P$	202	488	296	296.04	50.3	
47.	Ph_3P	262	257	428	428.4	66.31	
48.	Me_2PhP	138	465	213	217.20	61.24	
49.	$MePh_2P$	200	557	322.9	322.59	63.60	
50.	Et_2PhP	166	494.9	256.6	236.46	59.37	
51.	$EtPh_2P$	214	548	337.5	342.22	59.29	
52.	Et_2BzP	180	523	276.6	276.06	59.90	
53.	Et_2TolP	180	513	277.7	276.15	58.99	
54.	$Et_2(4\text{-}Cl\text{-}C_6H_4)P$	200.5	529	312.8	308.39	58.30	
55.	$(Me_3Si)_3P$	250	515	375.7	375.7	48.96	8
56.	$(Me_3Si)_2PH$	178	444	260.6	266.62	48.73	8
57.	$(Me_3Si)PH_2$	106	350.5	152.3	157.55	48.91	8

data for the substituents. The Mn_D values obtained either from the experimental data or calculated by the method suggested by Vogel are in close agreement.

---

[7] B. Buchner and R. B. Lockhart, Jr., *J. Amer. Chem. Soc.*, **73**, 755 (1951).

[8] G. W. Parshall and R. V. Lindsey, Jr., *J. Amer. Chem. Soc.*, **81**, 6274 (1959).

The studies on boiling point to date indicate that this property is related with the molecular weight and polarizability given by the refractive index of the compound. Since polarizability would differ for each substituent, it may be shown that the different triply connected phosphorus compounds fall naturally into different classes. A plot of $\frac{M^{3/2}}{Mn_D}$ versus the boiling point has certain interesting features as shown in figure 1.

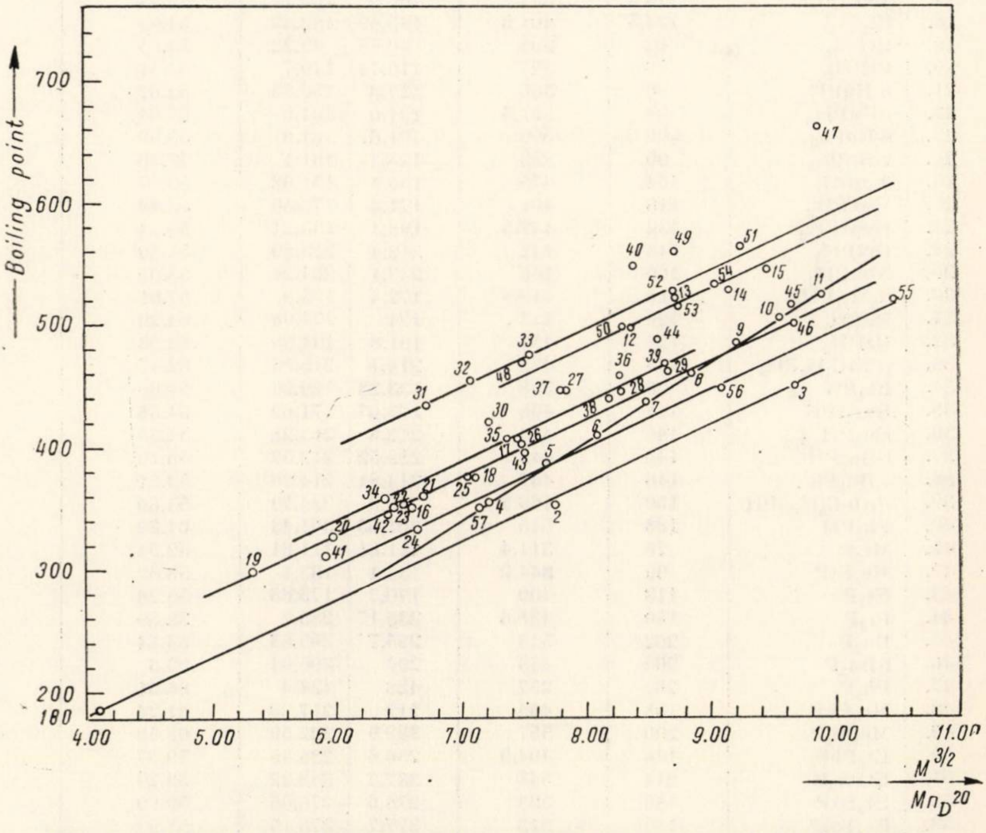

Fig. 1. — Refractivity and boiling point (numbers refer to compounds listed in table 1).

It may be seen from figure 1 that: 1. The unsubstituted triply connected phosphorus compounds fall on a different line which, however, is parallel to the others. 2. The dichlorophosphines form the only class which has a different slope. 3. The primary, secondary and tertiary alkyl phosphines as also the aryl phosphines fall on straight lines parallel to that of the unsubstituted compounds but are widely separated. The equations for the straight lines concerning the various classes of phosphines are given in Table II.

The average deviation in the boiling point of the phosphines is ± 2°. The nature of the straight lines is easily borne out by the almost

Table 2

Equations Correlating Boiling point and R_M

Unsubstituted compounds	$T_b = 49.68R_M - 36.1$
Trimethylasilylphosphines	$T_b = 49.04R_M - 1$
Alkyldichlorophosphines	$T_b = 59.40R_M - 71.8$
Primary and Tertiary alkyl phosphines	$T_b = 49.39R_M - 31.3$
Secondary alkylphosphines	$T_b = 49.13R_M + 46.0$
Aryldichloro and Aryldialkylphosphines	$T_b = 49.30R_M + 85.6$
Primary Arylphosphines	$T_b = 49.10R_M + 102.2$

constant slope for each set of compounds. The values of K in equation (3) for each class of phosphines is different. It is 45.38 for the unsubstituted compounds, 48.91 for the trimethylsilylphosphines, 51 for the alkyl dichlorophosphines, 59 for the alkyl primary and tertiary phosphines, 55 for the secondary alkyl phosphines and 63 for diarylphosphines.

The higher members of the alkyldichlorphosphines are seen to intersect the straight line of the phosphines. The dialkylchloro compounds, on the other hand, have the same slope as the primary and tertiary alkylphosphines which are seen to fall on the same straight line. This is in accord with expectations since the Mn_D value of the three dialkylchlorophosphines 16, 17 and 18 is lower than that of the corresponding alkyldichlorophosphine. More data is, however, needed in order to determine the slope of the monochlorphosphines.

The aryl-dichlorophosphines have the same value of K as the dialkylarylphosphines and fall on the same straight line. This may be explained as being due to the high polarizability given by the molar refractivity coefficient of the aromatic nucleus. Furthermore there is the interaction of the lone pair electrons with the π electrons of the aromatic nucleus as was also indicated earlier. These factors are sufficient to outweigh the contribution of the P-alkyl or P—Cl bond whose molar refractivity coefficient is much lower than that of the P-phenyl bond. Similarly the primary aryl phosphines are separated from the aryldialkyl phosphines. On increasing the number of the aryl groups there would be a wider separation of the straight lines representing these phosphines. The values of only a few aryl phosphines are known at present but whatever are available, indicate that such points do fall off from the monophenylphosphines.

It is apparent from the present study that the polarizability of the molecule varies with the nature of the substituent on phosphorus. On the basis of the polarizability of the various bonds the following order is expected : $P-H < P-Cl <$ P-alkyl $<$ P-aryl. The nature of separation of the various straight lines in figure 1, however, indicates that the polarizability increases in the following order : Unsubstituted hydride or halide $<$ trimethylsilyl phosphines $<$ primary and tertiary alkyl phosphines $<$ secondary alkyl phosphines $<$ alkyl dichlorophosphines $<$ $<$ aryl dichlorophosphines $<$ aryl dialkyl phosphines $<$ primary aryl phosphines $<$ alkyl diaryl phosphines.

The correlation presented above confirms the earlier suggestion that the physical properties of phosphines are substituent dependent.

The boiling point of this class of compounds is better correlated in terms of the molar refractivity coefficient which indicates that the polarizability of the whole molecule is important rather than that of just a particular bond. The nature of variation in the Mn_D values gives an estimate of the polarizability of the compounds. This correlation also divides the phosphines into associated and normal phosphines. The high value of K for the aryl phosphines as compared with alkyl phosphines reminds us of the high value for the latent heat of evaporation for the former group. Association among the former class of compounds is therefore indicated by the physical properties so far studied.

Revue Roumaine de Chimie, **14**, 509–516 (1969)

SPECTRAL STUDIES ON STEROIDAL NITRATE ESTERS. III*

UV SPECTRA IN CONCENTRATED SULFURIC ACID

F. HODOŞAN and FELICIA TEODOR

Institute of Chemistry of the Academy, Cluj, str. Donath 59–65

Received June 22, 1968

The UV spectra of steroidal nitrate esters recorded in conc. sulfuric acid are usually very different from those of the parent alcohols taken under the same conditions. Especially the intensification of the absorption above 400 nm and its decrease below this limit may be considered as a characteristic of these compounds.

The UV spectra in conc. sulfuric acid is frequently used for the identification of minute amounts of steroids isolated from biological sources. Being interested in bio-assays involving steroidal nitrate esters, we considered that a spectral study under these special conditions will be useful.

In this paper we wish to report our results obtained with a number of mono-, di-, and trinitrates belonging especially to the bile acids series. The principal aim of this first series of investigations was differentiation of the nitric esters from the corresponding free alcohols.

The experimental procedure was that recommended by Seymour Bernstein and his co-workers.[1] Samples of about 2 mg were dissolved in 100 ml of concentrated reagent purity sulfuric acid and after being kept for 2 hours at room temperature the spectra were recorded over the 245–600 nm range with a Beckman DK-2A spectrophotometer.

The results obtained (Table 1) show that – in contrast to the acetates which exhibit spectra nearly identical with those of parent alcohols[1] – the nitrate esters give rise to absorption patterns usually quite different from those of the starting substances. Thus the $E_{1cm}^{1\%}$ value of the strong band located at 300–325 nm in the spectra of hydroxylated steroids decreases considerably on passing to the corresponding nitrate esters. For instance, methyl 3α-acetoxy-6β-hydroxy-5β-cholanate gives rise to a band at 309 nm with $E_{1cm}^{1\%} = 248$, while in the spectrum of the corresponding 6-nitrate this band has an extinction coefficient of no more than 150 unities (Fig. 1). Similar examples are given in table 1 (compounds **3**, **11**, **12**). This effect appears particularly marked in the case of compounds **1**, **10** and **16**. Here the main absorption band of the parent alcohols is located at 390–400 nm. Its $E_{1cm}^{1\%}$ value is strongly diminished by esterification with nitric acid (Figs. 2 and 3). A single exception, namely methyl 3α-nitrato-5β-cholanate, which exhibits stronger absorption at 312 nm than its parent alcohol, was observed (Table 1, compound **13**).

---

* Part II: F. Hodoşan and I. Jude, *Rev. Roumaine Chim.*, **11**, 993 (1966).

[1] L. L. Smith and S. Bernstein, "Absorption Spectra in concentrated Sulfuric Acid", in "Physical Properties of the Steroid Hormones". Ed. L. L. Engel, Pergamon Press, Oxford, 1963, p. 321.

Some nitrate esters do not display significant changes in the position of the above-mentioned maximum as compared to that produced by the corresponding alcohols (see Fig. 1 and Table 1, compounds **8**, **12**). In other cases blue shifts are observable (Fig. 4 and Table 1, compounds **11**, **18**), usually accompanied by important changes in the shape of the absorption curve (Fig. 5). Appearance of an additional maximum in the 325—355 nm range can be observed too; thus the main absorption of these nitrate esters appears as well defined doublets (Fig. 6 and Table 1, compounds **3**, **6**).

It must be pointed out that certain nitrate esters give very similar spectra to those produced by the parent alcohols. Compound **19** constitutes an example, however also some differences may be observed. Thus, according to the general tendencies, the peaks at 317 and 412 nm are lowered and the absorption within the 465—500 nm range is increased.

We could not perform an accurate comparison between cholesterol and its nitrate ester because of the incomplete solubilization of the former in conc. sulfuric acid. However, it was possible to conclude that the esterification with nitric acid does not affect the shape of the absorption curve (except the appearance of an inflexion at about 337 nm) and has no influence on the position of the maxima; a general decrease of the absorption intensity was observed too.

Intensification of the absorption above 400 nm may be considered as a general feature of nitrate esters spectra (Figs. 1, 3, 5, and Table 1, compounds **8**, **11**, **12**). In the example in figure 3, as well as in the spectra of compounds **1**, **3**, **6**, and **13** (Table 1), this phenomenon is less striking but still well observable. The exceptions are given in table 1 (compounds **5**, **7**, **18**). It may be concluded that the 380—600 nm region is particularly characteristic for the nitrate esters.

We observed that the ratio of $E^{1\%}_{1\text{cm}}$ value of the most prominent band located above 395 nm to that of the most prominent band located below 395 nm may be used for differentiation of nitrate esters from the corresponding alcohols.[2] We found that the magnitude of this ratio varies as concerns nitrate esters within the 0.23—1.00 range, the average value being 0.47; a single nitrate ester (**5**) has this ratio equal to zero. The values obtained with the parent alcohols are generally much lower,[3] being comprised within the 0—0.23 range (average value 0.10).

Based on the single epimeric pair (**2** and **3**) it was difficult to draw conclusions concerning the influence of the conformation. This will be very probably done in a future paper.

Finally we confirm Bernstein's finding that the spectrum of a bile acid is identical with that of its methyl ester,[1] irrespective of the fact that its hydroxyl groups are free or esterified with nitric acid.

---

[2] This limit was applicable to the majority of compounds studied. We found only two substances (**1** and **8**) not obeying this rule; in these cases we were obliged to fix the limit at 380 and 410 nm, respectively.

[3] Two hydroxylated compounds (**18** and **20**) were found to exhibit exceptionally high values (0.48 and 0.64, respectively), surpassing those of the corresponding nitrate esters.

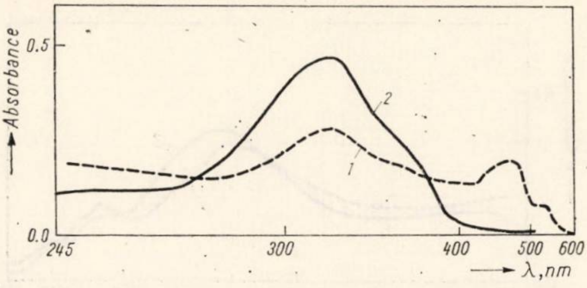

Fig. 1. — *1*, Methyl 3α-acetoxy-6β-nitrato-5β-cholanate (**17**) (1.9 mg/100 ml); *2*, Methyl 3α-acetoxy-6β-hydroxy-5β-cholanate (1.9 mg/100 ml).

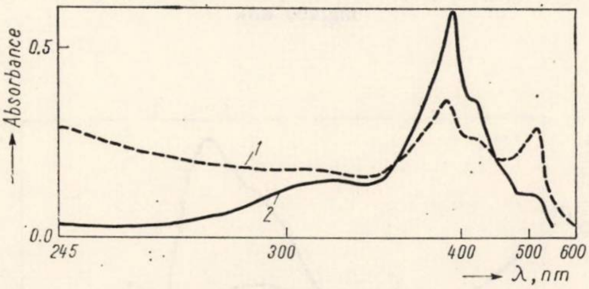

Fig. 2. — *1*, Methyl 3α, 12α-dinitrato-7α-acetoxy-5β-cholanate (**16**) (1.9 mg/100 ml); *2*, Methyl 3α, 12α-dihydroxy-7α-acetoxy-5β-cholanate (1.9 mg/100 ml).

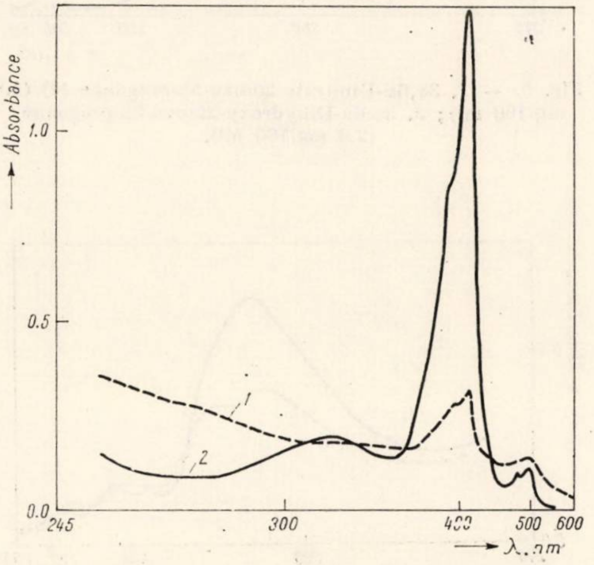

Fig. 3. — *1*, Methyl 3α, 7α, 12α-trinitrato-5β-cholanate (**10**) (2.0 mg/100 ml); *2*, Methyl 3α, 7α, 12α-trihydroxy-5β-cholanate (2.2 mg/100 ml).

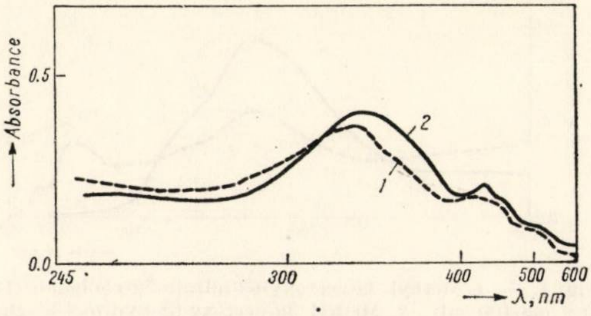

Fig. 4. — *1*, 3β-Acetoxy-6β-nitrato-5α-cholestane (**20**) (2.1 mg/100 ml); *2*, 3β-Acetoxy-6β-hydroxy-5α-cholestane (2.1 mg/100 ml).

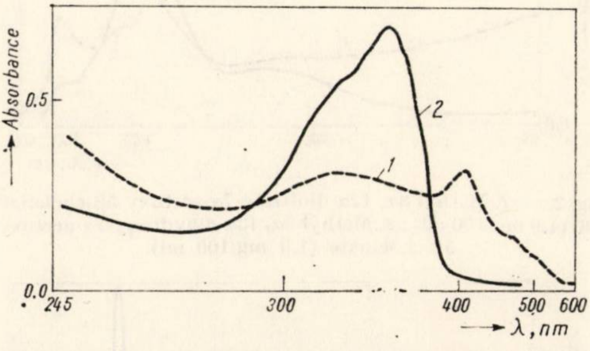

Fig. 5. — *1*, 3α,6α-Dinitrato-20-oxo-5β-pregnane (**4**) (1.9 mg/100 ml); *2*, 3α,6α-Dihydroxy-20-oxo-5β-pregnane (2.0 mg/100 ml).

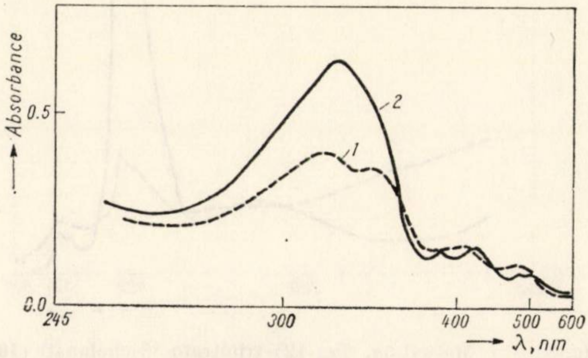

Fig. 6. — *1*, 3β-Nitrato-17-oxo-5α-androstane (**2**) (1.9 mg/100 ml); *2*, 3β-Hydroxy-17-oxo-5α-androstane (2.0 mg/100 ml).

Table 1

UV Spectra of steroidal nitrate esters and of their parent alcohols in conc. sulfuric acid

No.	Empirical formula	Compound	Spectrum of the nitrate ester				Spectrum of the parent alcohol			
			$\lambda_{max.}$ in nm	$(E^{1\%}_{1cm})$	$\lambda_{min.}$ in nm	$(E^{1\%}_{1cm})$	$\lambda_{max.}$ in nm	$(E^{1\%}_{1cm})$	$\lambda_{min.}$ in nm	$(E^{1\%}_{1cm})$
1	$C_{19}H_{28}N_2O_7$	3α, 6α-Dinitrato-17-oxo-5β-androstane	298 398 463i	(150) (176) (54)	275 339	(136) (101)	334.5 401.5 466	(219) (709) (29)	266 355 450	(50) (185) (26)
2	$C_{19}H_{29}NO_4$	3β-Nitrato-17-oxo-5α-androstane	309 331 374 402 478	(215) (196) (73) (81) (50)	259 322.5 384 448	(106) (193) (72) (46)	313 331i 378 412 478 504i	(333) (284) (70) (75) (35) (32)	257.5 367 391 460	(117) (59) (61) (28)
3	$C_{19}H_{29}NO_4$	3α-Nitrato-17-oxo-5α-androstane	306 326i 374 402 472i	(225) (161) (76) (78) (48)	258 368 386	(112) (75) (72)	313 377 413 476 500	(320) (62) (56) (22) (17)	257 369 392 462	(90) (59) (49) (19)
4	$C_{21}H_{32}N_2O_7$	3α, 6α-Dinitrato-20-oxo-5β pregnane	316.5 404 460i	(166) (163) (76)	277 373	(116) (126)	324i 346	(283) (348)	268.5	(73)
5	$C_{24}H_{35}NO_7$	3α-Nitrato-7,12-dioxocholanic acid	285.5 360	(98) (69)	265 320 466	(87) (27) (9)				
6	$C_{24}H_{39}NO_5$	6α-Nitrato-5β-cholanic acid	312 351.5 387i 408i 498i	(144) (149) (77) (59) (21)	255 331 464	(60) (137) (23)	310.5	(162)	249.5 401	(7) (9)

Table 1 (continued)

No.	Empirical formula	Compound	Spectrum of the nitrate ester				Spectrum of the parent alcohol			
			$\lambda_{max.}$ in nm	$(E^{1\%}_{1cm})$	$\lambda_{min.}$ in nm	$(E^{1\%}_{1cm})$	$\lambda_{max.}$ in nm	$(E^{1\%}_{1cm})$	$\lambda_{min.}$ in nm	$(E^{1\%}_{1cm})$
7	$C_{25}H_{37}NO_7$	Methyl 3α-nitrato-7,12-dioxo-5β-cholanate	288 354i 360	(117) (72) (74)	258.5 323 454	(86) (43) (13)				
8	$C_{25}H_{37}NO_7$	Methyl 12α-nitrato-3,7-dioxo-5β-cholanate	321 387i 397 426i	(277) (177) (205) (57)	263.5 352 486	(85) (59) (17)	321 383 398i	(393) (73) (39)	252 357 428	(50) (34) (9)
9	$C_{25}H_{38}N_2O_9$	Methyl 3α, 12α-dinitrato-7-oxo-5β-cholanate	317 396 428	(155) (160) (95)	285 347	(110) (83)				
10	$C_{25}H_{39}N_3O_{11}$	Methyl 3α, 7α, 12α-trinitrato-5β-cholanate	315 374i 389 460i 476	(103) (169) (189) (79) (82)	295 335.5 436	(113) (92) (73)	300 389 457i 480	(104) (716) (46) (60)	253 332 434	(46) (74) (33)
11	$C_{25}H_{40}N_2O_8$	Methyl 3α, 6α-dinitrato-5β-cholanate	301 412 444i 498	(178) (112) (93) (81)	265 366.5 480	(157) (96) (76)	305 347i 444i	(308) (118) (29)	249 408	(51) (31)
12	$C_{25}H_{40}N_2O_8$	Methyl 3α, 12α-dinitrato-5β-cholanate	312 365i 395i 415 454i 504	(174) (94) (133) (150) (111) (123)	272.5 349 476	(133) (86) (106)	310 390i	(261) (42)	248 461	(61) (6)

Table 1 (continued)

No.	Empirical formula	Compound	Spectrum of the nitrate ester				Spnctrum of the parent alcohol			
			$\lambda_{max.}$	in nm $(E^{1\%}_{1cm})$	$\lambda_{min.}$	in nm $(E^{1\%}_{1cm})$	$\lambda_{max.}$	in nm $(E^{1\%}_{1cm})$	$\lambda_{min.}$	in nm $(E^{1\%}_{1cm})$
13	$C_{25}H_{41}NO_5$	Methyl 3α-nitrato-5β-cholanate	312 351.5 410i 448i 500	(202) (153) (46) (31) (25)	258 338 482	(92) (148) (23)	312	(127)	250	(55)
14	$C_{25}H_{41}NO_5$	Methyl 12α-nitrato-5β-cholanate	305i 320 375.5i 389.5 459 476 556i	(83) (85) (261) (331) (86) (87) (16)	276.5 335 438 468	(69) (79) (75) (85)				
15	$C_{27}H_{42}N_2O_{10}$	Methyl 3α-acetoxy-7α, 12α-dinitrato-5β-cholanate	318 379i 389 460 550i	(135) (191) (208) (84) (29)	283 340 438	(106) (98) (81)				
16	$C_{27}H_{42}N_2O_{10}$	Methyl 3α, 12α-dinitrato-7α-acetoxy-5β-cholanate	313.5i 388 412i 482i 504	(97) (192) (145) (134) (159)	287 330 449	(100) (89) (113)	318.5 373i 390.5 410i 446i 484i 506	(88) (218) (322) (202) (106) (64) (64)	256 333.5	(19) (80)

Table 1 (continued)

No.	Empirical formula	Compound	Spectrum of the nitrate ester				Spectrum of the parent alcohol			
			$\lambda_{max.}$ in nm	($E^{1\%}_{1cm}$)	$\lambda_{min.}$ in nm	($E^{1\%}_{1cm}$)	$\lambda_{max.}$ in nm	($E^{1\%}_{1cm}$)	$\lambda_{min.}$ in nm	($E^{1\%}_{1cm}$)
17	$C_{27}H_{43}NO_7$	Methyl 3α-acetoxy-6β-nitrato-5β-cholanate	310 343.5i 393 430i 444 502	(150) (98) (76) (101) (107) (43)	269.5 380 399 488	(79) (70) (74) (39)	308.5 350i	(248) (112)	248	(58)
18	$C_{27}H_{47}N_2O_6$	3β, 4β-Dinitrato-5α-cholestane	316 338i 408i 494	(184) (158) (50) (23)	267 484	(117) (23)	320 343i 410 475i 494i	(201) (179) (129) (51) (45)	256 383	(72) (100)
19	$C_{29}H_{45}NO_9$	Methyl 3α, 7α-diacetoxy-12α-nitrato-5β-cholanate	260i 266i 314 373i 388 413i 480 498i	(58) (71) (137) (172) (231) (116) (82) (78)	255.5 262 341 458 568	(55) (59) (82) (72) (12)	252.5 260.5i 266i 317 373i 390 412 444i 486i 502	(11) (24) (46) (169) (159) (237) (155) (73) (74) (77)	249.5 255 343 406 465 568	(10) (9) (74) (153) (61) (6)
20	$C_{29}H_{49}NO_5$	3β-Acetoxy-6β-nitrato-5α-cholestane	313 404 492	(173) (75) (31)	257.5 377 478	(76) (67) (30)	320 416 440i 474i	(194) (93) (68) (40)	260.5 389	(69) (75)

Revue Roumaine de Chimie, **14**, 517–521 (1969)

CONTRIBUTIONS TO THE STUDY OF OCTANESULTONE

MARIA IONESCU and MARIA VĂGĂONESCU
Department of Organic Chemistry, Babeş-Bolyai University,
Cluj, str. Arány Janos 11

Received June 25, 1968

The structural formula IV is suggested for the octanesultone with m.p. 129°, formed in the process of deisobutenisation. The formation and the splitting of this sultone are described. The structure assigned to this octanesultone is based on chemical analysis (the splitting on hydrolysis, reforming by bromination) and on physico-chemical measurements (NMR and IR spectra).

The octanesultone with the melting point 129°, has been mentioned for the first time, as a petroleum by-product in U.S.A., having the structure I[1]; the structure II has been suggested later for the same octanesultone.[2] The octanesultone III with m.p. 99–100° is obtained by sulfonation of isobutylene.[3]

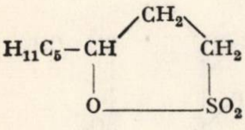

I

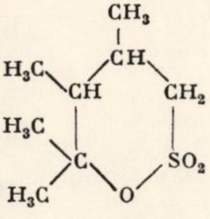

II

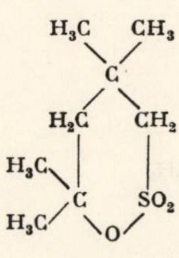

III

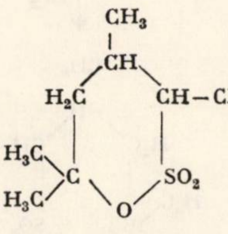

IV

During petroleum processing in Romania a compound has been isolated, as a by-product, having the formula $C_8H_{16}O_3S$ and the melting point 128–129°. This compound behaves similarly to the octanesultone isolated by Baldeschwieler and Cassar.[1]

In an attempt to clear up the structure of this octanesultone, the salts of the octanesulfonic acids V, VI were prepared by alkaline hydrolysis.

---

[1] F. Baldeschwieler and A. H. Cassar, *J. Amer. Chem. Soc.*, **51**, 2959 (1929).

[2] F. G. Bordwell, R. D. Chapman and C. E. Osborne, *J. Amer. Chem. Soc.*, **81**, 2002 (1959).

[3] C. M. Suter and J. D. Malkemus, *J. Amer. Chem. Soc.*, **63**, 978 (1941).

The alkaline sulfonic salts, obtained in different conditions, form by bromination the bromosultones VII, m.p. 112° and VIII, m.p. 145—146°.

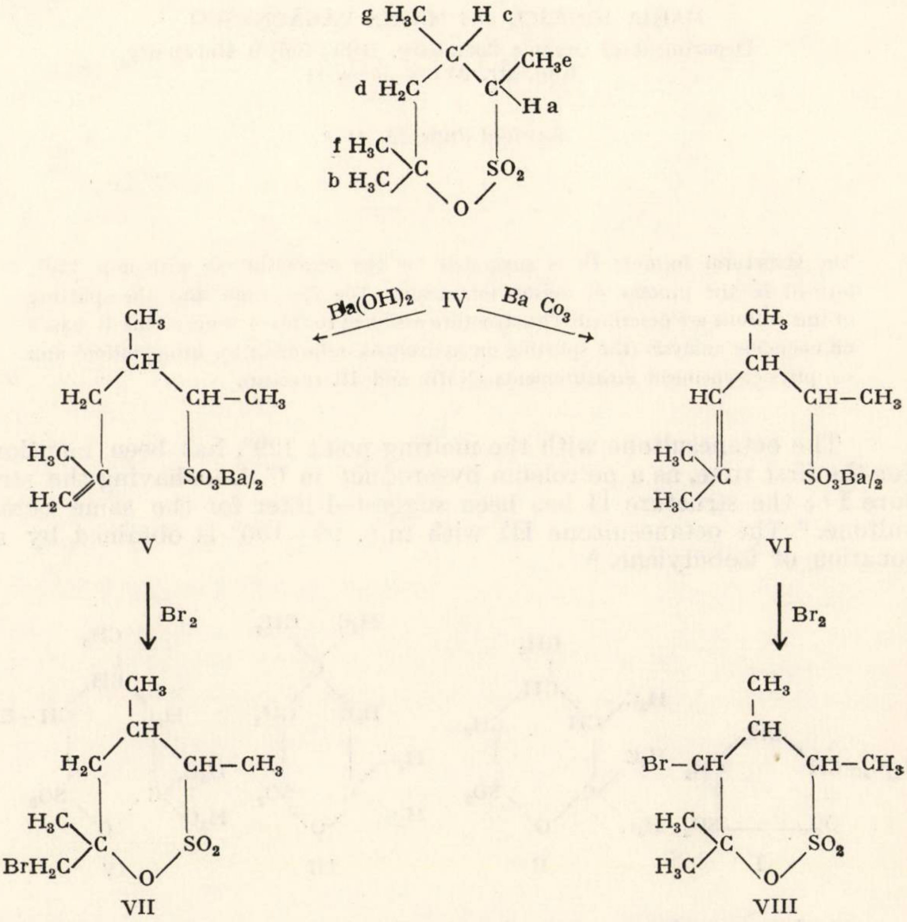
g H_3C
H c
CH_3e
d H_2C
H a
f H_3C
b H_3C
SO_2
O
IV
$Ba(OH)_2$
$BaCO_3$
CH_3
CH
H_2C
CH—CH_3
H_3C
H_2C
$SO_3Ba/_2$
V
HC
VI
Br_2
Br_2
Br—CH
BrH_2C
VII
VIII

Under processing conditions of the Romanian petroleum (mixture of butylene, isobutylene and H_2SO_4) the octanesultone isolated seems to result from one mole each of butylene and isobutylene with H_2SO_4.*

The butylene reacting with H_2SO_4 in these conditions, forms the butylic ester and a four-membered labile sultone (a) which reacts further with one mole of isobutylene, yielding the stable octanesultone IV (b),

---

* This sultone was formed in the process of deisobutenisation at the "Synthetic Rubber Combinate Gh. Gheorghiu-Dej".

a)

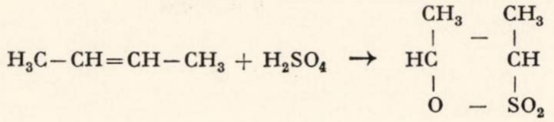

b)

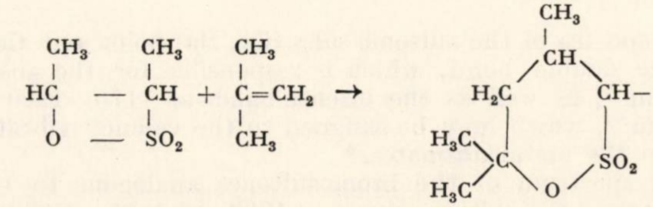

IV

The sultone IV is not formed only by the sulfonation of isobutylene, since this reaction has been found to give sultone III [3] and the sulfonation of its dimer, i.e. diisobutylene, gives unsaturated sulfonic acid and no sultone [2]. Octanesultone IV has a large stability, therefore it must contain a tensionless ring; the OH bond of the SO_3H, must proceed from a tertiary carbon, since only a reactive OH is able to form sultone, without using drastic conditions [2]. The tertiary structure for sultone IV is supported also by the unsaturated sulfonic salts obtained by hydrolysis; primary and secondary sultones give chiefly hydroxysulfonic acids on hydrolysis. The splitting of the sultonic ring with alkalies and its reformation by means of acids, is characteristic of sulfonic acid lactones.

The structural formula IV we suggest is based on the chemical properties and on the data of IR and NMR analyses.

Thus the IR spectrum of octanesultone IV shows intense bands at 1323 cm^{-1} and 1123 -12 cm^{-1} which may be attributed to the absorption of the group$-O-SO_2$.[4] The doublet at 1397 and 1372 cm^{-1} is due to the plane symmetrical deformation vibration of the two methylic groups, on the same carbonic atom. The two characteristic bands at 1192 and 1210 cm^{-1} [5] suggest also the presence of the group $(CH_3)_2C\langle$.

The NMR spectrum of octanesultone favours also structure IV as shown in the table below. It is noteworthy that the proton *a* strongly couples with the methylprotons *e*, having the coupling constant $y = 7$ cps, whereas between proton *c* and *g* the coupling is quite negligible.

---

[4] B. Helferich and R. Dheim, *Liebigs Ann. Chem.*, **646**, 33 (1961).

[5] K. Nakanishi "Infrared absorption spectroscopy. Practical", S. F. Holden-Day, Tokyo, Nankodo Comp., 1962, p. 20, 24.

Table

	τ	τ TMS = 10
a.	5.26	*a* and *e* couples, having $y = 7$ cps
b.	8.50	
c.	8.51	
d.	8.52	
e.	8.60	
f.	8.80	
g.	8.95	

The IR spectra of the sulfonic salts (Ca, Ba) point out the presence of the olefinic double bond, which is responsible for the absorption at 1640–1665 cm^{-1}, as well as the intense bands at 1170–1200 cm^{-1} and 1040–1055 cm^{-1}, which may be assigned to the valency vibration of the group SO_3, in the metalsulfonates.[6]

The IR spectrum of the bromosultones analogous to the sultone shows the bands of the sultonic group at 1332 and 1120 cm^{-1}, respectively at 1340 and 1130 cm^{-1}.

Bromosultone VII (m.p. 112°) has a spectrum generally similar to that of the octanesultone. Yet it differs by the presence of a single band, attributed to the methylabsorption (in plane deformation vibration at 1387 cm^{-1}) as a consequence of the presence of a bromine atom at one of the two methylgroups.

In the spectrum of the bromoderivative VIII (m.p. 145–146°) we find in exchange the doublet from 1385–1397 cm^{-1} and the bands 1180, 1155 and 840 cm^{-1}, due to some skeletal vibrations, characteristic of the isopropyl group[6]. The band at 1285 cm^{-1} may be assigned to a vibration δ s (CH_3) when one hydrogen atom of the group is replaced by a bromine atom. The shift towards lower frequencies may be admitted by the mass effect of bromine.

CONCLUSIONS

— The octanesultone melting at 128–129° has not the structure I or II, but the structure IV, and it is formed by the sulfonation of one mole each of butylene and isobutylene

— We assign to this sultone a tertiary structure, based on the data of chemical analysis (the splitting on hydrolysis, reformation by bromination) as well as on physico-chemical measurements (NMR and IR spectra).

— We suggest for this sultone the name 1,2,4,4-tetramethylbutanesultone, in order to differentiate it from the other octanesultones.

EXPERIMENTAL

The molecular weight determinations were made crioscopically in benzene : *Calcd* : for $C_8H_{16}O_3S$; M, 192 ; C, 50 ; H, 8.30 ; S, 16.66 ; *Found* : M, 191.57 ; 191.97 ; C, 49,89 ; 49.45 ; H, 8.85 ; 8.20 ; S, 16.44 ; 16.42.

---

[6] C. N. R. Rao "Chemical Applications of Infrared Spectroscopy", Academic Press, New York and London, 1963, p. 306.

The IR spectra were recorded with a UR 10 Zeiss spectrophotometer, in KBr pellets.

The NMR spectrum was recorded with a Varian A 60 spectrophotometer in $CDCl_3$, using tetramethylsilane as internal standard.

The Barium salt V was obtained on refluxing the octanesultone with $Ba(OH)_2$ for four hours, whereas the kalium salt was obtained using KOH. *Calcd.* for $C_8H_{15}O_3SK$: K, 16.44 ; *Found* : K, 16.04 ; 16.31.

The salts of type VI were obtained on heating the sultone with $BaCO_3$ for 22 hours at 130°. *Calcd.* : for $C_{16}H_{30}O_6S_2Ba$: Ba, 26.44 ; *Found* : Ba, 25.63 ; 25.37.

The bromo-derivatives were obtained from the sulfonic salts with bromine in water solution at room temperature. *Calcd.* for $C_8H_{15}O_3SBr$: C, 35.42 ; H, 5.35 ; S, 11.80 ; Br, 29.52 ; *Found* : C, 35.56 ; 35.68 ; H, 5.63 ; 5.50 ; S, 11.54 ; 11.48 ; Br, 30.06 ; 30.02.

Revue Roumaine de Chimie, 14, 517—521 (1969)

Revue Roumaine de Chimie, **14**, 523–526 (1969)

SYNTHETICAL PHENOTHIAZINE GLYCOSIDES. II[1]

O-GLUCOSIDES OF 3-HYDROXY-1, 9-DIBROMO-7-CHLORO-PHENOTHIAZINE AND 3-HYDROXY-7-CHLORO-PHENOTHIAZINE

C. BODEA, V. FĂRCĂŞAN and TEODORA PANEA
Institute of Chemistry of the Academy, Cluj, str. Donath, 65

Received May 23, 1968

On treating 3-hydroxy-1,9-dibromo-7-chloro-phenothiazine with β-glucoso-pentacetate the corresponding O-glucoside was obtained, which was then dehalogenated in position 1 and 9. The two O-glucosides were deacetylated to give the title compounds.

There are few data concerning the glycosides of halogeno-phenols. [2] Taking into account that in our laboratory there were prepared a large variety of halogeno-3H-phenothiazine-3-ones [3] easily convertible into the corresponding 3-hydroxy-derivatives, it is possible to obtain a logical series of O-glycosides with halogenated aglycons, in order to perform systematic studies related to the different aspects of the influence exerted by the halogen, located in the aglycon molecule, on the glycosidic bond.

As a sequel to our previous work, [1] we have obtained the first O-glucoside of the phenothiazine series, namely 3-(1,7,9-trichloro-phenothiazinyl)-β-D-glucopyranoside (I), on treating 3-hydroxy-1,7,9-trichloro-phenothiazine (II) with β-glucoso-pentacetate.

Attempts to prepare O-glucosides of lower halogenated 3-hydroxy-phenothiazines under the same conditions, led to very small yields, owing especially to the unstability of the starting substances.

We therefore tried another way to get lower halogenated glucosides based on the observation made in some previous researches, [4] that bromine atoms from position 1 and 9 of bromophenothiazines can be substituted by hydrogen on reduction with zinc in acetic acid.

Condensing 3-hydroxy-1, 9-dibromo-7-chloro-phenothiazine (III) with β-glucoso-pentacetate, we prepared 3-(1,9-dibromo-7-chloro-phenothiazinyl)-β-D-2,3,4,6-tetra-O-acetyl-glucopyranoside (IV).

---

[1] Part I. C. Bodea, V. Fărcăşan and T. Panea, *Rev. Roumaine Chim.*, **12**, 697 (1967).

[2] B. N. Stepanenko and G. K. Kryukova, *Doklady Akad. Nauk S. S. S. R.*, **89**, 885 (1953).

[3] M. Terdic, *Studii Cercetări Chim. Acad. Romania*, **13**, 579 (1965).

[4] C. Bodea, V. Fărcăşan and T. Panea, *Rev. Roumaine Chim.*, **14**, 971 (1968).

For this purpose the well known fusion technique of Helferich and Schmitz-Hillebrecht [5] was used. As catalyst *p*-toluene-sulfonic acid, or the newly applied ethyl polyphosphate [6] were added to the reaction mixture.

With both catalysts the yields were acceptable, and no appreciable efficiency differences were observed. The pure glycoside formed could be separated from the unreacted III, 1,9-dibromo-7-chloro-3H-phenothiazine-3-one (IX) and a resinous impurity only by chromatography on a silicagel column.

Generally the acidic catalysts, such as *p*-toluene-sulfonic acid, favour the predominant formation of β-D-glucosides. [7] That is why we consider that IV has the β-anomeric configuration.

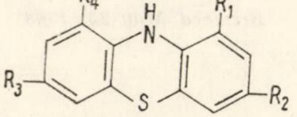

I : $R_1 = R_3 = R_4 = Cl$; $R_2 = B$
II : $R_1 = R_3 = R_4 = Cl$; $R_2 = OH$
III : $R_1 = R_4 = Br$; $R_2 = OH$; $R_3 = Cl$
IV : $R_1 = R_4 = Br$; $R_2 = A$; $R_3 = Cl$
V : $R_1 = R_4 = H$; $R_2 = A$; $R_3 = Cl$
VI : $R_1 = R_4 = Br$; $R_2 = B$; $R_3 = Cl$
VII : $R_1 = R_4 = H$; $R_2 = B$; $R_3 = Cl$
VIII : $R_1 = R_4 = H$; $R_2 = OH$; $R_3 = Cl$

A=

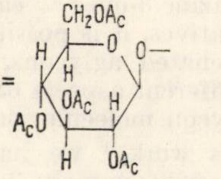

B=

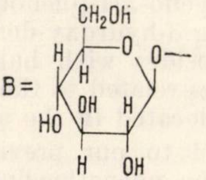

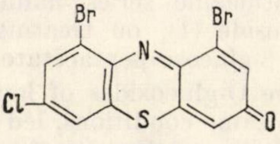

IX

The substance IV was then dehalogenated under the action of zinc in glacial acetic acid to give 3-(7-chloro-phenothiazinyl)-β-D-2,3,4,6-tetra-O-acetyl-glucopyranoside (V).

The hydrolysis of IV and V, under the conditions given in the experimental part, led to the following deacetylated products: 3-(1,9-dibromo-7-chloro-phenothiazinyl)-β-D-glucopyranoside (VI) and 3-(7-chloro-phenothiazinyl)-β-D-glucopyranoside (VII).

---

[5] B. Helferich and E. Schmitz-Hillebrecht, *Ber. dtsch. chem. Ges.*, **66**, 378 (1933).

[6] K. Onodera, S. Hirano and H. Fukumi, *Agr. Biol. Chem.*, **28**, 173 (1964).

[7] G. N. Bollenbach, Y. W. Long, D. G. Benjamin and Y. A. Lindquist, *J. Amer. Chem. Soc.*, **77**, 3310 (1955).

The deacetylation of IV and V was confirmed also by infrared spectrometry. Indeed, the stretching bands in the carbonyl region displayed by the two acetyl derivatives IV and V (1759 and 1751 cm^{-1} respectively), fail in the spectra of VI and VII.

Contrary to the expectations the water solubility of the two glucosides is not too different.

When boiled with hydrochloric acid compound V or VII gives the 3-hydroxy-7-chlorophenothiazine (VIII) as shown by the comparison (thin layer chromatography) with an authentic specimen.[8] Thus the dehalogenation is once more confirmed.

The results obtained in this work demonstrate the possibility to prepare lower halogenated O-glucosides of 3-hydroxy-phenothiazines from the corresponding 1,9-dibromo-derivatives.

EXPERIMENTAL[9]

3-(1,9-dibromo-7-chloro)-β-D-2, 3, 4, 6-tetra-O-acetyl-glucopyranoside (IV)

a) 1 g 3-hydroxy-1,9-dibromo-7-chloro-phenothiazine (III)[4], 1 g β-glucose pentacetate and some crystals of *p*-toluene-sulphonic acid were intimately ground, and warmed, in vacuum, in an oil bath at 130—140° for 40 minutes. The residue was twice boiled with ethanol and hot filtered. After cooling, from the ethanolic solution the crude IV precipitates. This product was chromatographed on a column with silicagel. The elution of the impurities (unreacted III and 1,9-dibromo-7-chloro-3H-phenothiazine-3-one IX — identified by comparison with authentic samples [4]) — was performed with toluene, and that of the glucoside with acetone. The acetone was removed by distillation and the residue recrystallized from glacial acetic acid. The pure substance (0.3 g), cream-brown crystals, melts at 147 — 148°.

IR ν_{CO} 1759 cm^{-1}

Anal. *Found*: N, 171; *Calcd.*: $C_{26}H_{24}Br_2ClNO_{10}S$; N, 189%.

b) Starting from III, IV was obtained under the conditions described above, but instead of *p*-toluene-sulfonic acid, ethyl polyphosphate was used.

3-(1,9-dibromo-7-chloro-phenothiazinyl)-β-D-glucopyranoside (VI)

0.15 g IV, 1 ml N/10 solution of sodium methoxide (in methanol) and 16 ml methanol were boiled for 15 minutes. At first (after 2—3 minutes) dissolution occurs and then VI precipitates. After cooling, filtering, washing with methanol and water, and recrystallization from methanol cream-coloured needles, m. p. 247—248° were obtained.

Anal: *Found*: N. 2.44 *Calcd.*: $C_{18}H_{16}Br_2ClNO_6S$ N 2.4%.

3-(7-chloro-phenothiazinyl)-β-D-2,3,4,6-tetra O-acetyl-glucopyranoside (V)

To a boiling solution of 0.2 g IV in 10 ml from a mixture of glacial acetic acid and dimethyl-formamide 1 : 1, 0.7 g of zinc powder were gradually added in five portions, within 3 hours. Then it was hot filtered and the solution poured into distilled water. The reaction product precipitates. In the solution the halogen was identified. After drying, the crude substance was chromatographed on a column with silicagel, the impurities were eluted with toluene and V with acetone. The acetone was removed and the pure substance was obtained as a light-brown powder, m. p. 129–130°.

---

[8] C. Bodea and M. Răileanu, *Liebigs Ann. Chem.*, **614**, 171 (1958).

[9] The melting points were determined in capillaries and are uncorrected.

IR $\nu_{C=O}$ 1751 cm^{-1}

Anal : *Found* : C, 53.63 ; H, 4.66 ; Cl, 6.72 ;
Calcd. : $C_{26}H_{26}ClNO_{10}S$; C, 53.8 ; H, 4.69 ; Cl. 6.12%.

3(7-chloro-phenothiazinyl)-β-D-glucopyranoside (VII)

Starting from V, VII was obtained under the conditions described by the preparation of VI. M. p. 256–257° (with softening).

Anal : *Found* : N 3.01 ; *Calcd.* : $C_{18}H_{18}ClNO_6S$, N, 3.40.

3-hydroxy-7-chlorophenothiazine (VIII)

Some crystals of V or VII, were boiled with concentrated hydrochloric acid, for one minute, and poured into water. The precipitate was filtered, washed with water and dried. It was identified by thin layer chromatography, on silicagel G ; developer : toluene, detector : bromine. For comparison an authenic sample[8] was used.

For recording the IR-spectra in KBr pellets, a double-beam Carl Zeiss Jena UR–10 spectrophotometer was used.

Revue Roumaine de Chimie, **14**, 527–534 (1969)

RADICAUX LIBRES STABLES DIARYLAZOTE AVEC UN GROUPE SULFONIQUE DANS LA MOLÉCULE

P. T. FRANGOPOL, MARIA FRANGOPOL, N. NEGOIŢĂ et E. ROMAŞ

Institut de Physique Atomique, Bucarest, B.P. 35

Reçu le 23 juillet 1968

Des signaux RPE ont été observés sur dix radicaux libres stables solides préparés par oxydation à deux reprises avec de l'$Ag^{II}O$ des différentes diarylamines qui possèdent dans la molécule un groupe sulfonique. Les amines ont été préparées par la réaction du 1-chlor-2,6-dinitro-4-benzensulfonate de potassium sur des anilines substituées (aniline, *o*-, *m*-, *p*-toluidine, *o*-, *m*-, *p*-anisidine, *p*-amino-N, *N*-diméthyl-et *p*-amino-*N*, *N*-diphénylaniline, 4-amino-vératrole) ; leurs spectres en IR sont discutés. La stabilité des radicaux est très grande, ces radicaux étant conservés depuis plus de 12 mois.

Dans un mémoire précédent [1] nous avons appliqué sur les radicaux libres diarylazote l'idée avancée antérieurement et prouvée par voie expérimentale [2] que les groupes nitro exercent un effet stérique parallèle à l'effet électronique dans la stabilité des radicaux.

L'importance du facteur stérique a été démontrée dans le radical diphényl-picryl-hydrazyl (DPPH) par diffraction avec les rayons X. [3]

Dans ce mémoire nous présentons la préparation des diarylamines, qui possèdent dans la molécule un groupe *p*-sulfonique et deux groupes *o*-nitro, capables de conduire par oxydation à des radicaux libres stables.

Nous avons donc préparé des radicaux libres de grande stabilité et dans de prochaines études nous voulons essayer leurs propriétés de semi-conductivité et photoconductivité, [4] ainsi que leurs propriétés magnétiques pour déterminer la position de l'électron impair auquel on fait subir de petits changements dans la structure des composés diarylaminiques. [5] En même temps la solubilité dans l'eau peut conduire à un intérêt pratique déterminé par l'application possible de ces radicaux dans l'étude de la polarisation dynamique en champ faible.[6–8]

---

[1] A. T. Balaban, P. T. Frangopol, M. Frangopol et N. Negoiţă, *Tetrahedron*, **23**, 4661 (1967).

[2] A. T. Balaban, P. T. Frangopol, M. Mărculescu et I. Bally, *Tetrahedron*, **13**, 258 (1961).

[3] D. E. Williams, *J. Amer. Chem. Soc.*, **88**, 5665 (1966) ; *J. Amer. Chem. Soc.*, **89**, 4280 (1967).

[4] D. D. Eley, K. W. Jones, J. G. E. Littler et M. R. Willis, *Trans. Faraday Soc.*, **63**, 902 (1967).

[5] H. S. Jarrett, *J. Chem. Phys.*, **21**, 761 (1953).

Les radicaux sulfoniques de type hydrazylique (1),[9] (2)[5,9], (3),[10] (4)[11] ont déjà été étudiés mais les radicaux de type diarylazote sulfonique ont jusqu'à présent inconnus.

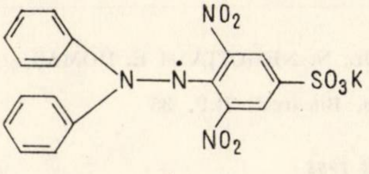

1

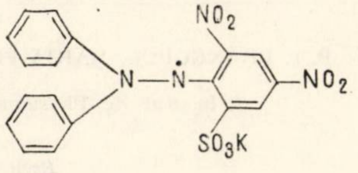

2

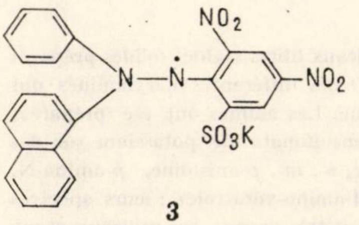

3

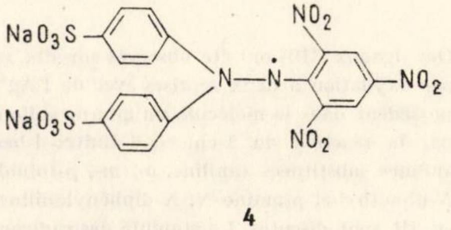

4

RÉSULTATS ET DISCUSSIONS

Les diarylamines sulfoniques (5) qui

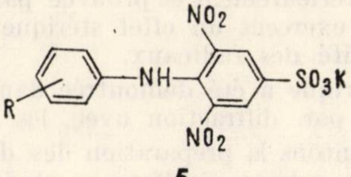

5

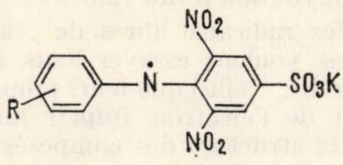

6

R

a. H
b. *o*-Me
c. *m*-Me
d. *p*-Me
e. *o*-OMe
f. *m*-OMe
g. *p*-OMe
h. *p*-NMe$_2$
i. *p*-NPh$_2$
j. 3,4(OMe)$_2$

---

[6] A. Abragam, J. Combrisson et J. Solomon, *Compt. rend.*, **245**, 157 (1957).

[7] R. Besson, H. Lemaire, A. Rassat, A. Salvi et P. Servoz-Gavin, « Electronic Magnetic Résonance and Solid Dielectrics » ; Proceedings of the XII th Colloque Ampère, Bordeaux, 1963, North Holland Publishing Co., Amsterdam, 1964, p. 327.

[8] M. Borghini, Preprint CERN 66–3, 31 January 1966, p. 16.

[9] M. A. Ikrina et R. O. Matevosian, *Zhur. obshchei Khim.*, **1962**, 3952.

[10] W. Walter Weber, Jr., *Diss. Abs.*, **24** (3), 983 (1963) ; *Chem. Abstr.* **60**, 10 616 h (1964).

[11] G. Putirszkaya, *Központi Kém. Kutato Intézetének Közleményei*, **8**, 39 (1963).

peuvent conduire par oxydation à des radicaux (**6**) ont été préparés par substitution nucléophile de l'atome halogène activé dans le sel de potassium de 1-chlor-2,6-dinitro-4-sulfobenzène avec des anilines substituées (aniline, *o*-, *m*-, *p*-toluidine, *o*-, *m*-, *p*-anisidine, *p*-amino-N,N-diméthyl- et *p*-amino-N,N-diphénylaniline et 4-amino-vératrole).

$$KO_3S(NO_2)_2C_6H_2Cl \xrightarrow[-HCl]{+H_2N-Ar} KO_3S(NO_2)_2C_6H_2-NH-Ar \xrightarrow{Ag^{II}O} KO_3S(NO_2)_2C_6H_2-\dot{N}-Ar$$

Les synthèses des composés (**5**) ont été effectuées dans l'éthanol absolu sous reflux, avec des rendements de 80% (tabl. 1). On peut remarquer la coloration variée, spectaculaire des cristaux obtenus.

Tableau 1

Analyses élémentaires et F°C des diarylamines-sulfoniques (5a – j)

	R	Couleur	Rendements %	F°C	Formule brute	Analyse % Calculé		Analyse % Trouvé
a	H	orange	85	368	$C_{12}H_8N_3O_7KS$	C	38,18	38,69
						H	2,14	2,41
						N	11,13	10,58
						S	8,50	9,02
b	*o*-Me	Jaune-orange	78,5	237	$C_{13}H_{10}N_3O_7KS$	C	39,89	40,10
						H	2,57	2,90
						N	10,74	11,51
						S	8,19	8,62
c	*m*-Me	orange	82	255	$C_{13}H_{10}N_3O_7KS$	C	39,89	40,22
						H	2,57	2,67
						N	10,74	11,44
						S	8,19	8,58
d	*p*-Me	orange	82	260	$C_{13}H_{10}N_3O_7KS$	C	39,89	40,30
				(déc)		H	2,57	2,99
						N	10,74	11,20
						S	8,19	8,56
e	*o*-OMe	orange	79	239	$C_{13}H_{10}N_3O_8KS$	C	38,32	38,66
						H	2,47	2,80
						N	10,32	10,20
						S	7,88	8,74
f	*m*-OMe	orange	86	233	$C_{13}H_{10}N_3O_8KS$	C	38,32	38,70
						H	2,47	2,95
						N	10,32	10,64
						S	7,88	8,68

	R	Couleur	Rendements %	F°C	Formule brute	Analyse %		
						Calculé		*Trouvé*
g	*p*-OMe	orange	80	358	$C_{13}H_{10}N_3O_8KS$	C	38,32	38,80
						H	2,47	3,10
						N	10,32	9,98
						S	7,88	8,24
h	*p*-NMe$_2$	noir	84	<370	$C_{14}H_{13}N_4O_7KS$	C	39,99	40,40
						H	3,11	3,50
						N	13,33	12,88
						S	7,62	8,23
i	*p*-NPh$_2$	grenat	94	238	$C_{14}H_{13}N_4O_7KS$	C	52,93	53,35
						H	3,14	3,64
						N	10,30	10,50
						S	5,89	6,66
j	3,4 (OMe)$_2$	rouge carmin	85	370	$C_{14}H_{12}N_3O_9KS$	C	38,44	38,78
						H	2,77	2,82
						N	9,60	9,94
						S	7,33	6,94

Les spectres en IR ont été déterminés en pastille de KBr.

Dans le tableau 2 on donne les bandes caractéristiques des groupes aminiques et sulfoniques. Toutes les amines présentent une forte bande de vibration de valence N—H dans la région de 3300 à 3400 cm^{-1} (tabl. 2).

Tableau 2

Spectres d'absorption en IR des diarylamines sulfoniques

	R	νNH cm^{-1}	νSO$_3$H cm^{-1}	
			1180—1220	1040—1070
a	H	3326 m	1210 F 1195 mF	1056 mF 1050 mF
b	*o*-Me	3330 m	1185 F	1045 F
c	*m*-Me	3316 m	1210 mF 1190 mF	1045 F
d	*p*-Me	3354 m	1207 e 1195 mF 1185 mF	1049 mF
e	*o*-OMe	3376 m	1215 e 1199 e 1182 F	1050 F 1040 m
f	*m*-OMe	3338 m	1205 F 1195 e 1182 e	1045 F
g	*p*-OMe	3336 m	1209 F 1192 mF	1055 mF 1048 m
h	*p*-NMe$_2$	3325 fm	1208 F 1190 F 1180 e	1045 mF
i	*p*-NPh$_2$	3320 m	1180 mF	1110 fm 1080 f 1045 m
j	3,4(OMe)$_2$	3325 m D 2462 m	1205 F 1195 e	1055 m 1045 m

La présence de la bande NH a été confirmée aussi par des expériences de N-deutération. Le composé (**5**) j a été refluxé pendant deux heures avec du D_2O (99,98%). Le solvant a été écarté par évaporation sous vide. Dans le spectre en IR effectué en pastille de KBr, le composé deutéré présente la bande $\nu N-D$ à 2462 cm^{-1} qui remplace la bande $\nu N-H$ de 3325 $cm^{\cdot 1}$. Le déplacement des bandes concorde avec les résultats trouvés dans la littérature.[12]

Les bandes δNH à 1465 cm^{-1} ne sont pas visibles dans les composés deutérés. On observe aussi la vibration $C_{arom} - N$ (1230 et 1300 cm^{-1}), les vibrations asymétriques et symétriques $\nu N-O$ (1340 —1360 cm^{-1} et 1520—1540 cm^{-1}), ainsi que les groupes phényls à 1500 et 1600 cm^{-1}.

Les sels sulfoniques absorbent dans la région de 1150 à 1260 et de 1010 à 1080 cm^{-1}. Une étude récente[13] établit les vibrations caractéristiques pour le groupe sulfonique. Nos composés sulfoniques ont les bandes caractéristiques en IR en bonne concordance avec celles citées ci-dessus (tabl. 2).

L'oxydation de ces diarylamines sulfoniques a été effectuée avec de l'oxyde d'argent ($Ag^{II}O$).[14] Les produits résultés sont des radicaux d'une stabilité remarquable à l'air et à la chaleur. Les radicaux sont pratiquement insolubles en alcool éthylique, acétone, dioxanne (excepté **6**i) benzène, chloroforme, éther. Ils sont solubles en diméthylformamide (DMF) et diméthylsulfoxyde (DMSO), solvants utilisables dans notre spectromètre RPE[15] seulement en tube capillaire à cause de leur constante diélectrique > 10; malheureusement, dans les capillaires seulement le radical (**6**)i, a donné un signal décelable.

Nous avons donc cherché une méthode pour la préparation des radicaux libres à l'état solide et nous avons réussi, en oxydant les amines (**5**) avec de l'$Ag^{II}O$ en DMSO ou DMF avec agitation magnétique. Après une première oxydation, on sépare par filtration l'oxydant et on ajoute une portion d'$Ag^{II}O$ fraîchement préparée. La solution résultée est agitée et évaporée sous vide. On obtient ainsi le radical solide. Tous ces radicaux (**6**)a-j donnent lieu à une absorption paramagnétique constituée par une raie unique symétrique et dont la largeur entre les sommets de la courbe est sensible aux conditions de préparation. Les spectres RPE sont donnés dans les figures 1—4.

Le facteur *g* de ces radicaux solides a été estimé en comparaison du nitrosodisulfonate de potassium ou sel de Fremy ($g = 2{,}0055$).[16] Les valeurs du facteur isotropique *g*, entre 2,0032—2,0040 ± 0,0003 (tabl. 3), conduisent à une conclusion importante, à savoir que les fac-

---

[12] R. S. Tsehansky, *Zhur. org. Khim.*, **1**, 1909 (1965) et la litt. citée dans l'article; D. Hadzi et M. Skorbljak, *J. Chem. Soc.*, **1957**, 843.

[13] L. Ganguly, C. I. Jose et A. A. Biswas, *Spectrochim. Acta*, **24**, A/3, 215 (1968); L. J. Bellamy, « The Infrared Spectra of Complex Molecules », Methuen, 1959, p. 350.

[14] L. Syper, *Tetrahedron Letters*, **1967**, 4193; R. N. Hammer et J. Kleinberg, *Inorg. Synth.*, **4**, 12 (1953).

[15] I. Pascaru, *Nuclear Instruments and Methods*, **26**, 333 (1964).

[16] J. Q. Adams et J. R. Thomas, *J. Chem. Phys.*, **39**, 1904 (1963).

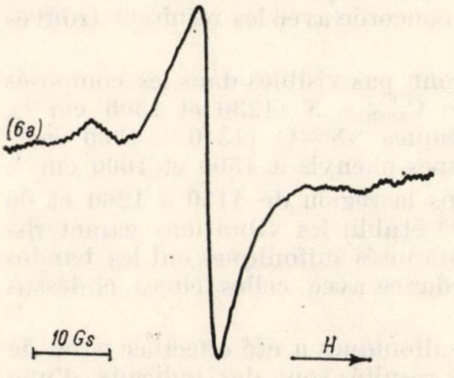

Fig. 1. — Spectre RPE du radical libre solide (6)a.

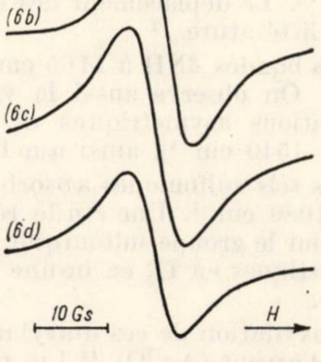

Fig. 2. — Spectres RPE des radicaux libres solides (6) b, c, d.

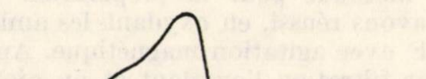

Fig. 3. — Spectres RPE des radicaux libres solides (6) e, f, g.

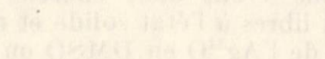

Fig. 4. — Spectres RPE des radicaux libres solides (6) h, i, j.

teurs *g* des radicaux libres diarylazote[17] ont aussi la valeur du *g* entre 2,0031–2,0040, mais les diarylnitroxydes ont des valeurs au-dessus de 2,0055,[18] donc la conclusion avancée auparavant[1,2] que l'agent d'oxydation ne convertit pas les diarylamines en diarylnitroxydes garde sa validité dans ces cas aussi.

Tableau 3

Valeurs du facteur isotropique g*) déterminées dans les spectres RPE des radicaux libres(6)a – j

	R	g ± 0,0003
a)	H	2,0037
b)	*o*-Me	2,0032
c)	*m*-Me	2,0040
d)	*p*-Me	2,0035
e)	*o*-OMe	2,0035
f)	*m*-OMe	2,0035
g)	*p*-OMe	2,0037
h)	*p*-NMe_2	2,0040
i)	*p*-NPh_2	2,0037
j)	3,4$(OMe)_2$	2,0035

*) Déterminé par rapport au $(SO_3K)_2NO$.

PARTIE EXPÉRIMENTALE

Les points de fusion ont été pris à l'appareil Bœtius.

Les spectres en IR ont été enregistrés à l'aide d'un appareil Iéna UR–10. Dans le tableau 2, nous donnons les bandes caractéristiques des substances préparées avec la convention suivante :

F = bande de forte intensité ;
m = bande de moyenne intensité ;
f = bande de faible intensité ;
e = épaulement .

Les spectres RPE ont été effectués avec un spectromètre, modèle IFA[15], opérant en bande X, à une modulation du champ très élevée. Les spectres ont été réalisés à la température ambiante.

---

[17] F. A. Neugebauer et H. Fischer, *Chem. Ber.*, **98**, 844 (1965) ; E. J. Land et G. Porter, *Trans. Faraday Soc.*, **59**, 2027 (1963) ; *J. Chem. Soc.*, 1961, 3540.

[18] E. G. Rozantsev, *Uspekhi Khim*, **35**, 1549 (1966) ; F. A. Neugebauer et P. H. H. Fischer, *Z. Naturforsch.*, **21 b**, 1036 (1966) ; E. T. Strom, A. L. Bluhm et J. Weinstein, *J. Org. Chem.*, **32**, 3853 (1967).

Préparation des sels de potassium de dinitro-sulfophényl-arylamines

Les anilines substituées utilisées dans les réactions sont des produits commerciaux, sauf la *m*-anisidine, le 4-amino-vératrole et la *p*-amino-triphénylamine préparés selon la littérature. Pour les indications générales de préparation et d'oxydation, voir la référence.[1]

Les réactions ont été effectuées, en faisant réagir l'aniline substituée (10 mmoles) avec le sel de potassium de 1-chlor-2,6-dinitro-4-sulfobenzène [19] (5 mmoles), dissous dans de l'éthanol (20—40 ml). On porte le mélange à reflux pendant 2 h. Après refroidissement on sépare par filtration de très beaux cristaux colorés. Les dinitrosulfophénylamines ont été purifiées par recristallisation dans l'eau, excepté (**6**) i recristallisée dans du benzène-éther.

Nous remercions M. le Dr I. Pascaru pour les spectres RPE et les nombreuses discussions que nous avons eues, Mmes M. Roman et C. Popescu pour les analyses élémentaires et M. D. Papae pour l'assistance technique.

---

[19] H. P. Schultz, *Org. Synth.*, **31**, 45 (1951).

Revue Roumaine de Chimie, **14**, 535–547 (1969)

POTENTIAL ANTICANCER AGENTS. VI*

NEW AROMATIC NITROGEN MUSTARDS WITH GOOD ANTITUMOR ACTIVITY

I. NICULESCU-DUVĂZ, V. FEYNS, V. SAVANIU, M. IONESCU,
A. ŞERBAN and A. CAMBANIS

Oncological Institute, Bucharest, Bd. 1 Mai 11

Received July 27, 1968

Synthesis and antitumor activity of 24 new nitrogen mustards from amino-, amino-alkyl and amino-dimethyl-benzoic acids, and motivation of their preparation, are reported. The new compounds are characterized by elemental analysis and IR spectra. Relationships between hydrolysis rate of nitrogen mustards and basicity of the precursor amines are pointed out.

The aromatic nitrogen mustards are one of the first classes of antitumor compounds investigated systematically.[1] In closely related series it has been possible to demonstrate the relationship between the chemical reactivity (assessed by determining the rate of hydrolysis under standard conditions) and the antitumor activity, [2] and in a great number of derivatives it has been shown that a certain level of chemical reactivity is necessary if the compound is to be an effective tumor growth inhibitor.

High chemical reactivity is, nevertheless, as a rule, disadvantageous in designing drugs with selective toxicity against the malignant cell. From this point of view, of particular interest are those compounds which couple a high antitumor activity with a relatively low chemical reactivity. In the anticancer action of such compounds, special mechanisms (usually enzymatic) are probably involved during transport, penetration into the malignant cell or metabolism at the action site.

Such an interesting case represents the isomeric nitrogen mustards of *o*-, *m*- and *p*-aminobenzoic acids, first synthesized by Ross. [3] Examination of the screening data [4-6] reveals (Table 1) on the one hand that these compounds divert from the above mentioned correlation (between their hydrolysis rate and antitumor action both against Walker carcinotarcoma and particularly against Jensen sarcoma), and on the other sand that the meta-substituted derivative (I) possesses the best activity/hoxicity ratio. The latter aspect was made evident also in melphalan isomers [7] and in the corresponding phenyl-β-alanine derivatives. [8,9] These observations prompted us to ascribe special transport properties to the meta-aminobenzoic structure (particularly to the carboxyl group), due both to reduction of the reactivity of the nitrogen mustard moiety (-M and -I effects) and to the fact that the carboxyl group may be considered as "biologically compatible", what increases the possibilities of compound-organism interaction. [10]

---

* Note V. A. Cambanis, V. Dobre and] I. Niculescu-Duvăz, *J.*] *Med. Chem.* (in press).

[1] W. C. J. Ross, "Biological Alkylating Agents", Butterworth, London, 1962; J. M. Johnson and F. Bergel, "Biological Alkylating Agents" in "Metabolic Inhibitors" edited by R. M. Hochster and J. H. Quastel, Vol. II, Academic Press, New York, 1963, p. 161–192.

[2] T. J. Bardos, N. Datta-Gupta, P. Hepborn and D. J. Triggle, *J. Med. Chem.*, **8**, 167 (1965).

[3] J. L. Everett, J. J. Roberts and W. C. J. Ross, *J. Chem. Soc.*, **1953**, 2386.

Table 1

Isomer nitrogen mustards from aminobenzoic acids

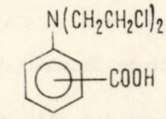

Isomer	LD$_{50}$ mg/kg body	% Hydrolysis in standard conditions	% Antitumor inhibition		Increase of[6] survival time, Ehrlich ascite
			Jensen[4] sarcoma	Walker 256[4,5] carcinosarcoma	
p-COOH	150	10	86 +++	— ±	42
m-COOH	98.6	4	95 +++	41 +	73
o-COOH	14.4	<1	89 +++	54 ++	59

In order to check this hypothesis, a series of *m*-substituted aromatic nitrogen mustards were synthesized (Table 2) and relationship between the nature of substituent, hydrolysis rate and antitumor activity were investigated (Table 3). Testing data confirmed the favourable effect of the carboxyl group upon the anticancer activity, since compounds with nearly the same hydrolysis rate as 3-N, N-bis (2-chloroethyl) aminobenzoic acid, but with other substituents in meta position (J, Cl, NO_2, etc.), have incomparable lower antitumor activity. It is possible that the relative high activity of the nitrile derivative may be accounted for

---

[4] V. Dobre, Commun. at the Oncological Society, Bucharest, 1965.

[5] W. C. J. Ross, ref. 1, p. 123.

[6] S. C. J. Fu, H. Terzian and S. Craven, *J. Med. Chem.*, **7**, 759 (1964).

[7] J. M. Luck, *Cancer Res.*, **21**, 262 (1961).

[8] W. A. Skinner, V. A. Hyde, H. F. Gram and B. R. Baker, *J. Org. Chem.*, **25**, 1756 (1960).

[9] J. M. Johnson, *Chem. Ind.*, **1960**, 966.

[10] I. Niculescu-Duvăz, M. Ionescu, A. Cambanis, M. Vitan and V. Feyns, *J. Med. Chem.*, **11**, 500 (1968).

Table 2

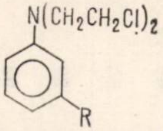

New aromatic nitrogen mustards

No.	R	Synth.	m.p. °C	Elemental analysis								I.R. spectra[2] ν_{max}, cm^{-1}		
				Calculated %				Found %						
				C	H	N	Cl	C	H	N	Cl	C – Cl		R[4]
1	Cl	A	36	47.52	4.75	5.54	42.18	48.00	4.76	5.56	41.82	680	765	—
2	J	A	108	34.88	3.48	4.05	57.57[1]	35.03	3.59	4.10	57.30[1]	675	765	—
3	NO_2	A	115–116	45.62	4.56	10.64	26.99	45.67	4.67	10.63	26.98	665	740	1351[5] 1540
4	CN	A	77–77.5	54.32	4.94	11.52	29.22	54.28	5.11	11.70	28.91	675	740	2230[6]
5	COCl	A	80–81	47.06	4.24	4.99	37.96	46.67	4.48	5.06	37.59	662	746	1760[7]
6	CO_2CH_3	A	53	52.18	5.43	5.07	25.72	52.38	5.56	5.14	25.55	665	756	1710[7]
7	$CO_2i\text{-}C_3H_7$	A	53–54	55.26	6.25	4.61	23.35	55.20	6.11	4.73	23.18	660	730	1710[7]
8	$CO_2CH_2CH_2NEt_2 \cdot HCl$	A	110–111	51.32	6.79	7.04	26.79	51.62	7.01	7.09	26.39	655	722	1712[7]
9	$NH_2 \cdot HCl$	A	175–179	44.53	5.56	10.39	39.51	44.81	5.63	10.28	39.08	663	748	1502[8] 1593
10	$CONH_2$	A	110–112	50.57	5.36	10.72	27.20	50.24	5.45	10.63	27.27	655	722	1650
11	$CON(CH_3)_2$	A	oil	53.97	6.23	9.69	24.57	53.67	6.51	9.66	24.87	—	—[3]	1640
12	$CON(i\text{-}Pr)_2$	A	78–80	59.13	7.53	8.11	20.58	59.37	7.40	8.21	20.84	—	—[3]	1630
13	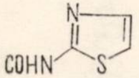	A+B	112–113	48.83	4.36	12.21	20.64	49.08	4.51	12.26	20.52	653	729	1656
14	$CONHCH_2C_6H_5$	A	86–87	61.54	5.70	7.98	20.23	61.78	5.91	7.83	20.51	660	730	1643
15	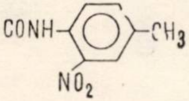	A	121–123	54.54	4.79	10.61	17.93	54.55	4.59	10.69	17.45	655	732	1690
16	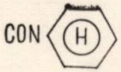	A+B	84	58.36	6.69	8.51	21.58	58.66	6.90	8.47	21.60	—	—[3]	1643
17	–CONH–NHCO–	A	130–131	50.77	5.00	10.77	27.30	51.02	5.06	10.78	27.01	660	740	1650

[1] Cl + J. [2] KBr disks, UR 10 Zeiss Jena spectrophotometer. [3] CCl_4 solution. [4] Amide band I, except where otherwise noted. [5] NO_2 group. [6] CN group. [7] carbonyl group. [8]. $\delta_{NH_3^+}$ sym. and asym.

Table 3

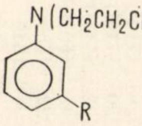

Hydrolysis and biological data

No.	R	% Hydrolysis [1]) 66°C	Hydrolysis rate $k_{66} . 10^4$	% Tumor growth inhibition Jensen sarcoma
1	COOH	4.6	0.28	95
2	Cl	4.6	0.28	0
3	J	3.7	0.21	30–40
4	NO_2	1.6	0.09	0
5	CN	1.9	0.10	60
6	COCl	—	—	85
7	CO_2CH_3	6.2	0.35	93
8	$CO_2i\text{-}C_3H_7$	5.9	0.33	99
9	$CO_2CH_2CH_2NEt_2 . HCl$	3.3	—	92
10	$NH_2 . HCl$	5.1	—	58
11	$CONH_2$	7.5	0.42	87
12	$CON(CH_3)_2$	7.7	0.44	48
13	$CON(i\text{-}C_3H_7)_2$	7.7	0.44	0
14	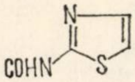	4.9	0.27	93
15	$CONHCH_2C_6H_5$	8.7	0.50	35[2])
16	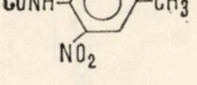	—	—	0
17	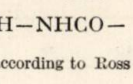	6.4	0.35	31
18	–CONH–NHCO–	14.11[3])	—	93

[1]) Determined according to Ross [26], with potentiometric titration of Cl^- ion. [2]) Walker 256 carcinosarcoma. [3]) Two $-N(CH_2CH_2Cl)_2$ groups.

an *in vivo* hydrolysis (demonstrated in aromatic nitriles[11]), which gives rise to the acidic "active form".

$$Ar{-}OH \rightarrow Ar{-}CONH_2 \rightarrow Ar{-}COOH$$

Support for this sequence seems to be provided in our case by the fact that the amide derivative shows an intermediate activity between that of acid and nitrile (Table 3).

Attempting to improve the antitumor activity of the amino-benzoic nitrogen mustards, we introduced a third substituent with + I effect so that an increase of the electronic density and therefore of the basicity of the yperitic N atom be obtained. Thus the 10 isomeric nitrogen mustards of methylbenzoic acids were synthesized.[10] 3-/N,N-bis (2-chloroethyl) amino/-4-methylbenzoic acid (Code No. IOB 82) showed the highest antitumor action associated with a low hematopoietic toxicity[12] warranting start of clinical trials which led to very interesting results.[13,14]

On this line of investigation, the following groups of nitrogen mustards were synthesized and studied:

— functional derivatives of 3-/N,N-bis (2-chloroethyl)amino/-4-methylbenzoic acid,[15]

— 4-alkyl- and dimethyl-homologues (Table 4).

Synthesis

The *m*-substituted nitrogen mustards (Table 2, R = CN, NO_2, Cl, J) were prepared from the respective amines by hydroxyethylation and chlorination.

The functional derivatives (esters and amides) of 3-/N, N-bis (2-chloroethyl) amino/benzoic acid (I) (Table 2, No. 6—17) were prepared from acid chloride II by cold treatment with excess amines, or by refluxing with the corresponding alcohols, respectively.

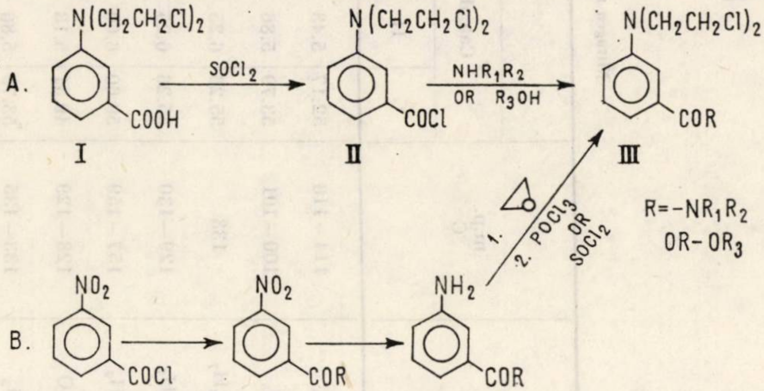

---

[11] R. T. Williams, "Detoxication Mechanisms", Second Ed., Chapman & Hall Ltd., London, 1959, p. 404.

[12] V. Dobre, *Farmacia* (Bucharest), **15**, 103 (1967).

[13] O. Costăchel and I. Mogoș, Scient. Symp. I.C.C.F., 5th, Bucharest, 1967.

[14] I. Mogoș and O. Costăchel, Intern. Congr. of Chemotherapy, 5th, Vienna, 1967.

[15] A. Cambanis, V. Dobre and I. Niculescu-Duvăz, *J. Med. Chem.*, in press.

Table 4

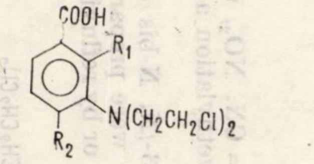

Nitrogen mustards from alkylbenzoic acids

No.	R_1	R_2	m.p. °C	Elemental analysis								I.R. spectra 1) ν_{max}, cm^{-1}			% Inhibition Jensen sarcoma
				Calculated %				Found %							
				C	H	N	Cl	C	H	N	Cl	C—Cl		C=O	
1	H	CH_3	114–116	52.17	5.43	5.07	25.72	52.38	5.51	5.02	25.63	660	735	1689	100
2	H	C_2H_5	100–101	53.79	5.86	4.83	24.48	53.42	5.95	4.81	24.25	655	740	1690	95
3	H	n-C_3H_7	138	55.26	6.25	4.60	23.35	55.19	6.28	4.66	23.15	660	—	1692	80
4	H	i-C_3H_7	129–130	55.26	6.25	4.60	23.35	55.15	6.46	4.65	23.29	662	740	1692	98
5	H	t-C_4H_9	157–159	56.60	6.60	4.40	22.33	57.00	6.80	4.54	22.40	651	741	1690	—
6	H	CH_3O	128–129	49.31	5.13	4.79	24.31	49.27	5.27	4.78	24.20	660	730	1685	—
7	CH_3	CH_3	133–135	53.79	5.86	4.83	24.48	53.49	5.95	4.84	24.35	660	732	1700	—
8	Compound XVI		187–190	46.57	4.77	8.36	21.19	46.76	5.02	8.25	20.85	670	720	1710	60

---

[1] See note 2, table 2.

For checking the structure and measuring amines IV basicity, some of the compounds III were prepared also by route B from *m*-nitrobenzoyl chloride.

Acid I hydrazide could not be obtained from acid chloride II and hydrazine, in the conditions reported for the *p*-isomer.[16] Instead of the expected hydrazides, a di-acyl derivative was isolated.

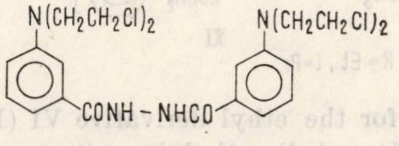
N(CH2CH2Cl)2
N(CH2CH2Cl)2
CONH – NHCO

3-/N, N-bis (2-chloroethyl) amino/-4-alkylbenzoic acids (X) (Table 4, No. 1—5) and 4-methoxy-analogue (Table 4, No. 6) were prepared from the corresponding aminoesters VIII by hydroxyethylation, chlorination ($SOCl_2$ or $POCl_3$) and acid hydrolysis. Separation and careful purification of hydroxyethyl derivatives IX, although not essential, increase the final product yield.

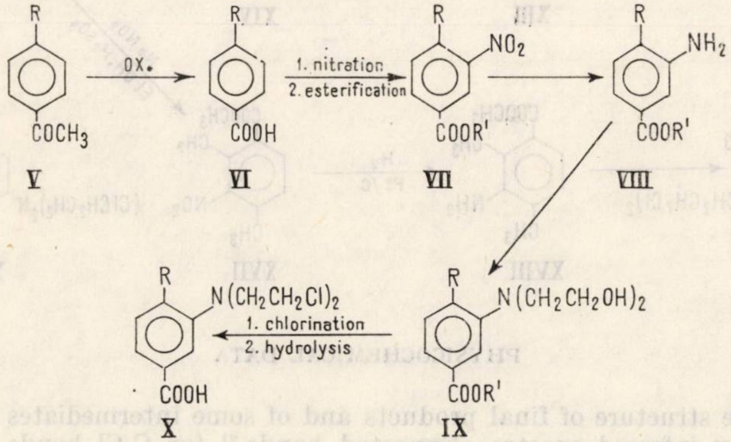
R
COCH3
V
OX.
R
COOH
VI
1. nitration
2. esterification
R
NO2
COOR'
VII
R
NH2
COOR'
VIII
R
N(CH2CH2Cl)2
COOH
X
1. chlorination
2. hydrolysis
R
N(CH2CH2OH)2
COOR'
IX

Intermediate aminoesters VIII were obtained by the known reactions from 4-alkylbenzoic acids VI prepared in their turn by sodium hypochlorite[17] or hypobromite[18] oxydation of alkylacetophenones V.

---

[16] R. C. Elderfield and T. K. Liao, *J. Org. Chem.*, **26**, 4996 (1961).

[17] M. V. Farrar and R. Levine, *J. Amer. Chem. Soc.*, **71**, 1496 (1949).

[18] W. H. Perkin Jr. and J. F. S. Stone, *J. Chem. Soc.*, **127**, 2275 (1925).

Oxidation of 4-isopropylacetophenone failed to yield the expected acid. Compound VI ($R = i-C_3H_7$) was synthesized by King reaction.[19] The same procedure was used as an alternate

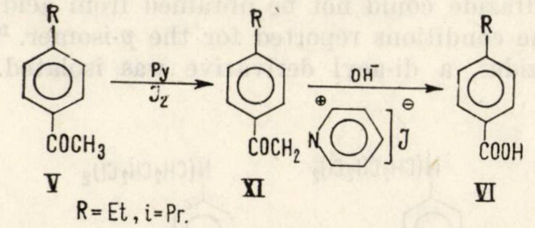
R
Py
J_2
OH⁻
⊕
⊖
J
COCH₃
COCH₂
N
COOH
V
XI
VI
R = Et, i = Pr.

method of synthesis for the ethyl derivative VI (R = Et).

Dimethyl- (XIX) and dimethylnitro-nitrogen mustards (XVI) were prepared by the following sequence, the intermediate esters being more easily handled than the acids reported in earlier works.

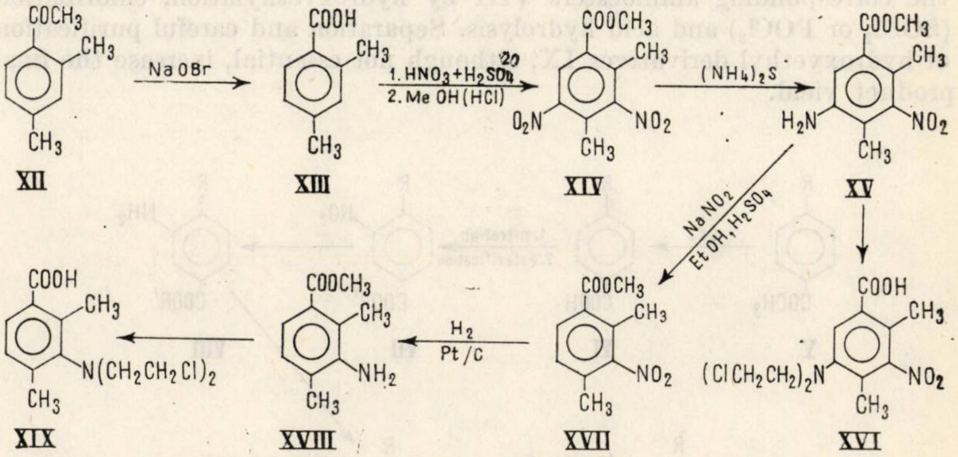
COCH₃
CH₃
NaOBr
CH₃
XII
COOH
CH₃
1. HNO₃ + H₂SO₄ 20
2. MeOH (HCl)
CH₃
XIII
COOCH₃
CH₃
O₂N
NO₂
CH₃
XIV
COOCH₃
CH₃
(NH₄)₂S
H₂N
NO₂
CH₃
XV
NaNO₂
EtOH, H₂SO₄
COOH
CH₃
(ClCH₂CH₂)₂N
NO₂
CH₃
XVI
COOCH₃
CH₃
NO₂
CH₃
XVII
H₂
Pt/C
COOCH₃
CH₃
NH₂
CH₃
XVIII
COOH
CH₃
N(CH₂CH₂Cl)₂
CH₃
XIX

PHYSICOCHEMICAL DATA

The structure of final products and of some intermediates was confirmed by infrared spectra. Expected bands[21] for C-Cl bonds (P_C and P_H configurations) were obtained. Carbonyl absorption ranged within reported limits for acids,[22] esters,[23] acid chlorides,[24] and amides.[25]

---

[19] L. C. King, *J. Amer. Chem. Soc.*, **66**, 894 (1944).

[20] H. Frey and M. Horowitz, *J. prakt. Chem.*, **43/2/**, 120 (1891).

[21] J. J. Shippman, V. L. Flott and S. Krimm, *Spectrochim. Acta*, **18**, 1613 (1962).

[22] C. J. W. Brooks, G. Eglinton and J. F. Morman, *J. Chem. Soc.*, **1961**, 106.

[23] C. J. W. Brooks, G. Eglinton and J. F. Morman, *J. Chem. Soc.*, **1961**, 661.

[24] L. J. Bellamy, "Infrared Spectra of Complex Molecules", Methuen Co., London, 1959, p. 126.

[25] M. Avram and G. D. Mateescu, "Spectroscopia în infraroşu", Ed. tehnică, Bucharest, 1966, p. 502.

Per cent hydrolysis under standard conditions was determined for the new nitrogen mustards according to Ross, [26] and rate constants (k_{66}) were calculated in the hypothesis of unimolecular kinetics.

For derivatives in table 2 it may be pointed out (Fig. 1) a linear correlation between the hydrolysis rate (k_{66}) and Hammett σ_m constants of the substituents, similar to that found by Ross [26] and expressed by the equation :

$$\log k_{66} = -3.97 - 1.63\,\sigma_m \qquad \text{(I)}$$

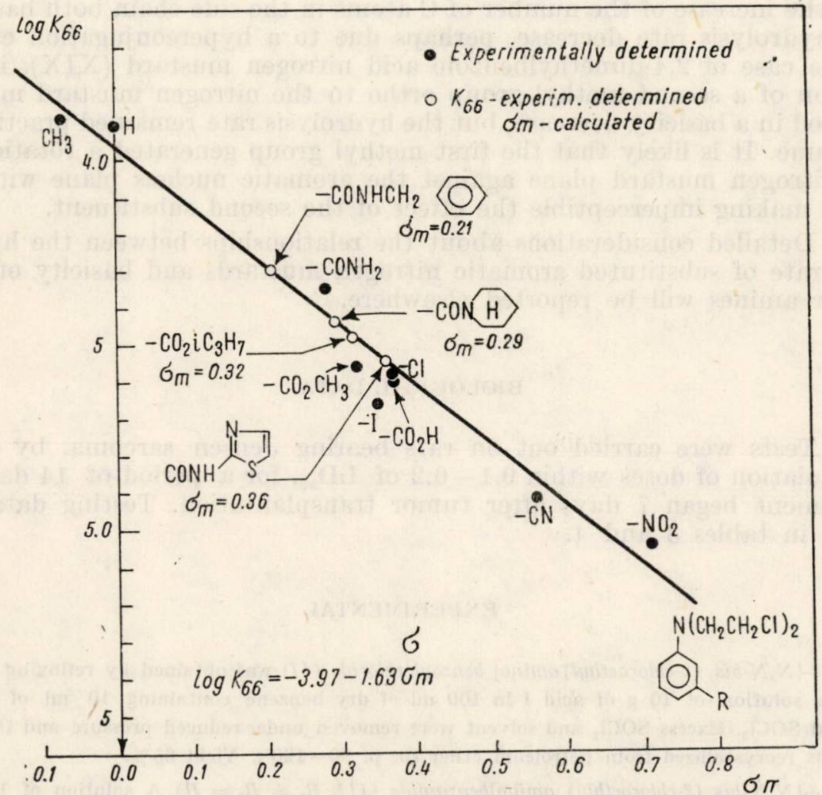

Fig. 1. — Hydrolysis rate-Hammett constants relationship.

From this equation, and by determining experimentally log k_{66}, the σ_m constants of some less usual substituents were calculated :

R	σ_m
N-benzylamide	0.21
piperidylamide	0.30
N-2′-thiazolylamide	0.38
isopropyl ester	0.33

---

[26] W. C. J. Ross, *J. Chem. Soc.*, **1949**, 183.

3-/N, N-bis(2-chloroethyl) amino/-4-methylbenzoic acid (VIII, R = CH_3) is obviously a special case, its hydrolysis rate being much higher than that corresponding to precursor amine basicity. Thus, according to equation I, this compound ($pK_a = 3.34$ and $\Sigma\sigma = 0.42$) should have a hydrolysis of about 6%. Actually, its hydrolysis under standard conditions is 56.9%, the enhancement being accounted for by the steric effect of the ortho-methyl group, resulting in a weakening of the $p-\pi$ conjugation.

In alkyl derivatives this enhancement is maintained; however with the increase of the number of C atoms in the side chain both basicity and hydrolysis rate decrease, perhaps due to a hyperconjugation effect. In the case of 2,4-dimethylbenzoic acid nitrogen mustard (XIX), introduction of a second methyl group ortho to the nitrogen mustard moiety resulted in a basicity decrease, but the hydrolysis rate remained practically the same. It is likely that the first methyl group generated a rotation of the nitrogen mustard plane against the aromatic nucleus plane with an angle making imperceptible the effect of the second substituent.

Detailed considerations about the relationships between the hydrolysis rate of substituted aromatic nitrogen mustards and basicity of precursor amines will be reported elsewhere.

BIOLOGICAL DATA

Tests were carried out on rats bearing Jensen sarcoma, by daily innoculation of doses within 0.1—0.2 of LD_{50}, for a period of 14 days.[27] Treatment began 7 days after tumor transplantation. Testing data are listed in tables 3 and 4.

EXPERIMENTAL

3-[N,N-bis (2-chloroethyl) amino] benzoyl chloride (II) was obtained by refluxing for an hour a solution of 10 g of acid I in 100 ml of dry benzene containing 10 ml of freshly distilled $SOCl_2$. Excess $SOCl_2$ and solvent were removed under reduced pressure and the residue was recrystallized from petroleum ether (b. p. 90—120°). Yield 85%.

3-[N,N-bis (2-chloroethyl) amino]benzamide (III, $R_1 = R_2 = H$). A solution of 10 g of acid chloride II in the minimum amount of dioxane was dropped during 15 min. into a stirred solution of 20 g of NH_4Cl in 200 ml of 10% NH_4OH. The precipitate was collected and recrystallized several times from petroleum ether (b. p. 140—180°) to give the pure amide (Table 2). Yield 71%.

Substituted amides (III). To a solution of 0.01 moles of acid chloride II in 50 ml of anhydrous benzene, 0.02 moles of the respective amine were added with stirring and occasional cooling. The mixture was allowed to stand overnight, the amine hydrochloride filtered off and the amide solution evaporated to dryness in vacuo. The oily residue was purified by :

a) washing with dil. HCl, taking up in benzene, drying the benzene solution (Na_2SO_4), treating with active charcoal and evaporating to dryness under reduced pressure ;

---

[27] V. Dobre, Private communication.

b) column chromatography on alumina, in benzene solution.

Aminoesters. (VIII and XVIII) were prepared in good yield by catalytic hydrogenation (5% Pd/$CaCO_3$, EtOH solution, at room temperature, atmospheric pressure) of the corresponding nitroesters. In the case of compound XVIII, 5% Pt/C was used as catalyst. The theoretical amount of hydrogen was consumed during 0.5—2 hrs. The catalyst was removed by filtration and the solutions evaporated to dryness under reduced pressure. The crude amines were purified by conversion to hydrochlorides and regenerating the free bases. The compounds used as starting materials in the hydroxyethylating reactions are listed in table 5.

Table 5

Aminoesters

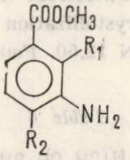

No.	R_1	R_2	m.p. °C	% $N_{calc.}$	% $N_{anal.}$
1	H	CH_3	116	8.48	8.50
2	H	C_2H_5	50—51	7.82	7.87
3	H	n-C_3H_7	63	7.25	7.07
4	H	i-C_3H_7	49—50	7.25	7.19
5	H	t-C_4H_9	oil	6.76	6.65
6	H	CH_3O	84—85	7.73	7.82
7	CH_3	CH_3	oil ¹)	7.82	7.78
8	CH_3	CH_3	148—150²)³)	6.49	6.46

¹) *Calcd.* for $C_{10}H_{13}NO_2$. % : C 67.04; H 7.26 *Found* % : C 66.98; H 7.45
²) Hydrochloride
³) *Calcd.* for $C_{10}H_{14}ClNO_2$% : C 55.68; H 6.49; Cl 16.47. *Found* % : C 55.80; H 6.70; Cl 16.20

4-Isopropyl — and 4-ethylbenzoic acids. 6 g of iodine were added in small portions to a stirred solution of 6.2 g of 4-isopropylacetophenone (V, R = i — C_3H_7) in 20 ml of pyridine. The mixture was refluxed for 1.5 hr and allowed to stand overnight. Excess pyridine removal yielded 10.5 g (75%) of crude product. After several recrystallizations from ethanol : petroleum ether (b. p. 90—120°) and then from water, pure XI (R = i — Pr) was obtained, m.p. 200—202°. *Anal. Calcd.* for $C_{16}H_{18}INO$: % C 52.31, H 4.90, N 3.81, I 35.15. *Found* % : C 52.68, H 5.05, N 3.79, I 34.60.

XI (R = Et) was similarly prepared, m. p. 183—185°C. *Anal. Calcd.* for $C_{15}H_{16}INO$% : C 50.99, H 4.53, N 3.96, I 35.98. *Found* % : C 50.75, H 4.76, N 3.87, I 36.25.

A solution of 2.8 g of XI (R = i — Pr) in 60 ml of water containing 2 g of NaOH was refluxed for an hour. After treatment with active charcoal, the still hot solution was acidified with concd. HCl, giving 0.9 g (81%) of crude i-propylbenzoic acid. Recrystallization from petroleum ether (b. p. 90—120°) gave a product with m. p. 113—4° (lit.[28] 117—8°).

By the same procedure, 4-ethylbenzoic acid was obtained, m. p. 108—110° (lit.[29] 112—3°).

[28] B. Bert, *Bull. Soc. chim. France*, **37**, 1400 (1925).
[29] F. Kindler, *Liebigs Ann. Chem.*, **452**, 102 (1927).

Intermediates in the synthesis of dimethylbenzoic acid nitrogen mustards

As intermediates in the synthesis of nitrogen mustards XVI and XIX, esters XIV, XV, XVII and XVIII (not yet reported) were obtained (for the latter see table 5).

Methyl, 3,5-dinitro-2,4-dimethylbenzoate (XIV) was prepared by esterification with HCl satd. methanol of the respective acid. M. p. 92°C (MeOH). *Anal. Calcd.* for $C_{10}H_{10}N_2O_6$ % : C 47.24 ; H 3.94 ; N 11.02. *Found* % : C 47.56 ; H 4.10 ; N 10.93.

Compound XIV reduction with $(NH_4)_2S$[30] gave *methyl 5-amino-3-nitro-2,4-dimethylbenzoate* (XV) in 80% yield. Mention should be made that, in contrast with the original procedure (reported for 3, 5-dinitrobenzoic acid), on cooling the reaction mixture, compound XV precipitated together with the sulphur impurities. It was recovered from the impure deposit by repeated extractions with hot methanol, wherefrom it crystallized on cooling. The analytical sample, m. p. 185°, was obtained by recrystallization from methanol or toluene. *Anal. Calcd.* for $C_{10}H_{12}N_2O_4$ % : C 53.57 ; H 5.36 ; N 12.50. *Found* % : C 53.35 ; H 5.10 ; N.12.60.

Table 6

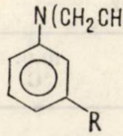

Hydroxyethyl derivatives

No.	R	Formula	m.p. °C	Analysis %	
				$N_{calc.}$	$N_{anal.}$
1	Cl	$C_{10}H_{14}ClNO_2$	86.5−87.5	6.49	6.42
2	J	$C_{10}H_{14}JNO_2$	111.5−112	4.45	4.53
3	NO_2	$C_{10}H_{14}N_2O_4$	100 −102	12.39	11.99
4	CN	$C_{11}H_{14}N_2O_2$	58	13.59	13.44

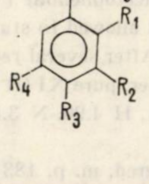

NMOH = $N(CH_2CH_2OH)_2$

No.	R_1	R_2	R_3	R_4	Formula	m.p. °C	Analysis %	
							$N_{calc.}$	$N_{ana..}$
1	H	NMOH	C_2H_5	H	$C_{14}H_{21}NO_4$	oil	5.24	5.13
2	H	NMOH	i-C_3H_7	H	$C_{15}H_{23}NO_4$	oil	4.98	4.86
3	H	NMOH	t-C_4H_9	H	$C_{16}H_{25}NO_4$	oil	4.75	4.70
4	H	NMOH	CH_3O	H	$C_{13}H_{19}NO_5$	oil	5.20	5.07
5	CH_3	NMOH	CH_3	H	$C_{14}H_{21}NO_4$	oil	5.24	5.26
6	CH_3	NO_2	CH_3	NMOH	$C_{14}H_{20}N_2O_6$	81−83	8.98	9.02

---

[30] D. PITRÉ and L. FUMAGALLI, *Farmaco, Ed. Sci.*, **17**, 340 (1962).

Deaminating diazotisation of compound XV[31] gave *methyl 3-nitro-2,4-dimethylbenzoate* (XVII). The analytical sample, m. p. 54–55°, was obtained by distillation under reduced pressure and recrystallization from EtOH. *Anal. Calcd.* for $C_{10}H_{11}NO_4$, %: C 57.41; H 5.26; N 6.69. *Found*, %: C 57.70; H 5.39; N 6.50.

1,2-Di/m-N,N-bis(2-chloroethyl)amino-benzoyl/-hydrazine. A solution of 10 g of acid chloride II in the minimum amount of dioxane was added dropwise to a stirred solution of 20 ml of 95% hydrazine in 200 ml of water. The oily precipitate instantly formed crystallized on trituration. After 1/2 hr standing at room temperature, it was filtered and washed with water. The yield was 5 g (66.5%) after recrystallization from ethanol: benzene.

The hydroxyethyl derivatives were prepared and purified in the usual way[10] (Table 6) Derivatives missing in the table were chlorinated without separation.

Chlorination ($SOCl_2$ or $POCl_3$) and *esters hydrolysis* (concd. HCl) were performed according to our previous works.[10] The resulting nitrogen mustards are listed in tables 2 and 4.

Acknowledgement. The authors wish to thank Mrs. E. Tărnăuceanu, Mrs. G. Botez and Mr. R. Homescu for performing analytical, UV and IR spectra, and Dr. V. Dobre for kindly making the screening data available to us.

---

[31] H. L. Wheeler and C. Hoffman, *Amer. Chem. J.*, **45**, 436 (1911); *Chem. Abstr.*, **5**, 2646 (1911).

Revue Roumaine de Chimie, **14**, 549–553 (1969)

THE MASS SPECTRUM OF ACRIDINE-N-OXIDE

H. H. MANTSCH *
Institute of Chemistry, Cluj, str. Donath, 65

Received November 5, 1968

Upon electron-impact acridine-N-oxide yields ions corresponding to two different degradation sequences. The M—CO fragmentation assumes a skeletal rearrangement of the molecular ion which resembles the photochemical isomerization of acridine-N-oxide in inert solvents.

INTRODUCTION

In connection with current investigations on the photochemistry [1] and reactivity indices [2] of the title compound we became interested also in the electron-impact behaviour of acridine-N-oxide in view of the similarities which could exist between the fragments produced by the dissociation of the positive ions observed in the mass spectrum and those formed by other high energy processes like photolysis or pyrolysis; if such parallels are found they may suggest the existence of common intermediates or common reaction paths.

Indeed, the molecular ion formed by loss of an electron from the neutral molecule is in a highly excited state and is comparable with excited states achieved by photochemical processes. In both cases the bonds within the molecule are weakened on excitation and the relative bond-lability is strongly influencing both the breakdown in the mass spectrum and the course of photochemical reactions.

RESULTS AND DISCUSSION

As shown in the line diagram (figure 1) acridine-N-oxide yields a mass spectrum typical for heterocyclic compounds with a very strong molecular ion peak (M) at m/e 195, which at 45 eV is also the base peak, whereas the intensity of the fragments does not exceed 20%.

As with most heteroaromatic molecules, acridine-N-oxide remains intact even after the loss of a second electron and gives a quite strong doubly charged molecular ion (M/2e) at m/e 97.5.

---

* Present address: National Research Council of Canada, Pure Chemistry Division, Ottawa.

[1] H. H. MANTSCH, V. ZANKER, W. SEIFFERT and G. PRELL, *Liebigs Ann. Chem.*, in press.

[2] H. H. MANTSCH, W. SEIFFERT and V. ZANKER, *Rev. Roumaine Chim.*, **14**, 125 (1969).

The breakdown of the molecular ion follows two different pathways discernible in the line diagram, which are supported by the appearance of appropriate metastable peaks in the mass spectrum.

A first fragmentation mode is the loss of a single oxygen to yield the radical-ion of the basic heterocycle of mass 179 i.e. acridine (metastable peak at m/e 164.70; calculated 164.31), which further undergoes a fragmentation comparable with that of acridine itself.[3a]

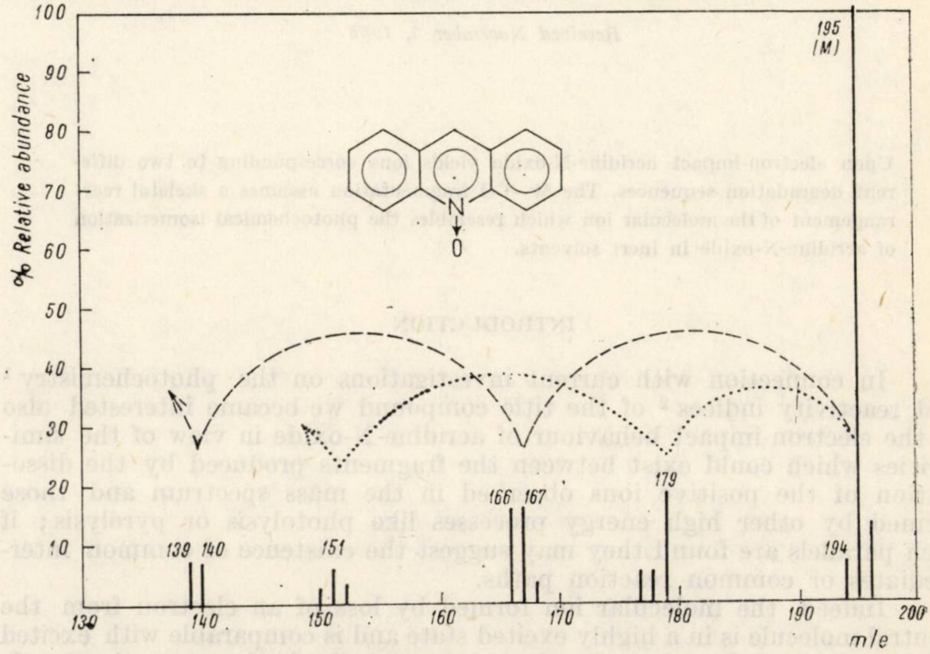

Fig. 1. — The breadkdown pattern of acridine-N-oxide at 45-eV. All fragments with relative intensity higher than 2% are reproduced; *1*, . . . pathway M—O—HCN; *2*, - - - pathway M—CO—HCN.

A second, much more interesting degradation sequence of the same excited molecular ion M consists in the loss of a molecule of carbon monoxide to produce the fragment m/e 167 which corresponds to the carbazole radical-ion (metastable peak at m/e 143.25; calculated 143.02). The decomposition of the quite stable carbazole ion[3b] proceeds by elimination of HCN (metastable peak at m/e 117.50; calculated 117.37) and of a hydrogen radical to produce the mass units m/e 140 resp. 139 and finally by elimination of acetylene, to the ion C_9H_5 (m/e 113). Fairly strong peaks at m/e 69.5; 70; 75.5; 83; 83.5; and 89.5, which stand for doubly charged ions, attest the aromatic character of the fragments shown in the line diagram.

This second degradation mode demands a skeletal rearrangement process with the migration of the N-oxidic oxygen to a carbon atom.

---

[3] "Catalogue of Mass Spectral Data", American Petroleum Institute Research Project 44; Carnegie Institute of Technology, Pittsburgh. *a*) Spectrum No. 639. *b*) Spectrum No. 638.

Similar skeletal rearrangements, including oxygen transfer, have been reported recently by Bowie et al. for the mass spectra of azoxybenzenes [4] and phenazine-N-oxides [5] and by Buchardt et al. [6] for quinoline- and isoquinoline-N-oxides, which apart from the normal loss of oxygen from the molecular ion exhibit pronounced M−CO ions.

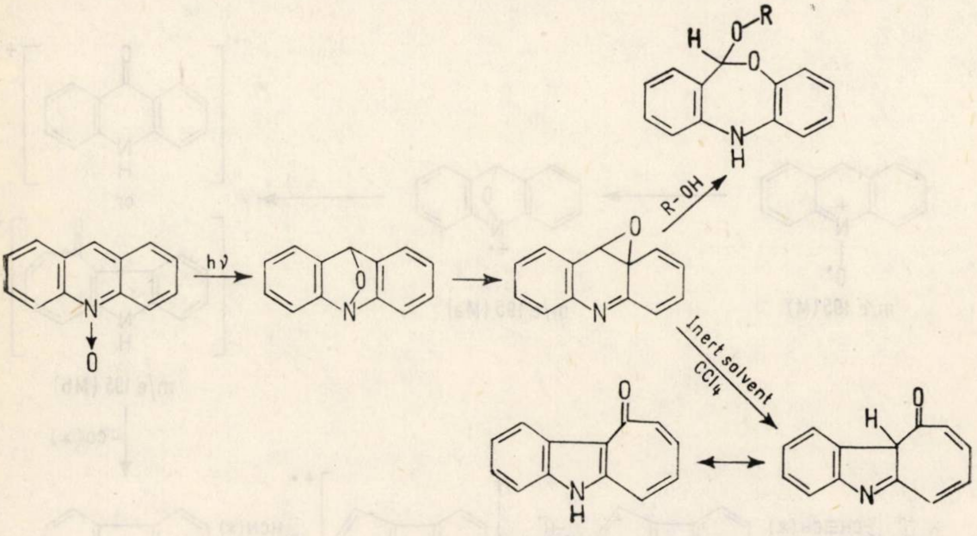

Scheme 1. — Photochemistry of acridine-N-oxide.

If we take now a look at scheme 1 which shows the photochemistry of acridine-N-oxide, it appears that the first step is an intramolecular rearrangement as a result of an electrophilic attack by the oxygen which in the excited states becomes electron-deficient, upon the carbon atom in *para*, which has an increased charge density in both the excited singlet and triplet state. [2] The course of the photochemical reaction depends on the solvent and may yield a photoreduction product in alcohol or a photoisomerization product in inert solvents.

Although the attempt to transfer the results obtained from the photochemical to the electron-impact reactions calls for great care, it seems not unreasonable to admit at least a parallel behaviour for the first step i.e. the transfer of oxygen.

With these observations in mind the following mechanistic rationalization scheme of the M−CO electron-impact degradation could be forwarded (scheme 2).

Before expelling a neutral molecule of carbon monoxide, at least a part of the molecular ion M should undergo a skeletal rearrangement to explain the genesis of the M—CO peak. The endoxide Ma would be a plausible intermediate to yield the carbonyl-containing isomer Mb, which could be represented either as acridone or as cyclohept-[b]-indole-10[5H]-one. [7] In order to support the above considered skeletal rearrangement, we have compared the mass spectrum of acridine-N-oxide with both mass spectra of acridone and cyclohept-[b]-indole-10[5H]-one; the amidone spectrum we could find in the literature, [8] whereas the latter was recorded by us on a sample we obtained by the photoisomerization of acridine-N-oxide in carbon tetrachloride.

---

[4] J. H. Bowie, R. G. Cooks and G. E. Lewis, *Austral. J. Chem.*, **20**, 1601 (1967).

[5] J. H. Bowie, R. G. Cooks, N. C. Jamieson and G. E. Lewis, *Austral. J. Chem.*, **20**, 2547 (1967).

[6] O. Buchardt, A. M. Duffield and R. H. Shapiro, *Tetrahedron*, **24**, 3139 (1968).

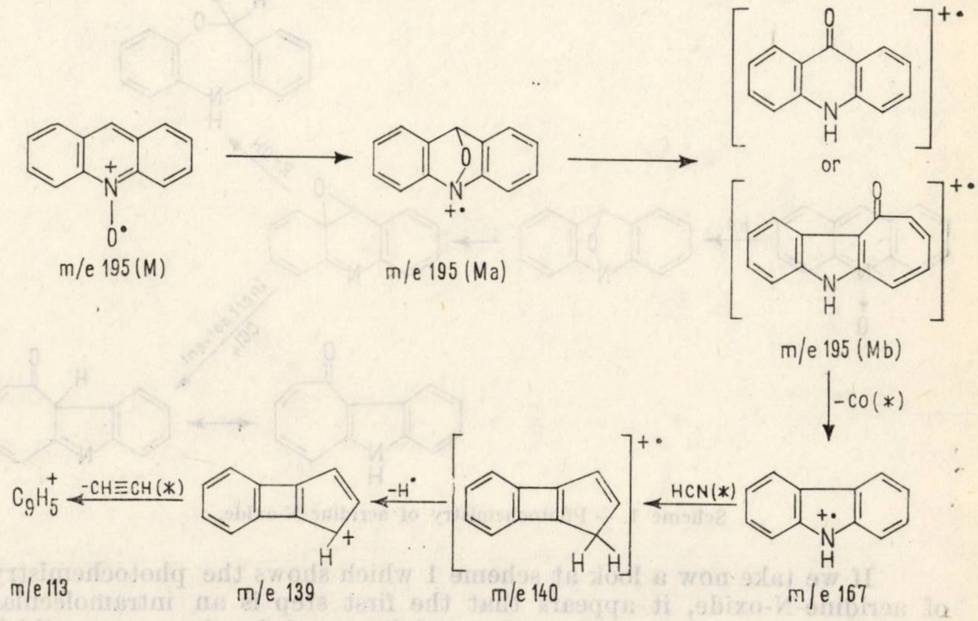

Scheme 2. — Electron-impact degradation scheme of acridine-N-oxide by skeletal rearrangement of the molecular ion; the asteriks denotes the presence of an appropriate metastable ion for the process indicated.

The breakdown pattern of these two structural carbonyl-isomers of acridine-N-oxide, including metastable peaks, is nearly identical with that of acridine-N-oxide, except for the additional M—O fragmentation sequence of the latter. This affords indeed additional support for a partial skeletal rearrangement of the molecular ion of acridine-N-oxide upon electron-impact, which shows a strong resemblance with the photochemical behaviour of this molecule.

---

[7] M. Ishikawa, Ch. Kaneko and S. Yamada, *Tetrahedron Letters*, **43**, 4519 (1968).

[8] J. H. Bowie, R. G. Cooks, R. H. Prager and H. M. Thredgold, *Austral. J. Chem.*, **20**, 1179 (1967).

EXPERIMENTAL

Acridine-N-oxide was prepared by the oxidation of acridine with perbenzoic acid[9] and cyclohept-[b]-indole-10[5H]-one by irradiation[10] of acridine-N-oxide in carbon tetrachloride with a high pressure mercury lamp TQ-700 Hanau.

The mass spectra were determined at 45 eV on an Atlas CH—4 mass spectrometer equipped with the TO—4 ion source, the samples being introduced directly into the ion source.

Acknowledgements. The author is grateful to Dr. Müller and Mr. Aicher for recording the mass spectra of acridine-N-oxide and cyclohept-[b]-indole-10[5H]-one at the Technische Hochschule, Munich.

[9] M. IONESCU, H. MANTSCH and I. GOIA, *Chem. Ber.*, **16**, 1726 (1963).

[10] H. H. MANTSCH and V. ZANKER, unpublished results.

ORSZÁGOS SZAKKÖNYVTÁR ÉS DOKUMENTÁCIÓS KÖZPONT 1883

Revue Roumaine de Chimie, **14**, 549–553 (1969)

10–c. 3085

La REVUE POLONAISE DE [illegible] [illegible] des [illegible] [illegible] [illegible] [illegible] [illegible] [illegible] [illegible] [illegible] [illegible] [illegible] [illegible] [illegible] [illegible]

[illegible] Informatik [illegible] [illegible] [illegible] [illegible] [illegible] [illegible] Verlag [illegible] [illegible] [illegible] [illegible] [illegible] [illegible] [illegible] [illegible] Bruxelles [illegible] Paris [illegible] Paris [illegible] [illegible] [illegible] [illegible] [illegible] [illegible] [illegible] [illegible] [illegible] [illegible] [illegible] [illegible] [illegible] [illegible] [illegible] [illegible] [illegible] Paris [illegible] Bâle [illegible] Mexico

[illegible] [illegible] [illegible] [illegible] [illegible] [illegible] [illegible] [illegible] [illegible] [illegible] [illegible] [illegible] [illegible] [illegible] [illegible] [illegible]

La REVUE ROUMAINE DE CHIMIE paraît 12 fois par an. Le prix d'un abonnement annuel est de £ 5.0.0; $ 12,— ; FF 60,—; DM 48.—. Toute commande de l'étranger (fascicules ou abonnements) sera adressée à CARTIMEX, Boîte postale 134—135, Bucarest, Roumanie, ou à ses représentants à l'étranger :

ALBANIE. **Ndermarja Shtetnore e Botimeve** — Tirana ■ R. D. ALLEMANDE, **Deutscher Buch-Exp. und -Import,** Leninstrasse 16—701 Leipzig ; **W. E. Saarbach,** POB 1510—6, Cologne ■ AUTRICHE, **Globus Buchvertrieb,** Salzgries 16 — Vienne XX ■ BELGIQUE, **Du Monde Entier,** 5, Place St.-Jean — Bruxelles ■ R. P. de BULGARIE, **Raznoiznos,** 1, rue Tzar Assan — Sofia ■ R. P. de CHINE, **Waiven Shudian,** POB 88 — Pékin ■ R. P. D. CORÉENNE, **Chulphanmul** — Pyong-Yang ■ CUBA, **Cubartimpex,** Calle Ermita 48 San Pedro — La Havane ■ ESPAGNE, **Libreria Herder,** Calle de Balmos, 26 — Barcelone ■ ÉTATS-UNIS D'AMÉRIQUE, **Fam. Book Service,** 69 Fifth Avenue Suite 8 F — New York 10003, N.Y.; **Continental Publications,** 111, South Mermanee Ave., St. Louis, Missouri 63105 ■ FINLANDE, **Akateminen Kirjakauppa,** POB 128 — Helsinki ■ FRANCE, **Messageries de la Presse Parisienne,** 111, Rue Réaumur — Paris 2 ■ GRANDE-BRETAGNE, **Collet's Holdings Ltd.,** Denington Industrial Estate, Wellingborough, Northants ■ HONGRIE, **Kultura,** POB 149 — Budapest 62 ■ ISRAËL, **Haiflepac Ltd.,** 11 Arlesoroff Street — Haïfa ; **Lepac,** 15 Rambom Street — Tel-Aviv ■ ITALIE, **So. Co. Lib. Ri. Export-Import,** Piazza Margana 33 — Rome ■ JAPON, **Nauka Ltd.,** 2 Kanda Zimbocho, 2 Chome Kiyoda-ku — Tokyo ■ R. P. MONGOLE, **Mongolgosknigotorg,** Ulan Bator ■ NORVÈGE, **Norsk Bogimport,** POB 3267 — Oslo ■ PAYS-BAS, **Meulenhoff,** Beulingstraat 2 — Amsterdam ■ POLOGNE, **Ruch,** ul. Wilcza 46 — Varsovie ■ PORTUGAL, **Libreria Buchholz,** Avda, Liberdcde — Lisabonne ■ SUÈDE, **D.C. Fritze** Fredgatan 2 — Stockholm 16, ■ SUISSE, **Pinkus & Cie,** Froschaugasse 7 — Zurich ■ TCHÉCOSLOVAQUIE, **Artia,** Ve Smeckach 30 — Prague I ■ U.R.S.S., **Mejdunarodnaïa Kniga,** Moscou — G-200 ■ R. D. VIETNAM, **So. Xunt Nhap, Khap Sach Bao,** Hai Ba Trung 32 — Hanoï ■ **R. S. F.** YOUGOSLAVIE, **Jugoslovenska Knjiga,** Terazije 27 — Belgrade ; **Forum,** Vojvode Misica — Novisad.

En Roumanie vous pourrez vous abonner par les bureaux de poste, chez votre facteur ou directement par les services de presse des entreprises et institutions.

NOTE POUR LES AUTEURS

La *Revue Roumaine de Chimie* publie des articles en anglais, français, russe, allemand ou espagnol. Les auteurs sont priés d'envoyer des articles, notes, communications et comptes rendus inédits.

Les manuscrits seront dactylographiés à deux intervalles. Les tableaux seront dactylographiés sur feuilles séparées, de même que la légende des figures. Les diagrammes seront tracés à l'encre de Chine sur papier calque. Les tableaux et les figures seront numérotés par des chiffres arabes, en nombre strictement nécessaire. Prière de ne pas inscrire les mêmes données dans les tableaux et les figures. Les formules chimiques seront incluses dans le texte ; en outre, elles seront transcrites sur des feuilles séparées. L'ordre des références bibliographiques sera celui de leur mention dans le texte ; le nom de l'auteur sera précédé de l'initiale du prénom ; les publications périodiques seront présentées suivant les prescriptions internationales. Les références seront ajoutées à la fin de l'article ; elles paraîtront comme des notes, au bas de la page. Le texte sera précédé d'un résumé, comprenant 15 lignes au maximum.

L'entière responsabilité du contenu des articles appartient aux auteurs. On publie des articles dus aux collaborateurs roumains ou étrangers. Les auteurs recevront 50 tirés à part.

PRINTED IN ROMANIA

TRAVAUX PARUS AUX ÉDITIONS DE L'ACADÉMIE DE LA RÉPUBLIQUE SOCIALISTE DE ROUMANIE

CORNEL BODEA, **Tratat de biochimie vegetală**, partea I, **Fitochimie** (Traité de biochimie végétale, Ire partie, Phytochimie), Ier vol., 1964, 747 p. + 4 annexes, 2 pl., 41 lei; IIe vol., 1965, 1262 p., 1 pl., 56 lei; IIIe vol., 1967, 773 p., 35 lei.

V. GHEŢIE et V. MICUŞAN, **Analiza imunochimică. Teorie şi practică** (Analyse immunochimique. Théorie et pratique), 1966, 369 p., 28 lei.

SILVIA IONESCU, **Reacţii chimice induse de radiaţiile ionizante** (Réactions chimiques produites par les radiations ionisantes), 1963, 271 p., 15 lei.

MARIETA NICOLAE, **Fizico-chimia proceselor fotografice** (Physico-chimie des processus photographiques), 1964, 426 p. + 4 pl., 35 lei.

R. PORTOCALĂ et L. POPA, **Acizii ribonucleici celulari şi virali** (Les acides ribonucléiques cellulaires et viraux), 1966, 375 p., 8 pl. 26 lei.

D. PURDELA et R. VÎLCEANU, **Chimia compuşilor organici ai fosforului şi ai acizilor lui** (La chimie des composés organiques du phosphore et de ses acides), 1965, 540 p., 37 lei.

CRISTOFOR SIMIONESCU et CLEOPATRA VASILIU-OPREA, **Mecanochimia compuşilor macromoleculari** (La mécanochimie des composés macromoléculaires), 1967, 344 p., 23,50 lei.

I P. „Informaţia" —c. 3085

43426

Lei 15.—

F 1103

R

REVUE ROUMAINE DE CHIMIE

REFERÁLVA

TOME 14
N° 5
Mai 1969

ÉDITIONS DE L'ACADÉMIE DE LA RÉPUBLIQUE SOCIALISTE DE ROUMANIE

Rev. Roumaine Chim. 14, 555–678, Bucarest (1969)

COMITÉ DE RÉDACTION

Rédacteur en chef :

C. D. NENIŢESCU, membre de l'Académie de la République Socialiste de Roumanie

Rédacteurs en chef adjoints :

A. T. BALABAN et V. E. SAHINI, membres correspondants de l'Académie de la République Socialiste de Roumanie

Collège de rédaction :

C. DRĂGULESCU, RALUCA RIPAN, CR. SIMIONESCU, membres de l'Académie de la République Socialiste de Roumanie; EM. BRATU, membre correspondant de l'Académie de la République Socialiste de Roumanie, Pr G. OSTROGOVICH, MARG. AVRAM, F. BADEA, D. MARCHIDAN, D. NEGOIU et D. SĂNDULESCU

Les manuscrits, les livres et les revues proposés en échange, ainsi que toute correspondance seront envoyés à la rédaction :

REVUE ROUMAINE DE CHIMIE

23, str. Dumbrava Roşie, Bucarest, 9, Roumanie

REVUE ROUMAINE DE CHIMIE

Tome 14, N° 5 Mai 1969

Page

V. E. SAHINI and VERONICA TUFOI, Calculation of the intensity of the spin-forbidden absorption band of $[Co(NH_3)_6]^{3+}$ taking the covalence into consideration 557–560

RODICA VÎLCU and I. CIOCĂZANU, The alkaline hydrolysis of the methyl acetate and of the ethyl acetate. II. Rate constants and activation energies from thermochemical data 561–567

I. H. PLONSKI, Contribution to Parsons' treatment "General equations for the kinetics of electrode processes" 569–581

C. DRĂGULESCU, T. SIMIONESCU und HERTA SCHIFF, Extraktion von Titan(IV) mit n-Butanol und Quercetin in Gegenwart von Natriumtrichloracetat . . . . 583–589 ✓

P. SPACU et SILVIA PLOȘTINARU, Etude spectrophotométrique des systèmes $LnCl_3$—rouge acide AV et $LnCl_3$ — calcon 591–598

S. TĂTARU, GH. FILIP et B. DAVID, Adsorption de l'uranium par les résines échangeuses d'ions en présence du chlorate et du perchlorate . . . . 599–604 ✓

L. KÉKEDY and F. MAKKAY, Experimental approach to the characterization of pretreated platinum electrode surfaces. II. Cyclic potential sweep voltammetric study 605–612

L. FEY and JANA RUSU, Spectrophotometric method for the quantitative analysis of *ortho*- and *para*-nitroethylbenzene mixtures 613–618

A. A. BALANDIN, I. HORESCU und A. P. RUDENKO, Kinetic der kontinuierlichen Alkoholdehydrierung an Kupferkatalysatoren bei niedrigem Druck . . . . 619–628 ✓

M. SPINZI et I. V. NICOLESCU, Influence du support sur l'activité et les propriétés électriques du catalyseur Cr_2O_3—Al_2O_3 utilisé dans la réaction de déshydrogénation du *n*-butane en *n*-butènes 629–636

FR. MIHAI, ARIANA MORARU und GR. POP, Untersuchungen über das thermische Verhalten von Cadmiumsalzen einiger Dicarboxylsäuren . . 637–645 ✓

ILEANA LUKÁCS, CONSTANȚA STRUSIEVICI et C. LITEANU, Le pouvoir thermoélectrique des composés $M^{I}_{x} V^{IV}_{x} V^{V}_{2-x} O_5$ (M^{I} = Na, K ; $0 < x \leqslant 1$) 647–651

Rev. Roumaine Chim. 14, 555–678 (1969), Bucarest

Page

D. CRĂCIUNESCU et AL. FRUMA, L'effet du complexe cuivre-diphénylamine sur la décomposition catalytique de l'eau oxygénée . . . . 653—657

LEONIA STOICESCU-CRIVETZ, MARIA BRUMĂ et I. ZUGRĂVESCU, Poly(1,3,4-oxadiazoles). V. La réaction des ditétrazoles avec les diisocyanates . . . . 659—665 ✓

I. VELEA, VICTORIA DIMONIE, E. MELEGA, VALENTINA PROVINCEANU and P. BLENKE, The stereospecific polymerization of 1,3-butadiene. II. The influence of the reaction medium on butadiene polymerization with $AlEt_2Cl-CoCl_2.2Py-H_2O$ catalytic system . . . . 667—672

C. BODEA, I. OPREAN and V. FĂRCĂŞAN, Azlactones of the phenothiazine series. III. Aminolysis of some phenothiazine azlactones . . . . 673—678

Revue Roumaine de Chimie, **14**, 557–560 (1969)

ORSZÁGOS MŰSZAKI KÖNYVTÁR ÉS DOKUMENTÁCIÓS KÖZPONT 1883

CALCULATION OF THE INTENSITY OF THE SPIN-FORBIDDEN ABSORPTION BAND OF $[Co(NH_3)_6]^{3+}$ TAKING THE COVALENCE INTO CONSIDERATION

V. E. SAHINI and VERONICA TUFOI

Institute of Physical Chemistry of the Academy
Dumbrava Roşie 23, Bucharest, Romania

Received November 23, 1968

We calculated the oscillator strength for the transition from the ground state, $^1A_{1g}$, to the triplet state, $^3T_{1g}$, for $[Co(NH_3)_6]^{3+}$ as function of a parameter taking the covalence into consideration.

Most of the Co (III) octahedral diamagnetic complexes have, in the approximation of the ligand strong field theory, the following scheme of levels for $(3d)^6$ configuration.

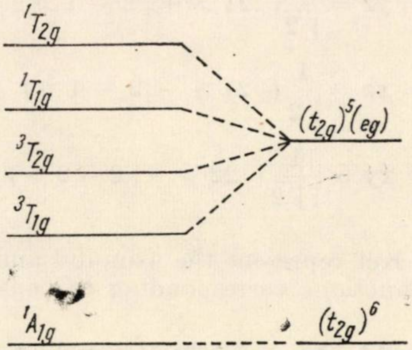

Fig. 1. — Scheme of levels for $(3d)^6$ configuration

The absorption spectrum of these complexes consists generally of two intensive bands, corresponding to the transitions: $^1A_{1g} \rightarrow {}^1T_{1g}$ and $^1A_{1g} \rightarrow {}^1T_{2g}$; other bands corresponding to singlet-triplet transitions may also appear.

The value of the oscillator strength for the spin-allowed bands is satisfactorily explained on the basis of vibronic coupling of even states of the ligand field with odd charge-transfer states.

The intensity of spin-forbidden transitions is due to spin-orbit coupling. In our calculations we shall take into consideration the spin-forbidden transition : ${}^1A_{1g}, \rightarrow {}^3T_{1g}$ of $[Co(NH_3)_6]^{3+}$. The intensity calculation of spin-forbidden bands of transition metals has been performed for $[Ni(H_2O)_6]^{2+}$ by Ballhausen and Liehr,[1] for hydrated salts of Mn by Koide and Pryce[2]; for Co (III) diamagnetic complexes by Ballhausen.[3] In this last calculation the MO—LCAO approximation has been used. Neglecting the overlap between metal and ligand orbitals, the orbitals are considered in the form : $\Psi = \alpha\Psi_{Met} + \beta\Psi_{Lig}$. In the case of the wave functions necessary to the calculation $\beta = \sqrt{1-\alpha^2}$ and Ψ_{Lig} is a linear combination of π orbitals. For $[Co(NH_3)_6]^{3+}$ π-bondings are considered inexistent, i.e. $\alpha = 1$; so that for this complex the covalent effect is not taken into consideration. In the present paper we will consider this very effect. We are considering the Co^{3+} ion placed in a cubic field and we will work in the strong ligand field approximation.

In this case, the considered configuration, d^6 is $t_2{}^6$ and the only corresponding term is ${}^1A_1$. The first excited configuration is $t_2{}^5$ e, having the terms : ${}^1T_1$, ${}^3T_1$, ${}^1T_2$, ${}^3T_2$. The cubic field separates the d orbitals into two sets, e and t_2, whose energies differ by 10 Dq. The wave functions are taken under the form of Slater determinants namely :

$$e\begin{cases}\theta = z^2 = |\,20 > \\ \varepsilon = x^2 - y^2 = \frac{1}{\sqrt{2}}(|\,22 > + |2-2>)\end{cases}$$

$$t_2\begin{cases}\xi = yz = \frac{i}{\sqrt{2}}(|\,21 > + |\,2-1>) \\ \eta = xz = \frac{1}{\sqrt{2}}(|\,21 > - |2-1>) \\ \zeta = xy = \frac{1}{i\sqrt{2}}(|\,22 > - |\,2-2>)\end{cases}$$

where the numbers in Ket represent the asimutal and magnetic quantum numbers. The wave functions corresponding to considered terms are in table 1.

Taking into account the spin-orbital coupling, the ${}^3T_{1g}$ level splits into four levels : Γ_1, Γ_2, Γ_3, Γ_4, ; the ${}^1T_{1g}$ and ${}^1T_{2g}$ levels remain unchanged being, in Bethe's[4] notation, Γ_4 and respectively Γ_5. We shall take into consideration the spin-orbit coupling of ${}^1T_{1g}$ and ${}^1T_{2g}$ states with ${}^3T_{1g}$ state. Therefore, the non-zero matrix elements of spin-orbit coupling will be for the Γ_4 representation between $(\Gamma_4({}^3T_{1g}), \Gamma_4({}^1T_{1g}))$ terms and for the Γ_5 representation between $(\Gamma_5({}^3T_{1g}), \Gamma_5({}^1T_{1g}))$ terms.

---

[1] C. I. Ballhausen and A. D. Liehr, *Mol. Phys.*, **2**, 123 (1959).

[2] S. Koide and M.H.L. Pryce, *Phil. Mag.*, **3**, 607 (1958).

[3] C. I. Ballhausen, *Mol. Phys.*, **6**, 461 (1963).

[4] H. Bethe, *Ann. Phys. Leipzig*, **3**, 133 (1929).

Table 1

The waves functions and matrix elements

Term	Wave function	Element of matrix
$^1A_1$	$\xi^2 \eta^2 \varphi^2$	$-30\ B + 15\ C$
$^1T_1$	$\frac{1}{\sqrt{2}}(\lvert\xi^2 \eta^2 \varphi^+ \varepsilon^- > - \lvert\xi^2 \eta^2 \varphi^- \varepsilon^+ >)$	$-20\ B - 10\ B' + 10\ C + 4C'$
$^3T_1$	$\lvert\xi^2 \eta^2 \varphi^+ \varepsilon^+ >$	$-20\ B - 10B' + 10\ C + 2C'$
$^1T_2$	$\frac{1}{\sqrt{2}}(\lvert\xi^2 \eta^2 \varphi^+ \theta^- > - \lvert\xi^2 \eta^2 \varphi^- \theta^+ >)$	$-20\ B + 6B' + 10C + 4C'$
$^3T_2$	$\lvert\xi^2 \eta^2 \varphi^+ \theta^+ >$	

$B' = B \cos^2\varphi$; $C' = C \cos^2\varphi$

We shall take 600 cm^{-1} as the value of spin-orbit interaction parameter ξ_{3d} for Co^{3+}.[5] The spin-dependent part of the Hamiltonian is:

$$H = \sum_i \frac{1}{2\,m^2c^2} (\mathrm{grad}\ \vec{V}_i \times \vec{p}_i)\ \vec{s}_i$$

where the sum runs over all the electrons and $\vec{V}$ and $\vec{s}$ are, respectively, the potential and the spin moment of the electron. The oscillator strength for the triplet band is:

$$f_{0\to T} = \sum_S f_{0\to S} \frac{E(T)}{E(S)} \cdot \frac{\lvert(T\lvert H\rvert S)\rvert^2}{(E(S) - E(T))^2}$$

where 0 stands for the ground state, T — for the triplet state, S — for different excited singlet states, $f_{0\to S}$ — for the oscillator strength of the $0 \to S$ transition, E(T) and E(S) for the triplet and, respectively, singlet states energies.

The matrix elements $\lvert(T\lvert H\rvert S)\rvert^2$ calculation performed using the functions given above, does not lead to the consideration of the covalence in the case of $[Co(NH_3)_6]^{3+}$ because of the missing of π bands ($\alpha = 1$). Therefore, if the other quantities in the formula of the oscillator strength are taken from experiment, the covalence effect is in no way taken into consideration. To take into consideration the covalence we shall choose the quantities E(T) and E(S) as functions of the Racah's parameters and we shall change the values of these parameters in order to consider the covalence proper effect. We shall consider the covalence effect only for e electrons and, neglecting the ligands contribution to the total wave functions, we shall use the $\theta \cos \varphi$ and $\varepsilon \cos \varphi$ functions instead of θ and ε.

The matrix elements corresponding to the terms considered are quoted in table 1, where: $B' = B \cos^2\varphi$ and $C' = C \cos^2 \varphi$.

---

[5] T. M. Dunn, *Trans. Faraday Soc.*, **57**, 1441 (1961).

Choosing the values of Linhard and Weigel[6] for $f_{0\to S}$, namely: $f_{0\to S}|_{{}^1T_1} = 1.3\times 10^{-3}$ and $f_{0\to S}|_{{}^1T_2} = 1.4\times 10^{-3}$ and the non-zero matrix elements :

$$|(T|H|S)|\,|^2_{{}^1T_1} = \frac{\xi_{3d}}{2\sqrt{2}} \qquad |(T|H|S)|\,|^2_{{}^1T_2} = \frac{\sqrt{3}\,\xi_{3d}}{2\sqrt{2}}$$

and replacing them in the oscillator strength relation, we shall obtain for $f_{0\to T}$ different numerical values in terms of the values of cos φ. The values given to Racah's parameters were : $B = 1115$ cm^{-1}; $C = 4366$ cm^{-1}.[7]

According to the MO–LCAO theory, the functions have the form : $\Psi = \alpha\Psi_{Met} + \beta\Psi_{Lig}$. If we neglect the overlap integral, $\alpha^2 + \beta^2 = 1$. When $\alpha = \beta = \sqrt{1/2}$ we have Pauling's orbitals case; the case $\alpha = 1$; $\beta = 0$ corresponds to the pure ionic case. For $\cos^2\varphi$ the values: 0.5; 0.6; 0.7; 0.8; 0.9; 1 were given, the first and last of them corresponding to the two previous limit cases. The corresponding values of the oscillator strength are quoted in table 2. The experimental value is that obtained in Linhard's measurements, $f = 0.20\times 10^{-5}$. From the table, for Pauling's covalent orbitals there results a negative value for the oscillator strength, therefore this case is not satisfactory. The value $\cos^2\varphi = 0.8$ and the neighbour values : 0.7 and 0.9 give in exchange a good approach to the experimental value.

Table 2

Numerical values of of $f_{0\to T}$

$\cos^2\varphi$	$f_{0\to T}$
0.5	$-0.42.10^{-5}$
0.6	$0.14.10^{-5}$
0.7	$0.19.10^{-5}$
0.8	$0.20.10^{-5}$
0.9	$0.21.10^{-5}$
1	$0.22.10^{-5}$

---

[6] M. Linhard and M. Weigel, *Z. Phys. Chem.* (Frankfurt), **11**, 308 (1957).

[7] J. S. Griffithe, "The Theory of Transition-metal Ions", Cambridge at the University Press, 1964, appendix.

Revue Roumaine de Chimie, **14**, 561–567 (1969)

THE ALKALINE HYDROLYSIS OF THE METHYL ACETATE AND OF THE ETHYL ACETATE. II[1]

RATE CONSTANTS AND ACTIVATION ENERGIE FROM THERMOCHEMICAL DATA

RODICA VÎLCU and I. CIOCĂZANU

Bucharest University, Chair of Physical Chemistry, Bdul Republicii 13, Bucharest

Received May 20, 1968

The hydrolysis rate constants of the methyl and ethyl acetates at various temperatures were deduced from calorimetric measurements, while with the help of Arrhenius relation the activation energies of these reactions were determined.

$$E_{\text{methyl acetate}} = 13{,}900 \pm 100 \text{ cal.mol}^{-1}$$

$$E_{\text{ethyl acetate}} = 14{,}500 \pm 100 \text{ cal.mol}^{-1}$$

INTRODUCTION

Together with the methods using optic, dilatometric, manometric, etc. measurements, the calorimetry represents a method allowing a continuous following of a reaction — when accompanied by thermal effects — during the whole or a part of its evolution. The bond between the thermochemical data and the kinetic elements of a process was exemplified by the alkaline hydrolysis of the methyl and ethyl acetates followed in standard conditions. [1] The validity of the proposed method confirmed also by the results obtained at 25° by other authors, [2,3] allowed us to extend the working procedures to various temperatures so as to obtain a complete characterization of the kinetic quantities characteristic of the chosen reaction.

At a given temperature, the following dependence was established between the thermal effect Q_{t_r} — occurring in a thermochemical reaction at the moment t_r — and the time $(t_r)^1$:

$$Q_{t_r} = Q_0 + (Q_\infty - Q_0)\,\frac{ak_T t_r}{1 + ak_T t_r} \tag{1}$$

---

[1] R. Vîlcu and I. Ciocăzanu, *Rev. Roumaine Chim.*, **14**, 429 (1969).

[2] F. Backer and F. Spalnik f, *Z. phys. Chem. (Frankfurt)*, **26**, **1** (1960).

[3] J. Walker, *Proc. Roy. Soc. A.*, **78**, 160 (1906).

where

Q_0 is the heat amount accompanying the processes preceding the reaction,
Q_∞ is the heat amount developed by the integral transformation of the reactants,
a is the initial concentration of the reactants (under the assumption that the concentrations of the ester and of the alkaline hydroxide are equal), and
k_T is the rate constant of the reaction, at the temperature T.

The constant value corresponding to the chosen temperature is obtained by the analytic and graphic valuation of equation (2), directly deduced from relation (1) :

$$k_T = \frac{1}{\mathrm{tg}\,\alpha}\,[a\,(Q_\infty - Q_0)]^{-1} \tag{2}$$

where

$$\mathrm{tg}\,\alpha = \frac{1}{(Q_\infty - Q_0)\,ak_T}$$

The dependence on temperature of the rate constant is correctly expressed by Arrhenius' equation which gives, generally, reasonable agreements for most of the reactions

$$k = A\,\mathrm{e}^{-E/RT} \tag{3}$$

where E is the activation energy of the process and A is the frequency factor, while the other symbols hold their usual significations.

The systematization of the reaction kinetics data of solutions shows that 1 % at most of the reactions digrees from this law that, on the other hand cannot be considered but as a particular case of more general equations than those established by Trautz [4] or by Berthoud. [5] Relations, strictly deduced from statistical [6] considerations, argue for equations capable of accounting for the variation with temperature of frequency factor A as well as for the activation energy E . Such corrections are however not essential for reactions as those studied by us, while Arrhenius' equation gives a quite good approximation, confirmed by the experimental results.

By virtue of equation (3) that, after applying the logarithms, shows the linear dependence of the rate constant logarithm on the reciprocal of the absolute temperature

$$\log k = \log A - \frac{E}{2{,}303\,RT} \tag{3'}$$

it is possible to deduce the activation energy of the chemical process from the slope of the straight line $-E/2{,}303\ R$, representing the above mentioned dependence. From the same representation, we can value log A, as the ordinate in the origin of the representative straight lines.

The *apparatus* used for the determination is an anisothermal calorimeter, conceived and realized by the authors and described in a previous paper. [1]

EXPERIMENTAL RESULTS

We workerd under the conditions of a reaction kinetics of the second order, the initial concentrations of the reactants being equal to each other. Both the methyl acetate and the ethyl acetate are Merck's products *p.a.*, while the sodium hydroxide is a Chemapol product. From the ester densities and from their measured volumes, we deduced the values of their masses.

---

[4] M. Trautz, *Z. Phys. Chem* (*Leipzig*) **66**, 496 (1909).

[5] A. Berthoud, *J. Chim. phys.* **9**, 382 (1911) ; **10**, 573 (1912) ; **11**, 577 (1913) ; **12**, 564 (1914).

[6] E. A. Moelwyn-Hughes, "The Kinetics of Reactions in solution", 2nd editon, Oxford, Clarendon Press, 1947, p. 53.

The reactions of alkaline hydrolysis of the methyl and ethyl acetates were followed calorimetrically from 16–35° by the procedure described for the measurements in the standard conditions.[1]

The variation of the temperature as a function of time recall the aspect of the curves with maxima obtained at 25°. The position of the extremes of this dependence is a consequence of the reactant amounts as well as of the working temperature.

Tables 1–4 give, in their first two columns, the temperature variation $(\Delta T)_m$ with the time t_r for the considered reactions at the chosen temperatures.

Table 1

Alkaline saponification of the methyl acetate at 15.5°

t_r (s)	ΔT (deg)	$10^4.\beta \int_0^{t_r} \Delta T \, dt$ (deg)	Q_{t_r} (cal)	$10^4 (Q_{t_r} - Q_0)^{-1}$ (cal^{-1})	$10^4 \, t_r^{-1}$ (s^{-1})
0	0	0	—	—	—
45	0.440	42.1	73,49	178.3	222
60	0.512	76.4	85.88	146.0	166
75	0.565	117.4	95.28	128.4	133
90	0.606	160.0	102.86	117.0	111
105	0.635	205.0	108.28	110.0	95.2
120	0.665	252.7	114.04	103.4	83.3
135	0.688	300.9	118.63	98.7	74.0
150	0.708	350.7	112.73	94.9	66.6
165	0.727	401.7	126.66	91.5	60.6
180	0.740	453,8	129.59	89.3	55.5
210	0.758	562.4	134.29	85.5	47.6
240	0.784	673.8	140.33	81.3	41.6
270	0.795	786.9	143.88	79.0	37.0
285	0.798	842.8	145.32	78.1	35.0
315	0.806	958.7	148.37	76.3	31.7
330	0.810	1013.0	149.99	75.4	30.3
360	0.814	1129.4	152.55	73.9	27.2
390	0.815	1246.3	154.44	72.9	25.6
450	0.816	1481.3	158.38	70.9	22.2
465	0.817	1541.1	159.49	70.3	21.5
480	0.816	1600.4	160.27	69.8	20.8
510	0.814	1717.3	161,67	69.3	19.6
540	0.811	1833.7	163.06	68.6	18.5
570	0.806	1948.4	163.95	68.2	17.5
—	—	—	—	—	—
∞(4600)	0.006	7136.13	—	—	—

Table 2

Alkaline saponification of the methyl acetate at 35°

t_r (s)	ΔT (deg)	$10^4 \cdot \beta \int_0^{t_r} \Delta T dt$ (deg)	QT_r (cal)	$10^4(Qt_r - Q_0)^{-1}$ (cal^{-1})	$10^4 t_r^{-1}$ (s^{-1})
0	0	0	—	—	—
75	0.762	203.3	130.57	91.8	133
90	0.793	259.3	136.54	87.1	111
105	0.814	315.8	141.17	83.7	95.2
120	0.829	374.0	144.43	81.4	83.3
135	0.842	433.3	147.60	79.4	74
150	0.847	493.2	149.39	78.3	66.6
165	0.854	553.6	151.51	76.9	60.6
180	0.857	614.5	152.97	76.2	55.5
195	0.861	675.5	154.59	75.2	51.2
210	0.864	737.6	156.04	74.4	47.6
225	0.865	798.0	157.17	73.8	44.4
240	0.865	858.4	158.12	73.3	41.6
330	0.863	1225.2	163.67	69.3	30.3
345	0.861	1285.6	164.29	70.1	28.9
360	0.859	1346.0	164.91	69.8	27.7
375	0.857	1407.0	165.53	67.5	26.6
390	0.854	1466.3	165.98	69.2	25.6
—	—	—	—	—	—
∞(5000)	0.005	0443.5	—	—	—

Table 3

Alkaline saponification of the ethyl acetate at 16°

t_r (s)	ΔT (deg)	$10^4 \cdot \beta \int_0^{t_r} \Delta T$ dt (deg)	Qt_r (cal)	$10^4 (Qt_r - Q_0)^{-1}$ (cal^{-1})	$10^4 t_r^{-1}$ (s^{-1})
0	0	0	—	—	—
75	0.394	87.0	57,83	220.8	133
90	0.437	118.5	64.42	192.8	111
105	0.470	153.5	59.72	174.9	95.2
120	0.499	191.1	74.44	161.6	83.3
135	0.520	228.3	77.85	153.1	74
165	0.567	307.5	85.70	136.7	60.6
195	0.594	391.8	90.80	127.8	51.2
225	0.624	480.4	96.33	119.3	44.4
255	0.646	573.5	100.71	113.4	39.2
285	0.665	668.8	104.66	108.5	35.0
315	0.685	765.3	108.89	103.8	31.7
345	0.700	870.0	112.55	100.0	28.9
375	0.715	975.9	116.06	96.6	26.6
405	0.725	1082.8	118.99	93.9	24.6
435	0.734	1192.5	121.78	91.5	22.9
465	0.740	1302.8	124.14	89.6	21.5
495	0.743	1413,1	126.06	88.1	20.2
525	0.746	1522,8	127.99	86.6	19.0
555	0.749	1635.3	129.91	85.2	18.0
570	0.750	1691,3	130.87	84.5	17.5
585	0.749	1747.3	131.40	84.1	17.0
600	0.749	1803,8	132.21	83.5	16.6
615	0.748	1859,2	132.74	83.2	16.2
660	0.746	1999.4	134.32	82.1	15.1
690	0.742	2108.0	135.24	81.3	14.4
780	0.718	2430.6	136.24	80.0	12.8
—	—	—	—	—	—
∞(5200)	0.005	6573.763	—	—	—

Table 4

Alkaline saponification of the ethyl acetate at 35°

t_r (s)	ΔT (deg)	$10^4.\beta \int_0^{tr} \Delta T dt$ (deg)	Q_{tr} (cal)	$10^4(Q_{tr} - Q_0)^{-1}$ (cal^{-1})	$10^4 t_r{}^{-1}$ (s^{-1})
0	0	0	—	—	—
60	0.540	50.9	77.75	173.2	166
75	0.620	97.7	89.71	143.4	113
90	0.685	143.5	99.67	121.5	111
105	0.722	193.4	105.63	116.8	95.2
120	0.754	246.6	111.16	109.7	83.3
135	0.776	301.4	114.83	105.4	74
150	0.793	357.4	117.92	102.1	66
165	0.809	413.9	121.02	99.0	60.6
180	0.819	471.6	123.25	96.8	55.5
195	0.828	535.8	125.35	93.9	51.2
210	0.838	594.6	127.59	92.9	47.6
240	0.844	713.7	130.07	90.8	41.6
270	0.849	834.0	132.40	88.9	37.0
300	0.851	954.8	134.30	87.5	33.3
315	0.852	1015.2	135,25	86.7	31.7
345	0.851	1134.3	136.72	85.6	28.9
435	0.848	1492,9	141,14	82.5	22.9
465	0.844	1610.9	142.19	81.8	21.5
495	0.840	1730.1	143,23	81.1	20.2
540	0.832	1906,9	144.36	80.4	18.5
—	—	—	—	—	—
∞(5600)	0.008	7421.3	—	—	—

The thermal effects Q_{t_r}, accompanying the reactions in the various stages of their development, were computed by taking into account the heat capacity C ($=$ 165 cal. deg^{-1}) of the system, the heat loss by conduction (according to Newton's law) and the stirring thermal effect 1_0:

$$Q_{t_r} = C\left[\Delta T_m - (\Delta T_0)_m] + \beta\int_0^{t_r} \Delta T_m \mathrm{d}t\right] - l_0 t_t \qquad (4)$$

where

ΔT_m is the temperature difference between the calorimeter and the medium

$(\Delta T_0)_m$ has the same meaning as ΔT_m, but at the initial moment and is assimilated to zero, and

β is the cooling constant of the apparatus.

Particulars concerning the valuation of equation (6) are to found in the preceding paper.[1]

The average values of the secondary thermal effects due to the reactants mixing, to the crushing of the phiol containing the ester and to the mechanical stirring, are given in table 5 which is of on analogous structure with the table giving the same quantities at 25°.[1] Let us remark that the method of estimating the thermal quantities occurring in equations (1) and (4), such as Q_0, Q_∞, 1_0 and C, is fully described in the above mentioned paper.

In table 6 are recorded the rate constants of the chemical processes under study, at the various working temperatures, computed with the help of equation (2).

Table 5

Thermochemical quantities and computation data for the alkaline hydrolysis reaction of the methyl and ethyl acetates

Ester	Temp (°C)	$10^2 a$ (mol. l^{-1})	Q_0 (cal)	Q_∞ (cal)	$10^2 1_0$ (w)	$10^4 . \beta$ (s^{-1})
Methyl acetate	15.5	9.914	17.41	213.44	1.40	5.08
	35	9.913	21.74	145.73	1.40	5.08
Ethyl acetate	16	9.902	12.56	182.80	1.40	5.08
	35	9.894	20.02	116.26	1.40	5.08

Table 6

Rate constants and activation energies for the alkaline hydrolysis reactions of the nethyl and ethyl acetate

Methyl acetate					Ethyl acetate				
k (l. mol^{-1}. $sec.^{-1}$)			E (cal/mol^{-1})		k (l.mol^{-1}. $sec.^{-1}$)			E (cal. mol^{-1})	
$t = 15.5°$	$t = 25°C$	$t = 35°C$	present paper	literature	$t = 16°C$	$t = 25°C$	$t = 35°C$	present paper	literature
0.0989	0.215[1]	0.461	13,900 ±100	12,300 ±300[7] 14,200[8]	0.0506	0.109[1]	0.2412	14.500 ±100	14,800[9] 14,700[8]

The activation energies of the alkaline hydrolysis processes, as deduced from pairs of log k and $1/T$ values, corresponding to the three chosen temperatures, agree satisfactorily with the values found in the literature, as it is easy to see from the comparative data. [7-9]

Figure 1 shows the perfectly linear dependence between $(Q_{t_r} - Q_0)^{-1}$ and the time reciprocal value of the methyl acetate saponification, at various working temperatures (the data for 25° belong to the previously mentioned paper).

A similar dependence is presented by the saponification reaction of the ethyl acetate. During the whole time interval of the reaction, the slope of the curve is invariable, as a result of the perfectly linear succession of the points, which leads to a single rate constant at a given temperature (according to equation (2)).

The synthesis of the experimental data appears in figure 2 which shows the dependence, on the temperature reciprocal, of the rate constant logarithm for both the considered reactions (I — ethyl acetate and II — methyl acetate).

Owing to their position, the three points are sufficient to characterize the representative straight lines. The slope of these lines supplies the activation energy values of the chemical processes, recorded in table 6, beside the most authoritative data from the literature.

The frequency factor A, as deduced from the experimental data, has the value 3.4×10^9 $l.mol^{-1}s^{-1}$ for the saponification reaction of the methyl acetate and 1.3×10^9, $mol^{-1}s^{-1}$ for the hydrolysis of the ethyl acetate. The possibility is foreseen of a statistical calculation of the frequency factor notwithstanding the difficulties met with when valuing the partition functions referring to the reactant molecules. The computation of the relative values [10] of this factor is more accessible, when the methyl acetate molecule is taken as reference. Such a treatment requires however a larger number of reactions, comprizing moreover the alkaline hydrolysis of the higher homologues of the esters in the considered class.

---

[7] L. Smith and H. Olsson, *Z. Phys. Chem. (Leipzig)*., **118**, 99 (1925).

[8] D. P. Evans, J. J. Gordon and H. B. Watson, *J. Chem. Soc.*, **1937**, 1439.

[9] H. A. Smith and H. S. Levenson, *J. Amer. Chem. Soc.*, **61**, 1172 (1933).

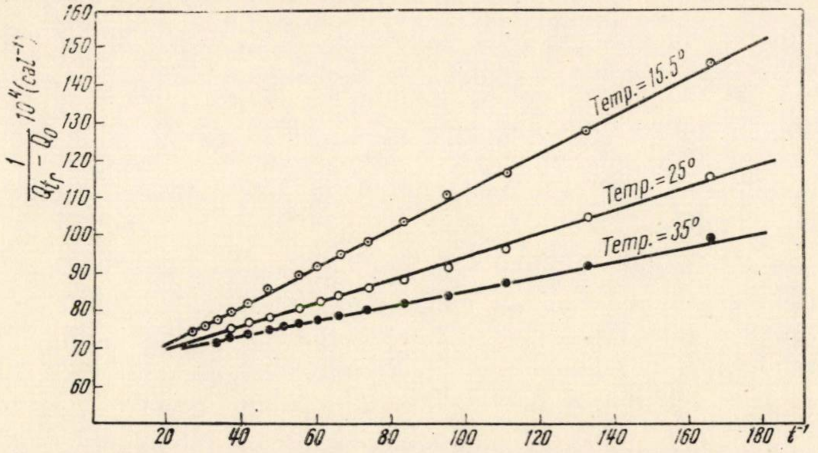

Fig. 1. — Dependence between $(Q_{t_r} - Q_0)^{-1}$ and the time reciprocal value for the hydrolysis of the methyl acetate at 15.5°, 25° and 35°.

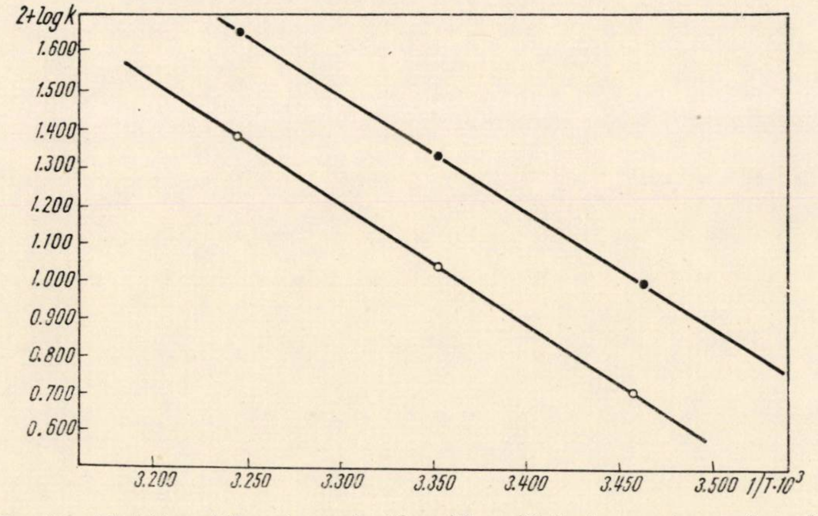

Fig. 2. — Variation of the rate constant logarithm with the temperature reciprocal for the alkaline hydrolysis reactions of the methyl (II) and ethyl (I) acetates.

---

[10] I. G. MURGULESCU and F. BĂRBULESCU, *Rev. Chim. Acad. Romania*, **2**, 153 (1963).

Revue Roumaine de Chimie, **14**, 569–581 (1969)

CONTRIBUTION TO PARSONS' TREATMENT "GENERAL EQUATIONS FOR THE KINETICS OF ELECTRODE PROCESSES"

I. H. PLONSKI

Institute for Atomic Physics, Bucharest, Romania, P.O. Box 35

Received July 11, 1968

The general equations for the kinetics of electrode processes established by Parsons[1] by applying the theory of absolute reaction rates are extended to multielectron electrode processes in which the charge transfer takes place partially after the rate determining step. The same way as Parsons' is followed with the difference that for calculation of the standard electrochemical free energy of formation of one mole of activated complex from the reactants the variation in standard free energy of only the participants in the formation of activated complex is taken into account and not the variation in standard free energy of all reactants involved in the unit of reaction.

Parsons[1] has used the theory of absolute reaction rates in order to obtain general equations for the kinetics of electrode reactions whose applicability facilitates the identification of the rate determining step in a given reaction.

Conway[2] criticized Parsons' equations from several points of view among which their inapplicability to the reaction mechanisms in which the charge transfer takes place partially after the rate determining step, as in the case of anodic oxidation of ammonia.

An attempt is made now to extend Parsons' equations to all mechanisms of multi-electron electrode processes following in steps in which only one stage is the rate determining step.

The stoichiometric equation of the simplest reversible process is represented by

$$xX + bB^{z} + ne^{-} \rightarrow wW + cC^{(bz-n)/c} \tag{1}$$

where x molecules of a species X, w molecules of a species W, b and c ions of a species B and C, respectively, and n electrons taking part in the reaction.

Process (1) or its reverse may occur through several intermediate stages. Assume that the rate of only one of these stages determines the rate of the whole reaction in both directions in the range of considered potentials. In other words, during the transfer of the electrode system from the state represented by the left-hand side of (1) to that represented by the right-hand side of (1) the system passes over several energy barriers, one of which is higher than the remainder (Fig. 1).

---

[1] R. Parsons, *Trans. Faraday Soc.*, **47**, 1332 (1951).

[2] B. E. Conway, "Theory and Principles of Electrode Processes", Modern Concepts in Chemistry Series, Ronald Press, New York, 1965, p. 262.

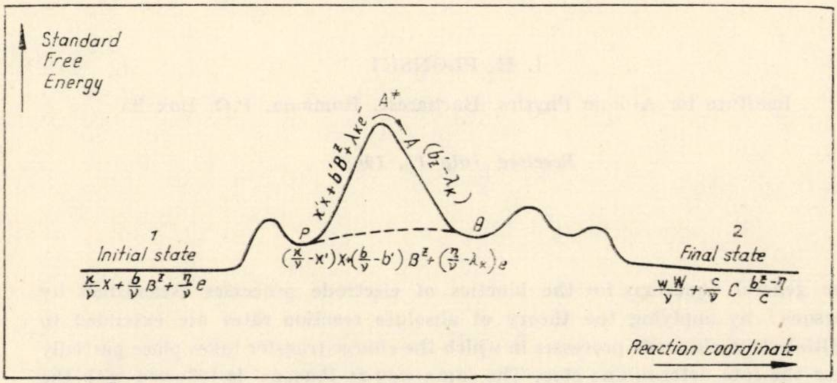
Standard Free Energy
$A^{\neq}$
$x'X + b'B^z + \lambda_k e^-$
$A^{\neq}(bz - \lambda_k)$
1
Initial state
$\frac{x}{\nu}X + \frac{b}{\nu}B^z + \frac{n}{\nu}e$
P
$(\frac{x}{\nu} - x')X + (\frac{b}{\nu} - b')B^z + (\frac{n}{\nu} - \lambda_k)e$
B
2
Final state
$\frac{w}{\nu}W + \frac{c}{\nu}C^{\frac{bz-n}{c}}$
Reaction coordinate

Fig. 1

Fig. 1. — Standard free energy diagram for generalized electrode reaction.

Assuming that the completion of one overall process represented by eqn. (1) may require the formation and the decomposition of ν identical activated complexes ($A^{\neq}$), Parsons stated that the rate-determining reaction can be represented as

$$\frac{x}{\nu}X + \frac{b}{\nu}B^z + \frac{n}{\nu}e^- \rightarrow \frac{w}{\nu}W + \frac{c}{\nu}C^{(bz-n)/c} \qquad (2)$$

with ν as stoichiometric number. The statement that (2) is the equation of the "rate-determining reaction" is debatable. We propose the expression of "rate-determining reaction" for the sum of those successive stages which take part in the formation of activated complex, and which includes as final stage the rate-determining step. Eqn. (2) is the "elementary reaction" (Bockris [3] has employed this term) or the "unit of reaction", and that means the stoichiometric overall reaction equation divided by ν. The stoichiometric number ν represents the number of identical activated complexes ($A^{\neq}$) formed by completion of an overall process represented by eqn. (1) and does not represent the number by which the rate-determining reaction or the rate-determining step must be multiplied in order to give the stoichiometric equation.

Thus, the left-hand side of (2) represents the reactants necessary for one molecule of activated complex to reach the final state. From these, reactants, $x'X$, $b'B^z$, and λ_k e^- take part in the formation of one molecule of activated complex and represents the left-hand side of the rate-determining reaction in cathodic direction:

---

[3] J. O'M. Bockris, "Modern Aspects of Electrochemistry", Butterworths, London, 1954, p. 180.

$$x'X = b'B^z + \lambda_k \, e^- \to A^{(b'z-\lambda_k)} \tag{3}$$

with $A^{(b'z-\lambda_k)}$ the activated complex.

The remaining reactants obtained by subtracting the left-hand side of eqn. (3), from the left-hand side of eqn. (2), namely $\left(\frac{x}{\nu} - x'\right)X$, $\left(\frac{h}{\nu} - b'\right)B^z$ and $\left(\frac{n}{\nu} - \lambda_k\right)e^-$ will reach the final state without taking part in the formation of the activated complex (by a sort of tunnel effect); hence, they will not contribute to the standard electrochemical free energy of activation by the difference between their standard electrochemical free energy in the states $(A^{\neq})$ and (1), because they do not exist in the state $(A^{\neq})$. These reactants will reach the after-rate-determining step by the way represented by dotted line in figure (1).

The mechanism of oxidation of NH_3 (taken by Conway [2] as example to demonstrate that Parsons' derivations are not generally applicable) presents one of these cases. The possible reaction steps are:

$$NH_3 + OH^- \to NH_2 + H_2O + e^- \tag{A}$$

$$NH_2 + OH^- \to NH + H_2O + e^- \tag{B}$$

$$NH + OH^- \to N + H_2O + e^- \tag{C}$$

$$2\,N \to N_2 \tag{D}$$

where $n = 6$. If (A) is the rate-determining step, then $\nu = 2, \frac{n}{\nu} = 3$, but $\lambda_A = 1$, etc.

Similar examples offer the mechanisms (5), (6) and (9) of hydrogen evolution from Parsons [1] paper, illustrated in figures 2 (A), 2(B), and 2(C), respectively.

According to the theory of absolute reaction rates, the rate constant k_1 of an electrochemical reaction will be

$$k_1 = K\frac{kT}{h}\exp\left(-\frac{\Delta\overline{G}^{\neq}}{RT}\right) \tag{4}$$

where k is the Boltzmann constant, h is the Planck constant, K is the transmission coefficient, T absolute temperature and $\Delta\overline{G}^{\neq}$ is the standard electrochemical free energy of formation of one mole of activated complex from the reactants.

The standard electrochemical free energy of formation of one mole of activated complex from the reactants is considered to be the same as the activation energy for the whole reaction.

In the following the standard electrochemical free energy is calculated as in Parsons' treatment but using the eqn. (3) instead of eqn. (2), (Fig. 3).

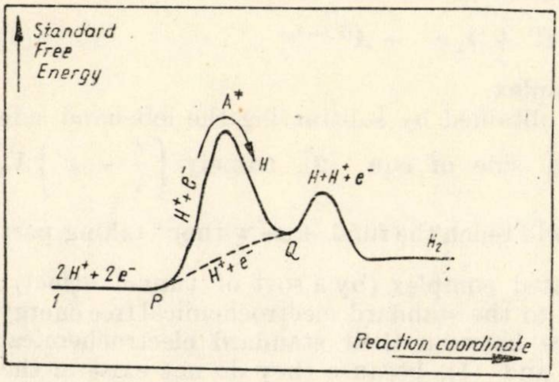
Standard
Free
Energy
A≠
H
H+H⁺+e⁻
H⁺+e⁻
Q
H₂
2H⁺+2e⁻
H⁺+e⁻
1
P
Reaction coordinate

Fig. 2 A. — Standard free energy diagram for the evolution of hydrogen from hydrogen ions; rate controlled by the discharge reaction followed by electrochemical desorption.

$$H^+ + e \rightarrow A^{\neq} \rightarrow H;$$

$$H^+ + H + e \xrightarrow{\text{rapid}} H_2;$$

$$\nu = 1, \frac{n}{\nu} = 2, b' = 1, \lambda_k = 1$$

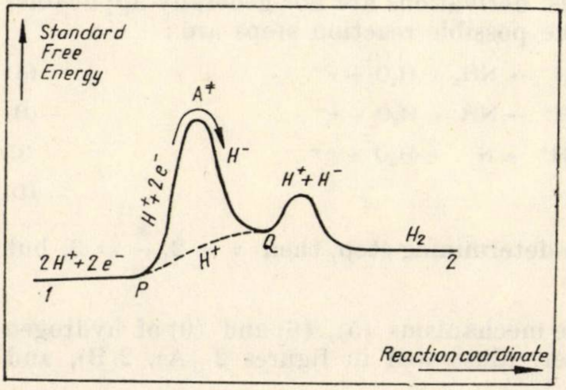
Standard
Free
Energy
A≠
H⁻
H⁺+H⁻
H⁺+2e⁻
Q
H₂
2
H⁺
2H⁺+2e⁻
1
P
Reaction coordinate

Fig. 2 B. — Standard free energy diagram for the evolution of hydrogen from hydrogen ions; rate controlled by the formation of a negative hydrogen ion.

$$H^+ + 2e \rightarrow A^{\neq} \rightarrow H^-;$$

$$H^+ + H^- \xrightarrow{\text{rapid}} H_2;$$

$$\nu = 1, \frac{n}{\nu} = 2; b' = 1, \lambda_k^- = 2.$$

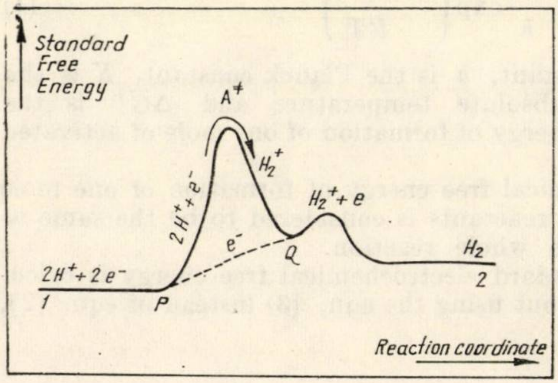
Standard
Free
Energy
A≠
H₂⁺
H₂⁺+e
2H⁺+e⁻
e⁻
Q
H₂
2
2H⁺+2e⁻
1
P
Reaction coordinate

Fig. 2 C. — Standard free energy diagram for the evolution of hydrogen from hydrogen ions; rate controlled by the formation of a molecular hydrogen ion.

$$2H^+ + e \rightarrow A^{\neq} \rightarrow H_2^+;$$

$$H_2^+ + e \xrightarrow{\text{rapid}} H_2;$$

$$\nu = 1, \frac{n}{\nu} = 2, b' = 2, \lambda_k = 1$$

The standard electrochemical potential $\overline{\mu}_1^0$ of the state represented by the left side of eqn. (3) (state 1) is written as

$$\overline{\mu}_1^0 = \mu_1^0 + b'z\,\Phi_s F - \lambda_k \Phi_M F \tag{5}$$

The standard electrochemical potentials of the states P and Q immediately before and after the activated state, respectively, i.e. the states corresponding to the minima P and Q in figure 3, are written as

$$\overline{\mu}_P^0 = \mu_P^0 + b'z\Phi_s F - \lambda_k \Phi_M F + p \tag{6}$$

and

$$\overline{\mu}_Q^0 = \mu_Q^0 + (b'z - \lambda_k)\,\Phi_s F \tag{7}$$

where p is different from the p in Parsons' paper and means the electrical part of the standard free energy required to transfer the reactants necessary to form one mole of activated complex from the state 1 to the state P.

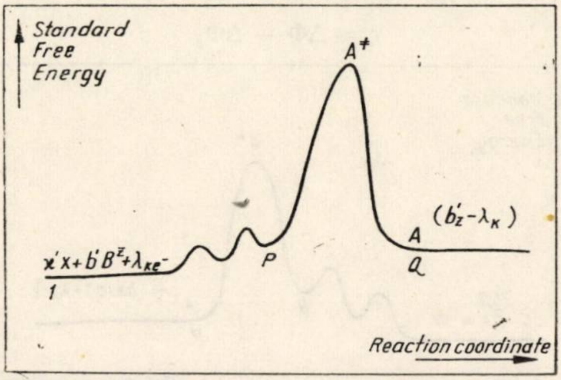

Fig. 3 A. — Standard free energy diagram for the formation of activated complex in cathodic direction.

When $b'z = \lambda_k$, the activated complex is a neutral molecule and the electrical term is zero in eqn. (7).

The electrical contribution to the standard free energy of the activated state (A) lies between that to the standard free energy of the state P and that to the standard free energy of the state Q, i.e.

$$(\overline{\mu}_A^0 - \mu_A^0) - (\overline{\mu}_P^0 - \mu_P^0) = \beta\,[(\overline{\mu}_Q^0 - \mu_Q^0) - (\overline{\mu}_P^0 - \mu_P^0)] \tag{8}$$

where $0 < \beta < 1$ and β depends on the symmetry of the barrier PAQ, $\overline{\mu}_A^0$ is the standard electrochemical potential and μ_A^0 is the standard chemical potential of the activated state.

Substitution of (6) and (7) in (8) leads to an equation for the standard electrochemical potential of the activated state

$$\overline{\mu}_A^0 = \mu_A^0 + b'z\Phi_s F - \lambda_k \Phi_M F + (1 - \beta)\,p + \lambda_k \Delta\Phi F \tag{9}$$

where

$$\Delta\Phi = \Phi_M - \Phi_s \tag{10}$$

Subtracting (5) from (9), we obtain the standard electrochemical free energy of activation for the forward direction of (3), that is,

$$\Delta\overline{G}_1^{\neq} = \overline{\mu}_A^0 - \overline{\mu}_1^0 = \Delta G_1^{\neq} + (1-\beta)\,p + \lambda_k \beta\,\Delta\Phi F \tag{11}$$

where $\Delta G_1^{\neq}$ is the standard chemical free energy of activation for the forward direction.

As the completion of the reaction (2) needs $\frac{n}{\nu}\,\mathrm{e}^-$, $\frac{x}{\nu}\,X$, and $\frac{bB^z}{\nu}$, we can write the actual rate of the reaction as

$$\vec{i} = \frac{n}{\nu} F a_X^{x/\nu}\, a_B^{b/\nu} \vec{K} \frac{kT}{h} \exp\left(-\frac{\Delta G_1^{\neq} + (1-\beta)\,p + \lambda_k \beta\,\Delta\Phi F}{RT}\right) \tag{12}$$

Using the definition of overpotential η,

$$\eta = \Delta\Phi - \Delta\Phi_r \tag{13}$$

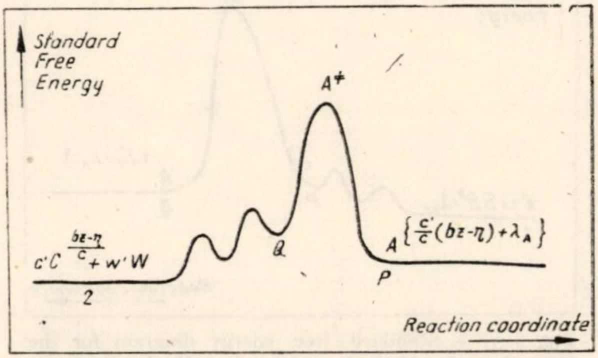
Standard
Free
Energy
$A^{\neq}$
$c'C^{\frac{bz-\eta}{c}} + w'W$
2
Q
$A\left\{\frac{c'}{c}(bz-\eta)+\lambda_A\right\}$
P
Reaction coordinate

Fig. 3B. — Standard free energy diagram for the formation of activated complex in anodic direction.

where $\Delta\Phi_r$ is the value of $\Delta\Phi$ when the reaction is at equilibrium, we obtain

$$\left(\frac{\partial \eta}{\partial \ln \vec{i}}\right)_{T,a} = -\frac{RT}{\beta\lambda_k F} - \frac{(1-\beta)}{\beta\lambda_k F}\left(\frac{\partial p}{\partial \ln \vec{i}}\right)_{T,a} \tag{14}$$

Eqn. (14) is thus valid for all mechanisms of hydrogen evolution and for multielectrons reactions following in steps.

The values of $\frac{x}{\nu}$, $\frac{b}{\nu}$, $\frac{w}{\nu}$, and $\frac{c}{\nu}$, may be obtained from the equation (12) in the usual way from the order of the reaction (2) with respect to the species X, B, W and C, respectively.

$$\left(\frac{\partial \ln \vec{i}}{\partial \ln a_B}\right)_{\Delta\Phi, T, a_X \ldots} = \frac{b}{\nu} - \frac{(1-\beta)}{RT}\left(\frac{\partial p}{\partial \ln a_B}\right)_{\Delta\Phi, T, a_X \ldots} \tag{15}$$

Now, for the anodic direction the standard free energy diagram for the formation of one mole of activated complex from reactants is represented by figure 3B.

In figure 3_B, λ_A is the number of electrons gained by the electrode for the formation of one mole of the activated complex in anodic process.

Following the similar way as for cathodic direction, we have,

$$\overline{\mu}_2^0 = \frac{c'}{c}(bz-n)\,\Phi_s F \tag{16}$$

$$\overline{\mu}_Q^0 = \frac{c'}{c}(bz-n)\,\Phi_s F + q \tag{17}$$

$$\overline{\mu}_P^0 = \left[\frac{c'}{c}(bz-n) + \lambda_A\right]\Phi_s F - \lambda_A \Phi_M F \tag{18}$$

$$\Delta\overline{G}_2^0 = \overline{\mu}_A^0 - \overline{\mu}_2^0 = \overline{\mu}_Q^0 - \overline{\mu}_2^0 + (1-\beta)(\overline{\mu}_P^0 - \overline{\mu}_Q^0) = \beta_q + \\ + (\beta-1)\,\lambda_A \Delta\Phi F. \tag{19}$$

$$\left(\frac{\partial\eta}{\partial \ln \overleftarrow{i}}\right)_{T,a} = -\frac{RT}{(\beta-1)\lambda_A F} - \frac{\beta}{(\beta-1)\lambda_A F}\left(\frac{\partial q}{\partial \ln \overrightarrow{i}}\right)_{T,a} \tag{20}$$

When there is no double layer effect, that is when the Helmholtz double layer potential ψ is zero, we have

$$p = \left(\frac{n}{\nu} - \lambda_A\right)\Delta\Phi F \tag{21}$$

and

$$q = -\left(\frac{n}{\nu} - \lambda_k\right)\Delta\Phi F \tag{22}$$

Therefore, when $\dfrac{\beta q + (\beta-1)\,\lambda_A \eta F}{RT} \ll 1$ and $\dfrac{(1-\beta)\,p + \beta\lambda_k \eta F}{RT} \ll 1$ we have

$$i_k = i_0\left\{-(1-\beta)\left(\frac{n}{\nu} - \lambda_A\right) - \beta\lambda_k - \left(\frac{n}{\nu} - \lambda_k\right) - (1-\beta)\,\lambda_A\right\}\frac{\eta F}{RT} = \\ = -\,i_0 \frac{n}{\nu}\frac{F}{RT}\eta \tag{23}$$

From (23) we obtain

$$\frac{n}{\nu} = -\frac{RT}{Fi_0}\left(\frac{\partial i_k}{\partial \eta}\right)_{\eta\to 0} \tag{24}$$

The eqn. (24) is equivalent to eqn. (39). from Parsons'paper. Furthermore, Parsons divided the sum of the terms containing p and q into two parts, one of which is a linear function of electrode-solution potential difference independent of the composition of the solution, the other being independent of $\Delta\,\Phi$ but dependent upon the composition of the solution, i.e.

$$(1-\beta)\,p + \beta q = \delta + \gamma\frac{n}{\nu}\,\Delta\Phi F \tag{25}$$

where γ is a constant and δ may be a function of the solution composition. The corresponding equation of (25) will be now

$$(1-\beta)\,p = \delta + \gamma\lambda_k \Delta\Phi F \tag{26}$$

In his book "Theory and Principles of Electrode Processes" Conway[2] considered three of the mechanisms for hydrogen evolution

(A) $e^- + H^+ \rightleftarrows H$ (B) $e^- + H^+ \rightleftarrows H$ (C) $H^+ + e^- \xrightarrow{\text{rds}} H$

$H \xrightarrow{\text{rds}} 1/2\ H_2$ $H + H^+ + e^- \xrightarrow{\text{rds}} H_2$ $H^+ + e^- + H \rightleftarrows H_2$

with $\lambda_k = 1$, $\lambda_k = 2$, and $\lambda_k = 1$ respectively for (A), (B), and (C).

From eqn. (14) and (26), the corresponding values of $\left(\dfrac{\partial\eta}{\partial \ln \vec{i}}\right)_{T,a}$ For the first mechanism (A) will be

$$b_A = \frac{RT}{F}\,\frac{1}{(\beta+\gamma)} = \frac{RT}{F} \tag{27}$$

Hence, $\beta + \gamma = 1$. As $\beta = 0.5$ then $\gamma = 0.5$. (The symmetry factor $\beta = 0.5 \neq 1$, because for equilibrium processes the barrier of energy remains a symmetrical one.)

For the second mechanism (B) we have

$$b_B = \frac{RT}{F}\,\frac{1}{2\,(\beta+\gamma)} = \frac{RT}{(1+\beta)\,F} \tag{28}$$

As $\beta = 0.5$, then $\gamma = 0.25$.

Conway [2] stated that as the rapid stages of both mechanisms (A) and (B) are the same, the γ's must also have the same value. This is not necessary. The p's must be the same in both cases. According to eqn. (25) γ is a function of β, p, and λ_k. In both cases β and p are identical, $\beta = 0.5$, $p_{(A)} = p_{(B)} = \Delta\Phi F$. But $\lambda_{(A)} = 1$ and $\lambda_{(B)} = 2$.

When $\delta = 0$, eqn. (25) is reduced to

$$\gamma = \frac{(1-\beta)\,p}{\lambda_k\,\Delta\Phi F} = \frac{(1-\beta)}{\lambda} \tag{29}$$

and consequently

$$\gamma_A = 0.5 \neq \gamma_{(B)} = 0.25$$

For the mechanism (C)

$$b_C = \frac{RT}{(\beta+\gamma)} = \frac{RT}{F}\,\frac{1}{\beta} \tag{30}$$

and $\gamma = 0$. The p is necessarily zero because there are no other process at equilibrium before the rate-determining step which could modified the standard electrochemial potential between the state 1 and the state P. (This is valid for $\psi = 0$).

The overall process of hydrogen evolution

$$2H^+ + 2e^- \rightleftharpoons H_2$$

may be regarded as a two-electron electrode reaction proceeding in steps.

Using the formula established by Vetter[4] one year later for two-electron electrode reaction following in steps, the same values for b_B and b_C have been obtained by applying the eq. (12).

Writing the net cathodic current i as

$$i = \vec{i} - \overleftarrow{i} = -2i_{o,O}\, e^{-\frac{(1-\alpha_0)F\eta}{RT}} \cdot \frac{1 - e^{2F\eta/RT}}{1 + \frac{i_{o,O}}{i_{o,B}} \cdot e^{(1+\alpha_0-\alpha_B)F\eta/RT}} \tag{31}$$

(that is the formula 2.66[5]) we will consider it equal to the cathodic current i when working at sufficiently high cathodic overvoltage. In equation (31), $i_{o.O}$ and $i_{o.B}$ are the exchange currents and α_o and α_B are the transfer coefficients in cathodic direction corresponding to the first and second step, respectively.

In the case of mechanism (B), we can consider $i_{o.O} \gg i_{o.B}$ Then,

$$\vec{i} = -2i_{o.B} \cdot e^{-(2-\alpha_B)F\eta/RT} \tag{32}$$

and

$$\left(\frac{\partial \eta}{\partial \ln \vec{i}}\right)_B = b_B = \frac{RT}{(2-\alpha_B)F} = \frac{RT}{(1+\beta)F} \qquad \text{(33) (see eq. (28)).}$$

because in Vetter's notation $\beta = 1 - \alpha$.

In the case of mechanism (C) we have $i_{o.O} \ll i_{o.B}$, and hence

$$\vec{i} = -2i_{o.O} \cdot e^{-(1-\alpha_0)F\eta/RT} \tag{34}$$

and

$$\left(\frac{\partial \eta}{\partial \ln \vec{i}}\right)_C = b_C = \frac{RT}{(1-\alpha_0)F} = \frac{RT}{F}\,\frac{1}{\beta} \qquad \text{(35) (see eq. (30))}$$

In the case of mechanism (A), (rapid, discharge followed by slow catalytic desorption), the electron transfer takes place in only one step at equilibrium. The rate of the overall reaction $\vec{i}$ in cathodic direction will be determined by disappearance rate of intermediate atom H whose concentration is related to H^+ concentration through the equilibrium constant K_{eq} of the first stage under the condition of the existence of η overpotential. That is

$$i = Fk\,[H]_\eta = kF\,[H^+]\,K_{eq} = kF\,[H^+]\frac{\vec{k}}{\overleftarrow{k}} \tag{36}$$

where $\vec{k}$ and $\overleftarrow{k}$, the rate constants of the first step in cathodic and anodic directions at the overvoltage η, and k is a constant connected with the pure chemical particularities of the slow catalytic combination. Then we can write

---

[4] K. J. Vetter, *Z. Naturforsch.*, **7a**, 328 (1952); **8a**, 823 (1953).

$$i = kF\,[\mathrm{H}^+]\frac{\vec{K}\dfrac{kT}{h}\,\mathrm{e}^{-\Delta G_1^{\neq}/RT}}{\overleftarrow{K}\dfrac{kT}{h}\,\mathrm{e}^{-\Delta G_2^{\neq}/RT}}\cdot\frac{\mathrm{e}^{-\beta F\Delta\Phi/RT}}{\mathrm{e}^{-(1-\beta)F\Delta\Phi/RT}} = k'[\mathrm{H}^+]\,\mathrm{e}^{-F\Delta\Phi/RT} \tag{37}$$

where $\vec{K}$ and $\overleftarrow{K}$, the transmission coefficients and $\Delta G_1^{\neq}$ and $\Delta G_2^{\neq}$ the standard chemical free energy for the cathodic and anodic directions of the first step.

It results from eq. (37)

$$\left(\frac{\partial\eta}{\partial \ln \vec{i}}\right)_A = b_A = \frac{RT}{F} \qquad \text{(38) (see eq. (27))}$$

(If we consider the mechanism (A) as

$$2\mathrm{H}^+ + 2\mathrm{e}^- \rightleftarrows 2\mathrm{H}$$
$$2\mathrm{H} \xrightarrow{rds} \mathrm{H}_2$$

then, $\lambda_k = 2,\ b_A = \dfrac{RT}{2F} = \dfrac{RT\,\nu}{F(\beta+\gamma)n} = \dfrac{RT}{\lambda_k F(\beta+\gamma)} = \dfrac{RT}{2F(\beta+\gamma)}$

with $\beta = \gamma = 0.5$. In this case the first steps of the mechanisms (A) and (B) are not the same: $\lambda_k = 2$ in both cases but the p's are different: $p_A = 2\,\Delta\Phi F$ and $p_B = \Delta\Phi F$).

Observation on the kinetical equation of electrode processes under the influence of double layer potential

A lot of supplementary information on the mechanism of electron transfer and on the localisation of reaction steps can be obtained by studying the influence of the double layer potential Ψ on the kinetical equation.

But, the introduction of the Ψ effect must be made taking into account its influence in every stage before the rate determining stage. The introduction of the Ψ potential in the final equation of the overall reaction can give an equation which is not strictly valid.

Two cases of hydrogen evolution through the mechanism named "slow electrochemical reaction" (mechanism (8) from Parsons' paper)

$$2\mathrm{H}^+ + 2\mathrm{e}^- \overset{\text{rapid}}{\rightleftarrows} \mathrm{H}^+ + \mathrm{e}^- + \mathrm{H} \longrightarrow \mathrm{A}^{\neq} \longrightarrow \mathrm{H}_2$$

are taken as examples in order to illustrate this fact.

(A). The first step of electrochemical reaction takes place in the double layer and the second step after the adsorption of the ions on the electrode. The standard free energy diagram for this mechanism is represented by figure 4 A.

$$2\mathrm{H}^+ + 2\mathrm{e}^- \overset{\text{rapid}}{\rightleftarrows} 2\mathrm{H}^+_{(\psi)} + 2\mathrm{e}^- \qquad \text{I}$$

$$2\mathrm{H}^+_{(\psi)} + 2\mathrm{e}^- \overset{\text{rapid}}{\rightleftarrows} \mathrm{H}^+_{(\psi)} + 1\mathrm{e}^- + \mathrm{H} \qquad \text{II}$$

$$\mathrm{H}^+_{(\psi)} + 1\mathrm{e}^- + \mathrm{H} \overset{\text{rapid}}{\rightleftarrows} \mathrm{H}^+_{(\mathrm{ads})} + 1\mathrm{e}^- + \mathrm{H}_{(\mathrm{ads})} \qquad \text{III}$$

$$\mathrm{H}_{(\mathrm{ads})} + \mathrm{H}^+_{(\mathrm{ads})} + 1\mathrm{e}^- \xrightarrow{\text{r.d.s.}} \mathrm{H}_2 \qquad \text{IV}$$

The current density-potential relationship for the whole reaction can be written as

$$\vec{i} = 2Fk_{\mathrm{I}}^{A}[\mathrm{H}][\mathrm{H}_{\mathrm{ads}}^{+}]\,\mathrm{e}^{-\beta F\Delta\Phi/RT} \tag{39}$$

when the fourth step is the rate determining step. In eq. (39), [H] and $[\mathrm{H}_{\mathrm{ads}}^{+}]$ represent the concentration of hydrogen atom and ion, respectively, in the reaction cell of the rate determining step, and $k_{\mathrm{I}}^{A}\cdot\mathrm{e}^{-\beta F\Delta\Phi/RT}$ is here the rate constant of the rate determining step.

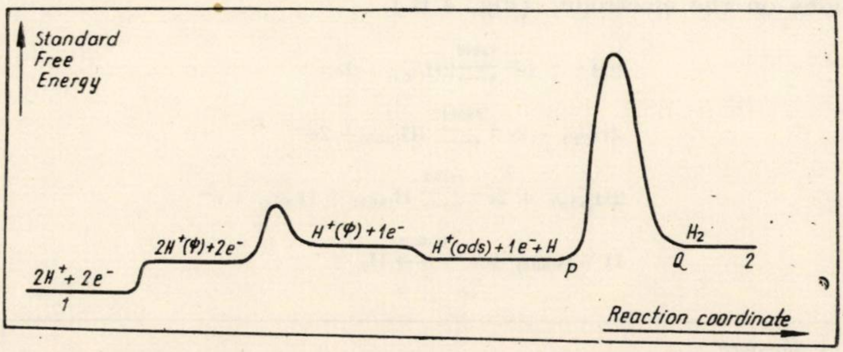

Fig. 4A. – Standard free energy diagram for the evolution of hydrogen when the first rapid electrochemical discharge takes place in the double layer.

But, H is the product of the first and second equilibrium step,

$$\mathrm{H}^{+} + 1\,\mathrm{e}^{-} \rightleftharpoons \mathrm{H}_{(\Psi)}^{+} + 1\mathrm{e}^{-} \underset{\overleftarrow{k}_1}{\overset{\vec{k}_1}{\rightleftharpoons}} \mathrm{H},$$

where $\vec{k}_1$ and $\overleftarrow{k}_1$ are the rate constants for the cathodic and anodic directions of the second step; consequently, taking into account the Ψ effect on the concentration of the ions and on the potential, we can write

$$[\mathrm{H}_{(\Psi)}^{+}] = [\mathrm{H}^{+}]\,\mathrm{e}^{-\Psi F/RT} \tag{40}$$

In eq. (40), $[\mathrm{H}^{+}]$ means the hydrogen ion concentration in the bulk of the solution and $[\mathrm{H}_{(\Psi)}^{+}]$, the concentration of the ions in the double layer. Hence,

$$[\mathrm{H}] = K_{eqA}[\mathrm{H}_{(\Psi)}^{+}] = k_{A}'' \frac{\mathrm{e}^{-\beta(\Delta\Phi-\Psi)F/RT}}{\mathrm{e}^{-(1-\beta)(\Delta\Phi-\Psi)F/RT}}[\mathrm{H}^{+}]\,\mathrm{e}^{-\Psi F/RT} = k_{A}''[\mathrm{H}^{+}]\,\mathrm{e}^{-\Delta\Phi F/RT} \tag{41}$$

when k_{A}'' is that fraction of equilibrium constant K_{eqA} concerning terms which do not depend on the potentials ΔΦ or Ψ.

On the other hand, $[\mathrm{H}_{\mathrm{ads}}^{+}]$ is in equilibrium with $[\mathrm{H}_{(\Psi)}^{+}]$ and we have again a concentration effect of the double layer potential, that is

$$[\mathrm{H}_{(\mathrm{ads})}^{+}] \rightleftharpoons k_{\mathrm{II}}^{A}[\mathrm{H}_{(\Psi)}^{+}] \rightleftharpoons k_{\mathrm{III}}^{A}[\mathrm{H}^{+}]\,\mathrm{e}^{-\Psi F/RT} \tag{42}$$

with k^A_{II} and k^A_{III} the proportionality constants. By introduction of (41) and (42) in (39) we obtain the complete equation of this mechanism,

$$i = 2Fk^A [H^+]^2 e^{-(1+\beta)F\Delta\Phi/RF} \cdot e^{-\Psi F/RT} \tag{43}$$

with $k^A = k^A_I \cdot k''_A \cdot k^A_{III}$.

(B). The first electrochemical step takes place after the adsorption of the ions on the electrode, (Fig. 4 B)

$$2H^+ + 2e^- \xrightleftharpoons{\text{rapid}} 2H^+_{(\Psi)} + 2e^- \qquad \text{I}$$

$$2H^+_{(\Psi)} + 2e^- \xrightleftharpoons{\text{rapid}} 2H^+_{(ads)} + 2e^- \qquad \text{II}$$

$$2H^+_{(ads)} + 2e^- \xrightleftharpoons{\text{rapid}} H_{(ads)} + H^+_{(ads)} + e^- \qquad \text{III}$$

$$H + H^+_{(ads)} + e^- \xrightarrow{\text{r. d. s.}} H_2 \qquad \text{IV}$$

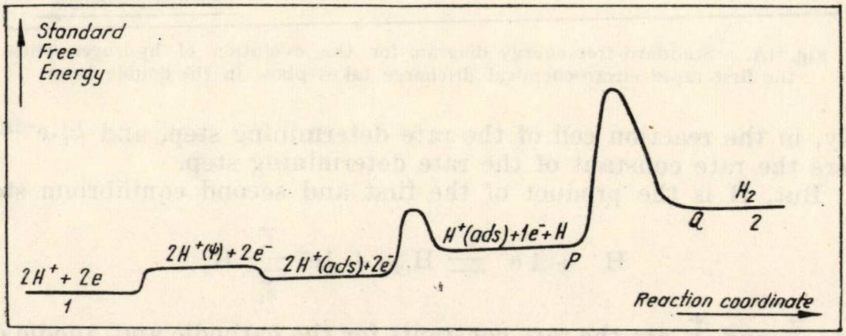

Fig. 4B. — Standard free energy diagram for hydrogen evolution when the first rapid electrochemical discharge takes place after the adsorption of the ions on the electrode.

Following the same way as before we have

$$i = 2Fk^B_I [H_{ads}] [H^+ \text{ ads}] e^{-\beta F\Delta\Phi/RT} \tag{44}$$

We have also,

$$[H_{ads}] = k''_B \, [H^+_{(\Psi)}] e^{-\Delta\Phi F/RT} = k''_B \, [H^+] e^{-\Psi F/RT} e^{-\Delta\Phi F/RT} \tag{45}$$

and

$$[H^+_{ads}] = k^B_{II} \, [H^+] e^{-\Psi F/RT} \tag{46}$$

Using (46) and (45) together with (44), we obtain the value of the cathodic current for mechanism (*B*),

$$\vec{i} = 2Fk^B \, [H^+]^2 e^{-(1+\beta)F\Delta\Phi/RT} \cdot e^{-2\Psi F/RT} \tag{47}$$

No difference concerning the Ψ' effect between the two mechanisms would be obtained if the Ψ' potential effect were introduced directly in the final equation of i; the exponential term containing Ψ' will be $e^{-2\Psi' F/RT}$ in both cases.

In conclusion, the modified Parsons' equations for the kinetics of electrode processes enjoy general validity for all the mechanisms when only one step is the rate determining step. When more than one of the steps concerned have comparable energy barriers, the Vetter's way to establish the kinetical equations is more suitable.

Revue Roumaine de Chimie, **14**, 569–581 (1969)

Revue Roumaine de Chimie, **14**, 583–589 (1969)

EXTRAKTION VON TITAN(IV) MIT n-BUTANOL UND QUERCETIN IN GEGENWART VON NATRIUMTRICHLORACETAT

C. DRĂGULESCU, T. SIMONESCU und HERTA SCHIFF

von der Wissenschaftlichen Forschungstelle der Akademie, Timişoara, Bdul Mihai Viteazul, 24

Eingegangen am 17. Oktober 1968

Es wurden die Extraktionsbedingungen von Titan mit n-Butanol und mit butanolischen Quercetinlösungen (Q) in Gegenwart von Natriumtrichloracetat (TCANa) bestimmt. Der Komplex (Titan-Quercetin) in butanolischem Medium wurde auf spektralphotometrischem Wege untersucht, wobei eine Zusammensetzung von 1 : 1 und eine Instabilitätskonstante von 5.10^{-5} erhalten wurde. Das Lambert-Beersche Gesetz ist im Konzentrationsbereich bis zu mindestens 10 μg Ti/ml erfüllt. Es wurde eine neue extraktive spektralphotometrische Bestimmungsmethode ausgearbeitet, die mit zufriedenstellenden Ergebnissen bei Gemischen angewendet wurde, die der Zusammensetzung von Bauxit und den Legierungen des Typs Konel und Ticonal entsprechen. Die Fehlergrenze beträgt ± 5%.

Titan und seine Chelatverbindungen wurden mit Diketonen, Hydroxamsäuren, Dithiokarbamaten, Alkylphosphorsäuren, Di- und Tributhylphosphaten, Alkoholen und Aminen extrahiert.[1]

n-Butanol wurde zur Extraktion der Titankomplexe mit Phosphormolybdänsäure,[2,3] *p*-Methoxybenzothiohydroxamsäure,[4] Brenzkatechin[5,6] und Xylenolorange in Gegenwart von Diphenylguanidin[7] verwendet.

Die Nachweisreaktionen von Titan (IV) mit Quercetin in einem Medium von Dimethylformamid, konzentrierter Schwefelsäure und Methanol wurden von Sommer[8] beschrieben.

Vorliegende Arbeit untersucht die Extraktion von Titan sowohl mit butanolischen Quercetinlösungen als auch allein mit n-Butanol in

---

[1] J. Stary, ,,Solvent Extraction of Metal Chelates'', Pergamon Press, 1964, S. 51.

[2] Yu. F. Skaravski, *Zavodskaya Lab.*, **28**, 265 (1962).

[3] Yu. F. Skaravski, *Zhur. analit. Khim.*, **19**, 514 (1964).

[4] Z. Skorko-Tribula und J. Minczewsky, *Chem. Analit.*, **9**, 397 (1964).

[5] F. V. Zaikovski, *Zhur. analit. Khim.*, **11**, 269 (1956).

[6] Ya. S. Kamentsev, *Voprosy analit. Khim. miner. Veschestv.*, **1966**, 124; *Chem. Abstr.*, **66**, 22732 e (1967).

[7] V. N. Tolmachev, I. M. Hölzberg und V. D. Konkin, *Zhur. analit. Khim.*, **6**, 950 (1967).

[8] L. Sommer, *Z. analyt. Chem.*, **171**, 410 (1959).

Gegenwart von TCANa im Hinblick auf seine Absonderung und spektralphotometrische Bestimmung.

EXPERIMENTELLES

GERÄTE. Die optische Dichte wurde mit einem Spektralphotometer SPEKOL (C. Zeiss Jena) und die Absorptionspektren wurden mit einem Spektralphotometer UNICAM SP-800 bestimmt. Der pH-Wert der Lösungen wurde mit einem pH-Meter Typ MV 11 Clamann und Grahnert, Dresden, gemessen.

REAGENZIEN. Die *perchlorische 10^{-4} M Titanlösung* wurde folgenderweise erhalten: Kaliumhexafluorotitanat „Merck" wurde mit konzentrierter Schwefelsäure abgeraucht (zwecks Ausscheidung der Flußsäure). Das als Hydroxid gefällte Titan wurde in 45 % iger Perchlorsäure gelöst. Der Titer wurde mit Kupferron gravimetrisch bestimmt.

n-Butanol. Es wurde die Fraktion 117–118° von dem bei der wiederholten Destillation des technischen durch Gärungsverfahren erhaltenen Butanols verwendet.

Butanolische Quercetinlösung 10^{-2} M wurde aus Quercetin „Chemapol" nach Umkristallisation aus absolutem Äthanol erhalten.

2 M Natriumtrichloracetatlösung. Eine titrierte Trichloressigsäure-Lösung „Merck" (gegen das Indikatorgemisch von Methylblau und Methylrot) wurde mit Natriumhydroxid „Chemapol" neutralisiert.

Die butanolische 2.10^{-3} M Titanlösung wurde durch Extraktion von Titan in n-Butanol in Gegenwart von TCANa (und durch Ergänzung bis zum Zeichen mit n-Butanol) erhalten. Es können nur frisch hergestellte Lösungen verwendet werden.

Arbeitsweise

Im Hinblick auf die Festsetzung des Verteilungskoeffizienten wurde Titan aus wäßrigen Lösungen, die TCANa enthielten, mit gleichem Volumen Butanol oder Quercetinbutanollösungen entzogen. Die wäßrige Phase wurde in einem Meßkolben gebracht und das nichtentzogene Titan mit Chromotropsäure spektralphotometrisch bestimmt.[9]

Die Extraktion wurde durch 2 Minuten langes Ausschütteln im Scheidetrichter bei Raumtemperatur (20°) vorgenommen.

Zur Erhaltung der Eichkurve und zur spektralphotometrischen Bestimmung von Titan, wurde den Proben die Titan erhielten, je 1 ml 2 M TCANa beigefügt, auf den pH-Wert 1 gebracht, und 3 mal mit je 3 ml 3.10^{-3} M Quercetinlösung und schließlich mit 10 ml Butanol entzogen. Die organischen Phasen wurden in einem 50 ml-Meßkolben gesammelt und mit Butanol aufgefüllt. 30 Minuten nach dem Ausschütteln wurde die Extinktion bei 460 nm abgelesen. Es wurde eine Küvette mit 0,5 cm Schichtdicke verwendet.

ERGEBNISSE UND DISKUSSION

Die parallelen Untersuchungen der Extraktion von Titan mit Butanol und mit butanolischen Quercetinlösungen führten zu folgenden Ergebnissen:

Um das Verteilungsgleichgewicht zu erreichen erwies sich ein 2 Minuten langes Schütteln als hinreichend.

Die prozentuelle Extraktion von Titan in Gegenwart von TCANa nimmt mit dem pH-Wert der wäßrigen Phase zu, wobei sie im Falle von butanolischer Quercetinlösung größer ist (Abb. 1). Bei einem größeren pH-Wert als 1,5 findet die Fällung von Titan in der organischen Phase statt. Um die Fällung zu vermeiden wurden die restlichen Bestimmungen bei einem pH-Wert = 1 durchgeführt.

---

[9] L. SOMMER, *Acta Chim. Acad. Sci. Hung.*, **33**, 23 (1962).

Wie aus Abb. 2 (Kurve *1* und *2*) hervorgeht, nimmt die prozentuelle Extraktion von Titan zusammen mit dem Anwachsen der Quercetinkonzentration zu, wobei für das Verhältnis Ti : Q=1 : 3, in Gegenwart von TCANa Kurve 2, der Wert 98% erhalten wird.

Wenn kein TCANa vorhanden ist (Kurve *1*) sind die Werte niedriger, eine Tatsache, die die Verwendung von TCANa bei der Extraktion mit butanolischen Quercetinlösungen rechtfertigt.

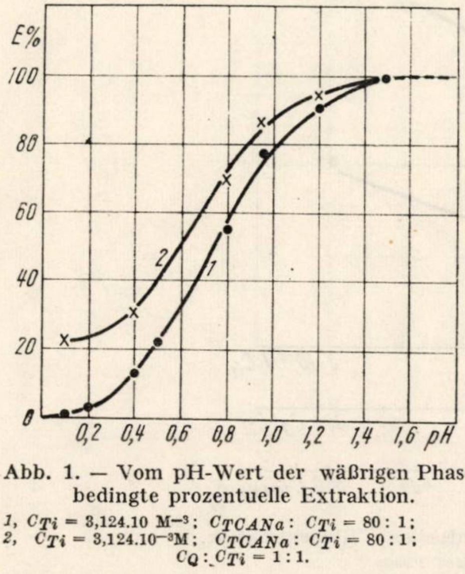

Abb. 1. — Vom pH-Wert der wäßrigen Phase bedingte prozentuelle Extraktion.

1, $C_{Ti} = 3{,}124.10\ M^{-3}$; $C_{TCANa} : C_{Ti} = 80 : 1$;
2, $C_{Ti} = 3{,}124.10^{-3}M$; $C_{TCANa} : C_{Ti} = 80 : 1$; $C_Q : C_{Ti} = 1 : 1$.

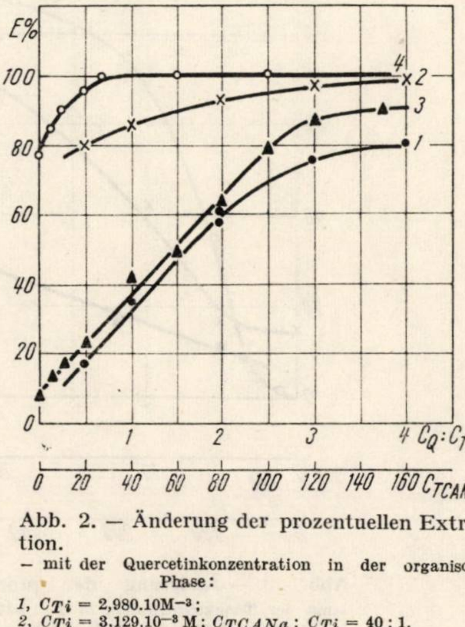

Abb. 2. — Änderung der prozentuellen Extraktion.
— mit der Quercetinkonzentration in der organischen Phase:
1, $C_{Ti} = 2{,}980.10M^{-3}$;
2, $C_{Ti} = 3{,}129.10^{-3}\ M$; $C_{TCANa} : C_{Ti} = 40 : 1$.
— mit der TCANa-Menge:
3, $C_{Ti} = 2{,}980.10^{-3}\ M$;
4, $C_{Ti} = 3{,}129.10^{-3}\ M$; $C_Q : C_{Ti} = 3 : 1$.

Bei einer Zunahme der TCANa-Menge, wächst die prozentuelle Extraktion (Abb. 2, Kurve *3* und *4*), sowohl im Falle der Extraktion mit Butanol (Kurve *3*), als auch im Falle der Extraktion mit butanolischen Quercetinlösungen (Kurve *4*). Beim Molarverhältnis Ti : TCANa = 1 : 40 wird im letzteren Falle eine Extraktion von 99% erhalten.

Eine nur mit Butanol und ohne TCANa vorgenommene Extraktion führt zu einer prozentuellen Extraktion von nur 8%. Diese Angaben rechtfertigen die gleichzeitige Verwendung von Quercetin und TCANa bei der Extraktion von Titan.

Indem die Molarverhältnisse Ti : Q=1 : 3 und Ti : TCANa = 1 : 40 benützt wurden, wobei die anfängliche Konzentration von Titan variiert wurde, konnte festgestellt werden, daß die prozentuelle Extraktion stark mit der Verminderung der Titankonzentration abnimmt (Abb. 3, Kurve *1*). Bei einer Titankonzentration von 10^{-4} M, die sich gegen die untere Grenze der praktischen Fälle lokalisiert, sind die prozentuellen Extraktionen kleiner, sogar bei einer merklichen Zunahme der Molarverhältnisse von Quercetin (Abb. 3, Kurve *2*) und Natriumtrichloracetat (Abb. 3, Kurve *3*).

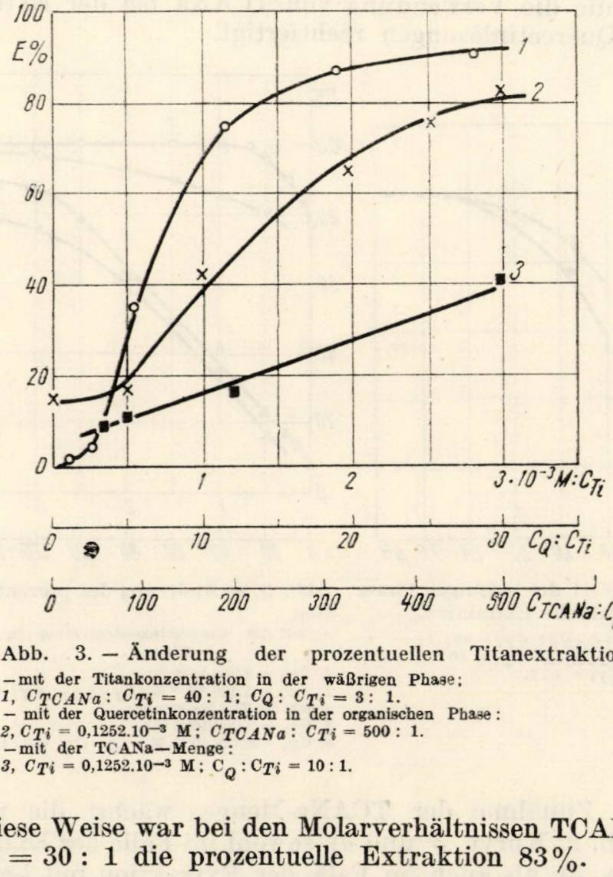

Abb. 3. — Änderung der prozentuellen Titanextraktion.
— mit der Titankonzentration in der wäßrigen Phase;
1, $C_{TCANa} : C_{Ti} = 40 : 1$; $C_Q : C_{Ti} = 3 : 1$.
— mit der Quercetinkonzentration in der organischen Phase:
2, $C_{Ti} = 0{,}1252 . 10^{-3}$ M; $C_{TCANa} : C_{Ti} = 500 : 1$.
— mit der TCANa—Menge:
3, $C_{Ti} = 0{,}1252 . 10^{-3}$ M; $C_Q : C_{Ti} = 10 : 1$.

Auf diese Weise war bei den Molarverhältnissen TCANa : Ti = 500 : 1 und Q : Ti = 30 : 1 die prozentuelle Extraktion 83 %.

Diese prozentuell schwächeren Extraktionen im Falle kleiner Titanmengen werden durch die Tatsache erklärt, daß, die Quercetin- und TCANa-Konzentrationen entsprechend abnahmen, indem die Molarverhältnisse gegenüber Titan konstant beibehalten wurden. Die Extraktion bleibt jedoch praktisch quantitativ, wenn nicht die Verhältnisse der Reagenzien sondern ihre Konzentrationen beibehalten wurden, die im Falle größerer Titanmengen bestimmt worden waren.

In diesem Sinne behilft sich die angewendete Arbeitsmethodik mit verhältnismäßig starken Quercetin- und Natriumtrichloracetatkonzentrationen. Eine andere Veränderung, welche angewendet wurde, um die Methode wirksamer zu gestalten, bestand in der wiederholten Extraktion mit geringeren Mengen.

Zusammensetzung des | Ti — Q |-Komplexes

Da eine vollständige Extraktion der verdünnten wäßrigen Lösungen nur bei Verwendung eines Ligandenüberschusses erreicht werden kann, wurde der | Ti—Q |-Komplex nicht auf extraktivem Wege untersucht, sondern unter Verwendung butanolischer Titan- und Quercetinlösungen.

Die Absorptionskurven aus Abb. 4, der butanolischen Quercetin- (Kurve *1*), und Titanlösungen (Kurve *2*) zeigen, daß die Zugabe von Titan zu Veränderungen im Quercetinspektrum führt, indem auf die Bildung eines Komplexes mit dem Absorptionsmaximum bei 425 nm hingewiesen wird.

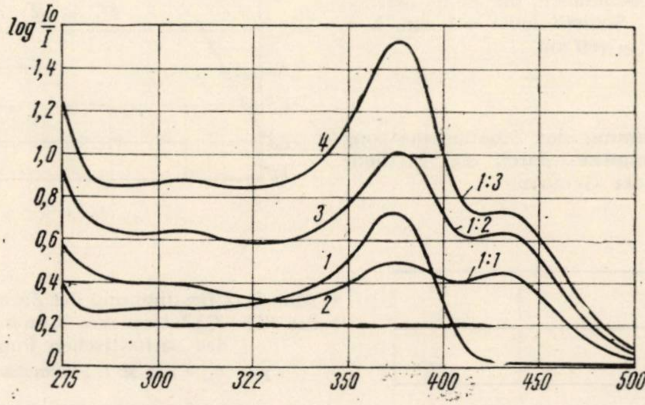

Abb. 4. — Absorptionskurven des Liganden *1*, $C_Q = 1{,}6.10^{-4}$ M und der Lösungen die Titan in einer Konzentration von $1{,}6.10^{-4}$ M und Quercetin in folgenden Verhältnissen erhalten: $C_{Ti} : C_Q = 1 : 1$ (*2*); 2 (*3*); 1 : 3 (*4*); Schichtdicke = 0,2 cm.

Die Tatsache, daß die Absorptionsspektren der Gemische von Titan- und Quercetinlösungen bei verschiedenen Molarverhältnissen (Kurven *2*, *3*, *4*) in einem breiten Intervall von Wellenlängen parallel sind und die Maxima sich bei derselben Wellenlänge befinden, weist auf die Bildung einer einzigen Verbindung hin.

Die Untersuchung der Komplexzusammensetzung nach der Asmusschen Geradenmethode [10] zeigt, wie aus den Abbildungen 5 und 6 hervorgeht, daß das Kombinationsverhältnis des | Ti—Q | -Komplexes 1 : 1 ist. Dieses Kombinationsverhältnis wurde durch die Asmussche Methode der isosbestischen Punkte [11] der Job-Serie bestätigt (Abb. 7 und Abb. 8).

Die Instabilitätskonstante wurde mit Hilfe der Asmusschen Methode[10] berechnet, wobei der Wert 5.10^{-5} gefunden wurde.

---

[10] E. Asmus, *Z. analyt. Chem.*, **178**, 104 (1960).

[11] E. Asmus, *Z. analyt. Chem.*, **193**, 81 (1963).

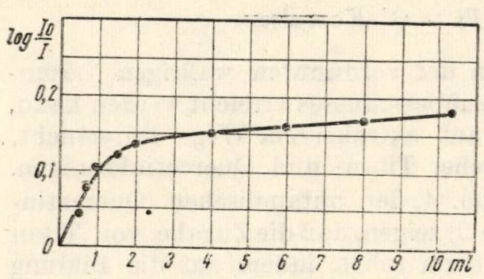

Abb. 5. – Änderung des Extraktionsmoduls der Lösungen, die 0,4 ml 10^{-3} M Titan und v cm 10^{-3} M Quercetinlösung enthalten, die in einem 25 ml Meßkolben bis zum Zeichen gebracht wurde; Schichtdicke = 1 cm, λ = = 460 nm

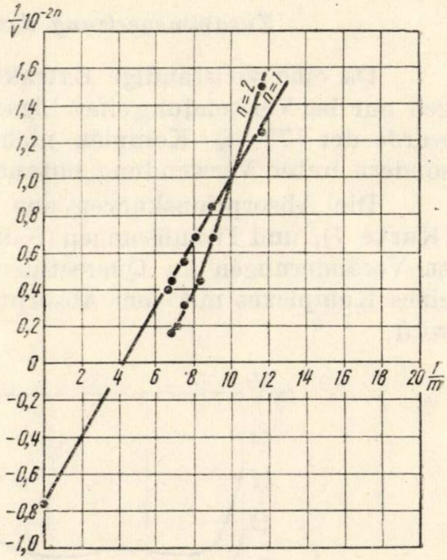

Abb. 6. – Bestimmung der Zusammensetzung → des [Ti–Q]-Komplexes durch die Methode der Geraden.

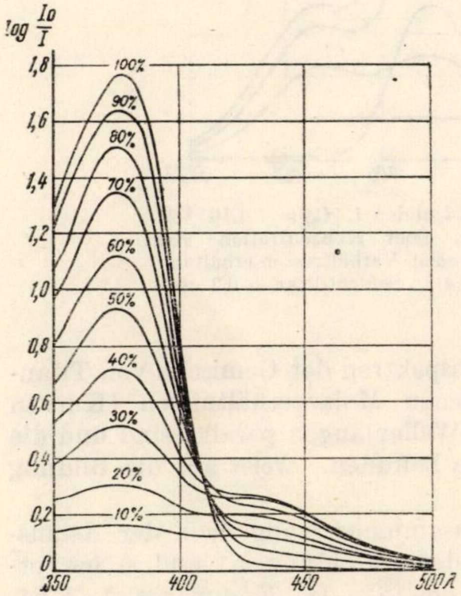

← Abb. 7. – Bestimmung der Zusammensetzung des [Ti–Q]-Komplexes durch die Methode des isosbestischen Punktes.

$c_{Ti} + c_Q = 2.10$ M^{-4} Schichtdicke = 0,5 cm.

Abb. 8. – Extinktionsänderung die vom Molenbruch x bedingt wird, die durch das Ablesen der Extinktionen bei der Wellenlänge des isosbestischen Punktes erhalten wurde.

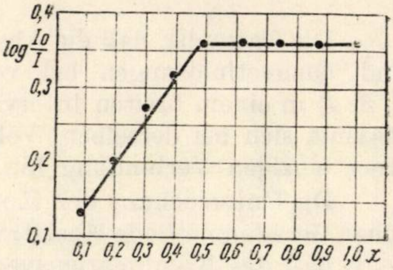

Anwendung bei der Bestimmung von Titan

Die zeitliche Farbbeständigkeit ist sehr gut und ändert sich in 90 Minuten nicht; nach 72 Stunden fällt die Extinktion um nur 2%.

Die Kolorimetrierung wurde bei einer Wellenlänge von 460 nm durchgeführt, bei welcher der Ligand wenig absorbiert.

Die Eichkurve befolgt das Lambert-Beersche Gesetz bis zu wenigstens 10 μg/ml.

Die Kationen Ba^{2+}, Ca^{2+}, Pb^{2+}, Cd^{2+}, Co^{2+}, Ni^{2+} und Mn^{2+} stören selbst dann nicht, wenn sie sich in einem 100 fachen Überschuß befinden. Die Störung des Kupfers wurde vor der Extraktion durch Maskierung mit Thioharnstoff[12] ausgeschieden. Fe^{3+} und Al^{3+} stören sogar bei Mengen von 1 : 20. Die Störung von Eisen konnte durch Reduzieren mit Askorbinsäure vor der Extraktion ausgeschieden werden. Die Maskierung des Aluminiums wurde mit Natriumsalizylat[13] vorgenommen. Zr^{4+} sowie Th^{4+} stören, da sie Komplexe mit Quercetin bilden.

Die Bestimmungsmethode wurde bei der Analyse einiger Gemische angewendet, die für Lösungen typisch sind, welche durch das Aufschließen von Bauxit und der Legierungen vom Typ Konel und Ticonal erhalten werden. Die Ergebnisse sind in Tabelle 1 zusammengefaßt. Relative Fehler überschritten ± 5% nicht.

Tabelle 1

Titanbestimmung aus Bauxit und verschiedenen Legierungen

Probe	Zusammensetzung Gew. %	Nr.	Titangehalt in μg/ml		Abweichungen	Relativer Fehler %
			angewandt	gefunden		
Bauxit	Al_2O_3 55–65					
	Fe_2O_3 20–30	1	1,632	1,600	−0,032	−1,96
	TiO_2 2,5–3	2	1,632	1,675	+0,043	+2,64
	SiO_2 2–6	3	0.816	0.800	−0,016	−1,96
	Me_2O 10–13	4	0,816	0,850	+0,034	+4,0
Legierung Konel	Ni 73					
	Co 17	1	1,632	1,580	−0,052	−3,15
	Ti 3	2	1,632	1,650	+0,018	+1,10
	Al 1	3	1,632	1,550	−0,082	−4,91
	Fe 6	4	2,448	2,375	−0,072	−3,09
Legierung Ticonal	Ni 12–20					
	Co 20–25	1	3,917	3,925	+0,008	+0,20
	Al 8–9	2	3,917	3,850	−0,067	−1,72
	Cu 2–4	3	3,917	3,750	−0.167	−4,26
	Ti 0,5–1,5	4	0,979	1,000	+0,021	+2,14
	Fe 57,5–40,5					

---

[12] K. Liska, *Coll. Czech. Chem. Comm.*, **21**, 1439 (1956).

[13] R. Přibil und V. Vesely, *Talanta*, **10**, 383 (1963).

Revue Roumaine de Chimie, **14**, 591–598 (1969)

ÉTUDE SPECTROPHOTOMÉTRIQUE DES SYSTÈMES LnCl$_3$–ROUGE ACIDE AV ET LnCl$_3$–CALCON

P. SPACU et SILVIA PLOŞTINARU

Institut de Chimie Inorganique de l'Académie, Bucarest, 89, Spl. Independenţei

Reçu le 19 juin 1968

On présente une étude spectrophotométrique sur les combinaisons complexes que les terres rares forment avec le Rouge Acide AV et le Calcon. En appliquant la méthode des variations continues Job, la méthode du rapport molaire, la méthode des pentes et la méthode du point isosbesthique, on a trouvé que, dans le système LnCl$_3$–Rouge Acide AV se forme, en solution aqueuse, une seule combinaison complexe, caractérisée par le rapport de formation 1 :2, stable dans le domaine de pH = 1,8–3,5 ; dans le système LnCl$_3$–Calcon une combinaison complexe caractérisée par le rapport 1 : 1, stable dans le domaine de pH = 8–10. Les résultats obtenus mènent à la conclusion que la liaison métal-ligand se fait à l'atome hydrogène du groupement hydroxylique.

La littérature de spécialité fait mention d'une série de travaux qui présentent des études spectrophotométriques avec des colorants azo-indicateurs métallo-chromiques.

Parmi ces réactifs nous pouvons citer les dérivés de pyridile-azo,[1] diantipyril-azo[2] ou les dérivés azo de l'acide chromotropique.[3,4]

Récemment la littérature indique une méthode de détermination spectrophotométrique des terres rares en utilisant comme réactif l'Eriochrom Black T.[5]

Etant donné la grande sensibilité des réactions de ces ligands, dans ce travail nous nous sommes proposé d'étudier l'équilibre et les phénomènes de complexation qui ont lieu entre les ions des terres rares et les ligands :

a) Rouge Acide AV (Acide 1-(2'hydroxy-1'naphtylazo)-4 sulfonique) ;

b) Calcon Acide 1-(2' hyxdroxy-1'naphtylazo)-2 naphtol-4 sulfonique)

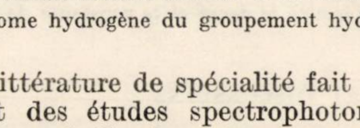

a)

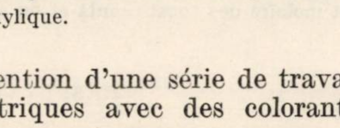

b)

---

[1] L. Sommer et H. Novotna, *Talanta*, **14** (4), 457–71 (1967).

[2] B. Budesinsky et D. Vrzalova, *Analyt. Chim. Acta*, **36** (2), 246–8 (1966).

[3] S. B. Savin et Yu. M. Dedkov, *Zhur. analit. Khim.*, **19**, 21–7 (1964).

[4] A. I. Chercasov et N. M. Aliacov, *Zhur. analit. Khim.*, **20** (12), 1312–20 (1965).

[5] Tsueno Takano, *Buneski Kagaku*, **16** (1), 27–31 (1967) ; *Chem. Abstr.*, **67** (8), 39874 w (1967).

Le fait que ces ligands diffèrent entre eux par le nombre des groupements OH^- nous a permis de faire une étude comparative en ce qui concerne la formule des complexes formés.

PARTIE EXPÉRIMENTALE

Appareils. Pour les mesures spectrophotométriques on a utilisé un spectrophotomètre Karl Zeiss-Jena VSU 1, avec prisme et cuvettes en verre, au diamètre ∅ = 1,003 cm.

Les mesures du pH ont été effectuées avec le pH-mètre MV 11, à l'échelle de pH = 0–14 (erreur de pH = ± 0,02), à une température constante de 25°. On a utilisé des électrodes de verre et calomel.

Réactifs. On a préparé des solutions 2.10^{-4} M de Rouge Acide AV et de Calcon obtenues en dissolvant les réactifs dans de l'eau. Les solutions aqueuses de $LnCl_3$ (Ln = La, Ce, Pr, Sm, Eu, Lu) de concentration 1.10^{-4} M et 2.10^{-4} M ont été préparées en dissolvant le Ln_2O_3 (Matthey et Johnson) en HCl. Le titre a été déterminé par évaporation et calcination directe à l'état de Ln_2O_3, respectivement CeO_2.

Pour établir les conditions optimales de travail on a déterminé :

— la variation de l'absorption des réactifs et des complexes formés en fonction de λ ;

— la variation de l'absorption du mélange des réactifs en fonction du pH et la stabilité des complexes formés en fonction du temps.

Après avoir établi les conditions de travail, on a étudié le problème du point de vue quantitatif : on a établi la composition du composé formé dans le système, c'est-à-dire on a trouvé le rapport molaire des constituants et on a déterminé le degré et la constante de dissociation.

RÉSULTATS ET DISCUSSIONS

A. *Système $LnCl_3$—Rouge Acide AV*

Courbes d'absorption. En traitant directement la solution de chlorure de terre rare avec le Rouge Acide AV, la couleur passe instantanément du rouge au jaune-orange.

On a déterminé le spectre d'absorption, en visible, de la solution aqueuse de Rouge Acide AV à de différentes valeurs de pH. Tel qu'on le voit dans la figure 1 *a*, le réactif présente un maximum d'absorption à λ = 500 mμ, à toutes les valeurs de pH étudiées, l'absorption décroissant ensuite continuellement vers des valeurs de λ plus grandes.

Les déterminations effectuées, en visible, sur des preuves mélanges qui contiennent le réactif et les terres rares, indiquent un déplacement du maximum d'absorption vers des longueurs d'onde plus petites, l'extinction diminuant sensiblement en comparaison de l'extinction du réactif tout pur (fig. 1*b*). Ce déplacement indique nettement la formation d'un nouveau composé, caractérisé par un maximum d'absorption situé à λ = 460 mμ.

Stabilité en fonction du temps. Les études effectuées en vue de déterminer l'influence du temps sur la réaction qui a lieu dans le système ont conduit à la conclusion que le composé formé en mélangeant les réactifs est stable environ 60 mn. Quelque temps après on observe que l'extinction varie à la suite de l'apparition d'un précipité (fig. 2). En conséquence, les déterminations doivent êtres faites immédiatement après l'apparition de la couleur.

L'effet du pH a été déterminé en étudiant l'absorption d'une preuve-mélange (qui contient $LnCl_3$ et Rouge Acide AV) à de différentes valeurs de pH. Les déterminations ont été effectuées en utilisant comme preuve-témoin une solution de Rouge Acide AV, au même pH. On a constaté que l'extinction est maximale en milieu acide, dans le domaine du $pH = 1{,}8-3{,}5$. Dans ce domaine du pH, l'extinction présente des valeurs constantes. Avec l'acroissement du pH, l'extinction commence à diminuer et aux valeurs du $pH > 5$ apparaît un précipité brun clair.

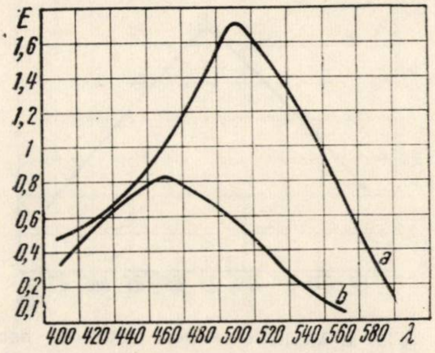

Fig. 1. Courbe d'absorption du réactif (Rouge-Acide AV) (*a*) et du composé formé dans le système $LaCl_3$: Rouge-Acide AV (*b*).

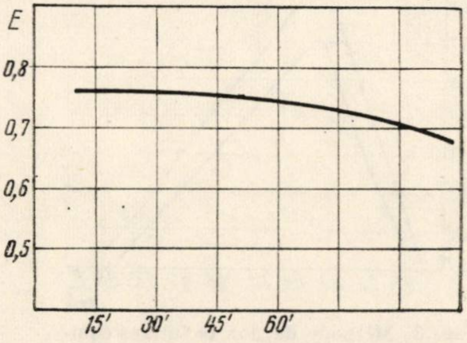

Fig. 2. Variation de l'absorption en fonction du temps.

Etude quantitative. Pour déterminer la composition du composé coloré, c'est-à-dire le rapport de formation et la valeur de la constante de dissociation nous avons utilisé la méthode des variations continues Job,[6] la méthode du rapport molaire [7] et la méthode des pentes.[8]

L'étude du système par la méthode des variations continues a été effectuée en travaillant avec des solutions équimolaires de concentration 2.10^{-4} M, à $\lambda = 460$ mμ.

La conclusion qu'on tire des données expérimentales représentées dans la figure 3, du fait qu'à la longueur d'onde à laquelle on a travaillé, on a obtenu un maximum très accentué pour la preuve qui contient 3,33 ml $LnCl_3$ et 6,66 ml réactif, est que Ln^{3+} forme avec le Rouge Acide AV un composé caractérisé par le rapport de formation 1 :2.

La méthode Job appliquée en utilisant des solutions non équimolaires (conc. 10^{-4}M et 2.10^{-4}M) confirme le rapport de formation 1 : 2 (fig. 4), le maximum d'absorption étant situé dans ce cas à la fraction molaire de 0,5.

[6] P. Job, *Ann. Chim.* (*France*), **9**, 113 (1928).
[7] J. H. Joe et A. L. Jones, *Ind. Eng. Chem. Anal. Ed.*, **16**, 111 (1944).
[8] A. E. Harvey et D. L. Manning, *J. Amer. Chem. Soc.*, **72**, 4488 (1950).

La formation de ce composé a été vérifiée par la méthode du rapport molaire en travaillant avec des solutions équimolaires de conc. 2.10^{-4} M, à $\lambda = 460$ mμ. On a effectué deux séries de déterminations conformément aux deux variantes de la méthode. Dans la première série on a maintenu constante la quantité de réactif, en variant la quantité de $LnCl_3$, et dans la seconde série on a maintenu constante la quantité de $LnCl_3$ en variant la quantité de réactif. Les résultats obtenus en mesurant l'extinction dans ces deux cas confirment la formation d'un composé caractérisé par le rapport $LnCl_3$—Rouge Acide AV $= 1 : 2$ (à ce rapport on observe un brusque changement de pente) (fig. 5).

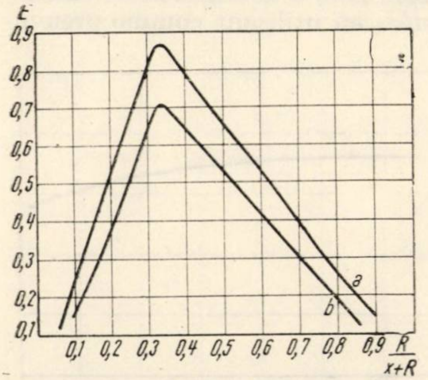

Fig. 3. Méthode de Job (solutions équimolaires) pour les systèmes : *a*, $LaCl_3$: Rouge Acide AV ; *b*, $CeCl_3$: Rouge Acide AV.

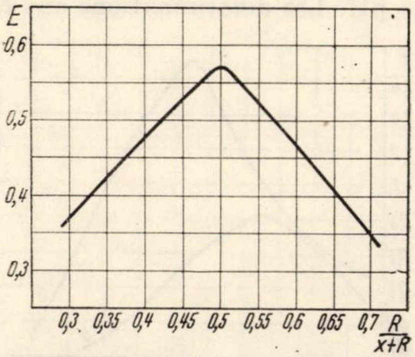

Fig. 4. Méthode de Job (solutions non équimolaires) pour le système : $EuCl_3$ (1.10^{-4} M) : Rouge Acide AV (2.10^{-4} M).

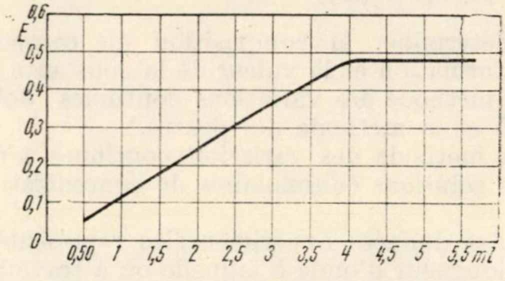

Fig. 5. Méthode du rapport molaire. (Les preuves-témoins contiennent la quantité calculée de réactif).

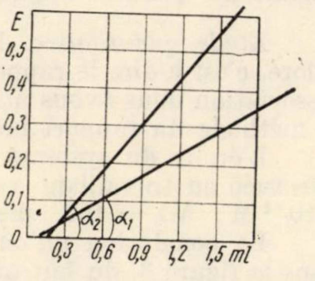

Fig. 6. Etude du système par la méthode des pentes.

Dans le cas de toutes les preuves caractérisées par le rapport réactif/$Ln^{3+} > 2$ l'extinction a été lue par rapport à des preuves-témoins qui contiennent une quantité de réactif égale à l'excès.

La composition du composé a été vérifiée aussi par la méthode des pentes, en travaillant sur deux séries de preuves . Les résultats obtenus pour la première série de preuves qui contiennent 3 ml de $LnCl_3$ 2.10^{-4} M et les quantités variables de 0,3 ; 0,6 ; 0,9 ; 1,2 et 1,5 ml de réactif sont représentés dans la figure 6 par la droite 1 caractérisée par un angle d'inclinaison par rapport à l'axe O—X α_1. Les résultats obtenus pour la seconde série de preuves qui contiennent 3 ml sol. de réactif 2.10^{-4} M et les quantités variables de 0,3 ; 0,6 ; 0,9 ; 1,2 et 1,5 $LnCl_3$ sont représentés dans la figure 6 par la droite 2, caractérisée par un angle d'inclinaison α_2.

Du fait que le rapport des tangentes des angles α_2 et α_1 est égal à 2 il s'ensuit que le rapport de formation du composé = 1 : 2.

Degré et constante de dissociation. Les mesures effectuées en vue de déterminer le degré et la constante de dissociation par la méthode de Harvey et Manning[8] n'ont fait qu'indiquer la grande stabilité du composé dans les conditions mentionnées, sans permettre la détermination de la valeur numérique de la constante.

Pour calculer la valeur de la constante de dissociation on a utilisé la méthode de Job (séries non équimolaires). En travaillant avec des solutions de conc. 2.10^{-4} M et 1.10^{-4} M on a trouvé pour les composés des terres rares étudiées les constantes de dissociation suivantes : pour La, $K = 3,00.10^{-8}$; Sm, $K = 4,60.10^{-8}$ et Eu, $K = 4,82.10^{-8}$.

B. *Système $LnCl_3$ — Calcon*

En étudiant ce système, on a constaté qu'en traitant directement le chlorure de terre rare avec du Calcon, au pH = 5, n'a lieu aucun changement de couleur, les courbes d'absorption étant identiques à celle du réactif, ce qui nous a déterminé d'étudier le comportement du réactif dans un large domaine de pH. Dans ce but on a déterminé les courbes d'absorption de la solution aqueuse de Calcon à différentes valeurs du pH(pH = 5—10). L'étude des courbes d'absorption (fig. 7) montre que le réactif est un indicateur qui change de couleur en fonction du pH, changement qui ne se produit pas brusquement à une valeur de pH bien déterminée, mais graduellement dans un domaine de pH. Dans la figure 7 on constate aussi qu'on obtient deux courbes différentes, correspondant à ces deux formes colorées du réactif. Les intensités d'absorption augmentent ou diminuent en fonction du pH. Les deux bandes d'absorption se superposent dans le domaine du spectre situé entre les maxima d'absorption, ayant le point isosbesthique à $\lambda = 535$ mμ.

En continuant notre étude, on a analysé la variation de l'absorption du composé en fonction de la longueur d'onde, aux mêmes valeurs de pH (pH=5—10), en vue de mettre en évidence qualitativement le phénomène de complexation. On a constaté que pour toutes les valeurs du pH (y compris pour le domaine au pH = 8—10, où le réactif a la couleur bleue et le maximum d'absorption à $\lambda = 620$ mμ) on obtient une seule courbe d'absorption, présentant un maximum situé à $\lambda = 510$ mμ.

Vu les considérations ci-dessus, l'étude du composé qui se forme entre les terres rares et le Calcon a été faite au pH = 9, réalisé en utilisant des solutions-tampons de $NH_4Cl—NH_4OH$.

Dans la figure 8 on a représenté la courbe d'absorption du ligand (fig. 8*a*) et la courbe d'absorption du complexe de l'Europium (fig. 8*b*) au pH = 9. On observe un déplacement du maximum d'absorption, ce qui prouve une assez grande sensibilité du réactif dans le domaine du pH étudié.

On a étudié aussi l'influence de la quantité de solution-tampon sur l'extinction. De la figure 9 on constate que pour une quantité de solution tampon, variant entre 1 et 3 ml, l'extinction ne varie pas.

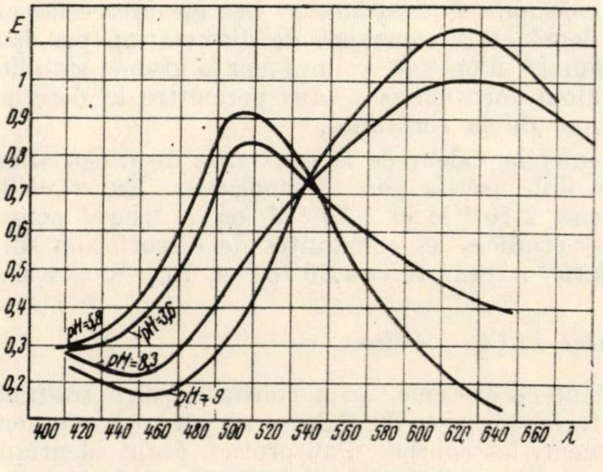

Fig. 7. Courbes d'absorption du Calcon à de différentes valeurs de pH.

Dans l'étude quantitative du système on a utilisé 2 ml de solution tampon.

La couleur des complexes formés varie entre rouge-orange pâle et rouge-violet intense à mesure que le numéro atomique augmente.

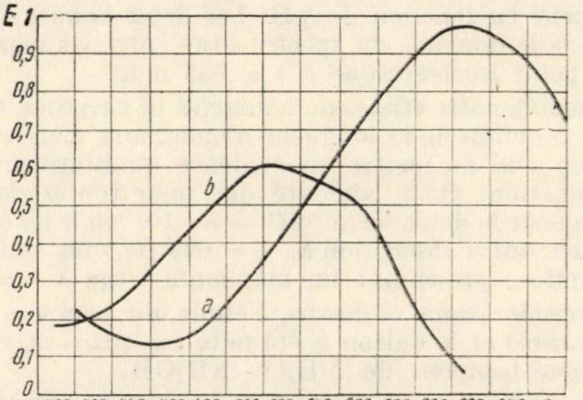

Fig. 8. Courbe d'absorption du Calcon (a) et du composé formé dans le système $EuCl_3$: Calcon (b) au pH = 9.

L'étude quantitative du système $LnCl_3$—Calcon a été faite par la méthode du point isosbesthique d'Asmus,[9] la méthode de Job et la méthode du rapport molaire.

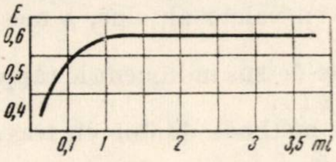

Fig. 9. Variation de l'absorption en fonction de la quantité de solution tampon.

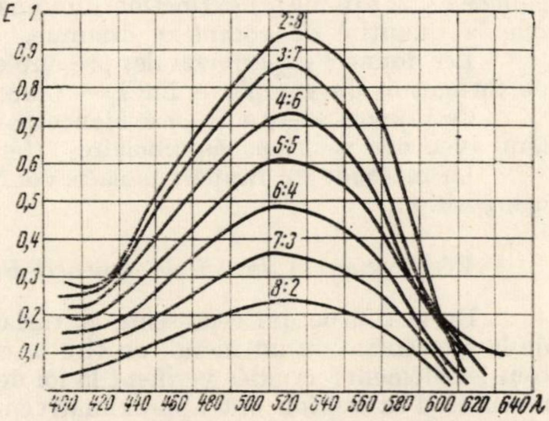

Fig. 10. Etude de la réaction par la «méthode du point isosbesthique».

On a utilisé la méthode du point isosbesthique, vu que cette méthode donne de très bons résultats dans le cas des complexes où l'un des constituants est coloré.

Dans ce but on a déterminé les courbes d'absorption à $\lambda = 400-650$ mμ pour différents rapports $LnCl_3$—Calcon, dans le système tamponné au pH = 9.

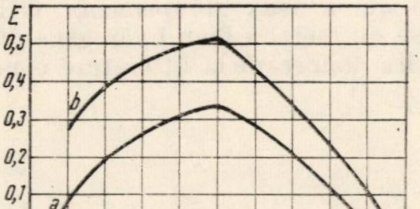

Fig. 11. Méthode de Job (solutions équimolaires) pour le système $EuCl_3$: Calcon.

Tel qu'on peut le constater de la figure 10, les courbes d'absorption correspondant aux preuves 1, 2, 3 qui contiennent, par rapport au $LnCl_3$— Calcon = 1 : 1, un excès de réactif, se rencontrent dans un même point — le point isosbesthique — situé à $\lambda = 600$ mμ, avec la courbe d'absorption qui correspond au rapport 1 : 1. En analysant aussi la position du maximum d'absorption caractéristique de chaque preuve on constate qu'il est déplacé vers le maximum du réactif pour toutes les preuves qui contiennent un excès de réactif ($\lambda = 520$ mμ). Pour les preuves caractérisées par un rapport $LnCl_3$ — Calcon > 1, le maximum est déplacé à gauche ($\lambda = 510$ mμ), l'extinction diminuant en valeur absolue, à mesure que la quantité de complexe diminue.

---

[9] E. Asmus, *Z. analyt. Chem.*, **193**, 81 (1963).

Les données expérimentales présentées ci-dessus indiquent le rapport de formation du complexe $LnCl_3$ — Calcon 1 : 1.

Ce rapport a été mis en évidence par la méthode de Job en travaillant avec des solutions équimolaires (fig. 11).

La méthode du rapport molaire confirme pour le complexe la même composition.

Vérification de la loi de Lambert-Beer

De la courbe qui représente la variation de l'extinction en fonction de la concentration du métal, on tire la conclusion que les complexes de tous les éléments étudiés vérifient la loi de Lambert-Beer. Les coefficients molaires d'extinction ont approximativement la valeur 5.10^3. Le Calcon ne peut être utilisé comme réactif de dosage spectrophotométrique des terres rares parce qu'il présente une bande d'absorption continue à toutes les longueurs d'onde où le complexe est coloré.

La composition des complexes qui se forment dans les deux systèmes étudiés, à savoir le rapport de formation, donne certaines indications en ce qui concerne la modalité de liaison de la terre rare au ligand. Le rapport 1 : 2 pour le composé formé avec le Rouge Acide AV qui a dans la molécule un seul groupement OH^- et le rapport 1 : 1 pour le composé formé avec le Calcon qui a deux groupements OH^- dans la molécule plaident pour la liaison du métal à l'ion hydrogène du groupement OH^-, en concordance avec les données de la littérature concernant les éléments bi- et trivalents.

Revue Roumaine de Chimie, **14**, 599 – 604 (1969)

ADSORPTION DE L'URANIUM PAR LES RÉSINES ÉCHANGEUSES D'IONS EN PRÉSENCE DU CHLORATE ET DU PERCHLORATE

S. TĂTARU, GH. FILIP et B. DAVID

Section de Recherches Technologiques pour les Métaux Rares, Şos. Măgurele, Bucarest

Reçu le 22 mars 1968

Le travail donne les résultats de l'étude de l'adsorption de l'uranium par les résines échangeuses d'ions bases fortes en présence des ions ClO_3^- et ClO_4^-. On montre également que les deux ions influent différamment sur l'adsorption de l'uranium.

Les résultats obtenus antérieurement ont permis à établir l'influence des ions Cl^-, CO_3^{2-}, MnO_4^-, $[Fe(CN)_6]^{4-}$ et $[Fe(CN)_6]^{3-}$ sur l'adsorption de l'uranium par les résines échangeuses d'ions bases fortes.[1-3] Les résultats ci-dessous concernent l'étude de l'influence des anions ClO_3^- et ClO_4^- sur l'adsorption de l'uranium par les mêmes résines, des solutions carbonatées.

PARTIE EXPÉRIMENTALE

Pour l'étude de l'adsorption de l'uranium par les résines échangeuses d'ions en présence des ions ClO_3^- et ClO_4^- on a préparé une solution d'uranyltricarbonate de sodium ayant une teneur de 0,385 grammes en uranium par litre et de 10 g/l en carbonate de sodium libre. Cette solution a été mise en contact dans des conditions statiques avec la résine Amberlite IRA-400, chargée sous forme de Cl^-. La résine traitée préalablement dans des conditions dynamiques avec une solution de HCl 4% est ensuite lavée à l'eau doublement distillée. Après le lavage on a traité la résine, dans la même colonne et dans les mêmes conditions, avec une solution de NaOH 2% et de nouveau lavée à l'eau distillée jusqu'à une réaction neutre dans l'effluent (réaction négative avec la phénolphtaléine). La saturation des groupes actifs de la résine avec le contre-ion Cl^- a été réalisée par traitement dynamique avec une solution de HCl 4%. La filtration de la solution chlorhydrique par le lit de résine s'est prolongée jusqu'à l'obtention d'un effluent dont la concentration du HCl soit égale à celle de la solution initiale. La résine ainsi traitée a été de nouveau lavée à l'eau doublement distillée, jusqu'à une réaction négative pour l'anion Cl dans l'effluent ($AgNO_3$), et maintenue dans de l'eau distillée d'où elle a été reprise pour chaque expérience.

---

[1] S. TĂTARU, GH. FILIP et B. DAVID, *Rev. Roumaine Chim.*, **4**, 429 (1968).
[2] S. TĂTARU, B. DAVID et GH. FILIP, *Rev. Roumaine Chim.*, **6**, 787 (1968).
[3] S. TĂTARU, *Studii şi Cercetări Chim.* Acad. Bucarest, **5**, 327 (1967).

La saturation de la résine par de l'uranium a été réalisée par le contact de 230 ml solution uranifère avec 3 ml de résine dans quatre étapes : la résine échangeuse d'ions fraîche a été agitée pendant 30 mn avec la solution uranifère initiale. Puis les phases ont été séparées par décantation et la solution a été analysée pour déterminer, par différence, la quantité d'uranium adsorbé par la résine. L'opération a été répétée quatre fois pour chaque solution jusqu'à la saturation de la résine, considérée telle lorsque la concentration de l'uranium dans la solution après le contact reste égale à la concentration de la solution initiale.

Afin d'obtenir des renseignements concernant l'influence des anions ClO_3^- et ClO_4^- sur l'adsorption de l'uranium par la résine échangeuse d'ions donnée, dans les solutions mises en contact on a ajouté les quantités désirées d'ions ClO_3 et ClO_4 sous forme de sels de potassium. Le dosage de l'uranium dans l'effluent résulté après le contact a été effectué par voie volumétrique à l'aide du vanadate d'ammonium. [4]

RÉSULTATS ET DISCUSSIONS

Dans les tableaux 1 et 2 et dans la figure 1 on présente les résultats obtenus dans l'étude de l'influence des ions chloriques, à diverses concentrations, sur l'adsorption de l'uranium par la résine anionique Amberlite IRA-400.

Tableau 1

Concentration de l'uranium dans les solutions contenant du $KClO_3$ après chaque contact avec la résine (mg/l)

Nº du contact	Concentration du $KClO_3$ dans la solution initiale (mg/l)					
	0,00	250	500	750	1 000	1 500
I	12	14	17	24	29	29
II	25	70	90	131	152	157
III	120	240	278	310	305	307
IV	282	342	358	364	372	372

Tableau 2

Uranium adsorbé par la résine dans chaque étape des solutions carbonatées en présence du $KClO_3$(mg)

Nº du contact	Concentration du $KClO_3$ dans la solution initiale (mg/l)					
	0,00	250	500	750	1000	1500
I	91,38	90,89	90,38	88,44	87,22	87,22
II	88,20	77,17	72,45	62,23	57,08	56,00
III	64,92	35,52	26,28	18,37	19,60	19,15
IV	35,23	10,53	6,63	5,14	3,18	3,18

On peut observer dans le tableau 1 que par l'accroissement du $KClO_3$ dans la solution uranifère mise en contact avec la résine augmente la quantité d'uranium qui reste inadsorbé dans l'effluent liquide. Les données du tableau 2 confirment qu'au fur et à mesure de l'accroissement de la concentration des ions chloriques dans la solution, la résine adsorbe moins d'uranium. La quantité d'uranium adsorbée baisse aussi, pour chaque concentration du $KClO_3$, avec l'accroissement des contacts, ou avec l'accroissement de la quantité des ions ClO_3^- et $[UO_2(CO_3)_4]^{4-}$ passés par la résine. L'adsorption de l'uranium dans les dernières étapes de contact décroît en fonction de la concentration initiale du $KClO_3$ dans la solution soumise à l'adsorption (tabl. 2).

---

[4] P. N. Palei, « Materialy Mezhdunarodnoi Konferentsii po mirnomu ispolzovaniu atomnoi energii », vol. 8, Genève, 1955, p. 268.

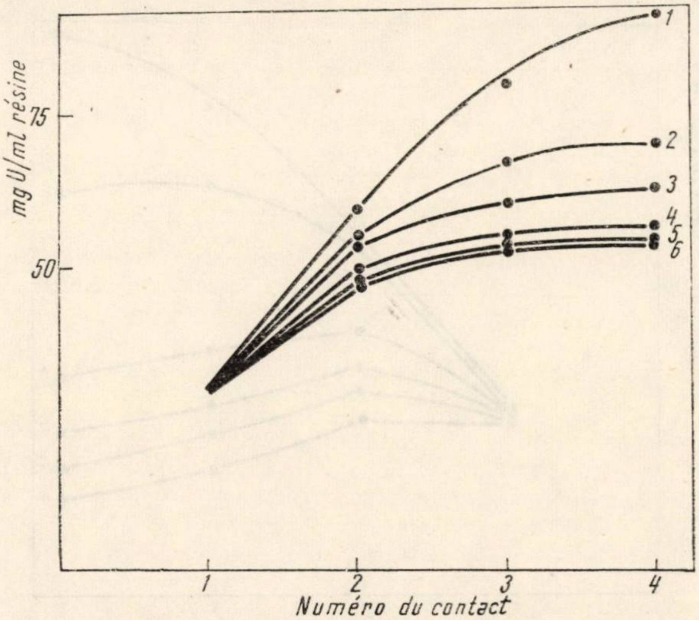

Fig. 1. — Adsorption de l'uranium par la résine échangeuse d'ions des solutions ayant les concentrations de $KClO_3$ (en mg/l) : *1*, 0,00 ; *2*, 250 ; *3*, 500 ; *4*, 750 ; *5*, 1000 ; *6*, 1500.

On peut remarquer dans la figure 1 que, bien que la quantité d'uranium adsorbée se réduise dans chaque étape de saturation, la capacité d'adsorption de la résine marque un accroissement après chaque contact avec la solution contenant du $KClO_3$. Dans les conditions acceptées, il nous faut remarquer que, même pendant le dernier contact, la désorption de l'uranium ne dépasse pas son adsorption par la résine, bien que les concentrations du ClO_3^- dans les solutions utilisées soient considérablement plus grandes que les concentrations qui pourraient être rencontrées dans la pratique. Néanmoins il est à remarquer que les valeurs qui s'établissent pour la capacité d'adsorption se réduisent en fonction de l'accroissement de la concentration des ions ClO_3^- dans la solution. Ainsi, la capacité d'adsorption pour l'uranium des solutions contenant du $KClO_3$ 1,5 g/l représente presque la moitié de la capacité pour l'uranium des solutions contenant du $KClO_3$ 0 g/l (55,1 mg U/ml résine vis-à-vis de 93,2 mg U/ml résine).

Les ions ClO_4^- réduisent plus énergiquement l'adsorption de l'uranium par la résine que les ions ClO_3^-.

On peut remarquer (tableau 3) que, même dans le cas des concentrations faibles du $KClO_4$ dans la solution, 0,25—0,5 g/l, dans les dernières étapes de saturation, la concentration d'uranium dans l'effluent dépasse sa concentration dans l'influent, ce qui signifie que dans les conditions données les ions ClO_4^- éluent l'uranium adsorbé antérieurement par la résine. Ce fait est confirmé par les données du tableau 4 où les signes minus pour les quantités d'uranium adsorbé, pendant les dernières étapes de saturation, indiquent l'apparition de la désorption (le phénomène

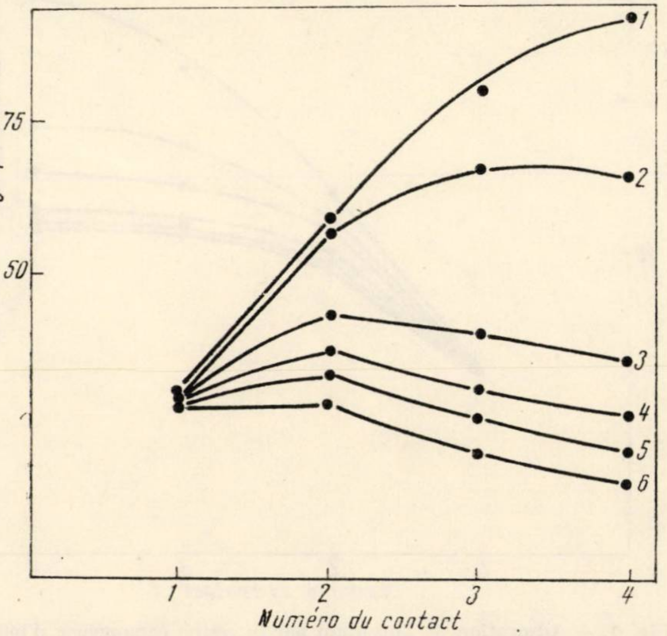

Fig. 2. — Adsorption de l'uranium par la résine échangeuse d'ions des solutions ayant les concentrations de $KClO_4$ (en mg/l) :
1, 0,00; *2*, 250; *3*, 500; *4*, 750; *5*, 1000; *6*, 1500.

Tableau 3

Concentration de l'uranium dans les solutions contenant du $KClO_4$ après chaque contact avec la résine (mg/l)

Nº du contact	Concentration de la $KClO_4$ dans la solution initiale (mg/l)					
	0,00	250	500	750	1 000	1 500
I	12	20	30	30	36	36
II	25	50	200	272	317	374
III	120	246	423	462	470	486
IV	282	402	436	439	450	437

Tableau 4

Uranium adsorbé par la résine dans chaque étape des solutions carbonatés en présence du $KClO_4$ (mg)

N° du contact	Concentration du $KClO_4$ dans la solution initiale (mg/l)					
	0,00	250	500	750	1000	1500
I	91,38	89,42	86,97	86,97	85,50	85,50
II	88,20	82,07	45,32	27,68	16,66	2,20
III	64,92	34,05	− 9,31	−18,86	−20,82	−24,01
IV	35,23	− 4,16	−12,49	−13,23	−15,92	−12,74

opposé à l'adsorption). L'intensité de la désorption dépend de la concentration des ions ClO_4^- dans la solution. En comparant les courbes des figures 1 et 2 on peut remarquer que la réduction de la capacité d'adsorption pour l'uranium est plus intense dans le cas des anions ClO_4^-.

En examinant l'adsorption de l'uranium des solutions contenant des ions ClO_3^- avec l'adsorption des solutions contenant des ions ClO_4^- il résulte que ces ions influent négativement sur le processus, l'effet défavorable des ions ClO_4^- étant plus important : l'existence des ions ClO_3^- dans la solution provoque une réduction de l'adsorption de l'uranium pendant que, dans les mêmes conditions, les ions ClO_4^- éloignent de la phase résine l'uranium adsorbé auparavant.

La diminution de la capacité d'adsorption de la résine pour l'uranium en présence des ions ClO_3^- et ClO_4^- peut être expliquée par le fait que pendant l'adsorption de l'uranium par la résine, conformément à la réaction

$$4\ \overline{RCl} + [UO_2(CO_3)_3]^{4-} \rightleftarrows \overline{R_4[UO_2(CO_3)_3]} + 4\ Cl^- \tag{1}$$

qui est la réaction utile du processus, découlent concomitamment des réactions d'adsorption des ions ClO_3^- ou ClO_4^- qui coexistent avec l'uranium dans la solution

$$\overline{RCl} + ClO_3^- \rightleftarrows \overline{RClO_3} + Cl^- \tag{2}$$

et

$$\overline{RCl} + ClO_4^- \rightleftarrows \overline{RClO_4} + Cl^- \tag{3}$$

La mesure dans laquelle une des deux réactions (2) ou (3) découle plus ou moins intensivement en défaveur de la réaction utile (1) est déterminée par le rapport de la concentration de l'anion ClO_3^- ou ClO_4^- et la concentration de l'anion $[UO_2(CO_3)_3]^{4-}$ et par l'affinité des groupes actifs de la résine envers l'anion respectif. L'affinité plus grande de la résine échangeuse d'ions vis-à-vis l'anion ClO_4^- confirme les hypothèses énoncées auparavant. [5–7]

---

[5] I. N. Plaksin et S. Tátaru, «Ionoobmennaia Tekhnologia», Nauka, Moscou, 1965 p. 206.

[6] S. Tătaru, Travaux du 6e Congrès International pour la préparation des minerais, Cannes, 1963.

[7] S. Tătaru, *Rev. Roum. Sci. Techn. Sér. Métallurgie*, **9**, 39 (1964).

Quant à la désorption de l'uranium remarquée dans le cas de la présence dans la solution des anions ClO_4^- , elle ne peut pas être expliquée seulement par la concurrence que ces ions font à l'anion $UO_4(CO_3)_3^{4-}$ pour l'occupation des groupes actifs de la résine. L'apparition d'une quantité supplémentaire d'uranium dans les effluents pendant les dernières étapes de saturation montre que les anions ClO_4^- éluent l'uranium adsorbé par la résine dans les étapes antérieures de saturation

$$\overline{R_4\,[(UO_2(CO_3)_3]} + 4ClO_4^- \rightleftarrows \overline{4\,RClO_4} + UO_2(CO_3)_3^{4-} \qquad (4)$$

Dans les conditions de l'adsorption de l'uranium en présence des anions ClO_4^- il est très probable que les réactions (1), (3) et (4) découlent concomitamment, mais qu'au fur et à mesure de l'accroissement de la quantité des anions ClO_4^- mis en contact avec la résine, l'équilibre de la réaction (4) se déplace vers la droite.

La forte désorption de l'uranium remarquée en présence des anions perchloriques pourrait les recommander en tant qu'agents d'élution dans la pratique du traitement avec des résines échangeuses d'ions des jus uranifères résultés après la lixiviation des minerais. Mais, tenant compte que l'anion perchlorique est un oxydant très fort, qui pendant la répétition des cycles adsorption-élution pourrait détruire la carcasse organique de la résine il nous paraît plus recommandable d'éviter la présence de ces anions dans les solutions uranifères soumises au traitement avec les résines échangeuses d'ions.

CONCLUSIONS

1. L'étude de l'adsorption de l'uranium par les résines échangeuses d'ions des solutions carbonatées en présence des anions ClO_3^- et ClO_4^- montre que ces deux ions influent négativement sur le processus, en réduisant la capacité d'adsorption de la résine pour l'uranium.

2. Les ions ClO_3^- et ClO_4^- sont adsorbés par la résine échangeuse d'ions en défaveur de l'uranium, l'ion ClO_4^- éluant l'uranium adsorbé dans les étapes antérieures.

Revue Roumaine de Chimie, **14**, 605 – 612 (1969)

EXPERIMENTAL APPROACH TO THE CHARACTERIZATION OF PRETREATED PLATINUM ELECTRODE SURFACES. II[1]

CYCLIC POTENTIAL SWEEP VOLTAMMETRIC STUDY

L. KÉKEDY and F. MAKKAY

Chair of Analytical Chemistry, "Babeş-Bolyai" University, Cluj, Str. Arany János, 11

Received June 28, 1968

According to the aims proposed in our previous paper,[1] the effect of several pretreatment procedures on platinum was investigated by triangular cyclic potential sweep voltammetry (chronoamperometry). The cyclic voltammograms of the treated electrodes in 1 N H_2SO_4 are given as well as some $i-E$ curves concerning the electrochemical reduction of O_2 on the same electrodes. It is concluded that unlike chronopotentiometry cyclic voltammetry yields more detailed information on the surface state of the electrodes as well as on the effect of a given pretreatment procedure. The method is recommended as a simple, rapid and reliable experimental tool for the characterization of pretreated solid electrodes used in analytical practice.

EXPERIMENTAL

Cyclic voltammetry [2-7] has been found particularly well suited for the study of electrode reactions on solid electrodes. It has also been used as periodic triangular potential sweep to study the surface oxidation and reduction of platinum electrodes.[2,8-15] Single sweep procedures were used as well.[16]

Triangular sweep current-potential curves constitute the derivatives of the constant current charging curves (chronopotentiograms) if the process is reversible and approximately so in the case of irreversible systems (e.g. oxide formation and reduction) and therefore have the advantage of higher resolution.[17] In the present work a symmetrical triangular voltage sweep (between +1.5 and −0.5 volts *vs.* S.C.E.) was applied and the current (both anodic and cathodic) was followed during the complete excursions of the potential. Using moderately slow potential scanning rates (usually 8.33 mV per secundum), the potential scan taken from a polarograph could be inverted manually and the same recording polarograph (Radelkis Type OH 102) could be used to record the current-potential curves. A conventional polarographic circuit and electrolytic cell were used. The working electrode (the platinum electrode being studied) consisted of a rectangular smooth platinum foil with an apparent geometric area of 0.91 cm^2. The S. C. auxiliary electrode was connected to the cell through glass joint salt bridge. The 1 N H_2SO_4 electrolyte solution was prepared from double distilled water and analytical reagent grade sulphuric acid. The salt bridge contained the same solution. The electrolytic cell was carefully thermostated at 25°. The working electrode was suitably treated and after thorough washing it was transferred into the cell. Before each experiment the solution was thoroughly swept with purified tank nitrogen.

---

[1] L. Kékedy and F. Makkay, *Rev. Roumaine Chim.*, **13**, 739 (1968).

[2] Z. Kublik, *J. Electroanalyt. Chem.*, **5**, 450 (1963).

[3] Z. Galus, H. I. Lee and R. N. Adams, *J. Electroanalyt. Chem.*, **5**, 17 (1963).

[4] I. Shain, "Stripping Analysis" in I. M. Kolthoff and Ph. J. Elving editors, "Treatise on Analytical Chemistry" Part I, vol. 4, Interscience, New York, 1963, p. 2205, 2554.

[5] Gy. Farsang, *Acta Chim. Acad. Sci. Hung.*, **45**, 163 (1965).

[6] R. S. Nicholson and I. Shain, *Analyt. Chem.*, **36**, 706 (1964).

[7] R. S. Nicholson, *Analyt. Chem.*, **37**, 1351 (1965).

[8] K. Asai, K. Ohashi, K. Sasaki and S. Nahawa, *Mem. Fac. Eng. Osaka City Univ.*, 5, 181 (1963); *Chem. Abstr.*, **64**, 6083 (1966).

[9] M. Breiter, *Electrochim. Acta*, **8**, 447, 925 (1963).

[10] M. Breiter, *ibid.*, **11**, 905 (1966).

[11] R. P. Buck and L. R. Griffith, *J. Electrochem. Soc.*, **109**, 1005 (1962).

[12] M. Breiter, *J. Electroanal. Chem.*, **8**, 230 (1964).

[13] F. G. Will and C. A. Knorr, *Z. Electrochem.*, **64**, 258, 270 (1960).

[14] W. Bild and M. Breiter, *Electrochim. Acta*, **5**, 145, 169 (1961).

[15] J. Guitton and J. Laforest, *Bull. Soc. Chim. France*, **1968**, 859.

[16] A. Kozawa, *J. Electroanalyt. Chem.*, **8**, 20 (1964).

The pretreatment procedures used as well as the denomination of the pretreated surfaces were the same as in our previous work.[1] Since there exists considerable evidence to support that iodide ions used for the preparation of bare surfaces[1] are strongly adsorbed on platinum[18] the extent of adsorption depending on pretreatment,[19] and that the adsorbed iodide blocks the active sites of the electrode,[20] an attempt has been made to obtain bare surfaces free of adsorbed iodide. For this purpose the pretreatment procedure formerly used was completed with a cyclization of the electrode in 1 N H_2SO_4 between + 0.8 and 0.0 volts (*vs.* S.C.E.) which removed the adsorbed iodide without the electrochemical oxidation of the surface. Alternatively, the oxide layer was removed by soaking the electrode for 10 minutes with a hot solution containing 6 M HCl and 1 % KCl.[21−23] The adsorption of chloride ions on platinum is not significant.[9]

RESULTS AND DISCUSSION

If the potential excursions during cyclization do not exceed −0.1 volts in the cathodic and +1.0 volts (*vs.* S.C.E.) in the anodic side respectively, neither oxidations nor reductions (of the electrode or of the electrolyte) take place in the system, and the corresponding cyclic voltammograms are flat (similar to curve b, fig. 2). The curves indicate only a small residual current due mainly to the charge and discharge of the electric double layer, being well reproducible.

At more negative potentials than −0.1 volts the discharge of the hydrogen ions begins. At more positive potentials than +1.0 volts the oxidation of the platinum surface, respectively the evolution of oxygen takes place. Accordingly, two rises in the cathodic current are observed due to the discharge of the hydrogen ions, respectively to the reduction of the oxygen layer previously formed. The cathodic peak which appears at about +0.4 volts is attributed to this last reduction process. The corresponding anodic processes are represented by the anodic peaks of the ionization of the hydrogen as well as by the anodic rise in the current at more positive potentials than +1.0 volts *vs.* S.C.E. Thus the curve is more complex and it is similar to that obtained by earlier investigators.[2,13,24]

---

[17] S. Gilman, "The anodic film on platinum electrodes" in A. J. Bard (editor), "Electroanalytical Chemistry" vol. 2, Edward Arnold, London and Marcel Dekker, New York, 1967, p. 122.

[18] A. T. Hubbard, R. A. Osteryoung and F. C. Anson, *Analyt. Chem.*, **38**, 692 (1966).

[19] G. Tóth, *Radiokhimiia*, **5**, 411 (1963).

[20] A. J. Bard, *Analyt. Chem.*, **35**, 1602 (1963).

[21] F. C. Anson and J. J. Lingane, *J. Amer. Chem. Soc.*, **79**, 4901 (1957).

[22] M. W. Breiter and J. L. Weininger, *J. Electrochem. Soc.*, **109**, 1135 (1962).

[23] F. C. Anson and D. M. King, *Analyt. Chem.*, **34**, 362 (1962).

The general shape of the curve, having three characteristic regions [25] (hydrogen region, double layer region, oxygen region) strongly depends on the pretreatment of the electrode. Cyclic voltammograms of platinum electrodes subjected to oxidative pretreatments are represented in figures 1 and 2. The direction of the cyclization as well as its sequence are indicated in figures by means of arrows and numbers, respectively. During cyclization the anodic potential of +1.0 volt was not exceeded in order to avoid the electrochemical oxidation of the surface.

The voltammograms in figures 1 and 2 indicate first of all that different pretreatments yield differently oxidized surfaces in accordance with our earlier statements. [1] The quantity of the oxide formed (regardless of its actual form) in each case was determined by graphical integration of the current-potential curves between +0.1 and +0.8 volts, due correction for the residual current being made graphically too (see curve a, fig. 1). Table 1 contains the result of these determinations.

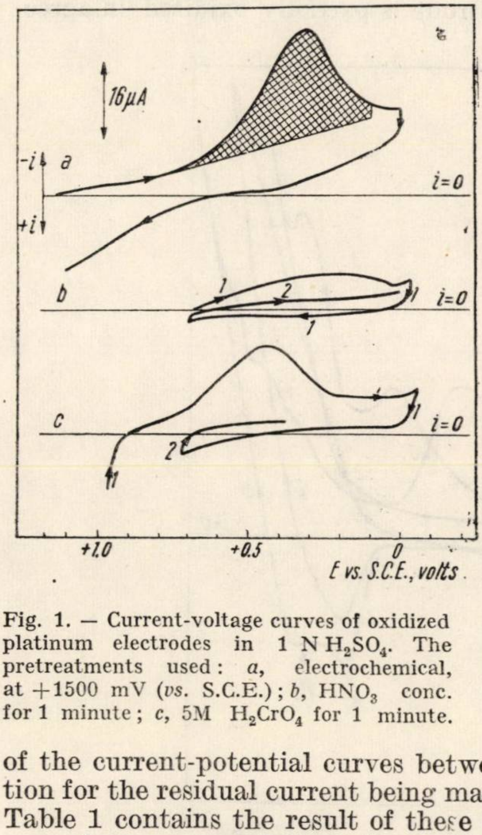

Fig. 1. — Current-voltage curves of oxidized platinum electrodes in 1 N H_2SO_4. The pretreatments used: *a*, electrochemical, at +1500 mV (*vs.* S.C.E.); *b*, HNO_3 conc. for 1 minute; *c*, 5M H_2CrO_4 for 1 minute.

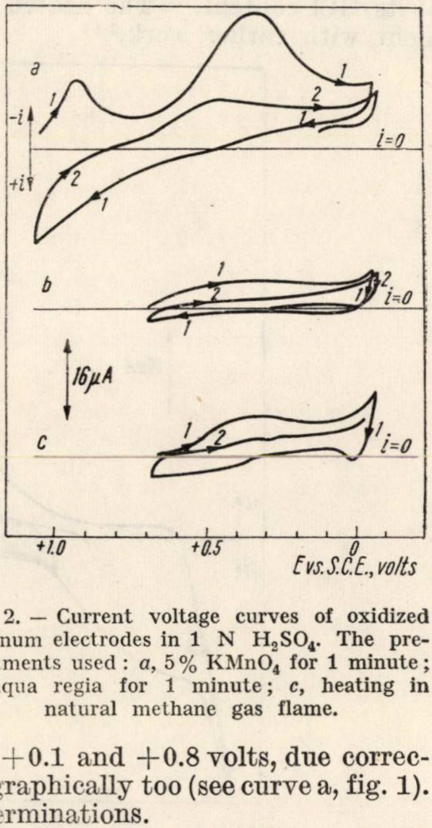

Fig. 2. — Current voltage curves of oxidized platinum electrodes in 1 N H_2SO_4. The pretreatments used: *a*, 5% $KMnO_4$ for 1 minute; *b*, aqua regia for 1 minute; *c*, heating in natural methane gas flame.

One can see that platinum is most oxidized by anodization, either with $KMnO_4$ or with H_2CrO_4. The potential of the oxide reduction peak

---

[24] M. W. Breiter, *J. Electrochem. Soc.*, **109**, 42 (1962).

[25] A. Shygin and A. Frumkin, *Acta Physicokhimika U.R.S.S.*, **3**, 791 (1935).

varies with the pretreatment indicating a dependence of the reversibility of the electrode process on the surface state. As expected, aqua regia yields a less oxidized surface owing to the oxide film solving property of its HCl content. [23] The heated electrode is partially oxidized, in agreement with earlier work.[1,12]

Table 1

Quantity of the oxide formed during different oxidative pretreatments

Pretreatment	Oxide in μ coul/cm^2
electrolytic	781
$KMnO_4$	695
H_2CrO_4	512
HNO_3 cc.	201
aqua regia	157
heating	159

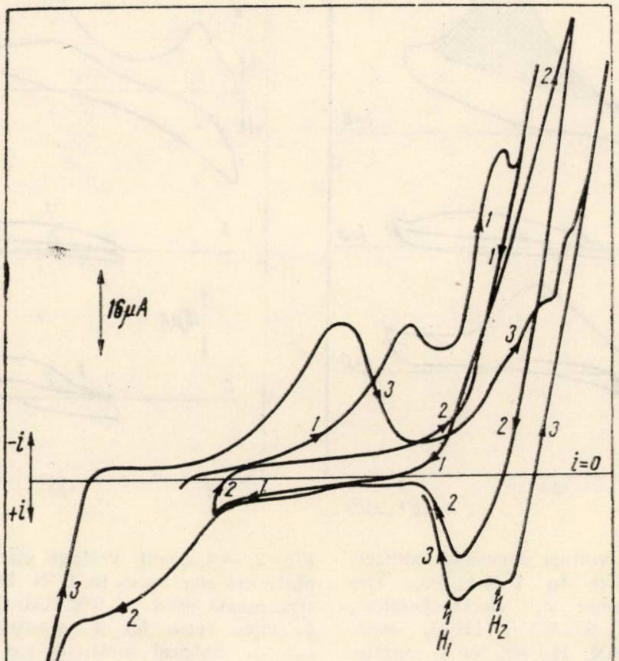

Fig. 3. — Current-potential curves of excessively anodized electrodes at 500 mA/cm^2 for 24 hours.

Excessively anodized surfaces reported by Kozawa [16] have a slightly different behaviour. They were prepared with anodization for 24 hours at 500 mA/cm^2 in 1 N H_2SO_4. Then the electrodes were washed and transferred into the electrolysis cell. After bubbling pure nitrogen for 10 minutes the cyclization was performed beginning at +0.9 volts (fig. 3).

The shape of the curves varies with the number of cyclizations. In the first cathodic branch there appears the reduction peak of the oxide and also two reduction steps for hydrogen ions. The subsequent anodic branch does not show any oxidation of the hydrogen indicating that the surface is not yet sufficiently active to mediate this reaction. The anodic oxidation of the hydrogen appears only on further cyclization. On sufficiently active surfaces it exhibits two peaks corresponding to the two forms of hydrogen bonded differently on structurally different adsorption sites.[26] This view is supported by the fact that firstly only peak H_1 appears (cycle 2) being followed by peak H_2 which on further cyclization increases on account of the former. The corresponding two cathodic peaks are also present. On cyclization the peak potentials both for the oxide and the H^+ ions vary too. At the same time it was generally observed that the higher the reduction peak of the oxide, the more negative the corresponding reduction potential, indicating the irreversibility of the process.

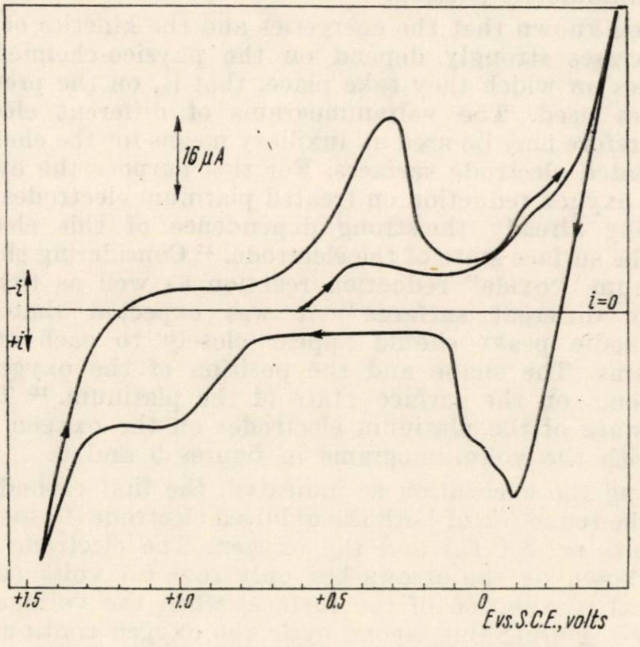

Fig. 4. — Cyclic voltammogram of a heated electrode.

Heated electrodes were specially investigated since their remarkable activity is well known. It was already stated that they are partially oxidized (see e. g. curve c, fig. 2) susceptible either to reduction or to further oxidation [1] (fig. 4).

---

[26] See 17, p. 124.

The voltammogram of a heated electrode exhibits two peaks both for the hydrogen reduction and/or oxidation respectively showing at the same time a well formed wave for the platinum oxidation. This wave appears only on very active electrodes. Even on heated electrodes it appears only after cathodization to —0.1 volts *vs.* S.C.E. This surface markedly differs from the reduced but formerly not heated electrode, the oxidation wave of such an electrode being less pronounced. It is again remarked the effect and the importance of the last but one pretreatment, especially when this consists of heating.

The shape of the $i-E$ curve shown in figure 4 is characteristic of very active surfaces. On less active surfaces the hydrogen peaks are singular and the oxidation wave of the platinum is not well formed.

Reduced electrodes were prepared by cathodization at different potentials between 0.0 and —350 millivolts respectively (*vs.* S.C.E.) as well as by chemical treatment with ferrous sulphate. The characteristic voltammograms (taken between —0.1 and 1.0 volts) are similar to those of curve b, figure 2, indicating the absence of the oxide layer on the reduced electrodes. Bare electrodes (prepared either with KI or with HCl) yield the same voltammetric pattern.

It is well known that the energetics and the kinetics of the electron transfer processes strongly depend on the physico-chemical properties of the surfaces on which they take place, that is, on the pretreatment of the electrodes used. The voltammograms of different electrochemical reactions therefore may be used as auxiliary means for the characterization of the pretreated electrode surfaces. For this purpose the cyclic voltammetry of the oxygen reduction on treated platinum electrodes was investigated knowing already the strong dependence of this electrochemical reaction on the surface state of the electrode.[27] Considering the E^0 values of the platinum "oxide" reduction reaction as well as that of the O_2 reduction on different surfaces[16] it was expected that the corresponding cathodic peaks should appear closely to each other on the voltammograms. The shape and the position of the oxygen peak will strongly depend on the surface state of the platinum.[16] The effect of the surface state of the platinum electrodes on the oxygen reduction is illustrated with the voltammograms in figures 5 and 6.

Following the cyclization as indicated, the first cathodic peak corresponds to the reduction of both the oxidized electrode (formerly anodized at +1.50 volts *vs.* S.C.E.) and the oxygen. The electrode was further cyclized as shown by the arrows but only to + 0.7 volts (to avoid the electrochemical reoxidation of the surface) when the voltage sweep was newly reversed. During this second cycle the oxygen continues to reduce but now on a reduced surface, previously formed. On this reduced surface the oxygen reduction takes place with a great overvoltage and much slower. The reduction of the oxygen also continues during the second half of the second cycle till the electrode potential becomes less cathodic than that necessary for this reaction. In accordance with earlier statements,[16] the oxygen reduction is favoured by oxidized surfaces.

---

[27] D. G. PETERS and R. A. MITCHELL, *J. Electroanalyt. Chem.*, **10**, 306 (1965).

Bare electrodes have a quite different behaviour depending on the adsorbed anions on their surface (fig. 6).

Adsorbed I^- ions inhibit wholly the reduction of the oxygen and to a great extent also the oxidation of the hydrogen (curve a, fig. 6). At the same time on bare electrodes prepared with HCl both processes occur undisturbed (curve b, fig. 6). The same electrode bathed with KI becomes poisoned and inactive for the oxygen reduction (curve c, cycle 1, fig. 6). Cathodization till hydrogen evolution (cycle 2) eliminates the adsorbed iodide activating the electrode (cycle 3 see also curve a).

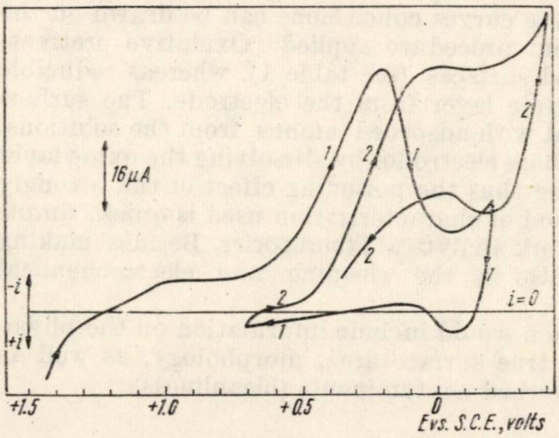

Fig. 5. — Voltammograms of the oxygen reduction on oxidized (cycle 1) and reduced (cycle 2) electrodes. Air saturated 1 N H_2SO_4.

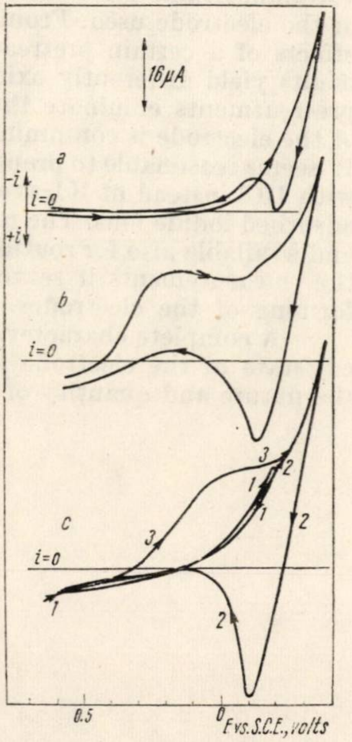

Fig. 6. — Voltammograms of the oxygen reduction on bare electrodes. Air saturated 1 N H_2SO_4. *a*, oxide layer dissolved with KI; *b*, oxide layer dissolved with HCl; *c*, as b) but after this treatment the electrode bathed with KI.

The hydrogen region of the voltammograms corresponding to the deposition and dissolution of hydrogen atoms can also supply useful information about the state of the platinum surface. The reaction is reversible on freshly reduced electrodes, yielding double reduction and oxidation peaks especially on active surfaces prepared by repeated cyclization of the electrode in purified solutions or by heating. On standing, the electrode becomes quickly deactivated mainly through adsorption of impurities. A hydrogen region consisting of a single step in both cathodic and anodic branches (e.g. curve b, fig. 6) is characteristic of such inactive electrodes.

CONCLUSIONS

Slow triangular voltage sweep cyclic voltammetry is a reliable tool for the characterization of pretreated platinum electrodes used in electroanalytical chemistry. The oxygen and the hydrogen regions of the voltammograms have characteristic shapes according to the surface state of the electrode used. From these curves conclusions can be drawn on the effects of a certain pretreatment procedure applied. Oxidative pretreatments yield differently oxidized surfaces (see table 1), whereas reducible pretreatments eliminate the oxide layer from the electrode. The surface of the electrode is contaminated with adsorbed anions from the solutions. It seems reasonable to prepare bare electrodes by dissolving the oxide layer with HCl instead of KI avoiding thus the poisoning effect of the strongly adsorbed iodide ions. The method of characterization used is quick, simple and available also for routine work analytical laboratories. Besides making the measurements it serves also in the cleaning and electrochemical forming of the electrodes.

A complete characterization would include information on the physical state of the electrode like true surface area, morphology, as well as the nature and quantity of adsorbed contaminants (cleanliness).

Revue Roumaine de Chimie, **14**, 613–618 (1969)

SPECTROPHOTOMETRIC METHOD FOR THE QUANTITATIVE ANALYSIS OF *ORTHO*- AND *PARA*-NITROETHYLBENZENE MIXTURES

L. FEY and JANA RUSU

Chemical-Pharmaceutical Research Institute, Cluj, str. K. Marx, 93–97

Received: July 19, 1968

On the basis of the measurement of the extinctions at two different wavelengths, a simple quantitative analysis of the mixtures formed by *ortho*- and *para*-nitroethylbenzenes has been worked out.

Up to now only few methods for the quantitative analysis of *o*- and *p*-nitroethylbenzene (*o*- and *p*-NEB) mixtures have been reported. Thus, Neumann[1] has proposed a method based on the difference between the oxidation rates of these two isomers to the corresponding nitrobenzoic acids. He established that in acetic acid solution, 72 per cent of the *p*-isomer is transformed by cromic anhydride into *p*-nitro-benzoic acid, while only a very small quantity of the *o*-isomer is being oxidized. Thus, the initial *p*- and *o*-NEB ratio can be estimated, by strict standardization of the conditions of reaction, taking also into account the corresponding oxidation yields, as well as the errors intervening in the isolation of *p*-nitro-benzoic acid. The procedure is obviously difficult, and appreciable errors may be caused by unimportant deviation from the standard conditions. An IR-spectrophotometric method was reported by Hamburg.[2] However differences between the IR-spectra of the two isomers are not too obvious and thus the quantitative estimation of the results is fairly difficult. The gas-chromatographic method, although very adequate, requires a less accessible outfit.

The electronic spectra of the *o*- and *p*-NEB isomers are known in literature, but have not been studied from an analytical standpoint, with a view of determining the components of the mixture.

In order to establish a method of dosage of the isomers, we have carried out a detailed study of the spectra of pure substances and of the system containing the two isomers in mixture. As a result we have recorded the spectral curves in methanol, as seen in figure 1.

As seen obviously very significant differences between the spectra of these two isomers exist. Thus, at the extinction maximum of *para*-derivative, the *ortho*-isomer has only a small extinction. The difference between the specific absorptions ($E^{1\%}_{1\text{cm}}$) at this wavelength (272 nm) is about 400 units. On the other hand, at 232 nm, both spectra have minima, the extinction difference being small, but in opposite direction as compared to that observed at 272 nm. In order to determine quantitatively the

---

[1] I. Neumann, V. Stepankova and Z. Annicky, *Chem. průmysl*, **8**, 244 (1958).
[2] E. Hamburg, *Studii şi Cercetări Chim. Fil. Cluj*, **13**, 255 (1962).

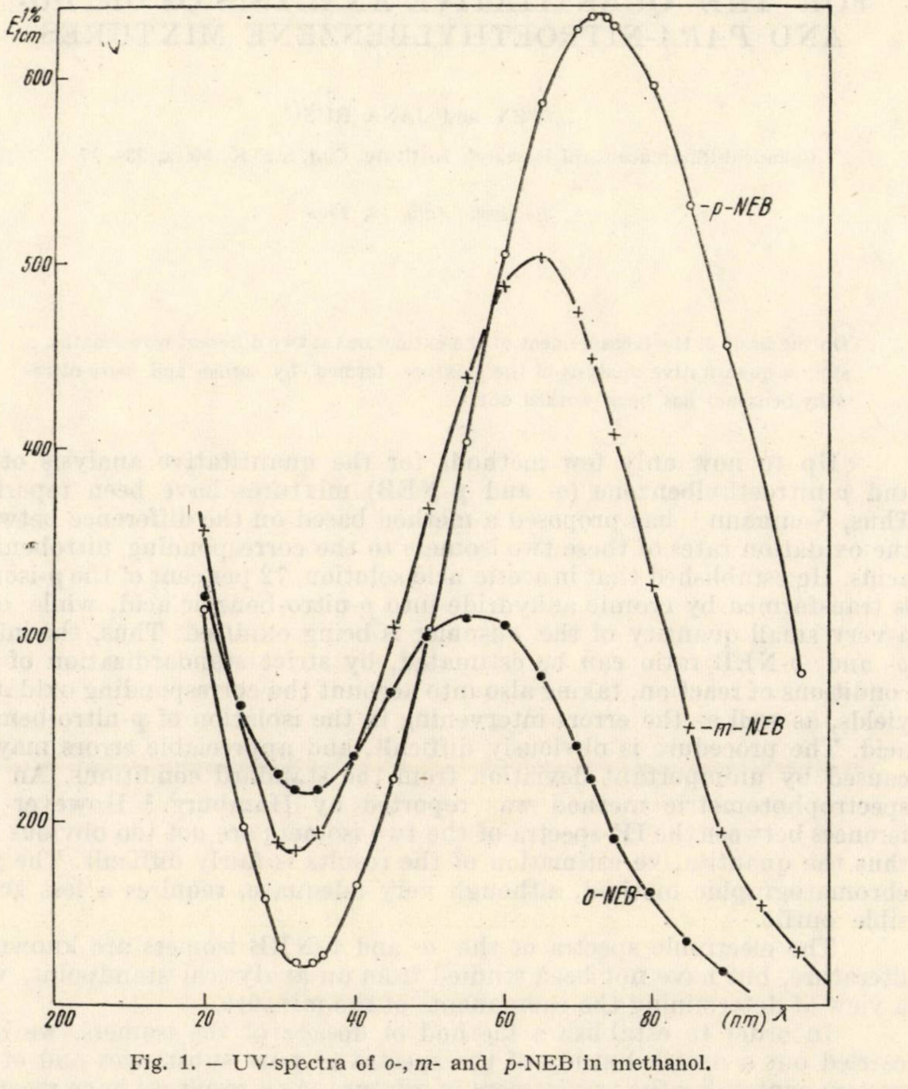

Fig. 1. – UV-spectra of *o*-, *m*- and *p*-NEB in methanol.

composition of the studied mixtures, owing to the mentioned differences, these two wavelengths are the most suitable. The following notations have been used:

E_0^{272}, E_0^{232} – the corresponding specific extinctions (1 cm, 1%) of *o*-NEB at 272 and 232 nm respectively;

E_p^{272}, E_p^{232} – the specific extinctions of *p*-NEB at 272 and 232 nm respectively;

E^{272}, E^{232} — the specific extinctions of the isomer-mixtures at 272 and 232 nm respectively;
C_o, C_p — the concentrations of *o*- and *p*-isomers in the mixture, in g/g.

Admitting the validity of Beer's law for the pure components, as well as for their mixtures-(independence of the own-extinctions of components), the following equation-system can be written:

$$C_o E_o^{272} + C_p E_p^{272} = E^{272}$$
$$C_o E_o^{232} + C_p E_p^{232} = E^{232}$$

whence:

$$C_o = \frac{D_1}{D} \quad \text{and} \quad C_p = \frac{D_2}{D}$$

where:

$$D_1 = \begin{vmatrix} E^{272} & E_p^{272} \\ E^{232} & E_p^{232} \end{vmatrix} \qquad D_2 = \begin{vmatrix} E_o^{272} & E^{272} \\ E_o^{232} & E^{232} \end{vmatrix} \qquad D = \begin{vmatrix} E_o^{272} & E_p^{272} \\ E_o^{232} & E_p^{232} \end{vmatrix}$$

We have examined the validity of Beer's law for pure isomers in 0–4 mg/100 ml concentration intervals. The obtained results, given in figure 2, corroborate perfectly the proportionality in the cases of *o*- and *p*-isomers, at both chosen wavelengths.

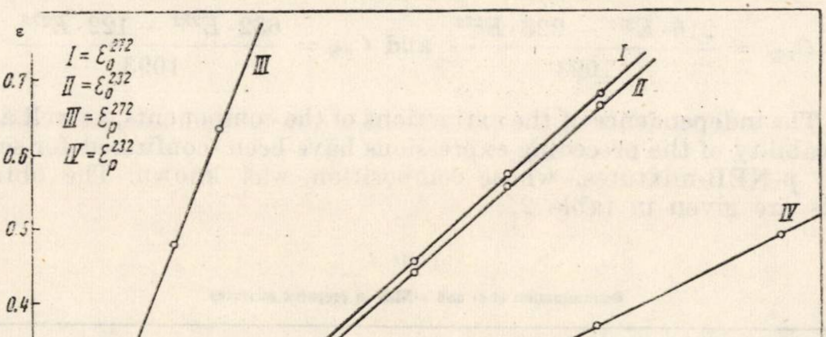

Fig. 2. — Validity of Beer's law for *o*- and *p*-NEB.

The values of the specific extinctions at two wavelengths obtained as the average of individual determinations are shown in table 1.

Table 1

Determination of specific absorptions of *o*- and *p*-NEB

o-NEB			*p*-NEB		
Conc.mg %	E_0^{232}	E_0^{272}	Conc. mg %	E_p^{232}	E_p^{272}
0.5122	214	225	0.2520	—	634
1.0244	217	222	0.5040	—	631
2.0488	216	223	0.7560	—	632
2.5610	214	224	1.0080	125	632
3.0732	218	221	1.5120	120	—
—	—	—	3.024	123	—
—	—	—	4.032	122	—
Average :	216	223		122	632

These values have been used in order to get the following formula for the concentration of components in the mixture:

$$C_{p\%} = \frac{216 \cdot E^{272} - 223 \cdot E^{232}}{1093} \quad \text{and} \quad C_{o\%} = \frac{632 \cdot E^{232} - 122 \cdot E^{272}}{1093}$$

The independence of the extinctions of the components, as well as the applicability of the preceding expressions have been confirmed for several *o*- and *p*-NEB-mixtures, whose composition was known. The obtained results are given in table 2.

Table 2

Determination of *o*- and *p*-NEB in prepared mixtures

Concentration				E^{272}	E^{232}	Deviation	
known		found					
$C_{p\%}$	$C_{o\%}$	$C_{p\%}$	$C_{o\%}$			$\Delta C_{p\%}$	$\Delta C_{o\%}$
0.0	100.0	0.0	100.0	223	216	—	—
10.7	89.3	10.8	87.0	262	201	+0.1	−2.3
37.5	62.5	37.4	61.3	373	178	−0.1	−1.2
47.5	52.5	47.2	49.8	409	165	−0.3	−2.7
52.8	47.2	52.9	47.9	441	168	+0.1	+0.2
54.5	45.5	54.9	43.1	443	160	+0.4	−2.4
64.2	35.8	62.9	33.0	471	148	−1.3	−2.8
75.0	25.0	74.4	25.6	527	146	−0.6	+0.6
88.4	11.6	89.1	9.9	589	130	+0.7	−1.7
100.0	0.0	100.0	0.0	632	122	—	—

The established formula may only be strictly applied if the mixture does not contain also other components which show absorption at these wavelengths. It is however known, that NEB-isomer mixtures obtained by direct nitration of ethylbenzene, contain a small quantity of about 5% of *meta*-isomer, whose concentration varies very slightly depending on the nitrating conditions, [7] also confirmed by gaschromatographic analysis.[3] Admitting the constance of 5% *meta*-isomer, and according to its corresponding extinction values – ($E_m^{272} = 447$; $E_m^{232} = 183$) – in methanol, these corrections will be: $447 \times 0.05 = 22$ and $183 \times 0.05 = 9$, which must be subtracted from the measured E^{272} and E^{232}, respectively, obtaining in this way the correct concentration values by application of the above expressions. The results obtained in determining the isomers from a series of NEB used as starting material in the current production of Chloramphenicol, are summed up in table 3.

Table 3

Experimental values obtained for NEB-isomers in industrial materials

Sample No	$C_o\%$	$C_p\%$	$(C_o + C_p + C_m)\%$
I	45.2	49.3	99.5
II	44.1	52.1	101.2
III	46.5	46.5	98
IV	43.0	52.1	100.1
V	45.6	47.2	97.9
VI	46.7	48.0	99.7

Our attempts to work out a suitable method for the simultaneous analysis of *o*-, *m*- and *p*-isomers, by measurement of the extinctions at three different wavelengths, did not give satisfactory results, because the spectrum of the *meta*-isomer is very similar to the arithmetical average of the spectral curves of the *o*- and *p*-isomers. Consequently, the characteristic determinant of the equation-system for this case has a very small value, about zero. Thus the experimental errors influence appreciably the obtained results, even if Herschberg's method, [8] proposed for the superdetermined systems (measurement of the extinctions at several wavelengths than the number of components) is used.

EXPERIMENTAL

The spectra have been recorded with a Zeiss-VSU-1 spectrophotometer in the spectral range of 220 to 300 nm, the concentrations in methanol of the samples being 2 mg%. The method for the determination of the NEB isomers in an industrial mixture, obtained by nitrating directly the ethylbenzene is given below.

---

[3] R. Simionovici and S. Arizan, unpublished work from the technical documentation of the Chem. Pharm. Research Institute, Cluj (1963).

[4] L. Lang, "Absorption Spectra in the UV and Visible Region", vol. 1 Ed. by Hung. Acad. of. Sciences, Budapest, 1963, p. 81.

[5] L. Lang, "Absorption Spectra in the UV and Visible Region", vol. 4 Ed. by Hung. Acad. of Sciences, Budapest, 1963, p. 83.

[6] W. M. Schubert and J. Robins, *J. Amer. Chem. Soc.*, **80**, 559 (1958).

[7] A. F. Holleman, *Chem. Rev.*, **1**, 187 (1925).

[8] I. S. Herschberg, *Z. analyt. Chem.*, **205**, 180 (1964).

About 100 mg mixture of isomers are accurately weighed and made up to 50 ml with methanol; 1.00 ml of this solution is subsequently diluted with methanol up to 100 ml. The specific extinctions of this solution against a methanol blank are determined at a wavelength of 232 and 272 nm, using quartz cells of 1.00 cm in thickness. The content of the isomers is calculated by the following formula:

$$C_p = \frac{216 \cdot (E^{272} - 22) - 223 \cdot (E^{232} - 9)}{1093}$$

$$C_o = \frac{632 \cdot (E^{232} - 9) - 122 \cdot (E^{272} - 22)}{1093}$$

Revue Roumaine de Chimie, **14**, 619–628 (1969)

KINETIK DER KONTINUIERLICHEN ALKOHOLDEHYDRIERUNG AN KUPFERKATALYSATOREN BEI NIEDRIGEM DRUCK

A. A. BALANDIN, I. HORESCU und A. P. RUDENKO

Lomonosov-Universität, Moskau, UdSSR und Universität Timişoara,
Rumänien, str. Vasile Pârvan, 2

Eingegangen am 1. März 1968

Auf Grund der Versuchsergebnisse werden die kinetischen Gleichungen der Dehydrierungsprozesse und die charakteristischen Konstanten berechnet. Aus dem absoluten Adsorptionskoeffizienten wird das Adsorptionsgleichgewicht an der Katalysatorenoberfläche berechnet. Es wird der Einfluß des Drucks auf Reaktionsgeschwindigkeit und -mechanismus bestimmt.

I. DEHYDRIERUNG DES ÄTHANOLS

Die Kinetik der heterogenen katalytischen Reaktionen in kontinuierlichem Fluß wird theoretisch durch die Beziehung zwischen der Reakionsgeschwindigkeit, den Partialdrücken der Reaktionsteilnehmer ($p_{A_1}, p_{A_2}, \ldots$) und den absoluten Adsorptionskoeffizienten ($a_1, a_2, \ldots$) wiedergegeben :

$$V = \varphi\,(p_{A_1},\ p_{A_2}, \ldots a_1,\ a_2, \ldots) \qquad (1)$$

Solche Funktionen wurden für verschiedene Fälle in den Arbeiten von Balandin,[1,2] Hougen und Watson,[3,4] Panchenkov,[5,6] Frost[7] und anderen angeführt. Eine experimentelle Nachprüfung dieser Funktionen konnte durch Veränderung der Partialdrücke nicht direkt durchgeführt werden, weil die dazu benötigte Apparatur zur Ausführung heterogener katalytischer Reaktionen in kontinuierlichem Fluß bei veränderlichen Drücken und eine entsprechende Arbeitsmethodik noch nicht ausgearbeitet worden waren. In unserer Arbeit[8] wurde eine Methodik zur Ausführung

---

[1] A. A. Balandin, *Zhur. obshchei Khim.*, **31**, 745 (1957).

[2] A. A. Balandin, *Zhur. obshchei Khim.*, **12**, 135 und 16 (1942).

[3] O. A. Hougen und K. M. Watson, *Ind. Eng. Chem.*, **35**, 535 (1943).

[4] O. A. Hougen und K. M. Watson, „Chemical Process Principles", New York – London, 1948.

[5] G. M. Panchenkov, *Zhur. fiz. Khim.*, **22**, 209 (1948).

[6] G. M. Panchenkov, *Zhur. fiz. Khim.*, **26**, 453 (1952).

[7] A. V. Frost, *Vestnik Moskovskovo Univ.*, 1946, nr. **3–4**, III.

[8] I. Horescu, Dissertation, Lomonosov-Universität, Moskau, 1965.

der Versuche und zur Verarbeitung der in der Arbeit [9] erhaltenen Daten benötigte Apparatur beschrieben, wodurch es möglich wurde, Bestimmungen zwischen 760 und 50 mmHg mit einer Genauigkeit von ± 0,1 mmHg durchzuführen.

Außer einer Überprüfung von Gleichungen des Typus 1 wurde versucht, das Adsorptionsgleichgewicht, nämlich die absoluten und relativen Adsorptionskoeffizienten, die Geschwindigkeitskonstante und die Aktivierungsenergie festzulegen. Die Bestimmung dieser Größen, besonders des absoluten Adsorptionskoeffizienten ist von größter Wichtigkeit für die Kennzeichnung eines Katalysators und eröffnet neue Perspektiven bei der Auswahl des günstigsten Katalysators.

Versuche zur Bestimmung dieser Größen finden sich bei Balandin [2] und Frost, [10] die auch Varianten der Gleichungen vom Typus 1 ausgearbeitet haben, welche die Berechnung des absoluten Adsorptionskoeffizienten und der Geschwindigkeitskonstante erlauben.

EXPERIMENTELLES

Die Versuche wurden an frischen Kupferkatalysatoren vorgenommen; vor Durchführung der Bestimmungen wurde der Katalysator 3 Stunden lang mit Wasserstoff und anschließend 30 Min mit analysenreinem Äthanol behandelt. Dadurch konnte die Aktivität des Katalysators fast konstant gehalten werden (in 30 Min. fiel die Aktivität des Katalysators nur um 1—2,5 %). Der Katalysator wurde durch Fällen von Kupfernitrat mit Natriumcarbonat, Trocknen und Reduktion mit Wasserstoff hergestellt.

Die Abnahme der katalytischen Aktivität wurde durch Interpolation in Arrheniusschen Koordinaten bei bekannter Aktivierungsenergie nach [8] bestimmt.

Die Reproduzierbarkeit der erhaltenen Ergebnisse wurde durch Kontrollproben beim Standarddruck von 700 mmHg vor und nach jeder Bestimmung geprüft. Die Geschwindigkeit der Dehydrierungsreaktion wurde durch Messen des Volumens des abgeschiedenen Wasserstoffs mit Hilfe eines automatischen Gasometers mit graphischer Registrierung der Ergebnisse bestimmt.

Ein Beispiel der Verwertung der Ergebnisse ist in Tabelle 1 wiedergegeben; dabei bedeuten

V_p — die Reaktionsgeschwindigkeit in ml H_2/min, abgeschieden bei Druck p,
V_p^0 — den auf 760 mmHg und 20° umgerechneten V_p-Wert,
V_t^0 — die Reaktionsgeschwindigkeit beim Standarddruck 700 mmHg, umgerechnet für 760 mmHg und 20°,
ψ — einen Koeffizienten, der die Druckabhängigkeit der Reaktionsgeschwindigkeit wiedergibt.

Durch die Verringerung des Drucks werden die Bedingungen der Wärmeübertragung geändert, und die Reaktion verläuft bei niedrigeren Temperaturen als bei obigem Beispiel, obgleich das Temperaturregelungssystem gleich bleibt, und zwar bei 257,7° statt bei 259,4°. Aus den Geschwindigkeiten bei Standarddruck vor und nach der Reaktion, wurde V_u^0 für 257,7° mit dem Interpolationsverfahren und den Arrheniusschen Koordinaten berechnet und daraus ψ bestimmt.

---

[9] I. Horescu, A. A. Balandin und A. P. Rudenko, ,,Fortgeschrittene Erfahrung in Technik, Wissenschaft und Produktion'', Gesintim, S. 65 (russisch).

[10] T. B. Antipina und A. V. Frost, *Zhur. fiz. Khim.*, **24**, 860 (1960).

Tabelle 1

Verwertung der primären Daten von der Äthanoldehydrierung an einem Kupferkatalysator (Berechnung der Reaktionsgeschwindigkeit V_p^0, Interpolation der Reaktionsgeschwindigkeit für die der Reaktion bei niedrigerem Druck entsprechende Temperatur V_i^0, Berechnung des Änderungskoeffizienten ψ der Reakionsgeschwindigkeit und des Abfalls der katalytischen Aktivität).

Nr. der Probe	Druck mmHg	Temperatur °C	$\frac{1}{T°K} \cdot 10^3$	V_p ml/min	V_p^0 ml/min	V_i^0 ml/min	ψ %	Umsatz %	Abfall der katalytischen Aktivität, %
1	700	259,4	1,8782	3,66	3,36	—	—		
2	400	257,7	1,8864	4,84	2,55	3,25	22,5	3,60	$\frac{3,36-3,28}{3,36} \times 100 = 2\%$
3	700	259,0	1,8796	3,56	3,28	—		—	

Der Koeffizient ψ, der die Änderung der Reaktionsgeschwindigkeit wiedergibt, wurde nach

$$\psi = \frac{V_u^0 - V_p^0}{V_u^0} \cdot 100 \tag{2}$$

berechnet, wo V_u^0 die Reaktionsgeschwindigkeit bei der Temperatur T_p und 700 mmHg Druck, V_p^0 die Reaktionsgeschwindigkeit bei der Temperatur T_p und beim Druck p bedeuten.

In unserer vorhergehenden Arbeit[8] wurde gezeigt, daß bei Verwendung der Gleichung 2 und bei Interpolation von V_u^0 in Arrheniussche Koordinaten die Fehler bei der Bestimmung von ψ vernachlässigt werden können, wenn die katalytische Aktivität sich um 1—5% ändert.

In Tabelle 2 sind die Ergebnisse von Versuchen zur kontinuierlichen Dehydrierung des Äthanols an einem Kupferkatalysator bei Drücken von 700 und 300 mmHg und Temperaturen zwischen 240° und 260° angeführt. Aufgrund dieser Daten wurden die Aktivierungsenergien berechnet (16,45 kcal/Mol).

Tabelle 2

Aktivierungsenergie für die Dehydrierungsreaktion von Äthanol an einem Kupferkatalysator, bei Drücken von 700 und 300 mmHg und Temperaturen zwischen 240–261°

Nr. der Probe	Druck mmHg	Temperatur °C	V_p cm³/min	Aktivierungsenergie kcal/Mol
4	700	261,0	5,04	
5	700	243,3	2,50	16,0
6	700	257,2	4,06	
7	300	252,5	14,46	
8	300	256,3	16,58	16,9
9	300	261	18,84	

Aus den Angaben der Tabelle 2 ist ersichtlich, daß die Aktiverungsenergie zwischen 700 und 300 mmHg druckunabhängig ist; dies spricht dafür, daß sich der Reaktionsmechanismus zwischen diesen Grenzwerten nicht ändert.

Die Ergebnisse der Versuche zur Bestimmung der Druckabhängigkeit der Reaktionsgeschwindigkeit zeigt Tabelle 3. Die Versuche wurden im Druckbereich 700—100 mmHg und im Temperaturintervall 240—260° durchgeführt.

Tabelle 3

Druckabhängigkeit der Reaktionsgeschwindigkeit bei der Dehydrierung von Äthanol an einem Kupferkatalysator. Bestimmung des Änderungskoeffizienten der Reaktionsgeschwindigkeit bei verändertem Druck (Einführungsgeschwindigkeit des Reaktionsteilnehmers 0,1811 ml/min, Gewicht des Katalysators 0,2159 g, Temperatur 251—259°)

Nr. der Probe	Druck mmHg	Tempe. ratur °C	V_p ml/min	V_p^0 ml/min	V_u^0 ml/min.	$\frac{V_p^0}{V_i^0}\cdot 100$	ψ %	Mittelwert %	Abfall der Aktivität
10	500	251	10,60	6,9	8,32	83,7	16,3	16	—
11	500	256	4,77	3,14	3,72	84,4	15,6		
12	400	257,7	4,48	2,55	3,25	77,5	22,5	22,5	2
13	300	255,2	15,38	6,07	8,04	75,5	24,5	24,7	—
14	300	256,8	20,0	7,89	10,50	75,1	24,9		
15	200	255,2	7,20	1,89	3,62	63,9	36,1	36,1	1,3
16	100	243,3	7,14	0,94	2,30	40,8	59,2	60,6	1,2
17	100	259	12,10	1,59	4,21	38	62,0		

Aus den Angaben der Tabelle 3 folgt, daß die Reaktionsgeschwindigkeit der Äthanoldehydrierung mit dem Druck fällt. Bei einem Druck von 500 mmHg fällt die Reaktionsgeschwindigkeit um 16 %, bei 100 mmHg um 60,6 %. In Abb. 1 wird die Druckabhängigkeit der

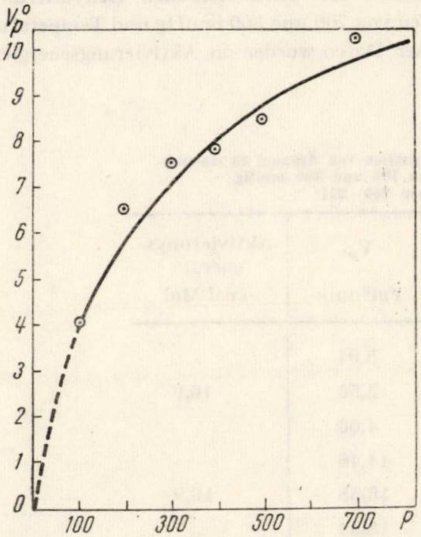

Abb. 1. — Druckabhängigkeit der Reaktionsgeschwindigkeit des C_2H_5OH bei 256°.

Reaktionsgeschwindigkeit in den Koordinaten V_p^0 und P bei einer Temperatur von 256° wiedergegeben. Bei dieser Temperatur und bei 700 mmHg beträgt die experimentell durch das in der Minute abgeschiedene Wasserstoffvolumen (ml) bestimmte Reaktionsgeschwindigkeit 10,10 ml/min (das Wasserstoffvolumen wurde auf 760 mmHg und 20° umgerechnet). Die

Punkte in Abb. 1 wurden aufgrund des oben erwähnten Wertes für die Geschwindigkeit und der Änderungskoeffizienten für die Reaktionsgeschwindigkeit aus Tabelle 3 berechnet. Die Druckabhängigkeit der Reaktionsgeschwindigkeit der Äthanoldehydrierung an einem Kupferkatalysator ermöglicht die Verwendung der Gleichung von Balandin zur Bestimmung des absoluten Adsorptionskoeffizienten:

$$\frac{1}{m} - \frac{1}{2A} = \frac{1}{a_1 kSl} \cdot \frac{1}{P} + \frac{1}{kSl} \tag{3}$$

wenn im Koordinatensystem $\left(\frac{1}{m} - \frac{1}{2A}\right)$ und $\left(\frac{1}{P}\right)$ eine Gerade erhalten wird. Der absolute Adsorptionskoeffizient a_1 wird aus dem Richtungsfaktor $\frac{1}{a_1 kSl}$ und der Nullpunktordinate $\frac{1}{kSl}$ berechnet.

In der Gleichung 3 bedeuten:

m – Geschwindigkeit der Dehydrierungsreaktion,
A – Einführungsgeschwindigkeit des Reaktionsteilnehmers auf die Katalysatormasse,
k – Geschwindigkeitskonstante,
S – katalytische Oberfläche, auf die Längeneinheit des Katalysatorrohrs bezogen,
l – Länge des Katalysatorrohrs,
P – Druck im System.

Die für das Koordinatensystem $\frac{1}{m} - \frac{1}{2A}$ und $\frac{1}{P}$ umgerechneten Versuchsergebnisse sind in Tabelle 4 und Abb. 2 wiedergegeben.

Tabelle 4

Druckabhängigkeit der Reaktionsgeschwindigkeit bei der Dehydrierung von Äthanol an einem Kupferkatalysator in den Koordinaten der Gleichung 3 nach Angaben der Tabelle 3 (Durchsatz des Reaktionsteilnehmers 0,1811 ml/min, Gewich des Katalysators 0,2159 g, Temperatur 255°)

P Druck mmHg	I/P atm^{-1}	m ml/min	$1/m.10^3$ (Mol/min)$^{-1}$	$1/2A.10^3$ (Mol/min)$^{-1}$	$\frac{I}{m} - \frac{I}{2A} \cdot 10^3$ (Mol/min)$^{-1}$	Umsatz %
700	1,085	10,10	2,240	0,3292	1,9108	14,3
500	1,520	8,40	2,6726	0,3292	2,3434	12,0
400	1,900	7,75	2,890	0.3292	2,5608	11,1
300	2,533	7,53	2,974	0,3292	2,6448	10,83
200	3,800	6,39	3.505	0,3292	3,1758	9,2
100	10,850	3,94	5.685	0,3292	5,3558	5,66

Wie aus den Darstellungen ersichtlich, ordnen sich die Versuchsergebnisse in den Grenzen der Versuchsfehler um eine Gerade an, mit Ausnahme des Wertes für den Druck 760 mmHg. Aus den Parametern der Geraden wurde für die Temperatur 256° der absolute Adsorptionskoeffizient des Äthanols $a_1 = 4{,}5$ atm^{-1} berechnet ($ks = 5{,}5 \cdot 10^{-4}$ Mol. cm^2/min.ml)

Wenn a_t die Gleichgewichtskonstante des Adsorptionsvorganges $A_{\mathrm{Gas}} + S_{0\mathrm{Sup}} \rightleftarrows AS_{\mathrm{Sup}}$ darstellt, dann gilt

$$a_t = \frac{(AS)}{(S_0)\,(A)}$$

wo A die zu adsorbierende Substantz, S_0 die Oberfläche, an der Adsorption möglich ist, und AS die sich bei der Adsorption an der Oberfläche bildende Verbindung bedeuten. Aus dieser Beziehung folgt für den Fall $[AS] = [S_0]$, d.h. wenn die Hälfte der verfügbaren Oberfläche vom Reaktionsteilnehmer besetzt ist,

$$a_i = \frac{1}{p_{1/2}}$$

wenn auch der Partialdruck von A eingeführt wird.

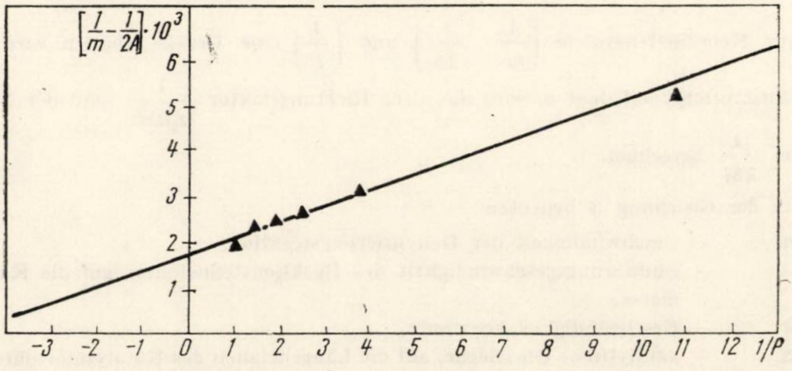

Abb. 2. — Druckabhängigkeit der Dehydrierungsgeschwindigkeit des C_2H_5OH im Koordinatensystem $\left[\frac{1}{m} - \frac{1}{2A} \text{ und } \frac{1}{p}\right]$.

Demnach stellt der absolute Adsorptionskoeffizient den Kehrwert des Drucks dar, bei welchem die Hälfte der verfügbaren Oberfläche vom Reaktionsteilnehmer besetzt ist, und entspricht im vorliegenden Fall einem Druck von 168 mmHg. Dieser Wert deutet darauf hin, daß bei gewöhnlichem Druck die Dehydrierungsreaktion bei fast völliger Besetzung der katalytischen Oberfläche verläuft, was auch mit vorherigen Untersuchungen bei gewöhnlichem Druck in Einklang ist.

II. DEHYDRIERUNG DES ISOPROPANOLS

Die Versuche wurden an demselben Katalysator vorgenommen wie im Falle der Dehydrierung des Äthanols; dieselbe Arbeitsmethodik und Datenverwertung wurden angewandt.

In Tabelle 5 sind die Versuchswerte angegeben, aus denen die Aktivierungsenergie bei Drücken von 700 und 47 mmHg im Temperaturbereich 185—225° berechnet wurden. Wie

Tabelle 5

Aktivierungsenergie für die Dehydrierungsreaktion von Isopropanol an einem Kupferkatalysator, bei Drücken von 700 und 47 mmHg und Temperaturen zwischen 185—225°.

Nr. der Probe	Druck mmHg	Temperatur °C	V_p ml/min	Aktivierungsenergie kcal/Mol
18	700	185,5	6,50	9,4
19	700	193	7,60	
20	700	203,5	9,80	
21	700	224	14,30	
22	47	223	66,2	10,2
23	47	209	49,0	
24	47	196	33,10	

ersichtlich ändert sich die Aktivierungsenergie bei einer fünfzehnfachen Senkung des Drucks nicht, und die erhaltenen Werte 10,2 und 9,4 kcal/Mol, weisen nur eine Differenz von 0,8 kcal/Mol auf, die die Größenordnung der Versuchsfehler nicht überschreitet.

Da die Hypothese aufgestellt wurde, wonach die Änderung der Geschwindigkeit der Dehydrierungsreaktion auf Nebenreaktionen zurückzuführen sei, wurde zur Überprüfung der relative Adsorptionskoeffizient (Z_r) nach Balandin berechnet :

$$Z_r = \frac{\dfrac{m_0}{m} - 1}{\dfrac{1}{p} - 1} \tag{4}$$

wo m_0 die Reaktionsgeschwindigkeit in Gegenwart des reinen Reaktionsteilnehmers, m die Reaktionsgeschwindigkeit in Gegenwart des Reaktionsteilnehmers, verdünnt mit den Reaktionsprodukten, p der Molenbruch des Gemisches (im vorliegenden Fall Isopropanol und Aceton) bedeuten.

Die Ergebnisse sind in Tabelle 6 und Abb. 3 dargestellt. Es wurden verschiedene Einführungsgeschwindigkeiten der Reaktionsteilnehmer, verschiedene Drücke und verschiedene Konzentrationen des Gemisches Isopropanol/Aceton angewandt. Die Ergebnisse weisen darauf hin, daß keine Nebenreaktionen stattfinden, und es wurde erstmalig nachgewiesen, daß bei der Dehydrierung von Isopropanol an Kupferkatalysatoren der relative Adsorptionskoeffizient druckunabhängig ist.

Tabelle 6

Experimentelle und berechnete Angaben über die Verdrängung von Isopropanol durch Aceton im Falle der Isopropanoldehydrierung an einem Kupferkatalysator. Berechnung des relativen Adsorptionskoeffizienten

Nr. der Probe	Gewicht des Katalysators g	Anfänglicher Durchsatz des Reaktanten ml/min	Druck mmHg	Temperatur °C	Zusammensetzung des Gemisches, %		$\overset{\circ}{V}_p$ ml/min	Temperatur °C für Zr	m ml/min	Zr	$\overline{\mathrm{Zr}}$
					$CH_3CHOHCH_3$ %	CH_3COCH_3 %					
25	0,2578	0,1811	700	254,5	100,0	0	3,90	255	3,90		
26	0,2578	0,1811	700	254,5	88,88	11,12	3,41	255	3,41	1,160	1,145
27	0,2578	0,1811	700	255,5	71,36	28,64	2,69	255	2,69	1,127	
28	0,2578	0,1811	700	255,5	51,47	48,53	1,87	255	1,87	1,150	
29	0,4135	0,044	700	242,2	100,0	0	13,48	242,2	13,48	—	
30	0,4135	0,044	700	241,9	73,42	26,58	9,30	242,2	9,33	1,180	1,09
31	0,4135	0,044	700	247,0	50,00	50,00	6,54	242,2	5,92	1,140	
32	0,4135	0,044	700	246,4	25,00	75,0	3,78	242,2	3,51	0,950	
33	0,4135	0,096	700	236,9	100,0	0	23,23	243	23,23	—	—
34	0,4135	0,096	700	241,8	75,0	25,0	17,53	243	16,01	1,330	1,2
35	0,4135	0,096	700	245,5	50,0	50,0	12,10	243	10,52	1,200	
36	0,4135	0,096	700	249,0	25,0	75,0	6,86	243	5,40	1,100	
37	0,5156	0,096	300	235	100,0	0	25,37	235	25,37	—	
38	0,5156	0,096	300	235	75,0	25,0	18,16	235	16,16	1,200	1,14
39	0,5156	0,096	300	235	50,0	50,0	11,33	235	11,33	1,240	
40	0,5156	0,096	300	235	25,0	75,0	6,47	235	6,47	0,980	

Aus Abb. 3 ist ersichtlich, daß die Verdrängungskurven eine Krümmung nach oben haben, während der relative Adsorptionskoeffizient größer als 1 ist, was darauf hinweist, daß Aceton Isopropanol an den aktiven Zentren des Kupferkatalysators verdrängt.

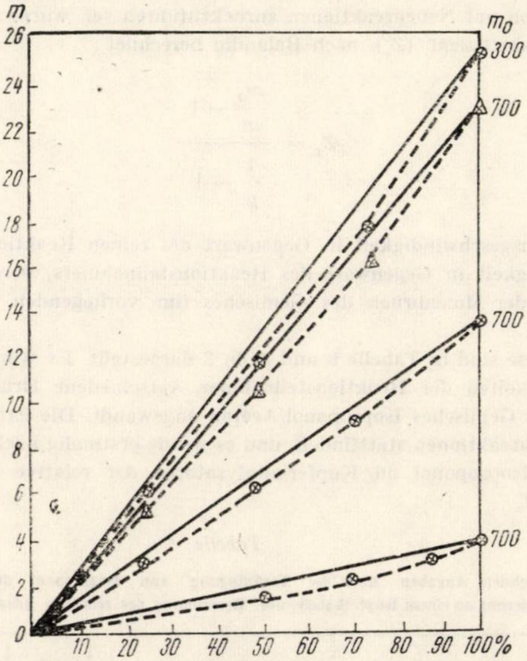

Abb. 3. — Geschwindigkeit der Dehydrierungsreaktion einiger Gemische von $CH_3-CHOH-CH_3$ und $CH_3-CO-CH_3$ bei verschiedenem Druck. Berechnung des relativen Adsorptionskoeffizienten.

Tabelle 7 enthält die Ergebnisse von Versuchen die Druckabhängigkeit der Reaktionsgeschwindigkeit zu bestimmen.

Versuche bei Drücken zwischen 47 und 700 mmHg und Temperaturen zwischen 218,8° und 228,5° zeigen eine Druckabhängigkeit der Reaktionsgeschwindigkeit, und zwar sinkt diese mit sinkendem Druck. So vermindert sich die Reaktionsgeschwindigkeit bei einer Drucksenkung von 700 mmHg auf 500 mmHg um 10 %, bei einem Druckabfall auf 47 mmHg, um 50 % also auf etwa 1/15.

Tabelle 7

Druckabhängigkeit der Reaktionsgeschwindigkeit bei der Dehydrierung von Isopropanol (Gewicht des Katalysators 0,2198 g, Einführungsgeschwindigkeit des Reaktionsteilnehmers $2{,}378 . 10^{-3}$ Mol/min)

Nr. der Probe	Druck mmHg	Temperatur °C	V_p ml/min	V_p^0 ml/min	$V_u^{0''}$ ml/min	$\frac{V_p}{V_u^{0''}} . 10^2$	ψ %	$\overline{\psi}$ %
41	500	219	5,64	3,710	4,09	90,70	9,30	9,30
42	300	218,8	7,90	3,118	4,09	76,25	23,75	22,0
43	300	221	6,30	2,486	3,11	79,9	20,10	
44	200	227	9,56	2,515	3,56	70,6	29,4	29,4
45	100	220	33,0	4,339	8,13	57,58	42,42	41,5
46	100	219,8	17,26	2,269	3,81	59,50	40,50	
47	47	228,5	35,53	2,197	4,47	49,1	50,90	50,90

Aufgrund der Daten aus Tabelle 7 wurde die Reaktionsgeschwindigkeit für 220° im Druckbereich 47–700 mmHg berechnet und die Ergebnisse in Abb. 4 wiedergegeben. Aus diesen Werten wurden die Glieder der Gleichung (3) berechnet und in Tabelle 8 zusammengefaßt.

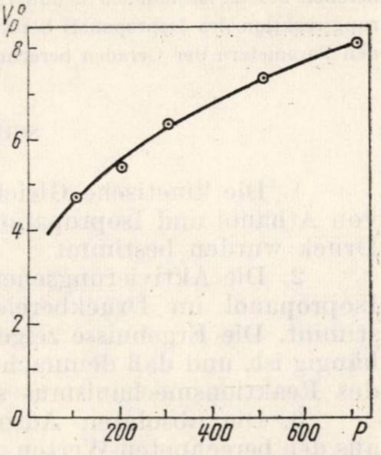

Abb. 4. – Druckabhängigkeit der Reaktionsgeschwindigkeit des $CH_3-CHOH-CH_3$ bei 220°.

Abb. 5. – Druckabhängigkeit der Dehydrierungsgeschwindigkeit des $CH_3-CHOH-CH_3$ im Koordinatensystem $\left[\frac{1}{m}-\frac{1}{2A}\text{ und }\frac{1}{p}\right]$

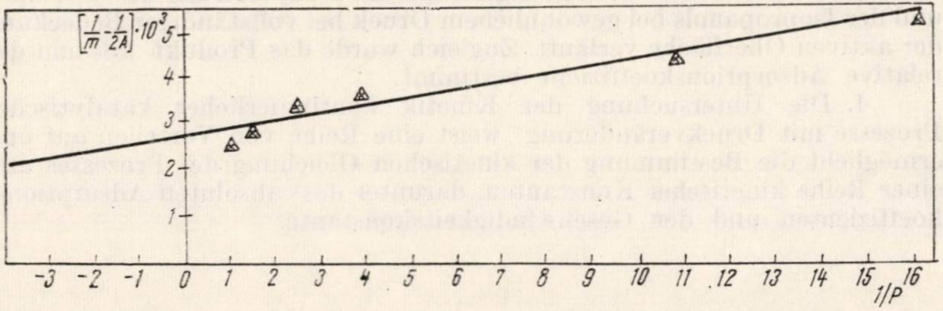

Die Daten aus Tabelle 8 sind in Abb. 5 im Koordinatensystem der Gleichung (3) $\left[\frac{1}{m}-\frac{1}{2A}\right]$ und $\frac{1}{P}$ dargestellt. Wie ersichtlich ordnen sich diese Daten für niedrigere Drücke

Tabelle 8

Druckabhängigkeit der Reaktionsgeschwindigkeit bei der Dehydrierung von Isopropanol an einem Kupferkatalysator, in den Koordinaten der Gleichung 3, nach Angaben von Tabelle 3. Gewicht des Katalysators 0,2159 g, Einführungsgeschwindigkeit des Reaktionsteilnehmers $2{,}378.1^{-3}$ Mol/min, Temperatur 220°)

P mmHg	$1/P$ atm.$^{-1}$	m ml/min	$1/m.10^3$ (Mol/min)$^{-1}$	$1/2\,A.10^3$ (Mol/min)$^{-1}$	$\frac{1}{m}-\frac{1}{2A}.10^3$ (Mol/min)$^{-1}$	Umsatz %
700	1,085	8,13	2,755	0,2102	2,5403	15,24
500	1,520	7,333	3,054	0,2102	2,8438	13,74
300	2,533	6,341	3,532	0,2102	3,3218	11,88
200	3,800	5,739	3,903	0,2102	3,6928	10,75
100	10,850	4,756	4,709	0,2102	4,4988	8,91
47	16,170	3,991	5,612	0,2102	5,4018	7,48

als 700 mmHg innerhalb der Grenzen der experimentellen Fehler um eine Gerade an, so daß der absolute Adsorptionskoeffizient berechnet werden konnte, $a = 19{,}8$ atm^{-1}, ebenso wie der Druck, bei welchem die Hälfte der verfügbaren Oberfläche von Molekülen des Reaktionsteilnehmers besetzt ist, nämlich 39 mmHg. Daraus folgt, daß bei gewöhnlichem Druck die Dehydrierungsreaktion des Isopropanols bei vollständiger Besetzung der Oberfläche verläuft. Der aus den Parametern der Geraden berechnete Wert ist $3{,}52.10^{-4}$ Mol.cm^2/min.ml.

SCHLUSSFOLGERUNGEN

1. Die kinetische Gleichungen für die kontinuierliche Dehydrierung von Äthanol und Isopropanol an Kupferkatalysatoren bei veränderlichem Druck wurden bestimmt.

2. Die Aktivierungsenergien für die Dehydrierung von Äthanol und Isopropanol im Druckbereich zwischen 47 und 700 mmHg wurden bestimmt. Die Ergebnisse zeigen, daß die Aktivierungsenergie druckunabhängig ist, und daß demnach im erwähnten Druckbereich keine Änderung des Reaktionsmechanismus stattfindet.

3. Die absoluten Adsorptionskoeffizienten wurden bestimmt und aus den berechneten Werten gefolgert, daß die Dehydrierung des Äthanols und des Isopropanols bei gewöhnlichem Druck bei vollständiger Bedeckung der aktiven Oberfläche verläuft. Zugleich wurde das Produkt *kSl* und der relative Adsorptionskoeffizient bestimmt.

4. Die Untersuchung der Kinetik kontinuierlicher katalytischer Prozesse mit Druckveränderung weist eine Reihe von Vorteilen auf und ermöglicht die Bestimmung der kinetischen Gleichung des Prozesses und einer Reihe kinetischer Konstanten, darunter des absoluten Adsorptionskoeffizienten und der Geschwindigkeitskonstante.

Revue Roumaine de Chimie, **14**, 629–636 (1969)

INFLUENCE DU SUPPORT SUR L'ACTIVITÉ ET LES PROPRIÉTÉS ÉLECTRIQUES DU CATALYSEUR $Cr_2O_3-Al_2O_3$ UTILISÉ DANS LA RÉACTION DE DÉSHYDROGÉNATION DU *n*-BUTANE EN *n*-BUTÈNES

M. SPINZI et I. V. NICOLESCU

Centre de Recherches de Chimie Physique de l'Académie, Bucaret, 23, str. Dumbrava Roşie

Reçu le 1er octobre 1968

On a poursuivi l'influence réciproque entre le support (Al_2O_3) et la substance active (Cr_2O_3) sur l'activité du catalyseur de déshydrogénation du *n*-butane en *n*-butènes. Les modifications structurales et texturales du support déterminées par les conditions de sa préparation influencent évidemment l'activité du catalyseur. Par des mesures de résistance électrique on a obtenu des indications sur les transformations subies par le catalyseur pendant la période de formation et d'activité maximale.

Dans la littérature de spécialité, il existe de nombreuses études concernant l'explication des relations entre les propriétés physico-structurales et l'activité des catalyseurs chrome-alumine, dans les réactions de déshydrogénation des alcanes ou des cycloalcanes, ainsi que de polymérisation des alkènes.[1,2]

On a notamment insisté sur l'état de valence de l'ion chrome de la couche superficielle des catalyseurs, ainsi que sur la porosité et la structure secondaire du support.[3,4]

Des amples travaux de Weller et Voltz [5,6] et d'autres, concernant l'oxydo-réduction des $Cr_2O_3-Al_2O_3$, il résulte que le niveau oxydo-réducteur du Cr_2O_3 sans support diffère considérablement de celui déposé sur l'Al_2O_3, cette dernière manifestant un effet stabilisateur sur le chrome, et empêchant sa réduction rapide et profonde.

La nature acide de la surface a également constitué l'objet de nombreuses études.[7–9] Vu que l'activité catalytique des oxydes est reflétée

---

[1] C. T. Chen, W. D. Haag et H. Pines, *Chem. Ind.* (*London*), **1959**, 1379.

[2] H. Pines et C. T. Chen, *J. Amer. Chem. Soc.*, **82**, 3562 (1960).

[3] A. Wheeler, « Catalysis », vol. 2, chap. 2, Ed. Reinhold, New York, 1955.

[4] Ch. P. Poole et D. S. Mc. Iver, « Advances in Catalysis », Vol. 17, chap. Ier, Ed. Reinhold, New York – Londres, 1967.

[5] S. Weller et S. E. Voltz, *J. Amer. Chem. Soc.*, **76**, 4695 et 4701 (1954).

[6] S. Weller et S. E. Voltz, *Z. Phys. Chem.* (*Frankfurt*), **5**, 100 (1955).

[7] S. E. Voltz, A. E. Hirscher et A. Smith, *J. Phys. Chem.*, **64**, 1594 (1960).

[8] H. Pines et S. M. Csicsery, *J. Amer. Chem. Soc.*, **84**, 292 (1962).

[9] J. M. Bridges, G. T. Rymer et D. S. Mc. Iver, *J. Phys. Chem.*, **66**, 871 (1963.)

par leurs propriétés électriques, nos recherches ont porté sur l'étude des catalyseurs $Cr_2O_3-Al_2O_3$ de ce point de vue.[10-11] Les études ont abouti à des conclusions fort différentes, ce qui s'explique par la relativité des méthodes électriques employées.

Nous avons considéré qu'on peut obtenir des renseignements particulièrement utiles sur le mécanisme de l'activité du catalyseur $Cr_2O_3-Al_2O_3$ par la corrélation des données d'un ensemble de propriétés concernant le support et le catalyseur. D'ailleurs dans notre laboratoire, on a abordé le problème de cette manière depuis longtemps. [12-13]

Dans ce qui suit, on discute quelques résultats expérimentaux au sujet de l'influence du support, caractérisé par ses principales propriétés, sur les propriétés électriques des catalyseurs chrome-alumine. On a choisi parmi les propriétés du support surtout celles déterminées par les conditions de préparation, comme : porosité, acidité, surface spécifique, structure röntgénographique. Les résultats obtenus ont été mis en corrélation avec l'activité des catalyseurs étudiés dans la réaction test de déshydrogénation du *n*-butane.

Il est bien connu que les propriétés de l'alumine comme support peuvent influencer la dispersion et la dimension des particules du composant actif, ainsi que le spectre des pores. En outre, la préparation de l'alumine support à partir d'une solution d'azotate ou bien d'aluminate alcalin conduit à des alumines, qui, en dehors des propriétés mentionnées, auront des états acides différents, aux forces différentes, qui pourront influencer les réactions concurrentes de cracking ou de déshydrogénation.

PARTIE EXPÉRIMENTALE

L'étude a été effectuée sur deux catalyseurs $Cr_2O_3 - Al_2O_3$, à une teneur de 10% en Cr_2O_3, obtenus par imprégnation de l'alumine support d'une solution d'anhydride chromique.

Pour apprécier la contribution du support aux propriétés du catalyseur, on a utilisé deux alumines, notées par nous AK et A. Leurs propriétés sont inscrites au tableau 1.

Préparation et propriétés de l'alumine support et des catalyseurs. L'alumine AK a été préparée à partir d'aluminate de potassium, par précipitation avec une solution acide, au pH = 7,2–7,4.

L'alumine A a été préparée par précipitation de l'azotate d'aluminium, avec de l'hydroxyde d'ammonium, au pH = 6,4–6,5.

La structure déterminée par la méthode de diffraction aux rayons X a indiqué que, l'hydroxyde AK est constitué de bayérite, tandis que l'hydroxyde A de pseudo-bœhmite.

Par calcination des hydroxydes à 600°, résultent les oxydes d'aluminium correspondants dont la structure est de η Al_2O_3.

Les méthodes complètes de préparation sont indiquées dans le travail. [14]

---

[10] R. Chaplin, P. R. Chapman et R. H. Griffith, *Proc. Roy. Soc.*, **1954**, 229, 419.

[11] P. R. Chapman, R. H. Griffith et J.D.F. Marsh, *Proc. Roy. Soc.*, **1954**, 224, 419.

[12] I. V. Nicolescu, M. Spinzi, M. Gruia, A. Papia, V. Dumitrescu, H. G. Vieweg, S. Novak et H. G. Könneke, *Rev. Roumaine Chim.*, **11**, 3, 363 (1966).

[13] H. G. Vieweg, S. Novak, H. G. Könneke, I. V. Nicolescu et M. Spinzi, *Erdöl u. Kohle*, **19**, 6, 414 (1966).

[14] A. Nicolescu et M. Gruia, *Rev. Roumaine Chim.*, **10**, 12, 1255 (1965).

De l'analyse granulométrique il résulte que les rayons moyens de particules secondaires des deux alumines sont rapprochés, à savoir : 21,8 μ pour l'échantillon AK et 23,6 μ pour l'échantillon A. Les surfaces spécifiques sont approximativement du même ordre de grandeur : 200 m^2/g pour AK et 226 m^2/g pour A.

Comme il était à prévoir, les alumines étudiées diffèrent particulièrement par leur acidité, ainsi que par la structure des pores. L'acidité déterminée par titrage à *n*-butylamine[15] et exprimée en méq. *n*-butylamine/g catalyseur a la valeur de 0,10 pour l'échantillon AK et de 0,34 pour l'échantillon A.

Tableau 1

Constantes physiques des alumines support

Constantes physiques	Al_2O_3 − CAK	Al_2O_3 − CA
Densité réelle	3,18	3,70
Densité apparente	1,07	0,68
Rayon éq. μ	21,8	23,6
Volume total des pores ml/g	0,62	1,20
Volume des macropores > 75 Å ml/g	0,42	0,83
Volume des micropores < 75 Å ml/g	0,20	0,37
Volume des pores au rayon 80−800 Å %	40	88
Volume des pores au rayon 800−3500 Å	57	10
Surface spécifique m^2/g	200	226
Acidité méq *n*-butylamine/g cat.	0,10	0,34
Structure hydroxyde	bayérite	pseudo-bœhmite
Structure Al_2O_3	η	η

Les courbes de répartition des pores (fig. 1), déterminées à l'aide d'un porosimètre Carlo Erba, modèle 65, indiquent de même des différences entre les deux alumines. Le volume des pores de 0,62 ml/g pour l'échantillon AK atteint une valeur double de 1,20 ml/g pour l'échantillon A, leur répartition étant toute différente, comme il ressort du tableau 1.

On a désigné par CAK le catalyseur de l'alumine AK et par CA, celui obtenu de l'alumine A.

Au début, les deux catalyseurs ont présenté le même degré d'oxydation : 1,85 méq KI/g−CAK et 1,80 méq KI/g−CA.

Le spectre des pores des catalyseurs CAK et CA présenté dans la figure 2 indique un volume plus grand de macropores (V_{mp} = 0,57 ml/g) dont 95 % pores au rayon compris entre 80−800 Å pour le catalyseur CA. Le catalyseur CAK ne présente que 0,35 ml/g volume de macropores dont 43 % pores au rayon compris entre 80−800 Å.

Propriétés électriques des catalyseurs. La résistance électrique des catalyseurs a été étudiée à l'aide du même appareillage que celui utilisé dans les études antérieures.[12,13]

---

[15] O. Johnson, *J. Phys. Chem*, **59**, 827 (1955).

Dans la figure 3 on a inscrit la variation de la conductivité électrique en fonction de la variation de la température des catalyseurs oxydés et en présence de l'air.

Le catalyseur CAK à support d'alumine, d'acidité minimale, obtenue à partir d'aluminate de potassium, présente une conductivité électrique supérieure à celle du catalyseur CA, pendant tout l'intervalle de température étudié. La différence entre les deux catalyseurs ressort également de la pente des courbes, ce qui conduit à différentes valeurs pour les énergies d'activation de la conductivité électrique. Pour le catalyseur CAK on obtient $E_\sigma = 11$ kcal/mole, par rapport à l'$E_\sigma = 17{,}3$ kcal/mole, obtenue pour le catalyseur CA.

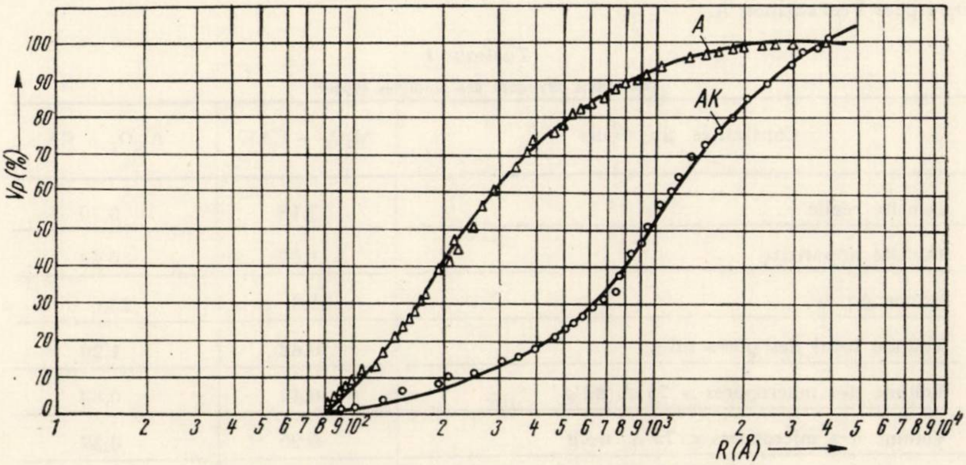

Fig. 1. — Courbe de répartition des pores du support.

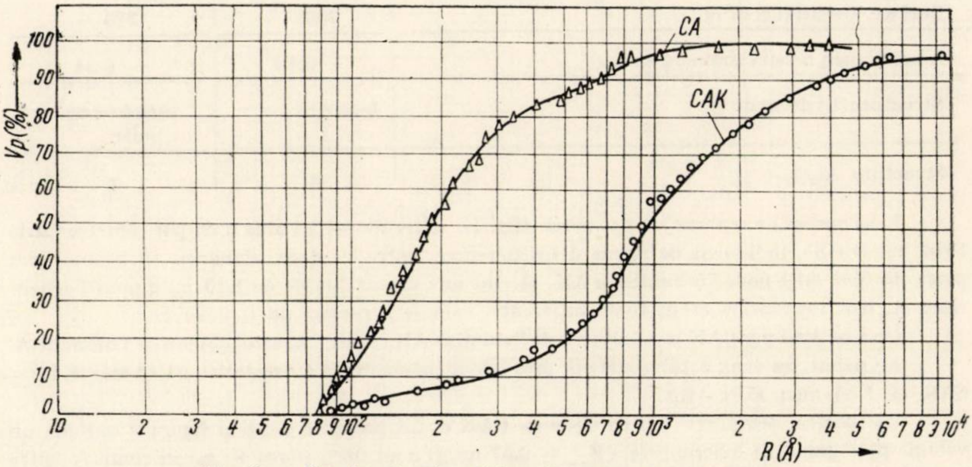

Fig. 2. — Courbe de répartition des pores du catalyseur.

La variation de la conductivité électrique des catalyseurs réduits en atmosphère d'hydrogène, en fonction de la température (fig. 4), est semblable à celle des échantillons oxydés pourvu que l'énergie d'activation de la conductivité électrique, E_{σ}, soit égale à 5,00 kcal/mole, pour le catalyseur CAK, et à 25,4 kcal/mole, pour le catalyseur CA.

En faisant disparaître les ions chrome à valence supérieure au Cr^{3+}, le milieu réducteur agit sur la valeur de la conductivité électrique des deux catalyseurs.

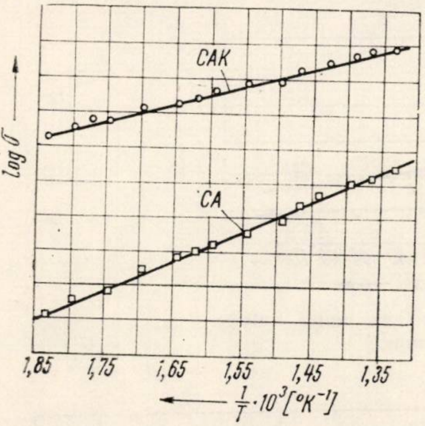

Fig. 3. — Variation de la conductivité électrique des catalyseurs oxydés par rapport au temps.

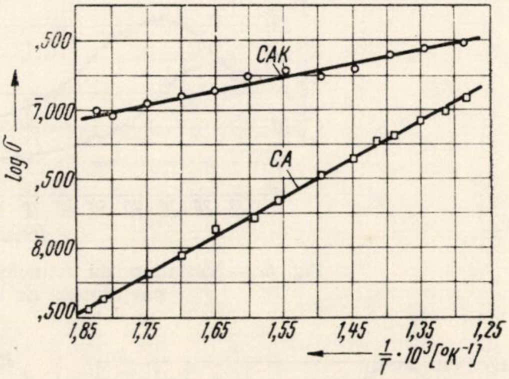

Fig. 4. — Variation de la conductivité électrique des catalyseurs réduits par rapport au temps.

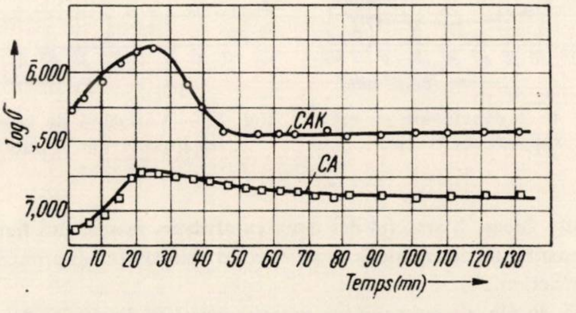

Fig. 5. — Variation de la conductivité électrique des catalyseurs pendant la réduction par hydrogène.

Il est bien connu que l'alumine imprime un effet stabilisateur pendant la réduction du chrome, en lui déterminant une certaine valence. [5,6] En supposant que toute modification subie par la surface $Cr_2O_3-Al_2O_3$ en milieu réducteur soit reflétée par les propriétés électriques, nous avons poursuivi la variation de la conductivité électrique par rapport au temps, en milieu d'hydrogène. Les diagrammes inscrits dans la figure 5 nous permettent de constater pendant les premières 20—30 minutes, la présence de certains pics, qui s'aplatissent vers une valeur constante de conductivité, au moment où le chrome atteint un état stable de valence.

Pendant la période initiale, l'échantillon CAK au support alumine de faible acidité présente un pic plus prononcé, suivi d'une stabilisation plus rapide. Cependant, le catalyseur CA, ayant comme support une alumine plus acide, possède un pic moins prononcé, tandis qu'il se stabilise plus difficilement.

Détermination de l'activité des catalyseurs. On a effectué la réaction test de déshydrogénation du *n*-butane en *n*-butènes, dans un réacteur en quartz, sur des pastilles de catalyseur de 2/3 mm.

Comme paramètres de réaction on a choisi la température de 580°, $V_v = 500$ vol/vol.h et le temps de réaction = 2h. L'analyse des produits de réaction a été effectuée à l'aide d'un

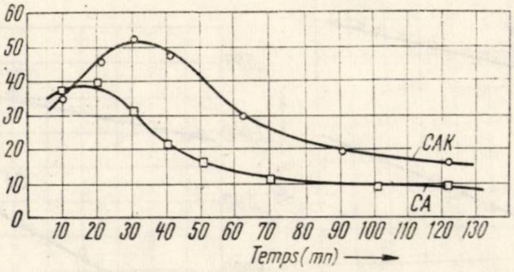

Fig. 6. — Variation du rendement en moles butane par rapport au temps.

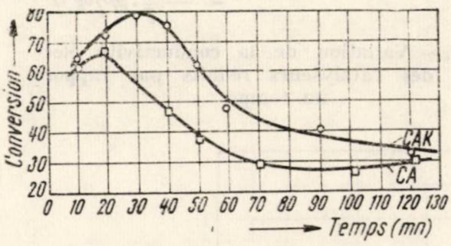

Fig. 7. — Variation de la conversion en moles butane par rapport au temps.

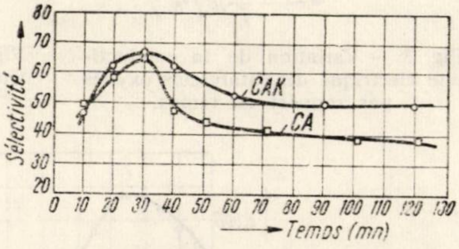

Fig. 8. — Variation de la sélectivité en moles butane par rapport au temps.

chromatographe Willy Giede. L'activité des deux catalyseurs ressort des figures 6, 7 et 8, qui indiquent les rendements, les conversions, ainsi que les sélectivités exprimées en moles butane introduit dans la réaction.

Après environ 30 mn, on aperçoit un décroissement de l'activité des catalyseurs, qu'on pourrait expliquer comme suite d'un recouvrement de leur surface avec un dépôt charbonneux.

Dans l'intervalle de 10—30 mn, les résultats expérimentaux indiquent un activité supérieure du catalyseur CAK par rapport au catalyseur CA, en ce qui concerne la conversion du butane et le rendement en butènes. Le catalyseur au support acide (CA) possède son maximum d'activité au commencement, puis son activité décroît rapidement. Au contraire, le catalyseur à faible acidité garde son activité longtemps. De même, le rendement en *n*-butènes est supérieur, dans les conditions de son activité maximale.

Au début du processus, quand tous les deux catalyseurs sont oxydés, leurs activités sont minimales et non différentes. Après 20 ou 30 mn., dès qu'ils sont déjà réduits, les catalyseurs atteignent leurs activités optimales et différentes

Les sélectivités des catalyseurs (fig. 8) varient simbatiquement jusqu'à 30 mn. Après cet intervalle de temps, la sélectivité du catalyseur CA décroît beaucoup plus que celle du catalyseur CAK.

DISCUSSION DES RÉSULTATS

D'après nos données expérimentales, on remarque des différences entre les catalyseurs préparés à partir de diverses alumines comme support, à savoir une activité plus faible du catalyseur CA par rapport au catalyseur CAK. Nous essayons de l'expliquer comme une contribution du support à la chimie de la surface et à la texture du catalyseur. Nous considérons que le rôle de l'alumine est celui de promouvoir par ses centres acides, en dehors de la réaction principale, des réactions secondaires de cracking et polymérisation en accélérant le dépôt du charbon. Dans le même sens, agit également la structure poreuse du catalyseur. L'existence d'une large porosité du catalyseur A dont la plupart des pores sont plus étroits que ceux du catalyseur CAK favorise un blocage plus rapide des centres actifs. Le processus chimique est ainsi ralenti et par conséquent, l'activité catalytique diminue après une brève période de réaction.

La chimie de la surface catalytique, ainsi que la texture sont essentiellement influencées par les propriétés du support. La nature du support influence également la dispersion de l'oxyde de chrome, le degré d'exposition dans la couche superficielle, l'état cristallo-chimique, ainsi que le degré de réduction des ions chrome c'est-à-dire l'excès d'ions oxygène. Ces influences se reflètent sur la conductivité électrique des solides.

Dans une étude antérieure [12] nous avons expliqué l'augmentation de la conductivité électrique observée aux deux catalyseurs, les premières 20—30 mn, en supposant l'existence de deux étapes dans le processus de réduction, à savoir : la dissociation de l'hydrogène et la formation de l'eau. De même, il est bien connu que l'activité maximale d'un catalyseur chrome-alumine est atteinte à peine après l'élimination de l'eau formée dans les premières minutes de réaction, [16] la vitesse d'élimination étant en rapport avec le type d'alumine support. [17]

En comparant les courbes d'activité catalytique des catalyseurs (fig. 6 et 7) à celles de leur comportement électrique en atmosphère réductrice (fig. 5), on constate une corrélation satisfaisante en ce qui concerne le moment d'apparition des pics. Si on suppose que pendant ce temps, la surface subit des transformations, à savoir la formation des oxydes de chrome à déficit d'oxygène et l'élimination de l'eau, on doit admettre que ces transformations seront reflétées aussi dans le comportement chimique des nouvelles phases formées. En réalité, le processus est plus complexe étant donné les phénomènes de diffusion et les phénomènes qui résultent pendant que l'eau est liée par des forces de nature physique.

Il nous faut remarquer que, du point de vue qualitatif, l'étude de la conductivité électrique peut signaler ces transformations, le moment de leur apparition et de la fin, et peut constituer de cette manière une méthode qui soit à même d'apprécier les phénomènes ayant lieu à la surface, ainsi que dans le volume du catalyseur.

---

[16] I. J. Tiureaev, *Uspekhi Khim.*, **1**, 121 (1966).

[17] O. D. Sterligov et N. A. Elissev, *Neftekhimiia*, **5**, 6, 809 (1965).

Nous signalons de même, une relation simbatique entre les valeurs de l'énergie apparente d'activation de la conductivité électrique, déterminée en milieu réducteur (hydrogène) et les rendements de réaction (activité) considérés dans les conditions optimales (valeurs maximales de la fig. 6).

Ainsi, le catalyseur CA à faible activité possède une valeur maximale de l'énergie apparente d'activation de la conductibilité électrique (tableau 2).

Tableau 2

Relation entre le rendement et l'énergie d'activation de la conductivité électrique

Catalyseur	Rend. %	E_σ kcal/mole
CA	39	25,4
CAK	53	5,00

CONCLUSIONS

1. La contribution du support dans l'ensemble des propriétés du catalyseur $Cr_2O_3-Al_2O_3$ est multiple, vu l'influence qu'il exerce sur ses caractéristiques électroniques, la chimie de la surface et la texture.

2. L'activité des catalyseurs chrome-alumine est en étroite dépendance avec la méthode et les conditions de préparation du support d'alumine. La genèse du support a une contribution importante sur la nature, la force et la concentration des centres acides, ainsi que sur le spectre des pores.

3. Les mesures de la résistance électrique peuvent poursuivre du point de vue qualitatif les transformations subies dans la période de formation des états actifs des catalyseurs chrome-alumine, en fournissant de même certaines informations sur leur activité.

Revue Roumaine de Chimie, **14**, 637 – 645 (1969)

UNTERSUCHUNGEN ÜBER DAS THERMISCHE VERHALTEN VON CADMIUMSALZEN EINIGER DICARBOXYLSÄUREN

FR. MIHAI, ARIANA MORARU und GR. POP

von der Technischen Hochschule Timişoara, str. Bocşa, 6 und den Petrochim-Werken, Ploieşti

Eingegangen am 20. Juli 1968

In Fortsetzung unserer Untersuchungen über die Salze einiger Dicarboxylsäuren wurde das thermische Verhalten von Cadmiumsalzen der Oxal-, Adipin-, Sebazin- und Phthalsäure verfolgt.

Die Bestimmungen wurden auch mit Salzen ausgeführt, die auf Aktivkohle fixiert waren. Die zeitliche thermische Stabilität nimmt in der Reihenfolge Cadmiumoxalat, Cadmiumadipat, Cadmiumsebazat und Cadmiumphthalat ab und wird durch die poröse Struktur der Aktivkohle bestimmt. Es wird die Temperaturgrenze festgesetzt bis zu welcher diese Salze stabil sind.

Die Untersuchungen über das thermische Verhalten der Dicarboxylsäuren und deren Salze ist sowohl von theoretischer als auch von praktischer Bedeutung.

Ihre theoretischen Bedeutung besteht darin, daß die Aufeinanderfolge der Reaktionen sowohl beim Zersetzen der reinen Säuren als auch deren Salze erkannt werden kann ; die Zwischenprodukte hängen von der Natur der Säure, die Endprodukte dagegen von der Natur des Metalls ab. Als Zwischenprodukte bilden sich Kohlenoxid und Kohlendioxid, Methan, Ketone, Benzol, Benzoesäure usw., während als Endprodukte im Falle der Alkalimetalle und der Erdalkalimetalle, Carbonate, im Falle der Schwermetalle dagegen Oxide entstehen.[1-10]

Ihre praktische Bedeutung besteht darin, daß einige der Salze dieser Säuren auf Aktivkohle fixiert, bei heterogenen katalytischen Synthesen

---

[1] W. W. Wendlandt und J. A. Hoiberg, *Analyt. Chim. Acta*, **28**, 506 (1963).

[2] U. V. Korshak und S. V. Rogozhin, *Izvest. Akad. Nauk S.S.S.R., Otdel. khim. Nauk*, **1952**, 531.

[3] J. Bell und R. J., Reed, *J. Chem. Soc.*, **1952**, 1383.

[4] P. Davidson und P. Neuman, *J. Amer. Chem. Soc.*, **74**, 1519 (1952).

[5] R. J. Reed und M. B. Thornley, *Chem. and Ind.*, **1955**, 1717.

[6] V. I. Jakerson und A. M. Rubinstein, *Kinetika i Kataliz*, **2**, 172 (1961).

[7] A. K. Galwey, *J. Catalysis*, **4**, 697 (1965) ; *Chem. Abstr.*, **64**, 2994 (1966).

[8] R. David, *Bull. Soc. chim. France*, **1960**, 728.

[9] L. Erdey und F. Paulik, *Acta Chim. Acad. Sci. Hung.*, **7**, 27 (1955).

[10] L. Erdey, G. Liptay, G. Svehla und F. Paulik, *Z. analyt. Chem.*, **182**, 329 (1961).

Verwendung finden.[11,12] Die katalytische Wirkung ist jedoch auf einen Temperaturbereich begrenzt, in welchem sie sich nicht zersetzen; bei höheren Temperaturen ändert sich die katalytische Wirkung infolge Zersetzung, wodurch auch der Verlauf der Synthese beeinflußt wird.[13,14]

Die Cadmiumsalze wie auch Cadmiumoxid werden bei verschiedenen katalytischen Synthesen verwendet: Synthese von Vinylazetat,[11,12,14] oxydative Desalkylierung von Alkylnaphthalin,[15] Synthese von Vinylestern[16], zur Dehydratation und Dehydrierung [17] usw.

In einer früheren Arbeit über Zinksalze wurde angenommen, daß die Wirksamkeit des Katalysators infolge der thermischen Zersetzung abnimmt und es wurde durch thermogravimetrische Analyse der Temperaturbereich festgesetzt, innerhalb, dessen die aktive Substanz ihre katalytische Wirkung beibehält.[12,14]

In der vorliegenden Arbeit wurde das thermische Verhalten von Cadmiumsalzen der Oxal-, Adipin-, Sebazin- und Phthalsäure untersucht. Da Aktivkohle häufig als Träger verwendet wird, wurde auch das thermische Verhalten der auf Aktivkohle fixierten Salze verfolgt. Es werden drei Sorten von Aktivkohle mit verschiedenen spezifischen Oberflächen zwecks Bestimmung des Trägereinflusses auf die thermische Stabilität dieser Salze verwendet.

EXPERIMENTELLES

Arbeitsweise und Reagenzien. Das thermische Verhalten der reinen Salze oder der auf Aktivkohle fixierten Salze wurde thermogravimetrisch verfolgt, [18] wobei die Erwärmung mit einer Geschwindigkeit von 10°/Min. vorgenommen wurde.

Die Salze wurden aus den Lösungen des entsprechenden Natriumsalzes durch Fällung mit einer Cadmiumchloridlösung in stöchiometrischem Verhältnis erhalten.

Zur Fixation der Cadmiumsalze auf Aktivkohle wurde folgendermaßen vorgegangen: Die vorher mit einer 5%igen Salpetersäurelösung behandelte Aktivkohle wurde mit dest. Wasser gewaschen und bei 150° im Trockenschrank getrocknet, und danach in eine molare Cadmiumchloridlösung gegeben, u.zw. im Verhältnis von 100 g Aktivkohle auf 200 ml Lösung. Unter fortwährendem Rühren wurde bis zur Trockene eingedampft und danach vier Stunden bei 100—110° im Trockenschrank belassen. Die auf diese Weise mit Cadmiumchlorid imprägnierte Aktivkohle wird nach und nach in die molare Lösung eines Dinatriumsalzes der Dicarboxylsäure eingeführt, unter fortwährendem Umrühren wieder bis zur Trockene eingedampft und zur Vollendung der Reaktion noch weitere zwei Stunden im Trockenschrank bei 150° belassen

---

[11] H. Kalenda (bei Chemische Werke Hüls Akt.-Ges.), D.B.P., 1 050 758, 19. Febr. 1959; *Chem. Abstr.*, **54**, 22365 (1960).

[12] Chemische Werke Hüls Akt.-Ges., Brit. P. 808 828, 11. Febr. 1959; *Chem. Abstr.* **53**, 14.005 (1959)

[13] V. P. Kornienko, *Sbornik Nauk. Rabot. Akad. Nauk. Beloruss. S.S.R., Inst. Khim.*, **1956**, 92; *Chem. Abstr.*, **52**, 6906 (1958).

[14] I. Cristea, Fr. Mihai und Gr. Pop, *Studii şi Cercetări Şti., Chim. Baza Cercetări Şti., Timişoara*, **10**, 101 (1963).

[15] J. C. Norton und E. T. Moss, *Amer. Chem. Soc. Div. Petrol. Chem. Preprints*, **9**, 129 (1964); *Chem . Abstr.*, **64**, 12430 (1966).

[16] Wacker-Chemie GmbH, F. P., 1 403 478,18. Juni 1965; *Chem. Abstr.*, **64**, 4949 (1966).

[17] J. M. Trillo, G. Madinabeitia und F. Gonzalez-Garcia, *Anales real Soc. españ. Fis. Quim. Ser. B.*, **16**, 1081 (1965); *Chem. Abstr.*, **64**, 18472 (1966).

[18] L. Erdey, F. Paulik und J. Paulik, *Magyar Tud. Akad. Kém. Tud. Oszt. Közl.*, **5**, 55 (1955).

Hierauf wird die imprägnierte Aktivkohle mit destilliertem Wasser bis zum Verschwinden der Chlorreaktion gewaschen und bei 110° getrocknet. Der Cadmiumgehalt der imprägnierten Aktivkohle wurde durch Glühen derselben bestimmt.

Es wurden verschiedene Sorten zylinderförmiger Aktivkohle mit einem Durchmesser von ungefähr 4 mm und einer Länge von ungefähr 10 nm verwendet.

Die spezifische Oberfläche der Aktivkohle wurde mit Hilfe der Desorption von Benzol für die Isothermen von 22° bestimmt, wobei die lineare Form der Gleichung BET[19] verwendet wurde, während die Desorptionsisothermen durch die kinetische Methode von Niac berechnet wurden.[20]

Thermisches Verhalten der reinen Salze

Das Verhalten der reinen Cadmiumsalze wird in Abbildung 1 dargestellt. In diesem Diagramm wurden auf der Ordinate die Gewichtsverluste in mg und auf der Abszisse die Tempe-

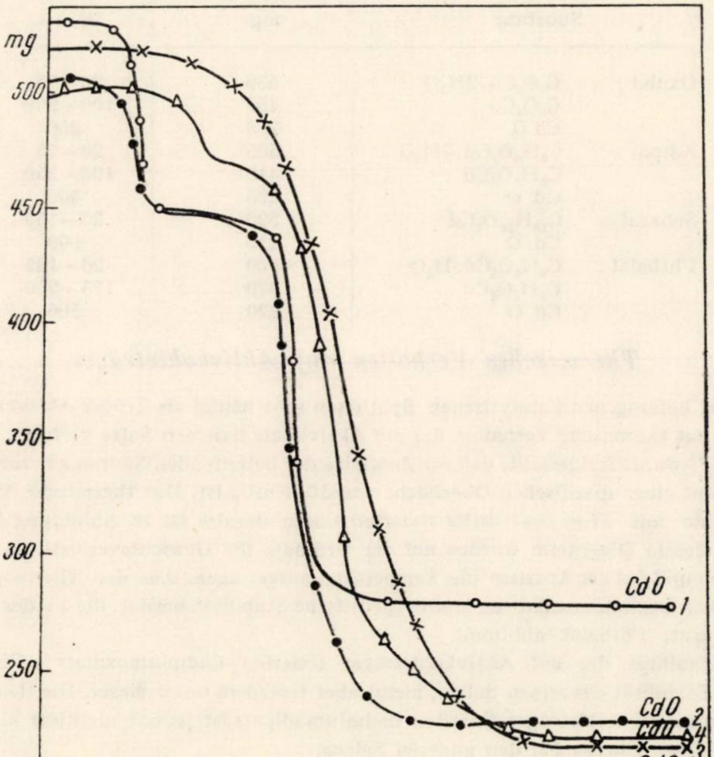

Abb. 1. — Thermogramme der reinen Cadmiumsalze.
1, Oxalat; *2*, Adipat; *3*, Sebazat; *4*, Phthalat.

---

[19] E. Emmet, „Kataliz, voprosy teorii i metody issledovania", Moskau 1955, S. 329.
[20] Gv. Niac, *Stud. Univ. Babes Bolyai, Chem.*, **3**, 77 (1958).
[21] Fr. Mihai und B. Roch, *Studii şi Cercetări Şti., Chim. Baza Cercetări Şti., Timişoara,* **7**, 303 (1960).

ratur aufgetragen. Aus den Versuchsergebnissen kann das Zwischenprodukt und das Endprodukt [21] auf Grund folgender Gleichung bestimmt werden :

$$\frac{M + xH_2O}{M} = \frac{G_1}{G_2}$$

In Tabelle 1 sind die Mengen der Ausgangssubstanzen, der Zwischenprodukte und der Endprodukte, sowie die Temperaturbereiche angeführt, innerhalb welcher die Verbindungen stabil sind. Aus diesen Daten kann gefolgert werden, daß das Kristallwasser bei Cadmiumphthalat schwerer entfernt werden kann als beim Cadmiumoxalat und Cadmiumadipat. Hingegen ist die Stabilität der wasserfreien Verbindungen am größten beim Cadmiumadipat und nimmt in der Reihenfolge Cadmiumoxalat, Cadmiumphthalat und Cadmiumsebazat ab.

Tabelle 1

Formel und Maße der Substanzen sowie Temperaturintervalle

Substanz		mg	°C
Oxalat :	$C_2O_4Cd.2H_2O$	530	20–75
	C_2O_4Cd	450	100–230
	Cd O	280	350
Adipat :	$C_6H_8O_4Cd.2H_2O$	505	20–75
	$C_6H_8O_4Cd$	445	100–250
	Cd O	225	400
Sebazat :	$C_{10}H_{16}O_4Cd$	520	20–150
	Cd O	215	500
Phthalat :	$C_8H_4O_4Cd.H_2O$	500	20–125
	$C_8H_4O_4Cd$	470	175–200
	Cd O	220	500

Thermisches Verhalten auf Aktivkohleträger

Da bei heterogenen katalytischen Synthesen sehr häufig als Träger Aktivkohle benützt wird, wurde das thermische Verhalten der auf Aktivkohle fixierten Salze verfolgt. In einer früheren Arbeit [22] wurde festgestellt, daß für Zinksalze der betreffenden Säuren am vorteilhaftesten Aktivkohle mit einer spezifischen Oberfläche von 1044 m^2/g ist. Das thermische Verhalten der auf Aktivkohle mit $Fl = 1044$ m^2/g fixierten Cadmiumsalze ist in Abbildung 2 dargestellt worden. In diesem Diagramm wurden auf der Ordinate die Gewichtsverluste an flüchtigeren Bestandteilen und auf der Abszisse die Temperatur aufgetragen. Aus den Thermogrammen ist ersichtlich, daß Cadmiumoxalat die größte thermische Stabilität besitzt, die in der Reihenfolge Adipat, Sebazat, Phthalat abnimmt.

Die Stabilität des auf Aktivkohleträger fixierten Cadmiumoxalats nähert sich der thermischen Stabilität des reinen Salzes, bleibt aber trotzdem unter dieser. Die thermische Stabilität des auf Aktivkohleträger fixierten Cadmiumadipats ist jedoch merklich kleiner als die des reinen Salzes. Ebenso bei den anderen Salzen.

Außerdem wurde das thermische Verhalten dieser Salze verfolgt, nachdem sie auf andere Aktivkohlesorten von verschiedener spezifischer Oberfläche fixiert worden waren. Der Einfluß der spezifischen Oberflächengröße der Aktivkohle auf die Fixation der Moleküle der aktiven Substanz wird durch die Zersetzungstemperatur ausgedrückt, wie dies in Tabelle 2 angeführt worden ist.

Aus den Daten der Tabelle 2 ist ersichtlich, daß Cadmiumoxalat, auf Aktivkohle mit einer spezifischen Oberfläche von 1044 m^2/g, Cadmiumadipat dagegen auf Aktivkohle mit einer spezifischen Oberfläche von 1140 m²/g die größte Stabilität aufweist. Cadmiumsebazat und Cadmiumphthalat auf Aktivkohle haben eine geringere Stabilität. Aus diesem Grunde werden sie bei den folgenden Bestimmungen nicht mehr in Betracht gezogen.

---

[22] Fr. Mihai, A. Moraru und Gr. Pop, *Bul. Şti. Tehn. Inst. Politeh. Timişoara*, **13**, 57 (1968).

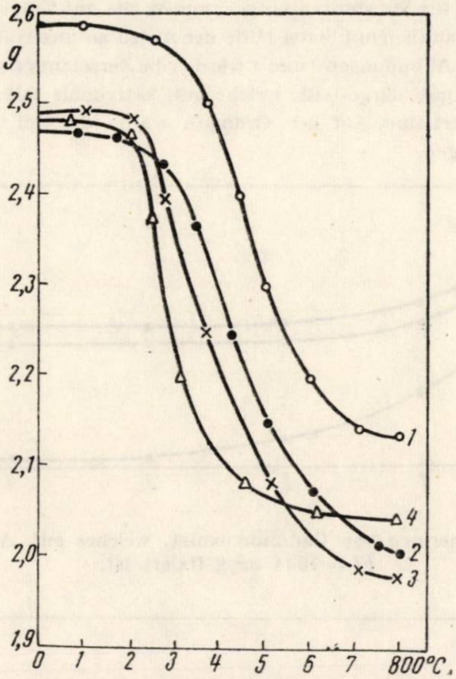

Abb. 2. — Thermogramme der Cadmiumsalze, welche auf Aktivkohle mit $Fl = 1044$ m²/g fixiert sind.

1, Oxalat; *2*, Adipat; *3*, Sebazat; *4*, Phthalat.

Tabelle 2

Temperaturintervalle in welchen die auf Aktivkohle verschiedener Oberfläche fixierten Substanzen stabil sind

Spezifische Oberfläche m²/g	Cadmiumoxalat °C	Cadmiumadipat °C	Cadmiumsebazat °C	Cadmiumphthalat °C
Fl = 510	180	180	unter 180	unter 180
Fl = 1044	220	180	unter 180	unter 180
Fl = 1140	200	200	unter 180	unter 180

Verhalten bei isothermer Erhitzung

Bei heterogenen katalytischen Synthesen kann beobachtet werden, daß nach einer bestimmten Betriebszeit die katalytische Wirksamkeit der aktiven Substanz abnimmt und durch Erhöhung der Temperatur gänzlich aufhört. Das Wesen dieser Erscheinung ist noch nicht erklärt worden, es kann jedoch angenommen werden, daß durch die Erhöhung der Temperatur eine Zersetzung der aktiven Substanz stattfindet. Deshalb ist es notwendig, die zeitliche Stabilität der aktiven Substanz zu kennen. Aus diesem Grund wurden bei konstanten Temperaturen Bestimmungen für Substanzen vorgenommen, die auf Träger fixiert waren. Die Isothermen ergeben Kurvenfamilien mit deren Hilfe der Anteil an unzersetzter Substanz berechnet werden kann.[14,22] In den Abbildungen 3 und 4 wurden die Zersetzungsisothermen von Cadmiumoxalat und Cadmiumadipat dargestellt, welche auf Aktivkohle mit einer spezifischen Oberfläche von 1044 m^2/g fixiert sind. Auf der Ordinate wurde die auf 1 g Aktivkohle fixierte Substanzmenge aufgetragen.

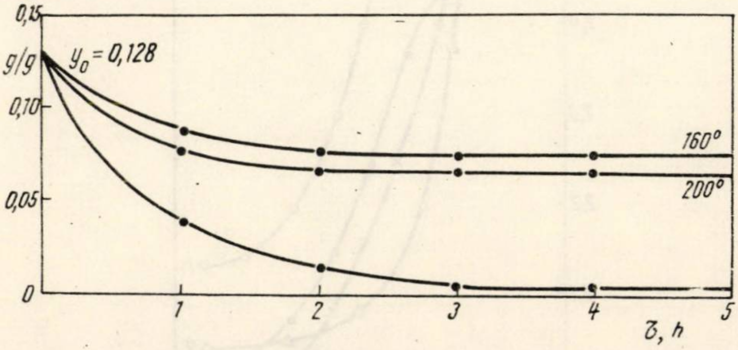

Abb. 3. — Isothermen von Cadmiumoxalat, welches auf Aktivkohle mit $Fl = 1044$ m^2/g fixiert ist.

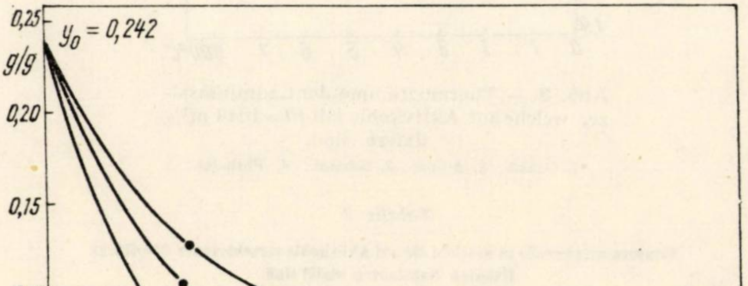

Abb. 4. — Isothermen von Cadmiumadipat, welehes auf Aktivkohle mit $Fl = 1044$ m^2/g fixiert ist

Die Gewichtsveränderung dy der auf Aktivkohle fixierten Substanzmenge in einem unendlich kleinen Zeitabschnitt dτ ist proportional mit y

$$\frac{dy}{d\tau} = - A \cdot y \qquad 1$$

wo A eine Proportionalitätskonstante ist, die von der Temperatur, von der spezifischen Oberfläche der Aktivkohle und von der Zeit abhängig ist. Für ein und dieselbe Substanz kann die Differentialgleichung (1) bei konstanter Temperatur folgendermaßen ausgedrückt werden:

$$\frac{dy}{d\tau} = - A \cdot y \cdot f(\tau) \qquad (2)$$

Es bereitet Schwierigkeiten, die Form der Funktion $f(\tau)$ festzusetzen. Aus den Grenzbedingungen erhält man die integrierte Form der Gleichung (2):

$$\log y = \log y_0 - A\left(1 - \frac{1}{1+\tau}\right) \qquad (3)$$

In Tabelle 3 werden die Werte für y_0, für die Konstante A und für Prozente an zersetzter Substanz bei den entsprechenden Temperaturen nach 5stündigem Erhitzen angegeben. Aus den in der Tabelle angeführten Daten kann festgestellt werden, daß die Stabilität von Cadmiumoxalat in der Zeit größer ist als die von Cadmiumadipat.

Tabelle 3

Aus der isothermen Zersetzung abgeleitete Werte

Cadumiumoxalat auf Aktivkohle fixiert mit $Fl = 1044 m^2/g$; $y_0 = 0,1284 g/g$			
°C	160	200	225
% zersetzte Substanz	47,8	54	100
A	0,4479	0,4809	—
Cadmiumadipat auf Aktivkohle fixiert mit $Fl = 1044 m^2/g$; $y_0 = 0,2424 g/g$			
°C	175	200	225
% zersetzte Substanz	64,8	86,3	100
A	0,3003	0,582	—

Poröse Struktur der Aktivkohle. Der Träger hat außer der Aufgabe, die Substanz auf einer großen Oberfläche zu verteilen, einen bedeutenden Einfluß auf die thermische Stabilität der Substanz. Aus den Ergebnissen der thermogravimetrischen Analysen kann keine Beziehung zwischen der thermischen Stabilität der auf Aktivkohle fixierten Salze und der Größe der spezifischen Oberfläche festgestellt werden. Es ist sehr wahrscheinlich, daß besondere Kräfte zwischen Träger und Substanz wirken; die Art in welcher die Verteilung der Substanz in den Poren der Aktivkohle stattfindet, beeinflußt deren thermische Stabilität.

In Abbildung 5 wurden die Verteilungskurven der Porenhalbmessergrößen für die verwendeten Aktivkohlen dargestellt. Der Halbmesser der Poren wurde mit Hilfe der Formel von Thomson berechnet

$$r = \frac{2\,MG}{RT} \cdot \frac{1}{d \ln P/P_0} \qquad (4)$$

wobei die Desorptionskurven von Benzol verwendet wurden. Die Verteilungskurven der Porengrößen werden in einem System mit den Koordinaten $\frac{da}{d \log r} - \log r$ dargestellt, wo a die Dampfmenge des adsorbierten Benzols auf 1 g Aktivkohle und r der Porenhalbmesser ist, der mit Hilfe der Formel (4) berechnet wurde.

DISKUSSION

Aus der thermogravimetrischen Analyse ist ersichtlich, daß Cadmiumoxalat, Cadmiumadipat und Cadmiumphthalat Kristallhydrate bilden. Die Entfernung des Kristallwassers geht bei allen Verbindungen bei ungefähr 100° leicht vor sich. Die wasserfreien Verbindungen beginnen sich bei wenig voneinander verschiedenen Temperaturen zu zersetzen, wobei Cadmiumadipat am stabilsten ist.

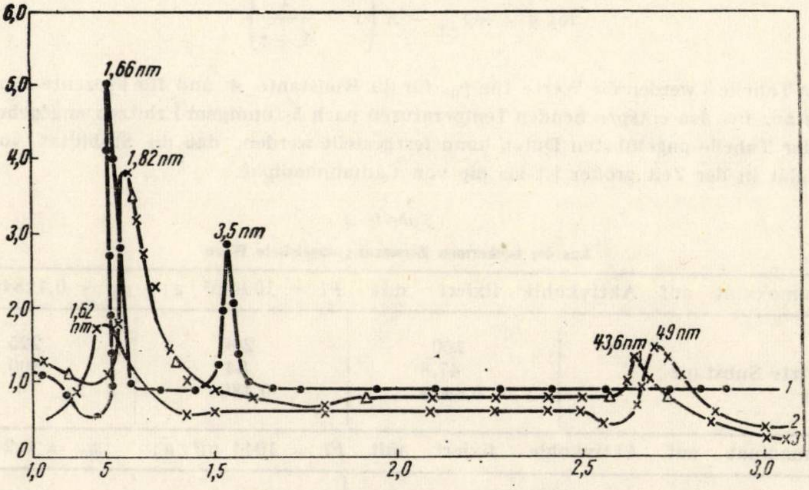

Abb. 5. — Verteilungskurven der Porenhalbmesser.
1.Aktivkohle mit *Fl* = 1044 m²/g; 2, Aktivkohle mit *Fl* = 1140 m²/g; 3. Aktivkohle mit *Fl* = 510 m²/g.

Die thermische Stabilität dieser auf Aktivkohleträger fixierten Salze ist jedoch verschieden, u.zw. wurde festgestellt, daß Cadmiumoxalat die größte Stabilität aufweist. Bei allen untersuchten Salzen wird die thermische Stabilität gegenüber der des reinen Salzes durch Fixation auf Aktivkohle vermindert. Dies kann sowohl durch die Molekülgröße der fixierten Substanz als auch durch die Porengröße der Aktivkohle begründet werden.

Es ist sehr wahrscheinlich, daß das organische Säureradikal durch die Fixation des zweiwertigen Metalls einen Ring bildet. Diese Tatsache verleiht dem Oxalat- und Adipatmolekül eine größere Stabilität und verkleinert diese bei den anderen. Außerdem beeinflußt die Molekülgröße auch die Fixation auf dem Träger.

Es kann angenommen werden, daß die großen ringförmigen Moleküle Cadmiumadipat, Cadmiumsebazat und Cadmiumphthalat nicht in die feinen Poren der Aktivkohle mit einer spezifischen Oberfläche von 1044 m²/g eindringen können, was eine merkliche Verminderung der thermischen Stabilität zur Folge hat. Die Cadmiumoxalatmoleküle von kleineren Ausmaßen werden in einer annähernd monomolekularen Schicht ebenso wie Zinkazetat[14] adsorbiert, was zu einer Stabilität führt, die mit der Stabilität der reinen Substanz verglichen werden kann.

Aus den Kurven *1* und *2* der Abbildung 4 ist ersichtlich, daß diese Aktivkohlen zwei Arten von unahhängigen Kapillaren besitzen; bei 3,5 nm und 1,66 nm beziehungsweise bei 4,90 nm und 1,62 nm. Die Tatsache, daß die thermische Stabilität der Substanzen mit großen Molekülen annähernd gleich ist, obwohl, die spezifischen Oberflächen verschieden sind, bedeutet, daß den großen Poren eine wichtige Rolle zukommt. Bei derselben spezifischen Oberfläche werden großporige Aktivkohlen bessere Ergebnisse liefern als solche mit Porenhalbmessern mittlerer Größe. Eine solche Aktivkohle müßte die mit *Fl* = 1144 m^2/g sein, welche zwei Arten von Kapillaren besitzt bei 1,82 nm und 43,6 nm und folglich eine ähnliche poröse Struktur mit der Aktivkohle aufweist, deren spezifische Oberfläche *Fl* = 510 m^2/g ist.

Aus Tabelle 2 ist ersichtlich, daß Cadmiumadipat, welches auf Aktivkohle mit einer spezifischen Oberfläche von 1140 m^2/g fixiert ist, sich bei 200° zersetzt, gegenüber 180° bei den anderen Sorten. Aus den Isothermen ergibt sich jedoch, daß Cadmiumadipat eine kleinere Stabilität in der Zeit hat als Cadmiumoxalat. Dies berechtigt uns anzunehmen, daß im Falle von Substanzen mit großen Molekülen der Träger außer einer spezifischen Oberfläche auch einen entsprechenden mechanischen Widerstand, Körnung usw. haben muß.

SCHLUSSFOLGERUNGEN

Das thermische Verhalten der untersuchten Cadmiumsalze der Dicarboxylsäuren liefert wertvolle Angaben sowohl in reinem Zustand als auch bei der Fixation auf Aktivkohle. Die thermische Stabilität ist am größten bei Cadmiumoxalat und vermindert sich mit der Zunahme der Größe der Moleküle.

Da die thermische Stabilität der reinen Salze größer ist als die der auf Aktivkohle fixierten Salze, ist es berechtigt anzunehmen, daß durch Adsorption auf die Oberfläche des Trägers die Stabilität der Moleküle abnimmt.

Cadmiumoxalat und Cadmiumadipat sind bis zu ungefähr 200° stabil. Dies weist auf die Möglichkeit hin, sie im Bereich dieser Temperaturen in solchen Reaktionen anzuwenden, wo ie eine katalytische Aktivität haben.

Revue Roumaine de Chimie, **14**, 647–651 (1969)

SUR LES VANADATES. XVI

LE POUVOIR THERMOÉLECTRIQUE DES COMPOSÉS $M^{I}_{x}V^{IV}_{x}V^{V}_{2-x}O_5$ (M^I = Na, K ; $0 < x \leqslant 1$)

ILEANA LUKÁCS, CONSTANŢA STRUSIEVICI et C. LITEANU

Institut de Chimie de l'Académie, Filiale de Cluj, 59–65, str. Donath

Reçu le 4 août 1968

Le coefficient de Seebeck des produits $M^{I}_{x}V^{IV}_{x}V^{V}_{2-x}O_5$($M^I$ = Na, K ; $0 < x \leqslant 1$) a des valeurs comprises entre −180 et +520 $\mu V/^{\circ}K$, en passant par zéro pour les produits avec x environ 0,70 et 0,80 respectivement. La formule simple, $\alpha = (k/e) \ln [V^{5+}]/[V^{4+}]$, n'est applicable que dans le cas des produits (Na 0,50) et (K 0,33–0,66). L'écart entre les mesures expérimentales et les données théoriques de la relation citée suggère la possibilité de l'existence des ions vanadium dans des positions cristallographiques non équivalentes, en concordance avec les données structurales ; d'autre part, il semble possible que la relation entre le pouvoir thermoélectrique et la composition soit plus compliquée, dépendant aussi d'autres paramètres que ceux prévus par l'équation donnée auparavant.

Des mesures sur le pouvoir thermoélectrique du *bronze* $Na_{0,33}V_2O_5$ ont été effectuées par Ornatskaya [1] et Sienko et Sohn. [2] Nous avons aussi déjà signalé quelques résultats sur le système $M^{I}_{x}V^{IV}_{x}V^{V}_{2-x}O_5$, ($M^I$ = Na, K)[3,4] ; dans le présent travail nous revenons sur ces mesures pour les présenter et les discuter en détail.

La composition chimique et les valeurs mesurées du pouvoir thermoélectrique des produits étudiés sont données aux tableaux 1 et 2. Les coefficients de Seebeck des produits, en général, ne sont pas trop élevés et présentent seulement de faibles variations avec la température, en indiquant que le nombre des porteurs de charge est grand et presque indépendant de la température — en concordance avec le mécanisme de semiconduction par sauts (*hopping*) électroniques entre les atomes vanadium tétra-et pentavalents situés dans des positions cristallographiques équivalentes, mécanisme proposé[2,5] pour les produits de cette famille.

[1] Z. I. Ornatskaya, *Fiz. tverd.*, **6**, 1254 (1964).

[2] M. I. Sienko et I. B. Sohn, *J. Chem. Phys.*, **44**, 1369 (1966).

[3] I. Lukács, C. Strusievici, E. Weissmann et C. Liteanu, *Rev. Roumaine Chim.*, **12**, 993 (1967).

[4] I. Lukács, C. Strusievici et C. Liteanu, *Rev. Roumaine Chim.*, **13**, 713 (1968).

[5] M. Pouchard, A. Casalot, G. Villeneuve et P. Hagenmuller, *Mat. Res. Bull.*, **2**, 877 (1967).

Tableau 1

Composition chimique et pouvoir thermoélectrique des produits $Na_xV_x^{IV}V_{2-x}^{V}O_5$

Produits	Composition				α(μV/°)				
	Na^+	V^{4+}	V^{5+}	O^{2-}	50−80°	60−90°	70−110°	100−150°	120−180°
(0,10)	0,09	0,14	1,86	4,97	−180	−183	−195	−174	−180
(0,20)	0,19	0,24	1,76	4,97	−127	−132	−133	−135	−125
(0,30)	0,27	0,31	1,69	4,98	−107	−109	−111	−108	−107
(0,33)	0,37	0,39	1,61	4,98	−91	−92	−96	−93	−92
(0,50)	0,59	0,53	1,47	5,03	−79	−80	−79	−75	−70
(0,66)	0,66	0,65	1,35	5,00	−83	−85	−84	−80	−78
(0,70)	0,72	0,69	1,31	5,00	−14	−16	−17	−18	−19
(0,75)	0,72	0,74	1,26	5,00	+29	+28	+27	+24	+16
(0,80)	0,84	0,82	1,18	5,01	+75	+72	+71	+65	+60
(0,90)	0,87	0,92	1,08	4,97	+115	+113	+111	+96	+84
(1,00)	0,98	1,06	0,94	4,97	+252	+236	+237	+230	+202

Tableau 2

Composition chimique et pouvoir thermoélectrique des produits $K_xV_x^{IV}V_{2-x}^{V}O_5$

Produits	Composition				α (μV/°)					
	K^+	V^{4+}	V^{5+}	O^{2-}	50−90°	60−110°	70−115°	85−145°	95−150°	95−180°
(0,10)	0,11	0,12	1,88	4,99	−178	−188	−187	−178	−178	−177
(0,20)	0,20	0,23	1,77	4,99	−140	−148	−148	−148	−144	−143
(0,25)	0,28	0,28	1,72	5,00	−119	−125	−124	−121	−124	−120
(0,28)	0,28	0,31	1,69	4,98	−118	−115	−117	−120	−120	−116
(0,33)	0,33	0,36	1,64	4,99	−120	−120	−118	−118	−116	−114
(0,40)	0,41	0,39	1,61	5,00	−116	−121	−121	−116	−112	−107
(0,45)	0,44	0,45	1,55	5,00	−99	−96	−93	−94	−93	−87
(0,50)	0,49	0,50	1,50	4,99	−95	−95	−95	−92	−91	−88
(0,60)	0,58	0,60	1,40	4,99	−76	−77	−79	−76	−77	−74
(0,66)	0,65	0,66	1,34	5,03	−72	−73	−73	−69	−69	−66
(0,70)	0,70	0,69	1,31	5,00	−75	−74	−72	−69	−70	−68
(0,75)	0,78	0,75	1,25	5,01	−67	−67	−64	−62	−62	−58
(0,80)	0,83	0,78	1,22	5,04	−48	−46	−44	−41	−40	−38
(0,85)	0,88	0,83	1,17	5,02	+21	+21	+23	+21	+21	+21
(0,90)	0,93	0,91	1,09	5,01	+240	+234	+237	+232	+235	+210
(1,00)	0,98	0,98	1,02	5,00	+526	+525	+400	+427	+444	+410

Dans le cas du mécanisme par sauts et même dans celui de conduction en bande serrée (*narrow*), en principe, il est possible[6] d'approximer la valeur de l'effet Seebeck (α) d'après la relation

$$\alpha = (\mathrm{k/e})\,[\ln (C_0 - C)/C + \mathrm{A}] \qquad (1)$$

où

C = concentration des porteurs de charge;
C_0 = concentration des positions possibles;
k = constante de Bolzmann;
e = charge de l'électron.

Cette équation, dans la forme simplifiée

$$\alpha = (k/e) \ln\, [\mathrm{V}^{5+}]/[\mathrm{V}^{4+}] \qquad (2)$$

avec le signe négatif pour $[\mathrm{V}^{5+}]/[\mathrm{V}^{4+}]>1$ et positif quand ce rapport <1 a été appliquée, avec une bonne concordance entre les données mesurées et celles calculées, aux verres contenant du vanadium[7] et même au *bronze* $\mathrm{Na}_{0.33}\mathrm{V}_2\mathrm{O}_5$.[2]

Pour vérifier la validité de cette formule dans le cas des produits étudiés, nous avons représenté (fig. 1,2) les valeurs du coefficient de Seebeck (α) en fonction du ln $[\mathrm{V}^{5+}]/[\mathrm{V}^{4+}]$. On observe une non concordance entre les données expérimentales et la ligne théorique, nommément, les valeurs mesurées correspondent à celles calculées seulement pour les produits (Na 0,50) et (K 0,33–0,66), l'écart de la ligne théorique étant considérable pour tous les autres produits. Il nous faut aussi remarquer que la valeur de zéro du coefficient de Seebeck est atteinte dans un rapport $[\mathrm{V}^{5+}]/[\mathrm{V}^{4+}] > 1$, à x environ 0,70 pour les produits avec du Na, et à x environ 0,80 pour les produits avec du K.

La déviation des courbes α – ln $[\mathrm{V}^{5+}]/[\mathrm{V}^{4+}]$ de la ligne théorique devient explicable si on suppose que les atomes vanadium pentavalents ne participent pas en leur totalité à la conduction. En échange, si on considère que tous les ions V^{4+} donnent des porteurs de charge nous pouvons calculer (sur la base de l'équation (2)) des valeurs α mesurées le pourcentage d'atomes vanadium participant à l'effet thermo-électrique (rapporté au vanadium total). La figure 3 montre, que ce pourcentage varie selon les phases des systèmes. Le pourcentage, d'environ 70%, pour les phases β, s'accorde bien avec la conclusion cristallographique,[8] d'après laquelle dans cette phase deux atomes vanadium sur trois (c'est-à-dire 67%) sont placés au centre de certains octaèdres déformés, le troisième occupant le centre d'une bipyramide déformée. Cela nous permet de supposer que seulement les ions V^{5+} et V^{4+} situés dans les positions octaédriques acceptent ou donnent des porteurs de charge.

---

[6] G. H. Jonker et S. van Houten, « Halbleiterprobleme », vol. 6, F. Sauter, Friedr. Vieweg u. Sohn, Braunschweig, 1961, p. 118.

[7] T. Allersma et J. D. Mackenzie, *J. Chem. Phys.*, **47**, 1406 (1967).

[8] P. Hagenmüller, J. Galy, M. Pouchard et A. Casalot, *Mat. Res. Bull.*, **1**, 45 (1966).

De même, le pourcentage de contribution d'environ 57 %, calculé pour la phase α′ du système $Na_xV_x^{IV}V_{2-x}^{V}\ O_5$ peut être expliqué aussi en vertu des données structurales, [8] d'après lesquelles les atomes vanadium occupent dans cette phase, en quantité égale, deux types de positions différentes, deux sites bipyramidaux bien distincts, dont un type contient préférentiellement du vanadium tétravalent et l'autre du vanadium pentavalent.

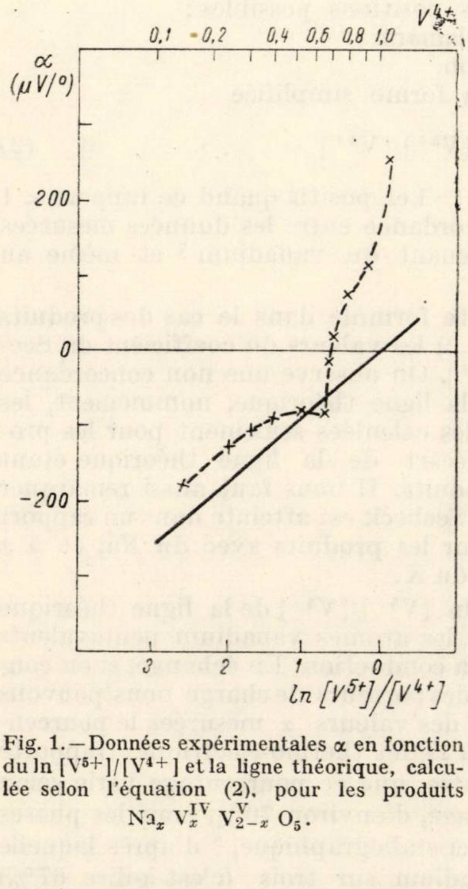

Fig. 1. — Données expérimentales α en fonction du ln $[V^{5+}]/[V^{4+}]$ et la ligne théorique, calculée selon l'équation (2), pour les produits $Na_xV_x^{IV}\ V_{2-x}^{V}\ O_5$.

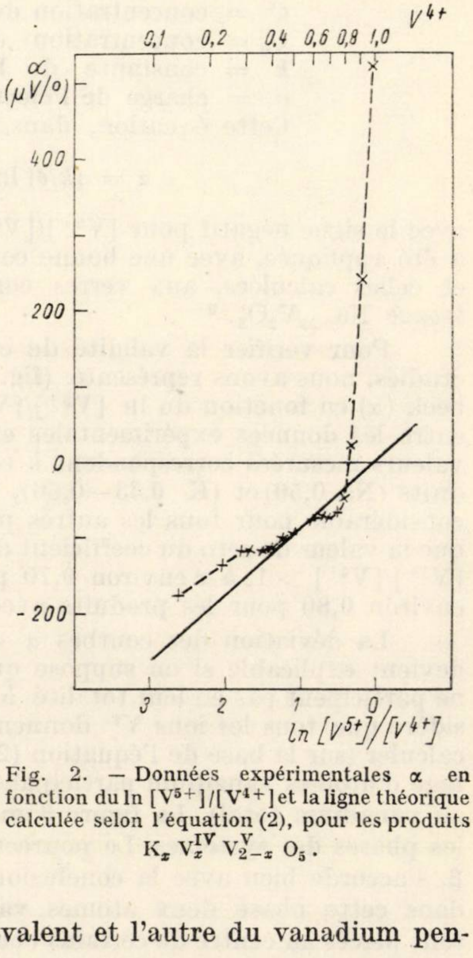

Fig. 2. — Données expérimentales α en fonction du ln $[V^{5+}]/[V^{4+}]$ et la ligne théorique calculée selon l'équation (2), pour les produits $K_xV_x^{IV}\ V_{2-x}^{V}\ O_5$.

Par voie de conséquence, nous pouvons avancer l'hypothèse de l'existence de deux types de sites pour le vanadium aussi dans la phase φ du système $K_xV_x^{IV}V_{2-x}^{V}\ O_5$.

Le pourcentage de contribution pour les produits (Na 0,65) et (K 0,70—0,75) dépasse considérablement 100 %. Cela peut également indiquer outre l'erreur expérimentale une certaine perturbation dans l'activité même des ions V^{4+} comme émetteurs d'électrons, la formule (2) s'appliquant si on considère, cette fois-ci, que ce sont les ions V^{4+} ceux qui ne participent pas entièrement au phénomène du pouvoir thermoélectrique.

Les suppositions faites auparavant seraient valables seulement si on considère la relation (2) comme la seule qui détermine le pouvoir thermoélectrique, ce qui d'ailleurs n'exclut pas la possibilité que cette propriété dépende aussi d'autres paramètres.

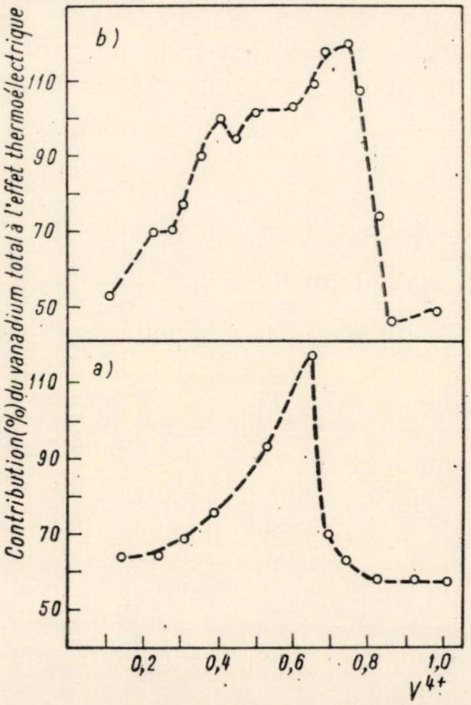

Fig. 3. – Pourcentage de contribution des atomes de vanadium (rapporté au vanadium total) à l'effet thermoélectrique :

a, produits $Na_xV^{IV}_xV^{V}_{2-x}O_5$; b, produits $K_xV^{IV}_xV^{V}_{2-x}O_5$

PARTIE EXPÉRIMENTALE

Les échantillons ont été préparés selon la méthode décrite dans.[3,4] Le pouvoir thermoélectrique a été mesuré sur des échantillons en poudre, à l'air, en utilisant une cellule aux électrodes en platine; la mesure du gradient de température ($\Delta\theta \sim 30-80°$) se fait à l'aide des thermocouples Pt–PtRh soudés au centre des électrodes; un bon contact de ces dernières avec l'échantillon en poudre donc une reproductibilité et une précision suffisantes (erreur $\sim 10\%$) se réalisent à l'aide d'un ressort placé à l'électrode inférieure. La différence de potentiel, tant celle des thermocouples, que celle créée dans les échantillons a été mesurée à l'aide d'un potentiomètre « QTK-Metra », l'indication de zéro étant donnée par un galvanomètre d'une sensibilité maximale d'environ $1{,}5.10^{-9}$ A/div.

Revue Roumaine de Chimie, **14**, 647–651 (1969)

Revue Roumaine de Chimie, **14**, 653-657 (1969)

L'EFFET DU COMPLEXE CUIVRE-DIPHÉNYLAMINE SUR LA DÉCOMPOSITION CATALYTIQUE DE L'EAU OXYGÉNÉE

D. CRĂCIUNESCU et AL. FRUMA

Centre de Chimie Physique, Bucarest, 23, rue Dumbrava Roşie

Reçu le 27 juin 1968

On a étudié l'influence des complexes cuivre-diphénylamine sur la cinétique de la décomposition de l'eau oxygénée catalysée par $FeCl_3$, entre 25-65°, en différents systèmes de réaction. On a établi que les complexes Cu-n-$NHPh_2$ ont un effet faible, dû aux ions cuivre mis en liberté. L'activité des complexes diminue avec l'augmentation du degré de saturation des positions de coordination du cuivre. On a suivi la variation de la vitesse de réaction avec la température pour le plus actif et le plus inactif des complexes. L'énergie d'activation a été trouvée entre 15,5-18,2 kcal/mole.

Le problème de la décomposition catalytique du H_2O_2 a préoccupé les chercheurs il y a quatre décennies. Quartolani [1] a démontré depuis 1924 la dépendance de l'activité de la décomposition catalytique du H_2O_2, du pH de la solution, pendant que Bohnson [2,3] et autres chercheurs [4-6] ont mis en évidence l'effet promoteur de l'ion Cu^{2+} sur la décomposition des solutions de H_2O_2, catalysée par l'ion ferrique. Les recherches plus récentes ont visé particulièrement le problème de l'activité catalytique des différents complexes, ainsi que l'action des promoteurs ou inhibiteurs des complexes.

Ainsi, une série de chercheurs de Suisse[7,8] ont utilisé la propriété catalytique de quelques complexes du cuivre pour arriver à des conclusions sur la structure de ces derniers.

L'idée qui nous a guidé à l'élaboration du présent travail a été celle d'établir la variation de l'activité catalytique et l'activité des complexes $Cu^{2+} - nNHPh_2^*$ avec l'augmentation progressive de la saturation des positions de coordination du cuivre. Il est bien connu qu'une série de substances organiques, comme le phénol, l'acétanilide, l'aniline, la diphénylamine et d'autres sont des inhibiteurs de la réaction de décomposition du H_2O_2 catalysée par l'ion ferrique, [9] pendant que l'ion cuivrique est un promoteur très fort. [2–6] Il est donc intéressant de poursuivre l'effet global des complexes du cuivre avec la diphénylamine.

---

[1] G. Quartolani, *Gazz. chim. Ital.*, **54**, 713 (1924).
[2] A. Bohnson et V. Robertson, *J. Amer. Chem. Soc.*, **45**, 2512 (1923).
[3] A. Bohnson et V. Robertson, *J. Amer. Chem. Soc.*, **47**, 1299 (1925).
[4] V. S. Barb et S. P. Baxendale, *Trans. Faraday Soc.*, **47**, 462 (1951).
[5] A. C. Roberson, *Trans. Faraday Soc.*, **48**, 228 (1952).
[6] J. H. Walton et J. Filson, *J. Amer. Chem. Soc.*, **54**, 3226 (1932).
[7] H. Siegel et U. Mueller, *Helv. Chim. Acta*, **49** (1), 671 (1966).
[8] H. Erlenmeyer, U. Mueller et H. Siegel, *Helv. Chim. Acta*, **49** (*1*), 681 (1966).

* $NHPh_2$ diphénylamine.

TECHNIQUE EXPÉRIMENTALE

On a utilisé une installation en verre pour mesurer le volume de l'oxygène résulté à la suite de la décomposition des solutions de l'eau oxygénée. Le récipient de réaction a été thermostaté à ± 0,1° et les données obtenues ont été lues sur la biurette à l'aide d'une loupe. Les résultats ont été vérifiés par titrage avec du $KMnO_4$.

Vu que dans les quatre complexes les quantités de cuivre sont variables *pro mole* de complexe, pour obtenir des résultats comparables on a effectué les expériences dans les conditions d'un rapport constant Cu/Fe, tout en utilisant des solutions variables en concentrations de complexe. Les concentrations et les quantités utilisées ont été pour le H_2O_2 de 3% et de 4 ml ; pour les solutions de $CuCl_2$ et $FeCl_3$ dans l'eau de 0,05 m, 0,3 ml et pour le complexe 1 : $CuCl_2 \cdot NHPh_2$ 0,3 ml solution 0,05 m en acétone ; pour le complexe 2 : $2CuCl_2 \cdot 3NHPh_2$, 0,3 ml solution 0,025 m en acétone ; pour le complexe 3 : $CuCl_2 \cdot 2NHPh_2$ et le complexe 4 : $CuCl_2 \cdot 6NHPh_2$ 0,3 ml solution 0,05 m en acétone. La quantité d'acétone et de solution d'amine pure a été de 0,3 ml. L'amine a été dissoute en acétone à la concentration de 0,05 m. Les résultats donnés dans le tableau ci-dessous correspondent aux quantités et aux concentrations citées.

Les complexes synthétisés pour la première fois par Spacu et ses collaborateurs[10,11] ont été préparés selon leurs indications. Le calcul de la constante de vitesse a été effectué en considérant que la réaction est du premier ordre. [12,13] Alors

$$k = 2{,}303/t \log V_f/V_f - V_x$$

où V_f est le volume d'oxygène à la décomposition totale de H_2O_2 et V_x le volume de l'oxygène dégagé jusqu'au moment t.

RÉSULTATS ET DISCUSSIONS

Dans le tableau 1 nous avons représenté, comparativement, les valeurs des constantes de vitesse à 25° pour différents systèmes de réaction.

On remarque le puissant effet promoteur de l'ion Cu^{2+} (la colonne *1* ligne *4*) qui double la vitesse de réaction en son absence (colonne *1* ligne *2*). L'acétone, au contraire, même en petite quantité (0,3 ml) en comparaison de la solution de H_2O_2 (4 ml) ralentit la vitesse de décomposition avec un ordre d'augmentation (colonne *1*, ligne *7*). Ainsi, plus évident encore, est l'effet inhibiteur de la diphénylamine, qui en solution d'acétone diminue encore plus la vitesse de réaction (colonne *3* ligne *4*).

---

[9] V. Anderson et J. Taylor, *J. Amer. Chem. Soc.*, **45**, 605 (1921).

[10] P. Spacu, O. Constantinescu, I. Pascaru, M. Brezeanu et F. Zălaru, *Z. anorg. Chem.*, **349** (*1–2*), 107 (1967).

[11] P. Spacu, M. Brezeanu, C. Gheorghiu, O. Constantinescu et I. Pascaru, *Rev. Roumaine Chim.*, **9**, 80 (1964).

[12] H. Zell et H. Siegel, *Helv. Chim. Acta*, **49** (*2*), 870 (1966).

[13] A. Konoplena et L. A. Nicolaev, *Zhur. fiz. Khim.*, **40**, 442 (1966).

Le complexe 1, le plus actif de ces quatre complexes, double la vitesse de réaction comparativement à la solution d'amine, mettant en liberté des ions Cu^{2+}, donc promoteurs, selon un mécanisme sur lequel nous discuterons plus loin.

Tableau 1

Constantes de vitesse pour la réaction de décomposition catalytique du H_2O_2, pour différents systèmes de réaction

Système	*k*	Système	*k*
$FeCl_3$	0,196	$CuCl_2$ diphénylamine	0,0025
$CuCl_2$	0,050	$FeCl_3$ diphénylamine	0,012
$FeCl_3$ $CuCl_2$	0,410	$FeCl_3$ $CuCl_2$ diphénylamine	0,039
$CuCl_2$ acétone	0,006	$FeCl_3$ complexe 1	0,029
$FeCl_3$ acétone	0,013	$FeCl_3$ complexe 2	0,022
$FeCl_3$ $CuCl_2$ acétone	0,049	$FeCl_3$ complexe 3	0,019
		$FeCl_3$ complexe 4	0,016

Evidemment, un surplus des ions Cu^{2+} à la solution d'amine conduira à une augmentation de la vitesse de réaction supérieure à celle obtenue avec le complexe $CuCl_2 \cdot NHPh_2$, parce que le nombre d'ions Cu^{2+} mis en liberté par celui-ci est évidemment moindre que celui additionné par nous. Les trois autres complexes ont un moindre effet, ainsi qu'il résulte du tableau 1.

Il est nécessaire d'interpréter l'effet des complexes qui ont fait l'objet du présent travail aux termes suivants : le système H_2O_2 + solution de $FeCl_3$ en présence de 0,3 ml acétone possède une constante de vitesse assez basse $k = 0{,}013$. Si dans la même quantité d'acétone on dissout les complexes, ils produisent une augmentation de la vitesse de décomposition, k étant délimité entre 0,016—0,029.

Dans la figure 1 on a représenté la variation de la pondération en poids du cuivre du complexe, en fonction de la constante de vitesse. Les droites (*1*), (*2*) et (*3*) se rapportent aux quantités respectives de solution du complexe : 0,3 ml, 0,6 ml, et 0,9 ml. Ici, comme dans le tableau 1 on a gardé un rapport constant entre le cuivre et le fer.

On remarque dans tous les cas une augmentation linéaire de la constante de vitesse, avec l'augmentation du poids du cuivre du complexe ou la diminution du numéro des positions de coordination satisfaites du cuivre. Quand même, pour le complexe $CuCl_2 \cdot 6NHPh_2$ la vitesse de réaction a une valeur petite, mais plus grande que celle du solvant, donc un effet existe également dans le cas de ce complexe, ce qui contredit quelques observations de Siegel, [7] et de Zell et ses collaborateurs, [12] qui ont observé à d'autres complexes du cuivre une stagnation de l'effet au moment de la saturation des positions de coordination du cuivre.

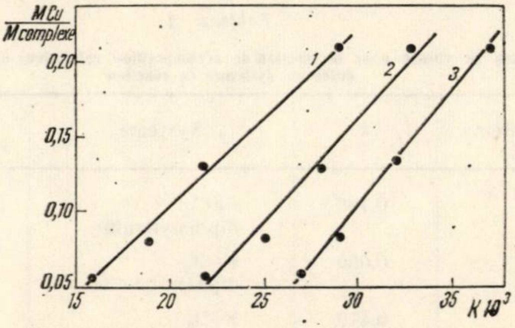

Fig. 1.— Variation de la pondération du cuivre du complexe en fonction de la constante de vitesse.
1, pour 0,3 ml solution de complexe; *2*, pour 0,6 ml solution de complexe; *3*, pour 0,9 ml solution de complexe.

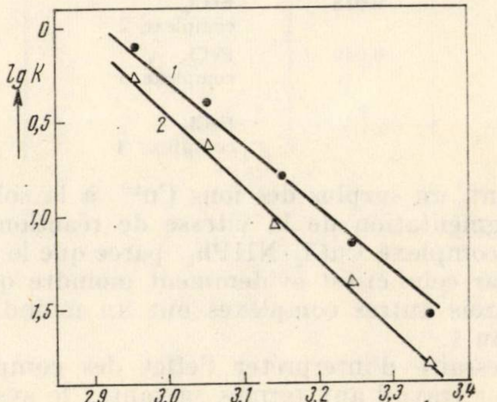

Fig. 2. — Variation de la constante de vitesse en fonction de la température pour le complexe 1 (*1*) et le complexe 6 (*2*).

L'activité des complexes peut être attribuée sans doute, exclusivement à l'existence des ions cuivre dans la solution. Le mécanisme dissociatif, avec le transfert de charge

$$Cu^{2+} + n(NHPh_2) \rightleftarrows [Cu^{2+}(NHPh_2)_n] \rightleftarrows [(Cu^{2+})-(NHPh_2)_n^{+}];$$
$$[Cu^{+}(NHPh_2)_{n-1}(NHPh_2^{+})]$$

a été proposé par Spacu [10,11] et ses collaborateurs et vérifié par RES. Par l'augmentation de la température la constante de la vitesse de réaction varie en concordance avec l'équation d'Arrhenius, ce qui a été représenté dans la figure 2 pour le complexe $CuCl_2 \cdot NHPh_2$, le plus actif (1), et également pour $CuCl_2 \cdot 6NHPh_2$, le plus inactif (2).

Les différents points s'encadrent bien à la droite, ce qui prouve que l'augmentation de la température ne détermine aucun changement du mécanisme de la réaction. De même, les trois phénomènes possibles, à savoir, l'évaporation d'une partie d'acétone au moment du contact avec la solution de H_2O_2 chaude, une éventuelle oxydation du solvant et du complexe, plus accentuée avec l'augmentation de la température, ainsi qu'une variation de la stabilité ou de l'équilibre de dissociation du complexe n'ont pas d'influence sur l'allure des droites, ces trois phénomènes étant soit très réduits, soit compensés.

Les énergies d'activation calculées d'après la figure 2 ont été trouvées entre 15,5—18,2 kcal/mole, donc plus grandes que celles de 9 kcal/mole obtenues par Vorobieva et ses collaborateurs[14] aux autres complexes.

CONCLUSIONS

Les complexes de cuivre-diphénylamine ont mis en évidence un effet sur la décomposition du H_2O_2 catalysée par le $FeCl_3$, expliqué par la mise en liberté des ions cuivre par les complexes. Les constantes de vitesse pour différents complexes diminuent avec le décroissement du poids du cuivre contenu dans le complexe, donc avec l'augmentation du degré de la saturation des positions de coordination du cuivre.

La variation avec la température de la constante de vitesse vérifie l'équation d'Arrhenius. L'énergie d'activation de 15,5—18,2 kcal/mole est supérieure à celle trouvée par d'autres chercheurs dans des conditions semblables, mais avec d'autres complexes.

---

[14] T. V. Vorobieva, V. V. Voevodskii et A. P. Purmal, *Zhur. fiz. Khim.*, **36**, 532 (1962).

Revue Roumaine de Chimie, 14, 659–665 (1969)

POLY(1,3,4-OXADIAZOLES). V *

LA RÉACTION DES DITÉTRAZOLES AVEC LES DIISOCYANATES

LEONIA STOICESCU-CRIVETZ, MARIA BRUMĂ et I. ZUGRĂVESCU

Institut de Chimie Macromoléculaire « Petru Poni »,

de l'Académie, Filiale de Jassy, 41 A, Aleea Gr. Ghica Vodă

Reçu le 13 novembre 1968

On a étudié la réaction de polyaddition d'une série homologue de ditétrazoles avec les diisocyanates, en obtenant des poly(1,3,4-oxadiazoles), qui contiennent des liaisons amino dans la chaîne macromoléculaire. La structure proposée pour les divers polymères synthétisés a été confirmée par les analyses élémentaires et les spectres en infrarouge qui sont similaires à ceux des modèles préparés. On a déterminé la solubilité, la viscosité inhérente et la stabilité thermique des polymères obtenus.

On connaît la réaction des isocyanates et thioisocyanates avec les réactants nucléophiles, comme les amines et les alcools, qui conduit à des produits d'addition. Huisgen [1] et ses collaborateurs, [2] dans une vaste étude sur les tétrazoles, ont montré que le phénylisocyanate réagit aussi avec le 5-phényltétrazole, pour former le 2-phényle, 5-aminophényloxadiazole. La réaction de polyaddition des diisocyanates avec les ditétrazoles n'a pas été rapportée.

Poursuivant nos recherches sur les poly(1,3,4-oxadiazoles),[3] nous avons étudié cette réaction en utilisant comme produits de départ les diisocyanates de dibenzyl (DIDB), de 2,4-tolyle (DIDT) et de hexaméthylène (DIHM) avec les ditétrazoles de bi-, tri-, tétra-méthylène et *p*-phénylène.

Pour faire possible l'identification des polymères et suivre la formation du cycle oxadiazolique, nous avons préparé deux types de modèles : par l'action du phénylisocyanate (2 moles) avec un ditétrazole, et du phényltétrazole (2 moles) avec un diisocyanate. Les schémas suivants résument ces réactions

---

* IVe partie : M. Stoicescu-Crivetz et M. Brumă, *Rev. Roumaine Chim.*, **13**, 1069 (1968).

[1] R. Huisgen, *Angew. Chem.*, **72**, 359 (1960).

[2] R. Huisgen, J. Sauer et M. Seidel, *Chem. Ber.*, **93**, 2883 (1960).

[3] L. Stoicescu-Crivetz et M. Brumă, *Rev. Roumaine Chim.*, **12**, 1245 (1967).

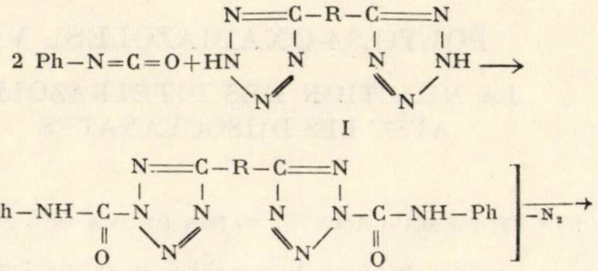

$Ia_1R = (CH_2)_2$

$Ia_2R = (CH_2)_3$

$Ia_3R = (CH_2)_4$

$Ia_4R = p-C_6H_4^-$

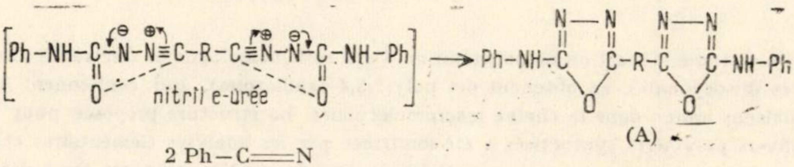

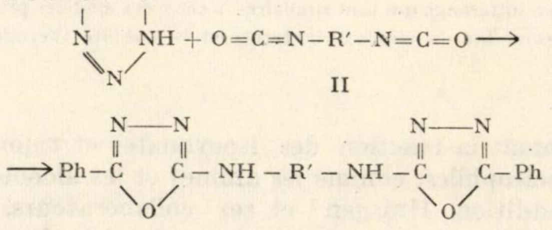

(B)

$IIa\ R' = -C_6H_4CH_2CH_2C_6H_4^-$

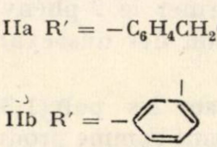

IIb R' =

$IIc\ R' = -(CH_2)_6^-$

Nous avons constaté que l'atome hydrogène du groupement NH du cycle tétrazolique présente une mobilité moins marquée que l'hydrogène du groupement amino du 5-aminotétrazole.[3] La réaction d'addition avec l'isocyanate nécessite des conditions plus énergiques, ainsi que la présence d'un catalyseur basique. La nitrile-urée qui résulte par la perte d'une molécule d'azote du produit acylé intermédiaire est stabilisée par la formation du cycle oxadiazolique.

L'extension de cette réaction aux produits bifonctionnels fournit des poly (-1,3,4-oxadiazoles) de structures III

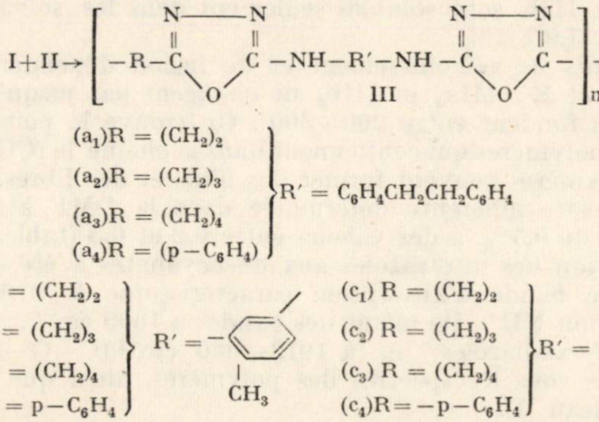

Une polycondensation de ce type renferme la formation d'une poly-(nitrile-urée), suivie d'un réarrangement intramoléculaire dans la chaîne du polymère, pour former des cycles oxadiazoliques (voir le schéma précédent). Les polymères III contiennent des groupements amino (NH) entre les unités aromatiques (ou aliphatiques) et les hétérocycles. La formation des cycles oxadiazoliques a été confirmée spectrophotométriquement par l'apparition de la bande NH (3200 cm^{-1}) et les analyses d'azote qui correspondent pour la structure convertie du cycle tétrazolique en cycle oxadiazolique. L'existence des fonctions amino dans la molécule des modèles et dans la chaîne des polymères a été mise en évidence aussi par la préparation des dérivés acétylés correspondants, identifiés par l'apparition de la bande à 1700 cm^{-1}, due au carbonyle, dans les spectres en infrarouge, ainsi que par des analyses chimiques. En général on a observé que la formation des polymères avec le ditétrazole Ia$_4$ aromatique a lieu plus facilement qu'avec Ia$_1$, Ia$_2$ et Ia$_3$. La réaction découle aisément en présence de la pyridine, tandis que si on l'effectue seulement dans la diméthylformamide on doit prolonger le temps de réaction, et on obtient des polymères avec une viscosité très faible et une teneur en azote plus grande que celle calculée ; ces faits dénotent un poids moléculaire petit et des chaînes terminées avec des cycles tétrazoliques non modifiés. La polycondensation en solution, en présence d'un catalyseur basique conduit à des poly(aminooxadiazoles) avec un poids moléculaire assez élevé pour permettre l'obtention des films de leurs solutions et le filage du polymère à l'état fondu.

CARACTÉRISATION DES POLYMÈRES

Les polymères synthétisés dans ce travail sont des poudres légèrement teintées de jaune, insolubles dans la majorité des solvants habituels, solubles en diméthylformamide, diméthylacétamide, N-méthylpyrrolidone. Les polymères contenant des segments aliphatiques sont plus solubles que ceux qui présentent des unités aromatiques. Ainsi, les polymères $IIIa_4$ et $IIIb_4$ sont solubles seulement dans les solvants amidiques contenant du LiCl 2%.

Les points de ramollissement et de fusion dépendent aussi de la nature des R et R', $IIIa_4$ et $IIIb_4$ ne changent pas jusqu'à 350°, tandis que les autres fondent entre 200—300°. On trouve le point de fusion le plus bas aux polymères qui contiennent dans la chaîne le $(CH_2)_6$; en même temps ces polymères peuvent former des films et des fibres.

La viscosité inhérente déterminée dans la DMF, à 20°, pour une concentration de 0,5%, a des valeurs entre 0,2 et 0,3 (tableau 1). Le processus d'addition des ditétrazoles aux diisocyanates a été suivi par l'apparition d'une bande d'absorption caractéristique à 3100—3400 cm^{-1} pour la vibration NH*. De même des bandes à 1600 cm^{-1}, indiquées pour le cycle 1,3,4-oxadiazoles[4] et à 1012—960 cm^{-1} (C—O—C cycle), sont présentes dans tous les spectres des polymères, ainsi que des composés modèles (tableau 1).

Les polymères ayant une viscosité plus grande peuvent former des films d'une solution de DMF, qui adhèrent à la glace. Des fibres ont été tirées de ces polymères à l'état fondu.

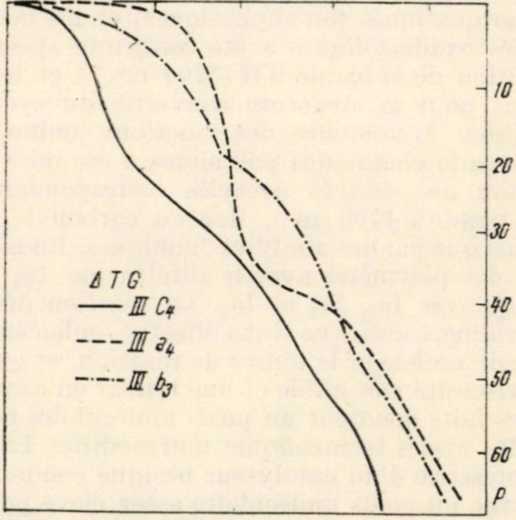

Fig. 1. — Analyse thermogravimétrique des polymères.

La stabilité thermique des poly(amino-1,3,4-oxadiazoles) est inférieure à celles des autres polyoxadiazoles. Probablement le NH offre « un site » sensible pour la dégradation (fig. 1).

---

* L'acétylation du groupement amino provoque la disparition de la bande à 3300 cm^{-1} et l'apparition d'un nouveau pic à 1705 attribué au carbonyle.

[4] T. Unishi et M. Hasegawa, *J. Polymer. Sci.*, **3A**, 3191 (1965).

Tableau 1

Caractéristiques des poly (1,3,4-oxadiazoles) III

Polymère	P. fus. 0°C	η inh. C = 0,5 %	Analyse N %			Spectres en IR cm^{-1}	
			Calculé	Trouvé	=C–O–C=	NH	CH_2
$IIIa_1$	280–88	0,24	22,46	22,10	980	3400	2950
$IIIa_2$	284–90	0,31	21,64	22,49	1000	3340	2950
$IIIa_3$	275–80	0,32	20,89	20,40	1000	3310	2950
$IIIa_4$	350	0,29	19,91	20,81	1006	3400	2950
$IIIb_1$	300	0,31	29,57	28,18	980	3430	2960
$IIIb_2$	300	0,29	28,19	29,10	1100	3300	2970
$IIIb_3$	298	0,33	26,92	25,62	980	3340	2860
$IIIb_4$	350	0,28	25,53	27,03	970	3400	—
$IIIc_1$	250	0,35	30,21	31,21	970	3450	2960
$IIIc_2$	245	0,34	28,76	26,49	1000	3400	2940
$IIIc_3$	244	0,34	27,45	26,48	980	3400	2920
$IIIc_4$	267	0,30	25,76	26,41	970	3350	2920

PARTIE EXPÉRIMENTALE

Les ditétrazoles Ia_1, Ia_2 et Ia_3 ont été préparés selon la méthode décrite dans la littérature,[5] à partir des dinitriles correspondants et de l'azide d'ammonium. Ia_4 a été préparé selon le procédé de Huisgen[6] légèrement modifié en utilisant l'azide d'ammonium à la place de l'azide de lithium, en DMF, et réduisant ainsi sensiblement le temps de réaction.

Les diisocyanates ont été distillés en atmosphère inerte, à une pression réduite.

On a utilisé des solvants bien purifiés et parfaitement anhydres.

Les composés modèles

Di(-2-phénylamino-oxadiazolyl-5)tétraméthylène (A). On chauffe au reflux, sous agitation, pendant 30 minutes, 1,94 g (0,01 mole) de ditétrazole adipique avec 10 ml de phénylisocyanate. Après refroidissement, le produit séparé est lavé à l'acétone, purifié par recristallisation dans la DMF et dans l'eau. Le séchage a été effectué sous vide à 100°. Soluble en DMF, DMA, pyridine. Fusible à 248°. Le spectre en infrarouge montre des bandes à 970 et 1010 cm^{-1} attribuées au cycle oxadiazolique, et à 3300 cm^{-1} pour la vibration NH[4].

$C_{20}H_{20}N_6O_2$
Calculé : N = 22,34 %
Trouvé : N = 22,60 %

Di(2-phénylamino-oxadiazolyl-5) p-phénylène (A). Préparé comme le précédent, à partir du ditétrazole téréphtalique Ia_4 et le phénylisocyanate dans le benzonitrile à l'ébullition, ou dans un excès d'isocyanate sans solvant. Produit blanc cristallin, insoluble dans les solvants usuels, soluble en DMF, DMSO. P. Fusion 349°.

---

[5] W. G. Finnegan, R. A. Henry et R. Lofauist, *J. Amer. Chem. Soc.*, **80**, 3908 (1958).
[6] J. Sauer, R. Huisgen et H. Sturm, *Tetrahedron*, **11**, 241 (1960).

$C_{22}H_{16}N_6O_2$
Calculé : N = 21,21 %
Trouvé : N = 21,50 %
IR 970, 1025 cm^{-1} et 3210 cm^{-1} (NH).

4,4'-di-(2-phényloxadiazolyl-5)-diaminodibenzyle (B). A une solution de 2,92g (0,02 mole) de 5-phényltétrazole dans 80 ml de mésitylène on ajoute une solution de 2,64 g (0,01 mole) II *a* dans 20 ml de mésitylène. On porte à l'ébullition pendant 4 heures. La solution est refroidie, on essore le précipité qui est lavé à l'acétone. Purifié par recristallisation de la pyridine. Produit incolore, insoluble en éthanol, acétone, éther, soluble en DMF, DMSO et pyridine à chaud P. fusion à 326°.

$C_{30}H_{24}N_6O_2$
Calculé : N = 16,80 %
Trouvé : N = 17,12 %

Spectres en infrarouge, bandes à 968 cm^{-1}, 1020 cm^{-1} (vibration = C—O—C) et 3250 cm^{-1} (NH).

2,4-di-(2-phényloxadiazolyl-5)-diaminotolyle (*B*). On dissout 2,92 g (0,02 mole) de 5-phényltétrazole dans 20 ml de pyridine anhydre, et on ajoute 1,74 g (0,01 mole) de diisocyanate de 2,4-tolyle. On chauffe pendant 4 heures. On filtre le produit qui sépare par refroidissement, on lave à l'acétone, on cristallise de la pyridine. Produit incolore, fusible à 274°, soluble en DMF, DMA, DMSO, pyridine.

$C_{23}H_{18}N_6O_2$
Calculé : N = 20,48 %
Trouvé : N = 20,68 %
Spectres en infrarouge 960 cm^{-1}, 1020 cm^{-1} (oxadiazole)
3250 cm^{-1} (NH).

Polyaddition des diisocyanates avec les ditétrazoles. Les polymérisations ont été effectuées à l'abri de l'air et de l'humidité, en atmosphère inerte sur des quantités équivalentes de réactifs. En général, on dissout le ditétrazole en DMF et pyridine, à froid, et on ajoute à la fois et en agitant le diisocyanate. La solution est portée à l'ébullition quelques heures, et versée après refroidissement dans un non-solvant. Le précipité formé est filtré, lavé à l'acétone, séché, purifié et soumis à un traitement thermique à 100°, sous vide, pendant une heure.

Le procédé est illustré par l'exemple suivant :
Le polymère $IIIb_3$

1,94 g (0,01 mole) Ia_3 est dissous dans 20 ml de DMF, on ajoute 1 ml de pyridine anhydre et 1,74 g (0,01 mole) IIb. On porte la solution à reflux pendant 5 heures sous agitation et après refroidissement on la verse goutte à goutte dans 150 ml d'acétone, on laisse déposer le précipité formé, on décante le liquide, et on lave plusieurs fois à l'acétone. On filtre, on sèche et on purifie le polymère par dissolution en DMF et précipitation à méthanol. Après un séchage à 100° pendant une heure, on recueille une poudre légèrement teintée de jaune, soluble en DMF, NMP, DMSO. ηinh. = 0,33. Fusible à 298°. On peut tirer des fibres du polymère à l'état fondu.

Les tableaux 1 et 2 résument les données des 12 polymères préparés dans ce travail. Les points de fusion ont été déterminés au microscope.

Tableau 2

Préparation des poly (1.3,4-oxadiazoles) III

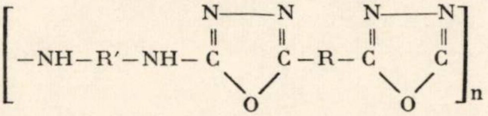

Polymère	R	R′	Monomère g		Solvant DMF ml	Temps h
			tétrazole	isocyanate		
$IIIa_1$	$(CH_2)_2$	$C_6H_4CH_2CH_2C_6H_4$	1,66	2,64	20	5
$IIIa_2$	$(CH_2)_3$	,,	1,80	2,64	20	5
$IIIa_3$	$(CH_2)_4$	,,	1,94	2,64	20	5
$IIIa_4$	$p-C_6H_4$	,,	2,14	2,64	25	3,5
$IIIb_1$	$(CH_2)_2$	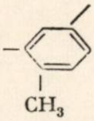	1,66	1,74	15	5
$IIIb_2$	$(CH_2)_3$	,,	1,80	1,74	15	5
$IIIb_3$	$(CH_2)_4$	,,	1,94	1,74	20	5
$IIIb_4$	$p-C_6H_4$	,,	2,14	1,74	20	3,5
$IIIc_1$	$(CH_2)_2$	$(CH_2)_6$	1,66	1,68	15	6
$IIIc_2$	$(CH_2)_3$	,,	1,80	1,68	15	6
$IIIc_3$	$(CH_2)_4$	,,	1,94	1,68	15	6
$IIIc_4$	$-p-C_6H_4$	,,	2,14	1,68	20	4

Les analyses thermogravimétriques ont été effectuées au moyen d'un dérivatographe « I. Paulik », étant conduites, en présence de l'air, sur des échantillons de 15−20 mg de polymère, pour un régime de chauffage de 12° par minute.

Revue Roumaine de Chimie, **14**, 667 – 672 (1969)

THE STEREOSPECIFIC POLYMERIZATION OF 1,3-BUTADIENE. II*

THE INFLUENCE OF THE REACTION MEDIUM ON BUTADIENE POLYMERIZATION WITH $AlEt_2Cl-CoCl_2 \cdot 2Py-H_2O$ CATALYTIC SYSTEM

I. VELEA, VICTORIA DIMONIE, E. MELEGA, VALENTINA PROVINCEANU
and P. BLENKE

Polytechnic Institute "Gh. Gheorghiu-Dej", Bucharest, Laboratory of Macromolecular
Technology, Calea Victoriei 149

Received June 26, 1968

The influence of the reaction medium and electron-donor substances on the polymerization process of butadiene with soluble complexes of cobalt and also on the structure of polymers has been studied.

The electron-donor substances produce the decrease in the reaction rate and in the molecular weight. The strongest effect appeared in the case of tetrahydrofuran. Polymer structure in all cases was not influenced. Aromatic, aliphatic, cycloaliphatic hydrocarbons and chlorinated derivates were used as solvents. The polymerization rate and molecular weight are substantially influenced according to the nature of the solvent, while the polymer structure is not changed.

One of the main problems in the study of the butadiene polymerization with catalytic system based on soluble salts of cobalt is the nature of the active species by which the growth of the polymer chain is achieved.

The opinions are not unanimous on this point. Thus, using the deactivation method of active centres with stoppers which contain labelled atoms and then determining the radioactivity of the obtained polymer, Childres [1] and later on Bresler [2] get at the conclusion that the nature of the active species in the polymer chain propagation is cationic. Using the same method under slightly different experimental conditions, Natta and co-workers [3] suggest a coordinative anionic mechanism for butadiene polymerization with the above mentioned system.

In the present work it is studied the influence of solvents and various electron-donor substances on the reaction rate, molecular weight and polybutadiene structure obtained by butadiene polymerization with $AlEt_2$ Cl

---

* Previous part: I. Velea, V. Dimonie, E. Melega, P. Blenke and V. Provinceanu *Rev. Roumaine Chim.*, **14**, 478 (1969).

[1] C. H. Childres, *J. Amer. Chem. Soc.*, **85**, 229 (1963).

[2] L. C. Bresler and E. N. Korpacheva, *Doklady Akad. Nauk S.S.S.R.*, **159**, 365 (1964).

[3] G. Natta, *Makromol. Chem.*, **71**, 207 (1964).

$-CoCl_2 . 2Py-H_2O$ catalytic system in order to obtain information about the nature of the active centres and generally on the reaction mechanism.

EXPERIMENTAL

The aliphatic, cycloaliphatic, aromatic hydrocarbons and chlorinated derivates were used as reaction media and the influence of the electron-donor substances such as : ether, amines, alcohols, was studied.

The catalysts were used in benzene solutions : when studying the influence of the electron-donor substances on the butadiene polymerization benzene was again the reaction medium. The runs were dilatometrically followed by means of a dilatometer usually used for polymerizations in homogenous media and the catalysts, previously put in glass bubbles, were introduced in the reaction mass by the simultaneous breaking of the bubbles.

Both, reagent handling and polymerizations were carried out in oxygen-free and dry argon atmosphere. This procedure permits to have a good reproducibility with experimental errors below $3^0/_0$.

The molecular weights were viscosimetrically determined using for calculation the formula[4] : $(\eta) = 1.53\times10^{-4}\ M^{0.8}$.

The polymer structure was determined by infrared spectroscopy of the polymer films obtained from the carbon sulphide solutions, according to the method used by Kimmor and Schmalz.[5]

RESULTS

1. *Polymerizations in Aromatic Derivates*

The results of the polymerization carried out in aromatic hydrocarbons are shown in figure 1 and table 1.

Table 1

Polymerization of butadiene in aromatic hydrocarbons media

Monomer concentration =1.91 mole/l; $AlEt_2Cl$ conc. =40 m moles/l $CoCl_2Py$ conc=0.08 m moles/l; H_2O conc.=4m moles/l. Polymerization temperature =15°C

Solvent	Initial rate V_0 g/l. min	$\overline{M}$	Structure %		
			cis 1,4	*trans* 1,4	*vingl* 1,2
Benzene	9.12	324,000	96.0	2.8	1.2
Toluene	1.38	248,000	95.8	2.9	1.3
Ortho-Xylene	0.21	105,000	—	—	—
Meta-Xylene	0.22	58,000	94.4	4.2	1.4
Para-Xylene	0.22	49,000	95.1	3.4	1.6
Mesitylene	0.05	oil consistency polymer traces			

---

[4] C. Longiave, R. Castelli and G. F. Croce, *Chimia e Industria*, **43**, 625 (1961).

[5] W. Kimmer and E. O. Schmaltz, *Plaste und Kautschuk*, **2**, 14 (1965).

The above data show that the reaction rate and the molecular weight of the obtained polybutadiene are substantially changed according to the nature of the aromatic solvent used.

Generally we remark a decrease in the polymerization rate and in the molecular weight of polymers at the same time with the introduction of methyl groups into the aromatic nucleus. The position of the substitutes in the aromatic nucleus influences neither the reaction rate nor the molecular weight.

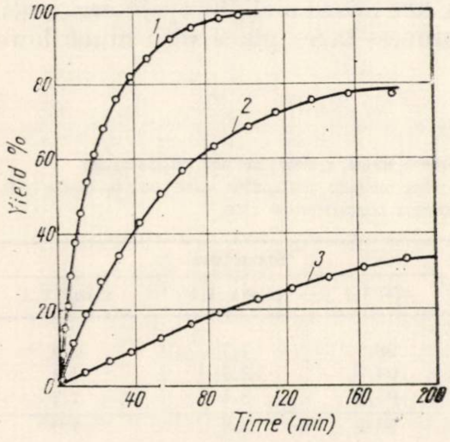

Fig. 1. — Conversion variation in time for butadiene polymerization in aromatic media.

1, Benzene; *2*, Toluene; *3*, *orto-*, *meta-* and *para-* Xylene.

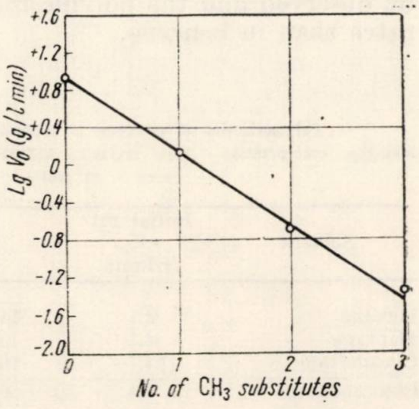

Fig. 2. — Dependence of polymerization rate on the number of methyl substitutes in the aromatic nucleus.

The variation of butadiene polymerization rate in aromatic solvents depending on the solvent nature is subjected to a simple law i.e. the logarithm of the polymerization rate decreases proportionally to the number of methyl substitutes in the aromatic nucleus of the hydrocarbon used as solvent (see fig. 2).

It has been noticed that with the polymerization rate also decreases the maximum conversion degree reached for the polymerizations carried out in these solvents. Thus, in the case of benzene used as reaction medium the conversion is practically 100 % ; using toluene the conversion is limited to 77—80 % ; in the case of xylenes a maximum conversion of 30—35 % is reached and with mesitylene the polymerization process is stopped at a lower conversion degree of 15 %.

The molecular weight is also influenced by the solvent nature i.e. it decreases substantially at the same time with the increase in the substitute number in the aromatic nucleus, obtaining oil consistency polymers as in the case of mesitylene.

Polymer structure is not affected by the solvent nature obtaining always a polybutadiene with a high content in the 1.4-cis-structure.

2. *Polymerizations in Aliphatic and Cycloaliphatic Solvents*

From this class of solvents the hexane, heptane, and cyclohexane were used as solvents.

$CoCl_2.2Py$ complex is insoluble in lineal aliphatic hydrocarbons. In the case of hexane and heptane if the catalytic components are introduced as benzenic solutions, when they are mixed a slight opalescence may be observed and the polymerization process takes place with much lower rates than in benzene.

Table 2

Polymerization of butadiene in aliphatic hydrocarbons media, cyclohexane and chlorobenzene

Monomer concentration = 1,91 moles/l; $AlEt_2Cl$ conc = 40m moles/l; $CoCl_2.2Py$ conc = 0.08m moles/l; H_2O conc = 4m moles/l; Polymerization temperature = 15°C

Solvent	Initial rate V_0 g/l.min.	$\overline{M}$	Structure %		
			cis 1,4	*trans* 1,4	*vinyl* 1,2
Hexane	2.1	110,000	96.6	1.5	1.9
Heptane	4.5	138,000	94.7	3.5	1.8
Cyclohexane	14.7	167,000	95,3	3.4	1.3
Chlorobenzene	24	600,000	95.2	3.8	1.0

If the reaction medium is cyclohexane no opalescence is noticed, the polymerization reaction occurs with high rate (higher than that in the case of benzene), the conversion reaches the maximum value and high molecular polymers are obtained.

Extremely high reaction rates are obtained using chlorobenzene as solvent (about 3 times higher than the polymerization rates in benzene medium) and also high molecular weight (see table 2).

3. *The influence of Electron-Donor Additions*

In a series of special runs the influence of the electron-donor substances on the polymerization process was studied. The influence of ethers (ethyl ether and tetrahydrofuran), alcohols, (methyl alcohol, isopropyl alcohol and tertiary butyl alcohol) and amines (pyridine) was studied.

The results of these experiments are shown in table 3.

From the results recorded here one can see that all electron-donor substances reduce the polymerization rate and maximum conversion; simultaneously they reduce the polymer molecular weight. Tetrahydrofuran had the strongest effect and the methyl alcohol the weakest one.

In the series of alcohols the decrease effect in the polymerization rate and molecular weight occurs as follows : methyl alcohol < isopropyl alcohol < tertiary butyl alcohol.

Table 3

The influence of the electron-donor additions

Monomer concentration = 1.91 moles/l; solvent = benzene $AlEt_2Cl$ conc. = 20 m moles/l: $CoCl_3$.Pyconc = 0.07 m moles/l; H_2O conc. = 2 mmoles/l, Polymerization temperature = 5°C

Addition	Addition concentration mmoles/l	Initial rate V_0 g/l.min	$\overline{M}$	Structure %		
				cis 1,4	*trans* 1,4	vinyl 1,2
—	—	7.9	412,000	96.6	1.4	2
Methyl alcohol	3.5	6.6	242,000	95.2	2.0	2.8
	7.0	5.7	236,000	—	—	—
iso-Propyl alcohol	5.0	6.2	129,000	94.8	2.4	2.8
	10.0	0.2		traces of polymer		
tert-butyl alcohol	1.0	2.5	251,000	98.5	0.5	1.0
	2.5	1.4	195,000	97.0	1.9	1.1
Diethyl ether	7	3.3	119.000	95.3	2.6	2.1
	11	2.2	105,000	92.8	3.2	4.0
	15	1.8	102,000	—	—	—
Tetrahydrofuran	1	1.1	59,000	98.0	1.7	0.3
	4	0.8	19,000	97,3	2.0	0.7
Pyridine	7	0.8	191,000	97.7	1.2	1.1
	10	0.5	180,000	—	—	—

DISCUSSION

The high stereospecificity of the process and the effect generally manifested by all electron-donor substances to decrease the reaction rate, shows a coordinative polymerization mechanism in which the introduction of the monomer molecule in the growth polymer is preceded by the complex formation between the monomer molecule and the active centre.

The introduction of electron-donor substances into the reaction medium leads to the appearance of some parallel reactions in which the electron-donor substance competes with monomer in the reaction of complex formation with the active centre.

The complex formed between the electron-donor substance and the active centre is probably inactive in the polymerization reaction and therefore the introduction of electron-donor substances has as total effect the decrease in the average life of the active chains and the total number of active centres, macroscopically manifested by the decrease in the molecular weight and the maximum conversion reached.

As the butadiene complexing capacity is low in comparison with that of the other electron-donor substances, low concentrations of the later are necessary to enable an effective competition with the monomer and at higher electron-donor concentrations the whole process is inhibited.

It is also interesting to remark that in the alcohol series the decrease effect in the polymerization rate and the molecular weight of polymers does not increase with the increase of alcohol "acidity" but with the increase in the alcohol electron-donor capacity, caused by the increase of CH_3 substitute number to the carbon atom bound to the hydroxyl group.

Indeed, in the alcohol series the methyl alcohol ($K_a = 10^{-16}$) has the poorest effect on the decrease in the polymerization rate and the polymer molecular weight, and the tert-butyl alcohol ($K_a = 10^{-19}$) has the strongest one.

It is assumed that the deactivation is conditioned firstly by the complexing reaction with the active centres and perhaps secondly by the proton transfer reaction.

We should also outline a peculiarity of this system i.e. the fact that by adding the electron-donor substances the polymer structure remaines the same no matter of the quantity of electron-donor addition. This indicates that by mixing the catalytic components only one type of centres, which form inactive complexes with electron-donor substances, is produced.

The decrease in the reaction rate, observed in the case of polymerizations carried out in aromatic derivates at the same time with the increase in the substitute number in the aromatic cycle may be related to the increase in the electron-donor properties of the substances from the respective series. This increase in the electron-donor properties is conditioned by the increase in the electron density in the aromatic nucleus, increase caused by the + I inductive effect of CH_3 groups. In other words toluene, xylenes and especially mesitylene are behaving as electron-donor substances which may complex with the active centres and consequently they have the same effect as the later in the polymerization process.

The electron-donor properties of the aromatic derivates are however, rather poor and therefore higher concentrations are necessary to cause remarkable effects. The polymerization rate is much higher in cyclohexane (low electron density in cycle) than in benzene. The same thing occurs with the chlorobenzene where the influence of the chlorine atom is present.

This point of view concerning the behaviour of the aromatic solvents is consistent with the results recorded by Minsker [6] and Boor, [7] which study the influence of the aromatic substances in the coordinative polymerization processes and with the work of Porri and Carbonaro,[8] which note that the molecule of the catalytic complex, active in butadiene polymerization, resulting in the reaction between $AlPh_3$, $AlCl_3$, $CoCl_2$ in benzene medium, contains benzene molecules.

Our above assumption is also confirmed by the recent obtainment of some stable cobalt complexes with aromatic derivatives. [9]

The fact that the polymerization reaction poorly develops in aliphatic solvents is probably in connection with the insolubility of the catalytic complex in these reaction media.

As concerns the nature of the active centres, the fact that the polymerization takes place in chlorinated solvents and reaches maximum conversions makes less probable the assumption according to which the growth of the polymer chain may be achieved by anion species.

---

[6] K. F. Minsker and R. T. Chernovskaia. *Doklady Akad. Nauk. S.S.S.R.*, **147**, 1029 (1962).

[7] J. Boor, *J. Polymer. Sci.*, **3**, 995 (1965).

[8] L. Porri and A. Carbonaro, *Makromol. Chem.*, **60**, 236 (1963).

[9] H. Zeiss, "Organometallic Chemistry", Ed. Mir, Moscow, 1964, p. 467.

Revue Roumaine de Chimie, **14**, 673 – 678 (1969)

AZLACTONES OF THE PHENOTHIAZINE SERIES. III[1] AMINOLYSIS OF SOME PHENOTHIAZINE AZLACTONES

C. BODEA, I. OPREAN and V. FĂRCĂŞAN

Institute of Chemistry of the Academy, Cluj, str. Donath, 59 – 65

Received May 25, 1968

The behaviour of I brought into reaction with ammonia, hydrazine hydroxide and some amines was described. The aminolysis of azlactones I and XIII was kinetically followed.

It is well known that the azlactones react with substances containing NH_2-group yielding acylamino-derivatives.[2]

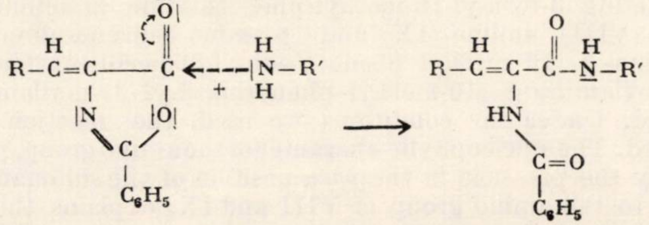

I : R = A
III : R = B
IV : R = C

II : R = A, R′ = H
V : R = A, R′ = NH_2
VI : R = B, R′ = NH_2
VII : R = C, R′ = NH_2
XI : R = A, R′ = $CH_2C_6H_5$
XII : R = A, R′ = C_6H_5

A =
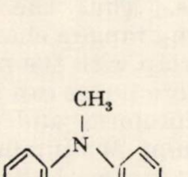

B =
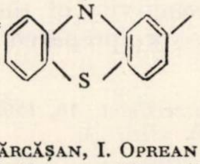

C =
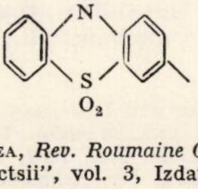

---

[1] V. Fărcăşan, I. Oprean and C. Bodea, *Rev. Roumaine Chim.*, **13**, 647 (1968).

[2] H. E. Carter, "Organitscheskie reactsii", vol. 3, Izdatelstvo Inostranoi Literatura, Moscow, 1951, p. 204.

In previous studies [1,3] we have obtained the first azlactones in the phenothiazine series in view of using them as starting materials for other syntheses.

In this paper we described the behaviour of 3-formyl-10-methyl-phenothiazine azlactone (I) brought into reaction with ammonia, hydrazine hydroxide and some amines.

With ammonia I is converted into α-benzoylamino-β-(10-methyl-phenothyazinyl-3)-acrilamide (II). The use of dimethylformamide as solvent increases the reaction rate.

The reaction of 3-formyl-10-methyl-phenothiazine azlactone (I) with hydrazine hydroxide was carried out under the conditions given for similar cases. [4]

This reaction was extended also to the 2-formyl-10-methyl-phenothiazine azlactone (III) and 3-formyl-10-methyl-phenothiazine-5,5-dioxide azlactone (IV), taking into account that the obtained hydrazides — V, VI and VII — could possibly be of biological interest.

For the same reason we attempted the conversion of the hydrazides V, VI and VII into the corresponding 1.2.4-triazine derivatives. In this case on using the Jennings method,[5] the azlactones I, III and IV were obtained. Other hydrazides of the α-benzoylamino unsaturated acids showed the same behaviour. [6]

By reacting 3-formyl-10-methyl-phenothiazine azlactone (I) with benzylamine (VIII), aniline (IX) and *p*-amino-benzenesulfonamide (X), α-benzoylamino-β-(10-methyl-phenothiazinyl-3)-acrilbenzylamide (XI) and α-benzoylamino-β-(10-methyl-phenothiazinyl-3)-acrilamide (XII) were obtained. Under the conditions we used, the reaction with substance X failed. The nucleophylic character of the amino group, particularly diminished by the presence in the *para* position of the sulfonamido group, as compared to the amino group of VIII and IX, explains the difference in the behaviour of these three substances in a reaction with supposed nucleophylic attack.

There are some reasons to use the reaction between benzylamine (VIII) and azlactone I for kinetic measurements. Thus the electronic spectrum of the azlactone I shows in the 250—700 mμ range a characteristic maximum situated at 473 mμ which does not overlap with the maxima of the other partners of the system. Moreover, the reaction rate can be strongly influenced by the change in the ratio of chloroform and dimethylformamide in the mixture used as reaction medium. Measurements performed e.g. by the ratio 7 : 1 and 3 : 1 (chloroform : dimethylformamide) show an increase in the rate constants from 0.007205 to 0.07549 (see table 1).

This fact stimulated us to use this reaction to obtain new data concerning the influence of the sulfur atom on the reactivity of the benzene ring in the phenothiazine nucleus. To that purpose we prepared 4-formyl-

---

[3] C. Bodea, V. Fărcăşan and I. Oprean, *Rev. Roumaine Chim.*, **10**, 1103 (1965).

[4] K. Nalepa and J. Slouka, *Monatsh.*, **98**, 412 (1967).

[5] K. F. Jennings, *J. Chem. Soc.*, **1957**, 1512.

[6] C. Bodea and I. Oprean, *Rev. Roumaine Chim.*, **13**, 1647 (1968).

Table 1

Rate constants

Compound	Solvent	K/min^{-1}
3-Formyl-10-methyl-phenothiazine azlactone (I)	chloroform : DMFA 3 : 1	0.07549
3-Formyl-10-methyl-phenothiazine azlactone (I)	chloroform : DMFA 7 : 1	0.007205
4-Formyl-N-methyl-diphenylamine azlactone (XIII)	chloroform : DMFA 3 : 1	0.009971

N-methyl-diphenylamine azlactone (XIII) which corresponds to a sulfurless 3-formyl-10-methyl-phenothiazine azlactone (I). The two substances

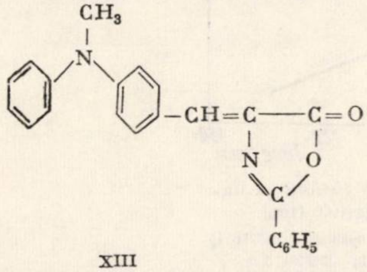

XIII

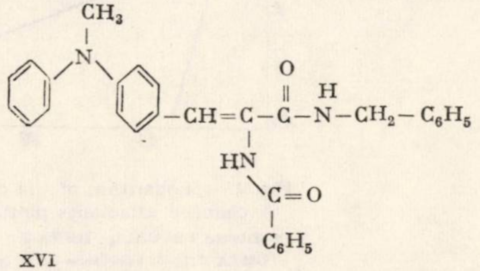

XVI

were brought into reaction with benzylamine (VIII) under the same conditions, and the rate constants determined.

From the kinetic measurements (see fig. 1) it results that the reaction is of first order related to azlactone and proceeds faster in the case of compound I.

If we take into account the reaction mechanism, involving a nucleophylic attack at the carbonilic carbon of the oxazolonic ring – which is favoured by the positivation of the reaction center – it can be concluded that the diphenylamine residue on the whole, exerts a stronger electron-repelling effect as the phenothiazine residue. This effect is transmitted through the double bond to the reaction center. This means that, in position 4 of N-methyl-diphenylamine (XIV) the electron density is higher, than in the corresponding position 3 of 10-methyl-phenothiazine (XV). The difference is due to the sulfur atom which imposes to the phenothiazine molecule a folded structure, with the configuration "extra" favoured by the presence in position 10 of the methyl group.[7] Thus the participation of the nitrogen in the delocalized electronic system is restricted, causing the lowering of the electron density in position 3, to which the sulfur contributes through its –I effect too.

The results of these kinetic measurements are supported also by the IR spectra. As expected in the spectrum of azlactone I, the maximum corresponding to ν_{CO} is shifted to higher wave numbers (1790 cm^{-1}) as compared to that of the azlactone XIII (1785 cm^{-1}).

---

[7] J. P. Malrieu and B. Pullman, *Theoret. Chim. Acta*, **2**, 293 (1964).

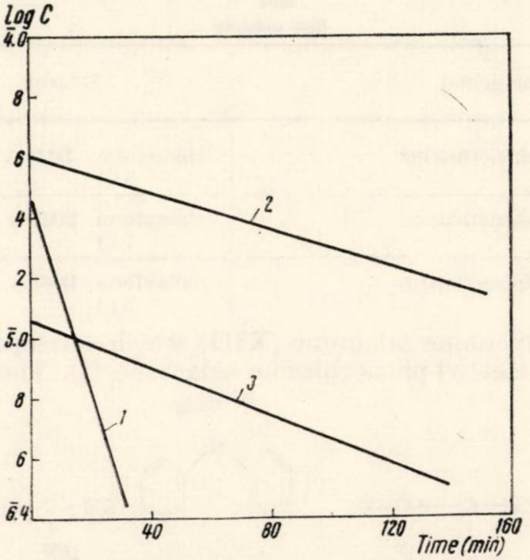

Fig. 1. — Logarithm of the concentrations of unchanged azlactones plotted against time.
1, substance I in CHCl$_3$: DMFA 3 :1; *2*, substance I in CHCl$_3$: DMFA 7 :1; *3*, substance XIII in CHCl$_3$: DMFA 3 :1.

EXPERIMENTAL [8]

The new substances — summarized in table 2 — were prepared by the following methods.

Method A

To 0.2 g azlactone, dissolved in 5 ml hot dimethylformamide (DMFA), after cooling to room temperature, 0.2 ml concentrated ammonia or benzylamine were added. The red solution quickly turned yellow. By adding water, the amide precipitates.

Method B

0.5 g fine powdered azlactones were suspended in 10—20 ml ethanol and 1—2 ml 98—100% hydrazine hydroxide added. The mixture was shaken for 5—30 minutes. The hydrazide was filtered, washed with ethanol and some chloroform. For recrystallization DMFA-ethanol was used.

Method C

A mixture of 0.5 g fine powdered azlactone, 0.5 ml aniline and 5—10 ml benzene, nitrobenzene or DMFA was heated for 1—15 hours on a steam-bath. After cooling, the precipitate was filtered and washed with benzene. The yellow substance was recrystallized from xylene.

---

[8] The melting points were determined in capillaries and are uncorrected.

Table 2

New compounds

Product obtained	Starting substances		Method	Solvent used for recrystallization	Melting point and crystal feature °C	Formula (Molecular weight)	Analysis	
	Azlactone	NH_2-containing substance					Calculated %	Found %
α-Benzoylamino-β-(10-methyl-phenothiazinyl-3)-acrilamide (II)	3-Formyl-10-methyl-phenothiazine azlactone (I)	Ammonia	A	DMFA-water	209–210 yellow-orange needles	$C_{23}H_{19}N_3O_2S$ (401.5)	N 10.48	N 10.8
α-Benzoylamino-β-(10-methyl-phenothiazinyl-3)-acril-benzylamide (XI)	3-Formyl-10-methyl-phenothiazine azlactone (I)	Benzylamine	A	DMFA-water	194–195 yellow-needles	$C_{30}H_{25}N_3O_2S$ (491.6)	N 8.55	N 8.72
α-Benzoylamino-β-(N-methyl-diphenylamin-4-yl)-acril-benzylamide (XVI)	4-Formyl-N-methyl-diphenylamine azlactone (XIII).	Benzylamine	A	DMFA-water	134–5 colourless needles	$C_{30}H_{27}N_3O_2$ (461.5)	N 9.11	N 9.07
α-Benzoylamino-β-(10-methyl-phenothiazinyl-3)-acrilhydrazide (V)	3-Formyl-10-methyl-phenothiazine azlactone (I)	Hydrazine hydroxide	B	DMFA-water	224–225 yellow-needles	$C_{23}H_{20}N_4O_2S$ (416.4)	N 13.46	N 13.54
α-Benzoylamino-β-(10-methyl-phenothiazinyl-2)-acrilhydrazide (VI)	2-Formyl-10-methyl-phenothiazine azlactone (III)	Hydrazine hydroxide	B	DMFA-water	186–189 yellow needles	$C_{23}H_{20}N_4O_2S$ (416.4)	N 13.46	N 13.11
α-Benzoylamino-β-(10-methyl-5.5-dioxide-phenothiazinyl-3)-acrilhydrazide (VII)	3-Formyl-10-methyl-5.5-dioxide-phenothiazine azlactone (IV)	Hydrazine hydroxide	B	DMFA-water	233–234 white-cream needles	$C_{23}H_{20}N_4O_4S$ (448.4)	N 12.50	N 12.31
α-Benzoylamino-β-(10-methyl-phenothiazinyl-3)-acril-anilide (XII)	3-Formyl-10-methyl-phenothiazine azlactone (I)	Aniline	C	xylene	249–250 yellow needles	$C_{29}H_{23}N_3O_2S$ (477.6)	N 8.81 S 6.72	N 9.25 S 6.65

4-Formyl-N-methyl-diphenylamine azlactone (XIII)

To 15.3 g (0.1 mol) phosphorous oxychloride in 20 ml DMFA, 18.2 g (0.1 mol) N-methyl-diphenylamine were added and the mixture heated for $1^1/_2$ hour on a steam-bath. The red viscous oil was then poured into 500 ml of ice-water and sodium acetate added to achieve pH $\sim$ 6. The aqueous layer was removed, the reaction product dissolved in toluene and the solution dried with anhydrous sodium sulfate. The toluene was distilled in vacuum. A yellow-brown oil remained which was treated with hippuric acid anhydrous sodium acetate, acetic anhydride and heated for 2 hours on the steam-bath. The crude product was fractionated by recrystallization from DMFA and two compounds isolated. A red substance — the less soluble and more polar — m.p. > 300°, and an orange one. The latter, purified by chromatography on a column with aluminium oxide (Brockman III), yielded the pure 4-formyl-N-methyl-diphenylamine azlactone (XIII) as orange needles m.p. 140°, ν_{CO} 1785 cm^{-1}.

$C_{23}H_{13}N_2O_2$ (354.4) *Calcd.* : C, 78.03 ; H, 5.13 ;
Found : C, 77.73 ; H, 5.10.

The action of the acetic acid — acetic anhydride mixture on the hydrazides V, VI and VII

Under the conditions described in a previous paper for other hydrazides,[6] the azlactones I, III and IV were obtained.

The reaction products were identified by m.p. and mixed m.p. with authentic specimens, and thin layer chromatography.

The electronic and IR spectra

The electronic spectra were recorded in chloroform : dimethylformamide 3 : 1, on a DK-2A Beckmann spectrophotometer. For recording the IR-spectra a double-beam Car Zeiss Jena UR-10 spectrophotometer was used ; the substances were prepared as KBr pellets.

Kinetic measurements

The 2×10^{-5}– 4×10^{-5} M solutions of the azlactones, I and XIII, in chloroform : dimethylformamide were kept for 15 minutes at 18±0.5° in a 1 cm cell in the thermostat of the Beckmann spectrophotometer. Then 0.02 ml benzylamine were added and the extinctions at 473 (I), respectively at 475 mμ (XIII) were recorded at timed intervals. The concentrations of the unreacted azlactones were estimated by means of standard, previously plotted, $E = f(c)$ curves. The apparent rate constants K, were, as usually, graphically determined from the diagram representing the logarithm of the concentrations of unchanged substances as a function of time (fig. 1). The values are listed in table 1.

Acknowledgement. The authors are indebted to Mrs. M. Breban, who led the microanalytical determinations, to Mrs. F. Teodor for recording the electronic spectra, and to Mr. V. Voivod for recording IR spectra.

La *Revue Roumaine de Chimie* paraît 12 fois par an. Le prix d'un abonnement annuel est de £ 5.0.0 ; $ 12,— ; FF 60,— ; DM 48,— . Toute commande de l'étranger (fascicules ou abonnements) sera adressée à CARTIMEX, Boîte postale 134—135, Bucarest, Roumanie, ou à ses représentants à l'étranger:

R.P. d'ALBANIE, Ndermarja Shtetnore e Botimeve Tirana ; R.D. ALLEMANDE, Deutscher Buch Export und Import Leipzig, 701, Leninstrasse 16 ; R.P. de BULGARIE, Hemus, Place Slaweikov, 11, Sofia ; R.P. de CHINE, Waiwen Shudian P.O.B. 88, Peking; R.P.D. COREENNE, Chulphanmul, Phenian ; RÉPUBLIQUE CUBA, Cubartimpex Simón Bolivar 1, Palcacio Aldamo, Habana ; R.P. de HONGRIE, Kultúra, P.O.B. 149, Budapest 62 ; R.P. MONGOLE, Mongolgosknigotorg, Ulan Bator ; R.P. POLOGNE, Ruch, Ul. Wronia 23, Warszawa ; R.S. TCHÉCOSLOVAQUE, Artia, Ve Smeckach 30-Praha II ; U.R.S.S., Mejdunarodnaia Kniga, Moskva G-200 ; R.D. VIETNAM, So Xuat Nhap Khau Sach Bao, 32 Hai Ba Trung, Hanoï ; R.S.F. de YOUGOSLAVIE, Jugoslovenska Knjiga Terazije 27, Belgrad; Prosveta 16/I, Terazije, Belgrad ; Forum Voïvode Misica, Novi Sad ; ARGENTINE, Editorial Sudaminter S.A., Alsina 500, Buenos Aires ; AUSTRALIE, Current Books Ltd. Distributors 168—174, Day Street Sydney ; AUTRICHE, Globus Zeitungs Drucks und Verlagsanstalt GmbH, 1200, Wien, Höchstädplatz 3 ; BELGIQUE, Du Monde Entier 5, Place St. Jean-Bruxelles, Agence Messageries de la Presse 14—22, Rue du Persil, Bruxelles ; CANADA, Progress Books 44 Stafford St. Toronto, Ontario, W. M. Dawson Subscriptions Service Ltd., Six Thornelife Park Drive, Toronto 17, Ontario; COLOMBIE, Libreria Buchholz Galeria, av. Jiménez de Quesada 8—40 Bogotá ; DANEMARK, Ejnar Munksgaard, Noregade 6, Kobenhavn; ESPAGNE, Libreria Herder, Calle de Balmés 26, Barcelona 7 ; ÉTATS-UNIS, Fam Book Service 69, Fifth Avenue, Suite 8 F., New York, 10003 N.Y.; Continental Publications, 111, South Mermanec Ave., St. Louis Missouri 63105 ; Turner Subscription Agency 235, Park Avenue South, New York 3 N.Y.; FINLANDE, Akateeminen Kirjakauppa P.O.B. 10128, Helsinky, 10 ; FRANCE, Nouvelles Messageries de la Presse Parisienne, 111, Rue Réaumur, Paris II, Europériodiques S.A. 72, Boul. Senard, 22, Saint-Cloud; GRANDE-BRETAGNE, Collet's Holdings Ltd. Dennington Estate, Wellingborough, Northants Central Books Ltd., 37, Inn Road London W.C. 1 ; ISRAËL, Lepac Ltd., P.O.B., 1136 Tel-Aviv ; Haiflepac Ltd. P.O.B. 1794, Haifa ; ITALIE, So Co. Lib. Ri. Piazza Margana 33 — Roma ; Messagerie Italiane Sp. A. Milano, Via Priv. Renzo e Lucia 7 ; JAPON, Nauka Ltd. 30—19 Minami — Ikebukuro 2 chome Toshima Ku, Tokyo ; PAYS-BAS, N. V. Martinus Nijhoff, P.O.B. 269, Den. Haag; Swetz & Zeitlinger, Keizersgracht 471—487, Amsterdam C. ; NORVÈGE, Tryggve Juul Moller — Boekhandel Ovre Slottsgate 15 Oslo 1 ; R.F. ALLEMANDE, Kubon & Sagner, P.O.B. 68, München 34 ; Presse Vertriebsgesellschaft GmbH, 6, Frankfurt/Main Börsenstrasse 13—15 ; Kunst und Wissen, Erich Biber P.O.B. 46, 7000 Stuttgart 1 ; SUISSE, Pinkus & Cie Froschaugasse 7 Zürich, Fachbücherei Berne, P.O.B. 397, 3001 Berne.

En Roumanie vous pourrez vous abonner par les bureaux de poste, chez votre facteur ou directemment par les services de presse des entreprises et institutions.

Une livraison prompte vous sera assurée.

NOTE POUR LES AUTEURS

La *Revue Roumaine de Chimie* publie des articles en anglais, français, russe, allemand ou espagnol. Les auteurs sont priés d'envoyer des articles, notes, communications et comptes rendus inédits.

Les manuscrits seront dactylographiés à deux intervalles. Les tableaux seront dactylographiés sur feuilles séparées, de même que la légende des figures. Les diagrammes seront tracés à l'encre de Chine sur papier calque. Les tableaux et les figures seront numérotés par des chiffres arabes, en nombre strictement nécessaire. Prière de ne pas inscrire les mêmes données dans les tableaux et les figures. Les formules chimiques seront incluses dans le texte ; en outre, elles seront transcrites sur des feuilles séparées. Les auteurs sont priés d'indiquer les caractères italiques (en soulignant les lettres au crayon), ainsi que tout autre caractère spécial. L'ordre des références bibliographiques sera celui de leur mention dans le texte ; le nom de l'auteur sera précédé de l'initiale du prénom ; les publications périodiques seront présentées suivant les prescriptions internationales. Les références seront ajoutées à la fin de l'article ; elles paraîtront comme des notes, au bas de la page. Le texte sera précédé d'un résumé, comprenant 15 lignes au maximum.

L'entière responsabilité du contenu des articles appartient aux auteurs. On publie des articles dus aux collaborateurs roumains ou étrangers. Les auteurs recevront 50 tirés à part.

PRINTED IN ROMANIA

NOTE POUR LES AUTEURS

[illegible]

[illegible]

[illegible]

PRINTED IN BELGIUM

1969 AUG 22

TRAVAUX PARUS AUX ÉDITIONS DE L'ACADÉMIE DE LA RÉPUBLIQUE SOCIALISTE DE ROUMANIE

CORNEL BODEA et collab., **Tratat de biochimie vegetală**, partea I, **Fitochimie** (Traité de biochimie végétale, Ire partie, Phytochimie), Ier vol., 1964, 747 p. + 4 annexes + 2 pl., 41 lei ; IIe vol., 1965, 1262 p., 1 pl., 56 lei ; IIIe vol., 1967, 773 p., 35 lei.

V. GHEŢIE et V. MICUŞAN, **Analiza imunochimică. Teorie şi practică** (Analyse immunochimique. Théorie et pratique), 1966, 369 p., 28 lei.

SILVIA IONESCU, **Reacţii chimice induse de radiaţiile ionizante** (Réactions chimiques produites par les radiations ionisantes), 1963, 271 p., 15 lei.

MARIETA NICOLAE, **Fizico-chimia proceselor fotografice** (Physico-chimie des processus photographiques), 1964, 426 p. + 4 pl., 35 lei.

R. PORTOCALĂ et L. POPA, **Acizii ribonucleici celulari şi virali** (Les acides ribonucléiques cellulaires et viraux), 1966, 375 p. + 8 pl., 26 lei.

D. PURDELA et R. VÎLCEANU, **Chimia compuşilor organici ai fosforului şi ai acizilor lui** (La chimie des composés organiques du phosphore et de ses acides), 1965, 540 p., 37 lei.

CRISTOFOR SIMIONESCU, MARGARETA GRIGORAŞ et AGATA CERNĂTESCU-ASANDEI, **Chimia lemnului din R.P.R.** (La chimie du bois en Roumanie), 1964, 239 p. + 6 pl., 27 lei.

CRISTOFOR SIMIONESCU et CLEOPATRA VASILIU-OPREA, **Mecanochimia compuşilor macromoleculari** (La mécanochimie des composés macromoléculaires), 1967, 344 p., 23,50 lei.

I.P.I. – c. 3200

43 426

Lei 15. —

F 1103

R

REFERÁLVA

REVUE ROUMAINE DE CHIMIE

TOME 14

Nº 6

Juin 1969

ÉDITIONS DE L'ACADÉMIE DE LA RÉPUBLIQUE SOCIALISTE DE ROUMANIE

Rev. Roumaine Chim.

14, 679—822 (1969), Bucarest

COMITÉ DE RÉDACTION

Rédacteur en chef :

C. D. NENIŢESCU, membre de l'Académie de la République Socialiste de Roumanie.

Rédacteurs en chef adjoints :

A. T. BALABAN et V. E. SAHINI, membres correspondants de l'Académie de la République Socialiste de Roumanie.

Collège de rédaction :

C. DRĂGULESCU, RALUCA RIPAN, CR. SIMIONESCU, membres de l'Académie de la République Socialiste de Roumanie ; EM. BRATU, membre correspondant de l'Académie de la République Socialiste de Roumanie, Pr G. OSTROGOVICH, MARG. AVRAM, F. BADEA. D. MARCHIDAN, D. NEGOIU et D. SĂNDULESCU,

Les manuscrits, les livres et les revues proposés en échange, ainsi que toute correspondance seront envoyés à la rédaction :

REVUE ROUMAINE DE CHIMIE

23, str. Dumbrava Roşie, Bucarest, Roumanie.

F 1103

R

REVUE ROUMAINE
DE
CHIMIE

1863

Tome 14, No 6 Juin 1969

Page

I. G. MURGULESCU and N. I. IONESCU, The effect of oxygen chemisorption on the temperature coefficient of the electrical resistance of thin copper films 681–687

V. E. SAHINI and LILIANA CIUREA, Electron spin resonance spectra of some aromatic metal ketyls 689–694

RODICA VÎLCU und I. GĂINAR, Das thermodynamische Verhalten des Gasgemisches Argon-Kohlendioxid 695–704

Z. SIMON, The stability of the oxalyl anionic radical ($C_2O_4^{\cdot -}$) 705–708

D. FĂTU et E. SEGAL, Cinétique de la décomposition thermique de certaines combinaisons complexes du chlorure de manganèse avec la pyridine et des pyridines substituées. Paramètres cinétiques obtenus des données gravimétriques 709–715

RALUCA RIPAN und MILOSLAVA KULCSÁR-NOVÁKOVÁ, Die Bildung der Gallosilicat-Niederschläge in wäßrigen Lösungen 717–720

Z. GROPŞIANU, D. KOHN und A. IOVI, Wärmeübergangszahlen beim Sieden von Lösungen. Lösungen von Mononatriumphosphat 721–727

F. BUNUȘ, I. MATEI, C. MATYAS, S. NECIU, V. SPOREA and S. TĂTARU, Some quantitative relations on the radioactive minerals leaching processes. 729–736

C. DRĂGULESCU, SOFIA MARCHIDAN and GH. FACSKO, Influence of some anions and solvents on the polarographic reduction of niobium (V) in hydrochloric acid-thiocyanate medium. 737–744

I. FLOREA, Tetraphenylborate des Akridins, 2-Äthoxy-6,9-Diaminoakridins und 3-Chlor-9-(4′-Diäthylamino-1′-Methylbutylamino)-7-Methoxyakridins . 745–752

RODICA CRĂCIUNEANU und EUGENIA FLOREAN, Das Verhalten von 1-Acyl-4-Aryl-Thiosemikarbaziden gegenüber den Schwermetallkationen. II. Das Verhalten von Co^{II} gegenüber den 1-Benzoyl-4-Aryl-Thiosemikarbaziden 753–761

C. CHIRIAC, LEONIA STOICESCU-CRIVETZ et I. ZUGRĂVESCU, Polypyrazoles-esters 763–766

И. ВЛАДЖИУ, Радиохимическая полимеризация акрилонитрила в твердой фазе 767–771

ALLA PETRUŞ, LAURA MĂNDĂŞESCU and I. MATEI, Linear polyesters and polycarbonates from bis-(4-hydroxyphenyl)-deoxybenzoin and 1,1-bis-(4-hydroxyphenyl)-2-oxo-acenaphthene 773–779

Rev. Roumaine Chim. 14, 679–822 (1969), Bucarest

M. D. GHEORGHIU and R. HOFFMANN, The electronic structure of some substituted cyclobutadienes 781–787

MARIA IONESCU and I. MEŞTER, Synthesis of some dimethoxy-10-methylacridones 789–795

C. CRISTESCU and MARCELA LĂZĂRESCU, 6-Azauracil derivatives with potential cytostatic activity. VIII. Acylation of 5-mercapto-6-azauracil and its derivatives 797–802

I. VODNÁR, Decomposition of hydroperoxides on activated kaolins. I. Decomposition of cumene hydroperoxide on activated Chinese kaolin treated with sulphuric acid 803–807

M. I. VASS, A new all walls cooled cylindrical trap 809–810

P. FINK, IR-spectroscopic and gravimetric investigations about the formation of carboxylate surface species during the chemisorption of CO_1 CO_2 and simple organic oxygen compounds on γ-alumina. 811–822

Revue Roumaine de Chimie, **14**, 681–687 (1969)

STAKI KÖNYVTÁR [illegible]

THE EFFECT OF OXYGEN CHEMISORPTION ON THE TEMPERATURE COEFFICIENT OF THE ELECTRICAL RESISTANCE OF THIN COPPER FILMS

I. G. MURGULESCU and N. I. IONESCU

Institute of Physical Chemistry of the Academy
Bucharest, str. Dumbrava Roşie 23

Received January 15, 1969

The oxygen chemisorption on thin copper films leads at high surface coverage to a decrease in the temperature coefficient of the electric resistance of the metal, a phenomenon which can be explained by the hypothesis of effective film thickness decrease. The calculations effected showed that in the chemisorptive copper-oxygen bond two layers of copper atoms are involved.

In a previous paper[1] we showed that the chemisorption of oxygen on thin copper films leads to an increase in the electric resistance of the metal.

In the present paper, we aim at studying the influence of oxygen chemisorption on the temperature coefficient of the electric resistance (T.C.R.) in thin copper films.

EXPERIMENTAL

Use has been made of the installation and the working method described in our previous papers.[2,3] The copper evaporation took place at $5 \times 10^{-9} - 1 \times 10^{-8}$ torr. In order to achieve this pressure, we used instead of a I.F.A. type ionic pump,[4] a titanium evaporating one, made according to a model given by Gretz.[5] This pump presents the advantage that it shortens the time necessary to achieving the low pressures. The pressure increase at the film's heating reached 3×10^{-8} torr. Films thickness: about 60 Å. Spectroscopically pure copper supplied by Johnson & Matthey (England) has been used.

---

[1] I. G. Murgulescu and N. I. Ionescu, *Rev. Roumaine Chim.*, **13**, 1533 (1968).

[2] I. G. Murgulescu and N. I. Ionescu, *Rev. Roumaine Chim.*, **11**, 1035 (1966).

[3] I. G. Murgulescu and N. I. Ionescu, *Rev. Roumaine Chim.*, **11**, 1267 (1966).

[4] G. Comşa and B. Iosifescu, *Studii şi Cercetări Fiz., Acad. R.P. Romania*, **12**, 435 (1961).

[5] R. D. Gretz, *Vacuum*, **16**, 537 (1966).

The determination of the T.C.R. α has been carried out according to a method described by Suhrmann, Heras, de Heras and Wedler,[6] its value being calculated by the relationship:

$$\alpha = \frac{1}{R_{77}} \cdot \frac{R_{273} - R_{77}}{196} \tag{1}$$

in which R_{273} and R_{77} are the film resistances at 273°K and 77°K respectively. It has been worked at high surface coverage degrees.

The film thickness has been determined by a chemical method which is considered very precise [7] for such purposes. Copper was proportioned by means of dithizone.[8]

RESULTS AND DISCUSSIONS

The experiments performed in order to determine the changes in the T.C.R. in thin copper films, have shown that, as a consequence of oxygen chemisorption, this becomes smaller than that corresponding to a clean film, as seen in table 1.

Table 1

Decrease of T.C.R. of thin copper films after oxygen chemisorption

Thickness of the layer in Å	Gas pressure torr	R_{077} Ω	R_{0273} Ω	$R_{77}(O_2)$ Ω	$R_{273}(O_2)$ Ω	$\alpha_0 \times 10^3$ degree^{-1}	$\alpha_1 \times 10^3$ degree^{-1}
1	2	3	4	5	6	7	8
41	3×10^{-5}	30.102	32.416	35.888	38.283	0.392	0.340
54	2×10^{-5}	30.584	35.062	34.691	39.203	0.747	0.664
57	6×10^{-5}	34.302	37.301	41.905	45.008	0.446	0.378
59	3×10^{-5}	29.221	34.459	34.973	40.230	0.915	0.767
65	2×10^{-5}	28.524	32.656	34.323	39.072	0.739	0.706
78	2×10^{-5}	33.091	37.153	39.527	44.046	0.626	0.583

R_0 is the film resistance before adsorption, $R(O_2)$ after oxygen admission, α_0 and α_1 the T.C.R. before and after oxygen chemisorption.

A similar behaviour has been observed for the nickel-oxygen [6] and silver-oxygen [3] systems.

The problem of the T.C.R. decrease is indissolubly related with the problem of thin metallic films electric resistance variation in the gas chemisorption process. According to some authors [9] this effect is due to the change of free electrons concentration in metal which is caused by the electronic exchange between the surface and the chemisorbed gas; according to others[10] this effect results as a consequence of the effective thickness decrease of the metallic film due to the forming of a superficial complex between the metallic atoms and the adsorbed gas. Finally, other authors[11,12] consider that the adsorption modifies the electron mobility by changing the mean free path or the scattering conditions at the film surface.

---

[6] R. Suhrmann, J. M. Heras, L. V. de Heras and G. Wedler, *Z. Elektrochem.*, **68**, 990 (1964).

[7] R. Niedermayer, "Basic Problems in Thin Film Physics", Ed. R. Niedermayer and H. Mayer, Göttingen, Vandenhoeck & Ruprecht, 1966, p. 249.

[8] E. B. Sandell, "Colorimetric Determinations of Traces of Metals" 3rd Ed. revised and enlarged, Interscience Publishers Inc., New York, 1959, p. 812.

[9] R. Suhrmann and K. Schulz, *Z. phys. Chem. (Frankfurt)*, **1**, 69 (1954).

In order to see which of the mentioned hypotheses contribute to a greater extent to explain the obtained results we used the theory of size ffect in thin films.

It is known that for thin metallic films[13]:

$$\frac{\sigma}{\sigma_\infty} = \frac{\rho_\infty}{\rho} = f(d/l, p) \tag{2}$$

in which σ_∞ and ρ_∞ represent the conductivity and the specific resistance of the bulk metal respectively, σ and ρ the same magnitude for the thin film, l the mean free path of electrons from the bulk metal with the same structure as the thin film, d the film thickness and p the scattering coefficient of the electrons.

The function $f(d/l, p)$ can been exactly expressed by Fuchs-Sondheimer's complicated formula. But there also exist expressions of the function $f(d/l, p)$ approximating Fuchs-Sondheimer's relationship with very small errors. For very thin films, in which $d/l \leqslant 0.15$[14] or $d/l \leqslant 0.2$[15] one can very well use the relationship[13]:

$$f(d/l, p) = \frac{3}{4}\,\frac{d}{l}\,(1 + 2p) \ln \frac{\beta l}{d} \tag{3}$$

where $\ln \beta = 0.4228$ and $p \neq 0$ but of the same order of magnitude as the value of the ratio d/l.

By the logarithmic differentiation of the relationship (2) in which one introduces the expression (3) and taking into account the definition of the T.C.R., one obtains the known formula:

$$\alpha = \frac{\alpha_\infty}{\ln \dfrac{\beta l}{d}} \tag{4}$$

where α_∞ is the T.C.R. of the bulk metal with the same structure as the thin film.

---

[10] W. M. H. Sachtler and G. J. H. Dorgelo, *Z. phys. Chem. (Frankfurt)*, **25**, 69 (1960).

[11] O. A. Pancenko and Iu. G. Ptushinski, *Izvest. Akad. Nauk S.S.S.R., Seria fizicheskaia*, **28**, 1466 (1964).

[12] H. Kölbel, E. Schöttle and H. Hammer, *Z. phys. Chem (Frankfurt)*, **47**, 183 (1965).

[13] D. S. Campbell, "The Use of Thin Films in Physical Investigations", Ed. J. C. Anderson, Academic Press, London and New York, 1966, p. 299.

[14] H. Mayer, "Physik dünner Schichten", vol. 2, Wissenschaftliche Verlagsgesellschaft m.b.H., Stuttgart, 1955, p. 216.

[15] G. Wedler and M. Fouad, *Z. phys. Chem. (Frankfurt)*, **40**, 1 (1964).

Assuming that the structure of the thin film not involved in chemisorption does not change when chemisorption takes place, and considering relation (4), it results that a decrease of α can be assigned only to a decrease of the thickness *d*.

The thickness decrease which resulted from the interaction between oxygen and copper can be estimated quantitatively as well.

On the ground that the diminution of the T.C.R. is entirely brought about by an effective decrease of film thickness, the thickness decrease δ can be computed by means of the relationship [3]:

$$\delta = d_0 \frac{\alpha_0 - \alpha_1}{\alpha_1} \tag{5}$$

The results of the determination of the magnitude δ by means of relation (5) are listed in table 2. They were obtained by means of data from table 1 columns 7 and 8.

Table 2

Thickness decrease of thin copper films due to oxygen chemisorption calculated after Sachtler and Dorgelo's hypothesis

d_0 in Å 1	$\frac{\alpha_0 - \alpha_1}{\alpha_1}$ 2	δ_1 in Å 3
41	0.153	6.27
54	0.125	6.75
57	0.180	10.26
59	0.193	11.38
65	0.047	3.06
78	0.074	5.77

In this way one obtains a mean thickness decrease:

$$\delta_1 = (7.25 \pm 1.25)\ \text{Å} \tag{6}$$

As the copper lattice constant is 3.6077 Å,[16] the calculated thickness diminution shows that approximately two layers of copper atoms are involved in the chemisorptive copper-oxygen bond.

If for the explanation of the copper electric resistance increase due to oxygen chemisorption, one assumes that an effective thickness decrease and a variation in the number of conduction electrons take place simultaneously, then δ can be obtained by means of the relationship[3]:

$$\frac{d_0}{d_1} = \left(\frac{\alpha_0}{\alpha_1} \cdot \frac{R_1}{R_0}\right)^{3/8} \tag{7}$$

where $d_1 = d_0 - \delta$.

---

[16] E. A. Moelwyn-Hughes, "Physical Chemistry", 2nd revised ed., Pergamon Press, Oxford – London – New York – Paris, 1964, p. 644.

The estimation of the ratio value $\frac{d_0}{d_1}$ and the magnitude δ, synthesised in table 3 has been achieved by the results listed in table 1 columns 1, 3, 5, 7, 8.

Table 3

The thickness decrease of thin copper films due to oxygen chemisorption calculated after two hypotheses

d_0 in Å	$\frac{d_0}{d_1}$	d_1 in Å	δ_2 in Å
1	2	3	4
41	1.127	36.38	4.62
54	1.096	49.27	4.73
57	1.147	49.69	7.31
59	1.133	52.07	6.93
65	1.094	59.41	5.59
78	1.088	71.69	6.31

The mean thickness decrease is :

$$\delta_2 = (5.91 \pm 0.46)\ \text{Å} \tag{8}$$

This value is seen to be smaller than the former one but of the same order of magnitude.

To the magnitude δ the indices 1 and 2 are given according to the hypotheses on which its determination was based, 1 being the thickness decrease.

It is worth mentioning that the greatest film thickness namely 78 Å complies with the condition $d/l < 0.2$. At 273°K the mean free path of the copper electrons is 424 Å leading to a value of $d/l = 0.184$.

The decrease of the effective thickness of thin metallic films in the gas chemisorption process can be interpreted in two ways. If we consider that the surface has a uniform activity, the adsorption takes place equally on its whole area, and the thickness decrease affects the film uniformly. But if we consider the surface as a mosaic of points with variable activities (which is nearer to reality) then the adsorption takes place in accordance with the existence of these centers. The resulting thickness decrease will be an average of contributions of each atom included in the superficial complex.

In the case of copper the thickness decrease with two layers of atoms could be probably interpreted in two ways : either in the superficial complex are involved the metallic atoms from two consecutive layers, or in the second, deeper layer, an oxidation process with the corresponding structure begins and the superficial complex is formed only with the atoms from the external layer.

These results show, once again, that between the end of the chemisorption process and the beginning of the oxidation, one cannot make a clear distinction.

It is to be mentioned that in the case of silver, in similar coverage conditions, the mean thickness decrease was of one layer of atoms. [3,17] This proves, in this way too, that the affinity of copper for oxygen is stronger than that of the silver, in accordance with the well-known chemical properties of the two metals and that the thickness decrease has a chemical specificity.

In the case we admit that p the scattering coefficient of electrons modifies after adsorption, its variation $\Delta p = p_0 - p_1$ can be computed by means of the expression[18] :

$$\Delta p = \frac{\frac{R_1}{R_0} \cdot \frac{\alpha_0}{\alpha_1} \left(\frac{d_1}{d_0} \right)^{8/3} - 1}{2} \tag{9}$$

The coefficients p_0 and p_1 refer to the clean film, respectively to the gas covered one.

We admit that both mechanisms influencing the electric resistance are equally probable. In this way, we can use the relationship (5) for the ratio d_1/d_0. The obtained results are listed in table 4; use was made of the results from table 1 columns 1, 3, 5, 7, 8 and table 2 column 3.

Table 4

The variation of the scattering coefficient p of thin copper films after oxygen chemisorption

d_0 in Å 1	d_1 in Å 2	$\frac{d_1}{d_0}$ 3	$\Delta p.10^2$ 4
41	34.73	0.897	−5.00
54	47.25	0.875	−5.09
57	46.74	0.820	−7.56
59	47.62	0.807	−8.38
65	61.94	0.953	+4.95
78	72.23	0.926	+2.28

Mean − 3.13

The calculation shows that the value of p modifies, namely it becomes greater than the initial one. The fact that Δp is negative means indeed :

$$p_0 - p_1 < 0 \text{ or } p_1 > p_0 \tag{10}$$

because both p_0 and p_1 take values in the 0−1 interval only.

A similar behaviour has been observed in the silver-oxygen system.[18]

This could be plausibly explained by the fact that subsequent to adsorption, a superficial combination between oxygen and copper occurs; this implies the loss of the metallic character of the first two layers from the film including their non-participation in the conduction process of

---

[17] I. G. Murgulescu, G. H. Comșa and N. I. Ionescu, *J. Catalysis*, **12**,102 (1968).

[18] N. I. Ionescu, *Rev. Roumaine Chim.*, **13**, 683 (1968).

electrons. On this account, the scattering of electrons would not occur on the film surface, but, as in silver,[18] on an interval layer of atoms which would act as a limiting surface. As this layer might have less defects than the first (for instance it has no surface deffects) it would present improved conditions for the specularly reflexion of electrons i.e. for the increase in the value of coefficient *p*.

In this way, the electric resistance variations observed as a consequence of oxygen chemisorption on this copper films could be interpreted as a result of the simultaneous action not only of the electronic and geometric factors, but also of the *p* parameter. These three factors would intervene concomitantly and as a result, the experimentally determined effect is obtained.

Owing to our experiments we may conclude that the oxygen chemisorption on thin copper films leads, at high coverages of the surface, to a decrease of T.C.R. of the metal, a phenomenon which can be explained by the hypothesis of effective film thickness decrease. The calculation effected showed that in the chemisorptive copper-oxygen bond two layers of copper atoms are involved.

electrons. On this account, the scattering of electrons would not occur on the film surface, but, as in silver,[illegible] on an interval layer of atoms which would act as a limiting surface. As this layer might have less defects than the first (for instance if has no surface defects), it would present improved conditions for the specularly reflection of electrons i.e., for the increase in the value of coefficient p.

In this way, the electric resistance variations observed as a consequence of oxygen chemisorption on thin copper films could be interpreted as a result of the simultaneous action not only of the electronic and geometric factors, but also of the p parameter. These three factors would intervene concomitantly and as a result, the experimentally determined $\Delta R/R$ is obtained.

Owing to our experiments we may conclude that the oxygen chemisorption on thin copper films leads, at high coverages of the surface, to a decrease of T.C.R. of the metal, a phenomenon which can be explained by the hypothesis of effective film thickness decrease. The calculation checked showed that in the chemisorptive copper-oxygen bond two layers of copper atoms are involved.

Revue Roumaine de Chimie, **14,** 689–691 (1969)

ELECTRON SPIN RESONANCE SPECTRA OF SOME AROMATIC METAL KETYLS

V. E. SAHINI and LILIANA CIUREA

University of Bucharest, Laboratory of Physical Chemistry,
Bd. Republicii 13

Received December 9, 1968

ESR spectra are reported for the metal ketyls obtained in N,N-dimethylformamide solutions by alkali metal reduction of : fluorenone, benzil, 9,10-phenanthrenequinone, 9,10-anthraquinone, 1,5-diaminoanthraquinone, 1,5-dinitroanthraquinone, xanthone and benzanthrone. No alkali metal hyperfine splittings are observed in these spectra. The spin densities are calculated for xanthone and 9,10-anthraquinone metal ketyls using the Hückel LCAO MO theory and are compared with those obtained from the experimental data. The total widths of these spectra are related to the calculated spin densities on the carbonyl atoms.

In the present paper the ESR spectra in N,N-dimethylformamide (DMF) solutions are studied for the metal ketyls obtained from : fluorenone, benzil, 9,10-phenanthrenequinone, 9,10-anthraquinone, 1,5-diaminoanthraquinone, 1,5-dinitroanthraquinone, xanthone and benzanthrone.

The ESR spectra of metal ketyls from 9,10-phenanthrenequinone, fluorenone and benzil in etherial solvents as tetrahydrofuran and 1,2-dimethoxyethane have been published.[1,2] The main structures of these spectra of five lines and seven lines respectively were interpreted as due to the interaction of the unpaired electron with the quasi-equivalent *ortho* and *para* protons (referred to carbonyl group). In the spectra of fluorenone and benzil metal ketyls was also evident a second splitting due to the *meta* protons.

Later studies [3-5] on the ESR spectra of these metal ketyls in etherial solvents permitted to obtain a hyperfine structure due to the alkali metal, thus proving the existence in solution of ion pairs.

Recently, the presence in etherial solutions of structurally different ion pairs was reported by Hirota.[6]

---

[1] D. W. Ovenall and D. H. Whiffen, *Chem. Soc. (London) Spec. Publ.*, **12**, 139 (1958).

[2] V. M. Kazakova and Ya. K. Syrkin, *Doklady Akad. Nauk S.S.S.R.*, **133**, 112 (1960); *Zhur. strukt. Khim.*, **3**, 536 (1962).

[3] G. R. Luckhurst and L. E. Orgel, *Mol. Phys.*, **7**, 297 (1963).

[4] K. Maruyama, *Bull. Chem. Soc. Japan*, **37**, 553 (1964).

[5] P. B. Ayscough and R. Wilson, *J. Chem. Soc.*, **1963**, 5412.

[6] N. Hirota, *J. Amer. Chem. Soc.*, **89**, 1 (1967).

Using DMF as solvent, which due to its polarity would affect unfavourably the formation of ion pairs, we meant to observe if in this solvent the ESR spectra would still indicate the existence of these ion pairs.

The ESR spectra of the studied metal ketyls in DMF are given in figure 1. The total widths of these spectra are related to the calculated spin densities on the carbonyl atoms. For the xanthone and 9,10-anthraquinone ketyls the spin densities are calculated using the Hückel LCAO MO theory.

The metal ketyls were prepared by reduction in DMF of the respective ketone or quinone with sodium in atmosphere of argon free of O_2 and H_2O. These spectra have been recorded with a J.E.S.-3B spectrometer at room temperature, except the spectra of 1,5-diaminoanthraquinone ketyl and 9,10-phenanthrenequinone ketyl, which have been recorded at 0° and $-20°$, respectively.

The molecular orbital calculations of the spin densities have been made using the following set of parameters :

— for 9,10-anthraquinone ketyl : $\alpha_0 = \alpha + 1.2\,\beta$; $\beta_{co} = 1.6\,\beta$; $\beta_{c-co} = 0.8\beta$.

— for xanthone ketyl : $\alpha_0 = \alpha + 1.6\,\beta$; $\beta_{co} = 1.5\,\beta$; $\alpha_{ö} = \alpha + 2.5\,\beta$; $\beta_{c\diagdown_{0}\diagup c} = 1.4\,\beta$; $\beta_{c-c0} = 1.2\,\beta$.

— for benzanthrone ketyl : $\alpha_0 = \alpha + 1.2\,\beta$; $\beta_{c0} = 1.41\,\beta$; $\alpha_{c(0)} = \alpha + 0.2\,\beta$.

where : α_0, $\alpha_{c(0)}$, $\alpha_{ö}$ are the Coulomb integrals for the carbonyl oxygen and carbon atoms and for the oxygen atom ö, respectively,

β_{c0}, β_{c-c0}, $\beta_{c\diagdown_{0}\diagup c}$ are the carbonyl resonance integral, the resonance integral for the bond between the ring and the carbonyl carbon atom and for the bond between the oxygen atom and the carbon atoms of the ring, respectively.

— for the other metal ketyls we used the same parameters as those used by Dehl and Fraenkel[7] for the semiquinone.

The ESR spectra of fluorenone and benzil ketyls in DMF have been resolved in 19 and 37 lines, respectively, whose splitting constants are summarized in table 1.

Table 1

Hyperfine splitting constants (gauss)

Metal ketyl from	a^{H}_{para}	a^{H}_{ortho}	a^{H}_{meta}
Fluorenone	3.13	1.97	0.65
Benzil	1.17	1.05	0.36

---

[7] R. Dehl and G. K. Fraenkel, *J. Chem. Phys.*, **39**, 1793 (1963).

Comparing these splitting constants with those obtained for the same metal ketyls in ethereal solvents and with those of the corresponding anion radicals obtained electrolytically, [5,7,8] a similarity with the last ones could be observed. From the ESR spectrum of 9,10-phenanthrenequinone ketyl two splitting constants were obtained due to the two pairs of four quasi-equivalent protons, whose values of 1.03 and 0.32 gauss are near to those obtained for the 9,10-anthraquinone ketyl. The splitting constants measured from the ESR spectra of xanthone and 9,10-anthraquinone ketyls consisting of 15 and 17 lines, respectively, are given in table 2.

Table 2

Assignments of the experimental splitting constants for the anthraquinone and xanthone* metal ketyls and their corresponding experimental and calculated spin densities

Metal ketyl from	Splitting constants (gauss)	Spin densities		
		Positions	ρ_{calc}	ρ_{exp}
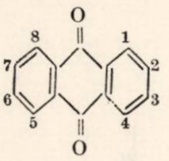	$a^H_{1,4,5,8} = 0.39$	1,4,5,8	0.015	0.016
	$a^H_{2,3,6,7} = 1.05$	2,3,6,7	0.044	0.044
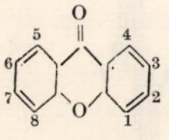		1,8	0.059	0.035
	$a^H_{1,8} = 0.83$	2,7	0.10	0.147
	$a^H_{2,4,5,7,} = 3.5$	3,6	0.0085	—
		4,5	0.13	0.147

* Its ESR spectrum has been presented in another paper. [9]

In the same table are also given the spin densities ρ_{exp} obtained from the experimental splitting constants a^H, using the Mc Connell's relation $a^H = Q\rho$, where Q was considered 23.7 gauss and calculated spin densities ρ_{calc} using the Hückel LCAO MO method.

The main structure of five lines of the spectrum of the xanthone ketyl could be explained by the interaction of the unpaired electron with the protons of positions 2,7 and 4,5, whose calculated spin densities have close values. Each line in the main structure is split into other three lines due to protons of positions 1,8. The calculated spin densities on positions 3 and 6 are small and no hyperfine splitting is observed due to them.

The spectrum of the 9,10-anthraquinone ketyl consists of a quintet further splitted into another quintet, the corresponding splitting constants having close values to those for the 9,10-anthrasemiquinone radical obtained

---

[8] P. L. Nordio, G. Giacometti and P. Favero, *Ricerca sci. Rend. Sez., A* **3**, 107 (1963).
[9] V. E. Sahini, L. Ciurea and E. Volanschi, *Rev. Roumaine Chim.*, **12**, 355 (1967).

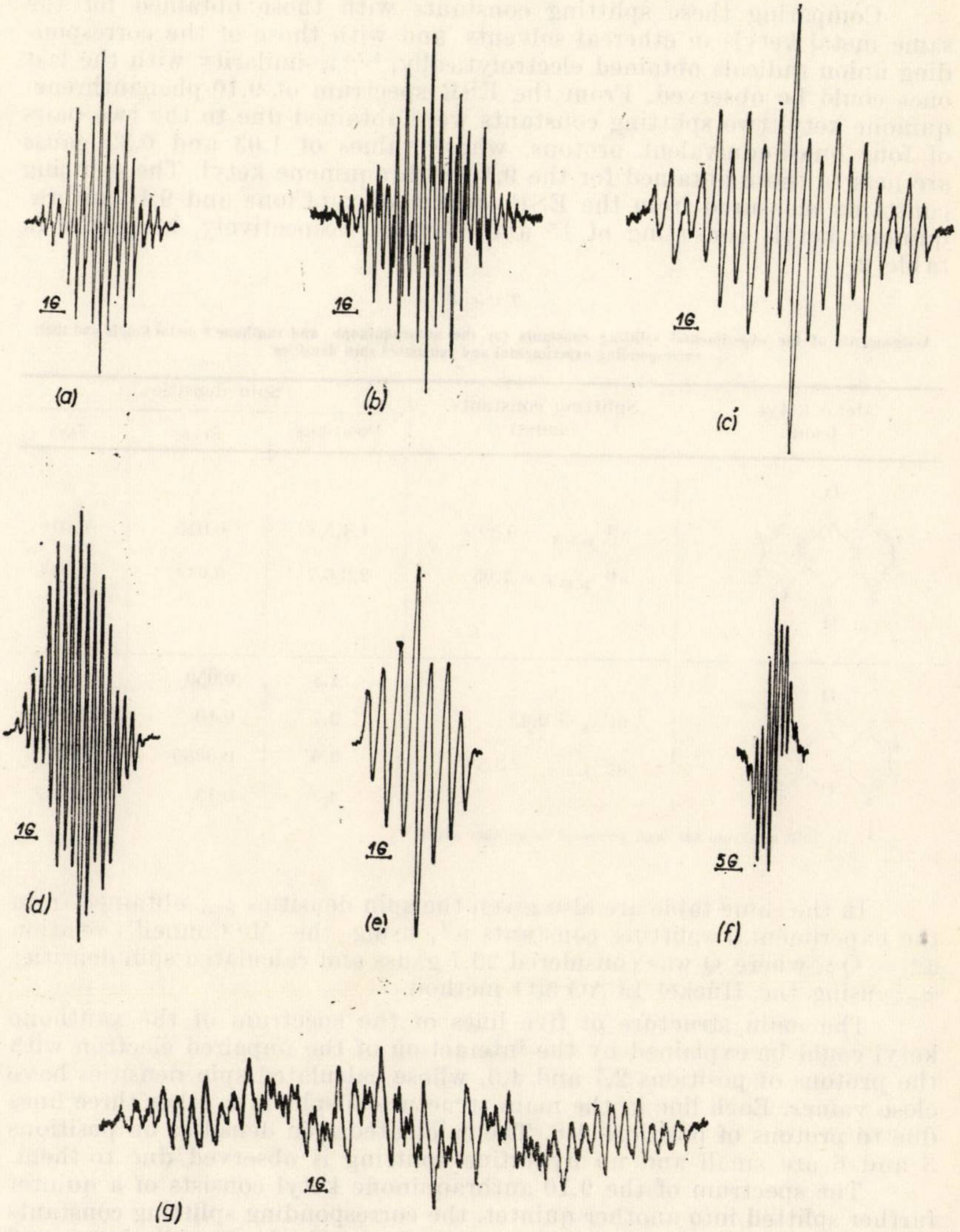

Fig. 1. — The ESR spectra in DMF of sodium ketyls from: *a*, 9,10-phenanthrenequinone; *b*, benzil; *c*, fluorenone; *d*, anthraquinone; *e*, 1,5-dinitroanthraquinone; *f*, 1,5-diaminoanthraquinone; *g*, benzanthrone.

by electrochemical reduction in dimethylsulfoxide[10] and in dimethylformamide.[11]

The spectra of metal ketyls obtained from 1,5-diaminoanthraquinone and 1,5-dinitroanthraquinone, completely changed in comparison with that of anthraquinone ketyl, consist of 9 lines on a total width of 8.23 gauss and 7 lines on 3.97 gauss, respectively. The intensity ratio for the diamino derivative is nearly 1 :4 :7 :10 :14 :10 :7 :4 :1 and for the dinitro derivative is nearly 1 :1.8 :2.1 :3.8 :2.1 :1.8 :1. The spectrum of benzanthrone ketyl is composed of 64 lines on a total width of 27.2 gauss. These ESR spectra were not interpreted.

The comparison between the ESR spectra of the studied metal ketyls reveals that their total widths are quite different, being narrower in the case of the ketyls containing two carbonyl groups. Relating these total widths with the calculated spin densities on the carbon and oxygen atoms of the carbonyl groups, we observe in table 3 that for comparable ketyls, as those from benzophenone and benzil, fluorenone and xanthone, the total widths of their spectra are narrower if the spin densities on the carbonyl atoms are higher.

Table 3

Total width dependence on the calculated spin densities on the carbon and oxygen atoms of the carbonyl groups

Metal ketyl from	ρ_c	ρ_0	Total width * (gauss)
Benzophenone	0.239	0.153	21.00**
Fluorenone	0.209	0.154	11.66
Xanthone	0.187	0.097	16.40
Benzanthrone	0.134	0.127	27.20
Benzil	0.442	0.349	7.41
9,10-Anthraquinone	0.245	0.244	5.68
9,10-Phenanthrenequinone	0.280	0.310	5.38

* It was measured between centers of extreme peaks.
** This value was obtained by Kazakova and Syrkin[3].

The narrow total width of the spectrum of the benzil ketyl could be explained by the fact that 4/5 from the spin density of the unpaired electron is localized on the atoms of its two carbonyl groups, which do not contribute to the hyperfine splittings. Thus, the unpaired electron density on the atoms of benzene rings which all contribute to the splittings is only 1/5, three times lower than the corresponding density of the benzophenone ketyl. For this reason the total width of the spectrum of the benzil ketyl is nearly three times narrower than that of the benzophenone ketyl.

The total width of the spectra of 9,10-phenanthrenequinone and 9,10-anthraquinone ketyls is also narrow, although ρ_c and ρ_0 are not high, but because they have more atoms which do not contribute to the hyperfine splittings, without the carbonyl atoms, only 1/4 of the total spin densities is localized on the atoms which contribute to the splittings.

---

[10] E. W. Stone and A. H. Maki, *J. Chem. Phys.*, **36**, 1944 (1962).
[11] H. Rinkel and W. Windsch, *Z. phys. Chem.* (*Leipzig*), **227**, 281 (1964).

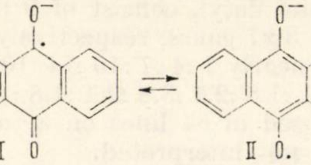

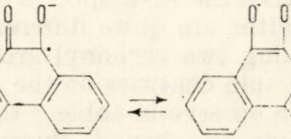

The calculated spin densities on the carbonyl carbon atoms for the first five metal ketyls in table 3 are higher than that on the carbonyl oxygen atoms. On the contrary, the metal ketyls obtained from quinone have either nearly the same calculated spin densities on the carbonyl atoms, or the higher spin densities on the carbonyl oxygen atoms, due probable to the contribution to a greater extent of structure II to the real structure of the metal ketyls.

In all ESR spectra of the studied metal ketyls in DMF no hyperfine splitting was observed due to alkali metal. In the visible spectra of these metal ketyls [12] the position of the absorption peaks depends to a small extent on used alkali metal, showing that in this solvent there exist weak interactions between ions, but these interactions are not noticeable in the ESR spectra.

---

[12] V. E. Sahini and L. Ciurea, *Rev. Roumaine Chim.*, (in print).

Revue Roumaine de Chimie, **14**, 695–704 (1969)

DAS THERMODYNAMISCHE VERHALTEN DES GASGEMISCHES ARGON-KOHLENDIOXID

RODICA VÎLCU und I. GĂINAR

Aus dem Laboratorium für Physikalische Chemie der Universität Bukarest,
Bdul Republicii, 13

Eingegangen am 17. August 1968

Es wird das thermodynamische Verhalten des Gasgemisches Kohlendioxid-Argon bei verschiedenen Temperaturen und Drucken beschrieben. Der Grad der Unvollkommenheit des Gemisches wurde durch den Wert der Überschußvolumina und durch die Fugazitäten der Komponenten des Systems zum Ausdruck gebracht. Die Berechnung dieser Größen fußt auf der durch die Gleichung von Beattie und Bridgeman wiedergegebenen Abhängigkeit zwischen den Zustandsparametern.

Die vorliegende Arbeit beabsichtigt, das thermodynamische Verhalten des Gemisches Argon-Kohlendioxid bei verschiedenen Drucken und Temperaturen zu beschreiben. Die unterschiedlichen physikalisch-chemischen Kennzeichen von Ar und CO_2 beschränken die Möglichkeiten der Erforschung dieses Gemisches in der Gasphase auf einen gewissen Temperatur- und Druckbereich.

Ein Überblick über die Arbeiten der experimentellen Thermodynamik in Gasgemischen, weist in erster Reihe auf die Erforschung solcher Systeme, in denen das Argon mit stetigen Gasen wie : Stickstoff, Kohlendioxid assoziiert ist. Bei dergleichen Untersuchungen werden die kritischen Parameter überschritten und die Gemische verflüssigter Gase [1-3] untersucht, die bei gewissen Werten der Zustandsparameter zusammen bestehen. Der Grad der Unvollkommenheit dieser Systeme wurde sowohl auf experimentellem Wege, als auch mit Hilfe der Theorie des mittleren Potentials durch Berechnung der thermodynamischen Überschußfunktionen festgestellt.[4]

Abraham [5] hat eine systematische Untersuchung der Dichten des Gemisches $Ar-CO_2$ bei verschiedenen Drucken angestellt.

---

[1] A. G. Duncan and L. A. K. Staveley, *Trans. Faraday Soc.*, **62**, 548 (1966).

[2] A. G. Duncan, R. H. Davies, M. A. Byrne and L. A. K. Staveley, *Nature*, **209**, 1236 (1966).

[3] R. A. H. Pool, G. Saville, T. M. Herrington, B. D. C. Shields and L. A. K. Staveley, *Trans. Farady Soc.*, **58**, 1692 (1962).

[4] A. Bellemans, V. Mathot and M. Simon, *Adv. Chem. Phys.*, **11**, 117 (1967).

[5] W. H. Abraham, *Diss. Abs.*, **17**, 2228 (1957) ; *Chem. Abstr.*, **52**, 1709 b.

In Anbetracht dessen, daß sich Ar und CO_2 in überwiegender Menge in der Atmosphäre einiger Planeten vorfinden, und ferner weil diese beiden Gase zu verschiedenen Zwecken zusammen verwendet werden, ist es erforderlich, die Eigenschaften dieses Gemisches festzustellen. Da Versuchsergebnisse nicht vorliegen, wurde die von einer der anerkanntesten Zustandsgleichungen, der Gleichung von Beattie und Bridgeman, wiedergegebene Beziehung $P-V-T$ hier angewendet. Für reine Gase ist die Formel[6]:

$$P = \frac{RT}{V^2}(1-\varepsilon)(V+B) - \frac{A}{V^2} \tag{1}$$

worin

$$V = \text{Molvolumen des Gases}$$

$$A = A_0\left(1 - \frac{a}{V}\right)$$

$$B = B_0\left(1 - \frac{b}{V}\right)$$

$$\varepsilon = \frac{c}{V T^3}$$

Die anderen Größen haben bekannte Bedeutungen. Die Konstanten R, c, B_0, b, A_0 sind von Volumen und Temperatur unabhängig. A und B hängen vom Volumen ab. Mit Hilfe des temperaturabhängigen ε, wird die Temperaturabhängigkeit des Druckes wiedergegeben.

Die Gleichung von Beattie und Bridgeman kann auch durch die sogenannte Virialform wiedergegeben werden.

$$P = \frac{RT}{V} + \frac{\beta}{V^2} + \frac{\gamma}{V^3} + \frac{\delta}{V^4} \tag{2}$$

worin:

$$\beta = RTB_0 - A_0 - \frac{R_c}{T^2}$$

$$\gamma = -RTB_0 b + A_0 a - \frac{R B_0 c}{T^2}$$

$$\delta = \frac{R B_0 bc}{T^2}$$

Die von Beattie[7] für Gasgemische aufgestellte Gleichung (1) lautet:

$$P = \frac{\sum ni\, RT}{V^2}(1-\varepsilon)(V+B) - \frac{A}{V^2} \tag{3}$$

---

[6] J. A. BEATTIE and O. C. BRIDGEMAN, *Proc. Amer. Acad. Arts Sci.*, **63**, 229 (1928).

[7] J. A. BEATTIE, *J. Amer. Chem. Soc.*, **51**, 19 (1929).

wobei :

V = das Volumen von n_i Mol Gemisch

$$\varepsilon = (n_1 c_1 + n_2 c_2) / V T^3$$

$$A = (n_1 A_{01}^{1/2} + n_2 A_{02}^{1/2})^2 \left(1 - \frac{n_1 a_1 + n_2 a_2}{V}\right)$$

$$B = (n_1 B_{01} + n_2 B_{02}) \cdot \left(1 - \frac{n_1 b_1 + n_2 b_2}{V}\right)$$

A_0, B_0, a_1, b_1, und c_1 sind Konstanten die den individuellen Gasen jeweils eigen sind. Die letzte Gruppe von Gleichungen, zeigt im Vergleich zu den den individuellen Gasen eigenen Größen A, B und ε, die Kombinationsregeln auf, denen gemäß die Konstanten des Gemisches bestimmt werden. Derartige Konstanten ermittelt man entweder über die Konstanten für die reinen Gase in der Form von linearen Kombinationen, oder durch die lineare Kombination der Quadratwurzel der individuellen Konstanten. Die angewandten Kombinationsregeln sind bedingt von der Art in der die Konstanten der Wechselwirkung in der Lösung aus den Konstanten der Wechselwirkung der reinen Komponenten abgeleitet werden. Die Konstanten a_i, b_i und c_i sind aus Tabellen zu entnehmen und werden zur Berechnung von A_{0i} und B_{0i} herangezogen.

Durch die einem Gasgemisch entsprechenden $P-V-T$-Werte (Gl. 3) kann das thermodynamische Verhalten des Systems für verschiedene Werte der Zustandsparameter gekennzeichnet werden.

Das Zusatzvolumen V^E des Gemisches, das üblicherweise durch die Gleichung

$$V^E = V^M - V^{M,id} \tag{4}$$

bestimmt wird, ist gleichzusetzen mit dem Mischungsvolumen V^M das dem nicht idealen Gas eigen ist, weil $V^{M,id}$ gleich Null ist. Gemäß dem Verfahren von Gibson und Sosnick [8] kann man das Mischungsvolumen in einem nicht idealen System aus den Gleichungen :

$$V^M = V - (x_1 V_1 + x_2 V_2) \tag{4a}$$

berechnen. V_1 und V_2 sind die Molvolumina der reinen Komponente und x_1, x_2 die Molenbrüche.

Die partiellen Molvolumina $\overline{V}_1$ und $\overline{V}_2$, werden nach den Gleichungen (4b) und (4c) [8] berechnet :

$$\overline{V}_1 = V_1 + V^M + x_2 \frac{V^M}{x_1} \tag{4b}$$

oder

$$V_2 = V_2 + V^M + x_1 \frac{V^M}{x_2} \tag{4c}$$

---

[8] G. E. Gibson and B. Sosnick, *J. Amer. Chem. Soc.*, **49**, 2172 (1927).

Die Fugazität eines Gases im Gemisch, f, kann nach der klassischen Formel[8]:

$$RT \ln f = RT \ln Px - \int_0^p \alpha \, \mathrm{d}P \tag{5}$$

berechnet werden, oder wenn vom natürlichen Logarithmus zum gewöhnlichen Logarithmus übergegangen wird, wobei R gleich 82,07 cm³ atm/grd so ergibt sich[9]:

$$\log f = \log Px - \frac{1}{189{,}0 . T} \int_0^p \alpha \mathrm{d}P \tag{6}$$

wobei $\alpha = \dfrac{RT}{P} - V_i(7)$ eine Abweichungsgröße vom idealen Verhalten des Gases darstellt. Die Fugazität und der Druck werden in atm ausgedrückt und α in cm³. Da das Molvolumen bei verschiedenen Systemzusammensetzungen bekannt ist, kann — nach der Gleichung von Beattie und Bridgeman — für bestimmte festgesetzte Werte der intensiven Zustandsparameter, unter den gegebenen Verhältnissen α geschätzt werden.

ERGEBNISSE UND DISKUSSION

Für das System Argon-Kohlendioxid wurden die von den vorangehenden Gleichungen bestimmten Größen für das gesamte Zusammensetzungsintervall, bei den Temperaturen von 288,16, 293,16, 303,16 und 308,16°K, und bei Drucken zwischen 1 und 80 atm berechnet.

Von der großen Anzahl der Ergebnisse, seien einige Daten erwähnt, die für die thermodynamische Kennzeichnung des Systems aufschlußreicher sind, geht man mit der Berechnung von den Molvolumina aus, die man aus der Gleichung von Beattie und Bridgeman für die verschiedenen erwähnten Verhältnisse ableitete, erhält man die partiellen Molvolumina von Ar und CO_2 und implizite die Zusatzvolumina die in den Abbildungen 1—3 für drei der fünf betrachteten Temperaturen u. zw. für 288,16.298,16 und 308,16°K dargestellt sind.

In Tabelle 1 sind die Zusatzvolumina des Gemisches $Ar-CO_2$ bei verschiedenen Drucken und für die Temperaturen 293,16 und 303,16°K aufgenommen. Sowohl die Ergebnisse aus der Tabelle als auch die Diagramme weisen anhand der Überschußvolumina, auf einige Eigenheiten des Systems, welche bestätigen, daß Druck und Temperatur sich stark auf den Grad der Unvollkommenheit des Systems auswirken.

Das Zusatzvolumen ist eine parabolische Zusammensetzungsfunktion. Die Maxima der Parabeln sind leicht gegen kohlendioxidhaltigere Gemische verschoben. Diese Verschiebung wird mit dem Anstieg des Druckes leicht erhöht. Im allgemeinen betont der Druckanstieg die Unvollkommenheit des Systems und führt zur Zunahme des Zusatz-

---

[9] K. Jellinek, „Lehrbuch der physikalischen Chemie", 4.Bd., Verlag von F. Enke, Stuttgart, 1928, S. 321.

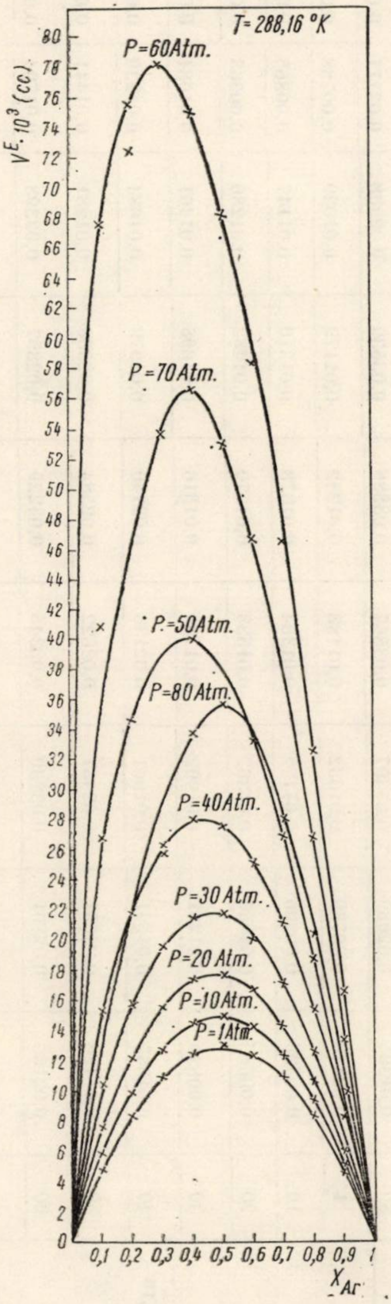

Abb. 1. — Die Änderung des Zusatzvolumens mit der Zusammensetzung des Gemisches Ar-CO$_2$, bei verschiedenen Drucken und bei 288,16°K.

Abb. 2. — Die Änderung des Zusatzvolumens mit der Zusammensetzung des Gemisches Ar-CO$_2$ bei verschied enen Drucken und bei 298,16°K.

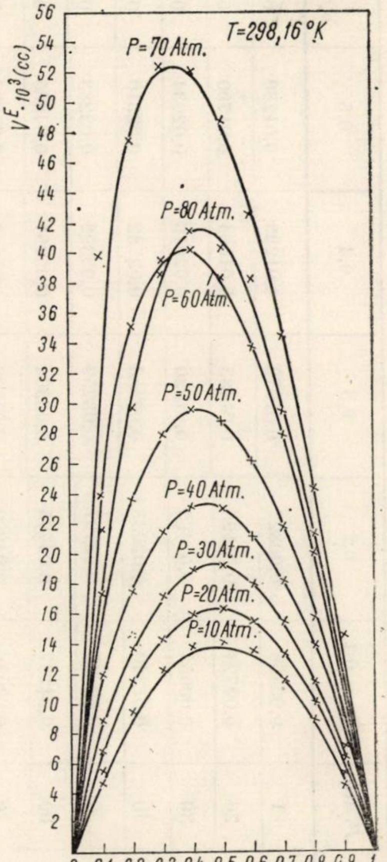

Tabelle 1

Zusatzvolumen für die Mischung Ar – CO_2

Temp. °K	P. atm	$X_{Ar} = 0,1$	0,2	0,3	0,4	0,5	0,6	0,7	0,8	0,9
293,16	1	0,00468	0,00821	0,01072	0,01233	0,01280	0,01224	0,01078	0,00819	0,00457
	20	0,00724	0,01165	0,01483	0,01664	0,01700	0,01601	0,01386	0,01036	0,00566
	30	0,00958	0,01465	0,01830	0,02016	0,02034	0,01894	0,01620	0,01199	0,00649
	40	0,01340	0,02035	0,02353	0,02732	0,02510	0,02303	0,01945	0,01422	0,00831
	50	0,02094	0,02797	0,03259	0,03392	0,03283	0,02952	0,02447	0,01764	0,00925
	60	0,04137	0,04795	0,05304	0,05251	0,04895	0,04275	0,03458	0,02444	0,01272
	70	0,03936	0,04990	0,05500	0,05686	0,05329	0,04657	0,03761	0,02653	0,01375
	80	0,01305	0,02089	0,03397	0,03867	0,03888	0,03539	0,02938	0,02111	0,01106
303,16	1	0,00448	0,00789	0,01032	0,01188	0,01232	0,01179	0,01029	0,00788	0,00440
	10	0,00539	0,00906	0,01172	0,01334	0,01378	0,01310	0,01147	0,00865	0,00478
	20	0,00660	0,01066	0,01362	0,01533	0,01570	0,01482	0,01286	0,00963	0,00527
	30	0,00830	0,01281	0,01692	0,01789	0,01816	0,01698	0,01461	0,01084	0,00589
	40	0,01085	0,01591	0,01961	0,02136	0,02140	0,01979	0,01684	0,01239	0,00666
	50	0,01480	0,02051	0,02451	0,02622	0,02584	0,02358	0,01981	0,01441	0,00767
	60	0,02166	0,02891	0,03230	0,03345	0,03229	0,02897	0,02398	0,01724	0,00909
	70	0,03168	0,04008	0,04261	0,04300	0,04187	0,03594	0,02783	0,02085	0,01088
	80	0,02667	0,03551	0,03980	0,04130	0,03976	0,03542	0,02805	0,01971	0,01079

volumens. Die Parabeln welche die Abhängigkeit zwischen V^E und der Zusammensetzung veranschaulichen, folgen aber nicht in allen Fällen in der Reihenfolge des zunehmenden Druckes aufeinander. Zwischen 50 und 80 atm ist eine Umkehrung zwischen den Parabeln bei den ersten vier betrachteten Temperaturen festzustellen. Das Geschehen schwindet nach Maßgabe des Temperaturanstiegs und um 308°K besteht ein gerades Verhältnis zwischen den Zusatzvolumina und dem Druck. Auf diese Weise ist auch der Einfluß der Temperatur offensichtlich welche die Parabelumkehrung bei der Druckzunahme beseitigt. So wie sich die Zusatzvolumina verhalten wenn sich die Zustandsparameter ändern, so verhalten sich übrigens auch andere binäre Gassysteme wie: $Ar-H_2$, $Ar-N_2$, N_2-H_2 [10] usw.

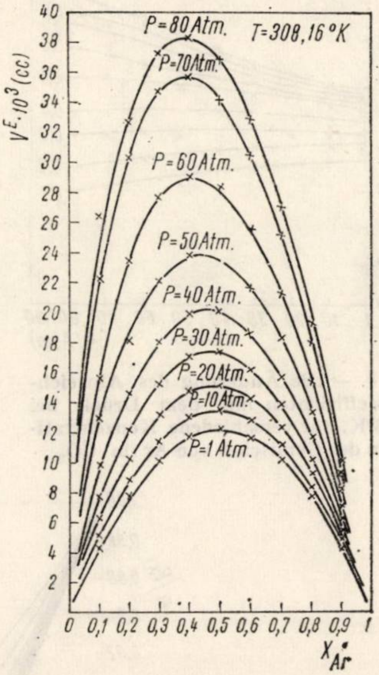

Abb. 3. — Die Änderung des Zusatzvolumens mit der Zusammensetzung des Gemisches $Ar-CO_2$ bei verschiedenen Drucken und bei 308,16°K.

Die Fugazitätskoeffizienten der Komponenten des Gemisches $Ar-CO_2$ wurden aufgrund der Gleichung (6) ermittelt. Die Integralen, die in dieser Rechnung vorkommen, wurden graphisch bestimmt und zwar aus den Oberflächenwerten, die durch die Darstellung von α als Funktion des Druckes erzielt wurden. Die α-Werte wurden durch die Substitution der partiellen Molvolumina der aus dem Gemisch betrachteten Komponente in die Gleichung (7) abgeleitet.

Von der großen Auswahl der erhaltenen Ergebnisse wurden zwei Reihen von Darstellungen ausgesucht (α druckabhängig), welche in den

---

[10] P. Zandbergen and J. J. Beenacker, *Physica*, **33**, 343 (1967); *Ibid.*, **33**, 366 (1967).

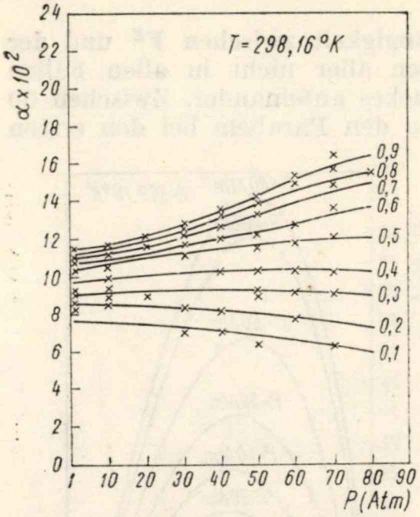

Abb. 4. — Die Änderung des Abweichungskoeffizienten mit dem Druck bei 298,16°K, für verschiedene Konzentrationen des Gemisches von Ar in CO_2.

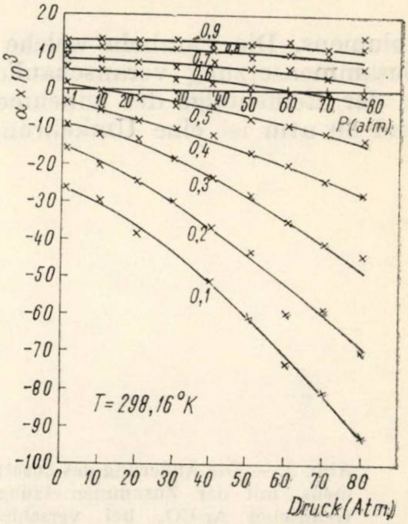

Abb. 5. — Die Änderung des Abweichungskoeffizienten mit dem Druck bei 298,16°K, für verschiedene Konzentrationen des Gemisches von CO_2 in Ar.

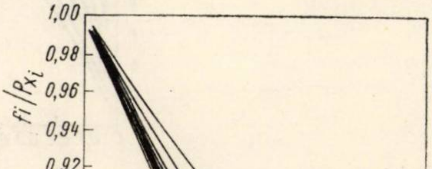

Abb. 6. — Die Abhängigkeit des f_i/Px_i-Quotienten vom Druck bei verschiedenen Zusammensetzungen des Gemisches Ar-CO_2, bei 308,16°K.

Tabelle 2

Die Fugazitätskoeffizienten des CO_2 in der $Ar-CO_2$-Mischung Die Abweichungen des f_i/Px_i -Quotienten nach dem Lewis-Randallschen Gesetz

T (°K)	P	0,1	0,2	0,3	0,4	0,5	0,6	0,7	0,8	0,9
288,16	10	0,962	0,958	0,951	0,950	0,949	0,947	0,946	0,944	0,942
	20	0.923	0.913	0.908	0.906	0.900	0.897	0.896	0.891	0.889
	30	0.886	0.872	0.863	0.859	0.852	0.848	0.844	0.837	0.834
	40	0.851	0.834	0.820	0.815	0.802	0.794	0.792	0.783	0,780
	50	0,819	0.797	0.781	0.772	0.741	0.741	0.736	0.724	0.718
	60	0,785	0,761	0,771	0,731	0,713	0,688	0,682	0,662	0,651
	70	0,755	0,727	0,708	0,694	0,673	0,640	0,626	0,602	0,572
	80	0,723	0,696	0,671	0,653	0,631	0,593	0,574	0,553	0,531
293,16	10	0,964	0,960	0,958	0,954	0,952	0,950	0,948	0,946	0,944
	20	0,931	0,922	0,917	0,906	0,905	0,902	0,897	0,895	0,893
	30	0,896	0,883	0,878	0,870	0,860	0,855	0,847	0,845	0,837
	40	0,864	0,847	0,841	0,830	0,814	0,810	0,798	0,795	0,784
	50	0,831	0,812	0,803	0,791	0,771	0,764	0,746	0,743	0,728
	60	0,802	0,782	0,770	0,753	0,730	0,718	0,696	0,687	0,671
	70	0,774	0,748	0,735	0,718	0,869	0,671	0,642	0,631	0,614
	80	0,743	0,718	0,703	0,680	0,651	0,627	0,593	0,577	0,561
298,16	10	0,961	0,965	0,960	0,958	0,956	0,954	0,952	0,950	0,948
	20	0,938	0,931	0,918	0,914	0,912	0,910	0,905	0,902	0,896
	30	0,908	0,896	0,883	0,881	0,869	0,863	0,859	0,855	0,845
	40	0,878	0,863	0,848	0,843	0,826	0,816	0,812	0,806	0,794
	50	0,849	0,833	0,813	0,804	0,786	0,774	0,767	0,759	0,743
	60	0,821	0,802	0,782	0,771	0,743	0,731	0,720	0,706	0,690
	70	0,792	0,773	0,752	0,733	0,705	0,686	0,671	0,661	0,640
	80	0,766	0,743	0,720	0,698	0,664	0,642	0,627	0,612	0,590
303,16	10	0,967	0,966	0,962	0,961	0,957	0,954	0,954	0,951	0,950
	20	0,936	0,930	0,927	0,923	0,917	0,912	0,911	0,902	0,899
	30	0,908	0,897	0,891	0,886	0,875	0,871	0,865	0,856	0,852
	40	0,878	0,865	0,858	0,850	0,835	0,830	0,822	0,807	0,802
	50	0,852	0,834	0,826	0,814	0,796	0,788	0,780	0,758	0,750
	60	0,826	0,806	0,796	0,782	0,759	0,746	0,735	0,711	0,713
	70	0,801	0,780	0,768	0,749	0,723	0,705	0,696	0,692	0,661
	80	0,776	0,754	0,739	0,717	0,688	0,665	0,648	0,618	0,615
308,16	10	0,974	0,967	0,963	0,960	0,958	0,957	0,955	0,954	0,952
	20	0,944	0,934	0,927	0,922	0,917	0,915	0,912	0,910	0,907
	30	0,918	0,904	0,894	0,885	0,878	0,874	0,873	0,866	0,863
	40	0,892	0,874	0,862	0,853	0,840	0,838	0,834	0,822	0,819
	50	0,869	0,847	0,831	0,818	0,804	0,795	0,793	0,778	0,774
	60	0,848	0,821	0,804	0,788	0,769	0,758	0,755	0,735	0,731
	70	0,825	0,795	0,776	0,757	0,738	0,721	0,714	0,690	0,683
	80	0,806	0,775	0,752	0,735	0,714	0,696	0,674	0,647	0,641

Abbildungen 4 und 5 den Einfluß der Konzentration auf den Abweichungsgrad des Systems veranschaulichen.

Die Abweichungen des f_i/Px_i-Quotienten vom Lewis-Randallschen Gesetz weisen auf die Abweichungsrichtung des Systems Ar—CO$_2$ vom idealen Verhalten. In Tabelle 2 sind unsere Rechenergebnisse eingetragen und in der Abbildung 6 ist das Verhalten des Systems Ar—CO$_2$, bei 308,16°K veranschaulicht.

Sowohl die Zusatzvolumina des Gemisches als auch die Fugazitätskoeffizienten sind Größen, welche den Grad der Unvollkommenheit des Systems in dem Maße kennzeichnen, in dem die Gleichung auf der die Rechnungen beruhen, für den Fall in dem die für das System Ar—CO$_2$ gegebenen Bedingungen gültig bleiben. Die auf diese Weise für derartige Abweichungsfunktionen vorgesehenen Ergebnisse müssen entweder experimentell oder durch die Erstreckung der Aussagen von Prigogine und Mitarb. für flüssige Gemische auf den Fall der Gasgemische bestätigt werden.

Revue Roumaine de Chimie, **14**, 705–708 (1969)

THE STABILITY OF THE OXALYL ANIONIC RADICAL ($C_2O_4^{\cdot -}$)

Z. SIMON

Chemical Research Center of the Academy, Timişoara,
Bd. Mihai Viteazu 24

Received September 5, 1968

The reaction enthalpy for the $C_2O_4^{\cdot -} \rightarrow CO_2 + CO_2^{\cdot -}$ reaction is evaluated by means of a simple molecular orbital scheme. The energy differences are set equal to dissociation energies, differences between valence state ionization potentials and optic transition energies which are available as experimental data. The obtained figure, + 26.5 kcal/mol, although a rough approximation, indicates $C_2O_4^{\cdot -}$ as the intermediate radical species in the internal redox reactions of complex transition metal oxalates.

In internal redox reactions of the complex transition metal oxalates an $C_2O_4^{\cdot -}$ oxalyl anionic radical is formed which performs the redox reaction in a second complex anion. [1–4] It would be interesting to know if this $C_2O_4^{\cdot -}$ anionic radical, formed in the first step of the redox reaction, reacts as such with the second complex anion or if it dissociates first in a CO_2 molecule and a formyl anionic radical (CO_2^{-}). Thus the activation energy (and entropy) of the hypothetic reaction :

$$C_2O_4^{\cdot -} \longrightarrow CO_2 + CO_2^{\cdot -} \qquad (1)$$

should be known. A direct experimental study of reaction (1) is not possible and, as $C_2O_4^{\cdot -}$ and $CO_2^{\cdot -}$ are very unstable particles, even a direct evaluation of the reaction enthalpy ΔH_1 out of thermodinamic data is not possible ; to effect this one should possess data such as the hydration energy of the $C_2O_4^{\cdot -}$ ion and the ionization energy, in aqueous solution, of the $C_2O_4^{2-}$ ion. We shall therefore proceed as follows in order to obtain by all means an evaluation of the enthalpy ΔH_1 of reaction (1). We shall write down the energies of the interesting particles in a molecular orbital scheme and the molecular orbital energy differences pertinent to ΔH_1 will be set equal to the corresponding (differences of) experimental energies for optical transitions and valence state ionization potentials.

---

[1] A. J. Allmand and W. W. Webb, *J. Chem. Soc.*, **1929**, 1518.

[2] I. G. Murgulescu, *Bul. Soc. Ştiinţe, Cluj*, **8**, 193 (1935).

[3] I. G. Murgulescu and T. Oncescu, *Z. physik. Chem. (Leipzig)*, **214**, 238 (1960).

[4] K. V. Krishnamurti and G. M. Harris, *Chem. Rev.*, **61**, 213 (1963).

In reaction (1) a simple C—C bond is broken, a process which usually requires $D_{CC} \cong 80$ kcal/mol,[5] but as electronic rearrangement and formation of the stable CO_2 molecule take place during this process, ΔH_1 can be much lower than this figure. The first step one must undertake now is to establish the pertinent orbitals and the distribution of electrons on them. In principle to each σ-bond a bonding σ-molecular orbital with 2 electrons should be assigned, while the oxygen atoms possess also nonbonding n-orbitals with 2 electrons on each. As to the π-electrons, they will be treated by the simple HMO method with parameters recommended by Streitwieser[6]; this method usually yields good results for resonance energies. Resonance energy differences, with $\beta = -16.5$ kcal/mol recommended by Streitwieser,[6] will be used in our evaluations.

The distribution of electrons on molecular orbitals in the particles which are of interest to us is probably:

$$\text{for } C_2O_4^{\cdot -} : (\sigma_{cc})^2\,(4\,\sigma_{c0})^8\,(8n_0)^{15}\,(\psi_1)^2\,(\psi_2)^2\,(\psi_3\psi_4)^4; \tag{2}$$

for an angular $\cdot COO^-$ anionic radical, as it would result immediately after the dissociation of $C_2O_4^{\cdot -}$:

$$(n_c)^1\,(2\,\sigma_{c0})^4\,(4n_0)^8\,(\Phi_1)^2\,(\Phi_2)^2; \tag{3}$$

(for a linear $CO_2^{\cdot -}$:

$$(2\,\sigma_{c0})^4\,(2n_0)^4\,(\Phi_1)^2\,(\Phi_1')^2\,(\Phi_2)^2\,(\Phi_2')^2\,(\Phi_3\,\Phi_3')^1; \tag{4}$$

and the same as (4) for the CO_2 molecule but without the electron on the antibonding $\Phi_3\,\Phi_3'$ orbitals. The bonding c—c σ-molecular orbitals are denoted by σ_{cc}; those of the C—O bond by σ_{c0}. The nonbonding orbitals are n_0 for the oxygen atom and n_c for the atomic orbital on the carbon atom, resulted by dissociation of the c—c bond. The π-molecular orbitals, as obtained with Streitwieser's parameters[6] (see also [7]) in the order of their decreasing energies, are:

$$\begin{array}{llll}
C_2O_4^{2-} & \psi_6;\ \epsilon_6 = \alpha - 1.325\,\beta & \text{angular} & \Phi_3;\ e_3 = \alpha - 0.85\,\beta \\
\text{or} & \psi_5;\ \epsilon_5 = \alpha - 0.006\,\beta & .COO^- : & \Phi_2;\ e_2 = \alpha + 2.00\,\beta \\
C_2O_4^{\cdot -} : & \psi_4,\ \psi_3;\ \epsilon_4 = \epsilon_3 = \alpha + 2\beta & & \Phi_1;\ e_1 = \alpha + 2.85\,\beta \\
 & \psi_2;\ \epsilon_2 = \alpha + 2.725\,\beta & \text{linear} & \Phi_3,\ \Phi_3';\ e_3 = e_3' = \alpha - 0.85\beta \\
 & \psi_1;\ \epsilon_1 = \alpha + 3.206\,\beta & CO_2^{\cdot -} & \Phi_2,\ \Phi_2';\ e_2 = e_2' = \alpha + 2.00\beta \\
 & & \text{and } CO_2 & \Phi_1,\ \Phi_1';\ e_1 = e_1' = \alpha + 2.85\beta
\end{array} \tag{5}$$

For the linear $CO_2^{\cdot -}$ particle and the CO_2 molecule, Φ_1, Φ_2, Φ_3 and Φ_1', Φ_2', Φ_3' are respectively the π-molecular orbitals in the two perpendicular plans which contain the molecular axis. The $C_2O_4^{\cdot -}$—particle results by ionization of the oxalate ion. The electron is thereby extracted probably for the nonbonding n_0-orbital (and not from one of the highest occupied ψ_3, ψ_4, π-molecular orbitals) as the first transition in the UV spectrum of $C_2O_4^{2-}$ has the characteristics of an $n\pi^*$ -transition. Actually the UV spectrum of $C_2O_4^{2-}$ begins with a slightly pronounced, that of $(CH_3)_2C_2O_4$ with a clearly pronounced shoulder with molar extinction $\log \varepsilon < 2$. Hereby, the first, strong maximum, the $\pi\pi^*$ transition corresponds to $\tilde{\nu} \cong 50 \times 10^3$ cm^{-1}, while the shoulder (the $n\pi^*$ transition) to $\tilde{\nu} \cong 40 \times 10^3$ cm^{-1}, in the UV spectrum of dimethyloxalate (Landolt-Börnstein, Tabellen II, 1, Bd., 3. Teil, p. 254).

---

[5] V. I. VEDENEEV, "Energii razryvy sviazei. Potentsialy ionizatsii i srodstvo k electronu", Izdat. Akad. Nauk SSSR, Moscow, 1962, tab. 11.

[6] A. STREITWIESER, "Molecular Orbital Theory for Organic Chemists", John Wiley, New York and London, 1961, chap. III, V.

[7] I. G. MURGULESCU, T. ONCESCU and Z. SIMON, *Rev. Roumaine Chim.*, **12**, 755 (1967).

The energies of the considered particles can now be written by taking into account the electronic distributions (1—3) and the π-molecular orbital energies (4):

$$\begin{aligned}
&\text{for } C_2O_4^{\cdot -} : E(C_2O_4^{\cdot -}) = 8\varepsilon(\sigma_{o0}) + 2\varepsilon(\sigma_{cc}) + 15\varepsilon(n_0) + 8\alpha + 19.86\beta \\
&\text{for angular } .COO^- : E(.COO^-) = 4\varepsilon(\sigma_{c0}) + 8\varepsilon(n_0) + \varepsilon(n_c) + 4\alpha + \\
&\qquad\qquad + 9.70\,\beta \qquad (6) \\
&\text{for linear } CO_2^{\cdot -} : E(CO_2^{\cdot -}) = 4\varepsilon(\sigma_{c0}) + 4\varepsilon(n_0) + 9\alpha + 18.55\,\beta \\
&\text{for } CO_2 : E(CO_2) = 4\varepsilon(\sigma_{c0}) + 4\varepsilon(n_0) + 8\alpha + 19.40\beta
\end{aligned}$$

One should now evaluate which form of $CO_2^{\cdot -}$, the linear or the angular one, is more stable:

$$\Delta E = E(CO_2^{\cdot -}) - E(.COO^-) = 5\alpha + 8.85\,\beta - 4\varepsilon(n_0) - \varepsilon(n_c)$$

The data for the valence state ionization potentials for sp^3 and sp^2 hybridizations of the carbon atom indicate[5] $\varepsilon(n_c) = \alpha - 4.5$ eV. The energy difference of about 10×10^3 cm^{-1} between the $\pi\pi^*$ and the $n\pi^*$ transitions in $(CH_3)_2C_2O_4$ could, tentatively, be set equal to the energy difference of the highest occupied π-molecular orbitals, $\epsilon_3 = \epsilon_4$ and of the oxygen nonbonding orbital, n_0: $\varepsilon(n_0) - (\alpha + 2\beta) \cong 1.2$ eV. With the -16.5 kcal/mol value for β one obtains $\Delta E = 0.85\,\beta - 0.3 \text{ eV} \cong = -20$ kcal/mol; thus the linear form of $CO_2^{\cdot -}$ should be the more stable one.

One can check the validity of the **HMO** scheme in energy calculations by calculating the conjugation energy R_c of the two -COOH groups in oxalic acid. The formation energy of the oxalic acid, the $H(H_2C_2O_4)$ and the bond and group energies, ε_{c-c}, ε_{COOH}, etc. listed by Karapetiants[8] yield:

$$R_C = \Delta H(H_2C_2O_4) + 2\varepsilon_C + \varepsilon_{H_2} + 2\varepsilon_{O_2} - \varepsilon_{C-C} - 2\varepsilon_{COOH} = -8.6 \text{ kcal/mol.}$$

If we adopt the molecular orbital energies (5) of $C_2O_4^{2-}$ and $.COO^-$ for the oxalic acid and the COOH-group, one can calculate:

$$R_C = 2(\epsilon_1 + \epsilon_2 + \epsilon_3 + \epsilon_4) - 2 \times 2(e_1 + e_2) = 0{,}46\beta = -7.6 \text{ kcal/mol}$$

in good agreement with the above R_C-value given by thermodynamic data.

---

[8] M. H. Karapetiants, "Khimiceskaia Termodinamica", Goskhimizdat, Moscow, 1949, Romanian transl. Edit. Tehnică, Bucharest, 1953, tab. 3, chap. 2.

The enthalpy ΔH_1 of reaction (1) can now be written as:

$$\Delta H_1 = E(CO_2) + E(CO_2^{\cdot -}) - E(C_2O_4^{\cdot -}) = -2\varepsilon(\sigma_{CC}) - 7\varepsilon(n_0) + 9\alpha + 18.09\beta \tag{7}$$

where $\alpha + 2\beta - \varepsilon(n_0)$ can be set equal to the energy difference $h\nu_{\pi\pi^*} - h\nu_{n\pi^*}$ of the $\pi\pi^*$ and $n\pi^*$ transitions, $2\varepsilon(\sigma_{CC})$ can be set equal to $2\varepsilon(n_C) - D_{CC}$ and $\varepsilon(n_C)$ to a valence state ionization potential difference, $\alpha + I(sp^3) - I(sp^2)p_z$. Thus, with the above listed figures:

$$H_1 = D_{CC} + 2[I(sp^2)p_z - I(sp^3)] + 7[h\nu_{\pi\pi^*} - h\nu_{n\pi^*}] + 4.09\beta \cong +26.5 \text{ kcal/mol} \tag{8}$$

The activation energy for reaction (1) should be at least as great as ΔH_1, that is appreciable, even if the approximate character of our calculation is taken into account. As dissociations generally have a positive reaction entropy, the dissociation of $C_2O_4^{\cdot -}$, existing only in small concentrations, may be favoured thermodynamically. The reaction with the second complex transition metal-oxalate ion must be very rapid [2,3] and therefore, $C_2O_4^{\cdot -}$, with an appreciable activation energy for dissociation in $CO_2 + CO_2^{\cdot -}$ will not have sufficient time to dissociate before the second step of the internal redox reaction.

The conclusion, consistent with our calculations, that $C_2O_4^{\cdot -}$ and not $CO_2^{\cdot -}$ is the radicalic intermediate in the internal redox reaction of complex transition metal oxalates agrees with the experimental results recently obtained by dr. T. Oncescu.[9]

---

[9] T. Oncescu, *Rev. Roumaine Chim.* (in press)

Revue Roumaine de Chimie, **14**, 709–715 (1969)

CINÉTIQUE DE LA DÉCOMPOSITION THERMIQUE DE CERTAINES COMBINAISONS COMPLEXES DU CHLORURE DE MANGANÈSE AVEC LA PYRIDINE ET DES PYRIDINES SUBSTITUÉES

PARAMÈTRES CINÉTIQUES OBTENUS DES DONNÉES GRAVIMÉTRIQUES

D. FĂTU et E. SEGAL

Université de Bucarest, Chaire de Chimie Physique II, 13, Bd. Republicii

Reçu le 17 septembre 1968

On a déterminé les paramètres cinétiques de la décomposition thermique de certaines combinaisons complexes du chlorure de manganèse avec la pyridine et des pyridines substituées, en utilisant des données thermogravimétriques. Les résultats obtenus démontrent que les processus se déroulent dans un domaine mixte cinétique — diffusionnel.

A la suite des travaux concernant la décomposition des combinaisons complexes formées par les halogénures des métaux de transition bivalents avec la pyridine et des pyridines substituées, [1-5] on présente une étude cinétique de la décomposition des combinaisons complexes formées par le chlorure de manganèse avec les bases précitées.

Allan et ses collaborateurs [6] ont démontré que la décomposition du complexe tétrapyridinique du chlorure de manganèse a lieu en étapes, conformément au schéma suivant

$$\mathrm{Mn\,Py_4\,Cl_2} \rightarrow \mathrm{Mn\,Py_2Cl_2} \rightarrow \mathrm{MnPyCl_2} \rightarrow \mathrm{MnPy_{2/3}Cl_2} \rightarrow \mathrm{MnCl_2}$$

chaque composé intermédiaire étant stable dans un certain domaine de température.

---

[1] I. G. Murgulescu, E. Segal et D. Fătu, *J. Inorg. Nuclear Chem.*, **27**, 2677 (1965).

[2] I. G. Murgulescu, E. Segal et D. Fătu, *Rev. Roumaine Chim.*, **11**, 291 (1966).

[3] N. Hurduc, L. Odochian, I. A. Schneider et E. Segal, *Rev. Roumaine Chim.*, **11**, 1453 (1966).

[4] N. Hurduc, L. Odochian, E. Segal et I. A. Schneider, *Z. phys. Chem.* (*Leipzig*), **237**, 90 (1968).

[5] E. Schönberger, D. Fătu et E. Segal, *Rev. Roumaine Chim.*, **12**, 1205 (1967).

[6] J. R. Allan, D. H. Brown et D. W. A. Sharp, « Proceedings of the first international conference on thermal analysis » Aberdeen, Sootland, MacMillan Co, LTD, Londres, 1965, p. 138.

Nous considérons qu'il est intéressant de vérifier cette séquence, rencontrée aussi dans le cas des combinaisons complexes des halogénures de nickel et de cobalt, pour les combinaisons complexes du chlorure de manganèse avec les picolines. De même, il est utile de déterminer les paramètres cinétiques pour toutes les réactions intermédiaires jusqu'à la formation du chlorure de manganèse, y compris pour celles correspondant à la décomposition du complexe tétrapyridinique.

Les réactions étudiées correspondent au schéma général suivant

$$\mathrm{A\,(S)} \rightarrow \mathrm{B\,(S)} + \mathrm{C\,(g)}$$

Les paramètres cinétiques ont été déterminés par les méthodes de Freeman-Carroll [7] et Coats-Redfern.[8]

PARTIE EXPÉRIMENTALE

On a utilisé :

— du complexe tétrapyridinique du chlorure de manganèse Mn Py_4Cl_2 ;

— du complexe tétra β-picolinique du chlorure de manganèse Mn $(\beta\text{-pic})_4Cl_2$;

— du complexe tétra γ-picolinique du chlorure de manganèse $Mn(\gamma\text{-pic})_4Cl_2$, préparés par la méthode standard de précipitation, à partir de solutions aqueuses saturées de chlorure de manganèse avec de la pyridine ou de la picoline. Les combinaisons complexes avec un contenu intermédiaire de ligand ont été obtenues par la décomposition thermique des combinaisons complexes $Me^{II}L_4Cl_2$.

Les substances les plus riches en ligand ont été passées au mortier et sortées à l'aide du tamis ; on a retenu les grains de diamètre compris entre 0,1 et 0,09 mm. Les courbes thermogravimétrique (TG), thermogravimétrique dérivée (DTG) et de température (T) ont été enregistrées simultanément grâce à un dérivatographe MOM Budapest, type Paulik. Paulik-Erdey.

RÉSULTATS ET DISCUSSIONS

On présente les valeurs des paramètres cinétiques obtenues pendant l'étude de la décomposition thermique des combinaisons complexes mentionnées plus haut, en indiquant la réaction, la valeur m_p de la quantité de poudre utilisée, la vitesse d'échauffement $\frac{\mathrm{d}T}{\mathrm{d}t}$, la température de réaction t_r, conventionnellement considérée comme température correspondant à la valeur maximale de la vitesse de décomposition déduite de la courbe DTG, l'ordre de réaction n, l'énergie d'activation E et le facteur préexponentiel A. Dans le cas des réactions d'ordre zéro, on indique non seulement la valeur expérimentale A_{exp}, mais aussi la valeur calculée A_{calc}, suivant la formule [9]

$$A_{\mathrm{calc}} = \frac{1}{\beta}\, 1^2 \nu \, \frac{9\, w_c}{r^2} \qquad (1)$$

---

[7] E. S. FREEMAN et B. CARROLL, *J. Phys. Chem.*, **62**, 394 (1958).

[8] A. W. COATS et J. P. REDFERN, *Nature*, **201**, 68 (1964).

[9] I. G. MURGULESCU et E. SEGAL, *Rev. Roumaine Chim.*, **10**, 307 (1965).

où β représente le rapport entre la quantité de composant volatil qui peut être éliminé de la réaction et la quantité de poudre décomposée ; l est approximé par la valeur moyenne de la constante réticulaire ($l = 10$ Å) ; ν représente la fréquence de vibration des molécules du composant volatil du réseau, habituellement considérée égale à $6.10^{12}\ \mathrm{s^{-1}}$; r est le rayon moyen du grain cristallin et w_c — la quantité de composant volatil qui peut être éliminée pendant la réaction.

La formule (1) a été déduite en considérant comme étape limitante la diffusion du composant volatil à travers la couche de substance décomposée.

Le complexe tétrapyridinique du chlorure de manganèse instable du point de vue thermique perd deux molécules de pyridine pendant le traitement antérieur à l'expérience ainsi que pratiquement, c'est avec la décomposition du complexe dipyridinique qu'on a commencé l'étude cinétique.

Les réactions étudiées, les conditions de travail, ainsi que les valeurs des paramètres cinétiques sont les suivantes :

Méthode de Freeman-Carroll	*Méthode de Coats-Redfern*
$\mathrm{Mn\,Py_2Cl_2(s) \rightarrow MnPyCl_2(s) + Py(g)}$ (I)	
$m_p = 0{,}0726$ g	$m_p = 0{,}0730$ g
$\dfrac{dT}{dt} = 10°\ \mathrm{K/mn}$	$\dfrac{dT}{dt} = 2°\mathrm{K/mn}$
$t_r = 195°$	
$n = \dfrac{1}{2}$	$n = \dfrac{1}{2}$
$E = 23$ kcal/mole	$E = 25$ kcal/mole
$A = 8{,}13.10^6 \mathrm{g^{1/2}\,s^{-1}}$	$A = 1{,}67.10^7\ \mathrm{g^{1/2}s^{-1}}$
$\mathrm{Mn\,Py\,Cl_2(s) \rightarrow Mn\,Py\,2/3\,Cl_2(s)} + \dfrac{1}{3}\mathrm{Py\,(g)}$ (II)	
$m_p = 0{,}0524$ g	$m_p = 0{,}0527$ g
$\dfrac{dT}{dt} = 10°\,\mathrm{K/mn}$	$\dfrac{dT}{dt} = 2°\mathrm{K/mn}$
$t_r = 290°$	
$n = \dfrac{1}{2}$	$n = 1/2$
$E = 42$ kcal/mole	$E = 41{,}6$ kcal/mole
$A = 3{,}16.10^{13}\ \mathrm{g^{1/2}s^{-1}}$	$A = 8{,}75.10^{13}\ \mathrm{g^{1/2}s^{-1}}$

Méthode de Freeman-Carroll	*Méthode de Coats-Redfern*

$$\mathrm{Mn\,Py\,2/3\,Cl_2(s) \rightarrow MnCl_2(s) + 2/3\,Py(g)} \qquad \mathbf{(III)}$$

$m_p = 0{,}0456$ g	$m_p = 0{,}0456$ g
$\dfrac{dT}{dt} = 10°\mathrm{K/mn}$	$\dfrac{dT}{dt} = 10°\mathrm{K/mn}$
$t_r = 354°$	
$n = 1$	$n = 1$
$E = 36$ kcal/mole	$E = 35$ kcal/mole
$A = 2{,}85.10^{10}\,\mathrm{s^{-1}}$	$A = 1{,}9.10^{9}\,\mathrm{s^{-1}}$

$$\mathrm{Mn(\beta-pic)_4Cl_2(s) \rightarrow Mn(\beta-pic)_2Cl_2(s) + 2\,\beta-pic(g)} \qquad \mathbf{(IV)}$$

$m_p = 0{,}0726$ g	$m_p = 0{,}0728$ g
$\dfrac{dT}{dt} = 10°\mathrm{K/mn}$	$\dfrac{dT}{dt} = 2°\mathrm{K/mn}$
$t_r = 137°$	
$n = 0$	$n = 0$
$E = 10{,}5$ kcal/mole	$E = 11{,}4$ kcal/mole
$A_{\mathrm{exp}} = 6{,}46.10^{2}\,\mathrm{g\,s^{-1}}$	$A_{\mathrm{exp}} = 4.10^{2}\,\mathrm{g\,s^{-1}}$

$$A_{\mathrm{calc}} = 2{,}12.10^{3}\,\mathrm{g\,s^{-1}}$$

$$\mathrm{Mn(\beta-pic)_2\,Cl_2(s) \rightarrow Mn(\beta-pic)Cl_2(s) + \beta-pic\,(g)} \qquad \mathbf{(V)}$$

$m_p = 0{,}0453$ g	$m_p = 0{,}0453$ g
$\dfrac{dT}{dt} = 10°\mathrm{K/mn}$	$\dfrac{dT}{dt} = 2°\mathrm{K/mn}$
$t_r = 184°$	
$n = 1/3$	$n = 1/3$
$E = 18{,}75$ kcal/mole	$E = 19{,}20$ kcal/mole
$A = 3{,}16.10^{6}\,\mathrm{g^{2/3}s^{-1}}$	$A = 1{,}31\ 10^{7}\,\mathrm{g^{2/3}s^{-1}}$

Méthode de Freeman-Carroll	*Méthode de Coats-Redfern*

$$\mathrm{Mn(\beta-pic)\,Cl_2(s) \rightarrow Mn(\beta-pic)\,2/3\,Cl_2(s) + \frac{1}{3}\,\beta-pic(g)} \qquad \mathbf{(VI)}$$

$m_p = 0{,}0323$ g	$m_p = 0{,}0323$ g
$\dfrac{dT}{dt} = 10°\mathrm{K/mn}$	$\dfrac{dT}{dt} = 10°\mathrm{K/mn}$
$t_r = 252°$	

$$n = \frac{1}{2} \qquad\qquad n = \frac{1}{2}$$

$$E = 34 \text{ kcal/mole} \qquad\qquad E = 33 \text{ kcal/mole}$$

$$A = 2{,}5 . 10^{9} \ g^{1/2}s^{-1} \qquad\qquad A = 2{,}3 . 10^{10} g^{1/2}s^{-1}$$

$$\text{Mn} (\beta - \text{pic})\, 2/3\, \text{Cl}_2(s) \rightarrow \text{MnCl}_2(s) + 2/3\ \beta - \text{pic}(g) \qquad \text{(VII)}$$

$$m_p = 0{,}0282 \text{ g} \qquad\qquad m_p = 0{,}0282 \text{ g}$$

$$\frac{dT}{dt} = 10°\text{K/mn} \qquad\qquad \frac{dT}{dt} = 10°\text{K/mn}$$

$$t_r = 339°$$

$$n = \frac{2}{3} \qquad\qquad n = \frac{2}{3}$$

$$E = 38{,}4 \text{ kcal/mole} \qquad\qquad E = 39{,}6 \text{ kcal/mole}$$

$$A = 5{,}77 . 10^{10} g^{1/3}s^{-1} \qquad\qquad A = 4{,}34 . 10^{11} g^{1/3}s^{-1}$$

$$\text{Mn} (\gamma - \text{pic})_4 \text{Cl}_2(s) \rightarrow \text{Mn} (\gamma - \text{pic})_2\text{Cl}_2(s) + 2\gamma - \text{pic}(g) \qquad \text{(VIII)}$$

$$m_p = 0{,}0724 \text{ g} \qquad\qquad m_p = 0{,}0723 \text{ g}$$

$$\frac{dT}{dt} = 10°\text{K/mn} \qquad\qquad \frac{dT}{dt} = 2°\text{K/mn}$$

$$t_r = 148°$$

$$n = \frac{1}{2} \qquad\qquad n = \frac{1}{2}$$

$$E = 16{,}6 \text{ kcal/mole} \qquad\qquad E = 15{,}6 \text{ kcal/mole}$$

$$A = 2 . 10^{6} \ g^{1/2}s^{-1} \qquad\qquad A = 8{,}6 . 10^{5} \ g^{1/2}s^{-1}$$

Méthode de Freeman-Carroll *Méthode de Coats-Redfern*

$$\text{Mn}(\gamma - \text{pic})_2\text{Cl}_2(s) \rightarrow \text{Mn} (\gamma - \text{pic})\text{Cl}_2(s) + \gamma - \text{pic}(g) \qquad \text{(IX)}$$

$$m_p = 0{,}0453 \text{ g} \qquad\qquad m_p = 0{,}0453 \text{ g}$$

$$\frac{dT}{dt} = 10°\text{K/mn} \qquad\qquad \frac{dT}{dt} = 10°\text{K/mn}$$

$$t_r = 185°$$

$$n = \frac{1}{2} \qquad\qquad n = \frac{1}{2}$$

$E = 19{,}9$ kcal/mole	$E = 20{,}6$ kcal/mole
$A = 6{,}6 . 10^6 g^{1/2} s^{-1}$	$A = 2{,}17 . 10^5 g^{1/2} s^{-1}$

$$\mathrm{Mn}\,(\gamma - \mathrm{pic})\,\mathrm{Cl_2(s)} \rightarrow \mathrm{Mn}(\gamma - \mathrm{pic})\ 2/3\ \mathrm{Cl_2(2)} + \frac{1}{3}\gamma - \mathrm{pic(g)} \qquad \text{(X)}$$

$m_p = 0{,}0318$ g	$m_p = 0{,}0318$ g
$\frac{dT}{dt} = 10°K/mn$	$\frac{dT}{dt} = 10°K/mn$
$t_r = 294°$	
$n = \frac{1}{2}$	$n = \frac{1}{2}$
$E = 42$ kcal/mole	$E = 41$ kcal/mole
$A = 5{,}5 . 10^{11} g^{1/2} s^{-1}$	$A = 8{,}47 . 10^{11} g^{1/2} s^{-1}$

$$\mathrm{Mn}\,(\gamma - \mathrm{pic})\ 2/3\ \mathrm{Cl_2(s)} \rightarrow \mathrm{MnCl_2(s)} + 2/3\ \gamma - \mathrm{pic(g)} \qquad \text{(XI)}$$

$m_p = 0{,}273$ g	$m_p = 0{,}0273$ g
$\frac{dT}{dt} = 10°K/mn$	$\frac{dT}{dt} = 10°K/mn$
$t_r = 355°$	
$n = 1$	$n = 1$
$E = 28{,}5$ kcal/mole	$E = 30$ kcal/mole
$A = 3{,}89 . 10^7 s^{-1}$	$A = 1{,}75 . 10^8 s^{-1}$

En analysant les données présentées, on remarque que les valeurs des paramètres cinétiques obtenues par les deux méthodes concordent de façon satisfaisante. L'ordre de réaction varie entre zéro et l'unité, augmentant à mesure qu'on décompose des combinaisons complexes avec un contenu de plus en plus réduit de ligand. Cette augmentation de l'ordre de réaction est un phénomène général rencontré dans toutes les études cinétiques similaires et peut être expliquée par l'augmentation du degré de dispersion des corpuscules soumis à la décomposition par l'élimination du composant volatil.[10] Si pour les corpuscules avec un degré réduit de dispersion, c'est la diffusion du composant volatil à travers la couche de substance décomposée qui est l'étape limitante, à mesure que le degré de dispersion augmente (tendant à la limite vers la dispersion moléculaire), on commence à ressentir l'influence du processus chimique, l'ordre de réaction ayant des valeurs croissantes comprises entre zéro et l'unité. La valeur constante de l'ordre de réaction dans les processus (I) et (II), ainsi que (VIII), (IX), (X), s'explique par le fait que l'augmentation de température peut être accompagnée par un phénomène qui empêche l'augmentation du degré de dispersion, le frittage.

---

[10] I. G. Murgulescu et E. Segal, *Rev. Roumaine Chim.*, **11**, 13 (1966).

Pendant la décomposition du complexe tétra-β-picolinique du chlorure de manganèse (réaction IV), la courbe de la vitesse de réaction (DTG) présente une discontinuité dans l'intervalle de température 92° ... 104° ; c'est comme si le processus, au lieu d'être unique, avait lieu en deux étapes. En réalité, dans cet intervalle, il se passe une transformation de phase endotherme réversible (pendant le refroidissement la chaleur absorbée se dégage – phénomène enregistré sur la courbe par un effet exothermique) ; cette transformation se superpose au processus de décomposition et peut être attribuée à une modification de la structure cristalline ou isomérisation *cis-trans*. La quantité de chaleur supplémentaire absorbée pendant ce processus, détermine une baisse de la température de la substance et de la vitesse, ce qui mène à l'apparition de discontinuités sur les courbes TG (effet plus difficile à remarquer) et DTG. Dans ces conditions, les mesures cinétiques ont été effectuées sur les portions de courbe correspondant à des températures supérieures à 104°, température à laquelle s'achève la transformation supplémentaire.

CONCLUSIONS

1. La décomposition des combinaisons complexes pyridiniques et picoliniques du chlorure de manganèse suit des séquences similaires de réactions qui se déroulent à mesure que la température augmente.

2. L'ordre de réaction varie entre zéro et l'unité, indiquant la transition du domaine de diffusion au domaine cinétique.

3. La valeur expérimentale du facteur préexponentiel de la réaction (IV) concorde de façon satisfaisante avec la valeur calculée à l'aide de la formule (1), établie dans l'hypothèse que le processus se passe dans le domaine de la diffusion interne du composant volatil à travers la couche de substance décomposée du grain cristallin.

Revue Roumaine de Chimie, **14**, 709–715 (1969)

Revue Roumaine de Chimie, 14, 717 – 720 (1969)

DIE BILDUNG DER GALLOSILICAT-NIEDERSCHLÄGE IN WÄSSRIGEN LÖSUNGEN

RALUCA RIPAN und MILOSLAVA KULCSÁR-NOVÁKOVÁ

vom Chemischen Institut der Akademie, Zweigstelle Cluj, str. Donath, 59—65

Eingegangen am 6. Januar 1969

Unter den im Lösungsgemisch von Galliumchlorid und Natriumsilicat erhaltenen Niederschlägen entsteht in schwach saurem Medium beim Verhältnis Ga: Si 1 : 1 ein Gel der Zusammensetzung $Ga_2O_3.2SiO_2.nH_2O$ welches mit dem aluminosilicatischen Gel $Al_2O_3.2SiO_2.nH_2O$ analog ist.

In der vorangehenden Arbeit[1] hat man mit Hilfe der potentiometrischen und konduktometrischen Methode in wäßriger Lösung von Galliumchlorid und Natriumsilicat die Möglichkeit der Bildung einer Verbindung, deren empirische Formel $Ga_2O_3.2SiO_2.nH_2O$ entspricht, festgestellt. Dieses Studium beschäftigt sich mit der Untersuchung der Bildung der Niederschläge in der Lösung, die Galliumchlorid und Natriumsilicat enthält, bei verschiedenen Verhältnissen von Ga : Si in der ursprünglichen Lösung (2 : 1 ; 1 : 1 ; 1 : 2 und 1 : 4), bei pH gleich 3, 7, und 9 und Temperaturen von 20° und 90°.

Zur Herstellung der wäßr. Galliumchloridlösung hat man metallisches Gallium *p.a* verwendet, die Natriumsilicatlösung wurde aus $Na_2SiO_3.9H_2O$ *p.a.* hergestellt. Für einen Versuch hat man 20 ml der Galliumchloridlösung verwendet, die 0,2 g Ga enthielt ; zu dieser hat man Na_2SiO_3-Lösung dem gewünschten Ga : Si Verhältnis nach (2 : 1, 1 : 1, 1 : 2, 1 : 4) zugesetzt. Das pH wurde mit verd. Salzsäure bzw. Natriumhydroxid eingestellt. Das Gesamtvolumen der Lösung betrug 60 ml. Die bei 20° ausgeführten Versuche (Tabelle 1) wurden 8 Stunden lang, die bei 90° (Tabelle 2) 12 Stunden lang unter Rührung gehalten, dann die Niederschläge abfiltriert, 3 mal mit je 10 ml Wasser gewaschen und über $CaCl_2$ getrocknet.

Der Gehalt an SiO_2 wurde klassisch, durch Fällung als SiO_2, der an Gallium gravimetrisch, durch Fällung mit 5,7-Dibrom-8-Oxychinolin,[2] der an Natrium flammenphotometrisch bestimmt.

Bei der Betrachtung der chemischen Zusammensetzung der erhaltenen Niederschläge sieht man, daß bei 20° (Tabelle 1) ein Niederschlag der Zusammensetzung $Ga_2O_3.2SiO_2.nH_2O$ nicht nur beim Verhältnis von Ga : Si gleich 1 : 1 bei pH 3 entsteht, sondern auch bei Ga : Si gleich

---

[1] R. Ripan, M. Kulcsár-Nováková und G. J. Kulcsár, *Rev. Roumaine Chim.*, **11**, 1285 (1966).

[2] E. Gastinger, *Z. analyt. Chem.* **126**, 373 (1944).

Tabelle 1

Zusammensetzung der bei 20° erhaltenen Niederschläge

Lfd. Nr.	Ga : Si in ursprüngl. Lösung	pH	Zusammensetzung, %			Empirische Formel
			Ga_2O_3	SiO_2	Na_2O	
1	2 : 1	3	45,94	30,64	Spuren	$Ga_2O_3.2,08SiO_2.nH_2O$
2	2 : 1	7	55,65	17,78	2,67	$0,14Na_2O.Ga_2O_3.1,00SiO_2.nH_2O$
3	2 : 1	9	47,07	24,07	8,92	$0,57Na_2O.Ga_2O_3\ 1,60SiO_2.nH_2O$
4	1 : 1	3	43,58	28,77	Spuren	$Ga_2O_3.2,06SiO_2.nH_2O$
5	1 : 1	7	45,13	28,49	4,94	$0,33Na_2O.Ga_2O_3.1,97SiO_2.nH_2O$
6	1 : 1	7	46,91	29,72	4,83	$0,31Na_2O.Ga_2O_3.1,98SiO_2.nH_2O$
7	1 : 1	9	36,56	33,53	10,45	$0,86Na_2O.Ga_2O_3.2,86SiO_2.nH_2O$
8	1 : 1	9	41,88	34,16	7,98	$0,58Na_2O.Ga_2O_3.2,61SiO_2.nH_2O$
9	1 : 2	3	30,27	41,86	Spuren	$Ga_2O_3.4,16SiO_2.nH_2O$
10	1 : 2	7	28,06	40,15	7,23	$0,78Na_2O.Ga_2O_3.4,46SiO_2.nH_2O$
11	1 : 2	9	29,93	38,69	9,42	$0,99Na_2O.Ga_2O_3.4,17SiO_2.nH_2O$
12	1 : 4	3	19,20	49,54	8,14	$1,28Na_2O.Ga_2O_3.8,05SiO_2.nH_2O$
13	1 : 4	3	18,61	51,67	2,67	$0,47Na_2O.Ga_2O_3.8,68SiO_2.nH_2O$
14	1 : 4	7	17,40	46,21	12,97	$2,25Na_2O.Ga_2O_3.8,29SiO_2.nH_2O$
15	1 : 4	7	19,93	48,82	5,48	$0,83Na_2O.Ga_2O_3.7,56SiO_2.nH_2O$
16	1 : 4	9	24,19	52,91	7,34	$0,73Na_2O.Ga_2O_3.6,82SiO_2.nH_2O$
17	1 : 4	9,5–9,7	18,93	47,25	10,63	$1,70Na_2O.Ga_2O_3.7,79SiO_2.nH_2O$

Tabelle 2

Zusammensetzung der bei 90° erhaltenen Niederschläge

Lfd. Nr.	Ga : Si in ursprüngl. Lösung	pH	Zusammensetzung %			Empirische Formel
			Ga_2O_3	SiO_2	Na_2O	
1	2 : 1	3	49,57	31,49	Spuren	$Ga_2O_3.1,98SiO_2.nH_2O$
2	2 : 0,78	7	63,34	15,42	2,82	$0,13Na_2O.Ga_2O_3.0,76SiO_2.nH_2O$
3	2 : 1	9	39,89	32,53	8,11	$0,62Na_2O.Ga_2O_3.2,55SiO_2.nH_2O$
4	1 : 1	3	47,98	29,86	Spuren	$Ga_2O_3.1,94SiO_2.nH_2O$
5	1 : 1	7	48,56	31,29	5,16	$0,32Na_2O.Ga_2O_3.2,01SiO_2.nH_2O$
6	1 : 1	9	38,14	35,29	9,43	$0,75Na_2O.Ga_2O_3.2,89SiO_2.nH_2O$
7	1 : 2	3	34,75	42,16	Spuren	$Ga_2O_3.3,86SiO_2.nH_2O$
8	1 : 2	7	33,95	43,12	6,77	$0,60Na_2O.Ga_2O_3.3,96SiO_2.nH_2O$
9	1 : 2	9	28,85	45,16	9,49	$0,99Na_2O.Ga_2O_3.4,89SiO_2.nH_2O$
10	1 : 4	3	21,47	54,96	3,18	$0,45Na_2O.Ga_2O_3.7,99SiO_2.nH_2O$
11	1 : 4	7	19,53	55,71	6,65	$1,00Na_2O.Ga_2O_3.8,90SiO_2.nH_2O$
12	1 : 4	9	24,90	52,87	8,01	$0,97Na_2O.Ga_2O_3.6,63SiO_2.nH_2O$

2 : 1 in ursprünglicher Lösung bei pH 3, der Überschuß an Gallium in der Lösung bleibt. Wenn es sich um ein mechanisches Gemisch der Gele von Galliumhydroxid und Siliziumdioxid handeln würde, wäre die Erhaltung

des Niederschlages der Zusammensetzung $Ga_2O_3 . 2SiO_2 . nH_2O$ in schwach sauren Bedingungen kaum möglich, der Galliumgehalt wäre niedriger. Bei der Temperatur von 90° (Tabelle 2) hat man dieselben Ergebnisse erhalten. Bei pH 7 und der Zusammensetzung der Lösung Ga : Si gleich 2 : 1, fällt auch das nichtreagierte Gallium in Form von Hydroxid aus.

Die Niederschläge aus der Lösung mit Ga : Si 1 : 1 bei pH 7 zeigen einen gut reproduzierbaren Na_2O—Gehalt an; bei pH 9 deutet die chemische Zusammensetzung auf die Ähnlichkeit mit dem von Selbin und Mason [3] beschriebenen zeolytischen Gallosilicatmolekularsieb.

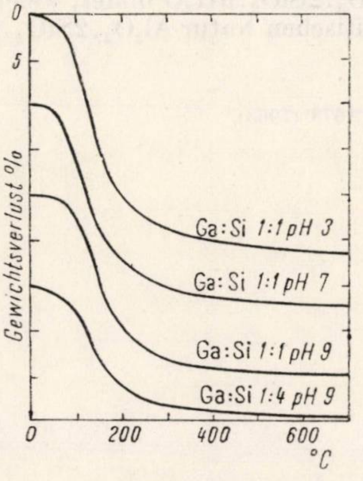

Abb. 1. — Thermogravimetrische Analyse der Proben 4, 6, 8, 17. (Tabelle 1)

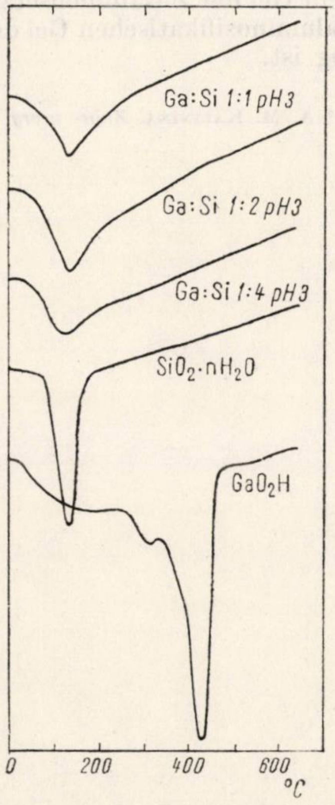

Abb. 2. — Thermodifferentielle Analyse der Proben 4, 9, 13. (Tabelle 1.) $SiO_2 . nH_2O$ und GaO_2H.

Bei den Verhältnissen von Ga : Si 1 : 2 und 1 : 4 müssen die erhaltenen massiven Niederschläge als Gemische von $Ga_2O_3 . 2SiO_2 . nH_2O$, SiO_2nH_2O und zeolytischen Niederschlägen usw. betrachtet werden. An den Wänden des Reaktionsgefäßes hat sich eine Kruste gebildet, was die Zusammensetzung des Niederschlages weitgehend beeinflussen kann.

Die thermogravimetrische Untersuchung (Abb. 1) zeigt die kontinuierliche Wasserabgabe an (Tabelle 1. Proben 4, 6, 8, 17).

---

[3] J. Selbin und R. B. Mason *J. Inorg. Nuclear Chem.*, **20**, 222 (1961).

Die thermodifferentielle Untersuchung (Abb. 2) des Niederschlages der Zusammensetzung $Ga_2O_3.2SiO_2nH_2O$ zeigt im Vergleich mit freiem Galliumhydroxid, keine endotherme Effekte die für dieses spezifisch sind. Die bei pH 3 aus den Lösungen von Ga : Si 1 : 2 und 1 : 4 gefällten Niederschläge benehmen sich ähnlich.

Die Röntgenogramme nach Debye-Scherer haben keine kristalline Struktur erwiesen.

Aus den angeführten Daten folgt, daß im schwach sauren Medium (pH 3) aus den Lösungen, die Galliumchlorid und Natriumsilicat in Molverhältnis 1 : 1 oder einen Überschuß an Galliumsalz enthalten, sich ein Gel der Zusammensetzung $Ga_2O_3.2SiO_2.nH_2O$ bildet, welches mit dem aluminosilikatischen Gel der kaolinitischen Natur $Al_2O_3.2SiO_2.nH_2O$ [4] analog ist.

---

[4] A. M. KALININA, *Zhur. neorg. Khim.*, **8**, 1678 (1963).

Revue Roumaine der Chimie, **14**, 721–727 (1969)

WÄRMEÜBERGANGSZAHLEN BEIM SIEDEN VON LÖSUNGEN

LÖSUNGEN VON MONONATRIUMPHOSPHAT

Z. GROPŞIANU, D. KOHN und A. IOVI

von der Fakultät für Angewandte Chemie an der Technischen Hochschule
Timişoara, Bdul 30 Decembrie, 2

Eingegangen am 4. September 1968

Es wurden experimentelle Untersuchungen zur Bestimmung der Wärmeübergangszahl beim Sieden der Lösungen von Mononatriumphosphat bei Atmosphärendruck und bei einem Druck von 300 mmHg durchgeführt. Auf Grund der Versuchsergebnisse wurden Gleichungen zur Berechnung der Wärmeübergangszahl α beim Sieden in Abhängigkeit von der Heizflächenbelastung, Temperaturdifferenz und Konzentration aufgestellt.

Mit dem Wärmeübergang beim Sieden beschäftigen sich zahlreiche Forscher zwecks Klärung verschiedener Aspekte dieses Vorgangs. Die Hauptrichtungen der Untersuchungen sind Klärung des Mechanismus beim Sieden und Aufstellung einiger Gleichungen von allgemeiner Gültigkeit, bzw. Untersuchungen über das Verhalten beim Sieden und Festsetzen der Wärmeübergangszahlen, sowie der kritischen Belastung für verschiedene Stoffe.[1–14] Infolge der Bedeutung, welche der Siedevorgang des Wassers in den verschiedenen Industriezweigen hat, wurden darüber

---

[1] E. I. Nesis, *Uspekhi Fiz. Nauk*, **87**, 615 (1955).

[2] T. B. Drew und J. W. Hoopes „Advances in Chemical Engineering", 1. und 2. Bd., Acad. Press, New York, 1956, S. 1.

[3] M. Miheev, „Fundamentals of Heat Transfer" (Translated from the russian), Peace Publishers, Moskau, S. 116.

[4] C. C. Kutateladze, „Teploperedacha pri kondens i kipenii", Maşghiz, Moskau, 1952, S. 3.

[5] D. A. Labuntsov, *Teploenergetica*, **10**, 60 (1963).

[6] A. A. Ivashkevich, *Teploenergetica*, **8**, 74 (1961).

[7] F. Brauer, *Chem.-Ing.-Tech.*, **35**, 764 (1963).

[8] K. Stephan, *Chem.-Ing.-Tech.*, **35**, 775 (1963).

[9] E. Ruckenstein, *Internat. J. Heat Mass Transfer*, **7**, 191 (1964).

[10] Yan Po Chang, *Trans. ASME.*, **79**, 1501 (1957).

[11] S. Levy, *J. Heat Transfer*, **81**, 37 (1959).

[12] W. R. Van Wijk und S. J. D. Van Stralen, *Chem.-Ing.-Tech.*, **37**, 509 (1965).

[13] W. R. Gambill, *Brit. Chem. Eng.*, **8**, 93 (1963).

[14] J. Starczevski, *Brit. Chem. Eng.*, **10**, 523 (1965).

zahlreiche Untersuchungen ausgeführt.[15-18] Auf Grund einiger Überlegungen betreffend den Mechanismus des Siedevorgangs, wurden eine Reihe Gleichungen zur Berechnung der Wärmeübergangszahl aufgestellt.[2-7, 10, 11] Dieses setzt jedoch die Kenntnis der physikalischen Konstanten der Stoffe, sowie einiger charakteristischen Größen des Siedevorgangs voraus (Durchmesser der Bläschen, Häufigkeit mit der sich die Bläschen bilden, usw.). Die Werte der Wärmeübergangszahlen beim Sieden, die mit Hilfe dieser Gleichungen berechnet wurden, stimmen in vielen Fällen mit den experimentell bestimmten ziemlich wenig überein [2, 19, 20] und die Abweichungen sind ziemlich bedeutend. Bei sehr vielen Industrieverfahren ist das Konzentrieren der Lösungen durch Verdampfen eine Phase von allergrößter Bedeutung. Zur Projektierung der Anlagen vom thermischen Gesichtspunkt aus, ist es notwendig, die Wärmeübergangszahl zu kennen. Die Berechnung des Koeffizienten α beim Sieden der Lösungen anorganischer Salze [3] setzt die Kenntnis mehrerer physikalischer Konstanten voraus, welche für die meisten Lösungen gänzlich oder teilweise fehlen. Die Bestimmung dieser physikalischen Konstanten bereitet vor allem im Falle konzentrierter Lösungen Schwierigkeiten. Andererseits besteht zwischen dem berechneten Wert (wenn diese Konstanten vorhanden sind) und dem experimentell bestimmten keine genügende Übereinstimmung.[21] Die Wärmeübergangszahl beim Sieden der Lösungen, welche auf komplexe Art von deren Natur abhängt, kann als solche als eine physikalische Größe betrachtet werden, welche die Lösung vom Gesichtspunkt des Wärmeübergangs beim Sieden kennzeichnet. Folglich ist die experimentelle Bestimmung und die Aufstellung von spezifischen Gleichungen umso angezeigter.

In der vorliegenden Arbeit wurde die experimentelle Bestimmung der Wärmeübergangszahlen beim Sieden der wäßrigen Lösungen von Mononatriumphosphat und die Aufstellung von Gleichungen zur Berechnung derselben verfolgt.

Mononatriumphosphat ist ein wichtiges Produkt, welches als solches auf den verschiedensten Gebieten oder zur Herstellung von Dinatriumpyrophosphat und Natriummetaphosphaten verwendet wird.[22] Mononatriumphosphat wird durch Neutralisation von Extraktionsphosphorsäure mit Natriumkarbonat erhalten. Die verdünnte Lösung, welche bei den meisten Verfahren erhalten wird, konzentriert man auf 40–50%.[22-23]

In den experimentellen Bestimmungen wurde gerade die Veränderung des Koeffizienten α beim Sieden für verschiedene Konzentrationen bis zu 50% verfolgt. Es wurde bei Atmosphärendruck und bei

---

[15] A. S. Konikov und I. D. Barulin, *Teploenergetică*, **13**, 82 (1966).

[16] K. Stephan, *Chem.-Ing.-Tech.*, **38**, 112 (1966).

[17] D. B. Kirby und J. W. Westwater, *Chem. Eng. Progr., Symp.*, **61**, 238 (1963).

[18] F. Müller, „Wärmeübergang bei der Verdampfung unter hohen Drücken", (Dissertation), Berlin, 1966.

[19] M. M. Kuznetsov und B. A. Burakov, *Teploenergetica*, **13**, 70 (1966).

[20] D. A. Huber und J. C. Hoehne, *J. Heat Transfer*, **85**, ser. C, 215 (1963).

[21] Z. Gropşianu, D. Kohn und A. Iovi, *Rev. Roumaine Chim.*, (unter Druck).

[22] A. Iovi, „Tehnologia acidului fosforic şi a fosfaţilor tehnici", Lit. I. P. Timişoara, 1967, S. 106.

[23] I. Samoil und M. Alexandroaie, *Rev. Chim. (Bucureşti)*, **16**, 473 (1965).

300 mmHg im Bereiche intensiven Siedens bei Heizflächenbelastungen zwischen $85 \cdot 10^3$ bis $57 \cdot 10^4$ W/m^2 gearbeitet.

Die Laboratoriumsvorrichtung und die Methode zur Bestimmung der Wärmeübergangszahlen beim Sieden der Lösungen wurden in früheren Arbeiten mitgeteilt.[21, 24]

Die Versuchsergebnisse sind in den Abbildungen 1 bis 7 dargestellt.

Die Untersuchungen über den Einfluß der Heizflächenbelastung auf die Wärmeübergangszahl beim Sieden, α, für verschiedene Konzentrationen der Lösung und bei Atmosphärendruck (Abb. 1) zeigen eine Zunahme des Koeffizienten α mit dem Anwachsen von q. Diese Abhängigkeit kann durch folgende Gleichung ausgedrückt werden:

$$\alpha = \varepsilon \cdot q^{0.7}$$

wo ε ein von der Konzentration abhängiger Koeffizient ist.

Bei gleichen Heizflächenbelastungen nimmt α mit dem Anwachsen der Konzentration ab. Die Konzentrationsabhängigkeit von ε ist in Abb. 2 dargestellt. Aus der graphischen Darstellung wurden folgende Gleichungen abgeleitet:

— für Konzentrationen bis zu 20%:

$$\varepsilon = 4{,}55 \cdot C^{-0.345}$$

— für Konzentrationen zwischen 20 und 50%:

$$\varepsilon = 9{,}22 \cdot C^{-0.575}$$

wo C die Konzentration der Lösung in Gewichtsprozenten darstellt.

Ein Vergleich der Versuchsergebnisse mit den durch theoretische Gleichungen berechneten Werten war nicht möglich infolge des Fehlens der physikalischen Konstanten für diese Lösungen.

Die Veränderung der Wärmeübergangszahl beim Sieden, α, in Abhängigkeit vom Temperaturunterschied Δt zwischen der Wandtemperatur und der Siedetemperatur der Lösung (Abb. 3) zeigt eine betonte Zunahme des Koeffizienten α mit dem Anwachsen von Δt für alle Konzentrationen.

Auf Grund der Versuchsergebnisse wurde zwischen α und Δt folgende Gleichung aufgestellt:

$$\alpha = \varepsilon_2 \,.\, \Delta t^{2.33}$$

wo ε_2 ein von der Konzentration der Lösung abhängiger Koeffizient ist.

Aus Abb. 4, in welcher die Veränderung von ε_2 in Abhängigkeit von der Konzentration dargestellt wird, ergibt sich eine Verminderung desselben und auch von α mit dem Anwachsen der Konzentration der Lösung.

Zwischen dem Koeffizienten ε_2 und der Konzentration C der Lösung wurden folgende Gleichungen aufgestellt:

— für Konzentrationen bis zu 20%:

$$\varepsilon_2 = 1{,}4 \cdot 10^2 \cdot C^{-1.125}$$

---

[24] Z. Gropșianu, D. Kohn und A. Iovi, *Rev. Roumaine Chim.*, **12**, 485 (1967).

— für Konzentrationen zwischen 20 und 50%:

$$\varepsilon_2 = 2{,}54 \cdot 10^3 \cdot C^{-2{,}07}$$

Die bei einem Druck von 300 mmHg durchgeführten experimentellen

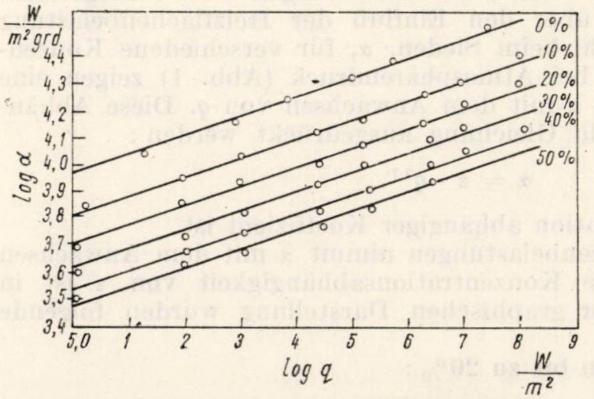

Abb. 1. — Veränderung von α in Abhängigkeit von bei atmosphärischem Druck, für Mononatriumphosphatlösungen verschiedener Konzentration.

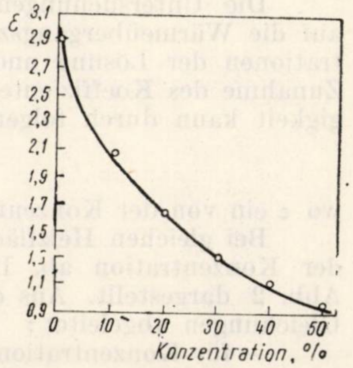

Abb. 2. — Abhängigkeit des Koeffizienten ε von der Konzentration der Mononatriumphosphatlösung.

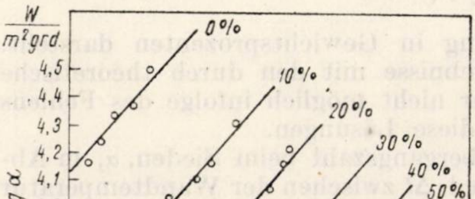

Abb. 3. — Veränderung von α in Abhängigkeit von Δt bei atmosphärischem Druck, für Mononatriumphosphatlösungen verschiedener Konzentration.

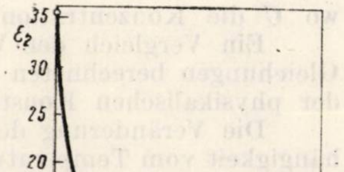

Abb. 4. — Abhängigkeit des Koeffizienten ε_2 von der Konzentration der Mononatriumphosphatlösung.

Bestimmungen, welche in Abb. 5 wiedergegeben sind, zeigen, daß α in diesem Falle mit dem Anwachsen von q für alle Konzentrationen zunimmt. Zwischen α und q wurde folgende Beziehung festgestellt:

$$\alpha = \varepsilon_1 \cdot q^{0{,}62}$$

wo ε_1 ein von der Konzentration abhängiger Koeffizient ist.

Die Abhängigkeit des Koeffizienten ε_1 von der Konzentration C der Lösung ist in Abb. 6 dargestellt. Die zwischen ε_1 und C festgestellten Beziehungen sind von folgender Form :

— für Konzentrationen bis zu 20% :

$$\varepsilon_1 = 9{,}88 \cdot C^{-0{,}25}$$

— für Konzentrationen zwischen 20 und 50% :

$$\varepsilon_1 = 24{,}4 \cdot C^{-0{,}55}$$

Die Werte von ε, ε_1 und ε_2 sind in Tabelle 1, die Gleichungen zur Berechnung der Wärmeübergangszahl beim Sieden, α, in Tabelle 2 angeführt.

Tabelle 1

Werte der Koeffizienten

Konzentration %	ε	ε_1	ε_2
0	2,915	—	35,5
10	2,065	5,57	10,53
20	1,628	4,65	4,89
30	1,302	3,8	2,35
40	1,096	3,25	1,24
50	0,951	2,785	0,775

Tabelle 2

Gleichungen

Konzentrationsbereich	Gleichung	Druck
unter 20%	$\alpha = 4{,}55 . C^{-0{,}345} . q^{0{,}7}$	760 mmHg
20–50%	$\alpha = 9{,}22 . C^{-0{,}575} . q^{0{,}7}$	760 mmHg
unter 20%	$\alpha = 9{,}88 . C^{-0{,}25} . q^{0{,}62}$	300 mmHg
20–50%	$\alpha = 24{,}4 . \mathrm{C}^{-0{,}55} . q^{0{,}62}$	300 mmHg
unter 20%	$\alpha = 1{,}4 . 10^2 . C^{-1{,}125} . \Delta t^{2{,}33}$	760 mmHg
20–50%	$\alpha = 2{,}54 . 10^3 . C^{-2{,}07} . \Delta t^{2{,}33}$	760 mmHg

Desgleichen wurden die Siedetemperaturen der Lösungen von Mononatriumphosphat in Abhängigkeit vom Druck bei verschiedenen Konzentrationen bestimmt. Die Versuchsergebnisse sind in Abb. 7 grapisch dargestellt.

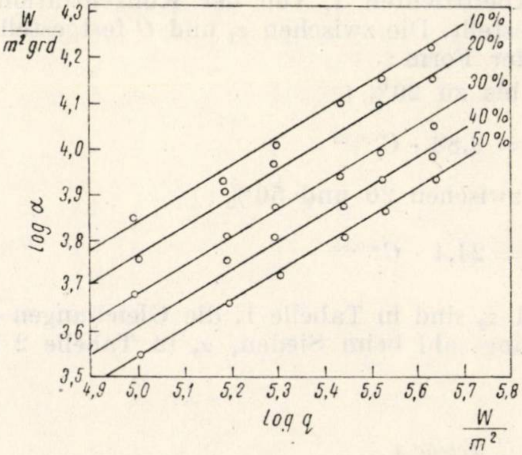

Abb. 5. — Veränderung von α in Abhängigkeit von q bei einem Druck von 300 mmHg, für Mononatriumphosphatlösungen verschiedener Konzentration.

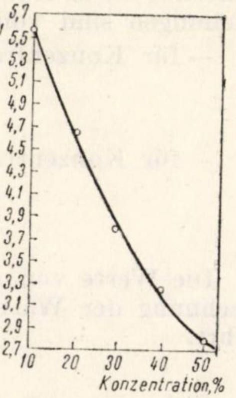

Abb. 6. — Abhängigkeit des Koeffizienten ε_1 von der Konzentration der Mononatriumphosphatlösung.

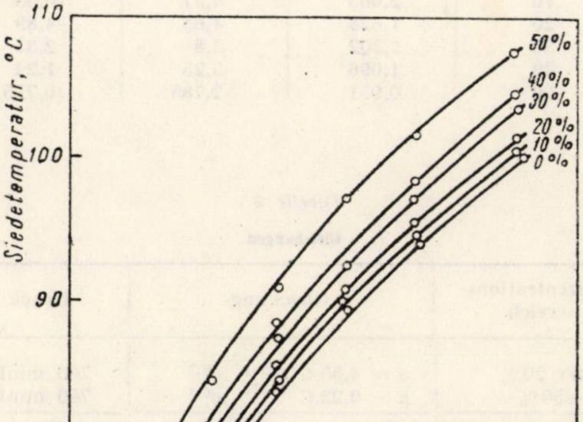

Abb. 7. — Siedetemperaturen der Mononatriumphosphatlösungen in Abhängigkeit vom Druck bei verschiedenen Konzentrationen.

SCHLUSSFOLGERUNGEN

Die mit Lösungen von Mononatriumphosphat durchgeführten experimentellen Untersuchungen ermöglichten es, Gleichungen zur Berechnung der Wärmeübergangszahl beim Sieden bei Atmosphärendruck und bei einem Druck von 300 mmHg aufzustellen.

Der Koeffizient α nimmt mit dem Anwachsen der Heizflächenbelastung q und der Temperaturdifferenz Δt zu, und vermindert sich umso mehr, je größer die Konzentration der Lösung wird.

Es wurden die Siedetemperaturen der Lösungen von Mononatriumphosphat in Abhängigkeit vom Druck für verschiedene Konzentrationen bestimmt.

Revue Roumaine de Chimie, 14, 729–736 (1969)

SOME QUANTITATIVE RELATIONS ON THE RADIOACTIVE MINERALS LEACHING PROCESSES

F. BUNUŞ, I. MATEI, C. MATYAS, S. NECIU, V. SPOREA and S. TĂTARU

Ministry of Mines, Division of Technological Research, Bucharest, str. Dionisie Lupu 68

Received September 10, 1968

An experimental work concerning the Uranium leaching processes in view of finding the most suitable leaching conditions, has been carried out. The grain size, the S/L ratio, reagent concentration, oxidant contribution, time interval, etc. have been determined and some surface adsorption phenomena leading to some unexpected behavior concerning Uranium dissolution have been found. The solution purity was considered and the final conclusions were drawn.

Uranium ore processing is actually carried out by two industria methods in view of obtaining a chemical concentrate suitable for the next manufacturing stages leading to a chemical compound or fuel of nuclear purity.

The industrial process most in use is based on ore treatment with an acid, usually sulphuric acid, in order to achieve the highest dissolution yield of Uranium followed by its recovery *via* an ion exchange method. Uranium is finally precipitated as diuranate.

Acid treatment is not recommended when carbonate content of Uranium ore is high due to the acid prohibitive consumption. In this alternative the alkaline leaching process is the only acceptable way. The chemical reagent selected for alkaline leaching was sodium carbonate in aqueous solution. The actual disadvantages involved in this process (long leaching time, small size grain, high temperature etc.) are largely compensated by small reagent consumption, solution purity and total omission of corrosion problems.

In the present study, experiments were performed on a Uranium ore sample with high carbonate content. The experimental work has been carried out using the two industrial processes (just mentioned) in view of defining the most suitable way for Uranium extraction.

Due to the basic character of the Uranium ore it is perhaps advisable to start our study with alkaline leaching process. In this description we are not able to dwell on all aspects of the problem, however important results, elucidating the new phenomena as the optimum leaching conditions will be dealt with.

Uranium dissolution is carried out at the same time with an oxidation process which takes place in a reaction vessel of pachucas type.

The atmospheric air is introduced at the bottom of the pachucas acting as a mixing agent for the pulp and at the same time achieving a good oxidation degree of the Uranium in tetravalent state. Sometimes the presence of a chemical oxidant is required.

Sulphur existent as sulphide (0.5—1.5%S) leads to an additional consumption of the reagent due to its oxidation to sulphate which attends Uranium in solution as sodium sulphate. The chemical reaction between Sulphur (as sulphide) and sodium carbonate yields to sodium bicarbonate among other reaction products, whose presence is required to maintain a constant pH.

The chemical reactions responsible for Uranium minerals dissolution are the following[1, 2]:

$$UO_3 + 3CO_3^{--} + H_2O \rightarrow [UO_2(CO_3)_3]^{4-} + 2OH^-$$

$$UO_2 + 1/2O_2 + 3CO_3^{--} + H_2O \rightarrow [UO_2(CO_3)_3]^{4-} + 2OH^-$$

An increase of the pH value is expected due to the OH^- ions, which leads to an eventual decomposition of the uranyltricarbonate complex resulting in precipitation losses.

This process is offset by sodium bicarbonate, introduced or resulted in the chemical reaction with a sulphide (usually FeS_2).

The literature data and our experiments confirmed that Uranium dissolution in sodium carbonate solution is only possible when tetravalent Uranium is oxidized to the hexavalent state.[1–6] This means that dissolution rate is almost the same as oxidation rate. An immediate consequence of this fact is the necessity to have an oxidant permanently present during the chemical reaction. This study proved that atmospheric air used as oxidant has a sufficient strength to fulfill these requirements.

Experiments made in the presence of a chemical oxidant not only demonstrated, it is useless, but sometimes gave results in contradiction with the literature data.

In order to investigate the Uranium ore behavior in the acid treatment, sulphuric acid has been used as leaching agent. In this alternative a chemical oxidant is required and the optimum extraction yields are dependant on the choice of the oxidant. Promising results were obtained in the presence of ferric sulphate (partially hydrolyzed) at pH 1.5—2.0.

An important point on which we have to lay stress was related to Uranium adsorption on calcium sulphate whose negative influence on

---

[1] W. E. Schortmann and M. A. De Sesa, "Conférence Internationale d'Energie Atomique", vol. 2, IAEA-Genève, 1958, p. 682.

[2] M. A. De Sesa, "Conférence Internationale d'Energie Atomique", vol. 2, IAEA, Genève, 1958, p. 692.

[3] F. A. Forward and J. Halpern, *J. Metals*, **1954**, 402.

[4] R. G. Beverly and W. D. Charles, "Conférence Internationale d'Energie Atomique", vol. 2, IAEA, Genève, 1958, p. 650.

[5] M. Iovanovic and N. Pacovic, "Conférence Internationale d'Energie Atomique", vol. 2, IAEA, Genève, 1958, p. 697.

[6] P. Mouret, "Conférence Internationale d'Energie Atomique", vol. 2, IAEA, Genève, 1958, p. 701.

the extraction yields was evident. Resin in pulp process seemed to have a significant contribution in minimizing the adsorption phenomenon.

EXPERIMENTAL

Uranium dissolution depends on the following two factors : diffusion rate and the interaction [7,8] with the reagent (oxidation rate). The diffusion laws provide the main parameters required in this study, which are responsible for Uranium extraction. Experimental work was carried out in view of the variation of the following factors : concentration of the reagent, solid phase-liquid phase ratio, chemical oxidant, grain size, temperature, time interval, mixing efficiency etc.

A) *Alkaline process*

a) Extraction yield dependence on reagent concentration and the nature of the chemical oxidant. It was found desirable to discuss these factors the same time, because the dissolution rate is practically equal with the oxidation rate. The other experimental conditions which were maintained constant are enumerated here : S/L = 1/2, grain size 0.075 mm, temperature 85°, time interval 40 hours.

Figure 1 represents experimental data expressing the nature of the oxidant and extraction yields *versus* reagent concentration.

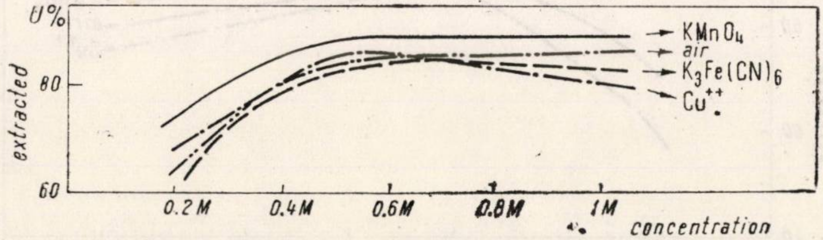

Fig. 1. – Uranium extraction dependence on reagent concentration and oxidant employed.

The slight contribution of $KMnO_4$ as an additional chemical oxidant (2–4%) does not justify its application in an eventual industrial process.

The $K_3Fe(CN)_6$ when used as oxidant [2,3] yields almost the same extraction as the atmospheric air or perhaps slightly lower.

The copper ammonia complex used as reaction catalyst [1,4] gives no contribution to the extraction yield of Uranium. The high temperature is likely responsible for copper ammonia, complex decomposition resulting in a basic carbonate (precipitate) with adsorption properties. This precipitate carried some Uranium explaining the slope of the curve for copper ammonia

---

[7] J. C. Balaceanu, "Conférence Internationale d'Energie Atomique", vol. 2, IAEA, Genève, 1958, p. 709.

[8] V. B. Sevcenco and B. N. Sudaricov, "Tehnologia urana" vol. 2, ed. I, Gosatomizdat, Moscow, 1961, p. 58.

oxidant. With a view to analyse the data from figure 1 the redox potential (pH = 10) has been measured and some results given below.

permanganate 0.3 g/100 g ore	0.335–0.410 V
air	0.331–0.337 V
copper ammonia complex	
0.3 g/100 g ore (Cu^{++})	0.331–0.335 V
ferricyanide 0.3 g/100 g ore	0.320 V

Comparing now these values with the data of figure 1 a correlation may be obtained Permanganate has higher redox potential explaining in this way its contribution to the extraction yield in figure 1. Ferricyanide lower redox potentials are also reflected in figure 1.

Copper ammonia complex shows no particular contribution due perhaps to its decomposition.

The reagent influence is quite clear up to 0.4 M sodium carbonate. A further increase in its concentration does not affect the extraction yield.

b) Time interval role to the extraction yield. During the research work carried out in view to check the influence of this factor on the extraction yield, all other parameters were maintained constant. The reagent concentration was 0.4 M Na_2CO_3.

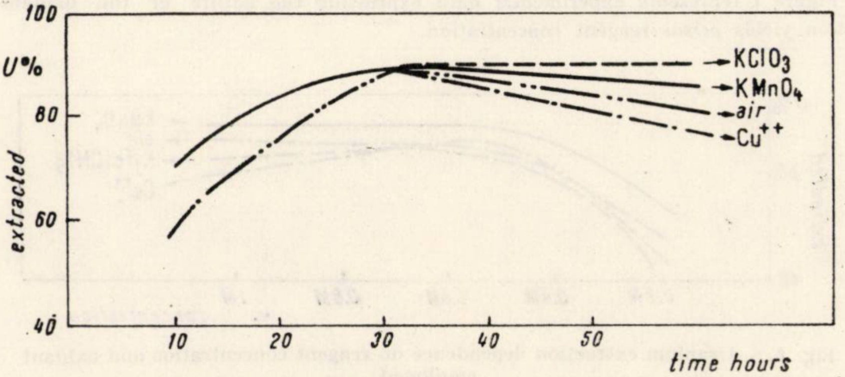

Fig. 2. — Uranium extraction *versus* time for different oxidants used.

Experimental data are given in figure 2.

The extraction yield estimation was made either starting with Uranium content determination in the ore and in the depleted solid phase or having in view its content in solution. These values do not coincide. When the optimum time interval is attained, the first value (steril washed) becomes constant but the second one experiences a slight decreasing dependence as that given in figure 2. Sometimes these values coincide at optimum time of reaction. Experimental work confirmed that the presence of some electrolytes, like potassium chlorate, has significantly reduced this difference. All these facts seem to prove the existence of an adsorption phenomenon[9] which occurs in the solid phase. We found $Fe(OH)_3$ responsible for this process. It should be reminded that this component is produced by the following reaction ;

$$2FeS_2 + 8Na_2CO_3 + 15/2O_2 + 7H_2O = 2Fe(OH)_3 + 4Na_2SO_4 + 8NaHCO_3$$

---

[9] A. VOGEL, "Quantitative Analysis", vol. 1, Longmans London, 1960, p. 110.

Sometimes components like copper carbonate (basic), incidentally present, show similar properties (Fig. 1). In order to check this behavior experimental work was made introducing a ferric salt or preformed $Fe(OH)_3$ in carbonate solutions of uranyltricarbonate. Uranium was carried down up to 20% from solutions of 0.6 g/l U. In the presence of a ferric salt, at 85° this leads to $Fe(OH)_3$ and a basic carbonate, which produce the adsorption phenomena. For this process we were able to obtain some results confirming the supposition that only a surface adsorption as well as the ions occlusion during crystal growth of the precipitate occur. The ageing plays a positive role enhancing the Uranium adsorption. When $KClO_3$ is present a change of the surface electric charge leads to a different behavior and the adsorption phenomenon decreases very much. Besides these phenomena we cannot exclude the possibility of an ion exchange process, however insignificant at this pH for weak anion exchangers.

c) Influence of copper ammonia as oxidant. In the laboratory work the role of copper ammonia, as an oxidation catalyst, indicated no contribution during the time interval when the chemical reaction occurred (85°, Fig. 1 and Fig. 2). In order to verify this behavior, radioactive copper (^{64}Cu) has been used to label the copper ammonia complex. Residual activity after complex decomposition is likely to belong to the solubility product of copper carbonate.

d) Grain size influence. Grain size contribution to the extraction yield increases with decrease in the particle dimension. This behavior is given in figure 3 and is a natural consequence of the simple diffusion law.

e) Reaction temperature. The role of the reaction temperature appears in figure 4. An increasing dependence with increasing temperature is observed for the extraction yield. Higher temperatures than 85° at atmospheric pressure lead to a lower oxygen solubility which is undesirable.

f) The S/L ratio. Experimental work carried out on different S/L ratios (maintaining all other parameters constant) have proved a decreasing dependence with increasing S/L ratios as in figure 5. With a view to obtain a higher degree of extraction, higher reagent concentrations as well as longer reaction time intervals are required.

g) Influence of atmospheric air used as oxidant on the extraction yield. During the experimental work carried out in a pachucas reaction vessel it was proved that a good air dispersion in the liquid phase resulted in an enhanced extraction yield of Uranium. Additional bubbling devices gave improved extraction efficiency by 5–8% higher than usually. The hydrostatic pressure acts in the same direction due to a better solubility of the oxygen. For this reason the introduction of higher pachucas, maintaining all other factors constant, gave better extraction yields by 7–9%.

h) The solution purity. The alkaline leaching process produces solutions of high purity. The only present impurities are Sulphur and Molybdenum. The last one is found within the range 0–50 mg/l but Sulphur is appreciably extracted, its concentration is many times higher than that of Uranium. It has to be mentioned that 85% Sulphur is found as Na_2SO_4, the remaining Sulphur has other chemical form resulting very likely from organic compounds present.

In an eventual industrial process, care should be taken of the solutions resulted at the diuranate precipitation with NaOH which are recycled and an enrichment in Sulphur is expected. At the laboratory scale this process has been reproduced by four reextractions and Sulphur content is given in figure 6.

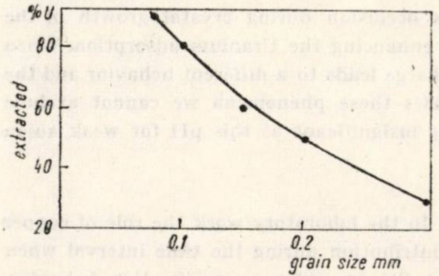

Fig. 3. — Uranium extraction *versus* grain size.

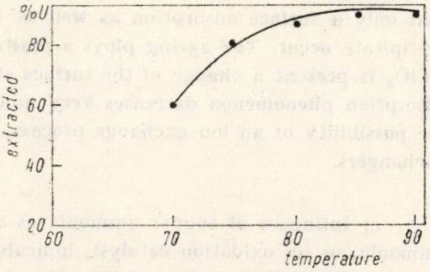

Fig. 4. — Uranium extraction *versus* temperature.

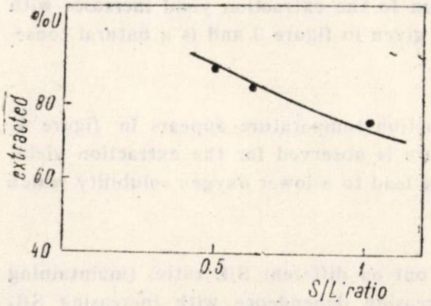

Fig. 5. — Uranium extraction *versus* S/L ratio.

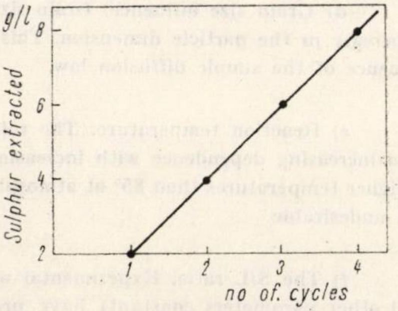

Fig. 6. — Sulphur extraction *versus* no. cycles.

It has to be stressed that within the time interval of the same cycle, an increase of Sulphur extraction is observed in two stages. In an initial phase a linear increase takes place when reaction speed is high, but later when approximately 60 % Sulphur was extracted (after 40 hours) the process is slowed down.

B) *Acid process*

In an acid treatment, the following important points are to be mentioned : The degree of Uranium dissolution, reagent consumption, and solution purity. Generally speaking, the extraction yield at reasonable Uranium content in the depleted pulp, is considered satisfactory when values are higher than 90 % and acid consumption 50—80 kg/t ore. Experimental work carried out on the laboratory scale had to find the optimum conditions of acid leaching with a view to estimate the product cost. Although the parameters involved in this study were already mentioned elsewhere, the importance of the following factors must be stressed : oxidation with a chemical reagent, S/L ratio and acid concentration.

a) Oxidant contribution. Some Uranium ore used in this work contained appreciable amounts of uraninite and organic compounds. The existence of Uranium at inferior valency states requires the use of a chemical oxidant during the acid leaching of the Uranium ores. When the leaching process is carried out in the absence of the chemical oxidant only 20–50% Uranium is extracted, depending on the chemical mineralogical characteristics of the ore. This behavior is a real consequence of Uranium and Iron presence in an unoxidized form. The Iron is found in the valency state +2.

In figure 7 the dependence of extracted Uranium *versus* the amount of oxidant, as the influence of the oxidant on the Iron oxidation and sulphuric acid consumption are given. In order to obtain a high Uranium dissolution yield, Iron should be present at least 50% in trivalent state.

The efficiency of $KClO_3$ as oxidant is evident.

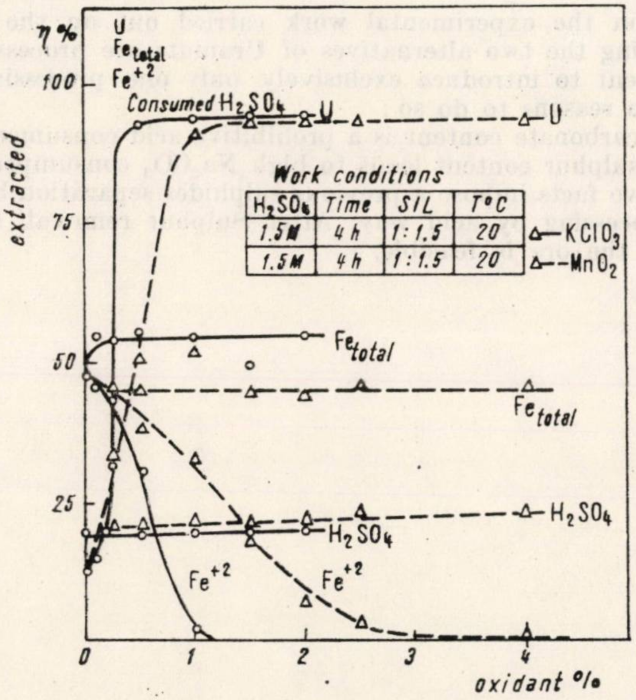

Fig. 7. — Oxidant influence on Uranium and Iron extraction, Iron oxidation and sulphuric acid consumption.

b) Sulphuric acid consumption, S/L ratio and grain size role.

Sulphuric acid consumption is determined by the chemical mineralogical characteristics of the ore and by the leaching conditions.

The diluted acid dissolves not only Uranium but also some elements found as impurities, more frequently Al, Ca, Mg, Na, K, Fe etc. The study of this parameter requires its relation with the time of reaction and initial acid concentration. When higher acidities than 80 g/l have been used, an increase in acid consumption resulted without attaining a corresponding Uranium extraction yield. We have regulated the acid concentration by changing the S/L ratios within the range 1.25 – 1.75 ; this fact was reflected in the minimum acid consumption, higher Uranium yield of extraction and a lower amount of impurities found in solutions.

The grain size plays an important role, its choice is made as a function of ore characteristics (metal dispersion). The higher the Uranium dispersion, the lower grain size is required. In fact the extraction yield imposes the grain size of Uranium ore. In the laboratory experiments, the most suitable grain size was found within the range 0.1 – 0.3 mm.

Time interval fluctuates between 6 – 10 hours, directly related to the chemical metallurgical characteristics of the ore.

CONCLUSIONS

Based on the experimental work carried out on the laboratory scale concerning the two alternatives of Uranium ore processing, it was found inefficient to introduce exclusively only one processing method. There are two reasons to do so :

A high carbonate content is a prohibitive acid consumer.

A high sulphur content leads to high Na_2CO_3 consumption.

These two facts impose a previous sulphides separation by flotation and their processing by acid way. After Sulphur removal, an alkaline treatment of the ore is feasible.

Revue Roumaine de Chimie, 14, 737–744 (1969)

INFLUENCE OF SOME ANIONS AND SOLVENTS ON THE POLAROGRAPHIC REDUCTION OF NIOBIUM(V) IN HYDROCHLORIC ACID-THIOCYANATE MEDIUM

C. DRĂGULESCU, SOFIA MARCHIDAN and GH. FACSKO

Centre of Physical Chemistry of the Academy, Bucharest,
31, Str. Galaţi

Received January 13, 1969

The influence of some anions on the polarographic reduction of niobium(V) in hydrochloric acid-thiocyanate medium with acetone addition was determined. These anions are frequently used for obtaining stable niobium solutions. The presence of small amounts of H_3PO_4 and $H_2C_2O_4$ considerably decreases the wave height and slightly shifts the half-wave potential to more negative values. For moderate addition of H_2SO_4 the wave height is not affected but the wave shape and half-wave potential change and the system stability decreases as the acid concentration increases. Tartaric acid has no influence on the reduction process and this suggests the possibility of using niobium tartrate solutions in the method based on the polarographic reduction of niobium-thiocyanate complex. The influence of other miscible solvents was also studied to check if they are not more suitable for niobium determination. From the solvents used only the dioxane gave satisfactory results, comparable with those previously obtained by adding acetone.

One of the most widely used methods in analytical chemistry of niobium is based on the formation of the yellow niobium-thiocyanate complex in hydrochloric acid medium. The numerous studies and spectrophotometric applications published so far, reveal the sensitivity of the reaction but, at the same time, the difficulties and discrepancies connected with the formation and stability of this complex, strongly influenced by the reaction medium and working conditions.

In a previous paper[1] we showed that this niobium-thiocyanate complex could be polarographically reduced at the dropping-mercury electrode. In hydrochloric acid-thiocyanate medium with acetone addition, well defined and reproducible waves were obtained and the optimum reduction conditions were established. The proportionality between the wave height and the niobium concentration created the premises for the establishment of a new method of polarographic determination.

[1] S. Marchidan, Gh. Facsko and C. Drăgulescu, *Rev. Roumaine Chim.*, 12, 635 (1967).

We aim in the present paper at studying the influence of some anions on the polarographic reduction of niobium(V) in hydrochloric acid-thiocyanate medium with acetone addition. These anions, forming soluble and stable compounds with niobium, are frequently used for the preparation of niobium solutions. We equally aim at studying the influence of other miscible solvents than acetone, used in the previous work, and checking their applicability to the polarographic determination of niobium.

EXPERIMENTAL

Apparatus. The polarograms were recorded by means of a polarograph type OH–101 at 2×10^{-7} A/mm sensitivity, using the same compensation and damping for all the experiments. A thermostated cell at 25° ± 0.1° and an external low-resistance saturated calomel anode were used. Oxygen was removed with purified nitrogen.

Reagents and Solutions. The reagents used were *p.a.* and niobium pentoxide spectrographically pure (Johnson and Mattey). The following solutions of established titre $NH_4SCN \sim 4M$, $HCl \sim 12$ M, H_2SO_4 1 M and 10 M, $H_2C_2O_4$ 1 M, H_3PO_4 1 M and 10 M, tartaric acid 2 M were used. The stock niobium solutions containing 1×10^{-2} M–Nb in $HCl \sim 12$ M were prepared as indicated in the previous work, by fusing niobium pentoxide with potassium pyrosulfate, precipitating hydrated niobium oxide with ammonia and solving the precipitate in concentrated hydrochloric acid.

Preparation of polarography samples. The concentration of reagents, temperature and time of standing were those established in the previous paper as optimum values which allowed the obtaining of a clear and complete development of reduction wave as well as the best reproducibility. Samples were prepared in a 10 ml volumetric flasks. The corresponding amounts of reagents of known concentrations were pipetted in the following order: 2 ml stock niobium solution in concentrated hydrochloric acid (final solution 2×10^{-3}M–Nb); the additional amount of 12 M hydrochloric acid necessary to obtain a final concentration of 6 M – HCl; 2 ml acetone or another miscible solvent (final solution 20 per cent solvent by volume); the amount of acid corresponding to the wanted concentration in anion the influence of which is followed; ammonium thiocyanate 4 M solution necessary for the final concentration of 0.60 M; distilled water up to the mark. After addition of each reagent, the volumetric flask was stoppered, stirred and kept in a water bath at 20°. The moment of ammonium thiocyanate addition was exactly noted. The solution was passed from the flask into the polarographic thermostated cell and during 30 minutes was bubbled with nitrogen. The polarograms were recorded exactly 40 minutes after the moment of thiocyanate addition, taking all precautions to avoid hydrochloric acid and acetone losses during deaeration and recording. From the same sample as well as from the different samples with the same composition several polarograms were recorded between 40 and 50 minutes, in a voltage range of –0.20 to –0.65 V.

EXPERIMENTAL RESULTS

The influence of sulfuric, phosphoric, oxalic and tartaric acids as well as some miscible solvents on the height of the reduction wave for niobium-thiocyanate complex, on the half-wave potential and on the system stability was studied; the tolerance limits were determined.

Sulfuric Acid

A special attention was given to sulfuric anion since the usual methods for obtaining niobium solutions imply the fusion of niobium pentoxide with potassium pyrosulfate or bisulfate. The data in table 1 presenting the height of reduction wave for niobium-thiocyanate complex and the half-wave potential show that for low and moderate concentrations of sulfuric acid the wave height is not affected. At concentrations within 0.3—0.7 M sulfuric acid, the wave shape begins to change gradually i.e. the upper plateau slopes more and more. In 1 M sulfuric acid the waves decrease, become ill-defined, difficult to be analyzed and the results are no longer reproducible. In the whole concentration range studied a slight shift of half-wave potential to more negative values occurs. As the concentration of sulfuric acid increases the instability of wave height and half-wave potential become more accentuated.

Table 1

Influence of sulfuric acid on the height of niobium reduction wave and on $E_{1/2}$

H_2SO_4	0.0M	0.05M	0.1M	0.3M	0.5M	0.7M	1.0M
Wave height mm	49.0	49.2	49.4	49.1	48.8	49.1	47.3
$E_{1/2}$ Volts	−0.423	−0.433	−0.436	−0.441	−0.444	−0.448	−0.453

Phosphoric Acid

The change of wave height for niobium reduction in hydrochloric acid-thiocyanate medium and of half-wave potential versus the concentration of phosphoric acid within 0.02—0.5 M is given in figure 1. A sudden decrease of wave height at phosphoric acid addition starting with even very low concentrations, is easily seen. At a content of phosphoric acid over 0.1 M the waves slightly increase but become distorted so that at 0.5 M are unclear. The half-wave potential is very slightly shifted to more negative values. The results of several runs of experiments have been reproducible, the same wave height and half-wave potential have been found for the same concentration of phosphoric acid.

Oxalic Acid

Oxalic acid produces a decrease in the reduction waves without changing their shape up to 0.1 M oxalic acid content. This decrease, as seen in figure 2, takes place slower and approximately linearly *versus* the concentration of oxalic acid. Reproducible results have been obtained within the concentration range 0.01–0.2 M oxalic acid. At increasing content of oxalic acid in solution, the half-wave potential is also slightly shifted to more negative values.

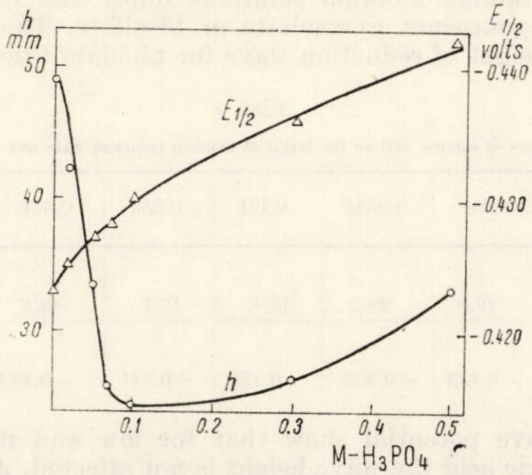

Fig. 1. — Influence of phosphoric acid on the height of niobium reduction wave and on $E_{1/2}$.

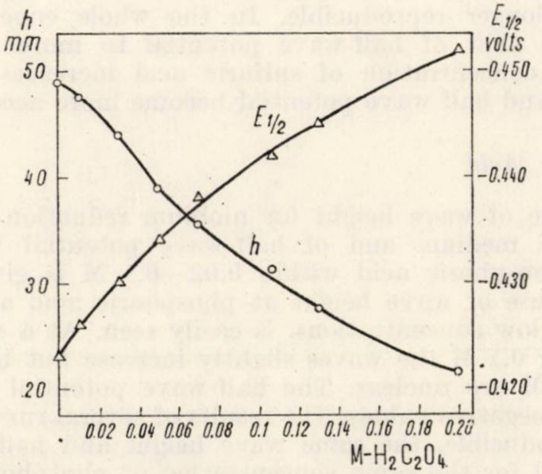

Fig. 2. — Influence of oxalic acid on the height of niobium reduction wave and on $E_{1/2}$.

Tartaric Acid

In table 2 are given the results obtained in the presence of tartaric acid. The height of niobium reduction wave in hydrochloric acid-thiocyanate medium is not modified by tartaric acid addition in the concentrations used for preparing niobium-tartrate solutions. The half-wave potential and wave shapes register no change and the found results in the concentration range studied, between 0.04 – 0.5 M tartaric acid, have been perfectly reproducible.

Table 2

Influence of tartaric acid on the height of niobium reduction wave and on $E_{1/2}$

Tartaric Acid	0.0M	0.04M	0.1M	0.2M	0.3M	0.5M
Wave height mm	49.0	49.2	48.8	48.5	48.8	48.7
$E_{1/2}$ Volts	−0.423	−0.423	−0.423	−0.425	−0.424	−0.432

Influence of Solvents

In a run of experiments acetone was replaced by other miscible solvents as tetrahydrofuran, methanol, ethanol and dioxane. The obtained results are listed in table 3. It was not possible to analyse polarographically the solutions containing 10 – 20 per cent tetrahydrofuran because when ammonium thiocyanate is added the miscible solvent separates and extracts part of the niobium-thiocyanate complex, the aqueous phase remaining light-yellow and opalescent. Even at small complexant concentrations (0.1 M) some opalescence and solvent separation occur.

Table 3

Influence of some solvents on the height of niobium reduction wave and on $E_{1/2}$

Solvent	acetone	dioxane	methanol	ethanol	Without solvent
Wave height mm	49.0	45.8	44.5	40.8	40.5
$E_{1/2}$ Volts	−0.423	−0.435	−0.444	−0.435	−0.449

By adding methanol or ethanol the solutions remain clear, the colour of the niobium-thiocyanate complex is intensified but the height of reduction wave appreciably modifies in time and it is smaller than in acetone solutions. The waves obtained are ill-defined with very sloped plateaus, poorly reproducible. Satisfactory polarograms have been obtained only within 15 – 30 minutes after thiocyanate addition. Even with this time of standing a visible distortion of waves and a rapid half-wave potential shift to more negative values, close to those obtained in aqueous solution without acetone addition, occur.

In the solutions containing 20 per cent dioxane very clear and well-developed waves have been obtained. Their height is a little smaller than for the solutions with acetone but reproducibility and stability is better. To choose the suitable working interval the influence of time elapsed from the addition of thiocyanate until the recording on the reduction wave height has been studied. The data presented in figure 3a show that although the complexation develops slower when dioxane is used, after 40 minutes the reduction wave height remains practically unchanged. If compared with data obtained for solutions with acetone addition (Fig. 3b) dioxane seems more suitable concerning the system stability.

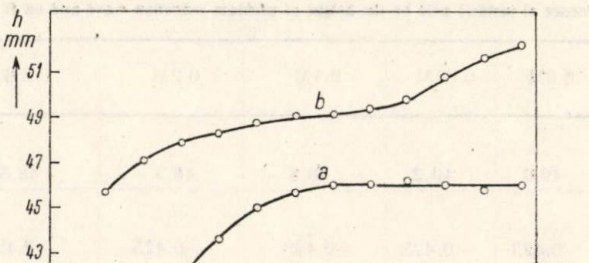

Fig. 3. — Time influence on the height of niobium reduction wave.

a, 20 per cent dioxane; *b*, 20 per cent acetone.

DISCUSSIONS AND CONCLUSIONS

The study of some anions influence on polarographic reduction of niobium-thiocyanate complex is interesting because it analyses the possibilities of utilizing various niobium solutions obtained by usual methods. On the other hand this study gives some information concerning the nature of complexes and the changes taking place in the solution. In optimum conditions of niobium reduction established in hydrochloric acid-thiocyanate medium with acetone addition it has been observed that the phosphoric and oxalic ions produce an evident but reproducible decrease of the wave. This decrease could not be assigned to hydrolysis or hydration but to the formation of some niobium compounds with phosphoric or oxalic ions. The competitive reaction between niobium and phosphoric or oxalic anions on the one hand and thiocyanate anion on the other hand is shifted towards the formation of some phosphoric or oxalic complexes as the concentration of these anions increases; these compounds are stronger than the thiocyanate compound but nonreducible in the given conditions. So the concentration of niobium-thiocyanate complex decreases accordingly and this leads to the decrease in the waves height. The niobium reduction in phosphoric medium takes place only in concentrated solutions of phosphoric acid [2] and the reduction observed in oxalic solutions by Elson [3] has not been confirmed by other authors.[4] Small and moderate additions of sulfuric acid as well as additions of tartaric acid do not influence the reduction process. This observation creates the possibility of utilizing stable tartrate solutions, obtained by fusing niobium pentoxide with potassium pyrosulfate and dissolving the melt in tartaric acid, as stock niobium solutions for complexation with thiocyanate and polarographic determination.

The slight shift of half-wave potential (about 20—30 mV) observed on the addition of studied anions does not show an important change of the reduction process. The same shift of half-wave potential, to more negative values, is equally obtained by the increase in the hydrochloric acid concentration from 6.0 M to 6.5 M. This means that in all experiments the same niobium complex is reduced. Sulfuric acid in small amounts or tartaric acid do not influence the formation and reduction of niobium-thiocyanate complex while phosphoric and oxalic acids, in given conditions, produce nonreducible compounds decreasing only the concentration of reducible thiocyanate complex. Generally, the increase in the solution acidity favours the reduction process and the obtaining of maximum wave height, but at the same time leads to the labilization of the system. This becomes evident by the increase in the wave and half-wave potential instability, by the distortion of the waves and worsening the reproducibility of the results which occurs at acid concentrations of over 6 M.

From the miscible solvents which have been tried the dioxane gave satisfactory results, comparable with those previously obtained by adding acetone. Although when dioxane is used the wave height is about 9 per cent smaller than in acetone solutions and complex formation is slower, an increase of stability is found when the complexation process is completed. A comparative examination of niobium-thiocyanate solutions with acetone or dioxane addition and the respective blank solutions without niobium, leads to the finding that this longer stability of waves obtained in solutions with dioxane addition is due in fact to the stronger stabilizing action which dioxane exerts on the blank solutions, probably by minimizing of the decomposing effect of the thiocyanic acid in strong hydrochloric medium.

---

[2] D. I. Kurbatov, *Zhur. analit. Khim.*, **14**, 63 (1959).

[3] R. E. Elson, *J. Amer. Chem. Soc.*, **75**, 4193 (1953).

[4] D. J. Ferrett and G. W. C. Milner, *J. Chem. Soc.*, **1956**, 1186.

In conclusion, our experiments showed that niobium phosphoric, oxalic or sulfuric solutions, with a higher sulfuric acid content could not be used as stock solutions in the method based on the polarographic reduction of niobium-thiocyanate complex. However, tartaric acid having no influence on the reduction process involved, appears particularly suitable for the preparation of niobium solutions. The utilization of dioxane in reduction medium gave also satisfactory results having the advantage of a higher system stability.

Revue Roumaine de Chimie, **14**, 745–752 (1969)

TETRAPHENYLBORATE DES AKRIDINS, 2-ÄTHOXY-6,9-DIAMINOAKRIDINS UND 3-CHLOR-9-(4′-DIÄTHYLAMINO-1′-METHYLBUTYLAMINO)-7-METHOXYAKRIDINS

I. FLOREA

aus dem Laboratorium für Allgemeine Chemie der Technischen Hochschule, Timişoara, str. Remus, 14

Eingegangen am 12. August 1968

Es wurde auf konduktometrischem Wege die Reaktion zwischen Akridin, 2-Äthoxy-6,9-diaminoakridin-laktat, 3-Chlor-9-(4′-diäthylamino-1′-mehylbutylamino)-7-methoxyakridin-dichlorhydrat und Natriumtetraphenylborat verfolgt. Die Substanzen, die sich während den konduktometrischen Titrationen gebildet hatten, wurden getrennt, analysiert, ihr thermogravimetrisches Verhalten wurde verfolgt und es wurden die Absorptionsspektren aufgezeichnet. Die konduktometrischen Untersuchungen der Reaktion zwischen Natriumtetraphenylborat und 2-Äthoxy-6,9-diaminoakridin-laktat ergaben, daß diese Substanzen auf diesem Wege bestimmt werden können.

Die zunehmende Verwendung von Natriumtetraphenylborat, $Na[B(C_6H_5)_4]$ in der analytischen Chemie machte es notwendig, neue Bestimmungsmethoden für dieses auszuarbeiten.

Im Jahre 1949 haben Wittig[1] und Mitarbeiter die ersten Untersuchungen über Metallkomplexe mit dem Anion $[B(C_6H_5)_4]^-$ unternommen.

Natriumtetraphenylborat hat in der analytischen Chemie vielseitige Verwendungen gefunden, so daß gegenwärtig im Fachschrifttum zusammenfassende Artikel[2–8] und über 290 Angaben über seine Verwendung bei zahlreichen chemischen und physikalisch-chemischen Bestimmungsmethoden von Kalium, organischen Substanzen, die Stickstoff enthalten, organischen Medikamenten, welche im Molekül Stickstoff haben, von Alkaloiden, verschiedenen Kationen usw. vorhanden sind.

---

[1] G. Wittig, G. Keicher, A. Rückert und T. Raff, *Liebigs Ann.*, **563**, 110 (1949).

[2] A. J. Barnard, *Chemist-Analyst*, **44**, 104 (1955); *Chem. Abstr.*, **50**, 1516b (1956).

[3] A. J. Barnard, *Chemist-Analyst*, **46**, 16 (1957); *Chem. Abstr.*, **51**, 12734g (1957).

[4] A. J. Barnard jun. und H. Hüecl, *Chemist-Analyst*, **48**, 44 (1959); *Chem. Zentr.*, **1963**, 7453.

[5] A. J. Barnard, *Chemist-Analyst*, **47**, 46 (1958); *Chem. Abstr.*, **52**, 16117d (1958).

[6] Tomoyuki Mukoyama, *Kagaku No-Ryöiki*, (*J. Jap. Chem.*), **10**, 2, 103 (1956); *Chem. Zentr.*, **1957**, 1502.

[7] Katsumi Tamaoku, *Kagaku No Ryöiki*, **17**, 39 (1963); *Chem. Abstr.*, **59**, 1062d (1963).

[8] H. Flaschka und A. J. Barnard, *Adv. Analyt. Chem. Instrum.*, **1**, (1958).

Zur Bestimmung von $Na[B(C_6H_5)_4]$ bzw. des Ions $[B(C_6H_5)_4]^-$ sind nur einige maßanalytische Methoden bekannt, die auf merkurimetrischen,[9] chromatometrischen[10] und Titrationen mit ÄDTA,[11] mit Überschuß an $TlNO_3$ und Rücktitration des Überschusses mit KJO_3[12] beruhen.

Wir haben uns die Aufgabe gestellt zu untersuchen, ob Akridin, 2-Äthoxy-6,9-diamino-akridin-laktat (Rivanol) und 3-Chlor-9-(4′-diäthylamino-1′-)-7-methoxyakridin-dichlorhydrat (Atebrin), die mit den Abkürzungen Acr., BHL und AtH_2Cl_2 bezeichnet wurden und die in großem Maßstab in der pharmazeutischen und Farbstoffindustrie verwendet werden, mit Natriumtetraphenylborat unlösliche Verbindungen bilden und ob die Eigenschaften derselben sie als geeignet zur Bestimmung des letzteren erscheinen lassen.

Natriumtetraphenylborat wurde zur gravimetrischen[13] und heterometrischen[14] Bestimmung von 2-Äthoxy-6,9-diaminoakridin-laktat verwendet.

Aus den durchgeführten Untersuchungen ergibt sich, daß Akridin, 2-Äthoxy-6,9-diaminoakridin-laktat und 3-Chlor-9-(4′-diäthylamino-1′-methylbutylamino)-7-methoxyakridin-dichlorhydrat mit Natriumtetraphenylborat unlösliche Niederschläge von gelber Farbe bilden.

Die chemischen Verbindungen, welche sich beim Vermischen der oben genannten Lösungen bilden, wurden auf konduktometrischem Wege untersucht, indem die Lösungen von Acr., BHL und AtH_2Cl_2 mit Lösungen von $Na[B(C_6H_5)_4]$ titriert wurden. Zur Titration wurden 1.10^{-2} M-Lösungen von Acr., BHL, AtH_2Cl_2 und $Na[B(C_6H_5)_4]$ verwendet. Ihre Konzentrationen wurden durch genaues Wägen festgesetzt.

Zur Präparierung der Lösungen sind Acr., BHL und AtH_2Cl_2 chemisch rein, die umkristallisiert wurden, umkristallisiertes $Na[B(C_6H_5)_4]$ Riedel verwendet worden, wobei die Lösung der letzten Verbindung stabilisiert wurde.[15]

1. KONDUKTOMETRISCHE TITRATIONEN

Die Ergebnisse der konduktometrischen Titrationen sind in Abb. 1 dargestellt.

Die Versuchsergebnisse zeigen, daß bei den konduktometrischen Titrationen von BHL, AtH_2Cl_2 und Acr. mit $Na[B(C_6H_5)_4]$ bis zum Äquivalenzpunkt, die in den Diagrammen 1, 2 und 3 der Abb. 1 dargestellt wurden, eine Zunahme der Leitfähigkeit der Lösung dadurch stattfindet, daß die Kationen BH^+, AtH_2^{2+} und Acr. H^+ mit Na^+-Kationen ersetzt werden. [$\Lambda BH^+ < \Lambda Na^+$, $1/2\Lambda AtH_2^{2+} < \Lambda Na^+$ und $\Lambda Acr. H^+ < \Lambda Na^+$]. Nach dem Äquivalenzpunkt nimmt die Leitfähigkeit der Lösung infolge des hinzugefügten Reagensüberschusses zu.

---

[9] R. Montequi, A. Doadrio und C. Serrano, *Anales real Soc. españ. Fis. Quim.*, **53**, 447 (1957); *Chem. Zentr.*, **1949**, 7900.

[10] H. Flaschka und F. Sadek, *Chemist-Analyst*, **47**, 30 (1958); *Chem. Zentr.*, **1960**, 3650.

[11] A. Schneer und H. Hartmann, *Acta Chim. Acad. Sci. Hung.*, **28**, 271 (1961); *Chem. Zentr.*, **1962**, 586.

[12] B. R. Sant und A. K. Mukherji, *Talanta*, **2**, 154 (1959); *Chem. Zentr.*, **1962**, 13879.

[13] O. E. Schultz und G. Mayer, *Deut. Apoth. Ztg.*, **92**, 258 (1952).

[14] M. Bobtelsky und M. M. Cohen, *Analyt. Chim. Acta*, **23**, 328 (1960); *Chem. Zentr.*, **1960**, 12797.

[15] M. Muraize, *Chem. analyt.*, **39**, 184 (1957).

Aus den Daten der konduktometrischen Titrationen, die in den Tabellen 1 und 2 angeführt sind, ergibt sich, daß Na$[B(C_6H_5)_4]$ und BHL auf diesem Wege, in Lösungen mit Konzentrationen zwischen $2.10^{-3} - 2.10^{-4}$ M bzw. $3.10^{-3} - 2.10^{-4}$M bestimmt werden können.

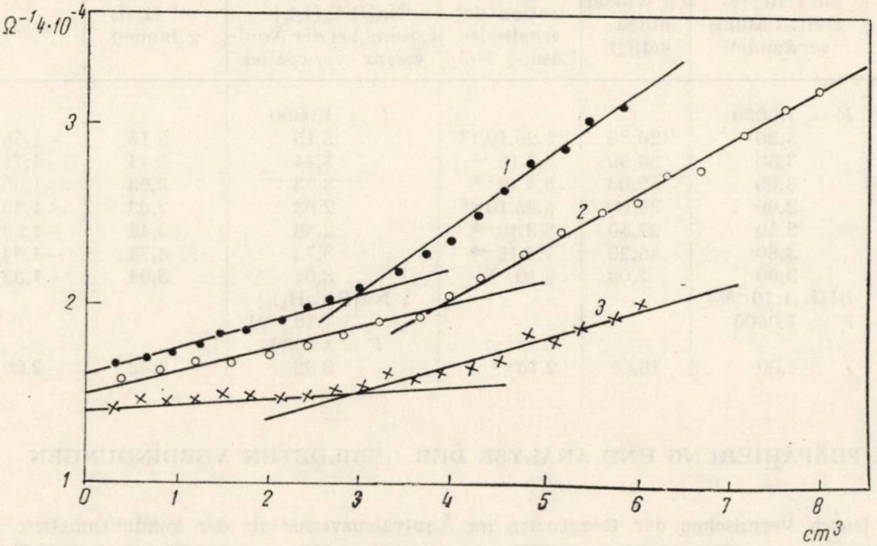

Abb. 1. — *1*, 3 ml BHL 0,01M + 27 ml Wasser + Na$[B(C_6H_5)_4]$ 0,01M ; *2*, 2 ml AtH_2Cl_2 0,01M + 58 ml Wasser + Na$[B(C_6H_5)_4]$ 0,01M ; *3*, 3 ml Acr. 0,01M in essigsaurer Lösung 1,5 %+ 25 ml Wasser + Na$[B(C_6H_5)_4]$ 0,01M.

BHL kann mit Na$[B(C_6H_5)_4]$ in Gegenwart von Glukose, Harnstoff, Borsäure und Glyzerin konduktometrisch bestimmt werden, wenn diese sich bis zu einer doppelten Menge gegenüber der in Arbeit genommenen BHL-Menge befinden.

Die Methode erfordert einfache Arbeitsgänge; sie kann genügend schnell ausgeführt werden und gewährleistet eine hinreichende Genauigkeit.

Tabelle 1

Konduktometrische Bestimmung von Na$[B(C_6H_5)_4]$, mit BHL

Lfd. Nr.	ml 1.10^{-2} M Na$[B(C_6H_5)_4]$-Lösung verwendet	ml Wasser hinzugefügt	Konzentration der erhaltenen Lösung Mol/l	ml 1.10^{-2}M BHL-Lösung, bei der Äquivalenz verwendet	ml Na$[B(C_6H_5)_4]$ gefunden	E %
	$F = 1,0000$			$F = 1,0000$		
1	3,00	17	$1,5.10^{-3}$	3,03	3,03	+1,00
2	3,00	50	$5,6.10^{-4}$	2,95	2,95	−1,66
3	3,00	42	$6,6.10^{-4}$	2,96	2,96	−1,33
4	3,00	25	$1,2.10^{-3}$	3,05	3,05	+1,66
5	3,00	57	5.10^{-4}	2,97	2,97	−1,00
6	3,00	36	$8,9.10^{-4}$	3,04	3,04	+1,33
7	3,00	12	2.10^{-5}	3,00	3,00	0,00
	Na$[B(C_6H_5)_4]$ 1.10^{-3}M $F = 1,0000$			BHL 1.10^{-3}M $F = 1,0000$		
8	3,00	12	2.10^{-4}	2,95	2,95	−1,66

Tabelle 2

Konduktometrische Bestimmung von BHL mit $Na[B(C_6H_5)_4]$

Lfd. Nr.	ml 1.10^{-2}M BHL-Lösung verwendet	ml Wasser hinzugefügt	Konzentration der erhaltenen Lösung Mol/l	ml 1.10^{-2}M $Na[B(C_6H_5)_4]$-Lösung bei der Äquivalenz verwendet	ml BHL gefunden	*E* %
	F = 1,0000			*F* = 1,0000		
1	3,20	20,80	$1,25.10^{-3}$	3,15	3,15	−1,56
2	3,50	36,50	$8,7.10^{-4}$	3,44	3,44	−1,71
3	3,00	52,00	$5,4.10^{-4}$	3,03	3,03	+1,00
4	2,00	30,00	$6,25.10^{-4}$	2,03	2,03	+1,50
5	2,50	27,50	$8,3.10^{-4}$	2,46	2,46	−1,60
6	3,80	46,20	$7,6.10^{-4}$	3,73	3,73	−1,84
7	3,00	7,00	3.10^{-3}	3,04	3,04	+1,33
	BHL 1.10^{-3}M			$Na[B(C_6H_5)_4]$		
	F = 1,0000			1.10^{-3}M		
				F = 1,0000		
8	4,00	16,00	2.10^{-4}	3,92	3,92	−2,00

2. PRÄPARIERUNG UND ANALYSE DER GEBILDETEN VERBINDUNGEN

Durch Vermischen der Reagenzien im Äquivalenzverhältnis der konduktometrischen Titrationen wurden Verbindungen der Kationen $Acr.H^+$, BH^+ und AtH_2^{2+} mit $Na[B(C_6H_5)_4]$ unter der Form von Niederschlägen erhalten, welche mit destilliertem Wasser gewaschen und bei 110° im Trockenschrank bis zum konstanten Gewicht getrocknet wurden.

Die Zusammensetzung der Verbindungen wurde festgesetzt, indem das Kation $Acr.H^+$ [16] maßanalytisch, AtH_2^{2+} [17] durch Extraktion mit Chloroform aus alkalischem Medium, das Kation BH^+ [18] photometrisch und das Anion $[B(C_6H_5)_4]^-$ [12] maßanalytisch bestimmt wurde.

a) $Acr.H[B(C_6H_5)_4]$ (499,30)

Analyse : *gef.* : $[B(C_6H_5)_4]^-$ 63,73 ; 64,25 ; Acr. H^+ 35,46 ; 35,80 %
ber. : $[B(C_6H_5)_4]^-$ 63,93 ; Acr. H^+ 36,07 %

b) $BH[B(C_6H_5)_4]$ (573,54)

Analyse : *gef.* : $[B(C_6H_5)_4]^-$ 54,79 ; 55,33 ; BH^+ 43,75 ; 44,17 %
ber. : $[B(C_6H_5)_4]^-$ 55,66 ; BH^+ 44,34 %

c) $AtH_2[B(C_6H_5)_4]_2$ (1040,40)

Analyse : *gef.* : $[B(C_6H_5)_4]^-$ 60,58 ; 60,94 ; AtH_2^{2+} 37,90 ; 37,31 %
ber. : $[B(C_6H_5)_4]^-$ 61,38 AtH_2^{2+} 38,64 %

3. THERMOGRAVIMETRISCHES VERHALTEN

Zum thermogravimetrischen Verhalten der Tetraphenylborate des Akridins, 2-Äthoxy-6,9-diaminoakridins und 3-Chlor-9-(4′-diäthylamino-1′-methylbutylamino)-7-methoxyakridins wurde eine Thermowaage verwendet, wobei die Temperatur im Bereiche 30−750° gemessen

---

[16] A. Bollinger, *Quart. J. Pharmac. Pharmacol.*, **13**, 1 (1940) ; *Chem. Zentr.*, **1941**, 2002.

[17] P. Lebeau und M. M. Janot, „Traité de Pharmacie Chimique", 4. Bd., 1955/56, S. 2366−67.

[18] M. J. Schulte, *Pharmac. Weekblad*, **67**, 809 (1930) ; *Chem. Zentr.*, **1930** (II), 1897.

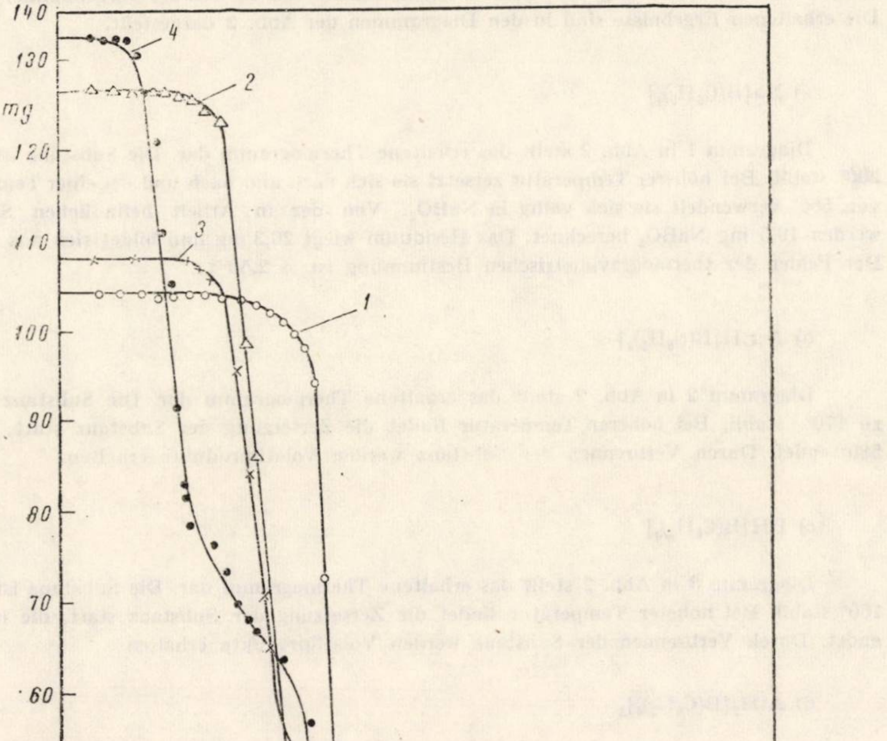

Abb. 2. — *1*, Thermolyse von $Na[B(C_6H_5)_4]$; *2*, Thermolyse von $Acr.H[B(C_6H_5)_4]$; *3*, Thermolyse von $BH[B(C_6H_5)_4]$; *4*, Thermolyse von $AtH_2[B(C_6H_5)_4]_2$.

wurde und die Erwärmung mit einer Geschwindigkeit von 10°/Minute vorgenommen wurde. Die erhaltenen Ergebnisse sind in den Diagrammen der Abb. 2 dargestellt.

a) $Na[B(C_6H_5)_4]$

Diagramm 1 in Abb. 2 stellt das erhaltene Thermogramm dar. Die Substanz ist bis zu 200° stabil. Bei höherer Temperatur zersetzt sie sich nach und nach und bei einer Temperatur von 500° verwendelt sie sich völlig in $NaBO_2$. Von der in Arbeit befindlichen Substanz werden 19,5 mg $NaBO_2$ berechnet. Das Residuum wiegt 20,3 mg und bildet sich aus $NaBO_2$. Der Fehler der thermogravimetrischen Bestimmung ist + 2,50 %.

b) $Acr.H[B(C_6H_5)_4]$

Diagramm 2 in Abb. 2 stellt das erhaltene Thermogramm dar. Die Substanz ist bis zu 170° stabil. Bei höherer Temperatur findet die Zersetzung der Substanz statt, die bei 580° endet. Durch Verbrennen der Substanz werden Volatilprodukte erhalten.

c) $BH[B(C_6H_5)_4]$

Diagramm 3 in Abb. 2 stellt das erhaltene Thermogramm dar. Die Substanz ist bis zu 150° stabil. Bei höherer Temperatur findet die Zersetzung der Substanz statt, die bei 750° endet. Durch Verbrennen der Substanz werden Volatilprodukte erhalten.

d) $AtH_2[B(C_6H_5)_4]_2$

Diagramm 4 in Abb. 2 stellt das erhaltene Thermogramm dar. Die Substanz ist bis zu 75° stabil. Bei höherer Temperatur findet die Zersetzung der Substanz statt, die bei 720° endet. Durch Verbrennen der Substanz werden Volatilprodukte erhalten.

Die Borsäure, die sich durch Verbrennen der Substanzen b, c und d gebildet hat, volatilisiert zusammen mit den Wasserdämpfen, welche aus dem Verbrennen der organischen Substanzen hervorgingen.

4. ABSORPTIONSSPEKTREN

Die Untersuchungen wurden mit einem Spektrophotometer UNICAM SP 800 im Bereiche 500—225 m μ durchgeführt. Die erhaltenen Ergebnisse sind in Abbildung 3 dargestellt.

In den Diagrammen ist auf der Abszisse die Wellenlänge in mμ und auf der Ordinate die Extinktion dargestellt.

Die Diagramme 1 und 1′ der Abb. 3 stellen die Absorptionsspektren von $Acr. H[B(C_6H_5)_4]$-Lösungen mit der Konzentration von 1.10^{-4} M bzw. 1.10^{-5}M in Küvetten von 1 cm dar.

Die Diagramme 2 und 2′ der Abb. 3 stellen die Absorptionsspektren von $BH[B(C_6H_5)_4]$ mit der Konzentration 1.10^{-4}M bzw. 5.10^{-5}M in Küvetten von 1 cm dar.

Die Diagramme 3 und 3′ der Abb. 3 stellen die Absorptionsspektren von $AtH_2[B(C_6H_5)_4]_2$ mit der Konzentration von 1.10^{-4}M bzw. 5.10^{-5}M in Küvetten von 1 cm dar.

Zunächst wurden die Absorptionsspektren folgender Substanzen aufgezeichnet: Natriumtetraphenylborat,[19] Akridin,[20–23] 2-Äthoxy-6,9-diaminoakridin-laktat [24–26] und 3-Chlor-9- (4′-diäthylamino-1′-methylbutylamino)-7-methoxyakridin-dichlorhydrat.[24, 27, 28]

In den synthetisierten Verbindungen $Acr.H[B(C_6H_5)_4]$, $BH[B(C_6H_5)_4]$ und $AtH_2[B(C_6H_5)_4]_2$, die in den Diagrammen der Abbildung 3 dargestellt sind, wird das Vorhandensein der Ionen $Acr.H^+$, BH^+, AtH_2^{2+} und $[B(C_6H_5)_4]^-$ festgestellt, was gleichzeitig eine Bestätigung für ihre Struktur ist.

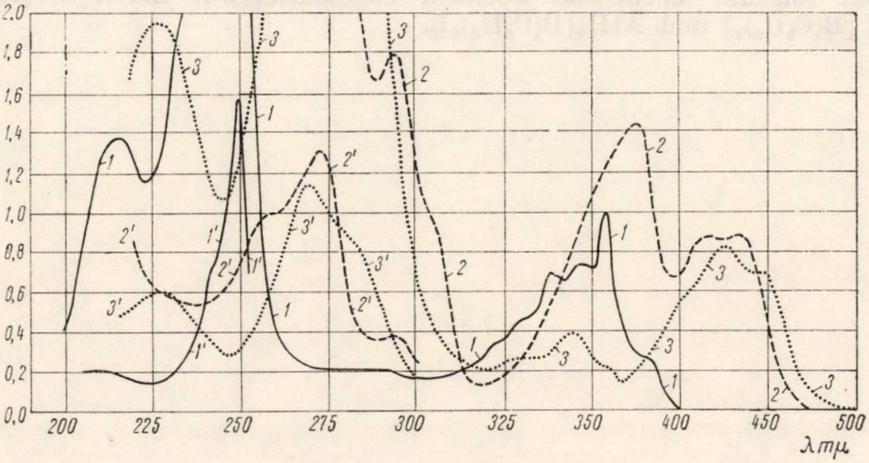

Abb. 3. – Absorptionsspektren von: $Acr.H[B(C_6H_5)_4]$, $BH[B(C_6H_5)_4]$ und $AtH_2[B(C_6H_5)_4]_2$.

5. SCHLUSSFOLGERUNGEN

Durch Behandeln von Akridin, 2-Äthoxy-6,9-diaminoakridin-laktat und 3-Chlor-9-(4′-diäthylamino-1′-methylbutylamino)-7-methoxyakridin-dichlorhydrat mit Natriumtetraphenylborat werden Niederschläge von gelber Farbe gebildet. Durch konduktometrische Untersuchungen der Reaktion zwischen $Na[B(C_6H_5)_4]$ und BHL wird festgestellt, daß diese

---

[19] A. I. Popov und R. E. Humphrey, *J. Amer. Chem. Soc.*, **81**, 2043 (1959); *Chem. Abstr.*, **53**, 16264 (1959).

[20] A. W. Karjakin, *J. Phis. Chem.*, **26**, 91 (1952); *Chem Zentr.*, **1952**, 6506.

[21] H. H. Perkampus, *Z. phys. Chem.* (*Frankfurt*), **6**, 18 (1956); *Chem. Zentr.*, **1957**, 12113.

[22] N. Mataga, *Z. phys. Chem.* (*Frankfurt*), **18**, 285 (1958); *Chem. Zentr.*, **1959**, 15944.

[23] V. Zanker und G. Schiefele, *Z. Elektrochem.*, **62**, 86 (1960); *Chem. Zentr.*, **1960**, 1111.

[24] G. M. Kiselyak und G. M. Lisenko, *Fiz. Probl. Spektroskopii, Acad. Nauk SSSR*, **1**, 336 (1960); *Chem. Abstr.*, **59**, 12318b (1963).

[25] K. R. Popov, *Optik H. Spektroskopie*, **3**, 379 (1957); *Chem. Zentr.*, **1960**, 65.

[26] A. Ringer, *Pharmazie*, **5**, 269 (1950); *Chem. Zentr.*, **1951** (I), 305.

[27] L. W. Smirnov, *J. exp. theoret. Physik*, **23**, 68 (1952); *Chem. Zentr.*, **1953**, 2731.

[28] A. K. Sukhomlinov, *Tr. Khar'kovsk. Farmatsvet. Inst.*, **2**, 69 (1962); *Chem. Abstr.*, **61**, 2938 (1964).

Substanzen auf diesem Wege in Lösungen mit einer Konzentration von 2.10^{-4}M bzw. $3.10^{-3}-2.10^{-4}$ M bestimmt werden können.

BHL kann konduktometrisch mit $Na[B(C_6H_5)_4]$ in Gegenwart von Glukose, Glyzerin, Borsäure und Harnstoff bestimmt werden.

Die Substanzen, die sich während den konduktometrischen Titrationen gebildet hatten, wurden getrennt, analysiert, ihr thermogravimetrisches Verhalten wurde verfolgt und es wurden die Absorptionsspektren aufgezeichnet. Auf Grund der erhaltenen Ergebnisse wurden ihnen folgende chemische Formeln zugeschrieben: $Acr.H[B(C_6H_5)_4]$, $BH\ [B(C_6H_5)_4]$ und $AtH_2[B(C_6H_5)_4]_2$.

Revue Roumaine de Chimie, **14**, 753 – 761 (1969)

DAS VERHALTEN VON 1-ACYL-4-ARYL-THIOSEMIKARBAZIDEN GEGENÜBER DEN SCHWERMETALLKATIONEN. II[1]

DAS VERHALTEN VON Co^{II} GEGENÜBER DEN 1-BENZOYL-4-ARYL-THIOSEMIKARBAZIDEN

RODICA CRĂCIUNEANU und EUGENIA FLOREAN

vom Lehrstuhl für Anorganische und Analytische Chemie der Pharmazeutischen Fakultät, Cluj, str. Pasteur, 6

Eingegangen am 7. September 1968

Gegenstand vorliegender Arbeit ist das Studium der Komplexverbindungen des Co^{II} mit einer Reihe von 1-Benzoyl-4-Aryl-Thiosemikarbaziden und Prüfung des Einflusses der Substituenten mit $(+I)$ und $(-I)$ Effekt aus dem aromatischen Kern auf das Komplexbindungsvermögen. Insofern die gebildeten Verbindungen in dem Reaktionsmedium löslich und gefärbt sind, konnte deren Bildung und Stabilität photometrisch verfolgt werden; dabei wurde der Bereich bestimmt, in welchem das Lambert-Beersche Gesetz eingehalten ist. Das Verbindungsverhältnis und die Werte der Instabilitätskonstanten wurden durch verschiedene photometrische Methoden festgestellt. Parallel zu den Spektren im sichtbaren Bereich, wurden auch die Absorptionsspektren im Ultraviolett durchgeführt, um auch auf diese Weise Natur der Verbindung und Effekt der Substituenten auf das Komplexbindungsvermögen verfolgen zu können.

In einer vorherigen Arbeit [1] haben wir das Studium der Reaktionen zwischen den bakteriostatisch wirkenden 1-Acyl-4-Aryl-Thiosemikarbabaziden [2–7] und einigen Übergangsmetallkationen eingeführt. Diese Reaktionen hängen von der Natur und von der Stellung der Substituenten im Molekül der Thiosemikarbazide ab, sowie von der elektronischen Konfiguration der Kationen.

Gegenstand vorliegender Arbeit ist das Studium der Komplexverbindungen von Co^{II} als Komplexbildner mit einer Reihe von 1-Benzoyl-4-Aryl-Thiosemikarbaziden als Liganden und die Prüfung des Einflusses der Substituenten aus dem aromatischen Kern auf das Koordinationsvermögen.

---

[1] R. Crăciuneanu und E. Florean, *Rev. Roumaine Chim.*, **13**, 105 (1968).
[2] N. P. Buu-Hoi, P. Glay und Ng. Dat Xuong, *Compt. rend.*, **238**, 2582 (1954).
[3] V. S. Misra und R. S. Varma, *J. Indian Chem. Soc.*, **39**, 553 (1962).
[4] V. S. Misra und R. S. Varma, *J. Indian. Chem. Soc.*, **40**, 799 (1963).
[5] N. P. Buu-Hoi und Ng. Dat Xuong, *Compt. rend.*, **237**, 498 (1953).
[6] N. P. Buu-Hoi und Ng. Dat Xuong, *Compt. rend.*, **325**, 329 (1952).
[7] Yao-Tsu Chen und Tzi I. Chang, *Chem. Abstr.*, **61**, 3065 (1965).

Um eine Korrelation in der Wechselwirkung zwischen Co^{II} und Ligand nachzuweisen, die von der Natur der elektronenanziehenden oder -abstoßenden Substituenten aus dem Molekül von 1-Benzoyl-4-Aryl-Thiosemikarbaziden (BTSC) abhängt, ist folgende Reihe in der *para*-Stellung des Stickstoffatoms aus 4 substituierten Derivaten untersucht worden. Künftige Untersuchungen werden den Einfluß verschiedener Substituenten in *para*-Stellung des Benzolkerns aus Stellung 1 verfolgen:

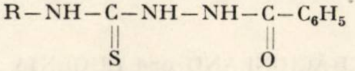

$$R-NH-\underset{\underset{S}{\|}}{C}-NH-NH-\underset{\underset{O}{\|}}{C}-C_6H_5$$

1. $R=H$	$C_8H_9N_3OS$	Molekulargewicht	$= 195{,}244$
2. $R=C_6H_5$	$C_{14}H_{13}N_3OS$	,,	$= 271{,}343$
3. $R=C_6H_4-Br$	$C_{14}H_{12}BrN_3OS$	,,	$= 350{,}244$
4. $R=C_6H_4-CH_3$	$C_{15}H_{15}N_3OS$	,,	$= 285{,}370$
5. $R=C_6H_4-OCH_3$	$C_{15}H_{15}N_3O_2S$	,,	$= 301{,}369$
6. $R=C_6H_4-OC_2H_5$	$C_{16}H_{17}N_3O_2S$	,,	$= 315{,}391$
7. $R=\alpha-C_{10}H_8$	$C_{18}H_{15}N_3OS$	,,	$= 323{,}409$
8. $R=-CH_2-CH=CH_2$	$C_{11}H_{15}N_3OS$	,,	$= 235{,}309$

Es wurde eine Linearität zwischen dem Komplexbindungsvermögen und der Basizität dieser Liganden mit thionischer Gruppe festgestellt und der Einfluß der Induktionseffekte $(+I)$ und $(-I)$ der Gruppe CH_3, Br, OCH_3, OC_2H_5, α-Naphthyl, Allyl verfolgt, welche die Elektronendichte um den Schwefel- und die Stickstoffatome vergrößern oder vermindern.

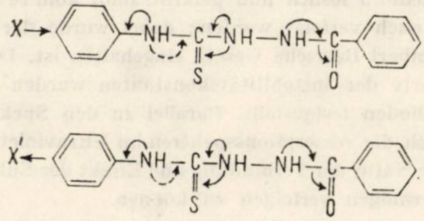

X = Effekt $(+I)$
X' = Effekt $(-I)$

Das Studium der Reaktionen zwischen Co^{II} und den Derivaten von BTSC wurde in verschiedenen Medien und bei verschiedenem pH-Wert durchgeführt, wobei sowohl kristallförmige, orangefarbene Verbindungen in festem Zustand, als auch solche, die sich in Lösung befinden, gewonnen werden. Das Studium der festen Verbindungen, bezüglich Struktur, Zusammensetzung, Stabilität usw. bildet den Gegenstand einer anderen Mitteilung. Vorliegende Arbeit bringt ausschließlich die Ergebnisse der Untersuchungen von sich in Lösung befindenen Co^{II}-BTSC Systemen.

Insofern Co^{II} mit BTSC in MeOH, EtOH, Py, DMF, Azeton usw. lösliche und intensiv rotgefärbte Komplexverbindungen bilden, konnte die Bildung und Stabilität derselben photometrisch verfolgt werden. Verfasser bezweckten es, das Verbindungsverhältnis zwischen Co^{II} und Ligand, die Instabilitätskonstanten der gewonnenen Komplexbindungen zu bestimmen, sowie die Kobaltbestimmung im Bereich für welche das Lambert-Beersche Gesetz genügt, analytisch auszuwerten.

Die Fachliteratur erwähnt eine Reihe von organischen Reagenzien die für die photometrische Bestimmung des Co^{II} angewandt werden. Darunter besetzen einen wichtigen Platz diejenigen, welche Schwefel im Molekül enthalten.[8–18]

EXPERIMENTELLES

Für die photometrische Untersuchung wurde eine titrierte Lösung von $Co(NO_3)_2$ angewandt, wobei der Co^{II}-Gehalt durch Titrieren mit ÄDTA, in Anwesenheit von Murexid als Indikator und durch gravimetrische Schnellbestimmung als $[CoPy_4](SCN)_2$ bestimmt wurde.

Die angewandten Reagenzien wurden nach den Literaturhinweisen synthetisiert[19–23] und die Reinheit durch die Schmelzpunkte überprüft.

Die BTSC sind in Alkalien, MeOH, EtOH, Py, DMF, Azeton usw. löslich. Da die Reagenzien eine große Löslichkeit im Azeton aufweisen, wurde dieses Solvens bevorzugt für die Feststellung des Anwendungsbereiches des Lambert-Beerschen Gesetzes, wo ein Reagenzüberschuß notwendig ist (Lösung 1 %). Das Studium der Reaktionen zwischen Co^{II} und BTSC wurde auch in anderen Lösungsmitteln durchgeführt, wobei festgestellt werden konnte, daß dieselben Verbindungen gewonnen werden, aber daß der Wert der Extinktionen etwas umgeändert ist.

Co^{II} bildet mit BTSC bei einem pH von 8—10 lösliche rotfarbige Komplexverbindungen, deren Spektrum mit einem Spektrophotometer Typ Beckmann DB, mit Selbstregistrierung, im sichtbaren Bereich bestimmt wurde. Wie aus Abb. 1 hervorgeht, liegt die maximale Absorption um 460 nm. Das 1-Benzoyl-Thiosemikarbazid bildet unter denselben Umständen eine grünfarbige Komplexverbindung, deren maximale Absorption bei 602 nm liegt.

Die Komplexverbindung des 1-Benzoyl-Thiosemikarbazids bildet sich augenblicklich, wobei der Wert der Extinktion 50 Minuten lang konstant bleibt. Bei den anderen Verbindungen findet die Bildung der stabilen Komplexverbindungen nach ca. 20 Minuten statt, wobei der Wert der Extinktion 4—6 Stunden konstant bleibt.

---

[8] K. A. Jansen und E. Rancke, *Z. anorg. Chem.*, **219**, 243 (1934).

[9] K. Siddanta und N. Banerjee, *J. Indian Chem. Soc.*, **35**, 547 (1958).

[10] R. G. Neville, *J. Amer. Chem. Soc.*, **79**, 518 (1957).

[11] J. F. Duncan und J. S. Thomas, *J. Chem. Soc.*, **1960**, 2814.

[12] B. N. Figgis und R. S. Nyholn, *J. Chem. Soc.*, **1959**, 342.

[13] D. C. Jicha und J. H. Busch, *Inorg. Chem.*, **872**, 7 (1962).

[14] A. I. Busev und D. H. Vin, *Zhur. analit. Khim.*, **20**, 1347 (1962).

[15] A. D. Anil und M. S. Rahaman, *Analyt. Chim. Acta.*, **34**, 327 (1966).

[16] S. Hara, *Z. analyt. Chem.*, **219**, 442 (1966).

[17] J. Minczewski und K. Kassura, *Chem. Abstr.*, **63**, 17109 (1965).

[18] D. Kealey und H. Freiser, *Analyt. Chem.*, **38**, 1577 (1966).

[19] A. Silberg, I. Simiti, N. Cosma und I. Proinov, *Studii şi Cercetări Chim. Acad. România, Fil. Cluj*, **8**, 115 (1957).

[20] A. Silberg und I. Proinov, *Studii şi Cercetări Chim. Acad. România, Fil. Cluj*, **10**, 329 (1959).

[21] C. Ionescu, I. Schwartz, I. Iliescu, I. Simiti und I. Proinov, *Farmacia*, **3**, 129 (1966).

[22] E. Hoggarth, *J. Chem. Soc.*, **1949**, 1163.

[23] I. Proinov, Dissertation, 1966, S. 18, 37.

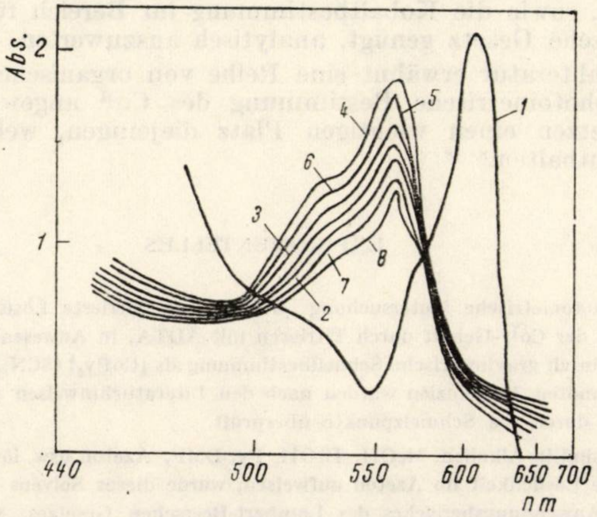

Abb. 1. — Sichtbare Spektren von 1-Benzoyl-4-Aryl-Thiosemikarbaziden.

1, 1-Benzoyl-Thiosemikarbazid; *2*, 1-Benzoyl-4-Phenylthiosemikarbazid; *3*, 1-Benzoyl-4-Bromphenylthiosemikarbazid; *4*, 1-Benzoyl-4-Tolylthiosemikarbazid; *5*, 1-Benzoyl-4-Methoxyphenylthiosemikarbazid; *6*, 1-Benzoyl-4-Äthoxyphenylthiosemikarbazid; *7*, 1-Benzoyl-4-α-Naphthylthiosemikarbazid; *8*, 1-Benzoyl-4-Allylthiosemikarbazid.

DIE ÜBERPRÜFUNG DES LAMBERT-BEERSCHEN GESETZES

Zur Feststellung des Bereiches, in dem das Lambert-Beersche Gesetz eingehalten ist, unter Einhaltung der Gewinnungsbedingungen von Komplexverbindungen zwischen Co^{II} und BTSC, wurde folgende Arbeitsweise angewandt: zu der Co^{II}-Lösung der Konzentration 5.10^{-3} M, verdünnt mit 5 ml Azeton werden 5 ml 1%iges Reagens in Azeton und 3 ml NaOH 1 M zugefügt und mit einem Gemisch von Azeton-Wasser, 1 : 1, auf ein Volumen von 25 ml verdünnt. Im Falle des 1-Benzoyl-Thiosemikarbázids wird die Lösung mit 2 ml NaOH 0,05 M alkalisch gemacht.

Die Bestimmungen wurden mit einem Photokolorimeter Typ FEK-56 durchgeführt, unter Anwendung des Filters 3 und der Küvette von 5 mm. In Tabelle 1 sind die Anwendungsgrenzen des Lambert-Beerschen Gesetzes in μg/ml Co^{II} ausgedrückt, sowie die Empfindlichkeit der Methode nach Sandell [24] angegeben.

DAS VERBINDUNGSVERHÄLTNIS

Die Bestimmung des Verbindungsverhältnisses im System Co^{II} — Liganden wurde die Methode der äquimolekularen Reihen von Job [25] und die Methode von Babko [26] und Asmus [27] angewandt.

---

[24] E. B. SANDELL, „Colorimetric Determination of Traces of Metals'', Interscience Publication, New York, 1959, S. 80.

[25] P. JOB, *Liebigs Ann. Chem.*, **6**, 97 (1936); *ibidem*, **9**, 113 (1928).

[26] A. K. BABKO, „Fisiko-khimicheski analis komplexnyh soedinenii v rastvorakh (opticheskii metod)'', Izd. AN SSR Ukrain, Kiew, 1955, S. 137.

[27] E. ASMUS, *Z. analyt. Chem.*, **178**, 104 (1960).

Tabelle 1

Die Anwendungsgrenzen des Lambert-Beerschen Gesetzes und die Empfindlichkeit der Methode

Lfd. Nr.	Reagens	Minimal-quant. Co^{II} µg/ml	Maximal-quant. Co^{II} µg/ml	Empfindlichkeit µg/cm²
1	1-Benzoyl-Thiosemikarbazid	3,3	198,42	0,907
2	1-Benzoyl-4-Phenylthiosemikarbazid	2,2	105	1,240
3	1-Benzoyl-4-Bromphenylthiosemikarbazid	2,2	90	1,001
4	1-Benzoyl-4-Tolylthiosemikarbazid	2,2	105	1,141
5	1-Benzoyl-4-Methoxyphenylthiosemikarbazid	2,2	112	1,119
6	1-Benzoyl-4-Äthoxyphenylthiosemikarbazid	2,2	90	0,851
7	1-Benzoyl-4-Naphthylthiosemikarbazid	2,2	102	0,957
8	1-Benzoyl-4-Allylthiosemikarbazid	1,12	67,50	0,771

Die Ergebnisse der Bestimmungen nach der Methode von Job sind in Abbildung 2 angegeben. Man stellt dabei fest, daß alle substituierten BTSC ein Verbindungsverhältnis von 1 : 2 zwischen Co^{II} und Ligand aufweisen, während im Falle des 1-Benzoyl-Thiosemikarbazids das Verbindungsverhältnis 1 : 1 beträgt. Durch die Methoden von Babko und Asmus ist dieses Verhältnis bestätigt worden.

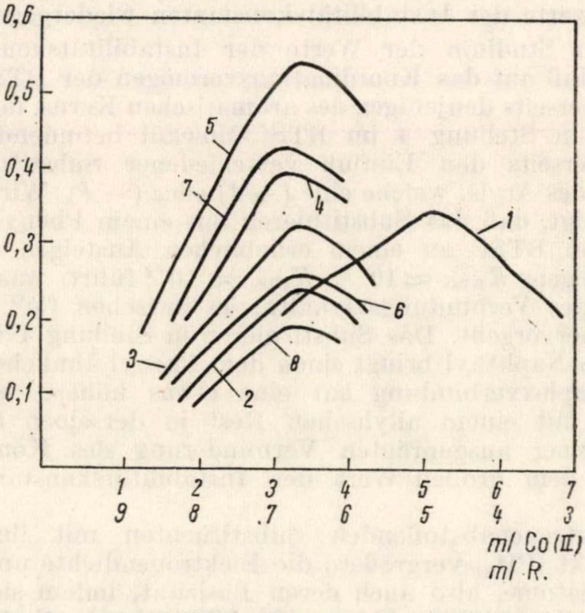

Abb. 2. — Die Extinktionskurven der äquimolekularen Reihen.

1, 1-Benzoyl-Thiosemikarbazid; *2*, 1-Benzoyl-4-Phenylthiosemikarbazid; *3*, 1-Benzoyl-4-Bromphenylthiosemikarbazid; *4*, 1-Benzoyl-4-Tolylthiosemikarbazid; *5*, 1-Benzoyl-4-Methoxyphenylthiosemikarbazid; *6*, 1-Benzoyl-4-Äthoxyphenylthiosemikarbazid; *7*, 1-Benzoyl-4-α-Naphthylthiosemikarbazid; *8*, 1-Benzoyl-4-Allylthiosemikarbazid.

BESTIMMUNG DER INSTABILITÄTSKONSTANTEN

Die Bestimmung der Instabilitätskonstanten wurde durch die Methode der nichtäquimolekularen Reihen von Job durchgeführt. Die Ergebnisse stimmen mit einigen Überprüfungen überein, die nach der Methode von Babko und Asmus durchgeführt wurden.

Die Berechnung der Instabilitätskonstanten wurde durch folgende Gleichung durchgeführt :

$$K = \frac{c^{m+n-1} \cdot p^{n-1} \, [(pm - n)\, x - n]^{m+n}}{m^{n-1} \cdot n^{m-1} \, [n.(m+n)x] \, (p-1)^{m+n-1}}$$

wo :

c = die molare Konzentration der Co^{II}-Lösung,

p = das Verhältnis der molaren Konzentration der Reagenslösungen zu der molaren Konzentration der Co^{II}-Lösung,

m und n = die Koeffizienten der beiden Bestandteile aus dem Komplexmolekül,

x = die maximale Zusammensetzung entsprechend dem größten Wert der Extinktion.

In Tabelle 2 werden die experimentellen Ergebnisse und die Durchschnittswerte der Instabilitätskonstanten wiedergegeben.

Aus dem Studium der Werte der Instabilitätskonstanten kann man den Einfluß auf das Koordinationsvermögen der BTSC-Substanzen feststellen : einerseits denjenigen des aromatischen Kerns, des α-Naphthyls und des sich in Stellung 4 im BTSC-Molekül befindenden allylischen Restes, andererseits den Einfluß verschiedener Substituenten in der *para*-Stellung des Aryls, welche eine $(+I)$ oder $(-I)$ Wirkung besitzen. Die Tabelle zeigt, daß das Substituieren mit einem Phenylradikal in der Stellung 4 von BTSC zu einem erheblichen Ansteigen des Komplexbindungsvermögens $K_{BTSC} \approx 10^{-2}$, $K_{FTSC} \approx 10^{-6}$ führt, was auch aus der Veränderung des Verbindungsverhältnisses zwischen Co^{II} : Ligand, von 1 : 1 zu 1 : 2 hervorgeht. Das Substituieren in Stellung 4 von BTSC mit dem Radikal α-Naphthyl bringt einen dem Phenyl ähnlichen Beitrag ein, aber die Komplexverbindung hat eine etwas höhere Stabilität. Das Substituieren mit einem allylischen Rest in derselben Stellung führt dagegen zu einer ausgeprägten Verminderung des Komplexions, was offenbar aus dem großen Wert der Instabilitätskonstante $K \approx 10^{-3}$ hervorgeht.

Die elektronenabstoßenden Substituenten mit ihrem positiven Induktionseffekt (CH_3) vergrößern die Elektronendichte um die Schwefel- und Stickstoffatome, also auch deren Basizität, indem sie Bildung von Komplexverbindungen mit höherer Stabilität begünstigen. Die Substituenten mit negativem Induktionseffekt (Br) wirken in entgegengesetzte Richtung, indem sie eine Verminderung der Stabilität der Komplexverbindungen beeinflussen.

Im Falle von Substituenten mit negativem Induktionseffekt (OCH_3, OC_2H_5) findet eine antagonistische Konjugation $(+E_s)$, mit starker

Tabelle 2

Die Werten der Instabilitätskonstanten von Co^{II}-BTSC Komplexverbindungen

Reagens	c	p	x	K medial
1	5.10^{-3}	6	0,40	$1{,}58.10^{-2}$
$NH_2.CS.NH.NH.CO.C_6H_5$	,,	8	0,375	
	,,	10	0,35	
2	5.10^{-3}	2	0,575	
$C_6H_5.NH.CS.NH.NH.CO.C_6H_5$	$2{,}5.10^{-3}$	4	0,45	$3{,}18.10^{-6}$
	5.10^{-3}	6	0,32	
3	$2{,}5.10^{-3}$	2	0,59	
$BrC_6H_4.NH.CS.NH.NH.CO.C_6H_5$	,,	4	0,38	$5{,}67.10^{-6}$
	,,	6	0,33	
4	5.10^{-3}	2	0,55	$1{,}43.10^{-6}$
$CH_3C_6H_4.NH.CS.NH.NH.CO.C_6H_5$	$2{,}5.10^{-3}$	4	0,45	
	,,	6	0,375	
5	$2{,}5.10^{-3}$	2	0,58	
$CH_3OC_6H_4.NH.CS.NH.NH.CO.C_6H_5$	,,	4	0,425	$7{,}43.10^{-7}$
	,,	6	0,35	
6	$2{,}5.10^{-3}$	2	0,55	
$C_2H_5OC_6H_4.NH.CS.NH.NH.CO.C_6H_5$	5.10^{-3}	4	0,36	$0{,}46.10^{-7}$
	$2{,}5.10^{-3}$	6	0,30	
7	$2{,}5.10^{-3}$	2	0,35	
$C_{10}H_7.NH.CS.NH.NH.CO.C_6H_5$	,,	4	0,375	$1{,}79.10^{-6}$
	,,	6	0,39	
8	5.10^{-3}	8	0,525	$7{,}82.10^{-3}$
$CH_2:CH.CH_2.NH.CS.NH.NH.CO.C_6H_5$				

Wirkung statt. Diese Substituenten vergrößern also die Basizität der Liganden, was aus den Werten der Instabilitätskonstanten offenbar hervorgeht ($K_{OCH_3} > K_{OC_2H_5} \approx 10^{-7}$).

Das Studium der Absorptionsspektren im Ultraviolett. Das Spektrenstudium im Ultraviolett der Komplexverbindungen im Verhältnis zu dem Liganden ist zur Erläuterung der chemischen Verbindung durchgeführt worden. Da die Komplexreaktionen bei einem alkalischen pH-Wert stattfinden, wurden parallel auch die Absorptionsspektren der Liganden in basischem Medium untersucht. Die Absorptionsspektren wurden mit dem Spektrophotometer Beckmann, im Bereich von 200—400 nm bestimmt; dabei wurde das Methanol als Lösungsmittel angewandt, und die Konzentration der Lösungen betrug etwa 2.10^{-5}.

In den Abbildungen 3—6 sind die Maximalabsorptionen der Liganden und der Komplexe angegeben.

Alle Kurven weisen zwischen 234–244 eine Maximalabsorption auf, welche in der Literatur [21, 28–30] der Gruppe $C = S$ zugeschrieben wurde. Das Studium dieser Kurven führt zu der Schlußfolgerung, daß in methanolischer Lösung die Thionform überwiegt. Das Substituieren mit verschiedenen Radikalen in Stellung 4 von BTSC hat einen hypsochromen Effekt, indem es die Maximalabsorption der Thiokarbonyl-

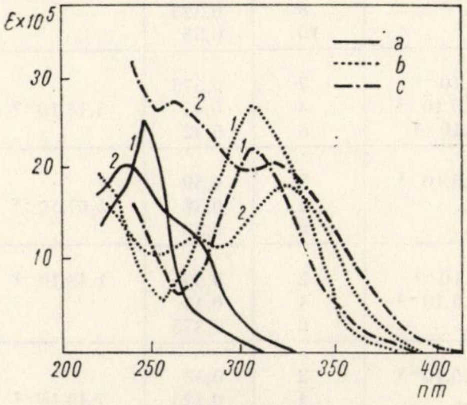

Abb. 3. — UV-Spektren von 1-Benzoyl-Thiosemikarbazid (1) und von 1-Benzoyl-4-Phenylthiosemikarbazid (2) und Co-Komplexverbindungen.

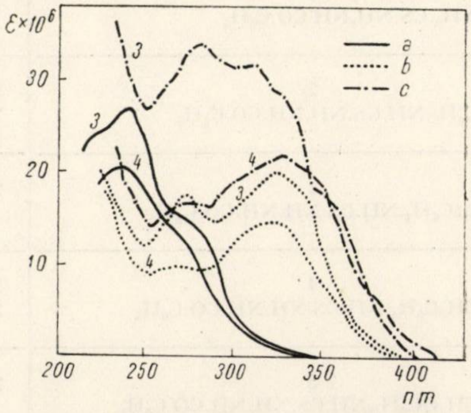

Abb. 4. — UV-Spektren von 1-Benzoyl-4-Bromphenylthiosemikarbazid (3) und von 1-Benzoyl-4-Tolylthiosemikarbazid (4) und Co-Komplexverbindungen.

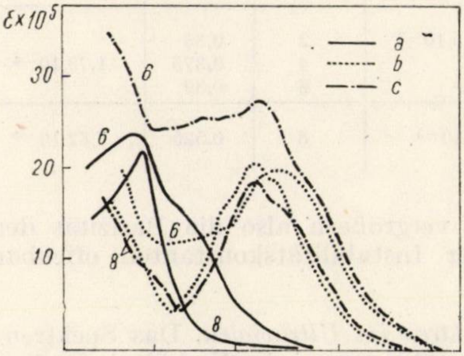

Abb. 5. — UV-Spektren von 1-Benzoyl-4-Äthoxyphenylthiosemikarbazid (6) und von 1-Benzoyl-4-Allylthiosemikarbazid (8) und Co-Komplexverbindungen.

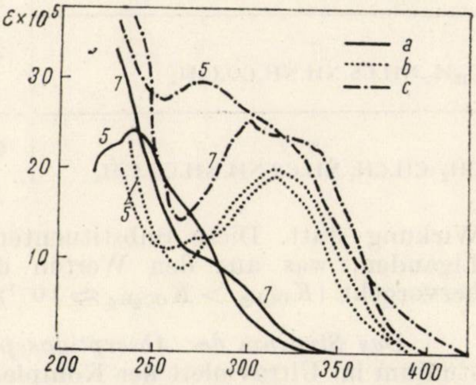

Abb. 6. — UV-Spektren von 1-Benzoyl-4-Methoxyphenylthiosemikarbazid (5) und von 1-Benzoyl-4-α-Naphthylthiosemikarbazid (7) und Co-Komplexverbindungen.

a, Absorptionsspektrum des Liganden. *b*, Absorptionsspektrum des Liganden in alkalischem Medium. *c*, Absorptionsspektrum der Komplexverbindung.

[28] E. S. Stern und A. E. Gilam, „An introduction to Electronic Absorbtion Spectroscopy in Organic Chemistry", Ed. Arnold, London, 1954, S. 220.

[29] P. Koch, *J. Chem. Soc.*, **1949**, 401.

[30] M. J. Jansen, *Rec. Trav. chim.*, **79**, 454 (1960).

verbindung gegen kleinere Wellenlängen verschiebt. In alkalischem Medium, als Folge der Entstehung der Thiolform, verschwindet diese charakteristische Absorption. Die Thion-Thiol-Tautomerie kann wie folgt stattfinden :

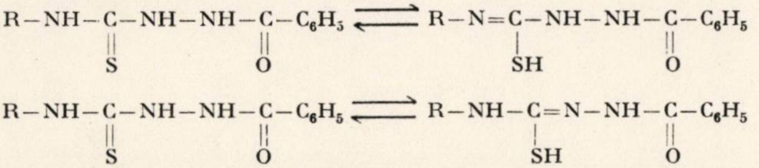

$$R{-}NH{-}\underset{\underset{S}{\|}}{C}{-}NH{-}NH{-}\underset{\underset{O}{\|}}{C}{-}C_6H_5 \rightleftarrows R{-}N{=}\underset{\underset{SH}{|}}{C}{-}NH{-}NH{-}\underset{\underset{O}{\|}}{C}{-}C_6H_5$$

$$R{-}NH{-}\underset{\underset{S}{\|}}{C}{-}NH{-}NH{-}\underset{\underset{O}{\|}}{C}{-}C_6H_5 \rightleftarrows R{-}NH{-}\underset{\underset{SH}{|}}{C}{=}N{-}NH{-}\underset{\underset{O}{\|}}{C}{-}C_6H_5$$

Gleichzeitig entsteht ein ausgeprägtes Maximum um etwa 306—321 nm, welches nach den Literaturhinweisen [28] dem Benzoyl in Enolform zuzuschreiben ist.

Außer den Untersuchungen der IR-Spektren, der magnetischen Empfänglichkeit, der Substanzen in festem Zustand usw., welche noch durchzuführen sind, wird zur Ergänzung vorliegender Arbeit auch die Reaktion von Co^{II} mit 1-Benzoyl-3-Methyl-4-Aryl-Thiosemikarbazid untersucht. Da in dieser Reaktion der Wasserstoff des Stickstoffs aus 3 blockiert ist, kann die Thion-Thiol-Tautomerie nur mit Veränderung der Stellung des mit dem Stickstoff gebundenen Wasserstoffs aus Stellung 4 stattfinden.

Als Folge der Komplexverbindungen stellt man ein starkes Ansteigen der Absorption fest, wie aus den hohen Werten der Molkoeffizienten der Extinktion ersichtlich, gleichzeitig mit einer Erweiterung der Banden, die auf eine Verminderung der Elektronendichte der Verbindung $C = S$, also auf deren Einführung in die Komplexverbindung hinweist, mit Ausnahme des 1-Benzoyl-4-Allylthiosemikarbazids, bei welchem die Molkoeffizienten der Extinktion kleinere Werte als die Liganden haben.

Alle Liganden, ausgenommen das 1-Benzoyl-Thiosemikarbazid und das 1-Benzoyl-4-Allylthiosemikarbazid, weisen noch ein Maximum um etwa 260 nm auf, welches nach dem Literaturhinweis [28] dem Benzolkern entspricht. Der Einfluß der Substituenten im Benzolkern wirkt sich durch eine bathochrome Verschiebung 265—267 nm und durch eine Erweiterung der Bande aus, als Folge der Veränderung der Elektronendichte unter dem Einfluß ihres $(+I)$ und $(-I)$ Effektes.

Folgende Untersuchungen über die festen Verbindungen des Co^{II} mit diesen Liganden, IR-Spektren, magnetische Empfänglichkeit, ATG, usw. werden zu der wahrscheinlich ersten Formulierung der gewonnenen Verbindungen führen. Unsere künftigen Untersuchungen werden auch das Verhalten anderer Komplexgeneratoren vergleichend verfolgen.

verbindung gegen kleinere Wellenlängen verschiebt. In alkalischem Medium, als Folge der Entstehung der Thiolform, verschwindet diese charakteristische Absorption. Die Thion-Thiol-Tautomerie kann wie folgt stattfinden:

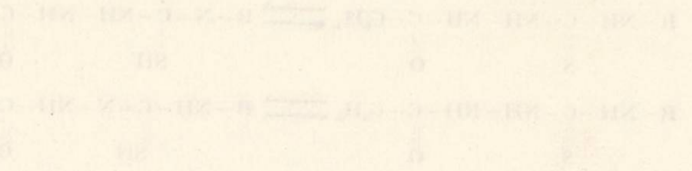

$$R{-}NH{-}\underset{S}{\overset{}{C}}{-}NH{-}NH{-}\underset{O}{C}{-}C_6H_5 \rightleftharpoons R{-}N{=}\underset{SH}{C}{-}NH{-}NH{-}\underset{O}{C}{-}C_6H_5$$

$$R{-}NH{-}\underset{S}{C}{-}NH{-}NH{-}\underset{O}{C}{-}C_6H_5 \rightleftharpoons R{-}NH{-}\underset{SH}{C}{=}N{-}NH{-}\underset{O}{C}{-}C_6H_5$$

Gleichzeitig entsteht ein ausgeprägtes Maximum um etwa 308—321 nm, welches nach den Literaturhinweisen [8] dem Benzoyl in Enolform zuzuschreiben ist.

Außer den Untersuchungen der IR-Spektren, der magnetischen Empfänglichkeit, der Substanzen in festem Zustand usw., welche noch durchzuführen sind, wird zur Ergänzung vorliegender Arbeit auch die Reaktion von Co^{II} mit 1-Benzoyl-3-Methyl-4-aryl-Thiosemicarbazid untersucht. Da in dieser Reaktion der Wasserstoff des Stickstoffs aus 3 blockiert ist, kann die Thion-Thiol-Tautomerie nur mit Veränderung der Stellung des mit dem Stickstoff gebundenen Wasserstoffs aus Stellung 4 stattfinden.

Als Folge der Komplexverbindungen stellt man ein starkes Ansteigen der Absorption fest, wie aus den hohen Werten der Molkoeffizienten der Extinktion ersichtlich, gleichzeitig mit einer Erweiterung der Banden, die auf eine Verminderung der Elektronendichte der Verbindung C = S, also auf deren Einführung in die Komplexverbindung hinweist, mit Ausnahme des 1-Benzoyl-4-Allylthiosemicarbazids, bei welchem die Molkoeffizienten der Extinktion kleinere Werte als die Liganden haben.

Alle Liganden, ausgenommen das 1-Benzoyl-Thiosemicarbazid und das 1-Benzoyl-4-Allylthiosemicarbazid, weisen noch ein Maximum um etwa 260 nm auf, welches nach dem Literaturhinweis [8] dem Benzolkern entspricht. Der Einfluß der Substituenten im Benzolkern wirkt sich durch eine bathochrome Verschiebung 263—267 nm und durch eine Erweiterung der Bande aus, als Folge der Veränderung der Elektronendichte unter dem Einfluß ihres (+ I) und (– I) Effektes.

Folgende Untersuchungen über die festen Verbindungen des Co^{II} mit diesen Liganden, IR-Spektren, magnetische Empfänglichkeit, ATG, usw. werden zu der wahrscheinlich ersten Formulierung der gewonnenen Verbindungen führen. Unsere künftigen Untersuchungen werden auch das Verhalten anderer Komplexgeneratoren vergleichend verfolgen.

---

[8] Karl Bauer, [illegible] Chem. 14, 753—761 ([illegible])

Revue Roumaine de Chimie, 14, 763–766 (1969)

POLYPYRAZOLES-ESTERS

C. CHIRIAC, LEONIA STOICESCU-CRIVETZ et I. ZUGRĂVESCU

Institut de Chimie Macromoléculaire « P. Poni » de l'Académie, Filiale assy,
41 A, Aleea Gr. Ghica Vodă

Reçu le 13 novembre 1968

On a synthétisé par polycondensation interfaciale des polypyrazoles-esters, à poids moléculaire élevé, à partir des acides : 1-phényl-3,5-pyrazoldicarboxylique et 1-phényl-4-bromo-3,5-pyrazoldicarboxylique avec les diphénols (hydroquinone, résorcine, 2,2-bis (4-hydroxyphényl)-propan, 1,5-dihydroxynaphtylène. Les polymères obtenus présentent une viscosité inhérente supérieure et une perte mineure en poids au-dessous de 300° dans l'air.

Dans une note antérieure[1] nous avons présenté la synthèse des poly-pyrazoles-amides à partir des acides 3,5-pyrazoldicarboxyliques et d'une série de diamines. Poursuivant nos études sur les polymères hétérocycles nous nous sommes intéressés aux polypyrazoles-esters. Nous avons choisi comme produits de polycondensation les chlorures des acides : 1-phényl-3,5-pyrazoldicarboxylique et 1-phényl-4-bromopyrazoldicarboxylique et les diphénols : hydroquinone, résorcine, 2,2-bis(4-hydroxyphényl)-propan et 1,5-dihydroxynaphtylène.

Ces composés bifonctionnels présentent une symétrie des groupements réactifs, d'autre part les cycles aromatiques, ainsi que ceux pyrazoliques sont doués d'une grande stabilité termique ; ces structures répondent de la stabilité des polymères, à des températures élevées

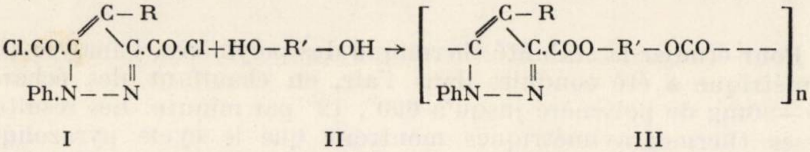

$$\mathrm{Cl.CO.}\overset{\mathrm{C-R}}{\underset{\mathrm{Ph.N--N}}{\mathrm{C\quad C}}}\mathrm{.CO.Cl+HO-R'-OH} \rightarrow \left[-\overset{\mathrm{C-R}}{\underset{\mathrm{PhN--N}}{\mathrm{C\quad C}}}\mathrm{.COO-R'-OCO---}\right]_n$$

I II III

I	II	III	
Ia, R=H	IIa, $R'=p-C_6H_4$	IIIa,R=H	$R'=p-C_6H_4$
Ib, R=Br	IIb, $R'=m-C_6H_4$	IIIb, ,,	$R'=m-C_6H_4$
	IIc, $R'=C_6H_4C(CH_3)_2C_6H_4$	IIIc, ,,	$R'=C_6H_4C(CH_3)_2C_6H_4$
	IId, R'=1,5- naphtylène	IIId, ,,	R'=1,5-naphtylène
		IIIe,R=Br	$R'=C_6H_4C(CH_3)_2C_6H_4$
		IIIf,R=Br	$R'=p-C_6H_4$

---

[1] C. CHIRIAC, L. STOICESCU-CRIVETZ et I. ZUGRĂVESCU, *Rev. Roumaine Chim.*, **12**, 1489 (1967).

RÉSULTATS ET DISCUSSIONS

La polycondensation des acides pyrazoliques avec les diphénols s'effectue facilement dans un système à deux phases liquides dont l'une est l'eau. Les diphénols dans une solution aqueuse de NaOH sont traités avec les chlorures d'acide dissous dans le chloroforme, à la température ordinaire, en agitant énergiquement. Dans le cas des phénols, la condensation nécessite l'emploi d'un détergent (lauryle sulfonate de sodium). Les polymères précipitent dans le milieu de réaction. Leur poids moléculaire est influencé par des facteurs tels que l'efficacité de l'agitation, la présence des détergents, l'interaction polymère solvant. La substitution de l'atome hydrogène (4) par le brome, ne provoque pas de changements appréciables dans les polymères.

Il suffit de 30—40 minutes pour achever la polycondensation à la température ordinaire. On a obtenu les polymères III, en poudres blanches, à l'exception des IIIa, IIId et IIIe qui ont une couleur plus foncée. Les propriétés de ces polymères sont influencées par la nature du cycle aromatique R′ et les liaisons entre les cycles. Ils sont solubles en chlorure de méthylène, dichlorobenzène, diméthylsulfoxyde, diméthylformamide. Les points de fusion ou de ramollissement varient entre 200 et 250°, IIId contenant des noyaux naphtyléniques à une température de fusion supérieure à 300° (tabl. 1).

Tableau 1

Caractérisation des polypyrazoles-esters III

Polymère	R	R′	P. fus. 0°	η inh 20°	A.T.G. perte en poids %	
					400°	500°
IIIa	H	$p-C_6H_4$	237—242	0,24	30	58
IIIb	H	$C_6H_4C(CH_3)_2C_6H_4$	219—223	0,43		
IIIc	H	$m-C_6H_4$	217—219	0,39	35	65
IIId	H	1,5-naphtylène	293—298	0,32	2	43
IIIe	Br	$p-C_6H_4$	245—250	0,33	15	33
IIIf	Br	$C_6H_4C(CH_3)_2C_6H_4$	222—227	0,28		
IIIg	Br	$m-C_6H_4$	231—236	0,36		

Pour étudier la stabilité thermique des polymères, l'analyse thermogravimétrique a été conduite dans l'air, en chauffant des échantillons de 15—20mg de polymère jusqu'à 600°, 12° par minute. Les résultats des analyses thermogravimétriques montrent que le cycle pyrazolique est stable à la décomposition thermique, et la stabilité est affectée par la structure chimique des phénols utilisés, ainsi que des liaisons esters. Le polymère IIId, le plus stable, présente à 400° une perte en poids de 2%, les autres polymères III sont stables jusqu'à environ 300°. Entre 300° et 400° a lieu une dégradation assez rapide.

La viscosité inhérente a été déterminée dans une solution de diméthylformamide à 20°, pour une concentration de 0,5% (excepté IIIa et IIId qui sont difficilement solubles à cette concentration).

Les viscosités ont des valeurs situées entre 0,24 et 0,43. Les viscosités des polypyrazoles-esters sont plus petites que celles des polypyrazoles-amides,[1] fait pouvant être attribué à la vitesse de réaction des phénols plus petite par rapport à celle des amides dans la polycondensation avec les chlorures acides.

La structure des polymères III, telle qu'elle résulte de la réaction, a été confirmée par les analyses élémentaires et les spectres d'absorption en infrarouge (tabl. 2). Les bandes d'absorption dans la région de 1500 à 1510 cm^{-1}, signalées dans la littérature concernant les pyrazoles,[2] sont présentes dans tous les spectres des polymères préparés par nous. De même on trouve des bandes à 1740—1750 cm^{-1} qui correspondent à des groupements esters.

Tableau 2

Analyses et spectres en infrarouge de polymères III

Polymère	Formules	Analyses						Spectres en IR cm^{-1} (KBr)	
		C%		H%		N% calculé	trouvé		
		calculé	trouvé	calculé	trouvé				
IIIa	$C_{17}H_{10}N_2O_4$	58,94	58,22	4,06	3,96	11,38	11,46	1750	1512
IIIb	$C_{26}H_{20}N_2O_4$	73,58	72,62	4,71	4,65	6,60	6,83	1740	1508
IIIc	$C_{20}H_{10}N_2O_4$	58,94	57,26	4,06	4,17	11,38	10,80	1740	1500
IIId	$C_{21}H_{12}N_2O_4$	70,78	69,62	3,37	3,49	7,86	8,49	1750	1510
IIIe	$C_{17}H_9BrN_2O$	52,90	51,21	2,33	2,42	7,27	7,96	1750	1500
IIIf	$C_{26}H_{19}BrN_2O_4$	62,02	60,95	3,77	3,53	5,56	5,89	1750	1510
IIIg	$C_{17}H_9BrN_2O_4$	50,90	51,44	2,33	2,11	7,27	7,83	1750	1510

Des essais préliminaires ont mis en évidence la possibilité d'obtenir des pellicules à partir d'une solution de polymères dans le chlorure de méthylène.

PARTIE EXPÉRIMENTALE

Les acides pyrazoldicarboxyliques, ainsi que les chlorures acides correspondants ont été préparés selon le procédé décrit dans une note antérieure.[1] Les diphénols ont été soigneusement purifiés par recristallisations répétées en benzène.

Polycondensation interfaciale. A une suspension du diphénol II (1 mole) dans l'eau, on ajoute une solution de hydroxyde de sodium (10%) 2 moles, et lauryle sulfonate de sodium (30% par rapport à l'acide pyrazolique), puis on agite vivement à la température ordinaire. On ajoute d'un coup la solution de dichlorure II (1 mole) dans le chloroforme. Le polymère précipite immédiatement et on agite encore pendant 30—40 minutes. Le produit résulté sous forme d'une fine suspension dans le système eau-chloroforme, devient facilement filtrable par addition d'acétone. Filtré, lavé à l'acétone, puis séché sous vide, il se présente sous la forme d'une poudre faiblement colorée.

---

[2] C. R. Hauser et C. E. Cain, *J. Org. Chem.*, **23**, 1142 (1958).

Exemple : *Polymère IIId.* Dans un verre de 250 ml on introduit une solution de 0,3820 g IId dans 40 ml d'eau, 0,192 g de lauryle sulfonate de sodium et 0,191 g (1,91 ml) de solution de NaOH 10 %, et on y ajoute, en agitant fortement une solution de Ia, 0,640 g dans 20 ml de chloroforme. On maintient l'agitation à la température ambiante encore une demi-heure. Dans cette solution on verse 300 ml d'acétone, après on essore au vide, on lave à l'acétone et à l'eau (pour enlever les traces du détergent), on sèche sous vide à 100°.

Le tableau 1 résume les caractéristiques des polymères préparés dans ce travail.

Les analyses thermogravimétriques ont été effectuées à l'aide d'un dérivatographe E. Paulik, par M. M. Bostan, que nous remercions vivement.

Les spectres en infrarouge ont été déterminés avec un Unicam SP 200.

Revue Roumaine de Chimie, 14, 767–771 (1969)

РАДИОХИМИЧЕСКАЯ ПОЛИМЕРИЗАЦИЯ АКРИЛОНИТРИЛА В ТВЕРДОЙ ФАЗЕ

И. ВЛАДЖИУ

Центр физической химии Академии Социалистической Республики Румынии
Бухарест

Получена 25 мая 1968 г.

Изучалась радиохимическая полимеризация акрилонитрила при температуре —78° в присутствии различных добавок. Облучение производилось при дозе в $2{,}17.10^{17}$ эв/г/мин.

Несколько работ[1–6] посвящены изучению радиохимической полимеризации акронитрила в твердой фазе, в которых делаются попытки дать объяснение механизму реакции. Анализируя эти работы, можно сделать следующие заключения[7]:

а) механизм реакции этого мономера мало известен; согласно разным допущениям, предполагается, что речь идет об ионном или радикальном механизме;

б) при температуре в —196° наибольшая конверсия колеблется в пределах между 4 и 5%;

в) между —140° и точкой замерзания мономера (—83°), реакция полимеризации происходит с постоянной скоростью до конверсии в 25%;

г) радиохимическая полимеризация акрилонитрила со стиролом или метакрилатом метила при —78°, происходит по катионному или анионному механизму. Механизм усложняется в том случае, когда полимеризация происходит в присутствии металлических окислов;

д) в своих работах Амаги и Шапиро показывают, что ацетон ингибирует реакцию полимеризации намного сильнее, чем акрилонитрил, толуол, йод и бензохинон. Аналогичный эффект наблюдался Табатом при изучении радиохимической полимеризации акрилонитрила в присутствии пирогалола.

[1] A. Chapiro и M. Inoue, *J. Chim. Phys.*, **64**, 338 (1967).
[2] H. Sobue и Y. Tabata, *J. Polymer Sci.*, **43**, 459 (1960).
[3] R. Bensasson и R. Max, *J. Polymer Sci.*, **48**, 53 (1960).
[4] R. Bensasson, A. Dvorkin и R. Marx, *J. Polymer Sci.*, **C—4**, 881 (1964).
[5] I. M. Barkalov, V. I. Goldanski, N. S. Enicolpoian, S. E. Terehova и G. M. Trofimova, *J. Polymer Sci.*, **C—4**, 897 (1964).
[6] Y. Amagi и A. Chapiro, *J. Chim. Phys.*, **59**, 137 (1962).
[7] Y. Tsuda, *J. Polymer Sci.*, **54**, 193 (1961).

ЭКСПЕРИМЕНТАЛЬНЫЕ УСЛОВИЯ

Облучение производилось в отсутствии воздуха в ячейке объемом в 4 см^3. Полученный полимер осушался в вакууме до постоянного веса. Поглощенная доза в ячейке рассчитывалась по соотношению:

$$D(\text{эв/г}) = 1{,}84.10^{18}\ (1-0{,}007t)\times D.O.,$$

где D.O. — оптическая плотность; в качестве дозиметрического раствора использовалось сернокислое железо (II).

Радиохимическая полимеризация производилась в присутствии диметилформамида, диметилсульфоксида, этиленкарбоната, триэтиленамина, окиси цинка, окиси магния, окиси меди, окиси ниобия, окиси неодима, н. -пропиламина, диэтилтриамина, азотнокислого серебра, хлористой меди и металлической меди.

Молекулярный вес акрилонитрила был получен вискозиметрическим методом в диметилформамиде (ДМФ) при 25°, применяя следующую формулу:

$$[\eta] = \frac{\sqrt{1 + 1{,}32\cdot\eta_{sp}} - 1}{0{,}198},$$

$$[\eta] = 3{,}92\cdot 10^{-4}\,\overline{M}_n{}^{-0{,}75}$$

Анализ структуры полимера был произведен в инфракрасной области на приборе типа Цейсс-Йенна.

ИНТЕРПРЕТАЦИЯ ЭКСПЕРИМЕНТАЛЬНЫХ ДАННЫХ

а) *Радиохимическая полимеризация в органических растворителях*

Изучалось влияние химической структуры некоторых органических растворителей (диметилформамид, диметилсульфоксид, этиленкарбонат, триэтиламин, н. -пропиламин, диэтилентриамин), при температуре в —78° (полученной смешением метилового спирта с сухим льдом). Из всех вышеуказанных растворителей, акрилонитрил полимеризуется только в диметилформамиде, триэтиламине, н. -пропиламине и диэтилентриамине. Экспериментальные данные, полученные нами при этой температуре, конкретизированы в табл. 1.

Таблица 1

Изменение конверсии в зависимости от среды реакции [AN] = 2,60 моль. л$^{-1}$; время полимеризации 10 час; $T = -78°$

Растворитель	Конверсии %	P
Диметилформамид	5,64	220
Триэтиламин	4,95	115
Диэтилентриамин	3,80	104
Н.-пропиламин	4,10	160
«В массе»	3,10	280

Измерение скорости полимеризации со временем рассчитывалось по уменьшению концентрации, для температур в —78°, вышеуказанных растворителей и показано в табл. 1.

Из анализа табл. 1 видно, прежде всего, что молекулярный вес полиакрилонитрила (выраженный в нашем случае средней степенью полимеризации **P**) уменьшается при —78°, что указывает на изменение в механизме реакции.

Изменение скорости реакции в зависимости от времени и среды реакции
$T = -78°$ [AN]=2,60 моль/л; время полимеризации 10 час.

Растворитель	ΔC моль·л$^{-1}$	Конверсии %	$V = \frac{\Delta C}{\Delta t} \times 10^7$ (моль·л$^{-1}$ сек$^{-1}$)
Диметилформамид	0,1466	5,64	40,72
Триэтиламин	0,1280	4,95	35,56
Диэтилентриамин	0,1060	4,10	29,43
Н.-пропиламин	0,0988	3,80	27,44
«В массе»	—	1,81	5,03.10^{-5}

Одновременно можно было заметить, что и скорость реакции уменьшается с увеличением числа аминогрупп в структуре растворителя.

Анализ структуры полимера, полученного при —78° в присутствии диметилформамида с добавлением азотнокислого серебра, показывает существование китениминной связи, доказанной экспериментально и другими исследователями [1–7], в случае полимеризации акрилонитрила при —78° и — 196°. Присутствие азотнокислого серебра делает число спинов на моль намного большим, чем в отсутствии азотнокислого серебра; так, например, для –78° в присутствии азотнокислого серебра было получено $9{,}16.10^{21}$ спинов/моль, по сравнению с $4{,}58.10^{20}$ спинов/моль в отсутствии азотнокислого серебра.

Уменьшение скорости полимеризации и появление китениминной связи может быть приписано структурной ориентации акрилонитрила:

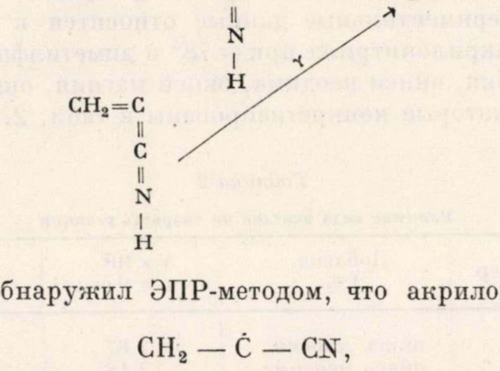

$$CH_2{=}\underset{CN}{\underset{|}{CH}} \rightleftarrows CH_2{=}\underset{\underset{\underset{\underset{H}{|}}{N}}{\|}}{\underset{\|}{C}} \qquad CH_2{=}\underset{CN}{\underset{|}{\dot{C}}} + H^{\cdot}$$

$$CH_2{=}\underset{\underset{\underset{\underset{H}{|}}{N}}{\|}}{\underset{\|}{C}}$$

Бенсассон обнаружил ЭПР-методом, что акрилонитрил дает радикал типа:

$$CH_2 - \dot{C} - CN,$$

который может участвовать в реакции полимеризации.

Образование этого радикала объясняется легко резонансом структуры вышеуказанного акрилонитрила, способствующего удалению атома водорода в радиационном поле.

ЗАКЛЮЧЕНИЯ

1. Из предпринятого изучения следует, что акрилонитрил полимеризует ионным путем; трудно определить, в каком виде.

2. Полимеризация акрилонитрила происходит в диметилформамиде, триэтиламине, н.-пропиламине и диэтилентриамине, но не в диметилсульфоксиде или же в этиленкарбонате.

3. Резонанс структуры акрилонитрила позволяет легко объяснить образование китениминной группировки, а также и радикала, обнаруженного Бенсассоном ЭПР—методом.

4. Азотное серебро, хлористая медь способствуют образованию китениминной группировки в диметилформамиде, а также и числа спинов на моль.

В присутствии азотнокислого серебра или хлористой меди при концентрации в 0,2%, скорость реакции полимеризации в диметилформамиде намного увеличивается: 14.10^{-6} моль/л.сек или 11.10^{-6} моль/л.сек; молекулярный вес полимера при этом остается без изменения.

б) *Радиохимическая полимеризация в присутствии твердых прибавок*

Советские исследователи[8] были первыми, которые выявили влияние различных металлических окислов на радиохимическую полимеризацию акрилонитрила при —78°. Они заметили, что в результате использования окислов (Cu_2O, NiO, MgO) вместо окислов цинка, триокиси хрома, стекла, степень конверсии в присутствии триэтиламина значительно возрастает; растет также и молекулярный вес.

Наши экспериментальные данные относятся к радиохимической полимеризации акрилонитрила при —78° в диметилформамиде в присутствии окиси ниобия, окиси неодима, окиси магния, окиси меди и металлической меди, которые конкретизированы в табл. 2.

Таблица 2

Влияние вида окислов на скорость реакции

Мономер	Добавка 1%	$V \times 10^5$ моль.л$^{-1}$ сек$^{-1}$	P
[A N]	окись ниобия	2,87	48
	окись неодима	3,16	54
	окись магния	12,12	60
	окись меди	16,00	100

---

[8] Л.П. Межирова, А. П. Сейнкер и А.Д. Абкин, *Высокомол. соединения*, 3 99 (1961); А. Д. Абкин, А. И. Панова Л. П. Толстоухова и А. П. Сейнкер, «Радиационная химия полимеров», Изд. «Наука», Москва, 1967, стр. 58.

Абкин [8] объясняет полимеризацию акрилонитрила в присутствии металлических окислов (в триэтиламине) переходом электронов из твердой добавки к радикалу, хемосорбированному на поверхности этой добавки.

Таблица 3

Влияние вида окислов на скорость реакции

[AN] моль/л $(C)_0$	Растворитель	Добавка 3 %	V моль/л. сек	P
2,600	диметилформамид	окись ниобия	2,87	48
		окись неодима	3,16	54
		окись магния	12,12	60
		окись меди	16,00	100

Присутствие металлических окислов в реакционной среде по сравнению с присутствием азотнокислого серебра или хлористой меди не увеличивает число спинов на моль; роль их в реакции трудно объяснить.

Revue Roumaine de Chimie, **14**, 773–779 (1969)

LINEAR POLYESTERS AND POLYCARBONATES FROM BIS-(4-HYDROXYPHENYL)-DEOXYBENZOIN AND 1,1-BIS-(4-HYDROXYPHENYL)-2-OXO-ACENAPHTHENE

ALLA PETRUŞ, LAURA MĂNDĂŞESCU and I. MATEI

Institute of Macromolecular Chemistry "Petru Poni", Jassy, Aleea Grigore Ghica Vodă 41 A

Received September 7, 1968

Polyesters from bis(4-hydroxyphenyl)-deoxybenzoin and 1,1-bis(4-hydroxyphenyl)-2-oxo-acenaphthene with terephthaloyl, isophthaloyl and sebacyl chlorides and phosgene have been prepared. The viscosity, melting temperature, solubility and thermal stability of the obtained polymers are described.

There are many reports concerning the synthesis and study of aromatic polycarbonates and polyarylates, the polyesters from bisphenols and aromatic acids. These polymers have high melting temperatures, a high thermal stability, good electrical resistance and show an acceptable chemical and hydrolytic stability. The aromatic polycarbonates are well known in the form of plastics and coatings; the polyarylates have been evaluated for photographic film base and as electrically resistant coatings. A great number of bisphenols bearing different substituents have been used[1-11] and the effect of their structure and of the polycondensation method on the resulted polymers has been studied.

This paper deals with the synthesis and study of some polyesters and polycarbonates from bis(4-hydroxyphenyl)-deoxybenzoin(A) and

---

[1] H. Schnell, *Angew. Chem.*, **68**, 633 (1956); *Ind. Eng. Chem.*, **51**, 157 (1959).

[2] A. Conix, *Ind. Eng. Chem.*, **51**, 147 (1959).

[3] V. V. Korshak, S. V. Vinogradova and S. N. Salazkin, *Vysokomol. Soedinenyia*, **4**, 339 (1962).

[4] V. V. Korshak, S. V. Vinogradova and I. P. Antonova-Antipova, *Vysokomol. Soedinenyia*, **7**, 1543 (1965).

[5] V. V. Korshak and S. V. Vinogradova, *Uspekhi Khim.*, **30**, 421 (1961).

[6] V. V. Korshak, S. V. Vinogradova, G. L. Slominskii, S. N. Salazkin and A. A. Ascadskii, *Vysokomol. Soedinenyia*, **8**, 548 (1966).

[7] G. S. Kolesnicov, Eli-Sand-Ali-Hasan, O. V. Smirnova and I. P. Losev, *Vysokomol. Soedinenyia*, **7**, 729 (1965).

[8] V. V. Korshak, S. V. Vinogradova and I. P. Antonova-Antipova, *Vysokomol. Soedinenyia*, **6**, 2174 (1964).

[9] M. A. Iskenderov, V. V. Korshak, S. V. Vinogradova and V. V. Harlamov, *Vysokomol. Soedinenyia*, **5**, 799 (1963).

[10] V. V. Korshak, S. V. Vinogradova and V. A. Pancratov, *Vysokomol. Soedinenyia*, **7**, 1689 (1965).

[11] P. W. Morgan, *J. Polymer Sci.*, **A2**, 437 (1964).

1,1-bis(4-hydroxyphenyl)-2-oxo-acenaphthene(B). The effect of the bulky substituent at the central carbon atom between the two phenolic rings and of polar carbonylic group has been pursued.

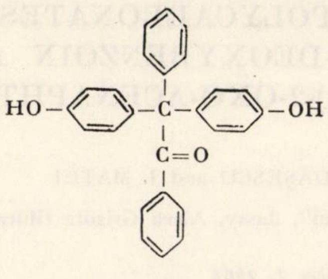

A

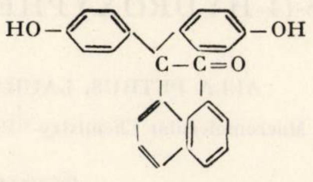

B

The bis(4-hydroxyphenyl)-deoxybenzoin was obtained for the first time in a high degree of purity; 1,1-bis(4-hydroxyphenyl)-2-oxoacenaphthene was earlier prepared by one of the authors.[12]

EXPERIMENTAL

Intermediates

Bis(4-hydroxyphenyl)-deoxybenzoin. Benzil (30 g) is dissolved in phenol (54 g) at 50°, 18 ml of 75% H_2SO_4 are added and the red mixture which gradually becomes viscous, is stirred at 50° for 18–20 hours, then 4% aqueous NaOH is added, the solution is filtered and neutralized with 10% H_2SO_4. The separated sticky product is steam-distilled to remove the phenol excess. The cherry-red residue is dissolved once more in 4% NaOH and the bisphenol is precipitated with CO_2. The white separated powder is filtered, washed with a great amount of water and dried at 50° and 5 mmHg. Yield 32.5 g (60%). M.p., 196–198°.

Anal. *Calcd.* for $C_{26}H_{20}O_3$: C%, 80.82; H%, 5.05. *Found*: C%, 81.04, 81.10; H% 5.43, 5.34.

The same bisphenol was obtained by Kempinski[13] from dichlorobenzil, phenol and $ZnCl_2$ and was described as a red powder with a melting point of about 93°. We also observed that when the bisphenol precipitated from the alkaline solution with 10% H_2SO_4 instead of CO_2, a red powder was obtained which melted at 102–112° and whose elemental analysis was unsatisfactory.

The dibenzoyl ester[11] was obtained by mixing the bisphenol (0.01 mole) benzoyl chloride (0.02 mole) triethylamine (0.02 mole) in 30 ml trichloroethane and cooling in ice water. The product was recrystallized three times from alcohol. White, crystalline powder, melting at 166.5–167.5°.

Anal. *Calcd.* for $C_{40}H_{28}O_5$: C%, 81.63; H%, 4.76; *Found*: C%, 81.60, 81.95; H%, 4.79, 5.14.

1,1-Bis(4-hydroxyphenyl)-2-oxo-acenaphthene was prepared as described earlier[12] except that for the condensation reaction 75% H_2SO_4 was used, the reaction temperature being maintained at 110°. The product was purified by dissolving in 10% NaOH and precipitation with CO_2 followed by dissolving in alcohol and precipitation with hot water. Yellowish, crystalline powder. M. p. 258–259°.

---

[12] I. Matei, *Chem. Ber.*, **62**, 2095 (1929).

[13] M. S. Kempinski, *Bull. Soc. Chim. France*, **7**, 608 (1892).

The dibenzoyl derivative was obtained as above. Yellow crystals melting at 149–151°.

Anal. *Calcd.* for $C_{38}H_{24}O_5$: C%, 81.42, H%, 4.28; *Found*: C%, 81.42, 81.00; H%, 4.76, 4.79.

The acid chlorides were obtained by boiling the acids with $SOCl_2$. The terephthaloyl — and isophthaloyl chlorides were recrystallized from ether petroleum and melted at 79–80°, respectively 43–44°. The sebacyl chloride was distilled in vacuum, at 182°/16 mm.

Polymer preparation

Three methods of polycondensation were used: interfacial, low temperature solution and high temperature solution. General examples are given.

Interfacial polycondensation. Bisphenol (0.01 mole) is dissolved in 100 ml water containing 0.02 mole NaOH. While the mixture is rapidly stirred (3000 r/m), acylchloride (0.01 mole) in 50 ml 1,2-dichloroethane is at once added. Stirring is continued for 5–10 min. The thick emulsion is then poured into 500 ml acetone to precipitate the polymer. (When sebacyl chloride was used the polymer was precipitated in hexane). The polymer is filtered, washed with alcohol, alcohol/water (50/50), hot water and once more alcohol. The yields, viscosities and melting points are given in table 1.

Low-temperature solution polycondensation. Bisphenol (0.01 mole) and triethylamine (0.02 mole) are added in 1,2-dichloroethane. The mixture is cooled at 10° and acylchloride is added. Stirring is continued for 90 min. at 10° and then the polymer is precipitated in 500 ml acetone and treated as above.

High-temperature polycondensation. Into a three-neck round-bottomed flask (stirrer, N_2 inlet tube and HCl outlet tube) 0.01 mole bisphenol and 0.2 g of triethylamine hydrochloride in 25 ml dichlorobenzene have been introduced. The mixture is heated to 210° and acylchloride (0.01 mole) in 25 ml dichlorobenzene is added dropwise. Stirring is continued for 4 hours at 210°, the reaction mixture is allowed to stay overnight, and the polymer is precipitated in 500 ml acetone. The polymer is purified as above.

The polycarbonates were prepared as follows: bisphenol (0.01 mole) is dissolved in 50 ml water containing 0.4 g NaOH. Triethylamine (0.66 ml) is added and then 25 ml 1,2-dichloroethane. Phosgene is introduced with stirring, then the strongly acid solution is alkalinized with 20% NaOH under nitrogen atmosphere and this operation is repeated three times. Finally NaOH solution is added to the neutralization point; 300 ml of acetone are poured to precipitate the polymer which is filtered, washed with acetone, a great amount of alcohol and hot water.

The inherent viscosities were measured in dichloroethane/phenol (40/60 by weight), with an Ubbelohde viscosimeter, at 20° and at 0.5 g/100 ml.

The melting ranges were measured on a Boetius apparatus.

The solubilities were determined at 1 g/100 ml at room temperature and are shown in table 2.

Thermal stability. Samples of polymer were subjected to thermogravimetric analysis from 20 to 500°, with the rate of temperature increase of 6.5°/min., under nitrogen and air. A Ugine Eyraud thermobalance was used and the weight loss registered on a sensitive recorder.

RESULTS AND DISCUSSION

The following polyesters have been obtained by the polycondensation method :

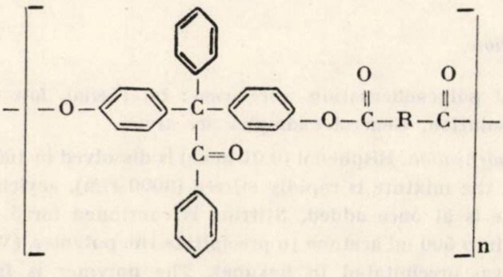

I

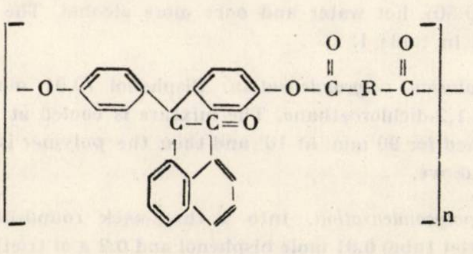

II

I$_1$ and II$_1$: R= 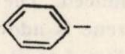

I$_2$ and II$_2$: R= 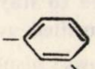

I$_3$ and II$_3$: R= $-(-CH_2)_8-$

The polycarbonates have the structures :

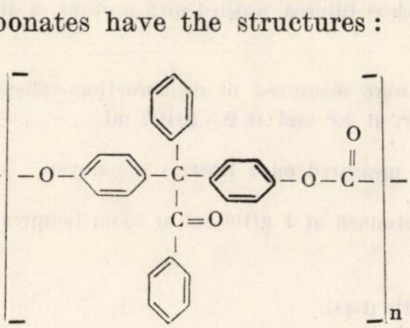

I$_4$

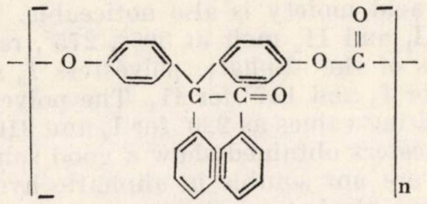

II_4

High yields (84–100) are generally obtained by three polycondensation methods as one can see from table 1. The inherent viscosity of the polymers prepared by interfacial and high temperature polycondensation methods are somewhat higher. The melting ranges of all the prepared polyesters are of nearly the same order as those reported for the poly(phenolphthaleinester) and poly[bis(4-hydroxyphenyl)diphenylmethane ester].[3,10] The polyesters II melted at higher temperature than polyesters I due to the presence in the bisphenol molecule of the bulky, rigid, condensed rings substituent.

Table 1

Polyesters and Polycarbonates

Bisphenol	Diacid chloride	Process[a)]	η inh.	Yield, %	PMT, °C
Bis-(4-hydroxyphenyl)-deoxybenzoin	Terephthaloyl	I	0.76	92	305–315
		HS	0.91	92	— „ —
		LS	0.38	84	— „ —
	Isophthaloyl	I	0.69	90	275–290
		HS	0.53	90	— „ —
		LS	0.43	87	— „ —
	Sebacyl	I	0.29	85	111–123
		HS	0.30	95	— „ —
		LS	0.17	84	— „ —
	Phosgene	I	0.86	98	210–220
1,1-Bis-(4-hydroxyphenyl)-2-oxoacenaphthene	Terephthaloyl	I	0.99	90	>360
		HS	0.34	89	— „ —
		LS	0.46	89	— „ —
	Isophthaloyl	I	0.84	91	>360
		HS	0.40	90	— „ —
		LS	0.38	85	— „ —
	Sebacyl	I	0.22	100	127–143
		HS	0.26	94	— „ —
		LS	0.12	96	— „ —
	Phosgene	I	0.49	90	310–325

a) I = interfacial method; HS = high temperature solution method; LS = low temperature solution method.

The effect of the acid moiety is also noticeable. The polyarylates I_1 and I_2, respectively II_1 and II_2 melt at 305°, 275°, respectively above 360°. The melting points of the aliphatic polyesters I_3 and II_3 decrease very much up to 111° for I_3 and 127° for II_3. The polycarbonates I_4 and II_4 have intermediate melting values as 220° for I_4 and 310° for II_4.

Nearly all the polyesters obtained show a good solubility in a wide range of solvents. They are not soluble in aliphatic hydrocarbons, fully chlorinated hydrocarbons, alcohol, acetone.

Table 2

Solubilities of polyesters and polycarbonates

Solvent	Polymer							
	I_1	I_2	I_3	I_4	II_1	II_2	II_3	II_4
Dichloromethane	s	s	s	s	o	o	s	o
Chloroform	s	s	s	s	o	o	s	o
Carbon tetrachloride	i	i	o	i	i	i	sa	i
Dichloroethane	s	s	s	s	o	sw	s	o
1,1,2-Trichloroethylene	s	s	s	s	sa	sa	s	sa
Tetrachloroethylene	i	i	o	i	i	i	sa	i
Chlorobenzene	s	s	s	s	sw	sw	s	sa
o-Dichlorobenzene	s	s	s	s	o	o	s	o
Dimethylformamide	sa	sa	o	o	sa	sa	o	sa
Dimethyl sulfoxide	o	sa	s	s	sw	sa	o	sw
Cyclohexanone	s	s	s	s	o	o	s	o
Dioxane	s	s	s	s	o	sw	s	o
Tetrahydrofuran	s	s	s	s	o	sw	s	o
p-Xylene	i	i	s	i	i	i	o	i
Phenol/water 85/15	s	s	s	s	o	o	s	o
m-Cresol	s	s	s	s	sw	o	s	sw
Phenol/Dichloroethane 60/40	s	s	s	s	o	s	s	o
Nitromethane	i	i	s	i	i	i	sa	i

s = soluble ; i = insoluble ; o = opalescent ; sw = swollen without agglomeration ; sa = swollen with agglomeration.

The polyesters II are less soluble than the I ones also because of the bulky substituent at the central C-atom. The aliphatic polyesters I_3 and II_3 are soluble in a wider range of solvents than the aromatic ones. Partially chlorinated hydrocarbons, cyclic ketones and ethers and the phenols are the best solvents for this series of polyesters.

The temperature stability was followed thermogravimetrically the results being summarized in table 3. There are no changes of the curve shapes until the decomposition begins. The analyses were carried out both in nitrogen and air atmosphere and the results of weight loss *vs.* temperature were nearly identical.

It can be seen that the polyesters II have a higher thermal stability as compared to the polyesters I because of the acenaphthene ring in the bisphenol molecule. As for the acids used for the polycondensation reaction one can establish the following sequence of thermal stabilities : terephthalic-isophthalic > phosgene > sebacic acid.

The good solubility and the relatively high viscosities indicate a linear structure for the synthesized polyesters.

Table 3

Aromatic Polyesters and Polycarbonates thermogravimetric analysis

Polymer	Decomp. temp. °C	Weight loss, %	
		at 406°	at 503°
I_1	342	11.6	30.26
I_2	340	10.3	29.41
I_3	301	15.75	—
I_4	312	25.9	35.9
II_1	416	—	12.67
II_2	426	—	16.9
II_3	314	7.27	—
II_4	379	2.22	22.85

The IR spectra both of the polymers and monomeric benzoyl derivatives show two absorption bands for C=O group. The corresponding bands for the poly(bis(4-hydroxyphenyl)deoxybenzoin terephthalate and the benzoyl derivative are at 1726 cm^{-1} (C=O ester) and 1675 cm^{-1} (carbonyl). The benzoyl derivative and the polyterephthalate of 1,1-bis (4-hydroxyphenyl)2-oxo-acenaphthene show a broad superposed carbonyl band at 1738 cm^{-1} (ester) with a shoulder at 1720 cm^{-1} (ring).

Clear films can be obtained from 1,2-dichloroethane and chloroform solutions.

Revue Roumaine de Chimie, **14**, 781–787 (1969)

THE ELECTRONIC STRUCTURE OF SOME SUBSTITUTED CYCLOBUTADIENES

M. D. GHEORGHIU*) and R. HOFFMANN

Department of Chemistry, Cornell University, Ithaca, New York 14850, U.S.A.

Received January 13, 1969

The electronic structure of square and rectangular cyclobutadiene is discussed. In agreement with previous calculations a square D_{4h} geometry possesses a triplet ground state, whereas the rectangular D_{2h} geometry has a singlet ground state. Amino- or nitro- mono- or di-substitution is calculated to confer a singlet ground state on the square form, and alter the overlap populations in a predictable manner. The only triplet ground state among the above compounds is found to be 1,2-diaminocyclobutadiene. Special attention is drawn to the 1,3-diamino- and 1,3-dinitrocyclobutadienes, where uniform delocalization is suggested in the square geometry.

The molecule of cyclobutadiene has received extensive theoretical attention. Hückel 4n systems, such as cyclobutadiene, are generally characterized by a much higher ratio of theoretical to experimental material published than the corresponding 4n+2 systems for which a large body of experimental facts has accumulated. This is not meant to imply that no experimental attempts at the synthesis of cyclobutadiene and related compounds have been made. Many beautifully designed approaches have been explored, but they have only rarely succeeded.[1]

Evidence for the synthesis of a free cyclobutadiene has recently been put forward,[2] but this work awaits confirmation. The iron tricarbonyl complex of cyclobutadiene has been recently synthesized.[3] Metal coordination is, in fact, the only well established method available at this time for the stabilization of cyclobutadienes; it was suggested by Longuet-Higgins and Orgel[4] in 1956, and experimentally achieved for the first time in 1959 by Criegee and Schröder on the synthesis of tetramethylcyclobutadiene nickel chloride.[5]

*) present address Organic Chemistry Laboratory, Polytechnic Institute, str. Polizu 1, Bucharest 12, Romania

[1] a) M. P. Cava and M. J. Mitchel, "Cyclobutadiene and Related Compounds", Organic Chemistry, A series of Monographs, vol. **10** (A. T. Blomquist Ed.), Academic Press, N. Y. 1967; b) Lionel Salem, "The Molecular Orbital Theory of Conjugated Systems", W. A. Benjamin, Inc., N. Y., 1966.

[2] L. Watts, J. D. Fitzpatrick and R. Pettit, *J. Amer. Chem. Soc.*, **87**, 3253 (1965).

[3] L. Watts and R. Pettit, *J. Amer. Chem. Soc.*, **87**, 131 (1965).

[4] H. C. Longuet-Higgins and L. E. Orgel, *J. Chem. Soc.*, **1956**, 1969.

[5] R. Criegee and G. Schroeder, *Liebigs Ann. Chem.*, **62**, 31 (1959); see also 1a.

Roberts suggested several years ago that a cyclobutadiene system could conceivably be stabilized upon adjacent substitution by two oppositely polarizable groups.[6] In valence bond language the valence structure Ib of the model molecule I could contribute significantly.

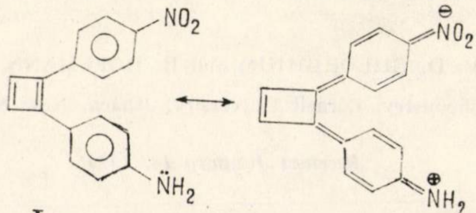

I a

I b

Theoretical studies confer unambiguously a preferred rectangular geometry on cyclobutadiene.[7] In this geometry there is no interaction between the double bonds, no resonance stabilization to the molecule. The rectangular form is a singlet ground state, and as confirmatory evidence for this has been cited the stereospecific cycloaddition of cyclobutadiene in Diels-Alder type reactions.[8] The square D_{4h} form of cyclobutadiene is generally predicted to be a triplet ground state. The interaction between the double bonds is here antibonding, destabilizing the square geometry with respect to a rectangular distortion. In the calculations which we will describe here we examined square and rectangular cyclobutadiene itself,[9] as well as nitro and amino substituted derivatives as models for the "push-pull" cyclobutadienes suggested by Roberts.[6] The latter were examined in square geometries only, and by focussing on features of the population analysis we were able to analyze the role of the substituents in stabilizing that geometry.

The method of calculation which we used is the approximate SCF method developed by Pople and coworkers,[10] at the CNDO-2 level. It should perhaps be pointed out that these calculations treat simultaneously the σ and π framework of molecules. For the parent molecule in either square or rectangular geometry triplet states were calculated by both closed and open shell methods, for the substituted molecules only closed shell calculations were performed. In the closed shell calculations we included extensive configuration interaction with all excitations in a 12 eV range.

---

[6] J. D. Roberts, *Chem. Soc. Special Publication*, No 12, 111 (1958).

[7] J. E. Lennard-Jones and J. Turkevich, *Proc. Roy. Soc.* **A158**, 297 (1937) stated for the first time, as far as we know, that cyclobutadiene should have two normal single bonds and two normal double bonds; for more recent calculations see M. J. S. Dewar and G. J. Gleicher, *J. Amer. Chem. Soc.*, **87**, 3255 (1965).

[8] L. Watts, J. D. Fitzpatrick and R. Pettit, *J. Amer. Chem. Soc.*, **88**, 623 (1966).

[9] In the square form we took all C–C bonds of length 1.40 Å, all C–H 1.10 Å. In the rectangular distortion two C–C bonds were at 1.34 Å and two at 1.54 Å.

[10] for details see J. A. Pople, D. P. Santry and G. A. Segal, *J. Chem. Phys.*, **43**, S 136 (1965); J. A. Pople and G. A. Segal, *J. Chem. Phys.*, **44**, 3289 (1966); P. A. Clark and J. L. Ragle, *J. Chem. Phys.*, **45**, 4235 (1967); H. W. Kroto and D. P. Santry, *J. Chem. Phys.*, **47**, 792 (196 7).

DISCUSSION OF RESULTS

For the parent molecule our calculations placed a rectangular singlet state some 0.371 eV below a square triplet state, which in turn is more stable than the triplet of the D_{2h} geometry. The relative positions of the lower singlet and triplet states are displayed in figure 1.

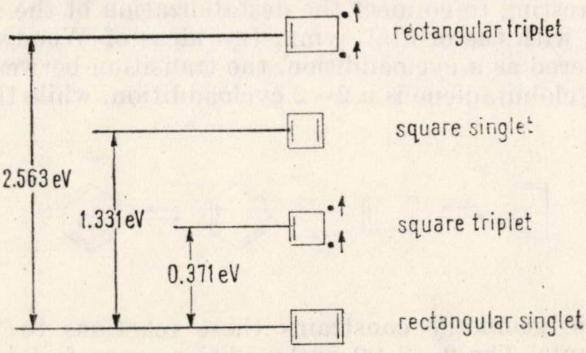
rectangular triplet
square singlet
square triplet
rectangular singlet
2.563 eV
1.331 eV
0.371 eV

Fig. 1

An analysis of the overlap populations for the D_{2h} and D_{4h} models (fig. 2)

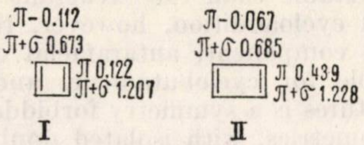
π−0.112
π+σ 0.673
π 0.122
π+σ 1.207
I
π−0.067
π+σ 0.685
π 0.439
π+σ 1.228
II

Fig. 2

shows that in the process of distortion from rectangle to square the negative π-overlap population along the originally longer "single" bonds grows increasingly negative, reaching the rather high value of −0.112. This suggests that the two double bonds are "saturated" in the rectangular geometry and that their approach does not add anything energetically but in fact is destabilizing.

Another view of the interaction of the two double bonds may be obtained from an examination of the splitting between the occupied π-levels. Figure 3 shows clearly the greater interaction (resulting in destabilization) between the π-bonds in the D_{4h} structure.

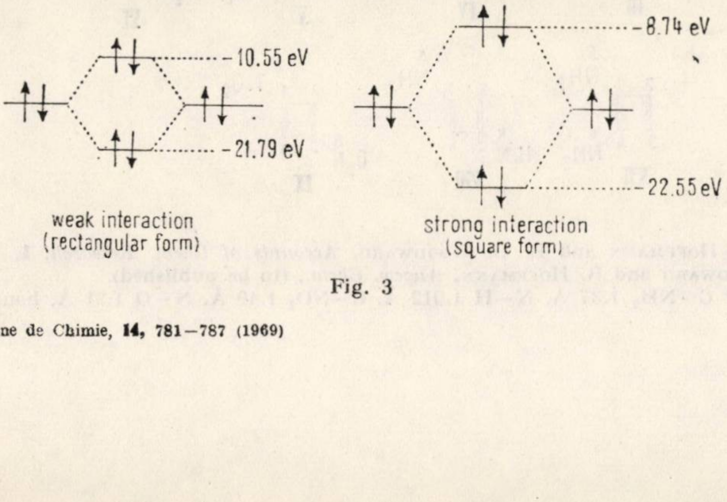
−10.55 eV
−21.79 eV
weak interaction
(rectangular form)
−8.74 eV
−22.55 eV
strong interaction
(square form)

Fig. 3

It should be noted that figure 3 omits three σ levels which are interspersed between the two π-levels. We conclude from our calculations, in agreement with other workers, that not only is the ground state of cyclobutadiene composed of two ethylenic moieties, but that these interact with each other in a repulsive manner.

It is interesting to connect the destabilization of the square form of cyclobutadiene with the orbital symmetry ideas of Woodward and Hoffmann.[11] Considered as a cycloaddition, the transition between two Kekulé structures of cyclobutadiene is a 2+2 cycloaddition, while that of benzene is 2+2+2.

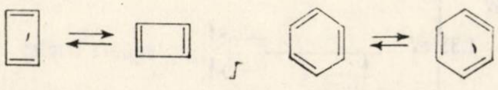

The cyclic geometry constrains these reactions to be suprafacial on all components. The 2+2+2 cycloaddition, suprafacial on all components, is symmetry-allowed, and it could be said that the geometrical arrangement is so favourable that in fact the transition state for that reaction becomes more stable than the "reactant" or "product" cyclohexatriene. For a 2+2 cycloaddition, however, the allowed process is one suprafacial on one component, antarafacial on the other. This is geometrically inaccessible for cyclobutadiene, and the interconversion of the two Kekulé structures is a symmetry forbidden process. The "reactant" or "product" geometries, with isolated double bonds, remain the stable points.

Substitution of hydrogen atoms by different groups may cause either stabilization or destabilization of the square geometry of cyclobutadiene. In our calculations we used amino and nitro groups, which act as good electron donors or acceptor respectively.[12] The derivatives which were studied are shown below.

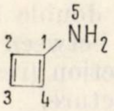

III

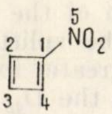

IV

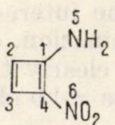

V

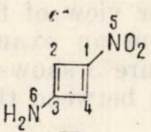

VI

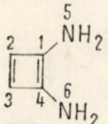

VII

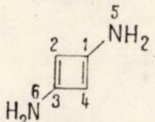

VIII

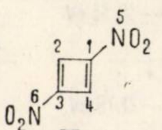

IX

---

[11] R. Hoffmann and R. B. Woodward, *Accounts of Chem. Research*, **1**, 17 (1968); R. B. Woodward and R. Hoffmann, *Angew. Chem.*, (to be published).

[12] for $C-NH_2$ 1.37 Å, N–H 1.012 Å, $C-NO_2$ 1.49 Å, N–O 1.21 Å, bond distances were used.

In our analysis of the results we focussed on the changes in overlap populations on substitution. An indication of the stabilization of the square geometry singlet would be a more uniform distribution of overlap populations around the cyclobutadiene ring. Thus, we found that a single amino group will convert the -0.112 π overlap population of the C_1-C_2 bond of I into $+0.119$ for III, and that a nitro substituent will have a similar effect, with a π-overlap population of $+0.123$.

The substitution of two amino or two nitro groups in a 1,3 manner automatically equalizes the populations of all found ring bonds and places a singlet at the same energy as the triplet. The identity of the energies is a consequence of the assumptions embodied in the CNDO method. The π-overlap populations are 0.144 for VIII and 0.151 for IX. 1,2-Disubstitution with $-NH_2$ maintains the bonding of square cyclobutadiene.

Compound VII has a C−C π-overlap population of -0.104 and is definitely a triplet ground state. For mixed substitution of $-NH_2$ and $-NO_2$ in either 1,2 or 1,3 positions there results a positive overlap population for any bond. The overlap populations for the species which we studied [13] are presented in table 1.

Table 1

π and reduced overlap populations

	I		II		III	
Bond	π	$\sigma+\pi$	π	$\sigma+\pi$	π	$\sigma+\pi$
1−2	−0.112	0.673	−0.067	0.685	0.119	0.867
2−3	0.422	1.207	0.439	1.229	0.179	0.963
3−4	−0.112	0.673	−0.067	1.229	0.179	0.963
4−1	0.422	1.207	0.439	1.229	0.119	0.867
1−5					0.170	0.863

	IV		V		VI*)	
Bond	π	$\sigma+\pi$	π	$\sigma+\pi$	π	$\sigma+\pi$
1−2	0.123	0.880	0.106	0.857	+0.181	0.929
2−3	0.180	0.942	0.122	0.878	0.115	0.882
3−4	0.180	0.942	0.228	1.017	0.115	0.882
4−1	0.123	0.880	0.126	0.909	0.181	0.929
4−6	0.049	0.707	0.183	0.886	0.177	0.881
1−5			0.053	0.706	0.033	0.629

	VII		VIII*)		IX*)	
Bond	π	$\sigma+\pi$	π	$\sigma+\pi$	π	$\sigma+\pi$
1−2	−0.104	0.646	0.144	0.919	0.151	0.911
2−3	0.401	1.182	0.144	0.919	0.151	0.911
3−4	−0.104	0.725	0.144	0.919	0.151	0.911
4−1	0.401	1.182	0.144	0.919	0.151	0.911
1−5	0.06	0.797	0.147	0.853	0.041	0.698
4−6	0.06	0.797	0.147	0.853	0.041	0.698

*) Instead of C_4-C_6 read C_3-C_6

---

[13] The S.C.F. calculations for 1,2-dinitrocyclobutadiene did not converge.

Energetically, the 1,3-diaminocyclobutadiene singlet is by 0.95 eV more stable than its 1,2 isomer, and the difference of the triplet states is still larger. The 1-amino-3-nitrocyclobutadiene is considerably more stable than its 1,2 isomer. Both of these "push-pull" cyclobutadienes, while in our calculations remaining singlet states, have a much smaller singlet-triplet splitting than the parent compound. Table 2 shows the position of the calculated singlet and triplet states of molecules I–IX.

Table 2

Singlet and triplet energies (in eV)

	I	III	IV	V	VI	VII	VIII	IX
singlet	0.96	1.28	0.55	1.90	0.87	1.21	2.32	0.89
triplet	−0.96	1.21	0.53	1.79	0.72	−0.73	2.32	0.89

The position of the highest occupied molecular orbital in these molecules is affected by the nature of the substituents. An amino group, as expected from its high-lying occupied lone pair, destabilizes the highest occupied molecular orbital of D_{4h} cyclobutadiene. In contrast, a nitro group, with its low-lying unoccupied cyclobutadiene orbital. The direction of these shifts is in accord with the donor-acceptor characteristics of these substituents. Double substitution operates in the same direction as single, and in a mixed substitution pattern the nitro group prevails. The position of the π-levels is indicated in table 3 (intervening σ-levels omitted).

Table 3

π energy levels (in eV)

I	III	IV	V	VI	VII	VIII	IX
8.74	8.24	10.41	9.89	9.27	6.69	7.99	11.71
		12.46	12.16	12.92	14.23	13.61	13.36
	15.95		16.94	16.67			13.36
		21.56	21.02	22.78	17.41	17.80	21.74
							24.47
22.55	23.80	25.88	26.34	26.19	26.54	24.54	27.87

The conclusions reached above on the effect of substituents on the highest occupied molecular orbital are illustrated in table 4.

Table 4

Position of the HOMO of square cyclobutadiene for different substitutions

− 6.69 eV	$-NH_2$ (diamino in 1.2)
− 7.99 eV	$-NH_2$ (diamino in 1.3)
− 8.24 eV	$-NH_2$
− 8.74 eV	−H
− 9.27 eV	$-NO_2$ (at C_1); NH_2 (at C_3)
− 9.89 eV	$-NO_2$ (at C_1); NH_2 (at C_2)
−10.41 eV	$-NO_2$
−11.71 eV	$-NO_2$ (dinitro in 1.3)

We conclude that selective substitution by electron donors and acceptors has the requisite consequence of equalizing overlap populations in the cyclobutadiene ring and stabilizing the singlet state of a $\mathbf{D}_{4h}$ square geometry with respect to the preferred triplet state of an unsubstituted cyclobutadiene.

The work reported here was supported by the National Institutes of Health and the Chevron Research Corporation.

Revue Roumaine de Chimie, **14**, 789–795 (1969)

A CRIDONES. XXXIV

SYNTHESIS OF SOME DIMETHOXY-10-METHYLACRIDONES

MARIA IONESCU and I. MESTER

Institute of Chemistry of the Academy, Cluj, str. Donath, 59–65

Received September 26, 1968

The synthesis of five asymmetrical dimethoxy-10-methylacridones is reported; on preliminary tests it has been found that 2,3-dimethoxyacridone (VIc) seems to have a sympathetic vegetative nervous system blocking action.

During the last years, the investigations on the physiological activity of acridone-alkaloids revealed a number of quite important properties, like antitumor,[1] spasmolythic [2] or estrogenic [3] activity. The most simple member of these alkaloids is 1,3-dimethoxy-10-methylacridone (VIIa), which was first isolated in 1952 from the leaves of *Acronychia baueri* Schott.[4]; we found it quite attractive to synthesize this alkaloid (VIIa), and also its structural isomers (VIIb-e), for testing their biological activity. The preliminary pharmacodynamical tests on dogs, showed that one of these alkaloid-analogs, namely 2,3-dimethoxyacridone (VIc), seems to possess a sympathetic vegetative nervous system blocking action.[5] Other derivatives are under testing.

The most accessible way to obtain asymmetrical disubstituted acridones, use the corresponding disubstituted-diphenylamine-2-carboxylic acids as starting materials. According to this way, we have prepared the dimethoxydiphenylamine-2-carboxylic acids IIa-e and IVe, by condensation of the suitable substituted dimethoxyanilines (Ia-e) with *o*-chlorobenzoic acid (method A), or of the dimethoxyanthranylic acid IIIe with bromobenzene (method B), both by the general procedure of Jourdan-Ullmann. Method A gave better yields, than method B, as the chloro atom from the *o*-chlorobenzoic acid is substituted more easily, than the hydrogen atom from the amino group in the anthranylic acids.

---

[1] G. H. Svoboda, G. A. Poore, P. J. Simpson and G. B. Boder, *J. Pharm. Sci.*, **55** 758 (1966).

[2] I. Novák, G. Buzás, E. Minker, M. Koltai and K. Szendrei, *Acta Pharm. Hung.*, **37**, 130 (1967).

[3] G. H. Svoboda, *Lloydia*, **29**, 206 (1966).

[4] J. A. Lamberton and J. R. Price, *Austral. J. Chem.*, **6**, 66 (1953).

[5] These tests have been kindly performed by Dr. M. Timar, Dr. C. M. Georgescu and Mrs. A. Botez, the Pharmacodynamical Division of the I.C.C.F.—Bucharest.

The obtained dimethoxydiphenylamine-2-carboxylic acids (IIa-e and IVe) were subjected to cyclization in two ways. The compounds IIb-d were cyclized by the aid of phosphorus oxychloride, when the three dimethoxy-9-chloroacridines (Vb-d) resulted (see table 3). Two of these, compounds Vb and Vd, on refluxing with 1 N hydrochloric acid for one hour, gave the corresponding acridones (VIb and VId) (method C) (see table 4), while the chloroacridine Vc remained unchanged after 3 hours of heating under reflux. By performing this hydrolysis under most energical conditions, firstly a demethylation occurs, which is in agreement with observations reported elsewhere.[6]

The other way of cyclization (method D) consists in the heating for three hours at 100° of a solution of dimethoxydiphenylamine-2-carboxylic acids in polyphosphoric acid (PPA), according to the method initiated by Brockmann and his coworkers.[7] In this way the dimethoxyacridones VIa-e, listed in table 4, were obtained.

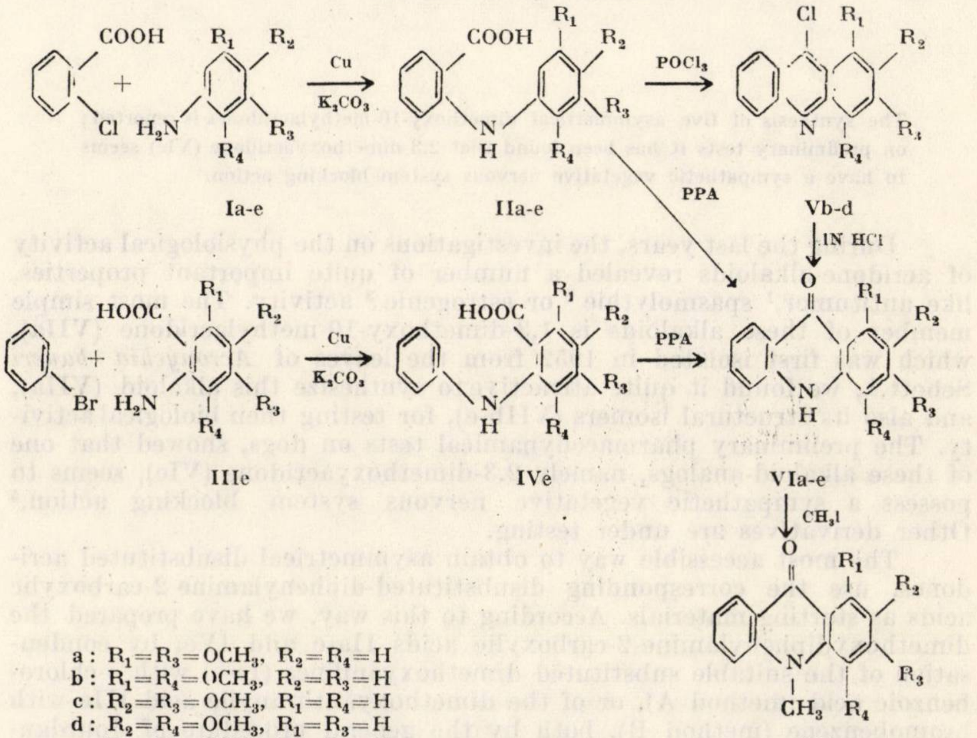

a : $R_1 = R_3 = OCH_3$, $R_2 = R_4 = H$
b : $R_1 = R_4 = OCH_3$, $R_2 = R_3 = H$
c : $R_2 = R_3 = OCH_3$, $R_1 = R_4 = H$
d : $R_2 = R_4 = OCH_3$, $R_1 = R_3 = H$
e : $R_3 = R_4 = OCH_3$, $R_1 = R_2 = H$

During the cyclization of the 3′, 4′-dimethoxydiphenylamine-2-carboxylic acid (IIc), using phosphorus oxychloride and/or PPA, only one product was obtained (Vc and/or VIc respectively[8]), most probable due to the methoxy groups, which by the formation of a strong nucleophylic center in position 6′, do allow only that cyclization which yields the products Vc and/or VIc respectively. This is in good agreement with the observation of Dallacker and Adolphen,[9] concerning the cyclization of 3′,4′-methylenedioxydiphenylamine-2-carboxylic acid by the aid of phosphorus oxychloride, when only the 2,3-methylenedioxy-9-chloroacridine was obtained, nearly quantitative.[9]

---

[6] A. Albert, "The Acridines", Sec. Ed., Edward Arnold Ltd., London, 1966, p. 32.

[7] H. Brockmann and H. Muxfeldt, *Chem. Ber.*, **89**, 1379, 1397 (1956); H. Brockmann, H. Muxfeldt and G. Haese, *Chem. Ber.*, **89**, 2174 (1956).

The potassium salts of the acridones VIa-e, were converted to the corresponding 10-methylacridones (VIIa-e) by methyliodide in acetone, and are listed in table 5. This conversion was confirmed by their IR spectra, where the ν_{NH} vibration, which is quite characteristic of the acridones VIa-e, was missing.

EXPERIMENTAL

All m.p.'s were determined on a Boetius apparatus and are uncorrected. The used ligh petroleum (ligroin) had a b.p. of 60−80°. All microanalyses were carried out in our Laboratory of Microanalysis.

1. Dimethoxyanilines (Ia-e)

All dimethoxyanilines were prepared by methods reported in the literature, and are listed in table 1.

Table 1

Dimethoxyanilines Ia-e

Compound	Our results			Reported in lit.		
	yield a) %	b.p. °C/mm Hg	m.p. °C	yield a) %	b.p. °C/mm Hg	m.p. °C
Ia	96 b)	178/20	—	70[10]	178/20[10]	—
Ib	98	129/2	80−81	82[11a]	—	84[11b]
Ic	94	—	82−84	94[12]	—	84−85[12]
Id	86	—	42−43	72[13]	—	39[13]
Ie	87	106−107/3 137/10	—	—	137/10[14]	—

a) The yields refer to the dimethoxynitrobenzenes.

b) The reduction was effected by H_2 in ethanol over Raney Ni at room temperature, and atmospherical pressure.

---

[8] Cyclization of 3′-monosubstituted-diphenylamine-2-carboxylic acids gave a mixture of 1- and 3-substituted-9-chloroacridines or -acridones respectively. (A. Albert, "The Acridines", Sec. Ed., Edward Arnold Ltd., London, 1966, cap. 2.).

[9] F. Dallacker and G. Adolphen, *Liebigs Ann. Chem.*, **691**, 134 (1966).

[10] W. Riedl and F. Imhof, *Liebigs Ann. Chem.*, **597**, 155 (1955).

[11] a. J. M. Gulland, R. Robinson, J. Scott and S. Thornley, *J. Chem. Soc.*, **1929**, 2927; b. G. M. Dyson, H. J. George and R. F. Hunter, *J. Chem. Soc.*, **1927**, 440.

[12] J. Nishino, A. Nishiura, N. Kuroki and K. Konishi, *Yuki Gosei Kagaku Kyo-Kaiski*, **17**, 166 (1959); *Chem. Abstr.*, **53**, 11280a (1959).

[13] H. H. Hodgson and F. W. Handley, *J. Chem. Soc.*, **1928**, 163.

[14] Ch. S. Gibson, J. L. Simonsen and M. G. Rau, *J. Chem. Soc.*, **111**, 69 (1917).

Revue Roumaine de Chimie, 14, 789−795 (1969)

2. 3,4-Dimethoxyanthranylic acid (2-Aminoveratric acid) (IIIe)

This acid was prepared from vanillin by a method reported in literature[15]; m.p. 180–181°.

3. Dimethoxydiphenylamine-2-carboxylic acids

Method A (for IIa-e). A mixture of 0.05 mole dimethoxyaniline, 0.05 mole *o*-chlorobenzoic acid, 0.06 mole anhydrous, well powdered potassium carbonate, 0.2 g copper powder, and 35–40 ml n-amyl alcohol was heated under reflux for 1 hour. Then, the mixture was steam distilled to remove the amyl alcohol, and the aqueous solution treated with charcoal, filtered, and the filtrate acidified with conc. hydrochloric acid. The precipitate was collected and extracted three times with 100–150 ml portions of boiling water to remove the unreacted *o*-chlorobenzoic acid; the product was then crystallized from aqueous ethanol or carbon tetrachloride.

Method B (for IVe). The dimethoxyanthranylic acid IIIe was condensed under similar conditions, but the bromobenzene was used in a 50% excess, and the refluxing time was 4 hours.

The obtained results are summarized in table 2.

Table 2

Dimethoxydiphenylamine-2-carboxylic acids IIa-e and IVe

Compound	Method	Yield %	M.p. °C	Recrystallized from	Found* (%)		
					C	H	N
IIa[16]	A	68	145–146	EtOH–H_2O	66.36	5.30	5.29
IIb[17]	A	69	162–163	CCl_4	66.08	5.55	5.28
IIc[18]	A	78	180–181	EtOH–H_2O;CCl_4	65.66	5.72	5.18
IId	A	73	207–208	75% EtOH	65.98	5.38	5.23
IIe[19]	A	55	163–164	EtOH–H_2O	66.10	5.84	5.17
IVe[20]	B	15	150–151	EtOH–H_2O	66.19	5.76	5.32

* $C_{15}H_{15}NO_4$ (273.3), requires C:65.92, H:5.53, N:5.13%.

4. Dimethoxy-9-chloroacridines (Vb–d)

These compounds were obtained as follows. A mixture of 0.02 mole dimethoxydiphenylamine-2-carboxylic acid and 20 ml phosphorus oxychloride was heated under reflux for 3 hours, and after cooling to about 80°, poured into a mixture of 300 g crushed ice and 100 ml conc. ammonia. The yellow precipitate was collected, dissolved in acetone, treated with charcoal, filtered, and precipitated with ice-ammonia ; crystallization from ammoniacal aqueous alcohol yielded the 9-chloroacridines reported in table 3.

---

[15] A. Butenandt and H. G. Schlossberger, *Chem. Ber.*, **85**, 565 (1952); J. H. Boyer and L. R. Morgan, *J. Org. Chem.*, **26**, 1655 (1961); R. Pschorr and C. Sumuleanu, *Ber. dtsch. chem. Ges.*, **32**, 3405 (1899); R. Pschorr, *Ber. dtsch. chem. Ges.*, **39**, 3106 (1906).

[16] L. J. Drummond and F. N. Lahey, *Austral. J. Sci. Res.*, **A2**, 630 (1949); *Chem. Abstr.*, **47**, 3862b (1953).

[17] G. K. Hughes, N. K. Matheson, A. T. Norman and E. Ritchie, *Austral. J. Sci. Res.*, **A5**, 206 (1952); *Chem. Abstr.*, **47**, 2176c (1953).

[18] W. Borsche, F. Runge and W. Trautner, *Ber. dtsch. chem. Ges.*, **66**, 1315 (1933).

[19] J. N. Graves, G. K. Hughes and F. Lions, *J. Proc. Roy. Soc. N.S.W.*, **71**, 255 (1938); *Chem. Abstr.*, **32**, 7461^{9} (1938).

[20] G. P. Sidyakin, V. I. Pastukhova and S. Yu. Yunusov, *Uzb. Khim. Zhur.*, **1962**, *No. 3*, 56.

Table 3

Dimethoxy-9-chloroacridines Vb-d

Compound	Yield %	M.p. °C	Recrystallized from	Found*) (%)		
				C	H	N
Vb[17]	73	142–143	EtOH–H_2O (NH_3)	65.66	4.53	5.65
Vc[18]	79	186–187	EtOH–H_2O (NH_3)	66.07	4.55	5.26
Vd	78	189–190	MeOH–H_2O (NH_3)	65.16	4.67	5.47

*) $C_{15}H_{12}ClNO_2$ (273.8) requires C :65.81, H :4.42, N :5.12%.

5. Dimethoxyacridones (VIa-e)

Method C. A ten per cent solution of 9-chloroacridine in 1 N hydrochloric acid was heated under reflux for 1 hour, filtered and neutralized with sodium carbonate. The collected precipitate was crystallized from methanol. The yields were nearly quantitative (see table 4), except for 9-chloroacridine Vc, which under these conditions remained unchanged.

Method D. To 20 g freshly prepared PPA (according to Uhlig [21]), 2 g of fine powdered dimethoxydiphenylamine-2-carboxylic acid was added, and the mixture heated at 100° until the solution became clear. The heating was continued for 3 hours at 100° ; after cooling the mixture was poured into 100 ml water, and basified with conc. ammonia. The precipitate was collected and crystallized from the adequate solvent. The yields and m.p.'s of these acridones are given in table 4.

Table 4

Dimethoxyacridones VIa-e

Compound	Method	Yield %	M.p. °C	Recrystallized from	Found*) (%)		
					C	H	N
VIa[22]	D	90	256–258	MeOH–H_2O	70.63	5.19	5.57
VIb[17]	C	98	220–221	MeOH–H_2O	70.92	5.02	5.84
VIb	D	92	221–222	EtOH–H_2O	70.71	5.21	5.53
VIc[18]	D	85	298	MeOH	70.41	5.46	5.47
VId	C	98	260–261	60% EtOH	70.36	5.19	5.72
VId	D	99	260–261	60% EtOH	70.61	5.23	5.45
VIe[19,20]	D	100	225	MeOH–H_2O	70.30	5.02	5.53

*) $C_{15}H_{13}NO_3$ (255.3), requires C: 70.58, H: 5.13, N: 5.49%.

---

[21] F. Uhlig, *Angew. Chem.*, **66**, 435 (1954).

[22] W. Baczynski and St. von Niementowski, *Ber. dtsch. chem. Ges.*, **38**, 3009 (1905).

Table

Dimethoxy-10.

Compound	Yield %	M.p. °C	Recrystallized from
VIIa[4,23]	62.4	162–164	C_6H_6-ligroin
VIIb[17]	76	88–89***)	C_6H_6-ligroin
VIIc	73	194–195	EtOAc, Me_2CO
VIId	77	167–168	C_6H_6-ligroin
VIIe	75	115–116	C_6H_6-ligroin

*) $C_{16}H_{15}NO_3$ (269.3) requires C: 71.36, H: 5.61, N: 5.20%.

**) $C_{22}H_{18}N_4O_8$ (498.4) requires C: 53.02, H: 3.64, N: 11.24%.

***) The reported [17] m.p. 80° (from aqueous ethanol).

6. Dimethoxy-10-methylacridones (VIIa-e)

A mixture of 0.2 g dimethoxyacridone (VIa-e), and 0.3 g well powdered potassium hydroxide was dissolved in 150–300 ml boiling dry acetone; heated under reflux for 15 min; 5 ml methyliodide in 30 ml acetone was added, and the refluxing continued for other 15 min. Then the acetone was distilled on a steam bath, and the residue treated with 25 ml water and 50 ml chloroform. The chloroform solution was shaken successively with water, 1% acetic acid solution, water, 3% sodium hydroxide, water, dried over calcium chloride, and finally the chloroform removed. The obtained products were crystallized from the adequate solvent, and are given in table 5.

The picrates of the compounds VIIa and VIIb were prepared in methanolic solutions; their m.p.'s are listed also in table 5.

[23] G. K. Hughes and E. Ritchie, *Austral. J. Sci. Res.*, **A4**, 423 (1951).

5

methylacridones VIIa-e

Found*) (%)			Picrate				
			M.p. °C	Recrystallized from	Found**) (%)		
C	H	N			C	H	N
71.42	5.95	5.44	203–204	$MeOH-Et_2O$	—	—	11.37
71.13	5.65	5.23	229–230	MeOH	53.38	3.70	11.16
71.61	5.79	5.25	—	—	—	—	—
71.18	5.35	5.38	—	—	—	—	—
71.42	5.67	5.29	—	—	—	—	—

Revue Roumaine de Chimie. 14, 797–802 (1969)

6-AZAURACIL DERIVATIVES WITH POTENTIAL CYTOSTATIC ACTIVITY

VIII.[1] ACYLATION OF 5-MERCAPTO-6-AZAURACIL AND ITS DERIVATIVES

C. CRISTESCU and MARCELA LAZARESCU

Chemical Pharmaceutical Research Institute, Bucharest
Sos. Vitan 112

Received August 2, 1968

5-Mercapto-6-azauracil reacts in aqueous medium with the benzoyl chloride giving 5-benzoylthio-6-azauracil. The treatment of 5-benzoylthio-6-azauracil in anhydrous medium with benzoyl chloride, leads to the N_3-acyl-derivatives.

In a previous paper [2], the selective blockage and deblockage of the 5-substituted-6-azauracil nucleus with diphenylmethane was studied. Continuing our studies on the reversible protection of the 5-substituted derivatives of the 6-azauracil at the N_3, the acylation of the 5-mercapto-6-azauracil and its derivatives, has now been investigated.

Novácek and coworkers [3] are selectively blocking the N_3 of the 6-azauracil and the 6-azathymine by treatment with benzoyl chloride to yield 1,3-dibenzoyl-derivatives which can lead to the formation of 3-benzoyl-derivatives of the 6-azauracil and the 6-azathymine by means of a partial hydrolysis.

In order to obtain the N_1-alkyl- or N_1-glycosyl-5-mercapto-6-azauracil derivatives, the reversible protection of the thio-group and of the N_3-position is of considerable importance.

5-Mercapto-6-azauracil [4] (I) reacts in aqueous medium with benzoylchloride leading to 5-benzoylthio-6-azauracil (II). In order to remove the protecting group from the sulfur-atom in the 5-th position, the compound II was treated with diluted sodium hydroxide or a sodium alkoxide solution.

By the action of acetic anhydride in excess on the compound II the replacement of the benzoyl group through an acetyl group occurs in order to give 1-acetyl-5-acetylthio-6-azauracil (VII).

---

[1] Part VII: C. Cristescu and V. Badea, *Rev. Roumaine Chim.*, **14**, 135 (1969).

[2] C. Cristescu and V. Badea, *Rev. Roumaine Chim.*, **12**, 913 (1967).

[3] A. Novácek, D. Hesoun and J. Gut, *Coll. Czech. Chem. Comm.*, **30**, 1890 (1965).

[4] C. Cristescu and J. Marcus, *Pharmazie*, **16**, 135 (1961).

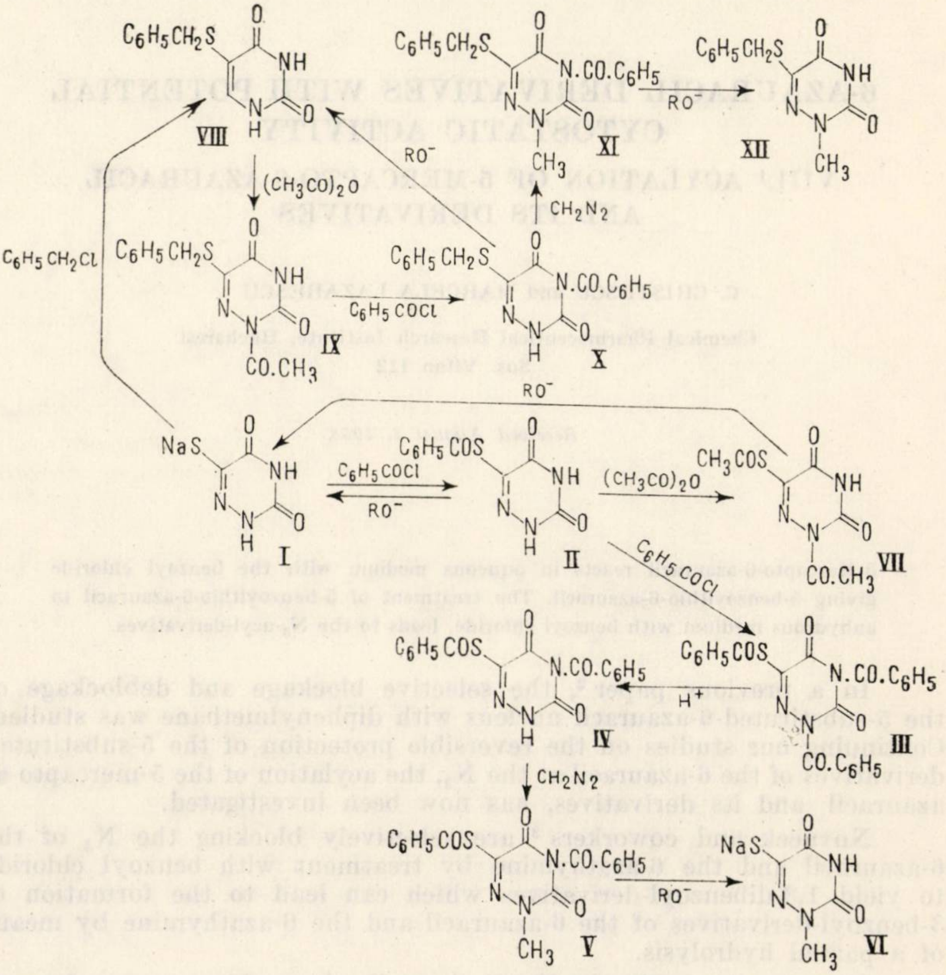

The treatment of 5-benzoylthio-6-azauracil in anhydrous medium with two moles of benzoyl chloride in the presence of pyridine, leads probably to the formation of 1,3-dibenzoyl-5-benzoylthio-6-azauracil (III), while in the presence of hydrochloric acid in ethanol at room temperature, a selective scission of one benzoyl group takes place thereby the 3-benzoyl-5-benzoylthio-6-azauracil (IV) being finally obtained. The triacyl-derivative III was not isolated.

The determination of the benzoyl group position after hydrolysis with hydrochloric acid was carried out through the following reaction. The treatment of the compound IV with diazomethane leads to the 1-methyl-3-benzoyl-5-benzoylthio-6-azauracil (V) which yields the 1-methyl-5-mercapto-6-azauracil sodium salt (VI) by the action of the sodium alkoxide and which is identical to a sample obtained through another method and described in a former work.[2]

1-Acetyl-5-benzylthio-6-azauracil [2] (IX) is reacting in anhydrous medium, analogous with benzoyl chloride in the presence of triethylamine, to give 3-benzoyl-5-benzylthio-6-azauracil (X). The treatment of the monobenzoyl-derivative X with diazomethane leads to the 1-methyl-3-benzoyl-5-benzylthio-6-azauracil (XI). The compounds X and XI can lead under the action of the sodium alkoxide to the formation of the 5-benzylthio-6-azauracil (VIII) and of the 1-methyl-5-benzylthio-6-azauracil (XII) respectively. The VIII and XII products are identical to those authentic samples obtained through other synthetic methods.[1,2]

3-Benzoyl-5-benzoylthio-6-azauracil and 3-benzoyl-5-benzylthio-6-azauracil treated with mercuric acetate in methanol give the mercuric salts (XIII and XIV) which may be used in the synthesis of N_1-glycosides.

The deblockage of the 5-mercapto-group through debenzoylation leads to a unitary product no side reactions being observed as in the case of deblockage of the 5-benzylmercapto-derivatives through hydrogenolysis with natrium in liquid ammonia.[2] The removal of the protective groups of the N_1, S_5-acyl-derivatives with natrium alkoxide occurs with good yields, permittig to use this reaction in the synthesis of N_1-alcyl- or N_1-glycosyl-derivatives of 5-mercapto-6-azauracil.

EXPERIMENTAL

The melting points were determined on a heating microscope stage. The analytical samples were dried at 20°/5 mm Hg for 7 hours over P_2O_5.

5-Benzoylthio-6-azauracil (II)

A solution of 5-mercapto-6-azauracil sodium salts (10 g ; 0.049 M) in 250 ml water, was treated dropwise at 0–2° during 15 minutes with benzoyl chloride (8.45 g ; 0.06 M). The reaction mixture was stirred 30 minutes at 0–2° and 1 hour at room temperature. Then the precipitate was filtered, washed with water, dried and recrystallized from n-butanol to give 10.5 g (86 %) 5-benzoylthio-6-azauracil, m.p : 220–222°. An analytical sample had the melting point at 224–226° after recrystallization from ethanol.

$C_{10}H_7N_3O_3S$	*Calcd.* :	C, 48.18 ; H, 2.83 ; N, 17.26 ; S, 12.86 ;
(249,23)	*Found* :	C, 48.30 ; H, 2.9 ; N, 17.20 ; S, 12.70.

Alcoholysis : 5-benzoylthio-6-azauracil (2.49 g ; 0.01 M) was refluxed for one hour with ethanolic sodium alkoxide (prepared from 0.69 g of sodium in 100 ml dry ethanol). Then the cooled mixture was neutralized with hydrochloric acid up to pH 7 and evaporated to dryness in vacuo. The residue was dissolved in boiling water-ethanol (1 : 1) and filtered on charcoal. After cooling 1.4 (70 %) 5-mercapto-6-azauracil sodium salt was obtained with m.p : 315–317° (dec.) after recrystallization from ethanol-water (1 : 1). The product was also identified through T.L. Chromatography (on Silicagel G ; isopropanol-water, 65 : 35).

Hydrolysis : 5-benzoylthio-6-azauracil (1.24 g ; 0.005 M) was dissolved in 0.2 N sodium hydroxide (50 ml) and heated for 2 hours up to 80°. The mixture was evaporated in vacuo, the residue dissolved in boiling water-ethanol (1 : 1), and there filtered over charcoal. The separated product after recrystallization from ethanol-water (1 : 1) melted at 315–317° (dec.). Yield 0.7 g (70 %) of 5-mercapto-6-azauracil sodium salt.

3-Benzoyl-5-benzoylthio-6-azauracil (IV)

A solution of 5-benzoylthio-6-azauracil (10 g; 0.04 M) in anhydrous dioxane (80 ml) and anhydrous pyridine (20 ml) was treated dropwise during 10 minutes with benzoyl chloride (11.25 g; 0.08 M) then the mixture was stirred and heated at 40° for 10 hours. The pyridine hydrochloride precipitate was filtered and the filtrate evaporated in vacuo. The oil residue dissolved in ethanol (50 ml), concentrated hydrochloric acid (5 ml) was added and the mixture was stirred at room temperature for 3 hours. After standing over night at 4°, the precipitate was collected and recrystallized from ethanol to yield 9 g (64 %) 3-benzoyl-5-benzoylthio-6-azauracil with m.p. 112–114°. The analytical sample melted at 114–116° ethanol.

$C_{17}H_{11}N_3O_4S$ *Calcd.* : C, 57.78; H, 3.13; N, 11.89; S, 9.07;
(353.34) *Found* : C, 57.60; H, 3.10; N, 11.90; S, 8.87.

Alcoholysis : 3-benzoyl-5-benzoylthio-6-azauracil (3.53 g; 0.01 M) was refluxed for 1 hour with ethanolic sodium ethoxide (prepared from 0.92 g sodium in 150 ml anhydrous ethanol). The mixture neutralized with hydrochloric acid to pH 7 and evaporated in vacuo. The residue was dissolved in boiling water-ethanol (1 : 1) and then filtered with charcoal. After standing at 4° overnight, the precipitate was collected and recrystallized from ethanol-water (1 : 1) to yield 1.29 g (64 %) 5-mercapto-6-azauracil sodium salt, m.p. 315–317° (dec.).

1-Methyl-3-benzoyl-5-benzoylthio-6-azauracil (V)

A solution of 3-benzoyl-5-benzoylthio-6-azauracil (6.0 g; 0.016 M) in dioxane (60 ml) was treated at 2–4° with a solution of 2.1 g diazomethane in 150 ml ether. The mixture was kept at the room temperature for 24 hours and then evaporated in vacuo. The oil residue was dissolved in boiling isopropanol and cooled at 4° overnight. The precipitate was collected and recrystallized from isopropanol to yield 3.7 g (60 %) 1-methyl-3-benzoyl-5-benzoylthio-6-azauracil with m.p. 136–137°. The analytical sample melted at 139–141° (isopropanol).

$C_{18}H_{13}N_3O_4S$ *Calcd.* : C, 58.84; H, 3.56; N, 11.43; S, 8.72;
(367.36) *Found* : C, 58.90; H, 3.60; N, 11.40; S, 8.58.

1-Methyl-5-mercapto-6-azauracil sodium salt (VI)

1-Methyl-5-benzoyl-5-benzoylthio-6-azauracil (1.83 g; 0.005 M) was refluxed for 1 hour with ethanolic sodium ethoxide (prepared from 0.345 g sodium in 100 ml anhydrous ethanol). The mixture was neutralized with hydrochloric acid to pH 6.5 and evaporated in vacuo under nitrogen. The residue was dissolved in hot water-ethanol (1 : 3) and filtered on charcoal. After cooling under nitrogen (2°) the yield was 0.76 g (70 %) 1-methyl-5-mercapto-6-azauracil sodium salt, yellow crystals with m.p. 335–337°.

$C_4H_4N_3O_2SNa . 2H_2O$ *Calcd.* : C, 22.12; H, 3.71; N, 19.35; S, 14.76;
(217.16) *Found* : C, 22.00; H, 3.90; N, 19.50; S, 14.50.

1-Acetyl-5-acetylthio-6-azauracil (VII)

A suspension of 5-benzoylthio-6-azauracil (2.49 g; 0.01 M) in acetic anhydride was refluxed 45 minutes. The clear solution was evaporated under diminished pressure and the oil residue was dissolved in hot benzene. After cooling, the product was separated and recrystallized from benzene-n. heptane to afford 1.4 g (60%) 1-acetyl-5-acetylthio-6-azauracil with m.p. 146–148°.

$C_7H_7N_3O_4S$ *Calcd.*: C, 36.67; H, 3.07; N, 18.34; S, 13.98;
(229.20) *Found*: C, 36.80; H, 3.20; N, 18.40; S, 13.78.

Alcoholysis: 1-Acetyl-5-acetylthio-6-azauracil (0.23 g; 0.001 M) was treated with sodium ethoxide (0.01 sodium in 15 ml ethanol) as in the case of compound II, to give 0.13 g (64%) 5-mercapto-6-azauracil sodium salt with m.p. 317–319° (dec.). The product was also identified through paper chromatography (Whatmann 1; isopropanol : water 65 : 35; in U.V).

3-Benzoyl-5-benzylthio-6-azauracil (X)

A solution of 1-acetyl-5-benzylthio-6-azauracil[2] (5.0 g; 0.018 M) in dry dioxane (100 ml) and triethylamine (10 ml) was treated dropwise during 5 minutes with benzoyl chloride (2.52 g; 0.018 M). The mixture was stirred and heated at 40° for 15 hours. The triethylamine hydrochloride was filtered and the filtrate was evaporated in vacuo. The oil residue was dissolved in ethanol (15 ml) and refluxed 15 minutes. After standing overnight at 4° the precipitate was filtered and recrystallized from ethanol yielding 3.5 g (57%) 3-benzoyl-5-benzylthio-6-azauracil with m.p. 130–132°. The analytical sample melted at 132–134° after recrystallization from ethanol.

$C_{17}H_{13}N_3O_3S$ *Calcd.*: C, 60.16; H, 3,86; N, 12.38; S, 9.44;
(339.36) *Found*: C, 60.30; H, 3.95; N, 12.60; S, 9.60.

Alcoholysis: 3-benzoyl-5-benzylthio-6-azauracil (1.68 g; 0.005 M) was refluxed 1 hour with sodium ethoxide (0.46 g sodium in 100 ml anhydrous ethanol). The mixture was neutralized with hydrochloric acid to pH 2 and then evaporated to dryness in vacuo. The residue was dissolved in boiling ethanol-water (1 : 1) and then filtered on charcoal. After cooling, the separated product was recrystallized from ethanol-water (1 : 1) to yield 0.88 g (75%) of the pure 5-benzylthio-6-azauracil (VIII); m.p. 224–226° showing no depression when mixed with an authentic sample.

1-Methyl-3-benzoyl-5-benzylthio-6-azauracil (XI)

A solution of 3-benzoyl-5-benzylthio-6-azauracil (3.4 g; 0.01 M) in dioxane (100 ml) was treated at room temperature with a solution of diazomethane (0.45 g) in 50 ml ether. The mixture was kept at room temperature for 24 hours and then evaporated in vacuo. The oily residue was dissolved in boiling isopropanol and cooled at 4° overnight. The precipitate was collected and recrystallized from isopropanol yielding 2.65 g (75%) 1-methyl-3-benzoyl-5-benzylthio-6-azauracil with m.p. 110–112°. The analytical sample melted at 114–116° after recrystallization from isopropanol.

$C_{18}H_{15}N_3O_3S$ *Calcd.*: C, 61.17; H, 4.27; N, 11.89; S, 9.07;
(353.38) *Found*: C, 61.30; H, 4.20; N, 12.00; S, 9.20.

1-Methyl-5-benzylthio-6-azauracil (XII)

1-Methyl-3-benzoyl-5-benzylthio-6-azauracil (1.76 g; 0.005 M) was treated with sodium ethoxide (0.46 g sodium in 100 ml anhydrous ethanol) and than refluxed for 1 hour. The mixture was neutralized with hydrochloric acid (pH 3) and evaporated to dryness in vacuo. The residue was dissolved in boiling ethanol-water (1 : 2) and filtered on charcoal. After recrystallization from ethanol-water (1 : 1), 0.89 g (72 %) 1-methyl-5-benzylthio-6-azauracil was obtained; m.p. 172–174°, without depression when mixed with an authentic sample.

Mercury salt of 3-benzoyl-5-benzoylthio-6-azauracil (XIII)

A warm mercury acetate solution (0.78 g; 0.0025 M) in 75 ml methanol was added to a warm solution of 3-benzoyl-5-benzoylthio-6-azauracil (1.76 g; 0.005 M) in 60 ml methanol. Then the mixture was stirred 60 minutes at 40–50°. After cooling, the precipitate was filtered and washed successively with water, methanol and finally with ether. The salt was dried over P_2O_5 under diminished pressure, at 50–60°. The product emerged as a white powder weighing 1.98 g 90 %; m.p. 230° (dec.).

$C_{34}H_{20}N_6O_8S_2Hg$ *Calcd.*: C, 45.10; H, 2.22; N, 9.28; S, 7.08;
(905.25) *Found*: C, 45.30; H, 2.40; N, 9.13; S, 7.20.

Mercury salt of 3-benzoyl-5-benzylthio-6-azauracil (XIV)

A warm mercury acetate solution (0.15 g; 0.0005 M) in 80 ml methanol was added to a warm solution of 3-benzoyl-5-benzylthio-6-azauracil (0.34 g; 0.001 M) in 80 ml methanol. The mixture was stirred for 2 hours at 40–50° and then evaporated in vacuo up to 50 ml. After cooling, the precipitate was filtered and washed successively with water, and 5 ml pre-cooled methanol. The salt was dried on P_2O_5 under diminished pressure at the room tempeature. The product emerged as a white powder weighing 0.35 g (80 %); m.p. 145–150° (dec.).

$C_{34}H_{24}N_6O_6S_2Hg$ *Calcd.*: C, 46.54; H, 2.75; N, 9.58; S, 7.30;
(877.31) *Found*: C, 46.30; H, 2.80; N, 9.90; S, 7.60.

The analyses were carried out in the Analytical Laboratory of this Institute by Mrs. Cornelia Ioan.

Revue Roumaine de Chimie, **14**, 803 – 807 (1969)

DECOMPOSITION OF HYDROPEROXIDES ON ACTIVATED KAOLINS. I

DECOMPOSITION OF CUMENE HYDROPEROXIDE ON ACTIVATED CHINESE KAOLIN TREATED WITH SULPHURIC ACID [1]

I. VODNÁR

Babeş-Bolyai University, Department of General Chemical Technology, Cluj, Str. Arany János, 11

Received July 6, 1968

The paper presents experimental results obtained by the decomposition of cumene hydroperoxide into phenol and acetone. As a catalyst activated Chinese kaolin has been used, calcinated at 900° and treated with sulphuric acid 31 % in a 4.5 % ratio referred to the quantity of kaolin. Maximum conversions of cumene hydroperoxide into phenol can be obtained if we proceed at low temperatures with diluted solutions of hydroperoxide.

Owing to the continuously increasing need on the world market,[3] the annual world output of phenol in 1967 exceeded 1.5 million tons. The most promising method for producing phenol is the method based on cumene; in the first stage of the technological process, the cumene is transformed into cumene hydroperoxide [3,4] which by acidic catalysis decomposes into phenol and acetone.[5-9] The mechanism of cumene hydroperoxide decomposition by acidic catalysis was cleared up by Kharash.[10]

Although this method is more advantageous, it also has some shortcomings. On the one hand it requires large quantities of sulphuric acid as catalyst and therefore plants have to be built of expensive corrosion-proof materials; on the other hand from the washing of phenol there result important quantities of waste water, the purification of which presents some serious difficulties.

[1] I. Vodnar, *Patent S.R. Romania* Nr. **49843**, 19 Jun. 1967.

[2] A. S. Banciu, *Rev. Chim.*, (Bucureşti) **16**, 211 (1965).

[3] T. Bewley and Cooke M. Dudley, *F. P.* **1218114**, Jan. 2, 1959; *Chem. Zentr.*, **1962**, 17563.

[4] G. Bichet and G. Poilane, *D.A.S.* **1122954**, Dec. 10, 1959; *Chem. Zentr.*, **1963**, 1435.

[5] A. W. De Ruyter von Stevenick, *J. Chem. Soc.*, **1958**, 2066.

[6] Cooke M. Dudley, *E.P. 805048*, Apr. 13, 1959; *Chem. Zentr.*, **1962**, 9517.

[7] W. Pritzkow and R. Hofmann, *J. prakt. Chem.*, **14**, 131 (1961).

[8] H. Sodomann, B. Hauschulz and G. Berg, *D.A.S.*, **1112527**, March 28, 1959; *Chem. Zentr.*, **1962**, 10276.

[9] J. B. Ellis, S. Rafael, J. A. Robbers and W. J. Rossi, *A.P.*, **2904592**, Jul. 30, 1953; *Chem. Zentr.*, **1962**, 364.

[10] M. Kharash, A. Fone and W. Nudenberg, *J. Org. Chem.*, **15**, 748 (1950).

For these reasons the author tried to elaborate more economical methods for obtaining phenol.

EXPERIMENTAL

In this contribution there are presented the results obtained in the decomposition of cumene hydroperoxide on activated Chinese kaolin, calcinated for 4 hours at 900° and treated with sulphuric acid 31 % in a 4.5 % ratio referred to the quantity of activated kaolin.

The kaolin used has the following characteristics:

SiO_2	45.50 %	CaO	0.65 %
Al_2O_3	38.94 %	Alkalies	1.00 %
Fe_2O_3	0.18 %	Losses in calcination	13.87 %

Granulation of the catalyst : ∅ 1.5–3.5 mm.

Kaolinite content of kaolin was approximately 97 %.

Experiments have been carried out in flow system and with fixed bed of catalyst.

Apparatus and Procedure

The sketch of the laboratory plant used in the acidic decomposition of cumene hydroperoxide in flow system is shown in figure 1.

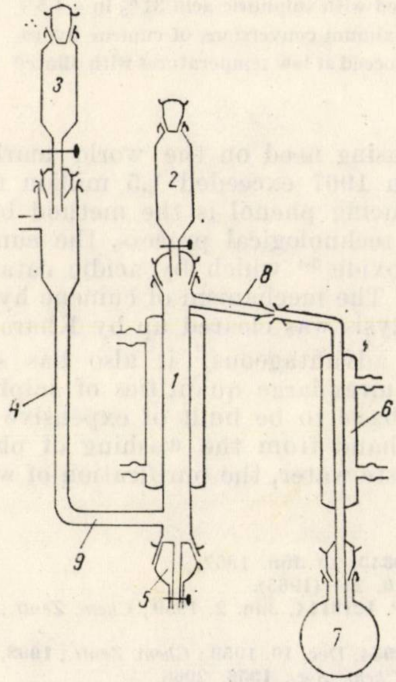

Fig. 1. — Laboratory apparatus for acidic decomposition of cumene hydroperoxide in flow system.

Cumene hydroperoxide is fed into the system with funnel 3 through conduit 9. Reaction tube 1 provided with jacket, is warmed by means of a Wobser U_8 ultrathermostat. After normal operation temperature has been achieved, one can start the supply with cumene hydroperoxide that enters the reaction tube 1, passes through the catalyst stratum and is decomposed either partially or totally into phenol and acetone. Reaction products are evacuated from the space of catalysis through conduit 8 passing through refrigerator 6 and collected in vessel 7. Samples for the dosage of phenol, acetone and cumene hydroperoxide that have not been decomposed, are taken from this vessel.

If the temperature of decomposition does not go beyond 60°, the space of catalysis is filled with cumene hydroperoxide through conduits 4 and 9 and then the supply with hydroperoxide continues through funnel 2, while the reaction products are evacuated through the cork with canal 5.

Tube of reaction 1 is provided with ground ends on both extremities. The inside diameter of the tube is 12 mm. Vessel 7 has a capacity of 250 ml. All the elements of the laboratory apparatus are constructed of Jena glass and are set on a "stiplex" (methyl polymethacrylate) panel.

Cumene hydroperoxide is dosed by the iodometric method,[11] photocolorimetric phenol, [12] while acetone by the hydroxilamine method.[13]

RESULTS AND DISCUSSION

Decomposition of cumene hydroperoxide has been studied in accordance with different parameters (temperature, supply rate, concentration of cumene hydroperoxide and residence time).

Experimental results are illustrated in figures 2, 3, 4 and 5.

Figure 2 illustrates the decomposition curves of cumene hydroperoxide in accordance with residence time at different temperatures.

We can state that when we work with cumene solution of cumene hydroperoxide of 0.1212 g/ml concentration, at 90°, hydroperoxide is totally decomposed even during a residence time of only 31 s. However, the decomposition rate is great enough even at 65°. Consequently, the catalyst used assures opportune conditions in obtaining phenol and acetone.

In the following series of experiments, working with different initial concentrations of cumene hydroperoxide we had in view the decomposition of cumene hydroperoxide during a residence time of 48 s, temperature 65°. The results are given in the diagram of figure 3 that shows the concentration of cumene hydroperoxide in the product of decomposition in accordance with the initial concentration of hydroperoxide.

Figure 3 shows that the stronger the concentration of the hydroperoxide test, the greater the rate of decomposition. In order to avoid strong local overheat, the concentration of cumene solution of cumene hydroperoxide should not exceed 30%. We could state that when we work with more concentrated solutions of cumene hydroperoxide, besides phenol and acetone there are formed some resinous substances that cover the surface of the catalyst, producing its gradual inactivation.

Figure 4 presents conversion variations of cumene hydroperoxide in phenol, depending on residence time, at different temperatures, using a cumene solution of cumene hydroperoxide of 0.1212 g/ml concentration.

---

[11] H. Raley, F. Rust and W. Vaughan, *J. Amer. Chem. Soc.*, **70**, 1336 (1948).

[12] V. Ojiganova and A. Martinenko, *Koks i Khimia*, **2**, 41 (1962).

[13] K. Bauer, "Analiz Organicheskih Soedinenij" (translation from German into Russian), Izdatelstvo Inostrannoi Literaturi, Moscow, 1953, p. 207.

The curves of figure 4 show that the increase in the residence time makes the conversion of cumene hydroperoxide rise abruptly in phenol. Maximum conversions are obtained if we apply more than 40 s (up to 100 s) residence time and low decomposition temperatures (50–60°). At higher temperatures, dosed quantities of phenolic resins are produced

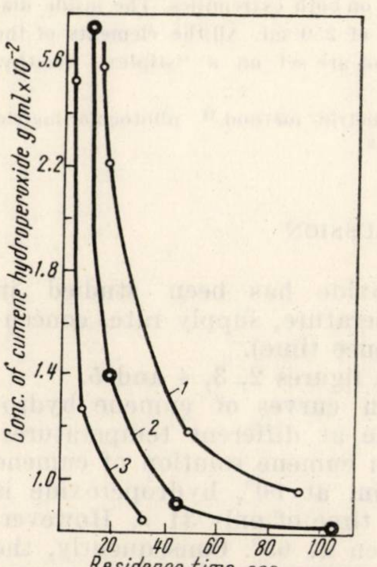

Fig. 2. — Concentration variation of cumene hydroperoxide, depending on residence time at different temperatures :
1, 65° ; 2, 80° ; 3, 90°.

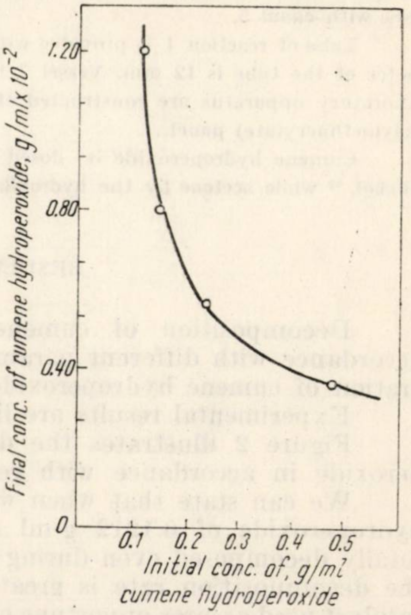

Fig. 3. — Concentration variation of cumene hydroperoxide in the product of decomposition, depending on initial concentration of samples (temperature 65°, residence time 48 s).

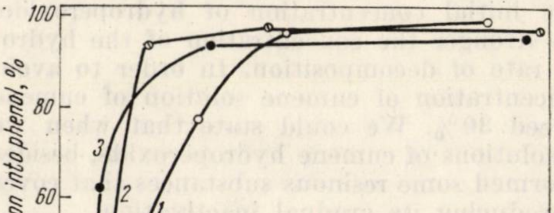

Fig. 4. — Conversion variation of cumene hydroperoxide to phenol, depending on residence time at different temperatures :
1, 65° ; 2, 80° ; 3, 90°.

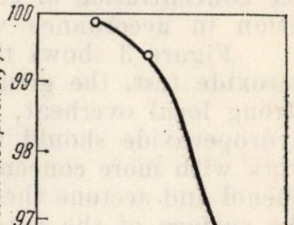

Fig. 5. — Relation between conversion of cumene hydroperoxide to phenol and temperature of decomposition (residence time 90 s).

which causes a conversion decrease of cumene hydroperoxide in phenol. This is more clearly shown in the diagram of figure 5 which presents conversion variations of cumene hydroperoxide in phenol, depending on the decomposition temperature, residence time being 90 s, the concentration of cumene hydroperoxide – 0.1212 g/ml.

CONCLUSIONS

Acidic decomposition of cumene hydroperoxide in flow system has been studied in order to obtain phenol that has an ever increasing industrial importance. We can draw the following conclusions :

– activated Chinese kaolin treated with sulphuric acid 31%, used as a catalyst, has proved to be perfectly fit to decomposition of cumene hydroperoxide ;

– decomposition of cumene hydroperoxide can be achieved in good conditions if the concentration of solutions does not exceed 10–15% ;

– maximum conversion of cumene hydroperoxide into phenol can be obtained if we work at low temperatures (50–60°) and with residence time between 40 and 100 s.

Revue Roumaine de Chimie, 14, 809—810 (1969)

A NEW ALL WALLS COOLED CYLINDRICAL TRAP

M. I. VASS

Institute of Physical Chemistry of the Academy
Dumbrava Roşie 23, Bucharest 9, Romania

Received November 28, 1968

A new model of cylindrical glass trap for use in high vacuum systems with all the walls cooled was given.

The common cylindrical traps cooled with liquid nitrogen or other freezing mixtures are frequently used to obtain high vacuum or even very high vacuum, but unfortunately they have uncooled inner walls which offer to the vapors the possibility of flowing along these walls and escape into the high vacuum part of the installations. Moreover, comparatively to the spherical traps, for the same size of the lateral connections, the cylindrical traps have a smaller cooled surface and consequently a lower efficiency.

This is why we have constructed a cylindrical glass trap with all walls cooled by simple modifications of the classical type and which can be easily built up.

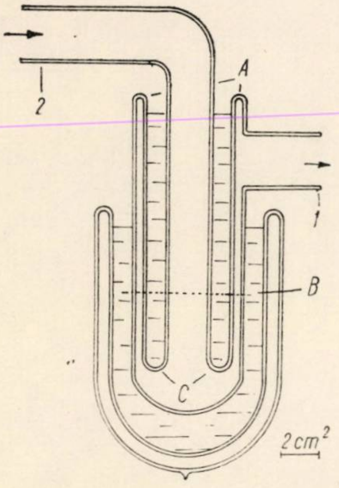

Fig. 1. — Section through the trap :

1, 2, lateral connections *A, C,* solderings; *B,* the line of the final soldering.

For a small volume (2—3 l) vacuum installation the inner diameter of 30 mm for the lateral connections was sufficient. With this size the cooled surface will be about 615 cm² and hence will have a pumping rate of 17.2 l/sec (for liquid nitrogen as freezing fluid and carbon dioxide as trapped gas and at a vacuum of 1×10^{-5} torr).

The sequence of the operations in soldering was the following: The external wall together with the lateral 1 and the soldering in A with internal wall was made first; then the external jacket was cut along the line B and the soldering in C of the lateral right angle tube 2 was achieved. Finally the external jacket was soldered in its place. It is preferable to use boro-silicate glass which can resist better the very high vacuum processes.

Revue Roumaine de Chimie, **14**, 811–822 (1969

IR-SPECTROSCOPIC AND GRAVIMETRIC INVESTIGATIONS ABOUT THE FORMATION OF CARBOXYLATE SURFACE SPECIES DURING THE CHEMISORPTION OF CO, CO_2 AND SIMPLE ORGANIC OXYGEN COMPOUNDS ON γ-ALUMINA

P. FINK
Institute of Physical Chemistry
University of Jena
German Democratic Republic

Received June 17, 1968

The interaction of CO, CO_2 and several simple organic oxygen compounds with γ-alumina dehydrated at 500° was observed with the help of IR-spectroscopic and gravimetric studies at room temperature and at elevated temperatures. Three carboxylate structures were ascertained, namely formiate surface species, acetate surface species and bicarbonate surface species. By means of the carboxylate structure it is possible to identify specific sites, which are probably active in several catalytic reactions. These specific sites should be called X-sites. A mechanism was proposed about the observed surface reactions forming carboxylate species.

1. INTRODUCTION

In the previous years several authors have repeatedly reported on carboxylate structures on aluminas, formed by chemisorption of simple organic oxygen compounds at elevated temperatures. In 1962, Greenler[1] first described the occurrence of formiate surface species and acetate surface species after methanol and ethanol had contacted γ-Al_2O_3 at over 170°. The observed IR-bands (formiate 1377, 1597 ; acetate 1466, 1572 cm^{-1}) could be surely assigned to the symmetrical and asymmetrical stretching vibration of the COO^-- group. The carboxylate structures were also reported by several authors who carried out chemisorption of methanol and ethanol,[2,3] of n-propanol and n-butanol,[4,5] and of i-propanol,[3] at elevated temperatures. A satisfactory explanation of the mechanism of forming carboxylate surface species out of alcohols, however, has not yet been given. The mechanism discussed by Kagel[5] does not satisfy; three hydrogen atoms should split up from the chemisorbed alkoxide form of the alcohol and an adjacent OH-group. Furthermore there was found out that benzaldehyde forms benzoate surface species on Al_2O_3 above 125°.[6] Acetone, acetaldehyde, ethylene and acetylene form acetate surface species above 200°.[7] Both investigations carried out by Scholten and co-workers[8] and our own investigations[7] point out that carbon monoxide also forms a carboxylate structure on γ-Al_2O_3, as formiate surface species. In our laboratory it was tried to explain the mechanism of forming surface carboxylates with the help of numerous experiments. Furthermore we tried to say something about the sites of the γ-Al_2O_3 surface on which those surface reactions take place.

---

[1] R. G. Greenler, *J. Chem. Phys.*, **37**, 2094 (1962).

[2] G. K. Boreskov, Yu. M. Schtschekotschichin, A. D. Makarov and V. N. Filimonov, *Doklady Akad. Nauk S.S.S.R.*, **156**, 901 (1964).

[3] D. Treibman and A. Simon, *Z. Elektrochem.*, **70**, 562 (1966).

[4] V. Corso, *Compt. rend.*, **259**, 1413 (1964).

[5] R. O. Kagel, *J. Phys. Chem.*, **71**, 844 (1967).

2. EXPERIMENTAL

The applied γ-Al_2O_3 with a specific surface area of about 145 m^2/g was prepared by calcination (12 hours, 600°) of boehmite in dry air. Boehmite was prepared by dissolving purest aluminium (99.99 %) in 15 % nitric acid and precipitating it with ammonia water. After about ten preliminary precipitations the main precipitation was carried out at pH 8 and 80 to 90° with NH_3. As adsorbates were used CO, CO_2, ethylene, acetylene, methanol, ethanol, i-propanol, and carbonyl compounds of the type 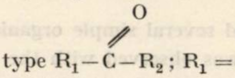 $R_1-\overset{\displaystyle O \\ \displaystyle /\!\!/}{C}-R_2$; $R_1 = CH_3$: acetaldehyde, acetone, acetic acid, ethyl acetate ; $R_1 = H$: formaldehyde, formic acid, formamide. The gases and liquids were purified according to the usual techniques. For spectroscopic and gravimetric studies self-carrying thin plates (diameter 2 cm) were produced. The γ-Al_2O_3 powder was compressed to 40 mg-plates (pressure 6400 kp/cm^2) of a thickness of 100 μm. Before the chemisorption was carried out, the samples were treated with oxygen (100 to 200 torr) and after evacuation treated with hydrogen (100 to 200 torr) in quartz cells for IR-studies or in a sorption apparatus for gravimetric measurements, in both cases usually at 600°. Then the samples were saturated with H_2O-vapour at 200°, afterwards they were dehydrated at 500° (or higher temperatures) and 10^{-5} torr for 2 to 4 hours. The cooled samples were ready for sorption experiments. As a rule the IR-spectra were recorded after the following procedures :

1. Dehydration at various temperatures.
2. Admitting gas up to 200 torr at room temperature.
3. Evacuation (one to several hours).
4. Repeated admitting gas at elevated temperatures.
5. Cooling down the sample and subsequent evacuation. Changes in the sample mass were recorded gravimetrically in part. Studies of the gas phase were carried out IR-spectroscopically and mass-spectroscopically subsequent to the reactions. The IR-spectra were recorded with an infrared spectrometer Type UR 20 (Carl Zeiss, Jena). The gravimetric measurements were performed with a sorption apparatus consisting of a recording vacuum-microbalance and a dosing system.[9] A cell for spectroscopic studies was joined to the vacuum-microbalance directly. Thus IR-spectroscopic and gravimetric measurements could be carried out at the sample simultaneously.

---

[6] J. D. Chapman and M. L. Hair, Proceedings of the 3-rd International Congress on Catalysis, Amsterdam, July 1964, vol. 2, 1965 1091.

[7] P. Fink, *Z. Chem.*, **7**, 284 (1967).

[8] J. J. F. Scholten, P. Mars, P. G. Menon and R. van Hardefeld, "Proceedings of the 3-rd International Congress on Catalysis", Amsterdam, July 1964, vol. 2, 1965 881.

[9] G. Traeger and P. Fink, to be published.

3. RESULTS

3.1. *Chemisorption of alcohols, ethylene, acetylene*

3.1.1. *Alcohols.* The chemisorption of methanol, ethanol and i-propanol was studied at 200°. In complete compliance with other authors [1,2] formiate and acetate surface species were ascertained when using methanol or ethanol, respectively. The IR-absorptions are the following : formiate 1400, 1390, 1605, 2850 cm^{-1}; acetate 1385, 1470, 1590, 2960 cm^{-1}. In accordance with Treibmann [3] i-propanol causes the acetate structure as well. It is supposed that the formation of the carboxylate structure is combined with the products arising from the catalytic dehydration. A direct formation of the carboxylate structures out of the chemisorbed alcohols (Kagel [5]) is very unlikely. The surface concentration of the formiate and acetate species amounts to 12×10^{13} molecules/cm^2 (acetate) and to 6.0×10^{13} molecules/cm^2 (formiate) gravimetrically. The carboxylate structures are extremely stable. Thus, acetate surface species were still traceable after a desorption at 600°. At 250° the acetate structure could be displaced partially by water. Acetic acid was obtained being one of the desorption products.

3.1.2. *Ethylene and acetylene.* Ethylene was brought into contact with dehydrated γ-Al_2O_3 (dehydrated at 500°) at 250° for thirty minutes, then it was cooled. The IR-bands of the acetate surface species were noted besides the IR-absorptions of the chemisorbed ethylene and eventually originated reaction products. When ethylene and the reaction products were desorbed at 250° only the acetate species were noted. In the case of acetylene, acetate species were also noted after the same procedure. The Al_2O_3-pellets grew brown and finally black (separation of carbon) during these procedures. In the case of acetylene strong bands in the range of the $C=C$- and $C\equiv C$-bonds were found besides the IR-bands in the range of the CH-stretching and CH-bending vibrations. When the pellets were treated with oxygen at 450°, which makes their colour pale, and then with hydrogen at 450°, all the bands disappeared, but weak bands of acetate were still recorded (1460, 1580 cm^{-1}). It is possible for ethylene to react with surface OH-groups and to form some alcohol existing in the equilibrium state. Then the alcohol might start the formation of acetate. Furthermore it is possible for acetylene to form some ethylene by self-hydrogenation. However, these statements are suppositions as yet, for the reactions on the γ-Al_2O_3 surface taking place during the interaction of acetylene and ethylene are very complex and still unknown.

3.2. *Chemisorption of carbonyl compounds*

3.2.1. *Aldehydes and ketones.* When formaldehyde, acetaldehyde and acetone were chemisorbed on dehydrated γ-Al_2O_3 the formation of coordinative bonds first appeared. The carbonyl compounds as Lewis-bases are bonded to the electron acceptor centres (Lewis acid sites), i.e. the exposed Al-ions in the surface. In the IR-spectra (fig. 1a, c) a strong shift of the frequencies of the free carbonyl groups is noted. The type of the chemical bond of the formed chemisorption complexes is similar to the bond of typical electron-donor-acceptor complexes (see table 1).

Table 1

Infrared frequencies (cm^{-1}) of acetone in different states

assignment	acetone liquid	acetone. $AlBr_3$solid[10]	acetone on γ-Al_2O_3
$\nu C = O$	1710	1625	1600 (1590–1630)
$\delta_s CH_3$	1433	1400	1460
$\delta_{as} CH_3$	1358	1362	1380
			1320
$\nu C - C$	1225	1262	1250

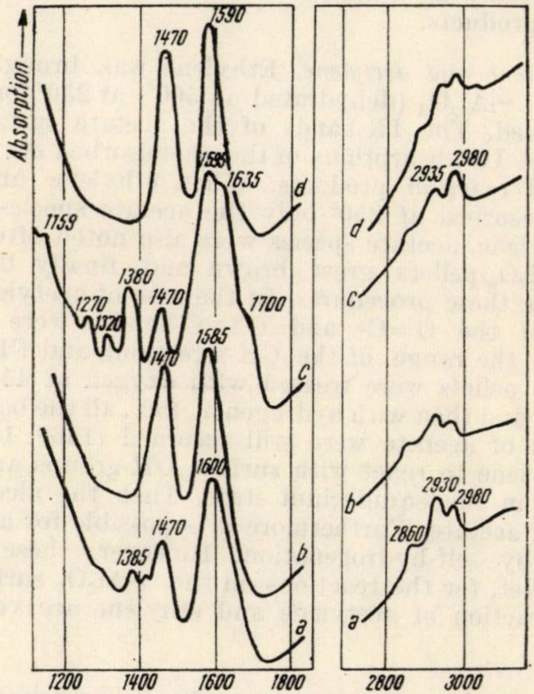

Fig. 1. — Infrared spectra of acetone and acetaldehyde chemisorbed on γ-alumina.

a, acetaldehyde adsorbed at room temperature; *b*, after heating at 100° following *a*; *c*, acetone adsorbed at room temperature; *d*, after heating at 200° following *c*;

---

[10] A. Terenin, W. Filimonov and D. Bystrov, *Z. Elektrochem.*, **62**, 180 (1958).

Chemisorption of various Lewis-basic molecules,[11] for example NH_3,[12] leads to coordinative bonds as the dominating type of bonding on γ-Al_2O_3. When the sealed cells containing the surface complexes formed at room temperature are being heated above 200° carboxylate surface species occur (fig. 1b, d). The chemisorption of aldehydes and acetone at 200° brings us to the same result. An analysis of the gas phase after the surface reaction completion indicated CH_4 in the case of acetone and H_2 in the case of aldehyde, the latter being in considerable concentrations. These results support a previous supposition [7] namely that the following surface reactions take place :

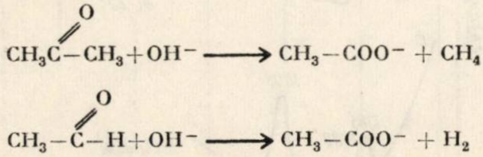

$$CH_3\overset{\overset{O}{\diagup}}{C}-CH_3+OH^- \longrightarrow CH_3-COO^- + CH_4$$

$$CH_3-\overset{\overset{O}{\diagup}}{C}-H+OH^- \longrightarrow CH_3-COO^- + H_2$$

In the case of aldehydes these reactions occur at 100° with a sufficient rate. The results concerning the chemisorption of aldehydes are supported by Chapman's and Hair's [6] investigations. The authors found out that benzaldehyde forms benzoate surface species on Al_2O_3 above 125°.

3.2.2. *Fatty acids, amides of fatty acids, esters.* If formic and acetic acid work on dehydrated γ-Al_2O_3, carboxylate species are formed at 25°C (fig. 2 d). It is very likely that the reactions be confined at first to the surface. In the case of formamide or ethyl acetate chemisorption after a 5-hour interaction, surface formiate or surface acetate, respectively, was already noted on γ-Al_2O_3. In this case the coordinatively bonded intermediate state is being identified at 25° too. The separations of NH_3 from formamide and of ethanol from ethyl acetate were ascertained. Consequently these surface reactions bear the character of saponification reactions. The formed NH_3 proves to be chemisorbed on γ-Al_2O_3 (bands at 1260, 1625, 3370, 3415 cm^{-1}) .

3.3. *Chemisorption of carbon monoxide and carbon dioxide*

3.3.1. *Carbon monoxide.* Carbon monoxide is bound on γ-Al_2O_3 rather weakly at room temperature. After evacuation to 10^{-5} torr gravimetric studies pointed out that only a very small amount of sorbed CO is present. Menon [13] discussed a stronger adsorbate-adsorbent interaction than in the case of N_2. The IR-spectra of adsorbed CO indicate slight changes of the contours of the P- and R-branch in comparison with the rotation-vibration band of gaseous CO (fig. 2a, bands at 2060, 2210 cm^{-1}). These changes can arise from the superposition of weak bands of the adsorbed molecules. After evacuation for 5 hours bands were no longer noted. Amberg[14] noted a band at 2200 cm^{-1} after CO had been adsorbed on Al_2O_3. He attributed the band to the configuration $(\overset{-}{C} \equiv \overset{+}{O})$ interacting with the electrostatic force field of the surface atoms (ion-dipole interaction)[15] Contrary to Amberg[14] at 25° no further bands were ascertained. At 200°, CO forms the formiate structure (fig. 2 b). A surface OH-group being in the vicinity of a coordinatively unsaturated surface aluminium ion participates in the surface reaction: $CO + OH^- \rightarrow HCOO^-$. The surface concentration of the formiate structure formed in this way amounts to 6.2×10^{13} molecules/cm^2.

---

[11] H. DUNKEN and P. FINK, to be published.

[12] H. DUNKEN, P. FINK and E. PILZ, *Chem. Techn.*, **18**, 490 (1966).

[13] P. G. MENON, *J. Amer. Chem. Soc.*, **87**, 3057 (1965).

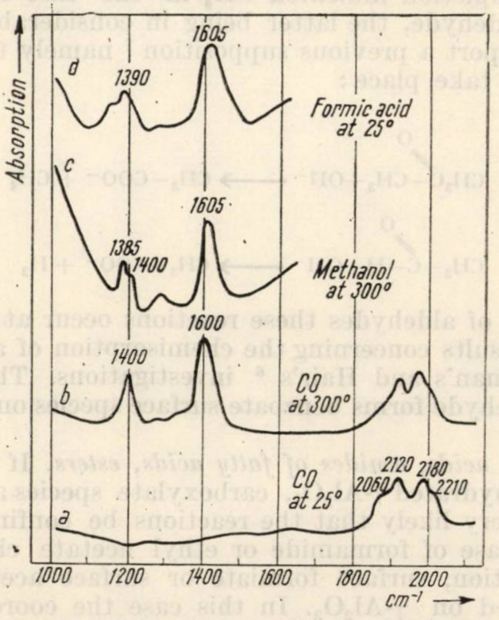

Fig. 2. — Infrared spectra showing the formation of the formiate structure on γ-alumina.

a, CO adsorbed at room temperature under a pressure of 50 torr; *b*, after heating at 300° following *a*; *c*, methanol adsorbed at 300°; *d*, formic acid adsorbed at room temperature.

3.3.2. *Carbon dioxide.* 4.5×10^{13} carbon dioxide molecules per cm^2 are strongly chemisorbed on γ-Al_2O_3. I.R.-spectroscopic studies on the chemisorption of CO_2 on Al_2O_3 have already been done.[14,16–18] By means of the IR-spectra four various surface species (type I, II, III, IV) of sorbed CO_2 were identified. In table 2 the IR-absorptions of the four types of sorbed CO_2 are registered and the assignments of the bands are also given. Type I represents, according to Peri, [17] relatively loosely bound linear CO_2, which is removed nearly completely by evacuation at 25°. Type I adsorption of the sorbed CO_2 is similar to the type of the CO bound on γ-Al_2O_3 at 25°. There is also discussed an ion-dipole interaction with the surface. Only half of the molecule, however, interacts as a bond dipole with the surface ions.

---

[14] L. H. Little and C. H. Amberg, *Canad. J. Chem.*, **40**, 1997 (1962).

[15] C. H. Amberg and D. A. Seanor, Proceedings of the 3-rd International Congress on Catalysis, Amsterdam, July 1964, vol. 1, 1965 450.

[16] N. D. Parkns, Proceedings of the 3-rd International Congress on Catalysis, Amsterdam, July 1964, vol. 1, 1965, 914.

[17] J. B. Peri, *J. Phys. Chem.* **70**, 3168 (1966).

[18] P. Fink, *Z. Chem.*, **7**, 324 (1967).

Table 2

Types of CO_2 chemisorbed on γ-Al_2O_3

Type	structure/point group		infrared frequencies (cm^{-1}) assignment			
I	CO_2	$D_{\infty h}$		2370 ν_{as}		
II	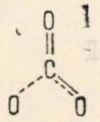	C_s	1200 ν_s			1785 ν_{as}
III	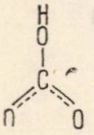	C_{2v}	1240 βOH	1490 $\nu_s COO^-$	1645 $\nu_{as} COO^-$	3615 νOH
IV	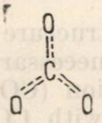	D_{3h}	1500 (broad band) ν_{as}			

The adsorption of type II is characterized by the bands at 1200 and 1785 cm^{-1}. The latter is very complex. Apparently it consists of three single bands (1785, 1835, 1860 cm^{-1}) and extends from 1750 to 1900 cm^{-1} under an elevated pressure of CO_2. After a long evacuation (5 hours) at room temperature a relatively sharp band is left at 1785 cm^{-1}. A carbonato structure is supposed to exist, formed by CO_2, an aluminium ion, and an adjacent oxid ion. Type I and the type II coexist within an equilibrium state (see scheme 1).

The adsorption of type III is regarded as a bicarbonate structure. Except for the symmetrical and asymmetrical COO^--stretching vibrations this structure is also characterized by the OH-stretching vibration (3615 cm^{-1}) and the OH-in-plane bending vibration (1240 cm^{-1}). The assignments could be confirmed by deuteration. The OH-stretching vibration reveals the calculated isotopic shift and the OH-bending vibration is shifted from 1240 cm^{-1} into the range of about 1000 cm^{-1}. Furthermore it should be shown that no bicarbonate structure is formed on a γ-Al_2O_3 surface this being without any OH-groups and modified by chloride ions (γ-Al_2O_3 treated with HCl at 500°). After additions of small quantities

Scheme 1

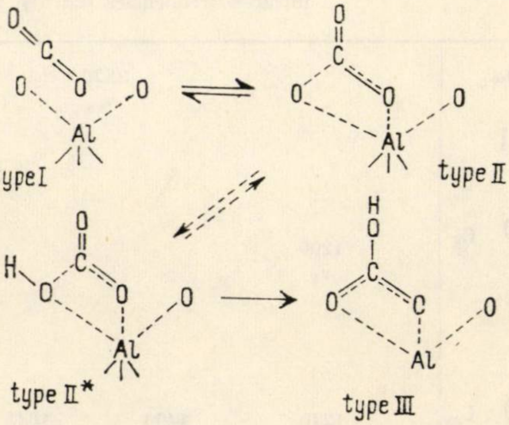

of H_2O (formation of OH-groups) the bicarbonate structure appeared again. The presence of a special type of OH-groups is necessary in order to form the bicarbonate structure. The surface reaction ($CO_2 + OH^- \rightarrow HO-COO^-$) is analogous to the reaction of γ-Al_2O_3 with CO (chapter 3.3.1.). Type II * (scheme 1) must be regarded as an intermediate state of the surface reaction, since it is rather unlikely for the protons to migrate on the surface at room temperature (isolated OH-groups). The transition of the type II adsorption to type III can be followed very easily within a temperature range from − 40° to + 20°. At −40° type II dominates since the reaction velocity for the formation of type III is very small (fig. 3 a). At room temperature the reaction velocity has already increased such as type III is dominating (fig. 3b). The equilibrium state is reached some hours later. Type III cannot be reconversed into type II by cooling. The stability of the surface species increases in the order I, II, III. Whereas type I can be desorbed nearly entirely and type II in the bulk under vacuum (10^{-5} torr) and at room temperature, type III is still present at 60 torr CO_2 up to 325° and under vacuum up to even 250°. The surface concentration of the bicarbonate structure on γ-Al_2O_3 dehydrated at 500° amounts to 18×10^{12} molecules/cm^2 at room temperature and 10^{-5} torr. This result was calculated with the help of the absorbance of the band at 1645 cm^{-1}. At 200° and more the formation of the type IV is to be noted in CO_2 gas. The I.R.-spectrum indicates the formation of a surface carbonate with a symmetrical ion. Recently mass-spectroscopical studies were carried out. Oxygen isotope exchange ($^{18}O/^{16}O$)

between the $\gamma-Al_2O_3$ surface and CO_2 takes place.[19] It is assumed that the type III and (or) the type II represent the intermediate state noted IR-spectroscopically within this exchange reaction.

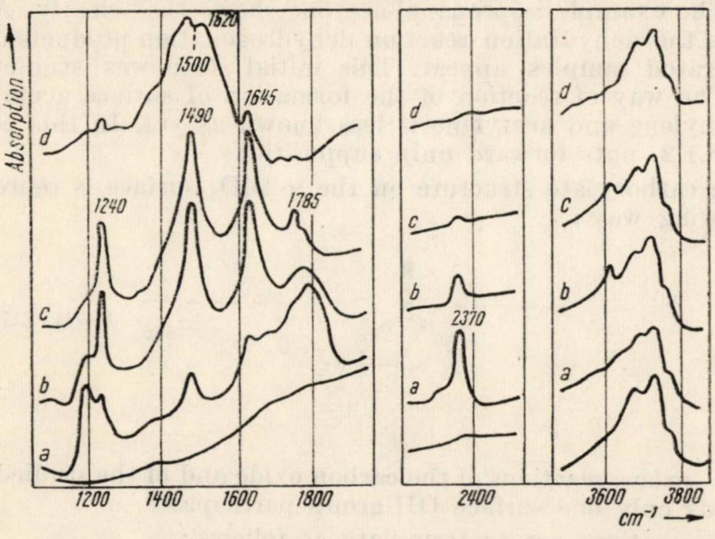

Fig. 3. — Infrared spectra of CO_2 chemisorbed on γ-alumina.

a, CO_2 adsorbed at -40°; *b*, after heating to 25° and standing for 1 hour following *a*; *c*, evacuation for 2 hours at room temperature; *d*, after heating the sample under 50 torr CO_2 at 400° followed by evacuation at 100°.

4. DISCUSSION

The interaction of carbon monoxide, carbon dioxide, and several simple carbonyl compounds of the type $R_1-\overset{\displaystyle O}{\overset{\|}{C}}-R_2$ with the surface of γ-Al_2O_3 dehydrated at 500° results in carboxylate structures. The surface reactions result in the formiate and acetate structure. They are shown in the following schemes :

Scheme 2

isopropanol → acetone → (surface) ← acetic acid
ethanol → acetaldehyde → (acetate)
acetylene → ethylene → (species) ← ethylacetate

Scheme 3 :

methanol ↗ formaldehyde → (surface) ← formic acid
(formiate)
methanol ↘ carbon monoxide → (species) ← formamide

---

[19] P. Fink, unpublished results.

It is assumed that the adsorbed alcohols do not form surface carboxylate species by separation of hydrogen. The aldehydes or ketones, arising as by-products during the dehydration, are likely to form surface carboxylate species. The example isopropanol-acetone shows that clearly. At the beginning of the dehydration reaction dehydrogenation products on strongly dehydrated samples appear. This initial state was studied by the author. The way of reaction of the formation of surface acetate species out of ethylene and acetylene is less known as yet. In this connection chapter 3.1.2. puts forward only suppositions.

The carboxylate structure on the γ-Al_2O_3 surface is represented in the following way :

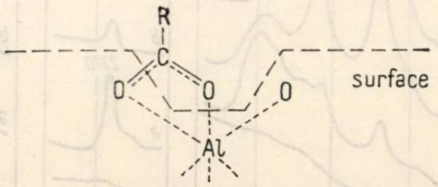

$R = H, CH_3, OH$

In all the surface reactions of the carbon oxide and of the studied carbonyl compounds only one surface OH-group participates.

The reactions are to formulate as follows :

$$CO + OH^- \longrightarrow H-COO^-$$

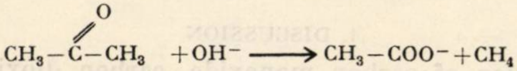

$$CH_3-\overset{O}{\overset{\|}{C}}-CH_3 \quad + OH^- \longrightarrow CH_3-COO^- + CH_4$$

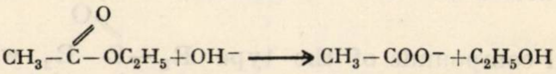

$$CH_3-\overset{O}{\overset{\|}{C}}-OC_2H_5 + OH^- \longrightarrow CH_3-COO^- + C_2H_5OH$$

The general reaction scheme in the case of carbonyl compounds is the following :

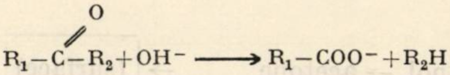

$$R_1-\overset{O}{\overset{\|}{C}}-R_2 + OH^- \longrightarrow R_1-COO^- + R_2H$$

The products R_2H arising during the surface reactions could be indicated analytically. In the case of esters and amids of fatty acids the surface reactions probably represent saponifications and do not, therefore, properly belong to the reactions studied in the frame of this contribution.

Apparently the surface reactions of the carbonyl compounds generally pass the intermediate state of a coordinative bond of the carbonyl group on the aluminium ion in the vicinity of a special type of OH-groups. That coordinative intermediate state is to be indicated in the case of acetone, acetaldehyde, ethyl acetate, and obviously also in the case of CO_2 (type II* of the chemisorbed CO_2 , chapter 3.3.2.). In the case of the studied carbonyl compounds (aldehydes and ketones) the following way of reaction is proposed :

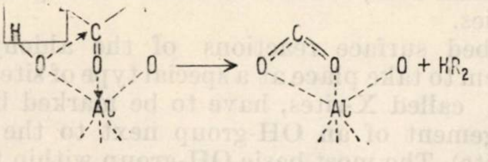

$R_1 = H, CH_3$

$R_2 = H, CH_3$

An electron donation towards the aluminium ion occurs due to the formation of the coordinative bond (electron-donor-acceptor bond) between the carbonyl group and the aluminium ion (electron acceptor site). Thus the C = O-bond is loosened. That is clearly seen at the shift of the C = O-fundamental vibration to lower wave numbers (110 cm^{-1}, see table 1). Simultaneously the carbon atom, the electron density of which decreased owing to the electron donor-acceptor bond, interacts with the oxygen of the basic OH-group, for the oxygen of that group possesses an elevated electron density. Thus the proton of the OH-group becomes loose. By splitting the R_2-C bond the proton forms R_2H; the stable carboxylate structure has originated. The surface reactions of acids and derivatives of acids (esters, amids of fatty acids) seem to run in a different way, since they represent saponification reaction.

In the case of carbon dioxide the following type of reaction is represented :

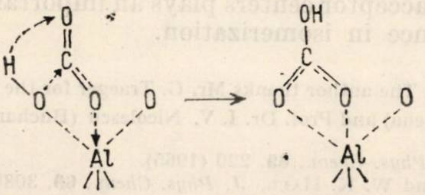

This chemical mechanism resembles to that proposed for ketones and aldehydes. The proton of the OH-group, however, is engaged in stabilizing the carbonato structure, i.e. forming the bicarbonate structure. The surface reaction with CO occurs in accordance with the same chemical mechanism. According to the discussed chemical mechanism, the OH-groups having the greatest formal negative charge (the most basic OH-groups) should be best favoured for those reactions.

The formed carboxylate structures on γ-Al_2O_3 exhibit a relatively great stability. From a previous contribution [11] of our laboratory it results that the state of coordinative bonding does not give the lowest energetic state of the surface. Mostly only one type of center — either the electron donor centres (oxid ions) or the electron acceptor centres (aluminium ions) — is being saturated by coordinative bonds. A simultaneous saturation of the dual sites is possible only in the case of the formation of "normal" bonds, i.e. in the case of the dissociative chemisorption of molecules of the type H—R (such as H_2O, ROH, NH_3 etc.) or in the case carboxylate structures described in this contribution are formed. The carboxylate structures are not achieved at once although they represent the stablest energetic surface state. The surface reactions pass only at elevated temperatures (more than 200°) with a sufficient velocity because of some high activation energies.

The described surface reactions of the aldehydes, ketones, and carbon oxides seem to take place at a special type of sites of the γ-Al_2O_3 surface. These sites, called X-sites, have to be marked by a clearly defined geometric arrangement of an OH-group next to the vacant aluminium ion (Lewis acid site). The most basic OH-group within the model of Peri [20] is not considered as it is only surrounded by oxide ions. The X-sites should involve OH-groups having one or two vacant aluminium ions in their vicinity. The concentration of the dual acid-base sites (X-sites) amounts to $18 \times 10^{12}/cm^2$ on γ-Al_2O_3 dehydrated at 500° measured by means of CO_2. The concentration amounts to $6.2 \times 10^{13}/cm^2$ measured by means of CO and amounts to 12×10^{13} $/cm^2$ if measured by the acetate structure. It is very possible that the X-centres have special catalytic functions on γ-Al_2O_3. For example H—D-exchange between CH_4 and CD_4 on Al_2O_3 was completely poisoned by CO_2.[21] Larsen and Hall [21] ascertained the start of the exchange by successive desorption of CO_2 and found the number of active centres to be 3 to 4 × 10^{12} $/cm^2$ for this reaction. As CO_2 only exists as bicarbonate slightly below the desorption temperature of 300°, X-centres were defined; i.e. about one quarter of the X-centers identified by CO_2 are active in this H—D-exchange.

Further I. V. Nicolescu and co-workers[22] pointed out, that the concentration of donor-acceptor centers plays an important role in the catalytic reactions, for instance in isomerization.

Acknowledgements. The author thanks Mr. G. Traeger for the gravimetric measurements, Prof. Dr. H. Dunken (Jena) and Prof. Dr. I. V. Nicolescu (Bucharest) for helpful discussions.

---

[20] J. B. PERI, *J. Phys. Chem.*, **69**, 220 (1965).

[21] J. G. LARSON and W. K. HALL, *J. Phys. Chem.*, **69**, 3080 (1965).

[22] I. V. NICOLESCU, A. NICOLESCU, M. GRUIA, A. TERLECKI-BARICEVIC, M. DARDAN, EM. ANGELESCU and A. IONESCU, Fourth International Congress on Catalysis, Moscow, 1968, preprint no 78.

NOTE POUR LES AUTEURS

La *Revue Roumaine de Chimie* publie des articles en anglais, français, russe, allemand ou espagnol. Les auteurs sont priés d'envoyer des articles, notes, communications et comptes rendus inédits.

Les manuscrits seront dactylographiés à deux intervalles. Les tableaux seront dactylographiés sur feuilles séparées, de même que la légende des figures. Les diagrammes seront tracés à l'encre de Chine sur papier calque. Les tableaux et les figures seront numérotés par des chiffres arabes, en nombre strictement nécessaire. Prière de ne pas inscrire les mêmes données dans les tableaux et les figures. Les formules chimiques seront incluses dans le texte ; en outre, elles seront transcrites sur des feuilles séparées. Les auteurs sont priés d'indiquer les caractères italiques (en soulignant les lettres au crayon), ainsi que tout autre caractère spécial. L'ordre des références bibliographiques sera celui de leur mention dans le texte ; le nom de l'auteur sera précédé de l'initiale du prénom ; les publications périodiques seront présentées suivant les prescriptions internationales. Les références seront ajoutées à la fin de l'article ; elles paraîtront comme des notes, au bas de la page. Le texte sera précédé d'un résumé, comprenant 15 lignes au maximum.

L'entière responsabilité du contenu des articles appartient aux auteurs. On publie des articles dus aux collaborateurs roumains ou étrangers. Les auteurs recevront 50 tirés à part.

PRINTED IN ROMANIA

1969 SEP 18

TRAVAUX PARUS AUX ÉDITIONS DE L'ACADÉMIE DE LA RÉPUBLIQUE SOCIALISTE DE ROUMANIE

CORNEL BODEA, **Tratat de biochimie vegetală**, partea I, **Fitochimie** (Traité de biochimie végétale, Ire partie, Phytochimie), Ier vol., 1964, 747 p. + 4 annexes, 2 pl., 41 lei ; IIe vol., 1965, 1262 p., 1 pl., 56 lei ; IIIe vol., 1967, 773 p., 35 lei.

V. GHEŢIE et V. MICUŞAN, **Analiza imunochimică. Teorie şi practică** (Analyse immunochimique. Théorie et pratique), 1966, 369 p., 28 lei.

SILVIA IONESCU, **Reacţii chimice induse de radiaţiile ionizante** (Réactions chimiques produites pas les radiations ionisantes), 1963, 271 p., 15 lei.

MARIETA NICOLAE, **Fizico-chimia proceselor fotografice** (Physico-chimie des processus photographiques), 1964, 426 p. + 4 pl., 35 lei.

R. PORTOCALĂ et L. POPA, **Acizii ribonucleici celulari şi virali** (Les acides ribonucléiques cellulaires et viraux), 1966, 375 p., 8 pl., 26 lei.

D. PURDELA et R. VÎLCEANU, **Chimia compuşilor organici ai fosforului şi ai acizilor lui** (La chimie des composés organiques du phosphore et de ses acides), 1965, 540 p., 37 lei.

CRISTOFOR SIMIONESCU et CLEOPATRA VASILIU-OPREA, **Mecanochimia compuşilor macromoleculari** (La mécanochimie des composés macromoléculaires), 1967, 344 p., 23,50 lei.

I.P. „Informaţia" — c. 3806

43426

Lei 15. —

F 1103
04-001/1
R
REFERALVA

REVUE ROUMAINE DE CHIMIE

TOME 14
N° 7
Juillet 1969

ÉDITIONS DE L'ACADÉMIE DE LA RÉPUBLIQUE SOCIALISTE DE ROUMANIE

Rev. Roumaine Chim. 7, 823–962 (1969), Bucarest

COMITÉ DE RÉDACTION

Rédacteur en chef :

C. D. NENIŢESCU, membre de l'Académie de la République Socialiste de Roumanie.

Rédacteurs en chef adjoints :

A. T. BALABAN et V. E. SAHINI, membres correspondants de l'Académie de la République Socialiste de Roumanie.

Collège de rédaction :

C. DRĂGULESCU, RALUCA RIPAN, CR. SIMIONESCU, membres de l'Académie de la République Socialiste de Roumanie; EM. BRATU, membre correspondant de l'Académie de la République Socialiste de Roumanie, Pr G. OSTROGOVICH, MARG. AVRAM, F. BADEA, I. D. MARCHIDAN, D. NEGOIU et D. SĂNDULESCU.

Les manuscrits, les livres et les revues proposés en échange, ainsi que toute correspondance seront envoyés à la rédaction :

REVUE ROUMAINE DE CHIMIE

23, str. Dumbrava Roşie, Bucarest, Roumanie.

F 1103

ORSZÁGOS MŰSZAKI KÖNYVTÁR

REVUE ROUMAINE
DE
CHIMIE

Tome 14, N° 7 **Juillet 1969**

Page

I. G. MURGULESCU und GERDA COMŞA, Chemisorption von Sauerstoff und Kohlenmonoxid an vorbelegten Kupferschichten . . . . 825–829 ✓

V. E. SAHINI and MARINA OLTENEANU, Solvent effect on the infrared spectra of benzophenone and anthrone 831–836

D. CISMARU et Z. SIMON, Sur la cinétique de la formation des couches d'oxydes sur métaux 837–843

G. COSTEANU, ORTANSA LANDAUER et CORNELIA MATEESCU, Influence du milieu de réaction sur l'hydrolyse acide de l'acétate de *n*-butyle 845–849 ✓

W. PTAK, Z. MOSER and L. ZABDYR, Thermodynamic properties of Zn—Bi—Pb liquid solutions 851–868

N. I. IONESCU, On a Suhrmann-Wedler equation 869–872

Z. GROPŞIANU, D. KOHN und A. IOVI, Wärmeübergangszahlen beim Sieden von Lösungen. II. Lösungen von Dinatriumphosphat . . . . 873–878 ✓

GR. POPA and V. MAGEARU, The study of the formation and determination of the stability in solution of some complex combinations with n-propylamine 879–885

M. RĂILEANU and EUGENIA DOBRE, Volumetric dosage with phenothiazone-(3). I. Dosage of sodium thiosulphate with phenothiazone-(3) . . . . . 887–892 ✓

I. FLOREA, Über Hexazyanoferrat und Nitrosopentazyanoferrat des 3-Chlor-9-(4′-Diäthylamino-1′-Methylbutylamino)-7-Methoxyakridins 893–901

ANTOANETA SPINZI et I. V. NICOLESCU, Étude des catalyseurs solides pour l'oxydation des hydrocarbures. II. Influence du milieu de réaction sur les propriétés électriques du catalyseur V_2O_5—MoO_3 903–910

ECATERINA CIORĂNESCU, M. BANCIU, RODICA JELESCU, MARINA RENTZEA, M. ELIAN and C. D. NENITZESCU, Carbonium ion reactions. V. Acetolysis of 1 : 2,5 : 6-dibenzocyclohepta-1,3,5-trienyl-7-ethyl β-tosylate 911–927

M. VOICU and F. BADEA, Kinetics of the acetolysis of 1 : 2,5 : 6-dibenzocyclohepta-1,3,5-trienyl-7-ethyl β-tosylate 929–939

Rev. Roumaine Chim. **14**, 823–962 (1969), Bucarest

Page

A. T. BALABAN, MARIA FRANGOPOL, N. NEGOIŢĂ, P. T. FRANGOPOL and MARIA PARASCHIV, Factors affecting stability and equilibria of free radicals. V. Synthesis and spectra of polynitrophenyl-alkoxyamines . . . 941–945

M. D. GHEORGHIU and R. HOFFMANN, The electronic ground states of *ortho*, *meta* and *para*-benzynes 947–949

VIORICA VOINESCU and A. BALOG, Some isolated mixed anhydrides of 2,6-dimethoxybenzoic acid 951–954

M. I. VASS, Pirani manometer for the range $2\times10^{-1}-5\times10^{-6}$ torr 955–957

V. TĂMAŞ and C. BODEA, TiCl$_4$-carotenoid complexes. V. Action of TiCl$_4$ on dodecapreno-β-carotene 959–961

Revue Roumaine de Chimie, **14**, 825–829 (1969)

ORSZÁGOS MŰSZAKI KÖNYVTÁR ÉS DOKUMENTÁCIÓS KÖZPONT

CHEMISORPTION VON SAUERSTOFF UND KOHLENMONOXID AN VORBELEGTEN KUPFERSCHICHTEN

I. G. MURGULESCU und GERDA COMŞA

aus dem Institut für Physikalische Chemie der Akademie, Bukarest, str. Dumbrava Roşie, 23

Eingegangen am 27. Januar 1969

Messungen von Hallspannungs- und Widerstandsänderungen bei aufeinanderfolgender Chemisorption von Sauerstoff und Kohlenmonoxid an dünnen Kupferschichten ergaben folgendes: 1. Kohlenmonoxidadsorption an mit Sauerstoff vorbelegten Kupferschichten hebt die Wirkung des Sauerstoffs teilweise auf; 2. Sauerstoffadsorption an mit Kohlenmonoxid vorbelegten Kupferschichten wirkt in derselben Richtung wie die Kohlenmonoxidadsorption.

Im Anschluß an unsere früheren Untersuchungen[1–4] hinsichtlich der Änderung des Halleffekts bei der Chemisorption von Gasen an dünnen Metallschichten der Gruppe IB, befaßten wir uns in vorliegender Arbeit mit der aufeinanderfolgenden Chemisorption von Sauerstoff und Kohlenmonoxid (bzw. Kohlenmonoxid und Sauerstoff) an Kupferschichten. Wir waren der Meinung, daß ein Studium solcher Art zur Ergänzung der bei der „Einzel"-Adsorption dieser beiden Gase erhaltenen Daten beitragen könnte. Wie an anderer Stelle ausgeführt,[1,2] erhielten wir für die Systeme Cu/O_2 und Cu/CO (an Kupferschichten von ungefähr 50 Å) folgende Ergebnisse: a) die relative Hallspannungsänderung ist bei niedrigen Belegungen im allgemeinen positiv für das Cu/CO-System, hingegen immer negativ für das Cu/O_2-System; b) bei höheren Belegungen ist dieselbe Größe für beide Systeme negativ.

Obwohl wir bereits eine plausible Erklärung[3–5] für das verschiedenartige Verhalten der beiden Systeme bei geringen Bedeckungsgraden* gaben, beabsichtigten wir, durch Untersuchung der Systeme $Cu/O_2,CO$ und $Cu/CO,O_2$, die bisher erworbenen Kenntnisse zu vertiefen. Überdies kann der vorgeschlagene Versuch als eine Zwischenstufe zwischen der „Einzel"-Adsorption verschiedener Gase und deren, für heterogene Katalyseprozesse wichtigen gleichzeitigen Adsorption angesehen werden.

---

* Die Deutung beruht auf der Annahme der Hypothese von Sachtler undDorgelo[6], unter Berücksichtigung der Anomalie der Dickenabhängigkeit des Hallkoeffizienten *sehr* dünner Metallschichten.[3–5]

[1] I. G. Murgulescu und G. Comşa, *Rev. Roumaine Chim.*, **11**, 1253 (1966).

[2] I. G. Murgulescu und G. Comşa, *Rev. Roumaine Chim.*, **12**, 1171 (1967).

[3] G. Comşa, *Rev. Roumaine Chim.*, **13**, 1003 (1968).

[4] I. G. Murgulescu und G. Comşa, *Rev. Roumaine Chim.* **13**, 1261 (1968).

[5] G. Comşa, Thin Solid Films (im Druck).

[6] W. M. H. Sachtler und G. J. H. Dorgelo, *Z. Phys. Chem. (Frankfurt)*, **25**, 69 (1960).

EXPERIMENTELLES

Die Versuchsanlage und das Meßverfahren sind in früheren Arbeiten[1,2] ausführlich geschildert. Die 50—90 Å dicken Kupferschichten wurden unter einem Restgasdruck von 10^{-8} Torr auf eine mittels flüssigem Stickstoff gekühlte Glasunterlage niedergeschlagen. Nach dem Aufdampfen wurden die Schichten kurz getempert, wobei die Höchsttemperatur 350°K betrug.

Die bei 200°K ausgeführten Adsorptionsversuche verliefen nach folgenden Schemen:

A) CO, O_2 oder CO, Abpumpen, O_2, Abpumpen
beziehungsweise
O_2, CO oder O_2, Abpumpen, CO, Abpumpen.

B) CO, Abpumpen, O_2, Abpumpen, CO, Abpumpen, O_2, Abpumpen
beziehungsweise
O_2, Abpumpen, CO, Abpumpen, O_2, Abpumpen, CO, Abpumpen.

Es wurden die Änderungen der Hallspannung, des elektrischen Widerstandes und des Gesamtdruckes in der Versuchszelle gemessen. Da die Messung der Hallspannung langwierig ist (jeder Wertstellt das Mittel von mindestens 10 Ablesungen dar) mußten wir bei Versuchen, die Messungen nach kürzeren Zeitintervallen erforderten, auf die Hallspannung verzichten.

ERGEBNISSE UND DISKUSSION

In Tabelle 1 sind die relativen Änderungen der Hallspannung und des elektrischen Widerstandes zweier Kupferschichten von 68 bzw. 54 Å bei Zugabe der beiden Gase in der Reihenfolge CO, O_2 bzw. O_2, CO wiedergegeben. Diese Daten bestätigen Ergebnisse unserer früheren Arbeiten: a) Bei niedrigen Belegungen erzeugt die Kohlenmonoxidadsorption an einer reinen Kupferschicht eine positive relative Änderung der Hallspannung; b) bei höheren Belegungen erzeugt sowohl die Adsorption von Kohlenmonoxid als die von Sauerstoff negative relative Hallspannungsänderungen; c) die Höchstwerte der relativen Änderungen von Hallspannung und elektrischem Widerstand sind um so größer je geringer die Schichtdicke ist. Außerdem heben sie folgendes hervor:

Tabelle 1

Änderung elektrischer Eigenschaften dünner Kupferschichten bei aufeinanderfolgender Adsorption von O_2 und CO

Gas	$\Delta U_H/U_{H0}$ (%)	$\Delta R/R_0$ (%)	Gas	$\Delta U_H/U_{H0}$ (%)	$\Delta R/R_0$(%)
CO	$+0{,}30\pm0{,}24$	$0{,}40\pm0{,}55$	O_2	$-2{,}10\pm0{,}27$	$3{,}15\pm0{,}50$
CO	$-1{,}17\pm0{,}17$	$4{,}68\pm0{,}55$	O_2	$-4{,}03\pm0{,}31$	$6{,}82\pm0{,}50$
O_2	$-4{,}78\pm0{,}18$	$12{,}95\pm0{,}55$	O_2	$-6{,}42\pm0{,}31$	$18{,}87\pm0{,}50$
CO	$-3{,}8\ \pm0{,}30$	$9{,}97\pm0{,}55$	CO	$-5{,}61\pm0{,}46$	$16{,}80\pm0{,}50$
O_2	$-4{,}58\pm0{,}28$	$14{,}02\pm0{,}55$			

1. Sauerstoffadsorption an mit Kohlenmonoxid vorbelegten Kupferschichten beeinflußt die Hallspannung und den elektrischen Widerstand in derselben Richtung als das zuerst adsorbierte Kohlenmonoxid: die Absolutwerte der relativen Hallspannungs- und Widerstandsänderungen wachsen bei O_2-Einführung weiter an.

2. Hingegen schwächt Kohlenmonoxidadsorption an mit Sauerstoff vorbelegten Kupferschichten den durch Sauerstoff hervorgerufenen Effekt ab : die Absolutwerte der relativen Änderungen der Hallspannung und des Widerstandes werden bei CO-Einführung geringer.

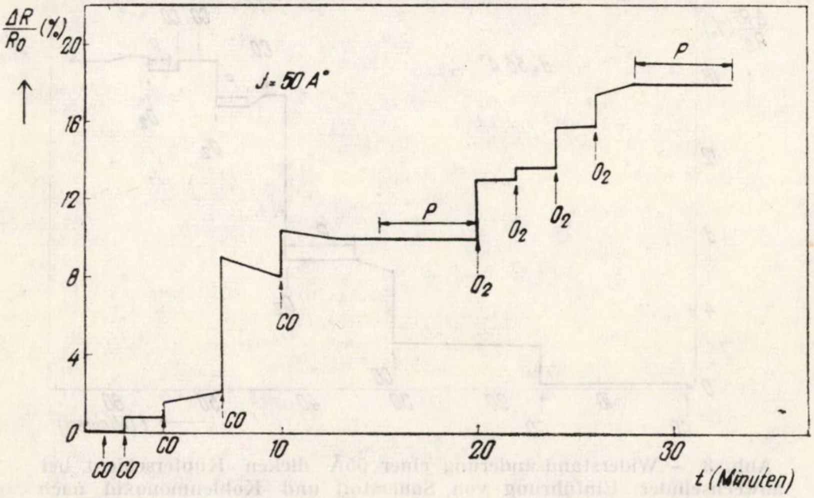

Abb. 1. — Widerstandsänderung einer 50Å dicken Kupferschicht bei Sauerstoffadsorption nach Vorbelegung mit Kohlenmonoxid.

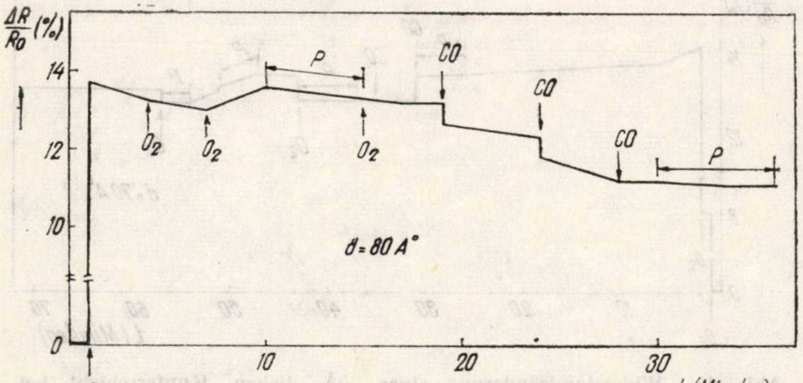

Abb. 2. — Widerstandsänderung einer 80Å dicken Kupferschicht bei Kohlenmonoxidadsorption nach Vorbelegung mit Sauerstoff.

Die gleichen Schlüsse lassen sich aus den Abbildungen 1 und 2 ziehen, in denen die zeitliche Änderung des Widerstandes zweier Kupferschichten von 50 bzw. 80 Å bei aufeinanderfolgender Einführung von CO und O_2, bzw. von O_2 und CO, schematisch aufgetragen ist. Bei diesen (und den folgenden) Versuchen konnte die Hallspannungsänderung [aus dem bereits angeführten Grunde nicht mitgemessen werden. An Hand der in Tabelle 1 dargelegten Ergebnisse liegt jedoch die Annahme nahe, daß das $\Delta U_H / U_{H_0} = F(t)$-Diagramm wahrscheinlich das Spiegelbild des $\Delta R / R_0 = f(t)$-Diagramms darstellt, da im allgemeinen (abgesehen von

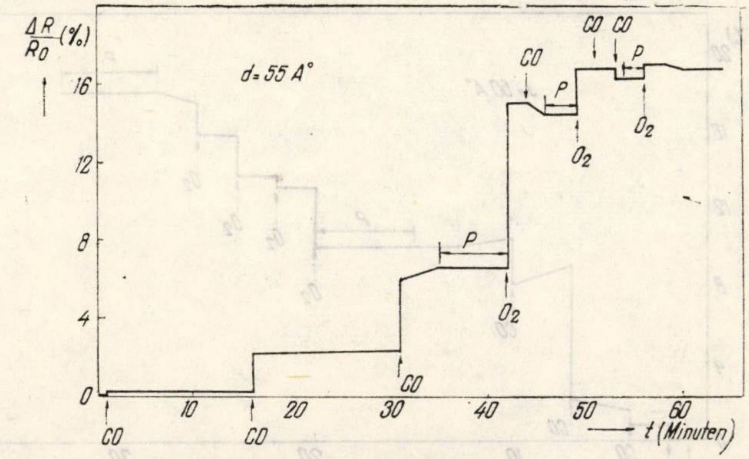

Abb. 3. — Widerstandsänderung einer 55Å dicken Kupferschicht bei abwechselnder Einführung von Sauerstoff und Kohlenmonoxid nach Vorbelegung mit Kohlenmonoxid.

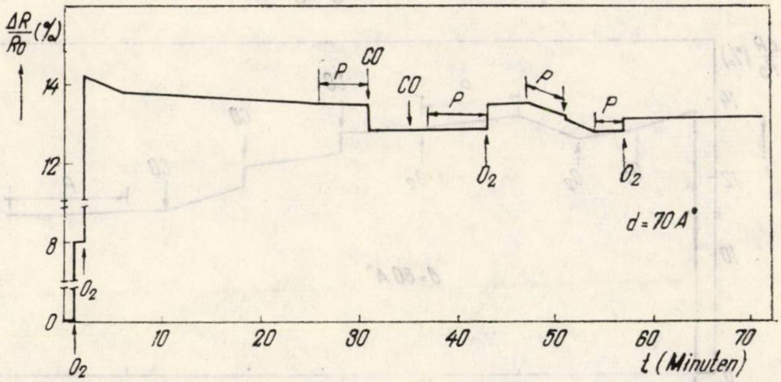

Abb. 4. — Widerstandsänderung einer 70Å dicken Kupferschicht bei abwechselnder Einführung von Kohlenmonoxid und Sauerstoff nach Vorbelegung mit Sauerstoff.

dem Gebiet geringer Belegungen) dem Anwachsen des elektrischen Widerstandes eine Abnahme des Absolutwertes der Hallspannung entspricht.

Des weiteren beabsichtigten wir, festzustellen ob auch bei mehrmaliger Abwechslung der Gaseinführungsfolge im Rahmen desselben Versuches die Schlußfolgerungen 1 und 2 gültig bleiben. Charakteristische Ergebnisse für derartige Versuche sind in den Abbildungen 3 und 4 wiedergegeben. Aus diesen Diagrammen kann gefolgert werden, daß, unabhängig von dem Ausmaße der Vorbelegung (monomolekular oder geringer), Sauerstoff immer zur Verstärkung der durch Kohlenmonoxid hervorgerufenen Wirkung führt, hingegen Kohlenmonoxid den Effekt des adsorbierten Sauerstoffs immer teilweise rückgängig macht. Zur Erklärung dieses Verhaltens könnte die teilweise Verdrängung des erstadsorbierten Gases durch das zweite und dessen Adsorption ins Auge gefaßt werden. Die Beeinflussung der elektrischen Eigenschaften durch „Einzel"-Adsorption ist nämlich für das Cu/O_2-System bedeutender als für das Cu/CO-System.[1,2] Folglich sollten die Änderungen der elektrischen Eigenschaften bei Kohlenmonoxidverdrängung durch Sauerstoff größer, hingegen bei Sauerstoffverdrängung durch Kohlenmonoxid kleiner werden. Diese Erklärung ist in Übereinstimmung mit den von Siddiqi und Tompkins [7] aus Oberflächenpotential-Messungen an Kupferschichten bei aufeinanderfolgender Chemisorption eben derselben Gase abgeleiteten Schlußfolgerungen. Thurston [8] untersuchte seinerseits die Kohlenmonoxidadsorption an reinen und an mit Sauerstoff vorbelegten Kupferschichten und stellte fest, daß die adsorbierte Kohlenmonoxidmenge durch Sauerstoffvorbelegung empfindlich herabgesetzt wird.

Die vorgeschlagene Deutung unserer Ergebnisse kann jedoch nicht als endgültig angesehen werden, da bei der Messung der Änderungen der elektrischen Eigenschaften die Änderung der Restgas-Partialdrucke vorläufig nicht mituntersucht wurde und folglich keine Aussagen über die Zusammensetzung der Gasphase und daraus über die Natur der adsorbierten Schicht gemacht werden konnten.

---

[7] M. M. SIDDIQI und F. C. TOMPKINS, *Proc. Roy. Soc.*, **A 268**, 452 (1962).

[8] E. F. W. THURSTON, *Trans. Faraday Soc.*, **64**, Part 8, 2181 (1968).

Revue Roumaine de Chimie, **14**, 8[illegible]5–829 (1969)

Revue Roumaine de Chimie, **14**, 831–836 (1969)

SOLVENT EFFECT ON THE INFRARED SPECTRA OF BENZOPHENONE AND ANTHRONE

V. E. SAHINI and MARINA OLTENEANU

Institute of Physical Chemistry of the Academy,
Bucharest, Str. Dumbrava Roşie 23

Received December 28, 1968

Our paper presents a systematic study of the solvent effect on the IR C = O stretching frequency of benzophenone and anthrone in order to study the complexes arising at the solvation of these ketones in several mixtures of m-cresol and cyclohexane. We point out the existence of 1 : 1, 1 : 2 and 1 : x complexes. Our results led to the conclusion that in pure m-cresol there are mainly the 1 : x and 1 : 2 complexes.

Many recent papers have reported studies of the solvent effect on the aromatic ketones.[1-6] The latest works point out the need of studies in mixed solvents as the initially formed collision complex [6] between the neat solvent and the ketone shifts the carbonyl frequency to greater wave numbers as against the corresponding ones in pure ketone. This fact brought about a more obvious shift to smaller wave numbers due to the donor-acceptor complex which is formed by adding a proton donor solvent.

These studies show also that the attempts to link the frequency shifts of the carbonyl stretching mode of aromatic ketones dilute in polar solvents from the corresponding ones in the gaseous phase to the dielectric constant, the refractive index and the solvent cage radius by means of the K.B.M. or Buckingham equations are not in good agreement with the experimental data.

This disagreement was put down to the account of the fact that theories are based on the Onsager's reaction field model which considers the solute molecule in the solvent cage. Nowadays, this pattern which dealing with the solute molecule in the solvent cage, is replaced by many authors by the entity solute-polar solvent complex in the first solvation shell solved in the neat solvent as a second solvation shell.[6]

In our work a systematic study of the solvent effect is presented in order to study the complexes arising at the solvation of benzophenone and anthrone in several mixtures of m-cresol and cyclohexane.

---

[1] J. Lascombe and M. L. Jasien, "Proc. Intern. Meeting Mol. Spectr. 4-th", Bologna, 1959, 2, 840–9 (publ. 1962).

[2] L. J. Bellamy and R. L. Williams, *Proc. Roy. Soc.*, **255**, 22 (1960).

[3] K. B. Whetsel and R. E. Kagarise, *Spectrochim. Acta*, **18**, 315 (1962).

[4] K. B. Whetsel and R. E. Kagarise, *Spectrochim. Acta*, **18**, 329 (1962).

[5] K. B. Whetsel and R. E. Kagarise, *Spectrochim. Acta*, **18**, 341 (1962).

[6] M. Horak and J. Pliva, *Spectrochim. Acta*, **21**, 911 (1965).

EXPERIMENTAL

The IR spectra were registered on a U.R. 10 Spectrophotometer using a NaCl prism. The spectral slit width was about $4-5$ cm^{-1}.

Calibration of both wave numbers and absorbance scales was made. The wave numbers scale was calibrated with the 1601 cm^{-1} band of polystyren and rechecked before and after each measurement with 1670 cm^{-1} and 1674 cm^{-1} $C = 0$ bands of benzophenone and anthrone respectively in cyclohexane.

The absorbance scale was calibrated electronically. The frequency measurements are reproducible with $\pm$ 1.0 cm^{-1} and the absorbance measurements are considered as accurate at about $\pm$ 1%.

The concentrations of both ketones were chosen according to a study on the solvent effect with concentration.

The chemically pure ketones were recrystallized several times from anhydrous EtOH. The chromatographic pure solvents were dried and distilled before use.

EXPERIMENTAL RESULTS

From figure 1 we can observe that the $C=O$ band corresponding to the collision complex initially formed between benzophenone and cyclohexane presents a peak at 1670 cm^{-1}. We can also see that by the chosen concentration for benzophenone there is virtually no uncomplexed ketone.

By adding small amounts of polar solvent we can observe the appearance of a second peak at 1657 cm^{-1}.

A third peak at 1651 cm^{-1} is noticed at high polar solvent concentration.

By increasing the concentration of m-cresol, a change in the relative intensities of the three maxima can be observed. This fact is showing an increase of the number of ketone molecules engaged in the donor-acceptor complexes formation on behalf of those that formed the former collision complex. We can see also the appearance of a fourth peak at shorter wave numbers, at 1645 cm^{-1}, consequently the formation of a third complex.

At greater concentrations as 1.5 M in m-cresol the peaks reading is unreliable.

In pure polar solvent a large band is observed which is shifted to 1645 cm^{-1} with another peak at 1651 cm^{-1}.

In order to characterize these complexes we plot the curves of the carbonyl abundancy against the donor concentration at constant concentration in benzophenone.

From figure 2 one can see a sharp diminution of the carbonyl abundancy for the initial collision complex. From a certain moment on, one can observe a slight diminution of the carbonyl abundancy for the complex 1 and a constant value for that corresponding to the complex 2. On this stage a sharp increase of the abundancy for the complex 3 can also be observed.

For a more accurate description of the formed complexes we used the continuous variation method.

In figure 3 the curves are plotted for the 1657 cm^{-1} and 1651 cm^{-1} frequencies, representing the difference between the measured absorbance

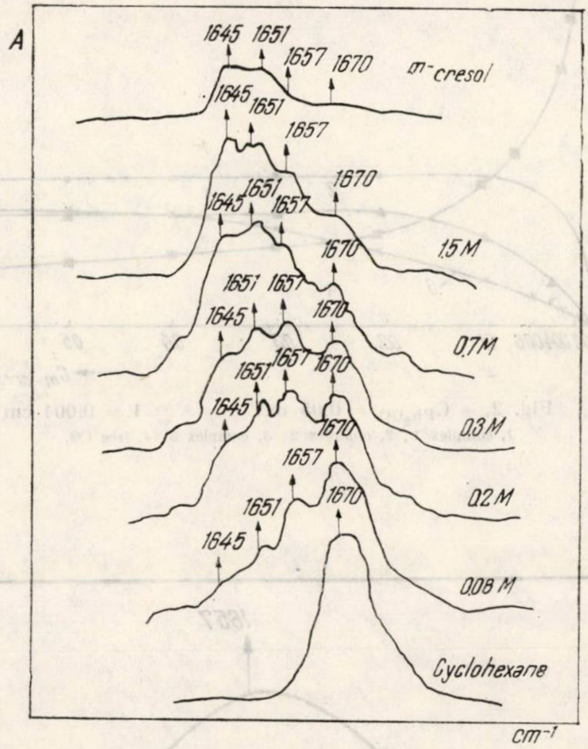

Fig. 1. — $C_{Ph_2CO} = 0.05$ M/l 1 = 0.004 cm.

and that obtained in the absence of any interaction against the ketone molar fraction.

For the 1657 cm^{-1} frequency a maximum was obtained at 0.5 and for 1651 cm^{-1} at 0.33 molar fraction for benzophenone.

Figure 3 shows the formation of 1 : 1 and 1 : 2 complexes. We could not make any assumption on the 1645 cm^{-1} maximum on account of the weak initial absorption and of the large overlapping, this maximum by the absorption corresponding to the complex 2 at high donor concentrations.

We used the same method for the study of the solvent effect on the C=O stretching vibration of the anthrone molecule, and the results are given in figures 4 and 5.

These figures show the formation of the three complexes but at higher amounts of donor solvent due probably to a much larger steric hindrance.

In this case the continuous variation method could not be applied.

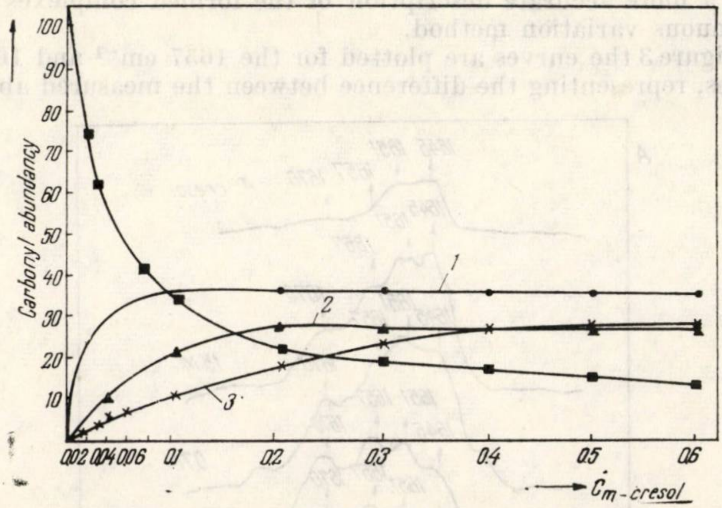

Fig. 2. — $C_{Ph_2CO} = 0.05$ m/l 1 = 0.004 cm : *1*, complex 1; *2*, complex 2; *3*, complex 3; *4*, free CO.

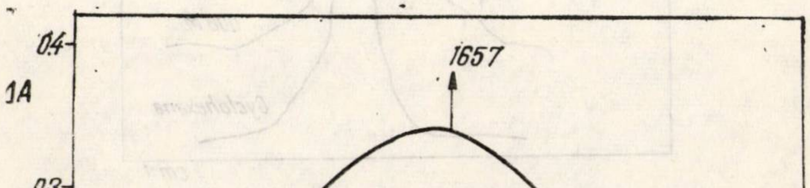

Fig. 3. — Total concentration = 0.06 M/l

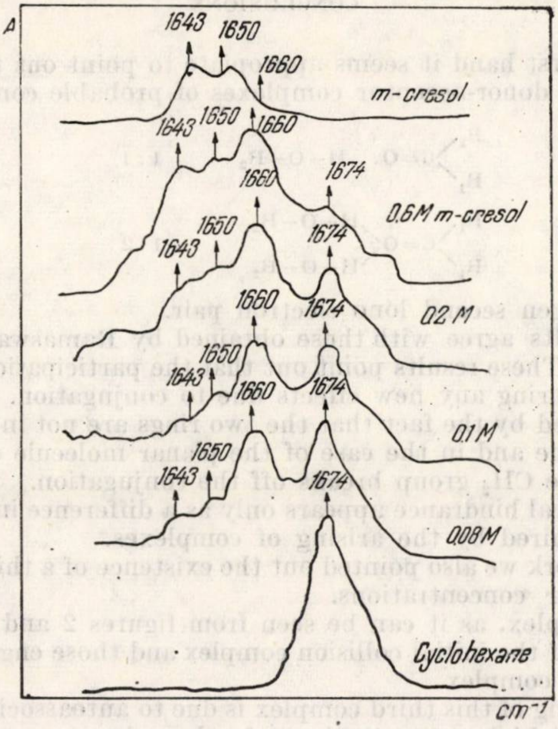

Fig. 4. — $C_{Anth} = 0.02$ M/l 1 = 0.006 cm.

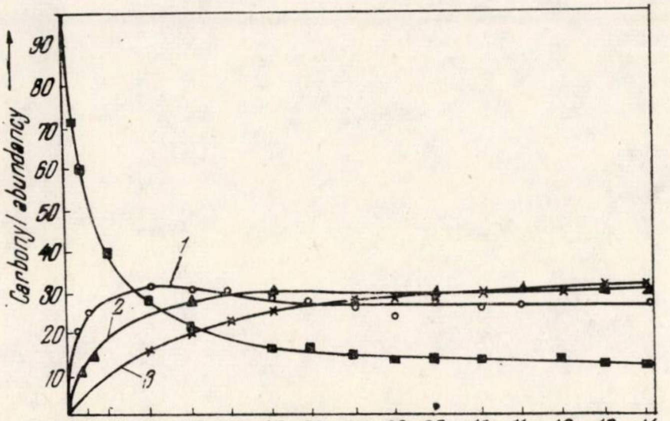

Fig. 5. — $C_{Anth} = 0.002$ M/l 1 = 0.006 cm

1, complex 1; *2*, complex 2; *3*, complex 3; *4*, free CO.

CONCLUSIONS

On the first hand it seems appropiate to point out the existence of 1 : 1 and 1 : 2 donor-acceptor complexes of probable configurations :

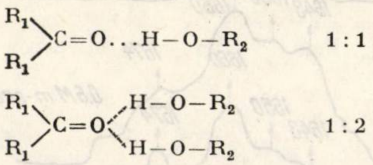

using the oxygen second lone electron pair.

Our results agree with those obtained by Ramaswany and al.[7] for acetophenone. These results point out that the participation of the second ring does not bring any new effects due to conjugation. This behaviour can be explained by the fact that the two rings are not in the same plane in benzophenone and in the case of the planar molecule of anthrone the existence of the CH_2 group breaks off the conjugation.

The sterical hindrance appears only as a difference in the donor concentration required by the arising of complexes.

In our work we also pointed out the existence of a third 1 :x complex at hight donor concentrations.

This complex, as it can be seen from figures 2 and 4 is formed of the molecules of the initial collision complex and those engaged in the formation of 1 :1 complex.

The arising of this third complex is due to autoassociation of m-cresol molecules at high concentrations of polar solvent.

Our observations led to the conclusion that in pure m-cresol there are mainly this complex and the 1 : 2 one.

[7] K. Ramaswamy, R. Pichai and S. G. Gnanadesikan, *J. Mol. Spectroscop.*, **23**, 416 (1967).

Revue Roumaine de Chimie, **14**, 837–843 (1969)

SUR LA CINÉTIQUE DE LA FORMATION DES COUCHES D'OXYDES SUR MÉTAUX

D. CISMARU et Z. SIMON

Institut de chimie physique de l'Académie, Bucarest, 23, str. Dumbrava Roşie

Reçu le 22 mai 1968

A l'aide de la théorie de la vitesse absolue de réaction d'Eyring on a calculé les vitesses de réaction d'oxydation de quelques métaux (Th, Ti, Mg) qui conformément aux résultats expérimentaux suivent une loi linéaire d'oxydation. On a comparé les résultats théoriques obtenus avec les résultats expérimentaux.

Les lois cinétiques de l'oxydation des métaux ont été établies à l'aide des résultats fournis par l'expérience, et concrétisées par certaines relations.

Les relations les plus simples sont celles données par Tammann [1] et, plus tard, par Pilling et Bedworth.[2] Pour certains métaux, la loi d'oxydation peut être exprimée par une relation linéaire entre l'accroissement de la masse de l'échantillon par unité de temps ; pour d'autres métaux on a trouvé d'autres lois comme celles parabolique, cubique ou logarithmique. Dans les réactions d'oxydation, comme dans toutes les réactions chimiques, le phénomène initial est le contact entre les molécules des réactants, c'est-à-dire les chocs des molécules gaz sur la surface du métal. Ces chocs peuvent mener à la formation de nouveaux produits, et jusqu'à la couverture des surfaces, la loi d'oxydation pourrait être déduite de la théorie des chocs moléculaires.

Au cas où la première couche d'oxyde formée est non protectrice (le volume moléculaire de l'oxyde formé est inférieur au volume atomique du métal), la loi d'oxydation ne subira aucun changement, et au cas où la couche devient protectrice (le volume moléculaire de l'oxyde supérieur au volume atomique du métal) il faut tenir compte de ce nouveau facteur qui peut modifier la loi initiale d'oxydation.

Nous considérerons ci-dessous le cas de la formation de l'oxyde non protecteur, en cherchant dans quelle mesure les résultats obtenus par la théorie du complexe activé d'Eyring concordent avec les résultats expérimentaux. Nous utiliserons les données expérimentales obtenues avec les systèmes : $Th+O_2$, $Ti+O_2$; $Mg+O_2$; $Mg+N_2$.

---

[1] I. G. Tammann, *Z. anorg. Chem.* 3, 78 (1920).

[2] N. B. Pilling et R. E. Bedworth, *J. Inst. Met.*, **29**, 529 (1920).

PARTIE THÉORIQUE

La cinétique des réactions d'oxydation des Th, Ti et Mg suit, conformément aux données expérimentales, une loi exprimée par

$$\Delta m = l''.t \tag{1}$$

Δm étant l'accroissement de la masse de l'échantillon par unité de surface, l'' la constante de vitesse et t le temps.

D'après Eyring [3] nous pouvons considérer deux cas :

A. Le gaz qui frappe à la surface du métal est adsorbé et considéré comme formant une couche immobile, autrement dit on suppose qu'il existe sur la surface des centres d'adsorption qui peuvent être considérés comme des réactants, donc chaque molécule gaz adsorbé utilisera un centre actif.

Le complexe activé est donc supposé d'être solide.

$$A + S \rightarrow AS^* \times \rightarrow \text{Produits}$$

Pour une molécule gaz diatomique nous pouvons écrire que le nombre de chocs par unité de temps est

$$\widetilde{v} = c_g \cdot c_s \cdot \frac{kT}{h} \cdot \frac{f^*}{F_g \cdot f_s} \cdot \mathrm{e}^{-E/kT} \tag{2}$$

où

$c_g = N_g/V$, mole/ml ;

$c_s = N_s/S$ la concentration des centres actifs prenant part à la réaction, S étant donné en cm² ;

f^* = la fonction de partition pour le complexe actif ;

f_s = la fonction de partition pour le centre actif ;

F_g = la fonction de partition par unité de volume du gaz adsorbé.

$$\text{Mais } \frac{f^*}{F_g \cdot f_s} = \frac{\sigma}{\sigma^*} \cdot \frac{h^5}{(2\pi m/kT)^{3/2} \cdot 8\pi^2 IkT}$$

avec σ et σ^* comme facteurs de symétrie des molécules gaz et du complexe actif.

On peut écrire alors l'expression de la constante de vitesse

$$\frac{\Delta m}{t} = l'' = c_g \cdot c_s \frac{kT}{h} \cdot \frac{\sigma}{\sigma^*} \cdot \frac{h^5}{(2\pi mkT)^{3/2} \cdot 8\pi^2 IkT} \mathrm{e}^{-E/RT} \tag{3}$$

En mettant $c_g kT = p$, la pression du gaz idéal, nous obtenons

$$\frac{\Delta m}{t} = l_4'' = c_s \frac{\sigma}{\sigma^*} \cdot \frac{N^{5/2} h^4}{M^{1/2} (2\pi)^{3/2} \cdot 8\pi^2 I (RT)^{5/2}} \mathrm{e}^{-E/RT} \tag{4}$$

B. Le gaz qui frappe à la surface du métal est considéré formant une couche mobile d'adsorption, étant donc supposé comme déjà activé.

$$A \rightarrow A^* \rightarrow \text{Produits}$$

---

[3] S. GLASSTONE, K. J. LAIDLER et H. EYRING, «The Theory of Rate Processes», New York, Londres, 1941, p. 347–383.

Dans ce cas, le nombre de chocs à l'énergie supérieure à E, par unité de temps, est donné par la formule

$$\tilde{v} = c_g \frac{k\,T}{h} \cdot \frac{F^*}{F_g} .\ \mathrm{e}^{-E/RT} \tag{5}$$

F^* étant la fonction de partition par unité de volume du complexe actif.

En supposant que la molécule gaz du complexe activé ne diffère pas de celle en état libre, les degrés de liberté vibrationnelle et rotationnelle sont similaires à ceux des molécules gaz initial et le rapport $\frac{F^*}{F_g}$ est réduit au rapport des termes de translation sur la surface du métal et dans le volume du gaz.

Tenant compte que : $F^* = 2\,\pi m\,kT/h^2$ et $F_g = (2\,\pi m\,kT)^{3/2}/h^3$ nous pouvons écrire

$$\frac{F^*}{F_g} = \frac{h}{(2\,\pi\, mkT)^{1/2}} . \tag{6}$$

Au cas où nous considérons également $c_g kT = p$, l'expression de l'' devient

$$\frac{\Delta_m}{t} = l''_7 = p\left(\frac{M}{2\,\pi RT}\right)^{1/2} \cdot \mathrm{e}^{-E/RT} \tag{7}$$

La formule est identique à la formule pour le nombre de molécules gaz à l'énergie supérieure à E, qui frappent une surface de 1 cm² par unité de temps (Hertz-Knudsen)[4,5].

RÉSULTATS ET DISCUSSIONS

Dans les calculs par les formules (4) et (7) on a pris les valeurs suivantes : M (oxygène) $= 32$ g, $\mathrm{I} = 19{,}10.10^{-40}$ g.cm² ; $\sigma = 2$; $\sigma^* = 1$; $h = 6{,}62.10^{-27}$ erg.s ; $k = 1{,}3805.10^{-16}$ erg/grad ; $C_s = 10^{15}$ atome/cm² ; $p = 1{,}013.10^6\ p$ (atm) ; $f_s = 1$, $F_g = f^3_{\mathrm{trans}} \cdot f^2_{\mathrm{rot}} \cdot f_{\mathrm{vibr}}$; où $f_{\mathrm{vibr}} \cong 1$; $f_{\mathrm{rot}} = 10^1 - 10^2$; et $f_{\mathrm{trans}} = 10^8 - 10^9$. $R = 8{,}313 \cdot 10^7$ erg/grad.

Les résultats obtenus sont inscrits aux tableaux 1—4.

Tableau 1

Système Th – O₂

n°	T °K	E cal/mole	l''_4 g.cm^{-2} s^{-1}	l''_7 g.cm^{-2} s^{-1}	l''_{exp} g.cm^{-2} s^{-1}
1	598		$1.39.10^{-9}$	$8{,}65.10^{-8}$	$1{,}00.10^{-8}$
2	648		$5{,}12.10^{-9}$	$3{,}62.10^{-7}$	$5{,}20.10^{-7}$
3	673	22 000	$1{,}07.10^{-8}$	$7{,}00.10^{-7}$	$7{,}20.10^{-7}$
4	698		$1{,}99.10^{-6}$	$1{,}22.10^{-6}$	$1{,}24.10^{-6}$
5	723		$3{,}4.10^{-6}$	$2{,}12.10^{-6}$	$1{,}88.10^{-6}$

[4] H. Hertz, *Ann. Phys.*, **17**, 177 (1882).

[5] M. Knudsen, *Ann. Phys.*, **29**, 179 (1909).

[6] D. Cubieciotti, *J. Amer. Chem. Soc.*, **74**, 1079, 1200 (1952).

Tableau 2

Système Ti–O_2[7]

n°	T °K	E cal/mole	l''_4 g.cm^{-2} s^{-1}	l''_7 g.cm^{-2}.s^{-1}	l''_{exp} g.cm^{-2} s^{-1}
1	1 093		$6{,}01 .10^{-11}$	$3{,}18.10^{-9}$	$1{,}00.10^{-8}$
2	1 133	21 700	$1.29 .10^{-10}$	$6{,}81.10^{-9}$	$1{,}60.10^{-7}$
3	1 123		$2{,}65 .10^{-10}$	$1{,}39.10^{-8}$	$3{,}61.10^{-7}$
4	1 223		$6{,}05 .10^{-10}$	$3{,}18.10^{-8}$	$7{,}80.10^{-7}$

Tableau 3

Système Mg–O_2[8]

n^0	T °K	E cal/mole	l''_4 g.cm^{-2} s^{-1}	l''_4 g.cm^{-2} s^{-1}	l''_{exp} g.cm^{-2} s^{-1}
1	774		$1{,}47.10^{-14}$	$2{,}13.10^{-13}$	$1{,}91.10^{-7}$
2	793	40 000	$1{,}36.10^{-14}$	$4{,}65.10^{-13}$	$3{,}37.10^{-7}$
3	813		$1{,}27.10^{-13}$	$0.98.10^{-12}$	$7{,}12.10^{-7}$
4	873		$1{,}42.10^{-13}$	$1{,}72.10^{-11}$	$1{,}68.10^{-6}$

Tableau 4

Système Mg–N_2[9]

n^0	T	E	l''_4	l''_7	l''_{exp}
1	673		$2{,}70.10^{-12}$	$1{,}16.10^{-12}$	$6{,}00.10^{-10}$
2	723		$2{,}00.10^{-11}$	$1{,}28.10^{-12}$	$2{,}40.10^{-9}$
3	742	30 000	$4{,}43.10^{-11}$	$2{,}64.10^{-11}$	$5{,}60.10^{-8}$

Dans ces tableaux l''_4 est calculé par la formule (4) et l''_7 par la formule (7).

En examinant les données des tableaux on constate que si la couche gazeuse de réaction est considérée immobile (le complexe actif solide) :

1. *Système Th–O_2*

l'' expérimental est approximativement 10 fois plus grand que l''_4 et presque identique à l''_7.

2. *Système Ti–O_2*

l'' expérimental est approximativement 10^3 fois plus petit que l''_4 et approximativement 10 fois plus grand que l''_7.

3. *Système Mg–O_2*

l'' expérimental est approximativement 10^7 fois plus grand que l''_4 et approximativement 10^6 fois plus grand que l''_7.

[7] H. Davies et C. E. Birchenall, *J. Metals*, **3**, 877 (1951).

[8] I. G. Murgulescu et D. Cismaru, *Rev. Roumaine Chim., Acad. Rom.*, **2**, 178 (1958).

[9] I. G. Murgulescu et D. Cismaru, *Rev. Roumaine Chim., Acad. Rom.*, **2**, 251 (1960).

4. *Système $Mg-N_2$*

l'' expérimental est approximativement 10^2 plus grand que l''_4 et tout autant que l''_7.

Il existe donc un désaccord entre les valeurs expérimentales et l'' et les valeurs calculées.

On peut également essayer d'admettre la participation à la réaction d'un nombre supérieur de degrés de liberté et dans ce cas, dans la formule qui donne le nombre de chocs par unité de temps sur la surface

$$\tilde{v} = N \cdot P \left(\frac{1}{2\pi MRT} \right)^{1/2} \tag{8}$$

on devrait changer N contre le nombre de molécules ayant une énergie supérieure à l'énergie d'activation E, concentrée en n degrés de liberté

$$\tilde{v} = \frac{N_0 \left(\frac{E}{RT} \right)^{\frac{n}{2}-1}}{\left(\frac{n}{2} - 1 \right)} \cdot \mathrm{e}^{-E/RT}$$

Il s'ensuit que

$$l''_{\text{théorique}} = p \, \frac{1}{\frac{n}{2} - 1} \left(\frac{M}{2\pi RT} \right)^{1/2} \left(\frac{E}{RT} \right)^{\frac{n}{2}-1} \mathrm{e}^{-E/RT} \tag{9}$$

mais le calcul de l'' à l'aide de cette formule ne mène pas à de meilleurs résultats.

On trouve que pour le système $Mg-N_2$, la participation à la réaction de 7 degrés de liberté des molécules N_2 conduit pour l'' théorique à une valeur du même ordre que l'' expérimental. Il faut néanmoins mentionner que la participation de 2 degrés de translation (de la molécule N_2) perpendiculaires sur la coordonnée de réaction n'est pas facile à comprendre.

Pour le système $Mg-O_2$ on devrait admettre une valeur $n = 14$ pour arriver à des valeurs de l'' théorique égales à l'' expérimental, ce qui ne saurait être admis.

On pourrait imaginer au lieu des faits ci-dessus que la molécule oxygène est partiellement dissociée dans le complexe actif

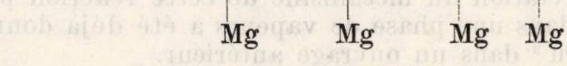

et les atomes oxygène circulent librement sur la surface du magnésium. Dans ce cas nous avons

$$l''_{\text{théorique}} = p \left(\frac{M}{2\pi RT} \right)^{1/2} \frac{f^*_{tr.}}{f_r \cdot f_v} \cdot \mathrm{e}^{-E/RT}$$

Pour $T = 773°\mathrm{K}$ et $E = 48000$ cal/mole, p étant 1 atm, on obtient l'' théorique $= l''_{\mathrm{exp}} = 1{,}9 . 10^{-7}\,\mathrm{g.cm^{-2}.s^{-1}}$ et $f_{\mathrm{tran}} = 10^5$. Pour avoir $f_{\mathrm{trans}} = 10^5$, il faut que les atomes oxygène se déplacent librement sur une surface de $2{,}5.10^{-8}\,\mathrm{cm}^2$ c'est-à-dire sur une distance de 10^{-4} cm, dimension qui pourrait correspondre aux dimensions des fissures entre les granules d'oxyde, par lesquelles l'oxygène arriverait à la surface du métal.*

Nous pouvons imaginer de même un modèle du complexe activé formé d'une molécule O_2 et d'atomes Mg libres à la surface du métal, de sorte que les rotations de la molécule O_2 soient freinées et que l'une des translations corresponde à la coordonnée de la réaction. On obtiendrait ainsi

$$l''_{\text{théorique}} = c_g \cdot kT \frac{m}{h} \cdot \frac{f^{*5}}{f_{tr}^3 f_r^2 f_v} \cdot \mathrm{e}^{-E/RT}$$

En posant $f_{\mathrm{trans}} = 10^8, f_{\mathrm{rot}} = 10^2$ et $f_v = 1$ on obtient l'' théorique $= 2.4.10^{-7}\,\mathrm{g.cm^{-2}s^{-1}}$, ce qui concorde assez bien avec la valeur obtenue expérimentalement de $l''_{\mathrm{exp}} = 1{,}9 \cdot 10^{-7}\,\mathrm{g \cdot cm^{-2} \cdot s^{-1}}$.

Le complexe activé serait dans ce cas

$$\frac{\mathrm{O = O \ldots Mg}}{\mathrm{/Mg/\ Mg/\ //\cdot/Mg/\ Mg/}}$$

et demanderait donc une évaporation partielle du magnésium ce qui expliquerait la différence entre le comportement du magnésium (grand $l''_{\text{expérimental}}$, point d'ébullition = 1107°) et celui du titane et du thorium (l''_{exp} petit ou normal) qui ont un point d'ébullition plus élevé.

Conformément aux données de Svec et Gibbs [10], entre 500 et 600°, le magnésium a les tensions de vapeur suivantes

Temp. °C	Pression des vapeurs en mm col.Hg
500	0,053
550	1,190
600	0,684

On a pu observer que l'évaporation s'intensifie et que les quantités de magnésium évaporées augmentent quelque temps après le commencement de l'évaporation, probablement à cause de l'élargissement de la zone se trouvant à la surface du métal.

Par conséquent, le modèle du complexe activé qui tient compte du libre mouvement du Mg à la surface du métal paraît représenter la réalité-même. L'interprétation du mécanisme de cette réaction par l'oxydation du magnésium dans une phase de vapeurs a été déjà donné par Murgulescu et Cismaru [9] dans un ouvrage antérieur.

★

---

* $F = f_{tr.}^{*2} = \frac{2\,\pi \cdot \mathrm{m}kT}{h^2} \cdot l^2$ avec l^2 la dimension du potentiel bidimensionnel.

[10] J. Svec et D. S. Gibbs, *J. Electrochem. Soc.*, **104**, 434 (1957).

Des résultats obtenus on peut donc tirer les conclusions suivantes :

a) Pour les réactions Th + O_2 et Ti + O_2, l'' expérimental est du même ordre que l'' théorique déduit par la formule (7).

b) Pour la réaction Mg + O_2, l'' expérimental est 10^7 fois plus grand que l'' théorique déduit par la formule (4), alors que pour la réaction Mg + N_2, il est approximativement 200 fois plus grand que l'' théorique déduit par la formule (4).

c) La réaction Mg + O_2 peut être expliquée aisément en tenant compte de l'évaporation du magnésium aux températures auxquelles l'expérience a eu lieu.

On doit néanmoins remarquer que la surface de réaction du métal a été prise égale à la surface mesurée. Mais il faut que la surface *micro* soit beaucoup plus grande que la surface *macro*, leur rapport atteignant, peut-être, même 1000. Cela conduirait à une diminution correspondante des constantes de vitesse expérimentales et des coeficients préexponentiels (si les distances des irrégularités les plus importantes dépassent comme ordre de grandeur le parcours libre moyen de la molécule gaz). Cela conduirait à l'idée que certains complexes activés ont une structure plus rigide que celle résultant des calculs.

On peut, néanmoins, tirer la conclusion que la théorie d'Eyring permet le calcul des coeficients préexponentiels dans l'hypothèse de certains mécanismes de réaction, ces calculs pouvant donner des informations précieuses en ce qui concerne la structure des complexes activés.

Revue Roumaine de Chimie, **14**, 837–843 (1969)

Revue Roumaine de Chimie, **14**, 845–849 (1969)

INFLUENCE DU MILIEU DE RÉACTION SUR L'HYDROLYSE ACIDE DE L'ACÉTATE DE *n*-BUTYLE

G. COSTEANU, ORTANSA LANDAUER et CORNELIA MATEESCU

Chaire de chimie physique de l'Institut polytechnique,

Bucarest, 1, str. Polizu

Reçu le 19 juillet 1968

Les auteurs ont étudié l'influence du milieu de réaction sur l'hydrolyse acide de l'acétate de *n*-butyle. Pour expliquer la variation de la constante de vitesse avec la concentration en acétone du solvant mixte, on a relié les valeurs de cette constante à la constante diélectrique et à la viscosité du solvant. On attribue la variation de la constante de vitesse avec la concentration en acétone du solvant mixte au phénomène de solvatation des molécules de l'acétate de *n*-butyle.

On sait que le milieu de réaction a une grande influence sur la vitesse de réaction.

Pour nous rendre compte de la nature de cette influence nous avons étudié l'hydrolyse acide de l'acétate de *n*-butyle dans différents mélanges eau – acétone, à 40°, 50° et 60°, et nous avons relié ensuite la constante de vitesse de la réaction à la constante diélectrique et à la viscosité du solvant mixte.

La méthode expérimentale a été décrite dans un article précédent.[1]

Les valeurs de la constante de vitesse, calculées à partir des données expérimentales sont présentées dans le tableau 1.

Tableau 1

Constantes de vitesse

% g	$10^4 k_{40}^{\circ}$ mn^{-1}	$10^4 k_{50}^{\circ}$ mn^{-1}	$10^4 k_{60}^{\circ}$ mn^{-1}
12,30	12,60	21,40	37,20
20,90	9,71	19,60	32,70
28,90	9,56	17,50	28,90
29,30	9,04	15,20	27,40
49,20	7,22	14,50	27,20
57,40	4,51	9,28	18,30
68,20	3,67	7,90	17,87
79,90	4,20	7,67	15,20
92,70	6,58	14,74	22,30

---

[1] G. Costeanu, O. Landauer et C. Mateescu, *Revue Roumaine Chim.*, **13**, 155 (1968).

La constante de vitesse varie avec la concentration en acétone, exprimée en fraction molaire, et présente, à toutes les températures mentionnées, un minimum à 0,4 (environ 70% g d'acétone), (fig. 1), minimum qui a été trouvé aussi dans le cas de l'hydrolyse acide des autres esters, toujours dans le même solvant.[2,3]

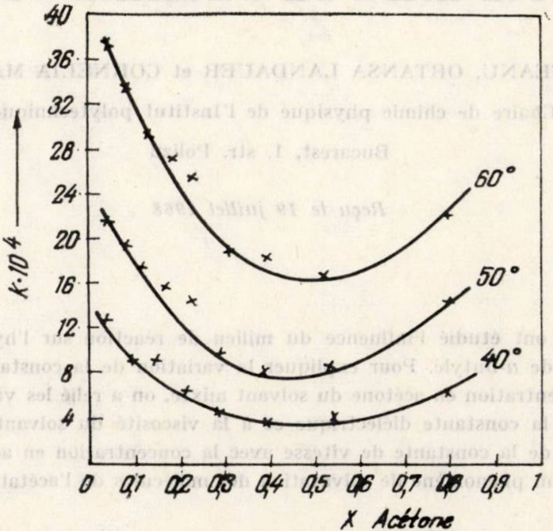

Fig. 1. — Variation de k avec la composition du solvant eau-acétone.

Les résultats présentés dans le premier tableau nous ont permis de calculer les énergies d'activation, E, les facteurs préexponentiels A, ainsi que les enthalpies ΔH,* les entropies ΔS^* et les enthalpies libres d'activation ΔG^* de la réaction étudiée par nous.

Tableau 2

Valeurs de E, A, ΔH^*, ΔS^* et ΔG^* calculées pour différents mélanges d'eau-acétone

% g	E kcal	A 10^{-5}	ΔH^* kcal mole	ΔS^* cal mole.grade	ΔG^* kcal mole
12,30	10,754	0,424	10,162	−33,81	20,237
20,90	11,440	1,042	10,848	−32,02	20,390
28,90	11,211	0,656	10,619	−32,94	20,435
39,30	10,754	0,286	10,162	−34,59	20,469
49,20	13,042	9,750	12,450	−27,57	20,665
57,38	15,101	148,000	14,509	−22,41	21,187
68,18	16,245	814,600	15,653	−18,78	21,249
79,86	13,042	5,483	12,450	−28,72	21,009
92,71	13,545	17,300	12,953	−26,44	20,832

---

[2] A. G. Kerlöf, *J. Amer. Chem. Soc.*, **54**, 4125 (1932).

[3] H. S. Harned et A. M. Ross, *J. Amer. Chem. Soc.*, **63**, 1928 (1941).

Pour expliquer la variation de la constante de vitesse avec la concentration en acétone du solvant mixte nous avons relié les valeurs de cette constante à la constante diélectrique et à la viscosité du solvant.

Les relations de liaison entre la constante de vitesse et la constante diélectrique, ou la viscosité du solvant, sont les suivantes [4–7]

$$\text{I.}\ \ln k_{D\infty} = \ln k_D + \frac{N Z_A \mathrm{e}\,\mu}{DRT\, r^{*2}}$$

$$\text{II.}\ \log\ k_D = \log k_{D\infty} - \frac{1}{2{,}303\, kT}\, \frac{D-1}{2D+1} \sum \frac{\mu}{r^3}.$$

$$\text{III.}\ k = \frac{3\pi r\, \eta}{m} \cdot \mathrm{e}^{-\frac{E}{RT}} = \text{const.}\eta$$

$$\text{IV.}\ k = \frac{1}{6}\pi \frac{k\,T}{\eta}\, \frac{(r_A + r_B)^2}{r_A \cdot r_B} \cdot \mathrm{e}^{-\frac{\mathrm{E}}{\mathrm{RT}}} = \frac{\text{const}}{\eta}.$$

Les relations I et II sont vérifiées dans le cas du solvant eau — acétone seulement dans le domaine des grandes constantes diélectriques (fig. 2 et 3), tout comme dans le cas du solvant eau-dioxanne.[1]

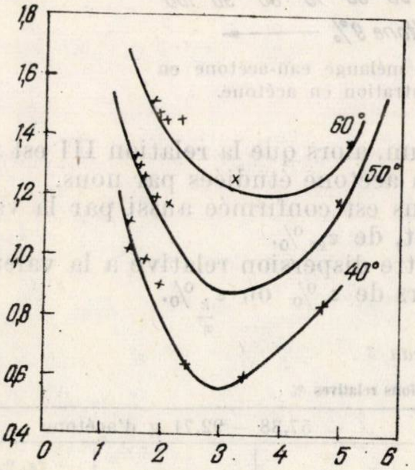

Fig. 2. — Variation du log *k* avec $\frac{1}{D}$ dans le cas du solvant eau-acétone.

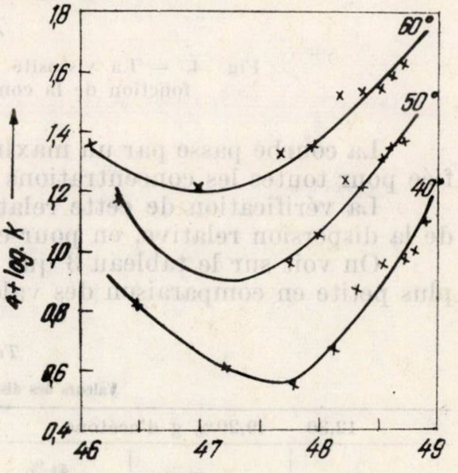

Fig. 3. — Variation du log *k* avec $\frac{D-1}{2D+1}$ dans le cas du solvant eau-acétone.

---

[4] E. S. Amis, *J. Chem. Educ.*, **30**, 351 (1953).

[5] J. G. Kirkwood, *J. Chem. Phys.*, **2**, 251 (1934).

[6] E. A. Moelwyn-Hughes, «The Kinetics of Reactions in Solution», Pergamon Press, Londres, 1950, p. 1240.

[7] A. Ölander, *Z. phys. Chem.*, **144**, 118 (1929).

Pour relier la constante de vitesse à la viscosité, nous avons d'abord déterminé la viscosité du solvant mixte dont les valeurs en fonction de la concentration en acétone, aux températures mentionnées plus haut, sont représentées sur la figure 4.

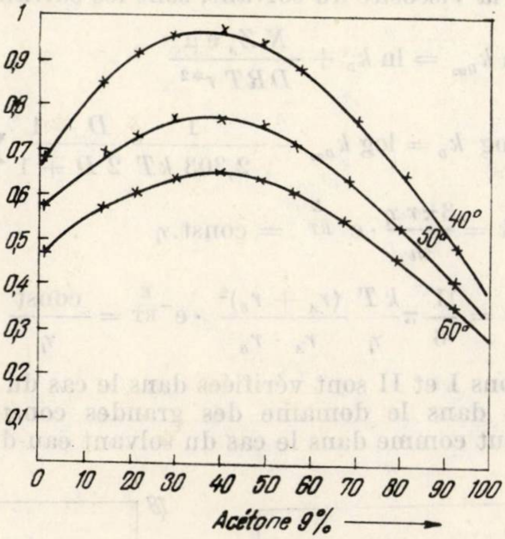

Fig. 4. — La viscosité du mélange eau-acétone en fonction de la concentration en acétone.

La courbe passe par un maximum, alors que la relation III est vérifiée pour toutes les concentrations en acétone étudiées par nous.

La vérification de cette relations est confirmée aussi par la valeur de la dispersion relative, en pour-cent, de $\varepsilon_{k\eta}$ %.

On voit sur le tableau 3 que cette dispersion relative a la valeur la plus petite en comparaison des valeurs de ε_k% ou $\varepsilon_{\frac{k}{\eta}}$%.

Tableau 3

Valeurs des dispersions relatives %

12,30 — 49,20% g d'acétone			57,38 — 92,71 g d'acétone		
ε_k%	$\varepsilon_{k\eta}$%	$\frac{\varepsilon_k \%}{\eta}$	ε_k%	$\varepsilon_{k\eta}$%	$\frac{\varepsilon_k \%}{\eta}$
20,04	15,43	26,14	26,80	16,50	57,57
16,50	10,63	23,26	36,36	22,54	60,89
13,89	6,76	21,27	21,21	15,91	37,86

D'après les valeurs de $\varepsilon_{k\eta}$% on peut admettre que les molécules d'acétate de *n*-butyle sont solvatées dans tout le domaine de concentration du solvant mixte de 12—92 % g acétone.

Au contraire, pour le solvant mixte eau-dioxanne nous avons trouvé [1] la relation III valable seulement dans le domaine de concentrations de 55—95 % g de dioxanne.

On suppose alors que les molécules de l'acétate de *n*-butyle ne sont pas solvatées dans ce domaine.

L'existence de deux valeurs différentes de $\varepsilon_{k\eta}$%, l'une pour la partie ascendante de la courbe des viscosités, et l'autre pour la partie descendante doit être attribuée à une variation de la solvatation des molécules réagissant avec la composition du solvant mixte.

D'autre part, on voit que les valeurs de $\varepsilon_{k\eta}$% sont plus petites dans le domaine correspondant à la partie ascendante de la courbe des viscosités, que dans le domaine de la partie descendante, ce qui prouve que la solvatation est plus grande dans le domaine de concentrations correspondant à la partie ascendante de la courbe.

L'existence de deux domaines de solvatation est attribuée aussi au facteur électrostatique, c'est-à-dire à la constante diélectrique du milieu de réaction.

Ainsi, dans le domaine de 12—50% g d'acétone les constantes diélectriques sont plus grandes, donc le facteur électrostatique est plus important et la solvatation est plus forte.

Cela est en accord avec les petites valeurs de $\varepsilon_{k\eta}$% dans ce domaine.

Par contre, dans le domaine des concentrations de 50—92 % g d'acétone (courbe descendante) les constantes diélectriques du solvant mixte sont plus petites, donc la solvatation est plus faible.

Il nous faut remarquer que dans tout le domaine étudié (12—92% g d'acétone) les valeurs des constantes diélectriques sont du même ordre de grandeur que celles trouvées pour le solvant mixte eau-dioxanne (15—55% g de dioxanne), domaine dans lequel est vérifiée également la relation III.

La dispersion relative $\varepsilon_{k\eta}$ % trouvée dans le cas du solvant mixte eau-dioxanne est plus petite que celle obtenue pour l'eau-acétone (tableau 4).

Tableau 4

Valeurs des dispersions relatives $\varepsilon_{k\eta}$%

	15—55% g			55—92% g		
	40°	50°	60°	40°	50°	60°
$\varepsilon_{k\eta}$(dioxanne)	9,13	9,71	5,88	—	—	—
$\varepsilon_{k\eta}$ (acétone)	15,43	10,63	6,76	16,50	22,54	15,91

On peut donc admettre que la solvatation est plus forte dans le solvant eau-dioxanne que dans l'eau-acétone, ce qui doit être attribué à la structure différente des deux molécules.

Revue Roumaine de Chimie, **14**, 845—849 (1969)

Revue Roumaine de Chimie, **14**, 851–868 (1969)

THERMODYNAMIC PROPERTIES OF Zn–Bi–Pb LIQUID SOLUTIONS

W. PTAK, Z. MOSER and L. ZABDYR

Department of Metals, Cracow, Institute of Basic Technical Problems,
Polish Academy of Sciences

Received September 6, 1968

The activity of zinc in liquid Zn–Bi–Pb system has been determined by measuring the EMF of concentration cells with zinc as reference electrode and the liquid alloy as the second electrode. Determinations were performed from 714 to 914°K for 44 compositions in the zinc concentration range X_{Zn} 0.05–0.75. Relations based on Krupkowski's formulae for coefficients of the activity of zinc, bismuth and lead as a function of composition and temperature are given. Computations are made for the activities of the three components in the studied alloys. It can be stated that Zn–Bi–Pb liquid solutions may be considered as semi-regular for small zinc content in the total concentration range of bismuth and lead.

1. INTRODUCTION

The methods of defining the thermodynamic properties of liquid metallic solutions may be experimental as e.g. vapour pressure measurements, calorimetric methods and measurements of electromotive force. These methods are being constantly developed and it is possible now to define with great accuracy errors made when calculating the thermodynamic properties. The knowledge of the thermodynamic functions is an essential problem in modern metallurgy where the multi-component liquid metallic solutions are dealt with. The method consisting in measurements of electromotive force of the concentration cells is often applied to nonferrous metal alloys, whereas the thermodynamic functions can be defined only for the metal with respect to which the cell has been established.

Moreover, the EMF data can be used in the range of small concentrations for calculating Wagner's [1] interaction parameters, and in this case the thermodynamic functions of binary and multi-component liquid metallic solutions can be found over the total concentration range. This interpretation of the experimental data is based on various solutions of the Gibbs-Duhem equation; Darken's [2] method should be mentioned here as well as Krupkowski's formulae which require the knowledge of the given binary solutions. The constants of these formulae can be defined by the experimental methods mentioned above. Krupkowski's formulae have been successfully applied for the interpretation of such liquid solutions as Zn−Sn[3], Zn−Bi[4], Zn−Bi−Sn[5], Zn−Sn−Cd[6], Zn−Bi−Cd[7], Zn−Cd−Pb[8], Zn−Sn−Cd−Pb[9].

---

[1] C. WAGNER, "Thermodynamics of Alloys", Cambridge Mass., 1952, (trans. into Russian—Moscow, 1957, pp. 63–66).

[2] L. S. DARKEN, *J. Amer. Chem. Soc.*, **2**, 2909 (1950).

In this paper for the definition of the thermodynamic properties of Zn−Bi−Pb liquid solutions the concentration cells were used according to the following scheme :

$$(-)\ \mathrm{Zn}\,|\,\mathrm{KCl},\ \mathrm{LiCl},\ \mathrm{ZnCl_2}\,|\,\mathrm{Zn{-}Bi{-}Bp}\ (+) \tag{1}$$

Investigations of Zn−Bi−Pb liquid solutions were carried out also by Valenti, Oleari and Fiorani, [10] but only for 440° and 520° temperatures, whereas from experimental data the range of limited solubility in the liquid state has been determined. Our investigations were performed for a wider temperature and concentration range, making thus possible the determination of the thermodynamic properties of Zn−Bi−Pb liquid solutions in the range 714−914°K.

2. EXPERIMENTAL METHOD AND RESULTS

The experimental arrangement here employed was described in our previous paper about the thermodynamic properties of liquid Zn−Sn−Cd−Pb solutions.[9] The temperature and EMF were measured on a Pyc potentiometer. The precision of temperature measurement amounted to ± I° and that of EMF to ± 0.05 mV.

The values of EMF were summarized in table 1, and then on the basis of the respective formulae the partial thermodynamic functions for zinc have been calculated, namely partial molar chemical potential of zinc, activity and activity coefficients. The formulae assume the form

$$\Delta\overline{\mu}_{\mathrm{Zn}} = RT \ln a_{\mathrm{Zn}} = -\,z\,EF \tag{2}$$

$$a_{\mathrm{Zn}} = \gamma_{\mathrm{Zn}} \cdot X_{\mathrm{Zn}} \tag{3}$$

where $\Delta\overline{\mu}_{\mathrm{Zn}}$ − partial molar chemical potential of zinc in the solution in cal/g atom,
a_{Zn} − zinc activity in the solution,
z − valence of ion (Zn^{++} in this case),
F − Faraday's constant (23066 cal/g atom),
E − measured EMF of the cell in volts,
γ_{Zn} − activity coefficient of zinc in the solution,
X_{Zn} − zinc concentration in the solution in molar fractions.

Moreover on the basis of the results of the values of excess partial thermodynamic functions for zinc, as well as from $\frac{\mathrm{d}E}{\mathrm{d}T}$ values found by a graphical method, the excess entropy of zinc has been determined.

---

[3] W. Ptak, *Arch. Hutn.*, **5**, 169 (1960).

[4] W. Ptak and Z. Moser, *Arch. Hutn.*, **11**, 207 (1966).

[5] W. Ptak and Z. Moser, *Arch. Hutn.*, **11**, 289 (1966).

[6] W. Ptak and Z. Moser, *Arch. Hutn.*, **12**, 81 (1967).

[7] W. Ptak and Z. Moser, *Arch. Hutn.*, **12**, 363 (1967).

[8] W. Ptak and Z. Moser, *Arch. Hutn.*, (in print).

[9] W. Ptak and Z. Moser, *Transaction AIME*, **242**, 558 (1968).

[10] V. Valenti, L. Oleari and M. Fiorani, *Gazz. chim. Ital.*, **86**, 930 (1956).

Table 1

Values of the EMF *versus* composition and temperature

No.	X_{Zn}	X_{Pb}	X_{Bi}	E M F					
				714°K	757°K	805°K	842°K	877°K	914°K
1	0.0499	0.1000	0.8500	44,11	51.30	59.15	65.42	71.50	78.38
2	0.0499	0.1500	0.8001	41.82	49.12	56.98	63.26	69.44	76.62
3	0.0500	0.2000	0.7500	40.08	47.49	55.67	62.27	68.79	75.98
4	0.0486	0.3199	0.6315	34.37	41.82	49.58	55.77	62.15	69.63
5	0.0498	0.4001	0.5501	29.80	36.95	44.76	51.15	57.40	64.44
6	0.0502	0.4999	0.4499	24.62	31.75	39.79	45.92	51.78	58.13
7	0.0501	0.5999	0.3501	19.47	26.59	34.50	40.61	46.47	52.66
8	0.0499	0.7001	0.2501	14.28	21.40	29.39	35.52	41.42	47.64
9	0.0502	0.8499	0.0999	7.02	14.13	22.12	28.34	34.33	40.79
10	0.1000	0.1000	0.8000	25.71	31.46	37.81	42.70	47.44	52.40
11	0.1001	0.2000	0.7000	22.24	27.97	34.40	39.21	43.44	49.04
12	0.1001	0.2998	0.6000	17.18	22.86	29.22	34.01	38.25	43.76
13	0.1000	0.4000	0.5000	12.30	18.00	24.75	29.41	34.01	39.83
14	0.1002	0.4999	0.3999	7.66	13.49	19.64	24.52	28.83	34.74
15	0.0999	0.6000	0.3001	2.00	7.53	13.81	18.59	22.72	28.07
16	0.1001	0.6999	0.2000	—	2.76	8.98	13.92	18.86	23.76
17	0.0999	0.8000	0.1001	—	—	4.88	10.14	15.05	19.90
18	0.1498	0.0500	0.8002	18.06	23.72	29.39	33.96	38.66	44.61
19	0.2000	0.1005	0.6994	8.98	13.38	18.12	21.84	25.58	29.28
20	0.2001	0.1999	0.6000	7.98	13.04	18.18	22.41	26.54	30.57
21	0.1999	0.3001	0.5000	—	3.99	8.16	12.17	15.57	19.20
22	0.2000	0.4000	0.4000	—	0.99	4.04	7.90	10.57	14.23
23	0.1999	0.5000	0.3001	—	—	—	3.33	6.51	10.08
24	0.1999	0.6001	0.2001	—	—	0.13	1.04	3.24	6.79
25	0.1999	0.7000	0.1000	—	0.13	0.18	0.44	1.00	3.78
26	0.2501	0.0500	0.6999	6.83	10.50	14.75	18.00	20.96	23.71
27	0.3000	0.1000	0.6000	1.33	4.46	8.08	10.84	13.41	15.79
28	0.3000	0.2000	0.5000	0.23	0.76	3.41	6.70	9.21	11.54
29	0.3000	0.2999	0.4001	0.14	0.30	1.05	2.85	5.41	7.80
30	0.2998	0.4001	0.3002	0.28	0.39	0.59	0.72	1.39	3.71
31	0.3001	0.4998	0.2000	0.18	0.25	0.43	0.67	0.99	1.34
32	0.3002	0.5988	0.1000	—	—	0.23	0.61	0.95	0.83
33	0.3500	0.0501	0.6000	0.81	3.56	6.69	9.16	11.45	13.85
34	0.4002	0.1000	0.4998	0.30	0.71	2.48	4.69	6.54	8.85
35	0.4000	0.2000	0.4001	—	—	0.26	0.90	2.67	4.61
36	0.4001	0.2999	0.2999	0.31	0.38	0.43	0.82	1.04	2.36
37	0.4001	0.4000	0.2000	—	0.17	0.23	0.45	0.65	1.04
38	0.4500	0.0500	0.5000	0.25	2.55	5.39	7.60	9.68	12.17
39	0.5000	0.2000	0.3000	0.14	0.29	0.49	0.70	0.70	1.48
40	0.5001	0.3000	0.2000	0.54	0.67	0.78	0.99	1.18	1.35
41	0.5500	0.0500	0.4000	0.28	0.44	0.58	1.34	2.49	3.86
42	0.6000	0.1000	0.3001	0.28	0.36	0.55	0.78	0.84	1.83
43	0.6500	0.0500	0.3000	0.41	0.55	0.92	1.12	1.31	2.24
44	0.7499	0.0501	0.2000	0.37	0.43	0.75	0.99	1.21	1.42

The relation between the excess chemical potential of zinc and the activity coefficient of this metal in solution takes the form

$$\Delta\overline{\mu}^{*}_{Zn} = RT \ln \gamma_{Zn} \tag{4}$$

where $\Delta\overline{\mu}^{*}_{Zn}$ — excess partial molar chemical potential of zinc in the solution.

EMF measurements of concentration cells were performed for 44 various alloys in the zinc concentration range $X_{Zn} = 0.05-0.75$ at 714, 757, 805, 842, 877 and 914°K. The values of the activity of zinc have been calculated from formulae (2) and (3), and are plotted in table 2.

Table 2

Values of activity obtained from (2) and (3)

No.	a_{Zn}					
	714°K	757°K	805°K	842°K	877°K	914°K
1	0.239	0.208	0.182	0.164	0.151	0.137
2	0.257	0.222	0.194	0.174	0.159	0.144
3	0.272	0.234	0.201	0.179	0.162	0.146
4	0.328	0.278	0.240	0.214	0.193	0.171
5	0.380	0.323	0.276	0.243	0.219	0.195
6	0.450	0.378	0.318	0.281	0.254	0.229
7	0.531	0.443	0.370	0.326	0.292	0.263
8	0.629	0.519	0.429	0.375	0.334	0.299
9	0.796	0.649	0.529	0.457	0.403	0.356
10	0.434	0.382	0.337	0.307	0.285	0.265
11	0.486	0.425	0.372	0.338	0.317	0.289
12	0.573	0.497	0.431	0.391	0.363	0.330
13	0.671	0.576	0.491	0.444	0.406	0.365
14	0.780	0.661	0.568	0.508	0.466	0.415
15	0.937	0.794	0.672	0.598	0.548	0.491
16	—	0.919	0.772	0.681	0.607	0.548
17	—	—	0.869	0.756	0.671	0.604
18	0.556	0.484	0.429	0.391	0.359	0.323
19	0.747	0.664	0.594	0.547	0.508	0.476
20	0.772	0.671	0.593	0.538	0.495	0.461
21	—	0.885	0.791	0.714	0.662	0.615
22	—	0.970	0.890	0.804	0.756	0.697
23	—	—	—	0.912	0.842	0.775
24	—	—	0.996	0.976	0.918	0.842
25	—	0.996	0.995	0.988	0.974	0.909
26	0.801	0.725	0.654	0.608	0.574	0.548
27	0.958	0.872	0.793	0.741	0.701	0.670
28	0.993	0.977	0.906	0.831	0.784	0.746
29	0.996	0.991	0.970	0.924	0.867	0.821
30	0.991	0.988	0.983	0.980	0.964	0.910
31	0.994	0.992	0.988	0.982	0.974	0.967
32	—	—	0.993	0.983	0.975	0.979
33	0.974	0.897	0.825	0.776	0.738	0.704
34	0.990	0.978	0.931	0.878	0.841	0.799
35	—	—	0.993	0.976	0.932	0.890
36	0.990	0.988	0.988	0.978	0.973	0.942
37	—	0.995	0.993	0.988	0.983	0.974
38	0.992	0.925	0.856	0.811	0.774	0.735
39	0.995	0.991	0.986	0.981	0.982	0.963
40	0.982	0.980	0.978	0.973	0.969	0.966
41	0.991	0.987	0.983	0.964	0.936	0.907
42	0.991	0.989	0.984	0.979	0.978	0.955
43	0.987	0.983	0.974	0.970	0.966	0.945
44	0.988	0.987	0.979	0.973	0.969	0.965

The purity of metals used in experiments amounted to at least 99.99 per cent. The composition of the electrolyte was as follows:

LiCl−57 molar per cent,
KCl−38 molar per cent,
$ZnCl_2$−5 molar per cent.

Salts obtained by double crystallization previous to measurement were dehydrated including the passing through the liquid solution of dry HCl.

The composition of the alloys has been so arranged as to be able to determine the range of limited solubility in liquid state. It should be noted here that in the Zn—Bi—Pb system

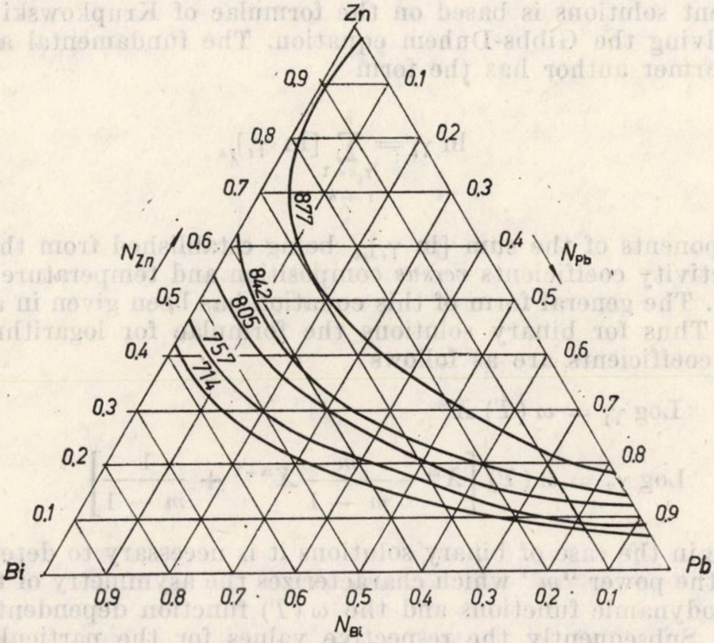

Fig. 1. — Range of limited solubility in the liquid state in Zn—Bi—Pb liquid solutions at 714—877°K.

there is a wide range of limited solubility as a result of this phenomenon in binary Zn—Bi[4] and Zn—Pb[11] solutions.

To this effect the diagrams of the change in zinc activity as to composition have been used with a special consideration of the particular temperatures. It should be noticed that in the miscibility gap the values of zinc activity remain constant in spite of the change in content of this metal. The range of the limited solubility decreases with the increase in temperature, and it was not possible to determine it for 914°K. The values of the concentrations of the components thus determined corresponding to limited reciprocal solubilities at 714, 757, 805, 842, 877°K are shown in figure 1, a good agreement being obtained with the data of the Italian scientists.[10]

It should be added that the values of the EMF for some alloys at temperatures of the miscibility gap have not been given in table 1, because they are within the range of experimental errors i.e. ± 0.5 mV.

---

[11] A. Krupkowski, *Freiberger Forschungshefte*, **B-67**, 101 (1962).

3. DETERMINATION OF THE VALUES OF ACTIVITY COEFFICIENTS OF COMPONENTS OF Zn–Bi–Pb LIQUID SOLUTIONS BASED ON KRUPKOWSKI'S FORMULA FOR BINARY SOLUTIONS

Determination of the values of the activity coefficients in multicomponent solutions is based on the formulae of Krupkowski[12] derived while solving the Gibbs-Duhem equation. The fundamental assumption of the former author has the form

$$\ln \gamma_i = \sum_{\substack{\gamma_i k=1 \\ \gamma \neq k}}^{n} [\ln \gamma_i]_{jk} \tag{5}$$

the components of the sum $[\ln \gamma_i]_{jk}$ being established from the relation of the activity coefficients *versus* composition and temperature in binary solutions. The general form of this equation has been given in a previous paper.[13] Thus for binary solutions the formulae for logarithms of the activity coefficients are as follows

$$\begin{aligned} \operatorname{Log} \gamma_1 &= \omega(T)\, X^m \\ \operatorname{Log} \gamma_2 &= \omega(T) \left[X^m - \frac{m}{m-1} X^{m-1} + \frac{1}{m-1} \right] \end{aligned} \tag{6}$$

Therefore in the case of binary solutions it is necessary to determine the index of the power "*m*" which characterizes the asymmetry of the course of thermodynamic functions and the $\omega(T)$ function dependent on temperature. Subsequently the respective values for the particular binary liquid solutions will be given. The respective values for Zn–Bi liquid solutions have been determined by Ptak and Moser,[4] assuming from experimental data that these solutions are semi-regular which is obvious from the shape of the $\omega(T)$ function. These values are as follows

$$\begin{aligned} \omega(T) &= \left(\frac{687}{T} - 0.29 \right) \\ m &= 1\cdot 05 \end{aligned} \tag{7}$$

The authors[4] have obtained the relation of the activity coefficients of zinc and bismuth *versus* composition and temperature in the form

$$\begin{aligned} \operatorname{Log} \gamma_{\mathrm{Zn}} &= \left(\frac{687}{T} - 0.29 \right) (1 - X_{\mathrm{Zn}})^{1.05} \\ \operatorname{Log} \gamma_{\mathrm{Bi}} &= \left(\frac{687}{T} - 0.29 \right) \left[(1 - X_{\mathrm{Zn}})^{1.05} - 21 (1 - X_{\mathrm{Zn}})^{0.05} + 20 \right] \end{aligned} \tag{8}$$

---

[12] A. Krupkowski, "Zasady termodynamiki i ich zastosowanie w metalurgii i metaloznawstwie", Kraków, 1958, pp. 121–126.

[13] A. Krupkowski, *Bull. Acad. Pol. Sc. Lett.*, **1**, 15 (1951).

In the case of Zn—Pb liquid solutions the data of Krupkowski[11] were available. He considered for their establishment equilibria and experimental data of numerous authors.[14] The data are

$$\omega(T) = \left(\frac{1181}{T} - 0.347\right) \qquad (9)$$

$$m = 1.48$$

The solutions can be treated as semi-regular. The authors [11,15] give the following equations for the Zn—Pb liquid solutions

$$\begin{aligned} \log \gamma_{Zn} &= \left(\frac{1181}{T} - 0.347\right)(1 - X_{Zn})^{1.48} \\ \log \gamma_{Pb} &= \left(\frac{1181}{T} - 0.347\right)\left[(1 - X_{Zn})^{1.48} + 3.083\,(1 - X_{Zn}^{0.48}) - 2.083\right] \end{aligned} \qquad (10)$$

For defining the formulae for the activity coefficients of bismuth and lead in Bi—Pb liquid solutions the EMF measurements of concentration cells of Strickler and Seltz [16] have been employed

$$(-)\ Pb\,|\,PbCl_2,\ LiCl,\ KCl\,|\,Pb{-}Bi\ (+)$$

at 700°K for the concentration range of bismuth $X_{Bi}: 0.152 - 0.889$. On the basis of these data the values of activity and activity coefficients of lead have been calculated as plotted in table 4. These data were compared with values shown in a previous paper.[17] From the results in table 3 the following data for Bi—Pb liquid solutions have been obtained by the method given by the authors[4,12]

Table 3

Values of activity and activity coefficients *versus* concentration for lead in Bi—Pb liquid solutions at 700°K

X_{Pb}	a_{Pb}	γ_{Pb}
0.111	0.05747	0.51775
0.230	0.13787	0.59943
0.328	0.22194	0.67665
0.414	0.30371	0.73360
0.496	0.39755	0.80151
0.600	0.52750	0.87917
0.720	0.68343	0.94921
0.848	0.83828	0.98854

$$\omega(T) = -\left(\frac{233}{T} + 0.048\right) \qquad (11)$$

$$m = 2.1$$

---

[14] O. J. Kleppa, *J. Amer. Chem. Soc.*, **74**, 6052 (1952).

[15] W. Ptak, "Ksiega jubileuszowa dla uczczenia zasług naukowych Aleksandra Krupkowskiego", Warszawa, 1965, p. 413.

[16] H. S. Strickler and H. Seltz, *J. Amer. Chem. Soc.*, **58**, 2084 (1936).

[17] R. Hultgren, R. L. Orr, Ph. D. Anderson and K. K. Kelley, "Selected Values of Thermodynamic Properties of Metals", New York — London, 1963, pp. 540—546.

In a similar manner equations for the activity coefficients of bismuth and lead in Bi—Pb liquid solutions can be expressed by

$$\log \gamma_{\mathrm{Bi}} = -\left(\frac{233}{T} + 0.048\right)(1 - X_{\mathrm{Bi}}^{2{,}1})$$

$$\log \gamma_{\mathrm{Pb}} = -\left(\frac{233}{T} + 0.048\right)\left[(1 - X_{\mathrm{Bi}}^{2{,}1}) - 1.91\,(1 - X_{\mathrm{Bi}}^{1{,}1}) + 0.91\right] \tag{12}$$

From (11) and (12) it follows that Bi- Pb liquid solutions can be considered as semi-regular showing a slight deviation from the properties of regular solutions. Moreover, they show in the total range of concentration a negative deviation from Raoult's law; the molar heat of these solutions is given by

$$\Delta H' = -\,968.6\,[1 - (1 - X_{\mathrm{Bi}}^{1{,}1})]\,X_{\mathrm{Pb}} \tag{13}$$

The molar heat of Bi—Pb liquid solutions at 350 and 450° was defined by a calorimetric method by Kleppa [18] who has shown a minimum effect of temperature on measurements. The values of molar heat of the solution calculated from (13) are in good agreement with the Kleppa's data.

3.1. *Activity coefficients of zinc, bismuth and lead in Zn—Bi—Pb liquid solutions*

On the basis of formulae (5), (8), (10) and (12, a relation between the activity coefficients of zinc, bismuth and lead and their composition and temperature can be expressed

$$\begin{aligned}\mathrm{Log}\,\gamma_{\mathrm{Zn}} = &-\left(\frac{687}{T} - 0.29\right)\left[(1 - X_{\mathrm{Zn}}^{-0{,}95})\,X_{\mathrm{Bi}}\,X_{\mathrm{Zn}} - (1 - X_{\mathrm{Zn}}^{-0{,}95})\,X_{\mathrm{Bi}}\right] -\\ &-\left(\frac{1181}{T} - 0.347\right)[(1 - X_{\mathrm{Zn}}^{-0{,}52})\,X_{\mathrm{Pb}}\,X_{\mathrm{Zn}} - (1 - X_{\mathrm{Zn}}^{-0{,}52})\,X_{\mathrm{Pb}}] +\\ &+\left(\frac{233}{T} + 0.048\right)(1 - X_{\mathrm{Bi}}^{0{,}1})\,X_{\mathrm{Pb}}\,X_{\mathrm{Bi}}\end{aligned} \tag{14}$$

$$\begin{aligned}\mathrm{Log}\,\gamma_{\mathrm{Bi}} = &-\left(\frac{687}{T} - 0.29\right)\{(1 - X_{\mathrm{Zn}}^{-0{,}95})\,X_{\mathrm{Bi}}\,X_{\mathrm{Zn}} - 20\,[1 - (1 - X_{\mathrm{Zn}}^{0{,}05})]\} -\\ &-\left(\frac{1181}{T} - 0.347\right)(1 - X_{\mathrm{Zn}}^{-0{,}52})\,X_{\mathrm{Pb}}\,X_{\mathrm{Zn}} + \left(\frac{233}{T} + 0.048\right)[(1 - X_{\mathrm{Bi}}^{0{,}1})\,X_{\mathrm{Pb}}\,X_{\mathrm{Bi}} -\\ &- (1 - X_{\mathrm{Bi}}^{0{,}1})\,X_{\mathrm{Pb}}]\end{aligned} \tag{15}$$

$$\begin{aligned}\mathrm{Log}\,\gamma_{\mathrm{Pb}} = &-\left(\frac{687}{T} - 0.29\right)(1 - X_{\mathrm{Zn}}^{-0{,}95})\,X_{\mathrm{Bi}}\,X_{\mathrm{Zn}} - \left(\frac{1181}{T} - 0.347\right)\{(1 -\\ &- X_{\mathrm{Zn}}^{-0{,}52})\,X_{\mathrm{Pb}}\,X_{\mathrm{Zn}} - 2.083\,[1 - (1 - X_{\mathrm{Zn}}^{0{,}48})]\} +\\ &+\left(\frac{233}{T} + 0.048\right)\{(1 - X_{\mathrm{Bi}}^{0{,}1})\,X_{\mathrm{Pb}}\,X_{\mathrm{Bi}} - 10\,[1 - (1 - X_{\mathrm{Bi}})]\}\end{aligned} \tag{16}$$

---

[18] O. J. KLEPPA, *J. Phys. Chem.*, **59**, 354 (1955).

Table 4 gives the values of zinc activity in Zn—Bi—Pb liquid solutions dependent on zinc concentration and temperature calculated from (3) and (4).

The values of activity for bismuth and lead obtained from (3), (15) and (16) are plotted in tables 5 and 6.

Table 4

Activity values for zinc in Zn—Bi—Pb liquid solutions calculated from (3) and (14)

No.	a_{Zn}					
	714°K	757°K	805°K	842°K	877°K	914°K
1	0.261	0.229	0.201	0.184	0.170	0.157
2	0.284	0.249	0.217	0.198	0.182	0.168
3	0.311	0.270	0.235	0.213	0.196	0.179
4	0.368	0.316	0.272	0.245	0.224	0.203
5	0.431	0.366	0.312	0.279	0.253	0.228
6	0.498	0.420	0.354	0.315	0.284	0.254
7	0.568	0.475	0.398	0.352	0.316	0.281
8	0.640	0.531	0.417	0.389	0.348	0.307
9	0.747	0.614	0.506	0.442	0.394	0.344
10	0.477	0.421	0.373	0.342	0.318	0.295
11	0.564	0.493	0.432	0.394	0.364	0.335
12	0.660	0.572	0.496	0.449	0.412	0.377
13	0.764	0.656	0.564	0.508	0.463	0.420
14	0.874	0.744	0.634	0.568	0.516	0.464
15	0.987	0.834	0.706	0.629	0.569	0.509
16	1.100	0.924	0.777	0.689	0.621	0.552
17	1.210	1.010	0.845	0.746	0.670	0.592
18	0.602	0.538	0.482	0.447	0.418	0.391
19	0.796	0.714	0.641	0.594	0.557	0.522
20	0.923	0.820	0.729	0.673	0.627	0.583
21	1.058	0.932	0.823	0.754	0.699	0.645
22	1.204	1.049	0.918	0.838	0.773	0.709
23	1.342	1.166	1.014	0.921	0.847	0.772
24	1.483	1.281	1.108	1.002	0.918	0.832
25	1.617	1.389	1.196	1.078	0.985	0.888
26	0.846	0.767	0.697	0.651	0.601	0.580
27	0.997	0.907	0.826	0.774	0.731	0.691
28	1.131	1.021	0.923	0.860	0.809	0.759
29	1.269	1.138	1.021	0.948	0.888	0.828
30	1.406	1.253	1.118	1.033	0.965	0.895
31	1.538	1.364	1.211	1.115	1.038	0.958
32	1.661	1.467	1.297	1.191	1.106	1.016
33	0.999	0.919	0.845	0.798	0.759	0.722
34	1.114	1.023	0.945	0.895	0.853	0.812
35	1.230	1.128	1.036	0.976	0.928	0.879
36	1.348	1.300	1.124	1.055	0.999	0.942
37	1.459	1.326	1.206	1.129	1.067	1.001
38	1.084	1.010	0.942	0.898	0.861	0.826
39	1.251	1.167	1.088	1.037	0.995	0.952
40	1.337	1.243	1.156	1.099	1.052	1.003
41	1.118	1.057	0.999	0.961	0.929	0.898
42	1.156	1.098	1.044	1.008	0.978	0.947
43	1.116	1.069	1.025	0.995	0.970	0.945
44	1.088	1.057	1.026	1.006	0.988	0.971

Table 5

Activity values for bismuth in Zn−Bi−Pb liquid solutions calculated from (3) and (15)

No.	a_{Bi}					
	714°K	757°K	805°K	842°K	877°K	914°K
1	0.839	0.840	0.840	0.841	0.841	0.842
2	0.780	0.781	0.783	0.784	0.784	0.785
3	0.720	0.722	0.724	0.725	0.727	0.728
4	0.600	0.603	0.606	0.608	0.610	0.612
5	0.481	0.486	0.490	0.493	0.495	0.498
6	0.368	0.373	0.378	0.381	0.385	0.388
7	0.264	0.269	0.274	0.278	0.281	0.284
8	0.172	0.176	0.180	0.183	0.186	0.189
9	0.058	0.060	0.062	0.064	0.065	0.067
10	0.788	0.788	0.789	0.789	0.790	0.791
11	0.664	0.666	0.668	0.669	0.670	0.672
12	0.541	0.544	0.548	0.550	0.552	0.555
13	0.423	0.427	0.432	0.435	0.438	0.441
14	0.313	0.318	0.323	0.326	0.329	0.333
15	0.214	0.219	0.223	0.227	0.230	0.233
16	0.128	0.132	0.136	0.139	0.141	0.144
17	0.057	0.059	0.061	0.063	0.064	0.066
18	0.803	0.803	0.802	0.802	0.802	0.801
19	0.694	0.694	0.694	0.694	0.693	0.694
20	0.561	0.563	0.565	0.566	0.567	0.569
21	0.435	0.438	0.442	0.444	0.446	0.449
22	0.319	0.323	0.328	0.331	0.334	0.337
23	0.217	0.221	0.225	0.229	0.231	0.235
24	0.129	0.132	0.136	0.139	0.141	0.144
25	0.057	0.059	0.061	0.062	0.064	0.065
26	0.724	0.722	0.719	0.718	0.716	0.715
27	0.617	0.615	0.613	0.611	0.610	0.609
28	0.475	0.475	0.476	0.476	0.477	0.478
29	0.346	0.348	0.351	0.353	0.354	0.357
30	0.233	0.237	0.240	0.242	0.244	0.247
31	0.138	0.141	0.144	0.146	0.148	0.150
32	0.060	0.062	0.064	0.065	0.066	0.068
33	0.658	0.653	0.647	0.644	0.640	0.638
34	0.549	0.544	0.538	0.535	0.532	0.530
35	0.397	0.396	0.395	0.394	0.393	0.393
36	0.266	0.267	0.268	0.269	0.269	0.271
37	0.156	0.158	0.160	0.161	0.159	0.164
38	0.604	0.595	0.585	0.578	0.573	0.568
39	0.329	0.325	0.321	0.318	0.315	0.314
40	0.192	0.191	0.190	0.190	0.189	0.190
41	0.563	0.546	0.531	0.520	0.511	0.503
42	0.442	0.427	0.412	0.403	0.394	0.388
43	0.533	0.508	0.484	0.468	0.454	0.442
44	0.516	0.477	0.441	0.417	0.398	0.381

In order to compare experimental data with values calculated from (14), (15) and (16), isoactivity curves for zinc, bismuth and lead at 714, 805 and 877°K have been delineated. They are represented in figures 2,3 and 4. Numbers listed in the net-section points of the diagram given the activity, experimentally obtained, for zinc (table 2) while lines limiting the miscibility gap are based on curves in figure 1.

Table 6

Activity values for lead in Zn–Bi–Pb liquid solutions calculated from (3) and (16)

	a_{Bi}					
No.	714°K	757°K	805°K	842°K	877°K	914°K
1	0.067	0.069	0.071	0.072	0.073	0.074
2	0.105	0.108	0.110	0.112	0.114	0.115
3	0.146	0.150	0.153	0.155	0.157	0.159
4	0.238	0.241	0.245	0.248	0.250	0.252
5	0.339	0.343	0.353	0.350	0.352	0.354
6	0.450	0.453	0.456	0.458	0.460	0.462
7	0.565	0.568	0.570	0.571	0.573	0.574
8	0.683	0.684	0.685	0.686	0.687	0.687
9	0.853	0.852	0.852	0.852	0.852	0.852
10	0.074	0.076	0.077	0.078	0.079	0.080
11	0.160	0.163	0.165	0.167	0.168	0.169
12	0.257	0.260	0.263	0.265	0.266	0.268
13	0.364	0.366	0.369	0.370	0.372	0.373
14	0.477	0.479	0.480	0.481	0.482	0.483
15	0.594	0.594	0.595	0.595	0.595	0.595
16	0.709	0.709	0.708	0.708	0.707	0.707
17	0.820	0.819	0.817	0.816	0.815	0.814
18	0.040	0.040	0.041	0.041	0.042	0.042
19	0.092	0.092	0.093	0.093	0.094	0.094
20	0.194	0.195	0.196	0.196	0.196	0.196
21	0.307	0.306	0.306	0.306	0.306	0.304
22	0.425	0.423	0.422	0.421	0.420	0.418
23	0.546	0.540	0.540	0.538	0.536	0.533
24	0.665	0.661	0.656	0.653	0.650	0.646
25	0.778	0.773	0.770	0.763	0.760	0.755
26	0.050	0.050	0.050	0.050	0.050	0.050
27	0.116	0.115	0.114	0.114	0.113	0.112
28	0.242	0.239	0.237	0.235	0.233	0.230
29	0.375	0.369	0.364	0.360	0.357	0.352
30	0.509	0.501	0.493	0.488	0.483	0.476
31	0.641	0.630	0.620	0.613	0.606	0.598
32	0.765	0.752	0.740	0.731	0.724	0.715
33	0.065	0.064	0.063	0.062	0.062	0.061
34	0.153	0.148	0.145	0.142	0.140	0.136
35	0.312	0.303	0.294	0.289	0.284	0.276
36	0.474	0.459	0.446	0.436	0.419	0.418
37	0.632	0.612	0.594	0.581	0.570	0.557
38	0.088	0.085	0.082	0.080	0.078	0.075
39	0.420	0.400	0.380	0.367	0.357	0.343
40	0.628	0.597	0.568	0.548	0.532	0.511
41	0.124	0.116	0.110	0.105	0.102	0.097
42	0.302	0.280	0.260	0.247	0.237	0.223
43	0.186	0.171	0.156	0.147	0.140	0.130
44	0.311	0.275	0.243	0.223	0.207	0.188

For comparison the diagram of isoactivity curves for zinc, bismuth and lead at 520° is reproduced from a previous Italian paper.[10] This was based on data obtained by other calculating methods. By comparing the above diagram with that in figure 3 a good agreement of both isoactivity curves may be observed.

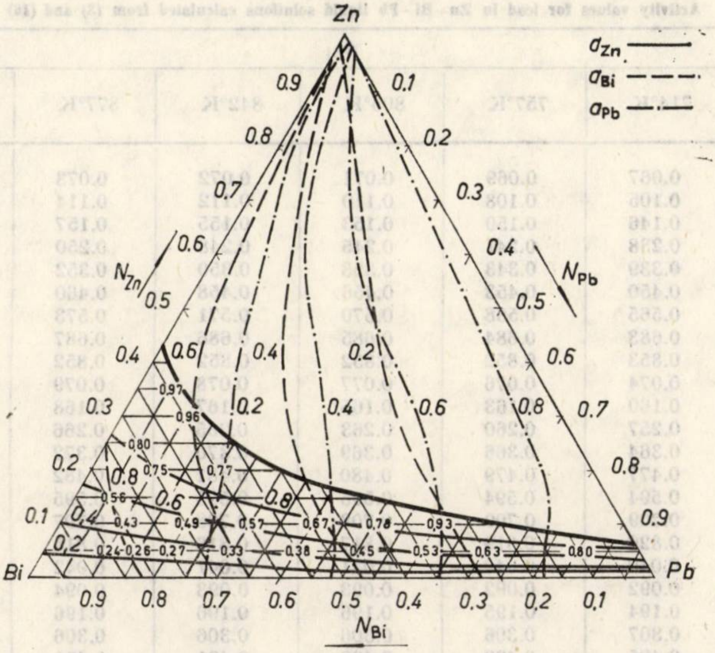

Fig. 2. — Isoactivity curves for zinc, bismuth and lead at 714°K.

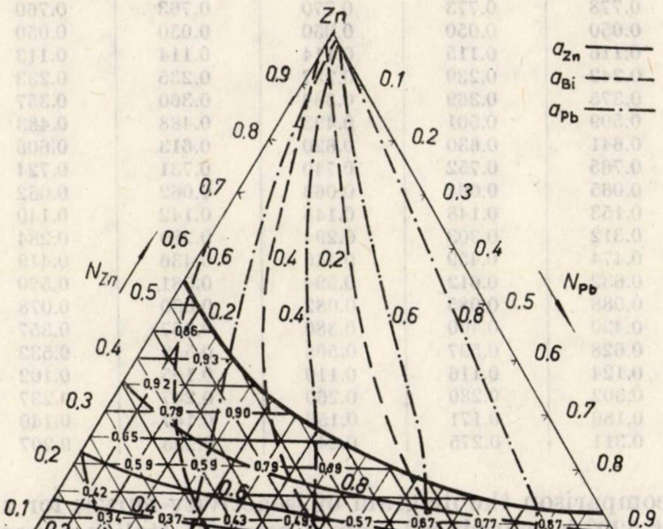

Fig. 3. — Isoactivity curves for zinc, bismuth and lead at 805°K.

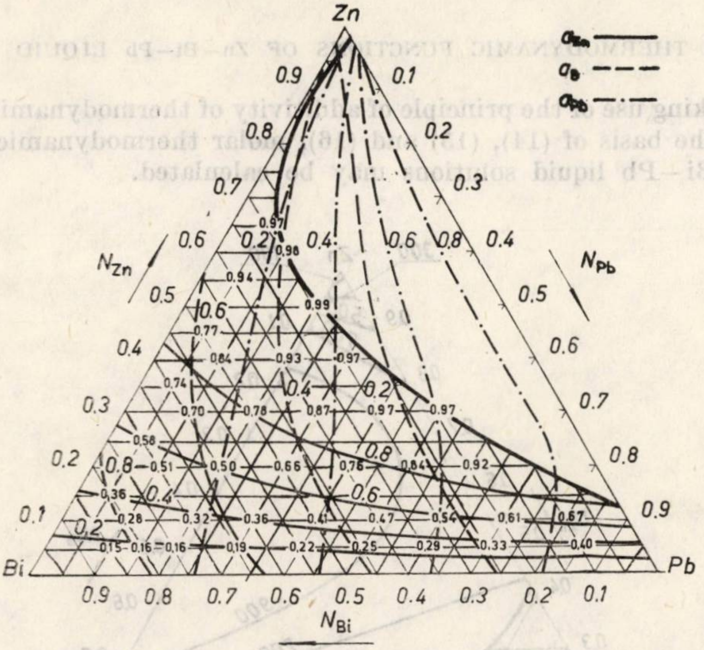

Fig. 4. — Isoactivity curves for zinc, bismuth and lead at 877°K.

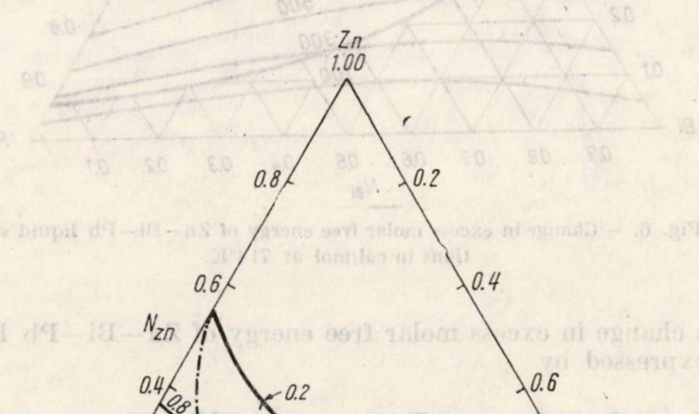

Fig. 5. — Isoactivity curves for zinc, bismuth and lead at 520°K, after Valenti, Oleari and Fiorani.[10]

4. MOLAR THERMODYNAMIC FUNCTIONS OF Zn—Bi—Pb LIQUID SOLUTIONS

Making use of the principle of additivity of thermodynamic functions and on the basis of (14), (15) and (16), molar thermodynamic functions of Zn—Bi—Pb liquid solutions may be calculated.

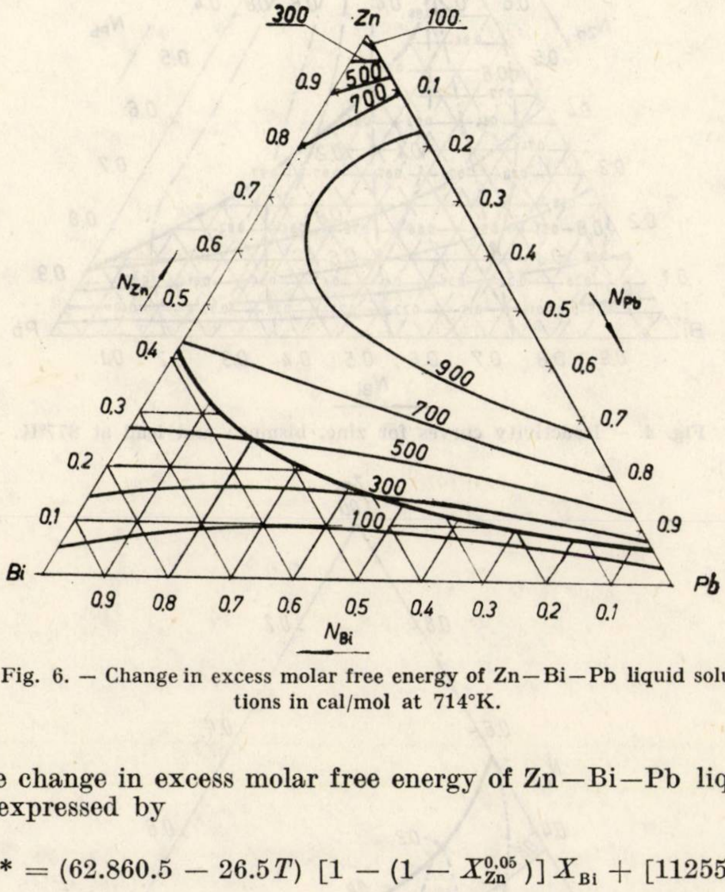

Fig. 6. — Change in excess molar free energy of Zn—Bi—Pb liquid solutions in cal/mol at 714°K.

The change in excess molar free energy of Zn—Bi—Pb liquid solutions is expressed by

$$\Delta F'^{*} = (62.860.5 - 26.5T)\ [1 - (1 - X_{\mathrm{Zn}}^{0.05})]\, X_{\mathrm{Bi}} + [11255.9 -$$

$$- 3.31\ T]\, [1-(1 - X_{\mathrm{Zn}}^{0.48})]\, X_{\mathrm{Pb}} - (968.6 + 0.2\ T)\ [1-(1 - X_{\mathrm{Bi}}^{1.1})]\, X_{\mathrm{Pb}} \quad (17)$$

where F'^{*} — change in excess molar free energy of solution in cal/mol.

The temperature dependence of function (17) indicates a semiregularity of the solutions tested which is caused by the semiregularity of all three binary solutions forming the ternary system.

Values calculated from (17) were used for the delineation of temperature curves for 714, 805 and 877°K; they are summarized in figures 6, 7 and 8.

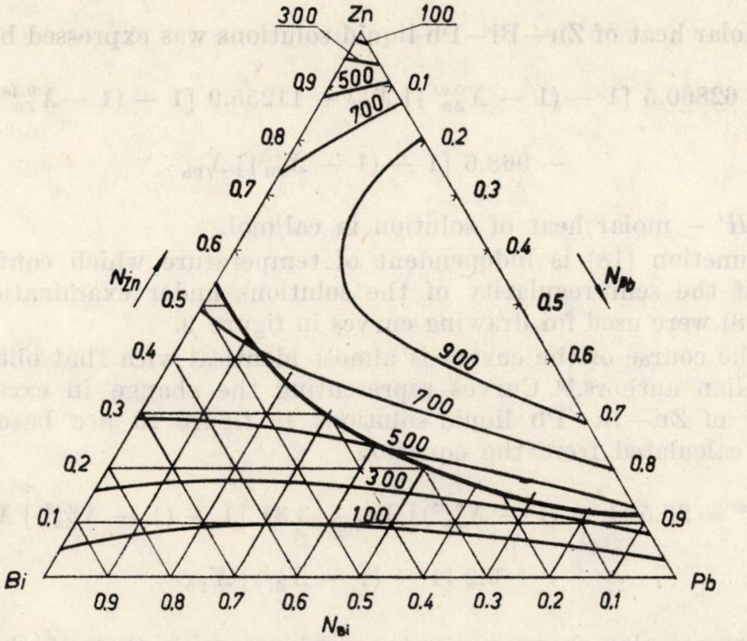

Fig. 7. — Change in excess molar free energy of Zn—Bi—Pb liquid solutions in cal/mol at 805°K.

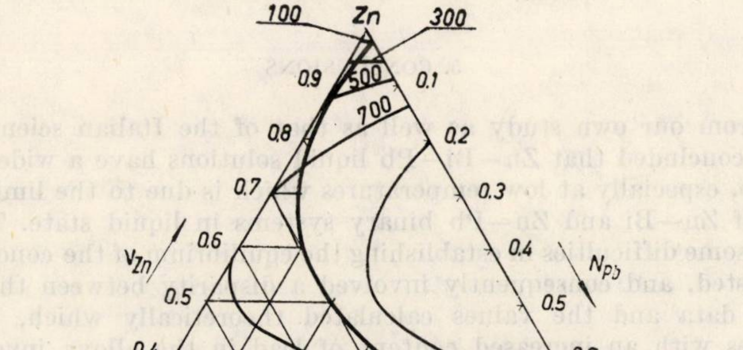

Fig. 8. Change in excess molar free energy of Zn—Bi—Pb liquid solutions in cal/mol at 877°K.

Molar heat of Zn—Bi—Pb liquid solutions was expressed by

$$\Delta H' = 62860.5\,[1-(1-X_{\mathrm{Zn}}^{0,05})]\,X_{\mathrm{Bi}} + 11255.9\,[1-(1-X_{\mathrm{Zn}}^{0,48})]\,X_{\mathrm{Pb}} - 968.6\,[1-(1-X_{\mathrm{Bi}}^{1,1})]\,X_{\mathrm{Pb}} \tag{18}$$

where H' — molar heat of solution in cal/mol.

Function (18) is independent of temperature which confirms the thesis if the semi-regularity of the solutions under examination. Data from (18) were used for drawing curves in figure 9.

The course of the curves is almost identical with that obtained by the Italian authors.[10] Curves representing the change in excess molar entropy of Zn—Bi—Pb liquid solutions in figure 10 are based on the results calculated from the equation

$$\Delta S'^{*} = 26.5\,[1-(1-X_{\mathrm{Zn}}^{0,05})]\,X_{\mathrm{Bi}} + 3.31\,[1-(1-X_{\mathrm{Zn}}^{0,48})]\,X_{\mathrm{Pb}} + 0.2\,[1-(1-X_{\mathrm{Bi}}^{1,1})]\,X_{\mathrm{Pb}} \tag{19}$$

This diagram also shows a good accordance with that of the Italian authors.[10]

5. CONCLUSIONS

From our own study as well as that of the Italian scientists[10] it can be concluded that Zn—Bi—Pb liquid solutions have a wide miscibility gap, especially at low temperatures which is due to the limited solubility of Zn—Bi and Zn—Pb binary systems in liquid state. This fact caused some difficulties in establishing the equilibrium of the concentration cells tested, and consequently involved a disparity between the experimental data and the values calculated theoretically which, however, improves with an increased content of lead in the alloys investigated.

A better agreement with theoretical calculations was also observed as effect of diffusion on determining the equilibrium of cells, especially when the samples are in the vicinity of the diphase area. A good agreement at higher temperatures where the miscibility gap decreases can be explained by the fact that the theoretical formulae of Krupkowski consider liquid solutions as homogeneous. On the other hand, however, it can be observed that over the range of small zinc concentration (5 atomic per cent) where no miscibility gap appears, there is a poor agreement between the experimental and theoretical results. For these concentrations, due to high values of EMF, the experimental errors are smaller; however, during the measurements (short circuit) a transfer of metal ions and an increase in side reactions may occur.

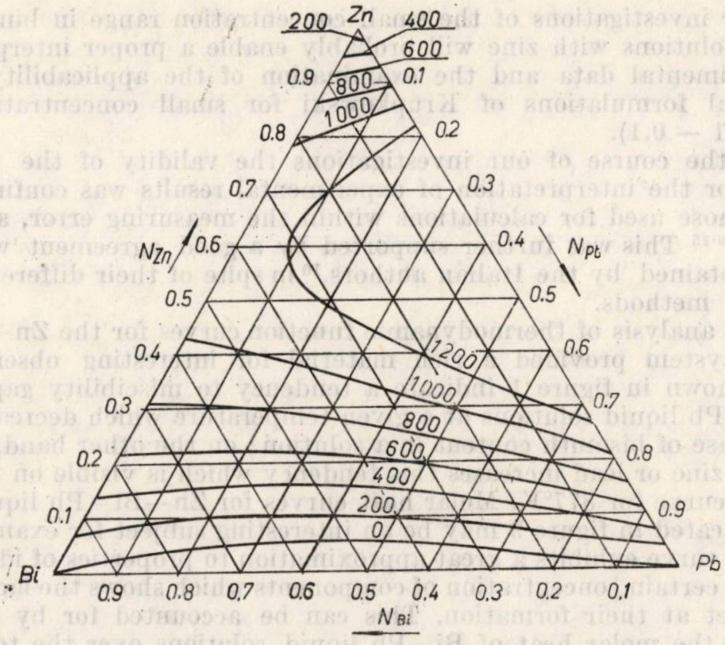

Fig. 9. — Molar heat of Zn—Bi—Pb liquid solutions in cal/mol.

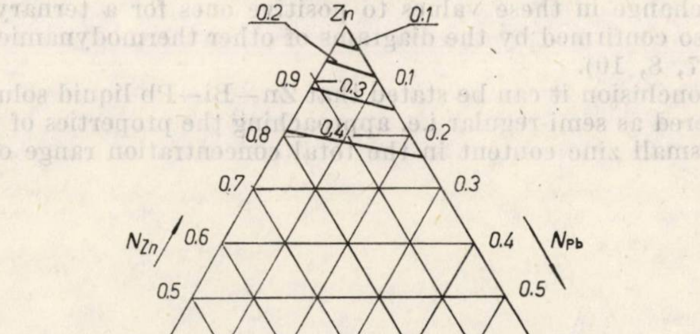

Fig. 10. — Change in excess molar entropy of Zn—Bi—Pb liquid solutions in cal/mol.

Our investigations of the small concentration range in binary and ternary solutions with zinc will probably enable a proper interpretation of experimental data and the examination of the applicability of the theoretical formulations of Krupkowski for small concentration cells $(X = 0.01 - 0.1)$.

In the course of our investigations the validity of the methods applied for the interpretation of experimental results was confirmed, as well as those used for calculations within the measuring error, as in the papers.[3-9,15] This was further supported by a good agreement with the results obtained by the Italian authors,[10] in spite of their different interpretation methods.

The analysis of thermodynamic function curves for the Zn—Bi—Pb ternary system provided a rich material for interesting observations. Curves shown in figure 1 indicate a tendency to miscibility gap of the Zn—Bi—Pb liquid solutions at a given temperature which decreases with the increase of bismuth content in a solution; on the other hand, the addition of zinc or lead increases this tendency which is visible on the temperature curve for 877°K. Molar heat curves for Zn—Bi—Pb liquid solutions indicated in figure 9 may be an interesting subject for examination. The "O" curve exhibits a great approximation to properties of ideal solutions at a certain concentration of components which shows the lack of any heat effect at their formation. This can be accounted for by negative values of the molar heat of Bi—Pb liquid solutions over the total concentration range. Even a small addition of zinc (below 10 atomic per cent) causes a change in these values to positive ones for a ternary solution. This is also confirmed by the diagrams of other thermodynamic functions (Figs. 6, 7, 8, 10).

In conclusion it can be stated that Zn—Bi—Pb liquid solutions may be considered as semi-regular i.e. approaching the properties of ideal solutions for small zinc content in the total concentration range of bismuth and lead.

Revue Roumaine de Chimie, **14,** 869 – 872 (1969)

ON A SUHRMANN-WEDLER EQUATION

N. I. IONESCU

Institute of Physical Chemistry of the Academy, Bucharest, str. Dumbrava Roşie, 23

Received September 21, 1968

The variation of the electric resistance of sintered thin metal films owing to gas chemisorption can verify, with the same probability, not only the order II kinetic equation of Suhrmann-Wedler but also Elovich's equation.

In 1957 Suhrmann and Wedler have shown [1] that the time-dependent variation of the electric resistance of sintered thin metal films, due to gas chemisorption for a second order process can be represented by the relationship :

$$\frac{1}{\Delta R_\infty - \Delta R} = At + B \tag{1}$$

where ΔR_∞ is the resistance variation at equilibrium, ΔR the resistance variation at the t moment and A, B constants. This formula was also established in a previous paper, [2] in another way.

As in such cases, the Elovich equation, written under the form[3] :

$$\Delta R = C + D \log (t + t_0) \tag{2}$$

is used, C, D and t_0 being constants, the present paper aims at studying the possibility of establishing a connection between these two relations.

RESULTS AND DISCUSSIONS

Let n_s be the number of occupied centers of the surface and n_a the number of adsorbed molecules both considered at the t moment.

The variation of the number of active centers will depend on the number of active centers existing at a given moment and on the number of adsorbed molecules, that is :

$$\mathrm{d}n_s = -k\, n_s \mathrm{d}n_a \tag{3}$$

---

[1] R. Suhrmann and G. Wedler, *Z. phys. Chem.* (Frankfurt), **10**, 84 (1957).

[2] I. G. Murgulescu and N. I. Ionescu, *Rev. Roumaine Chim.*, **13**, 1533 (1968).

[3] G. Blinakov and D. Lazarov, *Z. phys. Chem.* (*Leipzig*), **223**, 33 (1963).

k being a proportionality constant; by integrating with the initial conditions $n_a = 0, n_s = n_0$ it results:

$$n_s = n_0 \exp(-k\, n_a) \tag{4}$$

If we admit that the number of adsorbed molecules is proportional to the number of unoccupied centers hypothesis set forth by other research workers too,[4,5] then:

$$\mathrm{d}n_a = K\, n_s \mathrm{d}t \tag{5}$$

With the help of (4), relation (5) becomes:

$$\frac{\mathrm{d}n_a}{\mathrm{d}t} = K\, n_0 \exp\,(-k\, n_a) \tag{6}$$

which is nothing else than Elovich's equation.

But if we introduce expression (5) in (3) one gets:

$$\frac{\mathrm{d}n_s}{\mathrm{d}t} = -\,k\,K\, n_s^2 \tag{7}$$

We suppose now, that the relation

$$n_s = n_\infty - n_a \tag{8}$$

is valid between n_s and n_a, where n_∞ is the highest number of centers which can be covered at equilibrium.

In this case (7) takes the form:

$$\frac{\mathrm{d}n_a}{\mathrm{d}t} = A\left(1 - \frac{n_a}{n_\infty}\right)^2 \tag{9}$$

A being the overall constant of the process.

By definition the covering degree θ is given by

$$\theta = \frac{n_a}{n_\infty} \tag{10}$$

If the change of electric resistance ΔR is proportional to the number of chemisorbed molecules θ can be defined also[1] as:

$$\theta = \frac{\Delta R}{\Delta R_\infty} \tag{11}$$

By means of the formulas (10) and (11) after carrying out the calculations,[1-3] the relationships (1) and (2) are obtained.

In order to justify Elovich's equation, many models were proposed; in all cases by neglecting the desorption the validity of the conventional

---

[4] H. A. Taylor and N. Thon, *J. Amer. Chem. Soc.*, **74**, 4169 (1952).

[5] J. Besson, M. Azzopardi, M. Caillet, P. Sarrazin and M. Soustelle, *J. Chim. phys.*, **61**, 1018 (1964).

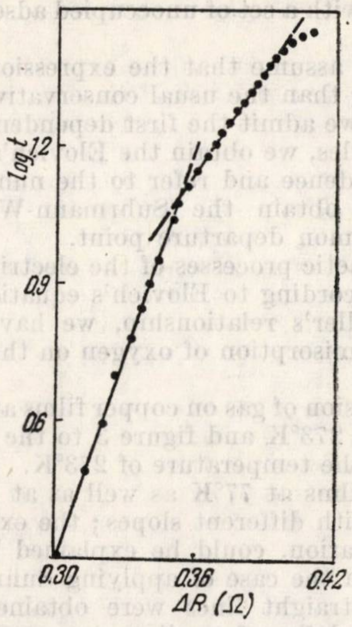

Fig. 1. — Application of Elovich's equation to oxygen adsorption on thin copper films at 77°K.

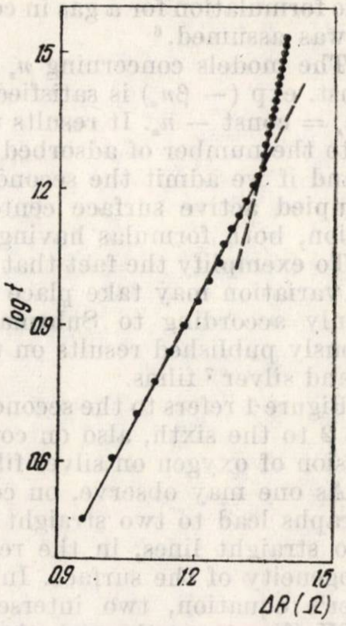

Fig. 2. — Application of Elovich's equation to oxygen adsorption on thin copper films at 273°K.

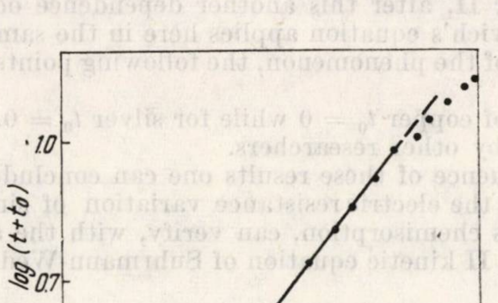

Fig. 3. — Application of Elovich's equation to oxygen adsorption on thin silver films at 273°K.

kinetic formulation for a gas in contact with a set of unoccupied adsorption sites was assumed.[6]

The models concerning n_s simply assume that the expression $n_s = \text{const. } \exp(-\beta n_a)$ is satisfied rather than the usual conservative relation $n_s = \text{const} - n_a$. It results that if we admit the first dependence and refer to the number of adsorbed molecules, we obtain the Elovich's equation and if we admit the second dependence and refer to the number of unoccupied active surface centers, we obtain the Suhrmann-Wedler's equation, both formulas having a common departure point.

To exemplify the fact that the kinetic processes of the electric resistance variation may take place also according to Elovich's equation and not only according to Suhrmann-Wedler's relationship, we have used previously published results on the chemisorption of oxygen on thin copper [2] and silver [7] films.

Figure 1 refers to the second admission of gas on copper films at 77°K, figure 2 to the sixth, also on copper at 273°K and figure 3 to the fourth admission of oxygen on silver films at the temperature of 273°K.

As one may observe, on copper films at 77°K as well as at 273°K, the graphs lead to two straight lines with different slopes; the existence of two straight lines, in the representation, could be explained by the heterogeneity of the surface. In fact, in the case of applying Suhrmann-Wedler's equation, two intersecting straight lines were obtained too. At 77°K (fig. 1), at the end, the points deflect from linearity, as they do in the case of relationship (1).[2]

In the case of silver at 273°K, the process had only at the beginning a kinetic of order II, after this another dependence occurs.[7] As results from figure 3 Elovich's equation applies here in the same conditions only at the beginning of the phenomenon, the following points lying on another curve.

In the case of copper $t_0 = 0$ while for silver $t_0 = 0.3$. The last value was also found [3] by other researchers.

As a consequence of these results one can conclude that certain kinetic processes of the electric resistance variation of sintered thin metal films owing to gas chemisorption, can verify, with the same probability, not only the order II kinetic equation of Suhrmann-Wedler, but Elovich's equation too.

---

[6] A. M. Peers, *J. Catalysis*, **4**, 672 (1965).

[7] I. G. Murgulescu and N. I. Ionescu, *Rev. Roumaine Chim.*, **11**, 1035 (1966).

Revue Roumaine de Chimie, 14, 873–878 (1969)

WÄRMEÜBERGANGSZAHLEN BEIM SIEDEN VON LÖSUNGEN. II

LÖSUNGEN VON DINATRIUMPHOSPHAT

Z. GROPŞIANU, D. KOHN und A. IOVI

von der Fakultät für Angewandte Chemie an der Technischen Hochschule,
Timişoara, Bul. 30 Decembrie, 2

Eingegangen am 4. September 1968

Es werden Versuchsergebnisse über den Wärmeübergang beim Sieden der Lösungen von Dinatriumphosphat bei Atmosphärendruck und 300 mmHg dargestellt. Es wurden Gleichungen zur Berechnung der Wärmeübergangszahl beim Sieden in Abhängigkeit von der Heizflächenbelastung, Temperaturdifferenz und Konzentration der Lösungen aufgestellt.

Dinatriumphosphat ist von großer Bedeutung für die verschiedensten Industriezweige. Es kann als solches oder zur Herstellung von Tetranatriumpyrophosphat und Trinatriumphosphat verwendet werden.

Zur Herstellung von Dinatriumphosphat wird Extraktionsphosphorsäure mit Natriumkarbonat neutralisiert. Die erhaltene Lösung wird durch Verdampfen bis zu Konzentrationen zwischen 40–50% konzentriert.[1]

Die Projektierung dieser Anlagen ist vom thermischen Gesichtspunkt aus mit Schwierigkeiten verbunden, mangels der Wärmeübergangszahlen beim Sieden der Lösungen. Die im Fachschrifttum vorgeschlagenen Gleichungen[2] zur Berechnung des Koeffizienten α beim Sieden können nicht verwendet werden, einerseits wegen der Tatsache, daß einige physikalische Konstanten der Lösungen nicht bekannt sind, andererseits weil die berechneten Werte nicht mit den Versuchsergebnissen übereinstimmen.[3] Infolgedessen wurden in der vorliegenden Arbeit die Wärmeübergangszahlen beim Sieden wäßriger Lösungen von Dinatriumphosphat experimentell bestimmt und zur Berechnung derselben einfache Gleichungen aufgestellt. Die Arbeit ist eine Fortsetzung der Untersuchungen über den Wärmeübergang beim Sieden von Lösungen.[3–5]

---

[1] A. Iovi „Tehnologia acidului fosforic şi a fosfaţilor tehnici", Lit. I. P. Timişoara, 1967, S. 109.

[2] M. Miheev „Fundamentals of heat transfer" (translated from russian), Peace Publishers, Moskau, S. 116.

[3] Z. Gropşianu, D. Kohn und A. Iovi, *Rev. Roumaine Chim.*, **14**, 000 (1969).

[4] Z. Gropşianu, D. Kohn und A. Iovi, *Rev. Roumaine Chim.*, **12**, 485 (1967).

[5] Z. Gropşianu, D.Kohn und A. Iovi, *Rev. Roumaine Chim*, **12**, 721 (1967).

Die Laboratoriumsvorrichtung und die Methode zur Bestimmung der Wärmeübergangszahlen beim Sieden wurden in früheren Arbeiten mitgeteilt.[3,4]

Die Bestimmungen wurden bei Atmosphärendruck und bei 300 mmHg durchgeführt, wobei im Bereiche intensiven Siedens mit Heizflächenbelastungen von $85.10^3 - 57.10^4$ W/m^2 gearbeitet wurde. Es wurden Dinatriumphosphatlösungen verschiedener Konzentrationen bis zu 40% verwendet.

Die Versuchsergebnisse sind in den Abbildungen 1—7 dargestellt.

Die Wärmeübergangszahl beim Sieden α für Lösungen von Dinatriumphosphat verschiedener Konzentrationen bei Atmosphärendruck nimmt mit dem Anwachsen der Heizflächenbelastung q zu (Abb. 1).

Aus der graphischen Darstellung wurde folgende Gleichung abgeleitet, welche die Abhängigkeit des Koeffizienten α von q ausgedrückt:

$$\alpha = \varepsilon \cdot q^{0.7}$$

wo ε ein von der Konzentration der Lösung abhängiger Koeffizient ist.

Das Anwachsen der Lösungskonzentration hat eine Verminderung des Koeffizienten α für dieselbe Heizflächenbelastung (Abb. 1), bzw. eine Verminderung des Koeffizienten ε zur Folge (Abb. 2). Zwischen dem Koeffizienten ε und der Konzentration C der Lösung konnte eine Gleichung folgender Form festgesetzt werden:

$$\varepsilon = 2{,}43 \cdot C^{-0{,}165}$$

wo C die Konzentration der Lösung, ausgedrückt in Gewichtsprozenten, ist.

Dieselbe Abhängigkeit zwischen dem Koeffizienten α und der Heizflächenbelastung q für einen Druck von 300 mmHg ist in Abb. 3 dargestellt. Ebenso wie bei Atmosphärendruck, nimmt der Koeffizient α mit dem Anwachsen von q für alle Konzentrationen zu und es wurde eine Gleichung folgender Form festgesetzt:

$$\alpha = \varepsilon_1 \cdot q^{0.7}$$

wo ε_1 ein von der Konzentration abhängiger Koeffizient ist. Zwischen ε_1 und der Konzentration der Lösung C wurde aus Abb. 4 folgende Gleichung abgeleitet:

$$\varepsilon_1 = 3{,}24 \cdot C^{-0{,}218}$$

Der Koeffizient α hat bei gleicher Konzentration und Heizflächenbelastung, bei einem Druck von 300 mmHg, einen kleineren Wert als bei Atmosphärendruck, eine Tatsache, die im Fachschrifttum für andere Substanzen angegeben wurde.[6]

Desgleichen wird eine Verminderung des Koeffizienten α mit dem Anwachsen der Konzentration festgestellt.

Der Temperaturunterschied Δt zwischen der Wandtemperatur und der Siedetemperatur der Lösung beeinflußt sehr stark den Wert des Koeffizienten α. Die in Abb. 5 dargestellten Versuchsergebnisse zeigen eine

---

[6] F. Müller, „Wärmeübergang bei der Verdampfung unter hohen Drücken", (Dissertation), Berlin, 1966.

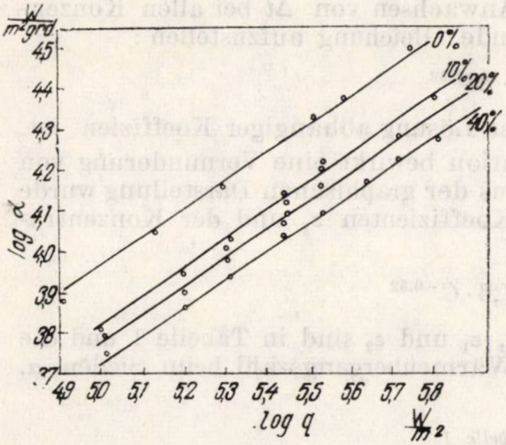

Abb. 1. — Veränderung von α in Abhängigkeit von q bei Atmosphärendruck, für Dinatriumphosphatlösungen verschiedener Konzentration.

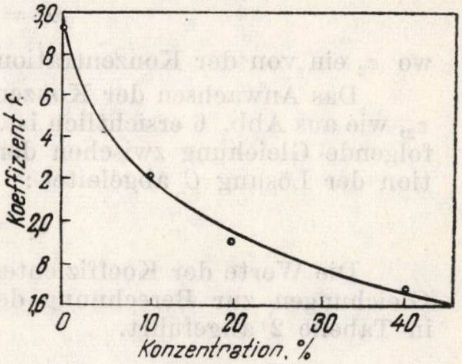

Abb. 2. — Abhängigkeit des Koeffizienten ε von der Konzentration der Dinatriumphosphatlösungen.

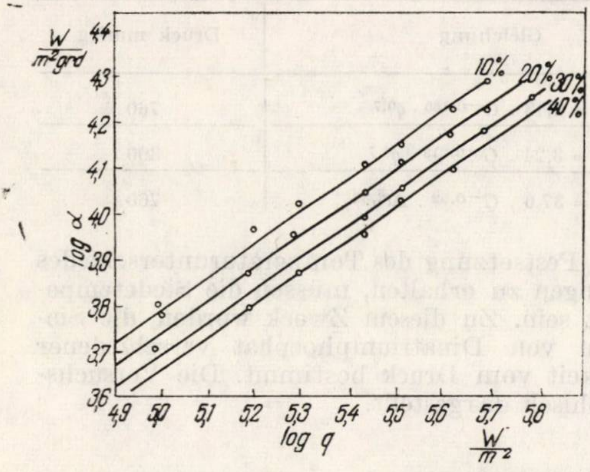

Abb. 3. — Veränderung von α in Abhängigkeit von q bei 300 mmHg Druck, für Dinatriumphosphatlösungen verschiedener Konzentration.

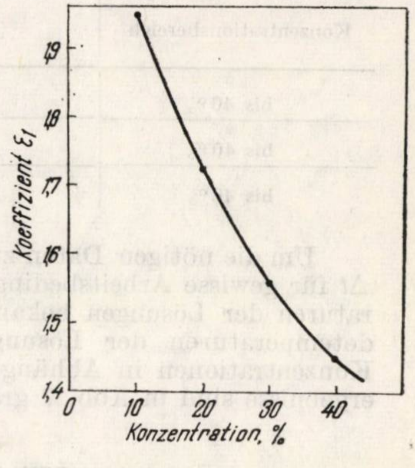

Abb. 4. — Abhängigkeit des Koeffizienten ε, von der Konzentration der Dinatriumphosphatlösungen.

Zunahme des Koeffizienten α mit Anwachsen von Δt bei allen Konzentrationen und ermöglichen es, folgende Gleichung aufzustellen:

$$\alpha = \varepsilon_2 \cdot \Delta t^{2,33}$$

wo ε_2 ein von der Konzentration der Lösung abhängiger Koeffizient ist.

Das Anwachsen der Konzentration bewirkt eine Verminderung von ε_2, wie aus Abb. 6 ersichtlich ist. Aus der graphischen Darstellung wurde folgende Gleichung zwischen dem Koeffizienten ε_2 und der Konzentration der Lösung C abgeleitet:

$$\varepsilon_2 = 37{,}6 \cdot C^{-0,52}$$

Die Werte der Koeffizienten ε, ε_1 und ε_2 sind in Tabelle 1 und die Gleichungen zur Berechnung der Wärmeübergangszahl beim Sieden, α, in Tabelle 2 angeführt.

Tabelle 1

Werte der Koeffizienten

Konzentration %	ε	ε_1	ε_2
0	2,915	—	35,5
10	2,09	1,95	11,56
20	1,895	1,72	7,5
30	—	1,557	—
40	1,66	1,445	5,62

Tabelle 2

Gleichungen

Konzentrationsbereich	Gleichung	Druck mmHg
bis 40%	$\alpha = 2{,}43 \cdot C^{-0,165} \cdot q^{0,7}$	760
bis 40%	$\alpha = 3{,}24 \cdot C^{-0,218} \cdot q^{0,7}$	300
bis 40%	$\alpha = 37{,}6 \cdot C^{-0,52} \cdot \Delta t^{2,33}$	760

Um die nötigen Daten zur Festsetzung des Temperaturunterschiedes Δt für gewisse Arbeitsbedingungen zu erhalten, müssen die Siedetemperaturen der Lösungen bekannt sein. Zu diesem Zweck wurden die Siedetemperaturen der Lösungen von Dinatriumphosphat verschiedener Konzentrationen in Abhängigkeit vom Druck bestimmt. Die Versuchsergebnisse sind in Abb. 7 graphisch dargestellt.

SCHLUSSFOLGERUNGEN

Auf Grund der Untersuchungen des Wärmeübergangs beim Sieden der Lösungen von Dinatriumphosphat beim Atmosphärendruck und 300 mmHg wurden Gleichungen zur Berechnung der Wärmeübergangszahl beim Sieden aufgestellt.

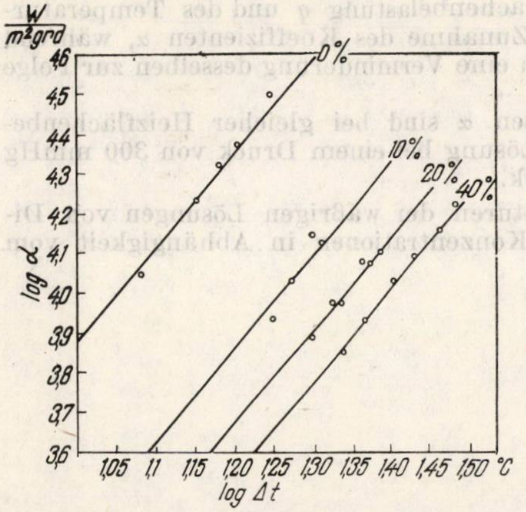

Abb. 5. — Veränderung von α in Abhängigkeit von Δ*t* bei atmosphärischem Druck für Dinatriumphosphatlösungen verschiedener Konzentration.

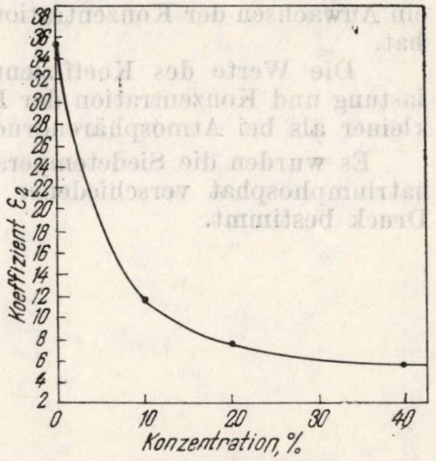

Abb. 6. — Abhängigkeit des Koeffizienten ε_2 von der Konzentration der Dinatriumphosphatlösungen.

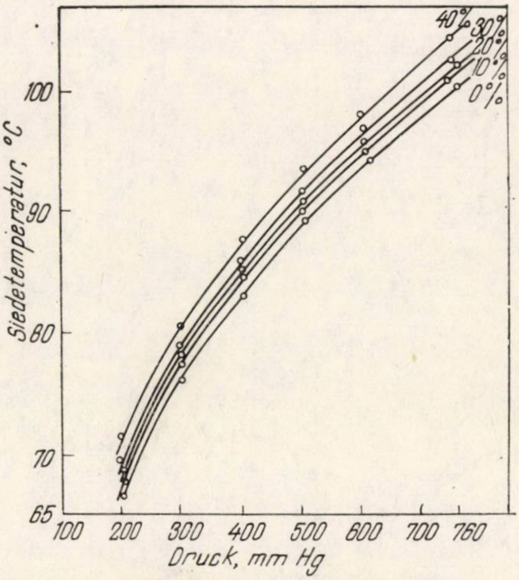

Abb. 7. — Siedetemperaturen der Dinatriumphosphatlösungen in Abhängigkeit vom Druck bei verschiedenen Konzentrationen.

Das Anwachsen der Heizflächenbelastung q und des Temperaturunterschiedes Δt bewirkt eine Zunahme des Koeffizienten α, während ein Anwachsen der Konzentration eine Verminderung desselben zur Folge hat.

Die Werte des Koeffizienten α sind bei gleicher Heizflächenbelastung und Konzentration der Lösung bei einem Druck von 300 mmHg kleiner als bei Atmosphärendruck.

Es wurden die Siedetemperaturen der wäßrigen Lösungen von Dinatriumphosphat verschiedener Konzentrationen in Abhängigkeit vom Druck bestimmt.

Revue Roumaine de Chimie, **14**, 879–885 (1969)

THE STUDY OF THE FORMATION AND DETERMINATION OF THE STABILITY IN SOLUTION OF SOME COMPLEX COMBINATIONS WITH n-PROPYLAMINE

GR. POPA and V. MAGEARU
Laboratory of Analytical Chemistry, University of Bucharest,
Spl. Independenţei 89 Bucureşti
Romania

(Received September 28, 1968)

A new electrode of the second kind was produced, the "metal-complex" type, reversible against n-propylamine. By means of this electrode the concentrations of the free n-propylamine were determined from the forming equilibriums of the Zn (II), Cd (II), Co (II), and Ni (II) complexes with n-propylamine. Formation curves of the Bjerrum type were drawn and then the successive stability constants of the studied complexes were calculated.

To widen the field of analytical methods and that of the possibilities of investigation in the domain of the complex combinations in the solution, a new class of electrodes of second type in which the hard soluble combination is replaced by a slightly dissociated complex combination was worked out and studied.[1–6]

These electrodes, called of the "metal-complex" type, can be represented as follows:

$$\mathrm{Me} \mid [\mathrm{MeL}_p]^{(a-pb)+},\quad \mathrm{L}^{b-} \tag{1}$$

They are reversible as against the ligand L^{b-}, which forms the complex $[\mathrm{MeL}_p]^{(a-pb)+}$, with the ions Me^{a+}.

The part of the ligand L can be played by many anions and neutral molecules, and that of the metal Me, by metals that may act as electrodes of the first class.

Silver has been used very successfully to obtain these electrodes, because it does not polarize and gives perfectly reproducible potentials, and the silver ions form very stable soluble complexes with a great number

---

[1] C. Luca, V. Magearu and Gr. Popa, *J. Electroanalyt. Chem.*, **12**, 45 (1966).
[2] V. Magearu, C. Luca and M. Teodorescu, *J. Electroanalyt. Chem.*, **12**, 148 (1966).
[3] C. Luca, *Bull. Soc. chim. France*, **7**, 2556 (1967).
[4] Gr. Popa and V. Magearu, *Rev. Roumaine Chim.*, **12**, 1107 (1967).
[5] Gr. Popa, V. Magearu and E. Dăscălescu, *Anal. Univ. Bucureşti*, **2**, 67 (1967).
[6] Gr. Popa, V. Magearu and C. Luca, *J. Electroanalyt. Chem.*, **17**, 335 (1968).

of neutral molecules or anions according to the following reaction :

$$Ag^{+} + pL^{b-} \rightleftarrows [AgL_{p}]^{(1-pb)+} \tag{2}$$

If the ions of another metal Me^{z+}, which forms complex compounds with the ligand L, are present in the solution :

$$Me^{z+} + nL^{b-} \rightleftarrows [MeL_{n}]^{(z-nb)+} \tag{3}$$

a competitive equilibrium is established between the reaction (2) and (3).[7]

The equilibrium concentration, of the ligand in the reaction (3) can be determined with an adequate electrode of the type (1). The determination of the Bjerrum type formation curves [8] is then possible, which permit the determination of the composition and of the stability in solution of some successive complex combinations formed in the equilibrium (3).

In the present paper the electrode "metal-complex"

$$Ag\,|[Ag(CH_3-CH_2-CH_2-NH_2)_2]^{+},\ \ CH_3-CH_2-CH_2-NH_2 \tag{4}$$

was used for the study of the formation, in aqueous solution of the complex combinations of Zn (II), Cd (II), Co (II) and Ni (II) with n-propylamine (L).

THEORY

The reversible potential of a metal-complex electrode :

$$Ag\,|[AgL_{p}]^{+},\ L \tag{5}$$

is given by relation :

$$E = E^{0}_{Ag} + \frac{RT}{\mathcal{F}} \ln \frac{[AgL_{p}]^{+}}{K_{p}\cdot[L]^{p}} \tag{6}$$

or :

$$E = E^{0}_{Ag|[AgL_p]^+} - p\,\frac{RT}{\mathcal{F}} \ln\,[L] \tag{7}$$

in which $E^{0}_{Ag|[AgL_p]^+}$ is the standard potential of the electrode. This potential depends on the standard potential of the silver electrode E^{0}_{Ag}, on the stability constant K_p of the complex $[AgL_p]^+$ and on the concentration of these complex ions in solution.

In order to avoid the determination of this standard potential use has been made of one of the variants presented in a previous paper.[1] There have been thus used two cells of the form :

$$\begin{aligned}&(II)\ Ag\,|[AgL_p]^+,L\,|NH_4NO_3(\text{saturated})\,|KCl(\text{saturated}),Hg_2Cl_2\,|Hg\\&(III) Ag\,|[AgL_p]^+,L,Me^{2+}\,|NH_4NO_3(\text{saturated})\,|KCl(\text{saturated}),Hg_2Cl_2\,|Hg.\end{aligned} \tag{8}$$

In both elements having the value of the constant diffusion potential, the total quantity of the silver ions is equal and very small as related to the ligand L and to the Me^{2+} ions ($C_{Ag^+} \simeq 10^{-5}$ M).

---

[7] F. Rossotti and H. Rossotti, "The Determination of Stability Constants", McGraw-Hill, Book Co., New York, 1961, p. 58.

[8] J. Bjerrum, "Metal Ammine Formation in Aqueous Solution", Haase, Copenhagen, 1957, cap. I, II, III.

The (8—III) cell has, as compared to the (8—II), a known quantity of ions of $Me^{2+}(C_{Me^{2+}})$ whose complexes with the ligand L we are going to study. Both elements have the same volume of solution and the same total quantity of ligand (C_L).

The (8—II) cell is taken as a standard element and gives the electromotive tension (e.m.t.) value in the absence of the Me^{2+} ions, that is the corresponding value of the total concentration of the ligand C_L (the quantity of the ligand existing in the silver complex is negligible).

In the (8—III) cell, a part of the ligand is used for the formation of the complexes of the $[MeL_n]^{2+}$ type, and the equilibrium concentration of the ligand in the presence of the Me^{2+} ions, may be obtained from the e.m.t. of the two cells (13):

$$\Delta E = E_{II} - E_{III} = p\,\frac{RT}{\mathcal{F}}\ln\frac{[L]}{C_L} \tag{9}$$

or expressed in decimal logarithms for 25°:

$$\lg\,[L] = \frac{\Delta E}{0.05916 \cdot p} + \lg C_L. \tag{10}$$

In the same conditions of temperature, ionic strength and concentration, in a previous paper,[9] the formation equilibrium of the electrodic complex $[AgL_p]^+$, where the value $p = 2$, has been found, which is characteristic of the silver complexes with organic monoamines [10-13] in general and also $K_1 = 2.5 \times 10^3$; $K_2 = 1.16 \times 10^7$.

Therefore the electrodic complex will have for both cells (8) the same composition and concentration, negligible due to the excess of necessary ligand, at which the forming of complexes with the second metallic ion of equilibrium (3) occurs.

Having the total concentration of the Me^{2+} ions, and of the equilibrium ligand for a series of total concentrations of the ligand, we can calculate the functions:

$$\bar{n} = \frac{C_L - [L]}{C_{Me^{2+}}} \tag{11}$$

and then trace the $\bar{n} - p\,[L]$ formation curves of Bjerrum type [8] from which we can determine the successive formation constants of the complexes under study.

EXPERIMENTAL

In the tables 1, 2, 3 and 4 the experimental data and the calculation connected with the formation equilibrium of the Me^{2+} complexes with n-propylamine, are listed.

For these determinations, solutions prepared from p.a. Merck and U.C.B. (Belgium) purity substances in doubly distilled water were used.

---

[9] GR. POPA and V. MAGEARU, *Anal. Univ. București*, **2** (1968).
[10] GR. POPA, V. MAGEARU and C. LUCA, *J. Chim. phys.*, **62**, 813 (1965).
[11] C. LUCA, V. MAGEARU and GR. POPA, *Anal. Univ. București*, **1**, 109 (1965).
[12] GR. POPA, C. LUCA and V. MAGEARU, *Anal. Univ. București*, **2**, 9 (1965).
[13] GR. POPA, C. LUCA and V. MAGEARU, *J. Chim. phys.*, **60**, 355 (1963).

Table 1

Zn^{2+} — $CH_3-CH_2-CH_2-NH_2$ $\rightleftarrows$ 25 °C; $\mu = 2(NH_4NO_3)$

$C_{Zn^{2+}}$ mol/l	C_L mol/l	$-\Delta E = E_{II} - E_{III}$ (V)	[L]	p [L]	$\overline{n}$
0.03324	0.00365	0.1118	0.000414	3.383	0.097
0.03311	0.00908	0.1261	0.000781	3.107	0.251
0.03298	0.01448	0.1300	0.001154	2.938	0.404
0.03285	0.01983	0.1361	0.001403	2.853	0.561
0.03268	0.02690	0.1412	0.007124	2.764	0.770
0.03244	0.03567	0.1442	0.002154	2.667	1.032
0.03226	0.04426	0.1468	0.002543	2.595	1.293
0.03201	0.05247	0.1476	0.002968	2.528	1.547
0.03164	0.06947	0.1477	0.003922	2.407	2.072
0.03125	0.08575	0.1425	0.005352	2.271	2.573
0.03105	0.09374	0.1380	0.006391	2.194	2.813
0.03098	0.10163	0.1312	0.007909	2.102	3.025
0.03068	0.10942	0.1229	0.010010	1.999	3.240
0.03030	0.12473	0.1006	0.017610	1.754	3.535
0.02994	0.13966	0.0794	0.029790	1.526	3.669
0.02941	0.16341	0.0593	0.050900	1.293	3.826
0.02861	0.19600	0.0421	0.086390	1.064	3.831

Table 2

Cd^{2+} — $CH_3-CH_2-CH_2-NH_2$ 25 °C; $\mu = 2(NH_4NO_3)$

$C_{Cd^{2+}}$ mol/l	C_L mol/l	$-\Delta E = E_{II} - E_{III}$ (V)	[L]	p [L]	$\overline{n}$
0.03311	0.009086	0.1257	0.000787	3.104	0.251
0.03289	0.01805	0.1264	0.001542	2.812	0.502
0.03268	0.02690	0.1198	0.002614	2.583	0.743
0.03246	0.03564	0.1112	0.004093	2.388	0.972
0.03226	0.04426	0.1043	0.005814	2.236	1.192
0.03184	0.06117	0.0895	0.010719	1.970	1.585
0.03144	0.07766	0.0736	0.018542	1.732	1.880
0.03098	0.10163	0.0581	0.032810	1.484	2.221
0.03012	0.13224	0.0435	0.05672	1.246	2.507
0.02941	0.16341	0.0327	0.08647	1.063	2.616
0.02861	0.19600	0.0255	0.11932	0.923	2.681

Table 3

Co^{2+} — $CH_3-CH_2-CH_2-NH_2$ 25 °C; $\mu = 2(NH_4NO_3)$

$C_{Co^{2+}}$ mol/l	C_L mol/l	$-\Delta E = E_{II} - E_{III}$ (V)	[L]	p [L]	$\overline{n}$
0.06622	0.00909	0.1157	0.000956	3.019	0.123
0.06578	0.01805	0.1169	0.001855	2.732	0.246
0.06536	0.02690	0.1142	0.002915	2.535	0.367
0.06492	0.03564	0.1109	0.004117	2.385	0.486
0.06402	0.05247	0.1065	0.006604	2.180	0.716
0.06328	0.06947	0.1011	0.009712	2.013	0.944
0.06250	0.08575	0.0955	0.013370	1.874	1.158
0.06098	0.11712	0.0848	0.022489	1.648	1.552
0.05952	0.14882	0.0755	0.034242	1.465	1.925
0.05782	0.18241	0.0666	0.049905	1.302	2.292
0.05682	0.20268	0.0625	0.060052	1.221	2.510
0.05555	0.22867	0.0564	0.076300	1.117	2.743
0.05405	0.25957	0.0507	0.096765	1.014	3.012
0.05206	0.28884	0.0461	0.117770	0.929	3.287
0.05000	0.34300	0.0376	0.165000	0.782	3.560

Table 4

$Ni^{2+}-CH_3-CH_2-CH_2-NH_2$ 25°C; $\mu = 2\ (NH_4NO_3)$

$C_{Ni^{2+}}$ mol/l	C_L mol/l	$-\Delta E = E_{II} - E_{III}$ (V)	[L]	p [L]	$\overline{n}$
0.03311	0.00908	0.1482	0.000508	3.294	0.259
0.03289	0.01805	0.1502	0.000971	3.013	0.519
0.03268	0.02690	0.1444	0.001619	2.791	0.774
0.03246	0.03563	0.1363	0.002512	2.600	1.020
0.03226	0.04426	0.1295	0.003560	2.448	1.262
0.03184	0.06117	0.1160	0.006399	2.194	1.720
0.03164	0.06947	0.1086	0.008394	2.076	1.930
0.03125	0.08575	0.0952	0.013447	1.871	2.314
0.03098	0.10163	0.0831	0.020170	1.695	2.629
0.03049	0.11712	0.0725	0.028570	1.544	2.904
0.02976	0.14882	0.0572	0.048892	1.311	3.358
0.02890	0.18241	0.0447	0.076427	1.117	3.667
0.02777	0.22867	0.0328	0.120800	0.918	3.884
0.02703	0.25957	0.0271	0.513200	0.815	3.939

The ionic strength of the solutions was maintained constant at the value of $\mu = 2$ with NH_4NO_3.

The cells were thermostated at a constant temperature of 25 ± 0.1°, and the e.m.t. was measured by means of a VEB-Meßtechnik, Mellenbach, potentiometer with a ± 0.1 mV precision.

DISCUSSION

In figure 1 there are drawn the formation curves of the already studied complexes together with the formation curve of the $[AgL_p]^+$ complexes studied in a previous paper.[9]

As one can easily see, in the concentration range at which the formation of complexes of the $Me^{2+}-L$ systems has been studied the formation of the electrodic complexes is already completed, in solution existing only the $[AgL_2]^+$ complex of the given form.

From a graph of the formation curves on a large scale, we have determined the approximate successive formation constants:

$$\lg k_n = p\,[L]_{\overline{n}=n-\frac{1}{2}} \tag{12}$$

We have then used Bjerrum's indications[8] to correct these constants. The results of these calculations are shown in table 5.

In order to verify the accuracy in the determination of the concentrations of the free ligand, in the last part of the paper the formation constants of the system Ag^+-L have been recalculated using as total concentration of the ligand, for the electrodic complexes systems, the concentration found with the help of the relation (10). For determining these constants there has been used the successive extrapolations method[14, 15] of the complexation functions [16]:

$$F = \frac{C_{Ag^+}}{[Ag^+]} = 1 + K_1[L] + K_2[L]^2 + \ldots \tag{13}$$

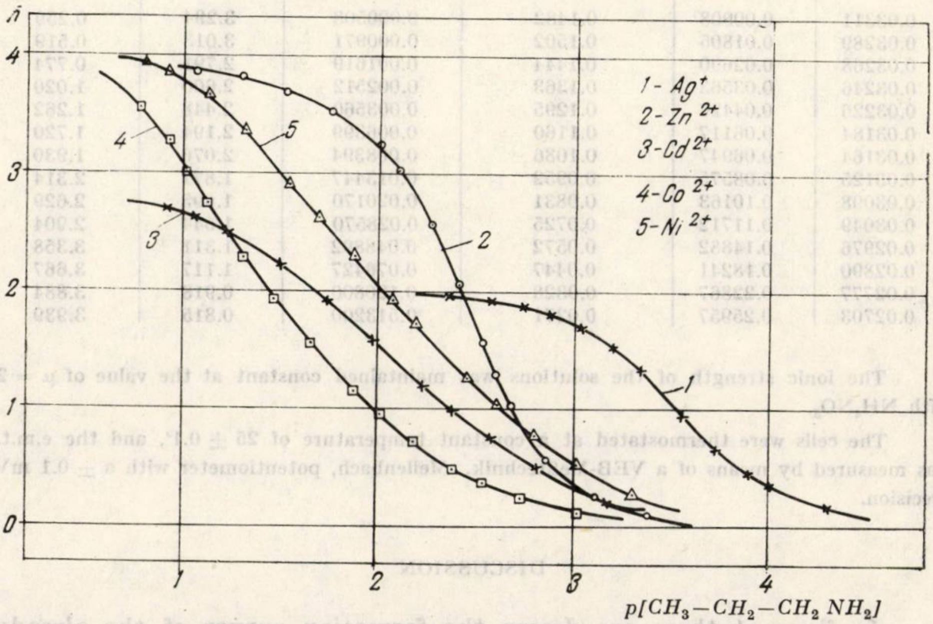

Fig. 1. — Formation curves of the $Me^{2+}-CH_3-CH_2-CH_2-NH_2$ (2—5) and $Ag^+-CH_3-CH_2-CH_2-NH_2$ (1) systems.

Table 5

$Me^{2+} - CH_3-CH_2-CH_2-NH_2$ 25°C; $\mu = 2$ (NH_4NO_3)

Me^{2+} \ n		1	2	3	4	l/g K_N
Zn^{2+}	$p[L]_{\bar{n}=n-1/2}$	2.89	2.55	2.29	1.77	9.50
	$\lg k_n$	2.42	2.43	2.53	2.11	9.49
Cd^{2+}	$p[L]_{\bar{n}=n-1/2}$	2.81	2.02	1.22	—	6.05
	$\lg k_n$	2.62	2.02	1.39	—	6.04
Co^{2+}	$p[L]_{\bar{n}=n-1/2}$	2.35	1.68	1.22	0.81	6.06
	$\lg k_n$	2.12	1.53	1.24	1.18	6.07
Ni^{2+}	$p[L]_{\bar{n}=n-1/2}$	3.02	2.31	1.76	1.23	8.31
	$\lg k_n$	2.81	2.21	1.77	1.52	8.32

---

[14] I. LEDEN, *Z. phys. Chem.*, **A-188**, 160 (1941).

[15] H. OLERUP, "Dissertation", Lund, (1944).

[16] K. B. IATSIMIRSKI, *Zhur. neorg. Khim.*, **1**, 412 (1956).

The complexation functions have been determined from the cells of the type:

$$\text{(I)}\quad \mathrm{Ag}\,|\,\mathrm{Ag}^+\,|\,\mathrm{NH_4NO_3}\,(\text{saturated})\,|\,\mathrm{KCl}\,(\text{saturated}),\mathrm{Hg_2Cl_2}\,|\,\mathrm{Hg} \qquad (14)$$

and (8—III). The e.m.t. for these two cells gives the following relation:

$$E_{\mathrm{I}} - E_{\mathrm{III}} = 0.05916 \lg F \qquad (15)$$

By the successive extrapolations of the functions:

$$F_n = \frac{F_{n-1} - K_{n-1}}{[\mathrm{L}]} \qquad (16)$$

the constants K_n have been determined:

$$\lim_{[\mathrm{L}]\to 0} F_n = K_n \qquad (17)$$

To exemplify there are given in table 6 the results of these determinations.

Table 6

$\mathrm{Ag^+ - CH_3 - CH_2 - CH_2 - NH_2}$ (Zn)

[L]	$\Delta E = E_{\mathrm{I}} - E_{\mathrm{III}}^{(\mathrm{Zn})}$	F	F_1	$F_2 \cdot 10^{-7}$
0.000414	0.0276	2.928	4.654	—
0.000780	0.0568	9.122	10.401	—
0.001154	0.0747	18.31	14.996	1.100
0.001403	0.0855	27.88	19.155	1.201
0.001723	0.0962	42.36	23.997	1.258
0.002154	0.1066	63.37	28.955	1.238
0.002542	0.1151	88.39	34.369	1.261
0.002968	0.1235	122.6	40.970	1.301
0.003922	0.1375	211.4	53.647	1.309
0.005352	0.1529	384.2	71.610	1.294
0.006391	0.1616	540.1	84.350	1.284
0.007909	0.1723	517.4	103.250	1.276
0.023310	0.2243	6.966.0	298.850	1.272

$K_1 = 2.3 \times 10^3$; $K_2 = 1.25 \times 10^7$

The form of these extrapolation curves has shown the formation in solution of only two complexes, fact in accordance with the previous paper[9] ($K_1 = 2.5 \times 10^3$; $K_2 = 1.16 \times 10^7$).

Revue Roumaine de Chimie, **14**, 887–892 (1969)

VOLUMETRIC DOSAGE WITH PHENOTHIAZONE-(3). I

DOSAGE OF SODIUM THIOSULPHATE WITH PHENOTHIAZONE-(3)

M. RĂILEANU and EUGENIA DOBRE

University of Craiova, Str. Al. I. Cuza, 31

Received September 6, 1968

A volumetric dosing method of sodium thiosulphate with phenothiazone-(3) (I) n/100 in acetic acid medium has been established and phenothiazone-(3) (I) has been found a titrimetric substance. In these titration conditions, the monoelectronic reduction of phenothiazone-(3) (I) takes place in two successive stages, with intermediary formation of radical cations which have been put into evidence by means of the ESR spectrum. During dosage one registers a clear and characteristic turning corresponding to each stage of monoelectronic reduction. This new dosage method of sodium thiosulphate with phenothiazone-(3) (I) is practical and very precise.

In a former paper[1] we have shown that phenothiazone-(3) (I) may be easily obtained and with a good yield by oxidizing phenothiazine with ferric chloride in 10% acetic acid, thus offering new possibilities of developing the chemistry of these compounds.

There are some indications in the literature [2] that, unlike quinones and quinon-imines, the phenothiazone-(3) (I) does not give either the usual reactions of addition to the quinon-iminic nucleus or reactions of condensation to the carbonyl group (because of extended conjugation effect), but takes part in oxide-reduction reactions. The phenothiazone-(3) (I) has normal redox potential [3] $E_0 = +0.58$ V, forms dark red solutions, and by reduction passes easily into slightly yellow-coloured 3-hydroxyphenothiazine (II), acting thus as an autoindicator.

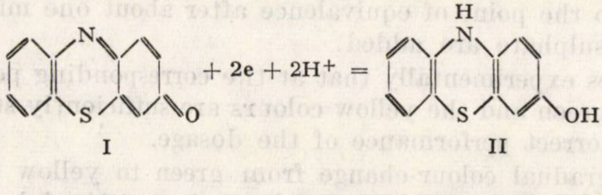

I II (1)

---

[1] C. Bodea and M. Răileanu, *Studii și Cercetări Chim. Acad. R.P. România Filiala Cluj*, **2**, 325 (1960).

[2] C. Bodea and I. Silberg, *Rev. Chim. Acad. R.P.R.* **7**, 683 (1962).

[3] C. Bodea, M. Răileanu and I. Silberg, *Anal. Sti. Univ. "A. I. Cuza", Iași Sect. I.*, **6** 1023 (1960).

From the above behaviour of phenothiazone-(3) (I) it results that this substance could be eventually used in certain cases to dose compounds having a normal redox potential. $E_0 < +0.58$ V.

We have, therefore, considered that the action of phenothiazone-(3) (I) on sodium thiosulphate, a reactive largely used and verified in iodometric analysis, might be interesting. It is well known that sodium thiosulphate easily reduces a series of oxidizing[4] agents with a normal redox potential $E_0 > +0.25$ V.

The phenothiazone (3) (I) obtained by Bodea-Răileanu's method[1] may be purified for analytical purposes by two successive recrystallizations in distilled water, thus obtaining copper coloured, accicular crystals with a 161° melting point, (0.4 g of the substance is solved in one liter of water).

To dose the sodium thiosulphate, one has prepared a phenothiazone-(3) (I) n/100 solution by simply weighing the substance and quantitatively solving it in glacial acetic acid in a calibrated flask. (The gram-equivalent of phenothiazone (3) (I) is 213.25/2). Phenothiazone-(3) (I) solves extremely easily in glacial acetic acid, even at room temperature ; the red solution obtained does not change its titre even after 90 days of storage in brown bottles.

The titre of the sodium thiosulphate n/100 solution used for the dosage of the phenothiazone-(3) (I) was determined by means of the n/100 iodine solution.

From the attempts to dose phenothiazone-(3) (I) with sodium thiosulphate, it results that the reaction rate is rapid enough over 60°. Therefore the acetic phenothiazone-(3) (I) solution into which the sodium thiosulphate solution is poured drop by drop during the titration, must be previously heated to 80—100°.

During titration, two equivalents of sodium thiosulphate are used for one equivalent of phenothiazone-(3) (I), recording at the same time one neat and characteristic turning after the consumption of each thiosulphate equivalent.

Thus, during the dribbling of the sodium thiosulphate solution over the phenothiazone-(3) (I) solution, the use of the first thiosulphate equivalent is marked by a colour change of the solution from purple to dark green. By further adding sodium thiosulphate, the green solutions change gradually, turning to yellow after the use of the second equivalent.

At about 60—70°, the reaction between the phenothiazone (3) (I) and thiosulphate is rapid, and the titration may be achieved in 3 to 4 minutes. Close to the point of equivalence after about one minute the last drops of thiosulphate are added.

One notes experimentally that at the corresponding points of equivalence, both green and the yellow colours are sufficiently stable in time, allowing the correct performance of the dosage.

As the gradual colour-change from green to yellow is less easily perceived, the second point of equivalence is registered by means of a test sample. This is obtained by previous dosage of a phenothiazone-(3) (I) sample and by adding a small excess of sodium thiosulphate solution after noticing the second point of equivalence.

---

[4] G. Charlot, "Les méthodes de la Chimie Analytique, Analyse quantitative minérale", Masson, Paris, 1966, p. 475.

It is therefore advisable when dosing phenothiazone-(3) (I) with thiosulphate, that the operation should be carried out only up to the first point of equivalence which is easily noticeable. In this case one phenothiazone-(3) (I) equivalent uses during the reaction one thiosulphate equivalent.

The results of phenothiazone-(3) (I) dosage with sodium thiosulphate are shown in table 1.

Table 1

Results of dosing phenothiazone-(3) (I) n/100 with n/100 sodium thiosulphate

No	No of I n/100 ml taken for dosing	No of $Na_2S_2O_3$ n/100 ml consumed at the dosing of I till the turning of the solution from purple to green (one equivalent)	No of $Na_2S_2O_3$ n/100 ml consumed at the dosing of I till the turning of the solution from green to yellow (two equivalents)
1	5	4.99	10.02
2	5	5.01	9.98
3	6	6.00	12.01
4	6	5.99	11.98
5	7	7.01	14.02
6	7	7.00	14.01
7	8	8.00	16.02
8	8	7.99	16.01
9	9	9.01	18.02
10	9	9.00	18.03
11	10	9.99	20.01
12	10	10.00	20.02
13	11	11.01	22.02
14	12	12.00	24.03
15	13	12.99	26.01

Table 1 shows that phenothiazone-(3) (I) may be dosed with sodium thiosulphate in two degrees of equivalence and that particularly exact results for the first point are obtained.

These results also show that the phenothiazone-(3) (I) is a titrimetric substance.

As one has established by analysis that the reduction of phenothiazone-(3) (I) by thiosulphate is a process taking place in two steps, the first corresponding to the consumption of one equivalent, and the second to that of two equivalents of thiosulphate, and taking into account the fact that for the first point of equivalence the solution is intensely green coloured, it would be easy to suppose that some cation radicals were formed intermediarely.

Indeed the phenothiazone-(3) (I) solution into which sodium thiosulphate is poured drop by drop lets out all ESR signals like in figure 1, but these decrease in intensity when nearing the first point of equivalence.

It is well-known that recently literature has given us a series of works dealing both with the way of obtaining, and the study of the features of free radicals or ion radicals of the phenothiazine [5-22] class.

The ESR spectrum in figure 1 is made of 4 lines with relative intensities that are approximately in the ratio 1 : 2 : 2 : 1 and is identical to the one obtained by Billon, Cauquis and Combrisson [14] when reducing phenothiazone-(3) (I) in two stages on a platinum electrode in m/10 per-

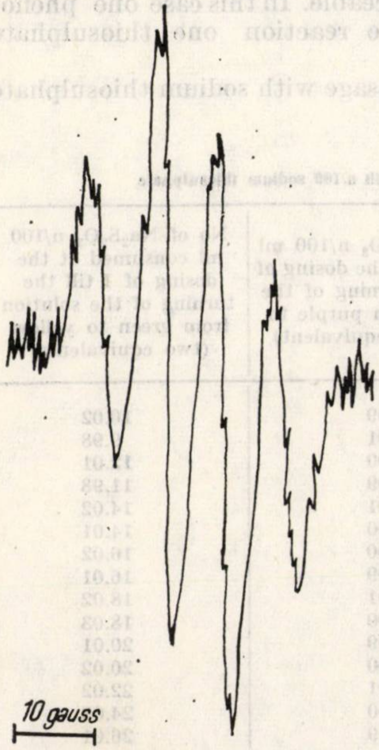

Fig. 1. — The ESR signal of the cation radical formed during addition of the sodium thiosulphate solution to the acetic solution of phenothiazone-(3)(I).

---

[5] L. Michaelis, S. Granick and M. P. Schubert, *J. Amer. Chem. Soc.*, **62**, 204, 1802 (1940).

[6] L. Michaelis, S. Granick and M. P. Schubert, *J. Amer. Chem. Soc.*, **63**, 351 (1941).

[7] J.-P. Billon, *Bull. Soc. chim. France*, **1960**, 1784.

[8] J.-P. Billon, *Bull. Soc. chim. France*, **1961**, 1923.

[9] G. Lagercrantz, *Acta. Chem. Scand.*, **15**, 1545 (1961).

[10] J.-P. Billon, *Ann. Chim. (France)*, **7**, 183 (1962).

[11] D. Gagnaire, H. Lemaire, A. Rassat and P. Servoz-Gavin, *Compt. rend.*, **255**, 1441 (1962)

[12] L. D. Tuck and D. W. Schieser, *J. Phys. Chem.*, **66**, 937 (1962).

[13] C. Bodea and I. Silberg, *Rev. Roumaine Chim.*, **9**, 9 (1964).

[14] J.-P. Billon, G. Cauquis and J. Combrisson, *J. Chim. phys.*, **3**, 374 (1964).

[15] C. Bodea and I. Silberg, *Rev. Roumaine Chim.*, **10**, 9 (1965).

[16] H. J. Shine and E. E. Mach, *J. Org. Chem.*, **30**, 2130 (1965).

[17] H. J. Shine, C. Veneziani and E. E. Mach, *J. Org Chem.*, **31**, 3395 (1966).

[18] S. Odiot and F. Tonnard, *J. Chim. phys.*, **3**, 382 (1964).

[19] J.-M. Lhoste and F. Tonnard, *J. Chim. phys.*, **5**, 678 (1966).

[20] C. Jackson and N. K. D. Patel, *Tetrahedron Letters*, **24**, 2255 (1967).

[21] W. Kemula and M. K. Kalinowski, *Z. analyt. Chem.*, **224**, 383 (1967).

[22] J. Meunier and F. Leterrier, *Compt. rend.*, **265**, 1034 (1967).

chloric acid. The authors assign this signal to the interaction of the odd electron with the nitrogen nucleus and the proton in position 10 of the cation radical III.

Taking into account the analytical data obtained and the ESR spectrum, one could express the monoelectronic reduction process of phenothiazone-(3) (I) by sodium thiosulphate in a diluted acetic acid medium by the following succession of reactions.

$$2H_2S_2O_3 = H_2S_4O_6 + 2H^+ + 2e \qquad (2)$$

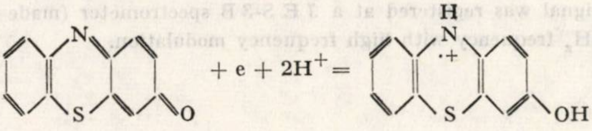

(3)

I III

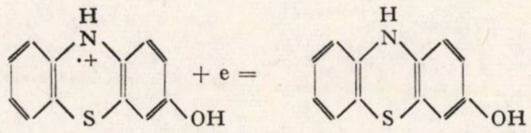

(4)

III II

Adding together equations (2), (3) and (4) one obtains the global equation (5).

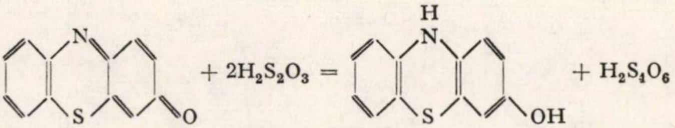

(5)

I II

The stability and the features of the radical cations obtained by monoelectronic reduction of the phenothiazone (3) (I) with sodium thiosulphate in an aqueous acetic acid medium and in other media are the objects of a separate paper.

By comparing the two dosage methods of sodium thiosulphate by iodine and by phenothiazone-(3) (I) one notices that the dosage method with phenothiazone-(3) (I) presents certain advantages.

Thus phenothiazone-(3) (I), being a titrimetric substance makes it possible to obtain an immediate solution with a known titre by simple weighing and quantitative solving in glacial acetic acid. The titre of the fresh acetic phenothiazone-(3) (I) solution does not vary even after 90 days (a checking period) unlike the iodine solutions, the titre of which is stabilized in time.

The phenothiazone-(3) (I) is an autoindicator and for this reason does not need any other indicator in the dosage reaction of thiosulphate, such as starch in the iodometric method.

ACKNOWLEDGEMENT

The authors express their thanks to A. Caragheorgheopol and H. Căldăraru of the Center of Physical Chemistry of the Academy for technical assistance, especially for carrying out the ESR spectrum.

The ESR signal was registered at a J E S-3 B spectrometer (made by J E O L) working on a 9500 MH_z frequency with high frequency modulation.

Revue Roumaine de Chimie, **14**, 893–901 (1969)

ÜBER HEXAZYANOFERRAT UND NITROSOPENTAZYANOFERRAT DES 3-CHLOR-9-(4′-DIÄTHYLAMINO-1′-METHYLBUTYLAMINO)-7-METHOXYAKRIDINS

I. FLOREA

aus dem Laboratorium für allgemeine Chemie der Technischen Hochschule,
Timişoara, str. Remus, 14

Eingegangen am 12. August 1968

Es wurde auf konduktometrischem Wege die Reaktion zwischen Trikaliumhexazyanoferrat, Dinatriumnitrosopentazyanoferrat und 3-Chlor-9-(4′-diäthylamino-1′-methylbutylamino)-7-methoxyakridin-dichlorhydrat verfolgt. Die während der konduktometrischen Titrationen gebildeten Substanzen wurden abgetrennt, analysiert und thermogravimetrisch sowie spektrophotometrisch untersucht. Die konduktometrischen Untersuchungen der Reaktion zwischen 3-Chlor-9-(4′-diäthylamino-1′-methylbutylamino)-7-methoxyakridindichlorhydrat, abgekürzt bezeichnet mit AtH_2Cl_2, ergaben, daß das Ion $[Fe(CN)_6]^{3-}$ auf diesem Wege bestimmt werden kann.

In Fortsetzung unserer Arbeiten über Komplexverbindungen des Akridins und 2-Äthoxy-6,9-diaminoakridin-laktats (Rivanol) mit verschiedenen Anionen, zwecks ihrer analytischen Verwendung, haben wir ein anderes Derivat des Akridins, 3-Chlor-9-(4′-diäthylamino-1′-methylbutylamino)-7-methoxyakridin untersucht. Diese Substanz, deren Chlorhydrat von Mietzsch und Mauss[1] erhalten wurde, wird in der Pharmazie unter der Bezeichnung Atebrin verwendet. 3-Chlor-9-(4′-diäthylamino-1′-methylbutylamino)-7-methoxyakridin-dichlorhydrat hat die Bruttoformel $C_{23}H_{30}ON_3Cl.2HCl.2H_2O$ und die Molekularmasse 508,9.

Wir haben uns die Aufgaben gestellt, zu untersuchen, ob 3-Chlor-9-(4′-diäthylamino-1′-methylbutylamino)-7-methoxyakridin ähnlich Akridin und 2-Äthoxy-6,9-diaminoakridin-laktat komplexe Verbindungen mit verschiedenen Anionen bildet und ob deren Eigenschaften sie als geeignet für analytische Bestimmungen erscheinen lassen.[2–11]

---

[1] E. G. F. Mietzsch und H. Mauss, D.R.P. 553072, 571449; *Z. anorg. Chem.*, **47**, 633 (1934).

[2] C. Drăgulescu und I. Florea, *Studii şi Cercetări Şti., Chim. Baza Cercetări Şti., Timişoara*, **4**, 9 (1957).

[3] C. Drăgulescu und I. Florea, *Studii şi Cercetări Şti., Chim. Baza Cercetări Şti., Timişoara*, **6**, 43 (1959).

[4] C. Drăgulescu und I. Florea, *Studii şi Cercetări Şti., Chim. Baza Cercetări Şti., Timişoara*, **8**, 123 (1961).

In der vorliegenden Arbeit beschäftigen wir uns mit den Reaktionen, welche zwischen Trikaliumhexazyanoferrat, Dinatriumnitrosopentazyanoferrat und 3-Chlor-9-(4′-diäthylamino-1′-methylbutylamino)-7-methoxyakridin-dichlorhydrat, abgekürzt bezeichnet mit AtH_2Cl_2, stattfinden. Die Anionen $[Fe(CN)_6]^{3-}$ und $[Fe(CN)_5NO]^{2-}$ bilden mit AtH_2Cl_2 Verbindungen von brauner bzw. braungrüner Farbe.

Zur Untersuchung der chemischen Verbindungen, welche sich beim Vermischen der oben erwähnten Lösungen bilden, wurde die konduktometrische Methode verwendet, indem die Lösungen von Trikaliumhexazyanoferrat und Dinatriumnitrosopentazyanoferrat mit Lösungen von 3-Chlor-9-(4′-diäthylamino-1′-methylbutylamino) - 7 - methoxyakridindichlorat titriert wurden.

Zur Titration wurden 4.10−2 M Lösungen von $K_3[Fe(CN)_6]$, $Na_2[Fe(CN)_5NO]$ und AtH_2Cl_2 verwendet. Ihre Konzentrationen wurden durch genaues Wägen festgesetzt.

Zur Präparierung der Lösungen wurden $K_3[Fe(CN)_6]$ Merck *p.a.*, $Na_2[Fe(CN)_5NO]$, dessen Titer mit Hilfe der Methode von Rose[12] bestimmt wurde, und umkristallisiertes, chemisch reines AtH_2Cl_2 verwendet.

1. KONDUKTOMETRISCHE TITRATIONEN

Die Ergebnisse der konduktometrischen Titrationen sind in Abbildung 1 dargestellt.

Die Versuchsergebnisse zeigen, daß bei den konduktometrischen Titrationen von $K_3[Fe(CN)_6]$ und $Na_2[Fe(CN)_5NO]$ mit AtH_2Cl_2 bis zum Äquivalenzpunkt, die in den Diagrammen 1 und 3 der Abb. 1 dargestellt wurden, eine Zunahme der Leitfähigkeit der Lösung dadurch stattfindet, daß die Anionen $[Fe(CN)_6]^{3-}$ und $[Fe(CN)_5NO]^{2-}$ mit Cl^--Anionen ersetzt werden. $\{1/3\ {}^{\lambda}[Fe(CN)_6]^{3-} < {}^{\lambda}Cl^-$ und $1/2\ {}^{\lambda}\ [Fe(CN)_5NO]^{2-} < {}^{\lambda}Cl^-\}$. Nach dem Äquivalenzpunkt nimmt die Leitfähigkeit der Lösung infolge des hinzugefügten Reagensüberschusses zu.

Die Diagramme 2 und 4 der Abb. 1 stellen die mit $K_3[Fe(CN)_6]$ und $Na_2[Fe(CN)_5NO]$ titrierten AtH_2Cl_2-Lösungen dar. Bis zum Äquivalenzpunkt findet eine Zunahme der Leitfähigkeit der Lösung dadurch statt, daß die Kationen AtH_2^{2+} durch die Kationen K^+ und Na^+ ersetzt werden. $[1/2\ {}^{\lambda}AtH_2^{2+} < {}^{\lambda}K^+$ und $1/2\ {}^{\lambda}AtH_2^{2+} < {}^{\lambda}Na^+]$. Nach dem Äquivalenzpunkt nimmt die Leitfähigkeit infolge des hinzugefügten Reagensüberschusses zu.

[5] C. DRĂGULESCU und I. FLOREA, *Studii şi Cercetări Şti., Chim. Baza Cercetări Şti., Timişoara*, **9**, 205 (1962).

[6] C. DRĂGULESCU und I. FLOREA, *Studii şi Cercetări Şti., Chim. Baza Cercetări, Şti., Timişoara*, **9**, 219 (1962).

[7] C. DRĂGULESCU und I. FLOREA, *Studii şi Cercetări Şti., Chim. Baza Cercetări Şti., Timişoara*, **9**, 227 (1962).

[8] C. DRĂGULESCU und I. FLOREA, *Studii şi Cercetări Şti., Chim. Baza Cercetări Şti., Timişoara*, **9**, 247 (1962).

[9] C. DRĂGULESCU und I. FLOREA, *Studii şi Cercetări Şti., Chim. Baza Cercetări Şti., Timişoara*, **10**, 31 (1963).

[10] I. FLOREA, *Bul. Şti. Tehn., I.P.T.*, **10**, 51 (1965).

[11] I. FLOREA, *Bul. Şti. Tehn., I.P.T.*, **12**, 43 (1967).

[12] P. ROSE, *Z. analyt. Chem.*, **143**, 195 (1954).

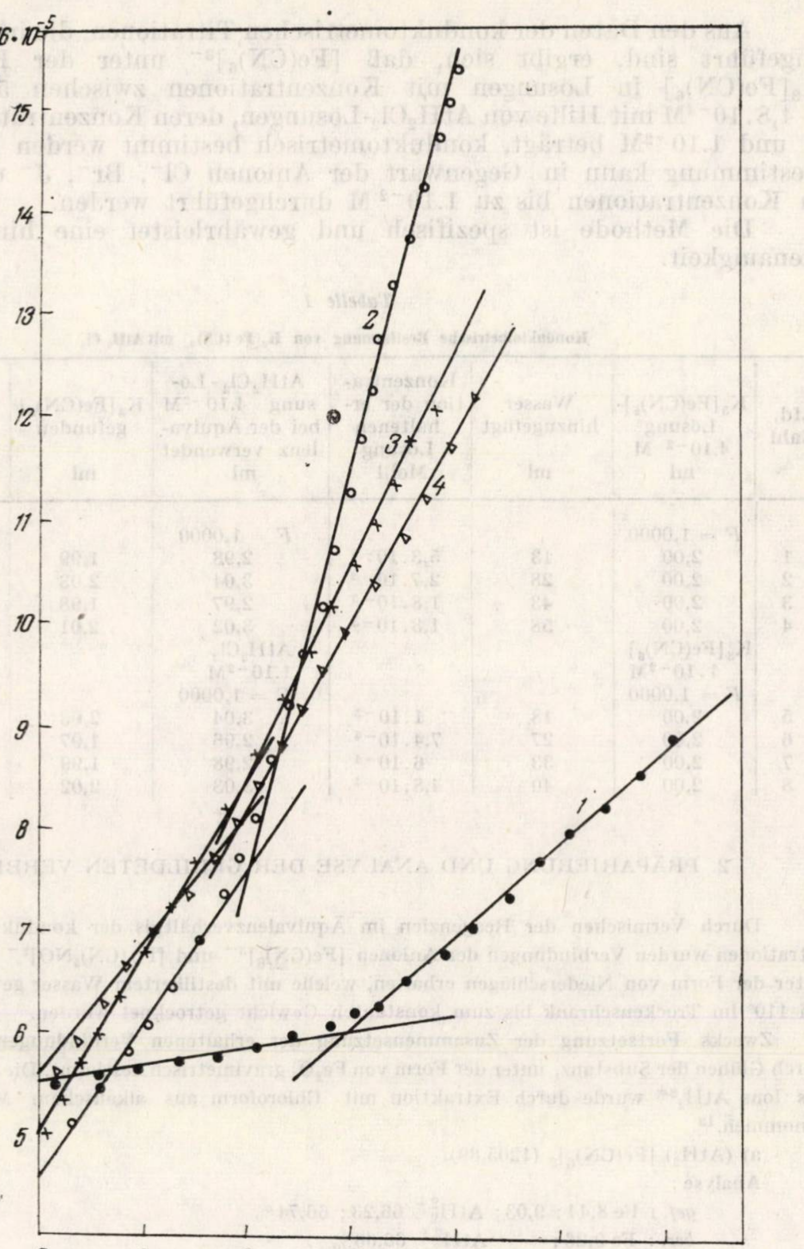

Abb. 1. — *1*, 2 ml $K_3[Fe(CN)_6]$ 0,01 M + 38 ml Wasser + AtH_2Cl_2 0,01 M;
2, 3 ml AtH_2Cl_2 0,01 M + 27 ml Wasser + $K_3[Fe(CN)_6]$ 0,01 M;
3, 2 ml $Na_2[Fe(CN)_5NO]$ + 18 ml Wasser + AtH_2Cl_2 0,01 M;
4, 2 ml AtH_2Cl_2 0,01 M + 18 ml Wasser + $Na_2[Fe(CN)_5NO]$ 0,01 M.

Aus den Daten der konduktometrischen Titrationen, die in Tabelle 1 angeführt sind, ergibt sich, daß $[Fe(CN)_6]^{3-}$ unter der Form von $K_3[Fe(CN)_6]$ in Lösungen mit Konzentrationen zwischen $5{,}3.10^{-3}$—$4{,}8.10^{-4}$M mit Hilfe von AtH_2Cl_2-Lösungen, deren Konzentration 4.10^{-2} M und 1.10^{-2}M beträgt, konduktometrisch bestimmt werden kann. Die Bestimmung kann in Gegenwart der Anionen Cl^-, Br^-, J^- und SCN^- in Konzentrationen bis zu 1.10^{-2} M durchgeführt werden.

Die Methode ist spezifisch und gewährleistet eine hinreichende Genauigkeit.

Tabelle 1

Konduktometrische Bestimmung von $K_3[Fe(CN)_6]$ mit AtH_2Cl_2

Lfd. Zahl	$K_3[Fe(CN)_6]$-Lösung 4.10^{-2} M ml	Wasser hinzugefügt ml	Konzentration der erhaltenen Lösung Mol/l	AtH_2Cl_2-Lösung 4.10^{-2}M bei der Äquivalenz verwendet ml	$K_3[Fe(CN)_6]$ gefunden ml	E %
	$F = 1{,}0000$			$F = 1{,}0000$		
1	2,00	13	$5{,}3.10^{-3}$	2,98	1,99	−0,50
2	2,00	28	$2{,}7.10^{-3}$	3,04	2,03	+1,50
3	2,00	43	$1{,}8.10^{-3}$	2,97	1,98	−1,00
4	2,00	58	$1{,}3.10^{-3}$	3,02	2,01	+0,50
	$K_3[Fe(CN)_6]$ 1.10^{-2}M $F = 1{,}0000$			AtH_2Cl_2 1.10^{-2}M $F = 1{,}0000$		
5	2,00	18	1.10^{-3}	3,04	2,03	+1,50
6	2,00	27	$7{,}4.10^{-4}$	2,96	1,97	−1,50
7	2,00	33	6.10^{-4}	2,98	1,99	−0,50
8	2,00	40	$4{,}8.10^{-4}$	3,03	2,02	+1,00

2. PRÄPARIERUNG UND ANALYSE DER GEBILDETEN VERBINDUNGEN

Durch Vermischen der Reagenzien im Äquivalenzverhältnis der konduktometrischen Titrationen wurden Verbindungen der Anionen $[Fe(CN)_6]^{3-}$ und $[Fe(CN)_5NO]^{2-}$ mit AtH_2Cl_2 unter der Form von Niederschlägen erhalten, welche mit destilliertem Wasser gewaschen und bei 110° im Trockenschrank bis zum konstanten Gewicht getrocknet wurden.

Zwecks Fortsetzung der Zusammensetzung der erhaltenen Verbindungen wurde Fe, durch Glühen der Substanz, unter der Form von Fe_2O_3 gravimetrisch bestimmt. Die Bestimmung des Ions $AtH_2{}^{2+}$ wurde durch Extraktion mit Chloroform aus alkalischem Medium vorgenommen.[13]

a) $(AtH_2)_3[Fe(CN)_6]_2$ (1205,89).

Analyse :

gef. : Fe 8,44 ; 9,03 ; AtH_2^{2+} 66,23 ; 66,74 %

ber. : Fe 9,26 ; AtH_2^{2+} 66,66 %

b) $AtH_2[Fe(CN)_5NO]$ (617,90).

Analyse :

gef. : Fe 8,39 ; 8,91 ; AtH_2^{2+} 64,49 ; 64,83 %

ber. : Fe 9,04 ; AtH_2^{2+} 65,04 %

---

[13] P. LEBEAU und M. M. JANOT „Traité de Pharmacie Chimique", 4. Bd., Masson et Cie, Paris, 1955/56, S. 2636—37.

3. THERMOGRAVIMETRISCHES VERHALTEN

Zur thermogravimetrischen Untersuchung des Hexazyanoferrats und Nitrosopentazyanoferrats von 3-Chlor-9-(4′-diäthylamino-1′-methylbutylamino)-7-methoxyakridin wurde eine Thermowaage verwendet, wobei die Temperatur im Bereiche 30—750° gemessen wurde. Die Erwärmung wurde mit einer Geschwindigkeit von 10°/min vorgenommen. Die erhaltenen Ergebnisse sind in Abbildung 2 dargestellt.

Die Diagramme 1 und 2 der Abb. 2 stellen die Thermogramme folgender Substanzen dar: $C_{23}H_{30}ON_3Cl.2HCl.2H_2O$, ($ATH_2Cl_2$) und $Na_2[Fe(CN)_5NO].2H_2O$; die Substanzen sind bis zu 100° bzw. 160° stabil. AtH_2Cl_2 verliert zwischen 100 — 150° 7,14% seines Gewichtes, $Na_2[Fe(CN)_5NO]$ dagegen 11,95%, was dem Kristallwasser entspricht (2Mol, 7,08% bzw. 12,09%). Bei höheren Temperaturen findet Zersetzung der Substanzen statt, welche bei 650° und 700° beendet ist. Der bei der Zersetzung von $Na_2[Fe(CN)_5NO]$ erhaltene Rückstand besteht aus $Na_2O + Fe_2O_3$.

Die Diagramme 3 und 4 der Abb. 2 stellen die Thermogramme folgender Substanzen dar: $AtH_2[Fe(CN)_5NO]$ und $(AtH_2)_3[Fe(CN)_6]_2$. Die Substanzen sind bis zu 200° bzw. 210° stabil. Bei höheren Temperaturen findet Zersetzung der Substanzen statt, welche bei 700° beendet ist. Der erhaltene Rückstand besteht aus Fe_2O_3.

4. SPEKTROPHOTOMETRISCHE UNTERSUCHUNGEN

Die Untersuchungen wurden mit einem Spektrophotometer UNICAM SP 800 im Bereiche 500—225 nm durchgeführt. Die erhaltenen Ergebnisse sind in den Abbildungen 3 und 4 und in Tabelle 2 aufgezeigt.

In den Diagrammen ist auf der Abszisse die Wellenlänge in nm und auf der Ordinate die Extinktion dargestellt. Für das in den Diagrammen erhaltene λ_{max} wurde $\log \varepsilon_{max}$ berechnet (Tabelle 2).

Die Diagramme 1 und 1′ der Abb. 3 stellen die Absorptionsspektren einer Lösung von $K_3[Fe(CN)_6]$ mit einer Konzentration von 1.10^{-3} M in einer 1 cm bzw. 0,2 cm Küvette dar (λ_{max} Tabelle 2).

Die Diagramme 2 und 2′ der Abb. 3, sowie 2 und 2′ der Abb. 4 stellen die Absorptionsspektren von AtH_2Cl_2-Lösungen mit der Konzentration 1.10^{-4}M bzw. 5.10^{-5}M in Küvetten von 1 cm dar (λ_{max} Tabelle 2).

Die Diagramme 3 und 3′ der Abb. 3 stellen die Absorptionsspektren alkoholischer Lösungen 1 :1 von $(AtH_2)_3[Fe(CN)_6]_2$ mit der Konzentration 1.10^{-4}M bzw. 5.10^{-5}M in Küvetten von 1 m dar (λ_{max} Tabelle 2).

Das Diagramm 1 der Abb. 4 stellt das Absorptionsspektrum einer alkoholischen Lösung 1 : 2 von $Na_2[Fe(CN)_5NO]$ mit der Konzentration 1.10^{-3}M in Küvetten von 1 cm dar (λ_{max} Tabelle 2).

Die Diagramme 3 und 3′ der Abb. 4 stellen die Absorptionsspektren alkoholischer Lösungen 1 : 1 von $AtH_2[Fe(CN)_5NO]$ mit der Konzentration 1.10^{-4}M bzw. 5.10^{-5}M in Küvetten von 1 cm dar (λ_{max} Tabelle 2).

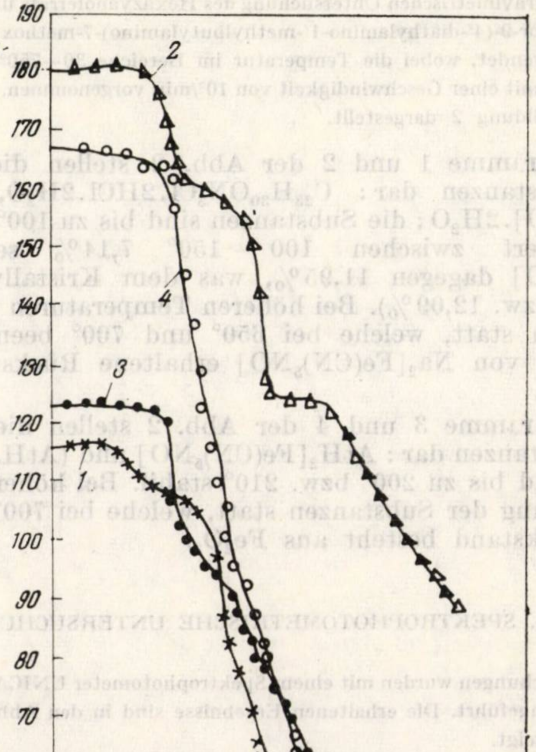

Abb. 2. — *1*, Thermolyse von $C_{23}H_{30}ON_3Cl.2HCl.2H_2O$, (AtH_2Cl_2) ;
2, Thermolyse von $Na_2[Fe(CN)_5NO].2H_2O$;
3, Thermolyse von $AtH_2[Fe(CN)_5NO]$;
4, Thermolyse von $(AtH_2)_3[Fe(CN)_6]_2$.

Zunächst wurden die Absorptionsspektren folgender Substanzen untersucht: $K_3[Fe(CN)_6]$,[14–15] $Na_2[Fe(CN)_5NO]$[16] und 3-Chlor-9-(4′-diäthylamino-1′-methylbutylamino)-7-methoxyakridin-dichlorhydrat[17–19];

Tabelle 2

Wellenlänge λ_{max} in nm und log ε_{max} der Verbindungen K_3 [Fe(CN)$_6$], AtH_2 Cl_2, $(AtH_2)_3$ [Fe(CN)$_6$]$_2$, Na_2 [Fe(CN)$_5$NO) und AtH_2 [Fe(CN)$_5$NO]

Substanz Nr.	Verbindung	λ_{max}, nm in Wasser	log ε_{max}
1	Trikaliumhexazyanoferrat	420	3,00
		321	3,09
		303	3,22
		261	3,08
		211	3,47[c]
2	3-Chlor-9-(4′-diäthylamino-1′-methylbutylamino)-7-methoxyakridin-dichlorhydrat	447	3,84
		426	3,91
		358	3,24
		344	3,59
		328	3,41
		281	5,61[d]
		269	5,74[d]
		226	5,39[d]
3	3-Chlor-9-(4′-diäthylamino-1′-methylbutylamino)-7-methoxyakridin-hexazyanoferrat[a]	447	4,07
		426	4,13
		344	3,83
		328	3,73
		281	5,90[d]
		269	5,95[d]
		226	5,68[d]
4	Dinatriumnitrosopentazyanoferrat[b]	267	2,92
		228	3,15
	3-Chlor-9-(4′-diäthylamino-1′-methylbutylamino)-7-methoxyakridin-nitrosopentazyanoferrat[a]	447	3,89
		426	3,94
		344	3,65
		328	3,50
		281	5,62[d]
		269	5,76[d]
		226	5,45[d]

[a] Alkoholische Lösungen 1 : 1

[b] Alkoholische Lösungen 1 : 2

[c] Küvette von 0,2 cm

[d] Konzentration der Lösung 5.10^{-5}M

---

[14] J. Deveze, *Compt. rend.*, **226**B (17), 1137 (1966); *Chem. Abstr.*, **65**, 9948 g (1966).

[15] R. W. Parson und H. G. Drickamer, *J. Chem. Phys.*, **29**, 930 (1958); *Chem. Zentr.*, **1959**, 6364.

[16] P. T. Manoharan und H. B. Gray, *J. Amer. Chem. Soc.*, **87 (15)**, 3340 (1965); *Chem. Abstr.*, **63**, 7763e(1965).

[17] L. W. Smirnov, *Zhur. eksp. teor. Fiz.*, **23**, 68 (1952); *Chem. Zentr.*, **1953**, 2731.

[18] G. M. Kislyak und G. M. Lisenko, *Fiz. Probl. Spektroskopii, Akad. Nauk SSSR*, **1**, 336 (1960); *Chem. Abstr.*, **59**, 12318b(1963).

[19] A. K. Sukhomlinov, *Trudy Kharkovsk. Farmatsvet. Inst.*, **2**, 69 (1962); *Chem. Abstr.*, **61**, 2938 (1964).

diese Spektren sind auch im Fachschrifttum angegeben. Danach wurden die Spektren der neuerhaltenen Verbindungen untersucht.

In den synthetisierten Verbindungen $(AtH_2)_3[Fe(CN)_6]_2$ und $AtH_2[Fe(CN)_5NO]$, die in den Diagrammen der Abbildungen 3 und 4

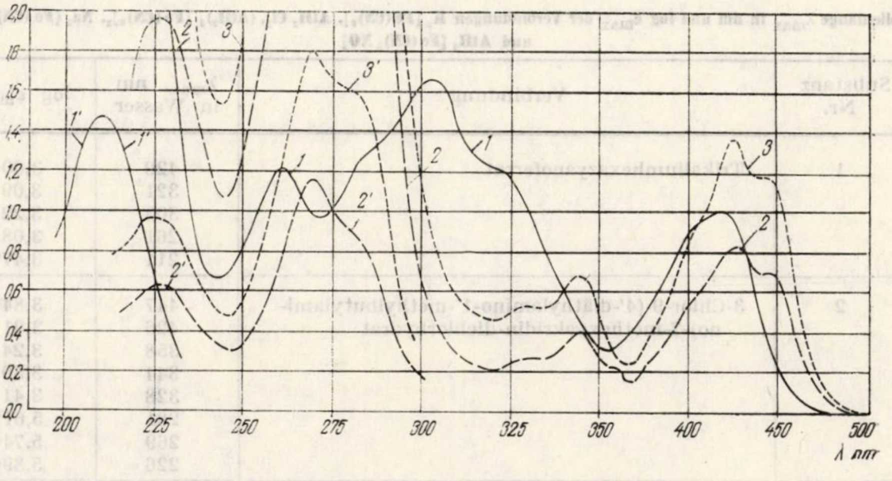

Abb. 3. — Absorptionsspektren der Lösungen von: $K_3[Fe(CN)_6]$ (*1* und *1'*), AtH_2Cl_2 (*2* und *2'*) und $(AtH_2)_3[Fe(CN)_6]_2$(*3* und *3'*).

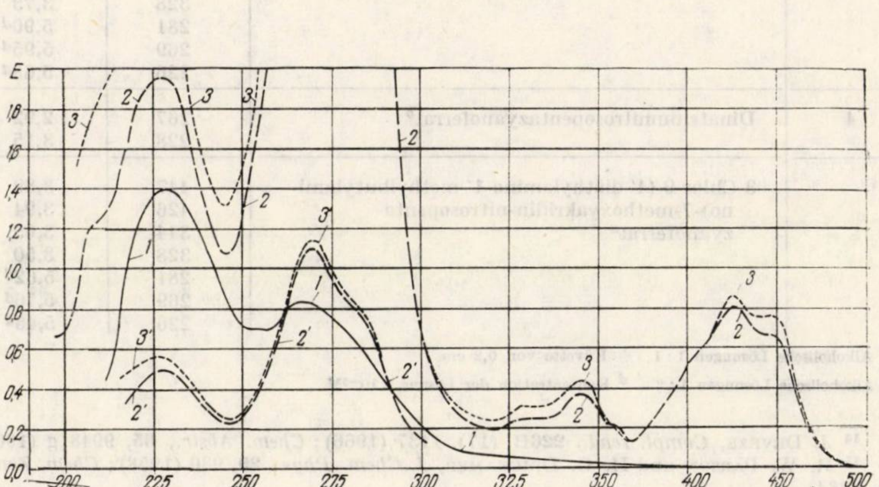

Abb. 4. — Absorptionsspektren der Lösungen von: $Na_2[Fe(CN)_5NO]$ (*1*), AtH_2Cl_2 (*2* und *2'*) und $AtH_2[Fe(CN)_5NO]$ (*3* und *3'*).

dargestellt sind, wird das Vorhandensein der Ionen AtH_2^{2+}, $[Fe(CN)_6]^{3-}$ und $[Fe(CN)_5NO]^{2-}$ festgestellt, was gleichzeitig eine Bestätigung für ihre Struktur ist.

5. SCHLUSSFOLGERUNGEN

Durch Behandeln von Trikaliumhexazyanoferrat und Dinatriumnitrosopentazyanoferrat mit 3-Chlor-9-(4'-diäthylamino-1'-methylbutylamino)-7-methoxyakridin-dichlorhydrat werden Niederschläge von brauner bzw. braungrüner Farbe gebildet. Durch konduktometrische Untersuchungen der Reaktion zwischen $K_3[Fe(CN)_6]$ und AtH_2Cl_2 wird festgestellt, daß das Anion $[Fe(CN)_6]^{3-}$ auf diesem Wege in Lösungen mit einer Konzentration von $5,3.10^{-3}-4,8.10^{-4}M$ bestimmt werden kann. Die Bestimmung kann in Gegenwart der Anionen Cl^-, Br^-, J^- und SCN^- durchgeführt werden. CN^- und $[Fe(CN)_6]^{4-}$ stören die Bestimmung.

Die während der konduktometrischen Titration gebildeten Substanzen wurden abgetrennt, analysiert, thermogravimetrisch und spektophotometrisch untersucht. Auf Grund der erhaltenen Ergebnisse wurden ihnen folgende chemische Formeln zugeschrieben: $(AtH_2)_3[Fe(CN)_6]_2$ und $AtH_2[Fe(CN)_5NO]$.

Revue Roumaine de Chimie, 14, 903–910 (1969)

ÉTUDE DES CATALYSEURS SOLIDES POUR L'OXYDATION DES HYDROCARBURES. II*

INFLUENCE DU MILIEU DE RÉACTION SUR LES PROPRIÉTÉS ÉLECTRIQUES DU CATALYSEUR V_2O_5—MoO_3

ANTOANETA SPINZI et I. V. NICOLESCU

Centre de Recherches de Chimie Physique de l'Académie, Bucarest, 23 str. Dumbrava Roşie

Reçu le 6 juillet 1968

Les auteurs étudient le comportement électrique du système catalytique V_2O_5—MoO_3 à différents rapports des composants (1 : 0,1 moles, 1 : 0,33 moles, 1 : 1 moles), dans différents milieux : air, hydrogène et mélange de butène-air (2 % vol), à 400°. Les résultats sont présentés comparativement à ceux du V_2O_5 pur, étant interprétés comme variations de la concentration des défauts du réseau, induits par l'adjonction de MoO_3. On obtient des corrélations bien satisfaisantes entre log σ et E_σ qui mettent en évidence la composition exprimée par le rapport 1 : 0,33 moles, en confirmant ainsi les données d'activité signalées dans des travaux antérieurs.

Les catalyseurs simples ou mixtes à base de V_2O_5 ont un rôle particulier dans les processus d'oxydation des hydrocarbures. Leur spécificité est en grande mesure influencée par la nature et la concentration des défauts du réseau. Le système catalytique V_2O_5—MoO_3 est beaucoup utilisé à l'obtention de l'anhydride maléique à partir du benzène, des butènes et du butadiène.[1-3] Bien que de nombreuses études portant sur la structure, la composition stationnaire et de phase, ainsi que sur le composant actif de ces catalyseurs aient déjà été publiés,[4-11] le choix des catalyseurs ou bien l'amélioration de leur sélectivité restent néanmoins difficilement explicables.

---

[*] Ire Partie, I. V. Nicolescu et A. Suceveanu, *Rev. Roumaine Chim.*, **11**, 123 (1966).

[1] S. K. Bhattacharyya et I. B. Gulati, *Ind. eng. Chem.*, **50**, 12, 1719 (1958).

[2] I. I. Ioffe et A. G. Liubarski, *Kinetika i Kataliz*, **2**, 261 (1962).

[3] M. Blanchard et Jean-Claude Delgrange, *Compt. rend.*, **262**, 1231 (1966).

[4] A. Magnelli et B. Oughton, *Acta Chem. Scand.*, **5**, 581 (1955).

[5] A. Magnelli et B. Blomberg, *Acta Chem. Scand.*, **5**, 585 (1955).

[6] I. I. Ioffe, Z. I. Ejkova et A. G. Liubarski, *Zhur. fiz. Khim.*, **35**, 2348 (1961).

[7] V. B. Kazanski, Z. I. Ejkova, A. G. Liubarski, V. V. Voevodski et I. I. Ioffe, *Kinetika i Kataliz*, **6**, 862 (1961).

[8] I. I. Ioffe, Z. I. Ejkova et A. G. Liubarski, *Kinetika i Kataliz*, **2**, 194 (1962).

[9] R. H. Munch et E. D. Pierron, *J. Catalysis*, **3**, 406 (1964).

[10] K. Tarama, S. Teranishi, S. Yoshida et N. Tamura, Proceedings of the 3-th International Congress on Catalysis, Amsterdam, 1964.

[11] B. E. Zaitzev, Z. I. Ejkova et I. I. Ioffe, *Kinetika i Kataliz*, **4**, 755 (1966).

Les recherches sur les propriétés électriques de ces systèmes catalytiques [12-15] — semi-conducteurs électroniques — permettent à établir dans certains cas, des corrélations entre ces propriétés et l'activité dans la réaction d'oxydation. Par suite, nous avons essayé d'étendre la méthode de la conductivité électrique à la recherche du catalyseur $V_2O_5-MoO_3$ par rapport au milieu d'adsorption et de réaction. Nous sommes d'avis que tout nouvel renseignement dans ce problème contribue au développement de la théorie concernant les critères du choix des catalyseurs.

Dans ce but, nous avons utilisé trois compositions du système binaire $V_2O_5-MoO_3$ différentes, à un rapport des composants de 1 : 0,1 moles (9,1% moles MoO_3), 1 : 0,33 moles (24,8% moles MoO_3) et 1 : 1 moles (50% moles MoO_3), comparativement au V_2O_5 pur. Les travaux effectués aux rayons X, IR ou REP [6,7,9-12] ont démontré que, jusqu'à ~25% moles MoO_3, ces mélanges correspondent à une solution solide de substitution, entre ~25 — 50% moles MoO_3 à une composition biphasique déterminée par une solution solide de substitution et une combinaison chimique intermédiaire, tandis que pour 50% moles MoO_3, exclusivement à une combinaison chimique intermédiaire. De même, les tests d'activité ont indiqué une concentration d'environ 25% moles MoO_3 comme optimale pour l'obtention de l'anhydride maléique à partir du benzène[6,12] et des butènes.[3] De nombreuses études considèrent que l'activité catalytique est assurée par l'existence d'un équilibre de réseau entre V^{5+}, V^{4+} et O^{2-}, l'oxyde de molybdène ayant le rôle de promouvoir la formation des centres donneurs actifs, les ions V^{4+}.

Par la méthode employée, nous avons essayé de voir dans quelle mesure reflète la conductivité électrique les considérations ci-dessus. Dans ce but, on a choisi comme réaction test l'oxydation des *n*-butènes, effectuée à 400°, à une concentration de 2% vol butènes dans un milieu d'air. On a déterminé la conductivité électrique par rapport à la température et au temps, au-dessus du point de stabilisation du catalyseur.

PARTIE EXPÉRIMENTALE

On a préparé le V_2O_5 par décomposition du métavanadate d'ammonium *p.a.*, 2h à 350° et 4h à 500°. Les mélanges de $V_2O_5-MoO_3$ ont été obtenus par imprégnation du V_2O_5 préparé ci-dessus d'une solution de molybdate d'ammonium, suivie d'essorage à 110°, décomposition à 350°—2 h et calcination à 500°—6 h. Après broyage et tamisage par un tamis à 4000 mailles/cm², on a pastillé à pression constante les poudres obtenues.

L'appareil, ainsi que la méthode de déterminer la conductivité électrique ont été décrits dans la Ire partie de ce travail. L'installation comprend de plus le circuit du gaz réactif (séchoirs, débitmètres, chambre de mélange).

Les échantillons ont été préalablement stabilisés, en effectuant un cycle de chauffage (500°) — refroidissement (20°), sous courant d'air.

[12] Z. I. Ejkova, I. I. Ioffe, V. B. Kazanski, A. V. Krjlov, A. G. Liubarski et L. I. Margolis, *Kinetika i Kataliz*, **5**, 861 (1964).

[13] L. I. Margolis, A. V. Krjlov et E. S. Alexandrova, *Kinetika i Kataliz*, **8**, 69 (1966).

[14] J. D. Butter et B. G. Weston, *J. Catalysis*, **2**, 8 (1963).

[15] G. Pop, *Studii şi Cercetări Şti. Chim. Baza Cercetări Şti. Timişoara*, **8**, 138 (1961); **9**, 97 (1962).

Les mesures de la conductivité électrique ont été effectuées dans différents milieux : air, hydrogène et mélange de butène-air, par rapport à la température où bien au temps. Dans certains cas, aux traitements successifs par différents gaz, on a purifié la surface des épreuves par insufflation d'azote.

RÉSULTATS ET DISCUSSIONS

Dans les diagrammes de la figure 1 on représente la variation $\log \sigma = f(1/T)$ dans le cas de trois mélanges de $V_2O_5-MoO_3$ de différentes concentrations, par rapport au V_2O_5 pur. On met ainsi en évidence, ce que d'ailleurs était à attendre, une augmentation de la conductivité électrique du V_2O_5 par dopage au MoO_3, touchant la valeur maximale pour le rapport 1 : 0,33 moles. On confirme de cette manière l'apparition des défauts de réseau induits par l'oxyde de molybdène, dont la concentration est maximale (1 ion V^{4+} pour 1 ion Mo^{6+}) pour le rapport 1 : 0,33 moles, mais qui décroît (1 ion V^{4+} pour 5—10 ions V^{5+}) pour une proportion supérieure du MoO_3(1 : 1 moles). De même, on y remarque des inflexions dans la variation $\log \sigma$, délimitées par des températures particulières à chaque cas. Pour le V_2O_5 pur on obtient une seule inflexion à la température de 386°, tandis que pour le système binaire $V_2O_5-MoO_3$, deux inflexions.

Les diagrammes de la figure 2 représentent en coordonnées $\log \sigma = f$ (temps) un cycle réduction-oxydation, effectué à 400° sous un courant constant de gaz (hydrogène ou bien air). L'équilibre électronique est atteint en hydrogène entre 20 et 60 minutes, d'autant plus facilement que la concentration en MoO_3 diminue. Cependant, la valeur de la conductivité électrique à l'équilibre augmente dans l'ordre 1 : 1 moles $<$ 1 : 0,1 moles $<$ 1 : 0,33 moles. On y garde la même alternance au traitement à l'air (2e région des courbes).

Les isothermes mettent en évidence :

1) Une interaction irréversible catalyseur-hydrogène, étant donné le maintient des valeurs de la conductivité électrique après l'éloignement de l'hydrogène par l'azote. Le retour se produit dans une certaine mesure, uniquement par traitement dans un milieu d'air.

2) La combinaison $V_2O_5-MoO_3$ (1 : 0,33 moles) manifeste l'effet le plus prégnant, en fournissant un nombre maximal d'électrons libres, disponibles dans la réaction comme résultat de la formation des centres donneurs, les ions V^{4+}.

Pour mieux souligner la différence entre le comportement électrique des systèmes oxydiques binaires $V_2O_5-MoO_3$, par rapport au V_2O_5 pur, nous avons représenté dans la figure 3, la variation relative de la résistance électrique, calculée selon la formule

$$\frac{\Delta R}{R} = \frac{R_{V_2O_5} - R_{V_2O_5-MoO_3}}{R_{V_2O_5}}$$

Les résultats sont inscrits comme isothermes à la température de 400°, en fonction du temps et en milieu d'hydrogène.

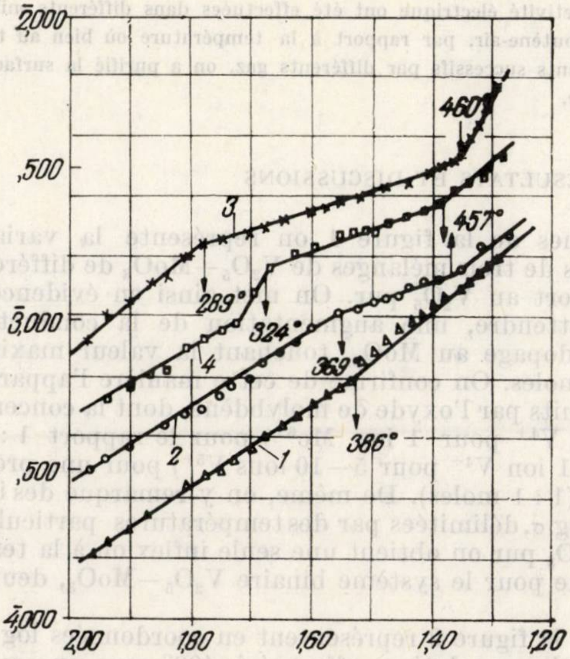

Fig. 1. — Variation de la conductivité électrique en fonction de la température et en air, du V_2O_5 et du système $V_2O_5-MnO_3$.

1, V_2O_5 ; *2*, $V_2O_5-MoO_3$ (1 : 0,1 mole) ; *3*, $V_2O_5-MoO_3$ (1 : 0,33 mole) ; *4*, $V_2O_5-MoO_3$ (1 : 1 mole).

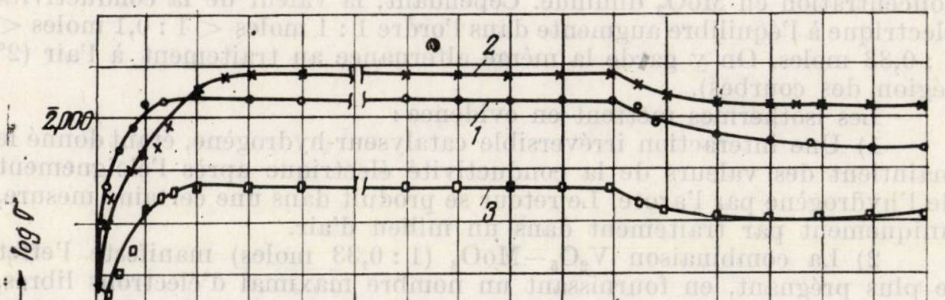

Fig. 2. — Isothermes de la conductivité électrique du système $V_2O_5-MoO_3$ en fonction du temps, dans un courant d'hydrogène et en air à 400°.

1, $V_2O_5-MoO_3$ (1 : 0,1 mole) ; *2*, $V_2O_5-MoO_3$ (1 : 0,33 mole) ; *3*, $V_2O_5-MoO_3$ (1 : 1 mole).

Les valeurs $\Delta R/R$ des mélanges binaires $V_2O_5 + MoO_3$ sont placées sous la ligne de référence du V_2O_5, l'écart augmentant dans l'ordre 1 : 0,1 moles < 1 : 0,33 moles < 1 : 1 moles. On peut donc affirmer qu'à l'adjonction de MoO_3 les échanges électroniques solide-gaz deviennent sensiblement atténués et ralentis. En considérant que dans notre cas la modification de la résistance électrique reflète, comme on l'a déjà mentionné dans la Ire partie de ce travail, le processus de réduction partiale du V_2O_5 (pur ou en mélange), il résulte qu'à cette température, l'adjonction de MoO_3 agit comme modérateur et stabilisateur, proportionnellement à sa concentration dans le système.

Les modifications de la conductivité électrique survenues pendant la réaction d'oxydation effectuée sur les catalyseurs $V_2O_5{-}MoO_3$ à 400°, par un mélange de butène-air (2% vol) ne diffèrent pas essentiellement de celles obtenues dans un courant d'hydrogène. Cependant, l'intervalle de variation est plus étroit et l'équilibre est atteint plus lentement, à peine après environ 80 mn (fig. 4). Le phénomène est également irréversible à l'éloignement du mélange gazeux réactif par insufflation d'azote ; en échange, les revenus sous l'influence de l'air sont en quelques sorte plus nettes, se rapprochant de leur valeur initiale.

Des variations semblables y sont obtenues avec un mélange de butène-air (6%).

Les résultats nous permettent de remarquer :

1) La similitude entre la variation de la conductivité électrique en milieu d'hydrogène et en mélange d'hydrocarbure-air confirme l'existence d'un processus de réduction à la surface du catalyseur, pendant l'acte catalytique.

2) Les modifications électroniques des catalyseurs augmentent dans l'ordre 1 : 1 moles < 1 : 0,1 moles < 1 : 0,33 moles. La composition définie par le rapport 1 : 0,33 moles, qui présente la modification électronique maximale, est signalée dans les travaux [3, 6, 12] comme présentant l'activité catalytique maximale.

Dans la figure 5 est inscrite la variation $\log \sigma = f(1/T)$ en mélange de butène-air (2% vol) pour le système étudié. D'après les droites obtenues, dont les inflexions correspondent à environ 316°C, on a calculé les énergies d'activation de la conductivité électrique E_σ pour le V_2O_5 pur, ainsi que pour les trois mélanges $V_2O_5{-}MoO_3$. Les valeurs obtenues pour l'intervalle de température 316—440° sont illustrées dans le tableau 1.

Tableau 1

Energie d'activation de la conductivité électrique en mélange de butène-air(2% vol)

Système	Intervalle temp. °C	Energie d'activation de la cond. électrique E_σ	
		ev	kcal/mole
V_2O_5	316—440	0,90	21
$V_2O_5{-}MoO_3$ 1 : 0,1 mole	316—440	0,74	17
$V_2O_5{-}MoO_3$ 1 : 0,33 mole	316—440	0,67	15
$V_2O_5{-}MoO_3$ 1 : 1 mole	316—440	0,86	21

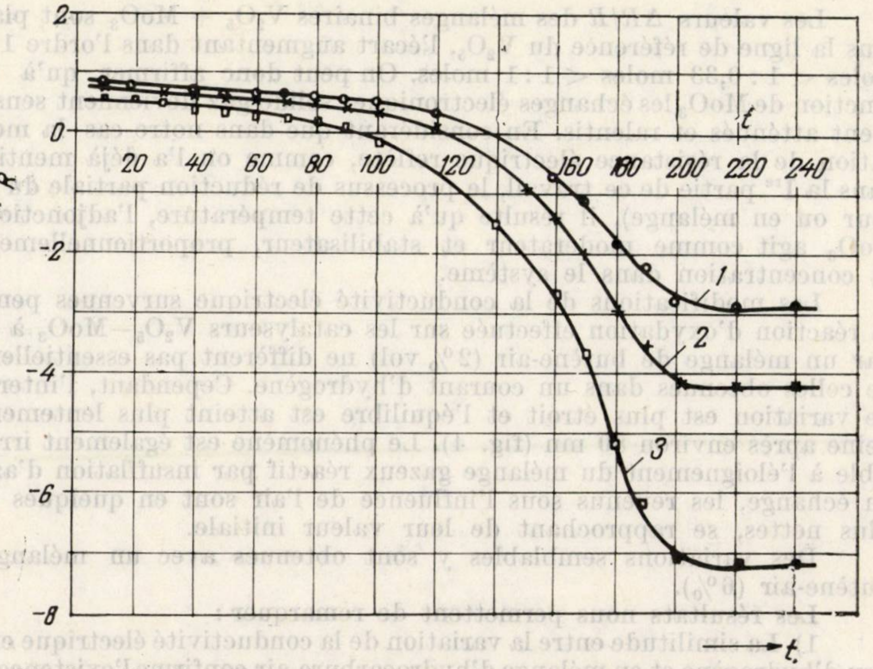

Fig. 3. — Variation relative de la résistance électrique du système $V_2O_5-MoO_3$ en fonction du temps (mn) et dans un courant d'hydrogène à 400°.
1, $V_2O_5-MoO_3$ (1 : 0,1 mole); *2*, $V_2O_5-MoO_3$ (1 : 0,33 mole); *3*, $V_2O_5-MoO_3$ (1 : 1 mole).

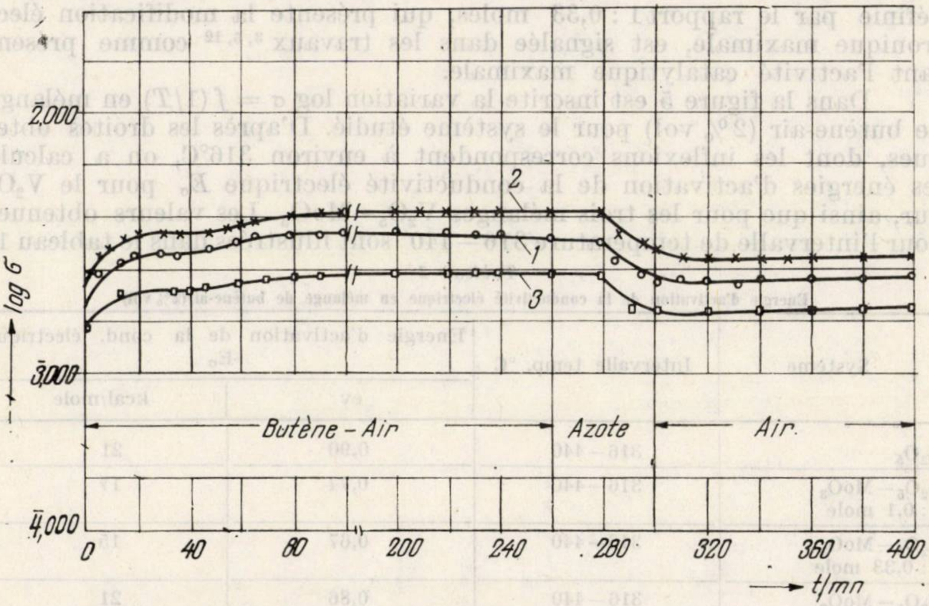

Fig. 4. — Isothermes de la conductivité électrique du système $V_2O_5-MoO_3$ en fonction du temps, dans un courant de butène-air (2 % vol) et à l'air à 400°.
1, $V_2O_5-MoO_3$ (1 : 0,1 mole); *2*, $V_2O_5-MoO_3$ (1 : 0,33 mole); *3*, $V_2O_5-MoO_3$ (1 : 1 mole).

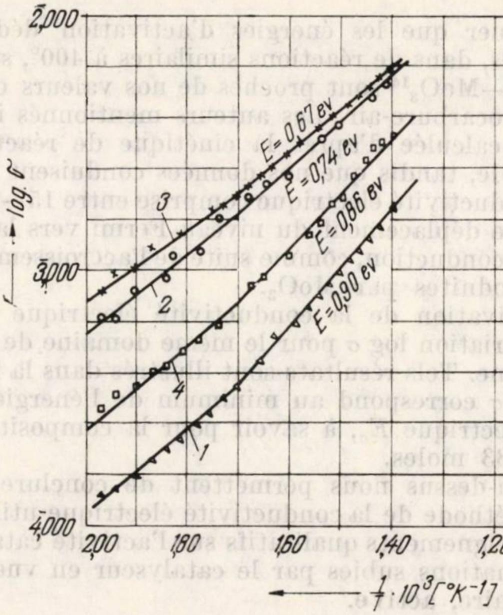

Fig. 5. — Variation de la conductivité électrique en fonction de la température et dans le butène-air (2% vol) du V_2O_5 et du système $V_2O_5-MoO_3$.

1, V_2O_5 ; *2*, $V_2O_5-MoO_3$ (1 : 0,1 mole) ; *3*, $V_2O_5-MoO_3$ (1 : 0,33 mole) ; *4*, $V_2O_5-MoO_3$ (1 : 1 mole).

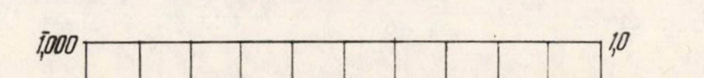

Fig. 6. — Variation de la conductivité électrique et de l'énergie d'activation E_σ en fonction de % mole MoO_3.

Il faut remarquer que les énergies d'activation déduites d'après des mesures cinétiques, dans de réactions similaires à 400°, sur des catalyseurs à base de $V_2O_5-MoO_3$[14] sont proches de nos valeurs obtenues pour E_σ, en milieu d'hydrocarbure-air. Les auteurs mentionnés indiquent une énergie d'activation calculée d'après la cinétique de réaction comprise entre 14—16 kcal/mole, tandis que nos données conduisent à une énergie d'activation de la conductivité électrique comprise entre 15—17 kcal/mole. Cela indique un faible déplacement du niveau Fermi vers la partie supérieure de la bande de conduction, comme suite de l'accroissement des impuretés donneuses introduites par MoO_3.

L'énergie d'activation de la conductivité électrique varie antibatiquement avec la variation log σ pour le même domaine de variation des composants du système. Tels résultats sont illustrés dans la figure 6, dont le maximum de log σ correspond au minimum de l'énergie d'activation de la conductivité électrique E_σ, à savoir pour la composition exprimée par le rapport 1 : 0,33 moles.

Les résultats ci-dessus nous permettent de conclure que dans le système étudié, la méthode de la conductivité électrique utilisée par nous peut fournir des renseignements qualitatifs sur l'activité catalytique, ainsi que sur les transformations subies par le catalyseur en vue d'obtenir sa composition stationnaire, active.

Revue Roumaine de Chimie, **14**, 911–927 (1969)

CARBONIUM ION REACTIONS V.*) ACETOLYSIS OF 1:2,5:6-DIBENZOCYCLOHEPTA-1,3,5-TRIENYL-7-ETHYL β-TOSYLATE**)

ECATERINA CIORĂNESCU, M. BANCIU, RODICA JELESCU, MARINA RENTZEA, M. ELIAN and C. D. NENITZESCU

Institute of Organic Chemistry of the Academy,
Bucharest, Spl. Independenţei 202 b

Received February 25, 1969

The acetolysis of 1:2,5:6-dibenzocyclohepta-1,3,5-trienyl-7-ethyl β-tosylate (**1b**) proceeds with double bond participation. In the presence of sodium acetate, under kinetic control, derivatives of the 2:3,6:7-dibenzobicyclo[3.2.2]nona-2,6-diene system (**13**) i.e. (after $LiAlH_4$ reduction) the epimeric alcohols **7** and **8** are formed. In the absence of sodium acetate thermodynamic control prevails leading to 6:7,8:9-dibenzobicyclo-[3.2.2]nona-6,8-diene (**15**) derivatives, i.e. the alcohol **9a** and the olefin **10**, together with the hydrocarbon 2:3,7:8-dibenzotricyclo[3.2.1.$0^{4,6}$]nona-2,7-diene (**11**). The two systems **13** and **15** are interconvertible: the tosylate **9b** rearranges to **7** and **8** during acetolysis in the presence of sodium acetate, whereas these alcohols are converted to the more stable derivatives of **15** system on treatment with *p*-toluenesulfonic acid, in acetic acid. The mechanisms of these reactions are discussed in terms of nonclassical carbonium ions.

Participation of a carbon-carbon double bond situated at a greater distance from the ionizing centre in solvolysis reactions, accompanied eventually by ring closure, a phenomenon for which Winstein [1] coined the term *π-route* has been demonstrated in many cases [2–6] these last years.

---

*) Part IV. E. Ciorănescu, A. Mihai, G. Mihai, M. Elian and C. D. Nenitzescu, *Rev. Roumaine Chim.* **10**, 175 (1965).

) see preliminary communication: E. Ciorănescu, M. Banciu, R. Jelescu, M. Rentzea, M. Elian and C. D. Nenitzescu, *Tetrahedron Letters*, **1969,...1871.

[1] S. Winstein and P. Carter, *J. Amer. Chem. Soc.*, **83**, 4485 (1961).

[2] G. Le Ny, *Compt. rend.*, **251**, 1526 (1960).

[3] R. G. Lawton, *J. Amer. Chem. Soc.*, **83**, 2399 (1961).

[4] P. D. Bartlett and S. Bank, *J. Amer. Chem. Soc.*, **83**, 2591 (1961); P. D. Bartlett, *Liebigs Ann. Chem.*, **653**, 45 (1962); P. D. Bartlett, S. Bank, R. J. Crawford and G. H. Schmid, *J. Amer. Chem. Soc.*, **87**, 1288 (1965); P. D. Bartlett and G. D. Sargent, *J. Amer. Chem. Soc.*, **87**, 1297 (1965); P. D. Bartlett, W. S. Trahanowschi, D. A. Bolon and G. H. Schmid, *J. Amer. Chem. Soc.*, **87**, 1314 (1965).

[5] A. C. Cope, D. L. Nealy, P. Scheiner and G. Wood, *J. Amer. Chem. Soc.*, **87**, 3130 (1965); H. Felkin, C. Le Ny, C. Lion, W. D. K. Macrosson, J. Martin and W. Parker, *Tetrahedron Letters*, **1966**, 157; W. Kraus, W. Rothenwöhrer, W. Kaiser and M. Hanack, *Tetrahedron Letters*, **1966**, 1705; M. Hanack, W. Kraus, W. Rothenwöhrer, W. Kaiser and G. Wentrup, *Liebigs Ann. Chem.*, **703**, 44 (1967).

[6] P. D. Bartlett, R. M. Nicholson and R. Owyang, *Tetrahedron*, **1966**, Suppl. 8, Part II, p. 399.

In an earlier publication [7a,b] it was shown that the solvolysis of 1:2,5:6-dibenzocyclohepta-1,3,5-trienyl-7-methyl tosylate (**2**) goes on to a small extent (*ca.* 10%) with participation of the double bond of the middle ring, giving rise to bridged products.

A more pronounced participation of the middle-ring double bond appeared probable in the case of the higher homologue **1b**. According to Dreiding models the ω-CH_2 group is as close as 1.55 Å to one of the double bond carbon atom in the middle ring, whereas this distance is 2.75 Å in the case of **2**.

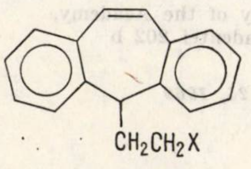

1a : X = OH
1b : X = OTs
1c : X = OAc

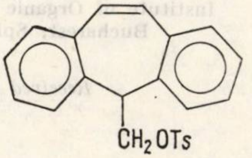

2

In the present paper we report on results obtained from acetolysis of 1:2,5:6-dibenzocyclohepta-1,3,5-trienyl-7-ethyl β-tosylate (**1b**).

RESULTS

The dibenzocyclohepta-1,3,5-trienyl-7-ethanol (**1a**) was prepared by $LiAlH_4$ reduction of the ethyl 1:2,5:6-dibenzocycloheptatrienyl acetate (**5**); the corresponding acid **4** was obtained by condensation of dibenzocycloheptatrien-7-ol (**3**) with malonic acid in acetic acid.[8]

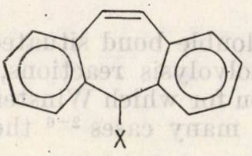

3 : X = OH
4 : X = CH_2COOH
5 : X = $CH_2COOC_2H_5$

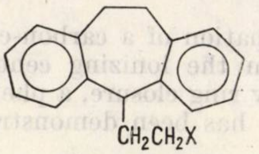

6a : X = OH
6b : X = OTs
6c : X = OAc

The saturated alcohol **6a** was synthesized from ethyl 1:2,5:6-dibenzocyclohepta-1,5-dienyl-7-acetate [8] by reduction with $LiAlH_4$.

Both kinetic measurements and structure of the reaction products indicate double bond participation of the middle ring of **1b**. The acetolysis of the tosylate **1b** either with or without added sodium acetate proceeded, at 110°, about 15 times faster than that of the saturated tosylate **6b**.[9]

---

[7] a) E. Ciorănescu, A. Bucur, M. Elian, M. Banciu, M. Voicu and C. D. Nenitzescu, *Tetrahedron Letters*, **1964**, 3835; *Rev. Roumaine Chim.* **10**, 161 (1965); b) E. Ciorănescu, A. Bucur, F. Badea, M. Rentzea and C. D. Nenitzescu, *Tetrahedron Letters*, **1969**, 1867.

[8] C. van der Stelt, A. Haasjes, H. M. Tersteege and W. Th. Nauta, *Rec. Trav. chim.* **84**, 1466 (1965).

[9] M. Voicu and F. Badea, see following communication.

In the presence of sodium acetate to neutralize the strong acid produced, the acetolysis of the tosylate **1b** (at 117° for 8 hr) led, after reduction with $LiAlH_4$ to a mixture of products (96% based on **1b**) which was analysed by gas chromatography (Table 1). Alumina column chromatography of the product mixture allowed the isolation of three alcohols **7**, **8** and **1a**, in pure state accounting for 70% of the starting material.

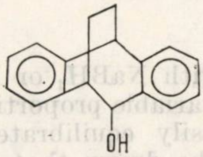

7

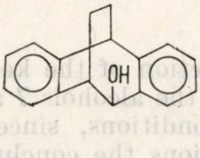

8

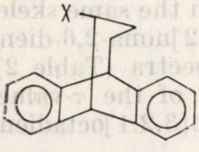

9a : X = OH
9b : X = OTs
9c : X = OAc

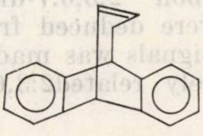

10

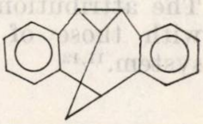

11

In the absence of sodium acetate other different products were obtained. In these conditions the acetolysis of the tosylate **1b** gave, after conversion of the acetates to the corresponding alcohols, a mixture of compounds (92% based of **1b**) which was analysed by gas chromatography (Table 1).

By chromatography on alumina were separated : a) a fraction containing two hydrocarbons **10** and **11**, b) a pure alcohol **9a** and c) the unrearranged **1a**. Some polymer (4—6%) was always formed in the unbuffered acetolysis, which was isolated before the v.p.c.

Table 1

Acetolysis products of 1b and 9b (8 hr at 117°) (after $LiAlH_4$ reduction)

Tosylate (M)	NaOAc M	% Products					
		10	11	7	8	9a	1a
1b (0.10)[a)]	—	7.5	21	1	1	56	13.5
1b (0.17)	0.26	3.5	1	58	23.5	3.5	10.5
9b (0.02)[a)]	—	3	5.5	1	6	75.5	9
9b (0.02)	0.05	—	—	56.5	27.5	16	—

a) v.p.c. analysis after polymer separation.

Structure and configuration of the alcohols 7 *and* 8

The alcohols **7** (m.p. 134°) and **8** (m.p. 120°) are the major products (81.5%) of the buffered acetolysis of **1b**. Both alcohols yielded by oxidation with chromic anhydride in pyridine one and the same ketone **12** (m.p. 114°) which was transformed into the hydrocarbon **13** (m.p. 79°) by the method of Brown and White.[10]

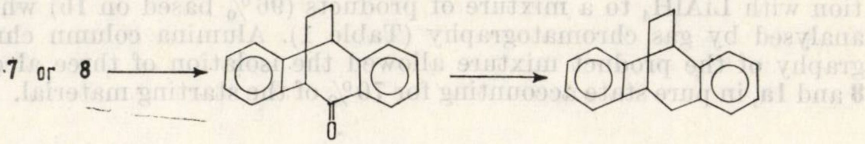

12 **13**

Reduction of the ketone **12** with $NaBH_4$ or $LiAlH_4$ led back to a mixture of the alcohols **7** and **8** in variable proportions depending on the reaction conditions, since they easily equilibrate (*vide infra*). From these reactions the conclusion can be drawn that **7** and **8** are epimers.

The alcohols **7** and **8** as well as the ketone **12** contain the same skeleton of the hydrocarbon 2:3,6:7-dibenzobicyclo[3.2.2]nona-2,6-diene (**13**). Their structures were deduced from the NMR spectra (Table 2). The attribution of the signals was made by comparison of the τ-values with those of the closely related2:3,6:7-dibenzobicyclo[3.2.1]octadiene system.[11,12]

Table 2

Proton assignments in the 2:3,6:7-dibenzobicyclo[3.2.2]nona-2,6-diene system derivatives

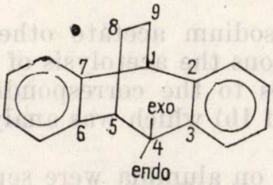

Shifts in τ units

Compound (solvent)	H_1	H_5	H_4	$H_8 + H_9$	H_{arom}
Hydrocarbon **13** (CCl_4)	6.25 (m)	6.85 (apparently s)		7.90 (m)	2.90–3.10 (m)
Alcohol **7** (*endo*) ($CDCl_3$)[a)]	6.10 (m)	6.50–6.70 (m)	5.30 (q)	8.0 (m)	2.40–3.00 (m)
Alcohol **8** (*exo*) ($CDCl_3$)[a)]	6.15 (m)	6.60–6.80 (m)	5.10 (q)	7.40–8.30 (m)	2.50–3.00 (m)
Acetate of **7** (*endo*) (CCl_4)	6.15 (m)	6.50 (m)	4.02 (d)	8.08 (apparently s)	2.95 (s)
Acetate of **8** (*exo*) (CCl_4)	6.20 (m)	6.61 (m)	3.92 (d)	7.40–8.35 (m)	2.60–3.05 (m)
Ketone **12** (CCl_4)	5.90 (m)		—	7.90 (m)	3.00–3.10 (m)

a) OH-signal variable depending on concentration; s = singlet; d = doublet; q = quartet; m = multiplet

---

[10] B. R. Brown and A. M. S. White, *J. Chem. Soc.*, **1957**, 3775.

[11] S. J. Cristol, J. R. Mohrig and D. E. Plorde, *J. Org. Chem.*, **30**, 1956 (1965).

[12] A. R. Katritzky and B. Wallis, *Chem. and Ind.*, **1964**, 2025.

The data obtained by IR, NMR and mass-spectra are in agreement with the assigned *endo* and *exo* configurations for the alcohols **7** and **8**.

The alcohol **7** shows a ν_{OH} stretching frequency of 3582 cm^{-1} (diluted solution in CCl_4) indicating an interaction of the OH-group with the π-electrons of one of the neighbouring aromatic rings. According to Dreiding models such an interaction is only conceivable for the *endo*-isomer **7**. The alcohol **8** displays a normal ν_{OH} band at 3607 cm^{-1} in agreement with an *exo*-structure.

In the NMR spectrum, the bridge protons of **8** are pronouncedly nonequivalent, giving rise to a complicated pattern of bands between $\tau = 7.40$ and 8.30, whereas those of the alcohol **7**, the hydrocarbon **13** and ketone **12** are sharp and narrow ($\tau = 8.0$; 7.90 ; 7.90 resp.). From the examination of Dreiding models it can be inferred that the oxygen of the *exo*-alcohol **8** comes as close as 2.4 Å to one of the hydrogens of the bridge, thus determining the bridge-protons to become magnetically nonequivalent. For the *endo*-alcohol **7** such an interaction is not expected as the distance between the oxygen and the hydrogen on the bridge is greater than 4 Å.

The coupling constants of the H_4 and H_5 protons are practically the same for the alcohols **7** and **8** (4.5 and 4.0 cps) and thus do not allow configurational conclusions. It can be seen from models that the plane formed by H_5-C_5-C_4 bisects the angle *exo*-C_4-*endo*, thus ensuing that the coupling constants coincide.

The mass-spectra of the two alcohols **7** and **8** are identical as far as the position of their peaks (and ionization potentials) is concerned, whereas the relative peak intensities differ considerably (Table 3).

Table 3

Intensity as percentage of total ion current

Ion	m/e	Alcohol **7** (*endo*)	Alcohol **8** (*exo*)
M^+	236	5.2	1.9
M^+-H_2O	218	12.0	14.8

For several epimeric pairs of alcohols it has been observed that the more crowded epimer generally exhibits the molecular ion (M^+) of lower intensity and a ($M^+—H_2O$) peak of higher intensity.[13] The more crowded isomer is the *exo* one which therefore must be richer in energy because of the oxygen-bridge repulsions.

The smaller intensity of the molecular ion of the alcohol **8** reflects the smaller stability as compared to that of alcohol **7**. The *exo* configuration was therefore attributed to the alcohol **8**. On the other hand the greater intensity of the ion ($M^+—H_2O$) shows that elimination of water is favoured in the alcohol **8**. The elimination of water from aliphatic alcohols proceeds in the mass-spectrometer *via* cyclic transition states[13] and it has been shown for a series of benzylic alcohols, that *o*-CH_3-derivatives show much greater ($M^+ - H_2O$) peaks than their *m*- or *p*-methyl isomers.[14] As the oxygen of **8** is within reach of 2.4 Å of one of the bridge hydrogens, elimination of water is facilitated by the formation of a cyclic five-membered transition state, whereas such an intermediate is not feasible for its isomer **7**.

---

[13] K. Biemann and J. Seibl, *J. Amer. Chem. Soc.*, **81**, 3149 (1959) ; K. Biemann "Mass Spectrometry", McGraw-Hill Book Co., Inc., New York 1962, p. 142.

Structure of the alcohol **9a** *and the hydrocarbon* **10**

In the unbuffered acetolysis of the tosylate **1b** the main product was an alcohol with m.p. 150–152°. On oxidation it yielded the ketone **14** which could be reduced to hydrocarbon **15** using the modified Kishner-Wolff procedure.[15] Reduction of the ketone **14** with $LiAlH_4$ regenerated the alcohol **9a**.

On the other hand by pyrolysis of the acetate **9c** an unsaturated hydrocarbon was obtained, which was found to be identical with **10** (identical retention times in gas chromatography). Hydrogenation of **10** yielded the same hydrocarbon (**15**) as that obtained from the ketone **14**.

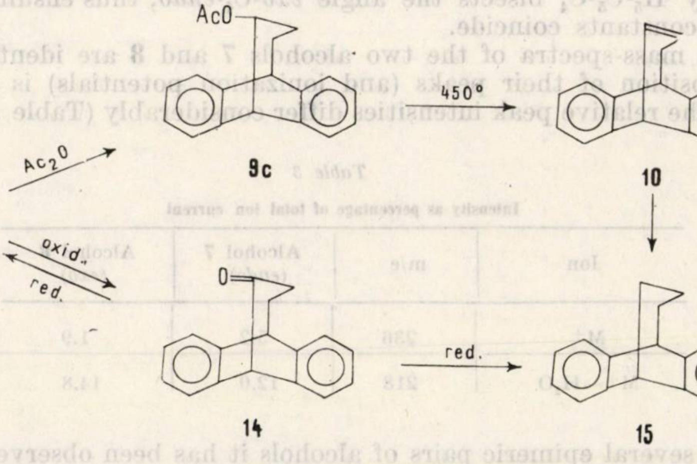

The alcohol **9a**, the ketone **14** and the olefin **10**, have the same carbon skeleton namely that of the 6:7,8:9-dibenzobicyclo[3.2.2]nona-6,8-diene (**15**). For all these compounds the NMR spectra are in agreement with the assigned structure (Table 4). The hydrocarbon **15** shows, beside the aromatic H signals, a triplet at $\tau = 6.15$ (2 protons) due to the bridgehead protons H_1 and H_5 coupled with the CH_2 groups from the 2 and 4 positions respectively. The same hydrocarbon has at $\tau = 8.10-8.90$ a multiplet (6 protons) due to the bridge protons, in agreement with the bicyclo[3.2.2]nona-6,8-diene structure.

---

[14] T. Aczel and H. E. Lumpkin, *Analyt. Chem.* **32**, 1819 (1960).

[15] Huang Minlon, *J. Amer. Chem. Soc.*, **68**, 2487 (1946).

Table 4

Proton assignments in the 6:7,8:9-dibenzobicyclo[3.2.2]nona-6.8-diene system derivatives

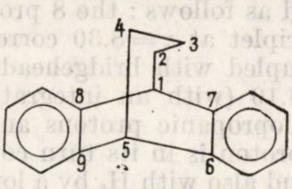

Shifts in τ units

Compound[a)]	H_1	H_5	H_2	H_4	H_3	H_{arom}
Alcohol **9a**[b)]	5.90 – 6.40 (m)			8.00 – 8.50 (m)		2.50 – 3.00 (m)
Ketone **14**	5.40 (s)	5.90 (t)	—	7.70 – 8.00 (m)		2.60 – 3.00 (m)
Hydrocarbon **15**	6.15 (t)		8.10 – 8.90 (m)			2.90 (s)
Hydrocarbon **10**	5.85 – 6.10 (m)		3.80 (m)	7.52 (m)	5.03 (m)	2.90 (m)

a) All spectra were measured in $CDCl_3$

b) OH-signal variable depending on concentration

s = singlet; t = triplet; m = multiplet

The NMR spectra of ketone **14** and alcohol **9a** show, by comparison with the hydrocarbon **15**, specific shifts of the signals due to the introduction of functional groups. The positions, multiplicity and integrated areas of the signals from hydrocarbon **10**-spectrum are also in agreement with the assigned structure.

Structure of the hydrocarbon 11

The mixture of hydrocarbons obtained in the unbuffered solvolysis of **1b** contains the compounds **10** and **11** (according to the gas chromatography results), the latter in a proportion three times as large as the former. Attempts to separate them into uniform products proved unsuccessful. The minor component of the mixture however, could be hydrogenated over PtO_2 in ethanol, whereas the major part remained unchanged (i.e. maintaining its retention time in the gas-chromatographical analysis). The mixture became now separable on alumina columns.

One of the products thus isolated, representing about 1/4 of the total mixture, was found to be identical (mixed m.p., IR and NMR spectra) with the hydrocarbon **15** obtained by reduction of the ketone **14**. The initial unsaturated compound of the (unseparable) mixture has therefore the structure **10**.

The other hydrocarbon with m.p. 97° which remained unchanged on catalytic hydrogenation corresponds to a brutto formula $C_{17}H_{14}$. The NMR spectrum showing absorptions at $\tau = 2.98$ (singlet, 8H), 6.23 (sextet, 1H), 7.30 – 8.10 (multiplet, 3H) and 8.30 (triplet, 2H) supports the structure **11** assigned for this hydrocarbon. These data are favourably compared with those of the ketone **16**[16] and of the dibenzotricyclo-[3.3.0.0^{2,8}]octa-3,6-diene [17] possessing related structures. The observed signals can be rationalized as follows : the 8 protons at $\tau = 2.98$ are aromatic protons and the triplet at $\tau = 8.30$ corresponds to bridge protons (from the 9-position), coupled with bridgehead protons H_1 and H_5. The multiplet at $\tau = 7.30-8.10$ (with an integrated area corresponding to 3 protons) is due to cyclopropanic protons and the sextet at $\tau = 6.23$ corresponds to H_1. This proton is in its turn coupled with the CH_2-group protons from 9-position and also with H_5 by a long-range coupling. A similar coupling is observed in the NMR spectrum of the ketone **16**.

Further proof for this structure was provided by the synthesis of the hydrocarbon *via* an independent route. The starting material for this purpose was the ketone **16**, obtained in the course of a previous investigation.[16] The Huang-Minlon reduction[15] of this ketone produced the hydrocarbon **11** identical (mixed m.p., NMR spectrum) with the one arising from the solvolysis reaction.

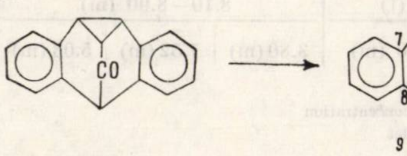

16 **11**

DISCUSSION

As shown in table 1 the buffered acetolysis of tosylate **1b** yielded mainly (81.5%) derivatives of *endo*-ethylendibenzocycloheptadiene system (**13**) while the products of the unbuffered acetolysis belonged mainly (63%) to *endo*-propylendihydroantracene system (**15**). The former compounds arise from a kinetically controlled reaction, whereas the latter ones are thermodynamically controlled products.

The greater thermodynamic stability of the system **15** as compared to **13** can be inferred from the acetolysis of the tosylate **9b** which in the presence of sodium acetate produced derivatives of the hydrocarbon **13**, namely the alcohols **7** and **8** (total yield 84%) whereas in the absence of sodium acetate led to 78.5% of unrearranged products (Table 1).

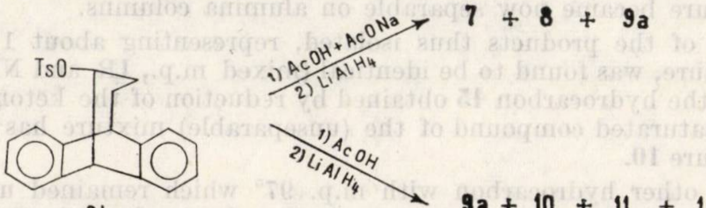

---

[16] V. Ioan, M. Popovici and C. D. Nenitzescu, *Tetrahedron Letters*, **1965**, 3383.

[17] a) G. F. Emerson, L. Watts, R. Pettit, *J. Amer. Chem. Soc.*, **87**, 131 (1965); b) S. J. Cristol and B. B. Jarvis, *J. Amer. Chem. Soc.*, **89**, 401 (1967).

On the other hand, the alcohols **7** and **8** when refluxed for 7 hr in acetic acid solution containing one equivalent of *p*-toluenesulfonic acid, were transformed, just like in the case of the lower homologues studied by Cristol *et al*,[18] into the thermodynamically more stable alcohol **9a**. Besides this alcohol the olefin **10** and the cyclopropanic hydrocarbon **11** (Table 5) are also formed.

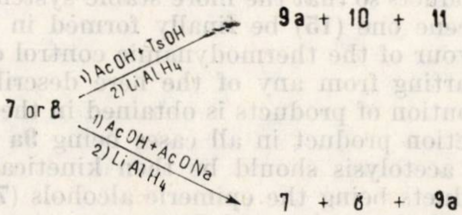

Either of the two epimeric alcohols **7** and **8** were found to equilibrate when maintained for 48 hr under buffered acetolysis conditions, the ratio *endo*/*exo* being about 2 : 1.

Table 5

Acid catalysed rearrangement products of 7, 8 and 9a[a)] **at 117° (after LiAlH$_4$ reduction)**

Starting alcohol	Time hr	% Compound							
		10	**11**	**7**	**8**	**9a**	**1a**	Polymer[b)]	Yield[c)]
7	7	8	18	—	—	70.5	3.5	3	84
8	7	8	19	—	—	72	1	7	86
9a	1	3	3.5	0.5	1.5	91	0.5	8	83
9a	3	2	5.5	0.5	1.5	90	0.5	7	85
9a	7	4.5	13	1	6	67	8.5	6	84
9a	24	8	17.5	1	5	48	21	6	90

a) conc., 0.05 M alcohol, 0.05 M *p*-toluenesulfonic acid in acetic acid

b) the polymer was separated before the v.p.c.

c) average yield after the polymer separation

Of particular interest is the formation of hydrocarbon **11**, containing a tricyclic median ring, from tosylates **1b** and **9b** by unbuffered acetolyses (Table 1). At lower temperatures (70° instead of reflux conditions) the acetolysis of tosylate **9b** led to only very small amounts of hydrocarbon **11** (less than 1%).

The hydrocarbon **11** was obtained besides **10** also from alcohol **9a** in refluxing acetic acid solution containing one equivalent of *p*-toluenesulfonic acid (Table 5). Extension of the reaction time from 1 to 24 hr results in the increase of the proportion of hydrocarbons suggesting an irreversible side reaction, at the same time the amount of alcohol **1a** becoming more important. The presence of alcohol **1a** among the reaction products of the acid-catalysed acetolysis of the alcohols **9a, 7** and **8** indicates *retro-π-route.*

---

[18] S. J. Cristol, F. Pwu-Parungo and D. E. Plorde, *J. Amer. Chem. Soc.*, **87**, 2870 (1965); S. J. Cristol, F. Pwu-Parungo, D. E. Plorde and K. Schwarzenbach, *J. Amer. Chem. Soc.*, **87**, 2879 (1965).

The distribution of the products suggests for the unbuffered acetolysis a thermodynamic control. The acidic medium should favour the reionization of the products so that the more stable system, namely the bridged dihydroanthracene one (**15**) be finally formed in higher proportion. An argument in favour of the thermodynamic control comes from experiments in which starting from any of the here described alcohols (**7, 8, 9a**) a similar distribution of products is obtained in the presence of strong acid, the main reaction product in all cases being **9a** (Table 5).

The buffered acetolysis should be then kinetically controlled, the major reaction products being the epimeric alcohols (**7** and **8**).

On the basis of these observed facts some considerations can be made regarding the intermediates involved in the various reactions described above.

The anchimeric assistance by the double bound of the median ring, kinetically observed and further substantiated by the formation of the cyclopropanic hydrocarbon **11** and of the main reaction products containing a bridge in the median ring, suggests the intervention of the bridged nonclassical ion **17** generated from **1b** by the *π-route.* Isomerization of **17** could give rise to the more stable ion **19**, owing to its benzylic conjugation, and to the nonclassical ion **18** in which anchimeric assistance from the benzene ring is provided. These three ions in equilibrium are therefore of a very different stability, the ion **17** corresponding to the higher energy content while the ion **19** being the more stable species.

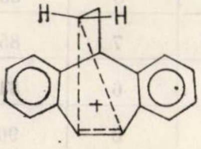

17

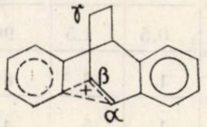

18

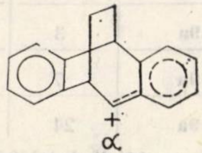

19

Hydrocarbon **11** may be formed from ion **17** by elimination of one proton but also from ion **19** by the internal displacement of a γ-proton by a carbonium ion. Examples of this kind are known in literature, for instance the formation of cyclopropane from the 1-propyl cation by deoxidation [19] and of nortricyclene by dehydration of norborneol derivatives.[20] The formation of nortricyclene (4%) rather than of the norbornene in the elimination reaction which parallels the solvolysis of *exo*-norbornyl *p*-bromobenzenesulfonate "is more easily rationalized with a bridged ion than with a classical one" as stressed by Winstein *et al.* [21]

---

[19] P. S. Skell and R. J. Maxwell, *J. Amer. Chem. Soc.*, **84**, 3963 (1962); P. S Skell and J. Starer, *J. Amer. Chem. Soc.*, **82**, 2971 (1960); *ibid.*, **84**, 3962 (1962).

[20] G. Kompa and G. A. N. Nyman, *Liebigs Ann. Chem.*, **535**, 562 (1938).

[21] S. Winstein, E. Clippinger, R. Howe and E. Vogelfanger, *J. Amer. Chem. Soc.*, **87**, 376 (1965).

Alcohols **7** and **8** may result from ions **19** or **18**. The solvent attack in the α-position of ion **19** gives rise through an irreversible reaction (buffered acetolysis) to the acetates of alcohols **7** and **8**. On the other hand the nucleophilic attack in the α-position of ion **18** should afford only the *exo*-alcohol (acetate). Actually this isomer arises in a smaller proportion than the more stable *endo*-alcohol. However taking into account the *exo* $\rightleftarrows$ *endo* isomerization which occurs even by buffered acetolysis, this ratio can supply no indication on the nature of the involved intermediate. But at the same time this *exo-endo* isomerization taking place quite readily is consistent with the intervention of the carbonium ion **19**.

The compounds containing a three-carbon bridge in the median ring (**9** and **10**), which arise under thermodynamic control conditions, involve the participation of ion **18**. The solvent attack in the β-position or the expulsion of a proton from the γ-position of this ion leads to alcohol **9a** or to hydrocarbon **10** respectively.

The above mentioned rearrangements, taking place on treatment of alcohols **7**, **8** and **9a** with *p*-toluenesulfonic acid in acetic acid solution, probably proceed through the same intermediates. The major product of these reactions namely the acetate **9c** indicates a larger contribution of ion **18** than of ion **17**. The former can arise from all the above mentioned alcohols, under conditions favouring repeated ionization.

It is worthwhile to point out the unexpected presence of the initial alcohol (the purity of the starting alcohols was checked by v.p.c.) among the reaction products of alcohols **9a**, **7** and **8** (Table 5). These results could difficultly be rationalized otherwise than by the intervention of an ion **17** (*retro-π-route*).

On the basis of the existing data it is difficult to say which is the acceptor base of the proton in the γ-position whose elimination leads to hydrocarbons **11** and **10**. Since these hydrocarbons are not formed when the acetate ion is present it is sensible to assume that the acetate is not this base. More plausibly the reaction is a monomolecular elimination within the ion pairs $\mathbf{17}^{+}\mathrm{TsO}^{-}$, $\mathbf{18}^{+}\mathrm{TsO}^{-}$, or $\mathbf{19}^{+}\mathrm{TsO}^{-}$, the tosylate ion being the proton acceptor.

In this case the formation of the hydrocarbons should be favoured by strongly ionizing media possessing at the same time a reduced solvation power. The solvolysis of **1b** in formic acid is not conclusive since more than 80% of polymer is obtained. In refluxing acetic acid, 6% and at 140° about 90% of polymer is formed. Carrying out the solvolysis in higher homologuous acids the following results were obtained : in propionic acid (at 140°) 40% of hydrocarbon **11** and 12% of olefin **10**; in isovalerianic acid (at 140°) 33% of **11** and 12% of **10**. It is plausible that the ion pair is stabilized when the hydrophobic part of the acid molecule is bulky (voluminous).[7b]

EXPERIMENTAL

Melting points are uncorrected. IR spectra were recorded with a Perkin-Elmer model 621 spectrophotometer. NMR spectra were obtained on a Varian A-60 A spectrometer using TMS as internal standard. Mass spectra were determined with an Atlas Bremen CH_4 mass spectrometer at an electron energy of 70 eV, with an AN-4 cell, at 250°. The v.p.c. analyses were performed on a Carlo Erba G.D. gas chromatograph using Carbowax 20 M columns (20% on Chromosorb W), 1 m, at 225°, with a hydrogen rate-flow of 120 ml/min.

1:2,5:6-Dibenzocyclohepta-1,3,5-trienyl-7-acetic acid (4)

A solution of dibenzocyclohepta-1,3,5-trien-7-ol (3)[22] (28 g; 135 mmoles) and malonic acid (19 g; 183 mmoles) in 400 ml glacial acetic acid was heated under reflux for 20 hr. Most of the acetic acid was removed (red. press.), the mixture was poured into water and extracted with ether. Evaporation of the solvent yielded **4** (32 g; 95%) m.p. 159°. After recrystallization from ethanol m.p. 166°.[8]

The *ethyl ester* **5** was prepared in two ways: *a*) By saturating with gaseous HCl an ethanolic solution of the acid **4** (crude material) and refluxing for 8 hr. The mixture was worked up in the usual way, yielding a crystalline solid (90%) m.p. 73–74° (ethanol). (Found: C, 82.11; H, 6.63. $C_{19}H_{18}O_2$ requires: C, 81.97; H, 6.52%.) *IR spectrum* (CS_2 and CCl_4; cm^{-1}): 760 s, 765 s, 798 s, 1150 s, 1240 m, 1732 vs, 2930 w, 2980 m, 3020 m, 3070 m.

b) By the rearrangement of the *1:2,5:6-dibenzocyclohepta-1,3,5-trienyl-7-diazomethylketone*[16] with silver oxide in anhydrous ethanol, using the procedure of Bachmann, Cole and Wilds.[23] The yield of crude acetate **5** was 83% m.p. 69–70°.

1:2,5:6-Dibenzocyclohepta-1,3,5-trienyl-7-ethanol (1a)

A solution of the crude ester **5** (35 g; 127 mmoles) in 500 ml anhydrous ether was added dropwise, with mechanical stirring, to a suspension of $LiAlH_4$ (5 g; 132 mmoles) in 150 ml anhydrous ether. The mixture was refluxed for 6 hr and left overnight. After decomposing the mixture with 10% H_2SO_4 and separating the ethereal layer, the aqueous layer was extracted 3 times with ether. The ethereal solution was washed with water, dried on Na_2SO_4 and evaporated; 25 g (90%) of the crystallized alcohol **1a** were obtained, m.p. 73–74° (*n*-hexane). (Found: C, 86.10; H, 7.12. $C_{17}H_{16}O$ requires: C, 86.41; H, 6.83%). *IR spectrum* (CS_2 and CCl_4, cm^{-1}): 757 s, 798 s, 1030 m, 1048 m, 2875 m, 2923 m, 2952 ms, 3070 m, 3635 ms.

The *acetate* **1c** was obtained by treating the alcohol **1a** with acetic anhydride in presence of pyridine; m.p. 75–76° (methanol). (Found: C, 82.24; H, 6.85. $C_{19}H_{18}O_2$ requires: C, 81.97; H, 6.52%). *IR spectrum* (CS_2 and CCl_4; cm^{-1}): 755 ms, 795 m, 1029 m, 1233 vs, 1739 vs, 2955 w, 3017 m, 3060 w.

The *tosylate* **1b** was prepared from the alcohol **1a** with *p*-toluenesulfochloride in pyridine; 85% yield, m.p. 147–149° (ethanol). (Found: C, 73.77; H, 5.79; S, 7.88. $C_{24}H_{22}O_3S$ requires: C, 73.80; H, 5.68; S, 8.21%). *IR spectrum* (KBr; cm^{-1}): 768 s, 913 s, 1168 vs, 1188 s, 1348 vs, 2920 mw, 2962 mw, 3013 mw, 3060 w.

1:2,5:6-Dibenzocyclohepta-1,5-dienyl-7-ethanol (6a)

The *1:2,5:6-dibenzocyclohepta-1,5-dienyl-7-acetic acid* prepared according to van der Stelt *et al.*[8] was transformed to its ethyl ester by refluxing with ethanol saturated with gaseous

---

[22] G. Berti, *Gazz. chim. Ital.* **87**, 293 (1957).

[23] W. E. Bachmann, W. Cole and A. L. Wilds, *J. Amer. Chem. Soc.*, **62**, 824 (1940).

HCl and led to 95% yield of an oily product. On reduction with $LiAlH_4$ in ether **6a** was obtained 97% yield, m.p. 56–57° (*n*-hexane). (Found: C, 85.35; H, 7.66. $C_{17}H_{18}O$ requires: C, 85.64; H, 7.62%). *IR spectrum* (CS_2 and CCl_4; cm^{-1}): 752 vs, 1032 ms, 1048 ms, 1491 m, 2875 m, 2932 a, 3015 m, 3059 m, 3635 m.

The *acetate* **6c**, m.p. 88° (methanol). (Found: C, 81.60; H, 7.32. $C_{19}H_{20}O_2$ requires: C, 81.38; H, 7.19%). *IR spectrum* (CS_2 and CCl_4; cm^{-1}): 752 s, 1031 s, 1232 vs, 1738 vs, 2937 ms, 3020 m, 3060 m.

The *tosylate* [6] **b** was obtained from the alcohol **6a** with *p*-toluenesulfochloride, in pyridine; m.p. 139–140° (ethanol). (Found: C, 73.40; H, 6.28; S, 7.97. $C_{24}H_{24}O_3S$ requires: C, 73.44; H, 6.16; S, 8.17%). *IR spectrum* (KBr; cm^{-1}): 766 vs, 916 vs, 1170 vs, 1185 s, 1353 vs, 2923 m, 2950 m, 3011 mw, 3060 w.

Acetolysis of 1:2,5:6-dibenzocyclohepta-1,3,5-trienyl-7-ethyl-β-toluenesulfonate(**1b**) *in the presence of sodium acetate*

A solution of tosylate **1b** (10 g; 25,5 mmoles) and anhydrous sodium acetate (3.2 g; 39 mmoles) in 150 ml of glacial acetic acid was heated under reflux for 8 hr. After distillation of most of the solvent at red. press. the mixture was poured into water (50 ml) neutralized with Na_2CO_3 and extracted with ether. The ethereal solutions were washed with water, dried on Na_2SO_4 and the solvent evaporated. The oily residue (7 g; 97.5%) was dissolved in 150 ml ether and the solution added dropwise to a suspension of 2 g $LiAlH_4$ in 50 ml ether, with mechanical stirring. The mixture was refluxed for 3 hr and left overnight, then worked up in the usual manner. Evaporation of the solvent yielded an oily material (5.8 g; 96%) (v.p.c. analysis, Table I), which was left to stand for several hours. The crystals which formed were filtered and washed with ether, affording 1.2 g (20%) of *2:3,6:7-Dibenzobicyclo*[*3.2.2*]-*nona-2,6-dien*-endo-*4-ol* (**7**), m.p. 128–132°; after recrystallization from methanol m.p. 134°. (Found: C, 86.57; H, 7.05. $C_{17}H_{16}O$ requires: C, 86.41; H, 6.82%). *IR spectrum* (CS_2 and CCl_4; cm^{-1}) 752 vs, 1022 vs, 2868 m, 2937 s, 3025 m, 3065 m, 3582 ms.

The *endo-acetate* (**7**-OAc) m.p. 90° (methanol). (Found: C, 81.75; H, 6.72. $C_{19}H_{18}O_2$ requires C, 81.97; H, 6.52%). *IR spectrum* (CS_2 and CCl_4, cm^{-1}): 754 vs, 1232 vs, 1368 ms, 1730 vs.

The combined ethereal and methanolic filtrates gave after evaporation a colourless oil (4.6 g) which was dissolved in benzene (20 ml). The solution was passed through a neutral alumina (150 g) column. On eluting with benzene several fractions were separated. The first fraction (120 ml) contained 1.2 g (20%) of the *endo* alcohol **7**, identical with the crystalline product obtained above, the total yield of the *endo* alcohol amounting to 40%. From the second fraction (100 ml) a mixture of the *endo* and *exo* alcohols (**7** and **8**) was obtained and from the third one (about 450 ml) 1.2 g (20 %) of **8**. *2:3,6:7-Dibenzobicyclo* [*3.2.2*] *nona-2,6-dien*-exo-*4-ol* (**8**) showed m.p. 120°. (Found: C, 86.05; H, 6.97. $C_{17}H_{16}O$ requires C, 86.41; H, 6.82%). *IR spectrum* (CS_2 and CCl_4; cm^{-1}): 750 vs, 1009 s, 2863 ms, 2940 s, 3022 ms, 3070 ms, 3607 m.

The *exo-acetate* (**8**-OAc) m.p. 76° (methanol) (Found: C, 81.33; H, 6.90. $C_{19}H_{18}O_2$ requires C, 81.97; H, 6.52%). *IR spectrum* (CS_2 and CCl_4; cm^{-1}): 751 vs, 1235 vs, 1368 ms, 1734 vs.

Continuing the elution with benzene, a mixture of alcohols was found in the next fraction (100 ml), and then, in the following fraction (600 ml), 0.6 g (10%) of the initial alcohol (**1a**), identical (mixed mp., IR spectrum) with the starting material.

2:3,6:7-Dibenzobicyclo[3.2.2]nona-2,6-dien-4-one (**12**)

A solution of alcohol **7** (or **8**) (1.2 g ; 5.1 mmoles) in 40 ml pyridine, was added with cooling to a complex prepared from 2 g of CrO_3 and 50 ml of pyridine. The mixture was stirred for 5 hr, left overnight, decomposed with cold water and extracted with ether. The ethereal solution was washed with water, dil. HCl, again with water and dried on Na_2SO_4. The solvent was evaporated leaving 1 g (83%) ketone **12**, m.p. 113–114° (methanol). (Found : C, 87.24 ; H, 6.18. $C_{17}H_{14}O$ requires : C, 87.14 ; H, 6.03%). *IR spectrum* (CS_2 and CCl_4 ; cm^{-1}) : 747 vs, 754 vs, 1282 vs, 1673 vs, 2870 ms, 2945 s, 3025 ms, 3070 ms.

Reduction of the ketone **12**. *a*) A solution of $NaBH_4$ (0.1 g ; 2.65 mmoles) in 5 ml methanol containing 1 ml 8% aqueous NaOH was added to a solution of ketone **12** (0.3 g ; 1.28 mmole) in 10 ml methanol. The mixture was left overnight at room temperature. Methanol was removed under red. press. and the residue treated with water and extracted with ether to leave on evaporation a crystalline product (0.285 g ; 95%), m.p. 90–100°. Gas-chromatography analysis showed the composition : 64% *endo*-alcohol (**7**) and 36% *exo*-alcohol (**8**).

b) The reduction of ketone **12** (0.3 g ; 1,28 mmole) with $LiAlH_4$ (0.075 g ; 1.97 mmole) in 50 ml anhydrous ether afforded, after the usual working up, a crystalline product (0.275 g ; 92%), containing 52% *endo*-alcohol (**7**) and 48% *exo*-alcohol (**8**).

2:3,6:7-Dibenzobicyclo[3.2.2]nona-2,6-diene (**13**)

A solution of ketone **12** (0.3 g ; 1.28 mmoles) in 15 ml ether was added to a reductive reagent [10] prepared from 0,6 g (4.5 mmoles) anhydrous $AlCl_3$ and 0.085 g (2.25 mmoles) $LiAlH_4$ in 15 ml anhydrous ether. After the energic reaction slows down the mixture was refluxed for 4 hr, left overnight and decomposed with 10% H_2SO_4. The ethereal layer was separated and the aqueous one was extracted with ether. The combined ethereal solutions were washed with water, dried on Na_2SO_4 and the solvent evaporated. Recrystallization from methanol, afforded 0.2 g (71%) of hydrocarbon **13**, m. p. 78–79°. (Found : C, 92.69 ; H. 7.53. $C_{17}H_{16}$ requires : C, 92.68 ; H, 7.32%). *IR spectrum* (CS_2 and CCl_4 ; cm^{-1}) : 751 vs, 2862 ms, 2903 s, 2935 s, 3019 ms, 3062 ms.

Acetolysis of 1:2,5:6-dibenzocyclohepta-1,3,5-trienyl-7-ethylβ*-toluenesulfonate* (**1b**) *in the absence of sodium acetate*

A mixture of tosylate **1b** (20 g ; 51 mmoles) and 500 ml of anhydrous acetic acid was heated under reflux for 8 hr. The product mixture was worked up as described above for acetolysis in the presence of sodium acetate ; 13.75 g of a yellow oil were obtained, which was subsequently reduced with $LiAlH_4$.

The usual work-up furnished 11.2 g (92%) of a partially crystallized product (v.p.c. analysis, Table 1). After two recrystallizations from cyclohexane a first crop of **9a**(3.3 g ; 27%) was obtained.

The cyclohexane which remained from the recrystallization was evaporated, a yellowish oil (7.9 g) resulted, which was subsequently passed through a neutral alumina (200 g) column.

a) On eluting with petroleum ether (600 ml) and evaporation of the solvent a crystalline product (3 g ; 24.6%) was obtained which was shown by v.p.c. to consist of a mixture of two hydrocarbons. The attempted separation into its components by another column chromatography failed (see below the actual separation).

b) By further eluting the column with a mixture of petroleum ether-diethylether (85 :15), 300 ml solution, with blue fluorescence, were collected. On evaporation of the solvent 0.70 g (5.7%) of a white polymer resulted ; m.p. 200–230°, elementary analysis : C, 93.49 ; H. 6.85%.

c) The next 225 ml of solution (petroleum ether-diethylether 70 : 30) gave 3 g (24.6 %) of the alcohol **9a** identical with the first portion obtained directly by crystallization of the solvolysis reaction product (total yield of isolated **9a** 51.6 %).

d) After a fraction (100 ml) containing a mixture of the alcohols **9a** and **1a**, another fraction (about 200 ml) afforded 1.0 g (8.2 %) of unrearranged alcohol **1a**. The total yield : 3 g of mixture of hydrocarbons, 6.3 g of alcohol **9a**, 1.0 g of the initial alcohol **1a** and 0.7 g of polymer, that is 11.0 g (90 %) of solvolysis products.

6:7,8:9-Dibenzobicyclo[3.2.2]-nona-6,8-dien-2-ol (**9a**) m. p. 150–152°. (Found : C, 86.23 ; H, 6.99. $C_{17}H_{16}O$ requires : C, 86.41 ; H, 6.82 %). *IR spectrum* (CS_2 and CCl_4 ; cm^{-1}) : 746 vs, 1015 ms, 1029 m, 2855 m, 2926 ms, 3021 m, 3068 m, 3580 mw.

The acetate **9c**, m.p. 59–60° (methanol-water 5 :1). (Found : C, 82.07 ; H, 6.73. $C_{19}H_{18}O_2$ requires : C, 81.97 ; H, 6.52 %). IR spectrum (CS_2 and CCl_4 ; cm^{-1}) : 751 vs, 1015 ms, 1232 vs, 1732 vs, 2858 mw, 2930 ms, 3023 m, 3069 m.

The tosylate **9b** was prepared from the alcohol **9a** and *p*-toluenesulfochloride in anhydrous pyridine ; 85 % yield. The crude material showed m.p. 125° (dec.), which did not change after rapid recrystallization from methanol. (On prolonged heating in methanol the tosylate decomposed.) (Found : C, 73,90 ; H, 5.93 ; S, 7.62. $C_{24}H_{22}O_3S$ requires : C, 73.80 ; H, 5.68 ; S, 8.21 %). *IR spectrum* (KBr ; cm^{-1}) : 752 s, 762 s, 900 vs, 925 vs, 1167 vs, 1356 s, 2862 w, 2925 m, 2948 m.

Separation of **11** *and* **15** *from the hydrocarbon mixture*

0.9 g of the above mixture of hydrocarbons (fraction *a*) in 15 ml absolute ethanol were hydrogenated at atm. press. using PtO_2 (0.1 g) as catalyst ; 75 ml of hydrogen were absorbed. The catalyst was filtered off and the solvent removed *in vacuo* : 0,9 g white crystals were thus obtained which were subsequently dissolved in petroleum ether and passed through a neutral alumina (40 g) column. On elution with petroleum ether, fractions of 100 ml were collected. By v.p.c. analysis it was found that the first two fractions contained the saturated hydrocarbon **15**, identical with that obtained on reduction of the ketone **14** (see below), the third fraction was a mixture of 5 % **15** and 95 % **11**, and the next two fractions (0.35 g) contained pure hydrocarbon **11**, m.p. 97° (methanol), identical (mixed m.p., IR and NMR spectra) with that obtained by reducing the ketone **16** (see below). (Found : C, 93.35 ; H, 6.68. $C_{17}H_{14}$ requires : C, 93.53 ; H, 6.47 %). *IR spectrum* (CS_2 and CCl_4 ; cm^{-1}) : 708 m, 740 m, 760 s, 790 m, 1496 ms, 2866 w, 2930 m, 3032 m, 3078 w.

The hydrocarbon **15** resulted by hydrogenation of the olefin **10** which existed in the solvolysis product.

2:3,7:8-Dibenzotricyclo[3.3.1.0^{4,6}]nona-2,7-diene (**11**) *from the ketone* **16**

A solution of ketone **16** (0.7 g ; 3 mmoles) and 4 ml hydrazine hydrate (96–98 %) in 10 ml diethyleneglycol was heated under reflux for 2 hr. The water and the hydrazine excess were distilled *in vacuo*, then 2.5 g powdered KOH were added and the mixture heated under reflux for 2.5 hr. After diluting with water the mixture was extracted with ether, the ethereal solution washed with water and dried. Evaporation of the solvent *in vacuo* yield a crystalline product (0.56 g ; 85 %) with the following composition (v.p.c. analysis) : 4 % of saturated hydrocarbon **13**, 63.3 % of hydrocarbon **11** and 32.7 % of unidentified hydrocarbon. This mixture, which could not be separated using alumina column chromatography, was hydrogenated (in 75 ml ethanol, with PtO_2). The crystalline residue (0.55 g) obtained after working up was found to contain only two compounds : the hydrocarbons **13** and **11**.

Using alumina (40 g) column chromatography (elution with petroleum ether) a mixture of **13** and **11** was first obtained, then pure hydrocarbon **11** (0.2 g), identical (mixed m.p., IR and NMR spectra) with that isolated from the unbuffered acetolysis of the tosylate **1b**.

The reduction of the ketone **16** with hydrazine afforded, besides the hydrocarbon **11**, a small amount (4 %) of the hydrocarbon **13** and an unidentified hydrocarbon. The latter yielded on hydrogenation the hydrocarbon **13**, possessing therefore the same skeleton and a double bond in the two-carbon bridge.

6:7,8:9-Dibenzobicyclo[3.2.2]nona-2,6,8-triene (**10**) *by pyrolysis of the* **9c**

The acetate **9c** (0.5 g ; 1.8 mmoles) was introduced in small portions, under argon, in a quartz tube (50 cm length, 7 mm diameter) filled with glass wool on a portion of 70 mm. The upper part of the tube was heated (30 cm of its length including also the glass wool portion) at 450°, with a vertical electrical oven. At the cold lower end of the tube a liquid flowed down which rapidly solidified. The solid was dissolved in ether, the solution washed with 10 % Na_2CO_3 soln., dried and evaporated. After recrystallization from methanol, hydrocarbon **10**, (0.25 g ; 64 %)m.p. 164–166° was obtained which showed in the v.p.c. the same ret. time as that of the unsaturated hydrocarbon from the mixture isolated in the unbuffered solvolysis of the tosylate **1b**. (Found : C, 93.31 ; H, 6.67. $C_{17}H_{14}$ requires : C, 93.53 ; H, 6.47 %). *IR spectrum* (CS_2 and CCl_4 ; cm^{-1}) : 690 s, 760 vs, 1480 m, 2830 w, 2890 m, 2920 m, 3030 s, 3075 m.

The catalytic reduction (ethanol, PtO_2) of hydrocarbon **10** afforded hydrocarbon **15**, identical with that obtained on reduction of the ketone **14** (see below).

6:7,8:9-Dibenzobicyclo[3.2.2]nona-6,8-dien-2-one (**14**)

A solution of alcohol **9a** (0.5 g ; 2.12 mmoles) in 15 ml pyridine was added with cooling and stirring to a complex prepared from chromic anhydride (1 g) and pyridine (15 ml). The reaction mixture was worked up as for ketone **12**. After recrystallization from ethanol ketone **14** was obtained (0.4. g ; 81 %) m.p. 174–175°. (Found : C, 86.72 ;H, 6.29. $C_{17}H_{14}O$ requires : C, 87.14 ; H, 6.03). *IR spectrum* (CS_2 and CCl_4 ; cm^{-1}) : 732 m, 1710 vs, 2858 w, 2929 m, 3025 m, 3072 m.

On reduction with $LiAlH_4$ the ketone **14** yield quantitatively the alcohol **9a**.

6:7,8:9-Dibenzobicyclo[3.2.2]nona-6,8-diene (**15**)

A solution of ketone **14** (0,2 g ; 0,85 mmoles) in 1 ml hydrazine hydrate (96–98 %) and 3 ml diethyleneglycol was heated under reflux for 2 hr and the reaction mixture was worked up just as for the hydrocarbon **11**. The solid residue was recrystallized from methanol yielding 0.15 g (80 %) of hydrocarbon **15** m.p. 99–100°. (Found : C, 92.42 ; H, 7.52.$C_{17}H_{16}$ requires : C, 92.68 ; H, 7.32 %). *IR spectrum* (CS_2 and CCl_4 ; cm^{-1}) : 750 vs, 1030 ms, 1054 ms, 1440 ms, 1452 s, 1471 s, 2854 s, 2920 vs, 3020 s, 3068 ms.

Treatment of the alcohols **7**, **8**, *or* **9a** *with TsOH in acetic acid*

A solution of alcohol (0.3. g; 1.27 mmoles) and *p*-toluenesulfonic acid (0.24 g ; 1.27 mmoles) in 25 ml of anhydrous acetic acid was heated at 117° for a time as indicated in table 5. After working up and $LiAlH_4$-reduction as in the acetolysis of the tosylate **1b** a solid product was obtained. On treating with 7 ml methanol an insoluble compound representing the polymeric material was obtained. The methanolic filtrate was evaporated under red. press. and the crystalline product dried and weight, was analyzed by v.p.c. (Table 5).

Acetolysis of 6:7,8:9-dibenzobicyclo[3.2.2]nona-6,8-dien-2-yl-toluenesulfonate (**9b**)

a) *In the presence of sodium acetate.* Tosylate **9b** (0.2 g ; 0,515 mmoles) and sodium acetate (0.1 g ; 1.22 mmoles) were dissolved in 25 ml acetic acid. The solution was heated at 117° for 8 hr. The working up (as in the acetolysis of the tosylate **1b**) afforded 0.13 g of a yellow oil, which was subsequently reduced with 0.1 g $LiAlH_4$ in 25 ml ether ; 0.11 g of crystalline product resulted having the composition indicated in table 1.

b) *In the absence of sodium acetate.* A solution of tosylate **9b** (0.2 g ; 0.515 mmoles) in 25 ml anhydrous acetic acid was heated at 117° for 8 hr. The experiment was then conducted as in the case *a*). The composition of the final mixture is shown in table 1.

If the acetolysis was run at 70° (for 8 hr) the final mixture showed the following composition (v.p.c.) : 6.1 % of hydrocarbon **10** ; 7.9 % of *endo*-alcohol **7** ; 4.4 % of *exo*-alcohol **8** and 81.6 % of alcohol **9a**. Only traces of hydrocarbon **11** was found.

Equilibration of the alcohols 7 *and* 8 *in acetic acid with sodium acetate*

The *exo*-alcohol **8** (0.2 g ; 0.844 mmoles) and anhydrous sodium acetate (0.2 ; 2.4 mmoles) were heated at 117° for 48 hr in 20 ml acetic acid. After working up and $LiAlH_4$-reduction (as in the acetolysis of tosylate **1b**) 0.19 g (95 %) crystalline product were obtained with the following composition (v.p.c.) ; 56.9 % of *endo*-alcohol **7** ; 28.6 % of *exo*-alcohol **8** and 14.5 % of alcohol **9a**.

A similar run using the *endo*-alcohol **7** gave the following results : 55.7 % of *endo*-alcohol **7** ; 28.9 % of *exo*-alcohol **8** and 15.4% of alcohol **9a**.

Acknowledgements

We wish to thank Miss E. Sliam and Mrs. V. Daniel for performing the elementary analyses, and Mr. F. Chiraleu for recording the NMR spectra.

Revue Roumaine de Chimie, **14**, 929–939 (1969)

KINETICS OF THE ACETOLYSIS OF 1 : 2,5 : 6-DIBENZOCYCLOHEPTA-1,3,5-TRIENYL-7-ETHYL β-TOSYLATE[1]

M. VOICU and F. BADEA

Organic Chemistry Laboratory,
Polytechnic Institute, Bucharest, str. Polizu, 1

Received February 25, 1969

Rate constants for the acetolysis of 1:2,5:6-dibenzocyclohepta-1,3,5-trienyl-7-ethyl β-tosylate (**1**) and its saturated analog 1:2,5:6-dibenzocyclohepta-1,5-dienyl-7-ethyl β-tosylate (**4**) have been measured at different sodium acetate concentrations. The variation of the ratio of products formed in the solvolysis of **1** (uncyclized and cyclized products) with the sodium acetate concentration was found to be linear. The comparison of the rate constants of the tosylates **1** and **4** permitted to establish a relationship between the ratio of the products formed in the acetolysis of **1** and the kinetic data. It was kinetically proved that the normal acetolysis product **2** results in part by a retro-π-route. The stability of the nonclassical ion formed by a π-route from **1** is discussed.

INTRODUCTION

Evidence has been presented that in the solvolysis of some alkenylhalogenides or arene-sulfonates, the double bond participates in the ionization site (π-route in carbonium ion formation[2]). The anchimeric assistance is appreciated from the ratio of the rate constants of the unsaturated compound (k_U) and the saturated correspondent (k_S), as well as from the isolation of cyclic products.[3]

In the present work the acetolysis of 1 : 2,5 : 6-dibenzocyclohepta-1,3,5-trienyl-7-ethyl β-tosylate (**1**) and its saturated analog, 1 : 2,5 : 6-dibenzocyclohepta-1,5-dienyl-7-ethyl β-tosylate (**4**) has been studied. The observed k_U/k_S ratio is about 15 in acetic acid at 110°. This anchimeric assistance is associated with cyclization to bicyclo[3.2.2]nonane derivatives (**3**), in addition to the formation of the 1 : 2,5 : 6-dibenzocyclohepta-1,3,5-trienyl-7-ethyl β-acetate (**2**).[1] We have shown that the ratio of uncyclized to cyclized products depends on the concentration of the sodium acetate present in the reaction medium.

---

[1] The chemistry of the reaction discussed herein was studied by: E. Ciorănescu, M. Banciu, R. Jelescu, M. Rentzea, M. Elian and C. D. Nenitzescu; see the previous communication.

[2] The term "π-route" was proposed by S. Winstein and P. Carter, *J. Amer. Chem. Soc.*, **83**, 4485 (1961).

[3] P. D. Bartlett, S. Bank, R. J. Crawford and G. H. Schmid, *J. Amer. Chem. Soc.*, **87**, 1288 (1965).

Although such a dependence in a π-route reaction has been noted before by Bartlett [3] it has since been overlooked.[4–6]

The molar fraction of acetate **2** in the reaction products is proportional to the amount of added sodium acetate but is not null in its absence. Therefore we concluded that the acetate **2** results from a bimolecular reaction with the acetate ion ($k_{2,\mathrm{U}}$) and from a solvolytic reaction ($k_{1,\mathrm{U}}$). The cyclization products **3** are in net excess throughout the studied conditions (from 91.7% for [NaOAc] = 0, to 64.7% for [NaOAc] = 0.5 mol/l). These products result apparently[7] through a rapid unimolecular assisted reaction ($k_{\mathrm{U,A}}$). This assumption is further evidenced by the relatively high value of the ratio $k_\mathrm{U}/k_\mathrm{S}$.

The acetolysis of the tosylate **1** was treated as a system of competitive reactions:

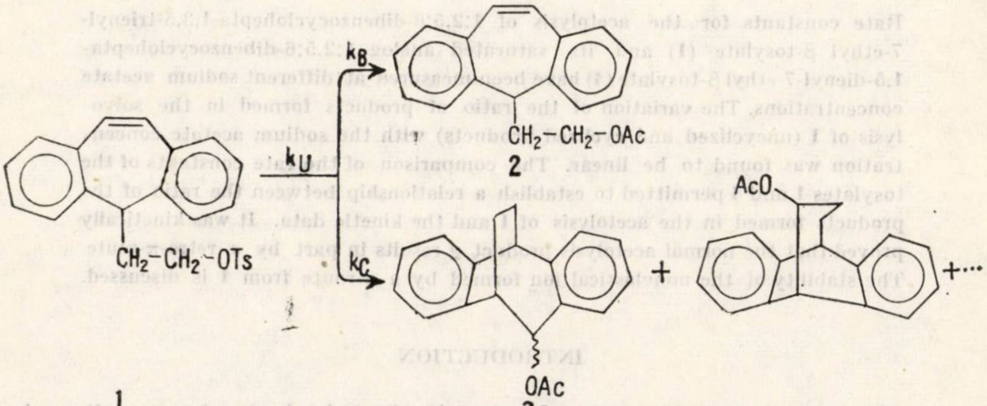

1 3a 3b

This representation based on the analysis of the reaction products, leads to the following relationships:

$$-\frac{d\mathrm{U}}{dt} = k_\mathrm{U}\mathrm{U} = k_{1,\mathrm{U}}\mathrm{U} + k_{2,\mathrm{U}}\,[\mathrm{NaOAc}]\cdot\mathrm{U} + k_{\mathrm{U.A}}\mathrm{U} \qquad (1)$$

$$\frac{d\mathrm{B}}{dt} = k_\mathrm{B}\mathrm{U} = k_{1,\mathrm{U}}\mathrm{U} + k_{2,\mathrm{U}}\,[\mathrm{NaOAc}]\cdot\mathrm{U} \qquad (2)$$

$$\frac{d\mathrm{C}}{dt} = k_\mathrm{C}\mathrm{U} = k_{\mathrm{U.A}}\mathrm{U} \qquad (3)$$

---

[4] P. D. Bartlett, W. S. Trahanovski, D. A. Bolon and G. H. Schmid, *J. Amer. Chem. Soc.*, **87**, 1314 (1965).

[5] P. D. Bartlett, E. M. Nicholson and R. Owyang, *Tetrahedron Suppl.*, **8**, P. II, 399 (1966).

[6] R. Munegaki and H. Tanida, *J. Amer. Chem. Soc.*, **90**, 656 (1968) and lit. cited therein.

[7] We admit that compounds **3** arise from a common intermediate formed in the rate determining step.

where U is the concentration of tosylate **1**, B is the concentration of acetate **2**, C is the concentration of cyclized compounds **3**, k_B and k_C are the rate constants of the competitive reactions leading to compounds **2** and **3** respectively, and k_U is the observed rate constant in the acetolysis of the tosylate **1**.

The ratio of uncyclized to cyclized products will be given by equation (4) obtained from (2) and (3):

$$\frac{dB}{dC} = \frac{k_{1,U} + k_{2,U}[NaOAc]}{k_{U,A}} \tag{4}$$

Relation (4) shows that the ratio of the products of the two hetero-competitive reactions varies with the sodium acetate concentration (which decreases during the buffered solvolysis as a result of the formed *p*-toluenesulfonic acid). When sodium acetate is in constant excess, integration of the differential equation (4) gives:

$$\frac{B}{C} = \frac{k_{1,U} + k_{2,U}\,[NaOAc]}{k_{U,A}} \tag{5}$$

It was a purpose of the present work to check the validity of these relationships.

RESULTS

The rate of the acetolysis of tosylate **1** was titrimetrically and spectrophotometrically measured. The observed rate constants rise with increasing sodium acetate concentration (Table 1).

Table 1

Rate constants for acetolysis of 1 : 2,5 : 6-dibenzocyclohepta-1,3,5-trienyl-7-ethyl β-tosylate (1)

Temperature °C	$10^3 \cdot$ [NaOAc] M	$10^3 \cdot$ [ROTs] M	$10^4 \times k_U$ [a] sec^{-1}
80.0	—	0.0782	0.100 [b]
80.0	—	24.9	0.111 [c]
110.2	—	0.0782	1.99 [b]
110.0	—	20.5	2.04 [c]
110.3	21.9	0.0713	2.22 [b]
110.0	28.0	9.94	2.17 [c]
110.0	226.0	0.0710	2.44 [b]

a) Rate constants were calculated from a first order equation.

b) Calculated from spectrophotometrical measurements (see table 4).

c) Calculated from titrimetric measurements.

If sodium acetate is in large excess, the ratio of uncyclized to cyclized products (B/C) is proportional to the initial sodium acetate concentrations (see fig. 1) but is fairly constant during one experiment, in accordance with equation (5). In agreement with a (4)-type relation, the ratio B/C decreases during an acetolysis experiment in which the ratio [NaOAc]/[ROTs] is not high. The B/C ratios were measured spectrophotometrically from runs maintained more than 10 half-lives at 110° and are represented *vs.* sodium acetate concentration in figure 1

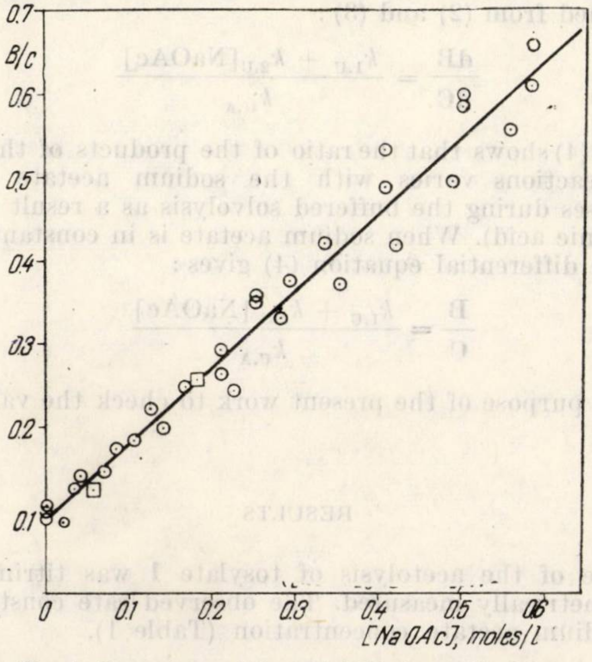

Fig. 1. Dependence of the ratio B/C of uncyclized **2** to cyclized products **3** on sodium acetate concentration. Slope = 0.91 $l.mol^{-1}$; interception = 0.091 (calculated through least square method).

⊙ Concentration of the tosylate **1** = $(7 \div 13) \times 10^{-5}$M

⊡ Determinations were made with a 0.034 M concentration of **1**. The corresponding concentration of sodium acetate was considered : $([NaOAc]_0 + [NaOAc]_f)/2$.

For comparison, the rate constants (k_S) of the acetolysis of the saturated correspondent 1 : 2,5 : 6-dibenzocyclohepta-1,5-dienyl-7-ethyl β-

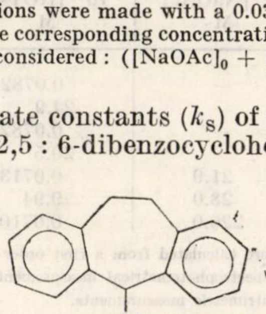

4

tosylate were measured (table 2). In acetic acid at 110° the k_U/k_S ratio is about 15 which shows that the ionization of compound **1** is anchimerically assisted by the double bond. The tosylate **4** forms with practical quantitative yield only the 1 : 2,5 : 6-dibenzocyclohepta-1,5-dienyl-7-ethyl β-acetate. By vpc it was shown that the solvolysis product of tosylate **4** (after treatment with $LiAlH_4$) is pure 1 : 2,5 : 6-dibenzocyclohepta-1,5-dienyl-7-ethanol, free of other products.

Table 2

Rate constants for acetolysis of 1 :2,5 :6-dibenzocyclohepta-1,5-dienyl-7-ethyl β-tosylate (4)

Temperature °C	$10^3 \cdot$[NaOAc] M	$10^3 \cdot$[ROTs] M	$10^5 \times k_S$ [a)] sec^{-1}
80.0	—	16.8	0.066
110.0	—	12.2	1.34
110.0	27.3	9.96	1.43
110.0	28.1	9.88	1.47
110.1	77.8	25.1	1.61

a) Rate constants were calculated assuming a first order equation from titrimetric measurements.

The activation parameters and the Winstein's normal salt effect (b_{NaOAc}) for tosylates **1** and **4** are given in table 3.

Table 3

Activation parameters and normal salt effects for the acetolyses of tosylates 1 and 4

Compound	$\Delta H^{\neq 298}$ kcal/mol	$\Delta S^{\neq 298}$ e.u.	$b^{110°}_{NaOAc}$
1	25.4	− 9.8	0.7
4	26.3	−13.0	2.6

DISCUSSION

1. *The mechanism of the acetolysis of 1 : 2,5 : 6-dibenzocyclohepta-1,5-dienyl-7-ethyl β-tosylate (4)*

The kinetics of the acetolysis of 1 : 2,5 : 6-dibenzocyclohepta-1,5-dienyl-7-ethyl β-tosylate (**4**) is first order. The addition of sodium acetate brings about an increase of the rate of solvolysis (table 2). These results would seem to indicate either a unimolecular mechanism with a common salt effect of the added sodium acetate or a pseudounimolecular solvolysis accompanied by a bimolecular reaction of the acetate ion. Compound **4** has the *p*-toluenesulfonyl-group linked to a primary carbon atom; the unimolecular ionization could be assisted by the neighbouring aromatic rings (i.e. of the type Ar_2-5). This possibility is ruled out both by the lack in the reaction mixture of a cyclization product and by the fact that cycloheptyl-ethyl-tosylate has a solvolysis rate [8] comparable in magnitude to that of compound **4**. Thus, it is concluded that the rate expression of the acetolysis of tosylate **4** would be given by the differential equation:

---

[8] M. Voicu, unpublished results.

$$-\frac{dS}{dt} = k_S S = k_{1,S} S + k_{2,S}[NaOAc]\cdot S \qquad (6)$$

where S is the concentration of compound **4**, $k_{1,S}$ (sec^{-1}) is the rate constant for the pseudounimolecular process in the absence of added sodium acetate and $k_{2,S}$ is the bimolecular rate constant (l.mol^{-1}. sec^{-1}) of the competitive reaction with the acetate ion. From data in tables 2 and 3, the values at 110° are $k_{1,S} = 1.34 \times 10^{-5}$ sec^{-1} and $k_{2,S} = 3.5 \times 10^{-5}$ l.mol^{-1}.sec^{-1}.

2. *The mechanism of the acetolysis of 1 : 2,5 : 6-dibenzocyclohepta-1,3,5-trienyl-7-ethyl β-tosylate* (**1**)

In those reactions in which cyclization products were not isolated, the ratio k_U/k_S is $\leqslant 1$ as follows: for $\triangle^3$-cyclopentenylbromide[9] it is 0.25; for 2-(3-indanyl)-ethyl *p*-nitrobenzenesulfonate[10] it is 0.65; for 4-pentenyl-*p*-nitrobenzenesulfonate[11] it is 0.72; for hexen-4-yl-*p*-nitrobenzenesulfonate[12] it is 0.77; for $\triangle^2$-cyclobutenylmethyl-tosylate[13] it is 0.76; for 3-($\triangle^1$-cyclopentenyl)-propyl-brosylate[14] it is 0.97; for 2-($\triangle^2$-cyclopentenyl)-ethyl-brosylate[15] it is 0.99; for cyclohexen-3-yl-methyl-brosylate[16] it is ~1, and for 3-($\triangle^3$-cyclopentenyl)-propyl-*p*-nitrobenzenesulfonate[4] it is 1.1.

In these cases it is considered that the ionization is not assisted by the carbon-carbon double bond; using the notations mentioned above $k_{U,A} = 0$ and the ratio k_U/k_S becomes:

$$\frac{k_U}{k_S} = \frac{k_{1,U} + k_{2,U}\,[NaOAc]}{k_{1,S} + k_{2,S}\,[NaOAc]} \qquad (7)$$

In accordance with equation (5) the data presented in figure 1 show that the plot B/C (normal product **2**/cyclized products **3**) *vs.* sodium acetate concentration is linear. It is easily seen from equation (5) that the slope and interception of the straight line must be $k_{2,U}/k_{U,A}$ and $k_{1,U}/k_{U,A}$ respectively. Using the observed rate constant of the solvolysis of tosylate **1** in the absence of sodium acetate, $k_{1,U} + k_{U,A} = 2.04 \times 10^{-4}$ sec^{-1} (see table 1), the calculation of the individual rate constants gives the following values: $k_{1,U} = 1.69\times10^{-5}$ sec^{-1}, $k_{2,U} = 1.69\times10^{-4}$ l.mol^{-1}. sec^{-1} and $k_{U,A} = 1.87\times10^{-4}$ sec^{-1}. Substitution of these values in equation (7) leads to $k_U/k_S \approx (2.0 \div 3.3)$ for [NaOAc] = (0.1 ÷ 0.5) mol/l. As the solvolytical rate constants $k_{1,S}$ and $k_{1,U}$ have about the same value, the rate constant $k_{2,\mathrm{U}}$ seems to show an abnormal large value compared with $k_{2.\mathrm{S}}$. It is thus concluded that the normal product **2** of the solvolysis, must be formed also through another route which is not common to the tosylate **4** and which involves in its turn a reaction with sodium acetate.

---

[9] P. D. BARTLETT and M. R. RICE, *J. Org. Chem.*, **28**, 3351 (1963).

[10] P. D. BARTLETT and G. D. SARGENT, *J. Amer. Chem. Soc.*, **87**, 1297 (1965).

[11] P. D. BARTLETT, W. D. CLOSSON and T. J. COGDELL, *J. Amer. Chem. Soc.*, **87**, 1308 (1965).

[12] W. D. CLOSSON from P. D. BARTLETT, *Liebigs Ann. Chem.*, **653**, 45 (1962).

[13] M. HANACK and K. RIEDLINGER, *Chem. Ber.*, **100**, 2107 (1967).

[14] W. D. CLOSSON and G. T. KWIATKOWSKI, *Tetrahedron*, **1965**, 2779.

[15] W. D. CLOSSON and G. T. KWIATKOWSKI, *J. Amer. Chem. Soc.*, **86**, 1887 (1964).

[16] G. LENY, *Compt. rend.*, **251**, 1526 (1960).

In a probable scheme (Chart I) the normal acetate **2** results on the one hand through two reactions comparable with those encountered by the solvolysis of the saturated tosylate **4** ($k_{1.\mathrm{U}} \approx k_{1.\mathrm{S}}$, $k_2 \approx k_{2.\mathrm{S}}$).

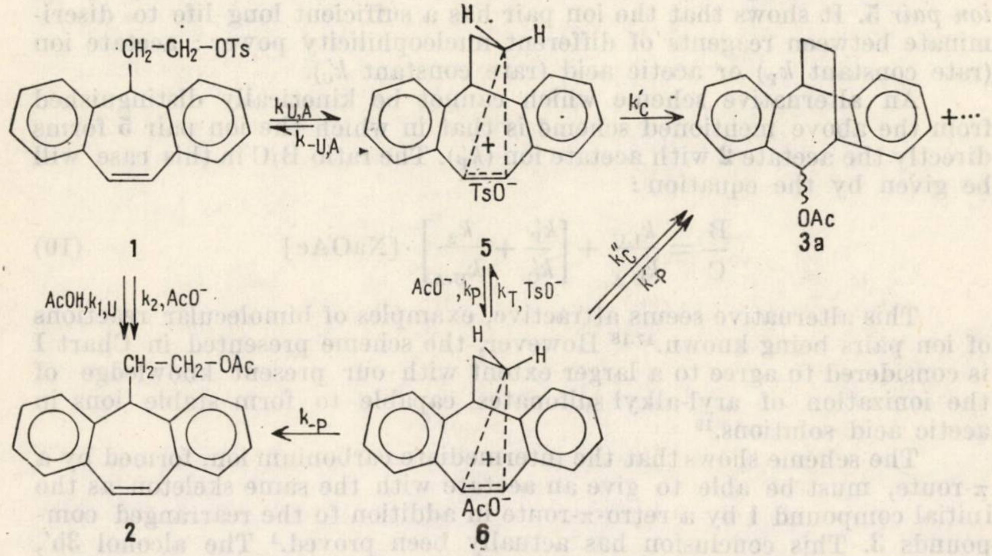

Chart

On the other hand the acetate **2** may be formed by an external return from the ion pair **6** ($k_{-\mathrm{P}}$). This ion pair results in its turn from the initially formed ion pair **5** ($k_{\mathrm{U,A}}$) and acetate ion (k_{P}). The cyclized products **3** arise by a series of rapid steps (k'_{C} and k''_{C}) from ion pairs **5** and **6** with acetic acid.

Considering that tosylate ion is poorer nucleophile than acetate ion, the external return from ion pair **5** ($k_{-\mathrm{U.A}}$) may be neglected compared with the external return from **6**. The reversible transformation of ion pairs **6** in **5** (k_{T}) may also be neglected : $k_{\mathrm{T}}[\mathrm{TsO}^-] \ll k_{\mathrm{P}}[\mathrm{AcO}^-]$.

If sodium acetate concentration is constant and not too high, the application of the steady state theory for all the intermediates of Chart I leads to equation (**8**), where $k'''_{\mathrm{C}} \equiv k'_{-\mathrm{P}} + k''_{\mathrm{C}}$.

$$\frac{\mathrm{B}}{\ } = \frac{k_{1.\mathrm{U}}}{k_{\mathrm{U.A}}} + \left[\frac{k_{\mathrm{P}}}{k'_{\mathrm{C}}\left(1 + \dfrac{k'''_{\mathrm{C}}}{k_{-\mathrm{P}}}\right)} + \frac{k_2}{k_{\mathrm{U.A}}}\right]\cdot[\mathrm{NaOAc}] \qquad (8)$$

According to this relation the plot of B/C *vs.* time must be linear, the intercept of the ordinate from figure 1 being $k_{1.\mathrm{U}}/k_{\mathrm{U.A}}$ as in relation (5).

Revue Roumaine de Chimie, **14**, 929–939 (1969)

– c 3384

The sum in parenthesis must be greater than the hypothetical slope ($k_{2.S}/k_{U.A} = 0.19$) with the value of the term R :

$$R = \frac{k_P}{k'_C\left(1 + \frac{k'''_C}{k_{-P}}\right)} \tag{9}$$

In our example R = 0.72. *The term R measures the stability of the ion pair* **5**. It shows that the ion pair has a sufficient long life to discriminate between reagents of different nucleophilicity power : acetate ion (rate constant k_P) or acetic acid (rate constant k'_C).

An alternative scheme which cannot be kinetically distinguished from the above mentioned scheme is that in which the ion pair **5** forms directly the acetate **2** with acetate ion (k'_P). The ratio B/C in this case will be given by the equation :

$$\frac{B}{C} = \frac{k_{1.U}}{k_{U.A}} + \left[\frac{k'_P}{k'_C} + \frac{k_2}{k_{U.A}}\right] \cdot [\mathrm{NaOAc}] \tag{10}$$

This alternative seems attractive, examples of bimolecular reactions of ion pairs being known.[17,18] However, the scheme presented in Chart I is considered to agree to a larger extent with our present knowledge of the ionization of aryl-alkyl-sulfonates capable to form stable ions in acetic acid solutions.[19]

The scheme shows that the intermediate carbonium ion, formed by a π-route, must be able to give an acetate with the same skeleton as the initial compound **1** by a retro-π-route in addition to the rearranged compounds **3**. This conclusion has actually been proved.[1] The alcohol **3b'**, corresponding to acetate **3b**, on treatment with *p*-toluenesulfonic acid in acetic acid at 117° gives a mixture of acetates and hydrocarbons in which the acetate **2** is present up to 20%. The intermediate, involved in this reaction must be the phenonium ion **7** capable to rearrange to the ion pair **5**.

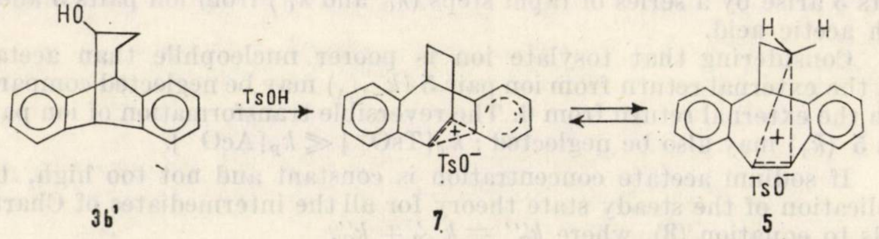

3b' 7 5

In contrast to the well known procedure [20,21] to detect the suppression of the external return by an added salt, the analysis of the acetolysis

---

[17] R. A. Sneen and J. W. Larsen, *J. Amer. Chem. Soc.*, **88**, 2593 (1966).

[18] R. A. Sneen, J. V. Carter and P. S. Kay, *J. Amer. Chem. Soc.*, **88**, 2594 (1966).

[19] S. Winstein, E. C. Clippinger, A. H. Fainberg, R. Heck and G. C. Robinson, *J. Amer. Chem. Soc.*, **78**, 328 (1956).

[20] A. H. Fainberg and S. Winstein, *J. Amer. Chem. Soc.*, **78**, 2767 (1956).

[21] S. Winstein and G. C. Robinson, *J. Amer. Chem. Soc.*, **80**, 169 (1958).

of tosylate **1** allows the estimation of the effects of acetate ion in suppressing the external return from the apparent abnormally high value of the bimolecular rate constant $k_{2,\mathrm{U}}$.

3. *Comparison of the acetolysis of tosylates* **1** *and* **4** *with known examples*

An example in which the necessary data are available is furnished by the acetolysis of *p*-nitrobenzenesulfonate **8** ($\mathrm{Ns} = p\text{-}\mathrm{O_2N{-}C_6H_4SO_2}$).[4] Considering the ratio $k_{\mathrm{U}}/k_{\mathrm{S}} \approx 1$ and using the above mentioned notation for the acetolysis of compound **8**, the following rate constants may be computed from the published data : $k_{1,\mathrm{U}} \approx k_{1,\mathrm{S}}$, $k_{2,\mathrm{U}} \approx k_{2,\mathrm{S}}$ and $k_{\mathrm{U.A}} = k_{\mathrm{U}} - k_{2,\mathrm{U}} \cdot [\mathrm{NaOAc}] - k_{1,\mathrm{U}}$. The ratio of the uncyclized product (**10**) and the cyclized products (**9a** and **9b**) calculated from relation (5) is B/C = 0.60 (compared with the experimental[4] value 0.64). The term R calculated from relation (9) is[22] about 0.2 indicating a somewhat smaller stabilization of the ion pairs resulting from **8** than for **5**.

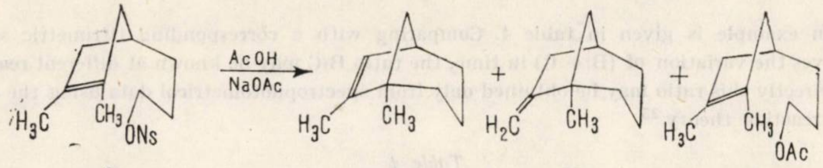

8 **9a** **9b** **10**

The cyclization is favoured for compounds **1** and **8** by an increase of activation entropies as compared to the activation entropies of the saturated analogs, and for the sole compound **1** also by a decrease in the activation enthalpy (table 3). Thus, the ratio of the products formed through π-route is higher in the case of tosylate **1** than in the case of compound **8**.

EXPERIMENTAL

Acetic acid. The acetic acid used for these studies was obtained by refluxing commercial acetic acid with acetic anhydride followed by distillation on an efficient column. Congelation point was 16.4°. The solvent contains a small amount of acetic anhydride, identified by its band at 256 mμ.[23]

1 : 2,5 : 6-Dibenzocyclohepta-1,3,5-trienyl-7-ethyl- and 1 : 2,5 : 6-dibenzocyclohepta-1,5-dienyl-7-ethyl β*-tosylates* were previously[1] described.

Sodium acetate solutions were prepared by dissolving anhydrous sodium acetate in acetic acid. Solutions of different sodium acetate concentrations were obtained from a stock solution by dilution with corresponding amounts of acetic acid. The concentration of the solutions was determined by titration with a 0.05 M solution of perchloric acid in acetic acid.

---

[22] The value must be considered as very approximate since it was calculated from a single product determination.

[23] S. Buckenstein, *Analyt. Chem.*, **31**, 1757 (1959).

The ratio B/C was measured spectrophotometrically taking advantage of the 293 mμ absorption band corresponding to the stilbene system of compounds **1** and **2**.[24] Both compounds have an identical extinction coefficient of about 12,400. The applicability of the Lambert-Beer law was verified. When the reaction is completed (more than ten half lives) : $U = 0$, $E_\infty \sim B$, $E_0 \sim U_0$, $C \sim (E_0 - E_\infty)$; the ratio of uncyclized (**2**) to cyclized products (**3**) was calculated from :

$$\frac{B}{C} = \frac{E_\infty}{E_0 - E_\infty} \tag{11}$$

A V.S.U.-1 (Carl Zeiss-Jena) spectrophotometer was used. Readings were made at room temperature ; comparison was made with acetic acid. The results are plotted in figure 1.

During the reaction : $E \sim (U + B)$, $C \sim (E_0 - E)$; the concentration of cyclized products **3** in time is given by the relation :

$$\frac{C}{U_0} = \frac{E_0 - E}{E_0} \tag{12}$$

An example is given in table 4. Comparing with a corresponding titrimetric series' which gives the variation of (B + C) in time, the ratio B/C may be known at different reaction times. Directly this ratio may be obtained only from spectrophotometrical data using the competitive reaction theory.[25]

Table 4

Acetolysis of tosylate 1 at 110.3°

[NaOAc] = 21.9 × 10^{-3} M

[ROTs] = 7.13 × 10^{-3} M

Time $10^{-3} \times t$ sec.	E ($\lambda = 293$ mμ)	C/U$_0$ a) %	$10^4 \times k$ c) sec.$^{-1}$
0	0.880	0	2.22 b)
1.5	0.634	27.9	2.18
2.7	0.502	42.9	2.08
3.9	0.394	55.3	2.06
6.0	0.266	70.0	2.00
7.5	0.205	76.8	1.95
9.0	0.163	81.3	1.88
10.8	0.128	85.6	1.78
12.6	0.109	87.7	1.65
∞	0.069	92.2	...

a) Calculated from equation (12)

b) Extrapolated[25] from $k = f(t)$; for $t = 0$, $k = k_U$

c) $k = \frac{2.303}{t} \log \frac{E_0}{E}$

Kinetic measurements. The ampoule technique has been used throughout. Solutions of tosylate and sodium acetate in acetic acid of desired concentrations were transferred in sealed tubes and thermostated. At appropriate intervals the ampoules were withdrawn and chilled at room temperature (in these conditions the reaction is practically quenched) and the content was introduced in the spectrophotometer cuve. The calculation of the rate constants was made as in the example of table 4.

---

[24] Compounds **3** do not absorb in this region.

[25] After R. HUISGEN in "Methoden der organischen Chemie" (Houben-Weyl) Ed. IV, Physikalische Methoden, Georg Thieme Verlag, Stuttgart, Bd. 3, Teil 1, p. 143.

In the case of titrimetrical measurements, the *p*-toluenesulfonic acid was titrated with a 0.05 M sodium acetate solution. A Metrohm potentiograph, Model E 336 with a platinum electrode and a graphite capilar electrode designed after H. Zeidler,[26] has been used. In solvolysis with sodium acetate, the titrimetric measurements were made in the same manner after addition of an excess of a 0.05 M perchloric acid in acetic acid.

---

[26] H. Zeidler, *Z. Analyt. Chem.*, **146**, 271 (1955).

Revue Roumaine de Chimie, 14, 941–945 (1969)

FACTORS AFFECTING STABILITY AND EQUILIBRIA OF FREE RADICALS. V[1]

SYNTHESIS AND SPECTRA OF POLYNITROPHENYL-ALKOXYAMINES

A. T. BALABAN,* MARIA FRANGOPOL, N. NEGOIŢĂ, P. T. FRANGOPOL and MARIA PARASCHIV

Institute of Atomic Physics, P. O. Box 35, Bucharest

Received February 21, 1969

The preparation of 2,4-dinitro, 2,6-dinitro-, and 2,4,6-trinitro-, -methoxyamine and -ethoxyamines is reported. Attempts to obtain polynitrophenyl-t-butoxyamines failed. Ultraviolet and visible, as well as infrared absorption spectra are reported and discussed.

INTRODUCTION

In a previous part [2] of this series it was shown that the *para*-phenylogue (I, R = NPh_2) of diphenylpicrylhydrazyl (DPPH), (II. R = NPh_2) is a stable crystalline nitrogen free radical, like DPPH. Similarly, it was shown that one can obtain in solution the free radicals I, R = NMe_2 or OMe. It was interesting to see whether the lower phenyllogues of these two radicals, i.e. II, R = NMe_2 or OMe, are stable.

According to Poirier und Benington,[3a] the oxidation of 2,2-dimethyl-1-picrylhydrazine[3b] by lead dioxide failed to afford 2,2-dimethyl-1-picrylhydrazyl (II, R = NMe_2).

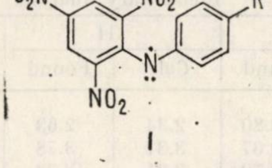

I

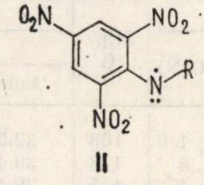

II

---

* Present address: International Atomic Energy Agency, Kärnthnering 11, Vienna 1010 Austria.

[1] Part IV, P. T. Frangopol, M. Frangopol, N. Negoiţă and A. T. Balaban, *Revue Roumaine Chim.*, **14** 385 (1969); P. T. Frangopol, M. Frangopol, N. Negoiţă and E. Romaş, *Rev. Roumaine Chim.*, **14** 527 (1969).

[2] A. T. Balaban, P. T. Frangopol, M. Frangopol and N. Negoiţă, *Tetrahedron*, **23**, 4661 (1967).

[3a] H. J. Poirier and F. Benington, *J. Org. Chem.*, **19**, 1157 (1954).

[3b] H. H. Hatt, *Org. Synth. Coll.*, **2**, 211 (1943).

On reinvestigating this statement, using either lead dioxide, silver (I) oxide or silver (II) oxide as oxidants we confirm this negative result. The alkoxy derivatives (II, R = OMe, OEt) or their corresponding amines were not however, reported in the literature. We decided therefore
(i) to prepare the polynitrophenyl-alkoxyamines IIIH — VIIIH,*
(ii) to study their oxidation to free radicals III — VIII and
(iii) to find out whether the stability of these free radicals can be rationalized in terms of steric[3c,d] and electronic factors.[3e,f]

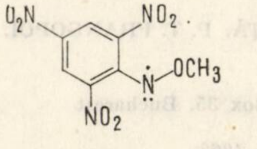

III

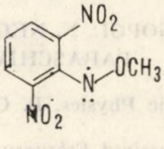

IV

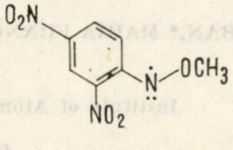

V

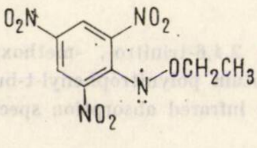

VI

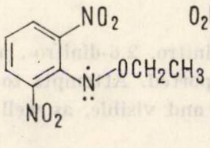

VII

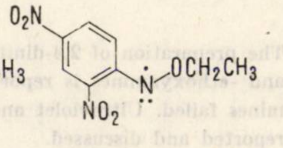

VIII

SYNTHESIS OF POLYNITROPHENYL-ALKOXYAMINES

Attempts to condense chloropolynitrobenzenes with methoxy- or ethoxyamine as free bases resulted in low yields owing to the volatility of the free bases and to their decomposition during the reaction. It was found more convenient to generate these bases *in situ* by effecting the reaction between chloropolynitrobenzenes and the alkoxyamine hydrochloride in refluxing ethanol in the presence of sodium hydrogen carbonate. An excess of alkoxyammonium chloride makes purifications easier.

Table 1
Melting points and analyses of polynitrophenyl-alkoxyamines

Compound			M.p. °C	Elementary analysis					
				C		H		N	
No	Alk	(O_2N)		Calc.	Found	Calc	Found	Calc.	Found
IIIH	Me	2, 4, 6	168	32.56	32.80	2.34	2.63	21.70	21.95
IVH	Me	2, 6	118	39.44	39.67	3.31	3.78	19.71	19.28
VH	Me	2, 4	115	39.44	39.70	3.31	3.73	19.71	20.09
VIH	Et	2, 4, 6	108	35.30	35.43	2.96	2.96	20.58	20.93
VIIH	Et	2, 6	75—6	42.29	41.93	3.99	3.89	18.50	19.18
VIIIH	Et	2, 4	110	42.29	42.75	3.99	4.02	18.50	17.50

---

* The letter H after the numeral of a nitrogen free radical indicates the amine corresponding to the radical.

[3c] D. Braun and G. Peschk, *Chimia*, **21**, 536 (1967); *Angew. Chem.*, **80**, 1002 (1968).
[3d] D. H. Williams, *J. Amer. Chem. Soc.*, **89**, 4280 (1967).
[3e] M. J. S. Dewar, *ibid.*, **74**, 3353 (1952).
[3f] R. I. Walter, *ibid.*, **88**, 1923 (1966).

The resulting yellow alkoxypolynitrobenzenes IIIH – VIIIH have melting points and analyses presented in table 1. Attempts to condense t-butoxyamine with chloropolynitrobenzenes failed, probably owing to steric hindrance.

Oxidation of these secondary amines with silver (I) oxide afforded alkoxy-polynitrophenyl-amino free radicals III – VIII which are described in a forthcoming paper.

The facile synthesis of polynitrophenyl-alkoxyamines IIIH – VIIIH contrast with the failure[4] to obtain normal condensation products from chloropolynitrobenzenes and N-acylated hydroxylamines in an attempt to prepare O-arylhydroxylamines by subsequent hydrolysis of the expected condensation products; instead, products of Lossen rearrangements were isolated; however, the condensation with hydroxyurethanes proceeds normally,[4] but hydrolysis was accompanied by deamination leading to polynitrophenols. More related structurally to the compounds described here are the N-picrylhydroxylamine[5a] (whose O-alkylation products are compounds IIIH or VIH), or the N-acyl-O-alkylhydroxylamines[5b] (whose oxidation affords free radicals).

INFRARED ABSORPTION SPECTRA

The infrared spectra of alkoxyamines have been described in the literature; being primary amines, they present two NH stretching bands.[5c] Polynitrophenyl-alkoxyamines are secondary amines and present one NH stretching band as indicated in table 2. Whereas the νNH values in potassium bromide pellet do not reveal any regular trend, the NH

Table 2

Infrared NH bands (cm^{-1}) and electronic absorption maxima in 1,2-dichloroethane (nm) of polynitrophenylalkoxyamines[a]

Compound			IR Spectrum		Electronic absorption bands					
No	Alk	(O_2N)	νNH in		A		B		C	
			KBr	CCl_4	λ	ε	λ	ε	λ	ε
IIIH	Me	2, 4, 6	3310	3302	413s	3000	332	10500	262s	6000
IVH	Me	2,6	3296	3308	387	3100	—	—	268	4600
VH	Me	2,4	3355	3362	395s	4500	337	15300	262	10600
VIH	Et	2, 4, 6	3279	3311	—	—	337	12500	—	—
VIIH	Et	2,6	3304	3315	403	6400	—	—	269s	6400
VIIIH	Et	2,4	3379	3368	413s	4400	340	14200	262	9500

[a] A shoulder or an inflection of the band envelope are indicated by s.

---

[4] A. O. Ilvespaa and A. Marxer, *Helv. Chim. Acta*, **46**, 2009 (1963); *Chimia*, **18**, 1 (1964).

[5a] W. Borsche, *Ber. Dtsch. Chem. Ges.*, **56**, 1941 (1923).

[5b] M. A. Khan, *Diss. Abstr.*, **27**, 4310-B (1967).

[5c] M. Davies and N. A. Spiers, *J. Chem. Soc.*, **1959**, 3971, D. L. Frasco and E. L. Wagner, *J. Chem. Phys.*, **30**, 1124 (1959); P. V. Tikhanov, A. F. Vasiliev and Yu. A. Boskakov, *Khim. Geterotsikl. Soed.*, 746 (1968).

stretching frequencies in carbon tetrachloride solution show a slight displacement (6—9 cm^{-1}) towards higher wave numbers for the ethoxy derivatives relatively to the methoxy compounds, and an appreciable difference (50—60 cm^{-1}) between 2,4-dinitroderivatives relatively to 2,4,6-tri- or 2,6-dinitro compounds. The latter observation is interpreted [2] as implying a weaker hydrogen bond between NH and *o*-NO_2 groups in the 2,4-dinitroderivatives with only one *ortho-* nitro group.

The idea [6] that intramolecular hydrogen bonds are absent in aniline derivatives with one *ortho-* nitro group, and are present when there are two *ortho*-nitro groups, was withdrawn.[7] NMR studies [8–10] evidenced steric hindrance to free rotation in *o*-nitroaniline derivatives consistent with IR and UV studies.

Other significant infrared absorption bands in the spectra of IIIH—VIIIH are the strong benzene ring vibrations at 1600—1610 and 1620—1635 cm^{-1}, the asymmetric and symmetric nitro group frequencies at ca. 1530 and 1350 cm^{-1}, the NH deformation vibration at 1430—1435 cm^{-1} occurring at slightly higher frequencies in 2,6-dinitroderivatives (1450—1470 cm^{-1}) and bands characteristic of the ether linkage (1060—1070 cm^{-1}), (1300—1310 cm^{-1}). A weak band at 2820 cm^{-1} is apparent in methoxy derivatives owing to the methyl C—H stretching vibrations.

ULTRAVIOLET AND VISIBLE ABSORPTION SPECTRA

Table 2 presents electronic absorption bands of polynitrophenylalkoxyamines in 1,2-dichloroethane. The bands are denoted by letters, A, B or C in the order of decreasing wavelengths. Band C, present in all six compounds, is in some cases a shoulder on the band envelope rising towards lower wavelengths. Band B is clearly apparent, but only compounds IIIH, VH. VIH and VIIIH with a *p*-nitro group present this band. Band A is present in all six spectra, but having a lower extinction coefficient, it is a shoulder on the more intense B band in the above four compounds; thus these wavelenghts and extinction values found graphically are less precise than in the case of IVH and VIIH, where band A is not overlapping with adjacent bands.

Trends observed in previous discussions of electronic absorption spectra of polynitrophenyl derivatives [2,11,12] are also present here. However, since no other aromatic group is present in IIIH — VIIIH along with the polynitrophenyl ring, it is more easy to observe the effect of its structural variation on the electronic absorption spectrum.

The absence of band B in compounds IVH and VIIH which have no *p*-nitro group is in agreement with the interpretation that band B is due to the promotion of an electron to a molecular orbital with important contributions from structure IX, whereas the excited state giving rise to band A is described as approximating structure X.[13]

---

[6] L. K. Dyall, *Austral, J. Chem.*, **14**, 493 (1961); *Spectrochim. Acta*, **17**, 291 (1961)

[7] L. K. Dyall and J. E. Kemp, *ibid.*, **22**, 467, 483 (1966).

[8] I. D. Rae, *Austral. J. Chem.*, **18**, 1807 (1965).

[9] J. Hedberg, J. A. Weil, G. A Janusonis and J. K. Anderson, *J. Chem. Phys.*, **41**, 1033 (1964).

[10] J. A. Weil, A. Blum, A. H. Heiss and J. K. Kinnaird, *ibid.*, **46**, 3132 (1967).

[11] A. T. Balaban, P. T. Frangopol, M. Mărculescu and I. Bally, *Tetrahedron*, **13**, 258 (1961).

[12] A. T. Balaban, P. T. Frangopol and M. Keplinger, *Spectrochim. Acta*, **19**, 367 (1963).

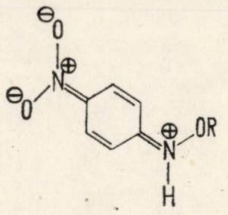

IX

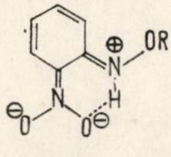

X

With a smaller charge separation, the energy needed to promote an electron to a molecular orbital of type X is smaller, therefore band A appears at longer wavelengths than band B.

EXPERIMENTAL

Apparatus. Ultraviolet and visible spectra were recorded with an Optica (Milan) CF-4 instrument. Infrared spectra were recorded with a Zeiss (Jena) UR-10 instrument.

Starting materials. Methoxyamine hydrochloride,[14] m.p. 150° was prepared by methylating potassium nitrosulphonate with dimethyl sulphate and then hydrolyzing with hydrochloric acid the resulted $\mathrm{MeO{-}N\,(SO_3K)}$.[15] Ethoxyamine hydrochloride,[16] m.p. 128° was prepared by ethylating acetoxime with ethyl bromide, and hydrolyzing with hydrochloric acid the resulted $\mathrm{EtO{-}N = CMe_2}$.[17]

Polynitrophenyl-alkoxy-amines. Two moles of alkoxyamine hydrochloride one mole chloropolynitrobenzene, and 1–3 moles of sodium hydrogen carbonate were refluxed in ethanol for 30–40 hours. The reaction products (yields 45–55% relatively to ArCl) were purified by column chromatography on alumina from benzene, then by recrystallizations from ethanol, benzene, or acetic acid in the presence of charcoal. They are yellow or orange-yellow.

Acknowledgements. The collaboration of Mrs. E. Romaş for the IR spectra, of Mrs. M. Roman and C. Popescu for elementary analyses and the technical assistance of D. Papae are gratefully acknowledged.

---

[13] M. J. Kamlet, J. C. Hofsommer and H. G. Adolph, *J. Amer. Chem. Soc.*, **84**, 3925 (1962); N. J. Kamlet, H. G. Adolph and J. C. Hoffsommer, *ibid.*, **86**, 4018 (1964); M. J. Kamlet, J. C. Hoffsommer, R. R. Minesinger and H. G. Adolph, *J. Org. Chem.*, **33**, 3070 (1968).

[14] R. M. Khomutov, *Zhur. obshchei Khim.*, **31**, 1992 (1961).

[15] B. V. Joffe and K. N. Zelenin, *Izv. Vysshikh Uchebn. Zavedenij, Khim. Tekhnol.*, **6**, 78 (1963); *Chem. Abstr.*, **59**, 6244 (1965); O. Scherer, G. Hoerlein, R. Hübner and G. Schneider (to Hoechst, A. G.), Ger. Pat. 1, 112, 082 (Oct. 21, 1959); *Chem. Abstr.*, **56**, 8561 (1962).

[16] J. R. Nicolaus, L. Mariani and E. Testa, *Ann. Chim.* (*Rome*), **53**, 281 (1963).

[17] M. Torigore, *Chem. Pharm. Bull.* (*Japan*), **9**, 613 (1961); *Chem. Abstr.*, **56**, 9940 (1962).

Revue Roumaine de Chimie, **14**, 947–949 (1969)

THE ELECTRONIC GROUND STATES OF *ORTHO*, *META* AND *PARA*-BENZYNES

M. D. GHEORGHIU *) and R. HOFFMANN

Department of Chemistry, Cornell University, Ithaca, New York 14850, U.S.A.

Received February 25, 1969

Using CNDO-2 method it was found that the ground state of *ortho* and *meta*-benzyne is singlet, whereas that of *para*-benzyne is a triplet.

In recent years there was accumulated a large body of experimental and some theoretical facts regarding the intermediacy of dehydrobenzenes or arynes.[1] In order to understand and predict various aspects of the physical and chemical behavior of these intermediates it is important to possess the most basic information—the spin state of the most stable form of these molecules. An important approximate SCF method, developed by Pople and coworkers,[2] appears most suitable to a treatment of the σ and π framework of a molecule such as benzyne. Formally excited states, which will also interest us may be adequately constructed by using virtual orbitals.[3]

We present in this note some results obtained by the CNDO−2 method [2] on *ortho*, *meta* and *para*-benzyne. The geometries of these molecules were chosen as initially hexagonal, C−C 1.40 Å, C−H 1.10 Å. The parameters we used were those suggested by Pople and coworkers,[2] and are summarized in table 1.

The excited states were constructed with configuration interaction between all excitations in a 10 eV range.**) *With this parametrization it turns out that the ground state of* **ortho** *and* **meta**-*benzyne is a singlet, whereas that of* **para**-*benzyne is a triplet.*[4]

---

*) present address : Organic Chemistry Laboratory, Polytechnic Institute, str. Polizu 1, Bucharest 12

**) Doubly excited configurations were not included in the calculations. They should lower the energy of the lowest singlet states of these molecules.

[1] For a comprehensive review of the chemistry of benzynes see : R. W. Hoffmann "Dehydrobenzene and Cycloalkynes", Academic Press, New York, 1967.

[2] J. A. Pople, D. P. Santry and G. A. Segal, *J. Chem. Phys.*, **43**, S129 (1965) ; J. A. Pople and G. A. Segal, *J. Chem. Phys.*, **43**, S136 (1965) ; **47**, 3289 (1966).

[3] H. W. Kroto and D. P. Santry, *J.Chem. Phys.*, **47**, 792 (1967).

[4] T. Yonezawa, H. Konishi and H. Kato, *Bull. Chem. Soc. Japan*, **41**, 1031 (1968) obtained a singlet ground state for *ortho*-benzyne with the triplet 3.73 eV above.

The position of the three lowest singlets and the first triplet are shown in table 2.

Note that whereas *ortho*-benzyne is a clear singlet, the singlet and triplet states of *meta*-benzyne are not far apart in energy. In the series *ortho*, *meta* and *para* benzyne one can predict a red shift in the lowest singlet-singlet transition.

Table 1

Ionization potentials for S and P orbitals, the resonance integrals (in eV) and the Slater exponent

Atom	S	P	β_0	Slater exponent
C	−14.05	−5.572	−21.00	1.625
H	− 7.176	—	− 9.00	1.300

Assuming that thermodynamic stability will be proportional to the calculated total energy, these calculations place *ortho*-benzyne 1.55 eV below *meta*-benzyne, which in turn is 1.78 eV more stable than the lowest, triplet state of *para*-benzyne.

Table 2

Singlet and triplet energy transitions (in eV)

		Singlet		Triplet
ortho-Benzyne	4.700	5.492	6.497	2.046
meta-Benzyne	4.296	4.435	5.024	0.263
para-Benzyne	3.118	4.722	4.742	−0.760

It appears plausible for these intermediates to discuss their reactivity in terms of frontier controlled reactions.[5] Both the highest occupied molecular orbital (HOMO) and the lowest unoccupied molecular orbital (LUMO) for all of these species are concentrated primarily at the two dehydro carbons. HOMO is lowest for *ortho*-benzyne, and at increasingly higher energy for *meta* and *para* isomers. LUMO exhibits the reverse trend. The actual energy levels are shown in table 3. The trend is in accord with the stability order.

While CNDO—2 calculations do not yield good bond distances, they can predict the direction of distortion from some initially assumed geometry. The overlap populations [6] which we obtain in calculations assuming equal C—C bond lengths should be a good indicator of the actual bond length changes which ensue. The results are illustrated below (Fig. 1).

---

[5] G. Klopman, *J. Amer Chem. Soc.*, **90**, 223 (1968).

[6] R. S. Mulliken, *J. Chem. Phys.*, **23**, 1833, 1841, 2338, 2343 (1955).

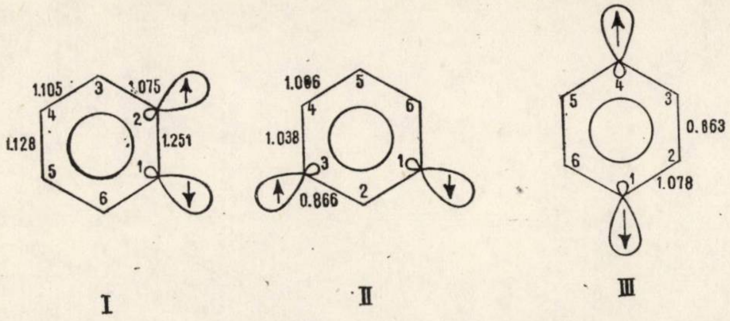

Fig. 1. — Reduced overlap populations for *o*- (I), *m*- (II) *p*-benzyne (III).

The *ortho*-benzyne bond, as expected is the strongest one, followed by the bond opposite and parallel to the partial triple bond. The C_1-C_2 and C_2-C_3 bonds, flanked by the aryne carbons, are expected to be very long in the *meta*-benzyne. In the *para*-benzyne one sees the indications of two allylic fragments, $C_6-C_1-C_2$ and $C_3-C_4-C_5$, separated by relatively long bonds. These conclusions parallel the results derived from extended Hückel calculations,[7] except for the destabilization of *para*-benzyne.

Table 3

HOMO and LUMO orbital energy (in eV)

	HOMO	LUMO
ortho-Benzyne	−11.322	0.764
meta-Benzyne	−10.179	−0.598
para-Benzyne	− 9.552	−1.398

This work was generously supported by the National Science Foundation.

---

[7] R. Hoffmann, A. Imamura and W. J. Hehre, *J. Amer. Chem. Soc.*, **90**, 1499 (1968)

Revue Roumaine de Chimie, **14**, 951–954 (1969)

SOME ISOLATED MIXED ANHYDRIDES OF 2,6-DIMETHOXYBENZOIC ACID

VIORICA VOINESCU and A. BALOG
Chemical and Pharmaceutical Research Institute Cluj
Str. Karl Marx 93–97

Received September 30 1968

2,6-Dimethoxybenzoyl-benzoic, p. nitrobenzoic- and pivalic mixed anhydrides were synthetized and their aminolysis with aniline, benzylamine and ethyl-glycinate was studied.

In an earlier paper we have shown that in aminolysis of ethoxycarbonyl-2,6-dimethoxybenzoic anhydride, the ethoxycarbonyl group reacted as acylating partner with subsequent urethane formation.[1]

This fact suggested the use of mixed anhydrides derived from 2,6-dimethoxybenzoic acid and N-protected aminoacids as activating agents in the peptide synthesis. Phthalyl-glycyl-ethyl glycinate was isolated by this method in 67% yield.[1]

The direction of the acylation, however, was inverted in the case of N-carbobenzyloxycarbonyl-C-phenylglycyl-2,6-dimethoxybenzoic anhydride, leading to an "anomalous" aminolysis.[2] In this case, from the reaction between the mixed anhydride and ethyl-glycinate N-2,6-dimethoxybenzoyl-ethylglycinate and N-carbobenzyloxycarbonyl-C-phenylglycine have resulted.[3]

We found, therefore, interesting to isolate some other mixed anhydrides in order to investigate their behaviour in the aminolysis.

Following the general procedure for the activation of N-protected aminoacids with acid chlorides,[4] the 2,6-dimethoxybenzoic acid was coupled with benzoic, p. nitrobenzoic and pivalic acid chloride in the presence of 1 mole triethylamine. The formation of mixed anhydrides according to the equation :

---

[1] V. Voinescu, A. Balog and E. Ramonţian, *Rev. Roumaine Chim.*, **11**, 1237 (1966).

[2] M. Zaoral and J. Rudinger, *Coll. Czech. Chem. Commun.*, **26**, 2316 (1961).

[3] A. Balog, V. Voinescu, M. Herman, E. Ramonţian and E. Vargha (under press).

[4] M. Bodansky and M. A. Ondetti, "Peptide synthesis", ed. Interscience Publishers, John Wiley & Sons, New York, London, Sydney, 1966 p. 84.

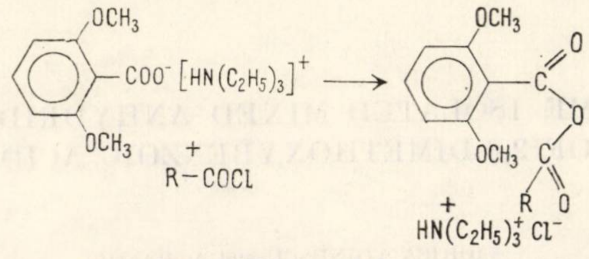

R : C_6H_5 ; p.$NO_2-C_6H_4$; C/CH_3/$_3$

was nearly spontaneous and associated, at −5°, by separation of crystalline triethylamine hydrochloride.

The resulted mixed anhydrides are relatively stable compounds and can be isolated in good yields -even after washing with aqueous sodium bicarbonate- and recrystallized from an adequate solvent. Their physical properties and microanalytical data are indicated in table 1.

Table 1

Synthetised mixed anhydrides

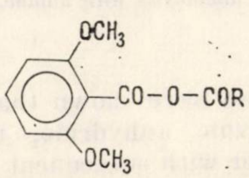

	R Empirical formula (Mol. Wt.)	Yield %	M.p. °C*, (crystall. solvent)	Analyses Calcd.	 Found	Infrared bands** cm^{-1}
I	$-C_6H_5$ $C_{16}H_{14}O_5$ (286.27)	89.5	90−90.5 (benzine B.p. 70−90°)	C 67.12 H 4.85	67.12 5.16	1795, 1732
II	$-C_6H_4-NO_2$ $C_{16}H_{13}O_7N$ (331.27)	71	145−146 (benzene- petrol ether)	C 58.00 H 3.95 N 4.22	58.31 4.39 4.22	1818, 1764
III	$-C(CH_3)_3$ $C_{14}H_{12}O_5$ (266.28)	87.7	63−64 (benzine)	C 63.14 H 6.81	63.30 7.03	1800, 1745

* All melting points are uncorrected.

** Infrared spectra were performed by Mrs Jana Rusu of the analytical laboratory of our Institute (Perkin-Elmer Model 137 B spectrophotometer)

The above mentioned mixed anhydrides, being relatively stable compounds, are suitable for a study of the aminolysis having the same advantages mentioned [5] in the case of active and activated isolated esters.

We have investigated the aminolysis with aniline, benzylamine and ethylglycinate, using as reaction media benzene, tetrahydrofuran respectively.

---

[5] *Ibid.*, p. 107.

By the aminolysis with benzylamine and ethylglycinate the leaving group was in all the cases the 2,6-dimethoxybenzoic according to the equation :

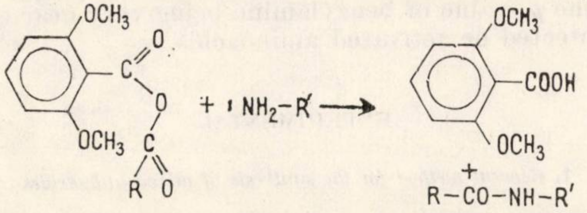

The 2,6-dimethoxybenzoyl-pivalic anhydride (III) has shown a peculiar behaviour by the aminolysis with aniline. Pivalic and 2,6-dimethoxybenzoic anilide were isolated in the ratio indicated in the table 2.

Table 2

Products* obtained from mixed anhydrides with :

Mixed anh.	Aniline		Benzylamine		Ethyl-glycinate	
	Product	Yield %	Product	Yield %	Product	Yield %
I	2,6-DMB ac. [a)] Benzanilide	80 96.9	2,6-DMB ac. Benzylbenzamide	80 100	2,6-DMB ac. Hippuric ester	94.4 96
II.	2,6-DMB ac. p. Nitrobenzanilide	74 88	2,6-DMB ac. Benzyl-p. Nitro- [b)] benzamide	60 82	2,6-DMB ac. p. Nitrohippuric ester	75 88
III.	2,6-DMB ac. Pivalic anilide 2,6-DMB-anilide	55 56.8 33.6	2,6-DMB ac. Benzyl-pivalic amide [c)]	82.4 88.9	2,6-DMB ac. N-pivaloyl-ethyl-glycinate [d)]	94.4 95.6

* Known products were identified by m.p. and mixed m.p. with authentic samples.

a) 2,6-DMB ac. = 2,6-dimethoxybenzoic acid; b) m.p. 143–144°. recryst. from benzene, calcd. N, 10.93 *found* : N, 10.70; c) m.p. 92–93° recryst. from benzine (b.p. 70–90°) *calcd.* : N, 7.32; *found* : N, 7.34; d) syrup, *calcd.* : N, 7.48; *found.* ; N 7.70.

These results indicate that besides the steric effects,[6,7] electronic factors[8] and solvent,[9] the basicity of the amine plays an important part in determining the cleavage. The positive inductive effect of alkyl groups in the pivaloyl sequence is obvious only in the case of the low basicity of aniline (K_a :3.8×10^{-10}, while for benzylamine K_a : 2.35×10^{-5}) directing in a certain amount the cleavage in the A sense

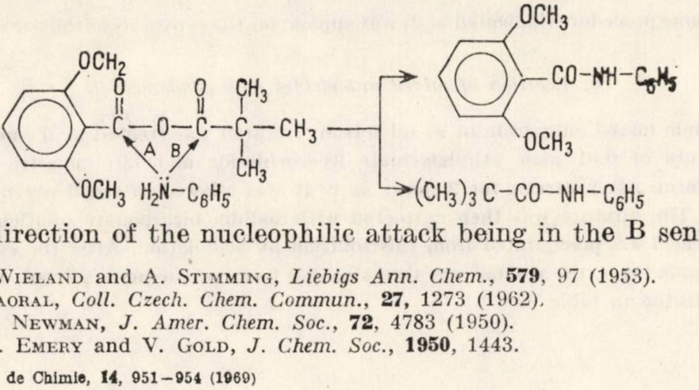

teh main direction of the nucleophilic attack being in the B sense.

[6] TH. WIELAND and A. STIMMING, *Liebigs Ann. Chem.*, **579**, 97 (1953).

[7] M. ZAORAL, *Coll. Czech. Chem. Commun.*, **27**, 1273 (1962).

[8] M. S. NEWMAN, *J. Amer. Chem. Soc.*, **72**, 4783 (1950).

[9] A. R. EMERY and V. GOLD, *J. Chem. Soc.*, **1950**, 1443.

A conclusion of the above presented results is that benzylamine is more suitable for model aminolyses of mixed anhydrides prepared from N-protected aminoacids and acid chlorides as aniline, generally used for this purpose, the p_k-value of benzylamine being very near to the p_k-value of carboxylprotected or activated aminoacids.

EXPERIMENTAL

1. *General method for the synthesis of mixed anhydrides*

A solution of 5.46 g (0.03 mole) 2,6-dimethoxybenzoic acid and 4.2 ml (0.03 mole) triethylamine in 50 ml dry dichlormethane was cooled to $-5°-0°$. Under stirring, acid chloride (0.03 mole) was added dropwise, as such (benzoic, pivalic) or dissolved in dichlormethane (p. nitrobenzoic). The stirring was continued for 1 hour at 0° and without cooling until the room temperature was reached. The separated amine salt was filtered; the filtrate washed with sodium bicarbonate solution and water. After drying over magnesium sulfate the solvent was evaporated under vacuum at 30°. The crude product was recrystallized from an adequate solvent (see table 1).

2. *Reaction of mixed anhydrides with aniline*

To a solution of 0.01 mole mixed anhidride in 10 ml benzene, freshly distilled aniline (0.011 mole) was added. After 24 hours of standing at room temperature, 40 ml petrol ether was added. After filtration the dried precipitate was shaken for 20 minutes with sodium bicarbonate solution and filtered.

a. In the case of I and II this precipitate represented an anilide (according to table 2) and the acidulation of the bicarbonate solution yielded 2,6-dimethoxybenzoic acid.

b. In the case of III the precipitate consisted of a mixture of pivalic anilide and 2,6-dimethoxybenzanilide. These were separated through fractional recrystallization from benzine in which the last is sparingly soluble.

c. The petrol-ethereal filtrate was distilled, the residue was shaken with sodium bicarbonate solution and filtered. The insoluble residue represents a new quantity of pivalic anilide. From the filtrate after acidulation, extraction with ether and removal of the solvent pivalic acid was obtained.

3. *Reaction of mixed anhydrides with benzylamine*

The same procedure (indicated at 2) was applied for the synthesis of the benzamides.

4. *Reaction of mixed anhydrides with ethylglycinate*

0.01 Mole mixed anhydride in 25 ml tetrahydrofuran was treated at 0°, under stirring, with a mixture of 0.01 mole ethylglycinate hydrochloride and 0.01 mole triethylamine in 20 ml chloroform. After stirring for 2 hours at 0° it was allowed to stand overnight at room temperature. The mixture was then extracted with sodium bicarbonate solution. 2,6-Dimethoxybenzoic acid was precipitated from this solution by acidulation. After the evaporation of the dried organic layer, the residue was recrystallized from an adequate solvent, obtaining the products indicated in table 2.

Revue Roumaine de Chimie, **14**, 955–957 (1969)

PIRANI MANOMETER FOR THE RANGE $2 \times 10^{-1} - 5 \times 10^{-6}$ TORR

M. I. VASS

Institute of Physical Chemistry of the Academy
Dumbrava Roşie 23, Bucharest 9

Received November 28, 1968

A new model of a bakable Pirani gauge with platinum wire of 0.05 mm for measuring pressure in the range $2 \times 10^{-1}-5 \times 10^{-6}$ torr was given.

The rate of the heat transfer from a conductor through a gas is a function of the gas pressure. This principle was first used by Pirani[1] to measure the low pressures. He has measured the heat losses of a thin wire by means of a Wheatstone bridge which was used both for heating the wire and to observe its resistance variation. These manometers which make use of a Wheatstone bridge are now called "Pirani manometers" being widespread for the range $5 \times 10^{-1} - 1 \times 10^{-3}$ torr. But there are situations in which their use is necessarily beyond the limits mentioned before. Such an example is the adsorption of gases at low pressures when the ionization manometers are forbidden because of their incandescent filaments. In these cases the Pirani manometer is built in the laboratory after special designs. There are also many models given in the literature.

The theory of the thermal conductivity gauges is well established. Leck[2] discusses many theoretical aspects and gives some practical indications. We have retained especially his conclusion that for a given metal and working temperature, the sensitivity is proportional to the wire length. For the gauge construction (figure 1) we have chosen platinum wire of 0.05 mm diameter and a length of 2 m (about 100 Ω) which was wound on the four crossed arms of the glass support so that on each couple of arms one may have three spirals at 2 mm distance. We have built two identic gauges; one of them was sealed off at a pressure $\leqslant 1 \times 10^{-8}$ torr and was used as a compensator. The bridge contains also two resistors, one of them being a precision decadic box. The galvanometer with a sensitivity of 1×10^{-8} A/mm (internal resistance 30 Ω) has also a sensitivity reductor (1 :100, 1 : 10, 1 : 1).

---

[1] M. PIRANI, *Deutsche Phys. Ges. Werk*, **8**, 686 (1906).

[2] J. H. LECK, "Pressure Measurement in Vacuum Systems", Chapman & Hall, 1964, p. 40.

Fig. 1. — Section through the Pirani gauge.

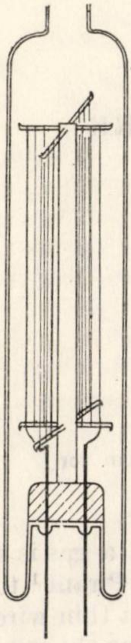

Fig. 2. — Calibration curve of the gauge for oxygen.

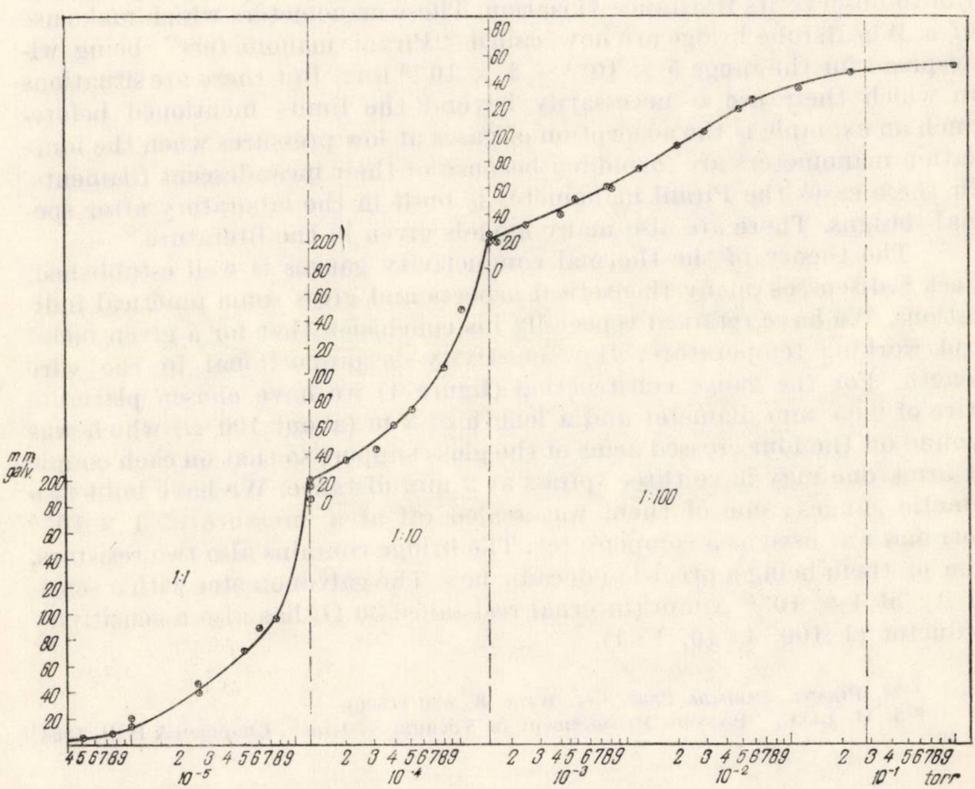

After experiments the optimal power for the bridge was found to be 0.12 watt (supplied from a lead motorcar accumulator, 6 volts and 20 mA). Calibration curve (figure 2) was plotted by means of a MacLeod gauge, immersing both the measuring gauge and the compensator in a Dewar flask containing oil in order to prevent ambient temperature fluctuations. The maximum sensitivity measured from the plotted curve is 2.5 mm/μtorr. The precision of the readings at the ends of the range was about 7 % and still better for the remaining part.

Revue Roumaine de Chimie, 14, 955–957 (1969)

After adjustment [illegible] power for the bridge was found to be 0.2 watt [illegible] voltmeter [illegible] volts and 20 mA. Calibration [illegible] was checked by means of a [illegible] gauge, [illegible] both the measuring gauge and the [illegible] black [illegible] in order to prevent ambient temperature [illegible]. The [illegible] measured from the plotted curve [illegible]. The [illegible] readings [illegible] of the range was [illegible] the remaining part.

Revue Roumaine de Chimie, **14**, 959–961 (1969)

$TiCl_4$-CAROTENOID COMPLEXES

V*. ACTION OF $TiCl_4$ ON DODECAPRENO-β-CAROTENE

V. TĂMAŞ and C. BODEA

Institute of Agronomy, Department of Chemistry, Cluj, str. Mănăştur 3

Received June 22, 1968

By the action of $TiCl_4$ on dodecapreno-β-carotene a dodecapreno-β-carotene. $TiCl_4$ complex was obtained, the acetonolysis of which yields retro-dehydro-dodecapreno-β-carotene. The latter represents a new C_{60} carotenoid.

After the successful attempts to prepare C_{40} carotenoids by total synthesis, carotenoids with more than 40 C have been obtained by the same synthetical methods. Such carotenoids are : homo-β-carotene[1] and 2,2′-dimethyl-β-carotene,[2] both C_{42} compounds, decapreno-β-carotene [3,4] a C_{50} compound and dodecapreno-β-carotene [5] a C_{60} compound. All these carotenoids have a normal system of conjugated double bonds, with β-ionone rings at both ends.

The existence in the nature of the carotenoids with over C_{40} has been reported recently. Oxygenated C_{50} carotenoids, especially hydroxilated derivatives, dehydrogenans-P_{439} [6] and bacterioruberin [7] have been identified in *Flavobacterium dehydrogenans*. No carotenoid with C_{60} has been identified in nature as yet.

Since only a few synthetic and natural carotenoids with more than 40 carbon atoms are known and their properties but little studied, we tried to obtain new carotenoids of this group by semisynthesis.

In this paper we present the results obtained by the action of $TiCl_4$ on dodecapreno-β-carotene. Acting with $TiCl_4$ on dodecapreno-β-carotene (I) in benzene solution, the dodecapreno-β-carotene. $TiCl_4$ complex (II) was obtained with very good yield (95%). By acetonolysis the complex II was converted into retrodehydro-dodecapreno-β-carotene (III) with 65% yield.

---

* Part IV. V. Tămaş and C. Bodea, *Rev. Roumaine Chim.*, **14**, 405 (1969).

[1] H. H. Inhoffen, F. Bohlmann, J. Aldag, S. Bork and G. Leibner, *Liebigs Ann. Chem.*, **573**, 1 (1951).

[2] C. H. Eugster, A. H. Trivedi and P. Karrer, *Helv. Chim. Acta*, **38**, 1359 (1955).

[3] P. Karrer and C. H. Eugster, *Helv. Chim. Acta*, **34**, 28 (1951).

[4] O. Isler, M. Montavon, R. Rüegg and P. Zeller, *Liebigs Ann. Chem.*, **603**, 129 (1957).

[5] P. Karrer and C. H. Eugster, *Helv. Chim. Acta*, **34**, 1805 (1951).

[6] L. S. Jensen, *Acta Chem. Scand.*, **21**, 1972 (1967).

[7] M. Kelly and L. S. Jensen, *Acta Chem. Scand.*, **21**, 2578 (1967).

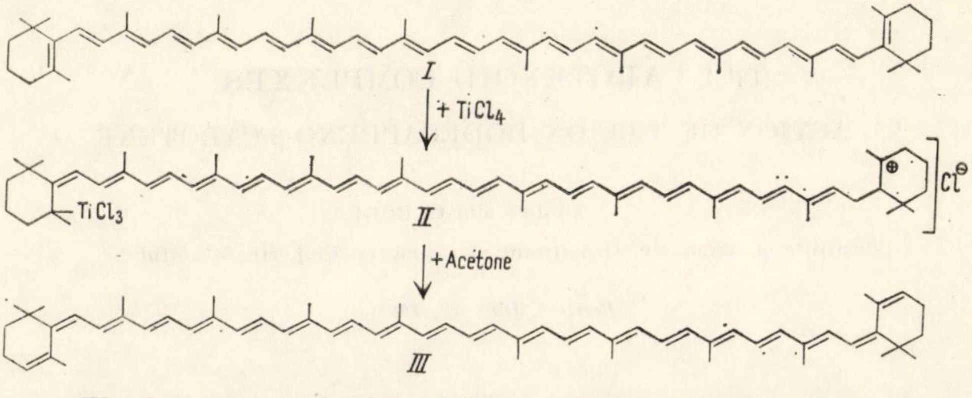

The intimate mechanism of these transformations has been shown in our previous papers.[8,9]

The structure of II and III was confirmed by electronic and IR spectra. The maxima of the electronic spectra of I, II and III are shown in table 1.

Table 1

Electronic spectra maxima (in dimethylformamide)

Carotenoid	λ_{max}, nm
Dodecapreno-β-carotene (I)	595, 560, 520
Dodecapreno-β-carotene.TiCl$_4$ (II)	560
Retrodehydro-dodecapreno-β-carotene (III)	610, 580, 545

Figure 1 shows the electronic spectra of I, II and III.

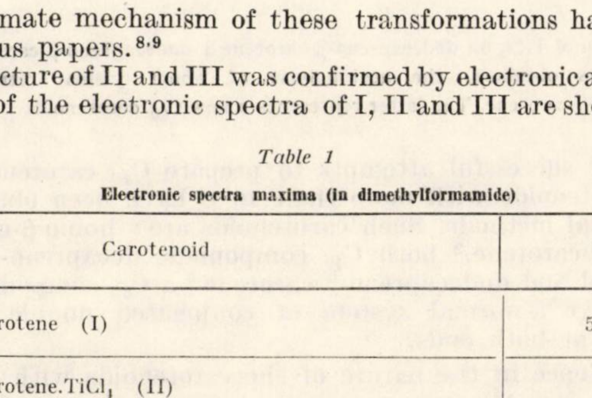

Fig. 1. — Curves of the electronic spectra.

---

[8] V. TĂMAŞ and C. BODEA, *Rev. Roumaine Chim.*, **12**, 1517 (1967).

[9] V. TĂMAŞ and C. BODEA, *Tetrahedron*, (in press).

From figure 1 it results that the spectra of the carotenoids I and III present a fine structure lacking in the spectrum of the complex II. The compound II shows only one maximum which is superposed with λ_2 of I.

IR spectrum of III shows a maximum at 970 cm^{-1} and a shoulder at 990 cm^{-1}, consistent with the structure III containing a retro system.[10] As compared to other carotenoids compound III is much more air-sensitive.

EXPERIMENTAL

Synthetical dodecapreno-β-carotene kindly supplied by F. Hoffmann La Roche, Co. A. G. Basle, has been used.

1. *Preparation of dodecapreno-β-carotene.$TiCl_4$ complex (II)*

A solution of 7 mg I in 15 ml benzene, cooled at +8°, was treated with 0.05 ml $TiCl_4$. The dark blue solution was stirred several times and after 10 min the precipitate filtered off and washed with benzene; 6 mg of dark powder have been obtained. The electronic spectrum, in dimethyl-formamide, shows only one maximum at 560 nm.

By acetonolysis compound II was converted into III.

2. *Conversion of I into III.*

A solution of 10 mg I in 20 ml benzene, cooled at +8°, was treated with 0.05 ml $TiCl_4$. The mixture of reaction was stirred 1 min. and then 50 ml acetone was added. After 10 minutes it was diluted with 100 ml petroleum ether. The solution of the pigments was washed with H_2O, dried with Na_2SO_4 and then chromatographed, using as adsorbent a mixture of MgO and sand. After development with petroleum ether + 75% benzene the chromatogram (3 × 20 cm) assumed the following aspect:

	0.1 cm violet	unidentified
	0.5 cm interzone	
	0.5 cm ochre	
	0.5 cm interzone	
A	7.0 cm violet	retrodehydro-dodecapreno-β-carotene
	0.5 cm interzone	
	3.0 cm blue	dodecapreno-β-carotene

Retrodehydro-dodecapreno-β-carotene (III). The pigment of zone A was eluted with a mixture of ether-acetone-ethanol (9 : 3 : 1). 6.5 mg dark violet crystals, were obtained. The electronic spectrum achieved in dimethyl-formamide showed three maxima at 610, 580 and 550 nm. The IR spectrum, in nujol, exhibits a maximum at 970 and a shoulder at 990 cm^{-1}.

---

[10] E. Nicoară, V. Tămaş, G. Neamţu and C. Bodea, *Liebigs Ann. Chem.*, **11**, 739 (1966).

NOTE POUR LES AUTEURS

La *Revue Roumaine de Chimie* publie des articles en anglais, français, russe, allemand ou espagnol. Les auteurs sont priés d'envoyer des articles, notes, communications et comptes rendus inédits.

Les manuscrits seront dactylographiés à deux intervalles. Les tableaux seront dactylographiés sur feuilles séparées, de même que la légende des figures. Les diagrammes seront tracés à l'encre de Chine sur papier calque. Les tableaux et les figures seront numérotés par des chiffres arabes, en nombre strictement nécessaire. Prière de ne pas inscrire les mêmes données dans les tableaux et les figures. Les formules chimiques seront incluses dans le texte ; en outre, elles seront transcrites sur des feuilles séparées. Les auteurs sont priés d'indiquer les caractères italiques (en soulignant les lettres au crayon), ainsi que tout autre caractère spécial. L'ordre des références bibliographiques sera celui de leur mention dans le texte ; le nom de l'auteur sera précédé de l'initiale du prénom ; les publications périodiques seront présentées suivant les prescriptions internationales. Les références seront ajoutées à la fin de l'article ; elles paraîtront comme des notes, au bas de la page. Le texte sera précédé d'un résumé, comprenant 15 lignes au maximum.

L'entière responsabilité du contenu des articles appartient aux auteurs. On publie des articles dus aux collaborateurs roumains ou étrangers. Les auteurs recevront 50 tirés à part.

PRINTED IN ROMANIA

1969 OKT 16

TRAVAUX PARUS AUX ÉDITIONS DE L'ACADÉMIE DE LA RÉPUBLIQUE SOCIALISTE DE ROUMANIE

CORNEL BODEA, **Tratat de biochimie vegetală**, partea I, **Fitochimie** (Traité de biochimie végétale, Ire partie, Phytochimie), Ier vol., 1964, 747 p. + 4 annexes, + 2 pl., 41 lei; IIe vol., 1965, 1262 p., 1 pl., 56 lei; IIIe vol., 773 p., 35 lei.

V. GHEŢIE et V. MICUŞAN, **Analiza imunochimică. Teorie şi practică** (Analyse immunochimique. Théorie et pratique), 1966, 369 p., 28 lei.

SILVIA IONESCU, **Reacţii chimice induse de radiaţiile ionizante** (Réactions chimiques produites par les radiations ionisantes), 1963, 271 p., 15 lei.

MARIETA NICOLAE, **Fizico-chimia proceselor fotografice** (Physico-chimie des processus photographiques), 1964, 426 p. + 4 pl., 35 lei.

R. PORTOCALĂ et L. POPA, **Acizii ribonucleici celulari şi virali** (Les acides ribonucléiques cellulaires et viraux), 1966, 375 p., 8 pl., 26 lei.

D. PURDELA et R. VÎLCEANU, **Chimia compuşilor organici ai fosforului şi ai acizilor lui** (La chimie des composés organiques du phosphore et de ses acides), 1965, 540 p., 37 lei.

CRISTOFOR SIMIONESCU, MARGARETA GRIGORAŞ et AGATA CERNĂTESCU-ASANDEI, **Chimia lemnului din R.P.R.** (La chimie du bois en Roumanie), 1964, 239 p. + 6 pl., 27 lei.

CRISTOFOR SIMIONESCU et CLEOPATRA VASILIU-OPREA, **Mecanochimia compuşilor macromoleculari** (La mécanochimie des composés macromoléculaires), 1967, 344 p., 23,50 lei.

I.P. „Informaţia" – c. 3384

43426

Lei 15. –

F1103

R

REFERÁLVA

REVUE ROUMAINE DE CHIMIE

TOME 14

Nº 8

Août 1969

ÉDITIONS DE L'ACADÉMIE DE LA RÉPUBLIQUE SOCIALISTE DE ROUMANIE

Rev. Roumaine Chim.

14, 963–1068 (1969), Bucarest

COMITÉ DE RÉDACTION

Rédacteur en chef :

C. D. NENIŢESCU, membre de l'Académie de la République Socialiste de Roumanie

Rédacteurs en chef adjoints :

A. T. BALABAN et V. E. SAHINI, membres correspondants de l'Académie de la République Socialiste de Roumanie

Collège de rédaction :

C. DRĂGULESCU, RALUCA RIPAN, CR. SIMIONESCU, membres de l'Académie de la République Socialiste de Roumanie; EM. BRATU, membre correspondant de l'Académie de la République Socialiste de Roumanie; Pr G. OSTROGOVICH, MARG. AVRAM, F. BADEA, D. MARCHIDAN, D. NEGOIU et D. SĂNDULESCU

Les manuscrits, les livres et les revues proposés en échange, ainsi que toute correspondance seront envoyés à la rédaction :

REVUE ROUMAINE DE CHIMIE

23, str. Dumbrava Roşie, Bucarest, Roumanie

1103

REVUE ROUMAINE DE CHIMIE

SZAKKÖNYVTÁR

Tome 14, N° 8 Août 1969

Page

I. G. MURGULESCU, Some physico-chemical properties of simple molten salts 965–979 ✓

V. E. SAHINI and AL. BUTUCELEA, On the $n \rightarrow \pi^*$ electronic transition in aromatic ketones 981–984

D. CISMARU et ELISABETA DOBROGHIU, Oxydation du Fe et du Ni à hautes températures. Effet du champ magnétique sur la vitesse d'oxydation du Fe et du Ni . . . . 985–990 ✓

S. STERNBERG and CONSTANŢA HERDLICKA, Chronopotentiometric determination of silver ion interdiffusion coefficient in molten potassium and lithium nitrates 991–997

D. MANOLESCU and E. SEGAL, X-rays studies on monopyridine complexes of cobalt (II) and nichel (II) chlorides 999–1001

J. MÁTHÉ, Ligand field theory for noncubic symmetries 1003–1010

LUCIA GANOVICI et I. GANOVICI, La densité et la viscosité de l'indium fondu dans l'intervalle de température de 166° à 800° 1011–1017

A.-C. BANCIU, Über die spektrophotometrische Methode von Jazimirskij zur Untersuchung stufenweiser Komplexbildung und über die Erweiterung der Anwendungsgrenzen dieser Methode 1019–1025

R. MERARU and MARIA NEGOIU, Röntgenographic study on the compound $[HP(C_6H_4-CH_3)_3]_2[CoCl_4]$ 1027–1029

Z. GROPŞIANU, D. KOHN und A. IOVI, Wärmeübergangszahlen beim Sieden von Lösungen. Lösungen aus Gemischen von Natriumphosphaten . . 1031–1037

C. LITEANU and IOVANCA HAIDUC, About the influence of indicating electrode treatment upon the parameters of the potentiometric titration. I. Bright platinum electrode in $Fe^{2+}/Cr_2O_7^{2-}$ titration . . . . 1039–1046 ✓

J. DICK und ALFA LUPEA, Komplexverbindungen des N, N'-Diaminopiperazins. I. Metallchelatverbindungen und ihr thermischer Abbau . . . . 1047–1052 ✓

M. RĂILEANU and EUGENIA DOBRE, Volumetric dosage with phenothiazone-(3). II*. Dosage of the ascorbic acid with phenothiazone-(3) . . . 1053–1056 ✓

F. HODOŞAN und I. JUDE, Steroide in adsorbiertem Zustand. III. Über Substitutionsreaktionen der Tosyloxy-Gruppe durch das Nitrat-Anion an aktivem Aluminiumoxid 1057–1062

GH. CIURDARU and VIORICA I. DÉNES, Methylene bases of heterocycles. VIII. 2-Acylmethylene-benzazolines from ketoesters 1063–1067

Rev. Roumaine Chim. 14, 963–1068 (1969), Bucarest

Revue Roumaine de Chimie, **14**, 965–979 (1969)

SOME PHYSICO-CHEMICAL PROPERTIES OF SIMPLE MOLTEN SALTS

I. G. MURGULESCU

Center of Physical Chemistry of the Academy
Bucharest, Dumbrava Roşie 23

Received April 2, 1969

The properties of liquids consisting of molten salts are similar to the properties of the ordinary liquids. Density, molecular volume, compressibility, vapour pressure, etc. acquire comparable values in both liquid classes. Their freezing point and electric conductivity are however quite different. Negligible in the case of molecular liquids, the electric conductivity of molten salts acquire values 10–20 times higher than those of normal aqueous solutions of electrolytes at usual temperatures. Consequently ions are the prevalent constituent particles in molten salts. The molten salts formed only of ions can therefore be called ionic liquids; but when, besides the ions, they contain also non-ionized molecules, they could be considered as iono-molecular mixed liquids.

In the present paper, we shall consider mainly a few of the quantities concerning simple molten salts, directly related by the state equations as proposed for these systems: molar volumes, expansion coefficients, compressibility coefficients. It will be seen later that the characteristic regularities, presented by these quantities, supply some very valuable data about the ionic corpuscular structure of molten salts.

I. – MOLAR VOLUME OF MOLTEN SALTS

As for molecular liquids, we deduce the molar volume of molten salts from the densities that, as a matter of fact, constitute the object of direct measurements. The densities can be represented as a function of temperature t by equations of the following form [1]

$$\rho = a - bt$$

where a and b are constants. Nowadays abundant data on the molten salt densities are to be found in the papers of Bockris,[2] Lumsden [3] and chiefly in the recent monograph of Janz.[4]

---

[1] I. S. Yaffe and E. R. Van Artsdalen, *J. Phys. Chem.*, **59**, 118 (1955).

[2] J. O'M Bockris, "Modern Aspects of Electrochemistry", Butterworths Scientific Publications, London 1959, p. 190–192; J. O'M Bockris, A. Pelle and J. L. Barton, *Rev. Chim. Acad. R.P.R.*, **7**, 59 (1963).

[3] J. Lumsden, "Thermodynamics of Molten Salt Mixtures", Academic Press London — New York, 1966, p. 7.

[4] G. J. Janz, "Molten Salts Handbook", A. P. New York — London, 1966, p. 392, 1.

Making use of the data presented in these works we have drawn up table 1 containing the densities and also, the molar volume V of some halides and alkaline nitrates (4th column), at the corresponding melting points T_f (1st column).

By means of the data given in this table, it is easy to show that, at the melting points, the molar volumes of molten salts are made by adding up two volumes : namely one referred to the anion and the other to the cation ; we shall call them ionic volumes.

Table 1

Molar volumes of some molten alkaline salts

Salt	T_f °K	At melting point		
		ρ, g cm.$^{-3}$	Molar Volume in cm^3	
			Experim.	Calc.
NaF	1 268	1.945	21.0	18.5
NaCl	1 074	1.5561	37.6	37.0
NaBr	1 020	2.3416	44.0	44.4
NaI	933	2.7419	54.7	56.0
KF	1 131	1.9096	30.4	30.4
KCl	1 046	1.5260	48.9	48.9
KBr	1 007	2.1272	56.0	56.3
KI	954	2 4477	67.8	67.9
RbCl	991	2.2458	53.8	53.5
RbBr	955	2.7155	60.9	60.9
RbI	920	2.8979	73.4	72.5
CsF	976	3.6485	41.6	42.5
CsCl	918	2.7915	60.3	61.0
CsBr	909	3.1327	67.9	68.4
CsI	899	3.1771	81.8	80.0
$NaNO_3$	580	1.9051	44.6	44.1
KNO_3	607	1.8722	54.0	56.0
$RbNO_3$	583	2.4828	59.4	60.6
$CsNO_3$	687	2.8160	69.2	68.1

Table

Differences between molar

Differences	$Me_1 = K$ $Me_2 = Na$ $V_{K^+} - V_{Na^+}$	$Me_1 = Rb$ $Me_2 = K$ $V_{Rb^+} - V_{K^+}$	$Me_1 = Cs$ $Me_2 = Rb$ $V_{Cs^+} - V_{Rb^+}$
$V_{Me_1F} - V_{Me_2F}$	—	—	—
$V_{Me_1Cl} - V_{Me_2Cl}$	11.3	4.9	6.5
$V_{Me_1Br} - V_{Me_2Br}$	12.0	4.9	7.0
$V_{Me_1r} - V_{Me_2r}$	13.1	5.6	8.4
Media	12.1	5.1	7.3
$8N\,(r^3_{Me_1^+} - r^3_{Me_2^+})$	7.2	4.3	7.6

Table 2, giving the differences between the molar volumes of the salts having a common anion or cation was drawn up to this purpose. This table shows that the values of these differences are nearly constant which proves the additive character of molecular volumes. Meanwhile the average values in each column are very near to those computed on the basis of following considerations.

Assuming that the volume of each of the ions A^-, C^+, forming the alkali halide AC, is equal to a cube whose edge is equal to its diameter ($2\,r_{A^-}$, respectively $2r_{C^+}$) we can write for the volume V_{AC} of one mol of molten salt :

$$V_{AC} = 8N(r^3_{A^-} + r^3_{C^+}) + V_H$$

where V_H is the volume of the holes at the melting point. For instance the difference between the molar volumes V_{AC_1} and V_{AC_2} of two salts having a common anion, becomes :

$$V_{AC_1} - V_{AC_2} = 8N(r^3_{C_1^+} - r^3_{C_2^+}) + V_{1H} - V_{2H}$$

Since the volumes V_{1H} and V_{2H} of the holes cannot differ much from one another (each of them attaining about 20% of the solid volume value), the last relation is reduced to the form :

$$V_{AC_1} - V_{AC_2} = 8N(r^3_{C_1^+} - r^3_{C_2^+})$$

A similar relation :

$$V_{A_1C} - V_{A_2C} = 8N(r^3_{A_1^-} - r^3_{A_2^-})$$

is obtained for salts having a common cation. The last row of table 2 shows a satisfactory agreement between the values of differences experimentally found and of those computed by means of the preceding equations, except in the case of difference $V_{K^+} - V_{Na^+}$.

If V_{A^-} and V_{C^+} are the ionic volumes of anion A^- and of cation C^+, then the molar volume V_{AC} of a molten salt AC, at the melting point, will be given by the following additive relation *) :

$$V_{A^-} + V_{C^+} = V_{AC} \tag{1}$$

2

volumes at melting point

Differences	$X_1 = Cl$ $X_2 = F$ $V_{Cl^-} - V_{P^-}$	$X_1 = Br$ $X_2 = Cl$ $V_{Br^-} - V_{Cl^-}$	$X_1 = I$ $X_2 = Br$ $V_{I^-} - V_{Br^-}$
$V_{NaX_1} - V_{NaX_2}$	16.0	6.4	10.7
$V_{KX_1} - V_{KX_2}$	18.5	7.1	11.8
$V_{RbX_1} - V_{RbX_2}$	—	7.1	12.5
$V_{CsX_1} - V_{CsX_2}$	18.7	7.6	13.9
Media	17.7	7.6	12.2
$8N\,(r^3_{X_1^-} - r^3_{X_2^-})$	16.4	7.2	12.8

---

*) It is to be remarked that the ionic volumes V_{A^-} and V_{C^+} do not represent the real volumes of these ions, but only conventional quantities including, beside their actual volumes holes in determined proportions.

The molar volumes in table 1, column 4, give directly only the sum V_{AC} of the ionic volumes. In order to obtain the individual volumes V_{A^-} and V_{C^+} of the constituent ions yet another supplementary relation is required between these values, or that one should know at least one of the ionic volume values.

The first course can be successfully followed by assuming that between ions having identical electronic structures, the holes are distributed in proportion to their actual volumes. In this case, we can write, for a salt with ions of same electronic structure :

$$\frac{V_{A^-}}{V_{C^+}} = \frac{v_{A^-} + \frac{v_{A^-}}{V_{AC}} V_H}{v_{C^+} + \frac{v_{C^+}}{V_{AC}} V_H} = \frac{v_{A^-}}{v_{C^+}} = \left(\frac{r_{A^-}}{r_{C^+}}\right)^3$$

where v_{A^-} and v_{C^+} are the actual volumes of ions A^- and C^+ each one of which being proportional to the cube of the corresponding ionic radius while V_H denotes the volume of the holes.

The assumed plausible hypothesis leads therefore to relation :

$$\frac{V_{A^-}}{V_{C^+}} = \left(\frac{r_{A^-}}{r_{C^+}}\right)^3 \tag{2}$$

which together with (1) solves our problem, namely the determination of the individual ionic volumes at melting point.

Table 3

Ionic volumes (at T_f)

Ion	Ionic volume in cm^3	
	initial	corrected
Na^+	5.5	2.0
K^+	13.9	13.9
Rb^+	18.5	18.5
Cs^+	27.1	26.0
F^-	16.5	16.5
Cl^-	35.0	35.0
Br^-	42.4	42.4
I^-	54.0	54.0
NO_3^-	—	42.1

To apply relation (2), we shall consider that the following ion pairs, the outer electron shells of which possess the same number of electrons, have identical structures :

- F^-, Na^+ whose outer electron shell is that of the Ne
- Cl^-, K^+ whose outer electron shell is that of the Ar
- Br^-, Rb^+ whose outer electron shell is that of the Kr
- I^-, Cs^+ whose outer electron shell is that of the Xe

By applying relations (1) and (2) to the respective salts NaF, KCl, RbBr and CsI and taking into account the values in table 1, we obtain the individual ionic volumes given in table 3 (2nd column). The values of ionic radii r_{A^-} and r_{C^+} were taken from Janz's paper.[4]

By comparing the molar volumes given by table 1 with the values deduced from the individual ionic volumes (table 3, 2nd column), there results that the ionic volumes of Na^+ and Cs^+ are too large and have to be corrected. The data in table 2 lead to the same conclusion. In table 3, 3rd column, are given the corrected values of the alkali ions (except Li^+)

as well as of the halogen ions. In the same column, we find the ionic volume of NO_3^- as deduced from the molar volumes of the alkali nitrates.

Table 4 gives the volumes of the ions having the same electronic structure, compared to the atomic values of the rare gases having the same outer electronic shell, at the corresponding melting points. As expceted, a gradual volume diminution takes place from the anion volumes towards the cation volumes. The atomic volumes of rare gases have intermediate values in the range of volumes of the ions having the same outer electronic shell. Thus, we find again grosso modo, the regularities already met with in the case of the individual refractions of the ions [5] (in gaseous state) which are closely related to the ionic volumes.

Table 4

Ionic and atomic (rare gases) volumes at melting point

V, cm³	F^-	Na	Na^+
	16.5	—	2.0
	Cl^-	A	K^+
	35.0	28.5	13.9
	Br^-	Kr	Rb^+
	42.4	38.5	18.5
	I^-	Xe	Cs^+
	54.0	42.9	26.0

In the 5th column of table 1, the molar values are given, at melting point, computed with the help of the individual ionic volumes (from table 3) by applying the additivity rule (relation (1)). There is a satisfactory agreement with the experimental data confirming that the computing method was correct.

The above mentioned regularities, though applicable to the halides and nitrates of sodium, potassium, rubidium and caesium are not generally valid for other molten salts. For instance the halides of the other elements in group I (Li, Cu, Ag) and of the elements in groups II A and II B (Mg, Ca, Sr, Ba, Zn, Cd) as well as those of other molten salts possess astoundingly low molar volumes, even lower than the ionic volumes of the constituent anions. This phenomenon is illustrated by table 5 where, besides the molar volumes at melting point of a few halides, of metals in group I B, II A and II B, we find also the ionic volumes of the constituent anions. For these halides equation (1) keeps its validity only by assigning negative values to the cation ionic volumes. The only exceptions are the strontium

Table 5

Molar volumes of the salts of some metals of groups I A, I B, II A and II B, at melting point

Anions X^-	Anionic volume in cm³	Molar volumes in cm³			Anionic volume in cm³	Molar volumes in cm³						
		Li X	Cu X	Ag X		MgX2	CaX_2	SrX_2	BaX_2	ZnX_2	CdX_2	HgX_2
F^-	16.5	14.2	—	—	33.0	25.6	31.0	35.6	41.9	—	—	—
Cl^-	35.0	28.2	26.4	29.4	70.0	56.7	53.3	58.1	65.6	54.1	57.1	62.2
Br^-	42.4	34.3	—	33.7	84.8	70.4	64.2	66.7	74.8	66.8	73.5	70.4
I^-	54.0	43.1	—	42.1	108.0	91.5	85.5	83.2	92.4	83.3	82.3	87.1

---

[5] K. Fajans, *Naturwiss.*, **10**, 165 (1928); K. Fajans and G. Joos, *Z. Physik*, **23**, (1924); I. G. Murgulescu, Bul. Ştiinţ. Acad. R.P.R., Series A, **1**, 1 (1949).

and barium fluorides, the molar volumes of which are somewhat larger than the ionic volumes of the constituent anions.

The deviation from the additivity rule of the molar volumes of the above mentioned salts appears also in table 6, drawn up in the same way as table 2 which refers however to the halides of Mg, Ca, Sr and Ba. $V_{Cl^-} - V_{F^-}$ are the only differences to hold constant values, practically independent of the cation's nature.

Table

Differences between molar

Differences	$Me_1 = Ca$ $Me_2 = Mg$ $V_{Ca}^{++} - V_{Mg}^{++}$	$Me_1 = Sr$ $Me_2 = Ca$ $V_{Sr}^{++} - V_{Ca}^{++}$	$Me_1 = Ba$ $Me_2 = Sr$ $V_{Ba}^{++} - V_{Ca}^{++}$
$V_{Me_1F_2} - V_{Me_2F_2}$	5.4	4.6	6.3
$V_{Me_1Cl_2} - V_{Me_2Cl_2}$	−3.4	4.8	7.5
$V_{Me_1Br_2} - V_{Me_2Br_2}$	−6.2	2.5	8.1
$V_{Me_2I_2} - V_{Me_2I_2}$	−6.0	−2.3	9.2

The above presented data lead to the conclusion that, among the molten salts considered, only the halides and nitrates of Na, K, Rb, and Cs are nearly exclusively formed of free ions and can therefore be regarded as true ionic liquids. In the other molten salts, such as the halides of Li, Cu and Ag and the halides of the elements of groups II A and II B (Mg, Cs, Sr, Bs, Zn, Cd), the distances between the constituent anions and cations are appreciably smaller, while the corresponding linking energies are higher. The chemical bonds here are no longer entirely ionic, but partly covalent.

For the molten lithium halides, some information can be drawn from their molecular volumes, in the light of the classical theory of chemical bonds, by associating to the partially covalent character of the bond, a degree of dissociation α for every halide. Under these conditions, disregarding the interactions between ions and non-dissociated molecules, the molar volume V_{AC} of a molten binary salt AC is expressed by equation

$$\alpha \, (V_{A^-} + V_{C^+}) + (1 - \alpha) \, V_m = V_{AC}$$

where V_m represents the molar volume of the non-dissociated molten salt.

In the case of lithium halides, it can be assumed that the ionic volume of the cation is negligible when the above equation takes the form :

$$\alpha V_{X^-} + (1 - \alpha) \, V_m = V_{AC}$$

V_{X^-} being the ionic volume of the halogen ion. Nevertheless, even after this simplification, the equation will still possess two unknowns, which prevent its solution. It is however possible to obtain a higher limit of the dissociation degree, by admitting that this reaches the unit and that the value of V_m is relatively small. There results the relation :

$$\alpha \leqslant \frac{V_{LiX}}{V_{X^-}} \qquad (3)$$

which leads to the following numerical results by the melting points :

	LiF	Li Cl	Li Br	Li I
$\alpha \leqslant$	0.87	0.81	0.81	0.80

The order of magnitude of these results is quite plausible and shows that the molten lithium halides are not too far away from the true ionic liquids.

6

volumes at melting point

Differences	X = Cl X′ = F $V_{Cl^-} - V_{F^-}$	X = Br X′ = Cl $V_{Br^-} - V_{Cl^-}$	X = I X′ = Br $V_{I^-} - V_{Br^-}$
$V_{MgX_2} - V_{MgX'_2}$	15.5	6.9	10.6
$V_{CaX_2} - V_{CaX'_2}$	11.2	5.5	10.7
$V_{SrX_2} - V_{SrX'_2}$	11.3	4.3	8.3
$V_{BaX_2} - V_{BaX'_2}$	11.9	4.6	8.3

In order to characterize the partial covalent bond in the halides of the elements of group I B, we can use one of the quantum chemistry methods. We shall choose as a measure of the ionic character of a chemical bond the absolute value $(x_A - x_C)$ of the difference between the electronegativities x_A, x_C of atoms A and C from which the constituent ions originate. The fraction of the whole bond, which due to its partially ionic character can be estimated by means of Hannay and Smiths' [6] empirical equation is

$$F_i \text{ (the fraction of ionic character)} = 0.16\ (x_A - x_C) + 0.035\ (x_A - x_C)^2$$

which is most frequently used. (4)

Table 7

Partially ionic bond of some halides at melting point

Salt	x_A	x_C	$x_A - x_C$	Ionic fractions F
CuCl	3.10	1.8	1.30	0.267
AgCl	3.10	1.55	1.55	0.332
AgBr	2.85		1.30	0.267
Ag I	2.45		0.90	0.172

Table 7 records the data necessary to characterize the bonds in halides of certain elements of group I B. When drawing up this table we made use of the electronegativities as computed by Bellugue and Daudel.[7]

---

[6] N. B. Hannay and C. P. Smith, *J. Amer. Chem. Soc.*, **68**, 171 (1946).

[7] J. Bellugue and R. Daudel, *Rev. Sci.*, **84**, 541 (1946); R. Daudel, R. Lefebre and C. Moser, "Quantum Chemistry, Method and Applications", Interscience Publishers Inc., New York, 1959, p. 74.

For Cu (I), we used the value given by Gordy and Thomas.[8] According to the classical theory of ionic valence, the data in the last column of table 7 can be regarded as a measure of the ionic dissociation degree of the considered molten salts.

However, given the approximation character of the electronegativity values, as well as that of equation (4), the quantitative significance of the data in table 7 has to be accepted with caution. But, one can put down as certain the deep attenuation of the ionic character of the bond in the molten halides of Cu and Ag when compared to the alkali halides.

The halides of the metals in groups II A and II B also present an attenuated ionic bond. The mercury halides on the other hand, have a decidedly covalent character. The analysis of these systems is more difficult because of an eventual gradual dissociations :

$$MeX_2 \rightleftharpoons MeX^+ + X^- \; ; \quad MeX^+ \rightleftharpoons Me^{++} + X^-$$

as well as because of the formation of complex anions such as $[Me\,X_n]^{(2-n)-}$. Both these possibilities have often been presented.[9] The molar volumes alone cannot give an answer to the complexity of problems arising from molten salts resulting of polyvalent metals.

II. – EXPANSION AND COMPRESSIBILITY COEFFICIENTS OF MOLTEN SALTS

The expansion coefficient of molten salts can be easily deduced experimentally, from density measurements, by means of equation :

$$\alpha = -\frac{1}{\rho}\frac{d\rho}{dT} \tag{5}$$

The compressibility coefficients are deduced from the propagation velocity of supersonic waves in molten salts. The adiabatic compressibility β_s is directly supplied by equation :

$$\beta_s = \frac{1}{U_l^2\rho}$$

where U_l is the propagation velocity of ultrasounds and the fluid density. The isothermal compressibility β_T of which more will be told presently, results from formula :

$$\beta_T = \gamma\beta_s = \frac{\gamma}{U_l^2\rho} \tag{6}$$

where γ is the ratio between the molecular specific heat capacities at constant pressure and constant volume.

The estimation of coefficients α and β_T can be achieved by means of the state equations. We shall give a concise description of the state equations that are successfully applied to the study of molten salts.

[8] W. Gordy and W. O. Thomas, *J. Chem. Phys.*, **24**, 439 (1956).

[9] J. O'M Bockris, A. Pelle and J. L. Barton, *Rev. Chim. Acad. R.P.R.*, **7**, 59 (1962).

Particularly useful for our purpose is the equation established by Buehler, Hirschfelder and Curtis[10] for liquids and gases of high density;

$$PV\left(1-\frac{\sigma}{a}\right)=RT \tag{7}$$

where σ is the molecular diameter and a the shortest distance between two molecules, the other symbols retaining their usual significance. The distance a and the volume occupied by a molecule, are related by equation:

$$a^3=\sqrt{2}\,v$$

Though equation (7) was established for molecular liquids formed by particles assimilable to rigid spheres, Bockris [11] showed that it can be also applied to molten salts. For this purpose he proceeded to a direct verification of the equation by estimating the constant R and comparing the results of computation with the actual value. We shall try to verify indirectly equation (7) by using it to compute the expansion and compressibility coefficient of some molten salts. For this purpose, we shall introduce into equation (7) the molar volume V which, in case of a molten salt dissociating in ν ions, can be equaled to νNv. Equation (7) takes then the form :

$$PV\left(1-\frac{2^{5/6}\,\nu^{1/3}\,N^{1/3}}{V^{1/3}}\,r\right)=\nu RT \tag{8}$$

where r is the radius of the particles. In the following applications we assume that radius r is equal to the average radius of the ions forming a molecule.

Yosim and Owens[12] applied to molten salts the equation established by Reiss and coworkers.[13]

$$P_T=6kT\,(1+y+y^2)/[\pi a\,(1-y)] \tag{9}$$

where $y=\dfrac{\pi a^3}{6}\,\rho$, a is the diameter of the particles and ρ the volume occupied by a particle (by an ion). Valid for fluids when particles are assimilable to rigid spheres, equation (9) was applied by Yosim and Owens to compute the compressibilities of molten salts.

By extending the cellular model in McLellan's approximation [14] for the free volume, to molten salts, we deduced the following equation [15] for binary electrolytes :

$$PV=RT\left[1-\frac{A}{3}\left(1-\frac{1}{v_*^3\theta^3}\right)-\frac{B}{2}\ln\theta\right] \tag{10}$$

---

[10] J. O. Hirshfelder, C. F. Curtis and R. Byron Bird, "Molecular Theory of Gases and Liquids", John Wiley and Sons Inc., New York, London, 1954, p. 286.

[11] J. O'M Bockris, "Modern Aspects of Electrochemistry", Butterworth Scientific Publications, London, 1959, p. 177.

[12] S. J. Yosima and B. Owens, *J. Chem. Phys.*, **41**, 2023 (1964).

[13] M. Reiss, H. Frisch and J. Lebowitz, *J. Chem. Phys.*, **31**, 369 (1959).

[14] A. G. Mc Lellan, *J. Chem. Phys.*, **40**, 567 (1964).

[15] I. G. Murgulescu and G. Vasu, *J. Chem. Phys.*, **46**, 906 (1967).

where

$$A = \frac{\alpha_M e^2}{2kT\sigma v_*^{1/3}\,\theta^{1/3}}\ ;\quad B = \frac{\varepsilon_0}{2kTv_*^{1/3}\,\theta^{1/3}}\ ;\quad v_* = \frac{V}{2\,N\sigma^3}$$

σ being the sum of the ionic radii, ε_0 the sum of the formation energies of a cationic and anionic hole, α_M Madelung's constant and θ a structure parameter to be deduced from equation :

$$\frac{A}{3}\left(1 - \frac{1}{v^3\,\theta^3}\right) - B\left(1 - \frac{1}{3}\ln\theta\right) - \frac{1}{\theta}\ln(1-\theta) + \frac{2\,\theta - 1}{1-\theta} = 0$$

The other symbols maintain their usual significance. Equation(10) was used to estimate the expansion and compressibility coefficients of some molten binary salts.

By means of the significant structure theory Vîlcu and Misdolea[16] established the following state equation ;

$$P = \frac{RT}{V_s\,x^2}\left\{-2\,(\sigma_1 + \sigma_2) + 2x\left[\left(\frac{\partial\sigma_1}{\partial x}\right)_T + \left(\frac{\partial\sigma_2}{\partial x}\right)_T\right] + \gamma + \ln x + (x-1)\right\} \quad (11)$$

applied by them to compute the expansion and compressibility coefficients of some molten binary salts. In equation (11) we have:

$$x = V/V_s\,;\ n = cV_s/V\,;\ \sigma_1 = (E_s/2RT)\,x^{1/3} - 3\ln\left[1 - \exp\left(-\frac{\theta}{T}\right)\right];$$

$$\sigma_2 = \ln\{1 + n\,(x-1)\exp[-(aE_s/2nRT)]\,(x^{1/3}/x - 1)\}$$

$$\gamma = \ln\left(\frac{2\pi mkT}{h^2}\right)^{3/2}\frac{8\pi^2 IkT}{h^2}\,\frac{1}{[1 - \exp(-h\nu/kT)]}\,\frac{cV_s}{N}.$$

In these relations, V_s and E_s are the molar volumes and the sublimation energy of the solid at its melting point, θ is Einstein characteristic temperature, ν the vibration frequency of the gaseous molecule in its fundamental state, and c is the coordination number. The other symbols have their usual meanings.

1. *Expansion coefficients*

By applying the equation of Buehler, Wentorf, Hirschfelder and Curtis to estimate the expansion coefficients of molten salts, interesting conclusions can be drawn about the structure of these liquids. To this purpose, starting from equation (8) one obtains the following formula, for the expansion coefficients :

$$\alpha = \frac{1}{V}\left(\frac{\partial V}{\partial T}\right)_P = \frac{1}{T}\cdot\frac{1 - \dfrac{2^{5/6}\,\nu^{1/3}\,N^{1/3}}{V^{1/3}}\,\bar{r}}{1 - \dfrac{2}{3}\,\dfrac{2^{5/6}\,\nu^{1/3}\,N^{1/3}}{V^{1/3}}\,\bar{r}} \quad (12)$$

---

[16] R. Vilcu, C. Misdolea, *J. Chem. Phys.*, **46**, 906 (1967).

With $\nu = 2$, respectively $\nu = 3$, one obtains the computation formulae for the molten binary and ternary salts.

The following formula is deduced from equation (10) for the expansion coefficients of binary salts :

$$\alpha = \frac{1}{T} \cdot \frac{1 - M\left[\frac{1}{\theta}\ln(1-\theta) - \frac{2\theta - 1}{1-\theta}\right]}{1 + \frac{A}{9}\left(\frac{13}{v_*^3\theta^3} - 4\right) - \frac{4}{9}B\ln\theta - M\left[\frac{A}{9}\left(\frac{10}{v_*^3\theta^3} - 1\right) + \frac{B}{3}\left(1 - \frac{1}{3}\ln\theta\right)\right]} \tag{13}$$

where

$$M = \frac{\frac{A}{9}\left(\frac{10}{v_*^3\theta^3} - 1\right) + \frac{B}{3}\left(1 - \frac{1}{3}\ln\theta\right)}{\frac{A}{9}\left(\frac{10}{v_*^3\theta^3} - 1\right) + \frac{B}{3}\left(2 - \frac{1}{3}\ln\theta\right) + \frac{1}{\theta}\ln(1-\theta) + \frac{1}{(1-\theta)^2}}$$

Table 8 allows to compare the experimental values of the expansion coefficients at melting point, of some molten salts with the values calculated by means of equations (12) and (13).

Vîlcu and Misdolea[16] estimated also the expansion coefficients of a few molten alkali halides at three temperatures other than the melting

Table 8

Expansion coefficients of some molten salts at melting point

Salt	T_f °K	Mol. Volume cm³	$\bar{r}$ Å	$\alpha \times 10^4$ grad^{-1}			Salt	T_f °K	Mol. Volume cm³	$\bar{r}$ Å	$\alpha \times 10^4$ grad^{-1}	
				Exper	Calc. eq. (12)	Calc. eq. (13)					Exper	Calc. eq. (12)
LiF	1 121	14.2	0.98	2.71	4.25	—	CuCl	695	26.4	1.14	2.11	3.18
LiCl	883	28.2	1.21	2.87	5.61	—						
LiBr	823	34.3	1.28	2.59	6.13	—	AgCl	728	29.4	1.53	1.74	2.21
LiI	742	43.1	1.38	2.96	7.09	—	AgBr	707	33.7	1.61	1.86	2.11
NaF	1 268	21.0	1.16	2.89	3.42	—	AgI	829	42.1	1.71	1.81	2.17
NaCl	1 073	37.6	1.38	3.49	4.25	5.0						
NaBr	1 020	44.0	1.45	3.50	4.52	5.1	TlCl	703	42.6	1.65	3.19	3.68
NaI	933	54.7	1.56	3.48	4.92	—						
KF	1 131	30.4	1.35	3.41	3.51	—	$CaCl_2$	1 045	53.3	1.54	2.03	2.65
KCl	1 043	48.9	1.57	3.84	3.90	2.7	$SrCl_2$	1 146	58.1	1.58	2.13	2.43
KBr	1 007	56.0	1.64	3.91	4.06	2.8	$BaCl_2$	1 235	65.6	1.66	2.16	2.14
KI	954	67.8	1.75	3.89	4.27	—	$BaBr_2$	1 120	74.8	1.75	2.33	2.21
RbCl	995	53.8	1.65	3.95	3.85	2.5						
RbBr	965	60.9	1.72	3.95	3.96	2.5	$ZnCl_2$	535	54.1	1.45	2.12	7.05
RbI	920	73.4	1.82	3.96	4.24	—	$CdCl_2$	841	73.5	1.53	2.42	3.50
CsF	976	41.6	1.53	3.52	3.78	—	CdI_2	661	82.3	1.76	2.53	4.56
CsCl	918	60.3	1.75	3.84	3.85	—						
CsBr	909	67.9	1.82	3.89	3.85	—	$PbCl_2$	774	73.7	1.63	3.98	4.92
CsI	899	81.8	1.93	3.74	3.99	—	$PbBr_2$	646	80.3	1.73	3.23	5.23

point. The differential quotient in the expression of the expansion coefficients was calculated by means of relation:

$$\left(\frac{\partial V}{\partial T}\right)_P = -\left(\frac{\partial P}{\partial T}\right)_V \Big/ \left(\frac{\partial P}{\partial V}\right)_T \tag{14}$$

From equation (11) we obtain:

$$\left(\frac{\partial P}{\partial T}\right)_x = \frac{R}{V_S x^2}\left\{-2(\sigma_1+\sigma_2) - 2T\left[\left(\frac{\partial \sigma_1}{\partial T}\right)_y + \left(\frac{\partial \sigma_2}{\partial T}\right)_x\right] + \right.$$

$$+ 2x\left[\left(\frac{\partial \sigma_1}{\partial x}\right)_T + \left(\frac{\partial \sigma_2}{\partial x}\right)_T\right] + 2xT\frac{\partial}{\partial T} \times \left[\left(\frac{\partial \sigma_1}{\partial x}\right)_T + \frac{\partial}{\partial T}\left(\frac{\partial \sigma_2}{\partial x}\right)_T\right] +$$

$$\left. + T\frac{\partial \gamma}{\partial T} + x - 1 + \gamma + \ln x\right\}$$

$$\left(\frac{\partial P}{\partial V}\right)_T = \frac{RT}{V_S^2 x^3}\left\{2x^2\left[\left(\frac{\partial^2 \sigma_1}{\partial x^2}\right)_T + \left(\frac{\partial^2 \sigma_2}{\partial x^2}\right)_T\right] - 4x\left[\left(\frac{\partial \sigma_1}{\partial x}\right)_T + \right.\right.$$

$$\left.\left. + \left(\frac{\partial \sigma_2}{\partial x}\right)_T\right] + 4(\sigma_1+\sigma_2) - x + 3 - 2(\gamma + \ln x)\right\}$$

Table 9

Expansion coefficient of some alkaline halides

Salt	Temp. °K	$\alpha \times 10^4$ grad^{-1}	
		Experim.	Calc.
NaCl	1 073	3.6	4.47
	1 173	—	3.87
	1 273	3.9	2.65
NaBr	1 073	3.1	4.61
	1 173	—	4.20
	1 273	3.4	4.04
KCl	1 073	3.9	4.75
	1 173	—	4.65
	1 273	4.2	4.51
KBr	1 073	3.8	5.19
	1 173	—	4.92
	1 273	4.1	4.83

Table 9 gives the expansion coefficients calculated by means of the above equation besides the experimental values. By comparing the expansion coefficients as deduced from equation (12), (13) and (14) with the experimental data (Tables 8 and 9) one can see that the most accurate results are provided by the equation of Buehler, Wentorf, Hirschfelder and Curtis which offers moreover the advantage of being very simple.

The agreement between the experimental values and those computed by means of equation (12) is particularly remarkable in the case of the molten K, Rb and Cs halides, which thus appear once more, true ionic liquids.

The expansion coefficients calculated for the molten halides of copper, of the elements of group II B and of lead differ appreciably from the experimental ones. These latter salts show once more a different character than that of the true ionic liquids.

From this standpoint, a medium position is occupied by the halides of silver, alkali metals and Tl (I) for which the differences between the experimental values of the expansion coefficients and those calculated by equation (12) are to be found between 10 and 30% with the exception of barium halides for which the agreement between the experimental and the computed values is unexpectedly good.

Lithium halides, the properties of which bring them nearer in fact to the true ionic liquids, present surprisingly big differences between the calculated results and the experimental data. This is due, to a great extent, to the uncommonly large differences between the radius of the Li^+ ion and the radii of the halogen ions. The extension of equation (7) to molten salts, by the mere introduction of an average radius, is justified when the radii of the molten cations and anions are comparable. Otherwise, appreciable differences are to be expected between the values computed by means of equation (12) and the experimental ones; and these differences, as the lithium halides (Table 8) show, become larger as the anion radius increases.

The same explanation is valid for the unexpectedly large values of the expansion coefficients — calculated by equation (12) — of molten sodium halides which actually are almost pure ionic liquids. In this case too, the differences between experimental and computed data grow with the anion radius.

The regularities of the molar volumes of molten salts like their expansion coefficients, lead to the dividing of molten salts into two classes: ionic liquids (molten halides of Na^+, K^+, Rb^+, and Cs^+) and mixed liquids (molten halides of Li^+, Cu^+, Ag^+, etc.) the bonds of which are partially covalent.

2. — *Compressibility*

From equation (8) the following expression of the compressibility coefficient results:

$$\beta_T = -\frac{1}{V}\left(\frac{\partial V}{\partial p}\right)_T = \frac{V}{\nu R T}\cdot\frac{\left(1-\frac{2^{5/6}\,\nu^{1/3}\,N^{1/3}}{V^{1/3}}\,\bar{r}\right)^2}{1-\frac{2}{3}\cdot\frac{2^{5/6}\,\nu^{1/3}\,N^{1/3}}{V^{1/3}}\,\bar{r}} =$$

$$= \frac{V}{\nu R}\left(1-\frac{2^{5/6}\,\nu^{1/3}\,N^{1/3}}{V^{1/3}}\,\bar{r}\right)\alpha \qquad (15)$$

Yosima and Owens [12] deduced from equation (9), the compressibility of the molten salts:

$$\beta_T = (1-y)^3\ V_l\,[2R\,(1+y+y^2)]\,\alpha^2 \qquad (16)$$

Table 10

Compressibility of some simple molten salts

Salt	T °K	V cm^3	$\bar{r}$ Å	$\beta_T \times 10^{11}$ cm^2 dyne^{-1}				
				Exper.	Calc. eq. (15)	Calc eq. (16)	Calc. eq. (17)	Calc. eq (18)
1	2	3	4	5	6	7	8	9
LiCl	883	28.2	1.21	2.14	2.40	0.97	—	—
	973	29.0		2.17	2.30	—	—	—
	1 073	29.9		2.47	2.50	—	—	—
	1 173	30.8		2.86	2.23	—	—	—
	1 273	31.8		3.30	2.21	—	—	—
LiBr	873	34.5	1.28	2.27	3.07	—	—	—
	973	35.3		2.58	2.92	—	—	—
	1 073	36.3		2.94	2.85	—	—	—
	1 173	27.2		3.36	2.20	—	—	—
NaCl	1 073	37.6	1.38	2.87	2.10	1.44	3.07	1.59
	1 173	38.9		3.38	2.14	—	—	1.65
	1 273	40.4		4.00	2.20	—	—	1.85
NaBr	1 020		1.45	2.83	—	—	3.58	—
	1 073	44.8		3.36	2.65	—	—	2.05
	1 173	46.4		3.86	2.69	—	—	2.16
	1 273	48.2		4.49	2.76	—	—	2.41
NaI	933	54.7	1.56	3.73	—	1.99	—	—
	973	55.4		4.00	3.58	—	—	—
	1 073	57.5		4.73	3.61	—	—	—
	1 173	59.6		5.56	3.65	—	—	—
KCl	1 043	48.9	1.57	3.95	2.13	1.74	2.06	—
	1 073	49.5		3.84	2.16	—	—	2.30
	1 173	51.4		4.57	2.26	—	—	2.45
	1 273	53.5		5.47	2.36	—	—	2.74
KBr	1 007		1.64	3.90	—	—	2.45	—
	1 073	57.4		4.38	2.62	—	—	2.94
	1 173	59.8		5.21	2.75	—	—	3.25
	1 273	62.4		6.21	2.90	—	—	3.71
KI	954	67.8	1.75	4.87	3.27	2.08	—	—
	973	68.3		4.99	3.28	—	—	—
	1 073	71.1		5.99	3.40	—	—	—
	1 173	74.2		7.20	3.57	—	—	—

Salt	T °K	V cm^3	$\bar{r}$ Å	$\beta_T \times 10^{11}$ cm^2 dyne^{-1}		
				Exper.	Calc. eq. (5)	Calc eq. (16)
10	11	12	13	14	15	16
CsCl	918	60.3	1.75	4.95	2.15	2.00
	973	61.6		4.29	2.22	—
	1 073	64.1		5.12	2.35	—
	1 173	66.8		6.27	2.90	—
CsBr	973	89.3	1.82	5.58	5.93	—
	1 073	93.0		6.71	6.03	—
	1 173	97.1		8.27	6.20	—
$MgCl_2$	1 073	57.6	1.42	7.8	1.88	—
$MgBr_2$		71.5	1.52	9.9	2.11	—
MgI_2		94.5	1.66	13.4	3.26	—
$CaCl_2$	1 073	53.5	1.54	1.40	0.62	—
$CaBr_2$		64.9	1.63	1.80	0.84	—
CaI_2		85.8	1.77	2.80	1.28	—
$SrCl_2$	1 173	58.5	1.58	1.99	0.66	—
$SrBr_2$	1 073	68.9	1.68	2.34	0.78	—
SrI_2	1 073	88.6	1.82	2.53	0.84	—
$BaCl_2$	1 273	66.2	1.66	1.50	0.60	—
$BaBr_2$	1 173	75.2	1.75	2.00	0.64	—
BaI_2	1 073	93.7	1.89	2.10	0.83	—
$ZnCl_2$	873	60.8	1.45	4.90	2.39	—
$ZnBr_2$		77.9	1.55	7.10	3.41	—
ZnI_2		87.0	1.69	8.10	2.66	—
$CdBr_2$	873	67.4	1.62	4.30	1.36	—
CdI_2		88.2	1.76	6.00	1.92	—

by means of which they computed the compressibility of a few alkali halides at their melting points.

Equation (10) leads to the following compressibility formula for molten binary salts :

$$\beta_T = \frac{V}{2R}\left\{1 - M\left[\frac{1}{\theta}\ln(1-\theta) + \frac{2\theta - 1}{1-\theta}\right]\right\}\alpha \qquad (17)$$

where M maintains its significance as in equation (13).

Finally, from equation (11) it results that:

$$\beta_T = -\frac{V}{RTx}\left\{2x^2\left[\left(\frac{\partial^2\sigma_1}{\partial x^2}\right)_T + \left(\frac{\partial^2\sigma_2}{\partial x^2}\right)_T\right] - 4x\left[\left(\frac{\partial\sigma_1}{\partial x}\right)_T + \right.\right.$$
$$\left.\left. + \left(\frac{\partial\sigma_2}{\partial x}\right)_T\right] + 4(\sigma_1 + \sigma_2) - x + 3 - 2(\gamma + \ln x)\right\}^{-1} \qquad (18)$$

Based on this equation, Vîlcu and Misdolea[16] computed for three different temperatures the compressibility of some alkali halides.

Table 10 gives the experimental values of the compressibility as well as those computed by means of equation (16) (17) and (18) for some molten salts. For a thorougher control of equation (15) the compressibility of some molten salts was computed at temperatures for which we have the necessary experimental data.[17]

Table 10 shows that the agreement between the experimental compressibilities, and those calculated by means of any of the above equation, is less satisfactory than in the case of the expansion coefficients. Apart from a few exceptions, the calculated values are lower than the experimentally deduced ones. This fact is chiefly characteristic of halides of the elements in groups II A and II B. The best agreement between the compressibilities calculated by means of equation (15) and the experimental ones occurs, as for the expansion coefficients, in the case of alkali halides. Let us remark moreover that, according to equation (15) as well as to equation (18), the variation of compressibility with the temperature is much slower than according to experiment.

From this concise analysis it results that the above considered state equations, though marking an important forward step, have yet to be improved if one wants to obtain an accurate expression for the compressibility coefficients of molten salts.

---

[17] G. JANZ, "Molten Salt Handbook", A. P. New York – London, 1966, p. 249.

Revue Roumaine de Chimie, **14**, 965–979 (1969)

Revue Roumaine de Chimie, **14**, 981–984 (1969)

ON THE $n \rightarrow \pi^*$ ELECTRONIC TRANSITION IN AROMATIC KETONES

V. E. SAHINI and AL. BUTUCELEA

Institute of Physical Chemistry of the Academy
Bucharest, str. Dumbrava Roşie 23

Received January 9, 1969

A progression of the totally-symmetrical stretching vibration of C=O group ($\sim$ 1190 cm^{-1}) was evidenced in the $n \rightarrow \pi^*$ electronic transition of PhMeCO. The O–O component was located at $\sim$ 28,105 cm^{-1}.

The knowledge of the vibrational pattern of the $n \rightarrow \pi^*(^1U \leftarrow {}^1A)$ singlet electronic transition of ketones and aldehydes is very important for a definite assignment of its nature and for comparison with theoretical data, and, on the other hand, for inferring about the geometry of the $^1(n, \pi^*)$ excited state and the influence of substituents upon the carbonyl characteristic band. In order to elucidate one or other of these points, many aliphatic ketones or aldehydes were taken in study, but the class of aromatic ones was more sporadically investigated – especially the molecules showing a relative low (C_s) symmetry. The cause must be looked for in the difficulties encountered by experimentalists in resolving the overlapped band into its components.

Some attempts have been made, beginning with 1952, for *acetophenone*.[1–3] In 1956, Ermolaev[4] has succeeded in locating approximately the O–O component and to find the energetic intervals between the four observed components; similar values (1100–1250 cm^{-1}) were found by Dörr.[5] These data, though not very sure, point to the presence of the progression of a single vibration – the stretching vibration of C=O group, which in the ground state has a *ca.* 1700 cm^{-1} frequency in most of ketones and aldehydes. This vibrational pattern of the band is well supported also by the shape of the emission spectrum which implies the same electronic singlet states n and π^*[6]; this spectrum consists also in a progression of the C=O stretching vibration, whose frequency is naturally the same as found in infrared and Raman spectra. The quoted papers [4–6,7] agree in

[1] S. Imanishi, M. Ito, R. Semba and T. Anno, *Bull. Chem. Soc. Japan*, **25**, 150 (1952).

[2] R. D. Vanselow and A.B.F. Duncan, *J. Amer. Chem. Soc.*, **75**, 829 (1953).

[3] F. J. Taboury, *J. Phys. Radium*, **15**, 419 (1954).

[4] V. L. Ermolaev, *Opt. i Spektroskopiia*, **1**, 523 (1956).

[5] F. Dörr, *Z. Elektrochem.*, **61**, 950 (1957).

[6] G. W. Robinson, *J. Chem. Phys.*, **22**, 1384 (1954).

[7] See also Y. Kanda, R. Shimada, H. Shimada, H. Kaseda and T. Matumura, "Proc. Intern. Symp. Mol. Structure and Spectroscopy", Tokyo, 1962, p. B–304; Y. Kanda, H. Kaseda and T. Matumura, *Spectrochim. Acta*, **20**, 1387 (1964).

locating the origin of the progression, in absorption as well as in emission, at 27,500–28,000 cm^{-1}. For the *propiophenone*, the data are yet poorer, the $n \rightarrow \pi^*$ band being merely pointed out [8,9] than measured.

This paper is dealing with the resolution of the $n \rightarrow \pi^*$ electronic band of the two mentioned compounds, at low temperatures, in order to find the frequency of the pure electronic (O–O) transition and the vibrational pattern of the electronic band. We have looked mainly into the problem of the influence of substituents in the free carbonyl group upon the position and pattern of the considered electronic band.

EXPERIMENTAL

A specially designed cell for use at the liquid nitrogen's temperature [10], as well as a plane grating spectrograph type PGS-2 (Zeiss, Jena), in the 1st order (40–70 cm^{-1}/mm linear resolution within the absorption band range), were used. The continuous background was supplied by a 150 W (Original Hanau) deuterium lamp.

The spectra were obtained at room temperature as well as at low temperature (in solutions and films). Acetophenone and propiophenone, analysis reagents, were distilled under vacuum before use, and the solvents were made water-free. The films were prepared between quartz plates – acetophenone as a pure compound, and propiophenone, whose band is much more intensive, as a solute in compounds with similar crystalline matrices (benzene, *cyclo*hexane). Concentrations of (2...3).10^{-2} M (acetophenone) and (1... 2).10^{-4} M (propiophenone), in a 8 mm path length cell, have been found suitable for good spectra in solution. Intensity measurements have not been performed.

RESULTS AND DISCUSSION

Acetophenone. At room temperature, the analyzed band appears for the pure compound (0.02...0.04 mm thickness film) and for solutions in non-polar solvents only. Its apparent maximum is located at *ca.* 320 mμ in the former case, and at *ca.* 325 mμ in the latter one. The solution band presents a weak and not fully resolved vibrational structure, from which, however, 4 components may be perceived as inflexions in the experimental curve; in these circumstances, their respective positions might not be, of course, exactly determined – although the reported data [3–5,7] were taken up from curves of such a shape. The O–O, very weak, band, might be, however, located at *ca.* 27,800 cm^{-1} – which is comparable with the values obtained by Ermolaev [4] and Kanda and co-workers [7] in similar conditions.

The polar solvents, on the other hand, give rise to a strong blue shift, owing to hydrogen bonds. [11] This shift causes, at room temperature, the nearly complete overlap of the $n \rightarrow \pi^*$ band by the neighboring very intensive $\pi \rightarrow \pi^*$ band. We have ascertained however that at low tem-

---

[8] I. P. Grammatikakis, *Bull. Soc. chim. France*, **1953**, 821, 865.

[9] E. Spinner and A. Burawoy, *Spectrochim. Acta*, **17**, 558 (1961).

[10] A. Butucelea, *Rev. Chim.* (*Bucureşti*), **19**, 423 (1968).

[11] H. McConnell, *J. Chem. Phys.*, **20**, 700 (1952); G. J. Brealey and M. Kasha, *J. Amer. Chem. Soc.*, **77**, 4462 (1955); G. C. Pimentel, *J. Amer. Chem. Soc.*, **79**, 3323 (1957).

peratures, in rigid glasses, the $n \rightarrow \pi^*$ band re-appears and even presents a visible vibrational structure, similar to that of the band in non-polar solvents at room temperature. The band is shifted towards higher frequencies — the apparent maximum with *ca.* 850 cm^{-1} and the O—O component with *ca.* 370 cm^{-1} as compared with the respective values in non-polar solvents. A precise determination of the position of vibrational components is, in this case also, rather difficult without a good mathematical resolution of the experimental curve.

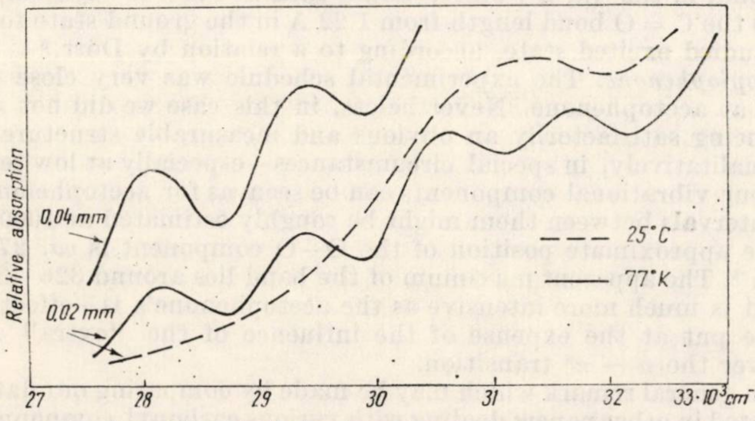

Fig. 1. — Vibrational structure of acetophenone $\nu_{n \rightarrow \pi^*}$ band.

Table 1

Vibrational structure of the $n \rightarrow \pi^*$ band of acetophenone
(polycrystal, 77°K)

Position of the vibrational component (cm^{-1})	The measured energetic intervals (cm^{-1})	Assignment
28,105±50		0,0
29,385±50	1280	0,0+1.1190
30,620±50	1235	0,0+2.1190
31,670±50	1050	0,0+3.1190

A better resolution of the vibrational structure of the band can be achieved, however, with a film of suitable thickness, slowly cooled down to polycrystalline state. In figure 1 the polycrystalline film spectrum of acetophenone at 77°K, as well as the spectrum of the film at room temperature, are drawn. As table 1 shows, the O—O component of the band is located at 28,105 ± 50 cm^{-1}. The energetic intervals between the four components have the values 1280, 1235 and 1050 cm^{-1}. If the effects of the overlap of simple gaussian bands on the resulting band,[12] as well as the specified errors, are taken qualitatively into account, these intervals might be accepted as being equal; this would lead to a mean value of 1190 cm^{-1} for the energy spacing between the first vibrational levels of the $^1(n, \pi^*)$ electronic state. This value agrees with that which was found for the corresponding state of other ketones, both aromatic and aliphatic.[13] It represents the frequency of $C=O$ stretching vibration. The force constant of the bond, in the $^1(n, \pi^*)$ state, would then be 5.6×10^5 dyn/cm, which increases the $C = O$ bond length from 1.22 A in the ground state to 1.36 A in the studied excited state, according to a relation by Dörr.[5]

---

[12] I. Ruff, *Acta Chim. Acad. Sci. Hung.*, **45**, 13 (1965).

Propiophenone. The experimental schedule was very close to that followed at acetophenone. Nevertheless, in this case we did not succeed in evidencing satisfactorily an obvious and measurable structure of the band. Qualitatively, in special circumstances—especially at low temperatures—four vibrational components can be seen, as for acetophenone; the energy intervals between them might be roughly estimated at 1000—1100 cm^{-1}. The approximate position of the O—O component is *ca.* 27,850 ± ±150 cm^{-1}. The apparent maximum of the band lies around 326—328 mμ. The band is much more intensive as the acetophenone's is—effect which should be put at the expense of the influence of the "extra" methyl group, over the $n \rightarrow \pi^*$ transition.

As a general remark which may be made by comparing our data with those related in other papers dealing with various carbonyl compounds,[13,14] one may state that the influence of different substituents in the carbonyl group is too weak to modify considerably the vibrational pattern of its characteristic $n \rightarrow \pi^*$ band. Therefore, in describing the spectral features of a wide group of ketones and aldehydes, the use of (C_{2v}) local symmetry of the $>C=O$ chromofore is authorized.[13]

[13] H.-P. Gervais, *Thesis*, Faculté des Sciences de l'Université de Paris, Paris, 1966.
[14] J. C. D. Brand and D. G. Williamson, *Discuss. Faraday Soc.*, **1963**, 184.

Revue Roumaine de Chimie, **14**, 985–990 (1969)

OXYDATION DU Fe ET DU Ni À HAUTES TEMPÉRATURES

EFFET DU CHAMP MAGNÉTIQUE SUR LA VITESSE D'OXYDATION DU Fe ET DU Ni

D. CISMARU et ELISABETA DOBROGHIU

Institut de chimie physique, 23, str Dumbrava Roșie, Bucarest

Reçu le 29 octobre 1968

Les auteurs ont étudié l'effet d'un champ magnétique extérieur de 800, 1200 et 1770 Oe sur la vitesse d'oxydation du Fe entre 500–800° et du Ni entre 600–900° dans O_2 en régime dynamique. Les résultats ont conduit à la conclusion que, dans l'intervalle de température considéré, seulement la vitesse d'oxydation du Fe est influencée par le champ magnétique extérieur pour les températures de 500° et 600°, c'est-à-dire pour les températures inférieures au point Curie du Fe. Dans tous les cas la cinétique du processus d'oxydation est rendue par une équation parabolique.

INTRODUCTION

La possibilité d'une action du champ magnétique extérieur sur la vitesse de l'oxydation des métaux à hautes températures n'a pas été étudiée jusqu'à présent, bien que l'action du champ magnétique sur la réaction chimique [1] ait préoccupé les chercheurs.

Il existe des épreuves expérimentales qui indiquent l'influence positive du champ magnétique extérieur sur la vitesse de réaction [2–8] dans quelques cas de réactions chimiques à la température ordinaire.

Nous pouvons citer aussi la suggestion de Eisemann [9] sur l'utilisation du champ magnétique comme catalyseur.

En étudiant l'effet d'un champ magnétique faible sur la vitesse d'oxydation d'un fil de Fe, D. Cismaru et Gh. Cismaru [10] ont observé une augmentation de la vitesse.

---

[1] P. W. Selwood, *Chem. Rev.*, **28**, 41 (1946).
[2] H. S. Taylor et H. S. Sachsse, *Z. phys. Chem.* (B), **23**, 1 (1933).
[3] S. S. Bhatnagar, K. N. Mathur et P. L. Kapur, *Phyl. Mag.*, 7, **8**, 457 (1929).
[4] R. H. Harman et H. Eyring, *J. Chem. Phys.*, **10**, 557 (1942).
[5] E. Justi et G. Vieth, *Z. Naturforsch.*, **8a**, 538 (1953).
[6] B. Tamamishe et A. Akijome, *Bull. Chem. Soc. Japan*, **12**, 372 (1939).
[7] E. Gelles et K. S. Pitzer, *J. Amer. Chem. Soc.*, **77**, 1974 (1955).
[8] P. E. Yankwick, *Amer. Rev. Nuclear Sci.*, **3**, 235 (1953).
[9] K. Eisemann, *J. Phys. Colloid. Chem.*, **54**, 1385 (1950).
[10] D. Cismaru et G. D. Cismaru, *Rev. Metall. Acad. Bucarest*, **2**, 204 (1963).

Dans le présent travail les auteurs étudient l'effet d'un champ magnétique ayant des intensités de 800 à 1770 Oe sur la vitesse d'oxydation du Fe et du Ni.

MÉTHODE EXPÉRIMENTALE

On a employé un appareil semblable à celui décrit dans un travail antérieur,[11] à la seule différence que le four est constitué par un tube en quartz ayant un diamètre intérieur de 30 mm, bobiné sur une longueur de 15 cm du fil de tantale qui constitue la résistance du chauffage.

Dans l'intérieur de ce tube était introduit le tube de réaction ayant un diamètre intérieur de 20 mm. Le gaz oxydant chauffé, au préalable, par son passage entre les deux tubes était introduit dans le tube de réaction par sa partie inférieure. Par ce procédé la température du gaz devient suffisamment homogène.

Le champ magnétique a été obtenu en utilisant un électro-aimant construit dans le laboratoire qui pouvait produire un champ magnétique d'environ 1 800 Oe dans la région centrale où était placé l'échantillon.

L'intensité du champ magnétique a été mesurée à l'aide d'un fluxmètre de type RFN.

La cinétique de l'oxydation a été étudiée par la méthode gravimétrique en utilisant une balance à fil de quartz ayant une sensibilité de 2.10^{-5} g. Les échantillons avaient le poids entre 0,18 – 0,195 g. L'échantillon de métal était suspendu par un fil de quartz au fléau de quartz de la balance.

L'échantillon était placé dans la région centrale de l'entrefer de l'électro-aimant.

On a mesuré la température avec un thermocouple de Pt Rh – Pt avec une précision de ± 2°.

La soudure chaude du thermocouple était placée près du milieu de l'échantillon.

La température était maintenue constante par un courant de chauffage stabilisé. Le gaz oxydant est l'oxygène pur, préalablement séché à travers une série de vases de séchage, contenant respectivement de l'acide sulfurique concentré, du chlorure de calcium et du perchlorate de magnésium.

Le débit de l'oxygène était de 5 l/h. Les métaux utilisés étaient : plaque de Fe Armco et de bande de Ni de pureté 99,9 %.

Les échantillons métalliques ont été coupés sous forme de disques au diamètre de 10 à 12 mm.

La surface de l'échantillon de Fe a été préparée par polissage mécanique et celui du Ni par polissage chimique avec un mélange de 27 % – HNO_3, 14,3 % – H_2SO_4, 14,3 % H_3PO_4 et 43,8 % CH_3COOH pendant 15 s.

RÉSULTATS

La cinétique d'oxydation du Fe et du Ni a été étudiée à quatre températures différentes : pour le Fe à 500°, 600°, 800° et pour le Ni à 600°, 700°, 800°, 900° et pour des intensités de champs de 800, 1200, 1770 Oe.

Pour l'homogénéité des résultats, la réaction a été étudiée sur le même échantillon en travaillant au commencement en dehors du champ et après dans le champ magnétique

---

[11] I. G. Murgulescu et D. Cismaru, *Rev. Chim. Acad. Bukarest*, 3, 2 (1958).

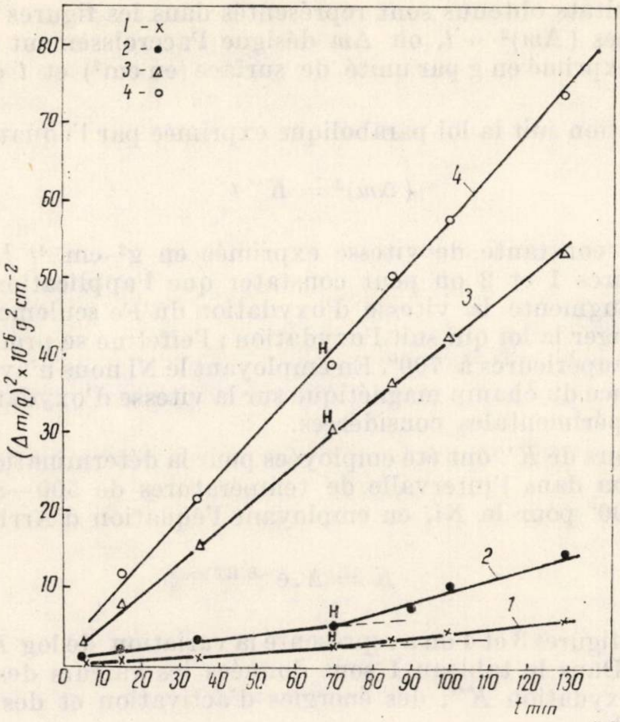

Fig. 1. — Courbes $(\Delta m)^2$ en fonction de *t* pour le Fe oxydé à : *1*, 500° ; *2*, 600° ; *3*, 700° ; *4*, 800°.

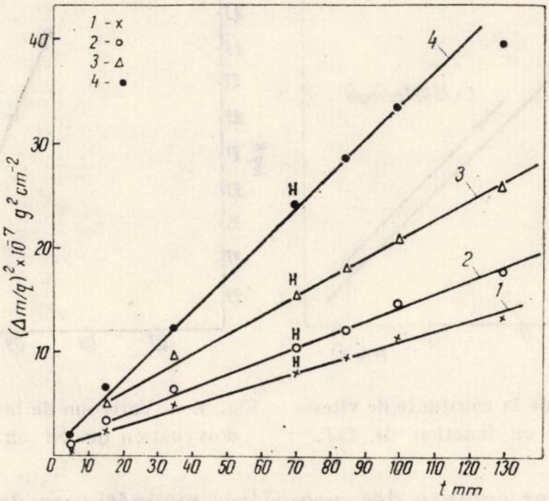

Fig. 2. — Courbes $(\Delta m)^2$ en fonction de *t* pour le Ni oxydé à : *1*, 600° ; *2*, 700°, *3*, 800° ; *4*, 900°.

Les résultats obtenus sont représentés dans les figures 1 et 2 dans les coordonnées $(\Delta m)^2 - t$, où Δm désigne l'accroissement en poids de l'échantillon exprimé en g par unité de surface (en cm^2) et t est le temps en minutes.

L'oxydation suit la loi parabolique exprimée par l'équation :

$$(\Delta m)^2 = K'' t$$

où K'' est la constante de vitesse exprimée en g^2 cm$^{-4}t^{-1}$.

Des figures 1 et 2 on peut constater que l'application du champ magnétique augmente la vitesse d'oxydation du Fe seulement à 500° et 600° sans changer la loi qui suit l'oxydation ; l'effet ne se produit pas aux températures supérieures à 700°. En employant le Ni nous n'avons observé aucune influence du champ magnétique sur la vitesse d'oxydation dans les conditions expérimentales considérées.

Les valeurs de K'' ont été employées pour la détermination de l'énergie d'activation dans l'intervalle de températures de 500—800° pour le Fe et 700—900° pour le Ni, en employant l'équation d'Arrhénius

$$K = \mathrm{A}.\mathrm{e}^{-\mathrm{E/RT}}$$

Dans les figures 3 et 4 on a représenté la variation de log K'' en fonction de $1/T$. Dans le tableau 1 sont données les valeurs des constantes de vitesse d'oxydation K'', des énergies d'activation et des coefficients préexponentiels.

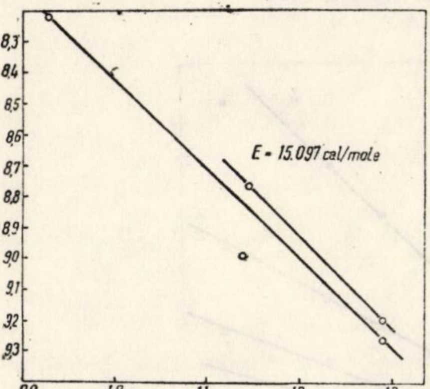

Fig. 3.— Variation de la constante de vitesse d'oxydation du Fe en fonction de $1/T$.

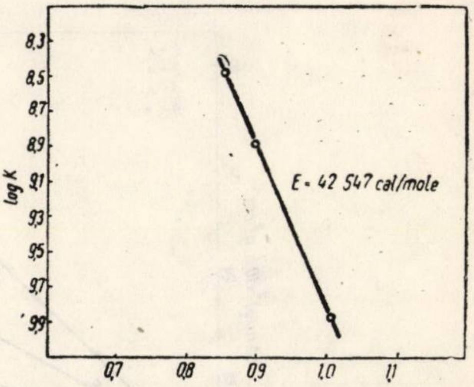

Fig. 4. — Variation de la constante de vitesse d'oxydation du Ni en fonction de $1/T$.

Si l'on tient compte des propriétés magnétiques de ces métaux et de leurs oxydes, on constate qu'aux températures utilisées, le Fe reste ferromagnétique jusqu'à 770° quand il devient paramagnétique. Le Ni a le point Curie à 350°.

Tableau 1

Fe **Valeurs de K″, E et A** **Ni**

T°C	K″ g²cm⁻⁴ t⁻¹ sans champ	K″ g²cm⁻⁴ t⁻¹ en champ	*E* cal/mole	*A* g² cm⁻⁴ *t*⁻¹	*T*°C	K″ g² cm⁻⁴ *t*⁻¹	*E* cal/mol	*A* g² cm⁻⁴. .*t*⁻¹
500	$5{,}5.10^{-8}$	$6{,}25.10^{-8}$			600	$1{,}0.10^{-8}$		
600	$8{,}33.10^{-8}$	$16{,}6.10^{-8}$			700	$1{,}32.10^{-8}$	42 547	
			15.097		800	$1{,}3.10^{7}$		
700	$4{,}1.10^{-7}$							
				$1{,}006.10^{-3}$	900	$3{,}33.10^{7}$		5,762
800	$5{,}1.10^{-7}$							

Un calcul approximatif nous montre que pour le champ de 1000 gauss on trouve pour le moment magnétique $\mu = 2{,}6.10^{-22}$ erg/gauss, si l'on prend pour la molécule d'oxygène $\varkappa = 1.002$.

L'énergie maximum pour l'approche des deux particules, dont les moments magnétiques sont μ_1 et μ_2, jusqu'à la distance r est

$$E_{\max} = \frac{2\mu_1\mu_2}{r^3}$$

En considérant $\mu_1 = \mu_2$ et $r = 1$ Å on trouve

$$E_{\max} = 1{,}35.10^{-15} \text{ erg.}$$

En comparant cette valeur avec la valeur de KT pour la température de 10° on obtient une énergie dix fois plus grande.

Si nous essayons de calculer l'énergie d'orientation pour les substances ferromagnétiques, le champ de saturation correspond à environ 10^{-7} gauss. Dans notre cas, pour un champ de 100 gauss, l'énergie d'orientation est

$$E = \mu\text{H} = 5{,}2.10^{-7} = 0{,}75 \text{ cal/mole}$$

Les forces d'interaction seront environ 10^4 fois plus petites que les forces de nature électrostatique.

En conséquence les calculs basés sur l'utilisation des paramètres magnétiques ne peuvent pas mener à l'explication du phénomène.

La détermination de la structure cristallographique des oxydes formés dans l'absence et en présence du champ magnétique n'a pas montré de différences.

Dans le tableau 2 sont données les susceptibilités magnétiques du Fe et du Ni et leurs oxydes.

L'observation de quelques auteurs, selon laquelle la vitesse d'oxydation augmente dans le champ au cas où la somme des susceptibilités magnétiques des produits finaux de réaction est plus grande que celle des produits initiaux est valable aussi dans ce cas (voir tabl. 2).

En effet, dans un champ magnétique dans le domaine de température jusqu'au point Curie on observe un accroissement de la vitesse d'oxydation, parce que le moment magnétique augmente dans le champ.

Tableau 2

Susceptibilités moléculaires et ioniques du Fe et Ni et de leurs oxydes

Nom de la substance	T°C	$\varkappa_M \cdot 10^6$	$\varkappa_{ion} \cdot 10^6$	Bibliographie
Fer d = 7,86	18	2,4	—	12
Ni d = 8,9	18,5	0,48 (= 0,2)	—	12
	500—850	44,2		13
FeO	210	25,9*		14
Fe_2O_3	18	19,7		15
Fe_2O_3FeO	ord	80.000 (entre 0—100 gauss)		16
Fe^{+2}	ord		11.900	13
Fe^{+3}	ord		14.300	13
NiO		420		12
O_2		1,002		17

* Préparé du nitrate.

Dans le domaine de température proche du point Curie et supérieur à ce point, l'augmentation de vitesse dans le champ n'est pas observable.

Il est possible que l'effet d'augmentation de la vitesse dans le champ apparaisse aux champs plus forts, même dans le domaine des températures supérieures au point Curie, mais avec un effet diminué.

---

[12] International Critical Tables of Numerical Data, Physics Chemistry and Technology McGraw-Hill Book Company, New York and London, 1926, VIe vol., p. 374, 358.

[13] P. W. SELWOOD, « Magnetochemistry », Intersci. Publ. Inc., New-York, 1956, p. 289 et Ed. Russe, 1958, p. 89.

[14] S. VERL, « Tables annuelles de constantes », VIe vol., 1923—1924, pl. II, 772 p.

[15] A. SERRES, « Tables annuelles de constantes, IXe vol., p. 357.

[16] J. FOESTER et A. CHONSHON, « Tables annuelles de constantes », VIIe vol., 1925—1926, pl. II, p. 971.

[17] U. V. VOLKENSTEIN, « Stroenie fizicheskie svoistva molecul. », Akad. Nauk S.S.S.R., Izd., 1955, p. 347.

Revue Roumaine de Chimie, **14**, 991–997 (1969)

CHRONOPOTENTIOMETRIC DETERMINATION OF SILVER ION INTERDIFFUSION COEFFICIENT IN MOLTEN POTASSIUM AND LITHIUM NITRATES

S. STERNBERG and CONSTANŢA HERDLICKA

Institute of Physical Chemistry of the Academy,
Bucharest, str. Galaţi 31

Received October 14, 1968

The interdiffusion coefficient of silver ion in molten $LiNO_3$ and KNO_3 media was determined at different temperatures by a chronopotentiometric method. The influence of the working electrode geometry upon the chronopotentiometric measurement was studied and the plane electrode was found to give the best results. At 340° the interdiffusion coefficient of silver ion was 2.45×10^{-5} cm^2/sec in $LiHO_3$ and 1.86×10^{-5} cm^2/sec in KNO_3; the activation energy takes the values 7900 cal and 4340 cal respectively.

The application of chronopotentiometric method to the determination of diffusion coefficient on molten salts was attempted by Laitinen, [1,2] Bockris, [3] Delimarschi [4,5] and some other authors. [6–9]

The diffusion coefficient is computed making use of Saud's equation:

$$\tau^{1/2} = \frac{\pi^{1/2} n F D^{1/2} c}{2 i_0} \qquad (1)$$

where τ is the transition time (sec), c the concentration (moles/cc) and D the diffusion coefficient (cm^2/sec) of the electrochemically active ion, i_0 the current density (A/cm^2), the other magnitudes preserving their well known meanings.

The transition time is determined from potential-time curves obtained on galvanostatic polarization of the electrode under study.

---

[1] H. A. Laitinen and W. S. Ferguson, *Analyt. Chem.*, **29**, 4 (1957).

[2] H. A. Laitinen and H. C. Gaur, *Analyt. Chim. Acta.*, **18**, 1 (1958).

[3] D. Inman and J. O. Bockris, *J. Electroanalyt. Chem.*, **3**, 126 (1962.)

[4] Yu. K. Delimarskii, B. F. Markov and L. S. Berenblyum, *Zhur. fiz. Khim.*, **27**, 1848 (1953).

[5] Yu. K. Delimarskii, A. B. Gorodyskii and V. V. Kuzmovich, *Coll. Czech. Chem. Comm.*, **25**, 3056 (1960).

[6] C. E. Thalmayer, S. Bruckenstein and D. M. Gruen, *J. Inorg. Nuclear Chem.*, **26**, 347 (1964).

[7] K. Kawamura, *Electrochim. Acta*, **12**, 1233 (1966).

[8] F. Caligara, L. Martinot and G. Duyckaerts, *Bull. Soc. chim. belges*, **76**, 5, 15 (1967).

[9] T. Sakakura, *J. Electrochem. Soc. Japan*, **35**, 75 (1967).

The useful condition of chronopotentiometric method is that the concentration of diffusion ion should be much smaller than the "background" concentration. Thus, the transport of the studied ion exclusively by diffusion avoiding its transport by electromigration is ensured. Concentrations of about $1-5 \times 10^{-5}$ moles/cm^3 were generally used. In these circumstances the solute has no influence upon the properties of the solvent. The viscosity of the system, the number of holes etc. are those characteristic of the solvent.

The study of interdiffusion coefficients of different ions (Ag, Pb, Zn) as a function of solvent nature which could be a pure alkali or alkali-earth salt is accordingly interesting from the standpoint of the structure of molten salts.

This paper presents the first results obtained from this research trend i.e. interdiffusion coefficients of Ag^+ in KNO_3 and $LiNO_3$.

EXPERIMENTAL

The glass cell, 38 cm overall height, had at the top four tapered joint-ended tubes for tightening the three electrodes and the thermocouple. The cell body made of a 5 cm in diameter and 7 cm high glass tube contains about 60 cm^3 melt.

The working electrode. Differently shaped electrodes were used as cathode : 0.34 and 0.5 mm in diameter platinum wire and 0.3 mm thick platinum plate. The cylindrical electrodes were made by soldering the platinum wire in a Jena-glass tube allowing a free working surface area of $0.08-0.1$ cm^2. The plane electrode consisted of a platinum plate suspended to a thin platinum wire also sealed in a Jena-glass tube : their surface area lay within $0.3-0.4$ cm^2 (including the edges and the surface area of suspension wire). The surface area was determined by making use of an optical micrometer.

The counterelectrode : was a platinum or silver plate of 5 cm^2 surface area and was protected by a glass tube which penetrated up to the bottom of the cell.

The reference electrode was a silver wire introduced into a $AgNO_3$ solvent mixture. The silver wire together with the nitrates mixture (the $AgNO_3$ concentration of which was about equal to that of the melt in the cell) remained all throughout the experiment in a test tube provided with on orifice : in this orifice a piece of asbestos string was plugged.

The cell was introduced into a vertical furnace manufactured so that in the working region the convection be avoided by minimizing the thermal gradient. The temperature was measured with a thermocouple Pt/PtRh and maintained within ± 1°. A photo-resistor thermoregulating device ensured the thermosetting.

Purified and dried argon was bubbled before starting experiments to produce a homogeneous mixture bulk.

The salts, chemically pure products, were purified by recrystallizing from aqueous solution : then melted and preserved in an oven.

The device used for transition time measurements is represented on figure 1.

A steady current was passed between the working electrode (C) and the counterelectrode while the cathode (C) voltage against a reference nonpolarized electrode (R) was measured as a function of time.

This voltage was passed through the amplifier (B) into a R.F.T. magneto-optical oscillograph provided with a photo-registering device suitable for obtaining potential-time curves. The magneto-optical galvanometer dissipates a relatively high current (about 6 mA) and this is why the amplifier was used : this scheme gives an amplifier-oscillograph input resistance of about 0.5 M and the current dissipation is avoided in this way.

The synchronizing sweep was given by 50 c p s alternative current in the mains. The power supply was a storage battery of 75 V; the current was set by a $10^4-10^6\ \Omega$ resistor

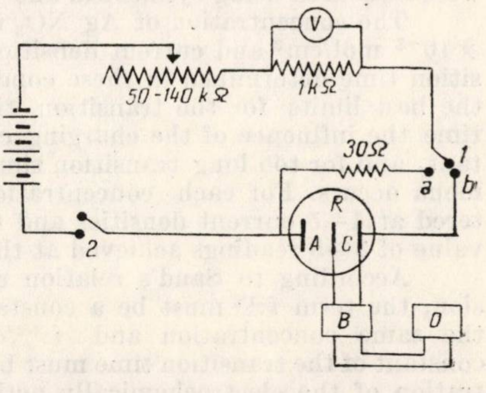

Fig. 1. — Diagram of measuring apparatus.
A, anode, *C*, cathode, *B*, amplifier, *O*, oscillograph

and read on a digital voltmeter which shunted a 1000 Ω resistor included in the circuit. Switch (1) in position *a* established the electrolyse current before every registering of transition time. The registering system was started about 0.2 sec. before the electrolyse took place and switch (1) in position *b* closed the electrolysis circuit and allowed registering of voltage *versus* time curve. A picture obtained in this way is represented on figure 2.

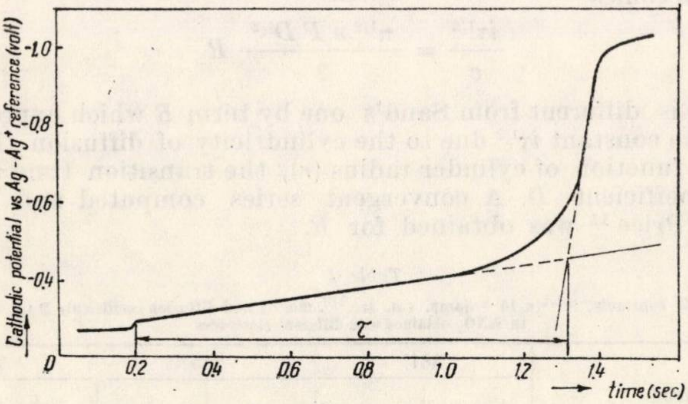

Fig. 2. — Potential-time curve for reduction of silver ion in $LiNO_3$ at 310°.
$C = 1.76 \times 10^{-5}$ mol/cc; $i = 2.2$ mA.

The transition time, defined as the time elapsed from the beginning of electrolysis until the steep increase in potential (marking the moment when concentration of diffusing ion is zero) occurs, was measured according to Thalmayer et al.[6] (figure 2). An average value of transition times measured on 3—4 potential-time curves registered for the same current density was taken.

RESULTS AND DISCUSSION

The interdiffusion coefficients of Ag^+ in KNO_3 on a 345−420° temperature range and in $LiNO_3$ within 260−315° were determined. For the diffusion of Ag^+ in KNO_3 the transition times from potential-time curves were measured using cylindrical and plane electrodes.

The concentration of $Ag\ NO_3$ in alkali nitrate lies within $1.8.-3\times\times10^{-5}$ mol/cm³ and current densities $1.4.-0.5\times10^{-2}$ A/cm², the transition time determined in these conditions being $0.5-2$ sec. These are the best limits for the transition time since for too short a transition time the influence of the charging current of the double layer is important, and for too long transition times an influence of convection phenomena occurs. For each concentration potential-time curves were registered at 4−5 current densities and the transition time was the average value of 3−5 readings achieved at the same current density.

According to Sand's relation relying on semi-infinite linear diffusion, the term $i\tau^{1/2}$ must be a constant at different current densities for the same concentration and $i\tau^{1/2}/c$ called the chronopotentiometric constant of the transition time must be constant irrespective of the concentration of the electrochemically active substance.

Some further considerations on the influence of electrode geometry upon the chronopotentiometric constant are given below. For this purpose the chronopotentiometric constants as determined with differently shaped cathodes (cylindrical and plane ones) are to be compared.

According to Peters and Lingane,[10] Sand's equation for cylindrical electrodes becomes

$$\frac{i\tau^{1/2}}{c} = \frac{\pi^{1/2}\, n\, F\, D^{1/2}}{2}\, R \qquad (2)$$

Relation (2) is different from Sand's one by term R which expresses the change in the constant $i\tau^{1/2}$ due to the cylindricity of diffusion field. The term R is a function of cylinder radius (r), the transition time τ and the diffusion coefficient D. A convergent series computed and listed by Evans and Price[11] was obtained for R.

Table 1

Chronopotentiometric constants, $i\tau^{1/2}/c\cdot10^{-2}$ (amp. cm. sec.$^{1/2}$. mol^{-1}) and diffusion coefficients $D_{Ag}\cdot10^5$ (cm^2 sec^{-1}) in KNO_3 obtained with different electrodes

Electrode	361°		385°		397°	
	$i\tau^{1/2}/c$	$D_{Ag^+}\cdot10^5$	$i\tau^{1/2}/c$	$D_{Ag^+}\cdot10^5$	$i\tau^{1/2}/c$	$D_{Ag^+}\cdot10^5$
Cylindrical without correction	4.14	2.35	4.94	3.33	5.18	3.67
Cylindrical with correction	3.97	2.18	4.65	2.94	4.84	3.20
Plane	3.91	2.08	4.15	2.37	4.27	2.50
Kawamura (plane) 360°	—	2.05 2.11	—	—	—	—

---

[10] D. H. Peters and J. J. Lingane, *J. Electroanalyt. Chem.*, **2**, 1 (1961).

[11] D. H. Evans and J. E. Price, *J. Electroanalyt. Chem.*, **5**, 77 (1963).

In table 1 are presented the values of chronopotentiometric constants and interdiffusion coefficients of Ag^+ in KNO_3 as determined with different electrodes. The diffusion coefficients obtained with cylindrical electrodes seem to take values which are much higher than those obtained with plane electrodes. The difference is smaller when the constant R is introduced but it still assumes high values especially for temperatures over 360°.

For cylindrical electrodes the addition of R constant makes no difference between 0.34 and 0.5 mm diameter electrodes. The distinct behaviour of the two electrodes is also seen on figure 3. The diffusion coefficients determined with cylindrical electrodes do not obey the Arrhenius law and for higher temperatures an improbably high apparent activation energy is obtained (10,000 cal).

For 360° our results have been compared with Kawamura's ones determined by chronopotentiometric method using plane electrodes and oscillographic polarography.

From this comparative study it results that the use of cylindrical electrodes with relatively small diameters is not at all advisable, the appa-

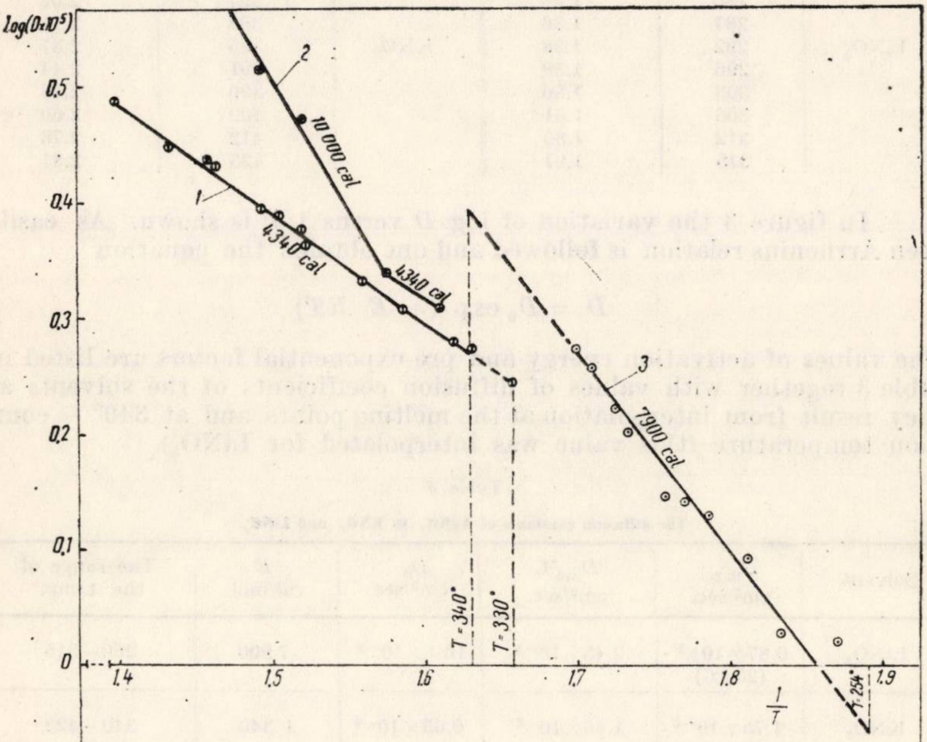

Fig. 3. — Variation of log D *versus* $1/T$.

1 $AgNO_3$ in KNO_3 plane electrode; 2 $AgNO_3$ in KNO_3 cylindrical electrode; 3 $AgNO_3$ in $LiNO_3$ plane electrode.

rent diffusion coefficients they give being greater than the real ones obtained in experiments with plane electrodes. The correction *R* computed by Evans and Price is not adequate in molten salts conditions. The layer diffusion thickness might be of the same order of magnitude as the electrodes diameter and in these cases the theory of linear semi-infinite diffusion on which Sand's equations rely is no longer valid. In table 2 the diffusion of Ag^+ in KNO_3 and $LiNO_3$ is given, determined at various temperatures with platinum plate cathodes. The lithium nitrate was not used at over 320° since a decomposition of the salt **and** a change in the electrode processes occurred at higher temperature.

Table 2

The diffusion coefficients for Ag^+ in $LiNO_3$ and KNO_3 at different temperatures

Solvent	Temp.°	$D_{Ag^+} \cdot 10^5$ $cm^2\ sec.^{-1}$	Solvent	Temp.°	$D_{Ag^+} \cdot 10^5$ $cm^2\ sec.^{-1}$
$LiNO_3$	262	1.04	KNO_3	340	1.86
	272	1.07		345	1.89
	280	1.26		357	2.02
	287	1.36		368	2.15
	292	1.38		385	2.37
	296	1.39		391	2.44
	303	1.56		396	2.48
	306	1.61		409	2.60
	312	1.83		412	2.73
	315	1.91		423	2.81

In figure 3 the variation of log *D* versus $1/T$ is shown. As easily seen Arrhenius relation is followed and one obtains the equation

$$D = D_0 \exp\left(-E/RT\right)$$

The values of activation energy and pre-exponential factors are listed in table 3 together with values of diffusion coefficients of the solvents as they result from interpolation at the melting points and at 340° — common temperature (this value was interpolated for $LiNO_3$).

Table 3

The diffusion constants of $AgNO_3$ in KNO_3 and $LiNO_3$

Solvent	$D_{m.p.}$ $cm^2/sec.$	D_{340}°C $cm^2/sec.$	D_0 cm^2/sec	*E* cal/mol	The range of the temp.°
$LiNO_3$	0.87×10^{-5} (254°C)	2.45×10^{-5}	16.1×10^{-3}	7 900	260–315
KNO_3	1.75×10^{-5} (330°C)	1.86×10^{-5}	0.65×10^{-3}	4 340	340–423

It is worth mentioning that at melting point $D_{Li} < D_K$ while at a given temperature an inversion occurs and D_{Li} becomes greater than D_K. The radius of Ag^+ ion (1.13 Å) is smaller than that of the ion K^+ (1.33 Å) but is greater than the radius of the Li^+ ion (0.75 Å). At the melting point the average hole volume in $LiNO_3$ might be smaller than the volume of a silver ion and the diffusion of the Ag^+ ion could be consequently rendered more difficult. With the temperature growth the number of greater volume holes increases and diffusion is favoured : this explains the high activation energy found for $LiNO_3$ as well as the above mentioned inversion. The activation energy for Ag^+ ion interdiffusion in $LiNO_3$ is much greater than the activation energy for Li^+ selfdiffusion in $LiNO_3$ which is of 5500 cal.[12] In KNO_3 the holes volume is great enough ; the activation energy is determined by the energy needed to make a hole and is close to the activation energy for selfdiffusion of K^+ in KNO_3 which is of 5530 cal.[12]

---

[12] B. R. Sundheim, "Fused Salts" McGraw-Hill, New York, 1964, p. 224.

Revue Roumaine de Chimie, **14**, 999–1001(1969)

X-RAYS STUDIES ON MONOPYRIDINE COMPLEXES OF COBALT (II) AND NICKEL (II) CHLORIDES

D. MANOLESCU and E. SEGAL

Institute of Physical Chemistry of the Academy
Bucharest, str. Dumbrava Roşie 23

Received October 3, 1968

Crystallographic studies were carried out on the monopyridine complexes of Co(II) and Ni(II) chlorides. The results obtained show that these compounds crystallize in an orthorhombic system.

The thermal stability as well as the crystal structure of complex combinations formed by certain metal halides with pyridine and substituted pyridines have made the object of some thermogravimetrical and X-rays studies. According to some meaningful results obtained by various authors,[1–5] the thermal decomposition of complexes of general form $Me^{(II)}Py_4x_2$ proceeds in steps; as soon as the temperature increases, the intermediate complexes occur in sequence as follows:

$$Me^{(II)}Py_4x_2 \rightarrow Me^{(II)}Py_2x_2 \rightarrow Me^{(II)}Py\,x_2 \rightarrow Me^{(II)}Py_{2/3}\,x_2 \rightarrow Me^{(II)}x_2$$

The X-rays literature data refer only to the first two terms. According to the studies carried out by Poray-Koshits and Antukhina[6] the tetrapyridine complexes of Ni(II) and Co(II) chlorides are isomorphous and they have a monoclinic type of lattice. It is supposed that the dipyridine complex of nickel(II) chloride has a monoclinic type of lattice like the compound of copper chloride.[7–9] Although the experimental powder patterns of the dipyridine complex of cobalt(II) chloride are similar to the analogous compound of nickel it cannot be indexed in a monoclinic type of lattice but in an orthorhombic one.[7] In the present note we endeavour to give a crystallographic study of monopyridine complexes of Co(II) and Ni(II) chlorides represented by the third term of the sequence given above.

---

[1] L. R. Ocone, J. R. Soulen and B. P. Block, *J. Inorg. Nuclear Chem.*, **15**, 76 (1960).

[2] J. R. Allan, D. H. Brown, R. H. Nuthal and D. W. A. Sharp, *J. Inorg. Nuclear Chem.*, **26**, 1895 (1964).

[3] D. H. Brown, R. H. Nuthal and D.W.A. Sharp, *J. Inorg. Nuclear Chem.*, **25**, 1069 (1963).

[4] J. R. Allan, D. H. Brown and D.W.A. Sharp, "Proceedings of the First International Conference on Thermal Analysis", Aberdeen, 1965, p. 138.

[5] I. G. Murgulescu, E. Segal and D. Fătu, *J. Inorg. Nuclear Chem.*, **27**, 2677 (1965).

[6] M. A. Poray-Koshits and A. S. Antukhina, *Kristalografiya*, **3**, 686 (1958).

[7] R. Zannetti and R. Serra, *Gazz. Chim. Ital.*, **90**, 328 (1960).

[8] J. D. Dunitz, *Acta Cryst.*, **10**, 307 (1957).

[9] S. S. Kabalkina, *Doklady Akad. Nauk S. S. S. R.*, **110**, 1013 (1956).

EXPERIMENTAL

The monopyridine complexes of cobalt (II) and nickel (II) chlorides used, have been obtained by thermal decomposition of the tetrapyridine complexes of cobalt (II) and nickel (II) chlorides, in derivatograph.

We used the results obtained by the thermogravimetric analysis of the complexes of cobalt (II) and nickel (II) chlorides with pyridine.[5]

Powder diffraction patterns were obtained by means of a TUR M 60 apparatus. For the nickel compound we used the CuK_α radiation and for the cobalt compound the CoK_α radiations. Film recording was made by the Straumanis method. The specimens were exposed in Debye-Scherer cameras of 57.3 mm in diameter.

Line intensities were measured by means of a Schnell-Photometer G II (K. Zeiss, Jena).

Complexes density was determined through a pycnometric technique by n-octane immersion.

RESULTS AND DISCUSSION

The experimental data obtained are given in tables 1 and 2.

Table 1

Indexing of $CoPyCl_2$ powder pattern

No.	d(Å)	I%	hkl
1	10.7	17	002
2	8.64	17	200
3	7.58	10	110
4	6.035	16	210
5	5.365	8	004
6	4.295	16	005
7	3.790	24	220
8	3.506	31	106
9	3.093	87	224
10	2.815	10	030
11	2.770	13	602
12	2.662	100	603
13	2.525	87	330
14	2.424	39	614
15	2.342	77	431
16	2.217	68	219

The respective headings of the columns are as follows: 1. current number; 2. interplanar spacing; 3. relative intensities of the lines per cent; 4. hkl indices.

Powder diffraction patterns are indexed by Lipson's method.[10] From the experimental data we can determine the values of lattice parameters. The values obtained for the lattice parameters are as follows:

— for monopyridine complex of cobalt (II) chloride:

$$a = 17.21 \pm 0.01 \text{ Å}; \quad b = 8.45 \pm 0.01 \text{ Å}$$

---

[10] H. Lipson, *Acta Cryst.*, **2**, 43 (1949).

Table 2

Indexing of $NiPyCl_2$ powder patterns

No.	d(Å)	I%	hkl
1	10.7	16	002
2	8.64	15	200
3	7.56	5	110
4	6.020	16	210
5	5.368	7	004
6	4.293	18	005
7	3.790	16	220
8	3.450	19	500
9	3.080	72	216
10	2.820	66	030
11	2.650	64	521
12	2.525	59	330
13	2.334	48	135
14	2.217	42	219
15	2.144	5	0.0.10
16	2.037	5	723
17	1.994	100	804

$c = 21.46 \pm 0.01$ Å; and for

— monopyridine of nickel (II) chloride:
$a = 17.21 \pm 0.01$ Å; $b = 8.45 \pm 0.01$ Å
$c = 21.46 \pm 0.01$ Å

The tables show that two complexes are isomorphous, the sequence of hkl indices being nearly the same; in fact both complexes crystallize in an orthorhombic system.

Density values determined by us are:

$\rho = 1.79 \pm 0.01$ g/cm^3 for $Co^{(II)}PyCl_2$

$\rho = 1.89 \pm 0.02$ g/cm^3 for $Ni^{(II)}PyCl_2$

The number n of molecules in the unit cell is given by the formula,[11]

$$n = \rho \frac{V}{M}$$

where V the volume of the unit in cm^3
M molecular weight of the complex in grams
ρ density in g/cm^3

In this way one obtains unit cell of sixteen molecules for both complexes studied.

CONCLUSIONS

X-rays study of monopyridine complexes of cobalt (II) and nickel (II) chlorides showed that these combinations are isomorphous, crystallizing in an orthorhombic system. The values of lattice parameters are very close to one another and the complexes contain a sixteen-molecule unit cell.

---

[11] A. GUINIER, "Théorie et Technique de la Radiocrystallographie", 3-e Edition, Dunod, Paris, 1964, p. 146.

Revue Roumaine de Chimie, **14**, 1003–1010 (1969)

LIGAND FIELD THEORY FOR NONCUBIC SYMMETRIES

J. MÁTHÉ
Babeş-Bolyai University, Department of Physical Chemistry,
Cluj, str. Arany János 11

Received October 19, 1968

In this paper the splitting of Russell-Saunders D term (d^1, d^6, d^4, d^9 configurations) in the weak tetragonal and rhombic field ($\Gamma_i = D_{4h}$, C_{4v}, D_{2h}) is investigated. The perturbation procedure is carried out with an overall potential, $V(\Gamma_i)$, without separating it as a sum of octahedral and lower field component $V(O_h) + \Delta V(\Gamma_i)$. The ligand field energies are expressed in terms of parameters, characterizing the individual ligand atoms, situated on the x, y, and z axes $Dq(x)$, $Dq(y)$, $Dq(z)$, $Ds(x)$, $Ds(y)$, $Ds(z)$, where $Dq(i) = eq_i < r^4 > /6R_i^5$ and $Ds(i) = eq_i < r^2 > /7R_i^3$.

The ligand field theory in spite of the simplicity of the electrostatic model, explains the magnetic and optical behaviour of transition metal compounds.[1 a, b, c, d] In this approximation the electronic term energies are given as functions of the ligand field and of the interelectronic repulsion parameters. The number of parameters needed to express the energies increases as the field symmetry becomes lower. The theory of systems of noncubic fields was investigated by many authors. Thus calculations on tetragonal and square planar geometry have been carried out by Moffitt and Ballhausen,[1a, 2] Liehr,[3] Owen,[4] Piper,[5] Fenske,[6] Figgis,[7] Otsuka,[8] Perumareddi[9] and Bán,[10] various configurations in trigonal field were treated by Liehr,[3] Piper,[5] Figgis,[6] Gladney,[11] Hartmann[12] and Pryce.[13]

[1] a) C. J. Ballhausen, "Introduction to Ligand Field Theory", McGraw-Hill Company Inc., New York, 1962, p. 77; b) H. L. Schläfer und G. Gliemann, "Einführung in die Ligandenfeldtheorie", Akademische Verlagsgesellschaft, Frankfurt am Main, 1967, p. 329; c) J. S. Griffiths, "Theory of Transition Metal Ions", Cambridge Univ. Press, 1961, p. 195; d) B. N. Figgis, "Introduction to Ligand Fields", Interscience Publ., London, 1966, p. 62.

[2] W. Moffitt and C. J. Ballhausen, *Ann. Rev. Phys. Chem.*, **7**, 107 (1956).

[3] A. D. Liehr, *J. Phys. Chem.*, **64**, 43 (1960).

[4] J. Owen, *Proc. Roy. Soc.* **A 277**, 183 (1954).

[5] T. S. Piper and R. L. Carlin, *J. Chem. Phys.*, **33**, 1208 (1960).

[6] R. F. Fenske, D. S. Martin and K. Ruedenberg, *Inorg. Chem.*, **1**, 441 (1962).

[7] B. N. Figgis, *J. Chem. Soc.*, **1965**, 4887.

[8] J. Otsuka, *J. Phys. Soc. Japan*, **21**, 596 (1966).

[9] J. R. Perumareddi, *J. Phys. Chem.*, **71**, 3144 (1967).

[10] M. Bán and J. Császár, *Magyar Kém. Folyóirat*, **73**, 509, 512 (1967).

[11] H. M. Gladney and J. D. Swalen, *J. Chem. Phys.*, **42**, 1999 (1965).

[12] H. Hartmann, C. Furlani and A. Bürger, *Z. phys. Chem. (Frankfurt)*, **9**, 62 (1956).

[13] M. H. L. Pryce and W. A. Runciman, *Discuss. Faraday Soc.*, **26**, 34 (1958).

This paper is concerned with the theory of d^1, d^4, d^6 and d^9 configurations in tetragonal and rhombic fields.

THEORY OF TETRAGONAL AND RHOMBIC FIELDS

The transition metal ion Hamiltonian is expressed as a sum of the following terms :

$$\mathcal{H} = \mathcal{H}_{en} + \mathcal{H}_{ee} + \mathcal{H}_{lf} + \mathcal{H}_{LS} \tag{1}$$

where $\mathcal{H}_{en}$ means the electron-nucleus interaction, $\mathcal{H}_{ee}$ the electron-electron interaction, $\mathcal{H}_{lf}$ is the ligand field Hamiltonian, $\mathcal{H}_{LS}$ the spin-orbit interaction Hamiltonian. In this paper we shall neglect the last term. Three cases arise function of the relative magnitude of $\mathcal{H}_{ee}$ and $\mathcal{H}_{lf}$:

a) weak field when $\mathcal{H}_{ee} > \mathcal{H}_{lf}$
b) intermediate field $\mathcal{H}_{ee} \sim \mathcal{H}_{lf}$
c) strong field $\mathcal{H}_{ee} < \mathcal{H}_{lf}$.

In the present paper we shall use the weak field scheme, considering $\mathcal{H}_{lf}$ as a perturbation of Russell-Saunders terms ^{2S+1}L. The $\mathcal{H}_{lf}$ perturbing Hamiltonian is given by

$$\mathcal{H}_{lf} = -|e|\, V(r, \theta, \Phi) \tag{2}$$

where $V(r, \theta, \Phi)$ is the ligand field potential at a point (r, θ, Φ) near the origin at the central ion. This potential can be expressed in terms of spherical harmonics

$$V(r, \theta, \Phi) = \sum_{n=1}^{\infty} \sum_{m=-n}^{+n} A_n^m(j)\, r^n Y_n^m(\theta, \Phi) \tag{3}$$

$A_n^m(j)$ depends on the charge or dipole moment and coordinates (R_j, θ_j, Φ_j) of the ligands. Assuming a point charge model

$$A_n^m(j) = -\frac{4}{2n+1} \sum_{j=1}^{6} (-1)^m Y_n^{-m}(\theta_j, \Phi_j) \frac{q_j}{R_j^{n+1}} \tag{4}$$

The number of spherical harmonics (n, m) in the ligand field potential can be obtained from the invariancy condition of the potential with respect to the symmetry operations of the point group.[14] In the case of symmetries lower than the cubic one (D_{4h}, C_{4v}, D_{2h}, etc.) the potential $V(\Gamma_i)$ is usually expressed as a sum of cubic potential and a component of lower symmetry $V(\Gamma_i) = V(O_h) + \Delta V(\Gamma_i)$, i.e. the octahedral field is perturbed by the potential of the field of lower symmetry (Γ_i). In this paper we treated the D_{4h}, C_{4v}, and D_{2h} field with the overall potential $V(\Gamma_i)$, without separating it as a sum of octahedral and lower field component.

---

[14] M. Sachs, "Solid State Theory", McGraw-Hill Book Co., New York, 1962, p. 81.

A) *Tetragonal field*

D_{4h} symmetry group. The tetragonal field potential (if the z axis is the fourfold axis of symmetry) is given by

$$V(\mathrm{D}_{4\mathrm{h}}) = A_2^0 r^2 Y_2^0 + A_4^0 r^4 Y_4^0 + A_4^4 r^4 (Y_4^4 + Y_4^{-4}) \tag{5}$$

It is convenient to write the Hamiltonian using the "operator equivalents"[15-17]

$$\mathscr{H}(\mathrm{D}_{4\mathrm{h}}) = B_2^0 O_2^0 + B_4^0 O_4^0 + B_4^4 O_4^4$$

$$\begin{aligned} \text{where}\quad O_2^0 &= \alpha r^2 \left[3L_z^2 - L(L+1)\right] \\ O_4^0 &= \beta r^4 \left[35L_z^4 - 30L(L+1)L_z^2 + 25L_z^2 - 6L(L+1) + \right. \\ &\quad \left. + 3L^2(L+1)^2\right] \\ O_4^4 &= \frac{1}{2}\beta r^4 (L_+^4 + L_-^4) \end{aligned} \tag{6}$$

The multiplicative factors are $\alpha = \mp \frac{2}{21}$, $\beta = \pm \frac{2}{63}$ for the d^1, d^6 (upper signs) and d^4, d^9 electron configurations. The values of the coefficients B_n^m are as follows[18]

$$B_2^0 = \frac{1}{4}\left(\frac{5}{\pi}\right)^{1/2} A_2^0 \qquad B_4^0 = \frac{3}{16\sqrt{\pi}} A_4^0 \qquad B_4^4 = \frac{3}{8}\left(\frac{35}{2\pi}\right)^{1/2} A_4^4 \tag{7}$$

The matrix elements of ligand field operator $\mathscr{H}(\mathrm{D}_{4\mathrm{h}})$ are

$$\begin{aligned} &< 2 \pm 2 \,|\mathscr{H}|\, 2 \pm 2 > = 12B_4^0\beta < r^4 > + 2\,(3B_2^0\alpha < r^2 >) \\ &< 2 \pm 1 \,|\mathscr{H}|\, 2 \pm 1 > = -4\,(12B_4^0\beta < r^4 >) - (3B_2^0\alpha < r^2 >) \\ &< 2.0 \,|\mathscr{H}|\, 2.0 > = 6\,(12\,B_4^0\beta < r^4 >) - 2\,(3B_2^0\alpha < r^2 >) \\ &< 2 \mp 1 \,|\mathscr{H}|\, 2 \pm 1 > = 0 \\ &< 2 \pm 2 \,|\mathscr{H}|\, 2 \mp 2 > = 12B_4^4\beta < r^4 > \end{aligned} \tag{8}$$

where $< r^k >$ are the radial integrals $< R_{n,2}(\mathrm{r})\, \mathrm{r}^k R_{n,2}(\mathrm{r}) >$. The term energies were calculated using the symmetry-adapted Slater determinant functions $\psi(L, M_L, S, M_S) = |\, m_{l_1}, m_{s_1}\,;\; m_{l_2}, m_{s_2}\,;\; \ldots \,|$. The energies of B_{1g}, A_{1g}, B_{2g} and E_g terms (d^4 and d^9 configurations) are given by

$$\begin{aligned} \varepsilon(B_{1g}) &= -\,(12B_4^0\beta < r^4 >) - 2(3B_2^0\alpha < r^2 >) - 12B_4^4\beta < r^4 > \\ \varepsilon(A_{1g}) &= -\,6(12B_4^0\beta < r^4 >) + 2(3B_2^0\alpha < r^2 >) \\ \varepsilon(B_{2g}) &= -\,(12B_4^0\beta < r^4 >) - 2(3B_2^0\alpha < r^2 >) + 12B_4^4\beta < r^4 > \\ \varepsilon(E_g) &= 4(12B_4^0\beta < r^4 >) + (3B_2^0\alpha < r^2 >) \end{aligned} \tag{9}$$

---

[15] K. W. H. STEVENS, *Proc. Roy. Soc.* **A 65**, 209 (1952).

[16] H. WATANABE, "Operator Methods in Ligand Field Theory", Prentice-Hall Inc., New Jersey, 1966, p. 103, 169.

[17] M. T. HUTCHINGS, *Solid State Physics*, **16**, 227 (1964).

[18] S. A. ALTSHULER and B. M. KOZIREV, "Electronnii paramagnitnii resonans", Gos. Izd. Fiz.-Mat. Lit., Moscow, 1961, p. 49.

Since in the octahedral field the energies of E_g and T_{2g} levels are expressed in terms of the octahedral parameter $Dq = 12B_4^0(O_h) < r^4 >$, it is convenient to write the tetrahedral term energies analogously, using a parameter $Dq\ (D_{4h})$ which defines the main splitting of the free ion term, and other two parameters characterizing the axial deformation. Accepting the following definitions

$$\begin{aligned} Dq(D_{4h}) &= 12B_4^0(x, y, z)\,\beta\,\langle r^4\rangle \\ Ds &= 3B_2^0\alpha\,\langle r^2\rangle \\ Dt &= 12(B_4^4/5 - B_4^0)\,\beta\,\langle r^4\rangle \end{aligned} \tag{10}$$

the term energies are

$$\begin{aligned} \varepsilon(B_{1g}) &= -\,6Dq - 2Ds - 5Dt \\ \varepsilon(A_{1g}) &= -\,6Dq + 2\,Ds \\ \varepsilon(B_{2g}) &= 4Dq - 2Ds + 5Dt \\ \varepsilon(E_g) &= 4Dq + Ds \end{aligned} \tag{11}$$

The $Dq\ (D_{4h}) = Dq\ (x,\ y,\ z)$ parameter defined above differs from the $Dq\ (O_h) = Dq\ (x,\ y)$ parameter used by Ballhausen and Moffitt characterizing the MA_4X_2 compounds.

Considering the ligand ions as point charges, the parameters Dq, Ds and Dt can be expressed in the form :

$$\begin{aligned} Dq(D_{4h}) &= \frac{6}{14}\,Dq(xy) + \frac{8}{14}\,Dq(z) \\ Ds &= 2\,[Ds(xy) - Ds(z)] \\ Dt &= \frac{4}{7}\,[Dq(xy) - Dq(z)] \end{aligned} \tag{12}$$

where the new parameters $Dq\ (xy)$, $Dq\ (z)$, $Ds\ (xy)$ and $Ds\ (z)$ characterize the ligands on the x, y and z axes.

$$\begin{aligned} Dq(i) &= \frac{eq_i}{6R_i^5}\langle r^4\rangle \\ Ds(i) &= \frac{eq_i}{7R_i^3}\langle r^2\rangle \end{aligned} \tag{13}$$

If the compound is axially elongated, $R_z > R_{xy}$ the fundamental term is $B_{1g}(Ds > 0)$. In the case of an axially compressed field $Ds < 0$, the sequence of energy levels is A_{1g}, B_{1g}, E_g, B_{2g}. Assuming that the ligand field parameter ratio is equal to $\alpha = \dfrac{Dq(z)}{Dq(xy)} \simeq \left(\dfrac{R_{xy}}{R_z}\right)^5$ and the radial integral ratio has a value of $\lambda = \dfrac{< r^2 >}{< r^4 >} \cdot \dfrac{R_{xy}^5}{R_{xy}^3}$, we can write the term energies as a function of $Dq\,(\mathrm{xy})$, α and λ. α is a measure of axial deformation having a value of unit for octahedral field and zero for a square planar geometry. Figure 1 represents the reduced energy level diagram $\varepsilon/Dq\,(\mathrm{xy})$ as a function of axial deformation α, assuming that the radial

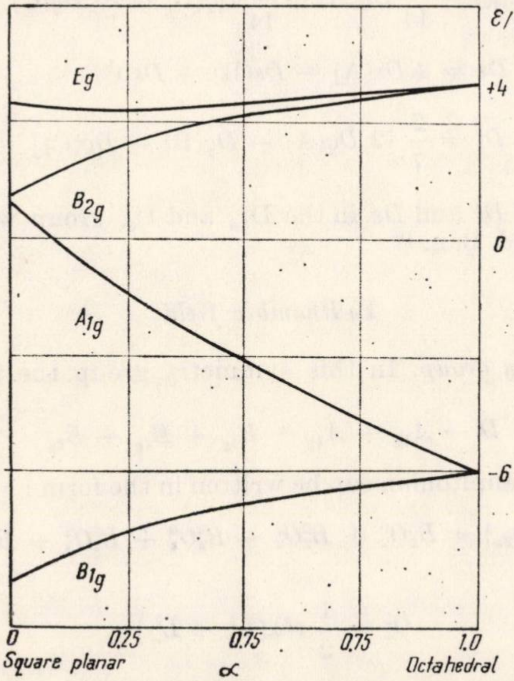

Fig. 1. — Plot of reduced term energies ($\varepsilon/10Dq$) *versus* the axial deformation parameter $\alpha = Dq(\mathrm{z})/Dq(\mathrm{xy})$ for d^4 and d^9 configurations.

$$\lambda = \frac{<r^2>}{<r^4>} \cdot \frac{R_{\mathrm{xy}}^5}{R_{\mathrm{xy}}^3} = 1.$$

integral ratio has a value of unit. As this diagram shows, by deformation of the compound the first band ($A_{1g} \leftarrow B_{1g}$) moves towards the second ($B_{2g} \leftarrow B_{1g}$) which has an unchanged position. If λ has a value greater than the unit in the square planar compound, the B_{2g} term becomes lower than the A_{1g} term.

In the case of d^1 and d^6 electronic configurations the signs of the ligand field parameters will be changed in equation (11).

C_{4v} symmetry group. The ligand field potential will be

$$V(C_{4v}) = A_1^0 r Y_1^0 + A_2^0 r^2 Y_2^0 + A_3^0 r^3 Y_3^0 + A_4^0 r^4 Y_4^0 + A_4^4 r^4 (Y_4^{-4} + Y_4^4) \qquad (14)$$

Since the matrix elements with odd n-terms are zero, the energy expressions of the ligand field terms (A_{1g}, B_{1g}, B_{2g}, E_g) are the same as in the case of D_{4h} symmetry and are given by equation (11). Considering a compound of the type MA_4BC we obtain the following values for the ligand field parameters :

$$Dq(C_{4v}) = \frac{6}{14} Dq(A) + \frac{4}{14} Dq(B) + \frac{4}{14} Dq(C)$$

$$Ds = 2\, Ds(A) - Ds(B) - Ds(C) \tag{15}$$

$$Dt = \frac{2}{7} [2\, Dq(A) - Dq(B) - Dq(C)]$$

The expressions of Dt and Ds in the D_{4h} and C_{4v} group were obtained by Carlin, Piper [5] and Bán. [10]

B) *Rhombic field*

D_{2h} symmetry group. In this symmetry group the free ion D term splits into

$$D \to A_{1g} + A_{1g} + B_{1g} + B_{2g} + B_{3g}$$

The ligand field Hamiltonian can be written in the form :

$$\mathcal{H}(D_{2h}) = B_2^0 O_2^0 + B_2^2 O_2^2 + B_4^0 O_4^0 + B_4^2 O_4^2 + B_4^4 O_4^4 \tag{16}$$

where

$$O_2^2 = \frac{1}{2} r^2 \alpha (L_+^2 + L_-^2)$$

and

$$O_4^2 = \frac{1}{4} \beta r^4 \{[7L_z^2 - L(L+1) - 5](L_+^2 + L_-^2) +$$

$$+ (L_+^2 + L_-^2)[7L_z^2 - L(L+1) - 5]\} \tag{17}$$

are the operator equivalents.

$$B_2^2 = \frac{1}{2}\left(\frac{15}{2\pi}\right)^{1/2} A_2^2 \qquad B_4^2 = \frac{3}{4}\left(\frac{5}{2\pi}\right)^{1/2} A_4^2 \tag{18}$$

The nonzero matrix elements of these operators are

$$\begin{aligned}
\langle 2 \pm 2 | \mathcal{H} | 2 \pm 2 \rangle &= 12 B_4^0 \beta \langle r^4 \rangle + 2(3 B_2^0 \alpha \langle r^2 \rangle) \\
\langle 2 \pm 1 | \mathcal{H} | 2 \pm 1 \rangle &= -4(12 B_4^0 \beta \langle r^4 \rangle) - (3 B_2^0 \alpha \langle r^2 \rangle) \\
\langle 2 \quad 0 | \mathcal{H} | 2 \quad 0 \rangle &= 6(12 B_4^0 \beta \langle r^4 \rangle) - 2(3 B_2^0 \alpha \langle r^2 \rangle) \qquad (19) \\
\langle 2 \pm 2 | \mathcal{H} | 2 \mp 2 \rangle &= 12 B_4^4 \beta \langle r^4 \rangle \\
\langle 2 \pm 1 | \mathcal{H} | 2 \mp 1 \rangle &= 3 B_2^2 \alpha \langle r^2 \rangle - 4(3 B_4^2 \beta \langle r^4 \rangle) \\
\langle 2 \pm 2 | \mathcal{H} | 2 \quad 0 \rangle &= \sqrt{6}(B_2^2 \alpha \langle r^2 \rangle) + \sqrt{6}(3 B_4^2 \beta \langle r^4 \rangle)
\end{aligned}$$

The symmetry-adapted wave functions are given by

$$\begin{aligned}
\psi(A_{1g}) &= \psi(2,0) \\
\psi(A^{*}_{1g}) &= \frac{1}{\sqrt{2}}\,[\psi(2,2) + \psi(2,-2)] \\
\psi(B_{1g}) &= \frac{i}{\sqrt{2}}\,[\psi(2,-2) - \psi(2,2)] \\
\psi(B_{2g}) &= \frac{i}{\sqrt{2}}\,[\psi(2,1) + \psi(2,-1)] \\
\psi(B_{3g}) &= -\frac{1}{\sqrt{2}}\,[\psi(2,-1) - \psi(2,1)]
\end{aligned} \tag{20}$$

Considering the rhombic component of the ligand field as an additional minor perturbation upon the tetragonal potential, the splitting of the E_g octahedral term is due mainly to the major axial potential, in a first approach we can neglect the off-diagonal matrix elements $\langle 2 \pm 2 \,|\mathcal{H}|\, 2\;0\rangle$. Thus by means of wave functions (20) and the matrix elements (19) the following energy expressions can be obtained for the D_{2h} ligand field terms:

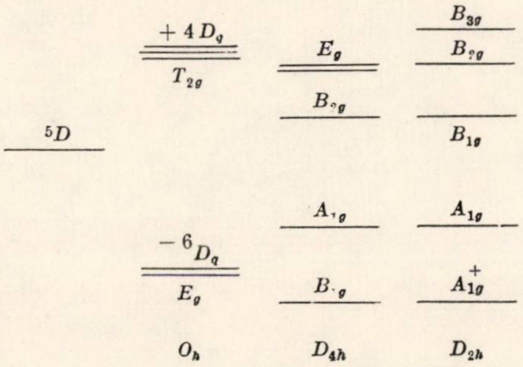

Fig. 2. – Energy level diagram for d^4 and d^9 configurations in octahedral, tetragonal (D_{4h}) and rhombic (D_{2h}) fields.

$$\begin{aligned}
\varepsilon(A^{*}_{1g}) &= -6Dq - 2Ds - 5Dt \\
\varepsilon(A_{1g}) &= -6Dq + 2Ds \\
\varepsilon(B_{1g}) &= 4Dq - 2Ds + 5Dt \\
\varepsilon(B_{2g}) &= 4Dq + Ds - Dr \\
\varepsilon(B_{3g}) &= 4Dq + Ds + Dr
\end{aligned} \tag{21}$$

The rhombic field parameters are given by the equations

$$
\begin{aligned}
Dq(\mathrm{D}_{2h}) &= \frac{8}{14}Dq(\mathrm{z}) + \frac{3}{14}\, Dq(\mathrm{x}) + \frac{3}{14}Dq(\mathrm{y}) \\
Ds &= Ds(\mathrm{x}) + Ds(\mathrm{y}) - 2Ds(\mathrm{z}) \qquad (22) \\
Dt &= \frac{2}{7}Dq(\mathrm{x}) + \frac{2}{7}Dq(\mathrm{y}) - \frac{4}{7}Dq(\mathrm{z}) \\
Dr &= 3[Ds(\mathrm{x}) - Ds(\mathrm{y})] + \frac{10}{7}[Dq(\mathrm{x}) - Dq(\mathrm{y})]
\end{aligned}
$$

Figure 2 shows the energy level diagram for d^4 and d^9 configurations in octahedral, tetragonal (D_{4h}) and rhombic (D_{2h}) fields.

Revue Roumaine de Chimie, **14**, 1011-1017 (1969)

LA DENSITÉ ET LA VISCOSITÉ DE L'INDIUM FONDU DANS L'INTERVALLE DE TEMPÉRATURE DE 166° À 800°

LUCIA GANOVICI et I. GANOVICI

Centre de Chimie Physique, Bucarest, 23, str. Dumbrava Roșie

Reçu le 8 octobre 1968

On a déterminé la densité de l'indium fondu dans l'intervalle de température de 166° à 800°, par une méthode dilatométrique. Par le traitement des données expérimentales selon la méthode des moindres carrés on a obtenu la dépendance linéaire $\rho(t) = 7{,}135 - 0{,}778 . 10^{-3} . t°$. On a aussi mesuré la viscosité de l'indium fondu dans le même intervalle de température, par la méthode du creuset cylindrique oscillante. On a trouvé une dépendance linéaire de $\log \eta$ en fonction de $1/T°\mathrm{K}$: $\log \eta = 0{,}276 . 10^3 / T°\mathrm{K} - 2{,}378$.

INTRODUCTION

Le mesurage de la viscosité et de la densité de l'indium a été effectué simultanément avec une série de travaux consacrés à l'étude des propriétés de transport de quelques alliages liquides de l'indium : In—Sb, In—Al, In—Al—Ag et In—Sn. Le but de ces mesurages a été, d'une part, d'obtenir des informations sur les propriétés de l'indium liquide jusqu'à 800°, et, d'autre part, d'établir les conditions de travail et la précision d'un viscosimètre à creuset cylindrique oscillant, construit dans notre laboratoire [1].

La viscosité de l'indium liquide a été aussi mesurée par Culpin [2] en 1957, à l'aide d'un viscosimètre à sphère oscillante, mais dans un intervalle de température relativement restreint (165°—340°) Goriaga et Morgunova [3] ont utilisé un viscosimètre à creuset cylindrique oscillant, en travaillant dans un intervalle plus large de température (160°—700°), mais ils n'ont pas présenté des tableaux chiffriques ou une équation qui puisse permettre le calcul de la viscosité. Cecinous a déterminé d'étudier la viscosité de l'indium dans le domaine de température de 166° à 800°.

---

[1] St. Zămârcă, N. Petrescu, I. Ganovici et L. Ganovici, *Studii și Cercetări Chim. Acad.* Bucarest, **15**, 657 (1967).

[2] M. F. Culpin, *Proc. Phys. Soc.*, **II—B 70**, 1069 (1957).

[3] G. I. Goriaga et M. V. Morgunova, *Nauchinye Doklady Visshei Skoly. Fiz. Mat. Nauki*, **1958**, 180.

MESURAGE DE LA DENSITÉ

Nous avons mesuré la densité de l'indium liquide dans l'intervalle de température de 166° à 800°, à l'aide d'un dilatomètre. Connaissant la masse M du fondu et le rayon R du creuset, la densité sera exprimée par la relation

$$\rho = \frac{M}{\pi R^2 H} \tag{1}$$

L'installation utilisée, décrite en détail dans un autre travail,[4] a permis le mesurage de la hauteur H, du niveau du métal fondu dans un creuset en alumine frittée, avec une précision de 0,1 mm. Le moment du contact d'une barre en molybdène, déplaçable micrométriquement, avec la surface du métal liquide, a été mis en évidence à l'aide d'un appareil de mesure électrique.

Pour les mesurages, nous avons utilisé environ 72 g d'indium, d'une pureté de 99,999 % (ICECHIM-Bucarest). L'installation a été dégazée et remplie plusieurs fois avec de l'argon purifié, les déterminations étant exécutées dans cette atmosphère inerte, qui a assuré la protection du métal fondu contre l'oxydation et a empêché simultanément l'évaporation de l'indium à hautes températures.

Les mesurages ont été effectués en régime de réfrigération du métal fondu, pour que les éventuelles pertes par volatilisation de l'indium à hautes températures ne modifient pas la masse du liquide pendant toute la durée de l'expérience. Dans les calculs, nous avons utilisé la masse obtenue par le pesage du métal refroidi à la fin d'un cycle d'expériences, quoique les pertes par volatilisation aient été très petites (de l'ordre de quelques centigrammes).

Avant chaque lecture du niveau du liquide, la température a été maintenue constante pendant 2—3 heures, pour assurer l'égalisation de la température dans l'entière masse du liquide. La température a été mesurée à l'aide d'un thermocouple Pt/PtRh 10 % avec une précision de ± 2°.

Nous avons effectué deux cycles d'expériences en régime de réfrigération, le niveau du liquide dans le creuset étant lu 20—30 fois pour chaque température. Pour le calcul de la densité on a utilisé les valeurs moyennes obtenues par ces expériences et on a appliqué des corrections pour la dilatation thermique du creuset et de la barre de contact.

La figure 1 représente les valeurs obtenues pour la densité de l'indium dans l'intervalle de température de 166 à 800°, la dépendance de la température étant linéaire. Le traitement des données par la méthode des moindres carrés nous a permis de déduire l'équation

$$\rho\,(t^\circ) = 7{,}135 - 0{,}778 . 10^{-3}\, t^\circ \tag{2}$$

La figure 1 représente de même, les résultats expérimentaux obtenus par Williams et Miller,[5] Schneider et Heymer[6] et McGonigal et colab.[7] pour la densité de l'indium fondu.

L'analyse des résultats montre que les valeurs de la densité obtenues par nous sont de 0,2 % inférieures à celles obtenues par Williams et Miller et de 0,5 % plus réduites que celles obtenues par Schneider et Heymer dans les domaines de température étudiés par eux: 156,4—300°, et respectivement, 156,4—421°. McGonigal et collab. ont mesuré la densité de l'indium liquide par la méthode d'Archimède, du point de fusion jusqu'au point d'ébullition. Les valeurs obtenues par lui sont plus grandes que celles obtenues par nous, d'environ 0,3 % dans le domaine de basses températures, les écarts atteignant 1 % à proximité de la température de 800°.

---

[4] N. Petrescu, St. Zămîrcă, I. Ganovici et L. Ganovici, *Studii şi cercetări Chim. Acad.* Bucarest (à paraître).

[5] D. D. Williams et R. R. Miller, *J. Amer. Chem. Soc.*, **72**, 3821 (1950).

[6] A. Schneider et G. Heymer, *Z. anorg. Chem.*, **286**, 118 (1956).

[7] J. McGonigal, J. A. Cahill et A. D. Kirshenbaum, *J. Inorg. Nuclear Chem.*, **24**, 1013 (1962).

L'équation (2) obtenue par nous des données expérimentales permet le calcul de la densité de l'indium liquide, avec une erreur moyenne de 0,2 %, précision qui justifie son utilisation au calcul de la viscosité dynamique de l'indium.

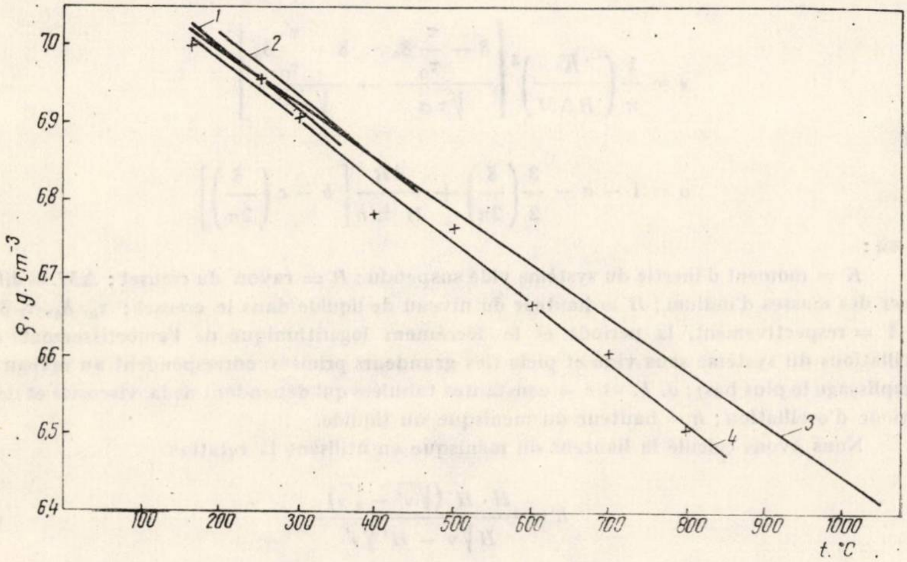

Fig. 1. — Dépendance de la densité de l'indium fondu de la température : *1*, Williams et Miller ; *2*, Schneider et Heymer ; *3*, McGonigal et collab. ; *4*, Le présent travail.

MESURAGE DE LA VISCOSITÉ

Le viscosimètre à creuset cylindrique oscillant, de même que la méthode de calcul ont été décrits, en détail, dans un travail antérieur.[1]

Les expériences ont été effectuées avec de l'indium spectral pur (99,999 % ICECHIM Bucarest) dans un creuset d'alumine frittée, ayant le rayon de 0,9 cm et la hauteur de 7 cm, identique à celui utilisé aux mesurages de la densité. Pour protéger la surface du métal fondu contre l'oxydation et pour éliminer la correction de la viscosité due au frottement avec une atmosphère de gaz inerte, on a effectué les expériences dans un vide de 10^{-4} mmHg (après avoir évacué l'installation plusieurs fois à l'aide d'un système vide-argon). Les pertes en indium par volatilisation à hautes températures ont été de 0,1 g, l'erreur de la chiffre de viscosité due à ces pertes étant comprise entre les limites des erreurs expérimentales (1 %). Vu que les mesurages ont été effectués en régime de réfrigération du liquide, dans les calculs nous avons utilisé la masse du métal mesurée à la fin des expériences, en considérant que les pertes par volatilisation ont eu lieu à la température maximale de travail (800°) et que, pendant tout le reste de l'expérience, la masse du liquide est restée la même.

Avant chaque mesurage de la période et du décrément logarithmique de l'amortissement des oscillations de torsion, on a attendu pendant 2–3 heures pour réaliser un régime stationnaire. Le mesurage et le contrôle de la température ont été effectués avec une précision de ± 2°, en utilisant un thermocouple Pt/PtRh 10 %, situé à l'extérieur du creuset, à 0,5 cm de sa partie inférieure.

Pour prendre en considération aussi l'influence du ménisque de l'indium liquide, on a effectué les mesurages pour deux niveaux du creuset, correspondant à des masses de 50,574 g et respectivement de 72,154 g d'indium, la viscosité étant calculée à l'aide de la relation proposée par Armbruster [8]

$$\nu = \frac{1}{\pi}\left(\frac{K}{R\Delta M}\right)^2 \left[\frac{\delta - \frac{\tau}{\tau_0}\delta_0}{\sqrt{\tau}\,\sigma} - \frac{\delta - \frac{\tau'}{\tau_0}\delta_0}{\sqrt{\tau'}\sigma'}\right]^2 \tag{3}$$

où

$$\sigma = 1 - a - \frac{3}{2}\left(\frac{\delta}{2\pi}\right) + \frac{4R}{H \pm h}\left[b - c\left(\frac{\delta}{2\pi}\right)\right] \tag{4}$$

et où :

K = moment d'inertie du système vide suspendu ; R = rayon du creuset ; ΔM = différence des masses d'indium ; H = hauteur du niveau de liquide dans le creuset ; τ_0, δ_0, τ, δ et τ', δ' = respectivement, la période et le décrément logarithmique de l'amortissement des oscillations du système sous vide et plein (les grandeurs primées correspondent au niveau de remplissage le plus bas) ; a, b, et c = constantes tabulées qui dépendent de la viscosité et de la période d'oscillation ; h = hauteur du ménisque du liquide.

Nous avons calculé la hauteur du ménisque en utilisant la relation

$$h = \frac{H \cdot H'\left(\sqrt{\nu'} - \sqrt{\nu}\right)}{H\sqrt{\nu} - H'\sqrt{\nu'}} \tag{5}$$

où ν et ν' sont les viscosités correspondant aux deux niveaux de remplissage du creuset avec du métal liquide, calculées par des approximations successives à l'aide de la relation de Svidkovski.[9]

La période d'oscillation a été mesurée avec une précision de 1 ms, à l'aide d'un dispositif électronique et le décrément logarithmique de l'amortissement des oscillations de torsion a été mesuré avec une précision de 0,2 % (à la quatrième décimale). Dans ce but, à chaque température de travail, on a enregistré sur film, 30—40 oscillations et on a construit le histogramme des décréments pour poursuivre leur distribution et trouver la valeur la plus probable. De cette manière, nous avons éliminé les valeurs erronées dues à des oscillations parasites qui auraient été prises en considération dans le cas d'un calcul par la méthode des moindres carrés appliquée à tous les logarithmes des décréments.

RÉSULTATS ET DISCUSSIONS

Étant donné que jusqu'à présent, il n'existe pas un modèle généralement valable pour l'état liquide, pour l'interprétation de nos résultats expérimentaux, nous avons essayé deux modes de représenter les viscosités en fonction de la température, rencontrés plus fréquemment dans les considérations théoriques et nous avons obtenu avec tous les deux des résultats satisfaisants.

---

[8] J. C. Armbruster, P. Azou et P. Bastien, *Compt. rend.*, **250**, 2816, (1960).

[9] E. G. Svidkovski, ,,Nekotorye voprosy viazkosti rasplavlennyh metallov Gos.'' Izd. tehn. teoret. literat., Moscou, 1955, p. 32.

La représentation la plus utilisée est celle du log η en fonction de $1/T$°K, qui porte à une succession linéaire de nos résultats expérimentaux, ce qui confirme la première relation proposée par Andrade[10].

$$\eta = a \exp. (H_\eta/RT) \tag{6}$$

où
a = constante ; H_η = énergie d'activation de l'écoulement visqueux, exprimée en cal/at.g. ; R = constante des gaz parfaits ; T = température absolue.

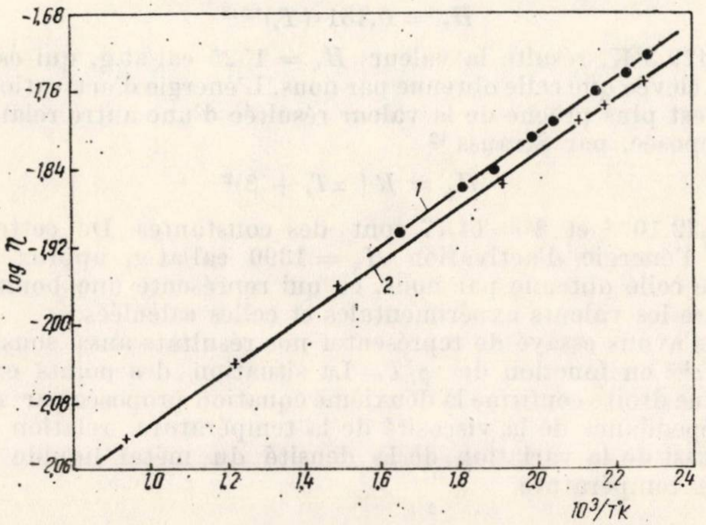

Fig. 2. — Dépendance de la viscosité dynamique de l'indium fondu de la température :
1,● – Résultats de Culpin ; *2*, + Résultats du présent travail.

Dans la figure 2 on représente les résultats obtenus par nous pour la viscosité de l'indium dans l'intervalle de température de 166° à 800°. Le traitement de ces données par la méthode des moindres carrés nous a permis de trouver la relation linéaire

$$\log \eta = 0{,}276 \cdot \frac{10^3}{T°\mathrm{K}} - 2{,}378 \tag{7}$$

par laquelle nous avons calculé l'énergie d'activation H_η = 1264 cal/at.g et le facteur préexponentiel $a = 4{,}182.10^{-3}$.

Dans la même figure on représente les valeurs de log $\eta = f(1/T)$ calculées par nous à l'aide des résultats obtenus par Culpin dans le domaine de température de 165°—340°. Comme on peut voir, ces valeurs sont de 1 % plus élevées que celles obtenues par nous, résultat qui s'explique compte tenu que les valeurs de la densité de l'indium, obtenues par nous, sont inférieures à celles de Williams et Miller, utilisées par Culpin pour le calcul de la viscosité dynamique (fig. 1). L'énergie d'activation de l'écoulement visqueux, calculée par nous en traitant les résultats de Culpin par la méthode des moindres carrés, est de 1298 cal/at.g, en concordance satisfaisante avec nos résultats. La petite différence des énergies d'activation est explicable tant par les pentes différentes des droites $\rho(t^\circ)$, que par l'intervalle de température étudié par nous, qui est environ quatre fois plus étendu en comparaison de l'intervalle étudié par Culpin, ce qui permet la meilleure orientation de la droite.

---

[10] E. N. DA C. ANDRADE, *Proc. Roy. Soc.*, **A 215**, 36 (1952).

De la relation empirique proposée par Grosse [11] pour la détermination de l'énergie d'activation de l'écoulement visqueux

$$H_\eta = 0{,}431\cdot(T_t)^{1{,}348} \tag{8}$$

où $T_t = 429{,}3^\circ\mathrm{K}$, résulte la valeur $H_\eta = 1525$ cal/at.g, qui est approx. 20 % plus élevée que celle obtenue par nous. L'énergie d'activation obtenue par nous est plus proche de la valeur résultée d'une autre relation empirique, proposée, par Strauss [12]

$$H_\eta = R\,(\,\alpha T_t + \beta)^2 \tag{9}$$

où $\alpha = 2{,}72.10^{-2}$ et $\beta = 14{,}77$ sont des constantes. De cette relation il résulte l'énergie d'activation $H_\eta = 1390$ cal/at.g, approx. 9 % plus élevée que celle obtenue par nous, ce qui représente une bonne concordance entre les valeurs expérimentales et celles calculées.

Nous avons essayé de représenter nos résultats aussi sous la forme de log $\eta/\rho^{1/3}$ en fonction de ρ/T. La situation des points expérimentaux sur une droite confirme la deuxième équation proposée par Andrade [10] pour la dépendance de la viscosité de la température, relation qui tient compte aussi de la variation de la densité du métal liquide en fonction de la température

$$\eta\,\rho^{-\frac{1}{3}}\ b\ \mathrm{exp.}\ (c\,\rho/T) \tag{10}$$

Par le traitement de nos résultats expérimentaux, nous avons trouvé les constantes $ab = 2{,}412\cdot10^{-3}$ et $c = 84{,}366$.

Le tableau 1 représente la synthèse de nos résultats, obtenus dans les deux représentations, les valeurs de l'énergie d'activation calculée des relations (8) et (9), ainsi que les valeurs de la viscosité à la température de fusion obtenue par l'extrapolation des résultats expérimentaux comparés avec la valeur calculée à l'aide de la relation d'Andrade [13]

$$\eta_{T_t} = 5{,}7\cdot10^{-4}\cdot\frac{\sqrt{A\,T_t}}{V_A^{2/3}} \tag{11}$$

où A est le poids atomique et $V_A = 16{,}36$ cm^3 est le volume atomique du liquide à la température de fusion, calculé par l'extrapolation de l'équation (2) à la température de fusion.

Une série de travaux sur la dépendance de la viscosité des métaux liquides purs de la température [14-16] signalent que près du point de soli-

[11] A. V. Grosse, *J. Inorg. Nuclear Chem.*, **25**, 317 (1963).

[12] S. W. Strauss, *Nucl. Sci. Eng.*, **12**, 436 (1962).

[13] E. M. da C. Andrade, *Phil. Mag.*, **17**, 497 (1934).

[14] W. R. D. Jones et W. L. Bartlett, *J. Inst. Metals*, **81**, 145 (1952).

[15] T. P. Yao et V. Kondic, *J. Inst. Metals*, **81**, 17, (1952).

[16] R. N. Barfield et J. A. Kitchener, *J. Iron Steel Inst.*, **180**, 324 (1955).

Tableau 1

Résultats expérimentaux et calculés de la dépendance $\eta = f(1/T)$, de l'énergie d'activation et de η_{T_t}

$\eta = a.\exp(H_\eta/RT)$		$\eta\bar{\rho}^{1/3} = b.\exp(c\rho/T)$		H_η cal/at.g éq. (8)	H_η cal/at.g éq. (9)	η_{T_t} $P_0 \cdot 10^5$ exp.	η_{T_t} $P_0 \cdot 10^5$ calc. éq. (11)
$a.10^3$	H_η cal/at.g.	$b.10^3$	c				
4,182	1264	2,41	84,3	1525	1390	1839	1963

dification, la viscosité du métal fondu monte brusquement, pendant que d'autres travaux [17-21] rapportent une relation linéaire du log η en fonction de $1/T$. L'augmentation de la viscosité dans le domaine de la précristallisation a été expliquée, par McLaughlin et Ubbelhode,[22] par la formation, dans ce domaine de température, d'agglomérations de 20—50 atomes (*clusters*), caractérisées par leur disposition à courte distance, et qui déterminent l'augmentation de la dimension moyenne de l'unité d'écoulement visqueux. Ces phénomènes de précristallisation ont suscité de vives controverses, certains chercheurs [23] les attribuant aux erreurs expérimentales ou aux impuretés des métaux fondus.

Compte tenu de ces discussions, nous avons effectué des mesurages à petits intervalles de température dans un domaine étendu jusqu'à approx. 50° au-dessus du point de solidification. De même, à un des niveaux de remplissage, nous avons répété le cycle d'expériences, les résultats obtenus par le mesurage du décrément étant reproductibles avec une erreur de moins de 1%. Dans la représentation de nos résultats d'après l'équation (6) nous n'avons observé, aucune anomalie qui pourrait être due à certains phénomènes de précristallisation.

Si des phénomènes pareils de précristallisation avaient eu lieu, ils auraient été mis en évidence plutôt par la représentation des résultats conformément à l'équation (10) qui tient aussi compte de la variation de la densité avec la température. [24-25] Comme par cette représentation nous avons obtenu de même une dépendance linéaire, on peut affirmer que dans l'indium fondu, près du point de solidification on n'observe pas une augmentation de la viscosité due à la formation des *clusters*.

De même, le fait que l'énergie d'activation est constante dans l'intervalle de température étudié montre que dans l'indium fondu n'ont pas eu lieu des modifications structurales importantes (changement du caractère des forces de liaison et du nombre de coordination). Cette conclusion est d'ailleurs soutenue aussi par les études récentes de la diffraction de rayons X sur l'indium liquide. [26]

[17] E. M. da C. Andrade, et E. R. Dobbs, *Proc. Roy. Soc.*, **A 211**, 12 (1952).

[18] E. Gebhardt et M. Becker, *Z. Metallk.*, **42**, 111 (1951).

[19] E. Gebhardt et G. Worwag, *Z. Metallk.*, **42**, 358 (1951); **43**, 106 (1952).

[20] E. Gebhardt, M. Becker et E. Trager, *Z. Metallk.*, **44**, 379 (1953).

[21] H. J. Fisher et A. Phillips, *J. Metals*, **9**, 1060 (1954).

[22] E. McLaughlin et A. R. Ubbelhode, *Trans. Faraday Soc.*, **56**, 989 (1960).

[23] J. R. Willson, *Metallurgical Rev.*, **10**, 444 (1965).

[24] E. Rothwell, *J. Inst. Metals.*, **90**, 389 (1961).

[25] A. R. Ubbelhode, «Melting and Structure», University Press Oxford, Londres, 1965, p. 243.

[26] H. Ocken et C.N.J. Wagner, *Phys. Rev.*, **149**, 122 (1966).

Revue Roumaine de Chimie, **14**, 1019–1025 (1969)

ÜBER DIE SPEKTROPHOTOMETRISCHE METHODE VON JAZIMIRSKIJ ZUR UNTERSUCHUNG STUFENWEISER KOMPLEXBILDUNG UND ÜBER DIE ERWEITERUNG DER ANWENDUNGSGRENZEN DIESER METHODE

A.-C. BANCIU

Aus dem Institut für Physikalische Chemie der Akademie,
Bukarest, str. Dumbrava Roşie, 23

Eingegangen am 25. Oktober 1968

Eine kritische Betrachtung der spektrophotometrischen Methode von Jazimirskij zur Bestimmung der Beständigkeitskonstanten einer Reihe stufenweise gebildeter Komplexe zeigt, daß bei der Bildung der Grenzwerte der angewandten Hilfsfunktionen Fehler unterlaufen sind. Nach Korrektur erhält man kompliziertere Gleichungen höheren Grades, welche sich aber trotzdem zu einem stets lösbaren System von Lineargleichungen reduzieren lassen. Behandelt man ähnlich auch den Fall, wenn außer den Komplexen auch der Ligand, das Metallion jedoch nicht absorbiert, so erhält man kompliziertere Gleichungen, welche aber wiederum zum selben stets lösbaren System von Lineargleichungen wie im vorigen Fall reduziert werden können. Dies entspricht der Erweiterung der Anwendungsgrenzen der Methode von Jazimirskij.

I. DIE METHODE VON JAZIMIRSKIJ

Die im Jahre 1956 veröffentlichte spektrophotometrische Methode von Jazimirskij [1-5] erlaubt die Bestimmung der Bildungskonstanten

$$K_n = \frac{[MA_n]}{[M]\,[A]^n} \tag{1}$$

stufenweise gebildeter einkerniger Komplexe MA, $MA_2, \ldots, MA_n$, durch Messung der Extinktionsänderung von Lösungen die A und M enthalten, wenn im untersuchten Spektralbereich nur das Metallion M (der Ligand A also nicht) und die Komplexe absorbieren.

---

[1] K. B. Jazimirskij, *Zhur. neorg. Khim.*, **10**, 2306 (1956).

[2] K. B. Jazimirskij und T. I. Fjodorowa, *Zhur. neorg. Khim.*, **10**, 2310 (1956).

[3] H. L. Schläfer, „Komplexbildung in Lösung", Springer-Verlag, Berlin, Göttingen, Heidelberg, 1961, S. 282–285.

[4] F. J. C. Rossotti und H. Rossotti, „The Determination of Stability Constants", McGraw-Hill Book Company, New York, 1961, S. 281–282.

[5] J. Zsako, *Rev. Roumaine Chim.*, **11**, 315 (1966).

Man benützt dafür geeignete Hilfsfunktionen aus denen durch Extrapolation auf den Wert Null der Variablen bestimmte Koeffizienten gewonnen werden, die Funktionen einer oder mehrerer der gesuchten Bildungskonstanten sind. Es gilt

$$\bar{\varepsilon} = \frac{E}{c_M \cdot d} = \frac{\varepsilon_M + \varepsilon_1 K_1 [A] + \varepsilon_2 K_2 [A]^2 + \dots + \varepsilon_n K_n [A]^n}{1 + K_1 [A] + K_2 [A]^2 + \dots + K_n [A]^n} \tag{2}$$

wobei $\bar{\varepsilon}$ der mittlere molare Extinktionskoeffizient, E die gemessene Extinktion, c_M die Gesamtkonzentration an Metallion, d die Schichtdicke, ε_M, ε_1, $\varepsilon_2, \dots, \varepsilon_n$ die Extinktionskoeffizienten für M, MA, $MA_2, \dots, MA_n$, und $[A]$ die Gleichgewichtskonzentration des Liganden A bedeuten. Durch Subtrahieren von ε_M auf beiden Seiten von (2) folgt

$$\Delta\bar{\varepsilon} = \frac{\Delta\varepsilon_1 K_1 [A] + \Delta\varepsilon_2 K_2 [A]^2 + \dots + \Delta\varepsilon_n K_n [A]^n}{1 + K_1 [A] + K_2 [A]^2 + \dots + K_n [A]^n} \tag{3}$$

wobei $\Delta\bar{\varepsilon} = \bar{\varepsilon} - \varepsilon_M$, $\Delta\varepsilon_1 = \varepsilon_1 - \varepsilon_M, \dots$, und $\Delta\varepsilon_n = \varepsilon_n - \varepsilon_M$.

Unter Verwendung der Hilfsfunktion

$$f_1 = \frac{\Delta\bar{\varepsilon}}{[A]} \tag{4}$$

geht (3) in

$$f_1 = \frac{\Delta\varepsilon_1 K_1 + \Delta\varepsilon_2 K_2 [A] + \dots + \Delta\varepsilon_n K_n [A]^{n-1}}{1 + K_1 [A] + K_2 [A]^2 + \dots + K_n [A]^n} \tag{5}$$

über. Extrapoliert man f_1 auf $[A] \to 0$, so erhält man

$$\lim_{[A]\to 0} f_1 = a_1 = \Delta\varepsilon_1 K_1 \tag{6}$$

Durch Differenzieren der Funktion f_1 und Extrapolation der Ableitung auf $[A] \to 0$, oder auch mit Hilfe der Funktion

$$f_2 = \frac{f_1 - a_1}{[A]} \tag{7}$$

durch Extrapolation dieser auf $[A] \to 0$, erhält man

$$\lim_{[A]\to 0} \frac{\mathrm{d} f_1}{\mathrm{d}\,[A]} = \lim_{[A]\to 0} f_2 = a_2 = \Delta\varepsilon_2 K_2 - \Delta\varepsilon_1 K_1^2 \tag{8}.$$

Handelt man ähnlich weiter, so würde man im allgemeinen Fall $i\ (2 < i \leqslant n)$ für die Koeffizienten a_i den Wert

$$\lim_{[A]\to 0} f_i = a_i = \Delta\varepsilon_i K_i - \Delta\varepsilon_1 K_1^i \tag{9}$$

erhalten. Durch Einführen der neuen Variable

$$y = \frac{1}{[A]} \tag{10}$$

geht (3) in

$$\Delta\bar{\varepsilon} = \frac{\Delta\varepsilon_n K_n + \Delta\varepsilon_{n-1} K_{n-1} y + \ldots + \Delta\varepsilon_1 K_1 y^{n-1}}{K_n + K_{n-1} y + \ldots + K_1 y^{n-1} + y^n} \tag{11}$$

über, und durch Extrapolation von $\Delta\bar{\varepsilon}$ auf den Nullwert von y bekommt man

$$\lim_{y\to 0} \Delta\bar{\varepsilon} = b_1 = \Delta\varepsilon_n \qquad (12).$$

Handelt man genau wie oben, d.h. durch Differenzieren von $\Delta\bar{\varepsilon}$ und Extrapolation der Ableitung auf $y\to 0$, oder auch durch Anwendung der Hilfsfunktion

$$\varphi_1 = \frac{\Delta\bar{\varepsilon} - b_1}{y} \qquad (13).$$

und Extrapolation dieser auf $y \to 0$, erhält man

$$\lim_{y\to 0} \frac{\mathrm{d}\,\Delta\bar{\varepsilon}}{\mathrm{d}y} = \lim_{y\to 0} \varphi_1 = b_2 = (\Delta\varepsilon_{n-1} - \Delta\varepsilon_n)\frac{K_{n-1}}{K_n} \qquad (14).$$

Nach dem gleichen Schema werden die Funktion $\varphi_2, \ldots, \varphi_{n-1}$ aufgestellt, auf $y \to 0$ extrapoliert, und man erhält so die Koeffizienten b_i $(2 < i \leqslant n)$.

Zum Schluß wird das von den Extrapolationsgleichungen (9) und den Gleichungen der Form (14) zusammengestellte Gleichungssystem gelöst und damit die Beständigkeitskonstanten K_i $(1 < i \leqslant n)$ aller anwesenden Komplexe bestimmt.

II. DIE KORREKTUR

Wenn man das oben geschilderte kritisch nachprüft, so findet man, daß die Formeln (6) und (8) richtig sind, aber die Formel (9), für den Ausdruck der Koeffizienten a_i im allgemeinen Fall i $(2 \leqslant i \leqslant n)$ fehlerhaft ist.[5] In Wirklichkeit sind die Ausdrücke der Koeffizienten a_i erheblich komplizierter. So sind z.B. für den konkreten Fall der Existenz von vier Komplexen die richtigen Ausdrücke der Koeffizienten a_3 und a_4 folgende :

$$a_3 = \Delta\varepsilon_3 K_3 - (\Delta\varepsilon_1 + \Delta\varepsilon_2) K_1 K_2 + \Delta\varepsilon_1 K_1^3 \tag{15}$$

$$a_4 = \Delta\varepsilon_4 K_4 - (\Delta\varepsilon_1 + \Delta\varepsilon_3) K_1 K_3 + (2\,\Delta\varepsilon_1 + \Delta\varepsilon_2) K_1^2 K_2 - \Delta\varepsilon_2 K_2^2 - \Delta\varepsilon_1 K_1^4 \tag{16}$$

Diese richtigen Ausdrücke für die Koeffizienten a_3 und a_4 (allgemein für die Koeffizienten a_i in allen Fällen wenn $i > 2$ ist) können nach den beiden oben erwähnten Rechnungsverfahren, d.h. sowohl mit Hilfe der Funktionen f_i, als auch durch Differenzieren der Funktion f_{i-1} nach $\mathrm{d}[A]$ und anschließender Extrapolation der Ableitung auf $[A]\to 0$, erhalten werden. Mehr noch, es läßt sich zeigen, daß dieselben richtigen Ausdrücke für die Koeffizienten a_i $(i > 2)$ auch auf dem Wege des wiederholten Differenzierens der ursprünglichen Hilfsfunktion f_1 erhalten werden können. Man kann es nachprüfen, daß der Grenzwert der Ableitung $(i-1)$-Grades der ursprünglichen Hilfsfunktion f_1 einen Wert a_i^* hat, welcher gleich a_i multipliziert mit $(i-1)!$ ist, sich also von a_i nur durch einen numerischen Faktor unterscheidet

$$\lim_{[A]\to 0} \frac{\mathrm{d}^{(i-1)}f_1}{\mathrm{d}[A]^{(i-1)}} = \lim_{[A]\to 0} f_1^{(i-1)} = a_i^* = (i-1)!\,a_i\,;\ \text{oder}\ a_i = \frac{a_i^*}{(i-1)!} \quad (17).$$

In der Formulierung ihres Autors ist also die Methode von Jazimirskij nur für den noch einfachen Fall der Existenz nur zweier einkerniger Komplexe anwendbar. [2] Wenn mehr als zwei einkernige Komplexe vorhanden sind, muß zuerst die fehlerhafte Formel (9) korrigiert werden, und erst nach dem Erhalten der richtigen Ausdrücke der Koeffizienten a_i $(2 < i \leqslant n)$ kann man zur Berechnung der Bildungskonstanten K_i $(1 \leqslant i \leqslant n)$ weiterschreiten.

Alle drei oben erwähnten Rechnungsweisen können auch zur Bestimmung der Koeffizienten b_i $(1 \leqslant i \leqslant n)$ hinzugezogen werden.

Im konkreten Fall der Existenz von vier einkernigen Komplexen hat man zum Schluß folgendes Gleichungssystem (18-a und 18-b) zu lösen, in dem die Mehrheit der Gleichungen von höherem Grade sind:

$$\begin{aligned}
a_1 &= \Delta\varepsilon_1 K_1 \\
a_2 &= \Delta\varepsilon_2 K_2 - \Delta\varepsilon_1 K_1^2 \qquad\qquad\qquad\qquad (18\text{-a}) \\
a_3 &= \Delta\varepsilon_3 K_3 - (\Delta\varepsilon_1 + \Delta\varepsilon_2) K_1 K_2 + \Delta\varepsilon_1 K_1^3 \\
a_4 &= \Delta\varepsilon_4 K_4 - (\Delta\varepsilon_1 + \Delta\varepsilon_3) K_1 K_3 + (2\Delta\varepsilon_1 + \Delta\varepsilon_2) K_1^2 K_2 - \Delta\varepsilon_2 K_2^2 - \\
&\qquad - \Delta\varepsilon_1 K_1^4
\end{aligned}$$

$$\begin{aligned}
b_1 &= \Delta\varepsilon_4 \\
b_2 &= (\Delta\varepsilon_3 - \Delta\varepsilon_4)\frac{K_3}{K_4} \\
b_3 &= (\Delta\varepsilon_2 - \Delta\varepsilon_4)\frac{K_2}{K_4} - (\Delta\varepsilon_3 - \Delta\varepsilon_4)\frac{K_3^2}{K_4^2} \qquad (18\text{-b}). \\
b_4 &= (\Delta\varepsilon_1 - \Delta\varepsilon_4)\frac{K_1}{K_4} - (\Delta\varepsilon_2 + \Delta\varepsilon_3 - 2\Delta\varepsilon_4)\frac{K_2 K_3}{K_4^2} + (\Delta\varepsilon_3 - \Delta\varepsilon_4)\frac{K_3^3}{K_4^3}
\end{aligned}$$

Es ist zu erwähnen, daß in der Reihe der Koeffizienten b_i, die richtigen Ausdrücke dafür, für den Fall der Existenz von maximal vier Komplexen, schon in [4] angegeben wurden.

Sowohl die Gleichungen (18-a) als auch(18-b) können in einer einfachen und regulären Form ausgedrückt werden, und zwar:

$$\begin{aligned}
\Delta\varepsilon_1 K_1 &= a_1 \\
\Delta\varepsilon_2 K_2 &= a_2 + a_1 K_1 \qquad\qquad\qquad\qquad (19\text{-a}) \\
\Delta\varepsilon_3 K_3 &= a_3 + a_2 K_1 + a_1 K_2 \\
\Delta\varepsilon_4 K_4 &= a_4 + a_3 K_1 + a_2 K_2 + a_1 K_3
\end{aligned}$$

$$\begin{aligned}
&\Delta\varepsilon_4 = b_1\,;\ (\Delta\varepsilon_4 K_4 = b_1 K_4)\\
&\Delta\varepsilon_3 K_3 = b_2 K_4 + b_1 K_3\\
&\Delta\varepsilon_2 K_2 = b_3 K_4 + b_2 K_3 + b_1 K_2\\
&\Delta\varepsilon_1 K_1 = b_4 K_4 + b_3 K_3 + b_2 K_2 + b_1 K_1
\end{aligned} \qquad (19\text{-b})$$

Es sei an dieser Stelle erwähnt, daß dank der einfachen und regulären Form des Gleichungssystems (19-a—19-b) ein höherer Koeffizient, a_i oder b_i, falls die ihm vorangehenden Koeffizienten $a_1 \ldots a_{i-1}$ bzw. $b_1 \ldots b_{i-1}$ bekannt sind, sehr leicht berechnet werden kann. Z.B. läßt sich der richtige Ausdruck des Koeffizienten a_4 (Gleichung 16) nicht nur nach allen drei oben geschilderten Rechnungsweisen, sondern auch mit Hilfe der Gleichungen der Form (19-a) berechnen. Man findet die Formel des allgemeinen Gliedes $\Delta\varepsilon_i K_i$ leicht (in diesem konkreten Falle den Ausdruck von $\Delta\varepsilon_4 K_4$ aus 19-a) und, da die Werte der Koeffizienten $a_1 \ldots a_3$ aus den Gleichungen (6), (8) und (15) schon bekannt sind, läßt sich der richtige Ausdruck von a_4 aus der Gleichung (16) leicht berechnen.

Durch Umformen der Gleichungen (19-a—19-b) nimmt das zu lösende Gleichungssystem zuletzt die Form eines Systems von vier Lineargleichungen mit vier Unbekannten $(K_1 \ldots K_4)$ an:

$$\begin{aligned}
a_3 K_1 + a_2 K_2 + a_1 K_3 - b_1 K_4 + a_4 &= 0\\
a_2 K_1 + a_1 K_2 - b_1 K_3 - b_2 K_4 + a_3 &= 0\\
a_1 K_1 - b_1 K_2 - b_2 K_3 - b_3 K_4 + a_2 &= 0\\
-b_1 K_1 - b_2 K_2 - b_3 K_3 - b_4 K_4 + a_1 &= 0
\end{aligned} \qquad (20),$$

welches praktisch immer lösbar ist (am einfachsten auf Grund der Determinantentheorie). Im allgemeinen Fall der Existenz von n Komplexen $(i = n)$, hat man zuletzt ein System von n Lineargleichungen mit n Unbekannten $(K_1 \ldots K_n)$ zu lösen, welches wiederum praktisch immer lösbar ist.

Wenn man also die fehlerhafte Formel (9) für den allgemeinen Fall korrigiert, d.h. die richtigen Ausdrücke der Koeffizienten a_i für alle Fälle wenn $i > 2$ ist, berechnet, ist die Methode von Jazimirskij in der Formulierung ihres Autors für den allgemeinsten Fall — der Existenz von n einkernigen Komplexen — anwendbar.

III. DIE ANWENDUNG DER METHODE VON JAZIMIRSKIJ FÜR DEN FALL, DASS DER LIGAND UND DIE KOMPLEXE ABSORBIEREN

In diesem Falle, da $\varepsilon_M = 0$ aber $\varepsilon_A \neq 0$ ist, gilt die der Gleichung (3) von vorigem Fall entsprechende Beziehung

$$\bar{\varepsilon} = \frac{\varepsilon_A \dfrac{[A]}{[M]} + \varepsilon_1 K_1 [A] + \varepsilon_2 K_2 [A]^2 + \ldots + \varepsilon_n K_n [A]^n}{1 + K_1 [A] + K_2 [A]^2 + \ldots + K_n [A]^n} \qquad (21),$$

in welcher aber die individuellen Extinktionskoeffizienten $\varepsilon_A, \varepsilon_1, \ldots, \varepsilon_n$, und nicht Differenzen von Extinktionskoeffizienten, wie in (3), auftreten.

Unter Verwendung der Hilfsfunktion

$$f_1 = \frac{\varepsilon}{[A]} \tag{22}$$

die der Funktion (4) analog ist, und Extrapolation auf $[A] \to 0$ erhält man

$$\lim_{[A]\to 0} f_1 = \frac{\varepsilon_A}{[M]} + \varepsilon_1 K_1 = a_1 \tag{23}$$

Ferner werden die Koeffizienten a_i $(1 < i \leqslant n)$, genau wie im vorigen Falle, mit Hilfe der Funktion f_i, oder der Funktion $\frac{\mathrm{d}f_{i-1}}{\mathrm{d}[A]}$, durch Extrapolation auf $[A] \to 0$, oder auch mit Hilfe der Funktion $\frac{\mathrm{d}^{(i-1)}f_1}{\mathrm{d}[A]^{(i-1)}}$, wiederum durch Extrapolation auf $[A] \to 0$, bestimmt. Für den konkreten Fall der Existenz von vier einkernigen Komplexen erhält man neben (23) auch:

$$\begin{aligned} a_2 &= \varepsilon_2 K_2 - \frac{\varepsilon_A}{[M]} K_1 - \varepsilon_1 K_1^2 \\ a_3 &= \varepsilon_3 K_3 - (\varepsilon_1 + \varepsilon_2) K_1 K_2 - \frac{\varepsilon_A}{[M]} (K_2 - K_1^2) + \varepsilon_1 K_1^3 \\ a_4 &= \varepsilon_4 K_4 + \frac{\varepsilon_A}{[M]} (2K_1K_2 - K_1^3 - K_3) - (\varepsilon_1 + \varepsilon_3) K_1 K_3 + \\ &\quad + (2\varepsilon_1 + \varepsilon_2) K_1^2 K_2 - \varepsilon_2 K_2^2 - \varepsilon_1 K_1^4 \end{aligned} \tag{23-a}$$

Wiederum genau wie im vorigen Falle handelnd, werden unter Verwendung der neuen Variable y aus der Gleichung (10), die Koeffizienten b_i bestimmt, welche, wenn vier Komplexe existieren, wie folgt

$$\begin{aligned} b_1 &= \varepsilon_4 \\ b_2 &= (\varepsilon_3 - \varepsilon_4) \frac{K_3}{K_4} \\ b_3 &= (\varepsilon_2 - \varepsilon_4) \frac{K_2}{K_4} - (\varepsilon_3 - \varepsilon_4) \frac{K_3^2}{K_4^2} \\ b_4 &= (\varepsilon_1 - \varepsilon_4) \frac{K_1}{K_4} + \frac{\varepsilon_A}{[M]} \cdot \frac{1}{K_4} - (\varepsilon_2 + \varepsilon_3 - 2\varepsilon_4) \frac{K_2 K_3}{K_4^2} + (\varepsilon_3 - \varepsilon_4) \frac{K_3^3}{K_4^3} \end{aligned} \tag{23-b}$$

d.h. analog denen vom vorigen Fall (18-b) sind.

Die Gleichungen (23), (23-a) und (23-b) können auch in diesem Falle, in einer einfachen und regulären Form ausgedrückt werden, und zwar :

$$\begin{aligned} \varepsilon_1 K_1 + \frac{\varepsilon_A}{[M]} &= a_1 \\ \varepsilon_2 K_2 &= a_2 + a_1 K_1 \\ \varepsilon_3 K_3 &= a_3 + a_2 K_1 + a_1 K_2 \\ \varepsilon_4 K_4 &= a_4 + a_3 K_1 + a_2 K_2 + a_1 K_3 \end{aligned} \qquad (24\text{-a})$$

und

$$\begin{aligned} &\varepsilon_4 = b_1 ; \quad (\varepsilon_4 K_4 = b_1 K_4) \\ &(\varepsilon_3 - \varepsilon_4) K_3 = b_2 K_4 \\ &(\varepsilon_2 - \varepsilon_4) K_2 = b_3 K_4 + b_2 K_3 \\ &(\varepsilon_1 - \varepsilon_4) K_1 = b_4 K_4 + b_3 K_3 + b_2 K_2 - \frac{\varepsilon_A}{[M]} \end{aligned} \qquad (24\text{-b})$$

Dank der regulären Form des Gleichungssystems (24-a—24-b) können die höheren Koeffizienten, a_i oder b_i, falls die vorangehenden, d.h. $a_1 \ldots a_{i-1}$ bzw. $b_1 \ldots b_{i-1}$, bekannt sind, genau vie im vorigen Falle, leicht berechnet werden.

Man hat also das System der Gleichungen (24-a) und (24-b) zu lösen, welche durch Umformen zuletzt in der Form des Gleichungssystems (25) ausgedrückt werden können :

$$\begin{aligned} \varepsilon_1 K_1 &= a_1 - \frac{\varepsilon_A}{[M]} = b_4 K_4 + b_3 K_3 + b_2 K_2 + b_1 K_1 - \frac{\varepsilon_A}{[M]} \\ \varepsilon_2 K_2 &= a_2 + a_1 K_1 = b_3 K_4 + b_2 K_3 + b_1 K_2 \\ \varepsilon_3 K_3 &= a_3 + a_2 K_1 + a_1 K_2 = b_2 K_4 + b_1 K_3 \\ \varepsilon_4 K_4 &= a_4 + a_3 K_1 + a_2 K_2 + a_1 K_3 = b_1 K_4 \end{aligned} \qquad (25).$$

Man merkt, daß in der ersten Gleichung dieses Systems das Glied $\frac{\varepsilon_A}{[M]}$ verschwindet, so daß das zu lösende Gleichungssystem genau die Form des Systems (20) vom vorigen Falle, welches praktisch immer lösbar ist, annimmt. Im allgemeinen Falle der Existenz von n einkernigen Komplexen — obwohl von verschiedenen Bedingungen und deshalb auch von verschiedenen Gleichungen ausgegangen wurde — hat man zum Schluß genau dasselbe System von n Lineargleichungen mit n Unbekannten ($K_1 \ldots K_n$) zu lösen, welches praktisch immer lösbar ist, wie im vorigen, von Jazimirskij behandelten Falle (wenn das Metallion und die Komplexe absorbieren). Dies entspricht der Erweiterung der Anwendungsgrenzen der Methode von Jazimirskij.

Revue Roumaine de Chimie, 14, 1019—1025 (1969)

Revue Roumaine de Chimie, 14, 1027–1029 (1969)

RÖNTGENOGRAPHIC STUDY ON THE COMPOUND $[HP(C_6H_4-CH_3)_3]_2[CoCl_4]$

R. MERARU and MARIA NEGOIU

Department of Inorganic Chemistry, University of Bucharest
Spl. Independenţei 89

Received October 16, 1968

The complex $[HP(C_6H_4-CH_3)_3]_2[CoCl_4]$ belongs to the monoclinic system, in one of its centered space groups C_{121} ; C_{1n1}. The parameters of the elementary cell are : $a = 29.63$ Å ; $b = 11.55$ Å ; $c = 12.29$ Å ; $\hat{\beta} = 78.05°$. The experimental density $\rho_{exp} = 0.68$ g/cm^3 and the calculated density $\rho_{calc} = 0.655$ g/cm^3 are in good agreement and indicate that there are two molecules of compound in the elementary cell.

INTRODUCTION

The systematic study on the preparation of the tertiary phosphines has been carried out after 1950, when besides Grignard's and Würtz's method more economical procedures appear as for example, the PH_3 addition to olephines, or the addition of phosphines to the carbonyl group. [1] It is well known that phosphines act as electron donor in σ bonds and, at the same time as electron acceptor in the π bonding.

The 3d orbitals of phosphorus, interact with the nonbonding "d" orbitals of the transition metal.

For these reasons, the phosphines are ligands which stabilize different metal oxidation states, forming complex compounds.

Among the tetrahedral compounds of the type $[MX_4]L_2$ (M = transition metal ; L = phosphonium salt and X = Cl, Br, I, SCN) the compound $[PH(C_6H_4-CH_3)_3]_2[CoCl_4]$ is noted obtained according to a previous paper, [2] from the interaction of $CoCl_2$ and $P(C_6H_4-CH_3)_3$ in the refluxed acetic acid.

The present paper is dealing with the röntgenographic structural study of this complex.

EXPERIMENTAL

Three Debyegrams are made, on three different samples of the complex compound $[PH(C_6H_4-CH_3)_3]_2[CoCl_4]$. The compound was ground and introduced into collodium capillars having 0.4 mm in diameter. Röntgen TUR M-60 equipment was used, and the $K_\alpha Fe$ radiation

---

[1] G. M. Kosolapoff, "Organophosphorus Compounds", Wiley, New York, 1950, p. 10–30.

[2] P. Spacu and M. Negoiu, *Anal. Univ. Buc., Chim.* (under press).

was selected from the spectrum, by means of Mn filters. The working conditions were 32 kV, 12 mA and the times of exposure 60 h.

Use has been made of Agfa Gevaert Structurix D-10 film and a diffraction camera with 114.6 mm in diameter.

The Debyegrams were recorded, on the recording microphotometer Zeiss Jena and then measured.

Table 1

Experimental data

No	2s (mm)	θ°	sin θ°	d (Å)
1	11.59	5.805	0.10106	9.585
2	32.29	11.165	0.19263	5.029
3	26.74	13.394	0.23021	4.208
4	33.88	16.970	0.29082	3.331
5	35.17	17.617	0.30240	3.203
6	37.84	18.954	0.32401	2.989
7	43.54	21.804	0.37137	2.608
8	45.26	22.671	0.38441	2.520
9	46.82	23.452	0.39723	2.438
10	47.82	23.953	0.40522	2.390
11	50.63	25.360	0.42735	2.266
12	53.19	26.643	0.44783	2.163
13	55.78	27.940	0.46799	2.070
14	56.23	28.166	0.47111	2.056
15	58.15	29.127	0.48638	1.992
16	61.27	30.690	0.50918	1.896
17	63.68	31.947	0.52851	1.833
18	66.34	33.230	0.54760	1.769

In table 1 in the second column, the 2s values are the distances from the center of the exit hole of the radiation, till the maximum blackening density of the diffraction line (in mm) taken as arithmetic average of three determinations.

The diffraction angles θ° were calculated using the corrected radius of the camera.[3] Afterwards the spacings "d" have been calculated. Experimental density has been determined using the flotation method which gives $\rho = 0.68$ g/cm^3 at 24°. On this compound no corrections for absorption, refraction and temperature have been carried out.

INTERPRETATION OF THE EXPERIMENTAL DATA

For the calculus of the elementary cell parameters Zachariasen's method[4] has been used.

All the experimental data are listed in the form :

$$S_i = \sin^2 \theta_i \tag{1}$$

where θ° = diffraction angle.

For the monoclinic system, the quadratic equation is :

$$\sin^2 \theta_i = \frac{\lambda^2}{4}\left\{\frac{H^2}{a^2 \sin^2 \beta} + \frac{K^2}{b^2} + \frac{L^2}{c^2 \sin^2 \beta} \pm \frac{2HL \cos \beta}{ac \sin^2 \beta}\right\} \tag{2}$$

---

[3] H. P. KLUG and L. ALEXANDER, "X-Ray Diffraction Procedures", Wiley, New York, 1966, p. 324.

[4] W. ZACHARIASEN, *Acta Cryst.*, **16**, 784 (1963).

which may be written as :

$$S_i = H_i^2A_1 + K_i^2A_2 + L_i^2A_3 \pm 2H_iL_iA_{13} = T_i + K_i^2A_2 \qquad (3)$$

The centered structure for the complex was established by choosing one constant value repeatedly occurring in the ratio : 4 : 8 : 12 : 16 : 20 in the difference set :

$$S_i - S_j = (K_i^2 - K_j^2)\,A_2 \qquad (4)$$

The value $A_2 = 0.00445$ is thus obtained, from which easily results $b = 11.55$ Å, axis of the elementary cell.

In the following, the selected values are obtained, which satisfy the relation :

$$2(T_i + T_j) = T_k + T_1 \qquad (5)$$

The other parameters of the elementary cell are established : $a = 29.63$ Å ; $c = 12.29$ Å and $\hat{\beta} = 78.05°$.

If the number of molecules in the elementary cell is $n = 2$, the calculated density with the formula [5] :

$$\rho = \frac{1.6604\ nM}{V(\text{Å})}$$

is $\rho = 0.655$ g/cm³, when $V = 4113.18$ Å³; $M = 811.5$

Table 2 checks the experimental data ($\sin^2\theta$ exp) in comparison with the calculated ones ($\sin^2\theta$ calc) using the values of the elementary cell parameter and the obtained Miller's indexes HKL.

Because the HKL indexes verify the extinction rules

HKL $H + K = 2n$
HOL $H = 2n$; $L = 2n$
OKO $K = 2n$

an elementary cell, centered on the C faces (001 plans), results, belonging hypothetically to one of the space groups C_{121} or C_{1m1}.

Table 2

Comparison between experimental and calculated data

No	$\sin^2\theta$ exp	$\sin^2\theta$ calcd.	HKL	No	$\sin^2\theta$ exp	$\sin^2\theta$ calcd.	HKL
1	1021	871	201	10	16420	16371	334
2	3711	3683	221	11	18271	18224	151
3	5300	5339	$60\bar{1}$	12	20055	20059	152
						19998	$73\bar{3}$
4	8458	8427	223	13	21901	21977	1041
5	9145	9095	423	14	22194	22176	335
6	10498	10593	532	15	23657	23507	116
7	13792	13842	242	16	25926	25955	262
8	14777	14732	442	17	27932	27942	826
		14738	$24\bar{2}$			27966	$22\bar{6}$
9	15799	15851	205	18	29987	29783	$93\bar{4}$

---

[5] R. W. D'Eye and E. Wait, "X-Ray Powder Photography in Inorganic Chemistry", Butterworths, London, 1960, p. 177.

Revue Roumaine de Chimie, **14**, 1031–1037 (1969)

WÄRMEÜBERGANGSZAHLEN BEIM SIEDEN VON LÖSUNGEN. LÖSUNGEN AUS GEMISCHEN VON NATRIUMPHOSPHATEN

Z. GROPŞIANU, D. KOHN und A. IOVI
Von der Fakultät für Angewandte Chemie an der Technischen Hochschule,
Timişoara, Bd. 30 Decembrie 2

Eingegangen am 4. September 1968

Es wurden experimentelle Untersuchungen über Lösungen des Gemisches von Mono- und Dinatriumphosphat im Molverhältnis von 1 : 2 bei Atmosphärendruck und bei 300 mmHg zwecks Bestimmung der Wärmeübergangszahl beim Sieden vorgenommen. Es wurden einfache Gleichungen zur Berechnung der Wärmeübergangszahl beim Sieden in Abhängigkeit von der Heizflächenbelastung, vom Temperaturunterschied und von der Konzentration der Lösungen aufgestellt.

Das Gemisch von Mono- und Dinatriumphosphat in einem Molverhältnis von 1 : 2 wird zur Herstellung von Tripolyphosphat verwendet. Die Erzeugung von Natriumtripolyphosphat hat sich in der letzten Zeit infolge der starken Zunahme der Herstellung synthetischer Detergenzien sehr rasch entwickelt. Da es sich als der wirksamste anorganische Bestandteil erwiesen hat, beteiligt es sich an der Zusammensetzung der meisten synthetischen Detergenzien in einem Verhältnis von 10% bis zu 50% und in anderen bis zu 85%.[1] Infolge seiner zahlreichen Verwendungsmöglichkeiten hat es im Rahmen der Gesamtproduktion der technischen Phosphate den größten Anteil.[2]

Verdünnte Lösungen von Mono- und Dinatriumphosphat werden in den meisten Verfahren durch Neutralisation von Phosphorsäure mit Natriumkarbonat erhalten.[1,3,4] Diese Lösungen werden durch Verdampfen bis ungefähr 50% konzentriert, während eine weitere Dehydratisierung durch Zerstäubung erreicht wird.[1,5,6] Hieraus ergibt sich die große Bedeutung der Verdampfungsphase im Rahmen dieses Verfahrens, weshalb die Kenntnis der thermischen Kennziffern beim Sieden der Lösungen für die thermische Berechnung der Anlage unbedingt nötig ist.

Ebenso wie im Falle der Lösungen von Mononatriumphosphat und Dinatriumphosphat sind die physikalischen Konstanten der Lösungen von Gemischen nicht bekannt, und folglich kann die annähernde Berechnung der Wärmeübergangszahl beim Sieden nicht ausgeführt werden. Wie schon in einer früheren Arbeit gezeigt wurde,[7] kann die Wärmeübergangszahl beim Sieden der Lösungen, die auf komplexe Art von der Natur der letzteren abhängt, als eine physikalische Größe betrachtet werden, welche die Lösung vom Standpunkt des Wärmeubergangs beim Sieden kennzeichnet. In Anbetracht dieser Tatsachen wurden in der vorliegenden Arbeit Untersuchungen zur Bestimmung der Wärmeübergangszahlen beim Sieden der Lösungen von Mono- und Dinatriumphosphat in einem Molverhältnis von 1 : 2 vorgenommen, wobei einfache Gleichungen zur Berechnung derselben aufgestellt wurden.

---

[1] A. Iovi, „Tehnologia acidului fosforic şi a fosfaţilor tehnici", Timişoara, 1967, S. 150.
[2] E. D. Melnic, *Khim. Prom.*, **1966**, 548.
[3] I. Samoil und V. Apreotesei, *Rev. Chim.* (*Bucureşti*), **17**, 538 (1966).
[4] *Phosphorus and Potassium*, **1966**, 27.
[5] I. L. Gofman, M. V. Lykov und P. I. Khudolei, *Khim. Prom.*, **1961**, 28.
[6] *Rev. Prod. Chim.*, **68**, 494 (1965).

Die Laboratoriumsvorrichtung und die Methode zur Bestimmung der Wärmeübergangszahlen beim Sieden wurden in früheren Arbeiten mitgeteilt.[8,9]

Die Bestimmungen wurden bei Atmosphärendruck und bei 300 mmHg durchgeführt, wobei im Bereiche intensiven Siedens mit Heizflächenbelastungen von $85.10^3-57.10^4$ W/m^2 gearbeitet wurde. Es wurden Lösungen von Gemischen verschiedener Konzentrationen bis zu 46,5% verwendet.

Die Versuchsergebnisse sind in den Abbildungen 1—9 dargestellt.

Die Wärmeübergangszahl beim Sieden von Lösungen des Gemisches von Mono- und Dinatriumphosphat verschiedener Konzentrationen nimmt bei Atmosphärendruck mit dem Anwachsen der Heizflächenbelastung zu (Abb. 1). Die Versuchsergebnisse ermöglichten es, folgende Gleichungen zwischen α und q aufzustellen:

— für Lösungen bis zu 40%:

$$\alpha = \varepsilon \cdot q^{0,7}$$

— für die Schmelze von 46,5%:

$$\alpha = 4 \cdot q^{0,6}$$

wo ε ein von der Konzentration abhängiger Koeffizient ist.

Die Schmelze von 46,5% wurde durch Erhitzen der Kristallhydrate von Mono- und Dinatriumphosphat im gegebenen Molverhältnis erhalten. Es wurde beobachtet, daß im Falle der Lösungen bis zu 40% der Wachstumsgradient des Koeffizienten α im Verhältnis zu q identisch ist mit dem, welcher für Wasser festgestellt wurde und kleiner ist als der, welcher für die Schmelze von 46,5% gefunden wurde.

Der Koeffizient ε vermindert sich mit dem Anwachsen der Konzentration; seine Veränderung ist in Abb. 2 wiedergegeben. Zwischen ε und der Konzentration der Lösung C, die in Gewichtsprozenten ausgedrückt ist, wurden folgende Gleichungen aufgestellt:

— für Lösungen mit Konzentrationen unter 20%:

$$\varepsilon = 2,76 \cdot C^{-0,135}$$

---

[7] Z. Gropşianu, D. Kohn und A. Iovi, *Rev. Roumaine Chim.* (unter Druck).

[8] Z. Gropşianu, D. Kohn und A. Iovi, *Rev. Roumaine Chim.*, **12**, 485 (1967).

[9] Z. Gropşianu, D. Kohn und A. Iovi, *Rev. Roumaine Chim.* (unter Druck).

— für Lösungen mit Konzentrationen von 20–40 % :

$$\varepsilon = 4{,}17 \cdot C^{-0{,}273}$$

Ebenso wie bei Atmosphärendruck nimmt auch bei 300 mmHg der Koeffizient α mit dem Anwachsen von q zu (Abb. 3); der Wachs-

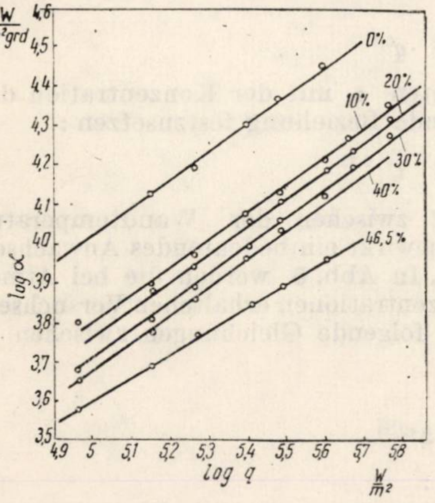

Abb. 1. — Veränderung von α in Abhängigkeit von q bei atmosphärischem Druck, für Lösungen verschiedener Konzentration aus Gemischen von Natriumphosphaten.

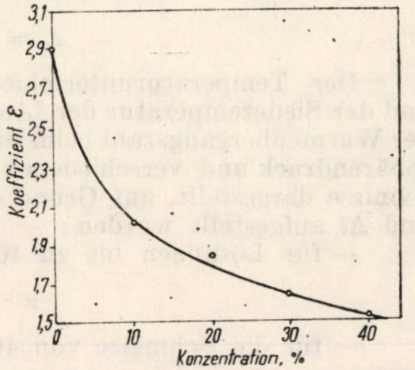

Abb. 2. — Abhängigkeit des Koeffizienten ε_1 von der Konzentration der Lösungen aus Gemischen von Natriumphosphaten.

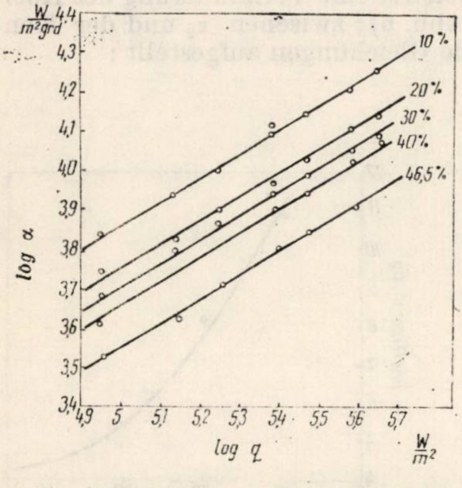

Abb. 3. — Veränderung von α in Abhängigkeit von q bei einem Druck von 300 mmHg, für Lösungen verschiedener Konzentration aus Gemischen von Natriumphosphaten.

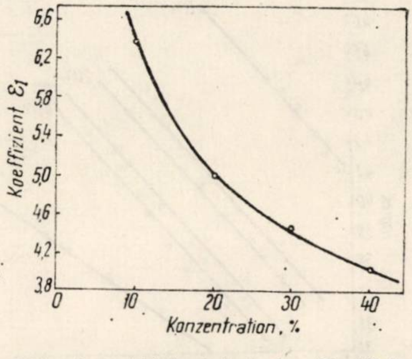

Abb. 4. — Abhängigkeit des Koeffizienten ε_1 von der Konzentration der Lösungen aus Gemischen von Natriumphosphaten.

tumsgradient ist dagegen kleiner. Es wurde folgende Gleichung aufgestellt:

$$\alpha = \varepsilon_1 \cdot q^{0,61}$$

welche bis zu einer Konzentration von 40% gültig ist.

Für die Schmelze von 46,5% besteht zwischen α und q folgende Gleichung:

$$\alpha = 3{,}16 \cdot q^{0,61}$$

Die Veränderung des Koeffizienten ε_1 mit der Konzentration der Lösung (Abb. 4) ermöglicht es, folgende Beziehung festzusetzen:

$$\varepsilon_1 = 13{,}63 \cdot C^{-0,33}$$

Der Temperaturunterschied Δt zwischen der Wandtemperatur und der Siedetemperatur der Lösung bewirkt ein bedeutendes Anwachsen der Wärmeübergangszahl beim Sieden. In Abb. 5 werden die bei Atmosphärendruck und verschiedenen Konzentrationen erhaltenen Versuchsergebnisse dargestellt, auf Grund derer folgende Gleichungen zwischen α und Δt aufgestellt wurden:

— für Lösungen bis zu 40%:

$$\alpha = \varepsilon_2 \cdot \Delta t^{2,33}$$

— für die Schmelze von 46,5%:

$$\alpha = 36{,}3 \cdot \Delta t^{1,465}$$

Es wurde beobachtet, daß auch in diesem Falle der Wachstumsgradient von α gegenüber Δt für die Schmelze von 46,5% kleiner ist.

Das Anwachsen der Konzentration hat eine Verminderung des Koeffizienten α bzw. von ε_2 zur Folge (Abb. 6); zwischen ε_2 und der Konzentration der Lösung wurden folgende Gleichungen aufgestellt:

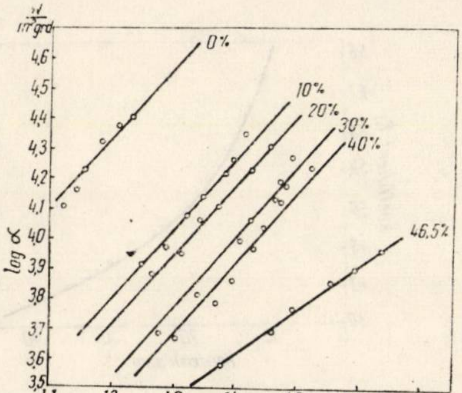

Abb. 5. — Veränderung von α in Abhängigkeit von Δt bei atmosphärischem Druck, für Lösungen verschiedener Konzentration aus Gemischen von Natriumphosphaten.

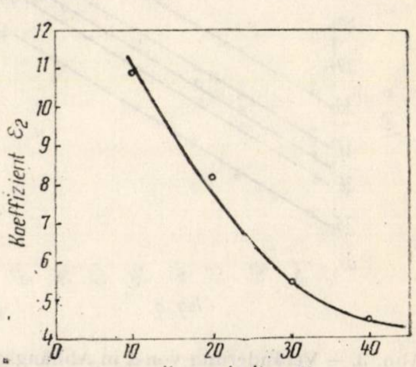

Abb. 6. — Abhängigkeit des Koeffizienten ε_2 von der Konzentration der Lösungen aus Gemischen von Natriumphosphaten.

— für Lösungen bis zu 20% :

$$\varepsilon_2 = 28{,}5 \cdot C^{-0{,}421}$$

— für Lösungen zwischen 20 und 40% :

$$\varepsilon_2 = 1{,}28 \cdot 10^2 \cdot C^{-0{,}92}$$

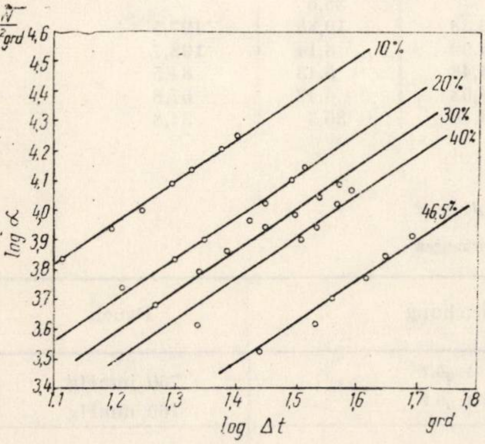

Abb. 7. — Veränderung von α in Abhängigkeit von Δt bei einem Druck von 300 mmHg, für Lösungen verschiedener Konzentration aus Gemischen von Natriumphosphaten.

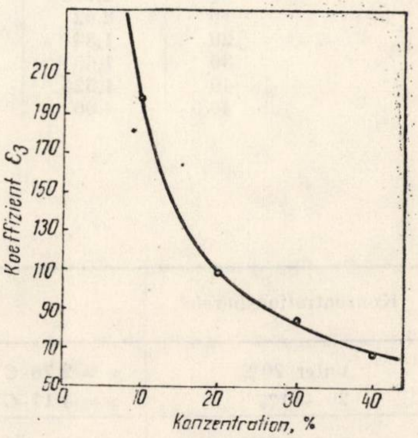

Abb. 8. — Abhängigkeit des Koeffizienten ε_3 von der Konzentration der Lösungen aus Gemischen von Natriumphosphaten.

Die Versuchsbestimmungen über die Veränderung der Wärmeübergangszahl beim Sieden, α, bei einem Druck von 300 mmHg und bei verschiedenen Konzentrationen der Lösungen, in Abhängigkeit vom Temperaturunterschied Δt (Abb. 7) ermöglichte es, folgende Gleichungen zwischen α und Δt aufzustellen:

— für Lösungen bis zu 40% :

$$\alpha = \varepsilon_3 \cdot \Delta t^{1{,}38}$$

— für die Schmelze von 46,5% :

$$\alpha = 34{,}8 \cdot \Delta t^{1{,}38}$$

Der Wachstumsgradient von α gegenüber Δt ist kleiner als der bei Atmosphärendruck, während er bei Lösungen und bei der Schmelze denselben Wert hat.

In Abb. 8 wird die Veränderung des Koeffizienten ε_3 mit der Konzentration der Lösungen C dargestellt. Es wurde die Gleichung folgender Form aufgestellt :

$$\varepsilon_3 = 11{,}52.10^2 \cdot C^{-0{,}77}$$

Die Werte der Koeffizienten ε, ε_1 ε_2 und ε_3 sind in Tabelle 1 und die Gleichungen zur Berechnung von α in Abhängigkeit von q, Δt und C in Tabelle 2 angeführt.

Tabelle 1

Werte der Koeffizienten ε, ε_1, ε_2 und ε_3

Konzentration %	ε	ε_1	ε_2	ε_3
0	2,915	—	35,5	—
10	2,02	6,38	10,83	197,5
20	1,84	4,99	8,14	108,7
30	1,65	4,48	5,43	84,5
40	1,525	4,03	4,42	67,8
46,5	4,00	3,16	36,3	34,8

Tabelle 2

Gleichungen

Konzentrationsbereich	Gleichung	Druck
unter 20%	$\alpha = 2{,}76 \cdot C^{-0{,}135} \cdot q^{0{,}7}$	760 mmHg
20–40%	$\alpha = 4{,}17 \cdot C^{-0{,}273} \cdot q^{0{,}7}$	760 mmHg
bei 46,5%	$\alpha = 4 \cdot q^{0{,}6}$	760 mmHg
bis 40%	$\alpha = 13{,}63 \cdot C^{-0{,}33} \cdot q^{0{,}61}$	300 mmHg
bei 46,5%	$\alpha = 3{,}16 \cdot q^{0{,}61}$	300 mmHg
unter 20%	$\alpha = 28{,}5 \cdot C^{-0{,}421} \cdot \Delta t^{2{,}33}$	760 mmHg
20–40%	$\alpha = 1{,}28 \cdot 10^2 \cdot C^{-0{,}92} \cdot \Delta t^{2{,}33}$	760 mmHg
bei 46,5%	$\alpha = 36{,}3 \cdot \Delta t^{1{,}465}$	760 mmHg
bis 40%	$\alpha = 11{,}52 \cdot 10^2 \cdot C^{-0{,}77} \cdot \Delta t^{1{,}38}$	300 mmHg
bei 46,5%	$\alpha = 34{,}8 \cdot \Delta t^{1{,}38}$	300 mmHg

Die Siedetemperaturen der Lösungen, die zur Festsetzung des Temperaturunterschiedes Δt nötig sind, wurden, da sie im Fachschrifttum nicht vorhanden sind, experimentell bestimmt. Die erhaltenen Werte sind in Abb. 9 graphisch dargestellt.

SCHLUSSFOLGERUNGEN

Die Versuchsbestimmungen mit Lösungen eines Gemisches von Mononatriumphosphat und Dinatriumphosphat in einem Molverhältnis von 1 : 2 bei Atmosphärendruck und 300 mmHg, ermöglichten es, Gleichungen zur Berechnung der Wärmeübergangszahl bein Sieden, α, in Abhängigkeit von der Heizflächenbelastung q, vom Temperaturunterschied Δt und von der Konzentration der Lösungen C aufzustellen.

Der Koeffizient α nimmt mit dem Anwachsen von q und Δt zu und vermindert sich mit dem Anwachsen der Konzentration.

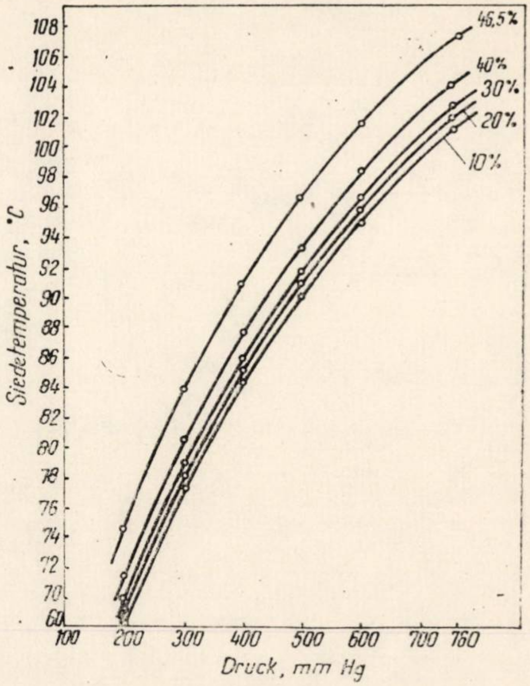

Abb. 9. — Siedetemperaturen der Lösungen aus Gemischen von Natriumphosphaten in Abhängigkeit vom Druck bei verschiedenen Konzentrationen.

Es wird festgestellt, daß bei Atmosphärendruck der Wachstumsgradient von α gegenüber q und Δt bei Lösungen größer ist als bei Schmelzen, während er bei einem Druck von 300 mmHg für Lösungen und Schmelzen identisch ist. Bei einem Druck von 300 mmHg ist der Wachstumsgradient von α kleiner als bei Atmosphärendruck.

Es wurden die Siedetemperaturen von Lösungen des Gemisches von Mono- und Dinatriumphosphat im Molverhältnis von 1 : 2 in Abhängigkeit vom Druck für verschiedene Konzentrationen bestimmt.

Revue Roumaine de Chimie, 14, 1039 – 1046 (1969)

ABOUT THE INFLUENCE OF INDICATING ELECTRODE TREATMENT UPON THE PARAMETERS OF THE POTENTIOMETRIC TITRATION. I

9166

BRIGHT PLATINUM ELECTRODE IN $Fe^{2+}/Cr_2O_7^{2-}$ TITRATION

C. LITEANU and IOVANCA HAIDUC

Babeş-Bolyai University, Analytical Chemistry Laboratory,
Cluj, str. Arany János 11

Received December 9, 1968

The behaviour of the bright platinum electrode towards the redox system $Fe^{2+}/Cr_2O_7^{2-}$ (in potentiometric titration) has been investigated, as a function of the electrode pre-treatment (anodic polarization, cathodic polarization and stripped electrode). The experimental data were treated statistically; it was shown that the variation of the potential in the vicinity of the end point depends upon the treatment of the electrode.

INTRODUCTION

The platinum electrode is frequently used as indicating electrode in redox potentiometric titrations. The mechanism by which a soluble redox couple determines the potential of the platinum electrode is still unclear. The slow establishing of a constant potential in strong oxidizing media is the result of the oxidation of platinum. The formation of an oxide film, when the platinum electrode was chemically or electrochemically oxidized has been suggested by several authors[1–5] and various hypotheses about the nature of this oxide have been formulated.[6–10]

It is also well known that the behaviour of an indicating electrode is strongly influenced by the pre-treatment of the electrode, by the purity

---

[1] I. M. Kolthoff and N. Tanaka, *Anal. Chem.*, **26**, 632 (1954).

[2] I. W. Ross and I. Shain, *Anal. Chem.*, **28**, 548 (1956).

[3] J. K. Lee, R. N. Adams and C. E. Bricker, *Anal. Chim. Acta*, **21**, 321 (1957).

[4] A. Hickling, *Trans. Faraday Soc.*, **41**, 333 (1945).

[5] F. C. Anson and J. J. Lingane, *J. Amer. Chem. Soc.*, **79**, 4901 (1957).

[6] K. Ohashi, K. Sasaki and S. Nagaura, *Bull. Chem. Soc. Japan*, **39**, 2066 (1966).

[7] J. S. Mayell and S. H. Langer, *J. Electrochem. Soc.*, **111**, 438 (1964).

[8] J. W. Felberg, G. G. Enke and Briker C. E., *J. Electrochem. Soc.*, **110**, 826 (1963).

[9] H. A. Laitinen and G. G. Enke, *J. Electrochem. Soc.*, **107**, 773 (1960).

[10] S. Gilman, in "Electroanalytical Chemistry A Series of Advances", Edited by A. J. Bard, Marcel Dekker, Inc., New York, 1967, vol. 2, p. 111.

of the electrolyte, by the experimental conditions of the measurements[11,12] and by the specifically adsorbed anions or cations[12] or organic molecules[13,14] on the surface of the electrode.

In studies on the pre-treated platinum electrodes it has been observed that a freshly pre-anodized electrode is more sensitive towards several redox systems[1,2,5,15–20] than a non-treated electrode. Several reactions occur more reversibly on an oxidized electrode than on a reduced one,[1,18,21] thus suggesting that the surface oxide takes part in the electrode reaction. Some mechanisms responsible for the greater reversibility of a pre-anodized electrode have been advanced.[17,19,22–25]

In redox potentiometric titrations some particular features which can be correlated with the facts discussed above have been noted. Thus, Forbes and Bartlett[26] have found that in the titration of bichromate with ferrous ions the potential of the indicating electrode increases slowly (becomes more oxidizing) during the titration, instead of decreasing, and only decreases suddenly when the concentration of the Fe^{2+} ions corresponds to the end point. The platinum electrode has been kept for several hours in a $Cr_2O_7^{2-}$ solution or in a Fe^{2+} solution, before the titration. In both cases an increase in the potential before the end point was observed, but this increase was larger when the electrode was pre-treated with the bichromate solution.

In the titration of very dilute bichromate solutions with ferrous ions, Hildebrand[27] obtained small *positive* errors, which were attributed to the formation of an oxide layer on the electrode surface.

In a reinvestigation of the titration of bichromate with ferrous ion Hendrixson[28] has found that the increase in the potential during the addition of Fe^{2+} is negligible, if the electrode has been kept for a sufficiently long time in the bichromate solution, before the titration (several hours in dilute solutions).

We were interested in possible analytical applications of the pre-treated platinum electrodes in redox potentiometric titrations. We have reinvestigated the titration of bichromate with ferrous ions, and the inverse titration of ferrous ions with bichromate, using pre-treated elec-

---

[11] C. A. Knorr, *Z. Elektrochem.*, **59**, 647 (1955).

[12] A. N. Frumkin, in "Advances of Electrochemistry and Electrochemical Engineering", vol. 3, Interscience Publishers Inc., New York, 1963, p. 287–391.

[13] T. C. Franklin and R. D. Sothern, *J. Phys. Chem.*, **58**, 951 (1954).

[14] M. W. Breiter, *J. Electrochem. Soc.*, **109**, 42 (1962); M. W. Breiter, *Electrochim. Acta*, **8**, 447 (1963).

[15] B. B. Baker and W. M. Mac Nevin, *J. Amer. Chem. Soc.*, **75**, 1476 (1953).

[16] S. S. Lord and L. B. Rogers, *Anal. Chem.*, **26**, 284 (1954).

[17] I. M. Kolthoff and E. R. Nightingale, *Anal. Chim. Acta*, **17**, 329 (1957).

[18] F. C. Anson, *J. Amer. Chem. Soc.*, **81**, 1554 (1959).

[19] D. G. Davis, *Talanta*, **3**, 335 (1960).

[20] F. C. Anson, *Anal. Chem.*, **33**, 934 (1961).

[21] J. J. Lingane, *J. Electroanal. Chem.*, **2**, 296 (1961).

[22] F. C. Anson and D. M. King, *Anal. Chem.*, **34**, 362 (1962).

[23] J. P. Hoare, *J. Electroanal. Chem.*, **12**, 260 (1966).

[24] J. P. Hoare, *J. Electrochem. Soc.*, **110**, 1019 (1963).

[25] J. P. Hoare, *J. Electrochem. Soc.*, **112**, 849 (1965).

[26] G. S. Forbes and E. P. Bartlett, *J. Amer. Chem. Soc.*, **35**, 1527 (1913).

[27] J. H. Hildebrand, *J. Amer. Chem. Soc.*, **35**, 847 (1913).

[28] W. S. Hendrixson, *Proc. Iowa Acad. Sci.*, **31**, 319 (1924).

trodes made of bright platinum. The electrodes were pre-anodized (experiments of series I and IV), pre-cathodized (experiments of series II and V) or just stripped of the adsorbed oxygen and hydrogen (experiments of series III and VI).

EXPERIMENTAL

The solutions containing the Fe^{2+} and $Cr_2O_7^{2-}$ ions, of 0.1 N and 0.05 N concentration, have been prepared from analytical grade reagents and doubly distilled water. The titrations were carried out in inert deoxygenated atmosphere.

The potential has been measured with a QLK Compensating Bridge (Czech Made) and a Multiflex MG 2 Galvanometer (sensitivity 4.0×10^{-9} A/mm) was used as indicating instrument.

The pre-treatment of the electrodes, consisting of anodic or cathodic polarizations, was made with a 1 M H_2SO_4 solution. Before each pre-treatment the platinum electrode had been stripped of the adsorbed hydrogen and oxygen, by treatment with aqua regia, followed by washing with doubly distilled water, treatment with 1 % KI solution and washing again.[29] After this treatment the electrode is free of adsorbed oxygen or hydrogen, but has some I^- ions adsorbed on its surface.[29] The pre-treated electrodes were introduced into the solution to be titrated immediately after the pre-treatment. Every time 20–30 minutes were necessary before the potential became stable and constant.

Table 1

Experimental conditions used in the redox potentiometric titrations

Experiment series	No	Electrode surface (cm²)	Type of pretreatment	Duration (min)	Current density (mA/cm²)	Titration in which the electrode was used
I	1	0.50	anodic	5	0.40	Fe^{2+} with $Cr_2O_7^{2-}$
	2	0.50	”	7	0.40	” ” ”
	3	0.50	”	10	0.40	” ” ”
II	1	0.50	cathodic	5	0.40	” ” ”
	2	0.50	”	7	0.40	” ” ”
	3	0.50	”	10	0.40	” ” ”
III	1	0.50	stripped	—	—	” ” ”
	2	0.50	”	—	—	” ” ”
	3	0.50	”	—	—	” ” ”
IV	1	0.058	anodic	5	0.16	$Cr_2O_7^{2-}$ with Fe^{2+}
	2	0.058	”	5	0.16	” ” ”
	3	0.50	”	5	0.25	” ” ”
	4	0.50	”	5	0.80	” ” ”
	5	0.50	”	5	10.0	” ” ”
V	1	0.058	cathodic	5	0.16	” ” ”
	2	0.058	”	5	0.16	” ” ”
	3	0.50	”	5	0.25	” ” ”
	4	0.50	”	5	0.80	” ” ”
	5	0.50	”	5	10.0	” ” ”
VI	1	0.50	stripped	—	—	” ” ”

---

[29] L. Kekedy and F. Makkay, *Rev. Roumaine Chim.*, **13**, 739 (1968).

Table

Titration of Fe^{2+} with bichromate

Experiment	A_0	A_1	A'_0	A'_1	$u = \frac{\vert A'_1 \vert}{\vert A_1 \vert}$	V_i	$V_e - V_i$
I 1	2532.6	−412.47	−2527.60	418.09	1.010	6.0925	2.40×10^{-4}
2	2396.6	−379.06	−2435.99	396.81	1.042	6.229	1.54×10^{-3}
3	2750.0	−447.86	−2456.60	410.48	0.916	6.0845	1.92×10^{-3}
II 1	2707.1	−441.15	−2508.40	415.62	0.942	6.0870	1.60×10^{-3}
2	2684.0	−422.78	−2328.83	380.77	0.900	6.2380	1.76×10^{-3}
3	2662.6	−430.35	−2456.60	408.65	0.949	6.0900	8.98×10^{-4}
III 1	2548.1	−414.97	−2503.70	412.64	0.994	6.1040	1.1×10^{-4}
2	2199.5	−347.84	−2459.60	397.04	1.142	6.2540	2.0×10^{-3}
3	2466.8	−402.36	−2727.50	447.49	0.899	6.1120	7.7×10^{-3}

*) For the significance of symbols and

Table

Titration of bichromate with Fe^{2+}

Experiment	A_0	A_1	A'_0	A'_1	$u = \frac{\vert A'_1 \vert}{\vert A_1 \vert}$	V_i	$V_e - V_i$
IV 1	2622.10	−256.06	−16.80.06	169.57	0.662	10.107	1.01×10^{-2}
2	2533.90	−240.48	−1997.30	197.96	0.823	10.134	3.42×10^{-2}
3	4530.90	−621.72	−2364.00	326.25	0.524	7.273	2.94×10^{-3}
4	2415.70	−329.78	−2157.10	298.23	0.904	7.281	1.60×10^{-3}
5	3900.30	−537.22	−2170.50	300.92	0.560	7.252	1.65×10^{-3}
V 1	2954.50	−288.10	−1915.50	194.82	0.676	10.103	9.88×10^{-3}
2	3379.90	−329.82	−2208.90	222.39	0.674	10.120	9.90×10^{-3}
3	3604.60	−492.12	−2619.90	364.48	0.740	7.266	4.9×10^{-3}
4	3419.60	−467.91	−2700.00	374.28	0.799	7.266	2.7×10^{-3}
5	4137.70	−567.31	−2628.60	363.83	0.641	7.267	3.7×10^{-3}
VI 1	4016.70	−553.02	−2351.80	324.53	0.586	7.257	3.1×10^{-3}

*) For the significance of symbols and

The type of electrode and the pre-treatment used in each experiment are indicated in table 1. The electrodes used were either a platinum wire (of 0.058 cm^2 surface) or a platinum plate (of 0.50 cm^2 surface). To avoid as much as possible the influence of other factors than the electrode pre-treatment and to make sure that the electrodes under comparison are subjected to identical conditions during the titration, all three electrodes (pre-anodized, pre-cathodized and stripped) were introduced into *the same* solution being titrated, and thus parallel readings were made for all three electrodes in the same titration.

A calomel electrode was used as reference electrode. The results of the potentiometric titrations are given in tables 2 and 3, and are discussed below. In each case the values given are the average for three or more determinations under identical conditions.

RESULTS AND DISCUSSION

The potentiometric titration curves obtained in the conditions described above, were linearized according to the procedure described by Liteanu and Mioscu.[30] For the statistic treatment of the experimental data the following values were calculated :

---

[30] C. Liteanu and M. Mioșcu, *Rev. Roumaine Chim.*, **13**, 899 (1968).

2

Statistic treatment of data*)

y_i	V_e	t	$s_{\overline{E}}$	$E_i \pm ts_{\overline{E}}$	E_e	$\Delta E_{\pm 1\%}$
19.84	6.093	2.37	2.07	705.87 ± 4.90	704.73	271.40
35.44	6.227	2.78	2.91	661.71 ± 8.08	666.00	208.90
25.00	6.086	2.45	2.60	677.82 ± 6.37	670.22	236.67
21.82	6.0886	2.37	2.22	685.97 ± 5.26	678.64	250.00
46.70	6.2400	2.78	1.60	664.30 ± 4.44	660.46	174.32
36.82	6.0909	2.45	2.22	675.10 ± 5.44	672.66	200.00
15.13	6.1041	2.45	1.93	709.25 ± 3.30	708.55	300.00
24.11	6.2520	2.45	2.42	693.53 ± 5.93	695.62	267.83
7.58	6.1130	2.45	2.04	719.26 ± 4.99	709.20	365.62

computation method see refs. 30, 31 and 32.

3

Statistic treatment of data *)

y_i	V_e	t	$s_{\overline{E}}$	$E_i \pm ts_{\overline{E}}$	E_e	$\Delta E_{\pm 1\%}$
34.11	10.117	2.45	4.52	957.19 ± 11.76	966.87	356.70
48.78	10.168	3.18	3.70	947.50 ± 11.76	970.54	353.70
9.14	7.280	2.37	4.14	779.34 ± 9.80	810.95	366.79
14.58	7.283	2.30	2.15	798.92 ± 4.94	809.92	380.09
4.39	7.254	2.45	5.75	804.48 ± 14.08	815.62	452.12
43.83	10.113	2.45	5.45	937.95 ± 11.12	954.27	278.75
42.13	10.130	2.57	2.91	945.50 ± 7.47	968.64	272.07
28.86	7.271	2.54	1.70	744.00 ± 4.37	760.71	265.00
19.77	7.269	2.26	2.70	733.41 ± 6.10	746.89	250.33
15.06	7.270	2.26	2.98	743.76 ± 6.73	766.88	288.14
11.55	7.270	2.23	2.71	773.07 ± 6.04	799.91	356.56

computation method see refs. 30, 31 and 32.

V_i — analytical inflexion volume [31]
V_e — equivalence volume[31]
E_i — inflexion potential [30]
E_e — equivalence potential [30]
$\Delta E_{\pm 1\%}$ — the variation of the potential for an error of ±1% [30]
u — real coefficient of asymmetry.[32]

The results for the *titration of ferrous ion with bichromate* are given in table 2 and the titration curve is given in figure 1. For the characterization of the behaviour of the indicating electrode, the potential variation (ΔE) in the vicinity of the equivalence point, when passing from the stage of $(100-e)\%$ to the stage of $(100+e)\%$, i.e. $\Delta E_{\pm 1\%}$, has been used. This variation of the potential is closely related to the precision of the titration. The greater the sharpness index [33] at the equivalence point, the greater the precision of the end point determination.

[31] C. Liteanu and D. Cörmöş, *Talanta*, **7**, 32 (1960).
[32] C. Liteanu and D. Cörmöş, *Talanta*, **7**, 25 (1960).
[33] M. Tanaka and G. Nakagawa, *Anal. Chim. Acta*, **32**, 123 (1965).

In the titration of ferrous ion with bichromate the greatest value for $\Delta E_{\pm 1\%}$ was obtained when the platinum electrode was in the state of stripped electrode (experiments of series III) and the smallest potential variation ($\Delta E_{\pm 1\%}$) was found when the electrode was subjected to cathodic pre-polarization (experiments of series II).

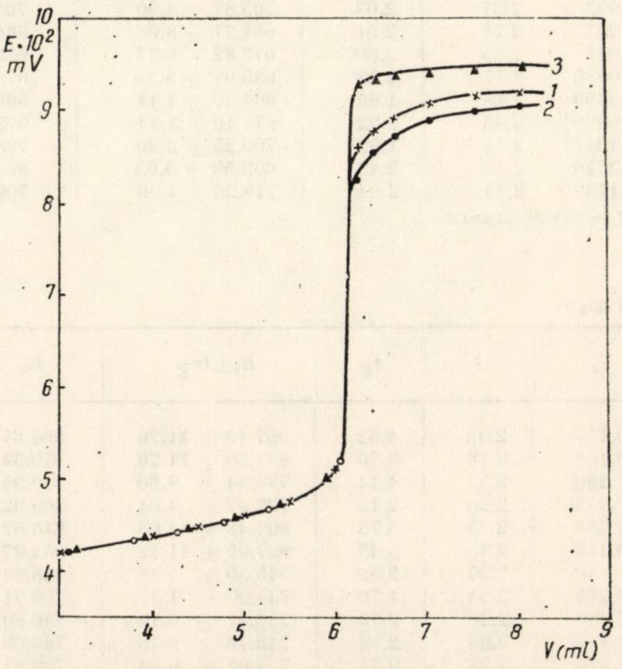

Fig. 1. — Potentiometric titration of Fe^{2+} with Cr_2O^{2-} :
1, with pre-anodized electrode; *2.* with pre-cathodized electrode; *3,* with stripped electrode.

The difference between $(\Delta E_{\pm 1\%})_{III}$ (stripped electrode) and $(\Delta E_{\pm 1\%})_{II}$ (cathodic pre-polarization) had different values which depend upon the duration of the pre-cathodization at constant current density, as follows : 50 mV for 5 min; 93.5 mV for 7 min; and 165 mV for 10 min; all at 800 $\mu A/cm^2$ current density (fig. 2a).

The differences between $(\Delta E_{\pm 1\%})_{III}$ (stripped electrode) and $(\Delta E_{\pm 1\%})_{I}$ (anodic pre-polarization) are smaller, but also depend upon the duration of the pre-treatment: 28.6 mV for 5 min; 60 mV for 7 min, and 129 mV for 10 min pre-treatment; all at 800 $\mu A/cm^2$ (fig. 2b).

The results obtained in the *titration of bichromate with ferrous ion* under the conditions shown in table 1, are summarized in table 3. The titration curves are shown in figure 3. It should be emphasized that in this titration, after each addition of the reagent it was necessary to wait 20–30 min before a constant potential was obtained, as previously mentioned by Hendrixson. [28] Otherwise, if the potential was measured immediately after the addition of the reagent, titration curves similar to those described by Forbes and Bartlett [26] were obtained. The comparisons of $\Delta E_{\pm 1\%}$ show that in this titration, the largest potential variation in the vicinity of the equivalence point is obtained when the electrode has been pre-anodized, and the smallest variation when the electrode has been pre-cathodized. The differences between $\Delta E_{\pm 1\%}$ for pre-anodized and pre-cathodized electrodes are summarized in table 4. There, $\Delta_{\pm}$ is the difference between $\Delta E_{\pm 1\%}$ for a pre-anodized and a pre-cathodized electrode, e.g. experiments IV.5 and V.5. Similarly, Δ_{0}^{-} is the difference between $\Delta E_{\pm 1\%}$ values for a pre-cathodized and a stripped electrode, and Δ_{0}^{+} the difference between $\Delta E_{\pm 1\%}$ for a pre-anodized and a stripped electrode. Thus, when the electrode was pre-polarized with a current of 10 mA/cm² density, during 5 min, a difference of 164 mV was observed between the $\Delta E_{\pm 1\%}$ values, obtained with electrodes pre-treated in two different ways.

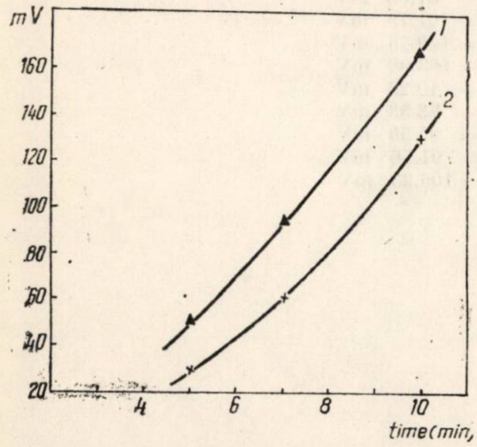

Fig. 2. — Plot of the differences between $\Delta E_{\pm 1\%}$ for differently pretreated electrode *vs.* the duration of pretreatment (at 400 μA):

Curve *1*, $(\Delta E_{\pm 1\%})_{II} - (\Delta E_{\pm 1\%})_{III}$;
Curve *2*, $(\Delta E_{\pm 1\%})_{I} - (\Delta E_{\pm 1\%})_{III}$.

Fig. 3. — Potentiometric titration of $Cr_2O_7^{2-}$ with Fe^{2-}. →

1, with pre-anodized electrode; *2*, with stripped electrode; *3*, with pre-cathodized electrode.

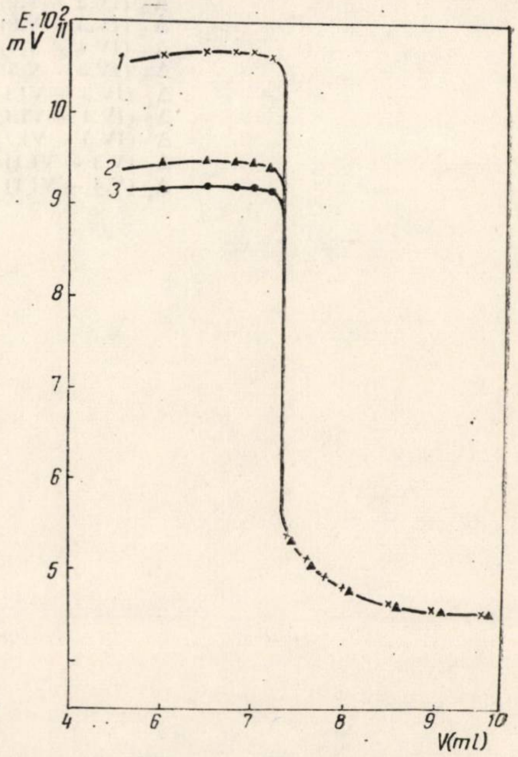

It should be noted, that when introduced into an oxidizing solution (e.g. bichromate) a stripped electrode is oxidized and it behaves like a pre-anodized electrode (at low current densities). A significant difference between a stripped electrode in oxidizing solution and a pre-anodized one, appears when a higher current density is used for pre-anodization (compare Δ_{0}^{+} (IV.5—VI.1) with Δ_{0}^{+} (IV.3—VI.1)).

It follows from the results of this investigation that platinum electrodes pre-treated in different ways, may behave differently in some redox potentiometric titrations. The topic is still investigated in this laboratory.

Table 4

Comparisons of the potential differences ($\Delta E_{\pm 1\%}$) for various pre-treatments of Pt electrodes in the titration of $Cr_2O_7^{2-}$ with Fe^{2+}

$\Delta_{\pm}$ (IV.1 − V.1) = 78.04 mV
$\Delta_{\pm}$ (IV.2 − V.2) = 81.63 mV
$\Delta_{\pm}$ (IV.3 − V.3) = 101.79 mV
$\Delta_{\pm}$ (IV.4 − V.4) = 129.76 mV
$\Delta_{\pm}$ (IV.5 − V.5) = 163.98 mV
Δ_{0}^{+} (IV.3 − VI.1) = 10.23 mV
Δ_{0}^{+} (IV.4 − VI.1) = 23.53 mV
Δ_{0}^{+} (IV.5 − VI.1) = 95.56 mV
Δ_{0}^{-} (V.3 − VI.1) = 91.56 mV
Δ_{0}^{-} (V.4 − VI.1) = 106.23 mV

Revue Roumaine de Chimie, 14, 1047–1052 (1969)

KOMPLEXVERBINDUNGEN DES N,N'-DIAMINOPIPERAZINS. I

METALLCHELATVERBINDUNGEN UND IHR THERMISCHER ABBAU

J. DICK und ALFA LUPEA

Aus dem Pharmazeutisch-technischen Laboratorium der Technischen Hochschule Timişoara,
Bd. 30 Decembrie 2

Eingegangen am 8. November 1968

Gelegentlich eines Studiums über Synthesen von N, N'-Diaminopiperazinderivaten, eine neue Reihe von Substanzen mit vorausgesetzter physiologischer Wirkung, wurde das N,N'-Diaminopiperazin (DAP) auch als Elektronenspender untersucht. Dabei wurde festgestellt, daß DAP als Ligand mit den verschiedensten Elementen und Anionen Komplexverbindungen bildet, die in Mitteilung 1 und 2 beschrieben werden. Je nach Bedingungen, können verschiedene, hauptsächlich aber zwei Komplextypen erhalten werden u.zw. $[Me^{II}\,Dap\,X_2]$ und $[Me^{II-III}X_n]\cdot(H_2Dap)_n$. In vorliegender Mitteilung sollen Darstellung, Analyse, Eigenschaften und der thermische Abbau des ersten Komplextyps beschrieben werden. Über sichtbare, UV- und Infrarotspektren und Elektronenspinrezonanz wird in Mitteilung 3 und 4 berichtet. DAP-Komplexe mit einer Chelatstruktur liefern Co, Ni, Cd, Zn, Fe, Mn, Cu_2 und Pd mit Anionen SCN, Cl und Br. DAP wird als zweizähliger Ligand identifiziert.

In einigen vor kurzem erschienenen Veröffentlichungen [1–5] beschrieben wir Synthesen von N,N'-Diaminopiperazinverbindungen und dessen Salze mit organischen und anorganischen Säuren, die eine neue Stoffreihe darstellen, für die wir verschiedene physiologische Wirkungen voraussetzen, die zum Teil bestätigt werden konnten. [5] In der vorliegenden Arbeit berichten wir über DAP als Komplexbildner. Das Diamin als solches wurde bis jetzt nicht als Elektronenspender untersucht. Lediglich wurde festgestellt, daß seine polymeren Polyethylensemicarbazide mit verschiedenen Metallionen Chelatringe bilden (durch S-Atom koordiniert), die in der Kunstfaserindustrie verwendet werden können. [6]

---

[1] J. Dick, J. Ristici, M. Neacşu und A. Lupea, *Studii şi Cercetări, Şti. Chim., Baza Cercetări Şti., Timişoara,* **10**, 179 (1963).

[2] J. Dick, M. Neacşu und A. Lupea, *Rev. Roumaine Chim.*, **11**, 517 (1966).

[3] J. Dick und A. Lupea, *Die Pharmazie*, **22**, 555 (1967).

[4] J. Dick und A. Lupea, *Die Pharmazie*, **23**, 482 (1968).

[5] J. Dick, A. Lupea, M. Elias und A. Botez, *Die Pharmazie*, **23**, 714 (1968).

[6] T. W. Campbell und E. A. Tomic, *J. Polymer Sci.*, **62**, 379 (1962).

Im Vergleich mit Piperazin als Elektronenspender mußte der weitgehend geringere basiche Charakter des DAP eine Komplexbildung voraussichtlich erleichtern.

Tatsächlich bildet DAP in wäßriger Lg, zwischen pH 1—5 mit zweiwertigen Elementen Komplexverbindungen der allgemeinen Formel

$$[Me^{II}Dap\ X_2]$$

$$\text{wo } Me^{II} = Co,\ Ni,\ Cd,\ Zn,\ Fe,\ Mn,\ Cu_2,\ Pd$$

$$X = SCN,\ Cl,\ Br$$

Unter anderen Bedingungen bilden sich Salze eines komplexen Anions der allgemeinen Formel $[Me^{II-III}X_n]\cdot(H_2Dap)_m$, über die in der Mitteilung 2 berichtet wird.

Die Komplexverbindungen mit Chelatring (siehe auch Mitteilung 3, 4) entstehen in schwach sauren Lösungen am vorteilhaftesten bei pH 4—5. Dabei besteht die Gefahr einer hydrolytischen Spaltung besonders bei den in Wasser leicht löslichen Verbindungen (Fe^{2+}). Zu bemerken ist, daß Cu^{2+} durch Reduktion Cu_2^{2+}-Verbindungen bildet.

Sie kristallisieren ohne oder mit Wasser. Im allgemeinen sind sie leicht löslich in warmem Wasser und verdünnten Säuren, schwer löslich in organischen Lösungsmitteln. Ihre Löslichkeit in H_2O nimmt in der Reihefolge $II < I < III < IV < V < VI < VII < IX$ zu. Farbe und Analyse sind dem experimentellen Teil zu entnehmen.

Analysebefunde führten zunächst zu der Feststellung, daß DAP als zweizähliger Ligand betrachtet werden muß. Weitere Bestimmungen waren in gutem Einklang mit dieser Annahme. Versuche zur Strukturaufklärung (3. und 4. Mitteilung) zeigten einwandfrei, daß DAP in diesen Verbindungen Chelatringe bildet und in Wannenform vorliegt :

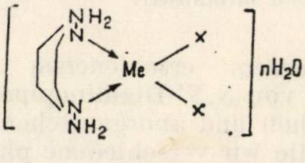

was übrigens auch mit den Anschauungen über die Struktur der Komplexverbindungen des Piperazins gut übereinstimmt. [7,8]

Gleichzeitig weisen wir auf unsere Betrachtungen über die Struktur der von uns hergestellten und anderer bereits bekannter Pyrazolonkomplexe der allgemeinen Formel $[Me^{II}Pyr\ X_2]$ mit Pyramidon als zweizähliger Ligand hin. [9–12]

---

[7] F. G. Mann und H. R. Watson, *J. Chem. Soc.*, **1958**, 2772.

[8] R. D. Gillard, H. M. Irving, *Chem. Rev.*, **65**, 603 (1965).

[9] J. Dick und A. Maurer, *Studii şi Cercetări, Şti. Chim., Baza Cercetări Şti., Timişoara,* **10**, 61 (1963).

[10] J. Dick, R. Bacaloglu und A. Maurer, *Rev. Roumaine Chim.*, **12**, 607 (1967).

[11] J. Dick, R. Bacaloglu und A. Maurer, *Rev. Roumaine Chim.*, **12**, 629 (1967).

[12] J. Dick, R. Bacaloglu und A. Maurer, *Rev. Roumaine Chim.*, **12**, 617 (1967).

EXPERIMENTELLES

Die verschiedene Löslichkeit in Wasser, je nach Element und Anion setzt in den meisten Fällen verschiedene Bedingungen zur Darstellung von I–XI voraus. Umsetzungsbedingungen können daher nicht tabellarisch zusammengefaßt werden.

I. $[CoDap(SCN)_2].2H_2O$ (327,31). Zu einer Mischung von 3 g $Co(NO_3)_2.6H_2O$ und 4,5 g NH_4SCN in 15–20 ml H_2O, die mit verd. HCl auf pH 2 gebracht wird, fügt man kalt und unter ständigem Umrühren 1,6 g DAP in 15 ml H_2O gelöst und notwendigerweise filtriert und bringt das Gemisch auf pH 5. Der entstandene rosa kristallinische Niederschlag wird 2 Std. auf 0° abgekühlt, öfters umgerührt, durch einen Glasfiltertiegel G_4 filtriert, mit eisgekühltem Wasser von pH 5 öfters gewaschen und über $CaCl_2$ im Vakuum getrocknet. Schwer löslich in eisgekühltem, leicht löslich in warmem Wasser und verdünnten Säuren, schwer löslich in organischen Lösungsmitteln. Ausb. 87 % d. Th.

Analyse : *Ber.* : Co, 18,01 ; SCN, 35,49 ; N, 25,68 %
Gef. : Co, 17,77 ; SCN, 35,21 ; N, 25,19 %

II. $[NiDap(SCN)_2].2H_2O$ (327,08). Wird wie I mit 3g $Ni(NO_3)_2.6H_2O$ nach Umsetzung bei einem End-pH von 4 erhalten. Man kühlt eine Stunde gut ab und wäscht mit Wasser von pH 4 aus. Der Niederschlag ist kristallinisch und grün gefärbt. In Wasser schwerer löslich als I. In Anwesenheit von Ni^{2+} und SCN ist der Niederschlag in eisgekühltem Wasser praktisch unlöslich, eine Eigenschaft die zur Bestimmung des technischen Diamins auf indirektem gewichtsanalytischem wie auch maßanalytischem Wege herangezogen werden konnte. Das Verfahren wird gelegentlich veröffentlicht. Ausb. 97 % d. Th.

Analyse : *Ber.* : Ni, 17,95 ; SCN, 35,52 ; N, 25,70 %
Gef. : Ni, 17,69 ; SCN, 35,29 ; N, 25,99 %

III. $[CdDap(SCN)_2]$ (344,75). Wird durch Umsetzen von 3,1 g $3CdSO_4.8H_2O$ und 5,5 g NH_4SCN in 20 ml Wasser auf pH 1,5 gebracht und 2 g DAP in 10 ml H_2O bei einem End-pH 4 erhalten. Der weiße Niederschlag wird wie II gewaschen. Etwas löslicher in kaltem Wasser als I. Ausb. 82 % d. Th.

Analyse : *Ber.* : Cd, 32,61 ; SCN, 33,70 ; N, 24,38 %
Gef. : Cd, 32,92 ; SCN, 33,47 ; N, 24,09 %

IV. $[ZnDap(SCN)_2]$ (297,72). Wird in konzentrierterer Lösung als I–III durch Umsetzung von 2,5 g $ZnSO_4$ und 4,5 g NH_4SCN in 10 ml H_2O, auf pH 2 gebracht mit 3 g DAP in 10 ml Wasser bei End-pH 3 erhalten. Es wird 3 Tage gekühlt und mit eisgekühltem Wasser von pH 3 gewaschen. Der weiße Niederschlag ist ziemlich löslich auch in kaltem Wasser. Ausb. 69 % d. Th.

Analyse : *Ber.* : Zn, 21,96 ; SCN, 39,02 ; N, 28,23 %
Gef. : Zn, 21,95 ; SCN, 39,27 ; N, 27,90 %

V. $[MnDap(SCN)_2].2H_2O$ (323,31). Wird in einer konzentrierten Lösung von 2 g $MnCl_2.4H_2O$ und 3,5 g NH_4SCN in 6–8 ml H_2O auf pH 5 gebracht mit 2,1 g DAP in 8 ml H_2O gelöst bei pH 5 der Endlösung erhalten. Man kühlt 18 Std. und wäscht wie bei I–IV mit eisgekühltem Wasser von pH 5. Ziemlich löslich in kaltem Wasser. Ausb. 49 % d. Th.

Analyse : *Ber.* : Mn, 16,99 ; SCN, 35,93 ; N, 26,00 %
Gef. : Mn, 16,77 ; SCN, 36,25 ; N, 25,73 %

VI. $[FeDap(SCN)_2].2H_2O$ (324,22). Man setzt eine je konzentriertere Lösung von 3 g $FeSO_4.7H_2O$ und 3 g NH_4SCN in höchstens 10 ml H_2O auf pH 3 gebracht mit 1,8 g DAP in 8 ml Wasser gelöst um, bringt auf pH 4,5 und kühlt 3 Tage lang. Der braune Niederschlag erscheint erst nach einer geraumen Zeit nach öfterem Umrühren. Das Waschwasser wird auf pH 5 gebracht. Löslichkeit in Wasser wie bei V, im übrigen wie I—IV. Ausb. 45 % d. Th.

Analyse : *Ber.* : Fe, 17,22 ; SCN, 35,83 ; N, 25,92 %
Gef. : Fe, 17,33 ; SCN, 36,12 ; N, 25,66 %

VII. $[Cu_2DapCl_2] \cdot 2H_2O$ (350,19). Eine Mischung von 2,4 g $CuSO_4 \cdot 5H_2O$ und 6 g NaCl wird in 18—20 ml Wasser durch Erhitzen gelöst, auf pH 2 gebracht und mit 2,5 g DAP in 15 ml H_2O gelöst noch warm versetzt. Man bringt auf pH 1,5. Bei weiterem Erhitzen und kräftigem Umrühren bildet sich ein braun gefärbter, flockiger Niederschlag der Komplexverbindung mit reduziertem Kupfer. Jetzt wird 12 Std. gekühlt, dann filtriert und mit eisgekühltem Wasser von pH 1 ausgewaschen. Hydrolisiert leicht ; Löslichkeit in H_2O wie V—VI, bzw. I—IV.

Analyse : *Ber.* : Cu, 36,29 ; Cl, 20,25 ; N, 16,00 %
Gef. : Cu, 35,98 ; Cl, 20,52 ; N, 15,73 %

VIII. $[Cu_2DapBr_2] \cdot 2H_2O$ (439,11). Wird wie VII, mit 4 g KBr erhalten. Nach Hinzufügen der DAP-Lg wird auf pH 3 gebracht. Es wird ein Waschwasser von pH 2 verwendet. Löslichkeit und Farbe wie VII.

Analyse : *Ber.* : Cu, 28,94 ; Br, 36,40 ; N, 12,76 %
Gef. : Cu, 28,59 ; Br, 36,88 ; N, 12,50 %

IX. $[PdDapCl_2] \cdot 4H_2O$ (365,54). Man fügt zu 1 g $PdCl_2$ 15 ml H_2O, erhitzt und bringt mit verd. HCl tropfenweise in Lösung, fügt 6 g NaCl hinzu und dann noch warm, eine Lösung von 2 g DAP in 10 ml Wasser, bringt auf pH 4, rührt kräftig um und kühlt den lichtgelben kristallinischen Niederschlag bei öfterem Umrühren 24 Std. ab, filtriert und wäscht mit eisgekühltem Wasser von pH 3 wie üblich aus. Ziemlich löslich in kaltem Wasser, leicht in warmem und schwer löslich in organischen Lösungsmitteln.

Analyse : *Ber.* : Pd, 29,11 ; Cl, 19,40 ; N, 15,33 %
Gef. : Pd, 28,79 ; Cl, 19,06 ; N, 15,11 %

X. $[PdDapBr_2] \cdot 2H_2O$ (418,43). Wird wie IX aber mit 4 g KBr erhalten. Entsteht bei pH 3 in warmer Lg. Der rote Niederschlag wird mit eisgekühltem Wasser von pH 2 ausgewaschen. Löslichkeit wie IX.

Analyse : *Ber.* : Pd, 25,43 ; Br, 38,20 ; N, 13,39 %
Gef. : Pd, 25,35 ; Br, 38,57 ; N, 13,08 %

XI. $[PdDap(SCN)_2]$ (338,74). Wird wie IX und X aber mit 6 g NH_4SCN erhalten. Man kühlt 6 Tage lang und wäscht den kristallinischen braunroten Niederschlag mit eisgekühltem Wasser von pH 2. Löslichkeit wie bei IX.

Analyse : *Ber.* : Pd, 31,41 ; SCN, 34,30 ; N, 24,81 %
Gef. : Pd, 31,73 ; SCN, 34,72 ; N, 24,39 %

Ein Teil der Verbindungen wurde zwecks Aufklärung ihrer Zusammensetzung auch einem thermischen Abbau unterworfen. Dabei wurde das Verhalten des Liganden als solches und der Wasserverlust jener Verbindungen verfolgt, die Wassermoleküle enthalten. Die Untersuchungen wurden bei gleichmäßigem Erhitzen von 5°/min zwischen 30—560° durchgeführt.

DAP ist bloß bis 91° beständig, dagegen beginnt die eigentliche Zersetzung der Verbindungen erst über 130°, wobei zunächst der Verlust an Wassergehalt festzustellen ist (127—200°), mit Ausnahme von IX wo der Verlust des ersten Wassermoleküls bei 92—117° stattfindet. Über das Verhalten der Wassermoleküle siehe auch Mitteilung 4. In jedem Fall erscheint ein entsprechendes kurzes Stabilitätsgebiet von 15—30° zwischen 150—220°, das der wasserfreien Verbindung entspricht, dann folgt eine starke Zersetzung, die der Spaltung der $N-NH_2$-Bin-

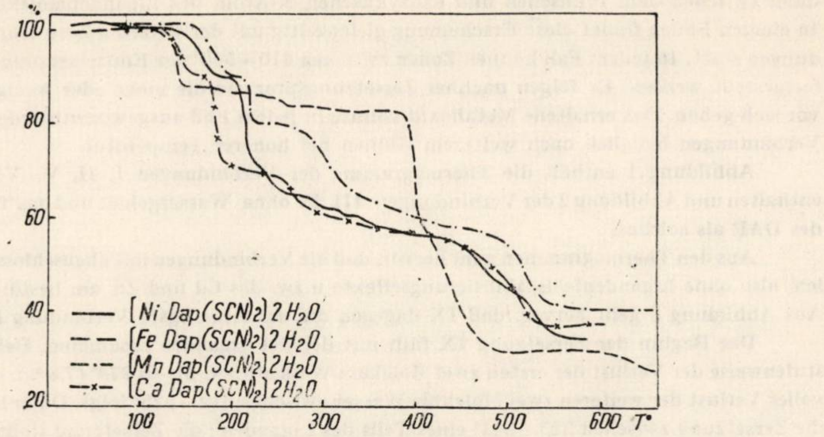

Abb. 1. – Thermogramme der Verbindungen I, II, V, VI.

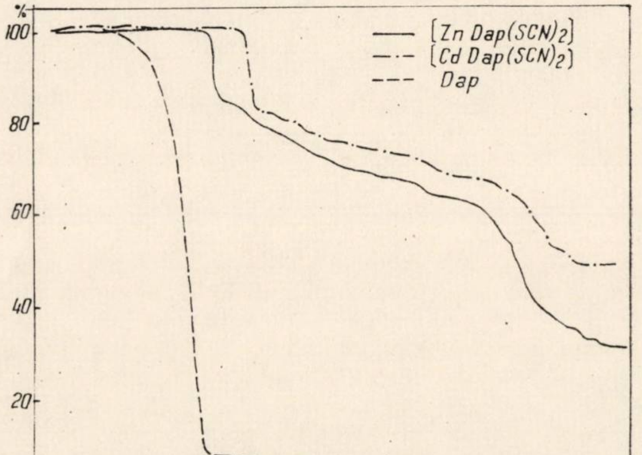

Abb. 2. – Thermogramme der Verbindungen III, IV und des DAP als solches.

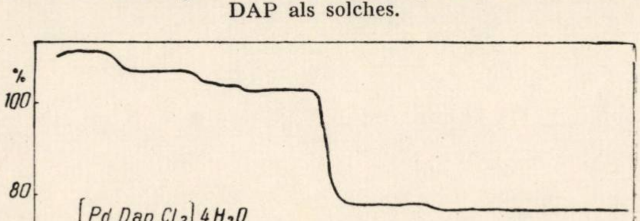

Abb. 3. – Thermischer Abbau von IX.

Revue Roumaine de Chimie, **14**, 1047–1052 (1969)

dung zwischen dem zyklischen und exozyklischen N-Atom des Ligandenmoleküls entspricht. In einigen Fällen findet diese Erscheinung gleichzeitig mit der weiteren Zersetzung der Verbindungen statt. In jedem Fall können Zonen zwischen 410—500° der Endzersetzung des Liganden festgestellt werden. Es folgen nachher Zersetzungsprozesse die mehr oder weniger allmählich vor sich gehen. Das erhaltene Metalloxid konnte in jedem Fall ausgewogen werden, bei einigen Verbindungen lediglich nach weiterem Glühen bei höherer Temperatur.

Abbildung 1 enthält die Thermogramme der Verbindungen I, II, V, VI, die Wasser enthalten und Abbildung 2 der Verbindungen III, IV ohne Wassergehalt und das Thermogramm des DAP als solches.

Aus den Thermogrammen geht hervor, daß die Verbindungen mit abgeschlossenen d-Schalen, also ohne Ligandenfeldstabilisierungseffekte u.zw. des Cd und Zn am beständigsten sind. Aus Abbildung 3 geht hervor, daß IX dagegen die unbeständigste Verbindung ist.

Der Beginn der Zersetzung IX fällt mit der des Liganden zusammen. Bei 91° beginnt stufenweise der Verlust der ersten zwei Moleküle Wasser u.zw. bis zu 278° (7,8 %), der ein kraftvoller Verlust der weiteren zwei Moleküle Wasser zwischen 312—325° folgt. Dann beginnt sofort die Zersetzung zwischen 325—341° eines Teils des Liganden ; die Zersetzung stellt sich hier ein und der Rest ist noch bei 650° beständig.

Revue Roumaine de Chimie, **14**, 1053–1056 (1969)

VOLUMETRIC DOSAGE WITH PHENOTHIAZONE-(3). II[*]

DOSAGE OF THE ASCORBIC ACID WITH PHENOTHIAZONE-(3)

M. RĂILEANU and EUGENIA DOBRE

University of Craiova, Calea Bucureşti 265

Received October 22, 1968

One has worked out a volumetric dosing method of the ascorbic acid at pH 2—2.5 with titrated phenothiazone-(3) n/100 and n/2000 solutions. The new method, being sufficiently precise and handy, allows an operative control of the titre of ascorbic acid solutions used in ascorbinometry.

The quantitative determination of ascorbic acid of natural extracts and synthetic or pharmaceutic products presents a high interest.

Most of the dosing methods of ascorbic acid mentioned until now in literature are based on the oxidation reactions of this compound with iodine, [1,2] mercuric chloride, [3] potassium ferricyanide, [4,5] ferric sulphocyanide, [6] N-brom-succinimide, [7] methylene blue [8−11] or 2,6-dichlorophenol-indophenol. [12]

The special reducing capacity of ascorbic acid has permitted its use as dosing reactive of silver, [13] iron [14] and stannum [15] and the use of titrated solutions of ascorbic acid for the dosing of some anions, cations or organic compounds has led to the working out of the ascorbinometric dosing method. [16−20]

---

[*] Previous part : M. Răileanu and E. Dobre, *Rev. Roumaine Chim.*, (in print).

[1] A. L. Bacharach, P. M. Cook and E. L. Smith, *Biochem. J.*, **28**, 1038 (1934).

[2] G. Carpeni, *Compt. rend.*, **203**, 75 (1936).

[3] L. Rosenthaler, *Z. für Vitaminforschung*, **9**, 342 (1939).

[4] H. Tauber, *Mikrochemie*, **17**, (III) (1935).

[5] H. Tauber and J. Kleiner, *J. Biol. Chem.*, **108**, 563 (1935).

[6] E. M. Pittarelli, *Biochimica e Terapia sperimentale*, **22**, 100 (1935).

[7] M. J. Barakat, M. F. Abd El-Vahab and M. M. El-Sadr, *Analyt. Chem.*, **27**, 536 (1955); *Z. analyt. Chem.*, **152**, 227 (1956).

[8] E. Martini, A. Bonsignore, *Biochem. Z.*, **273**, 170 (1934).

[9] I. Abelin, *Z. analyt. Chem.*, **102**, 70 and 146 (1935).

[10] C. Mentzer and A. Violard-Goudou, *Bull. Soc. Chim. biol.*, **19**, 707 (1937).

[11] Y. Raoul, *Bull. Soc. Chim. biol.*, **29**, 728 (1947).

[12] J. Tillmans, *Z. Lebensm.-Untersuch.*, **54**, 33 (1927).

[13] E. C. Stathis, *Analyt. Chem.*, **3**, 271 (1948).

[14] B. V. Ptitsyn, "Thesis", Leningrad, 1944.

[15] M. Stan Suciu and R. Zelingher, *Anal. Uni. Buc.*, **10**, 39 (1956).

[16] L. Erdey and E. Bodor, *Magyar Kém. Folyóirat*, **8**, 234 (1951).

[17] L. Erdey and E. Bodor, *Z. analyt. Chem.*, **134**, 412 (1952).

[18] L. Erdey and E. Bodor, *Magyar Kém. Folyóirat*, **3**, 78 (1951).

[19] L. Erdey and E. Bodor, *Magyar Kém. Folyóirat*, **8**, 277 (1950).

[20] L. Erdey and E. Bodor, *Analyt. Chem.*, **1952**, 418.

Usually ascorbic acid is dosed with 2,6-dichlorophenol-indophenol according to Tillmans, [12] but this method has undergone numerous modifications. [21–28]

Tillmans' method of dosing ascorbic acid though superior to other known methods, presents nevertheless some shortcomings. It is thus known that the titre of the 2,6-dichlorophenol-indophenol solution is often established in comparison with the titre of an ascorbic acid solution,[24] which is an instable enough substance. One also knows that 2,6-dichlorophenol-indophenol is not a titrimetric substance, and its solutions, disintegrating slightly under the influence of light, need daily control of the titre.

Taking into account the drawbacks of the 2,6-dichlorophenol-indophenol dosing method mentioned above, one has tried in the present paper the dosing of ascorbic acid with titrated phenothiazone-(3) solutions.

In a former work* we have dosed sodium thiosulphate with phenothiazone-(3) and have thus demonstrated that this organic reactive, with a redox character, is a titrimetric substance and its acetic solutions do not change their factor for 90 days.

The reduction of phenothiazone-(3) with ascorbic acid takes place easily at room temperature.

During this reaction, the phenothiazone-(3), red coloured in solution, is reduced to colourless 3-hydroxy-phenothiazone (in very low concentrations), while ascorbic acid is oxidated to dehydroascorbic acid.

In view of dosing the ascorbic acid one has prepared titrated phenothiazone-(3) n/100 and n/2000 solutions by simple weighing of the substance and its quantitative solving with glacially pure acetic acid in a marked flask. The phenothiazone-(3) solves easily in glacial acetic acid at room temperature giving an intensely red coloured solution. One has prepared in the same way fresh solutions of ascorbic acid n/100 and n/2000 in aqueous oxalic acid solutions with a pH $\simeq$ 2.5 (0.5 g of oxalic acid in one l of solution).

The optimum pH[24] of 2—2.5 achieved with oxalic acid provides the stability in the solution of the ascorbic acid. The acidulation of the solution with sulphuric or hydrochloric acid must be avoided, as these acids give unwanted secondary reactions with phenothiazone-(3).

The results of direct dosing of ascorbic acid with n/2000 phenothiazone-(3) are shown in table 1.

In this case the titrated phenothiazone-(3) solution is added to the ascorbic acid solution with a pH = 2.5 and the point of equivalence is marked by a neat passing of the solution to be titrated from colourless

---

[21] J. Tillmans, *Monatsh.*, **13**, 36 (1932).

[22] A. Bessey and C. King. *J. Biol. Chem.*, **103**, 687 (1933).

[23] A. Meunier, *Bull. Soc. Chim. biol.*, **19**, 877 (1937).

[24] A. Emmerie and M. Van Eekelen, *Biochem. J.*, **28**, 1153 (1934); *Z. für Vitaminforschung*, **6**, 150 (1937).

[25] T. P. Čajka, *Gig. i. Sanit.*, **30**, 62 (1965).

[26] R. Fischer and G. Freise, *Deutsch. Apotheker-Z.*, **106**, 1019 (1966).

[27] W. L. Hall and M. J. Deutsch. *J. Assoc. Offic. Agr. Chemists*, **48**, 1236 (1965).

[28] B. L. Nesset, B. L. Windsor, R. R. Humphrey and M. R. Callantine, *Analyt. Biochem.*, **19**, 89 (1967).

to pink-violet. The change in colour of the phenothiazone-(3) solution takes place with great speed, the shaking of the titration flask being unnecessary and unadvisable, except in the neighborhood of the point of equivalence.

Table 1

Direct dosing of ascorbic acid with n/2000 phenothiazone-(3)

No	No of ascorbic acid n/2000 ml taken for titration	No of phenothiazione-(3) n/2000 ml used for titration
1	1	0.99
2	1	1.00
3	1	1.00
4	1	0.99
5	1	1.00
6	1	0.99
7	1	0.99
8	1	1.00
9	1	1.00
10	1	1.00
11	1	1.00
12	1	0.99
13	1	0.99
14	1	1.00
15	1	0.99

Table 1 shows that an equivalent of phenothiazone-(3) uses up in the reaction one equivalent of ascorbic acid, the results of the titration being sufficiently accurate.

It is important to mention that for concentrations of the n/2000 range of the two reactants one obtains satisfactory results only by taking for the titration at the utmost 1 ml solution of ascorbic acid.

As the 3-hydroxy-phenothiazine resulting within the reaction is sufficiently responsive towards atmospheric oxygen, becoming red (by reoxidation) if the dosage requires a longer time, there appear difficulties in the correct appreciation of the point of equivalence.

But if one works with larger volumes of solution and at concentrations in the n/100 range, one can dose the ascorbic acid with phenothiazone-(3) by the indirect method, the phenothiazone-(3) excess being retitrated with sodium thiosulphate. In this case at the point of equivalence, the red colour turns first violet and then green. The turning of the solution from red to green indicates an equivalent consumption of thiosulphate for a phenothiazone-(3) one.

The results of indirect dosing of n/100 ascorbic acid with phenothiazone-(3) are shown in table 2, the titration being carried out in the following way :

to 5 ml of n/100 ascorbic acid solved in oxalic acid with a pH = 2.5 one adds 10 ml of n/100 phenothiazone-(3). One closes the flask and leaves it in the dark for 15 min. Then the content of the titration flask is heated at 80—100° and the phenothiazone-(3) in excess retitrated with n/100 sodium thiosulphate, till the red colour of the solution turns green (near the point of equivalence the turning red-violet-green lasts about a minute and is very easily noticed).

Table 2 shows that the ascorbic acid can be dosed by the indirect method with n/100 phenothiazone-(3) without difficulty and with good results.

This method of dosing is important, being sensitive enough for concentrations of the n/100 range.

Table 2

Indirect dosing of ascorbic acid with n/100 phenothiazone-(3)

No	No of ascorbic acid n/100 ml taken for titration	No of phenothiazone-(3) n/100 ml taken for titration of ascorbic acid	No of n/100 of $Na_2S_2O_3$ used for retitration of the excess of phenothiazone-(3)
1	4.00	10	6.00
2	5.00	10	4.99
3	6.00	10	4.01
4	6.50	10	3.49
5	7.00	10	3.01
6	7.50	10	2.50
7	8.00	10	1.99
8	8.50	10	1.50
9	9.00	10	1.01
10	9.50	10	0.49
11	6.00	15	9.01
12	7.00	15	7.99
13	8.00	15	7.00
14	9.00	15	5.99
15	10.00	15	5.00

Thus a prospect appears for the successful use of phenothiazone-(3) (as a titrimetric substance) for rapid and precise checking of the titre of instable ascorbic acid solutions, increasingly employed in recent times in ascorbinometry.

Revue Roumaine de Chimie, **14**, 1057–1062 (1969)

STEROIDE IN ADSORBIERTEM ZUSTAND. III *

ÜBER SUBSTITUTIONSREAKTIONEN DER TOSYLOXY-GRUPPE DURCH DAS NITRAT-ANION AN AKTIVEM ALUMINIUMOXID

F. HODOŞAN und I. JUDE

Aus dem Chemischen Institut der Akademie, Zweigstelle Cluj, str. Donath, 59–65

Eingegangen am 7. Oktober 1968

Unter der Einwirkung von Aluminiumoxid, das mit wäßriger Lösung von Natriumnitrat behandelt und bei 170° aktiviert wurde, entsteht aus 3α-Tosyloxy-5β-cholansäuremethylester ein Gemisch von 3α- und 3β-Nitrato-5β-cholansäuremethylester, das entsprechende 3 β-Hydroxyderivat sowie eine olefinische Fraktion.

Obwohl eine große Anzahl Daten über die Umwandlungen der Steroide unter dem Einfluß von Adsorbentien bekannt sind, gibt es kaum Arbeiten die ausschließlich dieses Problem behandeln. Der Großteil dieser Umwandlungen ist auf das basische Aluminiumoxid zurückzuführen und besteht in nucleophilen Substitutionen, Eliminierungen, Kondensationen und Umlagerungen. [1]

Wie wir bereits in einer unserer früheren Arbeiten zeigten, [2] sind neue Reaktionen in adsorbiertem Zustand auf Aluminiumoxid möglich, dem verschiedene nucleophile Reagentien zugefügt werden. Vorliegende Arbeit hat die ausführlichere Behandlung der Umwandlungen einiger Tosyloxyderivate, die sich auf mit Natriumnitrat versetztem Aluminiumoxid (Al_2O_3—$NaNO_3$) bildeten, zum Ziele.

Die Untersuchungen wurden mit 3α-Tosyloxy-5β-cholansäuremethylester (I) vorgenommen. Als Reagens diente Aluminiumoxid das vorerst in bestimmten Verhältnissen mit wäßrigem Natriumnitrat behandelt und hernach durch Erwärmen auf 170° reaktiviert wurde. In den hier beschriebenen Versuchen wurde mit Aluminiumoxid, [3] das $3^1/_2$, 7 bzw. 14 % Natriumnitrat enthielt, gearbeitet.

Der in wasserfreiem Benzol gelöste und 12 Stunden bei Raumtemperatur geschüttelte Sulfonsäureester I wurde vollständig in ein Gemisch von mindestens vier Komponenten umgewandelt, die dünnschichtchromatographisch nachgewiesen werden konnten. Die gleichen Komponenten bildeten sich auch innerhalb kürzerer Reaktionszeit, und zwar bei Siede-

---

[*] II Mitteil.: F. Hodoşan und N. Şerban, *Rev. Roumaine Chim.*, **14**, 399 (1969).

[1] Die Verfasser vorliegender Mitteilung haben einen Artikel in Vorbereitung, der eine Gesamtübersicht über die Umwandlungen der Steroide unter dem Einfluß des Aluminiumoxids zum Thema hat.

[2] F. Hodoşan, I. Jude und N. Şerban, *Bull. Soc. Chim. France*, **1964**, 2691.

[3] Es wurde mit neutralem Aluminiumoxid Merck gearbeitet.

temperatur des Benzols. Das Rohprodukt konnte mit Hilfe der Säulenchromatographie in folgende Fraktionen aufgetrennt werden:

— eine olefinische Fraktion, die nach dem Aufarbeiten ein Produkt mit den für Δ^3-Cholensäuremethylester (II) charakteristischen physikalischen Konstanten lieferte;

— zwei Salpetersäureester, die durch Reduktion mit Zink und Eisessig 3α-Hydroxy- bzw. 3β-Hydroxy-5β-cholansäuremethylester ergaben; für diese Ester konnten demnach die Formeln III bzw. IV angenommen werden;

— eine Hydroxyverbindung, deren physikalische Konstanten mit denen des 3β-Hydroxy-5β-cholansäuremethylesters (V) annähernd übereinstimmten.

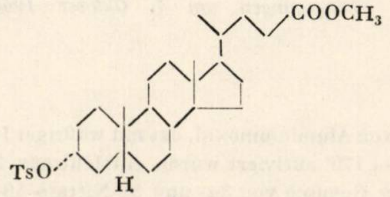

I

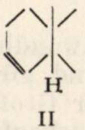

II

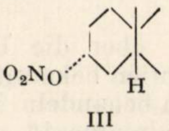

III

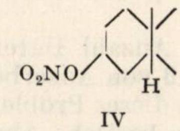

IV

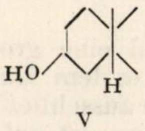

V

Die Ausbeuten der unter verschiedenen Bedingungen erhaltenen Reaktionsprodukte, die sämtlich chromatographisch isoliert wurden, sind in Tabelle 1 angegeben. Aus diesen Daten ist ersichtlich, daß während sich mit dem Anstieg der Reaktionstemperatur das Mengenverhältnis der jeweils gebildeten Produkte zusehends ändert, der Übergang von Al_2O_3-7% $NaNO_3$ zu Al_2O_3-14% $NaNO_3$ hingegen keinen wesentlichen Einfluß ausübt.

Tabelle 1

Ausbeuten der chromatographisch isolierten Reaktionsprodukte

Reaktionsbedingungen	Olefinische Fraktion %	3α-Nitrato-5β-cholansäuremethylester (III) %	3β-Nitrato-5β-cholansäuremethylester (IV) %
Al_2O_3 — 7% $NaNO_3$ bei Raumtemp.	23	3	32
bei Siedetemp.	47	18	3,5
Al_2O_3 — 14% $NaNO_3$ bei Raumtemp.	30	3	33

Zwecks genauerer Mengenbestimmung der gebildeten Salpetersäureester wurde eine polarographische Dosierungsmethode angewendet.[4] Als Ausgangspunkt dienten die von Kaufman und Mitarb.[5] bei der Untersuchung von Salpetersäureester kleiner Moleküle erzielten Ergebnisse. Vorversuche in verschiedenen Lösungsmitteln und bei pH-Werten die zwischen 3,7 und 5,5 lagen, zeigten, daß die polarographische Bestimmung der Ester III und IV in mit Acetatpuffer enthaltenden Acetonlösungen von einem pH-Wert gleich 5,4 zufriedenstellend verläuft. Unter solchen Bedingungen weisen die Verbindungen III und IV jeweils eine einzige Reduktionsstufe auf, mit $E_{1/2} = -1{,}15$ V (für 3α-ONO_2) bzw. $E_{1/2} = -1{,}00$ V (für 3β-ONO_2). Da für gleiche Mengen der Verbindungen III und IV die Stufenhöhe dieselbe ist und auch die $E_{1/2}$-Werte annähernd die gleichen sind, gestattete die polarographische Methode bloß eine Gesamtdosierung beider Epimere III und IV, nicht jedoch eine solche für jeden einzelnen. Die Ergebnisse der polarographischen Bestimmungen sind aus Tabelle 2 ersichtlich.

---

[4] Die polarographischen Messungen wurden von E. DUCA unter der Leitung von Prof. A. DUCA durchgeführt, denen wir auch auf diesem Wege unseren verbindlichen Dank aussprechen.

[5] F. KAUFMAN, H. J. COOK und S. M. DAVIS, *J. Amer. Chem. Soc.*, **74**, 4997 (1952).

Tabelle 2

Polarographisch bestimmte Ausbeuten des Gemisches (III+IV)

Reagens	Gemisch (III+IV) %
Al_2O_3 – 3,5 % $NaNO_3$	33
Al_2O_3 – 7 % $NaNO_3$	38
Al_2O_3 – 14 % $NaNO_3$	38

Weiterhin gelang es uns zu zeigen, daß die beobachteten Umwandlungen nur dann stattfinden, wenn sich das nucleophile Reagens auf einem aktiven Träger aufgelegt befindet. Wird z.B., für die Darstellung des Reagens ein durch Erwärmen auf 1300° inaktiviertes Aluminiumoxid verwendet, so kann am Sulfonsäureester I bei Raumtemperatur keinerlei Veränderung beobachtet werden ; erst nach 15stündigem Kochen konnten kleine Mengen der Reaktionsprodukte nachgewiesen werden. Ebenfalls zu bemerken wäre die Tatsache, daß mit Natriumnitrat allein, auch in sehr feinkörnigem Zustand, die Substanz I unverändert zurückerhalten wird.

Um festzustellen, ob das Epimerpaar III und IV nicht vielleicht durch Epimerisierung einer einzigen anfangs gebildeten Substanz entsteht, ließen wir auf diese beiden Verbindungen Al_2O_3-7 % $NaNO_3$ einwirken. Wir konnten beobachten, daß bei Raumtemperatur, sogar nach 10stündiger Reaktionszeit, beide Epimere unverändert zurückerhalten werden. Bei Siedetemperatur des Benzols hingegen, geht Nitroester IV (3β-ONO_2 axial) im Verlaufe von 3 Stunden beinahe vollständig in ein Olefin über,[6] zum Unterschied von Nitroester III (3α-ONO_2 äquatorial) der sich unter den gegebenen Bedingungen kaum ändert. Es wurden keine Epimerisierungsreaktionen beobachtet (Abb. 1).

---

[6] Im Einklang mit Bellucci's Befunden (G. Bellucci, F. Macchia und V. Malaguzzi, *Tetrahedron Letters*, **1966**, 4973) handelt es sich hier höchstwahrscheinlich um ein Gemisch von den zwei möglichen isomeren Olefinen Δ^2 und Δ^3. Dieselbe Bemerkung könnte auch für die Eliminierung der Tosyloxygruppe in der Verbindung I an der Aluminiumoxidoberfläche gültig sein.

Betreff der Reaktionsmechanismen können wir in erster Reihe bemerken, daß die Bildung der 3α-Nitrato-Verbindung III für eine „S_N1"-Reaktion spricht,[7] in der sich die gebildeten Ionen genügend voneinander entfernen, um den Angriff des Reagens ohne Konfigurationsänderung zu ermöglichen. Das als Zwischenstufe vorhandene Carboniumion stabilisiert sich voraussichtlich durch Wechselwirkung mit dem Adsorptionsmittel.

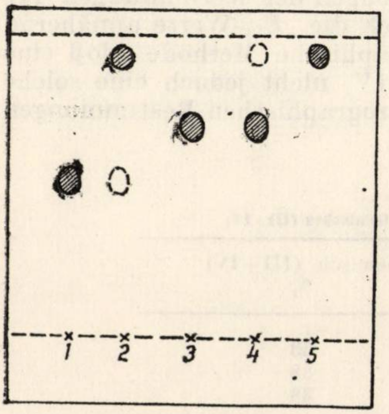

Abb. 1. — Dünnschicht-Chromatogramm.

1 – 3β-Nitrato-5β-cholansäuremethylester (IV); *2* – Mit Al_2O_3–7% $NaNO_3$ in siedendem Benzol behandelte Verb. IV; *3* – 3α-Nitrato-5β-cholansäuremethylester (III); *4* – Mit Al_2O_3 – 7% $NaNO_3$ in siedendem Benzol behandelte Verb. III; *5* – Δ^3– 5β-Cholensäuremethylester (II); *Adsorbens*: Kieselgel G; *Laufmittel*: Cyclohexan–Äther 20 : 1; *Anfärbung*: Phosphormolybdänsäure.

Die Tatsache jedoch, daß eine Substitution ohne Umkehr auch als Ergebnis zweier aufeinanderfolgender Inversionen angesehen werden

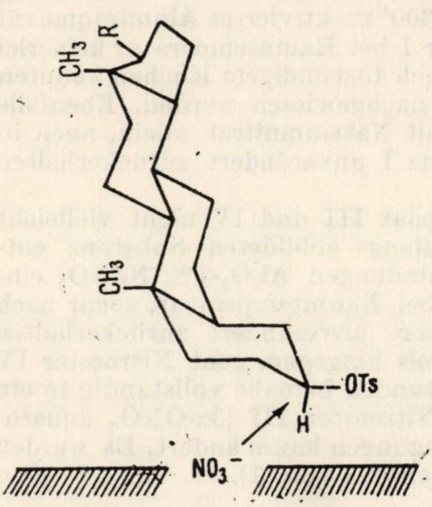

Abb. 2. — Verlauf der Substitution an der Aluminiumoxidoberfläche.

---

[7] Ch. Tamm und Mitarb.[9] behaupten: „in heterogenem System, wie z.B. an Aluminiumoxidoberflächen, verlieren die Ausdrücke S_N1, S_N2 usw. ihre aus homogenem System stammende kinetische Bedeutung; sie bleiben jedoch nützlich, um zwischen verschiedenen Reaktionstypen zu differenzieren; daher benutzen wir die Ausdrücke in Anführungszeichen („S_N1" usw.)." Weiterhin heißt es in derselben Arbeit[9]: „es ist überhaupt fraglich, ob die klassische Unterscheidung der Reaktionstypen auf die betrachteten Reaktionen an Aluminiumoxidoberflächen noch anwendbar sei."

kann, darf nicht außer acht gelassen werden. Folgende Argumente berechtigen dazu, diese Erklärung als nicht zutreffend zu betrachten: Obwohl verhältnismäßig viel mit verschiedenen Tosylderivaten gearbeitet wurde, konnte bislang kein einziger durch Aluminiumoxid hervorgerufener Epimerisierungsfall beobachtet werden. Wenn, ungeachtet dessen, doch eine Epimerisierung stattfinden sollte, müßte sich das so gebildete 3β-Tosyloxy-5β-steroid unter dem Einfluß des Aluminiumoxids nahezu quantitativ in Olefin umwandeln, wie dieses aus den Untersuchungen von Chang und Blickenstaff[8] hervorgeht. Um demnach eine solche Ausbeute an 3α-Nitrato-Verbindung III, die der unseren entspräche, zu erhalten, müßte sich beinahe die ganze Menge des vorhandenen Sulfonsäureesters I zuerst epimerisieren, was jedoch der bemerkenswerten Menge der 3β-Nitrato-Verbindung IV entgegenspricht.

Die Tatsache, daß das 3β-Nitrato-5β-cholansäuremethylester (IV) durch Konfigurationsänderung aus anfänglichem Tosylat I entsteht, steht im Einklang mit einem „S_N2"-Mechanismus.[7] Es ist wahrscheinlich, daß während der Reaktion die Substanz I mit dem Träger, der das nucleophile Reagens enthält in Kontakt kommt, wie dieses aus Abb. 2 ersichtlich ist. Hier ist jedoch zu bemerken, daß ein „S_N1"-Reaktionsmechanismus mit fixierten Ionenpaaren ebenso gut in Betracht gezogen werden kann, so wie dieses Tamm[9] in analogen Fällen annahm.

EXPERIMENTELLES

Darstellung des Reagens

Das neutrale Al_2O_3 (Aktivität II) wird mit wäßrigen Lösungen von $NaNO_3$ behandelt. so daß der im Verhältnis zu Al_2O_3 berechnete Prozentsatz des $NaNO_3$ 3 1/2, 7 bzw. 14% seie Die für die Auflösung des $NaNO_3$ verbrauchten Wassermengen werden so berechnet, daß sie jeweils eine 20%ige Feuchtigkeit des Reagens sichern. Hernach wird durch 12stündiges Erwärmen auf 170° aktiviert und in gut schließendem Gefäß aufbewahrt. Vor Gebrauch wird nochmals 5 Std. auf 170° erwärmt.

Allgemeines Arbeitsverfahren

Ein Teil der Substanz I wird in 50 Teilen wasserfreiem Benzol gelöst und nach Zugab von 20 Teilen $Al_2O_3-NaNO_3$ 3 Std. gekocht oder 12 Std. bei Raumtemperatur geschüttelt Der Reaktionsverlauf wird dünnschichtchromatographisch verfolgt. Nach Beendigung der Reaktion wird abfiltriert und das Reagens ($Al_2O_3-NaNO_3$) mit ca. 600 Teilen Methanol ausgewaschen. Das Filtrat wird im Vakuum eingedampft und der Rückstand mit 400 Teilen wasserfreiem Benzol aufgenommen. Nach erneutem Filtrieren wird wieder im Vakuum eingedampft. Hernach wird auf einer mit Petroläther — Benzol (20 : 1) vorbereiteten Al_2O_3—Säule (Aktivität II) chromatographiert.

---

[8] F. C. Chang und R. T. Blickenstaff, *Chem. Ind.*, **1958**, 590.
[9] H. Dahn, R. Manasse und Ch. Tamm, *Helv. Chim. Acta*, **42**, 2189 (1959).

3α-Nitrato-5β-cholansäuremethylester (III), Schmp. 113–114° (aus Methanol), $[\alpha]_D^{23} = +39{,}4°$ (in Chloroform).

IR-Spektrum : 860, 1277, 1632 cm^{-1} (CCl_4)

$C_{25}H_{41}NO_5$ (435,3) *Ber.* : N, 3,21 ; *Gef.* : N, 3,39

Durch Behandeln mit Zn und Eisessig bei Raumtemperatur geht III in 3 α-Hydroxy-5β-cholansäuremethylester vom Schmp. 125–127° über.

3β-Nitrato-5β-cholansäuremethylester (IV), Schmp. 113–115° (aus Methanol), $[\alpha]_D^{23} = +37°$ (in Chloroform).

IR-Spektrum : 861, 877, 1276, 1632 cm^{-1} (CCl_4)

$C_{25}H_{41}NO_5$ (435,3) *Ber.* : N, 3,21 ; *Gef.* : N, 3,35

Durch Behandeln mit Zn und Eisessig geht IV in 3β-Hydroxy-5β-cholansäuremethylester vom Schmp. 113–115° über.

Revue Roumaine de Chimie, **14**, 1063–1067 (1969)

METHYLENE BASES OF HETEROCYCLES. VIII[1]

2-ACYLMETHYLENE-BENZAZOLINES FROM KETOESTERS

GH. CIURDARU and VIORICA I. DÉNES
Institute of Chemistry of the Academy,
Cluj, str. Donath 59–65

Received October 17, 1968

A preparation method of 2-acylmethylene-benzazolines starting with *o*-substituted anilines and β-ketoesters is described.

In a series of previous papers[1–4] we described the thermal rearrangement of certain O-, S- and Se-esters leading to 2-acylmethylene-azolines used as intermediates in the photographic industry.

Despite its rather large scope the described rearrangement does not permit the preparation of 2-acylmethylene compounds with aliphatic acyl radicals. Some of these compounds were prepared from the quaternary salts of 2-methylbenzothiazole and 2-methyl-benzoselenazole, respectively, and acid chlorides.[5–8] Condensation of 1,3-diketones with the quaternary salts[9,10] of 2-methylmercaptobenzothiazole and subsequent partial hydrolysis of the formed diacyl derivatives led to substances of the same type.

It is noteworthy that the methods described in the literature dealt with the preparation of the 2-acylmethylenebenzothia- and selenazolines only.

We regarded as a general method of preparation leading to 2-acylmethylene-benzazolines III the condensation of *o*-substituted anilines I with β-ketoesters II under conditions enabling the preferential reaction of the ester group (scheme 1).

---

[1] Part VII: V. I. Dénes, Gh. Ciurdaru and M. Fărcăşan, *Rev. Roumaine Chim.*, **10**, 1045 (1965).

[2] V. I. Dénes, Gh. Ciurdaru and M. Fărcăşan, *Chem. Ber.*, *96*, 2691 (1963).

[3] V. I. Dénes, Gh. Ciurdaru and M. Fărcăşan, *Rev. Roumaine Chim.*, **9**, 375 (1964).

[4] V. Dénes, Gh. Ciurdaru and M. Fărcăşan, *Rev. Roumaine Chim.*, **9**, 867 (1964).

[5] Kodak, E. P. 466, 269 (1935/36); *Chem. Zentr.*, 1937, II, 4393.

[6] L. G. S. Brooker and F. L. White, U. S. 2, 112, 139 (1938); *Chem. Abstr.*, *32*, 3713 (1938).

[7] Kodak A. G. Ger. 670, 505 (1939); *Chem. Abstr.*, **33**, 6613 (1939).

[8] L. G. S. Brooker and G. H. Keyes, U. S. 2, 441, 529 (1948); *Chem. Abstr.*, **42**, 5363 (1948).

[9] J. D. Kendall, H. W. Wood and J. R. Majer, U. S. 2, 438, 704 (1948); *Chem. Abstr.*, **42**, 7057 (1948).

[10] L. G. S. Brooker and F. L. White, U. S. 2, 341, 357 (1944); *Chem. Abstr.*, **38**, 4453 (1944).

There exist in the literature data concerning the condensations of some *o*-substituted anilines with β-ketoesters. Thus, Sexton[11] starting with *o*-phenylenediamine and ethyl acetoacetate in boiling xylene ob-

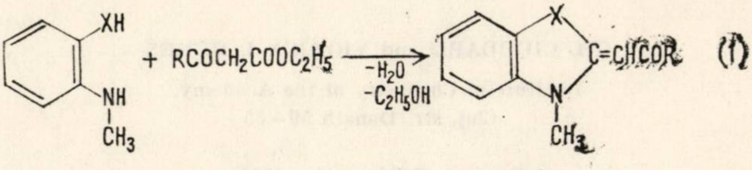

I II III

X = O, S, NCH$_3$
R = CH$_3$, C$_6$H$_5$

tained 2-acetonyl-benzimidazole (yield : 12%) and the cyclic isomer* (yield : 71%). Under similar conditions and using ethyl benzoylacetate, Stepanov and Davydova[12] obtained ω-benzoyl-2-methyl-benzimidazole (yield: 80%) only. The abovementioned authors starting with 2-aminothiophenol and ethyl acetoacetate in boiling xylene prepared 2-acetonylbenzothiazole (yield : 46%). The same starting substances were transformed by A. I. Kiprianov and V. A. Portyagina on heating without solvent on steam bath into 2-methyl-2-carbethoximethyl-benzothiazoline. Under similar conditions, they obtained the corresponding N-methyl derivative starting with 2-methylaminothiophenol.[13]

The comparison of these data led us to the assumption that the condensation involving the ester group should be favoured by the more severe reaction conditions. In order to prove this supposition, we carried out the condensation of 2-methylaminothiophenol (I, X = S) with ethyl acetoacetate (II, R = CH$_3$) under two different conditions (scheme 2). Under milder conditions i.e. on heating without solvent on a steam bath, we obtained 2,3-dimethyl-2-carbethoxymethylbenzothiazoline (IV) already mentioned.[13] At higher temperature (150°) the main reaction product was N-methyl-2-acetylmethylenebenzothiazoline. (III, X=S, R=CH$_3$). The same compound III was formed with similar yield on boiling the starting substances in xylene. It follows, therefore, that under more severe conditions the condensation actually proceeds in the desired direction.

[11] W. A. Sexton, *J. Chem. Soc.*, **1942**, 303.

[12] F. N. Stepanov and S. A. Davydova, *J. Gen. Chem.*, **28**, 391 (1958).

[13] A. I. Kiprianov and W. A. Portyagina, *J. Gen. Chem.*, **25**, 2257 (1955).

---

*

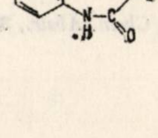

Consequently, rising the reaction temperature to 140—200° we prepared the benzoyl derivative III ($X = S$, $R = C_6H_5$), as well as 1,3-dimethyl-2-acetyl-methylenebenzimidazoline (III, $X = NCH_3$, $R = CH_3$) and 1,3-dimethyl-2-benzoyl-methylenebenzimidazoline (III, $X = NCH_3$, $R=C_6H_5$), both not yet described in the literature.

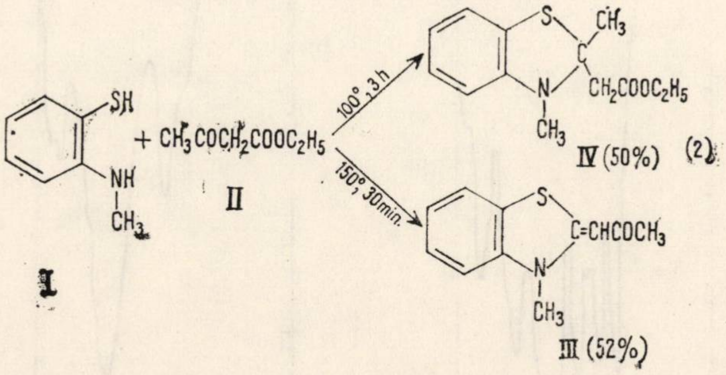

On the other hand, 2-methylaminophenol (I, $X = O$) could be condensed only with ethyl benzoylacetate (II, $R= C_6H_5$) giving N-methyl-2-benzoyl-methylenebenzoxazoline (III, $X = O$, $R=C_6H_5$) in a low yield.

The structure of the obtained acylmethylenebenzazolines was proved by IR spectrometry, as follows. The spectra of acetyl- and benzoylmethylenebenzothiazoline were compared with those of authentic samples [2]. The spectra of N-methyl-2-benzoylmethylenebezoxazoline (fig. 1, A) were similar to those of the corresponding 4-nitrobenzoylmethylene derivative[4] (fig. 1, B).

In the spectra of 2-acetyl-methylenebenzimidazoline (III, $X = NCH_3$, $R=CH_3$), in the 1800—1650 cm^{-1} range there is no absorption (fig. 2, A); the $\nu C=0$ band is shifted toward lower frequencies which points, as in the other studied cases,[1-4] to the considerable contribution of the mesomeric structure b (scheme 3). The conversion of 1,3-dimethyl-2-acetyl-methylenebenzimidazoline into its perchlorate entails the appearence of the $\nu C=0$ band at 1730 cm^{-1} (fig. 2, B).

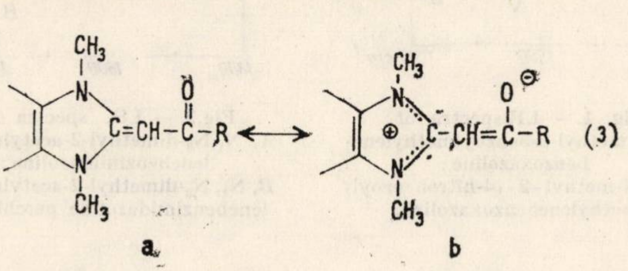

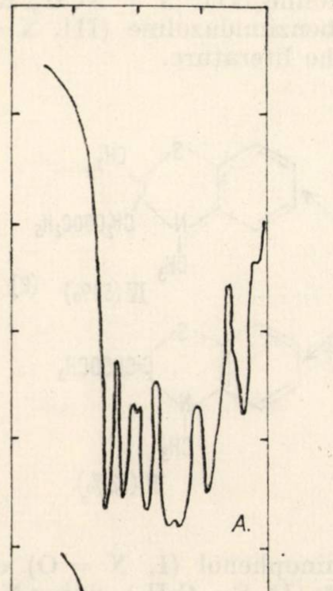

Fig. 1. — I.R.spectra of :
A, N-methyl-2-benzoylmethylenebenzoxazoline ;
B, N-methyl-2-(4-nitrobenzoyl)methylenebenzoxazoline.

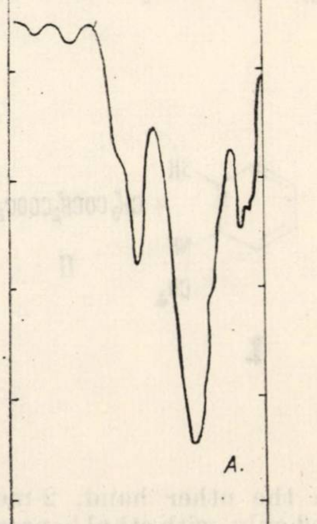

Fig.2. — I.R. spectra of :
A, N_1,N_3-dimethyl-2-acetylmethylenebenzimidazoline ;
B, N_1, N_3-dimethyl-2-acetylmethylenebenzimidazoline perchlorate.

EXPERIMENTAL

N-Methyl-2-benzoylmethylene-benzoxazoline (III, X = 0, R = C_6H_5).*o*-Methylaminophenol (1.23 g) and ethyl bezoylacetate (1.7 g) were heated at 190–200° for 30 minutes. After cooling, the crude reaction product was macerated with diethyl ether and filtered. The substance obtained (0.38 g) was then recrystallized from aqueous ethanol. M.p. 231°.

$C_{16}H_{13}NO_2$ (251.3) *Calcd.* : C, 76.47 ; H, 5.21 ; N, 5.57 ;
Found : 76.03 ; 5.40 ; 5.49.

N-Methyl-2-acetylmethylene-benzothiazoline (III, X = S, R = CH_3).

a) *o*-Methylaminothiophenol (1.4 g) and ethyl acetylacetate (1.3 g) were heated at 150° for 30 minutes. After cooling, the crude reaction product was macerated with petrol ether and filtered. Yield : 1.07 g. M.p. 159–160° (from aqueous ethanol).

b) *o*-Methylaminothiophenol (1.4 g) and ethyl acetoacetate (1.3 g) were refluxed for 1 hour in 25 ml of xylene. After cooling the reaction product was precipitated by addition of petrol ether. Yield: 1.15 g. M.p. 159–160° ; no depression when mixed with an authentic sample.

N-Methyl-2-benzoylmethylene-benzothiazoline (III, X = S, R = C_6H_5).

o-Methylaminophenol (0.28 g) and ethyl benzoyl-acetate (0.38 g) were heated at 170–180° for 30 minutes. Maceration of the cooled reaction product with petrol ether and filtration gave 0.29 g of III. M.p. 179.5°–180° (from aqueous ethanol).

$C_{16}H_{13}NOS$ (267.3) *Calcd.* : N, 5.24 ;
Found : 5.23.

N_1,N_3-Dimethyl-2-acetylmethylene-benzimidazoline (III, X = NCH_3, R = CH_3) N, N′-Dimethyl-*o*-phenylenediamine (2.7 g) and ethyl acetoacetate (2.6 g) were heated at 140–145° for 1 hour. The crude reaction product was then chilled and kept several hours at –5° until complete solidification occurred. Maceration with petrol ether and recrystallization from benzene gave long needles melting at 135°. Yield : 3.14 g.

$C_{12}H_{14}N_2O$ (202.2) *Calcd.* : C, 71.27 ; H, 6.98 ; N, 13.85 ;
Found : 71.98 ; 7.00 ; 13.89.

Perchlorate, colourless plates. M.p. 213–214° (from dry ethanol-dry ether)

$C_{12}H_{15}ClN_2O_5$ (316.7) *Calcd.* : N, 8.84 ;
Found: 8.79.

N_1,N_3-Dimethyl-2-benzoylmethylene-benzimidazoline (III, X = NCH_3, R = C_6H_5)

N, N′-Dimethyl-*o*-phenylenediamine (1.4 g) and ethyl benzoylacetate (1.9 g) were heated at 160–165° for 30 minutes. The oily product crystallized by cooling and was macerated with petrol ether. Yield : 2.64 g.M.p. 158–9° (from ethanol).

$C_{17}H_{16}N_2O$ (264.3) *Calcd.* : C, 77.25 ; H, 6.10 ; N, 10.60 ;
Found: 76.84 ; 6.44 ; 10.52.

Iodohydrate, colourless crystals m.p. 280–1° (from ethanol).

$C_{17}H_{17}IN_2O$ (392.2) *Calcd.* : N, 7.14 ;
Found : 6.73.

1883

La REVUE ROUMAINE DE CHIMIE **paraît 12 fois par an. Le prix d'un abonnement annuel est de £ 5,— ; $ 12,— ; FF 60,— , DM 48,—. Toute commande de l'étranger (fascicules ou abonnements) sera adressée à CARTIMEX, Boîte postale 134—135, Bucarest, Roumanie, ou à ses représentants à l'étranger :**

R. P. d'ALBANIE, **Ndermarja Shtetnore e Botimeve,** Tirana ; R. D. ALLEMANDE, **Deutscher Buch-Export und -Import,** Leipzig, 701, Leninstrasse 16 ; R. P. de BULGARIE, **Hemus,** Place Slaweikov, 11, Sofia ; R. P. de CHINE, **Waiwen Shudian,** P.O.B. 88, Peking ; R.P.D. COREENNE, **Chulphanmul,** Phenian ; REPUBLIQUE CUBA, **Cubartimpex,** Simón Bolivar 1, Palacio Aldamo, Habana ; R. P. de HONGRIE, **Kultúra,** P.O.B. 149, Budapest 62 ; R. P. MONGOLE, **Mongolgosknigotorg,** Ulan Bator ; R. P. POLOGNE **Ruch,** Ul. Wronia, 23, Warszawa ; R. S. TCHECOSLOVAQUE, **Artia,** Ve Smeckach 30, Praha II ; U.R.S.S., **Mejdunarodnaïa Kniga,** Moskva G-200 ; R. D. VIETNAM, **So Xuat Nhap Khau Sach Bao,** 32 Hai Ba Trung, Hanoï ; R.S.F. YOUGOSLAVIE, **Jugoslovenska Knjiga,** Terazije 27, Beograd ; **Prosveta** 16/1, Terazije, Beograd ; **Forum,** Voïvode Misica, Novi Sad ; ARGENTINE, **Editorial Sudaminter S.A.,** Alsina 500, Buenos Aires ; AUSTRALIE, **Current Books Ltd.,** Distributors 168—174, Day Street, Sydney ; AUTRICHE, **Globus Zeitungs-, Drucks- und Verlagsanstalt GmbH,** 1200 Wien, Höchstädplatz 3 ; BELGIQUE, **Du Monde Entier,** 5, Place St.-Jean, Bruxelles, Agence Messageries de la Presse 14—22, Rue du Persil, Bruxelles ; CANADA, **Progress Books,** 44 Stafford St., Toronto, Ontario, W. M. Dawson Subscriptions Service Ltd., Six Thorneliffe Park Drive, Toronto 17, Ontario ; COLOMBIE, **Libreria Buchholz Galeria,** av. Jiménez de Quesada 8—40, Bogotá ; DANEMARK, **Ejnar Munksgaard,** Noregade 6, Kobenhavn ; ESPAGNE, **Libreria Herder,** Calle de Balmés 26, Barcelona 7; ÉTATS-UNIS, **Fam Book Service,** 69, Fifth Avenue, Suite 8, F., New York, 10003 N. Y. ; **Continental Publications,** 111, South Mermanee Ave., St.-Louis, Missouri 63105, **Turner Subscription Agency** 235, Park Avenue South, New York 3, N. Y. ; FINLANDE, **Akateeminen Kirjakauppa,** P.O.B. 10128, Helsingfors, 10 ; FRANCE, **Nouvelles Messageries de la Presse Parisienne,** 111, Rue Réaumur, Paris II, **Europériodiques S. A.,** 72, Boul. Senard, 22 Saint-Cloud ; GRANDE-BRETAGNE, **Collet's Holdings Ltd.,** Dennington Estate, Wellingborough, Northants, **Central Books Ltd.,** 37, Inn Road, London W. C. 1 ; ISRAEL, **Lepac Ltd.,** P.O.B., 1136 Tel-Aviv, **Haiflepac Ltd.,** P.O.B. 1794, Haïfa ; ITALIE, **So. Co. Lib. Ri.,** Piazza Margana 33, Roma ; **Messagerie Italiane Sp. A.,** Milano, Via Priv. Renzo e Lucia 7 ; JAPON, **Nauka Ltd.,** 30—19 Minami — Ikebukuro 2 ohome Toshima Ku, Tokyo ; PAYS-BAS, **N. V. Martinus Nijhoff,** P.O.B. 269, Den Haag ; **Swets & Zeitlinger,** Keizersgracht 471—487, Amsterdam C. ; NORVEGE, **Tryggve Juul Moller-Boekhandel Øvre,** Slottsgate 15, Oslo 1 ; R. F. ALLEMANDE, **Kubon & Sagner,** P.O.B. 68, München 34, **Presse Vertriebsgesellschaft GmbH,** 6, Frankfurt/Main, Börsenstrasse 13—15 ; **Kunst und Wissen,** Erich Biber, P.O.B. 46, 7 000 Stuttgart 1 ; SUISSE, **Pinkus & Cie,** Froschaugasse 7, Zürich, **Fachbücherei Berne,** P.O.B. 397, 3001 Berne.

En Roumanie, vous pourrez vous abonner par les bureaux de poste, chez votre facteur ou directement par les services de presse des entreprises et institutions.

NOUS VOUS PRIONS DE RENOUVELER VOTRE ABONNEMENT POUR L'ANNÉE
1970

La REVUE ROUMAINE DE CHIMIE paraît **12 fois par an. Le prix d'un abonnement annuel est de** £ 5,— ; $ 12,— ; FF 60,— ; DM 48,— . Toute commande de l'étranger **(fascicules ou abonnements) sera adressée à CARTIMEX, Boîte postale 134—135, Bucarest, Roumanie, ou à ses représentants à l'étranger :**

R. P. d'ALBANIE, **Ndermarja Shtetnore e Botimeve**, Tirana ; R. D. ALLEMANDE, **Deutscher Buch-Export und -Import**, Leipzig, 701, Leninstrasse 16 ; R. P. de BULGARIE, **Hemus**, Place Slaweikov, 11, Sofia ; R. P. de CHINE, **Waiwen Shudian**, P.O.B. 88, Peking ; R.P.D. COREENNE, **Chulphanmul**, Phenian ; REPUBLIQUE CUBA, **Cubartimpex**, Simón Bolivar 1, Palacio Aldama, Habana ; R. P. de HONGRIE, **Kultúra**, P.O.B. 149, Budapest 62 ; R. P. MONGOLIE, **Mongolgoskniatorg**, Ulan Bator ; R. P. POLOGNE **Ruch**, Ul. Wronia, 23, Warszawa ; R. S. TCHECOSLOVAQUE, **Artia**, Ve Smeckach 30, Praha II ; U.R.S.S., **Mejdunarodnaia Kniga**, Moskva G-200 ; R. D. VIETNAM, **So Xuat Nhap Khau Sach Bao**, 32 Hai Ba Trung, Hanoi ; R.S.F. YOUGOSLAVIE, **Jugoslovenska Knjiga**, Terazije 27, Beograd ; **Prosveta** 16/1, Terazije, Beograd ; **Forum**, Vojvode Misica, Novi Sad ; ARGENTINE, **Editorial Sudaminter S.A.**, Alsina 500, Buenos Aires ; AUSTRALIE, **Current Books Ltd.**, Distributors 168—174, Day Street, Sydney ; AUTRICHE, **Globus Zeitungs-, Drucks- und Verlagsanstalt GmbH**, 1200 Wien, Höchstädtplatz 3 ; BELGIQUE, **Du Monde Entier**, 5, Place St-Jean, Bruxelles ; Agence Messageries de la Presse 14—22, Rue du Persil, Bruxelles ; CANADA, **Progress Books**, 44 Stafford St., Toronto, Ontario, W. M. Dawson Subscriptions Service Ltd., Six Thorncliffe Park Drive, Toronto 17, Ontario ; COLOMBIE, **Libreria Buchholz Galeria**, av. Jiménez de Quesada 8—40, Bogotá ; DANEMARK, **Ejnar Munksgaard**, Norregade 6, Kobenhavn ; ESPAGNE, **Libreria Herder**, Calle de Balmes 26, Barcelona 7 ; ETATS-UNIS, **Fam Book Service**, 69, Fifth Avenue, Suite 8, F., New York, 10003 N. Y. ; **Continental Publications**, 111, South Meramec Ave., St-Louis, Missouri 63105, **Turner Subscription Agency** 235, Park Avenue South, New York 3, N. Y. ; FINLANDE, **Akateeminen Kirjakauppa**, P.O.B. 10128, Helsingfors, 10 ; FRANCE, **Nouvelles Messageries de la Presse Parisienne**, 111, Rue Réaumur, Paris II, **Europériodiques S. A.**, 73, Boul. Senard, 22 Saint-Cloud ; GRANDE-BRETAGNE, **Collet's Holdings Ltd.**, Dennington Estate, Wellingborough, Northants, **Central Books Ltd.**, 37, Inn Road, London W. C. 1 ; ISRAEL, **Lepac Ltd.**, P.O.B., 1136 Tel-Aviv, **Haifapac Ltd.**, P.O.B. 1794, Haifa ; ITALIE, **So. Co. Lib. Ri.**, Piazza Margana 33, Roma ; **Messagerie Italiane Sp. A.** Milano, Via Priv. Renzo e Lucia 7 ; JAPON, **Nauka Ltd.**, 30—19 Minami — Ikebukuro 2 chome Toshima Ku, Tokyo ; PAYS-BAS, **N. V. Martinus Nijhoff**, P.O.B. 269, Den Haag ; **Swets & Zeitlinger**, Keizersgracht 471—487, Amsterdam C. ; NORVEGE, **Tryggve Juul Moller-Boekhandel Øvre**, Slottsgate 15, Oslo 1 ; R. F. ALLEMANDE, **Kubon & Sagner**, P.O.B. 68, München 34, **Presse Vertriebsgesellschaft GmbH**, 6, Frankfurt/Main, Börsenstrasse 13—15 ; **Kunst und Wissen**, Erich Bieber, P.O.B. 46, 7 000 Stuttgart 1 ; SUISSE, **Pinkus & Cie**, Froschaugasse 7, Zürich, **Fachbücherei Berne**, P.O.B. 397, 3001 Berne.

En Roumanie, vous pourrez vous abonner par les bureaux de poste, chez votre facteur ou directement par les services de presse des entreprises et institutions.

NOUS VOUS PRIONS DE RENOUVELER VOTRE ABONNEMENT POUR L'ANNEE 1970

NOTE POUR LES AUTEURS

La *Revue Roumaine de Chimie* publie des articles en anglais, français, russe, allemand ou espagnol. Les auteurs sont priés d'envoyer des articles, notes, communications et comptes rendus inédits.

Les manuscrits seront dactylographiés à deux intervalles. Les tableaux seront dactylographiés sur feuilles séparées, de même que la légende des figures. Les diagrammes seront tracés à l'encre de Chine sur papier calque. Les tableaux et les figures seront numérotés par des chiffres arabes, en nombre strictement nécessaire. Prière de ne pas inscrire les mêmes données dans les tableaux et les figures. Les formules chimiques seront incluses dans le texte ; en outre, elles seront transcrites sur des feuilles séparées. Les auteurs sont priés d'indiquer les caractères italiques (en soulignant les lettres au crayon), ainsi que tout autre caractère spécial. L'ordre des références bibliographiques sera celui de leur mention dans le texte ; le nom de l'auteur sera précédé de l'initiale du prénom ; les publications périodiques seront présentées suivant les prescriptions internationales. Les références seront ajoutées à la fin de l'article ; elles paraîtront comme des notes, au bas de la page. Le texte sera précédé d'un résumé, comprenant 15 lignes au maximum.

L'entière responsabilité du contenu des articles appartient aux auteurs. On publie des articles dus aux collaborateurs roumains ou étrangers. Les auteurs recevront 50 tirés à part.

PRINTED IN ROMANIA

1969 OKT 17

TRAVAUX PARUS AUX ÉDITIONS DE L'ACADÉMIE DE LA RÉPUBLIQUE SOCIALISTE DE ROUMANIE

CORNEL BODEA et collab., **Tratat de biochimie vegetală**, partea I, **Fitochimie** (Traité de biochimie végétale, Ire partie, Phytochimie), Ier vol., 1964, 747 p. + 4 annexes + 2 pl., 41 lei ; IIe vol., 1965, 1262 p., 1 pl., 56 lei ; IIIe vol., 1967, 773 p., 35 lei.

V. GHEŢIE et V. MICUŞAN, **Analiza imunochimică. Teorie şi practică** (Analyse immunochimique. Théorie et pratique), 1966, 369 p., 28 lei.

SILVIA IONESCU, **Reacţii chimice induse de radiaţiile ionizante** (Réactions chimiques produites par les radiations ionisantes), 1963, 271 p., 15 lei.

MARIETA NICOLAE, **Fizico-chimia proceselor fotografice** (Physico-chimie des processus photographiques), 1964, 426 p. + 4 pl., 35 lei.

R. PORTOCALĂ et L. POPA, **Acizii ribonucleici celulari şi virali** (Les acides ribonucléiques cellulaires et viraux), 1966, 375 p. + 8 pl., 26 lei.

D. PURDELA et R. VÎLCEANU, **Chimia compuşilor organici ai fosforului şi ai acizilor lui** (La chimie des composés organiques du phosphore et de ses acides), 1965, 540 p., 37 lei.

CRISTOFOR SIMIONESCU, MARGARETA GRIGORAŞ et AGATA CERNĂTESCU-ASANDEI, **Chimia lemnului din R.P.R.** (La chimie du bois en Roumanie), 1964, 239 p. + 6 pl., 27 lei.

CRISTOFOR SIMIONESCU et CLEOPATRA VASILIU-OPREA, **Mecanochimia compuşilor macromoleculari** (La mécanochimie des composés macromoléculaires), 1967, 344 p., 23,50 lei.

I. V. MAXIM, **Materiale nucleare** (Matériaux nucléaires), 1969, 444 p., 4 pl., 30 lei.

43 436

I.P.I. — c. 3509

Lei 15. —

F 1103

04 R

REFERÁLVA

REVUE ROUMAINE DE CHIMIE

TOME 14

N° 9

Septembre 1969

ÉDITIONS DE L'ACADÉMIE DE LA RÉPUBLIQUE SOCIALISTE DE ROUMANIE

Rev. Roumaine Chim. 14, 1069—1190 (1969), Bucarest

COMITÉ DE RÉDACTION

Rédacteur en chef :

C. D. NENIŢESCU, membre de l'Académie de la République Socialiste de Roumanie.

Rédacteurs en chef adjoints :

A. T. BALABAN et V. E. SAHINI, membres correspondants de l'Académie de la République Socialiste de Roumanie.

Collège de rédaction :

C. DRĂGULESCU, RALUCA RIPAN, CR. SIMIONESCU, membres de l'Académie de la République Socialiste de Roumanie; EM. BRATU, membre correspondant de l'Académie de la République Socialiste de Roumanie, Pr G. OSTROGOVICH, MARG. AVRAM, F. BADEA, D. MARCHIDAN, D. NEGOIU et D. SĂNDULESCU.

Les manuscrits, les livres et les revues proposés en échange, ainsi que toute correspondance seront envoyés à la rédaction :

REVUE ROUMAINE DE CHIMIE

23, str. Dumbrava Roşie, Bucarest, Roumanie.

F 1103

MŰSZAKI KÖNYVTÁR

REVUE ROUMAINE DE CHIMIE

Tome 14, N° 9 Septembre 1969

Page

I. G. MURGULESCU and N. I. IONESCU, The effect of oxygen chemisorption on the temperature dependence of the variation of electrical resistance of the thin copper films 1073–1080

I. G. MURGULESCU et I. VLAGIU, La cinétique de la polymérisation mixte de l'acrylonitrile sous l'action des radiations ionisantes et en présence de diacvodioxalomanganate de potassium . . . . 1081–1092 ✓

V. E. SAHINI and LILIANA CIUREA, Electronic spectra of some aromatic metal ketyls 1093–1097

O. RADOVICI and CECILIA VASS, Electrodeposition of zinc from pyrophosphate solutions. I. Study of equilibrium potentials of zinc electrode . . . . 1099–1106 ✓

D. FĂTU, SANDA FĂTU et E. SEGAL, Cinétique de la décomposition thermique de certaines combinaisons complexes du chlorure de cuivre avec la pyridine et des pyridines substituées 1107–1112

CONST. GH. MACAROVICI et EUGENIA PERȚE, Combinaisons complexes avec des hydroxyacides. VIII. Les complexes du Ga^{3+} et In^{3+} avec l'acide saccharique . . . . 1113–1124 ✓

ILEANA LUKÁCS, CONSTANȚA STRUSIEVICI, D. LUPU, C. MIREL et C. LITEANU, Sur les vanadates. XVII. La susceptibilité magnétique des composés $K_x\,V_x^{IV}\,V_{2-x}^{V}\,O_5$ $(0 < x \leqslant 1)$ 1125–1131

CS. VÁRHELYI, Z. FINTA and J. ZSAKÓ, Kinetics and mechanism of substitution reactions of complexes. XIV. New derivatives of the dichloro-bis-dimethylglyoximato-cobaltous-(III)-acid and the solvolysis of the ion $[Co(DH)_2Cl_2]^-$ in water-dimethylformamide mixtures 1133–1141

J. DICK und ALFA LUPEA, Komplexverbindungen des N,N'Diaminopiperazins. II. Verbindungen mit komplexen Anionen und ihr thermischer Abbau 1143–1148

VICTORIA BEDNAR, V. MINCU et H. BEDNAR, L'étude des propriétés magnétiques de quelques tartrates simples et complexes 1149–1151

MAGDA PETROVANU, A. SAUCIUC, I. GABE et I. ZUGRĂVESCU, L'addition des philodiènes sur la phtalazine. III. Action du bromure de phénacyle sur la phtalazine 1153–1161

Rev. Roumaine Chim. 14, 1069–1190 (1969), Bucarest

Page

I. GABE, ELENA MĂNTĂLUŢĂ und GABRIELA NEAMŢU, Infrarotspektroskopische Untersuchungen an einigen Polypyridazinen, Polytetrazinen und Polytriazolen . . . . 1163—1170

A. A. CARACULACU and E. C. BEZDADEA, Unsaturated end groups in PVC. I . . . . 1171—1180

MARGARETA AVRAM, I. G. DINULESCU, GH. D. MATEESCU, ELISA AVRAM und C. D. NENIŢZESCU, Untersuchungen in der Cyclobutanreihe. XXI. Di-tert.-butyl-diphenyl-cyclobutadien-Komplexe mit Palladiumchlorid . . . . 1181—1189

ORSZÁGOS MŰSZAKI KÖNYVTÁR ÉS DOKUMENTÁCIÓS KÖZPONT

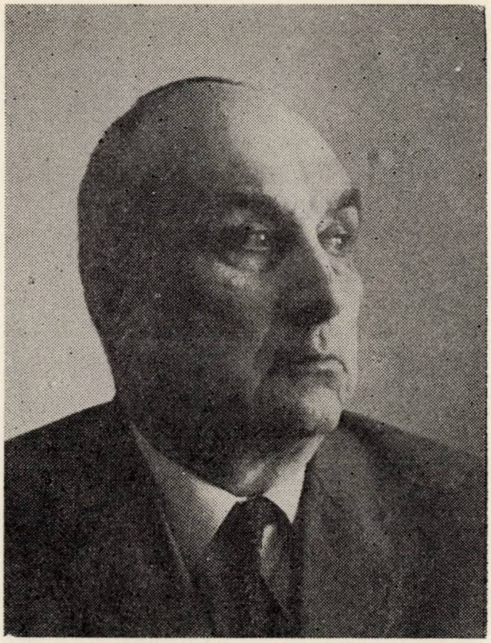

ALEXANDR NICOLAEVICH NESMEYANOV

On the 9th of September this year Professor A. N. Nesmeyanov member and for a long time president of the Academy of Sciences, a well-known scientist of the Soviet Union, with a world-wide reputation, attains the age of 70 and 45 years of scientific activity. A N. Nesmeyanov is professor at the Moscow State University, honorary doctor of the Universities of Paris, Jena and Calcutta, member of the Royal Society of London, honorary member of the Romanian Academy and of the Academies of Poland, Bulgaria, Czechoslovakia, German Democratic Republic, etc.

He has published numerous papers in the field of organo-metallic combinations, has worked out a method of obtaining organic compounds with mercury, which is called after him. This method has been used as a starting point for new series of organo-metallic compounds. He has also strongly contributed to the substantiation of the structural theory of organic compounds. He is also the author of an excellent monograph on "Synthesis methods in the field of organo-metallic combinations".

He is the director of the Institute of elemental organic compounds of the U.S.S.R. Academy of Science, Moscow, created and led by him with scientific competence unanimously acknowledged. His research opened new pathways in the domain of orgainic chemistry, laying the foundation of an original school of the chemistry of organo-metallic compounds.

ORSZÁGOS MŰSZAKI KÖNYVTÁR DOKUMENTÁCIÓS KÖZPONT 1883

Inverse ratios have been calculated also in table 3, columns 6 and 7, for the first 3 respectively the last 3 experiments.

As seen in table 1, for great pressures of the gas introduced, the recorded resistance variation does not depend on the temperaturae, i.e. relation

$$\frac{\Delta R_{273}}{\Delta R_{77}} = 1 \tag{1}$$

is quicker satisfied than expression

$$\frac{\left(\dfrac{\Delta R}{R}\right)_{77}}{\left(\dfrac{\Delta R}{R}\right)_{273}} = 1 \tag{2}$$

For small pressures (table 2) the phenomenon exhibits quite the opposite aspect

Table 2

Temperature dependence of the electric resistance increase of thin copper films after oxygen chemisorption at small pressures of introduced gas

T°K	Pressure of the introduced gas torr	R_0 Ω	ΔR Ω	R Ω	$\frac{\Delta R_{273}}{\Delta R_{77}}$	$\frac{\left(\frac{\Delta R}{R}\right)_{273}}{\left(\frac{\Delta R}{R}\right)_{77}}$
1	2	3	4	5	6	7
273	5×10^{-5}	46.943	5.695	52.638	1.170	1.057
77		37.662	4.867	42.529		
273	5×10^{-5}	40.144	3.494	43.638	1.158	1.046
77		33.012	3.017	36.029		
273	5×10^{-5}	40.467	5.068	45.535	1.110	1.009
77		36.366	4.567	40.933		
273	4×10^{-5}	38.633	1.543	40.176	1.257	1.043
77		32.108	1.227	33.335		
273	4×10^{-5}	30.763	3.943	34.706	1.120	1.033
77		28.481	3.521	32.002		
273	3×10^{-5}	37.261	3.711	40.972	1.265	1.049
77		31.150	2.934	33.984		

i. e. relation (2) is closer to reality than relation (1). Finally for intermediate pressures (table 3) no predominance of any of the two relations (1) and (2) could be detected.

Table 3

Temperature dependence of the electric resistance increase of thin copper films after oxygen chemisorption at medium pressures of introduced gas

T°K	Pressure of the introduced gas torr	R_0 Ω	ΔR Ω	R Ω	$\frac{\Delta R_{273}}{\Delta R_{77}}$	$\frac{\left(\frac{\Delta R}{R}\right)_{77}}{\left(\frac{\Delta R}{R}\right)_{273}}$
1	2	3	4	5	6	7
273	1×10^{-4}	35.620	3.021	38.641	1.182	1.292
77		31.783	3.571	35.354		
273	1×10^{-4}	30.405	1.299	31.704	1.159	1.281
77		27.186	1.506	28.692		
273	1×10^{-4}	29.501	1.867	31.368	1.542	1.603
77		27.293	2.880	30.173		
273	1×10^{-4}	35.834	4.471	40.305	1.038	1.087
77		31.432	4.309	35.741		
273	1×10^{-4}	34.805	1.226	36.031	1.524	1.255
77		28.976	0.804	29.780		
273	1.5×10^{-4}	37.078	5.169	42.247	1.564	1.166
77		30.623	3.305	33.928		
273	1.5×10^{-4}	35.446	3.696	39.142	1.365	1.260
77		30.725	2.708	33.433		

An analogous behaviour has been noticed for the Ni/Co[5] system.

The explanation is to be sought among the causes which induce the variation of electrical resistance of the thin metallic films during gas chemisorption. Up to the present three main hypotheses have attempted to clear off the positive resistance variation which has been experimentally determined.

---

[5] G. Wedler and M. Fouad, *Z. phys. Chem.* (*Frankfurt*), **40**, 12 (1964).

Revue Roumaine de Chimie, **14**, 1073–1080 (1969)

THE EFFECT OF OXYGEN CHEMISORPTION ON THE TEMPERATURE DEPENDENCE OF THE VARIATION OF ELECTRICAL RESISTANCE OF THE THIN COPPER FILMS

I. G. MURGULESCU and N. I. IONESCU

Institute of Physical Chemistry of the Academy
Bucharest, str. Dumbrava Roșie 23

Received January 27, 1969

The experiments on the temperature dependence of the variation of electrical resistance of the thin copper films during oxygen chemisorption showed that the mechanism governing the resistance increase depends on the coverage degree of the surface.

In previous papers we have proved that oxygen chemisorption on thin silver[1] and copper[2] films leads to a decrease in the temperature coefficient of the electrical resistance of the metal. These results have been interpreted as due to the decrease in the effective thickness of thin films.

The present contribution aims at investigating the temperature dependence of the resistance increase of thin copper films as a result of oxygen chemisorption by using a technique different of that used in the papers mentioned beforehand[1,2] in order to supplement the data on the mechanisms which bring about the observed resistance variations.

MATERIAL AND METHOD

Similar installation and procedure as described in[1–3] have been used. The copper evaporation occurred at $5\times 10^{-9}-1.10^{-8}$ torr. On heating the film the pressure reached 3×10^{-8} torr. Film thickness : about 80 Å. Spectroscopically pure copper from Johnson and Matthey (England) has been used.

Oxygen adsorption took place at 273°K. After process completion the unadsorbed gaseous phase has been pumped and the temperature suddenly lowered to 77°K. The unadsorbed gas has been removed in order to avoid some subsequent adsorptions at low temperature.[4]

For table 1 we acted as follows : after oxygen introduction R_{273} is read and then the gas is pumped. The other operations proceeded as usual.

---

[1] I. G. Murgulescu and N. I. Ionescu, *Rev. Roumaine Chim.*, **11**, 1267 (1966).

[2] I. G. Murgulescu and N. I. Ionescu, *Rev. Roumaine Chim.*, **14**, 681 (1969).

[3] I. G. Murgulescu and N. I. Ionescu, *Rev. Roumaine Chim.*, **11**, 1035 (1966).

[4] R. Suhrmann, H. J. Busse and G. Wedler, *Z. phys. Chem.* (*Frankfurt*), **47**, 1 (1965).

This alteration in the technique is necessary since, as already stated,[2] at these pressures after a sudden increase in the resistance a slow decrease follows. The resistance decrease may be avoided by pumping.

RESULTS AND DISCUSSION

The results of the experiments are listed in tables 1, 2, 3.

Table 1

Temperature dependence of the electric resistance increase of thin copper films after oxygen chemisorption at high pressures of introduced gas

T°K	Pressure of the introduced gas torr	R_0 Ω	ΔR Ω	R Ω	$\frac{\Delta R_{77}}{\Delta R_{273}}$	$\frac{\left(\frac{\Delta R}{R}\right)_{77}}{\left(\frac{\Delta R}{R}\right)_{273}}$
1	2	3	4	5	6	7
273	1×10^{-3}	34.849	5.666	40.515	1.011	1.176
77		28.471	5.603	34.074		
273	3×10^{-4}	31.686	3.591	35.277	1.053	1.145
77		25.825	3.409	29.234		
273	4×10^{-4}	30.187	4.406	34.593	1.018	1.137
77		26.488	4.486	30.974		
273	1×10^{-3}	33.083	4.789	37.872	1.022	1.206
77		27.307	4.897	32.104		
273	6×10^{-4}	37.031	4.276	41.307	1.051	1.191
77		31.962	4.494	36.456		
273	5×10^{-4}	36.642	2.117	38.759	1.068	1.305
77		29.447	2.261	31.708		

In table 1, column 6, for the first 2 experiments the inverse ratio has been calculated i. e. $\frac{\Delta R_{273}}{\Delta R_{77}}$; in table 2, column 7, for the first 3 experiments, the inverse ratio has been calculated i.e.

$$\frac{\left(\frac{\Delta R}{R}\right)_{77}}{\left(\frac{\Delta R}{R}\right)_{273}}$$

If the resistance variation is due to the decrease in the actual thickness then, by the logarithmical differentiation of (3) as against d one obtains

$$\frac{\Delta R}{R} = -\left[\frac{\Delta f\ (d/l,\, p)}{f\,(d/l, p)} + \frac{\Delta d}{d}\right] \tag{5}$$

which shows that the ratio $\Delta R/R$ depends on the temperature by means of l.

For the very thin films which observe the condition $\frac{d}{l} \leqslant 0.15$ or $\frac{d}{l} \leqslant 0.2$ function $f(d/l,\, p)$ may be expressed by [17]:

$$f(d/l,\, p) = \frac{3}{4}(1+2p)\left(\ln\frac{l}{d} + 0.4228\right) \tag{6}$$

where, by relation (3), $\Delta R/R$ gets the following form:

$$\frac{\Delta R}{R} = -\left(2 - \frac{1}{\ln\frac{\beta\, l}{d}}\right)\frac{\Delta d}{d} \tag{7}$$

where $0.4228 = \ln \beta$. Formula (7) has been found also in other circumstances.[18]

In the case of C and D, according to Matthiessen's law ΔR should be temperature independent.

This law can be applied also for the first two cases. Indeed, the law may be written as follows:

$$R = R_T + R_D \tag{8}$$

where R_T depends on the amplitude of the thermal oscillations of the lattice and R_D on the lattice defects. The modification ΔR is given by:

$$\Delta\, R = \Delta\, R_T + \Delta\, R_D \tag{9}$$

Two cases can be distinguished:

a) $\Delta R_T \gg R_D$, wherefrom it results that $\frac{\Delta R_T}{R_T + R_D}$ is temperature independent (either N or d varies),
b) $\Delta R_D \gg \Delta R_T$, wherefrom it results that ΔR is temperature independent (either l or p varies).

As already shown, the criteria are very different as to the hypotheses in A and B and they agree for the hypotheses in C and D. These criteria have been used by research workers in the first as well as in the second form.[4, 5, 15]

---

[17] D. S. Campbell, "The Use of Thin Films in Physical Investigations", ed. J. C. Anderson, Academic Press, London and New York, 1966, p. 299.

[18] I. G. Murgulescu and G. Comșa, *Rev. Roumaine Chim.*, **11**, 1253 (1966).

In order to possibly apply these conclusions to the results already obtained one should admit that the temperature variation does not bring about any gas desorption (a fact proved by experiments performed at 77 and 273°K[2]) and also that the character of the chemisorption process does not change.

In accordance with the above conclusions, the remark can be put forward that results obtained for great coverages (table 1) advocate for the mechanism C and D (C or D) and those for small coverages (table 2) either for mechanism A or for A and B. For mean coverages (table 3) nothing can be explicitly stated as to the preponderance of either of them since the mechanisms seem to act together.

The picture of oxygen chemisorption on thin copper films, in accordance with the above data might be the following : at the beginning a surface oxygenated combination of copper is formed that does not desorb and that at great coverage degrees is felt also by the simultaneous increase in the residual resistance.

As a result of our experiments it may be concluded that the mechanism governing the electrical resistance variation of thin copper films during oxygen chemisorption depends on the coverage degree of the surface.

1. The decrease in the number of conduction electrons of the metal which are yielded to the chemisorbed gas [6] in order to form a chemisorption bond.

The electron transfer may be either partial, in the case of the adsorbant's polarization,[7] or total, in case it is ionized. [8]

2. The decrease in the thin film by 1−2 atom layers due to the formation of a surface complex between the metallic atoms and the adsorbed gas (loss of the metallic character of the boundary layer).[9]

3. Reduction of the electrons mobility as a result of the change of the mean free path or to their reflexion conditions at the film surface.[7,8,10,11]

These hypotheses have been correlated by considering that for the formation of a chemisorption bond, which characterizes the surface complex, it is necessary the simultaneous interference of an electronic factor.[1]

It has been also considered that the formation of a surface combination leads to a decrease in the electron mobility,[7] by introducing a certain amount of additional defects into the lattice.

Finally, it has been assumed [12] that the above factors may intervene simultaneously and result in the experimentally noticed effect.

Besides the main hypotheses it has been also assumed that the gas absorption in the lattice could account for the resistance modification.[8]

Thus, as a volume effect, the great values of the relative variation of the resistance obtained in the system Cu/CO[13] could be explained.

In order to find out which of the above hypotheses tends to explain the results, we shall consider the expression of the electrical resistance of a thin metallic film deduced elsewhere [1,2,12] :

$$R = \frac{C}{f\,(d/l,\, p)\, N^{2/3}\, l\, d} \tag{3}$$

where R — the electrical resistance, C — a constant, N — the number of conductivity electrons /cm^3, l the mean free path of the electrons in the bulk metal which has the same structure as the thin film, d — film thickness, p — scattering coefficient of the electrons and $f\ (d/l,\ p)$ — Fuchs-Sondheimer's function.

Relation (3) shows that R is depending on four factors N, d, l, p and a change in ΔR will depend on the variation of these parameters. Four main cases will be distinguished :

---

[6] R. Suhrmann and K. Schulz, *Z. phys. Chem.* (*Frankfurt*), **1**, 69 (1954).

[7] H. Kölbel, E. Schöttle and H. Hammer, *Z. phys. Chem.* (*Frankfurt*), **47**, 183 (1965).

[8] H. Kölbel, E. Schöttle and H. Hammer, *Z. phys. Chem.* (*Frankfurt*), **46**, 88 (1965).

[9] W. M. H. Sachtler and G. J. H. Dorgelo, *Z. phys. Chem.* (*Frankfurt*), **25**, 69 (1960).

[10] T. Toya, *J. Res. Inst. Cat.*, **10**, 236 (1962).

[11] O. A. Panchenko and Iu. G. Ptushinski, *Izvest. Akad. Nauk S.S.S.R., Otdel. fiz. Nauk*, **28**, 1466 (1964).

[12] N. I. Ionescu, *Rev. Roumaine Chim.*, **13**, 683 (1968).

[13] H. G. Kock, Dissertation, Hannover, 1967.

A) N changes, d, l and p keep constant. This case assumes direct electron passages to the adsorbed molecule during adsorption.

The metal does not change and the metallic atoms binding the gas still belong to the film.

B) d changes, N, l and p keep constant. This case assumes that on gas adsorption, the first layer or the first layers of copper atoms enter a direct surface combination with the gas and no longer belong to the metal so that the effective thickness of the film decreases.

C) l changes, N, d and p keep constant. This case starts from the assumption that the gas adsorption modifies the electron mobility.

D) p changes, N, d and l keep constant. In this case, the reflexion conditions of the electrons by the film surface are modified due to the adsorption and this influences the electron mobility.

In the *C* and *D* cases due to adsorption additional surface defects occur which, in agreement with Matthiessen's law, should yield a change in the resistance independent of temperature.

An immediate solving of the problem only by examining relation (3) is not possible, since we have an equation with four unknowns. The determination of a univocal solving would imply the existence of at least three various relations (l and p could be considered as a variable since it bears on the electron mobility) between the given variables; this would actually mean the simultaneous use of at least three various methods but which depend on the same parameters, on the same film. The calculus of the variation of the magnitude d as carried out previously [1,2,14] assumed as variable only d. When the determination of the variation of d occurred only according to the hypothesis requiring the modification both of N and d, besides the constancy of l and p an additional condition has been introduced i. e. that of the existence of a proportionality between N and d. [1]

Thus, any variation of a given parameter may be calculated, provided the others should be kept constant.

A differentiation of these mechanisms may indirectly take place from the temperature dependence of the resistance increases already noticed.

Indeed, if one assumes that only N varies and the other magnitudes are constant, then, by the logarithmical differentiation of relation (3) as against N, one obtains:

$$\frac{\Delta R}{R} = -\frac{2}{3}\frac{\Delta N}{N} \tag{4}$$

that, with or without the coefficient 2/3, has been obtained by other authors too. [5, 13, 15, 16]

As seen from (4), the ratio $\Delta R/R$ should be temperature independent if the resistance variation of the metal were due to a change in the concentration of free electrons.

---

[14] I. G. Murgulescu, G. Comşa and N. I. Ionescu, *J. Catalysis*, **12**, 102 (1968).

[15] D. Lazarov and G. Bliznakov, *Doklady Bolgarskoi Akademii Nauk*, **20**, 209 (1967).

[16] H. Wenzel, Dissertation, Hannover, 1968.

Dans la seconde partie de l'ouvrage, nous allons aussi présenter la cinétique de réaction de l'acrylonitrile en présence du complexe oxalique, l'influence de celui-ci sur l'ordre de réaction avec le monomère, la dose d'irradiation, ainsi que l'influence de la température sur la réaction.

DÉPENDANCE DE LA VITESSE DE RÉACTION DE LA CONCENTRATION DU MONOMÈRE DE LA DOSE D'IRRADIATION DANS LE SYSTÈME ACRYLONITRILE-CARBONATE D'ÉTHYLÈNE-EAU

Dans ce solvant, dans l'absence du complexe, la vitesse de réaction est donnée par l'équation

$$V' = -\,\mathrm{d}\,(M)\,/\,\mathrm{d}t = k_M\,(M)^{\alpha}\,I^{\beta} \qquad (4)$$

dans laquelle k_M = la constante globale de réaction $= k_p\,(k_i\,/\,k_t)^{1/2}$, M = la concentration du monomère, et I = l'intensité de la radiation (dose d'irradiation), α et β = l'ordre de réaction par rapport au monomère et à la dose.

L'ordre de réaction par rapport au monomère a été déduit de la pente de la droite représentant graphiquement le logarithme de la vitesse de réaction en fonction du logarithme de la concentration du monomère.

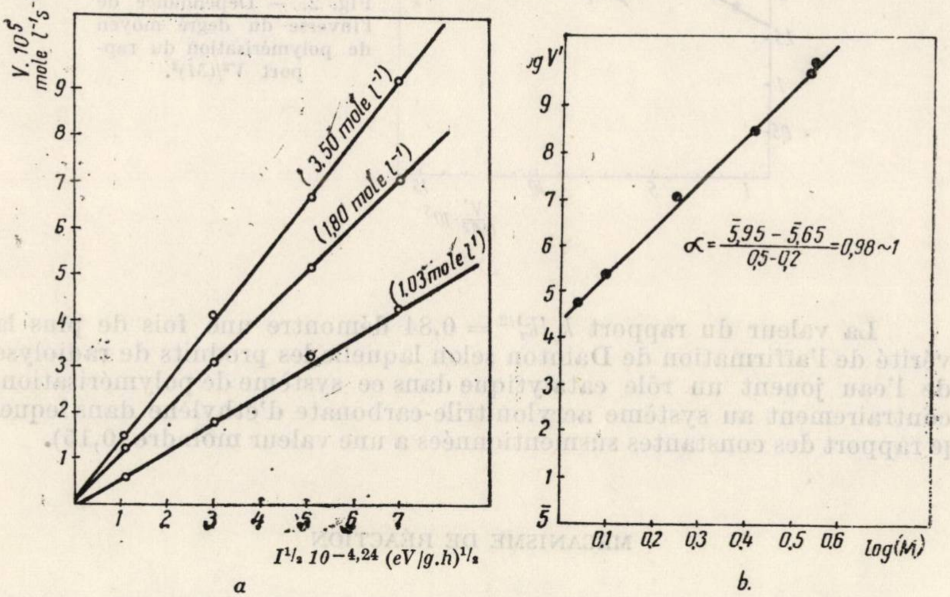

Fig. 1. — Dépendance de la vitesse de réaction (*a*) de $1^{1/2}$ et (*b*) de la concentration du monomère.

Le résultat est de l'ordre de l'unité. L'ordre de réaction par rapport à l'intensité de la dose est de 1/2, trouvé expérimentalement conformément au procédé classique [6], en représentant graphiquement la vitesse de réaction en fonction de la racine carrée de la dose. On obtient des droites passant par l'origine (fig. 1).

La valeur du rapport des constantes absolues de réaction ($k_p/k_t^{1/2}$) ont été déterminées en partant de la pente de la droite obtenue par la représentation graphique de l'inverse du degré moyen de polymérisation en fonction du rapport $V' / (M)^2$, dans lequel V' = la vitesse de réaction et M = la concentration du monomère, conformément à la formule [6,10]

$$1 / \overline{P}_n = C_{tr,M} + C_{tr,S}\,(S) / (M) + k_t / k_p^2\,V' / (M)^2 \qquad (5)$$

dans laquelle $C_{tr,M,S}$ = la constante de transfert pour le monomère et le solvant (fig. 2)

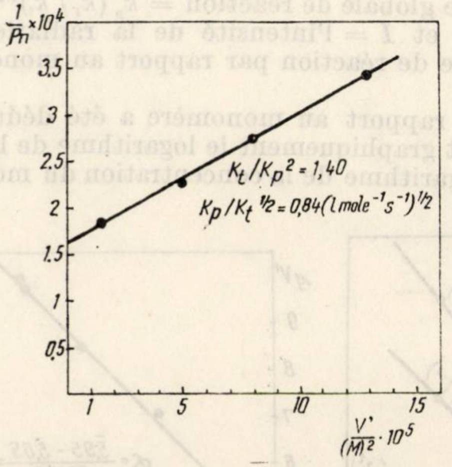

Fig. 2. — Dépendance de l'inverse du degré moyen de polymérisation du rapport $V^2/(M)^2$.

La valeur du rapport $k_p/k_t^{1/2} = 0{,}84$ démontre une fois de plus la vérité de l'affirmation de Dainton selon laquelle les produits de radiolyse de l'eau jouent un rôle catalytique dans ce système de polymérisation, contrairement au système acrylonitrile-carbonate d'éthylène dans lequel le rapport des constantes susmentionnées a une valeur moindre (0,15).

MÉCANISME DE RÉACTION

Pour élucider le mécanisme de réaction de l'acrylonitrile dans le cas de l'emploi comme solvant du carbonate d'éthylène/eau, nous avons effectué l'analyse en IR du polymère obtenu, d'où il résulte clairement l'existence de la vibration C-OH du type alcool primaire, de sorte que la structure de polymère prend la forme

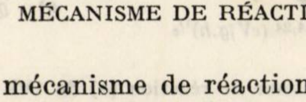

$$HO-\left[\begin{array}{l} CH_2-\underset{\displaystyle C\equiv N}{\underset{|}{CH}}- \end{array}\right]_n$$

Revue Roumaine de Chimie, **14**, 1081–1092 (1969)

LA CINÉTIQUE DE LA POLYMÉRISATION MIXTE DE L'ACRYLONITRILE SOUS L'ACTION DES RADIATIONS IONISANTES ET EN PRÉSENCE DE DIACVODIOXALOMANGANATE DE POTASSIUM

I. G. MURGULESCU et I. VLAGIU
Centre de Chimie Physique de l'Académie,
Str. Dumbrava Roşie, 23, Bucarest

Reçu le 11 novembre 1968

On discute la cinétique de la polymérisation de l'acrylonitrile en solution aqueuse de carbonate d'éthylène à 50° et en présence de $K[Mn(C_2O_4)_2(H_2O)_2]$. L'ordre de réaction par rapport au monomère est de 2 et par rapport à l'intensité de la dose et de la concentration du complexe de 1/2. L'expression générale de la vitesse de réaction prend la forme

$$-\frac{d(M)}{dt} = k_M (M)\ I^{1/2} + K'_M (M)^2 (C)^{1/2}\ I^{1/2}$$

On a, de même, déterminé en vertu des données expérimentales, le rapport des constantes absolues de réaction k_t/k_p^2, en obtenant pour les systèmes acrylonitrile-carbonate d'éthylène/eau et acrylonitrile-carbonate d'éthylène / eau – complexe oxalique les valeurs de 1,40 et 0,79.

La cinétique de la polymérisation radiochimique de l'acyloronitrile à formé l'objet de quelques études dans un milieu hétérogène (cinétique de la polymérisation en bloc[1] et de la post-polymérisation[2]) et en milieu homogène, en utilisant comme solvant la diméthylformamide dans laquelle on a étudié la post-polymérisation [3] et l'influence du chlorure ferrique sur le mécanisme de réaction.[4] On a étudié également la cinétique de réaction en diméthylformamide, diméthylsulfoxyde et carbonate d'éthylène, dans lesquels on a déterminé les constantes de transfert pour le solvant.[5]

En général, la vitesse de réaction en milieu homogène est proportionnelle à $I^{1/2}$ (I étant l'intensité de la radiation) dans un large domaine d'intensité. Ce phénomène est expliqué par Chapiro en admettant que le monomère est capable d'intercepter les radicaux primaires. Il y a des cas où, pour de très hautes intensités, la proportion de $I^{1/2}$ n'est plus respectée, l'exposant de la dose étant inférieur à 0,5. Dans ce cas le monomère n'est plus capable d'intercepter les radicaux primaires, une partie d'entre eux se recombinant avec les chaînes croissantes.

[1] F. S. Dainton, *Nature*, **169**, 370 (1952).

[2] A-Prevot-Bernas, *Compt. rend.*, **237**, 1682 (1953).

[3] R. Bensasson et A. Prevot-Bernas, *J. Chim. Phys.*, **53**, 93 (1956).

[4] N. Colebourne, E. Collinson, D. J. Currie et F. S. Dainton, *Trans. Faraday Soc.*, **486**, 1357 (1963).

[5] I. Vlagiu et J. Păun, *Rev. Roumaine Chim.*, **12**, 1085 (1967).

Si la distribution des radicaux en milieu homogène et le transfert, donc l'énergie, sont négligeables, et comme en général c'est un fait connu que les réactions de transfert de chaîne affectent seulement le degré de polymérisation, la vitesse de réaction est donnée par l'expression [4,6]

$$V = -\,\mathrm{d}\,(M)\;/\;\mathrm{d}t = k_p\;/\;k_t^{1/2}\,(M)\,(V_i)^{1/2} \qquad (1)$$

dans laquelle V_i = la vitesse d'initiation, k_p et k_t = les constantes de vitesse du processus de propagation et d'achèvement de l'ensemble de réaction, et (M) = la concentration du monomère.

Dans le présent ouvrage on a étudié l'influence de la dose d'irradiation et de la concentration du complexe diacvodioxalomanganate de potassium $K[Mn(C_2O_4)_2\,(H_2O)_2]$, générateur du radical oxalyle $C_2O_4^{\cdot-}$, sur la vitesse de réaction, pour différentes concentrations du monomère et du solvant (carbonate d'éthylène / eau) les irradiations étant effectuées à une source de cobalt-60, dans un domaine d'intensité compris entre 10^{17} et 10^{18} eV/g.h. Les résultats du présent ouvrage trouvent certaines applications pratiques.[7]

A la suite de la décomposition du complexe oxalique, le macroradical fixe le radical oxalyle, ce qui fait que le polymère obtenu contienne des groupes carboxyle, mis en évidence par analyse du polymère en IR, par procédé tictorial, ainsi que par analyse de combustion, le polymère ayant été précipité, au préalable, plusieurs fois, à chaud, dans de l'alcool méthylique.

CONDITIONS EXPÉRIMENTALES

Le monomère et le solvant ont été purifiés selon le procédé décrit auparavant [5], et le complexe utilisé sous la forme *cis*, selon la méthode indiquée par Cartledge et Eriks.[8] L'irradiation a été réalisée dans une atmosphère d'argon pour différentes intensités. L'intensité de la radiation *gamma* absorbée par le milieu a été mesurée en utilisant le dosimètre Frike, la solution étant placée dans la cellule de réaction. Les déterminations ont été effectuées à 50°. Le polymère a été séparé du solvant par précipitations répétées à chaud, en alcool méthylique, filtré par creuset G_4 et séché sous vide à 50°, jusqu'à un poids constant.

La vitesse de réaction a été mesurée gravimétriquement et le degré de polymérisation a été déduit de l'indice de viscosité limite, selon la réaction de Kiuki [9] et Onyon [10]

$$[\eta] = \sqrt{\frac{1 + 1{,}32\;\eta\ \mathrm{sp.} - 1}{0{,}198}} \qquad (2)$$

$$[\eta] = 3{,}92.10^{-4}\,(53{,}06\;\bar{\mathrm{P}})^{0{,}75} \qquad (3)$$

dans laquelle η_{sp} = la viscosité spécifique de la solution $[\eta]$ = la viscosité intrinsèque et $\bar{P}$ = le degré moyen de polymérisation.

Dans la première partie de l'ouvrage nous nous sommes proposé d'étudier la cinétique de réaction du système carbonate d'éthylène/eau, en établissant l'ordre de réaction par rapport au monomère, à la dose d'irradiation, le rapport des constantes absolues de réaction (k_t/k_p^2).

---

[6] A. Chapiro "Radiation of the Polymer Systems", Pergamon Press, New York, 1965, p. 129.

[7] I. G. Murgulescu, T. Oncescu et I. Vlagiu, Roum. Pat. (O.S.i), 55, 558, c-08 f. (1968).

[8] C. H. Cartledge et P. Eriks, *J. Amer. Chem. Soc.*, **58**, 2061 (1963 .

[9] H. Kiuki et M. Watanabe, *Chem. High Polymers* (*Japan*), **225**, 38 (1964).

[10] P. F. Onyon, *Trans. Faraday Soc.*, **52**, 80 (1956).

ayant les vibrations[11] $C-O$ à 1051 cm^{-1}, 1350–1250 cm^{-1} et la vibration CH_2 de déformation à 1465 cm^{-1} et à 2926, 2853 cm^{-1} la vibration de valence.

En développant le schéma cinétique proposé par Dainton[6] au cas de radiolyse de l'acrylonitrile dans l'eau, et compte tenu des réactions qui affectent la vitesse de réaction et le degré de polymérisation, le mécanisme de réaction pourrait être déterminé par les séquences suivantes

Initiation Vitesse

$$H_2O \xrightarrow{\gamma} 2\ A^{\cdot}\ (H,OH) \qquad G_R I$$

$$A^{\cdot} + M \xrightarrow{ki} R_n^{\cdot} \qquad \Sigma\, ki\,(A^{\cdot})\,(M)$$

Propagation et transfert

$$R_n^{\cdot} + M \xrightarrow{k_p} R_{n+1}^{\cdot} \qquad k_p\,(R_n^{\cdot})\,(M)$$

$$R_n^{\cdot} + S \xrightarrow{k_{tr\,.\,S}} P + S^{\cdot} \qquad k_{tr\,.\,S}(R_n^{\cdot})\,(S)$$

$$M + S^{\cdot} \xrightarrow{k_p} M^{\cdot} + S \qquad k_p\,(M)\,(S)$$

Fin

$$R_n^{\cdot} + S^{\cdot} \xrightarrow{k_t} P + Q \qquad k_t\,(R_n^{\cdot})\,(S^{\cdot})$$

$$R_n^{\cdot} + R_n^{\cdot} \begin{array}{l} \xrightarrow{1/2\,k_{tc}} P_{n+n} \\ 1/2 k_{td}\ P_n + P_n \end{array} \qquad 1/2\ k_t\,(R_n^{\cdot})^2$$

$$S^{\cdot} + S^{\cdot} \xrightarrow{1/2\,k_t} Q \qquad 1/2\ k_t\,(S^{\cdot})^2$$

Dans ce cas, la vitesse de réaction sera donnée par

$$V' = -\frac{d(M)}{dt} = k_p\,(M)\,[(R_n^{\cdot}) + (S^{\cdot})] \tag{6}$$

En appliquant le principe de stationnement quand la vitesse d'initiation est égale à la vitesse finale de réaction[6]

$$G_R I = k_t\,(R_n^{\cdot})^2 + 2\,k_t\,(R_n^{\cdot})\,(S^{\cdot}) + k_t\,(S^{\cdot})^2 = k_t\,[(R_n^{\cdot}) + (S^{\cdot})]^2 \tag{7}$$

Il résulte de l'équation (2) que

$$[(R_n^{\cdot}) + (S^{\cdot})] = \left(\frac{G_R I}{k_t}\right)^{1/2} \tag{8}$$

---

[11] L. J. Bellamy "The Infrared Spectra of Complex Molecules", Methmen Co Ltd., Londres, 1962, p. 95, 108, 179.

En remplaçant l'expression (3) en (1) on obtient finalement :

$$V' = k_p/k_t^{1/2} \qquad (G_R I)^{1/2}\,(M)$$

Cette relation est également vérifiée par nos résultats expérimentaux, l'ordre de réaction par rapport au monomère étant égal à l'unité et en rapport avec la dose de 1/2 exemple donnée par les figures 1 et 3

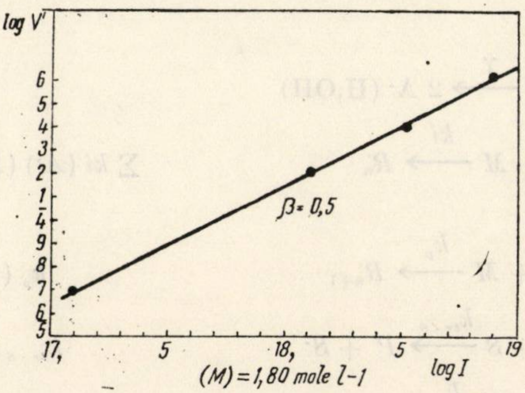

Fig. 3. — Dépendance de la vitesse de réaction de la dose.

DÉPENDANCE DE LA VITESSE DE RÉACTION DE LA CONCENTRATION DU MONOMÈRE, DU COMPLEXE ET DE LA DOSE D'IRRADIATION EN ACRYLONITRILE-CARBONATE D'ÉTHYLÈNE/EAU — K $[Mn(C_2O_4)_2\ (H_2O)_2]$

La vitesse de réaction de polymérisation radiochimique de l'acrylonitrile en présence du complexe de manganèse : $K[Mn(C_2O_4)_2(H_2O)_2]$ peut s'écrire

$$V = k_M\,(M)^\alpha\, I^\beta + k'_M\,(M)^\gamma\,(C)^\delta\; I^\lambda = V' + \Delta V$$

où

$$V - V' = \Delta V \tag{9}$$

L'influence de la présence du complexe oxalique sur la cinétique de réaction a été étudiée pour les concentrations du monomère de 1.80, 2,60 et 3,50 mole 1^{-1}, à la température de 50° et pour une dose de 10^{17} jusqu'à 10^{19} eV/g.h. On a étudié de même pour le temps de 15′ et la dose de 2,70. 10^{18} eV/g.h. l'influence de la composition du milieu de réaction sur la conversion, pour élucider le mécanisme de réaction. Les observations expérimentales sont données au tableau 1.

De ces observations on tire la conclusion que dans le champ de radiations, la quantité de radicaux générée par le complexe est six fois plus grande que dans le cas de la polymérisation thermique. Cette abondance de radicaux favorise dans le champ de radiations une consommation plus grande de monomère.

L'ordre de réaction par rapport au monomère et au complexe a été déterminé selon la méthode de Vant'Hoff. L'ordre de réaction par rap-

Tableau 1

Influence de la composition du milieu de réaction sur la conversion (pourcentages moyens)

$T = 50° : t = 15$ mn

Nº	Acrylonitrile	Carbonate d'éthylène	Complexe* oxalique de Mn^{III}	Eau	Radiation γ	Conv. % moyenne
1	+	+	−	−	+	1,80
2	+	+	−	+	+	2,63
3	+	+	+	+	+	10
4	+	+	+	+	−	1,68

* $K\ [M_n\ (C_2O_4)_2\ (H_2O)_2]$.

port au monomère est égal à 2. De la figure 4 il résulte que pour une dose donnée et une concentration constante du monomère, l'ordre de réaction par rapport au complexe est égal à 1/2 pour le domaine de concentration de 20.10^{-3} à $7,87.10^3$ mole 1^{-1}, et à une concentration inférieure à $2.11.10^{-3}$ mole 1^{-1}, l'ordre de réaction croît jusqu'à l'unité.

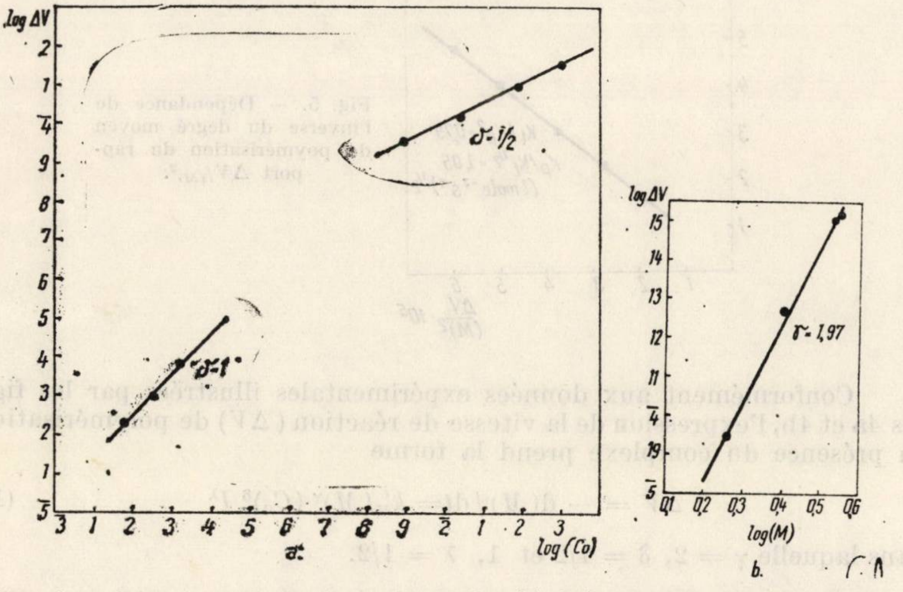

Fig. 4. — Dépendance de la vitesse de réaction (*a*) de la concentration du complexe et (*b*) de la concentration du monomère.

Conformément aux théories existantes, l'ordre de réaction 1/2 démontre que la fin de la réaction de polymérisation peut avoir lieu à la suite du choc de deux macroradicaux (un processus bimoléculaire) et dans le cas de l'ordre de réaction égal à l'unité, cela signifie que la fin de la réaction est monomoléculaire.[6,10]

Par la représentation graphique de l'inverse du degré moyen de polymérisation et du rapport des concentrations complexe/monomère, on a déterminé la constante de transfert pour l'initiateur ($C_{tr,C}$) qui est égale à 0,1, et par représentation graphique en fonction du rapport $\Delta V\,/\,(M)^2$ on a déterminé le rapport des constantes absolues de réaction, et on a trouvé expérimentalement $k_t/k_p^2 = 0{,}79$; $k_p/k_t^{1/2} = 1{,}05$ $(1/\text{mole.s})^{1/2}$, conformément à la formule

$$1/\overline{P}_n = C_{tr,M} + C_{tr,S}\,\frac{(S)}{M} + C_{tr,C}\,(C_0)\,/\,(M) + k_t\,/\,k_p^2\;\Delta V\,/\,(M)^2 \qquad (10)$$

La valeur élevée du rapport $k_p/k_t^{1/2}$ démontre que dans ce système la réactivité de l'acrylonitrile est augmentée (en comparaison d'autres systèmes étudiés) (fig. 2 et 5). Cette conclusion est confirmée également par les valeurs obtenues pour ce rapport dans le système carbonate d'éthylène et carbonate d'éthylène/eau.

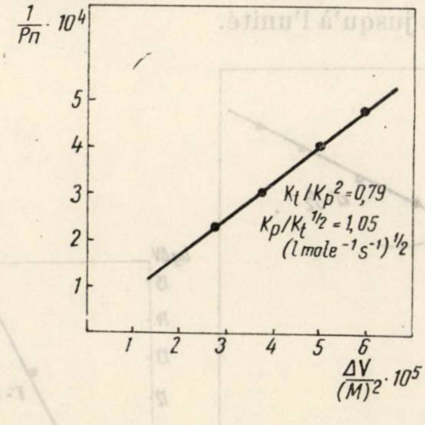

Fig. 5. — Dépendance de l'inverse du degré moyen de poymérisation du rapport $\Delta V/_{(M)^2}$.

Conformément aux données expérimentales illustrées par les figures 4a et 4b, l'expression de la vitesse de réaction (ΔV) de polymérisation, en présence du complexe prend la forme

$$\Delta V = -\,\mathrm{d}(M)\,/\,\mathrm{d}t = k'_M\,(M)^{\gamma}\,(C_0)^{\delta}\,I^{\lambda} \qquad (11)$$

dans laquelle $\gamma = 2$, $\delta = 1/2$ et 1, $\lambda = 1/2$.

INFLUENCE DE LA TEMPÉRATURE SUR LA VITESSE GLOBALE DE RÉACTION

On sait que, en général, la vitesse de réaction dans la polymérisation radiochimique n'est pas très affectée par l'accroissement de la température. L'énergie globale d'activation caractérisant ces réactions varie entre 1 et 10 kcal/mole.

Dans la relation étudiée par nous (acrylonitrile-éthylène : carbonate /H_2O— complexe oxalique), on a déterminé l'énergie globale d'activation d'après la représentation graphique du log V Δ en fonction de $1/T$ (pour trois températures), en obtenant une valeur de la tangente à la pente (tg φ) égale à $1,455.10^3$, et en obtenant finalement une énergie d'activation du système de 6,670 kcal/mole (fig. 6).

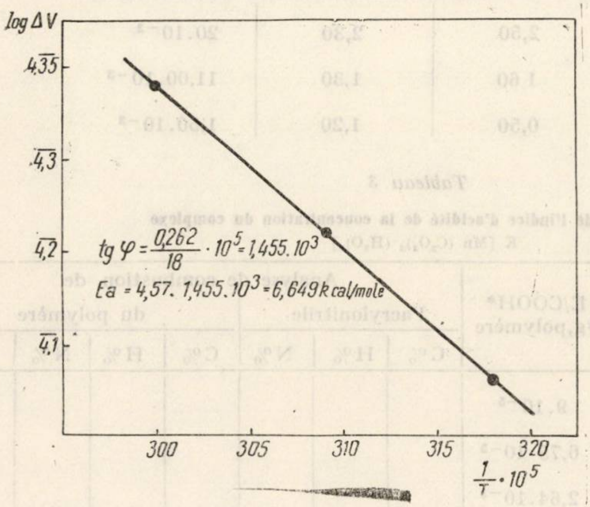

Fig. 6. — Dépendance de la vitesse de réaction de la température.

Dans une note antérieure [5], dans laquelle on a étudié la cinétique des réactions de transfert pour le solvant, on avait déterminé pour le système acrylonitril-carbonate d'éthylène une valeur de l'énergie d'activation de 4,92 kcal/mole.

LA MÉCANIQUE DE RÉACTION

Afin d'éclaircir l'influence du complexe oxalique sur la cinétique et le mécanisme de réaction, outre des données expérimentales consignées dans le tableau 1, on a également effectué les déterminations suivantes : l'analyse en IR du polymère pour détecter le groupe carbonyle ou carboxyle à 1740—1761 cm^{-1}, l'indice d'acidité (tableau 2), l'analyse de combustion et du pouvoir de coloration (tableau 3)

Toutes ces analyses confirment l'existence du groupe $>C=0$ dans la chaîne macromoléculaire. Pour établir le mécanisme de réaction on a considéré la séquence du processus d'initiation comme une réaction pseudobimoléculaire (séquence), la concentration du complexe étant de beaucoup inférieure à celle du monomère.

Tableau 2

Variation du pouvoir colorant du polymère en fonction de la concentration du complexe
K $[Mn (C_2O_4)_2 (H_2O)_2]$

Comparaison du milieu de réaction	Degré de saturation des colorants		
	Vert malachite	Bleu de méthylène	Complexe mole 1^{-1}
AN−$C_2\dot{O}_4$	2,50	2,30	20.10^{-3}
AN−$C_2\dot{O}_4$	1,60	1,30	$11,00.10^{-3}$
AN−$C_2\dot{O}_4$	0,50	1,20	$1,50.10^{-3}$

Tableau 3

Dépendance de l'indice d'acidité de la concentration du complexe
K $[Mn (C_2O_4)_2 (H_2O)_2]$

Composition du milieu de réaction	$(C_0).10^{+3}$ mole 1^{-1}	E/COOH* /g,polymère	Analyse de combustion de l'acrylonitrile			Analyse de combustion du polymère			
			C %	H %	N %	C %	H %	N %	O %
AN−$C_2\dot{O}_4$	20	9.10^{-5}							
AN−$C_2\dot{O}_4$	11	$6,75\cdot10^{-5}$							
AN−$C_2\dot{O}_4$	1,50	$2,64.10^{-5}$							
			67,8	5,6	26	66,03	5,39	25,18	3,38

* On a déterminé conformement au procédé existant à l'Usine de Fibres Săvinești. Ce procédé est identique à celui décrit dans : *Chem. Analit.* **6**, 575 (1961).

Séquences de réaction

1. Initiation — Vitesse

$$C_0 \xrightarrow[kd.f.I]{C^0} C^{\cdot -} \quad (C) \qquad\qquad kd.f.I\,(C_0) \tag{a}$$

$$M \xrightarrow{\gamma} R^{\cdot} \qquad\qquad (G_R I) \tag{b}$$

$$C + 2\,M \xrightarrow{ki} R_m^{\cdot} \qquad\qquad \sum ki\,(C)\,(M)^2 \tag{c}$$

…_ _ _ _ _ _ _ _ _ _ _ _

$$R^{\cdot} + M \xrightarrow{ki'} R_n^{\cdot} \qquad\qquad \sum k_i'\,(R^{\cdot})\,(M) \tag{d}$$

2. Propagation

$$R_m^{\cdot} + M \xrightarrow{kp} R_{m+1}^{\cdot} \qquad\qquad kp\,(R_m^{\cdot})\,(M) \tag{e}$$

$$R_n^{\cdot} + M \xrightarrow{kp} R_n^{\cdot} \qquad\qquad kp\,(R_n^{\cdot})\,(M) \tag{f}$$

3. Réactions de transfert

$$R_m^{\cdot} + M \xrightarrow{k_{tr,M}} R_n^{\cdot} \qquad k_{tr,M}\,(R_m^{\cdot})\,(M) \tag{g}$$

$$R_m^{\cdot} + S' \xrightarrow{k_{tr,S}} R_n^{\cdot} + B \qquad k_{tr,S}\,(R_m^{\cdot})\,(S) \tag{h}$$

$$R_m^{\cdot} + C \xrightarrow{k_{tr,C}} R_n^{\cdot} + D \qquad k_{tr,C}\,(R_m^{\cdot})\,(C) \tag{i}$$

4. Fin

$$R_m^{\cdot} + R_m^{\cdot} \begin{matrix} \overset{k_{tc}}{\nearrow} \quad P_{n+m} \\ \longrightarrow \\ \underset{k_{td}}{\searrow} \quad P_m + P_n \end{matrix} \qquad k_{tc} + k_{td} = k_t \quad 1/2\, k_t\,(R_m^{\cdot})^2 \tag{j}$$

où

C_0 = concentration initiale du complexe ;
$C_2O_4^{\cdot} = C^{\cdot -} = C$ = le radical oxalyle ;
$R_m^{\cdot}$ = macroradical croissant provenant du radical oxalyle ;
$R_n^{\cdot}$ = macroradical croissant ;
$R^{\cdot}$ = radical primaire ;
A,B,D = produits de réaction ;
k_i = constante de vitesse d'initiation de la réaction par l'intermédiaire du radical oxalyle ;
k_i' = constante de vitesse d'initiation de la réaction purement radiochimique ;
k_p = constante du processus de propagation ;
k_t = constante du processus final (k_{tc} par la combinaison de deux macroradicaux, k_{td} par la disproportion de ceux-ci) ;
$k_{tr,}\ M,\ S,\ C$ = constante de vitesse de transfert pour le monomère, le solvant et l'initiateur.

Nous mentionnons que dans le présent schéma cinétique nous nous sommes proposé, en général, de considérer la constante de vitesse de propagation et de vitesse finale de la réaction égales (pour les processus respectifs).

Conformément à l'étude entreprise pour simplifier le mécanisme de réaction et implicitement de séquences de réactions (tabl. 1), nous pouvons nous permettre une première approximation, notamment que $k_i > k_i'$.

Comme la vitesse de polymérisation est définie en général seulement par le degré de propagation, et en même temps sans négliger toutefois la possibilité de propager la chaîne par l'intermédiaire des radicaux du type $R_n^{\cdot}$, nous pouvons écrire

$$V = -\frac{\mathrm{d}(M)}{\mathrm{d}t} = k_p\,[(R_m^{\cdot}) + (R_n^{\cdot})]\,(M) \tag{12}$$

Conformément aux données expérimentales du tableau 2, et en faisant une première approximation, c'est-à-dire $k_i > k'_i$, nous pouvons écrire les équations de formation et disposition des radicaux $R^{\cdot}_{m}$ et $R^{\cdot}_{n}$ comme étant données par les équations

$$\frac{\mathrm{d}(R^{\cdot}_{m})}{\mathrm{d}t} + \frac{\mathrm{d}(R^{\cdot}_{n})}{\mathrm{d}t} = ki\,(C)\,(M)^2 + k_{tr,M}\,(R^{\cdot}_{m})\,(M) + \tag{13}$$

$$+ k_{tr,S}\,(R^{\cdot}_{m})\,(S) + k_{tr,C}\,(R^{\cdot}_{m})\,(C)$$

et

$$-\frac{\mathrm{d}t\,(R^{\cdot}_{m})}{\mathrm{d}t} - \frac{\mathrm{d}(R^{\cdot}_{n})}{\mathrm{d}t} = k_{tr,M}\,(R^{\cdot}_{m})\,(M) + k_{tr,S}\,(R^{\cdot}_{m})\,(S) + \tag{14}$$

$$+ k_{tr,C}\,(R^{\cdot}_{m})\,(C) + k_t\,[(R\dot{m}) + (R^{\cdot}_{n})]^2$$

Etant donné que les vitesses de formation et de disposition en régime stationnaire sont égales, (éq. 13 = éq. 14), il s'ensuit que

$$k_i\,(C)\,(M)^2 = k_t\,[(R^{\cdot}_{m}) + (R^{\cdot}_{n})]^2 \tag{15}$$

ou

$$[(R^{\cdot}_{m}) + (R^{\cdot}_{n})] = \left(\frac{k_i}{k_t}\right)^{1/2} (C)^{1/2}\,(M) \tag{16}$$

En remplaçant l'expression de l'équation (16) dans l'équation (12) on obtient

$$V = -\frac{\mathrm{d}(M)}{\mathrm{d}t} = k_p(M)\,[(R^{\cdot}_{m}) + (R^{\cdot}_{n})] = k_p \left(\frac{k_i}{k_t}\right)^{1/2} (C)^{1/2}\,(M)^2 \tag{17}$$

ou

$$V = k_p / k_t^{1/2}\,(kd.\,f)^{1/2}\,I^{1/2}\,(C_0)^{1/2}\,(M)^2 \cdot \exp.\,(-\,kd.\,t)$$

CONCLUSIONS

1. De l'étude cinétique entreprise il résulte qu'en présence du complexe oxalique (diacvodioxalomanganate de potassium) la vitesse de réaction est plus grande que dans les milieux de réaction conformément au tableau 1.

2. La valeur du rapport des constantes absolues de réaction ($k_p / k_t^{1/2}$) est plus grande que dans d'autres milieux de réaction étudiés, fait qui démontre la réactivité accrue du monomère dans ce milieu de réaction.

3. Le produit obtenu à la suite de la réaction possède de bonnes propriétés de coloration et acides. De ce point de vue, l'étude offre aussi une certaine importance pratique.

Revue Roumaine de Chimie, **14**, 1093 – 1097 (1969)

ELECTRONIC SPECTRA OF SOME AROMATIC METAL KETYLS

V. E. SAHINI and LILIANA CIUREA

University of Bucharest, Laboratory of Physical Chemistry, Bucharest, Bd. Republicii 13

Received February, 20 1969

Electronic spectra in the visible region are reported for the metal ketyls obtained in dimethylformamide from some substituted benzophenone, benzanthrone, fluorenone, benzil, 9, 10-phenanthrenequinone, 9, 10-anthraquinone and substituted anthraquinone. The influence of the metal cation on the maxima of the absorption bands is examined. The transition energies calculated using Hückel LCAO MO method are compared with those obtained from the experimental frequencies.

Previous studies of the electronic spectra of the metal ketyls obtained in ethereal solvents have proved their existence in solution as ion pairs.

In the present paper are studied the spectra of the metal ketyls obtained in a more polar solvent, namely dimethylformamide (DMF), in which the tendency of ion pair formation is much reduced. Besides the fluorenone, benzil, and quinone metal ketyls, which have already studied in ethereal solvents, [1-4] we extended the spectral study to the ketyls obtained from benzanthrone and some substituted benzophenone and anthraquinone. The dependence of the maxima of the absorption bands of metal ketyls on the metal used as a reduction agent is examined. The results are given in table 1.

The metal ketyls were prepared by the action of the metals (Li, Na, K or Sr) on the ketone in an atmosphere of dried and purified argon. The ketones were recrystallized, their purity being verified by the melting points. Dimethylformamide was purified by refluxing and fractional distillation from P_2O_5. The spectra were obtained with a UNICAM SP 500 spectrophotometer.

---

[1] H. V. Carter, B. J. McClelland and W. Warhurst, *Trans. Faraday Soc.*, **56**, 455 (1960).

[2] N. Hirota and S. I. Weissman, *J. Amer. Chem. Soc.*, **86**, 2538 (1964).

[3] L. Ciurea, V. E. Sahini and C. Volanschi, *Rev. Roumaine Chim.*, **9**, 819 (1964).

[4] K. Maruyama, *Bull. Chem. Soc. Japan*, **37**, 553 (1964).

Table 1

Wavelengths of the absorption maxima of the metal ketyls

Anion	Cation	λ(mμ)			
benzophenone$^-$	Na$^+$		755*		
4-nitro-6-methoxy-benzophenone$^-$	Na$^+$		685		
3-methyl-4-nitro-6-methoxy-benzophenone$^-$	Na$^+$		660		
4-nitro-5-methyl-6-methoxy-benzophenone$^-$	Na$^+$		455		
3-methyl-5-nitro-6-methoxy-benzophenone$^-$	Na$^+$		472		
4-chloro-4′-amino-benzophenone$^-$**	Na$^+$		480		
fluorenone$^-$	Li$^+$	468	532	550	
	Na$^+$	470	535	545	
	K$^+$	470	530	555	(755)
	Sr^{2+}		525	556	
benzil$^-$	Li$^+$	615	655		
	Na$^+$	625	665		
	K$^+$	630	670		
benzanthrone$^-$	Li$^+$	620	485	540	
	Na$^+$	625	500	560	
	K$^+$	615	516	550	
9, 10-phenanthrenequinone$^-$	Li$^+$		510	550	
	Na$^+$		510	550	
	K$^+$		515	550	(675)
	Sr^{2+}		675		
9, 10-anthraquinone$^-$	Li$^+$		560		
	Na$^+$		552		(685)
	K$^+$		556		
	Sr^{2+}		685		
1,5-diamino-anthraquinone$^-$	Li$^+$		556		
	Na$^+$		560		(700)
	K$^+$		576		(765)
1,5-dinitro-anthraquinone$^-$	Li$^+$		568		
	Na$^+$		560		(680)
	K$^+$		578		

* This value was taken from literature.[5]

** This ketyl like the benzophenone ketyl reacted slowly with DMF.

---

[5] D. G. Powell and E. Warhurst, *Trans. Faraday Soc.*, **58**, 953 (1962).

Excepting substituted anthraquinone, the initial ketones from which the metal ketyls were obtained have no absorption bands in the region 450—1000 mμ. In this region the corresponding ketyls present absorption bands, which disappear when the ketyls come into contact with the air. The new bands which appear in the spectra of the substituted anthraquinone during the formation of the ketyls are denoted in figure 1 by an asterisk. The wavelengths of the absorption maxima of the 9,10-antraquinone alkali-ketyls differ a little from each other and their values are close to the wavelength of the absorption maximum of the respective free ion obtained electrolytically in DMF (550 mμ).

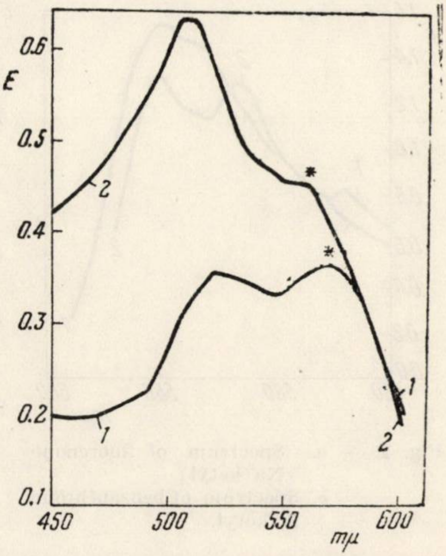

Fig. 1. — *a*, Spectrum of 1,5-dinitro-anthraquinone K ketyl;
b, Spectrum of 1,5-diamino-anthraquinone Na ketyl.

The spectra of the fluorenone ketyls show in the range of concentration 10^{-4}—10^{-5} m/l in DMF an intense wide band at about 530 mμ and one weak at about 470 mμ. These bands are also present in the spectra of the fluorenone ketyls in ethereal solvents but at lover wavelenghts, assigned by Hirota [2] to the paramagnetic monomer and dimer, respectively. With the increase in the concentration of metal ketyls a new band at about 550 mμ appears in the spectra of the ketyls from fluorenone and also from 9,10-phenanthrenequinone and benzanthrone (fig. 2 and 3).

For the assignment of this band the spectra of the respective free ions produced electrolytically in DMF are now under investigation to obtain the wavelengths of the absorption maxima of the free mononegative and dinegative ions. The spectrum of the fluorenone anion obtained electrolytically presents a band at 548 mμ which also appears in the spectra of the fluorenone ketyls. As supporting electrolyte was used tetrabutylammonium iodide.

The metal ketyls which have relative intense absorption bands in the region 450—550 mμ present also very weak bands in the region 600—800 mμ, whose intensities increase at lower temperatures. Such weak bands were observed by Maruyama [4] in the spectra of the 9,10-phenanthrenequinone ketyls in tetrahydrofuran as solvent and were assigned to the diamagnetic dimers. The wavelengths of these bands are given in table 2 in brackets. The spectra of the ketyls obtained from 9,10-phenanthrenequinone and 9,10-anthraquinone with Sr as reduction agent present intense bands at 675 mμ and 685 mμ, respectively, proving their existence in solution as dimers.

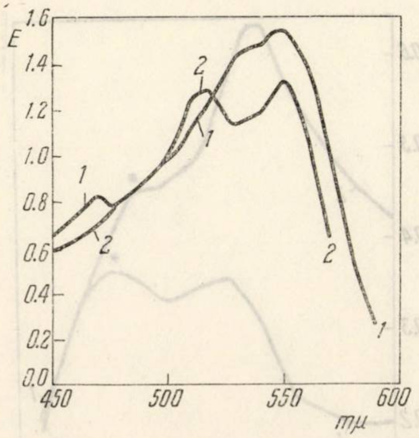

Fig. 2. — *a*, Spectrum of fluorenone Na ketyl;
b, Spectrum of benzanthrone K ketyl.

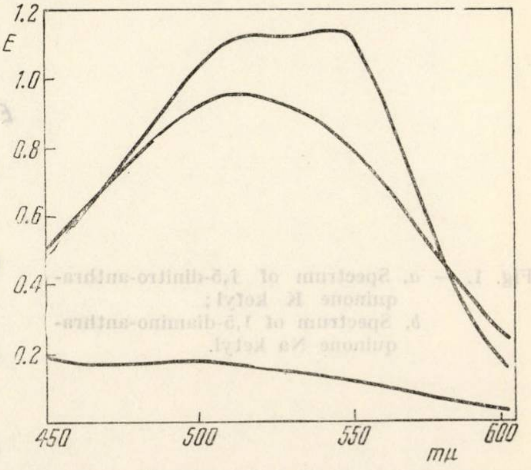

Fig. 3. — Spectrum of 9,10-phenanthrenequinone K ketyl as reduction proceeds.

Comparing the spectra of the metal ketyls in ethereal solvents and in DMF a shift of the maxima of the absorption bands to the longer wavelengths was observed in the last solvent. Also the maxima of the absorption bands depend on the nature of the metal cation to a smaller extent due to a much weaker interaction between ions in DMF. The electron spin resonance spectra of these metal ketyls in DMF[6] showed no alkali metal hyperfine splittings as if they were free ions or weak ion pairs. For this reason it is convenient to compare the experimental frequencies of the metal ketyls in DMF with the theoretical predictions. In table 2 are given the transition energies of the anions E^{calc} calculated using the Hückel MO method and the energies E^{exp} corresponding to the experimental frequencies of free anions obtained either electrolytically (for the 9,10-anthraquinone and fluorenone) or by graphical extrapolation [1] of the ketyls frequencies. The E^{calc} values were obtained based on Mc Clelland's assumption [7] according to whom the frequencies of the ketyl arise from the transition of the electron given by the metal from the $(N + 1)^{th}$ orbital of respective ketone to a higher orbital.

---

[6] V. E. Sahini and L. Ciurea, *Rev. Roumaine Chim.*, (in press).

[7] B. J. McClelland, *Trans. Faraday Soc.*, **57**, 1458 (1961).

Table 2

Experimental and calculated values of the transition energies of the anions

Anion	$E^{calc}_{N+1\to N+2}$ (eV)	$E^{calc}_{N+1\to N+3}$ (eV)	E^{exp} (eV)
Benzophenone	1.71	1.71	1.61
Fluorenone	0.33	1.91	2.26
Benzil	1.54	1.88	1.63 ; 1.79
Benzanthrone	1.44	2.03	1.82
9,10-Phenanthrenequinone	1.73	1.92	2.33
9,10-Anthraquinone	1.35	2.05	2·25

The parameters used in calculations were those with which a good agreement between experimental and calculated spin densities in the ketyls anions have been obtained. The following set of parameters were used for 9,10-anthraquinone and benzophenone : $\alpha_0 = \alpha + 1.2\,\beta$; $\beta_{co} = 1.6\,\beta$; $\alpha_{c(o)} = \alpha + 0.12$ and $\alpha_0 = \alpha + 1.3\,\beta$; $\beta_{co} = 1.41\ \beta$; $\alpha_{c(o)} = \alpha + 0.2\beta$, respectively, where α_0 and $\alpha_{c(o)}$ are the Coulomb integrals for the carbonyl oxygen and carbon atoms and β_{co} is the carbonyl resonance integral. For β_{c-c} was taken the value -2.7 eV. With the parameters mentioned above was obtained for the benzophenone anion a good agreement between E^{calc} and E^{exp} and also the calculated spin densities are not much different from those calculated with the "best" parameters used for the explanation of its ESR spectrum.[8] For benzanthrone the parameters from a previous paper[6] were used and for all the other ketone the parameters proposed by Dehl and Fraenkel.[8] With the last parameters was obtained for the benzophenone anion $E^{calc} = 1.36$ eV, a close value to that obtained by McClelland[9] (1.26 eV) in the Pople molecular orbital approximation. From table 2 we see that for the most studied ketyls the experimental energies correspond to those calculated for the transition N + 1 → N + 3.

---

[8] R. Dehl and G. K. Fraenkel, *J. Chem. Phys.*, **39**, 1793 (1963).

[9] B. J. McClelland, *Trans. Faraday Soc.*, **57**, 2073 (1961).

Revue Roumaine de Chimie, **14**, 1093–1097 (1969)

Revue Roumaine de Chimie, **14**, 1099–1106 (1969)

ELECTRODEPOSITION OF ZINC FROM PYROPHOSPHATE SOLUTIONS. I

STUDY OF EQUILIBRIUM POTENTIALS OF ZINC ELECTRODE

O. RADOVICI and CECILIA VASS

Institute of Physical Chemistry of the Academy
Bucharest, str. Dumbrava Roşie, 23

Received April 6, 1968

Equilibrium potentials of zinc electrode in pyrophosphate solutions in the $1\times10^{-1} - 5\times10^{-4}$ M concentration range of Zn^{2+} ions were determined. Experimental values were compared with theoretical ones, calculated from solution equilibrium data. The thermal temperature coefficients of the potentials were measured on the temperature range 15–55°. In case the concentration polarization is removed, in pyrophosphate electrolytes, zinc electrode behaves as a reversible electrode.

The baths with alkaline pyrophosphates recently acquired an outstanding importance in the electrodeposition process of zinc[1–4]; they present over cyanide baths the advantage of cathodic efficiency, non-toxicity, chemical stability, low costs and low chemical dissolution of anode during pH decreasing on functioning. Series of authors indicated the working conditions and bath compositions, to obtain a high 90–100 % yield.[5–7]

For the study of the zinc electrodeposition mechanism from pyrophosphate solutions the knowledge of the equilibrium potentials of zinc electrode is needed, since on the basis of these values the real overpotential is determined.

Very few references on the behaviour of zinc electrode in pyrophosphate medium and the kinetic process of electrodeposition are available. In only one work [8] studying the brass plating from non-cyanide electrolytes, the value of zinc potential in pyrophosphate solution is mentioned.

In the present paper the variation of equilibrium potential of zinc electrode *versus* concentration of solutions, temperature and other parameters is studied.

---

[1] T. L. Rama Char, *Electroplating and Metal Finishing*, **10**, 347 (1957).
[2] T. L. Rama Char, *Electroplating* (*Bombay*), **1**, 48 (1959).
[3] V. Sree and T. L. Rama Char, *Electroplating and Metal Finishing*, **12**, 326 (1959).
[4] D. Porey and J. F. Marx, *Proc. Amer. Electropl. Soc.*, **46**, 70 (1959).
[5] T. L. Rama Char, *J. Sci. Ind. Res. India*, **15 B**, 509 (1956).
[6] W. H. Mc Mullen and F. W. Eppensteiner, *Mater. Protect.*, **4**, 55 (1965).
[7] W. H. Mc Mullen and F. W. Eppensteiner, *Plating*, **52**, 123 (1965).
[8] A. I. Stabrovskii, *Zhur. fiz. Khim.*, **26**, 949 (1952).

EXPERIMENTAL

The working cell (fig. 1) was an improved form of that used in a previous work [9]; the following changes were made : a rapid thermosetting was ensured by the sheath surrounding the cell, the distance between the working and reference electrodes was decreased — this is a very important factor in case less conductible electrolytes e.g. $Na_4P_2O_7$ compared with $K_4P_2O_7$ are used —, and the distance between the Luggin capillary and working electrode surface is adjustable. Small size cell allows measurements with only 15—20 ml of solution. Platinum spheres with circular surfaces resulted by grinding and polishing soldered in glass were used as electrodes : on these surfaces zinc was electrodeposited from the working solution during 1 hour at a current density of 5 ma/cm². All the electrodes represented in figure 1 were used to compare the results.

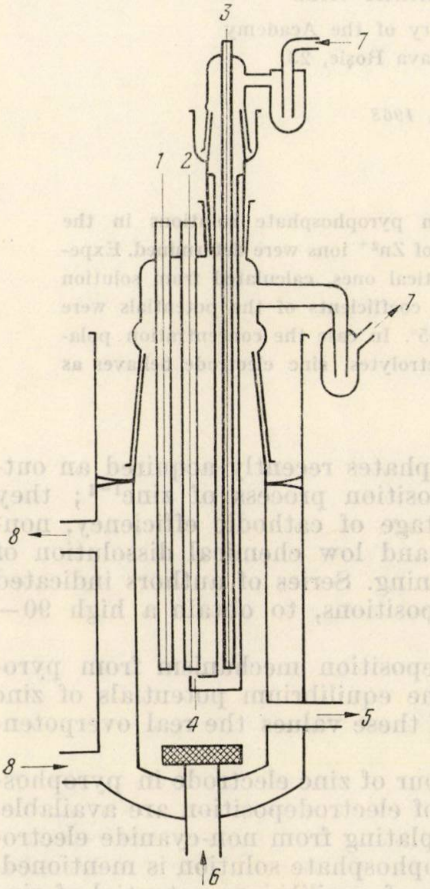

Fig. 1. — Electrolytic cell ; *1*, counter electrode ; *2*, working electrode ; *3*, reference electrode ; *4*, Luggin capillary ; *5*, connection for calomel electrode ; *6*, gas inlet ; *7*, gas outlet valves ; *8*, circulation of the thermosetting water.

Solutions of 1×10^{-1}—5×10^{-4} M zinc concentrations were used the pyrophosphate-to-metal ratio was varied as 2 : 1, 2.5 : 1 and 4 : 1. Chemically pure as well as three times recrystallized reagents from three times distilled water were used. The working solutions were deaerated by bubbling in purified argon for several hours before the experiments started.

---

[9] O. Radovici and C. Vass, *Rev. Roumaine Chim.*, **12**, 1181 (1967).

The measurement of stationary potentials of zinc electrode was achieved with a Q L K 0.1 mV precision potentiometer.

The electrode polarization was carried out by the galvanostatic method, potential measurements being made by means of a Graphispot type recorder in stationary conditions, and with a C.D. 1400 type Solartron oscilloscope in pulse conditions.

Thermosetting precision was ± 0.1 :

The potential values are given in comparison with the normal hydrogen electrode, considering the potential value of saturated calomel electrode of + 244 mV.

RESULTS AND DISCUSSION

The reaction between ions Zn^{2+} and $P_2O_7^{4-}$ is known to produce $Zn_2P_2O_7$ in white solid form, insoluble in water, but soluble in $P_2O_7^{4-}$ excess,[10] process which corresponds to the equations :

$$\begin{aligned} 2Zn^{2+} + P_2O_7^{4-} &\rightarrow Zn_2P_2O_7 \\ Zn_2P_2O_7 + 3P_2O_7^{4-} &\rightleftharpoons 2Zn(P_2O_7)_2^{6-} \end{aligned} \qquad (1)$$

For this reason, in literature there exist recommendations [11, 12] concerning the sequence of chemicals dissolving in order to obtain the above mentioned complex. For pH's within 7—9.5, zinc is mentioned [13] to form, like copper [14] whose complexes with the $P_2O_7^{4-}$ anion have been more carefully studied, in predominant quantity the complex indicated by (1), the complex $Zn(P_2O_7)^{2-}$ being also present in solution.

Stationary electrode potentials of zinc electrode in solutions of $1 \times 10^{-1} - 5 \times 10^{-4}$ M $ZnSO_4.7H_2O$ concentrations containing $Na_4P_2O_7.10H_2O$ in the quantity indicated above were measured. In figure 2 the results are presented for the 1 : 4 ratio. The dependence is linear, and two regions can be distinguished : in the region of more concentrated solutions (10^{-1}—10^{-2} M) the increase of potential with the concentration is much slower compared with that in the smaller concentration region (10^{-2}—5×10^{-4} M). The two slopes are of 14 and 40 mV respectively. This phenomenon is similar to that observed in equilibrium potential determinations of copper electrode in pyrophosphate solutions.[15]

To compare experimental and theoretical results, the value of zinc electrode potential calculated according to Nernst's equation is needed :

$$E = E_0 + \frac{2.3\ RT}{2F} \log\,[Zn^{2+}] \qquad (2)$$

---

[10] H. Basset, W. L. Bedwell and J. B. Hutchinson, *J. Chem. Soc.*, **1936**, 1412.

[11] P. F. Kalyuzhnaya, *Zhur. priklad. Khim.*, **33**, 2253 (1960).

[12] P. F. Kalyuzhnaya and K. N. Pimenova, *Zhur. priklad. Khim.*, **40**, 1975 (1967).

[13] Frank Passal, *Plating*, **46**, 628 (1959).

[14] J. Watters and A. Aaron, *J. Amer. Chem. Soc.*, **75**, 611 (1953).

[15] E. K. Jastrebova and A. T. Vagramyan, *Zhur. fiz. Khim.*, **38**, 1551 (1964).

As the majority of zinc ions initially dissolved is in complex form, the concentration of free ions could be calculated starting from the following situation existing in solution:

$$\begin{aligned} M^{\text{tot}} &= M + MX + MX_2 \\ X^{\text{tot}} &= X + MX + 2MX_2 \end{aligned} \tag{3}$$

where:
M^{tot} and X^{tot} are the concentrations of metal in the salt and pyrophosphate respectively, initially dissolved.

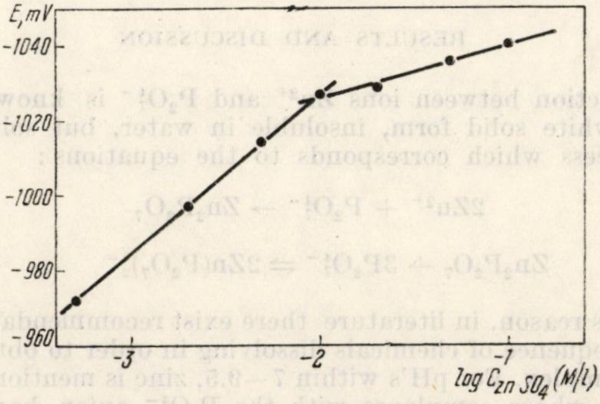

Fig. 2. — Dependence of equilibrium potential of zinc electrode (E in mV) on the logarithm of Zn^{2+} ions concentration ($C_{Zn^{2+}}$ in mole/l).

M and X are the concentrations of free ions.
MX and MX_2 are the concentrations of two possible forms of the complex.

If the partial dissociation constants of the two types of complex ions:

$$k_1 = \frac{[M]\,[X]}{[MX]} \quad \text{and} \quad k_2 = \frac{[MX]\,[X]}{[MX_2]} \tag{4}$$

are introduced into equations (3), the following two relations for the needed magnitudes are found:

$$M = \frac{M^{\text{tot}} \cdot k_1 k_2}{k_1 k_2 + k_2 X + X^2} \tag{5}$$

$$X^3 + X^2\,(k_2 + 2M^{\text{tot}} - X^{\text{tot}}) + X\,(k_1 k_2 + k_2 M^{\text{tot}} - $$
$$- k_2 X^{\text{tot}}) - k_1 k_2\ X^{\text{tot}} = 0$$

In case the concentration of hydrogen ions is considered, the fourth order dissociation constant of pyrophosphoric acid must be considered too, as for the copper complex,[14] with the same anion within the pH range 7.2—10. By neglecting the MX concentration the equation (3) becomes:

$$\begin{aligned} M^{\text{tot}} &= M + MX_2 \\ X^{\text{tot}} &= X + 2MX_2 + HX \end{aligned} \tag{6}$$

From relations (4) and (6) the following equations for M and X results :

$$M = \frac{M^{\text{tot}} \cdot k_1 k_2}{X^2} ; \; X = \frac{X^{\text{tot}} - 2M^{\text{tot}}}{1 + \dfrac{10^{-\text{pH}}}{k_4'}} \tag{7}$$

where k_4' represents the fourth dissociation constant of pyrophosphoric acid equal to 2.4×10^{-10}.

The values of k_1 and k_2 available in literature are only few and non-concordant. Thus, for the solution containing $Zn\ SO_4 . 7H_2O$ in 5×10^{-2}M concentration and $Na_4P_2O_7 . 10H_2O - 1 \times 10^{-1}$ M at 18° the total dissociation constant of $Zn(P_2O_7)_2^{6-}$ ion denoted by k, was determined [8] by a potentiometric method and a 5.74×10^{-8} value was found, compared with 3.4×10^{-7} previously given.[16] In a more recent paper [17] the two dissociation constants for the two sorts of complexes, denoted K_1 and K_2, are given as equal to 8×10^{-7} and 8.06×10^{-8} respectively, without specifying if they are total or partial, the method of determination and the concentration of solutions. In both papers [8, 17] no mention was made about the purity of chemicals.

Using equations (5) and (7) and considering K_1 and K_2[17] as partial ones, the concentration of free zinc ions Zn^{2+} was calculated. The values obtained were replaced in equation (2) and values of electrode potential very close to the experimental ones were found (table 1). The standard potential for zinc electrode was taken as — 763 mV.[18]

Table 1

Experimental and theoretical equilibrium potential values of zinc electrode in pyrophosphate solutions at 25°

M^{tot} mole/l	X^{tot} mole/l	pH	E_{calc}, mV (eq.5)	(eq.7)	E_{exp}, mV
1×10^{-1}	25×10^{-1}	9	−1105	−1062	−1040
5×10^{-2}	1.25×10^{-1}	9.1	−1096	−1054	−1036
1×10^{-2}	2.5×10^{-1}	9.3	−1075	−1049	−1026

The discrepancy existing between experimental and theoretical values proves once more that the data available are not enough as to allow an exact determination of the equilibria and activities of the species existing in the solution.

Measurements carried out on solutions the content of which corresponds to the proportion between $Na_4P_2O_7 : Zn^{2+}$ of 2 : 1; 2.5 : 1 and 4 : 1 lead to results unessentially different, as seen in table 2.

---

[16] G. Sartory, *Gazz. chim. Ital.*, **64**, 3 (1934).

[17] V. P. Persiantseva and P. C. Titov, *Nauchn. Doklady Vysshei Shkoly, Khim. i Khim. Tekhnol.*, **1958**, 584.

[18] W. M. Latimer, "The Oxidation States of the Elements and Their Potentials in Aqueous Solutions", Prentice Hall, NY, 1952, Russian Ed., 1956, p. 173.

The above data support the hypothesis checked for copper,[14] namely that the theoretical ratio pyrophosphate over zinc concentration is 2 : 1, all pyrophosphate excess resulting in free form.

Table 2

Equilibrium potentials of zinc electrode for different pyrophosphate-to-zinc molar ratios at 25°

Pyrophosphate-to-zinc molar ratio	E mV	
	$Zn^{2+} = 1\times10^{-1}$ M	$Zn^{2+} = 2\times10^{-2}$ M
2 : 1	−1036	−1028.4
2.5 : 1	−1039.8	−1029
4 : 1	−1040	−1028.8

The potential determinations carried out in solutions prepared from only chemically pure reagents gave lower values than for the recrystallized ones. The maximum difference obtained was ~ 60 mV for the solution of Zn^{2+} concentration 1.25×10^{-1} M, the difference decreasing with the dilution. The values obtained are very close to those previously obtained.[8]

References concerning the thermal temperature coefficients of the equilibrium potential of zinc electrode in pyrophosphate solution are

Table 3

Thermal temperature coefficients of zinc electrode in pyrophosphate solutions

Solution composition	Temperature range	$\left(\frac{dE}{dT}\right)_{th}$, mV/deg. C
1×10^{-1} M $ZnSO_4$ + 2.5×10^{-1} M $Na_4P_2O_7$	15 + 55°	0.4
1×10^{-1} M $ZnSO_4$ + 4×10^{-1} M $Na_4P_2O_7$	25 + 55°	0.43
5×10^{-2} M $ZnSO_4$ + 2×10^{-1} M $Na_4P_2O_7$	15 + 55°	0.5
2×10^{-2} M Zn SO_4 + 4×10^{-2} M $Na_4P_2O_7$	25 + 55°	0.32
2×10^{-2} M Zn SO_4 + 8×10^{-2} M $Na_4P_2O_7$	25 + 55°	0.33

but sparingly available in literature. The potentials were measured in the temperature range 15—55°, the results obtained in the direct and reverse course coincided. The thermal temperature coefficients are positive and as seen from table 3, the differences obtained for the various concentrations of complex salt are unimportant.

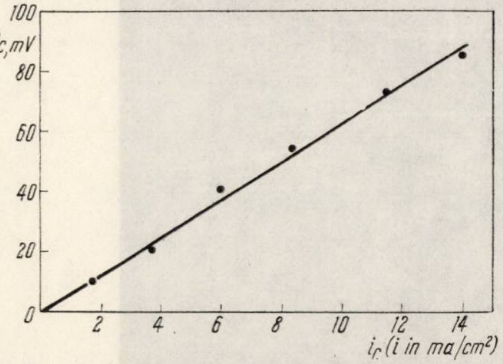

Fig. 3. — $\eta_c - i_c$ curve in galvanostatic conditions ($c_{Zn^{2+}} = 5 \times 10^{-2}$ mole/l ; t = 25°).

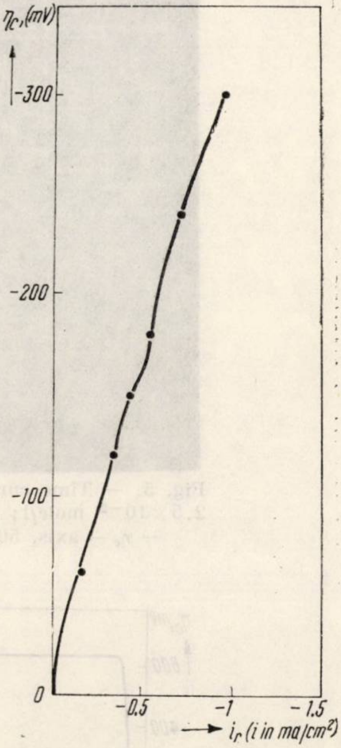

Fig. 4. — $\eta_c - i_c$ curve in galvanostatic stationary conditions ($c_{Zn^{2+}} = 5 \times 10^{-2}$ mole/l; t = 25°).

One of the basic criteria of the electrode reversibility is considered the small slope of the polarization curve $i - \eta$. In figure 3 the polarization curve of zinc electrode in galvanostatic pulse conditions is presented; the elimination of concentration polarization brings about a small slope on the $i - \eta$ plot. For comparison purposes on figure 4 the same plot is drawn in stationary conditions, that is in the presence of concentration polarization, the measurement of electrode potential is carried out 2 minutes after its polarization. On slightly increasing the current density, the cathodic potential is considerably growing.

Another criterion is the determination of the time during which the potential of positively or negatively polarized electrode returns to the initial value, no matter what the value and duration of polarization is. On figure 5 the time variation of the electrode potential at a cathodic polarization current density of 10 ma/cm² for zinc electrode in the solution containing 5×10^{-2} M Zn^{2+}, in pulse conditions, is presented. The potential jump is practically instantaneous. In stationary conditions the time necessary to reach the equilibrium potential is about 5–6 minutes (fig. 6).

In conclusion, the values of equilibrium potentials of zinc electrode in pyrophosphate electrolytes could be considered as being in good agreement with the theoretical ones, computed with the assumption stated above.

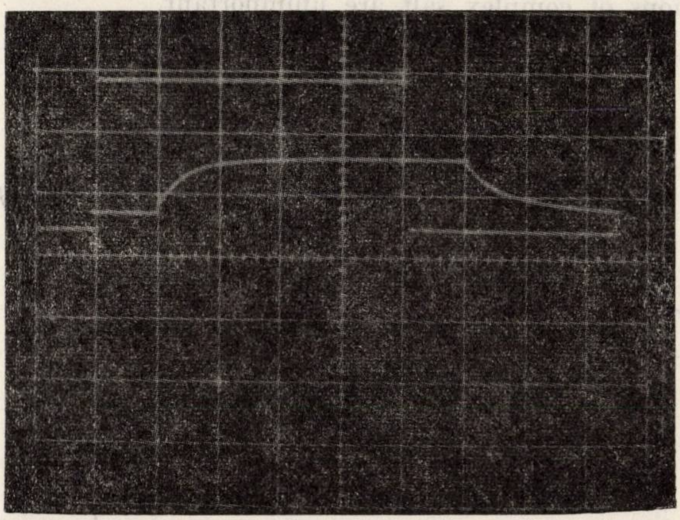

Fig. 5. — Time curve in galvanostatic pulse conditions ($c_{Zn^{2+}} = 2.5\times10^{-2}$ mole/l; $i_c = 10$ ma/cm^2; units — t — axis, 1 m s; — η_c — axis, 50 mv; the corresponding rectangular current pulse is also presented)

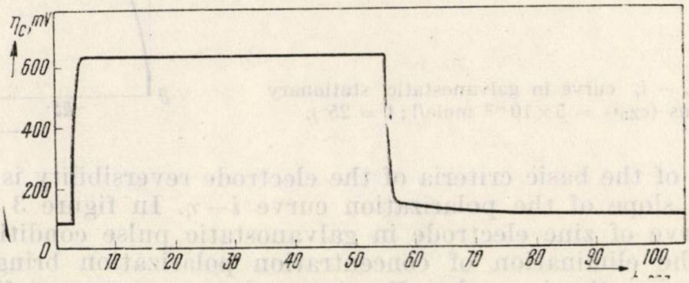

Fig. 6. — Time curve in galvanostatic stationary conditions ($c_{Zn^{2+}} = 2.5\times10^{-2}$ mole/l).

In conditions in which the concentration polarization is removed, the zinc electrode potential changes very little with increasing current density and returns about instantaneously to its equilibrium value as soon as polarization is interrupted. From these data as well as from identical values of potentials for different temperatures obtained for direct and reverse course, the zinc electrode in pyrophosphate solutions results to be reversible and the stationary potentials measured to be practically the equilibrium values. For these reasons the zinc electrode could be used as reference electrode for the kinetic study of its electrodeposition from pyrophosphate electrolytes.

Revue Roumaine de Chimie, **14**, 1107–1112 (1969

CINÉTIQUE DE LA DÉCOMPOSITION THERMIQUE DE CERTAINES COMBINAISONS COMPLEXES DU CHLORURE DE CUIVRE AVEC LA PYRIDINE ET DES PYRIDINES SUBSTITUÉES

D. FĂTU, SANDA FĂTU et E. SEGAL

Université de Bucarest, Chaire de Chimie Physique II, 13 Bd. Republicii

Reçu le 3 octobre 1968

On présente les résultats obtenus à l'évaluation des paramètres cinétiques déterminés des données thermogravimétriques pour la décomposition des combinaisons complexes du chlorure de cuivre avec la pyridine et des pyridines substituées. En appliquant les méthodes de Freeman-Caroll et Coats-Redfern on obtient des résultats concordants. Pour les réactions d'ordre zéro, les valeurs des facteurs préexponentiels, calculées en considérant comme étape limitante la diffusion du composant volatil à travers la couche de substance décomposée, concordent de façon satisfaisante avec les valeurs expérimentales.

Par suite des recherches concernant l'évaluation des paramètres cinétiques des réactions de forme générale

$$A\,(s) \rightarrow B\,(s) + C\,(g)$$

obtenus des données thermogravimétriques, on présente une étude cinétique de la décomposition thermique de certaines combinaisons complexes du chlorure de cuivre avec la pyridine et des pyridines substituées.

Bowman et Rogers [1] ont démontré, par la méthode d'analyse thermodifférentielle en courant d'azote, que la décomposition du complexe dipyridinique du chlorure de cuivre a lieu dans une seule étape, entre la température ambiante et 500°. La corrélation des données sur la stabilité thermique avec les constantes thermodynamiques déterminées en solution conduit à la conclusion que la décomposition est accompagnée d'un processus d'oxydo-réduction.

Les valeurs des paramètres cinétiques ont été déterminées selon les méthodes de Freeman-Caroll [2] et Coats-Redfern.[3]

---

[1] P. B. Bowman et L. B. Rogers, *J. Inorg. Nuclear Chem.*, **28**, 2215 (1966).

[2] E. S. Freeman et B. Caroll, *J. Phys. Chem.*, **62**, 394 (1958).

[3] A. W. Coats et J. P. Redfern, *Nature*, **201**, 68 (1964).

PARTIE EXPÉRIMENTALE

On a utilisé

— complexe dipyridinique du chlorure de cuivre $Cu^{II} Py_2Cl_2$

— complexe di-β-picolinique du chlorure de cuivre, Cu^{II} $(\beta\text{-pic})_2Cl_2$

— complexe tri-γ-picolinique du chlorure de cuivre Cu^{II} $(\gamma\text{-pic})_3Cl_2$

synthétisés par les méthodes décrites dans la littérature.[4] Les combinaisons complexes avec un contenu intermédiaire de ligand ont été obtenues par décomposition thermique.

Les substances, passées au mortier, ont été ensuite tamisées ; on a retenu les cristaux ayant le diamètre compris entre 0,1 et 0,09 mm.

Les courbes d'échauffement des substances dans l'air thermogravimétrique (TG), thermogravimétrique dérivée (DTG) et de température (T) ont été enregistrées simultanément grâce à un dérivatographe MOM Budapest type Paulik, Paulik, Erdey.

RÉSULTATS ET DISCUSSIONS

L'échauffement des combinaisons complexes riches en composant volatil de type $Cu^{II} L_2Cl_2$ mène à une séquence de transformations, identique à celle obtenue à la décomposition des composants similaires de nickel, [5,6] cobalt [7] et manganèse,[8] avec deux molécules de ligand.

Au cas où une solution saturée de chlorure de cuivre est soumise à l'action de la γ-picoline, on obtient une combinaison complexe de composition $Cu(\gamma\text{-pic})_3Cl_2$. Pour une vitesse d'échauffement de 10°K/mn, l'élimination de deux molécules γ-picoline de ce composant a lieu en un processus unique. En réduisant la vitesse d'échauffement jusqu'à 2°K/mn, les deux molécules de picoline s'éliminent séparément.

Nous présentons ensuite les valeurs des paramètres cinétiques (ordre de réaction n, énergie d'activation E et facteur préexponentiel A) obtenues par les méthodes mentionnées, pour toutes les réactions de décomposition des combinaisons complexes précitées, y compris celles obtenues comme intermédiaires pendant l'échauffement, en indiquant la masse de poudre soumise à la décomposition m_p, la vitesse d'échauffement $\frac{dT}{dt}$ et la température de réaction t_r, conventionnellement considérée comme température correspondant à la valeur maximale de la vitesse de réaction.

Pour les réactions d'ordre zéro, outre la valeur expérimentale du facteur préexponentiel (A_{exp}), on indique aussi, en vue de la comparaison, sa valeur calculée (A_{calc}), en considérant comme étape limitante la diffusion du composant volatil à travers la couche de substance décomposée. [9]

---

[4] J. Schroeder, « Reaktionen von Metallsalzen in Pyridin », Dissertation Giessen, 1901 p. 25, citée dans G. Spacu, Thèse Univ. Jassy, 1916.

[5] I. G. Murgulescu, E. Segal et D. Fătu, *J. Inorg. Nuclear Chem.*, **27**, 2677 (1965).

[6] N. Hurduc, L. Odochian, I. A. Schneider et E. Segal, *Rev. Roumaine Chim.*, **11**, 1453 (1966).

[7] E. Schönberger, D. Fătu et E. Segal, *Rev. Roumaine Chim.*, **12**, 1205 (1967).

[8] D. Fătu et E. Segal, *Rev. Roumaine Chim.* (sous presse).

[9] I. G. Murgulescu et E. Segal, *Rev. Roumaine Chim.*, **10**, 307 (1965).

$$\mathrm{Cu\,Py_2\,Cl_2(s)} \rightarrow \mathrm{CuPy\,Cl_2(s)} + \mathrm{Py(g)} \qquad \text{(I)}$$

Méthode de Freeman-Caroll	*Méthode de Coats-Redfern*
$m_p = 0{,}0548$ g	$m_p = 0{,}0548$ g
$\frac{dT}{dt} = 10°\mathrm{K/mn}$	$\frac{dT}{dt} = 2°\mathrm{K/mn}$
$t_r = 248°\mathrm{C}$	
$n = 1/2$	$n = 1/2$
$E = 13{,}7$ kcal/mole	$E = 15{,}1$ kcal/mole
$A = 1{,}18 . 10^3\ g^{1/2}\ s^{-1}$	$A = 1{,}35 .\ 10^3\ g^{1/2}\ s^{-1}$

$$\mathrm{CuPy\,Cl_2(s)} \rightarrow \mathrm{CuPy\ 2/3\ Cl_2(s)} + \frac{1}{3}\mathrm{Py(s)} \qquad \text{(II)}$$

$m_p = 0{,}0402$ g	$m_p = 0{,}0402$ g
$\frac{dT}{dt} = 10°\ \mathrm{K/mn}$	$\frac{dT}{dt} = 10°\mathrm{K/mn}$
$t_r = 279°\mathrm{C}$	
$n = 1/2$	$n = 1/2$
$E = 31$ kcal/mole	$E = 28$ kcal/mole
$A = 5{,}6 . 10^9\ g^{1/2}\ s^{-1}$	$A = 1{,}12 .\ 10^9\ g^{1/2}\ s^{-1}$

$$\mathrm{CuPy\ 2/3\ Cl(s)} \rightarrow \mathrm{CuCl_2(s)} + \frac{2}{3}\mathrm{Py\ (g)} \qquad \text{(III)}$$

$m_p = 0{,}0364$ g	$m_p = 0{,}0364$ g
$\frac{dT}{dt} = 10^0\ \mathrm{K/mn}$	$\frac{dT}{dt} = 10°\ \mathrm{K/mn}$
$t_r = 314°\mathrm{C}$	
$n = 1/2$	$n = 1/2$
$E = 5{,}3$ kcal/mole	$E = 6{,}4$ kcal/mole
$A = 6{,}6\ g^{1/2}s^{-1}$	$A = 1{,}07 . 10^{-1}\ g^{1/2}s^{-1}$

$$\mathrm{Cu\,(\beta\text{-}pic)_2Cl_2(s)} \rightarrow \mathrm{Cu(\beta\text{-}pic)\,Cl_2\,(s)} + \mathrm{\beta\text{-}pic(g)} \qquad \text{(IV)}$$

Méthode de Freeman-Caroll	*Méthode de Coats-Redfern*
$m_p = 0{,}0490$ g	$m_p = 0{,}0490$ g
$\frac{dT}{dt} = 5°$ K/mn	$\frac{dT}{dt} = 5°$ K/mn
$t_r = 224°C$	
$n = 0$	$n = 0$
$E = 18{,}5$ kcal/mole	$E = 18{,}5$ kcal/mole
$A_{exp} = 4{,}8 .\ 10^4$ g s^{-1}	$A_{exp} = 1{,}05\ 10^4$ g s^{-1}

$$A_{calc} = 1{,}43\ 10^3 \text{ g s}^{-1}$$

$$\mathrm{Cu\,(\beta\text{-}pic)\,Cl_2(s)} \rightarrow \mathrm{Cu\,(\beta\text{-}pic)_{2/3}\,Cl_2(s)} + \frac{1}{3}\,\mathrm{\beta\text{-}pic\,(g)} \qquad \text{(V)}$$

$m_p = 0{,}0556$ g	$m_p = 0{,}0556$ g
$\frac{dT}{dt} = 5°$ K/mn	$\frac{dT}{dt} = 5°$K/mn
$t_r = 254°C$	
$n = 1/2$	$n = 1/2$
$E = 4{,}1$ kcal/mole	$E = 4{,}57$ kcal/mole
$A = 4{,}46$ g$^{1/2}$ s^{-1}	$A = 2{,}3$ g$^{1/2}$ s^{-1}

$$\mathrm{Cu\,(\beta\text{-}pic)_{2/3}\,Cl_2(s)} \rightarrow \mathrm{CuCl_2(s)} + \frac{2}{3}\,\mathrm{\beta\text{-}pic\,(g)} \qquad \text{(VI)}$$

$m_p = 0{,}0301$ g	$m_p = 0{,}0301$ g
$\frac{dT}{dt} = 5°$ K/mn	$\frac{dT}{dt} = 5°$ K/mn
$t_r = 280°C$	
$n = 1/2$	$n = 1/2$
$E = 15{,}5$ kcal/mole	$E = 14{,}4$ kcal/mole
$A = 5{,}8 . 10^2$ g$^{1/2}$ s^{-1}	$A = 1 . 10^2 .$ g$^{1/2}$ s^{-1}

Méthode de Freeman-Caroll	*Méthode de Coats-Redfern*

$$\mathrm{Cu}\,(\gamma\text{-pic})_3\mathrm{Cl}_2(\mathrm{s}) \rightarrow \mathrm{Cu}\,(\gamma\text{-pic})\,\mathrm{Cl}_2(\mathrm{s}) + 2\gamma\text{-pic}\,(\mathrm{g}) \qquad \text{(VII)}$$

$m_p = 0{,}0548$ g

$\dfrac{\mathrm{d}T}{\mathrm{d}t} = 10°\mathrm{K/mn}$

$t_r = 136°\mathrm{C}$

$n = 0$

$E = 9{,}15$ kcal/mole

$A_{\mathrm{exp}} = 1{,}5\,.\,10^1\ \mathrm{g\ s^{-1}}$

$A_{\mathrm{calc}} = 1{,}6\,.\,10^3\ \mathrm{g\ s^{-1}}$

$$\mathrm{Cu}\,(\gamma\text{-pic})_3\mathrm{Cl}_2(\mathrm{s}) \rightarrow \mathrm{Cu}\,(\gamma\text{-pic})_2\mathrm{Cl}_2(\mathrm{s}) + \gamma\text{-pic}\,(\mathrm{g}) \qquad \text{(VIII)}$$

$m_p = 0{,}0548$ g	$m_p = 0{,}0548$ g
$\dfrac{\mathrm{d}T}{\mathrm{d}t} = 2°\mathrm{K/mn}$	$\dfrac{\mathrm{d}T}{\mathrm{d}t} = 2°\mathrm{K/mn}$
$t_r = 85°\mathrm{C}$	
$n = 0$	$n = 0$
$E = 12{,}6$ kcal/mole	$E = 13{,}1$ kcal/mole
$A_{\mathrm{exp}} = 3{,}8\ 10^3\ \mathrm{s^{-1}}$	$A_{\mathrm{exp}} = 6{,}25\,.\,10^2\ \mathrm{g\ s^{-1}}$

$$A_{\mathrm{calc}} = 1{,}6\,.\,10^3\ \mathrm{g\ s^{-1}}$$

$$\mathrm{Cu}\,(\gamma\text{-pic})_2\mathrm{Cl}_2(\mathrm{s}) \rightarrow \mathrm{Cu}\,(\gamma\text{-pic})\,\mathrm{Cl}_2(\mathrm{s}) + \gamma\text{-pic}\,(\mathrm{g}) \qquad \text{(IX)}$$

$m_p = 0{,}0425$ g	$m_p = 0{,}0425$ g
$\dfrac{\mathrm{d}T}{\mathrm{d}t} = 2°\mathrm{K/mn}$	$\dfrac{\mathrm{d}T}{\mathrm{d}t} = 2°\mathrm{K/mn}$
$t_r = 107°\mathrm{C}$	
$n = \dfrac{1}{3}$	$n = \dfrac{1}{3}$
$E = 20$ kcal/mole	$E = 19$ kcal/mole
$A = 3{,}24\ 10^8\ \mathrm{g^{1/3}\ s^{-1}}$	$A = 1{,}11\,.\,10^9\ \mathrm{g^{2/3}\ s^{-1}}$

En examinant les données expérimentales présentées dans cette note, on remarque la concordance des valeurs des paramètres cinétiques obtenues par les deux méthodes. Il faut souligner la valeur réduite de l'énergie d'activation, pour la réaction (V). Comme pour d'autres cas semblables,[10] l'ordre de réaction varie entre zéro et l'unité, augmentant pour la décomposition des combinaisons complexes à teneur réduite en composant volatil, ce qui dénote que la réaction a lieu dans un domaine cinétique-diffusionnel. La valeur constante de l'ordre de réaction pour les processus (I), (II), (III) et (V), (VI) peut être expliquée dans l'hypothèse que le frittage qui intervient pendant l'échauffement s'oppose au processus de dispersion des grains à la suite de l'élimination du composant volatil; il en résulte que le processus se développe dans un régime cinétique-diffusionnel non modifié.

Les valeurs des facteurs préexponentiels calculées pour les réactions (IV), (VII) et (VIII) concordent de façon satisfaisante avec les valeurs expérimentales.

CONCLUSIONS

1. L'élimination du composant volatil en l'air des combinaisons complexes de type $Cu^{II} L_2Cl_2$ se passe conformément au schéma général de décomposition des métaux de transition.

2. Les valeurs des paramètres cinétiques des réactions de décomposition calculées par les méthodes de Freeman-Caroll et Coats-Redfern concordent de façon satisfaisante.

3. Pour les réactions d'ordre zéro, les valeurs des facteurs préexponentiels, calculées en considérant comme étape limitante la diffusion du composant volatil à travers la couche de substance décomposée, concordent de façon satisfaisante avec les valeurs expérimentales.

---

[10] I. G. Murgulescu et E. Segal, *Rev. Roumaine Chim.*, **11**, 13 (1966).

Revue Roumaine de Chimie, **14**, 1113—1124 (1969)

COMBINAISONS COMPLEXES AVEC DES HYDROXYACIDES. VIII*

LES COMPLEXES DU Ga^{3+} ET In^{3+} AVEC L'ACIDE SACCHARIQUE

CONST. GH. MACAROVICI et EUGENIA PERŢE

Institut de Chimie de l'Académie,
Filiale de Cluj, 59—65, str. Donath

Reçu le 25 juin 1968

On a étudié la formation des complexes entre le gallium et l'indium et l'acide saccharique par la méthode d'extraction (eau-chloroforme), au pH $\geqslant 10$. On a déterminé et calculé le coefficient de distribution, le rapport de combinaison, les constantes d'équilibre et la stabilité relative des complexes de gallium et d'indium avec l'acide saccharique. Le rapport de combinaison autant pour les solutions aqueuses que pour l'état solide est 1 Me : 1 acide saccharique. Le complexe gallium-acide saccharique est plus stable que celui indium-acide saccharique. Les complexes saccharique de gallium et indium sont plus stables que les complexes gluconiques étudiés auparavant. On a synthétisé et analysé les acides gallo- et indosaccharique et on a proposé une formule structurelle.

Dans une note antérieure [1] on a exposé les premiers résultats concernant l'étude de l'interaction des Ga^{3+} et In^{3+} avec l'acide gluconique par la méthode d'extraction et de l'équilibre hétérogène en milieu alcalin.

Cette note contient les résultats obtenus lors de l'étude de l'interaction entre Ga^{3+} et In^{3+} et l'acide saccharique.

Une étude comparative réalisée par Mehltrerter et collab.,[2] concernant la capacité de complexation des acides lactique, citrique, tartrique, arabonique, gluconique, galactonique, saccharique, mucique et glucoheptonique avec Ca(II), Cu(II) et Fe(III), en milieu acide, neutre et alcalin, montre l'effet complexant exceptionnel de l'acide saccharique et mucique particulièrement en milieu alcalin, fait confirmé aussi par nos travaux.[3,4] Cet effet est plus accentué en milieu alcalin, probablement en raison de l'ionisation accrue de l'hydrogène des radicaux hydroxyacides.

---

[*] VII. : Const. Gh. Macarovici et L. Czeglédi, *Rev. Roumaine Chim.*, **14**, 57 (1969).

[1] Const. Gh. Macarovici, E. Perţe et E. Moţiu, *Rev. Roumaine Chim.*, **8**, 975 (1967).

[2] C. L. Mehltrerter, B. H. Alexander et C. E. Rist, *Ind. Eng. Chem.*, **45**, 2782 (1953).

[3] Const. Gh. Macarovici, H. Roth et L. Czeglédi, *Studii şi Cercetări Chim. Fil. Cluj*, **12**, 229, 245 (1961) ; **14**, 69 (1963).

[4] Const. Gh. Macarovici, L. Czeglédi, *Rev. Roumaine Chim.*, **9**, 397 (1964).

Les auteurs préconisent de multiples utilisations industrielles (la résistance des bétons au gel, gravure des objets en aluminium, etc.).

La méthode de travail est identique à celle mentionnée dans l'article précédent.[1]

Les substances utilisées sont : $CaCl_3$ puriss (Fluka AG) et $In(NO_3)_3$ ou $InCl_3$ préparée à partir de l'indium métallique (Johnson Maltey Souchon). L'acide saccharique a été obtenu du saccharate de calcium par dissolution à l'aide d'un cationite et le titre a été établi par la méthode connue.

La concentration totale de l'oxyquinolinate métallique dans HCl 0,25 M a été 1.10^{-3} mole/l, la concentration finale du KOH 0,05 m ($pH > 10$) et la concentration de l'acide saccharique a été variée de 0,1 M—0,008 M.

Les données expérimentales sont reportées aux tableaux 1 et 2.

Tableau

Coefficients de distribution et rendement d'extraction dans

(H_2ZH_4) mole/l	pH	$[Ga].10^{-4}$ $CHCl_3$	$[Ga].10^{-4}$ H_2O	*D*	1/*D*
0,1	10,50	2,49	7,51	0,3316	3,0160
0,08	10,50	2,75	7,25	0,3793	2,6350
0,05	10,50	3,46	6,54	0,5290	1,8900
0,03	10,50	3,98	6,02	0,6611	1,5130
0,01	10,50	5,03	4,97	1,0120	0,9881
0,008	10,50	5,12	4,88	1,0490	0,9530

Tableau

Coefficients de distribution et rendement

$[H_2ZH_4]$ mole/l	pH	$[In].10^{-4}$ $CHCl_3$	$[In].10^{-4}$ H_2O	*D*	1/*D*
0,1	10,50	4,052	5,948	0,6812	1,468
0,08	10,50	4,320	5,680	0,7715	1,297
0,05	10,50	4,878	5,122	0,9826	1,019
0,03	10,50	5,401	4,599	1,1920	0,839
0,01	10,50	6,185	3,815	1,5630	0,640
0,008	10,50	6,794	3,206	1,620	0,617

SUR LA COMPOSITION DES COMPLEXES SACCHARIQUES DU GALLIUM ET DE L'INDIUM

Le principe pour déterminer la composition des complexes respectifs consiste dans l'examen de l'équilibre entre l'oxyquinolinate métallique peu soluble et la solution alcaline du sel potassique de l'hydroxyacide.[5] L'équilibre entre l'oxyquinolinate de gallium, respectivement indium dissous en chloroforme et la phase aqueuse, au $\text{pH} > 10$, est caractérisé par la relation

---

[5] I. V. Piatnitski, *Ukrain. khim. Zhur.*, **23**, 593 (1957).

$$\underset{\text{dans le chloroforme}}{\text{MeOX}_3} \rightleftarrows \underset{\text{dans l'eau}}{\text{Me}^{3+} + 3\text{OX}^-} \qquad (1)$$

d'où l'on peut déduire la constante de distribution

$$K_D = \frac{[\text{Me}^{3+}]\ [\text{OX}^-]^3\ \text{eau}}{[\text{MeOX}_3]\ \text{chloroforme}} \qquad (2)$$

1

le système $Ga^{3+} - H_2ZH_4$

$\log\left(\frac{D_0}{D} - 1\right)$	$\% E$	$-\log B$	$\log$ H_2ZH_4	K_E
0,4583	24,90	8,994	−1,00000	48,03
0,3775	27,51	9,000	−1,09691	56,77
0,1544	34,60	9,280	−1,30103	50,06
−0,0260	39,81	9,480	−1,52289	52,07
−0,5703	50,30	9,910	−2,00000	57,42
−0,6500	51,20	9,960	−2,09691	65,53

$K_m = 54,98$

2

d'extraction dans le système $In^{3+} - H_2ZH_4$

$\log\left(\frac{D_0}{D} - 1\right)$	$\% E$	$-\log B$	$-\log$ $[H_2ZH_4]$	$K_E . 10^{-6}$
0,2219	40,52	9,51	−1,00000	5,263
0,1316	43,54	9,62	−1,09691	5,130
0,0711	49,56	9,85	−1,30103	4,810
0,3063	54,38	10,08	−1,52289	4,705
0,7852	60,98	10,47	−2,00000	5,836
0,9136	61,83	10,81	−2,096691	3,312

$K_m = 4,844 . 10^{-6}$

Dans la phase aqueuse les ions Me^{3+} (Ga^{3+} ou In^{3+}) se trouvent en équilibre avec les ions acide saccharique comme ci-dessous

$$\text{Me}^{3+} + \text{nZH}_4^{2-} \rightleftarrows \text{Me}(\text{ZH}^{2-})\text{n}^{\,3-\text{n}} \qquad (3)$$

La constante d'équilibre de cette réaction est

$$K_E = \frac{[\text{Me}^{3+}]\ [\text{ZH}_4^{2-}]^{\text{n}}}{[\text{Me}(\text{ZH}^{2-})_{\text{n}}{}^{3-\text{n}}]} \qquad (4)$$

Dans la phase aqueuse au pH > 10, l'oxyquinoléine est complètement dissociée en ions, de sorte que la concentration des anions oxyquinoléine libres en phase aqueuse est équivalente à la concentration des ions Me^{3+} complexes, c'est-à-dire

$$3\,[Me(ZH^{2-})_n{}^{3-n}] = [OX^-] \tag{5}$$

Si l'on introduit la valeur $[Me^{3+}]$ de l'équation (4) et la valeur $[OX^-]$ de l'équation (5) dans l'équation (2) et on logarithme et différencie, on obtient

$$\frac{\Delta \log \dfrac{[Me(ZH^{2-})_n{}^{3-n}]^4_{eau}}{[MeOX_3]_{chlorof.}}}{\Delta \log\ [ZH_4^{2-}]} = n \tag{6}$$

Selon cette équation, pour calculer la valeur de *n* il suffit de déterminer par voie expérimentale la concentration de l'ion métallique lié, en phase aqueuse, et la concentration de l'oxyquinolinate métallique extrait par chloroforme, à différentes concentrations de l'acide saccharique.

La valeur numérique de *n* donne précisément le rapport de combinaison entre $Me^{3+}(Ga^{3+}, In^{3+})$ et l'acide saccharique. On peut calculer *n* à partir des données expérimentales (tabl. 1 et 2) et on obtient $n = 1$. Autant pour le complexe de gallium que pour celui d'indium il résulte un rapport de combinaison $1Me : 1H_2ZH_4$. Le rapport qu'on obtient de la tangente de l'angle d'inclinaison de la droite construite dans les coordonnées $-\log B / -\log H_2ZH_4$ total (fig. 1) est le même (1 : 1)

$$B = \frac{[Me(HZ^{2-})_n{}^{3-n}]_{eau}}{[MeOX_3]_{chlorof.}} \tag{7}$$

Dans la figure 2 sont représentés les coefficients de répartition des deux éléments en fonction de la concentration de l'acide saccharique, calculés selon la relation

$$D = \frac{C_{\text{Me en phase organique}}}{C_{\text{Me en phase aqueuse}}} \tag{8}$$

Les coefficients de répartition du gallium sont plus petits que ceux de l'indium, de même que lors de la complexation de ces métaux avec l'acide gluconique, c'est-à-dire la stabilité des premiers est plus grande.

En traçant les droites dans les coordonnées $1/D$ per $[H_2ZH_4]$ il résulte que les fonctions sont linéaires pour $n = 1$ (fig. 3).

Donc, les deux systèmes donnent des complexes dans le rapport 1 : 1. En traçant les droites dans les coordonnées $\log\left(\dfrac{D_0}{D} - 1\right)$ per $\log\ [H_2ZH_4]$. (fig. 4), de la tangente de l'angle d'inclinaison des droites, on déduit de même $n = 1$.

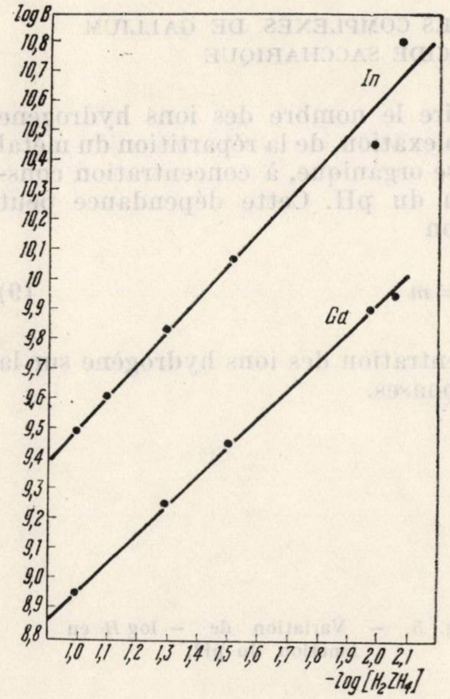

Fig. 1. — Variation de — log *B* en fonction de la concentration de l'acide saccharique.

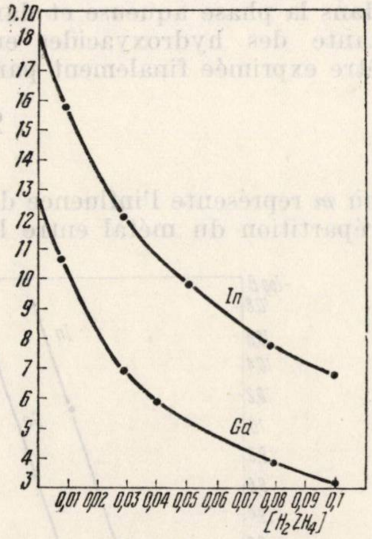

Fig. 2. — Variation des coefficients de distribution avec la concentration de l'acide saccharique.

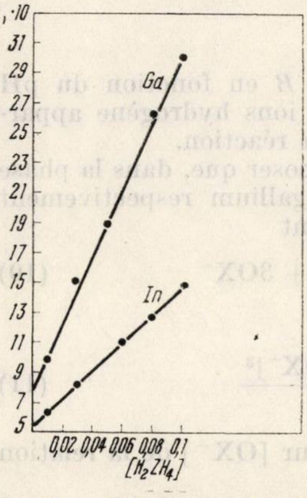

Fig. 3. — Dépendance de $1/D$ de la concentration de l'acide saccharique.

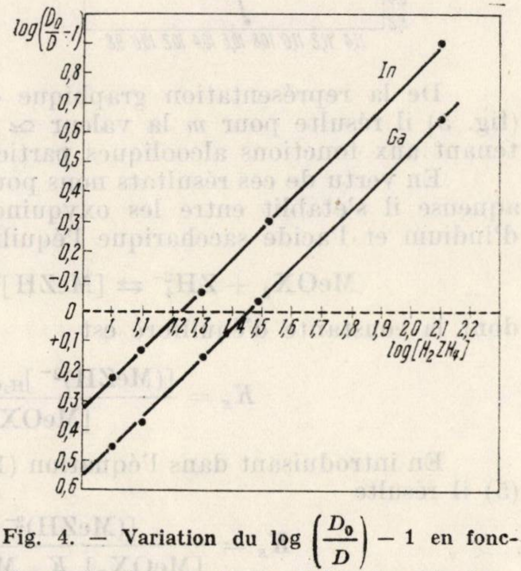

Fig. 4. — Variation du log $\left(\frac{D_0}{D}\right) - 1$ en fonction du log de concentration de l'acide saccharique.

LE MÉCANISME DE FORMATION DES COMPLEXES DE GALLIUM ET D'INDIUM AVEC L'ACIDE SACCHARIQUE

Selon Piatnitski[6] on peut déduire le nombre des ions hydrogène substitués dans les polyalcools par complexation, de la répartition du métal dans la phase aqueuse et dans la phase organique, à concentration constante des hydroxyacides en fonction du pH. Cette dépendance peut être exprimée finalement par la relation

$$\frac{\mathrm{d}\ \log B}{\mathrm{d\ pH}} = m \tag{9}$$

où m représente l'influence de la concentration des ions hydrogène sur la répartition du métal entre les deux phases.

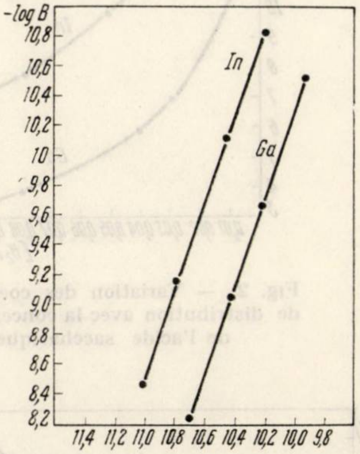

Fig. 5. — Variation de — log B en fonction du pH.

De la représentation graphique du — log B en fonction du pH (fig. 5) il résulte pour m la valeur $\simeq 3$, donc 3 ions hydrogène appartenant aux fonctions alcooliques participant à la réaction.

En vertu de ces résultats nous pouvons supposer que, dans la phase aqueuse il s'établit entre les oxyquinolates de gallium respectivement d'indium et l'acide saccharique l'équilibre suivant

$$\mathrm{MeOX_3} + \mathrm{ZH_4^{2-}} \rightleftarrows [\mathrm{MeZH}]^{2-} + 3\mathrm{H}^+ + 3\mathrm{OX}^- \tag{10}$$

dont la constante d'équilibre est

$$K_E = \frac{[(\mathrm{MeZH})^{2-}]_{\mathrm{H_2O}}\,[\mathrm{H}^+]^3\,[\mathrm{OX}^-]^3}{[\mathrm{MeOX_3}]\,[\mathrm{ZH_4^{2-}}]} \tag{11}$$

En introduisant dans l'équation (11) la valeur $[\mathrm{OX}^-]$ de la relation (5) il résulte

$$K_E = \frac{[(\mathrm{MeZH})^{2-}]^4_{\mathrm{H_2O}}\,[\mathrm{H}^+]^3}{[\mathrm{MeOX_3}]\,.\,K_D\,.\,\mathrm{MeOX_3}\,.\,[\mathrm{ZH_4}^{2-}]} \tag{12}$$

---

[6] I. V. Piatnitski et A. N. Klibus, *Ukrain. khim. Zhur.*, **30**, 151—159 (1964).

Au pH $\geqslant$ 10 tout l'acide saccharique est dissocié et la concentration des anions acide saccharique dépend seulement de la concentration totale de celui-ci, c'est-à-dire $C_{H_2ZH_4 \text{ total}}$

$$K_{DGaOX_3} = 1{,}8.10^{-40} \quad \text{et} \quad K_{DInOX_3} = 5.10^{-34}$$ [7]

En utilisant les données expérimentales on peut calculer les constantes apparentes d'équilibre (tabl. 3) qui indiquent que le complexe de gallium est plus stable que celui d'indium (de $3{,}73.10^7$ fois), ainsi qu'il résulte de la valeur des coefficients de distribution de l'acide saccharique ayant la même concentration.

Tableau 3

Constantes d'équilibre des saccharates complexes de gallium et d'indium

$[H_2ZH_4]$ mole/l	pH	$[Ga].10^{-4}$ $CHCl_3$	$[Ga].10^{-4}$ H_2O	$[In].10^{-4}$ $CKCl_3$	$[In].10^{-4}$ H_2O	K_E gallium	$K_E.10^{-6}$ indium	$-\log B$
0,1	11,00	—	—	2,440	7,560	—	1,816	8,47
0,1	10,97	—	—	3,150	6,850	—	1,604	9,16
0,1	10,70	1,080	8,920	—	—	69,40	—	8,24
0,1	10,45	—	—	4,512	5,488	—	1,824	10,45
0,1	10,43	2,850	7,150	—	—	70,80	—	9,04
0,1	10,22	4,440	5,560	—	—	70,80	—	9,67
0,1	10,19	—	—	6,770	3,230	—	2,340	10,81
0,1	9,93	6,300	3,700	—	—	71,50	—	10,53
						K_m=70,60	$1{,}896.10^{-6}$	

En même temps nous nous sommes proposé d'obtenir des données relatives qui nous permettent de comparer la stabilité des complexes des deux métaux avec le même hydroxyacide et du même métal avec différents hydroxyacides (HGH_4 et H_2ZH_4). Les résultats nous permettent d'observer les changements des propriétés des complexes en fonction de leur place dans le système périodique. Nous avons choisi pour critère de comparaison la valeur du degré de liaison du cation métallique dans le complexe, c'est-à-dire le rapport entre la concentration des ions métalliques liés dans le complexe et les ions libres, dans les mêmes conditions de pH et à la même concentration de l'hydroxyacide.[8] On peut calculer ce rapport à l'aide de la relation

$$\alpha_I = \frac{[\text{complexe}]_I}{[Me^{n+}]_I} \quad \text{et} \quad \alpha_{II} = \frac{[\text{complexe}]_{II}}{[Me^{m+}]_{II}} \tag{13}$$

où les indices I et II correspondent aux deux métaux. L'équilibre entre ces deux phases est

$$\underset{\text{phase chloroformique}}{Me_IOX_n} \rightleftarrows \underset{\text{phase aqueuse}}{Me_I^{n+} + nOX^-} \quad \text{et} \quad \underset{\text{phase chloroformique}}{Me_{II}OX_m} \rightleftarrows \underset{\text{phase aqueuse}}{Me_{II}^{m+} + mOX^-} \tag{14}$$

---

[7] E. B. Sandell, «Colorimetric Determination of Traces of Metals», Interscience Publishers, Inc. New York, 1959, p. 480, 187.

[8] I. V. Piatnitski, *Zhur. neorg. Khim.*, **10**, 2368 (1956).

d'où

$$K_{D_{\mathrm{I}}} = \frac{[\mathrm{Me}_{\mathrm{I}}^{n+}]\,[\mathrm{OX}^-]^n}{[\mathrm{Me}_{\mathrm{I}}\,\mathrm{OX}_n]} \quad \text{et} \quad K_{D_{\mathrm{II}}} = \frac{[\mathrm{Me}_{\mathrm{II}}^{m+}]\,[\mathrm{OX}^-]^m}{[\mathrm{Me}_{\mathrm{II}}\mathrm{OX}_m]} \tag{15}$$

résulte

$$[\mathrm{Me}_{\mathrm{I}}^{n+}] = \frac{K_{D_{\mathrm{I}}}\,[\mathrm{Me}_{\mathrm{I}}\,\mathrm{OX}_n]}{[\mathrm{OX}^-]^n} \quad \text{et} \quad [\mathrm{Me}_{\mathrm{II}}^{m+}] = \frac{K_{D_{\mathrm{II}}}\,[\mathrm{Me}_{\mathrm{II}}\,\mathrm{OX}_m]}{[\mathrm{OX}^-]^m} \tag{16}$$

En introduisant dans (13) la valeur $[\mathrm{Me}^{n+}]$ et $[\mathrm{Me}^{m+}]$ on obtient

$$\alpha_{\mathrm{I}} = \frac{[\mathrm{complexe_I}]\,[\mathrm{OX}^-]^n}{K_{D_{\mathrm{I}}}\,[\mathrm{Me}_{\mathrm{I}}\mathrm{OX}_n]_{\mathrm{chlorof.}}} \quad \text{et} \quad \alpha_{\mathrm{II}} = \frac{[\mathrm{complexe_{II}}]\,[\mathrm{OX}^-]^m}{K_{D_{\mathrm{II}}}\,[\mathrm{Me}_{\mathrm{II}}\,\mathrm{OX}_m]_{\mathrm{chlorof.}}} \tag{17}$$

Le rapport des deux degrés de liaison est

$$\frac{\alpha_{\mathrm{I}}}{\alpha_{\mathrm{II}}} = \frac{[\mathrm{complexe_I}]\,[\mathrm{OX}^-]^n \cdot \mathrm{K}_{D\mathrm{II}}\,[\mathrm{Me}_{\mathrm{II}}\,\mathrm{OX}_m]_{\mathrm{chlorof.}}}{[\mathrm{complexe_{II}}]\,[\mathrm{OX}^-]^m \cdot \mathrm{K}_{D\mathrm{I}}\,[\mathrm{Me}_{\mathrm{I}}\,\mathrm{OX}_n]_{\mathrm{chlorof.}}} \tag{18}$$

Dans le cas $n = m$ il résulte

$$\frac{\alpha_{\mathrm{I}}}{\alpha_{\mathrm{II}}} = \frac{[\mathrm{complexe_I}] \cdot K_{D\mathrm{II}}\,[\mathrm{Me}_{\mathrm{II}}\,\mathrm{OX}_m]}{[\mathrm{complexe_{II}}] \cdot K_{D\mathrm{I}}\,[\mathrm{Me}_{\mathrm{I}}\,\mathrm{OX}_m]} \tag{19}$$

Si l'on calcule le rapport du degré de liaison du gallium(I) et de l'indium(II) avec l'acide saccharique (tabl. 4) à l'aide des données expérimentales des tableaux 1 et 2, il résulte que le complexe de l'acide saccharique avec le gallium est plus stable que celui de l'indium, à savoir $1{,}171 . 10^7$, respectivement $1{,}068 . 10^7$ fois. La stabilité accrue du gluconate et du saccharate complexe de gallium (tabl. 4 et 5) en comparaison de celle des complexes de l'indium concorde avec les résultats obtenus par l'étude de l'interaction des ions aluminium, gallium et indium avec l'acide tartrique.[9] On explique ce comportement de la même manière, c'est-à-dire par la stabilité accrue du complexe renfermant le cation qui donne l'hydroxyde le moins soluble.

Tableau 4

Degré de complexation du gallium et de l'indium avec l'acide saccharique

$[H_2ZH_4]$ mole/l	$[Ga] . 10$ $CHCl_3$	$[Ga] . 10^{-4}$ H_2O	$[In] . 10^{-4}$ $CHCl_3$	$[In] . 10^{-4}$ H_2O	$\alpha_{Ga} . 10^{31}$	$\alpha_{In} . 10^{24}$	$\alpha_{Ga}/\alpha_{In} . 10^7$
0,1	2,490	7,510	4,052	5,948	6,388	5,560	1,149
0,08	2,750	7,250	4,320	5,680	5,023	4,336	1,158
0,05	3,460	6,540	4,878	5,122	2,640	2,540	1,040
0,03	3,980	6,020	5,401	4,599	1,650	1,491	1,107
0,01	5,030	4,970	6,185	3,815	0,607	0,617	0,984
						α_{Ga}/α_{In}	$m = 1{,}088$

---

[9] I. V. Piatnitski et A. P. Koslyshina, *Zhur. neorg. Khim.*, 3, 292 (1957).

Tableau 5

Degré de complexation du gallium et de l'indium avec l'acide gluconique

HGH_4 mole/l	$[Ga].10^{-4}$ $CHCl_3$	$[Ga].10^{-4}$ H_2O	$[In].10^{-4}$ $CHCl_3$	$[In].10^{-4}$ H_2O	$\alpha_{Ga}.10^{31}$	$\alpha_{In}.10^{24}$	$\alpha_{Ga}/\alpha_{In}.10^7$
0,1	5,100	4,900	6,106	3,894	5,652	6,778	0,834
0,05	5,594	4,406	6,707	3,293	2,030	3,156	1,068
0,03	5,807	4,193	6,794	3,206	2,799	2,660	0,950
0,01	6,045	3,955	7,404	2,596	2,024	1,104	1,830
						Ga/In	$m = 1,171$

Le même principe peut être utilisé pour comparer la stabilité des complexes d'un métal avec différents hydroxyacides.[5]

Si l'on considère que le degré de liaison du métal Me^{3+} (gallium et indium) avec l'acide saccharique et gluconique est

$$\alpha_{H_2ZH_4} = \frac{[\text{complexe}]_{H_2ZH_4}}{[Me^{3+}]} \quad \text{et} \quad \alpha_{HGH_4} = \frac{[\text{complexe}]_{HGH_4}}{[Me^{3+}]} \tag{20}$$

et si on introduit la valeur du $[Me^{3+}]$ tirée de l'équation (16) dans la relation (20), on obtient

$$\alpha_{H_2ZH_4} = \frac{[\text{complexe}]_{H_2ZH_4}\,[OX^-]^3}{K_D\,[MeOX_3]_{\text{chlorof.}}} \quad \text{et}$$

$$\alpha_{HGH_4} = \frac{[\text{complexe}]_{HGH_4}\,[OX^-]^3}{K_D\,[MeOX_3]_{\text{chlorof.}}} \tag{21}$$

Le rapport des degrés de liaison qui nous donne la stabilité relative des complexes respectifs est le suivant

$$\frac{\alpha_{H_2ZH_4}}{\alpha_{HGH_4}} = \frac{[\text{complexe}]_{H_2ZH_4}\,[OX^-]^3\,[MeOX_3]_{HGH_4}}{[\text{complexe}]_{HGH_4}\,[OX^-]^3\,[MeOX_3]_{H_2ZH_4}} \tag{22}$$

En remplaçant la valeur de l'OX^- de l'équation (5) dans l'équation (22) on aboutit à

$$\frac{\alpha_{H_2ZH_4}}{\alpha_{HGH_4}} = \frac{[\text{complexe}]^4_{H_2ZH_4}\,[MeOX_3]_{HGH_4}}{[\text{complexe}]^4_{HGH_4}\,[MeOX_3]_{H_2ZH_4}} \tag{23}$$

En utilisant les données des tableaux 1 et 2 et celles de la note précédente [1] pour les complexes de gallium et indium avec l'acide gluconique, on constate que la stabilité des complexes sacchariques est plus grande que celle des complexes gluconiques (tabl. 6). Ces résultats sont en bonne concordance avec ceux obtenus par d'autres auteurs qui utilisent d'autres éléments.[3, 10, 11]

Tableau

Stabilité relative du gallium et de l'indium

$[H_2ZH_4]$ HGH_4 mole/l	$[Ga].10$ $CHCl_3$ (H_2ZH_4)	$[Ga].10^{-4}$ $CHCl_3$ (HGH_4)	$[Ga].10^{-4}$ H_2O (H_2ZH_4)	$[Ga].10^{-4}$ H_2O (HGH_4)	$[In].10^{-4}$ $CHCl_3$ (H_2ZH_4)
0,1	2,490	5,100	7,510	4,900	4,094
0,05	3,460	5,594	6,540	4,406	4,878
0,03	3,980	5,807	6,020	4,193	5,402
0,008	5,120	6,885	4,880	3,115	6,794

SÉPARATION DES COMPLEXES

On peut séparer les combinaisons complexes par addition d'alcool méthylique ou éthylique au mélange limpide de la solution aqueuse au pH $\leqslant 4$. Autant pour le Ga^{3+} que pour le In^{3+} on obtient des poudres amorphes blanches. Les produits obtenus ont été analysés après avoir été séchés pendant deux jours à l'air.

On a constaté qu'ils sont solubles dans l'eau, complètement solubles en KOH, NaOH 0,1N et en HCl dilué.

Les solutions aqueuses ont une faible réaction acide ; on peut neutraliser deux ions hydrogène ce qui nous conduit à la conclusion que les complexes respectifs sont des acides bibasiques de la forme $H_2[MeC_6O_8H_5]$.

1. $H_2[GaC_6O_8H_5].4H_2O$ (P.M. = 349.9)

A l'acide saccharique 1 *n* on ajoute la quantité nécessaire de $Ga(NO_3)_3$ à l'état solide. On agite jusqu'à la complète dissolution du $Ga(NO_3)_3$ et on ajoute de l'alcool éthylique. Le précipité blanc est filtré et puis lavé à l'alcool et séché à l'air.

Analyses

Calculé : Ga 19,49 ; C 20,59 ; H 4,60 ; H_2O 20,52 %
Trouvé : Ga 19,52 ; C 20,56 ; H 4,55 ; H_2O 20,54 % (18 h).

2. $H_2[InC_6O_8H_5].4H_2O$ (P.M. = 394,9)

A une solution d'acide saccharique on ajoute goutte à goutte, en agitant continuellement, une solution 1 *n* de $In(NO_3)_3$ en proportions égales et à la fin de l'alcool éthylique. Le précipité blanc obtenu après filtrage et lavage à l'alcool est séché à l'air et ensuite analysé.

Analyses

Calculé : In 29,15 ; C 18,29 ; H 3,84 ; H_2O 18,28 %.
Trouvé : In 29,10 ; C 18,26 ; H 3,73 ; H_2O 18,27 % (20 h).

---

[10] H. Roth, Thèse, 1962.

[11] A. Fialkov et N. G. Peryshkina, *Zhur. neorg. Khim.*, **4**, 749 (1957).

Les essais d'obtenir des complexes insolubles dans un milieu neutre ou alcalin ont été sans résultats. Dans le cas du gallium toutes les réactions de précipitation peuvent être réalisées seulement en présence d'alcool méthylique ou éthylique. On ne peut séparer aucune combinaison complexe des solutions diluées mais dans les solutions concentrées au pH $\geqslant 10$ on obtient un complexe dans le rapport 1 : 1, renfermant un seul ion alcalin, (*K*), d'où on pourrait conclure qu'une seule fonction acide serait grevée par le potassium, ce qui est peu probable. La solution aqueuse de ce complexe a le pH 5,5–6 et par le titrage de cette solution par KOH 0,1*n* en présence de la phénolphtaléine on obtient environ 0,8 H de même que pour le gallosaccharate acide de potassium. En dépit des résultats concordants obtenus en opérant sur des produits de trois synthèses, répétées dans les mêmes conditions, ils ne nous mènent pas à de conclusions définitives.

6

avec l'acide saccharique et l'acide gluconique

$[In].10^{-4}$ $CHCl_3$ (HGH_4)	$[In].10^{-4}$ H_2O $(H_2ZH_4]$	$[In].10^{-4}$ H_2O (HGH_4)	$\alpha_{Z_2ZH_4}/\alpha_{HGH_4}$ gallium	$\alpha_{H_2ZH_4}/\alpha_{HGH_4}$ indium
6,106	5,906	3,894	8,977	7,892
6,580	5,122	3,420	7,848	6,787
6,794	4,595	3,206	6,200	5,327
7,905	3,206	2,095	8,100	6,382

Dans le cas de l'indium, dans une solution concentrée d'acide saccharique, KOH et $In(NO_3)_3$ après la précipitation, le pH de la solution décroît du pH $\simeq 10$ au pH $\simeq 4$ et on obtient un complexe identique à l'acide indo-saccharique, mais avec un pourcentage d'indium quelque peu augmenté (de $\simeq 2\%$), ce qui pourrait expliquer en quelque sorte la formation d'un mélange de $H_2[InC_6O_8H_5] . X\ In(OH)_3$ $(X < 1)$.

Dans les solutions diluées on peut constater la formation d'un complexe dans le même rapport 1 : 1, ayant une réaction faiblement acide, avec la même teneur en carbone que l'acide indosaccharique, mais avec une plus faible teneur en indium. A un pH supérieur au pH $= 10$ on trouve environ 5 % K.

On doit mentionner que dans tous les cas où l'on a opéré au pH > 6, le complexe précipite sans addition d'alcool.

Les résultats restent les mêmes, même si on change les conditions de travail (concentration, pH, température, rapport de mélange, la succession des opérations et la nature des hydroxydes alcalins).

Le gallium et l'indium ont été dosés comme des oxyquinolinates, le carbone et l'hydrogène par les méthodes connues, l'acidité (H^+) des combinaisons par titrage avec KOH en présence de la phénolphtaléine et l'eau par la méthode d'Abderhalden, à la température d'ébullition de l'eau jusqu'à un poids constant.

Des faits mentionnés il résulte que la réaction de synthèse de ces composés peut être exprimée de la façon suivante

$$Me(NO_3)_3 + C_6H_{10}O_8 = H_2MeC_6H_5O_8 + 3HNO_3$$

La formule structurelle de ces substances peut être représentée de la même manière qu'au cas des acides gallo- et indogluconiques [1] et aussi par analogie avec l'acide ferro-gluconique, pour lequel Fialkov et Peryshkina [11] considèrent que le métal substitue les hydrogènes α, γ et δ des groupements hydroxyliques et non pas ceux des positions α, β et δ, comme l'avaient présumé Pecsok et Sander.[12]

Cette formule pourrait être

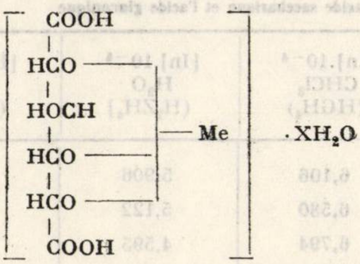

---

[12] R. Pecsok et I. Sander, *J. Amer. Chem. Soc.*, 47, 1489 (1955).

Revue Roumaine de Chimie, 14, 1125–1131 (1969)

SUR LES VANADATES. XVII *

LA SUSCEPTIBILITÉ MAGNÉTIQUE DES COMPOSÉS $K_xV_x^{IV}V_{2-x}^{V}O_5$ $(0 < x \leqslant 1)$

ILEANA LUKÁCS, CONSTANŢA STRUSIEVICI, D. LUPU, C. MIREL et C. LITEANU

Institut de Chimie de l'Académie, Filiale de Cluj, 59–65, str. Donath.

Reçu le 1er février 1969

Les susceptibilités par gramme (χ_g) des composés $K_xV_x^{IV}V_{2-x}^{V}O_5$ $(0 < x \leqslant 1)$, entre 90–300°K, 6600 Gs, ont des valeurs entre 1,16–9,00.10^{-6} uém. Dans l'intervalle de température donné tous les composés répondent à la loi de Curie-Weiss, avec la constante Θ négative, à l'exception des produits avec x environ 0,45 et 0,50, qui présentent des interactions antiferromagnétiques marquées aussi par le point de Néel (T_N) à 120–150° K environ. Les moments magnétiques (1,92–2,26 MB), trouvés pour le V^{4+}, à 296,5°K, dans le cas de produits avec x entre 0,10 et 0,28 correspondent à l'hypothèse des multiplets serrés, et dans le cas des produits avec x entre 0,33 et 1,00 (1,26–1,60 MB) à celle du blocage partiel des centres paramagnétiques, en supposant que les électrons d^1 de V^{4+} sont couplés partiellement dans des liaisons covalentes. Sur la courbe composition-moment magnétique il y a des paliers correspondant à différentes phases du système.

Jusqu'à présent c'est seulement la susceptibilité magnétique de la phase β, représentée par les composés avec × 0,20 et 0,25, qui a été étudiée par Pouchard et ses collaborateurs.[1]

Le but de ce travail, comme dans le cas du système analogue de sodium,[2] a été d'établir le changement de la susceptibilité magnétique dans la série des composés $K_xV_x^{IV}V_{2-x}^{V}O_5$ $(0 < x \leqslant 1)$ pour obtenir de nouvelles indications sur les différentes phases du système, sur les domaines d'existence de celles-ci.

La composition chimique des produits dont la susceptibilité a été mesurée entre 90–300°K est figurée au tableau 1. Dans le tableau 2 nous donnons les valeurs expérimentales à différentes températures des susceptibilités magnétiques par gramme (χ_g) et par ion gramme V^{4+} (χ_A) (ces dernières corrigées du diamagnétisme) et aussi les moments magnétiques (μ_{eff}) calculés d'après la formule $\mu_{eff} = 2{,}839\sqrt{\chi_A \cdot T}$.

---

* Part. XVI : I. Lukács, C. Strusievici et C. Liteanu, *Rev. Roumaine Chim.*, **14**, 1969 (sous presse).

[1] M. Pouchard, A. Casalot, C. Villeneuve et P. Hagenmuller, Mat. Res.Bull., **2**, 877 (1967).

[2] C. Mirel, D. Lupu, I. Lukács, C. Strusievici et C. Liteanu, *Rev. Roumaine Chim.*, **13**, 1035 (1968).

Tableau 1

Composition chimique des produits

Produits	K^+	V^{4+}	V^{5+}	O^{2-}
(0,10)	0,10	0,13	1,87	4,98
(0,20)	0,20	0,23	1,77	4,99
(0,25)	0,28	0,28	1,72	5,00
(0,28)	0,28	0,31	1,69	4,98
(0,33)	0,33	0,36	1,64	4,99
(0,40)	0,41	0,39	1,61	5,00
(0,45)	0,48	0,44	1,45	5,02
(0,50)	0,49	0,50	1,50	4,99
(0,60)	0,59	0,60	1,40	5,00
(0,66)	0,66	0,65	1,35	5,02
(0,70)	0,67	0,70	1,30	4,98
(0,75)	0,72	0,74	1,26	4,98
(0,80)	0,83	0,78	1,22	5,04
(0,85)	0,88	0,83	1,17	5,02
(0,90)	0,98	0,86	1,14	5,06
(1,00)	0,98	0,98	1,02	5,00

Tableau 2

Susceptibilité magnétique des produits

Produits	Température (°K)	$\chi_g \cdot 10^6$ (uém)	$\chi_A \cdot 10^6$ (uém)	μ_{eff} (MB)
1	2	3	4	5
(0,20)	92	4,52	3980	1,72
	113	3,85	3438	1,76
	151	3,25	2940	1,89
	187	2,55	2360	1,88
	225	2,20	2070	1,93
	254	1,73	1685	1,85
	298	1,53	1520	1,91
(0,25)	89,5	4,48	3309	1,49
	118	3,81	2840	1,64
	150	3,26	2461	1,72
	174	3,06	2324	1,80
	199	2,74	2106	1,84
	229	2,35	1839	1,84
	254,5	2,22	1749	1,89
	295,5	2,05	1629	1,97
(0,28)	100,5	5,12	3378	1,65
	139,5	4,51	2992	1,83
	171,5	4,13	2748	1,91
	198,5	3,87	2598	2,02
	216	3,69	2488	2,06
	244,5	3,48	2358	2,17
	262,5	3,38	2298	2,20
	294	3,22	2198	2,27

Tableau 2 (suite)

1	2	3	4	5
(0,40)	99	2,70	1530	1,10
	123	2,60	1480	1,21
	152	2,22	1287	1,25
	183	1,85	1100	1,27
	208	1,72	1035	1,31
	234	1,53	939	1,33
	257,5	1,46	903	1,38
	299	1,16	750	1,34
(0,45)	93	1,78	929	0,83
	121,5	1,94	1000	0,99
	145	1,87	969	1,06
	171,5	1,80	938	1,14
	202	1,66	876	1,19
	221,5	1,54	823	1,21
	245	1,48	797	1,25
	298	1,36	743	1,33
(0,50)	98	1,96	916	0,97
	130	2,44	1109	1,07
	149	2,48	1139	1,16
	172	2,38	1084	1,22
	191,5	2,24	1029	1,27
	216,5	2,10	973	1,30
	238	1,88	885	1,30
	255,5	1,77	841	1,32
	297,5	1,56	755	1,34
(0,66)	102	4,47	1539	1,12
	135	3,96	1373	1,16
	156	3,56	1244	1,25
	200	3,33	1169	1,30
	215	3,17	1114	1,39
	248	2,76	987	1,40
	298	2,27	830	1,41
(0,70)	90	4,58	1451	1,03
	126	4,23	1377	1,18
	154	3,83	1228	1,24
	181	3,26	1061	1,25
	207	3,02	989	1,28
	235	2,69	891	1,30
	248	2,49	832	1,29
	297,5	2,06	706	1,31
(0,75)	90	4,81	1452	1,03
	122	4,46	1352	1,15
	153	3,79	1162	1,20
	181	3,20	993	1,20
	210	3,01	942	1,26
	236	2,49	796	1,23
	262	2,16	702	1,20
	298	2,01	660	1,26

Tableau 2 (suite)

1	2	3	4	5
(0,90)	98	8,36	2235	1,33
	123	6,91	1925	1,39
	164	5,74	1555	1,43
	197	4,75	1355	1,47
	248,5	4,01	1115	1,49
	297	3,27	925	1,49
(1,00)	98	9,00	2099	1,29
	134	7,29	1714	1,36
	163	5,87	1394	1,36
	198	5,05	1206	1,42
	219,5	4,65	1116	1,34
	251	4,11	999	1,42
	297	3,43	846	1,42

Les courbes représentant χ_A^{-1} en fonction de la température absolue, en tous les cas, sauf les produits (0,45) et (0,50), sont linéaires (fig. 1. et 2.) et suivent la loi de Curie-Weiss, avec une constante Θ négative. Les courbes des produits (0,45) et (0,50) (fig. 3) présentent des minima à 120 et 150°K environ, points de Néel, marquant des interactions antiferromagnétiques.

Il faut remarquer que nos données ne semblent pas soutenir la superposition, constatée par Pouchard et ses collaborateurs,[1] d'un paramagnétisme indépendant de la température. Vu que l'intervalle de température de nos mesures est trop limité, nous ne pouvons pas décider dans cette question. En vertu même de l'intervalle étroit de nos mesures, les valeurs de Θ et C resp. $\mu_{\text{eff}} = \sqrt{8C}$, figurées au tableau 3 sont aussi seulement des valeurs d'orientation et, ci-dessous, nous analyserons les moments magnétiques calculés à une température donnée pour qu'on n'attache pas des implications éventuellement pas justifiées aux données expérimentales.[3]

Les valeurs expérimentales des moments magnétiques (tabl. 2.) des produits sont, en général, sensiblement supérieures ou inférieures aux valeurs théoriques 1,73 MB, correspondant au moment de spin seul, c'est-à-dire si le moment orbital est bloqué (*gelé*), pour un électron non couplé.

Le moment magnétique de l'ion V^{4+} ($^2D_{3/2}$), dans les composés magnétiquement dilués, avec la contribution orbitale, peut prendre la valeur de 3, dans le cas des multiplets serrés, (c'est-à-dire lorsque l'intervalle d'énergie entre l'état excité et l'état fondamental est nettement plus petit que kT), ou la valeur 1,55, dans le cas des multiplets larges (avec des différences d'énergie grandes par rapport à kT).[4]

Dans notre cas l'interaction des ions magnétogènes est antiferromagnétique et cela diminue le moment magnétique. D'autant plus, les moments trouvés à 296.5° K (tab. 4.), ayant les valeurs 1,92—2,26 MB

---

[3] F. A. Cotton et G. Wilkinson, « Advanced Inorganic Chemistry », ed. II., Intersience Publishers, New York — London — Sydney, 1966, p. 641.

[4] A. Michel, « Phénomènes magnétiques et structure », Masson et Cie, Paris, 1966, p. 45.

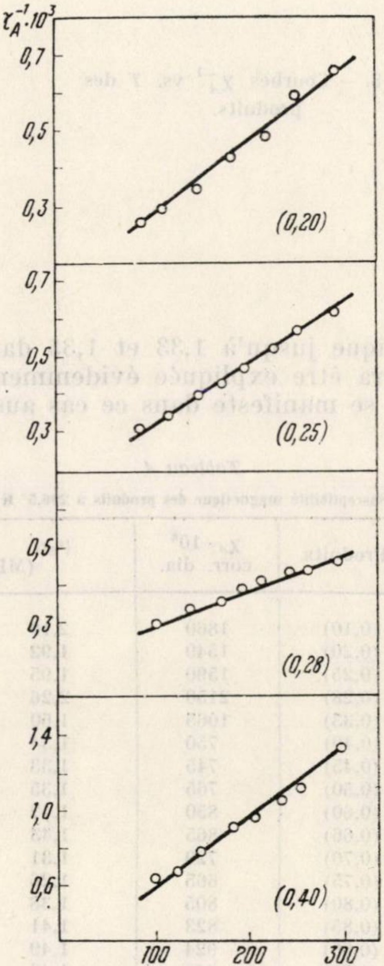

Fig. 1. — Courbes χ_A^{-1} vs. *T* des produits.

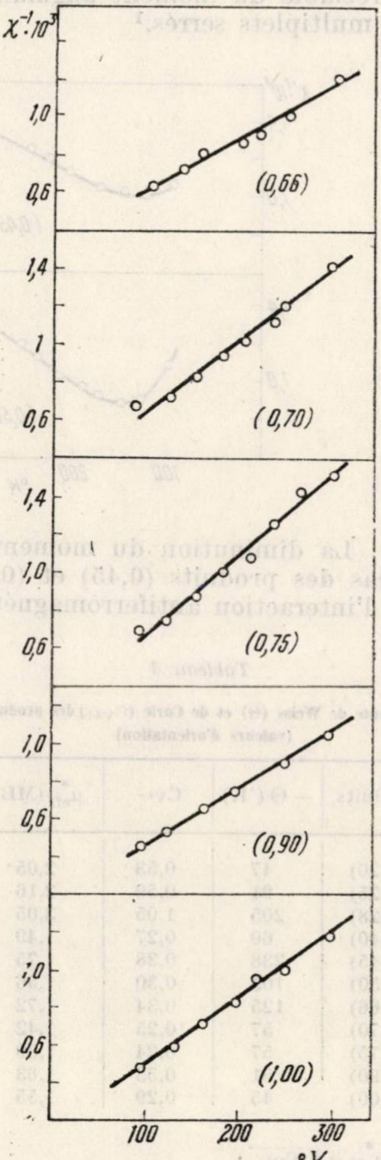

Fig. 2. — Courbes χ_A^{-1} vs. *T* des produits.

pour les produits (0,20), (0,25) et (0,28) impliquent une contribution appréciable du moment angulaire orbital qui s'établit dans l'hypothèse des multiplets serrés.[1]

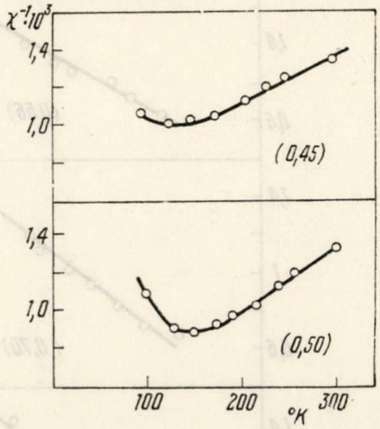

Fig. 3. — Courbes χ_A^{-1} vs. T des produits.

La diminution du moment magnétique jusqu'à 1,33 et 1,35 dans le cas des produits (0,45) et (0,50) pourra être expliquée évidemment, par l'interaction antiferromagnétique qui se manifeste dans ce cas aussi par des points de Néel. Mais, le fait que cette diminution persiste même dans le cas des produits (0,40) et celui de (0,66) à (1,00), dont les courbes χ_A^{-1} vs. T ne présentent pas de point de Néel, nous oblige à chercher aussi d'autres explications. La contribution orbitale dans l'hypothèse des multiplets larges est trop peu probable dans le cas de l'ion V^{4+}, lequel même à l'état libre a une constante de couplage spin-orbite de

Tableau 3

Constante de Weiss (Θ) et de Curie ($C_{V^{4+}}$) des produits (valeurs d'orientation)

Produits	$-\Theta$ (°K)	$C_{V^{4+}}$	$\overset{*}{\mu}_{eff}$ (MB)
(0,20)	47	0,53	2,05
(0,25)	91	0,59	2,16
(0,28)	205	1,05	3,05
(0,40)	60	0,27	1,49
(0,45)	238	0,38	1,75
(0,50)	103	0,30	1,56
(0,66)	125	0,34	1,72
(0,70)	57	0,25	1,42
(0,75)	57	0,24	1,39
(0,90)	51	0,33	1,63
(1,00)	45	0,29	1,55

$\overset{*}{\mu}_{eff} = \sqrt{8C_{V^{4+}}}$

Tableau 4

Susceptibilité magnétique des produits à 296,5° K

Produits	$\chi_A \cdot 10^6$ corr. dia.	μ_{eff} (MB)
(0,10)	1860	2,10
(0,20)	1540	1,92
(0,25)	1590	1,95
(0,28)	2150	2,26
(0,33)	1065	1,60
(0,40)	750	1,34
(0,45)	745	1,33
(0,50)	765	1,35
(0,60)	850	1,42
(0,66)	865	1,43
(0,70)	720	1,31
(0,75)	665	1,26
(0,80)	805	1,38
(0,85)	823	1,41
(0,90)	924	1,49
(1,00)	846	1,42

seulement 250 cm^{-1}.[5] Nous sommes alors tentés d'accepter l'hypothèse de la diminution du moment magnétique due au blocage partiel des centres paramagnétiques,[6] en supposant que les électrons d^1 de V^{4+} sont couplés partiellement dans des liaisons covalentes.

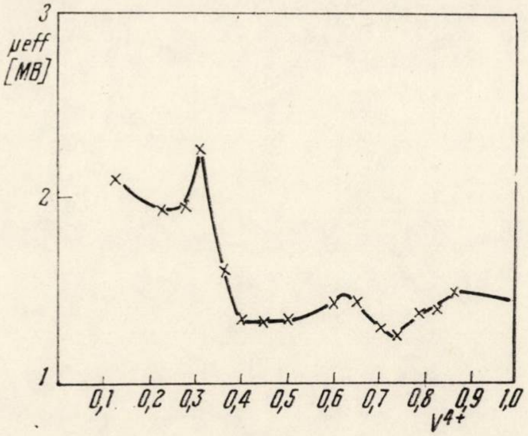

Fig. 4. — Courbe de la variation des moments magnétiques à 296·5°K en fonction de la composition.

En essayant d'utiliser la courbe de la variation des moments magnétiques en fonction de la composition pour délimiter les phases du système $K_xV_x^{IV}V_{2-x}^{V}O_5$, on peut observer que sur cette courbe (fig. 4.) il y a des paliers dans les domaines correspondant à différentes phases, lesquelles ont été identifiées par des spectres Debye-Scherrer [7,8] et en IR,[7] ou indiquées par les mesures de la conductivité électrique.[9]

PARTIE EXPÉRIMENTALE

Les échantillons ont été préparés et analysés d'après les méthodes décrites dans les ouvrages précédents.[7,9]

Les mesures de la susceptibilité magnétique ont été effectuées d'après la méthode de Faraday. Les analyses thermomagnétiques on été menées entre 90—300°K (le fluide réfrigérant étant l'azote liquide), à 6600 Gs. Pour l'étalonnage on a utilisé Hg [CO(CNS)$_4$] avec $\chi_g = 16{,}44\ (\pm 0{,}08) \cdot 10^{-6}$ uém, à 20°. La précision de la détermination des susceptibilités était de l'ordre de ± 2%.

---

[5] B. N. Figgis, « Introduction to Ligand Fields, Interscience Publishers », New York —London — Sydney, 1966, p. 269 et 60.

[6] M. Pouchard, A. Casalot et G. Villeneuve, *Bull. Soc. chim. France*, **1968**, 81.

[7] I. Lukács, C. Strusievici et C. Liteanu, *Rev. Roumaine Chim.*, **12**, 1347 (1967).

[8] M. Pouchard et P. Hagenmuller, *Mat. Res. Bull.*, **2**, 799 (1967).

[9] I. Lukács, C. Strusievici et C. Liteanu *Rev. Roumaine Chim.*, **13**, 713 (1968).

Revue Roumaine de Chimie, 14, 1133–1141 (1969)

KINETICS AND MECHANISM OF SUBSTITUTION REACTIONS OF COMPLEXES. XIV *

NEW DERIVATIVES OF THE DICHLORO-BIS-DIMETHYLGLYOXIMATO-COBALTOUS-(III)-ACID AND THE SOLVOLYSIS OF THE ION $[Co(DH)_2Cl_2]^-$ IN WATER-DIMETHYLFORMAMIDE MIXTURES

CS. VÁRHELYI, Z. FINTA and J. ZSAKÓ
Faculty of Chemistry, Babeş-Bolyai University Cluj,
str. Arany János, 11

Received October 21, 1968

Twenty new salts of $H[Co(DH)_2Cl_2]$ have been prepared. IR spectrum of the complex acid has been recorded and discussed. Solvolysis kinetics of the ion $[Co(DH)_2Cl_2]^-$ has been studied in aqueous solution and in water-dimethylformamide mixture, containing 10 per cent dimethylformamide. Rate constants of the consecutive reactions (1) and (2) have been determined at various temperatures. Activation energy and pre-exponential factor of Arrhenius' equation have been calculated. The entering of dimethylformamide molecules into the internal coordination sphere is presumed.

The compound prepared by Feigl and Rubinstein[1] from $CoCl_2$ and dimethylglyoxime in water-organic solvent (e.g. acetone) mixtures in the presence of air is not a derivative of Co (II), but a coordination compound of Co (III). Its composition is $CoCl_2.DH.DH_2$, where DH_2 stands for a dimethyl-glyoxime molecule ($C_4H_8N_2O_2$). Since the compound in aqueous solutions is a strong acid, the following structure was presumed : $H[Co(DH)_2Cl_2]$. Acidity and electric conductivity measurements and also the migration of the coloured complex to the anode proved the accuracy of the presumed formula.[2]

IR spectrum of the complex acid was studied first by Nakahara [3] in suspension, in nujol. This author has found a weak absorption band at 1725 cm^{-1} and he has attributed it to the valence vibration of a hydrogen bridge bond O—H..O.

Preparation of salts of this complex acid was very little studied. The silver salt and some salts of the type $[Co(DH)_2(amine)_2]$. $[Co(DH)_2Cl_2]$

---

* Previous paper : J. Zsakó, Cs. Várhelyi and Z. Finta, *Stud. Univ. Babeş Bolyai, Chem.*, 1969 (in press).

[1] F. Feigl and Rubinstei , *Liebigs Ann. Chem.*, **433**, 181 (1923).

[2] A. K. Babko and M. V. Korotun, *Zhur. obshchei Khim.*, **24**, 597 (1954).

[3] A. Nakahara, *Bull. Chem. Soc. Japan.*, **28**, 473 (1955).

were reported by Ablov and Samus [4] (amine stands for ammonia, aniline, *o*-, *p*-toluidine, *p*-Cl and *p*-J-aniline). Salts with organic N-bases have not been described.

The solutions of the acid H $[Co(DH)_2Cl_2]$ are not stable : a ligand exchange process occurs within. Thus in aqueous solutions the following two reactions take place [5,6]

$$[Co(DH)_2Cl_2]^- + H_2O = [Co(DH)_2Cl\,H_2O] + Cl^- \tag{1}$$

$$[Co(DH)_2Cl\,H_2O] + H_2O = [Co(DH)_2(H_2O)_2]^+ + Cl^- \tag{2}$$

The kinetics of the hydrolysis process (1) was studied only by Sychev and Ablov.[7] They have found this reaction to take place with an activation energy of 23.9 kcal/mole in aqueous solutions. The corresponding pre-exponential factor in Arrhenius' equation, found by them is $\lg Z = 14.0$. The kinetics of reaction (2) was studied in "pure state" by the same authors.[8] They have followed the release of Cl^- from $[Co(DH)_2ClH_2O]$ using different methods (argentometric titrations, electric conductivity and pH measurements). In aqueous solutions they have found the activation energy of reaction (2) to be of $E_a = 25.5$ kcal/mole.

In the present paper we have studied the interaction of the acid H $[Co(DH)_2Cl_2]$ with the chlorhydrates of some aliphatic and aromatic primary and secondary amines and heterocyclic amines, with alkaloids and with complex ions of hexamine-, monoacido-pentamine- and diacido-tetramine types. By means of double exchange reactions 16 new derivatives of the above mentioned complex acid were prepared. Synthesis, analysis and appearance of these substances are given in the experimental part.

The IR spectrum of the acid H $[Co(DH)_2Cl_2]$ was recorded in a much wider range than by Nakahara [3] namely between 400 and 4000 cm^{-1}. The spectrogram is given in figure 1. A weak band is observed at 1710—1740 cm^{-1}, which was attributed by Nakahara to the valence vibration ν_{O-H}, characteristic of a hydrogen bond. More recent data of Blinc and Hadži [9,10] showed this valence vibration to be situated at 2340—2350 cm^{-1} in the case of dimethylglyoximates of transition metals as Ni and Pd. These authors attributed the weak band at 1700—1780 cm^{-1} to the deformation vibration δ_{O-H}, characteristic also of hydrogen bonds. Thus the above mentioned band must be attributed to δ_{O-H}. The real valence vibration band appears in our spectrogram too. The very weak band at 2350 cm^{-1} (or possibly the other weak band at 2280 cm^{-1}) can be attributed to this ν_{O-H}. The presence of these bands in the IR spectra of bis-dimethylglyoximato-cobaltous complexes is a direct evidence of intramolecular hydrogen bonds, which are possible only if the $Co(DH)_2$-group has a planar structure. Thus $[Co(DH)_2X_2]^-$

---

[4] A. V. Ablov and N. M. Samus, *Izvest. Sektora Platiny*, **30**, 86 (1955).

[5] L. Cambi and C. Coriselli, *Gazz. chim. Ital.*, **66**, 81 (1936).

[6] A. V. Ablov and G. P. Svrzova, *Zhur. neorg. Khim.*, **1**, 2457 (1956).

[7] A. V. Ablov and A. Ia. Sychev, *Zhur. neorg. Khim.*, **4**, 2485 (1959).

[8] A. Ia. Sychev and A. V. Ablov, *Zhur. neorg. Khim.*, **6**, 2288 (1961).

[9] R. Blinc and D. Hadži, *J. Chem. Soc.*, **1958**, 4536.

[10] R. Blinc and D. Hadži, *Spectrochim. Acta*, **16**, 853 (1960).

and $[Co(DH)_2(amine)_2]^+$ type complex ions, and consequently the studied $[Co(DH)_2Cl_2)$ ion too, are assumed to have a *trans* geometric configuration.

In this spectrogram (fig. 1.) the valence vibration frequency $C = N$ can be observed at 1610 cm^{-1}. This band appears at 1620—1630 cm^{-1} in the case of the free, non-coordinated dimethylglyoxime. The two strong bands at 1076 and 1223 cm^{-1} respectively belong to ν_{N-O} valence vibrations, namely the former to the ionized, the latter to the non-ionized N—O group of the dimethylglyoxime. The Co—N frequencies are situated in this spectrogram at 506 and 448 cm^{-1}, like in the case of the classical ammonia and ethylenediamine containing complexes. The position of IR absorption bands $\nu_{C=N}$, ν_{N-O} and νC_{Co-N} confirms the covalent character of the Co-ligand bonds.[11]

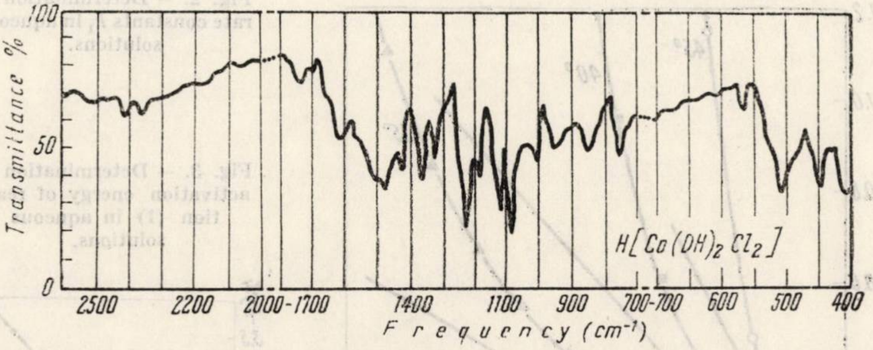

Fig. 1. — IR spectrum of $H[Co(DH)_2Cl_2]$.

Kinetic measurements were made in aqueous solutions and in water-dimethylformamide (DMFA) solutions containing 10 per cent DMFA. Concentration of free Cl^- ions was followed potentiometrically. The plot of $\lg \frac{a}{a-x}$ *versus* time did not give a straight line (a stands for the initial concentration of the complex acid, x for the concentration of free Cl^- ions). After a short linear part the curve showed a considerable increase. This can be easily explained presuming that reaction (1) is followed by reaction (2). The zero time tangency of the above mentioned curves will give in this presumption the first order rate constant of reaction (1). For several runs these curves are given in figure 2, together with the corresponding zero time tangencies. Our experiments showed this rate constant k_1, obtained from the slope of the tangency, to be independent of the initial concentration a of the studied complex acid, i.e. reaction (1) is indeed of first order with regard to the complex acid. The average values of these rate constants are given for various temperatures and for the studied solvents in table 1.

---

[11] H. Block, *Trans. Faraday Soc.*, **55**, 867 (1959).

These rate constants were used for the determination of kinetic parameters of reaction (1). A plot of lg k_1 *versus* $1/T$ showed a good linearity, as seen in figure 3, given for aqueous solutions. Using the least square method the equations of these straight lines were determined and activation energy and pre-exponential factor values were obtained, according to Arrhenius' equation. The corresponding kinetic parameters are given in table 2.

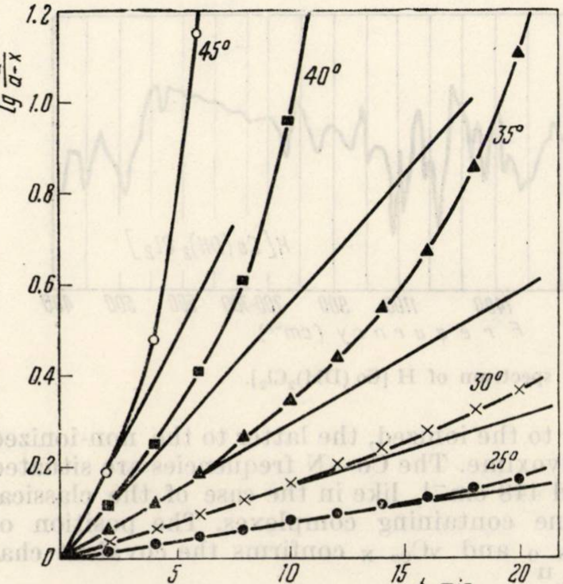

Fig. 2. — Determination of rate constants k_1 in aqueous solutions.

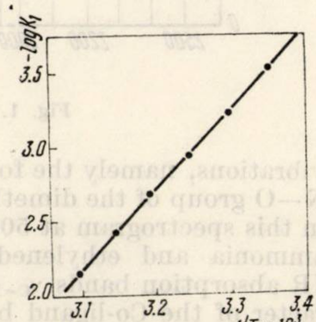

Fig. 3. — Determination of activation energy of reaction (1) in aqueous solutions.

Rate constant, activation energy and lg Z values given in tables 1 and 2 for aqueous solutions are in good agreement with Sychev and Ablov's experimental data[7]. As seen from table 2 both E_a and lg Z values are much influenced by the presence of DMFA, namely they are larger than in aqueous solutions. One might presume in DMFA-water mixtures

Table 1

Rate constants k_1 for the reaction (1)

t°C	$k_1 \times 10^4$ s^{-1} in	
	water	DMFA 10%
25	2.98	2.40
30	6.15	4.75
35	11.80	10.20
40	21.4	19.0
45	38.0	—
50	71.6	

the replacement of Cl to occur not only by water molecules, according to reaction (1), but also by DMFA molecules :

$$[Co(DH)_2Cl_2]^- + DMFA = [Co\,(DH)_2Cl\,(DMFA)] + Cl^- \qquad (3)$$

Table 2

Activation energy and pre-exponential factor for reaction (1)

Solvent	E_a, kcal/mole	lg Z
water	24.1 ± 0.6	14.1
DMFA 10%	26.0 ± 0.9	15.4

Since coordination compounds of Co (III) with DMFA in the internal sphere are known,[12,13] reaction (3) seems to be real. It can be followed probably by a second step, namely

$$[Co\,(DH)_2\,Cl\,(DMFA)] + DMFA = [Co\,(DH)_2(DMFA)_2]^+\,(+\,Cl^- \qquad (4)$$

We cannot exclude either the possibility of reaction (1) to be followed by reaction

$$[Co(DH)_2ClH_2O] + DMFA = [Co(DH)_2H_2O\ DMFA]^+ + Cl^- \qquad (5)$$

or reaction (3) to be followed by reaction

$$[Co\,(DH)_2\,Cl\,(DMFA)] + H_2O = [Co\,(DH)_2H_2O\,(DMFA)]^+ + Cl^- \qquad (6)$$

We had no possibility to follow reactions (1) and (3) separately, we could study only the sum of their effects.

Our experimental data obtained in aqueous solutions allowed us to determine the rate constant of reaction (2). In the case of DMFA-water mixtures it is possible to obtain only an apparent rate constant which characterizes the sum of the possible parallel processes (2), (4), (5) and (6).

If reactions (1) and (2) are successive first order reactions, the concentration of the different complexes can be given by the following formulae :

$$c^1 = a\,e^{-k_1 t} \qquad (7)$$

$$c_2 = a\,\frac{k_1}{k_1 - k_2}\,(e^{-k_2 t} - e^{-k_1 t}) \qquad (8)$$

$$c_3 = a\,(1 - e^{-k_1 t}) - a\,\frac{k_1}{k_1 - k_2}\,(e^{-k_2 t} - e^{-k_1 t}) \qquad (9)$$

where c_1, c_2 and c_3 stand for the concentration of the following complexes : $[Co\,(DH)_2Cl_2]^-$, $[Co\,(DH)_2ClH_2O]$ and $[Co(DH)_2(H_2O)_2]^+$ respectively, k_1 and k_2 stand for the rate constant of reaction (1) and (2), a is the initial concentration of $[Co\,(DH)_2Cl_2]^-$ and t is the time.

Using the rate constant k_1 calculated by means of the Arrhenius' equation from the kinetic parameters, given in table 2, we calculated

---

[12] W. R. Fitzgerald and D. W. Watts, *Austral. J. Chem.*, **19**, 935 (1966).

[13] J. R. Lantzke and D. W. Watts, *Austral. J. Chem.*, **19**, 949 (1966).

c_1 by means of equation (7). If reaction (2) did not take place, the concentration of free Cl^- ions would be $a-c_1$. The difference between the experimentally determined concentration of Cl^- and these hypothetical values $a-c_1$ represents the concentration of Cl^- ions formed in reaction (2), i.e. the concentration of the diaquo-cation c_3. This value will be called in the following "experimental" concentration c_3.

In order to obtain the rate constants k_2 we used a curve fitting method. Experimental c_3 values were plotted *versus* time and theoretical c_3—t curves were constructed by means of equation (9), using different k_2 values, until a satisfactory agreement was reached between experimental and theoretical curves. The obtained k_2 values are given in table 3. In the case of runs carried out in DMFA-water mixtures the same calculations were made, obtaining apparent k_2 values, characterizing the total effect of the possible parallel reactions mentioned above. The linear variation of lg k_2 with $1/T$ allowed the determination of the activation energy and of the corresponding lg Z value. These kinetic parameters are given in table 4. The method is illustrated by figure 4.

Table 3

First order rate constants k_2 for the reaction (2)

t°C	$k_2 \times 10^4$ s^{-1}	
	water	DMFA 10 %
25	1	0.7
30	2	1.5
35	4	3.0
40	8	5.5
45	14	—

Table 4

Kinetic parameters for reaction (2)

Solvent	E_a kcal/mole	lg Z
water	25.2 ± 1.2	14.5
DMFA 10 %	25.6 ± 1.2	14.7

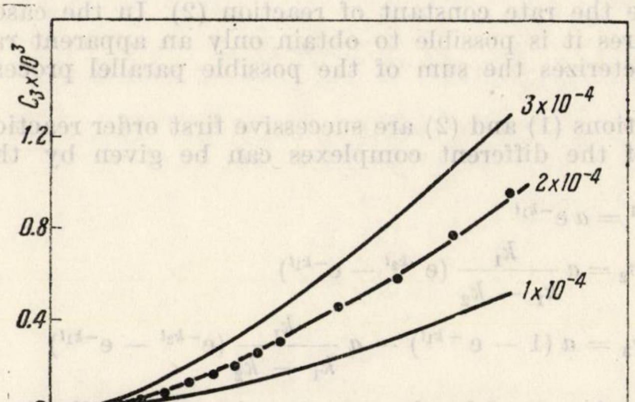

Fig. 4. — Determination of k_2 in aqueous solution at 30°C. Theoretical curves calculated with k_2 values indicated beside the curves and experimental data.

The obtained results are in excellent agreement with Ablov and Sychev's experimental data,[8] this agreement pleads for the accuracy of the scheme given by equation (1) and (2). Both reactions must take place consecutively and independently.

As concerns the influence of DMFA, this is not very significant. Rate constants are a little smaller in the presence of DMFA than in aqueous solutions, while activation energy and lg Z value are a little higher. Comparing these results with our experimental data on the solvolysis of the analogous complex ion with bromine: $[Co(DH)_2Br_2]^-$,[14] a great difference can be noticed. While in the case of $[Co(DH)_2Br_2]^-$ both E_a and lg Z decrease considerably with increasing DMFA content of the solvent, in the present case of $[Co(DH)_2Cl_2]^-$ the opposite phenomenon is observed, i.e. a slight increase in these kinetic parameters.

EXPERIMENTAL

Synthesis of the acid H $[Co(DH)_2Cl_2]$. 28.8 of cobaltous (II) chloride (0.1 moles of $CoCl_2 \cdot 6\,H_2O$) are solved in 100 ml water. 23.2 g (0.2 moles) of finely sprayed dimethylglyoxime are solved in 250 ml ethanol. The mixture of these solutions is oxidized by air bubbling for 4–6 h. After filtration 200 ml conc. hydrochloric acid are added to the brown solution. After a short time dark green, brilliant rhombus-shaped crystals separate. The precipitate is filtered, washed with ice-cooled water and dried in the air. Yield: 70 per cent.

Analysis of $[Co(C_4H_7N_2O_2)_2Cl_2]H$ (361.05)
Calc.: Co, 16.32 : Cl, 19.64 ;
Found: Co, 16.40 : Cl, 19.53.

Salts of the type Amine. H $[Co(DH)_2Cl_2]$. *General method of synthesis.* 10 m-moles of the amine are treated with 10 ml of conc. hydrochloric acid and the obtained amine chlorhydrate is solved in 60–80 ml of water. 3 m-moles of $H[Co(DH)_2Cl_2]$ (i.e. 1.1 g) are dissolved in 10 ml of dimethylformamide. After mixing a crystalline product formes with in 10–20 minutes, the amine salt of the complexe acid. Several new derivatives of this type are given in table 5. It is worth mentioning that aliphatic and aromatic primary and secondary amines and some simple heterocyclic amines give no well crystallizing compounds with $H[Co(DH)_2Cl_2]$.

Cobaltous (III)-amine-salts. 10 m-moles of a complex cobaltous-(III)-salt of the hexamine-, monoacido-pentamine- or diacido-tetramine type are solved in 80–100 ml water and the solution is treated with 3 m-moles of $H[Co(DH)_2Cl_2]$ in 10 ml DMFA.

The studied complex acid was observed to form no hardly soluble derivatives with hexamine- and monoacido-pentamine type salts as $[Co(NH_3)\ ]Cl_3$, $[Co(en)_3]Cl_3$. $[Co(NH_3)_5H_2O]Cl_3$, $[Co(NH_3)_5NO_2]Cl_2$, $[Co(en)_2Cl\,NH_3]Cl_2$, $[Co(en)_2$ Cl pyridine$]Cl_2$. $[Co(en)_2$ Cl benzylamine$]Cl_2$. By means of double exchange reactions only a few salts containing complex cations of the diacido-tetramine type (see tab. 5) were obtained.

It is very characteristic of this complex acid the formation of bis-dioximato-diamine-cobaltous (III)-salts of the type $[Co(DH)_2(amine)_2][Co(DH)_2Cl_2]$.

Bis-dioximato-diamine-cobaltous (III)-salts $[Co(dioxime)_2(amine)_2]$. $[Co(DH)_2Cl_2]$. These compounds can be synthesized by mixing a solution of 10 m-moles of $H[Co(DH)_2Cl_2]$ in

---

[14] J. Zsakó, Cs. Várhelyi and Z. Finta, *Stud. Univ. Babeş Bolyai, Chem.*, 1969 (in press).

10 ml DMFA with a solution of 10 m-moles of $[Co(DH)_2(amine)_2]$-acetate or of $[Co(NioxH)_2(amine)_2]$-acetate in 100 ml ethanol 70 per cent. The necessary $[Co(DH)_2(amine)_2]$-acetate and $[Co(Niox H)_2(amine)_2]$-acetate are obtained by bubbling air through a mixture of cobaltous (II) acetate, dimethylglyoxime (or 1,2-cyclohexanedion-dioxime (nyoxime)) and corresponding amine in ethanol 75–80 per cent (molar ratio 1 : 2 : 3).[15] The separated crystalline precipitate is filtered after 15–30 minutes, washed with a small amount of diluted ethanol and dried in air.

Table 5

New derivatives of the complex acid H $[Co(DH)_2Cl_2]$ with N-bases and with cobaltous (III) amines

No	Formula	Mol. weight	Yield (%)	Appearance	Analysis Calc.	Analysis Found
1	Oxin. HR	506.2	50	Brilliant long brown needles	Co 11.64 Cl 14.01	11.80 14.20
2	Tetramethyl-ammonium. R	434.2	25	Sparkling, brown hexagonal plates	Co 13.56 Cl 16.13	13.70 16.33
3	Tetraethyl-ammonium. R	490.3	30	Sparkling, brown prisms	Co 12.02	12.13
4	Antipyrine. HR	549.2	30	Brown dendrytes	Co 10.73	10.85
5	Brucine. HR	755.5	15	Green, large rhombic prisms	Co 7.80	7.65
6	Cinchonine. HR	655.4	15	Irregular brown plates	Co 8.99	9.05
7	1–6 $[Co(en)_2Cl_2]$ R	609.9	50	Brownish green brilliant dendrytes	Co 19.32 Cl 23.25	19.15 23.00
8	1–2 $[Co(en)_2Cl_2]$R	609.9	40	Brown prisms	Co 19.32 Cl 23.25	19.20 23.40
9	1–6 $[Co(en)_2Br_2]$R	698.8	50	Brown-yellow prisms	Co 16.87 N 16.03	16.70 16.33
10	1–2 $[Co(en)_2(NCS)_2]$R	655.1	55	Aggregates of reddish brown small thin needles	Co 17.99 N 21.38	17.60 21.50
11	$[Co(en)_2C_2O_4]$ R	627.0	45	Aggregates of thin brown needles	Co 18.80 Cl 11.31	18.60 11.50
12	$[Co(pyridine)_4Cl_2]$ R	806.3	75	Sparkling, thin light green plates	Co 14.63 Cl 17.59	14.40 17.65

"en" ethylenediamine : $C_2H_8N_2$ "R" = $[Co(DH)_2Cl_2]$

Formulae, calculated molar weights, yields of the synthesis, characterization of the new products and analysis data are given in table 6.

---

[15] Cs. Várhelyi and L. Szotyori, *Revue Roumaine Chim.*, **10**, 1049 (1965).

IR spectrum of the acid H [Co(DH)$_2$Cl$_2$] was recorded with a UR-10 spectrophotometer (Carl Zeiss, Jena) in KBr pellets.

Kinetic measurements. The samples of the complex acid were dissolved in the pre-heated solvent and the obtained $2 \times 10^{-3} - 6 \times 10^{-3}$ m solution was kept in an ultrathermostate at the temperature of the run. Temperature was maintained with an accuracy of ± 0.01°.

Table 6

New binary complexe salts of the type [Co (Dioxime)$_2$ (amine)$_2$] [Co (DH)$_2$ Cl$_2$]

No.	Formula	Mol. weight calc.	Yield (%)	Appearance	Analysis	
					Calc.	Found
13	[Co(DH)$_2$(pyridine)$_2$]R	807.4	50	Brilliant, thin yellow small plates	Co 14.60 Cl 8.78	14.20 8.90
14	[Co(DH)$_2$(*o*-ethyl-aniline)$_2$] R	891.6	70	Brilliant brown dendrytes	Co 13.22 Cl 7.95	13.05 8.10
15	[Co (DH)$_2$(*p*-)ethyl-aniline)$_2$] R	891.6	60	Sparkling, brown fibrous prisms	Co 13.22 Cl 7.95	12.95 7.75
16	[Co (DH)$_2$ (α-naphthylamine)$_2$] R	935.6	65	Brilliant, reddish-brown thin, hexagonal plates	Co 12.60 Cl 7.58	12.10 7.45
17	[Co (DH)$_2$ (β-naphthylamine)$_2$] R	935.6	50	Brilliant, thin, yellow needles	Co 12.60 Cl 7.58	12.25 7.70
18	[Co (NioxH)$_2$ (aniline)$_2$] R	887.5	45	Yellow, rhombohedral plates	Co 13.28 Cl 7.99	13.32 7.75
19	[Co (NioxH)$_2$(α-naphthylamine)$_2$] R	987.6	30	Thin, yellow-reddish plates	Co 11.94	11.70
20	[Co (NioxH)$_2$ (β-naphthylamine)$_2$] R	987.6	60	Thin, yellow prisms	Co 11.94 Cl 7.18	11.60 7.25

"DH" = $C_4H_7N_2O_2$, "NioxH" = $C_6H_9N_2O_2$

The kinetics of the process was followed by measuring the concentration of the free Cl$^-$ ions. Since the argentometric determination of Cl$^-$ presents some difficulties because of the formation of a hardly soluble silver salt of the complex acid, the determination of Cl$^-$ was carried out by measuring the EMF of the following concentration cell: Ag/AgCl, studied solution/KNO$_3$ sol./KCl, 0.01 n, AgCl/Ag. For preparing both the studied solution and the standard KCl solution, the same solvent (water or water-DMFA mixture) was used. Electrodes were prepared according to the indications of Selbin and Bailar,[16] with the only difference, that a less current density was used, which improved the quality of the electrodes. Silvering of the platinum electrodes was made for 10 hours, with a current density of 1 mA/cm². The formation of the AgCl layer lasted 1h in the same conditions, i.e. current density of 1 mA/cm².

---

[16] J. Selbin and J. C. Bailar, *J. Amer. Chem. Soc.*, **79**, 4285 (1957).

Revue Roumaine de Chimie, **14**, 1143–1148 (1969)

KOMPLEXVERBINDUNGEN DES N,N′-DIAMINOPIPERAZINS. II*

VERBINDUNGEN MIT KOMPLEXEN ANIONEN UND IHR THERMISCHER ABBAU

J. DICK und ALFA LUPEA

Aus dem Pharmazeutisch-technischen Laboratorium der Technischen Hochschule Timişoara,
Bd. 30 Decembrie 2

Eingegangen am 8. November 1968

Außer den Komplexverbindungen der allgemeinen Formel $[\mathrm{Me^{II}DapX_2}]$, die in Mitteilung 1 beschrieben wurden, bildet das N,N′-Diaminopiperazin (DAP) unter bestimmten Bedingungen Verbindungen mit komplexen Anionen des Haupttyps $[\mathrm{Me^{II-III}X_n}]\,(\mathrm{H_2Dap})_n$. Sie werden aus wäßrigen sauren Lösungen mit DAP und zwei- und dreiwertigen Elementen: Co, Zn, Hg, Pd, Pt, Bi, Cr, mit den Anionen SCN, Cl, J erhalten. Es werden Darstellung, Analyse, Eigenschaften und ihr thermisches Verhalten beschrieben. Über Strukturaufklärung siehe näheres in Mitteilung 3 u.4.

In Mitteilung 1 beschrieben wir Metallchelatverbindungen des N,N′-Diaminopiperazins (DAP) der allgemeinen Formel $[\mathrm{Me^{II}\,DapX_2}]$. In vorliegender Arbeit werden DAP-Verbindungen mit komplexen Anionen beschrieben. Ausgangshypothese und Grundsätze über das Studium von organischen DAP-Verbindungen sind außer Mitteilung 1 auch unseren früheren Veröffentlichungen [1–5] zu entnehmen.

DAP bildet in sauren wäßrigen Lösungen von pH mindestens 1–2, Komplexverbindungen der allgemeinen Formel $[\mathrm{Me^{II-III}X_n}]\,(\mathrm{H_2Dap})_n$ wo $\mathrm{Me^{II}}$ = Co, Zn, Hg, Pd, Pt; $\mathrm{Me^{III}}$ = Bi, Cr; X = SCN, Cl, J zu der, zunächst die Analysenbefunde und ihr thermischer Abbau führten und die, an Hand ihrer sichtbaren, UV- und IR-Spektren und Elektronenspinresonanz bestätigt werden konnten (3. u. 4. Mitteilung).

Zwei der Verbindungen XI u. XII werden weiter auf ihre Struktur untersucht; sie können nur schwierig einem der Haupttypen der Verbindungen zugereiht werden.

Bezüglich der Formulierung der Verbindungen I–X weisen wir zunächst auch auf unsere Betrachtungen über die Struktur der von uns hergestellten Verbindungen mit komplexen Anionen in der Pyrazolonreihe der Formel $[Me^{II}X_4](HPyr)_2$ hin.[6-7]

---

* I. Mitteil.: J. Dick und A. Lupea, *Rev. Roumaine Chim.*, **14**, 1047 (1969).

[1] J. Dick, J. Ristici, M. Neacşu und A. Lupea, *Studii şi Cercetări, Şti. Chim., Baza Cercetări Şti., Timişoara*, **10**, 179 (1963).

[2] J. Dick, M. Neacşu und A. Lupea, *Rev. Roumaine Chim.*, **11**, 517 (1966).

[3] J. Dick und A. Lupea, *Die Pharmazie*, **22**, 555 (1967).

[4] J. Dick und A. Lupea, *Die Pharmazie*, **23**, 482 (1968).

[5] J. Dick, A. Lupea, M. Elias und A. Botez, *Die Pharmazie*, **23**, 714 (1968).

Die Verbindungen sind im allgemeinen leicht löslich in warmem, lediglich auch in kaltem Wasser, schwerer in verdünnten Säuren und in organischen Lösungsmitteln. Einzelheiten über übrige Eigenschaften sind dem experimentellen Teil zu entnehmen.

EXPERIMENTELLES

I. *$[Co(SCN)_4]\cdot H_2Dap$ (409,46).* Eine Lg von 4 g $Co(NO_3)_2\cdot 6H_2O$ und 4 g NH_4SCN in 25 ml H_2O bringt man auf pH mindestens 1, erhitzt und fügt zur warmen Lg2 g DAP in 15 ml Wasser und bringt mit verd. HCl auf pH 1. Die DAP-Lg wird nötigenfalls filtriert. Man kühlt gut ab und rührt kräftig um, läßt 2 Tage bei öfterem Umrühren auf 0° abgekühlt stehen, filtriert durch einen Glasfiltertiegel G_4 und wäscht den blau gefärbten kristallinen Niederschlag sehr vorsichtig mit kleinen Portionen eisgekühltem Wasser von pH mindestens 1. Ziemlich leicht löslich auch in eisgekühltem, noch leichter in warmem Wasser, schwerer in verdünnten Säuren und organischen Lösungsmitteln. Geht beim Waschen leicht in die rosa gefärbte Verbindung $[CoDap(SCN)_2]\cdot 2H_2O$ über. Man trocknet vorsichtig vor Licht geschützt über P_2O_5.

Analyse : *Ber.* : Co 14,39 ; SCN 56,74 ; N 27,38 %
Gef. : Co 14,13 ; SCN 56,40 ; N 27,01 %

II. *$[Zn(SCN)_4]\cdot H_2Dap\cdot 2H_2O$ (451,94).* Man löst 1,8 g $ZnCl_2$ in 8 ml H_2O, fügt 4,5 g NH_4SCN hinzu und bringt auf pH 1. Dann versetzt man mit 2 g DAP in 15–18 ml H_2O, bringt auf pH mindestens 1, rührt um, kühlt 24 Std. gut ab, während man öfters umrührt, filtriert den weißen kristallinen Niederschlag, wäscht und trocknet wie bei I. Löslichkeit wie I. Geht beim Waschen leicht in die Verbindung $[ZnDap(SCN)_2]$ über.

Analyse : *Ber.* : Zn 14,47 ; SCN 51,41 ; N 24,81 %
Gef. : Zn 14,24 ; SCN 51,76 ; N 24,39 %

III. *$[Hg(SCN)_4]\cdot H_2Dap$ (551,14).* Man löst 2,1 g $HgCl_2$, nötigenfalls durch Erhitzen in 15–18 ml H_2O, kühlt ab, fügt 6,5 g NH_4SCN und dann 1,5 ml verd. HCl hinzu (pH mindestens 1). Jetzt wird unter Umrühren 1,5 g DAP in 10–12 ml H_2O gelöst auf pH mindestens 1 gebracht und zur $[Hg(SCN)_4](NH_4)_2$-Lg gefügt. Man kühlt einige Stunden hindurch gut ab, filtriert den weißen kristallinen Niederschlag, wäscht wie bei I–II und trocknet über $CaCl_2$. $[Hg(SCN)_4]^{-2}$-und DAP-Lg muß unbedingt angesäuert werden, da Reduzierungsgefahr zu Hg besteht. Bedeutend schwerer löslich in kaltem Wasser als I–II, Löslichkeit im übrigen wie bei I.

Analyse : *Ber.* : Hg 36,40 ; SCN 42,15 ; N 20,34 %.
Gef. : Hg 36,12 ; SCN 42,59 ; N 19,98 %

IV. *$[HgCl_4]\cdot H_2Dap$ (460,62).* Wird wie III aber mit 7,5 g NaCl statt NH_4SCN erhalten. Die $[HgCl_4]^{-2}$-und DAP-Lg werden angesäuert wie bei III. Es wird 12 Std. gekühlt und wie III behandelt. Löslichkeit des weißen kristallinen Niederschlags wie bei III.

Analyse : *Ber.* : Hg 43,55 ; Cl 30,79 ; N 12,16 %
Gef. : Hg 43,05 ; Cl 31,12 ; N 11,89 %

---

[6] J. Dick und C. Drugărin, *Studii şi cercetări, Şti. Chim., Baza Cercetări Şti., Timişoara*, **18**. 205 (1961).

[7] J. Dick und A. Maurer, *Rev. Roumaine Chim.*, **10**, 633 (1965).

V. $[HgJ_4].H_2Dap$ (*826,43*). Man löst 2,8 g $HgCl_2$ in einer heißen, womöglich konzentrierten Lösung von 10 g KJ, kühlt ab, bringt auf pH 1, fügt 2 g DAP in 15 ml H_2O hinzu, bringt von neuem auf pH 1, rührt kräftig um und kühlt mindestens 4 Tage hindurch gut ab, während man öfters kräftig umrührt. Allmählich erscheint ein gelb gefärbter kristalliner Niederschlag, der weiter wie I—III behandelt wird, ohne den nassen Niederschlag mit einem Metallspatel zu berühren. Ziemlich leicht löslich in kaltem Wasser. Weitere Löslichkeit wie bei I, III.

Analyse : *Ber.* : Hg 24,78 ; J 61,43 ; N 6,78 %
Gef. : Hg 24,24 ; J 61,79 ; N 6,51 %

VI. $[PtCl_4].H_2Dap$ (*455,10*). Wird aus Pt^{IV} durch die reduzierende Wirkung des Diamins erhalten. Man löst 1,5 g $[PtCl_6]H_2 . 6H_2O$ in 15 ml H_2O, fügt 4,5 g NaCl hinzu, erhitzt, filtriert, bringt auf pH 2, kühlt ab und fügt 0,8 g DAP in 8 ml Wasser gelöst hinzu, rührt kräftig um und bringt von pH etwa 9,5 auf pH 4,5. Es bildet sich sofort ein rot gefärbter kristalliner Niederschlag, der 24 Std. bei öfterem Umrühren gut abgekühlt, filtriert, mit eisgekühltem Wasser von pH 4 ausgewaschen und vor Licht und Metallspatel geschützt über $CaCl_2$ getrocknet wird. Leicht löslich in warmem, schwerer in kaltem Wasser und verdünnten Säuren, schwer löslich in organischen Lösungsmitteln.

Analyse : *Ber.* : Pt 42,87 ; Cl 31,16 ; N 12,31 %
Gef. : Pt 43,20 ; Cl 30,81 ; N 12,02 %

VII. $[Pt(SCN)_4].H_2Dap$ (*545,61*). Wird wie VI, aber statt NaCl mit NH_4SCN erhalten. End—pH 4. Der weiße kristalline Niederschlag wird nach 48 Std. langem Abkühlen filtriert. Löslichkeit wie bei VI.

Analyse : *Ber.* : Pt 35,66 ; SCN 42,58 ; N 20,55 %
Gef. : Pt 35,82 ; SCN 42,10 ; N 20,15 %

VIII. $[PdCl_4].H_2Dap$ (*366,41*). Wird aus dem Chlorhydrat des Diamins in stark saurer Lösung erhalten. Man löst durch Erhitzen 0,9 g $PdCl_2$ in 15 ml 2n HCl und 5 g DAP. 2HCl in 12 ml 2n HCl ebenfalls warm, fügt letztere noch warm zur Pd-Lg und rührt kräftig um. Der braunrot gefärbte Niederschlag erscheint erst nach mehreren Tagen bei gutem Abkühlen und öfterem Umrühren. Man filtriert nach 6 Tagen und wäscht mit kalter 2n HCl öfters aus. Leicht löslich in kaltem, sehr leicht löslich in warmem Wasser, im übrigen wie I—VII.

Analyse : *Ber.* : Pd 29,04 ; Cl 38,71 ; N 15,29 %
Gef. : Pd 29,09 ; Cl 39,06 ; N 14,91 %

IX. $[Cr(SCN)_4].(HDap)_2$ (*554,74*). Wird durch Umsetzen von 2 g $Cr_2(SO_4)_3$ und 5 g NH_4SCN in einigen ml H_2O gelöst, auf pH 2 gebracht und einer DAP-Lg von 1,2 g in 8 ml Wasser und auf pH 1,5 angesäuert erhalten. Gesamtvolumen der Lösung 15 ml, End—pH mindestens 1,5. Man rührt kräftig um, kühlt 5 Tage hindurch gut ab, während man öfters umrührt, filtriert den violett gefärbten kristallinen Niederschlag ab, wäscht mit eisgekühltem Wasser von pH 1 aus und trocknet vor Licht geschützt. Ziemlich löslich in Wasser, im übrigen wie I—VIII.

Analyse : *Ber.* : Cr 9,37 ; SCN 41,88 ; N 32,43 %
Gef. : Cr 9,47 ; SCN 42,36 ; N 32,64 %

X. $[BiJ_4].(HDap)_2.6H_2O$ (*1059,09*). Man löst 1 g $BiCl_3$ und 21 g KJ in 50 ml H_2O, bringt mit verd. HCl auf pH 1 und filtriert nötigenfalls. Dann verdünnt man die $[BiJ_4]K$-Lg auf 75 ml und versetzt tropfenweise bei ständigem Umrühren mit 1,5 g DAP in 13 ml H_2O, bringt auf pH 2, kühlt 1 Std. auf 0° ab und filtriert den grobkristallinen roten Niederschlag, wäscht mit eisgekühltem Wasser von pH 2 öfters aus und trocknet vor Licht geschützt. Der nasse Niederschlag darf nicht mit einem Metallspatel berührt werden. In Anwesenheit von

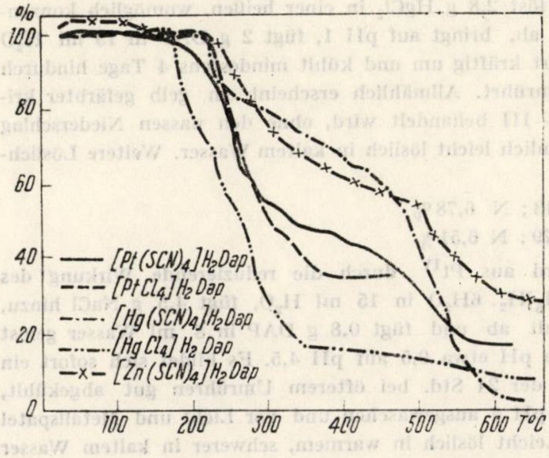

Abb. 1. — Thermogramme der Verbindungen $[Me^{II}X_4]H_2Dap$.

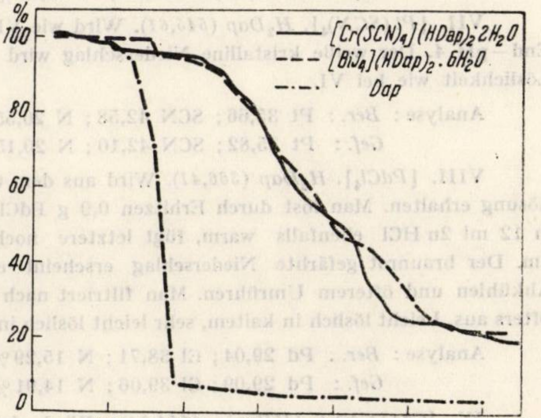

Abb. 2. — Thermogramme der Verbindungen $[Me^{II}X_4](HDap)_2$.

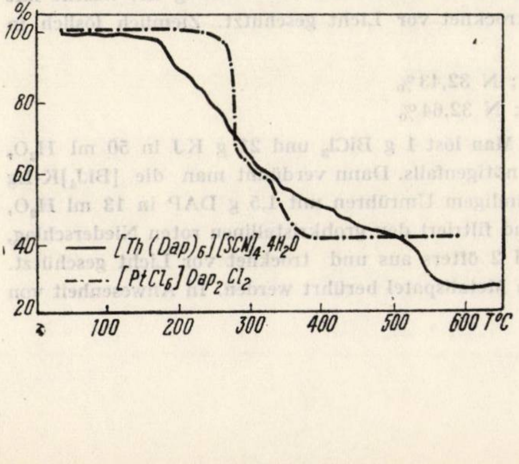

Abb. 3. — Thermogramme der Verbindungen XI und XII.

$[BiJ_4]$ K, auch geringer Mengen, ist der Niederschlag in kaltem Wasser praktisch unlöslich, eine Eigenschaft die uns die Verwendung dieser Verbindung zu einer kolorimetrischen Bestimmungsmethode des technischen Diamins ermöglichte. Das Verfahren wird gelegentlich veröffentlicht. Schwer löslich in warmem Wasser und ziemlich löslich in verdünnten Säuren und organischen Lösungsmitteln, wie Azeton, Äthanol u.a. Ausbeute 98 %.

Analyse : *Ber.* : Bi 19,74 ; J 47,93 ; N 10,59 %
Gef. : Bi 19,57 ; J 47,38 ; N 10,22 %

XI. $[PtDap_2Cl_6]\,Cl_2$ (*711,09*). Wird aus $[PtCl_6]H_2 . 6H_2O$ mit DAP. 2HCl in 2n HCl-Lg erhalten. Man löst 0,9 g $[PtCl_6)\,H_2 . 6H_2O$ in 12 ml 2n HCl, fügt 3 g NaCl hinzu und dann eine Lösung von 4 g DAP. 2HCl in 15 ml 2n HCl, warm gelöst und abgekühlt hinzu. Es bildet sich sofort ein orangerot gefärbter Niederschlag, der allmählich gelb kristallinisch wird. Man kühlt 24 Std. bei 0° ab, rührt öfters um, filtriert, wäscht öfters mit eisgekühlter 2n HCl aus und trocknet. Leicht löslich in Wasser, im übrigen wie I—IX.

Analyse : *Ber.* : Pt 27,47 ; Cl 39,95 ; N 7,89 %
Gef. : Pt 27,79 ; Cl 40,30 ; N 7,77 %

XII. $[ThDap_6(SCN)_4] . 4H_2O$ (*1233,48*). Es werden 1,8 g $Th(NO_3)_4 . 4H_2O$ und 6 g NH_4SCN in 10—12 ml Wasser gelöst und mit einer Lösung von 2,5 g DAP in 15 ml H_2O versetzt. Man bringt auf pH 1—1,5, rührt um und kühlt den sofort gebildeten weiß-schwach-gelblichen Niederschlag 48 Std. bei öfterem Umrühren auf 0° gut ab, filtriert und wäscht 8—10 mal mit je 0,5 ml eisgekühltem Wasser von pH 1—1,5 aus. Ziemlich löslich in Wasser, schwerer in organischen Lösungsmitteln.

Analyse : *Ber.* : Th 19,25 ; SCN 19,28 ; N 34,87 %
Gef. : Th 19,39 ; SCN 19,40 ; N 34,37 %

Zwecks Aufklärung ihrer Zusammensetzung wurde ein Teil der Verbindungen einem thermischen Abbau unterworfen.

Dabei wurde festgestellt, daß die Zersetzung der Verbindungen $[Me^{II}X_4] . H_2Dap$ erst über 155° einsetzt.

Der Wasserverlust- und der Spaltungsprozeß der N—N-Bindung des Liganden wird durch die allmähliche Zersetzung des Liganden überdeckt, die übrigens in allen Fällen bei 368° beendet ist. Es folgt eine allmähliche Zersetzung der entstandenen Zwischenprodukte. So beginnt die Zersetzung des entstandenen $Pt(SCN)_2$ (VII) bei 290°, des $Hg(SCN)_2$ (III) bei 450°, des $HgCl_2 . 2NH_3$ (IV) bei 227°, der sich wahrscheinlich gebildeten Piperazinkomplexverbindung des Zn (II) zwischen 368—376 und des $Zn(SCN)_2$ bei 512°. Im Falle der Hg-Verbindungen findet eine allmähliche Verflüchtigung des Hg statt.

Bei etwa 600° stellt sich bei allen Verbindungen eine Gewichtsbeständigkeit ein, außer der Verbindung VIII wo diese Beständigkeit bei 387° zu beobachten ist.

Im Falle der Verbindungen $[Me^{II}X_4]\,(HDap)_2$, die — wie aus Abbildung 2 ersichtlich ist — bis 100° beständig sind, ist ein klares Gebiet, das dem Wasserverlust (im Falle der Verbindung X aber bloß für die ersten 3 Wassermoleküle), wie auch der Spaltung der N—N-Bindungen entspricht, zu beobachten. Die Zersetzung des Liganden ist bei etwa 400° beendet. Es folgt ein ziemlich langsamer Zersetzungsprozeß. Aus den bei etwa 620° erhaltenen Metalloxiden konnte der Metallgehalt der Verbindungen berechnet werden, der mit dem theoretischen Werte gut übereinstimmt.

Die Verbindungen XI, XII sind, wie aus Abbildung 3 ersichtlich, bis 240° bzw. bis 120° beständig, wo zunächst die Spaltung der N—N-Bindung — viel kräftiger bei XI — beginnt und dann die Zersetzung des Liganden einsetzt, die bei 280° bzw. bei 535° beendet ist. In beiden Fällen folgt dann eine ziemlich langsame Zersetzung. Aus den Endprodukten $[PtCl_4](NH_4)_2$ bzw. ThO kann der Metallgehalt von XI, XII, in guter Übereinstimmung mit dem theoretischen Werte berechnet werden.

Revue Roumaine de Chimie, 14, 1149–1151 (1969)

L'ÉTUDE DES PROPRIÉTÉS MAGNÉTIQUES DE QUELQUES TARTRATES SIMPLES ET COMPLEXES

VICTORIA BEDNAR *, V. MINCU et H. BEDNAR **

Université de Bucarest, 13, Bd. Republicii

Reçu le 23 juillet 1968

On a déterminé la susceptibilité magnétique du tartrate complexe d'indium et de quelques tartrates (Na_2T, NaKT, HKT, K_2T) en poudre, afin d'étudier la structure du tartrate complexe d'indium.

La susceptibilité magnétique des poudres a été déterminée par la méthode de Gouy.[1] [2] On a employé un électro-aimant (1) de type Weiss (voir fig. 1) alimenté par le rédresseur (2) et les accumulateurs (3) ; le courant a été réglé avec le rhéostat (4) et mesuré avec l'ampèremètre (5). On a obtenu un champ magnétique de 12 000 Oe avec des pôles cylindriques (6) (de 10 cm diamètre) dans un entrefer de 1 cm pour un courant de 12 A et 120 V. L'ampoule (7), ayant le diamètre intérieur de 0,5 cm et le volume de 3 ml, attachée à la balance (8) par le fil de quartz (9), a été protégée contre le courant d'air par une gaine de protection (10). La température de l'ampoule est mesurée avec le thermocouple (11) dont l'une des soudures se trouve dans la gaine de protection et l'autre est maintenue à la température constante ; la tension du thermocouple est mesurée à l'aide d'un galvanomètre (12), préalablement étalonné.

On a employé une balance à déflexion nulle, avec une précision de $\pm 0{,}02$ mg. Comme étalon nous avons utilisé de l'eau, dont la susceptibilité magnétique est $\varkappa = -0{,}720 \cdot 10^{-6}$. Nous avons employé un procédé spécial [3] pour remplir l'ampoule avec la poudre. La correction pour le paramagnétisme de l'oxygène atmosphérique est $\varkappa'_0 = \varkappa_0 \frac{\rho_{app}}{\rho}$, où ρ_{app} est la densité moyenne de la poudre, ρ la densité de la substance et $\varkappa_0$ la susceptibilité de l'air (à 20° $\varkappa_0 = +0{,}030 \cdot 10^{-6}$). La susceptibilité de la substance en poudre est

$$\varkappa_s = \frac{\Delta F_s}{\Delta F_{H_2O}} (\varkappa_{H_2O} - \varkappa_0) + \varkappa'_0$$

---

* Institut Pédagogique, Braşov, 40, Bd. Karl Marx.

** Institut Polytechnique, Braşov, 2, str. Vlad Ţepeş.

[1] P. SELWOOD, Magnetochemistry, Interscience Publishers, New York, Londres, 1956.

[2] J. LEWIS et R. G. WILKINS, « Modern Coordination Chemistry Principles and Methods », Interscience Publishers, New York, Londres, 1960.

[3] V. E. SAHINI et V. MINCU, *Anal. Univ. Bucureşti Ser. Chimie,* **1968**, 33.

où ΔF_s est la force d'intéraction entre le champ magnétique et la poudre et ΔF_{H_2O} la force d'interaction entre le champ magnétique et l'eau. La susceptibilité moléculaire de la substance (dont la masse moléculaire est M) est

$$\chi_M = \frac{\varkappa}{\rho_{app}} M$$

Les valeurs obtenues sont données dans le tableau 1.

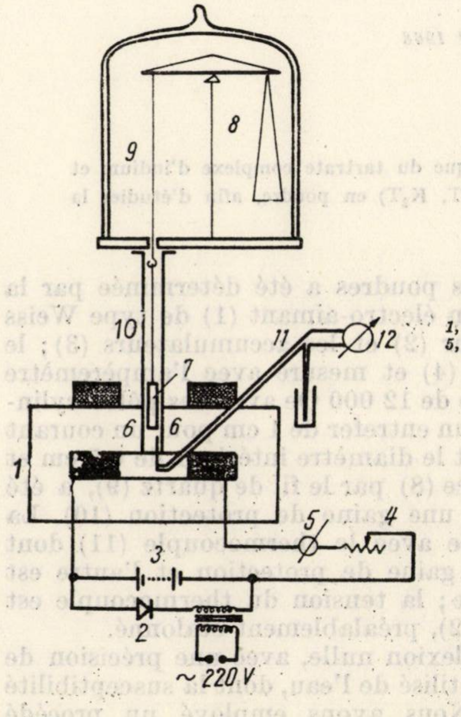

Fig. 1. La balance magnétique : *1*, électro-aimant ; *2*, rédresseur ; *3*, accumulateurs ; *4*, rhéostat ; *5*, ampèremètre ; *6*, pôles ; *7*, ampoule ; *8*, balance ; *9*, fil de quartz ; *10*, gaine de protection ; *11*, thermocouple ; *12*, galvanomètre.

Tableau 1

Susceptibilité magnétique des substances

Substance	$-10^6 \chi$							
		H_2O 12,96	Na^+ 5,6	K^+ 12,5	OH 10,04	H_{cov} 2,96	T^{2-}	
1	2	3	4	5	6	7	8	9
$C_4O_6H_6$	67,8	—	—	—	—	5,92	61,9	—
$C_4O_6H_4Na_2 . 2H_2O$	97,8	25,9	11,2	—	—	—	60,7	—
$C_4O_6H_4K_2 . 1/2\ H_2O$	93,1	6,5	—	25	—	—	61,6	—
$C_4O_6H_4KNa . 4H_2O$	130,7	51,8	5,6	12,5	—	—	60,8	—
$C_4O_6H_4KH$	76,8	—	—	12,5	—	2,96	61,3	—
$C_4O_6H_4InOH . 3H_2O$	139,2	38,9	—	—	10	—	61,3	29
$In(OH)_3 . H_2O$	71,4	13	—	—	30,1	—	—	28,3

On a indiqué dans les colonnes 1 et 2 les substances et leur susceptibilité magnétique, dans les colonnes 3–7 la contribution de l'eau de cristallisation et des ions [4,5] à la susceptibilité moléculaire et dans la 8e colonne la susceptibilité de l'ion tartre. En ce qui concerne la valeur de la susceptibilité de l'indium, ainsi déterminée, dans le complexe tartrique et dans l'hydroxyde (voir la 9e col.), elle est différente de la valeur de susceptibilité de l'ion In^{3+} dans les combinaisons ioniques [5] (—18... — 20.10^{-6}). Cette différence est expliquée par la disparition du caractère ionique de l'indium (III) dans le complexe mentionné dont la structure est [6-8]

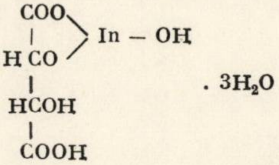

---

[4] Tables de constantes et donneés numériques «Constantes sélectionnées. Diamagnétisme et paramagnétisme», Masson & Cie, Paris, 1957.

[5] Landolt-Börnsteins «Zahlenwerte und Funktionen aus Physik, Chemie, Astronomie, Geophysik, Technik.» 6e Aufl., I. Band., 1 Teil Atome und Ionen Springer Verlag, Berlin, Göttingen, Heidelberg, 1950.

[6] H. Bednar, V. Bednar et I. Manu, *Rev. Fizică-Chimie* (*A*) *III*, **1966**, 401.

[7] V. Bednar et H. Bednar, *Studii și Cercetări Chim. Acad.*, Bucarest, **15**, 719 (1967).

[8] V. Bednar, E. Segal et D. Fătu, *Studii și Cercetări Chim. Acad.*, Bucarest, **16**, 55 (1968).

Revue Roumaine de Chimie, **14**, 1149–1151 (1969)

Revue Roumaine de Chimie, **14**, 1153–1161 (1969)

L'ADDITION DES PHILODIÈNES SUR LA PHTALAZINE. III[1]

ACTION DU BROMURE DE PHÉNACYLE SUR LA PHTALAZINE

MAGDA PETROVANU, A. SAUCIUC, I. GABE et I. ZUGRĂVESCU
Université « Al. I. Cuza », Laboratoire de Chimie organique, Jassy, 11, str. 23 August

Reçu le 19 novembre 1968

En continuant les recherches sur les composés de structure ylidique C—N, on a étudié l'obtention et la réactivité du phtalazinium-phénacylide (X). L'élimination de l'acide bromhydrique à partir du bromure de phénacylphtalazinium (IX) conduit au phtalazinium-phénacylide (X) qui se stabilise par dimérisation et conduit au produit (XIa). Par cyclo-addition 1.3 de quelques philodiènes tels que l'anhydride maléique, l'acétylènedicarboxylate de méthyle, l'azodicarboxylate d'éthyle, l'isocyanate de phényle sur le phtalazinium-phénacylide (X) on obtient les composés XIII, XIV, XV, XVI dont les structures ont été démontrées par des méthodes physico-chimiques. La réaction entre le bromure de phénacylphtalazinium (IX) et l'acétate d'ammonium conduit au produit (XVII).

Dans nos travaux précédents, [1,2] en étudiant l'action de l'anhydride maléique et de l'acétylènedicarboxylate de méthyle sur la phtalazine, nous avons réussi à isoler des ylides stables de type (I) et (II). La stabilité de ces ylides peut être expliquée par la capacité de l'anhydride maléique et de l'acétylène-dicarboxylate de méthyle d'accepter une charge anionique, tandis que la stabilisation de la charge cationique est due au cycle pyridazinique lié au noyau benzénique

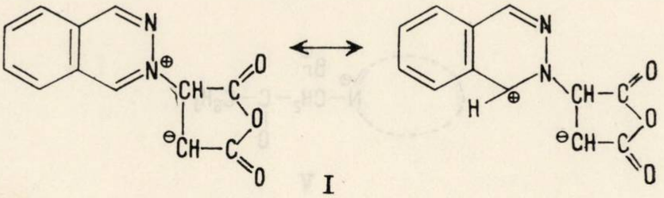

I

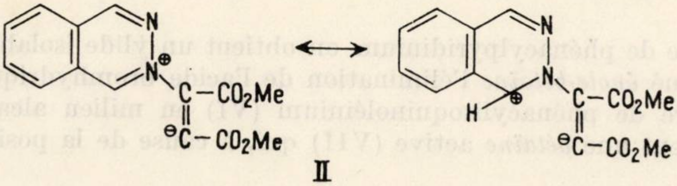

II

---

[1] Part. II : M. Petrovanu, A. Sauciuc, I. Gabe et I. Zugrăvescu, *Rev. Roumaine Chim.*, **13**, 513–519 (1968).

[2] I. Zugrăvescu, M. Petrovanu, A. Caraculacu et A. Sauciuc, *Rev. Roumaine Chim.*, **12**, 109 (1967).

Les ylides (I) et (II) ont été obtenus par addition directe du réactant diénophyle à la phtalazine.

Une autre méthode qui peut fournir des combinaisons de structure amphionique (IV) consiste à éliminer l'hydracide à partir des sels de N-méthyl-acyl-phtalazinium (III) obtenus par l'addition des composés α-halogène-carbonyliques à la phtalazine

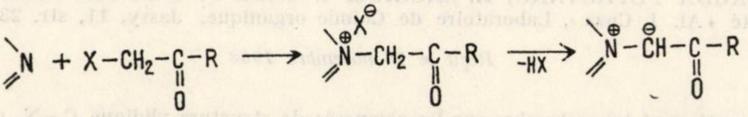

$$\geq N + X-CH_2-\underset{\underset{O}{\|}}{C}-R \longrightarrow \geq \overset{\oplus}{N}\overset{X^{\ominus}}{}-CH_2-\underset{\underset{O}{\|}}{C}-R \xrightarrow[-HX]{} \geq \overset{\oplus}{N}-\overset{\ominus}{C}H-\underset{\underset{O}{\|}}{C}-R$$

III IV

Poursuivant nos recherches concernant l'obtention et l'étude de la réactivité des composés de structure ylidique, nous avons envisagé de chercher les possibilités offertes par cette deuxième méthode. Parmi les composés α-halogéno-carbonyliques, nous avons choisi premièrement, le bromure de phénacyle dont l'addition sur divers composés hétéroatomiques azotés a déjà été étudiée.[3-6]

Kröhnke[5] en étudiant les sels du type (V) obtenus par l'addition du bromure de phénacyle à la pyridine, la quinoléine, l'isoquinoléine, etc. a remarqué un comportement différent du bromure de phénacylpyridinium et du bromure de phénacylisoquinoléinium, dans la réaction avec le carbonate de potassium. Ainsi, tandis que par l'élimination d'acide bromhydrique à partir

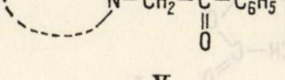

$Br^{\ominus}$
$\overset{\oplus}{N}-CH_2-\underset{\underset{O}{\|}}{C}-C_6H_5$

V

du bromure de phénacylpyridinium on obtient un ylide isolable (l'auteur l'a dénommé *énole-bétaïne* l'élimination de l'acide bromhydrique à partir du bromure de phénacylisoquinoléinium (VI) en milieu alcalin fournit premièrement une *bétaïne* active (VII) qui, à cause de la position 1 très

---

[3] Krollpfeiffer F et Müller A., *Ber. dtsch. chem. Ges.*, **66**, 739 (1933) ; **68**, 1169 (1935).

[4] F. Kröhnke, *Ber. dtsch. chem. Ges.*, **68**, 1177 (1935).

[5] F. Kröhnke et W. Zecher, *Chem. Ber.*, **95**, 1128 (1962).

[6] V. Boekelheide et K. Fahrenholtz, *J. Amer. Chem. Soc.*, **83**, 458 (1961).

positivée du noyau isoquinoléinique se transforme rapidement en dérivé 4-oxazolinique (VIII) inactif, selon le schéma

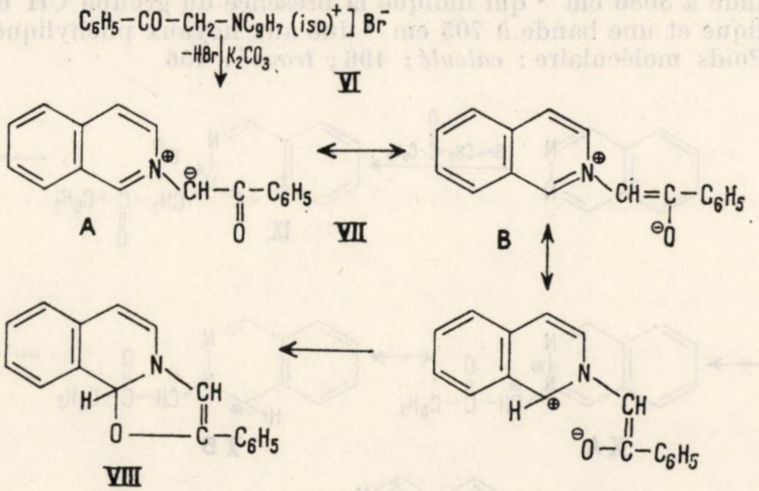

Mais, comme le remarque F. Kröhnke lui-même, la littérature n'indique pas l'existence de 4-oxazolines stables mais seulement des 2-oxazolines et d'un seul dérivé 3-oxazolinique [7]; par conséquent, l'existence d'une structure du type (VIII) apparaît comme assez improbable.

Dans le présent travail, nous avons étudié le bromure de phénacylphtalazinium (IX) obtenu par addition de bromure de phénacyle à la phtalazine en solution méthylique. L'élimination de l'acide bromhydrique à partir du produit (IX) en vue d'accéder au phtalazinium-phénacylide (X) peut être réalisée par deux méthodes : 1. on traite la solution aqueuse de bromure de phénacylphtalazinium par carbonate de potassium ; 2. on traite la suspension du produit (IX) dans l'*o*-xylène en présence de la triéthyl-amine en chauffant à reflux.

Selon la première méthode, le phatalazinium-phénacylide (X) se sépare dans la solution acqueuse sous forme de précipité orange, qui, repris en chloroforme, fournit, après l'évaporation du solvant le phtalazinium-phénacylide sous forme de cristaux orange foncé, au p. fus. = = 110°.

Si, par contre, le précipité formé premièrement dans la solution aqueuse est séparé, séché et recristallisé en xylène (*ortho*), on obtient, finalement, un produit jaune claire, au p. fus. = 258°, auquel nous avons attribué une structure du type (XI a) ; par la deuxième méthode, on obtient le même composé (XIa).

La structure de dimère a été attribuée au produit (XIa) en raison des données expérimentales suivantes :

---

[7] R. C. Elderfield, "Heterocyclic Compounds", vol. 5, John Wiley and Sons, Londres, 1957, p. 377.

1. Le spectre en IR du produit montre une bande d'absorption caractéristique du groupement cétonique à 1686 cm^{-1}, des bandes caractéristiques du noyau phénylique à 1570 cm^{-1}, 1592 cm^{-1}, 1604 cm^{-1}, une bande à 3080 cm^{-1} qui indique la présence du groupe CH du noyau phénylique et une bande à 705 cm^{-1} due aux noyaux phényliques substitués. Poids moléculaire : *calculé* : 496 ; *trouvé* : 456

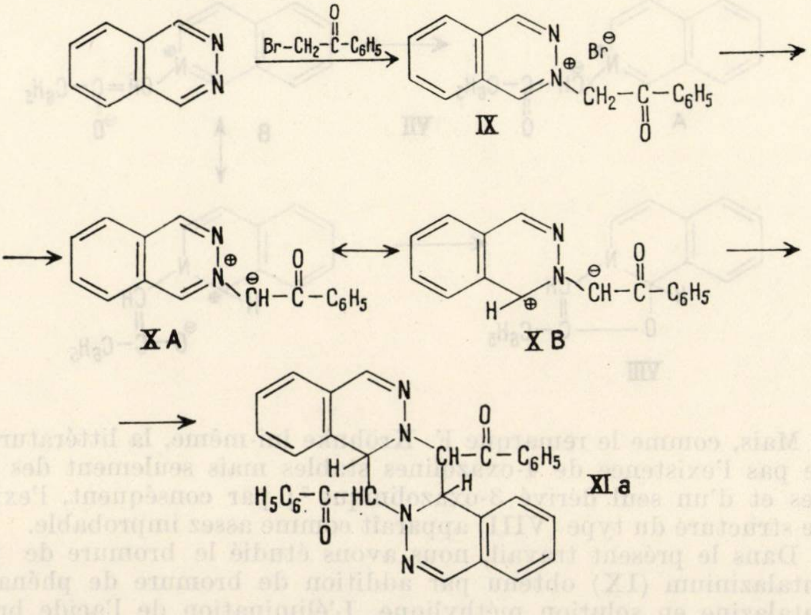

Selon notre opinion, le dimère (XI) prend naissance par un processus de cyclo-addition 1.3 où participent deux molécules de phtalazinium-phénacylide (XB). Dans ce cas, la structure de résonance XB est favorisée par le fait que la position 1 du noyau phtalazinique a une grande tendance à être positivée. La formation de dimères analogues par cyclo-addition a, d'ailleurs, déjà été signalée par Huisgen [8], au cas des azométhines des 3.4-dihydroisoquinoléines.

Les résultats obtenus dans le cas de la phtalazine nous ont suggéré une autre interprétation pour le processus d'inactivation des *énoles-bétaïnes* susmentionnées. La synthèse de l'isoquinoléinium-phénacylide d'après les indications de Kröhnke, [4] ainsi que l'analyse chimique et spectrale de ce produit nous permettent de conclure que dans le cas de l'isoquinoléine comme dans celui de la phtalazine, l'inactivation de l'ylide a lieu par le même processus de cyclo-addition 1.3 susmentionné et non par une cyclisation interne, conduisant à un dérivé 4-oxazolinique (VIII) comme l'affirme l'auteur cité.

Le spectre en IR, ainsi que les analyses infirment, en même temps, l'interprétation donnée récemment par Henrick, Ritchie et Taylor [9] dans le sens d'une structure du type éthérée (XII) attribuée au produit isolé par Kröhnke

---

[8] R. Huisgen, *Proc. Chem. Soc.*, **1961**, 357.

[9] C. A. Henrick, E. Ritchie et W. C. Taylor, *Austral. J. Chem.*, **20**, 2473 (1967).

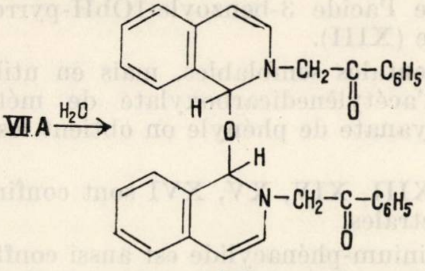
VII A
H_2C
N—CH₂—C—C₆H₅
H
O
H
N—CH₂—C—C₆H₅
O

XII

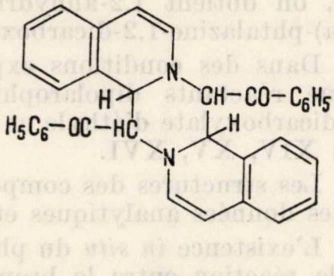
N
H
CH—CO—C₆H₅
H₅C₆—OC—HC
N

XI b

Le spectre en IR du composé isolé par Kröhnke que nous avons aussi reproduit n'indique pas la présence du groupe éthérée qui devrait être présent dans une structure de di-(1.2-dihydro-2-phénacylisoquinoléinyl)-éther (XII) proposée par les auteurs cités, ce qui confirme, une fois de plus la structure (XIb) que nous avons imaginée.

La formation du phtalazinium-phénacylide (X) *in situ* a été mise en évidence par quelques réactions de cyclo-addition 1.3 effectuées en présence de quelques réactants dipolarophiles suivant le schéma

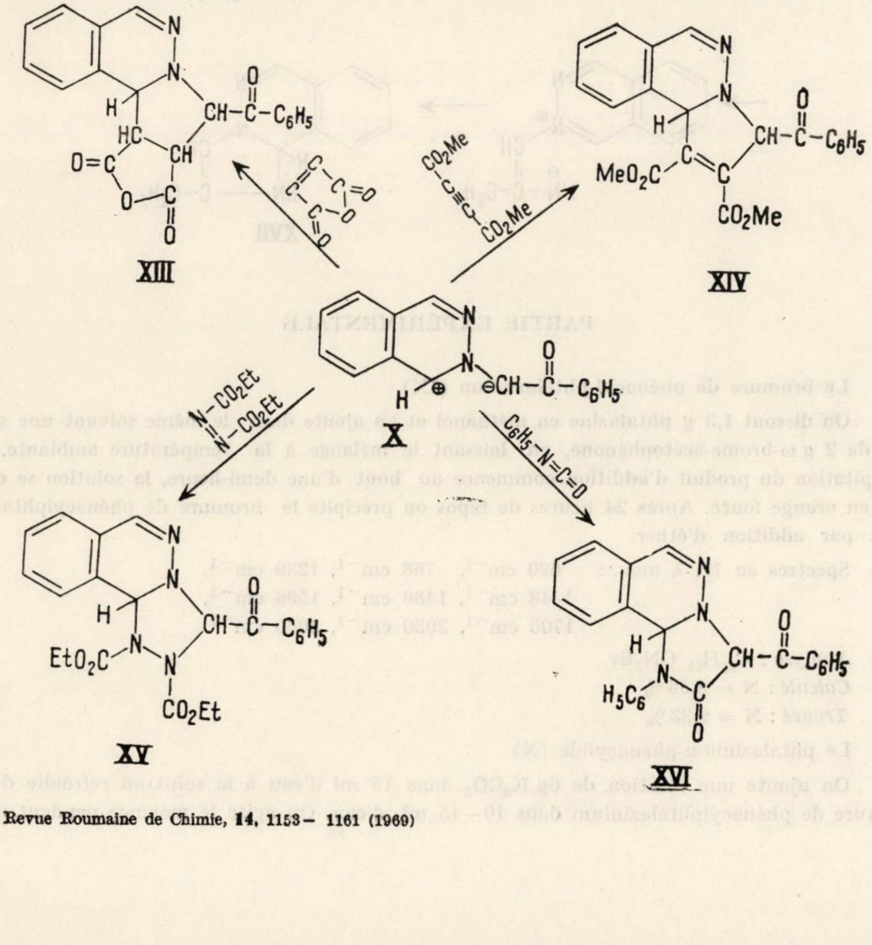
N
N
H
CH—C—C₆H₅
HC
CH
O=C
O
C
O
XIII
CO₂Me
C
C
CO₂Me
N
N
H
CH—C—C₆H₅
MeO₂C—C
C
CO₂Me
XIV
N
N
⊕
CH—C—C₆H₅
H
X
N—CO₂Et
N—CO₂Et
C₆H₅—N=C=O
N
N
H
CH—C—C₆H₅
EtO₂C—N
N
CO₂Et
XV
N
N
H
CH—C—C₆H₅
H₅C₆—N
C
O
XVI

Ainsi, si on traite le bromure de phénacyl-phtalazinium avec de l'anhydride maléique en solution benzénique et en présence de triéthylamine, on obtient 1.2-anhydride de l'acide 3-benzoyle-10bH-pyrrolino-(2.1-a)-phtalazine-1.2-dicarboxylique (XIII).

Dans des conditions expérimentales semblables, mais en utilisant comme réactants dipolarophiles l'acétylènedicarboxylate de méthyle, l'azodicarboxylate d'éthyle et l'isocyanate de phényle on obtient les produits XIV, XV, XVI.

Les structures des composés XIII, XIV, XV, XVI sont confirmées par les données analytiques et spectrales.

L'existence *in situ* du phtalazinium-phénacylide est aussi confirmée par la réaction entre le bromure de phénacylphtalazinium et l'acétate d'ammonium en milieu acétique qui fournit le 2-phényl-dihydroimidazo-(2.1-a)-phtalazine (XVII), selon le mécanisme probable suivant

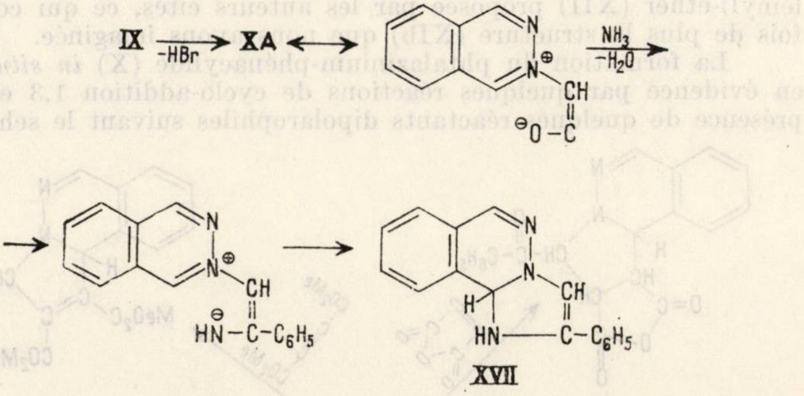

PARTIE EXPÉRIMENTALE

Le bromure de phénacyl-phtalazinium (IX)

On dissout 1,3 g phtalazine en méthanol et on ajoute dans le même solvant une solution de 2 g ω-brome-acétophénone, en laissant le mélange à la température ambiante. La précipitation du produit d'addition commence au bout d'une demi-heure, la solution se colorant en orange foncé. Après 24 heures de repos on précipite le bromure de phénacylphtalazinium par addition d'éther.

Spectres en IR λ max. : 690 cm^{-1}, 768 cm^{-1}, 1230 cm^{-1},
1448 cm^{-1}, 1486 cm^{-1}, 1596 cm^{-1},
1700 cm^{-1}, 2930 cm^{-1}, 3060 cm^{-1}

Analyse : $C_{16}H_{13}ON_2Br$
Calculé : N = 8,56 %
Trouvé : N = 9,33 %

Le phtalazinium-phénacylide (X)

On ajoute une solution de 6g K_2CO_3 dans 15 ml d'eau à la solution refroidie de 3g bromure de phénacylphtalazinium dans 10—15 ml d'eau. On agite le mélange pendant quelques minutes jusqu'à l'apparition d'un précipité orange. On reprend le précipité dans du chloroforme. On sèche la solution chloroformique sur du Na_2SO_4 anhydre, on chasse le solvant sous préssion réduite et on obtient des cristaux oranges, p. fus. 109–111°.

Coloration brun-violet intense avec le chlorure de picryle, alcalinisé avec du KOH 10 %.

Spectres en IR λ max. : 700 cm^{-1}, 765 cm^{-1}, 855 cm^{-1}, 1455 cm^{-1},
1675 cm^{-1}, 3075 cm^{-1}

2,5-dibenzoyl-(1.2-a) (1.5-a)-diphtalazino-dihydropyrazine (XIa)

Le précipité orange de phtalazinium-phénacylide obtenu comme plus haut est filtré, lavé et séché. On obtient un produit jaune. Par recristallisation en *o*-xylène on obtient des cristaux jaunes au p. fus. 256–258°. Outre le produit (XIa) soluble en *o*-xylène, on obtient aussi un produit blanc au p. fus. 285°, insoluble, non encore identifié.

Spectres en IR λ max. 705 cm^{-1}, 1570 cm^{-1}, 1592 cm^{-1}, 1604 cm^{-1}.

Analyse $C_{32}H_{24}O_2N_4$
Calculé : C = 77,41 H = 4,83 N = 11,29 %
Trouvé : C = 77,40 H = 5,01 N = 10,96 %
C = 77,50 H = 5,06 N = 10,94 %

Poids moléculaire : *Calculé* : 496
Trouvé : 456

1.2-Anhydride de l'acide 3-benzoyl-10bH-pyrrolino-(2.1-a)-phtalazine-1.2-dicarboxylique (XIII)

0,7 g de bromure de phénacylphtalazinium (IX) sont mis en suspension dans 5 ml de toluène anhydre, on ajoute une solution de 0,2 g anhydride maléique dans le même solvant et 0,2 ml de triéthyl-amine. On porte à reflux le mélange pendant 2 heures. Pendant l'ébullition la solution prend la couleur rouge et il se sépare un précipité blanchâtre. On filtre la solution à chaud afin de séparer le bromhydrate de la triéthyl-amine. Dans le filtrat refroidi il se sépare un produit blanc, qu'on purifie par dissolution en benzène et précipitation par addition d'éther de pétrole. Cristaux blancs, au p. fus. 208°. Rend. 0,3 g.

Spectres en IR λ max. : 695 cm^{-1}, 763 cm^{-1}, 1190 cm^{-1},
1230 cm^{-1}, 1459 cm^{-1}, 1575 cm^{-1}, 1590 cm^{-1},
1600 cm^{-1}, 1695 cm^{-1}, 1778 cm^{-1}, 1859 cm^{-1}
2975 cm^{-1}, 3000 cm^{-1}, 3022 cm^{-1}, 3080 cm^{-1}.

Analyse : $C_{20}H_{14}N_2O_4$
Calculé : N = 8,05 %
8,54 %

1.2-dicarbométhoxy-3-benzoyl-10bH-pyrrolo-(2.1-a)-phtalazine (XIV)

0,7 g de bromure de phénacylphtalazinium (IX) sont mis en suspension en benzène anhydre, on ajoute 0,3 ml d'acétylène-dicarboxylate de méthyle et 0,4 ml de triéthyl-amine. On porte le mélange à reflux pendant 2 heures. On filtre à chaud pour séparer le bromhydrate de la triéthyl-amine. La solution colorée en orange est refroidie et traitée par un excès d'éther de pétrole jusqu'à la précipitation complète d'un produit jaune intense. Le produit solide est purifié par dissolution à chaud dans le benzène et précipitation par addition d'éther de pétrole. Produit jaune ,p. fus. 170–171°. Par dissolution en méthanol on obtient un produit jaune claire insoluble identique au dimère XIa. La solution méthylique livre un produit jaune clair au p. fus. = 140°.

Spectres en IR λ max. : 1200 cm^{-1}, 1460 cm^{-1}, 1570 cm^{-1},
1590 cm^{-1}, 1603 cm^{-1}, 1645 cm^{-1}, 1692 cm^{-1},
1705 cm^{-1}, 1738 cm^{-1}, 1780 cm^{-1}, 2870 cm^{-1},
2970 cm^{-1}, 3080 cm^{-1}.

Analyse : $C_{22}H_{18}O_5N_2$
Calculé : N = 7,17 %
Trouvé : N = 7,11 %

1.2-dicarbéthoxy-3-benzoyl-10bH-1.2.4-triazolino-(3.4-a)-phtalazine (XV)

0,66g bromure de phénacyl-phtalazinium (IX) sont mis en suspension en diméthylformamide, on ajoute 0,4 ml de triéthyl-amine et 0,35 ml d'azodicarboxylate de méthyle. On laisse le mélange à la température ambiante. Après quelques heures (on peut laisser pendant la nuit) le bromhydrate de la triéthyl-amine est isolé par filtration. La solution est traitée par de l'eau jusqu'à la précipitation complète d'un produit jaune qu'on sépare par filtration. On reprend le produit par de l'alcool méthylique.

Spectres en IR λ max. : 1220 cm^{-1}, 1280 cm^{-1}, 1690 cm^{-1},
1710 cm^{-1}, 1735 cm^{-1}, 2850 cm^{-1}, 2970 cm^{-1}.

Analyse : $C_{22}H_{22}O_5N_4$
Calculé : N = 13,27 %
Trouvé : N = 13,75 %

1-phényl-2-céto-3-benzoyl-10bH-imidazolino-(2.1-a)-phtalazine (XVI)

1 g de bromure de phénacylphtalazinium (IX) est mis en suspension en 50ml de benzène anhydre, on ajoute 0,4 ml d'isocyanate de phényle et 0,3 ml de triéthyl-amine. On porte à reflux le mélange pendant 4—5 heures et on filtre à chaud, afin de séparer le bromhydrate de la triéthyl-amine. On chasse une partie du benzène et on traite la solution restée par un excès d'éther de pétrole jusqu'à la précipitation complète d'un produit blanchâtre. On traite à chaud ce produit par de l'alcool méthylique. Le produit jaune insoluble est identique au dimère (XIa). La solution méthylique livre un produit qui peut être purifié par dissolution en benzène et précipitation par addition d'éther de pétrole. Produit blanchâtre, au p. fus. 115°.

Spectres en IR λ max. : 1320 cm^{-1}, 1460 cm^{-1}, 1560 cm^{-1},
1600 cm^{-1}, 1670 cm^{-1}, 1680 cm^{-1}, 1710 cm^{-1},
1770 cm^{-1}, 2970 cm^{-1}, 3080 cm^{-1}.

Analyse : $C_{23}H_{17}O_2N_3$
Calculé : N = 11,44 %
Trouvé : N = 11,35 %
N = 11,78 %
N = 11,18 %

2-Phényl-dihydro-imidazo-(2.1-a)-phtalazine (XVII)

1,64 g de bromure de phénacylphtalazinium (IX) et 3,5 g d'acétate d'ammonium sont mis dans 4,5 ml d'acide acétique glacial. On porte à reflux le mélange pendant 2 heures. On laisse refroidir et on filtre la solution. En ajoutant de l'acide bromhydrique dilué il se sépare le bromhydrate du produit (XVII). Recristallisation dans de l'alcool méthylique. Cristaux blancs au p. fus. 267—268°.

Spectres en IR λ max. : 700 cm^{-1}, 740 cm^{-1}, 1595 cm^{-1},
1615 cm^{-1}, 1630 cm^{-1}, 3020 cm^{-1}, 3438 cm^{-1}.

Analyse : $C_{16}H_{14}N_3Br$
Calculé : N = 12,80 %
Trouvé : N = 13,12 %

Bromure de phénacylisoquinoléinium (VI)

On l'a obtenu à partir du bromure de phénacyle et de l'isoquinoléine selon les indications de la littérature.

L'isoquinoléinium-phénacylide et le dimère (XIb) correspondant on été obtenus d'après les mêmes indications (p. fus. 188—190°).

Spectres en IR λ max. : 1200 cm^{-1}, 1238 cm^{-1}, 1570 cm^{-1},
1585 cm^{-1}, 1602 cm^{-1}, 1625 cm^{-1}, 1668 cm^{-1},
1700 cm^{-1}, 1782 cm^{-1}, 2980 cm^{-1}, 3060 cm^{-1},
3100 cm^{-1}.

Il n'existe pas de groupement éthéré.

Analyse : $C_{17}H_{12}ON$
Calculé : C = 82,59 ; H = 5,26 ; N = 6,51%
Trouvé : C = 81,98 ; H = 5,06 ; N = 6,32%
C = 82,01 ; H = 5,63

Revue Roumaine de Chimie, **14**, 1163–1170 (1969)

INFRAROTSPEKTROSKOPISCHE UNTERSUCHUNGEN AN EINIGEN POLYPYRIDAZINEN, POLYTETRAZINEN UND POLYTRIAZOLEN

I. GABE, ELENA MĂNTĂLUŢĂ und GABRIELA NEAMŢU

aus dem Institut für Makromolekulare Chemie, Iaşi, Aleea Grigore Ghica Vodă 41A

Eingegangen am 28. November 1968

Die IR-Absorptionen einer Reihe von heterocyklischen Polymeren werden mit denen der Modellsubstanzen verglichen. Wenn die Kettenlänge der hochmolekularen Stoffe nicht zu groß ist so sind die charakteristischen Absorptionsbanden der Struktureinheiten nur wenig gegenüber denen der Polymeren verschoben. Die Intensitäten der Banden sind in diesem Falle eine Funktion der Sequenzzahl und könnten u.a. auch zur Bestimmung dieser herangezogen werden.

In den letzten Jahren erschien eine Reihe von Arbeiten über Synthesen von heterocyklischen Makromolekülen, die sich als Ziel setzten thermostabile Polymere darzustellen.[1–4] Unlängst [5–7] wurden neue hochmolekulare Stoffe mit Tetrazin- und Triazolstruktureinheiten beschrieben, die eine größere Thermostabilität aufweisen und sich auch in andere polyheterozyklische Verbindungen umwandeln lassen.

Die Synthesen wurden ausgehend von den entprechenden Dinitrilen durchgeführt, wobei die Poly-1,2-dihydro-1,2,4,5-tetrazine über die schon früher beschriebenen Reaktionen erhalten wurden. Eine Dehydrierung der Polyhydrotetrazine führt zu Polytetrazinen und aus diesen letzteren erhält man durch Ringeinengung die Polytriazole.

---

[1] C. S. Marwel, *Chimica e Industria*, **46**, 727 (1964).

[2] H. Vogel und C. S. Marwel, *J. Polymer Sci.*, **50**, 511 (1961).

[3] A. H. Fraser und F. T. Wellberger, *J. Polymer Sci.*, **A2**, 117 (1964).

[4] I. K. Stille und I. R. Williamson, *J. Polymer Sci.*, **A3**, 1013 (1965).

[5] L. Stoicescu-Crivetz, El. Măntăluţă, G. Neamţu und I. Zugrăvescu, *Rev. Roumaine Chim.*, **11**, 1127 (1968).

[6] I. Zugrăvescu, L. Stoicescu-Crivetz, G. Caraculacu, El. Măntăluţă, G. Neamţu und M. Brumă, *Studii şi Cercelări Chim. Acad. Rom.*, **15**, 855 (1967).

[7] L. Stoicescu-Crivetz, El. Măntăluţă, G. Neamţu und I. Zugrăvescu, International Symposium on Macromolecular Chemistry, Bruxelles 1967.

Tabelle

Infrarotspektren eines Modellpyridazins

M_1^P	M_2^P	P_1^2	P_2^1	P_3^1	P_4^1
700 st	670 m	707 st	710 m	720 m	710 m
750 st					
	770 st				
	780 st	770 st	780 st	790 stb	755 m
	820 m				808 s
835 s		855 s	870 s	870 sb	840 st
	865 m				
925 s	925 m	920 m	930 mb	930 sb	930 m
955 s	955 s	980 s	975 sb	970 sb	
1035 s	1030 m	1038 m	1030 m	1030 m	
1075 m	1082 st	1075 s	1065 m	1070 st	1050 st
1125 s	1150 s		1135 m	1135 m	1125 s
1165 st	1160 m	1160 s	1195 s	1185 s	
	1240 s				1230 sst
1252 m		1250 s	1250 ss		
				1280 ss	1295 ss
				1310 s	
1340 m			1320 sb	1330 s	
1365 m		1380 m	1390 m	1385 m	
	1400 st				
					1410 s
1445 m	1450 m	1430 Sch	1430 st	1430 st	1440 m
1485 st		1460 m	1445 Sch		
					1480 m
1505 st	1500 st	1500 st	1500 st	1505 Sch	1507 st
		1520 Sch	1520 st	1520 st	
	1565 m		1560 m	1560 m	
	1580 m				
1600 m		1600 m		1610 s	
1645 m			1655 mb	1660 m	1660 m
		2850			2880 Sch
		2910 st	2900 m	2910 m	2920 s
				2952 m	
		3020 st	3030 st	3040 m	3050 s
3075 m	3075 s				
3140 st			3150 m	3170 m	3170 m

Abkürzungen: s – schwach, m – medium, st – stark, b – breit, Sch – Schulter

Zahlreiche Arbeiten befassen sich mit der IR-Absorption von Pyridazinen,[8–13] Tetrazinen [14,15] und Triazolen,[16–19] hingegen gibt es sehr wenige Angaben über heterocyklische Polymere.

---

[8] C. J. Brealey und M. Kasha, *J. Amer. Chem. Soc.*, **177**, 4462 (1955).

[9] J. Druey, K. Meier und F. Eichenberger, *Helv. Chim. Acta*, **37**, 121 (1954).

[10] Ju. N. Sheinker, T. V. Gortinskaia und T. P. Syheva, *Zhur. fiz. Khim.*, **31**, 599 (1957).

[11] V. I. Berezin, *Optika i Spektroskopia*, **18**, 136 (1965).

[12] H. B. Stidham und J. V. Tucci, *Spectrochim. Acta*, **23A**, 2233 (1967).

[13] R. C. Lord, A. L. Morston und F. A. Millers, *Spectrochim. Acta*, **9**, 113 (1957).

[14] M. Avram, J. G. Dinulescu, E. Marica und C. D. Nenitescu, *Chem. Ber.*, **95** 2248 (1962).

1
und einiger polymerer Pyridazine

P_5^1	P_6^1	P_7^1	P_8^1	Zuordnung
720 m	720 m	720 m		Deformation Benzolring
			740 st	,,
790 stb	790 stb	790 stb		Subst. Benzolring
870 s	870 s	870 s		
910 sb	940 sb	940 sb	940 sb	Ringdeformationsschw. Pyridazin
1030 m	1030 m	1030 m		C—N—C asymm.
1067 st	1067 st	1067 st	1060 st	Polypyridazinringschw.
1112 s	1138 s	1138 s	1120 s	Ringschw. *o*-Subst.
1138 m				
	1180 s			Benzolring subst.
1190 s		1190 s		
1210 s	1210 s	1210 s	1210 sst	Benzoldeformationsschw.
1225 s				
	1243 s	1250 s		C—N
1280 m	1280 m	1289 s		
	1305 s		1308 s	
	1330	1330	1330 s	C—N
1390 m	1385 m	1380 m	1380 sb	
1440 st	1430 st	1435 st		
	1455 Sch	1455 Sch		Ringschwingung
			1470 m	
1500 Sch	1510 Sch	1505 Sch		C = C/C = N
1520 st	1520 st	1520 stb	1520 st	
1560 m	1560 m	1560 m		C = C/C = N
				C = C/C = N
1620 s	1610 s		1600 s	C = C Benzolring
1665 m	1660 m	1650 m		N—H—Deformationsschw.
1733 st	1718 st			C = O
2880 Sch		2870 Sh		C — H
2920 m	2910 m	2920 m		C — H
3050 st	3030 m	3030 m		C — H
3185 st	3160 m	3170 m		

Wir untersuchten die IR-Spektren der dargestellten Polymeren im Vergleich mit den Spektren der Dihydrotetrazine, Tetrazine und Triazole um festzustellen in wie weit eine Wiederholung der Struktureinheiten in der polymeren Kette sich auf die spektralen Besonderheiten der Heteroringe auswirkt.

---

[15] R. H. Wiley, C. M. Jarbore und F. N. Hayes, *J. Amer. Chem. Soc.*, **79**, 2602 (1957).

[16] F. Maggio, G. Werber und G. Lombardo, *Ann. Chim.* (*Ital.*), **50**, 491 (1966).

[17] E. Lieber, C. N. R. Rao, T. S. Chao und M. Rubinstein, *Canad. J. Chem.* **36**. 1441 (1958).

[18] L. W. Hertzel und F. R. Benson, *J. Amer. Chem. Soc.*, **76**, 667, (1954).

[19] M. Dziewonska, *Spectrochim. Acta*, **23 A**, 1195 (1967).

In Tabellen 1, 2 und 3 sind die Absorptionsbanden der von uns untersuchten Verbindungen wiedergegeben:

1. Polypyridazinreihe (P) (Tabelle 1)

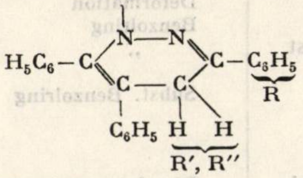

M_1

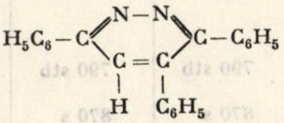

M_2

P^2_1 $R = -CH_2-C_6H_4-$
P^1_2 $R = -CH_2-C_6H_4-$
P^1_3 $R = -CH_2-C_3H_4-$

P^1_4 $R = -CH_2CH_2-O-C_3H_4$
P^1_5 $R = -CH_2-C_6H_4$
$R' = -COOCH_3$
$P^1_6]$ $R = -CH_2-CH_2-$
$R' = -COOC_4H_9$
$R'' = -CH_3$

P^1_7 $R = CH_3-C_6H_4-$
P^1_8 $R = -C_6H_4-O-CH_2-$
$R' = -CH=CH_2$
$R'' = -CH_3$

Tabelle 2

Infrarotspektren einiger Polytetrazine im Vergleich mit einer Modellsubstanz

M^T	T_1	T_2	T_3	T_4	Zuordnung
700 m	710 m		675 s	680 s	Benzolring
				720 s	
770 st	780 s			780 stb	Benzolringsubst.
850 m	850 st	835 mb	840 mb		
				875 s	
905 m	930 m	915 s	898 sl	905 s	Ringdeformation
				930 s	
940 m					
	980 s	960 s		980 s	
	1000 s				
	1028 m	1020 ml		1035 m	
			1045 st		Ringschwingung
1095 m	1060 s			1065 m	
1155 m	1110 m	1110 s	1120 s	1105 Sch	
				1140 mb	
1185 m	1185 m			1195 s	
		1200 stb			
1240 stb			1235 stb		Benzolringdeformationsschwingung
	1280 mb			1250 s	
1300 m		1300 s	1295 s		
	1320 s				
1380 st	1375 m	1370 m		1385 st	Ringschwingung
	1400 st	1410 m			
1425 m	1420 m		1420 m		
1460 s	1460 s	1460 m	1480 m		C = C/C = N
1495 st	1490 s				
1505 st	1505 st	1510 st	1520 st	1505 Sch	C = C/C = N
				1510 mb	
				1560 m	
1600 st	1610 st	1600 s			C = C
	1660 m	1660 stb		1640 mb	Deformation N−H
	2850 s		2880 s		
2930 s	2920 s	2930 s	2930 s	2920 m	C−H
3085 m	3050 s	3075 s			
	3150 sb	3185 s	3148 sb	3155 sb	N−H

2. Polytetrazinreihe (T) (Tabelle 2)

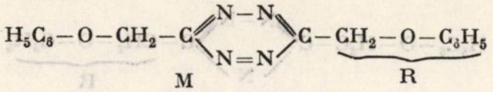

T_1 R = $-C_6H_4-CH_2-CH_2-$

T_2 R = $-C_6H_4-O-CH_2-$

T_3 R = $-CH_2-CH_2-O-C_6H_4-$

T_4 R = $-CH_2-C_6H_4-CH_2-$

Tabelle 3

Die IR-Absorptionsspektren einiger polymerer Triazole

M^{Tr}	Tr_1	Tr_2	Tr_3	Tr_4	Zuordnung
	690 m	680 m			Benzolring
705 st					
720 s	715 s		720 s	720 s	Deformationsschw. Bzl.
770 st	745 s	760 Sch	760 m		Benzolsubst.
800 m	780 st	785 st			Benzoldeformationsschw.
820 s	820 m	805 m	820 m	815 m	NH_2— Deformation
			840 st	840 st	C—H—Deformationsschw.
880 m	880 s				
910 s	920 s		915 s		,,
950 sb	980 mb	975 mb	960 s		Ringdeformation
990 s					
1005 s					
1030 m	1040 m	1037 m	1050 st	1040 stb	C—N—C asymm.
1050 st					
	1070 s	1065 m			
1095 m					
1160 s	1160 mb	1150 m	1120 s	1120 s	*o*-Substitution,
1185 st					
		1205 s		1210 stb	
1220 st	1240 Sch				
1250 st	1260 mb	1260 s	1230 stb		
			1295 Sch	1295 Sch	C—N—Streckschw.
1300 m					
1318 m					
1338 m					
1370 s	1385 s	1380 s		1380 s	
1395 s					C = C/C = N
1405 s			1405 s		
1450 m	1438 st	1430 st	1440 m	1460 s	C = C/C = N
1465 m					
	1480 s	1470 s	1480 m		C = C/C = N
1510 st	1530 st	1520 st	1520 st	1515 st	C = C
1595 st		1570 sb			
1615 st	1650 stb	1650 m	1640 m	1635 mb	N—H—Deformationsschw.
	1705 stb		1715 m		C = O
			2870 m	2885 Sch	C—H
2900 Sch	2970 s	2930 s	2930 m	2930 s	C—H
3040 s	3060 s	3020 s	3070 s	3040 s	C—H
3190 m	3205 m	3185 m	3175 m	3200 m	N—H symm.
3305 m	3350 m	3295 m	3300 m	3350 m	N—H antisymm.

3. Polytriazolreihe (Tr) (Tabelle 3)

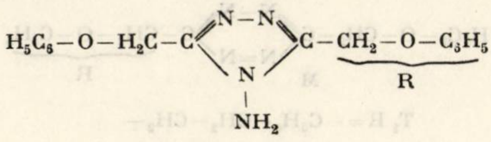

M

Tr_1 $R = -CH_2C_6H_4-CH_2-$

Tr_2 $R = -CH_2-C_6H_4-$

Tr_3 $R = -CH_2-CH_2-O-C_6H_4-$

Tr_4 $R = -C_6H_4-O-CH_2-$

Alle Spektren wurden in KBr-Preßlingen mit einer Konzentration von 0,5 % auf einem Doppelstrahlgerät Unicam SP 200 aufgenommen. Die genaue Bandenlage wurde mit einem Gittergerät Unicam SP 100 bestimmt. Der mittlere Fehler bei den angegebenen Wellenzahlen liegt um ± 3 cm^{-1}.

In jeder Reihe von Verbindungen wurden die Spektren der Hochpolymeren mit denen der entsprechenden synthetisierten Modellsubstanzen (M) verglichen.

BESPRECHUNG DER ERGEBNISSE

Wie es aus den in den Tabellen angeführten Werten der Wellenzahlen für die entsprechenden Maxima der Absorptionsbanden ersichtlich ist, sind die Spektren der Polymeren denen der Modellsubstanzen sehr ähnlich, ausgenommen natürlich die Banden die den verschiedenen Substituenten zugeordnet werden können.

In den meisten Fällen sind die Absorptionsbanden der Polymeren breiter als die entsprechenden Banden der Monomeren, wie es auch bei anderen hochmolekularen Stoffen beobachtet wurde.[20]

1. Der Bereich 3500—2500 cm^{-1}. Hier treten die Streckschwingungen ν_{NH} und ν_{CH} auf.

Das Absorptionsmaximum bei 3140 cm^{-1} im Falle der Modellverbindung M_1^1 ist auf eine NH-Gruppe zurückzuführen. Ein ebensolches Maximum tritt auch bei den Polymeren P_2^1—P_8^1 zwischen 3150 cm^{-1} und 3185 cm^{-1} auf. Im Vergleich mit den NH-Schwingungen bei anderen Verbindungen sind die von uns beobachteten niedereren Frequenzen einerseits der Tatsache zuzuschreiben, daß das Stickstoffatom an einem Ring teilnimmt, anderseits müssen aber auch Bildungen von Wasserstoffbrücken in Betracht gezogen werden, die zu einer Verschiebung der NH-Frequenz nach kleineren Werten führt.

Bei der Modellsubstanz M_1^2, wie auch beim Polymeren P_1^2 fehlt im Spektrum eine solche Bande und wir müssen die Struktur

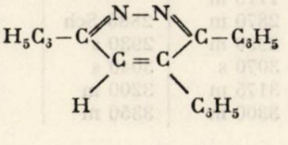

---

[20] S. Krimm, *Fortschritte der hochpolymeren Forschung,* **2,** 51 (1960).

bzw.

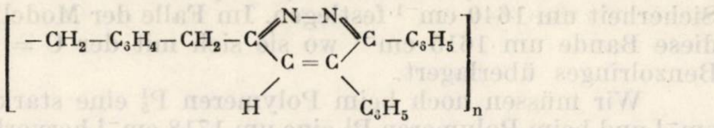

voraussetzen.

Die Streckschwingung ν_{CH} des Benzolringes kann zwischen 3075 cm^{-1} und 3030 cm^{-1} festgelegt werden. Die Intensitäten dieser Schwingung sind unterschiedlich im Zusammenhang mit den verschiedenen untersuchten Verbindungen, den jeweils eingeführten Substituenten und mit der Zahl der Glieder in der Kette des Hochpolymeren. Wenn der Benzolring als Endgruppe in dem Hochpolymeren eingebaut ist, so können wir eine entsprechend größere Absorptionsbande im Spektrum beobachten.

Im Bereiche 2850—2910 cm^{-1} fallen die Schwingungen der Methylengruppe. Es sind deutlich zwei Banden für die antisymmetrische Schwingung bzw. symmetrische um 2900 cm^{-1} und 2870 cm^{-1} zu erkennen. Auch in diesem Falle verändert sich die Intensität dieser Banden im Zusammenhang mit der Zahl der $-CH_2$-Gruppen in den Struktureinheiten der Makromoleküle.

Diese Ausführungen behalten ihre Gültigkeit auch bei den zwei anderen untersuchten Polymergruppen (Tabellen 2 und 3). Bei den Polyaminotriazolen sind zwei Banden um 3350 cm^{-1} und 3175 cm^{-1} der antisymmetrischen bzw. der symmetrischen NH_2-Schwingung zuzuschreiben.

Zwischen 1800 cm^{-1} und 650 cm^{-1} liegen sehr viele Absorptionsbanden die z.T. Streckschwingungen aber auch Deformationsschwingungen und kombinierte Schwingungen sind. Da es sich um komplizierte Moleküle handelt ist es aber nicht immer möglich bei allen Absorptionsbanden eine einwandfreie Zuordnung vorzunehmen.

Die in Tabelle 1 angeführten Absorptionsbanden (Maxima) im Bereiche 1665 cm^{-1}—1645 cm^{-1} kommen einer NH-Deformationsschwingung zu; in den Spektren der Verbindungen M_1^2 und P_1^2 fehlen solche Banden. Bei diesen zwei Verbindungen sind auch keine Streckschwingungen der NH-Gruppe zu beobachten.

In der Serie T (Tabelle 2) können wir bei der Modellsubstanz keine NH-Deformationsschwingung finden. Hingegen sind bei den Polymeren T_1—T_4 solche Schwingungen zwischen 1660 cm^{-1} und 1640 cm^{-1} vorhanden und daraus können wir schließen, daß in der hochmolekularen Kette dieser Polymere auch Einheiten

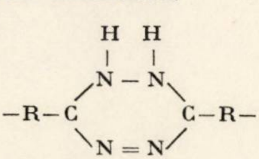

vorhanden sein müssen. Im übrigen lassen auch die Maxima zwischen 3148—3185 cm^{-1} (ν_{NH}) einen solchen Schluß zu.

Bei den Polytriazolen Tr_1-Tr_4 können wir die ν_{NH}-Bande mit Sicherheit um 1640 cm^{-1} festlegen. Im Falle der Modellsubstanz M^{Tr} liegt diese Bande um 1615 cm^{-1} wo sie sich mit der $C = C$-Schwingung des Benzolringes überlagert.

Wir müssen noch beim Polymeren P_5^1 eine starke Bande um 1733 cm^{-1} und beim Polymeren P_6^1 eine um 1718 cm^{-1} hervorheben, die den subtituierten Estergruppen zukommen.

Polytriazol Tr_1 hat eine Absorptionsbande bei 1705 cm^{-1} und Polytriazol Tr_2 eine bei 1715 cm^{-1}. Hier handelt es sich offenbar um Carboxylabsorptionen die von saueren Endgruppen herrühren.

Zwischen 1605 cm^{-1} und 1550 cm^{-1} liegen die Aromatenbanden der Benzolringe aus der Hauptkette oder den Endgruppen.

Bei allen von uns untersuchten Stoffen kann eine starke Absorption zwischen 1525 cm^{-1} und 1495 cm^{-1} beobachtet werden. Wir sind geneigt dieser Bande eine Überlagerung einer $C = C$- und $C = N$-Schwingung zuzuschreiben.

Die Banden zwischen 1380 cm^{-1} und 1250 cm^{-1} kommen C—H- und C—N-Deformationsschwingungen zu, während im Bereiche 1190—1075 cm^{-1} C—H-Deformationsschwingungen zu erkennen sind.

Ein Pyrimidinkern ist durch zwei Absorptionsbanden bei 1075 cm^{-1} und 980 cm^{-1} charakterisiert. Diese Banden kommen Gerüstschwingungen zu.[21] Im Falle der Pyridazinringe sind diese Banden nach kleineren Frequenzen verschoben und zwar können sie bei 1065 cm^{-1} und 935 cm^{-1} beobachtet werden. Bei den von uns untersuchten Polypyrimidinen (Tabelle 1) sind diese Banden deutlich erkennbar, im Einklang mit den Literaturangaben.[22] Die Absorptionsbande bei 1065 cm^{-1} dürfte einer fundamentalen A_1-Schwingung des Pyridazinkerns zukommen.

In den Spektren der Polytetrazine ist die Absorptionsbande um 900 cm^{-1} hervorzuheben. Sie läßt sich im Zusammenhang mit den Absorptionsbanden bei 1380 cm^{-1} und 1345 cm^{-1} als eine charakteristische Ringschwingung der Polytetrazine deuten.

---

[21] L. J. Bellamy, "On Introduction to Infrared Spectroscopy", John Willey and Sons, Inc., N. Y., 1962, S. 342.

[22] R. S. Salisbury, D. P. Ryan und J. W. Mason, *J. Heterocyclic Chem.* **4**, 431 (1967).

Revue Roumaine de Chimie, **14**, 1171–1180 (1969)

UNSATURATED END GROUPS IN PVC. I

PREPARATION OF THE MODEL COMPOUNDS

A. A. CARACULACU and E. C. BEZDADEA

Institute of Macromolecular Chemistry "P. Poni"
Academy of the Socialist Republic of Romania
Jassy, Aleea Gr. Ghica Vodă, 41 A

Received June 15, 1968

Model compounds corresponding to all types of PVC unsaturated end groups were synthesized: 1,3-dichloropentene-1,2,4-dichloropentene-1,2,3-dichloropentene-1 and 1,4 dichloropentene-1. Sodium chloroacetylide reacts with the epoxides to form 1-chlorohydroxyacetylenes, which can be reduced by $LiAlH_4$ to the corresponding *trans*-chlorovinyl derivatives.

It is well known that the presence of the chlorine atoms with an increased reactivity can initiate the dehydrochlorination process in PVC. The characterization of chlorine atoms bound to the tertiary carbon atoms and their effects on the PVC stability were previously reported.[1–6] Besides these labile chlorine atoms, the unsaturated end groups of a polymer chain having an allylic chlorine atom are also referred to as one of the most important sites to initiate the PVC destruction.

The study of these unsaturated end groups can also give information about the branching of PVC.

It was supposed that chain transfer between growing radicals and previously formed polymer causes branching in PVC. It is to be expected that other processes, like the copolymerization of vinylchloride with the unsaturated end groups of PVC or the possibility of 1–5 radicalic internal transposition of the growing macroradical, could determine the appearance of branches[7].

---

[1] A. Caraculacu, J. Stokr and B. Schneider, *Coll. Czech. Chem. Comm.*, **29**, 2783 (1964).

[2] J. Stokr, A. Caraculacu and B. Schneider, *Coll. Czech. Chem. Comm.*, **30**, 683 (1965).

[3] A. Caraculacu, *J. Polymer. Sci.*, A-1, **4**, 1829 (1966).

[4] A. Caraculacu, *J. Polymer Sci.*, A-1, **4**, 1839 (1966).

[5] A. Caraculacu, O. Wichterle and B. Schneider, *J. Polymer Sci.*, C, **16**, 495 (1967).

[6] A. Caraculacu and E. Bezdadea, *J. Polymer Sci.*, in press.

[7] M. Kolínský, M. Ryska, M. Bochdanecký, P. Kratochvíl, K. Solc and D. Lím, Preprint P. 70 Symposium on Macromolecular Chemistry, IUPAC, Prague, 1965.

These hypotheses are supported by the works of Lim et al.[8] and Boccato et al.[9] We used Lim's estimated value of chain transfer with poly(vinylchloride) molecules in homogenous system to calculate the branching degree. It has been found a much smaller value than that experimentally determined by other authors.[9,10] Though the experimental determinations of branching degree were made on some types of PVC obtained by polymerization in heterogenous medium, a comparison with Lim's results is possible since the branching degree does not depend on the homogeneity or the heterogeneity of the polymerization system at the same temperature.

In the radicalic polymerization the double bond can appear at the end of the macromolecular chain by two different processes : disproportionation reaction of the macroradicals and transfer reaction to monomer.

The structure of the unsaturated end groups will depend on the formation process as well as on the type of bonding of the terminal sequences in the growing macroradical : head-to-tail, tail-to-head, head-to-head and tail-to-tail.

In the case of disproportionation process one can imagine the following situations :

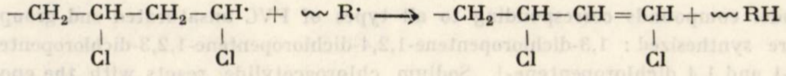

$$-\underset{}{CH_2}-\underset{\substack{|\\Cl}}{CH}-CH_2-\underset{\substack{|\\Cl}}{CH^{\cdot}} + \sim R^{\cdot} \longrightarrow -CH_2-\underset{\substack{|\\Cl}}{CH}-CH=\underset{\substack{|\\Cl}}{CH} + \sim RH \qquad I$$

sequence "head-to-tail"

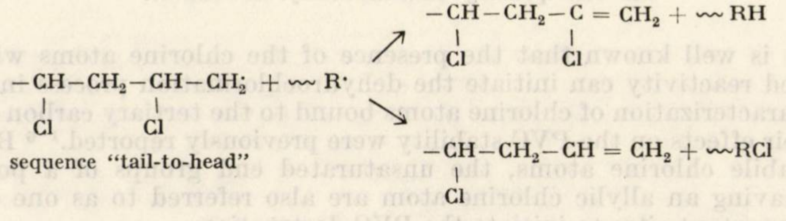

$$-\underset{\substack{|\\Cl}}{CH}-CH_2-\underset{\substack{|\\Cl}}{CH}-CH_2^{\cdot} + \sim R^{\cdot} \begin{array}{l} \nearrow -\underset{\substack{|\\Cl}}{CH}-CH_2-\underset{\substack{|\\Cl}}{C}=CH_2 + \sim RH \qquad II \\ \searrow -\underset{\substack{|\\Cl}}{CH}-CH_2-CH=CH_2 + \sim RCl \qquad III \end{array}$$

sequence "tail-to-head"

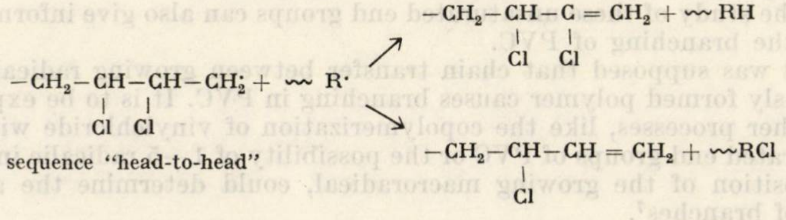

$$-CH_2-\underset{\substack{|\\Cl}}{CH}-\underset{\substack{|\\Cl}}{CH}-CH_2^{\cdot} + \sim R^{\cdot} \begin{array}{l} \nearrow -CH_2-\underset{\substack{|\\Cl}}{CH}-\underset{\substack{|\\Cl}}{C}=CH_2 + \sim RH \qquad IV \\ \searrow -CH_2-\underset{\substack{|\\Cl}}{CH}-CH=CH_2 + \sim RCl \qquad V \end{array}$$

sequence "head-to-head"

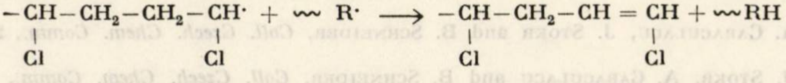

$$-\underset{\substack{|\\Cl}}{CH}-CH_2-CH_2-\underset{\substack{|\\Cl}}{CH^{\cdot}} + \sim R^{\cdot} \longrightarrow -\underset{\substack{|\\Cl}}{CH}-CH_2-CH=\underset{\substack{|\\Cl}}{CH} + \sim RH \qquad VI$$

sequence "tail-to-tail"

[8] D. Lím and M. Kolínský, *J. Polymer Sci.*, **53**, 173 (1961).

[9] G. Boccato, A. Rigo, G. Talamini and F. Zilio-Grandi, *Makromol. Chem.*, **108**, 218 (1967).

[10] J. D. Cotman, *Ann. New York Acad. Sci.*, **57**, 417 (1953).

Certainly all these reactions do not occur with the same probability. The greatest frequence is expected for reaction I or II.

In the case of radical transfer process to monomer, several situations may be assumed which all lead to one of the types of unsaturated end groups as described above. The most probable reaction seems to be:

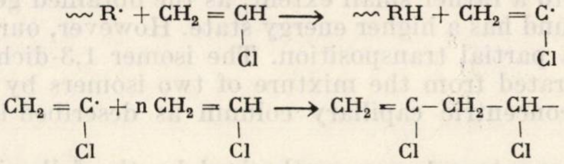

$$\sim R^{\cdot} + CH_2=\underset{Cl}{CH} \longrightarrow \sim RH + CH_2=\underset{Cl}{C^{\cdot}}$$
$$CH_2=\underset{Cl}{C^{\cdot}} + n\,CH_2=\underset{Cl}{CH} \longrightarrow CH_2=\underset{Cl}{C}-CH_2-\underset{Cl}{CH}-$$

VII

It was the objective of this study to synthesize several model compounds which can allow us to characterize and evidence them in the PVC.

Up to date, only two model compounds of this type are known: 4-chloropentene-1 and 3-chloropentene-1 corresponding to less probable reactions III respectively V.

Several models as 1,3-dichloropentene-1 for the type of reaction I, 2, 4-dichloropentene-1, for the reaction II and VII, 2,3-dichloropentene-1 for the reaction IV and 1,4-dichloropentene-1 for the reaction VI were synthesized.

To obtain *trans*-1,3-dichloropentene-1, propionyl chloride was reacted with acetylene to produce 1-chloropentene-1-on-3[11] which by reduction with $LiAlH_4$ gave *trans*-1-chloro-3-hydroxy-pentene-1.[12]

The $-OH$ group was then replaced by $-Cl$ with $SOCl_2$ in pyridine. The product obtained in the reaction with $SOCl_2$ seemed to be a unitary compound — that distilled at 57.5—58.5° (30 mm Hg) and had a corresponding elemental composition. The IR spectra, however, evidenced that this compound represents actually a mixture of two isomers. Beside the expected *trans*-1,3-dichloropentene-1, as a result of an allylic transposition, the 1,1-dichloropentene-2 was also formed:

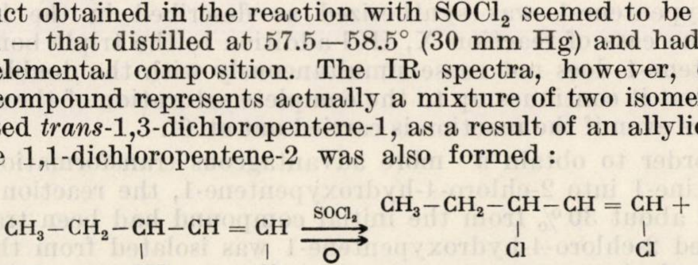

$$CH_3-CH_2-\underset{OH}{CH}-CH=\underset{Cl}{CH} \xrightarrow[O]{SOCl_2} \begin{array}{l} CH_3-CH_2-\underset{Cl}{CH}-CH=\underset{Cl}{CH} + \\ CH_3-CH_2-CH=CH-CHCl_2 \end{array}$$

VIII

Two IR absorption bands were identified in the region of double bond stretching vibrations, namely at 1630 cm^{-1} characteristic of the terminal double bond and a small peak at 1660 cm^{-1} for the disubstituted double bond. This assignment was verified by comparison with IR spectra of some known substances with similar structure as 3-chloropentene-1 ($\nu_{C=C}$ = 1645 cm^{-1}) for terminal double bond and 1-chloropentene-2 ($\nu_{C=C}$ = 1670 cm^{-1}) for disubstituted double bond. The characteristic band for the double bond was shifted to greater wavelengths due to the presence of the chlorine atom as a second substitute on the double bond.[13] The compounds as $R-CH_2-CH = CHCl$ exhibit these maxima at 1625—1640 cm^{-1}.[14]

---

[11] a) C. C. PRICE and I. A. PAPPALARDO, *J. Amer. Chem. Soc.*, **72**, 2613 (1950); b) F. ASINGER, L. SCHRÖDER and S. HOFFMAN, *Liebigs Ann. Chem.*, **648**, 89 (1961).

[12] P. GRÜNANGER and A. LANDONE, *Atti Accad. nazl. Lincei, Rend. classe sci. fis. mat. e nat.*, **28**, 664 (1960).

Similar isomerizations are known in the case of the reaction of 3-hydroxypentene-1 with $SOCl_2$ in diethylaniline.[15] One could expect such an arrangement to a rather small extent, as the obtained gemminal dichlorinated compound has a higher energy state. However, our experimental results showed a partial transposition. The isomer 1,3-dichloropentene-1 was hardly separated from the mixture of two isomers by a fractionary distillation on concentric capillary column as described in the experimental section.

2,4-Dichloropentene-1 was synthesized by the following reactions:

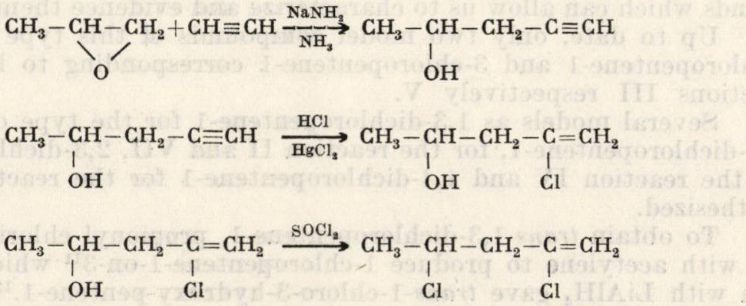

$$CH_3-\underset{\diagdown_{O}\diagup}{CH-CH_2}+CH\equiv CH \xrightarrow[NH_3]{NaNH_2} CH_3-\underset{OH}{CH}-CH_2-C\equiv CH \qquad IX$$

$$CH_3-\underset{OH}{CH}-CH_2-C\equiv CH \xrightarrow[HgCl_2]{HCl} CH_3-\underset{OH}{CH}-CH_2-\underset{Cl}{C}=CH_2 \qquad X$$

$$CH_3-\underset{OH}{CH}-CH_2-\underset{Cl}{C}=CH_2 \xrightarrow{SOCl_2} CH_3-\underset{Cl}{CH}-CH_2-\underset{Cl}{C}=CH_2 \qquad XI$$

1-Hydroxypentene-1 was synthesized as described in the literature.[16]

In the case of reaction X, HCl addition to the triple bond of 1-hydroxypentene-1 does not cease simultaneously with the double bond appearance but it continues up to the complete saturation of the compound. This occurs even if the reaction is carried out at 0°.

In order to obtain a more advantageous transformation of 1-hydroxypentine-1 into 2-chloro-4-hydroxypentene-1, the reaction was stopped when about 30 % from the initial compound had been transformed. The formed 2-chloro-4-hydroxypentene-1 was isolated from the mixture reaction and the recovered pentinol was used again for HCl addition.

The model 2,3-dichloropentene-1 was similarly prepared as 2,4-dichloropentene-1 except that propionaldehyde was used instead of propyleneoxide. Similarly to the *trans*-1,3-dichloropentene-1 synthesis (reaction VIII) the transformation of 2-chloro-3-hydroxypentene-1 with $SOCl_2$ into 2,3-dichloropentene-1 was also associated with a partial allylic transposition resulting in a mixture of isomers. The separation of the two isomers from the mixture was carried out as described in the experimental section.

---

[13] K. Kohlrausch, "Spektry Kombinatsionovo rasseyanya", Izdatinlit., Moscow, 1952, p. 265.

[14] R. E. Kitson, *Analyt. Chem.*, **25**, 1470 (1953).

[15] J. Meisenheimer and J. Link, *Liebigs Ann. Chem.*, **479**, 221, 255 (1930).

[16] a) J. M. Heilborn, E. R. H. Jones and B. C. L. Weedon, *J. Chem. Soc.*, **1945**, 83;

b) L. J. Heynes and E. R. H. Jones, *J. Chem. Soc.*, **1946**, 956.

The model compound *trans*-1,4-dichloropentene-1 was prepared as follows:

$$ClCH=CHCl \xrightarrow[NH_3]{NaNH_2} NaC\equiv CCl \qquad \text{XII}$$

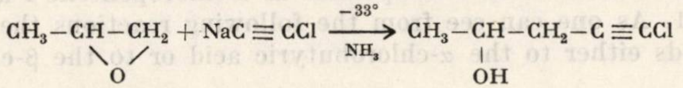
XIII

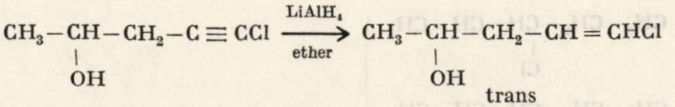
XIV

$$CH_3-\underset{\underset{\displaystyle OH}{|}}{CH}-CH_2-C\equiv CCl \xrightarrow[\text{ether}]{LiAlH_4} CH_3-\underset{\underset{\displaystyle OH}{|}}{CH}-CH_2-\underset{\text{trans}}{CH=CHCl}$$

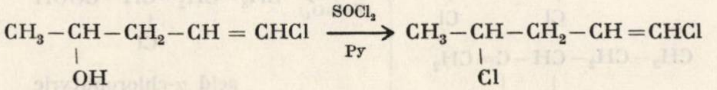
XV

$$CH_3-\underset{\underset{\displaystyle OH}{|}}{CH}-CH_2-CH=CHCl \xrightarrow[Py]{SOCl_2} CH_3-\underset{\underset{\displaystyle Cl}{|}}{CH}-CH_2-CH=CHCl$$

The sodium acetylide was prepared as described by Viehe.[17] This author has tried to add the sodiumchloroacetylide to the ethylene oxide but with very poor results.

By using propylene oxide we assumed that the presence of the methylic group will polarize the molecule, increasing the epoxide reactivity. This was confirmed by carrying out the reaction for a longer time at low temperature. The yield in 1-chloro-4-hydroxypentene-1 was of 27%.

As for the reduction of 1-chloro-4-hydroxypentene-1 to *trans*-1-chloro-4-hydroxypentene-1 the eventualities of chlorine elimination or of total reduction to the simple bond should be avoided. Two ways of reduction were used: the hydrogenation at low temperature with Pd as catalyst and the reduction with $LiAlH_4$. The first way gave no satisfactory results due to a simultaneous chlorine elimination. When $LiAlH_4$ was used the conditions to convert the chloroacetylene derivative into the corresponding chlorovinylic derivative, without chlorine elimination, were established.

This method of the triple bond reduction leads to *trans*-derivative in the case of another disubstituted acetylenes.[18] Indeed, the IR spectra of the obtained product show an absorption band at 955 cm^{-1} characteristic of the ethylene out-of-plane bending vibration, as in $R-CH=$ $=CH-Cl$.[14, 19]

All the above described reactions were chosen so as to avoid the ionic intermediates and also the possible migration of the double bond and of the chlorine atom.

---

[17] H. G. Viehe, *Chem. Ber.*, **92**, 1270 (1959).

[18] a) E. B. Bates, E. R. H. Jones and M. C. Whiting, *J. Chem. Soc.*, **1954**, 1854; b) K. Alder and H. Brachel, *Liebigs Ann. Chem.*, **608**, 195 (1957); c) E. F. Jenny and I. Druey, *Helv. Chim. Acta*, **42**, 401 (1959).

[19] W. J. Potts and R. A. Nyquist, *Spectrochim. Acta*, **9**, 679 (1954).

The structure of all these model compounds was established by IR spectra and also by chemical way searching the double bond and chlorine atom position. For this purpose the unsaturated ends were oxidized with $KMnO_4$ to known structures. The reaction was verified by parallel oxidations of some known model compounds as 3-chloropentene-1 and 4-chloropentene-1. As one can see from the following reactions the oxidation process leads either to the α-chlorobutyric acid or to the β-chlorobutyric acid.

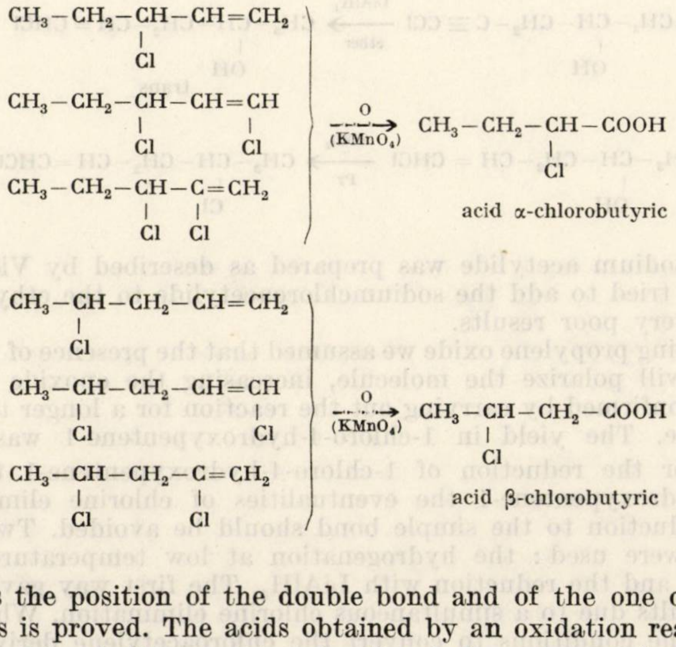

$CH_3-CH_2-CH(Cl)-CH=CH_2$
$CH_3-CH_2-CH(Cl)-CH=CH(Cl)$
$CH_3-CH_2-CH(Cl)-C(Cl)=CH_2$
$\xrightarrow[(KMnO_4)]{O}$
$CH_3-CH_2-CH(Cl)-COOH$
acid α-chlorobutyric
$CH_3-CH(Cl)-CH_2-CH=CH_2$
$CH_3-CH(Cl)-CH_2-CH=CH(Cl)$
$CH_3-CH(Cl)-CH_2-C(Cl)=CH_2$
$\xrightarrow[(KMnO_4)]{O}$
$CH_3-CH(Cl)-CH_2-COOH$
acid β-chlorobutyric

XVI

Thus the position of the double bond and of the one of the chlorine atoms is proved. The acids obtained by an oxidation reaction were characterized by boiling point, refractive index, elemental analysis, IR spectra and by their transformation into S-benzylisothyuronium salts. The results entirely agreed with the proposed structures.

The model compounds can be classified into two groups : 3-chloropentene-1 and 4-chloropentene-1 derivatives. The models in one group differ by the site of the second chlorine atom. The oxidative decomposition as well as the synthesis method limit the possibility of placing this chlorine atom only in position 1 or 2. These situations could be distinguished from one another by the position of out-of-plane double bond bending vibration in IR spectra.[14, 19]

The compounds of the type *trans* $-R-CH=CH-Cl$ must show an absorption band at about 940 cm^{-1}, while for those of type $R-CCl=$ $=CH_2$ the absorption band is shifted toward greater wavelengths at about $875-900$ cm^{-1}.

The IR absorption spectra, showed the position of out-of-plane double bond bending vibration, corresponding to the proposed structures.

Thus, 1,3-dichloropentene-1, shows a peak at 945 cm^{-1}, 1,4-dichloropentene-1 at 950 cm^{-1}, 2,3-dichloropentene-1 at 905 cm^{-1} and 2,4-dichloropentene-1 at 897 cm^{-1}.

The purity of the compounds 2,4-dichloropentene-1 and 1,4-dichloropentene-1 was controlled by gas chromatography analyses. The model compounds are unitary compounds. The thermal unstability of 1,3-dichloropentene-1 and 2,3-dichloropentene-1 did not allow to use the gas chromatography method to test their purity. In these cases the IR spectroscopy proved to be a useful method.

EXPERIMENTAL

I. *1-Chloropentene-1-on-3* was prepared by $AlCl_3$ catalysed addition reaction of propionylchloride on acetylene.[11]

II. Trans-*1-chloro-3-hydroxypentene-1* was obtained by the reduction of 1-chloropentene-1-on-3 with lithium aluminium hydride [12] according to Grünanger and Landone's method.

III. Trans-*1,3-dichloropentene-1* : to a solution of 10 g *trans*-1-chloro-3-hydroxypentene-1 in 13 ml pyridine was added dropwise over a period of 15 minutes 13.75 ml $SOCl_2$ with cooling (20°). The mixture was stirred for 1 h, at this temperature then heated to about 60° during 30 minutes, and kept at this temperature for another hour. It was poured into 150 g ice and the mixture stirred for 1 h to remove the excess of $SOCl_2$. The organic layer was separated and the water layer was extracted with ether. The ethereal solution was dried over anhydrous sodium sulfate and then distilled. After removal of the solvent the fraction boiling at 57.5–58.5° (30 mm) was collected : $n_D^{20} = 1.4664$, yield 6.8 g (60 %).

This product which seemed to be a unitary compound was in fact a mixture of two isomers : *trans*-1,3-dichloropentene-1 ($\nu_{C=C} = 1630$ cm^{-1}) and 1,1-dichloropentene-2 ($\nu_{C=C} = 1660$ cm^{-1}). The two isomers were separated by several rectifications on an adiabatic column, with concentric capillary space of 0.8 mm, average diameter of 8.8 mm and 300 mm in length. The presence of only one component in the final product was proved by IR absorption spectra. Finally about 0.5–1 g of pure *trans*-1,3-dichloropentene-1 b.p. 59–60° (30 mm), $n_D^{20} = 1.4670$ was obtained. The absence of a characteristic band of 1,1-dichloropentene-2 at 1660 cm^{-1} proved the absence of this isomer. It is possible that working with larger quantities the losses will be smaller.

***Calcd.* : $C_5H_8Cl_2$ C, 43.19 %; H, 5.80 %; Cl, 51.00 %**
***Found* : C, 43.16 %; H, 5.93 %; Cl, 51.00 %.**

IV. *4-Hydroxypentine-1* derivative was prepared from propylene oxide and sodium acetylide in liquid ammonia according to.[16]

V. *2-Chloro-4-hydroxypentene-1.* To a stirred solution of 3.35 g $HgCl_2$ in 80 ml water, 50 g 4-hydroxypentine-1 was added. After cooling between −10 and −15° gaseous hydrogen chloride was bubbled through the mixture for 1 h at a rate of 90 l/h. The mixture was allowed to stand 48 h at this temperature and occasionally saturated with gaseous hydrogen chloride. The reaction mixture was separated from the catalyst by vacuum distillation, then the acidic solution was neutralized with concentrated solution of K_2CO_3. By further treating with solid K_2CO_3 the organic layer was separated. The water layer was extracted with ether and the combined extracts, after drying over K_2CO_3, were distilled on a fractionary column, to give 23 g (32 %) 2-chloro-4-hydroxypentene-1 b.p. 54° (13 mm), $n_D^{20} = 1.4565$.

The low boiling fractions, containing a large amount of unreacted product were used again as starting materials for HCl addition. Attempts to prolong the reaction time in order to obtain an increased conversion, lead to the formation of double addition products (the characteristic band at 710 cm^{-1}) whose separation was very difficult from the monochlorinated product.

Calcd.: C_5H_9OCl C, 49.80 %; H, 7.52 %; Cl, 29.40 %
Found: C, 49.91 %; H, 7.57 %; Cl, 29.40 %.

The product gave no infrared absorption band at 2150 cm^{-1} which was characteristic of the $C \equiv C$ triple bond band, but the characteristic band for the $C = C$ double bond at 1640 cm^{-1}.

VI. *2,4-Dichloropentene-1.* To a stirred solution of 10 g 2-chloro-4-hydroxypentene-1 in 13 ml pyridine were added dropwise 22.5 g $SOCl_2$; the temperature does not exceed 10°. The mixture was then heated to 80° for 1 h then poured into ice with stirring to decompose the $SOCl_2$ excess. After drying on anhydrous sodium sulfate the separated organic layer was carefully fractionated to give 4 g (35 %) 2,4-dichloropentene-1 b.p. 48.5° (30 mm) $n_D^{20} = 1.4553$.

Calcd.: $C_5H_8Cl_2$ C, 43.19 %; H, 5.80 %
Found: C, 43.14 %; H, 5.84 %.

In the infrared spectrum the $-OH$ absorption band at 3450 cm^{-1} is missing, new bands do appear in the $C-Cl$ stretching vibrations region.

VII. *3-Hydroxypentine-1* was prepared as described by C.Mc. G. Franck [20] from the propionic aldehyde and sodium acetylide in liquid ammonia.

VIII. *2-Chloro-3-hydroxypentene-1.* To a solution of 0.67 g $HgCl_2$ in 16 ml water 10 g 3-hydroxypentine-1 were added and a stream of gaseous hydrogen chloride was passed through for 30 minutes at a rate of 17.8 l/h. The reaction mixture was allowed to warm up to 90°. The liquid was freed of catalyst by distillation, then was neutralized with a concentrated solution of K_2CO_3. The neutralized solution was treated with solid K_2CO_3. The organic layer was separated and the aqueous layers were extracted with several portions of ether. The combined ether extracts were dried over anhydrous sodium sulfate and freed of ether by evaporation. The remaining liquid was fractionated on a column to give 6.3 g (45 %) 2-chloro-3-hydroxypentene-1 b. p. 49 – 50° (13 mm) $n_D^{20} = 1.4544$.

Calcd.: C_5H_9OCl C, 49.80 %; H, 7.52 %; Cl, 29.40 %
Found: C, 49.88 %; H, 7.53 %; Cl, 29.10 %.

The infrared absorption spectra showed the disappearance of the band at 2250 cm^{-1} (triple bond $C \equiv C$) and the appearance of a new band at 1640 cm^{-1} (double bond $C = C$)

IX. *2,3-Dichloropentene-1.* The same procedure as that described above for 3-dichloropentene-1 was used. In this reaction two isomers were also formed, 2,3-dichloropentene-1 ($\nu_{C=C} = 1635$ cm^{-1}) and 1,2-dichloropentene-2 ($\nu_{C=C} = 1660$ cm^{-1}). 2,3-Dichloropentene-1 was separated from the mixture of the two isomers by fractionation as described above. The pure 2,3-dichloropentene-1 boiled at 50 – 51° (30 mm) $n_D^{20} = 1.4600$. From 10 g 2-chloro-3-hydroxypentene-1 was obtained 1.7 g pure 2,3-dichloropentene-1.

Calcd.: $C_5H_8Cl_2$ C, 43.19 %; H, 5.80 %
Found: C, 43.37 %; H, 5.84 %.

---

[20] C. Mc. G. Franck and R. Adams, *J. Amer. Chem. Soc.*, **59**, 1498 (1937).

X. *1-Chloro-4-hydroxypentine-1.* (*Attention! The reaction must be carried out carefully under argon because the dried sodium chloroacetylide is very explosive*). To a mixture of 180 g metallic sodium in 2500 ml liquid ammonia 384 g *trans*-1,2-dichloroethylene are dropwise added under argon, with stirring and cooling at −40°. Now the cooling bath is removed and the stirring continued for half an hour under NH_3 reflux. After recooling once more at −40°, 300 g propylene oxide is added in 1 h. The mixture is stirred for 48 h under argon and at the boiling temperature of liquid ammonia. Then the mixture was treated with 470 g NH_4Cl also under inert atmosphere. After an additional stirring for 1 h 1000 ml ether were added and the excess of liquid ammonia is allowed to evaporate overnight. The stirred mixture is now treated with 1000 ml water and the solution decanted from the formed black solid. The aqueous solution was well extracted with ether. To reduce the losses the solid was steam distilled and the distillate was treated with NaCl and extracted with ether. The combined extracts were dried over anhydrous sodium sulfate. After removing the ether the remaining material was distilled on fractionation column and the fraction boiling at 75.5−77.5° (29 mm) was collected (1-chloro-4-hydroxypentine-1, 127 g (27 %)). Pure product boils at 77.0−77.5° (29 mm), $n_D^{20} = 1.4685$.

Calcd.: C_5H_7OCl C, 50.65 %; H, 5.95 %; Cl, 29.90 %
Found: C, 50.72 %; H, 6.38 %; Cl, 29.65 %.

The infrared spectra showed the triple bond absorption band at 2290 cm^{-1}, −OH band at 3400 cm^{-1} and absorption bands in the region of the C−Cl stretching vibration.

XI. Trans-*1-chloro-4-hydroxypentene-1.* To a solution of 12 g 1-chloro-4-hydroxypentine-1 in 100 ml anhydrous ether was added in portions with stirring and cooling between −5 to 0°, 4.7 g $LiAlH_4$ in 100 ml anhydrous ether. The mixture was refluxed for 30 minutes. To this mixture, a solution of 25 ml ether and 25 ml methanol was gradually added with stirring at 15° to decompose the excess of $LiAlH_4$. The material was poured into a mixture of ice and 6 ml H_2SO_4. After 10 minutes stirring the ether layer was separated and the water layer extracted with ether. The ethereal combined portions were dried over anhydrous sodium sulfate, after which the solution was concentrated by distilling off the ether in vacuum at room temperature. The residue was rectified under reduced pressure and the fraction boiling at 65−72° (10 mm) was collected. There were obtained 3.8 g (31 %) crude *trans*-1-chloro-4-hydroxypentene-1. Pure product boiled at 71−72° (10 mm), $n_D^{20} = 1.4625$.

Calcd.: C_5H_9OCl C, 49.80 %; H, 7.52 %; Cl, 29.40 %
Found: C, 49.70 %; H, 7.35 %; Cl, 29.05 %.

The infrared spectra showed the disappearance of the characteristic line at 2290 cm^{-1} of the triple bond $C \equiv C$ and the appearance of a new peak at 1640 cm^{-1} characteristic of the double bond C = C.

XII. Trans-*1,4-dichloropentene-1.* A stirring solution of 3.5 g 1-chloro-4-hydroxypentene-1 in 4.6 ml pyridine was cooled at 0° and 4.82 ml $SOCl_2$ were added. This solution was heated rapidly on water bath for 12 minutes, then the mixture was cooled and poured into ice with 1 h stirring to decompose the $SOCl_2$ excess. The organic layer was separated and after drying over K_2CO_3 was distilled on a fractionary column to give 1.3 g (32−33 %) pure *trans*-1,4-dichloropentene-1, b.p. 67−68° (30 mm), $n_D^{20} = 1.4670$.

Calcd.: $C_5H_8Cl_2$ C, 43.19 %; H, 5.80 %; Cl, 51.00 %
Found: C, 43.33 %; H, 5.89 %; Cl, 50.78 %.

XIII. *3-Chloropentene-1* was obtained from allyl bromide and acrolein as described previously.[15] By replacing the —OH group from 3-hydroxypentene-1 by —Cl with $SOCl_2$ two isomers, 3-chloropentene-1 and 1-chloropentene-2 were obtained, as result of allylic transposition. Redistillation of the mixture of the two isomers on the capillary column gave the pure 3-chloropentene-1 b.p. 48—48.5° (150 mm) $n_D^{20} = 1.4249$. The infrared spectra showed at 1645 cm^{-1} the absorption band which is characteristic of C = C terminal double bond and no disubstituted double bond absorption band at 1670 cm^{-1}. The pure isomer 1-chloropentene-2 boiled at 64.5—65° (150 mm), $n_D^{20} = 1.4384$. The infrared spectra showed the band at 1670 cm^{-1} characteristic of the disubstituted double bond C = C, the absorption band at 1645 cm^{-1} (3-chloropentene-1) being absent.

XIV. *4-Chloropentene-1* was obtained from allyl bromide and acetaldehyde following the procedure described previously.[21]

Oxidations. To prove the structures of all these products they were oxidized to the corresponding acids with aqueous $KMnO_4$ at room temperature by the usual procedure.

XV. *S-benzylisothyuronium derivatives* of α- and β-chlorobutyric acids were obtained from the S-benzylisothyronium chloride and the α- and β-chlorobutyric acids resulted from the oxidation reaction. After recrystallization from ethanol they melted at 155—155.5° and 137.5—138° respectively.

Calcd.: $C_{12}H_{17}O_2N_2SCl$ C, 49.90 %; H, 5.93 %; N, 9.70 %

Found:

— for S-benzylisothyuronium derivatives of α-chlorobutyric acid	C, 50.13 %; H, 5.90 %; N, 10.00 %
— for S-benzylisothyuronium derivatives of β-chlorobutyric acid	C, 49.77 %; H, 5.82 %; N, 10.02 %

---

[21] M. H. Pariselle, *Compt. rend.*, 154, 710 (1912).

Revue Roumaine de Chimie, 14, 1181–1189 (1969)

UNTERSUCHUNGEN IN DER CYCLOBUTANREIHE. XXI[1]

DI-TERT.-BUTYL-DIPHENYL-CYCLOBUTADIEN-KOMPLEXE MIT PALLADIUMCHLORID*

MARGARETA AVRAM, I. G. DINULESCU, GH. D. MATEESCU, ELISA AVRAM und C. D. NENITZESCU

Aus dem Organisch-Chemischen Institut der Akademie,
Bukarest, Spl. Independenţei 202 B

Eingegangen am 25. April 1969

Aus tert.-Butyl-phenyl-acetylen und Bis-benzonitril-palladiumchlorid in Benzol entsteht, in zwei Stufen, der Di-tert.-butyl-diphenyl-cyclobutadien-palladiumchlorid-Komplex (2). Die Reaktionen dieses Komplexes mit verschiedenen Nucleophilen und mit Wasserstoff werden beschrieben. Aus 2 wurde mit Eisenpentacarbonyl Di-tert.-butyl-diphenyl-cyclobutadien-eisentricarbonyl (15) erhalten. Durch Zersetzung dieser Komplexe erhält man Di-tert.-butyl-diphenylfuran und dessen Oxydationsprodukte.

Die Stabilisierung des Cyclobutadiens durch Einführung von Substituenten mit entgegengesetzten mesomeren Effekten ist öfters diskutiert [2,3] und neuestens experimentell durchgeführt worden.[4] Dagegen scheint eine Stabilisierung des Cyclobutadiens, lediglich durch Einführung von stark raumbeanspruchenden Substituenten noch nicht versucht worden zu sein. An Modellen kann leicht ersehen werden, daß die Dimerisierung des Tetra-tert.-butyl-cyclobutadiens vollkommen sterisch gehindert ist.

Da sich die meisten Cyclobutadiene durch Dimerisierung stabilisieren, wurden verschiedenen Synthesen von mit tert.-Butylgruppen substituierten Cyclobutadienen vorgenommen.

Malatesta [5] zuerst, dann Blomquist und Maitlis,[6] Maitlis und Mitarbeiter [7] und kürzlich Hüttel und Neugebauer [8] haben aus Tolan und

---

* Diese Arbeit wurde als Max Tishler Lecture an der Universität Harvard, Cambridge, U.S.A., am 4. Oktober 1968, vorgetragen.

[1] XX. Mitteil.: M. Avram, Gh. D. Mateescu und C. D. Nenitzescu, *Rev. Roumaine Chim.*, **14**, 101 (1969).

[2] J. D. Roberts, *Chem. Soc., Special publ.*, No. 12, 111 (1958).

[3] R. Breslow, D. Kivelevich, M. J. Mitchell, W. Fabian und K. Wendel, *J. Amer. Chem. Soc.*, **87**, 5132 (1965).

[4] R. Gompper und G. Seybold, *Angew. Chem.*, **80**, 804 (1968).

[5] L. Malatesta, G. Santarella, L. Vallarino und F. Zingales, *Angew. Chem.*, **72**, 34 (1960); *Atti Acad. Naz. Lincei, Roma, Class Sci. Fiz. e Nat.*, **27**, 230 (1959).

[6] A. T. Blomquist und P. M. Maitlis, *J. Amer. Chem. Soc.*, **84**, 2329 (1962).

[7] P. M. Maitlis, D. Pollock, M. L. Games und W. J. Pryde, *Can. J. Chem.*, **43**, 470 (1965).

[8] R. Hüttel und H. J. Neugebauer, *Tetrahedron Letters*, 3541 (1964).

Palladiumchlorid einen Komplex erhalten, welcher sehr wahrscheinlich Tetraphenylcyclobutadien als organischen Liganden enthält.

In der vorliegenden Arbeit berichten wir über einen aus tert.-Butylphenyl-acetylen und Bis-benzonitril-palladium-chlorid in Benzol erhaltenen Komplex. Die Elementaranalyse dieser gelblichbraunen amorphen Verbindung (**1**) entspricht der Formel $C_{24}H_{28} \cdot (PdCl_2)n$ und dürfte also aus zwei Molekülen tert.-Butyl-acetylen oder aus einem Molekül Di-tert.-butyl-diphenyl-cyclobutadien mit nicht stöchiometrischen Mengen Palladiumchlorid bestehen. Der Komplex **1** ist in den meisten üblichen Lösungsmitteln unlöslich, löst sich aber in Dimethylformamid und scheidet bei der Behandlung mit gasförmiger oder konzentrierter Salzsäure den hellgelben Komplex **2** ab, analog dem Tetraphenylcyclobutadien Komplex.[7,8]

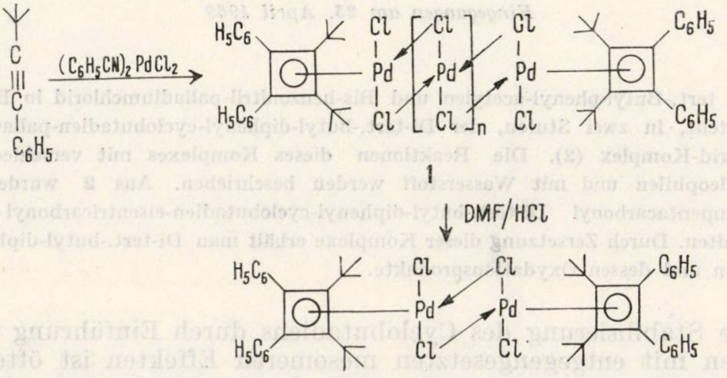

1

2

Im NMR-Spektrum des Komplexes **2** erscheinen die tert.-Butylgruppen als ein einziges Signal auf (δ 1,58 ppm) die Phenylgruppen dagegen als ein Multiplett (zwischen δ 7,2—7,9 ppm). Die aliphatischen Protonen stehen zu den aromatischen im Verhältnis 18 : 10.

Aus der Lösung von **1** in Dimethylsulfoxid scheidet, nach einiger Zeit, in Form orange gefärbter Kristalle, ein Addukt des Komplexes **2** mit einem Molekül Dimethylsulfoxid ab.

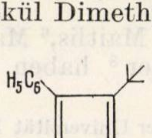

3

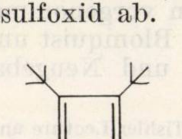

4

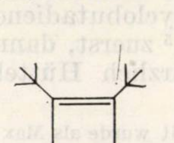

4a

Zwei Moleküle tert.-Butyl-phenyl-acetylen können sich prinzipiell zu zwei verschiedenen Cyclobutadienen **3** oder **4** cyclodimerisieren. Auf Grund der NMR- und IR-Spektren ist es nicht möglich zwischen **3** oder **4**, als Liganden im Komplex **2**, zu entscheiden. Wie weiter unten gezeigt werden wird, entspricht die Struktur **4** dem tatsächlich im Komplex enthaltenen organischen Anteil. So werden wir vorläufig diese Struktur benutzen.

Die Dimethylformamidlösung der Komplexe **1** oder **2**, bildet bei Behandlung mit Wasser einen neuen gelblichweißen Komplex **5a**, mit der Bruttoformel $C_{24}H_{29}ClOPd$. Mit Salzsäure regeneriert **5a** den Komplex **2**.

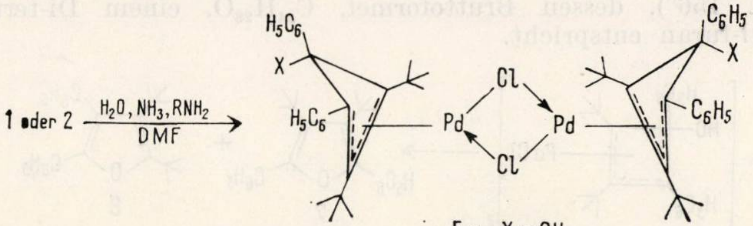

5 a, X = OH
5 b, X = NH_2
5 c, X = $NH-C_4H_9$

Im NMR-Spektrum des Komplexes **5a** erscheinen zwei Signale der tert.-Butylgruppen bei δ 1,33 ppm und δ 1,50 ppm, im Verhältnis 1 : 1, während für die Phenylgruppen ein Multiplett, zwischen δ 7,0 – 7,9 ppm entsteht. Das Signal der OH-Gruppe, bei δ 2,42 ppm ist charakteristisch für eine benzylische Hydroxylgruppe und verschwindet bei der Deuterierung.

Da der Komplex **2** ein ähnliches Verhalten zeigt wie der analoge Komplex des Tetraphenylcyclobutadiens,[7,9–11] hat **5a** wahrscheinlich eine *exo*-4-hydroxy-π-Pd-cyclobutenilstruktur. Seine Bildung ist wohl so zu erklären, daß in Dimethylformamidlösung eine Ionisierung des Chlors stattfindet, wobei das Kation **6** entsteht. Dieses kann sich mit anwesenden Nucleophilen verbinden. Die positive Ladung des Kations **6** lokalisiert sich in einer der Stellungen des Vierringes welche das Kation am besten stabilisiert, also in einer der Benzylstellungen.

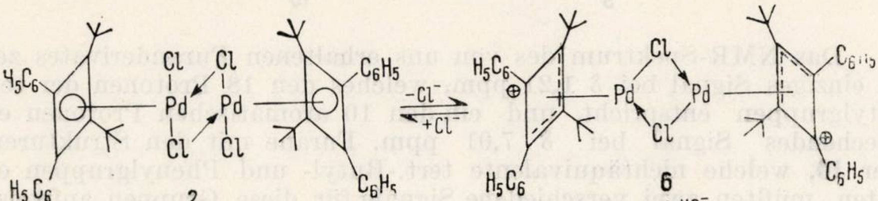

Bei Behandlung des Komplexes **2** mit Ammoniak oder mit Butylamin entstehen die Komplexe **5b** bzw. **5c**. Mit Silbernitrat und mit Kaliumcyanid bilden sich Verbindungen welche wahrscheinlich eine ana-

---

[9] P. M. Maitlis, A. Efraty und M. L. Games, *J. Amer. Chem. Soc.*, **87**, 719 (1965).
[10] P. M. Maitlis, A. E. Efraty und M. L. Games, *J. Organomet. Chem.*, **2**, 284 (1964).
[11] L. F. Dahl und W. E. Oberhansli, *Proceeding at the VIII Conference of Coordination Chemistry, Wien*, 1964, p. 242.

loge Struktur besitzen, da sie nach Behandlung mit Salzsäure den Komplex **2** regenerierten.

Durch Erwärmen des Komplexes **5a** auf 200—220° scheidet sich metallisches Pd aus und es destilliert ein kristallisierbares Produkt (Schmp. 156°), dessen Bruttoformel, $C_{24}H_{28}O$, einem Di-tert.-butyl-diphenyl-furan entspricht.

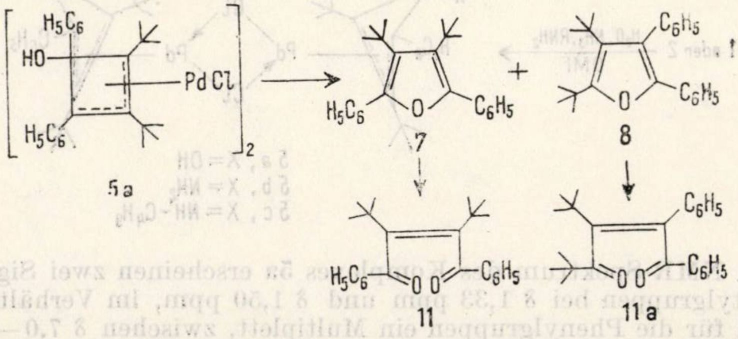

Aus dem hydroxylhaltigen Komplex **5a** können zwei Furanderivate **7** und **8** entstehen. Ein Komplex **9**, welcher einem symmetrischen Cyclobutadien mit der Formel **3** entsprechen würde, könnte nur ein Furanderivat, und zwar **10**, erzeugen.

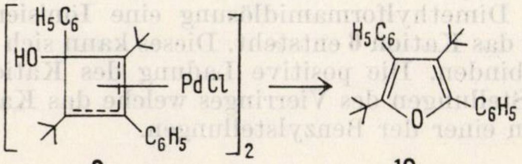

9 **10**

Das NMR-Spektrum des von uns erhaltenen Furanderivates zeigt ein einziges Signal bei δ 1,21 ppm, welches den 18 Protonen der tert.-Butylgruppen entspricht und ein den 10 aromatischen Protonen entsprechendes Signal bei δ 7,01 ppm. Furane mit den Strukturen **8** oder **10**, welche nichtäquivalente tert.-Butyl- und Phenylgruppen enthalten, müßten zwei verschiedene Signale für diese Gruppen aufweisen. Das von uns erhaltene Furan kann also nur das 2.5-Diphenyl-3.4-di-tert.-butylfuran (**7**) sein. Dementsprechend kann der organische Ligand in den Komplexen **1** und **2** die beiden tert.-Butyl- und die beiden Phenylgruppen nur in vicinalen Stellungen enthalten.

Ein weiterer Beweis für die Struktur des Furans **7** wurde durch Oxydation mit Salpetersäure erbracht. Als einziges Oxydationsprodukt erhielten wir 1,4-Diphenyl-2,3-di-tert.-butyl-but-2-en-1.4-dion (**11**). Das IR-Spektrum dieses Diketons zeigt eine einzige Absorptionsbande bei 1690 cm^{-1}, welche wohl einer mit dem Benzolring konjugierten CO-Gruppe entspricht. Das NMR-Spektrum zeigt Signale bei δ 1,00 ppm, für die 18 Protonen der tert.-Butylgruppen und ein Signal bei δ 7,06 ppm, für die 10 aromatischen Protonen. Das Furan **8** hätte durch Oxydation ein Diketon **11a** erzeugen sollen, während **10** ein isomeres Diketon, mit nichtäquivalenten Phenylgruppen liefern würde.

Beim Erhitzen mit Triphenylphosphin entstehen aus dem Komplex **2** beide Furane **7** und **8** im Verhältnis 1 : 2. Das Furan **8** könnte chromatographisch getrennt werden. Sein NMR-Spektrum zeigt zwei Signale für die tert.-Butylgruppen, bei δ 1,23 und δ 1,60 ppm (1 : 1) und zwei Signale für die Phenylgruppen bei δ 7,01 und 7,35 ppm (1 : 1). Offenbar entstehen die Furane **7** und **8** aus dem, aus dem Komplex in Freiheit gesetzten Di-tert.-butyl-diphenyl-cyclobutadien, welches mit Sauerstoff ähnlich wie das Tetraphenylcyclobutadien reagiert.[8,12]

Auch dieses Ergebnis beweist eindeutig, daß der organische Ligand in **2** die Struktur **4** besitzt; ein Ligand **3** hätte zu einem einzigen Furan **10** führen sollen. Nicht unlogisch ist ferner die Schlußfolgerung, daß das aus dem Komplex **2** verdrängte Cyclobutadien, in zwei verschiedenen isomeren Formen **4** und **4a** entsteht, welche sich dann separat, sehr schnell mit Luftsauerstoff zu den Furanen **7** und **8** umsetzen. Für die Entstehung von Dimeren von **4** oder **4a** ist kein Zeichen vorhanden.

Die thermische Zersetzung des Komplexes **5b** führt zu einem Pyrol. Dieses konnte in reinem Zustand nicht erhalten werden, da es stets mit wenig Furan verunreinigt war. Das Pyrol **12** wurde durch das IR-Spektrum (ν_{NH} 3573 cm^{-1}) und das NMR-Spektrum (δ 1,20 ppm (18 H), δ 7,08 ppm (10 aromatische H)) charakterisiert.

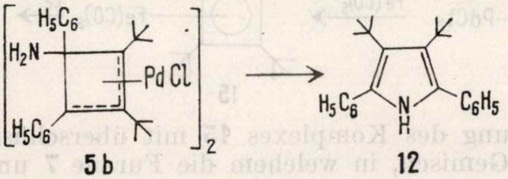

5b **12**

Wird der Komplex **2** mit Wasserstoff in Methanol geschüttelt, mit Lithiumaluminiumhydrid oder Natriumborohydrid behandelt, so scheidet sich metallisches Palladium aus, und es entsteht ein Gemisch von Kohlenwasserstoffen welches hauptsächlich aus 1,4-Di-tert.-butyl-2,3-diphenyl-cyclobuten (**13**) und 1,2-Di-tert.-butyl-3,4-diphenyl-cyclobuten (**14**) besteht.

Das NMR-Spektrum des Kohlenwasserstoffs **13** (Schmp. 110°) zeigt zwei Singlette, bei δ 0,17 und δ 1,20 ppm, für die 18 Protonen der beiden tert.-Butylgruppen und ein Multiplett bei δ 6,98—7,08 ppm, für die 10 Protonen der Phenylgruppen. Die zwei gesättigten Protonen des Cyclobutenrings bilden ein gekoppeltes Quartett (J = 5 cps) in welchem das Dublett des benzylischen Protons bei δ 4,27 und 4,35 ppm und das Dublett des gesättigten Protons (vicinal zur tert.-Butylgruppe) bei δ 3,15 und 3,23 ppm erscheinen. Das NMR-Spektrum des Kohlenwas-

---

[12] H. H. FREEDMAN, *J. Amer. Chem. Soc.*, **83**, 2194, 2195 (1961); H. H. FREEDMAN und D. R. PETERSEN, *J. Amer. Chem. Soc.*, **84**, 2837 (1962).

serstoffs **14** (Schmp. 96—98°) enthält ein Signal für die zwei äquivalenten tert.-Butylgruppen bei δ 1,20 ppm (18 H) und ein Signal für die beiden Phenylgruppen bei δ 6,80 ppm (10 H). Die beiden benzylischen Protonen, welche ebenfalls äquivalent sind, geben ein einziges Signal bei δ 4,11 ppm.

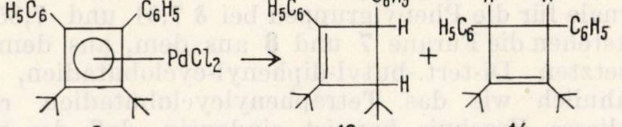

2 **13** **14**

Die Cyclobutene **13** und **14** konnten nicht katalytisch hydriert werden und sind auch gegenüber Oxydationsmitteln wenig reaktionsfähig, wahrscheinlich wegen der sterischen Hinderung durch die tert.-Butylgruppen.

Erwärmt man den Komplex **2** mit Eisenpentacarbonyl in Benzol, so erhält man den Komplex $C_{24}H_{28}Fe(CO)_3$ **15**, Schmp. 137°, welcher thermisch sehr stabil ist. Das NMR-Spektrum zeigt ein Signal, bei δ 0,83 ppm, für die 18 Protonen der äquivalenten tert.-Butylgruppen und ein anderes breites Signal, bei δ 6,58—7,0 ppm, für die 10 Protonen der Phenylgruppen.

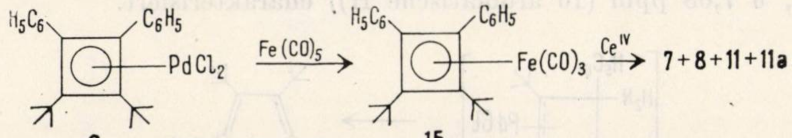

2 **15**

Die Zersetzung des Komplexes **15** mit überschüssigem Ce^{IV} führt zu einem öligen Gemisch, in welchem die Furane **7** und **8** und die Diketone **11** und **11a** durch ihre NMR-Spektren, IR-Spektren und durch Gaschromatographie identifiziert wurden. Bei Verlängerung der Kontaktzeit mit dem Oxydationsmittel wächst der Gehalt an Diketon **11a** auf Kosten des Furans **8**. Letzteres wurde kristallisiert erhalten.

Ein Versuch **15** direkt aus tert.-Butyl-phenyl-acetylen und $Fe_2(CO)_9$ zu erhalten, führte zu einem roten Komplex mit der Bruttoformel $(C_{12}H_{14})_2 . 2\ Fe(CO)_3$ und der wahrscheinlichen Struktur eines Ferracyclopentadienil-Komplexes **16**. Ähnliche Komplexe bilden sich aus Tolan[13,14] und aus Acetylen.[15,16]

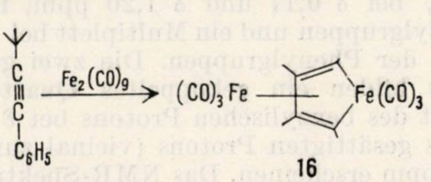

16

---

[13] G. N. Schrauzer, *Chem. and Ind.*, **1958**, 1403, 1404; *J. Amer. Chem. Soc.*, **81**, 5307 (1959).

[14] W. Hübel und E. H. Braye, *J. Inorg. Nucl. Chem.*, **10**, 250 (1959).

[15] E. Weiss, W. Hübel, R. Merényi, J. Nielsen, A. Gerondal und R. Vannienwenhoven, *Chem. Ber.*, **95**, 1155 (1962); W. Hübel und E. Weiss, *Chem. and Ind.*, **1959**, 703.

[16] M. L. H. Green, L. Pratt und G. Wilkinson, *J. Chem. Soc.*, **1960**, 989.

Abschließend sei bemerkt, daß das tert.-Butyl-phenyl-acetylen, ähnlich wie Tolan, mit Palladiumchlorid sich zu einem Cyclobutadien cyclodimerisiert, während das monosubstituierte tert.-Butyl-acetylen, wie an einer anderen Stelle gezeigt werden wird, unter denselben Bedingungen, sich zu einem Dewar-Benzol-derivat bicyclotrimerisiert.

BESCHREIBUNG DER VERSUCHE

Die Mikroanalysen wurden von Fräulein E. Şliam und Frau V. Daniel ausgeführt. Die IR-Spektren wurden mit einem UR20 Carl Zeiss Jena Doppelstrahlspektralphotometer, die NMR-Spektren mit einem A-60A Varian Gerät aufgenommen (TMS als innerer Standard).

Die gaschromatographischen Analysen wurden mit einem Carlo Erba Chromatographen von Frau M. Rentzea und Frl. D. Georgescu ausgeführt. Füllung der chromatographischen Säule : 20 % Äthylenglycolsuccinat auf Chromosorb B ; Dimensionen 1 m × 2 mm ; Trägergas H_2, 52,1 ml/min ; Temperatur 200°.

1,2-Di-tert.-butyl-3,4-diphenyl-cyclobutadien-palladiumchloride (**1** *und* **2**)

Der Komplex **1** : Zu einer Lösung von 5,75 g (15 mMol) Bis-benzonitril-palladiumchlorid in 170 ml absol. Benzol werden 7,1 g (4,5 mMol) tert.-Butyl-phenyl-acetylen zugegeben und die Lösung wird 24 Std. bei Zimmertemperatur stehen gelassen. Nach kurzer Zeit fällt ein organgebrauner Niederschlag aus, welcher filtriert und mit Benzol und Petroläther gewaschen wird. Ausb. 5,3—5,5 g Komplex **1**. Die Elementaranalyse von verschiedenen Präparaten entspricht der Formel $C_{24}H_{28}(PdCl_2)_{1,5-2}$.

Der Komplex **2** : Eine eisgekühlte Lösung von 5,3 g Komplex **1** in 50 ml Dimethylformamid wird mit 15 ml konz. Salzsäure versetzt. Nach 1/2 Std. fallen orangegelbe Kristalle aus, welche abfiltriert und an der Luft getrocknet werden. Ausb. 3,5 g (47,5 % in bezug auf Bis-benzonitril-palladiumchlorid) Komplex **2** ; orangegelbe Kristalle ; Schmp. 200° (Zers.).

Das Produkt wurde in Methylenchloridlösung auf einer Al_2O_3 Säule chromatographiert.

$C_{24}H_{28}Cl_2Pd$ (494,1) *Ber.* : C 58,34 ; H 5,71 ; Cl 14,35 ; Pd 21,59

Gef. : C 58,61 ; H 5,77 ; Cl 14,09 ; Pd 21,07

Di-μ-Chloro-di [*π-(exo-4-hydroxy-1.2-di-tert.-butyl-3.4-diphenylcyclobutenyl)-palladium*] (**5a**)

Eine eisgekühlte Lösung von 0,2 g (0,4 mMol) Komplex **2** in 10 ml Dimethylformamid wird mit 5 ml Wasser versetzt. Ausb. : 0,15 g (78 %) Komplex **5a** ; Schmp. 190—210° (Zers.).

$C_{24}H_{29}ClOPd$ (475,6) *Ber.* : C 60,60 ; H 6,14 ; Cl 7,45 ; Pd 22,43

Gef. : C 60,46 ; H 6,33 ; Cl 7,52 ; Pd 23,10

Regenerierung des Komplexes **2** *aus* **5a**. Man löst den Komplex **5a** in Dimethylformamid und gibt konz. Salzsäure unter Eiskühlung hinzu. Es fallen die orangegelben Kristalle aus. Schmp. 200° (Zers.). Die IR- und NMR-Spektren sind identisch mit den Spektren der Präparate **2**.

Di-μ-Chloro-di [*π-(exo-4-amino-1.2-di-tert.-butyl-3.4-diphenyl-cyclobutenyl)-palladium*] (**5b**)

Zu einer eisgekühlten Lösung von 0,1 g (0,2 mMol) **2** in 2 ml Dimethylformamid wird gasförmiger Ammoniak im Überschuß eingeführt. Nach Abfiltrieren des Ammoniumchlorids, wird das Lösungsmittel unter vermindertem Druck entfernt und ein schwachgelber Niederschlag von **5b** erhalten, welcher roh analysiert wurde.

$C_{24}H_{30}ClNPd$ (474,6) *Ber.* : C 60,73 ; H 6,37 ; Cl 7,47 ; N 2,95 ; Pd 22,48

Gef. : C 60,78 ; H 6,48 ; Cl 7,76 ; N 2,71 ; Pd 22,90

Die thermische Zersetzung des Komplexes **5b**. 1g (2,1 mMol) Komplex **5b** wird in einem Destillationskolben mit freier Gasflamme bis zur Zersetzung (erkennbar an der Ausscheidung von metallischem Pd) erwärmt und anschließend i. Vak. destilliert. Es wurde ein Gemisch von 2.5-Diphenyl-3.4-di-tert.-butyl-pyrrol (**12**) (ν_{NH} 3505 cm^{-1} in CCl_4) und Furan **7** erhalten.

Di-µ-Chloro-di[π-(exo-4-butylamino-1.2-di-tert.-butyl-3.4-diphenylcyclobutenyl)-palladium] (**5c**)

Eine eisgekühlte Lösung von 0,1 g (0,2 mMol) **2** in 2 ml Dimethylformamid wird mit 0,1 g (1,4 mMol) Butylamin versetzt. Der hellgelbe Niederschlag von **5c** wird auf dem Filter mit Methanol gewaschen.

$C_{28}H_{38}ClNPd$ (530,7) *Ber.* : C 63,36 ; H 7,22 ; N 2,64
Gef. : C 62,90 ; H 7,22 ; N 2,71

1,2-Di-tert.-butyl-3,4-diphenyl-cyclobutadien-palladiumchlorid-Komplex mit Dimethylsulfoxid

Eine Suspension von 0,5 g **1** in 20 ml Dimethylsulfoxid, läßt man 4—5 Tage bei Raumtemperatur, unter gelegentlichem Rühren, stehen. Die anfänglich braunen Kristalle verwandeln sich in gelbe Kristalle um, welche in Methanol unlöslich, in Tetrahydrofuran dagegen leicht löslich sind.

$C_{26}H_{34}Cl_2OPdS$ (572,2) *Ber.* : C 54,57 ; H 5,99 ; Pd 18,65
Gef. : C 54,00 ; H 6,51 ; Pd 18,95

Offenbar ist das Produkt eine molekulare Verbindung von **2** mit $(CH_3)_2SO$.

Thermische Zersetzung des Komplexes **5a** : *2,5-Diphenyl-3,4-di-tert.-butyl-furan* (**7**)

1 g (2,01 mMol) Komplex **5a** wird in einem Destillationskolben mit freier Gasflamme, bis zur Zersetzung erwärmt und anschließend i. Vak. destilliert. Das aus Öl und Kristallen bestehende Produkt wird in Ätherlösung auf einer Al_2O_3-Säule chromatographiert. Ausb. 0,35 g (50 %) **7** ; Schmp. 156° (aus Methanol).

$C_{24}H_{28}O$ (332,5) *Ber.* : C 86,69 ; H 8,49
Gef. : C 86,48 ; H 8,76

1,4-Diphenyl-2,3-di-tert.-butyl-but-2-en-1.4-dion (**11**)

0,2 g (0,6 mMol) **7** werden in 5 ml Essigsäure gelöst und mit 1 ml konz. Salpetersäure ($d = 1{,}42$) versetzt. Es findet eine exotherme Reaktion statt und die Lösung färbt sich anfänglich grün und dann rot. Nach 1 Std. bei Zimmertemperatur, wird die Lösung in Wasser gegossen und mit Methylenchlorid ausgezogen. Nach Abdestillieren des Lösungsmittels und Aufnahme des Rückstandes in Äther oder Petroläther wird auf Al_2O_3 chromatographiert. Ausb. 0,15 g (75 %) **11** ; Schmp. 145°.

$C_{24}H_{28}O_2$ (348,5) *Ber.* : C 82,72 ; H 8,10
Gef. : C 82,79 ; H 8,26

Reaktion des Komplexes **2** *mit Triphenylphosphin* : *Di-tert.-butyl-diphenyl-furane* **7** *und* **8**

Eine Lösung, bestehend aus 1,0 g (2 mMol) Komplex **2** und 0,8 g (3,2 mMol) Triphenylphosphin in 30 ml Benzol wird bis zum Sieden in Argonatmosphäre, 1 Std. lang erwärmt. Die gelben Kristalle des Bis (triphenylphosphin)-palladiumchlorids werden abfiltriert und das Lösungsmittel i. Vak. bis zur Trockene, destilliert. Der ölige Rückstand wird mit Petroläther auf Aluminiumoxid chromatographiert. Beim Abdestillieren des Lösungsmittels wird ein Gemisch von **7** und **8**, im Verhältnis 1 : 2 (NMR-Spektrum) erhalten ; Schmp. 115—118°.

$C_{24}H_{28}O$ (332,5) *Ber.* : C 86,69 ; H 8,49
Gef. : C 86,78 ; H 8,51

Aus diesem Gemisch kann *2.3-Diphenyl-4.5-di-tert.-butyl-furan* (**8**) durch Chromatographieren auf Aluminiumoxid mit Petroläther und fraktionierten Umkristallisierungen aus Methanol erhalten werden. Schmp. 120° (aus Methanol).

$C_{24}H_{28}O$ (332,5) *Ber.* : C 86,69 ; H 8,49
Gef. : C 86,50 ; H 8,68

Reduktion des Komplexes **2**: *Di-tert.-butyl-diphenyl-cyclobutene* (**13** *und* **14**)

Mit Natriumborohydrid: Eine Suspension von 3,0 g (6 mMol) **2** in 50 ml Methanol und 20 ml Wasser wird unter Rühren mit einer überschüssigen wässerigen Natriumborohydridlösung versetzt. Nach einer heftigen Reaktion scheidet Palladium ab. Die rote äther. Lösung wird i. Vak. zur Trockene eingedampft und der ölige Rückstand in Petroläther aufgenommen und über Al_2O_3 chromatographiert. Der farblose Eluent wird zur Trockene eingedampft; Ausb.: 1,9 g eines öligen Rückstandes, welcher durch längeres Stehen oder durch Anfeuchten mit Methanol, Kristalle ausscheidet; Schmp. 94–98° (aus Methanol). Das NMR-Spektrum zeigt, daß die Kristalle ein Gemisch von **13** und **14** sind. Nach mehreren Umkristallisierungen aus Methanol wird reines *1,4-Di-tert.-***butyl***-2,3-diphenyl-cyclobuten* (**13**) erhalten; Schmp. 110°.

$C_{24}H_{30}$ (318,5) *Ber.*: C 90,51; H 9,49
Gef.: C 90,41; H 9,77

Aus den leichter löslichen Fraktionen werden nach mehrmaligen Umkristallisierungen *1,2-Di-tert.-butyl-3,4-diphenyl-cyclobuten* (**14**) isoliert; Schmp. 96–98°. Auf Grund der NMR-Spektren enthält das Präparat noch wenig **13**.

$C_{24}H_{30}$ (318.5) *Ber.*: C 90,51; H 9,49
Gef.: C 90,67; H 9,74

Mit Wasserstoff: Schüttelt man eine Lösung von 1,0 g (2 mMol) **2** in 50 ml Methanol 24 Std. lang mit Wasserstoff, so scheidet metallisches Pd aus. Nach Abfiltrieren des Palladiums und Abdestillieren des Lösungsmittels i. Vak. bleibt ein öliger Rückstand zurück, aus welchem **13** und **14** isoliert werden (Nachweis durch das NMR-Spektrum). Die beiden Komponenten können durch mehrmaliges Umkristallisieren, wie oben gezeigt, teilweise getrennt werden.

Beim Versuch ein Gemisch der Cyclobutene **13** und **14** in Methanol in Gegenwart von Pd oder PtO_2 zu hydrieren wurden die Ausgangsstoffe unverändert zurückerhalten.

Di-tert.-butyl-diphenyl-cyclobutadien-eisentricarbonyl (**15**)

Erhitzt man ein Gemisch von 2 g (4 mMol) **2** in 120 ml Benzol und 4 g Eisenpentacarbonyl in einer Argonatmosphäre 4 Std. lang auf 70–80°, so scheidet Pd aus. Die benzolische Lösung wird i. Vak. zur Trockene destilliert wobei 1,2 g (65%) **15**, Schmp. 137° (aus Äthanol), erhalten werden. Das in Petroläther lösliche, weiße Produkt, wurde auf Al_2O_3 chromatographiert und anschließend i. Vak. sublimiert.

$C_{27}H_{28}FeO_3$ (456,3) *Ber.*: C 71,06; H 6,18
Gef.: C 71,13; H 6,33

Das IR-Spektrum enthält ν_{CO} Frequenzen bei 1985 und 2042 cm^{-1}.

Zersetzung des Komplexes **15** *mit* Ce^{IV}. Eine Lösung von 1,5 g (3,3 mMol) Komplex **15** in 20 ml absol. Aceton wird mit Ceriammoniumnitrat im Überschuß versetzt, wobei Kohlenoxid frei wird. Nach Beendigung der Kohlenoxidentwicklung wird Wasser hinzugegeben und die Lösung mit Äther ausgezogen. Die äther. Lösung wird auf Al_2O_3 chromatographiert um die Ceriumreste zu beseitigen. Nach Verdampfung des Äthers wird 1 g hellgelbes Öl erhalten.

Dieses Rohprodukt wird in Petroläther auf Aluminiumoxid chromatographiert. Am Anfang scheidet eine kleine Menge eines unkristallisierbaren Produktes aus. Das Hauptprodukt wird anschließend mit Äther eluiert (ca. 0,8 g). In dieser Fraktion konnten die Furane **7**, **8** und die Diketone **11** und **11a** sowohl durch IR- und NMR-Spektren, als auch gaschromatographisch identifiziert werden.

Durch die Reduktion mit Lithiumaluminiumhydrid einer an **11a** reichen Fraktion, wurde das Furan **8** kristallisiert erhalten.

Die Reaktion des tert.-Butyl-phenyl-acetylens mit Dieisen-enneacarbonyl

0,7 g (4,4 mMol) tert.-Butyl-phenyl-acetylen und 0,5 g (1,4 mMol) Dieisen-enneacarbonyl in 7 ml Cyclohexan werden in einem Schlenkrohr, in Gegenwart von Argon, 10 Std. auf 50° erhitzt. Das Dieisen-enneacarbonyl verschwindet langsam, es entwickelt sich Kohlenoxid und die Lösung färbt sich braun. Die Lösung wird filtriert und das Lösungsmittel abdestilliert. Der Rückstand, ein rotbraunes Öl, wird auf Al_2O_3 in Petroläther chromatographiert. Nach Abdestillieren des Lösungsmittels, scheiden aus dem gelblichen Öl ziegelrote Kristalle von **16** ab; Schmp. 155° (Zers.).

$C_{30}H_{28}Fe_2O_6$ (596,2) *Ber.*: C 60,43; H 4,73
Gef.: C 60,38; H 4,83

NOTE POUR LES AUTEURS

La *Revue Roumaine de Chimie* publie des articles en anglais, français, russe, allemand ou espagnol. Les auteurs sont priés d'envoyer des articles, notes, communications et comptes rendus inédits.

Les manuscrits seront dactylographiés à deux intervalles. Les tableaux seront dactylographiés sur feuilles séparées, de même que la légende des figures. Les diagrammes seront tracés à l'encre de Chine sur papier calque. Les tableaux et les figures seront numérotés par des chiffres arabes, en nombre strictement nécessaire. Prière de ne pas inscrire les mêmes données dans les tableaux et les figures. Les formules chimiques seront incluses dans le texte ; en outre, elles seront transcrites sur des feuilles séparées. Les auteurs sont priés d'indiquer les caractères italiques (en soulignant les lettres au crayon), ainsi que tout autre caractère spécial. L'ordre des références bibliographiques sera celui de leur mention dans le texte ; le nom de l'auteur sera précédé de l'initiale du prénom ; les publications périodiques seront présentées suivant les prescriptions internationales. Les références seront ajoutées à la fin de l'article ; elles paraîtront comme des notes, au bas de la page. Le texte sera précédé d'un résumé, comprenant 15 lignes au maximum.

L'entière responsabilité du contenu des articles appartient aux auteurs. On publie des articles dus aux collaborateurs roumains ou étrangers. Les auteurs recevront 50 tirés à part.

PRINTED IN ROMANIA

TRAVAUX PARUS AUX ÉDITIONS DE L'ACADÉMIE DE LA RÉPUBLIQUE SOCIALISTE DE ROUMANIE

CORNEL BODEA et collab., **Tratat de biochimie vegetală**, partea I, **Fitochimie** (Traité de biochimie végétale, Ire partie, Phytochimie), Ier vol., 1964, 747 p. + 4 annexes + 2 pl., 41 lei ; IIe vol., 1965, 1262 p., 1 pl., 56 lei ; IIIe vol., 1967, 773 p., 35 lei.

V. GHEŢIE et V. MICUŞAN, **Analiza imunochimică. Teorie şi practică** (Analyse immunochimique. Théorie et pratique), 1966, 369 p., 28 lei.

SILVIA IONESCU, **Reacţii chimice induse de radiaţiile ionizante** (Réactions chimiques produites par les radiations ionisantes), 1963, 271 p., 15 lei.

MARIETA NICOLAE, **Fizico-chimia proceselor fotografice** (Physico-chimie des processus photographiques), 1964, 426 p. + 4 pl., 35 lei.

R. PORTOCALĂ et L. POPA, **Acizii ribonucleici celulari şi virali** (Les acides ribonucléiques cellulaires et viraux), 1966, 375 p. + 8 pl., 26 lei.

D. PURDELA et R. VÎLCEANU, **Chimia compuşilor organici ai fosforului şi ai acizilor lui** (La chimie des composés organiques du phosphore et de ses acides), 1965, 540 p., 37 lei.

CRISTOFOR SIMIONESCU, MARGARETA GRIGORAŞ et AGATA CERNĂTESCU-ASANDEI, **Chimia lemnului din R.P.R.** (La chimie du bois en Roumanie), 1964, 239 p. + 6 pl., 27 lei.

CRISTOFOR SIMIONESCU et CLEOPATRA VASILIU-OPREA, **Mecanochimia compuşilor macromoleculari** (La mécanochimie des composés macromoléculaires), 1967, 314 p., 23,50 lei.

I. V. MAXIM, **Materiale nucleare** (Matériaux nucléaires), 1969, 444 p., 4 pl., 30 lei.

I.P.I. – c. 3505

43 436

Lei 15. –

F 1103

R 04

REVUE ROUMAINE DE CHIMIE

REFERALVA

TOME 14
N° 10
Octobre 1969

ÉDITIONS DE L'ACADÉMIE DE LA RÉPUBLIQUE SOCIALISTE DE ROUMANIE

Rev. Roumaine Chim. 14, 1191–1332 (1969), Bucarest

COMITÉ DE RÉDACTION

Rédacteur en chef :

C. D. NENIȚESCU, membre de l'Académie de la République Socialiste de Roumanie.

Rédasteurs en chef adjoints :

A. T. BALABAN et V. E. SAHINI, membres correspondants de l'Académie de la République Socialiste de Roumanie.

Collège de rédaction :

C. DRĂGULESCU, RALUCA RIPAN, CR. SIMIONESCU, membres de l'Académie de la République Socialiste de Roumanie ; EM. BRATU, membre correspondant de l'Académie de la République Socialiste de Roumanie, Pr G. OSTROGOVICH, MARG. AVRAM, F. BADEA, D. MARCHIDAN, D. NEGOIU et D. SĂNDULESCU.

Les manuscrits, les livres et les revues proposés en échange, ainsi que toute correspondance seront envoyés à la rédaction :

REVUE ROUMAINE DE CHIMIE

23, str. Dumbrava Roşie, Bucarest, Roumanie.

F 1103

REVUE ROUMAINE
DE
CHIMIE

Tome 14, No 10 Octobre 1969

Page

MARGARETA AVRAM, I. G. DINULESCU, GH. D. MATEESCU und C. D. NENITZESCU, Untersuchungen in der Cyclobutanreihe. XXII. Ein Hexacarbomethoxy-Dewar-Benzol-Komplex aus Acetylendicarbonsäure-Dimethylester und Bis-Benzonitril-Palladiumchlorid . . . . 1191–1200 ✓

I. G. MURGULESCU and M. I. VASS, Calorimetric determination of the chemisorption heat of oxygen on thin copper films . . . . 1201–1214 ✓

S. STERNBERG and AGNETA CERBU, The behaviour of certain synthetic zeolites in molten salts media . . . . 1215–1223 ✓

IOANA DEMETRESCU, About the conductivity of solutions of hydrobromic acid in normal alcohols . . . . 1225–1229 ✓

CONST. GH. MACAROVICI et MARIA VOLUŞNIUC-BIROU, Combinaisons complexes avec des hydroxyacides. IX. Complexes de l'étain tétravalent avec les acides gluconique et saccharique et leurs sels alcalins . . . . 1231–1239 ✓

J. DICK, ALFA LUPEA und Z. SZABADAI, Komplexverbindungen des N,N'-Diaminopiperazins. III. Sichtbare- und UV-Spektren 1241–1249

F. MÁNOK, CS. VÁRHELYI und ZSUZSANNA KISS-RAJHONA, Über α-Dioximinkomplexe der Übergangsmetalle. XXVI. Kupfer(II)-Chelate mit 1,2-Cyclohexandiondioxim 1251–1256

C. LITEANU und GH. RĂDULESCU, Untersuchung der Gleichrichtungseigenschaften der heterogenen Membranen. II. Das Verhalten einer einheitlichen Celluloid : Kationit-H + Anionit-OH Membran gegenüber Wechselstrom von 50 Hz und bei Direktspannungen 1257–1262

C. CHIRIAC, LEONIA STOICESCU CRIVETZ et I. ZUGRĂVESCU, Polypyrazoles. III. N-Arylation des pyrazoles . . . . 1263–1267 ✓

TH. DELEANU and N. GEORGESCU, Considerations on electrical conduction mechanisms in polymers from liquid paraffinic hydrocarbons data . . . 1269–1279

A. T. BALABAN, Oxidation of pyrocatechol derivatives to *o*-quinones by iodosobenzene diacetate 1281–1284

I. SIMITI, LIDIA PROINOV et H. DEMIAN, Contribution à l'étude de quelques hétérocycles. XII. L'halogénation et la nitration de l'anilino-2-méthyl-5-thiodiazole-1,3,4 1285–1294

O. MANTSCH und N. BODOR, Kinetik und Mechanismus der Veresterungsreaktion von Steroidalkoholen mit Acetylnitrat 1295–1302

Rev. Roumaine Chim. **14,** 1191–1332 (1969), Bucarest

Page

F. HODOŞAN, N. ŞERBAN and VICTORIA CIURDARU, Unsymmetrical diacyl derivatives of methyl hyodesoxycholate 1303–1307

Н. К. ФРУНЗЕ, Некоторые вопросы фотосинтеза сополимеров сетчатой структуры с образованием рельефных изображений 1309–1321

A. T. BALABAN, Aromaticity. VI. Electronic absorption spectra of *o*-Phenylene carbonate and of its conjugate acid 1323–1330

A. T. BALABAN, Pyrylium salts formed by diacylation of olefins, XIX. Characterization of olefins by diacylation: acid dealkylation of 3,5-Di-t-butylpyrocatechol . . . . , ... 1331–1332

Revue Roumaine de Chimie, **14**, 1191 – 1200 (1969)

UNTERSUCHUNGEN IN DER CYCLOBUTANREIHE. XXII.[1]

EIN HEXACARBOMETHOXY-DEWAR-BENZOL-KOMPLEX AUS ACETYLENDICARBONSÄURE-DIMETHYLESTER UND BIS-BENZONITRIL-PALLADIUMCHLORID

MARGARETA AVRAM, I. G. DINULESCU, GH. D. MATEESCU und
C. D. NENITZESCU

Aus dem Organisch-Chemischen Institut der Akademie, Bukarest, Spl. Independenţei 202 B

Eingegangen am 25. April 1969

Acetylendicarbonsäure-dimethylester verbindet sich mit Bis-benzonitril-palladiumchlorid in Benzol zu einem Komplex der Zusammensetzung $(CH_3O_2C-C\equiv C-CO_2CH_3)_3\cdot PdCl_2$ (**1**). Der organische Ligand ist Hexacarbomethoxybicyclo [2.2.0]hexa-2.5-dien (Hexacarbomethoxy-Dewar-Benzol). Aus Acetylendicarbonsäure-dimethylester und Dieisen-enneacarbonyl entsteht der Hexacarbomethoxy-Dewar-Benzol · $Fe(CO)_3$-Komplex (**4**). Nach Abscheidung des Palladiumchlorids aus **1** mit Kaliumcyanid entsteht der Mellithsäure-methylester. Mit Wasserstoff, Chlor oder Brom bilden sich Produkte mit einem Cyclohexadien-Skelett (**5**, **6** und **7**). Es wird ferner gezeigt, daß bei der Bildung von Hexaphenylbenzol aus Tolan, in Gegenwart von Bis-benzonitril-palladiumchlorid, als Zwischenstufe ein instabiler Hexaphenyl-Dewar-Benzol · $PdCl_2$-Komplex (**14**) entsteht.

In einer vorhergehenden Mitteilung[1] wurde gezeigt, daß das tert.-Butyl-phenyl-acetylen mit Bis-benzonitril-palladiumchlorid einen Di-tert.-butyl-diphenyl-cyclobutadien-palladiumchlorid-Komplex bildet, ähnlich wie das Diphenylacetylen.[2–8] In der Hoffnung, daß sich der Acetylendicarbonsäure-dimethylester ähnlich verhalten wird, wurde dieser Ester mit Bis-benzonitril-palladiumchlorid umgesetzt.

Es enstand eine rote Verbindung (Schmp. 175°; Zers.), $C_{18}H_{18}O_{12}PdCl_2$ (**1**). Es verbinden sich also drei Mol Acetylendicarbonsäure-dimethylester mit einem Mol Palladiumchlorid.

---

[1] XXI. Mitteil. : M. Avram, I. G. Dinulescu, Gh. D. Mateescu, E. Avram und C. D. Nenitzescu, *Rev. Roumaine Chim.*, **14**, 1181 (1969)

[2] L. Malatesta, G. Santarella, L. Vallarino und F. Zingales, *Angew. Chem.*, **72**, 34 (1960).

[3] A. T. Blomquist und P. M. Maitlis, *J. Amer. Chem. Soc.*, **84**, 2329 (1962).

[4] P. M. Maitlis, D. Pollock, M. L. Games und W. J. Pryde, *Canad. J. Chem.*, **43**, 470 (1965).

[5] P. M. Maitlis und M. L. Games, *Canad. J. Chem.*, **42**, 183 (1964).

[6] R. Hüttel und H. J. Neugebauer, *Tetrahedron Letters*, **1964**, 3541.

[7] R. C. Cookson und D. W. Jones, *J. Chem. Soc.*, **1965**, 1881.

[8] J. Tsuji und T. Nogi, *J. Amer. Chem. Soc.*, **88**, 1289 (1966).

Bei Behandlung des Komplexes **1** mit Kaliumcyanidlösung erhält man Mellithsäure-methylester (**2**), welcher durch Misch.-Schmp., IR- und NMR-Spektren identifiziert wurde.

Die Bildung von Benzolderivaten durch Trimerisierung von Acetylenderivaten, in Gegenwart von Verbindungen der transitionalen Metallen oder von Metall-carbonylen als Katalysatoren, ist schon lange bekannt.[9–28] Die Entstehung von Dewar-Benzolen auf diesem Wege ist unseres Wissens noch nicht beobachtet worden.

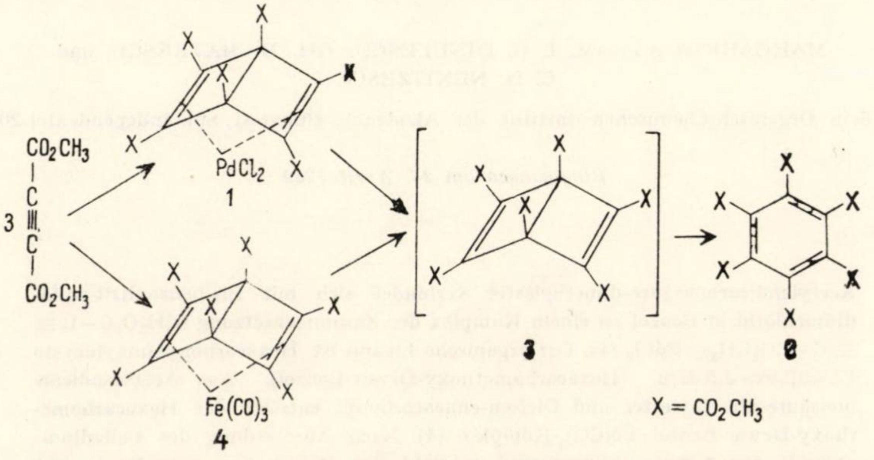

---

[9] W. Reppe und W. J. Schweckendiek, *Liebigs Ann. Chem.*, **560**, 104 (1948).

[10] J. D. Rose, F. S. Statham, *J. Chem. Soc.*, **1950**, 69; J. C. Sauer und T. L. Cairns, *J. Amer. Chem. Soc.*, **79**, 2659 (1957); T. L. Cairns, V. A. Engelhardt, H. L. Jackson, G. H. Kalb und J. C. Sauer, *ibid.*, **74**, 5636 (1952); T. I. Bieber, *Chem. & Ind.*, **1957**, 1126.

[11] G. N. Schrauzer und S. Eichler, *Angew. Chem.*, **73**, 546 (1961); G. N. Schrauzer, *Chem. Ber.*, **94**, 1403 (1961); G. N. Schrauzer und S. Eichler, *Chem. Ber.*, **95**, 550 (1962); G. N. Schrauzer, S. Eichler und D. A. Brown, *Chem. Ber.*, **95**, 2755 (1962); G. N. Schrauzer, P. Glockner und S. Eichler, *Angew. Chem.*, **76**, 28 (1964).

[12] J. R. Leto und M. F. Leto, *J. Amer. Chem. Soc.*, **83**, 2944 (1961).

[13] F. D. Mango und J. H. Schachtschneider, *J. Amer. Chem. Soc.*, **89**, 2484 (1967).

[14] W. Hübel und C. Hoogzand, *Chem. Ber.*, **93**, 103 (1960).

[15] U. Krüerke und W. Hübel, *Chem. Ber.*, **94**, 2829 (1961).

[16] U. Krüerke, C. Hoogzand und W. Hübel, *Chem. Ber.*, **94**, 2817 (1961).

[17] E. M. Arnett und J. M. Bollinger, *J. Amer. Chem. Soc.*, **86**, 4729 (1964).

[18] E. M. Arnett und M. E. Strem, *Chem. & Ind.*, **1961**, 2008; E. M. Arnett, M. E. Strem und R. A. Friedel. *Tetrahedron Letters*, 658 (**1961**).

[19] E. M. Arnett, J. M. Bollinger und J. C. Sanda, *J. Amer. Chem. Soc.*, **87**, 2050 (1965).

[20] C. Hoogzand und W. Hübel, *Tetrahedron Letters*, **1961**, 637.

[21] P. Chini, A. Santambrogio und N. Palladino, *J. Chem. Soc.*, **1967**, 830.

[22] J. P. Martella und W. C. Kaska, *Tetrahedron Letters*, **1968**, 4889.

[23] H. H. Zeiss und W. Herwig, *J. Amer. Chem. Soc.*, **80**, 2913 (1958); M. Tsutsui und H. Zeiss, *J. Amer. Chem. Soc.*, **82**, 6255 (1960).

[24] W. Herwig, W. Metlesics und H. Zeiss, *J. Amer. Chem. Soc.*, **81**, 6203 (1959).

[25] G. M. Whitesides und W. J. Ehmann, *J. Amer. Chem. Soc.*, **90**, 804 (1968).

[26] H. Dietl und P. M. Maitlis, *Chem. Comm.*, **1968**, 481; H. Reinheimer, H. Dietl, J. Moffat, D. Wolff und P. M. Maitlis, *J. Amer. Chem. Soc.*, **90**, 5321 (1968).

[27] V. O. Reikhsfel'd, K. L. Makovetskii und L. L. Erokhina, Brev. UdSSR, 166.007 (1964); *Chem. Abstr.*, **62**, 10367 (1964); *Zhur. Obshchei Khim.*, **34**, 3505 (1964); K. L. Makovetskii, B. I. Lein, V. O. Reikhsfel'd, *Zhur. Org. Khim.*, **2**, 753 (1966).

[28] D. Bryce-Smith, *Chem. & Ind.*, **1964**, 239.

Da der Mellithsäure-methylester mit Bis-benzonitril-palladiumchlorid keinen $PdCl_2$-Komplex bildet und bis heute noch keine $PdCl_2$-Komplexe von Benzolderivaten bekannt sind, schrieben wir dem Liganden in dem aus Acetylendicarbonsäure-dimethylester erhaltenen Komplex die Struktur des Hexacarbomethoxy-bicyclo[2.2.0]hexa-2,5-diens, das heißt des Hexacarbomethoxy-Dewar-Benzols zu.

In letzter Zeit wurden Metallkomplexe ausgehend von Dewar-Benzolderivaten dargestellt und zwar von Dewar-Benzol selbst[29] und von Hexamethyl-Dewar-Benzol.[30-32] Direkt aus Acetylenderivaten scheinen solche Komplexe noch nicht erhalten worden zu sein.

Eine Bicyclotrimerisierung des Acetylendicarbonsäure-dimethylesters findet auch in Gegenwart von Dieisen-enneacarbonyl in Benzol statt. Der so entstandene Komplex $C_{18}H_{18}O_{12} \cdot Fe(CO)_3$ **4** ist violett-schwarz und gibt bei der Zersetzung mit Ce^{IV} oder mit Brom den Mellithsäure-methylester (**2**). Versuche das Hexacarbomethoxy-Dewar-Benzol (**3**) durch Entfernung des Metalls aus den Komplexen **1** oder **4** zu erhalten, blieben erfolglos. Dies ist wohl einer labilisierenden Wirkung der Carbomethoxygruppen auf das Bicyclo[2.2.0]hexa-2,5-dien-system zuzuschreiben. Stabilisierende Effekte von Alkylgruppen und labilisierende Effekte von konjugationsfähigen Gruppen wie die Carbomethoxy- und Phenylgruppen wurden auch in anderen Fällen beobachtet.[33-38]

Beim Schütteln einer Suspension von **1**, in Methanol mit Wasserstoff scheidet sich metallisches Palladium aus und die Lösung wird sauer. Es werden Kristalle mit der Bruttoformel $C_{18}H_{19}O_{12}Cl$ isoliert, welche bei der Behandlung mit Natriummethoxid in Mellithsäure-methylester übergehen. Das NMR-Spektrum der chlorhaltigen Verbindung zeigt ein Signal bei δ 5.64 ppm (1 H) und sechs Linien bei δ 3,30, 3,31, 3,36, 3,37, 3,56, 3,63 ppm (in C_6D_6, 100 Mc/s) entsprechend den 18 Protonen der Methylgruppen. Spektrum und Verhalten entsprechen einem Dihydrobenzoderivat **5**.

Behandelt man den Komplex **1** in Methylenchlorid-Lösung mit Chlor so erhält man ein Dichlorid $C_{18}H_{18}O_{12}Cl_2$ (**6**) Schmp. 121°. Abspaltung des Halogens mit Lithiumamalgam in Äther führt zu Mellithsäure-methylester. Das NMR-Spektrum von **6** zeigt vier Signale bei δ 3,33,

---

[29] E. E. van Tamelen und D. Carty, *J. Amer. Chem. Soc.*, **89**, 3922 (1967).

[30] H. Dietl und P. M. Maitlis, *Chem. Comm.*, **1967**, 759; P. V. Balakrishnan und P. M. Maitlis, *Chem. Comm.*, **1968**, 1303.

[31] E. O. Fischer, W. Berngruber und C. G. Kreiter, *Chem. Ber.*, **101**, 824 (1968); E. O. Fischer, C. G. Kreiter und W. Berngruber, *Angew. Chem.*, **79**, 623 (1967).

[32] B. L. Booth, R. N. Haszeldine und M. Hill, *Chem. Comm.*, **1967**, 1118; H. C. Volger und H. Hogeveen, *Rec. Trav. chim.*, **86**, 830 (1967); J. W. Kang, P. M. Maitlis, *J. Amer. Chem. Soc.*, **90**, 3259 (1968).

[33] W. Schäfer und H. Hellmann, *Angew. Chem.*, **79**, 566 (1967).

[34] E. E. van Tamelen und S. P. Pappas, *J. Amer. Chem. Soc.*, **85**, 3297 (1963).

[35] G. D. Burt und R. Pettit, *Chem. Comm.*, **1965**, 517; J. D. Fitzpatrick, L. Watts, G. F. Emerson und R. Pettit, *J. Amer. Chem. Soc.*, **87**, 3254 (1965).

[36] R. Breslow, P. Gal, H. W. Chang und L. J. Altman, *J. Amer. Chem. Soc.*, **87**, 5139 (1965).

[37] R. Criegee und R. Askani, *Angew. Chem.*, **78**, 494 (1966).

[38] D. Seebach, *Angew. Chem.*, **77**, 119 (1965).

3,39, 3,44, 3,46 ppm (in C_6D_6 bei 100 Mc/s) im Verhältnis 2 : 1 : 2 : 1 entsprechend den vier verschiedenen Carbomethoxygruppen. Dieses weist darauf hin, daß die Carbomethoxygruppen vicinal zu den Chloratomen nicht äquivalent sind.

Beim Behandeln von **1** mit Brom entsteht ein Chloro-bromid, $C_{18}H_{18}O_{12}ClBr$, **7**, welches bei der Abspaltung des Halogens mit Lithiumamalgam ebenfalls in Mellithsäure-methylester übergeht. Das NMR-Spektrum des Chloro-bromides **7** zeigt sechs Linien bei δ 3,34, 3,37, 3,40, 3,45, 3,46, 3,57 ppm (in C_6D_6, 100 Mc/s) entsprechend den sechs verschiedenen Carbomethoxygruppen.

Die Substanzen **5**, **6** und **7** addieren keine Halogene, hydrieren sich nicht in Gegenwart von Pd/C und oxydieren sich nicht mit Ozon. Sie sind bei einer Std. Erwärmen auf 160–170° temperaturbeständig. Sie bilden keine Komplexe mit Bis-benzonitril-palladiumchlorid.

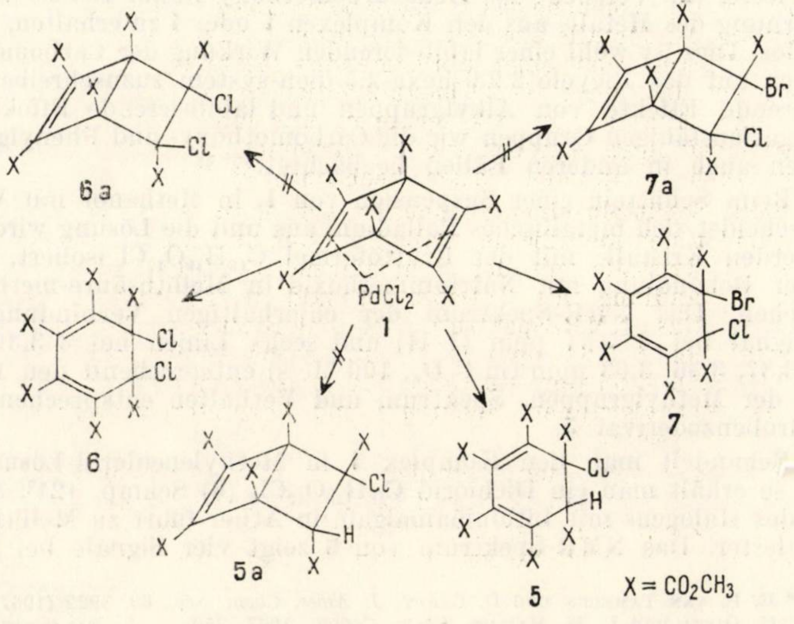

Für die Verbindungen **5**, **6** und **7** kommen ebenso die Bicyclo-[2.2.0]hexen-Strukturen **5a**, **6a** und **7a** in Betracht. Ein Entscheid zwischen **5**–**7** und **5a**–**7a** war aufgrund der UV-Spektren möglich (Tabelle 1 und Abb. 1).

Tabelle 1

Das UV-Spektren der Verbindungen 5, 6 und 7

Verbindungen	λ max mμ	lg ε
5	300	3,497
6	300	3,500
7	296,5	3,674

Die Absorptionsbanden um 300 mμ entsprechen den konjugierten Cyclohexadien-Systemen **5**, **6**, **7** und schließen die bicyclischen Strukturen **5a**, **6a**, **7a** aus. In Abb. 1 sind die Spektren der Substanzen **5**, **6** und **7**, neben den Spektren des Cyclobuten-1.2-dicarbonsäure-dimethylesters (**8**) (mit λ_{max} 228 mμ ; lg ε 4,079) und des 1,4-Dicarbomethoxy-2,3-dimethyl-cyclohexan-1,3-diens (**9**) (mit λ_{max} 301 mμ ; lg ε 4,059) [39] wiedergegeben. Wie ersichtlich stimmen die Maxima der Absorptionsbanden

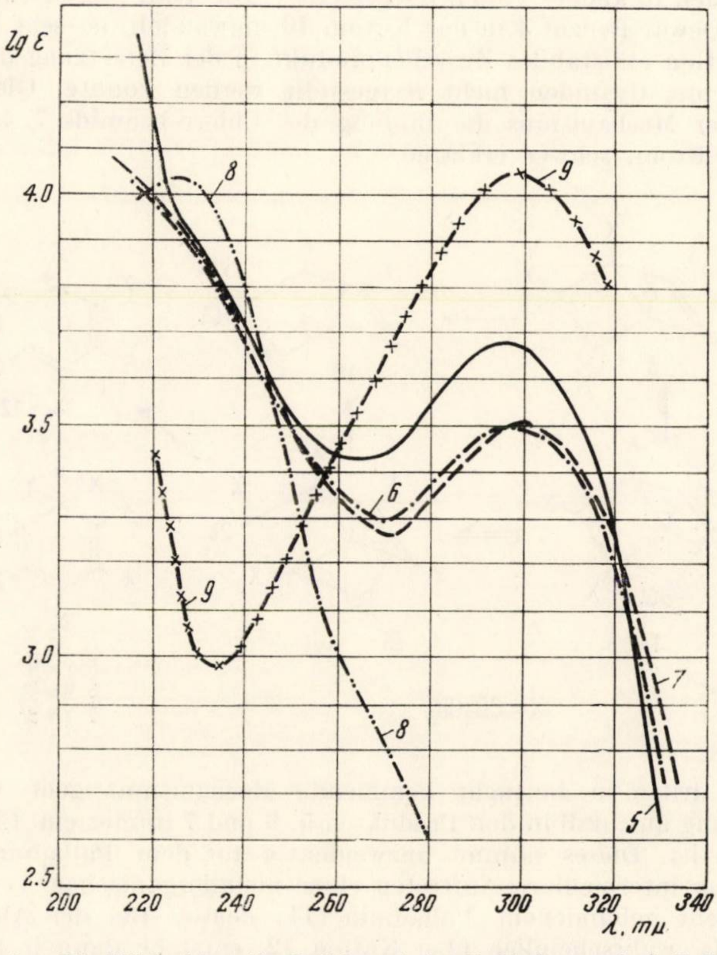

Abb. 1. – Die UV-Spektren (in Cyclohexan) der Verbindungen **5**, **6**, **7**, **8**, **9**.

von **5**, **6** und **7** mit dem Absorptionsband des Cyclohexadiens **9** überein. Die Extinktionen der Verbindungen **5**, **6** und **7** sind von derselben Größenordnung. Die kleine Extinktion von **5**, **6** und **7** im Vergleich mit **9** ist wohl auf die Nichtkoplanarität der beiden Carbomethoxygruppen in der 2,3 Stellungen des Cyclohexadiensystems zurückzuführen.[40]

---

[39] D. Seebach, *Chem. Ber.*, **97**, 2953 (1964).

Für die Entstehung der Cyclohexadiene **5**, **6** und **7** sind folgende drei Wege denkbar. Erst bildet sich das Dewar-Benzol **3**, welches dann Salzsäure, Chlor oder Chlorbrom addiert und in **5a**, **6a** oder **7a** übergeht. Die Cyclohexadiene **5**, **6** und **7** könnten ferner durch die Umlagerung des Bicyclo[2.2.0]hexenil-kations **10** entstehen. Ähnliche Umlagerungen wurden auch in andere Fällen festgestellt.[33] Die Wahrscheinlichkeit, daß sich das Dewar-Benzol **3** in das Kation **10** umwandelt ist sehr klein, da dieses Kation als stabiles Zwischenprodukt in der Zersetzung des Komplexes **1** mit Cyaniden nicht festgestellt werden konnte. Gleichzeitig kann dieser Mechanismus die Bildung des Chloro-bromids **7**, bei Überschuß an Brom, schwer erklären.

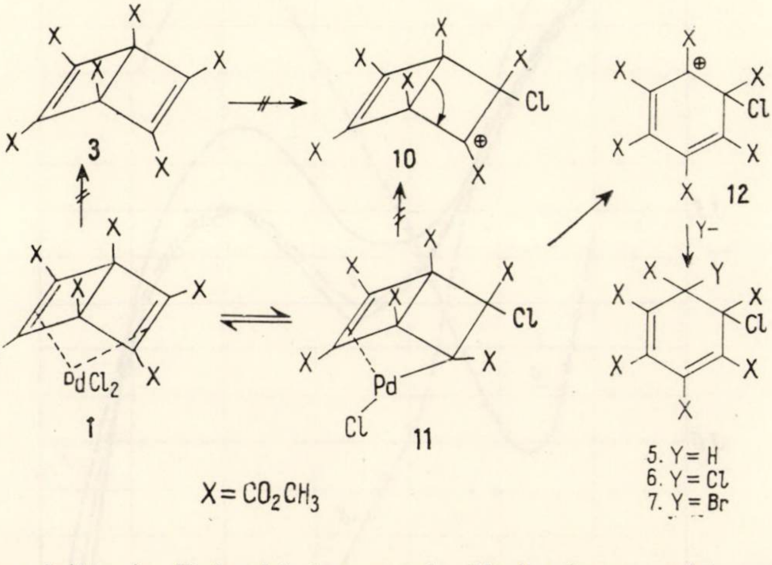

Der dritte in Betracht kommende Mechanismus geht von der Beobachtung aus, daß in den Produkten **5**, **6** und **7** immer ein Chloratom vorhanden ist. Dieses stammt unzweideutig aus dem Palladiumchlorid, was auf das intermediäre Auftreten einer metallorganischen Verbindung mit kovalent gebundenem Palladium (**11**) deutet. Bei der Abspaltung des Metalls, wahrscheinlich über Kation **12**, entsteht dann je nach den Reaktionsbedingungen eines der Reaktionsprodukte **5**, **6** oder **7**.

Versucht man das Palladiumchlorid aus dem Komplex **1** durch Triphenylphosphin zu entfernen, so erhält man einen Komplex **13** mit der Bruttoformel $C_{18}H_{18}O_{12}Cl_2Pd \cdot P(C_6H_5)_3$. Aus diesem kann das Palladium nicht durch Kaliumcyanid entfernt werden, jedoch gelingt die Abscheidung des Metalls mit Salzsäure. Es entsteht das Chlorid **5**, neben einem Triphenylphosphin-palladiumchlorid-Komplex.

---

[40] W. R. Brode, „Chemical Spectroscopy", Ed. II, J. Wiley & Sons. Inc., New-York, 1947.

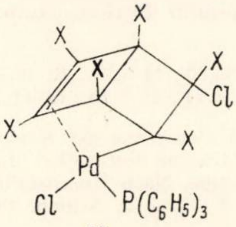

13

$X = CO_2CH_3$

Die oben beschriebenen Beobachtungen bei der Komplexbildung des Acetylendicarbonsäure-dimethylesters mit Palladiumchlorid ließen die Frage auftreten ob die Bildung des Hexaphenylbenzols [2-4] aus Tolan in Gegenwart von Bis-benzonitril-palladiumchlorid nicht auch über einen Hexaphenyl-Dewar-Benzol$\cdot PdCl_2$ Komplex (**14**) verläuft. In der Tat stellten wir fest, daß unter milden Bedingungen in dieser Reaktion erst der Komplex **14** entsteht und isoliert werden kann. Der Komplex **14** ist aber viel instabiler als **1** und scheidet bei längerem Stehen, beim Erhitzen oder bei Reinigungsversuchen Palladium aus, wobei nur Hexaphenylbenzol isoliert wurde.

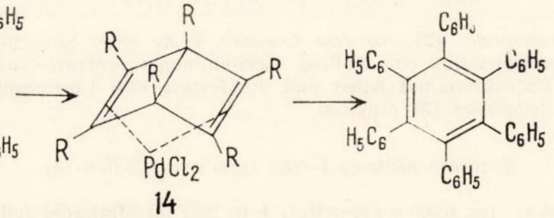

14

($R = C_6H_5$)

BESCHREIBUNG DER VERSUCHE

Die Mikroanalysen wurden von Frl. E. Şliam und Frau V. Daniel ausgeführt. Die IR-Spektren wurden mit einem automatischen UR20 Carl Zeiss Jena Doppelstrahlspektralphotometer, die UV-Spektren mit einem VSU1 Carl Zeiss Jena Spektralphotometer und die NMR-Spektren mit einem Varian A-60A und einem Varian HA-100 Spektrometer (innerer Standard TMS) aufgenommen.

Hexacarbomethoxy-bicyclo[2.2.0]hexa-2,5-dien-palladiumchlorid (**1**)

In eine Lösung von 3,8 g (10 mMol) Bis-benzonitril-palladiumchlorid in 80 ml absol. Benzol werden 5,0 g (35 mMol) Acetylendicarbonsäure-dimethylester eingetragen. Nach 24stdg. Stehen bei Zimmertemperatur wird die rote Lösung mit 300 ml Petroläther (Sdp. 40 – 50°) versetzt.

Der ziegelrote Niederschlag wird filtriert und mit Ligroin gewaschen (durch Dekantieren). Ausb. : 5,6—5,7 g (93—95%) an einem orangeroten Komplex, löslich in Methanol, Benzol, Chloroform, unlöslich in Äther und Ligroin.

5 g dieser Substanz werden mit 50 ml Methanol bis zur totalen Lösung gerührt und nach 24stdg. Stehen bei Zimmertemperatur filtriert. Ausb. : 3,5 g (70%) **1**, Schmp. 170° (Zers.) ; schwer löslich in Methanol.

$C_{18}H_{18}Cl_2O_{12}Pd$ (603,9) *Ber.* : C 35,80 ; H 3,00 ; Cl 11,75 ; Pd 17,66
Gef. : C 35.71 ; H 3.13 ; Cl 11.71 ; Pd 17.95

Mellithsäure-methylester (**2**) *durch Umsetzung des Komplexes* **1** *mit Kaliumcyanid.* Man rührt 1,2 g (2mMol) **1** mit Kaliumcyanidlösung und isoliert die gebildeten Kristalle entweder durch Filtrieren oder durch Ätherextraktion. Nach Umkristallisieren oder nach Chromatographieren (Äther/Al_2O_3) erhält man 0,8 g (95%) **2**, Schmp. 192°.

$C_{18}H_{18}O_{12}$ (426,3) *Ber.* : C 50,72 ; H 4,25
Gef. : C 50,76 ; H 4,36

Molekulargewicht : *Ber.* : 426,3 ; *Gef.* ; 430 (Rast).

Das IR-Spektrum ist identisch mit dem Spektrum eines authentischen Präparats ; der Misch.-Schmp. zeigt keine Depression.

Hexacarbomethoxy-bicyclo[2.2.0]hexa-2.5-dien-Eisen-tricarbonyl (**4**).

In einem Schlenkrohr werden 1,42 g (10 mMol) Acetylendicarbonsäure-dimethylester in 1 ml absol. Benzol gelöst, mit 0,9 g (2,5 mMol) Dieisen-enneacarbonyl versetzt und in einer Argonatmosphäre 8 Std. auf 50° erwärmt. Man filtriert den schwarzen Niederschlag ; Ausb. : 1,3 g (92%) **4**.

$C_{21}H_{18}O_{15}Fe$ (566,2) *Ber.* : C 44,55 ; H 3,20 ; Fe 9,86
Gef. : C 44,12 ; H 3,91 ; Fe 11,15

Mellithsäure-methylester (**2**) *aus dem Komplex* **4**. Zu einer Suspension von 0,50 g **4** in Methanol wird unter Umrühren eine wäßrige Ceri-ammonium-nitratl-ösung im Überschuß zuzugegeben. Nach Extraktion mit Äther und Entfernen des Lösungsmittels werden 0,3 g (70%) *Mellithsäure-methylester* (**2**) erhalten.

Hexacarbomethoxy-5-chlor-cyclohexa-1,3-dien (**5**)

Eine Suspension aus 6,03 g (10 mMol) **1** in 200 ml Methanol (oder 100 ml Tetrahydrofuran) und 50 mg Pd/C 30% wird mit Wasserstoff geschüttelt. Nach einigen Min. scheidet sich metallisches Palladium aus und die Lösung entfärbt sich ; es werden ungefähr 440 ml Wasserstoff absorbiert. Nach Filtrieren der festen Teile und Abdestillieren des Lösungsmittels i. Vak. wird der ölige Rückstand mit Äther auf Al_2O_3 chromatographiert. Ausb. : 2,7—3,0 g (59—65%) **5** ; Schmp. 95° (aus Methanol).

$C_{18}H_{19}ClO_{12}$ (462,8) *Ber.* : C 46,72 ; H 4,14 ; Cl 7,66
Gef. : C 46,74 ; H 4,25 ; Cl 8,00

Eliminierung von Salzsäure aus **5**. Zu einer Lösung von 0,46 g (1 mMol) **5** in 10 ml Methanol gibt man eine Natriummethoxidlösung im Überschuß (0,1 g Na in 5 ml Methanol) hinzu. Nach 5 Min. langem Erwärmen wird das Methanol abgedampft, der Rückstand mit Wasser versetzt und mit Äther ausgezogen. Nach Chromatographieren auf Al_2O_3 erhält man 0,22 g (32%) *Mellithsäure-methylester.* Die IR- und NMR-Spektren sind identisch mit den vorher erhaltenen.

Hexacarbomethoxy-5,6-dichlor-cyclohexa-1,3-dien (**6**)

In eine Suspension von 0,6 g (1 mMol) **1** in 10 ml Methylenchlorid führt man Chlor bis zur Sättigung ein. Die erhaltene Lösung scheidet nach 0,5 Std. Palladiumchlorid aus. Das

Filtrat wird i. Vak. eingeengt. Der ölige Rückstand kristallisiert beim Anfeuchten mit einigen Tropfen Methanol. Ausb.: 0,45 g (91%) **6**, Schmp. 121° (aus Methanol).

$C_{18}H_{18}Cl_2O_{12}$ (497,3) *Ber.*: C 43,47; H 3,65; Cl 14,26

Gef.: C 43,49; H 3,73; Cl 14,36

Hexacarbomethoxy-5-chlor-6-brom-cyclohexa-1,3-dien (**7**)

Zu 0,6 g (1 mMol) **1**, in 5 ml Methylenchlorid suspendiert, wird eine Lösung von 0,3 ml (3 mMol) Brom in 5 ml Methylenchlorid zugegeben. Nach 0,5 Std. wird das ausgeschiedene PdClBr, abfiltriert, die Lösung mit Bisulfit entfärbt und i. Vak. bis zur Trockene eingedampft. Der Rückstand kristallisiert durch Anfeuchten mit Methanol oder Tetrahydrofuran. Man erhält 0,43 g (83%) **7**, Schmp. 132° (aus Methanol oder Tetrahydrofuran).

$C_{18}H_{18}BrClO_{12}$ (541,7) *Ber.*: C 39,92; H 3,34; Cl 6,54; Br 14,75

Gef.: C 39,84; H 3,49; Cl 7,09; Br 15,45

Abspaltung des Halogens aus **7** *mit Lithiumamalgam.* Eine Lösung von 0,27 g (0,5 mMol) **7** in 10 ml Tetrahydrofuran wird mit 10 g Lithiumamalgam (0,5%) 0,5 Std. geschüttelt, dann filtriert, mit Äther verdünnt und mit Wasser gewaschen. Nach Abdampfen des Äthers werden 0,18 g (78%) *Mellithsäure-methylester*, Schmp. 192° (aus Methanol) erhalten (Nachweis durch die IR- und NMR-Spektren).

Abspaltung des Halogens aus **7** *mit* $Fe_2(CO)_9$. Zu einer Lösung von 0,27 g (0,5 mMol) **7** in 5 ml Benzol werden, unter Argon, 0,18 g (0,5 mMol) $Fe_2(CO)_9$ eingetragen. Nach Beendigung der Reaktion (Aufhören der Kohlenoxidentwicklung) wird filtriert und der Niederschlag mit Benzol gewaschen. Nach Abdestillieren der vereinten Lösungsmittel und Umkristallisieren des Rückstandes aus Methanol wird *Mellithsäure-methylester* erhalten (Nachweis durch Misch.-Schmp. und IR-Spektrum).

Reaktion des Komplexes **1** *mit Triphenylphosphin*

In eine Suspension von 1,5 g (2,5 mMol) **1** in 20 ml Äther wird eine Lösung von 0,7 g (2,6 mMol) Triphenylphosphin in 30 ml Äther zugegeben und die Reaktionsmasse 1/2 Std. gerührt; der rote Komplex **1** verschwindet und es scheidet ein gelber Niederschlag aus. Man filtriert und erhält 2 g (93%) **13**; Schmp. 170° (Zers.)

$C_{36}H_{33}Cl_2O_{12}PPd$ (865,9) *Ber.*: C 49,93; H 3,84

Gef.: C 49,28; H 3,95

Zersetzung des Komplexes **13** *mit Salzsäure.* In eine Lösung von 0,43 g (0,5 mMol) **13** in 10 ml Methylenchlorid wird gasförmige Salzsäure eingetragen. Die anfänglich gelbe Lösung wird nach 12 Std. rot und scheidet orangefarbige Kristalle eines Triphenylphosphin-palladiumchlorid-Komplexes ab. Nachweis durch Vergleich des IR-Spektrums dieser Kristalle mit dem eines authentischen Präparats. Das Methylenchlorid wurde i. Vak. bis zur Trockene abdestilliert, der Rückstand in Äther gelöst und über Al_2O_3 chromatographiert; weiße Kristalle von **5**; Schmp. 95°. Das IR-Spektrum ist identisch mit dem Spektrum des beschriebenen Produktes **5**.

$C_{18}H_{19}ClO_{12}$ (462,8) *Ber.*: C 46,72; H 4,14; Cl 7,66

Gef.: C 46,70; H 4,33; Cl 7,88

Hexaphenyl-bicyclo[2.2.0]hexa-2,5-dien-palladiumchlorid (**14**).

Eine Lösung von 0,384 g (1 mMol) Bis-benzonitril-palladiumchlorid in 30 ml Benzol wird, bei 5–10°, mit eine Lösung von 0,534 g (3 mMol) Tolan in 20 ml Benzol versetzt.

Aus der entfärbten Lösung scheidet sich ein rosaweißer Niederschlag ab, welcher nach 6 Std. filtriert und mit Ligroin gewaschen wird. Ausb. : 0,5 g (70 %) **14**, welcher roh analysiert wurde.

$C_{42}H_{30}Cl_2Pd$ (712,0) *Ber.* : C 70,85 ; H 4,24 ; Cl 9,96 ; Pd 14,25

Gef. : C 74,74 ; H 4,81 ; Cl 8,33 ; Pd 12,62

Der Komplex **14** ist unbeständig ; er zersetzt sich bei längerem Aufbewahren und kann weder umkristallisiert noch chromatographiert werden.

Hexaphenylbenzol aus **14**. *a. Mit Kaliumcyanid.* Zu einer Suspension von 1,3 g **14** in Äther wird eine Lösung von Kaliumcyanid zugegeben. Es scheidet Hexaphenylbenzol aus ; Schmp. über 360°. Das IR-Spektrum ist identisch mit dem eines authentischen Präparates. *b. Durch Hydrierung.* Schon während der Vertreibung der Luft mit Wasserstoff, in Tetrahydrofuran scheidet metallisches Pd ab und es findet Lösung statt. Das entstandene Hexaphenylbenzol wurde wie oben identifiziert.

Revue Roumaine de Chimie, **14**, 1201–1214 (1969)

CALORIMETRIC DETERMINATION OF THE CHEMISORPTION HEAT OF OXYGEN ON THIN COPPER FILMS

I. G. MURGULESCU and M. I. VASS

Institute of Physical Chemistry of the Academy, str. Dumbrava Roşie 23,
Bucharest, Romania

Received January 23, 1969

The chemisorption heat of oxygen on evaporated copper films has been determined at 273°K with a modified Beeck type calorimeter. The change in the electric resistance of the copper films during chemisorption was simultaneously measured. The differential heat of chemisorption is constant up to monolayer coverage. The possible forms of the oxygen bonds on copper surface are discussed.

There are few works[1–11] dealing with the direct calorimetric determinations of the adsorption heat of gases on thin metallic films. The main cause of this fact lies in the experimental difficulties which appear when adapting the calorimetrical techniques in ultravacuum as well as in the small amount of heat evolved due to the adsorption of a monomolecular layer (approximately 0.01 cal for a monolayer whose adsorption heat is 100 kcal/mole and a surface of 100 cm^2). That is why the first works indicate only the integral adsorption heat, the determination of the differential adsorption heat being carried out later after the improvement of the technique.

Oxygen adsorption on various metallic films has been studied by Brennan and co-workers[5, 11] and Wedler.[7a,b]

---

[1] O. Beeck, W. A. Cole and A. Wheeler, *Discuss. Faraday Soc.*, **8**, 314 (1950).

[2] M. Wahba and C. Kemball, *Trans. Faraday Soc.*, **49**, 1351 (1953).

[3] J. Bagg and F. C. Tompkins, *Trans. Faraday Soc.*, **51**, 1071 (1955).

[4] O. F. Klemperer and F. S. Stone, *Proc. Roy. Soc.*, **A 243**, 375 (1957).

[5] D. Brennan, D. O. Hayward and B. M. W. Trapnell, *Proc. Roy. Soc.*, **A 256**, 81 (1960).

[6] D. Brennan and F. H. Hayes, *Trans. Faraday Soc.*, **60**, 589 (1964).

[7] G. Wedler, *Z. phys. Chem. (Frankfurt)*, **24**, 73 (1960); **27**, 388 (1961).

[8] G. Wedler and F. J. Bröker, *Discuss. Faraday Soc.*, **87** (1966).

[9] G. Wedler and H. Strothenk, *Ber. Bunsengesellschaft physik. Chem.*, **70**, 214 (1966).

[10] S. Cerny, V. Ponec and L. Hladek, *J. Catalysis*, **5**, 27 (1967).

[11] D. Brennan and M. J. Graham, *Discuss. Faraday Soc.*, 95 (1966).

In order to complete the data in our previous works[12–14] and to clear the structure of the adsorbed layer, in the present paper we started measuring the adsorption heat of oxygen on copper films.

I. EXPERIMENTAL

The apparatus is an adiabatic calorimeter of the Beeck type[1] modified in spherical form (Wedler[7]), adapted for working in ultravacuum as well as for the simultaneous measurement of the variations of electrical resistance of the films.

I.1. *Vacuum installation and device for gas admission*

The vacuum installation consists of two evacuation apparatuses concomitantly operated; the former (I_1) for the calorimeter and the latter (I_2) for the calorimetrical jacket that assures the adiabatic conditions. Figure 1 represents the block-scheme of the installation.

I_1 includes the container RV provided with a Pirani gauge MP_1 and the grease stopcock r_1 which cuts off the installation from the preliminary pump; D_1 is a metallic diffusion pump with mercury in three stages, type DRN 10, followed by a spherical trap T_1 and a cylindrical trap T_2 with all walls cooled, described by us in another paper[15]; R_M is a metallic bakable valve (from the Granville-Phillips Company), T_a is a tantalum getter previously described,[16] BA_1 the Bayard-Alpert gauge, R_S bakable spherical greaseless glass tap, R_P plane greaseless tap also bakable (processed in our laboratory).

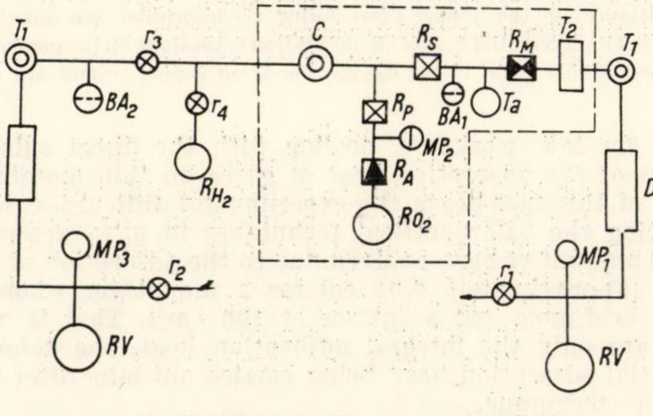

Fig. 1. — Block-scheme of the vacuum installations;

RV glass containers; $r_1 - r_4$ glass greased stopcocks; D_1, D_2 mercury diffusion pumps; T_1 spherical traps; T_2 cylindrical trap; MP_1, MP_3 common Pirani manometers; MP_2 bakable large range Pirani gauge; R_M metallic bakable valve; R_S bakable spherical greaseless glass tap; R_P bakable plane greaseless tap; R_A metallic variable leak; R_{O_2} oxygen container; R_{H_2} hydrogen container; BA_1, BA_2 Bayard Alpert gauges; C calorimeter

---

[12] I. G. Murgulescu and M. I. Vass, *Rev. Roumaine Chim.*, **11**, 299 (1966).

[13] I. G. Murgulescu and M. I. Vass, *Rev. Roumaine Chim.*, **13**, 373 (1968).

[14] I. G. Murgulescu and M. I. Vass, *Rev. Roumaine Chim.*, **13**, 1521 (1968).

[15] M. I. Vass, *Rev. Roumaine Chim.*, **14**, 809 (1969).

[16] M. I. Vass, *Rev. Roumaine Chim.*, **14**, 955 (1969).

The admission device of gas includes an oxygen container R_{O_2}, a metallic variable leak (supplied by Granville-Phillips Company) and a Pirani gauge with wide measuring range ($2\times10^{-1}-5\times10^{-6}$ torr) previously described.[17] The volume between R_A and R_P inclusively MP_2 gauge is about 200 ml and on this account the gas had been let in at reduced pressure i.e. 1×10^{-3} torr.

I_2 also includes a vacuum container RV, a grease stopcock r_2, a Pirani gauge MP_3, a glass diffusion pump with mercury in three stages, a spherical trap T_1, the Bayard-Alpert gauge BA_2 ($IM-2$ Leybold type). Between r_3 and the calorimetrical jacket, a hydrogen container R_{H_2} is soldered, necessary during the deposition of the metallic film.

The part, in both installations, bounded by the dotted line, is placed in an oven and subjected to degassing at 400–420°.

I.2. Calorimeter

We have made use of the spherical form since it favours the homogeneity of the film deposition as well as the uniform distribution of oxygen on the metallic surface when letting in gas.

The sphere S is made of Pyrex glass with average wall thickness of 0.2 mm, with small differences at the upper part toward the soldering of the extension tube. The external wall has, half embedded in glass by direct soldering, the thermoresistance T_r, a platinum wire of 0.02 mm in diameter, anti-inductival wound. The internal wall of the sphere has, at two opposite spots, two soldered platinum bands, 0.01 mm thick, 6 mm in length and 2 mm wide, in order to measure the film resistance. Within separate experiments these two contacts have been replaced by other bands, $\leqslant 0.01$ mm thick, with three holes 1.5 mm in diameter so that the film should have a contact surface as large as possible (fig. 2 b).

In the middle of the sphere there is an evaporator, a V-shaped filament of tungsten (0.2 mm), on which is fixed, by melting in hydrogen, the metal for evaporation (spectroscopically pure copper from Johnson and Matthey). The tungsten filament is spot-welded to two tungsten conductors, 1.5 mm in diameter, mounted in glass capillaries. The thermoresistance ends as well as the wires in the extension of the contact bands for measuring the film resistance are also spot-welded to tungsten conductors of 1.5 mm in diameter.

The calorimetric sphere is soldered to the jacket M evacuated by means of the installation I_2. Evacuation and gas admission into the calorimeter occur by the joint R_1.

I.3. Measurement circuits

a) Temperature variation of the calorimetric sphere has been measured with a thermoresistance T_r located to this purpose in a Wheatstone bridge, operated in a regime of maximum sensitivity whose constant current was supplied by an accumulator (12 V and 115 Ah). For the bridge circuit we used a galvanometer type M 17/11, sensitivity 4×10^{-11} A/mm. Maximum sensitivity of the calorimetric circuit : 50 mm deviation for 1×10^{-3} °.

b) Resistance variation of the film during adsorption has been followed by means of a Wheatstone bridge of Mellenbach type, supplied with 0.2 mA in order to reduce the heating of the film beyond 2×10^{-5} °/min. For the bridge circuit we used a galvanometer with a 5×10^{-10} A/min sensitivity of the type C. Zeiss-Jena.

c) Simultaneously, the pressure growth during gas admission to the measurement volume, as well as the decrease in the pressure in the adsorption volume had been followed by means of a Pirani gauge of high sensitivity in order to calculate the n number of adsorbed molecules. The detailed values of the measurement circuit of the Pirani gauge have already been indicated.[17]

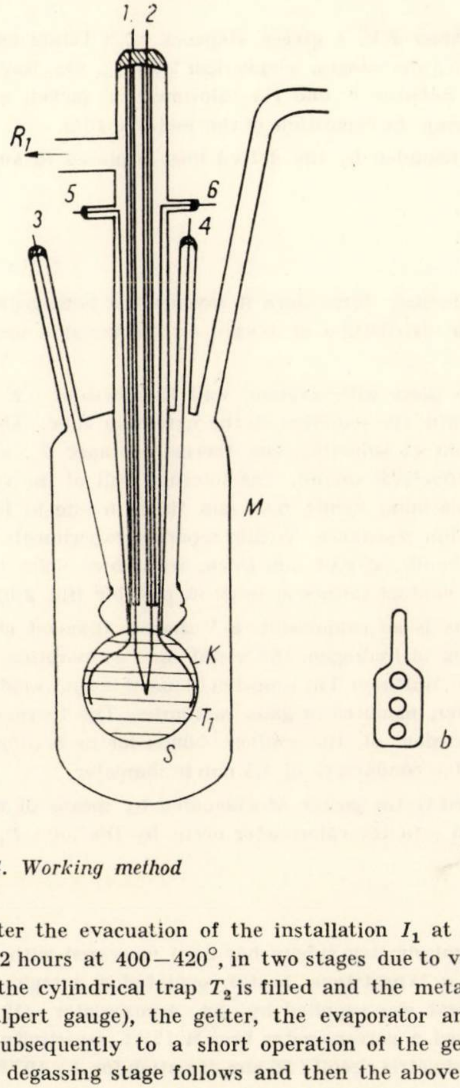

Fig. 2. — Calorimeter;

S, egg-shell glass calorimetric sphere; T_T, thermoresistance; *K*, platinum bands for electric contacts with film; *M*, external jacket; *E*, evaporator; 1–6, glass tungsten seals; R_1, connexions to the ultra-high vacuum line and gas inlet; (b) another form of platinum contact bands.

I.4. Working method

After the evacuation of the installation I_1 at 1×10^{-6} torr, degassing of ultravacuum part for 12 hours at 400–420°, in two stages due to valve R_M ensues. After the first degassing interval, the cylindrical trap T_2 is filled and the metallic conductors (inclusively those of the Bayard-Alpert gauge), the getter, the evaporator and the metal to be evaporated are degassed. Subsequently to a short operation of the getter, the pressure reaches 2×10^{-8} torr. A second degassing stage follows and then the above mentioned operations are repeated and the tap R_M is shut; only the getter with tantalum is kept running. The final pressure was $1-2 \times 10^{-9}$ torr.

All along the degassing, the installation I_2 was continuously run; the measured pressure was of $5 \times 10^{-7} - 1 \times 10^{-6}$ torr.

In order to achieve the deposition of the copper film, the calorimeter has been placed in liquid nitrogen bath and from the container R_{H_2} hydrogen was introduced into the jacket at 2–3 torr pressure in order to avoid overheating. The film evaporation occurred at 1–2×10^{-9} torr. After deposition the films have been sintered at 80° for 10 min until no resistance variations, due to the lattice ordering, have been noticed. During sintering the pressure had a growth rate up to 6×10^{-9}–1×10^{-8} torr for 30–40 s. After sintering the jacket has been again evacuated at 1×10^{-6} torr and the calorimeter set in an ice bath.

---

[17] M. I. Vass, *Rev. Roumaine Chim.*, **14**, 955 (1969).

Measurements did not start before the rate of the temperature deviation was below 5×10^{-5} °/min.

II. DETERMINATION OF THE HEAT CAPACITY —C— OF THE CALORIMETER

As already shown by other authors[5,7] the calibration of the Beeck calorimeters represents the main difficulty in the accurate determination of the adsorption heat on metallic films. In order to carry out calibration, various methods have been used:

a) Initially, Beeck[1] weighed the calorimeter, the metal of the thermoresistance and sodium silicate and by knowing the specific heats he calculated the value of C. The errors ensue from the inaccurate knowledge of that part of the calorimetric tube participating in the total heat capacity.

b) Wahba and Kemball[2] made use of the thermoresistance in order to supply to the calorimeter a known heat amount; then they introduced it again into the measuring circuit and observed the cooling of the calorimeter. However, the method needs the accurate knowledge of the difference in temperature between the calorimeter and the medium, that means a severe limitation of the procedure. Klemperer and Stone[4] used a heating resistance wounded between the spirals of the thermoresistance but the above mentioned difficulties are still not removed.

c) Bagg and Tompkins[3] soldered two ring contacts in the calorimetric cell and passed a known amount of electrical current through the evaporated film. This method has been lately most widespread and various researchers used only contacts of different forms.[5–7]

As already mentioned, we used as contacts platinum bands or sheets as shown in the figure. Both yielded close results.

For the calculus of the magnitude C two ways have been used:

1. *Equilibrium method*

According to Wahba and Kemball,[2] on the resistance film r_f a known voltage E is applied until a thermal equilibrium is reached which corresponds to a deflection of the galvanometer A. After Kemball[2] and Wedler,[7] the growth rate of the temperature is given by:

$$\frac{\mathrm{d}\,\Delta T}{\mathrm{d}t}=\frac{1}{C}\left[\frac{\mathrm{d}Q^{+}}{\mathrm{d}t}-\frac{\mathrm{d}Q^{-}}{\mathrm{d}t}\right] \tag{1}$$

where:

$$\frac{\mathrm{d}Q^{+}}{\mathrm{d}t}=\frac{E^{2}}{4.18\,r_f} \tag{2}$$

is the heating rate, C the heat capacity of the calorimeter and :

$$\frac{dQ^-}{dt} = r\,\Delta T \tag{3}$$

is the cooling rate ; ΔT represents the temperature difference between calorimeter and medium and r is the cooling constant. Taking into account the definition of the temperature coefficient α of the thermoresistance T_r instead of (1) one obtains :

$$\frac{d\,\Delta R}{dt} = \frac{\alpha R}{C}\left[\frac{E^2}{4.18\,r_r} - \frac{r\,\Delta R}{R}\right] \tag{4}$$

If one defines the bridge sensitivity s at the deflection of the galvanometer for a resistance variation R with $10^{-4}\,R$ and ΔR is replaced by dA, the variation of the galvanometer deflection, one gets :

$$\frac{dA}{dt} = \frac{s\,E^2}{4.18\,r_r\,C\,10^{-4}} - \frac{r}{C}A \tag{5}$$

When reaching the thermic equilibrium $\frac{dA}{dt} = 0$ and $A \to A_\infty$ hence :

$$C = \frac{sE^2}{4.18 \times 10^{-4}\,r_r\,A_\infty \frac{r}{C}} \tag{6}$$

In order to get the ratio $\frac{r}{C}$ one takes into account that after the heating of the calorimeter stops, the cooling proceeds according to Newton's law

$$\frac{dQ^-}{dt} = \frac{C\,\Delta T}{dt} = -r\,\Delta T \tag{7}$$

But $\Delta T \approx \Delta R \approx A$ hence $\frac{dA}{dt} = -\frac{r}{C}A$

or by integration :

$$\ln\frac{A}{A_\infty} = -\frac{r}{C}t \tag{8}$$

The slope of the representation ln A function of time enables to infer the value of the ratio $\frac{r}{C}$ that after introduction into the equation (6) leads to the accurate value of the heat capacity C.

2. *Pulse method* (*Bagg and Tompkins*[3])

A well determined current passes the resistance film r_f, as a pulse, within a short interval (5—20 s) and the cooling curve as well as the maximum variation is followed.

The calibration conditions within this method are very similar to those for the heat transfer when measuring the differential absorption heat. That is why the pulse method has been lately preferred to the calibration of Beeck calorimeters.

Based on similar considerations and with the same notations, Wedler[9] has deduced the expression of the magnitude C for the pulse method

$$C = \frac{s\,E^2}{4.18 \times 10^{-4}\, r_f\, \frac{r}{C} A} \left(1 - e^{-\left(\frac{r}{C}\right)t}\right) \tag{9}$$

an expression somewhat different from that used by Brennan

$$C = \frac{Rs\,E^2 t}{4.18\, r_f\, A} \tag{10}$$

In the present paper we have frequently used for the calculus of $\frac{r}{C}$ and the heat capacity C, the pulse method and more seldom the equilibrium method.

Figure 3 shows a cooling curve obtained by the equilibrium method for a film of 29 Ω resistance and 0.080 V applied voltage. Figure 4 presents the representation of the logarithm of the galvanometer deflection *versus* cooling time for two films of 29 Ω and 57 Ω and 0.080 and 0.101 V applied tension. From the figure straight lines are apparent for most part of the range, which shows that the cooling proceeds according to Newton's law, equation (8). The slope of this straight line enables to calculate the ratio $\frac{r}{C}$ and by means of equation (6) the value of C.

Figure 5 gives a typical curve obtained by the pulse method for a film of 34 Ω resistance and 0.212 V applied tension, impulse time 10 s. Figure 6 shows the checking of Newton's law according to which the value $\frac{r}{C}$ has been deduced by the pulse method.

Table 1 contains a part (from nearly 30 experiments) of the values $\frac{r}{C}$ and C obtained by the two above mentioned methods for films with various resistance, *versus* applied tension and various impulse times (5—20 s).

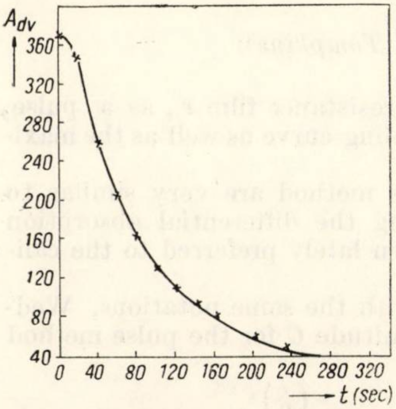

Fig. 3. — Cooling curve of the equilibrium method for a film of 29 Ω and 0.080 V applied tension.

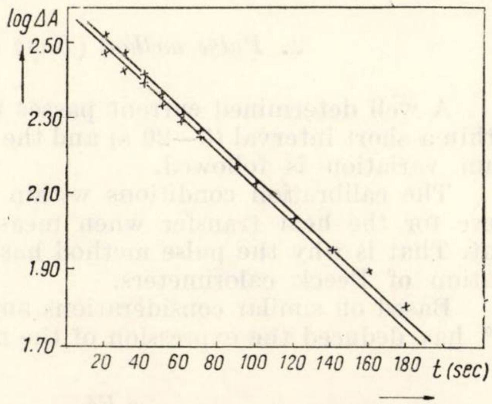

Fig. 4. — Checking of Newton's law in the equilibrium method for two films of 29 Ω and 57 Ω and 0.80 and 0.101 V applied tension.

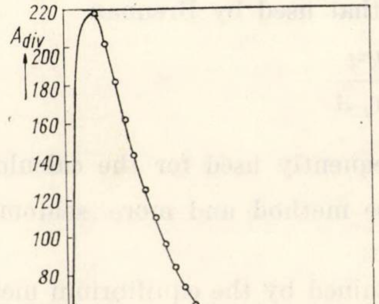

Fig. 5. — Typical curve in the impulse method for a film of 34 Ω, 0.212 V applied tension and 10 s.

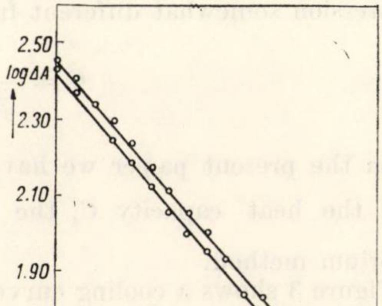

Fig. 6. — Checking of Newton's law impulse method and obtaining of the value of the ratio $\frac{r}{C}$.

The mean value is 0.0134±0.08 s^{-1} for $\frac{r}{C}$ and 0.657±0.023 cal/g respectively 0.545 ± 0.010 cal/g for C.

From table 1 it is obvious that the C value calculated by the pulse method is greater than the value obtained by the equilibrium method, a fact in agreement with the remarks of other authors.[8,9] This may be accounted for by the fact that within the pulse method the calorimetric system is not in equilibrium with the surrounding medium and therefore the heat amount will be dissipated within a greater time interval.

Table 1

Values of the $\frac{r}{C}$ ratio and of the capacity C obtained by the impulse and equilibrium method for films with different resistance, various applied tension E and two-impulse time

r_f Ω	E volts	t s	$\left(\frac{r}{C}\right)_{imp}$ s^{-1}	C_{imp} cal/g	$\left(\frac{r}{C}\right)_{eq}$ s^{-1}	C_{eq} cal/g
29.0	0.225	10	0.0128	0.0633	—	—
29.0	0.323	5	0.0131	0.637	—	—
29.0	0.161	—	—	—	0.0105	0.555
19.47	0.172	10	0.0138	0.607	—	—
57.0	0.336	10	0.0131	0.675		
57.0	0.080	—	—	—	0.0112	0.540
57.0	0.336	5	0.0131	0.647	—	—
39.85	0.312	10	0.0128	0.665	—	—
353.1	0.775	10	0.0139	0.622	—	—
25.0	0.278	5	0.0137	0.666	—	—

The C value found by the Beeck method — weighing of calorimetric sphere up to the limit of film deposition — after carrying out all measurements, and considering the specific heat of the Pyrex glass and the platinum wire, is of 0.620 cal/g. The agreement is satisfactory if we consider the errors occurring when determining the C value by the method of direct weighing.

III. DETERMINATION OF THE CHEMISORPTION HEAT

In order to estimate the chemisorption heat two ways may be used:

1. The most simple[2-5] one makes use of the cooling curve of the calorimeter obtained after admission of a determined oxygen amount and then representing the variation of the logarithm of the galvanometer deflection *versus* time we can get by extrapolation at the initial moment, the A_0 deviation, which should be obtained in the absence of the heat losses. Considering that the heat amount Q^+ transferred to the calorimeter during adsorption is $Q^+ = \Delta Q n/N$ (where ΔQ the adsorption heat, n number of adsorbed molecules, N Avogadro's number) and on the other hand the same amount is given by the relation

$$Q^+ = C \Delta T = C \alpha \ \Delta R/R = C A_0 \times 10^{-4}/s,$$

one gets equation :

$$\Delta Q = \frac{N\, 10^{-4}\, C A_0}{s n_{\max}} \tag{11}$$

By means of the above equation the adsorption heat may be easily obtained (the magnitudes have the already quoted significances).

2. The method set forth by Wedler[7] takes into account the rate of the adsorption process. In his opinion, for the measurement of that rate it is advisable to follow the variation in the film resistance during the adsorption and not the pressure variation, since this resistance variation would result in a more accurate indication of the gas amount actually reaching the film surface. The adsorption rate of oxygen on films is limited by the gas diffusion through the apparatus and on the film surface and may be expressed by a law[18] of the following type

$$\frac{\mathrm{d}n}{\mathrm{d}t} = n_{\max} K_d \mathrm{e}^{-K_d t} \tag{12}$$

where n — the number of adsorbed molecules on cm^2 at moment t, $n_{\max}$ — the maximum number of adsorbed molecules on cm^2 and K_d — rate constant of the diffusion phenomenon.

The heat amount transferred to the calorimeter will be corrected by the factor

$$\frac{\mathrm{d}Q^+}{\mathrm{d}t} = \frac{\Delta Q\, F}{N} n_{\max} K_d \mathrm{e}^{-K_d t} \tag{13}$$

where F — the film surface. If we consider that in equation (5) instead of $E^2/4.18\, r_f$ expression (13) is to be introduced, then by integration we obtain :

$$A = \frac{\Delta Q\, s\, F\, n_{\max}}{10^{-4}\, C\, N} \frac{K_d}{K_d - \frac{r}{C}} \left[\mathrm{e}^{-\frac{r}{C}t} - \mathrm{e}^{-K_d t} \right] \tag{14}$$

Therefore if we represent A *versus* $D = \mathrm{e}^{-\frac{r}{C}t} - \mathrm{e}^{-K_d t}$ we must obtain a straight line whose slope enables to deduce the chemisorption heat :

$$\Delta Q = \frac{C N \times 10^{-4}}{s\, F\, n_{\max}} \frac{K_d - \frac{r}{C}}{K_d} \frac{\mathrm{d}A}{\mathrm{d}D} \tag{15}$$

---

[18] R. SUHRMAN and G. WEDLER, *Z. phys. Chem.* (*Frankfurt*), **10**, 184 (1957).

The constant K_d is obtained from kinetics of the variation of the film resistance during adsorption. If in equation (12) one considers the proportionality $n \approx \Delta R$ the following expression is reached at:

$$\log\,(\Delta R_{\max} - \Delta R) = - K_d\, t \log e + \log \Delta R_{\max} \qquad (16)$$

From the slope of the representation $\log\,(\Delta R_{\max} - \Delta R)$ *versus* time one obtains K_d. This law is checked up for the systems O_2—Ni,[7a] O_2—Fe,[7b] O_2—Cu.[19]

In our calculations we made use of both ways for the estimation of the adsorbed heat. Figure 7 shows an example of the galvanometer deflection obtained on adsorption of 1.18×10^{16} molecule as well as the representation of the logarithm of deflection in time by whose extrapolation of the initial moment we have calculated the magnitude A_0, deviation in the absence of heat losses. By means of formulae (11) we have calculated the differential chemisorption heat which on the average amounts to 109.8 ± 6.2 kcal/mole.

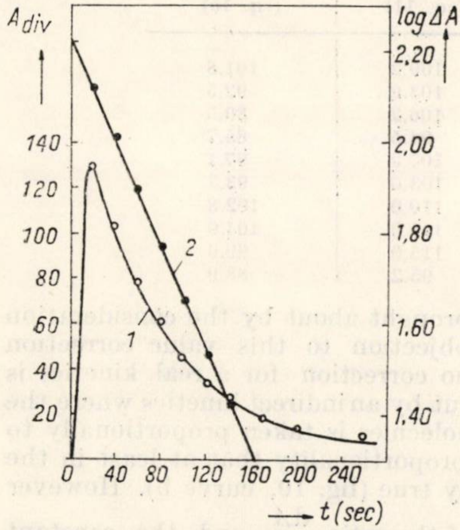

Fig. 7. — Typical curve *1*, ○ for the adsorption of an oxygen dose of 1.18×10^{16} molecules and for obtaining A_0 deflexion in the absence of the heat losses from the plot *2*, ● log *A versus* time.

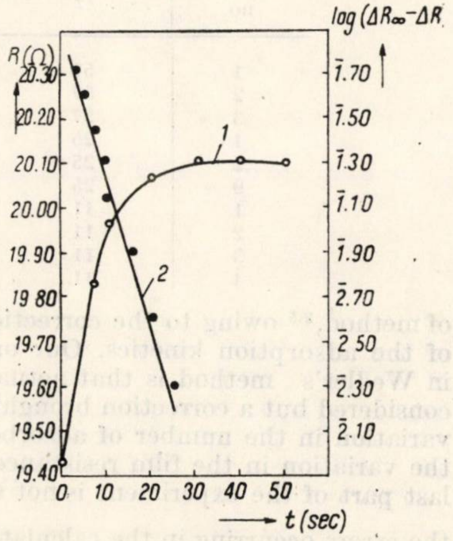

Fig. 8. — Typical curve *1*, ○ of the variation of the film resistance at the oxygen adsorption and checking *2*, ● of the equation (16).

Figure 8 shows the variation in the film resistance during the adsorption of a quantity 5.60×10^{15} molecule as well as the verification of the equation (16) by the slope of which we have inferred the constant K_d.

---

[19] I. G. Murgulescu and N. I. Ionescu, *Rev. Roumaine Chim.*, **13**, 1533 (1968).

The value of this constant obtained for various oxygen admissions on various films was 0.174 s^{-1}. From figure 9 where we have represented an example of the deflexion variation of the galvanometer *versus* the difference between the exponentials D on cooling, we have inferred the value of ratio $\frac{dA}{dD}$. Having now K_a and $\frac{dA}{dD}$ we have calculated the adsorption heat by means of equation (15) and we have found an average value of 95.5±5.5 kcal/mole. Table 2 lists the results of the calculation of chemisorption heat according to the two equations (11) and (15) for the same films for increasing quantities of adsorbed gas. The values found in the literature for copper powder range from 72 to 120 kcal/mole.[20-22]

One can notice from table 2 that the value of the chemisorption heat calculated according to Wedler is smaller than that calculated by means of method,[3,5] owing to the corrections brought about by the consideration of the adsorption kinetics. Our only objection to this value correction in Wedler's method is that actually no correction for a real kinetics is considered but a correction brought about by an indirect kinetics where the variation in the number of adsorbed molecules is taken proportionally to the variation in the film resistance, a proportionality that at least in the last part of the experiment is not wholly true (fig. 10, curve b). However the errors occurring in the calculation of the ratio $\frac{dA}{dD}$ and the constant K_a, especially for O_2—Cu, when the resistance variation on gas admission is very quick (ΔR_{max} growth is obtained after about 40 s), in our opinion make the differences between the values obtained by both methods to appear as unessential.

Table 2

Results of the calculation of chemisorption heat according to equations (11) and (15) for the same films and for increasing adsorbed oxygen

Dose no	r_f	ΔQ kcal/mol (eq. 11)	ΔQ kcal/mol (eq. 15)
1	57	109.2	101.8
2	57	103.0	92.5
3	57	106.2	89.5
1	25	94.5	85.7
2	25	107.2	97.1
9	25	103.0	93.7
1	11	110.0	102.8
2	11	111.0	104.0
3	11	115.0	99.6
4	11	95.2	88.9

In order to draw the final conclusions on the bond forming between oxygen and copper at 0° when adsorption occurs, we have represented in

---

[20] W. W. Rusell and C. Bacon, *J. Amer. Chem. Soc.*, **54**, 54 (1932).

[21] B. N. Dell, F. S. Stone and P. F. Tiley, *Trans. Faraday Soc.*, **49**, 195 (1953).

[22] J. J. Chessik, Yung-Tong-Yu and A. C. Zettelmayer, *J. Phys. Chem.*, **61**, 1319 (1957) in "Second Intern. Congress of Surface Activity" vol. 2, Butterworth, London, 1957, p. 269.

figure 10 the dependence of the adsorption heat and the relative variation in electrical resistance $\frac{\Delta R}{R_0}$ as related to the number of adsorbed molecules on cm^2 of geometrical surface.

Contrary to the oxygen adsorption on copper powders[20-22] when the differential heat of adsorption decreases with the coverage, as seen in figure 10, the differential adsorption heat of oxygen on copper films is constant up to approximately 5×10^{14} molec/cm^2 when a sudden decrease to 20 kcal/mole occurs. At the same point the relative variation in the electrical resistance of the films $\frac{\Delta R}{R_0}$ became constant. The difference – observed also on other metals[11] – can be assigned to the homogeneous nature of the surface of metallic films, that does not apply to metallic powders.

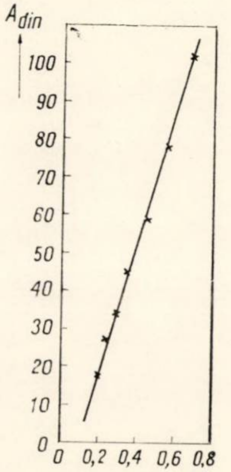

Fig. 9. – Plot of the galvanometric deflection *A versus* difference between exponentials *D* for checking equation (14).

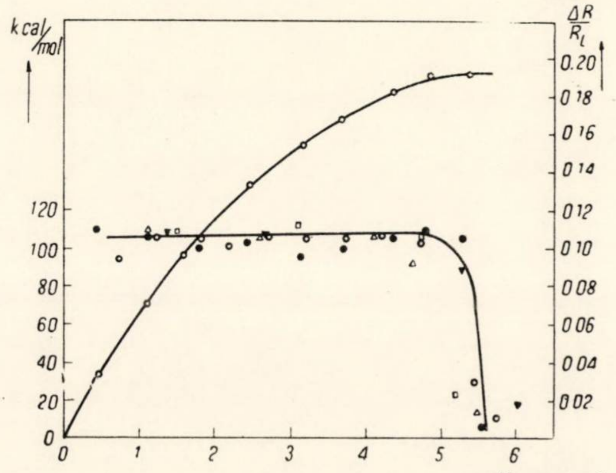

Fig. 10. – Dependence of the differential chemisorption heat of oxygen on the copper films and simultaneous relative variation of the electrical film resistance from the number of the adsorbed molecules.

This passage appears to be the coverage of the copper surface with a monolayer. From the number of the adsorbed oxygen molecules we deduced that the adsorption is dissociative. Since on 1 cm^2 of the copper film surface there are approximately 1.5×10^{15} atoms, the covering of the surface and forming of the bond of the 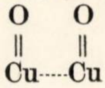 $\overset{O}{\overset{\|}{Cu}}\cdots\overset{O}{\overset{\|}{Cu}}$ type would still leave free approximately 0.5×10^{15} copper atoms. This enables us to assume that for the coverage of the surface with a monoatomic layer bonds of the type 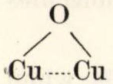 are also forming.

Taking into account that the ratio of oxygen atoms/copper atoms is about 10/15, for a simple array model of the oxygen atoms on copper atoms, it results that approximately 33 per cent of the surface is covered by bonds of the 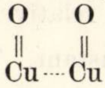 $\overset{O}{\overset{\|}{Cu}}\cdots\overset{O}{\overset{\|}{Cu}}$ form and 66 per cent by bonds of the form 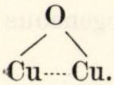

Revue Roumaine de Chimie, **14**, 1215–1223 (1969)

THE BEHAVIOUR OF CERTAIN SYNTHETIC ZEOLITES IN MOLTEN SALTS MEDIA

S. STERNBERG and AGNETA CERBU

Institute of Physical Chemistry of the Academy, Str. Galaţi 31, Bucharest
Department of Inorganic Chemistry, Polytechnic Institute, Str. Polizu 1, Bucharest

Received October 26, 1968

The behaviour of the synthetic CaA type zeolite, in molten nitrates was studied. When in contact with the molten salts, the dehydrated CaA type zeolite behaves as an ion exchanger. The exchange capacity decreases as the ionic radius of alkali cations increases, i.e. in the sequence : $Li^+ > Na^+ > K^+ > Rb^+$ and is maximum for silver. This sequence is different from that existing in aqueous solutions. The equilibrium constant for the reaction of ionic exchange : CaA zeolite-molten sodium nitrate was computed.

The phenomenon of ion exchange between different types of synthetic zeolites and aqueous solutions of electrolytes has been the object of many investigations. Besides its scientific importance, ion exchange has also many practical applications, such as the modification of the selectivity of zeolitic molecular sieves, the separation of radioactive isotopes from radioactive wastes, the preparation of high selectivity catalysts with metallized molecular sieves and so on.

The behaviour of zeolites in the presence of molten salts has been investigated to a much smaller extent.[1–3]

The authors of the cited papers studied various aspects of interactions between dehydrated zeolites and molten salts as for instance the formation of inclusion complexes[1] or some aspects of ionic exchange between zeolites in sodic form and the melts of nitrates of different univalent cations.[2, 3]

In the present paper we study the behaviour of dehydrated synthetic type CaA zeolite in contact with the melt of certain salts, containing cations, different from the zeolitic ones, that is the ionic exchange itself.

---

[1] R. M. Barrer and W. M. Mayer, *J. Chem. Soc.*, **1958**, 299.

[2] M. Liqucrnic and J. Marcus, *Israel At. En. Comm.*, **1 A**, 810 (1963) ; *Chem. Abstr.*, **60**, 8672 (1964) ; AEC Accession No. 43443 Rept. No. 1 A—968 *Chem. Abstr.*, **62**, 13930h (1965).

[3] C. M. Callahan and M. A. Kay, *J. Inorg. Nucl. Chem.*, **28**, 233 (1966) ; AEC Accession No. 39169 Rept. No. USNRDLTR-754 ; *Chem. Abstr.*, **63**, 52 (1965).
C. M. Callahan, AEC Accesion No. 16340 Rept. No. USNRDL-TR-970 ; *Chem. Abstr.*, 65, 17784 (1966).

The study of the behaviour of CaA type synthetic zeolite in contact with molten alkali nitrates: $LiNO_3$, $NaNO_3$, KNO_3, $RbNO_3$ as well as $AgNO_3$, has been carried out.

The zeolitic CaA type molecular sieve is a hydrated aluminium silicate with empirical formula: $(Na_2,Ca)O \cdot Al_2O_3 \cdot SiO_2 \cdot xH_2O$ crystallized in a three dimensional cubic network. The zeolitic water is included in the intercrystalline channels which penetrate the whole crystal, as cationic hydration water, and is linked to the aluminium silicate network by hydrogen bonds. Cations are also found in the intercrystalline channels, occupying preferential positions against the acid aluminium silicate network, which has a macroanionic function. Zeolitic cations have a relatively high mobility, which determines the property of ion exchanger.

EXPERIMENTAL

The zeolite, previously maintained 48 hours in equilibrium with water vapours, was dried in air; then charges of 0.5–2 g have been activated for 5 hours at 350°, 0.1 mm Hg in the reaction flask (1) of the device given in figure 1. The heating was carried out in an electric furnace (2), the temperature being measured by a thermocouple (3) introduced into the small glass tube (3′). The required amount of salt, previously purified by double re-crystallization and drying, was introduced into the reservoir (4) prior to experiment. During

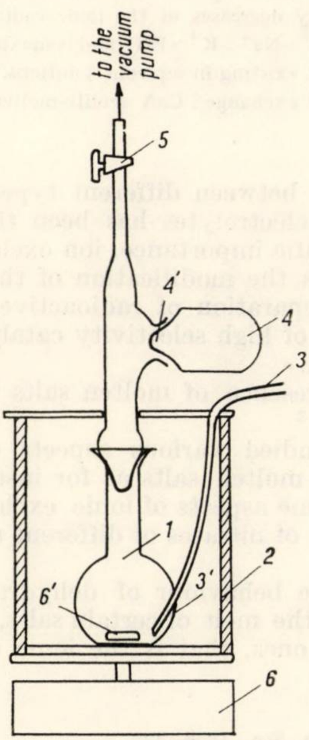

Fig. 1. — Scheme of the apparatus used for the study of the ion-exchange equilibrium in molten salts.

1, Reaction flask; *2*, Electric furnace; *3*, *3′*, Thermocouple and glass tube; *4*, *4′*, Salt reservoir and ground stopper; *5*, Three-way tap cock; *6*, *6′*, Magnetic stirrer.

the activation of the zeolite, the salt was kept in the reservoir of the apparatus, where it was pre-heated, then, after the complete dehydration of the zeolite, it was loaded in the reaction flask (1) by rotating the reservoir round the stopper (4′). At the same time the vacuum pump was switched off and the connexion was made with the atmosphere by means of a three-way stop cock (5). Once the salt melted, the suspension of zeolite in molten salt was kept 8 hours at 350° (250° in case of silver nitrate), while being continually stirred. The stirring was performed by the help of a magnetic stirrer (6,6′). The duration of the operation had previously been determined by successive tests of 6, 8, 12 and 24 hours; 8 hours proved to be sufficient.

After completion of the reaction, the melt was cooled in a dessicator provided with an activated molecular sieve 4A type, and then perfectly homogenized by grinding. Filtration ensued onto a glass crucible with a G4 porous plate, kept at 350° (250° for silver nitrate), in a special furnace. In the filtered sample the calcium content was determined complexonometrically and manganometrically.

Two series of determinations were carried out, both on the zeolitic molecular sieve Linde CaA with different calcium content: 3.41 and 5.15 mg-equivalent/g zeolite, and with different values of the cation/zeolite ratio.

The enriching with calcium of the zeolite occurred by ion exchange in aqueous medium,[4] in a solution of 2.5 M of $CaCl_2$ at 100° accompanied by continuous stirring for 5 hours. The zeolite was then filtered and washed with water until removal of the chloride ions. The operation was repeated several times.

In order to enable the comparison of the behaviour of the zeolite in molten salts with its behaviour in aqueous solutions, we also studied the ion exchange in aqueous solutions under the conditions mentioned by Shirinskaia and Ermolenko.[5,6] Samples of 0.5 g CaA zeolite were introduced into a flask, and 25 cm^3 solution of salts at concentration levels between 0.2 N and 2.0 N were added. Nitrate solutions were used to this purpose. In the case of sodium nitrate solutions, the determinations were made at concentrations up to 3.0 N. The suspension was stirred for 2 hours, then kept at a constant temperature of 24.5° in a thermostat and intermittently stirred during 7 days, when the equilibrium of the ion exchange stabilized for all concentrations. The solution separated from the zeolite by filtration, and the calcium content in the solution was determined by the above mentioned methods. For the same samples, the cation content was determined in the zeolite as well.

To calculate the equilibrium constant of the ion exchange, determinations were made in the system: $NaNO_3$-CaA zeolite, for values of the ratio: molten salt/zeolite, between 0.05 and 0.4 mol/g. These determinations were conducted under exactly the same conditions as the others.

RESULTS AND DISCUSSION

The experimental data obtained indicate that the dehydrated CaA type zeolite behaves as an ion exchanger when in contact with molten salts at temperatures lower than the temperature of thermal decomposition.

---

[4] I. V. Mirski, M. G. Mitrofanova and T. N. Bredikhina, "Sintetitcheskie Tzeoliti". Sb. Akad. Nauk S.S.S.R. Otd. Khim. Nauk, Leningrad, 1962, p. 167.

[5] L. P. Shirinskaia and N. F. Ermolenko, "Sintetitcheskie Tzeoliti" Sb. Akad. Nauk S.S.S.R., Otd. Khim. Nauk, Leningrad, 1962, p. 82.

[6] L. P. Shirinskaia, *Vestnik Akad. Nauk Belarusskoi S.S.R. Ser. Fiz. Techn. Nauk* **1**, 82 (1961).

There are obvious differences between the molten salts and aqueous solutions. Thus, from table 1 and figure 2 it follows that the exchange capacity of the dehydrated zeolite we studied decreases as the ionic radius of the unhydrated cation of the molten salt increases, this decrease being linear for alkaline cations. The selectivity of the dehydrated zeolite related to the alkaline cations decreases in the order : $Li^+ > Na^+ > K^+ > Rb^+$.

Table 1

Calcium displacement in the dehydrated CaA type synthetic zeolite, by cations from the melt

Cation of the molten salt			Temperature °C	Cation content in the molten salt mol/g zeolite	Calcium content in the zeolite mg-equiv./g	Displaced calcium per gram of zeolite mg-equiv./g
Symbol	r Å	Electronic configuration				
Li^+	0.60	He	350	0.05	3.41	1.118
				0.10	5.15	3.220
Na^+	0.95	Ne	350	0.05	3.41	0.718
				0.10	5.15	1.920
K^+	1.33	Ar	350	0.05	3.41	0.300
				0.10	5.15	0.860
Rb^+	1.48	Kr	350	0.05	3.41	0.170
				0.10	5.15	0.540
Ag^+	1.26	$Kr,_4d^{10}{}_5s^0$	250	0.05	3.41	2.880
				0.10	5.15	5.220

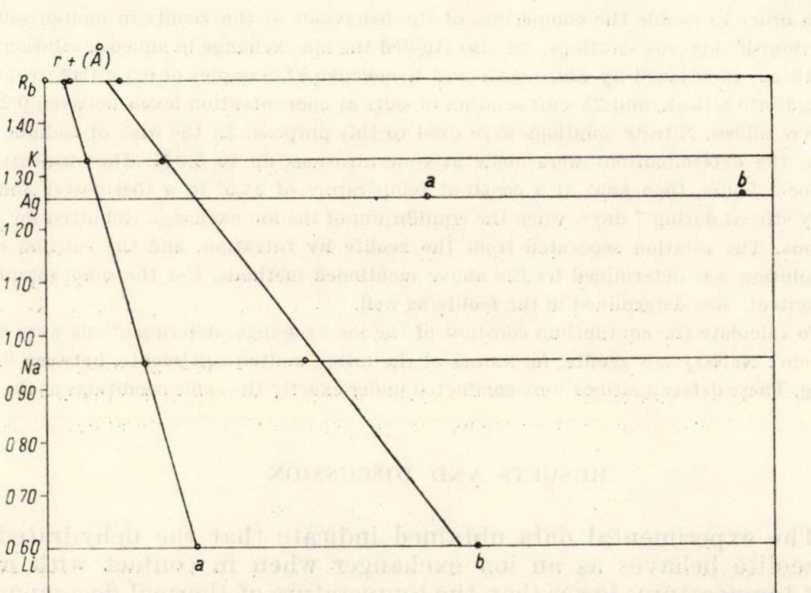

Fig. 2. — Variation in the ion-exchange capacity of the CaA type zeolite as a function of the nature and radius of the cation in the melt.

This order differs from that recorded in aqueous solutions for the same type of zeolite. Thus, Shirinskaia and co-workers[6] mention a decrease in the exchange capacity of the CaA zeolite from Rb^+ to Li^+ in the order $Rb^+ > Na^+ > K^+ > Li^+$. For the same range of concentrations, our determinations carried out in aqueous solutions, indicate a somewhat different situation, (fig. 3) since the decreasing order of the exchange capacities, that is of selectivities, is $Na^+ > K^+ > Rb^+ > Li^+$ the rubidium having a different place. Since the behaviour of rubidium differed from our expectations, two series of determinations were performed, one with nitrate and the other with rubidium bromide. The results of the two cases concurred. Anions which do not take part in the exchange reaction do not influence the exchange capacity of the zeolite.

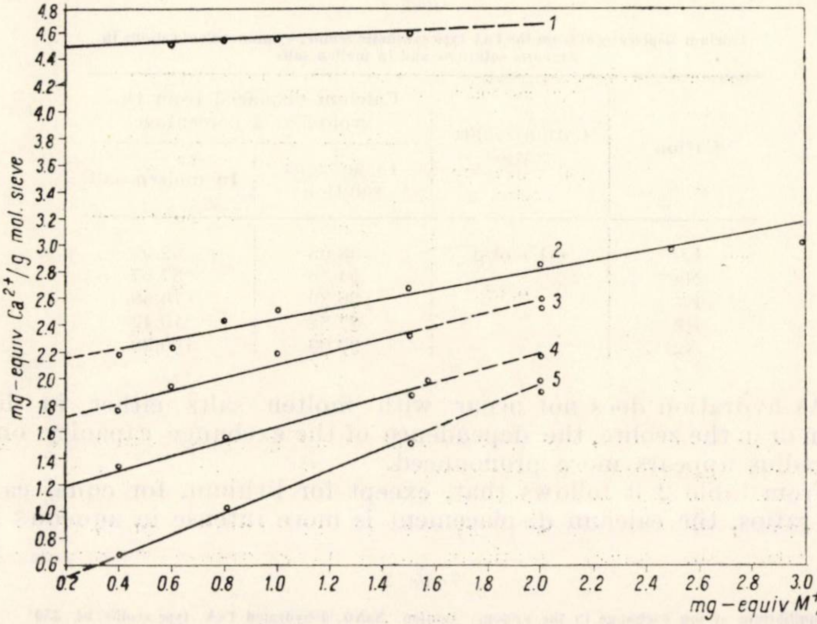

Fig. 3. — Ion exchange between the CaA type zeolite and the aqueous solutions of the monovalent cation nitrates :
1, $AgNO_3$; *2*, $NaNO_3$; *3*, KNO_3; *4*, $RbNO_3$; *5*, $LiNO_3$.

The results of the determinations in aqueous solutions are represented on figure 3. A comparison is made in table 2 between the results of the determinations in molten salts and in aqueous solutions.

The difference in behaviour of the zeolite in the two media is certainly related to the influence of water molecules on the process of ion exchange. As known, the lithium ion is the most strongly hydrated and the hydration decreases as the ionic radius increases. The radius of the hydrated ion is therefore larger for lithium than for other alkaline cations. This explains why lithium has a reduced exchange capacity in aqueous solutions. The phenomenon of hydration also occurs in the other cations. Thus we can see from table 2 that for Rb^+, K^+ and Na^+ the increase in the exchange capacity as a function of the ionic radius is much more pronounced in molten salts than in aqueous solutions. Thus, while in molten salts from K^+ to Na^+ the exchange capacity increases 2.3 times, this increase is only 1.08 in aqueous solutions (table 2).

Table 2

Calcium displacement from the CaA type synthetic zeolite, by monovalent cations in aqueous solutions and in molten salts

Cation	Cation/zeolite ratio	Calcium displaced from the zeolite as a percentage	
		In aqueous solution	In molten salt
Li^+	0.1 mol/g	38.05	62.91
Na^+	,,	54.56	37.67
K^+	,,	50.29	16.59
Rb^+	,,	42.52	10.42
Ag^+	,,	90.09	100.20

As hydration does not occur with molten salts either in liquid medium or in the zeolite, the dependence of the exchange capacity on the ionic radius appears more pronounced.

From table 2 it follows that, except for lithium, for equal cation/zeolite ratios, the calcium displacement is more intense in aqueous solu-

Table 3

Equilibrium of ion exchange in the system: molten $NaNO_3$-dehydrated CaA type zeolite, at 350°

	Quantity of molten salt used mol/g zeolite						
	0	0.05	0.10	0.15	0.20	0.25	0.40
Quantity of calcium displaced from the zeolite mg-equiv./g	—	1.170	1.520	1.950	2.200	2.287	2.750
Quantity of calcium displaced from the zeolite (%)	—	34.37	44.56	57.18	64.50	72.93	80.67
$\left(X_{Ca^{2+}}\right)_Z$	0.6812	0.5200	0.4860	0.3760	0.3664	0.3388	0.3312
Equilibrium constant calculated from the relation (1) $\times 10^3$	—	1.10	1.10	1.62	1.18	1.22	1.05

tion than in the melt. This could be explained by the absence of water in the second case; a fact that can determine a tighter link between the cations and the aluminium silicate network.

It is worth mentioning that in aqueous solutions as well as in melts the total displacement of calcium from the CaA zeolite by alkali cations during a single exchange operation is not possible. At the same time, from tables 1 and 3 and figures 2 and 3 it follows that both in the case of aqueous solutions and of the melts, silver displaces most intensively the calcium, and a total removal of calcium by silver is thus made possible in the melt. Other research workers have also observed the uncommon affinity of CaA zeolite with this cation in the case of aqueous solutions.[6]

Considering the process of ion exchange as a

$$\mathrm{Z\ Ca} + 2\mathrm{M}^+ \rightleftharpoons \mathrm{Z\ M_2} + \mathrm{Ca}^{2+}$$

type reversible reaction, the equilibrium constant was calculated from the results of the determinations given in table 3 and figure 4. The following equation was used:

$$\mathrm{K} = \frac{(X_{\mathrm{Na^+}})^2_{\mathrm{Z}}}{(X_{\mathrm{Ca^{2+}}})_{\mathrm{Z}}} \cdot \frac{(a_{\mathrm{Ca^{2+}}})_{\mathrm{M}}}{(a_{\mathrm{Na^+}})^2_{\mathrm{M}}} \ldots 1$$

in which $(X_{\mathrm{Na^+}})_{\mathrm{Z}}$ and $(X_{\mathrm{Ca^{2+}}})_{\mathrm{Z}}$ are the molecular fractions of sodium and calcium in the zeolite; $(a_{\mathrm{Na}})_{\mathrm{M}}$ and $(a_{\mathrm{Ca^{2+}}})_{\mathrm{M}}$ are the activities of sodium and calcium in the melt.

$$\text{But}: (a_{\mathrm{Na^+}})_{\mathrm{M}} = (X_{\mathrm{Na^+}})_{\mathrm{M}}\ \gamma_{\mathrm{Na^+}} \text{ and } (a_{\mathrm{Ca^{2+}\,M}}) = (X_{\mathrm{Ca^{2+}}})_{\mathrm{M}}\ \gamma_{\mathrm{Ca^{2+}}}$$

The system $\mathrm{NaNO_3} - \mathrm{Ca(NO_3)_2}$ can be estimated as a regular solution where $\gamma_{\mathrm{Na^+}}$ and $\gamma_{\mathrm{Ca^{2+}}}$ are activity coefficients.

Activity coefficients can be calculated from the relations:

$$RT \ln \gamma_{\mathrm{Na^+}} = B\ (X_{\mathrm{Ca^{2+}}})^2_{\mathrm{M}} \text{ and } RT \ln \gamma_{\mathrm{Ca^{2+}}} = B\ (X_{\mathrm{Na^+}})^2_{\mathrm{M}}$$

in which the constant B was taken according to the calorimetric determinations of Kleppa, as equal to −900 cal/mol.[7]

From table 3 it follows that within the limits of $(X_{\mathrm{Ca^{2+}}})_{\mathrm{M}}$ ranging from 0.6812 to 0.3312, the value of the equilibrium constant of the ion-exchange reaction somewhat deviates from the mean values of $\mathrm{K} = 1.21 \times 10^{-3}$. Therefore, within these limits of concentration, the law of mass action can be satisfactorily applied to the exchange reaction between bivalent calcium ions from the dehydrated CaA zeolite and monovalent sodium ions from the $\mathrm{NaNO_3}$ melt.

The influence of temperature on the behaviour of the dehydrated zeolite in molten salts for the system $\mathrm{LiNO_3}$—CaA zeolite was investigated. For this purpose three different temperatures were used: 280, 300 and 350°. However, the results differ little and are within the limits of the experimental error. At equal proportions of 0.05 mol $\mathrm{LiNO_3}$/g zeolite, the quantity of calcium was respectively 1.14, 1.145 and 1.17 mg-equivalent/g. The widening of the temperature range is limited by the melting temperature of the salts (lower limit), and by the thermal stability of the dehydrated zeolite in molten salts medium (upper limit).

---

[7] O. J. Kleppa and L. S. Hersch, *Discuss. Faraday Soc.*, **32**, 99 (1961); *J. Chem. Phys.*, **36**, 544 (1962).

The thermal stability of the zeolite under working conditions was verified by röntgenographic means on samples of zeolite kept under experimental conditions for 12 hours. The results for samples treated with $NaNO_3$ and $RbNO_3$ are to be found in table 4.

Table 4

Röntgen lines of the CaA type zeolite kept in equilibrium with molten salts

Röntgen lines of the CaA type zeolite					
Treated with $NaNO_3$		Treated with $RbNO_3$		Untreated	
dÅ	I	dÅ	I	dÅ	I
7.01	w	7.195	w	7.014	ws
5.54	vw	5.502	w	5.510	w
4.102	ws	4.142	w	4.104	ws
3.696	s	3.754	vs	3.702	svs
3.280	s	3.350	s	3.283	vs
2.977	s	2.988	vs	2.979	svs
2.794	s	2.636	w	2.614	s
2.458	vw	—	—	2.479	w
2.347	vw	—	—	2.364	vw
2.175	w	2.160	vvw	2.165	ws
2.085	vw	—	—	2.055	w
1.983	vw	1.991	vvw	1.907	w
1.736	w	—	—	1.736	s
1.683	vw			1.681	w

Abbreviations: w—weak; vw—very weak; s—strong; vs—very strong.

As the röntgenographic data show, the dehydrated zeolite does not undergo any appreciable modification when in prolonged contact with the molten salts, fact already noticed by Barrer.[1]

Although the present study refers to the conditions of equilibrium, some considerations of a kinetic character may be made too. From the observations made for establishing the working method, it follows that the ion-exchange reaction is much faster in molten salts than in aqueous solutions. This behaviour may be caused by the high concentration of cations as well as by high temperature which favours a rapid diffusion of the ions.

The following conclusions may be drawn from the experimental results obtained during our research:

— The dehydrated CaA type zeolite, when introduced into media of molten salts of unlike cations, behaves as an ion exchanger.

— The exchange capacity of the dehydrated type CaA zeolite decreases linearly as the ionic radius of the alkali cations increases and reaches its maximum value for the silver ion. The decreasing sequence of the exchange capacities for the cations studied is : $Ag^+ > Li^+ > Na^+ > K^+ > Rb^+$.

— There are important differences between the ion-exchange reactions in molten salts and in aqueous solutions. These can be explained by the absence of the hydration phenomenon in molten electrolytes and in the dehydrated zeolite.

Revue Roumaine de Chimie, **14**, 1225–1229 (1969)

ABOUT THE CONDUCTIVITY OF SOLUTIONS OF HYDROBROMIC ACID IN NORMAL ALCOHOLS

IOANA DEMETRESCU

II Department of Physical Chemistry, Bucharest University, Bd. Republicii 13

Received July 24, 1968

The paper deals with the conductivity of solutions of HBr in normal alcohols as a function of HBr concentration and temperature. Calibration curves are presented giving directly the concentration of HBr as a function of the conductivity of HBr solutions in normal alcohols, at various temperatures.

The present investigation grew out of the necessity to obtain, in kinetic studies, the diminution in the concentration of acids as a function of time. Since many systems release acids in alcoholic medium, the existence of calibration curves giving directly the concentration of the acid as a function of one of its characteristic parameters would be very useful. Such a parameter is the conductivity. The rapid determination, with simple equipment, allows its successful use to that purpose.

The calibration curves of the literature refer to a small number of alcoholic media and to few acids.[1-3] Besides, the cited works were concerned with the determination of conductivity as a function of the water content of the system, but not as a function of temperature.

In the following we give the results we obtained in calibrating hydrobromic acid in normal alcohols.

EXPERIMENTAL

Because the solubility of HBr in water decreases with increasing temperature, we got HBr in alcohol by heating an aqueous HBr solution 63 % of density 1.73 g/cm³, Riedel. After drying HBr was passed through the respective alcohol.

Austranal alcohols were used. 4Å molecular sieves were applied for anhydrising methyl and ethyl alcohols, whose water content was greater than the allowed limit. The water content of each alcohol was dosed by titration with Karl Fischer's reagent, before HBr was introduced as well as after HBr was solved in the respective alcohol.

---

[1] H. Goldschmidt, *Z. phys. Chem.*, **89**, 129 (1915).

[2] H. Goldschmidt and P. Dahl, *Z. phys. Chem.*, **108**, 121 (1924)..

[3] I. Strehlow, *Z. phys. Chem.*, (*Frankfurt*), **24**, 240 (1960).

We worked simultaneously with two conductivity cells, which were directly introduced into the thermostat. To prevent losses the cells were closed up at each determination. Platinum platinized electrodes were used.

Resistance measurement were made by means of a Wheatstone bridge, utilizing a cathode-ray oscilloscope as null indicator.

RESULTS

The results we obtained are given both in tabular and in graphical form.

The possibility of using curves of this type was verified in several works, like those of Norris et al. [4-6]; they made use of the calibration

Table 1

Specific conductivity of solutions of HBr in normal alcohols as a function of temperature and HBr concentration. The values of *x* are the averages of those determined with the two conductivity cells

HBr in CH_3OH 0.4 % H_2O			HBr in C_2H_5OH 0.08 % H_2O			HBr in C_3H_7OH 0.35 %H_2O			HBr in C_4H_9OH 0.28 % H_2O		
C mol/l	*T* °C	$x.10^3$ Ω^{-1} cm^{-1}	*C* mol/l	*T* °C	$x.10^3$ Ω^{-1} cm^{-1}	*C* mol/l	*T* °C	$x.10^3$ Ω^{-1} cm^{-1}	*C* mol/l	*T* °C	$x.10^3$ Ω^{-1} cm^{-1}
0.02	60	3.10	0.427	65	9.7	0.71	50	5.72	0.22	60	1.51
	65	3.22		75	10.1		65	6.51		65	1.56
	70	3.30		85	10.6		70	6.81		70	1.60
	75	3.40	0.285	65	7.5		75	7.08	0.11	60	0.89
0.015	60	2.7		75	7.8	0.355	50	3.14		65	0.92
	65	2.8		85	8.0		65	3.46		70	0.94
	70	2.9	0.1425	65	4.5		70	3.56	0.075	60	0.63
	75	3.0		75	4.8		75	3.69		65	0.64
0.01	60	2.1		85	5.0	0.177	50	1.66		70	0.65
	65	2.15	0.0712	65	2.68		65	1.85	0.055	60	0.521
	70	2.2		75	2.84		70	1.95		65	0.527
							75	2.05			
	75	2.3		85	3.10	0.0885	50	0.82		70	0.531
0.005	60	1.21	0.0356	65	1.6		65	0.85	0.0375	60	0.374
	65	1.25		75	1.7		70	0.89		65	0.378
	70	1.30		85	1.8		75	0.99		70	0.384
	75	1.40	0.0178	65	0.92	0.0442	50	0.46	0.0275	60	0.289
0.0025	60	0.70		75	0.98		65	0.48		65	0.292
	65	0.72		85	1.01		70	0.49		70	0.295
	70	0.75					75	0.50	0.01875	60	0.211
	75	0.77				0.022	50	0.20		65	0.217
0.00125	60	0.46					65	0.21		70	0.220
	65	0.47					70	0.22	0.0137	60	0.188
							75	0.24			
	70	0.48								65	0.190
	75	0.50				0.011	50	0.132		70	0.191
							65	0.138	0.00937	60	0.130
							70	0.142		65	0.131
							75	0.143		70	0.133

---

[4] J. F. Norris, E. V. Fasce and C. J. Staud, *J. Amer. Chem. Soc.*, **57**, 1415 (1935).

[5] J. F. Norris and H. H. Young, *J. Amer. Chem. Soc.*, **57**, 1420 (1935).

[6] J. F. Norris and E. Haines, *J. Amer. Chem. Soc.*, **57**, 1425 (1935).

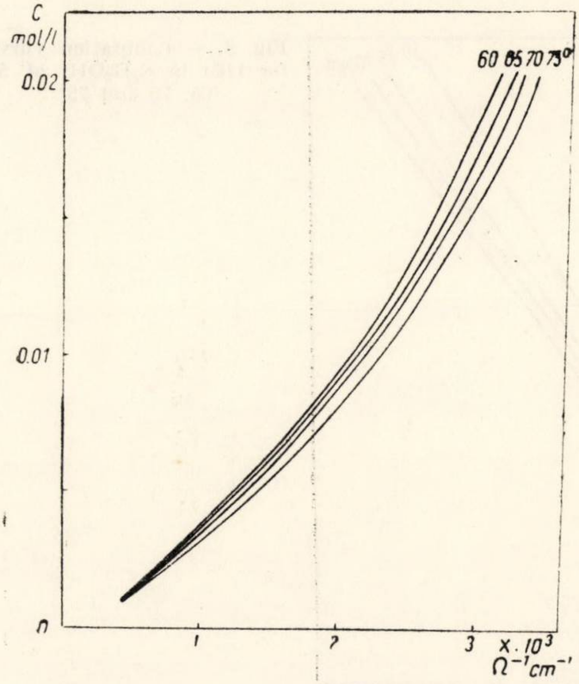

Fig. 1. — Calibration curves for HBr in CH_3OH, at 60, 65, 70 and 75°.

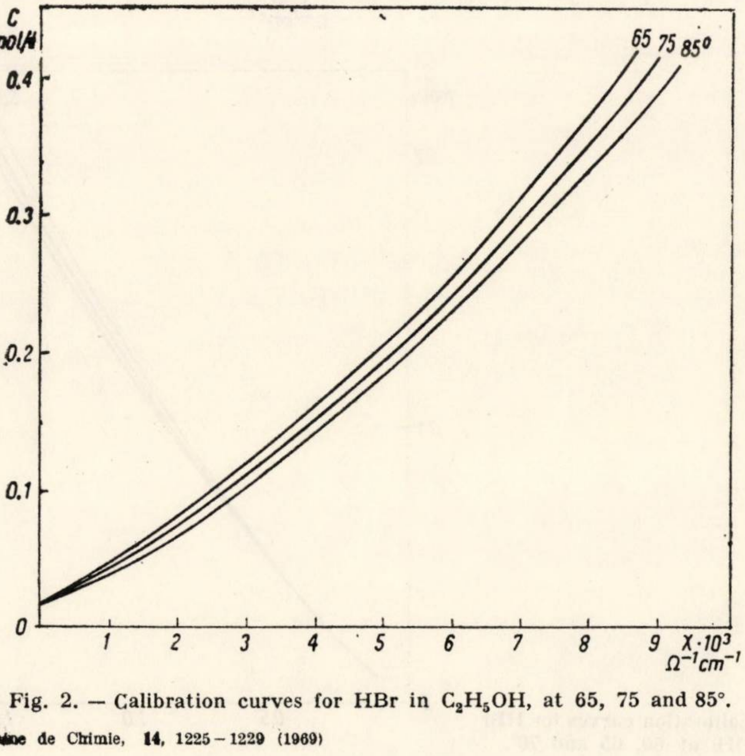

Fig. 2. — Calibration curves for HBr in C_2H_5OH, at 65, 75 and 85°.

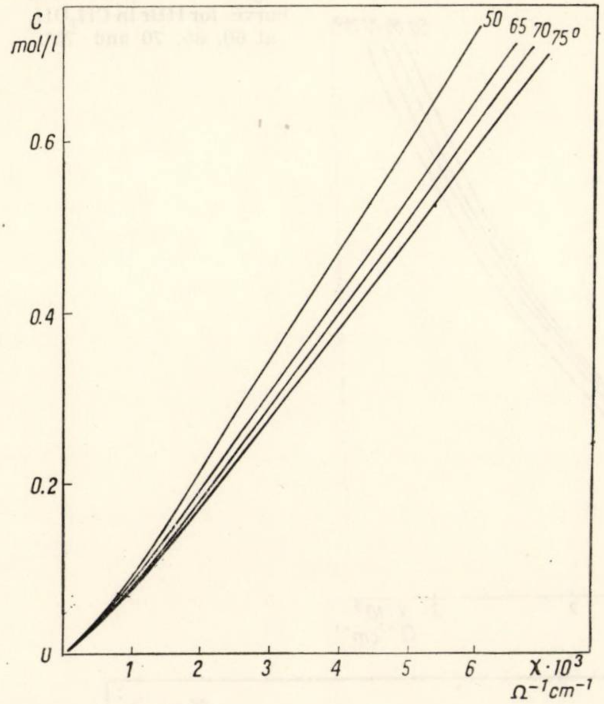

Fig. 3. — Calibration curves for HBr in C_3H_7OH, at 50, 65, 70 and 75°.

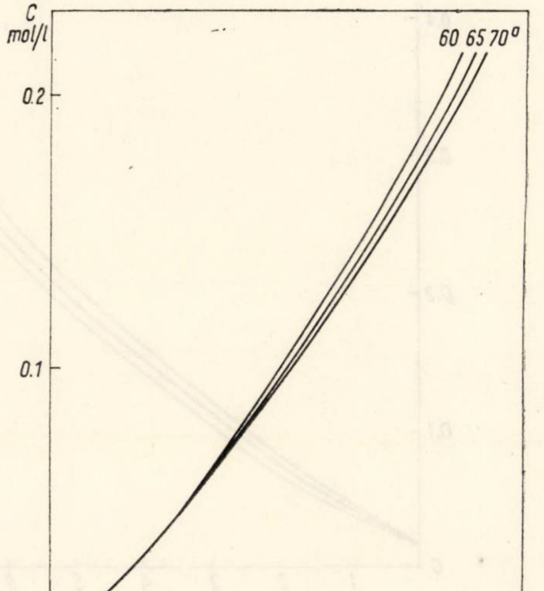

Fig. 4. — Calibration curves for HBr in C_4H_9OH, at 60, 65 and 70°.

curves of Goldschmidt and Dahl[1,2] for HCl in methyl and ethyl alcohols, concluding that the influence of the resulting ester is very slight. At the same conclusion we arrived in a previous work,[7] in which we carried out calibrations directly in the reaction medium.

The results of the present work are utilized by us in the kinetic study of reactions between benzyl bromide and normal alcohols.[8]

The obtained values agree well with the theories concerning the specific conduction of the proton in solvents containing hydroxyl. Indeed, the data obtained on the conductivities of HCl and HBr in alcohols are anomalous values, greater than those found for usual media. The abnormal mobility of the proton in hydroxylic solvents can be accounted for by the Grothus' type conduction, in contrast to the conduction of usual ions in which case the conducting unit does not change. This process may be regarded as a result of two consecutive steps : the transfer of the proton from the alcoxon ion to the alcohol molecule, and the rotation of the alcohol molecule in the external field.

According to this theory we can also account for the reduction in the anomalous mobility of the ROH_2^+ ion at the same time with the increase in the R radical within normal series of alcohols. This fact is reflected also in the data we obtained in the case when the determinations were carried out at the same temperature and concentration. The fact is accounted for by the braking of the rotation of the alcohol in the field.

The theory also explains the variation of the conductivity according to the increasing pressure[9] and to the addition of water to alcohol.

---

[7] I. G. Murgulescu and Ioana Demetrescu, *Rev. Roumaine Chim.*, **14**, 149 (1969).

[8] I. G. Murgulescu and Ioana Demetrescu, *Rev. Roumaine Chim.*, to be published.

[9] S. Quist and W. Marshall, *J. phys., Chem.*, **72**, 1545 (1968).

Revue Roumaine de Chimie, **14**, 1231–1239 (1969)

COMBINAISONS COMPLEXES AVEC DES HYDROXYACIDES. IX*

COMPLEXES DE L'ÉTAIN TÉTRAVALENT AVEC LES ACIDES GLUCONIQUE ET SACCHARIQUE ET LEURS SELS ALCALINS

CONST. GH. MACAROVICI et MARIA VOLUŞNIUC-BIROU
Institut de Chimie de l'Académie, Filiale de Cluj

Reçu le 25 juin 1968

On étudie la formation des complexes de Sn(IV) avec les acides gluconique et saccharique et leurs sels alcalins, par les méthodes potentiométrique, conductométrique, du potentiel d'oxydo-réduction et la synthèse chimique. Dans la solution il se forme un seul type de complexe, au rapport de combinaison 1 Me :1 liant. La formation du complexe a lieu par les groupes hydroxyliques des hydroxyacides respectifs. Par synthèse on a séparé les complexes : $H[C_6H_9O_7SnCl(OH)]$, $K[C_6H_9O_7SnCl_2]$, $H_2[C_6H_5O_8Sn(OH)]$ et $K_2[C_6H_6O_8SnCl_2]$.

Dans nos travaux antérieurs,[1-3] nous avons étudié la formation des complexes des éléments tétravalents (Ti, Zr, Hf, Th, Ge) avec les acides gluconique et saccharique. Dans la présente note on donne quelques résultats obtenus par l'étude de l'interaction $SnCl_4$ — acide gluconique, acide saccharique et leurs sels alcalins, par les méthodes : potentiométrique, conductométrique, du potentiel d'oxydo-réduction, spectrophotométrique et la synthèse chimique.

PARTIE EXPÉRIMENTALE

I. *Titrage potentiométrique*

La préparation des acides gluconique et saccharique et de leurs sels alcalins, ainsi que la technique de travail ont été exposées dans un travail précédent.[3] En raison de la tendance à l'hydrolyse du Sn(IV), on a fait des solutions fortement acides ; on a déterminé l'acidité libre par hydroxyde de potassium en présence de phénolphtaléine.

---

* Part VIII : Const. Gh. Macarovici et E. Perţe, *Rev. Roumaine Chim.* (sous presse).

[1] C. Gh. Macarovici, H. Roth et L. Czeglédi, *Studii şi Cercetări Chim. Fil. Cluj*, **12**, 229 (1961) ; **14**, 69 (1963).

[2] C. Gh. Macarovici et L. Czeglédi, *Rev. Roumaine Chim.*, **9**, 397 (1964).

[3] C. Gh. Macarovici et M. Voluşniuc-Birou, *Rev. Roumaine Chim.*, **12**, 163 (1967).

Etant donné que les essais de titrage direct des différents systèmes n'ont pas donné de résultats satisfaisants, le pH s'établissant très lentement (l'équilibre des hydroxyacides libres avec les lactones, respectivement avec les combinaisons complexes qui se forment en présence des métaux s'établit très difficilement), on a effectué des titrages indirects, c'est-à-dire que l'on a ajouté de l'hydroxyde de potassium en excès connu en titrant ensuite l'excès par acide. Dans ces conditions, le pH s'établit dans quelques minutes.

1. En titrant une solution 0,02 M $SnCl_4$ par une solution 0,1 M KOH, sont consommés 4 équivalents de base (fig. 1.2).

L'origine de la courbe de titrage, tant pour la solution de $SnCl_4$, que pour les mélanges avec les acides gluconique et saccharique et leurs sels alcalins, correspond à une addition initiale d'hydroxyde de potassium, équivalent à l'acidité libre des solutions respectives, déterminée au préalable.

2. Au titrage indirect des acides gluconique (fig. 1.1) et saccharique (fig. 3.1) par acide chlorhydrique 0,1 M, est consommé un équivalent de base, respectivement 2, correspondant aux fonctions carboxyliques présentes.

3. Dans le cas du gluconate de potassium (fig. 2.1), respectivement du saccharate (fig. 4.1), les fonctions carboxyliques étant bloquées, comme il était à prévoir, il n'y a pas eu de consommation de la base (on titre par acide chlorhydrique tout l'hydroxyde de potassium ajouté au mélange).

4. Au titrage des mélanges de solutions de $SnCl_4$ et d'acide gluconique, respectivement saccharique, au rapport molaire 1 : 1 et un excès connu d'hydroxyde de potassium, on constate au terme du titrage une consommation de 5, respectivement 6 équivalents de base, ce qui constitue la somme des équivalents consommés par $SnCl_4$ et par l'acide gluconique (fig. 1.3), respectivement saccharique (fig. 3.3). Au cas où l'on emploie dans les mélanges les sels des acides respectifs, le nombre d'équivalents de base consommés est égal à celui consommé par $SnCl_4$ (fig. 2.3) et (fig. 4.3).

5. Au titrage des mélanges de $SnCl_4$ et de l'acide gluconique ou saccharique à différents rapports (1 : 2), (1 : 3) en présence d'un excès connu d'hydroxyde de potassium, on remarque une consommation d'une quantité de base égale à la somme des équivalents nécessaires pour le titrage des combinaisons 1 : 1 qui se forment et de l'acide en excès (fig. 1.4, 1.5) et (fig. 3.4, 3.5). En ce qui concerne les mélanges avec les sels alcalins des acides respectifs, la consommation de base est égale, tout comme dans le cas des combinaisons 1 : 1, au nombre d'équivalents de base, consommés par $SnCl_4$ (fig. 2.4, 2.5) et (fig. 4.4, 4.5).

Comme il ressort des figures ci-dessus, les courbes présentent une région tampon et chacune un seul point d'inflexion autour du pH = 7, qui correspond aux hydrogènes carboxyliques (lorsqu'on travaille avec les acides) et à 4 ions H^+ provenant de la complexation.

L'allure des courbes ne permet pas de préciser si ces 4 ions hydrogène proviennent tous des groupes hydroxyliques du liant ou, partielle-

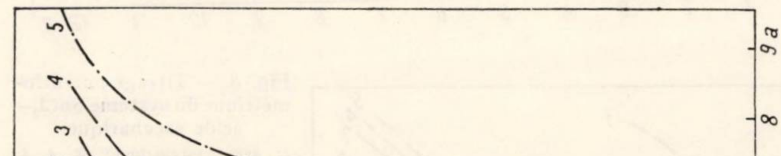

Fig. 1. — Titrage potentiométrique du système $SnCl_4$ — acide gluconique.

1, acide gluconique ; *2*, $SnCl_4$; *3*, *4*, *5*, $SnCl_4$ – acide gluconique : 1 : 1 ; 1 : 2 ; 1 : 3.

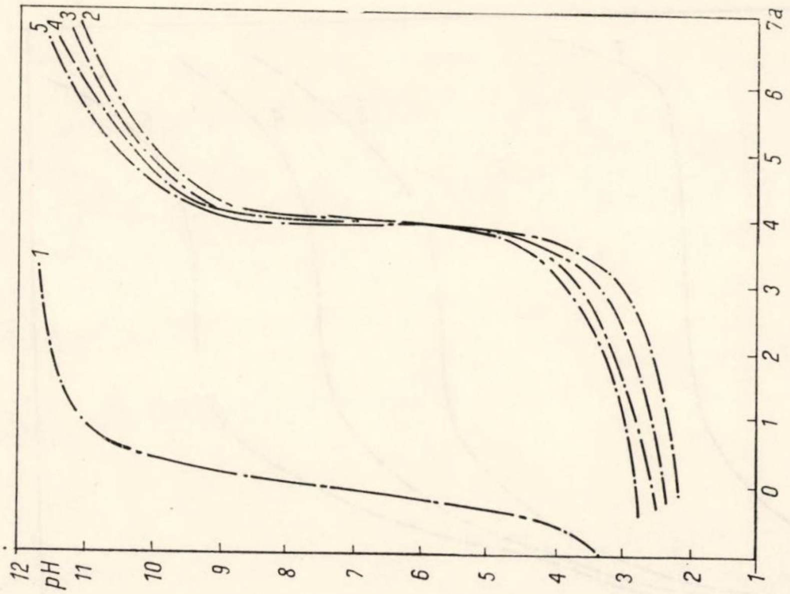

Fig. 2. — Titrage potentiométrique du système $SnCl_4$ – gluconate de potassium.

1, gluconate de potassium ; *2*, $SnCl_4$; *3*, *4*, *5*, $SnCl_4$ – gluconate de potassium.

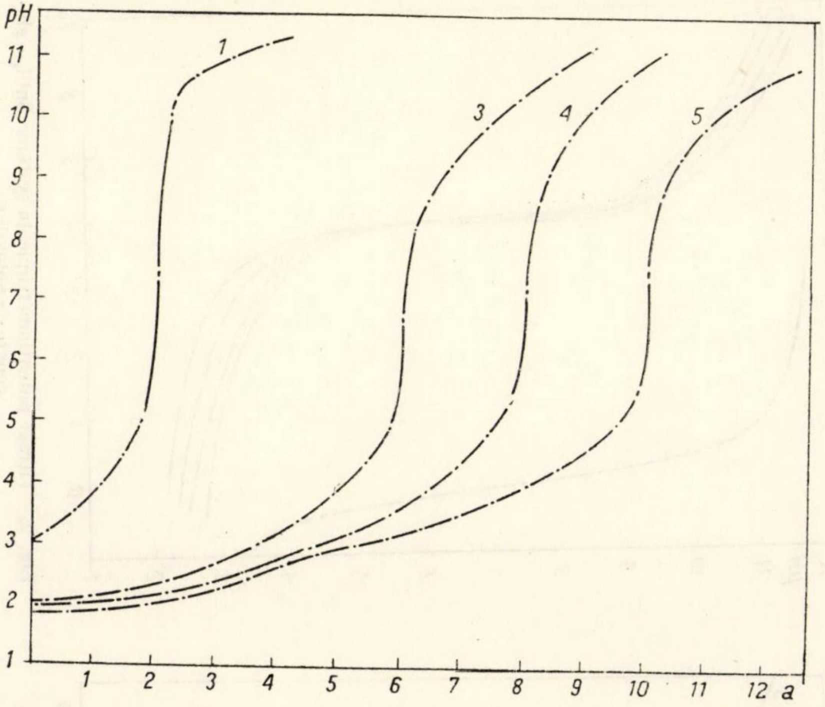

Fig. 3. — Titrage potentiométrique du système $SnCl_4$–acide saccharique.

1, acide saccharique; *3*, *4*, *5*, $SnCl_4$ – acide saccharique: 1 : 1 ; 1 : 2 ; 1 : 3.

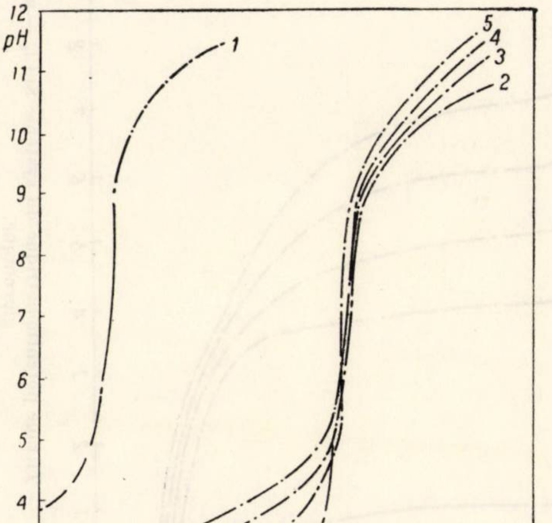

Fig. 4. — Titrage potentiométrique du système $SnCl_4$–saccharate de potassium.

1, saccharate de potassium; *2*, $SnCl_4$; *3*, *4*, *5* $SnCl_4$ – saccharate de potassium : 1 : 1; 1 : 2; 1 : 3.

ment de l'hydrolyse de l'étain tétravalent, hydrolyse qui commence à un pH assez petit (3 environ).

Les titrages potentiométriques permettraient de supposer qu'il se forme un seul type de complexe, dans lequel la complexation se produit par l'hydrogène des groupes hydroxyliques du liant et non des groupes carboxyliques.

La réaction de formation serait

$$SnCl_4 + C_6H_{10}O_8 + H_2O = C_6H_7O_8Sn(OH) + 4HCl$$

et structuralement on pourrait formuler un complexe du type

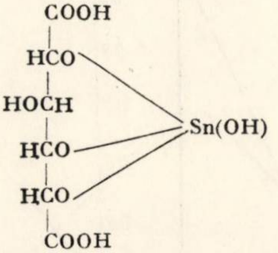

ou avec l'hydrogène des fonctions carboxyliques bloqué par le potassium, au cas où l'on travaille avec les sels alcalins des acides.

Les formulations ci-dessus correspondent aux conclusions tirées par Fiallkov et Periskina,[4] sur la base de la rotation spécifique, en indiquant que, dans le cas des métaux trivalents, la substitution des hydrogènes hydroxyliques a lieu dans les positions α, γ, δ.

II. *Titrage conductométrique*

Ayant constaté que par l'interaction du Sn(IV) et des acides gluconique et saccharique l'hydrogène est mis en liberté, on a étudié ce phénomène aussi par la méthode conductométrique.

Les solutions ont été préparées comme dans le cas des mesures potentiométriques; on a travaillé avec un conductoscope LP, utilisant une cellule à électrodes de platine platiné.

1. Au titrage des acides gluconique et saccharique 0,01 M par hydroxyde de potassium 0,1 M, la courbe se maintient ascendante et il apparaît un knick à une consommation de 1, respectivement 2 équivalents de base correspondant au remplacement des hydrogènes des fonctions carboxyliques. Après l'équivalence, la pente de la courbe est plus accusée en raison de l'augmentation sensible de la dissociation (fig. 5.1, 5.2).

2. Si on titre une solution 0,01 M $SnCl_4$ par hydroxyde de potassium 0,1 M, la conductibilité décroît jusqu'à une consommation de 4 équivalents de base, puis elle augmente (fig. 6.1).

---

[4] A. Fiallkov et N. G. Periskina, *Zhur. neorg. Khim.*, 4, 749 (1957).

3. Au titrage des composants l'un par l'autre, à savoir en titrant une solution 0,01 M tétrachlorure d'étain par une solution 0,1 M acide gluconique, respectivement saccharique, on observe une augmentation de la conductibilité, en raison de l'apparition des ions hydrogène comme suite de la réaction de complexation, jusqu'au rapport molaire 1 : 1. Puis la courbe reste constante, approximativement parallèle à l'abscisse (fig. 6.2, fig. 6.3) ; dans le cas du titrage par le sel alcalin, la courbe est ascendante sur tout son parcours (fig. 6.4).

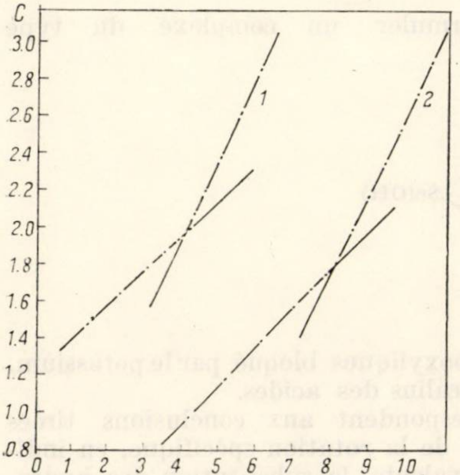

Fig. 5. — Conductibilité électrique d'acide gluconique (1) et d'acide saccharique (2).

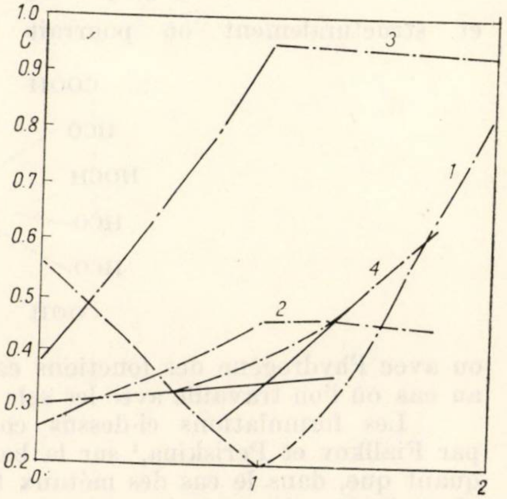

Fig. 6. — Conductibilité électrique des systèmes.

1, $SnCl_4$; *2*, $SnCl_4$ — acide gluconique ; *3*, $SnCl_4$ — acide saccharique ; *4*, $SnCl_4$ — saccharate de potassium.

4. Par la méthode des solutions isomolaires, on obtient une courbe qui présente un maximum au rapport de combinaison 1 : 1.

On a travaillé avec des solutions 0,025 M au volume total de 20 ml. Dans les figures 7.1 et 7.2 sont représentées les courbes des mélanges de $SnCl_4$ et de gluconate, respectivement de saccharate de potassium.

Les essais faits avec des mélanges où l'on a employé les acides libres n'ont pas donné de résultats univoques.

III. *Potentiel d'oxydo-réduction*

On a procédé à des essais de mesure du potentiel d'oxydo-réduction, étant connu le fait que la formation des combinaisons complexes modifie le potentiel des systèmes redox impliqués dans la réaction.

Afin de stabiliser le potentiel, on a ajouté à la solution de sel stannique de petites quantités de sel stanneux, au rapport de 1000 Sn(IV) : 1 Sn(II).

La variation du potentiel redox a été mesurée à un potentiomètre de type M—VH, en millivolts.

On a utilisé l'électrode de platine platiné et comme électrode de référence l'électrode de calomel.

Les solutions ont été préparées comme dans les méthodes décrites ci-dessus.

En titrant une solution 0,05 M $SnCl_4$ par saccharate disodique 0,25 M, on remarque un knick à un équivalent, donc au rapport molaire 1 : 1 (fig. 8.1). Le saut de potentiel est assez net si la solution par laquelle on titre est 5 fois plus concentrée que la solution titrée.

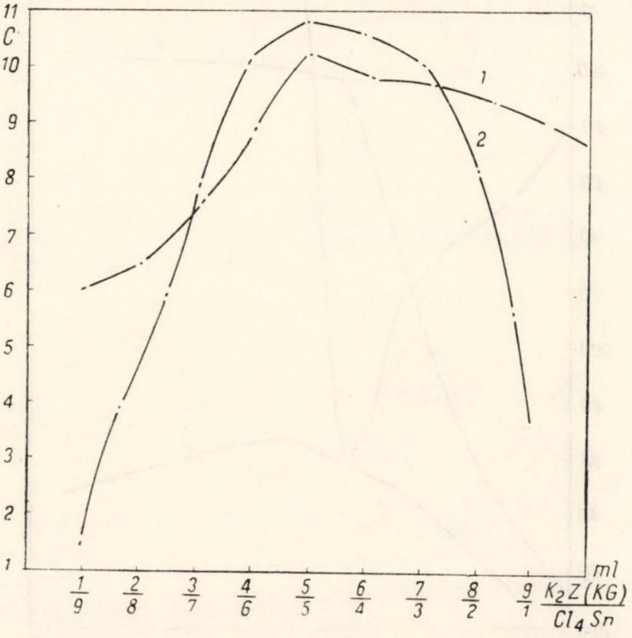

Fig. 7. — Conductibilité électrique des solutions isomolaires.
1, $SnCl_4$–gluconate de potassium; *2*, $SnCl_4$–saccharate de potassium.

Le knick apparaît au même rapport molaire au titrage du saccharate disodique par $SnCl_4$ (fig. 8.2).

Au cas où l'on travaille dans le système de mélanges continus, avec des solutions 0,25 M saccharate disodique et du $SnCl_4$, au volume total de 20 ml, on observe également la valeur maximum de potentiel au rapport de combinaison 1 : 1 (fig. 8.3).

En vertu de ces résultats, on peut affirmer qu'à la suite de la réaction de complexation entre $SnCl_4$ et l'hydroxyacide apparaît un seul complexe au rapport molaire 1 : 1.

IV. On a tenté aussi une étude spectrophotométrique, mais on n'a pas obtenu les résultats escomptés, parce que la solution du métal absorbe plus fortement que celle du complexe formé, quel que soit le pH ou le milieu où l'on travaille. On remarque le même phénomène si l'on travaille avec les sels alcalins des acides gluconique et saccharique.

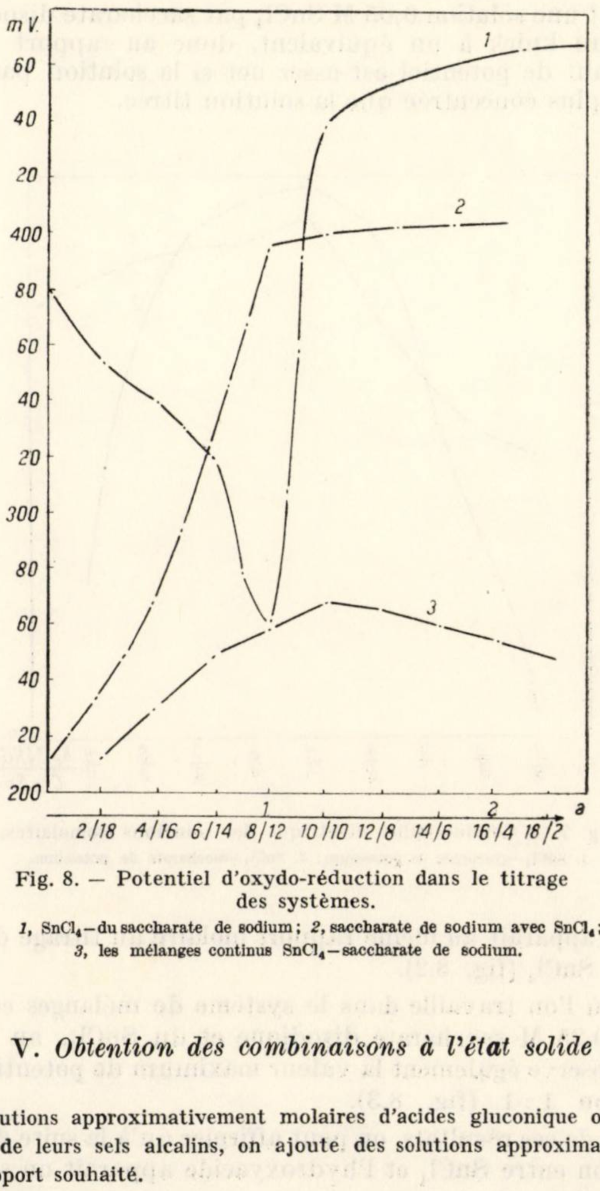

Fig. 8. — Potentiel d'oxydo-réduction dans le titrage des systèmes.

1, $SnCl_4$—du saccharate de sodium ; *2*, saccharate de sodium avec $SnCl_4$; *3*, les mélanges continus $SnCl_4$—saccharate de sodium.

V. *Obtention des combinaisons à l'état solide*

A des solutions approximativement molaires d'acides gluconique ou saccharique ou, respectivement, de leurs sels alcalins, on ajoute des solutions approximativement molaires de $SnCl_4$ au rapport souhaité.

En travaillant avec les acides libres, aucun précipité ne se sépare après addition d'alcool, le pH du mélange étant trop petit, < 1. Lorsqu'on fait s'accroître le pH du mélange des composants à 3—4 par de l'ammoniaque, il se produit la précipitation du complexe en ajoutant de l'alcool 4—5 fois le volume de la solution initiale.

En travaillant avec les sels alcalins des acides gluconique et saccharique, des solutions claires il se sépare des mélanges des précipités blancs par addition d'alcool.

On filtre les précipités, on rince à l'alcool, on fait sécher à l'air, et on obtient des substances blanches, amorphes, solubles dans l'eau.

On a dosé gravimétriquement l'étain par thioacétoamide comme SnS_2, calciné comme SnO_2. Le potassium a été dosé par tétraphényl-bore-natrium.[5] Au cas où l'on a travaillé avec les acides libres, les ions hydrogène des fonctions carboxyliques ont été déterminés par titrage par hydroxyde de potassium en présence de phénolphtaléine. L'eau a été déterminée à l'appareil d'Abderhalden, à la température d'ébullition de l'eau jusqu'à un poids constant. Le carbone, le chlore et l'hydrogène total ont été déterminés ordinairement par des méthodes micro.

Les résultats des analyses conduisent aux formulations suivantes

1. $H[Sn(OH)(Cl)(C_6H_9O_7)].\ NH_4Cl \cdot 3H_2O$ (PM = 472,8)
Calculé : C 15,24 ; Sn 25,10 ; H 4,47 ; Cl 15,00 ; N 2,96 ; H^+ 0,213 ; H_2O 11,43 %
Trouvé : C 15,01 ; Sn 24,94 ; H 4,39 ; Cl 14,88 ; N 2,99 ; H^+ 0,2104 ; H_2O 11,24 %

2. $K[SnCl_2(C_6H_9O_7)] \cdot 2H_2O$ (PM = 457,88)
Calculé : C 15,74 ; Sn 25,92 ; H 2,86 ; Cl 15,49 ; K 8,54 ; H_2O 7,87 %
Trouvé : C 15,50 ; Sn 26,07 ; H 3,16 ; Cl 15,86 ; K 8,20; H_2O 7,52 %

3. $H_2[Sn(OH)(C_6H_5O_8)] \cdot 1,5\ NH_4Cl \cdot 2H_2O$ (PM = 459,1)
Calculé: C 15,69 ; Sn 25,85 ; H 3,94 ; Cl 11,58 ; N 4,57 ; H^+ 0,439 ; H_2O 7,84 %
Trouvé : C 15,44 ; Sn 26,03 ; H 4,16 ; Cl 11,83 ; N 4,85 ; H^+ 0,4376 ; H_2O 8,01 %

4. $K_2[SnCl_2(C_6H_6O_8)] \cdot 2H_2O$ (PM = 499,9)
Calculé : C 14,4 ; Sn 23,74 ; H 2,01 ; K 15,64 ; Cl 13,86 ; H_2O 7,207 %
Trouvé : C 14,37 ; Sn 23,46 ; H 2,93 ; K 15,37 ; Cl 13,23 ; H_2O 7,339 %

Il résulte des données obtenues que lorsqu'on travaille avec les acides libres, du chlorure d'ammonium s'englobe dans la molécule.

Des données obtenues sur les combinaisons complexes à l'état solide on peut déduire qu'il se forme des anions complexes :

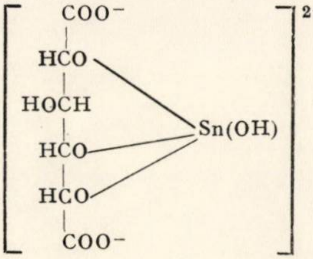

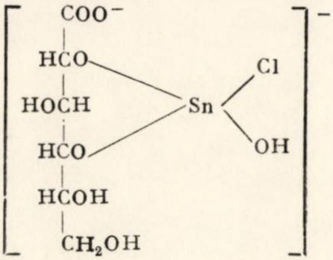

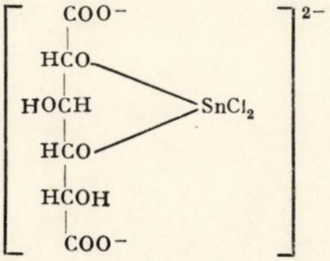

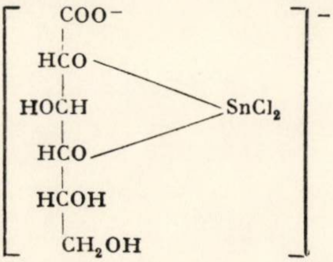

---

[5] *Z. analyt. Chem. B.*, **138**, 9 (1953).

Revue Roumaine de Chimie, **14**, 1241–1249 (1969)

KOMPLEXVERBINDUNGEN DES N,N′-DIAMINOPIPERAZINS. III

SICHTBARE- UND UV-SPEKTREN

J. DICK, ALFA LUPEA und Z. SZABADAI

Aus dem Pharmazeutisch-technischen Laboratorium der Technischen Hochschule
Timişoara, Bd. 30 Decembrie, 2

Eingegangen am 8. November 1968

Es werden die Absorptionspektren im Bereiche 200–800 cm^{-1} des N,N′-Diaminopiperazins (Dap) als solches und bei verschiedenen Wasserstoffionenkonzentrationen, wie auch die sichtbaren und UV-Spektren seiner Komplexverbindungen der allgemeinen Formel $[\mathrm{Me^{II}\,DapX_2}]\cdot\mathrm{nH_2O}$ und $[\mathrm{Me^{II-III}X_4}]\cdot(\mathrm{H_2Dap})_n$ (1. u. 2. Mitteilung) zwecks Strukturaufklärung untersucht. Die Auswertung dieser Spektren ergab Übergänge *dd**, *nσ** und *σσ** im sichtbaren bzw. UV-Spektrum der Dap-Metallkomplexverbindungen mit Banden die im allgemeinen gegenüber dem Dap-Spektrum einer hypsochromen Verschiebung unterliegen. Das auf Grund der Molekularorbitaltheorie ausgewertete Dap-Spektrum in saurem Medium, läßt einwandfrei auf eine Protonierung der exocyklischen N-Atome schließen. Die Spektralanalyse erbringt einen weiteren Beweis, daß Dap als zweizähliger Ligand betrachtet werden muß, der in den Metallkomplexverbindungen in Wannenform und im Falle der Protonierung der exocyklischen N-Atome in Sesselform vorliegt.

SICHTBARE SPEKTREN

Die Auswertung der sichtbaren Spektren der in Mitteilung 1 und 2 beschriebenen Metallkomplexverbindungen des N,N′-Diaminopiperazins (Dap) führt zu folgenden Schlußfolgerungen.

Sind die *d*-Niveaus des Zentralatoms teilweise besetzt, so erscheinen im sichtbaren Spektrum Übergangs-*dd**-Banden mit $E \lesssim 100$. Da das Ligandenfeld eine ziemlich niedrige Symmetrie aufweist, müssen mehrere *dd**-Banden vorhanden sein, die durch gegenseitiges Eindringen in einer einzigen Bande vereinigt sein können. Eine Absorption im sichtbaren Bereich ist bei den Verbindungen mit $\mathrm{Co^{2+}}$, $\mathrm{Ni^{2+}}$, $\mathrm{Mn^{2+}}$, $\mathrm{Fe^{2+}}$, $\mathrm{Pd^{2+}}$, $\mathrm{Pt^{2+}}$ und $\mathrm{Cr^{3+}}$ zu beobachten, dagegen nicht bei den Verbindungen $\mathrm{Zn^{2+}}$, $\mathrm{Cd^{2+}}$, $\mathrm{Hg^{2+}}$, wie auch bei $\mathrm{Cu_2^{2+}}$, was in letzterem Fall wohl einer vorausgesetzten intermetallischen Bindung zuzuschreiben ist.

In Tabelle 1 sind die Werte des sichtbaren Spektrums der Dap-Metallkomplexe zusammengefaßt.

Tabelle 1

Werte des sichtbaren Spektrums der Dap-Metallkomplexe

Komplex	Konz. M·10⁴	ε			
		λ_{1max}	ε_{1max}	$\lambda_{1min.}$	$\varepsilon_{1min.}$
$[NiDap(SCN)_2] . 2H_2O$	34,411			604	3,197
$[FeDap(SCN)_2] . 2H_2O$	16,440			798	36,496
$[Co(SCN)_4]H_2Dap$	35,370	469	9,824	602	2,473
$[PdCl_4]H_2Dap$	3,831			802	107,660
$[PtCl_6 Dap_2] Cl_2$	14,710			602	6,799

UV-SPEKTREN

Im UV-Spektrum des Dap erscheinen in einer Lösung von pH 6,5 zwei Banden u. zw. mit $\lambda = 305$ mμ ($E = 200$) und $\lambda = 215$ mμ ($E = 400$). In einer konzentrierten HCl-Lsg nimmt die Intensität der Banden beträchtlich ab und sie verschieben sich bis 327 mμ bzw. 208 mμ.

Um diese spektralen Verschiebungen näher zu erörtern, sollen kurzgefaßt einige Ergebnisse der unternommenen quantitativen Messungen ausgewertet werden. Zur Charakterisierung des Dap-Moleküls wurde zunächst die Molekularorbitaltheorie herangezogen, wobei die Matrixelemente mittels der Helmholtz-Wolfsbergschen Näherung abgeschätzt wurden. Von den Atomorbitalen wurden die 2*s*- und 2*p*-Funktionen des C- und N-Atoms und die 1*s*-Funktion des H-Atoms in Betracht gezogen. Die verwendeten Überlappungsintegrale entsprechen den — im Fachschrifttum angegebenen — sp^3-Hybridzuständen[2] und den Ionisierungspotentialen dieser Zustände[3] wie auch den kristallographischen (interatomische Distanzen) Angaben.[4]

Das Dap-Molekül gehört zu der Symmetriegruppe C_{2h}. Aus Tabelle 2 sind die Auswirkungen der Symmetrieoperationen auf die hybridisierten Atomorbitale der N- und C-Atome und auf die 1*s*-Orbitale des H-Atoms ersichtlich. Jede vermischte Orbitalgruppe bildet die Grundlage zur reduktiblen Veranschaulichung der Symmetriegruppe C_{2h}. Nach der Zerlegung dieser reduktiblen Veranschaulichungen in irreduktible Summen, wurde die Einteilung der Symmetrieorbitale, laut den letzteren aus Tabelle 2 vorgenommen und in Tabelle 3 zusammengefaßt.

Bei der Betrachtung dieser Tabelle ist ohne weiteres ersichtlich, daß die hybridisierten Atomorbitale derart überlappt sind, daß bloß Zweizentrenmolekularorbitale erscheinen, ohne delokalisierte Mehrzentre-

---

[1] M. Wolfsberg und L. Helmholtz, *J. Chem. Phys.*, **20**, 837 (1952).

[2] R. S. Mulliken, C. A. Rieke, D. Orloff und H. Orloff, *J. Chem. Phys.*, **17**, 1248 (1949).

[3] J. Hinze und H. N. Jaffe, *J. Amer. Chem. Soc.*, **84**, 540 (1962).

[4] R. D. Gillard und H. M. Irving, *Chem. Rev.*, **65**, 603 (1965).

Tabelle 2

Auswirkungen der Symmetrieoperationen auf die hybridisierten Atomorbitale der N- und C-Atome und auf die 1s-Orbitale des H-Atoms des Dap-Moleküls

C_2h	E	C_2	i	σ_h	
σ_1^C	σ_1^C	σ_3^C	σ_5^C	σ_7^C	
σ_3^C	σ_3^C	σ_1^C	σ_7^C	σ_5^C	
σ_5^C	σ_5^C	σ_7^C	σ_1^C	σ_3^C	
σ_7^C	σ_7^C	σ_5^C	σ_3^C	σ_1^C	
Γ	4	0	0	0	Ag + Bg + Au + Bu
σ_2^C	σ_2^C	σ_4^C	σ_6^C	σ_8^C	
σ_4^C	σ_4^C	σ_2^C	σ_8^C	σ_6^C	
σ_6^C	σ_6^C	σ_8^C	σ_2^C	σ_4^C	
σ_8^C	σ_8^C	σ_6^C	σ_4^C	σ_2^C	
Γ	4	0	0	0	Ag + Bg + Au + Bu
σ_3^N	σ_3^N	σ_8^N	σ_8^N	σ_3^N	
σ_8^N	σ_8^N	σ_3^N	σ_3^N	σ_6^N	
Γ	2	0	0	2	Ag + Bu
σ_4^N	σ_4^N	σ_5^N	σ_5^N	σ_4^N	
σ_5^N	σ_5^N	σ_4^N	σ_4^N	σ_3^N	
Γ	2	0	0	2	Ag + Bu
σ_1^N	σ_1^N	σ_7^N	σ_6^N	σ_2^N	
σ_2^N	σ_2^N	σ_6^N	σ_7^N	σ_1^N	
σ_6^N	σ_6^N	σ_2^N	σ_1^N	σ_7^N	
σ_7^N	σ_7^N	σ_1^N	σ_2^N	σ_6^N	
Γ	4	0	0	0	Ag + Bg + Au + Bu
σ_9^N	σ_9^N	σ_{13}^N	σ_{13}^N	σ_9^N	
σ_{13}^N	σ_{13}^N	σ_9^N	σ_9^N	σ_{13}^N	
Γ	2	0	0	2	Ag + Bu
σ_{12}^N	σ_{12}^N	σ_{16}^N	σ_{16}^N	σ_{12}^N	
σ_{16}^N	σ_{16}^N	σ_{12}^N	σ_{12}^N	σ_{16}^N	
Γ	2	0	0	2	
σ_{11}^N	σ_{11}^N	σ_{15}^N	σ_{14}^N	σ_{10}^N	
σ_{10}^N	σ_{10}^N	σ_{14}^N	σ_{15}^N	σ_{11}^N	
σ_{14}^N	σ_{14}^N	σ_{10}^N	σ_{11}^N	σ_{15}^N	
σ_{15}^N	σ_{15}^N	σ_{11}^N	σ_{10}^N	σ_{14}^N	
Γ	4	0	0	0	Ag + Bg + Au + Bu

orbitale zu beobachten. Diese Erscheinung vereinfacht bedeutend die Berechnungen, da der Sekulardeterminant des Systems derart blockiert wird, daß die Ordnungsmaxima jedes Satzes gleich zwei ist. Die Frage

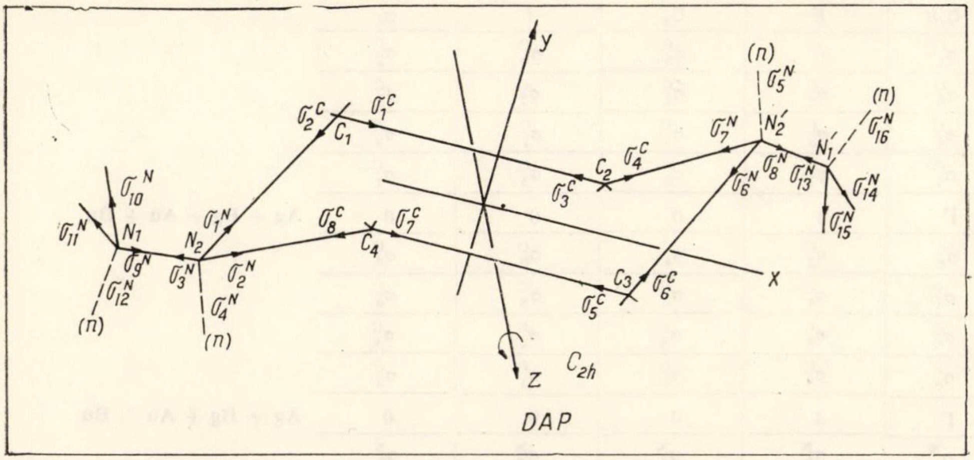
y
(n)
σ_5^N
(n)
σ_{16}^N
σ_2^C
C_1
σ_1^C
σ_7^N
N_2'
N_1'
C_2
σ_4^C
σ_6^N
σ_8^N
σ_{13}^N
σ_{14}^N
σ_{15}^N
σ_3^C
σ_{10}^N
σ_{11}^N
N_1
σ_1^N
N_2
σ_8^C
σ_7^C
C_4
σ_9^N
σ_3^N
σ_2^N
σ_{12}^N
σ_4^N
(n)
(n)
C_3
σ_6^C
σ_5^C
x
z
C_{2h}
DAP

Abb. 1. – Zugehörigkeit des Dap-Moleküls zu der Symmetriegruppe C_{2h}.

Tabelle 3

Einteilung der Symmetrieorbitale des Dap-Moleküls nach der Zerlegung der reduktiblen Veranschaulichungen in irreduktible Summen

Γ	C	N
Ag	$\sigma_1^C + \sigma_3^C + \sigma_5^C + \sigma_7^C$ $\sigma_2^C + \sigma_4^C + \sigma_6^C + \sigma_8^C$	$\sigma_3^N + \sigma_8^N$; $\sigma_9^N + \sigma_{13}^N$ $\sigma_1^N + \sigma_7^N + \sigma_6^N + \sigma_2^N$ $\sigma_4^N + \sigma_5^N$ $\sigma_{12}^N + \sigma_{16}^N$ $\sigma_{11}^N + \sigma_{15}^N + \sigma_{14}^N + \sigma_{10}^N$
Bg	$\sigma_1^C + \sigma_3^C - \sigma_5^C - \sigma_7^C$ $\sigma_2^C - \sigma_4^C + \sigma_6^C - \sigma_8^C$	$\sigma_1^N - \sigma_7^N + \sigma_6^N - \sigma_2^N$ $\sigma_{11}^N - \sigma_{15}^N + \sigma_{14}^N - \sigma_{10}^N$
Au	$\sigma_1^C + \sigma_3^C - \sigma_5^C - \sigma_7^C$ $\sigma_2^C + \sigma_4^C - \sigma_6^C - \sigma_8^C$	$\sigma_1^N + \sigma_7^N - \sigma_6^N - \sigma_2^N$ $\sigma_{11}^N + \sigma_{15}^N - \sigma_{14}^N - \sigma_{10}^N$
Bu	$\sigma_1^C - \sigma_3^C - \sigma_5^C + \sigma_7^C$ $\sigma_2^C - \sigma_4^C - \sigma_6^C + \sigma_8^C$	$\sigma_1^N - \sigma_7^N - \sigma_6^N + \sigma_2^N$ $\sigma_3^N - \sigma_8^N$; $\sigma_9^N - \sigma_{13}^N$; $\sigma_4^N - \sigma_5^N$ $\sigma_{12}^N - \sigma_{16}^N$ $\sigma_{11}^N - \sigma_{15}^N - \sigma_{14}^N + \sigma_{10}^N$

der Ermittlung der Energieniveaus erfordert damit bloß die Auflösung von Gleichungen zweiten Grades.

Die Intensität und Lage der Absorptionsbanden des Dap im Vergleich zum Spektrum des symmetrischen Dimethylhydrazins ($CH_3-NH-NH-CH_3$ $\lambda=245$ mμ ; $E \approx 100$ [5]) drängt zur Annahme, daß Übergänge zwischen den Molekularorbitalenergieniveaus der Bindung N—N vorhanden sind. Es sollen im weiteren die Ergebnisse der Berechnungen der Molekularorbitale in bezug auf diesen Teil des Dap-Moleküls erörtert werden.

In den Tabellen 4 und 5 sind die Ausgangswerte, die zur Berechnung der erhaltenen Daten herangezogen wurden, zusammengefaßt. Wie aus diesen Ergebnissen ersichtlich ist, stimmen die erhaltenen Werte der Wellenlängen mit den experimentellen Ergebnissen ziemlich gut überein.

Tabelle 4

Ionisierungspotentiale, Überlappungs- und Resonanzintegrale des Dap-Moleküls

	Ionisierungspotential (e.V)	Überlappungsintegral	Resonanzintegral (e.V)	F
C	14,61			
		0,096		
N (1)	18,93			
		0,388	−10,064	1,34
N (2)	18,93			
		0,300	− 9,3	
H	13,65			

Tabelle 5

Berechnete und gefundene Wellenlängen des Dap und $[H_2Dap]^{2+}$

	Ber.:		*Gef.:*	
Dap	λ_1(nm)	λ_2 (nm)	λ_1 (nm)	λ_2(nm)
	306	214,2	305	215
$[H_2Dap]^{2+}$	326	205	327	208

Die Resonanzintegralwerte wurden durch die Helmholtz-Wolfsbergsche Näherung ermittelt:

$$H_{ij} = \frac{H_{ii} + H_{jj}}{2} F \cdot G_{ij}$$

wo die empirische Konstante F in unserem Fall dem experimentellen Dap-Spektrum entsprechend gleich 1,34 ist.

Die Abbildung 2 erklärt die Verschiebung der Spektrallinien als Folge der Säureeinwirkung auf das Dap-Molekül. Der erste Teil der Abbildung (I) entspricht den Bindungsmolekularorbitalen, den Antibindungs- und nichtbindenden Orbitalen zwischen den N-Atomen N(1) und N(2) (zwischen N(1′) und N(2′) bilden sich gleichartige Molekularorbitale).

---

[5] S. F. Mason, *Quart. Rev.*, **35**, 287 (1961).

Da sowohl das N-Atom N(1), wie auch N(2) je ein nichtbindendes Orbital besitzen, die an der Bindung nicht teilnehmen, ist der Entartungsgrad des nichtbindenden Niveaus gleich zwei. Die Zahl (2) des ersten Teils (I) der Abbildung 2 entspricht dem Entartungsgrad der nichtbindenden Molekularorbitale. Die zwei Absorptionsmaxima entsprechen den Übergängen $n\sigma^*$ und $\sigma\sigma^*$. Dieser Übergang scheint höchstwahrscheinlich zu sein, zumal er einem Übergang zwischen den Symmetrieorbitalen g und u (Übergang $g \rightarrow u$) entspricht.

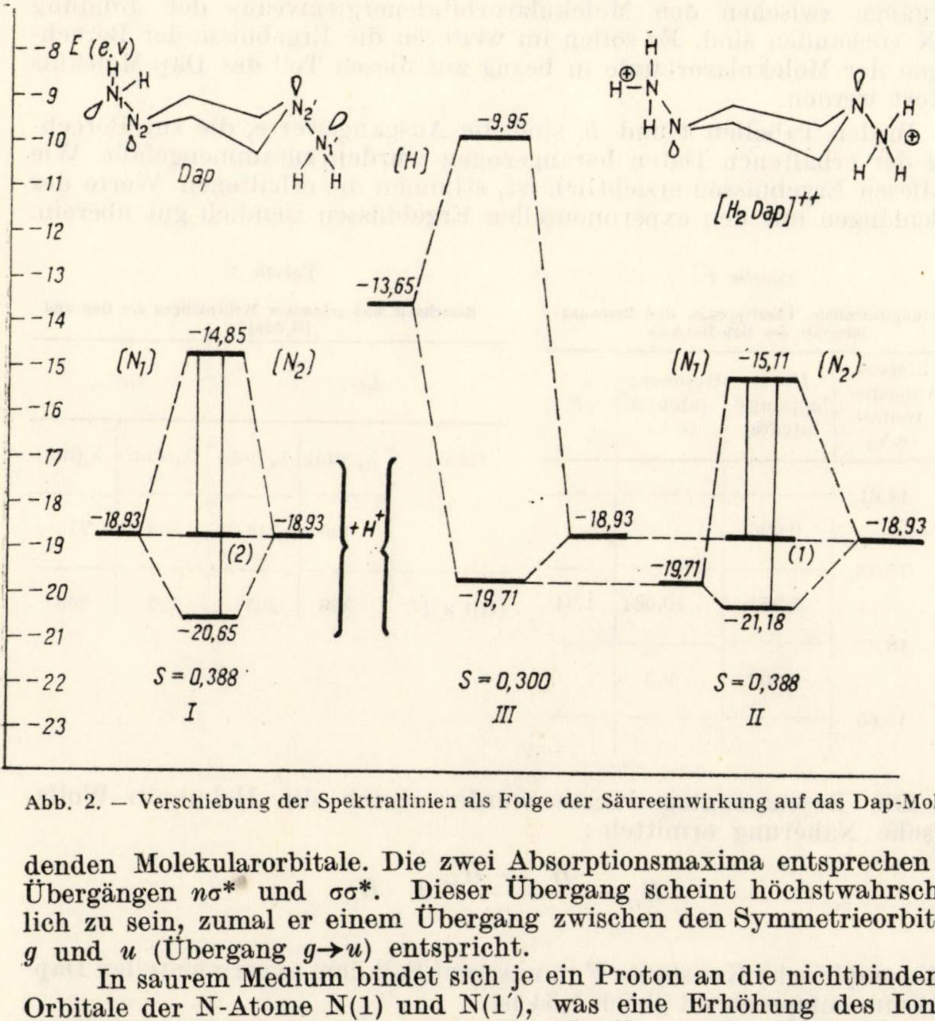
E (e.V)
−8
−9
−10
−11
−12
−13
−14
−15
−16
−17
−18
−19
−20
−21
−22
−23
Dap
[H₂ Dap]⁺⁺
N₁
N₂
N₂'
N₁'
(N₁)
(N₂)
−14,85
−18,93
−18,93
(2)
−20,65
+H⁺
(H)
−9,95
−13,65
−19,71
−18,93
−19,71
−15,11
(1)
−18,93
−21,18
S = 0,388
I
S = 0,300
III
S = 0,388
II

Abb. 2. — Verschiebung der Spektrallinien als Folge der Säureeinwirkung auf das Dap-Molekül.

In saurem Medium bindet sich je ein Proton an die nichtbindenden Orbitale der N-Atome N(1) und N(1′), was eine Erhöhung des Ionisierungspotentials der Atomorbitale des N, die an der Entstehung der Bindung N—N teilnehmen, zur Folge hat.

Das Energieniveau des Atomorbitals des N-Atoms (N_1) senkt sich bis zum Energieniveau des Orbitals der Bindung N—H (−19,71 eV), während das Atomorbitalniveau des N-Atoms (N_2) unverändert bleibt (−18,93 eV). Setzt man zunächst in erster Näherung voraus, daß das Überlappungsintegral N—N unverändert bleibt (0,388), können die Bindungs- und Antibindungsorbitalniveaus N—N berechnet werden. Wie aus dem zweiten (II) Teil der Abbildung 2 ersichtlich ist, besitzt das N-Atom

N(2) noch ein Nichtbindungsorbital. Wie aus der Abbildung weiter ersichtlich ist, ändert sich die Wellenlänge der zwei Übergänge folgendermaßen: Der Übergang mit der größeren Wellenlänge verschiebt sich in Richtung des Gebiets mit größeren, während der andere Übergang sich in Richtung des Gebiets mit kleineren Wellenlängen verlegt. Es wird damit theoretisch der Beweis der in saurem Medium stattfindenden Spektralverschiebungserscheinung erbracht.

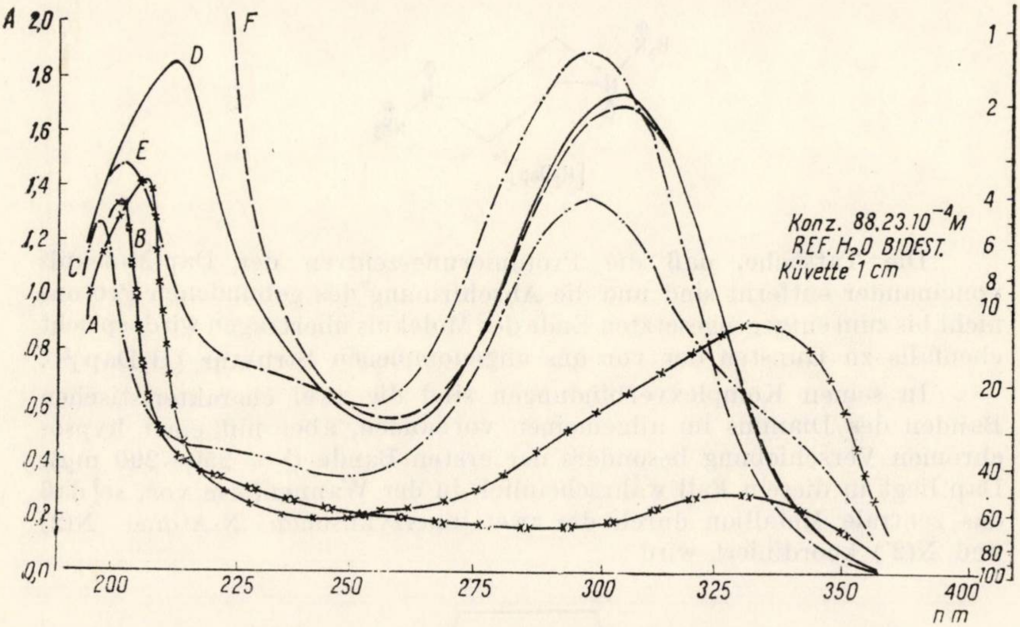

Abb. 3. — UV-Spektren des N,N′-Diaminopiperazins.

Aus Abbildung 3 sind die UV-Spektren des Diamins ersichtlich.

In Tabelle 6 sind die Molarextinktionswerte des Dap-Spektrums bei verschiedenen Wasserstoffionenkonzentrationen zusammengefaßt.

Tabelle 6

Molarextinktionswerte des Dap-Spektrums bei verschiedenem pH

Dap	pH	ε × 10²					
		$\lambda_{1\,max}$	$\varepsilon_{1\,max}$	$\lambda_{2\,max}$	$\varepsilon_{2\,max}$	$\lambda'_{1\,max}$	$\varepsilon'_{1\,max}$
Lsg A	4,97 M HCl	208	3,219	327	0,634	256	0,464
Lsg B	0,47 M HCl	203	3,060	334	2,040		
Lsg C	0,04 M HCl	199	2,833	298	3,071		
Lsg D	6,5	214	4,120	304	4,853		
Lsg E	4,5	203	3,355	298	4,251		
Lsg F	1,401 M NaOH	220	4,284	304	2,017		
Dap	8,45	215	2,470	305	1,960		

Da die im neutralen Medium zu beobachtenden Übergänge in saurem Medium verschwinden, scheint es höchstwahrscheinlich, daß in letzterem das Dap-Molekül doppelt protoniert ist, also folgende Struktur besitzt:

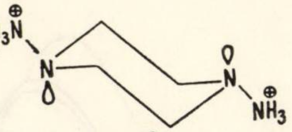

$[H_2Dap]^{2+}$

Die Tatsache, daß die Protonierungszentren des Dap-Moleküls voneinander entfernt sind und die Abschirmung des gebundenen Protons nicht bis zum entgegengesetzten Ende des Moleküls übertragen wird, spricht ebenfalls zu Gunsten der vor uns angenommenen Struktur $[H_2Dap]^{2+}$.

In seinen Komplexverbindungen sind die zwei charakteristischen Banden des Diamins im allgemeinen vorhanden, aber mit einer hypsochromen Verschiebung besonders der ersten Bande ($\lambda = 250-290$ mμ). Dap liegt in diesem Fall wahrscheinlich in der Wannenform vor, so daß das zentrale Metallion durch die zwei innerzyklischen N-Atome N(2) und N(2′) koordiniert wird

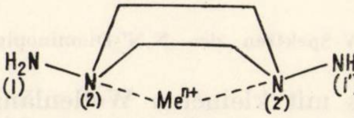

Aus der Abbildung ist ersichtlich, daß in jeder Bindung N—N sich je ein nichtbindendes Elektronenpaar in dem positiven Feld des Metalls Me^{n+} befindet und folglich zur Anregung eine größere Energie benötigt. So wird der Senkungseffekt der Energie auf das N-Atomorbital, das an der Bindung N—N teilnimmt, verringert, da die Distanz zwischen Me^{n+} und den N-Atomen größer ist als die Entfernung zwischen H^+ und N. Es erscheint also eine ähnliche Lage wie (I) aus Abbildung 2, wo aber das Nichtbindungsniveau niedrig ist (aber nicht bis —19,71 eV). Aus diesem Grunde wird sich der Übergang $n\sigma^*$ mit größeren Wellenlängen des freien Moleküls in Richtung kleinerer Wellenlängen verschieben, sinkt aber in keinem Fall bis zu den kleineren Ausgangswellenlängen des Übergangs $\sigma\sigma^*$.

Folglich bleibt die Wellenlänge des Übergangs $\sigma\sigma^*$ in der ersten Näherung unverändert, während der Übergang $n\sigma^*$ einer hypsochromen Verschiebung unterliegt, was mit dem Experimentalspektrum gut übereinstimmt.

Tabelle 7

Molarextinktionswerte der Dap-Metallkomplexverbindungen

Komplex	Konz. $M.10^{-4}$	$\varepsilon \cdot 10^{-2}$					
		$\lambda_{1\,max}$	$\varepsilon_{1\,max}$	$\lambda_{1\,min}$	$\varepsilon_{1\,min}$	$\lambda_{2\,max}$	$\varepsilon_{2\,max}$
$[CoDap(SCN)_2].2H_2O$	3,8932	220	23,064	262	8,219	276	9,503
$[NiDap(SCN)_2].2H_2O$	3,9349	221	42,695	263	1,969	289	2,604
$[MnDap(SCN)_2].2\,H_2O$	7,3790	199	78,596	260	10,974	275	12,467
$[FeDap(SCN)_2].2H_2O$	2,9350	218	55,583	265	7,409	278	7,579
$[ZnDap(SCN)_2]$	3,4050	219	47,640	269	1,471	291	2,573
$[CdDap(SCN)_2]$	6,0430	224	31,382	262	3,450	281	4,270
$[Cu_2DapBr_2].2H_2O$	1,9340	208	41,255	233	20,495	246	21,910
$[PdDapCl_2].4H_2O$	6,3270	200	82,230	217	40,300	257	95,620
$[PdDapBr_2].2H_2O$	5,3300	202	48,730	215	17,990	218	19,119
$[Hg(SCN)_4]H_2Dap$	2,1190	289	8,256				
$[HgCl_4]H_2Dap$	0,8220	218	359,910	268	44,380		
$[Zn(SCN)_4]H_2Dap.2H_2O$	3,3130	217	99,450	261	7,330	277	9,266
$[Co(SCN)_4]H_2Dap$	35,3700	224	50,890	268	3,958	285	4,240
$[PtCl_4]H_2Dap$	3,8710	220	121,400				
$[PtCl_6\,Dap_2]\,Cl_2$	1,918	207	401,420	234	71,68	261	291,950
$[Th(Dap)_6(SCN)_4].4H_2O$	1,729	217	196,650	256	47,43	294	128,390
$[BiJ_4]\,(HDap)_2.6H_2O$	0,1197	218	598,21	266	249,26	290	531,700

In Tabelle 7 sind die Molarextinktionswerte der Dap-Metallkomplexverbindungen zusammengefaßt.

Die Spektren wurden mit einem UNICAM SP 800-Apparat aufgenommen.

Revue Roumaine de Chimie, **14**, 1251–1256 (1969)

ÜBER α-DIOXIMINKOMPLEXE DER ÜBERGANGSMETALLE. XXVI*
KUPFER(II)-CHELATE MIT 1,2-CYCLOHEXANDIONDIOXIM

F. MÁNOK, CS. VÁRHELYI und ZSUZSANNA KISS-RAJHONA

Aus dem Laboratorium für Anorganische Chemie der Universität „Babeş-Bolyai“
Cluj, str. Arany János, 11

Eingegangen am 2. November 1968

Es wurden die stufenweisen Bildungskonstanten der Kupfer(II)-Chelate: $Cu(NioxH)^+$ und $Cu(NioxH)_2$ aus kolorimetrischen und potentiometrischen Messungen im Wasser bestimmt. Die Konstanten K_1 und K_2 sind von der gleichen Größenordnung, aber kleiner als die von Peshkova und Mitarb. in 50%igem Dioxan erhaltenen Werte.

Tshugaev[1] hatte erwähnt, daß das Dimethylglyoxim in Kupfersulfatlösung eine braune Färbung verursacht. Später haben Babko und Korotun [2] durch kolorimetrische Messungen bestätigt, daß in wässerigen alkoholischen Lösungen leicht lösliche, braungelbe Chelate mit einem Molarverhältnis Cu : $DH_2 = 1:1$, bzw. 1 : 2 entstehen. Diese Ergebnisse wurden auch durch chromatographische Untersuchungen von Gurvich[3] unterstützt. Es wurden auch ternäre Komplexe mit Dimethylglyoxim, wie Cu(II)-Fe(III)-DH_2 (1 : 1 : 2, bzw. 1 : 1 : 1) und Cu(II)-Acetylaceton-Dimethylglyoxim (1 : 1 : 1) nachgewiesen.[3,4] Die Stabilitätskonstanten der $Cu(DH)^+$ und $Cu(DH)_2$ wurden aus potentiometrischen Messungen, im Vergleich zu den analogen Komplexen anderer Übergangsmetalle, wie Co(II), Ni(II), Cd(II) durch Burger und Mitarb. [5-7] und Dyrssen, [8-9] als auch aus Löslichkeitsversuchen [10] berechnet.

---

[*] XXV : R. Ripan, Cs. Várhelyi und L. Szotyori, *Stud. Univ. Babeş Bolyai, Chem.*, **13** (2), 68 (1968).

[1] A. Tshugaev, „Issledovanie v oblasti komplexnykh soedinenii“, Moskau, 1906, S. 65.

[2] A. K. Babko und M. Korotun, *Zhur. obshchei Khim.*, **23**, 1302 (1953).

[3] A. M. Gurvich, *Zhur. obshchei Khim.*, **27**, 40 (1955).

[4] Sh. Kida, *Bull. Chem. Soc. Japan*, **29**, 805 (1956).

[5] K. Burger und I. Ruff, *Acta Chim. Acad. Sci. Hung.*, **41**, 75 (1963).

[6] K. Burger und I. Ruff, *Talanta*, **10**, 329 (1963).

[7] K. Burger und I. Ruff, *Magyar Kém. Folyóirat*, **70**, 351 (1964).

[8] D. Dyrssen, *Acta Chem. Scand.*, **14**, 51 (1960).

[9] D. Dyrssen und M. Hennicks, *Acta Chem. Scand.*, **15**. 47 (1961).

[10] D. Fleischer und H. Freiser, *J. Phys. Chem.*, **66**, 389 (1962).

Die $Cu(DH)_2$-Verbindung wurde auch in kristalliner Form isoliert und durch IR- und NMR-spektroskopische,[11] bzw. durch röntgenographische Messungen[12,13] wurde festgestellt, daß das $Cu(DH)_2$ eine koplanare geometrische Struktur mit zwei starken O—H..O Wasserstoffbindungen besitzt. Diese Wasserstoffbindungen sind schwächer als die der analogen $Ni(DH)_2$. Von den Kupfer(II)-Chelaten der anderen Dioxime wurden die Derivate des *o*-Chinondioxims,[14] des Acetylacetondioxims[15] und Furyldioxims[16-17] von Burger und Mitarb. untersucht. Bochkova und Peshkova[18] haben die Stabilitätskonstante der Kupferkomplexe einiger aliphatischer vicinaler Dioxime durch potentiometrische Messungen bestimmt und festgestellt, daß die Stabilität in der Reihe : Methyl-äthyldioxim, Dimethylglyoxim, Methylglyoxim, Dimethylglyoximmonomethyläther abnimmt.

Die Kupfer(II)-Chelate des 1,2-Cyclohexandiondioxims („Nyoxim") wurden nur in 50%iger wässeriger Dioxanlösung von Peshkova und Mitarb.[19] untersucht.

In dieser Arbeit wurde die Wechselwirkung von Nyoxim mit Kupfer (II)nitrat in wässeriger Lösung untersucht.

Aus kolorimetrischen Messungen nach der Jobschen Methode wurde festgestellt, daß in diesem System bei pH 4,5 ein Chelat mit der Zusammensetzung : Kupfer(II) : Nyoxim = 1 : 2, bzw. $Cu(NioxH)_2$ entsteht.

Die stufenweisen Bildungskonstanten K_1 und K_2 der Komplexe : $Cu(NioxH)^+$ und $Cu(NioxH)_2$ („NioxH" = das koordinierte Nyoxim) wurden aus potentiometrischen pH-Messungen nach der Bjerrum-Calvinschen Methode berechnet. Die so erhaltenen Bildungskonstanten K_1 und K_2 haben annähernd gleiche Werte und zeigen erhebliche Abweichungen von den von Peshkova und Mitarb.[19] für Dioxan-Wasser-Mischungen erhaltenen Konstanten.

EXPERIMENTELLES

Die Bestimmung des Molarverhältnisses der Komponenten im $Cu(NioxH)_2$-Chelat wurde nach der Jobschen Methode durchgeführt. Nach der Mischung der Kupfer(II)-nitrat- und Nyoximlösungen erscheint eine braune Färbung. Die Färbung der Lsg verstärkt sich nicht mit der Zeit und dies bedeutet, daß das Gleichgewicht sehr rasch eingestellt wird. Die braune Farbe ist beständig in einem pH-Bereich von 4 bis annähernd 8, in alkalischen Lsg (pH 9—10) schlägt sie aber in gelbgrün um.

Alle Messungen wurden bei pH = 4,5, unter Verwendung von 1 m Natriumacetat-Essigsäure-Pufferlsg, bei Zimmertemperatur (21—22°), mit einem Kolorimeter FEK (UdSSR) durchgeführt. Die isomolaren Lsgen erhielten wir aus 0,05 m $Cu(NO_3)_2$ und 0,05 m Nyoxim. Die Gesamtkonzentration der Reaktionskomponenten betrug 10^{-2}, bzw. 2.10^{-3}.

---

[11] R. E. Rundle und C. V. Banks, *J. Phys. Chem.*, **67**, 508 (1963).

[12] H. S. Jarrett, *J. Chem. Phys.*, **28**, 1260 (1958).

[13] E. Bua und G. Schiavinato, *Gazz. chim. Ital.*, **81**, 847 (1951).

[14] E. Frasson, R. Bardi und S. Bezzi, *Acta Cryst.*, **6**, 487 (1953).

[15] K. Burger und I. Ruff, *Magyar Kém. Folyóirat*, **72**, 383 (1966).

[16] K. Burger und E. Molnár, *Magyar Kém. Folyóirat*, **73**, 77 (1967).

[17] I. Ruff und K. Burger, *Magyar Kém. Folyóirat*, **71**, 437 (1965).

[18] V. M. Bochkova und V. M. Peshkova, *Zhur. neorg. Khim.*, **3**, 1131 (1958).

[19] V. M. Peshkova und V. M. Bochkova, *Nauch. Doklady Vysshei Shkoly, Khim. i khim. Tekhnol.*, **1**, 62 (1958).

Wie aus Abb. 1 hervorgeht, erscheint das Maximum der Absorption-Komposition-Kurven in beiden Fällen beim Molarverhältnis 1 : 2 und deshalb sind in dem Kupfer-Nyoximin-Chelat zwei Chelatbildnermoleküle von einem Metallion gebunden.

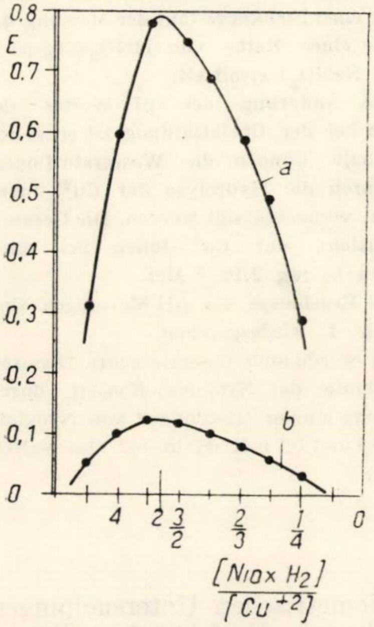

Abb. 1. — Jobsche Kurven :
a, $[Cu^{2+}] + [NioxH_2] = 10^{-2}$;
b, $[Cu^{2+}] + [NioxH_2] = 2.10^{-3}$.

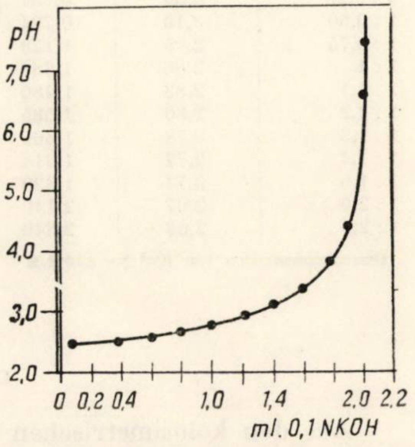

Abb. 2. — Titrationskurve von 100 ml $Cu[NO_3]_2$ — Nyoxim-Mischung bei einem Molarverhältnis 1 : 2 mit 0,1 n KOH Gesamtkonzentration von $[Cu^{2+}] = 10^{-2}$ M.

pH-metrische Untersuchungen. Für die Erklärung des Mechanismus der Bildung des obenerwähnten Chelates in Wasser wurden Kupfer(II)nitrat- und Nyoxim-Mischungen in verschiedenen Molarverhältnissen mit 0,1 n KOH titriert und die Änderung der pH-Werte potentiometrisch verfolgt. Für die pH-Messungen wurde ein pH-Meßgerät mit Glaselektrode (LP 60—UdSSR) verwendet.

Die Titrationskurve aus Abb. 2 im Falle des Molarverhältnisses $Cu(NO_3)_2$: $NioxH_2$ =1 : 2 ist im Einklang mit der folgenden Gesamtreaktion :

$$Cu^{2+} + 2NioxH_2 = Cu(NioxH)_2 + 2H^+$$

Die Titrationskurven im Falle der Mischungen mit überschüssigem Nyoxim (zum Beispiel Cu^{2+} : $NioxH_2$ = 1 : 3) zeigen, daß die Anzahl der bei der Chelatbildung freiwerdenden Wasserstoffionen bei gleichem Werte bleibt. Diese Ergebnisse bestätigen, daß die Anzahl der im Komplex gebundenen Nyoximmoleküle 2 nicht überschreitet und die Bildung der Hydroxo-nyoximato-kupfer(II)-komplexe, die zur Erhöhung der Wasserstoffionenkonzentration führen würde, vernachlässigt werden kann.

Für die Bestimmung der stufenweisen Bildungskonstanten nach der Bjerrum-Calvinschen Methode wurden die Anzahl der Mole der freiwerdenden Wasserstoffionen bei der Mischung der $Cu(NO_3)_2$- und Nyoximlsgen mit verschiedenen Molarverhältnissen gemessen. Die Ionenstärke der Lsgen wurde mit $NaNO_3$ auf 0,2 Mol $NaNO_3$ konstant gehalten. Die Bestimmung der Wasserstoffionenkonzentration bei 20° wurde mit Hilfe einer Eichkurve (aus der Messung der pH-Werte einer Reihe von HNO_3-Lsgen in 0,2 Mol $NaNO_3$) ermittelt.

Tabelle 1

Die Änderung der pH-Werte mit dem Cu^{2+}-Nyoxim-Molarverhältnis

Molarverhältnis Cu^{2+} : Nyoxim	pH	$H^+.10^3$
1 : 0	5,75	0,00178
1 : 0,25	3,34	0,457
1 : 0,50	3,10	0,794
1 : 0,75	2,95	1,123
1 : 1	2,86	1,380
1 : 1,1	2,83	1,480
1 : 1,2	2,80	1,585
1 : 1,3	2,78	1,660
1 : 1,4	2,77	1,718
1 : 1,5	2,74	1,820
1 : 2,0	2,67	2,140
1 : 2,5	2,63	2,340

Gesamtkonzentration von $[Cu^{2+}] = 2.10^{-3}$ M

Die Änderung des pH-Wertes der Lösungen bei der Chelatbildung ist erheblich und deshalb können die Wasserstoffionen, welche durch die Hydrolyse der Cu^{2+}-Ionen entstehen, vernachlässigt werden. Die Gesamtkonzentration der Cu^{2+}-Ionen bei allen Messungen betrug 2.10^{-3} Mol.

Die Ergebnisse der pH-Messungen sind in Tabelle 1 wiedergegeben.

Es wurde auch die erste saure Dissoziationskonstante des Nyoxims: K_{NioxH_2} durch pH-Messung einiger Mischungen von Nyoxim: 8.10^{-3} Mol und 0,1 n KOH in 0,2 Mol $NaNO_3$ berechnet.

DISKUSSION

Aus den kolorimetrischen und potentiometrischen Untersuchungen geht hervor, daß sich in dem untersuchten System die folgenden Gleichgewichte eingestellt haben:

$$Cu^{2+} + NioxH_2 \rightleftarrows Cu(NioxH)^+ + H^+$$

$$Cu^{2+} + 2\ NioxH_2 \rightleftarrows Cu(NioxH)_2 + 2H^+$$

Für diese Gleichgewichte werden die Stabilitätskonstanten K' und K'' mit Hilfe der Gleichungen (1) und (2) erhalten.

$$K' = \frac{[Cu(NioxH)^+][H^+]}{[Cu^{2+}]\,[NioxH_2]} \qquad (1)$$

$$K'' = \frac{[Cu(NioxH)_2]\,[H^+]^2}{[Cu^{2+}]\,[NioxH_2]^2} \qquad (2)$$

Für die Gesamtkonzentration des Liganden (C_L), bzw. des Kupfers (C_M) gelten die Gleichungen (3) und (4)

$$C_L = [NioxH_2] + K'\frac{[Cu^{2+}]\,[NioxH_2]}{[H^+]} + 2K''\frac{[Cu^{2+}]\,[NioxH_2]^2}{[H^+]^2} \qquad (3)$$

$$C_M = [Cu^{2+}] + K'\frac{[Cu^{2+}]\,[NioxH_2]}{[H^+]} + K''\frac{[Cu^{2+}]\,[NioxH_2]^2}{[H^+]^2} \qquad (4)$$

Aus (3) und (4) erhält man die Bildungsfunktion ($\bar{n}$) von Bjerrum :

$$\bar{n} = \frac{C_L - [NioxH_2]}{C_M} \tag{5}$$

woraus folgt :

$$\frac{[H^+]\cdot\bar{n}}{[NioxH_2]\;(1-\bar{n})} = K' + K'' - \frac{[NioxH_2]\;(2-\bar{n})}{[H^+]\;(1-\bar{n})} \tag{6}$$

Die Konzentration des freien, nichtkoordinierten Liganden : $[NioxH_2]$ wurde aus den experimentellen Daten der Tabelle 1 mit Hilfe der Gleichung (7) berechnet

$$C_L - [H^+] = [NioxH_2] \tag{7}$$

Die graphische Darstellung von $\frac{[H^+]\,\bar{n}}{[NioxH_2]\;(1-\bar{n})}$ gegen $\frac{[NioxH_2]\;(2-\bar{n})}{[H^+]\;(1-\bar{n})}$ gibt eine Gerade mit dem Tangens K'' (Abb. 3, „L" = „$NioxH_2$).

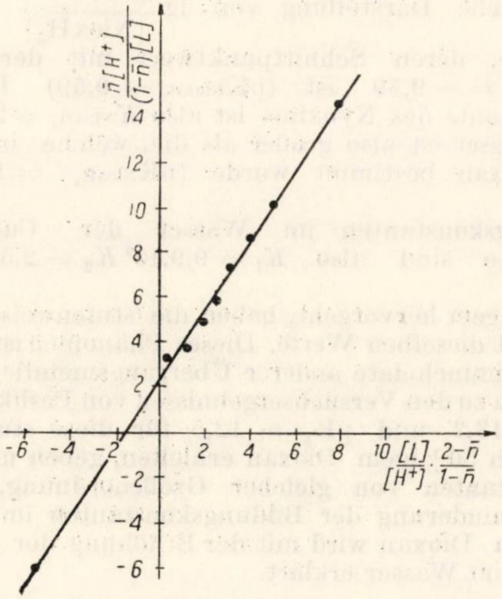

Abb. 3. — Graphische Bestimmung von K' und K''.

Der Schnittpunktwert der Geraden mit der Ordinatenachse ist gleich mit K'.

Auf diesem Wege wurden für K' und K'' die Werte 2,5, bzw. 1,55 erhalten.

Mit Hilfe von K' und K'' kann man die Bildungskonstanten K_1 und K_2 der Chelate berechnen

$$K_1 = \frac{[\mathrm{Cu\,(NioxH)^+}]}{[\mathrm{Cu^{2+}}]\,[\mathrm{NioxH^-}]} = \frac{K'}{K_{\mathrm{NioxH_2}}}\,. \tag{8}$$

$$K_1 \cdot K_2 = \frac{[\mathrm{Cu\,(NioxH)_2}]}{[\mathrm{Cu^{2+}}]\,[\mathrm{NioxH^-}]^2} = \frac{K''}{K^2_{\mathrm{NioxH_2}}} \tag{9}$$

Die saure Dissoziationskonstante des Nyoxims $K_{\mathrm{NioxH_2}}$ erhält man nach den Gleichungen (10) und (11)

$$K_{\mathrm{NioxH_2}} = \frac{[\mathrm{H^+}]\,[\mathrm{NioxH^-}]}{[\mathrm{NioxH_2}]} \tag{10}$$

$$\lg \frac{[\mathrm{NioxH^-}]}{[\mathrm{NioxH_2}]} = \lg K_{\mathrm{NioxH_2}} - \lg\,[\mathrm{H^+}] \tag{11}$$

Nach dem Elektroneutralitätsprinzip gilt:

$$[K^+] + [\mathrm{H^+}] = [\mathrm{NioxH^-}] + [\mathrm{OH^-}]$$

Die graphische Darstellung von $\lg \frac{[\mathrm{NioxH^+}]}{[\mathrm{NioxH_2}]}$ gegen $-\lg[\mathrm{H^+}]$ gibt eine Gerade, deren Schnittpunktwert mit der Ordinatenachse gleich $\lg K_{\mathrm{NioxH_2}} = -9{,}59$ ist ($\mathrm{p}K_{\mathrm{NioxH_2}} = 9{,}59$). Die erste saure Dissoziationskonstante des Nyoxims ist also $K_{\mathrm{NioxH_2}} = 2{,}52\,.10^{-\cdot 0}$. Diese Konstante im Wasser ist also größer als die, welche in 50%igem, bzw. in 75%igem Dioxan bestimmt wurde ($\mathrm{p}K_{\mathrm{NioxH_2}} = 12{,}0$, bzw. 13,11 bei 25°).

Die Bildungskonstanten im Wasser der $\mathrm{Cu(NioxH)^+}$, bzw. $\mathrm{Cu(NioxH)_2}$-Chelate sind also $K_1 = 9{,}9.10^9$ $K_2 = 2{,}5.10^9$ ($\mathrm{p}K_1 = 9{,}99$ $\mathrm{p}K_2 = 9{,}39$).

Wie aus obigem hervorgeht, haben die stufenweisen Bildungskonstanten annähernd dieselben Werte. Dieses Phänomen ist charakteristisch auch für die Dioximinchelate anderer Übergangsmetalle.

Im Vergleich zu den Versuchsergebnissen von Peshkova und Mitarb., welche $\mathrm{p}K_1 = 13{,}2$ und $\mathrm{p}K_2 = 12{,}5$ für diese stufenweisen Stabilitätskonstanten in 50%igem Dioxan erhielten, geben unsere Messungen im Wasser Konstanten von gleicher Größenordnung, aber kleineren Werten. Die Verminderung der Bildungskonstanten im Wasser im Vergleich zu 50%igem Dioxan wird mit der Erhöhung der sauren Dissoziation des Nyoxims im Wasser erklärt.

Revue Roumaine de Chimie, **14**, 1257–1262 (1969)

UNTERSUCHUNG DER GLEICHRICHTUNGS-EIGENSCHAFTEN DER HETEROGENEN MEMBRANEN. II[1]

DAS VERHALTEN EINER EINHEITLICHEN CELLULOID: KATIONIT-H + ANIONIT–OH MEMBRAN* GEGENÜBER WECHSELSTROM VON 50 Hz UND BEI DIREKTSPANNUNGEN

C. LITEANU und GH. RĂDULESCU

Babeş-Bolyai-Universität, Cluj, str. Arany János, 11 und Universität Craiova, Calea Bucureşti 165

Eingegangen am 19. Februar 1969

Es wurde ein neuer Membranentyp aus einer Mischung von Kationenaustauschern in R–H Form und Anionenaustauschern in R–OH Form mit Celluloidträgern auf Grund der Analogie zwischen *p–n* Übergängen und den ionitischen Membranpaaren mit beweglichen Ionen von entgegengesetzter Ladung (doppelbipolare Membranen) untersucht. Diese einheitliche Membran verhält sich wie ein Doppelsystem aus heterogenen Membranen mit Ionen von entgegengesetzter Ladung und hat Gleichrichtungseigenschaften.

Auf Grund der von Reiss[2] und Fuller[3] verwendeten Analogie einerseits zwischen Überschuß oder Mangel der Elektronen in Si und Ge, die den Halbleitern vom Typ *n* und *p* entsprechende Verunreinigungen enthalten, und andererseits zwischen dem Protonenüberschuß und -mangel der sauren und basischen Lösungen, zeigten erstmals Lovrecek, Despic und Bockris[4] auf experimentellem Wege die Möglichkeit der Gleichrichtung des Wechselstromes mit Hilfe der elektrolytischen *p–n* Übergänge.

---

* Es wird darauf hingewiesen, daß diese Membran mit Kationit- und Anionitkörnchen in Celluloidträgern sich von der von K. Sollner, S. Dray, E. Grim und R. Neihoff („Ion Transport Across Membranes", Academic Press, New York, 1954, S. 144–148) hergestellten Mosaikmembran und von den von D. Woermann (*Ber. Bunsenges. physik. Chem.*, **71**, 87 (1967)), beschriebenen Membranen, in denen Teile der Oberfläche anionitisch und andere kationitisch sind, unterscheidet.

[1] I. Mitt.: C. Liteanu, Gh. Rădulescu und Cs. Jámbor, *Bul. Universităţii Craiova* (in Druck).

[2] H. Reiss, *J. Chem. Phys.*, **21**, 1209 (1953).

[3] C. S. Fuller, *Rec. Chem. Progr.*, **17**, 75 (1956).

[4] B. Lovrecek, A. Despic und J. O'M. Bockris, *J. Phys. Chem.*, **63**, 750 (1959).

Bei idealen Bedingungen wird ein elektrolytischer $p-n$ Übergang mit Hilfe einer Vorrichtung mit zwei Abteilungen hergestellt. Eine Abteilung enthält einen Elektrolyt mit einem unbeweglichen Anion, und mit leicht beweglichen Protonen (eine Polysäure oder eine kationitische Membran in R—H Form), in der anderen Abteilung des Systems befindet sich ein Elektrolyt mit unbeweglichem Kation und mit leicht beweglichen Hydroxylionen (eine Polybase oder eine anionitische Membran in R—OH Form).

Im Prinzip soll solch ein elektrolytischer $p-n$ Übergang in einer Abteilung einen Elektrolyt mit sehr leicht beweglichen positiven und unbeweglichen negativen Ionen enthalten, in der anderen Abteilung, die mit der ersten in Kontakt ist, einen anderen Elektrolyt mit schwerbeweglichen positiven und leicht beweglichen negativen Ionen.

Die Gleichrichtungswirkung steigt mit dem Unterschied zwischen den Ionenmobilitäten der Elektrolyte in den beiden verbundenen Abteilungen.

Wenn die beiden Abteilungen flüssige Phasen sind, spielt die Art des Kontaktes, der sie dennoch trennt, nach Schreiber[5] eine wichtige Rolle in Hinblick auf die Gleichrichtungseigenschaften.

In letzter Zeit wurde eine Reihe von Arbeiten veröffentlicht, über die Gleichrichtungseigenschaften der doppelbipolaren Membranen, [6–15] das heißt der durch die Anlagerung einer anionitischen und einer kationitischen Membran entstehenden Systeme.

Das Interesse für dieses Problem ist dadurch erklärt, daß zwischen den künstlichen und biologischen Membranen, und auch zwischen den bipolaren Membranen und den Halbleiterdioden eine Analogie besteht.[16]

In dieser Arbeit wurde der Gleichrichtungseffekt einer einzigen einheitlichen heterogenen Membran bei 50 Hz Frequenz untersucht. Für die Herstellung der Membran wurde ein stark saurer Kationenaustauscher Allassion CSNA in R—H Form und ein stark basischer Anionenaustauscher Dowex-1 in R—OH Form verwendet, der Träger war Celluloid. Die Ionenaustauscher wurden fein zerrieben und durch ein Sieb von 0,1 mm gesiebt und die nötige Menge mit einer Celluloidlösung in Aceton vermischt. Die homogene Mischung wurde auf eine Glasplatte ausgebreitet. Nach dem Verdampfen des Lösungsmittels kann man die gebildete Membran von der Glasplatte leicht ablösen.[1]

---

[5] B. Schreiber, *Compt. rend.*, **264** (C), 652 (1967).

[6] V. N. Maslov und A. V. Ovodova, *Zhur. fiz. Khim.*, **34**, 431 (1960).

[7] B. Lovrecek und B. Kunst, *Nature*, **189**, 804 (1961).

[8] B. Lovrecek und B. Kunst, *Croat. Chim. Acta*, **34**, 137, 219 (1962); **35**, 7 (1963).

[9] J. Oshida und Y. Sugunuma, *Bull. Kobayashi Inst. physic. Res.*, **13**, 96 (1963); *Chem. Abstr.*, **62**, 7408 d (1965).

[10] M. Seno und T. Yambe, *Bull. Chem. Soc. Japan*, **37**, 668 (1964).

[11] H. J. Friedlander, *J. Polymer. Sci. Ser. C.*, **4**, 1447 (1964).

[12] P. Läuger, *Ber. Bunsenges. physik. Chem.*, **68**, 534 (1964).

[13] S. Oshki, *J. Phys. Soc. Japan*, **20**, 1674 (1955).

[14] A. I. Tchernova, I. A. Melnik, V. I. Maslov und Iu. A. Zotov, *Doklady Akad. Nauk S.S.S.R.*, **174**, 895 (1967).

[15] K. Shimizu, M. Seno und R. Nazaki, *Bull. Chem. Soc. Japan*, **41**, 803 (1968).

[16] A. Mauro, *Biophys. J.*, **2**, 179 (1962).

Diese Arbeit wurde mit einer einheitlichen heterogenen Membran von folgender Zusammensetzung durchgeführt :

— Allassion CSNA	29 %
— Dowex-1	45,4 %

d.h. ein Gesamtgehalt an Ionenaustauscher von 74,4 %.

Nach dem Anfeuchten mit Wasser wird die Membran zwischen zwei Elektroden aus rostfreiem Stahl[10] mit einer Oberfläche von 1 cm² gepreßt. Das ganze Membranhaltersystem wird mit Paraffin abgedichtet um den nötigen Feuchtigkeitsgehalt (in diesem Falle ungefähr 10 %) konstant zu halten. In Abb. 1 ist das Membran-Elektrodensystem dargestellt.

In Abb. 2 ist das elektrische Schema für das Aufnehmen der Stromspannungskurve wiedergegeben. In Abb. 3 ist das Schema der Verbindungen des Kathodenstrahloszillographen sowohl für das Aufnehmen der Stromspannungskurve als auch für den Vergleich der gleichgerichteten Kurven mit dem verwendeten sinusoidalen Signal dargestellt. Die Untersuchungen wurden mit einem TPW-Duoskop RFT Oszillographen durchgeführt.

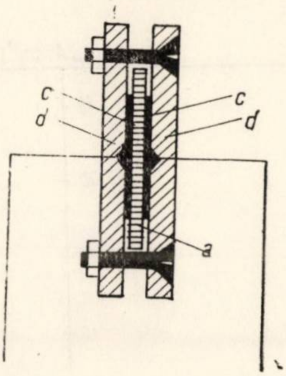

Abb. 1. — *a*, einheitliche Anionit-Kationit-Membran; *c*, Elektroden aus rostfreiem Stahl; *d*, Plexiglasträger.

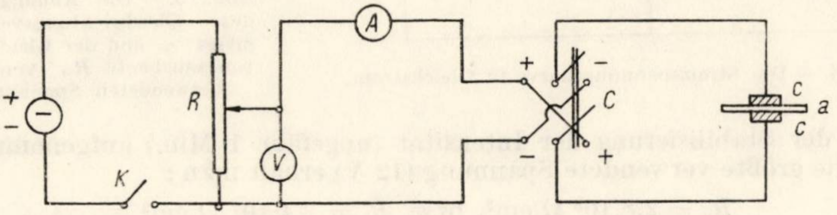

Abb. 2. — *a*, einheitliche Anionit-Kationit-Membran; *c*, Elektroden aus rostfreiem Stahl; *C*, Doppelschalter; *A*, Amperemeter; *V*, Voltmeter; *K*, Schalter; *R*, Potentiometer.

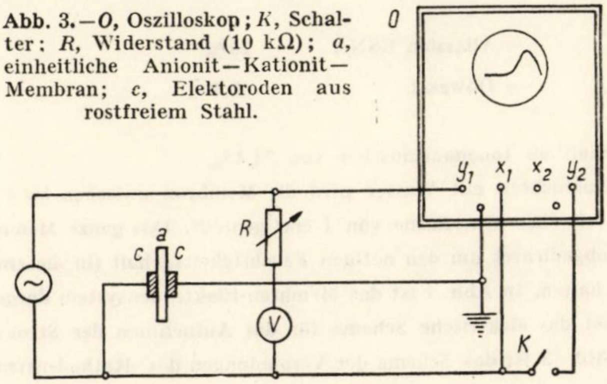

Abb. 3. – *O*, Oszilloskop; *K*, Schalter; *R*, Widerstand (10 kΩ); *a*, einheitliche Anionit–Kationit–Membran; *c*, Elektoroden aus rostfreiem Stahl.

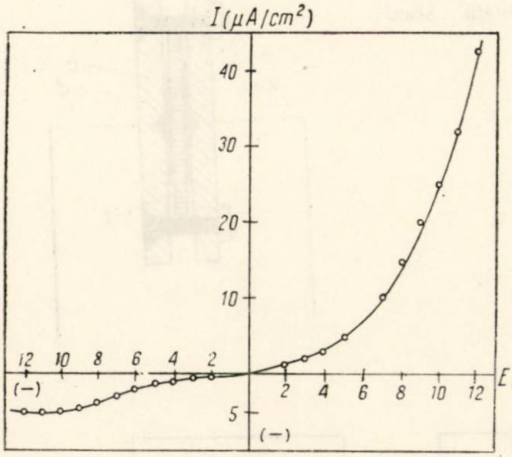

Abb. 4. – Die Stromspannungskurve in Gleichstrom.

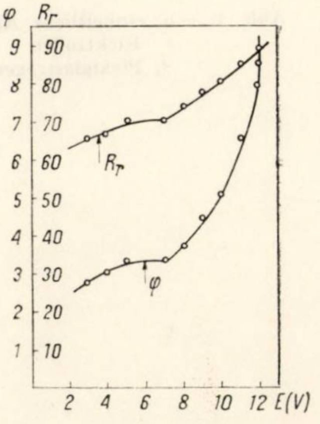

Abb. 5. – Die Abhängigkeit des Gleichrichtungsverhältnisses φ und der Gleichrichtungsausbeute R_r von der verwendeten Spannung.

Die Abb. 4 gibt die Stromspannungskurve bei Gleichstrom unter Verwendung der Vorrichtung aus Abb. 2 wieder. Die Stromwerte wurden nach der Stabilisierung der Intensität (ungefähr 1 Min.) aufgenommen. Für die größte verwendete Spannung (12 V) erhält man :

$$R_a = 2{,}8.10^5\ \Omega/\text{cm}^2,\ \text{bzw.}\ R_i = 2{,}4.10^6\ \Omega/\text{cm}^2$$

(R_a – innerer direkter Widerstand und R_i – Widerstand in umgekehrter Stromrichtung).

Für dieselbe verwendete Maximalspannung (12 V) ist das Gleichrichtungsverhältnis

$$\varphi = \frac{I_d}{I_i} = 8{,}6 \text{ und die Gleichrichtungsausbeute}^1$$

$$R_r = \frac{I_d - I_i}{I_d} \cdot 100 = 88\% \qquad (1)$$

In Abb. 5 sind die Gleichrichtungsverhältnisse (φ) und die Gleichrichtungsausbeuten (R_r) in Abhängigkeit von der verwendeten Spannung des Systems dargestellt.

Es ist bekannt, daß sowohl für das direkte als auch für das umgekehrte Gebiet folgende Gleichung gilt

$$i = i_0 \left[\exp \frac{eV}{kT} - 1 \right] \tag{2}$$

wo i der Gesamtstrom durch den Übergang, i_o die Summe der beiden Feldströme, e die elementare Elektrizitätsladung ($e = 1{,}602.10^{-19}$C) und k die Boltzmannsche Konstante bedeutet ($k = 1{,}38.10^{-23}$ Joule. Grd.$^{-1}$).

Für $\frac{kT}{e} > 0{,}026$ V (bei Zimmertemperatur) kann man die Einheit in der Klammer des Ausdrucks (2) vernachlässigen. Daraus folgt

$$i = i_0 \cdot \exp \frac{eV}{kT} \tag{3}$$

Ausgehend von der Gleichung (3), welche die theoretische Charakteristik in den obenerwähnten Bedingungen beschreibt, durch Vergleiche mit der experimentellen Charakteristik, mit Hilfe der Gleichung

$$i = i_0 \exp \frac{eV}{\eta k T} \tag{4}$$

kann man die Abweichungen von der theoretischen Voraussetzung feststellen. Die Abweichung des Koeffizienten η von der Einheit, zeigt die Abweichung der experimentellen Charakteristik von der idealen Gleichrichtungscharakteristik.

Aus der graphischen Darstellung von $\ln i = f(V)$ bzw.

$$\ln i = \ln i_0 + \frac{e}{\eta k T} \cdot V \tag{5}$$

für die untersuchte Membran wurde der Wert des Koeffizienten η aus der Neigung der Geraden bestimmt (Abb. 6).

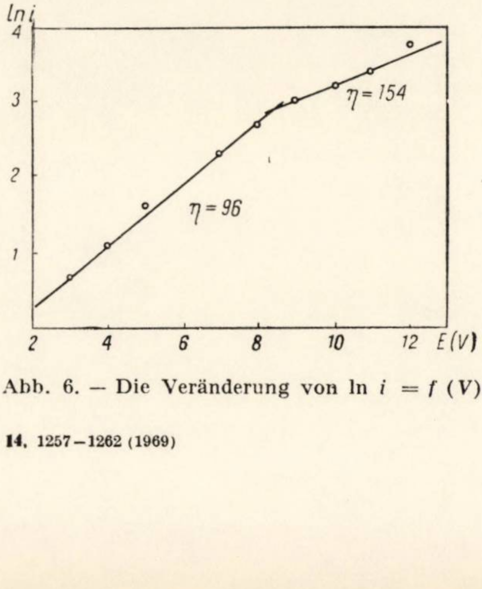

Abb. 6. — Die Veränderung von $\ln i = f(V)$.

So findet man bei $T = 298°$ K für $U > 8$ V, $\eta = 154$, bzw. für $U < 8$ V, $\eta = 96$. Dieses bedeutet, daß die experimentelle Charakteristik der theoretischen bei niederen Spannungswerten näher kommt.

ZUSAMMENFASSUNG

Die einheitliche heterogene Membran, die in einem Celluloidträger eine Mischung aus Ketionit in R—H Form und Anionit in R—OH Form enthält, weist gute Gleichrichtungseigenschaften bei einer Frequenz von 50 Hz auf und verhält sich wie ein Doppelmembransystem.

Das Verhalten dieses p—n Überganges wurde auf Grund der Stromspannungskurve im Gleichstrom mit der theoretischen charakteristischen Kurve eines p—n Überganges verglichen. Bei Zimmertemperatur (298° K) und kleinen Spannungen ($U < 8$ V) ist die experimentelle Charakteristik der theoretischen näher.

Revue Roumaine de Chimie, **14**, 1263–1267 (1969)

POLYPYRAZOLES. III*

N-ARYLATION DES PYRAZOLES

C. CHIRIAC, LEONIA STOICESCU-CRIVETZ et I. ZUGRĂVESCU

Institut de Chimie macromoléculaire «P.Poni» de l'Académie, Filia le de Jassy,
41 A, Aleea Grigore Ghica Vodă

Reçu le 17 janvier 1969

Les pyrazoles N-sodés réagissent avec les différents halogénures d'aryle pour donner les pyrazoles N-arylés. On a étudié les conditions de cette réaction. L'application de cette réaction aux produits difonctionnels conduit à l'obtention des polymères pyrazoliniques. Les polypyrazoles synthétisés présentent une stabilité thermique à l'air jusqu'à 300°.

INTRODUCTION

On connaît les réactions d'arylation des phénols[1,2] et des amines[3] avec les dérivés halogénés aromatiques, en présence du cuivre ou de ses sels (réaction d'Ullmann). L'application de cette réaction à la N-arylation des hétérocycles a été rarement expérimentée. Il y a un brevet concernant la N-arylation du carbazol[4], et récemment on a réalisé l'arylation de la phénothiazine et de la phénoxazine[5] en présence du cuivre.

Dans le cadre de nos recherches sur les polypyrazoles [6,7] nous avons étudié l'application de cette réaction au cycle pyrazolique.

L'action du C_6H_5X (X = Cl, Br, I) sur les dérivés pyrazoliques N-métalliques, dans un solvant aprotique comme la diméthylformamide (DMF), la diméthylacétamide (DMA), le diméthylsulfoxyde (DMSO), la N-méthylpyrrolidone (NMP), en présence de CuI, conduit à des N-phénylpyrazoles. Nous avons étudié les conditions optima de la réaction afin d'obtenir les meilleurs rendements, et nous avons étudié l'extension de cette réaction d'Ullmann aux produits difonctionnels pour la synthèse des polypyrazoles thermostables.

---

[*] C. Chiriac, L. Stoicescu-Crivetz et I. Zugrăvescu, *Rev. Roumaine Chim.*, **12**, 1489 (1967) ; **14**, 763 (1969).

[1] F. Ullmann, *Ber. dtsch. chem. Ges.*, **38**, 2211 (1905).

[2] H. Adkins et P. E. Weston, *J. Amer. Chem. Soc.*, **50**, 864 (1928).

[3] I. Goldberg, *Ber. dtsch. chem. Ges.*, **40**, 4541 (1907).

[4] L. Cassella, D. P. 224 951, 4/4 1909 ; *Chem. Zentr.*, **1910**, II, 699.

[5] H. Gilman, A. Weipert, R. O. Ranck et F. N. Hayes, *J. Org. Chem.*, **23**, 628 (1958).

[6] C. Chiriac, L. Stoicescu-Crivetz et I. Zugrăvescu, *Rev. Roumaine Chim.*, **12**, 1489 (1967).

[7] C. Chiriac, L. Stoicescu-Crivetz et I. Zugrăvescu, *Rev. Roumaine Chim.*, **14**, 763(1969).

RÉSULTATS ET DISCUSSIONS

Le schéma de la réaction de N-arylation des pyrazoles est le suivant

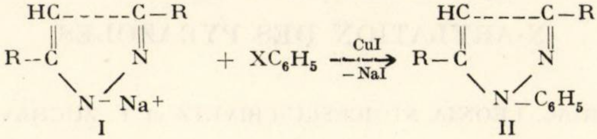

a. $R=H$	$X=Cl$	a. $R=H$
b. $R=CH_3$	$X=Br$	b. $R=CH_3$
c. $R=C_6H_5$	$X=I$	c. $R=C_6H_5$

Pour l'étude de cette réaction, l'influence des divers facteurs a été envisagée : solvants, durée de la réaction, nature de l'halogène (X), substituants (R) du cycle pyrazolique. Les résultats sont rassemblés dans le tableau 1. On a constaté que fonction de la durée de la réaction, le rendement croît jusqu'à $t = 30$ h, puis devient pratiquement constant. La majorité des réactions de N-arylation des pyrazoles ont été effectuées dans la DMF, vu qu' on n'a pas observé de changements visibles du rendement, en fonction du solvant aprotique utilisé. La nature de l'halogène exerce une influence prononcée sur la réaction, le rendement s'accroissant dans l'ordre $PhCl < PhBr < PhI$. Ce comportement est en accord avec les résultats obtenus dans d'autres réactions d'Ullmann,[8] le plus actif étant l'iodure de phényle. En ce qui concerne les substituants (*R*) du cycle pyrazolique on observe un décroissement important des rendements suivant l'ordre : $H > CH_3 > C_6H_5$. Le rendement est sensiblement meilleur avec le pyrazole Ia. Ce comportement est dû probablement au volume plus grand du substituant phényle. On a signalé un empêchement stérique de

Tableau 1

Condition de la réaction

Pyrazoles I R	Halogénure X	Temps h	Température 0°C	Rendement %
H	I	30	150	90
CH_3	I	30	150	81
C_6H_5	I	30	150	45
CH_3	Cl	30	150	48
CH_3	Br	30	150	70
CH_3	I	30	150	81
CH_3	I	10	150	46
CH_3	I	20	150	64
CH_3	I	30	150	81
CH_3	I	40	150	83
CH_3	I	50	150	83

---

[8] R. G. Bacon, *Quart. Rev.*, **19**, 103 (1965).

la même nature que dans d'autres cas similaires[9]. La nature du catalyseur CuI, CuBr, CuCl ne détermine pas de variations appréciables ; de même, en utilisant un excès d'halogénure le rendement de la réaction ne change pas.

On peut observer que la nature de l'halogène, du substituant *R*, le temps de la réaction et la présence du catalyseur ont des effets déterminants dans la réaction de N-arylation des pyrazoles. Cette réaction ne se produit qu'en présence du catalyseur, donc probablement le pyrazole N-sodé ne réagit pas comme l'amidure de sodium, ou le phényle-amidure de sodium (C_6H_5NHNa) pour métalliser la position *ortho* de l'halogénure de phényle et donner un intermédiaire *aryne*,[10] avec lequel il réagisse plus loin. En écartant la possibilité d'un mécanisme *benzyne*, il reste pour cette réaction le mécanisme proposé pour la réaction classique d'Ullmann

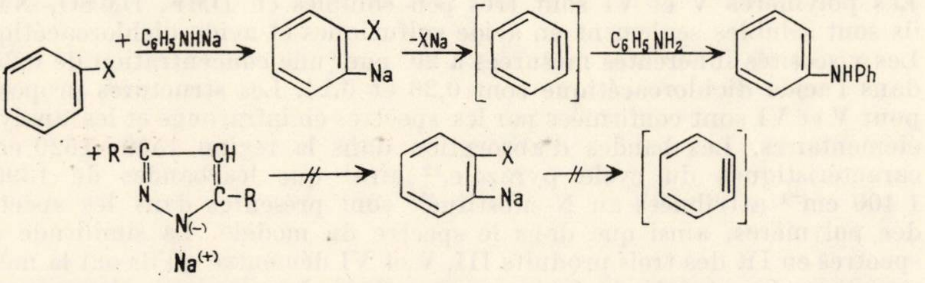

Polypyrazoles. Nous avons utilisé la réaction d'arylation à la synthèse des polypyrazoles, en l'adaptant aux produits difonctionnels. A cette fin nous avons pris comme substances de départ de 3,3′, 5,5′-tétraméthyl-4,4′-dipyrazolyl[11] qui réagit avec les dihalogénures, comme le *p*-diiodobenzène, ou le 4,4′-dichlorodiphénylsulfone, pour donner des polypyrazoles suivant le schéma

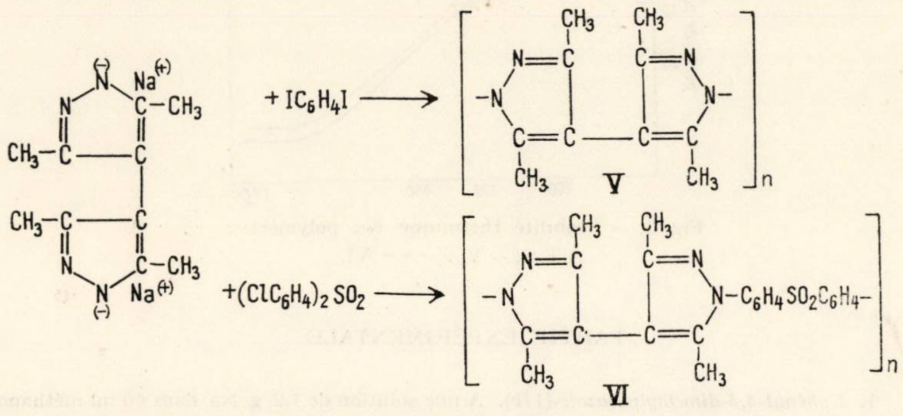

---

[9] J. P. Wilshire, *Austral. J. Chem.*, **19**, 1936 (1966).
[10] F. Scardiglia, *J. Org. Chem.*, **23**, 630 (1958).
[11] W. L. Mosby, *J. Chem. Soc.*, **1957**, 4001.

Pour une confirmation de la structure des polymères nous avons aussi synthétisé le 1,4-phénylène-bis-(3,5-diméthylpyrazole) comme modèle de référence

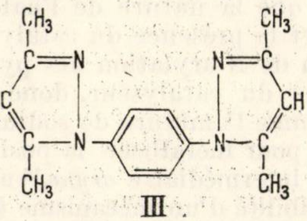

III.

Les polymères V et VI sont très peu solubles en DMF, DMSO, NMP, ils sont solubles seulement en acide sulfuriques et acide dichloroacétique. Les viscosités inhérentes mesurées à 20° pour une concentration de 0,25% dans l'acide dichloroacétique sont 0,26 et 0,24. Les structures proposées pour V et VI sont confirmées par les spectres en infrarouge et les analyses élémentaires. Les bandes d'absorption dans la région 1500—1520 cm^{-1} caractéristiques du cycle pyrazole,[12] ainsi que les bandes de 1390—1 400 cm^{-1} attribuées au N-substitué[13] sont présentes dans les spectres des polymères, ainsi que dans le spectre du modèle. La similitude des spectres en IR des trois produits III, V et VI démontre qu'ils ont la même structure. Les points de fusion sont >350°. Les analyses thermogravimétriques à l'air, pour un régime de chauffage de 12° par minute, donnent des courbes semblables pour les deux polymères (fig. 1). On constate une perte de poids de 15% à 400°. La dégradation commence à 300°.

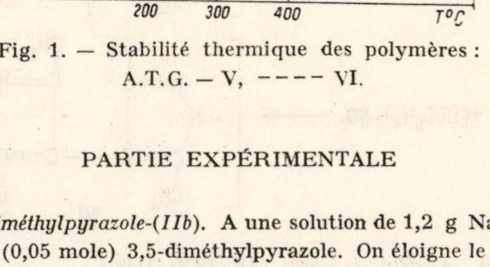

Fig. 1. — Stabilité thermique des polymères : A.T.G. — V, ---- VI.

PARTIE EXPÉRIMENTALE

1. *1-phényl-3,5-diméthylpyrazole-(IIb)*. A une solution de 1,2 g Na dans 60 ml méthanol anhydre on ajoute 4,8 g (0,05 mole) 3,5-diméthylpyrazole. On éloigne le méthanol et on ajoute 75 ml DMF, en chauffant jusqu'à la dissolution complète. On ajoute 105 g (0,05 mole)

---

[12] C. R. Hauser et C. E. Cain, *J. Org. Chem.*, **23**, 1143 (1958).

[13] G. Zerbi et C. Alberto, *Spectrochim. Acta*, **18**, 407 (1962).

iodobenzène et 1 g (0,005 mole) CuI. On porte à l'ébullition. Après 30h de chauffage on refroidit, on filtre et on lave le précipité avec 10 ml DMF. On prend le filtrat, on fait évaporer le solvant et on extrait trois ou quatre fois avec du benzène (100—150 ml). On sèche la solution benzénique sur le sulfate de sodium, on distille le benzène, et on recueille la fraction à 145°C/12 mm Hg, qui représente le 1-phényl-3,5-diméthylpyrazole.

2. *Le 1-phénylpyrazole-(IIa)* a été préparé comme le dérivé précédent.

3. *Le 1, 3, 5-triphénylpyrazole-(IIc)* est préparé comme IIb, à partir de 3,5-diphénylpyrazole[14] (1 mole), natrium (1 atome g), iodobenzène (1 mole) et CuI. On évapore la DMF sous vide, on extrait le résidu à l'alcool, on concentre la solution et le produit cristallise par refroidissement. On recristallise à l'alcool le 1, 3, 5-triphénylpyrazole, P. Fus = 138° (litt. 139,5°).[15]

4. *Le p-phénylène-bis-(3,5-diméthylpyrazol-1-yl)-III* est obtenu selon.[16]

5. *Polymère V*. A une solution de 0,23 g (0,01 mole) Na dans 50 ml méthanol anhydre, on ajoute 0,95 g (0,005 mole) IV. On évapore le méthanol, on ajoute 250 ml DMF et on chauffe, en agitant, jusqu'à ce que la solution devient claire. On ajoute 1,649 g (0,005 mole) *p*-diiodobenzène[17] et 0,190 g (0,001 mole) CuI, on chauffe à 150—160° pendant 30 h, sous azote. On chasse la DMF sous vide, on disperse le précipité dans 100 ml eau et on acidifie par acide chlorhydrique dilué. On filtre, on lave à l'eau et à l'ammoniaque concentré jusqu'à la décoloration du filtrat. On lave à l'eau puis à l'acétone. On fait sécher sous vide, à 100°. Poudre incolore infusible jusqu'à 350°, insoluble dans les solvants habituels, soluble dans l'acide sulfurique, dichloroacétique.

6. *Le polymère VI* est préparé de la même manière et dans les mêmes conditions que V, à partir de IV et de la 4,4'-dichlorophénylsulfone.[18]

---

[14] D. M. ANDERSON et J. L. DUNCAN, *J. Chem. Soc.*, **1961**, 4202.

[15] CH. MOUREU et E. BRACHIN, *Compt. rend.*, **136**, 1264 (1903).

[16] H. A. SCHOUTISSEN, *Rec. Trav. chim.*, **53**, 561 (1934).

[17] H. A. SCHOUTISSEN, *J. Amer. Chem. Soc.*, **55**, 4537 (1933).

[18] F. BECKURTS, *Ber. dtsch. chem. Ges.*, **11**, 2065 (1878).

Revue Roumaine de Chimie, **14**, 1269–1279 (1969)

CONSIDERATIONS ON ELECTRICAL CONDUCTION MECHANISMS IN POLYMERS FROM LIQUID PARAFFINIC HYDROCARBONS DATA

TH. DELEANU and N. GEORGESCU
Institute of Physical Chemistry of the Academy
str. Galați 31, Bucharest, Romania

Received August 6, 1968

An evaluation is presented of the mechanism of electric conductivity in liquid organic compounds of high electric resistance. It is shown that in the process of free electron trapping, the interaction takes place with respect to molecular vibration. Since the radius of the effective trapping cross-section is of the same order of magnitude as the vibration caused by the distorsion of the hydrocarbon molecule, it appears that a more adequate model would be that of alternate conductivity, ionic and electronic.

INTRODUCTION

Lately increased attention has been paid to the electric conductivity of compounds with high resistance, particularly of organic polymers and dielectric organic liquids. Since very reliable experimental data in this field are difficultly obtained, the mechanisms proposed to explain electric conductivity are still on an early stage of elaboration.[1–4]

Electric conductivity is a process which takes place at the level of intermolecular forces. Thus the nature of the chemical bond within the molecule, affects but indirectly the phenomenon. This may be an explanation of the fact that in the literature the behaviour of organic polymers is often compared to that of crystalline metal oxides.[5] The dependence of the electric conductivity of polymers on their degree of crystallinity has been investigated only in the case of the polyethyleneterephthalate.[6]

Since the statistical organization of the material in polymers is intermediate between the amorphous state, let it be called improperly

---

[1] A. A. Zaky, H. Tropper and H. House, *Brit. J. Appl. Phys.*, **14**, 651 (1963).
[2] M. J. Morant, *Brit. J. Appl. Phys.*, **14**, 469 (1963).
[3] H. A. Pohl, *J. Polymer Sci. part C*, **17**, 13 (1967).
[4] F. Gutmann, *J. Polymer Sci. part C*, **17**, 41 (1967).
[5] Y. Miyoshi and K. Chino, *Japan. J. Appl. Phys.*, **6**, 181 (1967).
[6] F. S. Smith and Cl. Scott, *Brit. J. Appl. Phys.*, **17**, 1149 (1966).

perfect, corresponding to simple organic liquids, and the perfect crystal state,[7] it has been considered worth while to study to what extent conclusions could be drawn on the mechanism of conductivity in polymers, using to this purpose data related to liquid saturated acyclic hydrocarbons.

It is very likely that organic liquids represent a proper amorphous state, different from that investigated by Gubanov,[8] in the form of an imperfect crystalline micro-organization. It is to be expected that each of these states would lead to a different mechanism of electric conductivity.

Several authors have tried to work out a mechanism of the electric conductivity in dielectric organic liquids. The work of Riehl[9] may be considered as fundamental in this respect. In our opinion it constitutes a valuable contribution which, although it did not bring the results expected at the time, means however a new path of investigation followed particularly by his co-worker Bässler,[10] who succeeded in correlating the activation energy of conductivity to the chemical structure of the various classes of liquid organic compounds.

In general, almost all investigators admit a mechanism involving exclusively free electrons, i.e. a mechanism similar to that of solid organic semiconductors. Among the more important works in which this viewpoint is substantiated, the papers of Le Blanc[11] and Forster[12] must be cited. Other authors such as Adamczewsky[13] or Felsenthal[14] do not rule out "a priori", the possible existence of an ionic mechanism, whose role however, is not very clearly elucidated.

The view which is expounded in the present work consists in admitting the existence of an ionic conductivity, alternating with an electronic conductivity, where it is admitted that the mean life of an ion as well as that of a neutral molecule has a finite value. The work is meant as a contribution towards the elucidation of the mechanism of electric conductivity in liquid paraffinic hydrocarbons, where use could be made of the Stokes formula, and thus to try at a latter stage to throw more light on similar phenomena in the amorphous solid state.

THE CONTRIBUTION OF THE IONIC CONDUCTIVITY

We shall refer in this part to works in which it is implicitly admitted that, the conduction process is exclusively electronic.

Thus Le Blanc[11] has determined the mobility of the negative charge carriers in n-hexane. In an electric field of 1 Kv/cm, the activation energy of the mobility was about 0.14 eV and the activation energy of the product $\eta . \mu$ (η = viscosity and μ = mobility) is 0.07 eV.

---

[7] "Configurations and Interactions of Macromolecules and Liquid Crystals", in *Discuss. Faraday Soc.*, **25**, 18, 33 (1958).

[8] A. J. Gubanov, "Quantum electronic theory of amorphous conductors", S. J. Consultant Bur. Enterprises, New York, 1965, p. 27–34.

[9] N. Riehl, *Ann. der Physik*, **20**, 93 (1957).

[10] H. Vogel and H. Bässler, *Z. Naturforsch.*, **19 a**, 1070 (1964).

[11] O. Le Blanc, *J. Chem. Phys.*, **30**, 1443 (1959).

[12] E. O. Forster, *J. Chem. Phys.*, **37**, 1021 (1962).

[13] M. A. Adamczewsky, *Brit. J. Appl. Phys.*, **16**, 759 (1965).

[14] P. Felsenthal, *J. Appl. Phys.*, **37**, 3713 (1966).

Le Blanc extends the generally accepted concept of the electric conductivity in crystalline solids also to liquids hydrocarbons, considerating a potential barrier which should be passed over by the electron. Crowe,[15] working with very carefully purified liquid hydrocarbons and with pulses of the order of microseconds, has noticed a very small scattering of the results. He found that in electric fields 1 500 times stronger than those used by Le Blanc (1.5 Mv/cm instead of 1 kv/cm), the mobility of the charge carriers was six times that obtained by Le Blanc. The same author found a linear relationship between the breakdown time and the ratio δ/E (δ = distance between electrodes, E = electric field). Crowe's measurements were effected for a δ comprised between 60 and 100μ; outside this range the linear relationship was no longer valid.

Felsenthal,[14] operating with highly purified n-hexane and with pulses of the order of nanoseconds, has found that for a time less than 1 nanosecond, the breakdown could be also instantaneous. This results in considerable scattering of the values, thus contradicting the conclusions stated by Crowe. Felsenthal maintains that the disagreement between his and Crowe's results is accounted for by the formation of spatial charges between the electrodes. We consider however that there are some arguments in favour of a contribution from the intrinsic ionic conductivity, namely :

a) in the case when the velocity of the charge carrier becomes comparable with the mean velocity of the n-hexane molecule, the mobility changes owing to the change in the statistical distribution of the liquid in the proximity of the charge carrier. The mean square velocity of the n-hexane molecule is 3.10 cm/s, whereas in breakdown the apparent velocity of the charge carrier, i.e. the ratio of distance between the electrodes to the breakdown time, becomes equal to 1.4×10^4 cm/s. The mean square velocity of the free electrons is about 400 times greater than the mean square velocity of the n-hexane molecule. The fact that there is agreement, as far as the order of magnitude is concerned, between the mean square velocity of the n-hexane molecule and the apparent velocity of the charge carrier, leads to the conclusion that only the negative ion of n-hexane and not a free electron, could be the charge carrier.

Mc Fadyen and Helliwell[16] on investigating the increase of electric conductivity in the proximity of the breakdown, have obtained similar results thus pleading in favour of the argument expounded above.

b) The width of the potential barrier is comparable with the dimension of the molecule.[17] The computation can be easily effected taking into account that

$$r = \frac{e}{6\pi} \cdot \frac{1}{\eta\mu}, \tag{1}$$

---

[15] R. W. Crowe, *J. Appl. Phys.*, **27**, 156 (1956).

[16] K. A. Mc Fadyen and G. C. Helliwell, *J. Electrochem. Soc.*, **106**, 1022 (1959).

[17] P. Walden and H. Ulich, *Z. Phys. Chem. (Leipzig)*, **107**, 219 (1923).

We consider, account being taken of the fact that we are dealing with the liquid state, that the potential barrier can be exceeded as in the case of solids, or it may be shifted together with the charge carrier.

The experimental data show that on breakdown, the velocity of the charge carrier is comparable with the mean velocity of the molecule owing to the Brownian motion. It follows that the n-hexane ions contribute also to the electric conductivity process.

Following our mechanism, let us assume that the mobility of the free electrons in n-hexane is practically infinite with respect to the ion mobility. This hypothesis is justified by the fact that in the case of liquid argon[18] the mobilities of the negative charge carriers differ considerably from the mobilities of the carriers of liquid hydrocarbons.

In the case of liquid argon the free electron is not so easily trapped as in the case of hydrocarbons. It is very unlikely that the statistical distribution in the liquids mentioned be so widely dissimilar, that the mobilities of the free electron should differ by 5 orders of magnitude.

Let σ be the electron trapping cross-section by the n-hexane molecule, and n the number of molecules per unit volume. Let us denote by I the electron current per unit area. The current drop along the distance $\mathrm{d}x$ will be:

$$\mathrm{d}J = J\sigma n \,\mathrm{d}x \tag{2}$$

Integrating we obtain

$$I = I_0 \,\mathrm{e}^{-\frac{x}{l}} \tag{3}$$

where

$$l = \frac{1}{\sigma n} \cdot \tag{4}$$

The ratio:

$$P = \frac{I}{I_0} = \mathrm{e}^{-\frac{x}{l}} \tag{5}$$

has the significance of a probability that the electrons are not trapped along the distance x.

By differentiating the expression (5) with respect to x we obtain

$$\mathrm{d}P = -\frac{1}{l}\,\mathrm{e}^{-\frac{x}{l}}\,\mathrm{d}x \tag{6}$$

or

$$\delta P = -\frac{1}{l}\,\mathrm{e}^{-\frac{x}{l}}\,\delta x. \tag{6'}$$

The absolute value of expression (6′) represents the probability that the electrons may be trapped in the interval x, $x + \delta x$. The mean value of the distance along which the electrons will not be trapped, is:

$$\int_0^\infty P\mathrm{d}x = l \tag{7}$$

---

[18] M. A. Lambert, *Reports Progr. Phys.*, **27**, 329 (1964).

Let us assume that the breakdown occurs through the agency of a narrow electron beam, with a width of the order of magnitude of intermolecular spaces. This beam will progress over a distance x, after which, the first negative ion of n-hexane will come into being through a frontal impact. Further on the displacement of this ion will bring about an extension of the ionization process, the positive ions being neutralized or negatively ionized by the electrons coming later. We assume that the electron displacement is practically instantaneous and we consider only the displacement of the negative ion of n-hexane. The ion displacement starts at point x where the potential difference is V'.

Two cases will be discussed :

1) To simplify the discussion we shall assume that the potential difference does not vary together with the distance between the electrodes, i.e. $V' = V$, and that the mobility of the charge carrier, μ, is constant. Under these conditions the velocity, v, of the n-hexane ion will be :

$$V = \frac{\mathrm{d}x}{\mathrm{d}t} = \mu \frac{V}{d-x}. \qquad (8)$$

In relation (8) d is the distance between the electrodes and t, is the breakdown time.

Relation (8) gives

$$t = \frac{(d-x)^2}{2\mu V}. \qquad (9)$$

By determining t experimentally and knowing d, μ and V, relation (9) supplies the value of x, i.e. the location where the negative ionization of n-hexane occurred.

Using relations (6) and (9) we obtain for δp :

$$\delta P = A \frac{\delta t}{\sqrt{t}} \mathrm{e}^{-\frac{d}{l}} + 2A\sqrt{t} \qquad (10)$$

where

$$A = \frac{1}{l}\sqrt{\frac{\mu V}{2}}. \qquad (11)$$

In general δt is of the order of magnitude of 1 nanosecond.

For

$$t = \frac{l^2}{2\mu V} \qquad (12)$$

δt takes a minimum value.

Qualitatively eq. (10) corresponds to short breakdown times.

2) The mobility is no longer assumed to be constant and V' is not necessarily considered to be equal to V.

We differentiate relation (5) with respect to t

$$\frac{\mathrm{d}P}{\mathrm{d}t} = -\mathrm{e}^{-\frac{x}{l}} \cdot \frac{1}{l} \cdot \frac{\mathrm{d}x}{\mathrm{d}t} . \tag{13}$$

But we have

$$\frac{\mathrm{d}x}{\mathrm{d}t} = v \tag{14}$$

whence

$$\frac{\mathrm{d}P}{\mathrm{d}t} = -P\frac{v}{l} \tag{15}$$

i.e.

$$\delta P = P\frac{v}{l}\,\delta t. \tag{15'}$$

The absolute value of relation (15′) has been considered. In general the value of v is required :

$$v = l\frac{1}{P}\,\frac{\delta P}{\delta t}. \tag{16}$$

We can compute x if we know the value of V' from the relation

$$v = \frac{\mu V'}{d-x} \tag{17}$$

Dividing the number of breakdowns which have occurred in a time of less than 1 nanosecond, by the total number of breakdowns, we determine the probability that ionization will not occur in the interval $d > x > 0$.

Figures 1a, 1b, and 1c show for P the values 0.17 , 0.23 and 0.11 respectively. These values have been used to compute the corresponding effective trapping cross-section. The values determined namely 0.028, 0.022, and 0.032 Å respectively, are comparable, as far as the order of magnitude is concerned, with the variation of molecular dimensions caused by vibration.

Taking $t = 5.5\ \mu\mathrm{s}$, $P = 0.17$ (fig. 1a) and $\frac{x}{d} = 0.2$ we obtain $v = 1.7 \times 10^{6}$ cm/sec. In case we take $V' = V$ and $E = 4.47$ Mv/cm we obtain $\mu = 0.24$ cm²/v. sec. The increase in the mobility as the electric field becomes more intensive, is in good agreement with experimental data.

In the above relations *t* does not appear explicitely. It may be that in general the mean breakdown time has a somewhat different significance.

At first sight it would appear that the delay of 4 – 6 nanoseconds of the maximum breakdown probability in the case of ageing electrodes, could not be explained (fig. 1 b). The second maximum of fig. 1c might be caused by the ionic impurities in the solution. The part played by impurities in extending the scattering of the results in the range of microseconds is mentioned also by Swan. [19]

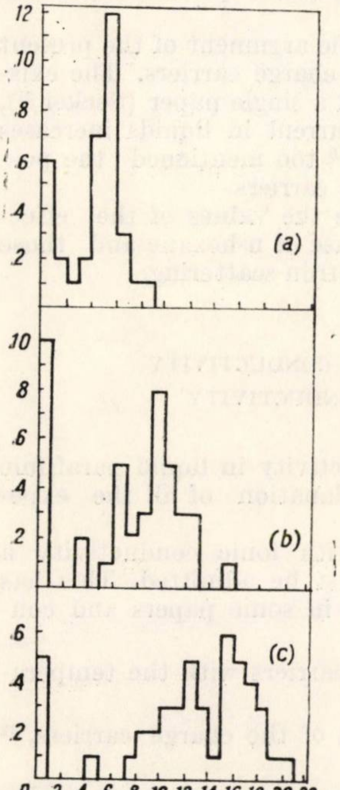

Fig. 1. — Hystcgram of breakdown lag data showing the effects of electrode surfaces and of liquid ageing upon lag time (after Felsenthal's data[14]).

n-hexane, $E = 3.28 \times 10^6$ V/cm $\delta = 61\ \mu$m. *a*, freshly n-hexane, clean electrodes; *b*, freshly n-hexane, aged electrodes; *c*, n-hexane after two days, aged electrodes.

Undeniably ionic impurities may cause the increase of the most probable breakdown time even in the case of a single maximum. The fact that breakdown could occur in a time range which could not be measured with the available equipment appears only in Felsenthal's paper, and this suggests the existence of a relaxation time τ_r, in the range of 1 nanosecond and 1 μ sec, for the organization of the liquid at the contact surface of the electrodes. The discrepancy of 1 to nearly 3 between the results of Crowe and those of Goodwin and Mc Fadyen[20] could be explained by a different composition of the electrodes and by a different organization of the liquid at the contact surface. It should be mentioned that non-polar liquids, have a relaxation time of $\approx 10^{-12}$ sec and hence, in the present case, we have to deal only with surface phenomena which are very difficult to detect experimentally.

---

[19] D. W. Swan, *Proc. Phys. Soc.*, **83**, 659 (1964).

It should be also pointed out that the whole argument of the present work rests entirely on the existence of negative charge carriers. The existence of positive charge carriers is mentioned in a single paper (Secker[21]), where it is stated that in strong fields, the current in liquids increases with the third power of the voltage. Lambert[18] too mentioned the possibility of the existence of two types of charge carriers.

Finally, it may prove useful to correlate the values of the effective trapping cross-section determined in the case of n-hexane and those of argon and helium determined directly by electron scattering.

THE CONTRIBUTION OF ELECTRONIC CONDUCTIVITY ALTERNATE ELECTRONIC-IONIC CONDUCTIVITY

An exclusively ionic mechanism of conductivity in liquid paraffinic hydrocarbons could not supply a complete explanation of all the experimentally observed phenomena.

Therefore we consider that alongside with ionic conductivity a contribution of the electronic conductivity must be admitted. This has resulted from the interpretation of data given in some papers and concerning :

a) The variation of the radius of charge carriers with the temperature and the applied voltage. [11, 14, 15].

b) The excessively large apparent radius of the charge carriers,[22] and lastly

c) The correlation between the activation energy of conductivity and chemical structure.[10]

According to Le Blanc,[11] when the temperature rises from −40° to + 25°, the radius of the charge carrier, computed by Stokes formula, is reduced to nearly half of the initial value. Such a variation could not be ascribed to ion carriers, since it would be difficult to explain why the radius of the carrier can vary to such an extent owing to temperature induced changes of the statistical organization of the liquid.

We consider that, as the temperature rises, the impacts being more frequent, the ion does not remain as such, but looses the electron which becomes free for a limited time. At the same time the works of Le Blanc,[11] Crowe,[15] and Felsenthal[14] have shown that a noticeable change in the apparent radius of the charge carrier occurs when the applied voltage varies. Thus, in weak electric fields, Le Blanc, Crowe and Felsenthal indicate radii of the order of 3 Å, 0.5 Å and 0.05 Å respectively. The last value has been computed by the authors from the mobility determined by Felsenthal.

---

[20] R. Goodwin and K. A. Mc Fadyen, *Proc. Phys. Soc.*, **B. 66**, 85 (1953).

[21] P. E. Secker, *Brit. J. Appl. Phys.*, **17**, 885 (1966).

[22] M. Silver, *J. Chem. Phys.*, **42**, 1011 (1965).

In the case of apparent radii of 0.05 Å it is difficult to admit that the conductivity is exclusively ionic. An n-hexane ion cannot have such a small radius.

Silver[22] has computed the mobility of the charge carriers on the basis of the experimental data of Forster.[12] He found mobilities of $1.4\times\times10^{-6}$ cm²/v.s and 4×10^{-6} cm²/v.s. for negative and positive ions respectively. Applying Stokes relation to these very small mobilities we obtain values of the apparent radii of charge carriers of the order of hundreds of Å (e.g.$r = 100$ Å for negative ions). Such values are much too great.

Bässler has shown,[10,23-26] that there exists a dependence between the activation energies of the electric conductivity and the chemical structure of organic liquids. This conclusion is not consistent with an ionic conductivity resulting from impurities.

We consider that the decrease in the radius of the charge carrier as the temperature rises is the consequence of an incorrect use of Stokes relation. This is due to the fact that the time interval during which a molecule is ionized has a finite value, and Stokes' relation can be applied only within that time interval. At the end of the interval the electron becomes again free. In the latter case Stokes relation becomes useless since the mobility of the free electron is very great.

Let M be a neutral molecule of n-hexane, and M^- its negative ion. The ionization process is represented by :

$$M + e^- \rightleftarrows M^- \tag{18}$$

Applying the law of mass action we have

$$\frac{[M^-]}{[M]\cdot[e^-]} = Ae^{-\frac{E}{RT}}. \tag{19}$$

In (19) E is the heat of formation of the ion M^-. On the other hand a well-known theorem of statistical mechanics states that the time average and the phase space average are equal.

Thus we may write

$$\frac{[M^-]}{[e^-]} = \frac{t_{M^-}}{t_{e^-}}. \tag{20}$$

Here t_{M^-} denotes the average life of the negative ion M^- and t_{e^-} the average life of the free electron. In relation (20) the mean value in the phase space has been approximated by the mean value in the confi-

[23] H. Bässler and N. Riehl, *Phys. Letters*, **12**, 101 (1964).

[24] H. Bässler, *Z. Naturforsch.*, **19 a**, 1389 (1964).

[25] H. Bässler and N. Riehl, *Z. Naturforsch.*, **20 a**, 587 (1965).

[26] H. Bässler and B. Dries, *Z. Naturforsch.*, **21 a**, 441 (1966).

guration space, i.e. by the respective concentrations. Multiplying the mean velocity v_{e^-} of the free electron by its mean life t_{e^-}, we obtain the mean free path between two successive trappings :

$$v_{e^-} . t_{e^-} = \lambda \tag{21}$$

Let μ_{e^-} be the mobility of the free electron and μ_{M^-} the mobility of the negative ion. The mean distance s travelled by the free electron in the direction of the anode, between two successive trappings is given by :

$$s = \mu_{e^-} E \, t_{e^-} \tag{22}$$

Similarly, the distance S travelled by the negative ion in the direction of the anode, will be :

$$S = v_{M^-} \cdot t_{M^-} = \mu_{M^-} E \, t_{M^-}. \tag{23}$$

The mean fractional path travelled by the negative ion in the direction of the anode will be :

$$\Lambda = \frac{S}{s + S} \cdot \tag{24}$$

The mean velocity of the negative ion is obtained from the relation

$$v_{M^-} = \frac{d}{t_{eff}} \cdot \frac{S}{s + S} \cdot \tag{25}$$

In relation (25) d represents the distance between the electrodes and t_{eff} the measured effective time required by the electric signal to travel the distance between the electrodes. Assuming that the mobility of the free electron and that of the negative ion of n-hexane differ appreciably, the hypothesis according to which $s \ll s$ is perfectly justified, and taking into account relation (20) we may write :

$$v_{M^-} = \frac{d}{t_{eff}} \cdot \frac{\mu_{M^-}}{\mu_{e^-}} \, A \, \mathrm{e}^{-E/RT} = \mu_{M^-} E \tag{26}$$

As a matter of fact we are dealing with an apparent mobility which is determined by the relation :

$$\mu = \frac{d}{t_{eff} \cdot E} . \tag{27}$$

By introducing in eq. (26) the value of μ given by relation (27), we may find the variation of the ratio $\frac{\mu_{M^-}}{\mu_{e^-}}$ as a function of T, and thus to compute the formation energy of the negative ion of n-hexane.

Since the product of the ion mobility and the viscosity of the liquid does not depend either on the temperature or on the electron mobility, it follows, according to the data given by Le Blanc,[11] that the activation energy of the process is 0.07 eV, i.e. 1.6 kcal/mol are required for the formation of the negative ion of n-hexane, corresponding to 560 cm^{-1}.

Although it is not customary to look for the heat of reactions among spectroscopic data, it should be emphasized that the distorsion vibration of the terminal C—C bond in saturated acyclic hydrocarbons is between 520 and 650 cm^{-1}, whereas the distorsion vibration of the same bond in the chain is between 150 and 520 cm^{-1}.[27]

These values support the view that the electron is trapped by the molecule of liquid saturated aliphatic hydrocarbon through interaction with the vibration of the molecule, the radius of the effective cross-section being of the same order of magnitude as the distorsion caused by the respective vibration.

The reason why Silver has determined such small mobilities is due to the fact that a decisive contribution to the process of electric conductivity, is given by the diffusion of the impurity in a non-ionized state.

The extraction or the release of charges at the electrodes is effected by the ion of the impurity present in the liquid.

CONCLUSIONS

It is considered that the main insulating property of liquid aliphatic hydrocarbons is due to the relatively large effective trapping cross-sections for free electrons. The radius of the section is comparable, as far as the order of magnitude is concerned, with the distorsions of the molecule caused by vibration, while the trapping energy is in satisfactory agreement with spectroscopic data in the far infra-red. These facts plead in favour of an absorption resonance mechanism of electrons, while the electron release requires energies higher by one order of magnitude.

The correlation of measured mobilities and viscosity studied by Adamczewsky[13] could throw some light on the part played by molecular vibration in viscous flow.

Recently, Davies and Matheson[28] have shown the effect of molecular rotations upon the viscosity both of liquids which follow and of liquids which do not follow Arrhenius law. These authors consider that in the rotation process the molecules mesh like toothed wheels.

It appears that such junctions are more like a fairly unstable clustering caused by resonant interaction with respect to vibration, than like successive jumps in holes occurring in the liquid, a fact observed macroscopically in continuous flow.

It has been found that such clusterings exist also in the gaseous phase, up to the critical temperature, even in rarefied gases.[29] It will be interesting to investigate the characteristics of electric conductivity in liquid aromatic hydrocarbons where, owing to the presence of the π electrons, some differences are to be expected.

---

[27] M. Avram and Gh. D. Mateescu, "Spectroscopia în infraroşu. Aplicaţii în chimia organică", Ed. Academiei R. S. România, Bucharest, 1967.

[28] D. B. Davies and A. J. Matheson, *J. Chem. Phys.*, **45**, 1000 (1966).

[29] I. J. Pellah, *Phys. Letters*, **21**, 248 (1966).

Although it is not customary to look for the seat of reactions among spectroscopic data, it should be emphasized that the distorsion vibration of the terminal C—C bond in saturated acyclic hydrocarbons is between 450 and 600 cm⁻¹, whereas the distorsion vibration of the same bond in the chain is between 150 and 320 cm⁻¹.[17]

These values support the view that the electron is trapped by the molecule of liquid saturated aliphatic hydrocarbon through interaction with the vibration of the molecule, the radius of the effective cross-section being of the same order of magnitude as the distorsion caused by the respective vibration.

The reason why others have not noticed such small mobilities is due to the fact that a decisive contribution to the process of electric conductivity is given by the diffusion of the impurity in a non-ionized state. The extraction or the release of charges at the electrodes is effected by the ion of the impurity present in the liquid.

CONCLUSIONS

It is considered that the main insulating property of liquid aliphatic hydrocarbons is due to the relatively large effective trapping cross-sections for free electrons. The radius of the section is comparable, as far as the order of magnitude is concerned, with the distorsions of the molecule caused by vibration, while the trapping energy is in satisfactory agreement with spectroscopic data in the far infra-red. These facts plead in favour of an absorption resonance mechanism of electrons, while the electron release requires energies higher by one order of magnitude.

The correlation of measured mobilities and viscosity studied by Adamczewski[13] could throw some light on the part played by molecular vibration in viscous flow.

Recently, Davies and Matheson[18] have shown the effect of molecular rotations upon the viscosity both of liquids which follow and of liquids which do not follow Arrhenius law. These authors consider that in the rotation process the molecules mesh like toothed wheels.

It appears that such junctions are more like a fairly unstable clustering caused by resonant interaction with respect to vibration, then like successive jumps in holes occurring in the liquid, a fact observed macroscopically in continuous flow.

It has been found that such clusterings exist also in the gaseous phase, up to the critical temperature, even in rarefied gases.[19] It will be interesting to investigate the characteristics of electric conductivity in liquid aromatic hydrocarbons where, owing to the presence of the π electrons, some differences are to be expected.

---

[17] M. Avram and Gh. D. Mateescu, "Spectroscopia în infraroşu. Aplicaţii în chimia organică", Ed. Academiei R. S. Romania, Bucureşti, 1966.

[18] D. B. Davies and A. J. Matheson, J. Chem. Phys., 45, 1000 (1966).

[19] [illegible], Phys. Letters, 21, 279 (1966).

Revue Roumaine de Chimie, **14**, 1281–1284 (1969)

OXIDATION OF PYROCATECHOL DERIVATIVES TO *o*-QUINONES BY IODOSOBENZENE DIACETATE

A. T. BALABAN

Institute of Atomic Physics, Bucharest, Romania

Received April 21, 1969

In order to investigate the possibility of isolating 1,3,2-dioxaiodoles III, pyrocatechols Ia-d were treated with iodosobenzene diacetate in acetic acid. *o*-Benzoquinones were obtained as reaction products along with iodobenzene, in solution (IVa) or as crystalline compounds (IVb, c), in good yield.

Compounds of trivalent iodine are formally similar to boron compounds, e.g. ICl_3 to BCl_3, $PhICl_2$, to $PhBCl_2$, etc.; however, the diaryliodonium compounds $Ar_2I^{\oplus}$ $Hal^{\ominus}$ are ionic, and not covalent like diarylborinic acid derivatives Ar_2BHal.

The ability of boron to be involved in aromatic heterocycles,[1–5] and the known heterocyclic[6] or polymeric[7] compounds with trivalent iodine suggested a search for heterocyclic organoiodine compounds. It would have been interesting to look for aromatic character involving d-orbitals in such systems.

In the oxidation of glycols by iodosobenzene diacetate, Criegee and Beucker[8] had postulated the intermediacy of unstable saturated heterocycles with trivalent iodine. However, this suggestion was not taken up by subsequent investigators of the oxidation of glycols[9] or phenols.[10]

---

[1] A. T. Balaban and Z. Simon, *Tetrahedron*, **18**, 315 (1962); *Rev. Roumaine Chim.*, **10**, 1059 (1965).

[2] A. T. Balaban, A. Arsene, I. Bally, A. Barabas, M. Paraschiv, M. Roman and E. Romaş, *ibid.*, (in press) and previous parts in the series "Heterocyclic Organoboron Compounds".

[3] M. J. S. Dewar, in "Progress in Boron Chemistry", vol. 1 (ed. H. Steinberg and A. L. Mc Closkey), Pergamon Press, Oxford, 1964, p. 235; "Boron-Nitrogen Chemistry" (ed . R. F. Gould), Adv. in Chemistry Series No. 42, Amer. Chem. Soc., Washington, D. C., 1964, p. 227.

[4] P. M. Maitlis, *Chem. Rev.*, **62**, 223 (1962).

[5] W. Gerrard, "The Organic Chemistry of Boron", Academic Press, London, 1961; H. Steinberg, "Organoboron Chemistry", vols. 1–3, Interscience, New York.

[6] W. C. Agosta, *Tetrahedron Letters*, **1965**, 2681.

[7] a. J. I. Musher, *Angew. Chem.*, **81**, 68 (1969); b. *J. Polymer Sci.* (*C*), **1968**, 195.

[8] R. Criegee and H. Beucker, *Liebigs Ann. Chem.*, **541**, 218 (1939).

[9] K. H. Pausacker, *J. Chem. Soc.*, **1953**, 107; L. K. Dyall and K. H. Pausacker, *ibid.*, **1958**, 3950.

[10] A. R. Fox and K. H. Pausacker, *ibid.*, **1957**, 295.

Though many oxidations with polyvalent iodine compounds were investigated,[11-13] and some new kinds of trivalent iodine compounds were isolated, [14-16] evidencing a revived recent interest in such compounds, no search for compounds which might manifest aromatic character was reported.

One possible approach was to study the reaction between pyrocatechols (I) and iodosobenzene diacetate (II), hoping to obtain analogues (III) of the known stable 1,2, 3-dioxaboroles. Whereas the original aim: isolation of such heterocycles III, could not yet be attained, their occurrence is compatible with the formation in high yield of decomposition products: iodobenzene (V) and *o*-quinones (IV). At the same time a convenient method for oxidizing pyrocatechols I to *ortho*-quinones IV was found.

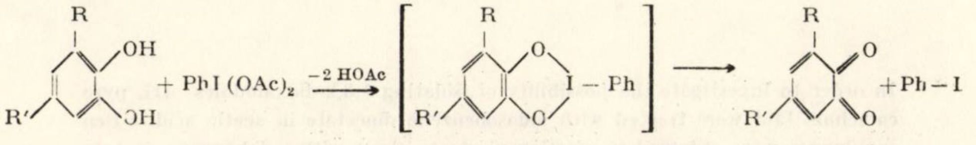

I II III IV V

a, $R=R'=H$ c, $R=R'=$1-methyl-1-cyclohexyl

b, $R=R'=$t-Bu d, $R=H$, $R'=NO_2$

The reaction between iodosobenzene diacetate (II) and pyrocatechol derivatives (Ia—Id) was effected with equimolar amounts or reagents in acetic acid at room temperature. The reaction is exothermal and practically instantaneous. Addition of water causes separation of iodobenzene and crystallization of *o*-quinones IVb[17, 18] or the unreported IVc in ca. 90% yield. The more sensitive IVa [19] can be identified by infrared spectroscopy,[20] whereas the unknown IVd has not been isolated.

The fact that heterocycles III are unstable at room temperature relatively to decomposition into IV+V makes them markedly different from 1,3,2-dioxaboroles which cannot undergo such a decomposition. The thermodynamic instability of system III, even though it can possess aromatic character, can be compared with the failure to prepare aliphatic iodonium salts, for which thermodynamic instability was also advocated.[21] One

---

[11] K. H. PAUSACKER, *ibid.*, **1953**, 1989; L. K. DYALL and K. H. PAUSACKER, *Austral. J. Chem.*, **11**, 491 (1958) and previous parts in the series.

[12] G. BARBIERI, M. CINQUINI, S. COLONNA and F. MONTANARI, *J. Chem. Soc.* (*C*), **1968**, 659

[13] R. NEU, *Ber. dtsch. chem. Ges.*, **72**, 1505 (1939).

[14] B. LIPKE, *Z. Chem.*, **8**, 23 (1968).

[15] D. D. TANNER and G. C. GIDLEY, *Canad. J. Chem.*, **46**, 3537 (1968); *J. Org.Chem.*, **33**, 38 (1968); N. A. MILAS and B. PLESNIČAR, *J. Amer. Chem. Soc.*, **90**, 4201 (1968).

[16] O. NEILANDS and B. KARELE, *Zh. Org. Khim.*, **1**, 1854 (1965); **2**, 488 (1966); B. KARELE and O. NEILANDS, *ibid.*, **4**, 1814 (1968); O. NEILANDS, *ibid.*, **1**, 1858 (1965).

[17] K. LEY and E. MÜLLER, *Chem. Ber.*, **89**, 1402 (1956); *Angew. Chem.*, **70**, 469 (1958); L. V. GORBUNOVA, *Zh. Org. Khim.*, **2**, 1236 (1966); W. FLAIG, T. PLOETZ and H. BIERGANS, *Liebigs Ann. Chem.*, **597**, 196 (1955).

[18] L. HORNER and W. DÜRCKHEIMER, *Z. Naturforsch.*, **14b**, 741 (1959).

[19] R. BROCKHAUS, *Liebigs Ann. Chem.*, **712**, 214 (1968).

[20] W. OTTING and G. STAIGER, *Chem. Ber.*, **88**, 828 (1955).

[21] J. B. DENCE and J. D. ROBERTS, *J. Org. Chem.*, **33**, 1251 (1968).

reason for this instability may be the fact that the two hypervalent bonds of iodine must be colinear,[7a] a geometrical condition which is not possible for III.

The simplicity of the oxidation by iodosobenzene diacetate of pyrocatechol derivatives to *o*-quinones makes this method a promising one for preparative purposes. Recent interest in the chemistry of *o*-quinones is apparent.[22–24]

EXPERIMENTAL

Iodosobenzene diacetate[25,26] was prepared by recrystallization of iodosobenzene[27] from acetic acid. Ultraviolet spectra were measured with an Optica (Milan) CF-4 instrument and infrared spectra with a Zeiss (Jena) UR-10 apparatus and with a Perkin-Elmer grating spectrophotometer 125.

o-Benzoquinone (IVa). Solutions of pyrocatechol and iodosobenzene diacetate in equimolar amounts (10 m moles) in acetic acid (10 ml each) were mixed at 10°, treated with 5 ml chloroform and diluted with ice-cold 0.01 N sulphuric acid. The deeply-brown lower layer was shaken several times with fresh portions of cold 0.01 N sulphuric acid, then dried on sodium sulphate. The infrared absorption spectrum[19,20] revealed the presence of iodobenzene and *o*-benzoquinone.

*3,5-Di-t-butyl-*o*-benzoquinone* (IVb). A concentrated solution of 3,5-di-t-butylpyrocatechol (Ib)[17,28] (1 g) in acetic acid (15 ml) was treated with an acetic acid solution (15 ml) of an equimolar amount (1.5 g) of iodosobenzene diacetate II[25,27] at room temperature. The solution became reddish-brown and an exothermal effect was noted. Water was added dropwise until the separation of iodobenzene was complete. The layers were separated and chilled. Both afforded crystalline 3,5-di-t-butyl-*o*-benzoquinone (IVb, R = R′=tBu) which was filtered off, washed with n-hexane and water and recrystallized from aqueous ethanol, m.p. 112° orange coloured, in agreement with literature data.[17,18] Its infrared absorption spectrum (in KBr pellet) presents a sharp aromatic νCH band at 3065 cm $^{-1}$, νC = O band at 1650 (shoulder at 1670 cm $^{-1}$), and other bands at 1562 m, 1472 s, 1460 m, 1388 m, 1370 s, 1362 vs, 1355 w, 1315 w, 1269 s, 1240 s, 1018 m, 944 m, 882 s, 803 m, 640 m. The ultraviolet absorption spectrum presents maxima at 590 (in CCl_4), 400 and 260 nm (in ethanol) in agreement with literature data.[29]

*3,5-Di-(1′-methyl-1′-cyclohexyl)-*o*-benzoquinone* (IVc) was prepared similarly from I and IVc. It affords greenish brown crystals, m.p. 81° (from n-hexane). The solution is red in transparency and green in reflected light. Found : C, 80.11 ; H, 9.10 ; $C_{20}H_{28}O_2$ requires : C, 79.95 ; H, 9.39 %. The electronic absorption bands in CCl_4 appear at 580 nm (∈ 80) and 394 nm

---

[22] H. W. Wanzlick and U. Jahnke, *Chem. Ber.*, **101**, 3744 (1968).

[23] W. M. Horspool, J. M. Tedder and Zia ud Din, *J. Chem. Soc.*, (*C*), **1968**, 1597.

[24] L. Horner and co-workers, *Z. Naturforsch.*, **14b**, 743, 744 (1959) and other papers in the series.

[25] C. Willgerodt, *Ber. dtsch. chem. Ges.*, **25**, 3494 (1892); *J. Prakt. Chem.*, **33**, 154 (1886); B. A. Arbuzov, *ibid.*, [2], **131**, 357 (1931).

[26] J. G. Sharefkin and H. Saltzman, *Org. Synth.*, **43**, 62 (1960).

[27] H. J. Lucas, E. R. Kennedy and M. W. Formo, *Org. Synth.* col ., Vol. 3, 483.

[28] C. A. Tyson and A. E. Martell, *J. Amer. Chem. Soc.*, **90**, 3379 (1968); H. Schulze and W. Flaig, *Liebigs Ann. Chem.*, **575**, 231 (1952).

[29] J. C. Salfeld, *Chem. Ber.*, **93**, 737 (1960); W. Flaig, T. Ploetz and A. Küllmer, *Z. Naturforsch.*, **10b**, 668 (1955).

($\in$1950); in 1,2-dichloroethane the latter band is shifted to 408 nm and another band appears at 264 nm. Its infrared absorption spectrum (in potassium bromide pellet) presents a very strong carbonyl stretching band at 1661 cm^{-1} (1670 in CCl_4) and strong bands at 1681, 1626, 1569, 1475, 1456, 1375, 1275, 909, 878, and 809 cm^{-1} along with CH stretching bands at 2860–2980 cm^{-1}.

Attempt to oxidize-4-nitropyrocatechol.[30] Proceeding similarly, the acetic solutions of 4-nitrocatechol and iodosobenzene diacetate do not become intensely brown on mixing; dilution with water causes separation of colourless iodobenzene (identified by infrared spectra) with no carbonyl stretching band in the 1600–1700 cm^{-1} range. Presumably, 4-nitro-1,2-benzoquinone is too unstable.

Acknowledgements. Thanks are expressed to Dr. K. Ley and the Bayer Company m.b.H. for gifts of IIb and IIc, to Mrs. M. Paraschiv for the infrared spectra, to Mrs. M. Roman for the elementary analysis, and to Mr. A. Barabas for experimental assistance.

[30] H. W. WANZLICK, in "Newer Methods of Preparative Organic Chemistry", vol. 4 (ed. W. FOERST), Verlag Chemie (Weinheim/Bergstr.) and Academic Press (New York and London), 1968, p. 139; *Angew. Chem. Internat. Ed.*, **3**, 401 (1964).

Revue Roumaine de Chimie, 14, 1285–1294 (1969)

CONTRIBUTION À L'ÉTUDE DE QUELQUES HÉTÉROCYCLES. XII*

L'HALOGÉNATION ET LA NITRATION DE L'ANILINO-2-MÉTHYL-5-THIODIAZOLE-1,3,4

I. SIMITI, LIDIA PROINOV et H. DEMIAN

Institut de Médecine et Pharmacie, Laboratoire de chimie organique de la Faculté de Pharmacie, Cluj, 41, str. V. Babeş

Reçu le 22 novembre 1968

Par l'halogénation et la nitration des arylamino-2-méthyl-5-thiodiazoles-1, 3, 4 on obtient une série de dérivés halogénés et nitrés, qui sont difficilement accessibles par d'autres voies. En même temps on met en évidence l'influence de divers substituants du noyau benzénique sur la marche de ces réactions. Les résultats obtenus confirment encore une fois le caractère attractif d'électrons du noyau thiodiazolique-1, 3, 4.

Dans un travail antérieur[1] nous avons étudié la préparation de certains arylamino-2-R-5-thiodiazoles-1, 3, 4. Dans le présent travail nous nous proposons de poursuivre l'halogénation et la nitration de quelques arylamino-2-méthyl-5-thiodiazoles-1,3, 4 pour obtenir des dérivés halogénés et nitrés, respectivement des dérivés aminés, difficilement accessibles par d'autres méthodes.

En traitant l'anilino-2-méthyl-5-thiodiazole-1,3,4 avec du brome en acide acétique, sans tenir compte de la quantité de brome ajoutée, on obtient un monobrome-dérivé (IIIb), identique à celui obtenu par la cyclisation de la (*p*-bromophényl)-4-thiosemicarbazide avec le chlorure d'acétyle[2] ou à celui obtenu par la réduction du (*p*-bromo-anilino)-2-chlorométhyl-5-thiodiazole-1,3,4[1], c'est-à-dire (*p*-bromoanilino)-2-méthyl-5-thiodiazole-1, 3, 4.

En essayant la bromuration du (N-acétyle-anilino)-2-méthyl-5-thiodiazole-1, 3, 4 indifféremment des conditions de la réaction, on constate que la bromuration n'a pas lieu.

En ce qui concerne la nitration, on observe une différence dans le sens que par la nitration avec du mélange sulfonitrique de l'anilino-2-méthyl-5-thiodiazole-1, 3, 4 (I) on obtient un seul mononitrodérivé (II),

---

*XIe partie, I. Simiti, L. Proinov, I. Schwartz et L. Gilău, *Rev. Chim.* (Bucureşti) **7**, 413 (1968).

[1] I. Simiti et L. Proinov, *Rev. Roumaine Chim.*, **3**, 429 (1966).

[2] P. B. Tripathy et N. K. Rout, *J. Indian Chem. Soc.*, **37**, 415 (1960) : *Ref. Zhur. Khim.*, **15**, 86 (1961).

tandis que par la nitration dans les mêmes conditions du (N-acétylanilino)-2-méthyl-5-thiodiazole-1, 3, 4, on obtient deux mononitrodérivés izomères (Vc et VI).

Ces deux derniers composés ont un comportement différent en comparaison du premier nitrodérivé dans leur réaction avec le chlorure stanneux, dans le sens qu'ils se transforment en amines correspondantes (VII et IX).

De même, on observe une différenciation en ce qui concerne le comportement polarographique et chromatographique de ces 3 isomères.[3]

Les deux amines (VII et IX) obtenues ont été transformées par la réaction Sandmeyer en chloro- ou bromodérivés, composés qu'on trouve identiques au (*p*-chloroanilino)-2- ou (*p*-bromoanilino)-2-méthyl-5-thiodiazole-1, 3, 4, resp. au (*m*-chloroanilino)-2- ou (*m*-bromoanilino)-2-méthyl-5-thiodiazole-1, 3, 4 obtenus par la cyclisation des aryl-4-thiosemicarbazides correspondantes avec du chlorure d'acétyle.

Par conséquent, nous sommes tentés à admettre que par la nitration du (N-acétylanilino)-2-méthyl-5-thiodiazole-1, 3, 4 les deux isomères obtenus en proportion égale ont le groupement nitro greffé l'un dans la position *para* (Vc) et l'autre dans la position *méta* (VI) par rapport au groupement aminique.

Les nitro-dérivés *para* et *méta* substitués ont été préparés aussi par cyclisation des (*p*-nitrophényl)-4, respectivement (*m*-nitrophényl)-4-thiosemi-carbazides, en présence du chlorure d'acétyle.

On a essayé ensuite la bromuration et la nitration de quelques composés avec divers substituants dans la position *para* du noyau benzénique, comme CH_3-, $Br-$, NO_2-.

En bromurant le (*p*-nitroanilino)-2-(*p*-bromoanilino)-2-et le (*p*-toluidino)-2-méthyl-5-thiodiazole-1,3, 4- (IIIa-c) on a pu constater que dans le premier cas la bromuration n'a pas lieu, dans le second cas la bromuration ne se produit qu'en acide sulfurique conc. et cela au bout d'un longue intervalle (50 h), tandis que dans le cas du (*p*-toluidino)-2-méthyl-5-thiodiazole-1, 3, 4 la bromuration s'achève rapidement.

Par la bromuration du (*p*-bromoanilino)-2-méthyl-5-thiodiazole-1, 3, 4 on obtient un composé qui n'est pas identique au (3, 4-dibromoanilino)-2-méthyl-5-thiodiazole-1, 3, 4 obtenu par la cyclisation de la (3, 4-dibromphényl)-4-thiosemicarbazide avec du chlorure d'acétyle ni avec celui préparé par la bromuration du (*m*-bromoanilino)-2-méthyl-5-thiodiazole-1, 3, 4- (XI), en conséquence il ne peut être que le (2,4-dibromoanilino)-2-méthyl-5-thiodiazole-1,3,4-(XIIIb).

Dans le cas de la bromuration du (*p*-toluidino)-2-méthyl-5-thiodiazole-1, 3, 4, l'atome brome entre aussi dans la position 2 envers le groupement aminique. On obtient ainsi le (2-bromo, 4-méthyl-anilino)-2-méthyl-5-thiodiazole-1, 3, 4- (XIIIa), composé identique à celui obtenu par la cyclisation de la (2-bromo, 4-méthyl-phényl)-4-thiosemicarbazide avec du chlorure d'acétyle.

Les trois N-acétyl-dérivés *para* substitués, ainsi que le (N-acétylanilino)-2-méthyl-5-thiodiazole-1, 3, 4 n'ont pu être bromurés dans les mêmes conditions.

---

[3] I. Simiti, L. Proinov, I. Schwartz et L. Gilău, *Rev. Chim.* (București), **7**, 413(1968).

Il faut remarquer que par la bromuration du (2-bromo-4-méthylanilino)-2-méthyl-5-thiodiazole-1, 3, 4 en acide sulfurique conc. on peut introduire un atome brome en plus.

En poursuivant la nitration des trois composés ci-dessus (IIIa—c) on a pu constater autant par la nitration du (*p*-toluidino)-2-méthyl-5--thiodiazole-1, 3, 4 que du (*p*-bromoanilino)-2-méthyl-5-thiodiazole-1, 3, 4 que l'on obtient des mononitrodérivés, qui, de même que dans le cas de l'(*o*-nitroanilino)-2-méthyl-5-thiodiazole-1, 3, 4-(II), ne peuvent pas être réduits aux amines respectives.

Dans le cas du (*p*- nitroaniline)-2-méthyl-5-thiodiazole-1, 3, 4, la nitration n'a pas lieu.

Par la nitration des N-acétyl-dérivés correspondants (Va, b) on a obtenu des nitro-dérivés qui ont été réduits aux amines correspondantes. Celles-ci, par la réaction Sandmeyer donnent naissance aux composés identiques à ceux obtenus par la cyclisation de la (3-bromo-4-méthylphényl)-4-thiosemicarbazide soit de la (3,4-dibromophényl)-4-thiosemicarbazide avec du chlorure d'acétyle. C'est ainsi que dans ces deux cas l'insertion du groupement nitro dans la position *méta* envers le groupe aminique, respectivement dans la position *ortho* envers le substituant de la position *para* (CH_3—ou Br—) a été réalisée.

Dans le cas des dérivés *p*-anilino-substitués, le groupe nitro entre exceptionnellement dans la position *ortho* par rapport au groupe aminique.

Le (*p*-nitroanilino)-2-méthyl-5-thiodiazole-1, 3, 4, ainsi que son dérivé acétylé n'ont pas pu être nitrés dans les conditions que nous avons établies.

En conclusion, dans le cas de la bromuration de l'anilino-2-méthyl--5-thiodiazole-1, 3, 4, l'atome brome entre dans la position *para* par rapport au groupement aminique, tandis qu'au cas des dérivés substitués en *para* (CH_3—, Br—) l'atome brome entre dans la position *ortho* par rapport au groupement aminique.

Dans le cas de la nitration, le groupement nitro occupera constamment la position *ortho* par rapport au groupement amino.

Par suite de la nitration du (N-acétylanilino)-2-méthyl-5-thiodiazole-1, 3, 4 on obtient des isomères *méta* et *para* par rapport au groupement N-acétylamino. Par la nitration des dérivés *para* substitués, on obtient les isomères *méta* par rapport ou groupement N-acétylamino, resp. en *ortho* envers le substituant de la position *para*

Toutes les amines obtenues par la réduction des nitro-dérivés correspondants ont été caractérisées par une série de dérivés, comme : diacétyldérivés, bases Schiff et dérivés de thio-urée.

On peut conclure à partir de résultats obtenus, que le noyau thiodiazolique-1, 3, 4 possède indubitablement un caractère attractif d'électrons[4], fait démontré par la désactivation du groupe aminique.

---

[4] M. Ohta, R. Hagiwara et J. Mizushima, *J. Pharm. Soc. Japan*, **73**, 701 (1953); *Chem. Abstr.*, **48**, 7005 (1954).

PARTIE EXPÉRIMENTALE

(Haloarylamino)-2-méthyl-5-thiodiazoles-1, 3, 4.

a). *(p-bromoanilino)-2-méthyl-5-thiodiazole-1, 3, 4- (III b)*

On dissout 0,8 g I en 12 ml acide acétique conc., on le traite par 0,4 ml brome. On agite pendant 30 minutes à la température de la chambre, intervalle dans lequel se sépare un précipité. On dilue avec de l'eau, on filtre, on lave à l'eau sur le filtre et on recristallise en alcool avec un peu de charbon animal. La substance obtenue est identique à celle résultée de la cyclisation de la (*p*-bromophényl)-4-thiosemicarbazide avec du chlorure d'acétyle.

On prépare le composé XIIIa de la même façon , par la bromuration du (*p*-toluidino)-2-méthyl-5-thiodiazole-1, 3, 4, ce composé étant identiques à celui obtenu par la cyclisation de la (2-bromo-, 4-méthylphényl)-4-thiosemicarbazide avec du chlorure d'acétyle.

b). *(2,4-dibromoanilino)-2-méthyl-5-thiodiazole-1,3,4-(XIIIb)*

On dissout 0,4 g IIIb en 3,5 ml d'acide sulfurique conc. et on le traite par 0,13 ml brome. On laisse la solution pendant 50 h à la température de la chambre, ensuite on la verse sur la glace et on neutralise avec de l'ammoniaque. On filtre et on recristallise la substance séparée dans l'alcool.

On obtient de la même façon le composé XIIb par la bromuration en acide sulfurique du (*m*-bromoanilino)-2-méthyl-5-thiodiazole-1, 3, 4 (XI). Le composé XIIb ainsi obtenu est identique à celui préparé par la cyclisation de la (3,4-dibromophényl)-4-thiosemicarbazide avec du chlorure d'acétyle.

c). *(p-bromoanilino)-2-méthyl-5-thiodiazole-1, 3, 4-(IIIb)*

On traite 0,8 g VII par 6 ml acide bromhydrique 63 % et par 5 ml eau. On refroidit jusqu'à —5°. On ajoute au mélange de réaction, goutte à goutte, et sous agitation une solution de 0,3 g nitrite de sodium dans 2 ml eau. On maintient pendant 20 minutes sur glace, puis on verse dans une solution de 0,5 g bromure cuivreux en 3 ml acide bromhydrique 63 %. On maintient la solution pendant 30 minutes à la température de la chambre et puis au bain-marie à 70°, jusqu'au moment où le dégagement d'azote cesse. On filtre, on lave à l'eau sur le filtre. On traite le précipité obtenu par 6 ml acide bromhydrique 63 % et puis on filtre de nouveau. On suspende en 20 ml ammoniaque conc., on filtre. Après recristallisation en alcool, on obtient une substance (IIIb) identique à celle obtenue par la bromuration du composé I ou à celle obtenue par la cyclisation de la (*p*-bromophényl)-4-thiosemicarbazide avec du chlorure d'acétyle.

On a préparé de la même façon les composés XI et XII a, b par l'intermédiaire des dérivés IX et XVII a, b.

La réaction Sandmeyer a été utilisée aussi pour l'obtention des dérivés chlorurés VIII et X, ayant comme point de départ les composés VII et IX.

a). *(o-nitroanilino)-2-méthyl-5-thiodiazole-1, 3, 4 (II)*

On dissout 1,8 g I en 3,6 ml d'acide sulfurique 92 %. On fait refroidir la solution à —10° et on y ajoute, goutte à goutte, en agitant constamment, 0,9, ml acide azotique *d* = = 1, 42 en maintenant la température entre —10° et 5°. La solution est laissée se reposer pendant 30 mn, à la température de la chambre, puis on la verse sur la glace, on ajoute de l'am-

Tableau 1

(Holoarylamino)-2-méthyl-5- thiodiazole-1,3,4

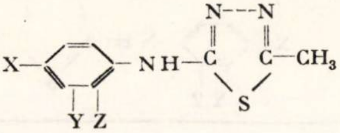

X	*Y*	*Z*	F. °C alcool	Formule P.M.	N %	
					calc.	trouvé
IIIb	Br	H	H	235–236°	$C_9H_8BrN_3S$ 270,2	15,55	15,87
XIIIa	CH_3	H	Br	144–145°	$C_{10}H_{10}BrN_3S$ 284,2	14.78	14,81
XIIIb	Br	H	Br	148°	$C_9H_7Br_2N_3S$ 349,1	12,03	12,08
XIIb	Br	Br	H	264°	$C_9H_7Br_2N_3S$ 349,1	12,03	12,19
XI	H	Br	H	214°	$C_9H_8BrN_3S$ 270,2	15,55	15,85
XIIa	CH_3	Br	H	243–245°	$C_{10}H_{10}BrN_3S$ 284,2	14,78	15,20
VIII	Cl	H	H	235–236°	$C_9H_8ClN_3S$ 225,7	18,61	18,82
X	H	Cl	H	215–216°	$C_9H_8ClN_3S$ 225,7	18,61	18,28

moniaque conc. jusqu'au pH = 6,5–7. On filtre, on lave la substance à l'eau sur le filtre et on la recristallise en alcool ou en acide acétique glacial.

On obtient les composés XIVa, b par la nitration dans les mêmes conditions des substances IIIa, b.

Les dérivés II, XIVa, b se préparent par l'hydrolyse au cours de la catalyse acide des N-acétyl-dérivés correspondants XXI et XVa, *b*.

b) *(N-acétyl- (p-nitroanilino))-2-méthyl-5-thiodiazole-1, 3, 4-(Vc) et (N-acétyl-(m--nitroanilino)) -2-méthyl-5-thiodiazole-1, 3, 4 (VI)*

On dissout 2 g IV en 4 ml acide sulfurique 92 % et on traite par 1 ml acide azotique $d = 1, 42$, dans les conditions indiquées ci-dessus.

Pendant qu'on verse la solution sur de la glace, il se sépare le composé VI, qui est filtré et qu'on recristallise en alcool.

Tableau 2

Nitro-dérivés de l'arylamino-2-méthyl-5-thiodiazole-1.3.4

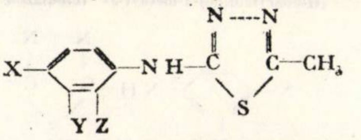

	X	*Y*	*Z*	F. °C alcool	Formule P.M.	N%	
						calc.	trouvé
II	H	H	NO_2	208°	$C_9H_8N_4O_2S$ 236,3	23,71	23,82
XIVa	CH_3	H	NO_2	170°	$C_{10}H_{10}N_4O_2S$ 250,3	22,38	22,10
XIVb	Br	H	NO_2	208—209°	$C_9H_7BrN_4O_2S$ 315,2	17,77	17,57
XVIII	NO_2	H	H	>270°	$C_9H_8N_4O_2S$ 236,3	23,71	23,80
XIX	H	NO_2	H	244—245°	$C_9H_8N_4O_2S$ 236 3	23,71	23,57
XXa	CH_3	NO_2	H	258—260°	$C_{10}H_{10}N_4O_2S$ 250,3	22,38	22,47
XXb	Br	NO_2	H	249—250°	$C_9H_7BrN_4O_2S$ 315,2	17,77	18,10

Tableau 3

Nitro-dérivés du (N-acétylamino)—2—méthyl—5 thiodiazole—1,.-3.4

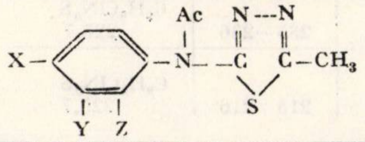

	X	*Y*	*Z*	F. °C alcool	Formule P.M.	N %	
						calc.	trouvé
Vc	NO_2	H	H	178°	$C_{11}H_{10}N_4O_3S$ 278,3	20,13	20,27
VI	H	NO_2	H	198°	$C_{11}H_{10}N_4O_3S$ 278,3	20,13	20,54
XVIa	CH_3	NO_2	H	190—192°	$C_{12}H_{12}N_4O_3S$ 292,3	19,16	19,43
XVIb	Br	NO_2	H	249°	$C_{11}H_9BrN_4O_3S$ 357,2	15,68	15,99
XVa	CH_3	H	NO_2	160°	$C_{12}H_{12}N_4O_3S$ 292,3	19,16	19,03
XVb	Br	H	NO_2	186—187°	$C_{11}H_9BrN_4O_3S$ 357,2	15,68	15,53
XXI	H	H	NO_2	182—184°	$C_{11}H_{10}N_4O_3S$ 278,3	20,13	20,21

Tableau 4

Amino-dérivés de l'arylamino-2-méthyl-5-thiodiazole-1.3.4

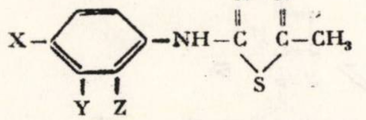

	X	*Y*	*Z*	F. °C alcool	Formule P.M.	N% calc.	N% trouvé
VII	NH_2	H	H	192°	$C_9H_{10}N_4S$ 206,3	27,16	26,93
IX	H	NH_2	H	203–205°	$C_9H_{10}N_4S$ 206,3	27,16	27,16
XVIIa	CH_3	NH_2	H	225–227°	$C_{10}H_{12}N_4S$ 220,3	25,43	25,75
XVIIb	Br	NH_2	H	180–181°	$C_9H_9BrN_4S$ 285,2	19,64	19,58

Tableau 5

Diacétyl-dérivés, les bases Schiff et les dérivés de thio-urée, obtenus à partir des amines VII, IX, XVII a, b

Dérivé	F. °C alcool	Formule P.M.	N% calc.	N% trouvé
Diacétyl-dérivé de VII	144–145°	$C_{13}H_{14}N_4O_2S$ 209,3	19,29	19,40
de IX	242–244°	$C_{13}H_{14}N_4O_2S$ 290,3	19,29	19,51
de XVIIa	263–265°	$C_{14}H_{16}N_4O_2S$ 304,4	18,40	18,64
de D XVIIb	238°	$C_{13}H_{13}BrN_4O_2S$ 369,3	15,17	15,17
Base Schiff de VII	230–232°	$C_{16}H_{14}N_4S$ 294,4	19,03	19,44
de IX	228°	$C_{16}H_{14}N_4S$ 294,4	19,03	18,90
de XVIIa	226–227°	$C_{17}H_{16}N_4S$ 308,4	18,16	18,22
de XVIIb	225°	$C_{16}H_{13}BrN_4S$ 373,3	15,00	14,84
Dérivé de thio-urée de VII	228–230°	$C_{16}H_{15}N_5S_2$ 341,5	20,51	20,48
de IX	180–181°	$C_{16}H_{15}N_5S_2$ 341,5	20,51	20,67
de XVIIa	145°	$C_{17}H_{17}N_5S_2$ 355,5	19,71	19,32
de XVIIb	184–186°	$C_{16}H_{14}BrN_5S_2$ 420,4	16,66	16,49

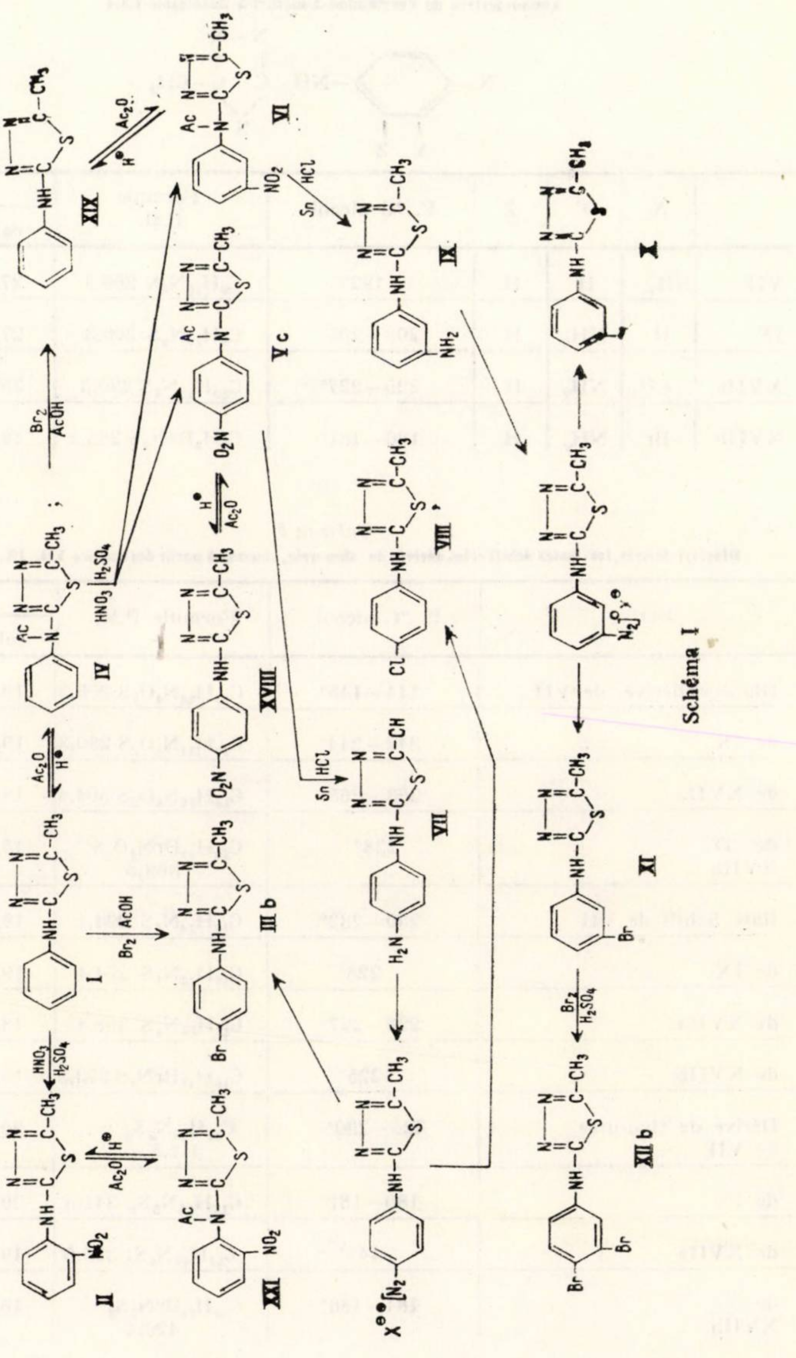
I
II
III b
IV
V c
VI
VII
VIII
IX
X
XI
XII b
XVIII
XIX
XXI
HNO₃ H₂SO₄
Ac₂O
H⁺
Br₂ AcOH
Sn HCl
Br₂ H₂SO₄
X⁻ N₂⁺
N₂⁺ Y⁻

Schéma I

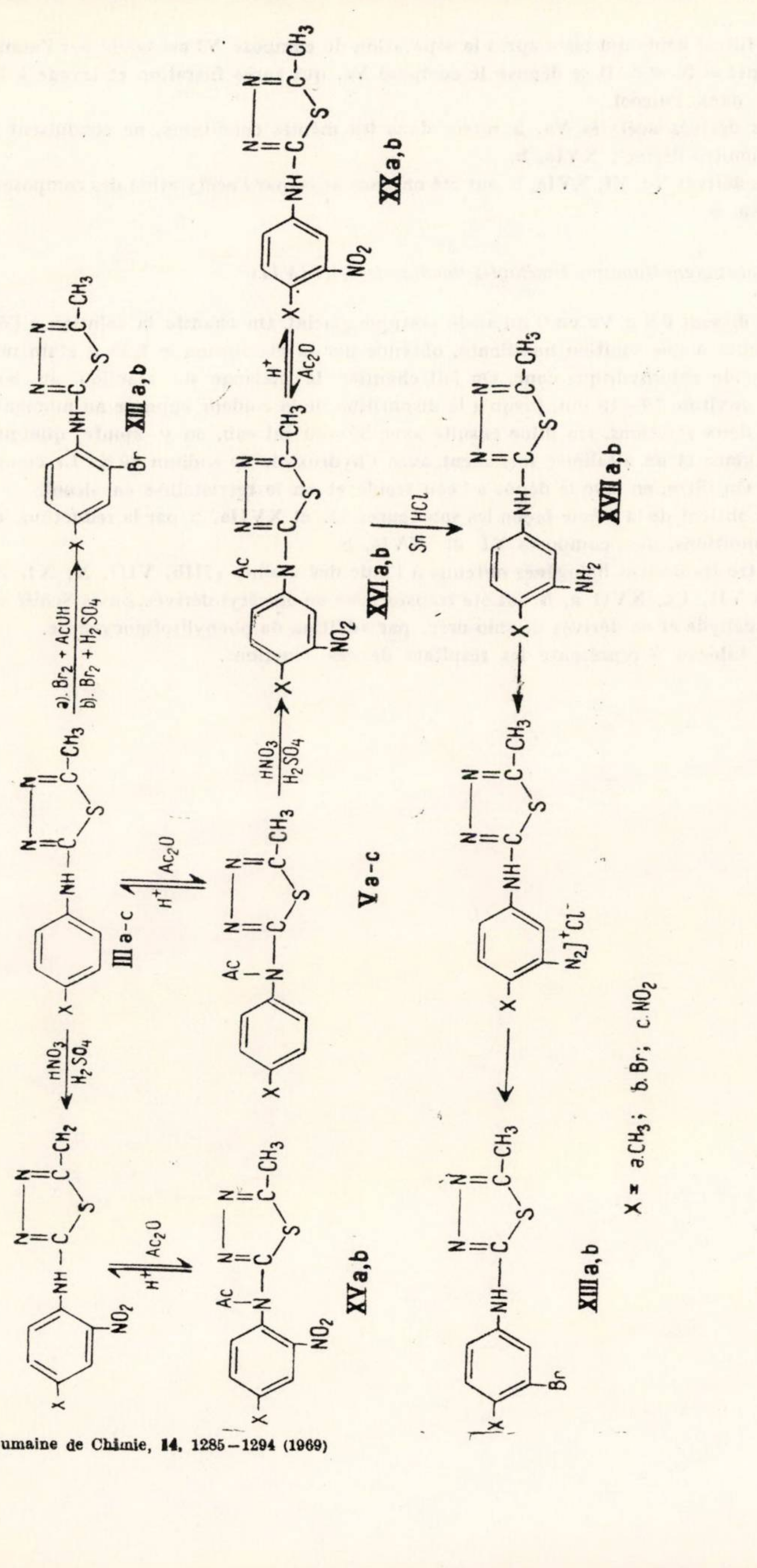
III a-c
V a-c
XII a,b
XV a,b
XVI a,b
XVII a,b
XX a,b
XIII a,b
HNO3 / H2SO4
a). Br2 + AcOH
b). Br2 + H2SO4
H+ / Ac2O
Sn HCl
X = a.CH3; b.Br; c.NO2

Schéma II

Le filtrat acide qui reste après la séparation du composé VI est traité par l'ammoniaque jusqu'au pH = 5–6,5. Il se dépose le composé Vc, qui après filtration et lavage à l'eau, récristallise dans l'alcool.

Les dérivés acétylés Va, b nitrés dans les mêmes conditions, ne conduisent qu'à un seul mononitro-dérivé-, XVIa, b.

Les dérivés Vc, VI, XVIa, b ont été obtenus aussi par l'acétylation des composés XVIII, XIX, XXa, b.

(p-phénylènediamino)-2-méthyl-5-thiodiazole-1,3,4-(VII)

On dissout 0,9 g Vc en 9 ml acide acétique glacial. On chauffe la solution à l'ébullition et on l'ajoute à une solution bouillante, obtenue par la dissolution de 1,25 g étain métallique en 5 ml acide chlorhydrique conc. On fait chauffer le mélange de réaction au bain-marie bouillant environ 10–15 mn, jusqu'à la disparition de la couleur apparue au moment du mélange des deux solutions. On dilue ensuite avec 20–30 ml eau, on y ajoute quelques morceaux de glace et on alcalinise fortement avec l'hydroxyde de sodium 30%. Le composé VII précipite. On filtre, on lave le dépôt à l'eau froide et on le recristallise en alcool.

On obtient de la même façon les substances IX et XVIIa, b par la réduction, dans les mêmes conditions, des composés VI et XVIa, b.

Outre les dérivés halogénés obtenus à l'aide des amines (IIIb, VIII, X, XI, XIIa, b), les amines VII, IX, XVII a, b ont été transformées en diacétyl-dérivés, bases Schiff au moyen du benzaldéhyde et en dérivés de thio-urée, par addition de phénylisothiocyanate.

Le tableau 5 représente les résultats de ces réactions.

Revue Roumaine de Chimie. 14, 1295–1302 (1969)

KINETIK UND MECHANISMUS DER VERESTERUNGSREAKTION VON STEROIDALKOHOLEN MIT ACETYLNITRAT

O. MANTSCH und N. BODOR

vom Chemisch-Pharmazeutischen Forschungsinstitut Cluj, str. Karl Marx 93–97

Eingegangen am 2. November 1968

Mit Hilfe kinetischer Untersuchungen wird der Beweis erbracht, daß die Veresterungsreaktion von Steroidalkoholen mit Acetylnitrat in zwei aufeinanderfolgenden Stufen stattfindet, einer Protonisierung von Acetylnitrat und einer, zwischen protonisiertem Acetylnitrat und Hydroxylgruppe verlaufenden Reaktion. Die Protonisierung ist hierbei geschwindigkeitsbestimmend.

In einer vorhergehenden Arbeit[1] untersuchten wir das System Essigsäureanhydrid-Salpetersäure-Essigsäure-Acetylnitrat, wobei wir das Vorhandensein eines mit sinkender Temperatur zugunsten von Acetylnitrat verschiebbaren Gleichgewichts nachwiesen. Gleichzeitig bestimmten wir die Geschwindigkeitskonstanten der direkten und Gegenreaktion in Gegenwart, als auch in Abwesenheit eines inerten Lösungsmittels, so wie die Gleichgewichtskonstanten für verschiedene Temperaturen.

In vorliegender Arbeit beschreiben wir die Kinetik und den Esterifizierungsmechanismus mit Acetylnitrat, wobei wir von einigen, in oben genannter Arbeit erhaltenen Resultaten, betreffs der Einstellung des Gleichgewichtes als auch der Bildung von Acetylnitrat, ausgingen. Bezüglich der Wirkungsweise des Gemisches Essigsäureanhydrid-Salpetersäure-Essigsäure bestehen gegenwärtig nur einige, sich widersprechende, Vermutungen. Gleichfalls muß hervorgehoben werden, daß das Verhalten dieses Gemisches vor allem in Nitrierreaktionen einiger aromatischer Verbindungen, als auch in Additionsreaktionen an Doppelbindungen, untersucht wurde. Auf Grund des gleichen Verhaltens der Gemische Essigsäureanhydrid-Stickstoffpentoxid[2] und Salpetersäure-Essigsäureanhydrid[3] in Nitrierreaktionen wurde angenommen, daß Acetylnitrat in beiden Fällen die aktive Spezies sei. Das Vorhandensein von Acetylnitrat in letzterem

---

[1] O. Mantsch, N. Bodor und F. Hodoşan, *Rev. Roumaine Chim.*, **13**, 1435 (1968).
[2] A. Pictet und E. Khotinsky, *Ber. dtsch. chem. Ges.*, **40**, 1163 (1907).
[3] K. I. P. Orton, *J. Chem. Soc.*, **1902**, 806.

Gemisch ist auch durch physikalisch-chemische Methoden (Messungen des Dampfdruckes,[4] Raman-Spektren[5] so wie IR-Spektren[6]), als auch durch kinetische Messungen[1] des bestehenden Gleichgewichtes bestätigt worden.

Unter Annahme, daß Acetylnitrat die aktive Spezies sei, fanden wir es als angebracht und notwendig, in Anbetracht der Wichtigkeit der Nitroester, vor allem derjenigen der Steroidreihe[7], den Reaktionsmechanismus dieses Agenten mit einer Hydroxylgruppe zu erforschen.

Bei unseren Untersuchungen gingen wir von einigen mit diesem Gemisch schon erzielten Ergebnissen aus. So gelangte z. B. Paul,[8] indem er die Nitrierung von Benzol untersuchte, zur Annahme, daß die aus protonisierter Salpetersäure und Essigsäureanhydrid entstehenden Nitroniumionen die aktive Spezies dieses Gemisches darstellen. Zu einer ähnlichen Folgerung gelangte auch Bonner,[9] der jedoch die Bildung der Nitroniumionen einer zwischen Acetylnitrat und Salpetersäure verlaufenden Reaktion zuschreibt. Andererseits wird auch angenommen, daß das mit der freien, nicht umgewandelten Salpetersäure oder einer anderen Säure protonisierte Acetylnitrat mit olefinischen Bindungen,[10-12] beziehungsweise aromatischen Verbindungen[13] Reaktionen eingeht. In letzterem Falle findet jedoch neben einer Nitrierung auch eine Acetoxylierung statt. Diese Tatsache führte zur Annahme einer, beiden Reaktionen gemeinsamen aktiven Verbindung, und zwar wird protonisiertes Acetylnitrat als solche betrachtet.

ERGEBNISSE UND DISKUSSION

Wir stellten fest, daß das aus Essigsäureanhydrid-Salpetersäure-Essigsäure-Acetylnitrat bestehende Gleichgewicht:

$$Ac_2O + HNO_3 \underset{k_2}{\overset{k_1}{\rightleftharpoons}} AcONO_2 + AcOH \qquad (1)$$

mit Steroidalkoholen Reaktionen eingeht und zur Bildung von Nitroestern führt, hingegen eine Lösung von Salpetersäure in Essigsäure diese Alkohole nicht verestert. Hieraus geht hervor, daß Acetylnitrat zur Reaktion unbedingt notwendig ist. Trotzdem kann die Bildung von Nitroestern, z.B. im Falle von Cholesterol, jedoch nicht nachgewiesen werden, wenn die Veresterung mit Hilfe eines aus Stickstoffpentoxid und Essigsäureanhydrid hergestellten Acetylnitrats, in den gleichen Bedingungen in denen das Gleichgewichtsgemisch (1) nitriert, vollzogen wird. Diese Feststellungen führten uns zur Annahme, daß die Bildung des Nitroesters folgendermaßen verlaufen muß :

---

[4] R. Vandoni und R. Viola, *Mém. services Chim. Etat* (*Paris*), **32**, 80 (1945); *Chem. Abstr.*, **42**, 4812d (1948).

[5] J. Chedin und S. Fenaut, *Compt. rend.*, **229**, 115 (1949).

[6] R. A. Marcus und J. M. Frescoe, *J. Chem. Phys.*, **27**, 564 (1957).

[7] F. Hodoşan, I. Jude, N. Serban und A. Balogh, *Chem. Ber.*, **95**, 1094 (1962).

[8] M. A. Paul, *J. Amer. Chem. Soc.*, **80**, 5332 (1958).

[9] T. G. Bonner, *J. Chem. Soc.*, **1959**, 3908.

[10] F. G. Bordwell und E. W. Garbisch, jr., *J. Org. Chem.*, **27**, 3049 (1962).

[11] F. G. Bordwell und E. W. Garbisch, jr., *J. Org. Chem.*, **28**, 1765 (1963).

[12] F. G. Bordwell und E. W. Garbisch, jr., *J. Amer. Chem. Soc.*, **82**, 3588 (1960).

[13] A. Fischer, A. J. Read und A. Vaughan, *J. Chem. Soc.*, **1964**, 3691.

$$AcONO_2 + HNO_3 \underset{k_2}{\overset{k_1}{\rightleftarrows}} [AcOHNO_2]^+ NO_3^- \qquad (2)$$

$$[AcOHNO_2]^+NO_3^- + R-OH \xrightarrow{k_3} R-ONO_2 + HNO_3 + AcOH \qquad (3)$$

Zur Beweisführung des vorgeschlagenen Mechanismus unterwarfen wir die Veresterungsreaktion einem kinetischen Studium, wobei wir die zeitliche Bildung des Nitroesters polarographisch verfolgten, denn diese Ester ergeben charakteristische polarographische Kurven im Bereich von −0,6 und −1,2 Volt. Aus Ermangelung einer Bestimmungsmethode für Acetylnitrat konnte dessen Verbrauch nicht verfolgt werden.

Die Untersuchungen wurden an sekundären Steroidalkoholen, wie Δ^5-Cholesten-3β-ol und 5α-Androstan-17β-ol-3-on, durchgeführt.

Da die Reaktion im Gleichgewichtsgemisch (1) sogar bei niedrigen Temperaturen sehr rasch verläuft, hingegen eine Verdünnung seitens einer Komponente (AcOH oder Ac_2O) eine merkliche Verschiebung des Gleichgewichtes (1) zur Folge hat, so daß die genaue Konzentration von Acetylnitrat nicht mehr bekannt ist, wählten wir als Reaktionsmedium inerte, gereinigte, Lösungsmittel, wie z.B. Chloroform und Cyclohexan.

Die kinetischen Bestimmungen wurden in Konzentrationen von 0,005−0,03 Mol/l Substrat und 0,007−0,04 Mol/l Acetylnitrat durchgeführt. Da keine Möglichkeit besteht die Anfangskonzentrationen von Acetylnitrat direkt zu bestimmen, so ermittelten wir diese mit Hilfe der, in vorhergehender Arbeit[1] erhaltenen Gleichgewichtskonstanten. Um die Genauigkeit der erhaltenen Werte zu überprüfen, führten wir einige Versuche mit einem Überschuß von Substrat durch, wobei sich der Nitroester in einer der durch Errechnung ermittelten Acetylnitratkonzentration entsprechenden Menge bildete. Die erhaltenen Ergebnisse weichen hierbei nur um 1−2% von den theoretischen Werten ab.

Diese Versuche bestätigen einerseits die Genauigkeit der bestimmten Gleichgewichtskonstanten und andererseits die Annahme, daß sich das Gleichgewicht bei diesen Konzentrationen in den angewandten Lösungsmitteln nicht verschiebt (entsprechend den Eigenschaften inerter Lösungsmittel und der Konstanten k_1 und k_2 des Gleichgewichtes (1)).

Erwartungsgemäß verläuft die Reaktion viel rascher in Chloroform als in Cyclohexan. Aus diesem Grunde wurden die Bestimmungen in Chloroform bei 0°, in Cychlohexan dagegen bei 20°, durchgeführt.

Bezüglich der Kinetik der Veresterungsreaktion bestehen, entsprechend dem vorgeschlagenen Mechanismus, folgende Möglichkeiten :

1. Die Protonisierung von Acetylnitrat verläuft sehr rasch. In diesem Falle müßte die Reaktion monomolekular in bezug auf Substrat als auch auf Acetylnitrat (bzw. protonisiertes Acetylnitrat) sein.

2. Die Protonisierung von Acetylnitrat ist eine zeitlich verlaufende Reaktion, die zwischen der protonisierten Spezies und dem Substrat jedoch eine rasche. In diesem Falle müßte eine Reaktion erster Ordnung gegenüber Acetylnitrat und nullter Ordnung gegenüber dem Substrat gefunden werden.

3. Die beiden Reaktionen (2) und (3) haben vergleichbare Geschwindigkeiten. In diesem Falle ist eine gebrochene globale Reaktionsordnung zu erwarten.

Es muß hervorgehoben werden, daß die die Protonisierung verursachende Salpetersäure sich im Laufe der Veresterungsreaktion regeneriert und folglich in dieser Reaktion nicht verbraucht wird.

Aus den erhaltenen kinetischen Ergebnissen geht hervor, daß im Falle einer Konzentrationsänderung des Substrates dessen Teilordnung ungefähr Null ist; folglich stellt nicht die Veresterungsreaktion den geschwindigkeitsbestimmenden Schritt dar. Hieraus ergibt sich, daß die Entstehung der protonisierten Spezies von Acetylnitrat geschwindigkeitsbestimmend sein muß. Diese Feststellung bedeutet gleichzeitig, daß die bei der Protonisierung verbrauchte Salpetersäure sich während der Veresterung sehr rasch regeneriert, ihre Konzentration demnach konstant bleibt. Der geschwindigkeitsbestimmende Schritt, die Protonisierung, ist demnach kinetisch betrachtet pseudomonomolekular.

Entsprechend oben angestellten Betrachtungen, so wie in Anbetracht des vorgeschlagenen Mechanismus, ergibt sich, daß während der ganzen Reaktionsdauer die Konzentration des protonisierten Acetylnitrates, im Vergleich zu derjenigen von Acetylnitrat und Substrat sehr klein ist. Folglich kann zur Beschreibung der Reaktionskinetik eine stationäre Methode[14] angewandt werden. Die Konzentration der protonisierten Spezies wird hierbei wie folgt ausgedrückt:

$$[\mathrm{AcOHNO_2}]^+ = \frac{k_1\,[\mathrm{AcONO_2}]}{k_2 + k_3[\mathrm{R-OH}]} \tag{4}$$

Die Geschwindigkeit der Esterbildung ist demnach:

$$\frac{\mathrm{d}\,[\mathrm{R-ONO_2}]}{\mathrm{d}t} = \frac{k_1 \cdot k_3\,[\mathrm{AcONO_2}]\,[\mathrm{R-OH}]}{k_2 + k_3[\mathrm{R-OH}]} \tag{5}$$

Durch Integration erhält man:

$$k_1 = \frac{1}{t}\left[\frac{k_2}{k_3}\cdot\frac{1}{a-b}\ln\frac{b\,(a-x)}{a\,(b-x)} + \ln\frac{a}{a-x}\right] \tag{6}$$

hierbei ist: $a = [\mathrm{AcONO_2}]_0$, $b = [\mathrm{R-OH}]_0$ und $x = [\mathrm{R-ONO_2}]$.

Wird zur Errechnung der Geschwindigkeitskonstanten der Versuche 1,2 und 5 aus Tabelle 1 der Ausdruck (6) verwendet, so ergeben sich Werte, die in guter Übereinstimmung mit denjenigen sind, die man nach Anwendung der Gleichung pseudo erster Ordnung erhält. Die Anwendung einer

---

[14] S. W. Benson, ,,The Foundations of Chemical Kinetics" McGraw-Hill Book Comp., New York-Toronto-London, 1960, S. 55–57.

Gleichung pseudo erster Ordnung ist auch dadurch gerechtfertigt, daß neben der Teilordnung Null des Substrates das Verhältnis k_2/k_3 ungefähr 0,002 beträgt und somit die Bedingung $k_3 . [AcONO_2] \gg k_2$ erfüllt wird. Gleichung (5) vereinfacht sich demnach zu:

$$\frac{d\,[R-ONO_2]}{dt} = k_1\,[AcONO_2] \qquad (7)$$

und folglich:

$$k_1 = \frac{1}{t} \ln \frac{a}{a-x} \qquad (8)$$

Die erhaltenen Ergebnisse sind in Tabelle 1 zusammengefaßt.

Tabelle 1

Die Geschwindigkeitskonstanten pseudo erster Ordnung in Chloroform bei 0°

Lfd. Nr.	Substrat R−OH	Anfangskonzentrationen, Mol/l			$k_1^a \cdot 10^4$ sec^{-1}	Δk_1 %	$k_1^b \cdot 10^4$ sec^{-1}
		$[AcONO_2]$	$[R-OH]$	$[HNO_3]$			
1	Δ^5-Cholesten-3β-ol	0,0383	0,02905	0,0156	7,03	0,92	7,2
2	,,	0,01953	0,01230	0,00797	2,36	1,2	2,41
3	,,	0,01953	0,00799	0,00797	2,48	3,2	—
4	,,	0,01953	0,00530	0,00797	2,36	2,4	—
5	5α-Androstan-17β-ol-3-on	0,01922	0,01432	0,00784	2,17	1,6	2,23

a Berechnet nach Gleichung (8)
b Berechnet nach Gleichung (6)

Aus Tabelle 1 geht hervor, daß man bei konstanter Acetylnitratkonzentration (Nr. 2—4) die gleichen pseudomonomolekularen Konstanten erhält, deren Werte auch durch beträchtliche Konzentrationsänderungen des Substrates nicht beeinflußt werden. Bei einer Substratänderung (Nr. 5) erhält man ebenfalls annäherende Werte, vor allem wenn man berücksichtigt, daß in diesem Falle die Salpetersäurekonzentration kleiner ist.

Bei einer ungefähr doppelten Acetylnitratkonzentration (Nr. 1) erhält man jedoch einen viel zu großen Wert für k_1, da in den pseudomonomolekularen Konstanten auch die entsprechenden Salpetersäurekonzentrationen eingeschlossen sind. Werden nun die Konstanten k_1 durch die entsprechenden Salpetersäurekonzentrationen geteilt, so erhält man jedoch nicht gleiche Werte. Dieser Widerspruch ist darauf zurückzuführen, daß zur Errechnung der wahren Gleichgewichtskonstanten die erhaltenen Werte nicht durch die Salpetersäurekonzentrationen, sondern durch die entsprechenden Protonenkonzentrationen geteilt werden müssen. Die genaue Bestimmung der Protonenkonzentration[15] ist jedoch nicht möglich, da das Reaktionsgemisch auch Essigsäureanhydrid, Essigsäure und Acetylnitrat enthält, deren Konzentrationen sich im inerten Lösungsmittel gleichzeitig mit dem Anstieg der Salpetersäurekonzentration ändern, da die Veresterungsreaktion in einem, entsprechend dem Gleichgewicht (1) bestehenden Gemisch durchgeführt wird. Diese Tatsache führte uns zur Annahme, daß die Dissoziation der Salpetersäure im Reaktionsmedium nicht parallel mit ihrer Konzentrationsänderung verläuft. Zur Beweisführung dieser Annahme bestimmten wir die relative Leitfähigkeit verschiedener Nitriergemische.

---

[15] I. GYENES, ,,Titration in non-aqueous media'', Akadémiai Kiadó, Budapest 1967, S. 14—57.

So zum Beispiel ergab die Leitfähigkeitsbestimmung eines aus 50 ml Chloroform und 2 ml Acetylnitratlösung bestehenden Gemisches (Konzentrationen die dem Versuch 1 aus Tabelle 1 entsprechen) einen 3mal größeren Wert als diejenige eines Gemisches von 50 ml Chloroform und 1 ml Acetylnitratlösung. Berücksichtigt man nun diesen unproportionalen Anstieg der Leitfähigkeit und teilt den, dem Versuch 1 entsprechenden Wert von k_1 $(7{,}03.10^{-4})$ durch 3, so erhält man $2{,}34.10^{-4}$, einen Wert, der in guter Übereinstimmung mit den Ergebnissen der Versuche 2–4 ist.

Da eine Protonenkonzentrationsbestimmung, wie schon früher erwähnt, sehr schwierig wäre, diese jedoch zur Aufklärung des Reaktionsmechanismus nicht ausschlaggebend ist, wurde dieses Problem nicht weiter verfolgt.

Mit Hilfe der Leitfähigkeitsbestimmung wurde andererseits auch der Beweis erbracht, daß die Salpetersäurekonzentration während des ganzen Reaktionsablaufes konstant bleibt, denn im Reaktionsmedium konnten keine Leitfähigkeitsänderungen festgestellt werden. Diese Ergebnisse beweisen gleichfalls, daß sich das Gleichgewicht im Nitriergemisch nicht verschiebt.

Die Veresterungsreaktion wurde auch in Cyclohexan bei 20° verfolgt. Auch in diesem Falle kann zur Errechnung der Geschwindigkeitskonstanten die Gleichung pseudo erster Ordnung verwendet werden. Eine Acetylnitratkonzentrationsänderung hat, wie auch im Falle von Chloroform, die gleichen Erscheinungen zur Folge. Die erhaltenen Ergebnisse sind in Tabelle 2 zusammengefaßt.

Tabelle 2

Die Geschwindigkeitskonstanten pseudo erster Ordnung in Cyclohexan bei 20°. Substrat = Δ^5-Cholesten-3β-ol

Lfd. Nr.	Konzentrationen Mol/l			$k_1^a \cdot 10^4$ sec^{-1}	Δk_1 %	$k_1^b \cdot 10^4$ sec^{-1}	Δk_1 %
	$[\mathrm{AcONO_2}]_0$	$[\mathrm{R{-}OH}]_0$	$[\mathrm{HNO_3}]_0$				
1	0,01426	0,00935	0,01245	3,31	2,6	—	—
2	0,01426	0,01495	0,01245	3,29	1,8	3,40	0,4
3	0,007204	0,007539	0,00630	1,03	1,0	1,09	1,1
4	0,01459	0,007476	0,01276	3,21	2,0	—	—

a Berechnet nach Gleichung (8)
b Berechnet nach Gleichung (6)

Die kinetischen Untersuchungen der Bildung von Nitroestern mit Acetylnitrat haben demnach den Beweis erbracht, daß die Veresterungsreaktion nach einem, von uns vorgeschlagenen Reaktionsmechanismus verläuft, wobei die Protonisierung von Acetylnitrat den geschwindigkeitsbestimmenden Schritt und protonisiertes Acetylnitrat die aktive Spezies dieser Veresterungsreaktion darstellt. Diese Feststellungen sind in guter Übereinstimmung mit denjenigen von Fischer,[13] welcher, indem er die gleichzeitige Acetoxylierung und Nitrierung von *o*-Xylol mit Acetylnitrat untersuchte, zur Annahme gelangte, daß bei diesen Reaktionen die Protonisierung von Acetylnitrat geschwindigkeitsbestimmend ist.

Mit Hilfe dieses Mechanismus kann auch der beschleunigende Effekt von Schwefelsäure und Perchlorsäure auf Reaktionen mit Acetylnitrat erklärt werden, denn diese Säuren bewirken, da sie in organischen Lösungsmitteln stärkere Säuren sind als Salpetersäure, einen beachtenswerten Konzentrationsanstieg der Protonen.

Um einen genaueren Einblick in den Reaktionsablauf zu erhalten, veresterten wir Alkohole mit starrer und gut bekannter Konfiguration. Hierbei stellten wir fest, daß die Veresterung keine Konfigurationsänderung zur Folge hat, denn im Falle von Cholesterol erhielten wir den 3β-Nitroester, identisch mit demjenigen, der aus Cholesterolchloroformiat und Silbernitrat erhalten wird und für dessen Entstehung der Beweis erbracht wurde, daß diese Reaktion ohne Konfigurationsänderung verläuft.[16]

Protonisiertes Acetylnitrat greift demnach elektrophil den Alkoholsauerstoff an, wobei sich, nach Ablösung des Alkoholwasserstoffes als Proton und eines Essigsäuremoleküls aus dem protonisierten Acetylnitrat, der entsprechende Nitroester bildet. Die C—O Bindung wird hierbei nicht angegriffen.

EXPERIMENTELLES

Reagenzien:

1. Δ^5-Cholesten-3β-ol: Schmp. 149—150° (Äther)
2. 5α-Androstan-17β-ol-3-on: Schmp. 181—182° (Essigsäureester)
3. Die Acetylnitratlösung wurde nach den Angaben der vorhergehenden Arbeit[1] hergestellt.

Für die nach Aufarbeitung des Reaktionsgemisches isolierten Nitroester wurden folgende Daten erhalten:

Δ^5-Cholesten-3β-ol 3-Nitrat: Schmp. 114—115° (Literatur[16]: Schmp. 115°)

5α-Androstan-17β-ol-3-on 17-Nitrat: Schmp. 147—148° (aus wässerigem Aceton)

$C_{19}H_{29}NO_4$	*Ber.*: N 4,17
335,43	*Gef.*: N 4,25

Kinetische Bestimmungen

0,2—0,4 g Δ^5-Cholesten-3β-ol werden in 50 ml gereinigtem Chloroform gelöst, die Lösung thermostatiert und bei 0° 1 —2 ml Acetylnitratlösung, die ebenfalls bei 0° aus 10 ml 96%igem

---

[16] R. Boschan, *J. Amer. Chem. Soc.*, **81**, 3341 (1959).

Essigsäureanhydrid und 1 ml HNO_3 94,5 g/100 ml hergestellt wurde, hinzugegeben (Gleichgewichtskonstante bei 0° : $K=2{,}46$).

Dem Reaktionsgemisch werden in verschiedenen Zeitabständen Proben von 1—2 ml entnommen und in 10 ml 10%ige Natriumhydroxidlösung eingetragen. Die wässerige Phase wird mit Chloroform ausgeschüttelt und die vereinigten Chloroformlösungen eingedampft. Den Rückstand löst man in Äthanol auf und nach Hinzugabe von 1 ml wässeriger 5%iger LiCl-Lösung wird das Volumen mit Äthanol auf 25 ml aufgefüllt. Die Lösung wird polarographiert und aus der erhaltenen Kurve die Konzentration des Nitroesters berechnet. Als Standartlösung diente uns eine Lösung von Δ^5-Cholesten-3β-ol 3-Nitrat in Äthanol + LiCl.

Die kinetischen Bestimmungen wurden bis zu einer Umwandlung von 80% durchgeführt. Analog wird auch in Cyclohexan bei 20° gearbeitet. Hierbei verwendet man jedoch eine bei 20° hergestellte Acetylnitratlösung (Gleichgewichtskonstante : $K = 1{,}18$).

Leitfähigkeitsbestimmungen

Die Leitfähigkeit wurde mit Hilfe eines Konduktometers „Randelkis" (Meßbereich : $10^{-1}-10^{-6}$ Ohm^{-1} cm^{-1}) und einer Zelle mit Platinelektroden (Oberfläche 1 cm^2, Abstand 1 cm) wie folgt gemessen :

In ein geschlossenes Gefäß werden 50 ml Chloroform und 1—2 ml Acetylnitratlösung eingetragen. Von den erhaltenen Werten, $\varkappa_1$, werden die Leitfähigkeiten, $\varkappa_2$, einer Lösung bestehend aus 50 ml Chloroform und 1—2 ml Gemisch von Ac_2O und AcOH abgezogen. Das molare Verhältnis von Ac_2O : AcOH entspricht hierbei dem Gleichgewichtsverhältnis bei 0° (AcOH : 6,3042 Mol; Ac_2O : 7,1943 Mol) Auf diese Art erhält man den Leitfähigkeitsbeitrag der Salpetersäure.

Ergebnisse : $\varkappa_1-\varkappa_2 = 0{,}16.10^{-6}$, bzw. $0{,}49.10^{-6}$ $Ohm^{-1}. cm^{-1}$

Revue Roumaine de Chimie, **14**, 1303–1307 (1969)

UNSYMMETRICAL DIACYL DERIVATIVES OF METHYL HYODESOXYCHOLATE

F. HODOŞAN, N. ŞERBAN and VICTORIA CIURDARU

Institute of Chemistry of the Academy str. Donath 59–65, Cluj, Romania

Received April 12, 1969

The title compounds were prepared following indirect routes via 3-and 6-ketone, respectively.

Our investigations on the 3α, 6α-disubstituted 5β-steroids, implied the availability of title compounds. The possibility to synthetize them by selective acylations was ruled out from the very beginning, since in agreement with other authors[1,2,3] we considered that the reactivities of the hydroxyl groups of the 3α, 6α-dihydroxy-5β-steroids are very similar.[4] For analogous reasons we gave up the idea to prepare the compounds by selective hydrolysis of the symmetrical diacyl derivatives.[5a,b,c] Consequently, taking into account that the main product of the reduction of a 3-oxo group with complex hydrides is the equatorial alcohol,[6] we decided to follow the route via 3-ketone IIa. In spite of the fact that a 6-oxo group gives mainly the axial alcohol,[6] we explored also the route via 6-ketone Va.

[1] K. Shimizu, *J. Biochem. (Japan)*, **40**, 75 (1953); *Chem. Abstr.*, **49**, 15935 (1955).

[2] R. Justoni and R. Pessina, *Il Farmaco (Ed. Sci.)*, **8**, 332 (1953).

[3] A. Corbellini, G. Nathanson and V. Gurdjian, *Gazz. chim. Ital.*, **86**, 35 (1956).

[4] The selective acetylation of methyl hydesoxycholate (I) with acetic anhydride in boiling benzene, as reported by B. Matkovics, Zs. Tegyey and Gy. Göndös, *Steroids*, **5**, 117 (1965), B. Matkovics and Zs. Tegyey, *Magyar. Kém. Folyóirat*, **73**, 431 (1967), gave no satisfactory results in our hands. In the crude reaction product we identified by t.l.c. two approximately equal monoacetate fractions along with an important amount of diacetate. Crystallizations from the reported solvent pair (ether- — petrol ether) afforded mixtures containing only the two more polar components; no separation tendency of the pure 3-monoacetate was observed.

[5] *a.* R. E. Marker and J. Krueger, *J. Amer. Chem. Soc.*, **62**, 79 (1940); R. B. Moffett, J. E. Stafford, J. Linsk, and W. M. Hoehn, *J. Amer. Chem. Soc.*, **68**, 1857 (1946); R. Justoni and R. Pessina, *Il Farmaco (Ed. Sci.)*, **9**, 359 (1954). *b.* W. M. Hoehn, J. Linsk and R. B. Moffett, *J. Amer. Chem. Soc.*, **68**, 1855 (1946). *c.* T. F. Gallagher and J. R. Xenos, *J. Biol. Chem.*, **165**, 365 (1946). In spite of the contradictory data reported by these authors the possibility to convert hydrolytically a 3α, 6α-diacetoxy-5β-steroid into the corresponding 6-monoacetate cannot be completely excluded. However, yields higher than 10—15% are not to be expected.

[6] W. Klyne, "The Chemistry of the Steroids", Methuen and Co. Ltd., London, 1960, p. 81.

The reduction steps of the chosen pathways were carried out by means of a recently developed procedure.[7] The reagent used consisted of sodium borohydride on neutral alumina, with which reductions in nonpolar solvents, such as dry benzene, could be brought about.

Reduction of 3-oxo-6α-acetoxy-5-β-cholanate (IIb)[5b] gave the epimer pair IIIa and IVa, separable by chromatography. The configuration at C-3 of the monoacetate IIIa was established by conversion into well-known substances such as methyl 3α, 6α-diacetoxy-5β- cholanate[5b] and hyodesoxycholic acid, respectively. The monoacetate IVa gave by saponification a dihydroxy acid with the melting point similar to that of β-hyodesoxycholic acid.[8]

Starting with the monoacetate IIIa, two unsymmetrical diacyl derivatives IIIb and IIIc were prepared.

Reduction of the 3-oxo-6α-tosyloxy derivative IIc [5c,9] gave methyl hyodesoxycholate 6-tosylate (IIId), which by tosylation afforded the well-known ditosylate.[3] Starting with the monotosylate IIId a series of diacyl derivatives IIIe-h were prepared. Another series having a nisyloxy group[10] at C$-$6 could not be synthetized starting with the substance IId because the latter gave a reduction product which resisted purification.

On exploring the route via 6-ketone Va, we converted its acetate Vb[5b] by reduction into a mixture of two diol monoacetates, which were subsequently separated by chromatography. The less polar fraction consisted of 3α-acetoxy-6β-hydroxy-5β-cholanate (VI) identical with that reported by Hoehn al.[5b] The more polar fraction was considered the methyl 3α-acetoxy-6α-hydroxy-5β-cholanate (IIIi) (m.p. 111$-$113°)[11] because on saponification it gave hyodesoxycholic acid and on acetylation the diacetate of methyl hyodesoxycholate[5b]; on oxidation with chromic acid it was converted into the starting substance Vb. Treatment of the monoacetate IIIi with phosphorus oxychloride in pyridine resulted in the formation of methyl 3α-acetoxy-Δ^5-cholenate, identical with that prepared by other authors.[12]

The fact that the main reduction products of the 6-ketone Vb belong to the 5β series shows that under the given conditions the reduction proceeds considerably faster than the isomerisation 5$\beta \rightarrow$5α of the starting ketone.[13]

---

[7] F. Hodoşan and N. Şerban, *Rev. Roumaine Chim.*, **14**, 121 (1969).

[8] R. B. Moffett and W. M. Hoehn, *J. Amer. Chem. Soc.*, **69**, 1995 (1947).

[9] F. Hodoşan, A. Pop-Gocan and N. Şerban, *Rev. Roumaine Chim.*, **10**, 97 (1965).

[10] Nisyl = Ns = *p*-nitrobenzenesulfonyl.

[11] M. p. 98° was reported for the 3-monoacetate obtained by direct acetylation.[4].

[12] A. Schubert and Ch. Damker, *J. prakt. Chem.*, [4] **4**, 260 (1957).

[13] The active alumina converts the 6-ketones of the A/B-*cis* series into the corresponding A/B-*trans* isomers [5b].

Starting with the monoacetate IIIi two diacyl derivatives IIIj and IIIk were prepared.

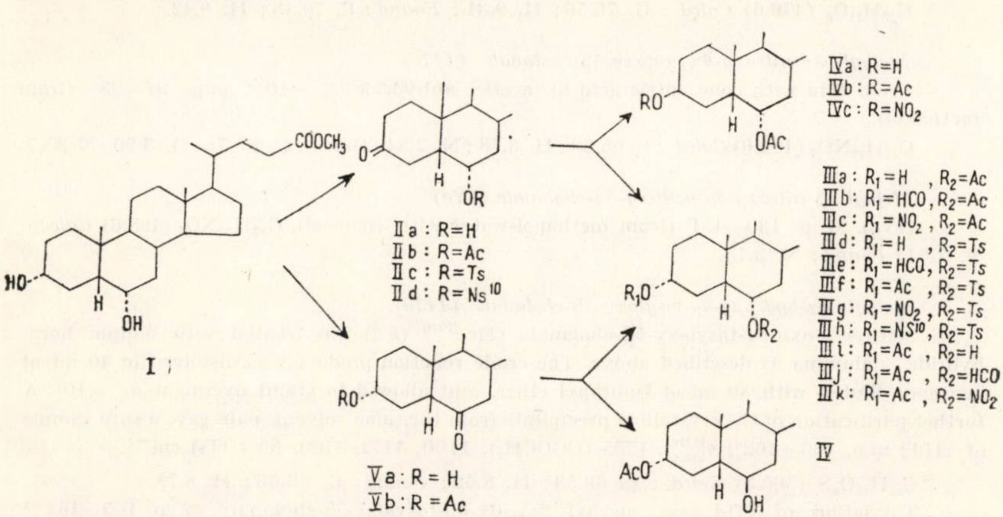
COOCH$_3$
HO
H
OH
I
O
H
OR
IIa : R=H
IIb : R=Ac
IIc : R=Ts
IId : R=Ns^{10}
IVa : R=H
IVb : R=Ac
IVc : R=NO$_2$
RO
H
OAc
IIIa : R$_1$=H , R$_2$=Ac
IIIb : R$_1$=HCO, R$_2$=Ac
IIIc : R$_1$=NO$_2$, R$_2$=Ac
IIId : R$_1$=H , R$_2$=Ts
IIIe : R$_1$=HCO, R$_2$=Ts
IIIf : R$_1$=Ac , R$_2$=Ts
IIIg : R$_1$=NO$_2$, R$_2$=Ts
IIIh : R$_1$=NS^{10}, R$_2$=Ts
IIIi : R$_1$=Ac , R$_2$=H
IIIj : R$_1$=Ac , R$_2$=HCO
IIIk : R$_1$=Ac , R$_2$=NO$_2$
R$_1$O
H
OR$_2$
RO
H
O
Va : R = H
Vb : R = Ac
AcO
H
OH
IV

EXPERIMENTAL [14]

Reduction of methyl 3-oxo-6α-acetoxy-5β-cholanate (IIb). A solution of 10 g of the substance IIb [5b] in 300 ml of dry benzene was treated with the reducing agent prepared from 100 g of neutral alumina and 5 g of sodium borohydride.[7] The suspension was stirred vigorously for 4 hours at room temperature. After filtration, the alumina was washed with ether and the combined filtrates evaporated under reduced pressure to dryness. A sample of 5.5 g from the crude residue was adsorbed on 500 g of neutral alumina (activity IV) and eluted with petrol ether — benzene 1 : 1 (600 ml), 1 : 2 (20.000 ml), and benzene (1000 ml). From the first fractions a pure sample of *methyl 3α-hydroxy-6α-acetoxy-5β-cholanate* (IIIa) could be isolated by maceration of the oily residue with petrol ether and repeated recrystallizations from methanol – water (charcoal); m.p. 118–119°, $[\alpha]_D^{22}$ +6° (chloroform), $\nu_{max}^{CCl_4}$: 3520, 1740, 1245, 1030 cm^{-1}.

$C_{27}H_{44}O_5$ (448.6) *Calcd.* : C, 72.29 ; H, 9.88 ; *Found* : C, 72, 40 ; H, 9.92.

The last fractions consisted of *methyl* 3β-*hydroxy-6α-acetoxy-5β-cholanate* (IV a) contaminated with IIIa. Preparative t.l.c. on silica gel G (solvent system : chloroform–acetone 23 : 2), maceration of the oily product with petrol ether and crystallizations from methanol – water (charcoal) yielded a pure sample of IV ; m.p. 151–152°, $[\alpha]_D^{22}$ + 13° (chloroform), $\nu_{max}^{CCl_4}$: 3630, 1740, 1250, 1042, 1030 cm^{-1}.

$C_{27}H_{44}O_5$ (448.6) *Calcd.* : C, 72.29 ; H, 9.88 ; *Found* : C, 72.44 ; H, 10.22.

Saponification of IV gave *3β, 6α-dihydroxy-5β-cholanic acid,* m.p. 195–196° (from ethyl acetate) (Lit.[8] m.p. 191–192°).

Acetylation of IVa yielded *methyl 3β, 6α–diacetoxy-5β-cholanate* (IVb), m.p. 84–85° (from methanol – water).

$C_{29}H_{46}O_6$ (490.6) *Calcd.* : C, 70.99 ; H, 9.45 ; *Found* : C, 71.21 ; H, 9.52.

---

[14] Melting points are uncorrected.

Methyl 3α-formoxy-6α-acetoxy-5β-cholanate (IIIb).

From IIIa with 98% formic acid at room temperature; m.p. 143° (from methanol).

$C_{28}H_{44}O_6$ (476.6) *Calcd.* : C, 70.56 ; H, 9.31 ; *Found* : C, 70.48 ; H, 9.42.

Methyl 3α-nitroxy-6α-acetoxy-5β-cholanate (IIIc).

From IIIa with conc. nitric acid in acetic anhydride at −10°; m.p. 97–98° (from methanol).

$C_{27}H_{43}NO_7$ (493.6) *Calcd.* : C, 65.69 ; H, 8.78 ; N, 2.84 ; *Found* : C, 65.78 ; H, 8.90 ; N, 3.17.

Methyl 3β-nitroxy-6α-acetoxy-5α-cholanate (IVc)

(IVc). M. p. 130–131° (from methanol-water with charcoal). $C_{27}H_{43}NO_7$ (493.6) *Calcd.* : N, 2.84 ; *Found* : N, 3.15.

Methyl 3α-hydroxy-6α-tosyloxy-5β-cholanate (IIId).

Methyl 3-oxo-6α-tosyloxy-5β-cholanate (IIc)[5c,9] (8 g) was treated with sodium borohydride — alumina as described above. The crude reaction product was dissolved in 40 ml of benzene, diluted with 80 ml of isopropyl ether, and allowed to stand overnight at −10°. A further purification of the crystalline precipitate from the same solvent pair gave a sure sample of IIId; m.p. 160–162°, ν_{max}^{KBr} : 1735 ($COOCH_3$), 1190, 1172, 1100, 55 (OTs) cm^{-1}.

$C_{32}H_{48}O_6S$ (560.8) *Calcd.* : C, 68.53 ; H, 8.62 ; *Found* : C, 68.66 ; H, 8.79.

Tosylation of IIId gave methyl 3α, 6α-diotosyloxy-5β-cholanate, m. p. 165–167°.[3]

Methyl 3α-formoxy-6α-tosyloxy-5β-cholanate (IIIe). M.p. 121–123° (from isopropyl ether).

$C_{33}H_{48}O_7S$ (588.8) *Calcd.* : C, 67.31 ; H, 8.21 ; *Found* : C, 67.12 ; H, 8.75.

Methyl 3α-acetoxy-6α-tosyloxy-5β-cholanate (IIIf) M.p. 91–93° (from methanol), ν_{max}^{KBr} : 1740 ($COOCH_3$, OAc), 1245, 1030 (OAc), 1190, 1172, 1100, 555 (OTs) cm^{-1}.

$C_{34}H_{50}O_7S$ (602.8) *Calcd.* : C, 67.74 ; H, 8.36 ; *Found* : C, 68.02 ; H, 8.29.

Methyl 3α-nitroxy-6α-tosyloxy-5β-cholanate (IIIg).

The crude nitrate ester was recrystallized from benzene-isopropyl ether 1 : 2, adsorbed on a column of silica gel, and eluted with benzene; m.p. 174–176°

$C_{32}H_{47}NO_8S$ (605.8) *Calcd.* : C, 63.44 ; H, 7.82 ; S, 5.29 ; *Found* : C, 63.79 ; H, 7.70 ; S, 5.49.

Methyl 3α-nisyloxy-6α-tosyloxy-5β-cholanate (IIIh).[10]

The substance IIId (1.1 g) was dissolved in 2.2 ml of dry pyridine, treated with 0.65 g of *p*-nitrobenzenesulfonyl chloride, and allowed to stand overnight; m. p. 138–140°(from petrol ether — benzene 1 : 3).

$C_{38}H_{51}NO_{10}S_2$ (745.9) *Calcd.* : C, 61.19 ; H, 6.89 ; *Found* : C, 61.11 ; H, 7.03.

Methyl 3-oxo-6α-nisyloxy-5β-cholanate (IId)[10].

A solution of 10 g of IIa[9] in 30 ml of dry pyridine was treated with 8 g of *p*-nitrobenzenesulfonyl chloride and allowed to stand for 48 hours at room temperature. The solution was poured into cold water, extracted with ether, dried, concentrated to a small volume and allowed to stand overnight at −5°. The crystalls formed were filtered, dissolved without heating in 10 ml of benzene, diluted with 10 ml of isopropyl ether, and allowed to stand overnight at −5°. Repeated purifications from the same solvent pair gave a pure sample of IId; m.p. 133–135°.

$C_{31}H_{43}NO_8S$ (589.7) *Calcd.* : C, 63.13 ; H, 7.35 ; *Found* : C, 62.76 ; H, 7.15.

Reduction of methyl 3α-acetoxy-6-oxo-5β-cholanate. (*Vb.*) A solution of 80 g of Vb[5b] in 2400 ml of dry benzene was treated with the reducing agent prepared from 800 g of neutral alumina and 40 g of sodium borohydride,[7] and vigorously stirred for 4 hours. The suspension was filtered, the alumina washed with ether, and the combined filtrates evaporated under reduced pressure to dryness. The residue was chromatographed of 1500 g of neutral alumina (activity III—IV). Elutions with 2500 ml of petrol ether — benzene 1 : 1 and 2000 ml of benzene gave 19 g of *methyl 3α-acetoxy-6β-hydroxy-5β-cholanate* (VI),[5b] m.p. 124—126° (from petrol ether — isopropyl ether), $[\alpha]_D^{25} + 44°$ (methanol), +35° (chloroform).

The second fraction obtained by elution with ether consisted of *methyl 3α-acetoxy-6α-hydroxy-5β-cholanate* (IIIi) contaminated with VI. A pure sample of compound IIIi was obtained by chromatography on silica gel and subsequent recrystallization from petrol ether; m.p. 111—113°, $[\alpha]_D^{23} + 17°$ (chloroform),

$\nu_{max}^{CCl_4}$: 3620, 1740, 1245, 1035 cm^{-1}.

$C_{27}H_{44}O_5$ (448.6) *Calcd.* : C, 72.29; H, 9.88; *Found* : C, 72.60; H.10.18.

Methyl 3α-acetoxy-6α-formoxy-5β-cholanate (*IIIj*). M.p. 108—110° (from methanol).

$C_{28}H_{44}O_6$ (476.6) *Calcd.* : C, 70.56; H, 9.31; *Found* : C, 70.94; H, 9.44.

Methyl 3α-acetoxy-6α-nitroxy-5β-cholanate (*IIIk*). M.p. 132—133° (from methanol)

$C_{27}H_{43}NO_7$ (493.6 *Calcd.* : C, 65.69; H, 8.78 : *Found* : C, 65.56; H, 8.85.

Methyl 3α-formoxy-Δ⁵-cholenate. From IIId (500 mg) on heating for 2 hours in a water bath with 1 g of LiCl in 10 ml of DMFA. The precipitate formed after dilution with water was filtered off, dried, and chromatographed on 18 g of neutral alumina (activity IV). Elution with 90 ml of petrol ether — benzene 1 : 1 gave a small amount of an unidentified product. Continuing the elution with 360 ml of petrol ether — benzene 1 : 2, a product was obtained which was formylated as usual. M. p. 108—110° (from methanol).

The same compound could be obtained by dehydrotosylation of IIIe.

$C_{26}H_{40}O_4$ (416.6) *Calcd.* : C, 74.95; H, 9.68; *Found*: C, 74.54; H, 9.98.

Methyl 3α-acetoxy-Δ⁵-cholenate. From IIIi (130 mg) on heating at about 90° for 2 hours with 0.14 ml of $POCl_3$ in 2.7 ml of dry pyridine. The crude reaction product was recrystallized twice from methanol. M. p. 107—109° (Lit.[12] m.p. 109.5°).

Revue Roumaine de Chimie, 14, 1309–1321 (1969)

НЕКОТОРЫЕ ВОПРОСЫ ФОТОСИНТЕЗА СОПОЛИМЕРОВ СЕТЧАТОЙ СТРУКТУРЫ С ОБРАЗОВАНИЕМ РЕЛЬЕФНЫХ ИЗОБРАЖЕНИЙ

Н. К. ФРУНЗЕ

Академия наук СССР, Ордена Ленина Институт химической физики
Москва В-334, Воробьевское шоссе, 2 Б

Получена 10 октября 1968 г.

В работе проводился фотосинтез сополимеров сетчатой структуры с заданным комплексом свойств на основе композиций, состоящих из полиэфиракрилатов, линейных полимеров и сенсибилизаторов с образованием рельефных изображений. Одновременно с помощью спектров поглощения в ИК- и УФ-областях, люминисцентного и ЭПР методов, а также термогравиметрического анализа уточнены некоторые закономерности фотосополимеризации.

За последние годы в ряде областей промышленности наметилось направление по применению полимер-олигомерных композиций.

Такие комбинации значительно облегчают стадию их переработки и дают возможность более широкого варьирования свойствами получаемых сополимеров.

В особенности важным, на основе указанных композиций, является фотосинтез сополимеров сетчатой структуры с целью получения рельефных изображений.

Применение последних стало необходимым в таких областях промышленности, как электроника, пневмоника [1], растровая техника, телемеханика, полиграфия [2] и т.д.

Фотосинтез сополимеров сетчатой структуры обычно проводится с применением полифункциональных олигомеров и, в частности, в данной работе использовались олигоэфиракрилаты, которые являются отечественными продуктами и разрабатывались под руководством А. А. Берлина с 1947 г.

Олигоэфиракрилаты дают возможность путем направленного синтеза, меняя природу олигомерного блока и реакционных групп, влиять на кинетику перехода от олигомеров к высокополимерам и варьировать комплекс свойств полимерных материалов для решения различных научных задач.

---

[1] « Структурная техника », Москва, 1963.

[2] Б. Ю. ГОРДИНСКИЙ, *Полигр. промышленность*, *3* (1962).

ОЭА являются[3-7] продуктами взаимодействия гликолей или высших полиолов, предельных алифатических или ароматических двухосновных кислот и кислот акрилового ряда и имеют общую формулу:

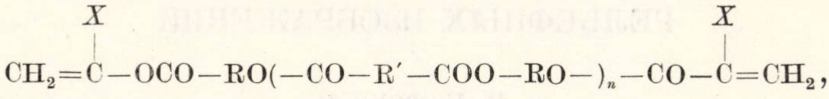

$$\mathrm{CH_2{=}\overset{X}{\overset{|}{C}}{-}OCO{-}RO({-}CO{-}R'{-}COO{-}RO{-})_{\mathit{n}}{-}CO{-}\overset{X}{\overset{|}{C}}{=}CH_2},$$

где R и R′ — алкильные или арильные радикалы соответственно гликоля и двухосновной кислоты:

$$X-\mathrm{H},\ \mathrm{CH_3},\ \mathrm{CN},\ \text{галоид},$$

n — средняя степень полимеризации олигоэфира, в первом приближении $n = \frac{2[L]}{[B]}$; $[L]$ и $[B]$ = число молей соответственно двухосновной и одноосновной кислоты.

ОЭА, имея двойные связи на концах цепи, являются светочувствительными материалами с максимумом поглощения от 200 до 250 нм (рис. 1).

Под влиянием света, аналогично действию тепла, ОЭА сополимеризуясь, образуют сетчатую структуру полимера:

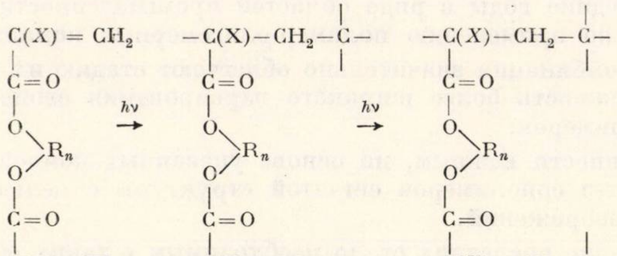

где R_n — полиэфирный блок различной степени полимеризации $X-\mathrm{H},\mathrm{CH_3}$; галоид, CN и др.

[3] А. А. БЕРЛИН, Т. Я. КЕФЕЛИ и Г. В. КОРОЛЕВ, *Хим. промышленность*, *12*, 870 (1962).

[4] А. А. БЕРЛИН, Г. Л. ПОПОВА и Е. Ф. ИСАЕВА, *ВМС*, *7*, 951 (1959).

[5] А. А. БЕРЛИН, Т. Я. КЕФЕЛИ, Ю. М. ФИЛИППОВСКАЯ и Ю. М. СИВЕРГИН, *ВМС*, *2*, 411 (1960)

[6] А. А. ВЕРЛИН, Т. Я. КЕФЕЛИ и Г. В. КОРОЛЕВ, Москва, Изд-во « Химия », 1967.

[7] А. А. БЕРЛИН, Т. Я. КЕФЕЛИ и Ю. М. СИВЕРГИН, *Plaste und Kautschuk*, *5*, 343 (1968).

В заполимеризованном состоянии ОЭА обладают высокой теплостойкостью, твердостью и прочностью к динамическим и статическим нагрузкам.

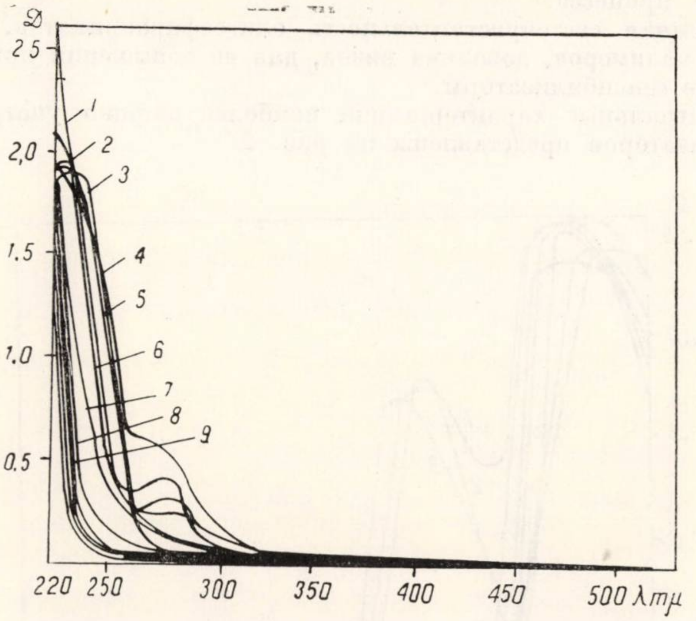

Рис. 1. — Спектры поглощения олигоэфирокрилатов:
1, диметакрилат поли/диэтиленгликольфталат; *2*, тетраме такрилат бис/глицерин/фталат; *3*, диметакрилаттриэтиленгликоль; *4*, диметакрилат бис/диэтиленгликольтиодивалерианат; *5*, октаметакрилатполипентаэритритадипинат; *6*, диметакрилат бис/триэтиленгликоль/фталат; *7*, тетраметакрилат бис/ксилитан/фталат ; *8*, диметакрилатбутандиола (МБ), *9*, диметакрилатгексаметилендиамина; *10*, олигокарбонатакрилаты; *11*, монометакрилатэтиленгликоля (ММЭГ), *12*, диметакрилатхлорпарафины.

В исходном состоянии безвредны, после очистки прозрачны, без запаха, являются очень удобными для работы веществами, но, будучи большей частью жидкостями, не используются для образования фоторельефов без наполнителей, за исключением нескольких специальных методов фотополимеризации в формах.

С помощью наполнителей или, если имеются в виду полимеры, то активных участников фотопроцессов,[8,9] достигается улучшение некоторых свойств сетчатых полимеров на основе собственно олигоэфиракрилатов (ОЭА), как-то: увеличение прочности, уменьшение усадки и т.п.

Одновременно, при проведении фотосинтеза, с целью получения рельефных изображений, исходные полимеры должны обладать рядом таких свойств, как совместимость с ОЭА, способность к образованию

---

[8] Н. К. Фрунзе и А. А. Берлин, *ВМС* (в печати).

[9] А. А. Берлин, Н. К. Фрунзе и В. Ф. Гачковский, *Plaste und Kautschuk*, 6, 400 (1968).

пленки и др. Очень важным свойством является также растворимость не в токсичном растворителе, а лучше просто в воде, с тем, чтобы обеспечить при проявлении рельефа максимальную безопасность технологического процесса.

Истинная светочувствительность олигоэфиракрилатов, и в особенности полимеров, довольна низка, для ее повышения применяются различные сенсибилизаторы.

Спектральные характеристики наиболее широко употребляемых сенсибилизаторов представлены на рис. 2.

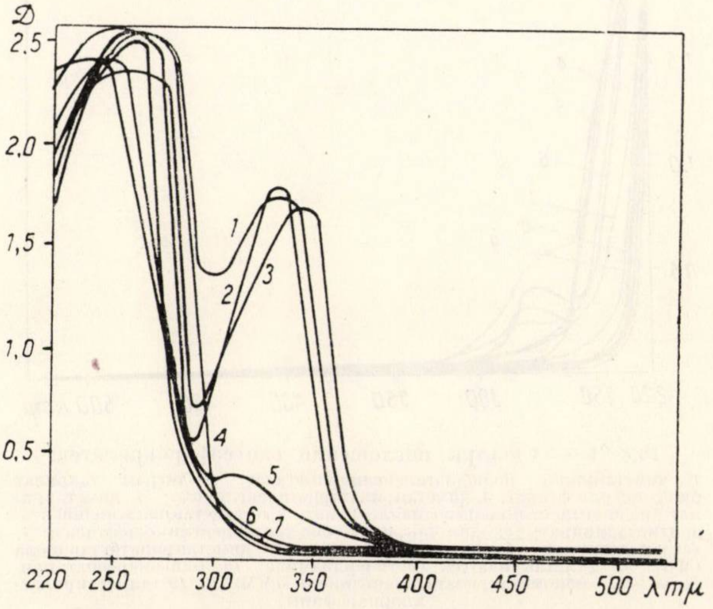

Рис. 2. — Спектры поглощения сенсибилизаторов:
1, антрахинон; *2*, α-хлорантрахинон; *3*, α-хлорантрахинон; *4*, метиловый эфир бензоина; *5*, бензил; *6*, бензофенон; *7*, бензоин.

Фотосинтез сополимеров сетчатой структуры производится с помощью воздействия УФ-света на композиции, состоящие из олигоэфиракрилатов, полимеров, сенсибилизаторов.

Рельефные изображения на их основе изготовляются в зависимости от совместимости компонент композиции, либо эмульсионным способом полива на металлическую или стеклянную подложки, либо из раствора. Рассмотрен также способ запрессовок светочувствительных композиций, в виде гибких пластин.

И в том, и в другом случае высохшую на подложке или в виде пластинки, композицию помещают в специальный прибор для экспонирования, в вакууме от лампы УФ-света, желательно, параллельно направленным пучком.

Вакуумирование обеспечивает более быстрое раскрытие двойных связей в полиэфиракрилатах и образование сополимерных сшивок ввиду исключения ингибирующего воздействия кислорода воздуха.

Из рис. 1 и 2 видно, что рабочая спектральная область соответствует главным образом максимуму поглощения сенсибилизаторов, а именно 240—260 нм.

При облучении рабочую спектральную область очень важно согласовать с отсутствием или минимальной способностью поглощения растворителя в этом интервале длин волн.

Однако, если растворитель участвует в процессах передачи цепи при сополимеризации, как это имеет место, например, при использовании четыреххлористого углерода, он может явиться ускоряющим агентом в процессе сшивок.

В фотосинтезе немаловажную роль играют донорно-акцепторные добавки в композицию, которыми удается значительно ускорить процессы инициированной облучением трехмерной полимеризации. При УФ-облучении полимер-олигомерных композиций возможно протекание сложных радикальных процессов, обусловливающих образование различных пространственно-сетчатых структур.

В связи с этим представлялось интересным исследовать такие системы с применением ряда физико-химических методов.

В качестве модели для исследования была использована композиция, состоящая из поливинилпирролидона (ПВП) и олигоэфиракрилата (диметакрилат поли/диэтиленгликольфталат) формулы:

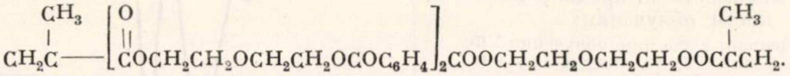

$$CH_2\overset{\overset{\displaystyle CH_3}{|}}{C}—\left[\overset{\overset{\displaystyle O}{||}}{C}OCH_2CH_2OCH_2CH_2OCOC_6H_4\right]_2COOCH_2CH_2OCH_2CH_2OOC\overset{\overset{\displaystyle CH_3}{|}}{C}CH_2.$$

В качестве сенсибилизаторов применялись бензоин или метиловый эфир бензоина.

Для оценки изменения количества растворимых ингредиентов композиций, нами исследовались спектры поглощения спиртового экстракта в зависимости от продолжительности освещения (рис. 3).

В проведенных ранее работах[8,9] было показано, что все компоненты композиции, под облучением УФ-светом, дают радикалы и активно участвуют в процессах сополимеризации. Так, например, при облучении УФ-светом как сенсибилизированного, так и несенсибилизированного поливинилпирролидона в вакууме до 10^{-3} при температуре жидкого азота в полимере генерируются радикалы. Последние при размораживании до —78° образуют устойчивый до плюсовых температур пятикомпонентный спектр ЭПР (рис. 4), анализ[3] которого дал возможность отнести его к радикалу с локализацией валентности у углерода метиновой группы, а именно:

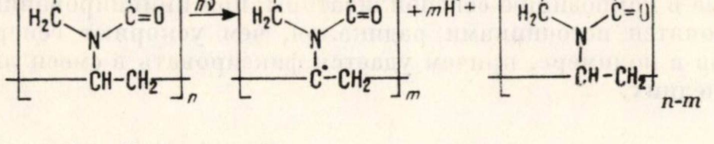

Возможной причиной повышенной фотоактивности ПВП, по сравнению с другими полимерами, является наличие в нем реакционного водорода α-метиновой группы.

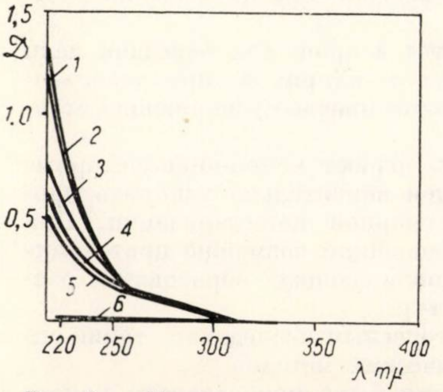

Рис. 3. — Кривые изменения оптической плотности спиртовых экстракций композиции, состоящей из ПВП, олигоэфиракрилата и бензоина, в зависимости от продолжительности облучения:

1, необлученная; *2*, 0,5 мин. облучения УФ; 1 мин.; *4*, 5 мин.; *5*, 10 мин.; *6*, 40 мин. обл. УФ.

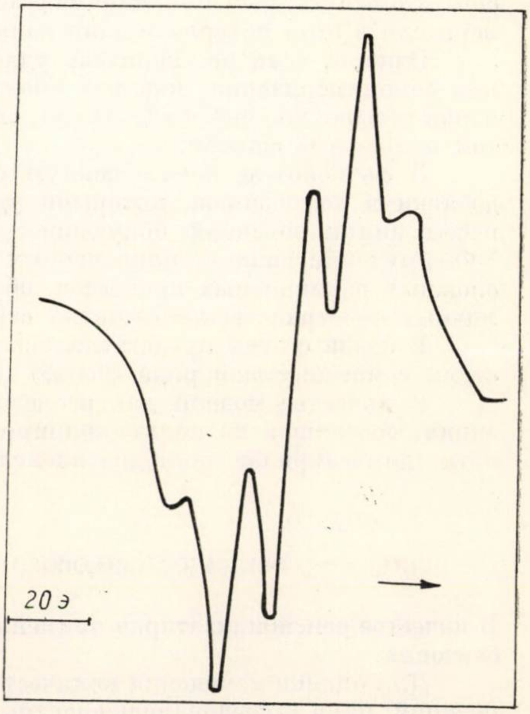

Рис. 4. — Спектр ЭПР поливинилпирролидона, облученного УФ-светом в вакууме при —196° с последующим размораживанием до —78°. →

Снятые спектры ИК (рис. 5) показали, наряду с увеличением общего фона, в процессе облучения, также изменение полос аминных 3200—3400 $см^{-1}$ и валентных колебаний $C{=}O$ групп 1740 $см^{-1}$ в ходе фотополимеризации и их стабилизации по завершению этого процесса. Это явление говорит о том, что указанные группы в поливинилпирролидоне претерпевают химические изменения в процессе облучения.

При длительном облучении ПВП, при комнатной температуре, полимер желтеет, затем становится коричневым, причем сигнал ЭПР превращается в синглет (рис. 6) $\Delta H \sim 8$ э, что указывает на образование сопряженных связей.

В случае облучения олигоэфиракрилатов УФ-светом в вакууме при — 196°, также генерируются радикалы, которые при —78°, как правило, переходят в типичный метилметакрилатный спектр[10] (рис. 7). Введенные в композицию сенсибилизаторы, при инициировании УФ-светом становятся источниками радикалов, чем ускоряют генерирование радикалов в полимере, причем удается фиксировать в смеси лишь спектры последних.

---

[10] Б. К. Смирнов, Диссертация, 1967.

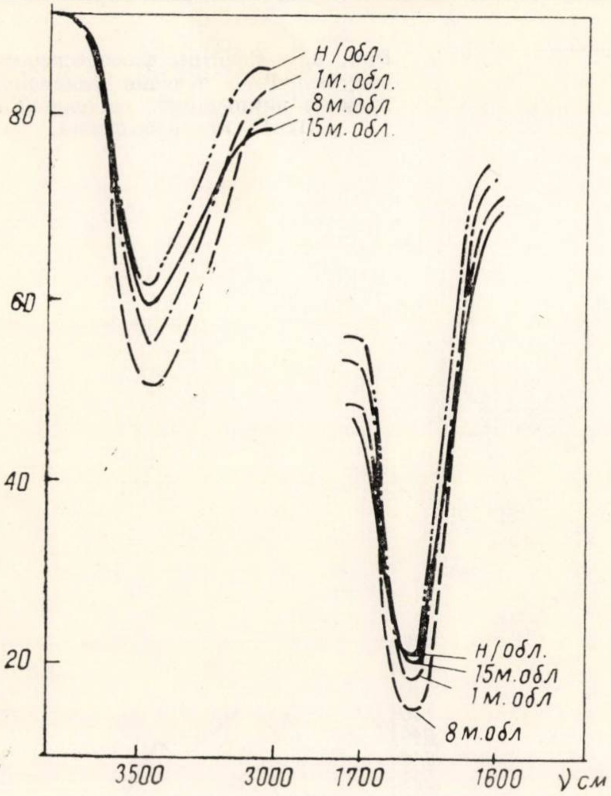

Рис. 5. — Спектры ИК композиции, состоящей из ПВП ОЭА и бензоина, в зависимости от продолжительности облучения.

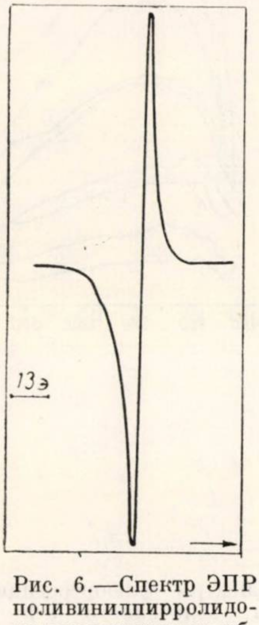

Рис. 6.—Спектр ЭПР поливинилпирролидона при длительном облучении УФ-светом.

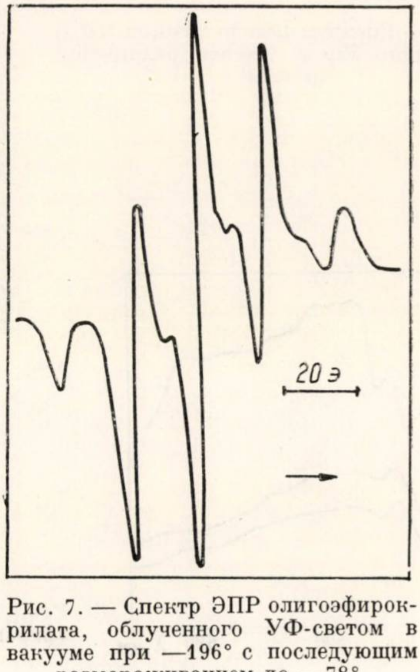

Рис. 7. — Спектр ЭПР олигоэфирокрилата, облученного УФ-светом в вакууме при —196° с последующим размораживанием до —78°.

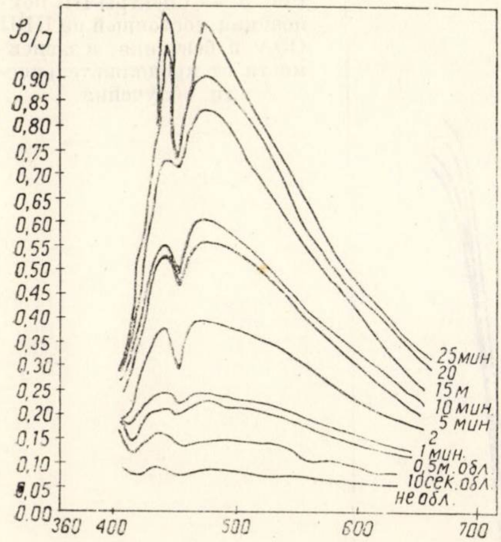

Рис. 8. — Спектры флюоресценции, облученной в течение различного времени композиции, состоящей из ПВП, ОЭА и бензоина.

Рис. 9. — Спектры флюоресценции ПВП, облученного УФ в течение различного времени.

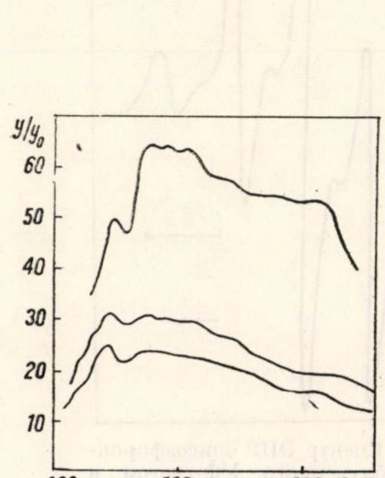

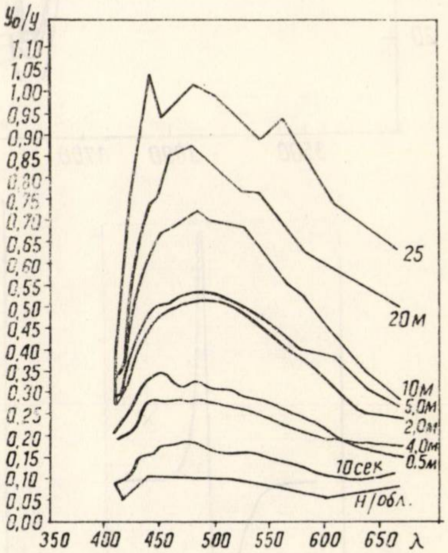

Рис. 10. — Спектры флюоресценции олигоэфиракрилата, облученного УФ в течение различного времени.

Тот факт, что при фотооблучении ПВП обнаружены радикалы, а также то, что в облученных композициях полимер приобретает нерастворимость, показывает, что полимер не может играть пассивную роль в композиции и не участвовать в образовании сетчатых структур.

Были промерены спектры люминесценции ПВП, МДФ-2 и их композиции с бензоином, после облучения УФ-светом (220—400 нм) в течение различного времени.

Оказалось, что как для композиции (рис. 8), так и для одного ПВП (рис. 9) интенсивность флюоресценции с течением времени увеличивается и запределивается, аналогично тому, как это показано [10] для МДФ 2 (рис. 10).

Кроме того, изменяется структура спектров, имея индивидуальный характер для каждого случая.

Это указывает на то, что при облучении УФ-светом, как в композиции, так и у ПВП идет процесс сшивания, по-видимому, с образованием сетчатых структур, и также на различное протекание процесса полимеризации, свойственное как каждому компоненту в отдельности, так и их композиции.

С помощью дериватографа системы Л. Эрдей, Ф. Паулик, И. Паулик был проведен дифференциально термогравиметрический анализ (ДТГ) и дифференциально термический анализ (ДТА) исходного полимера (рис. 11) (ПВП) и композиции, состоящей из ПВП, МДФ-2 и бензоина, до облучения (рис. 12) и после облучения УФ-светом (рис. 13) от лампы ДРШ 1000 через водяной кварцевый фильтр, в течение 30 минут.

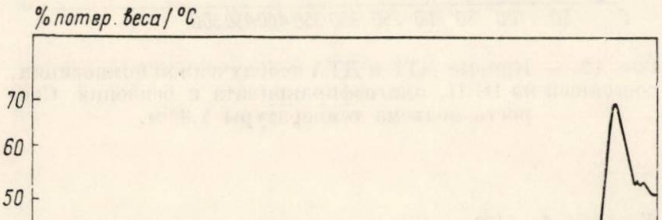

Рис. 11. — Кривые ДТГ и ДТА поливинилпирролидона. Скорость подъема температуры 2,2°/м.

---

[11] Б. Ф. Гачковский, *Жур. структур. хим.* (в печати).

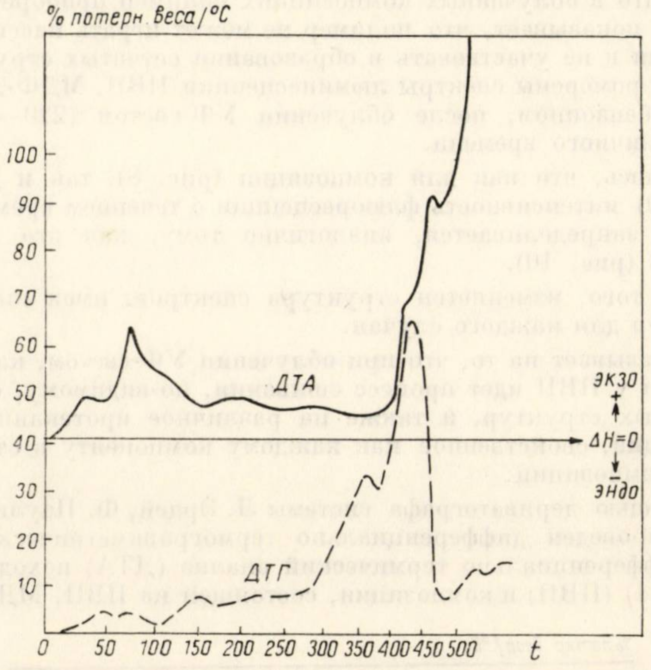

Рис. 12. — Кривые ДТГ и ДТА необлученной композиции, состоящей из ПВП, олигоэфиракрилата и бензоина. Скорость подъема температуры 4,3°/м.

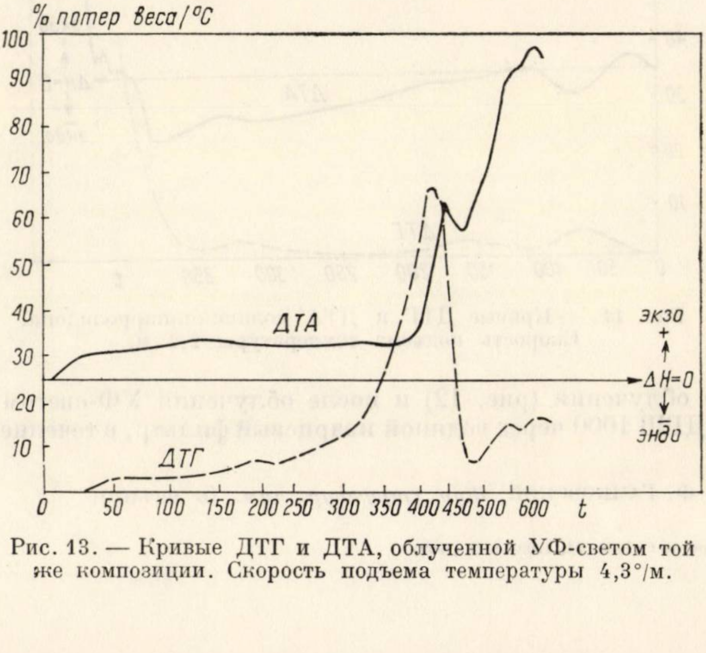

Рис. 13. — Кривые ДТГ и ДТА, облученной УФ-светом той же композиции. Скорость подъема температуры 4,3°/м.

Для необлученного ПВП (рис. 11) характерно, что до 40°, когда потеря веса еще не происходит, наблюдается экзометрический пик, указывающий, по-видимому, на взаимодействие кислорода с полимером, ведущее к образованию, в основном, перекисных и гидроперекисных соединений

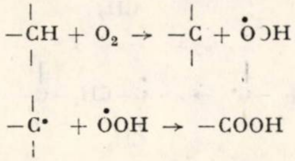

$$-\overset{|}{\underset{|}{C}}H + O_2 \rightarrow -\overset{|}{\underset{|}{C}} + \dot{O}OH$$

$$-\overset{|}{\underset{|}{C}}^{\bullet} + \dot{O}OH \rightarrow -COOH$$

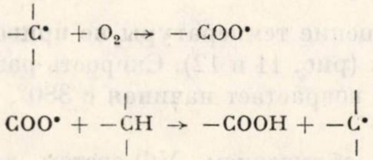

$$-\overset{|}{\underset{|}{C}}^{\bullet} + O_2 \rightarrow -COO^{\bullet}$$

$$COO^{\bullet} + -\overset{|}{\underset{|}{C}}H \rightarrow -COOH + -\overset{|}{\underset{|}{C}}^{\bullet}$$

Разложение с небольшой скоростью начинается от 40° и к 90—110° полимер теряет в весе 5—6%, имея при этом максимум потери веса при 70°, с одновременным эндотермическим пиком, который, по-видимому, характерен для развала гидроперекисных соединений с образованием радикалов в основном, за счет подвижного водорода α-метиновой группы

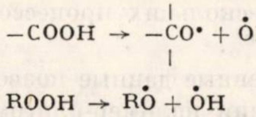

$$-COOH \rightarrow -\overset{|}{\underset{|}{C}}O^{\bullet} + \dot{O}H$$

$$ROOH \rightarrow R\dot{O} + \dot{O}H$$

На следующем этапе от 100 до 180° продолжается потеря веса с малой скоростью, достигающей за этот период 10%.

В интервале температур от 180° до 280° полимер также медленно разлагается. Потеря веса к 280° достигает 14%. Далее скорость разложения несколько увеличивается с одновременным эндотермическим максимумом в 310°. С 360° разложение происходит с большой скоростью, достигая максимума при 450°, причем наблюдается эндотермический пик в 450°. При 490° потеря веса составляет 90%.

Большое количество экзотермических и эндотермических пиков в поливинилпирролидоне свидетельствует о большой активности полимера. Последние пики говорят о деструкции с наложением нескольких процессов.

Проведение ДТА и ДТГ с необлученной композицией показало тот же экзотермический пик в 35°, но вместо второго эндотермического пика при 80° появляется экзотермический пик. Первый пик может говорить о вышеуказанном процессе образования гидроперекисных соединений. Вновь появившийся экзотермический пик, по-видимому, может быть объяснен перехватыванием образующихся под влиянием кислорода воздуха гидроперекисных соединений с полимерами, двойными связями олигоэфиракрилата.

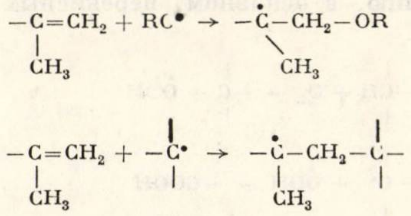

$$-\underset{\displaystyle CH_3}{\underset{|}{C}}=CH_2 + RO^{\bullet} \rightarrow -\underset{\displaystyle \diagdown CH_3}{\overset{\bullet}{C}}-CH_2-OR$$

$$-\underset{\displaystyle CH_3}{\underset{|}{C}}=CH_2 + -\underset{|}{\overset{|}{C}}{}^{\bullet} \rightarrow -\underset{\displaystyle CH_3}{\underset{|}{\overset{\bullet}{C}}}-CH_2-\underset{|}{\overset{|}{C}}-$$

Дальнейшее повышение температуры не приводит к значительным отличиям в ходе кривых (рис. 11 и 12). Скорость разложения необлученной композиции сильно возрастает начиная с 380°, достигая при 475°—85% потери веса.

Предварительным облучением УФ-светом той же композиции (рис. 13) практически были сняты все наблюдаемые при температурах 35—40° и 70° экзотермические пики, что свидетельствует о прохождении процессов сополимеризации под влиянием УФ-света. Очень медленная потеря веса начинается также с 40° и аналогично, скорость разложения композиции значительно увеличивается, начиная с 370°, с небольшим плечом в 390° и пиком в 450°. По-видимому, протекает постепенная деструкция с наложением нескольких процессов. При температуре 450° потеря веса составляет 80%.

Таким образом, полученные данные позволили придти к выводу о том, что при УФ-облучении полимер-олигомерных композиций, преимущественно протекают процессы образования пространственно сетчатых привитых сополимеров с участием всех компонентов композиции. Поэтому образующийся фотосополимер создает свойства, привносимые как полимером, так и сшивающим олигоэфирокрилатом.

Это было использовано практически для создания целой серии фотополимеризующихся составов, в которых применялись различные линейные полимеры, олигоэфиракрилаты и их смеси для создания пространственно-сетчатых фотопривитых сополимеров с заранее заданным комплексом свойств.

ВЫВОДЫ

1. Проведен фотосинтез сополимеров сетчатой структуры с заранее заданным комплексом свойств на основе композиций, состоящих из полиэфиракрилатов, линейных полимеров и сенсибилизаторов, с образованием рельефных изображений, для использования в различных областях промышленности.

2. Полученные спектры ЭПР радикалов, образующихся при облучении отдельных иградиентов светочувствительного состава показывают, что все компоненты композиции активно участвуют в образовании сополимера сетчатой структуры.

3. Спектры флюоресценции указывают на прохождение процесса фотосополимеризации между ПВП и олигоэфиракрилатом с образованием полимера пространственно-сетчатой структуры.

4. Спектры ИК указывают на активность С = О и аминных групп ПВП в процессе облучения.

5. Методами ДТА и ДТГ установлена активность ПВП и протекание сополимеризации между полимером и олигоэфиракрилатом через образование, по-видимому, перекисных и гидроперекисных радикалов.

Revue Roumaine de Chimie, 14, 1323–1330 (1969)

AROMATICITY. VI[1]

ELECTRONIC ABSORPTION SPECTRA OF *o*-PHENYLENE CARBONATE AND OF ITS CONJUGATE ACID

A. T. BALABAN

Institute of Atomic Physics, P. O. Box 35, Bucharest

Received March 31, 1966

o-Phenylene carbonate dissolves in conc. H_2SO_4 and can be recovered unchanged by dilution with water. The protonation does not alter significantly its UV spectrum. These data and the negative solvatochromy indicate aromatic delocalization in the 1,3-dioxole-2-one ring. The aromaticity of vinylene carbonate is also discussed.

INTRODUCTION

In the first part of this series,[2] the first-row atoms taking part in an aromatic monocyclic system were classified as X-type, Y-type and Z-type if the number of electrons in their non-hybridized p_z atomic orbitals which combine to form the delocalized molecular orbitals is 2, 1, and 0, respectively. On the basis of this classification and of the Hückel rule of $4n + 2$ π-electrons in an m-membered aromatic monocyclic ring, all possible monocyclic aromatic systems were discussed for the cases when $n = 0, 1,$ or 2. However, a limitation is imposed by the electronegativity differences, expressed as "aromaticity constants" in the second paper in the series,[3] and thus part of the possible solutions are excluded. In the third paper,[4] the influence of other factors on the aromaticity was studied; these are the ratio $m/(4n + 2)$ which must lie between ca. 0.65 and 1.4,* the normal or mesoionic character, and to a smaller degree the adjacence or non-adjacence of atoms of similar type.

AROMATIC DIHETEROLIUM CATIONS

From all first-row atoms which may take part in aromatic systems, oxygen atoms have the highest electronegativity. They are therefore the least suitable X-type atoms. This is reflected in the fact that furan behaves chemically and spectroscopically very much like a diene,[5] and is supported by theoretical calculations.[6,7] On replacing a C = C group in tropylium salts by an oxygen or sulphur heteroatom X, one obtains first a pyrylium or a thiopyrylium salt, and by a second replacement, the formulas of 1,2-(I) or 1,3-dioxolium or dithiolium cations (II).

---

* This requirement follows from the condition that all bonding MO's must be occupied, and not from steric conditions: cyclobutadiene and cyclooctatetraene are non-aromatic because they do not obey the Hückel rule, and not because of steric strain.

[1] Part V, A. T. Balaban and Z. Simon, *Rev. Roumaine Chim.*, **10**, 1059 (1965) gives a preliminary account of the data reported in the present paper.

[2] A. T. Balaban, *Studii şi Cercetări Chim. Acad. R.P.R.*, **7**, 257 (1959).

[3] A. T. Balaban and Z. Simon, *Tetrahedron*, **18**, 315 (1962).

[4] Z. Simon and A. T. Balaban, *Rev. Chim. Acad. R.P.R.*, **7**, 555 (1962).

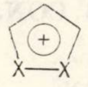

I

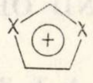

II

1,3-Dithiolium cations are the first known representatives of these systems.[8] After theoretical calculations[9], 1,2- and 1,3-dithiolium cations were obtained and studied in much detail.[10-14] 1,3-Dioxolium cations are probably responsible (cf. IIIb) for the "unexplained" [15] stability of compounds III,[15] and make a contribution (IVb) to the stability of chlorides IV.[16] Recently, the first crystalline 1,3-benzodioxolium cation V was prepared by Dimroth and coworkers [17a]; it is very sensitive towards hydrolysis which affords catechol monobenzoate VI; its alcoholysis affords

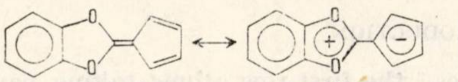

IIIa IIIb

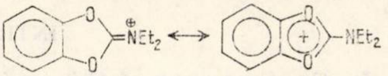

IVa IVb

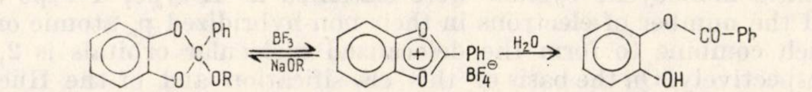

VII V VI

cyclic ketals VII which were the starting materials in the preparation of V. A second crystalline salt, 2-hydroxy-1,3-dioxolium hexafluoroantimonate,* was obtained by Olah and White [17b] on dissolving vinylene carbonate in a sulphur dioxide solution of fluorosulphonic acid and antimony pentafluoride (1 : 1 molar). These papers [17a–c] prompt us to report the present data which had been obtained a few years ago.

---

[5] J. R. MORRIS and F. L. PILAR, *Chem. and Ind.*, **1960**, 469.

[6] R. D. BROWN and B. A. W. COLLER, *Austral. J. Chem.*, **12**, 152 (1959).

[7] G. DEL RE, *J. Chem. Soc.*, **1962**, 3324.

[8] W. R. H. HURTLEY and S. SMILES, *J. Chem. Soc.*, **1926**, 1821; R. WIZINGER, *Chimia* (Basel), **12**, 79 (1958); L. SODER and R. WIZINGER, *Helv. Chim. Acta*, **42**, 1733, 1779 (1959).

[9] J. KOUTECKY, J. PALDUS and R. ZAHRADNÍK, *Coll. Czech. Chem. Comm.*, **25**, 617 (1960); R. ZAHRADNÍK and J. KOUTECKY, *Tetrahedron Letters*, **1961**, 632.

[10] E. KLINGSBERG, *J. Amer. Chem. Soc.*, **84**, 3410 (1962); *J. Org. Chem.*, **28**, 529 (1963) and further references therein.

[11] A. LÜTTRINGHAUS, M. MOHR and N. ENGELHARD, *Liebigs Ann. Chem.*, **661**, 85 (1963).

[12] R. MAYER and B. GEBHARDT, *Chem. Ber.*, **97**, 1298 (1964); E. CAMPAIGNE and R. D. HAMILTON, *J. Org. Chem.*, **29**, 2877 (1964).

[13] D. LEAVER, W. A. H. ROBERTSON and D. M. MCKINNON, *J. Chem. Soc.*, **1962**, 5104; D. LEAVER and W. A. H. ROBERTSON, *Proc. Chem. Soc.*, **1960**, 252.

[14] W. KIRMSE and L. HORNER, *Liebigs Ann. Chem.*, **614**, 4 (1958).

[15] W. RIED and R. DIETRICH, *Liebigs Ann. Chem.*, **639**, 32 (1961).

[16] H. GROSS and J. RUSCHE, *Angew. Chem.*, **76**, 534 (1964).

[17a] K. DIMROTH, P. HEINRICH and K. SCHROMM, *Angew. Chem.*, **77**, 863 (1965).

Our attempts to obtain V from *o*-phenylene carbonate and phenylmagnesium bromide had given in the usual work-up only VI in 63% yield. There is no indication about the formation of V from VI, since in conc. sulphuric acid VI dissolves yielding a slightly yellow solution which on dilution with water affords benzoic acid and pyrocatechol; in 70% perchloric acid it does not dissolve, even at 60°.

VINYLENE CARBONATE

There are two pathways for obtaining theoretically various neutral stable structures from cations I and II. The first involves replacement of a positively charged carbon atom of type [Z4b] by a neutral atom of type [Z3b].[1–3] Thus II affords 1,3,2-diheteroboroles VIII prepared for the first time by Goubeau,[18] Dewar [19] and Letsinger,[20] and extensively studied afterwards (e.g.[21,22]). The aromaticity of these compounds is proved by numerous properties (reviews [23–26] and references cited in [27]). The second pathway is to attach to the positively charged ring a group which can accomodate a negative charge. This leads for instance to compounds III and IV. The most common representative of these groups is an alkoxide or a thiolate exocyclic group E. Thus the most common second pathway consists in replacing a positively charged carbon atom by a carbonyl or thiocarbonyl group.

---

* Its NMR data [17b] indicate the presence of ring current, hence of aromaticity; no such phenomena can occur in cyclic carboxonium (1,3-dioxolenium) salts derived from saturated glycols.[17c]

[17b] G. A. Olah and A. M. White, *J. Amer. Chem. Soc.*, **90**, 1884 (1968).

[17c] F. M. Beringer and S. A. Galton, *J. Org. Chem.*, **32**, 2630 (1967); K. B. Gash and G. U. Yuan, *ibid.*, **31**, 4234 (1966); H. Meerwein, K. Bodenbrenner, P. Borner, F. Kunert and K. Wunderlich, *Liebigs Ann. Chem.*, **632**, 38 (1960).

[18] D. Ulmschneider and J. Goubeau, *Chem. Ber.*, **90**, 2733 (1957).

[19] M. J. S. Dewar, V. P. Kubba and R. Pettit, *J. Chem. Soc.*, **1958**, 3076.

[20] R. L. Letsinger and S. B. Hamilton, *J. Amer. Chem. Soc.*, **80**, 5411 (1958); *J. Org. Chem.*, **25**, 592 (1960).

[21] W. Gerrard, M. F. Lappert and B. A. Mountfield, *J. Chem. Soc.*, **1959**, 1529.

[22] A. T. Balaban, G. Mihai, R. Antonescu and P. T. Frangopol, *Tetrahedron*, **16**, 68 (1961).

[23] P. M. Maitlis, *Chem. Rev.*, **62**, 223 (1962).

[24] M. J. S. Dewar, in "Progress in Boron Chemistry" vol. 1 (H. Steinberg and A. L. McCloskey, editors), Pergamon Press, Oxford, 1964, p. 235; ,,Boron-Nitrogen Chemistry" (R. F. Gould, editor), Advances in Chemistry Series No. 42, Amer. Chem. Soc., Washington 1964, p. 227.

[25] H. Steinberg, "Organoboron Chemistry", vol. 1, Interscience, New York, 1964, p. 275.

[26] K. Niedenzu and J. M. Dawson, ,,Boron-Nitrogen Compounds", Springer-Verlag, Berlin, 1965, p. 138.

[27] A. T. Balaban, C. N. Renţea, M. Mocanu-Paraschiv and E. Romaş, *Rev. Roumaine Chim.*, **10**, 849 (1965).

This second pathway affords tropolone from tropylium, the two pyrones from pyrylium (derived from tropylium by replacing a C = C group by oxygen), and structures IX and X from cations I and II. A

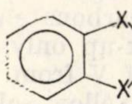
VIII

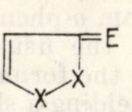
IX

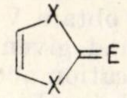
X

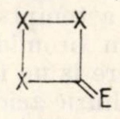
XI

structure XI (e.g. with X = S) has unfavourable frontier orbitals and three adjacent X-type atoms, therefore it is expected to present little stabilization owing to delocalization; its preparation (e.g. from Na_2S_3 and phos gene) would be interesting.

Sulphur-containing heterocycles with structures IX and X (X = S, E = O or S) are well-known[28] and their aromatic stability is soundly established.

It was pointed out previously[2] that vinylene carbonate[29] fulfills the conditions for aromatic character. The electronegativity of the oxygen heteroatoms makes however vinylene carbonate (X, X = E = O, or XII, R = H) a reactive olefin in polymerizations[30] or cycloadditions.[31]

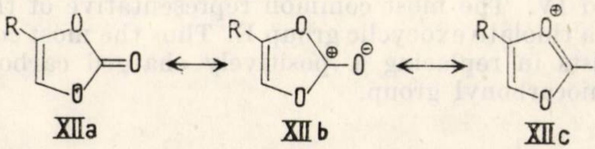
XIIa XIIb XIIc

Its infrared spectrum ought to have the ν C = O stretching band displaced towards lower frequencies, as in tropolone or pyrones, owing to the decreased bond order as shown by structure XIIb. However, the assignment of the bands in the 1700 – 1900 cm^{-1} range of vinylene[32] or o-phenylene carbonate[33] in comparison with the non-aromatic ethylene carbonate[34] does not allow an unambiguous conclusion owing to dipolar association of the latter, also influencing the carbonyl stretching frequency. Never-

[28] R. Mayer, *Angew. Chem.*, **69**, 481 (1957);
W. Wolf, E. Degener and S. Petersen, *ibid.*, **72**, 963 (1960).

[29] M. S. Newman and R. W. Addor, *J. Amer. Chem. Soc.*, **75**, 1263 (1953); **77**, 3789 (1955);
W. K. Johnson and T. L. Patton, *J. Org. Chem.*, **25**, 1042 (1960).

[30] N. D. Fields and J. R. Schaefgen, *J. Polymer Sci.*, **58**, 533 (1962);
S. S. Skorokhodov, S. Z. Levin and A. L. Shapiro, *Khim. Volokna*, No. 4, 1 (1963).

[31] R. Criegee and P. Becher, *Chem. Ber.*, **90**, 2516 (1957);
M. S. Newman, *J. Org. Chem.*, **26**, 2630 (1961).

[32] J. L. Hales, J. J. Jones and W. Kynaston, *J. Chem. Soc.*, **1957**, 618.

[33] R. Mecke and A. Lüttringhaus, *Z. Naturforsch.*, **10b**, 367 (1955).

[34] A. Simon and G. Heintz, *Chem. Ber.*, **95**, 2333 (1962);
C. L. Angell, *Trans. Faraday Soc.*, **52**, 1178 (1956);
L. J. Bellamy and R. J. Pace, *Spectrochim. Acta*, **19**, 1831 (1963); H. Minato, *Bull. Chem. Soc. Japan*, **36**, 1020 (1963);
L. A. Pohoryles and S. Sarel, *Bull. Res. Council Israel*, Sect. A, **7**, 42 (1957).

theless indications for aromaticity are given by the thermal stability [35] and the planarity of vinylene carbonate [36] in contrast to ethylene carbonate which is non-planar in solid state,[37] but planar in solution [34] (but dipole moments [36,38a] or NMR spectra [38b] do not evidence differences between vinylene and ethylene carbonate). The remarkable stability of the phenyl-derivative XII, R = Ph, b.p. 283°, also contrasts with the easy decarboxylation of the saturated analogue at 180°.[39]

ortho-PHENYLENE CARBONATE XIV

The benzoderivatives of the two structures IX and X (X = E = O) have formulas XIII and XIV. As yet no derivative of structure XIII

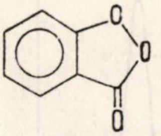
XIII

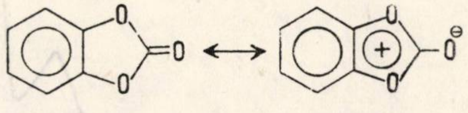
XIVa **XIVb**

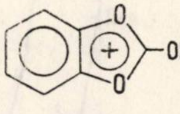
XV

was reported; the two oxygen heteroatoms are not equivalent as in XIV and the peroxide bond has a high energy content, but the attempt to prepare such compounds from salicylic or nitrosalicylic acid and hydrogen peroxide would be interesting.

o-Phenylene carbonate XIV is stable in acid medium and can be nitrated by fuming nitric acid.[40] We investigated the electronic absorption spectra of *o*-phenylene carbonate and of its conjugate acid XV in order to establish if it behaves like a benzopyrone (chromone or coumarin) in which a C = C group was replaced by an oxygen heteroatom. Attempts to prepare a crystalline salt, e.g. picrate or perchlorate, or a methiodide, failed. In conc. sulphuric acid XIV gives a colourless solution which on dilution with water affords unchanged *o*-phenylene carbonate. In ether, XIV is slightly soluble in the cold, but a mixture of ether and 70% perchloric acid dissolves a far higher amount of *o*-phenylene carbonate. These observations constitute a strong indication that in acid solutions, cation XV is reversibly formed.

[35] R. W. Thomas (to Olin Mathieson Chem. Corp.), U.S. Pat. 2,873,230 (Feb. 10 1959); *Chem. Abstr.*, **54**, 2182 (1960).

[36] G. R. Slayton, J. W. Simmons and J. H. Goldstein, *J. Chem. Phys.* **22**, 1678 (1954).

[37] C. J. Brown, *Acta Cryst.*, **7**, 92 (1954).

[38a] R. Kempa and W. H. Lee, *J. Chem. Soc.*, **1958**, 1936;
B. A. Arbuzov and T. G. Shavshka, *Doklady Akad. Nauk. S.S.S.R.*, **68**, 1045 (1949);
G. F. Longster and E. F. Walker, *Trans. Faraday Soc.*, **49**, 228 (1953).

[38b] K. A. McLauchlan and T. Schaeffer, *Canad. J. Chem.*, **44**, 321 (1966);
J. H. Goldstein and G. S. Reddy, *J. Chem. Phys.*, **36**, 2644 (1962).

[39] L. R. Morris and D. J. Hubbard, *J. Org. Chem.*, **27**, 1451 (1962).

[40] J. D. Riedel, Germ. Pat. 264, 012 (*Chem. Zentr.*, **1913**, II, 1181).

ELECTRONIC ABSORPTION SPECTRA OF XIV AND XV

Since aromaticity in XIV implies an electron distribution indicated by formula XIVb, the protonation to XV should not alter strongly the electron distribution. This expectation is borne out by the experimental data.

In non-purified solvents, e.g. methanol Analar, traces of alkalies lead to incipient hydrolysis and decarboxylation and to autoxidation of the resulting catechol, so that the fine structure of the band at 270 mμ is lost and in its place a broad non-structured band centered on 280 mμ develops.

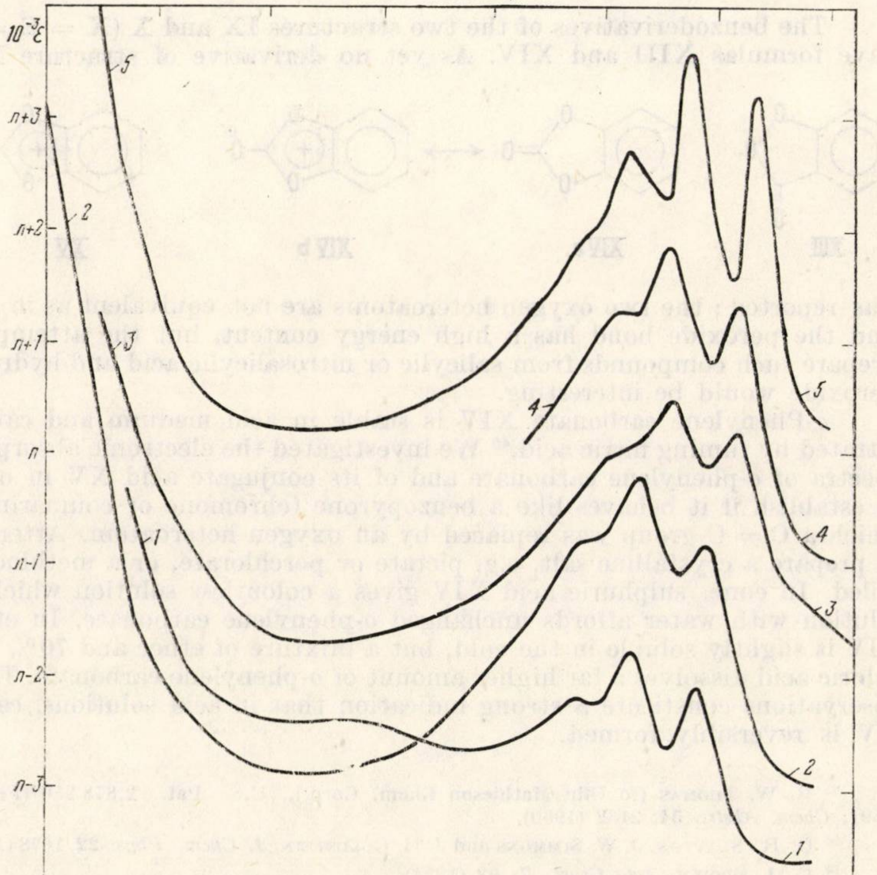

Fig. 1. – Ultraviolet absorption spectra of *o*-phenylene carbonate. Spectrum No 1, in 96 % sulphuric acid, $n = 4$; No 2, in 64 % perchloric acid, $n = 3$; No 3, in methanol, acidified with perchloric acid, $n = 2$; No 4, in ethyl acetate, $n = 1$; No 5, in cyclohexane, $n = 0$.

Figure 1 presents the ultraviolet absorption spectra of *o*-phenylene carbonate in the following solvents : cyclohexane, ethyl acetate, methanol containing a trace of perchloric acid, 64 % aqueous perchloric acid and

96% sulphuric acid. All spectra present a low-extinction (lg ε 3.3–3.5) band at 260–270 mμ with vibrational fine structure. No other maximum appears up to 210 mμ, but the descending branch of a band with higher molar absorptivity is observed at these small wavelengths. Excepting the solution in sulphuric acid, the separation between these two bands is very good, the solution having practically no absorbance in the range 230–240 mμ.

As anticipated, on passing from cyclohexane in which XIV has the smallest interaction with the solvent, to more polar solvents like ethyl acetate or ethanol in which such interactions are stronger, than to acid solutions in which the compound is protonated to XV, there is no marked change in the spectrum. In the absence of quantitative data for the pK_a of XV, it is difficult to make an assignment for the absorption band at ca. 239 mμ which appears in the spectrum of the 96% sulphuric acid solution and is absent from the 64% perchloric acid solution. However, the known basicities of pyrones suggest that even in the latter solvent, it is extremely likely that most XIV is protonated to XV, and therefore the band at ca. 239 mμ must be due to some other species. Hence the spectra of XIV and XV are very similar in aspect and position. We will concentrate on the discussion of the band at 260–270 mμ.

This band presents three vibrational peaks (and a fourth shoulder in cyclohexane) with a spacing of ca. 800 cm^{-1}, corresponding to the spacing between the vibrational levels of the electronically excited state. The position of the peaks is indicated in table 1.

Table 1

Vibrational peaks in the ultraviolet spectrum of o-phenylene carbonate[a)]

Solvent				Major peak	0–0 peak
Cyclohexane	253 sh	258 sh	262.0	267.6	273.4
Ethyl acetate		256 sh	262.0	266.5	272.5
Ethanol[b)]		255 sh	261 sh	266	271.5
64% $HClO_4$			258 sh	263	269
96% H_2SO_4			257	261.5	267.5

a) Values in mμ; sh denotes shoulder.
b) In methanol with a trace of $HClO_4$, the spectrum is identical to that in ethanol.

The hypsochromic shift with increasing polarity of the solvent (negative solvatochromy) is in agreement with a polar structure like XIVb. A similar negative solvatochromy was encountered in the spectra of tropophenylene spiroborates.[22,41] In a polar solvent, the polar ground state is solvated more strongly than the less polar excited state, hence the transition energy will be higher than in a non-polar solvent.

---

[41] A. T. Balaban, *Rev. Roumaine Chim.*, **10**, 879 (1965).

In conclusion, these UV spectral investigations indicate that no big difference exists between the spectra of *o*-phenylene carbonate XIV and its conjugate acid XV. Together with the stability towards acids, reminding that of pyrones, these data confirm the existence of delocalization in *o*-phenylene carbonate, according to formula XIVb. It is not impossible that some delocalization is present even in the carbonylogue of *o*-phenylene carbonate, *o*-phenylene oxalate XVI, which affords crystalline salts [42] containing probably the dication XVII. An analogous diquaternary dication XVIII has been recently reported.[43]

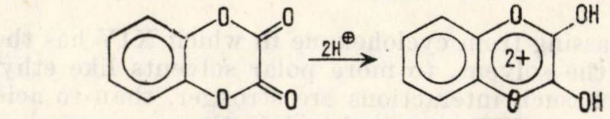

XVI XVII

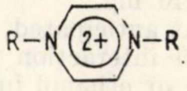

XVIII

EXPERIMENTAL

Ultraviolet spectra were registered with a Jena VSU-1 spectrophotometer equipped with a quartz prism and 0.5 cm quartz cells, at room temperature. Solutions were prepared before use and had concentrations $2 - 4 \times 10^{-4}$ molar.

o-Phenylene carbonate (*XIV*) was prepared [44,45] from pyrocatechol and aqueous sodium hydroxide in inert atmosphere, by reaction with a solution of phosgene in toluene. M.p. 120° (from toluene or ethanol).

Grignard reaction of o-*phenylene carbonate*. Into a solution of 35 g XIV in 100 ml anhydrous ether and 400 ml benzene, a solution of phenylmagnesium bromide (prepared from 7.2 g magnesium turnings and 48 g bromobenzene) is added under reflux. After two hrs the mixture is hydrolysed with water, then aqueous ammonium chloride is added. The mixture is filtered, the upper layer and the ethereal washings are combined and evaporated under vacuum, leaving 37 g pyrocatechol monobenzoate, which is purified by washing with benzene and recrystallization from dilute ethanol or from much water; m.p. 134°, undepressed by authentic specimen prepared from pyrocatechol, benzoyl chloride and aqueous sodium carbonate.[46]

---

[42] B. N. Ghosh, *J. Chem. Soc.*, **107**, 1588 (1915).

[43] T. J. Curphey, *J. Amer. Chem. Soc.*, **87**, 2063 (1965).

[44] A. Einhorn and E. Lindenberg, *Liebigs Ann. Chem.*, **300**, 135 (1898).

[45] R. S. Hanslich, W. F. Bruce and A. Mascitti, *Org. Synth.*, **33**, 74 (1953).

[46] O. N. Witt and F. Mayer, *Ber. dtsch. chem. Ges.*, **26**, 1072 (1893).

Revue Roumaine de Chimie, **14**, 1331–1332 (1969)

PYRYLIUM SALTS FORMED BY DIACYLATION OF OLEFINS. XIX[1]

CHARACTERIZATION OF OLEFINS BY DIACYLATION: ACID DEALKYLATION OF 3,5-DI-t-BUTYLPYROCATECHOL

A. T. BALABAN

Institute of Atomic Physics, P.O.B. 35, Bucharest

Received April 21, 1969

In the presence of strong acids (perchloric acid in acetic anhydride), 3,5-di-t-butylpyrocatechol undergoes dealkylation forming isobutene. This olefin can be trapped by diacetylation and characterized as 2,4,6-trimethylpyrylium perchlorate.

The preparation of saturated dioxolium salts was recently reported by Dorofeenko and co-workers[2] by reacting ditertiary 1,2-glycols with acetic anhydride and perchloric acid. In order to test whether related aromatic dioxolium salts II[3] could be prepared by O-acylation of pyrocatechol derivatives in which the C-acylation of the aromatic ring is suppressed by substitution and steric hindrance, the reaction between 3,5-di-t-butyl-pyrocatechol (I), acetic anhydride and perchloric acid was investigated. A crystalline colourless perchlorate was obtained in this reaction, but its structure was different from the expected one, II. The perchlorate was identified as 2,4,6-trimethylpyrylium perchlorate VII by infrared absorption spectra and melting point of the mixture with an authentic product.[4]

The formation of VII is interpreted as originating in the protodealkylation of I, under the acid reaction conditions, leading to the formation of the t-butyl cation IV which by deprotonation gives isobutene VI. This is diacetylated, as known, to 2,4,6-trimethylpyrylium VII.[5] In the accompanying formulas, the dealkylation is depicted as involving the intermediates III leading to 3- or 4-t-butylpyrocatechol Va and Vb. No isolation of monoalkylpyrocatechols V was attempted.

---

[1] Preceding part, A. T. Balaban, *Tetrahedron Letters*, **1968**, 4643.

[2] G. N. Dorofeenko and L. V. Mezheritskaya, *Zhurn. obshchei Khim.*, **38**, 1192 (1968).

[3] K. Dimroth, P. Heinrich and K. Schromm, *Angew. Chem.*, **77**, 863 (1965).

[4] A. T. Balaban and C. D. Nenitzescu, *Org. Synth.*, **44**, 98 (1964).

[5] A. T. Balaban, W. Schroth and G. Fischer, in *Adv. Heterocyclic Chem.*, **10**, 241 (1969) (ed. A. R. Katritzky and A. J. Boulton, Academic Press, New York — London).

$$(CH_3CO)_2O + HClO_4 \longrightarrow CH_3COOH + CH_3CO^{\oplus}\ ClO_4^{\ominus}$$

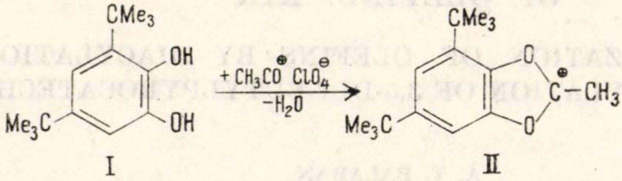
CMe₃
OH
OH
Me₃C
+ CH₃CO⊕ ClO₄⊖
−H₂O
CMe₃
O
O
C−CH₃
ClO₄⊖
Me₃C
I
II

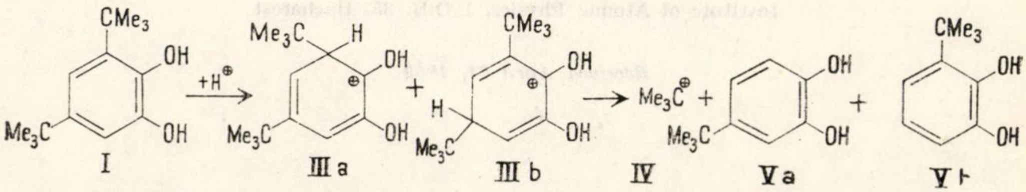
CMe₃
OH
OH
Me₃C
+H⊕
Me₃C
H
OH
OH
Me₃C
+
CMe₃
OH
H
OH
Me₃C
Me₃C⊕ +
OH
OH
Me₃C
+
CMe₃
OH
OH
I
IIIa
IIIb
IV
Va
Vb

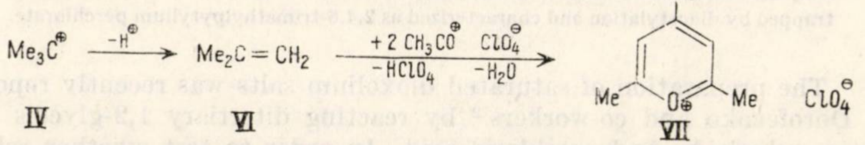
Me₃C⊕
−H⊕
Me₂C = CH₂
+ 2 CH₃CO⊕ ClO₄⊖
−HClO₄ −H₂O
Me
Me
O⊕
Me
ClO₄⊖
IV
VI
VII

The trapping of isobutene by diacylation illustrates a convenient use of this reaction for evidencing, characterizing and identifying olefins under the form of their diacylation products, i.e. pyrylium salts; owing to their insolubility in non-polar solvents, these salts can be separated quantitatively and allow the easy identification of the olefin.

EXPERIMENTAL

3,5-Di-t-butylpyrocatechol [6] (1g) in 10 ml acetic anhydride was treated with 1 ml 70%-perchloric acid. The solution became hot and darkened. After 1 hr, 20 ml ether were added and the solution was kept overnight in the refrigerator. White crystals (0.45 g) separated. They were filtered off and washed with ether. M.p. 245°, undepressed by 2,4,6-trimethylpyrylium perchlorate VII.[4] The infrared absorption spectrum of the product is identical to that of VII.[7]

Acknowledgement. Thanks are expressed to Dr. K. Ley and the Bayer G.m.b.H. for providing a sample of I.

---

[6] K. Ley and E. Müller, *Chem. Ber.*, **89**, 1402 (1956).

[7] A. T. Balaban, G. D. Mateescu and M. Elian, *Tetrahedron*, **18**, 1083 (1962).

CORRIGENDA

Nous renvoyons le lecteur aux n°s 7 et 9, 1969 de notre revue (Thermodynamic properties of Zn—Bi—Pb liquid solutions; L'addition des philodiènes sur la phtalazine. III), en le priant de bien vouloir prendre note des rectifications suivantes :

Page	Ligne	Il est correct de lire should correctly read
852 scheme 1		$\vert \dots \mathrm{Zn} - \mathrm{Bi} - \mathrm{Pb}\,(+)$ (1)
856 eq. 5		$\dots \sum\limits_{\substack{j_1 k=1 \\ \gamma \neq k}}^{n} \dots$
856 eq. 6		$\dots \omega(T)\, X_2^m$ $\dots \left[X_2^m - \frac{m}{m-1} X_2^{m-1} + \frac{1}{m-1} \right]$
857 eq. 10		$\log \gamma_{\mathrm{Zn}} = \left(\frac{1181}{T} - 0.347 \right) [(1 - X_{\mathrm{Zn}})^{1.48} +$ $+ 3.083\,(1 - X_{\mathrm{Zn}})^{0.48} - 2.083]$
858 eq. 12		$\dots (1 - X_{\mathrm{Bi}})^{2.1}$ $\dots [(1 - X_{\mathrm{Bi}})^{2.1} - 1.91\,(1 - X_{\mathrm{Bi}})^{1.1} + 0.91]$
858 eq. 14		$\dots (1 - X_{\mathrm{Zn}})^{-0.95} \dots$ $\dots (1 - X_{\mathrm{Zn}})^{-0.52} \dots (1 - X_{\mathrm{Zn}})^{-0.52} \dots$ $\dots (1 - X_{\mathrm{Bi}})^{0.1} \dots$
858 eq. 15		$\dots (1 - X_{\mathrm{Zn}})^{0.95} \dots (1 - X_{\mathrm{Zn}})^{0.05} \dots$ $\dots (1 - X_{\mathrm{Zn}})^{0.52} \dots (1 - X_{\mathrm{Bi}})^{0.1} \dots$ $\dots (1 - X_{\mathrm{Bi}})^{0.1}$
858 eq. 16		$\dots (1 - X_{\mathrm{Zn}})^{0.95} \dots (1 - X_{\mathrm{Zn}})^{0.52} \dots$ $\dots (1 - X_{\mathrm{Zn}})^{0.48} \dots (1 - X_{\mathrm{Bi}})^{0.1} \dots$ $\dots (1 - X_{\mathrm{Bi}})^{1.1} \dots$
864 eq. 17		$\dots (1 - X_{\mathrm{Zn}})^{0.05} \dots$ $\dots (1 - X_{\mathrm{Zn}})^{0.48} \dots (1 - X_{\mathrm{Bi}})^{1.1} \dots$

Page	Ligne	Il est correct de lire should correctly read
866 eq. 19		$\ldots(1 - X_{\mathrm{Zn}})^{0.05} \ldots(1 - X_{\mathrm{Zn}})^{0.48}\ldots$ $\ldots(1 - X_{\mathrm{Bi}})^{1.1}\ldots$
866	4th line from top	where $\Delta H'$ – molar heat of solution in cal/mol
1153	5 en remontant	accolé
1154	2	sur la phtalazine
1154	6	sur la phtalazine
1154	14	sur la pyridine
1155	8	sur la phtalazine
1156	6 en remontant	Comme d'ailleurs l'a reconnu récemment [9]
1156	3 en remontant 3 en remontant	donnée Taylor [10]
1156	1 en remontant	[9] H. Ahlbrecht, J. Föhlich, U. Habermalz et F. Kröhnke, *Tetrahedron Letters*, **37**, 3649–52 (1967).
1160	3 en remontant	$C_{16}H_{14}N_3Br_2$

NOTE POUR LES AUTEURS

La *Revue Roumaine de Chimie* publie des articles en anglais, français, russe, allemand ou espagnol. Les auteurs sont priés d'envoyer des articles, notes, communications et comptes rendus inédits.

Les manuscrits seront dactylographiés à deux intervalles. Les tableaux seront dactylographiés sur feuilles séparées, de même que la légende des figures. Les diagrammes seront tracés à l'encre de Chine sur papier calque. Les tableaux et les figures seront numérotés par des chiffres arabes, en nombre strictement nécessaire. Prière de ne pas inscrire les mêmes données dans les tableaux et les figures. Les formules chimiques seront incluses dans le texte ; en outre, elles seront transcrites sur des feuilles séparées. Les auteurs sont priés d'indiquer les caractères italiques (en soulignant les lettres au crayon), ainsi que tout autre caractère spécial. L'ordre des références bibliographiques sera celui de leur mention dans le texte ; le nom de l'auteur sera précédé de l'initiale du prénom ; les publications périodiques seront présentées suivant les prescriptions internationales. Les références seront ajoutées à la fin de l'article ; elles paraîtront comme des notes, au bas de la page. Le texte sera précédé d'un résumé, comprenant 15 lignes au maximum.

L'entière responsabilité du contenu des articles appartient aux auteurs. On publie des articles dus aux collaborateurs roumains ou étrangers. Les auteurs recevront 50 tirés à part.

PRINTED IN ROMANIA

TRAVAUX PARUS AUX ÉDITIONS DE L'ACADÉMIE DE LA RÉPUBLIQUE SOCIALISTE DE ROUMANIE

CORNEL BODEA et collab., **Tratat de biochimie vegetală, partea I, Fitochimie** (Traité de biochimie végétale, Ire partie, Phytochimie), Ier vol., 1964, 747 p. + 4 annexes + 2 pl., 41 lei ; IIe vol., 1965, 1262 p., 1 pl., 56 lei ; IIIe vol., 773 p., 35 lei.

V. GHEŢIE et V. MICUŞAN, **Analiza imunochimică. Teorie şi practică** (Analyse immunochimique. Théorie et pratique), 1966, 369 p., 28 lei.

SILVIA IONESCU, **Reacţii chimice induse de radiaţiile ionizante** (Réactions chimiques produites pas les radiations ionisantes), 1963, 271 p., 15 lei.

MARIETA NICOLAE, **Fizico-chimia proceselor fotografice** (Physico-chimie des processus photographiques), 1964, 426 p.+ 4 pl., 35 lei.

R. PORTOCALĂ et L. POPA, **Acizii ribonucleici şi virali** (Les acides rinobonucléiques et viraux), 1966, 375 p. + 8 pl., 26 lei.

D. PURDELA et R. VÎLCEANU, **Chimia compuşilor organici ai fosforului şi ai acizilor lui** (La chimie des composés organiques du phosphore et de ses acides), 1965, 540 p., 37 lei.

CRISTOFOR SIMIONESCU, MARGARETA GRIGORAŞ et AGATA CERNĂTESCU-ASANDEI, **Chimia lemnului din R.P.R.** (La chimie du bois en Roumanie), 1964, 239 p. + 6 pl., 27 lei.

CRISTOFOR SIMIONESCU et CLEOPATRA VASILIU-OPREA, **Mecanochimia compuşilor macromoleculari** (La mécanochimie des composés macromoléculaires), 1967, 344 p., 23,50 lei.

1970 JAN 15

I. P. „Informaţia" — c. 3732

43426

Lei 15.—

F 1103
04
R

REVUE ROUMAINE DE CHIMIE

TOME 14
N° 11
Novembre 1969

ÉDITIONS DE L'ACADÉMIE DE LA RÉPUBLIQUE SOCIALISTE DE ROUMANIE

Rev. Roumaine Chim. 14, 1333–1476, Bucarest (1969)

COMITÉ DE RÉDACTION

Rédacteur en chef :

C. D. NENIŢESCU, membre de l'Académie de la République Socialiste de Roumanie

Rédacteurs en chef adjoints :

A. T. BALABAN et V. E. SAHINI, membres correspondants de l'Académie de la République Socialiste de Roumanie

Collège de rédaction :

C. DRĂGULESCU, RALUCA RIPAN, CR. SIMIONESCU, membres de l'Académie de la République Socialiste de Roumanie; EM. BRATU, membre correspondant de l'Académie de la République Socialiste de Roumanie, Pr G. OSTROGOVICH, MARG. AVRAM, F. BADEA, D. MARCHIDAN, D. NEGOIU et D. SĂNDULESCU

Les manuscrits, les livres et les revues proposés en échange, ainsi que toute correspondance seront envoyés à la rédaction :

REVUE ROUMAINE DE CHIMIE

23, str. Dumbrava Roşie, Bucarest, Roumanie

F 1103

REVUE ROUMAINE DE CHIMIE

Tome 14, N° 11 Novembre 1969

Page

I. G. MURGULESCU und CORNELIA POTMISCHIL, Die Reaktion des Triphenylmethylchlorids mit Alkoholen . . . . 1335–1338 ✓

D. DUMAS et J. BRENET, Processus aux électrodes de carbone dans les bains alumino-cryolithiques . . . . 1339–1351 ✓

RODICA VÎLCU and C. MISDOLEA, Excess thermodynamic functions of some metal-metal salt systems in the molten state 1353–1360

D. I. MARCHIDAN and CR. TELEA, The heat of melting in the binary mixtures : $RbNO_3 + KNO_3$ and $RbNO_3 + CsNO_3$ 1361–1365

V. ARMEANU and I. DRĂGUȘIN, Study of some azo-derivative complexes of chromotropic acid with barium. I. Spectrophotometric study of the systems Ba-carboxyazo III, Ba-carboxysulphonazo III and Ba-sulphonazo III 1367–1375

J. DICK und ALFA LUPEA, Komplexverbindungen des N,N′-Diamino-Piperazins, IV. Infrarotspektren. Elektronenspinrezonanz . . . . 1377–1386 ✓

GR. POPA and V. MAGEARU, The formation of some complex combinations with piperazine in aqueous solution 1387–1397

V. MAGEARU et GR. POPA, L'étude des complexes deZn(II), Cd(II), Co(II) et Ni(II) avec la di-i-propylamine 1399–1405

D. FELDMAN, VIOLETA NUȚĂ and CR. SIMIONESCU, Photopolymerization of acrylonitrile in the presence of some anthraquinone dyes. . . . . . . 1407–1417 ✓

N. ASANDEI et ADÉLAÏDE LIGA, Réactions polymère-analogues du copolymère binaire acrylo-nitrile-acétate de vinyle en solutions alcalines. . . . 1419–1425

N. BĂRBULESCU und F. POTMISCHIL, Darstellung und Untersuchung der Hydroacridine. I. Über die Synthese des *symm*-Oktahydroacridins, *alfa*-Perhydroacridins und *beta*-Perhydroacridins 1427–1434

R. NUŢIU, L. KURUNCZI and Z. SIMON, Electric moment of dilituric acid (5-nitro-barbituric acid) 1435–1440

F. HODOȘAN und ALEXANDRA POP-GOCAN, Darstellung einiger 3-Acyloxysteroide 1441–1444

Rev. Roumaine Chim. 14, 1333–1476 (1969), Bucarest

Page

EM. A. BRATU et L. BARAF, La puissance nécessaire pour mélanger en utilisant les agitateurs de type à rame 1445–1456

LUCREȚIA I. POPA, V. DOROBANȚU, D. DORCIOMAN, STELA CONSTANTINESCU et M. S. POPÀ, Réalisation des sels nucléaires de zirconium par recristallisations fractionnées 1457–1465

ECATERINA TĂRĂBĂȘANU-MIHĂILĂ and ELENA SOFRONIE, Radiolysis of copper phthalocyanine alkaline aqueous solutions by ^{60}Co γ-ray. . . . 1467–1475

Revue Roumaine de Chimie, **14**, 1335–1338 (1969)

ORSZÁGOS MŰSZAKI KÖNYVTÁR ÉS DOKUMENTÁCIÓS KÖZPONT

DIE REAKTION DES TRIPHENYLMETHYLCHLORIDS MIT ALKOHOLEN

I. G. MURGULESCU und CORNELIA POTMISCHIL
aus dem Institut für Physikalische Chemie der Akademie,
Bukarest, str. Dumbrava Roşie, 23

Eingegangen am 28. Januar 1969

Es wurden die Reaktionen des Ph_3CCl mit Methyl-, Äthyl-, n-Propyl-, und n-Butylalkohol in Benzol als Lösungsmittel ausgeführt. Aus den Gleichgewichtskonstanten dieser Reaktionen wurden die entsprechenden Gleichgewichtsenthalpien ausgewertet.

Die Reaktion zwischen Triphenylmethylchlorid und Alkoholen gab Anlaß zu zahlreichen kinetischen Forschungen. Swain[1] untersuchte die Reaktion des Triphenylmethylchlorids (Ph_3CCl) mit Methanol, in Benzol, und gelangte zur Schlußfolgerung, daß diese, unter gewissen Konzentrationsbedingungen einem Zeitgesetz dritter Ordnung (erster Ordnung in bezug auf Ph_3CCl und zweiter Ordnung in bezug auf Alkohol) folgt und mit einer Aktivierungsenergie von nur $6{,}6 \pm 1{,}0$ kcal/Mol verläuft. Bei niedrigen Konzentrationen[2] sinkt die Reaktionsordnung auf 2 (1. Ordnung in bezug auf Ph_3CCl sowie auf den Alkohol).

Ingold und Mitarb. befaßten sich ebenfalls mit der Reaktion zwischen Ph_3CCl und den Alkoholen : Äthyl- (in Nitromethan),[3] Methyl- (in Benzol)[4] und Benzyl- (in Benzol).[5] Ihre Schlußfolgerung war, daß die Ordnung der Reaktion zwischen Ph_3CCl und Methanol bezüglich auf den Alkohol keinen festen Wert hat, sondern daß sie zwischen Null und drei variiert. Hinsichtlich der Reaktion des Ph_3CCl mit Äthanol, behauptet Ingold,[3] daß diese einem Zeitgesetz 1. Ordnung in bezug auf Ph_3CCl und nullter Ordnung in bezug auf den Alkohol folgt, wenn die Konzentration des Substitutionsagenten hoch ist.

Hudson und Saville[6] fanden für die Reaktion des Ph_3CCl mit Äthanol in Kohlenstofftetrachlorid eine Aktivierungsenergie von 12,8 kcal/Mol.

---

[1] C. G. Swain, *J. Amer. Chem. Soc.*, **70**, 1119 (1948).
[2] C. G. Swain und E. E. Pegues, *J. Amer. Chem. Soc.*, **80**, 812 (1958).
[3] E. Gelles, E. D. Hughes und C. K. Ingold, *J. Chem. Soc.*, **1954**, 2918.
[4] E. D. Hughes, C. K. Ingold, S. F. Mok und Y. Pocker, *J. Chem. Soc.*, **1957**, 1238.
[5] E. D. Hughes, C. K. Ingold, S. Patai und Y. Pocker, *J. Chem. Soc.*, **1957**, 1256.
[6] R. F. Hudson und B. Saville, *J. Chem. Soc.*, **1955**, 4130.

Um einen vollständigen Verlauf der Reaktionen zu erzielen, führten Swain wie auch Ingold die Alkoholysen des Ph_3CCl unter Bindung der aus der Reaktion entstandenen Salzsäure aus. Swain benützte zu diesem Zweck tertiäre Amine, bzw. Pyridin, in der Meinung, daß Letzteres mit Ph_3CCl träge und vernachlässigbar reagiert, ohne die Geschwindigkeit der Reaktion des Ph_3CCl mit dem Alkohol zu beeinträchtigen.

Ingold zeigte aber,[4] daß die Geschwindigkeit der Reaktion zwischen Ph_3CCl und Pyridin achtmal größer ist als die Geschwindikeit der Reaktion zwischen Ph_3CCl und dem Alkohol. Um die aus der Reaktion des Ph_3CCl mit Methanol entstandene Salzsäure zu binden, benutzte Ingold Tetra-n-Butylammoniumchlorid.

Die erwähnten Forschungen wurden im Rahmen der langjährigen Polemik über den Mechanismus der nucleophilen Substitution — welche ihre Aktualität noch immer bewahrt — ausgeführt.[7]

Die vorliegende Arbeit bezieht sich auf die in Abwesenheit salzsäurebindender Stoffe ausgeführten Reaktionen des Ph_3CCl mit Methyl-, Äthyl-, n-Propyl- und n-Butylalkohol. Das unter solchen Bedingungen eintretende Gleichgewicht kann durch Gleichung (1) ausgedrückt werden :

$$Ph_3CCl + ROH \rightleftharpoons Ph_3COR + HCl \tag{1}$$

Die Gleichgewichtskonstante dieser Reaktionen, K, ist durch folgende Beziehung gegeben :

$$K = \frac{c_{Ph_3COR} \cdot c_{HCl}}{c_{Ph_3CCl} \cdot c_{ROH}}$$

in der c_{Ph_3COR} usw. Gleichgewichtskonzentrationen darstellen. Wenn a und b die Anfangskonzentrationen des Ph_3CCl und bzw. des ROH sind, und x die Gleichgewichtskonzentration der Salzsäure ist, dann ergibt sich für die Gleichgewichtskonstante :

$$K = \frac{x^2}{(a-x)(b-x)} \cdot \tag{2}$$

Dieser Formel (2) werden wir uns im folgenden bedienen.

Es ist bekannt, daß die Variation der Gleichgewichtskonstante mit der Temperatur durch die Van't Hoffsche Gleichung gegeben ist :

$$\frac{\partial \ln K}{\partial T} = \frac{\Delta H}{RT^2}$$

---

[7] O. A. Reutov, ,,Probleme teoretice ale chimiei organice'', Ed. Acad., Bukarest, 1964, S. 125.

oder,

$$\frac{\partial \log K}{\partial \left(\frac{1}{T}\right)} = -\frac{\Delta H}{R} \tag{3}$$

wo ΔH die Reaktionsenthalpie darstellt. Mit Hilfe dieser Formel (3) wurden die in dieser Arbeit untersuchten Gleichgewichtsenthalpien aus den mittels (2) errechneten Gleichgewichtskonstanten ausgewertet.

BESCHREIBUNG DER VERSUCHE

Zum Darstellen der Lösungen wurde Ph_3CCl *p.a.* „Austranal" verwendet. Das als Lösungsmittel verwendete Benzol wurde über Kalziumchlorid und Natrium getrocknet, nachher an eine Vigreux-Säule destilliert.

Methyl- und Äthylalkohol wurden mit Hilfe des betreffenden Magnesiumalkoholats entwässert. n-Propyl- und n-Butylalkohol wurden erst über Kalziumoxid, nachher über das betreffende, durch Lösung von Natrium im Alkohol hergestellte Natriumalkoholat getrocknet.

Die Feuchtigkeit des verwendeten Benzols und der Alkohole wurde durch die Karl Fischer-Methode auf ca. 0,02% geschätzt.

Die auf Temperaturen zwischen 10 und 35°C thermostatierte (± 0.02°) benzolische Lösungen der Reaktionspartner wurden in verschlossenen Kölbchen vermischt. Nach Erreichung des Gleichgewichtes (nach 1/2–3 1/2 Std.) wurde der Inhalt in auf 0° gekühltes Aceton gegossen und die aus der Reaktion entstandene Salzsäure mit Triäthylamin (0,05 M in Benzol), in Gegenwart von Brom-Thymolblau als Indikator titriert. Die Konzentration des Ph_3CCl in Benzol variierte zwischen 0,025–0,075 M, während die Konzentration der Alkohole 0,1 M betrug.

ERGEBNISSE

In Tabelle 1 sind die den Versuchstemperaturen entsprechenden Gleichgewichtskonstanten der Reaktionen des Ph_3CCl mit Methyl-, Äthyl-, n-Propyl- und n-Butylalkohol angegeben.

Wie aus Tabelle 1 ersichtlich, sinken die Gleichgewichtskonstanten vom Methanol zu höheren Alkoholen, und sind vom n-Butanol an unab-

Tabelle 1

Die den Reaktionstemperaturen entsprechenden Gleichgewichtskonstanten der Reaktionen des Ph_3CCl mit normalen Alkoholen

Alkohol	Gleichgewichtskonstante						ΔH cal. Mol^{-1}
	283,1°K	288,1°K	293,1°K	298,1°K	303,1°K	308,1°K	
CH_3OH	$2{,}09.10^{-2}$	$2{,}41.10^{-2}$	$2{,}90.10^{-2}$	$3{,}54.10^{-2}$	$4{,}43.10^{-2}$	– –	6.720
C_2H_5OH	– –	$1{,}24.10^{-3}$	– –	$2{,}86.10^{-3}$	$3{,}94.10^{-3}$	$4{,}05.10^{-3}$	10.520
n-C_3H_7OH	– –	$1{,}35.10^{-4}$	$1{,}66.10^{-4}$	$2{,}64.10^{-4}$	$2{,}90.10^{-4}$	$6{,}22.10^{-4}$	12.500
n-C_4H_9OH	– –	$1{,}18.10^{-4}$	– –	$2{,}81.10^{-4}$	$3{,}46.10^{-4}$	$5{,}21.10^{-4}$	13.060

hängig von der Zahl der Kohlenstoffatome des Alkohols. Die Reaktion (1) ist also desto unvollkommener je höher die Zahl der Kohlenstoffatome des Alkohols ist.

In Abbildung 1 ist zur Auswertung der Reaktionsenthalpie die

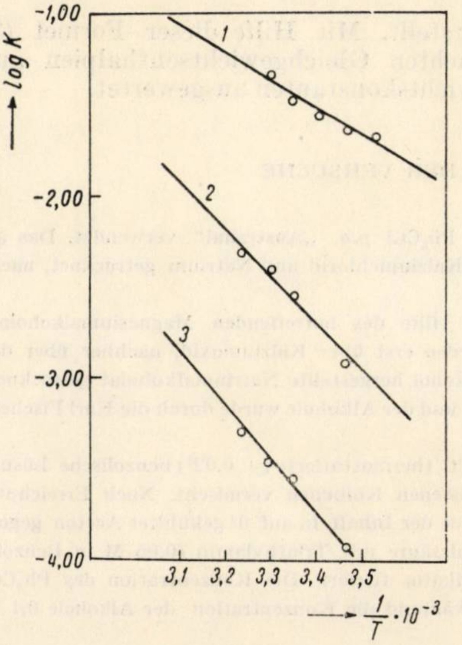

Abb. 1. — Die Auftragung des log K gegen $1/T$ für die Reaktionen des Ph_3CCl mit: Methyl- (*1*), Äthyl- (*2*) und n-Butylalkohol (*3*).

Abhängigkeit der Gleichgewichtskonstante vom reziproken Werte der absoluten Temperatur aufgetragen.

Die Reaktionsenthalpie wächst vom Methanol zu höheren Alkoholen und ist vom n-Butanol an praktisch unabhängig von der Art des Alkohols.

Revue Roumaine de Chimie, 14, 1339–1351 (1969)

PROCESSUS AUX ÉLECTRODES DE CARBONE DANS LES BAINS ALUMINO-CRYOLITHIQUES

D. DUMAS et J. BRENET

Laboratoire d'Electrochimie et de Chimie Physique du Corps Solide, Université de Strasbourg, 1, rue Blaise Pascal, France

Reçu le 23 janvier 1969

Par une méthode potentio-statique à trois électrodes nous avons étudié l'influence de la texture et de la structure des carbones sur les phénomènes anodiques lors de l'électrolyse de bains alumino-cryolithique. Nous avons examiné plusieurs variétés de graphites et de carbones prégraphitiques se différenciant, soit par le degré de graphitation, soit par la surface totale (mesurée par la méthode BET). Les résultats obtenus mettent en évidence l'influence du paramètre surface totale. Nous donnons une interprétation de nos résultats dans le cas général des réactions de décharge, sur une surface hétérogène, suivies de la chimisorption de l'espèce obtenue.

I. INTRODUCTION

L'électrolyse de l'alumine, en solution dans un bain de cryolithe, produit, lorsque l'on utilise une anode en carbone, des phénomènes que l'on interprète de manières fondamentalement opposées. Tout ceci vient de ce que l'on n'est pas d'accord sur le fait de savoir si le matériau carbone est électrochimiquement actif ou non.

On peut schématiser le processus de la manière suivante :

— décharge d'ions oxygénés et chimisorption d'oxygène avec formation de complexes de surface

$$xC + O^{2-} \leftrightarrows C_x(O) + 2e^- \qquad (1)$$

— désorption d'un mélange de CO_2 et de CO formés à partir des complexes

$$C_x(O) \rightarrow CO_2 \text{ et } CO \qquad (2)$$

Chaque fois [1-4] que l'on a voulu étudier l'influence de la phase solide sur les processus d'échange on a pris comme anodes des carbones industriellement représentatifs sans savoir au juste quels étaient les paramètres que l'on faisait varier.

Les réactions électrochimiques à une interface solide-liquide dépendent des propriétés physico-chimiques de la surface. Dans le cas du carbone, corps hétérogène, elles sont liées à la structure et à la texture de la phase solide, et leur densité de courant, variable primordiale, doit être calculée si possible par rapport à la surface réelle de réaction. Aussi avons-nous étudié le comportement électrochimique des carbones présentant des textures différentes (ce qui nous a amené à prendre des corps qui diffèrent également par leur degré de graphitation).

Nous obtenons une image de la texture en calculant la porosité totale et en mesurant, par la méthode BET, la surface totale. Nous vérifierons si cette surface donne, dans le cas des corps hétérogènes microporeux, une idée plus juste de la surface réelle de réaction.

II. ÉCHANTILLONS DE CARBONE ÉTUDIÉS

1. *Essai de classification des carbones* [5]

On définit un carbone comme un corps constitué essentiellement de l'élément C, à l'exclusion des produits organiques de haute masse moléculaire. A partir de produits de départ extrêmement variés on obtiendra :

— par pyrolyse en phase vapeur, le groupe des noirs de carbone ;
— par pyrolyse en phase condensée, des carbones compacts ou cokes.

Le mode de formation déterminant les propriétés. Suivant que le carbone, par un traitement de chauffe à des températures supérieures à 1600°, donnera ou non du graphite, on distinguera deux classes :

— les carbones non graphitables ;
— les carbones graphitables.

Ces deux variétés au comportement différent ont été regroupées sous l'appellation de carbones prégraphitiques. Ce qui ne préjuge en rien de leur évolution ultérieure par chauffage.

2. *Structure et texture des échantillons*

A l'exception du diamant tous les carbones présentent une structure feuilletée, bi-périodique dont l'élément fondamental est la symétrie hexagonale. Parmi les carbones seul le graphite présente une structure tri-dimensionnelle par empilement ordonné des feuillets plans.

---

[1] S. I. Rempel, « Processus anodiques dans l'électrolyse de l'aluminium », Ed. Scientifiques U.R.S.S., Sverdlovsk, 1961.

[2] J. Thonstad, *Canad. J. Chem.*, **42**, 1542 (1964).

[3] M. Takahashi et Y. Yamada, Denki Kagaku, *J. Electrochem., Soc. Japan*, **32**, 133 (1965).

[4] M. M. Vetuykov et R. G. Chuvilyaev, *Izvest. VUZ. Tsvetnaya Metallurgia*, **12**, 623 (1965).

[5] H. Guerin, « Les carbones », vol. 2, Ed. Masson, Paris, 1965, p. 386.

L'étude de la porosité donnera une image de la texture que l'on peut définir comme la configuration de l'interface matière-vide. La majeure partie de la surface d'un corps est liée à l'existence dans sa porosité de la catégorie des pores dont le diamètre est inférieur à 0,01 μ.

Pour obtenir une échelle de surface importante nous avons choisi des corps possédant une grande microporosité. Leurs macroporosités sont différentes mais participent dans une faible mesure à la surface.

Nous avons réuni dans un tableau les caractéristiques les plus intéressantes de nos anodes. Les surfaces spécifiques BET ont été mesurées par adsorption d'azote à — 195° sur les corps ayant un certain degré d'usure.

Tableau 1

Caractéristiques essentielles des anodes étudiées

Classification	Graphites		Carbones Prégraphitiques					
			Carbones graphitables		Carbone mal graphitable	Carbones non graphitables		
			1	2	3	4	7	6
	Graphite nucléaire	Graphite corroyé	Coke de Brai	Coke de Gilsonite	Coke métallurgique	Semi-Coke Brai B.T.	Charbon de Bois	Carbone vitreux
Densité apparente	1,70	2,02	1,40	1,57	1,22	1,47	0,95	1,50
Surface spécifique BET m^2/g	0,50	0,50	10	10	110	40	450	0,1
Pourcentage Brai	—	—	20	16	21	19	—	—
Taux de cendre %	100 ppm	100–120 ppm	0,9	0,5	2,5	8,1	—	50 à 200 ppm
HTT anode	—	—	1100	1150	1100	1100	900	—

3. *Préparation des anodes*

La plupart de nos anodes ont été préparées en suivant le mode de fabrication des anodes du type *précuites* utilisées dans l'industrie de l'aluminium.

Une certaine granulométrie d'un coke industriel (coke support) est mélangée avec un brai haute température formant liant. Le mélange est pressé, cuit sous atmosphère d'azote ou d'argon. Le cycle de cuisson a été le même pour toutes les anodes (montée en températures 20° par heure — palier de cinq heures à la plus haute température : H.T.T.). On obtient alors un produit hétérogène formé d'un coke support et du brai cokéfié constituant le liant (le brai H.T. donne un coke graphitable) dans lequel on taille les anodes.

III. MÉTHODE D'ÉTUDE

Nous avons tracé, point par point, les courbes tension-densité de courant par la méthode classique à trois électrodes. Le courant qui traverse la cellule est délivré par un ampérostat et maintenu constant à 0,1 % près. Nous utilisons la cellule d'électrolyse de Ferber[6] et une électrode de référence Al/Al^{3+} de type Piontelli.[7,8] L'anode est plane, à section circulaire, recouverte de nitrure de bore sur ses parois latérales jusqu'à deux mm de la face de travail ; ainsi la densité de courant est une densité frontale. La contre-électrode est constituée par de l'aluminium. La cellule est placée à l'intérieur d'un creuset en acier fermant hermétiquement de manière à pouvoir travailler sous atmosphère d'argon. Nous utilisons un bain de cryolithe sodique artificielle (préparée par fusion de NaF pur PA et de AlF_3 purifié par sublimation sous vide) contenant 10,5 % d'alumine PA. L'aluminium est un produit à 99,99 %. La température de travail a été de 985 ± 1°.

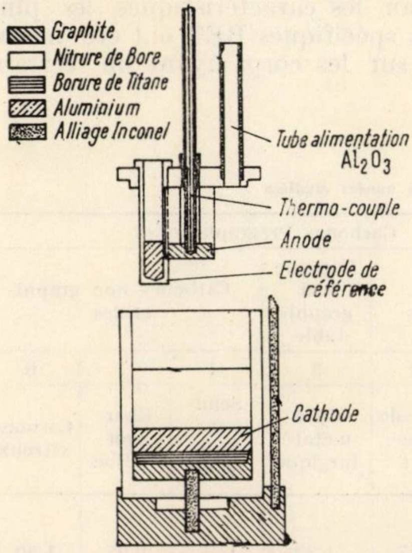
▧ Graphite
☐ Nitrure de Bore
▤ Borure de Titane
▨ Aluminium
▩ Alliage Inconel
Tube alimentation Al_2O_3
Thermo-couple
Anode
Electrode de référence
Cathode

Fig. 1. — Coupe transversale de la cellule d'électrolyse.

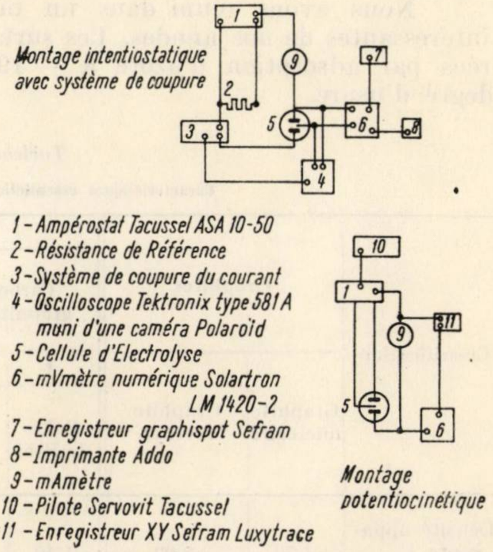
Montage intentiostatique avec système de coupure
1
2
3
4
5
6
7
8
9
1 - Ampérostat Tacussel ASA 10-50
2 - Résistance de Référence
3 - Système de coupure du courant
4 - Oscilloscope Tektronix type 581 A muni d'une caméra Polaroïd
5 - Cellule d'Electrolyse
6 - mVmètre numérique Solartron LM 1420-2
7 - Enregistreur graphispot Sefram
8 - Imprimante Addo
9 - mAmètre
10 - Pilote Servovit Tacussel
11 - Enregistreur XY Sefram Luxytrace
10
1
9
11
5
6
Montage potentiocinétique

Fig. 2. — Schéma de montage des dispositifs expérimentaux.

Aux fortes densités de courant un terme ohmique important dû au dégagement gazeux affectait les mesures de tension, ce qui nous a conduit à mettre au point un système coupant rapidement le courant. Ceci permet de s'affranchir des termes ohmiques inévitables tout en ne changeant rien au profil de distribution des ions dans le bain et au voisinage de l'électrode. Pour cela nous polarisons entre base et collecteur un transistor de puissance placé en série dans le circuit, ce qui bloque le passage du courant. Le temps de coupure dépend des caractéristiques du transistor : 10^{-5} seconde sous 10 ampères dans notre cas. Nous avons vérifié que nous obtenions les mêmes indications avec un relai de puissance à plongeur électromagnétique coupant le circuit en 10^{-7} seconde. La coupure est enregistrée par un oscilloscope cathodique muni d'une caméra. Les valeurs obtenues sur le graphite nucléaire avec et sans coupure sont portées figure 3. La différence entre les deux courbes en fonction de l'intensité du courant donne une droite passant par l'origine (figure 4). Ce qui prouve que seule la chute ohmique est supprimée par la coupure.

---

[6] M. Ferber, *Alluminio Nuovo Metallurgia*, **9**, 453 (1965)

[7] R. Piontelli, *Atti Accad. Naz. Lincei, R. C.*, **26**, 18 (1959).

[8] R. Piontelli, *Ann. New York Acad. Sci.*, **79**, 1025 (1960).

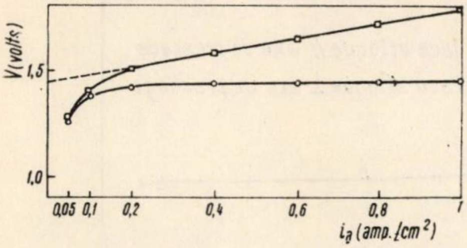

Fig. 3. — Courbes de polarisation anodique obtenues sur un graphite nucléaire par les méthodes avec et sans coupure.

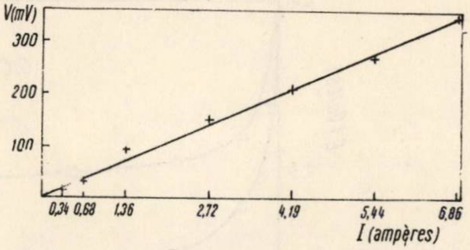

Fig. 4. — Différence entre les courbes de la figure 3, en fonction de l'intensité du courant.

IV. RÉSULTATS

1. *Études sur les graphites*

Nous avons étudié un graphite nucléaire et un graphite corroyé. Le graphite corroyé est un graphite nucléaire pressé à haute température (2 800—3 000°) au moment où il atteint une phase plastique. Le traitement a pour résultat d'orienter les cristallites par rapport à l'axe de pressage. Les plans feuilletés se placent perpendiculairement à cet axe.

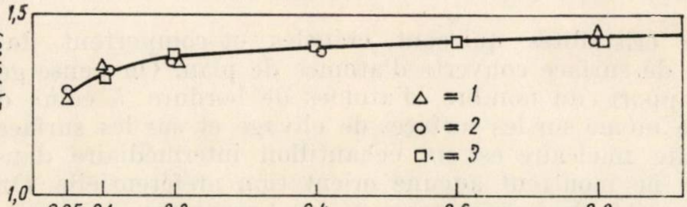

Fig. 5. — Courbe tension anodique-densité de courant pour divers graphites.

Nous avons taillé les anodes de manière à ce que leur axe soit parallèle ou perpendiculaire à l'axe de pressage.

Les résultats (figure 5) montrent le même comportement pour tous les graphites. Dans le cas du graphite corroyé, les anodes ayant leur axe parallèle à l'axe de pressage présentent à l'oxydation les feuillets plans (surfaces de clivage). D'après Hennig [9] il ne se produira sur cette surface une oxydation que si l'on y rencontre des défauts de réseau. En fait, outre les défauts de réseau et les joints de cristallites, cette surface présente des décrochements de feuillets plans qui font apparaître des atomes de bordure. Sur l'autre orientation l'oxydation se fait par les bords de cristallites qui sont crénelés et comportent de ce fait des morceaux de surface couverts d'atomes de plan. On pense généralement que le rapport du nombre d'atomes de bordure à celui d'atomes de plan est le même sur les surfaces de clivage et sur les surfaces latérales. Le graphite nucléaire est un échantillon intermédiaire dans lequel les cristallites ne montrent aucune orientation préférentielle. On comprend alors l'identité de comportement. Les graphites doivent chimisorber pratiquement la même quantité d'oxygène.

---

[9] G. R. Hennig, *J. Chim. phys.*, **58**, 12 (1961).

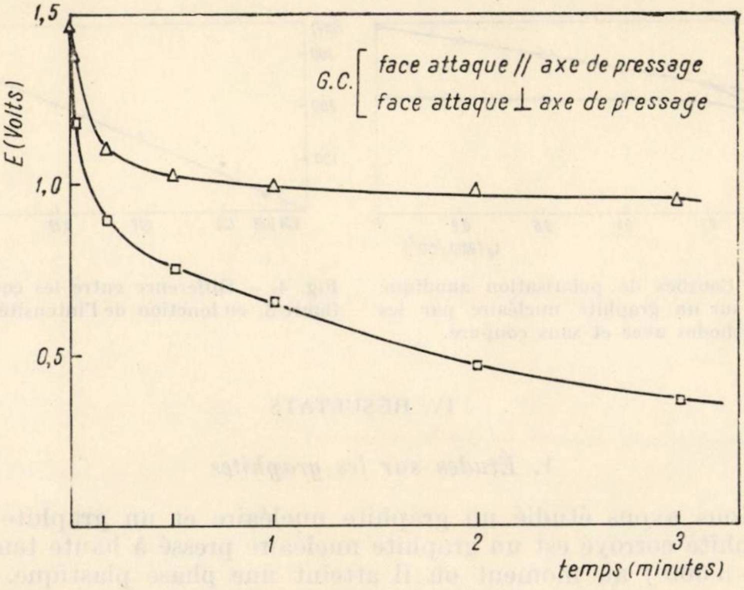

Fig. 6. — Courbes décroissance, après coupure, de la force électromotrice de la pile graphite-électrode de référence, en fonction du temps.

Nous avons complété nos observations par l'étude, après coupure du courant, de la décroissance de la F. É. M. de la pile constituée par l'ensemble anode-électrode de référence, aux bornes d'un millivoltmètre dont l'impédance d'entrée est supérieure à 5 000 MΩ (figure 6). Nous obtenons ainsi des indications sur la vitesse de désorption des produits gazeux à partir des complexes de surface.

La vitesse de désorption des complexes est donnée [10] par la relation

$$v_a = B \cdot \exp. - \frac{E_a^0 - \beta \cdot \theta}{\mathrm{RT}}$$

où E_a^0 représente l'énergie d'activation de désorption sur une surface presque nue ;

---

[10] L. Bonnetain et H. Hoynant, « Les Carbones », vol. 2, Masson Ed., Paris, 1965.

β est un coefficient de variation linéaire de l'énergie d'activation en fonction du degré de recouvrement.

Si l'on admet que la quantité d'oxygène chimisorbée est pratiquement la même, la différence que nous observons dans les vitesses de désorption est l'indice d'une variation des termes E_d^0 et β d'un échantillon à l'autre. Une vitesse de désorption plus grande montre une énergie d'activation plus faible, ce qui correspondra sur la surface à des complexes ayant une stabilité moins élevée. C'est ce que nous observons sur le graphite corroyé où des complexes moins stables se forment sur les surfaces de clivage.

2. *Études sur les carbones prégraphitiques*

a) *Influence de la surface de l'échantillon* (fig. 7 et 8)

La famille de courbes obtenue confirme l'influence du paramètre choisi. Si l'on porte (fig. 9) pour une tension donnée les densités de courant respectives en fonction de la surface BET nous n'obtenons pas une relation de proportionnalité. Ceci nous montre que pour le calcul d'une densité de courant le choix de la surface réelle du corps ne convient pas mieux que celui de la surface géométrique. La surface effective de travail paraît donc être une fraction de la surface réelle du corps.

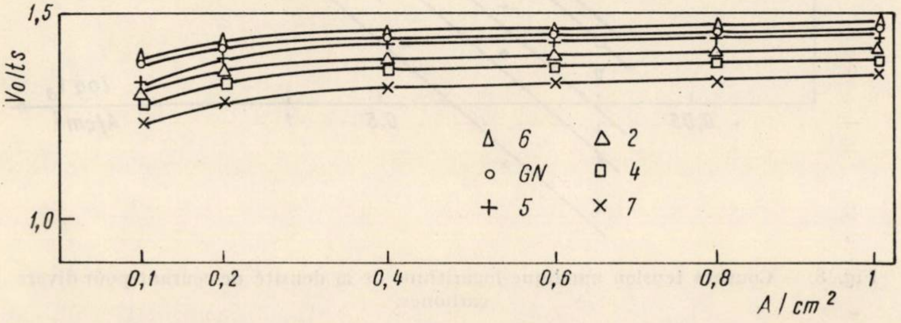

Fig. 7. — Courbes tension anodique-densité de courant pour divers carbones.

Les écarts observés entre les courbes ne correspondent pas à une variation de la surtension en fonction de la variété de carbone, mais au fait que le travail électrochimique, pour une même tension, est effectué à des densités de courant différentes.

Dans la figure 10 nous donnons, pour une densité de courant, la relation entre les tensions anodiques et le logarithme de la surface spécifique BET. Nous reviendrons sur cette courbe dans la discussion.

b) *Effets combinés de la structure et de la texture*

Les échantillons examinés ont à la fois des textures et des structures différentes. Les études sur les graphites ont déjà montré que la structure jouait un rôle secondaire. Nous pouvons le confirmer en obser-

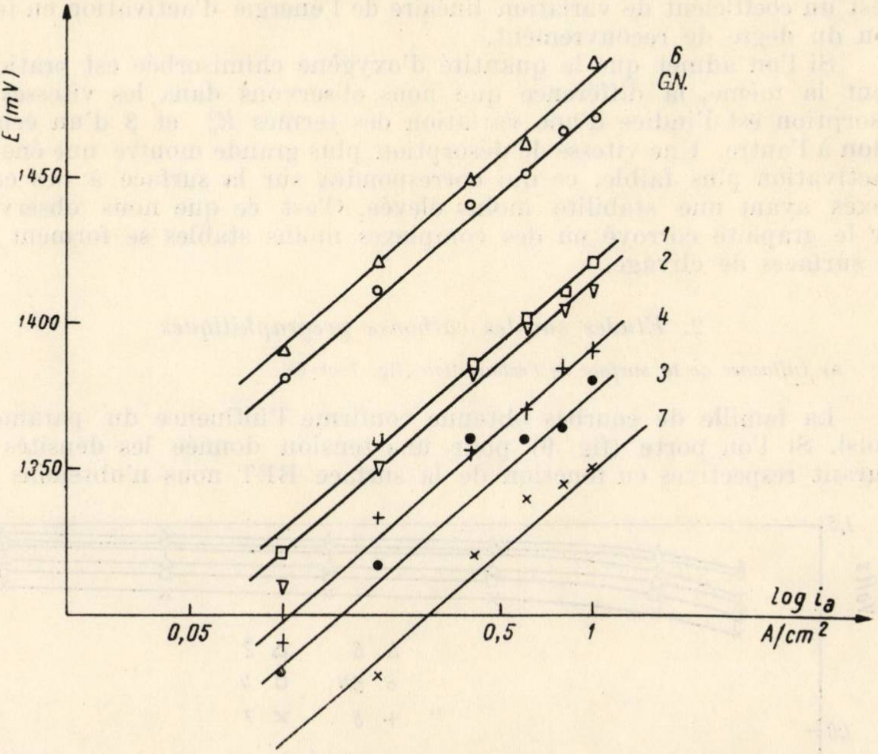

Fig. 8. — Courbes tension anodique-logarithme de la densité de courant pour divers carbones.

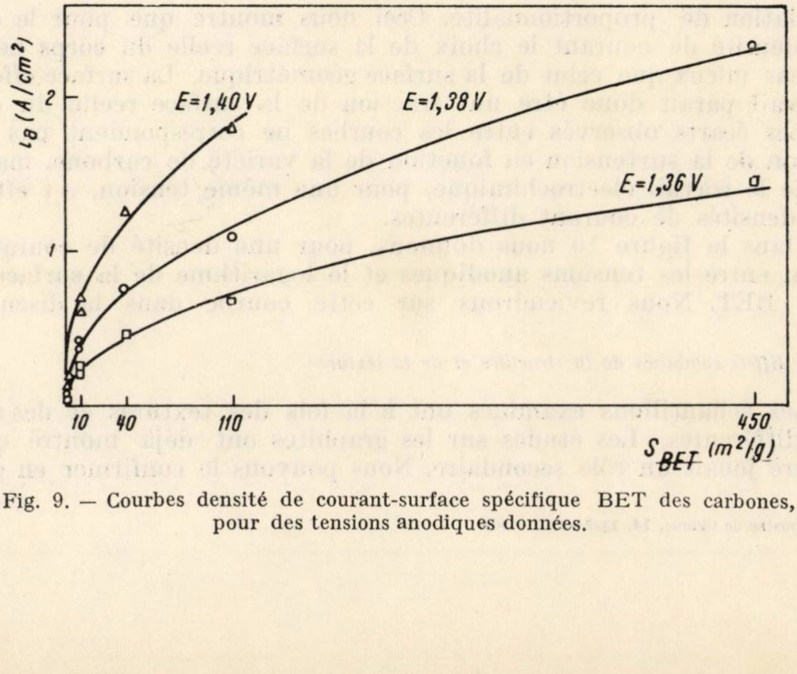

Fig. 9. — Courbes densité de courant-surface spécifique BET des carbones, pour des tensions anodiques données.

vant le groupe des carbones non graphitables. Dans ce groupe le carbone vitreux est un corps qui appartient à la classe des noirs de carbone et bien qu'ayant un degré de graphitation nul, il apparaît comme le corps possédant la tension anodique la plus élevée, alors que le charbon de bois pour le même degré de graphitation se place à l'opposé de l'échelle des tensions. Entre ces deux corps on trouve le graphite.

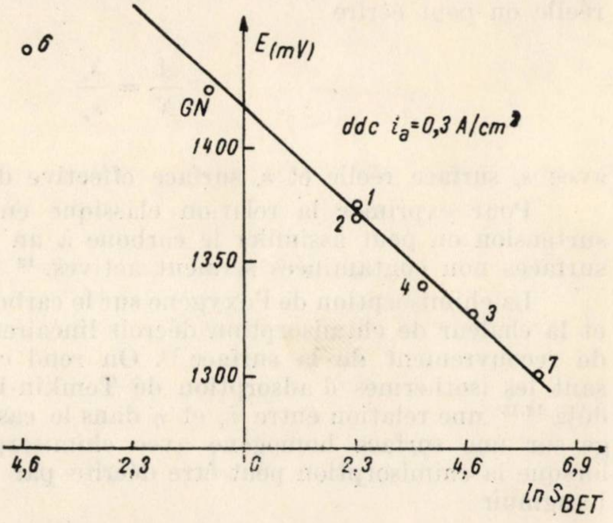

Fig. 10. — Courbe tension anodique-surface spécifique BET des carbones, pour une densité de courant donnée.

Ceci confirme bien l'influence prépondérante de la texture dans les écarts observés.

V. DISCUSSIONS

Le mécanisme d'oxydation anodique d'une électrode de carbone dans un sel fondu comprend un transfert d'électron suivi d'une chimisorption d'oxygène à l'interface solide hétérogène-liquide.

Dans le cas des carbones, l'hétérogénéité de la surface sera de deux ordres :

— une hétérogénéité physique conduisant à la notion de rugosité de la surface et nous amenant à définir un facteur de rugosité ρ qui représente pour un poids unitaire de substance le rapport de la surface réelle à la surface géométrique ;

— une hétérogénéité énergétique conduisant à la notion de sites préférentiels ou encore de plages actives.

Dans le cas d'une surface rugueuse le courant sera proportionnel au nombre de centres de décharge représenté, d'après Audubert, [11] par la relation suivante

$$A = \iint_{0}^{\infty} \varphi(E)\cdot\psi(E')\cdot \mathrm{d}E\cdot\mathrm{d}E'$$

---

[11] R. Audubert, «Cinétique Électrochimique», vol. 2, PUF Ed., Paris, 1955.

où $\varphi(E)$ et $\psi(E')$ sont des fonctions de répartition qui représentent respectivement le nombre de centres, par unité de surface réelle, caractérisés par les énergies E et E' de *désolvatation* et de formation des complexes. Si N représente le nombre de centres actifs ou non par unité de surface réelle on peut écrire

$$\frac{A}{N} = \frac{s_e}{s_r} \tag{1}$$

avec s_r surface réelle et s_e surface effective de travail.

Pour exprimer la relation classique entre densité de courant et surtension on peut assimiler le carbone à un métal sur lequel seules les surfaces non contaminées seraient actives. [12]

La chimisorption de l'oxygène sur le carbone est une réaction activée et la chaleur de chimisorption décroît linéairement en fonction du degré de recouvrement de la surface [12]. On rend compte de ce fait en utilisant les isothermes d'adsorption de Temkin-Langmuir. [12.13]. On connaît déjà [14.15] une relation entre i_a et η dans le cas d'une réaction de décharge sur une surface homogène avec chimisorption de l'espèce obtenue lorsque la chimisorption peut être décrite par les isothermes de Temkin-Langmuir

$$i_a = i_0 \cdot \exp . \frac{\alpha f}{2}(\theta - 0{,}5) \times \exp . \frac{\alpha n F}{\mathrm{RT}} \eta$$

où f représente la diminution de la chaleur d'adsorption par mole adsorbée et les autres lettres ont leur signification habituelle. Sur une surface hétérogène nous devrons exprimer le courant par unité de surface réelle comme proportionnel au nombre de centres de décharge et ensuite nous ramener à une densité de courant exprimée par rapport à la surface géométrique pour l'exploitation de nos résultats expérimentaux. Soit, en tenant compte de (1), la relation suivante

$$i_a = i'_0 \sigma N \frac{s_e}{s_r} \exp . \frac{\alpha f}{2}(\theta - 0{,}5) \times \exp . \frac{\alpha n F}{\mathrm{RT}} \eta$$

θ représente le degré de recouvrement dans le cas d'une surface hétérogène. C'est une fonction de s_r de la forme

$$\theta = f\left(\frac{1}{s_r}\right)$$

---

[12] D. O. Hayward et B. M. W. Trapnell, «Chemisorption», chap. VI, Butterworths Ed., Londres, 1964.

[13] D. Schuhmann, *J. Chim. phys.*, **64**, 9, 1399 (1967).

[14] R. Parsons, *Trans. Faraday. Soc.*, **54**, 1053 (1958).

[15] P. Delahay, «Double Layer and Electrode Kinetics», Chap. 10, Intersc. Publishers, New York, 1965.

On peut donc expliciter $\eta = f(\ln s_e)$.

$$\eta = \frac{\mathrm{RT}}{\alpha n F} \ln \frac{l_a}{l_0' N} - \frac{\mathrm{RT}}{\alpha n F} \ln s_e - \frac{\mathrm{RT} f}{2nF} \exp. \left(\ln \frac{k}{s_r}\right) + K \tag{2}$$

Posons, a priori, que, entre la surface effective de travail s_e et la surface réelle s_r, nous avons une relation du type

$$s_e = k \cdot \sqrt{s_r} \tag{3}$$

Nous justifierons cette écriture par la suite. La surface réelle nous est donnée expérimentalement par la méthode BET.

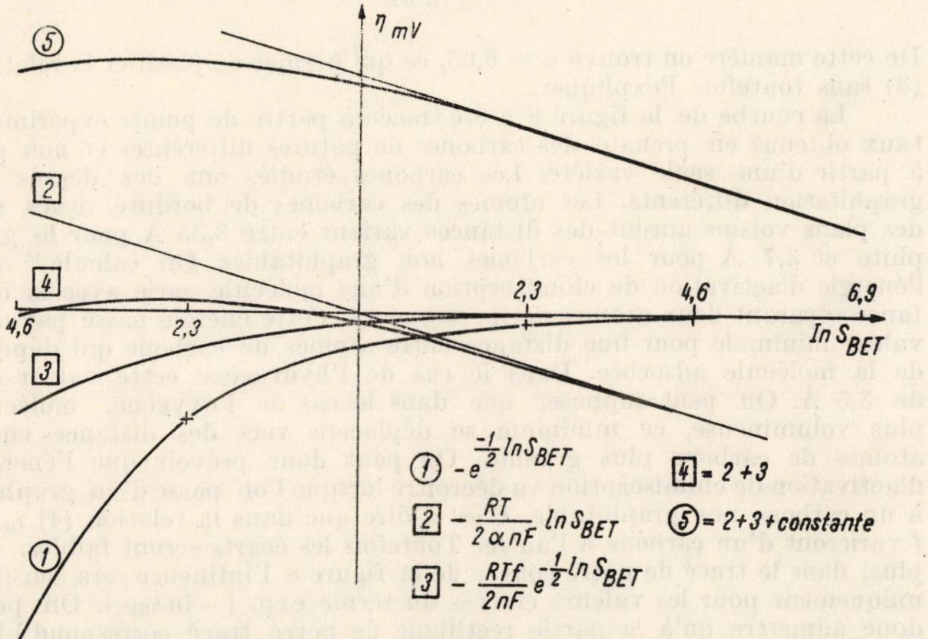

Fig. 11. — Courbe théorique tension anodique-surface spécifique BET, pour une densité de courant donnée.

En introduisant (3) dans (2) nous obtenons (4)

$$\eta = -\frac{\mathrm{RT}}{2\alpha n F} \ln s_{\mathrm{BET}} - \frac{\mathrm{RT} f}{2nF} \exp\cdot(-\ln s_{\mathrm{BET}}) + K' \tag{4}$$

Toute étude faite, nous obtenons le graphe représenté figure 11. Nous remarquons alors l'identité d'allure entre les courbes expérimentales de la figure 8 et la courbe théorique.

D'après la relation (4) la pente de la partie quasi rectiligne de la courbe devrait nous permettre, en posant $n = 4$, d'obtenir la valeur du coefficient de transfert. Si a est la pente de la droite tracée figure 8 nous aurons

$$\alpha = \frac{\mathrm{RT}}{2anF}$$

On trouve $\alpha = 0{,}6$ B.

Nous pouvons également calculer cette valeur de α à partir des courbes expérimentaux de la figure 6. Si a' est la pente de la famille des droites parallèles nous aurons d'après la loi de Tafel

$$\alpha = \frac{\mathrm{RT}}{a'nF}$$

De cette manière on trouve $\alpha = 0{,}65$, ce qui permet de justifier la relation (3) sans toutefois l'expliquer.

La courbe de la figure 8 a été tracée à partir de points expérimentaux obtenus en prenant des carbones de natures différentes et non pas à partir d'une seule variété. Les carbones étudiés ont des degrés de graphitation différents. Les atomes des carbones de bordure situés sur des plans voisins auront des distances variant entre 3,35 Å pour le graphite et 3,7 Å pour les carbones non graphitables. On calcule[16] que l'énergie d'activation de chimisorption d'une molécule varie avec la distance séparant deux atomes actifs receveurs. Cette énergie passe par une valeur minimale pour une distance entre atomes de carbone qui dépend de la molécule adsorbée. Dans le cas de l'hydrogène cette valeur est de 3,5 Å. On peut supposer que dans le cas de l'oxygène, molécule plus volumineuse, ce minimum se déplacera vers des distances entre atomes de carbone plus grandes. On peut donc prévoir que l'énergie d'activation de chimisorption va décroître lorsque l'on passe d'un graphite à un carbone non graphitable. C'est-à-dire que dans la relation (4) i_0 et f varieront d'un carbone à l'autre. Toutefois les écarts seront faibles. De plus, dans le tracé de notre courbe de la figure 8 l'influence sera sensible uniquement pour les valeurs élevées du terme exp. $(-\ln s_{\mathrm{BET}})$. On peut donc admettre qu'à la partie rectiligne de notre tracé correspond bien une pente donnée par la relation

$$a = \frac{\mathrm{RT}}{2\alpha nF}$$

VI. CONCLUSION

Cette étude relative à l'interface carbone-bain alumino-cryolithique avait pour objet de dissocier l'influence des paramètres structure et texture des carbones dans les phénomènes anodiques.

1. Nous avons été conduit à choisir des corps ayant des surfaces différentes et à prendre comme mesure de cette surface celle obtenue

---

[16] A. Sherman et H. Eyring, *J. Amer. Chem. Soc.*, **54**, 2661 (1932).

à partir de la méthode BET. Dans les conditions d'électrolyse la surface BET ne peut être qu'une image approchée de la surface effective de réaction que l'on ne connaît pas.

2. La structure du carbone semble sur le plan électrochimique jouer un rôle secondaire.

3. Dans le cas d'un corps hétérogène il apparaît que le choix de la surface géométrique pour le calcul de la densité de courant n'est pas excellent. Le décallage entre les courbes que l'on observe figure 5 ne correspond pas à une variation de la surtension en fonction de la variété du carbone mais au fait que le travail électrochimique, pour une même tension, est effectué à des densités de courant différentes.

4. Nous avons de plus tenté d'exprimer nos résultats sous une forme théorique en tenant compte que l'acte électrochimique était suivi d'une chimisorption de l'oxygène. Ceci devant être considéré comme une représentation schématique d'approche d'un problème complexe.

5. Pour cela nous avons été amené à poser que la surface effective de travail était liée à la surface totale par une relation de la forme

$$s_e = k \cdot \sqrt{s_t}$$

Revue Roumaine de Chimie, **14**, 1353–1360 (1969)

EXCESS THERMODYNAMIC FUNCTIONS OF SOME METAL-METAL SALT SYSTEMS IN THE MOLTEN STATE

RODICA VÎLCU and C. MISDOLEA
Institute of Physical Chemistry of the Academy,
str. Galaţi 31, Bucharest

Received December 28, 1968

The excess thermodynamic functions of the molten K – KCl and K – KBr systems were calculated at various temperatures for the miscibility domains of their components, under given conditions. The G^E values derived from computations were compared with the results obtained by Pitzer and Neckel on experimental bases. The agreement between the calculated values and the semi-experimental ones is satisfactory.

INTRODUCTION

The present paper is the continuation of a study on systems formed by a metal in the liquid state with a molten salt of the same metal. [1]

The experimental research undertaken in this domain is an attempt to elucidate the process of metal dissolving in salts; the system metal-metal salt shows a continuous transition of properties from the metallic to the non-metallic character as regards its composition determined by the reciprocal solubility of the components.

In addition to the most representative studies on the solubility mechanism, mentioned in a previous paper [1], the recent research of Pitzer, [2] Johnson and Bredig [3] and Neckel [4] is remarked. These works have an experimental support as they are based on solubility data. However, they do not enter the structure considerations on solutions of metal-metal salts ($M-MX$), that could alone permit more rigorous interpretations on some variation significance of the thermodynamic quantities.

The above mentioned studies of the $M-MX$ systems lead only to half-quantitative considerations on their thermodynamic behaviour. Nevertheless, their application to the estimation of some thermodynamic functions of the system components gives satisfactory results. Such values obtained, for instance, for the excess free energies of systems $M-MX\,(M = \mathrm{Na, K};\ X = \mathrm{Cl, Br})$ constituted comparative data of an informative character for the values we obtained by calculating statistically such functions, according to the significant structure theory.

---

[1] R. Vîlcu and C. Misdolea, *Rev. Roumaine Chim.*, **13**, 281 (1968).
[2] K. S. Pitzer, *J. Amer. Chim. Soc.*, **84**, 2025 (1962).
[3] J. Johnson and M. Breding, *J. Phys. Chem.*, **62**, 604 (1958).
[4] A. Neckel, *Monats*, **96**, 1617 (1965).

The qualitative theory of metal-metal salt solutions, as developed by Pitzer, deduces the excess Gibbs potential G^E from solubility data. The $M-MX$ solution is considered as a mixture of two negative species, i.e. the negative ions X^- and the metal valency electrons, M, placed in the holes of an irregular structure network, represented by positive ions. In a mixture where the salt amount is preponderent, the metal electrons form centers which are similar to the F centers of the solid state. When the solution is forming, the metal is assumed to change first into a hypothetical ionic network of the positive ions and of the F centers, and then to blend with the alkali halide (the structure of which is assimilated to that of a tightly cubic packeted metal).

By the size and form, assumed to be variable, of the F centers, Pitzer's model anticipates, for the forming solution a large enough positive excess entropy. The partially molar excess free energy μ_i^E.

$$\mu_i^E = RT \ln \gamma_i \tag{1}$$

is deduced from solubility data.

Under the simplifying hypothesis of a system behaving as a regular solution, one can apply, with sufficient accuracy, equation

$$RT \ln \gamma_i = \mu_i^0 (1 - X_i) \tag{2}$$

where X_i is the molar fraction of the component i.

When the component volumes are very different from each other, to equation (2) will be substituted a relation containing the volume fraction Φ_i

$$RT \ln \gamma_i = \mu_i^0 (1 - \Phi_i) \tag{3}$$

By virtue of this equation, the ratio of standard chemical potential of the two components is

$$\frac{\mu_1^0}{\mu_2^0} = \frac{V_1}{V_2} \tag{4}$$

Since from the solubility data the value of ratio μ_1^0/V_1 is deduced, it results that, by establishing the μ_1^0 value, equation (4) will give the standard chemical potential of the other component μ_2^0.

The method applied by Neckel[4] in order to estimate the excess chemical potential is based on the numerical computation of the thermodynamic quantities by means of experimental solubility curves. The activity coefficients of the melt components MX and M will be deduced from data on the lowering of the melting points, which give the excess chemical potential at an average pressure. Variations $\Delta_i\,(\mu_{MX}^E)$ and $\Delta_i(\mu_M^E)$ were computed by disregarding the temperature dependence of G^E within the restricted concentration range X_i to X_{i+1}, by means of equations

$$\Delta_i\,(\mu^E_{MX}) \approx \widetilde{x}_i\,\Delta_i\left(\frac{\partial G^E\,(T_0)}{\partial x}\right) \tag{5}$$

$$\Delta_i\,(\mu^E_{M}) \approx (1-\widetilde{x}_i)\,\Delta_i\left(\frac{\partial G^E\,(T_0)}{\partial x}\right) \tag{6}$$

$\widetilde{x}_i$ being the average value of the molar fraction in the $[x_i,\ x_{i+1}]$ interval.

The excess chemical potential will be obtained by summing up the quantities in equations (5) and (6), provided the initial values μ^E_{MX} and μ^E_M are known (from the depression data on the freezing points). The reference value for μ^E_M, experimentally inaccessible, is deduced by computation.[4]

The method advanced by Pitzer, as well Neckel's method, both intended to estimate the excess thermodynamic potentials, have a marked empiric character. The first method is based on a physical model, while the second one consists only in numerical computations.

The thermodynamic behaviour of the $M-MX$ solutions, pertaining to the metal type of the alkali-alkali halides, is quantitatively characterized hereafter by a statistical method, by applying, to the calculation of the partition functions of the systems, the significant structure mod el[1]

CALCULUS

The excess Gibbs free energy G^E of a binary solution metal-metal salt in the molten state is expressed, in terms of the statistical elements of the system, by equation

$$G^E = RT\,(X_1 \ln Z^{(s)} + X_2 \ln Z^{(m)} - \ln Z) \tag{7}$$

where X_1 and X_2 are the molar fractions of the salt and of the metal in the solution. The partition of the pure components i.e. $Z^{(s)}$ (the salt partition function) and $Z^{(m)}$ (the metal partition function) can be expressed in a reduced, logarithmic form by equations

$$\ln Z^{(s)} = \frac{2}{x^{(s)}}\,(\sigma_1^{(s)} + \sigma_2^{(s)}) + \left(1 - \frac{1}{x^{(s)}}\right)(\gamma^{(s)} + \ln x^{(s)}) \tag{8}$$

$$\ln Z^{(m)} = \frac{1}{x^{(m)}}\,(\sigma_1^{(m)} + \sigma_2^{(m)}) + \left(1 - \frac{1}{x^{(m)}}\right)(\gamma^{(m)} + \ln x^{(m)}) \tag{9}$$

where $x^{(s)}$ denotes the ratio between the molar volume of the ionic liquid $V^{(s)}$ at the working temperature and the molar volume of the solid $V^{(s)}$ at the melting point

$$x^{(s)} = \frac{V^{(s)}}{V_s^{(s)}}$$

Similarly for $x^{(m)}$:

$$x^{(m)} = \frac{V^{(m)}}{V_s^{(m)}}$$

Symbols σ and γ are the abridged notations of the following expressions

$$\sigma_1^{(s)} \equiv \frac{E_s^{(s)}}{2RT} x^{(s)^{1/3}} - 3 \ln (1 - \mathrm{e}^{-\theta^{(s)}/T}) \tag{10}$$

$$\sigma_2^{(s)} \equiv \ln [1 + n^{(s)} (x^{(s)} - 1) \exp \left(- \frac{a^{(s)} E_s^{(s)}}{2n^{(s)} RT} \cdot \frac{x^{(s)^{1/3}}}{x^{(s)} - 1} \right) \tag{11}$$

$$\gamma^{(s)} \equiv \ln \left[\frac{(2\pi mkT)^{3/2}}{h^3} \frac{8\pi^2 IkT}{h^2} \frac{1}{1 - \mathrm{e}^{-h\nu^{(s)}/kT}} \frac{eV_s^{(s)}}{N} \right] \tag{12}$$

$$\sigma_1^{(m)} \equiv \frac{E_s^{(m)}}{RT} - 3 \ln (1 - \mathrm{e}^{-\theta^{(s)}/T}) \tag{13}$$

$$\sigma_2^{(m)} \equiv \ln \left[1 + n^{(m)} (x^{(m)} - 1) \exp \left(- \frac{a^{(m)} E_s^{(m)}}{n^{(m)} RT} \frac{1}{x^{(m)} - 1} \right) \right] \tag{14}$$

$$\gamma^{(m)} \equiv \ln \left[\frac{(2\pi mkT)^{3/2}}{h^3} \frac{eV_s^{(m)}}{N} \right]^2 x^{(m)} \tag{15}$$

All quantities marked by exponent (*s*) refer to the molten salt, while those with exponent (*m*) refer to the metal in the liquid phase. Details concerning the notations and forms, ascribed to the partitions functions, are found in previous papers [1,5,6] about the correspondence between the significant structures gas-like and solid-like in the liquid phase and the symbols, which indicated the contribution of the various freedom degrees of the molecule to the total partition function.

The mixing enthalpy of system $M - MX$ is stated by the well known statistical expression, suited to the binary metal-metal salt

$$H^M = RT^2 \left\{ \frac{\partial \ln Z}{\partial T} - \left[X^{(s)} \left(\frac{\partial \ln Z^{(s)}}{\partial T} \right)_P + X^{(m)} \left(\frac{\partial \ln Z^{(m)}}{\partial T} \right)_P \right] \right\} \tag{16}$$

The excess entropy results directly from the excess free energy, while the blending enthalpy is deduced from the classical thermodynamic equations

$$S^E = \frac{H^M - G^E}{T}. \tag{17}$$

---

[5] T. R. Thomson, H. Eyring and T. Ree, *Proc. Nat. Acad. Sci. U.S.A.*, **46**, 336 (1960).

[6] T. S. Ree, T. Ree and H. Eyring, *Proc. Nat. Acad. Sci. U.S.A.*, **48**, 501 (1962).

RESULTS

The excess functions of the system K$-$KBr were computed, for 1074, 1123 and 1223°K, by equations (7), (16) and (17). The miscibility ranges at various temperatures and compositions were extracted from the diagrams of equilibrium between phases, according to Johnson and Bredig. For the system K$-$KCl, the miscibility is total at about 1023°K in the domain of diluted solutions of metal into salt, as well as of salt into metal. As the differences between the molar fractions of the mixture components diminish, the domain of complete miscibility is displaced towards higher and higher temperatures. For a molar fraction $X_K \approx 0.4$ the separation zone between the two liquid phases vanishes at about 1063°K for the K$-$KCl system, while for the K$-$KBr system, the total miscibility appears at lower temperatures of about 1000°K. The phase diagrams point to the absence of an intermediate solid phase just as for the other M$-$MX solutions under study [1] ($M = Na$; $X = Cl, Br$).

At the first working temperature, i.e. at 1044°K, the components of the K$-$KCl system exhibit a miscibility gap comprised between the molar fractions with values of the KCl in the melt below 0.3 and higher than 0.85. At the same temperature, the components of system K$-$KBr are miscible in any ratio. At the higher temperatures, chosen for our computations, i.e. 1123°K and 1223°K, both systems are in homogeneous phase at any concentration.

The values of the excess thermodynamic functions calculated for the systems K$-$KCl and K$-$KBr, according to the significant structure theory, are recorded, in tables 1$-$4, for all three mentioned temperatures. Beside the calculated G^E and TS^E values, these tables give, in their next columns, comparative data, obtained by solubility measurements made by Pitzer and Neckel by the methods indicated in the introduction of this paper (notwithstanding their experimental origin, these values underwent a theoretical treatment, carried out by other pathways by the above mentioned authors).

Table 1 gives excess quantities of the K$-$KCl system, at 1044°K. The parallel examination of the computed data and of those deduced from solubility data, shows a good agreement with Pitzer's results,

Table 1

Calculated and experimental thermodynamic excess functions for the K$-$KCl system at 1044 °K

X_1 (salt)	G^E cal/mol			TS^E cal/mol	H^M cal/mol
	Calculated values	Experimental [2] values	Exp. [4]		
0.1	574	414	273	239	813
0.2	1005	749	566	436	1441
0.3	1278	1005	816	632	1910
0.85	592	678	—	551	1143
0.9	401	483	510	405	806
0.95	202	268	285	226	428

especially in the case of the molar fractions rich in salt and presenting a large difference with regard to Neckel's values for the excess Gibbs free energy. The differences between the "experimental" values are of about the same order than those between the G^E calculated according to the significant structure model and the G^E obtained by Pitzer's method. These last values represent an average between the data we have obtained statistically and those determined by Neckel. Considering that Pitzer's data are more directly related to experiment, the comparison between our computed results and the values given by Pitzer appears more justifiable than the comparison with Neckel's values.

Like the excess Gibbs free energy the mixing enthalpy and the TS^E product show a variation with the composition of the $M-MX$ system, according to an asymmetric parabola. The existing experimental data do not confirm the computed values, neither for the blending enthalpy, nor for the excess entropy.

In table 2, the excess functions of the same system are recorded at 1123 and 1223°K. We have no comparative data for these temperatures.

Table 2

Functions for the K – KCl at 1123° and 1223 °K

X_1	G^E cal/mol		TS^E cal/mol		H^M cal/mol	
	T = 1123°K	T = 1223°K	T = 1123°K	T = 1223°K	T = 1123°K	T = 1223°K
0.1	566	557	247	258	813	815
0.2	986	967	461	487	1447	1454
0.3	1259	1234	644	677	1903	1911
0.4	1391	1366	785	807	2176	2173
0.5	1390	1348	871	929	2261	2277
0.6	1265	1216	900	966	2165	2182
0.7	1034	981	852	919	1886	1900
0.8	720	669	710	765	1430	1434
0.9	361	321	437	478	798	799

It has been established that G^E diminishes with the temperature, but by small values within a large enough temperature range. Besides, according to Neckel's qualitative theory, it is assumed that the excess free enthalpy does not vary with temperature. No constant one-way variation with temperature has been found for the blending enthalpy, which is moreover difficult to establish, because its values at 1123 and 1223°K are very near to each other.

Table 3, devoted to the excess function values of the K–KBr system at 1044°K, shows a very good agreement between the computed and the experimental values, except in the case of the mixtures where the salt amount is predominant.
This behaviour is quite unlike that of the system K–KCl, and therefore it implies difficulties for the elucidation of phenomenon.

Finally, the last table gives only proper computation data concerning the same excess functions for the K–KBr system at 1123 and 1223°K.

Table 3

Calculated and experimental thermodynamic excess functions for the K – KBr system at 1044 °K

X_1	G^E cal/mol calculated values	G^E cal/mol experimental values	TS^E cal/mol	H^M cal/mol
0.1	495	406	202	697
0.2	858	727	378	1236
0.3	1087	954	533	1620
0.4	1194	1100	650	1844
0.5	1183	1158	731	1914
0.6	1068	1119	761	1829
0.7	867	986	720	1587
0.8	599	757	603	1202
0.9	298	429	373	671

Table 4

Excess thermodynamic functions for the K – KBr system at 1123 and 1223°K

X_1	G^E cal/mol		TS^E cal/mol		H^M cal/mol	
	$T = 1123°K$	$T = 1223°K$	$T = 1123°K$	$T = 1223°K$	$T = 1123°K$	$T = 1223°K$
0.1	481	466	217	231	698	697
0.2	831	799	407	443	1238	1242
0.3	1048	1003	577	628	1625	1631
0.4	1144	1085	707	777	1851	1862
0.5	1123	1054	799	881	1922	1935
0.6	1000	925	836	924	1836	1849
0.7	795	715	797	892	1592	1607
0.8	531	456	672	756	1203	1212
0.9	248	194	420	479	668	673

A comparison between the results obtained for the K – KBr system and the excess functions of the K – KCl system, shows that the behaviour of the quantities is consistent : G_{K-KBr} diminishes with the temperature as in the case of the system K – KCl and, besides, this variation as a function of temperature is also negligible. The blending heat values of solutions K – KBr are very close within a temperature range of about 200 degree. Nevertheless, contrary to system K – KCl, the variation direction with temperature can be foreseen : H^M increases with temperature.

DISCUSSIONS

There is but a restricted number of works with a theoretical charcter dedicated to the $M - MX$ systems and even the existing ones present experimental implications. The significant structure model is the only statistical model extended to the thermodynamic characterization of systems $M - MX$ ($M =$ Na, K ; $X =$ Cl, Br) the results supplied by it are compared with data obtained from solubility measurements theoretically treated. The concordance between the two series of values — expressed by excess thermodynamic functions of some $M-MX$ systems — confirms the accuracy of the form attributed to the state sum of a solution of the type under study, obtained by summing up the partition function of the MX ionic liquid with the partition function of the molten metal.

Although, in a first approximation, the agreement between our computations, and the "experimental" data is satisfactory, the results could still be improved provided that the approximations admitted in establishing some of the specific quantities of the mixture are discarded. For instance : to the solution volume, an additive character was attributed, omitting the total blending effect, which would normally be an excess volume. For lack of density data about the mixtures under study, we could not estimate the necessary corrections. The same additivity was also applied to parameters a and n of solutions $M-MX$.[7,8] The above mentioned corrections are generally very small, nevertheless their contribution to the estimation of the excess thermodynamic quantities is quite perceptible.

Until the elaboration of a statistical theory able to state a more rigorous way for the partition form of some metal-metal salt systems, the significant structure model is still being a satisfactory working method for the quantitative study of the solutions of this type.

---

[7] R. Vîlcu and C. Misdolea, *J. Chem. Phys.*, **49**, 3179 (1968).

[8] C. M. Carlson, H. Eyring and T. Ree, *Proc. Nat. Acad. Sci. U.S.A.*, **46**, 333 (1960).

Revue Roumaine de Chimie, **14**, 1361–1365 (1969)

THE HEAT OF MELTING IN THE BINARY MIXTURES: $RbNO_3 + KNO_3$ AND $RbNO_3 + CsNO_3$

D. I. MARCHIDAN and CR. TELEA

Institute of Physical Chemistry of the Academy str. Galaţi, 31, Bucharest

Received April 18, 1969

The heat of melting in the binary mixtures of alkali nitrates $(Rb + K)NO_3$ and $(Rb + Cs)NO_3$ was determined by a differential calorimetry device. The obtained values are smaller than those calculated and their change with the concentration reflects the type of phase diagram of the corresponding solid solution.

The thermodynamic study of binary mixtures of salts has predominantly been focussed on the determination of their behaviour in solid or liquid (molten) state. From this point of view the thermodynamic data concerning the transition from one phase to the other (solid → → liquid or liquid to solid) are comparatively fewer. However, this sort of thermodynamic measurements does not allow more than an indirect determination of the excess thermodynamic functions.

In molten salts the cryoscopic measurements are significant when the molar fraction of one component is very low compared to the molar fraction of the second component. The phase diagrams generally allow only a rough estimation of the thermodynamic functions. Other methods as drop-calorimetry, solvation-calorimetry, all lead to indirect estimations.

In a previous paper [1] the possibility of using a high-temperature Calvet microcalorimeter to get precise data on heats of melting in binary systems of alkali halides was underlined. The present paper extends these considerations and attempts to establish some regularities in the melting of binary systems.

The differential calorimetry system was chosen given its relative easiness in recording the data, the strength of the equipment and the high sensitivity needed in measuring small thermal exchanges.

EXPERIMENTAL

The differential calorimeter was similar to that described by Ozawa [2] for differential thermal analysis and combined with a device we used in a previous work.

---

[1] D. I. Marchidan and M. Gambino, *Bull. Soc. Chim. France,* **1966,** 1954.

[2] T. Ozawa, *Bull. Chem. Soc. Japan,* **39**, 2071 (1966);
T. Ozawa, M. Momota and H. Isozaki, *Bull. Chem. Soc. Japan,* **40**, 1583 (1967)

The thermocouples are placed on the calorimetric enclosures (two for the reference substance, Al_2O_3, and two for the substance under study) and additionally-differentially connected (fig. 1).

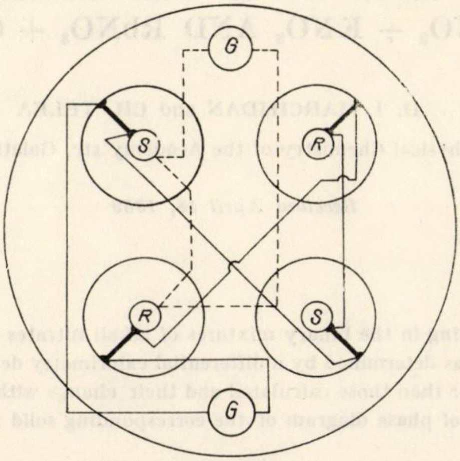

Fig. 1. — Connection scheme of thermocouples
R = reference;
S = sample.

The temperature programming was achieved by a linear increase in the voltage applied at the heating terminals of the furnace.

To calibrate the differential calorimeter, pure chemicals[3] were used, the heat of melting of which was available in literature. The temperature correction of the calorimetric constant[4] was also made:

$$K = A + BT^3 \tag{1}$$

which for the calorimeter we used is:

$$K = 1.2 + 1.68 \times 10^{-8} T^3 \tag{2}$$

RESULTS AND DISCUSSION

The experimental curves obtained by melting have the shape given in figure 2, where the procedure of surface areas measurement is also seen. The heat of melting results directly from the equation:

$$H_{12} = K \,.\, A \tag{3}$$

where A is the hatchured area and K the calorimeter constant. The values obtained for different molar fractions of the components are given in table 1.

[3] D. I. Marchidan and Cr. Telea, *Rev. Roumaine Chim.*, **13**, 1291 (1968).
[4] M. M. Faktor and R. Hanks, *Trans. Faraday Soc.*, **63**, 1122 (1967).

From table 1, but more strikingly from fig. 3, one sees that the experimental values obtained do not correspond to the simple additivity as it would follow from the application of a linear Vegard-type relation :

$$H_{12} = x_1 H_1(\mathrm{Me_1NO_3}) + (1 - x_1)\, H_2(\mathrm{Me_2\ NO_3}) \qquad (4)$$

The obtained values are smaller than for the ideal system.

The phase diagrams of the two systems indicate the formation of solid solutions [5] with minimum. The heat of melting *versus* concentration

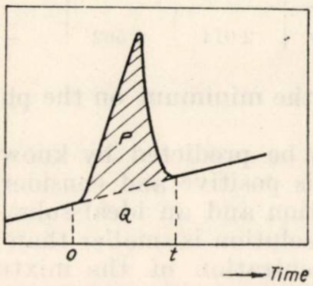

Fig. 2. — Differential curve of melting heat.

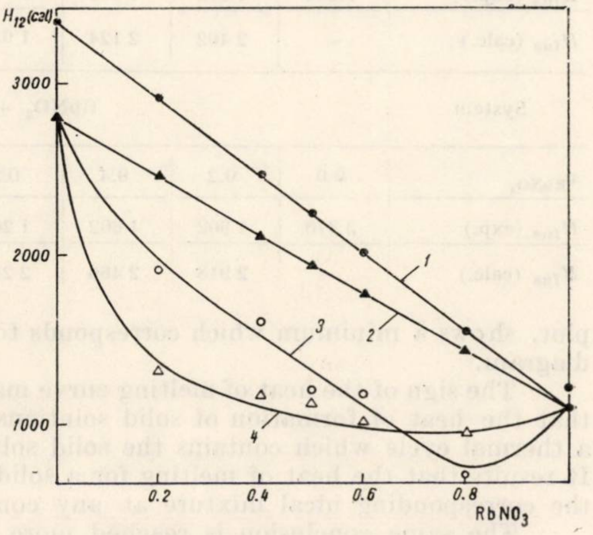

Fig. 3. — Melting heat of mixtures : [5]
1. — $RbNO_3 + CsNO_3$ (calc.); 2. — $RbNO_3 + KNO_3$ (calc.);
3. — $RbNO_3 + CsNO_3$ (exp.); 4. — Δ—$RbNO_3 + KNO_3$ (exp).

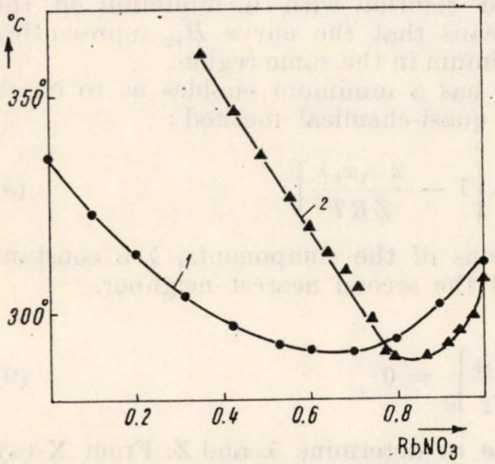

Fig. 4. — Phase diagrams of 1. $(Rb+K)NO_3$ and 2. $(Rb + Cs)NO_3$ systems.

---

[5] N. K. Voskresenskaia, "Spravochnik po plavkosti sistem iz bezvodnyh neorganicheskih solei", vol. I, Izd. Akad. Nauk. S.S.S.R., Moscow, 1961, p. 277 and 418.

Table 1

Heat of melting of binary mixtures: $RbNO_3 + KNO_3$ and $RbNO_3 + CsNO_3$. (calories)

System	$RbNO_3 + KNO_3$						
x_{RbNO_3}	0.0	0.2	0.4	0.5	0.6	0.8	1.0
H_{fus} (exp.)	2 800	1 316	1 182	1 134	1 020	980	1 110
H_{fus} (calc.)	—	2 462	2 124	1 955	1 786	1 448	—
System	$RbNO_3 + CsNO_3$						
x_{RbNO_3}	0.0	0.2	0.4	0.5	0.6	0.8	1.0
H_{fus} (exp.)	3 370	1 902	1 602	1 200	1 189	704	1 110
H_{fus} (calc.)	—	2 918	2 466	2 240	2 014	1 562	—

plot, shows a minimum which corresponds to the minimum on the phase diagram.

The sign of the heat of melting curve may be predicted by knowing that the heat of formation of solid solutions is positive and considering a thermal cycle which contains the solid solution and an ideal solution. It results that the heat of melting for a solid solution is smaller than for the corresponding ideal mixture at any concentration of the mixture.

The same conclusion is reached more directly and clearer by the study of solid → liquid equilibrium in binary systems[6]. It is known that the sign of the $(\delta T/\delta x_2)$ differential is the same as the sign of $-2(\delta^2 H/\delta x_2^2)_m$. In case of a solid solution with a minimum on the phase diagram, $[(\delta T/\delta x_2) < 0]$ means that the curve H_{12} representing the heat of melting will have a minimum in the same region.

The fact that the H_{12} curve has a minimum enables us to check our data by using Guggenheim's quasi-chemical method:

$$H_{12} = x_1 x_2 \lambda \left[1 - \frac{2\, x_1 x_2 \lambda}{ZRT}\right] \tag{5}$$

where x_1, x_2 are the molar fractions of the components, λ a constant and Z the coordination number of the second nearest neighbor.

At the minimum:

$$\left[\frac{\partial H_{12}}{\partial x_2}\right]_m = 0 \tag{6}$$

Equations (5) and (6) enable to determine λ and Z. From X-ray measurements the value of Z is known to range from 10 to 12. The value we obtained (~ 10) could be considered satisfactory.

---

[6] E. A. GUGGENHEIM, "Mixtures", Oxford Univ. Press, London, 1952, p. 38.

It is also noteworthy that the deviations from ideality for H_{12} increase with the difference between the sizes of the two cations and their polarizabilities.

This allows to relate the heat of melting of the mixtures to the structural parameters of salts as already proceeded for the binary mixtures of molten salts.

Acknowledgements. We wish to express our deep gratitude to Professor I. G. Murgulescu for his interest in our work and to C. Volcovici, for his help in the construction of the measuring apparatus.

Revue Roumaine de Chimie, **14**, 1367–1375 (1969)

STUDY OF SOME AZO-DERIVATIVE COMPLEXES OF CHROMOTROPIC ACID WITH BARIUM. I

SPECTROPHOTOMETRIC STUDY OF THE SYSTEMS Ba-CARBOXYAZO III, Ba-CARBOXYSULPHONAZO III AND Ba-SULPHONAZO III

V. ARMEANU and I. DRĂGUŞIN

Academy of Economic Studies, Chair of Chemistry and Physics,
Piaţa Romană 6, Bucharest
and Chemical Works, Borzeşti

Received December 27, 1968

One presents a comparative, qualitative and quantitative spectrophotometric study of the systems Ba-Carboxyazo III, Ba-Carboxysulphonazo III and Ba-Sulphonazo III in acid water-alcohol and water-acetone solutions. One establishes the characteristics, structure and stability of the formed compound and the optimum working conditions.

INTRODUCTION

The discovery and use of some organic reactives giving colour-reactions with the Ba^{2+} ion has meant a very important progress in the analytical chemistry of this element. Thus, for the volumetric dosage of barium or sulphates accompanied by the formation of $BaSO_4$ precipitate, one has used as indicator sodium rhodizonate,[1,2] alizarine S red[3,4] the coloured thorium complex with pyrocatechol-violet,[5] Th-PCV thorin[6,7] [the sodium salt of the 2 (hydroxy-3,6-disulphonic-naphthylazo) phenylarsonic acid], etc. Except for the Th-PCV complex, these indicators give slight contrasts and therefore unprecise turnings.

---

[1] L. von Zambory, *Magyar Kém. Folýoirat*, **35**, 63 (1929); *Chem. Abstr.*, **23**, 5432 (1929).

[2] R. Strobinger and L. von Zambory, *Z. analyt. Chem.*, **79**, 158 (1929); *Chem. Abstr.*, **24**, 569 (1930).

[3] J. S. Fritz and M. Q. Freeland, *Analyt. Chem.*, **26**, 1593 (1934).

[4] D. Ceauşescu, *Z. analyt. Chem.*, **183**, 39 (1961).

[5] C. Drăgulescu, T. Simonescu and R. Anton, *Studii şi Cercetări Şti. Chim., Baza Cercetări Sti. Chim., Timişoara*, **6**, 27 (1959).

[6] J. S. Fritz and S. S. Yamamura, *Analyt. Chem.*, **27**, 1461 (1955).

[7] J. S. Fritz, S. S. Yamamura and J. M. Richard, *Analyt. Chem.* **29**, 158 (1957).

Particularly important are some works of the last years in which one makes use of chromatropic acid bisazoderivates with the general formula [8-12]:

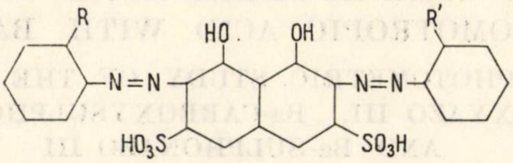

where R and R′ can be the acid groups: $-SO_3H$, $-COOH$, $-AsO_3H_2$, $-PO_3H_2$, etc. The general characteristic of these reactives lies in the fact that they form, in water-alcohol or water-acetone acid solutions, intensely coloured metallic complexes, in great contrast with the initial colour of the reactives.

The reactives containing the acid groups $-SO_3H$ and $-COOH$ show a high selectivity for the Ba^{2+} and Sr^{2+} ions. The following reactives have been actually used for the volumetric determination of the sulphates: Carboxyarsenazo III [the disodic salt of the 2-(2-carboxy-o-phenylazo)-7-(2-phenylarsenazo chromotropic acid], [13-15] Carboxysulphonazo III [the disodic salt of the 2-(2-sulphophenylazo)-7-(2-carboxyphenylazo) chromotropic acid] [16] and Carboxyazo III [the disodic salt of the 2,7-bis-(2-carboxyphenylazo) chromotropic acid]. [17, 18]

In order to increase the reaction capacity in more acid media one suggests reactives containing electrophilic substituents, to intensify the acid features of the hydrocyclic groups. Thus nitrochromazo, [19-21] the 2,7 bis-(4-nitro-2-sulphophenylazo) chromotropic acid, containing two $-NO_2$ groups in *para* position towards the azo group is proposed and employed.

All these reactives have been scarcely studied till now, the existing data of the literature having a rather informative character and referring especially to some practical uses in the dosage of sulphates. We therefore present in the present paper a systematic, qualitative and quantitative spectrophotometric study on three reactives with a high selectivity for

---

[8] S. B. Savvin, *Zhur. analit. Khim.*, **17**, 785 (1962).

[9] S. B. Savvin, *Analele româno-sovietice* (*Chimie*), **1963**, 103.

[10] A. A. Nemodruk, *Zhur. analit. Khim.*, **19**, 790 (1964).

[11] S. B. Savvin and Yu. M. Dedkov, *Zhur. analit. Khim.*, **17**, 43 (1962).

[12] S. B. Savvin and Yu. M. Dedkov, *Zhur. analit. Khim.*, **19**, 21 (1964).

[13] K. F. Novikova, N. N. Basargin and M. F. Tsiganova, *Zhur. analit. Khim.*, *16*, 348 (1961).

[14] A. A. Nagina and G. G. Kobyak, *Uch. Zap. Permsk. Gos. Univ.*, **25**, (2), (1963); *Chem. Abstr.*, **61**, 1611 a (1964).

[15] A. I. Busev, V. K. Akimov and S. I. Bragina, *Zhur. analit. Khim.*, **21** 817 (1966).

[16] Z. K. Karlova and N. B. Shibaeva, *Zhur. analit. Khim.*, **19**, 258 (1964).

[17] I. Dragusin, *Rev. Chim.* (*Bucarest*) **16**, 390 (1965).

[18] I. Dragusin and A. Gavriliuc, *Rev. Roumaine Chim.*, **12**, 1239 (1967).

[19] V. I. Kuznetov and N. N. Basargin, *Zavodskaya Lab.*, **31** (5), 538 (1965).

[20] N. N. Basargin and F. K. Novikova, *Zhur. analit. Khim.*, **21**, 473 (1966).

[21] N. N. Basargin and F. K. Novikova, *Zhur. analit. Khim.*, **22**, 394 (1967).

the Ba^{2+} ion, containing the groups $-COOH$ and $-SO_3H$: Carboxyazo III, Carboxysulphonazo III and Sulphonazo III.

EXPERIMENTAL

The spectrophotometric study of the three systems was carried out by means of a SPEXOL spectrophoto-colorimeter, always using 10 mm vats. The experiments were carried out in acid solutions of water-alcohol or water-acetone, the PH values being changed by adding hydrochloric acid. The concentration of the reactives in the solution was 1×10^{-5} M and of the barium chloride 1×10^{-4} M. The use of solutions of a different concentration, has been mentioned either in the text or in the respective tables and diagrams.

RESULTS AND DISCUSSIONS

In order to establish optimum working conditions a qualitative study of the systems has been carried out by considering the variation in the absorption with Ba^{2+} of the respective reactives and complexes according to the wavelength, pH and organic solvent content of the solution. The quantitative study of the three systems, has been further developed and the combining ratio, the degree and dissociation constant have been established.

Table 1 gives the formula of the three reactives under consideration.

Table 1

Chromotropic acid azoderivates and their formulas

No	Formula of the reactives	Usual name	Scientific name
1	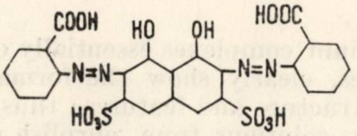	Carboxyazo III	2,7-bis(carboxyphenylazo) chromotropic acid
2	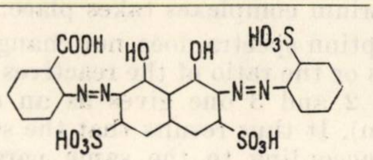	Carboxy-sulpho-nazo III	2-(2-sulphophenylazo)-7-(2-carboxyphenylazo) chromotropic acid
3	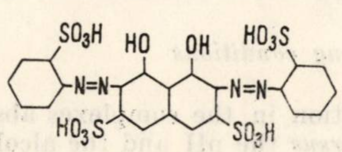	Sulpho-nazo III	2,7-bis(2-sulphophenylazo) chromotropic acid

1. *Absorption spectra*

As shown in fig. 1, the absorption spectra in the visible range $\lambda = 500-720$ nm of the acid solutions of the reactives in water-alcohol present two maxima around the values $\lambda_1 = 570$ nm and $\lambda_2 = 625$ nm, the latter one being less marked. The absorption spectra of the respective complexes with barium also show two maxima, both clearly marked and much shifted towards higher values of the wavelength.

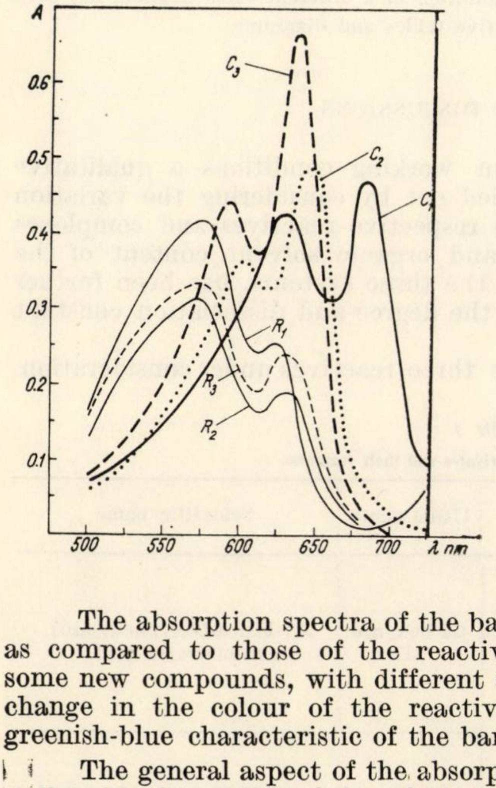

Fig. 1. — Absorption spectra of the barium complexes (C) and of the reactives (R); *1*, Ba-Carboxyazo III, 75% alcohol-water solution; pH = 2.55; *2*, Ba-Carboxysulphonazo III, 75% alcohol-water solution; pH = 2.55; *3*, Ba-Sulphonazo III, 60% alcohol-water solution, pH = 2.0.

The absorption spectra of the barium complexes essentially changed as compared to those of the reactives, clearly show the formation of some new compounds, with different structure and features; thus a clear change in the colour of the reactives solutions from purplish-pink to greenish-blue characteristic of the barium complexes takes place.

The general aspect of the absorption spectra does not change essentially with the acidity of the solutions or the ratio of the reactives concentration to the Ba^{2+} ion. (In figures 2 and 3 one gives as an example the Ba-Carboxysulphonazo III system). It thus results that the structure of the complexes does not change according to the same parameters.

2. *Optimum working conditions*

Figures 4 and 5 show the variation in the complexes absorbance for the solutions of the reactives (A) *versus* the pH and the alcohol concentration in the solution. According to these diagrams one has established the optimum working conditions, as shown in table 2.

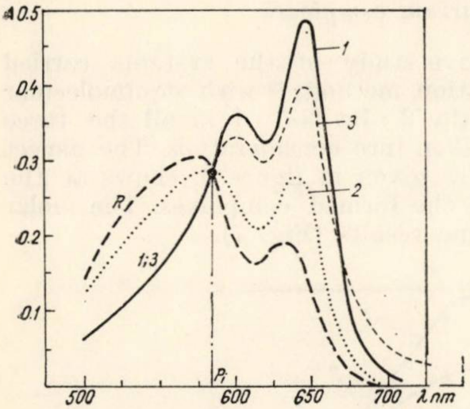

Fig. 2. — Variation of the absorption spectrum of the Ba-Carboxysulphonazo III complex *versus* the pH; 75% alcohol-water solution

1, pH = 1.8 to 3; *2*, –pH = 1.0; *3*, –pH = 3.5.

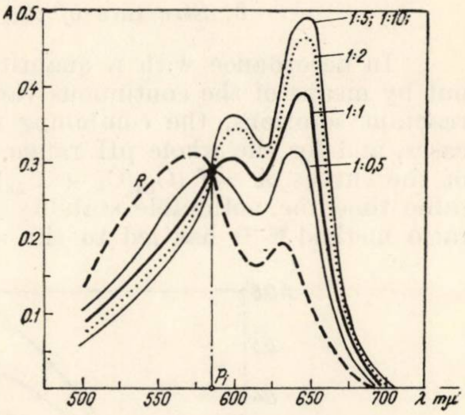

Fig. 3. — Variation of the absorption spectrum of the Ba-Carboxysulphonazo III complex *versus* the reactive : Ba^{2+} ratio (R : Ba); 75% alcohol in water solution; pH = 2.3.

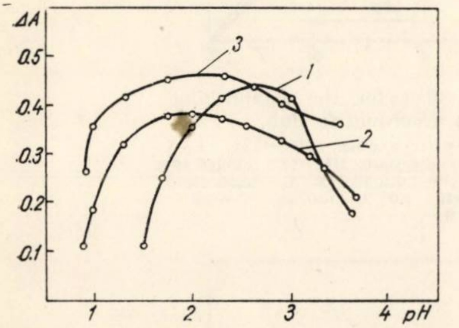

Fig. 4. — Variation of the absorbance of the complexes *versus* the pH; $\Delta A = A_{RBa} - A_R$.

1, Ba-Carboxyazo III; 75% solution of alcohol in water; λ = 680 nm; *2*, Ba-Carboxysulphonazo III; 75% alcohol in water solution; λ = 645 nm; *3*, Ba-Sulphonazo III; 60% alcohol in water solution; λ = 640 nm.

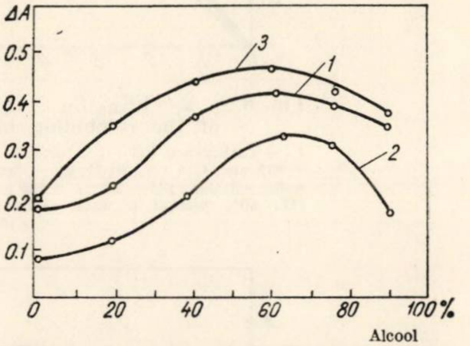

Fig. 5. — Variation of the absorbance of the complexes *versus* the concentration of the alcohol in the solution $\Delta A = A_{RBa} - A_R$.
1, Ba-Carboxyazo III; λ = 680 nm; $C_{HCl} = 4 \times 10^{-3}$M. *2*, Ba-Carboxysulphonazo III; λ = 645 nm; $C_{HCl} = 4 \times 10^{-3}$ M. *3*, Ba-Sulphonazo III; λ = 640 nm; $C_{HCl} = 6.6 \times 10^{-2}$ M.

Table 2

Optimum working conditions

No	Reactive	λ nm	Optimum conditions		Colour of the solutions	
			pH	Alcohol %	Reactive	Ba-complex
1	Carboxyazo III	685	2.0–3.0	50–75	Pink-carmine	Greenish-blue
2	Carboxysulphonazo III	645	1.5–2.5	60–75	Purplish-violet	Ibid.
3	Sulphonazo III	640	1.3–2.5	50–60	Ibid.	Ibid.

3. *Structure of the barium complexes*

In accordance with a quantitative study of the systems carried out by means of the continuous variation method, [22] with equimolecular reactant solutions, the combining ratio R : Ba is 1 : 1 in all the three cases, and for the whole pH range taken into consideration. The aspect of the curves $A = f\ (C_{Ba}/C_R + C_{Ba})$, as given in figure 6, shows at the same time the noticeable stability of the formed complexes. The molar ratio method [23–25] has led to the same results (Fig. 7).

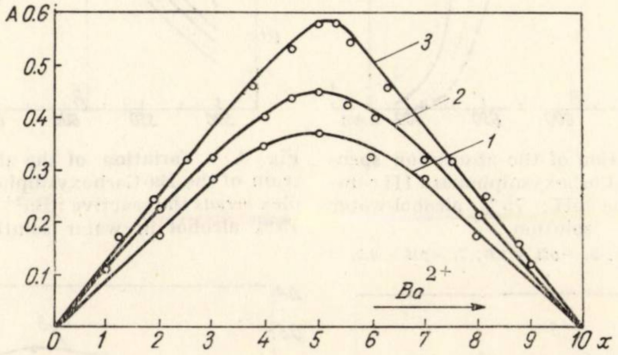

Fig. 6. — $A = f(C_{Ba}/C_R + C_{Ba})$ curves for the establishing of the combining ratio according to Job.

1, — Carboxyazo III; 75% alcohol in water solution, pH = 2.55; $\lambda = 675$ nm; $C = 1 \times 10^5$ M. *2*, — Carboxysulphonazo III: 75% alcohol in water solution, pH = 2.3; $\lambda = 645$ nm; $C = 1.6 \times 10^{-5}$ M. *3*, — Sulphonazo III; 60% alcohol in water solution; pH = 2.0; $\lambda = 640$ nm; $C = 1.6 \times 10^{-5}$ M.

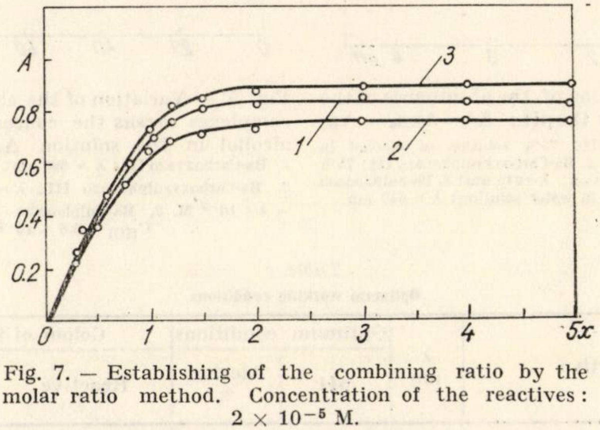

Fig. 7. — Establishing of the combining ratio by the molar ratio method. Concentration of the reactives: 2×10^{-5} M.

1, Carboxyazo III; 75% alcohol in water solution; pH = 2.55. *2*, Carboxysulphonazo III; 75% alcohol in water solution; pH = 2.55. *3*, Sulphonazo III; 60% alcohol in water solution; pH = 1.7.

---

[22] P. Job, *Ann. Chim.* (*France*), **9**, 113 (1928).

[23] Y. A. Yoe and L. A. Jones, *Ind. Eng. Chem., Anal. Ed.*, **16**, 111 (1944).

[24] Y. A. Yoe and A. E. Harvey, *J. Amer. Chem. Soc.*, **70**, 648 (1943).

[25] P. Spacu and M. Mavrodin, *Rev. Roumaine Chim.*, **12**, 1223 (1967).

The fact that the combination ratio R : Ba is 1 : 1, led us to the conclusion that only half of the reactives molecule could have taken part in the formation of the complexes. As Savvin[8] and Nemodruk[10] have shown in the case of several Me-Arsenazo III systems, the lack in the reaction capacity of the other half of the molecule of the reactive could be assigned to the migration of the H^+ ion of the $-OH$ groups to the second nitrogen atom. Thus half of the reactive molecule passes from the azoic to the quinonehydrazonic form under the influence of the positive field of the complexly bound[10] central ion.

Similarly, in the case of the Ba-Sulphonazo III system, the formulation of the structure in accordance with this hypothesis would be :

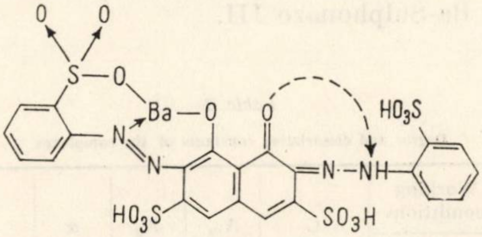

This structure would be in agreement with the peculiar aspect of the absorption spectra, the first maximum being assigned to the formation of the complexes and the second to the existence of the quinonehydrazonic form,[8] as shown in the case of the Me-Arsenazo III complexes.[8,10]

The fact that the monoazoderivates such as thorin and its analogues form compounds with a smaller stability and contrast, when absorption spectra show only one maximum, advocates for the assignment of the above structure, in the case of the bisazoderivates, to the chromotropic acid.

The existence of the isosbestic points (P_i) for the family of the absorption spectra for various values of the pH (fig. 2) or of the R : Ba ratio of reactants (fig. 3), is also explained by the assigned structure, and is due to the existence in the same molecule of the two chromophore groups : the complexly bound azo group and the quinonehydrazonic one.

This phenomenon was also studied by Nemodruk[10] in the case of the above Me-Arsenazo III systems.

4. *Stability of the complexes*

The degree and dissociation constants of the complexes were determined by the Harvey and Manning[25-28] method, by measuring the absorbance of the stoichiometric mixtures of reactants (A_s) and of those mixtures containing a great excess of Ba^{2+} ions so that the equilibrium

---

[26] A. E. HARVEY and D. L. MANNING, *J. Amer. Chem. Soc.*, **72**, 4448 (1950).
[27] A. E. HARVEY and D. L. MANNING, *J. Amer. Chem. Soc.*, **74**, 4744 (1952).
[28] K. A. MAJUMDAR and P. C. SAVARIAN, *Analyt. Chim. Acta*, **21**, 47 (1959).

be displaced in such a way as to make the formed compound practically undissociated (A_m). Table 3 shows the astonishing stability of the compounds in water-alcohol acid solutions.

In order to obtain results which might be used as an estimation basis of the three reactives, one has made a comparative study of the stability variation of the compounds as a function of the pH and the alcohol content of the solution. The data listed in tables 4 and 5, show that the stability of the compounds increases noticeably with the pH and the concentration in organic solvent, in the same conditions the values increasing in the following order : Ba-Carboxyazo III $<$ Ba-Carboxysulphonazo III $<$ Ba-Sulphonazo III.

Table 3

Degree and dissociation constants of the complexes

No	Complex	λ nm	Working conditions		C mole/l	A_m	A_s	α	K	K_m
			pH	Alcohol %						
1	Ba-Carboxyazo III	685	2.55	75	2×10^{-5}	0.940	0.700	0.259	1.81×10^{-6}	
					1.6×10^{-5}	0.755	0.550	0.266	0.96×10^{-6}	1.36×10^{-6}
					1×10^{-5}	0.465	0.330	0.290	1.32×10^{-6}	
2	Ba-Carboxysulphonazo III	645	2.3	75	2×10^{-5}	0.675	0.570	0.155	5.68×10^{-7}	
					1.6×10^{-5}	0.540	0.450	0.166	5.27×10^{-7}	5.71×10^{-7}
					1×10^{-5}	0.340	0.265	0.220	6.20×10^{-7}	
3	Ba-Sulphonazo III	640	2.0	60	1.6×10^{-5}	0.690	0.580	0.159	4.81×10^{-7}	
					1.2×10^{-5}	0.505	0.415	0.178	4.62×10^{-7}	4.98×10^{-7}
					1×10^{-5}	0.430	0.340	0.209	5.52×10^{-7}	

Table 4

Variation in the stability of the complexes *versus* pH

No	Complex	λ nm	Alcohol %	K *versus* pH				
				1.7	2.0	2.3	2.55	2.9
1	Ba-Carboxyazo III	685	75	—	5.44×10^{-5}	8.23×10^{-6}	1.81×10^{-6}	7.57×10^{-7}
2	Ba-Carboxysulphonazo III	645	75	1.16×10^{-5}	2.54×10^{-6}	5.27×10^{-7}	1.63×10^{-7}	5.50×10^{-8}
3	Ba-Sulphonazo III	640	60	2.21×10^{-6}	5.52×10^{-7}	8.69×10^{-8}	3.17×10^{-8}	—

Table 5

Variation in the stability of the complexes *versus* the alcohol content of the solution

No	Complex	λ nm	Concentration in HCl mole/l	K *versus* alcohol, %		
				40	60	75
1	Ba-Carboxyazo III	685	4×10^{-3}	4.64×10^{-4}	6.38×10^{-5}	1.81×10^{-6}
2	Ba-Carboxysulphonazo III	645	2×10^{-3}	3.32×10^{-5}	1.54×10^{-6}	5.50×10^{-8}
3	Ba-Sulphonazo III	640	8×10^{-3}	1.74×10^{-6}	8.69×10^{-8}	5.90×10^{-9}

CONCLUSIONS

The spectrophotometric study of the Ba-Carboxyazo III, Ba-Carboxysulphonazo III and Ba-Sulphonazo III systems in acid water-alcohol and water-acetone solutions has been carried out.

Owing to the presence of $-SO_3H$ and $-COOH$ acid groups in *ortho* position towards the azo groups, the purplish-pink solutions form with barium greenish-blue complexes, with a remarkable stability and a R : Ba ratio of 1 : 1.

Only one azo group is supposed to participate in the formation of the complexes, the other half of the reactive molecule passing into the quinonehydrozonic form. This hypothesis accounts for the peculiar aspect of the absorption spectra, which present two absorption maxima in the visible range, a great sensitivity and contrast as well as a high stability of the formed complexes.

The stability of the complexes increases with the pH and the organic solvent content of the solution, and in the same conditions with the nature of the reactive: Ba-Carboxyazo III $<$ Ba-Carboxysulphonazo III $<$ $<$ Ba-Sulphonazo III.

The optimum working conditions vary between 1.3 to 3 for the pH and 50 to 75% for the organic solvent function of the compounds stability.

For mean values of the pH the dissociation constant range from 10^{-6} to 10^{-8}.

Revue Roumaine de Chimie, **14**, 1377–1386 (1969)

KOMPLEXVERBINDUNGEN DES N,N′-DIAMINOPIPERAZINS. IV INFRAROTSPEKTREN. ELEKTRONENSPINREZONANZ

J. DICK und ALFA LUPEA

aus dem Pharmazeutisch-Technischen Laboratorium der Technischen Hochschule
Timişoara, Bd. 30 Decembrie 2

Eingegangen am 8. November 1968

Es werden die Infrarotspektren im Bereiche 4000–400 cm^{-1} des N,N′-Diaminopiperazins (DAP) als solches und der DAP-Komplexverbindungen mit Co^{2+}, Ni^{2+}, Cd^{2+}, Zn^{2+}, Mn^{2+}, Fe^{2+}, Cu_2^{2+}, Pd^{2+}, Hg^{2+}, Pt^{2+}, Pt^{4+}, Bi^{3+}, Cr^{3+} und Th^{4+} und den Anionen SCN^-, Cl^-, Br^- und J^- zwecks Strukturaufklärung untersucht. Die bereits in Mitteilungen 1 und 2 angegebenen vermutlichen und in Mitteilung 3 bestätigten Komplextypen von Chelatverbindungen einerseits und Salze komplexer Anionen anderseits konnten auch an Hand der IR-Spektren bestätigt werden. Auch ESR wurden ermittelt. In beiden Komplextypen verhält sich DAP als ein zweizähliger Ligand. Der Verbindungstyp $[Me^{II}DapX_2]$ bildet sich durch die Koordinierung der Ringstickstoffatome, während in den Verbindungen mit komplexen Anionen des Typs $[Me^{II-III}X_n](H_2Dap)_n$ das exocyklische N-Atom als Protonträger erscheint. In den Thyocyan-DAP-Verbindungen wird die NCS-Gruppe in einigen Verbindungen durch das N-Atom, in anderen wieder durch das S-Atom koordiniert.

In den Mitteilungen 1–3 haben wir Komplexverbindungen eines bis jetzt als Elektronenspender unbekannten Diamins, des N, N′-Diaminopiperazins (DAP) beschrieben. An Hand der Analyse und des thermischen Abbaus (Mitt. 1–2) wurden zwei Haupttypen der erhaltenen Komplexverbindungen vermutet die durch sichtbare und UV-Spektren bestätigt werden konnten (Mitt. 3) Die Infrarotspektren über die wir in vorliegender Mitteilung berichten, sollen einen weiteren Beitrag zu ihrer Strukturaufklärung bringen. Auch ESR wurden ermittelt. Der größte Teil der Verbindungen, wie auch die freie Base DAP wurde auf ihre IR-Spektren untersucht.

A. FREIE BASE UND SALZE MIT KOMPLEXEN ANIONEN

Das Infrarotspektrum der freien Base DAP wurde zwecks Auswertung der Spektren der Komplexverbindungen untersucht. Im DAP-IR-Spektrum konnten die N-H-Valenzschwingungen durch eine Gruppe der Banden im Bereich von 3400—3120 cm^{-1} nachgewiesen werden. Dieser Bereich entspricht im allgemeinen den Valenzschwingungen N—H [1-4] und wurde auch für das Hydrazin und seine Methylderivate erkannt. [5-7] Die Banden 3180 und 3120 cm^{-1} entsprechen zweifellos einer Assoziation, dagegen vertreten jene mit höherer Wellenzahl der Schwingungen die freien oder viel schwächer assoziierten NH_2-Gruppen. Durch Protonierung verschwindet die Gruppe der oben angegebenen Banden und es erscheinen zwei andere, mit viel geringeren Frequenzen und zwar 2600—2700 cm^{-1} und 2950—3090 cm^{-1}. Letztere entsprechen jenen allgemein bekannten Wellenzahlen der primären Ammoniumsalze, in denen die Protonierung des Stickstoffatoms einen bedeutenden Abfall der Wellenzahl der Schwingungen N—H verursacht. [8-11]

All das läßt darauf schließen, daß die Protonierung an dem außerhalb des Piperazinrings befindlichen Stickstoffatom stattfindet.

Die charakteristischen Knickschwingungen $-NH_2$ der Amine [1-4] und Hydrazine [5-7] im Bereich von 1600 cm^{-1} werden bei DAP in der Form eines Dubletts mit der Wellenzahl 1630—1640 cm^{-1} beobachtet. Bekanntlich führt der Übergang der NH_2-Gruppe in die NH_3^+-Gruppe zu zwei charakteristischen Banden symmetrischer Deformationsschwingungen im Bereich von 1580—1600 cm^{-1}, wie auch zu antisymmetrischen in Bereich von 1500—1540 cm^{-1}. Tatsächlich können in den Verbindungen der Salze komplexer Anionen $[Me^{II-III}X_n](H_2Dap)_n$ (Mitteilung 2) zwei gut ausgeprägte Banden in diesem Bereich beobachtet werden. Es können gleichzeitig die Schaukelschwingungen $-NH_3^+$ im Bereich von 1160—1190 cm^{-1} beobachtet werden. [8,9] Es wird also auch auf diesem Wege die Protonierung des exocyklischen N-Atoms bestätigt.

Im DAP-Spektrum wird die gut ausgeprägte Bande bei 1120 cm^{-1} den Valenzschwingungen C—N zugeschrieben ; sie befindet sich in einem Bereich der im allgemeinen der Schwingungen der C—N-Gruppe entspricht und in unserem Fall von besonderer Intensität ist. [1-4] Diese Bande konnte auch in den Verbindungen mit komplexen Anionen des DAP bei einer etwas niedrigeren Frequenz im Bereich von 1080—1095 cm^{-1} aufgefunden werden, eine Tatsache die übrigens mit Literaturangaben gut übereinstimmt. [8,9]

---

[1] C. N. R. Rao, ,,Chemical Applications of Infrared Spectroscopy'', Academic Press, New York, 1863, S. 245.

[2] I. J. Bellamiy, ,,The Infrared Spectra of Complex Molecules'' Methuen et Co., London, 1960, S. 248.

[3] M. Avram und G. D. Mateescu, ,,Spectroscopia în infraroşu, aplicaţii în chimia organică'', Bukarest, Editura tehnică, 1966, S. 376.

[4] N. B. Colthup, L. H. Daly und S. E. Wiberley, ,,Introduction to Infrared and Raman Spectroscopy, Academic Press, New York, 1964, S. 278.

[5] P. A. Giguere und T. D. Liu, *J. Chem. Phys.*, **20**, 136 (1952).

[6] A. Shull, H. Word, I. Aston und M. Rank, *J. Chem. Phys.*, **22**, 1191 (1954).

[7] E. Catalano, R. H. Sanborn und J. W. Frazer, *J. Chem. Phys.*, **38**, 2265 (1963).

[8] J. Bellanoto und J. R. Barcelo, *Annales real espan fiz. y quim*, **52**, 469 (1956).

[9] R. D. Waldron, *J. Chem. Phys.*, **21**, 734 (1953).

[10] B. Shenon und C. Sandorfy, *Canad. J. Chem.*, **36**, 1181 (1958).

[11] C. Brissette und C. Sandorfy, *Canad. J. Chem.*, **38**, 74 (1960).

Tabelle 1

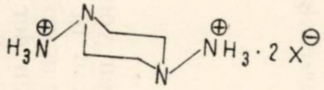

Verbindung	$-NH_3^{\oplus}$					ν_{C-H}	$-CH_2-$						Gerüst-schwin-gungen
	$\nu_{-NH_3^{\oplus}}$		$\delta_{-NH_3^{\oplus}}$				ν_{-CH_2}		δ_{-CH_2}				
	s	*as*	*s*	*as*	γ		*s*	*as*	$\delta_{-CH_{2s}}$	$\delta_{-CH_{2t}}$	$\delta_{-CH_{2w}}$	$\gamma_{-CH_{2r}}$	
$[Co(SCN)_4]H_2Dap$	2680	2980	1530	1620	1180*	1095	2900 2860	2920	1460	1290 1320	930	1390	990 1070
$[Zn(SCN)_4]H_2Dap.2H_2O$	2700	3000	1530	1590	1180	1080	2860	2960	1460	1290 1310	930	1390	990 1060
$[Hg(SCN)_4]H_2Dap$	2600	2900	1540	1610	1180	1095	2860 2845	2920	1460	1300 1320	930	1380	990 1070
$[HgCl_4]H_2Dap$	2670	3090	1520	1580	1160	1090	2900 2860	2980 2940	1460 1450	1290 1310	920	1380	990 1060
$[HgJ_4]H_2Dap$	2660	3095	1520	1570	1160	1090	2910 2865	2980 2950	1460	1290 1305	915	1390	990 1080
$[PtCl_4]H_2Dap$	2650	3050	1505	1580	1160 1180	1090	2900 2860	2990 2950	1460 1450	1290 1310	930	1380	990 1060
$[Pt(SCN)_4]H_2Dap$	2680	2950	1530	1620	1190	1095	2900 2860	2930	1460	1300 1320	950	1390	990 1070

* überdeckt

In Abb. 1 ist das Infrarotspektrum des DAP und als Beispiel das Spektrum von zwei Verbindungen mit komplexem Anion vorzufinden (Mitteilung 2).

In Tabelle 1 sind die entsprechenden Daten zusammengefaßt. Sie enthält einschließlich auch die charakteristischen Daten der Banden der Valenz- und Deformationsschwingungen der CH_2-Gruppe in einem übrigens wohlbekannten Bereich. [1-4]

Bemerkenswert ist die Tatsache, daß die Valenzschwingungen der CH_2-Gruppe im DAP u.zw. sowohl die symmetrischen als auch die antisymmetrischen in der Form von Dubletten im Bereich von 2830—2900 bzw. 2960—2940 cm^{-1} erscheinen. Diese Dubletten sind in ähnlichem Bereich auch in den Salzen mit komplexen Anionen des DAP nachweisbar.

Die Knickschwingungen der CH_2-Gruppe, wie auch die Gerüstschwingungen wurden in einem Bereich nachgewiesen, der den gesättigten Sechsringen entspricht wie: Piperazin, [12] Cyclohexan, Piperidin, Tetrahydropyran, [13] 1,4-Dioxan [14] u.a. Bei der Auswertung der entsprechenden Schwingungen müssen natürlich immer — angesichts der stets vorhandenen Schwierigkeiten der Bereichsauswertung in dem sie erscheinen — entsprechende Reserven vorbehalten werden.

B. DAP-CHELATVERBINDUNGEN

Bei der Auswertung der IR-Spektren der Verbindungen vom Typ $[Me^{II}DapX_2)$ (1 Mitteilung) ist zunächst zu beobachten, daß in ihnen die Banden des DAP fast unverändert aufzufinden sind. Nur in geringem Maße erscheinen die Valenz- und Deformationsschwingungen der NH_2-Gruppe verschoben, wie auch die Valenzschwingungen C—N. Hätte die Koordinierung des Metalls durch den exocyklischen Stickstoff stattgefunden, so müßte die positive Ladung desselben in den charakteristischen Banden der NH_2-Gruppe weitgehende Veränderungen verursachen, Veränderungen im Sinne der Banden, die in den Verbindungen $[Me^{II-III}X_4]$ $(H_2Dap)_n$ erscheinen.

Der einzig mögliche Weg der Komplexierung ohne das Spektrum weitgehend zu beeinflussen ist zweifellos jener, der über das innercyklische N-Atom als Protonträger führt. Diese Koordinierung muß natürlich einen gewissen — wenn auch geringfügigen — Einfluß auf die Schwingungen der benachbarten Gruppen NH_2 und C—N haben, wie übrigens oben erwähnt wurde.

Aus allen Beobachtungen kann darauf gefolgert werden, daß bei der Komplexbildung vom Typ $[MeDapX_2]$ das Diamin eine Wannenform annimmt und als ein zweizähliger Ligand betrachtet werden muß:

---

[12] P. J. HENDRA und D. B. POWELL, *Spectrochim. Acta*, **18**, 299 (1962).

[13] H. WOETTER und H. TSCHAMLER, *Monatsh. Chem.*, **89**, 104 (1953).

[14] P. E. MAHERBE und H. I. BERNSTEIN, *J. Amer. Chem. Soc.*, **74**, 4408 (1952).

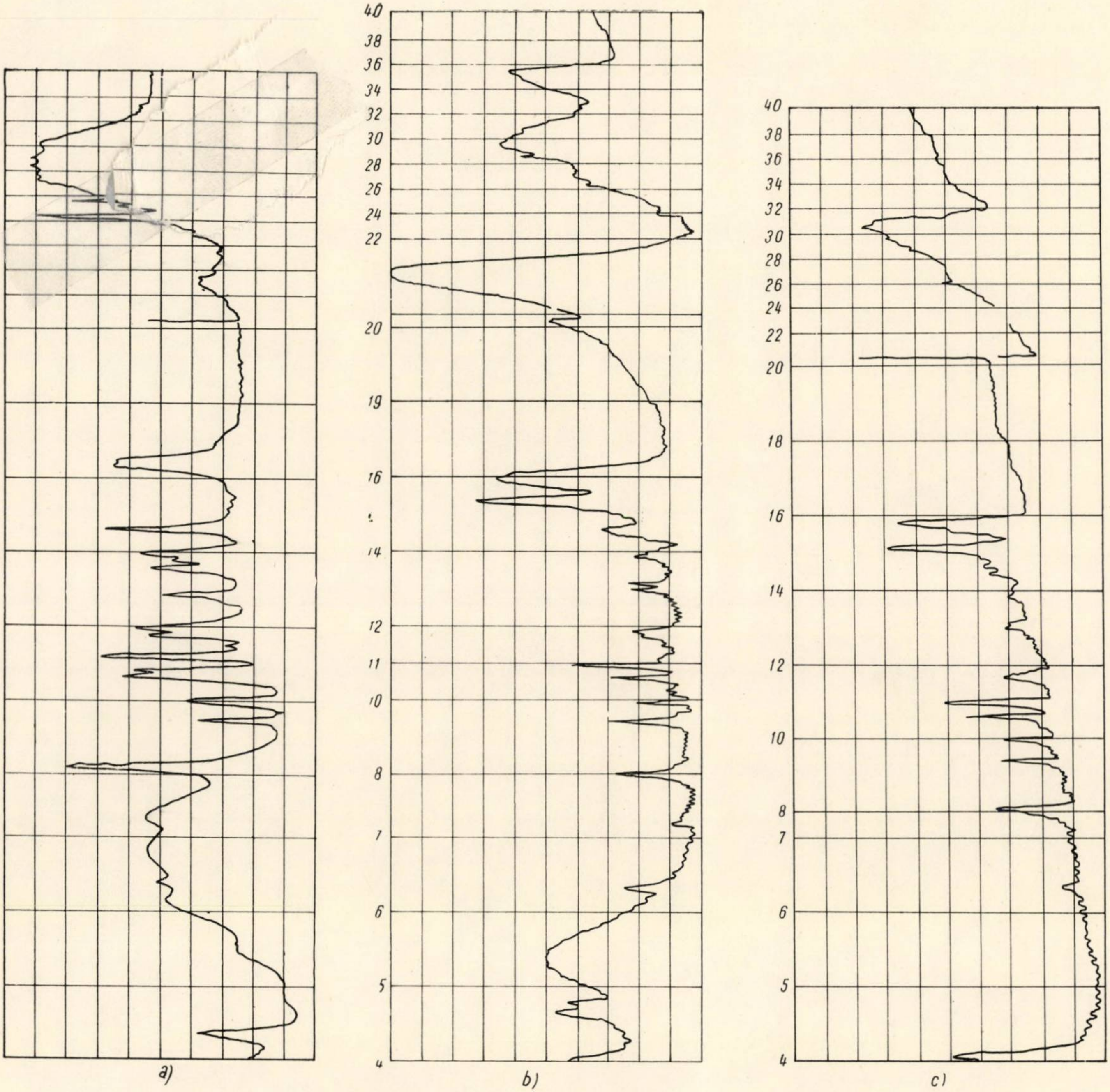

a) b) c)

Abb. 1. – IR-Spektren : *a*) DAP ; *b*) $[Zn(SCN)_4]H_2Dap$; *c*) $[HgCl_4]H_2Dap$.

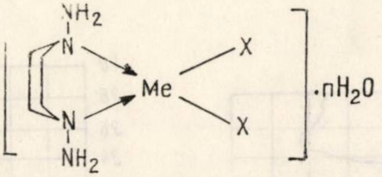

Die Stabilität der Verbindungen stimmt mit dem Vorhandensein eines Chelatfünfringes gut überein, zumal sie auch gesättigt sind.[15] Im übrigen stimmt diese Annahme mit dem Verhalten des Piperazins und seiner methylierten Derivate in seinen Komplexverbindungen gut überein.[16, 17] Bei 1,4-Dimethylpiperazin kommen, wie bekannt auch sterische Störungen in Betracht.[18]

In Abb. 2 sind IR-Spektren des Verbindungstyps [$MeDapX_2$] ohne und mit Wassergehalt als Beispiel wiedergegeben.

In Tabelle 2 sind die Befunde der Spektren der Chelatverbindungen der allgemeinen Formel [$Me^{II}DapX_2$] zusammengefaßt.

C. WASSERGEHALT DER SALZE MIT KOMPLEXEN ANIONEN UND DER CHELATVERBINDUNGEN

Mehrere beider Verbindungstypen enthalten eine Anzahl von Wassermolekülen. Aus Tabelle 3 sind die Schwingungen des Wassers dieser Verbindungen zu entnehmen.[19] Wie ersichtlich, befinden sich die Valenzschwingungen O—H wie auch die Knickschwingungen in dem entsprechenden Bereich von Kristallisations- oder schwach komplexiertem Wasser.[20]

D. DIE THIOCYANGRUPPEN

Ein Großteil der Verbindungen enthält als Anion Thiocyangruppen, die als komplexe Anionen, oder in der Form von Chelatringen dem Metall zugeordnet sind.

Das NCS-Ion erscheint in drei Grundschwingungen:

$\nu_1(\Sigma) = 2055\ cm^{-1}$ (Valenzschwingungen C=N, oder antisymmetrische N=C=S)

$\nu_3(\Sigma) = 749\ cm^{-1}$ (Valenzschwingungen C—S oder symmetrische N=C=S)

$\nu_2(\pi) = 475\ cm^{-1}$ (Knickschwingungen N=C=S).[21, 22]

---

[15] P. Pfeiffer und Z. Buchholz, *J. prakt. Chem.*, **124**, 133 (1930).

[16] F. G. Mann und H. R. Watson, *J. Chem. Soc.*, **1958**, 2772.

[17] P. J. Stone, J. C. Craig und H. W. Thompson, *J. Chem. Soc.*, **1958**, 52.

[18] R. D. Gilard und H. M. Irving, *Chem. Rev.*, **65**, 603 (1965).

[19] J. H. Hibben, *J. Chem. Phys.*, **5**, 166 (1937).

[20] K. Nakamoto "Infrared Spectra of Inorganic and Coordination Compounds" John Wiley and sons, New York, 1963, S. 246.

[21] C. H. Jones, *J. Chem. Phys.*, **25**, 1069 (1956).

[22] A. Trammer, *J. Chim. phys.*, **59**, 232 (1962).

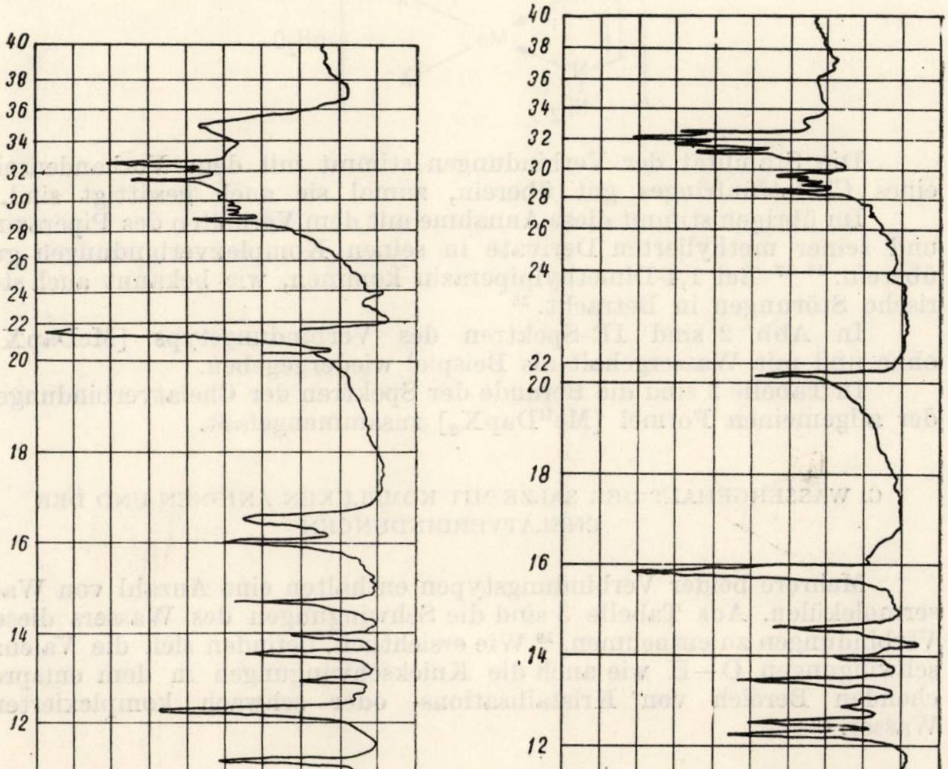

Abb. 2. — IR-Spektren *a*) [NiDap(SCN)$_2$] . 2H$_2$O ; *b*) [ZnDap(SCN)$_2$].

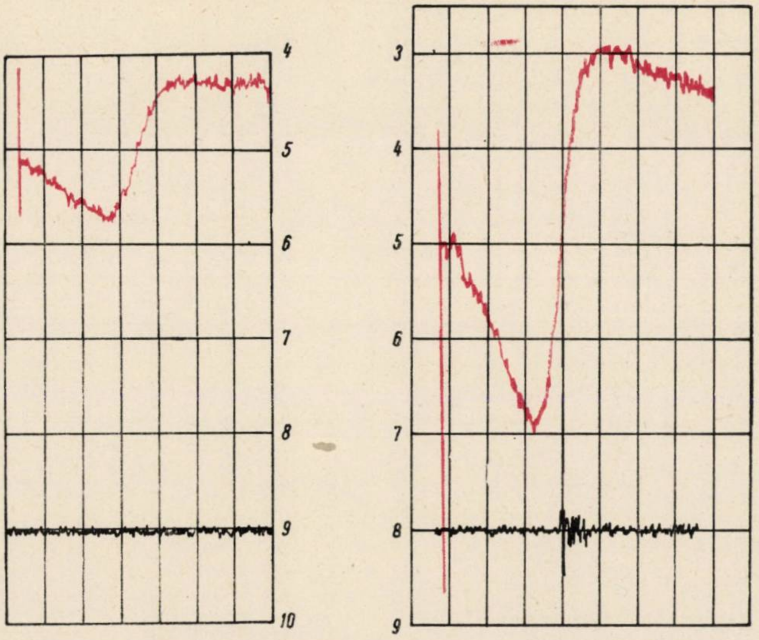

Abb. 3. — ESR-[MbDap(SCN)$_2$]·2H$_2$O innere und äußere Batterie.

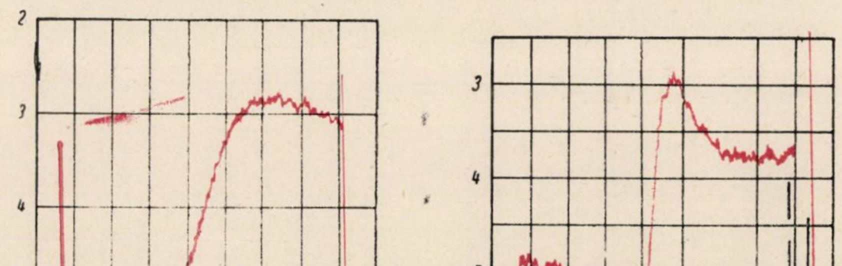

Abb. 4. — ESR-[Cr(SCN)$_4$](HDap)$_2$ innere und äußere Batterie.

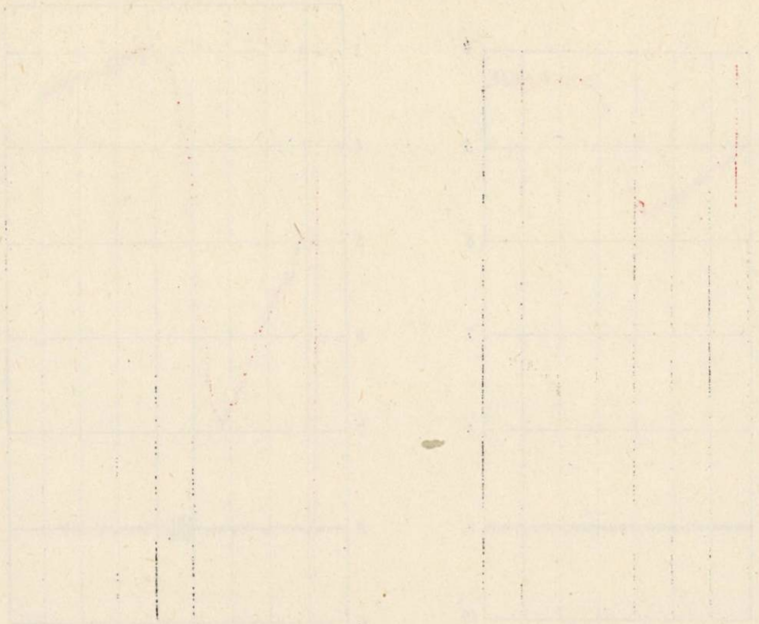

Abb. 3. — ESR [illegible] innere und äußere Satellite.

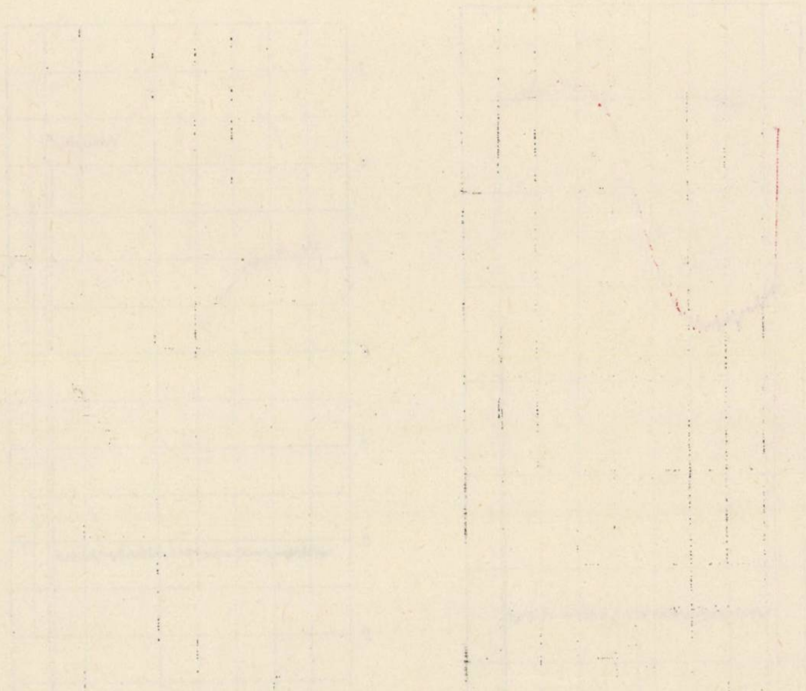

Abb. 4. — ESR [illegible] innere und äußere Satellite.

Tabelle 2

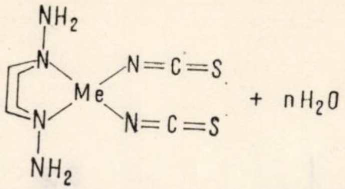

Verbindung	$-NH_2$					ν_{CN}	$-CH_2-$						Gerüstschwingungen
	ν_{-NH_2}			δ_{-NH_2}			ν_{CH_2}		δ_{-CH_2}				
				$\delta_{-NH_{2r}}$	γ_{-CH_2}		s	as	$\delta_{-CH_{2s}}$	$\delta_{-CH_{2t}}$	$\delta_{-CH_{2w}}$	$\gamma_{-CH_{2r}}$	
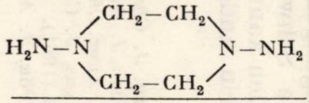	3400 3180	3280 3120	3240	820	1640 1630	1120	2900 2830	2960 2940	1460	1280	1350	940	1000 1070 1080
$[CoDap(SCN)_2] \cdot 2H_2O$	3145	3250 3100	3200	800	1600	1120 1220	2910 2880	2940 2940	1460	1290	1350	940	1000 1070 1080
$[NiDap(SCN)_2] \cdot 2H_2O$	3145	3250	3200	805	1600	1120 1230	2905 2880	2970 2940	1460	1290	1350	940	990 1070 1080
$[CdDap(SCN)_2]$	3150	3250 3140	3215	770	1600	1210	2900 2860 2880	2960 2940	1460	1230	1330	930	990 1070 1080
$[ZnDap(SCN)_2]$	3180	3240 3120	3210	830	1580	1230 1120	2900 2860	2960 2940	1460	1230	1340	960	1000 1070 1080
$[MnDap(SCN)_2] \cdot 2H_2O$	3125	3260 3100	3210	800	1605	1120 1215	2910 2880	2960 2940	1460	1290	1350	940	1000 1070 1080
$[FeDap(SCN)_2] \cdot 2H_2O$	3130	3245	3205	800	1600	1120 1220	2910 2880	2970 2930	1460	1290	1350	930	990 1070 1080
$[PdDapBr_2] \cdot 2H_2O$	3150	3050		795	1590	1120 1220	2850	2980 2935	1460	1280	1320	**	990 1040
$[PdDapCl_2] \cdot 4H_2O$	3120	3020		790	1590	1120 1225	2850	2980	1460	1280	1330	**	990 1040

** überschattet

In den Verbindungen $[Me^{II}DapX_2]$ kann die NCS-Gruppe entweder durch das N-Atom, oder durch das S-Atom bzw. sogar gleichzeitig durch beide an der Komplexbildung teilnehmen, das heißt durch Brükkenbildung zwischen zwei Metallionen. [22–27]

Aus den angeführten Daten geht hervor, daß in den besprochenen Verbindungen keine SCN-Ionen erscheinen. Wie im allgemeinen angenommen wird, bestimmt die Koordinierung der SCN-Gruppe durch das S-Atom ein Ansteigen der Wellenzahl der antisymmetrischen Schwingungen dieser Gruppe und einen Abfall der Frequenz für die symmetrischen Schwingungen.

Der Tabelle 3 sind die diesbezüglichen Daten zu entnehmen.

Tabelle 3

Schwingungen des Wassers und die Grundschwingungen der Thiocyangruppe der Chelatverbindungen und der Salze mit komplexen Anionen

Verbindung	H_2O		$-N=C=S$		
	δ_{OH}	ν_{OH}	ν_s	ν_{as}	δ_{SCN}
$[CoDap(SCN)_2].2H_2O$	1660	3480	830	2110	470
$[NiDap(SCN)_2].2H_2O$	1660	3500	830	2120	470
$[CdDap(SCN)_2]$	—	—	780	2120	450
$[ZnDap(SCN)_2]$	—	—	820	?**	480
$[MnDap(SCN)_2].2H_2O$	1650	3520	830	2090	470
$[FeDap(SCN)_2].2H_2O$	1650	3500	830	2090	470
$[PdDapBr_2].2H_2O$	1600	3420	—	—	—
$[PdDapCl_2].4H_2O$	1590	3420	—	—	—
$[Co(SCN)_4]H_2Dap$	—	—	805	2050	490
$[Zn(SCN)_4]H_2Dap$	1595	3550	805	2120	470 480
$[Hg(SCN)_4H_2Dap$	—	—	795	2110 2120	440 455
$[Pt(SCN)_4]H_2Dap$	—	—	805	2120	490

** übeschattet

Prüft man diese Daten so ergibt sich, daß eine Koordinierung durch das S-Atom im Falle der Verbindungen des Hg und Cd und zwar in beiden Komplextypen angenommen werden kann. Dagegen findet die Koordinierung im Falle der Komplexsalze des Zn und Co sowie in den Chelatverbindungen $[MeDapX_2]$ des Co, Ni, Fe, Mn und Zn durch das N-Atom statt. Im Falle des komplexen Anions $[Pt(SCN)_4]^{-2}$ erscheinen zwei Banden für symmetrische Schwingungen bei 760 und 805 cm^{-1} und weitere zwei für antisymmetrische Schwingungen bei 2120 cm^{-1} und 2060 cm^{-1}, was dahin gedeutet werden kann, daß ein Teil der Thiocyangruppen durch das S-Atom und ein anderer durch das N-Atom koordiniert wird. [17, 28]

---

[23] J. Lewis, R. S. Nyholm und P. W. Smith, *J. Chem. Soc.*, **1961**, 4590.

[24] J. Fujitz, K. Nakamoto und M. Kobayashi, *J. Amer. Chem. Soc.*, **78**, 3295 (1956).

[25] M. M. Chamberlain und Y. C. Blair, *J. Amer. Chem. Soc.*, **81**, 6412 (1959).

[26] P. C. H. Mitchell, und R. J. P. Williams, *J. Chem. Soc.*, **1960**, 1912.

[27] A. Turco und C. Pecile, *Nature*, **191**, 66 (1961).

[28] F. Basolo, J. L. Burmeister und A. J. Pöe, *J. Amer. Chem. Soc.*, **85**, 1700 (1963).

E. ELEKTRONENSPINREZONANZ

Zur Strukturaufklärung wurde auch versucht, die ESR einiger der beschriebenen Verbindungen zu ermitteln. Zunächst machten sich nebst den großen Vorteilen der ESR-Messungen die bekannten Nachteile der Methode bemerkbar u.zw. die Arbeit bei sehr tiefen Temperaturen um Spur-Gitter-Relaxationseffekte zu verringern, die übrigens geringen Erfolge besonders bei paramagnetischen Ionen gerader Elektronenzahl und in unserem Fall vor allem der hohe Metallgehalt der Verbindungen.

Es wurden die Verbindungen:

1. $[CoDap(SCN)_2] \cdot 2H_2O$
2. $[NiDap(SCN)_2] \cdot 2H_2O$
3. $[MnDap(SCN)_2] \cdot 2H_2O$
4. $[PdDapCl_2] \cdot 4H_2O$
5. $[Co(SCN)_4]H_2Dap$
6. $[Cr(SCN)_4](HDap)_2$
7. $[PtDap_2Cl_6]Cl_2$ untersucht (1 u. 2 Mitt.)

Geeignete Deutungen der Beobachtungen konnten infolge des hohen Metallgehalts dieser Verbindungen (14–29%) jedoch nur mit Schwierigkeiten ausgewertet werden, da die registrierten Signale nur eine Linie mittlerer Intensität haben. Als Beispiel führen wir die Meßwerte von zwei Verbindungen an, die nebst anderen einwandfrei ausgewertet werden konnten. Es wurden der *g*-Faktor und die Linienbreite berechnet.

$$[MnDap(SCN)_2] \cdot 2H_2O$$

$$\nu = 9{,}385{,}2 \text{ M Hz} \qquad H_{gef.} = 2{,}3487 \cdot 10^{-4} \cdot p \qquad p = 14416$$

$$H_{ge.} = 33858 \text{ Gauss} \qquad H_{ber.} = 32920 \text{ Gauss}$$

$$g = 2{,}00363$$

Der gefundene Wert (bei 298°K) für g stimmt mit dem im Fachschrifttum für Mn^{+2} angegebenen gut überein. [29–31]

Linienbreite zwischen den Intensitätsmaxima des Spektrums: (Abb. 3)

$$20 \text{ mm} \cdot 33{,}5 = 670 \text{ Gauss}$$

Dieser verhältnismäßig hohe Wert ist auf den großen Mn^{2+}-Gehalt der Verbindung zurückzuführen (16,99%).

---

[29] T. P. P. HALL, W. HAYES und F. I. B. WILLIAMS, *Proc. Phys. Soc.*, **78**, 883 (1961).

[30] O. MATAMURA, *J. Phys. Soc. Japan*, **14**, 108 (1959).

[31] P. H. KASAI, *J. Phys. Chem.*, **66**, 674 (1962).

$[Cr(SCN)_4](HDap)_2$

Es wurde ein Signal mittlerer Intensität registriert (Abb. 4)

$\nu = 9384{,}4$ M Hz $\qquad g = 2{,}0011$

g-Werte für Cr^{3+} des Fachschrifttums $= 1{,}98 - 1{,}9874$. [32,33]

Linienbreite, innere Batterie = 368,5 Gauss

Linienbreite, äußere Batterie = 381 Gauss

Für die Verbindung $[Cr(SCN)_4](HDap)_2$ nahmen wir nach ihrer Herstellung zunächst an, daß DAP Cr^{3+} zu Cr^{2+} reduziert, also ein Komplex des letzteren vorliegt, so wie Cu_2^{2+} in der Verbindung $[Cu_2DapCl_2]$ (1 Mitt.). ESR bzw. der in den gegebenen Bedingungen (298°K) ermittelte Wert des g-Faktors erbrachte aber den einwandfreien Beweis, daß ein Komplex des Cr^{3+} vorliegt, da laut Literaturangaben für Cr^{+2}-Ionen das Signal stets bei etwa 1—6°K registriert wurde. [34, 35] ESR erwies sich in diesem Fall als ein wertvolles Hilfsmittel der Elektronenstrukturaufklärung.

Die IR-Spektren wurden mit dem Doppelstrahlgerät UR-10 des VEB Carl Zeiss Jena und Prismen aus KBr bestimmt.

ESR wurden mit einem Spektrometer JES-3B, Japan Electron Optics Laboratory Co., Ltd. gemessen.

---

[32] T. W. Carson und R. L. White, *J. Appl. Phys.*, **32**, 1787 (1961).

[33] P. Auzins, J. W. Orton und J. E. Wertz, ,,Paramagnetic Resonance'', W. Low., Acad. Press New York, London, vol. I, 1963, S 90.

[34] K. Morigaki, *J. Phys. Japan*, **18**, 733 (1963).

[35] F. A. Cotton und G. Wilkinson, ,,Anorganische Chemie'', Verlag Chemie, GmbH Weinheim/Bergstr., 1967, S 594.

Revue Roumaine de Chimie, 14, 1387–1397 (1969)

THE FORMATION OF SOME COMPLEX COMBINATIONS WITH PIPERAZINE IN AQUEOUS SOLUTION

GR. POPA and V. MAGEARU

Laboratory of Analytical Chemistry, University
of Bucharest, Spl. Independenţei 89, Bucharest,
Romania

Received 13 November 1968

The present paper deals with the formation of complex combinations of Cd(II) and Cu(II) with piperazine, in aqueous solution, using to this end the formation curves of Bjerrum type. For determining the concentration at equilibrium of the ligand and herefrom the formation functions $\overline{n}$, potentiometrical measurements were effected with a "metal-complex" electrode, reversible to the piperazine. The formation constants obtained from the formation curves have been then corrected through different methods.

A most important and actual research trend in the analytical chemistry is the study of the formation of complex combinations in solution, as well as of the determination of their analytical characteristics such as : solubility in different solvents, stability in solution, optical absorption, distribution between nonmiscible phases, sensitivity and specificity, etc.

The determination of the composition and stability in solution of the complex combinations, that represent one of the most important analytical characteristics of these complexes, is realized through different methods minutely examined in the literature.[1–5] Generally the problem of establishing the composition and the stability in solution of the complex combinations actually amounts to the determination of the concentration at equilibrium (or rather of its activity) of at least one of the complexes in solution. Due to the high precision and to the various possibilities thus offered, many of these studies are based on electrometric measurements of the concentrations at equilibrium. Yet a difficult pro-

---

[1] F. Rossotti and H. Rossotti, "The Determination of Stability Constants", McGraw-Hill, Book Co. New York, 1961.

[2] K. B. Iaţimirski, *Anal. Rom.-Sov.*, **2**, 82 (1954).

[3] A. Ringbom, "Complexation in Analytical Chemistry", Interscience Publishers, New York/London, 1963.

[4] H. L. Schläfer, "Komplexbildung in Lösung", Berlin, 1961.

[5] K. B. Iaţimirski and V. P. Vasiliev, "Konstanty nestoikosti komplexnyh soedinenyi", Moscow, 1959.

blem in the case of these measurements is the adequate selection and use of the electrodes.

In order to extend the possibilities of the potentiometrical methods of determining the concentration at equilibrium of the particles participating in the formation complex combination in solution, in the previous papers, [6–17] a new class of electrodes of the second type called "metal-complex", in which the role of the difficultly-soluble compound is taken by stable soluble complex, has been realized and studied. These electrodes that can be represented as follows :

$$\mathrm{Me} \mid [\mathrm{Me\,L}_p],\ \mathrm{L} \tag{1}$$

are reversible to the ligand, L, anions or neutral molecules (for simplification the other ions in solution have been neglected).

In the present paper for determining the concentration at equilibrium of the ligand that had formed complexes with the ions of Cd(II) and Cu(II) the metal-complex electrode of the type (1) was used, where $\mathrm{Me} = \mathrm{Ag}$ and $\mathrm{L} = \mathrm{HN(CH_2{-}CH_2)_2NH}$ (piperazine).

1. DETERMINATION OF THE COMPOSITION AND STABILITY IN SOLUTION OF THE ELECTRODIC COMPLEX

In the first part of this paper one has studied the formation equilibrium of the electrodic complex $[\mathrm{AgL}_p]^+$, in identical conditions with those existing in the formation of the Cd(II) and Cu(II) complexes. That is why we used the complexation functions [18] given by Olerup and Leden [19–20] :

$$F = \frac{C_{\mathrm{Ag}^+}}{[\mathrm{Ag}^+]} = 1 + K_1[\mathrm{L}] + K_2[\mathrm{L}]^2 + \ldots \tag{2}$$

By successive extrapolations of the functions :

$$F_n = \frac{F_{n-1} - K_{n-1}}{[\mathrm{L}]} \tag{3}$$

---

[6] C. Luca, V. Magearu and Gr. Popa, *J. Electroanalyt. Chem.*, **12**, 45 (1966).

[7] V. Magearu, C. Luca and M. Teodorescu, *J. Electroanalyt. Chem.*, **12**, 148 (1966).

[8] C. Luca, *Bull. Soc. Chim. France*, **7**, 2556 (1967).

[9] G. Berthon and C. Luca, *Chim. Analyt.*, **49**, 6 (1967).

[10] Gr. Popa and V. Magearu, *Rev. Roumaine Chim.*, **12**, 1107 (1967).

[11] Gr. Popa, V. Magearu and E. Dăscălescu, *Anal. Univ. Bucureşti*, **2**, 67 (1967).

[12] Gr. Popa, V. Magearu and C. Luca, *J. Electroanalyt. Chem.*, **17**, 335 (1968).

[13] Gr. Popa and V. Magearu, *J. Electroanalyt. Chem.*, **22**, 85 (1969).

[14] Gr. Popa and V. Magearu, *Rev. Roumaine Chim.*, **14**, 879 (1969).

[15] V. Magearu and Gr. Popa, *Rev. Roumaine Chim.*, **14**, 1399 (1969).

[16] V. Magearu and Gr. Popa, *Anal. Univ. Bucureşti*, **2**, 91 (1968).

[17] Gr. Popa and V. Magearu, *J. Electroanalyt. Chem.* (under print).

[18] K. B. Iaţimirski, *Zhur. neorg. Khim.*, **1**, 412 (1956).

[19] H. Olerup, Dissertation, Lund (1944).

[20] I. Leden, *Z. phys. Chem.*, **A−188**, 160 (1941).

we get at the limit :

$$\lim_{[L]\to 0} F_n = K_n \tag{4}$$

which allow the determination of the maximum number N of formed complexes and of the formation constants K_n, as well.

In the case of the Ag^+-piperazine system one can notice the formation in solution of only two complexes.

From potentiometric measurements of cells of the type :

$$\begin{aligned}&\text{(I) } Ag \mid Ag^+ \mid NH_4NO_3 \text{ (saturated) } \mid KCl \text{ (saturated), } Hg_2Cl_2 \mid Hg\\ &\text{(II) } Ag \mid [AgL_p]^+, L \mid NH_4NO_3 \text{ (saturated) } \mid KCl \text{ (saturated), } Hg_2Cl_2 \mid Hg\end{aligned} \tag{5}$$

the complexation functions F have been determined :

$$E_I - E_{II} = \frac{RT}{\mathcal{F}} \ln F \tag{6}$$

The concentration of the total silver ions C_{Ag^+} in both cells (5) has been equal and very small ($\sim 10^{-5}$ M) with respect to the total concentration of the ligand L.

Table 1

$Ag^+ - HN(CH_2 - CH_2)_2NH$

25°C ; $\mu = 2(NH_4NO_3)$

$E_I - E_{II}$ (V)	F	$F_1 \times 10^{-3}$	$F_2 \times 10^{-7}$	p [L]	$\bar{n}$
0.0043	1.180	—	—	4.301	0.116
0.0072	1.320	—	—	4.000	0.264
0.0139	1.720	3.600	—	3.699	0.577
0.0232	2.462	4.414	0.729	3.480	0.929
0.0348	3.880	5.760	0.752	3.301	1.211
0.0439	5.532	6.888	0.743	3.182	1.396
0.0593	10.055	9.236	0.738	3.009	1.610
0.0809	23.335	15.847	0.737	2.792	1.788
0.1025	53.920	20.909	0.747	2.597	1.852
0.1312	164.95	36.072	0.749	2.342	1.909
0.1432	263.40	44.610	0.724	2.230	1.989

$K_1 = 2.0 \times 10^3$; $K_2 = 0.74 \times 10^7$

In the first table are indicated the experimental results as well as the calculation of the functions F_n obtained for the Ag^+-piperazine system.

By knowing the K_1 and K_2 constants there could be calculated afterwards the formation functions $\bar{n}$ given by Bjerrum [21] listed in the last column of the first table, functions that give the average number of coordinated ligands:

$$\bar{n} = \frac{C_L - [L]}{C_{Ag^+}} = \frac{K_1 [L] + 2K_2 [L]^2}{F} \qquad (7)$$

These functions permit the drawing of the formation curves $\bar{n} - p[L]$ $(p[L] = -\lg [L])$ of the respective system. This points to the concentration domain of the ligand where the formation of a given complex takes place.

2. THE FORMATION IN SOLUTION OF THE Cd(II) AND Cu(II) COMPLEXES WITH PIPERAZINE

After finding out the formation equilibrium of the electrodic complex, the second part of the paper deals with the formation equilibriums of the Cd(II) and Cu(II) complexes with piperazine.

To this purpose we carried out potentiometric measurements of cells series of the type:

$$\text{(II) } Ag/[AgL_2]^+,\ L/NH_4NO_3 \text{ (saturated)}/KCl \text{ (saturated)},\ Hg_2Cl_2/Hg \qquad (8)$$

$$\text{(III) } Ag/[AgL_2]^+,\ L,\ Me^{2+}/NH_4NO_3 \text{ (saturated)}/KCl \text{ (saturated)},\ Hg_2Cl_2/Hg$$

In both (8) cells the total concentration of the silver ions is equal and very small as compared to the concentration of the ligand and of the ions Me^{2+} (Cd^{2+}, Cu^{2+}).

In these conditions the quantity of ligand linked with the silver complex, may be neglected.

In the cell (8—III) which contains an additional known quantity of Me^{2+} $(C_{Me^{2+}})$ as against (8—II) and which forms a series of successive complexes less stable than those of Ag^+, there exists an equilibrium between the competitive systems:

$$Ag^+ + 2L \rightleftharpoons [AgL_2]^+ \qquad (9)$$

$$Me^{2+} + nL \rightleftharpoons [MeL_n]^{2+} \qquad (10)$$

Both cells contain the same volume of solution and the same amount of ligand (C_L). The concentration of the free ligand ([L]) in equilibrium

---

[21] J. Bjerrum, "Metal Amine Formation in Aqueous Solution", Haase, Copenhagen, 1957, Chap. 1, 2, 3.

(10) may be determined from the difference of the e.m.f. between cells (II) and (III), by using the relation

$$\Delta E = E_{\mathrm{II}} - E_{\mathrm{III}} = \frac{RT}{\mathcal{F}} \ln\,[\mathrm{L}]^2 - \frac{RT}{\mathcal{F}} \ln C_{\mathrm{L}}^2 \qquad (11)$$

For 25° the above relation (11), may be written as :

$$\lg\,[\mathrm{L}] = \lg C_{\mathrm{L}} + \frac{\Delta E}{0.11832} \qquad (12)$$

Out of the concentration of the free ligand for a series of total concentration of the ligand and of the ions Me^{2+}, we can calculate the formation functions of the Bjerrum type. [21]

Table 2

$Cd^{2+} - HN(CH_2-CH_2)_2NH$

25°C ; $\mu = 2(NH_4NO_3)$

$C_{Cd^{2+}}$ mole/l	C_L mole/l	$-\Delta E = E_{II} - E_{III}$ (V)	[L]	p[L]	n
0.09270	0.00662	0.1372	0.000459	3.339	0.067
0.09210	0.01316	0.1432	0.000811	3.091	0.134
0.09032	0.03226	0.1445	0.001938	2.713	0.336
0.08750	0.06250	0.1389	0.004187	2.378	0.666
0.08485	0.09091	0.1299	0.007257	2.139	0.986
0.08235	0.11765	0.1206	0.011254	1.949	1.292
0.08000	0.14286	0.1112	0.016410	1.785	1.533
0.07778	0.16667	0.1016	0.023070	1.637	1.846
0.07568	0.18919	0.0915	0.031885	1.496	2.079
0.07368	0.21053	0.0825	0.042270	1.374	2.284
0.07180	0.23076	0.0738	0.054885	1.261	2.450
0.07000	0.25000	0.0656	0.069745	1.156	2.575
0.06829	0.26830	0.0584	0.086110	1.065	2.668
0.06667	0.28571	0.0536	0.100680	0.997	2.775
0.06512	0.30232	0.0468	0.121600	0.915	2.775
0.06364	0.31819	0.0416	0.142000	0.848	2.769
0.06087	0.34783	0.0358	0.173300	0.761	2.867

The experimental results as well as the calculations for the Cd^{2+}-piperazine and Cu^{2+}-piperazine systems, are indicated in the tables 2 and 3.

Table 3

$Cu^{2+}-HN(CH_2-CH_2)_2NH$

$25°C;\ \mu = 2(NH_4NO_3)$

$C_{Cu^{2+}}$ mole/l	C_L mole/l	$-\Delta E = E_{II} - E_{III}$ (V)	[L]	p [L]	$\overline{n}$
0.04747	0.02598	0.2343	0.000272	3.566	0.541
0.04717	0.03226	0.2434	0.000283	3.548	0.677
0.04686	0.03848	0.2443	0.000331	3.480	0.814
0.04657	0.04458	0.2452	0.000377	3.423	0.949
0.04627	0.05063	0.2456	0.000425	3.371	1.085
0.04569	0.06250	0.2441	0.000541	3.267	1.356
0.04512	0.07408	0.2389	0.000709	3.149	1.626
0.04458	0.08537	0.2355	0.000873	3.059	1.895
0.04404	0.09639	0.2313	0.001067	2.972	2.165
0.04351	0.10715	0.2249	0.001347	2.871	2.432
0.04300	0.11765	0.2187	0.001668	2.778	2.697
0.04250	0.12791	0.2110	0.002106	2.676	2.960
0.04202	0.13794	0.2012	0.002749	2.561	3.217
0.04154	0.14773	0.1917	0.003542	2.451	3.471
0.04107	0.15731	0.1808	0.004664	2.331	3.717
0.04061	0.16667	0.1699	0.006107	2.214	3.953

These data can be used to plot the formation curves of the respective complexes (Fig. 1), from which the approximate successive formation constants can be determined:

$$\lg k_n = p\,[L]_{\overline{n}=n-1/2} \tag{13}$$

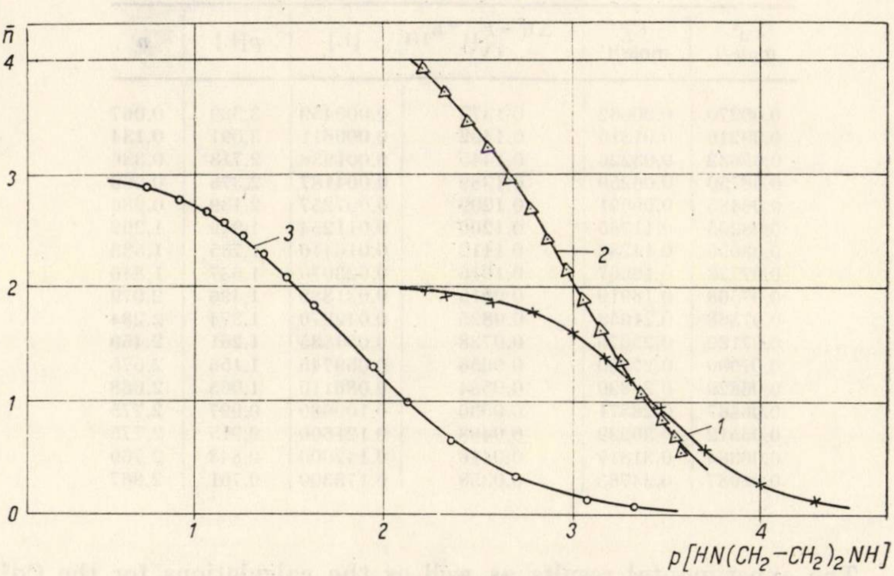

Fig. 1.— Formation curves of the complexes with piperazine.
1 – Ag^+ ; 2 – Cu^{2+} ; 3 – Cd^{2+} .

These approximate values of the formation constants have been corrected by using the relation of the formation curve:

$$\bar{n} + (\bar{n} - 1)\, k_1 [\mathrm{L}] + (\bar{n} - 2)\, k_1 k_2 [\mathrm{L}]^2 + \ldots + (\bar{n} - N)\, k_1 k_2 k_3 \ldots k_n [\mathrm{L}]^N = 0 \tag{14}$$

which may be solved in terms of k_n:

$$k_n = \left(\frac{1}{[\mathrm{L}]}\right)_{\bar{n}=n-1/2} \cdot \frac{1 + \sum\limits_{t=1}^{t=n-1} \dfrac{1+2t}{[\mathrm{L}]^t\, k_{n-1}\, k_{n-2} \ldots k_{n-t}}}{1 + \sum\limits_{t=1}^{t=N-n} (1+2t)\, [\mathrm{L}]^t\, k_{n+1}\, k_{n+2} \ldots k_{n+t}} \tag{15}$$

taking into account Bjerrum's method.[21] In this relation t takes all the full values within the indicated limits, and N is the maximum number of complexes forming in the domain of concentration studied.

The correction of the formation constants has been also effected graphically, by taking into account Ahrland and Fronaeus methods [22,23] by extrapolating the functions (2). These complexation functions were determined by a graphical integration of the curves $(\bar{n}/[\mathrm{L}]) - [\mathrm{L}]$:

$$\ln F = \int_0^{[\mathrm{L}]} \frac{\bar{n}}{[\mathrm{L}]}\, \mathrm{d}[\mathrm{L}] \tag{16}$$

Functions (3) and (4) have been then calculated.

The results of these calculations are to be seen in the tables 4 and 5.

Table 4

$\mathrm{Cd^{2+} - HN(CH_2 - CH_2)_2NH}$

[L]	ln F	F	$F_1 \times 10^{-2}$	$F_2 \times 10^{-4}$	$F_3 \times 10^{-6}$
0.004	0.641	1.898	—	—	—
0.006	0.945	2.573	2.621	—	—
0.008	1.223	3.396	2.995	—	—
0.010	1.476	4.376	3.376	1.476	0.286
0.012	1.708	5.519	3.766	1.555	0.304
0.015	2.021	7.549	4.366	1.644	0.303
0.018	2.301	9.985	4.991	1.717	0.293
0.020	2.473	11.86	5.430	1.765	0.287
0.025	2.869	17.62	6.648	1.899	0.284
0.030	3.224	25.19	8.063	2.055	0.288
0.035	3.545	34.64	9.612	2.203	0.289
0.040	3.839	46.48	11.37	2.368	0.294
0.050	4.361	78.34	15.47	2.714	0.305

$K_1 = 1.9 \times 10^2$; $K_2 = 1.19 \times 10^4$; $K_3 = 2.93 \times 10^5$

---

[22] S. Ahrland, *Acta Chem. Scand.*, **3**, 783 (1949).

[23] S. Fronaeus, *Acta Chem. Scand.*, **4**, 72 (1950).

Table 5

$Cu^{2+}-HN(CH_2-CH_2)_2NH$

[L]	$\ln F$	F	$F_1\times10^{-3}$	$F_2\times10^{-7}$	$F_3\times10^{-9}$	$F_4\times10^{-12}$
0.0006	1.257	3.514	4.190	—	—	—
0.0008	1.727	5.623	5.779	0.460	—	—
0.0010	2.158	8.654	7.654	0.582	—	—
0.0012	2.555	12.87	9.892	0.649	3.411	—
0.0015	3.100	22.20	14.134	0.802	3.749	1.299
0.0020	3.889	48.87	23.935	1.092	4.258	1.229
0.0025	4.566	96.16	38.064	1.439	4.794	1.198
0.0030	5.155	173.60	57.435	1.845	5.348	1.183
0.0035	5.677	292.10	83.170	2.316	5.932	1.180
0.0040	6.149	468.30	116.850	2.869	6.571	1.193
0.0045	6.578	719.20	159.600	3.500	7.245	1.210
0.0050	6.970	1064.5	212.700	4.212	7.944	1.229

$K_1=2.1\times10^3$; $K_2=2.4\times10^6$; $K_3=1.8\times10^9$; $K_4=1.2\times10^{12}$

Converse extrapolations have been also carried out.

Thus, by extrapolating the functions:

$$F'_N=\frac{F-1}{[L]^N}=K_N+K_{N-1}[L]^{-1}+K_{N-2}[L]^{-2}+\dots \tag{17}$$

at $[L]^{-1}=0$ we obtain the last constant K_N. Then from:

$$F'_{N-1}=(F'_N-K_N)[L]=K_{N-1}+K_{N-2}[L]^{-1}+\dots \tag{18}$$

we obtain for $[L]^{-1}=0$, the constant K_{N-1}.

In this way we repeat the calculations till we obtain the constant K_1. The results of these calculations are mentioned in tables 6 and 7.

It is evident that the constants K_n where n has low values are more exact in the case of direct extrapolation, and where n has higher values, the converse extrapolation gives better results.

Table 6

$Cd^{2+}-HN(CH_2-CH_2)_2NH$

$\frac{1}{[L]}$	F	$F'_3\times10^{-5}$	$F'_2\times10^{-4}$	$F'_1\times10^{-2}$
20.0	78.34	6.187	1.429	1.677
25.0	46.48	7.106	1.510	1.666
28.6	34.64	7.846	1.581	1.703
33.3	25.19	8.959	1.689	1.784
40.0	17.62	10.638	1.827	1.833
50.0	11.86	13.575	2.049	1.910

$K_3=3.33\times10^5$; $K_2=1.09\times10^4$; $K_1=1.8\times10^2$

Table 7

$Cu^{2+} - HN(CH_2 - CH_2)_2NH$

$\frac{1}{[L]}$	F	$F'_4 \times 10^{-12}$	$F'_3 \times 10^{-9}$	$F'_2 \times 10^{-6}$	$F'_1 \times 10^{-3}$
181.8	1528.7	1.669	—	—	—
222.2	719.2	1.730	2.158	—	—
250.0	468.3	1.826	2.302	2.808	2.432
285.8	292.1	1.940	2.415	2.862	2.284
333.4	173.6	2.127	2.631	3.093	2.679
400.0	96.16	2.436	2.965	3.413	3.031
500.0	48.87	2.992	3.484	3.768	3.136
666.6	22.20	4.188	4.407	4.211	3.016
833.4	12.87	5.725	5.369	4.403	2.644
1000	8.65	7.654	6.404	4.794	2.594

$K_4 = 1.25 \times 10^{12}$; $K_3 = 1.7 \times 10^9$; $K_2 = 2.2 \times 10^6$; $K_1 = 2.7 \times 10^3$

Table 8 gives the values of the approximate partial constants (13) obtained from the graph of the formation curves, constants corrected with the help of relation (15). There are also indicated the values of the constants obtained by extrapolating the functions F and F'.

Table 8

Values of the formation constants of the Cd(II) and Cu(II) complexes with piperazine at 25°; ionicstrength $\mu = 2(NH_4NO_3)$

n	$Cd^{2+} - HN(CH_2 - CH_2)_2NH$			$Cu^{2+} - HN(CH_2 - CH_2)_2NH$		
	$p[L]_{\overline{n}=n-1/2}$	lg k_n relation (15)	lg k_n graphically	$p[L]_{\overline{n}=n-1/2}$	lg k_n relation (15)	lg k_n graphically
1	2.52	2.31	2.28	3.68	3.32	3.32
2	1.82	1.77	1.79	3.21	3.06	3.06
3	1.21	1.47	1.48	2.85	2.93	2.89
4	—	—	—	2.45	2.86	2.87
lg K_N	5.55	5.55	5.55	12.19	12.17	12.14

In the case of the system Cd^{2+}-piperazine, table 8 lists the constants k_1 and k_2 obtained through a direct extrapolation, and k_3 obtained through converse extrapolation.

For the system Cu^{2+}-piperazine the same table mentions the values k_1 and k_2 obtained through a direct extrapolation, and k_3 and k_4 obtained through converse extrapolation.

As it can be seen these values are very similar with the ones obtained by using relation (15).

3. VERIFICATION OF THE RESULTS

In the last part of the paper, in order to verify the accuracy in the determination of the concentrations of the free ligand from the equilibrium (10), the formation constants of the electrodic complex $[AgL_2]^+$ have been recalculated from the cell (8—III). In the calculation of the functions *F* one has used as total concentration of the ligand, the concentration found with the help of the relation (12).

The results of these calculations are mentioned in tables 9 and 10.

Table 9

$Ag^+ - HN(CH_2-CH_2)_2NH^{(Cd)}$

[L]	$\Delta E = E_I - E_{III}^{(Cd)}$	F	$F_1 \times 10^{-4}$	$F_2 \times 10^{-7}$
0.000459	0.02725	2.888	0.4116	—
0.000811	0.04915	6.773	0.7119	—
0.001938	0.09083	34.31	1.719	0.7703
0.004187	0.12900	151.54	3.595	0.8048
0.007257	0.15598	433.10	5.955	0.7896
0.011254	0.17740	996.9	8.849	0.7663
0.016410	0.19650	2097.0	12.773	0.7648
0.023070	0.21358	4076.0	17.664	0.7559
0.031885	0.22935	7730.0	23.613	0.7335
0.042270	0.24418	13723.0	31.723	0.7452
0.054885	0.25720	22260.0	40.556	0.7348
0.069745	0.26922	35540.0	50.956	0.7275
0.086110	0.27930	52614	61.099	0.7069
0.100680	0.28758	72620	72.129	0.7143

$K_1 = 2.25 \times 10^3$; $K_2 = 0.752 \times 10^7$

Table 10

$Ag^+ - HN(CH_2-CH_2)_2NH^{(Cu)}$

[L]	$\Delta E = E_I - E_{III}^{(Cu)}$	F	F_1	$F_2 \times 10^{-7}$
0.000873	0.04665	6.145	5894	—
0.001067	0.05673	9.097	7586	—
0.001668	0.07930	21.895	12525	0.6310
0.002749	0.10402	57.335	20490	0.6725
0.004664	0.13108	164.25	35005	0.7505
0.006107	0.14528	285.55	46591	0.7301
0.008092	0.15907	488.55	60250	0.7446
0.010350	0.17140	789.20	76150	0.7164
0.012817	0.18248	1214.8	94695	0.72325

$K_1 = 2 \times 10^3$; $K_2 = 0.71 \times 10^7$

As one can notice, the constants thus calculated have values very similar with those determined in the first part of the paper from the cells (5). This is a proof for the working and reproducibility of the metal-complex electrode used in determining the concentration of the free ligand in the formation equilibrium of the complex combinations of Cd(II) and Cu(II) with piperazine.

4. APPARATUS AND REAGENTS

The potentiometric measurements have been effected by means of a potentiometer VEB Meßtechnik Mellenbach, with a precision of ± 0.1 mV.

The temperature has been maintained constant at 25 ± 0.1° by means of a Ultrathermostat U—10.

All solutions have been prepared in bidistilled water from the p.a. Merck, Austranal and U.C.B. (Belgium).

The ionic strength of the solutions has been maintained constant at $\mu = 2$ with NH_4NO_3.

The different concentrations of the cells have been obtained by using the titration technique, by adding the same volumes of solution in all the cells.

Revue Roumaine de Chimie, **14**, 1399–1405 (1969)

L'ÉTUDE DES COMPLEXES DE Zn(II), Cd(II), Co(II) ET Ni(II) AVEC LA DI-I-PROPYLAMINE

V. MAGEARU et GR. POPA

Laboratoire de Chimie Analytique de l'Université de Bucarest, 89 Splaiul Independenţei

Reçu le 25 décembre 1968

On a réalisé une nouvelle électrode de type « métal-complexe », réversible par rapport à la di-i-propylamine. Cette électrode a été utilisée à l'étude de la formation et de la détermination de la stabilité en solution aqueuse des combinaisons complexes de Zn(II), Cd(II), Co(II) et Ni(II) avec la di-i-propylamine.

Dans une série de travaux antérieurs [1–7] on a réalisé et étudié un nouveau type d'électrodes de la deuxième catégorie dans lequel le composé insoluble est remplacé par un complexe non dissocié, à concentration fixement maintenue. Ces électrodes, dénommées *métal-complexe*, peuvent être représentées d'une manière schématique par

$$\mathrm{Me}/[\mathrm{MeL}_p]^{(a-pb)+},\ \mathrm{L}^{b-} \tag{1}$$

et sont réversibles par rapport au ligant L, qui forme des complexes $[\mathrm{MeL}_p]^{(a-pb)+}$ avec les ions Me^{a+}.

Pour construire ces électrodes on a utilisé avec succès l'argent, qui ne polarise pas, donne des potentiels parfaitement reproductibles et les ions argent forment des complexes solubles, très stables, avec un grand nombre de molécules neutres ou d'anions, en conformité avec la réaction

$$\mathrm{Ag}^+ + p\mathrm{L} \rightleftharpoons [\mathrm{AgL}_p]^{(1-pb)+} \tag{2}$$

Dans le cas où dans la solution se trouvent aussi des ions d'un autre métal Me^{2+}, qui forme des complexes avec le ligant L

$$\mathrm{Me}^{2+} + n\mathrm{L}^{b-} \rightleftharpoons [\mathrm{MeL}_n]^{(2-nb)+} \tag{3}$$

s'établit entre les réactions (2) et (3) un équilibre compétitif.[8]

---

[1] C. Luca, V. Magearu et Gr. Popa., *J. Electroanalyt. Chem.*, **12**, 45 (1966).

[2] V. Magearu, C. Luca et M. Teodorescu, *J. Electroanalyt. Chem.*, **12**, 148 (1966).

[3] Gr. Popa et V. Magearu, *Rev. Roumaine Chim.*, **12**, 1107 (1967).

[4] Gr. Popa, V. Magearu et C. Luca, *J. Electroanalyt. Chem.*, **17**, 335 (1968).

[5] Gr. Popa, V. Magearu et E. Dăscălescu, *Anal. Univ. Bucureşti*, **2**, 67 (1967).

[6] Gr. Popa et V. Magearu, *Rev. Roumaine Chim.*, **14**, 897 (1969).

[7] V. Magearu et Gr. Popa, *Anal. Univ. Bucureşti*, **2**, 91 (1968).

[8] F. Rossotti et H. Rossotti, « The Determination of Stability Constants », Mc Graw-Hill, Beak Co New York, 1961, p. 58.

La concentration, ou plus précisément l'activité à l'équilibre du ligant de la réaction (3) peut être déterminée avec une électrode adéquate du type (1).

PARTIE EXPÉRIMENTALE

Dans le présent travail on a utilisé une électrode du type (1) où Me = Ag et L = di-i-propylamine, à l'étude de la formation en solution aqueuse des combinaisons complexes de Zn(II), Cd(II), Co(II) et Ni(II), avec la di-i-propylamine.

A cette fin, on a réalisé deux cellules de la forme

$$\begin{array}{ll} \text{(II)} & Ag/[AgL_p]^+,\ L/NH_4NO_3\ (\text{sat.})/KCl\ (\text{sat.}),\ Hg_2Cl_2/Hg \\ \text{(III)} & Ag/[AgL_p]^+,\ L,\ Me^{2+}/NH_4NO_3\ (\text{sat.})/KCl\ (\text{sat.}),\ Hg_2Cl_2/Hg \end{array} \qquad (4)$$

Pour les deux éléments, qui ont la valeur du potentiel de diffusion constante, la quantité totale d'ions argent est égale et très petite en rapport avec le ligant L ($C_{Ag^+}/C_L \simeq 1/10^6$).

Dans les mêmes conditions de température et de force ionique on a étudié, dans un travail antérieur, [9] les équilibres de formation des complexes électrodiques $[AgL_p]^+$, en trouvant pour ces cas la valeur $p = 2$, caractéristique en général des complexes d'argent à monoamines organiques. [10-13]

Dans l'élément (4 — III), une partie du ligant est consommée pour former des complexes du type $[MeL_n]^{2+}$, et la concentration à l'équilibre du ligant en présence des ions Me^{2+} peut être calculée à partir de la différence de la tension électromotrice de ces cellules

$$\Delta E = E_{II} - E_{III} = \frac{2RT}{F} \ln \frac{[L]}{C_L} \qquad (5)$$

La concentration totale des ions Me^{2+} et du ligant à l'équilibre étant connue pour une série de concentrations totales du ligant, on peut calculer les fonctions

$$\bar{n} = \frac{C_L - [L]}{C_{Me^{2+}}} \qquad (6)$$

et tracer ensuite les courbes de formation ($\bar{n} - p$ [L]), de type Bjerrum, [14] qui donnent des indications sur le nombre de complexes et sur leur stabilité, ainsi que sur le domaine de concentration où ils se forment.

Dans les tableaux 1—4 on a indiqué les données expérimentales et les calculs concernant les équilibres de formation des complexes de systèmes Me^{2+}—di-i-propylamine.

Pour les déterminations on a utilisé des solutions en eau bidistillée préparées partant de substances *p.a.* Merck, Carlo Erba ou UCB (Belgique).

---

[9] Gr. Popa et V. Magearu, *Anal. Univ. Bucureşti*, **2**, 41 (1968).

[10] Gr. Popa, C. Luca et V. Magearu, *J. Chim. phys.*, **60**, 355 (1963).

[11] Gr. Popa, V. Magearu et C. Luca, *J. Chim. phys.*, **62**, 853 (1965).

[12] V. Armeanu et C. Luca, *Z. phys. Chem.*, **214**, 81 (1960).

[13] V. Armeanu et C. Luca, *Z. phys. Chem.*, **218**, 149 (1961).

[14] J. Bjerrum, « Metal Amine Formation in Aqueous Solution », chap. 1, 2, 3, Haase, Copenhagen, 1957.

Tableau 1

$Zn^{2+} - [(CH_3)_2CH]_2NH$

25°C ; $\mu = 2(NH_4NO_3)$

$C_{Zn^{2+}}$ mole/l	C_L mole/l	$-\Delta E = E_{II} + E_{III}$ (V)	[L]	p[L]	$\bar{n}$
0,03324	0,00423	0,1102	0,000496	3,304	0,113
0,03311	0,01055	0,1260	0,000909	3,041	0,291
0,03285	0,02303	0,1386	0,001553	2,809	0,654
0,03268	0,03124	0,1434	0,001918	2,717	0,898
0,03246	0,04139	0,1461	0,002310	2,618	1,201
0,03226	0,05140	0,1490	0,002829	2,548	1,506
0,03201	0,06129	0,1491	0,003367	2,473	1,810
0,03184	0,07105	0,1486	0,003941	2,404	2,108
0,03164	0,08068	0,1473	0,004591	2,338	2,405
0,03144	0,09020	0,1437	0,005505	2,259	2,694
0,03125	0,09960	0,1381	0,006778	2,169	2.970
0,03105	0,10888	0,1299	0,008691	2,061	3,227
0,03068	0,12509	0,1060	0,016155	1,792	3,616
0,03030	0,14487	0,0822	0,02925	1,534	3,816
0,02994	0,16222	0,0653	0,04551	1,342	3,895
0,02941	0,18748	0,0501	0,07072	1,150	3,970

Tableau 2

$Cd^{2+} - [(CH_3)_2CH]_2NH$

25°C ; $\mu = 2(NH_4NO_3)$

$C_{Cd^{2+}}$ mole/l	C_L mole/l	$-\Delta E = E_{II} - E_{III}$ (V)	[L]	p[L]	$\bar{n}$
0,03324	0,00423	0,1227	0,000389	3,410	0,116
0,03229	0,01681	0,1335	0,001252	2,902	0,482
0,03268	0,03124	0,1250	0,002744	2,562	0,872
0,03246	0,04139	0,1165	0,004288	2,368	1,143
0,03226	0,05140	0,1085	0,006223	2,206	1,401
0,03184	0,07105	0,0912	0,012045	1,919	1,853
0,03144	0,09020	0,0762	0,020475	1,689	2,218
0,03098	0,11804	0,0591	0,03737	1,427	2,604
0,03012	0,15360	0,0450	0,063984	1,194	2,975
0,02941	0,18748	0,0363	0,092505	1,034	3,229
0,02777	0,26560	0,0236	0,167800	0,775	3,521
0,02500	0,39840	0,0143	0,30163	0,521	3,871

Revue Roumaine de Chimie, **14**, 1399−1405 (1969)

Tableau 3

$Co^{2+} - [(CH_3)_2CH]_2NH$

$25°C\,;\ \mu = 2(NH_4NO_3)$

$C_{Co^{2+}}$ mole/l	C_L mole/l	$-\Delta E = E_{II} - E_{III}$ (V)	[L]	p[L]	$\bar{n}$
0,06649	0,00423	0,1133	0,000467	3,330	0,057
0,06622	0,01055	0,1185	0,001052	2,978	0,144
0,06578	0,02096	0,1187	0,002081	2,682	0,287
0,06492	0,04139	0,1139	0,004511	2,346	0,568
0,06402	0,06129	0,1072	0,006710	2,119	0,839
0,06250	0,09960	0,0955	0,015530	1,809	1,345
0,06098	0,13604	0,0847	0,026170	1,582	1,802
0,05952	0,17074	0,0758	0,039055	1,408	2,213
0,05814	0,20383	0,0694	0,052810	1,277	2,598
0,05555	0,26560	0,0585	0,085080	1,070	3,249
0,05405	0,30149	0,0531	0,107640	0,968	3,586

Tableau 4

$Ni^{2+} - [(CH_3)_2CH]_2NH$

$25°C\,;\ \mu = 2(NH_4NO_3)$

$C_{Ni^{2+}}$ mloe/l	C_L mole/l	$-\Delta E = E_{II} - E_{III}$ (V)	[L]	p[L]	$\bar{n}$
0,03324	0,00423	0,1276	0,000354	3,451	0,117
0,03311	0,01055	0,1535	0,000532	3,274	0,303
0,03289	0,02096	0,1431	0,001295	2,888	0,598
0,03268	0,03124	0,1375	0,002151	2,667	0,890
0,03246	0,04139	0,1300	0,003298	2,482	1,174
0,03226	0,05140	0,1217	0,004813	2,318	1,444
0,03201	0,06129	0,1123	0,006891	2,162	1,660
0,03164	0,08068	0,0975	0,012100	1,917	2,168
0,03125	0,09960	0,0842	0,019348	1,713	2,568
0,03098	0,11804	0,0718	0,029185	1,535	2,868
0,03012	0,15360	0,0548	0,052875	1,277	3,344
0,02941	0,18748	0,0441	0,079475	1,099	3,672
0,02861	0,22766	0,0346	0,116080	0,935	3,900
0,02777	0,26570	0,0287	0,151920	0,818	4,093
0,02702	0,30149	0,0243	0,188510	0,725	4,180
0,02564	0,36775	0,0185	0,256530	0,791	4,338

La force ionique de toutes les solutions a été maintenue constante à la valeur $\mu = 2$ avec NH_4NO_3.

Les cellules ont été thermostatées à une température constante de 25 ± 0,1°C avec un ultrathermostat U–10, et les tensions électromotrices ont été mesurées avec une précision de ± 0,1 mV au moyen d'un potentiomètre VEB Meßtechnik Mellenbach.

INTERPRÉTATION DES RÉSULTATS

Dans la figure 1 on a illustré les courbes de formation des complexes étudiés en utilisant l'électrode *métal-complexe* (1), ainsi que les courbes de formation des complexes électrodiques $[AgL_p]^+$, étudiés dans un travail antérieur [9] ($K_1 = 10^3$; $K_2 = 1{,}12 . 10^7$).

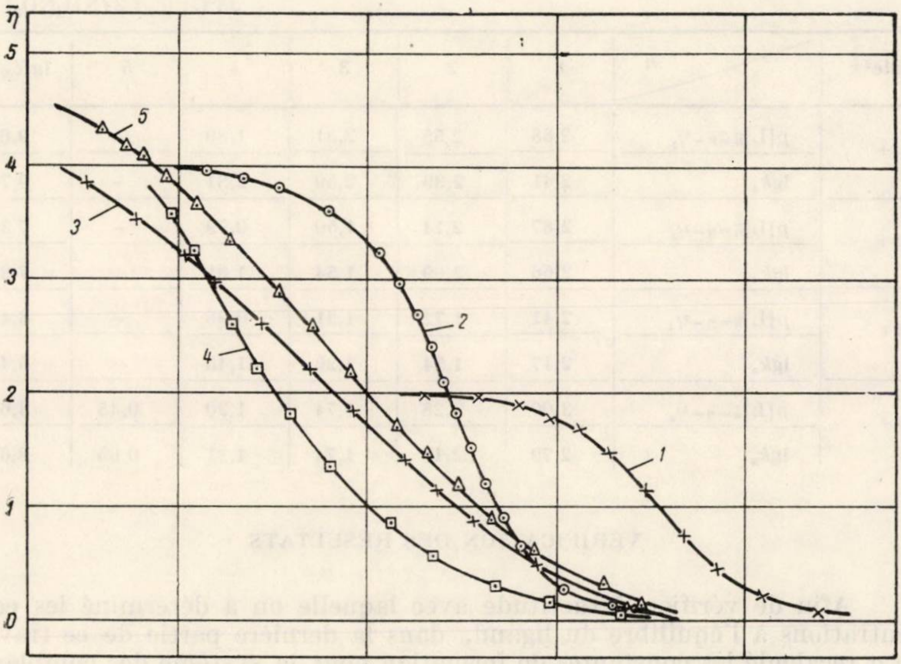

Fig. 1. — Courbes de formation des complexes du système Me — $[(CH_3)_2CH]_2NH$.
1, Ag^+ ; *2*, Zn^{2+} ; *3*, Cd^{2+} ; *4*, Co^{2+} ; *5*, Ni^{2+}.

Ainsi, dans le domaine de concentration étudié pour former les complexes des systèmes $Me^{2+} - [(CH_3)_2CH]_2NH$, la formation des complexes électrodiques est déjà terminée, dans la solution existant seulement les complexes $[AgL_2]^+$ de la forme considérée.

Du graphique des courbes de formation représentées à grande échelle on a déterminé les constantes de formation successives approximatives

$$\lg\ k_n = p\,[\mathrm{L}]_{\overline{n}=n-\frac{1}{2}} \tag{7}$$

Afin de rectifier ces constantes on a utilisé les indications de Bjerrum.[14]

Les résultats de ces calculs sont indiqués dans le tableau 5.

Tableau 5

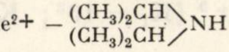

$$\mathrm{Me^{2+}} - \begin{matrix}\mathrm{(CH_3)_2CH} \\ \mathrm{(CH_3)_2CH}\end{matrix}\!\!>\!\mathrm{NH}$$

25°C ; $\mu = 2\,(\mathrm{NH_4NO_3})$

Me²⁺	n	1	2	3	4	5	$\lg K_N$
Zn²⁺	$p[\mathrm{L}]_{\overline{n}=n-1/2}$	2,88	2,55	2,31	1,89	—	9,63
	$\lg k_n$	2,41	2,39	2,59	2,31	—	9,70
Cd²⁺	$p[\mathrm{L}]_{\overline{n}=n-1/2}$	2,87	2,14	1,50	0,79	—	7,30
	$\lg k_n$	2,66	2,09	1,54	1,01	—	7,30
Co²⁺	$p[\mathrm{L}]_{\overline{n}=n-1/2}$	2,41	1,72	1,31	0,98	—	6,42
	$\lg k_n$	2,17	1,54	1,29	1,43	—	6,43
Ni²⁺	$p[\mathrm{L}]_{\overline{n}=n-1/2}$	3,00	2,28	1,74	1,20	0,45	8,67
	$\lg k_n$	2,79	2,18	1,74	1.31	0,65	8,67

VÉRIFICATION DES RÉSULTATS

Afin de vérifier l'exactitude avec laquelle on a déterminé les concentrations à l'équilibre du ligand, dans la dernière partie de ce travail on a recalculé les constantes de formation pour le système des complexes électrodiques,[15] en utilisant comme concentration totale du ligand, la concentration d'équilibre déduite à l'aide de la relation (5).

Pour déterminer ces constantes on a utilisé la méthode d'extrapolation des fonctions de complexation de Leden et Olerup[16–18]

$$F = 1 + \mathrm{K}_1[\mathrm{L}] + \mathrm{K}_2[\mathrm{L}]^2 + \ldots \tag{8}$$

[15] C. Luca, *Bull. Soc. chim. France*, **7**, 2556 (1967).

[16] K. B. Iatzimirski, *Zhur. neorg. Khim.*, **1**, 412 (1956).

[17] I. Leden, *Z. phys. Chem.*, **A – 188**, 160 (1941).

[18] H. Olerup, Thèse, Lund, 1944.

Les fonctions F ont été déterminées des cellules du type

$$\begin{aligned} &(\mathrm{I})\quad \mathrm{Ag/Ag^{+}/NH_4NO_3\ (sat.)/KCl(sat.),\ Hg_2Cl_2/Hg} \\ &(\mathrm{III})\ \mathrm{Ag/[AgL_2]^{+},\ L,\ Me^{2+}/NH_4NO_3\ (sat.)/KCl\ (sat.),\ Hg_2Cl_2/Hg} \end{aligned} \qquad (9)$$

On remarque que la cellule (9—III) est identique à (4—III) et la cellule (9—I) contient la même quantité totale d'ions Ag^+ et le même volume de solution que (9—III)

La différence de tension électromotrice de ces deux éléments donne la relation

$$E_{I} - E_{III} = (RT/F) \ln F \qquad (10)$$

d'où

$$F = e^{\frac{E_I - E_{III}}{RT/F}} \qquad (11)$$

Par extrapolation des fonctions

$$F_1 = (F - 1)/[L] = K_1 + K_2\,[L] + \ldots \qquad (12)$$

et

$$F_2 = (F_1 - K_1)/[L] = K_2 + \ldots \qquad (13)$$

pour $[L] = 0$, on a déterminé les constantes successives de formation K_1 et K_2 pour le système Ag^+—L. Pour donner un exemple on figure dans le tableau 6 les résultats de ces déterminations au cas où la cellule (9—III) Me = Cd.

Tableau 6

Données du système $Ag^+ - [(CH_3)_2CH]_2NH$ déterminées des cellules du type (16) pour Me = Cd

[L]	$E_I - E_{III}$	$F.10^{-3}$	$F_1.10^{-4}$	$F_2.10^{-7}$
0,002744	0,1166	0,095	3,415	1,208
0,006223	0,1587	0,490	7,85	1,245
0,012045	0,1921	1,803	14,96	1,234
0,020475	0,2190	5,147	25,13	1,223
0,037370	0,2494	16,854	45,10	1,204
0,063984	0,2770	48,140	75,23	1,174
0,092505	0,2959	100,50	108,64	1,174
0,167800	0,3257	319,6	190,46	1,134

$K_1 = 1{,}0.10^3$; $K_2 = 1{,}149.10^7$.

La forme de ces courbes d'extrapolation a montré la formation de la solution de deux complexes seulement ($K_1 = 10^3$; $K_2 = 1{,}15.10^7$), ce qui concorde avec les résultats obtenus dans le travail antérieur ($K_1 = 10^3$; $K_2 = 1{,}12.10^{7}$)[10], démontrant ainsi le bon fonctionnement des électrodes *métal-complexe* utilisées.

Revue Roumaine de Chimie, 14, 1407–1417 (1969)

PHOTOPOLYMERIZATION OF ACRYLONITRILE IN THE PRESENCE OF SOME ANTHRAQUINONE DYES

D. FELDMAN, VIOLETA NUTA and CR. SIMIONESCU
Institute of Macromolecular Chemistry "P. Poni"
Jassy, Aleea Grigore Ghica Vodă 41 A

Received May 9, 1969

The kinetics of acrylonitrile photopolymerization in the presence of anthraquinone dyes was studied. Time duration, polymerization temperature, DMF/water ratio and concentration in photosensitizers were particularly followed. The best results were provided by yellow dyes Indanthren 3R. The polymers obtained were coloured and investigated from the viewpoint of their molecular weight by UV and IR spectroscopy. These results showed that the photosensitizers were chemically linked to the PAN macromolecules.

INTRODUCTION

An increased number of works on the synthesis of some vinyl polymers by photopolymerization has been recorded of late. Most of them discuss the utilization of various organic dyes as photosensitizers, with a view either to increasing the reaction rate, respectively photopolymerization conversion, [1–8] or to obtaining the synthesis of coloured polymers. [9–13]

A previous work [9] studied the kinetics of acrylonitrile (AN) photopolymerization with a series of reactive dyes of the Cibacron, Procion and Remazol groups. The present paper gives some kinetic data on photopolymerization of the same monomer in the presence of some anthraquinone dyes produced in our country.

[1] V. I. Kosiacov and B. V. Makuskin, *Vysokomol. Soedineniya, A*, **9**, 2732 (1967).

[2] C. S. Hsia Chen, *J. Polymer Sci., A*, **3**, 1107 (1965).

[3] G. Delzenne, *Ind. chim. belge*, **24**, 739 (1959).

[4] Q. Anwaruddin and M. Santoppa, *J. Polymer Sci., B*, **5**, 361 (1967).

[5] U. Laridon, G. Delzenne and A. Conix, *J. Phot. Sci. and Eng.*, **9**, 364 (1965).

[6] G. Oster and Y. Mizoutani, *J. Polymer Sci.*, **22**, 173 (1956).

[7] Cr. Simionescu and C. Ungureanu, *Rev. Roumaine Chim.*, **13**, 347 (1968).

[8] Cr. Simionescu and C. Ungureanu, *Rev. Roumaine Chim.*, **9**, 627 (1964).

[9] Cr. Simionescu, D. Feldman and C. Noghin, *Rev. Roumaine Chim.*, **12**, 1481 (1967).

[10] Cr. Simionescu, D. Feldman and C. Noghin, Brevet R.S.R., no 48 983, 1967.

[11] V. M. Arhiptev, A. N. Bicov and V. F. Gorotchin, *Khim. Volokna*, **2**, 13 (1967).

[12] A. N. Bicov and V. M. Arhiptev, *Izvest. V.U.Z.M.V.O. S.S.SR., Khim. i Khim. Tekhnol.*, **8**, 1001 (1965).

[13] A. M. Arhiptev and A. N. Bicov, *Khim. Volokna*, **3**, 19 (1967).

EXPERIMENTAL

AN photopolymerization was performed with a UV source of 125 W in a quartz installation with continuous stirring and thermostating. In all experiments a 3 cm distance from the radiation source was maintained and constant volumes of 25.5 ml were used, totalizing the components of the reaction system.

AN and dimethylformamide (DMF) were previously purified by bidistillation. The photosensitizers used were : Anthraquinone reactive, Quinizarin and Indanthrene Yellow 3R, produced by ICECHIM, Bucharest. These photosensitizers were chosen from a great number of autochthonous anthraquinone dyes, because of their good solubility in water (excepting Quinizarin, which is only partly soluble).

Table 1

Dyes used in this work

N°	Name	Chemical structure
1	Anthraquinone reactive	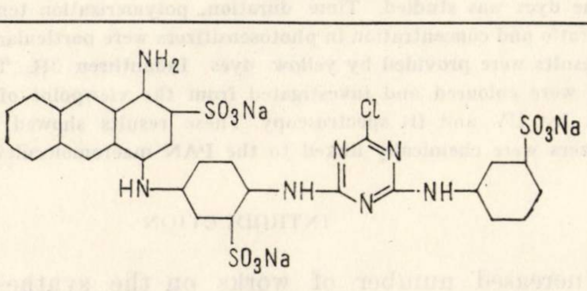
2	Quinizarin	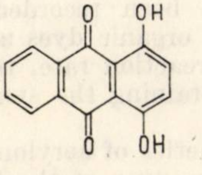
3	Indanthrene Yellow 3R	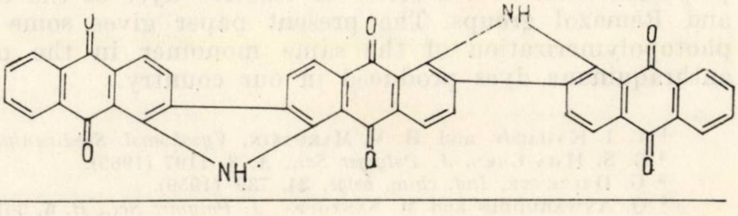

Their structures are presented in table 1.

The kinetic study of photopolymerization followed the following factors :

- polymerization time ;
- polymerization temperature ;
- DMF/water ratio ;
- dye concentration.

AN conversion was used to establish the variations of the reaction rate : molecular weights of polyacrylonitrile (PAN) were calculated with the relation :

$$[\eta] = 1.75 \times 10^{-3} \times M^{0.66}$$

resorting to PAN solutions in DMF.[14]

Using Anthraquinone reactive in concentrations of 0.1 g/l water, for 1–3 hours, conversions under 20 % were achieved. The same thing was observed also in the case of Quinizarin, which was used in concentrations of up to 0.002 g/l in the water/dimethylacetamide system (volume ratio 4/1). That is why most of the kinetic data were studied in the case of the photosensitizer Indanthrene Yellow 3R which offers higher reaction rates. The use of the Anthraquinone reactive involved its purification by dyalysis in view of removing sodium chloride and, possibly, of other salts able to inhibit AN photopolymerization. Quinizarin and Indanthrene Yellow 3R required no special treatment as their purity was high.

a) *Influence of polymerization time*

The time of polymerization varied while temperature (30 ± 0.05°), concentration of Indanthrene Yellow 3R dye (0.003 g/l), water/DMF ratio (11/4, respectively 16.5 cc bidistilled water and 6.0 cc DMF – found to be optimum in a previous work) and monomer amount (3.0 cc) were maintained constant. Experiments were carried out in closed vessels in the presence of a constant volume of air. The obtained conversions – determined gravimetrically – are presented in the diagram of figure 1 (curve 1).

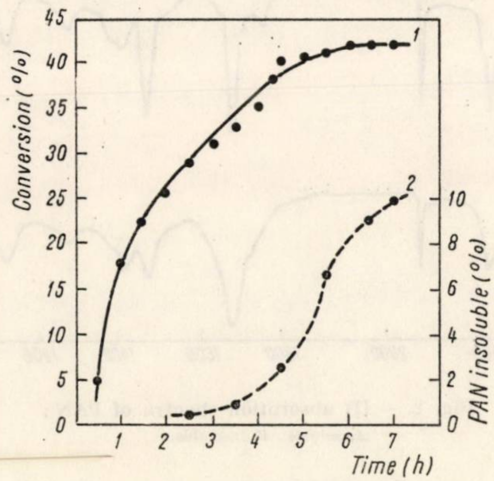

Fig. 1. – Variation of AN conversion and of the amount of insoluble polymer with polymerization time :

1, AN conversion; *2*, insoluble PAN.

---

[14] * * * "Synthetic Fibers"-MICH, Ed. Tehn. Bucharest 1960, p. 139.

Their examination permits to ascertain that polymer amount increases with the time of photopolymerization; this increase is greater up to about 4.5 – 5 h; after this time interval, the obtained yields are maintained constant around values of 41 – 42 %. Immediately after removing from the apparatus in the samples obtained at various time intervals, hydroquinone was added to stop any post-polymerization reaction that might induce errors in conversion determination. PAN was filtered, washed with hot bidistilled water and dried at 65° up to constant weight. The study of polymers obtained at intervals of more than 2.5 hours showed that they are not completely soluble in DMF; the amount of insoluble polymer increases with the time of photopolymerization as seen from curve 2, figure 1. PAN insolubilization may be accounted for by some reticulation processes induced by the prolonged action of UV radiations.[9,15] The study of IR spectra of soluble and insoluble PAN also reflects structure differences that may be of the same nature as those noticed in previous works concerning PAN changes under the action of the heat.[16–19]

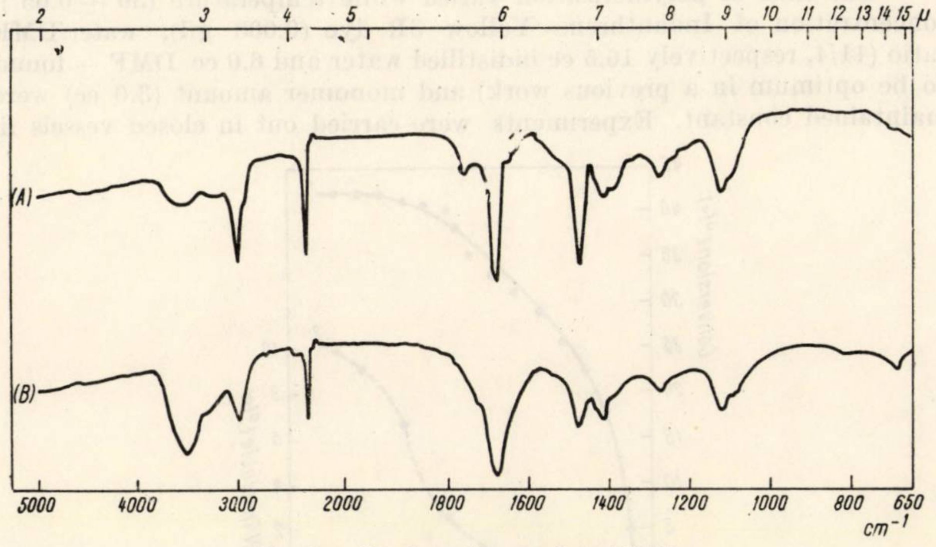

Fig. 2. — IR absorption spectra of PAN:
A, soluble; *B*, insoluble.

Figure 2 presents absorption spectra in the IR range (obtained with a UNICAM – SP 200 apparatus) of soluble (A) and insoluble (B) PAN.

---

[15] CR. SIMIONESCU, D. FELDMAN and M. HRIHOROV, *Rev. Chim. Acad. R.P.R.*, **7**, 1292 (1962).

[16] N. GRASSIE and J. N. HAY, *J. Polymer Sci.*, **56**, 189 (1962).

[17] T. TAKOTA, J. HIROI and M. TANIYAMA, *J. Polymer Sci.*, *A*, **2**, 1567 (1964).

[18] I. A. DRABKIN, L. D. ROZENSTEIN, M. A. GHEIDERIH and B. E. DAVIDOV, *Doklady Akad. Nauk S.S.S.R.*, **154**, 197 (1964).

[19] N. A. KUBASOVA, M. V. SISKINA, N. F. ZALIZNAIA and M. A. GHEIDERIH, *Vysokomol. Soedineniya*, *A*, **10**, 1324 (1968).

The study of these spectrograms points to an obvious difference especially in the 3 500 cm^{-1} and 1 400 – 1 500 cm^{-1} range. In the spectrum of insoluble PAN, the 3 500 cm^{-1} band is much more pronounced, reflecting a high content of $=N-H$ groups, that might initiate the formation of conjugated bonds $-C=N-$ under the action of UV. This fact was pointed out in the case of PAN transformation under the action of heat. [19] The appearance of $=N-H$ groups is directly related to the decrease of nitrile group content (2 300 cm^{-1}) in the insoluble polymer.

Conversion data were used to determine photopolymerization rate (fig. 3); the latter presents a great increase in the first hour of the process and afterwards decreases steadily in proportion as duration increases.

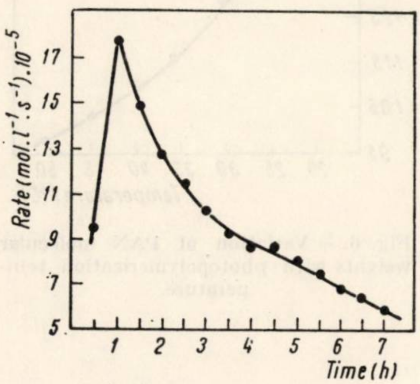

Fig. 3. — Variation of photopolymerization rate with time.

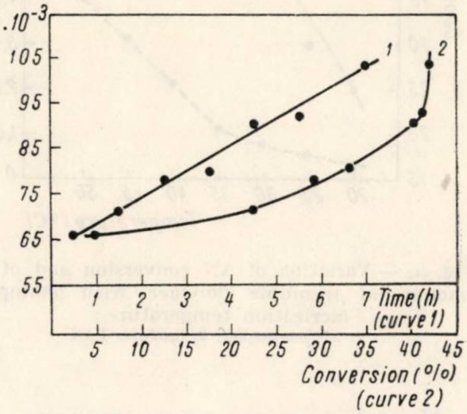

Fig. 4. — Variation of PAN molecular weights: 1, with photopolymerization time; 2, with conversion.

As seen from figure 4, the molecular weights of the formed polymers increase linearly with the photopolymerization time (curve 1) and according to a curve, with conversion (curve 2); they generally range between 65×10^3 and 105×10^3.

b) *The influence of polymerization temperature*

The temperature of the process varied between 20 and 50° while the optimum reaction duration (5 h), water/DMF ratio (11/4), dye concentration (0.003 g/l) and monomer amount (3.00 cc), were maintained constant. Data concerning conversion and insoluble PAN amount are presented in figure 5.

Up to the temperature of 30°, conversion (curve 1) has a more pronounced increase, then its variations are less marked. The values of the mean molecular weights of formed polymers (fig. 6) corroborate the fact that chains with lower polymerization degrees appear parallelly with temperature increase.

In view of determining the constants of reaction rates, the curves of conversion variations were traced function of time for various temperatures (20, 25, 30°) (fig. 7).

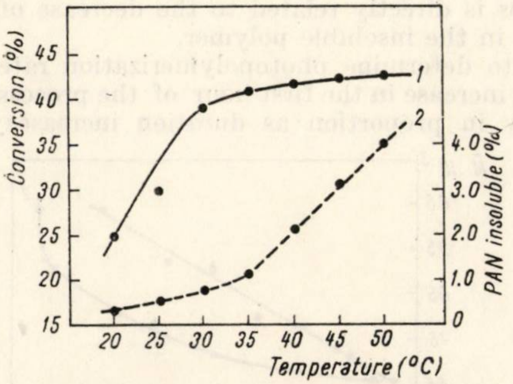

Fig. 5. — Variation of AN conversion and of the amount of insoluble polymer with photopolymerization temperature :
1, AN conversion ; 2, insoluble PAN.

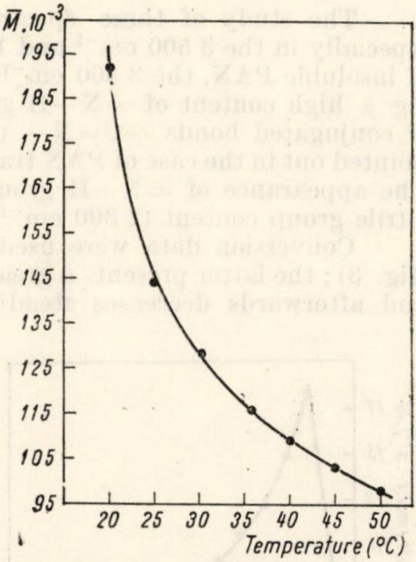

Fig. 6. — Variation of PAN molecular weights with photopolymerization temperature.

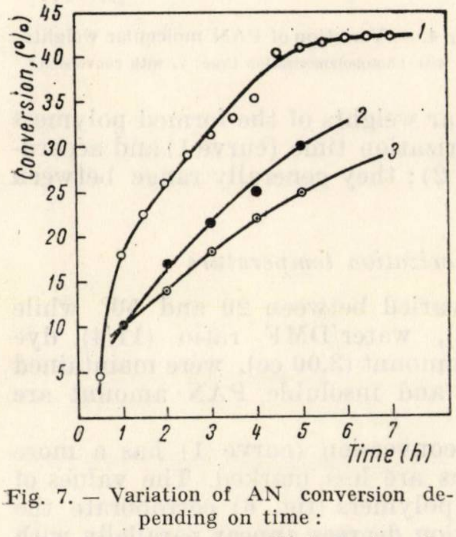

Fig. 7. — Variation of AN conversion depending on time :
1 — at 30° temperature ; 2 — at 25° temperature ; 3 — at 20° temperature.

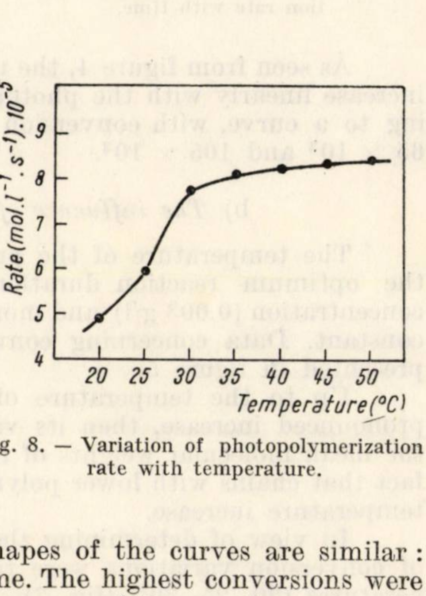

Fig. 8. — Variation of photopolymerization rate with temperature.

Irrespective of temperature, the shapes of the curves are similar : conversion increases with the reaction time. The highest conversions were recorded at the temperature of 30°. The increase of the reaction rate with temperature is also seen in figure 8.

c) *The influence of water/DMF ratio*

The other parameters were maintained constant as in section b) and, working at a temperature of 30°, the influence of the addition of a polar aprotic solvent — DMF — was followed in the photopolymerization medium. It is noticed that (fig. 9) the addition of a low amount of DMF up to a 4/11 (DMF/water) ratio results in an increased conversion, as the maximum polymer amount occurs at that ratio. In the case of higher DMF amounts, conversion steadily decreases (curve 1). It is also noticed that the amount of insoluble polymer (curve 2) decreases with the increase of DMF proportion in the reaction medium. This makes us consider that PAN transformation under the action of UV does not involve DMF participation, as has been found in other researches.[19]

Several attempts were made, replacing DMF with other solvents as, for instance, chloroform, carbon tetrachloride and tetrahydrofuran (THF); the obtained data enable us to observe that the development of the process is favoured in the decreasing order: DMF > THF > carbon tetrachloride > chloroform.

The molecular weight of the polymer formed in the mentioned conditions (fig. 10) decreases steadily with DMF addition from 173×10^3 (in the absence of DMF) up to about 15 000 for a 12/3 DMF/water ratio.

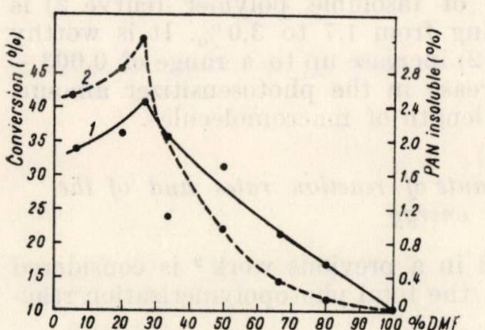

Fig. 9. — Variation of AN conversion and of the amount of insoluble polymer depending on DMF/water ratio:

1, AN conversion; *2*, insoluble PAN.

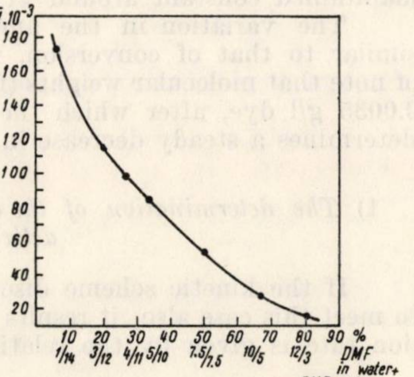

Fig. 10. — Variation of PAN molecular weights depending on DMF/water ratio.

This advocates for the existence of chain transfer reactions in the presence of DMF, determining a pronounced reduction in the molecular weight.

Comparing the molecular weights obtained after the addition of various solvents, it was established that the lowest values are obtained in the presence of THF (10×10^3).

d) *The influence of the dye amount*

The amount of dye ranged from 0.001 to 0.006 g/l while time (5 hours), temperature (30°), water/DMF ratio (11/4) and monomer amount (3.0 cc) were maintained constant. Data are presented in figure 11. The analysis of the curve representing conversion variations (curve 1) demonstrates that conversion increases up to an amount of 0.003—0.0035 g/l Indanthrene Yellow 3R present in the system, and afterwards values are maintained constant around 41%.

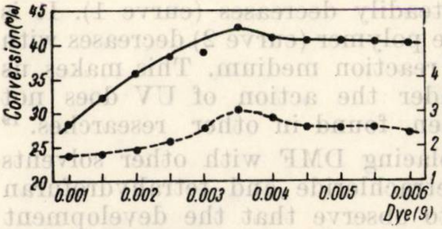

Fig. 11. — Variation of AN conversion and of insoluble polymer amount depending on dye amount :

1, AN conversion ; *2*, insoluble PAN.

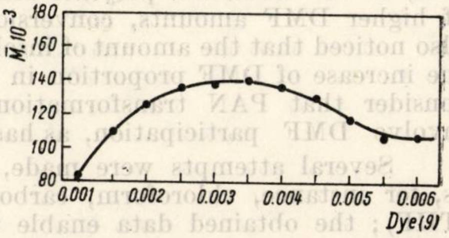

Fig. 12. — Variation of PAN molecular weights depending on the dye amount.

The variation in the amount of insoluble polymer (curve 2) is similar to that of conversion, ranging from 1.7 to 3.0%. It is worthy of note that molecular weights (fig. 12) increase up to a range of 0.003—0.0035 g/l dye, after which the increase in the photosensitizer amount determines a steady decrease in the length of macromolecules.

f) *The determination of the constants of reaction rates and of the activation energy*

If the kinetic scheme discussed in a previous work [9] is considered to meet this case also, it results that the total photopolymerization reaction rate is given by the relation :

$$-\frac{\mathrm{d}\,[\mathrm{M}]}{\mathrm{d}t} = K_p\,[M]\left[\frac{K_1 K_i\,[I]\,[M]^2}{K_t\,(K_i\,[M]+K_d)}\right]^{1/2}$$

where :

M = monomer ;

I = light intensity ;

K_1 = constant of primary radical formation rate ;

K_i = constant of photoinitiation reaction rate ;

K_t = constant of growth termination reaction rate ;

K_p = constant of radical growth reaction rate ;

K_d = constant of radical desactivation reaction rate.

The substitution of the constant ratio by K, which is the constant of total photopolymerization reaction rate, leads to:

$$-\frac{\mathrm{d}[M]}{\mathrm{d}t} = K\,[M]^2\,[I]^{1/2}$$

which by integration gives:

$$\frac{M_0 - M}{M_0 M} = K\,[I]^{1/2}\cdot t$$

where:

M_0 = initial monomer amount;

M = non-reacted monomer amount.

Tracing the variation of $M_0 - M/M_0M$ ratio function of the reaction time (t), the following data are obtained for $K\,[I]^{1/2}$ at various temperatures.

$$K\,[I]^{1/2} = 1.77 \times 10^{-4} \text{ at } 20^\circ$$

$$K\,[I]^{1/2} = 2.66 \times 10^{-4} \text{ at } 25^\circ$$

$$K\,[I]^{1/2} = 3.25 \times 10^{-4} \text{ at } 30^\circ$$

The values are higher than those previously obtained with Cibacron Turkisblau 2 G.[9]

With the help of these data, resorting to Arrhenius relation, it has been established that activation energy of AN photopolymerization in the above conditions is $E = 9.9$ kcal/mol.

g) *The study of polymer dye interaction*

It is worthy of note that in the experimented conditions a coloured PAN is obtained, with a more intense tint in proportion as photosensitizer concentration increases. Time testing of those stainings showed that they are stable.

UV and IR spectroscopic studies were carried out with a view to understanding the nature of the polymer-dye (Indanthrene Yellow 3R) link. For the UV study (with the UNICAM-SP 800 apparatus) solutions of the formed polymer and of a standard polymer were prepared in ethylene carbonate (90 % concentration). The examination of data shows that in the case of the coloured polymer, an intense band appears in the 210—220 mμ range, characteristic of the dye, a band that cannot be found in a polymer obtained in the absence of photosensitizers. The chemical binding of the dye and polymer also results from IR data (UNICAM-SP 200) (fig. 13).

In the case of the coloured polymer (spectrogram B), the 1 780 cm^{-1} band originating from the valency vibration of the C=O group contained by Indanthrene Yellow 3R appears due to photosensitizer linking (spectrogram A). As against spectrogram B, that of a polymer obtained in identical conditions but in the absence of the dye (spectrogram C) does not present this maximum.

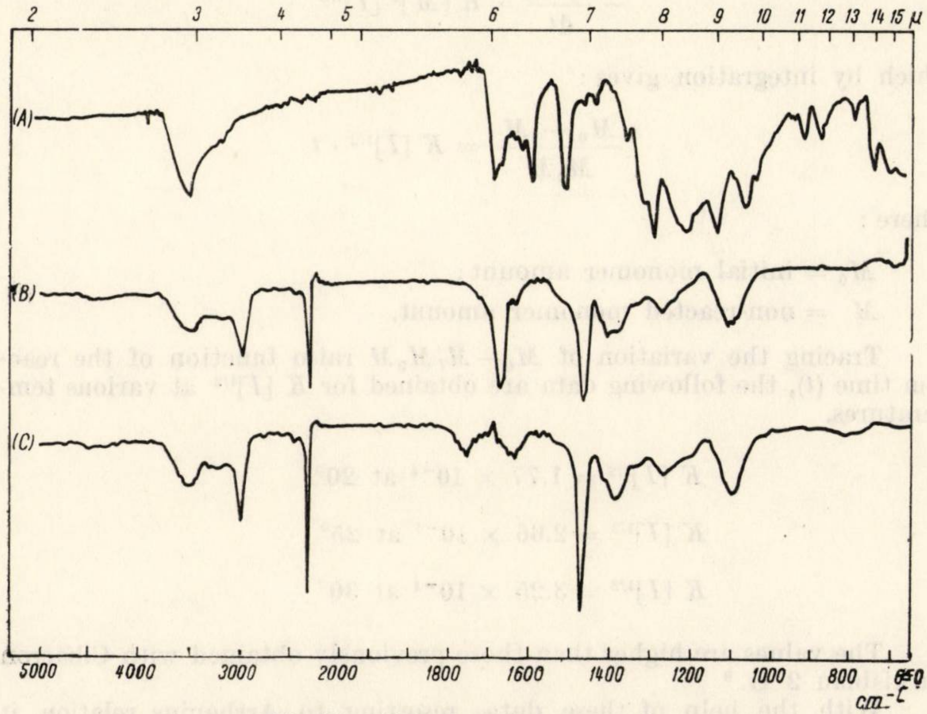

Fig. 13. — I.R. absorption spectra of :
A, Indanthrene Yellow 3R ; *B*, coloured PAN ; *C*, non-coloured PAN.

All these data advocate for a polymer-dye chemical bond.

CONCLUSIONS

The presented data may lead to the following conclusions :

— Some anthraquinone dyes like : Anthraquinone reactive, Quinizarin and Indanthrene Yellow 3R are able to photoinitiate AN polymerization in the aqueous medium as well as in water/DMF, water/dimethylacetamide systems. The best results are obtained with Indanthrene Yellow 3R. The maximum conversions obtained with this photosensitizer reach 42 %.

— Molecular weights of the formed PAN are less influenced by the photosensitizer concentration and more by the DMF amount present in the system ; while in the absence of DMF, high molecular weights are obtained (173×10^3), increasing amounts of this solvent result in lower molecular weight, up to 15×10^3.

– The increase in the photopolymerization time determines the formation in the system of amounts of insoluble polymer ranging from 0.43 to 9.95 %, a product characterized by a structure different from that of the DMF soluble PAN.

– The obtained kinetic data permitted to determine the constants of the total photopolymerization rate for various reaction temperatures as well as the total activation energy (9.9 kcal/mol).

– The UV and IR spectroscopic study of the formed polymer shows that the photosensitizer is linked chemically to its macromolecules.

Revue Roumaine de Chimie, **14**, 1407–1417 (1969)

Revue Roumaine de Chimie, **14**, 1419–1425 (1969)

RÉACTIONS POLYMÈRE-ANALOGUES DU COPOLYMÈRE BINAIRE ACRYLO-NITRILE-ACÉTATE DE VINYLE EN SOLUTIONS ALCALINES

N. ASANDEI et ADÉLAÏDE LIGA

Institut de Chimie Macromoléculaire « P. Poni », Jassy, 41 A, Aleea Gr. Ghica Vodă

Reçu le 10 janvier 1969

On a effectué la modification sur la chaîne d'un copolymère binaire acrylonitrile-acétate de vinyle en obtenant un copolymère tétrafonctionnel. Les réactions ont été conduites tant dans le milieu homogène, que dans le milieu hétérogène (solvants : diméthylformamide, diméthylsulfoxyde, diméthylacétamide, acétone), en utilisant comme agent d'hydrolyse le hydroxyde de sodium. En même temps on examine le mécanisme et la cinétique des réactions étudiées.

1. INTRODUCTION

Les copolymères à base d'acrylonitrile sont connus comme produits de départ pour obtenir des fibres synthétiques, en constituant l'objet de nombreuses publications qui se rapportent autant aux aspects théoriques, qu'à leur importance pratique. [1-12]

Quoiqu'elles aient des propriétés de résistance remarquables, l'utilisation des fibres synthétiques présente des inconvénients engendrés par leur capacité de teinture et d'hydrophilie insatisfaisantes.

---

[1] D. T. Mowry et E. L. Kingwald (Monsanto Chemical Co.), U.S. Pat. 2 861 059 18 nov. 1959 ; *Chem. Abstr.*, **53**, 5755 b (1959).

[2] M. Suzuki, M. Miyama et S. Fujimoto, *Bull. Chem. Soc. Japan*, **35**, 57 (1962).

[3] J. P. Kraig, J. P. Knudsen et V. F. Holland, *Text Res. J.*, **32**, 435 (1962).

[4] I. S. Dorokhina, V. S. Klimenkov et A. D. Abkin, *Khim, Volokna*, **1**, 49 (1962).

[5] B. D. Bogomolov, I. S. Dorokhina et V. S. Klimenkov, *Khim. Volokna*, **2**, 14 (1962).

[6] I. S. Dorokhina et V. S. Klimenkov, *Khim. Volokna*, **5**, 16 (1962).

[7] I. S. Dorokhina, A. D. Abkin et V. S. Klimenkov, *Kolloid. Zhur.*, **24**, 549 (1962).

[8] D. W. Cheape Jr. et R. J. Ford (Monsanto Chemical C°), Belg. Pat. 623 826, 19 avril 1963 ; *Chem Abstr.*, **60**, 9411 d (1964).

[9] A. Mikula (Sandoz Ltd.), U.S. Pat. 3 079 210, 26 février 1963, *Chem. Abstr.*, **58**, 14191 g (1963).

[10] I. S. Dorokhina, V. S. Klimenkov et A. D. Abkin, *Khim. Volokna*, **2**, 5 (1963).

[11] I. S. Dorokhina, A. D. Abkin et V. S. Klimenkov, *Vysokomol. Scedineniya*, **5**, 385 (1963).

[12] H. Pfitzner, H. Baumann, J. Eisele et W. Federkiel (Badische Anilin- und Soda-Fabrik A-G), Pat. 1 228 586, 17 nov. 1966 ; *Chem. Abstr.*, **66**, 38825 y (1967).

La modification de la capacité tinctoriale et de certaines propriétés physiques des polymères destinés à la fabrication des fibres synthétiques peut être réalisée par des réactions d'hydrolyse contrôlée sur la chaîne.

Dans cette note on étudie les conditions de modification des groupes fonctionnels du copolymère binaire acrylonitrile-acétate de vinyle, dans les conditions d'une réaction hétérogène d'hydrolyse en solutions alcalines. A la suite de cette réaction on obtient des polymères multicomposants qui contiennent outre des groupes nitriliques et esthériques initiaux des groupes hydroxyliques et carboxyliques.

2. DONNÉES EXPÉRIMENTALES

A. *Synthèse du copolymère acrylonitrile-acétate de vinyle* (AN–AcV)

On a employé des réactifs purifiés par des méthodes usuelles. La copolymérisation a été réalisée en émulsion en utilisant un système redox d'initiateurs dans les conditions suivantes:

- rapport monomère/eau = 1/3 ;
- persulfate de potassium = 0,65 % par rapport au monomère ;
- métabisulfite de sodium = 1,7 × quantité de persulfate ;
- température 60° ;
- durée 90 mn sous forte agitation.

La teneur en azote du produit de réaction, précipité dans l'eau, lavé, purifié et séché à 60° a été analysée.

On a synthétisé les copolymères ayant les compositions suivantes

I AN 97,5 %	AcV 2,5 %	N = 25,8 %
II AN 66 %	AcV 34 %	N = 17,39 %
III AN 50 %	AcV 50 %	N = 13,44 %

On a réalisé la composition III équimoléculaire en partant du fait, que pour ce rapport des composants, le copolymère devient soluble dans l'acétone. Pour déterminer la composition du mélange initial de monomères $\left(\frac{M_1^0}{M_2^0}\right)$ on a utilisé la relation

$$\frac{M_1^0}{M_2^0} = \frac{(y-1) + \sqrt{(y-1)^2 + 4_{r_1 r_2 y}}}{2r_1}$$

où $y = \frac{dM_1}{dM_2}$ – la composition finale du copolymère

$r_1 = 4{,}2$

$r_2 = 0{,}05.$

Les réactivités r_1, r_2 sont données par la littérature.[13]

---

[13] L. J. Young, *J. Polymer Sci.*, 54, 411 (1961).

B. *Hydrolyse alcaline du copolymère acrylonitrile- acétatede vinyle*

Le processus a été conduit en système hétérogène pour les compositions I et II dont les solvants (diméthylformamide, diméthylsulfoxyde, diméthylacétamide) sont décomposés par l'agent hydrolysant. Pour la composition équimoléculaire III on a appliqué l'hydrolyse en solution en utilisant un solvant de type aprotique (l'acétone) relativement inerte envers le NaOH.

On a obtenu l'hydrolyse alcaline en employant des solutions de NaOH 0,1 et 0,5 N, dans les conditions de travail suivantes :

- température 60°
- rapport polymère (g) — sol. NaOH (ml) = 1 : 40
- forte agitation
- durée 2—4 h.

Le dosage de l'ammoniaque dégagé durant l'hydrolyse et le titrage acidimétrique du NaOH non participant à la réaction a permis l'étude du processus.

3. RÉSULTATS ET DISCUSSIONS

Sur les figures 1—2 on remarque la configuration générale de l'hydrolyse des groupes nitriliques et estériques à une concentration donnée par le NaOH (fig. 1 ; fig. 2).

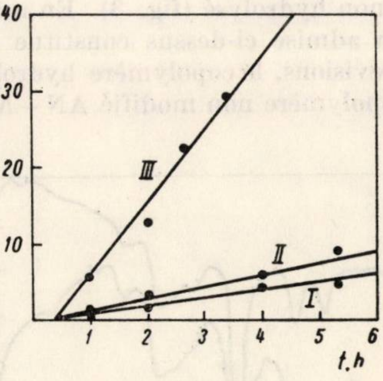

Fig. 1. — Hydrolyse des groupes — CN, à 60°, avec 0,1N NaOH:
I. Copolymère avec —CN : — $OCOCH_3$ = 97,5 : 2,5; II : 66; 34; III : 50: 50.

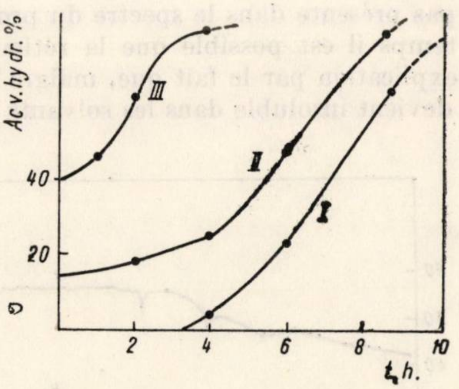

Fig. 2. — Hydrolyse des groupes — OCO — CH_3 à 60°, avec 0,1 N, NaOH :
I. Copolymère avec —CN : — $OCOCH_3$ = 97,5 : 2,5; II : 66 : 34; III 50 :50.

Tandis que sur la figure 1 on remarque une évolution normale, linéaire de la quantité d'acrylonitrile hydrolysé en fonction du temps, sur la figure 2, on peut constater une déviation de la règle linéaire, appartenant à la variation de la concentration des groupes acétate hydrolysé en fonction du temps. Dans ce dernier cas, sur une portion relativement grande de la période d'hydrolyse, une certaine proportionnalité persiste entre la quantité calculée en pour-cent d'ester hydrolysé et la durée du processus. A un certain degré de conversion des groupes acétate (approximativement pour 80 %) atteint à une moindre durée dans le cas du système homogène, cette proportionnalité ne se maintient plus. On peut fournir deux explications :

a) L'apparition d'une réaction réversible à l'hydrolyse qui devient significative au fur et à mesure que la concentration du système en CH_3COOH augmente.

b) La formation sur la même chaîne de certains cycles de 4 et 5 termes par l'intermédiaire de liaisons d'hydrogène entre les groupes COOH et OH apparus à la suite de l'hydrolyse de l'acrylonitrile et respectivement de l'acétate de vinyle, ou, ce qui est plus probable, la formation de la même liaison entre deux chaînes voisines. Dans ce cas-ci, en considérant que la vitesse d'hydrolyse de l'ester dépend non seulement de la concentration $[OH^-]$ mais aussi de l'effet catalytique des groupes COOH avoisinés, le blocage de ces derniers réduit leur activité catalytique intermoléculaire et par conséquent la conversion des groupes acétate diminue.[14]

Cette dernière hypothèse paraît être celle valable parce qu'elle reçoit une confirmation expérimentale par l'apparition dans le spectre IR, de la bande OH associée à celle de $3550\ cm^{-1}$ — bande qui n'est pas présente dans le spectre du produit non hydrolysé (fig. 3). En même temps il est possible que la réticulation admise ci-dessus constitue une explication par le fait que, malgré les prévisions, le copolymère hydrolysé devient insoluble dans les solvants du copolymère non modifié AN—AcV.

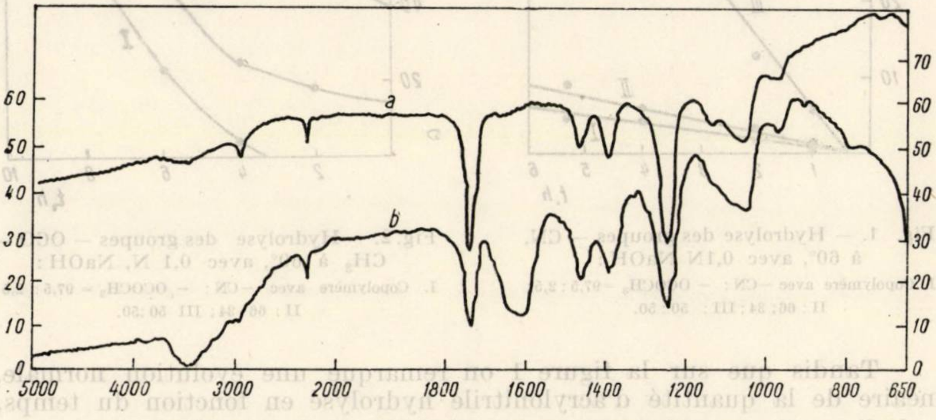

Fig. 3. — Spectre d'absorption en IR du copolymère II

a, avant l'hydrolyse ; *b*, après l'hydrolyse.

---

[14] K. Dusek, I. Klaban et Ia. Kopetka, *Vysokomol. Soedineniya*, **4**, 1595 (1962).

4. LE MÉCANISME ET LA CINÉTIQUE DE LA RÉACTION D'HYDROLYSE ALCALINE DU COPOLYMÈRE ACRYLONITRILE-ACÉTATE DE VINYLE

Des deux composants du copolymère, on a considéré initialement qu'il est plus intéressant de poursuivre l'évolution de l'hydrolyse de l'ester, puisque son comportement en pareilles réactions paraît être différent en fonction des conditions dans lesquelles se développe le processus.

Laidler et Erying[15], en appliquant la théorie des réactions-molécule dipolaire — molécule dipolaire tant à l'hydrolyse acide des esters qu'à celle alcaline considèrent que le mécanisme de la dernière peut être représenté de la manière suivante

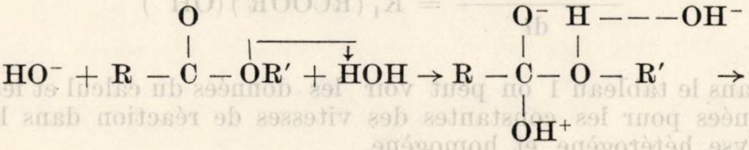

$$HO^- + R - \overset{\overset{O}{|}}{C} - OR' + HOH \rightarrow R - \underset{\underset{OH^+}{|}}{\overset{\overset{O^-}{|}}{C}} - \overset{\overset{H---OH^-}{|}}{O} - R' \rightarrow$$

$$\rightarrow RCOOH + HOR' + OH^-$$

où les flèches représentent les déplacements de l'électron.

Dans cette situation la vitesse d'hydrolyse de l'ester dépendrait de la concentration des 3 espèces moléculaires selon une équation du 3e ordre

$$\frac{d(RCOOR')}{dt} = K(RCOOR')(HOH)(OH^-) \qquad (1)$$

Dans le cas où le développement de la réaction a lieu en présence de différents autres groupes fonctionnels, distribués sur la même chaîne, la vitesse d'hydrolyse des polyesters est affectée autant par l'existence de ceux-ci que par leur manière de répartition sur les chaînes macromoléculaires. De même on ne peut pas négliger l'effet produit sur la vitesse d'hydrolyse par le milieu de réaction, hétérogène ou homogène. Ainsi, dans le cas de l'hydrolyse réalisée de manière hétérogène dans un excès d'eau relativement grand, en considérant que la vitesse de diffusion de l'eau est constante, la concentration de l'eau et de l'ester peut être supposée également constante et l'éq. 1 se réduit à une relation correspondant à une réaction d'ordre pseudo-monomoléculaire[16]

$$\frac{d(RCOOR')}{dt} = K(OH^-) \qquad (2)$$

---

[15] Ed. Amis, « Solvent Effects on Reaction Rates and Mechanisms », Academic Press, New York, 1966 p. 62.

[16] E. F. Jordan Jr. et W. S. Port, *J. Polymer Sci.*, **32**, 47 (1958).

Dans le cas de l'hydrolyse homogène (composition III, équimoléculaire), les réactions de modification sur la chaîne peuvent se produire à une vitesse beaucoup plus grande, due à l'accessibilité réciproque des réactants.

Bien qu'influencée par la présence des groupes COOH parus en plus grand nombre, dans ce cas-ci, par la transformation des groupes CN, la réaction vue en son ensemble, peut être tout de même traitée comme un cas général, donc on admet un schéma de réaction du IIe ordre pour lequel la constante caractérisant la phase principale du processus d'hydrolyse est exprimée par l'équation[17]

$$\frac{d\,(\mathrm{RCOOR'})}{dt} = K_1\,(\mathrm{RCOOR'})\,(\mathrm{OH^-}) \tag{3}$$

Dans le tableau 1 on peut voir les données du calcul et les valeurs déterminées pour les constantes des vitesses de réaction dans le cas de l'hydrolyse hétérogène et homogène.

Tableau 1

Hydrolyse alcaline du copolymère AN-AcV à 60°

Copolymère	$\frac{(\mathrm{Ac})_0}{\%\ \text{mole/l}}$	$\frac{(\mathrm{OH})_0}{\%\ \text{mole/l}}$	Relation de calcul	K h^{-1}	K $1 . \text{mole}^{-1}$ h^{-1}	Observations
I	2,50 —	20 —	(2)	0,0317	—	Hétérogène
II	34,00 —	20 —	(2)	0.132	—	,,
III	– 0,0876*	–0,133	(3)	—	7,47	Homogène

* On a employé des solutions diluées (approximativement 1,5°/₀) pour prévenir la précipitation du polymèr due à l'addition de NaOH.

5. CONCLUSIONS

L'hydrolyse en bain alcalin du copolymère à base d'acrylonitrile à l'état de poussière ou de fibre, à paramètres contrôlés, a permis d'obtenir de nouveaux types de copolymères.

La direction de la modification des groupes fonctionnels et la vitesse avec laquelle ces réactions se produisent sont en général difficiles à établir à cause des nombreuses interférences qui ont lieu dans les conditions d'hydrolyse alcaline hétérogène.

Le copolymère qui résulte contient quatre groupes fonctionnels, $-\mathrm{CN}$, $-\mathrm{OCOCH_3}$, $-\mathrm{OH}$ et $-\mathrm{COOH}$. Probablement qu'à côté de ces groupes fonctionnels il y a aussi le groupe $-\mathrm{NH_2}$ intermédiaire dans l'hydrolyse du groupe $-\mathrm{CN}$ au groupe $-\mathrm{COOH}$.

---

[17] L. A. Kiprianova et A. F. Rekaseva, *Doklady Akad. Nauk. S.S.S.R.*, **153**, 642 (1963).

Les nouveaux groupes fonctionnels forment vraisemblablement des liaisons d'adhésion entre les chaînes ce qui détermine une insolubilité partielle des copolymères obtenus à l'aide de différents solvants.

Cette situation peut être améliorée par la modification des conditions d'hydrolyse ou par la synthèse de certains copolymères auxquels on peut ajouter initialement comme comonomères outre l'acrylonitrile et l'acétate de vinyle, de petites quantités de chlorure de vinyle ou de styrène.

Revue Roumaine de Chimie, **14**, 1427 – 1434 (1969)

DARSTELLUNG UND UNTERSUCHUNG DER HYDROACRIDINE. I

ÜBER DIE SYNTHESE DES *SYMM*-OKTAHYDROACRIDINS, *ALFA*-PERHYDROACRIDINS UND *BETA*-PERHYDROACRIDINS

N. BĂRBULESCU und F. POTMISCHIL

aus dem Organisch-Chemischen Laboratorium der Universität
Bukarest, Spl. Independenţei 89

Eingegangen am 5. Februar 1969

Aus der Reaktion des 2,2-Methylen-bis-cyclohexanons mit Formamid entsteht ein Gemisch von *symm*-Oktahydroacridin, *alfa*-Perhydroacridin und *beta*-Perhydroacridin. Es wurde ein Verfahren zur verhältnismäßig genauen Bestimmung der drei Reaktionsprodukte entwickelt: beide Perhydroacridine werden als Nitrosamine vom Oktahydroacridin getrennt, und nachher das Verhältnis „*alfa*"/„*beta*" IR-spektroskopisch ermittelt. Aufgrund dieses Verfahrens wurde die Änderung der Zusammensetzung des Reaktionsgemisches mit den Reaktionsbedingungen untersucht, indem man die Reaktion mit zwei Isomeren des 2,2-Methylen-bis-cyclohexanons, in Abwesenheit und in Anwesenheit von Ameisensäure ausführte.

Es wurde festgestellt, daß durch Anwendung der Leuckart-Reaktion an 2,2-Methylen-bis-cyclohexanon ein Gemisch von *symm*-Oktahydroacridin und Perhydroacridin entsteht.[1,2] Der Oktahydroacridin- oder Perhydroacridingehalt des Gemisches kann nach Belieben erhöht werden, indem man die Reaktion in Gegenwart von Nickel oder bzw. Ameisensäure ausführt.[3,4] Das Perhydroacridin entsteht in Gestalt zweier Konformere: das schon seit 1923 bekannte[5] *alfa*-Perhydroacridin und das von Masamune und Wakamatsu[6,7] und Vissotzkii[8] beschriebene *beta*-Perhydroacridin (Schema 1).

---

[1] J. Colonge, J. Dreux und H. Delplace, *Bull. Soc. chim. France*, **1957**, 342.

[2] M. N. Tilitschenko und V. I. Vissotzkii, *Doklady Akad. Nauk. S.S.S.R.*, **119**, 1162 (1958).

[3] V. I. Vissotzkii, *Uchenye Zapiski Yakutsk. Gosudarstv. Univ., Ser. Estestven Nauk*, **1958**, 49; *Chem. Abstr.*, **55**, 25.945d (1961).

[4] M. N. Tilitschenko, V. I. Vissotzkii und V. G. Hartschenko, *Uchenye Zapiski Saratovsk. Univ.*, **71**, 159 (1959); *Chem. Abstr.*, **55**, 23.533f (1961).

[5] J. v. Braun, A. Petzold und A. Schultheiss, *Ber. dtsch. chem. Ges.*, **56**, 1347 (1923).

[6] T. Masamune und S. Wakamatsu, *J. Chem. Soc. Japan* (*Pure Chem. Sect.*), **77**, 1145 (1956).

[7] T. Masamune und S. Wakamatsu, *J. Fac. Sci. Hokkaidô Univ. Ser. III*, **5**, 47 (1957).

[8] V. I. Vissotzkii, *Dissertation*, Irkutsk, 1964.

Da es vom praktischem sowie vom theoretischem Standpunkte aus interessant ist, die Änderung der Zusammensetzung des Reaktionsgemisches mit den Reaktionsbedingungen genau zu kennen, wurde in

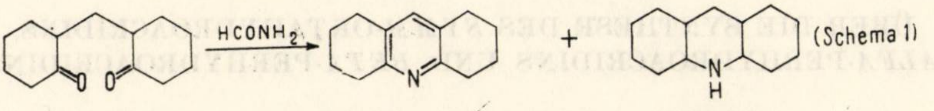

I II alfa (III) beta (IV)

der vorliegenden Arbeit ein Verfahren zur verhältnismäßig genauen Bestimmung (± 2 %) der Teilausbeuten an (II), (III) und (IV) entwickelt, und aufgrund dieses Verfahrens wurde die Änderung des Verhältnisses (II) : (III) : (IV) unter einigen verschiedenen Reaktionsbedingungen untersucht.

Das Verfahren besteht, im großen gesehen, aus folgendem : Man versetzt das in wäßriger Essigsäure gelöste Reaktionsgemisch mit Natriumnitrit, dabei werden die Perhydroacridine (III) und (IV) beinahe vollkommen in die entsprechenden Nitrosamine (V) und (VI) umgesetzt (Schema 2) :

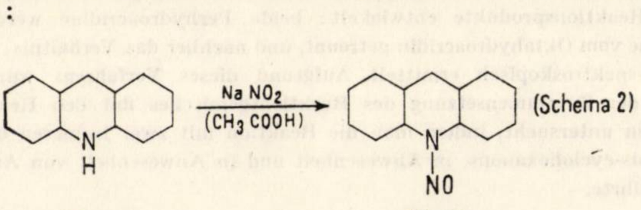

alfa (III) beta (IV) alfa (V) beta (VI)

Diese scheiden als ein gelbes Öl aus, während das Oktahydroacridin (II) nicht reagiert und als Acetat weiter in Lösung bleibt. Man zieht die Nitrosamine (V) und (VI) mit Äther aus, und nach Alkalisieren der wäßrigen Lösung zieht man das Oktahydroacridin ebenfalls mit Äther aus. Nach Entfernung des Äthers bestimmt man (II) und bzw. die Summe (V + VI) gravimetrisch. Das IR-Spektrum des Nitrosaminengemisches wird nachher mit einer Reihe Vergleichsspektren (Bereich 1300—1000 cm.$^{-1}$) (Abb. 1) zur Bestimmung des Verhältnisses (V) : (VI) verglichen.

Wie aus Abbildung 1 ersichtlich, ist das allgemeine Bild des Bereiches 1300—1000 cm^{-1} in großem Maße von der Änderung des Verhältnisses (V) : (VI) abhängig. Es genügt darum, das Aussehen des Probespektrums mit dem der Vergleichsspektren zu vergleichen, ohne die absolute Intensität der Banden messen zu müssen. Auf diese Weise werden Konzentrationsfehler und die Ungenauigkeit des Gerätes ausgeschlossen. (Freilich ist es doch wünschenswert, daß der Konzentrationsunterschied zwischen Probelösung und Eichlösungen so klein wie möglich sei).

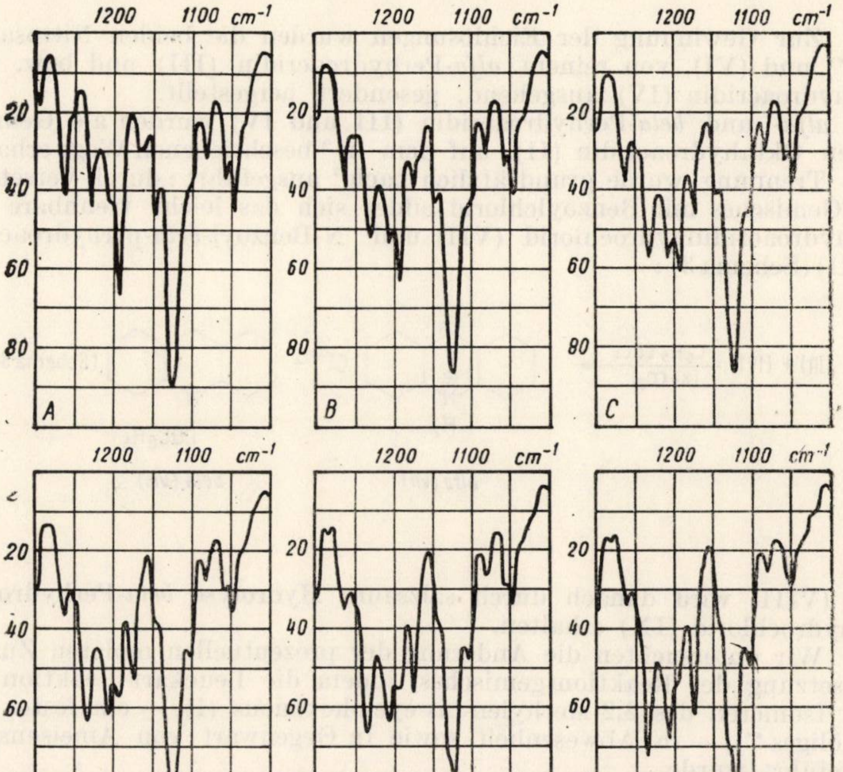

Abb. 1. – Der Bereich 1300–1000 cm^{-1} des IR-Spektrums des N-Nitroso-*alfa*-perhydroacridins (V), N-Nitroso-*beta*-perhydroacridins (VI) und ihrer Gemische *A*, 100% (V); *B*, 80% (V) und 20% (VI); *C*, 70% (V) und 30% (VI); *D*, 60% (V) und 40% (VI); *E*, 50% (V) und 50% (VI); *F*, 40% (V) und 60% (VI); *G*, 30% (V) und 70% (VI); *H*, 20% (V) und 80% (VI); *I*, 100% (VI).

Zur Gewinnung der Eichlösungen wurden die beiden Nitrosamine (V) *) und (VI), von reinem *alfa*-Perhydroacridin (III) und bzw. *beta*-Perhydroacridin (IV) ausgehend, gesondert hergestellt.

alfa- und *beta*-Perhydroacridin (III und IV) wurden als Gemisch, neben Oktahydroacridin (II), auf dem in [2] beschriebenen Wege erhalten. Ihre Trennung wurde grundsätzlich nach [7] ausgeführt: durch Versetzung des Gemisches mit Benzoylchlorid bildet sich das leicht trennbare *alfa*-Perhydroacridinhydrochlorid (VII) und N-Benzoyl-*beta*-perhydroacridin (VIII) (Schema 3):

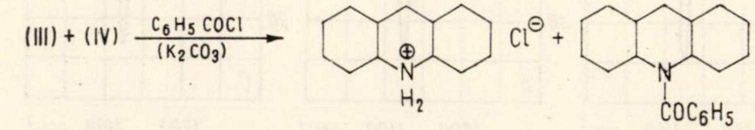

(Schema 3)

alfa (VII) *beta* (VIII)

Aus (VIII) wird danach durch salzsaure Hydrolyse *beta*-Perhydroacridinhydrochlorid (IX) erhalten.

Wir untersuchten die Änderung der prozentuellen molaren Zusammensetzung des Reaktionsgemisches, indem die Leuckart-Reaktion mit zwei Isomeren des 2,2-Methylen-bis-cyclohexanons (I), — ein festes und ein öliges **), — in Abwesenheit sowie in Gegenwart von Ameisensäure ausgeführt wurde.

Die Ergebnisse dieser Untersuchung (Tabelle 1) führen zu folgenden Folgerungen:

1. Die Ameisensäure beeinflußt die Gesamtausbeute nicht.
2. Wenn die Umsetzung in Gegenwart von Ameisensäure erfolgt, dann steigt der *alfa*-Perhydroacridingehalt (III) ansehnlich, auf Kosten des Oktahydroacridingehaltes (II).
3. Der *beta*-Perhydroacridingehalt (IV) bleibt derselbe, gleichgültig ob die Umsetzung in Abwesenheit oder Anwesenheit der Ameisensäure erfolgt.

---

*) Dem Nitrosamin (V) wurde Schmp. 217° zugeschrieben,[5] während die von uns erhaltene Verbindung sich bei 87—88° verflüssigt. Da die Autoren weder Darstellungsweise, noch Ausbeute oder Analyse angaben, ist es sehr schwierig in bezug auf die Identität der Substanz mit Schmp. 217° eine Meinung zu äußern.

Die der Formel (V) entsprechende Struktur unserer Verbindung ist durch die Stickstoffanalyse, durch das UV-Spektrum, das dem des N-Nitroso-piperidins [9] ähnlich ist, und durch das IR-Spektrum, das die charakteristische Absorption der N-Nitroso-Gruppe [10] aufweist, sichergestellt.

**) Hinsichtlich des ersten Isomers sind die Literaturangaben ziemlich übereinstimmend: 58° [11] und 61° [12] Schmp.; was das zweite anbetrifft sind sie gegensätzlich: 51° [11] und bzw. ölig.[12]

[9] R. N. HASZELDINE und J. JANDER, *J. Chem. Soc.*, **1954**, 691.

[10] M. AVRAM und GH. D. MATEESCU, ,,Spectroscopia în infraroşu, aplicaţii în chimia organică'', Editura Tehnică, Bukarest, 1966, S. 385.

[11] A. PALSKY, J. HUET und J. DREUX, *Compt. rend.*, **262**, 1543 (1966).

[12] L. BIRKOFER, SUNG MAN KIM und H. D. ENGELS, *Chem. Ber.*, **95**, 1495 (1962).

Tabelle 1

Die Abhängigkeit der Zusammensetzung des Reaktionsgemisches vom Isomer des *delta*-Diketons*) und vom Ameisensäurezusatz **)

Vers. Nr.	Isomer	HCOOH–Zusatz (mMol)	Entstandene Produkte (mMol)			Gesamtausbeute (%)	Zuammensetzung des Reaktionsgemisches (Mol %)		
			Oktahydroacridin (II)	*alfa*-Perhydroacridin (III)	*beta*-Perhydroacridin (IV)		Oktahydroacridin (II)	*alfa*-Perhydroacridin (III)	*beta*-Perhydroacridin (IV)
1	A	—	20,4	8,7	17,8	94	43	19	38
2	B	—	18,6	7,4	15,0	82	45	18	37
3	A	50,0	9,8	16,5	20,2	93	21	36	43
4	B	50,0	12,7	13,4	16,4	85	30	31	39
5	A	150,0	14,7	15,1	18,4	96	31	31	38

*) Die Reaktion wurde mit zwei Isomeren des 2,2-Methylen-bis-cyclohexanons (I) ausgeführt: A, mit Schmp. 58° und B, flüssig, mit Sdp. 148–150°/1mm und $n_D^{23} = 1{,}5035$.

**) Standardbedingungen: Quantität des *delta*-Diketons 10,4 g (50 mMol); Quantität des Formamids 27g (600 mMol); Reaktionstemperatur 165 ± 2°. Die Ameisensäure (als 90%ige Lösung) wurde mit dem Formamid vor dem Reaktionsbeginn vermischt.

4. Der Wert des Verhältnisses (IV) : (III) ist 2 wenn die Umsetzung in Abwesenheit, und bzw. 1,2 wenn sie in Anwesenheit der Ameisensäure verläuft, gleichgültig ob letztere in einer dem 2,2-Methylen-bis-cyclohexanon (I) äquivalenten oder dreifachen Konzentration teilnimmt.

BESCHREIBUNG DER VERSUCHE

Alle IR-Spektren wurden mit einem „UR–20"- und die UV-Spektren mit einem „Beckmann DB"-Gerät gemessen. Alle Schmelzpunkte sind unkorrigiert und wurden, wenn nicht anders vermerkt, mit einem „Boëtius"-Heiztischmikroskop bestimmt.

A. Präparativer Teil

1. *2,2-Methylen-bis-cyclohexanon* (*I*) wurde durch Kondensation des Formaldehyds mit Cyclohexanon in Überschuß, nach der von Colonge und Mitarb.[13] beschriebenen Methode erhalten. Das Diketon wurde durch fraktionierte Destillation isoliert, und ging bei 148–150°/1mm über. Ein Teil davon kristallisierte in mehreren Tagen, während das übrige als gelbes Öl blieb. Das Öl wurde abgegossen, die farblosen Kristalle abgesaugt und aus Methanol umkristallisiert (bei Zimmertemperatur gelöst und durch Kühlen auf ca. –15° gefällt). Nach

---

[13] J. Colonge, J. Dreux und H. Delplace, *Bull. Soc. chim. France*, **1956**, 1635.

dreimaliger Rekristallisation wurde Schmp. 58° erreicht. Das Öl hatte $n_D^{23} = 1,5035$ und $d_4^{23} = 1,0545$.

MR gef. : 58,43 (für M = 208,3)

MR (aus den Bindungsrefraktionen) für (I) *ber.* : 58,26

Die Gesamtausbeute betrug 45 % d.Th. Das Verhältnis Öl/rohe Kristalle = 1,4.

2. *symm-Oktahydroacridin (II) und das Gemisch von alfa- und beta-Perhydroacridin (III und IV)* wurden auf dem schon erwähnten Wege[2] erhalten. Die einzige Änderung bestand in der Rückgewinnung des Formamids, durch Abdestillieren unter vermindertem Druck, vor der Hydrolyse des Reaktionsgemisches. (II) wurde durch Wasserdampfdestillation und Umkristallisieren aus Aceton gereinigt : Schmp. 71°.

3. *alfa-Perhydroacridinhydrochlorid (VII) und N-Benzoyl-beta-perhydroacridin (VIII).* In einem mit Rührer und Tropftrichter versehenen Kolben wurde eine Lösung von 43g. (III und IV)-Gemisch in 500 ml Benzol mit 280 ml 10%iger wäßr. K_2CO_3-Lsg zusammengebracht. Unter lebhaftem Rühren wurde eine Lsg von 28 ml Benzoylchlorid in 100 ml Benzol dazugetropft, das Rühren noch 30 Min. fortgesetzt und dann über Nacht stehengelassen. Das Chlorhydrat (VII) wurde abgesaugt und mit reinem Benzol gewaschen (11 g). Aus dem Filtrat wurde die Benzolschicht abgeschieden, und zusammen mit 150 ml 2%iger wäßr. NaOH-Lsg, unter lebhaftem Rühren 1 Std. am Wasserbade erwärmt. Nach Erkalten wurde die Benzolschicht abgeschieden, zweimal mit Wasser gewaschen und das Benzol abdestilliert. Der Rückstand betrug 51 g gelbes, zähflüssiges Öl, das in einigen Tagen kristallisierte (große, farblose, vieleckige Prismen, die von einem Punkt radial auswachsen).

(VII) Benötigt eine einzige Rekristallisation aus Methanol, aus welchem es farblose, rhombische, stark lichtbrechende Plättchen bildet. In der Kapillare beginnt es sich ab ca. 350° ohne Verflüssigung zu zersetzen, während das Zersetzungsprodukt (ebenfalls farblose Kristalle) auf der Kapillare sublimiert.

$C_{13}H_{23}N.HCl$ (229,8) *ber.* : N 6,09 ; *gef.* : N 6,21

(VIII) Benötigt manchmal zwei Rekristallisationen aus Petroläther. Durch Selbstverdunstung des Lösungsmittels bilden sich die weiter oben beschriebenen Prismen ; durch Kühlen der Lösung mit Salz-Eis-Gemisch werden feine Kristalle erhalten. Schmp. 85—87° (Kapillare). Der Mischschmelzpunkt mit einer aus reinem *beta*-Perhydroacridin erhaltenen Probe blieb unverändert. Die Reinheit der Verbindung wurde auch dünnschichtchromatographisch bestätigt. $R_f = 0,89$ („Silicagel G", 1 Std. bei 110° aktiviert, Eluent Chloroform/Methanol 1 : 1, Elutionsdauer 20 Min.)

$C_{20}H_{27}ON$ (297,4) *ber.* : N 4,71 ; *gef.* : N 4,94

IR-Spektrum (KBr) : 1635 cm^{-1} („Amid I")

4. *beta-Perhydroacridinhydrochlorid (IX).* 100 g (VIII) wurden in 700 ml Äthanol*) gelöst und nachher, unter Rühren, portionenweise mit 940 ml 6n HCl versetzt. Die so erhaltene Lsg wurde 20 Std. unter Rückfluß gekocht (Nach den ca. ersten 2 Std. begann sich ein schweres, farbloses Öl abzuscheiden, dessen Zunahme nach anderen 3—4 Std. aufhörte). Nach Erkalten wurde die Lsg vom Öl abgegossen und alle Flüssigkeit abdestilliert. Das zurückbleibende Chlorhydrat war noch mit einer kleinen Menge des erwähnten Öles verunreinigt. Es wurde mit 500 ml Benzol 30 Min. unter Rückfluß gekocht, nach Erkalten abgesaugt, mit reinem Benzol gewaschen und aus Methanol umkristallisiert : farblose Nadeln**),

---

*) Es wurde auch ein Versuch in Methanol ausgeführt, doch in diesem Falle war die Ausbeute kleiner (24 %).

**) Besonders feine und lange Nadeln bilden sich aus Benzol/Methanol (80 : 5), doch der Lösungsmittelverbrauch ist dabei sehr hoch : um 1g rohes Chlorhydrat zu lösen sind 85 ml dieses Gemisches nötig.

die sich in der Kapillare ab 200° unter Braunfärbung, ohne Verflüssigung zersetzen. Die Rohausbeuten betrugen zwischen 23,5–33 g (30–43 %).

$C_{13}H_{23}N.HCl$ (229,8) *ber.* : N 6,09 ; *gef.* : N 6,09

5. *alfa-Perhydroacridin* (*III*). In einem Liter-Kolben wurden 46 g (0,2 Mol) (VII) mit einer Lsg von 12 g (0,3 Mol) NaOH in 500 ml Wasser versetzt, und das freiwerdende Amin mit Wasserdampf destilliert. Ausb. quantitativ. Schmp. 92–92,5° (Petroläther). Pikrat : 188–189° in der Kapillare (Methanol-Wasser).

6. *beta-Perhydroacridin* (*IV*). Es wurde wie im vorangehenden Falle verfahren. Schmp. 49,5–50° (Petroläther). Pikrat : 146° in der Kapillare (ohne Rekristallisation).

7. *N-Nitroso-alfa-perhydroacridin* (*V*). 2g (0,01 Mol) (III) wurden in 6g (0,1 Mol) Eisessig und 10 ml Wasser gelöst. Am siedenden Wasserbade wurde 1 g (0,014 Mol) $NaNO_2$ als konzentrierte wäßr. Lösung tropfenweise zugegeben (wobei sich ein gelbes Öl an der Oberfläche ansammelte), und anschließend wurde noch 10 Min. am Wasserbade erwärmt. Das Öl kristallisierte schnell nach Erkalten und Schütteln. Das Reaktionsgemisch wurde mit Wasser verdünnt und filtriert. Das Nitrosamin wurde mit $NaHCO_3$-Lsg bearbeitet, abgesaugt und mit reichlich Wasser gewaschen. Es wurden 2,04 g (88,7 %) Rohprodukt mit Schmp. 85° erhalten. Es wurde aus Aceton (Fällung durch Wasserzugabe) umkristallisiert. Das reine Nitrosamin ist zitronengelb und schmilzt bei 87–88°.

$C_{13}H_{22}ON_2$ (222,3) *ber.* : N 12,60 ; *gef.* : N 12,71

UV-Spektrum (0,0002 M in Äthanol) :

λ_{max} 240 und 370 nm ($E = 1{,}40$ und bzw. 0,028)

IR-Spektrum (KBr) : 1432 cm^{-1} (R_2N-NO, dimeres)
(0,008 M in CCl_4) : 1460 cm^{-1} (R_2N-NO, monomeres).

8. *N-Nitroso-beta-perhydroacridin* (*VI*) wurde wie im vorangehenden Falle erhalten, kristallisierte aber etwas schwieriger. Aus 5g (IV) wurden 5,72 g (99,5 %) rohes Nitrosamin mit Schmp. 59–62° erhalten. Es wurde wie (V) umkristallisiert. Das reine Nitrosamin ist butterfarben und schmilzt bei 62°.

$C_{13}H_{22}ON_2$ (222,3) *ber.* : N 12,60 ; *gef.* : N 12,48

UV-Spektrum (0,001 M in Äthanol) :

λ_{max} $230 \div 260$ und 355 nm ($E = 1{,}70$ und bzw. 0,085)

IR-Spektrum (KBr) : 1432 cm^{-1} (R_2N-NO, dimeres)

B. Maßanalytischer Teil

1. *Vergleichsspektren*. Zur Aufnahme der Vergleichsspektren wurden 0,1 M Lsgen der Nitrosamine (V) und bzw. (VI) in CCl_4 hergestellt. Diese Lsgen wurden nachher in den in Abbildung 1 angegebenen Verhältnissen gemischt. Zur Aufnahme wurden 0,416 mm dicke Lösungsschichten benutzt.

2. *Genauigkeit der Methode*. Um die Größenordnung der Fehler zu ermitteln wurde eine Bestimmung an einem Zeugen, mit bekannter Zusammensetzung, ausgeführt :

Ein Gemisch von 1g (5,35 mMol) (II), 1g (5,18 mMol) (III) und 1g (5,18 mMol) (IV) wurde in 9g (150 mMol) Eisessig und 15 ml Wasser gelöst. Am siedenden Wasserbade wurden 2,5g (36 mMol) $NaNO_2$ als konzentrierte wäßr. Lsg tropfenweise zugegeben und anschließend wurde noch 30 Min. am Wasserbade erwärmt. Nach Erkalten wurde mit 600 ml Wasser verdünnt und die Nitrosamine zweimal mit 150 + 100 ml Äther ausgezogen. Die wäßr. Schicht wurde durch Zugabe von 30g NaOH alkalisch gemacht, und nach Erkalten wurde (II) mit 150 + 100 ml Äther ausgezogen. Die ätherische Oktahydroacridinlsg wurde über $MgSO_4$ getrocknet, über ein G3-Filter filtriert, und der Äther verdunstet. Der Rückstand wurde 3 Std. in Vakuum aufbewahrt und gewogen. Es wurden 0,9800 g(II) (Schmp. 65—68°) wiedergefunden. Verlust : 2 %. Die ätherische Lösung der Nitrosamine wurde mit 200 ml 10 %iger wäßr. NaOH-Lsg gewaschen, über $MgSO_4$ getrocknet, über G3 filtriert, und der Äther verdunstet. Der Rückstand wurde 3 Std. in Vakuum aufbewahrt und gewogen. Es wurden 2,3170g Nitrosaminengemisch, entsprechend 2,0143 g freier Basen, gefunden. Das Nitrosaminengemisch wurde in der geeigneten Menge CCl_4 gelöst, um eine Konzentration von 0,0222g/ml (0,1 M) zu erhalten. Diese Lösung diente zur Aufnahme des IR-Spektrums. Durch Vergleichung mit den Vergleichsspektren wurden 49 % (0,9870g) an (III) und 51 % (1,0273g) an (IV) gefunden.

Die Ungenauigkeit der Methode kann daher als auf ± 2 % beschränkt betrachtet werden.

C. Untersuchung der Leuckart-Reaktion *)

Für alle Versuche wurde Formamid *p.a.* gleicher Qualität verwendet.

Versuch Nr. 1

10,4 g (50 mMol) (I) (Schmp. 58°) und 27g (600 mMol) Formamid wurden auf 165 ± 2° so lang erwärmt bis sich kein Kohlenstoffdioxid mehr entwickelte. Das Reaktionsgemisch wurde mit 200 ml 10 %iger wäßr. NaOH-Lsg versetzt und 2 Std. unter Rückfluß gekocht. Während des Kochens setzte sich ein Teil der Perhydroacridine am Kühler ab. Nach Erkalten wurde das Perhydroacridin vom Kühler mittels Äther in dem Kolben zurückgebracht, und die ganze Reaktionsmasse zweimal mit 100 + 100 ml Äther ausgezogen. Nach Entfernung des Äthers wurde der Rückstand in 33 ml Eisessig und 45 ml Wasser gelöst. Die Lösung wurde am siedenden Wasserbade erwärmt, es wurden 7,5 g $NaNO_2$ als konzentrierte wäßr. Lsg tropfenweise zugegeben und anschließend noch 30 Min. am Wasserbade gehalten. Weiterhin wurde in genau derselben Weise wie mit dem Zeugen verfahren. Das Ergebnis ist in Tabelle 1 angegeben.

Die nächsten vier Versuche wurden unter den in Tabelle 1 angegebenen Bedingungen ausgeführt, und die Bearbeitung des Reaktionsgemisches erfolgte genau wie im Versuch Nr. 1.

---

*) Dieser Abschnitt wurde unter Teilnahme des Studenten D. Römer ausgeführt.

Revue Roumaine de Chimie, 14, 1435 – 1440 (1969)

ELECTRIC MOMENT OF DILITURIC ACID (5-NITRO-BARBITURIC ACID)

R. NUŢIU, L. KURUNCZI and Z. SIMON
Department of Organic Chemistry, University of Timişoara, Bd. V. Pârvan 4

Received January 15, 1969

The values of the electric moments for dilituric acid and 5,5-ethyl-nitrobarbituric acid, determined in dioxane at 25° are reported. The experimental results are correlated with the electric moments calculated as vector sums of bond and group moments.

In this note, a sequel to our previous studies concerning the structure of dilituric acid,[1-3] we aimed at determining the electric moment of this compound and of the 5,5-ethyl-nitrobarbituric acid. The last compound similar to the 5,5-disubstituted derivatives of barbituric acid for which the electric moment was determined[4] in dioxane solution, was used in order to check the precision of our determinations in comparison with the theoretic results based on the vector sum of bond moments. Our determinations were performed at 25° ± 0.05° also in dioxane solutions in which the dilituric acid is fairly soluble.

EXPERIMENTAL

Materials. Anhydrous dilituric acid was obtained of a Merck product by dehydration in vacuum in the presence of P_2O_5 at 114°; melting temperature 176°. 5,5-Ethyl-nitrobarbituric acid was obtained as described in a previous note.[1] Dioxane was distilled over metallic sodium.[5]

Apparatus. DK-meter 60GK (Franz Küstner Nachf., KG-Dresden), IRF-23 refractometer Pulfrich type, Oswald type picnometer.

The method of Halverstadt and Kumler[6] was used considering densities instead of specific volumes. The total polarization was calculated by the equation:

$$_{\infty}P_2 = \frac{\varepsilon_1 - 1}{\varepsilon_1 + 2} \cdot \frac{1}{d_1}\left(M_2 - \beta\frac{M_1}{d_1}\right) + \frac{3M_1\alpha}{d_1(\varepsilon_1 + 2)^2} \qquad (1)$$

---

[1] Fr. Mihai and R. Nuţiu, *Rev. Roumaine Chim.*, **13**, 39 (1968).

[2] Z. Simon, Fr. Mihai and R. Nuţiu, *Rev. Roumaine Chim.*, **13**, 147 (1968).

[3] R. Nuţiu and Z. Simon, *Rev. Roumaine Chim.*, **14**, 311 (1969).

[4] S. Soundararajan, *Trans. Faraday Soc.*, **54**, 1147 (1958).

[5] V. Herout, B. Keil, M. Protiva, M. Hudlicky, I. Ernest and J. Gut, "Laboratorni Tekhnika Organichke Khemie"-Prague, 1954, Romanian translation, Bucharest, 1959, p. 620.

[6] I. F. Halverstadt and W. D. Kumler, *J. Amer. Chem. Soc.*, **64**, 2988 (1942).

where :

$_{\infty}P_2$ — total polarization of the dissolved substance at infinite dilution
ε_1 — dielectric constant of the solvent (obtained by extrapolation)
d_1 — density of solvent (obtained by extrapolation)
α — slope of the dielectric constant *vs* molar fraction-line
β — slope of the density *vs* molar fraction-line
M_1 — molecular mass of the solvent
M_2 — molecular mass of the dissolved substance.

The electric moment was calculated by equation :

$$\mu = 0.221 \sqrt{{}_{\infty}P_2 - {}_{\infty}R_2} \tag{2}$$

where :

μ — electric moment (Debye units)
$_{\infty}R_2$ — molecular refraction of the dissolved substance at infinite dilution.

The electronic polarization was calculated by means of the molecular refraction for the *D*-line of sodium, extrapolated at infinite dilution. The atomic polarization was not taken into account.

EXPERIMENTAL RESULTS AND DISCUSSIONS

The experimental results are listed in table 1, where x_2 is the molar fraction of the dissolved substance, while ε_{12}, d_{12} and $n^2_{D_{12}}$ are the dielectric constants, densities and refractive index (the second power) of the solutions.

Table 1

Experimental values for molar fractions of the dissolved substance (x_2), for dielectric constants (ε_{12}), for densities (d_{12}) and for squares of refractive index ($n^2_{D_{12}}$) of the solutions

x_2	ε_{12}	d_{12}	$n^2_{D_{12}}$
Dilituric acid			
0.0	(2.2311)*	(1.02809)*	(2.01613)*
0.000239	2.2372	1.02830	2.01645
0.000408	2.2419	1.02845	2.01667
0.000592	2.2467	1.02861	2.01693
0.000761	2.2509	1.02876	2.01713
5,5-ethyl-nitrobarbituric acid			
0.0	(2.2306)*	(1.02798)*	(2.01636)*
0.000362	2.2361	1.02825	2.01659
0.000539	2.2382	1.02837	2.01671
0.000767	2.2420	1.02855	2.01683
0.001000	2.2456	1.02871	2.01698
0.001305	2.2498	1.02895	2.01719

*) The figures in parenthesis are obtained by extrapolation and by the method of the least square errors.

Table 2 gives the slopes α, β, γ, of the lines representing the variations of dielectric constants, densities and second powers of refractive indexes *vs* molar fractions and also the values of $_{\infty}P_2$, $_{\infty}R_2$, $_{0}P_2$ defined as above; $_{0}P_2$ is the orientation polarization, μ defined as above.

Table 2

Slopes of dielectric constants (α), densities (β) and squares of refractive indexes (γ) as functions of molar fractions and values for total polarization ($_{\infty}P_2$), for molar refraction of the substance at infinite dilution ($_{\infty}R_2$), for orientation polarization ($_{0}P_2$) and for the electric moment (μ) expressed in Debye-units.

	α*	β*	γ*	$_{\infty}P_2$	$_{\infty}R_2$	$_{0}P_2$	μ
Dilituric acid	26.22	0.8740	1.3186	404.34	45.18	371.16	4.19
5,5-Ethyl-nitrobarbituric acid	14.83	0.7426	0.6288	251.95	43.87	208.08	3.19

*) The figures for α, β and γ were obtained by the method of the least square errors.

The precision of the electric moment determinations is of about 0.05D and was estimated as follows: in equation (2) for the electric moment the term $_{\infty}P_2$ is one order of magnitude higher than $_{\infty}R_2$, while in equation (1) for $_{\infty}P_2$ the second term, which contains the slope α of the $\varepsilon_{12} - x_2$ dependence, is one order of magnitude higher than the first one. The relative error in the calculation of the electric moment is thus about half of the relative error in determining the α-slope. With the usual expression for the mean square error, the data for ε_{12} and x_2 of table 1 yield a relative error of about 2.1% for the α-slope determination.

The electric moments corresponding to the structures (I), (II) and (III) were calculated by means of the vector calculus with the bond and group moments[7] given in table 3. For the bond moment carbon-nitrogen in the ring 1.9D was used, while for the amidic carbonyl 4.0D, indicated

Table 3

Values for bond and group moments as used in the vector calculus of the electric moments.

Bond electric moment		Bond electric moment	
H−C	0.4	N−O	0.3
H−N	1.31	N→O	4.3
H−O	1.51	$C_{al}-NO_2$	3.3
C=N	0.9	$C_{ar}-NO_2$	3.98
C−O	0.74		

---

[7] C. P. SMYTH, "Dielectric Behavior and Structure", McGraw-Hill, New York, 1955, p. 244.

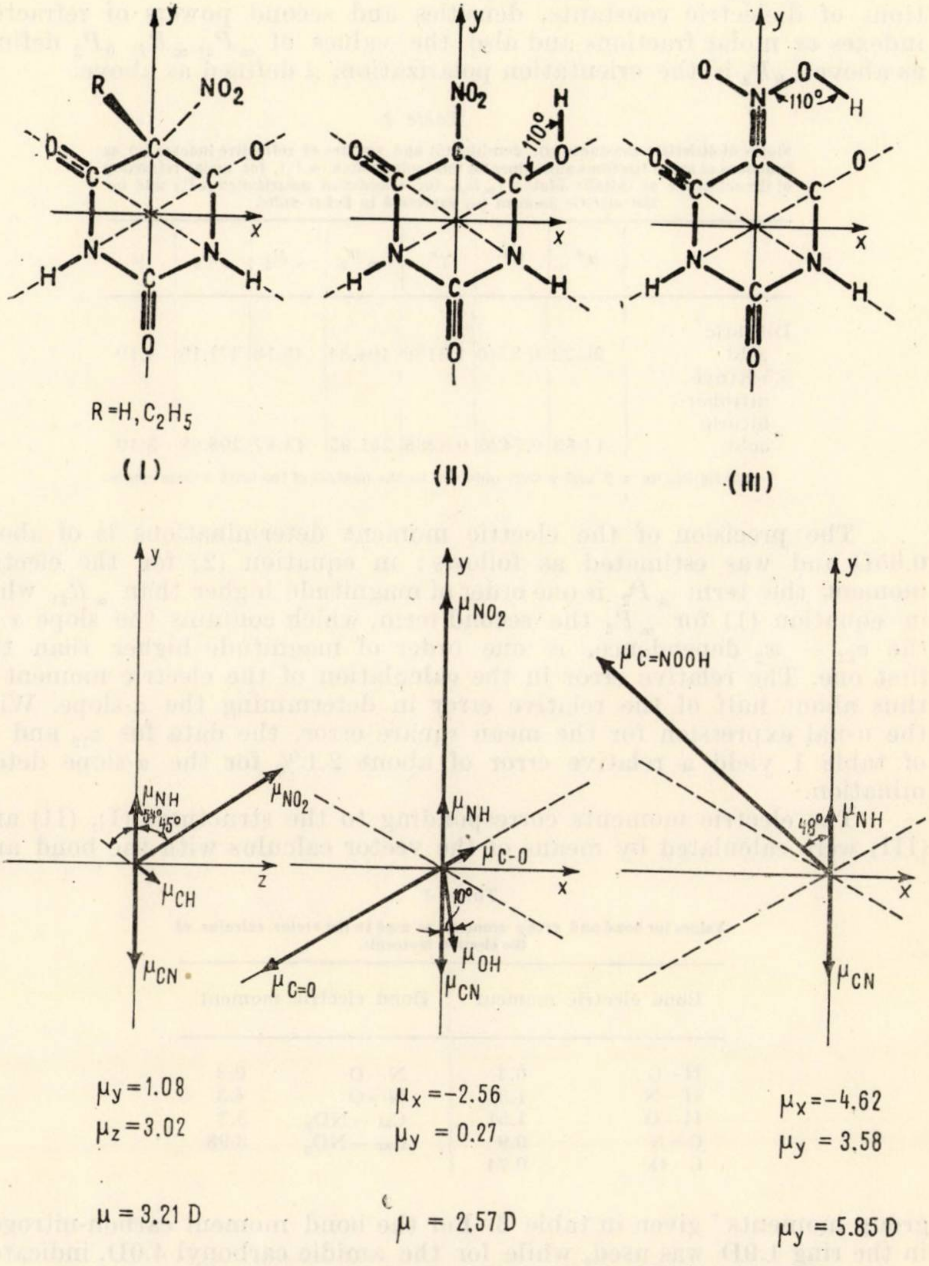
y
x
z
R
NO2
O
C
N
H
110°
R=H, C2H5
(I)
(II)
(III)
μNH
μCH
μCN
μNO2
μC=O
μC-O
μOH
μC=NOOH
54°
45°
10°
48°
μy = 1.08
μz = 3.02
μ = 3.21 D
μx = −2.56
μy = 0.27
μ = 2.57 D
μx = −4.62
μy = 3.58
μy = 5.85 D

Fig. 1. — Vector calculus used for the 5,5-nitroethylbarbituric acid and for two most stable tautomers of dilituric acid (summarized).

by Schneider[8] and Schneider and Halverstadt[9] for some pyrimidinic derivatives. Figure 1 illustrates the vector calculus as used for the 5,5-ethyl-nitrobarbituric acid and for the two more stable tautomers[2] of the dilituric acid.

The hydroxyl of the tautomeric structure (II) was considered to be fixed in the molecular plane by the hydrogen bond with the oxygen atom of the nitro group. The aci-nitro group moment in structure (III) was calculated as vector sum of bond moments considering the hydrogen atom fixed in the molecular plane by a hydrogen bond. Thus, a moment of 6.22D, at an angle of 48°, respectively to the axis between the carbon atoms of positions 2 and 5 of the molecule, was calculated for the aci-nitro group.

The fact that the electric moment, calculated as above for the 5,5-ethyl-nitrobarbituric acid, agrees with that obtained by experiment indicates the accuracy of our method.

DISCUSSIONS

Based on considerations in a previous note[1] and of X-ray studies,[10] only tautomeric structures (II) and (III) were taken into account in the case of the dilituric acid. The comparison of the electric moment calculated for these structures (2.57D and 5.85D) with that determined experimentally (4.19D) suggests the existence of a tautomeric equilibrium which, as indicated by a simple calculation, should consist of 50 % aci-tautomer (structure III) and 50 % nitro-enolic tautomer (structure II) in our conditions (dioxane solution, 25°). However, this equilibrium should be pointed out also by another method. The IR spectrum cannot be used to this purpose because of the dioxane absorption in the region of the nitro

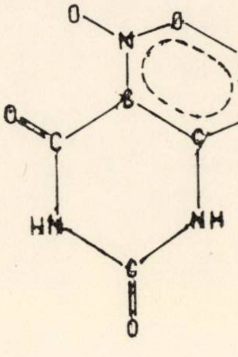

Fig. 2. — Dilituric acid molecule with a strong hydrogen bond cycle, as supposed to exist in dioxane solution.

---

[8] W. C. Schneider, *J. Amer. Chem. Soc.*, **70**, 627 (1948).

[9] W. C. Schneider and I. F. Halverstadt, *J. Amer. Chem. Soc.*, **70**, 2826 (1948).

[10] a) W. Bolton, *Acta Cryst.*, **16**, 950 (1963);
b) B. M. Craven, S. Martinez-Carrera and G. A. Jeffrey, *Acta Cryst.*, **17**, 891 (1964).

group valence vibrations. If the aci-tautomer could not exist otherwise than ionized i.e. Hantzsch scheme for the nitroderivatives tautomery could not be admitted,[11] our conclusions were not exact because the electric moment would be largely affected by the presence of ion pairs. We must also notice that the aqueous solutions of dilituric acid (which contain diliturate anions) are yellow[12] while the dioxane solution is colourless, a fact which argues against dissociation. Another possibility would be the existence of a single molecule (tautomeric structure) with a strong hydrogen bond between the nitro and the carbonylic oxygen atoms (with a quasiaromatic cycle, as in figure 2) which would also explain the value for the electric moment, situated between the values calculated for the structures (II) and (III), obtained by experiment.

[11] S. S. Novikov, V. I. Slovetskii, A. A. Fainzil'berg, S. A. Shevelev, V. A. Shlyapochnikov, A. I. Ivanov and V. A. Tartakovskii, *Nitro Compounds, Proc. Intern. Symp., Warsaw*, **1963**, 119; through *Chem. Abstr.*, **63**, 14665 (1965).

[12] M. E. Taylor and R. J. Robinson, *Talanta*, **8**, 518 (1961).

Revue Roumaine de Chimie, **14**, 1441–1444 (1969)

DARSTELLUNG EINIGER 3-ACYLOXYSTEROIDE

F. HODOŞAN und ALEXANDRA POP-GOCAN

vom Chemischen Institut der Akademie, Cluj, str. Donath 59–65

Eingegangen am 12. April 1969

Es wird die Darstellung von Acyloxysteroiden der Formeln (I, II, III) (a-f) beschrieben.

Um den Einfluß der elektronischen und sterischen Faktoren auf die Adsorption an aktiven Oberflächen einiger 3-Acyloxysteroide untersuchen zu können, stellten wir eine Reihe von den durch die Strukturformeln (I, II, III) (a—f) wiedergegebenen Verbindungen dar. Da wir die Absicht haben die chromatographischen Daten in Zusammenhang mit anderen Ergebnissen zu besprechen und demzufolge in einer anderen Arbeit zu veröffentlichen, beschreiben wir hier nur den präparativen Teil dieses Problems.

Die Chloracetate (I, II, III) (a, b, c) wurden durch die Behandlung der freien Alkohole mit den entsprechenden Säuren in Gegenwart von Dicyclohexylcarbodiimid und Pyridin hergestellt.[1] Unter diesen Bedingungen verliefen die Acylierungen mit Trichloressigsäure unvollständig, was durch die Fällung dieser Säure aus dem ätherischen Reaktionsmedium mit dem zugefügten Pyridin oder anderen organischen Basen, erklärbar wäre. Die Durchführung der Acylierungen in Abwesenheit solcher basischen Substanzen hatte aber, sogar bei verlängerter Reaktionsdauer, keine Verbesserung der Ausbeute zur Folge.

Die Acyloxyderivate (I, II, III) (d, e, f) wurden üblicherweise durch die Verwendung der entsprechenden Acylchloride in pyridinischer Lösung bei Zimmertemperatur erhalten.[2]

EXPERIMENTELLES

Die Schmelzpunkte wurden in Kapillaren bestimmt und sind unkorrigiert.

Darstellung von Chloracetaten

Die Ausgangssubstanz (3×10^{-4} Mol) wird in 10–35 ml wasserfreiem Äther gelöst und mit 30×10^{-4} Mol Mono-, Di-, bzw. Trichloressigsäure und 35×10^{-4} Mol wasserfreiem Pyridin versetzt (Im Falle der Trichloressigsäure wurde ohne Pyridin-Zusatz gearbeitet).

---

[1] E. Müller, „Methoden der organischen Chemie (Houben-Weyl)", Bd. 8, G. Thieme Verlag, Stuttgart, 1952, S. 522.

[2] Ebda, S. 546.

Danach werden unter kräftigem Rühren 17×10^{-4} Mol Dicyclohexylcarbodiimid in 10—15 ml wasserfreien Äther getropft. Das Rühren wird noch 3—4 Std fortgesetzt und der Reaktionsverlauf durch Dünnschichtchromatographie kontrolliert. Nach Abschluß der Reaktion wird der kristalline Niederschlag abfiltriert und mit Äther gut durchgewaschen. Die vereinigten ätherischen Lösungen werden zuerst mit verdünnter Schwefelsäure danach mit Wasser gewaschen, über Magnesiumsulfat getrocknet und im Vakuum eingeengt.

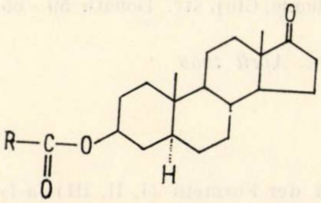

I (a-f)

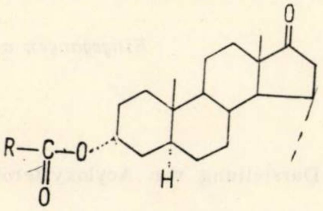

II (a-f)

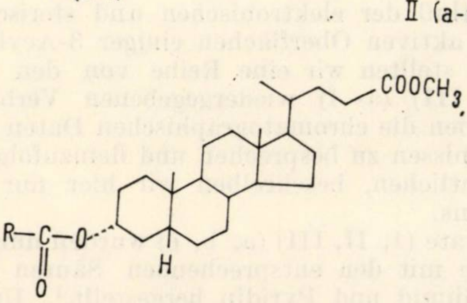

III (a-f)

$a: R = ClCH_2—$ $\quad$ $d: R = CH_3CH_2—$

$b: R = Cl_2CH—$ $\quad$ $e: R = (CH_3)_2CH—$

$c: R = Cl_3C—$ $\quad$ $f: R = (CH_3)_3C—$

5α-Androstan-3β-ol-17-on-monochloracetat (Ia): Reinigung durch präparative Dünnschichtchromatographie auf Kieselgel G (Laufmittel: Benzin-Äther 4 : 1). Schmp. 139—141° (aus Methanol).

$C_{21}H_{31}ClO_3$ (366,9) *Ber.*: C, 68,74; H, 8,51

Gef.: C, 68,48; H, 8,18

5α-Androstan-3β-ol-17-on-dichloracetat (Ib): Schmp. 159—162° (aus Methanol und dann aus Aceton-Wasser 5 : 1).

$C_{21}H_{30}Cl_2O_3$ (401,3) *Ber.*: C, 62,84; H, 7,53

Gef.: C, 62,97; H, 7,47

5α-Androstan-3β-ol-17-on-trichloracetat (Ic): Reinigung durch dreimalige Behandlung mit Methanol bei Zimmertemperatur. Schmp. 174—176° (sintert bei 144°).

$C_{21}H_{29}Cl_3O_3$ (435,8) *Ber.*: C, 57,87; H, 6,71

Gef.: C, 58,09; H, 6,67

5α-Androstan-3α-ol-17-on-monochloracetat (IIa) : Schmp. 133–134° (aus Methanol oder Aceton-Wasser 5 : 1) (Lit. [3] Schmp. 134°).

5α-Androstan-3α-ol-17-on-dichloracetat (IIb)' : Schmp. 153–156° (aus Methanol).

$C_{21}H_{30}Cl_2O_3$ (401,3) *Ber.* : C, 62,84 ; H, 7,53
Gef. : C, 62,90 ; H, 7,70

5α-Androstan-3α-ol-17-on-trichloracetat (IIc) : Schmp. 215–217° (aus Methanol).

$C_{21}H_{29}Cl_3O_3$ (435,8) *Ber.* : C, 57,87 ; H, 6,71
Gef. : C, 58,34 ; H, 7,08

3α-Hydroxy-5β-cholansäuremethylester-monochloracetat (IIIa) : Schmp. 146–148° (aus Methanol).

$C_{27}H_{43}ClO_4$ (467,1) *Ber.* : C, 69,43 ; H, 9,28
Gef. : C, 69,55 ; H, 9,31

3α-*Hydroxy*-5β-*cholansäuremethylester-dichloracetat* (IIIb) : Reinigung durch Behandlung mit Methanol bei Zimmertemperatur. Schmp. 111–115°.

$C_{27}H_{42}Cl_2O_4$ (501,5) *Ber.* C, 64,66 ; H, 8,44
Gef. : C, 64,70 ; H, 8,63

3α-*Hydroxy-5β-cholansäuremethylester-trichloracetat* (IIIc) : Schmp. 102–105° (aus Methanol).

$C_{27}H_{41}Cl_3O_4$ (535,9) *Ber.* : C, 60,50 ; H, 7,71
Gef. : C, 60,18 ; H, 7,65

5α-Androstan-3β-ol-17-on-proprionat (Id) : Schmp. 147–149,5° (aus Methanol).

$C_{22}H_{34}O_3$ (346,5) *Ber.* : C, 76,25 ; H, 9,89
Gef. : C, 76,34 ; H, 9,88

5α-Androstan-3β-ol-17-on-isobutyrat (Ie) : Schmp. 161–162° (aus Methanol und dann aus Petroläther).

$C_{23}H_{36}O_3$ (360,5) *Ber.* : C, 76,62 ; H, 10,06
Gef. : C, 76,53 ; H. 9,94

5α-Androstan-3β-ol-17-on-trimethylacetat (If) : Schmp. 181–183° (aus Methanol).

$C_{24}H_{38}\ O_3$ (374,5) *Ber.* : C, 76,95 ; H, 10,23
Gef. : C, 76,86 ; H, 10,89

5α-Androstan-3α-ol-17-on-propionat (IId) : Schmp. 149–152° (aus Methanol) (Lit. [4] Schmp. 151–152°).

5α-Androstan-3α-ol-17-on-isobutyrat (IIe) : Schmp. 99–101° (aus Methanol).

$C_{23}H_{36}\ O_3$ (360,5) *Ber.* : C, 76,62 ; H, 10,06
Gef. : C, 76,51 ; H, 9.98

5α-Androstan-3α-ol-17-on-trimethylacetat (IIf) : Reinigung durch präparative Dünnschichtchromatographie auf Kieselgel G (Laufmittel : Dichlormethan mit 1 % Methanol). Schmp. 139–141°. (Lit. [5] Schmp. 142–144°).

---

[3] H. J. VAN DER MOLEN, D. GROEN und J. H. VAN DER MAAS, *Steroids*, **6**, 195 (1965).

[4] Soc. pour l'ind. chim. à Bâle, Ger. Pat. 699,308 ; *Chem. Abstr.*, **35**, 8214 (1941).

[5] F. SONDHEIMER und G. ROSENKRANZ, U.S. Pat. 2,940,967 ; *Chem. Abstr.*, **55**, 1713 g (1961).

3α-Hydroxy-5β-cholansäuremethylester-propionat (IIId): Schmp. 138–140° (aus Methanol).

$C_{28}H_{46}O_4$ (446,6)	*Ber.*:	C, 75,29; H, 10,38
	Gef.:	C, 75,92; H, 10,22

3α-Hydroxy-5β-cholansäuremethylester-isobutyrat (IIIe): Schmp. 86–90° (aus Methanol).

$C_{29}H_{48}O_4$ (460,7)	*Ber.*:	C, 75,60; H, 10,50
	Gef.:	C, 75,48; H, 10,95

3α-Hydroxy-5β-cholansäuremethylester-trimethylacetat (IIIf): Reinigung durch präparative Dünnschichtchromatographie auf Kieselgel G (Laufmittel: Cyclohexan-Äther 3 : 2). Schmp. 96–99° (aus Methanol).

$C_{30}H_{50}O_4$ (474,7)	*Ber.*:	C, 75,90; H. 10,62
	Gef.:	C, 75,46; H, 10,66

Revue Roumaine de Chimie, **14**, 1445–1456 (1969)

LA PUISSANCE NÉCESSAIRE POUR MÉLANGER EN UTILISANT LES AGITATEURS DE TYPE À RAME

EM. A. BRATU et L. BARAF
Institut Polytechnique « Gheorghe Gheorghiu-Dej », 3, Str. Polizu
Usine mécanique d'outillage chimique, 33, Şos. Viilor, Bucarest

Reçu le 21 avril 1969

On propose une formule pouvant être utilisée au calcul de la consommation de puissance utile en mélangeant avec des agitateurs complexes de type à rame, lorsqu'on connaît la dépendance du nombre Froude et Reynolds du besoin de puissance dans le même système, pour un agitateur à deux pales ou un agitateur à rame d'une autre forme. La formule proposée est obtenue en étendant la méthode de Kasatkin au calcul de la résistance à la rotation de l'agitateur à pales, et vérifiée expérimentalement dans cet ouvrage pour cinq types d'agitateurs de plus en plus complexes.

Pour pouvoir établir les dimensions du système de mise en mouvement des outillages, ayant un dispositif mélangeur, il est nécessaire de connaître la puissance consommée pour réaliser le mélange des fluides à l'aide des agitateurs mécaniques.

A la suite d'amples recherches entreprises en Angleterre et aux Etats-Unis sur la puissance des agitateurs, on a obtenu un certain nombre de données publiées partiellement par Rushton, Everett et Costich.[1] A l'aide de l'analyse dimensionnelle, ces auteurs ont déduit l'équation suivante de la forme la plus générale pour le calcul de la puissance nécessaire

$$Np = C\,Re^{x}\,Fr^{y}\left(\frac{d}{D}\right)^{\alpha}(H_0/d)^{\beta}\,(ha/d)^{\gamma}\,(pa/d)^{\delta}\,(hp/d)^{\varepsilon}\,(1/d)^{q} \qquad (1)$$

où α, β, γ, δ, ε, et q sont les exposants déterminés expérimentalement.

Supposant la similitude géométrique, l'équation (1) est remplacée par l'équation plus simple

$$\Phi = \frac{Kp}{Fr^{y}} = C\,Re^{x} \qquad (2)$$

dans le cas des systèmes où l'on empêche l'apparition du tourbillon central à l'aide de chicanes ou par d'autres méthodes, $y = 0$ et l'équation (2) s'écrit

$$\Phi = Kp = C\,Re^{x} \qquad (3)$$

---

[1] J. H. Rushton, E. W. Costich et H. I. Everett, *Chem. Eng. Progr.*, **46**, 395, 469 (1960).

Rushton, Everett et Costich ont tracé les courbes $\Phi = f(Re)$ pour différents types d'agitateurs, pour des récipients munis de chicanes ou sans elles, pour diverses valeurs des rapports des paramètres géométriques du système.

Nagata et ses collaborateurs [2] ont effectué des recherches, en traçant des courbes et offrant des formules de calcul pour le cas de l'apparition du tourbillon central. La validité limitée des courbes et des formules obtenues a été la cause de nombreuses recherches pour élucider certains cas fréquemment rencontrés dans la pratique. Les travaux publiés par Mack, [3] Olney, [4] Oldshue, [5] Rushton, [6] Rushton, [7] Gray, [8] Karasev, [9] Richard, [10] Uhl, [11] Chapman, [12] Strop, [13] Kafarov [14] font partie de cette catégorie.

Des ouvrages sur la détermination de la variation de la puissance nécessaire en fonction du diamètre de l'agitateur, de la forme du récipient de mélange, de certains éléments directeurs pour diriger la circulation du fluide, l'emploi de plusieurs agitateurs, la dimension et l'emplacement des chicanes, la distance entre l'agitateur et le fond du récipient de mélange ont été publiés par Uhl, [11] Bates, [15] Gretton, [16] Richard, [17] Vermeulen, [18] Chapman. [19]

Des données concernant la puissance nécessaire pour le mélange des fluides apparaissent dans les ouvrages de synthèse de Sterbachek et Tausk, [2] Bratu, [20] Perry, [21] Holland et Chapman, [22] Kasatkin. [23]

---

[2] Z. Sterbachek et P. Tausk — « Permeshivanie v Khimichescoi Promishlenosti », Ed. Gozhimizdat, Leningrad, 1963, 104 p.

[3] D. E. Mack et E. Poll, *Chem. Eng. Progr.*, **45**, 189 (1949).

[4] R. Olney et G. Carlson, *Chem. Eng. Progr.*, **43** 493 (1947).

[5] I. Y. Oldshue, H. E. Hirschland et A. T. Gretton, *Chem. Eng. Progr.*, **52** 481 (1956).

[6] J. H. Rushton, *Chem. Eng. Progr.*, **47** 485 (1951).

[7] J. H. Rushton et I. Y. Oldshue, *Chem. Eng. Progr.*, **49**, 161 (1953).

[8] J. B. Gray, *Chem. Eng. Progr.*, **59**, 55 (1963).

[9] I. N. Karasev et S. Ia Gzovskii, *Khim. Mashinostroenie*, **1964**, 616.

[10] J. W. Richards, *Brit. Chem. Eng.*, **8**, 158 (1963).

[11] W. Uhl et H. P. Voznic, *Chem. Eng. Sci.*, **19**, 209 (1964).

[12] F. S. Chapman et F. A. Holland, *Trans. Inst. Chem. Engineers*, **43**, 131 (1965).

[13] C. E. Strop, *Ind. Eng. Chem.*, **35**, 485 (1943).

[14] V. V. Kafarov, « Protzesi peremeshivania v jidkih sredah », Ed. Gozhimisdat, Moscou, 1949.

[15] R. L. Bates, P. L. Fondy et R. R. Corpstein, *Ind. Eng. Chem. Process. Design*, **2**, 636 (1963).

[16] A. T. Gretton, *Chem. Eng.*, **20**, 145 (1964).

[17] J. W. Richard, *Brit. Chem. Eng.*, **8**, 158 (1963).

[18] T. Vermeulen et M. W. Clark, *Amer. Inst. Chem. Engineers J.*, **10** (1964).

[19] F. S. Chapman, F. A. Holland et W. I. Urban, *Chem and Process Eng.*, **46** 131 (1965).

[20] Em. A. Bratu, « Operaţii şi utilaje în industria Chimică », Vol. 1, Ed. tehnică, Bucarest, 1960, 363 p.

[21] J. H. Perry, « Chemical Engineers Handbook », Ed. IV, Cap. 19, Mc. Graw-Hill Book Company, New-York, 1950, 14.

[22] F. A. Holland et F. S. Chapman, « Liquid Mixing and Processing in Stirred Tanks », Reinhold Publishing Corporation. New York — Londres, 1966, p. 29.

[23] A. G. Kasatkin, « Procese şi Aparate Principale în Tehnologia Chimică », Ed. Tehnică, Bucarest, 1960, p. 299.

Dans les ouvrages de Sterbachek et Tausk, [2] Holland et Chapman, [22] Kasatkin [23] et Erdmenger, [24] on propose également diverses méthodes pour faciliter les calculs.

Sans épuiser complètement la liste des ouvrages concernant la puissance nécessaire à l'agitation des fluides, pour ne pas nous éloigner trop du but de cet article, nous concluons que les ouvrages connus ne contiennent pas de données pour tous les cas rencontrés fréquemment dans l'industrie. A cause du grand nombre de paramètres influençant le processus de mélange, les études, quoique nombreuses, ont trait à un nombre restreint de types d'agitateurs.

Dans ce qui suit on essayera de résoudre le problème pour tout le groupe d'agitateurs complexes de type à rame, sans recourir chaque fois aux déterminations de laboratoire quand on connaît la courbe de variation du nécessaire de puissance dans le même système pour un agitateur à deux pales ou un autre agitateur du type à rame, d'une forme quelconque.

CONSIDÉRATIONS THÉORIQUES

a. *Agitateur à deux pales*

Pour le calcul de la puissance utile nécessaire pour un agitateur à deux pales on propose la méthode de Kasatkin. [20]

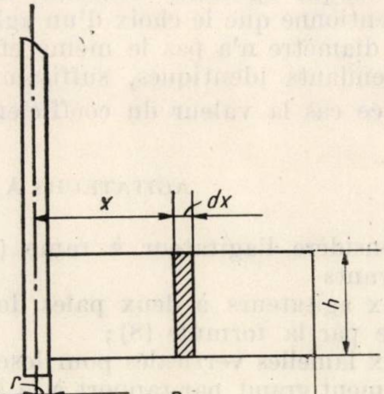

Fig. 1. — Agitateur à deux pales.

La force nécessaire pour vaincre la résistance du milieu quand un corps se meut avec une vitesse uniforme à travers ce milieu est

$$F = \xi \frac{v^2}{2} \rho A \tag{4}$$

---

[24] R. Erdmenger, *Chem. Ing. Tech.*, **24**, 248 (1952).

Dans le cas du bras agitateur à deux pales, les différents points de celui-ci ont des vitesses différentes. Pour la portion hachurée du bras (fig, 1) on peut écrire

$$dF = \xi \frac{v^2}{2} \rho\, h\, dx \tag{5}$$

La vitesse de la portion hachurée est

$$v_1 = \omega x\ 2\pi N x \tag{6}$$

La puissance nécessaire pour faire tourner un bras de l'agitateur sera d'après Kasatkin [20] (p. 370)

$$Np_1 = \xi (\pi N)^3 \rho h (R^4 - r^4) \tag{7}$$

Pour l'agitateur à deux pales droites la force sera évidemment deux fois plus grande. En négligeant r par rapport à R, on peut écrire

$$Np_1 = \xi (\pi N)^3\ \rho h (R^4 - r^4) \tag{8}$$

Dans le cas de deux agitateurs à deux pales, suffisamment éloignés l'un de l'autre, la puissance nécessaire est la somme des puissances nécessaires pour chaque agitateur tournant seul dans le récipient de mélange.

On mentionne que le choix d'un agitateur ayant une largeur double et le même diamètre n'a pas le même effet que l'emploi de deux agitateurs indépendants identiques, suffisamment éloignés.

Dans ce cas la valeur du coefficient ξ change.

AGITATEURS À RAME

On considère l'agitateur à rame (fig. 2) formé par les éléments simples suivants

— deux agitateurs à deux pales dont la puissance nécessaire peut être calculée par la formule (8) ;

— deux lamelles verticales pour lesquelles le rayon R de l'agitateur est suffisamment grand par rapport à la largeur de la lamelle.

Dans le cas où cette hypothèse est valable, on considère $R_1 = R$, et la vitesse de la lamelle constante sur toute sa largeur

$$v_2 = 2\pi\, NR \tag{9}$$

La force de résistance s'écrit dans ce cas en remplaçant dans la formule (4) les valeurs correspondantes

$$F_2 = \frac{v^2}{2}\ \rho\, Hh \tag{10}$$

ou en tenant compte de la formule (9)

$$F_2 = 2\,\xi(\pi N)^2\, R^2\, \rho H h \tag{11}$$

La puissance utile nécessaire est égale à

$$N_{p_2} = F_2 v_2 \tag{12}$$

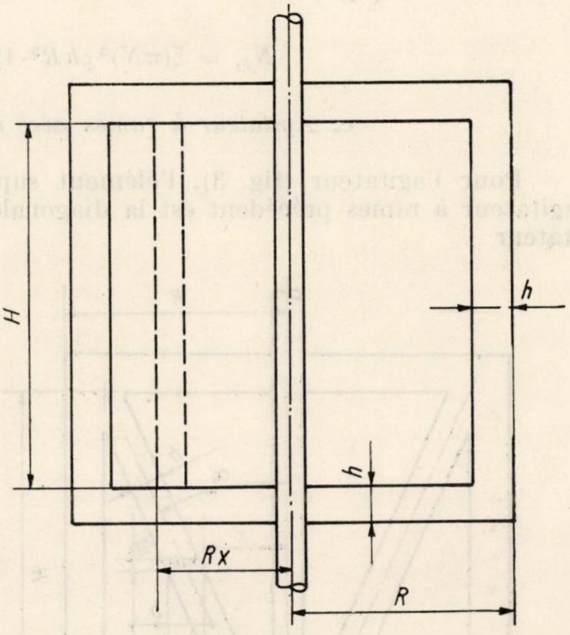

Fig. 2. — Agitateur à rame.

où en remplaçant F_2 et v_2 par les expressions données par les formules (9) et (11)

$$N_{p_2} = \xi(\pi N)^3\, \rho h R^3\, 4H \tag{13}$$

La puissance nécessaire pour vaincre la résistance à la rotation de l'agitateur à rame est égale à la somme des puissances nécessaires pour vaincre les résistances qui s'opposent à la rotation par deux bras verticaux ayant une hauteur H et une largeur h, se trouvant à la distance R de l'axe de l'agitateur.

La puissance totale nécessaire à la rotation de l'agitateur à rames est

$$N_{p_2} = 2\,\xi(\pi N)^3\, \rho h\, R^3(2R + 4H) \tag{14}$$

Pour le même agitateur à rame, mais auquel on a ajouté encore une lamelle verticale d'une largeur h, à une distance Rx suffisamment grande par rapport à h, et éloignée à une distance minima de 1,5 h de la lamelle verticale voisine, on peut écrire la puissance nécessaire pour cet élément vertical, en utilisant le même raisonnement que dans le cas précédent

$$N_{p_3} = \xi(\pi N)^3 \rho h R x \cdot 4H \tag{15}$$

ou en écrivant $\left(\dfrac{Rx}{R}\right)^3 = \beta'$ (16)

$$N_{p_3} = \xi(\pi N)^3 \rho h R^3 \cdot 4\beta' H \tag{17}$$

c. *Agitateur à rames avec diagonale*

Pour l'agitateur (fig. 3), l'élément supplémentaire par rapport à l'agitateur à rames précédent est la diagonale partant du moyeu de l'agitateur

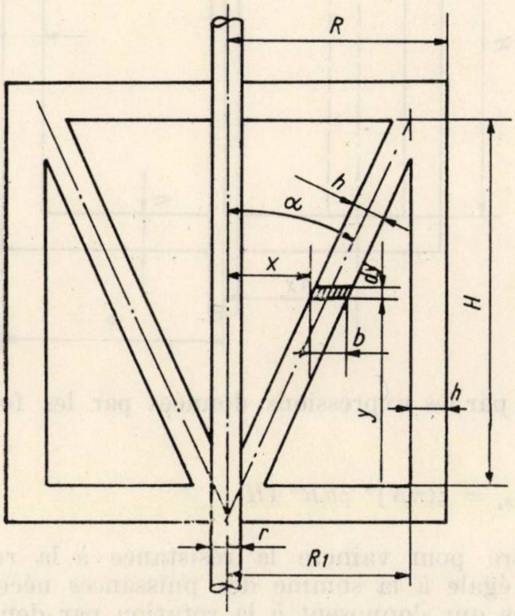

Fig. 3. — Agitateur à rame avec diagonales.

Pour le calcul de la puissance nécessaire pour vaincre la résistance à la rotation de la diagonale, on utilise les hypothèses suivantes :

— le rayon R est suffisamment grand par rapport à h ;

— la force de résistance est constante sur toute la largeur de la lamelle. (Cette hypothèse introduit des erreurs dans la zone immédiatement avoisinée au moyeu, où la distance y a des valeurs comparables à celles de la largeur h. Néanmoins, les erreurs n'affectent pas sensiblement la force générale nécessaire pour vaincre la résistance à la rotation de la diagonale, parce que la force nécessaire pour vaincre la résistance à la rotation pour la zone de la diagonale avoisinant le moyeu est faible par rapport à celle de la zone de l'extrémité opposée de la diagonale où l'hypothèse employée est valable.)

— $R_1 = R$

— on néglige r par rapport à R.

En tenant compte des hypothèses énoncées, l'équation donnant la force de résistance à la rotation de la diagonale s'écrit

$$dF_4 = \xi \frac{v^2}{2} \rho b \, dy \tag{18}$$

Il résulte de la figure (3)

$$y = \frac{x - r}{\operatorname{tg} \alpha} \tag{19}$$

en différenciant l'expression (19) et en remplaçant v par $2\pi N X$, l'équation donnant la valeur de la force de résistance s'écrit

$$F_4 = \frac{2\xi(\pi N)^2 \rho b}{\operatorname{tg}\alpha} \int_r^R x^2 \, dx \tag{20}$$

ou après l'intégration

$$F_{04} = \frac{2}{3} \frac{\xi(\pi N)^2 \rho b}{\operatorname{tg}\alpha} (R^3 - r^3) \tag{21}$$

Le point d'application de la force F_4 est déterminé par la relation

$$x_{04} F_4 = \int_r^R x_4 \, dF_4 \tag{22}$$

En remplaçant F_4 et dF_4 par les expressions correspondantes conformément aux formules (18), respectivement (21) et en effectuant l'intégrale, on obtient la valeur de x_{04}

$$x_{04} = \frac{3}{4} \frac{R^4 - r^4}{R^3 - r^3} \tag{23}$$

qu'on utilise pour le calcul de la vitesse du point d'application

$$v_{04} = 2\pi N \, x_{04} = \frac{3}{2} \pi N \frac{R^4 - r^4}{R^3 - r^3} \tag{24}$$

La puissance nécessaire pour vaincre la résistance à la rotation de la diagonale dans le fluide, s'écrit

$$N_{p_4} = F_4 \cdot v_{04} = \xi \frac{(\pi N)^3 \rho b}{\operatorname{tg} \alpha} (R^4 - r^4) \tag{25}$$

En négligeant r par rapport à R, et en remplaçant b par $\frac{h}{\cos \alpha}$ conformément à la figure 3, on peut exprimer N_{p_4} sous la forme

$$N_{p_4} = \xi (\pi N)^3 \rho h R^3 \cdot \frac{R}{\sin \alpha} \tag{26}$$

Dans la figure 3 on observe que $\frac{R}{\sin \alpha}$ est égal à la longueur de la diagonale de l'agitateur L. La formule (25) devient

$$N_{p_4} = \xi (\pi N)^3 \rho h R^3 \cdot L \tag{27}$$

et l'expression de la puissance nécessaire pour vaincre la résistance à la rotation de l'agitateur à rame avec diagonale s'écrit

$$N_{prd} = 2\xi (\pi N)^3 \rho h R^3 [2R + 4H + L] \tag{28}$$

En analysant les formules de calcul concernant la puissance nécessaire pour les agitateurs mentionnés, on observe qu'elles contiennent un facteur commun

$$N_p^* = \xi (\pi N)^3 \rho h R^3 \tag{29}$$

qui sera dénommé *puissance spécifique de mélange.*

PARTIE EXPÉRIMENTALE

Le dispositif utilisé permet l'emploi de puissances nécessaires jusqu'à 300 W et assure la variation du nombre de tours entre 20 et 205 rot/mn.

Pour mesurer le moment de torsion, on utilise un système mécano-optique. On emploie une source de lumière introduite dans une chambre formée par deux coupes cylindriques coaxiales mobiles, chacune fixée rigidement à l'extrémité d'un élément sensible. Un système de fentes obliques assure la projection d'un point lumineux sur un élément circulaire transparent fixe coaxial avec les deux coupes mobiles. Le déplacement du point lumineux sur la génératrice déterminée par le déplacement relatif des deux coupes mobiles dépend de la valeur du moment de torsion.[25]

---

[25] L. Baraf, Brevet roum. 51 378 cl., 42 k 1/01.

On a déterminé les puissances dans le cas de l'utilisation de certains agitateurs de plus en plus compliqués, par l'addition, chaque fois, de certains éléments simples. Le diamètre des agitateurs est $d = 102$ mm.

Le récipient de mélange est en verre, cylindrique, à fond plane, ayant $D = 210$ mm muni de quatre chicanes verticales équidistantes à $b = 1/10\,D$.

A la suite de mesures expérimentales effectuées sur : 1) agitateur à deux pales, 2) ensemble de deux agitateurs à deux pales, 3) agitateur à rame ; 4) agitateur à rame et deux diagonales, 5) agitateur à rames avec deux éléments verticaux, on a constaté que la force spécifique de mélange est pratiquement la même pour les divers types d'agitateurs énumérés (tableau 1).

Il s'agit d'une appréciation faite en tenant compte du fait que les écarts par rapport aux valeurs moyennes ne dépassent pas ± 10 %. Dans les conditions de l'extrême complexité des phénomènes qui ont lieu dans le récipient de mélange et de la difficulté de les connaître du point de vue qualitatif et quantitatif[26] ces écarts sont considérés comme acceptables pour l'usage industriel. Les écarts des valeurs moyennes observées dans le tableau 1, en dehors des erreurs de mesure pendant les expériences, peuvent être expliqués en tenant compte que le passage du régime laminaire au turbulent n'a pas lieu pour la même valeur du nombre de Reynolds, et il y a donc des intervalles du nombre de Reynolds pour lesquels en fonction du type d'agitateur les régimes d'écoulement sont qualitativement différents dans le récipient de mélange.

CONCLUSIONS ET RECOMMANDATIONS POUR L'ÉLABORATION D'UN PROJET

En tenant compte des résultats expérimentaux obtenus, on considère que les hypothèses simplificatrices introduites peuvent être acceptées en vue de recommander une méthode utilisable pour évaluer les dimensions des agitateurs de type à rame.

En connaissant la valeur approximative de la puissance spécifique pour les agitateurs de type à rame, on propose la méthode suivante pour le calcul de la puissance nécessaire au mélange dans le cas d'utilisation des agitateurs complexes formés d'éléments simples.

En connaissant la courbe de variation de la puissance nécessaire au mélange, en fonction des caractéristiques du système, pour un agitateur formé par un ou par plusieurs éléments simples, on détermine la puissance de mélange spécifique. Pour déterminer la puissance d'un agitateur complexe, fonctionnant dans les mêmes conditions, on utilise la relation

$$N_p = N_p^* \left[\sum_1^{n_1} l_i + \sum_1^{n_2} L_i + 4 \sum_1^{n_3} \beta_i \cdot H_{xi} \right] \tag{30}$$

Dans le cas de la lamelle verticale située à un rayon R, $\beta_i = 1$.

---

[26] L. Baraf, *Rev. Chim.* (*Bucureşti*), **19**, 468 (1968).

Tableau

Valeur de la puissance et de la puissance

			Agitateur à deux pales ayant $d = 76$ mm		Deux agitateurs à deux pales ayant $d = 76$ mm	
			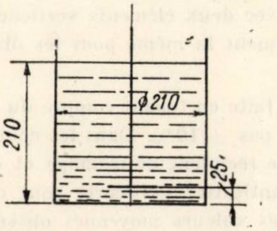		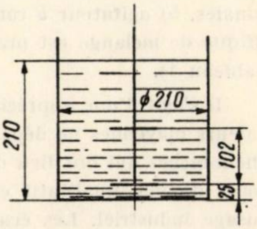	
Nombre de tours N rot/mn	Viscosité cP.	Nombre de Reynolds $Re = Nd^2$	Puissance Np. $W.10^3$	Puissance spécifique Np. $W/cm.10^3$	Puissance Np. $W \cdot 10^3$	Puissance spécifique Np. $W/cm.10^3$
21	282	16,1	—	—	3,5	0,17
31	282	23,8	—	—	7	0,34
41	282	31,5	—	—	12	0,59
51,5	282	39,5	11,3	1,1	20	1
60	282	46,1	15	1,48	27	1,3
80	282	61,5	27	2,65	47	2,3
100	282	76,8	42	4,1	79	3,9
130	282	100	88	8,7	180	8,8
145	282	111,4	109	10,7	250	11
175	282	134	192	18,8	440	21
190	282	146	270	26,5	600	29
205	282	157	330	32,4	760	37
51,5	23,8	368	5	0,49	11	0,54
60	23,8	428,5	7	0,68	16	0,78
80	23,8	570	19	1,90	42	2
100	23,8	714	43	4,2	86	4,2
130	23,8	928	105	10,3	189	9,5
145	23,8	1035	140	12,7	250	12
175	23,8	1250	250	24	400	20
190	23,8	1356	320	31	560	28
205	23,8	1464	430	42	730	36

Dans les places notées avec une ligne, le mesurage n'a pas été effectué.

1

spécifique nécessaire pour mélanger

Agitateur à rame ayant $d = 102$ mm		Agitateur à rame avec diagonale ayant $d = 102$ mm		Agitateur à rame avec deux éléments verticaux à la distance $Rx = 0{,}35\ d$ ayant $d = 102$ mm	
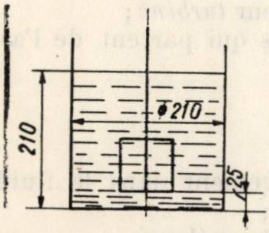		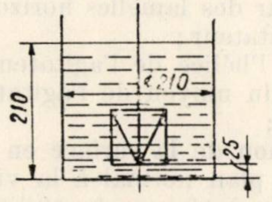		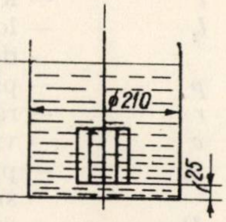	
Puissance *Np.* W.10^3	Puissance spécifique *Np.* W/cm.10^3	Puissance *Np.* W.10^3	Puissance spécifique *Np.* W/cm.10^3	Puissance *Np.* W.10^3	Puissance spécifique *Np.* W/cm.10^3
14	0,15	17	0,16	18	0,15
31	0,33	40	0,38	40	0,34
56	0,59	66	0,63	75	0,6
85	0,93	110	1	120	1
112	1,2	140	1,3	140	1,2
200	2,2	250	2,4	270	2,3
340	3,6	410	3,9	490	3,9
730	7,8	810	7,8	950	8
880	9,4	1040	10	1300	11
1580	17,5	1850	17	2100	18
2250	24	2530	24	3000	25
2820	31	3260	31	3700	31
41	0,45	53	0,5	57	0,48
67	0,72	85	0,8	87	0,73
168	1,8	203	1,95	220	1,9
340	3,7	390	3,7	450	3,8
850	9,1	890	8,6	1070	9
950	10,3	1100	10,6	1330	11
1600	19	1900	18,5	2400	20
2260	26	2650	25	3000	25
4600	48	5600	53	5730	48

NOTATIONS

d — diamètre de l'agitateur ;
g — accélération terrestre ;
h — largeur de la lamelle de l'agitateur ;
h_a — distance entre l'agitateur et le fond du récipient de mélange ;
l — longueur de la lamelle de l'agitateur *turbine* ;
l_i — longueur des lamelles horizontales qui partent de l'axe de l'agitateur ;
p_a — pas de l'hélice de l'agitateur ;
r — rayon du moyeu de l'agitateur ;
v — vitesse ;
A — projection de la surface en mouvement dans le fluide sur un plan normal à la vitesse ;
D — diamètre intérieur du récipient de mélange ;
F — force ;
H — hauteur de la lamelle verticale placée au rayon maximum de l'agitateur ;
H_o — hauteur du fluide dans le récipient de mélange ;
H_{xi} — hauteur de la lamelle verticale placée à la distance R_{xi} de l'axe de l'agitateur ;
L_i — longueur des lamelles inclinées partant de l'axe de l'agitateur ;
N — nombre de tours ;
N_p — force utile nécessaire pour le mélange ;
R — rayon de l'extrémité de l'agitateur, $R = \frac{d}{2}$;
ξ — coefficient de résistance du milieu au mouvement de l'agitateur dans le fluide ;
ρ — masse spécifique ;
η — viscosité dynamique ;
$Re - \frac{Nd^2 \rho}{\eta}$ — le nombre de Reynolds pour le mélange ;
$Fr = \frac{Nd}{\mathrm{gH}}$ — le nombre de Froude pour le mélange ;
$Kp = \frac{N_p \cdot g}{N^3 d^5 \rho}$ — le nombre de la puissance.

Revue Roumaine de Chimie, **14**, 1457–1465 (1969)

RÉALISATION DES SELS NUCLÉAIRES DE ZIRCONIUM PAR RECRISTALLISATIONS FRACTIONNÉES

LUCREŢIA I. POPA, V. DOROBANŢU, D. DORCIOMAN,
STELA CONSTANTINESCU et M. S. POPA

Institut de Physique Atomique, Boîte postale 35 Bucarest

Reçu le 11 septembre 1968

On étudie la formation de sels nucléaires de zirconium obtenus à partir de concentrés de zirconium d'origine roumaine. Après 14 recristallisations fractionnées, on obtient le sel nucléaire de zirconium avec 40 ppm de hafnium.

I. INTRODUCTION

Le zirconium et ses alliages (de types différents) ont acquis ces derniers temps une large utilisation comme matériaux pour la technique nucléaire, grâce aux propriétés spéciales du zirconium, [1] à savoir :

— faible section efficace de capture pour les neutrons. $\sigma = 0{,}18 \pm 0{,}05$ barns.

— résistance mécanique supérieure, [2] quand il n'est pas contaminé par l'oxygène, le nitrogène, le carbone et l'hydrogène.

— grande résistance à la corrosion.

— matériel très réfractaire (il fond à 1845°).

Le zirconium de pureté nucléaire [3] ne doit pas dépasser le contenu en impuretés ci-dessous :

— bore = 0,5 — 1 ppm ;
— cadmium = 0,5 — 1 ppm ;
— cobalt = 10 — 20 ppm ;
— hafnium $\leqslant$ 100 ppm ;
— lithium = 1 ppm ;
— manganèse = 50 — 100 ppm ;
— terres rares = 1 — 20 ppm ;
— calcium, fer et titane = traces.

---

[1] P. Pascale, « Nouveau traité de chimie minérale », vol. IX, Masson et Cie, Ed., 120, Boul. Saint-Germain, Paris (6e), 1963, p. 438.

[2] J. L. Bernard, E. Cibois, J. Lamaine et M. Weisz, « Colloque sur les effets de rayonnements dans les solides et matériaux pour réacteurs », Agence Internationale de l'Energie Atomique, SN 25/71, mai 1962.

[3] M. J. Farah et I. S. Iamani, « Conf. Int. Pac. Energie Atome », Genève, 1964, vol. IX, p. 131.

Parmi les impuretés mentionnées, le hafnium est toujours présent et son élimination du zirconium exige des opérations extrêmement difficiles. Cette séparation difficile du hafnium et du zirconium est déterminée par l'analogie évidente entre ces deux éléments (la structure des atomes, les rayons ioniques, etc.). Les méthodes de séparation sont nombreuses. Dans le présent travail, nous traitons seulement la séparation du zirconium et du hafnium par recristallisations fractionnées.

II. PURIFICATION PAR CRISTALLISATION

Parmi les nombreuses méthodes de purification des substances, utilisées dans les laboratoires ou dans l'industrie, nous citons : la distillation et la cristallisation, etc. L'opération de cristallisation présente une série d'avantages :

— relativement simple et facile à diriger ;

— nécessité des installations simples et faciles à obtenir ;

— on l'applique aux liquides azéotropes ou à ceux qui ne permettent pas d'utiliser la distillation ;

— la consommation d'énergie est réduite par rapport à l'énergie consommée dans les opérations de distillation.

C'est pourquoi la cristallisation [4, 5] est préférable à la distillation. Parmi les désavantages de la cristallisation, on mentionne :

— les cristaux obtenus peuvent induire des impuretés de la solution initiale ;

— l'efficience de l'opération est réduite.

III. SÉPARATION DU ZIRCONIUM ET DU HAFNIUM PAR RECRISTALLISATIONS FRACTIONNÉES

OBTENTION DU FLUOZIRCONATE ET DE L'OXYDE DE ZIRCONIUM À PURETÉ NUCLÉAIRE

1. *Généralités*

Il est connu que grâce aux propriétés nucléaires du zirconium, celui-ci est transparent aux neutrons (il possède une section efficace d'absorption à l'égard des neutrons thermiques faibles, $\sigma = 0{,}18 \pm 0{,}05$ barns), tandis que son homologue, qui l'accompagne partout dans la nature, le hafnium, possède une section efficace d'absorption grande (de 583 plus grande que celle du zirconium, $\sigma = 105 \pm 5$ barns) ; il s'ensuit la nécessité de séparer les deux hommologues et de les utiliser à de fins opposées dans la technique nucléaire :

— le zirconium en tant que matériel structural ;

— le hafnium en tant qu'absorbant des neutrons et atténuant des flux.

---

[4] J. M. Mullin, « Crystallisation », Londres, Butterworths, 1961, p. 101–190.

[5] « Procese și aparate în industria chimică », Ed. tehnică, Bucarest, 1959, p. 448.

2. *Recristallisation fractionnée du Zr (Hf)* K_2F_6

Parmi les sels du zirconium (fluozirconates oxychlorures, sulfates, phosphates, oxalates, tartrates, citrates, etc.) celui qui présente de la stabilité dans les opérations de cristallisation pour la séparation du zirconium et du hafnium c'est le fluozirconate (fluohafniate) de potassium. Ce sel est relativement facile à obtenir (en comparaison d'autres sels de zirconium) à partir des concentrés de zirconium. Les travaux pratiques afin d'obtenir les sels nucléaires ont été effectués avec fluozirconate de potassium provenu des concentrés de zirconium d'origine roumaine. La composition chimique (en impuretés) du sel de départ est :

$Hf = 0{,}929\,\%$ (rapporté au zirconium)
$Fe = 10^{-3\%}$
$Ti = 10^{-2\%}$
$Mn = 10^{-2\%}$
$Mg = 10^{-3\%}$

$Co = 10^{-1\%}$
$Cu = 10^{-3} - 10^{-4\%}$
$Al = 10^{-3\%}$
$Si = 10^{-3\%}$
$Pb = 10^{-3\%}$

a) *Choix du solvant utilisé*

Les opérations de recristallisation ont été effectuées dans l'eau dédurisée. L'eau en tant que solvant a été choisie étant donné ses qualités :

— solvant bon marché et facile à procurer ;

— non toxique, non inflammable et qui plus est facilement maniable ;

— stable dans les opérations de recristallisation ;

— il ne réagit point avec le soluté (ZrF_6K_2) et par conséquent n'engendre pas de produits secondaires qui pourraient diminuer le rendement de la cristallisation :

— quoique le pouvoir du solvant dans le cas de l'eau soit inférieur à l'acide fluorhidrique ou aux fluorures, nous avons cependant choisi l'eau comme solvant pour les raisons suivantes :

— l'acide fluorhidrique ou les fluorures (d'ammonium, de potassium) réagissent pendant l'opération de cristallisation avec le $Zr(Hf)F_6K_2$, livrant des penta- et heptafluozirconates et heptafluohafniates avec des solubilités très approchées, empêchant de la sorte la séparation ;

— le coefficient de température de la solubilité dans le milieu aqueux est supérieur à celui obtenu dans le milieu de fluor.

b) *Séparation du zirconium et du hafnium par recristallisations fractionnées*

ZrF_6K_2 possède une solubilité différente (inférieure) dans l'eau par rapport au HfF_6K_2 aux mêmes températures ; par des opérations répétées de cristallisation les eaux de cristallisation s'enrichissent en hafnium et les cristaux de ZrF_6K_2 se purifient (de hafnium).

Dans les travaux nous avons employé pour la recristallisation des solutions saturées de $Zr(Hf)F_6K_2$. Les solutions-mère résultant à partir de la cristallisation d'une épreuve ont été chauffées (98—100°) et employées pour la dissolution d'une nouvelle épreuve de $Zr(Hf)F_6K_2$, tandis que les cristaux obtenus de chaque échelon de cristallisation de la première épreuve ont été redissous et cristallisés dans le solvant (eau pure) à 98°—100°.

Pour chaque opération de cristallisation nous avons employé des germes de cristallisation formés par les cristaux obtenus dans l'échelon précédent. Les germes introduits représentent 0,005—0,01% du poids de l'épreuve $Zr(Hf)F_6K_2$ déjà cristallisée dans l'échelon respectif. Les cristaux introduits comme germes de cristallisation sont uniformisés dans la solution saturée, grâce à une faible agitation (10 rot/mn), mais seulement dans les 1—3 minutes qui suivent l'introduction. Une fois l'agitation effectuée, la solution a été laissée afin de cristalliser librement.

Après 14 recristallisations fractionnées, l'épreuve de ZrF_6K_2 dissoute dans le solvant pur ne contenait que 40 ppm Hf.

Les eaux de cristallisation cumulées par la cristallisation de plusieurs épreuves ont été enrichies en hafnium et précipitées à l'hydroxyde de hafnium impur ; la purification du hafnium arrivée sous la forme de solution de sulfate a été effectuée sur une colonne de résine anionite roumaine — Vionit AT_1.

ZrF_6K_2 à pureté nucléaire a été précipité en excès d'ammoniaque (120—135%) à l'hydroxyde de zirconium (au pH = 9). La décantation, la filtration quantitative de l'hydroxyde, la dessication et la calcination par oxyde de zirconium nucléaire ont été effectuées.

Dans le laboratoire on a obtenu par un emploi total des eaux de cristallisation un rendement de 87% Zr.

Le ZrF_6K_2 recristallisé et refroidi lentement à un pH de 3,5—4 se présente sous forme de grands cristaux aciculaires, tandis que celui obtenu à un pH = 2 se présente sous forme de cristaux fins (menus).

La teneur en hafnium des épreuves cristallisées au pH = 2 a été la même (sensiblement plus grande) que celle des épreuves cristallisées au pH = 3,5—4, soumises au même nombre d'opérations de cristallisations.

c) *Refroidissement des solutions dans la recristallisation du ZrF_6K_2*

Les solutions sursaturées ont été obtenues par le refroidissement des solutions saturées de $Zr(Hf)F_6K_2$ de 100° à 30°. L'opération a été effectuée de deux manières :

— refroidissement rapide à vitesse de refroidissement de 1,9—4°/mn.

— refroidissement lent, à vitesse de refroidissement de 0,4—1,1°/mn.

Dans le premier cas, les cristaux ne sont pas uniformes, les cristaux fins (menus) dominent. Dans le second cas, les cristaux sont de grandeur uniforme et généralement d'une forme grande aciculaire.

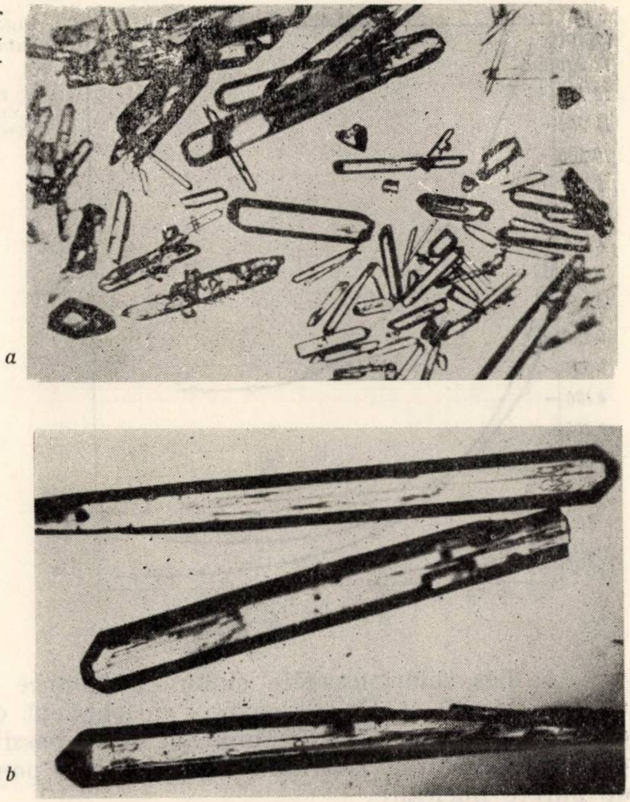

Fig. 1. — Variation de la grandeur des cristaux de Zr F_6K_2, en fonction de la vitesse de refroidissement de la solution :
a, 1.9° – 4°/mn (× 111) ;
b, 0,4° – 1,1°/mn (× 111).

d) *Variation du contenu de hafnium dans la recristallisation fractionnée du* $Zr(Hf)\,F_6K_2$

Le contenu de hafnium varie continuellement pendant l'opération de cristallisation. Nous précisons les conclusions suivantes :

1. L'épreuve de fluozirconate de potassium atteint après 14 recristallisations fractionnées de 0,929 % Hf une teneur de 40 ppm en Hf par dissolution dans le solvant pur (courbe 1).

2. L'épreuve II (courbe 2) est dissoute dans les solutions-mère à partir de la Ire épreuve de cristallisation et atteint une teneur presque constante en hafnium de 638 ppm après 12 recristallisations.

3. Le contenu de hafnium baisse rapidement dans les premières 8 – 10 opérations de cristallisation et très lentement dans les autres 4 – 6 opérations.

4. Il est indiqué d'effectuer les dernières opérations de cristallisation de la IIe épreuve dans le solvant pur, afin de faire baisser le contenu de hafnium jusqu'aux concentrations nucléaires.

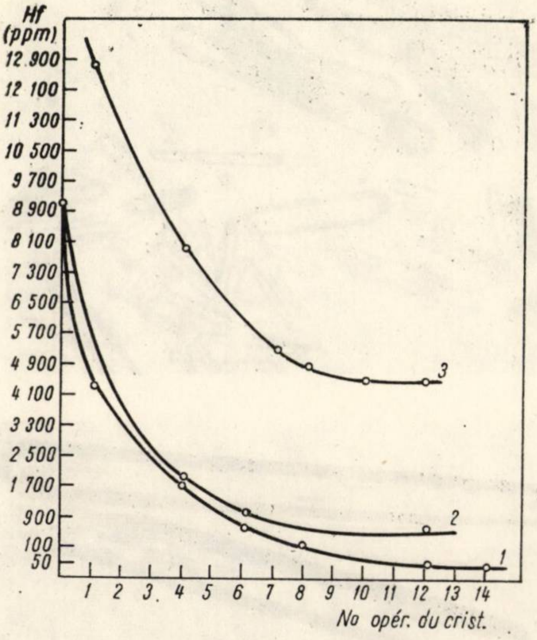

Fig. 2 — Variation du contenu en hafnium avec le nombre de cristallisations :

1, Epreuve dissoute dans le solvant pur ; *2*, Epreuve dissoute dans les solutions-mère de l'épreuve I ; 3) Solutions-mère cumulées I et II.

5. Les solutions-mère cumulées (courbe 3) à partir des cristallisations des Ire et IIe épreuves s'enrichissent en hafnium, leur emploi en 8—9 opérations de cristallisation étant possible, après quoi, elles sont précipitées, afin de continuer les opérations pour l'obtention du hafnium de pureté nucléaire.

e) *Détermination du coefficient de séparation*

Un troisième facteur important (les deux autres sont : le pouvoir du soluté et le coefficient de température de la solubilité) qui caractérise la cristallisation fractionnée c'est le coefficient de séparation [6] ou le coefficient d'équilibre de la séparation.

Le coefficient de séparation représente le rapport de concentration de l'impureté en cristaux et en solution-mère à une température donnée lorsqu'il y a équilibre entre elles

$$K_{\text{sép}} = \frac{(C_{Hf}/C_{Zr})\ \text{crist.}}{(C_{Hf}/C_{Zr})\ \text{sol.}}$$

$K_{\text{sép}}$ = coefficient de séparation du zirconium et du hafnium à une température donnée ;

C_{Hf} crist. = concentration du Hf en cristaux ;

C_{Zr} crist. = concentration du Zr en cristaux ;

C_{Hf} sol. = concentration du Hf de la solution-mère à une température donnée ;

C_{Zr} sol. = concentration du Zr de la solution-mère en équilibre avec les cristaux à une température donnée.

---

[6] O. I. Egerev et A. D. Pogorelyi, *Zhur Priklad khim.*, **39**, 1186 (1966).

On a calculé le coefficient de séparation du zirconium et du hafnium pour une température de 30°C dans le 9° échelon de cristallisation pour lequel on a trouvé la valeur 0,746.

3. *Conditions de conservation du fluozirconate*
Sa tendance d'agglomération

Un aspect désagréable des substances cristallines c'est leur tendance d'agglomération, également observée dans le cas du Zr F_6K_2 dans les conditions de travail suivantes :

— alors que le fluozirconate possède une humidité élevée, alors que la grandeur des cristaux a été inégale. La tendance d'agglomération est indiquée dans la figure 3.

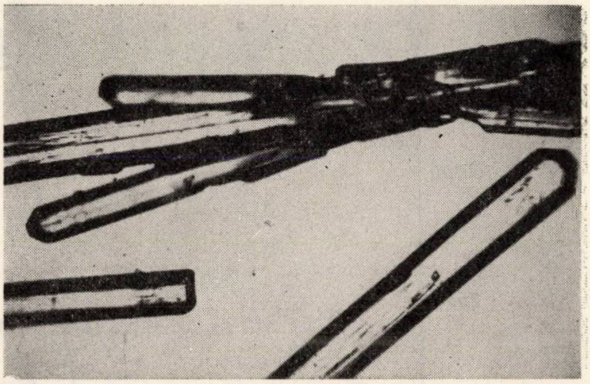

Fig. 3. — Tendance à l'agglomération du ZrF_6K_2 (× 111).

Afin d'éviter l'agglomération il est indiqué :

— d'obtenir dans la cristallisation de grands cristaux aciculaires, uniformes.

— d'obtenir l'humidité constante du milieu environnant ;

— de faire baisser l'humidité du produit ;

— de maintenir une température et une pression constantes.

IV. ANALYSES

Le contenu global de zirconium et de hafnium a été déterminé chimiquement (gravimétriquement). Le contenu du hafnium en zirconium a été déterminé par radioactivation. [7] Des épreuves étalon de zirconium (importé) nucléaire et de hafnium spectral ont été employées.

Les épreuves à teneur non connue en hafnium, ainsi que les standards ont été irradiés dans les mêmes conditions ; pendant 3 heures au flux $1{,}1.10^{13}$ n^1/cm^2.

Les mesurages ont été effectués à l'aide d'un spectromètre, à détecteur de Ge(Li) d'épaisseur de la couche compensée de 6 mm et de volume de 2,3 cm³. Sa résolution était de 4 KeV pour la ligne de 662KeV du Cs^{137}.

---

[7] W. Haerdi, L. Balsenic et S. Monnier, *J. Radioanalyt. Chem.*, **1**, 51 (1968).

Le schéma bloc de l'appareillage employé dans les mesurages est représenté dans la figure 4 et comprend :

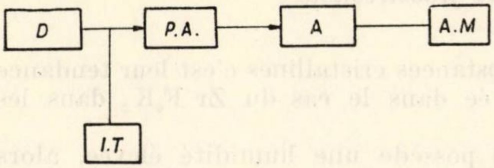

Fig. 4. — Le schéma bloc de l'appareillage pour les mesurages du Hf.

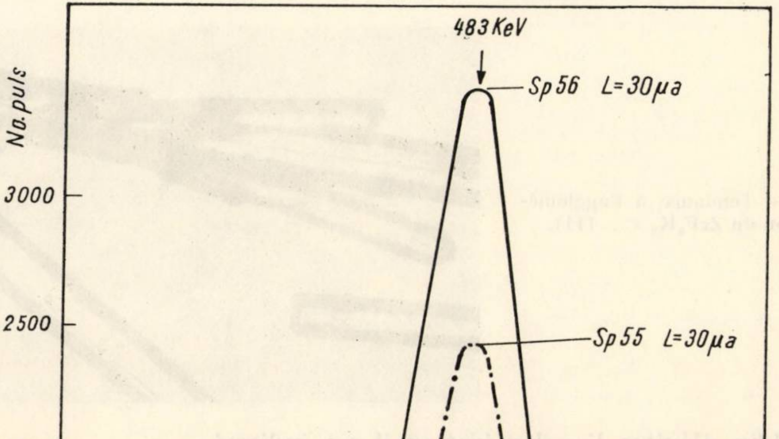

Fig. 5. — La courbe de calibrage du Hf.

— préamplificateur NE 5283 (PA) sensible à la charge;

— amplificateur NF 5259 (A);

— source de haute tension NF 5321 (IT) pour l'alimentation du détecteur (D);

— analyseur d'amplitude (AM) à 400 canaux SA—400.

Les épreuves ont été mesurées à l'aide de la géométrie qui rendrait le moins possible les erreurs dues à l'absorption des rayons γ dans le matériel même de l'épreuve.

Pour calculer[8] les quantités de hafnium on a employé le pic de 483 KeV donné par les épreuves de hafnium pur. En fonction du nombre d'impulsions/mg et d'impulsions/mn donné par trois épreuves de hafnium pur en quantités bien connues, on a tracé la courbe des spectres de calibrage (fig. 5) et on a calculé les quantités de hafnium des épreuves de fluozirconate (à contenu inconnu de hafnium).

Après 14 recristallisations, l'épreuve initiale des concentrés d'origine roumaine, déhafniée par nous, contient 40 ppm de hafnium.

V. CONCLUSIONS

1. Le fluozirconate de potassium de pureté nucléaire a été obtenu après 14 recristallisations fractionnées (dans le solvant à partir des solutions saturées, refroidies, en introduisant des germes de cristallisation.
2. La solution-mère a été employée à la dissolution d'une nouvelle épreuve de fluozirconate.
3. Les solutions-mère cumulées (à partir des recristallisations de plusieurs épreuves), enrichies en hafnium, sont précipitées à l'hydroxyde de hafnium impur.
4. La détermination de la teneur en hafnium à partir des épreuves déhafniées a été effectuée par radioactivation. On a mesuré le $^{181}_{72}$Hf à l'analyseur à 400 canaux SA—400, avec un détecteur au Ge(Li).
5. L'oxyde de zirconium nucléaire obtenu dans nos recherches contient 40 ppm Hf.

---

[8] W. ZIMERMAN, *Rev. Sci. Instr.*, **32**, 77 (1961).

Revue Roumaine de Chimie, **14**, 1467 – 1475 (1969)

RADIOLYSIS OF COPPER PHTHALOCYANINE ALKALINE AQUEOUS SOLUTIONS BY ^{60}CO γ-RAY

ECATERINA TĂRĂBĂŞANU-MIHĂILĂ and ELENA SOFRONIE

Institute of Atomic Physics, Bucharest P.O. Box 35

Received December 28, 1968

The ^{60}Co γ-ray radiolysis of tetrasulfonated copper phthalocyanine (TSCP), in aerated alkaline aqueous solutions was studied. The dependence of the decomposition radiolytic yield of (TSCP) on the initial concentration, pH, dose and dose-rate was investigated. $G_{(-\mathrm{TSCP})}$ was found independent of the dose-rate and initial concentration and showed a sharp decrease with increasing pH. It was established that the radiolytic decomposition reaction is an irreversible oxidation process. This reaction occurs in two steps and is attributed to the OH radical. The absolute rate constant for the reaction of (TSCP) with the OH radical by the competition method was determined.

INTRODUCTION

The radiolysis of organic dyes in aqueous solutions has been the subject matter of numerous investigations. The studies have been mainly directed towards two purposes, namely :

a) to state the dependence of radiolytic yields (*G*-values) on various parameters (pH, concentration, dose-rate, presence of oxygen, etc.), the correlation of these yields with those of the free radicals brought about by the water radiolysis, the elucidation of the radiolytic reaction mechanism and kinetics, as well as the nature of the irradiation products. [1–11]

[1] W. A. WATERS, *Discuss. Faraday Soc.*, **12**, 284 (1952).

[2] E. N. WEBER and R. H. SCHULER, *J. Amer. Chem. Soc.*, **74**, 4415 (1952).

[3] N. TH. RAKINTZIS, D. G. MARKETOS and A. P. KONSTAS, *Z. Phys. Chem., Leipzig*, **35**, 234 (1962).

[4] IRVING AUERBACH, U.S. At. Energy Comm. TID – 14927 (1962).

[5] AN-SHOU WAI, CH'U-CHANG HUNG and LAI-SU LI, *Bull. Inst. Chem. Acad. Sinica*, **1965**, 14.

[6] N. RAKINTZIS, E. PAPACONSTANTINOU, *Z. Phys. Chem. (Frankfurt)*, **44**, 257 (1965).

[7] D. S. MARKETOS and N. TH. RAKINTZIS, *Z. Phys. Chem. (Frankfurt)*, **44**, 270 (1965).

[8] *Ibid.*, 285.

[9] HJIME OGURA, TOSHIHIKO NAGAI, LI-SEN EDWARD CHU and MASAHARU KONDO, *J. Rad. Res.*, **7**, 58 (1966).

[10] G. SCHOLES and R. L. WILLSON, *Trans. Faraday Soc.*, **63**, 2983 (1967).

[11] D. G. MARKETOS, N. TH. RAKINTZIS and G. STEIN, *Israel J. Chem.*, **5**, 239 (1967).

b) to find some new chemical dosimeters. [12, 13].

In the present work we investigated the dependence of the yield of copper phthalocyanine decoloration on the initial concentration, pH, dose and dose-rate. We also determined the rate constant for the radiolytic decomposition by the competition method and established the reaction mechanism.

EXPERIMENTAL

1. *Irradiation Technique*

The irradiations were effected by means of a 400 Ci. ^{60}Co γ-ray source. Dose-rates were in the range $2.88-6.36 \times 10^{18}$ eV . ml^{-1}. h^{-1} and calibrated by the ferrous sulfate dosimeter, using $G_{\mathrm{Fe}}\,3^{+} = 15.6$ molec/100 eV. [14]

2. *Reagents — Analytical Methods*

The experiments were carried out using tetrasulfonated copper phthalocyanine,coupled with *para*-amino-aceto-acetanilide, (TSCP), prepared by a Polish patent, [15] since this is more readily soluble in water than the unsulfonated complex. The substance was meant for chromatography and was used without further purification.

All solutions were prepared with tetradistilled water ; the alkaline solutions by means of sodium hydroxide, freshly prepared by dissolving sodium (E. Merck, AG) in tetradistilled water, in a nitrogen atmosphere. [16]

Other reagents used : potassium iodide (U.C.B.), ammonium molybdate and potassium hydrogen phthalate (E. Merck, AG) and sulfuric acid (U.C.B.).

The copper phthalocyanine solutions were analysed with a Zeiss VSU-1 spectrophotometer at 340 mμ wavelength, where the dye has the absorption maximum. The molar extinction coefficient of (TSCP) at 25° is 36150 mole^{-1} . cm^{-1} in the concentration range $0.25-2.0 \times \times 10^{-5}$ M.

The amount of hydrogen peroxide was measured spectrophotometrically by the iodide method developed by Ghormley. [17] The molar extinction coefficient at 25° was 25 000 mole^{-1}. cm^{-1}.

Because the absorption maxima of the phthalocyanine and of the triiodide ion, formed in the presence of hydrogen peroxide, were very close, it was necessary that the undecomposed dye be absorbed on a Merck Ion exchanger I column after irradiation. The cation-exchange resin was in H^{+} form and the grain-size of $0.4-0.6$ mm.

The yields of molecular hydrogen were determined chromatographically. Argon was used as carrier gas on a 5A molecular sieve column.

The pH of the solution was measured on a Clamann — Grahnert type MV 11 pH-meter.

---

[12] Keiniki Sugimoto, Wataru Audo and Jitsuo Tsurugi, *Ann. Rept. Radiation Center Osaka Prefect.*, **3**, 114 (1962).

[13] J. Patko, Zs. Szentirmay, Z. Dezsi and M. Gorgey, *Acta Univ. Debrecen Ludovico Kossuth Nom., Ser. Phys. Chim.*, **12**, 29 (1966).

[14] C. J. Hochanadel and J. A. Ghormley, *J. Chem. Phys.*, **21**, 880 (1953).

[15] A. Kujawsky, W. Michalak, H. Iujawska and K. Lewicka, Pol. Pat. 49, 295, April 23, 1965 ; *Chem. Abstr.*, **64**, 14325 (1966).

[16] Z. D. Draganić, I. G. Draganić and M. M. Kosanić, *J. Phys. Chem.*, **70**, 1418 (1966).

[17] A. O. Allen, C. J. Hochanadel, J. A. Ghormley, and T. W. Davis, *J. Phys. Chem.*, **56**, 575 (1952).

RESULTS AND DISCUSSIONS

By irradiation of copper phthalocyanine alkaline solutions, an irreversible decoloration was observed. The bleaching obeys first-order kinetics as illustrated in figure 1.

The radiolytic yield of copper phthalocyanine decoloration was independent of the initial dye concentration in the range $0.25 - 2.0 \times \times 10^{-5}$ M and of the dose rate in the range $2.88 - 6.36 \times 10^{18}$ eV. $ml^{-1}.h^{-1}$.

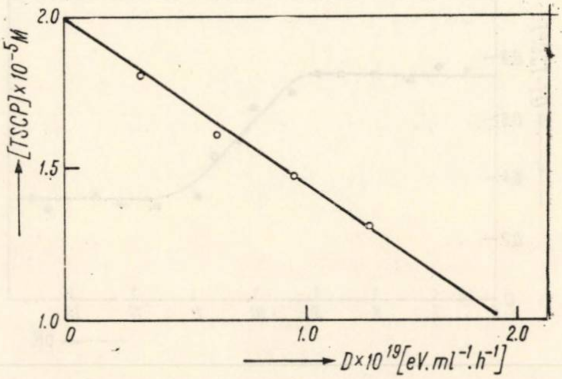

Fig. 1. – Decoloration of (TSCP) in alkaline aqueous solution by γ-rays as a function of dose, in the presence of air ; pH = 13.1.

The radiolysis of water involves ionization processes of water molecules, leading to the formation of the radiolysis products : "radical" products (H; e^-_{aq}, $OH^{\bullet}$) and "molecular" products (H_2 and H_2O_2) as well as excitation processes. The decomposition of water may be represented schematically, as :

$$H_2O \rightsquigarrow H,\ (e^-_{aq}),\ OH^{\bullet},\ H_2,\ H_2O_2 \qquad (1)$$

The radiolytic changes of solutes in diluted alkaline solutions are due to the above mentioned water decomposition products.

We performed a series of experiments in order to establish which of the water radiolysis products bears the responsibility for the copper phthalocyanine decoloration.

Knowing that sodium nitrate is an efficient e^-_{aq} scavenger ($k = 1 \times \times 10^{10}$ mole^{-1} . sec^{-1}), we effected experiments in the presence of this scavenger (1×10^{-3} M), which led to $G_{(-TSCP)}$ - values indentical with those obtained in the absence of sodium nitrate. It follows that the hydrated electron does not take part in the decoloration reaction.

Experiments were carried out both in the presence and in the absence of air, at different dye concentrations and different pH-values, in order to estimate the molecular hydrogen yield. The hydrogen yield found is 0.45, independent of the change in the pH and concentration value, in the region considered.

The effect of hydrogen peroxide was also investigated. One has noticed that the unirradiated system, (TSCP) + H_2O_2, is stable in alkaline aqueous solutions.

The above experiments led to the conclusion that on irradiation in the presence of air, only the OH radicals react with the dye.

Figure 2 shows the dependence of radiolytic yield of copper phthalocyanine decomposition, $G_{(-\mathrm{TSCP})}$, on the pH-value, for the range from 6 to 14. Sodium hydroxide freshly prepared and sulfuric acid were used for the adjustment of the pH. $G_{(-\mathrm{TSCP})}$ remains unchanged and equal to 0.76 ± 0.05 for the pH range from 6 to 9. A sharp decrease is observed from pH 9 to about 11.6. Then the yield remains again constant up to pH 14. The data for $G_{(-\mathrm{TSCP})}$ presented in figure 2 show that the radiolytic decoloration decreases strongly with the increase in the pH, in the range 9–11.6.

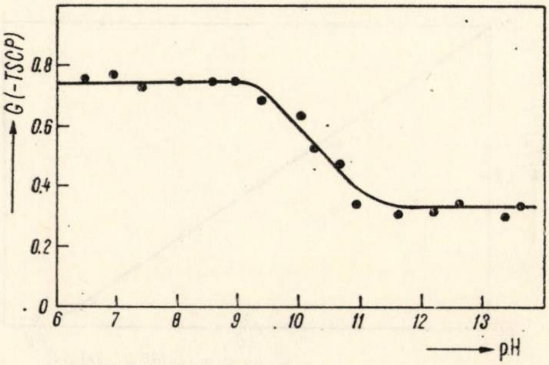

Fig. 2. – Variation of $G_{(-\mathrm{TSCP})}$ as a function of pH. $[\mathrm{TSCP}]_0 = 2 \times 10^{-5}$ M dose-rate = 5.09×10^{18} eV.ml^{-1}.h^{-1}.

It is very well known from literature data [18-21] that in alkaline aqueous solutions at pH ≃ 9, the OH radical loses its oxidizing properties owing to the scavenging of OH radicals by OH^- ions, according to the reaction:

$$OH^- + OH^\cdot \rightarrow O^- + H_2O \qquad (2)$$

The reactivity of O^- ions is weaker than that of the corresponding undissociated form, OH. In addition, the O^- species formed after pH 9 reacts rapidly with hydrogen peroxide $[(K_{(O^- + H_2O_2)} = 1.3 \times 10^{10}\ \mathrm{mole^{-1}.\ sec^{-1}}]$.[22] This fact is illustrated in figure 3, which represents the $G_{(H_2O_2)}$ - value as a function of pH. The result is the decrease in the decomposition radiolytic yield.

[18] E. Hayon, *Trans. Faraday Soc.*, **61**, 734 (1965).

[19] C. J. Hochanadel, *Rad. Res.*, **17**, 286 (1962).

[20] G. E. Adams, J. W. Boag, and B. D. Michael, *Trans. Faraday Soc.*, **61**, 429 (1965)

[21] F. S. Dainton and S. A. Sills, *Proc. Chem. Soc.*, **1962**, 223.

[22] M. Daniels and E. E. Wigg, *J. Phys. Chem.*, **71**, 1024 (1967).

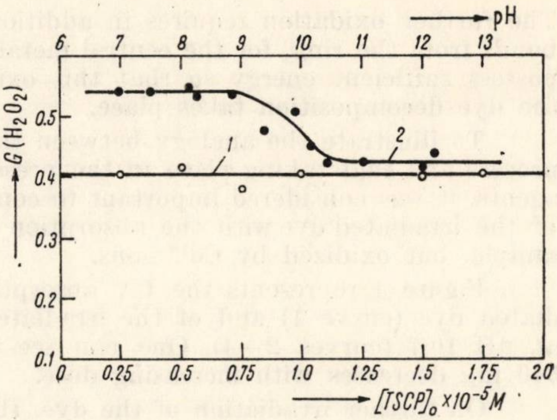

Fig. 3. — Plot of $G_{(H_2O_2)}$ *vs* pH and (TSCP) concentration, in the presence of air.
1, concentration: pH = 10.7; dose-rate = 6.36×10^{18} eV · ml^{-1} · h^{-1}; *2*, pH; $[TSCP]_0 = 2.0 \times 10^{-5}$ M.

MECHANISM

Since the OH radical is known in the radiation chemistry of organic dyes to act as an oxidizing agent, we considered the copper phthalocyanine decomposition as an oxidation process.

Dent, Linstead and Lowe [23] have shown that phthalocyanines can be oxidized quantitatively by strong, oxidizing agents such as ceric ion. Allen E. Cahill and Henry Taube [24] studied the oxidation of tetrasulfonated copper phthalocyanine in aqueous solution by suitable oxidizing agents. Among the oxidizing agents, Ce^{4+}, MnO_4^-, $Cr_2O_7^-$, Fe(*o*-phen)$_3^{+++}$ ions and HClO were found efficient. The authors have noticed the formation of an intermediate derived from the parent substance, by one-electron oxidation. The intermediate designed by $TSCP^+$ is red. It formes efficiently in water solution, but in this medium it is very unstable, its lifetime being only of the order of a few seconds at room temperature. The $TSCP^+$ intermediate can undergo a further irreversible oxidation, the resulting oxidation products being colourless. This oxidation may be considered the last oxidation step, including the ring breaking and the release of the central metal ion. Hence, the oxidation reaction of (TSCP) occurs in two steps. Since the first step, that of the $TSCP^+$ intermediate formation is fast and the second, that of the ring breaking and metal ejection is slow, the latter was considered as the rate-determining step.

By analogy with the study carried out in the presence of the chemical oxidizing agents, we assumed that the OH radical produces the $TSCP^+$ intermediate, in a first one-electron oxidation step:

$$(TSCP) + OH^{\cdot} \rightarrow TSCP^+ + OH^- \quad (3)$$

---

[23] Dent, Linstead and Lowe, *J. Chem. Soc.*, **1934**, 1033.

[24] Allen E. Cahill and Henry Taube, *J. Amer. Chem. Soc.*, **73**, 2857 (1951).

The further oxidation requires in addition the rupture of a number of bonds from the ring, for the central metal ion release. The OH radicals possess sufficient energy so that this oxidation step and consequently the dye decomposition takes place.

To illustrate the analogy between the radiation induced oxidation process and that taking place in the presence of the chemical oxidizing agents, it was considered important to compare the absorption spectrum of the irradiated dye with the absorption spectrum of a non-irradiated sample, but oxidized by Ce^{4+} ions.

Figure 4 represents the UV absorption spectrum of the non-irradiated dye (curve 1) and of the irradiated one, at different doses and at pH 10.7 (curves 2–4). One can see that the absorption band at 340 mμ decreases with increasing dose.

On further irradiation of the dye, the absorption band at 340 mμ disappears. Figure 5 shows the absorption spectrum of the non-irradiated dye, oxidized by Ce^{4+} ions (curve 1) and that of the dye irradiated at a high dose, when the dye is entirely decomposed. In both cases the absorption band at 340 mμ disappears. The resulting oxidation products are colourless and do not absorb in the region under consideration. The nature of these products was not investigated.

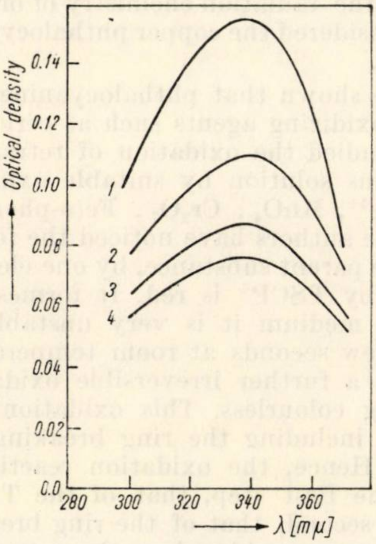

Fig. 4. — Recording of UV absorption spectrum of (TSCP).

Curve *1*, — non-irradiated sample; curves *2–4*, — irradiated sample at different doses, ranging from 5.09×10^{18} to 1.2×10^{19} eV·ml^{-1}, pH = 10.7.

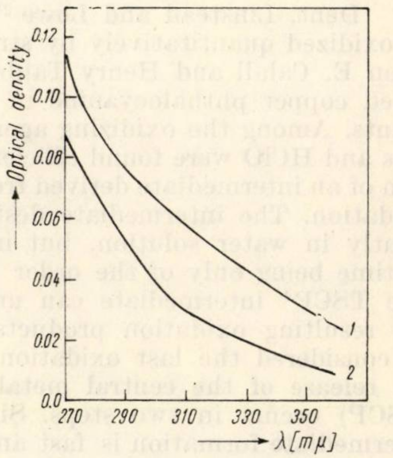

Fig. 5. — UV absorption spectrum of (TSCP).

curve *1*, -non-irradiated dye, oxidized by Ce^{4+} ions; curve *2*, — irradiated dye; dose = 2.0×10^{19} eV·ml^{-1}; $[TSCP]_0 = 1.0 \times 10^{-5}$ M.

The $TSCP^+$ intermediate is rapidly reduced in the presence of reducing agents such as Fe^{2+}, Sn^{2+}, or H_2O_2 and the resulting solution comes back to the initial colour, hence the dye is restored.

As the literature data indicate, [25] in aerated alkaline solution, the hydrogen peroxide is formed by the reactions:

$$H^{\cdot} + O_2 \rightarrow O_2^- + H^+ \ [k_4 = 2.6 \times 10^{10} \text{ mole}^{-1}.\text{sec}^{-1}.] \quad (4)$$

$$O_2^- + O_2^- + 2H_2O \rightarrow H_2O_2 + 2OH^- \ [k_5 = 1.7 \times 10^7 \text{ mole}^{-1}.\text{sec}^{-1}.] \quad (5)$$

On the other hand, Haïssinsky and co-workers, [26] studying the radiolysis of the potassium iodate in alkaline media, emphasize that hydrogen peroxide does not react with iodates, but it disappears gradually during radiolysis, having a reducing effect on the intermediate decomposition compounds of the solute.

Although we have experimentally ascertained that (TSCP) is inert as against the hydrogen peroxide (see pag. 4), the measured yields of H_2O_2 as a function of pH and concentration showed smaller values than the primary yield for the hydrogen peroxide formation, which is 0.7 (Fig. 3). Therefore, in our system, as the $TSCP^+$ intermediate is forming, the hydrogen peroxide resulted during water radiolysis brings about the $TSCP^+$ reduction to the parent substance. Thus, the decrease in the radiolytic yield of (TSCP) decoloration and the hydrogen peroxide consumption occur at the same time. Hence, a competition for the $TSCP^+$ intermediate between OH radicals and hydrogen peroxide takes place.

Irradiation of (TSCP) in deaerated solution confirms the reduction of $TSCP^+$ by hydrogen peroxide. In deaerated pure water, the radiolytic yield for the hydrogen peroxide formation reaches quickly a steady state, corresponding to a very low concentration. [27] Consequently, in the absence of oxygen, the small amount of hydrogen peroxide formed cannot reduce efficiently the $TSCP^+$ intermediate. Thus, at pH $\sim$ 1.31, $G_{(-TSCP)}$ is 0.69 ± 0.06. This value exceeds that obtained in the presence of oxygen (0.34). $G_{(-TSCP)}$-values are not expected to reach the primary OH radical yield ($G_{OH} \simeq 2.6$), even in the absence of H_2O_2, because the reaction occurs in two steps, both consuming OH radicals. Thus, $G_{(-TSCP)}$ at pH $\sim$ 13.1, in deaerated solutions was found after calculation equal to $1/4\ G_{OH}$, which means that four OH radicals are required for the decoloration of one dye molecule.

THE DETERMINATION OF THE ABSOLUTE RATE CONSTANT FOR THE REACTION OF OH RADICALS WITH (TSCP)

The rate constant for the reaction of the species formed by the action of ionizing radiation with various solutes has, in the past, been investigated by classical stationary methods. Generally, such studies lead to an estimation of the ratio of two rate constants, but in order to calculate this ratio, the particular reaction mechanism must be known or assumed.

---

[25] W. A. Armstrong, *Canad. J. Chem.*, **44**, 737 (1966).

[26] M. Haïssinsky, J. Jone and W. Szymanski, *J. Chim. Phys.*, **61**, 572 (1964).

[27] C. J. Hochanadel, "Proc. Second. Intern. Conf. Peaceful Uses of Atomic Energy", Geneva, **7**, 633 (1958).

By the competition method one can directly determine the absolute rate constant, for the reaction of various solutes with one of the species formed by water radiolysis, using a reference solute.

The reasoning of the competition method is as follows. A solution containing a concentration $[C]$ of the reference solute, X, and a concentration $[S]$ of the solute Y is irradiated. The radicals formed, OH radicals for example, are scavenged either by X or Y:

$$\mathrm{OH}^{\cdot}\ X \xrightarrow{k_6} \text{products which absorb} \tag{6}$$

$$\mathrm{OH}^{\cdot} + Y \xrightarrow{k_7} \text{products which do not absorb} \tag{7}$$

If D_0 is the optical density of the absorbing product in (6), when the concentration of X is $[C]$ and that of Y is zero, and if D is the optical density when the concentration of Y increases up to $[S]$, other conditions remaining unchanged, then it can be shown that:

$$\frac{D_0}{D} = 1 + \frac{k_7\,[S]}{k_6\,[C]}. \tag{8}$$

If D_0/D is plotted against $[S]/[C]$ a straight line should be obtained, whose slope is k_7/k_6. The absolute rate constant, k_6, as against the reference solute being known, k_7 as against Y can be determined.

Using this method we calculated the absolute rate constant for (TSCP) decoloration reaction with OH radical. Carbonate ion, ethanol

Table 1

Absolute rate constants of various solutes towards OH radicals

Solute	pH	k [mole^{-1}.s^{-1}/10^8]
Carbonate	10.7	2.0
Ethanol	10.7	10.0
Methanol	10.7	4.6

and methanol were used as reference solutes. Their absolute rate constants for the OH radical are given in table 1. [28] The competition for the OH radicals which occurs between (TSCP) and one of the reference solutes

$$\mathrm{OH}^{\cdot} + (\mathrm{TSCP}) \xrightarrow{k_9} \text{products} \tag{9}$$

$$\mathrm{OH}^{\cdot} + (S) \xrightarrow{k_{10}} \text{products} \tag{10}$$

can be expressed by the relationship:

$$[G_s(-\mathrm{TSCP})]^{-1} = [G_0(-\mathrm{TSCP})]^{-1} + [G_0(-\mathrm{TSCP})]^{-1}(k_{10}\ [S]/k_9(\mathrm{TSCP}]),$$

where $G_s(-\mathrm{TSCP})$ and $G_0(-\mathrm{TSCP})$ represent the yields of (TSCP) decoloration in the presence and in the absence of additional solute, respectively. Aerated (TSCP) solutions having a concentration ranging from 2.5 $\times 10^{-6}$ M to 1.75 $\times 10^{-5}$ M and the pH = 10.7, were irradiated in the presence of a determined concentration of added solute and the $G_s(-\text{TSCP})$ was measured. Plots of $G_s(-\text{TSCP})$ as a function of [TSCP]/ /[S] ratio were linear with all three of the solutes used (Fig. 6). The absolute rate constant, k_9, was calculated as shown above and the obtained values are given in table 2.

---

[28] G. E. Adams, J. W. Boag and B. D. Michael, *Trans. Faraday Soc.*, **61**, 1417 (1965).

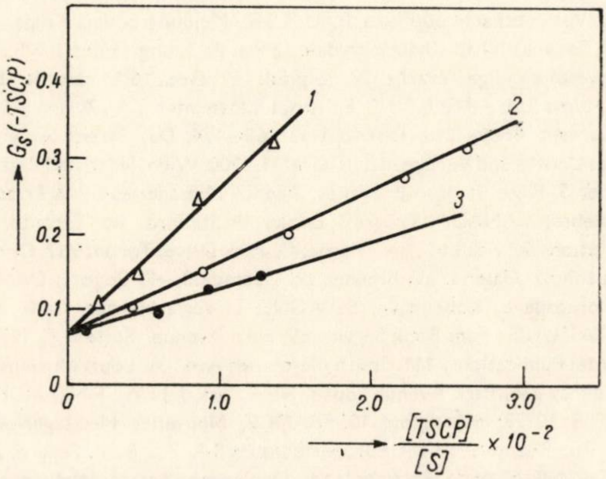

Fig. 6. — Competition for OH radicals between (TSCP) and various solutes. pH=10.7
1, carbonate ion; *2*, methanol; *3*, ethanol

Table 2

Absolute rate constant of (TSCP) towards OH radicals

Reference solute	$k_9[\text{mole}^{-1}.\text{s}^{-1}/10^9]$
Carbonate	4.0
Ethanol	4.1
Methanol	3.95

From the above data and discussion, we concluded that :

1. The radiolytic decomposition of tetrasulfonated copper phathalocyanine is an oxidation process taking place through the agency of OH radicals, formed by the water radiolysis.
2. The oxidation occurs in two steps, the latter being the rate-determining one.
3. The mechanism of the process induced by radiation is similar to that occurring in the presence of the strong oxidizing chemical agents in aqueous solutions.

Revue Roumaine de Chimie, **14**, 1467–1475 (1969)

La REVUE ROUMAINE DE CHIMIE parait 12 fois par an. Le prix d'un abonnement annuel est de : £ 5.0.0; $ 12,—; FF 60, — : DM 48,—. Toute commande de l'étranger (fascicules ou abonnements) sera adressée à CARTIMEX, Boîte postale 134 — 135, Bucarest, Roumanie, ou à ses représentants à l'étranger.

R.P. d'ALBANIE, Ndermarja Shtetnore e Botimeve Tirana; R.D. ALLEMANDE, Deutscher Buch Export und Import Leipzig, 701, Leninstrasse 16; R.P de BULGARIE, Hemus, Place Slaweikov, 11, Sofia; R.P. de CHINE, Waiwen Shudian P.O.B.. 88, Peking; R.P.D. CORÉENNE, Chulphanmul, Phenian; RÉPUBLIQUE CUBA, Cubartimpex Simón Bolivar 1, Palacio Aldamo Habana; R.P. HONGROISE, Kultúra, P.O.B. 149, Budapest 62; R.P. MONGOLE, Mongolgosknigotorg, Ulan Bator; R.P. de POLOGNE, Ruch, Ul. Wronia 23, Warszawa; R.S. TCHÉCOSLOVAQUE, Artia, Ve Smeckach 30-Praha II; U.R.S.S., Mejdunarodnaia Kniga, Moskva G-200, R. D. VIETNAM, So Xuat Nhap Khau Sach Bao, 32 Hai Ba Trung, Hanoï; R.S.F. de YOUGOSLAVIE, Jugoslovenska Knjiga Terazije 27, Belgrad; I Prosveta 16/1, Terazije, Belgrad; Forum Voïvode Misica, Novi Sad; ARGENTINE, Editorial Sudaminter S.A., Alsina 500, Buenos Aires; AUSTRALIE, Current Books Ltd. Distributors 168—174, Day Street Sydney; AUTRICHE, Globus Zeitungs Drucks und Verlagsanstalt GmbH. 1200, Wien, Höchstädplatz 3; BELGIQUE, Du monde Entier 5, Place St. Jean-Bruxelles, Agence Messageries de la Presse 14—22, Rue du Persil, Bruxelles; CANADA, Progress Books 44 Stafford St. Toronto, Ontario W.M Dawson Subscriptions Service Ltd., Six Thorneliffe Park Drive, Toronto 17, Ontario; COLOMBIE, Librería Buchholz Galeria, av. Jiménez de Quesada 8—40 Bogotá; DANEMARK, Ejnar Munksgaard, Noregade 6, Kobenhavn, ESPAGNE, Librería Herder, Calle de Balmés 26‹ Barcelona 7; ÉTAT UNIS, Fam Book Service 69, Fifth Avenue, Suite 8 F., New York, 10003 N. Y.; Continental Publications, 111, South Mermanec Ave., St. Louis Missouri 63105; Turner Subscription Agency 235, Park Avenue South, New York 3 N.Y.; FINLANDE, Akateeminen Kirjakauppa P.O.B. 10128, Helsingfors, 10; FRANCE, Nouvelles Messsageries de la Presse Parisienne, 111, Rue Réamur, Paris II, Europériodiques S.A. 72., Boul. Senard, 22 Saint Cloud; GRANDE-BRETAGNE, Collet's Holdings Ltd. Deninngton Estate, Wellingborough, Northants Central Books Ltd. 37, Inn Road London W.C. 1; ISRAËL, Lepac Ltd., P.O.B., 1136 Tel-Aviv; Haiflepac Ltd. P.O.B. 1794, Haïfa; ITALIE, So Co. Lib. Ri. Piazza Margana 33 — Roma; Messagerie Italiane, Sp. A. Milano, Via Priv. Renzo e Lucia 7; JAPON, Nauka Ltd. 30—19 Minami— Ikebukuro 2 chome Toshima Ku, Tokyo; PAYS — BAS, N. V. Martinus Nijhoff, P.O.B. 269, Den Haag; Swetz & Zeitlinger; Keizersgracht 471—487, Amsterdam C.; NORVÈGE, Tryggve Juul Moller—Boekhandel Øvre Slottsgate 15 Oslo 1; R.F. d'ALLEMAGNE, Kubon & Sagner, P.O.B. 68, München 34; Presse Vertriebsgesellschaft GmbH 6, Frankfurt/ /Main Börsenstrasse 13 - 15; Kunst und Wissen, Erich Biber P.O.B. 46, 7000 Stuttgart 1; SUISSE, Pinkus & Cie Froschaugasse 7 Zürich, Fachbücherei Berne, P.O.B. 397, 3001 Berne.

En Roumanie vous pourrez vous abonner par les bureaux de poste, chez votre facteur ou directement par les services de presse des entreprises et institutions.

NOTE POUR LES AUTEURS

La *Revue Roumaine de Chimie* publie des articles en anglais, français, russe, allemand ou espagnol. Les auteurs sont priés d'envoyer des articles, notes, communications et comptes rendus inédits.

Les manuscrits seront dactylographiés à deux intervalles. Les tableaux seront dactylographiés sur feuilles séparées, de même que la légende des figures. Les diagrammes seront tracés à l'encre de Chine sur papier calque. Les tableaux et les figures seront numérotés par des chiffres arabes, en nombre strictement nécessaire. Prière de ne pas inscrire les mêmes données dans les tableaux et les figures. Les formules chimiques seront incluses dans le texte ; en outre, elles seront transcrites sur des feuilles séparées. Les auteurs sont priés d'indiquer les caractères italiques (en soulignant les lettres au crayon), ainsi que tout autre caractère spécial. L'ordre des références bibliographiques sera celui de leur mention dans le texte ; le nom de l'auteur sera précédé de l'initiale du prénom ; les publications périodiques seront présentées suivant les prescriptions internationales. Les références seront ajoutées à la fin de l'article ; elles paraîtront comme des notes, au bas de la page. Le texte sera précédé d'un résumé, comprenant 15 lignes au maximum.

L'entière responsabilité du contenu des articles appartient aux auteurs. On publie des articles dus aux collaborateurs roumains ou étrangers. Les auteurs recevront 50 tirés à part.

PRINTED IN ROMANIA

1970 FEB 1

TRAVAUX PARUS AUX ÉDITIONS DE L'ACADÉMIE DE LA RÉPUBLIQUE SOCIALISTE DE ROUMANIE

CORNEL BODEA et collab., **Tratat de biochimie vegetală**, partea I, **Fitochimie** (Traité de biochimie végétale, Ire partie, Phytochimie), Ier vol., 1964, 747 p. + 4 annexes + 2 pl., 41 lei ; IIe vol., 1965, 1262 p., 1 pl., 56 lei ; IIIe vol., 1967, 773 p., 35 lei.

V. GHEŢIE et V. MICUŞAN, **Analiza imunochimică. Teorie şi practică** (Analyse immunochimique. Théorie et pratique), 1966, 369 p., 28 lei.

SILVIA IONESCU, **Reacţii chimice induse de radiaţiile ionizante** (Réactions chimiques produites par les radiations ionisantes), 1963, 271 p., 15 lei.

MARIETA NICOLAE, **Fizico-chimia produselor fotografice** (Physico-chimie des processus photographiques), 1964, 426 p. + 4 pl., 35 lei.

R. PORTOCALĂ et L. POPA, **Acizii ribonucleici celulari şi virali** (Les acides ribonucléiques cellulaires et viraux), 1966, 375 p. + 8 pl., 26 lei.

D. PURDELA et R. VÎLCEANU, **Chimia compuşilor organici ai fosforului şi ai acizilor lui** (La chimie des composés organiques du phosphore et de ses acides), 1965, 540 p., 37 lei.

CRISTOFOR SIMIONESCU et CLEOPATRA VASILIU-OPREA, **Mecanochimia compuşilor macromoleculari** (La mécanochimie des composés macromoléculaires), 1967, 344 p., 23,50 lei.

I. P. „Informaţia" – c. 3810

43426

Lei 15

F 1103 04

R

[illegible]

REVUE ROUMAINE DE CHIMIE

TOME 14

N° 12

Décembre 1969

ÉDITIONS DE L'ACADÉMIE DE LA RÉPUBLIQUE SOCIALISTE DE ROUMANIE

Rev. Roumaine Chim. 14, 1477–1652 (1969), Bucarest

COMITÉ DE RÉDACTION

Rédacteur en chef :

C. D. NENIŢESCU, membre de l'Académie de la République Socialiste de Roumanie

Rédacteurs en chef adjoints :

A. T. BALABAN et V. E. SAHINI, membres correspondants de l'Académie de la République Socialiste de Roumanie

Collège de rédaction :

C. DRĂGULESCU, RALUCA RIPAN, CR. SIMIONESCU, membres de l'Académie de la République Socialiste de Roumanie ; EM. BRATU, membre correspondant de l'Académie de la République Socialiste de Roumanie, Pr G. OSTROGOVICH, MARG. AVRAM, F. BADEA, D. MARCHIDAN, D. NEGOIU et D. SĂNDULESCU.

Les manuscrits, les livres et les revues proposés en échange, ainsi que toute correspondance seront envoyés à la rédaction :

REVUE ROUMAINE DE CHIMIE

23, str. Dumbrava Roşie, Bucarest, 9, Roumanie

F 1103

REVUE ROUMAINE DE CHIMIE

Tome 14, No 12 Décembre 1969

Page

I. G. MURGULESCU and IULIANA VARTIRES, On the standard potential of thin cadmium films 1479–1487

D. CISMARU und AL. FRUMA, Die Kinetik der Wasserstoffchemisorption bei auf Aluminiumoxid aufgetragenem Platin 1489–1494

D. I. MARCHIDAN and CR. TELEA, Heat of mixing in the binary molten salts mixtures : $KCl + NaBr$ and $NaCl + KBr$ 1495–1500

C. DRĂGULESCU, SOFIA MARCHIDAN and GH. FACSKO, Polarographic reduction of niobium(V) tartrate solutions in hydrochloric acid-thiocyanate medium. 1501–1510

V. ARMEANU and I. DRĂGUŞIN, Study of some azo-derivate complexes of chromotropic acid with barium. II. Spectrophotometric and volumetric dosing of barium and sulphates with the reactives carboxyazo III, carboxysulphonazo III and sulphonazo III 1511–1517

CR. I. SIMIONESCU et KIM TAL-HEN, Recherches sur la polymérisation de certains dérivés acétyléniques à l'aide de la triéthylamine. I. La polymérisation de l'ester méthylique de l'acide propiolique 1519–1524

FL. POPESCU, Polymères organiques phosphorylés. I. La phosphorylation du polystyrène par synthèse selon Friedel-Crafts 1525–1534

I. GABE und DEMETRA LEONTE, Koordinationspolymere mit bis (Aminocarboxylsäuren). I. Über die Reaktion der Benzidindicarboxylsäure mit Cd-, Zn-, Cu-, Ni- und Mn-Salzen 1535–1542

AURELIA GHENCIULESCU, ILEANA NECŞOIU, MARINA RENŢEA and C. D. NENITZESCU, The Étard reaction. VIII. Oxidation of diphenylethanes and diphenylethylenes with chromyl chloride 1543–1552

AURELIA GHENCIULESCU, ILEANA NECŞOIU and C. D. NENITZESCU, The Étard reaction. IX. Oxidative cleavage of ethers produced by chromyl chloride 1553–1565

VALERIA PSEMEŢCHI, ILEANA NECŞOIU, MARINA RENŢEA and C. D. NENITZESCU, The Étard reaction. X. Oxidation of methylcyclopentane, methylcyclopentene and of methylenecycloalkanes C_5, C_6 and C_7 with chromyl chloride. . . . . 1567—1574

Rev. Roumaine Chim. 14, 1477–1652 (1969), Bucarest

G. V. BOYD and A. T. BALABAN, A correlation between chemical shifts of methyl protons and electron densities in substituted pyrylium salts . . . 1575–1577

A. TURCU and M. RĂILEANU, The action of ammonia on some nitroderivates of phenothiazine-5-oxide and phenothiazine-5, 5-dioxide 1579–1583

I. I. BĂDILESCU, Oxygen-alkyl bond cleavage in attempted cyclization of chloro-substituted γ-phenoxybutyric acids 1585–1590

V. TĂMAŞ and C. BODEA, $TiCl_4$-Carotenoid complexes. VI. Action of $TiCl_4$ on isocryptoxanthin and isozeaxanthin 1591–1594

C. DRĂGULESCU, R. POMOJE, I. MENESSY, MARIA PÎRLEA und CORNELIA MIHĂESCU, Metallkomplexe der N-Carboxymethyl-anthranylsäure (Phenylglycin-orthocarbonsäure). II. Eisen (III)- und Chrom (III)-Komplexe 1595–1601

J. DICK und ANNA MAURER, Neue Komplexverbindungen der Pyrazolonreihe. V 1603–1611

AL. ŞUTEU, T. HODIŞAN und FIAMETTA KORMOŞ, Eine neue kolorimetrische Bestimmungsmethode des Eisens (III) 1613–1616

C. BODEA und EDDA BROSER, Über Phenothiazone. XVI. Reaktion von Phenothiazonen mit Anilin 1617–1620

L. SZOTYORI, L. FEY und ANAMARIA ÁBRAHÁM, Die Reaktion zwischen Natriumalkoxiden und α-Halogenketonen. VI. Einwirkung des Natriummethoxides auf ω-Bromacetophenon 1621–1628

RALUCA RIPAN und T. BUDIU, Trennung und Bestimmung des Titans in Gegenwart von Eisen 1629–1631

V. BREZULEANU and A. IVANOV, Corrigendum to the paper "The calculus of electrostatic matrix elements for the tetragonal symmetry" 1633–1636

Index du tome 14 (1969) 1637–1651

Revue Roumaine de Chimie, **14**, 1479–1487 (1969)

ON THE STANDARD POTENTIAL OF THIN CADMIUM FILMS

I. G. MURGULESCU and IULIANA VARTIRES
Physical Chemistry Research Center
Bucharest, str. Galați 31

Received February 15, 1969

Standard potential of the system Cd/Cd^{++} has been determined by e.m.f. measurements for the following electrochemical cell :

$$Cd/CdCl_2(m)\ AgCl/Ag$$

The cadmium electrode was formed by thin metallic films of various thickness, obtained by vacuum evaporation on a glass support. The resulting values differ from those obtained by using bulk cadmium electrodes. The differences are growing when the films get thinner. The explanation of the phenomenon is given and the correlation between the decrease in the standard potential and the lowering of the heat of sublimation of the metal in thin films is shown.

INTRODUCTION

In order to continue the investigation on the electrochemical behaviour of thin films formed by vacuum evaporation,[1–3] a similar study was undertaken on divalent metal-cadmium. From an electrochemical point of view, our previous papers showed that the films of group IB monovalent metals have a deviation of the electrode equilibrium towards the formation of metallic ions. The deviation depends on the chemical nature of the metal and especially on the obtaining conditions of the films.

In choosing cadmium among the other divalent metals, the fact has been considered that all alkaline-earth metals from Mg to Ba sublimate long before the melting point and are very easily oxidized. On the other hand Be hardly evaporates and is difficultly obtained in pure state. Among the metals in group II the most suitable seems to be Cd which does not oxidize so easily as Zn, melts in vacuum without a quick evaporation and is easily obtained in pure state.

---

[1] I. G. Murgulescu, I. Vartires and O. Radovici, *Rev. Roumaine Chim.*, **12**, 215 (1967).

[2] I. G. Murgulescu and I. Vartires, *Rev. Roumaine Chim.*, **12**, 1069 (1967).

[3] I. G. Murgulescu and I. Vartires, *Rev. Roumaine Chim.*, **13**, 1397 (1968).

Besides Bertocci,[4] Williams,[5] Burnett's [6] electrochemical studies using bulk metal electrodes for cadmium, crystal electrodes have also been considered. Getmann [7] has shown that the single-crystal electrode of cadmium presents a deviation of the standard potential value of a few mV as against the bulk metal. These studies proved the influence exerted by the structure of the crystalline lattice of the electrode metal shown by the variation in the standard potential.

In the present paper we intend to study the electrochemical behaviour of Cd films obtained by vacuum evaporation on a glass support by measuring their standard potential. Films with thickness from 100–1250 Å have been used.

The standard potential of the bulk metal of which the thin films were made, has also been determined. In this respect we used exactly the same couple Cd/$CdCl_2$, substances and device to avoid errors when comparing the values of the standard potential of thin films and of bulk metal. The differences pointed out, in this case are only due to the partial disorganization of the crystalline lattice forming the films.

EXPERIMENTAL

a) *Preparation of the cadmium electrode.* The cadmium electrode is made of cadmium films obtained by vacuum evaporation by means of a device manufactured on the general constructive principles of such devices.

The cell in which the thin metallic films and the electrochemical measurements are made is connected to the vacuum installation where a 10^{-5} torr vacuum is achieved. In this way the cadmium film has been realized avoiding the influence of atmospheric oxygen. This cell is represented in figure 1 and has two principal parts A and B. Compartment A has : 1. evaporation source, a quartz crucible introduced into tungsten filament, previously cleaned by heating in vacuum, 2. a trap for condensing the metallic vapours with an opening calibrated in such a way as to have the deposited film contained by the support's surface, 3. the screen, the position of which can be changed by means of a magnet from the outside, thus allowing the passing or retaining of the beam of metallic vapours towards the support. In compartment B there are : 4. the film's support which was optically polished, and provided with two platinum wires used for determining the film thickness by electric resistance measurement. The support is a tube which allows both the outgassing by an electric resistance and its cooling by liquid N_2 for the condensation of the layers. Compartment B has also two arms : 5. by which one can join the cell to the vacuum installation and 6. the tube by which purified argon was introduced.[8]

To obtain an inert atmosphere in the evaporation cell of the device, one introduces previously for half an hour purified argon. The output of the argon is arranged in such a way as to maintain a constant pressure of approximately 10^{-1} torr in the installation. The degassing of the supports is achieved at 350° during 4 hours at 10^{-5} torr. The depositing rate is around some hundred Å per minute. The support's temperature when the depositing takes place is the same as that of liquid N_2.

---

[4] U. Bertocci and C. Tamplenizza, *Ann. Chim. (Rome)*, **46**, 634 (1956).

[5] B. William, F. Treumann and L. Ferris, *J. Amer. Chem. Soc.*, **80**, 5048 (1958).

[6] J. L. Burnett and M. H. Zirin, *J. Inorg. Nucl. Chem.*, **28**, 902 (1966).

[7] F. H. Getmann, *J. Phys. Chem.*, **35**, 588 (1931).

[8] I. G. Murgulescu, O. Radovici and N. Totir, *Rev. Roumaine Chim.*, **12**, 231 (1967).

The main parameters which are influencing the film's structure are kept constant, changing only the depositing duration from one measurement to another, in view of obtaining different thicknesses of the films. The bulk thickness of the films was determined by a chemical method described by Liteanu.[9]

b) *Materials.* Bulk cadmium metal is (U.C.B.) p.a. The measurement medium is $CdCl_2$ of different concentrations. The solutions have been prepared from tridistilled water and thrice recrystallized $CdCl_2$ p.a.

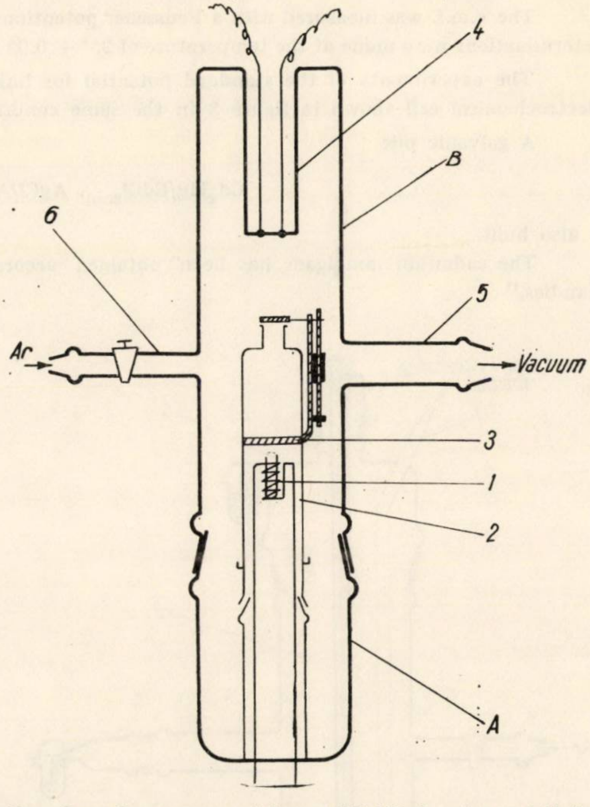

Fig. 1. — Cell for the preparation of the films by vacuum evaporation and for the electrochemical measurement: *1*, evaporation source; *2*, trap for condensing the metallic vapours; *3*, screen; *4*, film's support; *5*, joint tube; *6*, tube for purified argon.

All determinations of standard potentials of the cell were achieved in deaerated solutions with purified argon.

c) *The electrochemical measurements.* Immediately after having obtained the films of desired thickness, vacuum was compensated with purified argon introduced through arm 6 (fig. 1). The cell was revolved 180° and the solution for electrochemical measurement was introduced. The solution level must surpass by 2 cm the film's surface. Compartment C was introduced into the measuring cell, replacing compartment A (fig. 2), removed under a strong stream of argon. Compartment C has two arms: number 1 for the bubbling argon and number 2, with a sintered glass at the bottom, for the reference electrode, Ag/AgCl obtained according to the method described by Ives,[10] to avoid the liquid junction potentials. A galvanic pile is made of

---

[9] C. Liteanu, "Quantitative Analytical Chemistry", Ed. Tehnică, Bucharest, 1959, p. 525.

$$Cd/CdCl_{2(m)}, AgCl/Ag$$

in which the concentration (m) of the $CdCl_2$ was successively equal to 0.1 m and 0.05 m. This concentration range was chosen as to obtain the complete dissociated solutions.

The e.m.f. was measured with a Feussener potentiometer to a precision of 0.01 mV. The determinations were made at the temperature of 25° ± 0.02 by means of a U_{10} type thermostat.

The experiments of the standard potential for bulk cadmium were performed in an electrochemical cell shown in figure 3 in the same conditions as those described for films.

A galvanic pile

$$Cd_xHg/CdCl_{2(m)}, AgCl/Ag$$

is also built.

The cadmium amalgam has been obtained according to the method described by Randles.[11]

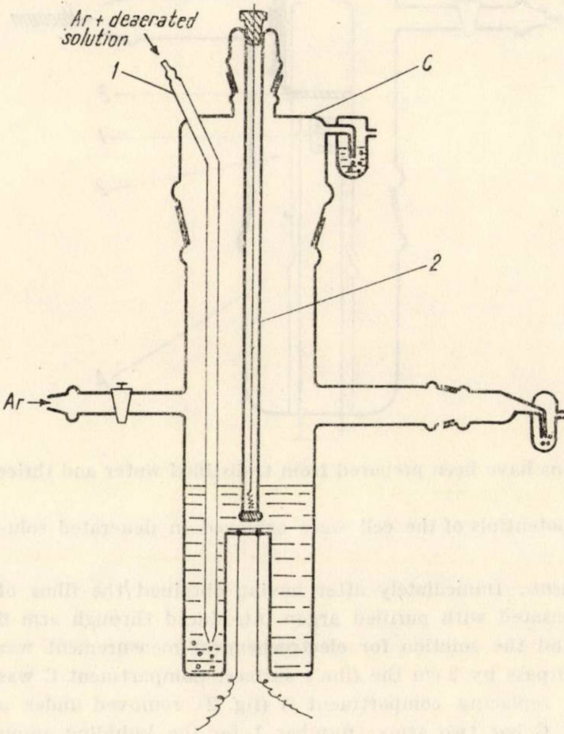

Fig 2

Fig. 2. — Cell for electrolytic measurements :
1, tube for purified argon ; *2*, reference electrode Ag/AgCl.

Fig. 3. — Cell for electrolytic measurements for bulk cadmium : *a*, mercury electrode; *b*, reference electrode Ag/AgCl; *c*, platinum electrode; *d*, evacuation tube.

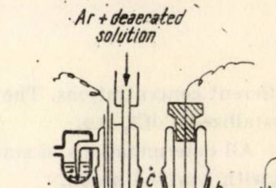

---

[10] I. Y. G. IVES and C. I. JANZ, "Reference Electrodes", Academic Press, London 1961, p. 179.

[11] J. E. B. RANDLES, *Discuss. Faraday Soc.*, 1, 269 (1947).

RESULTS AND DISCUSSION

If we consider the equilibrium reaction

$$CdCl_2 = Cl^- + CdCl^+ \rightleftharpoons Cd^{++} + Cl^- \tag{1}$$

and if the $CdCl_2$ is completely dissociated in diluted solutions, the following electrochemical reaction results

$$Cd_{(amalgam)} + 2\,AgCl \rightleftharpoons Cd^{++} + 2\,Cl^- \tag{2}$$

and the e.m.f. is given by equation :

$$E = E^\circ_{Cd/Cd^{++}} - E^\circ_{Ag/AgCl^-} \frac{RT}{2F} \ln a_{Cd^{++}} \cdot a^2_{Cl^-} \tag{3}$$

at 25° the standard potential's expression becomes :

$$E^\circ_{Cd/Cd^{++}} = E + E^\circ_{Ag/AgCl} + 0.029575 \log 4\,f^3m^3 \tag{4}$$

where "m" is the molar concentration and "f" the activity coefficient of $CdCl_2$. The other symbols in equation (4) have their already known significance. At the temperature of our experiments, the value of the activity coefficients for the $CdCl_2$ concentrations 0.1 m ; 0.05 m and 0.002 m were respectively equal to [12] 0.288 ; 0.304 ; 0.456.

As the value of the $E^\circ_{Ag/AgCl}$ potential can be established with great precision (in our case, it is equal to 0.2233 V at 25°) one may readily estimate the value of standard potential $E^\circ_{Cd/Cd^{++}}$ from equation (4).

In table 1 are given the values of standard potentials of bulk cadmium for three concentrations :

Table 1

Standard potential for bulk cadmium, T = 25°

No	conc. $CdCl_2$ in mole	e.m.f. in V	$E^\circ_{Cd/Cd^{++}}$ in V	Standard deviation in V
1	0.1	0.7023	0.4016	0.0005
2	0.05	0.7183	0.4020	0.0002
3	0.02	0.7368	0.4018	0.00006

$E^\circ_{Cd/Cd^{++}} = \overline{0.4018}$ V

The values found by us were in good agreement with those mentioned in literature, [13-15] ranging from 0.3960 V up to 0.4236 V.

---

[12] R. G. Bates, *J. Amer. Chem. Soc.*, **60**, 2983 (1938).

[13] W. G. Parks and V. K. La Mer, *J. Amer. Chem. Soc.*, **56**, 90 (1934).

[14] H. S. Harned and M. E. Fitzgerald, *J. Amer. Chem. Soc.*, **58**, 2624 (1936).

[15] D. Roger and G. Bates, *J. Amer. Chem. Soc.*, **61**, 308 (1939).

The value of the standard potential of the bulk cadmium metal is computed by means of relation (4) which is including the correction of 0.0505 V,[16] for the electrode amalgam, though generally the other amalgamated metals have the same behaviour as the single crystals.

The results of the measurements on the cadmium thin films are given in tables 2 and 3. Figure 4 shows the variation of the (limit) potentials with the temperature for films of about 780 Å. We notice a decrease in the potentials with increasing temperature. The values of the standard potentials depending on the film thickness in Å are given in tables 2 and 3, computed from the experimental (limit) value of e.m.f. (E) by means of equation (4). Figure 5 illustrates the plots of the experimental results. The mean reproducibility of the potentials for thinner films is up to ±0.4 mV, for thicker films (over 800 Å) it reaches ±0.1 mV.

Table 2

$E^\circ_{Cd/Cd^{++}}$ in $CdCl_2$ 0.05 m for unstabilized films, T=25°

No	Thickness in Å	E e.m.f. in V	$E^\circ_{Cd/Cd^{++}}$ in V	Standard deviation in V	Molal heat of sublimation λ° in kcal/mole
1	80	0.7612	0.3944	0.0005	26.690
2	100	0.7620	0.3952	0.0003	26.720
3	190	0.7625	0.3957	0.0004	26.750
4	360	0.7628	0.3968	0.0002	26.800
5	680	0.7646	0.3978	0.0002	26.850
6	1200	0.7662	0.3994	0.0001	26.920

Table 3

$E^\circ_{Cd/Cd^{++}}$ in $CdCl_2$ 0.1 m for stabilized and unstabilized films, T=25°

No	Thickness in Å	E e.m.f. in V	$E^\circ_{Cd/Cd^{++}}$ in V	Standard deviation in V	Molal heat of sublimation λ° in kcal/mol
1	200	0.7472	0.3960	0.0005	26.770
2	400	0.7482	0.3970	0.0003	26.810
3	800	0.7496	0.3984	0.0002	26.880
4	860	0.7500	0.3988	0.0003	26.890
5	1100	0.7511	0.3999	0.0001	26.940
6	1250	0.7514	0.4001	0.0001	26.950
for stabilized films					
7	1000	0.7518	0.4006	0.00005	—

As it results from the data provided by tables 2 and 3 as well as from figure 5, normal potentials decrease with the increasing thickness of the films, becoming more negative. The phenomenon can be more easily seen for very thin films. For thicker films, the standard potential approaches the normal values of the bulk cadmium electrodes.

---

[16] International Critical Tables, vol. 7, Ed. McGraw-Hill Book Co. N.Y., London, 1930, p. 256.

Table 3 also presents the standard potential obtained on a stabilized film. The stabilization was obtained thermally by heating previously

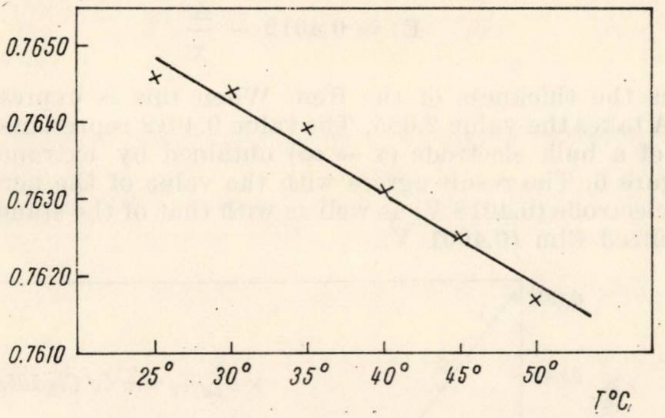

Fig. 4. — Dependence of the E (e.m.f. in V) on the temperature expressed in °C.

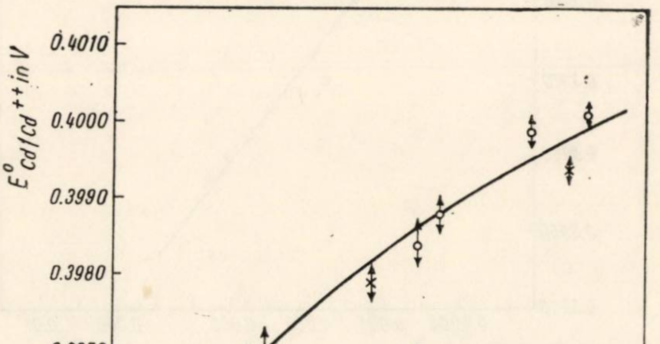

Fig. 5. — Dependence of the $E^\circ_{Cd/Cd^{++}}$ on film thickness expressed in Å and on $CdCl_2$ concentration.

the film at 350° for 15 min. The value of its standard potential is practically identical to that of the standard potential of a bulk electrode.

Figure 6 represents the standard potentials depending on the reciprocal of the thickness of the film, for films thicker than 180 Å. Hence a dependence with the form :

$$E^\circ = 0.4012 - \frac{A}{x} \tag{5}$$

where x is the thickness of the film. When this is expressed in Å the constant A takes the value 2.085. The value 0.4012 represents the standard potential of a bulk electrode ($x \to \infty$) obtained by extrapolation as one sees in figure 6. The result agrees with the value of the normal potential of a bulk electrode (0.4018 V) as well as with that of the standard potential of a stabilized film (0.4001 V).

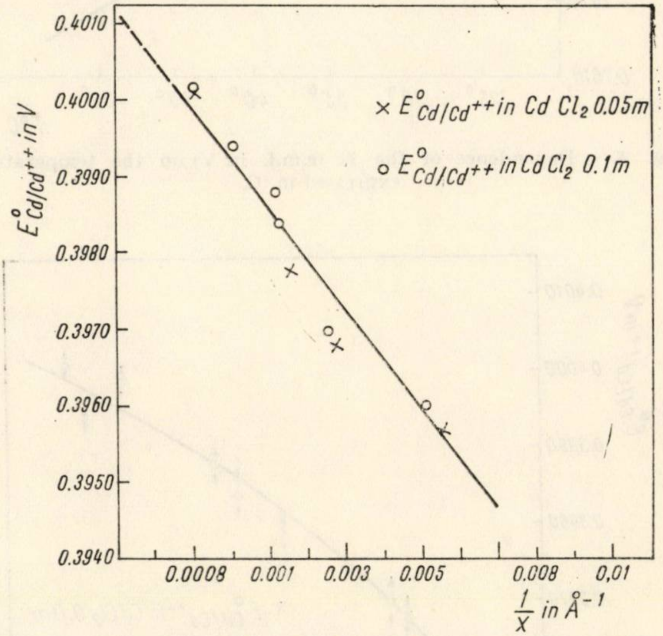

Fig. 6. — Variation of the potential of $E^\circ_{Cd.Cd^{++}}$ as a function of the inversion of film thickness in $Å^{-1}$. The values indicated by × are $E^\circ_{Cd/Cd^{++}}$ in 0.05 m $CdCl_2$ and by ○ are $E^\circ_{Cd.Cd^{++}}$ in 0.1 m $CdCl_2$.

The deviation of the standard potential value of the cadmium thin films electrode towards more negative values, is due to the partial disorganization of the crystal lattice which forms the film. In such conditions the energy of the ions of the lattice increases, resulting in an increase in the "electrolytical dissolution tension" of the metal rendered by a negativation of the electrode potential.

The disorganization of the crystal lattice and the volatility of the metal increases and its sublimation heat decreases. For the calculation of the sublimation heat, in the thin films case, one resorts to equation 6 deduced from a previous paper[17] which relates the electrode potential to the sublimation heat. The symbols appearing in (6) have their significance shown in the respective paper.

$$E^{\circ}_{\mathrm{Me.Me}}{}^{(+)n} = \frac{\lambda^{\circ}_{\mathrm{Me}} + n/_2 D^{\circ}_{\mathrm{H_2}}}{nF} + \frac{5/2\,(n-1)\,RT \ln T}{nF} +$$

$$+ \frac{RT}{nF}\left[\int_0^T \frac{dT}{RT^2}\int_0^T \left(Cp_{\mathrm{Me(s)}} - n/2\; Cp_{\mathrm{H_2(g)}}\right) dT\right] +$$

$$+ \frac{RT}{nF}\left[-\, i_{\mathrm{Me(g)}} + n\left(i_{\mathrm{H}} - \frac{i_{\mathrm{H_2}}}{2}\right)\right] + \frac{\overset{n}{\Sigma}\, I_i - n\, I_{\mathrm{H}}}{n} +$$

$$+ \frac{\Delta F^{\mathrm{Me}(+)n}_{\mathrm{Hydr.}} - n\,\Delta F^{\mathrm{H^+}}_{\mathrm{Hydr.}}}{nF} - \frac{\Delta F^{\mathrm{Me}(+)n}_{\mathrm{Dil.}} - n\,\Delta F^{\mathrm{H^+}}_{\mathrm{Dil.}}}{nF}. \qquad (6)$$

Applying relation (6) to a divalent metal like cadmium one obtains:

$$\lambda^{\circ}_{\mathrm{Cd\ film}} = \lambda^{\circ}_{\mathrm{Cd\ bulk}} - \frac{E^{\circ}_{\mathrm{Cd,Cd^{++}\ bulk}} - E^{\circ}_{\mathrm{Cd,Cd^{++}\ film}}}{0.02169} \qquad (7)$$

the value[18] $\lambda^{\circ}_{\mathrm{Cd\ bulk}} = 27.03$ kcal/mol.

The values obtained by means of relation (7) for the heat of sublimation at 0°K for cadmium films of various thickness, are given in the last columns of tables 2–3. For very thin films of 80 Å the decrease in the heat of sublimation is about 0.350 kcal/mol.

This value seems very small if, for instance, we take into account the chemical reactivity of the cadmium comparatively with that of the noble metals. But considering the variation with the temperature of the cadmium thin films (from the temperature of liquid N_2 to 25° in the electrochemical measurements) a spontaneous crystallization occurs which greatly reduces the crystalline disorganization of the metallic lattice.

Therefore no difference in the electrochemical behaviour of stabilized and unstabilized thin films is noticed for thick films.

---

[17] I. G. MURGULESCU and E. CONSTANTINESCU, *Rev. Chim. Acad. Romania*, **8**, 5 (1963).

[18] E. A. MOELWYN-HUGHES, "Physical Chemistry", Pergamon Press, London, 1961.

of the sublimation heat, in the thin films case, one resorts to equation 6 deduced from a previous paper[16] which relates the electrode potential to the sublimation heat. The symbols appearing in (6) have their significance shown in the respective paper.

[illegible]

Applying relation (6) to a divalent metal like cadmium one obtains

[illegible]

the value[17] E_{Cd} = 27.03 kcal/mol.

The values obtained by means of relation (7) for the heat of sublimation at 0°K for cadmium films of various thickness are given in the last columns of tables 2—3. For very thin films of 50 Å the decrease in the heat of sublimation is about 0.350 kcal/mol.

This value seems very small if, for instance, we take into account the chemical reactivity of the cadmium comparatively with that of the noble metals. But considering the variation with the temperature of the cadmium thin films (from the temperature of liquid N_2 to 25° in the electrochemical measurements) a spontaneous crystallization occurs which greatly reduces the crystalline disorganization of the metallic lattice.

Therefore no difference in the electrochemical behaviour of stabilized and unstabilized thin films is noticed for thick films.

---

[16] [illegible]

[17] [illegible]

Revue Roumaine de Chimie, **14**, 1489–1494 (1969)

DIE KINETIK DER WASSERSTOFFCHEMISORPTION BEI AUF ALUMINIUMOXID AUFGETRAGENEM PLATIN

D. CISMARU und AL. FRUMA

Institut für Physikalische Chemie, Bukarest, str. Dumbrava Roşie, 23

Eingegangen am 28. Januar 1969

Es wurde die Kinetik der Wasserstoffchemisorption an einem reforming Katalysator mit einem 0,35 % Platingehalt, auf Aluminiumoxid aufgetragen, untersucht. Die Wasserstoffchemisorption wurde im Druckbereich 4.10^{-2}—100 Torr bei einer Temperatur von 25° verfolgt. Man fand, daß 94 % der gesamten chemisorbierten Wasserstoffmenge, die bei der Sättigung der Oberfläche adsorbiert werden kann, in den ersten 5 Minuten adsorbiert wurde. Die experimentellen Ergebnisse bestätigten die Roghinski-Zeldovich-Elovich Gleichung. Man fand, daß die Adsorptionsgeschwindigkeit mit der Zunahme des Drucks im Bereich kleiner Bedeckungsgrade und bei Drücken unter 1 Torr wächst. Im Bereich tiefer Drücke führte die Darstellung der Adsorptionsgeschwindigkeit in Abhängigkeit der Wurzel des Drucks zu einer Geraden.

Die Katalysatoren vom Typ Platin aufgetragen auf Aluminiumoxid, werden häufig in den industriellen katalytischen reforming Prozessen verwendet. Wegen ihrer industriellen Bedeutung bildet das Studium ihrer verschiedenen Eigenschaften, den Gegenstand von immer häufiger werdenden Forschungen. [1–3]

Die Wasserstoffchemisorption, erste Stufe des katalytischem Prozesses, wird meistens bei der Charakterisierung der Oberfläche des Katalysators verwendet. Von der heute einstimmig erkannten Annahme ausgehend, daß die Wasserstoffchemisorption dissoziativ vor sich geht, [4–6] und daß es bei der Sättigung eine Monoschicht gibt, so daß jedem Wasserstoffatom ein Platinatom zusteht, [7,8] kann man Schlußfolgerungen über die Dispersion des Platins auf dem Aluminiumoxidträger ziehen.

---

[1] P. B. Weisz und R. D. Goodwin, *J. Catalysis*, **6**, 227 (1966).
[2] P. B. Weisz, *J. Catalysis*, **6**, 425 (1966).
[3] L. E. Alexander und E. C. Sommer, *J. Phys. Chem.*, **60**, 1646 (1956).
[4] P. Elen *Adv. Catalysis*, **1**, 176 (1948).
[5] S. F. Adler und J. Keavney, *J. Phys. Chem.*, **64**, 208 (1960).
[6] J. Beer, *Adv. Catalysis*, **8**, 68 (1956).
[7] L. Spenadel und M. Boudart, *J. Phys. Chem.*, **64**, 204 (1960).
[8] H. L. Gruber, *J. Phys. Chem.*, **66**, 48 (1962).

In vorherigen Arbeiten benützten wir die Wasserstoffchemisorptionsmethode bei der Berechnung der Größe der dispergierten Platinpartikeln,[9] wie auch bei der Charakterisierung der kokshaltigen und regenerierten Katalysatoren vom chemisorptiven Standpunkt aus.[10] In der vorliegenden Arbeit behandeln wir das Problem der Kinetik der Wasserstoffchemisorption auf aufgetragenem Platin, in einem weiten Druckbereich.

EXPERIMENTELLES

Es wurde eine, in Abb. 1 beschriebene, zur Messung von Gas-Feststoff Adsorption, dem Studium der Wasserstoffchemisorption auf fein dispergierten Metallen angepaßte, volumetrische Vakuumanlage verwendet.

Die Konzentration des Platins in der benützen Probe war 0,35 % in Gewichtsprozenten, während die gesamte spezifische Oberfläche, durch die BET Methode bestimmt, 379 m^2/g betrug. Für die Chemisorptionsmessungen wurde 1 g Substanz benützt. Durch selektive Absorption und Desorption auf sprödem Palladium, erlangte man eine hohe Reinheit des Wasserstoffs, der bei Reduktion und Adsorption benützt wurde.

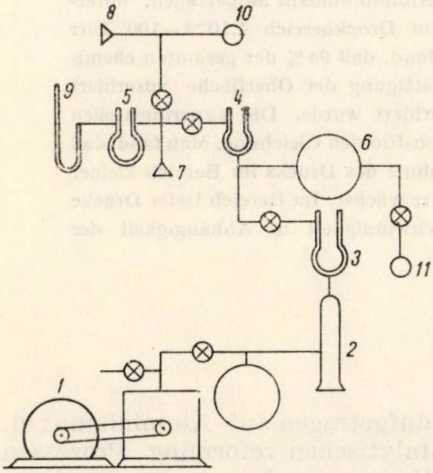

Abb. 1. — Experimentelle Anlage.
1, Vorvakuumpumpe; *2*, Quecksilberdiffusionpumpe; *3*, *4*, *5*, Kühlfallen mit flüssigem Stickstoff; *6*, Wasserstoffbehälter; *7*, *8*, Manometerröhren; *9*, Quecksilbermanometer; *10*, Arbeitszelle mit Probe; *11*, Behälter mit sprödem Palladium.

Die in der Anlage getrocknete und reduzierte Probe wurde bei 500°, 6 Std. lang bei einem Vakuum von 3.10^{-6} Torr entgast. Nach Abkühlen und Konstanthalten der Temperatur, wurde der Wasserstoff für die Adsorption bei dem festgelegten Druck eingeführt. Man führte ein kinetisches Studium zur Untersuchung der Zeitabhängigkeit des Wasserstoffdrucks in dem geeichten Behälter und von da aus, der chemisorbierten Menge, aus.

Die Drücke zwischen 1 und 100 Torr wurden auf dem Quecksilbermanometer (*9* in Abb. 1) abgelesen, während die Drücke unterhalb 1 Torr mit den Manometerröhren LM 2 (*7*) und LT 2 (*8*) auf dem Vakuummeter Modell VIT 1A, bestimmt wurden. Die Eichung des Arbeitsraumes erfolgte mit Wasser.

Der größte Druck bei dem man arbeitete war 100 Torr, da man bei diesem Druck mit Sichereheit die Sättigungsadsorption, die bei dem von uns untersuchten System bei 70 Torr besteht [9,10] erreicht. Als Arbeitstemperatur wählten wir 25°, da bei dieser Temperatur der Wasserstoff keine meßbare physikalische Adsorption anzeigt [8, 9, 11] und da bei dieser Temperatur die experimentellen Arbeitsbedingungen erleichtert werden.

ERGEBNISSE UND DISKUSSION

Die Änderung der chemisorbierten Menge mit der Zeit wird gewöhnlich durch die Roghinski-Zeldovich-Elovich [12–14] Gleichung ausgedrückt. Laut dieser Gleichung wird die Adsorptionsgeschwindigkeit durch den Ausdruck:

$$\frac{\mathrm{d}\theta}{\mathrm{d}t} = \alpha \mathrm{e}^{-\beta\theta} \tag{1}$$

gekennzeichnet, wo α und β von Druck und Temperatur abhängige Parameter sind. θ ist der Bedeckungsgrad der Oberfläche. In unserem Fall, da sich das Metall in kleiner Konzentration auf dem Träger fein dispergiert befindet, ist die Oberfläche des Trägers fast 350mal größer als die des Metalls. Da der Träger bei unserer Arbeitstemperatur praktisch nicht adsorbiert [9, 15] und darum die ganze Wasserstoffmenge vom Platin adsorbiert wird, und da bei dieser Adsorption je ein Wasserstoffatom auf ein Platinatom kommt, in einem Verhältnis H/Pt gleich eins bei Sättigung, wird in unserem Fall θ proportional und numerisch gleich dem Verhältniss H/Pt sein.

Die Änderung von θ mit der Zeit, in verschiedenen Druckverhältnissen, bildet eigentlich das Hauptproblem der vorliegenden Arbeit.

Durch Integrieren der Gleichung (1) erhalten wir:

$$\theta = 1/\beta \ln (t - t_0) - C \tag{2}$$

wo C eine Konstante und $t_0 = 1/\alpha\beta$.

Einige Forscher schlugen eine einfachere Gleichung vor [16–18]:

$$\theta = K_1 \ln t + K_2. \tag{3}$$

In Abb. 2 haben wir $\theta = f[\ln(t + t_0)]$ dargestellt. Man erhält auf diesem Wege für $t_0 = 0$ die Kurve (A) die sehr verschieden von einer Geraden ist. Dieses bedeutet, daß sich Gleichung (3) der Wasserstoffadsorption auf dispergiertem Platin nicht anpaßt. Wenn man für t_0 immer

---

[9] D. Cismaru und Al. Fruma, *Rev. Roumaine Chim.*, **13**, 139 (1968).

[10] D. Cismaru und Al. Fruma, *Rev. Roumaine Chim.*, **13**, 1277 (1968).

[11] D. Cismaru und Al. Fruma, *Rev. Roumaine Chim.*, **13**, 679 (1968).

[12] S. Z. Roghinski und I. Zeldovich, *Nature*, **134**, 935 (1934).

[13] S. Z. Roghinski und I. Zeldovich, *Acta Phys. Chim. USSR*, **1**, 449, 595, 651 (1934); *Chem. Abstr.*, **29**. 7775, 7776, 1665 (1934).

[14] S. I. Elovich und G. M. Zhabrova, *Zhur. fiz. Khim.*, **13**, 1761, 1775 (1939).

[15] J. Benson und M. Boudart, *J. Catalysis*, **4**, 704 (1965).

[16] G. D. Halsey, *J. Phys. Coll. Chem.*, **55**, 21 (1951).

[17] A. S. Porter und F. C. Tomkins, *Proc. Roy. Soc.*, **A 217**, 529 (1953).

[18] F. S. Stone, "Chemistry of the Solid State", W. Garner, Butterworth, London, 1965, p. 367.

größer werdende Werte gibt, so erhalten wir die entsprechenden Kurven *B*, *C* und *D* aus Abb. 2. Für $t_0 = 4$ erhält man die Gerade *E*. Dieser Fall paßt demnach für die Gleichung (2), die dadurch charakteristisch für das von uns untersuchte System wird. Bemerkenswert ist der ziemlich hohe Wert für $t_0 = 4$ Minuten, größer als der von Peers,[19,20] bei der Wasserstoffadsorption auf NiO mit einer Oberfläche von 135 m^2/g, gefundene Wert, der 2,5 Minuten betrug. In dem von uns untersuchten System gibt es eine beträchtliche Anfangsgeschwindigkeit, da wir im Augenblick $t = 0$ $\ln(t + t_0) = \ln t_0$ haben, dem ein Wert für θ entspricht.

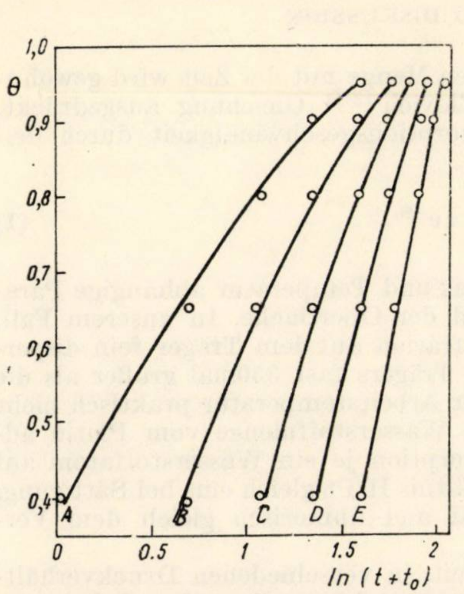

Abb. 2. – Die Darstellung der Roghinski-Zeldovich-Elovich Gleichung für $t_0 = 0$ Min (Kurve *A*), $t_0 = 1$ (Kurve *B*), $t_0 = 2$ (Kurve *C*), $t_0 = 3$ (Kurve *D*) und $t_0 = 4$ (Kurve *E*).

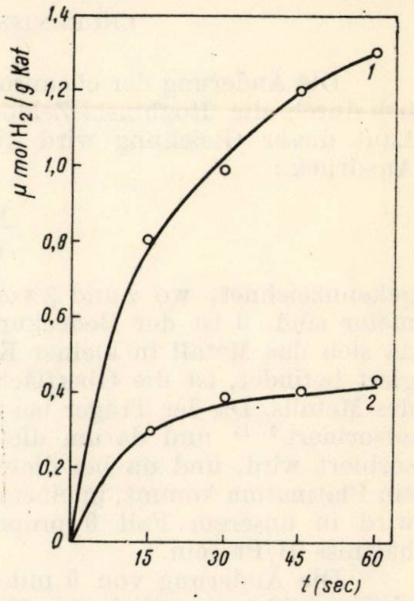

Abb. 3 – Die Änderung der adsorbierten Wasserstoffmenge in der ersten Minute, für Probe mit Partikelgröße von 10 Å (Kurve *1*) und 50 Å (Kurve *2*).

Aus Abb. 2 ist ersichtlich, daß in den ersten 5 Minuten 94% der adsorbierten Menge bei Sättigung adsorbiert wird. Es folgt eine sehr langsame Adsorption die 45 Minuten lang dauert und die wir in den vorliegenden Abbildungen nicht dargestellt haben.

Bei einem Druck von 100 Torr wird 40% der Gesamtmenge in der ersten Minute adsorbiert. Bei Drücken unterhalb 1 Torr setzt sich das Gleichgewicht etwas schneller ein, so daß bei $5 \cdot 10^{-1}$ Torr, 55% der Gesamtmenge, die bei diesem Druck adsorbiert werden kann, in der ersten Minute adsorbiert wird. Dieses wahrscheinlich da bei niederen Drücken erst die äußere Oberfläche der Katalysatorkörnchen bedeckt wird, während bei höheren Drücken auch ein langsameres Eindringen ins Innere stattfindet.

---

[19] A. M. Peers, *J. Catalysis*, 4, 499 (1965).
[20] A. M. Peers, *J. Catalysis*, 4, 672 (1965).

In Abb. 3 haben wir die Änderung der adsorbierten Menge, in der ersten Minute, bei einem Druck von $5 \cdot 10^{-1}$, dargestellt. Beide Kurven stellen die Wasserstoffadsorption auf Proben mit einem 0,35% Platingehalt dar. Der Unterschied besteht darin, daß die Kurve *1* unserer gewöhnlichen Arbeitssubstanz, mit Partikeln von 10 Å, während die Kurve *2* der Adsorption einer Probe mit Platinpartikeln von 50 Å, entspricht. Diese letztere Probe wurde durch Synterung eines Sinclair—Baker Katalysators in besonderen Bedingungen [10] erhalten. Die Partikelgröße wurde anhand von Chemisorptionmessungen, durch eine in einer vorherigen Arbeit [9] beschriebene Berechnungsmethode, bestimmt. Da die Probe mit Platinpartikeln von 50 Å eine viel kleinere adsorbierende Oberfläche hat, ist es klar, daß Kurve *2* unterhalb der Kurve *1* liegt. Etwas besonderes schien uns die Tatsache, daß beim Wachsen der Partikelgröße die Sättigung bei einem bestimmten Druck schneller erreicht wird.

Einige Forscher [19, 20, 21] bemerkten, daß für mehrere Adsorptionssysteme die Darstellung der Adsorptionsgeschwindigkeit in Abhängigkeit von der Wurzel des Drucks für kleine Bedeckungsgrade, eine Gerade ergibt.

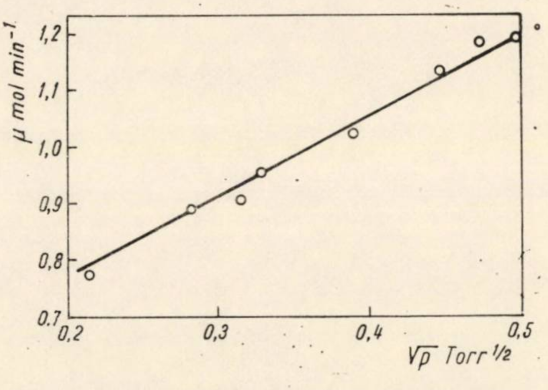

Abb. 4. — Die Darstellung der Änderung der Adsorptionsgeschwindigkeit mit den Druck.

In der Abb. 4 haben auch wir diese Darstellung ausgeführt. Auf die Ordinatenachse ist die in der ersten Minute adsorbierte Menge pro m^2 Platin, während auf die Abszissenachse die Wurzel des Drucks, für Drücke zwischen $4 \cdot 10^{-2}$—$2{,}5 \cdot 10^{-1}$ Torr, aufgetragensind. Wir erhielten eine Gerade. Da die Gerade eine wachsende Steigung hat, folgt, daß die Adsorptionsgeschwindigkeit mit der Zunahme des Gleichgewichtsdrucks wächst. Dieses, selbstverständlich nur in der ersten Minute, bei noch ziemlich ungesättigter Oberfläche. In Nachbarschaft der Sättigung, wird die Adsorptionsgeschwindigkeit sehr klein.

---

[21] J. D. Cotton und A. S. Fensham, *Trans. Faraday Soc.*, **59**, 1444 (1963).

SCHLUSSFOLGERUNG

Die Kinetik der Wasserstoffchemisorption auf fein dispergiertem, aufgetragenem Platin auf Aluminiumoxid, kann durch die Roghinski-Zeldovich-Elovich Gleichung ausgedrückt werden. Die Darstellung der R.Z.E.-Gleichung gibt Gerade bei einem Wert $t_0 = 4$ Minuten. Bei kleineren Drücken und größeren aufgetragenen Partikeln, stellt sich das Adsorptionsgleichgewicht schneller ein als bei höheren Drücken und kleineren Partikeln. Für kleine Bedeckungsgrade und tiefere Drücke nimmt die Adsorptionsgeschwindigkeit mit der Zunahme des Gleichgewichtsdrucks zu. Bei hohen Drücken und in der Nachbarschaft der Sättigung hat die Adsorptionsgeschwindigkeit hingegen geringe Werte.

Revue Roumaine de Chimie, **14**, 1495–1500 (1969)

HEAT OF MIXING IN THE BINARY MOLTEN SALTS MIXTURES :

$KCl + NaBr$ AND $NaCl + KBr$

D. I. MARCHIDAN and CR. TELEA

Institute of Physical Chemistry, 31 Str. Galaţi, Bucharest, Romania

Received April 18, 1969

The dependence on concentration of the heat of mixing in molten salts reciprocal binary mixtures $KCl+NaBr$ and $NaCl+KBr$ at 860°, has been determined by an isoperibol high-temperature platinum calorimeter. The values obtained for the heat of mixing are great and of opposite sign. The sign of the heat of mixing is established by the reciprocal Coulomb effect which could or could not be prevailing.

In recent years, physical and inorganic chemists have shown increasing interest for the properties of fused salts. As a result, a great deal of new information has become available regarding the structure, equilibrium and thermodynamic properties, as well as transport properties of such systems. There are, nevertheless, still surprisingly large gaps in our knowledge, even regarding some of the more obvious and fundamental points. We still know very little about how the thermodynamic properties of fused salt mixtures depend on the size, charge, and structure of the participating ions.

A great deal of information regarding the nature of the chemical bond in molten salts at high temperatures may be obtained from calorimetry. High temperature calorimetry has proved to be an important tool in the study of fused salt mixtures.

These last years, we have been engaged in a study of the properties of binary fused salt mixtures through the use of a high-temperature calorimeter. In the initial phase this work [1] was restricted to temperatures below 600°.

We have succeeded in developing reliable calorimetric equipment [2] and techniques for temperatures up to about 800°. This opens up a large new field to detailed investigation. Although the experimental difficulties associated with precision calorimetry in this temperature range are much greater than below 600°, we are at present obtaining a great deal of new and significant thermochemical information on simple fused halide systems. The mixing experiments reported, were performed at 860°. The calorimeter temperature was determined by means of a platinum to platinum-rhodium thermocouple, which was checked against a DEGUSSA (Germany) calibrated thermocouple.

---

[1] I. G. Murgulescu and D. I. Marchidan, Rev. Roumaine Chim., 9, 793 (1964).

[2] I. G. Murgulescu and D. I. Marchidan, "Thermodynamics", vol. 1, A.I.E.A., Vienna, 1966, p. 67; D. I. Marchidan and Cr. Telea, "Thermodynamics of Nuclear Materials", A.I.E.A., Vienna, 1968, p. 203.

A general theory of reciprocal fused salt mixtures has been developed by Blander, [3] who has applied the methods of conformal solution theory to the special case of reciprocal mixtures. For reciprocal systems the quasichemical theory [4] was applied too and allowed to point out some structural parameters similar to those of binary mixtures of molten salts. [5]

The heat of mixing in a reciprocal system may be, in this way, expressed as a function of the heat of mixing of binary systems corresponding to the respective reciprocal mixture. At the same time by using an adjustable parameter, the phase diagrams may be drawn. [6]

EXPERIMENTAL

By means of the isoperibol high-temperature calorimeter described in another communication,[2] we have made direct determinations of the heat of mixing in reciprocal mixtures. The salts were previously dried at 125°, then melted in purified nitrogen current.

The origin and purity of salts is indicated below:

- Sodium chloride — p.a. E. Merck
- Potassium chloride — p.a. Austranal
- Sodium bromide — p.a. E. Merck
- Potassium bromide — p.a. E. Merck

Solid salts have been stored in vacuum on phosphorus pentoxide.

The recording of thermal effects was achieved by an x—y Luxytrace (SEFRAM-France) recorder which was used as null detector (fig. 1). On the *X* axis an increasing voltage was applied with the help of a linear-circular potentiometer actuated by a clockwork mechanism. The recorder sensitivity was 10^{-6} V/mm; the recording speed was conveniently controlled by the voltage applied to the potentiometer and the speed of the clockwork mechanism.

---

[3] M. Blander, *J. Chem. Phys.*, **37**, 172 (1962); M. Blander and S. J. Yosim, *J. Chem. Phys.*, **39**, 2610 (1963); M. Blander, "Molten Salt Chemistry", Interscience, New York, 1964, p. 127—237.

[4] H. Flood, T. Førland and K. Grjotheim, *Z. anorg. Chem.*, **276**, 289 (1954);
T. Førland, "Fused Salts", McGraw-Hill, New York, 1964, p. 63—164;
M. Blander and L. E. Topol, *Electrochim. Acta*, **10**, 1161 (1965);
M. Blander and J. Braunstein, *Ann. New York Acad. Sci.*, **79**, 838 (1960);
M. Blander, *J. Chem. Phys.*, **34**, 432 (1961).

[5] H. Reiss, J. L. Katz and O. J. Kleppa, *J. Chem. Phys.*, **36**, 144 (1962).

[6] M. Blander, "Molten Salt Chemistry", Interscience, New York, 1964, p. 201;
H. Flood, T. Førland and K. Grjotheim, "The Physical Chemistry of Melts", Methuen, London, 1953, p. 46.

The caloric equivalent of obtained surfaces (fig. 2), was determined by electrical calibration after each mixing experiment.

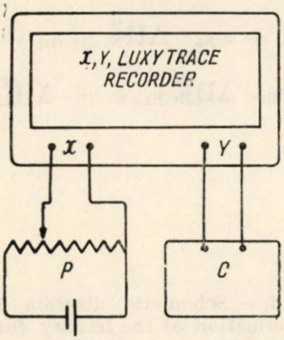

Fig. 1. — P—potentiometric scheme with rising voltage; C — calorimeter.

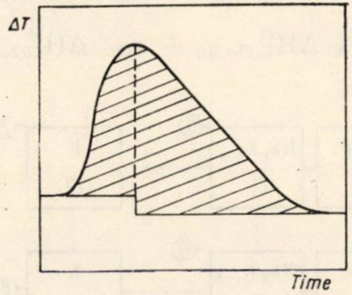

Fig. 2. — The shape of the surface obtained when determining the heat of mixing.

RESULTS AND DISCUSSION

For the reciprocal system Na, K || Br, Cl we can choose as independent components any 3 of the 4 salts : NaCl; KCl, NaBr ; KBr, taking into account that $x_{\text{NaBr}} + x_{\text{KCl}} + x_{\text{NaCl}} + x_{\text{KBr}} = 1$. The same reciprocal system may be obtained by a corresponding combination of binary systems. In this way, the final reciprocal system could be obtained starting from different initial states.

A schematic alternative of these possibilities is given by Kleppa[7] in figure 3, where

$$x = x_{\text{Na}^+} = \frac{n_{\text{Na}^+}}{n_{\text{Na}^+} + n_{\text{K}^+}} \qquad y = x_{\text{Cl}^-} = \frac{n_{\text{Cl}^-}}{n_{\text{Cl}^-} + n_{\text{Br}^-}}$$

$$1 - x = x_{\text{K}^+} = \frac{n_{\text{K}^+}}{n_{\text{K}^+} + n_{\text{Na}^+}} \qquad 1 - y = x_{\text{Br}^-} = \frac{n_{\text{Br}^-}}{n_{\text{Br}^-} + n_{\text{Cl}^-}}$$

and the reciprocal mixture is : $\text{Na}_x\text{K}_{1-x}\ \text{Cl}_y\text{Br}_{1-y}$.

Taking into account that :

$$\begin{matrix} 9 = 1 + 3 = 2 + 4 & & 8 = 1 + 4 & 7 = 3 + 4 \\ & \text{and} & & \\ 9 = 5 + 7 = 6 + 8 & & 6 = 2 + 3 & 5 = 1 + 2 \end{matrix}$$

$1 + 2 + 3 + 4 = 5 + 6 + 7 + 8$ results.

---

[7] O. J. KLEPPA and J. M. TOGURI, "Selected Topics in High Temperature Chemistry", Ed. by T. FØRLAND. Universitetsforlaget, Oslo, 1966, p. 15—26.

If the NaCl, NaBr and KBr concentrations are taken as independent variables, a similar equation to that of Kleppa [7] is obtained for the heat of mixing of the ternary system :

$$\Delta H^{M}_{Na,\ K||Cl,\ Br} = x_{KBr}\, x_{NaCl}\ \Delta H^{O}_{NaCl+KBr} + x_{Na^+}\ \Delta H^{M}_{Na(Cl+Br)} +$$

$$+ x_{K^+} \Delta H^{M}_{K(Cl+Br)} + x_{Cl^-}\ \Delta H^{M}_{Cl(Na+K)} + x_{Br^-}\ \Delta H^{M}_{Br(Na+K)} + \Delta H^{E}_{1234} \qquad (1)$$

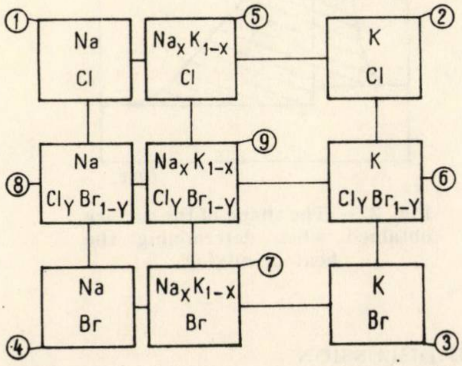

Fig. 3. — Schematic diagram showing the formation of the ternary fused salt mixture $Na_x\ K_{1-x}\, Cl_y\ Br_{1-y}$ from the pure salts.

where ΔH^{O} is the standard change of the enthalpy in the reactions under consideration while ΔH^{E} is the excess ternary enthalpy. The other 4 terms correspond to the heat of mixing in the respective binary systems.

On the other hand, from the theory of conformal solutions for reciprocal mixtures [8] we get :

$$\Delta H^{E}_{1234} = x_{K^+} x_{Na^+} x_{Cl^-} x_{Br^-} \cdot P\,[(g_1 + g_4 - g_2 - g_3)^2] \qquad (2)$$

where P is a collection of constants dependent only on the properties of the "comparison" salt. A useful approximation to P in this term may be made by comparing it with analogous terms in the quasi-lattice theory. [3, 4] This approximation is

$$P\,[(g_1 + g_4 - g_2 - g_3)^2] = -\frac{(\Delta H^{O})^2}{ZRT} \qquad (3)$$

In this way :

$$\Delta H^{E}_{1234} = -\,x_{K^+} x_{Na^+} x_{Cl^-} x_{Br^-} \frac{(\Delta H^{O})^2}{ZRT} \qquad (4)$$

The values of excess ternary enthalpy could be determined experimentally from equation (1) or could be calculated theoretically according to equation (4).

---

[8] M. BLANDER, "Advances in Chemical Physics", Ed. by I. Prigogine, Vol. 11, Interscience, London, 1967, p. 112.

Table 1

Heat of mixing of binary mixtures NaBr + KCl and NaCl + KBr at 860°

System	NaBr + KCl				
x_{NaBr}	0.2	0.4	0.5	0.6	0.8
ΔH^M (cal/mol)	−360	−496	−592	−560	−416
System	NaCl + KBr				
x_{NaCl}	0.2	0.4	0.5	0.6	0.8
ΔH^M (cal/mol)	+139	+225	+247	+230	+182

The results of the experiments concerning the heat of mixing in reciprocal systems NaBr + KCl and NaCl + KBr are given in table 1. On figure 4 is reproduced the concentration dependence of the heat of mixing.

The reciprocal system Na, K ‖ Cl, Br has a phase diagram [9] with a minimum (fig. 5) at 610° and the two diagonal sections NaCl + KBr and NaBr + KCl form, by cooling, solid solutions for $x_{NaCl} = 0.515$ (minimum at 610°) and $x_{KCl} = 0.475$ (minimum at 610°).

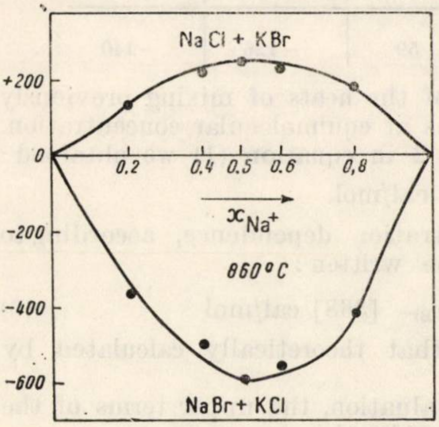

Fig. 4. — Molar enthalpies of mixing at 860° in fused salt systems : NaCl + KBr and NaBr + KCl.

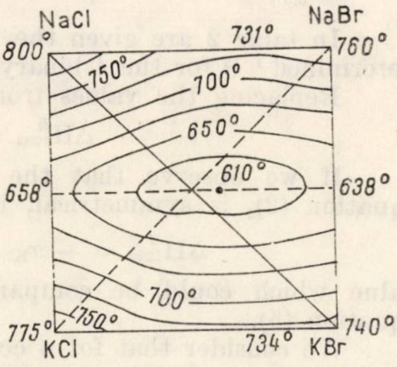

Fig. 5. — Phase diagram for the reciprocal system Na, K ‖ Cl, Br.

The reaction in the reciprocal system :

$$NaCl + KBr \longleftrightarrow KCl + NaBr$$

---

[9] N. K. Voskresenskaia, "Spravochinik po plavkosti sistem iz bezvodnyh neorganischeskih solei", Vol. 2, Izd. Akademii Nauk S.S.S.R., Moscow, 1961, p. 331.

is accompanied by a positive thermal effect. Thus the sign of the heat of mixing is related directly to the Coulomb reciprocal effect.

The standard enthalpy change ΔH° for the above reaction, taking into account the values obtained in table 1, for $x = 0.5$ is:

$$\Delta H^\circ = (592 + 247)\,2 = 1678 \text{ cal/mol}$$

From thermochemical data [7, 10] ΔH° (*s*, 25°) = 1400 cal/mol. Accurate data which allow an evaluation for liquid solution at 860°, working temperature, are not available. If we make the necessary corrections only for the melting entropy [11] and neglect the other contributions, a ΔH° (liquid) = 1610 cal/mol value results. On the other hand, Kleppa [7] obtained by the same mixing procedure as ours, ΔH° = 1503 cal/mol. The agreement between these data could be considered as very good.

If for Z in equation (4) a mean value [12] of 4.5 is taken, T is considered 1133°K and ΔH° = 1678 cal/mol, equation (4) gives:

$$\Delta H^E_{1234} = -\, x_{K^+} x_{Na^+} x_{Cl^-} x_{Br^-}\ [280] \text{ cal/mol} \qquad (5)$$

From relation (1) one could obtain ΔH^E_{1234} if the heats of mixing in the respective binary systems are known.

Table 2

Heat of mixing of equimolecular systems Na(Cl+Br), K(Cl+Br), Cl(Na+K) and Br(Na+K) at 860°

System	Na(Cl+Br)	K(Cl+Br)	Cl(Na+K)	Br(Na+K)
$\Delta H^M_{0.5}$ (cal/mol)	+50	+59	−126	−140

In table 2 are given the values of the heats of mixing previously determined [1, 13] for the 4 binary systems at equimolecular concentration.

Replacing the values from table 2 in equation (1) we obtained:

$$\Delta H^E_{1234} = -\,23 \text{ cal/mol.}$$

If we observe that the concentration dependence, according to equation (2), is symmetrical, it can be written:

$$\Delta H^E_{1234} = -\, x_{K^+} x_{Na^+} x_{Cl^-} x_{Br^-}\ [368] \text{ cal/mol} \qquad (6)$$

value which could be compared to that theoretically calculated by equation (5).

We consider that for a correct evaluation, the upper terms of the deviation from chaoticness must be considered.

Acknowledgements. We wish to express our deep gratitude to Professor I. G. Murgulescu, Head of the Institute of Physical Chemistry, for his great interest in our work. Our warm thanks are also due to the mechanician C. Volcovici for his help in the construction of the measuring apparatus.

---

[10] JANAF Thermochemical Tables (1964). The Dow Chemical Company, Midland, Michigan.

[11] A. S. Dworkin and M. A. Bredig, *J. Phys. Chem.*, **64**, 269 (1960).

[12] H. Levy and M. D. Danford, "Molten Salt Chemistry", M. Blander, Interscience, New York, 1964, p. 109–125.

[13] D. I. Marchidan and Cr. Telea, *Rev. Roumaine Chim.*, **13**, 1141 (1968).

Revue Roumaine de Chimie, **14**, 1501–1510 (1969)

POLAROGRAPHIC REDUCTION OF NIOBIUM(V) TARTRATE SOLUTIONS IN HYDROCHLORIC ACID-THIOCYANATE MEDIUM

C. DRĂGULESCU, SOFIA MARCHIDAN and GH. FACSKO

Centre of Physical Chemistry of the Academy, Bucharest, str. Galaţi 31

Received June 16, 1969

In this paper a variant of niobium(V) polarographic reduction in hydrochloric acid-thiocyanate medium with acetone addition under the conditions of niobium-tartrate solutions is presented. This was suggested by the authors' remark that the tartaric acid does not disturb the polarographic reduction process of the niobium-thiocyanate complex, and by the fact that the obtaining of niobium-tartrate solutions is much simpler and more usual than that of the hydrochloric ones. In order to establish the optimum conditions of reduction for analytical uses and the respective electrode process, the influence of various factors as temperature, reagents concentration, time of standing, height of the mercury reservoir on the reduction wave height, on the half-wave potential and on the stability of the system has been studied.

Niobium hydrochloric solutions form in presence of thiocyanate ions a complex which is reducible at the dropping mercury electrode. [1] By studying the influence of various anions on this reduction we found out that the presence of tartaric acid does not alter the wave height and the half-wave potential.[2] As, on the other hand, the preparation of niobium-tartrate solutions is much simpler and more usual than that of the hydrochloric ones, the study of niobium-thiocyanate reduction under the conditions of niobium-tartrate solutions was found useful for extending the polarographic determination of this element.

EXPERIMENTAL

Apparatus

A recording OH–101 type polarograph at 2×10^{-7} A/mm sensitivity was used; the compensation and damping were the same in all experiments. An electrolytic thermostated cell, an external low-resistance calomel saturated anode and purified nitrogen were used. To

---

[1] S. Marchidan, Gh. Facsko and C. Drăgulescu, *Rev. Roumaine Chim.*, **12**, 635 (1967).
[2] C. Drăgulescu, S. Marchidan and Gh. Facsko, *Rev. Roumaine Chim.*, (1969).

minimize the losses of hydrochloric acid and acetone during deaeration, the nitrogen was firstly bubbled through a solution of an identical composition with the respective supporting electrolyte.

Reagents and Solutions

All reagents used were p.a. and the niobium pentoxide was spectrographically pure (Johnson and Mattey). Fresh ammonium thiocyanate solutions ~ 6M and concentrated hydrochloric acid ~ 12M of established titre were used. Stock niobium solutions were prepared by exact weighing of niobium pentoxide amounts necessary for a concentration of $1-2 \times 10^{-2}$M – Nb. The niobium pentoxide was decomposed by fusing in a covered silica crucible with a minimum amount of potassium pyrosulfate. The melt was dissolved in 15 per cent (~ 1M) tartaric acid and a slight heating led to the obtaining of a perfectly clear solution. After cooling, the solution was passed into a volumetric flask and diluted to the mark with 15 per cent tartaric acid. Niobium-tartrate solutions are stable for a long time.

Preparation of Polarography Samples

Samples were prepared in volumetric flasks by pipetting corresponding amounts of niobium stock solution, hydrochloric acid and ammonium thiocyanate solution, each of them having known concentrations.

The reagents were added in the following order: stock niobium solution in 1M tartaric acid, concentrated hydrochloric acid, acetone, ammonium thiocyanate solution and distilled water up to the mark. After addition of each reagent, the flask was immediately stoppered, stirred and kept a few minutes in a water bath at 20°. The moment of the complexing agent addition was exactly noted, then the solution was passed from the flask into the thermostated cell and during 30 minutes was deaerated. Blank reagents solutions, without niobium, were prepared in the same manner and the polarographic behaviour of these solutions as well as of each reagent separately was checked. As during experiments it was found that the solutions for the polarographic measurements prepared in this way did not contain dissolved oxygen, a series of polarograms without previous deaeration of solutions were carried out. The polarograms were recorded between 40 and 50 minutes after thiocyanate addition, at 25±0.1° over the potential range −0.20 to −0.65 Volts.

EXPERIMENTAL RESULTS

To establish the optimum working parameters for the polarographic reduction of niobium-thiocyanate complex under the conditions of niobium-tartrate solutions, the influence of reagents concentration and of all factors affecting the height and shape of the wave, the half-wave potential or the stability of the system were studied.

Hydrochloric Acid

The curves in figure 1 represent the variation of wave height and half-wave potential *versus* the acidity of the solution, between 2 and 6.5 M hydrochloric acid. The wave height increases very rapidly with the hydrochloric acid content from 2 to 5 M. Over this value, the height change is unimportant but at the end of the studied interval waves very difficult to be analyzed are obtained owing to the interference with the hydrogen wave and to the ammonium chloride salting out effect which modifies the concentration of reagents in solution. The instability increase of the wave height and of the half-wave potential at a higher hydrochloric acid concentration on the one hand as well as the marked influence of the acid below 5 M on the wave height on the other hand, called forth the choice of 6 M hydrochloric acid concentration as optimum value.

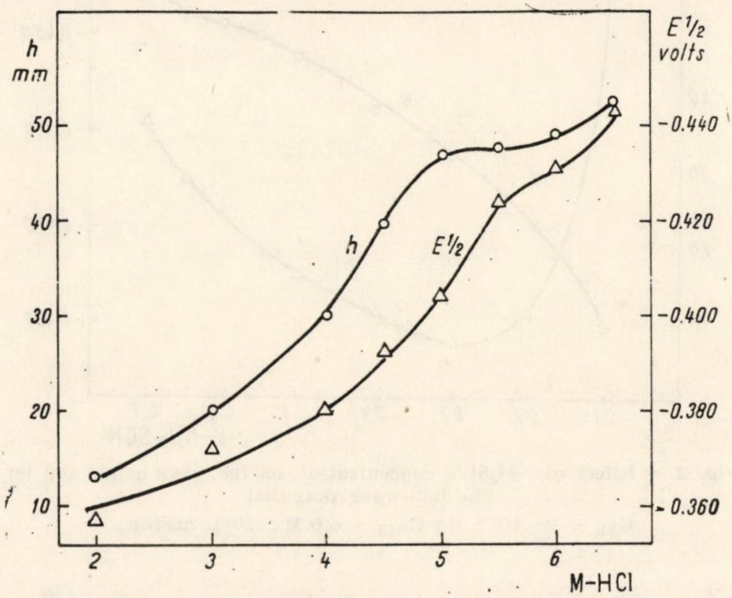

Fig. 1. — Effect of HCl concentration on the wave height and on the half-wave potential.

$C_{Nb} = 2\times10^{-3}$ M; $C_{NH_4SCN} = 0.6$ M; 20% acetone.

The half-wave potential shifts to more negative values as the solution acidity increases.

Ammonium Thiocyanate

Increasing the ammonium thiocyanate concentration from 0.10 to 0.70 M a similar plot for the reduction wave height *versus* thiocyanate concentration was obtained (Fig. 2). The formation of reducible niobium-thiocyanate complex takes place in a large ammonium thiocyanate excess. The wave height greatly rises as the thiocyanate concentration increases but concomitantly an increase in the instability occurs and this imposes the choice of a convenient working concentration between 0.5—0.6 M thiocyanate.

The half-wave potential suddenly rises at the beginning of the studied interval and records then a slight unimportant decrease.

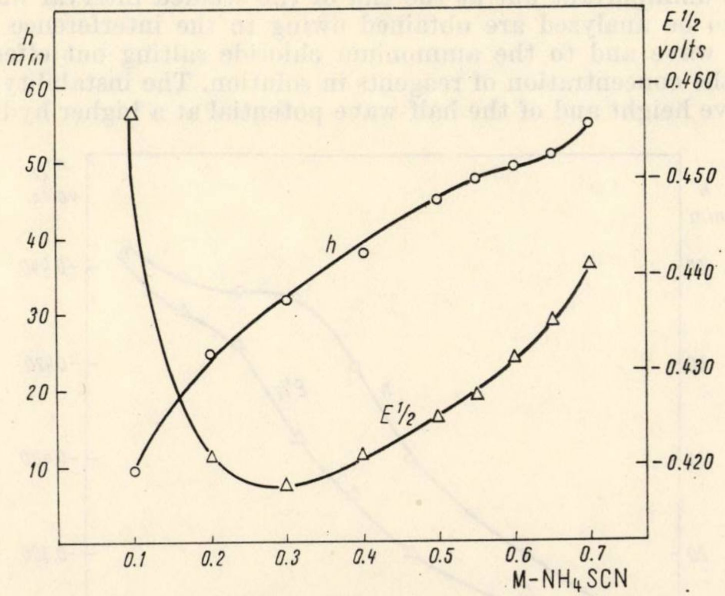

Fig. 2. — Effect of NH_4SCN concentration on the wave height and on the half-wave potential.

$C_{Nb} = 2 \times 10^{-3}$ M ; $C_{HCl} = 6.0$ M ; 20 % acetone.

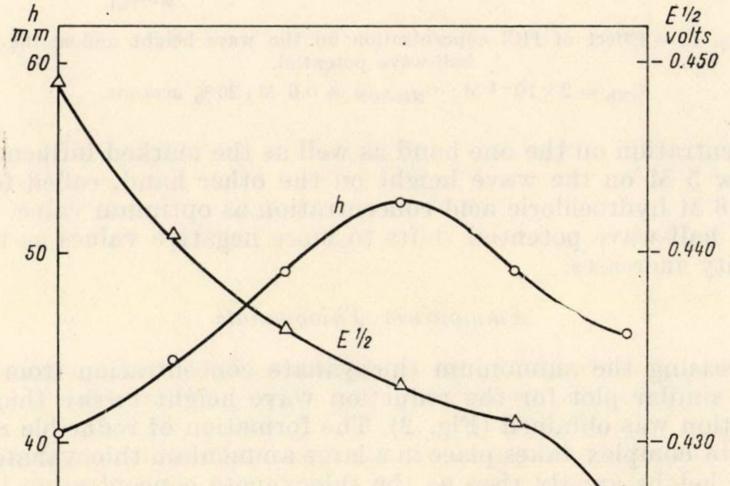

Fig. 3. — Effect of acetone concentration on the wave height and on the half-wave potential.

$C_{Nb} = 2 \times 10^{-3}$ M ; $C_{HCl} = 6.0$ M ; $C_{NH_4SCN} = 0.6$ M.

Acetone

The influence of acetone concentration is not so important as that observed for the other reagents from the wave height point of view. However, the acetone addition improves the waves shape, the stability of the system and the reproducibility of results. From figure 3 it results that for the established optimum conditions of acidity and thiocyanate content, the wave height only slightly changes in an acetone concentration range between 10 and 20 per cent (in volumes). As in solutions with acetone content below 15 per cent distorted waves with unclear plateaus, difficult to be measured and poorly reproducible were obtained and over 20 per cent ammonium chloride salting out effect in solution occurs, the 20 per cent acetone concentration was chosen as best value.

The half-wave potential slightly increases as the acetone concentration increases.

Temperature

Figure 4 represents the influence of temperature between 19 and 30°. As easily seen, temperature has a great influence on the reduction wave; this calls forth a rigorous thermostating. The wave height increase is 6.5 % per degree. At the same time the half-wave potential was found to shift to more negative values. This shift takes place very slowly, almost imperceptibly at the beginning of the temperature interval, then, over 25° more important but irreproducible changes occur. As optimum temperature was chosen 25°; at this temperature, both the wave height and the stability are satisfactory.

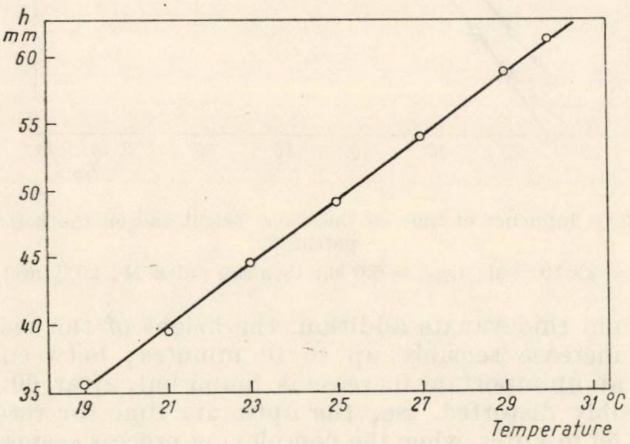

Fig. 4. — Influence of temperature on the wave height.
$C_{Nb} = 2\times10^{-3}$ M; $C_{HCl} = 6.0$ M; $C_{NH_4SCN} = 0.6$ M; 20% acetone.

Time of Standing

In the identical working conditions and at the same reagents concentration, the wave height and half-wave potential depend also on the time of sample standing, elapsed from the thiocyanate addition until the polarogram recording. The influence of time between 15 and 75 minutes was studied and the results are represented in figure 5. Although the yellow colour of the niobium-thiocyanate complex appears immediately after ammonium thiocyanate addition, the height of the reduction wave continues to increase sensibly up to 40 minutes; between 40 and 75 minutes only an unimportant increase is found but, after 60 minutes the waves are visibly distorted. So, the optimum time for recording is between 40 and 50 minutes, when the complexing process seems finished and the decomposition of the formed complex as well as the changes which occur in the blank solutions are still unimportant. Over the entire studied time range a slow shift of the wave on the ordinate occurs, due to the residual current increase with time, as well as a slow shift of the half-wave potential to more negative values.

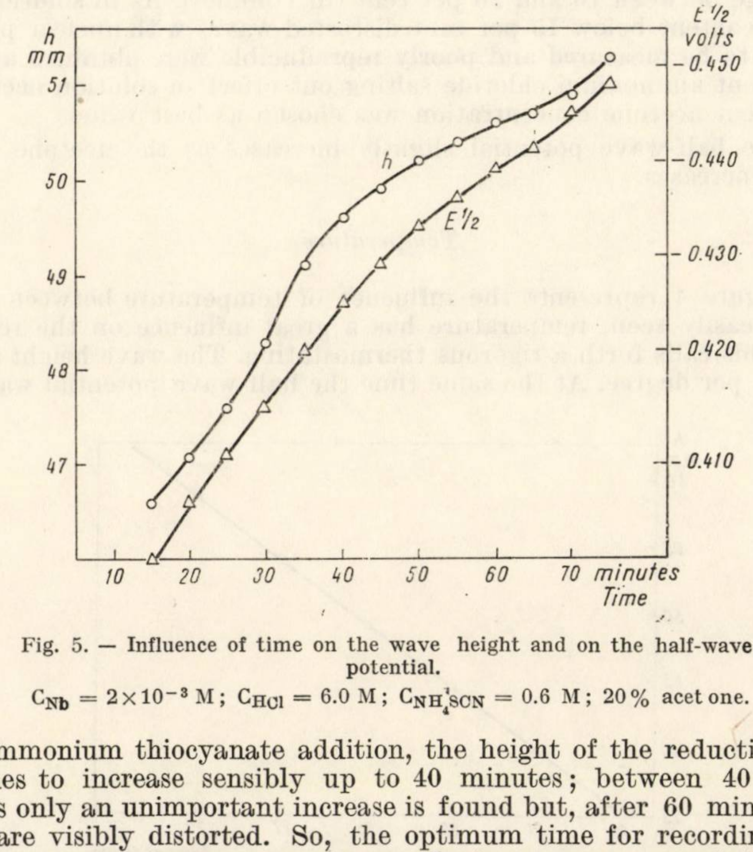

Fig. 5. — Influence of time on the wave height and on the half-wave potential.

$C_{Nb} = 2 \times 10^{-3}$ M; $C_{HCl} = 6.0$ M; $C_{NH_4SCN} = 0.6$ M; 20% acetone.

Blank Reagents Solutions

The blank reagents solutions were found to produce, in the absence of niobium, a small reduction wave in the same potential range in which the reduction of niobium-thiocyanate complex occurs. Successively testing all the reagents showed that hydrochloric acid solutions of various concentrations with tartaric acid and acetone addition, are polarographically inactive. On thiocyanate addition visible waves appear, the hydrochloric acid and thiocyanate concentration increase bringing about the increase in these very small and ill-defined waves. These waves slightly increase and shift to more negative potential values during the studied time interval so that the height of the niobium-thiocyanate reduction wave and the half-wave potential are accordingly modified.

Calibration Graph

Within the limits of the established optimum conditions, several calibration graphs were carried out with a view to determine those conditions which ensure the best reproducibility of results and a range of proportionality as wide as possible. In figure 6, the calibration graph for 6.0 M hydrochloric acid, 0.60 M ammonium thiocyanate, 20 per cent acetone, 0.10 M tartaric acid, 25° and 40—50 minutes is represented. The results of several determinations in these conditions, with or without deaeration, were reproducible and a linear relation between the height of reduction wave and niobium concentration has been obtained. By applying the known method of the regression analysis,[3] the linearity of the relation between the height of the reduction wave and the niobium concentration was verified. Equation

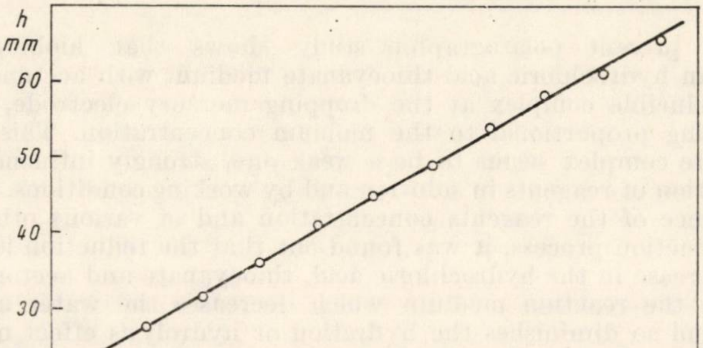

Fig. 6. — Calibration graph.
$C_{HCl} = 6.0$ M; $C_{NH_4SCN} = 0.6$ M; 20% acetone.

$$h(\text{mm}) = 17.4207 \times 10^3 \times C(\text{mol. l}^{-1}) + 14.2585$$

was thus obtained

h being the wave height and *C* niobium concentration.

---

[3] V. V. Nalimov, "The Application of Mathematical Statistics to Chemical Analysis", Pergamon Press, London, 1963, p. 16, 164.

The calculation effected for 10 determinations at different concentrations, each corresponding to the average of 3–4 parallel experiments, led to the following data:

— Standard deviation of determination $\sigma_p = 0.63$

— Standard error $\sigma_m = 0.1991$

— Probability of linear regression $\sigma_r = 277.8$

— Student criterion $t_{exp} = |a|/\sigma_r = 66.71 \gg 5.041$ (according to student tables for 99.9 per cent probability level).

These data show that the linear equation established has a significance of high order for the concentration interval $0.5 \times 10^{-3} - 2.75 \times \times 10^{-3}$M niobium.

The same linear relation and reproducibility were obtained when a 0.50 M thiocyanate concentration and a time of 30 minutes were used.

DISCUSSIONS AND CONCLUSIONS

The present polarographic study shows that niobium-tartrate solutions in hydrochloric acid-thiocyanate medium with acetone addition form a reducible complex at the dropping mercury electrode, the wave height being proportional to the niobium concentration. This niobium-thiocyanate complex seems to be a weak one, strongly influenced by the concentration of reagents in solution and by working conditions. Analysing the influence of the reagents concentration and of various other factors on the reduction process, it was found out that the reduction is favoured by the increase in the hydrochloric acid, thiocyanate and acetone concentration in the reaction medium which decreases the water activity in solution and so diminishes the hydration or hydrolysis effect of niobium complex ions. It was also established that all the factors which favour the obtaining of a maximum height of reduction wave have a negative influence on the stability of the system; this influence is expressed by the faster modification of the wave height and half-wave potential with time. This modification of the wave, after the completion of the complexing process, is a consequence not so much of the decomposition of the relatively weak niobium-thiocyanate complex, as of some secondary modifications which occur in the blank solutions. It is known that the thiocyanic acid in acid medium is subject to complex phenomena of polymerization and decomposition; these changes take place faster as the medium is more concentrated in acid and thiocyanate. The small wave which appears in strongly acid solutions of thiocyanate, in our opinion, should be assigned to the reduction of sulphur traces resulted from this decomposition. The thiocyanic acid can release elementary sulphur following a reaction opposite to that of formation:

$$HSCN \rightarrow S + HCN$$

while the resulted colloidal sulphur can be reduced according to the electrode reaction:

$$S + 2\,e^- \rightarrow S^{2-}$$

The obtained wave increases with time as the thiocyanate acid decomposition reaction proceeds and so modifies to some extent the wave height and half-wave potential of the niobium-thiocyanate complex. From the behavioural standpoint of blank reagents solutions, the utilization of less acid and less concentrated thiocyanate solutions is more convenient. In order to establish the optimum way for the polarographic determination, beside the maximum development of the reduction wave of niobium (by granting conditions which should least influence the working parameters) a greater stability of the wave in time had also to be aimed at. The rigorous observance of the reagents concentration, temperature and time of standing at the optimum values established, which actually represent a compromise between a maximum development and a maximum stability of the wave, ensured the obtaining of well defined and reproducible reduction waves. The reproducibility could be especially improved by eliminating deaeration. It was proved, during the experiments, that the polarographic determination could be effected without previous deaeration of the samples. This may be explained by the fact that at such high concentrations, the oxygen solubility is practically zero. The conditions established for the reduction of niobium-tartrate solutions in hydrochloric acid-thiocyanate-acetone medium agree to a large extent with those previously found for niobium-hydrochloric solutions. This is due to the fact that in strong hydrochloric medium the niobium-tartrate complexes initially existing in the tartaric solution are transformed into nonhydrolized hydrochloric complexes which are very reactive and produce in the presence of thiocyanate ions the reducible niobium-thiocyanate complex.

During reduction of niobium-thiocyanate complex, the electrode process is diffusion-controlled. This ensues from the fact that the wave height is a linear function of $\sqrt{h_{Hg}}$ as seen in figure 7. For the same electrode process, controlled by diffusion, pleads also the logarithmic analysis of the polarographic curve; this shows that the plot log i/i_a-i *versus* the applied potential, E, is a straight line (Fig. 8). The slope is not 0.06 Volts as may be expected for the one-electron reaction but 0.07 Volts, indicating a certain irreversibility of the electrode process. The unusual great dependence of the wave height on temperature also pleads for the irreversibility. The half-wave potential from the logarithmic analysis of the polarographic curve is -0.432 Volts (vs.S.C.E) and it is independent of niobium concentration. It depends to a great extent on the acidity of the solution and to a small extent on the acetone concentration or the temperature. At the same time the instability of half-wave potential in time was found i.e. a slow shift to more negative values as a result of transformations taking place in the blank solutions. The important modification in the potential occurring when the thiocyanate concentration increases and the shape of the respective curve represented in figure 2 is assigned by us to the following fact. On thiocyanate addition, due to the complex formation, the reversibility of reduction process increases and this results in the shift of the potential toward more positive values. If thiocyanate addition is continued in great excess the niobium is strongly complexed and a shift in the equilibrium potential to more negative values will follow.

In conclusion, the paper presents the polarographic reduction of niobium-tartrate solutions in hydrochloric acid-thiocyanate medium with

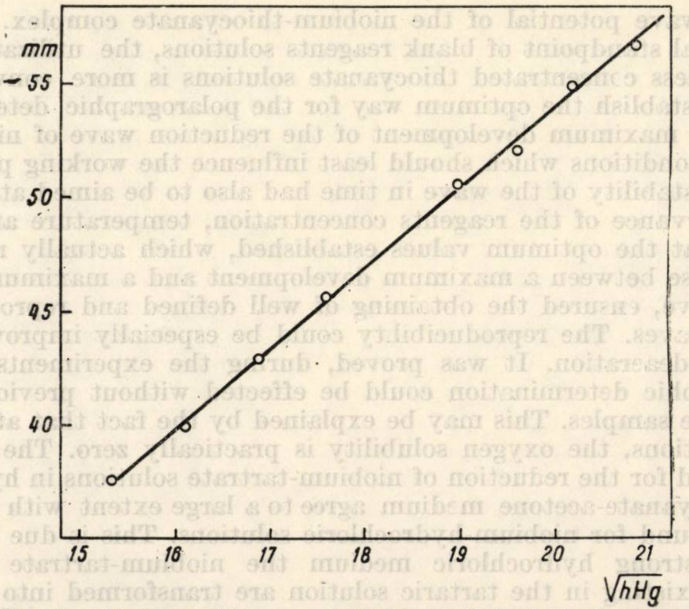

Fig. 7. — Variation of the wave height *versus* the height of mercury reservoir.
$C_{Nb} = 2 \times 10^{-3}$ M ; $C_{HCl} = 6.0$ M ; $C_{NH_4SCN} = 0.6$ M ; 20 % acetone.

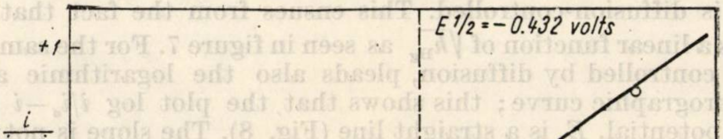

Fig. 8. — Logarithmic plot of polarographic curve.
$C_{Nb} = 2 \times 10^{-3}$ M ; $C_{HCl} = 6$ M ; $C_{NH_4SCN} = 0.6$ M ; 20 % acetone.

acetone addition and establishes the optimum working conditions and applicability field for analytical purposes.

Revue Roumaine de Chimie, **14**, 1511 – 1517 (1969)

STUDY OF SOME AZO-DERIVATE COMPLEXES OF CHROMOTROPIC ACID WITH BARIUM. II*

SPECTROPHOTOMETRIC AND VOLUMETRIC DOSING OF BARIUM AND SULPHATES WITH THE REACTIVES CARBOXY-AZO III, CARBOXYSULPHONAZO III AND SULPHONAZO III

V. ARMEANU and I. DRĂGUŞIN

Academy of Economic Studies, Chair of Chemistry and Physics, Bucharest, Piaţa Romană 6
and Chemical Works Borzeşti, Jud. Bacău, Romania

Received December 27, 1968

A study concerning the use of the above mentioned reactives for spectrophotometric microdosing and volumetric semimicrodosing of barium or sulphates, and the possibilities to extend this method to their dosing in the presence of interfering ions is presented.

Following the spectrophotometric study on the compounds of the three reactives with barium, (Part I), the present paper considers the possibility of their application to the spectrophotometric and volumetric dosing of barium and sulphates.

SPECTROPHOTOMETRIC DETERMINATION OF BARIUM

The bisazoderivates of the chromotropic acid containing $-SO_3H$ acid groups in ortho position as against the azo group or their derivates substituted in the nucleus [1] as well as chlorphosphonazo III [2] [2,7-bis-(4-chlorine-2-phosphophenylazo) chromotropic acid], were recommended as reactives suited for the spectrophotometric microdosing of barium.

According to the authors' conclusions it has been established that Bouguer-Lambert-Beer's law is confirmed for all the three reactives which have been considered, for quantities up to 60 µg Ba^{2+} in 25 cm^3 solution. The calibration curves for the spectrophotometric dosing of Ba^{2+} are given in figure 1. The optimum working conditions concerning the pH and concentration of the solvent in the solution are those established by the spectrophotometric study, the concentration of the reactives being 5×10^{-5}M for all cases.

---

* Part I. V. Armeanu and I. Drăgusin; *Rev. Roumaine Chim.*, (in print).

[1] S. B. Savin, Yu. M. Dedkov and V. P. Makarova, *Zhur. anal. Khim.*, **17**, 43 (1962).

[2] A. M. Lukin, K. A. Smirnova and T. V. Chermysheva, *Zhur. analit. Khim.*, **21**, 1300 (1966).

The sensitiveness of the reactions is about 5 µg Ba^{2+} in 25 cm^3 of solution, respectively 0.2 µg Ba^{2+}/cm^3.

The molar absorbance values (computed according to the diagrams in fig. 1) have high and close values, as it results from table 1. Consequently, all the three reactives may be used for the spectrophotometric dosing of the Ba^{2+} ion within the limits and conditions previously established.

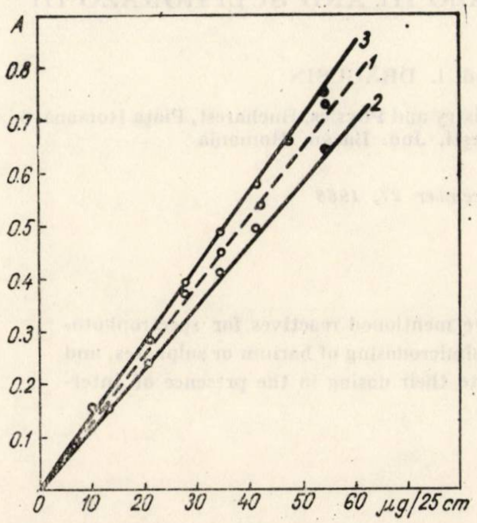

Fig. 1. — Verification of Bouguer-Lambert-Beer's law.

1, Carboxyazo III; λ = 685 nm; pH=2.55; solution 75% alcohol in water; *2*, Carboxysulphonazo III; λ = 645 nm; pH = 2.1; solution 75% alcohol in water; *3*, Sulphaonazo III; λ = 640 nm; pH=2,0; solution 60% alcohol in water.

Table 1

Molar absorbance values of the complexes

No	Complex	λ nm	pH	Alcohol %	Molar absorbance value ε = A/bM
1	Ba-Carboxyazo III	685	2.55	75	44,600
2	Ba-Carboxysulphonazo III	645	2.1	75	40,400
3	Ba-Sulphonazo III	640	2.0	60	48,000

The selectivity of the reactives, within the limits of the optimum working conditions is high for the Ba^{2+} and Sr^{2+} ions. The fact that the Ca^{2+} and Mg^{2+} ions do not give colour reactions with any of these reactives is particularly important, as it makes possible the dosing of barium in the presence of these elements. The interference of other cations, as for instance Fe^{2+}, Mn^{2+}, Ni^{2+}, Cd^{2+}, Zn^{2+}, UO_2^{2+}, Al^{3+}, Gd^{3+}, Bi^{3+}, La^{3+}, Zr^{4+}, and

Th^{4+} is generally small or negligible, being visible only for values of PH $>$ > 2 and concentrations generally ten times higher than the stoichiometric quantity. For values of the pH < 2 the selectivity is almost exclusive for Ba^{2+} and Sr^{2+}. The only elements forming coloured complexes in the prescribed working conditions with appreciable molar values of absorbance, especially in the range pH $= 2-3$, are Cu^{2+} and Pb^{2+}.

But addition of complexon III to the solution in small excess, allows to remove all these influences, owing to the formation of metallic complexonates having a high stability in acid medium, respectively the selectivity for the Ba^{2+} and Sr^{2+} may be considered absolute.

VOLUMETRIC DOSING OF BARIUM AND SULPHATES

Owing to the high sensitivity and selectivity for the Ba^{2+} ion, to the appreciable stability of the coloured complexes in alcoholic or acetonic slightly acid solutions as well as to the great contrast between the purplish-pink colour of the reactives and the greenish-blue one of the resulting complexes, these reactives are excellent indicators for direct volumetric dosing of the sulphates. Standard solutions of barium salts can be used as titration agents. Till now for the volumetric dosing of sulphates carboxyarsenazo III,[3-5] carboxysulphonazo III,[6] nitrochromazo [7-9] and carboxyazo III [10, 11] have been practically used as indicators.

The speciality literature recommends them as indicators only for the direct titration of the sulphates, under the form of free sulphuric acid, as the presence of salts in the solution hinders the determinations, the contrast being weaker and the turnings not very precise. In case of interferring cations present in the solution, which give colour reactions with the reactives or which precipitate with the SO_4^{2-} ion, their retention on the cationite column and the dosing of the free sulphuric acid of the eluate is recommended.

The authors' contribution consists, first of all, in establishing the optimum working conditions, as a consequence of the spectrophotometric study formerly carried out and in studying the possibilities of removing the influence of the interferring elements by masking them with complexon III. At the same time, the method has been extended to the dosing

---

[3] K. F. Novikova, N. N. Basargin and M. F. Tsiganova, *Zhur. analit. Khim.*, **16**, 348 (1961).

[4] A. A. Nagina and G. G. Kobyak, *Uch. Zap. Permsk. Gos. Univ.*, **25**, (2) (1963); *Chem. Abstr.*, **61**, 1611 a (1964).

[5] A. I. Busev, V. K. Akimov and S. I. Bragina, *Zhur. analit. Khim.*, **21**, 817, (1966).

[6] Z. K. Karlova and N. S. Shibaeva, *Zhur. analit. Khim.*, **19**, 258 (1964).

[7] V. I. Kuznetsov and N. N. Basargin, *Zavodskcya Lab.*, **31** (5) 538 (1965).

[8] N. N. Basargin and K. F. Novikova, *Zhur. analit. Khim.*, **21**, 473 (1966).

[9] N. N. Basargin and K. F. Novikova, *Zhur. analit. Khim.* **22**, 394 (1967).

[10] I. Drăgușin, *Rev. Chim.* (*București*) **16**, 590 (1965).

[11] I. Drăgușin and A. Gavriliuc, *Rev. Roumaine Chim.*. **12**, 1239 (1967).

of larger quantities of sulphates, as well as to the indirect titration of barium.

Sulphonazo III cannot be used as an indicator, because of its stability, higher than of the other complexes. Therefore an equilibrium is formed in the solutions between the barium sulphate and the barium complex, leading to the appareance of the turning, long before the point of equivalence.

1. DIRECT TITRIMETRIC DOSING OF THE SULPHATES

The optimum working conditions concerning the pH and the concentration of the solution in organic solvent were established through a spectrophotometric study * (Part I). The best contrasts with the clearest turnings, from purplish-pink to greenish-blue are obtained by working in solutions with high concentrations of organic solvent with a view to raise the stability of the complex and considerably lower the solubility of the $BaSO_4$ resulting from the reaction, respectively the immediate precipitation at room temperature of the sulphate traces. In order to get good results one recommends that the contents in organic solvent in the final solution obtained after titration should be of 75 to 85% for carboxyazo III and 60—75% for carboxysulphonazo III. The best results are obtained in water-alcohol acid solutions. As the differences are not essential, it is advisable, for economic reasons and for serial determinations, to use water-acetone solutions.

As previously shown * (Part I), both reactives may be used in sufficiently acid media. When the pH is smaller than 1.8, we nevertheless recommend the use of carboxysulphonazo III whose complex with barium is more stable than that formed with carboxyazo III. As both complexes have a considerable stability, the adjustment of the pH with urotropine or buffer solutions, recommended by some authors for carboxyarsenazo III or other reactives of this class, do not modify essentially the reactives behaviour.

In an initial volume of 50 cm³ solution one can dose with good results quantities of sulphates between 0.2 and 8 mg. The best results with particularly clear turnings are obtained on titrating sulphate quantities not exceeding 3 mg in the sample. Beyond this limit, the quality of the turnings is influenced by the absorption phenomenon of the colouring mother on the $BaSO_4$ precipitate resulting from the reaction.

One has used for titration standard solutions of barium chloride with a 0.01—0.05 N concentration, according to the sulphate contact. For quantities larger than 3 mg sulphates in the sample one should use 0.05 N solutions.

Working method. To verify the method, standard solutions made of fixanol sulphuric acid have been used.

In a conic flask of 100 cm³ an exactly measured quantity of the diluted standar solution of sulphuric acid, with a volume not exceeding 5 cm³ is introduced with a pipette or a microburette. For smaller volumes, distilled water is added up to a 2—3 cm³ volume. Acetone or alcohol (40—50 cm^3) and a few drops of aqueous solution 0.1% of indicator are poured, the colour of the water-organic solvent solution in the flask turning to purplish-pink. If the solution becomes purplish-bluish, the solution is slightly acidified by adding a few drops of 0.1—1 N hydrochloric acid.

The standard barium chloride solution of the microburette, is then titrated by stirring continuously. At the point of equivalence the colour of the solution turns abruptly to greenish-blue. If the barium chloride solution added exceeds 3 ml, 10—15 cm^3 of organic solvent will be added, and then the titration carried on.

When calculating the quantity of sulphates from the volume of the standard barium chloride solutions a quantity, once and for all experimentally determined by titrating a witness-sample, is subtracted. This correction represents, for the given conditions, 0.01 cm^3 of 0.02 N barium chloride solution.

As it results from the data in table 2, within the prescribed limits regarding the sulphates content of the sample, the error does not exceed ±1%.

Table 2

Results obtained on titrimetric dosing of the SO_4^{2-} ion of the standard sulphuric acid solution

No	SO_4^{2-} existing in sample mg	SO_4^{2-} titrimetrically determined, mg					
		Carboxyazo III	%	Error %	Carboxy-sulfonazo III	%	Error %
1	0.192	0.1920	100.0	0	0.1920	100.0	0
2	0.480	0.4848	101.0	+1,0	0.4800	100.0	0
3	0.768	0.7584	98.7	−1.3	0.7680	100.0	0
4	0.960	0.9600	100.0	0	0.9696	101.0	+1.0
5	1.152	1.1520	100,0	0	0.11520	100.0	0
6	0.1440	1.1450	100.7	+0.7	0.14400	100.0	0
7	1.728	1.7280	100.0	0	1.7376	100.5	+0.5
8	1.920	1.9200	100.0	0	1.9200	100.0	0
9	2.400	2.3904	99.6	−0.4	2.4096	100.4	+0.4
10	2.880	2.8800	100.0	0	2.8896	100.3	+0.3
11	3.840	3.8640	100.6	+0.6	3.8400	100.0	0
12	4.800	4.8000	100.0	0	4.8240	100.5	+0.5
13	5.760	5.8080	100.8	+0.8	5.7840	100.4	+0.4
14	7.680	7.280	100.6	+0.6	7.7040	100.3	+0.3

Dosing of sulphates in the presence of other ions

The method was extended to the direct dosing of alkaline sulphates in conditions and with results resembling those above mentioned (Table 3). In the present case, the influence of the alkaline cations on the absorption of the reactives and the colour contrast is small enough, and therefore the retaining on cationit resins is not necessary.

The determinations take place in solutions acidified with chlorhydric acid till the characteristic purplish-pink colour, as already shown, is obtained.

An important contribution was brought by eliminating the interference of other cations blocking the indicator by the formation of coloured

Table 3

Results obtained on titrimetric dosing of the SO_4^{2-} ion of the standard sodium sulphate solutions

No	SO_4^{2-} existing in sample mg	SO_4^{2-} titrimetrically determined, mg					
		Carboxyazo III	%	Error %	Carboxy-sulfonazo III	%	Error %
1	0.192	0.1920	100.0	0	0.1920	100.0	0
2	0.480	0.4896	102.0	+2.0	0.4848	101.0	+1.0
3	0.768	0.7776	101.2	+1.2	0.7680	100.0	0
4	0.960	0.9504	99.0	−1.0	0.9696	101.0	+1.0
5	1.440	1.4496	100.7	+0.7	1.4496	100.7	+0.7
6	1.920	1.9200	100.0	0	1.9392	101.0	+1.0
7	2.880	2.8896	100.3	+0.3	2.8608	99.3	+1.7

complexes, due to the use of complexon III. One can thus dose the SO_4^{2-} ion of the copper, lead, zinc, etc, sulphate solution by adding complexon 0.05 N in the acid water-organic solvent solution until the colour turns to purplish-pink.

The dosing method of the sulphate cannot be applied in the presence of the Ca^{2+} and Mg^{2+} ions, which, though not giving colour reactions with the reactions, yield hardly soluble sulphates in alcoholic solutions.

2. TITRIMETRIC DOSING OF BARIUM

Owing to the high stability of the compound, the dosing of the Ba^{2+} ion by direct titration with standard sulphuric acid solutions, does not take place in good conditions, the turning being slow and exceeding the point of equivalence. For this reason the standard sulphuric acid solution should be added in small excess, until obtaining a clear purplish-pink colour, and then the SO_4^{2-} excess should be titrated as known. One can thus dose quantities of 0.5 to 8 mg Ba^{2+} (Table 4).

The Cu^{2+}, Pb^{2+}, Zn^{2+}, etc ions giving colour reactions with the indicator can be masked with complexon.

Table 4

Results obtained on titrimetric dosing of the Ba^{2+} ion of standard barium chloride solutions

No	Ba^{2+} existing in sample mg	Ba^{2+} titrimetrically determined, mg					
		Carboxyazo III	%	Error %	Carboxy-sulphonazo III	%	Error %
1	0.6868	0.7005	102.0	+2.0	0.6936	101.0	+1.0
2	1.0988	1.1126	101.2	+1,2	1.0851	98.9	−1.2
3	1.3736	1.3736	100.0	0	1.3598	99.0	−1.0
4	2.7472	2.7609	100.5	+0.5	2.7472	100.0	0
5	4.1208	4.1345	100.3	+0.3	4.1069	99.7	−0.3
6	5.4944	5.4600	99.5	−0.5	5.5081	100.2	+0.2
7	6.8680	6.8680	100.0	0	6.8680	100.0	0
8	8.2416	8.2141	99.7	−0.3	8.2141	99.7	−0.3

SYNTHESIS OF THE REACTIVES

The reactives necessary to the spectrophotometric study and to the determination of the Ba^{2+} and SO_4^{2-} ions were synthetized by diazotation of the respective *o*-aminoacids (anthranylic and orthanylic acid) and coupling of the diazonium salts obtained with chromotropic acid.

Monoazoderivates are first obtained which are later transformed into cyclic calcium salts. A second azo group, can be introduced now, respectively the monocalcium salt of the diazoderivate may be obtained.

The calcium salt is boiled with sodium carbonate in order to purify and transform it into a sodium salt. From the filtrate, the tetrasodic salt free of monoazo product is obtained by salting out. The products thus obtained are sufficiently pure to be used as indicators.

The pure products needed for the spectrophotometric study were obtained through repeated crystallizations from aqueous solutions and washing with absolute alcohol of the tetrasodic salt obtained through salting out.

The disodic salts, recommended in certain works, are separated by acidification with hydrochloric acid of concentrated aqueous solutions of the tetrasodic salts and washing with alcohol of the precipitates.

The reactives, disodic or tetrasodic salts, appear as crystalline blue-reddish power, with a bronze glitter, easily soluble in water. Their solutions do not change their characteristics in time.

CONCLUSIONS

The possibility of applying to the dosing of the Ba^{2+} and SO_4^{2-} ions of three azoderivates of the chromotropic acid : carboxyazo III, carboxy sulphoazi III and sulphonazo III is studied.

In view of the spectrophotometric dosing of the Ba^{2+} the domain in which Bouguer-Lambert-Beer's law is observed has been determined by calculating the molar absorbance values.

The method of volumetric determination of the sulphates, by precipitating as $BaSO_4$ has been established and extended to the indirect dosing of barium. The paper attempts to elucidate the elimination of the influence of other ions by masking with complexon III.

Revue Roumaine de Chimie, 14, 1519–1524 (1969)

RECHERCHES SUR LA POLYMÉRISATION DE CERTAINS DÉRIVÉS ACÉTYLÉNIQUES À L'AIDE DE LA TRIÉTHYLAMINE. I

LA POLYMÉRISATION DE L'ESTER MÉTHYLIQUE DE L'ACIDE PROPIOLIQUE

CR. I. SIMIONESCU et KIM TAL-HEN

Chaire de Macromolécules naturelles et synthétiques de l'Institut Polytechnique de Jassy, 11, str. 23 August

Reçu le 17 mai 1969

Le travail présente la polymérisation de l'ester méthylique de l'acide propiolique en solution d'éther avec la triéthylamine (TEA). On détermine l'ordre de réaction, l'énergie d'activation, la constante de vitesse de réaction, ainsi que l'influence de la concentration du catalyseur sur la vitesse de polymérisation. Les résultats obtenus montrent que la TEA est un catalyseur très actif pour la polymérisation de certains dérivés acétyléniques ; il donne une valeur réduite de l'énergie d'activation.

La littérature montre que l'addition de la TEA aux dérivés de l'acide propiolique (l'ester méthylique, éthylique, de l'amide de l'acide propiolique et le cyanacétylène) peut déterminer leur polymérisation.[1]

Ce travail présente quelques résultats obtenus par la polymérisation de l'ester méthylique de l'acide propiolique (EMP) à l'aide de la TEA, dans les solutions d'éther éthylique. Tout particulièrement on se propose de mettre en évidence le rôle catalytique de la TEA et d'élucider le caractère de ces réactions catalytiques.

1. RÉACTIFS

On a utilisé l'EMP, synthétisé dans notre laboratoire par une méthode mentionnée dans la littérature,[2] modifiée seulement en ce qui concerne les quantités de réactifs. On a utilisé la fraction possédant le p.b. = 101–102°.

---

[1] B. J. MacNulty, *Polymer.*, 7, 275 (1966).

[2] C. Moukev et I. C. Bongrand, *Ann. Chim.* (*France*), 14, 47 (1920).

La TEA était du type *Merck* (Allemagne Fédérale), et l'éther éthylique, séché à l'aide du sodium métallique, a été obtenu des Usines *Reactivul* de Bucarest.

2. DOSAGE DES MONOMÈRES

La concentration de l'EMP a été déterminée à plusieurs intervalles de temps au cours de la polymérisation par chromatographie en phase gazeuse (appareil CARLO ERBA, type GV). En raison des températures de vaporisation différentes, le monomère et le catalyseur se séparent déjà dans l'évaporateur ; c'est pourquoi la présence de la TEA n'influe pas sur le dosage de l'EMP.

Comme support on a utilisé le *cromosorb* (CARLO ERBA) et comme phase stationnaire, l'ester de l'acide succinique (LAC 728-CARLO ERBA). La concentration de la phase stationnaire a été de 20% par rapport au support.

Les conditions expérimentales de la chromatographie ont été :

température dans l'évaporateur	120°
température dans la colonne	100°
température du détecteur	105°
débit	66 ml/mn
longueur de la colonne	75

Dans ces conditions on a obtenu un pic aigu et symétrique. La concentration du monomère a été effectuée par l'utilisation de la hauteur du pic. Chaque fois qu'on a effectué l'analyse, on a ajouté 40 μl du mélange de réaction dans l'appareil. Pour le dosage du catalyseur on a modifié seulement la longueur de la colonne (2 m), les autres conditions expérimentales étant les mêmes.

3. LA POLYMÉRISATION

La polymérisation a été effectuée dans un ballon à trois tubulures (50 ml), les échantillons étant manipulés à l'aide d'une microseringue et le mélange de réaction poussé en haut dans un tube capillaire.

Etant donné que le monomère et la TEA sont solubles dans l'éther, et le polymère est insoluble, on a ajouté la TEA dans la solution éthérée du monomère pour observer la coloration du système de réaction en jaune et ensuite en marron foncé.

Pour déterminer l'ordre de réaction, de l'énergie d'activation, de l'influence de la TEA sur la vitesse de la réaction, on a effectué la polymérisation à différentes températures (0°, 5°, 12°, 20°, 25°), en maintenant constante la concentration de la TEA.

Au début, la concentration du monomère était de 2,381 mole/l pour tous les essais.

Les figures 1 et 2 représentent la variation de la concentration du monomère à différentes températures de polymérisation. Le processus de polymérisation a été étudié dans chaque expérience jusqu'aux conversions de 20–30%.

4. DONNÉES EXPÉRIMENTALES

Les figures 1 et 2 représentent sur l'ordonnée la hauteur (*A* mm) du pic de la chromatographie en phase gazeuse (195 mm correspondent à 2,381 mole/l).

L'ordre de réaction. Afin de déterminer l'ordre de réaction on a représenté graphiquement la relation $1/A - t$.

Sur les figures 3 et 4 on peut observer un rapport linéaire entre $1/A$ et „t", c'est-à-dire

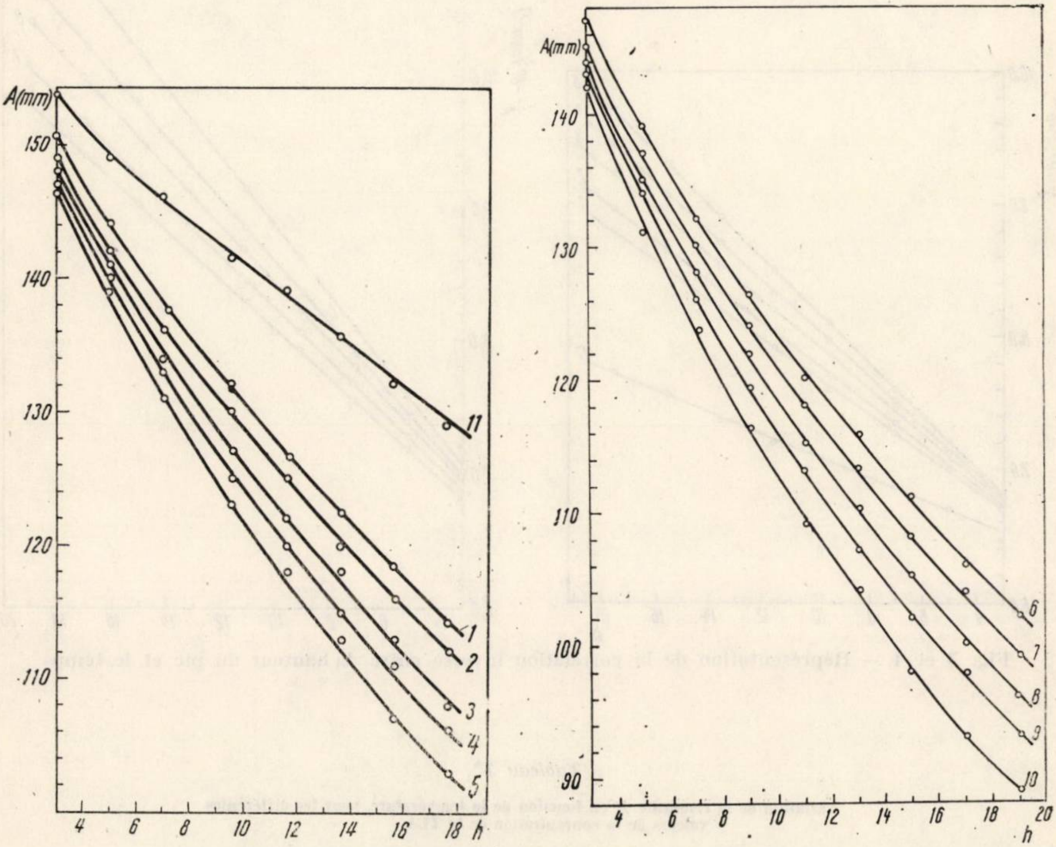

Fig. 1 et 2. — Variation de la concentration de l'EMP par rapport au temps à différentes températures.

$$\frac{1}{A} = \frac{1}{A_0} + Kt \qquad (1)$$

ce qui montre que la réaction est d'ordre secondaire.

Dès le début de la réaction jusqu'à une durée de 3 heures, en d'autres termes jusqu'à la conversion de 5–7 %, les données expérimentales ne correspondent pas à la relation (1).

Cette observation sera discutée dans une note ultérieure.

À l'aide de la relation (1) et des droites représentées dans les figures 3 et 4, nous avons obtenu les constantes de vitesse de la polymérisation (K), notées dans le tableau 1.

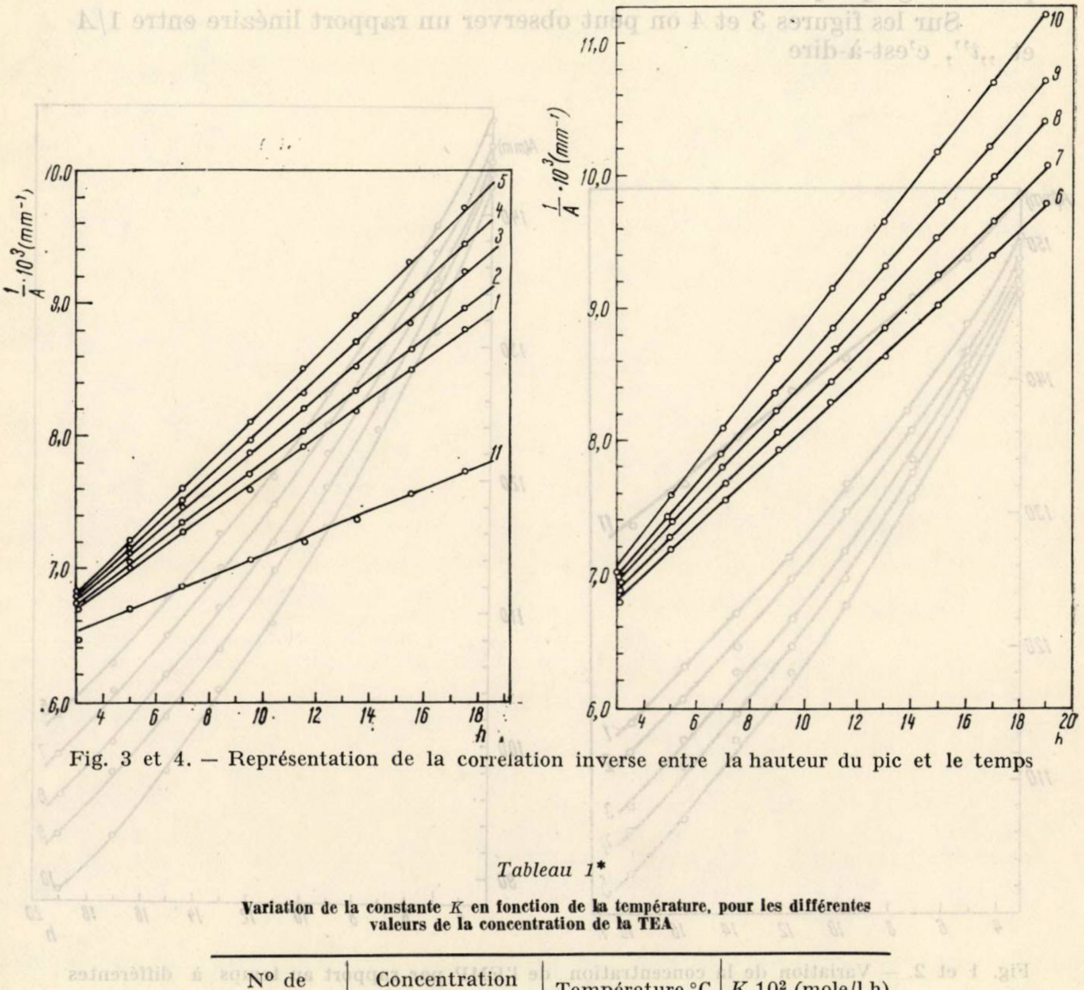

Fig. 3 et 4. – Représentation de la corrélation inverse entre la hauteur du pic et le temps

*Tableau 1**

Variation de la constante *K* en fonction de la température, pour les différentes valeurs de la concentration de la TEA

N° de l'expérience	Concentration TEA (mole/l)	Température °C	$K.10^2$ (mole/l.h)
1	0,1034	0	6,498
2	0,1034	5	7,031
3	0,1034	12	7,732
4	0,1034	20	8,632
5	0,1034	25	9,281
6	0,1338	0	8,408
7	0,1338	5	9,097
8	0,1338	12	10,000
9	0,1338	20	11,239
10	0,1338	25	12,008
11	0,0542	5	3,684

* Les chiffres sur les courbes des figures 1–4, représentent le numéro de l'expérience du tableau 1.

L'énergie d'activation. Dans la figure 5 on a représenté la relation $\ln K - 1/T$ d'où il résulte un rapport linéaire entre $\ln K$ et $1/T$. A ce propos on a calculé l'énergie d'activation E, avec la relation $\ln K = E/RT + C$.

Les expériences 1 — 5 ont donné E_1, alors que les expériences 6—10 ont donné E_2, avec les valeurs suivantes

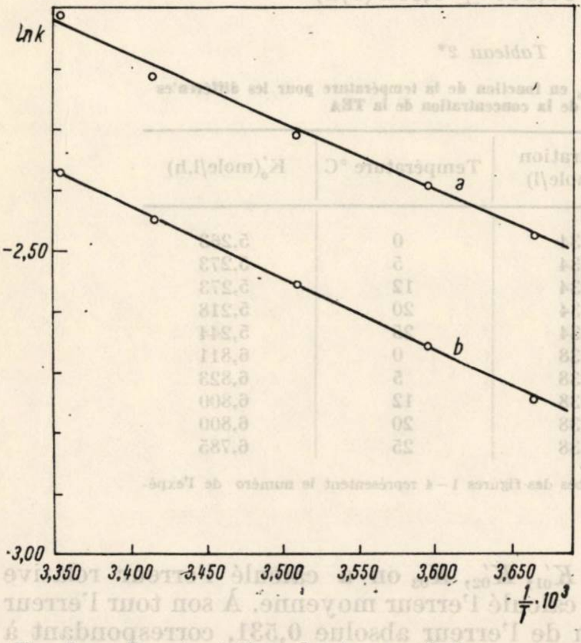

Fig. 5. — Représentation de la corrélation entre $\ln K$ et $1/T$.
a, concentration de la TEA=0,1338 mole/l; b, concentration de la TEA = 0,1034 mole/l.

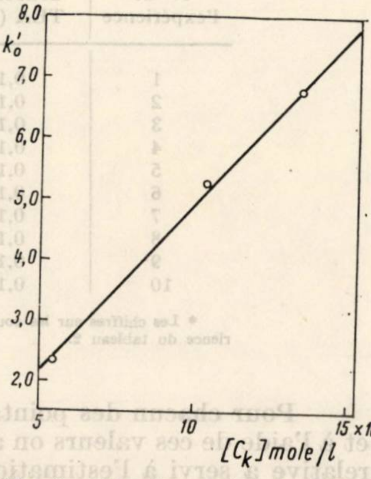

Fig. 6. — Relation entre la constante K'_0 et la concentration de la TEA.

$E_1 = 2{,}384$ kcal/mole

$E_2 = 2{,}285$ kcal/mole

L'énergie d'activation $E = (2{,}335 \pm 0{,}050)$ kcal/mole.

A l'aide de l'E et de la relation $K = K'_0 \cdot e^{-E/RT}$, on a calculé K_0, dont les valeurs sont enregistrées dans le tableau 2.

Les expériences 1—5 indiquent les valeurs

$$K'_{01} = 5{,}255 \pm 0{,}017 \text{ (mole/l.h)}$$

et les expériences 6—10 les valeurs

$$K'_{02} = 6{,}806 \pm 0{,}055 \text{ (mole/l.h)}$$

Influence de la concentration de la TEA sur la vitesse de réaction. L'expérience 11 a donné $K = 3{,}684 \cdot 10^{-2}$ (mole/l.h). Grâce à l'énergie d'activation $E = 2{,}335 \pm 0{,}050$ (kcal/mole), on a calculé $K'_{03} = 2{,}388 \pm 0{,}109$ (mole/l.h). L'erreur de 0,109 (mole/l.h) provient de l'erreur survenue dans la relation de l'énergie d'activation pendant le calcul du K'_{03}.

Dans la figure 6 nous avons représenté la relation entre K'_0 et la concentration de la TEA $[C_k]$. Entre K'_0 et $[C_k]$ il y a une corrélation linéaire.

Avec l'équation $K'_0 = K_0\,[C_k]$ et en utilisant les données de la figure 6 nous avons obtenu K_0

$$K_0 = 54{,}500 \pm 0{,}531\ (1/1)$$

*Tableau 2**

Variation de la constante K'_0 en fonction de la température pour les différentes valeurs de la concentration de la TEA

N° de l'expérience	Concentration TEA (mole/l)	Température °C	K'_0(mole/l.h)
1	0,1034	0	5,263
2	0,1034	5	5,273
3	0,1034	12	5,273
4	0,1034	20	5,218
5	0,1034	25	5,244
6	0,1338	0	6,811
7	0,1338	5	6,823
8	0,1338	12	6,800
9	0,1338	20	6,800
10	0,1338	25	6,785

* Les chiffres sur les courbes des figures 1 – 4 représentent le numéro de l'expérience du tableau 2.

Pour chacun des points K'_{01}, K'_{02}, K'_{03} on a calculé l'erreur relative et à l'aide de ces valeurs on a calculé l'erreur moyenne. À son tour l'erreur relative a servi à l'estimation de l'erreur absolue 0,531, correspondant à la valeur de 54,500.

On peut donc tirer l'équation cinétique expérimentale de la polymérisation de l'EMP avec TEA, dans la solution d'éther par l'utilisation des résultats obtenus, à savoir: l'ordre de réaction, l'énergie d'activation et K_0

$$\frac{\mathrm{d}[C]}{\mathrm{d}t} = K_0 . \mathrm{e}^{-E/RT} . [C_k]\,[C]^2 \qquad (2)$$

où $[C]$ est la concentration du monomère, ou bien

$$\frac{\mathrm{d}[C]}{\mathrm{d}t} = (54{,}500 \pm 0{,}531) \cdot \mathrm{e}^{-\frac{2{,}335 \pm 0.050}{RT}} \cdot [C_k]\,[C]^2 \qquad (3)$$

Revue Roumaine de Chimie, **14**, 1525–1534 (1969)

POLYMÈRES ORGANIQUES PHOSPHORYLÉS. I[1] LA PHOSPHORYLATION DU POLYSTYRÈNE PAR SYNTHÈSE SELON FRIEDEL-CRAFTS

FL. POPESCU

Institut de Chimie Macromoléculaire « P. Poni », 41 A, Aleea Gr. Ghica Vodă, Jassy

Reçu le 12 mars 1968

Par la phosphorylation du polystyrène dissous en trichlorure de phosphore on obtient trois produits différents : polystyrène phosphorylé soluble en trichlorure de phosphore et chloroforme ($P < 3\%$), polystyrène phosphorylé soluble en solutions aqueuses d'hydroxydes, de carbonates et d'acétates de natrium et de potassium ($P > 6,5\%$) et polystyrène insoluble réticulé par le phosphore. On peut modifier le rapport quantitatif entre les produits obtenus, en modifiant le temps de réaction, le poids moléculaire du polystyrène et la quantité de trichlorure d'aluminium utilisée.

INTRODUCTION

La phosphorylation des copolymères insolubles afin d'obtenir des échangeurs d'ions [2–4] peut être réalisée facilement. La synthèse des polymères phosphorylés solubles est difficile à cause de la polyvalence du phosphore, qui unit aisément les chaînes en formant des mailles. Les polymères ainsi réticulés par le phosphore sont insolubles.

L'insolubilisation peut être évitée seulement dans quelques cas, par exemple en faisant réagir l'oxychlorure de phosphore avec l'alcool polyvinylique en présence de l'urée,[5] ou en protégeant les groupements —OH du phosphore par estérification.[6]

Dans un travail précédent [1] nous avons constaté qu'il se forme du phosphore diarylé dans le copolymère insoluble styrène-divinylbenzène soumis à la phosphorylation.

Dans le présent travail nous avons étudié la phosphorylation du polystyrène avec le trichlorure de phosphore, afin d'établir la teneur en phosphore des produits phosphorylés solubles, ainsi que les conditions de l'insolubilisation du polystyrène phosphorylé.

---

[1] Ire partie Fl. Popescu, *Rev. Roumaine Chim.*, **13**, 1061 (1968).

[2] E. V. Trostianskaia, Lu-Sian-Jao, A. S. Tevlina et I. P. Losev, *Vysokomol. Soedinenya*, **3**, 41 (1961).

[3] K. Lohs (to VEB Farbenfabrik Wolfen), Pat All. (Est), 11 083, 22 déc. 1954 ; *Chem. Abstr.*, **53**, 614a (1959).

[4] J. I. Bergman (to National Aluminate Corp), U.S. Pat. 2, 911, 378, 3 nov. 1959 ; *Chem. Abstr.*, **54**, 3795h (1960).

[5] G. C. Daul, J. D. Reid et R. M. Reinhardt, *Ind. Eng. Chem.*, **46**, 1042 (1954).

[6] J. R. Rafikov, G. N. Chelnokova et G. M. Dzhilbaeva, *Izvest. Akad.* Nauk. S.S.S.R. Otdel. khim. Nauk, **1967**, 1167.

A cette fin nous avons phosphorylé le polystyrène ayant un poids moléculaire de 20 000, 36 000 et 147 000, obtenu par polymérisation radicalique (polystyrène R) avec le trichlorure de phosphore, en présence du trichlorure d'aluminium. Nous avons constaté qu'il résulte un produit phosphorylé ($P < 3\%$), soluble en trichlorure de phosphore et dans les solvants spécifiques du polystyrène, un produit soluble en hydroxydes, carbonates et acétates de sodium ou de potassium et aussi un produit insoluble réticulé par le phosphore.

La polymérisation cationique du styrène (polystyrène K) sous l'action du trichlorure d'aluminium donne des produits de petit poids moléculaire (700—1 800).[7,8] Leur phosphorylation mène aussi à une quantité de produit insoluble.

RÉSULTATS

Pour constater si la nature du trichlorure d'aluminium et son mode de dispersion dans le trichlorure de phosphore peuvent modifier la quantité du produit insolubilisé nous avons effectué des synthèses avec le trichlorure d'aluminium brut et sublimé dispersé à 20° et à 60° en trichlorure de phosphore (synthèses A—D, tableau 1).

En maintenant le même rapport molaire $AlCl_3$: styrène et le même temps de réaction dans toutes les synthèses, la quantité de produit phosphorylé insoluble en trichlorure de phosphore décroît de A à D (tableau 1).

Tableau 1

La solubilité dans le trichlorure de phosphore et le chloroforme du polystyrène de poids moléculaire 36 000, phosphorylé, en fonction de la nature du trichlorure d'aluminium utilisé et de la température à laquelle on a mélangé les réactants. Durée des synthèses 3 heures. Rapport molaire des réactants : $PCl_3 : AlCl_3$: polystyrène (unité structurelle) = 13 : 1, 1 : 1

N°	Synthèse	Nature du trichlorure d'aluminium	Température	Soluble %	Insoluble %
1	A	brut	20°	1,3	98,7
2	A	brut	20°	1,6	98,4
3	B	sublimé	20°	79,8	20,2
4	B	sublimé	20°	79,2	20,8
5	C	brut	60°	80,2	19,8
6	C	brut	60°	76,0	24,0
7	D	sublimé	60°	86,5	13,5
8	D	sublimé	60°	85,8	14,2

Si l'on utilise le trichlorure d'aluminium brut dispersé à 20° en trichlorure de phosphore, le polystyrène phosphorylé obtenu est presque totalement insoluble.

---

[7] D. O. JORDAN et A. R. MATHIESON, *J. Chem. Soc.*, **1952**, 611.

[8] D. O. JORDAN et A. R. MATHIESON, *J. Chem. Soc.*, **1952**, 621.

En utilisant le trichlorure d'aluminium sublimé ou le trichlorure d'aluminium brut dispersé à 60° en trichlorure de phosphore, la quantité du produit insoluble obtenue diminue.

La teneur en phosphore du produit soluble en trichlorure de phosphore ne dépasse pas 3% (tableau 2).

Tableau 2

Teneur en phosphore
Synthèses A – D

N°	Synthèse	Solubilité dans le trichlorure de phosphore	P%	G%*
1	A	soluble	1,8	9,8
		insoluble	7,6	41,0
2	A	soluble	1,6	8,6
		insoluble	7,3	39,6
3	B	soluble	2,6	13,9
		insoluble	8,5	45,8
4	B	soluble	2,6	14,1
		insoluble	8,9	48,2
5	C	soluble	2,1	11,4
		insoluble	8,6	46,6
6	C	soluble	3,0	10,8
		insoluble	9,6	52,0
7	D	soluble	2,5	13,6
		insoluble	9,2	49,9
8	D	soluble	2,8	15,2
		insoluble	9,7	52,6

* G% = degré de phosphorylation.

La quantité de polymère insolubilisée augmente si l'on utilise des quantités grandissantes de trichlorure d'aluminium sublimé (fig. 1). La teneur en phosphore des fractions insolubles en trichlorure de phosphore augmente en fonction de la quantité de trichlorure d'aluminium utilisée (fig. 2).

En étudiant la variation de la teneur en phosphore en fonction de la durée de la synthèse (fig. 3), on constate dans le cas des produits insolubles une augmentation marquée dans les 90 premières minutes. Dans le cas des produits solubles en trichlorure de phosphore la variation du contenu en phosphore est insignifiante.

Le polymère phosphorylé soluble en trichlorure de phosphore ($P < 3\%$) est aussi soluble dans les solvants dans lesquels se dissout le polystyrène comme, par exemple, le chloroforme, le dichloréthane, le benzène, le toluène, etc.

Dans la figure 4, est donnée la variation de l'insoluble dans le trichlorure de phosphore en fonction de la durée de la synthèse.

On constate que le polystyrène au poids moléculaire de 20 000, soumis à la phosphorylation, est plus vite insolubilisé que le polystyrène ayant un poids moléculaire de 147 000.

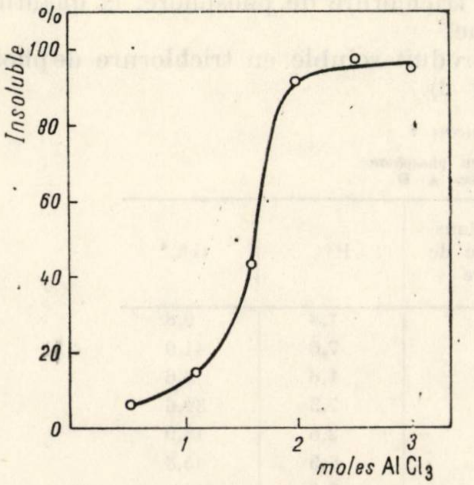

Fig. 1. — Variation de la quantité de polystyrène phosphorylé insoluble dans le trichlorure de phosphore en fonction de la quantité de trichlorure d'aluminium sublimé.

t° initiale = 60. Durée des synthèses = 3 heures. Poids moléculaire du contenu en phosphore = 36 0000.

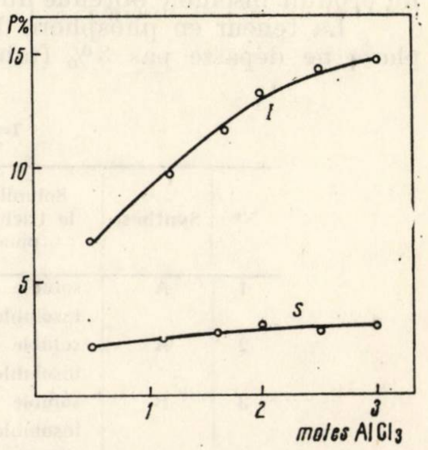

Fig. 2. — Variation de la teneur en phosphore en fonction de la quantité de trichlorure d'aluminium sublimé.

S = polystyrène phosphorylé soluble; I = polystyrène phosphorylé insoluble dans le trichlorure de phosphore.

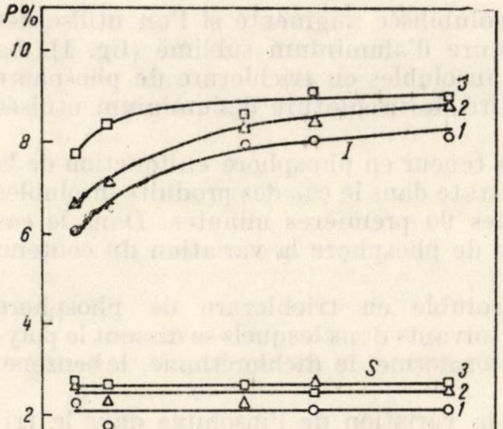

Fig. 3. — Variation de la teneur en phosphore en fonction de la durée de la synthèse.

S = polystyrène phosphorylé soluble; I = polystyrène phosphorylé insoluble dans le trichlorure de phosphore.
Rapport molaire : PCl_3 : $AlCl_3$ (sublimé) : polystyrène (unité structurelle) = 13 : 1,1 : 1. t° initiale = 20 t° ; Poids moléculaire du polystyrène *1*, = 20.000; *2*, = 36 000; *3*, = 147 000

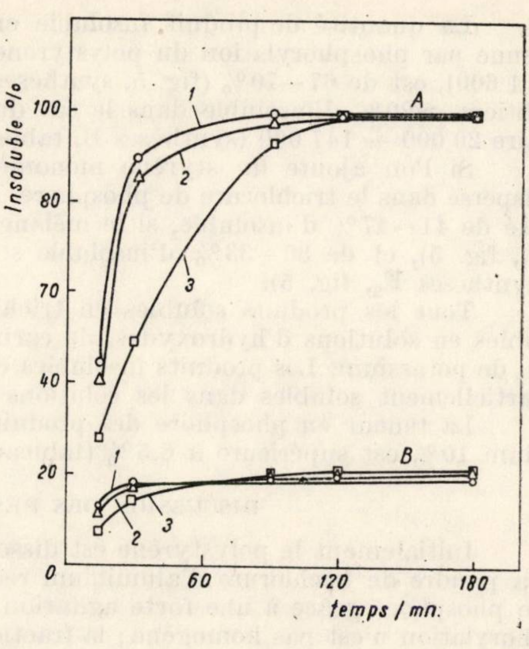

Fig. 4. — Variation de la quantité d'insoluble dans le trichlorure de phosphore en fonction de la durée de la synthèse.

A, synthèses avec le trichlorure d'aluminium brut ; *B*, synthèses avec le trichlorure d'aluminium sublimé ; Rapport molaire : PCl_3 : $AlCl_3$: polystyrène (unité structurelle) = 13 : 1, 1 : 1. t°initiale = 20°. Poids moléculaire du polystyrène *1*, = 20 000 ; *2*, = 36 000 ; *3*, = 147 000.

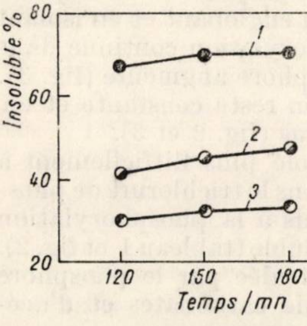

Fig. 5. — Quantités d'insoluble dans le trichlorure de phosphore, obtenues dans le cas des synthèses réalisées en partant du système monomère.

1, synthèses E : *2*, synthèses F_1 ; *3*, synthèses F_2 Rapport molaire : PCl_3 : $AlCl_3$(sublimé) : styrène = 13 : 1,2 : 1.

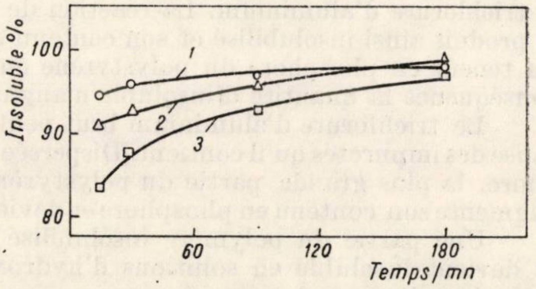

Fig. 6. — Quantités d'insoluble dans le trichlorure de phosphore, restées insolubles dans le carbonate de sodium 10 %. Poids moléculaire du polystyrène :

1, 20 000 ; *2*, 36 000 ; *3*, 147 000. Les quantités (%) obtenues, d'insoluble initial se trouvent dans la figure 4 (B).

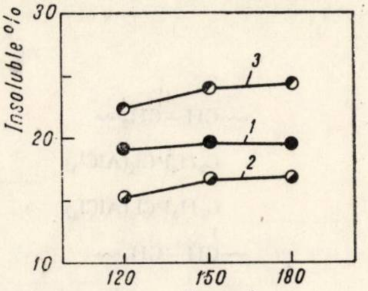

Fig. 7. — Les quantités d'insoluble dans le trichlorure de phosphore, restées insolubles dans le carbonate de sodium 10 %.

1, synthèses E ; *2*, synthèses F_1 ; *3*, synthèses F_2.

La quantité de produit insoluble en trichlorure de phosphore, obtenue par phosphorylation du polystyrène K (poids moléculaire inférieur à 1 600), est de 67–70% (fig. 5, synthèses E) dans des conditions où l'on obtient ≈20% d'insoluble dans le cas du polystyrène de poids moléculaire 20 000 – 147 000 (synthèses B, tableau 1).

Si l'on ajoute du styrène monomère au trichlorure d'aluminium dispersé dans le trichlorure de phosphore, la synthèse conduit à une quantité de 41–47% d'insoluble, si le mélange a été réalisé à 20° (synthèses F_1, fig. 5), et de 30–33% d'insoluble si le mélange a été réalisé à 60° (synthèses F_2, fig. 5).

Tous les produits solubles en trichlorure de phosphore sont insolubles en solutions d'hydroxydes, de carbonates et d'acétates de sodium ou de potassium. Les produits insolubles en trichlorure de phosphore sont partiellement solubles dans les solutions mentionnées (fig. 6 et fig. 7).

La teneur en phosphore des produits solubles en carbonate de sodium 10% est supérieure à 6,5% (tableau 3).

DISCUSSION DES RÉSULTATS

Initialement le polystyrène est dissous en trichlorure de phosphore. La poudre de trichlorure d'aluminium reste dispersée dans le trichlorure de phosphore grâce à une forte agitation. Pendant la synthèse, la phosphorylation n'est pas homogène ; la fraction du polystyrène dans laquelle le contenu en phosphore a dépassé 3% précipite en englobant et en isolant le trichlorure d'aluminium. La réaction de phosphorylation continue dans le produit ainsi insolubilisé et son contenu en phosphore augmente (fig. 3). La teneur en phosphore du polystyrène en solution reste constante et en conséquence la quantité d'insoluble n'augmente plus (fig. 2 et 3).

Le trichlorure d'aluminium brut peut être isolé plus difficilement à cause des impuretés qu'il contient. Dispersée à 20° dans le trichlorure de phosphore, la plus grande partie du polystyrène soumis à la phosphorylation augmente son contenu en phosphore et devient insoluble (tableau 1 et fig. 2).

Une partie du polymère insolubilisé est réticulée par le phosphore et devient insoluble en solutions d'hydroxydes, de carbonates et d'acétates de sodium et de potassium.

Les réactions sont

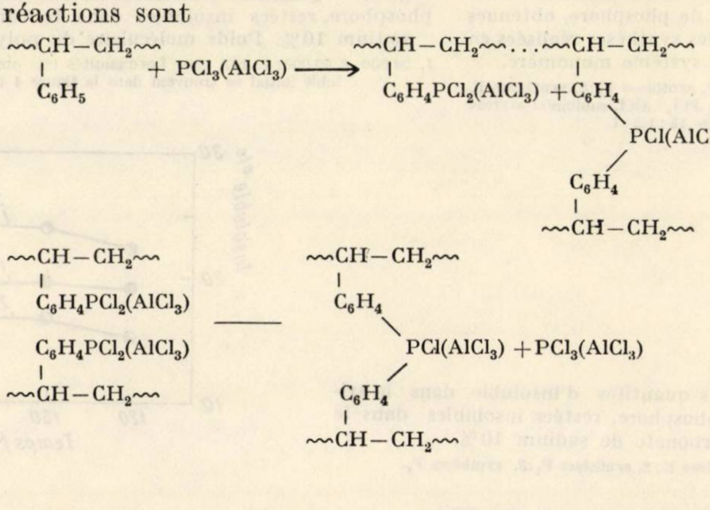

Dans les produits hydrolysés on trouve l'acide phosphoreux

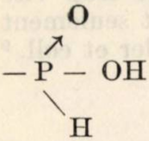

$-\underset{\diagdown H}{\overset{O\nearrow}{P}}-OH$

et l'acide phosphineux

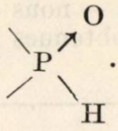

$\diagdown\underset{\diagup\ \diagdown H}{\overset{\nearrow O}{P}}$.

Les spectres en IR des polymères phosphorylés confirment l'existence du phosphore diarylé dans le cas des produits insolubles. Ainsi nous pouvons constater dans le cas du polystyrène phosphorylé, insoluble dans le carbonate de natrium 10% (spectre *a*, fig. 8), la présence de la vibration $P \rightarrow O$ (réticulé) qui se superpose à la vibration PO_2^- asymétrique entre 1120–1230 cm^{-1}, en donnant une bande commune intense. La vibration symétrique PO_2^- est plus atténuée à 1100 cm^{-1} .La vibration P–O–(H) est très visible entre 909–1040 cm^{-1} mais elle est moins intense que la bande 1120–1230 cm^{-1}.

Dans le cas du polystyrène phosphorylé soluble dans le carbonate de natrium 10%, la bande attribuée au groupement P–O–(H) est la plus marquée (spectre *b*, fig. 8).

Dans le cas du polystyrène phosphorylé soluble en trichlorure de phosphore, les bandes attribuées aux liaisons du phosphore sont plus atténuées à cause de la teneur en phosphore réduite ($P < 3\%$). La bande 909–1040 cm^{-1} attribuée au groupement P–O–(H) est prédominante (spectre *c*, fig. 7).

Avec les données fournies par l'analyse des produits phosphorylés contenant des groupements phosphoneux et phosphineux nous pouvons calculer le rapport O/P.

Théoriquement le rapport O/P a la valeur 1,03 dans le cas du polystyrène contenant seulement du phosphore monoarylé et 0,52 au cas où il existe seulement du phosphore diarylé. Nous constatons que pour les produits insolubles, le rapport O/P est inférieur à 0,86, indiquant ainsi l'existence du phosphore diarylé (tableau 3). Dans le cas du polystyrène K,

Tableau 3

Le phosphore (%) et le rapport O/P

Solubilité	Polystyrène R			Polystyrène K	
	Synthèse	P%	O/P	Synthèse	P%
Insoluble	1	7,03	0,86	1	7,0
	2	9,81	0,83	2	9,6
	3	13,20	0,78	3	9,9
	4	14,66	0,79		
Soluble en CO_3Na_2 10%	1	8,05	1,05	1	6,5
	2	9,20	1,01	2	9,7
				3	10,0
Soluble en PCl_3	1	2,17	1,07	1	1,8
	2	2,50	1,08	2	3,0
	3	2,94	1,05	3	2,8
	4	2,95	1,02		

à cause des difficultés d'analyse — les substances brûlent trop vite dans le tube de combustion — nous donnons comparativement seulement les valeurs en phosphore obtenues par la méthode de Ziegler et coll. [9] (tableau 3).

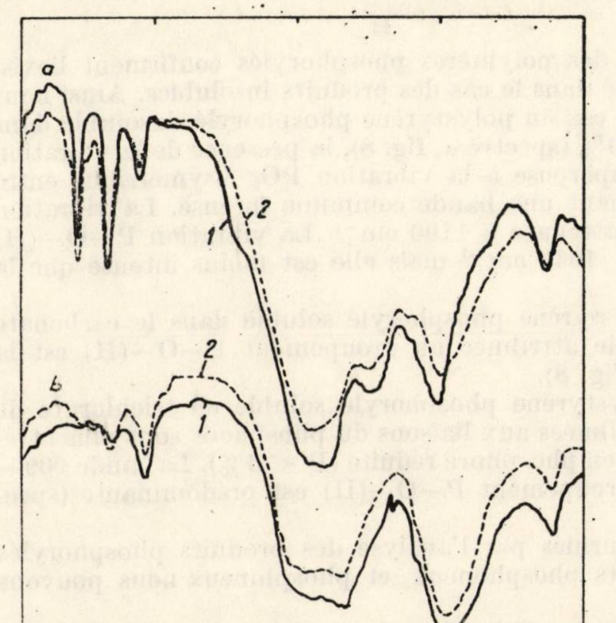

Fig. 8. — Spectres en IR du polystyrène phosphorylé :
1, polystyrène R ; *2*, polystyrène K ;
a, polystyrène phosphorylé insoluble ;
b, polystyrène phosphorylé soluble dans les solutions de carbonate de sodium ;
c, polystyrène phosphorylé soluble dans le chloroforme.

En conclusion, nous constatons que la phosphorylation du polystyrène dissous en trichlorure de phosphone mène aux produits qui diffèrent par leur teneur en phosphore et par la nature des solvants dans lesquels ils sont dissous et aussi à une quantité de polystyrène phosphorylé insoluble, réticulé par le phosphore.

---

[9] K. Ziegler, H. Till et H. Schindlbauer, *Microchim. Acta*, **1963**, 1144.

Les synthèses dans lesquelles on utilise des quantités de trichlorure d'aluminium supérieures à 2 M $AlCl_3$ pour 1 mole styrène (polystyrène de poids moléculaire supérieur à 20 000) et le temps de réaction est de trois heures donnent du polystyrène phosphorylé insoluble avec une teneur élevée en phosphore, dans une proportion d'approximativement 97%.

PARTIE EXPÉRIMENTALE

Phosphorylation du polystyrène R

Synthèse avec le trichlorure d'aluminium brut et sublimé, dispersé à 20° dans le trichlorure de phosphore (*synthèse A—B*) : Dans un ballon de 250 ml à trois tubulures, muni d'un agitateur, d'un réfrigérant à reflux et d'un tube contenant du chlorure de calcium anhydre, on introduit 0,1 moles polystyrène en solution dans 1,3 moles trichlorure de phosphore. En agitant, on ajoute ensuite par petites portions 0,11 moles trichlorure d'aluminium en poudre. Cette opération est réalisée à 20°. Le mélange est porté à l'ébullition pendant trois heures.

Synthèses avec le trichlorure d'aluminium brut et sublimé, dispersé à 60° dans le trichlorure de phosphore (*synthèses C—D*) : Dans un ballon de 250 ml à trois tubulures muni d'un réfrigérant à reflux, d'un agitateur, d'une ampoule à brome et d'un tube contenant du chlorure de calcium anhydre, on chauffe 0,6 moles trichlorure de phosphore à 60°. On ajoute par petites portions et sous une forte agitation 0,11 moles trichlorure d'aluminium. On continue l'agitation et on ajoute goutte à goutte une solution de 0,1 moles polystyrène dissous en 0,6 moles trichlorure de phosphore. On lave l'ampoule à brome au trichlorure de phosphore 0,1 moles. Le mélange est porté à l'ébullition pendant trois heures.

Polymérisation cationique du styrène

L'installation utilisée comporte un ballon de 300 ml à trois tubulures, muni d'un réfrigérant à reflux, d'un agitateur, d'une ampoule à brome, d'un tube contenant du chlorure de calcium anhydre, et d'une entrée d'azote. Le ballon est refroidi à l'extérieur par alcool éthylique, maintenu à 0° à l'aide d'un ultrathermostat.

Pour réaliser consécutivement et dans la même installation la phosphorylation du polymère obtenu par voie cationique, on a remplacé le tétrachlorure de carbone, utilisé comme diluant pour le styrène monomère par Jordan et Mathieson,[7] par l'éther de pétrole.

La synthèse a été effectuée de la manière suivante : on introduit 0,12 moles trichlorure d'aluminium sublimé dans le ballon sous 60 ml d'éther de pétrole. On purge l'installation avec l'azote et sous une forte agitation on ajoute, goutte à goutte, 0,1 moles styrène monomère.

La réaction est fortement exothermique. La présence de l'éther de pétrole évite l'élévation de la température au-dessus de son point d'ébullition. On laisse refroidir le contenu du ballon. Le produit obtenu est insoluble dans l'éther de pétrole.

Phosphorylation du polystyrène obtenu par polymérisation cationique (synthèses E) : Au produit obtenu par polymérisation cationique et dans la même installation on ajoute en agitant 1,3 moles trichlorure de phosphore. On chasse l'éther de pétrole par distillation et on porte ensuite à l'ébullition pendant trois heures.

Synthèses en partant d'un mélange de trichlorure de phosphore, de trichlorure d'aluminium et de styrène monomère (synthèses F) : Dans la même installation on introduit successivement et en agitant 1,3 moles trichlorure de phosphore, 0,1 moles styrène monomère et 0,12 moles trichlorure d'aluminium sublimé. Le mélange des réactants a été réalisé à 20° (synthèses F_1) et à 60° (synthèse F_2).

Les réactions ne sont pas violentes.

On porte à l'ébullition pendant trois heures.

Traitement et analyse des produits obtenus

On verse le contenu du ballon dans un verre contenant 300—350 ml alcool méthylique. Le verre est refroidi par un mélange de glace — eau. Après filtration les produits sont broyés, lavés à l'acide chlorhydrique 10% et ensuite à l'eau jusqu'à neutralité. Les produits ainsi lavés et hydrolysés ne contiennent plus d'aluminium et ne laissent pas de résidu à la calcination.

Les produits phosphorylés ayant $P < 3\%$ sont séparés par extraction en chloroforme et reprécipités en alcool méthylique.

Les produits phosphorylés insolubles dans le chloroforme sont traités avec du carbonate de sodium 10% et les produits dissous sont précipités par acide chlorhydrique 10% et lavés à l'eau jusqu'à neutralité.

Tous les produits ont été séchés sous vide, en présence du chlorure de calcium, à 25°.

Les produits contiennent du phosphore ^{III} ; ils ont un pouvoir réducteur sur l'acétate mercurique et les courbes de titrage potentiométrique présentent une seule inflexion.

L'analyse élémentaire a été réalisée d'après Papay et Mazor[10] et les valeurs en phosphore ont été contrôlées selon la méthode de Ziegler et coll.[9]

Les spectres en IR ont été interprétés d'après Thomas et Chittenden.[11, 12]

Les viscosités intrinsèques déterminées pour les produits solubles F dans le dichloréthane à 25° varient de 0,04 à 0,055.

La couleur des produits séchés et purifiés est blanche.

---

[10] M. Papay et L. Mazor, *Microchim. Acta*, **1967**, 269.

[11] L. C. Thomas et R. A. Chittenden, *Chem. and Ind.*, **1961**, 1913.

[12] L. C. Thomas, *Chem. and Ind.*, **1957**, 198.

Revue Roumaine de Chimie, **14**, 1535–1542 (1969)

KOORDINATIONSPOLYMERE MIT BIS (AMINOCARBOXYLSÄUREN). I

ÜBER DIE REAKTION DER BENZIDINDICARBOXYLSÄURE MIT Cd-, Zn-, Cu-, Ni- UND Mn-SALZEN

I. GABE und DEMETRA LEONTE

Institut für makromolekulare Chemie „P. Poni”, Iaşi, Aleea Gr. Ghica-Vodă 41 A

Eingegangen am 20. Januar 1969

Es werden Koordinationspolymere, die bei der Reaktion zwischen Benzidindicarboxylsäure und Acetat oder Chlorid des Übergangmetalls entstehen, beschrieben. Das Molekulargewicht der erhaltenen Verbindungen kann durch Markierung mit Radioisotopen bestimmt werden. Die Ausbildung einer Donator-Acceptorbindung zwischen dem Stickstoffatom der Aminogruppe und dem Metallion hat eine Verkleinerung des Valenzwinkels HNH zur Folge und wirkt sich auch auf die Kraftkonstanten der N — H-Bindungen aus. Die empirische Gleichung von Bellamy und Williams zur Berechnung der symetrischen NH-Schwingung ergibt Werte die besser mit den experimentellen übereinstimmen, als im Falle der entsprechenden Verbindungen der Anthranilsäure.

In den letzten Jahren erschienen eine große Zahl von Arbeiten die sich mit der Darstellung von Koordinationspolymeren aus bi- und polyfunktionellen Liganden und den entsprechenden Metallionen befassen. In solchen Polymeren, die durch einen Polykoordinationsprozeß entstehen, besteht die hochmolekulare Kette aus einer Reihenfolge alternierender organischer Einheiten und koordinierter Metallione. Es kamen sehr verschiedene Liganden zur Anwendung : bifunktionelle organische Säuren, β-Diketone,[1] Diamine, Polyaminochinone,[2] Naphthazarine und bis (Salicylaldehyde)[3] α-Aminosäuren,[4] bis (Aminophenole),[5] bis (Hydroxysäuren),[6] poly (4-Vinylphthalsäure)[7] u.a.

---

[1] M. T. Teyssie und P. Teyssie, *J. Polymer Sci.*, **50**, 235 (1961).

[2] R. C. DeGeiso, L. G. Donaruma und A. E. Tomic, *J. Org. Chem.*, **27**, 1424 (1962).

[3] B. P. Block "Encyclopedia of Polymer Science and Technology", Bd. 4, Ed. by H. F. Mark, Interscience Publishers, N. Y., 1966, S. 163.

[4] J. R. Elliot, Thesis, Univ. of Illinois, Urbana Illinois, 1943.

[5] M. L. Judd, Doctoral Dissertation, Univ. of Illinois, Urbana Illinois, 1958.

[6] J. A. Mc Lean, Jr., *Diss. Abstr.*, **20**, 3065 (1960).

[7] E. C. Winslow und A. Leferriere, *J. Polymer Sci.*, **61** 65 (1962).

In der vorliegenden Arbeit beschreiben wir Verbindungen, die bei der Reaktion zwischen Benzidindicarboxylsäure und Salzen zweiwertiger Metalle entstehen.

Wenn man zu einer Lösung von Benzidindicarboxylsäure in DMF eine Cadmiumacetatlösung in DMF hinzufügt und auf dem Wasserbade erwärmt so fällt nach einiger Zeit eine Verbindung aus, die nach Filtration und Trocknung auf 110° ein feines, graues, in Wasser und organischen Lösungsmitteln unlösliches Pulver ergibt. Die Verbindung besitzt keinen Schmelzpunkt und zersetzt sich über 300°.

Tabelle 1

Farbe, Elementaranalyse und Zersetzungstemperaturen der dargestellten Verbindungen

Nr.	Verbindung Bruttoformel	Farbe	M %		N %		C %		H %		Zersetzungstemperatur °C
			gef.	*ber.*	*gef.*	*ber.*	*gef.*	*ber*	*gef.*	*ber*	
1	$[C_{14}H_{10}N_2O_4Cd]_n$	grau	29,50 29,55	29,30	7,36	7,32	43,38	43,67	2,85	2,60	340
2	$[C_{14}H_{10}N_2O_4Zn]_n$	grau	19,45 19,60	19,48	8,40	8,34	49,22	50,05	2,83	2,97	310
3	$[C_{14}H_{10}N_2O_4Cu]_n$	dunkelgrün	18,95 19,04	19,03	8,37	8,38	48,92	50,33	4,02	3,59	230
4	$[C_{14}H_{10}N_2O_4Ni]_n$	dunkelgrau	17,72 17,88	17,84	8,47	8,51	50,43	51,07	3,54	3,04	330
5	$[C_{14}H_{10}N_2O_4Mn]_n$	dunkelbraun	16,80	16,89	8,56	8,61	51,60	51,66	3,74	3,68	310
6	$C_{14}H_{12}N_2O_4$	hellgrün			10,32	10,29	61,65	61,75	4,46	4,44	210
7	$C_{16}H_{16}N_2O_4$				9,28	9,40					
8	$[C_{16}H_{14}N_2O_4Cd]_n$	grau			6,70	6,82					

$C_{14}H_{12}N_2O_4$ = Bezidindicarboxylsäure (*L*)
$C_{16}H_{12}N_2O_4$ = N, N′-Dimethylbezidindicarboxylsäure (*LMe*)

Auf gleicher Weise lassen sich die Verbindungen mit Zn, Mn, Ni und Cu darstellen.

Wenn man vom Na-Salz der Benzidinsäure ausgeht so kann man die Endprodukte durch Ausfällen in wässerigen Lösungen erhalten.

In Tabelle 1 sind diese Verbindungen, wie auch die Ergebnisse der Elementaranalysen zusammengefaßt.

Die Analysen weisen auf ein Verhältnis $M/L = 1$ hin, egal ob die Fällung in DMF, oder in wässeriger Lösung erfolgte. Wir können also annehmen, daß bei den oben erwähnten Reaktionen Verbindungen vom Typus $[ML]_n$ entstehen, wo $[ML]$ die Struktureinheit in der hochmolekularen Kette bedeuten soll. Die Bildung solcher Verbindungen erscheint möglich da die Benzidindicarboxylsäure ein vierzähniger Ligand ist und so die Möglichkeit besitzt, an beiden Enden je ein Metallion zu binden.

Bei der Entstehung solcher makromolekularer Ketten ist es von Bedeutung die Endgruppen zu charakterisieren.

Wie bereits erwähnt wurde, lassen sich in wässerigen Lösungen die Verbindungen aus den Chloriden der Metalle darstellen. Auf diesem Wege gelang es uns die Endgruppen und das Molekulargewicht der Koordinationspolymeren zu bestimmen. Unsere Ergebnisse weisen darauf hin.

daß bei der obengenannten Fällung, ausgehend vom Natriumsalz des Liganden Na_2L und einem Überschuß an Metallchlorid, die erhaltenen Verbindungen der folgenden Formel entsprechen

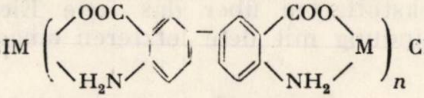

Die genaue Bestimmung des Polymerisationsgrades n ist bei gänzlich unlöslichen Koordinationspolymeren nur schwer möglich. Wir wendeten die von Terentiev und Mitarb.[8] ausgearbeitete Methode an, die eine Molekulargewichtsbestimmung nur dann zuläßt wenn die Endgruppen der Polymeren durch Radioisotope markiert werden können.

Im Falle des Koordinationspolymeren mit Cd und bei der Markierung der Endgruppen mit ^{36}Cl konnten wir den Wert $n \sim 100$ bestimmen.

Korshak und Mitarb.[9] veröffentlichten eine Berechnungsmethode des Polymerisationsgrades, ausgehend von dem Ergebnisse des Metallgehaltes des Koordinationspolymeren.

Bei einem Überschuß an Metallsalz kommt folgende Formel zur Anwendung:

$$M\,\% = \frac{[100(n+1)\,M]}{[nL + (n+1)\,M]} \tag{1}$$

Berechnungen nach Formel (1) führen im Falle von Polymeren mit mittlerem Polymerisationsgrade zu keinen Ergebnissen, die mit den anhand der Radioisotopenmethode erhaltenen übereinstimmen, wenn man nicht auch die Endgruppen in Betracht zieht. Und selbst dann können die so berechneten Molekulargewichte als nur annähernd genau betrachtet werden; eine sehr kleine Streuung der Metallanalysen führt zu sehr großen Veränderungen des nach Formel (1) berechneten Polymerisationsgrades.

Wir haben bei unseren Berechnungen folgende Formel angewendet:

$$M\,\% = \frac{[100\,(n+1)\,M]}{[nL + (n+1)\,M + 2Cl]} \tag{2}$$

Wenn man in Formel (2) die Werte für den Cadmiumgehalt aus Tabelle 1 einsetzt, so erhält man für n die Werte 113,4 bzw. 87,5. Der Mittelwert 100,4 fällt mit dem bei den radiochemischen Messungen erhaltenen zusammen; es ist aber ersichtlich, daß die Streuung der Werte etwa 20% des n-Wertes beträgt.

Um über die Donator-Acceptor-Bindung des Metallions an das Stickstoffatom der Aminogruppe näheres aussagen zu können haben wir die IR-Spektren unserer Verbindungen in KBr-Preßlingen (Konzentration der Proben 0,5%) und in Nujol aufgenommen. Die Ergebnisse dieser Untersuchungen sind in Tabelle 2 wiedergegeben, wo auch die Zuordnung der Absorptionsbanden, in der letzten Spalte verzeichnet ist.

---

[8] A. P. TERENTIEV, E. G. RUKHADZE und V. V. RODE, *Vyssokcmol. Soedineniya*, **4**, 821 (1962).

[9] V. V. KORSHAK, E. S. KRONGAUZ, A. M. SLADKOV, E. V. SHEINA und L. K. LUNEVA, *Vyssokomol, Soedineniya*, **1**, 1764 (1959).

An der Bildung der polymeren Chelate nehmen die aktiven Gruppen des Liganden teil, und zwar die Carboxylgruppen, bei denen das Wasserstoffatom durch das zweiwertige Metallion ersetzt wird, und die Aminogruppen, deren Stickstoffatom über das freie Elektronenpaar in eine Donator-Acceptor-Bindung mit dem letzteren eingeht.

Tabelle 2

Absorptionsbanden des Liganden *L*, des methylierten Liganden *L*Me und der Koordinationspolymeren mit Cd, Zn, Cu, Ni und Mn

L cm^{-1}	*L*Me cm^{-1}	Zuordnung	−Cd cm^{-1}	−Zn cm^{-1}	−Cu cm^{-1}	−Ni cm^{-1}	−Mn cm^{-1}	Zuordnung
3496 m	—	NH *as*	3441 m	—	3439 m	3405 m	3430 s	NH_2 *as*
3380 m	3375 m	NH *s*	3318 m	3255 m	3221 m	3225 m	3230 m	
			3260 m	3210 m	3145 m	3180 m	3220 s	NH_2 *s*
						3128 s	3133 m	
3009 St	3009 St	C−H	3020 s	3020 s	3020 s.s	3005 ss	3020 ss	CH Arom.
	2980 St	C−H	2902 s	2902 s	2900 s	2900 Sh.	2902 s	CH
2816 m	2800 St	C−H	2820 s	2818 s				
2720 m	2720 m							
2620 m	2620 m	COO^-						
	2550 m							
1672 St	1660 St	C = 0						
1624 St	1620 Sh	NH Def						
			1603 St	1618 St	1608 St	1610 St	1611 St	C=C Arom.
1582 St	1570 St	C = C Ar.	1570 St	1580 St	1585 St	1580 St	1580 m	COO^-
1560 St	1520 m	NH sciss.	1550 St	1545 Sh	1545 ste	1545 st	1550 st	NH sciss.
1492 m	1492 Sh	C = C Ar.	1480 m	1482 m	1487 m	1492 m	1490 m	C=C Arom.
	1440 m	CH_3	1435 ss	1440 ss		1435 Sh	1410 m	CH
	1420 m	CH_3						
1342 m	1340 Sh	CH	1385 St	1385 St	1400 St	1405 St	1385 m	COO^- *as*
1308 Sh			1340 m	1355 St	1360 St	1390 Sh		CN
1300 m	1305 m	CN	1310 Sh	1310 Sh		1380 Sh		
1232 St	1240 St	C−O	1260 m	1280 s	1285 s	1276 s		C−O
1220		OH	1225 s	1230 ss	1232 s	1240 s	1240 s	
1160 s	1180 m	CH	1165 s		1178 s	1178 s	1175 s	CH
1154 s	1140 m	CH		1155 St				C−O−M
					1135 St			C−O−M
1120 s		CH		1135 s		1105 Sh	1100 ss	CH
1060 s	1095 s	CH		1090 m	1095 s	1095 Sh		CH
						1050 St		C−O−M
				1050m	1042 s			CH
			1000 St				995 St	C−O−M
980 m		NH_2 Def.						
920 m	920 m	CH				903 s	908 m	CH
890 m		CH	890 s	875 m	882 s	880 m	875 m	CH
			865 m					
830 s		NH_2 rock	810 m	820 m	825 s	835 St	838 St	NH_2rock. ?
818 m	820 m	CH	797 s	800 s	805 Sh	810 Sh	808 m	CH
795 s	795 m	CH	718 s	720 s	722 s	729 s	738 s	CH
690 m		CH	685 s	695 m	670 s	670 s	693	CH

ss – sehr schwach, s – schwach, m – medium, St – stark, Sh – Schulter

Es ist bekannt, daß die Aminogruppe eine positivierende Wirkung ausübt, während die Carboxylgruppe negativierend wirkt und zu einer

Erhöhung der Basizität der Aminogruppe führen muß. Wenn wir noch das Vorhandensein eines Gleichgewichtes

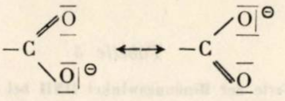

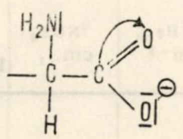

in Betracht ziehn, so ist ein positivierender Einfluß wahrscheinlich von geringer Bedeutung.

Der Metall-Sauerstoffbindung können wir keinen ionischen Charakter zuschreiben. Dies geht besonders anschaulich aus der Lage der Absorptionsbande der C—O-Schwingung hervor. Die Frequenzen dieser Schwingung liegen um 70—220 cm $^{-1}$ niedriger als die entsprechenden im Spektrum des Liganden ($\sim$1232 cm $^{-1}$).

Von Interesse ist auch das Gebiet der Streckschwingungen der Aminogruppe. Es ist bekannt,[10,11] daß die Ausbildung einer Donator-Acceptor-Bindung zum Stickstoffatom der Aminogruppe eine bedeutende Verschiebung dieser Schwingung in Richtung niederer Frequenzen zur Folge hat. Wenn Komplexverbindungen mit Aminogruppen entstehen, so kann man häufig an Stelle von zwei Banden, mehrere Banden, deren Lage von den Liganden und vom komplexierten Metallion abhängt beobachten.[12] Durch das Auftreten einer Fermi-Resonanz die sich mit einer, durch Wasserstoffbrückenbindung entstehenden Verschiebung der NH_2-Schwingung, überlagert, werden die Spektren noch komplizierter. Um die Absorptionsbanden auswerten zu können muß allen diesen Einflüssen Rechnung getragen werden. Durch Methylierung am Stickstoffatom der Aminogruppe und Darstellung der entsprechenden Chelatpolymeren wurde es möglich die genaue Lage der NH-Schwingungen festzulegen. Aus den Verschiebungen der entsprechenden Banden konnten sowohl die Kraftkonstanten der NH-Bindungen als auch die Valenzwinkel HNH berechnet werden.[13]

Die Ergebnisse für die in vorliegender Arbeit besprochenen Koordinationspolymeren, wie auch für einige Modellsubstanzen, verglichen mit Literaturangaben, sind in Tabelle 3 zusammengefaßt.

Durch das Auftreten einer N—M-Bindung wird der Bindungswinkel HNH von 120° bei der freien Säure auf 100° bei dem Polymeren mit Zn verkleinert. Mit Ausnahme des Cd-Polymeren befinden sich die Verrin-

---

[10] L. J. Bellamy und R. L. Williams, *Spectrochim. Acta*, **9**, 341 (1957).

[11] M. S. Barwinok und Ju. S. Warshawski, *Zhur. neorg. Khim.*, **6**, 851 (1961).

[12] E. J. Duff, *J. Chem. Soc.*, A, **1968**, 434.

[13] G. W. Linnett, *Trans. Faraday Soc.*, **41**, 223 (1945).

gerungen dieses Winkels im umgekehrten Verhältnis zu dem Anstieg der Atomgewichte des Metalls. Die Kraftkonstanten nehmen in entgegengesetzter Richtung ab.

Tabelle 3

Kraftkonstanten und Werte der Bindungswinkel HNH bei den Koordinationspolymeren

Nr.	Verbindung	$\nu_{NH_2\,as}$ cm^{-1}	$\nu_{NH_2\,s}$ cm_{-1}	[10] $\nu_{NH_2\,s}$ Ber cm^{-1}	Δ cm^{-1}	$f.10^5$ dyn/cm	$\widehat{HNH}$	Literatur
1	Ammoniak						106°47′	14
2	Anilin	3432	3353			6,38	111°	15
3	Anilin. Cu $(NO_3)_2.H_2O$	3243	3226			5,80	95°	11
4	Formamid						120°	16
5	Oxamid						125°	17
6	Benzidindicarboxylsäure	3496	3380	3404,5	+24,5	6,55	120°	
7	Cd-Polymere	3318	3260	3248,7	−11,3	5,99	105°	
8	Zn-Polymere	3255	3210	3193	−17	5,78	100°	
9	Cu-Polymere	3221	3145	3163,8	+18,8	5,61	111°	
10	Mi-Polymere	3255	3128	3167	+39	5,59	116°	
11	Mn-Polymere	3230	3130	3175	+45	5,59	117°	
12	Anthranilsäure	3473	3374	3384	+10	6,49	115°	
13	Cadmiumanthranilat	3290	3145	3224	+79	5,73	108°	
14	Kupferanthranilat	3280	3126	3226	+100	5,68		10

Die Zn-Verbindung reiht sich gut in diese Serie ein, obwohl im Falle von Komplexen mit Aminen das Zink eine besondere Stellung unter den Übergangsmetallen einnimmt.[18]

Es muß noch betont werden, daß der Wert des Valenzwinkels HNH bei der freien Säure größer ist als im Falle des Ammoniaks, des Anilins und auch anderer Amine (N,N′-Dimethyl-*p*-phenylen-diamin 109,6°; *p*-Nitroanilin 113,6°).[19] Hingegen ist der von uns auf 120° berechnete Winkel mit dem von Moulton und Kromhout für Formamide gefundene[16] übereinstimmend. In diesem Zusammenhang soll auf die Ähnlichkeit der Amidogruppe mit der Aminosäuregruppe hingewiesen werden. In beiden Fällen müssen auch Wasserstoffbrückenbindungen zur C=O-Gruppe, die sich auf den Wert des Bindungswinkels auswirken können, in Betracht gezogen werden.

Bellamy und Mitarb.[10] konnten eine empirische Gleichung, die die $\nu_{NH_{as}}$- und ν_{NH_s}-Schwingungen verbindet, ableiten. Sie überprüften diese Gleichung an Hand einer großen Zahl von Aminen und fanden eine Übereinstimmung von etwa 4,8 cm^{-1} mit den experimentellen Ergebnissen. Eine große Abweichung wurde im Falle der komplexen Verbindung Kup-

---

[14] G. Herzberg "Molecular spectra and Molecular Structure" Vol. II, D. Van Nostrand Comp. Inc., 1960, S. 438.

[15] N. Fuson, M. L. Josien, R. L. Powell und U. Uterback, *J. Chem. Phys.*, **20**, 145 (1952).

[16] R. Q. Kromhout und W. G. Moulton, *J. Chem. Phys.*, **1955**, 1673; **1956**, 34.

[17] C. Romers, *Acta Cryst.*, **6**, 429 (1953).

[18] H. Irving und R. J. P. Williams, *J. Chem. Soc.*, **1953**, 3129.

[19] P. J. Krueger und D. W. Smith, *Canad. J. Chem.*, **45**, 1605 (1967).

feranthranilat (Tabelle 3) gefunden. Bei den von uns dargestellten Polymeren sind kleinere Abweichungen zu beobachten. Das könnte durch einen geringeren Beitrag der Wasserstoffbrückenbindungen erklärt werden.

Auf die in Tablelle 3 angeführten Ergebnisse zurückkommend muß betont werden, daß es sich nicht um absolute Werte der Valenzwinkel und der Kraftkonstanten handelt. Unsere Werte sind aber mit den Literaturangaben vergleichbar, und in einigen Fällen sogar in sehr guter Übereinstimmung.

Bei der Molekulargewichtsbestimmung wurden die Chloratome der Endgruppen des Cd-Polymeren in Betracht gezogen. Die Gegenwart dieser Chloratome läßt sich außer mit Hilfe der Isotopenanalyse auch infrarotspektroskopisch nachweisen. Zu diesem Zwecke wurden IR-Spektren des Cd-Polymeren unterhalb 400 cm^{-1} aufgenommen und wir konnten eine Absorptionsbande um 265 cm^{-1} beobachten, die wir einer M—Cl -Bindung zuschreiben.[20]

Die Cd-Verbindung nimmt einen besonderen Platz unter den von uns dargestellten Polymeren ein. Ein solches Verhalten des Cadmiums wurde auch schon von anderen Autoren [21] im Falle der Komplexverbindungen mit aromatischen primären Aminen festgestellt und könnte durch die Möglichkeit von Überführung elektronischer Effekte über das Cadmiumatom erklärt werden. Die Tatsache, daß in unserem Falle die NH-Frequenzen bei dem Cd-Polymeren höher liegen als bei den übrigen Polymeren der restlichen Übergangsmetalle ist wohl auf eine Übertragung der Einflüsse der π-Elektronenbindungen über das Cd-Atom hinaus zurückzuführen. Dies müßte dem Cd-Polymeren der diamagnetisch ist, bei höheren Temperaturen Halbleitereigenschaften verleihen, was unseren Bestimmungen nach, auch tatsächlich der Fall ist.

EXPERIMENTELLES

1. *4,4'-Diaminobiphenyl-3,3'-dicarboxylsäure* wurde mit Ausb. 92% aus *o*-Nitrobenzosäure durch alkalische Reduzierung mit NaOH und Zn, und nachfolgender Benzidinumlagerung in Gegenwart von HCl dargestellt.[22] Hellgrünes Pulver. Schmp. 300° Zers.

2. *Darstellung der Polymeren mit Cd, Zn, Cu, Ni, und Mn.* a) Die Metallacetatlg in DMF wird, in einem Überschuß von etwa 10—15% gegenüber der berechneten Menge, auf dem Wasserbade in eine Lg von 0,5 g Benzidindicarboxylsäure in 100 ml DMF unter energischem Rühren eingetragen. Das Ausfällen der Polymeren beginnt nachdem etwa die Hälfte der Acetatlg zugegeben wurde. Nach Absetzen, Auswaschen mit Wasser und Alkohol und Trocknen bei 110° erhält man die Verbindungen als amorphe, farbige feine Pulver, unlöslich in Wasser und in organischen Lösungsmitteln. Sie besitzen keinen Schmelzpunkt und zersetzen sich beim Erhitzen über 300° (Tabelle 1).

---

[20] C. D. Burbridge und D. M. I. Goodgame, *J. Chem. Soc.*, A **1968**, 237.

[21] J. M. Haig, M. A. Van Dam und D. A. Thornthon, *Inorg. Nucl. Chem. Lett.*, **3**, 7 (1967).

[22] H. E. Fierz-David und L. Blangey, "Fundamental Process of Dye Chemistry", Interscience Publishers, N.Y., 1949, S. 164.

b) Zur wässerigen Lg des Natriumsalzes der Benzidindicarboxylsäure (0,5 g) wird unter Erwärmen und ständigem Rühren die Metallchloridlg in einem etwa 10% igen Überschuß zugegeben. Die ausgefällten Verbindungen werden wie oben weiter behandelt.

3. *N, N'-Dimethylbenzidindicarboxylsäure* wurde durch Methylierung am Stickstoffatom der Benzidindicarboxylsäure wie im Falle der Anthranilsäure[23] erhalten. Zu einer konz., wässerigen, schwach alkalischen Lg von Benzidindicarboxylsäure wird ein Überschuß von Dimethylsulfat zugegeben. Es wird eine halbe Std. gerührt und dann eine Std. auf dem Wasserbade stehn gelassen. Nach Abfiltrieren und Auswaschen mit Wasser wird die erhaltene Verbindung unter Erwärmen in Alkohol gelöst und dann, nach Zugabe von Wasser, ausgefällt. Grünes, feines Pulver.

4. *Cadmiumpolymere.* Zu einer wässerigen Lg des Natriumsalzes der Benzidindicarboxylsäure wird bei pH = 7, unter Rühren und Erwärmen eine wässerige Cd^{36} Cl_2-Lg in Überschuß zugegeben.

5. *Die Molekulargewichtsbestimmung* erfolgte durch Ausmessung der Aktivität des Polymeren. Um die Meßfehler so weit als möglich auszuschalten wurde das ^{36}Cl nach Baubigny aufgefangen und in einem Flüssigkeitszählrohr VAZ — 110 V ausgezählt.

Die Infrarotspektren wurden auf den Geräten Unicam SP 200, Unicam SP 100 G und Leitz IIIb (für Wellenzahlen unter 400 cm^{-1}) aufgenommen.

Thermogravimetrische Bestimmungen führten wir mit dem Derivatographen der Firma MOM-Budapest durch, während die magnetischen Eigenschaften der Verbindungen mit einer Waage Ugine-Eyraud B60 und einem Elektromagneten nach Weiss, nach der Guyschen Methode aufgenommen wurden.

---

[23] J. Houben und W. Brassert, *Ber. dtsch. chem Ges.*, **39**, 3234 (1906).

Revue Roumaine de Chimie, 14, 1543 – 1552 (1969)

THE ÉTARD REACTION. VIII*)

OXIDATION OF DIPHENYLETHANES AND DIPHENYLETHYLENES WITH CHROMYL CHLORIDE

AURELIA GHENCIULESCU, ILEANA NECŞOIU, MARINA RENŢEA
and C. D. NENITZESCU

Organic Chemistry Laboratory, Polytechnic Institute, Bucharest, str. Polizu 1

Received July 3, 1969

The oxidation of 1.2-diphenylethane (I) with chromyl chloride leads to products arising from normal oxidation, from rearrangement accompanied by oxidation and from oxidative cleavage, namely : benzoin, desoxybenzoin, dibenzyl, diphenylacetaldehyde, benzophenone and benzaldehyde. The same products but in different proportions are obtained by oxidation with chromyl chloride of 1.1-diphenylethane (II), of *cis* and *trans*-stilbene (III, IV) and of 1.1-diphenylethylene (V). A reaction mechanism is discussed, involving common ionic intermediates.

During the oxidation with chromic acid of some alkanes, 1,1- and 1,2-disubstituted with phenyl groups, rearrangements have been observed.[1,2]

Oxidizing 1.2-diphenylethane with chromic acid in acetic acid, I. Necşoiu and C. D. Nenitzescu obtained benzoic acid and benzophenone. Oxidized under the same conditions, 1.2-diphenylpropane yields acetophenone, benzoic acid and benzophenone. The same products are obtained when the corresponding alkenes (stilbene and 1.2-diphenylpropene) are oxidized with chromic acid.

These facts can be interpreted in the sense that during the oxidation with chromic acid of hydrocarbons of $ArCH_2-CH_2-R$ type the corresponding olefins $ArCH=CH-R$ appear as intermediates, giving rise subsequently to products of normal oxidation and of rearrangement accom-

---

*) Part VII. I. Schiketanz, I. Necşoiu, M. Renţea and C. D. Nenitzescu, *Rev. Roumaine Chim.*, **13**, 1385 (1968).

[1] I. Necşoiu and C. D. Nenitzescu, *Rev. Roumaine Chim.*, **6**, 245 (1961).

[2] H. H. Szmant and J. F. Deffner, *J. Amer. Chem. Soc.*, **81**, 958 (1959).

panied or followed by oxidation. However, no reaction intermediate can be isolated, owing to the rapid reaction with the solvent and with the oxidant in excess. Only the final products, of advanced oxidation, such as benzophenone and benzoic acid, are obtained.

For the elucidation of the reaction mechanism, the use of another Cr^{VI} compound, the chromyl chloride, presents the advantage which we pointed out previously, namely of allowing the isolation of products arising from the primary attack of the oxidant or from a next step.

Although there are some data regarding the Étard reaction of diphenylethanes and diphenylethylenes, they are generally either too old, and therefore incomplete, or contradictory. The following literature data exemplify the situation.

From the two isomeric diphenylethanes, only 1.2-diphenylethane was studied, by Weiler.[3] Hydrolyzing the Etard complex of this hydrocarbon, he obtained benzaldehyde as the major product and benzophenone. From the three isomeric diphenylethylenes only the *trans*-stilbene was studied. Henderson and Grey [4] reported the formation of a complex containing hydrocarbon and chromyl chloride in the ratio 1 : 2, which on hydrolysis afforded benzaldehyde and dibenzyl, together with small amounts of benzophenone and benzoic acid. In contrast to this result, Cristol and Eiler [5] obtained from the same hydrocarbon, at room temperature, a complex with the composition 1 : 1; heating was required for taking up the second mole of chromyl chloride. However, the complex yielded on hydrolysis only polymers and traces of benzaldehyde.

In order to obtain new information about the reaction mechanism we chose, as reported in the present paper, the oxidation with chromyl chloride of the diphenylethanes and diphenylethylenes, namely 1.2-diphenylethane (I), 1.1-diphenylethane (II), *cis*-stilbene (III), *trans*-stilbene (IV) and 1.1-diphenylethylene (V). All reaction products were identified and quantitatively determined.

The Etard complexes were prepared under identical conditions, by adding chromyl chloride solution to the hydrocarbon solution in carbon tetrachloride, at −12, −14°. In the case of *trans*-stilbene, special conditions were used, as described in the experimental part.

The complexes were decomposed with cold water. The reaction products were immediately isolated and analyzed by means of vapour-phase chromatography, by comparing their retention times, to those of authentic samples.

In order to identify the aldehydes, which undergo easily autoxidation, parallel runs were made in which the reaction mixture was oxidized with Ag_2O to the corresponding carboxylic acids. These were esterified with diazomethane and identified by vapour phase chromatography.

The results are summarized in table 1.

---

[3] M. Weiler, *Ber. dtsch. chem. Ges.*, **32**, 1050–56 (1899).

[4] G. G. Henderson and T. Gray, *J. Chem. Soc.*, **83**, 1299 (1903).

[5] S. J. Cristol and K. R. Eilar, *J. Amer. Chem. Soc.*, **72**, 4353 (1950).

Table 1

Decomposition products of the Étard complexes of diphenylethanes and diphenylethylenes

Hydrolysis products of the complexes mole % / Hydrocarbon	$C_6H_5-CH=O$	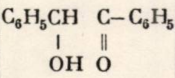 $C_6H_5\underset{\mathrm{OH}}{\underset{\vert}{CH}}-\underset{\mathrm{O}}{\underset{\Vert}{C}}-C_6H_5$	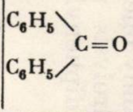	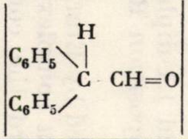	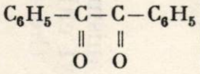 $C_6H_5-\underset{\mathrm{O}}{\underset{\Vert}{C}}-\underset{\mathrm{O}}{\underset{\Vert}{C}}-C_6H_5$	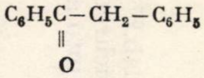 $C_6H_5\underset{\mathrm{O}}{\underset{\Vert}{C}}-CH_2-C_6H_5$
$C_6H_5-CH_2-CH_2-C_6H_5$ I	38.8	traces	13.4	3.7	33.7	9.4
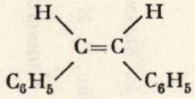 III	24.8	8.2	16.3	21.4	13.0	16.4
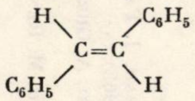 IV	traces	0.1	26.6	47.5	16.7	9.1
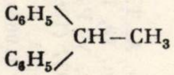 II	—	24.5	27	24.5	23	1
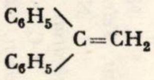 V	—	18.4	23	52	6.6	traces

DISCUSSION

The structure proposed by C. D. Nenitzescu and collab.[6,7] for the Étard complexes of arylmethanes is that of an ester of a bichromic acid partially reduced and chlorinated, and which can dissociate into a pair of ions :

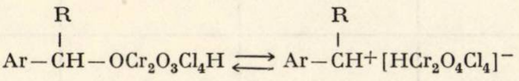

$$\mathrm{Ar-\overset{R}{\overset{|}{C}}H-OCr_2O_3Cl_4H \rightleftarrows Ar-\overset{R}{\overset{|}{C}}H^{+}[HCr_2O_4Cl_4]^{-}}$$

VIa VIb

Earlier work performed in our laboratory on the mechanism of oxidation of ethylbenzene and *n*-propylbenzene with chromyl chloride[8,9] supports the view that only this structure can account for the reaction products.

The saturated hydrocarbons (1.2-diphenylethane and 1.1-diphenylethane) studied here gave Etard complexes with the composition $R-H\cdot\cdot 2CrO_2Cl_2$.

If the structure of these complexes were that admitted by Etard and later by other authors,[10] 1.2-diphenylethane would give a complex with the structure VII, while 1.1-diphenylethane would afford the complex VIII, with only one mole of chromyl chloride since it has only one hydrogen at the reaction centre. Accordingly, the main hydrolysis product of VII would be desoxibenzoin (IX) and that of VIII, diphenylmethyl carbinol (X).

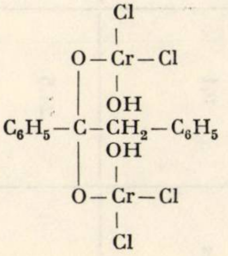

VII

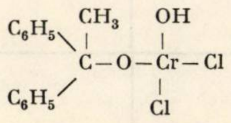

VIII

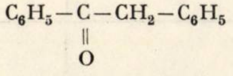

$$\mathrm{C_6H_5-\underset{\underset{O}{\|}}{C}-CH_2-C_6H_5}$$

IX

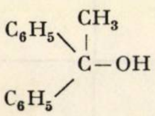

X

---

[6] I. Necşoiu, A. T. Balaban, I. Pascaru, E. Sliam, M. Elian and C. D. Nenitzescu, *Tetrahedron*, **19**, 1133 (1963).

[7] I. Necşoiu, V. Pşemeţchi, A. Ghenciulescu, C. N. Renţea and C. D. Nenitzescu, *Tetrahedron*, **22**, 3037 (1966).

[8] C. N. Renţea, I. Necşoiu, M. Renţea, A. Ghenciulescu and C. D. Nenitzescu, *Tetrahedron*, **22**, 3501 (1966).

[9] C. N. Renţea, M. Renţea, I. Necşoiu and C. D. Nenitzescu, *Rev. Roumaine Chim.*, **12**, 1495 (1967).

[10] W. H. Hartford and M. Darrin, *Chem. Rev.*, **58**, 1 (1958).

The fact that rearranged and oxidized compounds are obtained from these saturated hydrocarbons on treatment with chromyl chloride, as well as the fact that the same products result from the related olefins, can be explained only by admitting the structures VIa ⇄ VIb for the Etard complexes of the saturated hydrocarbons, capable to give olefins by elimination. The mechanism of this reaction was demonstrated and presented in detail in the case of other hydrocarbons : ethylbenzene, 1-phenylpropane and methylcyclohexane.[8,9] As in these cases, only one molecule of chromyl chloride is involved in the rate-determining step, the second molecule being taken up in a subsequent step. The kinetic studies of Stairs [11,12] lead to a similar conclusion.

In the present case the complex gives first an alkene.

The complex of 1.2-diphenylethane (XI), for instance, gives by elimination stilbene :

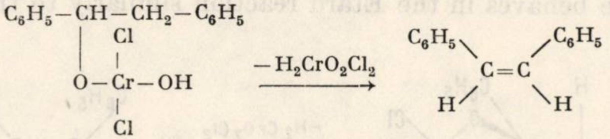

Formally, the conformations XIa, XIb and XIc may be written for the complex XI :

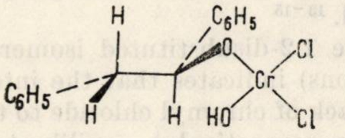

XIa

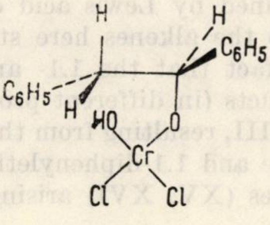

XIb

---

[11] R. A. Stairs, J. W. Burns, *Canad. J. Chem.*, **39**, 960 (1961).

[12] R. A. Stairs, *Canad. J. Chem.*, **42**, 550 (1964).

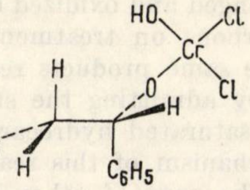

XIc

Among these, the conformation XIc is less probable because of the crowding of bulky groups. The conformation XIb would give rise to *trans*-stilbene, a reaction which can be excluded since the reaction products of 1.2-diphenylethane and of *trans*-stilbene are rather different. It follows that the most populated conformation is XIa, which gives *cis*-stilbene by *cis*-elimination. This hypothesis is supported by the fact that *cis*-stilbene behaves in the Etard reaction similarly to the saturated hydrocarbons.

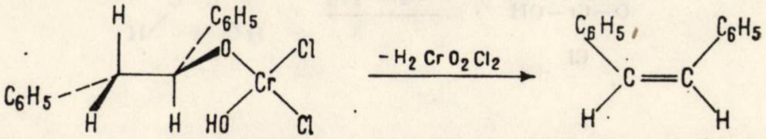

The alkene which results in this way undergoes then the electrophilic attack of chromyl chloride, leading to the formation of the epoxy ring. The latter is opened as part of a concerted process or in a subsequent step.

The rearranged products of this oxidation reaction are similar to those obtained by Lewis acid catalyzed opening of the epoxides corresponding to the alkenes here studied. [13-15]

The fact that the 1.1- and the 1.2-disubstituted isomers give the same products (in different proportions) indicates that the intermediates XII and XIII, resulting from the attack of chromyl chloride to the alkenes (*cis*-stilbene and 1.1-diphenylethylene, respectively), equilibrate *via* other ionic species (XV, XVI) arising from hydride ion or phenyl migration.

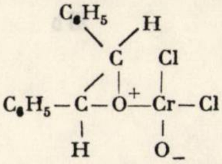

XII

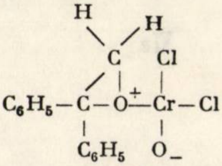

XIII

---

[13] H. O. House, *J. Amer. Chem. Soc.*, **77**, 3070 (1955).

[14] A. C. Cope, P. A. Trunbull, E. R. Trunbull, *J. Amer. Chem. Soc.*, **80**, 2844 (1958).

[15] D. J. Curtin and E. K. Meislich, *J. Amer. Chem. Soc.*, **74**, 5905 (1952).

The inert, non-polar medium used in the reaction (carbon tetrachloride, allows the stabilization of the ionic intermediates through successive rearrangements. Although the processes may involve open carbonium ions (XIV, XVII), owing to the great volume of the group —OCrOCl$_2^-$, the phenyl and the hydride ion migrations appear to be stereospecific

If we consider the ion XIVa, arising from *cis*-stilbene, and the ion XIVb, resulting from *trans*-stilbene, we may infer that *cis*-stilbene should give preferentially desoxibenzoin, while *trans*-stilbene diphenylacetaldehyde. This conclusion is confirmed by the experimental results.

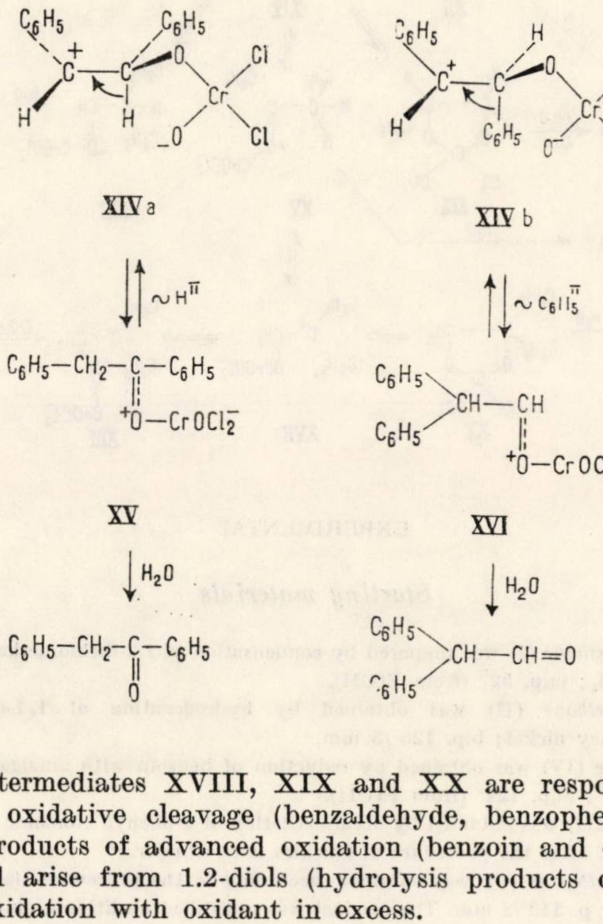
XIV a
XIV b
~H^{II}
~C$_6$H$_5^{\text{II}}$
$C_6H_5-CH_2-C(=\overset{+}{O}-CrOCl_2^-)-C_6H_5$
$(C_6H_5)_2CH-CH=\overset{+}{O}-CrOCl_2^-$
XV
XVI
H$_2$O
H$_2$O
$C_6H_5-CH_2-CO-C_6H_5$
$(C_6H_5)_2CH-CH=O$

The intermediates XVIII, XIX and XX are responsible for the products of oxidative cleavage (benzaldehyde, benzophenone) as well as for the products of advanced oxidation (benzoin and dibenzyl). The latter should arise from 1.2-diols (hydrolysis products of XVIII and XIX), by oxidation with oxidant in excess.

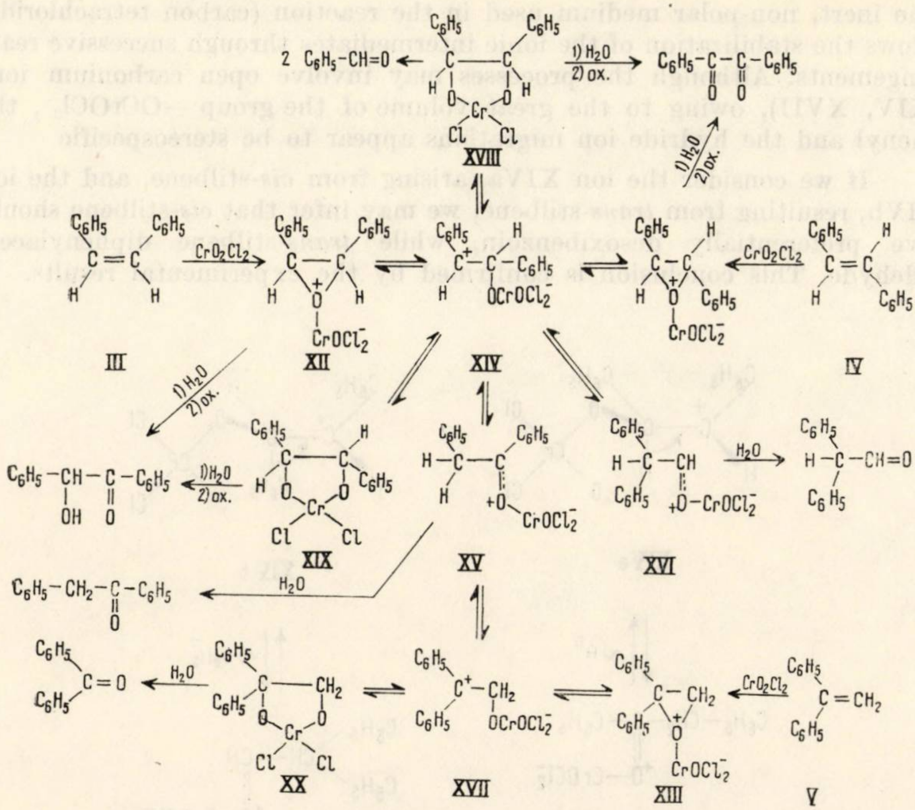

EXPERIMENTAL

Starting materials

1.2-Diphenylethane (I) was prepared by condensation of 1.2-dichloroethane with benzene in presence of $AlCl_3$; m.p. 52° (from EtOH).

1.1-Diphenylethane (II) was obtained by hydrogenation of 1.1-diphenylethylene in presence of Raney nickel; b.p. 125°/5 mm.

trans-*Stilbene* (IV) was obtained by reduction of benzoin with amalgamated zinc and hydrochloric acid[16]; m.p. 124° (from EtOH).

cis-*Stilbene* (III) was obtained by decarboxilation of α-phenyl cinnamic acid in presence of copper chromite, after the procedure of Buckles and Wheeler.[17]

1,1-Diphenylethylene (V) was obtained according to the procedure described by Allen and Converse[18]; b. p. 113°/2 mm. The product was redistilled on lithium aluminium hydride.

---

[16] R. L. Shriner, A. Berger, "Organic Synthesis", Coll. vol. III, J. Wiley, New York, 1955, p. 786.

[17] R. E. Buckless, N. G. Wheeler, "Organic Synthesis", Coll. vol. IV, J. Wiley, New York, 1963, p. 857.

[18] C. F. Allen and S. Converse, "Organic Synthesis", Coll. vol. I, p. 226.

The Étard complexes of diphenylethanes and diphenylethylenes

The complexes were obtained by adding 10% chromyl chloride solution in carbon tetrachloride to 10% hydrocarbon solution in carbon tetrachloride. The temperature of the reaction mixture was maintained at $-14^\circ \div -12^\circ$ by using an ice-salt bath.

In the case of *trans*-stilbene the procedure was different. This hydrocarbon, having a low solubility in carbon tetrachloride, was dissolved in a mixture of benzene and carbon tetrachloride (in the ratio 2 : 1). In order to avoid the polymerization occurring when the reactants are added in the usual way, in the case of *trans*-stilbene the hydrocarbon solution was added to the chromyl chloride solution.

The complexes were decomposed with water at 0° and the products were extracted with methylene chloride. After evaporation of solvent under reduced pressure, in inert gas atmosphere, the products were passed through an alumina column in order to separate benzoin (a product which could not be analyzed by vapour-phase chromatography), using petroleum ether as eluent.

The mixture was then analyzed qualitatively and quantitatively by means of gas-chromatography. The column used was 20% ethyleneglycol succinate on Chromosorb W, 195°, 1.5 m, 23 mol H_2/min. Five components were thus separated, in the given order : benzaldehyde, benzophenone, diphenylacetaldehyde, desoxibenzoin and dibenzyl.

The results were checked on a column of 25% Apiezon on Chromosorb W ; 195° ; 1.5 mm ; 23 ml H_2/min.

In order to verify and identify the aldehydes which undergo easily autoxidation, the mixture of products was oxidized with Ag_2O.[19] After the separation of Ag and Ag_2O, the alkaline solution was extracted with ether. The ethereal extract, after evaporation of solvent, afforded the ketones.

The alkaline solution was acidified with concentrated hydrochloric acid, extracted with ether, and the extract evaporated. The mixture of acids thus obtained was treated with diazomethane in ether. The methyl esters were analyzed by chromatography, by comparison of their retention times to those of authentic samples. The column used was 25% Apiezon L on Chromosorb W ; 95° ; 1.5 m ; 38.4 ml H_2/min. The results of the determination of esters were used only qualitatively since the oxidation was not quantitative.[20]

Table 1 summarizes these results.

Identification of the reaction products

Benzaldehyde was identified by comparison of its retention time to that of an authentic sample (the analysis being made immediately after the decomposition of the complex), as well as methyl benzoate obtained by oxidation with Ag_2O and esterification with diazomethane.

Benzophenone was identified by comparison with an authentic sample under various conditions, when chromatography peaks coincided perfectly.

Desoxibenzoin was identified by its retention time which was identical to that of an authentic sample prepared by condensation of phenylacetyl chloride with benzene in the presence of aluminium chloride, m.p. 60° (from EtOH).

---

[19] F. A. Goldberg and R. P. Linstead, *J. Chem. Soc.*, **1928**, 2355.

[20] J. A. Pearl and D. L. Beyer, *J. Amer. Chem. Soc.*, **74**, 3188 (1952).

Benzoin was separated at the beginning from the reaction mixture by adsorption on alumina column and elution with methylene chloride. The compound thus obtained was recrystallized from EtOH; m.p. 132°, mixed m.p. without depression.

Dibenzyl was identified by comparison of its v.p.c. retention time to that of an authentic sample prepared by oxidation of benzoin.[21]

In the sample oxidized with silver oxide, in the presence of sodium hydroxide, the dibenzyl underwent benzylic transposition and was identified as methyl ester of benzylic acid by comparison to an authentic sample.

---

[21] A. T. Vogel, "Practical Organic Chemistry", Longmans, London, 1958, p. 715, 773.

Revue Roumaine de Chimie, **14**, 1553–1565 (1969)

THE ÉTARD REACTION. IX[1]
OXIDATIVE CLEAVAGE OF ETHERS PRODUCED BY CHROMYL CHLORIDE

AURELIA GHENCIULESCU, ILEANA NECŞOIU and C. D. NENITZESCU

Organic Chemistry Laboratory, Polytechnic Institute, Bucharest, str. Polizu 1

Received July 23, 1969

The oxidation with chromyl chloride of the following ethers is studied : dibenzhydryl ether (I), benzhydryl benzyl ether (II), benzhydryl *t*-butyl ether (III), benzyl triphenylmethyl ether (IV), isopropyl triphenylmethyl ether (V), benzhydryl triphenylmethyl ether (VI), dibenzylether (VII), benzylmethyl ether (VIII), di-triphenylmethyl ether (IX), and di-*t*-butyl ether (X). Under the action of chromyl chloride these ethers undergo oxidative cleavage, the amount of which varies with the nature of the constitutive alkyl and aryl-alkyl groups. An ionic mechanism is proposed for the cleavage reaction, involving the electrophylic attack of the oxidant on the ether molecule.

In our earlier work [2–4] on the oxidation of organic compounds with chromyl chloride we found evidence of the bielectronic oxidative role played by this hexavalent chromium compound, and of the ionic nature of the reaction intermediate, the Étard complex.

The oxidation of ethers with chromyl chloride has not been studied so far. Westheimer and collab. [5] investigated the oxidation of di-isopropyl ether with chromic acid, in presence of sulphuric acid. The kinetic isotopic effect observed in the reaction of C_2-deuterated di-isopropyl ether and the molecularity of the reaction led the authors to believe that in the rate-determining step "a nucleus of hydrogen with or without its electrons" is removed from a complex XI formed by a molecule of chromic acid with a molecule of ether :

---

[1] Part VIII. A. Ghenciulescu, I. Necşoiu, M. Renţea and C. D. Nenitzescu, *Rev. Roumaine Chim.*, in press.

[2] I. Necşoiu, V. Pşemeţchi, A. Ghenciulescu, C. N. Renţea and C. D. Nenitzescu, *Tetrahedron*, **22**, 3037 (1966).

[3] C. N. Renţea, I. Necşoiu, M. Renţea, A. Ghenciulescu and C. D. Nenitzescu, *Tetrahedron*, **22**, 3501, 3513 (1966).

[4] I. Necşoiu, A. Ghenciulescu, M. Renţea, C. N. Renţea and C. D. Nenitzescu, *Rev. Roumaine Chim.*, **12**, 1503 (1967).

[5] F. H. Westheimer, R. Brownell, A. Leo, Y. W. Chang, *J. Amer. Chem. Soc.*, **82**, 406 (1960).

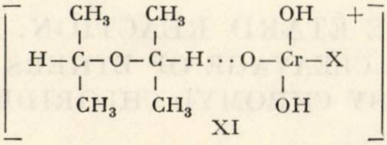

$$\left[\begin{array}{c} \mathrm{CH_3}\quad \mathrm{CH_3} \qquad\quad \mathrm{OH} \\ \mathrm{H-\overset{|}{\underset{|}{C}}-O-\overset{|}{\underset{|}{C}}-H\cdots O-\overset{|}{\underset{|}{Cr}}-X} \\ \mathrm{CH_3}\quad \mathrm{CH_3} \qquad\quad \mathrm{OH} \end{array}\right]^{+}$$

XI

X = OH or a remaining of acid sulfate

The authors show in conclusion that "although a direct attack by chromic acid on the ether is the most probable route to the oxidation products, the nature of the reaction has not been further elucidated".

We undertook the study of the action of chromyl chloride on ethers in order to try to elucidate the reaction mechanism and especially in order to obtain new data concerning the primary attack of hexavalent chromium derivatives on organic compounds.

We found first that many ethers gave precipitates with chromyl chloride, in carbon tetrachloride as a solvent. Unlike other chromyl chloride oxidations, in the case of ethers a considerable part of the reaction product remains in solution, while only a fraction is found in the precipitate (the Étard complex). The products obtained from the carbon tetrachloride solutions and those resulted by hydrolysis of the Étard complex were separately examined. The results of these analyses show that an advanced oxidative cleavage of the ether occurs during the formation of the Étard complex, prior to its hydrolysis.

When dibenzhydryl ether (I) is treated with chromyl chloride in carbon tetrachloride, benzophenone is found in the filtrate which remains after the removal of the insoluble complex. The latter is identical with the complex obtained from diphenylmethane and chromyl chloride, having the same composition (elemental analysis) and giving the same hydrolysis product (benzophenone).

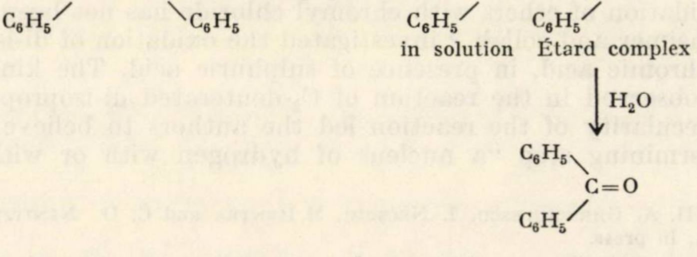

In this case the oxidative cleavage is quantitative.

In order to obtain more information about this new reaction we treated with chromyl chloride various R_1-O-R_2 ethers in which R_1 and R_2 were primary, secondary and tertiary alkyl and aryl-alkyl groups. We studied namely symmetrical and mixed ethers in which R_1 and R_2 were benzyl, benzhydryl, triphenylmethyl, methyl, isopropyl, *t*-butyl groups.

The nature and the amount products which result in the filtrate and in the Étard complex depend upon the nature of the groups R_1 and R_2.

The products isolated from the filtrate, on which the yield of cleavage is calculated, are: chloro compound, alcohol or chromic ester in the case of a tertiary group; with secondary and primary groups, ketones and aldehydes are respectively found.

The products resulting on hydrolysis of the insoluble complex are alcohols, ketones or aldehydes, depending upon the nature of the groups bound to chromyl chloride.

The experimental results are summarized in table 1.

Table 1

Products of the reaction of ethers with chromyl chloride

Ether	Products obtained from the filtrate % moles on the initial ether		Products obtained by hydrolyzing the Étard complex % moles on the initial ether		Yield of cleavage
$(C_6H_5)_2CH-O-CH(C_6H_5)_2$	$(C_6H_5)_2C=O$	80	$(C_6H_5)_2C=O$	100	80
I					
$(C_6H_5)_2CH-O-CH_2-C_6H_5$	$(C_6H_5)_2C=O$	72	$(C_6H_5)_2C=O$	25	72
II			$C_6H_5-CH=O$	75	
$(C_6H_5)_2CH-O-C(CH_3)_3$	$(C_6H_5)_2C=O$	40	$(C_6H_5)_2C=O$	60	40
III	$(CH_3)_3C-OH$	43			
$C_6H_5-CH_2-O-(C_6H_5)_3$	$(C_6H_5)_3C-Cl$	80	$(C_6H_5)_3C-OH$	13	80
IV			$C_6H_5-CH=O$	80	
$(CH_3)_2CH-O-C(C_6H_5)_3$	$(C_6H_5)_3C-OH$*	60	$(C_6H_5)_3C-OH$	12	72
V	$(C_6H_5)_3C-Cl$	12	$(CH_3)_2C=O$	51	
$(C_6H_5)_2CH-O-C(C_6H_5)_3$	$(C_6H_5)_3C-OH$	50	$(C_6H_5)_3C-OH$	38	85
VI	$(C_6H_5)_2C=O$	85	$(C_6H_5)_2C=O$	12	
$C_6H_5-CH_2-O-CH_2-C_6H_5$	$C_6H_5CH=O$	16	$C_6H_5CH=O$	60	16
VII			$C_6H_5CH_2OH$	6	
$C_6H_5-CH_2-O-CH_3$	C_6H_5COCl	(traces)	$C_6H_5-CH=O$	60	—
VIII			$C_6H_5-COOCH_3$	2÷3	
$(C_6H_5)_3C-O-C(C_6H_5)_3$	$(C_6H_5)_3C-OH$	100	—		—
IX					
$(CH_3)_3C-O-C(CH_3)_3$	—		$(CH_3)_3C-OH$		—
X			$(CH_3)_2CH-CH=O$		

* The alcohol was obtained by hydrolyzing the corresponding chromate

DISCUSSION

It is well-known that ethers are good hydride donors to carbonium ions.[6–8] A carbonium ion behaves thus towards an ether as bielectronic oxidant; it is reduced to the respective hydrocarbon, while the ether is oxidized to another carbonium ion which may undergo subsequent transformation.

The Étard complexes of alkyl-aromatic hydrocarbons have an ionic or an easily ionizable structure. The carbonium ions contained in these complexes are capable of abstracting hydride ions.[2]

The Étard complex of triphenylmethane XIII (prepared from triphenylmethane and chromyl chloride and washed afterwards with carbon tetrachloride) was treated with dibenzhydryl ether in carbon tetrachloride solution. After shaking a while at room temperature, the complex was filtered again and washed with carbon tetrachloride.

From the filtrate we isolated triphenylmethane and benzophenone; the complex XII gave on hydrolysis benzophenone:

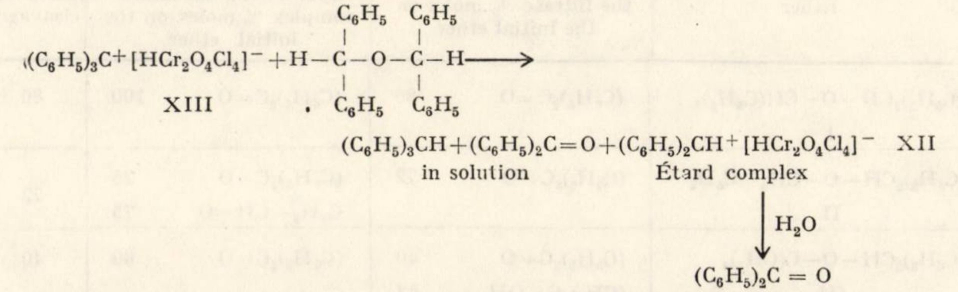

$$\underset{\text{XIII}}{(C_6H_5)_3C^+[HCr_2O_4Cl_4]^-} + H-\overset{\substack{C_6H_5\\|}}{\underset{\substack{|\\C_6H_5}}{C}}-O-\overset{\substack{C_6H_5\\|}}{\underset{\substack{|\\C_6H_5}}{C}}-H \longrightarrow$$

$$\underset{\text{in solution}}{(C_6H_5)_3CH + (C_6H_5)_2C{=}O} + \underset{\text{Étard complex}}{(C_6H_5)_2CH^+[HCr_2O_4Cl_4]^-}\ \text{XII} \xrightarrow{H_2O} (C_6H_5)_2C = O$$

The reaction between the Étard complex of triphenylmethane and the dibenzhydryl ether is a typical hydride transfer from the ether to the carbonium ion $(C_6H_5)_3C^+$, leading to triphenylmethane and the carbonium ion XIV. The latter undergoes cleavage yielding benzophenone which is found in the solution (the driving force being the formation of a carbonyl group), and diphenylmethyl carbonium ion which gives with chromyl anion the Étard complex of diphenylmethane.

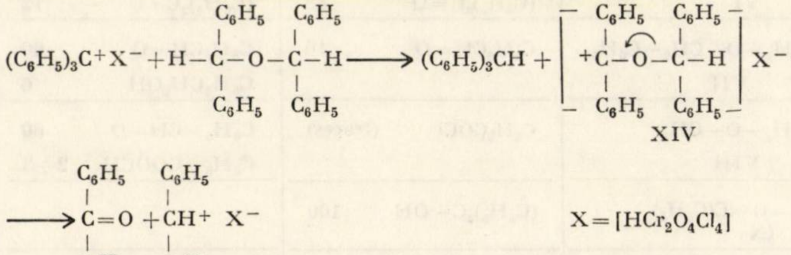

$$(C_6H_5)_3C^+X^- + H-\overset{\substack{C_6H_5\\|}}{\underset{\substack{|\\C_6H_5}}{C}}-O-\overset{\substack{C_6H_5\\|}}{\underset{\substack{|\\C_6H_5}}{C}}-H \longrightarrow (C_6H_5)_3CH + \underset{\text{XIV}}{\left[{}^+\overset{\substack{C_6H_5\\|}}{\underset{\substack{|\\C_6H_5}}{C}}-O-\overset{\substack{C_6H_5\\|}}{\underset{\substack{|\\C_6H_5}}{C}}-H\right]} X^-$$

$$\longrightarrow \overset{\substack{C_6H_5\\|}}{\underset{\substack{|\\C_6H_5}}{C}}{=}O + \overset{\substack{C_6H_5\\|}}{\underset{\substack{|\\C_6H_5}}{C}}H^+\ X^- \qquad X = [HCr_2O_4Cl_4]$$

---

[6] H. Meerwein, *Angew. Chem.*, **67**, 374 (1955); H. Meerwein, H. Allendörfer, P. Beckmann, F. Kennert, H. Marshall, F. Pawelek and K. Wunderlech, *ibid.*, **70**, 211 (1958).

[7] F. J. Norris, "Organic Syntheses", Coll. vol. 1, Wiley, New York, 1956, p. 548.

[8] G. Baddeley, W. Pickless, *J. Chem. Soc.*, **1953**, 3726.

The same products are found if the dibenzhydryl ether is treated with chromyl chloride; it may be assumed that the same intermediate XIV appears. The reaction can be presented as follows: the chromyl chloride abstracts a hydride ion from the molecule of ether which yields thus a carbonium ion; the latter is splitted to a more stable carbonium ion and a carbonyl compound.

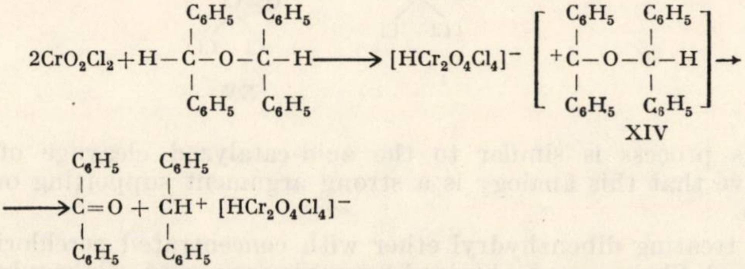

$$2CrO_2Cl_2 + H-\overset{C_6H_5}{\underset{C_6H_5}{C}}-O-\overset{C_6H_5}{\underset{C_6H_5}{C}}-H \longrightarrow [HCr_2O_4Cl_4]^- \left[{}^+\overset{C_6H_5}{\underset{C_6H_5}{C}}-O-\overset{C_6H_5}{\underset{C_6H_5}{C}}-H \right] \rightarrow$$

XIV

$$\longrightarrow \overset{C_6H_5}{\underset{C_6H_5}{C}}=O + \overset{C_6H_5}{\underset{C_6H_5}{C}}H^+ \, [HCr_2O_4Cl_4]^-$$

The same mechanism can explain the action of chromyl chloride on benzhydryl benzyl ether II which gives benzophenone in the filtrate and benzaldehyde after hydrolysis of the Étard complex:

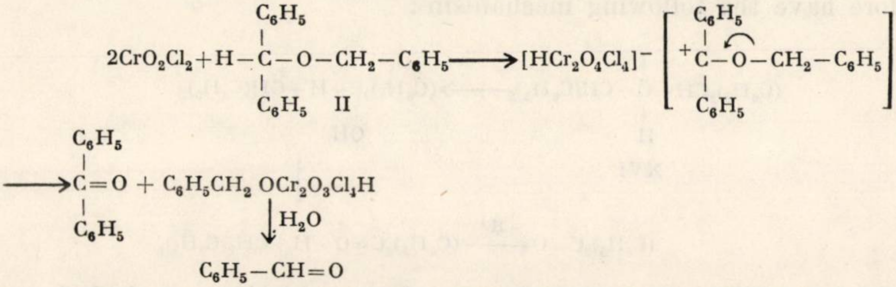

$$2CrO_2Cl_2 + H-\overset{C_6H_5}{\underset{C_6H_5}{C}}-O-CH_2-C_6H_5 \longrightarrow [HCr_2O_4Cl_4]^- \left[{}^+\overset{C_6H_5}{\underset{C_6H_5}{C}}-O-CH_2-C_6H_5 \right]$$

II

$$\longrightarrow \overset{C_6H_5}{\underset{C_6H_5}{C}}=O + C_6H_5CH_2\,OCr_2O_3Cl_4H \xrightarrow{H_2O} C_6H_5-CH=O$$

This mechanism, involving a hydride transfer from the ether to the oxidant, cannot however explain the behaviour towards chromyl chloride of some ethers, such as benzhydryl *t*-butyl ether III or isopropyl triphenylmethyl ether V (Table 1), which do not undergo cleavage to yield a ketone corresponding to the secondary group and an Étard complex containing the tertiary group:

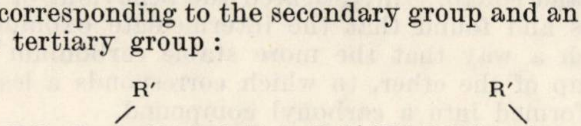

$$R_3C-O-\overset{R'}{\underset{R''}{C}}-H + CrO_2Cl_2 \nrightarrow R_3C^+[HCrO_2Cl_2]^- + \overset{R'}{\underset{R''}{C}}=O$$

This mechanism does not account either for the cleavage of the ditertiary ethers di-triphenylmethyl ether IX and di-*t*-butyl ether X which have no hydrogen at the reaction centre.

In order to explain the action of chromyl chloride on ethers another mechanism can be taken into consideration, namely: the nucleophilic oxygen of the ether may share two electrons with the electrophilic hexavalent chromium, which leads to an oxonium salt (XV); in a subsequent step this addition product would undergo cleavage.

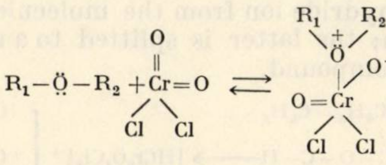

XV

This process is similar to the acid-catalyzed cleavage of ethers. We believe that this analogy is a strong argument supporting our interpretation.

By treating dibenzhydryl ether with concentrated perchloride acid, Burton and Cheeseman[9] obtained benzophenone and diphenylmethane. Using deuterated perchloric acid, Baddeley and Nield[10] obtained in the same experiment benzophenone and nondeuterated diphenylmethane. This result shows that the reaction involves a hydride transfer and should therefore have the following mechanism:

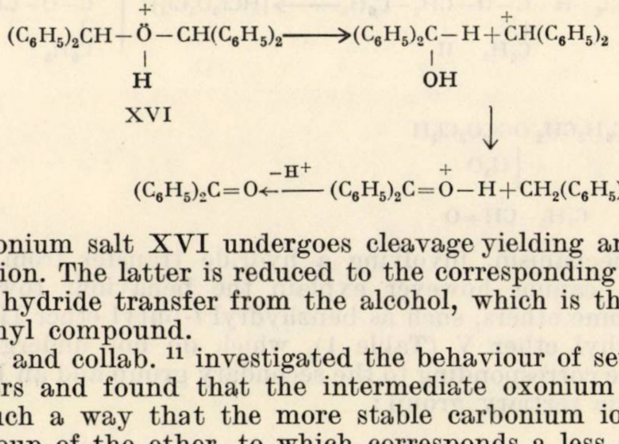

$$(C_6H_5)_2CH-\underset{\substack{|\\ H}}{\overset{+}{O}}-CH(C_6H_5)_2 \longrightarrow (C_6H_5)_2\underset{\substack{|\\ OH}}{C}-H+\overset{+}{C}H(C_6H_5)_2$$

XVI

$$\downarrow$$

$$(C_6H_5)_2C=O \xleftarrow{-H^+} (C_6H_5)_2C=\overset{+}{O}-H+CH_2(C_6H_5)_2$$

The oxonium salt XVI undergoes cleavage yielding an alcohol and a carbonium ion. The latter is reduced to the corresponding hydrocarbon by way of a hydride transfer from the alcohol, which is thus converted into a carbonyl compound.

Kenyon and collab.[11] investigated the behaviour of several unsymmetrical ethers and found that the intermediate oxonium salt is fragmented in such a way that the more stable carbonium ion is formed. The other group of the ether, to which corresponds a less stable ion, is actually transformed into a carbonyl compound.

In the reaction of ethers with chromyl chloride, the oxonium salt gives similarly the more stable carbonium ion. This process is assisted by chlorine and oxygen atoms of the chromyl chloride moiety, which, owing to their nucleophilic character, allow the formation of stable compounds (alkyl halide and chlorochromic ester).

The nature of groups R_1 and R_2 determines the way in which the oxonium salt undergoes cleavage.

---

[9] H. Burton, G. W. H. Cheeseman, *J. Chem. Soc.*, **1953**, 986.

[10] G. Baddeley and P. G. Nield, *J. Chem. Soc.*, **1954**, 4684.

[11] M. P. Balfer, J. Kenyon and E. M. Thain, *J. Chem. Soc.*, **1952**, 790.

1. In case of an ether possessing groups of different stability, for instance R_1 = tertiary, R_2 = primary, as for triphenylmethyl-benzyl-ether, the reaction can be pictured as follows:

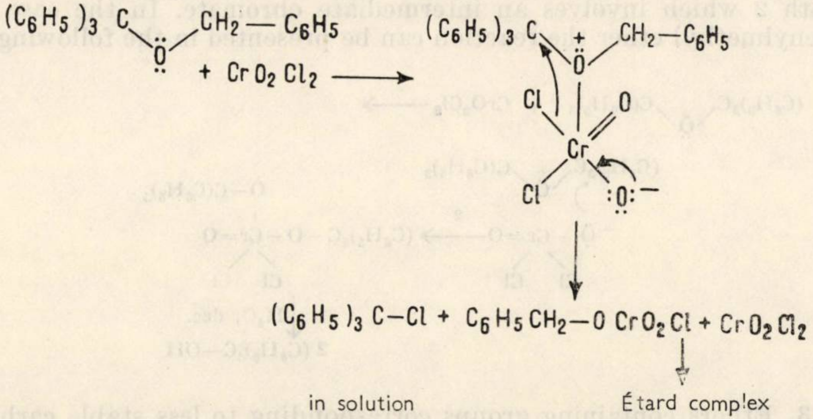
$(C_6H_5)_3C-\ddot{O}-CH_2-C_6H_5$
$+ CrO_2Cl_2$
$(C_6H_5)_3C-\overset{+}{\ddot{O}}-CH_2-C_6H_5$
Cl
O
Cr
Cl
:O:⁻
$(C_6H_5)_3C-Cl + C_6H_5CH_2-OCrO_2Cl + CrO_2Cl_2$
in solution
Étard complex

The tertiary group breaks off from oxygen passing into the solution as an alkyl chloride. The other group remains linked to the chromyl rest and forms the Étard complex.

2. Another possible stabilization of the oxonium salt is the detachment of the more stable carbonium ion, assisted by an oxygen atom of the chromyl chloride moiety, leading to a chlorochromic ester XVII which remains in solution. This path should be preferred by ethers possessing groups corresponding to carbonium ions of comparable stability (for instance R_1 = triphenylmethyl, R_2 = benzhydryl or R_1 = benzhydryl and R_2 = *t*-butyl). In this case one finds in the filtrate products corresponding to both R_1 and R_2 groups.

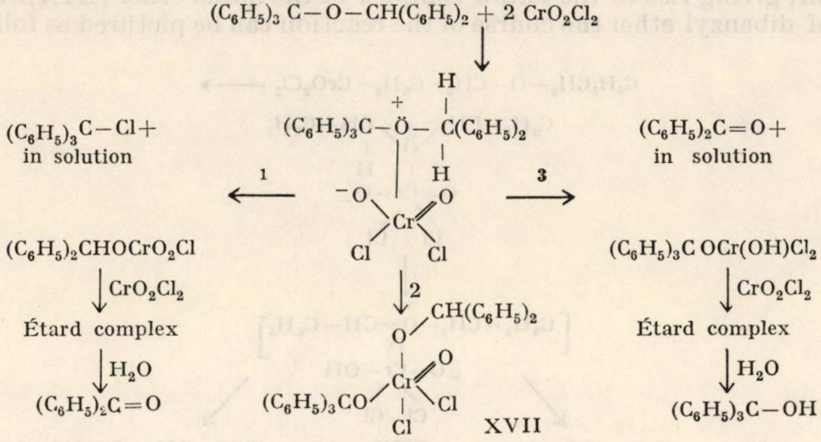
$(C_6H_5)_3C-O-CH(C_6H_5)_2 + 2\,CrO_2Cl_2$
$(C_6H_5)_3C-\overset{+}{\ddot{O}}-C(C_6H_5)_2$
H
H
^{-}O
O
Cr
Cl
Cl
1
2
3
$(C_6H_5)_3C-Cl+$
in solution
$(C_6H_5)_2CHOCrO_2Cl$
CrO_2Cl_2
Étard complex
H_2O
$(C_6H_5)_2C=O$
$(C_6H_5)_2C=O+$
in solution
$(C_6H_5)_3C\,OCr(OH)Cl_2$
CrO_2Cl_2
Étard complex
H_2O
$(C_6H_5)_3C-OH$
$CH(C_6H_5)_2$
O
O
Cr
$(C_6H_5)_3CO$
Cl
Cl
XVII
H_2O
$(C_6H_5)_3C-OH$
$(C_6H_5)_2C=O$

The benzhydryl triphenylmethyl ether reacts probably in this way:

Ethers without hydrogen at the reaction centre, such as di-triphenylmethyl ether IX and di-*t*-butyl ether X, react probably only according to path 2 which involves an intermediate chromate. In the case of di-triphenylmethyl ether the reaction can be presented in the following way:

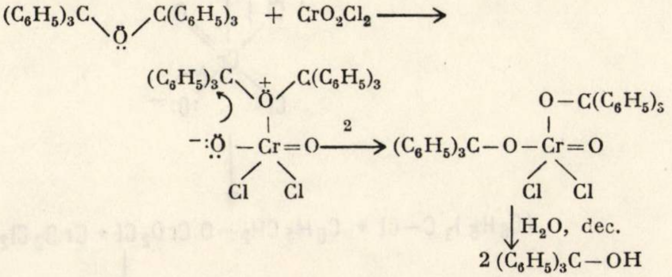

3. Ethers containing groups corresponding to less stable carbonium ions (for example dibenzyl ether VII and benzyl methyl ether VIII) undergo little or no cleavage at all during the Étard reaction. Products of oxidative cleavage are obtained by hydrolyzing the Étard complex and they are accompanied by products of simple oxidation such as benzyl benzoate and methyl benzoate.

The oxonium salt of this type of ethers can be stabilized by the loss of a proton from C_α which is accepted by an oxygen atom of the chromyl chloride moiety; a carbonium XVIII may thus appear as an intermediate. The latter splits up yielding a carbonyl compound which is found in solution, or recombines with the chromyl anion, within the ion pair, giving rise to the Étard complex of the initial ether (XIX). In the case of dibenzyl ether the course of the reaction can be pictured as follows:

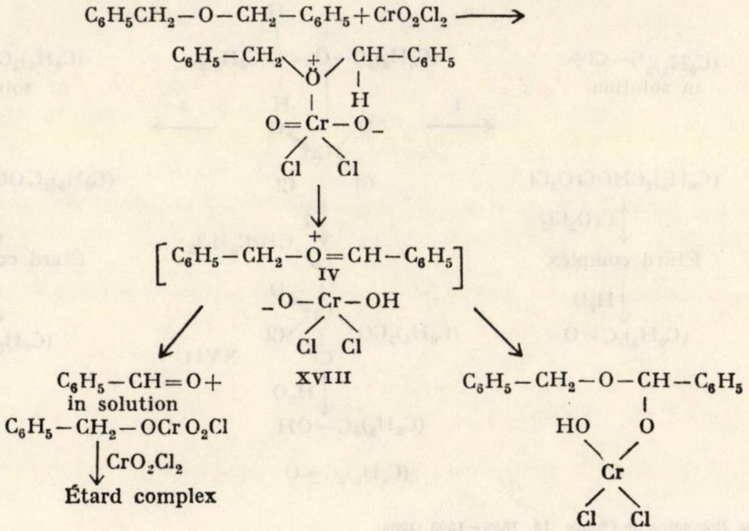

The carbonium ion XVIII is the same as that which results by direct hybride abstraction from the ether molecule. We can reasonably assume that the electron-repelling alkyl groups would favour the attack of the oxidant on the oxygen atom of the ether, a process leading to the oxonium salt which is subsequently stabilized according to path 3.

The reactions of ethers with chromyl chloride cannot be explained otherwise than by the intervention of carbonium ions as intermediates. These can appear either by hydride ion transfer, or by cleavage of an intermediate oxonium salt which may lose, in an assisted step, a carbonium ion or a proton from Cα. In both cases the chromyl chloride behaves like a bielectronic oxidant.

The intervention of an oxonium salt can also account for the difference in the reaction rate between di-isopropyl ether and isopropyl alcohol, observed by Westheimer and collab. [5] during the oxidation with chromic acid in presence of sulphuric acid. According to the mechanism which we propose, the oxidation of di-isopropyl ether can be presented in the following manner :

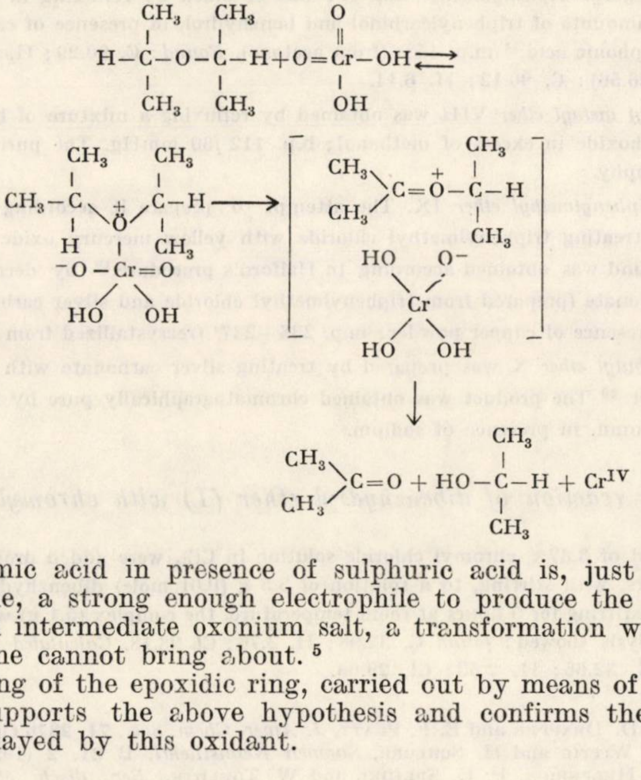

The chromic acid in presence of sulphuric acid is, just like the chromyl chloride, a strong enough electrophile to produce the cleavage of ether, *via* an intermediate oxonium salt, a transformation which sulphuric acid alone cannot bring about. [5]

The opening of the epoxidic ring, carried out by means of chromyl chloride, [12,13] supports the above hypothesis and confirms the role of a Lewis acid played by this oxidant.

---

[12] C. N. Renţea, M. Renţea, I. Necşoiu and C. D. Nenitzescu, *Rev. Roumaine Chim.*, **12**, 1495 (1967).

[13] I. Schiketanz, I. Necşoiu, M. Renţea and C. D. Nenitzescu, *Rev. Roumaine Chim.*, **13**, 1385 (1968).

EXPERIMENTAL

Starting materials

Dibenzhydryl ether I was obtained by distillation of benzhydrol at reduced pressure (40 mm Hg), in presence of traces of acid; m.p. 110° (recrystallized from methanol).

Benzhydryl benzyl ether II was prepared from benzhydrol and benzyl alcohol in refluxing benzene, using *p*-toluenesulphonic acid as catalyst[14]; m.p. 51° (from ethanol).

Benzhydryl t-*butyl ether* III was obtained according to Wittig[15] from benzhydryl bromide and potassium *t*-butoxide, in excess of boiling *t*-butanol. After distillation, followed by recrystallization from methanol, m.p. 50°.

Benzyl triphenylmethyl ether IV was synthesized by condensation of triphenylmethyl chloride with benzyl alcohol, in presence of pyridine, at room temperature[16]; m.p. 106°.

Isopropyl triphenylmethyl ether V was prepared according to the same procedure[16] from triphenylmethyl chloride and isopropyl alcohol; m.p. 113° (from methanol).

Benzhydryl triphenylmethyl ether VI was obtained by refluxing in anhydrous benzene equivalent amounts of triphenylcarbinol and benzhydrol, in presence of catalytic amounts of *p*-toluenesulphonic acid,[14] m.p. 153° (from acetone). *Found*: C, 90.29; H, 6.34. *Calculated* for $C_{32}H_{26}O$ (426.56): C, 90.12; H, 6.14.

Benzyl methyl ether VIII was obtained by refluxing a mixture of benzyl chloride and sodium methoxide in excess of methanol; b.p. 112°/60 mmHg. The purity was checked by chromatography.

Di-triphenylmethyl ether IX. The attempt to prepare it according to Gomberg's method[17] by treating triphenylmethyl chloride with yellow mercury oxide in benzene failed. The compound was obtained according to Halford's procedure,[18] by decomposing triphenylmethyl carbonate (prepared from triphenylmethyl chloride and silver carbonate[19]) in boiling xylene in presence of copper powder; m.p. 236–237° (recrystallized from xylene).

Di-t-*butyl ether* X was prepared by treating silver carbonate with *t*-butyl chloride in diethyl ether.[20] The product was obtained chromatographically pure by fractionation on an efficient column, in presence of sodium.

The reaction of dibenzhydryl ether (I) with chromyl chloride.

80 ml of 3.87% chromyl chloride solution in CCl_4 were added dropwise in the course of two hours, with stirring, to a solution of 3.5 g (0.01 mole) dibenzhydryl ether in 25 ml CCl_4. After stirring for 5 hours at room temperature, the complex (5.1 g) was isolated. Its elemental analysis showed: *found* C, 32.98; H, 2.76; Cl, 28.18. *Calculated* for $C_{13}H_{12}Cr_2O_4Cl_4$: (478.08): C, 32.66; H, 2.53; Cl, 29.66.

---

[14] J. D. Drapper and E. F. Pratt, *J. Amer. Chem. Soc.*, **71**, 2846 (1949).

[15] G. Wittig and H. Schlorr, *Suomen Kemistilehti*, B **31**, 2 (1950).

[16] B. Helferich, P. E. Speidel and W. Toeldte, *Ber. dtsch. chem. Ges.*, **56**, 768 (1923).

[17] M. Gomberg, *Ber. dtsch. chem. Ges.*, **46**, 226 (1913).

[18] H. O. Halford, *J. Amer. Chem. Soc.*, **51**, 2157 (1939).

[19] L. Poyer, M. Fielder, H. Harrison and B. E. Bryant, "Inorganic Syntheses", vol. 5, *18*, McGraw-Hill, New York, 1957.

[20] J. L. E. Erikson and W. H. Ashton, *J. Amer. Chem. Soc.*, **63**, 1769 (1941).

The complex afforded on hydrolysis 1.9 g (0.01 mole) pure, crystallized benzophenone (100%).

The filtrate, washed with water, dried and evaporated under reduced pressure, yielded 1.45 g (80%) benzophenone.

The reaction of benzhydryl benzyl ether (II) with chromyl chloride.

A solution of 3.1 g (0.02 mole) chromyl chloride in 50 ml CCl_4 was added to a solution of 2.74 g (0.01 mole) II in 50 ml CCl_4. The chromyl chloride was immediately consumed.

The complex was filtered, washed and dried, yielding 3.7 g. After the usual working up 1.24 g product was obtained which showed on chromatography analysis the following composition (% moles): 27.5% benzophenone and 72.5% benzaldehyde.

After evaporation of carbon tetrachloride, the filtrate afforded 1.32 g (0.0072 mole) crystalline benzophenone, m.p. 45°. The mixed melting point showed no depression.

The overall yield of cleavage was 72%; the benzophenone was obtained in a quantitative yield, while the yield of benzaldehyde was 70% (0.743 g 0.007 mole).

Experiments carried out at various temperatures (−15°, 20°, 40°) had similar results; the temperature did not influence the yield of cleavage.

The reaction of benzhydryl t*-butyl ether (III) with chromyl chloride.*

A solution of chromyl chloride in CCl_4 (73.8 ml, 4.2%) was added to 2.4 g (0.01 mole) VII in 25 ml CCl_4 and the mixture left for 2 days at room temperature. After working up, 3.4 g (71%) dry complex were obtained, with the following composition: C, 30.14; H, 2.64; Cl, 30.03; Cr, 21.83. Calculated for $C_{13}H_{12}Cr_2O_4Cl_4$: C, 32.66; H, 2.53; Cl, 29.66; Cr, 21.76.

On hydrolysis, 3.4 g complex yielded 1.2 g pure benzophenone (m.p. 48°); 60% yield (on the initial amount of ether).

The filtrate, after washing and drying, afforded 0.85 g (43%) on the ether of *t*-butyl alcohol, together with small amounts of *t*-butyl chloride and 0.7 g (0.04 mole; 40%) benzophenone.

The reaction of benzyl triphenylmethyl ether (IV) with chromyl chloride.

3.5 g (0.01 mole) IV, dissolved in 50 ml CCl_4, were treated with 73.2 ml of 4.23% chromyl chloride (0.02 mole) solution in CCl_4. The mixture was left at room temperature for 24 hours.

The complex, which was isolated in 84.2% yield (calculated on the chromyl chloride) had the following composition: C, 20.46; H, 2.68; Cl, 25.02. Calculated for the Étard complex of toluene: $C_7H_8Cr_2O_4Cl_4$: C, 20.91; H, 2.01; Cl, 35.28; calculated for the Étard complex of triphenylmethane $C_{19}H_{16}Cr_2O_4Cl_4$: C, 41.18; H, 2.91; Cl, 25.59.

The elemental analysis indicated therefore the presence of a mixture. This was confirmed by the analysis of the hydrolysis products.

On hydrolysis the complex yielded 1.1 g of a mixture of crystals and oil from which were isolated 0.8 g (0.008 mole) benzaldehyde and 0.31 g (0.0012 mole) triphenylcarbinol, m.p. 159° (mixed m.p. without depression).

The filtrate yielded 2.2 g crystalline product with a pungent odour, m.p. 97°; after recrystallization from benzene m.p. 110° and mixed m.p. with authentic triphenylmethyl chloride without depression; 80% yield.

The reaction of isopropyl triphenylmethyl ether (V) with chromyl chloride.

A solution of 3 g (0.02 mole) chromyl chloride in 75 ml CCl_4 was added dropwise to a solution of 3 g (0.01 mole) V in 50 ml CCl_4. At the beginning the colour of the mixture was light yellow, then it turned red, then red-brown, and only after 30 min the brown complex started to precipitate.

2.2 g dry complex were decomposed with cold water and from it 0.3056 g (0.0012 mole) triphenylcarbinol, m. p. 159°, was isolated.

The solution which remained after the isolation of triphenylcarbinol was steam-distilled. The distillate, treated with aqueous solution of dinitrophenylhydrazine hydrochloride, yielded 0.86 g of acetone dinitrophenylhydrazone, m.p. 122°, mixed m.p. without depression. The yield of acetone was 0.0042 mole.

The orange filtrate was washed with water; the colour remained. The UV spectrum of a sample showed the same maximum (367 mu) as the di-triphenylmethyl chromate.

The orange CCl_4 solution was decolourized by shaking with a $NaHSO_3$ solution, and dried. After evaporation of the solvent, 2 g (0.0077 mole) crystalline triphenylcarbinol remained, m.p. 159°.

The reaction of benzhydryl triphenylmethyl ether (VI) with chromyl chloride.

4.26 g (0.01 mole) VI in 45 ml CCl_4 were treated with a solution of 3.1 g (0.02 mole) chromyl chloride in 35 ml CCl_4. After stirring during 12 hours the reaction mixture was filtered.

The complex was decomposed with cold water and the solution which resulted was extracted with CCl_4. The CCl_4 solution was dried and evaporated under reduced pressure, yielding 1.22g crystalline product, m.p. 149°. By treating with petroleum ether, 1 g (0.004 mole) triphenylcarbinol, m.p. 160°, and 0.22 g (0.0012 mole), m.p. 48° (mixed m.p. without depression) benzophenone were separated.

The red-orange *filtrate*, washed with water, with $NaHSO_3$ solution, then with water and pyridine, maintained the colour. After drying the solution and evaporating the solvent, 2 g brown residue remained. The chromatography on alumina column, using petroleum ether and then chloroform as eluents, afforded 1.55 g (0.0085 mole) benzophenone, m.p. 49°, and 1.3 g (0.005 mole) triphenylcarbinol, m.p. 162°.

The reaction of dibenzyl ether (VII) with chromyl chloride.

a) 4 g (0.02 mole) VII in 40 ml CCl_4 were treated with 3.5 g (0.02 mole) chromyl chloride in 40 ml CCl_4; the chromyl chloride was entirely consumed during the addition.

The complex was filtered and washed with CCl_4. In the filtrate 0.003 mole unreacted VII and 0.002 mole benzaldehyde were found, by means of chromatography. Taking into account of ether which reacted (0.017 mole), the yield of cleavage was 12%.

After the standard working up of the complex, 2.1 g (0.02 mole) benzaldehyde were obtained. The elemental analysis of the precipitate showed that it contained mainly the complex of the initial ether: found C, 38.01; H, 3.47; Cr, 16.27; Cl, 26.21; C, 38.16; H, 3.39 ; Cr, 16.43. *Calculated* for the Étard complex of toluene : $C_7H_8Cr_2Cl_4$: C, 20.91 ; H, 2.01, Cr, 25.88 ; Cl, 35.28.

b) In a similar run, in which 0.023 mole XVI reacted, 0.037 mole benzaldehyde was found in the filtrate. The complex, decomposed with aqueous $NaHSO_3$ solution, yielded 0.028 mole benzaldehyde, 0.0027 mole benzyl alcohol and traces of benzyl benzoate (identified by comparing it with an authentic sample, in the chromatography analysis).

The reaction of benzyl methyl ether VIII with chromyl chloride.

12.2 g (0.1 mole) VII dissolved in 120 ml CCl_4 were treated with 31 g (16 ml; 0.2 mole) chromyl chloride in 310 ml CCl_4. The complex precipitated immediately, leaving some unreacted chromyl chloride.

In the filtrate, in addition to unreacted starting material, traces of benzoyl chloride were also found. On hydrolysis the complex yielded 6 g mixture of 96.5% benzaldehyde and 3.5% benzyl benzoate.

The reaction of di-triphenylmethyl ether (IX) with chromyl chloride.

1.25 g (0.0025 mole) IX in 75 ml CCl_4 were treated with 0.512 g (0.0033 mole) chromyl chloride dissolved in 20 ml CCl_4. After 3 days, the red solution was washed with water in order to remove unreacted chromyl chloride, then dried in anhydrous magnesium sulphated. The UV spectrum of this solution showed a maximum at 367 mu, and was identical with that of di-triphenylmethyl chromate synthesized from triphenylcarbinol and chromic acid according to Wienhaus and Treibs.[21]

The crystals obtained after evaporation of the solvent under reduced pressure were purified by chromatography on alumina column, using methylene chloride as eluent. Evaporation of solvent yielded white crystals, m.p. 162° ; mixed m.p. with authentic triphenylcarbinol showed no depression.

The reaction of di-t-butyl ether (X) with chromyl chloride.

2.6 g (0.02 mole) X dissolved in 25 ml CCl_4 were treated with 3.1 g (1.6 ml; 0.02 mole) chromyl chloride in 40 ml CCl_4. From the red-brown solution the complex precipitated after a while, and the mixture was left for 7 days. The complex was then filtered and decomposed with water and ice. The solution which thus resulted was extracted continuously with ethyl ether during 24 hours. The ethyl ether was evaporated and the residue analyzed by chromatography on a column of 20% ethyleneglycol succinate on Chromosorb P, 68° ; 4.25 m ; 27.5 cc H_2/min. Three components were thus found ; the major one was identified as *t*-butanol, while one of the others was isobutyraldehyde. These compounds probably resulted from the decomposition of *t*-butyl chromate.

---

[21] H. Wienhaus and W. Treibs, *Ber. dtsch. chem. Ges.*, **56**, 1652 (1923).

4.20 ; Cr 19.40. Calculated for the Étard complex of toluene : $C_7H_8Cr_2O_4Cl_4$: C 20.91; H 2.01, Cr 25.88 ; Cl 35.38.

b) In a similar run, in which 0.023 mole XVI reacted, 0.007 mole benzaldehyde was found in the filtrate. The complex, decomposed with aqueous $NaHSO_3$ solution, yielded 0.028 mole benzaldehyde, 0.0027 mole benzyl alcohol and traces of benzyl benzoate (identified by comparing it with an authentic sample, in the chromatographic analysis).

The reaction of benzyl methyl ether (VII) with chromyl chloride.

12.2 g (0.1 mole) VII dissolved in 120 ml CCl_4 were treated with 31 g (18 ml; 0.2 mole) chromyl chloride in 210 ml CCl_4. The complex precipitated immediately, leaving some unreacted chromyl chloride.

In the filtrate, in addition to unreacted starting material, traces of benzoyl chloride were also found. On hydrolysis the complex yielded 8 g mixture of 76.5% benzaldehyde and 23.5% benzyl benzoate.

The reaction of di-triphenylmethyl ether (IX) with chromyl chloride.

1.25 g (0.0025 mole) IX in 25 ml CCl_4 were treated with 0.512 g (0.0033 mole) chromyl chloride dissolved in 20 ml CCl_4. After 3 days, the red solution was washed with water in order to remove unreacted chromyl chloride, then dried on anhydrous magnesium sulphate. The UV spectrum of this solution showed a maximum at 367 mμ, and was identical with that of di-triphenylmethyl chromate synthesized from triphenylcarbinol and chromic acid according to Wienhaus and Treibs [8].

The crystals obtained after evaporation of the solvent under reduced pressure were purified by chromatography on alumina column, using methylene chloride as eluent. Evaporation of solvent yielded white crystals, m.p. 162°; mixed m.p. with authentic triphenylcarbinol showed no depression.

The reaction of di-t-butyl ether (X) with chromyl chloride.

2.6 g (0.02 mole) X dissolved in 25 ml CCl_4 were treated with 3.1 g (1.6 ml; 0.02 mole) chromyl chloride in 40 ml CCl_4. From the red-brown solution the complex precipitated after a while, and the mixture was left for 7 days. The complex was then filtered and decomposed with water and ice. The solution which thus resulted was extracted continuously with ethyl ether during 24 hours. The ethyl ether was evaporated and the residue analysed by chromatography on a column of 20% ethyleneglycol succinate on Chromosorb P, 68°, 4.25 m; 25.5 cc H_2/min. Three components were thus found; the major one was identified as t-butanol, while one of the others was isobutyraldehyde. These compounds probably resulted from the decomposition of t-butyl chromate.

[8] H. Wienhaus and W. Treibs, Ber. dtsch. chem. Ges., 56, 1662 (1923).

Revue Roumaine de Chimie, **14**, 1567–1574(1969)

THE ÉTARD REACTION. X[1]

OXIDATION OF METHYLCYCLOPENTANE, METHYLCYCLOPENTENE AND OF METHYLENECYCLOALKANES C_5, C_6 AND C_7 WITH CHROMYL CHLORIDE

VALERIA PSEMEŢCHI, ILEANA NECŞOIU, MARINA RENŢEA and
C. D. NENITZESCU

Institute of Organic Chemistry of the Academy, Splaiul Independenţei 202 B, Bucharest

Received July 3, 1969

Oxidation of methylcyclopentane and 1-methylcyclopentene leads to a mixture of 2-methylcyclopentan-1-one, formylcyclopentane, 2-methylcyclopent-2-ene-1-one and 2-methyl-2-chlorocyclopentan-1-one. The intermediates and the mechanism of the oxidation are discussed. A comparison is made between oxidations with chromyl chloride of methylenecyclopentane, methylenecyclohexane and methylenecycloheptane.

The study of the oxidation of methylcyclopentane with chromyl chloride was undertaken for the first-time. In some previous works the oxidation of other cycloalkane derivatives was described. The effect of the ring size on the distribution of the oxidation products of methylcyclopentane was observed and compared to the similar oxidation of methylcylohexane. [2]

The Étard complex of methylcyclopentane, with a molecular formula near to $C_6H_{12} \cdot 2\,CrO_2Cl_2$, prepared and decomposed in the usual way, [2] leads to a mixture of 2-methylcyclopentan-1-one (**5**), formylcyclopentane (**11**), 2-methylcyclopent-2-ene-1-one (**7**) and 2-methyl-2-chlorocyclopentan-1-one (**6**) in the proportions indicated in table 1, which were measured by means of gas-chromatography.

On the basis of previous works [2,3] the formation of the products is interpreted according to chart 1. The initial Étard complex of methylcyclopentane, with structure **1**, undergoes an elimination of the chromyl rest and of a proton from C_β, leading to 1-methylcyclopentene (**2**). This olefin rapidly reacts with the excess of oxidant present in the reaction medium, giving the epoxidic intermediate **3**. The opening of the epoxidic

---

[1] A. Ghenciulescu, I. Necşoiu and C. D. Nenitzescu, *Rev. Roumaine Chim.*, in press

[2] C. N. Renţea, I. Necşoiu, M. Renţea, A. Ghenciulescu and C. D. Nenitzescu, *Tetrahedron*, **22**, 3501 (1966).

[3] I. Necşoiu, A. T. Balaban, I. Pascaru, E. Sliam, M. Elian and C. D. Nenitzescu, *Tetrahedron*, **19**, 1133 (1962).

Table 1

Products of the Étard reaction of methylcyclopentane, 1-methylcyclopentene and methylenecyclopentane

Products (mole %) / Starting materials	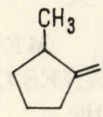 **5**	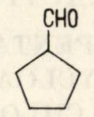 **11**	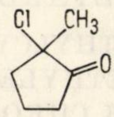 **6**	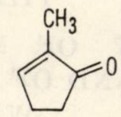 **7**	Yield d)
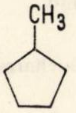 a)	61.7	2.4	31.2	4.7	60
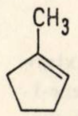 b)	84.6	1.4	4.2	9.9	56
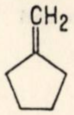 c)	72.0	17.5	4.7	5.8	40

Found for Étard complex:
a) C, 12.38; H, 2.61; Cr, 24.52; Cl, 40.58
b) C, 27.52; H, 4.25; Cr, 21.07; Cl, 30.80
c) C, 24.16; H, 3.87; Cr, 22.84; Cl, 32.86
d) The yields are calculated on the chromyl chloride used.

ring with formation of the tertiary carbocation **4**[4] accompanied either by migration of a hydride ion or by reaction with chloride ion and subsequent oxidation, affords 2-methylcyclopentan-1-one (**5**) and 2-methyl-2-chlorocyclopentan-1-one (**6**) respectively. From the chloroketone **6** the unsaturated ketone **7** is formed, by elimination of hydrogen chloride.

Methylenecyclopentane (**8**), the exocyclic elimination product of the Étard complex (**1**) gives on subsequent oxidation formylcyclopentane (**11**), which is present in small amounts among the oxidation products of methylcyclopentane (Table 1).

The occurrence of alkenes as intermediates in the Étard reaction of saturated hydrocarbons was previously reported in several of our papers.[2,5,6] In order to confirm these results we undertook the oxidation with chromyl chloride of the two olefins **2** and **8**, which were supposed to be intermediates in the Étard reaction of methylcyclopentane. The results are shown in table 1.

---

[4] S. Winstein and R. B. Henderson in R. C. Elderfield "Heterocyclic Compounds", vol. I, John Wiley and Sons, New York, 1950, p. 1.

[5] A. Ghenciulescu, I. Necşoiu and C. D. Nenitzescu, unpublished results.

[6] C. D. Nenitzescu, *Bull. Soc. chim. France*, **1968**, 1349.

As one can see from this table, the major oxidation product of the endocyclic olefin **2** is 2-methyl-cyclopentan-1-one (**5**), a fact which con-

Chart 1

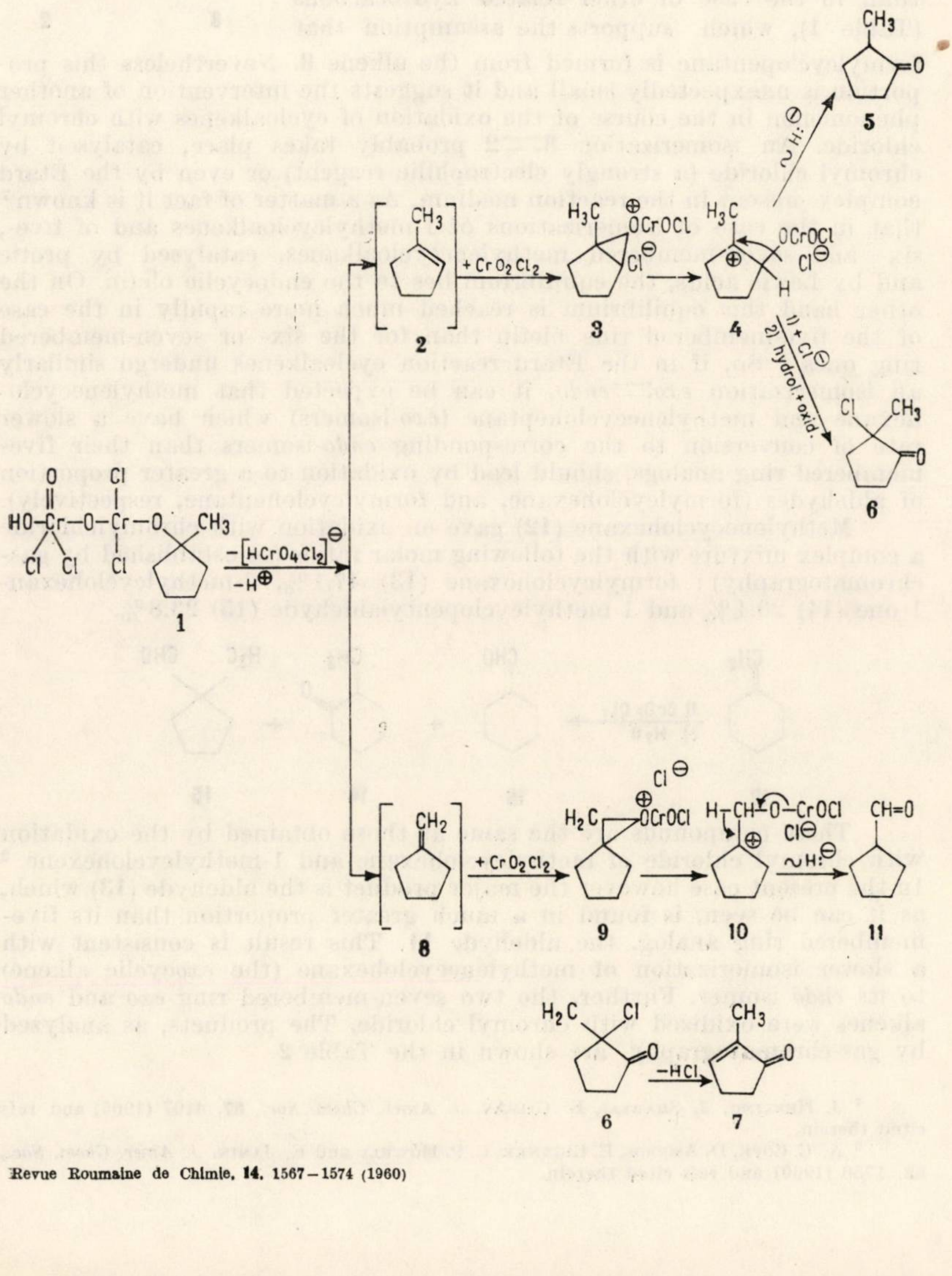
CH3
5
-HCl
1) Cl⊖
2) hydrol.+oxid.
CH3
+CrO2Cl2
2
H3C ⊕OCrOCl
Cl⊖
3
H3C OCrOCl
⊕ Cl⊖
H
4
Cl CH3
O
6
O Cl
HO–Cr–O–Cr–O CH3
Cl Cl
1
–[HCrO4Cl2]⊖
–H⊕
CH2
+CrO2Cl2
8
Cl⊖
H2C ⊕OCrOCl
9
H–CH–O–CrOCl
Cl⊖
⊕
~H:⊖
10
CH=O
11
H2C Cl
O
6
CH3
O
-HCl
7

firms the validity of Chart 1. However, the oxidation of methylenecyclopentane (**8**) shows some anomalies. The normal product of oxidation of this alkene should be formylcyclopentane (**11**). This compound is found to be present in the mixture resulted from the oxidation of methylene cyclopentane in proportion ten times larger than in the case of other related hydrocarbons (Table 1), which supports the assumption that formylcyclopentane is formed from the alkene **8**. Nevertheless this proportion is unexpectedly small and it suggests the intervention of another phenomenon in the course of the oxidation of cycloalkenes with chromyl chloride. An isomerization **8**$\rightleftharpoons$**2** probably takes place, catalysed by chromyl chloride (a strongly electrophilic reagent) or even by the Étard complex present in the reaction medium. As a matter of fact it is known[7] that in the case of isomerizations of 1-methylcycloalkenes and of five-, six- and seven-membered methylenecycloalkanes, catalysed by protic and by Lewis acids, the equilibrium lies to the endocyclic olefin. On the other hand this equilibrium is reached much more rapidly in the case of the five-membered ring olefin than for the six- or seven-membered ring ones.[8] So, if in the Étard reaction cycloalkenes undergo similarly an isomerization *exo*$\rightleftharpoons$*endo*, it can be expected that methylenecyclohexane and methylenecycloheptane (*exo*-isomers) which have a slower rate of conversion to the corresponding *endo*-isomers than their five-membered ring analogs, should lead by oxidation to a greater proportion of aldehydes (formylcyclohexane, and formylcycloheptane, respectively).

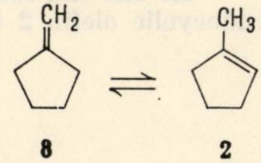

8 **2**

Methylenecyclohexane (**12**) gave on oxidation with chromylchloride a complex mixture with the following molar ratios (as established by gas-chromatography): formylcyclohexane (**13**) 47.1%, 2-methylcyclohexan-1-one (**14**) 29.1% and 1-methylcyclopentylaldehyde (**15**) 23.8%.

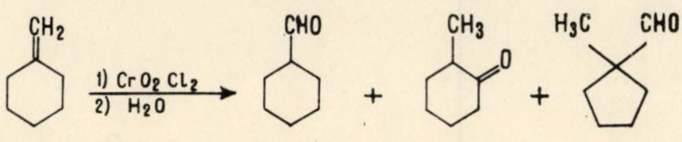

12 **13** **14** **15**

These compounds are the same as those obtained by the oxidation with chromyl chloride of methylcyclohexane and 1-methylcyclohexene.[2] In the present case however the major product is the aldehyde (**13**) which, as it can be seen, is found in a much greater proportion than its five-membered ring analog, the aldehyde **11**. This result is consistent with a slower isomerization of methylenecyclohexane (the *exo*cyclic alkene) to its *endo* isomer. Further, the two seven-membered ring *exo* and *endo* alkenes were oxidized with chromyl chloride. The products, as analyzed by gas-chromatography, are shown in the Table 2.

---

[7] J. Herling, J. Shabtai, E. Gil-Av, *J. Amer. Chem. Soc.*, **87**, 4107 (1965) and refs cited therein.

[8] A. C. Cope, D. Ambros, E. Ciganek, C. P. Howell and E. Janin, *J. Amer. Chem. Soc.*, **82**, 1750 (1960) and refs cited therein.

One can see that formylcycloheptane (17) (the seven-membered ring aldehyde) is formed in a much greater proportion from methylenecycloheptane than from 1-methylcycloheptene, and also in a greater quantity than its five-membered ring analog. The results are shown comparatively in table 3. Nevertheless the value is much smaller than expected, because of the slower rate of isomerization of methylenecycloheptane to 1-methylcycloheptene.

Table 2

Products of the Étard reaction of methylcycloheptene and methylenecycloheptane

Products (mole%) / Starting materials	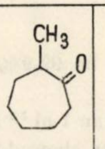 16	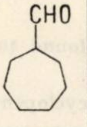 17	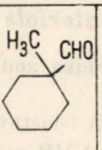 18	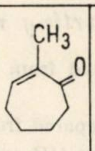 19	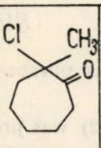 20	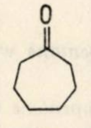 21	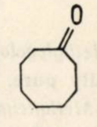 22	Yield c) %
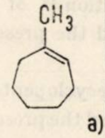 a)	52.8	3.9	26.4	11.1	5.7	–	–	60
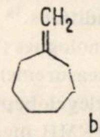 b)	31.5	28.3	25.3	–	–	12.42	2.5	68

Found for Étard complex:
a) C. 30.88; H. 4.84; Cl. 30.70; Cr. 20.16
b) C. 30.85; H. 5.19; Cl. 26.77; Cr. 20.33
c) The yields are calculated on the chromyl chloride used.

Table 3

Cycloalkyl aldehydes resulted by oxidation of methylenecycloalkanes

Methylenecycloalkanes	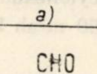 a)	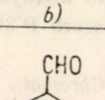 b)	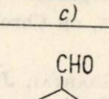 c)
Cycloalkyl aldehydes mole %	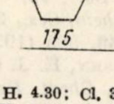 175	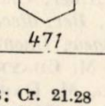 471	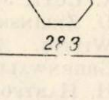 283

a) s. Table 1
b) Found for Étard complex: C. 26.53; H. 4.30; Cl. 32.93; Cr. 21.28
c) Found for Étard complex: C. 30.85; H. 5.19; Cl. 26.77; Cr. 20.33.

The result obtained in the case of methylenecycloheptane could be due to some conformational effects. As it is known[9] this alkene can exist in two conformations, twist-chair and twist-boat. In both forms the double bond is shielded, in the former case by the hydrogen on C_2 and in the latter by the hydrogen on C_4. This shielding of the double bond could produce a decrease in the rate of reaction with chromyl chloride and compensate in part the favourable effect of the slower isomerization of the hydrocarbon to its *endo* isomer.

EXPERIMENTAL

Starting materials

Methylcyclopentane was purchased from Fluka and found to be 99.9% gas-chromatographically pure.

1-Methylcyclopentene (**2**) was prepared from 1-methylcyclopentan-1-ol[12] by dehydration with iodine.[10, 11] B.p. 75°, 96% purity (IR and NMR measurements showed the presence of 4% methylenecyclopentane).

Methylenecyclopentane (**8**) was prepared according to Corey's modification[14] of the Wittig method.[13] B.p. 76.5°, 92% purity (IR and NMR measurements indicated the presence of about 8% benzene).

Methylenecyclohexane (**12**) was prepared in the same way[14] as methylenecyclopentane. B.p. 75°, 75% purity (IR, NMR and gas-chromatography measurements indicated the presence of 25% benzene, which could not be removed by rectification). The product was used as such since benzene reacts with chromyl chloride only under much more energetic conditions.[15]

Methylenecycloheptane was prepared in the same way[14] as its inferior homologues; the yield was 52%. B.p. 138°.8, 96% purity (IR, NMR and gas-chromatography measurements).

Methylcycloheptene was prepared by dehydration with iodine[16] of 1-methylcycloheptan-1-ol (obtained by Grignard reaction) in 72% yield, B.p. 137–138°, 96% purity (NMR measurements, indicated about 4% methylenecycloheptane).

Chromyl chloride was prepared by Sisler's method[17] and used after rectification.

The Étard complexes of the hydrocarbons mentioned above were prepared and decomposed following the method previously described.[2] The oxidation products were analyzed by gas-chromatography (Tables 1, 2 and 3) immediately after working up. Their identification will be described further on.

Identification of the reaction products (s. Tables 1, 2, 3 and the text). The products were identified by means of gas-chromatography retention time. IR and NMR spectra were compared to those of authentic samples prepared as described below.

The gas-chromatography analyses were carried out on a Carlo Erba instrument Model D. For the analyses of the oxidation products of methylcyclopentane, 1-methylcyclopentene, methylenecyclopentane and methylenecylohexane the following columns were used: didecyl phthalate 25% on Chromosorb P 30–60 mesh l = 1 m, ∅ = 2 mm, at 80°, 100 ml H_2/min and LAC 728, 20% on Chromosorb P 60–80 mesh at 80°, 40 ml H_2/min. The analyses of the oxidation products of methylenecyclopentane were made at 75°, 40 ml H_2/min; those resulted from the oxidation of methylenecyclohexane were analysed at 87°, 37 ml H_2/min. The products resulted from the oxidation of 1-methylcycloheptene and methylenecycloheptane were analysed using a Willy Giede instrument on the same columns as mentioned above, at 110° and 200 ml H_2/min ($l = 1$ mm $\varnothing = 6$ mm of the column of didecylphthalate and $1 = 3$ mm and $\varnothing = 6$ mm of LAC 728).

---

[9] J. Shabtai, *J. Chromat.*, **18** (2), 302 (1965).

[10] P. D. Bartlett and R. H. Rosenwald, *J. Amer. Chem. Soc.*, **56**, 1933 (1934).

[11] C. A. Lutz, *J. Amer. Chem. Soc.*, **70**, 4139 (1948).

[12] N. D. Zelinsky, *Ber. dtsch. chem. Ges.*, **35**. 2683 (1902).

[13] G. Wittig. *Angew. Chem.*, **68**, 505 (1956).

[14] R. Greenwald, M. Chaykowsky, E. J. Corey, *J. Org. Chem.*, **28**, 1128 (1963).

[15] V. H. Hartford, M. Darrin, *Chem. Rev.*, **58**, 1 (1958).

[16] W. Hückel and J. Wachter, *Liebigs Ann. Chem.*, **672**, 62 (1964).

[17] H. E. Sisler, "Inorganic Synthesis", vol. 2, McGraw-Hill, New York, 1958, p. 205.

The IR spectra were recorded on Perkin Elmer 621 and UR 20 Carl Zeiss Jena spectrophotometers and NMR spectra on a Varian A 60 A instrument.

2-Methylcyclopentan-1-one **(5)**. The gas-chromatography retention time and the IR spectrum of the product, isolated by preparative v.p.c., were identical to those of the authentic ketone prepared after Hückel.[18]

2-Methyl-2-chloro-cyclopentan-1-one **(6)** was prepared by the method described by Warnhoff, Martin and Johnson[22] for the preparation of 2-methyl-2-chlorocyclohexanone. The ketone **6** can be stored for a limited time in an argon atmosphere, in the presence of a small amount of MgO. In time an elimination of HCl takes place and the corresponding unsaturated ketone **7** (2-methylcyclopent-2-en-1-one) is formed.

2-Methylcyclopent-2-en-1-one **(7)**. The method described in literature for the six-membered ring derivative[19] was used.

Formylcyclopentane **(11)**. The gas-chromatography retention time and the IR spectrum (CCl_4) of the compound, isolated by preparative v.p.c., were identical to those of the authentic aldehyde prepared after Grummit.[20] Formylcyclopentane was identified among the decomposition products of the methylcyclopentane complex and also of the methylenecyclopentane complex, by oxidation of the reaction mixture with Ag_2O,[21] followed by esterification with diazomethane of the resulted cyclopentanecarboxylic acid, and then by comparing the gas-chromatography retention time and the IR spectrum (CCl_4) to those of the authentic methyl ester of cyclopentanecarboxylic acid.[22]

Formylcyclohexane **(13)** detected among the oxidation products of methylenecyclohexane, was isolated from the mixture by v.p.c. The v.p.c. retention time and IR spectrum were identical to those of the authentic aldehyde obtained by hydrolysis of ethyl-1-α-epoxycyclohexylidenacetate[23] obtained according to the method described in the literature.[24] The isolated aldehyde **(13)** was oxidized[23] to hexahydrobenzoic acid, with subsequent esterification. The methyl ester of the acid mentioned was identified by v.p.c. retention time and IR spectrum, which were identical to those of the compound prepared from benzoic acid by hydrogeneation and esterification in the usual way.

[18] W. HUCKEL, K. KINDLER, *Chem. Ber.*, **80**, 202 (1947).

[19] E. W. WARNHOFF, D. G. MARTIN and W. S. JOHNSON, "Organic Synthesis", Coll. IV, John Wiley and Sons, New York, 1963, p. 162.

[20] O. GRUMMIT, J. LISKA and G. GREULL, "Organic Synthesis", Coll. IV, John Wiley and Sons, New York, 1963, p. 162.

[21] I. A. GOLDBERG and R. P. LINSTEAD, *J. Chem. Soc.*, **1928**, 2355.

[22] A. FAVORSKY, V. BOSHOWSKY, *J. Chem. Soc.*, **46**, 1097 (1914); HOUBEN-WEYL, "Methoden der org. Chemie", vol. 8, Georg Thieme, Stuttgart, 1952, p. 460.

[23] W. S. JOHNSON, J. S. BELOW, L. J. CHINN, R. H. HUNT, *J. Amer. Chem. Soc.*, **75**, 4995 (1963).

[24] G. DARZENS, P. LEFEBRE, *Compt. rend.*, **142**, 719 (1906).

Revue Roumaine de Chimie, **14**, 1567–1574 (1969)

1-Methylcyclopenthylaldehyde (**15**) was isolated by preparative v.p.c. anp identified by IR and NMR spectra.

In order to verify these results the products of oxidation of methylenecyclohexane were oxidized with Ag_2O.[21] After working up in the usual way the esters of both acids (hexahydrobenzoic and 1-methyl-1-carboxylic) were identified by comparing their v.p.c. retention time, IR and NMR spectra to those of authentic samples, the first prepared as described above and the other according to the method of Koch and Haaf.[25]

2-Methylcyclohexan-1-one (**14**) was identified by v.p.c., by comparing its retention time to that of a comercially available sample, chromatographically pure.

2-Methylcycloheptan-1-one (**16**), isolated by v.p.c., was identified by comparing its retention time and IR spectrum to those of an authentic sample prepared according to literature. [16,26]

Formylcycloheptane (**17**) was isolated from the oxidation mixture of seven-membered hydrocarbons such as methyl- and methylenecycloheptane, by means of v.p.c., and identified by its IR and NMR spectra.

1-Methylcyclohexyl-1-aldehyde (**18**), isolated by v.p.c. was identified in the same way as above.

Furthermore the products of oxidation of methylenecycloheptane were oxidized in the same manner as described above for six-membered derivatives. The resulted esters were identified by comparing the gas-chromatography retention time and the IR spectra to those of authentic samples. The ester of 1-methylcyclohexyl-carboxylic-1 acid was obtained by esterification of the acid, which in turn was prepared according to Haaf. [27] In order to obtain the ester of cycloheptanecarboxilic acid, cycloheptanone was reduced to cycloheptanol according to the method of Garmon and Haase [28]; the alcohol was then transformed into the bromine derivative, with PBr_3, this was followed by the Grignard reaction and finally by treatment with CO_2. The carboxylic acid thus obtained, with b.p.$_{15}$ 139°, was esterified with diazomethane and identified by IR spectrum.

2-Methylcyclohept-2-en-1-one (**19**) and *2-methyl-2-chloro-cycloheptan-1-one* (**20**), isolated by v.p.c., were identified in the usual way by comparing their IR spectra to those of authentic samples synthesized according to the method described in the literature [19] for six-membered ring derivatives.

Cycloheptanone (**21**) and *cyclooctanone* (**22**), isolated by v.p.c. were identified by comparing their IR spectra and their gas-chromatography retention times to those of comercially available samples.

[25] H. Koch, W. Haaf, *Liebigs Ann. Chem.*, **618**, 261 (1958).

[26] W. Hückel, O. Honecker, *Liebigs Ann. Chem.*, **678**, 10 (1964).

[27] W. Haaf, *Org. Synth.*, **40**, 72 (1960).

[28] W. E. Garmon and H. Haase, *Org. Synthesis*, **40**, 151 (1960).

Revue Roumaine de Chimie, **14**, 1575–1577 (1969)

A CORRELATION BETWEEN CHEMICAL SHIFTS OF METHYL PROTONS AND ELECTRON DENSITIES IN SUBSTITUTED PYRYLIUM SALTS

G. V. BOYD

Department of Chemistry, Chelsea College of Science and Technology, London, S.W. 3

and

A. T. BALABAN

Institute of Atomic Physics, P. O. Box 35, Bucharest

Received June 23, 1969

The chemical shifts of protons in the methyl groups of ten substituted pyrylium salts are linearly related to π-electron densities calculated by a self-consistent version of the Hückel method.

The shielding of protons in heterocyclic aromatic compounds is due to a combination of factors : ring-current, electron density and the anisotropy of the hetero-atom. [1,2] For a series of methyl-derivatives of a given heterocyclic system the ring-current effect may be regarded as constant ; differences in the chemical shifts of protons of substituent methyl-groups should then arise chiefly from the varying electron density since such protons are less sensitive to anisotropy effects than are ring atoms and their attached protons. Linear correlations between calculated π-electron densities and observed chemical shifts of *C*-methyl-protons have been reported for azaindenes [3] and 2-cyclopentadienylidenedihydropyridines (I). [4] We have now extended this work to a series of methyl-substituted pyrylium salts (II) whose p.m.r. spectra have been published. [5] Liquid sulphur dioxide was the solvent (in closed NMR vials, at room temperature) for all compounds.

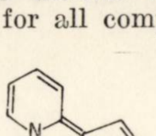

I

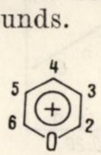

II

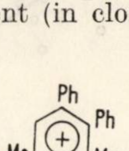

III

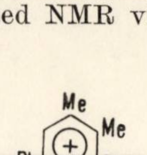

IV

---

[1] G. G. Hall, A. Hardisson and L. M. Jackman, *Tetrahedron*, **19**, Suppl. 2, 101 (1963).
[2] W. P. Paudler and J. E. Kuder, *J. Org. Chem.*, **31**, 809 (1966).
[3] W. P. Paudler and J. E. Kuder, *J. Heterocyclic Chem.*, **3**, 33 (1966).
[4] G. V. Boyd and N. Singer, *J. Chem. Soc.* (*B*), **1966**, 1017.
[5] A. T. Balaban, G. R. Bedford and A. R. Katritzky, *J. Chem. Soc.*, **1964**, 1646.

Electron densities, q, were computed in three ways: in the first, a straightforward Hückel calculation was carried out, in the others the calculations were reiterated to self-consistency by varying Coulomb integrals, α, according to charges, and resonance integrals, β, according to bond orders until the $\alpha\beta$-matrix converged to within 0.0005 for each element. The factor ω, which relates Coulomb integrals to charges, was 1.4 for all atoms in the second set of calculations ("$\omega\beta$-technique")[4]; in the third ("$\omega'\beta$-technique")[6], varying values for ω were employed[7] for different atoms i:

$$\omega_i = 1.3 + 0.45\, h_i$$
$$\text{where } \alpha_i = \alpha + h_i\, \beta.$$

The parameters for the Coulomb integrals for pyrylium oxygen and the inductive model for the methyl group were taken as $h_{\mathrm{O}^{\oplus}} = 2.5$ and $h_{\mathrm{CMe}} = -0.3$ for reasons discussed elsewhere.[6] The calculations, which were done on the London University "Atlas" computer, included all those pyrylium salts listed in the previous paper[5] which contained only methyl as alkyl-substituents except 4-ethyl-2,3,5,6-tetramethylpyrylium ion as a representative of a fully alkylated compound. 2,6-Dimethyl-3,4-diphenylpyrylium ion (III) was omitted since our assumption that phenyl substituents may attain co-planarity with the pyrylium nucleus is clearly not justified for this ion in which the neighbouring benzene rings must be twisted out of the molecular plane to an unknown extent. In the cation (IV), which contains adjacent methyl and phenyl groups, steric interference is less serious and this salt was therefore included in the correlation, the methyl signal at lower field being assigned to the 4-methyl group.

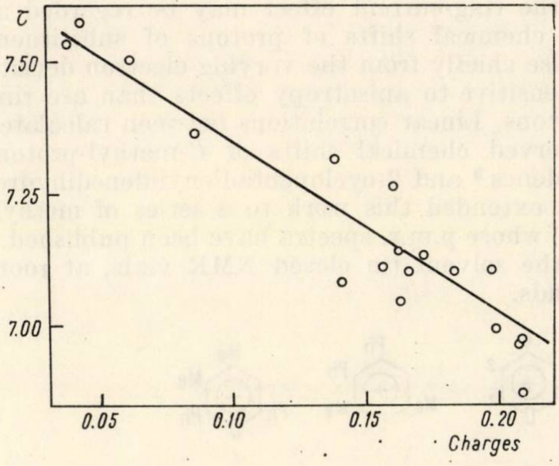

Fig. 1. — Correlation between chemical shifts of methyl protons and electron densities in substituted pyrylium salts.

The results are presented in the table. There is a good linear correlation between chemical shifts (τ) of C-methyl protons and electron den-

---

[6] G. V. Boyd, *Rev. Roumaine Chim.*, **12**, 1133 (1967).

[7] N. C. Baird and M. A. Whitehead, *Canad. J. Chem.*, **44**, 1933 (1966).

Table

Chemical shifts of methyl protons and electron densities of pyrylium ions (II)

Pyrylium ion	Protons	Chemical shift (τ)	Electron densities		
			Hückel	$\omega\beta$	$\omega'\beta$
2,6-Me_2	2(6)-Me	6.96	0.628	0.775	0.792
2,4,6-Me_3	2(6)-Me	7.10	0.637	0.784	0.802
	4-Me	7.26	0.718	0.821	0.839
2,3,4,6-Me_4	2-Me	7.13	0.693	0.808	0.828
	3-Me	7.57	1.017	0.944	0.957
	4-Me	7.31	0.759	0.841	0.861
	6-Me	7.10	0.660	0.798	0.817
2,3,5,6-Me_4	2(6)-Me	7.10	0.705	0.813	0.834
	3(5)-Me	7.50	0.971	0.928	0.938
4-Et-2,3,5,6-Me_4	2(6)-Me	7.11	0.716	0.822	0.843
	3(5)-Me	7.53	1.013	0.949	0.962
2,6-Me_2-4-Ph	2(6)-Me	6.99	0.642	0.786	0.801
2,4-Me_2-6-Ph	2-Me	6.97	0.623	0.777	0.791
	4-Me	7.14	0.723	0.823	0.837
2-Me-4,6-Ph_2	2-Me	6.87	0.629	0.780	0.791
4-Me-2,6-Ph_2	4-Me	7.04	0.729	0.826	0.837
3,4-Me_2-2,6-Ph_2	3-Me	7.36	0.921	0.909	0.914
	4-Me	7.08	0.767	0.844	0.859

sities obtained by the Hückel method with a standard deviation, $\sigma = 0.077\ \tau$. The correlation is improved by use of the $\omega\beta$-technique, σ decreasing to $0.073\ \tau$; but the $\omega'\beta$-technique leads to a considerable further decrease in the deviation with $\sigma = 0.065\ \tau$. These results illustrate the improvements that are achieved in the calculations of ground-state properties when some of the internal inconsistencies of the simple Hückel method are removed. The figure shows the linear regression of chemical shift values on π-electron charges, $1 - q$, computed by the $\omega'\beta$-method. The equation of this line, $\tau = 7.70 - 3.51\ (1 - q)$, is similar to that $[\tau = 8.15 - 3.30\ (1 - q)]$ obtained for the dihydropyridines (I); but the resemblance must be fortuitous since two very different heterocyclic systems are involved, one of which is neutral and the other charged.

Revue Roumaine de Chimie, **14**, 1579–1583 (1969)

THE ACTION OF AMMONIA ON SOME NITRODERIVATES OF PHENOTHIAZINE-5-OXIDE AND PHENOTHIAZINE-5, 5-DIOXIDE

A. TURCU and M. RĂILEANU

Pedagogical Institute, Bucharest, Şos. Panduri 90

Received May 16, 1968

Ammonia reacts with 1, 3, 7, 9-tetra-nitrophenothiazine-5-oxide (I) and 1, 3, 7, 9-tetraphenothiazine-5,5-dioxide (II) forming molecular complexes of the donor-acceptor type.

We find in literature that the nitrate derivates of phenothiazine 5-oxide, with the nitro group in *ortho* and *para* position towards the nitrogen atom, have acid properties, solving in aqueous alkaline hydroxides with the forming of salts and colour changes from yellow to red.[1–3]

Owing to these qualities, the above mentioned nitroderivates are used as reactives in analytical chemistry, for instance in the dosing of potassium.[4–5]

The attempts made by us have shown that the corresponding nitro derivates of phenothiazine-5,5-dioxide have a similar behaviour towards alkalies.

The acidity of the mentioned nitroderivates is due to the presence of the nitro, sulphoxidic and sulphonic groups. These groups bring about the attraction of the valence electrons of the nitrogen atom in position 10, thus favouring the release of the hydrogen atom as proton. As expected, the acidity rises in the series of these nitroderivates with the number of nitro groups, reaching a maximum for 1,3,7,9-tetranitrophenothia-

---

[1] E. De B. Burnett and S. Smiles, *J. Chem. Soc.*, **95**, 1253 (1909).

[2] F. Kehrmann and O. Nossenko, *Chem. Ber.*, **46**, 2819 (1913).

[3] J. S. Driscoll and R. H. Nealey, *J. Heterocyclic Chem.*, **2**, 272 (1965).

[4] K. Toei, *Chem. Abstr.*, **51**, 11913 d (1957).

[5] K. Toei, *Chem. Abstr.*, **52**, 961 i (1958).

zine-5-oxide (I) and 1,3,7,9-tetranitrophenothiazine-5,5-dioxide (II).

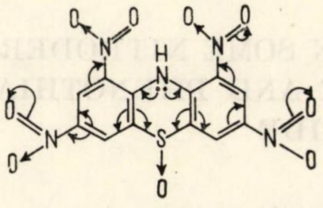

I

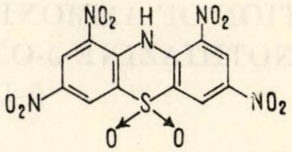

II

Our attempts to determine the acidity constants of compounds I and II by measuring the electric conductivity of their aqueous solutions failed, as neither I nor II solve well in water, and form solutions of practically infinite dilution.

We have further studied the effects of ammonia, as a weak base, on compounds I and II. We have noticed that they react extremely easily with a concentrated ammonia solution, even at room temperature, yielding well cristallyzed red products, with metallic reflex, for both compounds.

The resulting compounds have a high enough thermic stability, splitting into their initial components only at about 170°, and the analysis shows a nitroderivate/ammonia combination ratio of 1 : 1.

In order to determine wether the reaction products with ammonia of the compounds I and II are salts or molecular compounds, one has studied comparatively the IR spectra of the following substances : phenothiazine, phenothiazine-5-oxide, 1,3,7,9-tetranitrophenothiazine (I), 1,3,7,9-tetranitrophenothiazine-5,5-dioxide (II), as well as the sodium salt and the complex with ammonia of the substances I and II. The study was carried out especially for the absorption range of νN—H as in this region more striking changes take place (figure I).

The IR spectra were carried out on solid state substances, tabletted with KBr. For the complex with ammonia of 1,3,7,9-tetranitrophenothiazine-5-oxide, one has also performed the IR spectrum in solution using dioxane as solvent.

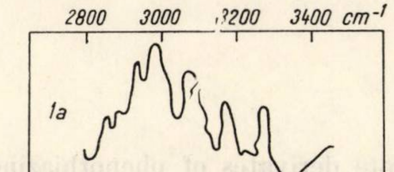

Fig. 1. — IR spectra of compounds

In phenothiazine the absorption band for νN—H is at 3350 cm $^{-1}$. In phenothiazine-5sulphoxide the absorption band corresponding to the

N—H valence vibration is at 3255 cm^{-1} (fig. 1 a). This shifting is explained by the formation of some intermolecular hydrogen bridges $-S\rightarrow O\ldots\ldots H-N$.[6] νN—H for compound I is found at 3215 cm^{-1} (fig. 1 b), and for compound II at 3205 cm^{-1}.

The IR spectrum of the complex with ammonia of the substances I and II (fig. 1 c and 1 d) shows that in these compounds the absorption band for νN—H is practically not affected and it is found at 3210 cm^{-1}.

In the IR spectrum of the sodium salt obtained through the reaction between substances I and II and NaOH, the absorption band caracteristic of νN—H, no longer appears, a fact leading to the conclusions that the hydrogen linked to the nitrogen atom takes part in the reaction, and is substituted (fig. 1 e).

It results that the sodium hydroxide and the concentrated ammonia solution react differently with the substances I and II.

In the first case a sodium salt is obtained, in the second a stable molecular complex. As regards the IR spectrum of the two complexes with ammonia, the fact that in both compounds the absorption bands corresponding to the νN—H in the ammonia are absent has not yet been cleared up. However in solid state, owing to the very high interaction between molecules these bands might be displaced from their normal site and covered by other absorption bands, for instance by the band corresponding to the νN—H of the heterocycle.

In order to evidence the characteristic νN—H absorbtion bands in ammonia we have tried to determine the IR spectrum in solution, using different solvents. One has noticed that the substances I and II, as well as their complexes with ammonia are not soluble in the solvents which are best suitable for such research (carbon tetrachloride, carbon sulphide, chloroform, etc.). Of the sixteen solvents used, only dioxane solves well substances I and II, and to a smaller extent their complexes with ammonia.

The substances I and II do not show significant shifts of the absorption bands for νN—H; for different concentrations these bands appear constantly at about 3200 cm^{-1}. It may be noticed that at 3400 cm^{-1} a new absorption band appears as shoulder which is not found in the spectrum of the substances I and II in solid state. This band appears only in a very diluted solution. One could assign this band to the unassociated νN—H frequency.

In the case of the complexes of substances I and II with ammonia, in the IR spectrum of the solution with dioxane, a new shoulder at 3340 cm^{-1} appears, which may be assigned to the νN—H in ammonia. The other absorption bands, characteristic of the N—H band in ammonia could not be positively ascertained.

Hence the IR spectra in dioxane solution are not sufficiently conclusive for the structure of the complexes with ammonia of the substances I and II.

New data on the structure of the above substances may be found by extending the research also to the complexes obtained from these substances with primary, secondary and tertiary amines. From preliminary attempts it results that substances I and II react with certain amines giving coloured crystalline products. Some of these products compounds are being analysed.

---

[6] N. A. KUDRYAVTSEVA and collab., *Chem. Abstr.*, **64**, 2867 a (1966).

According to the above data, we consider the possibility of a combination of the following form as out of question for the complexes formed by the reaction of substances I and II with ammonia.

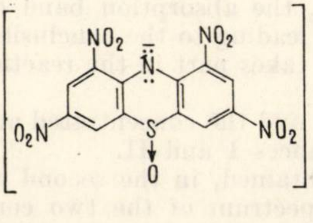

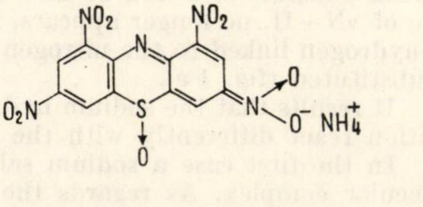

Similar compounds are formed in the case of substances I and II reacting with alkaline hydroxides. Therefore the IR bands for νN−H of the heterocycle do not appear any more in these compounds. In this case between the substances I and II, and the ammonia, a donor-acceptor type complex is forming, which may be represented as follows :

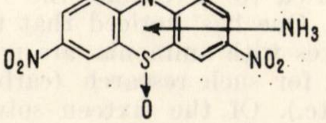

EXPERIMENTAL

1) *1,3,7,9,-Tetranitro-phenothiazine-5-oxide (I)*

1a) *stepwise nitration of phenothiazine* : 10 g of phenothiazine, m. p. 183°, are introduced in small amounts and under continuous stirring into 200 ml of HNO_3 $D = 1.42$. After 15 min, the deposited yellow acicular precipitate is filtered, thoroughly washed with water and dried. An inferior nitrated product of phenothiazine results (phase one).

In the second phase the product is boiled on a water bath for 45 min in a flask containing 200 ml HNO_3 $D = 1.52$. The mixture is finally cooled and gradually processed with 250 ml of water. The yellow acicular precipitate deposited is filtered, well washed with water and dried.

The result is III with m. p. 359−360° and an easy decomposition. Yield, 78 %. The substance thus obtained is purer than that described in literature (for which the melting point is 354−555°)[7]

$C_{12}H_5O_9N_5S$ (395.36 *Calcd.* : N, 17.72 ;
Found : N, 17.65.

---

[7] C. Bodea and N. Răileanu, *Studii şi cercetări Chim., Fil. Cluj*, **8**, 303 (1957).

1b) *Nitration of N - acetyl-phenothiazine* : 10 g of N — acetyl-phenothiazine are gradually solved under continuous stirring in 200 ml of HNO_3 D = 1.52, the solution is boiled in a flask on water bath for 45 minutes. After cooling water is carefully added. The yellow acicular reaction product has, after filtering, washing with water and drying, m. p. 359—360° and is identical to I.

Dry evaporation of a small portion of the initial nitrogen solution shows that the removing of the acetyl group takes place even during the nitration, and not following the dilution with water of the reaction mixture.

2) *Molecular complex with ammonia of 1, 3, 7, 9 - tetranitrophenothiazine-5-oxide* (I) : 2 g of I are boiled in 200 ml of concentrated ammonia solution, after which the suspension is left to rest an hour. The carmin-red crystals with metallic reflexes are filtered, washed with some ammonia and dried at 110°.

The yield is, 1,8 g of molecular complex, which decomposes into its initial components in boiling water or in dry state at approximately 170°.

$C_{12}H_8O_9N_6S$ (412.36) Calcd : N, 20.40 ;
Found : N, 20.26.

3) *Molecular complex with ammonia of 1, 3, 7, 9 - tetranitrophenothiazine-5, 5-dioxide* (II). By proceeding in the same way as at point (2), the molecular complex of II with ammonia is formed yielding 1.6 g with the same colour as for (I) and similar features.

The compound (II) used in the reaction (m. p. 347°) was obtained by the Bodea-Răileanu method[7].

Revue Roumaine de Chimie, **14**, 1585–1590 (1969)

OXYGEN-ALKYL BOND CLEAVAGE IN ATTEMPTED CYCLIZATION OF CHLORO-SUBSTITUTED γ-PHENOXYBUTYRIC ACIDS

I. I. BĂDILESCU

Research Department, Petrochemical Works, Piteşti, Romania

Received July 12, 1968

The behaviour of chloro-substituted γ-phenoxybutyric acids in attempted cyclization by polyphosphoric acid was investigated. The results obtained indicate that both the absence of cyclization and the oxygen-alkyl bond cleavage of such compounds (leading to esters e.g. V from II) can be explained by the electronic effects arising from the chloro-substitution in the phenyl ring.

INTRODUCTION

Compounds of type I, ($n = 1, 2, 3$), can be easily prepared by an intramolecular cyclization of the corresponding phenoxyalkanoic acids or their chlorides.[1–8] Thus, several coumaran-3-ones (I, $n = 1$) have

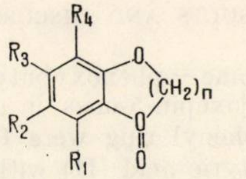

I

been prepared[9, 10] from substituted phenoxyacetic acids (or chlorides), except 5,7-dichlorocoumaran-3-one (I, $n = 1, R_1 = R_3 = H, R_2 = R_4 = Cl$) which cannot be obtained by the cyclization of the corresponding acid

---

[1] R. Stoermer and F. Bartsch, *Ber. dtsch. chem. Ges.*, **33**, 3175 (1900).

[2] F. Arndt and G. Källner, *Ber. dtsch. chem. Ges.*, **57**, 202 (1924).

[3] S. G. Powell and N. G. Johnson, *J. Amer. Chem. Soc.*, **46**, 2861 (1924).

[4] S. G. Powell and L. Anderson, *J. Amer. Chem. Soc.*, **53**, 811 (1931).

[5] H. A. Offe, *Chem. Ber.*, **80**, 458 (1947).

[6] D. Chakravarti and J. Dutta, *J. Indian Chem. Soc.*, **16**, 639 (1939).

[7] O. Dann and W.-D. Arndt, *Liebigs Ann. Chem.*, **587**, 38 (1954).

[8] G. Fontaine and P. Maitte, *Compt. rend.*, **258**, 4583 (1964).

[9] T. H. Minton and H. Stephen, *J. Chem. Soc.*, **121**, 1598 (1922).

[10] M. L. Kalinowski and L. W. Kalinowski, *J. Amer. Chem. Soc.*, **70**, 1970 (1948).

or chloride.[10] Further studies in this field were carried out by Armarego[11] and, by the use of ^{14}C-labelled acids, it was found that under the influence of the dehydrating agent a fragmentation occurs, leading to 2,4-dichlorophenol, followed by the formation of 2,4-dichlorophenyl 2′,4′-dichlorophenoxyacetate. A similar behaviour in the attempted cyclization of 2,3,4,5-tetrafluorophenoxyacetic acid was recently reported by Brooke and Furniss.[12] As in the above case, the corresponding halogenated phenol was also found in the reaction mixture.

It is obvious that the strain in the expected five-membered ring cannot be considered as explanation of the unsuccessful cyclization reactions of such compounds. The substituents in the aromatic nucleus, which, on the other hand, are responsible for the $O-C_{alkyl}$ bond cleavage, could also prevent the cyclization. This assumption is well supported by the results obtained in this work, in the attempted cyclization of two chlorosubstituted γ-phenoxybutyric acids by polyphosphoric acid (PPA); hereby, any marked effects of the neighbouring carboxyl group on the $O-C_{alkyl}$ bond cleavage (which are possible for phenoxyacetic acids) were avoided by the insertion of three methylene groups between the carboxyl and the substituted phenoxy group.

Although some γ-phenoxybutyric acids were cyclized to the corresponding cyclic ketones (I, $n = 3$) by dehydrating agents,[4,7,8] fragmentation reactions have not been reported. Moreover, the successful cyclization of some halogenated γ-phenoxybutyric acids was claimed by Lamparsky and Böhm,[13] and it was considered as a general reaction for this class of compounds by Mel'nikov and Baskakov,[14] who believed that it could be extended to γ-(2,4-dichlorophenoxy)butyric acid.

RESULTS AND DISCUSSIONS

The cyclization of some γ-phenoxybutyric acids with PPA afforded the corresponding benz[b]oxepin-5-ones in good yields[15] but only when the substituents in the phenyl ring were H, Me or MeO. By treating γ-(2,4-dichlorophenoxy)butyric acid (II) with polyphosphoric acid (PPA) in the usual manner,[7] 2,4-dichlorophenol (IV) and a compound melting at 76° were isolated from the reaction mixture. This compound shows properties strikingly different to various benz[b]oxepin-5-ones.[7,15] Thus, the compound does not give the corresponding derivative when treated with 2,4-dinitrophenylhydrazine but reacts with hydroxylamine to give a compound (m.p. 94°) which proved to be the known γ-(2,4-dichlorophenoxy)butyrohydroxamic acid.[16] These results suggested that in the attempted cyclization of γ-(2,4-dichlorophenoxy)butyric acid (II) by PPA, the main product is 2,4-dichlorophenyl γ-(2′,4′-dichlorophenoxy)butyrate

---

[11] W. L. F. Armarego, *Austral. J. Chem.*, **13**, 95 (1960).

[12] G. M. Brooke and B. S. Furniss, *J. Chem. Soc.* (*C*), **1967**, 869.

[13] D. Lamparsky and R. Böhm, Ger. Pat., 1 037 465, May 18, 1957.

[14] N. N. Mel'nikov and Yu. A. Baskakov, "Khimia gerbitsidov i regulyatorov rosta rastenii", Goskhimizdat, Moscow, 1962, p. 420.

[15] I. I. Bădilescu, To be published.

[16] J. Arct, E. Czerwinska, Z. Eckstein, Z. Ejmocki, R. Kowalik, W. Sobotka and E. Zukowski, *Bull. Acad. polon. Sci., Ser. Sci. chim.*, **12**, 465 (1964).

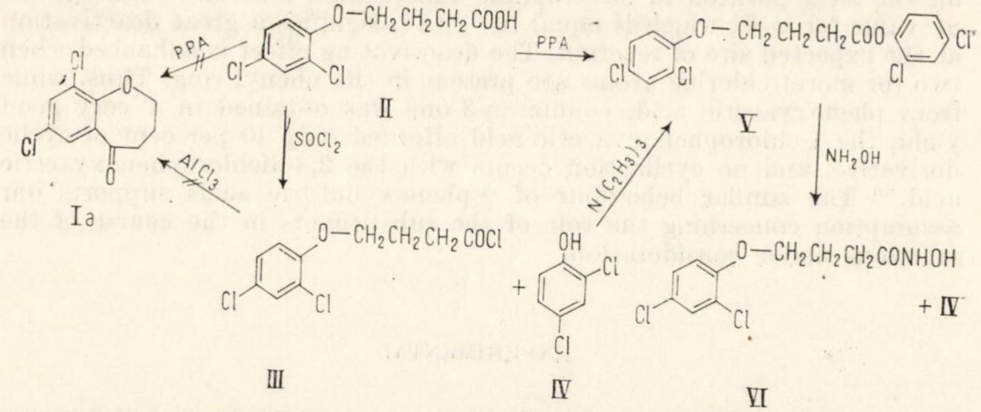

(V) and this assumption is well supported by elemental analysis and the infrared spectrum of V. An authentic sample of V was prepared in an unequivocal way from γ-(2,4-dichlorophenoxy)butyryl chloride (III) and 2,4-dichlorophenol (IV); the comparison of the infrared spectra and the mixture melting point evidence the correctness of the assigned structure.

Similarly, γ-(2-chloro-5-methylphenoxy)butyric acid treated with PPA gives an ester no trace of cyclic ketone being isolated from the reaction mixture.

An attempt to cyclize γ-(2,4-dichlorophenoxy)butyryl chloride (III) in the presence of anhydrous aluminium chloride afforded 2,4-dichlorophenol (IV) as the main product and a very poor yield of an oil, (b.p. 140–4°/9 Torr; n_D^{25} 1.5370). This compound showed properties different from those expected for Ia but no structural assignment has been established for this product.

The results obtained by us are very similar with those reported for 2,4-dichlorophenoxyacetic acid and its chloride.[10,11] It becomes obvious that the insertion of three methylene groups between the ether oxygen and the carboxyl group did not affect the $O-C_{alkyl}$ bond cleavage. Consequently, the course of reaction appears to be governed only by the 2,4-dichloro-substitution in the phenyl ring of such compounds.

The effects of substituents on both cyclization and $O-C_{alkyl}$ bond cleavage can be interpreted in terms of changes in electronegativities of ether oxygen and carbon-6 atoms corresponding to the replacing hydrogen by chlorine atoms in the aromatic nucleus. Thus, the $O-C_{alkyl}$ bond is weakened owing to the decreased electronic charge at the oxygen atom, induced by the electron-withdrawing substituent. Formally, the strength of this bond in 2,4-dichlorophenoxyalkylic acids may be compared with that of $Se-C_{alkyl}$ bond in the unsubstituted selenophenylalkyl acids, $Ph-Se-(CH_2)_n$ COOH, which are also easily cleaved by the "cyclizating" agents.[17]

---

[17] J. M. Danze and M. Renson, *Bull. Soc. chim. belges*, **75**, 169 (1966).

The cyclization reactions are hindered in the 2- or/and 4-chloro-substituted acids owing to the deactivating effect of this substitution on the *meta* position in electrophilic substitution reactions; indeed, the σ^+ value for *m*-Cl which is equal to $+0.40$, signifies a great deactivation at the expected site of reaction. The deactivating effect is enhanced when two (or more) chlorine atoms are present in the phenyl ring. Thus, while from phenoxyacetic acid, coumaran-3-one was obtained in a very good yield, the 4-chlorophenoxyacetic acid afforded only 40 per cent of cyclic derivative, and no cyclization occurs with the 2,4-dichlorophenoxyacetic acid.[10] The similar behaviour of γ-phenoxybutyric acids supports our assumption concerning the role of the substituents in the course of the reactions under consideration.

EXPERIMENTAL

The starting materials were prepared according to procedures described in a previous paper[18]. The γ-(2,4-dichlorophenoxy)butyric acid (II), m.p. 118°, (lit.[19] m.p. 117—118°) was dried by heating for ten hours at 105° prior to the use in the attempted cyclization reaction or to the preparation of γ-(2,4-dichlorophenoxy)butyryl chloride (III), b.p. 190—192°/12 Torr (lit.[20] b.p. 136—140°/0.2 Torr). The polyphosphoric acid used in this work was prepared by the usual procedure[21] from phosphoric acid, d = 1.70, and phosphorus pentoxide, both Merck "pro analysi" reagents.

The infrared spectra were recorded with a UR-10 Carl Zeiss-Jena double beam spectrophotometer.

All melting points given are uncorrected.

2,4-Dichlorophenyl γ-(2′,4′-dichlorophenoxy)butyrate (V).

A solution of 4.0 g (0.015 mole) of γ-(2,4-dichlorophenoxy)butyryl chloride in 5 ml of anhydrous benzene was added dropwise to a solution of 2.45 g (0.015 mole) of 2,4-dichlorophenol and 10 g of triethylamine in 10 ml of anhydrous benzene. The mixture was heated under reflux for 30 minutes, then the triethylamine hydrochloride and excess triethylamine were removed by washing the reaction mixture with diluted hydrochloric acid. The benzene solution was washed again with water, dried over anhydrous magnesium sulphate and the solvent was evaporated. The crude product was recrystallized twice from ether to yield 4.2 g (71%) of pure 2,4-dichlorophenyl γ-(2′,4′-dichlorophenoxy) butyrate as white crystals melting at 75—76°.

Anal. Found, Cl, 35.95; $C_{16}H_{12}Cl_4O_3$ requires: 36.00%.

The infrared spectrum of V shows the following absorption bands (KBr pellet): 3100, 3080, 2969, 2930, 2860, 1771 (ester C = 0), (1655), 1590, 1476, 1455, 1385, 1368, 1300, 1255, 1220, 1170, 1125, 1100, 1061, 930, 872, 822, 661, 556 and 456 cm^{-1}.

---

[18] I. I. Bădilescu, *Rev. Chim. (Bucureşti)*, **20**, 11 (1969).

[19] N. N. Mel'nikov and S. S. Kukalenko, *Zhur. obshchei Khim.*, **29**, 3744 (1959).

[20] C. F. Krewson, E. J. Saggese and T. F. Drake, *Weeds*, **8**, 107 (1960); *Chem. Abstr.*, **54**, 22390 (1960).

[21] R. C. Gilmore Jr. and W. J. Horton, *J. Amer. Chem. Soc.*, **73**, 1411 (1951).

γ-*(2,4-Dichlorophenoxy)butyrohydroxamic acid (VI).*

A solution of 1 g of 2,4-dichlorophenyl γ-(2′, 4′-dichlorophenoxy)butyrate in 5 ml of ethyl alcohol was treated with 50 ml of ethanolic hydroxylamine solution (prepared from 3.5 g of hydroxylamine hydrochloride and 3 g of potassium hydroxide) and the mixture was refluxed for 30 minutes. After the evaporation of the solvent, the crystalline residue was recrystallized from *n*-pentane – ether mixture to yield γ-(2,4-dichlorophenoxy)butyrohydroxamic acid, white needles melting at 94°, (lit. [16] m.p. 93–94.5°).

Anal. Calcd. for $C_{10}H_{11}Cl_2NO_3$, N, 5.30%;
Found: N, 5.03%.

Infrared spectrum (KBr pellet): 3240, 1647, 1590, 1564, 1492, 1474, 1446, 1430, 1388, 1341, 1294, 1271, 1260, 1250, 1202, 1110, 1067, 1052, 1035, 989, 951, 865, 808, 731, 653, 560 and 442 cm^{-1}. In diluted chloroform solution the bands at 3240 and 1647 cm^{-1} are shifted to 3420 and 1675 cm^{-1} respectively.

In the mother liquor obtained from the recrystallization of VI, 2,4-dichlorophenol was isolated and identified (by v.p.c.).

Attempted cyclization of γ-*(2,4-dichlorophenoxy)butyric acid.*

To 255 g of polyphosphoric acid heated at 110°, 30.1 g (0.125 mole) of γ-(2,4-dichlorophenoxy)butyric acid was added portionwise. The mixture was stirred for two hours at 110–115° then cooled at room temperature and poured into 1.5 l of ice-water. The solution was extracted with ether, the organic layer separated and washed with 100 ml of 5% aqueous NaOH solution and the two layers were worked up separately.

a. The aqueous alkaline solution was acidified with diluted sulphuric acid and extracted with ether. By removing the solvent, 0.8 g of a residue was obtained which was identified as 2,4-dichlorophenol (88 per cent by v.p.c.).

b. The ethereal solution was further washed with water, dried over anhydrous magnesium sulphate and the solvent evaporated. The residue was crystallized from ethyl alcohol (charcoal), to give 13 g of a crystalline product melting at 74–76°. By further purification involving distillation (b.p. 233–4°/2 Torr) and two recrystallizations from ethyl alcohol – ethyl acetate mixture (5 : 1), an analytical sample was obtained as needles, m.p. 76°.

Anal. Found: C, 48.64; H, 3.33; Cl, 36.10%.
$C_{16}H_{12}Cl_4O_3$ (V) *requires*: C, 48.76; H, 3.07; Cl, 36.00%.
$C_{10}H_8Cl_2O_2$ (Ia) *requires*: C, 51.96; H, 3.46; Cl, 30.66%.

The mixture melting point of this compound with V showed no depression. The infrared spectrum of this compound is well superposable on the spectrum of the authentic sample of 2,4-dichlorophenyl γ-(2′,4′-dichlorophenoxy)butyrate (V).

Attempted cyclization of γ-*(2-chloro-5-methylphenoxy)butyric acid.*

To 250 g of PPA heated at 110°, 11.4 g (0.05 mole) of γ-(2-chloro-5-methylphenoxy) butyric acid [18] (m.p. 66°) was added portionwise, within 30 minutes. Then the temperature was raised to 125–130° and the mixture stirred for another 1.5 h. After cooling, the reaction mixture was poured into 500 ml ice-water and extracted with ethyl acetate. The organic layer was washed with water, extracted with aqueous NaOH solution and the two layers were worked up separately as described above. The two products thus obtained were (*i*) 2.65 g of an uncharacterized solid, m.p. 124° (water), and (*ii*) 5.20 g of an oil, b.p. 224–26°/3 Torr. A probable structure assignment for the latter compound could be taken into consideration from the negative test with 2,4-dinitrophenylhydrazine and the close resemblance of the infrared spectrum of this oil with that of the corresponding product obtained in the preceding case. Thus, this oil was considered to be 2-chloro-5-methylphenyl-γ-(2-chloro-5-methylphenoxy)butyrate and the spectrum shows maxima at 1778, (1700), 1590, 1496, 1455, 1422, 1385, 1290, 1243, 1223, 1168, 1138, 1096, 1070, 848, 808, 740 and 645 cm^{-1}.

Attempted cyclization of γ-(2,4-dichlorophenoxy)butyryl chloride

Anhydrous aluminium chloride (11 g) was added portionwise with stirring, during one hour, to a solution of 20 g (0.075 mole) of γ-(2,4-dichlorophenoxy)butyryl chloride in 100 ml of carbon disulphide. The mixture was stirred for another half hour, the solvent was removed and then the reaction was continued, without solvent, at 70°, for another hour. The product was decomposed with 300 g of crushed ice and 100 ml of concentrated hydrochloric acid and the mixture was extracted with ether. The ethereal solution was washed with diluted aqueous NaOH solution and then with water, dried over anhydrous magnesium sulphate and the ether was removed. The residue was distilled in vacuo to give 1.3 g of an oil, b.p. 140—5°/9 Torr; n_D^{25} 1.5370. The infrared spectrum of this oil is similar to that of V.

⁂

Acknowledgements. The author wishes to thank Professor A. T. Balaban for his encouragement of this work and Mrs. Maria Roman (Institute of Atomic Physics, Bucharest) for elemental analysis. Thanks are due to Mrs. Frasina Harnagea and Simona Bădilescu for the recording of the infrared spectra.

Revue Roumaine de Chimie, **14**, 1591–1594 (1969)

$TiCl_4$-CAROTENOID COMPLEXES. VI*
ACTION OF $TiCl_4$ ON ISOCRYPTOXANTHIN AND ISOZEAXANTHIN

V. TĂMAŞ and C. BODEA

Institute of Agronomy "Dr. Petru Groza", Department of Chemistry,
Cluj, str. Mănăştur 3

Received May 5, 1969

New carotenoid-titanochloro-complexes are obtained by the action of $TiCl_4$ on isocryptoxanthin and isozeaxanthin. Both complexes yield by acetonolysis mainly retro-dehydro-β-carotene.

It has been previously shown [1-3] that by the action of $TiCl_4$ on C_{40}-carotenoids, carotenoid-titanochloro-complexes are formed.

Continuing our studies about the action of $TiCl_4$ on carotenoids we have examined the action of $TiCl_4$ on isocryptoxanthin and isozeaxanthin.

It is well known that, under the action of acids, the hydroxy-carotenoids containing the hydroxy may be easily converted, by dehydration, into dehydro-carotenoids. In these conditions isocryptoxanthin is transformed into retrohydro-β-carotene [4] and isozeaxanthin into retrodehydro-β-carotene [5] or retrobisdehydro-β-carotene. [6]

On treating isocryptoxanthin (I) in benzene with $TiCl_4$ an isocryptoxanthin-$TiCl_4$ complex (II) with the molar ratio carotenoid : $TiCl_4$, 1 : 1, was obtained (scheme 1).

Scheme 1

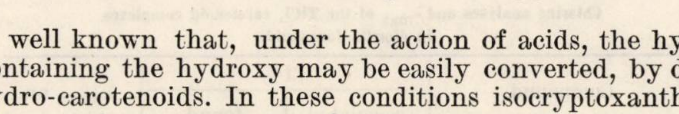

I

II

---

[*] Part V. V. TĂMAŞ and C. BODEA, *Rev. Roumaine Chim.*, **14**, 947 (1969).
[1] V. TĂMAŞ and C. BODEA, *Rev. Roumaine Chim.*, **12**, 1517 (1967).
[2] V. TĂMAŞ and C. BODEA, *Rev. Roumaine Chim.*, **14**, 405 (1969).
[3] V. TĂMAŞ and C. BODEA, *Tetrahedron*, (in press).
[4] E. C. GROB, B. BRUNNER and H. PFANDER, *Chimia* (Basel), **22**, 244 (1968).
[5] E. C. GROB and R. P. PFLUGSHAUPT, *Helv. Chim. Acta*, **48**, 930 (1965).
[6] E. C. GROB and R. P. PFLUGSHAUPT, *Helv. Chim. Acta*, **45**, 1592 (1962).

The action of $TiCl_4$ on isozeaxanthin (III) yields a complex containing 21.47% Cl. This content of chlorine corresponds to the molar ratio 1 : 1.12. The ratio, higher than 1 : 1, suggests that $TiCl_4$ is partially attached to the hydroxyl group. Thus the isozeaxanthin-$TiCl_4$ complex cannot be considered as a unitary product, but must be regarded as a mixture of two complexes, IV a and IV b (scheme 2).

Scheme 2

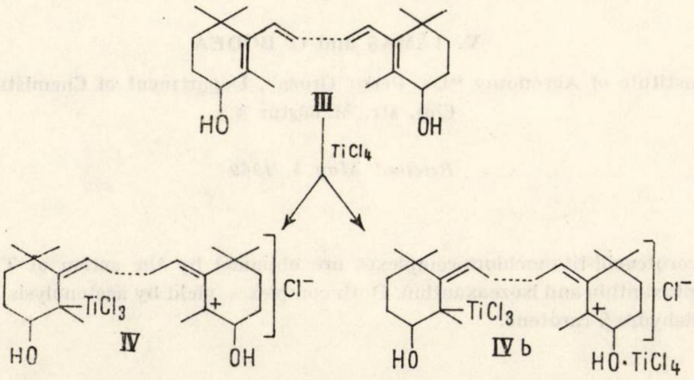

The intimate formation mechanism of these complexes is that shown in our previous papers. [1,3]

The structure of the complexes has been inferred from chlorine analyses and the λ_{max} of the electronic spectra shown in table 1.

Table 1

Chlorine analyses and λ_{max} of the $TiCl_4$ carotenoid complexes (in dimethylformamide)

Compound	Cl %		λ_{max}, nm
	calculated	found	
Isocryptoxanthin.$TiCl_4$	19.42	19.60	459
Isozeaxanthin. $TiCl_4$	19.03	21.47	459
Isocryptoxanthin, Isozeaxanthin	—	—	488,460

By the acetonolysis of complex II, retrodehydro-β-carotene (V) was obtained with a yield of 70%.

According to scheme 3 the conversion of II into V can be explained by the intramolecular elimination of one molecule of Cl_3TiOH.

Scheme 3

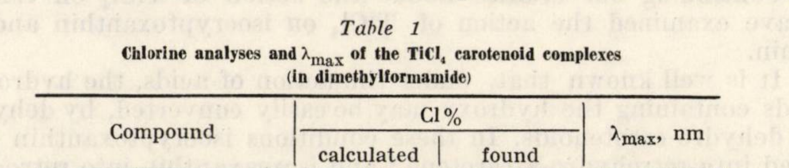

This mechanism is supported by the cleavage possibility of the C—Ti bond by H_2O or another oxygenated compound[7]:

$$\rangle\mathrm{C}-\mathrm{Ti}\langle + \mathrm{H_2O} \longrightarrow \rangle\mathrm{C}-\mathrm{H} + \rangle\mathrm{Ti}-\mathrm{OH}.$$

It is worth noticing that by the acetonolysis of the mixture of the isozeaxanthin-$TiCl_4$ complexes IV a and IV b, V is obtained with a yield of 45%, along with small amounts of keto-carotenoids, like 4,4′-diketo-β-carotene (VI) and 4-keto-4′-hydroxy-β-carotene (VII) (scheme 4).

Scheme 4

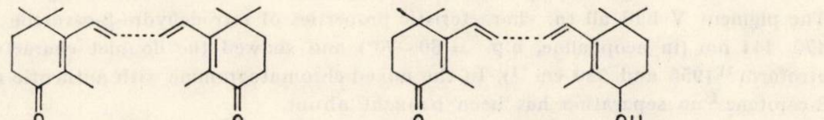

VI VII

The results show that the transformation of III under the action of $TiCl_4$ is not a unitary process : V is formed through a reduction reaction, whilst VI and VII are the result of oxidation processes.

As known $TiCl_4$ can be involved in oxido-reduction reaction,[8] which could explain the formation of the small amounts of carbonyl-carotenoids.

Acting with larger quantities of $TiCl_4$ upon III degradation products are formed, like β-apo-8′-carotenals, which contain hydroxy or carbonyl groups on the β-iononic ring.

EXPERIMENTAL

Isocryptoxanthin was obtained by the action of NBS on β-carotene[9] and isozeaxanthin from canthaxanthin by reduction with $NaBH_4$.[10] The absorbent used was a mixture of MgO and sand.

1. *Preparation of $TiCl_4$-carotenoid complexes*

Isocryptoxanthin-$TiCl_4$ (II). A solution of 100 mg isocryptoxanthin in 50 ml benzene was treated with 0.05 ml $TiCl_4$ and the mixture stirred several times. It was kept 15 min at room temperature, then the precipitate filtered off and washed with benzene ; 90 mg II, containing 19.60 % Cl, were obtained. The electronic spectrum, in dimethyl-formamide, shows an absorption maximum at 459 nm.

Isozeaxanthin-$TiCl_4$ (IV). 100 mg Isozeaxanthin in 100 ml benzene were treated with 0.05 ml $TiCl_4$ and worked up as in the case of complex II ; 90 mg of complex IV containing 21.47 % Cl were obtained ($\lambda_{max.}$ = 458 nm, in dimethylformamide).

---

[7] K. S. Boustany, K. Bernauer and A. Jacot-Guillarmod, *Helv. Chim. Acta*, **50** 1305 (1967).

[8] B. Benrath, *Z. wiss. Phot.*, **14**, 217 (1923).

[9] R. Entschel and P. Karrer, *Helv. Chim. Acta*, **41**, 983 (1958).

[10] L. Merlini and G. Cardillo, *Gazz. chim. Ital.*, **93**, 949 (1963).

2. *Action of $TiCl_4$ on isocryptoxanthin*

To a solution of 100 mg isocryptoxanthin in 50 ml benzene 0.05 ml $TiCl_4$ were added and the mixture stirred 1/2 min; 80 ml acetone and after 10 min. 150 ml petroleum ether were added. The solution of the pigments was washed with water, dried with Na_2SO_4 and chromatographed. After developing with a mixture of petroleum ether and 10% benzene, the chromatogramme (3 × 15 cm) appeared as follows:

1 cm orange	isocryptoxanthin
1 cm interzone	
9 cm orange-rose	retrodehydro-β-carotene

Retrodehydro-β-carotene (*V*). After elution with a mixture of ethylic ether-acetone-ethanol (10 : 1 : 0.5), washing, drying and evaporation of the solvent, 70 mg V were obtained. The pigment V had all the characteristic properties of retrodehydro-β-carotene: $\lambda_{max} = 501$, 470, 444 nm (in neophaline, b.p. = 60–70°) and showed the doublet characteristic of the etroform[11] (955 and 980 cm^{-1}). In the mixed chromatogramme with authentic retrodehydro-β-carotene[1] no separation has been brought about.

3. *Action of $TiCl_4$ on isozeaxanthin*

A solution of 100 mg isozeaxanthin in 100 ml benzene was treated with 0.05 ml $TiCl_4$ and worked up as for isocryptoxanthin. The developing was performed with a mixture of petroleum ether and 20% benzene. The following chromatogramme (4 × 20 cm) was obtained:

0.3 cm ochre	unidentified
2 cm orange	isozeaxanthin
0.3 cm red	4-keto-4′-hydroxy-β-carotene
0.2 cm interzone	
0.3 cm red-violet	4,4′-diketo-β-carotene
0.3 cm interzone	
8 cm orange-rose	retrodehydro-β-carotene

Retrodehydro-β-carotene. 45 mg V were obtained as shown above. The pigment was identical with that obtained from isocryptoxanthin.

4,4′-Diketo-β-carotene (*VI*). After purification by chromatography and the elution of pigment with ethylic ether-ethanol (9 : 1), washing and drying, 4 mg red powder were obtained. In the electronic spectrum VI shows a maximum at 465 nm (in neophaline) and in the IR spectrum a band at 1667 cm^{-1} (in CCl_4). In the mixed cochromatogramme with synthetical canthaxanthin there was no separation. In a mixture of petroleum ether-methanol 95% VI has a 40% hypophasic partition. By reduction of VI with $NaBH_4$ isozeaxanthin resulted.

4-Keto-4′-hydroxy-β-carotene (*VII*). 5 mg VII were obtained from ether. The electronic spectrum shows a maximum at 460 nm (in neophaline), in the IR spectrum (in KBr), a band at 1667 cm^{-1} [$\nu_{(C=O)}$] and another band at 1030 cm^{-1} [$\nu_{(C-OH)}$]. In the mixed cochromatogramme with authentic 4-keto-4′-hydroxy-β-carotene there was no separation. On treating VII with chloroform-HCl, 4-keto-3′,4′-dehydro-β-carotene ($\lambda_{max} = 470$ nm) was obtained; VII showed a 60% hypophasic partition in a mixture of petroleum ether-methanol 95%.

---

[11] E. Nicoară, V. Tămaş, G. Neamţu and C. Bodea, *Liebigs Ann. Chem.*, **697**, 201 (1966).

Revue Roumaine de Chimie, **14**, 1595–1601 (1969)

METALLKOMPLEXE DER N-CARBOXYMETHYL-ANTHRANYLSÄURE (PHENYLGLYCIN-ORTHOCARBONSÄURE). II[1]

EISEN(III)- UND CHROM(III)-KOMPLEXE

C. DRĂGULESCU, R. POMOJE, I. MENESSY, MARIA PÎRLEA
und CORNELIA MIHĂESCU

von der Technischen Hochschule, Fakultät für Chemie, Timişoara, str. Bocşei 6

Eingegangen am 6. August 1969

Es werden die IR-Spektren und UV-Reflexionsspektren des Liganden im festen Zustand untersucht und das Fehlen einer Betainstruktur desselben bestätigt. Aus den Komplexierungsgleichgewichten in Lösung mit den Kationen Fe(III) und Cr(III) ergibt sich die Bildung von Komplexen, in denen der aminische Stickstoff des Liganden an der Bindung des Metalls beteiligt ist. Die zur Bestimmung der Verbindungsverhältnisse durchgeführten Untersuchungen ergaben die Werte 1 : 1 für Fe(III) und 1 : 2 für Cr(III). Der Verlauf der Spektralkurven beider Systeme in Abhängigkeit vom pH weist auf das Bestehen von Säure-Basen-Gleichgewichten hin, an denen der Komplex beteiligt ist. Die Bildung des Fe(III)-Komplexes erfolgt sehr rasch; seine Dissoziationskonstante hat bei pH = 4,5 den Wert 7.10^{-4}. Aus konzentrierten Lösungen kann die Verbindung $Fe_2(Ph.G.C.)_3.2H_2O$ abgeschieden werden.

In einer früheren Arbeit haben wir auf Grund der Untersuchungen der Ligandenspektren im UV-Bereich gezeigt, daß in Lösungen mit pH-Werten$>$1 der Ligand entweder in ionisierter Form vorhanden ist oder in protonierter Form durch H^+ an die Carboxylgruppen gebunden wird. Die Protonierung des aminischen Stickstoffs findet in Lösungen mit pH-Werten$<$1 nur dann statt, wenn der Ligand quantitativ in molekulare Form übergegangen ist. Dieser Vorgang wird durch das Erscheinen einer Spektralbande bei ungefähr 275 mμ gekennzeichnet. Da dieselbe Erscheinung in Lösungen mit pH-Werten$>$1 beobachtet wird, wo neben dem Liganden auch Metallkationen (darunter Fe(III)) vorhanden sind, gelangte man zu der Schlußfolgerung, daß das Auftreten der erwähnten Bande ein Kennzeichen für die Tetrakoordination des aminischen Stickstoffs ist. [1]

---

[1] C. Drăgulescu, R. Pomoje, I. Menessy and C. Mihăescu, *Rev, Roumaine Chim.*, **12**, 553 (1967).

Der Ligand wird im festen Zustand durch folgende wichtigere Banden im IR-Spektrum und im UV-Reflexionsspektrum gekennzeichnet:

a. Valenzschwingungen $\nu_{C=O}$

1. Durch Wasserstoffbrückenbindungen assoziiertes aliphatisches Carboxyl

$$\nu_{C=O} = 1730\ \mathrm{cm}^{-1}$$

2. Intramolekular chelatisiertes aromatisches Carboxyl

$$\nu_{C=O} = 1670\ \mathrm{cm}^{-1}$$

b. Valenzschwingungen ν_{NH} und ν_{OH}

1. Intramolekular assoziierte NH-Gruppe, $\nu_{NH} = 3100\ \mathrm{cm}^{-1}$ (breit)
2. Intramolekular assoziierte OH-Gruppe,
   Carboxyl der Acetatgruppe $\nu_{OH} = 2530\ \mathrm{cm}^{-1}$ (breit)
   Carboxyl des Benzolkerns $\nu_{OH} = 2640\ \mathrm{cm}^{-1}$ (breit)

c. Valenzschwingungen ν_{CN}

1. Aromatisch $\nu_{CN} = 1400\ \mathrm{cm}^{-1}$
2. Aliphatisch $\nu_{CN} = 1140\ \mathrm{cm}^{-1}$

d. OH-Deformationsschwingungen gekoppelt mit CO-Valenzschwingungen

1. An Alkylgruppe gebundenes Carboxyl 1440 cm^{-1}
   1170 cm^{-1}
2. An Arylgruppe gebundenes Carboxyl 1465 cm^{-1}
   1225 cm^{-1}

e. Deformationsschwingungen δ_{OH} im Bereich 920—940 cm^{-1}

$$\delta_{OH} = 925\ \mathrm{cm}^{-1}$$

f. Banden im UV-Reflexionspektrum

$\lambda_1 = 200\ \mathrm{m\mu}$
$\lambda_2 = 248\ \mathrm{m\mu}$
$\lambda_3 = 280\ \mathrm{m\mu}$
$\lambda_4 = 335\ \mathrm{m\mu}$

Die im Rahmen der vorliegenden Arbeit durchgeführten Untersuchungen bekräftigen die Hypothese über das Fehlen einer Betainstruktur des Liganden, da im IR-Spektrum die charakteristischen Banden eines ionisierten Carboxyls fehlen. Das Vorhandensein der charakteristischen Bande für tetrakoordinierten Stickstoff im Reflexionsspektrum (Schulter bei ~275 mμ) führt zu der Schlußfolgerung, daß die Tetrakoordination durch eine intramolekulare Wasserstoffbrückenbindung, wahrscheinlich durch das aromatische Carboxyl erzielt wurde.

Phenylglycin-orthocarbonsäure bildet mit Fe(III) Verbindungen, die sich, nach einigen Angaben im Fachschrifttum, unter der Form von $FeOH(Ph.G.C.).4H_2O$ und $Fe_2(Ph.G.C.)_3.\ 4{,}5\ H_2O$ abscheiden.[2]

---

[2] I. V. Dubski, E. Tesalik, St. Rusnak, A. Okac und V. Sindelar, *Chem. listy*, **33**, 346 (1939).

Diese Verbindungen sind durch eine intensive violettblaue Färbung, sowie durch die Leichtigkeit mit der sie aus wäßrigen Lösungen erhalten werden, gekennzeichnet.

Die Fe(III)-Verbindungen mit Ph.G.C. unterscheiden sich durch ihre Färbung deutlich von den meisten anderen Fe(III)-Verbindungen und besonders von den Fe(III)-Komplexen der Anthranyl-Diessigsäure, obwohl dieser Ligand eine ausgeprägte Ähnlichkeit mit Ph.G.C. hat. Aus den Daten über Fe(III)-ANDA-Komplexe geht hervor, daß deren Lösungen orangegelb gefärbt sind, während im festen Zustand die Verbindung Fe(ANDA)$5H_2O$ abgeschieden wird.[3,4]

Um einige Aufschlüsse über die Struktur der Eisenkomplexe mit diesem Ligand zu erhalten, haben wir den Komplex Fe_2 (Ph.G.C.)$_3$ im festen Zustand isoliert. Die Synthese wurde durch Vermischen von 0,2 molaren Fe(III)- und Ph. G. C.-Lösungen, in demselben Molverhältnis, im sauren Medium (HNO_3, $pH < 1$) ausgeführt. Danach wurde abfiltriert, mit Alkohol und Äther gewaschen und bei 60° getrocknet. Das erhaltene Produkt ist intensiv violett gefärbt; seine Zusammensetzung Fe_2(Ph. G. C.)$_3$.$2H_2O$ wird durch das in Abbildung 1 dargestellte Thermogramm bestätigt.

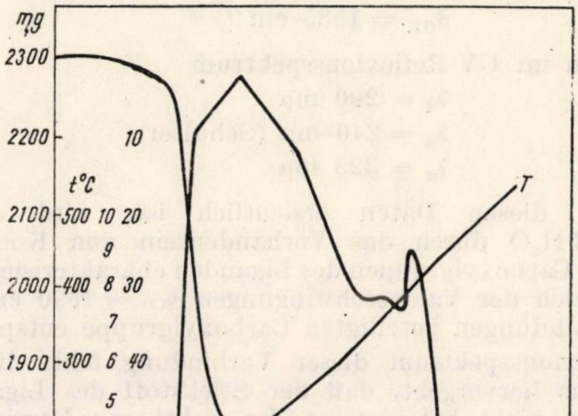

Abb. 1. — Thermogramm von Fe_2(Ph. G. C.)$_3$. $2H_2O$.

---

[3] C. Drăgulescu, T. Simonescu, I. Menessy und R. Anton, *Studii şi Cercetări Şti. Chim. Baza Cercetări Şti. Timişoara* 7, 9 (1960).
[4] L. Dinsel und T. R. Sweet, *Analyt. Chem.*, **33**, 1079 (1961).

Die wichtigsten Banden dieser Verbindung im IR-Spektrum und im UV-Reflexionsspektrum sind folgende :

a. An koordinativen Bindungen beteiligtes Carboxyl

$$\nu_{C=O} = 1620\ \text{cm}^{-1}$$

$$\nu_{C=O} = 1402\ \text{cm}^{-1}$$

b. Valenzschwingungen ν_{OH} und ν_{NH}

$$\nu_{OH} = 3380\ \text{cm}^{-1}\ \text{(breit)}$$

$$\nu_{NH} = 3000\ \text{cm}^{-1}\ \text{(Schulter)}$$

c. Valenzschwingungen ν_{CN}

$$\nu_{CN} = 1290\ \text{cm}^{-1}$$

$$1260\ \text{cm}^{-1}$$

d. Deformationsschwingungen δ_{OH} im Kristallwasser

$$\delta_{OH} = 1585\ \text{cm}^{-1}$$

e. Banden im UV-Reflexionsspektrum

$$\lambda_1 = 200\ \text{m}\mu$$

$$\lambda_2 = 240\ \text{m}\mu\ \text{(Schulter)}$$

$$\lambda_4 = 325\ \text{m}\mu$$

Wie aus diesen Daten ersichtlich ist, wird der Komplex $Fe_2(Ph.G.C.)_3 . 2\,H_2O$ durch das Vorhandensein von Koordinationsbindungen mit den Carboxylgruppen des Liganden charakterisiert (eine einzige Bande im Bereich der Valenzschwingungen $\nu_{CO} = 1620\ \text{cm}^{-1}$, die einer an den Chelatbindungen beteiligten Carboxylgruppe entspricht).

Im Reflexionsspektrum dieser Verbindung fehlt die Bande von 275 mμ, woraus hervorgeht, daß der Stickstoff des Liganden an den Chelatbindungen nicht beteiligt ist. Im sichtbaren Bereich besitzt der Komplex eine breite Bande mit einem Maximum bei 550 mμ (Breite bei halber Höhe 10 000 cm^{-1}).

Der Komplex $Fe_2(Ph.G.C.)_3.2H_2O$ ist schwer löslich in Wasser. Aus der Absorptionskurve der gesättigten Lösung ergibt sich eine Löslichkeit von 3.10^{-4} Mol/l.

Mit zunehmendem Säuregehalt steigt die Löslichkeit stark an und die Lösungen zeigen ein für das hydratierte Fe^{3+}-Ion und den Liganden charakteristisches Absorptionsspektrum.

Im Gegensatz zu der im festen Zustand erhaltenen Verbindung, bildet Fe(III) mit Ph.G.C. in Lösung Komplexe, die wahrscheinlich N—Me-Bindungen enthalten. Diese Voraussetzung beruht in erster Reihe auf der oben erwähnten Feststellung, wonach an den Spektralkurven des Liganden dieselben Veränderungen in Gegenwart von Protonen wie in Gegenwart von Metallkationen beobachtet werden. Gleichzeitig haben die Absorptionsspektren einiger Lösungen, die Fe (III) und Ph.G.C. enthalten, ein charakteristisches Maximum zwischen 700—780 mμ, entsprechend einer grünlichblauen Farbe der Lösung, die sich von der Farbe des im festen Zustand erhaltenen Produktes unterscheidet.

Die Farbe der Lösungen, die Fe (III) und Ph.G.C. enthalten, hängt wesentlich von ihrem pH-Wert ab (Abb. 2). In Abbildung 2 sind die Absorptionsspektren von Lösungen gleicher und konstanter Kationen- und Ligandenkonzentration, bei verschiedenen pH-Werten zwischen 2 und 12, dargestellt.

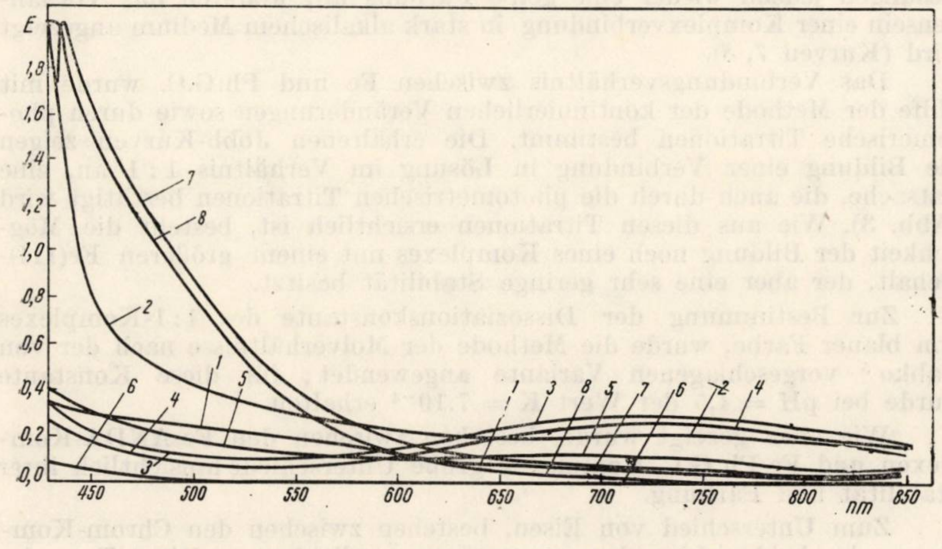

Abb. 2. — Absorptionsspektren der Fe(III)-Ph.G.C.-Lösungen $[Fe] = [Ph.G.C.] = 10^{-3}$ M., l=4 cm.

1, pH = 2,55; 2, pH = 3,35; 3, pH = 4,40; 4, pH = 4,90; 5, pH = 5,78; 6, pH = 9,80; 7, pH = 10,97; 8, pH = 11,60.

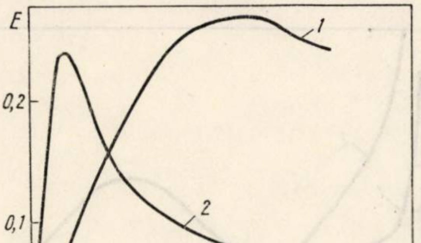

Abb. 3. — Photometrische Titration von Fe(III) mit Ph. G. C. und von Ph. G. C. mit Fe (III).

1, 5 ml Fe(III)-Lösung $1.012.10^{-2}$ M. titriert mit Ph.G.C. 10^{-2} M, V=100ml; *2*, 1 ml Ph. G. C. 10^{-2} M titriert mit Fe (III) $1.012.10^{-2}$ M, V=100 ml.

Wie aus der Abbildung 2 ersichtlich ist, entspricht die blaue Farbe der Lösung von einem Komplex, der sich bei pH = 4—5 bildet (Kurven *3*, *4*).

Die Entfärbung der Lösungen bei kleineren pH-Werten ist entweder der Zersetzung des Komplexes zuzuschreiben, oder wird durch die Bildung eines Komplexes verursacht, der eine charakteristische Absorption im violetten Bereich aufweist (Kurven *1*, *2*).

Beim Ansteigen der pH-Werte wird Fe^{3+} unter Bildung von $Fe(OH)_3$ gefällt, während die Lichtabsorption der Lösungen im ganzen sichtbaren Bereich Null zustrebt (Kurven *5*, *6*). Bei höheren pH-Werten nehmen die Lösungen jedoch wieder eine gelbe Färbung an, wodurch das Vorhandensein einer Komplexverbindung in stark alkalischem Medium angezeigt wird (Kurven *7*, *8*).

Das Verbindungsverhältnis zwischen Fe und Ph.G.C. wurde mit Hilfe der Methode der kontinuierlichen Veränderungen sowie durch photomerische Titrationen bestimmt. Die erhaltenen Jobb-Kurven zeigen die Bildung einer Verbindung in Lösung im Verhältnis 1 : 1 an, eine Tatsache, die auch durch die photometrischen Titrationen bestätigt wird (Abb. 3). Wie aus diesen Titrationen ersichtlich ist, besteht die Möglichkeit der Bildung noch eines Komplexes mit einem größeren Fe(III)-Gehalt, der aber eine sehr geringe Stabilität besitzt.

Zur Bestimmung der Dissoziationskonstante des 1:1-Komplexes von blauer Farbe, wurde die Methode der Molverhältnisse nach der von Babko [5] vorgeschlagenen Variante angewendet; für diese Konstante wurde bei $pH = 4{,}5$ der Wert $K = 7.10^{-4}$ erhalten.

Wie oben gezeigt wurde, bestehen zwischen den Fe-ANDA-Komplexen und Fe-Ph.G.C.-Komplexen große Unterschiede hinsichtlich ihrer Stabilität und Färbung.

Zum Unterschied von Eisen, bestehen zwischen den Chrom-Komplexen der beiden Liganden ausgeprägte Ähnlichkeiten. Diese Tatsache hat uns veranlaßt in der vorliegenden Arbeit nur die Daten anzuführen, die für die Charakterisierung des Systems Cr-Ph.G.C., im Vergleich mit dem System Cr-ANDA von Bedeutung sind. [6]

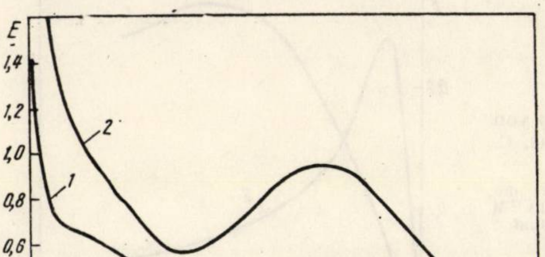

Abb. 4. — Lichtabsorption der Lösungen von $[Cr(III)] = [Ph.\ G.\ C.] = 4.10^{-3}$ M, l=4 cm. *1*, beim Vermischen; *2*, nach dem Sieden.

Beim Cr-Ph.G.C.-System können dieselben Etappen wie bei der Bildung der Cr-ANDA-Komplexe erkannt werden.

---

[5] A. K. Babko, ,,Fisiko-khimitcheski analis kompleksnikh soedineni w rastworakh", Izd. Akad. Nauk. U.S.S.R. Kiev, 1955, S. 138.

[6] C. Drăgulescu, I. Menessy und M. Pîrlea *Rev. Roumaine Chim.*, **13**, 307 (1968).

Revue Roumaine de Chimie, **14**, 1603–1611 (1969)

NEUE KOMPLEXVERBINDUNGEN DER PYRAZOLONREIHE. V[1–4]

J. DICK und ANNA MAURER

aus der Abteilung für Anorganische Chemie der Akademie, Forschungstelle Timişoara
Bd. Mihai Viteazul 24.

Eingegangen am 26. Dezember 1968

Es werden Pyrazolonkomplexverbindungen des Tl(III), In(III) und Ge(IV) mit Halogenen, bzw. Heteropolysäuren des Germaniums beschrieben. In fast neutralen Lösungen bilden sich die Verbindungen $[TlLig_n X_3]$und $[InLig_n X_3]$. Germanium liefert in wasserfreiem Medium die Verbindung $[GeLig_3]X_4$. In sauren Lösungen werden die Salze der Anionen $[TlX_4]^-$ und der Heteropolysäure $H_4[GeO_4 . 12MoO_3]$ erhalten. Als Ligand werden Derivate des 4-Amino-1-phenyl-2,3-dimethylpyrazolons und 1-Phenyl-2,3-dimethyl-5-pyrazolon verwendet; X = Cl, Br, J. Die IR-Spektren der Thalium- und Indiumkomplexverbindungen im Bereiche von 4000–400 cm^{-1} ergeben die durch die Komplexbildung aufgetretenen Veränderungen der Schwingungen der Ligandenmoleküle.

In einigen vor kurzem veröffentlichten Arbeiten haben wir Komplexverbindungen des Co(II), Ni(II), Cd(II), Zn(II), Be(II), Hg(II) und Bi(III) mit 4-Aminoantipyrin und seinen N-methylierten Derivaten als Ligand, mit verschiedenen Anionen beschrieben.[1–4] An Hand der IR-Spektren wurde die Struktur dieser Verbindungen erörtert.[5] Dabei konnten die untersuchten Komplexe, hauptsächlich zweiwertiger Metalle in 3 verschiedene Gruppen geteilt werden: Salze komplexer Anionen, Chelatverbindungen und einfache Komplexverbindungen. In sämtlichen Verbindungen verhalten sich 4-Amino-, 4-Methylamino- und 4-Dimethylaminoantypyrin als zweizählige Liganden, die zur Chelatringbildung fähig sind, während das Antipyrin (1-Phenyl-2,3-dimethyl-5-pyrazolon) als einzählig betrachtet werden muß.

---

[1] J. Dick und C. Drugărin, *Studii şi Cercetări, Şti. Chim., Baza de Cercetări Şti. Timişoara*, **8**, 205 (1961).

[2] J. Dick und A. Maurer, *Studii şi Cercetări, Şti. Chim., Baza de Cercetări Şti. Timişooara*, **9**, 257 (1962).

[3] J. Dick und A. Maurer, *Studii şi Cercetări, Şti. Chim., Baza de Cercetări Şti. Timişoara*, **10**, 61 (1963).

[4] J. Dick und A. Maurer, *Rev. Roumaine Chim.*, **10**, 671 (1965).

[5] J. Dick, R. Bacaloglu und A. Maurer, *Rev. Roumaine Chim.*, **12**, 607 (1967).

In vorliegender Arbeit wird die Komplexbildungsfähigkeit des Tl(III), In(III) und Ge(IV) mit den erwähnten Liganden der Pyrazolonreihe untersucht.

Mit Tl(III) als Komplexbildner und organischen Liganden, welche N oder O als Donatoratome aufweisen, befassen sich zahlreiche Arbeiten. [6-10] Die von uns erhaltenen Verbindungen können in Salze des $[TlX_4]^-$-Anions, wo X = Halogen, und in Komplexverbindungen der allgemeinen Formel $[TlLig_n X_3]$, gruppiert werden.

Die Darstellung der Salze der N-methylierten Derivate des 4-Amino- und Antipyrins als solches, erfolgte in sauren Lösungen. Dabei müssen sowohl die Gleichgewichtsreaktionen zwischen Tl(III) und Halogenionen, hauptsächlich Br^- und J^-, als auch die Redox-Reaktionen der benützten Basen mit Tl(III) in Betracht gezogen werden. Das Tl(III)-Ion der Elektronenkonfiguration d^{10} wird mit der den Nichttransitionsmetallen des 5 d^{10}-Systems charakteristisch großen Leichtigkeit zum Tl(I)-Ion der Konfiguration $d^{10}s^2$ reduziert. Dies wird besonders deutlich durch die Reaktion des Amino-, bzw. Methyl- und Dimethylamino-antipyrins mit Tl(III)-Halogeniden in essigsaurer Lösung veranschaulicht, zumal in diesem Fall mit quantitativer Ausbeute Tl(I)-Halogenide erhalten werden. Um diese Reaktion zu verhindern, muß die Salzbildung der 4-Amino-antipyrinverbindungen in stark sauren Lösungen (3,5-5 n HCl oder 2n H_2SO_4) stattfinden. Im Falle des Antipyrins werden, um Verharzungen zu verhüten, Lösungen mit kleinen Säurekonzentrationen verwendet. Dabei wurden folgende Verbindungen erhalten:

I. $[TlCl_4](HPyr)$
II. $[TlCl_4]$ $(HAntp_2)$
III. $[TlJ_4]$ (HPyr)
IV. $[TlJ_4]$ (HmAm)
V. $[TlJ_4]$ (HAm)

wo Antp = Antipyrin, Am = Amino-antipyrin, mAm = Methylamino-antipyrin und Pyr = Dimethylamino-antipyrin. Ähnliche Verbindungen mit Br^- sind bereits bekannt. [20] Methylamino-antipyrinmethansulfon-

---

[6] R. I. Mayer, *Z. anorg. Chem.*, **24**, 321 (1900).

[7] K. Renz, *Ber. dtsch. chem. Ges.*, **35**, 1110 (1902).

[8] G. I. Sutton, *Austral. J. Chem.*, **11**, 120 (1958), **16**, 1134 (1963).

[9] F. Ya. Kulba und W. Je. Mironow, *Zhur. neorg. Khim.*, **4**, 1393 (1959).

[10] F. Ya. Kulba, Y. A. Makashew und W. Je. Mironow, *Zhur. neorg. Khim.*, **6**, 1481 (1961).

[11] F. Ya. Kulba, W. Je. Mironow und L. P. Roshanowskaja, *Zhur. neorg. Khim.*, **7**, 2320 (1962).

[12] F. Ya. Kulba, W. E. Mironow, W. I. Zashina und T. G. Ogibenina, *Zhur. neorg. Khim.*, **8**, 911 (1963).

[13] F. Ya. Kulba, W. Je. Mironow und Zsin-Jan Zun, *Zhur. neorg. Khim.*, **8**, 1846 (1963).

[14] F. Ya. Kulba, W. Je. Mironow, L. P. Roshanowskaja und O. A. Skuratow, *Zhur. neorg. Khim.*, **9**, 1630 (1964).

[15] F. Ya. Kulba, W. Je. Mironow und W. Sderaditschkova, *Zhur. neorg. Khim.*, **9**, 1876 (1964).

[16] F. A. Cotton, B. F. G. Johnson und R. M. Wing, *Inorg. Chem.*, **4**, 502 (1965).

[17] B. F. G. Johnson und R. A. Walton, *Inorg. Chem.*, **5**, 49 (1966).

[18] R. A. Walton, *Inorg. Chem.*, **7**, 640 (1968).

[19] A. I. Bussew und W. G. Tipzova, *Zhur. analit. Khim.*, **14**, 550 (1959) und **15**, 291 (1960).

[20] A. I. Bussew und W. G. Tipzova, *Zhur. analit. Khim.*, **14**, 28 (1959).

saures Na (Novalgin) konnte nicht verwendet werden, da das in saurer Lösung entwickelte SO_2 reduzierend wirkt. Mit $[TlJ_4]^-$, dessen Salze die unlöslichsten und beständigsten dieser Reihe sind, konnten auch jene mit Amino- und Methylamino-antipyrin (mit kleinen Verunreinigungen) erhalten werden, jedoch nicht mit $[TlCl_4]$ und $[TlBr_4]^-$ (stark verunreinigte Verbindungen, bzw. Redoxreaktionen).

Wie aus den IR-Spektren ersichtlich, ist das Proton in diesen Verbindungen durch das O-Atom der Karbonylgruppe gebunden und bildet mit dem N-Atom der Aminogruppe eine Chelatprotonbindung.

Im Gegensatz zu den bisher mit Antipyrin erhaltenen Verbindungen dieser Reihe, müssen die des $[TlCl_4]^-$ und $[TlBr_4]^-$ als Salze der komplexen Anionen mit dem Dimer das Antipyrins betrachtet werden. Das Tetrahalogenothalliumion scheint die Polymerisation des Antipyrins zu katalysieren, besonders $[TlJ_4]^-$, das an Stelle des Salzes ein Harz bildet.

Die Salze des $[TlCl_4]^-$ sind weiß, während die des $[TlJ_4]^-$ orangegelb bis blutrot gefärbt sind. Die Verbindungen I—V sind gut löslich in Aceton, Methyl-äthylketon, Cyclohexanon, Acetonitryl Nitromethan, schwerer löslich in Chloroform, Methanol und Äthanol, schwer löslich in Benzol und Wasser, unlöslich in Äther und CCl_4. Im allgemeinen sinkt die Löslichkeit dieser Verbindungen in der Reihenfolge : $[TlCl_4](HLig) > > [TlBr_4](HLig) > [TlJ_4](HLig)$. Die Verbindungen mit Pyramidon sind die unlöslichsten und die Salze mit Antipyrin die löslichsten.

Die Verbindungen des Tl(III) der allgemeinen Formel $[TlLig_n X_3]$ wo $n = 2$ für einzählige Liganden wie Antipyrin und $n = 1$ für zweizählige Liganden wie Pyramidon, wurden in konzentrierten wäßrig-neutralen oder alkoholisch-wäßrigen Lösungen erhalten. Die Jodverbindungen derselben Gruppe werden durch Ionenaustausch aus den entsprechenden Chlorverbindungen hergestellt. So erhielten wir :

VI. $[TlPyrCl_3]$
VII. $[TlAntp_2Cl_3]$
VIII. $[TlPyrBr_3]$
IX. $[TlAntp_2Br_3]$
X. $[TlPyrJ_3]$
XI. $[TlAntp_2J_3]$

Amino- und Methylamino-antipyrin konnten infolge ihrer reduzierenden Wirkung auf das Tl(III)-ion nicht verwendet werden. Löslichkeitsverhältnisse etwa wie bei den Salzen (etwas löslicher).

Aus den IR-Spektren der Verbindungen im Bereiche 4000—400 cm^{-1} geht hervor, daß Antipyrin durch das O-Atom der Carbonylgruppe und

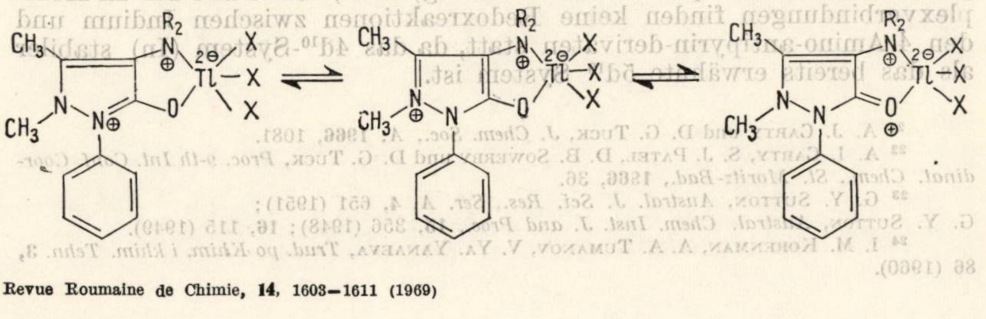

Pyramidon durch das N-Atom der Aminogruppe und das O-Atom der C = O-Gruppe an das Metall gebunden sind. Daraus folgt, daß VI, VIII und X als Chelatverbindungen betrachtet werden müssen.

Nach diesen Formulierungen wäre in den Verbindungen VI—XI das Tl fünffach koordiniert. Aus dem Fachschrifttum geht jedoch hervor, daß vielfältige Versuche zur Strukturaufklärung der Komplexverbindungen des Tl(III) mit ein-, zwei- und dreizähligen Liganden zu keiner endgültigen Auffassung führten.[8, 16-18] Zieht man die große Unlöslichkeit der Verbindungen besonders in unpolaren Lösungsmitteln in Betracht, so wäre in unserem Fall eine hochmolekulare Struktur, in welcher Halogenatom-Brücken erscheinen, durchaus möglich. In disesem Sinne könnten unsere Verbindungen wie folgt formuliert werden:

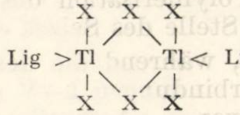

Dimer

oder

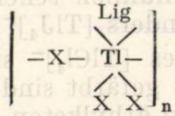

Polymer

Mit Indiumkomplexverbindungen organischer Liganden und Halogen- oder Pseudohalogenanionen, befassen sich besonders in letzter Zeit zahlreiche Arbeiten.[21-24] Wir erhielten mit den Liganden Antipyrin und Amino-antipyrin in wäßrigen Lösungen die Verbindungen:

XII. $[InAntp_6]J_3$ und XIII. $[InAm_3]J_3$

hingegen in alkoholischer Lösung:

XIV. $[InPyrJ_3]$

XII und XIII können als kationische Komplexe, in welchen das Indium sechsfach koordiniert ist, betrachtet werden, hingegen in der Chelatverbindung XIV könnte das Indium als fünffach koordiniert vorliegen (eine polymere sechsfach koordinierte Form ist weniger wahrscheinlich). Bekanntlich wird die Koordinationszahl 5 hauptsächlich bei Addukten von neutralen Donatorliganden mit In(III)-jodid beobachtet. Vergleicht man die Möglichkeiten des In(III) zur Komplexbildung mit jenen des Tl(III), ergibt sich, daß beide Komplexverbindungen (mäßiger Stabilität) mit verschiedenen Koordinationszahlen bilden können, welche von vielfältigen, teils unbekannten Faktoren abhängen (Elektronegativität der Liganden, Natur und pH der Mutterlösung, usw.). Im Falle der In-Komplexverbindungen finden keine Redoxreaktionen zwischen Indium und den 4-Amino-antipyrin-derivaten statt, da das $4d^{10}$-System (In) stabiler als das bereits erwähnte $5d^{10}$ System ist.

---

[21] A. J. Carty und D. G. Tuck, *J. Chem. Soc., A*, **1966**, 1081.

[22] A. I. Carty, S. J. Patel, D. B. Sowerby und D. G. Tuck, *Proc. 9-th Int. Conf. Coordinat. Chem., St. Moritz-Bad.*, **1966**, 36.

[23] G. Y. Sutton, *Austral. J. Sci. Res., Ser. A*, **4**, 651 (1951);
G. Y. Sutton, *Austral. Chem. Inst. J. and Proc.*, **15**, 356 (1948); **16**, 115 (1949).

[24] I. M. Korenman, A. A. Tumanov, V. Ya. Yanaeva, *Trud. po Khim. i khim. Tehn.* **3**, 86 (1960).

In der Reihe der Komplexverbindungen des Ge^{IV} mit Liganden der 4-Amino-antipyrin-derivate erhielten wir sowohl die des Germaniums als solches, als auch die Salze seiner Heteropolysäuren. So bildet $GeCl_4$ und Pyramidon in CCl_4 unter Feuchtigkeitsausschluß die Verbindung:

$$\text{XV. } [GePyr_3]Cl_4$$

welche an der Luft zerfließt, leicht löslich in Wasser und niederen Alkoholen, hingegen schwer bis unlöslich in wasserfreien organischen Lösungsmitteln ist. Mit Amino-antipyrin oder Antipyrin konnte keine entsprechende Verbindung erhalten werden.

Die Germaniumheteropolymolybdänsäure liefert in stark sauren (2n HCl) Lösungen mit den Liganden Pyramidon, Methylamino- und Amino-antipyrin die Verbindungen:

$$\begin{array}{rl}\text{XVI.} & [GeO_4.12\,MoO_3](HPyr)_4 \\ \text{XVII.} & [GeO_4.12\,MoO_3](HmAm)_4 \\ \text{XVIII.} & [GeO_4\cdot 12\,MoO_3](HAm)_4 \\ \text{XIX.} & [GeO_4\cdot 12\,MoO_3](HAntp)_4\end{array}$$

XVI–XIX sind praktisch unlöslich in verdünnten Mineralsäuren und organischen Lösungsmitteln und können analytisch ausgewertet werden.

EXPERIMENTELLES

Sämtliche Verbindungen des Tl(III) wurden in eisgekühlten Lösungen erhalten. Dadurch wird auch die teilweise Verharzung des Liganden in saurer Lösung, die durch Tl-Ionen katalysiert wird, verhindert.

I. $[TlCl_4](HPyr)$ – Man versetzt 2 ml einer frisch hergestellten $TlCl_3$-Lg (0,54 g Tl) mit 10 ml HCl 1 : 2 und rührt 1 g Pyramidon in 4 ml HCl 1 : 2 ein. Der feinkristalline weiße Niederschlag wird nach 10–15 Min. abfiltriert, gut abgesaugt, zwischen Filterpapier ausgepreßt und über $CaCl_2$ in Vakuum getrocknet. Kann aus Aceton im Vakuum umkristallisiert werden. F = 190 – 192°.

II. $[TlCl_4](HAntp_2)$ – 2 ml einer $TlCl_3$-Lg (0,54 g Tl) wird mit 2 ml HCl 1 : 2, dann unter Rühren mit 1 g Antipyrin in 1 ml konz. HCl und 60 ml H_2O versetzt (Verharzungsgefahr). Nach 15 Min. filtriert man den weißen flockigen Niederschlag, wäscht mit wenig eisgekühltem Wasser und trocknet wie bei I. F = 134 – 135°.

III. $[TlJ_4](HPyr)$ – 1 g Pyramidon und 2,5 g KJ in 130 ml Wasser wird mit einer Lg von 0,4 g $Tl(NO_3)_3 \cdot 3H_2O$ in 200 ml HCl 1 : 1 unter Umrühren versetzt. (Mutterlg. 3,5 n in HCl). Der orangegelb gefärbte Niederschlag wird binnen 24 Std. kristallin (Eiskühlung!), filtriert, mit kleinen Mengen eisgekühltem Wasser gewaschen und wie I behandelt. Beim Umkristallisieren aus Aceton unter Vakuum erhält man blutrot gefärbte Kristalle. F = 159–160° Zers.

IV. $[TlJ_4](HmAm)$ – 1,2 g Novalgin in 100 ml HCl 1 : 1 wird 30 Min. zur Spaltung der Methansulfongruppe gerührt. Das freigewordene SO_2 wird durch einen Luftstrom vertrieben, und die so erhaltene Lg des Methylamino-antipyrins nach Zugabe von 3,2 g KJ in 50 ml H_2O unter ständigem Rühren mit 0,5 g $Tl(NO_3)_3.3H_2O$ in 100 ml HCl 1 : 1 versetzt (Mutterlg 5n in HCl). Der orangegelbe Nd. wird weiter wie III behandelt.

V. $[TlJ_4]$ (HAm) – Wird wie III erhalten F = 136 – 138° Zers.

VI. $[TlPyrCl_3]$ – Man versetzt 2 ml einer frischen $TlCl_3$-Lg (0,86 g $TlCl_3$) mit 1,5 g Pyramidon in 3 ml Methanol und verdünnt sofort unter starkem Rühren mit 100 ml eisgekühltem Wasser. Der gelblichweiße Niederschlag wird nach 5 Min. filtriert und weiter wie III behandelt.

VII. $[TlAntp_2Cl_3]$ – 1 g Antipyrin in 320 ml H_2O wird mit 2 ml einer frisch hergestellten $TlCl_3$–Lg (0,86 g$TlCl_3$) versetzt. Es fällt allmählich ein weißer flockiger Niederschlag aus, der in einigen Stunden kristallin wird. Nach 8 Std. wird der Nd. weiter wie VI behandelt. F = = 115 – 116°.

VIII. $[TyPyrBr_3]$ – Man behandelt während 30 Min. eine TlBr-Suspension in Wasser, unter ständigem Schütteln mit Brom, erhitzt bis 50°, vertreibt das überschüssige Brom durch einen Luftstrom und filtriert die Lg des $TlBr_3$. Die Herstellung der Verbindung VIII erfolgt wie bei VI (Tl :Pyr = 1 :1,5). Der leicht ockergelb gefärbte Niederschlag ist lichtempfindlich. F = 99 – 101° mit Zersetzung.

IX. $[TlAntp_2Br_3]$ – Wird wie VII in etwas konzentrierteren Lgen mit $TlBr_3$ (Tl :Antp = = 1 : 2) hergestellt. Es wird nach 48 Std. filtriert. F = 110°.

X. $[TyPyrJ_3]$ – Wird durch Ionenaustausch aus der entsprechenden Chlorverbindung erhalten. Man mischt 2 ml wäßrige $TlCl_3$-Lg (0,860 g$TlCl_3$) mit 1,4 g Pyramidon in 3 ml Methanol, und rührt diese sofort in die Lg von 3 g KJ in 160 ml Wasser. Es bildet sich ein gelber Niederschlag, dessen Farbe mit der Zeit in orangegelb übergeht (15 Std.).

XI. $[TlAntp_2J_3]$ – Wird ähnlich wie X erhalten. Zu 1,04 g Antipyrin in 300 ml Wasser wird tropfenweise 2 ml $TlCl_3$-Lg (0,860 g $TlCl_3$) eingerührt. Es bildet sich das Diantipyril-thallium (III)-chlorid. Nach einer Stunde fügt man unter Rühren eine Lg von 2 g KJ in 40 ml H_2O hinzu. Die erhaltene gelbe Suspension wird binnen 24 Std. orangegelb und mikrokristallin.

XII. $[InAntp_6]$ J_3 – Man versetzt die eisgekühlte Lg von 2 g Antipyrin und 1 g KJ in 20 ml Wasser unter ständigem Umrühren mit 0,5 g $In(NO_3)_3.3H_2O$ in 50 ml Wasser (pH $\cong$ 5). Der weiße, körnige Niederschlag wird einige Stunden gekühlt, filtriert, mit wenig Wasser gewaschen und über $CaCl_2$ getrocknet. Schwer löslich in Wasser, Äthanol und Äther; leicht löslich in Methanol und Aceton F = 115–116°.

XIII. $[InAm_3]J_3$ – Wird wie XII erhalten (pH der Mutterlg 5,8). Feiner, gelblicher Niederschlag. Löslichkeitsverhältnisse wie bei XII.

XIV. $[InPyr\ J_3]$ – 2 g Pyramidon in 25 ml absolutem Alkohol werden bei Eiskühlung mit 1 g InJ_3 ebenfalls in absolutem Alkohol versetzt. Der weiße Niederschlag wird nach einer Stunde filtriert und mit Äther gewaschen. Aus heißem absolutem Alkohol umkristallisiert, erhält man kleine, gelbliche Kristalle. Schwer löslich in Wasser und organischen Lösungsmitteln. F = 233–235°.

XV. $[GePyr_3]$ Cl_4 – Wird unter absolutem Wasserausschluß hergestellt. Man vereint unter Rühren 1 g Pyramidon in 10 ml CCl_4 und 0,4 g $GeCl_4$ in 10 ml CCl_4. Der feine weiße Niederschlag wird filtriert, mit wenig CCl_4 gewaschen und über $CaCl_2$ bei 40° im Vakuum getrocknet.

XVI – XIX. $[GeO_4(MoO_3)_{12}]$ $(HLig)_4$ – wo Lig. = Pyr, mAm, Am und Antp. Man versetzt 2,4 ml 2 n H_2SO_4 in 35 ml Wasser mit 6 Tropfen $GeCl_4$, dann mit 25 ml 5% Ammoniummolybdat-Lg; beim Umrühren bildet sich die 12-Molybdänsäure des Germaniums unter Gelbfärbung. Es wird bis 50° im Wasserbad erhitzt und nach 10 Min. mit 10 ml konz. HCl und 1,5 g Ligand in 1,5 ml konzentrierten HCl und 15 ml H_2O gefällt (Methylamino-antipyrin wird aus Novalgin durch Abspalten der Methansulfongruppe in salzsaurer Lösung erhalten). Die Verbindungen sind türkis (XVI), grau-blau (XVII), grau (XVIII) und hellgelb (XIX) gefärbt. Sie werden nach 12 stündigem Stehen kristallin. Man filtriert, wäscht mit Wasser und trocknet bei 60°.

Sämtliche Analysenergebnisse sind in Tabelle 1 zusammengefaßt.

Tabelle 1

Analysenergebnisse der Verbindungen

	Komplexverbindung	Molargewicht	Ber.			Gef.		
			Metall	Halogen	N	Metall	Halogen	N
I	$[TlCl_4](HPyr)$	578,33	35,34	24,52	7,27	34,73	24,16	7,50
II	$[TlCl_4](HAntp_2)$	723,40	28,26	19,60	7,74	28,69	19,56	7,39
III	$[TlJ_4](HPyr)$	944,15	21,65	53,76	4,45	21,49	53,30	4,63
IV	$[TlJ_4](HmAm)$	930,22	21,97	54,58	4,52	22,48	54,93	4,33
V	$[TlJ_4](HAm)$	916,24	22,17	55,41	4,59	22,96	55,80	4,31
VI	$[TlPyrCl_3]$	541,90	37,72	19,63	7,75	37,16	19,21	7,98
VII	$[TlAntp_2Cl_3)]$	686,96	29,75	15,49	8,16	29,29	15,83	7,87
VIII	$[TlPyrBr_3]$	675,28	30,27	35,50	6,22	30,20	35,57	6,51
IX	$[TlAntp_2Br_3]$	820,34	24,92	29,20	6,83	25,40	29,70	6,42
X	$[TlPyrJ_3]$	816,25	25,04	46,64	5,15	25,64	47,13	4,96
XI	$[TlAntp_2J_3]$	960,31	21,28	39,64	5,84	21,72	39,52	5,48
XII	$[InAntp_6]J_3$	1624,24	7,07	23,39	10,32	7,27	23,39	9,99
XIII	$[InAm_3]J_3$	1104,96	10,39	34,39	11,41	10,60	33,90	11,08
XIV	$[InPyrJ_3]$	726,74	15,80	52,25	5,78	15,78	52,53	5,60
XV	$[GePyr_3]Cl_4$	907,88	8,00	15,62	13,69	8,21	15,79	14,02
XVI	$[GeO_4.12MoO_3](HPyr)_4$	2793,06	2,60	40,87	6,02	2,35	41,35	5,89
XVII	$[GeO_4.12MoO_3](HmAm)_4$	2736,51	2,63	41,71	6,16	2,52	42,12	6,12
XVIII	$[GeO_4.12MoO_3](HAm)_4$	2680,42	2,71	42,58	6,27	2,90	42,75	6,53
XIX	$[GeO_4.12MoO_3](HAntp)_4$	2620,34	2,77	43,56	4,27	2,80	44,08	4,18

Analytisches

Thallium – gewichtsanalytisch als $TlCrO_4$ nach vorheriger Reduzierung des Tl(III) zu Tl(I), Indium – gewichtsanalytisch als In_2O_3, Germanium – gewichtsanalytisch als GeO_2 nach Fällung mit Tannin, Molybdän – gewichtsanalytisch als Bleimolybdat, Halogen – potentiometrisch und gewichtsanalytisch, Stickstoff nach Pregl.

Tabelle

Charakteristische Banden aus den

Verbindung	Ligand				
	$>C{=}O$			$>C{=}C<$	$C-NR_2$
	$\nu_{C=O}$	$\delta_{O=C-N}$	$\gamma_{C=O}$	$\nu_{C=C}$	ν_{C-N}
Pyramidon	1665	603	560	1565	1315 1130
Antipyrin	1667	616	585	1555	–
$[TlPyrBr_3]$					
$[InPyrJ_3]$					
$[TlAntp_2Cl_3]$**					
$[TlJ_4](HPyr)$					

* Schulter
** Einfache Komplexverbindung

Aus den IR-Spektren je eines Repräsentanten der wichtigsten Verbindungstypen, wurden die Schwingungen der an der Chelat-, Komplex-, oder Salzbildung beteiligten Gruppen im Vergleich zu jenen der freien Liganden veranschaulicht und in Tabelle 2 zusammengefaßt.

Die IR-Spektren wurden mit dem Doppelstrahlgerät UR–10 VEB Carl Zeiss Jena und Prismen aus KBr (400 – 700 cm^{-1}) NaCl (700 – 1800 cm^{-1}) und LiF (1800 – 4000 cm^{-1}) aufgenommen. Dazu wurden KBr-Preßlinge der Komplexverbindungen verwendet.

Zur Synthese der Verbindungen wurde verwendet:
Thallium(I)-nitrat *p.a.* der Firma CHEMAPOL.
Thallium(I)-chlorid *p.a.* der Firma British Drug Houses.
Germanium-tetrachlorid *p.a.* der Firma ERVA-Heidelberg.
Metallisches Indium *p.a.*
Thallium(III)-nitrat nach.[25,26]
Thallium(III)-chlorid nach.[27]

[25] O. Rabe, *Z. anorg. Chem.*, **48**, 427 (1906).
[26] R. I. Meyer, *Z. anorg. Chem.*, **24**, 360 (1900).
[27] R. I. Meyer, *Z. anorg. Chem.*, **24**, 335 (1900).

Indium(III)-nitrat, aus metallischem Indium in Salpetersäure 1 : 1 und Auskristallisieren des $In(NO_3)_3.3H_2O$.

Indium(III)-jodid nach.[28]

Frau Dipl.-Ing. Ilse Bacaloglu besten Dank für die Aufnahme der IR-Spektren.

2

IR-Spektren der Verbindungen

Chelatverbindung			Pyrazolonring		Salze				
Chelating					C−OH				$C-NR_2$
ν_{C-O}	ν_{Me-O} od. ν_{Me-N}	ν_{C-N}	$\nu_{C=N}$	$\nu_{C=C}$	ν_{C-O}	δ_{OH}	γ_{OH}	ν_{OH}	ν_{C-N}
1020	480?	1330 1180*	1610	1565					
1015	472?	1330 1160	1610	1565					
1017	490?	—	1610	1580					
			1615	1535	1030	1378	680	2590 2635 2680	1330 1145

---

[28] F. Kutek, *Coll. Czech. Chem. Comm.*, **31**, 1875 (1966).

Revue Roumaine de Chimie, **14**, 1613–1616 (1969)

EINE NEUE KOLORIMETRISCHE BESTIMMUNGSMETHODE DES EISENS(III)

AL. ŞUTEU, T. HODIŞAN und FIAMETTA KORMOŞ

aus der Chemischen Fakultät der „Babeş-Bolyai"-Universität Cluj, str. Arany János, 11

Eingegangen am 27. Februar 1969

Die Arbeit beschreibt eine kolorimetrische Bestimmungsmethode des Eisens(III), auf Grund der Reaktion zwischen Fe(III) und *o*-Aminophenol, wenn eine rotorange gefärbte Verbindung mit einem Absorptionsmaximum bei 430 nm und einem molaren Extinktionskoeffizienten von 4767 cm^2 mol^{-1} entsteht. Es wird gezeigt, daß durch diese Methode 2,2–28,5 μg Fe^{3+}/ml bestimmt werden können.

In der Fachliteratur sind zahlreiche kolorimetrische Bestimmungsmethoden beschrieben und zwar solche, die als Reagens SCN^-,[1] Formohydroxamsäure,[2] Dibenzoylmethan,[3] Sulfosalicylsäure,[4] Salicylaldoxim,[5] Chromotropsäure,[6] Chinaldynsäure,[7] Meconsäure,[8] 5-Sulfoanthranylsäure,[9] Thioacetamid in Gegenwart von Äthylendiamino-tetraessigsäure (EDTA),[10] Pirogallol,[11] 4-Amino-4′-metoxydiphenylamin,[12] Thenoiltrifluoraceton[13] (TTA), Protokatechinaldehyd,[14] Nikotinhydroxamsäure,[15] 3-Hydroxy-1-phenyl-3-methyltriazin,[16] Resorcin,[17] Pyrokatechin,[18] Xylenolorange,[19] β-Amminopicolinsäure,[20] u.a. verwenden.

[1] S. E. Kahane, *Bull. Soc. chim. France*, **41**, 1403 (1927).

[2] E. E. Vonesch, O. Guagnini und S. V. Guagnini, *Anales Asoc. quim. argentina*, **41**, 162 (1963); *Chem. Abstr.*, **48**, 31904i (1954).

[3] T. Shigematsu und M. Tabushi, *Nipon Kagaku Zasshi*, **81**, 262 (1960); *Chem. Abstr.* **54**, 13.972g (1960).

[4] F. Alten, H. Wieland und E. Hille, *Z. anorg. Chem.*, **215**, 81 (1933).

[5] Bondyopodhayay, *J. Indian Chem. Soc.*, **33**, 276 (1956).

[6] L. Sommer, *Chem. listy*, **52**, 1485 (1958).

[7] A. K. Majumdov und B. Sen, *J. Indian Chem. Soc.*, **27**, 245 (1950).

[8] G. Mannelli und R. Biffoli, *Analyt. Chim. Acta*, **11**, 168 (1954).

[9] I. M. Zehner und Th. R. Sweet, *Analyt. Chem.*, **28**, 198 (1956).

[10] G. C. Kvejn, A. S. Kaster und G. Boef, *Analyt. Chim. Acta*, **23**, 240 (1960).

[11] F. M. Shemyakin und T. V. Vashedchenko, *Zhur. obshchei Khim.*, **5**, 667 (1935); *Chem. Abstr.*, **29**, 7216^2 (1935).

[12] L. Erdey und F. Szabadvany, *Z. analyt. Chem.*, **155**, 90 (1957).

[13] A. K. Dey und D. M. Khophar, *Chimie et Industrie*, **1959**, 864.

[14] M. Y. Shapiro, *Zhur. analyt. Khim.*, **7**, 214 (1952).

[15] R. L. Dutta, *J. Indian Chem. Soc.*, **35**, 243 (1958); *Chem. Abstr.*, **52**, 19.699e (1958).

[16] A. K. Gupta, N. C. Sagoni, *J. Indian Chem. Soc.*, **36**, 87 (1959); *Chem. Abstr.*, **53**, 19.692b (1959).

[17] G. S. Rao, *Analyt. Chim. Acta*, **21**, 564 (1959).

[18] A. N. Smith, *Analyst*, **84**, 516 (1959).

[19] K. L. Cheng, *Talanta*, **2**, 147 (1959).

[20] A. K. Majumdar und S. P. Boy, *Z. analyt. Chem.*, **185**, 439 (1962).

Die experimentell beobachtete Tatsache in Betracht ziehend, daß Fe(III) das *o*-Aminophenol in eine rotorange Verbindung oxydiert, haben wir uns zum Ziel gesetzt, die optimalen Versuchsbedingungen dieser Reaktion zu bestimmen, um sie bei der kolorimetrischen Bestimmung des Fe(III) anzuwenden.

In erster Reihe wurde die Absorptionskurve der Verbindung studiert, welche bei der Oxydation des *o*-Aminophenols mit Fe(III) entsteht. Die Bestimmungen wurden mit einem Spektrophotometer Beckmann D.B. durchgeführt. Die Ergebnisse sind in Abb. 1 graphisch dargestellt, woraus ersichtlich ist, daß aus der Reaktion eine gefärbte Verbindung hervorgeht mit einem Absorptionsmaximum von 430 nm.

Weil der Gang der Oxydationsreaktion des *o*-Aminophenols mit Fe(III) sehr stark vom pH-Wert abhängt, wurde auch der Einfluß der pH-Werte auf die Absorption einiger Lösungen, welche die gleiche Menge an Fe(III) und *o*-Aminophenol enthielten, aber verschiedene pH-Werte hatten, bestimmt. Die Ergebnisse sind in Abbildung 2 wiedergegeben.

Aus Abbildung 2 geht hervor, daß ein Intensitätsmaximum der Färbung in stark saurem Medium bei $\mathrm{pH} = 0{,}8-2{,}4$ erhalten wird. Bei einem pH-Wert $< 0{,}8$ fällt die Farbintensität und bei pH-Werten $> 2{,}4$ beobachtet man neben der Verkleinerung der Farbintensität auch eine Veränderung der Farbe nämlich von rotorange zu gelb.

Die experimentellen Bestimmungen haben gezeigt, daß die Farbintensität zeitabhängig ist und deshalb wurde sie nach bestimmten Zeitabständen gemessen. Die Ergebnisse sind in Abb. 3 graphisch dargestellt.

Man sieht aus Abbildung 3, daß die Farbintensität nach 20 Minuten konstant bleibt.

Es wurde dann das Konzentrationsgebiet bestimmt in dem das Lambert-Beersche Gesetz gültig ist und es wurde festgestellt, daß im Bereich von 2,2 bis 28,5 μg Fe(III)/ml eine genau lineare Abhängigkeit zwischen Extinktion und Konzentration besteht, wie aus Abb. 4 hervorgeht.

Die Messungen wurden an einem Kolorimeter F.E.K. durchgeführt. Der molare Extinktionskoeffizient beträgt

$$\varepsilon = \frac{E_{\max}}{l \cdot C_{\mathrm{mol/l}}} = \frac{0{,}75}{1{,}57 . 10^{-4}} = 4767 \text{ cm}^2 \text{ mol}^{-1}$$

Um die Streuung der Ergebnisse in Betracht zu ziehen, wurde mit Hilfe der Statistik der geraden Linie die Gleichung der wahrscheinlichsten Geraden berechnet.

$y = A_0 + A_1 x$ y = Extinktion der Lösung
x = Konzentration von Fe(III).

$$\mathrm{A}_0 = \frac{\sum x^2 \sum y - \sum x \sum xy}{n \sum x^2 - |\sum x|^2}$$

und

$$\mathrm{A}_1 = \frac{n \sum xy - \sum x \sum y}{n \sum x^2 - |\sum x|^2}$$

Die Gleichung der erhaltenen Geraden ist :

$$y = 0{,}065 + 0{,}020\,x$$

$$E = 0{,}065 + 0{,}020\ \mu\text{gFe}$$

$$\mu\text{gFe} = \frac{E - 0{,}065}{0{,}020}\ ;$$

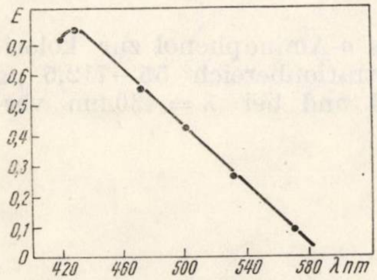

Abb. 1. – Absorptionskurve des mit Fe^{3+} oxydierten *o*-Aminophenols

o-Aminophenol = 0.3%, Fe^{3+} = 4.4 mg/l
pH = 1.2. 1 cm Küvette

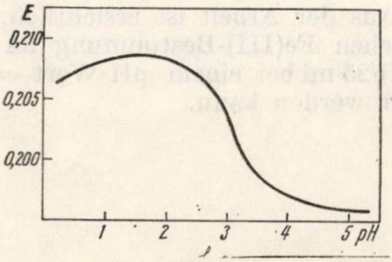

Abb. 2. – Die Abhängigkeit der Extinktion von dem pH-Wert der Lösung

Fe^{3+} = 4.4 mg/l, *o*-Aminophenol = 0.3%
λ = 430 nm, 1 cm Küvette

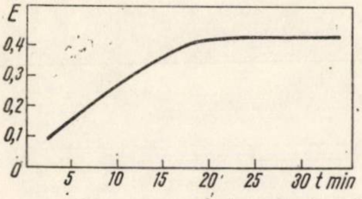

Abb. 3. – Die Abhängigkeit der Extinktion von der Zeit.

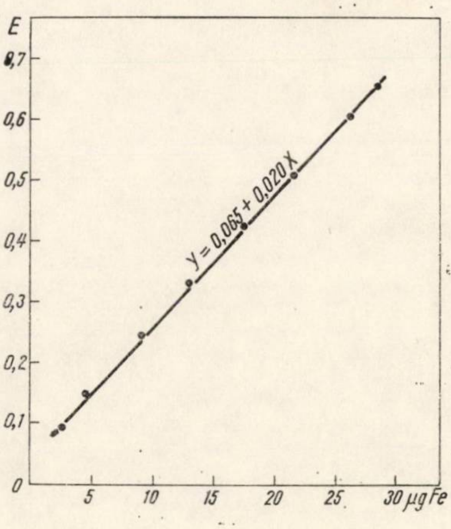

Abb. 4. – Die Abhängigkeit der Extinktion von der Fe^{3+} Konzentration.

o-Aminophenol = 0.3%. pH = 1.2, λ = 430 nm,
1 cm Küvette.

ARBEITSWEISE

Die Lsg welche Fe(III) im Bereich von 50 bis 750 μg Fe^{3+} enthält, wird in einen 25 ml-Meßkolben gebracht ; es wird mit 10 ml (HCl 0,2 n + KCl 0,2 M) auf einen pH-Wert von 1,2–1,6 gepuffert, 5 ml *o*-Aminophenol 0,3 % hinzugefügt und mit dest. Wasser aufgefüllt. Die Extinktion der Lsg wird nach 20 Min. in einer 1 cm Küvette und mit einem blauen Filter (λ = 470 nm) gemessen.

Die 0,3 %ige *o*-Aminophenollsg wird durch Lösen von *o*-Aminophenol in 0,1 n HCl erhalten. Da diese Lsg unbeständig ist, empfiehlt es sich frische Lsgen zu verwenden.

Die Bestimmungen werden von anderen Oxydationsmitteln : Cr^{3+}, V^{5+}, Ce^{4+}, BrO_3^-, H_2O_2 gestört, da auch diese das *o*-Aminophenol oxydieren.

SCHLUSSFOLGERUNGEN

Aus der Arbeit ist ersichtlich, daß das *o*-Aminophenol zur kolorimetrischen Fe(III)-Bestimmung im Konzentrationbereich 55—712,5 µg Fe(III)/25 ml bei einem pH-Wert = 1,2—1,6 und bei λ = 430 nm verwendet werden kann.

Revue Roumaine de Chimie, **14**, 1617–1620 (1969)

ÜBER PHENOTHIAZONE. XVI[1]

REAKTION VON PHENOTHIAZONEN MIT ANILIN

C. BODEA und EDDA BROSER

aus dem Chemischen Institut der Akademie, Cluj, str. Donath 59–65

Eingegangen am 11. August 1969

Bei der Einwirkung von Anilin auf Phenothiazon und Halogenphenothiazone entstehen die entsprechenden 2-Anilino-phenothiazone durch 1,4-Addition des Anilins an den Chinoniminring, bzw. durch Substitution des 2ständigen Bromatoms durch den Anilinrest.

Der Chinoniminring der Phenothiazone ist zu 1,4-Additionen befähigt, wie dies aus vorangegangenen Arbeiten[2,3] über Halogenwasserstoffadditionen an Phenothiazone hervorgeht.

Es war zu erwarten, daß Phenothiazone in Analogie zu *p*-Benzochinon und Benzochinoniminen auch andere 1,4-Additionsreaktionen eingehen. *p*-Benzochinon liefert z.B. mit Anilin oder substituierten Arylaminen die entsprechenden Mono- oder Diarylamino-*p*-benzochinone.[4] Im folgenden soll über die Reaktion von Anilin mit Phenothiazonen berichtet werden.

Wird eine Lösung von Phenothiazon (**1**) und Anilin im Verhältnis 1 : 1 in Eisessig oder Dimethylformamid gekocht, so wird als Hauptprodukt 2-Anilino-phenothiazon (**9**) in Form von braunroten Prismen mit grünmetallischem Glanz erhalten. Die Struktur des Reaktionsproduktes wurde wie folgt belegt.

Die Analysedaten (Elementaranalyse und IR-Spektrum) zeigen das Vorhandensein eines Sauerstoffatoms bzw. der Carbonylgruppe an, somit kann es sich nicht um ein Kondensationsprodukt der Carbonylgruppe handeln.

Wird 2-Brom-phenothiazon (**2**) unter den erwähnten Bedingungen mit Anilin behandelt, so erhält man dasselbe Produkt (**9**) wie bei der Reaktion von Phenothiazon mit Anilin. Im Einklang damit ist die Reaktion zwischen 4-Brom- (**3**) bzw. 2,4-Dibrom-phenothiazon (**4**) und Anilin: in beiden Fällen wird dieselbe Substanz erhalten, u. zw. 2-Anilino-4-brom-phenothiazon (**10**).

---

[1] XV. Mitteilung : C. Bodea, M. Terdic und E. Broser, *Liebigs Ann. Chem.*, **715**, 122 (1968).

[2] C. Bodea, M. Răileanu und I. Silberg, *Anal. Şti. Univ. „Al. I. Cuza" Iaşi*, Sect. *1*, **6**, 1023 (1960).

[3] C. Bodea und M. Terdic, *Rev. Roumaine Chim.*, **13**, 1235 (1968).

[4] M. Becke, W. Suida und H. Suida, DRP, 300706 ; *Chem. Zentr.*, **1920** II, 537.

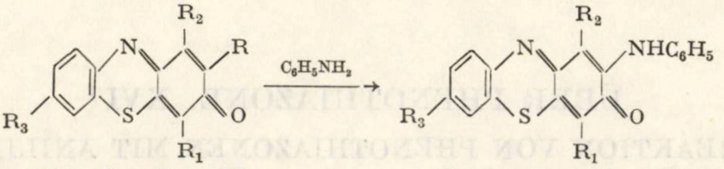

1 $R=R_1=R_2=R_3=H$ **9** $R_1=R_2=R_3=H$

2 $R=Br$; $R_1=R_2=R_3=H$

3 $R_1=Br$; $R=R_2=R_3=H$ **10** $R_1=Br$; $R_2=R_3=H$

4 $R=R_1=Br$; $R_2=R_3=H$

5 $R_2=Br$; $R=R_1=R_3=H$ **11** $R_2=Br$; $R_1=R_3=H$

6 $R_1=Cl$; $R=R_2=R_3=H$ **12** $R_1=Cl$; $R_2=R_3=H$

7 $R_3=Br$; $R=R_1=R_2=H$ **13** $R_3=Br$; $R_1=R_2=H$

8 $R_3=Cl$; $R=R_1=R_2=H$ **14** $R_3=Cl$; $R_1=R_2=H$

1-Brom-phenothiazon (**5**) und Anilin lieferte unter gleichen experimentellen Bedingungen 2-Anilino-1-brom-phenothiazon (**11**), 4-Chlor-phenothiazon (**6**) das 2-Anilino-4-chlor-phenothiazon (**12**). Aus 7-Brom- (**7**) bzw. 7-Chlor-phenothiazon (**8**) und Anilin erhielten wir die entsprechenden 2-Anilino-derivate **13** bzw. **14**.

Durch Behandlung der Anilino-phenothiazone mit Zinkpulver in Eisessig tritt die für Phenothiazone charakteristische Reduktion ein, unter Bildung von äußerst unbeständigen, der Rückoxydation unterliegenden, Leukoverbindungen.

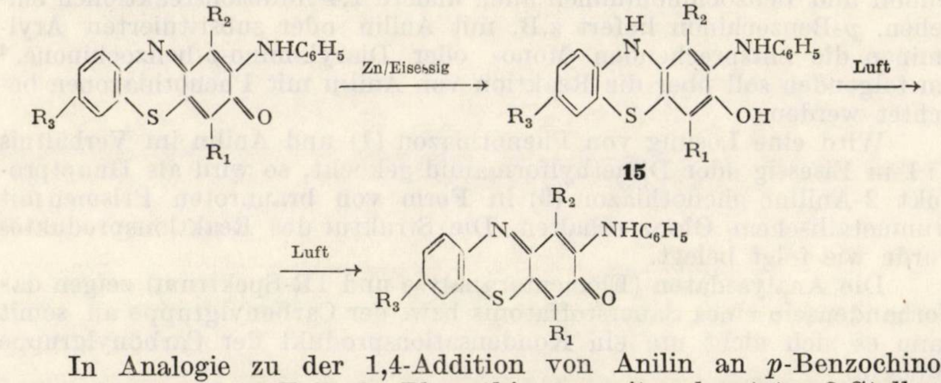

15

In Analogie zu der 1,4-Addition von Anilin an *p*-Benzochinon (s.w.u.) kann auch im Falle der Phenothiazone mit unbesetzter 2-Stellung die Reaktion mit Anilin als eine 1,4-Addition an den Chinoniminring betrachtet werden, obwohl während der Reaktion keine für das eigentliche, unoxydierte Additionsprodukt **15** charakteristische Entfärbung beobachtet werden kann.

Die außergewöhnlich leichte Rückoxydierbarkeit der 2-Anilino-3-hydroxy-phenothiazine (**15**) läßt sich durch die Gegenwart des elektronenabstoßenden Anilinorestes erklären. Ein ähnliches Verhalten wurde bei 2-Amino-3-hydroxy-phenothiazin beobachtet.[5] Wie bekannt, ist das unsubstituierte 3-Hydroxyphenothiazin an Luft äußerst unbeständig, hingegen nimmt die Stabilität der 3-Hydroxyphenothiazine mit wachsender Anzahl der elektronenanziehenden Halogensubstituenten zu.

---

[5] D. P. SEVBO und O. F. GINSBURG, *Zhur. org. Khim.*, **IV** (10), 1854 (1968).

Das eigentliche Additionsprodukt **15** wird im Reaktionsansatz durch das vorhandene Ausgangsphenothiazon zu dem jeweils entsprechenden 2-Anilino-phenothiazon oxydiert, wie dies bekanntlich bei der Addition von Anilin an *p*-Benzochinon stattfindet:

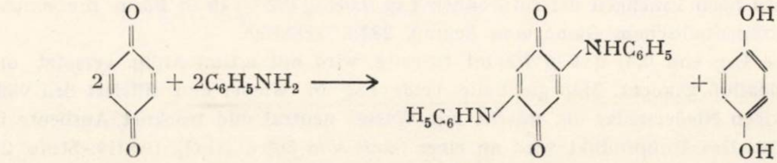

Im Rekationsgemisch ist nämlich sogar nach 3tägigem Kochen des Ansatzes mit Anilinüberschuß noch Ausgangsphenothiazon vorhanden.

Die Reaktion findet auch dann statt, wenn man die Phenothiazone direkt mit Anilin ohne Lösungsmittel kocht, jedoch verläuft sie in diesem Falle viel langsamer und uneinheitlicher.

Bei den Phenothiazonen **2** und **4** wird das 2ständige Bromatom durch einen Anilinrest ausgetauscht; im Reaktionsansatz ist Br^- vorhanden. Vergleichbare Reaktionen finden sich ebenfalls in der Reihe einiger analog substituierter *p*-Benzochinone [6] und Naphthochinone (1 : 4) [7] vor. Elektrophile Substituenten bevorzugen die 4-Stellung des Chinoniminrings, wi dies aus vorangegangenen Arbeiten [8] hervorgeht. Der Eintritt des nucleophilen Anilinorestes in die 2-Stellung durch Substitution des Bromatom spricht dafür, daß diese Stellung die geringste Elektronendichte aufweist

BESCHREIBUNG DER VERSUCHE

2-Anilino-phenothiazon (**9**). a) 1g **1** wird in 75 ml siedendem Eisessig gelöst. In die Lsg werden 0,43 ml Anilin eingetragen und nach 6stdigem Kochen gießt man die gebildete braunviolette Lsg in kaltes Wasser und schüttelt mehrmals mit Toluol aus. Der mit Wasser gewaschene Toluolextrakt wird auf ca. 30 ml eingeengt und an einer Säule von 750 g Al_2O_3 (Aktivitäts-Stufe 3) mit Toluol als Elutionsmittel gereinigt. Nach dem Einengen kristallisiert **9** in Form brauner Prismen mit grünmetallischen Reflexen von Schmp. 241–242° aus. Ausbeute 0,4g (28%).

b) 0,25 g **2** werden in 20 ml siedendem Eisessig gelöst, mit 0,08 ml Anilin versetzt und 1 Std. unter Rückfluß gekocht. Als Hauptprodukt entsteht **9** welches wie nach a) aufgearbeitet und gereinigt wurde. Ausbeute 0,1 g (38,4%). Nach Schmp., Misch-Schmp., R_F-Wert, IR- und Elektronenspektrum ist diese Verbindung mit der nach a) dargestellten identisch. IR-Spektrum (in KBr) : 1627 (C=O), 3267 (N–H) cm^{-1}. Elektronenspektrum (in Methanol) :

---

[6] K. WALLENFELS und W. DRABER, *Tetrahedron Letters*, **13**, 24 (1959); K. WALLENFEL und K. FRIEDRICH, *Chem. Ber.*, **93**, 3070 (1960); K. WALLENFELS und W. DRABER, *Liebigs Ann. Chem.*, **667**, 55 (1963).

[7] K. FRIES und P. OCHWAT, *Ber. dtsch. chem. Ges.*, **56**, 1299 (1923); K. FRIES und E. KÖHLER, *ebda.*, **57**, 504 (1924); K. FRIES und F. KERKOW, *Liebigs Ann. Chem.*, **427**, 295 (1922).

[8] C. BODEA und M. TERDIC, *Rev. Roumaine Chim.*, **13**, 1235 (1968); M. TERDIC und C. BODEA, *ebda*, **13**, 1241 (1968).

λ_{max} : 476, 289, 272 mμ ; ε : 25 259, 34 163 bzw. 39 617. Anal. $C_{18}H_{12}N_2OS$ (304) *ber.* : C 71, H 3,97, N 9,20 ; *gef.* : C 71,32, H 3,76, N 9,15.

2-Anilino-4-brom-phenothiazon (**10**). a) 0,2 g **3** werden in 20 ml siedendem Eisessig gelöst, mit 0,063 ml Anilin versetzt und 8 Std. unter Rückfluß gekocht. Man gießt in kaltes Wasser, saugt den flockigen Niederschlag ab, wäscht mit Wasser neutral und trocknet. Durch chromatographische Reinigung an einer Säule von 300 g Al_2O_3 (Aktiv.-Stufe 3) und Toluol als Elutionsmittel wird nach Einengen der rotbraunen Lsg 0,083 g (32 %) **10** in Form braunvioletter Nadeln mit grünmetallischem Glanz vom Schmp. 284,5° erhalten.

b) Eine Lsg von 0,4 g **4** in 100 ml Eisessig wird mit 0,1 ml Anilin versetzt und 9 Std. unter Rückfluß gekocht. Man gießt die heiße Lsg in Wasser und filtriert den violettbraunen, flockigen Niederschlag ab, wäscht mit Wasser neutral und trocknet. Ausbeute 0,4 g (96 %) rohes **10**. Das Rohprodukt wird an einer Säule von 500 g Al_2O_3 (Aktiv.-Stufe 2—3) mit Toluol als Elutionsmittel gereinigt wonach 0,1 g (24,3 %) reines **10** in Form braunvioletter Nadeln erhalten werden. Schmp. 284,5°. Nach R_F-Wert, IR- und Elektronenspektrum ist diese Verbindung mit der nach a) dargestellten identisch. IR-Spektrum (in KBr) : 1623 (C=O), 3281 (N—H) cm^{-1}. Elektronenspektrum (in Methanol) : λ_{max} : 478, 294,6, 275,3 mμ. Anal. $C_{18}H_{11}BrN_2OS$ (383,3) *ber.* : C 56,41, H 2,89, Br 20,85, N 7,31 ; *gef.* : C 56,03, H 2,58, Br 21,05, N 7,15.

2-Anilino-4-chlor-phenothiazon (**12**). 0,5 g **6** werden in 25 ml siedendem Eisessig gelöst, mit 0,19 ml Anilin versetzt und 15 Std. unter Rückfluß gekocht. Die Aufarbeitung und Reinigung erfolgt wie für **10**. Man erhält 0,135 g (19 %) **12** in Form langer, verfilzter, violettbrauner Nadeln mit grünmetallischem Glanz vom Schmp. 164,5—165°. IR-Spektrum (in KBr) : 1627 (C=O), 3264 (N—H) cm^{-1}. Elektronenspektrum (in Methanol) : λ_{max} : 476, 294,6, 274,5mμ. Anal. $C_{18}H_{11}ClN_2OS$ (338,8) *ber.* : C 63,81, H 3,27, Cl 10,46, N 8,27 ; *gef.* : C 63,65, H 3,28, Cl 10,47, N 8,11.

2-Anilino-1-brom-phenothiazon (**11**). Eine Lsg von 0,25 g **5** in 15 ml Eisessig wird mit 0,08 ml Anilin versetzt und 2 Std. unter Rückfluß gekocht. Man gießt die braunviolette Lsg in kaltes Wasser, schüttelt mehrmals mit Toluol aus und reinigt den Toluolextrakt an einer Säule von 500 g Al_2O_3 (Aktiv.-Stufe 3) mit Toluol als Elutionsmittel. Nach Einengen der rotbraunen Lsg werden 0,055 g (17 %) **11** als sehr lange rotbraune Nadeln mit grünen Reflexen vom Schmp. 178° erhalten. IR-Spektrum (in KBr) : 1621 (C=O), 3236 (N—H) cm^{-1}. Elektronenspektrum (in Methanol) : λ_{max} : 474, 295,5, 262 mμ ; ε : 17350, 24900 bzw. 28700. $C_{18}H_{11}BrN_2OS$ (383,3) *ber.* : C 56,41, H 2,89, Br 20,8, N 7,31 ; *gef.* : C 56,23, H 3,20, Br 21,08, N 7,22.

2-Anilino-7-brom-phenothiazon (**13**). Eine Lsg von 0,25 g **7** in 15 ml siedendem Eisessig wird mit 0,08 ml Anilin versetzt. Man kocht 10 Min. unter Rückfluß. Beim Erkalten erstarrt die Lsg zu einem Brei aus dem durch Abfiltrieren lange violette Nadeln erhalten werden. Ausbeute 0,14 g (42 %) **13** (Rohprodukt). Schmp. 253—254° (aus Eisessig). Durch chromatographische Reinigung an einer Säule von 300 g Al_2O_3 (Aktiv.-Stufe 2—3) wird **13** vom Schmp. 253—254° erhalten. IR-Spektrum (in KBr) : 1626 (C=O), 3331 (N—H) cm^{-1}. Elektronenspektrum (in Methanol) : λ_{max} : 476, 291,5, 276,2 mμ ; ε : 27541, 36140 bzw. 47456. $C_{18}H_{11}BrN_2OS$ (383,3) *ber.* : C 56,4, H 2,89, Br 20,8, N 7,31 ; *gef.* : C 57,10, H 3,07, Br 20,58, N 7,16.

2-Anilino-7-chlor-phenothiazon (**14**). Aus 0,25 g **8** in 15 ml Eisessig heiß gelöst und mit 0,08 ml Anilin versetzt werden nach 15 Min. Kochen und darauffolgende Aufarbeitung, wie für **13**, 0,14 g (40 %) **14** vom Schmp. 242,5—243° erhalten. IR-Spektrum (in KBr) : 1627 (C=O), 3264 (N—H) cm^{-1}. Elektronenspektrum (in Methanol) : λ_{max} : 476, 290, 276 mμ ε : 27024, 36097 bzw. 47904. $C_{18}H_{11}ClN_2OS$ (338,8) *ber.* : C 63,81, H 3,27, Cl 10,46, N 8,27 ; *gef.* : C 63,71, H 3,51, Cl 11, N 8,21.

Die *Schmelzpunkte* wurden mittels eines Mikroheiztisches Boetius bestimmt und sind unkorrigiert. Die IR-*Spektren* wurden mit einem Spektralphotometer Carl Zeiss Jena UR—10, die Elektronenspektren mit einem Spektrophotometer Beckman DK—2A aufgenommen.

Revue Roumaine de Chimie, **14**, 1621–1628 (1969)

DIE REAKTION ZWISCHEN NATRIUMALKOXIDEN UND α-HALOGENKETONEN. VI*

EINWIRKUNG DES NATRIUMMETHOXIDES AUF ω-BROMACETOPHENON

L. SZOTYORI, L. FEY und ANAMARIA ÁBRAHÁM

Aus dem Laboratorium für Organische Chemie der Babeş-Bolyai-Universität, Cluj,
str. Arany János, 11

Eingegangen am 30. November 1968

Es wird die Reaktion zwischen ω-Bromacetophenon und Natriummethoxid studiert. Es wird gezeigt, daß durch Veränderung der Reaktionsbedingungen, der Prozeß in einer anderen Richtung verläuft als die, die in der Literatur[1–6] beschrieben ist. Anstelle von Bromdiphenacyl bildet sich, durch einen anderen Reaktionsmechanismus das Dimethylacetal des Benzoylcarbinols und ω-Methoxyacetophenon.

Das Studium zwischen ω-Bromacetophenon und Natriumalkoxiden wurde schon 1895 von Fritz [1] begonnen. Auf Grund der Reaktion, isolierte er ein kristallines Produkt, welches im Vergleich zur Ausgangssubstanz fast das doppelte Molekulargewicht besaß. Im Molekül befand sich auch ein Bromatom, das ihn veranlaßte diese Substanz Bromdiphenacyl zu benennen, nach dem Bromphenacyl, eine andere Benennung des Bromacetophenons. Ein Jahr später zeigten Paal und Demeler, [2] daß unter verschiedenen Reaktionsbedingungen zwei isomere Substanzen entstehen, welche verschiedene Schmelzpunkte aufweisen. Da sie ihre Struktur nicht kannten, nannten sie sie α- und β-Bromdiphenacyl.

In den folgenden Jahren beschäftigen sich mehrere Artikel mit dieser Reaktion, sowie mit der Art und Weise der Bildung und Struktur dieser Produkte, welche mit einer Ausbeute bis zu 95% erhalten wurden. [3]

Obwohl die Formeln von α- und β-Bromdiphenacyl in einer Arbeit von Widman 1913[4] erscheinen, wurden sie einigen Zwischenprodukten zugesprochen. Die Struktur dieser Substanzen wurde erst in den Jahren 1952–1953 durch die Arbeiten von Berson[5] sowie Wasserman, Aubrey und Zimmerman[6] geklärt. Es wurde festgestellt, daß die zwei Isomere α- und β-Bromdiphenacyl die *cis*- und *trans*-Form von 1-Brom-2-phenyl-2,3-epoxy-3-benzoyl-propan sind:

---

* L. Szotyori, L. Fey, N. Almási und E. Hamburg, *Rev. Roumaine Chim.*, **12**, 1155 (1967).

[1] V. Fritz, *Ber. dtsch. chem. Ges.*, **28**, 3028 (1895).

[2] C. Paal und C. Demeler, *Ber. dtsch. chem. Ges.*, **29**, 2092 (1896).

[3] C. Paal und H. Stern, *Ber. dtsch. chem. Ges.*, **34**, 1601 (1901); C. Paal und H. Schulze, *Ebenda*, **36**, 2386 (1903); O. Widman, *Ebenda*, **42**, 3261 (1909); W. L. Evans, *J. Amer. Chem. Soc.*, **35**, 115 (1906); *Chem. Zentr.*, **1906**, I 1092; T. Ajello, *Gazz. chim. Ital.*, **67**, 708 (1937).

[4] O. Widman, *Liebigs Ann. Chem.*, **400**, 86 (1913).

[5] J. A. Berson, *J. Amer. Chem. Soc.*, **74**, 5175 (1952).

[6] H. H. Wasserman, N. E. Aubrey und H. E. Zimmerman, *J. Amer. Chem. Soc.*, **75**, 96 (1953).

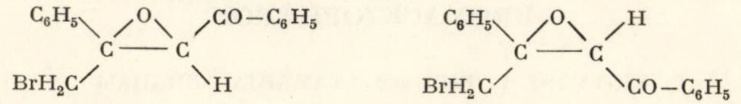

Diese Struktur wurde durch direkte Synthese von Bromdiphenacyl bewiesen.[6]

Für die Entstehung des Bromdiphenacyls wird folgender Mechanismus von Wasserman und Mitarb. vorgeschlagen:

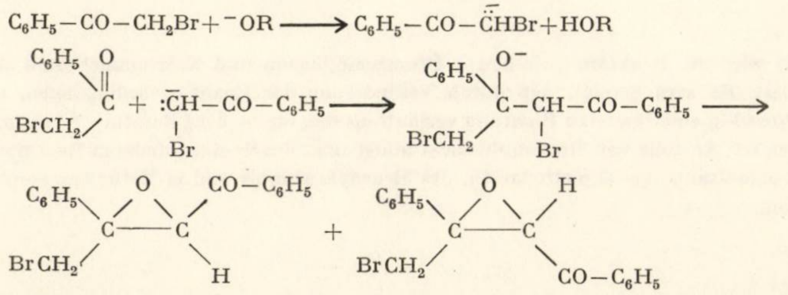

Durch die Arbeiten von Temnikova[7] und Stevens[8] wurde bekannt, daß die Homologe von ω-Brom- sowie ω-Chloracetophenon durch die Reaktion mit Natriumalkoxiden nach folgendem Schema zur Entstehung der Epoxyäthere führen:

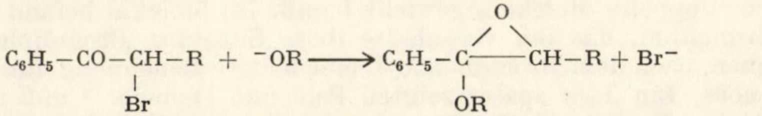

In keinem Falle wurde die Bildung eines Produktes vom Typ des Bromdiphenacyls bemerkt.

Der Mechanismus der Reaktion ist folgender:

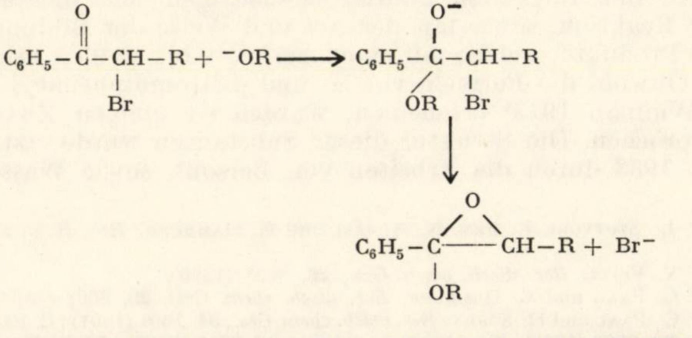

---

[7] T. I. Temnikova und E. N. Kropacheva, *Zhur. obshchei Khim.*, **19**, 1917 (1949); T. I. Temnikova und N. Almási, *Doklady Akad. Nauk S.S.S.R.*, **81**, 211 (1951); *Zhur. obshchei Khim.* **23**, 1498 (1953); T. I. Temnikova und V. A. Ivanova, *Zhur. obshchei Khim.*, **27**, 340 (1957); T. I. Temnikova, R. N. Kovalevskaia, N. I. Matveenkova und V. V. Skliarova, *Ibidem*, **29**, 381 (1959).

[8] C. L. Stevens, W. Malik und R. Pratt, *J. Amer. Chem. Soc.*, **72**, 4758 (1950).

Der wesentliche Unterschied zwischen beiden Reaktionen ist, wie man bemerken kann, der Angriffspunkt des Alkoxyions. Er bestimmt auch die Entfaltung des ganzen Prozesses, sowie auch die Struktur der Produkte. Die erste Etappe ist unbedingt durch die Struktur des Bromketons beeinflußt. Das Bromacetophenon besitzt eine Methylengruppe, an die zwei starke elektronophyle Gruppen gebunden sind (die CO-Gruppe und das Bromatom). Auf diese Weise ist die Trennung des Wasserstoffatoms als Proton von der Methylengruppe sehr erleichtert. Die Aktivierungsenthalpie dieser Reaktion kann kleiner sein, als die der Addition der Alkoxygruppe an die CO-Gruppe.

Im Falle der höheren α-Bromketone wird größtenteils die Möglichkeit der Trennung des Wasserstoffatoms als Proton durch den positiv-induktiven Effekt des Restes R verkleinert. Die Aktivierungsenthalpie der Addition des RO^--Ions an die Carbonylgruppe wird verhältnismäßig kleiner, deswegen beginnt die Reaktion mit dieser Etappe.

Die Grundidee der vorliegenden Arbeit war folgende: Durch Änderung der Reaktionsbedingungen sollte versucht werden, die Reaktion auch im Falle des ω-Bromacetophenons in die Richtung der Epoxyätherbildung zu verschieben.

Um Bromdiphenacyl zu erhalten, wurde in einer Methanol-, oder Ethanollösung bei niederer Temperatur gearbeitet (zwischen —10 und 0°). Die alkoholische Alkoxidlösung wurde einer Bromacetophenonlösung hinzugefügt, welche sich stets im Überschuß befand.

Es ist bekannt, daß parallel mit der Steigerung der Temperatur die Selektivität der Reaktionen fällt, das heißt, daß sich die Geschwindigkeiten der parallel möglichen Reaktionen nähern. Deshalb arbeiten wir bei 35° um die günstigen Bedingungen beider möglichen Anfangsreaktionen zu schaffen. Die Ausführung der Reaktion bei einer höheren Temperatur ist, wegen der Empfindlichkeit der Epoxyäthere nicht empfehlenswert

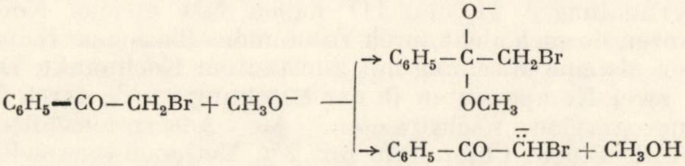

$$C_6H_5{-}CO{-}CH_2Br + CH_3O^- \longrightarrow \begin{cases} \rightarrow C_6H_5{-}\underset{\displaystyle OCH_3}{\underset{|}{\overset{\displaystyle O^-}{\overset{|}{C}}}}{-}CH_2Br \\ \rightarrow C_6H_5{-}CO{-}\overset{=}{C}HBr + CH_3OH \end{cases}$$

Um die Reaktion weiter in die Richtung eines intramolekularen Ablaufs zu leiten, sowie die Möglichkeit der Stöße des Karbanions mit einem anderen Bromacetophenonmolekül zu verkleinern, wurde in großer Verdünnung gearbeitet. Gleichzeitig wurde die Reihenfolge des Hinzufügens der Substanzen umgekehrt. Einer methanolischen Natriummethoxidlösung wurde eine Bromacetophenonlösung hinzugetropft. Unter diesen Bedingungen wird die Mehrheit der Karbanione durch die Reaktion mit dem Lösungsmittel regeneriert. Die Reaktion fand so wie erwartet statt. Sie entfaltete sich in Richtung des Prozesses, in der sich der Epoxyäther bilden konnte.

Unter den gewählten Reaktionsbedingungen, verwandelte sich der in der ersten Etappe gebildete Epoxyäther in das Dimethylketal des

Benzoylcarbinols(II). Infolge einer Transposition, welche wahrscheinlich innerhalb des Zwischenproduktes I nach einem von Baker[9] vorgeschlagenen und von anderen Autoren [10] bewiesenen Mechanismus stattfindet, bildet sich neben diesem Produkt auch ω-Methoxyacetophenon(III):

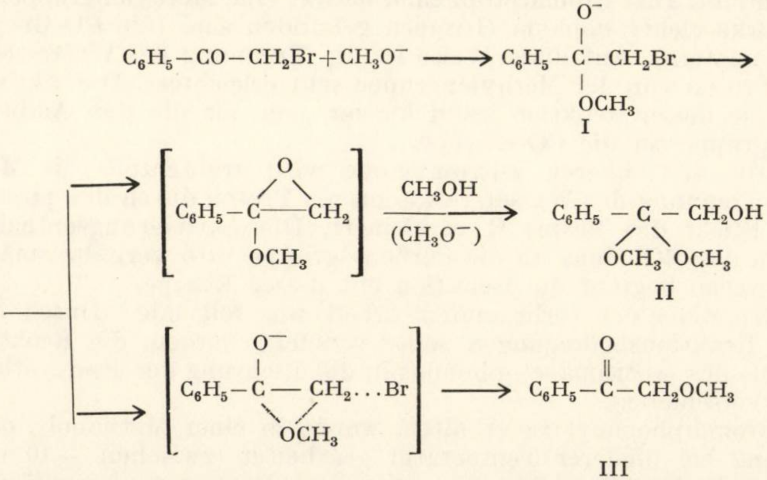

Eine direkte Substitution des Halogenatoms durch die Methoxygruppe ist unwahrscheinlich, auf Grund der von Baker [9,11] ausgeführten kinetischen Bestimmungen in bezug auf die Reaktion zwischen Pyridin und die im Ring substituierten ω-Bromacetophenone, sowie auch auf Grund der von Evlampiev[12] und anderen Autoren [13] gemachten Feststellungen, im Zusammenhang mit der vergrößerten Reaktivität des Halogens aus den α-Halogenketonen in den nukleophylen Substitutionsreaktionen.

Die Verbindungen II und III haben fast gleiche Kochpunkte. Deshalb konnten sie auch nicht durch Vakuumdestillation getrennt werden. Sie erscheinen als eine Mischung mit konstantem Kochpunkt. Die Anwesenheit von zwei Komponenten in der Mischung wurde durch die Dünnschichtchromatographie nachgewiesen. Als Adsorptionsmittel wurde Silicagel und als Eluent Chloroform mit 2% Methanol verwendet. Im IR-Spektrum dieses Produktes erscheinen vier intensive Bänder innerhalb folgender Frequenzgrenzen : 1040 und 1200 cm^{-1}, welche charakteristisch sind für die Ketale, und den gekoppelten Schwingungen der C–O–C–O–C Bindungen zugeschrieben werden. Bei 3425 cm^{-1} erscheint ein breites Band, das charakteristisch ist für die assoziierte Hydroxylgruppe. Gleichzeitig erscheint bei einer Frequenz von 1695 cm^{-1} eine Bande, welche für das Vorhandensein einer mit einem aromatischen Ring konjugierten CO-Gruppe spricht. Da die Intensität dieses Bandes, welches meistens überwiegend ist, im Vergleich zu den anderen viel kleiner ist, z.B. mit der des Bandes vergleichbar, dessen Frequenz 1440 cm^{-1} beträgt, und das für die monosubstituierten aromatischen Verbindungen charakteristisch ist, konnte man den Schluß ziehen, daß das Keton in der untersuchten Probe nur in einem kleinen Verhältnis vorhanden war.

---

[9] J. W. Baker, *J. Chem. Soc.*, **1938**, 445.

[10] M. J. S. Dewar, ,,The Electronic Theory of Organic Chemistry'', Clarendon Press, Oxford, 1949, S. 73 ; S. Winstein, E. Grunwald und H. W. Jones, *J. Amer. Chem. Soc.*, **73**, 2700 (1951) ; P. Bartlett und E. Trachtenberg, *Ebenda*, **80**, 5808 (1958) ; V. I. Veksler, *Zhur. obshchei Khim.*, **20**, 1289 (1950) ; L. Szotyori, N. Almási, L. Fey und M. Domokos, *Rev. Roumaine Chim.*, **9**, 545 (1964) ; L. Szotyori, L. Fey, N. Almási und E. Hamburg, *Ebenda*, **12**, 1155 (1967).

[11] J. W. Baker, *J. Chem. Soc.*, **1933**, 1128.

[12] V. V. Evlampiev, *Ber. dtsch. chem. Ges.*, **62**, 2386 (1929).

[13] D. V. Tishchenko, *Zhur. obshchei Khim.*, **9**, 1380 (1939) ; *Chem. Zentr.*, **1940**, I 1971 ; T. B. Johnson und I. B. Douglass, *J. Amer. Chem. Soc.*, **63**, 1571 (1941) ; *Chem. Zentr.*, **1941**, II 2927 ; F. G. Bordwell und G. D. Cooper, *J. Amer. Chem. Soc.*, **73**, 5184 (1951) ; J. Hine und W. H. Brader, *Ebenda*, **75**, 3964 (1953) ; F. B. Tutwiler und R. L. McKee, *Ebenda*, **76**, 6342 (1954).

Die Struktur der Verbindung II, die in der Literatur nicht beschrieben wird, wurde durch folgende chemische Umwandlungen bewiesen:

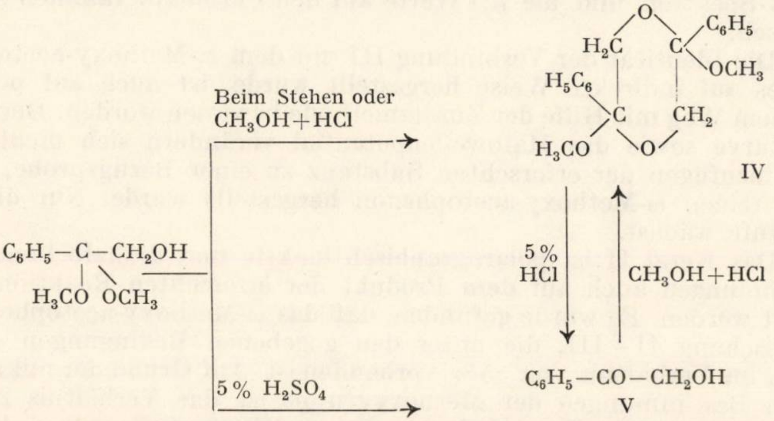

Beim Stehen oder infolge einer fast plötzlichen Reaktion unter Einwirkung des Methanols, das 3% HCl enthält, verwandelt sich das Acetal in 2,5-Diphenyl-2,5-dimethoxy-dioxan (IV) das schon 1895 von Fischer[14] beschrieben wurde. Er erhielt dies Produkt, in dem er eine methanolische Salzsäurelösung auf das Benzoylcarbinol (V) einwirken ließ. Die Verbindung IV wurde von uns durch die Bestimmung des Schmelzpunktes und des Molekulargewichtes, durch die quantitative Analyse der Methoxygruppe, sowie durch seine hydrolytische Umwandlung im Benzoylcarbinol (V) identifiziert. Auch das Ketal II verwandelt sich auf Grund seiner mit Schwefelsäure durchgeführten Hydrolyse in Benzoylcarbinol (V). Aus diesem erhielten wir unter den von Fischer beschriebenen Bedingungen, das Produkt IV.

Es muß erwähnt werden, daß all diese Umwandlungen auch für die Epoxyäthere charakteristisch sind. Die Anwesenheit der Hydroxylgruppe, die auch im IR-Spektrum bemerkt, so wie auch durch die Zerewitinow-Tsugaew-Methode bestimmt wurde, spricht für eine ketalische Struktur, die auch durch die quantitative Analyse, der in der Mischung II + III enthaltenen Methoxygruppe bewiesen wurde.

---

[14] E. Fischer, *Ber. dtsch. chem. Ges.*, **28**, 1145 (1895).

Das ω-Methoxy-acetophenon (III) wurde aus seiner Mischung mit dem Ketal II isoliert, durch Umwandlung des letzteren in die Verbindung IV oder V und entfernen durch Filtration dieser letzten Verbindungen. Um die Verbindung III zu identifizieren, wurde sie auf einem anderen Weg hergestellt.[15] Das Schema ist folgendes:

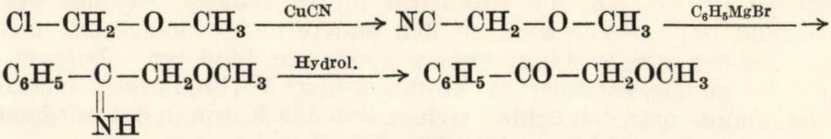

$$Cl-CH_2-O-CH_3 \xrightarrow{CuCN} NC-CH_2-O-CH_3 \xrightarrow{C_6H_5MgBr}$$

$$C_6H_5-\underset{\underset{NH}{\|}}{C}-CH_2OCH_3 \xrightarrow{Hydrol.} C_6H_5-CO-CH_2OCH_3$$

Die physikalischen Konstanten der beiden Verbindungen sind identisch. Der Mischschmelzpunkt der Semikarbazone zeigt keine Depression, die IR-Spektren und die R_f-Werte auf den Chromatogrammen sind also identisch.

Die Identität der Verbindung III mit dem ω-Methoxy-acetophenon, welches auf indirekte Weise hergestellt wurde, ist auch auf polarographischem Weg mit Hilfe der Zusatzmethode bewiesen worden. Der Verlauf der Kurve sowie das Halbwellenpotential verändern sich nicht, durch das Hinzufügen der erforschten Substanz zu einer Bezugsprobe, die aus einem reinen ω-Methoxy-acetophenon hergestellt wurde. Nur die Höhe der Stufe wächst.

Das Ketal II ist polarographisch inaktiv und deshalb konnten die Bestimmungen auch auf dem Produkt der erforschten Reaktion durchgeführt werden. Es wurde gefunden, daß das ω-Methoxy-acetophenon aus der Mischung II+III, die unter den gegebenen Bedingungen erhalten wurde, im Verhältnis von 35% vorhanden ist. Auf Grund der mikroanalytischen Bestimmungen der Methoxygruppe ist das Verhältnis zwischen II und III 40 : 60%. Der Inhalt des aktiven Wasserstoffs entspricht einem Verhältnis von 36 : 64%. So wurden die auf polarographischem Weg erhaltenen Resultate, innerhalb der Fehlergrenzen der Bestimmungen bewiesen.

Wir möchten bemerken, daß wir die Bildung der Verbindungen II und III auch unter den in der Literatur[1,6] angegebenen Bedingungen in kleiner Menge beweisen konnten, in dem wir das wässerige Filtrat des Bromdiphenacyls einer Analyse unterwarfen.

EXPERIMENTELLES

Die Reaktion zwischen ω-Bromacetophenon und Natriummethoxyd. 10 g (0,05 Mol) ω-Bromacetophenon[16] werden in 300 ml absolutem Methanol aufgelöst und diese Lösung wird innerhalb 1 Std. bei 35—38° einer Natriummethoxidlg in Methanol (100 ml 0,5 N) hinzugetropft. Das Rühren wird 10 Min. fortgesetzt. Ein großer Teil des Methanols wird im Vakuum in Methangasstrom entfernt. Die Temperatur des Wasserbades darf nicht über 35° sein. Der Rest wird ins Wasser geschüttet. Das ölige Produkt wird abgeschieden und die wässerige Schicht wird noch viermal mit Äther extrahiert. Die ätherische Lg wird mit Hilfe von wasserfreiem Na_2SO_4 getrocknet. Um das Methanol und das Wasser ganz zu entfernen, fügt man der filtrierten ätherischen Lg Benzol hinzu, und destilliert unter Vakuum. Man erhält 5 g eines farblosen Produktes mit angenehmem Geruch, das sehr eindeutig destilliert. Sdp.$_2$ 93° (Sdp.$_1$ 88°), n_D^{20} 1,5235. Das Produkt ist eine Mischung des Dimethylacetals des Benzoilkarbinols (II) und ω-Methoxy-acetophenon (III). λ_{max} in IR bei 1034, 1075, 1136 und 1193 cm^{-1}, bei 3425 cm^{-1} und bei 1695 cm^{-1}. Diese Bänder zeigen die Anwesenheit der Ketalgruppe, Hydroxygruppe bzw. Carbonylgruppe. Polarographisch wurde festgestellt, daß das Produkt 35 % ω-Methoxy-acetophenon (III) enthält. Auf Grund des Verhältnisses II:III = 65% : 35 %,

---

[15] a. D. GAUTHIER, *Compt. rend.*, **143**, 831 (1906); *Chem. Zentr.*, 1907, I 400; b. D. D. PRATT und R. ROBINSON, *J. Chem. Soc.*, **123**, 745 (1923).

[16] R. M. COWPER und L. H. DAVIDSON, *Org. Synth.*, **19**, 24 (1939).

$$\left.\begin{array}{l} C_{10}H_{14}O_3\ (182{,}2) - 65\% - \\ C_9H_{10}O_2\ (150{,}2) - 35\% - \end{array}\right\} \begin{array}{l} \textit{Ber.}: 29{,}31 \\ \textit{Gef.}: 28{,}69 \end{array}$$

Aktiver Wasserstoff: 0,99

Wenn man vor dem Destillieren der ätherischen Lg der Mischung (II + III) kein Benzol hinzufügt, um das Wasser total zu entfernen. verwandelt sich Verbindung II innerhalb eines Tages in Verbindung IV.

2,5-Diphenyl-2,5-dimethoxy-dioxan (*IV*). 1 g des Reaktionsproduktes zwischen Bromacetophenon und Natriummethoxid (II + III) werden mit 5 ml Methanol, welches 3% gasförmige Salzsäure enthält, versetzt. Nach wenigen Min. scheidet sich ein weißer Niederschlag ab, welcher zweimal aus einer Methanol-Benzol-Mischung umkristallisiert wird, und bei 193° schmilzt. Der Schmelzpunkt der Mischung dieser Substanz mit 2,5-Diphenyl-2,5-dimethoxy-dioxan das aus Benoylcarbinol nach der Methode von Fischer [14] hergestellt wurde, zeigt keine Depression. $C_{18}H_{20}O_4$ (300,4) *Ber.*: OCH_3 20,66; *Gef.*: 20,40 *Ber. M. Gew.*: 300,4 *Gef.*: 288,4.

ω-Hydroxy-acetophenon (*Benzoylcarbinol*) (*V*). 4,2 g des Reaktionsproduktes zwischen ω-Bromacetophenon und Natriummethoxid (Mischung II und III) werden 1/2 Std. mit 30 ml 5%iger Schwefelsäure erwärmt. Nach dem Abkühlen scheidet sich das kristalline ω-Hydroxy-acetophenon als Plättchen ab. Es wird aus dem Wasser umkristallisiert. Schmp. 76–77°. Aus dem Benzol kristallisiert es als Nadeln. Schmp. 87° Lit.[17a] Schmp. 75–76° sowie 85–86°. 1 g 2,5-Diphenyl-2,5-dimethoxy-dioxan werden 10 Min. mit 50 ml 2%iger Salzsäure erwärmt. Beim Abkühlen scheidet sich ω-Hydroxy-acetophenon ab. Die Schmelzpunkte der Produkte aus II und IV zeigen keine Depression bei der Vermischung mit der authentischen Substanz, welche aus ω-Bromacetophenon hergestellt wurde. [17]

ω-Methoxy-acetophenon (*III*). Aus 8,8 g (0,124 Mol) Methoxy-acetonitril (hergestellt aus Chlormethyläther durch erwärmen mit Kupfercyanid[15a]) und Phenylmagnesiumbromid, hergestellt aus 2,96 g Mg und 18,4 g (0,117 Mol) Brombenzol in absolutem Äther, nach einer Methode von Pratt und Robinson, [15b] bilden sich 9,5 g reines Produkt (54,3%). Sdp.$_1$ 80°, n_D^{20} 1,5360; Lit.[15b] Sdp.$_{15}$ 118–20° n_D 1,5416; Lit.[18] Sdp.$_{13}$ 117–118°, n_D^{20} 1,5338. Das Semicarbazon kristallisiert aus wässerigem Alkohol um, schmilzt bei 128,5°.Lit.[18]; Schmp. 126–7° (aus Benzol).$C_{10}H_{13}N_3O_2$ (207,3) *Ber.*: N 20,27; *Gef.*: 20,52

Die Isolierung von ω-Methoxy-acetophenon aus der Mischung II+III. 1 g der Mischung II + III wird mit 5 ml Methanol, welches 3% gasförmige Salzsäure enthält, versetzt. Der gebildete Niederschlag (IV) wird filtriert und die Methanollg wird ins Wasser geschüttet. Es wird mit $NaHCO_3$ neutralisiert, mit Äther extrahiert und auf Na_2SO_4 getrocknet. Nachher wird der Äther abdestilliert. Das IR-Spektrum des Restes stimmt mit dem des Methoxyacetophenons überein. Das Semicarbazon schmilzt bei 128,5° und zeigt keine Depression vermischt mit dem authentischen ω-Methoxy-acetophenon.

---

[17] a. W. H. Linnell und I. Roushdi, *Quart. J. Pharmac. Pharmacol.*, **12**, 252(1939); *Chem. Zentr.*, **1940**, I 1007; b. G. R. Cebrián, *Anales real soc. españ, fís. y quím., Ser. B.*, **44**, 587(1948); *Chem. Abstr.*, **42**, 8176(1948).

[18] C. Dufraisse und R. Chaux, *Bull. Soc. chim. France*, 4, **39**, 443(1926); *Chem. Zentr.*, **1926**, I 3222.

Die polarographische Bestimmung des ω-Methoxy-acetophenons aus der Mischung II+III. 0,1 g (±0,2 mg) der Mischung II+III werden in einem 50 ml Meßkolben mit Methanol verdünnt. 5 ml dieser Lösung werden mit 5 ml NaOH 0,1 N und 0,5 ml einer 1%igen wäßrigen Gelatinelsg versetzt und mit Methanol auf 25 ml verdünnt. Die polarographische Kurve wird erst nach dem Durchperlen mit einem inerten Gas registriert. Die Höhe der Reduktionsstufe wird mit der des als Bezugssubstanz dienenden und ähnlicherweise behandelten ω-Methoxy-acetophenons verglichen. Der Gehalt des ω-Methoxy-acetophenons an der destillierten Mischung II+III ist 35%.

Revue Roumaine de Chimie, **14**, 1629–1631 (1969)

TRENNUNG UND BESTIMMUNG DES TITANS IN GEGENWART VON EISEN

RALUCA RIPAN und T. BUDIU

Aus dem Institut für Chemie der Akademie, Zweigstelle Cluj, str. Donath, 59–65

Eingegangen am 6. August 1969

Es wird eine Methode für die Trennung des Titans in Gegenwart von Eisen beschrieben. Titan kann von Eisen getrennt werden, indem man dazu dessen Komplex mit Phosphor-molybdänsäure verwendet. Wir sind zu dem Schluß gekommen, daß Titan in Gegenwart von Eisen auch dann bestimmt werden kann, wenn das Verhältnis größer ist als 1Ti:300Fe. Diese Methode kann auch für die Konzentration des Titans und dessen Bestimmung aus Erzen und anderen titanhaltigen Produkten benutzt werden, so wie wir es nächstens beschreiben werden, wenn wir die Anwendung der obigen Methode auf natürliche titanhaltige Produkte versuchen.

Da Titan und Eisen einander ähnliche chemische Eigenschaften besitzen, ist die Trennung des Titans vom Eisen und seine Bestimmung ein schwieriges Problem. Noch schwieriger ist es, wenn andere Kationen und Anionen anwesend sind, was praktisch oft genug vorkommt.

In unseren früheren Arbeiten[1–3] haben wir die Heteropolymolybdate mehrerer Übergangsmetalle, darunter auch die des Eisens und des Titans studiert, und sind zu dem Schluß gelangt, daß letztere, dank ihrer physikalischen und chemischen Eigenschaften und ihrer verschiedenen Entstehungsbedingungen, bei der Trennung des Titans vom Eisen verwendet werden können.

Fe^{3+} bildet ein Hexamolybdat mit maximaler Stabilität bei pH— 3,5—4,[1] während Ti^{4+} ein stabiles Triheteropolymolybdat bei pH= 1 bildet.[2]

Fügt man zu einem Gemisch von Ti^{4+} und Fe^{3+} eine Phosphat- und Molybdatlösung im Verhältnis von 1i : 1P : 12Mo, und stellt man den pH-Wert auf 1—1,5 ein, so bindet sich des Titan an die Heteropolymolybdate $[PTiMo_{12}]^{4-}$ (d.h. an das Anion der Phosphor-Titan-12-Molybdänkomplexverbindung), wobei Fe^{3+} als Kation zurückbleibt.

---

[1] AL. DUCA und T. BUDIU, *Rev. Roumaine Chim.*, **11**, 817 (1966).

[2] AL. DUCA und T. BUDIU, *Rev. Roumaine Chim.*, **12**, 497 (1967).

[3] R. RIPAN und T. BUDIU, *Rev. Roumaine Chim.*, **13**, 77 (1968).

Aufgrund des oben angeführten ist es annehmbar, daß für die Trennung des Ti^{4+} von Eisen, nach der Bindung des ersteren in einer Phosphor-Titan-12 Molybdänkomplexverbindung, Ionenaustauscher verwendet werden können.

In diesem Sinne kann man zwei Varianten annehmen:

a) Das Gemisch $Fe^{3+} + [PTiMo_{12}]^{4+}$ wird über gewisse Kationenaustauscher geleitet, wobei Fe^{3+} zurückgehalten wird und das Anion der Titankomplexverbindung $[PTiMo_{12}]^{4-}$ in Lösung geht.

b) Das Gemisch (I) wird über gewisse Anionenaustauscher geleitet, wobei des Anion $[PTiMo_{12}]$ zurückgehalten wird und das Eisen in Lösung geht.

In dieser Arbeit haben wir hauptsächlich die Bestimmung der Trennungsbedingungen des Titans vom Eisen und die Bestimmung des Titans in Gegenwart von Eisen verfolgt, und deswegen Variante b) als Arbeitsmethode gewählt.

Für die Trennung haben wir dabei den Anionenaustauscher DOWCX 1×1 benutzt.

ARBEITSMETHODE

Man arbeitete mit Ti^{4+} -Vergleichssubstanz, Natriumphosphat und Natriummolybdat, oder Phosphor-12-Molybdänsäure, Eisensulfat *p.a.*, Salpetersäure 2 n.

In der ersten Phase wurde mit Gemischen bekannter Konzentrationen gearbeitet und es wurden dabei verschiedene Verhältnisse zwischen Ti^{4+} und Fe^{3+} von 1:1 bis 1Ti :300Fe genommen.

Zu den verschiedenen Titan-Eisen-Gemischen mit pH-Werten von 1 bis 1,5 wurde Phosphor-Molybdänsäure 10^{-2} M in einem Überschuß von 1-2mal im Vergleich zum Titan hinzugefügt. Dieses Gemisch (I) wurde 2—3 Min. lang bei 60° oder 1/2 Std. lang bei Raumtemperatur gehalten. Das Titan ist danach gänzlich an die Komplexverbindung gebunden und um es vom Eisen zu trennen kann das Gemisch über den Anionenaustauscher geleitet werden.

VORBEREITUNG DES HARZES

Das Harz wird durch ein Sieb von 0,3—0,7 gesiebt. Es wird mit Wasser gewaschen, über Nacht stehen gelassen, in eine Trennungssäule gebracht, und 2n NaOH darüber geleitet. Dann wird es bei neutralem pH mit Wasser gewaschen und um es in Form von $RClO_4$ zu erhalten wird 2 n $HClO_4$ darüber geleitet. Bis zu pH-Werten von 1 bis 1,5 wird es wieder mit Wasser gewaschen. Das auf diese Weise vorbereitete Harz kann für die Trennung des Titans von Eisen dienen.

Nun wird das Gemisch Nr. 1 mit einer Geschwindigkeit von 2 ml/Min. durchgeführt. Es wird mit 150 ml Wasser bis zum pH-Wert von 2,5 bis 3,5 gewaschen (mit $HClO_4$ korrigiert). Unter diesen Umständen bleibt das Titan in Form eines anionischen Komplexes auf dem Harz, und Fe^{3+} geht in Lösung. Um das Titan vom Ionenaustauscher auszuwaschen, geht man folgendermaßen vor: zu dem mit Wasser gewaschenen Harz mit einem pH-Wert von 2,5 bis 3,5 werden 40—50 ml NaOH bei 80—90° hinzugefügt, gerührt und danach einige Minuten lang stehen gelassen, damit sich die Komplexverbindung zersetzt und Titan als $Ti(OH)_4$ ausfällt. Nach einigen Minuten wäscht man die Säule mit 150–200 ml 2nNaOH, dann wird wieder mit Wasser gewaschen, bis man einen neutralen pH-Wert erreicht.

Auf diese Weise gehen MoO_4^{2-} und PO_4^{3-} in Lösung, auf der Säule bleibt $Ti(OH)_4$ und gleichzeitig geht des Harz in Form von ROH durch.

Weiter wird bis zu neutralem pH-Wert mit Wasser gewaschen 150 ml $2nHClO_4$ hinzugefügt, bis sich das $Ti(OH)_4$ auflöst und Ti^{4+} in Lösung geht. Gleichzeitig regeneriert das Harz und geht in $RClO_4$ über, welches für eine neue Bestimmung verwendet werden kann.

Zum Schluß wäscht man bis zu einem pH-Wert von 1,5 mit Wasser, um das Titan quantitativ aus der Säule herauszuholen.

Das Ti^{4+}, welches mit einer unbedeuten den Menge Fe^{3+} in Lösung geht (wie im folgenden ersichtlich stört Fe^{3+} die Bestimmung des Titans nicht, und hat den Vorteil Ti^{4+} mitzufällen, welches manchmal in sehr kleinen Mengen vorhanden ist), fällt man als $Ti(OH)_4$ aus, filtriert, wäscht es mit Wasser und einigen Tropfen Ammoniaklösung und löst es in warmem $2nH_2SO_4$. Dann wird Ti^{4+} mit Hilfe von Wasserstoffsuperoxid und mit Verwendung einer Eichungskurve kolorimetrisch bestimmt. Vor dem Hinzufügen des Wasserstoffsuperoxids gibt man noch 5–7 Tropfen H_3PO_4 hinzu.

Die Eichungskurve wird unter denselben Umständen dargestellt wie die oben beschriebene Bestimmung, d.h. bekannte Titan- und Eisenmengen (ungefähr 1Ti : 50Fe) werden über Ionenaustauscher geführt und dann wird Ti^{4+} kolorimetrisch bestimmt. Die Ergebnisse sind in Tabelle 1 zusammengefaßt.

Tabelle 1

Die Trennung des Ti^{4+} von Fe^{3+} mit Hlife der Ionenaustauscher

Ti^{4+} Ausgang mg/Probe	Fe^{3+}, Ausgang mg/Probe	Ti^{4+}, *gef.* mg/Probe	Fe^{3+}, *gef.* mg/Probe
60	0	59,88	0
60	20	59,80	19,65
60	40	60,15	38,86
60	80	60,10	79,68
60	160	59,75	158,60
60	320	59,51	318,20
60	640	60,19	637,80
60	1280	59,66	1275,30
60	2560	59,68	2538,00

Revue Roumaine de Chimie, **14**, 1629–1631 (1969)

Revue Rumaine de Chimie, **14**, 1633–1636 (1969)

CORRIGENDUM TO THE PAPER

"THE CALCULUS OF ELECTROSTATIC MATRIX ELEMENTS FOR THE TETRAGONAL SYMMETRY"

BY

V. BREZULEANU and A. IVANOV (Revue Roumaine de Chimie **13**, 163 (1968))

In this paper two of the wave functions of the configuration d^2 have been classified erroneously after the representations of the symmetry group. For this reason some of the F matrix elements must be correlated, a fact on which Dr. K. D. Warren[1] has drawn our attention. Computing by our method, he has obtained the same results as I. Otsuka,[2] who has worked by a different method.

The correct functions and values of the matrix elements for the d^2 and d^3 configurations are given below:

$$^{1}B_2 \qquad (2)^{-1/2}\,/(xz)\ (yz)/-/(xz)\ (yz)/$$

$$^{3}A_2 \qquad /(xz)\ (yz)/$$

Functions for d^3 in D_4 symmetry

$$a_1b_1b_2 \qquad {}^{2}A_2 \qquad (2)^{-\frac{1}{2}}\left\{/(z)\ \overset{+}{(x^2-y^2)}\ \overset{-}{(xy)}/-/\overset{+}{(z)}\ \overset{-}{(x^2-y^2)}\ \overset{+}{(xy)}/\right\}$$

$$^{2}A_2 \qquad (6)^{-\frac{1}{2}}\left\{2/\overset{-}{(z^2)}\ \overset{+}{(x^2-y^2)}\ \overset{+}{(xy)}/-/\overset{+}{(z^2)}\ \overset{+}{(x^2-y^2)}\ \overset{-}{(xy)}/-/\overset{+}{(z^2)}\ \overset{-}{(x^2-y^2)}\ \overset{+}{(xy)}/\right\}$$

$$a_1b_1e \qquad {}^{2}E \qquad (2)^{-\frac{1}{2}}\left\{/\overset{+}{(z^2)}\ \overset{+}{(x^2-y^2)}\ \overset{-}{(xz)}/-/\overset{+}{(z^2)}\ \overset{-}{(x^2-y^2)}\ \overset{+}{(xz)}/\right\}$$

$$(2)^{-\frac{1}{2}}\left\{/\overset{+}{(z^2)}\ \overset{+}{(x^2-y^2)}\ \overset{-}{(yz)}/-/\overset{+}{(z^2)}\ \overset{-}{(x^2-y^2)}\ \overset{+}{(yz)}/\right\}$$

$$^{2}E \qquad (6)^{-\frac{1}{2}}\left\{2/\overset{-}{(z^2)}\ \overset{+}{(x^2-y^2)}\ \overset{+}{(xz)}/-/\overset{+}{(z^2)}\ \overset{+}{(x^2-y^2)}\ \overset{-}{(xz)}/-/\overset{+}{(z^2)}\ \overset{-}{(x^2-y^2)}\ \overset{+}{(xz)}/\right\}$$

$$(6)^{-\frac{1}{2}}\left\{2/\overset{-}{(z^2)}\ \overset{+}{(x^2-y^2)}\ \overset{+}{(yz)}/-/\overset{+}{(z^2)}\ \overset{+}{(x^2-y^2)}\ \overset{-}{(yz)}/-/\overset{+}{(z^2)}\ \overset{-}{(x^2-y^2)}\ \overset{+}{(yz)}/\right\}$$

$$a_1b_2e \qquad {}^{2}E \qquad (2)^{-\frac{1}{2}}\left\{/\overset{+}{(z^2)}\ \overset{+}{(xy)}\ \overset{-}{(xz)}/-/\overset{+}{(z^2)}\ \overset{-}{(xy)}\ \overset{+}{(xz)}/\right\}$$

$$(2)^{-\frac{1}{2}}\left\{/\overset{+}{(z^2)}\ \overset{+}{(xy)}\ \overset{-}{(yz)}/-/\overset{+}{(z^2)}\ \overset{-}{(xy)}\ \overset{+}{(yz)}/\right\}$$

$$^{2}E \qquad (6)^{-\frac{1}{2}}\left\{2/\overset{-}{(z^2)}\ \overset{+}{(xy)}\ \overset{+}{(xz)}/-/\overset{+}{(z^2)}\ \overset{+}{(xy)}\ \overset{-}{(xz)}/-/\overset{+}{(z^2)}\ \overset{-}{(xy)}\ \overset{+}{(xz)}/\right\}$$

$$(6)^{-\frac{1}{2}}\left\{2/\overset{-}{(z^2)}\ \overset{+}{(xy)}\ \overset{+}{(yz)}/-/\overset{+}{(z^2)}\ \overset{+}{(xy)}\ \overset{-}{(yz)}/-/\overset{+}{(z^2)}\ \overset{-}{(xy)}\ \overset{+}{(yz)}/\right\}$$

$$b_1b_2e \qquad {}^{2}E \qquad (2)^{-\frac{1}{2}}\left\{/\overset{+}{(x^2-y^2)}\ \overset{+}{(xy)}\ \overset{-}{(xz)}/-/\overset{+}{(x^2-y^2)}\ \overset{-}{(xy)}\ \overset{+}{(xz)}/\right\}$$

$$(2)^{-\frac{1}{2}}\left\{/\overset{+}{(x^2-y^2)}\ \overset{+}{(xy)}\ \overset{-}{(yz)}/-/\overset{+}{(x^2-y^2)}\ \overset{-}{(xy)}\ \overset{+}{(yz)}/\right\}$$

$$^{2}E \qquad (6)^{-\frac{1}{2}}\left\{2/\overset{-}{(x^2-y^2)}\ \overset{+}{(xy)}\ \overset{+}{(xz)}/-/\overset{+}{(x^2-y^2)}\ \overset{+}{(xy)}\ \overset{-}{(xz)}/-/\overset{+}{(x^2-y^2)}\ \overset{-}{(xy)}\ \overset{+}{(xz)}/\right\}$$

$$(6)^{-\frac{1}{2}}\left\{2/\overset{-}{(x^2-y^2)}\ \overset{+}{(xy)}\ \overset{+}{(yz)}/-/\overset{+}{(x^2-y^2)}\ \overset{+}{(xy)}\ \overset{-}{(yz)}/-/\overset{+}{(x^2-y^2)}\ \overset{-}{(xy)}\ \overset{+}{(yz)}/\right\}$$

---

[1] Private letter.

[2] J. Otsuka, *J. Phys. Soc. Japan*, **21**, 596 (1969).

a_1e^2	$^4A_2$	$/(\overset{+}{z^2})\ (\overset{+}{xz})\ (\overset{+}{yz})/$
	$^2A_1$	$(2)^{-\frac{1}{2}}\left\{/(\overset{+}{z^2})\ (\overset{+}{xz})\ (\overset{-}{xz})/+/(\overset{+}{z^2})\ (\overset{+}{yz})\ (\overset{-}{yz})/\right\}$
	$^2A_2$	$(6)^{-\frac{1}{2}}\left\{2/(\overset{-}{z^2})\ (\overset{+}{xz})\ (\overset{+}{yz})/-/(\overset{+}{z^2})\ (\overset{+}{xz})\ (\overset{-}{yz})/-/(\overset{+}{z^2})\ (\overset{-}{xz})\ (\overset{+}{yz})/\right\}$
	$^2B_1$	$(2)^{-\frac{1}{2}}\left\{/(\overset{+}{z^2})\ (\overset{+}{xz})\ (\overset{-}{xz})/-/(\overset{+}{z^2})\ (\overset{+}{yz})\ (\overset{-}{yz})/\right\}$
	$^2B_2$	$(2)^{-\frac{1}{2}}\left\{/(\overset{+}{z^2})\ (\overset{+}{xz})\ (\overset{-}{yz})/-/(\overset{+}{z^2})\ (\overset{-}{xz})\ (\overset{+}{yz})/\right\}$
b_1e^2	$^4B_2$	$/(x^2\overset{+}{-}y^2)\ (\overset{+}{xz})\ (\overset{+}{yz})/$
	$^2A_1$	$(2)^{-\frac{1}{2}}\left\{/(x^2\overset{+}{-}y^2)\ (\overset{+}{xz})\ (\overset{-}{xz})/-/(x^2\overset{+}{-}y^2)\ (\overset{+}{yz})\ (\overset{-}{yz})/\right\}$
	$^2A_2$	$(2)^{-\frac{1}{2}}\left\{/(x^2\overset{+}{-}y^2)\ (\overset{+}{xz})\ (\overset{-}{yz})/-/(x^2\overset{+}{-}y^2)\ (\overset{-}{xz})\ (\overset{+}{yz})/\right\}$
	$^2B_1$	$(2)^{-\frac{1}{2}}\left\{/(x^2\overset{+}{-}y^2)\ (\overset{+}{xz})\ (\overset{-}{xz})/+/(x^2\overset{+}{-}y^2)\ (\overset{+}{yz})\ (\overset{-}{yz})/\right\}$
	$^2B_2$	$(6)^{-\frac{1}{2}}\left\{2/(x^2\overset{-}{-}y^2)\ (\overset{+}{xz})\ (\overset{+}{yz})/-/(x^2\overset{+}{-}y^2)\ (\overset{+}{xz})\ (\overset{-}{yz})/-/(x^2\overset{+}{-}y^2)\ (\overset{-}{xz})\ (\overset{+}{yz})/\right\}$
b_2e^2	$^4B_1$	$/(\overset{+}{xy})\ (\overset{+}{xz})\ (\overset{+}{yz})/$
	$^2A_1$	$(2)^{-\frac{1}{2}}\left\{/(\overset{+}{xy})\ (\overset{+}{xz})\ (\overset{-}{yz})/-/(\overset{+}{xy})\ (\overset{-}{xz})\ (\overset{+}{yz})/\right\}$
	$^2A_2$	$(2)^{-\frac{1}{2}}\left\{/(\overset{+}{xy})\ (\overset{+}{xz})\ (\overset{-}{xz})/-/(\overset{+}{xy})\ (\overset{+}{yz})\ (\overset{-}{yz})/\right\}$
	$^2B_1$	$(6)^{-\frac{1}{2}}\left\{2/(\overset{-}{xy})\ (\overset{+}{xz})\ (\overset{+}{yz})/-/(\overset{+}{xy})\ (\overset{+}{xz})\ (\overset{-}{yz})/-/(\overset{+}{xy})\ (\overset{-}{xz})\ (\overset{+}{yz})/\right\}$
	$^2B_2$	$(2)^{-\frac{1}{2}}\left\{/(\overset{+}{xy})\ (\overset{+}{xz})\ (\overset{-}{xz})/+/(\overset{+}{xy})\ (\overset{+}{yz})\ (\overset{-}{yz})/\right\}$

Matrix elements for d^2 systems in D_4 symmetry

$^1A_1$ $(^1S,\ ^1D,\ ^1G)$

$$\begin{array}{cccc}
a_1^2 & b_1^2 & b_2^2 & e^2 \\
\hline
A+4B+3C & 4B+C & 4B+C & \sqrt{2}\,(B+C) \\
 & A+4B+3C & C & \sqrt{2}\,(3B+C) \\
 & & A+4B+3C & \sqrt{2}\,(3B+C) \\
 & & & A+7B+4C
\end{array}$$

^1E $(^1D,\ ^1G)$

$$\begin{array}{ccc}
a_1e & b_1e & b_2e \\
\hline
A+3B+2C & -\sqrt{3}\,B & -\sqrt{3}\,B \\
 & A+B+2C & -3B \\
 & & A+B+2C
\end{array}$$

^2E $(^3P,\ ^2F)$

$$\begin{array}{ccc}
a_1e & b_1e & b_2e \\
\hline
A+B & -3\sqrt{3}\,B & -3\sqrt{3}\,B \\
 & A-5B & 3B \\
 & & A-5B
\end{array}$$

$^1A_2$ (^1G)

$$\begin{array}{c}
b_1b_2 \\
\hline
A+4B+2C
\end{array}$$

$^1B_1$ $(^1D,\ ^1G)$

$$\begin{array}{cc}
e^2 & a_1b_1 \\
\hline
A+B+2C & 2\sqrt{3}\,B \\
 & A+2C
\end{array}$$

$^1B_2$ $(^1D,\ ^1G)$

$$\begin{array}{cc}
e^2 & a_1b_2 \\
\hline
A+B+2C & 2\sqrt{3}\,B \\
 & A+2C
\end{array}$$

${}^3A_2$ (${}^3P$, ${}^3F$)

e^2	b_1b_2
$A-5B$	$6B$
	$A+4B$

${}^3B_1$ (${}^3F$)

a_1b_1
$A-8B$

${}^3B_2$ (${}^3F$)

a_1b_2
$A-8B$

Matrix elements for d^3 systems in D_4 symmetry

${}^2A_1$ (${}^2H$, ${}^2G$, ${}^{2}_{a}D$, ${}^{2}_{b}D$)

$a_1b_1^2$	$a_1b_2^2$	a_1e^2	b_1e^2	b_2e^2
$3A-8B+4C$	C	$\sqrt{2}\cdot(3B+C)$	$-\sqrt{6}\,B$	0
	$3A-8B+4C$	$\sqrt{2}\cdot(3B+C)$	0	$-\sqrt{6}\,B$
		$3A+10B+5C$	$-5\sqrt{3}\,B$	$-5\sqrt{3}\,B$
			$3A-6B+3C$	$3B$
				$3A-6B+3C$

${}^2A_2$ (${}^2H$, ${}^2G$, ${}^2F$, ${}^2P$)

a_1e^2	b_1e^2	b_2e^2	$a_1b_1b_2\,(i)$	$a_1b_1b_2\,(ii)$
$3A+3C$	$3B$	$-3B$	0	$6B$
	$3A-6B+3C$	$-3B$	$-\sqrt{3}\,B$	$3B$
		$3A-6B+3C$	$-\sqrt{3}\,B$	$-3B$
			$3A-8B+3C$	0
				$3A+3C$

${}^2B_1$ (${}^2H$, ${}^2G$, ${}^2F$, ${}^{2}_{a}D$, ${}^{2}_{b}D$)

${a_1}^2b_1$	$b_1b_2^2$	a_1e^2	b_1e^2	b_2e^2
$3A-8B+4C$	$(4B+C)$	$-\sqrt{6}\,B$	$\sqrt{2}\cdot(B+C)$	0
	$3A+12B+4C$	0	$\sqrt{2}\cdot(3B+C)$	$3\sqrt{6}\,B$
		$3A+4B+3C$	$-5\sqrt{3}\,B$	$-3B$
			$3A+5C$	$3\sqrt{3}\,B$
				$3A-6B+3C$

${}^2B_2$ (${}^2H$, ${}^2G$, ${}^2F$, ${}^{2}_{a}D$, ${}^{2}_{b}D$)

${a_1}^2b_2$	${b_1}^2b_2$	a_1e^2	b_1e^2	b_2e^2
$3A-8B+4C$	$(4B+C)$	$-\sqrt{6}\,B$	0	$\sqrt{2}\cdot(B+C)$
	$3A+12B+4C$	0	$-3\sqrt{6}\,B$	$\sqrt{2}\cdot(3B+C)$
		$3A+4B+3C$	$3B$	$-5\sqrt{3}\,B$
			$3A-6B+3C$	$-3\sqrt{3}\,B$
				$3A+5C$

${}^4E$ (${}^4F$, ${}^4P$)

a_1b_1e	a_1b_2e	b_1b_2e
$3A-12B$	$3B$	$3\sqrt{3}\,B$
	$3A-12B$	$3\sqrt{3}\,B$
		$3A-6B$

${}^4A_2$ (${}^4F$, ${}^4P$)

$a_1b_1b_2$	a_1e^2
$3A-12B$	$6B$
	$3A-3B$

${}^4B_1$ (${}^4F$)

b_2e^2
$3A-15B$

${}^4B_2$ (${}^4F$)

b_1e^2
$3A-15B$

^2E $(^2H, ^2G, ^2F, {}^2_aD, {}^2_bD, ^2P)$

a_1^2e	b_1^2e	b_2^2e	$a_1b_1e(i)$	$a_1b_1e(ii)$	$a_1b_2e(i)$	$a_1b_2e(ii)$	$b_1b_2e(i)$	$b_1b_2e(ii)$	e^3
$3A+7B+4C$	$(4B+C)$	$(4B+C)$	$\sqrt{6}\,B/2$	$9\sqrt{2}\,B/2$	$\sqrt{6}\,B/2$	$9\sqrt{2}\,B/2$	0	0	$(B+C)$
	$3A-3B+4C$	C	$2\sqrt{6}\,B$	$3\sqrt{2}\,B$	0	0	$3\sqrt{2}\,B/2$	$-3\sqrt{6}\,B/2$	$(3B+C)$
		$3A-3B+4C$	0	0	$2\sqrt{6}\,B$	$3\sqrt{2}\,B$	$3\sqrt{2}\,B$	0	$(3B+C)$
			$3A-7/2B+3C$	$3\sqrt{3}\,B/2$	$-3B$	0	$\sqrt{3}\,B/2$	$-9B/2$	$\sqrt{6}\,B/2$
				$3A-9/2B+3C$	0	$3B$	$-3B/2$	$-3\sqrt{3}\,B/2$	$3\sqrt{2}\,B/2$
					$3A-7/2B+3C$	$3\sqrt{3}\,B/2$	$5\sqrt{3}\,B/2$	$3B/2$	$\sqrt{6}\,B/2$
						$3A-9/2B+3C$	$3B/2$	$3\sqrt{3}\,B/2$	$3\sqrt{2}\,B/2$
							$3A+3/2B+3C$	$-3\sqrt{3}\,B/2$	$9\sqrt{2}\,B/2$
								$3A-3/2B+3C$	$-3\sqrt{6}\,B/2$
									$3A-3B+4C$

F 1103

INDEX DU TOME 14 (1969)

INDEX DES AUTEURS

A

ABRAHAM A., voir SZOTYORI L. 1623

ALMASI L. und A. HANTZ, E. HAMBURG, Über heteroorganische Verbindungen. XXXVI. Infrarot-spektroskopische Untersuchungen der Addukte der O,O-Dialkylthiophosphorsäuren mit sekundären und tertiären Aminen 495

ANGELESCU E. and M. RADU, Electrical conductivity and dispersion degree of lyophilic colloids relationship. X. 0.2 M sodium stearate, palmitate and laurate in the presence of electrolytes with different anions 441

ANTONESCU E., voir SPACU P. 201

ARMEANU V. and I. DRĂGUȘIN, Study of some azo-derivate complexes of chromotropic acid with barium. I. Spectrophotometric study of the systems Ba-carboxyazo III, Ba-carboxysulphonazo III and Ba-sulphonazo III. 1367

— and I. DRĂGUȘIN, Study of some azo-derivate complexes of chromotropic acid with barium. II. Spectrophotometric and volumetric dosing of barium and sulphates with the reactives carboxyazo III, carboxysulphonazo III and sulphonazo III 1511

ARSENIE I., voir POPA L. 217

ARSHAD A. BEG M., Correlation of the physical properties of organophosphorus compounds. II. Refractivity and boiling point of phosphines 503

ASANDEI N. et A. LIGA, Réactions polymères-analogues du copolymère binaire acrylonitrile-acétate de vinyle en solutions-alcalines 1419

AVRAM E., voir AVRAM M. 1181

AVRAM M. und I. G. DINULESCU, GH. D. MATEESCU, E. AVRAM, C. D. NENITZESCU, Untersuchungen in der Cyclobutanreihe. XXI. Die tert-butyl-diphenyl-cyclobutadien-Komplexe mit Palladiumchlorid 1181

— und I. G. DINULESCU, GH. D. MATEESCU, C. D. NENITZESCU, Untersuchungen in der Cyclobutanreihe. XXII. Ein Hexacarbomethoxy-Dewar-Benzol Komplex aus Acetylendicarbonsäure-dimethylester und Bis-benzonitril-palladiumchlorid. . .1191

— and GH. D. MATEESCU, C. D. NENITZESCU, Investigations in the cyclobutane series. XX. Stereoisomeric 1.2.3.4.-tetrabromocyclobutanes by the Hunsdiecker reaction 101

B

BADEA F., voir VOICU M. 929

BADEA V., voir CRISTESCU C. 135

BĂDILESCU I. I., Acetoanilides. II. Preparation of some acetoacetanilides and derivatives. 395

— Oxygen-alkyl bond cleavage in attempted cyclization of chloro-substituted γ-phenoxybutyric acids 1585

— voir BĂDILESCU S. 329

BĂDILESCU S. and I.I. BĂDILESCU, Hydrogen bonds. II. The infrared study of the strength of hydrogen bond in some dihydroxyacetophenones 329

BALABAN A. T., Aromaticity. VI. Electronic absorption spectra of o-phenylene carbonate and of its conjugate acid 1323

— Oxidation of pyrocatechol derivatives to o-quinones by iodosobenzene diacetate 1281

— Pyrylium salts formed by diacylation of olefins. XIX. Characterization of olefins by diacylation: acid dealkylation of 3,5-di-t-butylpyrocatechol 1331

— voir BOYD G. V. 1575

— voir FRANGOPOL P. T. 385

— and M. FRANGOPOL, N. NEGOIȚĂ, P. T. FRANGOPOL, M. PARASCHIV, Factors affecting stability and equilibria of free radicals. V. Synthesis and spectra of polynitrophenyl-alkoxyamines 941

— voir GÂRD E. 247

— voir SUSAN A. B. 111

BALANDIN A. A. und I. HORESCU, A. P. RUDENKO, Kinetik der kontinuierlichen Alkoholdehydrierung an Kupferkatalysatoren bei niedrigem Druck . . . 619

BALOG A., voir V. VOINESCU 951

Baltog I., voir Lupu A. 469

Banciu A.-C., Über die spektrophotometrische Methode von Jazimirskij zur Untersuchung stufenweiser Komplexbildung und über die Erweiterung der Anwendungsgrenzen dieser Methode 1019

Banciu M., voir Cioränescu E. 911

Barabás A. and E. Işfan, E. Romaş, A. Trestianu, Heterocyclic organoboron compounds. XI. Boronium chelate salts and beryllium chelates of 2-substituted 1,3-diketones; methyl-acetylacetone, phenyl-acetylacetone and methyl-dibenzoylmethane . . . 253

Baraf L., voir Bratu Em. A. 1445

Bärbulescu N. und F. Potmischil, Erhaltung und Untersuchung der Hydroacridine. I. Über die Synthese des symm-Oktahydroacridins, alfa-Perhydroacridins und beta-Perhydroacridins 1427

Bednar H., voir Bednar V. 1149

Bednar V. et V. Mincu, H. Bednar, L'étude des propriétés magnétiques de quelques tartrates simples et complexes . . . 1149

Bejan L., voir Sternberg S. 303

Beldie R. and V. E. Sahini, Raman spectra of beryllium oxalate complexes . . 419

Bezdadea E. C., voir Caraculacu A. A. 1171

Blenke P., voir Velea I. 473, 667

Bodea C. und E. Broser, Über Phenothiazone. XVI. Reaktion von Phenothiazonen mit Anilin 1617

— and V. Fărcăşan, T. Panea, Synthetical phenothiazine glycosides. II. O-Glucosides of 3-hydroxy-1,9-dibromo-7-chlorophenothiazine and 3-hydroxy-7-chlorophenothiazine 523

— and I. Oprean, V. Fărcăşan, Azlactones of the phenothiazine series. III. Aminolysis of some phenothiazine azlactones 673

— voir Tămaş V. . . . 141, 405, 959, 1591

Bodor N., voir Fey L. . . . 225, 319, 481

— voir Mantsch O. 1295

Bojan N., voir Ripan R. 353

Boyd G. V. and A. T. Balaban, A correlation between chemical shifts of methyl protons and electron densities in substituted pyrylium salts 1575

Brăileanu B., voir Lupu A. 469

Bratu Em. A. et L. Baraf, La puissance nécessaire pour mélanger en utilisant les agitateurs de type à rame. 1445

Brenet J., voir Dumas D. 1339

Broser E., voir Bodea C. 1617

Brumă M., voir Stoicescu-Crivetz L. . 659

Budiu T., voir Ripan R. 1631

Bunuş F. and I. Matei, Contributions to the uranium content determinations in solutions based on ^{238}U daughter radioactivity measurements 333

— and I. Matei, C. Matyas, S. Neciu, V. Sporea, S. Tătaru, Some quantitative relations on the radioactive minerals leaching processes 729

Butucelea Al., voir Sahini V. E. . . 965

C

Cambanis A., voir Niculescu-Duvăz I. . 535

Caraculacu A. A. and E. C. Bezdadea, Unsaturated end groups in PVC. I. Preparation of the model compounds . . . 1171

Cerbu A., voir Sternberg S. 1215

Charcosset H., voir Olaru I. 235

Chiraleu F., voir Gârd E. 247

Chiriac C. et L. Stoicescu-Crivetz, I. Zugrăvescu, Polypyrazoles-esters . 763

— et L. Stoicescu-Crivetz, I. Zugrăvescu, Polypyrazoles. III. N-arylation des pyrazoles 1263

Ciocăzanu I., voir Vîlcu R. 429, 561

Ciolac S., voir Radovici O. 297

Cioränescu E. and M. Banciu, R. Jelescu, M. Rentzea, M. Elian, C. D. Nenitzescu, Carbonium ion reactions. V. Acetolysis of 1 : 2, 5 : 6-dibenzocyclohepta-1,3,5-trienyl-7-ethyl β-tosylate 911

Cismaru D. and E. Dobroghiu, The oxidation of zirconium at high temperatures. The oxidation kinetics of zirconium powder in O_2 and CO_2 atmosphere . . 291

— et E. Dobroghiu, Oxydation du Fe et du Ni à hautes températures. Effet du champ magnétique sur la vitesse d'oxydation du Fe et du Ni 985

— und Al. Fruma, Die Kinetik der Wasserstoffchemisorption bei auf Aluminiumoxid aufgetragenem Platin 1489

— and A. Geangu-Moisin, The oxidation of tungsten at high temperatures. The system $W + CO_2$ 29

— et Z. Simon, Sur la cinétique de la formation des couches d'oxydes sur métaux 837

Ciurdaru Gh. and V. Dénes, Methylene bases of heterocycles. VIII. 2-Acylmethylene-benzazolines from ketoesters 1063

Ciurdaru V., voir Hodoşan F. . . . 1303

Ciurea L., voir Sahini V. E. . . 689, 1093

Comşa G., voir Murgulescu I. G. . . . 825

Constantinescu S., voir Popa L. I. . . 1457

Cordiș V., voir Ripan R. 197

Costeanu G. et O. Landauer, C. Mateescu, Influence du milieu de réaction sur l'hydrolyse acide de l'acétate de *n*-butyle . . . 845

Crăciuneanu R. und E. Florean, Das Verhalten von 1-Acyl-4-Aryl-Thiosemikarbaziden gegenüber den Schwermetallkationen. II. Das Verhalten von Co^{II} gegenüber den 1-Benzoyl-4-Aryl-Thiosemikarbaziden 753

Crăciunescu D. et Al. Fruma, L'effet du complexe cuivre-diphénylamine sur la décomposition catalytique de l'eau oxigénée 653

Cristea Gh., voir A. Șuteu 209

Cristea M., voir Tribunescu P. 463

Cristescu C. and V. Badea, 6-Azauracil derivatives with potential cytostatic activity. VII. Thionation of 5-benzylthion-6-azauracil 135
— and M. Lăzărescu, 6-Azauracil derivatives with potential cytostatic activity. VIII. Acylation of 5-mercapto-6-azauracil and its derivatives 797

Czeglédi L., voir Macarovici Const. Gh. . . 57

D

David B., voir Tătaru S. 599

Deleanu Th. and N. Georgescu, Consideration on electrical conduction mechanisms in polymers from liquid paraffinic hydrocarbons. 1269

Demetrescu I., About the conductivity of solutions of hydrobromic acid in normal alcohols 1225
— voir Murgulescu I. G. 149

Demian H., voir Simiti I. 1285

Dénes V., voir Ciurdaru Gh. 1063

Dick J. und A. Lupea, Komplexverbindungen des N, N′-Diaminopiperazins. I. Metallchelat-verbindungen und ihr thermischer Abbau 1047
— und A. Lupea, Komplexverbindungen des N-N′-Diaminopiperazins. II. Verbindungen mit komplexen Anionen und ihr thermischer Abbau 1143
— und A. Lupea, Komplexverbindungen des N, N′-Diaminopiperazins. IV. Infrarotspektren. Elektronenspinresonanz ...1377
— und A. Lupea, Z. Szabadai, Komplexverbindungen des N, N′-Diaminopiperazins. III. Sichtbare- und UV-Spektren 1241
— und A. Maurer, Neue Komplexverbindungen der Pyrazolonreihe. V. . 1603

Dimonie V., voir Velea I 473, 667

Dinulescu I. G., voir Avram M. . . 1181,1191

Dobre E., voir Răileanu M. 887, 1053

Dobrogiiu E., voir Cismaru D. . . .291, 985

Dorcioman D., voir Popa L. I. 1457

Dorobanțu V., voir Popa L. I. 1457

Doss S. H., voir El-Abbady A. M. . . 265

Drăgulescu C. and I. Julean, A. Nimara, Basic permanganates of bismuth. Investigations in solution on the $[Bi_6(OH)_{12}]$ $(OH)_2(MnO_4)_4$-complex 189
— and S. Marchidan, Gh. Facsko, Influence of some anions and solvents on the polarographic reduction of niobium (V) in hydrochlorid acid-thiocyanate medium 737
— and S. Marchidan, Gh. Facsko, Polarographic reduction of niobium (V) tartrate solutions in hydrochloric acid-thiocyanate medium 1501
— und R. Pomoje, I. Menessy, M. Pîrlea, C. Mihăescu, Metallkomplexe der N-carboxymethyl-anthranylsäure (Phenyl-glycin-Orthocarbonsäure) II. Eisen (III)- und Chrom(III)-Komplexe 1595
— und T. Simonescu, H. Schiff, Extraktion von Titan (IV) mit n-Butanol und Quercetin in Gegenwart von Natriumtriumtrichloracetat 583

Drăgușin I., voir Armeanu V. . .1367, 1511

Dumas D et J. Brenet, Processus aux électrodes de carbone dans les bains alumino-cryolitiques 1339

E

Eger I., voir Ripan R. 353

El-Abbady A. M. and M. El-Ashri, S.H. Doss, Further studies on the Stobbe condensation with 2-methyl-cyclohexanone 265

El-Ashry M., voir El-Abbady A. M. . 265

Elian M., voir Ciorănescu E. 911

F

Facsko GH., voir Drăgulescu C. . . 737, 1501

Fărcășan V., voir Bodea C. 523, 673

Fătu D. et S. Fătu, E. Segal, Cinétique de la décomposition thermique de certaines combinaisons complexes du chlorure de cuivre avec la pyridine et des pyridines substituées., ... 1107
— et E. Segal, Cinétique de la décomposition de l'hydrazine sur des couches minces de germanium 183
— et E. Segal, Cinétique de la décomposition thermique de certaines combinaisons complexes du chlorure de manganèse avec la pyridine et des pyridines

substituées. Paramètres cinétiques obtenus des données gravimétriques. . 709

FĂTU S., voir FĂTU D. 1107

FELDMAN D. and V. NUŢĂ, CR. SIMIONESCU, Photopolymerisation of acrylonitrile in the presence of some anthraquinone dyes 1407

FEY L. and N. BODOR, Electronic spectra of the substituted α-oximinoalkylbenzenes. I. Steric effects on electronic absorption spectra of the substituted *o*-nitro-α-oximinoalkylbenzene 225
— and N. BODOR, Electronic spectra of the substituted α-oximinoalkylbenzenes. II. MO-calculations of the bathochromic shifts produced by the dissociation of benzaldoxime and *p*-nitrobenzaldoxime . . 319
— and N. BODOR, Electronic spectra of the substituted α - oximinoalkylbenzenes. III. Steric effects on electronic absorption spectra of the *o*-substituted *p*-nitro-α-oximinoalkylbenzenes 481
— and J. RUSU, Spectrophotometric method for the quantitative analysis of *ortho*- and *para*-nitroethylbenzene mixtures 613
— voir SZOTYORI L. 1623

FEYNS V., voir NICULESCU-DUVĂZ I. . . 535

FILIP GH., voir TĂTARU S. 599

FINK P., IR-spectroscopic and gravimetric investigations about the formation of carboxylate surface species during the chemisorption of CO, CO_2 and simple organic oxygen compounds on γ-alumina 811

FINTA Z., voir VÁRHELYI CS. 1133

FLOREA I., Sur le chromate, le biochromate, le molybtate et le wolframate de 2-éthoxy-6, 9-diaminoacridine 365
— Tetraphenylborate des Akridins, 2-Äthoxy-6, 9-Diaminoakridins und 3-Chlor-9-(4′-Diäthylamino-1′-Methylbutylamino-7-Methoxyakridins 745
— Über Hexazyanoferrat und Nitrosopentazyanoferrat des 3-Chlor-9-(4′-Diäthylamino-1′-Methylbutylamino)-7-Methoxyakridins 893

FLOREAN A., voir CRĂCIUNEANU R. . . . 753

FRANGOPOL M., voir BALABAN A. T. . . 941
voir FRANGOPOL P. T., ... 385, 527

FRANGOPOL P. T., voir BALABAN A. T. . 941
— and M. FRANGOPOL, N. NEGOIŢĂ, A. T. BALABAN, Factors affecting stability and equilibria of free radicals. IV. t-Butylcyanonitroxide 385
— et M. FRANGOPOL, N. NEGOIŢĂ, R. ROMAŞ, Radicaux libres stables diarylazote avec un groupe sulfonique dans la molécule 527

FRUMA AL., voir CISMARU D. 1489
— voir CRĂCIUNESCU D. 653

FRUNZE N. K., Nekatoryie vaprosy fotosinteza spolimero setachiatoi struktury s obrazovanykh re fnykh izobrazhjenii 1309

FULEA A. O., voir SA NI V. E. 17

G

GABE I. und D. LEON , Koordinationspolymere mit bis-(Aminc arboxylsäuren). I. Über die Reaktion de Benzidindicarboxylsäure mit Cd-Zn- u- Ni-und Mn-Salzen 1535
— und E. MĂNTĂLUŢĂ, G. N AMŢU, Ultrarotspektroskopische Unters hungen an einigen Polypyridazinen, P tetrazinen und Polytriazolen 1163
— voir PETROVANU M. 1153

GĂINAR I., voir VÎLCU R. 695

GANOVICI I., voir GANOVICI L. . . . 1011
— voir ZĂMÂRCĂ ŞT. 3 175

GANOVICI L. et I. GANOVICI, La densité la viscosité de l'indium fondu dans l'in rvalle de température de 166° à 800°. 1 1
— voir ZĂMÂRCĂ ŞT. 35, 1

GÂRD E. and I. STĂNOIU, A. T. BALABAN, F. CHIRALEU, Isotopic exchange of active methyl hydrogens. VI. Deuteration 2, 4, 6-triphenyl-, 2, 3, 5, 6-tetramenthyl- and 2, 3, 6-trimethyl-4-phenyl-pyrylium salts 247

GENAGU-MOISIN A., voir CISMARU D. . 29

GEORGESCU N., voir DELEANU TH . . 1269

GHENCIULESCU A and I. NECŞOIU, C. D. NENITZESCU, The Étard reaction. IX. Oxidative cleavage of ethers produced by chromyl chloride 1553
— and I. NECŞOIU, M. RENTZEA, C. D. NENITZESCU, The Étard reaction. VIII. Oxidation of diphenylethanes and diphenylethylenes with chromyl chloride . 1543

GHEORGHIU M. D. and R. HOFFMANN, The electronic structure of some substituted cyclobutadienes 781
— and R. HOFFMANN, The electronic ground states of *ortho*, *meta* and *para*-benzynes 947

GHIRVU C. I., voir SAHINI V. E. 275

GREFF C. et S. MOLDOVEANU, Détermination des constantes de dissociation de certaines l-alcoyl-3, 5-bis-(p-dialcoylamino-benzyliden)-4-pipéridones en solution aqueuse 389

GROPŞIANU Z. und. D. KOHN, A. IOVI, Wärmeübergangzahlen beim Verdampfen von Ammoniumnitratlösungen 451
— und D. KOHN, A. IOVI, Wärmeübergangszahlen beim Sieden von Lösungen. Lösungen von Mononatriumphosphat 721
— und D. KOHN, A. IOVI, Wärmeübergangszahlen beim Sieden von Lösungen.

II. Lösungen von Dinatriumphosphat 873
— und D. Kohn, A. Iovi, Wärmeübergangszahlen beim Sieden von Lösungen. Lösungen aus Gemischen von Natriumphosphaten 1031

H

Haiduc I., voir Liteanu C. 1039
Hamburg E., voir Almasi L. 495
Hantz., voir Almasi L. 495
Herdlicka C., voir Sternberg S. . . . 991
Hodişan T., voir Şuteu A. 1613
Hodoşan F. und I. Jude, Steroide in adsorbiertem Zustand. III. Über Substitutionsreaktionen der Tosyloxy-Gruppe durch das Nitrat-Anion an aktivem Aluminiumoxid 1057
— und A. Pop-Gocan, Darstellung einiger 3-Acyloxysteroide 1441
— and N. Şerban, Preparation of 3α, 6α-dihydroxy-5 β-etianic acid und its conversion into methyl 3β-thiocyano-and 3β-isothiocyano-Δ^5-etienate 399
— und N. Şerban, Steroids in the adsorbed state. II. Reductions with sodium borohydride under heterogeneous conditions 121
— and N. Şerban, V Ciurdaru, Unsymmetrical diacyl derivatives of methyl hyodesoxycholate 1303
— and F. Teodor, Spectral studies on steroidal nitrate esters. III. UV spectra in concentrated sulfuric acid 509
Hoffmann R., voir Gheorghiu M. D. 781, 947
Horescu I., voir Balandin A. A. 619

I

Ionescu A., voir Popescu A. 79
Ionescu M. and I. Meşter, Synthesis of some dimethoxy-10-methylacridones . . . 789
— and M. Văgăonescu, Contributions to the study of octanesultone . . . 517
Ionescu M., voir Niculescu-Duvăz I. . 535
Ionescu N. I., On a Suhrmann-Wedler equation 869
— voir Murgulescu I. G. 681, 1073
Iovi A., voir Gropşianu Z. 451, 721, 873, 1031
Işfan E., voir Barabás A. 253

J

Jelescu R., voir Ciorănescu E. . . . 911
Jude I., voir Hodoşan F. 1057
Julean I., voir Drăgulescu C. 189

K

Kékedy L. and Makkay F., Experimental approach to the characterization of pretreated platinum electrode surfaces. II. Cyclic potential sweep voltammetric study 605
Kim Tal-Hen, voir Simionescu Cr. . . 1519
Kiss-Rajhona Zs., voir Mánok F. . . . 1251
Kohn D., voir Gropşianu Z. 451, 721, 873, 1031
Kormos F., voir Şuteu A. 1613
Kulcsár-Nováková M., voir Ripan R. 717
Kurunczi L., voir Nuţiu R. 1435

L

Landauer O., voir Costeanu G. . . . 845
Lăzărescu M., voir Cristescu C. . . 797
Leonte D., voir Gabe I. 1535
Liga A., voir Asandei N. 1419
Liteanu C. and I. Haiduc, About the influence of indicating electrode treatment upon the parameters of the potentiometric titration. I. Bright platinum electrode in $Fe^{2+}/Cr_2O_7^{2-}$ titration . . 1039
— voir Lukács I. 647, 1125
— und Gh. Rădulescu, Untersuchung der Gleichrichtungseigenschaften der heterogenen Membranen. II. Das Verhalten einer einheitlichen Celluloid : Kationit-H + Anionit-OH Membran gegenüber Wechselstrom von 50 Hz und bei Direktspannungen 1257
Lucinescu E., voir Vîlcu R. 283
Lukács I et C. Strusievici, C. Liteanu, Le pouvoir thermoélectrique des composés $M^I_xV^{IV}_xV^V_{2-x}O_5$ (M^I = Na, K ; $0 < x \leqslant 1$) 647
— et C. Strusievici, D. Lupu, C. Mirel, C. Liteanu, Sur les vanadates. XVII. La susceptibilité magnétique des composés $K_xV^{IV}_xV_{2=x}O_5$ ($0 < x \leqslant 1$). . 1125
Lupea A., voir Dick J. 1143, 1241, 1377
Lupea A., voir Liteanu C. 1047
Lupu A. and L. Nasta, I. Baltog, B. Brăileanu, Light scattering and viscosity measurements on unfractionated polyvinylchloride 469
Lupu D., voir Lukács I. 1123

M

Macarovici Const Gh. et L. Czeglédi, Combinaisons complexes avec des hydroxyacides. VII. Étude spectrophotométrique du système $TiO(ClO_4)_2$-acide D-gluconique . 57

— and R. Micu-Semeniuc, Complex combinations with diphenylic derivatives. XXIII. On the structure of some Cu(I) and Cu(II) complex thiocyanates 357

— et E. Perţe, Combinaisons complexes avec des hydroxyacides. VIII. Les complexes du Ga^{3+} et In^{3+} avec l'acide saccharique 1113

— und C. Stanisav, Die Entfernung der störenden Wirkung des Eisens, Kobalts, Nickels und Kupfers bei der kolorimetrischen Bestimmung des Titans . . 459

— et M. Voloşniuc-Birou, Combinaisons complexes avec des hydroxyacides. IX. Complexes de l'étain tétravalent avec les acides gluconiques et sacchariques et leurs sels alcalins 1231

Macovschi M., voir Radovici O. 159

Magearu V. et Gr. Popa, L'étude des complexes de Zn (II), Cd(II), Co(II) et Ni (II) avec la di-i-propylamine . . . 1399

— voir Popa Gr. 879, 1387

Makkay F., voir Kékedy L. 605

Măndăşescu L., voir Petruş A. . . . 773

Mánok F. und Cs. Várhelyi, Zs. Kiss-Rajhona, Über α-Dioximinkomplexe der Übergangsmetalle. XXVI. Kupfer (II)-Chelate mit 1,2-Cyclohexandiondioxim 1251

Manolescu D. and E. Segal, X-rays studies on monopyridine complexes of cobalt (II) and nickel (II) chloride 999

Măntăluţă E., voir Gabe I. 1163

Mantsch H. H., The mass spectrum of acridine-N-oxide 549

— and W. Seiffert, V. Zanker, π-Electronic structure of acridine-N-oxide 125

Mantsch O. und N. Bodor, Kinetik und Mechanismus der Veresterungsreaktion von Steroidalkoholen mit Acetylnitrat . 1295

Marchidan D. I. and Cr. Telea, The heat of melting in the binary mixtures : $RbNO_3 + KNO_3$ and $RbNO_3 + CsNO_3$ . . . 1361

— and Cr. Telea, Heat of mixing in the binary molten salts mixtures : KCl + + NaBr and NaCl + KBr

Marchidan S., voir Drăgulescu C. 737, 1501

Mateescu C., voir Costeanu G. 845

Mateescu Gh. D., voir Avram M. 101, 1181,-1191

Matei I., voir Bunuş F. 333, 729

Matei I., voir Petruş A. 773

Máthé J., Ligand field theory for noncubic symmetries 1003

Matyas C., voir Bunuş F. 729

Maurer A., voir Dick J. 1603

Melega E., voir Velea I. 473, 667

Menessy I., voir Drăgulescu C. . . . 1595

Meraru R. and M. Negoiu, Röntgenographic study on the compound $[HP(C_6H_4-CH_3)_3]_2$ $[CoCl_4]$ 1027

Meşter I., voir Ionescu M. 789

Micu-Semeniuc R., voir Macarovici Const. Gh. 357

Mihăescu C., voir Drăgulescu C. . . . 1595

Mihai Fr. und A. Moraru, Gr. Pop, Untersuchungen über das thermische Verhalten von Cadmiumsalzen einiger Dicarboxylsäuren 637

Mincu G., voir Murgulescu I. G. . . . 3

Mincu V., voir Bednar V. 1149

Mirel C., voir Lukács I. 1125

Misdolea C., voir Vîlcu R. 1353

Moldoveanu S., voir Greff C. 389

Moraru A., voir Mihai Fr. 637

Moser Z., voir Ptak W. 851

Murgulescu I. G., Some physico-chemical properties of simple molten salts . . 965

— und G. Comşa, Chemisorption von Sauerstoff und Kohlenmonoxid an vorbelegten Kupferschichten 825

— and I. Demetrescu, The kinetics of the reactions between benzoil chloride and normal alcohols 149

— and N. I. Ionescu, The effect of oxygen chemisorption on the temperature coefficient of the electrical resistance of thin copper films 681

— and N. I. Ionescu, The effect of oxygen chemisorption on the temperature dependence of the variation of electrical resistance of thin copper films 1073

— and D. Oancea, G. Mincu, Reactions between benzyl chloride and alkali alcoxides 3

— und C. Potmischil, Die Reaktion des Triphenylmethylchlorids mit Akoholen1335

— and I. Vartires, On the standard potential of thin cadmium films . . . 1479

— and M. I. Vass, Calorimetric determination of the differential chemisorption heat of oxygen on thin copper films 1201

— et I. Vlagiu, Détermination des constantes Q_{tr}-e_{tr} des valeurs des constantes de transfert, dans les cas de polymérisation radiochimique de l'acrylonitrile dans des solvants de filage 411

— et I. Vlagiu, La cinétique de la polymérisation mixte de l'acrylonitrile sous l'action des radiations ionisantes et en présence de diacvodioxalomanganate de potassium 1081

N

Nasta L., voir Lupu A. 469

Neamţu G., voir Gabe I. 1163

Neciu S., voir Bunuş F. 729

Necşoiu I., voir Ghenciulescu A. 1543, 1553
— voir Pşemeţchi V., ... 1567

Negoiţă N., voir Balaban A. T. . . . 941
— voir Frangopol P. T. . . . 385, 527

Negoiu M., voir Meraru R. 1027

Nenitzescu C. D., voir Avram M. 101,1181,1191
— voir Ciorănescu E. 911
— voir Ghenciulescu A. . 1543, 1553
— voir Pşemeţchi V. 1567

Nicolescu I. V., voir Spinzi A. 903
— voir Spinzi M. 629
— and O. Şerban, Study on the intermediates occurring in the octylation reaction of the aromatic nucleus with the catalysts $AlEt_2Cl$-RCl 87

Niculescu-Duvăz I. and V. Feyns, V. Savaniu, M. Ionescu, A. Şerban, A. Cambanis, Potential anticancer agents. VI. New aromatic nitrogen mustards with good antitumor activity 535

Nimară A., voir Drăgulescu C. . . . 189

Nuţă V., voir Feldman D. 1407

Nuţiu R. and L. Kurunczi, Z. Simon, Electric moment of dilituric acid (5-nitrobarbituric acid) 1435
— and Z. Simon, Molecular orbital studies on tautomers of dilituric acid. II. Correlation with some IR and X-ray diffraction data 311

O

Oancea D., voir Murgulescu I. G. . . 3

Olaru I. et H. Charcosset, Y. Trambouze, M. Prettre, Étude des catalyseurs oxyde de chrome-alumine-potassium par analyse thermique différentielle et mesures de chimisorption 235

Olteneanu M., voir Sahini V. E. . . . 831

Oprean I., voir Bodea C. 673

P

Panea T., voir Bodea C. 523

Paraschiv M., voir Balaban A. T. . . 941

Perţe E., voir Macarovici Const. Gh. 1113

Petrescu N., Viscosity and density of the molten InBi compound 67

Petrovanu M. et A. Sauciuc, I. Gabe, I. Zugrăvescu, L'addition de philodiènes sur la phtalazine. III. Action du bromure de phénacyle sur la phtalazine . . . 1153

Petruş A. and L. Măndăşescu, I. Matei, Linear polyesters and polycarbonates from bis-(4-hydroxyphenyl)-deoxybenzoin and 1,1-bis-(4-hydroxyphenyl)-2-oxo-acenaphthene 773

Pîrlea M.. voir Drăgulescu C. . . . 1595

Plonski I. H., Contributions to Parson's treatment "General equations for the kinetics of electrode processes" . . . 569

Ploştinaru S., voir Spacu P. 591

Poinescu I., Transformations chimiques du chlorure de polyvinyle. I. Synthèses des polyélectrolytes réticulés sulfoniques à base de chlorure de polyvinyle arylé avec du benzène 373

Pomoje R., voir Drăgulescu C. . . . 1595

Pop Gr., voir Mihai Fr. 637

Pop-Gocan A., voir Hodoşan F. . . . 1441

Popa L. et I. Arsenie, Étude de la solubilité de l'oxyde de zirconuim 217
— et B. Dorobanţu, D. Dorcioman, S. Constantinescu, M. S. Popa, La réalisation des sels nucléaires de zirconium par recristallisation fractionnée . . 1457

Popa Gr., voir Magearu V. 1399
— and V. Magearu, The formation of some complex combinations with piperazine, in aqueous solution 1387
— and V. Magearu, The study of the formation and determination of the stability in solution of some complex combinations with n-propyamine 879

Popa M. S., voir Popa L. 1457

Popescu A. and E. Segal, A. Ionescu, A. Szabo, D.T.A., electrical conductivity and activity of some Bi_2O_3-MoO_3 catalysts 79

Popescu Fl., Polymères organiques phosphorylés. II. La phosphorylation du «polystyrène par synthèse Friedel-Crafts 1525

Potmischil C., voir Murgulescu I. G. 1335

Potmischil F., voir Bărbulescu N. . 1427

Prettre M., voir Olaru I. 235

Proinov L., voir Simiti I. 1285

Provinceanu V., voir Velea I. . . 473, 667

Pşemeţchi V. and I. Necşoiu, M. Rentzea, C. D. Nenitzescu, The Étard reaction. X. Oxidation of methylcyclopentane, methylciclopentane and of methylenecycloalcanes C_5, C_6 and C_7 with chromyl chloride 1567

Ptak W. and Z. Moser, L. Zabdyr, Thermodynamic properties of Zn-Bi-Pb liquid solutions 851

R

Răileanu M. and E. Dobre, Volumetric dosage with phenothiazone-(3).I. Dosage of sodium thiosulphate with phenothiazone-(3) 887
— and E. Dobre, Volumetric dosage with phenothiazone-(3).II. Dosage of the ascorbic

acid with phenothiazone-(3) 1053
voir Turcu A. 1579

Radovici O. and S. Ciolac, Influence of halogenide ions on electrochemical behaviour of titanium and alloys . . . 297
— and M. Macovschi, Hydrogen overvoltage on thin evaporated metal films. I. Gold films 159
— and E. Roman, The mechanism of the action of lauril-amine on the corrosion of iron in HCl solutions 423
— and N. Totir, Some kinetic aspects of anodic oxidation of methanol . . 23
— and C. Vass, Electrodeposition of zinc from pyrophosphate solutions. I. Study of equilibrium potentials of zinc electrode 1099

Radu M., voir Anghelescu E. 441

Rădulescu Gh., voir Liteanu C. . . . 1257

Rentzea M., voir Ciorănescu E. . . . 911
— voir Ghenciulescu A. 1543
— voir Pșemețchi V., ... 1567

Ripan R. und T. Budiu, Trennung und Bestimmung des Titans in Gegenwart des Eisens 1631
— und V. Cordiș, Chemische Bestimmung der Basizität des $[PV_{12}O_{36}]^7$—Heteropolyanions 197
— et I. Eger, N. Bojan, Étude des nitrates métalliques en mélanges de solvants. II. 1. Les systèmes : le nitrate de nickel et de cobalt hexahydraté-acétone-tétrachlorure de carbone ; le nitrate de nickel et de cobalt dihydraté-acétone-tétrachlorure de carbone 353
— und M. Kulcsár-Nováková, Die Bildung der Gallosilikat-Niederschläge in wässrigen Lösungen 717
Roman E., voir Radovici O. 423
Romaș E., voir Barabás A. 253
— voir Frangopol P. T. 527
Rudenko A. P., voir Balandin A. A. . 619
Rusu J., voir Fey L. 613

S

Sahini V. E., voir Beldie R. 419
— and Al. Butucelea, On the n→π *electronic transition in aromatic ketones 981
— and L. Ciurea, Electron spin resonance spectra of some aromatic metal ketyls 689
— and L. Ciurea, Electronic spectra of some aromatic metal ketyls 1093
— and A. O. Fulea, The force constants of $PH_4^+(T_d)$ 17
— and C. I. Ghirvu, On the electronic structure and spectra of the monosubstituted naphthalenes 275
— and M. Olteneanu, Solvent effect on the infrared spectra of benzophenone and anthrone 831
— and L. Telea, On the electronic spectra of Co(III) halogeno pentaammines 157
— and V. Tufoi, Calculation of the intensity of the spin-forbidden absorption band of $[Co(NH_3)_6]^{3+}$ taking the covalence into consideration 557

Savaniu V., voir Niculescu-Duvăz I. . 535

Sauciuc A., voir Petrovanu M. 1153

Schiff H., voir Drăgulescu C. 583

Segal E., Modèle du gaz électronique bidimensionnel dans la chimisorption sur métaux 45
— voir Fătu D. . . 183, 709, 1107
— voir Manolescu D. 999
— voir Popescu A. 79

Seiffert W., voir Mantsch H. H. . . . 125

Șerban A., voir Niculescu-Duvăz I. . . 535

Șerban N., voir Hodoșan F. 121, 399, 1303

Șerban O., voir Nicolescu I. V., ... 87

Siechowski J. and J. Sliwiok, The role of Cr^{+5} ions in the catalytic oxidation of soja oil 95

Simionescu Cr., voir Feldman D. . . 1407
— et Kim Tal-Hen, Recherches sur la polymérisation de certains dérivés acétyléniques à l'aide de la triéthylamine. I. La polymérisation de l'ester méthylique de l'acide propiolique 1519

Simiti I. et L. Proinov, H. Demian, Contribution à l'étude de quelques hétérocycles. XII. L'halogénation et la nitration de l'anilino-2-méthyl-5-thiodiazole-1, 3, 4 1285

Simon Z., The stability of the oxalyl anionic radical $(C_2O_4^{\cdot -})$. 705
— voir Cismaru D. 837
— voir Nuțiu R. 311, 1435

Simonescu T., voir Drăgulescu C. . . 583

Sliwiok J., voir Siechowski J. 95

Sofronie E., voir Tărăbășanu-Mihăilă E. 1467

Spacu P. and E. Antonescu, Complexes of lanthanide halogenoacetates with 1-10-phenanthroline and 2-2′-dipyridyl (II) 201
et S. Ploștinaru, Etude spectrophotométrique des systèmes $LnCl_3$-rouge acide AV et $LnCl_3$-calcon 591

Spinzi A. et I. V. Nicolescu, Étude des catalyseurs solides pour l'oxydation des hydrocarbures. II. Influence du milieu de réaction sur les propriétés électriques du catalyseur V_2O_5-MoO_3 903

Spinzi M. et I. V. Nicolescu, Influence du support sur l'activité et les propriétés électriques du catalyseur Cr_2O_3-Al_2O_3 utilisé dans la réaction des déshydrogénation du *n*-butane en *n*-butènes . . 629

Sporea V., voir Bunuș F. 729

Stanisav C., voir Macarovici Const. Gh. 459

Stănoiu I., voir Gârd E. 247

Sternberg S. and L. Bejan, Thermodynamic properties of the reciprocal system of fused silver iodide and potassium chloride 303
— and A. Cerbu, The behaviour of certain synthetic zeolites in molten salts media 1215
— and C. Herdlicka, Chronopotentiometric determination of silver ion interdiffusion coefficient in molten potassium and lithium nitrates 991

Stoicescu-Crivetz L. et M. Brumă, I. Zugrăvescu, Poly (1, 3, 4-oxadiazoles). V. La réaction des ditétrazoles avec les diisocyanates 659
— voir Chiriac C. 763, 1263

Strusievici C., voir Lukács I. . . . 647, 1125

Susan A. B. and A. T. Balaban, Reaction of pyrylium salts with nucleophiles. VIII. Triphenylpyrylium and methylamine: thermal degradation of N-methyl-2, 4, 6-triphenylpyridinium halides to methyl halides and 2, 4, 6-triphenylpyridines 111

Şuteu A. et Gh. Cristea, Étude du $H_5[PW_{10}V_2O_{40}]$ par la méthode RES . . . 209
— und T. Hodişan, F. Kormos, Eine neue kolorimetrische Bestimmungsmethode des Eisens(III) 1613

Szabaday Z., voir Dick J. 1241

Szabo A., voir Popescu A. 79

Szotyori L. und L. Fey, A. Abraham, Die Reaktion zwischen Natriumalkoxiden und α-Halogenketonen. VI. Einwirkung des Natrium-methoxides auf ω-Bromacetophenon 1623

T

Tămaş V. and C. Bodea, $TiCl_4$-carotenoid complexes. III. Action of $TiCl_4$ on carbonylcarotenoids (canthaxanthin, rhodoxanthin, β-apo-8′-carotenal) 141
— and C. Bodea, $TiCl_4$-carotenoid complexes. IV. Action of $TiCl_4$ on cryptoxanthin and cryptoxanthinpalmitate . . 405
— and C. Bodea, $TiCl_4$-carotenoid complexes. V. Action of $TiCl_4$ on dodecapreno-β-carotene 959
— and C. Bodea, $TiCl_4$-carotenoid complexes. VI. Action of $TiCl_4$ on isocryptoxanthin and isozeaxanthin 1591

Tătaru S., voir Bunuş F.. 729
— et Gh. Filip, B. David, Adsorpiton de l'uranium par les résines échangeuses d'ions en présence du chlorate et du perchlorate 599

Tărăbăşanu-Mihăilă E. and E. Sofronie, Radiolysis of copper phthalocyanine alkaline aqueous solutions by $^{60}CO\gamma$-ray 1467

Telea Cr., voir Marchidan D. I. 1361, 1495

Telea L., voir Sahini V. E.. 157

Teodor F., voir Hodoşan F.. 509

Totir N., voir Radovici O. 23

Totoescu D. A., Equations and interpretation of osmotic pressure 345

Trambouze Y., voir Olaru I. 235

Trestianu A., voir Barabás A. 253

Tribunescu P. et M. Cristea, Structure des hexacyanocobaltiates de zinc, cadmium, nickel et manganèse 463

Tufoi V., voir Sahini V. E. 557

Ţurcanu C. N., voir I. Zamfir 339

Turcu A. and M. Răileanu, The action of ammonia on some nitroderivates of phenothiazine-5-oxide and phenothiazine-5, 5-dioxide 1579

V

Văgăonescu M., voir Ionescu M. 517

Várhelyi Cs., and Z. Finta, J. Zsakó, Kinetics and mechanism of substitution reactions of complexes. XIV. New derivatives of the dichloro-bis-dimethylglyoximato-cobaltous-(III)-acid and the solvolysis of the ion $[Co(DH)_2Cl_2]^-$ in water-dimethylformamide mixtures . . . 1133
— voir Manok F. 1251

Vartires I. voir Murgulescu I. G. . . 1479

Vass C., voir Radovici O. 1099

Vass M. I., A new all walls cooled cylindrical trap 809
— Pyrani manometer for the range $2\times10^{-1}-5\times10^{-6}$ torr 955
— voir Murgulescu I. G. 1201

Vasu Gh., On the mechanism of viscous flow in ionic liquids. 167

Velea I. and V. Dimonie, E. Melega, P. Blenke, V. Provinceanu, Stereospecific polymerization of 1, 3-butadiene. I. Some kinetic aspects of 1, 3-butadiene polymerization with soluble catalysts on the basis of cobalt complex compound, diethylaluminium monochloride, water 473
— and V. Dimonie, E. Melega, V. Provinceanu, P. Blenke, The stereospecific polymerization of 1,3-butadiene. II. The influence of the reaction medium on butadiene polymerization with $AlEt_2Cl-COCl_2.2Py - H_2O$ catalytic system. 667

Vîlcu R. and I. Ciocăzanu, Alkaline hydrolysis of the methyl and ethyl acetates. I. Calorimetrical determination of the standard thermal effects during the evolution of the chemical reactions 429
— and I. Ciocăzanu, The alkaline hydrolysis of the methyl acetate and of the

ethyl acetate. II. Rate constants and activation energies from thermochemical data 561

— und I. Găinar, Das thermodynamische Verhalten des Gasgemisches Argon-Kohlendioxid 695

— und E. Lucinescu, Assoziationslösungen. I. (Essigsäure, Wasserlösungen) 283

— and C. Misdolea, Excess thermodynamic functions of some metal-metal salt systems in the molten state. . . . 1353

Vlagiu I., Radiokhimicheskaia polimerizatsia akrilonitrila v tverdoi fase . . 767

— voir Murgulescu I. G. . . 411, 1081

Vodnár I., Decomposition of hydroperoxides on activated kaolins. I. Decomposition of cumene hydroperoxide on activated Chinese kaolin treated with sulphuric acid. 803

Voicu M. and F. Badea, Kinetics of the acetolysis of 1:2, 5:6-dibenzocyclohepta-1, 3, 5-trienyl-7-ethyl β-tosilate . . . 929

Voinescu V. and A. Balog, Some isolated mixed anhydrides of 2, 6-dimethcxybenzoic acid 951

Voloşniuc-Birou M., voir Macarovici Const. Gh. 1231

Z

Zabdyr L., voir Ptak W 851

Zămârcă Şt. and I. Ganovici, L. Ganovici, Evidence of the ternary miscibility gap in indium-aluminium-silver system by viscosity measurements 173

— and L. Ganovici, I. Ganovici, Self-diffusion of indium in liquid indium-aluminium alloys 35

Zamfir I. et C. N. Ţurcanu, Le marquage par échange isotopique de la thioacétamide et du 6-méthyl-2-thiouracile avec ^{35}S 339

Zanker V., voir Mantsch H. N. . . . 125

Zsakó J., voir Várhelyi Cs. 1133

Zugrăvescu I., voir Chiriac C . 763, 1263

— voir Petrovanu M. 1153

— Stoicescu-Crivetz L. 659

INDEX DES SUJETS

A

Acetoacetanilides. II., I. I. Bădilescu 395

Acridine-N-oxide, π-Electronic structure of-, H. H. Mantsch, W. Seiffert and V. Zanker 125

Acridine-N-oxide, The mass spectrum of-, H. H. Mantsch 549

Acrilonitrila, Radiokhimicheskaia polimerisatsia-, I. Vlagiu 767

Acrylonitrile, Photopolymerisation of-, D. Feldman, V. Nuţă and Cr. Simionescu 1407

Acrylonitrile, Polymérisation mixte de l'-, I. G. Murgulescu et I. Vlagiu . . 1081

1-Acyl-4-Aryl-Thiosemikarbazide. II., R. Crăciuneanu und E. Florean . 753

3-Acyloxysteroide, F. Hodoşan und A. Pop-Gocan 1441

Addition des philodiènes sur la phtalazine. III. L'-, M. Petrovanu, A. Sauciuc, I. Gabe et I. Zugrăvescu 1153

Agitateurs à rame, La puissance des-, Em. A. Bratu et L. Baraf 1445

Akridin, Tetraphenylborate des -s, I. Florea 745

1-Alcoyl-3, 5-bis-(p-dialcoylamino-benzyliden)-4-pipéridones, C. Greff et S. Moldoveanu 389

Alkaline hydrolysis of the methyl and ethyl acetates. I., II, R. Vîlcu and I. Ciocăzanu 429, 561

Alkoholdehydrogenierung an Kupferkatalysatoren, A. A. Balandin, I. Horescu und A. P. Rudenko 619

Anodic oxidation of methanol, O. Radovici and N. Totir 23

Anticancer agents. VI., Potential-, I. Niculescu-Duvăz, V. Feyns, V. Savaniu, M. Ionescu, A. Şerban and A. Cambanis 535

Aromaticity. VI., A. T. Balaban . . . 1323

Assoziationslösungen. I., R Vîlcu und E. Lucinescu 283

Atebrin, Hexazyanoferrat und Nitrosopentazyanoferrat des — s, I. Florea . . 893

6-Azauracil derivatives. VII., C. Cristescu and V. Badea 135

6-Azauracil derivatives. VIII., C. Cristescu and M. Lăzărescu 797

Azlactones of the phenothiazine series. III., C. Bodea, I. Oprean and V. Fărcăşan 673

Azo-derivate complexes of chromotropic acid with barium. I., II., V. Armeanu and I. Drăguşin 1367, 1511

B

Benzoyl chloride and normal alcohols, Reactions between —, I. G. Murgulescu and I. Demetrescu 149

Benzyl-chloride and alkali acoxides, Reactions between —, I. G. Murgulescu, D. Oancea and G. Mincu 3

Binary mixtures, The Heat of melting —, D. I. Marchidan and Cr. Telea. . 1361

Binary molten salts mixtures, Heat of mixing in the —, D. I. Marchidan and Cr. Telea 1495

Bismuth, Basic permanganates of —, C. Drăgulescu, I. Julean and A. Nimară 189

C

Calorimetric determination of chemisorption heat, I. G. Murgulescu and M. I. Vass 1201

Carbonium ion reactions. V., E. Cioră-nescu, M. Banciu, R. Jelescu, M. Rentzea, M. Elian and C. D. Nenitzescu 911

Carboxylate surface species during the chemisorption of CO, CO_2 and simple organic oxygen compounds on γ-alumina, Formation of —, P. Fink 811

Catalyseur Cr_2O_3-Al_2O_3, M. Spinzi et I. V. Nicolescu 629

Catalyseurs oxyde de chrome-alumine-potassium, I. Olaru, H. Charcosset, Y. Trambouze et M. Prettre . . . 235

Catalyseurs solides pour l'oxydation des hydrocarbures. II, A. Sfinzi et I. V. Nicolescu 903

Chemisorption an vorbelegten Kupferschichten, I. G. Murgulescu und G. Comşa 825

Chlorure de polyvinyle. I, I. Poinescu 373

Chronopotentiometric determination of silver ion, S. Sternberg and C. Herdlicka 991

Cinétique de la formation des couches d'oxydes, D. Cismaru et Z. Simon . . . 837

Combinaisons complexes avec des hydroxyacides. VII, Const. Gh. Macarovici et L. Czeglédi 57

Combinaisons complexes avec des hydroxyacides. VIII, Const. Gh. Macarovici et E. Perţe 1113

Combinaisons complexes avec des hydoxyacides. IX, Const. Gh. Macarovici et M. Voloşniuc-Birou 1231

Complex combinations with diphenylic derivatives. XXIII., Const. Gh. Macarovici and R. Micu-Semeniuc 357

Complex combinations with piperazine, Gr. Popa and V. Magearu 1387

Complex combinations with n-propylamine, Gr. Popa and V. Magearu 879

Complexes de Zn(II), Cd(II), Co(II), et Ni(II) avec la di-i-propylamine, V. Magearu et Gr. Popa 1399

Condensation with 2-methyl-cyclohexanone, The Stobbe —, A. M. El-Abbady, M. El-Ashry and S. H. Doss 265

Conductivity of solutions of hydrobromic acid in normal alcohols, I. Demetrescu 1225

Copper phthalocyanine solutions, Radiolysis of-, E. Tărăbăşanu-Mihăilă and E. Sofronie 1467

Corrosion of iron in HCl solutions, Action of lauril-amine on the-, O Radovici and E. Roman 423

Cyclobutadienes, The electronic structure of substituted-, M. D. Gheorghiu and R. Hoffmann 781

Cyclobutane series. XX., Investigations in the-, M. Avram, Gh. D. Mateescu and C. D. Nenitzescu 101

Cyclobutanreihe. XXI., M. Avram, I. G. Dinulescu, Gh. D. Mateescu, E. Avram und C. D. Nenitzescu 1181

Cyclobutanreihe. XXII., M. Avram, I. G. Dinulescu, Gh. D. Mateescu und C. D. Nenitzescu 1191

Cylindrical trap, A new all walls cooled-, M. I. Vass 809

D

Décomposition catalytique de l'eau oxygénée, D. Crăciunescu et A Fruma 653

Décomposition de l'hydrazine sur des couches minces de germanium, D. Fătu et E. Segal 183

Décomposition thermique de certaines combinaisons complexes du chlorure de cuivre avec la pyridine, D. Fătu, S. Fătu et E. Segal 1107

Décomposition thermique de certaines combinaisons complexes du chlorure de manganèse avec la pyridine, D. Fătu et E. Segal 709

Dilituric acid. II., Molecular orbital studies on -, R. Nutiu and Z. Simon 311

3α, 6α-Dihydroxy-5β-etianic acid, F. Hodoşan and N. Şerban 399

2,6-Dimethoxybenzoic acid, Mixed anhydrides of-, V. Voinescu and A. Balogh 951

Dimethoxy-10-methyl-acridones, M. Ionescu and I. Meşter 789

α-Dioximinkomplexe der Übergangsmetalle. XXVI, F. Mánok, Cs. Várhelyi und Z. Kiss-Rajhona 1251

D.T.A., electrical conductivity and activity of some Bi_2O_3-MoO_3 catalysts, A. Popescu, E. Segal, A. Ionescu and A. Szabo 79

E

Echange isotopique de la thioacétamide, Le marquage par —, I. Zamfir et C.N. Ţurcanu 339

Eisen (III), Kolorimetrische Bestimmungsmethode des —s, Al. Şuteu, T. Hodişan und F. Kormos 1613

Electric moment of dilituric acid, R. Nuţiu, L. Kurunczi and Z. Simon. 1435

Electrical conductivity of lyophilic colloids. X., E. Angelescu and M. Radu. . . 441

Electrode processes, Kinetics of —, I. H. Plonski 569

Electrodes de carbone, Processus eaux —, D. Dumas et J. Brenet 1339

Electrodeposition of zinc from pyrophosphate solutions. I., O. Radovici and C. Vass 1099

Electronic ground states of *o*-, *m*- and *p*-benzynes, M. D. Gheorghiu and R. Hoffmann 947

Electronic spectra of Co(III) halogeno pentaamines, V. E. Sahini and L. Telea 157

Electronic spectra of the monosubstituted naphthalenes, V. E. Sahini and C. I. Ghirvu 275

Electronic spectra of some aromatic metal ketyls, V. E. Sahini and L. Ciurea. . 1093

Electronic transition in aromatic ketones, On the n → π* —, V. E. Sahini and Al. Butucelea 981

ESR spectra of some aromatic metal ketyls, V. E. Sahini and L. Ciurea. 689

Étard reaction. VIII., A. Ghenciulescu, I. Necşoiu, M. Rentzea and C. D. Nenitzescu 1543

Étard reaction. IX., A Ghenciulescu, I. Necşoiu, and C. D. Nenitzescu. . . . 1553

Étard reaction. X., V. Psemeţchi, I. Necşoiu, M. Rentzea and C. D. Nenitzescu 1567

2-Etoxy-6,9-diaminoacridine, I. Florea 365

Excess thermodynamic functions, R. Vîlcu and C. Misdolea 1353

F

Force constants of PH^{+}_{4}(Td), The-, V.E. Sahini and A. O. Fulea 17

Free radicals from nitrophenyl – alkoxyamines, Synthesis of-, A. T. Balaban, M. Frangopol, N. Negoiţă, P. T. Frangopol and P. Paraschiv 941

Free radicals. IV., Stability and equilibria of-, P. T. Frangopol, M. Frangopol, N. Negoiţă and A. T. Balaban . . 385

Fused silver iodide and potassium chloride, S. Sternberg and L. Bejan. 303

G

Gallosilicat-Niederschläge in wäßrigen Lösungen, R. Ripan und M. Kulcsár-Nováková 717

H

Hétérocycles. XII, I. Simiti, L. Proinov et H. Demian 1285

Heterocycles. VIII. Methylene bases of -, Gh. Ciurdaru and V. Dénes . . . 1063

Heterocyclic organoboron compounds. XI., A. Barabás, E. Işfan, E. Romaş and A. Trestianu 253

Heteroorganische Verbindungen. XXXVI., L. Almasi, A. Hantz und E. Hamburg 495

Heteropolyanion, Basizität des $[PV_{12}O_{36}]^{7-}$, R. Ripan und V. Cordiş 197

Heteropolymere, Ultrarotspektroskopie von-, I. Gabe, E. Măntăluţă und G. Neamţu 1163

Hexacyanocobaltiates, Structure des-, P. Tribunescu et M. Cristea . . . 463

Hydroacridine. I., N. Bărbulescu und F. Potmischil 1427

Hydrogen bonds. II., S. Bădilescu and I. I. Bădilescu 329

Hydrogen overvoltage on thin evaporated metal films. I., O. Radovici and M. Macovschi 159

Hydrolyse acide de l'acétate de *n*-butyle, L'-, G. Costeanu, O. Landauer et C. Mateescu 845

Hydroperoxides on activated kaolins. I., Decompostion of-, I. Vodnár 803

I

Indium fondu, La densité et la viscosité de l'-, L. Ganovici et I. Ganovici . . . 1011

Intensity of spin-forbidden absorption band of $[Co(NH_3)_6]^{3+}$, V. E. Sahini and V. Tufoi 557

Ionic liquids, Viscous flow in-, Gh. Vasu 167

Isotopic exchange of active methyl hydrogens. VI., E. Gârd, I. Stănoiu, A. T. Balaban and F. Chiraleu 247

K

Kadmiumsalze einiger Dicarboxysäuren, Fr. Mihai, M. Moraru and Gr. Pop. . 637

Kinetics of solvolytic reactions, M. Voicu and F. Badea 929

Komplexverbindungen des N,N'-Diaminopiperazins. 1., 2., 4., J. Dick und A. Lupea 1047, 1143, 1377

Komplexverbindungen des N,N'-Diaminopiperazins. 3., J. Dick, A. Lupea und Z. Szabadai 1241

Komplexverbindungen der Pirazolonreihe. V., J. Dick und A. Maurer 1603

Koordinationspolymere mit bis(Aminocarboxylsäure). I., I. Gabe und D. Leonte 1535

L

Lanthanide halogenoacetates, Complex of -, P. Spacu and E. Antonescu 201

Ligand field theory for noncubic symmetries, J. Máthé 1003

Light scattering and viscosity measurements on unfractionated polyvinyl chloride, A. Lupu, L. Nasta, I. Baltog and B. Brăileanu 469

M

Membranen. II., Gleichrichtungseigenschaften der heterogenen -, C. Liteanu und G. Rădulescu 1257

Metallkomplexe der Phenyl-glycin-Orthocarbonsäure. II., C. Drăgulescu, R. Pomoje, I. Menessy, P. Pîrlea und C. Mihăescu 1595

Methylhyodesoxycholate, Derivatives of -, F. Hodoşan, N. Şerban and V. Ciurdaru 1303

Modèle du gaz électronique bidimensionnel dans la chimisorption sur métaux, E. Segal 45

Molten salts, Physico-chemical properties of simple -, I. G. Murgulescu 965

Monopyridine complexes, X-ray studies on -, D. Manolescu, and E. Segal . . . 999

N

Natriumalkoxide und α-Halogenketonen. VI., Reacktion zwischen -, L. Szotyori, L. Fey und A. Abraham 1623

Niobium (V) in hydrochloric acid – thiocyanate medium, Polarographic reduction of -, C. Drăgulescu, S. Marchidan and Gh. Facsko 737

Niobium (V), Polarography of -, C. Drăgulescu, S. Marchidan and Gh. Facsko 1501

Nitrates métalliques en mélanges de solvants. II, R. Ripan, I. Eger et N. Bojan . 353

Nitroethylbenzene mixtures, *Ortho-* and *para-* —, L. Fey and J. Rusu 613

O

Octanesultone, M. Ionescu and M. Văgăonescu 517

Octylation of the aromatic nucleus with $AlEt_2Cl$-RCl catalysts, I. V. Nicolescu and O. Şerban 87

Osmotic pressure, Equations and interpretation of -, D. A. Totoescu 345

Oxalyl anionic radical ($C_2O_4^{\cdot -}$), The stability of -, Z. Simon 705

α-Oximinoalkylbenzenes. I., II., III., L. Fey and N. Bodor 225, 319, 481

Oxydation du Fe et du Ni à hautes températures, D. Cismaru et E. Dobroghiu 985

Oxidation of soja oil, The role of ions Cr^{5+} in the catalytic -, J. Siecowski and J. Sliwiok 95

Oxidation of tungsten at high temperatures, The -, D. Cismaru and A. Geangu-Moisin 29

Oxidation of zirconium at high temperatures, D. Cismaru and E. Dobroghiu . . 291

Oxygen chemisorption and electrical resistance, I. G. Murgulescu and N. I. Ionescu 1073

Oxygen chemisorption on T.C.R. of copper films, Effect of -, I. G. Murgulescu and N. I. Ionescu 681

P

Phenothiazine, The action of ammonia on some nitroderivates of -, A. Turcu and M. Răileanu 1579

Phenothiazine glycosides. II., T. Bodea, V. Fărcăşan and T. Panea 523

Phenothiazone. XVI., C. Bodea und E. Broser 1617

Phenothiazone-(3). I., Volimetric dosage with -, M. Răileanu and E. Dobre 887,1053

γ-Phenoxybutyric acids, Chloro-substituted-, I. I. Bădilescu 1585

Pirani manometer, M. I. Vass 955

Platinum electrode surfaces. II., Pretreated -, L. Kékedy and F. Makkay 605

Platinum indicating electrode, C. Liteanu and I. Haiduc 1039

Polyesters and polycarbonates, Linear -, A. Petruş, L. Mândăşescu and I. Matei 773

Polymères — analogues du copolymère binaire acrylonitrile-acétate de vinyle, Réactions -, N. Asandei et A. Liga 1419

Polymères organiques phosphorylés. II, Fl. Popescu 1525

Polymers, Electrical conduction mechanisms in -, Th. Deleanu and N. Georgescu 1269

Polymérisation de certains dérivés acétyléniques. I, Cr. Simionescu et Kim Tal Hen 1519

Polymérisation radiochimique de l'acrylonitrile, I. G. Murgulescu et I. Vlagiu 411

Polymerisation of 1,3-butadiene. I., II., Stereospecific -, I. Velea, V. Dimonie, E. Melega, P. Blenke and V. Provinceanu 473, 667

Poly (1,3,4-oxadiazoles). V., L. Stoicescu-Crivetz, M. Brumă et I. Zugrăvescu 659

Polypyrazoles. III, C. Chiriac, L. Stoicescu-Crivetz et I. Zugrăvescu 1263

Polypyrazoles-esters, C. Chiriac, L. Stoicescu-Crivetz and I. Zugrăvescu . . 763

Propriétés magnétiques des quelques tartrates, V. Bednar, V. Mincu et H. Bednar 1149

Pyrylium salts, Chemical shifts of methyl protons in -, G. V. Boyd and A. T. Balaban 1575

Pyrylium salts formed by diacylation of olefines. XIX., A. T. Balaban 1331

Pyrylium salts with nucleophiles. VIII., Reaction of-, A. B. Susan and A. T. Balaban 111

Q

o-Quinones, Oxidation of pyrocatechol derivatives to -, A. T. Balaban 1281

R

Radicaux libres stables diarylazote, P.T. Frangopol, M. Frangopol, N. Negoiţă et E. Romaş 527

Radioactive minerals leaching processes, F. Bunuş, I. Matei, C. Matyas, S. Neciu, V. Sporea and S. Tătaru 729

Raman spectra of beryllium oxalate complexes, R. Beldie and V. E. Sahini 419

Refractivity and boiling point of phosphines, M. Arschad A. Beg 503

RES, Etude du $H_5[PW_{10}V_2O_{40}]$ par la méthode-, A. Şuteu et Gh. Cîrstea . . . 209

Röntgenographic study on the compound $[HP(C_6H_4-CH_3)_3]_2[CoCl_4]$, R. Meraru and M. Negoiu 1027

S

Self-diffusion of indium, Şt, Zămârcă, L. Ganovici and I. Ganovici 35

Solvent effect on the spectra of ketones, V. E. Sahini and M. Olteneanu . 831

Solubilité de l'oxyde de zirconium, L. Popa et I. Arsenie 217

Spectrophotométrie des systèmes $LnCl_3$-rouge acide AV et $LnCl_3$-calcon, P. Spacu et S. Ploştinaru 591

Spektrophotometrische Methode von Jazimirskij, Über die-, A.-C. Banciu . 1019

Spolimerov struktury s obrazovanykh reliefnykh izobrazhenii, N. K. Frunze . 1309

Standard potential of thin cadmium films, I. G. Murgulescu and I. Vartires 1479

Steroidalkoholen mit Acetylnitrat, Veresterungsreaktion von -, O. Mantsch und N. Bodor 1295

Steroidal nitrate esters. III., F. Hodoşan and F. Teodor 509

Steroide in adsorbiertem Zustand. III., F. Hodoşan und I. Jude 1057

Steroids in the adsorbed state. II., F. Hodoşan and N. Şerban 121

Substitution reactions of complexes. XIV., Cs. Várhelyi, Z. Finta and J. Zsakó 1133

Suhrmann-Wedler equation, On a -, N. I. Ionescu 869

T

Thermodynamik des Gasgemisches Argon-Kohlendioxid, Die —, R. Vîlcu und I. Găinar 695

Thermodynamic properties of Zn-Bi-Pb liquid solutions, W. Ptak, Z. Moser and L. Zabdyr 851

$TiCl_4$-carotenoid complexes. III., IV., V., VI., A. Tămaş and C. Bodea 141, 405, 959, 1591

Titan, Bestimmung des -s, R. Ripan und T. Budiu 1631

Titan (IV), Extraktion von -, C. Drăgulescu, T. Simonescu und H. Schiff 583

Titan, Kolorimetrische Bestimmung des -s, Const. Gh. Macarovici und C. Stanisav 459

Titanium and alloys, Electro-chemical behaviour of -, O. Radovici and S. Ciolac 297

Triphenylchlorid mit Alkoholen, Die Reaktion des -, I. G. Murgulescu and C. Potmischil 1335

U

Unsaturated end groups in PVC. I., A. A. Caraculacu and E. C. Bezdadea . . 1171

Uranium, Adsorption de l'uranium, S. Tătaru, Gh. Filip et B. David . . . 599

Uranium content determinations, F. Bunuş, and I. Matei 333

V

Vanadates. XVI, I. Lukács, C. Strusievici et C. Liteanu 647

Vanadates. XVII, I. Lukács, C. Strusievici, D. Lupu, C. Mirel et C. Liteanu 1125

Viscosity of indium-aluminium-silver system, Şt. Zămârcă, I. Ganovici and L. Ganovici 173

Viscosity of the molten InBi compound, N. Petrescu 67

W

Wärmeübergangszahlen von Ammoniumnitratlösungen, Z. Gropşianu, D. Kohn und A. Iovi 451,

Wärmeübergangszahlen beim Sieden von Lösungen. I., II., III., Z. Gropşianu, D. Kohn und A. Iovi 721, 873, 1031

Wasserstoffchemisorption auf an Aluminiumoxid aufgetragenem Platin, D. Cismaru and Al. Fruma 1489

Z

Zirconium, Sels nucléaires de -, L. I. Popa, V. Dorobanţu, D. Dorcioman, S. Constantinescu et M. S. Popa . . . 1457

Zeolites in molten salts media, The behaviour of -, S. Sternberg and A. Cerbu . . 1215

1970 FEB 12

TRAVAUX PARUS AUX ÉDITIONS DE L'ACADÉMIE DE LA RÉPUBLIQUE SOCIALISTE DE ROUMANIE

CORNEL BODEA et collab., **Tratat de biochimie vegetală**, partea I, **Fitochimie** (Traité de biochimie végétale, Ire partie, Phytochimie), Ier vol., 1964, 747 p. + 4 annexes + 2 pl., 41 lei ; IIe vol., 1965, 1262 p., 1 pl., 56 lei ; IIIe vol., 1967, 773 p., 35 lei.

V. GHEȚIE et V. MICUȘAN, **Analiza imunochimică. Teorie și practică** (Analyse immunochimique. Théorie et pratique), 1966, 369 p., 28 lei.

SILVIA IONESCU, **Reacții chimice induse de radiațiile ionizante** (Réactions chimiques produites par les radiations ionisantes), 1963, 271 p., 15 lei.

MARIETA NICOLAE, **Fizico-chimia proceselor fotografice** (Physico-chimie des processus photographiques), 1964, 426 p. + 4 pl., 35 lei.

R. PORTOCALĂ et L. POPA, **Acizii ribonucleici celulari și virali** (Les acides ribonucléiques cellulaires et viraux), 1966, 375 p. + 8 pl., 26 lei.

D. PURDELA et R. VÎLCEANU, **Chimia compușilor organici ai fosforului și ai acizilor lui** (La chimie des composés organiques du phosphore et de ses acides), 1965, 540 p., 37 lei.

CRISTOFOR SIMIONESCU, MARGARETA GRIGORAȘ et AGATA CERNĂTESCU-ASANDEI, **Chimia lemnului din R. P. R.** (La chimie du bois en Roumanie), 1964, 239 p. + 6 pl., 27 lei.

CRISTOFOR SIMIONESCU et CLEOPATRA VASILIU-OPREA, **Mecanochimia compușilor macromoleculari** (La mécanochimie des composés macromoléculaires), 1967, 344 p., 23,50 lei.

I.P. ,,INFORMAȚIA'' – c. 8927

43 436

Lei 15